

OXFORD PSYCHOLOGY SERIES NO. 29

Binocular Vision and Stereopsis

IAN P. HOWARD

BRIAN J. ROGERS

BINOCULAR VISION AND STEREOPSIS



OXFORD PSYCHOLOGY SERIES

Editors

Nicholas J. Mackintosh
Daniel Schacter
Anne Treisman

James L. McGaugh
Timothy Shallice
Lawrence Weiskrantz

1. *The neuropsychology of anxiety: an enquiry into the functions of the septohippocampal system*
Jeffrey A. Gray
2. *Elements of episodic memory*
Endel Tulving
3. *Conditioning and associative learning*
Nicholas J. Mackintosh
4. *Visual masking: an integrative approach*
Bruno G. Breitmeyer
5. *The musical mind: the cognitive psychology of music*
John Sloboda
6. *Elements of psychophysical theory*
Jean-Claude Falmagne
7. *Animal intelligence*
Edited by Lawrence Weiskrantz
8. *Response times: their role in inferring elementary mental organization*
R. Duncan Luce
9. *Mental representations: a dual coding approach*
Allan Paivio
10. *Memory, imprinting, and the brain*
Gabriel Horn
11. *Working memory*
Alan Baddeley
12. *Blindsight: a case study and implications*
Lawrence Weiskrantz
13. *Profile analysis*
D. M. Green
14. *Spatial vision*
R. L. DeValois and K.K. DeValois
15. *The neural and behavioural organization of goal-directed movements*
Marc Jeannerod
16. *Visual pattern analyzers*
Norma V. Graham
17. *Cognitive foundations of musical pitch analysis*
C. L. Krumhansl
18. *Perceptual and associative learning*
G. Hall
19. *Implicit learning and tacit knowledge*
A. S. Reber
20. *Neuromotor mechanisms in human communication*
D. Kimura
21. *The frontal lobes and voluntary action*
R. E. Passingham
22. *Classification and cognition*
W. Estes
23. *Vowel perception and production*
B. S. Rosner and J. B. Pickering
24. *Visual stress*
A. Wilkins
25. *Electrophysiology of mind*
Edited by M. Rugg and M. Coles
26. *Attention and memory: an integrated framework*
N. Cowan
27. *The visual brain in action*
A. D. Milner and M. A. Goodale
28. *Perceptual consequences of cochlear damage*
B. C. J. Moore
29. *Binocular vision and stereopsis*
I. P. Howard and B. J. Rogers

Binocular Vision and Stereopsis

Ian P. Howard

*Centre for Vision Research
York University*

Brian J. Rogers

*Department of Experimental Psychology
Oxford University*

OXFORD PSYCHOLOGY SERIES
NO. 29

New York Oxford
OXFORD UNIVERSITY PRESS • CLARENDON PRESS
1995

Oxford University Press

Oxford New York
Athens Auckland Bangkok Bombay
Calcutta Cape Town Dar es Salaam Delhi
Florence Hong Kong Istanbul Karachi
Kuala Lumpur Madras Madrid Melbourne
Mexico City Nairobi Paris Singapore
Taipei Tokyo Toronto
and associated companies in
Berlin Ibadan

Copyright © 1995 by Oxford University Press, Inc.

Published by Oxford University Press, Inc.,
198 Madison Avenue, New York, New York 10016

Oxford is a registered trademark of Oxford University Press, Inc.

All rights reserved. No part of this publication may be reproduced,
stored in a retrieval system, or transmitted, in any form or by any means,
electronic, mechanical, photocopying, recording, or otherwise,
without the prior permission of Oxford University Press.

Library of Congress Cataloging-in-Publication Data
Howard, Ian P.

Binocular vision and stereopsis/
Ian P. Howard, Brian J. Rogers.

p. cm. Includes bibliographical references and index.
ISBN 0-19-508476-4
1. Binocular vision. 2. Depth perception.
I. Rogers, Brian J. II. Title.
QP487.H68 1995 612.8'4—dc20 94-45728

9 8 7 6 5

Printed in the United States of America
on acid-free paper

Acknowledgments

We are specially grateful to Antonie Howard for her careful editing of the whole book. We thank Christopher Tyler for his critical reading of eight chapters and the following people for making useful comments on particular chapters, Richard Abadi, Peter Bishop, Gregory DeAngelis, Casper Erkelens, Ralph Freeman, Stuart Judge, Suzanne McKee, Robert O'Shea, Izumi Ohzawa, Hiroshi Ono, Jack Pettigrew, David Regan, Arnulf Remole, Nicholas Wade, Roger Watt, and Jeremy Wolfe. Our thanks are also due to Mark Bradshaw for creating many of

the random-dot stereograms, to Rachel Christophers for help in editing, to Mark Bradshaw, Rita Fanfarelli, and Alan Ho for preparing figures and to Teresa Manini for secretarial help. We are also grateful for many invaluable discussions with members of our respective vision groups at York and in Oxford and to the speakers and participants at the Advanced Workshop on Stereoscopic Vision and Optic Flow in June 1993 for sharing their most recent research findings.

This page intentionally left blank

Contents

Chapter 1	Introduction.....	1
Chapter 2	Binocular correspondence and the horopter.....	31
Chapter 3	Sensory coding.....	69
Chapter 4	The physiology of binocular vision.....	105
Chapter 5	The limits of stereoscopic vision.....	149
Chapter 6	Matching corresponding images.....	195
Chapter 7	Types of disparity	235
Chapter 8	Binocular fusion and rivalry.....	313
Chapter 9	Binocular masking and transfer	349
Chapter 10	Vergence eye movements	381
Chapter 11	Stereo constancy and depth cue interactions	427
Chapter 12	Depth contrast and cooperative processes	461
Chapter 13	Spatiotemporal aspects of stereopsis.....	535
Chapter 14	Vision in the cyclopean domain.....	585
Chapter 15	Development and pathology of binocular vision.....	603
Chapter 16	Binocular and stereoscopic vision in animals.....	645
References		658
Subject Index.....		732

This page intentionally left blank

BINOCULAR VISION AND STEREOPSIS

This page intentionally left blank

Introduction

1.1 General introduction	1
1.1.1 About the book	1
1.1.2 Binocular vision and stereopsis	2
1.1.3 Types of binocular stimuli and processes	2
1.1.4 Cyclopean procedures	3
1.2 Historical background	4
1.2.1 History of physiological optics and vision	4
1.2.2 History of ideas of stereoscopic vision	13
1.3 Stereoscopic Techniques	24
1.3.1 Types of stereoscope	24
1.3.2 Three-dimensional imagery	26
1.3.3 Autostereograms	26

1.1 GENERAL INTRODUCTION

1.1.1 About the book

This book is a survey of knowledge about binocular vision, with an emphasis on its role in the perception of a three-dimensional world. Our primary interest is biological vision, we mention machine vision and computational models only where they contribute to an understanding of the living system. Clinical material is reviewed insofar as it throws light on normal functioning.

When a key term is first introduced and defined it is printed in bold type. The pages on which we define key terms are printed in bold in the subject index, which serves as a glossary. The page numbers where references are mentioned are entered in italics in the reference list at the end of the book. This list serves as the author index. Throughout the book we suggest experiments we think could decide theoretical issues. These suggestions are printed in italics.

The stereograms presented in this book can be fused with the aid of the stereoscope provided. For readers using free fusion, the stereograms may be fused by diverging or converging the eyes. For many demonstrations it does not matter whether the eyes converge or diverge, and only one stereogram pair is provided. When the effect depends on the sign of disparity, two stereogram pairs are provided—one pair for readers who prefer to converge the eyes and the other for readers who prefer to diverge. Sometimes we ask readers to attend to both the fused

image created by convergence and that created by divergence, to experience the effects of a change in the sign of disparity.

In learning to free fuse it helps if the eyes are converged on a pencil point held at the correct distance between the stereogram and the eyes. Some people find the correct vergence angle more easily when they look through a piece of transparent plastic with grid lines. For divergence, one may place a piece of clear plastic over the stereogram and fixate the reflection of a point of light seen beyond the plane of the stereogram. The correct distance can be found by observing how the images of the two pictures move toward each other as the pencil or sheet of plastic is moved in depth. After some practice, readers will find that they can converge or diverge by the correct amount without an aid. Note that when two dichoptic pictures are free fused, one sees a monocular version of each picture on either side of the fused image. The presence of three pictures confirms that correct vergence has been achieved. Free fusion is a skill well worth acquiring, since it is often the only way to achieve fusion with displays presented at vision conferences.

Previous books on stereopsis and binocular vision include Ogle (1964), Ogle et al. (1967), Julesz (1971), Gulick and Lawson (1976), Solomons (1978), and Regan (1991). Books on vergence and binocular vision include Noorden (1990) and Schor and Ciuffreda (1983). Reviews of stereopsis and binocular vision have been provided by Arditi (1986), Tyler (1983, 1991), and Patterson and Martin (1992).

1.1.2 Binocular vision and stereopsis

Strictly speaking, all animals with two eyes have binocular vision. Even animals with laterally placed eyes are able to integrate the information from the two eyes and almost all animals have some region of binocular overlap. But the term “**binocular vision**” is usually reserved for those animals who possess a large area of binocular overlap and use it to code depth. In addition to its role in depth perception, binocular vision provides some other advantages. Performance on basic visual tasks such as detection, resolution, and discrimination is slightly better with both eyes open (see Section 9.2.1). Many complex visual tasks, such as reading, detecting camouflaged objects, and eye-hand coordination are also performed more effectively with two eyes than with one, even when the visual display contains no depth (Jones and Lee 1981; Sheedy et al. 1986). Ballistic prehensile movements of the hand toward binocularly viewed targets show shorter movement times, higher peak velocities, and more accurate final position than those towards monocularly viewed targets, with monocular cues to distance present (Servos et al. 1992). Binocular vision confers some advantage when available during only the planning stage of the motion or only the execution stage (Servos and Goodale 1994). Convergence of the two visual axes on an object of interest helps us attend to the fixated object and disregard objects lying nearer or further away (see Section 12.5).

The term “**stereoscopic vision**” means literally, “solid sight” and refers to the visual perception of the three-dimensional structure of the world, when seen by either one eye or two. Monocular cues to depth include differential focusing, perspective, image overlap, shading, and motion parallax. There are two exclusively binocular cues to depth—the vergence position of the eyes and binocular disparity. Binocular disparity, or binocular parallax, is the difference in the positions and shapes of the images in the two eyes due to the different vantage points from which the eyes view the world. The term “**binocular stereopsis**” is often used for the impression of depth arising from binocular cues. Unless otherwise specified we use the term “**stereopsis**” for the impression of depth arising from binocular disparity.

Stereopsis greatly enhances the ability to discriminate differences in depth. Under the best conditions we can detect the depth between an object and a fixated object when the disparity between the images of the nonfixated object is 2 to 6 arcsec, in angular terms. We will see in Chapter 13 that the only monocular cue providing this degree of precision is

that of monocular motion parallax created by moving the head from side to side. Binocular disparity and monocular parallax are closely related, since the successive views obtained by moving the head from side to side through the interocular distance provide the same information as the simultaneous views obtained by the two eyes with the head stationary. Binocular stereopsis does not necessarily aid in the performance of all depth-related tasks. For instance, the task of recognizing a familiar shape when it is rotated to very different orientations in three-dimensional space may be performed just as well by people who lack binocular stereopsis as by people with normal vision (Klein 1977).

We will see in Chapter 16 that the eyes of some animals have a fixed angle of vergence. For these animals, the magnitude of the disparity between the images of an object is an invariant function of the distance of the object from the point of convergence. Since the convergence distance is fixed, disparity has a fixed scaling with respect to the absolute distance of the object from the eyes. The ability to judge depth on this basis is referred to as **range-finding stereopsis**, since it works like a range finder. The eyes of humans and many other animals change their angle of vergence so that the two visual axes intersect on the object of particular interest. The images of the fixated object have zero disparity. The disparity in the images of an object at another distance has a sign that depends on whether the object is nearer or further away than the fixated object and a magnitude that is proportional to its depth relative to the fixated object. Disparity therefore provides information only about the relative depth between the two objects and not about the distance of either object from the viewer. For isolated objects, absolute depth must be indicated by information other than disparity. We will see in Section 7.6.7 that the pattern of disparity over an extended surface provides information about the absolute distance of the surface, even when no other information is available. The absolute disparity between the images of a particular object or between the retinal images as a whole controls vergence movements of the eyes. However, as we emphasize throughout the book, the perception of depth does not depend on absolute disparities but rather on patterns of relative disparity over surfaces or between sets of objects.

1.1.3 Types of binocular stimuli and processes

Several terms referring to binocular vision are in common use, but their meanings vary from author to author. The terms “**binocular vision**” and “**stereoscopic vision**” have already been defined.

The **binocular visual field** is that part of the visual field common to both eyes. A **binocular stimulus** is one seen by both eyes at the same time or by the two eyes in rapid succession. There are two basic types of binocular stimulus—dioptic and dichoptic. A **dioptic stimulus** is a single distal stimulus seen by both eyes. Although a dioptic stimulus may produce distinct retinal images in the two eyes, because of the different positions of the eyes, we will assume that a dioptic stimulus produces identical monocular images. **Dichoptic stimuli** are distinct distal stimuli, one presented to one eye and one to the other, over which an experimenter has separate control. Dichoptic displays are typically created in a stereoscope, but they can also be created by placing different optical devices, such as prisms or filters, before the eyes. The images of distinct objects fused by diverging or converging the eyes are also dichoptic images.

A binocular visual process is any process in the visual system engendered by stimuli arising in the two eyes. We distinguish three levels of binocular processing. The simplest is **interocular judgments** in which a person compares stimuli received in different eyes. For instance, one may compare the length of a line seen by one eye with the length of a line seen by the other eye. In this type of binocular processing, one stimulus is not affected by the other—the stimuli do not interact, they are simply compared. The task is essentially the same when both stimuli are presented to the same eye, so that binocular processing is not essential to its performance.

The second level comprises processes that are **not exclusively binocular**. This type of process occurs when dichoptic stimuli in the binocular field interact to generate a distinct visual impression not evident when either stimulus is viewed alone, but is evident when the two stimuli are combined in the same eye. For instance, in the Poggendorff illusion, collinear oblique lines appear non-collinear when a pair of vertical lines is placed between them. This illusion is evident when the oblique lines are presented to one eye and the parallel lines to the other. Thus, the dichoptic form of the illusion depends on processes occurring after the inputs from the two eyes are combined, that is, on central processes. The illusion is also evident, however, when the parts of the illusion are presented to the same eye, so that the illusion does not depend exclusively on binocular processes and, with monocular viewing, may not be exclusively central.

The third level of consists of **exclusively binocular processes**. An exclusively binocular process is one that occurs only when inputs from the two eyes are combined and is not evident when the same

stimuli are combined in one eye. An exclusively binocular process depends on a central mechanism activated only by binocular inputs. For example, the sensation of depth arising from static binocular disparity is an exclusively binocular process. Binocular rivalry produced by combining distinct images in the two eyes is also exclusively binocular. The detection of binocular disparity, as a process for detecting differences in spatial location, is not exclusively binocular because the difference in location of two dichoptic stimuli is evident when the same stimuli are combined in one eye. However, the psychophysical properties of the two processes are not identical and we have physiological evidence that some cells in the visual cortex are specialized for detecting binocular disparity and that this mechanism differs from that involved in the spatial discrimination of monocular stimuli. Thus, in some respects the detection of disparity is an exclusively binocular process. Binocular lustre created by dichoptic combination of different luminances is an exclusively binocular effect (Section 8.3.1). Dichoptic colour mixing has some features in common with monocular colour mixing, but in other respects it is exclusively binocular (Section 8.2).

1.1.4 Cyclopean procedures

The term “cyclopean” is difficult to define because different authors have used it in different ways. The Cyclops was a one-eyed giant in Homer's *Odyssey*, and the term is used to describe a birth defect in which there is only one central eye. Galen used the concept of the cyclopean eye to refer to the optic chiasma where he believed the images from the two eyes fused to form a single impression. Helmholtz used the term “cyclopean eye” to denote the point midway between the eyes which serves as a centre of reference for headcentric directional judgments (Section 14.5). This concept was first developed by Alhazen in the eleventh century but he used the term “centre” rather than cyclopean eye. Julesz generalized the term “cyclopean” to denote the central processing of visual information, that is, processing at a level after inputs from the two eyes are combined. As used by Julesz (1971), the term seems to have the same connotation as “central processing” as opposed to “retinal processing”. Julesz defined a cyclopean stimulus in a “weak sense” as one in which the centrally processed visual feature is evident in the monocular image. He defined a cyclopean stimulus in a “strong sense” as one in which the feature is not evident in the monocular image. We use the term in the strong sense to refer to a stimulus formed centrally but not on either

retina—it can be said to bypass the retinas. A cyclopean phenomenon or a cyclopean task is based on a cyclopean stimulus and therefore necessarily involves processes occurring at or beyond the primary visual cortex. A **cyclopean procedure** involves the use of a cyclopean phenomenon or task and allows one to infer that a process is cortical.

Three types of cyclopean procedure exist; that is, there are three ways to present a stimulus to the visual cortex without there being a corresponding stimulus on the retina.

1. *Paralysis of an eye.* For instance, if a bright light is presented to one eye and the afterimage is still visible after that eye has been pressure paralyzed, one must conclude that afterimages can be generated at a central site.

2. *Direct stimulation of the visual cortex.* The visual cortex can be stimulated directly by an electric current and the subject reports the resulting visual phosphenes. Fortification illusions of migraine are a naturally occurring cyclopean stimulus, since they arise from a direct disturbance of the visual cortex.

3. *Use of dichoptic stimuli.* This procedure may be called a **dichoptic cyclopean procedure**. Since this is the only cyclopean procedure discussed in this book, when we use the term "cyclopean procedure" we mean dichoptic cyclopean procedure. Many subtypes of dichoptic cyclopean procedure exist and are described in several chapters, particularly Chapters 9 and 15.

1.2 HISTORICAL BACKGROUND

1.2.1 History of physiological optics and vision

The Greeks

The Greeks were apparently the first to enquire into the nature of vision. Many Greek philosophers, including Alcmaeon of the Pythagorean school (early fifth century BC), Plato (ca. 427-347 BC), Euclid (ca. 300 BC), Hipparchus (160-125 BC), and Ptolemy (ca. AD 150), followed the suggestion made by Empedocles (5th century BC) that light leaves the eye in the form of a cone of straight rays with its base in the pupil. These rays were believed to sense the surfaces upon which they fall, in the same way that the fingers feel an object. The light emanating from the eyes coalesces with external light to create an effective optical medium through which motions of anything it comes in contact with are transported to the mind and generate visual sensations. Several early theorists regarded the image that can be seen reflected in a person's cornea as crucial to the visual

process, presumably believing that it represented the image seen by the eye. This became known as the emanation theory of sight. This theory was designed to solve the problem of how the visual world is externalized and seen in its proper size. In touch, the problems of external reference and proper size are solved because the fingers touch external objects and the impression formed on the skin by an object is the same size as the object. The idea that the eye is a source of light may have been inspired by the flash seen when a finger is pressed against the eye in dark surroundings—the pressure phosphene. Other Greek philosophers, including Aristotle (384-322 BC), Democritus (b. ca. 460 BC), and Epicurus (342-270 BC) rejected the idea of light emanating from the eyes and believed that objects continuously emit corpuscular images of themselves (*éidola* or *simulacra*) that move in straight lines into the eye through the intermediate translucent medium, which Aristotle called the diaphanous medium. Early theorists believed the crystalline lens to be the primary source of visual sensations, which were then conveyed to the brain. Aristotle described how an object upon which the gaze is fixed appears double when the eyes are caused to misconverge by pressing against one eye with the finger (see Beare 1906; 1931). This is perhaps the earliest known reference to binocular disparity.

The earliest known book on optics is Euclid's *Optics*, which was written in Alexandria in about the year 300 BC. Burton (1945) has produced an English translation. The book consists of seven definitions, or postulates, and about 60 theorems. The seven postulates establish that light proceeds from the eye in straight lines in the form of a cone with its apex centred on the eye. Only objects on which the cone of light falls are visible. Objects subtending a larger angle appear larger, those intersecting higher rays are seen above those intersecting lower rays, and those intersecting rays to the left are seen to the left of those intersecting rays to the right. The seventh postulate states that objects upon which more rays fall are seen more clearly.

The theorems build on these postulates, each linking a geometrical property of light rays with a visual sensation. Nevertheless, Euclid proved each theorem as if it were a statement in geometry. Today we would express these theorems as statements linking the geometry of light rays to the shape and position of retinal images rather than to sensations. In these terms, Euclid's theorems and proofs are still valid, except for his statements about emission of rays of light from the eye. Table 1.1 lists several of Euclid's theorems, with added corresponding statements in terms of the geometry of the retinal image.

Table 1.1. A selection of Euclid's theorems with equivalent statements

Euclid's theorem	Restatement in terms of retinal image
For a horizontal surface located above eye level, the parts further away appear lower.	More distant objects on a ceiling plane project on the retina above nearer objects.
An arc of a circle placed on the same plane as the eye appears as a straight line.	An arc in a plane containing the nodal point projects on the retina as a straight line.
When the eye approaches a sphere, the part seen will be less, but will seem to be more.	When the eye approaches a sphere, less of its surface will project on the retina but the image will increase in area.
For a sphere with a diameter smaller than the distance between the eyes, more than the hemisphere will be seen.	For a sphere with a diameter smaller than the interocular distance, the cyclopean image extends beyond half the sphere.
When the eye moves nearer to an object, the object will appear to grow larger.	The size of the image of an object is inversely proportional to the distance of the object from the eye.
When objects move at equal speed, those more remote seem to move more slowly.	The angular velocity of an object moving at constant linear velocity is inversely proportional to its distance from the eye.

Today we distinguish between the geometry of retinal images (physiological optics) and accounts of visual sensations (psychophysical functions), because we know that a given retinal image produces different sensations depending on the context. Euclid described sensations because he knew nothing about the retinal image and also because he confirmed his theorems by observation and wished to explain visual sensations, not merely images.

Euclid believed that a fixed number of rays is emitted from the eye so that, with increasing distance, a small object becomes invisible because it falls between rays. We would say that there is a fixed number of receptors, which limits the spatial sampling of the image.

Euclid was aware that the world looks slightly different when viewed by each eye in turn, and realized that two eyes see more of a solid object, such as a sphere, than either eye alone.

Claudius Ptolemy (ca. AD 127-165) the famous Greek-speaking astronomer, optician, and geographer of Alexandria, wrote the five-volume work *Optica*, of which the first volume is lost. He adopted Euclid's ideas but insisted that light rays form a continuous bundle rather than a discrete set separated by spaces, as Euclid postulated. He also contributed

two ideas (1) that light is a form of energy and (2) that the apex of the cone of light is at the centre of the curvature of the cornea.

Galen (ca. AD 129-201) was born in Pergamon, Asia Minor and was educated in Pergamon, Smyrna, and Alexandria. He later practiced medicine in Rome, where he became a friend of Emperor Marcus Aurelius. His book *De usa partium corporis humani* (On the uses of parts of the human body), which he completed in AD 175, is available in English translation. This consists of 17 books with Book 10 devoted to the eyes. Herophilus of Alexandria described the anatomy of the eyeball and optic nerve in about 300 BC. Rufus of Ephesus (ca AD 50), also working in Alexandria, first described the optic chiasma. Galen did not dissect humans, but rather pigs, goats, and tailless apes and he sometimes erroneously generalized his findings to humans. He based his anatomy of the eye on Herophilus. A spherical lens at the centre of the eye was considered to be the essential organ of vision and an extension of the brain. It has been suggested that the lens was placed in this position because it tends to migrate there in the dead eye. Galen also proposed that each optic nerve is a hollow tube which projects from the rear surface of the lens to the lateral cerebral ventricle on its own

side of the brain. He referred to these ventricles as the thalami, meaning "inner chambers" but overlooked the nucleus which we now call the thalamus. For Galen, "visual spirit", or *pneuma*, is conveyed from the brain to the eye along the hollow optic nerve where it leaves the eye and interacts with the surrounding air to form a sentient medium that extends to distant objects. He argued that the lens is the principal organ of sight. The visual spirit conveys visual sensations from the lens along the optic nerve to the cerebral ventricles, where it mixes with the "animal spirit". The animal spirit was believed to be generated in the base of the brain from "vital spirit" arriving from the heart. The animal spirit was stored in the ventricles, from where it was thought to circulate through nerves to different parts of the body. The brain was regarded as the seat of "reason", or "mind".

Galen believed that the meeting of the optic nerves in the chiasma united impressions from the two eyes into a single experience and concentrated the flow of visual spirit into one eye when the other eye was closed. This idea gave rise to the notion of a cyclopean eye located at the chiasma. We shall see later in this section that this idea was not overthrown until the seventeenth century. We now talk about the cyclopean eye to refer to the fact that we judge the directions of objects as if we see from a single eye midway between the eyes (see Section 14.5).

Galen adopted Euclid's optics and described binocular parallax and how each eye sees distinct parts of an object, which are then combined into a unified visual impression. Several pages of Book 10 contain a condescending explanation of why he does not give the geometry of light rays and binocular vision. He claimed that his readers would not understand geometry and would hate him for explaining it. The little geometry he does provide is inaccurate and vague. One wonders whether it was Galen himself who did not understand geometry.

Several lenses dating from Greek and Roman times have been excavated. They seem to have been used to focus the sun's rays to make fire, and Pliny mentions their use in cauterising. Seneca described how letters could be magnified by a ball of glass filled with water (see Needham 1962, p. 118; Polyak 1957). The Chinese appear to have made lenses from rock-crystal or glass to focus the sun's rays as early as the third century. The foundations of the science of refraction, or dioptrics, were laid in Greek and Roman times. Phenomena due to refraction, such as the apparent bending of a half-submerged object and the magnification of objects seen through a bottle of water, were well known. Ptolemy was the first to investigate refraction quantitatively. He measured the

relationship between the angle of incidence and the angle of refraction for various combinations of transparent media and concluded that the ratio of these two angles was constant for a given combination. This is approximately true for small angles. The correct rule, that the ratio of the sines of the angles is constant for a given pair of media, was not discovered until 1621 by Willebrord Snell, professor of mathematics at Leiden. A full account of image formation by a lens was first provided in 1611 by Kepler .

The Arabs

During the middle ages there was virtually no scientific enquiry in Europe. The neo-Platonist school in Athens was disbanded in AD 529 by Justinian, the Emperor of Byzantium, and the scholars took refuge in Persia and Syria. After the westward expansion of Arabic civilization from its centres in Egypt, Damascus, and Baghdad in the eighth century, Arabic (and Jewish) centres of learning were established as far west as Sicily and Spain. Many books that had been translated from Greek into Arabic or had been written by Arabic scholars were subsequently translated into Latin, leading to a revival of learning in Europe in the thirteenth century. This revival laid the foundation for the Renaissance and the growth of modern science.

The first great Arab scholar was Abu Yusuf Ya'quib ibn Ishaq al-Kindi, who was born in the late eighth century in the city of al-Kufa. He worked in Baghdad under the patronage of the caliphs and died in about 866. He wrote about 260 books, one of which, entitled *De aspectibus* in Latin translation, was on optics. This became a popular textbook in Islam and its influence lasted for hundreds of years. Al-Kindi believed that everything in the world produces rays in all directions like a star, and this radiation binds the world into a network in which everything acts on everything else to create natural effects. Al-Kindi adopted Euclid's geometrical approach to vision and conducted experiments with shadows to establish the rectilinear propagation of light. In spite of this theoretical approach, and in spite of his experiments, he clung to the emanation theory of vision.

Avicenna (Abu Ali al-Husain ibn Abdullah ibn Sina, AD 980-1037) is the best known Arabic natural philosopher. He discussed vision in several books which still exist. He was mainly concerned with refuting the emanation theory of vision in all its forms. He adopted Aristotle's theory of visual optics and Galen's ideas on visual anatomy (see Lindberg 1976 for a discussion of Al-Kindi, Avicenna, and other Arabic scholars).

Of the Arabic scholars, Alhazen (Abu Ali Al-Hazan ibn Al-Hazan ibn Al-Haytham) made the most significant contributions to optics and vision (see ten Doesschate 1962). He was born in Basra in about AD 965 and died in Cairo in about 1040. In his autobiography he lists ninety-two of his own works, more than sixty of which have survived. Sixteen works were on optics. In the seven books constituting his great synthetic work, the *Book of Optics* (*Kitāb al-manāzir*), he set out to examine the science of vision systematically, using mathematics and experimental observation. Alhazen was familiar with Ptolemy's *Optics* and used the same division of the subject into vision from rectilinear rays, vision by reflection, and vision by refraction. Alhazen's work was ignored in the Arabic world during the 250 years after his death, but in the twelfth century the *Book of Optics* was translated into Latin with the name *Perspectiva*, perhaps by Gerard of Cremona. It became the principal source for the subject in Europe until the seventeenth century. The book was translated into English by Sabra in 1989.

Alhazen firmly rejected the emanation theory of vision and described how rays of light enter the eye from sources of light and from objects that reflect and refract light. In the Aristotelian intromission theory, a visible object issues a copy of itself to the eye. This raises the problem of how multiple copies can be sent to a multitude of eyes over an extended period. It also raises the problem of how a copy of a large object can enter the pupil. In solving these problems, Alhazen adopted al-Kindi's idea that light radiates in all directions from each point of an object. Instead of an object issuing copies of itself, each point on an object emits or reflects light in all directions. He thus laid the foundations of modern geometrical optics.

The Muslim religion forbade dissection, so Alhazen had to base his ideas of the anatomy of the eye on Galen, but he rejected Galen's ideas of light. He described the surface of the cornea and the front surface of the lens as concentric and stated that rays of light entering the pupil converge on the common centre of curvature and then diverge to form an inverted and reversed image on the rear surface of the lens. The common centre was placed at the centre of rotation of the eye so that he believed that the rear surface of the lens is mounted on the hollow optic nerve and that the process of sentience begins at this interface and continues in the fluid-filled cavity of the nerve. Figure 1.1 shows a diagram of the eyes and visual pathways from the earliest known copy of Alhazen's book.

Alhazen compared the eye to a "dark chamber" into which light enters through a small hole to form

an inverted image without the aid of refraction. He was clearly referring to what we now call the pinhole camera, or *camera obscura* (see Hammond 1981, for a history of this instrument). The pinhole camera works because the aperture is so small that only a narrow beam of light passes from any point on the object to a given point in the image. Alhazen described how an eclipse of the sun can be safely observed by looking at the image produced by a small hole in the wall of a dark chamber and understood that the image is sharp only when the hole is small. The invention of the *camera obscura* is usually credited to Roger Bacon or Leonardo da Vinci. Alhazen realized that the pupil is too large to allow the eye to work as a pinhole camera. Although he did not understand image formation by a lens, he realized that clear vision requires that each point on the recipient surface in the eye receives light from only one point in the visual field. He was thus confronted with the problem of how light from each object forms a distinct image on the surface of the lens without being diluted by rays from other objects. His clear statement of this fundamental problem is perhaps Alhazen's greatest achievement in vision. He came close to solving the problem when he speculated on the possible role of refraction (p. 116; see Lindberg 1976, p. 76). A full solution along these lines was not forthcoming until Kepler provided a theory of image formation in 1611. The solution Alhazen adopted was that an image is formed on the rear surface of the lens only by rays that strike the cornea and front surface of the lens at right angles. He argued that the surface of the cornea and the front surface of the lens are concentric, so rays striking the two surfaces at right angles pass through the common centre before forming an image on the rear surface of the lens. We now know that there is some truth to Alhazen's idea, because light rays normal to the retinal surface are more likely to enter visual receptors than are rays at any other angle. This is the Stiles-Crawford effect, described in Section 4.1.1.

Alhazen realized that the image on the rear of the lens would be inverted and reversed. To avoid the problem he proposed that the rays are refracted at the rear surface of the lens, seemingly to form an erect image in the head of the optic nerve, although his description of this process is very hazy (p. 116). Like Galen, he believed that the coherent pattern of rays is conveyed along the hollow tube of each optic nerve to the optic chiasma where the images from the two eyes fuse into a single image and the primary act of seeing occurs. He realized that the rectilinear propagation of light rays determines the spatial integrity of the image but that once the "image" is conveyed into the curved optic nerve its

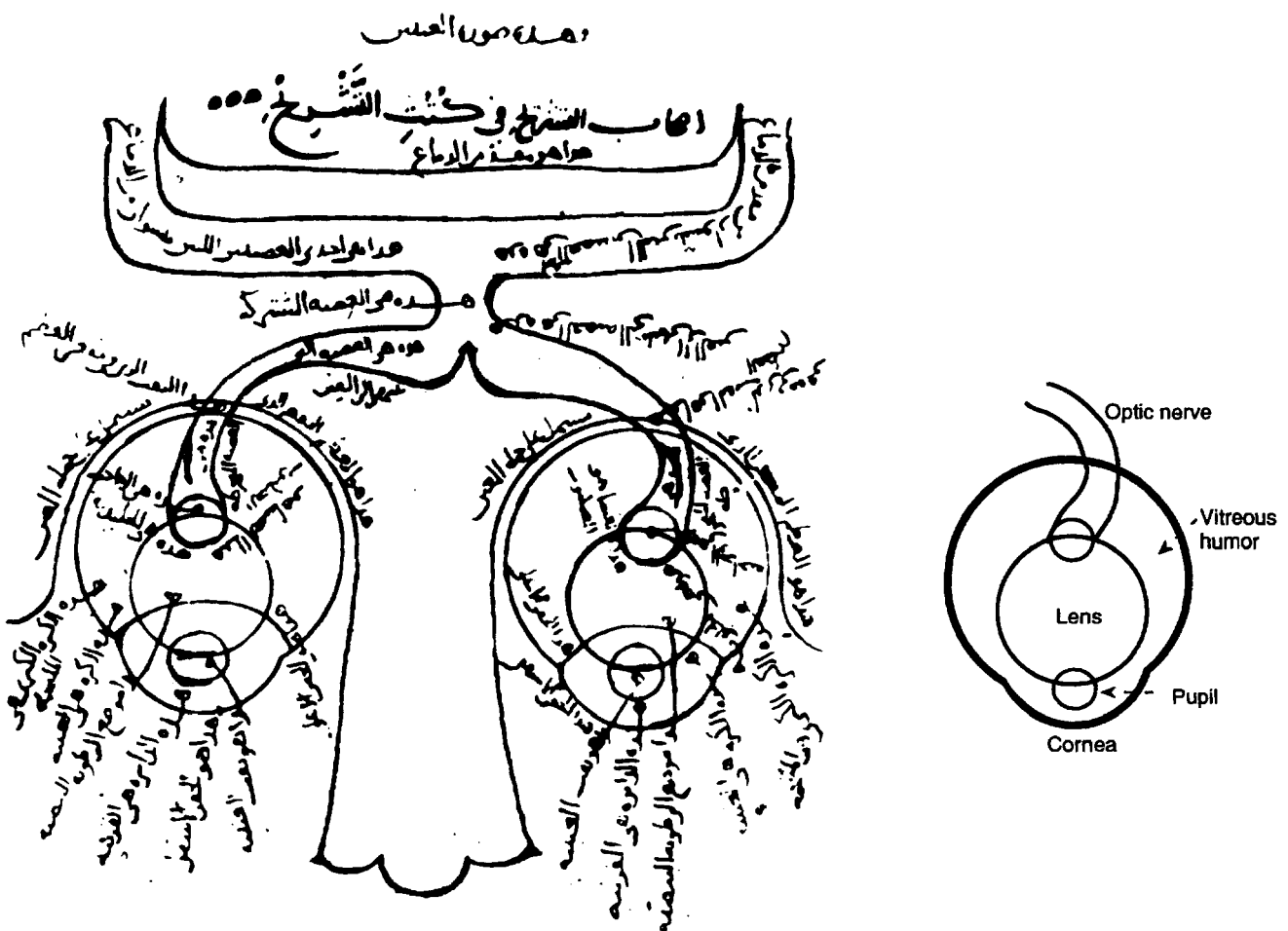


Figure 1.1. Alhazen's diagram of the visual system.

This diagram is from the *Book of Optics* (*Kitāb al-manāzir*) by Alhazen, copied by his son-in-law in 1083 from an earlier version. It is the oldest extant diagram of the visual system. (MS No. 3212 in the Faith Library in Istanbul.) The diagram on the right provides a key to the parts.

spatial integrity depends on retention of the relative order of parts rather than on rectilinear propagation. He had no idea how this could be achieved in what he believed to be a fluid medium. Alhazen's ideas on basic visual processes, erroneous though they were in many ways, set the stage for subsequent developments in physiological optics and, ultimately, for Kepler's account of image formation.

Alhazen described visual masking (p. 97), dark adaptation and afterimages (p. 51), induced visual motion (261), size constancy (p. 177), shape constancy (208), the contribution of eye movements to the perception of motion (p. 193), and the role of the ground plane in the perception of distance (p. 179), an idea revised by Gibson in 1950. Alhazen's ideas on binocular vision are reviewed in Section 1.2.2.

Alhazen described how perception beyond direct sensation requires inference and experience,

although at an unconscious level (p. 136). His views are very similar to Helmholtz's theory of unconscious inference. Alhazen also described a third level of perceptual recognition in which conscious knowledge plays a part. Alhazen expressed ideas very similar to what we now refer to as the preattentive and attentive stages of perception (p. 209). Although Alhazen's book inspired many commentaries and derivatives, it was not superseded until the early seventeenth century.

Medieval and Renaissance Europe

The thirteenth century saw some revival of interest in science. Roger Bacon, the "doctor admirabilis" (1210-1292), studied in Oxford and Paris and was familiar with the works of Euclid, Aristotle, Galen, and Alhazen. In his *Opus Major* of 1268 he mentions that people with weak eyes can use a lens for

reading. His writings on vision are largely commentaries on the writings of Alhazen. The same can be said of other thirteenth-century scholars such as Vitello (1230-70), who lived in Poland and wrote his own book with the title *Perspectiva*—the first European treatise on optics (1270), and John Peckham, (1240-91) Archbishop of Canterbury (ten Doeschate 1962). In the fourteenth century the disastrous plague—the black death—brought most scientific enquiry to a halt. Learning in Europe became dominated by scholastic explorations of implications of classical learning for Christian doctrine and the exercise of dialectical skills.

Spectacles were first made in about the year 1285 by an unknown person, probably a worker in glass in Pisa, Italy. The earliest written reference to spectacles is in notes for a sermon delivered by the Dominican Friar, Giordano da Rivalto, in the church of Santa Maria Novella in Florence on Wednesday, February 23rd, 1306. The earliest known work of art depicting spectacles is a portrait at Treviso of Hugh St. Cher painted by Tommaso da Modena in 1352. Since Hugh St. Cher died well before the painter was born and more than 20 years before spectacles were invented, the spectacles in the portrait are an anachronism. Rosen (1956) has provided an interesting account of spurious claims that spectacles were invented in Venice, in England by Roger Bacon, in Belgium by Bacon transformed into a Walloon, and in Germany. Magnifying lenses were used in China in the twelfth century for reading illegible documents and possibly for fine engraving but do not seem to have been used as spectacles until the early Ming dynasty in the fifteenth century (Needham 1962, p. 119).

During the sixteenth century several people, including Girolamo Cardano, professor of mathematics in Milan and Daniele Barbaro, a Venetian architect, improved the camera obscura by replacing the small hole with a biconvex lens. The resulting instrument was used for observing eclipses of the sun, for popular amusement, and in art (see Hammond 1981). In modern times it has become the projector and with the addition of light-sensitive film—the camera (Gernsheim 1969).

The artists of the Italian renaissance revived interest in vision. The art of drawing in linear perspective is credited to Filippo Brunelleschi (1377-1446) of Florence, although some Roman frescos have almost perfect perspective (Little 1971). Lynes (1980) has written an interesting interpretation of Brunelleschi's contribution in which he concludes that Brunelleschi succeeded by drawing on the surface of a polished sundial rather than by using geometrical principles. The first account of the geometry of drawing in

perspective was first provided in 1435 in Leon Battista Alberti's (1404-1472) *Della Pittura*. Leonardo da Vinci and others rapidly improved the geometrical methods, although a full understanding of the mathematics of perspective had to wait for Desargues and Pascal in the eighteenth century. Albrecht Dürer brought knowledge of drawing in perspective to northern Europe in 1505, although he had an imperfect understanding of the geometry (see Ivins 1973). For accounts of the development of perspective in art, see White (1967), Edgerton (1975), Kubovy (1986), and Pirenne (1970). Renaissance artists were preoccupied with representing three-dimensional scenes on a flat surface. This directed their attention to monocular cues to depth, which can be represented in a picture, and away from binocular cues.

The following passage from Leonardo da Vinci (1452-1519) has been viewed as the first suggestion that light travels as waves rather than corpuscles, as earlier writers believed. He wrote,

Just as the stone thrown into water becomes the centre and cause of various circles, and sound made in the air spreads out in circles, so every body placed within the luminous air spreads itself out in circles and fills the surrounding parts with an infinite number of images of itself, and appears all in all and all in each part. (cited in Keele 1955)

In Lindberg's (1976) opinion, this was merely an analogy describing the propagation of images, and said nothing about how light itself is propagated. Be that as it may, the preceding quotation essentially reaffirms Al-Kindi's principle of universal radiation. Like Alhazen, Leonardo proved that light from many objects passes through each point of space by showing that many objects produce distinct images through the same pinhole in the pinhole camera. He then proved that light from any one object is in each location of space by showing that several images of the same object are produced simultaneously by several pinholes. Leonardo had little knowledge of the anatomy of the eye. He compared the eye with a camera obscura, believing that an inverted image is produced in the centre of the eye by light passing through the pupil but that the rays cross again by reflection or refraction to form an erect image on the head of the optic nerve. Leonardo observed the changes in pupil size accompanying changes in illumination but failed to observe pupil changes accompanying changes in accommodation. He had the erroneous idea that the larger the pupil the larger the appearance of the object. Leonardo's writings on vision had no effect because they were in

private hands until 1636 and were not studied seriously until the end of the eighteenth century.

Giovanni Battista della Porta (ca. 1535-1615) of Naples was a flamboyant collector and investigator of natural wonders, a playwright, and translator of Greek texts. His father's house in Naples was a centre for philosophers, musicians, and poets. Giovanni founded a group calling themselves *Otiosi* (Men of Leisure). Each member was required to have made a new discovery in natural science. This was the first scientific society of modern times. At the age of 23 he wrote *Magiae naturalis* (1558), a collection of wonders, recipes, and remedies, and one of the most popular books of its time, which was translated into English in 1658. In his major work on optics, *De refractione optice parte libri novem* (1593) he dealt with refraction and expounded Alhazen's view that an image is formed on the lens by perpendicular rays in the manner of a camera obscura but added his own view that this happened only after a second inversion of the image by reflection from the back of the eye, which acted as a concave mirror. He was apparently the first to give an account of binocular rivalry between differently shaped images in the two eyes. He was aware that a lens placed in the aperture of a camera obscura improves the image and he obtained an erect image by use of a concave mirror. He failed to apply this knowledge to the eye, preferring to believe that the image is formed on the lens of the eye. He was the first to use the camera obscura for drawing, simply by tracing round the image.

The modern study of human anatomy was initiated by Andreas Vesalius who was born in Brussels in 1514 and studied medicine in Paris, Louvain, and Padua where, the day after his graduation at the age of 25, he was appointed to the chair of anatomy and surgery (see O'Malley 1964). In 1544 he became physician to the Emperor Charles V in Madrid, which prevented him from engaging in further research. After the abdication of Charles V in 1559, Vesalius hoped to return to his chair in Padua but was forbidden to do so by the new Emperor, Philip II. In 1564 Vesalius made a pilgrimage to Jerusalem. On the return journey, stormy weather forced him to land on the island of Zante, where he became sick and died in miserable circumstances. His great work *De Corporis Humani Fabrica* (*On the Structure of the Human Body*) was published in 1543, when he was 29 years old. It contains many fine anatomical drawings, including drawings of the eye, based on his own dissections and presented in the form of woodcuts made by a master engraver. Vesalius could not confirm that the optic nerve was hollow, as required by Galen's theory that it transported visual spirits. In spite of this and his critical attitude toward classical

anatomy, Vesalius did not question the doctrine of animal spirits, which persisted until after Kepler. He suggested that the retina is the sensitive organ of sight but produced no evidence in favour of this view. Like Galen, Vesalius believed that the optic pathways project to the lining of the most anterior of the three cerebral ventricles. Leonardo da Vinci, who injected wax into the cerebral ventricles to obtain a more accurate idea of their shape, concluded more correctly that the optic pathways end in the posterior ventricle (see Keele 1955).

Eustachio (1520-1574), in his *Tabulae Anatomicae*, was the first person to recognize that the optic pathways do not project directly to the brain but first pass to the posterior part of the thalamus (the lateral geniculate nucleus), although his discovery was ignored for more than 150 years.

The idea that the retina rather than the lens is the site of image formation was expressed by Abn Rushd, a Spanish-Arab scholar of the thirteenth century (Polyak 1957), and hinted at by Vesalius in 1543. But Felix Platter, an anatomist in Basel (1536-1614), was the first to state the principle clearly and produce supporting anatomical evidence in his *De corporis humani structura et usu* of 1583, although his account lacked a clear statement of the dioptric principles of image formation. The honour of that discovery belongs to Kepler.

Kepler

Johannes Kepler (1571-1630) was born in the city of Weil of Lutheran parents. He studied at the University of Tübingen, intending to become a Lutheran clergyman, but instead took a teaching position in mathematics at the Protestant seminary at Graz. In 1600 he became the assistant to the astronomer Tycho Brahe at the court of Rudolf II in Prague. When Brahe died a year later he succeeded him as court mathematician and astrologer. He later became a mathematician in Linz, and finally in Rostock. In the seventeenth century, science, and particularly astronomy and mathematics, was emerging from the mystical, hermetic tradition of thought with which they had been inextricably combined. Kepler's attitude toward astrology was ambivalent. He cast horoscopes for the Emperor but once remarked that the wayward daughter, astrology, had to support the honest dame astronomy. Although some of his theoretical speculations were inspired by mystical concepts derived from the Hermetic-Cabalistic (magical) tradition, he, like Marin Mersenne in France, was among the first to state clearly the distinction between testable scientific hypotheses and mystical speculation and between the use of mathematics to describe natural phenomena and its use in

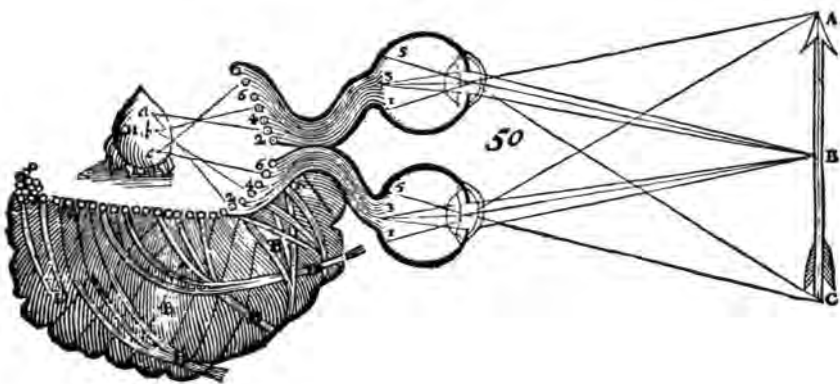


Figure 1.2 Descartes' diagram of the visual system.

The formation of the images is based on Kepler. Each optic nerve projects to the lining of the ipsilateral cerebral ventricle, an idea taken from Galen. Pairs of corresponding points from the two ventricles converge in the pineal gland to form a unified impression. (From Descartes' *Tractatus de Homine* 1664.)

mystical numerology. This becomes clear in his famous dispute with Robert Fludd, a writer within the magical tradition (Yates 1964).

In the year 1604, while in Prague, Kepler set out for the first time the geometrical principles of image formation on the retina in *Ad vitellionem paralipomena* and later in his book *Dioptrice* (1611). He established the modern principles of dioptrics and put physiological optics on a firm foundation. As his starting point Kepler considered the two problems raised by Alhazen—the problem of the inverted image produced in the eye and the problem that each part of the image plane receives light from every point in the visual field.

At first Kepler was disposed to accept Alhazen's solution to the inverted image problem by positing a second inversion, but he soon abandoned this idea. He concluded that a mental process was responsible for seeing the image in its correct orientation, which is tantamount to saying that he left the problem unsolved. It was left to the Dubliner William Molyneux (1692, p. 105), in his *Treatise of Dioptricks*, to propose the correct answer to the problem, which is that the perceptual system does not have access to the absolute orientation of the retinal image but only to information about its orientation with respect to inputs from other sensory modalities. Bishop Berkeley (1709) also stated the correct solution to the problem of the inverted image. For an account of empirical investigations of the effects of inverting the retinal image, see Howard (1982).

With regard to the second problem, Kepler rejected Alhazen's solution of allowing only normal rays to enter the eye on the grounds that there would be no way to distinguish between normal rays and slightly refracted rays. By analyzing the

paths of light rays through a lens, he arrived at the correct solution, which he then applied to the eye. Light radiating out from any point on a visible object is refracted by the lens to form a converging cone of light which comes to a point in the image plane. Light radiating from any other point on the object converges in another point in the image. There is thus a one-to-one mapping of object points onto image points and therefore no stray refracted light rays dilute the image. He concluded that an inverted and left-right reversed picture of the visual scene is projected on the retina. He derived his ideas of the anatomy of the eye and in particular that the retina is the site of image formation from Platter's *De corporis humani structura et usu*. He had no idea that the refractive power of the lens could change. The problem of the inverted image continued to trouble him, but he concluded that the problem would be solved by considering visual processes beyond the retina. Like Alhazen, Kepler realized that optical principles could not apply beyond the retina because the optic nerve is not straight and contains opacities. He clung to Galen's notion of visual spirits but admitted that he knew nothing about visual processes beyond the retina, only insisting that they were not optical.

Christopher Scheiner, a Jesuit friar who lived in Bavaria (1579-1650), provided the first experimental proof that a miniature inverted image is formed on the retina. He observed the image directly by cutting away the back of a bull's eyeball. Knowledge about the structure of the retina had to wait until the microscope was developed in the seventeenth century.

Descartes

René Descartes (1596-1650) was born of Jewish parents near Tours in France. He lived in Paris for a

time and travelled as a soldier before settling down in Holland to devote himself to mathematics and philosophy. In his *Traité de l'homme* (*Treatise on Man*), published in 1664, he adopted Kepler's ideas of image formation but retained Galen's notions of animal spirits and ventricular projection. He believed that each optic nerve projects to its own side of the brain, thus moving the site where inputs from the two eyes form a united image back from the chiasma into the brain. He contributed the idea that each fibre in the optic nerve projects from a location in each retina to a specific location on the lining of the ipsilateral cerebral ventricle, as shown in Figure 1.2. From there he proposed that each point from one eye projects to the same location in the pineal gland as the corresponding point from the other eye, to form a unified impression of a single object. Although Alhazen had proposed that corresponding inputs are combined into a unitary image, Descartes gave a more precise account of the topographical projection of corresponding visual inputs onto a surface in the brain, albeit the wrong one.

Newton

By the sixteenth century it was generally believed that visual inputs from the two eyes do not fuse in the chiasma, as Galen had proposed, but that each optic nerve passes ipsilaterally to the brain, where fusion occurs. We now know that, in man, the inputs from only the temporal half of each retina project ipsilaterally. Inputs from the nasal half of each retina cross over, or decussate, in the optic chiasma and project to the contralateral half of the brain. Isaac Newton in his *Opticks* (1704) was the first to propose that visual inputs segregate in this way. He wrote,

Are not the species of objects seen with both eyes united where the optick nerves meet before they come into the brain, the fibres on the right side of both nerves uniting there, and after union going thence into the brain in the nerve which is on the right side of the head, and the fibres on the left side of both nerves uniting in the same place, and after union going into the brain in the nerve which is on the left side of the head, and these two nerves meeting in the brain in such a manner that their fibres make but one entire species or picture, half of which on the right side of the sensorium comes from the right side of both eyes through the right side of both optic nerves to the place where the nerves meet, and from thence on the right side of the head into the brain, and the other half on the left side of the sensorium comes in like manner from the left side of both eyes. (p. 346)

He went on explain that this is true only of animals with frontal vision and that the optic nerves of

animals with laterally placed eyes do not meet in this way. He conceived of each optic nerve as a multitude of "solid, pellucid and uniform Capillamenta" which transmit vibrations caused by light to "the place of sensation" in the brain.

Newton believed that corresponding fibres fuse in the chiasma so that the brain receives only one nerve from each pair of corresponding retinal points. He thus returned to Galen's concept of the cyclopean eye. He stated that similar images falling on corresponding points fuse to give the impression of a single object and are seen as double when they fall on noncorresponding points. Newton also realized that dissimilar stimuli falling on corresponding points rival rather than fuse. He wrote, "they cannot both be carried on the same pipes into the brain; that which is strongest or most helped by phantasy will there prevail, and blot out the other." (quoted in Harris 1775). John Taylor (1738) produced some anatomical evidence that nerve fibres from the two eyes remain distinct until they reach the brain but, as we shall now see, the matter was not settled until 1870.

Microscopic structure of the visual system

Although the microscope was invented in the seventeenth century, it was not until the early nineteenth century that the details of retinal structure began to be clearly understood. Heinrich Müller (1854), professor of anatomy at Würzburg, Bavaria, was the first to identify the outer segments of the rods and cones as the site of photosensitivity. He measured the parallactic displacement of the shadows of retinal blood vessels for a given motion of a light source, and from this computed the distance that the receptive layer must lie behind the vessels. This distance was the same as the anatomically determined distance between the layer containing the rods and cones and that containing the blood vessels. The synaptic organization of the retinal layers was revealed in great detail by Santiago Ramón y Cajal (1852-1934), working in Madrid (see Ramón y Cajal 1937). These structures are described in Section 4.1.1.

The anatomical confirmation of hemidecussating pathways was provided in 1870 by Bernhard von Gudden, an eminent neuroanatomist and professor of psychiatry in Zürich and Munich (Duke-Elder 1968a). Von Gudden conspired with a group of politicians to have King Ludwig II of Bavaria certified insane and incarcerated in Schloss Berg. On the second day of incarceration, in June 1886, the king asked von Gudden to take a walk with him by Lake Starnberg. Both men were later found drowned in shallow water. It is generally believed that the king killed von Gudden and then drowned himself, but this was never proved (Blunt 1970).

Herman Monk (1839-1912), professor of physiology in Berlin, established the occipital cortex as the site of the primary visual cortex. For a review of other early studies on the visual pathways and cortex see Polyak (1957).

1.2.2 History of ideas of stereoscopic vision

The realization after Kepler that the retinal image is two-dimensional and inverted caused people to wonder how we perceive an erect three-dimensional world. Since ancient times, artists had struggled with the related problem of how to represent three-dimensional space in a picture. This preoccupation with pictorial space led to an emphasis on monocular cues to distance. Euclid knew that the eyes have different views of three-dimensional objects, and Aristotle noted that one sees double images when a finger presses against one eye. But the problem that double images raised in peoples' minds was how we form an impression of a single visual world, despite these differences between the two images. The binocular disparities and double images were regarded as something to be overcome rather than made use of.

It is amazing that the simple facts about binocular stereoscopic vision were not fully appreciated until about 150 years ago. One reason for this ignorance is that even with one eye closed a rich variety of monocular information is available for coding depth. Thus, the importance of binocular stereopsis is not apparent with casual observation of everyday scenes.

Alhazen on binocular vision

In his *Book of Optics* Alhazen followed Galen in explaining that we have two eyes so that when one is harmed the other remains intact, and he added that two eyes beautify the face (p. 102). In chapter 2 of the third book he clearly described the concept of corresponding points in the image planes of the eyes. He explained how one sees a single object when images fall on corresponding points and two objects when they fall on noncorresponding points. Like Aristotle and Galen, he mentioned that an object appears double when one eye is pushed by the finger, and like Galen, pointed out that when the visual axes converge on a point they lie in one plane, the plane we now call the plane of regard. He stated that the two eyes always move together and by an equal amount, so that the visual axes converge on the object of interest. This idea lay dormant until the nineteenth century when Hering developed the principle of equal innervation (see Section 10.6.1). Alhazen called the line extending from the chiasma

to the fixation point the "common axis" and the point in the chiasma where images from the two visual axes converge "the centre". Alhazen explained that images from an object near the intersection of the visual axes project to corresponding points in the two image planes and appear single, but that an object in the frontal plane well to one side of the fixation point appears double, because the angles it subtends to the two eyes are unequal. He thus realized that the locus of fused images is not the frontal plane. It is a pity that he did not go one step further and apply Euclid's geometry to show that it is a circle passing through the fixation point and the two eyes. We will see that this development had to wait until 1811. He stated that small differences in visual angle are tolerated without diplopia. We now refer to this tolerated disparity as Panum's fusional area (see Section 8.1). He explained that an object above or below the fixation point in the midline is not seen double, because its distance from the two eyes is the same and it therefore projects equal angles to the two eyes. This idea anticipates the modern concept of the vertical horopter (see Section 2.7). He then discussed double images produced by an object nearer or further away than the fixation point, with both the object and the fixation point in the median plane. He wrote,

If the eyes perceive another object closer to or farther away than that on which the two axes meet, . . . that object will be differently situated with reference to the eyes in direction. Because if it lies between the two axes, then: it will be to the right of one of them and to the left of the other; the rays drawn to it from one eye will be to the right of the axis and those drawn to it from the other eye to the left of the axis; therefore its position relative to the eyes will differ in respect of direction. The forms (images) of such an object will occur in differently situated places in the eyes; . . . will proceed to two different places in the cavity of the common nerve . . . and thus will be two non-coincident forms (p. 237).

He invited the reader to view lines on a board extending horizontally from the bridge of the nose, as shown in Figure 1.3. He described the following visual impressions.

An object at point *I* does not appear double if it is not too far from the plane *TKH* in which the eyes are converged but an object at *Q*, well away from the plane of convergence, appears double. He was thus aware of what we now call Panum's fusional area. Objects closer to or farther than the fixation point (points *L* and *F*) appear double and on opposite sides of the fixated object when they are between the visual axes, and on the same side of the fixated

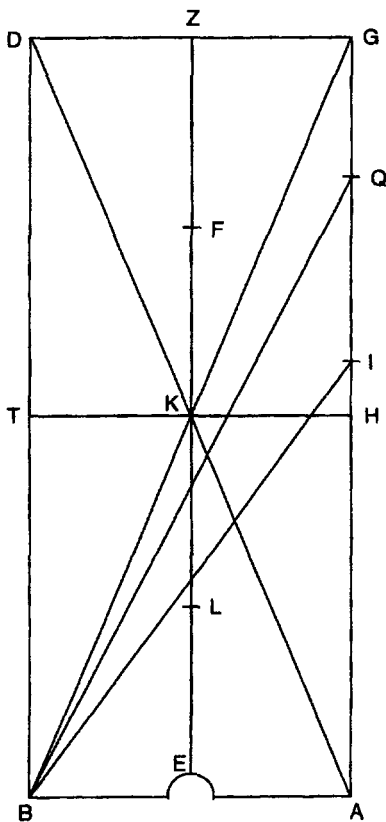


Figure 1.3. Alhazen's geometry of binocular vision.

The board is held horizontally with the bridge of the nose at *E*, the eyes at *B* and *A*, and fixation on *K*. Small objects are placed at *K*, *F*, *L*, *I*, and *Q*. The line *EZ* appears like a cross passing through *K*. Lines *BG* and *AD* appear as four lines with the two centre lines superimposed down the midline. Objects *F* and *L* produce double images, one on either side of the midline. Object *Q* produces double images, on the same side of the midline. Object *I* produces double images that are too near together to be seen as two. Objects at *T* and *H* appear single but objects more eccentric on the same frontal plane appear double. (From Alhazen's *Book of optics*, trans. Sabra, 1989, p. 238.)

object when they are outside the visual axes (point *Q*). Here he established the basic facts about diplopia. Small objects, *T* and *H*, in the same frontal plane as the fixation point appear single when not too far from the fixation point but double when well to the side. He proved this by showing that the angle between an eccentric object and the median plane was not the same for the two eyes. He thus proved that the locus of fused images for a given viewing distance does not lie in a frontal plane. He did not go on to establish the true locus of fused images. As we will see, that step had to wait until 1811.

A line, *EZ*, down the centre of the board appears as two lines intersecting in the fixation point, *K*. Finally, two lines, *AD* and *BG*, extending diagonally from each eye and intersecting in the fixation point appear as four lines, with the centre two appearing close together along the median plane of the head.

He explained that these two lines appear in the centre because they lie on the visual axes and therefore share a common visual direction in the fused image. This shared visual direction lies along the "common axis" that bisects the angle between the two visual axes and intersects the "centre". He wrote,

The reason why two of the four appear closer together is this: when the two visual axes meet at the middle object, then each of the two diameters will be perceived by the eye next to it through rays that are very close to the visual axis; thus their forms (images) will be very close to the centre within the common nerve (the chiasma) and their point of intersection will be at the centre itself, and thus the diameters will appear very close to the middle (the median plane) (p. 242).

Alhazen's "centre" is now called the "egocentre" and his "common axis" is called the "cyclopean axis". These ideas of Alhazen on binocular vision have been totally ignored. They did not resurface until Wells gave an account of cyclopean visual direction in his *Essay upon Single Vision with Two Eyes*, written in 1792, 87 years before Hering wrote his account in 1879. Neither of these authors acknowledged Alhazen's contribution (see Section 14.5).

After Alhazen there were no advances in knowledge about binocular vision until the seventeenth century. Leonardo da Vinci (1452-1519), in his book *Trattato della Pittura*, wrote,

A painting, though conducted with the greatest art and finished to the last perfection, both with regard to its contours, its lights, its shadows and its colours, can never show a relieveo equal to that of the natural objects, unless these be viewed at a distance and with a single eye.

He went on to describe how an object obscures from each eye a different part of the distant scene. This had been described by Euclid, but unlike Euclid, da Vinci described it as a source of information about depth (see Keele 1955; Strong 1979).

Aguilonius

Franciscus Aguilonius (François D'Aguilon) was born in Brussels in 1546, the son of the secretary to King Philip II. He became a Jesuit priest in 1586 and died in Antwerp in 1617. He taught logic, syntax, and theology and was charged with organizing the teaching of science in Belgium. In 1613 he published part one of a three-part work on optics designed to synthesize the work of Euclid, Alhazen, Vitello, Roger Bacon, and others. He died before completing the other parts. The published work consisted of six books with the title. *Opticorum Libri Sex*.

In his treatment of visual optics and perception he followed the order of topics discussed in Alhazen's book. His ideas on binocular vision were presented in book 2. He was aware that binocular vision improves the sense of depth, as the illustration from his book, shown in Figure 1.4a, reveals. He adopted Galen's idea of the cyclopean eye located in the chiasma and one of the illustrations in his book shows putti dissecting the cyclopean eye after having removed it from a cadaver, as shown in Figure 1.4b.

Aguilonius introduced the term "horopter" to describe the locus in space within which both fused and diplopic images appear to lie. The word is derived from the Greek words "horos" meaning "boundary", and "opter" meaning "observer". Aguilonius presented the diagram shown in Figure 1.5a and wrote,

Let the centres of sight be at A and B which the straight line AB connects. The optic axes AC and BC come together at C, and through C, parallel to AB runs a straight line, DE.

He called this line the horopter and went on to state,

The appearance of all those objects placed in the plane (of regard) assume places for themselves. For example, F is a visible object, the optic radii AF and BF join at F, but they carry beyond the image of the object, until they site it in the horopter as in a common terminus and station, where the twin sites of H and G are placed. In this way, the horopter is the terminus of all things which exist beyond and on this side of the junction of the optic radii (p.111).

By a similar argument he stated that the double images, K and L, produced by object I beyond the point of fixation are also seen in the horopter.

We now use the term "horopter" to refer to the locus in space within which an object must lie to appear fused. Thus, one cannot credit Aguilonius with the discovery of the horopter as we now use the term. Aguilonius built an instrument to measure the spacing of double images in the horopter as he defined it, which was fancifully illustrated by Rubens (Figure 1.4c). In the actual instrument, the vertical plane could be moved to different distances from the observer.

It seems from Ruben's illustration, from Figure 1.5a, and from Aguilonius' account that he used his instrument to plot the projected positions of disparate images rather than the locus of fused images. Aguilonius maintained that the horopter defined this way is a frontal plane passing through the point of convergence. He probably believed this because the double images of objects well outside the frontal plane appeared to lie in the frontal plane. We will

see in Chapter 2 that the horopter, defined as the locus of fused images, is approximately a circle passing through the point of convergence and the two eyes—the Vieth-Müller circle. Alhazen had already proved in the eleventh century that the locus of fused images is not the frontal plane, although he did not establish the shape of this locus. Aguilonius had read Alhazen and cited him four times. However, he did not refer to this proof or to Alhazen's demonstrations on the limits of fusion and cyclopean vision. In fact, as far as we can determine, nobody has cited this aspect of Alhazen's work.

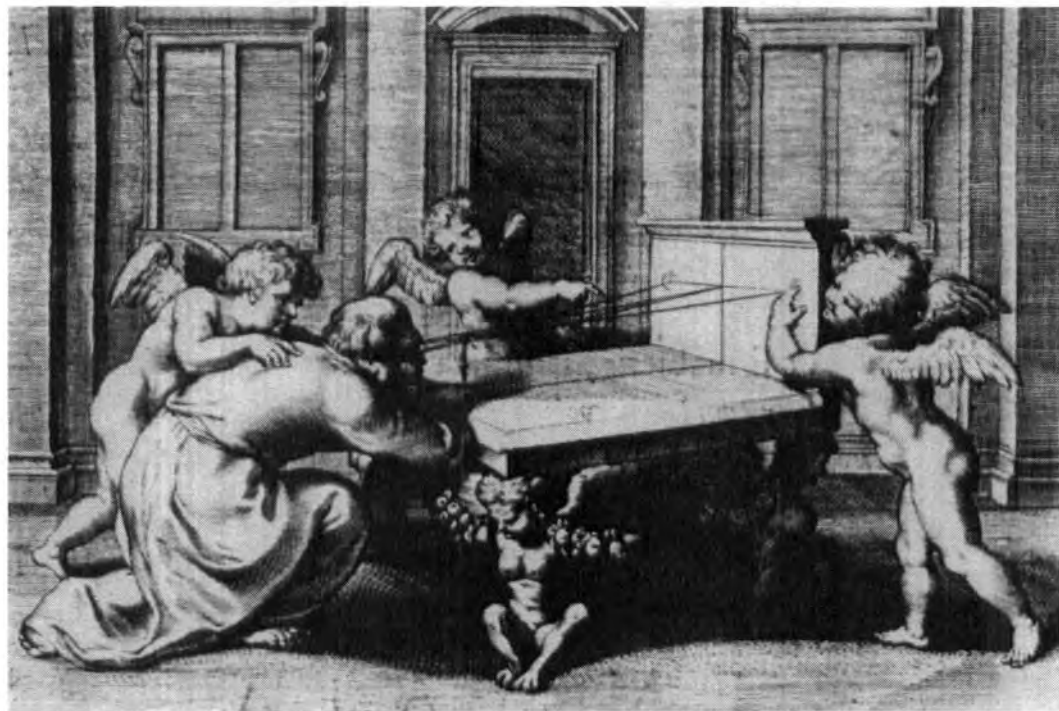
On page 156 of his book Aguilonius produced the drawing shown in Figure 1.5b, accompanied by the following statement;

If objects fall upon different radii, it can happen that things at different distances can be seen at equal angles. If point C be directly opposite the eyes, A and B, with a circle drawn through the three points, A, B, and C. By theorem. 5 of Euclid's Fourth book, any other point D on its circumference which lies closer to the observer than C, will subtend an angle ADB which will equal angle ACB by theorem 21 of Euclid's Third. Therefore, objects at C and at D are judged equally far from the eye. But this is false, because point C is farther away than D. Therefore a judgment of distance is false when based on the angles between converged axes, quod erat probandum.

At first glance it looks as though Aguilonius discovered the geometrical horopter more than 200 years before Vieth and Müller! However, it is clear from this quotation that he was concerned to prove that objects equidistant from an eye do not subtend equal angles to the two eyes. He thought of his circle as the locus of equal angles of convergence of visual lines rather than as the locus of zero disparity. It would have been an easy step to prove that these are theoretically the same thing but Aguilonius did not take that step, probably because he did not have a clear conception of how light rays are projected onto the retinas. His eyes are represented only by points. The Aguilonius book appeared 2 years after Kepler's *Dioptrice* but it seems that Aguilonius was not aware of Kepler's work on the formation of the retinal image. In spite of the fact that Alhazen had already proved that the locus of fused images does not lie in the frontal plane, the idea of a frontal-plane horopter persisted until the middle of the nineteenth century when, as we will see in Chapter 2, Vieth used the same Euclidean theorems to prove that, theoretically, the locus of equal angles of binocular subtense is the locus of fused images and both are a circle passing through the centres of the eyes. He was apparently unaware of the Aguilonius contribution.



(a) A one-eyed man underestimating the distance of a stick illustrates the general point that binocular vision aids in the perception of distance.



(b) A demonstration of the horopter as defined by Aguilonius. The eyes are converged on a point on the vertical plane, which is therefore seen single, and the disparate images of the small sphere in front of the plane are shown projected on the far plane. (Reproduced from *Opticorum Libri Sex*, shelf mark Savile 0.2, pp. 151 and 195 in the Bodleian Library, University of Oxford.)

Figure 1.4. Rubens' illustrations from Aguilonius (1613).

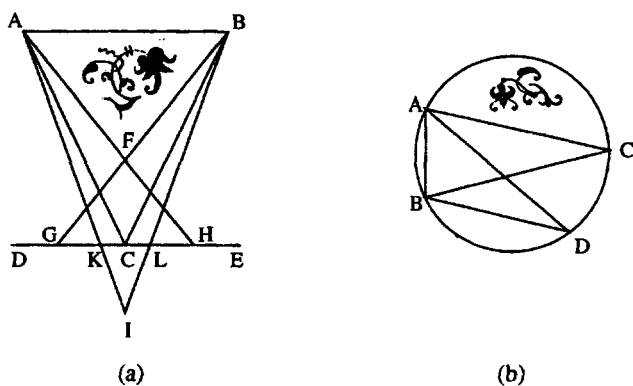


Figure 1.5. Diagrams from Aguilonius (1613).

(a) The horopter, defined as the plane in which double images appear to lie (p. 111). The eyes are at *A* and *B* and are converged on point *C* on a frontal plane, *DE*, defined as the horopter. An object at *F* produces disparate images, which project onto the plane of the horopter at *G* and *H*. The images of an object at *I* project to *K* and *L*.

(b) The locus of equal convergence of visual lines (p. 156). The eyes are at *A* and *B* and points on a circle through the eyes project equal angles to the two eyes.

The seventeenth and eighteenth centuries

Other writers in the seventeenth and eighteenth centuries, including Rohault (1671), Nicholas Malebranche (1674), and Robert Boyle (1688), clearly stated that binocular vision contributes to the impression of visual depth. Like Aguilonius, they noted that it is more difficult to reach accurately for an object with one eye than with two. Rohault noted that after losing one eye people recover the ability to judge the distances of objects and suggested that they use parallax generated by moving the head from side to side. This suggests that he was aware of the use of binocular parallax by people with two eyes. Sébastien Le Clerc (1679), an authority on perspective, clearly described the differences between the images of a solid object in the two eyes but did not relate these differences to the perception of depth. Smith (1738) in his *Compleat system of opticks*, described how he sighted a distant object between the points of a vertical pair of dividers about 6 cm apart. When the dividers were placed at the correct distance, the inner pair of diplopic images fused to create the impression of a rod extending down the midline from the hand to the distant object. This is essentially the same effect that Alhazen had observed when looking at the fused image of lines extending out from the two eyes. Porterfield (1759) produced drawings of an object as seen by each eye. Joseph Harris, Master of the Mint in London, who died in 1764, made drawings of crossed and uncrossed disparities arising from objects nearer and further than the point of fixation, as had Aguilonius

before him. He realized, as had da Vinci, that binocular parallax contributes to the impression of depth, not only between an object and its background, but also within a single object, as revealed in the following passage from his *Treatise of Optics*, published in 1775, 11 years after his death.

And by the parallax on account of the distance betwixt our eyes, we can distinguish besides the front, part of the two sides of a near object . . . and this gives a visible relieu to such objects, which helps greatly to raise or detach them from the plane, on which they lie. Thus, the nose on a face, is the more remarkably raised by seeing each side of it at once. These observations, I say, are of use to us in distinguishing the figures of small and near object; and when the breaks, prominences and projections are more considerable, we do not want them. The distances betwixt the legs of a chair, are visible many yards off, and the projection of a building is visible still farther. But as the distance is increased, different degrees of eminances, cavities, et cetera, disappear one after another. (p. 171)

It is also clear from this passage that Harris realized that disparity information is scaled by absolute distance. He seems to have been the first to realize this. He used the term "horopter" in its modern sense as the locus of objects producing fused images. However, he believed the horopter to be a frontal surface. He also wrote; "An object that is a little out of the plane (of the horopter), may yet appear single. . . . it will also shift its place by winking either eye, and looking at it with both eyes." (p. 113). This is description of Panum's fusional area, written 700 years after Alhazen had made the same point and 80 years before the account provided in 1858 by Peter Ludvig Panum, professor of physiology at Kiel University. The quotation also clearly states the principle of parallactic motion, although a similar observation had been made by Galen.

The Vieth-Müller circle

Vieth (1818) was the first to specify clearly the geometry of corresponding points and of the horizontal horopter as the locus of objects producing fused images. He wrote,

*Firstly it is correct and established from common experience, that point *P* in Fig. 2 (Figure 1.6) towards which both eyes are directed, or at which both visual axes intersect is seen singly.*

*Whether the so-called corresponding points *M* and *N*, or more specifically, whether these images of a point *X* are equidistant or at unequal distances from *A* and *B*, the images of point *P*, that depends on whether the angles *o* and*

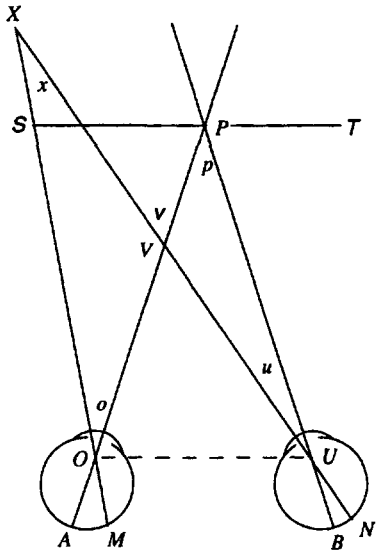


Figure 1.6. Drawing used by Vieth (1818).

Vieth used this drawing to prove that the horizontal horopter is a circle passing through the optical centre of each eye (O and U) and fixation point P . Points A and B represent the foveas and are therefore corresponding points. Points M and N represent the images of point X and fall on corresponding points when M is as far from A as N is from B . This is true when angles o and u are equal. But angles o and u are equal when angles x and p are equal, since they belong to similar triangles OXV and UPV . Angles x and p are equal when they fall on the circumference of a circle passing through O and U , since angles subtended on a circle by common chord OU are equal. Line ST is the frontal-plane.

u at the pupil are equal or unequal. However, $o = v - x$ and $u = v - p$. Therefore, . . . if x is equal to p , then o is equal to u .

Thus, in that condition, where the angles p and x are equal, the images M and N are equidistant from A and B , and this case occurs when X lies on the circumference of a circle, which passes through O and U and P , because all angles on this circumference are subtended by the same chord OU .

Here Vieth applied the same geometrical theorems that Aguilonius used to establish the isovergence locus, to establish the locus of single vision—the horopter. Instead of a frontal plane through the fixation point, the horopter is a circle through the fixation point and the centre of each eye. Vieth went on to write,

Thus, if by the expression corresponding points one understands such points which lie in the same direction in both eyes, and are equidistant from A and B which seems to me the correct meaning, and one asserts one sees that thing singly whose images fall on such corresponding points, then, according to this rule, one sees that thing singly which is situated within the boundary of a sphere

which passes through O , U , P , hence, not what lies in the plane ST , which one has called the horopter.

Here Vieth incorrectly generalized his principle of corresponding points in claiming that the horopter is a sphere rather than a circle. Not all angles subtended by a chord on the surface of a sphere are equal. As we will see in Chapter 2, the theoretical horopter for parallel visual axes is an infinite toroid formed by sweeping the horopter circle about the interocular axis. Prévost (1843) first pointed out that when the visual axes are converged, the horopter is not a surface but a horizontal circle and a vertical line in the median plane of the head (see Section 2.7).

Vieth went on to state, as had Alhazen in the eleventh century, that an object positioned between the visual axes projects images on opposite sides of the image of the fixated object, whereas an object to either side of the two visual axes produces images that fall on the same side of the image of the fixation point. He also stated, as others had before him, that an object nearer than the fixation point produces images which are crossed with respect to the fixation point and an object beyond the fixation point produces uncrossed images. These ideas are explained more fully in Section 2.3.1.

Johannes Müller (1826) produced a similar and independent analysis, but became aware of Vieth's work, which he acknowledged in his paper. The theoretical horizontal horopter is now known as the Vieth-Müller circle. Müller had the horopter passing through the centres of the two lenses. He discussed binocular disparity in the context of fusion and rivalry of binocular images and concluded that the differences between the images in the two eyes were too small to be detected. In 1843, 5 years after Wheatstone reported that disparate images produce a sensation of depth, Müller agreed that disparity is involved in the perception of depth. Volkmann (1836) first specified the geometrical assumptions underlying the theoretical horopter, and Helmholtz in 1866 generalized the geometry of the horopter over the visual field (Helmholtz 1909). For more details on the history of the horopter, see Shipley and Rawlings (1970a).

Wheatstone

Sir Charles Wheatstone (see Figure 1.7) was born near Gloucester, England, in 1802. As a young man he made and sold musical instruments, but he also wrote some scientific papers on acoustics. One of his inventions gave rise to the accordion. Throughout his life he contributed to many fields, including chronometry, optics, cryptography, and telegraphy, and he invented many useful devices before his



Figure 1.7. Sir Charles Wheatstone.
An engraving from a photograph from the *Illustrated London News* (1868, 52, p. 145). (Reproduced by permission of Illustrated London News Picture Library.)

death in Paris in 1875. In 1834 he became professor of experimental physics at King's College, London. Towards the end of 1832 he had two stereoscopes made by Murray and Heath, opticians in London. One was a mirror stereoscope and the other a prism stereoscope (see Gernsheim 1969). But he became involved with the electric telegraph and waited until 1838 before reporting the details of construction of the mirror stereoscope and his experiments with the new instrument to the Royal Society (Wheatstone 1838). He called his new instruments stereoscopes although Aguilonius had used the word "stéréoscopique" in 1613 to denote binocular vision. He stated the principle of the stereoscope thus,

It being thus established that the mind perceives an object of three dimensions by means of the two dissimilar pictures projected by it on the two retinas, the following question occurs. What would be the visual effect of simultaneously presenting to each eye, instead of the object itself, its projection on a plane surface as it appears to that eye? To pursue this inquiry it is necessary that means should be contrived to make the two pictures, which must necessarily occupy different places, fall on similar parts of both eyes. (p. 373)

His mirror stereoscope consisted of two mirrors at right angles and two vertical picture holders

(Figure 1.8a). In a later version, shown in Figure 1.8b, the two halves could be rotated to change the angle of convergence. He described twenty pairs of pictures, or stereograms, that appeared solid when viewed in his stereoscope. These included a series of points stepped in depth, a cube, a cone, and a pyramid, as shown in Figure 1.9. He observed that all these shapes appeared flat when the pictures in the two eyes were the same and appeared in reverse depth when the pictures with disparity were reversed to the two eyes.

The essence of any stereoscope is that it allows one to control the inputs to the two eyes separately. An experimenter can thus isolate binocular variables and study their effects quantitatively—it provides an experimenter with dichoptic control. With his new instrument Wheatstone demonstrated the relationship between binocular disparity and depth perception. His stereoscope with adjustable arms allowed him to vary convergence while keeping disparity constant, and thus show that impressions of depth do not depend on disparity alone. The invention of the stereoscope was the crucial event that inaugurated the modern study of stereoscopic vision.

In 1852 Wheatstone presented a second paper to the Royal Society in which he described the pseudoscope which reverses the inputs to the two eyes, thus reversing the sign of disparity and making concave surfaces appear convex. In a communication to the Microscopical Society, Wheatstone (1853) described a binocular microscope made by a Capuchin monk, Père Chérubin d'Orléans, in 1677 and presented to the Dauphin of France. Chérubin d'Orléans also made a binocular telescope in 1671. However, each image in these instruments was inverted so that it created a pseudostereoscopic effect in which the sign of disparity was inverted. Wheatstone also drew attention to a binocular microscope made by Riddell (1853) to which additional erecting eye pieces were added to produce a true stereoscopic effect (see Wade 1981). These devices were not stereoscopes because the stimuli were simply objects viewed by both eyes. Dubbosq and Claudet attempted to combine the stereoscope with moving photographic pictures to produce moving three-dimensional pictures (see Gernsheim 1969). William Shaw (1861) combined a thaumatrope, which produced an impression of a moving object from a sequence of images on a revolving drum, with a mirror stereoscope to produce a moving stereoscopic picture. One of his displays was of a moving train. He called this instrument the "stereotrope" and showed it at the International Exhibition of 1862. In February of 1860, P. H. Desvignes registered a patent of a similar device and also used a train as one of his pictures.

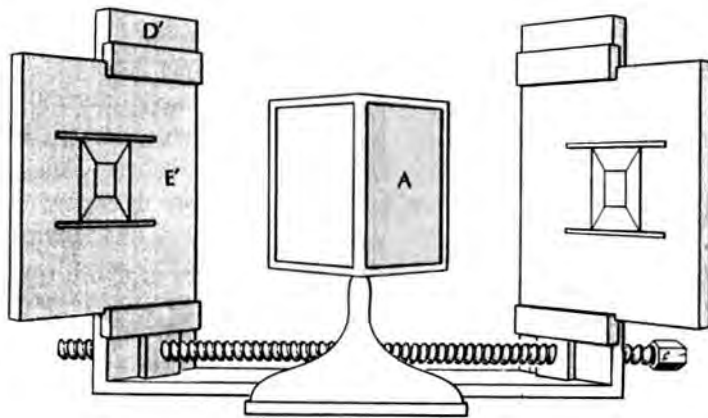


Figure 1.8. Wheatstone's first mirror stereoscope. (From Wheatstone 1838.)

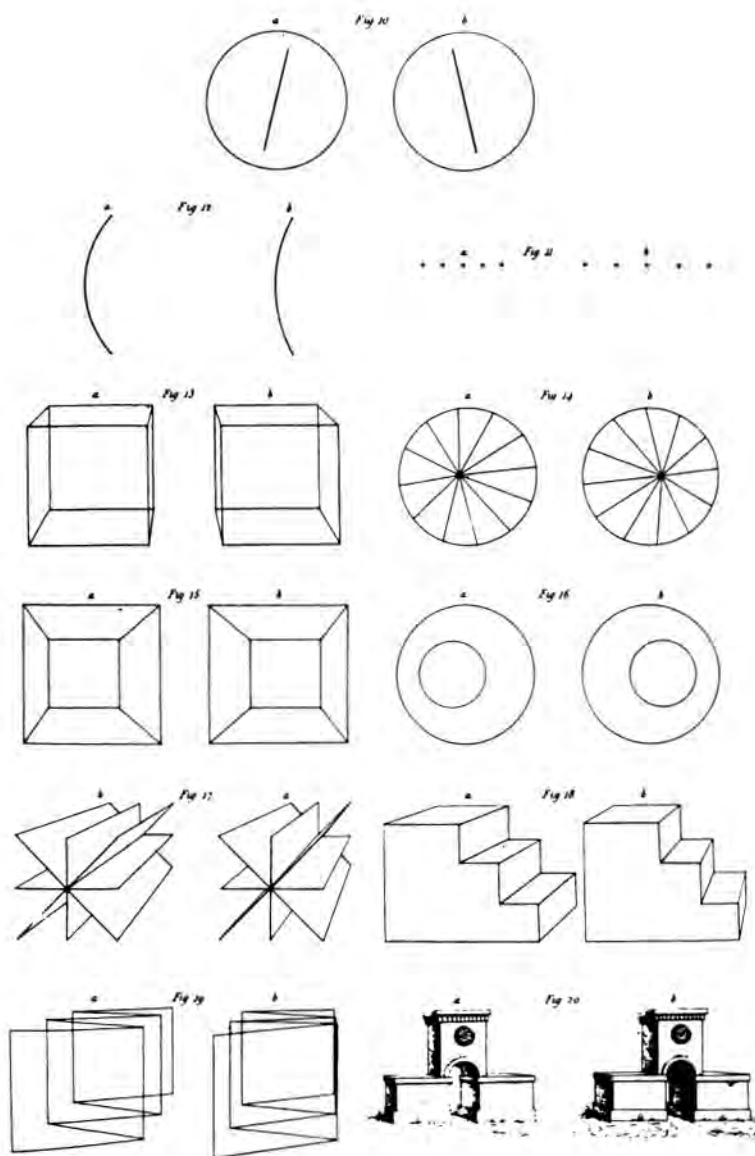


Figure 1.9. Wheatstone's stereograms.
(From Wheatstone, Philosophical Transactions of the Royal Society, 1838.)



Figure 1.10. Sir David Brewster.

An engraving from a photograph in the *Illustrated London News* (1868, 52, p. 189). (Reproduced by permission of the *Illustrated London News Picture Library*.)

Brewster and stereoscopic photography

Sir David Brewster (see Figure 1.10) was born in Jedburgh, Scotland, in 1781, the son of the rector of Jedburgh grammar school and died in 1868. He wrote many scientific papers on optics, especially on the polarization of light, and invented the kaleidoscope. He was a scientific editor, college principal at St. Andrews University, Principal of Edinburgh university, and secretary to the Royal Society of Edinburgh. Brewster witnessed Wheatstone's demonstration of his mirror stereoscope at the Royal Society and bought a model with which he began his own experiments. In 1849 he described to the Royal Society of Edinburgh a stereoscope in which two side-by-side pictures were placed in a box and viewed through prisms which fused and magnified the images. A description was also included in his book on stereoscopes published in 1856. Brewster made his original stereoscope by cutting a convex lens in half and arranging each half with its vertical cut edge on the temporal side of an eye. A picture of an early instrument is shown in Figure 1.11. An example of one of the earliest stereograms produced for the prism stereoscope is shown in Figure 1.12a. The prism, or lenticular, stereoscope is still referred

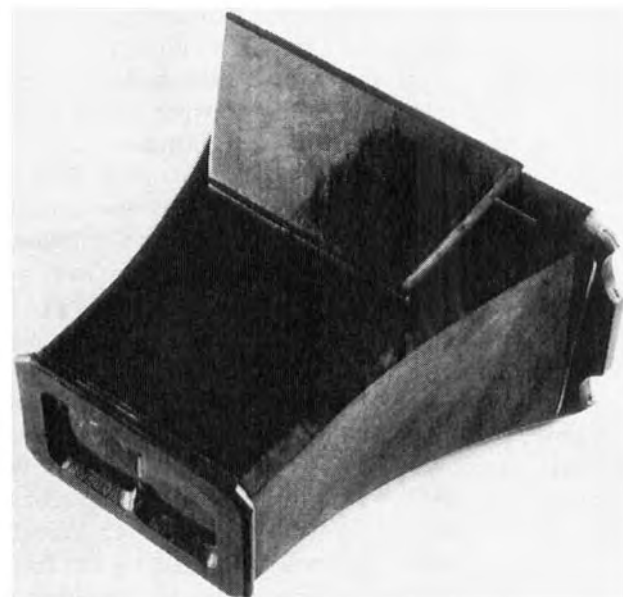


Figure 1.11. Brewster's prism stereoscope.

This early model has fixed prisms, later models have adjustable eyepieces. A mirror in the hinged panel reflects light onto the stereogram.

to as the Brewster stereoscope, although Wheatstone had one made in 1832.

Brewster wrote an anonymous letter to the *Times* in October 1856 in which he disputed Wheatstone's claim to the invention of the stereoscope and the principle upon which it was founded. Wheatstone effectively refuted Brewster and the two men engaged in an acrimonious correspondence in the newspaper. In 1859 Brewster attacked Wheatstone again, claiming that two similar drawings by the seventeenth century artist Jacopo Chimenti were a stereogram. But it was generally agreed that the differences between the drawings were accidental and not related to binocular disparity. A lively account of the debate between these two men is provided by Wade and Ono (1985) and Ono and Wade (1985), and the works of Wheatstone and Brewster have been edited by Wade (1983).

Joseph Niépce produced the first photograph in about 1826 and Louis Daguerre produced his first successful daguerreotype photograph in 1837. In 1841 Wheatstone employed two photographers to help him produce the first photographic stereogram which was a portrait of Charles Babbage. By 1846 stereoscopic photographs were being sold in a shop in Soho Square, London. However, stereoscopic photography did not arouse much interest because inexpensive stereoscopes were not available. Brewster took his prism stereoscope to Paris in 1850 and engaged the interest of the optician Jules Duboscq who built a number of them. These stereoscopes were

shown in London at the Great Exhibition of 1851 and one was made specially for Queen Victoria who took a great interest in the device. Within three months nearly a quarter of a million prism stereoscopes were manufactured and sold in London and Paris. Duboscq patented the prism stereoscope in 1852, but the patent was successfully challenged and annulled in 1857. Stereoscopic views of the Great Exhibition of 1851, such as those shown in Figure 1.12b, were particularly popular because people who could not get to London were able to see the exhibits. The photographer Claudet devoted himself to the improvement of stereoscopic photography and patented a folding pocket version of the prism stereoscope. A rotary stereoscope holding 50 or 100 views was made in England in 1854. A hand-held version of the prism stereoscope designed by Oliver Wendell Holmes in 1863 was mass produced by his friend Joseph Bates as a popular item of home entertainment. It is readily available in antique shops and is still manufactured.

In 1854 George Swan Nottage, a man of humble origin and limited education, founded the London Stereoscopic Company. By 1858 the company had sold over half a million stereoscopes and its travelling photographers had produced 100,000 stereoscopic photographs of famous places from many parts of the world. Nottage died in 1885, a wealthy and honoured man. Stereoscopic photography was introduced into the United States by William and Frederick Langenheim in 1854 who founded the American Stereoscopic Company in New York in 1861. By 1862 more than a thousand professional photographers were producing stereoscopic photographs, which were sold by the million. Until the advent of the cinema, the stereoscope was the optical wonder of the age, allowing people to see the world in the comfort of their own living rooms. See Darrah (1964) and Gernsheim (1969) for more details on the history of stereoscopic photography. In 1992 there was a dramatic resurgence of interest in stereoscopy with the advent of the random-dot autostereogram, described in Section 1.3.3.

In 1960 Bela Julesz, introduced the random-dot stereogram which allows one to create an impression of depth in the absence of all monocular cues and a three-dimensional object which is not visible in either monocular image. This technique had a profound effect on research into mechanisms of stereoscopic vision (see Section 5.2.3).

Discovery of the physiological basis of stereopsis
Before the 1960's many visual scientists believed that binocular stereopsis did not arise from the conjunction of visual inputs at an early stage of visual

processing, but from high-level cognitive processes. This idea was motivated by the belief that only higher mammals have stereoscopic vision and the observation that the three-dimensional appearance of the world does not change appreciably when one eye is closed. Helmholtz (1893, p. 262) wrote,

We therefore learn that two distinct sensations are transmitted from the eyes, and reach consciousness at the same time and without coalescing; that accordingly the combination of these two sensations into a single perceptual picture of the external world is not produced by any anatomical mechanism of sensation, but by a mental act.

He realized that stereopsis depends on the registration of disparities but argued that;

the coincidence of localization of the corresponding pictures received from the two eyes depends upon the power of measuring distances of sight which we gain by experience.

This view stemmed from his empirical theory of vision and his associated theory of unconscious inference, summed up in his dictum;

we always believe that we see such objects as would, under conditions of normal vision, produce the retinal image of which we are actually conscious.

Sherrington, also, concluded from his work on binocular flicker that monocular images are processed independently and that the final synthesis is "mental".

Ramón y Cajal (1911) proposed that inputs from corresponding regions of the two retinas converge on what he called "isodynamic cells", and that this mechanism forms the basis of unified binocular vision. This idea received experimental verification when Hubel and Wiesel (1959, 1962) reported that the receptive fields of binocular cells in the visual cortex of the cat occupy corresponding positions in the two eyes. If a binocular cell had identical receptive fields, identically positioned, in each eye, it would respond optimally to stimuli with zero binocular disparity, and depth could not be recovered from its output. This was the gist of Helmholtz's argument against the idea of convergence of visual inputs. The problem would be solved if there were cells specifically tuned to similar images in slightly different positions in the two eyes. Different cells would be optimally tuned to different disparities. Simple as this idea is, it was not proposed until 1965. This is probably because the idea of any cortical cell being tuned to a specific stimulus feature was not in vogue until 1959 when Hubel and Wiesel discovered

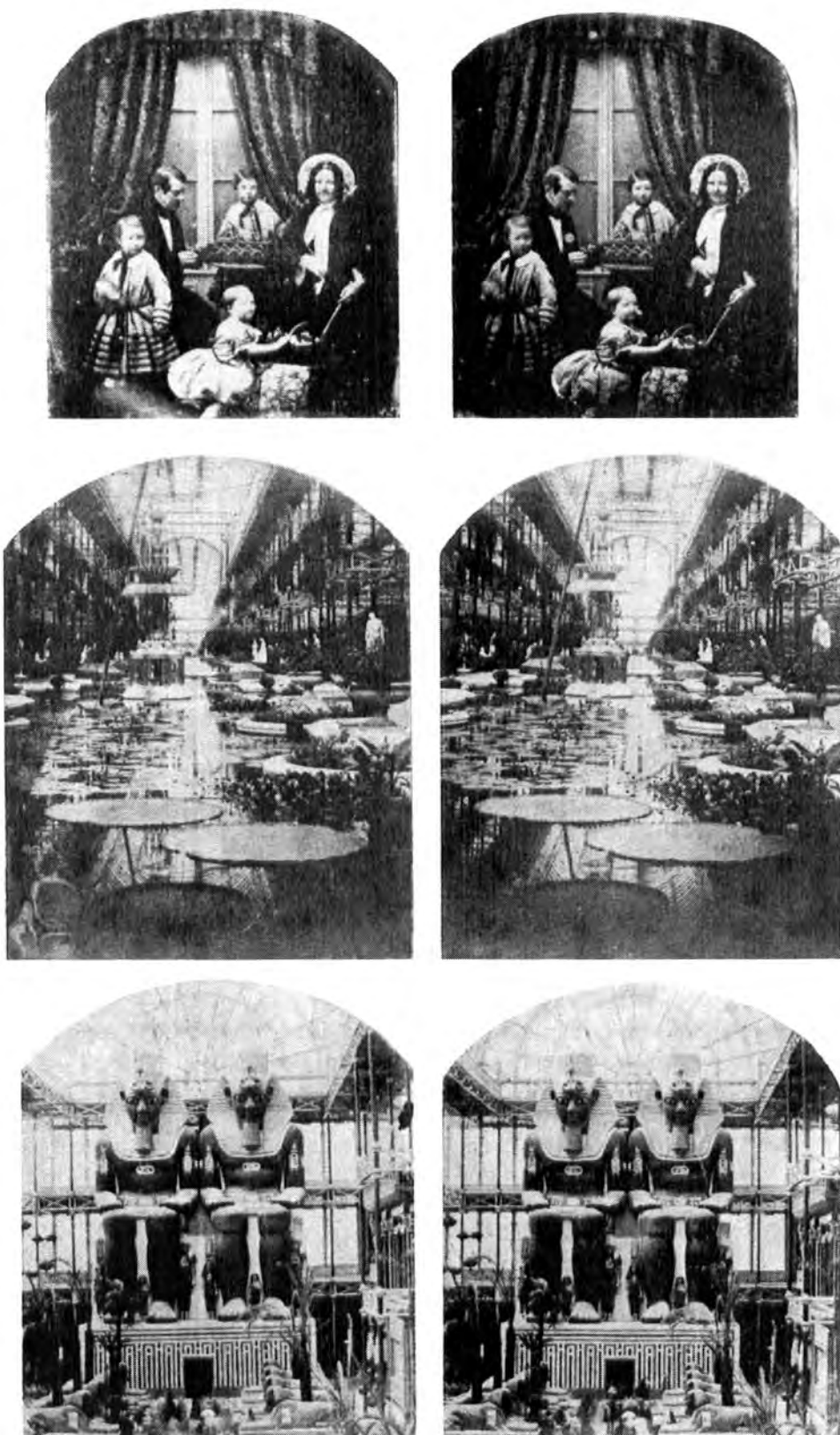


Figure 1.12. Early photographic stereograms.

The top stereogram is the Wheatstone family photographed by Antoine Claudet probably in the mid 1850's. (Reproduced by permission of the National Portrait Gallery.)

The lower stereograms are views of the Great Exhibition of 1851 in the Crystal Palace, London. These stereograms should be viewed with the stereoscope or with divergent fusion.

cortical cells tuned to stimulus orientation and movement. Hubel and Wiesel reported that the receptive fields of binocular cells occupy corresponding positions in the two eyes and thus failed to find disparity-sensitive cells. But they did not have close control over positions of the eyes and it is not clear from their report whether they had thought of binocular cells devoted to the detection of disparity.

It seems that the idea of disparity detectors at an early stage of visual processing was first proposed by Jack Pettigrew in his undergraduate thesis written in the University of Sydney in 1965. He got the idea while inspecting a Julesz random-dot stereogram and mentioned it to his supervisor Peter Bishop who was working on binocular cells in the cat visual cortex, but not with this particular idea in mind. Bishop, suggested to Pettigrew that he repeat Hubel and Wiesel's experiments on the visual cortex of the cat using a Risley prism to control the disparity of the images from a single display rather than using separate stimuli for each eye. The search for binocular cells selectively tuned to different disparities was beset with the problem of ensuring that the images in the two eyes were in binocular register. Pettigrew solved this problem by paralyzing the extraocular eye muscles with gallamine and curare.

Bishop took Pettigrew's thesis to a Conference in California in 1966 and showed it to Horace Barlow who had just set his graduate student, Colin Blakemore, the task of looking for disparity detectors. Barlow invited Pettigrew to work with him and Blakemore at Berkeley. The three of them confirmed the presence of disparity-sensitive cells in the visual cortex of the cat and reported their findings in 1967 (Barlow et al. 1967). They found that certain binocular cells in the visual cortex of the cat respond selectively to line and bar stimuli having a particular binocular disparity, that is, stimuli normally produced by an object at a given distance from the plane of fixation. Similar findings, based on work done between 1965 and 1967, were reported about the same time from the University of Sydney, Australia by Pettigrew, Nikara, and Bishop (1968). The history of these discoveries is described by Bishop and Pettigrew (1986) and subsequent developments are described in Section 4.4. Disparity detectors in the primary visual cortex of the monkey were first reported in 1977 by Gian Poggio and his coworkers at the University in Baltimore.

For more details on the history of visual optics and binocular vision see Lindberg (1976), Polyak (1957), and Gulick and Lawson (1976). Wade (1987) provides a particularly interesting account of the development of the stereoscope.

1.3 STEREOSCOPIC TECHNIQUES;

1.3.1 Types of stereoscope

The mirror stereoscope

The optical features of the mirror stereoscope are shown in Figure 1.13a. Mirror stereoscopes are often referred to as Wheatstone stereoscopes. Displays of up to 90° of visual angle can be viewed in a mirror stereoscope, which is the most precise and versatile type of stereoscope for research purposes. If the mirrors are replaced by semisilvered mirrors, a stereoscopic image formed by the combination of the two side displays is combined with a display presented in the frontal plane. If the side displays are mounted on arms hinged about a point beneath each eye, the subject's position of vergence can be controlled. Clinical instruments used in orthoptics, such as amblyoscopes and synoptoscopes, are essentially mirror stereoscopes, with adjustable vergence and devices for controlling the luminance and size of each image (see Section 10.2.3).

The prism stereoscope

In Brewster's original prism stereoscope, dichoptic displays were printed side by side about 6.5 cm apart on a rectangular card and viewed through two base-out prisms, as shown in Figure 1.13b. The partition between the eyes allows each eye to see only half of the stereogram. Magnifying lenses incorporated into the prisms enlarge the picture and allow one to accommodate on the stereogram. For this reason, this type of stereoscope is also known as a lenticular stereoscope.

Prisms cause vertical lines to appear curved. In the prism stereoscope, the apparent curvature is in opposite directions in the two eyes and causes a rectangular grid to appear concave, a fact first noticed by Antoine Claudet (1856). This problem is overcome by omitting the prisms, as in the stereoscope included with this book. In this stereoscope each eye sees through the centre of a complete convex lens, which allows the viewer to accommodate on the images at close distance but does not displace the image. This lens is not essential, and fusion of any of the stereograms in this book is facilitated by simply holding a card about 20 cm long between the eyes so that each eye sees only its own half image. To fuse the images without prisms, the eyes must diverge beyond the plane of the stereogram but most people have no difficulty doing this since the partition between the eyes removes the tendency to remain converged in the plane of the stereogram. With a partition, the images can be fused only by divergence, whereas without the partition, the images can

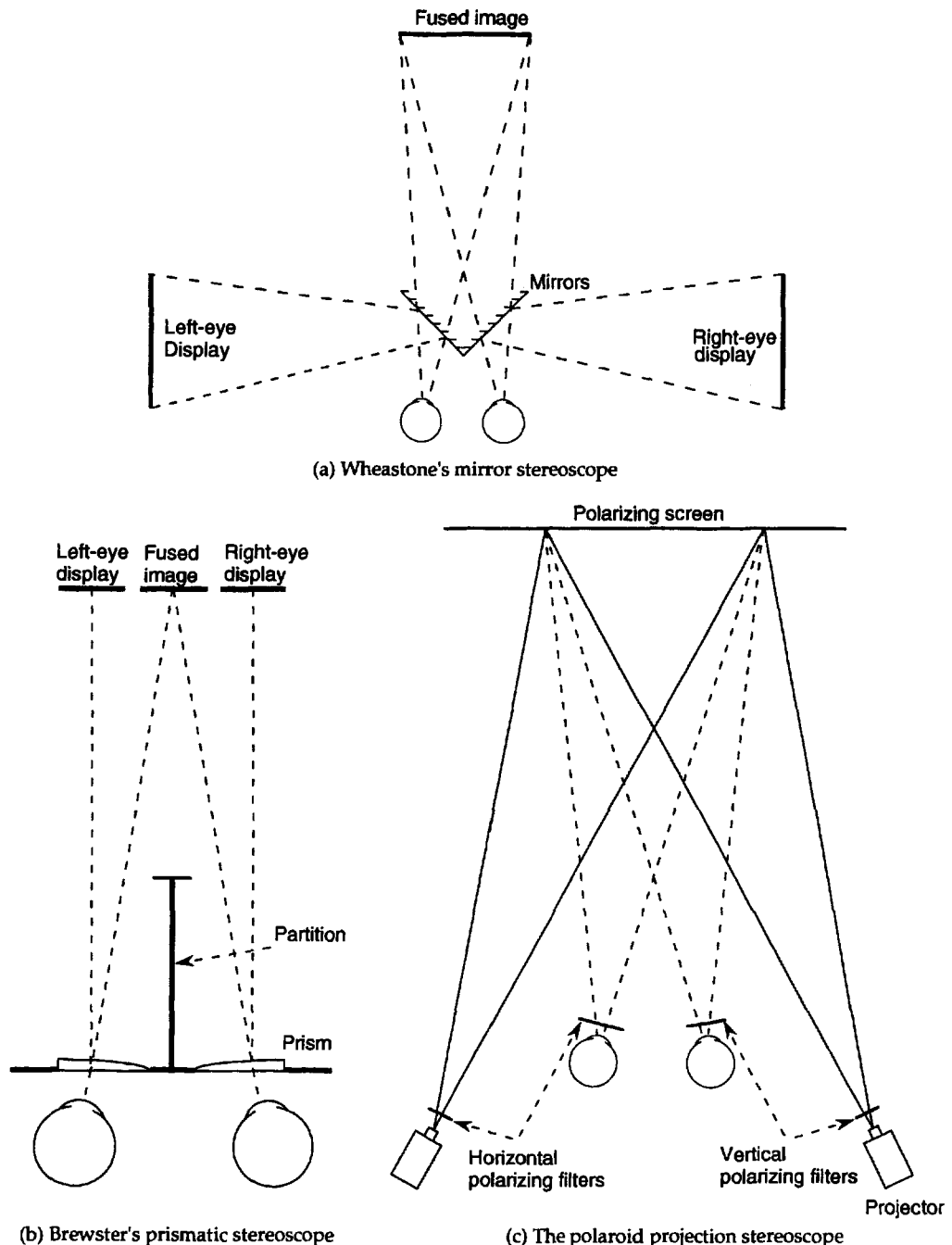


Figure 1.13. The optical features of various types of stereoscopes.

be fused by either convergence or divergence, once the tendency to converge in the plane of the stereogram is overcome. Thus, the essential element in a prism stereoscope is the partition rather than the prisms.

The size of picture that can be placed in a prism stereoscope is limited by the interocular distance, which subtends about 20° of visual angle at a viewing distance of 20 cm. Pictures taken with a stereoscopic camera through wide-angle lenses encompass

a broad view of the scene but suffer from severe fish-eye distortion. However, if the distorted pictures are viewed in a Brewster stereoscope through similar wide-angle lenses, an undistorted wide-angle view of the original scene can be seen. Stereoscopes constructed in this way are available commercially

Anaglyphs

The anaglyph process was patented by Louis Ducos du Hauron in September 1891, although a similar

process was described by the Frenchman J. C. d'Almeida in 1858 and the German W. Rollmann in 1853 (see Gernsheim 1969). In anaglyph stereoscopy, slides of dichoptic displays are projected on a screen, one through a green filter and one through a red filter. Otherwise, red and green pictures are printed one on top of the other on the same sheet of paper. The subject wears red and green filters with the red-filtered eye seeing only the green picture and the green-filtered eye seeing only the red picture. There is some loss of resolution and some colour rivalry with anaglyph pictures and the method cannot be used when the colour of the display is important.

The polaroid stereoscope

The polaroid stereoscopic system was first described by J. Anderson in 1891 (see Gernsheim 1969). Dichoptic displays are projected onto the same screen through two projectors with oppositely oriented polaroid filters (Figure 1.13c). The viewer uses cross-polarized spectacles so that the left eye sees only the picture projected by the projector on the left and the right eye only that projected by the projector on the right. The screen must have an aluminized surface, since other types of screen do not preserve the plane of polarization of reflected light. There is no limitation on the size of display, but polaroid filters dim the image and attenuate the light to the other eye by only 1 to 1.5 log units.

The shutter stereoscope

In a shutter system, the dichoptic pictures are presented in rapid alternation on a computer monitor. The subject views the display through electro-optic shutters that alternately occlude the two eyes in phase with the alternation of the display. Some flicker is evident with the frame speed of 30 Hz used on most computers. This can be avoided with more expensive systems running at 60 Hz in each eye.

1.3.2 Three-dimensional imagery

Slice-stacking stereo imagery

A three-dimensional picture can be built up by scanning an optical display with a flexible mirror (varifocal mirror) vibrating at 30 Hz in response to an acoustic signal. The system was developed by A. C. Traub of the Mitre Corporation in 1970 (see Okoshi 1976). The viewer looks into the mirror set at 45° to the screen of a cathode-ray tube. The vibration changes the focal length of the mirror to focus the image on the cathode-ray tube at various distances within a defined volume. For each position of the mirror the appropriate part of the scanned picture is imaged by the mirror. The image is scanned twice in

each complete vibration of the mirror, producing an effective scan frequency of 60 Hz. The effect is equivalent to that produced by tracing out a three-dimensional form by rapid movements of an LED. Fine continuous gradations of depth can be created limited only by the bandwidth of the cathode-ray tube and the persistence of the phosphor. However, only green phosphors are of sufficiently short duration. The changing focal length of the mirror introduces unwanted changes in the size of the image. These distortions can be compensated for in computer generated images. Since the image is truly three-dimensional, it produces true parallax when viewed from different vantage points and also the correct changes in accommodation when convergence changes.

Computer-generated holography

Three-dimensional images can also be built up by holography (Tricoles 1987). Until recently, moving holographic images could not be created in real time because of the heavy computational load. There has been some progress in solving this problem (see McKenna and Zeltzer 1992). Coloured holograms have been created but at the cost of lower resolution. Like image-stacking displays, holograms produce true parallax, that is, the form of the image changes appropriately with changes in vantage point. They also provide correct changes in accommodation. Jones and Aitken (1994) have compared the data requirements of different types of three-dimensional imaging system.

1.3.3 Autostereograms

An autostereogram is a picture that appears three-dimensional without the aid of a stereoscope.

Parallax stereograms

In a parallax autostereogram, pictures of the left- and right-eye views of a scene are arranged in vertical strips and combined into a single picture in which right-eye and left-eye strips alternate. The object is first photographed from two vantage points with a plate of fine vertical slits placed over the film. A similar slit plate is placed over the composite developed picture. Since the periodicity of the picture strips corresponds to the periodicity of the slits in the slit plate, each eye sees only its own image when the stereogram is viewed from the correct distance. The geometry of a parallax autostereogram is depicted in Figure 1.14. The image seen by a particular eye through each slit is centred on a line of sight passing through the slit. The intersections of lines of sight from the two eyes through neighbouring slits

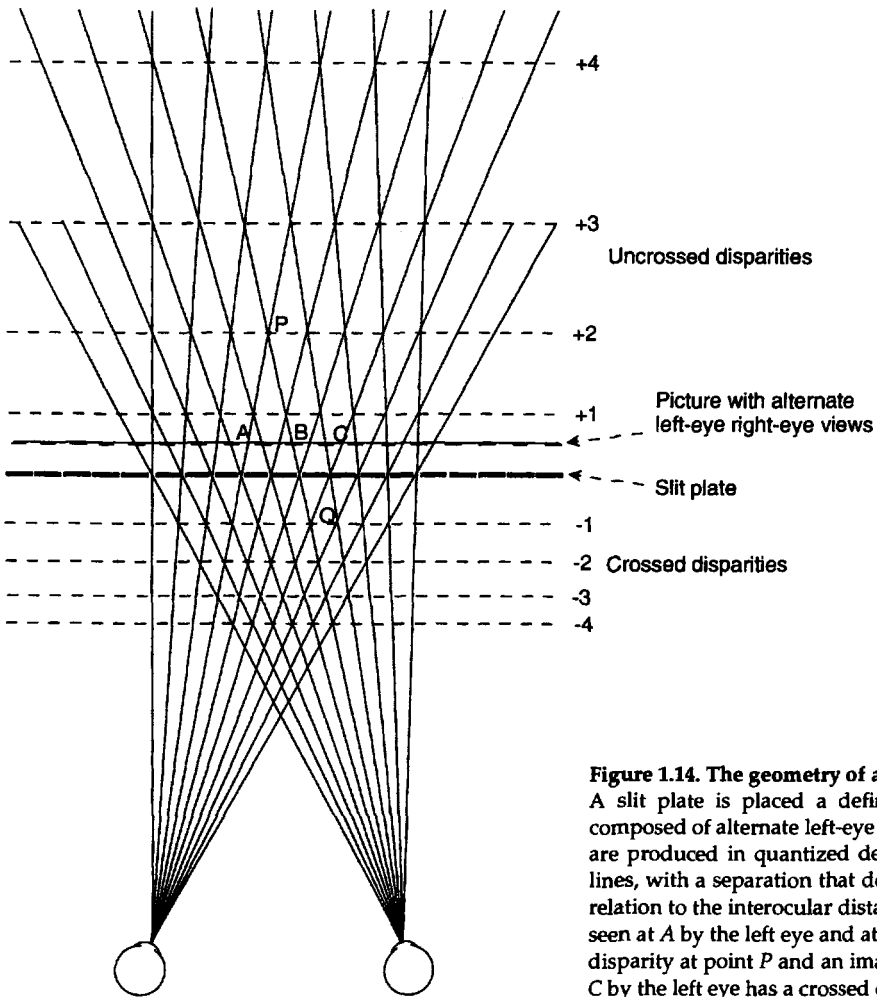


Figure 1.14. The geometry of a parallax stereogram.

A slit plate is placed a defined distance in front of a picture composed of alternate left-eye and right-eye vertical strips. Images are produced in quantized depth levels, indicated by the dotted lines, with a separation that depends on the spacing of the slits in relation to the interocular distance. For instance, a picture element seen at A by the left eye and at B by the right eye has an uncrossed disparity at point P and an image seen at B by the right eye and at C by the left eye has a crossed disparity at point Q.

define the first depth plane. The second depth plane is defined by the set of intersections through every second slit, and the third depth plane by intersections of lines through every third slit, and so on for other depth planes. Thus, the perceived image consists of discrete depth planes of increasing separation. The separation between the depth planes depends on the spacing of the slits in relation to the interocular distance and on the distance between the slit plate and picture. The viewing distance is governed by these same factors.

The parallax autostereogram was patented by F. E. Ives in 1903. Projection systems based on this principle were used in the cinema but had several drawbacks, including darkening of the image, image diffraction, and dependence on viewing position.

Lenticular-sheet stereograms

In a lenticular-sheet autostereogram, photographs are taken through multiple vertical cylindrical lenses so that the picture is composed of narrow vertical stripes arranged in alternating left-eye right-eye columns. A sheet of transparent plastic with multiple

vertical cylindrical lenses moulded into its surface is placed over the picture plane at the focal length of the lenses so that each image point produces a parallel beam (imaged at infinity). The periodicity of the vertical lenses allows each eye to see only one of the interleaved pictures. The geometry of lenticular-sheet autostereograms is similar to that for parallax stereograms, as depicted in Figure 1.14. By using several pairs of cameras and projectors, more than one pair of images may be registered behind each lens, allowing one to create images that can be viewed with parallax from different positions (McAllister and Robbins 1987). Lenticular stereograms have two advantages over parallax stereograms; they produce a brighter image, since there are no occlusions, and the effects of diffraction are less severe. They do not need a viewing instrument and are used commercially for picture postcards. However, the pictures are subject to chromatic aberration in the lenses and require the viewer to be approximately in the correct position. Projection systems using lenticular sheets have been developed but sheets for large pictures are expensive and

several projectors are required. A lenticular sheet can be placed over a computer-generated display (see McKenna and Zeltzer 1992). The construction and projection of lenticular-sheet stereograms are described in detail in Okoshi (1976).

Random-dot autostereograms

With a little training a person can learn to converge or diverge the eyes so as to fuse dichoptic pictures placed side by side. This is known as **free fusion**. The stimuli can be no wider than the angle through which the viewer can voluntarily converge or diverge the eyes. This limitation is overcome in the random-dot autostereogram, described next.

When a repetitive pattern, such as that shown in Figure 11.1, is viewed with both eyes, the images can be fused with various angles of convergence. As convergence changes, the images come into correspondence at every multiple of the spatial period of the pattern. The pattern appears closer and smaller when the eyes are converged, and larger and more distant when they are diverged. This is the wallpaper effect. Brewster (1844a, 1844b) created relative depth by introducing small horizontal deviations of opposite sign into adjacent elements of a repeating pattern. In 1970 Masayuki Ito, a Japanese graphic designer, produced the autostereogram shown in Figure 1.15, using four bands of random-dot patterns. In 1977 Alfons Schilling, a Swiss-American artist now living in Vienna, produced the autostereogram shown in Figure 1.16 (Sakane 1994). These autostereograms produce simple squares or rectangles in depth. In 1979 Christopher Tyler, with the help of computer programmer Maureen Clarke, showed that almost any stereoscopic figure can be generated by programming a computer to produce suitably designed deviations of a repetitive pattern of random dots (Tyler and Clarke 1990).

Figure 1.17 illustrates a simple method for constructing a random-dot autostereogram. The spaces between the outer dots (d_1) are slightly larger than those between the nine inner dots (d_2). When the eyes converge or diverge by distance d_1 , the outer dots remain fused but a disparity of $d_1 - d_2$ is created between the images of the inner dots. The inner dots therefore appear nearer or farther away than the outer dots, depending on whether the eyes diverge or converge. When the eyes converge by $2d_1$, a disparity of $d_1 - d_2$ is created, where the inner dots in one eye overlap the outer dots in the other eye, and a disparity of $2(d_1 - d_2)$ is created between the images of the remaining inner dots. This creates three layers of dots, arranged in a pyramid. With each increase of vergence of d_1 , an extra depth layer is added to the pyramid. In autostereograms created by changing

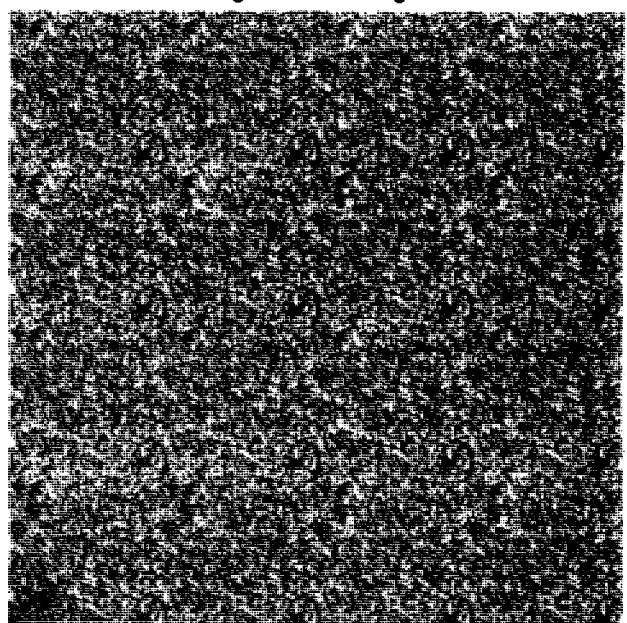


Figure 1.15. Autostereogram drafted by Masayuki Ito in 1970. An array of squares is produced when the eyes misconverge on the vertical display and an array of rectangles when the display is rotated 90°. (From Sakane 1994.)

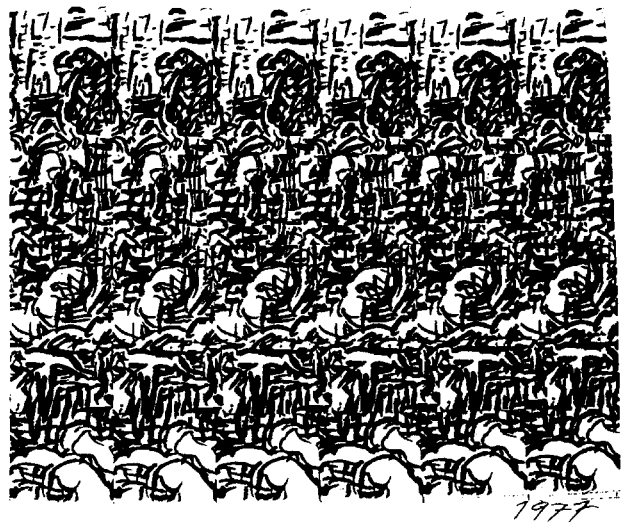


Figure 1.16. Autostereogram drawn by Alfons Schilling in 1977. Recessed and elevated rectangles are seen when the two dots are fused. (From Sakane 1994.)

the dot-pattern spacing, disparate regions are visible in each image and differential dot densities provide a monocular cue to depth.

In a truly cyclopean random-dot autostereogram extra dots are added and subtracted from a repeating random-dot sequence, keeping the spacing constant. Figure 1.18 shows a one-dimensional random-dot autostereogram consisting of a random sequence of twenty black and white dots repeated five times. An extra white dot has been added to the



Figure 1.17. An autostereogram based on differential spacing of elements.

The spaces between the outer dots (d_1) are slightly larger than those between the nine inner dots (d_2). When the eyes diverge or converge by distance d_1 , the outer dots remain fused but a disparity of $d_1 - d_2$ is created between the inner dots. This causes the inner dots to appear in a different depth plane.



Figure 1.18. The principle of the random-dot autostereogram.

An extra white dot has been added to the third repeating sequence of 20 black and white dots. When the eyes are converged or diverged by the period of the dot sequence, the central sequence of dots stands out from the surrounding dots.

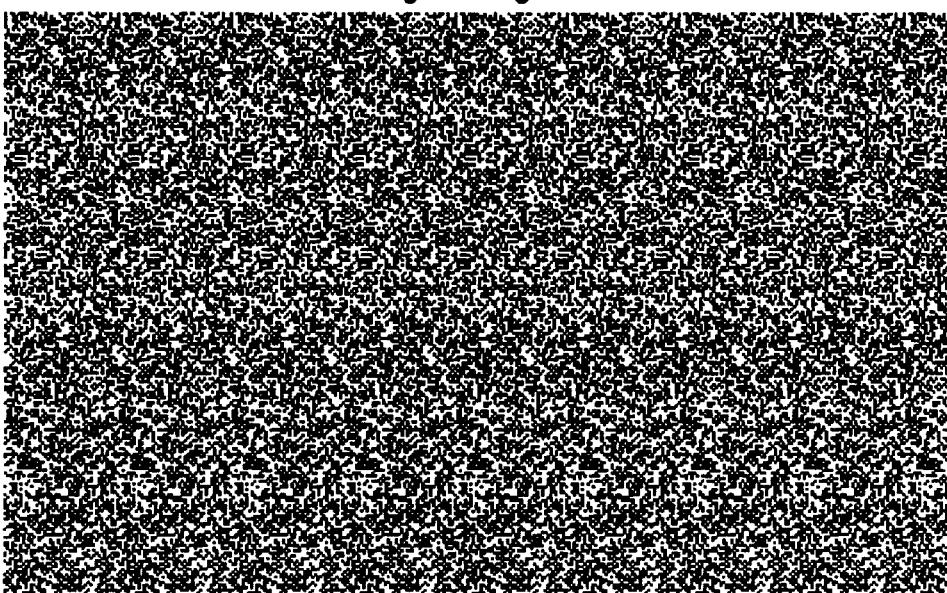


Figure 1.19. An autostereogram of a rectangle.

A single rectangle emerges from a background when the eyes converge or diverge by the distance between the two dots. Three layers emerge when convergence changes by two dot intervals. Four layers emerge with an extra interval of convergence.

third sequence. When the eyes converge or diverge by the width of the twenty-dot sequence, the sequence containing twenty-one dots in one eye is superimposed on a sequence containing twenty dots in the other eye, causing this region to appear displaced in depth relative to the other dots in the display. In a two-dimensional random-dot autostereogram, the random sequence of dots is different in each row, but the width of the basic sequence is the same in all the rows. Depth is created by adding or subtracting dots in selected regions of each row, keeping dot density constant. For instance, in Figure 1.19 the repetition cycle is thirty-two black or white dots wide, and a raised region is created in certain rows by decreasing the repetition cycle to thirty dots

in that region. A rectangle in relief is created by appropriate adjustment of the region in each row that is decreased to the thirty-dot cycle. Thus the repetition cycle is thirty dots within the raised rectangle and thirty-two dots in the surrounding region. If the eyes converge by thirty-two dots, a crossed disparity two dots wide is created in the region with a thirty-dot cycle and the raised rectangle is seen. When the eyes converge by sixty-four dots an added central region is created in which the disparity is four dots wide. The impression now is of a raised rectangle superimposed on a larger raised rectangle. For every thirty-two element increase in convergence, an extra plane of depth is created. The autostereogram in Figure 1.20 (see after page 310) creates an annulus-

shaped valley. See Tyler and Clarke (1990) for further information on the construction of auto-stereograms. A short history of the subject is provided in the book *Stereogram*, (Cadence Books, San Francisco in 1994.) Stork and Rocca (1989) describe a computer program for generating autostereograms.

Practical uses of stereograms

Stereograms have many practical uses outside the vision laboratory. During the second world war stereoscopic photographs of enemy territory revealed the presence of structures, such as rocket sites, that were not evident in ordinary photographs. Stereoscopic photographs of clouds reveal their structure and relative height. When a forged bank note is stereoscopically fused with a genuine bank note slight differences become visible as surface relief. Stereograms of complex organic molecules help chemists to visualize their structure.

One of the most active applications of stereopsis is in the design of stereoscopic imaging devices for virtual reality systems. In a virtual reality system

two light-weight monitors are carried on a helmet and viewed through lenses which magnify the images to create a binocular field about 60° wide with flanking monocular fields. The display is coupled to the movements of the head to allow the viewer to look around the virtual environment. Objects in the display may be coupled to the movements of the hand as detected by sensors in a glove to allow the viewer to manipulate virtual objects or to initiate motion of the self through the virtual space. This technology is reviewed by Earnshaw et al. (1993) and Burdea and Coiffet (1994). In a related technology, video cameras convey stereoscopic information to a monitor some distance away. The operator can then control machinery in a remote or dangerous environment such as a mine, a fire, or a radioactive site or a surgeon can control instruments in inaccessible parts of the body (see Diner and Fender 1993).

Another active field of applied stereoscopy is in the design of artificial visual systems for robots (SPIE 1992; Harris and Jenkin 1993).

Binocular correspondence and the horopter

2.1 The visual fields.....	31
2.2 Visual pathways and decussation	33
2.3 Binocular correspondence.....	35
2.3.1 Basic geometry of binocular correspondence.....	35
2.3.2 Coordinate systems for binocular disparity.....	37
2.3.3 Disparity gradients	40
2.3.4 Physiological and empirical correspondence.....	41
2.3.5 The Keplerian projection.....	43
2.4 Correspondence Stability	46
2.4.1 Stability of normal correspondence.....	46
2.4.2 Anomalous correspondence.....	46
2.4.3 Monocular diplopia.....	47
2.5 The theoretical horopter	48
2.5.1 The theoretical optic-array horopter.....	48
2.5.2 The theoretical point horopter	49
2.5.3 Line horopters.....	52
2.6 Empirical horizontal horopter	53
2.6.1 The fusion horopter.....	53
2.6.2 The midfusional-zone horopter.....	54
2.6.3 The maximum stereoscopic acuity horopter	54
2.6.4 The nonius horopter.....	55
2.6.5 The zero-motion horopter	56
2.6.6 The zero-vergence horopter.....	57
2.6.7 Equal-distance and frontal-plane horopters.....	57
2.7 Empirical vertical horopter	60
2.8 Anisometropia and aniseikonia	62
2.8.1 Relation of anisometropia to aniseikonia	62
2.8.2 Measurement of aniseikonia	64
2.8.3 Adaptation to aniseikonia.....	67

2.1 THE VISUAL FIELDS

Any system of lenses that produces an image has an anterior nodal point and a posterior nodal point, both of which lie on the optic axis. For analytic purposes one can assume that any ray of light entering an optical system passes through the anterior and posterior nodal points and emerges with its direction unchanged. For most purposes one can assume that the two nodal points of the human eye coincide at a point on the optic axis 17 mm in front of the retina (see Figure 2.28). Thus, for a given state of focus of the eye, the **nodal point** is that location through which pass all straight lines that join points in the object plane to their corresponding points in the image plane on the retina. Any such straight line is a **visual line**, and the nodal point is

where all visual lines intersect. The fovea is the central region of the retina where visual acuity is highest. The visual line through the fixation point and centre of the fovea is the **visual axis**. The line through the centres of the optical components of the eye is the **optic axis**. The pupillary line passes through the centre of the pupil and is orthogonal to the corneal surface. The visual axis in the human eye is at an angle of about 5° to the optic axis. It is displaced from the optic axis because the pupil is not quite central with respect to the cornea and lens. For most purposes it is convenient to specify the position of an eye by the position of its nodal point. One can construct the retinal image produced by any object by drawing straight lines from each point on the object through the nodal point. The nodal point is also referred to as the **station point**.

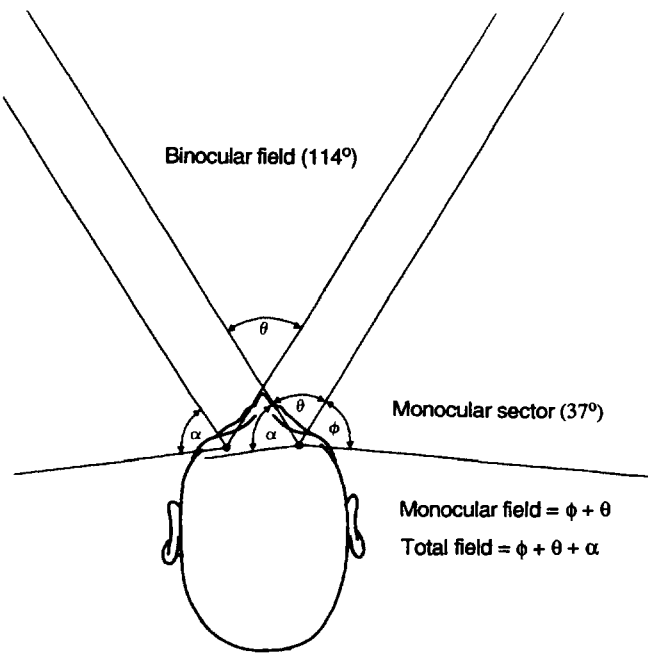


Figure 2.1. The visual fields.

Angle θ is the extent of the binocular visual field. Angles α and ϕ are the extents of the monocular sectors of the visual field at infinity. For each eye, the sum of the binocular field and the monocular sector is the monocular visual field. The total visual field is the sum of the monocular sectors and the binocular field.

The **optic visual field** is the solid angle subtended at the anterior nodal point of the stationary eye by the region of space from which light refracts through the lens. The **retinal visual field** of an eye is the solid angle subtended at the nodal point by that region of space from which light falls on the retina. See Hughes (1977) for a fuller discussion of these concepts. We can get around the problem of deciding which of these boundaries determines the visual limits of the field by defining the **monocular visual field** as the solid angle within which an object is visible to a stationary eye. Strictly speaking, the nose and orbital ridge are in the visual field, but the boundary is usually set to exclude them. The **distal stimulus** is the geometrical layout of light sources, illuminated surfaces, and transparent media within the visual field that determine the physical features of the light converging on a defined station point. The **optic array** is the cone of light rays that enters the eye from the whole distal stimulus. It is also the distal stimulus described in terms of the angles subtended at the eye by objects in the visual field. The transformation of the optic array due to movements of the distal stimulus relative to the eye is the **optic flow field**. The optic array defines the disposition and spectral profile of light sources visible from a fixed station point,

without considering the effects that the optics of the eye or the properties of the visual system might have on how things are imaged. The retinal image of a given distal stimulus is the **proximal visual stimulus**. The proximal stimulus thus takes account of the optical properties of the eye as they affect the distribution of light in the image. After the image has been transduced into neural impulses, we can talk about the neural image, or afferent visual signal. The chromatic selectivity of the receptors, the properties of the transduction process, and the anatomical features of the retina now impose themselves on the visual input.

The monocular visual field of the stationary eye extends about 95° in the temporal direction and about 56° in the nasal direction (Fischer and Wagenaar 1954). The **total visual field** is the solid angle subtended at a point midway between the two eyes by all those points in space visible to either eye or both. It extends laterally about 190° in humans when the eyes are stationary and about 290° if they are allowed to move. If the head moves on the stationary body, the total visual field extends through almost 360°. The **binocular visual field** is the portion of the total field within which an object must lie to be visible to both eyes for a given position of the eyes. The binocular visual field is flanked by two monocular sectors within which objects are visible to only one eye. Each monocular sector extends about 37° laterally from the temporal boundary of the orbital ridge to the boundary of the binocular field at infinity (see Figure 2.1). Each monocular visual field is the sum of the binocular field and the monocular sector for that eye. The left and right boundaries of the binocular field, formed by the nose, are about 114° apart when the eyes converge symmetrically and less when they converge on an eccentric point. The horizontal extent of the binocular visual field in the 3-month-old human infant has been estimated as 60° and that in the 4-month-old infant as 80° (Finlay et al. 1982). With the eyes in a straight ahead position, the upper boundary of the binocular field, formed by the orbital ridges, extends about 50° above the line of sight. The lower boundary extends about 75° below the line of sight. The blind spot, the region where the optic nerve leaves the eye, is devoid of receptors. The projection of the blind spot in the visual field is about 3° in diameter and falls about 12 to 15° into the temporal hemifield. Hence, there are two monocular islands within the binocular field, one on each side of the point of convergence. The **binocular field of fixation** is the area within which binocular fixation is possible by moving the eyes but not the head (see Sheni and Remole 1986).

A monocular stimulus is one seen by only one eye, because it falls outside the binocular field or on the blind spot of the other eye or because one eye is closed. Stimuli falling in the binocular field and visible to both eyes are **binocular stimuli**. Section 1.1 explained that there are two types of binocular stimuli, dioptic and dichoptic. A dioptic stimulus is a single visual object seen in essentially the same way by the two eyes, although the images in the two eyes may differ in shape or position because the eyes are not converged on the object or because the optical properties of the eyes differ, as in aniseikonia.

Dichoptic stimuli are visual displays under dichoptic control. An experimenter has dichoptic control when, by external manipulation, he or she can control the stimulus reaching one eye independently of that reaching the other eye. There are two basic procedures for gaining dichoptic control. The first is to present distinct stimuli to the two eyes in a stereoscope or by an equivalent procedure such as free fusion; the other is to place different filters or lenses in front of the two eyes.

2.2 VISUAL PATHWAYS AND DECUSSTATION

The axons of ganglion cells leave the eye to form the **optic nerve**. Each nerve has a diameter of 3 to 4 mm and contains about one and a quarter million axons. After passing out of the retina at the optic disc, the optic nerve travels about 5 cm to end in the **optic chiasma**. In primates and many other mammals, axons from the nasal hemiretinas **decussate** at the chiasma, that is, they cross over to the other side. The word "decussate" comes from the Latin *decussare*, meaning to divide in the form of a cross. Thus axons from the temporal half of the left eye join decussated axons from the nasal half of the right eye to form the **left optic tract**, and axons from the temporal half of the right eye join decussated axons from the nasal half of the left eye to form the **right optic tract**. Thus, inputs from the two eyes with similar local signs are brought together. Collateral branches of optic-tract axons go to the superior colliculus, the pretectum by way of the accessory optic tract, and other subcortical areas.

Each optic tract leaves the chiasma and terminates on its own side in a part of the thalamus known as the **lateral geniculate nucleus (LGN)**. Within each LGN inputs from the two eyes remain in distinct layers, or **laminae**, where they synapse with relay cells. Axons of the relay cells leave the LGN on each side and fan out to form the **optic radiations** which course backwards and upwards to

terminate in the visual cortex in the ipsilateral occipital lobe of the cerebral cortex (see Figure 2.2). Thus, axons from the right half of each eye project to the right occipital lobe and those from the left half of each eye project to the left occipital lobe. Because of the reversal of each retinal image, the left half of the visual field (left hemifield) is represented in the right cerebral hemisphere and the right hemifield is represented in the left hemisphere. Chapter 4 deals with the organization of laminae in the LGN and visual cortex, and Chapter 15 deals with their development.

The crossing over of inputs from the nasal half of each retina in the chiasma is known as **hemidecussation**. The optic nerves in submammalian

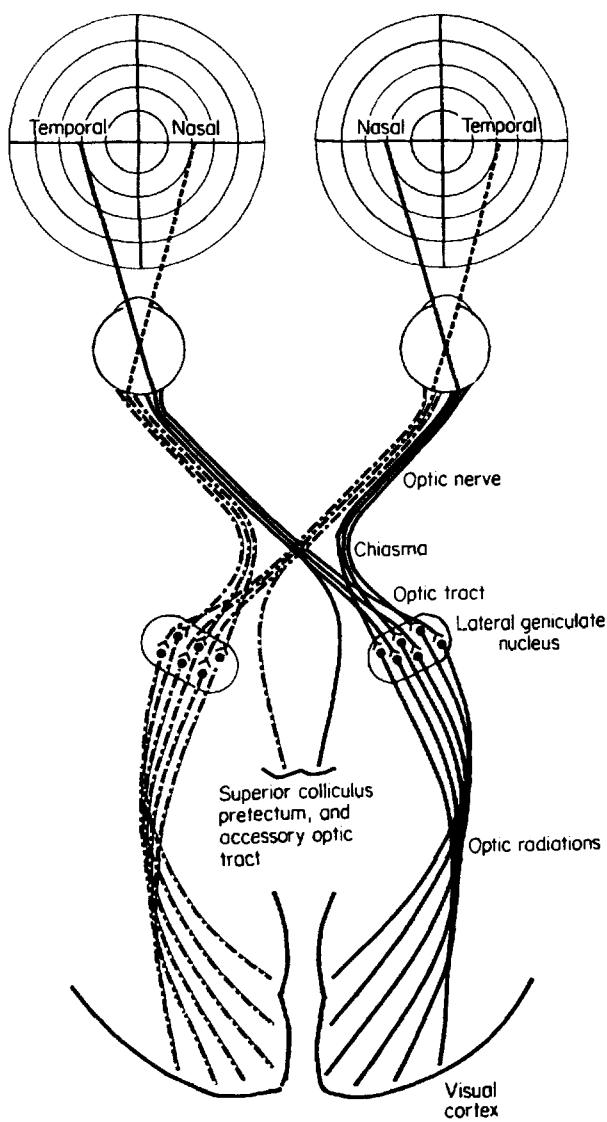


Figure 2.2. The visual pathways.

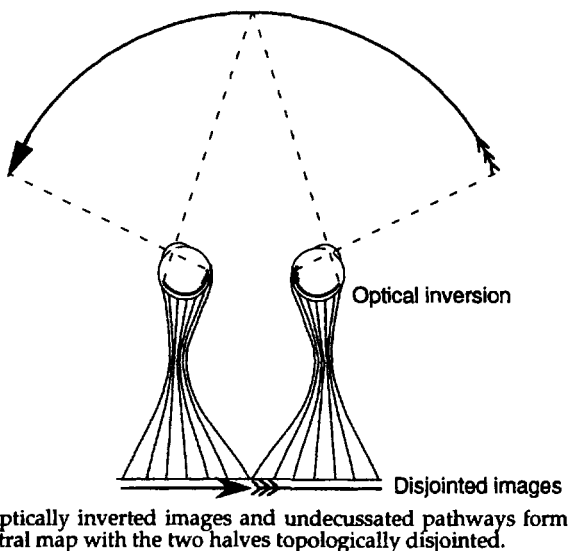
Axons from the right half of each eye (left visual hemifield) project to the right occipital lobe and those from the left half of each eye (right visual hemifield) project to the left occipital lobe.

vertebrates decussate fully, so that full decussation must be the primitive condition. Ramón y Cajal (1911) proposed that full decussation evolved to preserve the spatial integrity of the central neural map of the images from the two eyes. Because of the optical inversion of each retinal image, there is a disruption of the continuity of the central mapping across the hemispheres when the pathways are undecussated, as in Figure 2.3a. The central map is continuous when the pathways decussate, as in Figure 2.3b. The spatial integrity of the internal map is not important as such, since spatial location is coded in terms of fibre connections and patterns of firing, not in terms of spatial maps. However, transcallosal fibres connect spatially adjacent regions on either side of the midline so that visual stimuli in the midline region can be processed. These connections are shorter with decussated than with undecussated pathways. It is believed that the crossing over of visual inputs to the opposite visual cortices led to the crossing over of the motor pathways so that visual inputs from a given half of space control the movements of limbs on the same side of the body. Nobody has proposed a better explanation of visual and motor decussation.

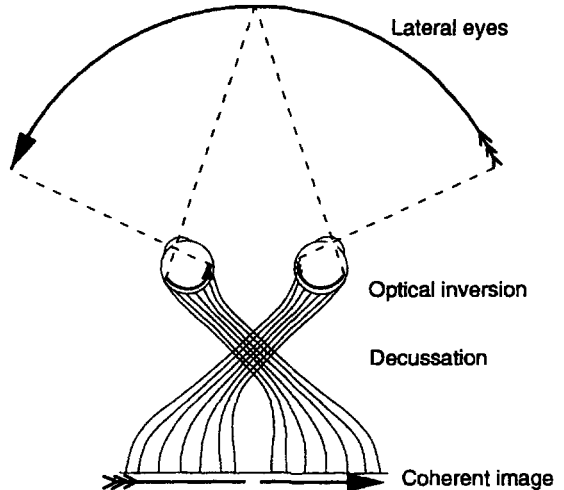
Hemidecussation

Hemidecussation of the optic nerves occurs only in mammals, but not in all mammals. In those in which it does occur, the ratio of uncrossed to crossed fibres, which has a minimum value of 0 and a maximum value of 1, is proportional to the size of the binocular visual field, which in turn depends on the extent to which the eyes are located in a frontal position. This relationship is known as the **Newton-Müller-Sudden law**. Thus, in the rabbit the proportion of uncrossed fibres is almost zero, in the horse about one-eighth, in the dog one-fourth, in the cat one-third, and in primates, including man, one-half (Walls 1963, p. 321). In primates, the boundary between decussating and nondecussating ganglion cells falls approximately along the midvertical meridian of the eye. In nonprimate mammals, the position of this boundary varies according to the type of ganglion cell, with some types of cell remaining fully decussated whether they arise in the nasal or in the temporal retina (Leventhal et al. 1988). We will see in Chapter 16 that in birds such as the pigeon hemidecussation occurs beyond the thalamus.

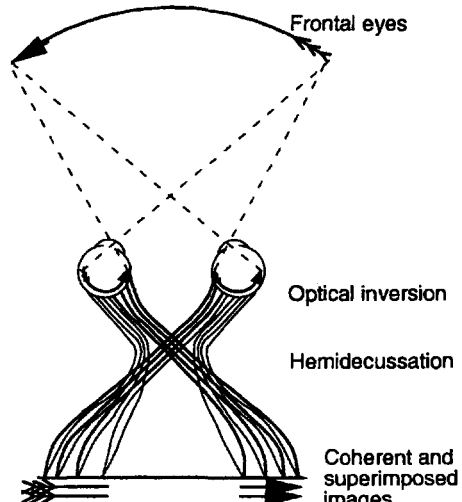
One important function of hemidecussation is to bring inputs from the same part of the binocular visual field to the same location in the brain, as illustrated in Figure 2.3c. This allows the visual system to compare inputs from roughly corresponding regions of the two retinas with a minimum length of



(a) Optically inverted images and undecussated pathways form a central map with the two halves topologically disjointed.



(b) A coherent central map is formed when the visual pathways decussate in lateral-eyed animals.



(c) In frontal-eyed animals, hemidecussation forms coherent and superimposed images.

Figure 2.3. Undecussated, decussated, and hemidecussated visual pathways. (Adapted from Ramón y Cajal 1911.)

connections and provides the basis for detecting binocular disparities and hence for binocular stereoscopic vision. The other function of hemidecussation is in the control of binocular eye movements. When the gaze moves over the visual scene, the eyes must move together to ensure that light from the same points in the visual scene projects to corresponding points in the two retinas (see the next section for a definition of corresponding points).

Binocular inputs are not essential for coordinated shifts of gaze, since the eyes move through equal angles even when only one eye is open (see Section 10.6.1). Even opposed movements of the eyes, which allow the visual axes to converge on an object of interest at a particular distance, occur when only one eye is open. However, binocular disparity is sufficient to initiate vergence eye movements, and the control of directional shifts of gaze and vergence is more precise when both eyes are open (see Chapter 10).

Stereoscopic vision is particularly well developed in mammals with frontal eyes, such as the cat and monkey. We will see in Chapter 4 that, in these animals, visual inputs from corresponding regions in the two eyes converge on binocular cells in the visual cortex, which are tuned to binocular disparity. There is also evidence of disparity-tuned binocular cells in some mammals with laterally placed eyes and small binocular fields, such as the rabbit, sheep, and goat. Some nonmammalian species, such as some insects, amphibians, and birds, have frontal vision and perhaps some binocular range-finding (see Chapter 16).

The binocular field and the associated mechanism of corresponding points are not necessary for the perception of a unified visual field. Animals with a binocular field suffer diplopia when the mechanisms responsible for conjunctive and disjunctive eye movements are damaged, as in strabismus. Animals with laterally placed eyes, which have only a small binocular field, are less affected by diplopia. They no doubt experience a unified panoramic visual field, which may extend 360°. We humans experience a unified visual field when the nasal half of each eye's visual field is occluded. A simple way to demonstrate this is to hold up against the nose an occluder just wide enough to make the nasal limit of vision for one eye coincide with the nasal limit for the other eye. Three fingers are about the correct width. The visual field seen with such an occluder looks complete although it is composed of only abutting monocular temporal hemifields.

Sections 4.1 and 15.1 provide more details about the visual pathways.

2.3 BINOCULAR CORRESPONDENCE

2.3.1 Basic geometry of binocular correspondence

The eyes are, on average, about 6.5 cm apart and therefore see things from different vantage points. This causes the optic arrays and images of a three-dimensional object to differ in the two eyes. For instance, the left eye sees more of the left side of a three-dimensional object and the right eye more of the right side. Side-to-side differences in the positions of similar images in the two eyes are called **horizontal disparities**, and can produce a compelling sensation of three-dimensionality. Differences in the up-down positions of similar binocular images are known as **vertical disparities**. These occur when the eyes are out of vertical alignment and under a variety of other circumstances. It is usually assumed that vertical disparities play no part in stereopsis, but in Chapter 7 we will see that this view must be revised. Differences in the orientations of two similar images are **orientation disparities**. We refer to a rotation of the whole image in one eye with respect to that in the other as a **cyclodisparity**. One can also describe orientation disparities as spatial gradients of horizontal or vertical disparity. We will deal with the role of disparities in depth perception after discussing the concepts of corresponding points and binocular disparity in more detail.

For each anatomically defined point in the binocular portion of the retina of one eye there is one and only one **corresponding point** in the retina of the other eye. One can define corresponding points geometrically, anatomically, or psychophysically. Images in the two eyes that fall on corresponding points have **zero binocular disparity** and, when they are similar, produce a sensation of one object. Similar images that fall on noncorresponding points are **disparate images**.

When the disparity between a pair of similar images exceeds a certain value we see two images—referred to as **diplopia**. We describe a disparity in terms of its horizontal and vertical components. However, we will see in the next section and in Chapter 7 that the precise specification of these components depends on the choice of coordinates. The **horopter** is the locus of points in space that project images to corresponding points in the two retinas for a given position of the eyes. The concept of the horopter is discussed in more detail in the next section. For the time being, let it be assumed that it is a circle passing through the point of fixation and the nodal points of both eyes. This is the Vieth-Müller circle.

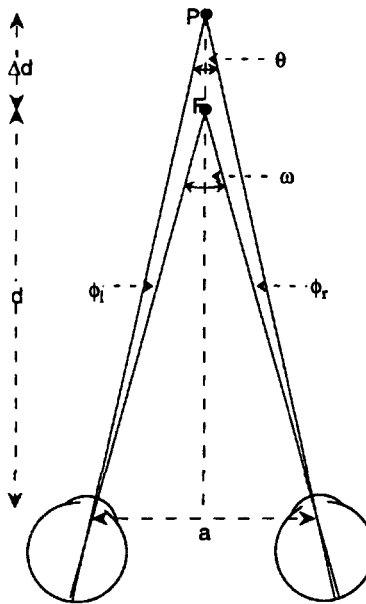


Figure 2.4. Binocular disparity.

The angles and distances used to define the binocular disparity of a point, P , with respect to a fixation point, F , at distance d from the eye. Δd is the distance between F and P , a is the interocular distance. Angle θ is the binocular subtense of P and ω is the binocular subtense of F .

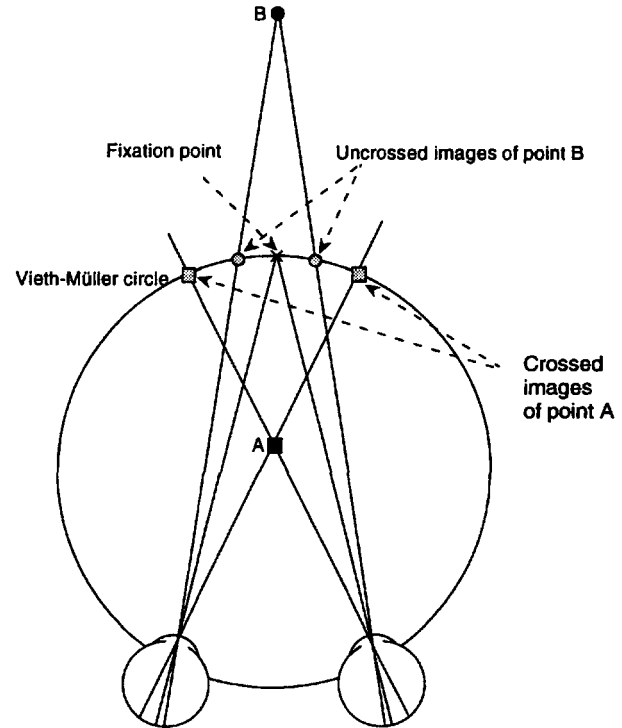


Figure 2.5. Crossed and uncrossed disparities.

The images of point A are crossed because their visual lines cross inside the horopter. The images of point B are uncrossed because their visual lines cross beyond the horopter.

Geometrical corresponding points can be defined in terms of corresponding visual lines within the optic array, as we will see in Section 2.5.1, or in terms of corresponding retinal points. Corresponding retinal points have the same positions on two idealized spherical retinas that are superimposed. Imagine two identical eyes, each with a fovea and a horizontal meridian. The congruence of the nodal points, fovea, and horizontal meridians brings all other pairs of geometrically defined corresponding points into congruence.

Figure 2.4 illustrates the geometrical definition of disparity. The visual axes converge on point F and a second point P is placed some distance beyond F . The visual angle between the image of P in the left eye and the fovea is ϕ_l , signed positive if P is to the right of the fixation point. The same angle in the right eye is ϕ_r , signed in the same way. The **binocular disparity** of the images of F is zero since each image falls on a fovea. The angular disparity, η , of the images of P is $\phi_l - \phi_r$. If ω is the binocular subtense of point F and θ is the binocular subtense of point P , one can easily prove that $\eta = \omega - \theta$. In other words, the angular disparity between a pair of objects is equal to the binocular subtense of one object minus the binocular subtense of the other.

An object nearer to an observer than the horopter produces images with **crossed horizontal disparity**

in the two eyes, because visual lines from the images intersect nearer than the Vieth-Müller circle. This is also known as convergent disparity. With monocular viewing, a midline object with crossed disparity appears on the opposite side of the point of convergence.

An object beyond the horopter produces images with **uncrossed disparity** because their visual lines intersect beyond the Vieth-Müller circle. This is also known as divergent disparity. In monocular viewing, a midline object with uncrossed disparity appears on the viewing-eye side of the point of convergence. Figure 2.5 depicts these relationships, with the double images placed on the horopter.

We shall now derive a simple expression for angular disparity, with symmetrical convergence. Let the eyes be converged on point F in the median plane of the head at distance d , as in Figure 2.4. Point P is another point in the median plane, a small distance, Δd , beyond point F . The image of P is ϕ_r degrees of visual angle to the left of the fovea in the right eye and ϕ_l degrees to the right of the fovea in the left eye. For objects in the median plane $\phi_l = \phi_r$. The total disparity, η , is therefore 2ϕ degrees. By elementary geometry $\phi = \omega/2 - \theta/2$. If the interpupillary distance is a ,

Table 2.1 Coordinate systems used to measure binocular disparity

Type of coordinates	Components
Polar coordinates	Meridional angle
Elevation-azimuth	Horizontal lines of longitude
Latitude-longitude	Horizontal lines of latitude
Bilongitude axes	Horizontal lines of longitude
Bilatitude axes	Horizontal lines of latitude

$$\tan \frac{\omega}{2} = \frac{a}{2d} \quad \text{and} \quad \tan \frac{\theta}{2} = \frac{a}{2(d + \Delta d)}$$

For small angles, the tangent of an angle is equal to the angle in radians. Therefore,

$$\eta = 2\phi \approx \frac{a}{d} - \frac{a}{d + \Delta d} \quad \text{or} \quad \eta \approx \frac{a\Delta d}{d^2 + d\Delta d}$$

Since $d\Delta d$ is usually small by comparison with d^2 we can write

$$\eta = \frac{a\Delta d}{d^2} \quad \text{in radians} \quad (1)$$

Thus, for large distances of symmetrical convergence, the absolute disparity between the images of an object is proportional to the interpupillary distance and to the distance in depth of the object from the point of convergence. It also follows from this expression that the disparity produced by an object at a given distance from the fixation point is inversely proportional to the square of the distance of the fixation point from the eyes. In other words, the depth between two objects required to produce a given disparity increases as the square of the distance of the objects from the observer. If Δd is the smallest discriminable difference in depth between P and F then η is a measure of stereoaquity. In the preceding analysis we assumed that the eyes are converged on point F . However, if we define η as the difference in disparity between any two points rather than as the disparity of point P relative to the fixation point, then the relationships described by formula (1) are independent of convergence, given that the points are close to the median plane of the head. Disparities

produced between points in eccentric positions are discussed later in this chapter.

2.3.2 Coordinate systems for binocular disparity

Any two corresponding points, however defined, remain congruent whatever coordinate frame we use to measure their retinal locations. However, the measurement of a distance between two noncorresponding points requires the specification of a system of retinal coordinates. There are five retinal coordinate systems to choose from, as set out in Table 2.1. They are discussed and illustrated in Section 7.1.

Polar coordinates

Retinal positions in the single eye are most commonly specified in perimetric or polar coordinates; a set of concentric circles centred on the fovea is used to specify the angle of eccentricity, θ , and a set of meridians passing through the fovea is used to specify meridional angle, ϕ , counterclockwise with respect to the normally horizontal meridian, as shown in Figure 7.5. Polar coordinates are appropriate for specifying **polar disparities**, that is, disparities defined in terms of orientation, and radial magnitude. Locally, horizontal disparity is the difference between $\theta \cos \phi$ in the two retinas and vertical disparity is the difference between $\theta \sin \phi$ in the two retinas.

One can express horizontal and vertical components more directly in one of the other retinal coordinate systems. These systems include a horizontal and a vertical set of reference lines on the retina. The horizontal set consists of either lines of longitude or lines of latitude, and the vertical set may also consist of either lines of longitude or lines of latitude, making four systems altogether. **Lines of longitude** are meridians, or

great circles, between poles at opposite ends of a diameter of the eye and **lines of latitude** are parallel circles over the surface of the retina, each parallel to the equator.

Mixed latitude-longitude systems

The system consisting of horizontal lines of longitude and vertical lines of latitude measures retinal location in terms of elevation and azimuth, respectively (see Figure 7.3). The system consisting of horizontal lines of latitude and vertical lines of longitude measures location in terms of latitude and longitude, like locations on the surface of the earth (Figure 7.2). A 90° rotation changes one into the other. These coordinate systems are related to the Helmholtz and Fick coordinate systems used to specify eye positions but, whereas the Helmholtz and Fick systems are anchored gimbal-fashion to the head, those described here are anchored to the retina.

Bilongitude axes

For the present, we define binocular disparity in terms of horizontal and vertical lines of longitude (Figure 7.1). The **monocular plane of regard** is the plane containing the visual axis and the normally horizontal meridian of the eye. The **monocular elevation** (or depression) of a point on the retina is the dihedral angle (λ) between the plane of regard and the **plane of elevation**, that is, the plane containing the nodal point and the horizontal meridian on which the image of the point lies. **Vertical meridians** run between poles at opposite ends of the normally vertical diameter of the eye. The midsagittal plane of an eye contains the visual axis and the normally vertical meridian of the eye. The **azimuth** of a point is the dihedral angle between the midsagittal plane of the eye and the plane containing the vertical meridian on which the image of the point lies. The direction of any point in space with respect to the principal meridians of the retina is specified by its elevation and azimuth.

The horizontal disparity between a pair of images in the two eyes is the difference between the azimuth of the image in one eye and the azimuth of the image in the other eye. Similarly, the vertical disparity between two images is the difference between their elevations. The orientation of a line on the retina is specified in terms of **radial meridians** that run between poles on the eyeball at opposite ends of the visual axis. Finally, the cyclodisparity between two lines is the angle between the two radial meridians on which the lines fall. Coordinates consisting of horizontal and

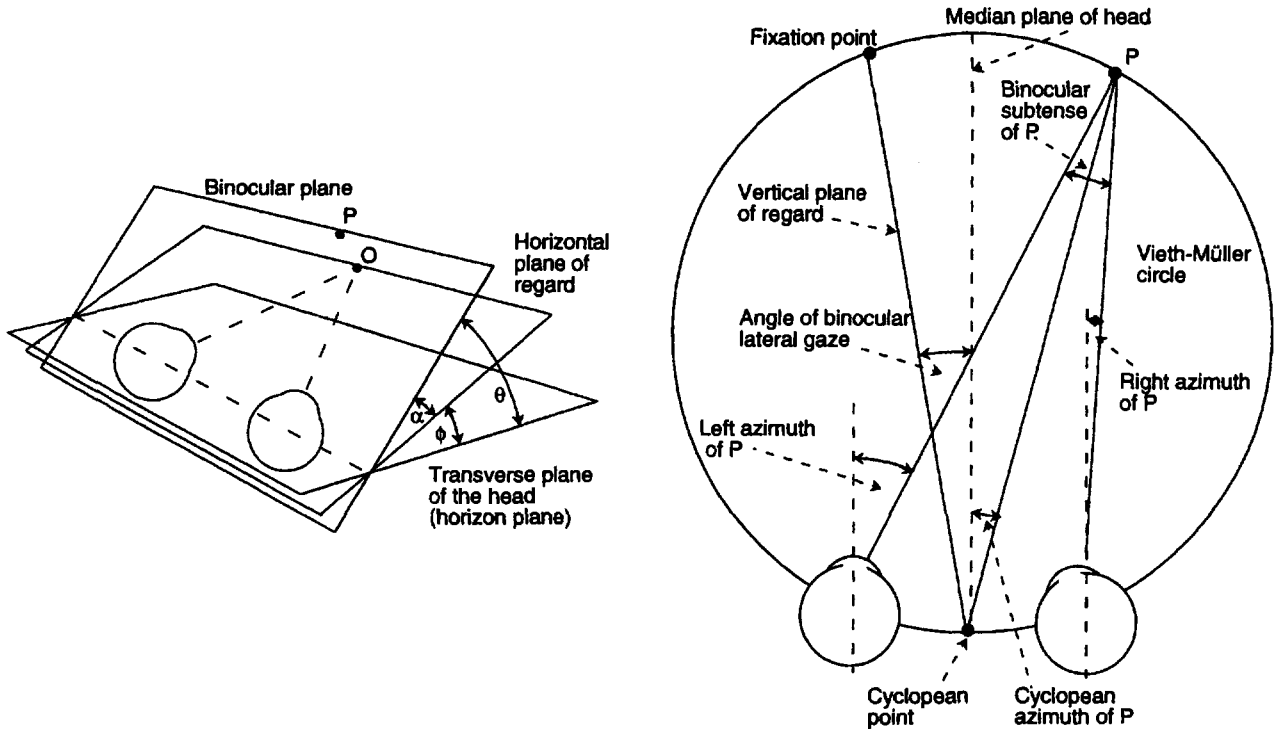
vertical lines of latitude, is discussed in Section 7.1.1.

One cannot specify precisely any of these coordinate systems in terms of natural retinal landmarks, since there is no precise way to determine the normally vertical or normally horizontal meridian of an eye. Nevertheless, geometrically defined corresponding points are useful for an initial theoretical analysis, as long one realizes that the results may not predict the results of psychophysical experiments exactly.

Cyclopean coordinates

When investigating binocular visual direction and binocular eye movements, it is useful to specify the positions of points with respect to a single set of coordinate axes. We refer to these as **cyclopean coordinates**. The line joining the nodal points of the two eyes is the **interocular axis**, and the point on the interocular axis midway between the eyes is the **cyclopean point**. Cyclopean elevation and azimuth are defined with respect to the cyclopean point. Cyclopean coordinates can be within an oculocentric framework (relative to landmarks of the cyclopean eye) or within a headcentric framework (relative to landmarks fixed to the head). The cyclopean eye and the egocentre discussed in Section 14.5 are closely related.

In a bilongitudinal system we cannot derive the bipolar elevation of a point in space by combining the monocular elevations because the elevations of all points coincide only when the eyes are converged at infinity and in orientational alignment. Instead, we define a set of **horizontal binocular planes**. Each plane contains the nodal points of the two eyes and a specified point in space. The **horizontal plane of regard** is the binocular plane containing the two visual axes, assuming they intersect. The **horizon plane** is the binocular plane orthogonal to the plane of the face. The plane of regard cuts each retina in its midhorizontal meridian. These are corresponding meridians for all angles of convergence, but only when the eyes are in torsional alignment. Any other binocular plane cuts the two retinas in horizontal meridians an equal distance above or below the midhorizontal meridian. These **epipolar meridians** are corresponding retinal meridians only when the visual axes are parallel and the eyes are in torsional alignment. The **cyclopean elevation** of a point in headcentric space is the dihedral angle between the horizon plane and the binocular plane containing the point P (angle θ in Figure 2.6a). The cyclopean elevation of a point is often referred to as its bipolar elevation. The cyclopean elevation of a point relative to



(a) The cyclopean elevation of a point P in headcentric coordinates is the angle θ between the transverse plane of the head (horizon plane) and the horizontal plane of regard containing the point. Angle ϕ is the binocular elevation of the plane of regard, and angle α is the oculocentric angle of elevation of point P with respect to the plane of regard.

(b) The cyclopean azimuth of point P is the dihedral angle between the median plane of the head and the vertical plane containing the point and the cyclopean point midway between the eyes. The cyclopean azimuth of point P is the mean of the two monocular azimuth angles of that point.

Figure 2.6. Cyclopean coordinates.

retinal coordinates of a cyclopean eye (an eye centred on the cyclopean point) is the dihedral angle between the binocular plane containing the point and the plane of regard (angle α). The elevation of binocular gaze is the angle between the plane of regard and the horizon plane (angle ϕ).

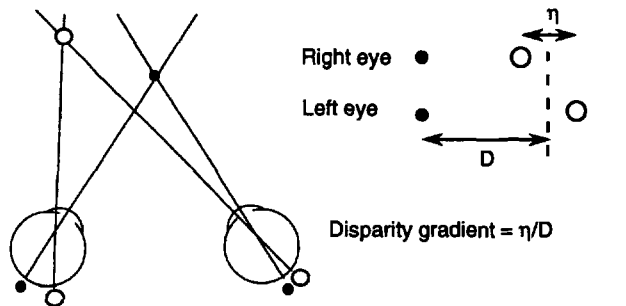
The eyes are an interocular distance apart within the horizon plane so that the monocular azimuth of a point in space cannot be the same for the two eyes in both magnitude and sign except at infinity. Instead, we define a set of **vertical binocular planes**. Each vertical binocular plane is at right angles to the horizon plane and contains the cyclopean point and a specified point in space. The **vertical plane of regard** is the vertical binocular plane containing the point of fixation. The median plane of the head is the vertical binocular plane contained in the mid-sagittal plane of the head.

The **cyclopean azimuth** of a point in headcentric coordinates is the dihedral angle between the median plane of the head and the vertical binocular plane containing the point, as shown in Figure 2.6b. It is approximately equal to half the

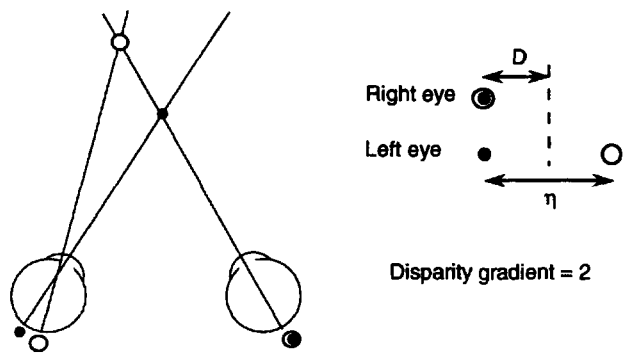
sum of the two monocular azimuth angles of the point. The cyclopean azimuth of a point with respect to coordinates of a cyclopean retina is the angle between the vertical binocular plane containing the point and the vertical plane of regard. The **angle of binocular lateral gaze** is the angle between the vertical plane of regard and the median plane of the head.

In summary, one can fully specify the headcentric position of a point in cyclopean coordinates by its elevation relative to the transverse plane of the head and its azimuth relative to the median plane of the head, both referred to the cyclopean point. The position of a point with respect to the cyclopean eye is specified by its elevation with respect to the horizontal plane of regard and its azimuth with respect to the vertical plane of regard.

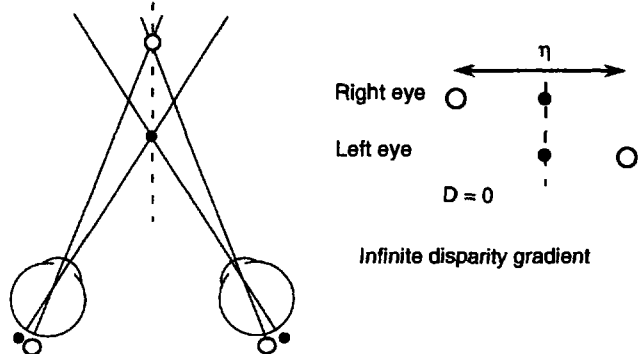
For any two points on a circle passing through the two nodal points (the Vieth-Müller circle), the algebraic sum of their cyclopean azimuths is equal to the angle that the two points subtend at the nodal point of either eye. The **binocular subtense**, or **bipolar parallax**, of a point is the angle subtended



(a) Two objects with a disparity gradient of less than 2.



(b) Two objects on a visual line of one eye have a disparity gradient of 2. The visual line may, or may not, be a visual axis.



(c) Two objects on a hyperbola of Hillebrand have a disparity gradient approaching infinity.

Figure 2.7. Disparity gradients.

A disparity gradient is the angular disparity, η , between the images of two objects divided by their angular separation, D . The separation is the angle between the mean direction of the images of one object and the mean direction of the images of the other object. In this case, one object is a fixated black dot and the other object is a circle producing disparity, η , and with a mean direction indicated by vertical dotted lines.

at the point by the two nodal points and is equal to the difference between the two monocular azimuth angles of that point. When the eyes precisely converge on a point, the bipolar azimuth is the angle of convergence. Note that the bipolar azimuth of a point does not involve the cyclopean point. All points on any circle passing through the two nodal points have the same binocular subtense. This

follows from the fact that all angles subtended by a chord of a circle at the circumference are equal.

Cyclopean coordinates cannot specify absolute values of binocular disparity, because they are not defined in oculocentric coordinates. However, they can specify patterns of relative disparity. They are useful for specifying the directions of objects in binocular space (see Section 14.5) and for specifying binocular eye movements (see Section 10.1).

2.3.3 Disparity gradients

A disparity gradient, G , is the difference in binocular disparity, η , between the images of two objects divided by the difference between the mean direction of the images of one object and the mean direction of the images of the other object, D , as shown in Figure 2.7a. Thus, $G = \eta/D$. The disparity gradient between a pair of points lying along a horizontal meridian relates the horizontal disparity between them to their lateral angular separation. The disparity gradient between a pair of points lying along a vertical meridian relates the horizontal disparity between them to their vertical angular separation. Points lying on the horopter have a disparity gradient of zero. Points lying along any other isodisparity locus also have a zero gradient. Points lying along a visual line of one eye have a horizontal disparity gradient of 2, as shown in Figure 2.7b. A line containing points with a disparity gradient of 2 has a slant relative to the median plane of the head that varies as a function of the interocular distance and the eccentricity of the visual line on which the line lies. The horizontal disparity gradient cannot exceed 2 for points on an opaque vertical surface, because beyond this value the surface is invisible to one eye. Two objects with a horizontal disparity gradient of 2 correspond to Panum's limiting case. The objects form only one image in the eye with which they are aligned, and two images in the other eye (see Section 12.4). Points lying along a hyperbola of Hillebrand (locus of isoversion) produce a disparity gradient approaching infinity, as shown in Figure 2.7c. The images of one such object have the same mean direction as the images of the other object, so that the lateral separation between the two mean positions is zero.

A set of points in space for which the disparity between successive dots is a constant proportion of their lateral separation is a linear disparity ramp. Note that the set of points forming a linear disparity ramp are not collinear because disparity decreases with the square of the distance whereas the lateral separation between points decreases in proportion to distance. A disparity ramp has a

disparity gradient, as defined earlier; a **depth**, which is the disparity difference between the near and far edges of the ramp; a **lateral extent**, which is the angular subtense between the mean position of the images of the near edge and the mean position of the images of the far edge of the ramp. A disparity ramp also has an **image density**, which is the number of points for each 1° of visual angle (spatial frequency), and a **surface density**, which is the number of points per visual angle when the display is viewed head on. A disparity ramp also has an orientation when projected into a frontal plane; it can be horizontal, vertical, or at an oblique angle. Burt and Julesz (1980) used the term "**dipole angle**" to refer to the angle that a disparity ramp makes with the horizontal in a frontal plane. A constant disparity gradient is the first spatial derivative of disparity. In Section 7.7 we discuss higher-order spatial derivatives of disparity.

A visual line is any straight line through the pupil and the nodal point. The visual axes are the principal visual lines. **Corresponding visual lines** are two visual lines, one for each eye, that project to corresponding points in the two retinas. We call the region between any two intersecting corresponding visual lines an **inter-visual-line region**. The inter-visual-line region between the visual axes is the **inter-visual-axis region**.

Consider two small objects, *A* and *B*, within the inter-visual-line region and on a line passing through the fixation point. The images of the two objects in the left eye (A_L and B_L) are in reversed left-right order with respect to the images of the objects in the right eye (A_R and B_R), as can be seen in Figure 6.22. In other words, the relative order, or topological continuity, of corresponding images is not preserved for objects having a disparity gradient greater than 2. But the relative order is not necessarily preserved if the gradient is less than 2. In general, a pair of objects lying on any straight line that passes through the intersection of two visual lines and contained in the space between the two vertical planes containing those visual lines do not preserve the relative order of images in the two eyes. Such lines can have a disparity gradient of less than 2 if they do not lie in the plane of two corresponding visual lines. This rule applies to objects within the region between any pair of corresponding visual lines and not only to objects between the visual axes. For all other pairs of objects, the image of *A* is to the left of the image of *B* in both eyes, and the topology is preserved.

Objects lying along a line that intersects the fixation point and lies in the space between the two

vertical planes containing the visual axes have another distinctive property. When the eyes fixate on one of the objects, the images of the other fall on opposite sides of the vertical retinal meridians. Thus, the images of any nonfixated object lying within the space between the vertical planes that contain the visual axes project to opposite cerebral hemispheres (see Section 4.3). The disparate images of any object lying outside this region project to the same side of the brain.

2.3.4 Physiological and empirical correspondence

Corresponding points could be defined as those that project to the same binocular cell in the primary visual cortex. According to this definition the receptive field of a cortical cell in one eye corresponds to the receptive field of the same cell in the other eye. But some cortical cells detect images that fall on noncorresponding points, as defined geometrically. These are the so-called disparity detectors discussed in Chapter 4. Therefore, the physiological criterion based on the monocular receptive fields of binocular cells does not provide a satisfactory definition of corresponding points.

We defined geometrical corresponding points by the criterion of congruence, either of visual lines or of retinal points. The criterion of congruence can be considered in terms of two orthogonal components—radial and meridional. Geometrical corresponding points are radially congruent because, for any pair, the point in one eye has the same retinal eccentricity as that in the other eye. Geometrical corresponding points are also meridionally congruent (isotropic) because, for any pair, the point in one eye lies on the same meridian through the fovea as that in the other eye. Geometrical corresponding points need not be homogeneously distributed.

Empirical corresponding points are those on which similar images must fall to satisfy a psychophysical criterion, such as singleness of vision or nonius alignment. These psychophysical criteria, described later, provide the experimental basis for the determination of the empirical horopter. Several investigators have claimed that empirical corresponding points are not congruent along the horizontal meridians. They claim that points in the temporal hemiretinas are relatively compressed with respect to the corresponding points in the nasal hemiretinas (see Figure 2.16). However, we argue in Section 2.6.7 that the data supporting this conclusion are open to other interpretations. Empirical corresponding points are not meridionally congruent—they are anisotropic. The anisotropy of empirical corresponding points is

illustrated by the fact that, when corresponding horizontal meridians are aligned by a psychophysical procedure, corresponding vertical meridians defined psychophysically are extorted about 2° (see Section 2.7). In other words, corresponding vertical meridians are sheared with respect to corresponding horizontal meridians, when both are defined psychophysically.

The point in space where the two visual axes intersect is the point of convergence. However, for many people the eyes are slightly misconverged when they attempt to fixate an object, although not to the extent of causing the object to appear double. This condition is **fixation disparity** (see Section 10.2.4). With no fixation disparity, the images of a binocularly fixated object fall on the foveas, and it is believed that the centres of the foveas constitute one pair of corresponding points. However, the part of the eye used for fixation may not coincide exactly with the centre of the fovea defined in some other way, such as the part of the retina with the highest acuity. We discuss this issue further in Sections 2.4.2 and 10.2.4.

For any point of convergence, the horopter is a region in space within which stimuli must lie if they are to stimulate corresponding points. The definition of the horopter depends on the criterion used to specify correspondence, as we see later. An object outside the horopter produces images which are disparate, either vertically, horizontally, or both.

There is a range of disparities within which two similar images, one in each eye, are experienced as a single object. This is Panum's fusional area, and images falling within it are referred to as **fused images** (Panum 1858). The angular subtense of Panum's fusional area depends on several factors, including retinal eccentricity and characteristics of the stimulus and surrounding stimuli (see Section 8.1). We experience binocular images falling outside Panum's fusion as double, or diplopic. When dissimilar images fall on or near corresponding points, they do not fuse but rather exhibit **binocular rivalry**, in which we see the two images in alternation (see Section 8.3).

A person with a squint, or strabismus, cannot converge the visual axes onto an intended object. Therefore the images of all objects fall on noncorresponding points and things appear double. Strabismics of long standing avoid double vision by suppressing the input from one eye when both eyes are open or by modifying the pattern of binocular correspondence (see Section 2.4.2). Often, the suppressed eye has reduced acuity and other visual defects, a condition known as **strabismic amblyopia** (see Section 15.7).

2.3.5 The Keplerian projection

Consider a horizontal row of small dot-shaped objects lying on the horizontal horopter, such as points 1, 2, and 3 in Figure 2.8. Two corresponding visual lines, one from each eye, intersect in each object. Each of these objects produces images with zero disparity. Images with zero disparity are also produced by any pair of objects lying on a pair of corresponding lines, not merely by a single object lying on the horopter. These are known as **false matches**. For instance, objects *A* and *B* produce images with the same zero disparity as object 2. Objects *A* and *B* also produce images which fall on noncorresponding points. Lines passing through distinct objects in the horopter intersect in a point outside the horopter. An object on this intersection point produces images with a disparity equal to the angular separation between the two objects on the horopter. For instance, object *B* in Figure 2.8 produces images with a disparity equal to the angular separation between objects 2 and 3. In general, for any two objects lying in a horizontal plane, a unique single object in a distinct depth plane produces images with the same disparity. Conversely, for any single object there is an infinite set of pairs of objects which produce images with the same disparity as those produced by the single object.

A diagram showing the set of intersections of visual lines to a set of identical objects on the horizontal horopter is a **Keplerian projection**. For N objects in distinct visual directions, there are N^2 points of intersection of visual lines. These N^2 points specify all possible pairwise combinations of the images of the set of objects. Put another way, the Keplerian projection defines the set of possible correspondences plus the set of possible disparities between the images of a set of objects. Binocular images that arise from the same object are **correctly matched images**. Correctly matched images may not be identical, since they may arise from a solid object. On the other hand, incorrectly matched images may be identical since they may arise from distinct but identical objects. Binocular images, correctly matched or not, that fall on corresponding points in the two retinas are **corresponding images**. Binocular images that are stereoscopically linked by the visual system, whether or not they are correctly matched and whether or not they fall on corresponding points, are **stereoscopically matched images**. We see objects in their proper depth relationships only if the visual system links correctly matched images and not incorrectly matched images. Any other combination of binocular images produces illusory impressions of relative depth.

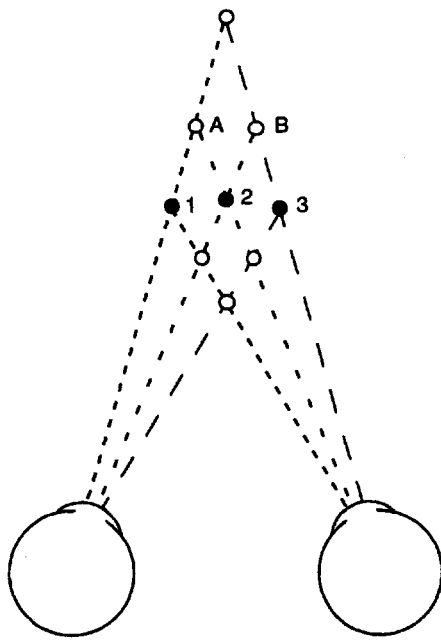


Figure 2.8. The Keplerian projection.

The solid dots represent three objects lying in the horopter. Similar dotted lines represent pairs of corresponding visual lines. The circles represent the positions of objects that would produce images with the same disparities. For instance, an object at B produces images with an uncrossed disparity equal to the angular separation between the images of objects 2 and 3 on either retina. Objects at A and C produce a fused pair of images equivalent to those produced by object B, in addition to unpaired images in each eye in the directions of objects 1 and 3.

For a regular array of objects along the horizontal horopter, the set of correctly matched images produces zero disparities and forms the zero level of the Keplerian projection, which is the horopter. Sets of incorrectly matched images occur at each of a series of levels, nearer than and beyond the zero level. The apparent objects formed by linking non-matching images are **ghosts**, or false matches. There has been a good deal of discussion about how the visual system avoids seeing ghosts. The problem of how the visual system makes appropriate stereoscopic links, known as the **binocular correspondence problem**, is discussed in Chapter 6. The present section provides only a preliminary account.

Simple image-matching rules

For an irregular array of objects in the neighbourhood of the horopter, two matching rules usually guarantee appropriate matches of images: (1) images that are closest to each other in the binocular field are matched (**nearest-neighbour rule**), and (2) once two images are matched, other matches for either of those images are forbidden (**unique-matching rule**).

When the eyes converge out of the plane of a regular array of dots (see Figure 2.9a), the two sets of images slide over each other until they come into correspondence at the first level in the Keplerian projection. When the eyes converge more, the images coincide at the second level. At each level of convergence, the dots appear to get smaller and nearer, and at each level of divergence beyond the zero level they appear to larger and further away. This is the **wallpaper illusion** first described by Smith in 1738.

One can observe an interesting variation of the wallpaper illusion by steadily fixating an inclined regular pattern of dots, as in Figure 2.9 (Piggins 1978; Odom and Chao 1987). The surface breaks up into a set of inclined planes with a depth step between each plane. Within each plane, the dots in one eye fuse with their nearest neighbours in the other eye to create the impression of an inclined plane. At the boundary between one plane and the next, the nearest-neighbour match suddenly shifts to dots relatively shifted one interdot spacing. Tyler (1980) reported that a display of vertical lines in a frontal plane appears to break up into distinct planes. This happens because the vertical horopter inclines top away (see Section 2.7) so that a frontal display of vertical lines inclines with respect to the locus of zero disparity. Readers may observe that the display of dots in Figure 2.9 more readily break up into distinct planes when it is inclined bottom away than when it is inclined top away.

The unique-matching rule ensures that the visual system does not match an image in one eye simultaneously with more than one image in the other eye. This means that if the visual system matches images falling on a pair of intersecting visual lines, it does not match the image on either of those lines and that on any other line. For an array of dots on the horizontal horopter, the nearest-neighbour and unique-matching rules ensure that we see do not see multiple "ghost" images.

Image matching determined by convergence

The nearest-neighbour and unique-matching rules are not sufficient to ensure appropriate image matches for objects at different distances. Consider the simplest case of two vertical pins, one behind the other in the median plane, in front of a featureless background, as shown in Figure 2.10. When the eyes converge on point A, well beyond the two pins, the left eye sees the images of the pins on the right of A and the right eye sees them on the left, making a total of four images. In other words, the images of both pins have crossed disparity. The distance

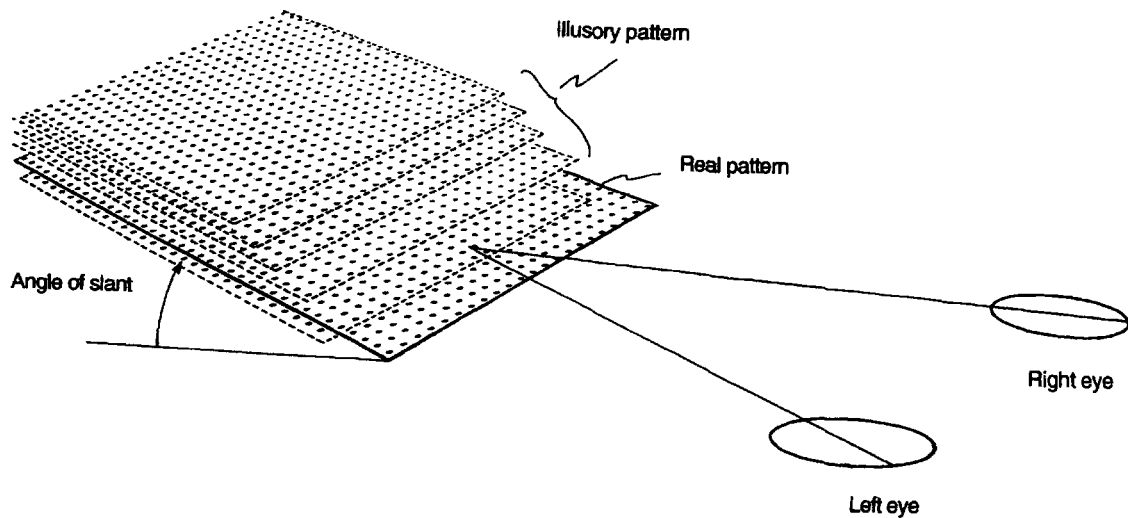
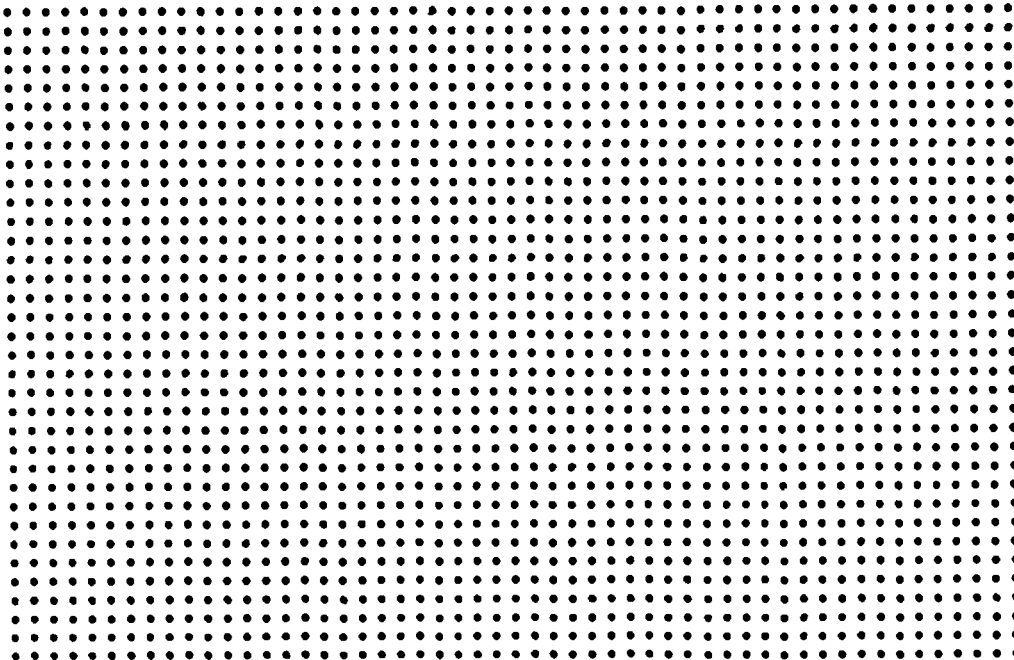


Figure 2.9. A variation of the wallpaper effect.

When the pattern of dots is viewed at an angle of about 10° to the plane of regard, the surface breaks up into several layers stepped in depth, as depicted in the lower diagram. At the boundary between one step and the next, the nearest-neighbour match of the images in the two eyes suddenly shifts to dots relatively shifted one interdot spacing. (Figure designed by S. Nakamizo and H. Ono.)

between these pairs of images may be too great for the disparity detection system. The images have an indeterminate depth somewhere beyond the actual pins, and their apparent direction conforms to the rules of egocentric direction (see Section 14.5). Their appearance beyond the actual pins is probably due to the effect of far convergence.

We also see four images when the eyes converge on point C, well in front of the two pins, except that

now the pairs are uncrossed and appear somewhere in front of the actual rods. When the eyes converge on the far pin, the images of this pin fuse and those of the near pin remain in crossed disparity. Similarly, when the eyes converge on the near pin the images of this pin fuse and we see the images of the far pin with an uncrossed disparity. The generally accepted view is that the crossed or uncrossed disparities cause the nonfixated pin to appear in front

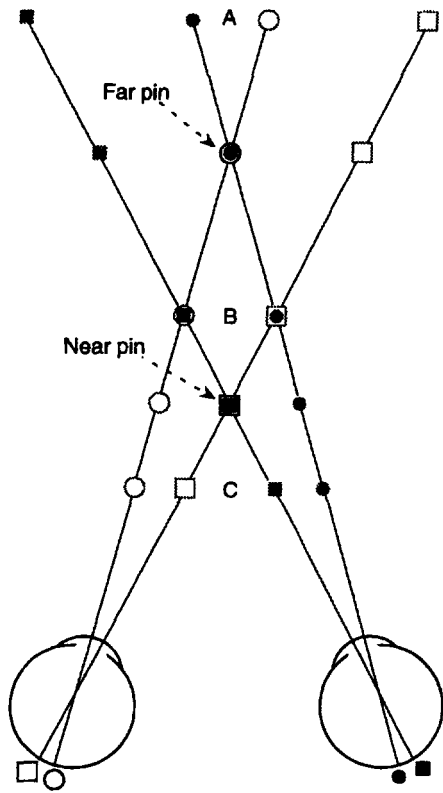


Figure 2.10. The double-nail illusion.

Two pins are held in the median plane about 30 cm from the eyes, with one pin about 2 cm further away than the other. Four images are seen when the eyes are converged at distance A or C. When the far pin is fixated, its images are fused and the near pin is seen with a crossed disparity. When the near pin is fixated, the far pin is seen with an uncrossed disparity. When convergence is at B, about halfway between the pins, the two pairs of images are matched inappropriately to form an impression of two pins side by side. A third pin between the other two helps bring the point of fixation to the intermediate position.

of or beyond the far pin. This view may need qualifying because in both cases, a pair of fused images separates the disparate images, which complicates the task of linking the disparate images (the images are topologically disrupted). We argue that the impression of depth in these cases is not due solely to the disparity between the unfused images, but mainly to disparity induced into the fused images by vergence caused by the stimulus asymmetry. We defer further discussion of this point to Section 12.4.6.

There remains one special case; convergence on point B, midway between the two pins. Normally the eyes converge on one or other pin, and it is difficult to hold convergence midway between them. A small fixation point at the half way point helps. However, if the pins are about 1 cm apart in depth at a distance of about 30 cm, the gaze tends to slip into a point between them even when no fixation

point is provided. The image of the near pin in the left eye fuses with the image of the far pin in the right eye, and vice versa. There are no unfused images and hence no disparities with respect to the plane of convergence. This acts as a strong vergence lock since both pairs of images fuse rather than just one pair, as in any other way of matching the images. The appearance created is of two pins, side by side in the plane of fixation (Cogan 1978). This is the **double-nail illusion** (Krol and van de Grind 1980; Mallot and Bideau 1990). It is somewhat misleading to call it an illusion because there is no information, other than that provided by accommodation, that distinguishes between a side-by-side pair of pins and an in-line pair of pins—the two situations create identical proximal stimuli (Ono 1984). The side-by-side pins are ghost images in the sense that they arise from inappropriately matched images. However, we do not see them at the same time as pins in other positions and the unique-matching rule is preserved. If the pins differ in shape, the illusion does not work because the images of an in-line pair of pins are no longer identical to those of a side-by-side pair. If one pin is taller than the other, the images of the top of the taller pin form a disparate pair and, as Krol and van de Grind reported, this part of the pin appears to float out of the plane of convergence to the location in depth appropriate to the disparity of its images. If the two pins are tilted slightly in a frontal plane in opposite directions, one sees two side-by-side pins inclined in depth in opposite directions. This is to be expected, because the proximal stimuli for the two situations are identical.

We know of no conclusive evidence that the visual system simultaneously registers multiple matches between images when each image in one eye has a matching image in the other eye (see Section 6.2.2 for details). There is some dispute about whether double-duty matching occurs when there is only one image in one eye and two in the other, a stimulus configuration known as Panum's limiting case. Section 12.4.6 deals with this issue.

This discussion reveals a third matching rule, namely, that the visual system matches only similar images. We call this the **similarity rule**. We now have three matching rules, the nearest-neighbour rule, the unique-matching rule, and the similarity rule. In most situations, these three rules in conjunction with changes in convergence are sufficient to ensure that images in the two eyes match correctly and that we do not see ghosts arising from multiple-matches. However, more complex stimuli require other matching rules, as we will see in Chapter 6.

2.4 CORRESPONDENCE STABILITY

2.4.1 Stability of normal correspondence

Evidence suggests that binocular correspondence can change in people with normal vision under three circumstances. The first is a change in the eccentricity of gaze or vergence. Section 2.8.3 deals with this topic. In the second circumstance there are fluctuations in the vergence position of the eyes during fixation. Section 10.5.3 deals with this topic. The third circumstance is the order in which one applies tests of binocular correspondence, as discussed in Section 8.1.8. Binocular correspondence also changes in people with strabismus, as we see in the next section.

2.4.2 Anomalous correspondence

The misalignment of the two visual axes in strabismus causes diplopia. The visual system adapts to chronic diplopia in two ways. One is for the inputs from the nondeviating eye to suppress those from the deviating eye when both eyes are open. In severe strabismus, in which one eye persistently deviates and the other remains fixated on the intended object, the deviating eye becomes amblyopic. Amblyopia involves a severe loss of visual acuity especially in the central visual field. It is believed that inputs from the deviating eye lose or weaken their connections to cortical cells. In alternating strabismus, sometimes one eye and sometimes the other eye deviates, and either eye can be used for fixation. Under these circumstances, both eyes have normal acuity presumably because they both retain inputs to cortical cells. Nevertheless, stereopsis is deficient, although it is normal in the peripheral visual field of some alternating strabismics.

The second way in which the visual system adapts to diplopia is by the development of **anomalous retinal correspondence (ARC)**, that is, a shift in the relative local signs of corresponding regions in the two retinas. The angular extent of anomalous correspondence is the **angle of anomaly** or simply **angle A**. When the angle of anomaly is the same over the visual field it is harmonious anomalous correspondence, and when it varies from one part of the visual field to another it is inharmonious anomalous correspondence. Anomalous correspondence may be unstable and may alternate with normal correspondence. Sometimes anomalous correspondence operates at the same time as normal correspondence so that a given retinal location has two local sign values with respect to the corresponding point in the other eye. Under these

circumstances the patient experiences monocular diplopia when looking at a single object with the deviant eye or binocular triplopia when looking with both eyes. Monocular diplopia is discussed in the next section.

Several orthoptic tests are available for measuring anomalous correspondence, including the Hering-Bielchowsky afterimage test, the Bagolini striated glasses test, and Cüpper's correspondence test (see Griffin 1976; Schor 1991). They all involve the alignment of calibrated dichoptic images. The angle of the strabismic deviation is first determined. The angle of anomaly is the angle through which the subject separates dichoptic images so they appear fused, minus the angle of strabismic deviation. In the afterimage test the patient first fixates the centre of a vertical streak of light with one eye and then the centre of a horizontal streak of light with the other eye. The centre of each streak is blank. The degree of anomalous correspondence is the angular offset of the two blank regions in the two afterimages. The validity of the test depends on how accurately the patient fixates when the clinician impresses the afterimage on each fovea, but eye movements occurring after impression of the afterimages do not affect the measurement.

Anomalous correspondence can also be measured with the aid of Maxwell's spot, which is an entoptic dark spot seen in blue light. In people with normal vision Maxwell's spot is centred on the fovea and moves with the eyes. In the amblyopic eye of a sample of eleven strabismic amblyopes the spot was between 5 and 20 arcmin to one side of the fixation point and esotropes saw two Maxwell's spots, suggesting that for them the foveas did not correspond (Flom and Weymouth 1961). Anomalous correspondence produces characteristic distortions of the horizontal horopter (Flom 1980).

Strabismic amblyopes and strabismic alternators commonly show one pattern of adaptation to diplopia in the central retina and a different pattern in the peripheral retina. Suppression develops in the central retina, destroying stereopsis but leaving a normal pattern of retinal correspondence, whereas anomalous correspondence develops in the periphery, leaving some coarse stereopsis intact (Sireteanu and Fronius 1989). Because the receptive fields in the central visual field are small, corresponding receptive fields become relatively well separated in space when the eyes are strabismic. Since anomalous correspondence cannot cope with completely separated receptive fields, the system adapts to diplopia by suppressing the input from one eye. In the peripheral visual field, receptive fields are large so that a given pair of receptive

fields may continue to overlap in space even with a strabismus. The mechanism of anomalous correspondence, which probably involves setting up different matching subregions within pairs of large receptive fields, is thus able to cope in peripheral regions.

There has been some dispute about the extent to which normal correspondence is reestablished after surgical correction of strabismus. There are various methods for treating anomalous correspondence after surgery, including periods of occlusion of the deviated eye, the use of prisms, and the use of orthoptic exercises (Burian 1951). Some investigators reported rapid changes in the pattern of correspondence after surgery (Bagolini 1967), while some patients had diplopia after surgery, even though they did not experience double vision before surgery (Azar 1965). There is a higher incidence of the development of normal correspondence in patients for whom the strabismus was overcorrected, especially when esotropia was converted into exotropia (Rutstein et al. 1991). Bagolini (1967) and Schor (1991) review the whole question of anomalous correspondence in clinical practice.

McCormack (1990) recorded evoked potentials from the primary visual cortex of human subjects with anomalous correspondence but found no evidence of changes in the relative positions of receptive fields in the two eyes. This procedure may not be sensitive enough to detect shifts responsible for anomalous correspondence.

Grant and Berman (1991) recorded from single binocular cells in area 17 and in the lateral suprasylvian area of cats reared with varying degrees of surgically induced strabismus. For angles of anomaly over 10°, severe loss of binocular cells occurred and the receptive fields of remaining binocular cells did not alter their relative positions in the two eyes. Cats with mild strabismus (less than 10°) had a normal number of binocular cells and the relative positions of receptive fields in the two eyes shifted. However, this anomalous correspondence was evident in the suprasylvian area but not in area 17.

2.4.3 Monocular diplopia

A person with monocular diplopia sees two points of light when only one is present. The condition can be due to (1) an abnormality in the optics of the eye, such as irregular cornea, defective pupil, dislocation or refractive irregularities of the lens, entoptic bodies, and detached retina, and (2) lesions of the occipital lobe, cerebellum, or oculomotor centres (Gerstmann and Kestenbaum 1930; Klein and Stein

1934), (3) anomalous correspondence due to strabismus. The condition is rare, even among squinters.. Worth (1903) found only four cases among 2,000 squinters. It also occurs in bitemporal hemianopia, possibly due to the shift of normal fixation which this condition induces (Kubie and Beckmann 1929). Monocular diplopia was first reported by Javal (1865), but it was not until 1898 that Bielschowsky pointed out the significance of the condition in relation to anomalous correspondence.

The usual explanation of monocular diplopia associated with anomalous correspondence is that the old pattern of correspondence coexists with the new pattern so that a point on the retina of the good eye has the same space value as two points in the retina of the deviating eye. An object imaged on the retina of the deviating eye is seen in two locations because of the double local sign. This usually happens in the period following surgical correction for strabismus. Cases have been described in which there was monocular diplopia in both eyes (Purdy 1934; Cass 1941; Lewis 1944) but the condition is usually restricted to the deviating eye or to an eye in which the deviation has been corrected. The image with anomalous visual direction is usually dim relative to the image seen in its normal position. Ramachandran et al. (1994a) found that the dim image of a diplopic pair appears about one-third of a second later than the normal image and lags behind the normal image when the visual stimulus is moved. They also found in two patients with intermittent exotropia that the degree of monocular diplopia varied as a function of the position of the stimulus in the visual field (Ramachandran et al. 1994b).

Tschermark (1899), who was strabismic, experienced monocular diplopia only when he attempted to fixate with a closed eye an object seen by the open eye. Morgan (1955) described a patient who could squint at will and who had monocular diplopia only when she did so. Ramachandran et al. described a patient with intermittent exotropia who experienced monocular diplopia only when she voluntarily allowed one eye to deviate. When her eyes were properly aligned, afterimages of vertical lines impressed one above and one below the fovea appeared aligned but as she allowed one eye to deviate the afterimages appeared to move apart. These reports suggest that the remapping of local sign can be conditional on the vergence position of the eyes and hence on proprioception from the extraocular muscles or on oculomotor efference.

Ramachandran et al. (1994a) impressed an afterimage of a patch of vertical grating on one eye and a patch of horizontal grating on the

corresponding location in the other eye. When the eyes were aligned, the gratings rivalled in the usual way, but they continued to rival when one eye was deviated so that the afterimages no longer appeared superimposed. Thus binocular rivalry occurred between dichoptic images that did not appear superimposed. This suggests that rivalry occurs before the process that assigns egocentric direction to images in the two eyes.

Bielschowsky (1898) superimposed in one eye the normal image of a red patch on the weak image of a green patch. The patches rivalled like two dichoptic patches instead of producing the hue one expects when differently coloured images are combined in the same eye. In a patient examined by Purdy (1934) the distinct colours of superimposed normal and weak images in the same eye did not mix or rival but appeared to be present simultaneously.

Ramachandran et al. (1994a) made similar observations on a patient with intermittent exotropia. A patch of vertical lines was superimposed on the weak diplopic image of a patch of horizontal lines in the same eye. The subject experienced mosaic rivalry rather than the checkerboard pattern obtained when two orthogonal gratings are superimposed in the same eye. These effects are related to the phenomenon of monocular rivalry discussed in Section 8.3.8.

2.5 THEORETICAL HOROPTER

The **horopter** is the locus of points in space which project images onto corresponding points in each retina. The horopter is best understood by considering it in two parts; the **horizontal horopter**, sometimes called the longitudinal horopter, which normally lies in the horizontal plane of regard; and the **vertical horopter**, which lies in the median plane. Considered together the two parts are the **space horopter** (Solomons 1975a). The space horopter based on corresponding points is also known as the **point horopter** in contrast to an horopter based on lines, which is known as a **line horopter**.

Tyler (1991) has reviewed the properties of the theoretical point horopter. Unless otherwise stated, we use the term "horopter" to refer to the point horopter. There are two ways to consider the theoretical space horopter. First, one can define the horopter wholly in terms of congruence between the two optic arrays. We call this the theoretical **optical horopter**. Second, one can define the horopter in terms of congruence between the two retinas. This is the **theoretical point horopter**.

2.5.1 The theoretical optic-array horopter

In deriving the **optic-array horopter**, one represents each eye by a nodal point and lines passing in any direction through a nodal point are visual lines. The visual axis of each eye is the **principal line** which defines the origin of the coordinate system. One set of visual lines, including the principal line, lies in the **horizontal plane**, and one set lies in the **vertical plane**. The lines form a coherent set referred to as the **optic array**—when the principal line moves, the whole array moves. When the principal lines and the horizontal planes of the two eyes are superimposed, any visual line in one eye and the line with which it is congruent in the other eye are **corresponding visual lines**. In this scheme, correspondence is defined by congruence of visual lines. From a position of congruence, let the two nodal points be separated horizontally by a specified distance. The line joining the two eyes is the **interocular axis** and the plane at right angles to the interocular axis midway between the eyes is the **median plane**. The optic-array horopter is simply the locus of points in space where corresponding visual lines intersect.

When the visual axes are parallel, corresponding lines in the two vertical planes intersect in a vertical line at infinity. This is the **vertical optic-array horopter at infinity**. Also, with parallel visual axes, corresponding lines in the two coplanar horizontal planes intersect in an infinitely large circle contained in the same plane and passing through the two eyes (the proof is given later). This is the **horizontal optic-array horopter at infinity**, or **Vieth-Müller circle**. Similarly, the corresponding lines in any other pair of coplanar planes intersect in a Vieth-Müller circle at infinity. The optic-array horopter at infinity is therefore an infinitely large toroid formed by sweeping a Vieth-Müller circle round the interocular axis.

Let each optic array rotate about a vertical axis through the nodal point so that the two visual axes converge on a point and the horizontal planes remain coplanar. This point is the **fixation point**, and the angle between the visual axes is the **vergence angle**. In Figure 2.11 the fixation point, F , necessarily lies on the horopter. Any other point, P , in the horizontal plane is the intersection of corresponding visual lines if each of those lines is at the same angle, θ , from a visual axis. Since triangles FON_1 and PON_2 are similar, this will be true when the binocular subtense of F is the same as that of P . But the angles are equal when F and P lie on a circle through the two eyes, since angles subtended by a chord onto the circumference of a circle are equal.

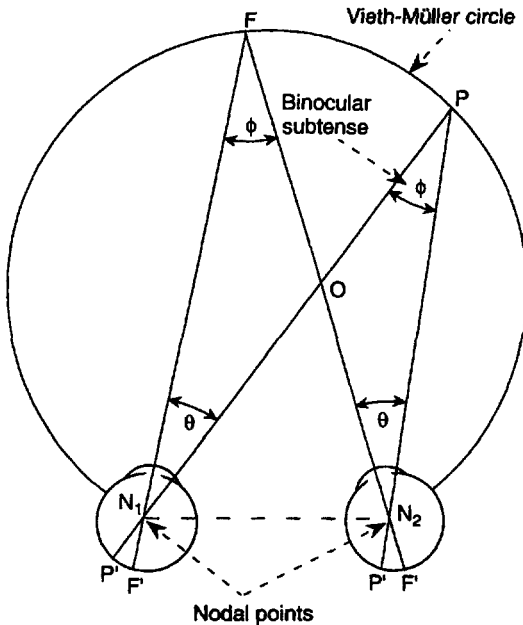


Figure 2.11. Basic geometry of the horizontal horopter.

When the eyes are converged on point F , the images, F' , fall on the foveas and have zero disparity. Let ϕ be the binocular subtense of point F and let a circle pass through F and the nodal points of the eyes (the Vieth-Müller circle). Any other point, P , on the circle also has a binocular subtense of ϕ , since all points on this circle are projections from a common chord. Since the opposite angles at O are equal, the angles θ must also be equal. Therefore the images of point P stimulate corresponding points with respect to the images of point F . The Vieth-Müller circle therefore defines the locus of points having zero disparity.

This circle is therefore the theoretical horizontal horopter, or Vieth-Müller circle (see Section 1.2.2). The point of fixation may be at any location on a given Vieth-Müller circle without affecting the location of the circle. We will see later that the Vieth-Müller circle does not pass through the fixation point when the optic arrays are rotated about the principal lines.

When the visual axes converge, the horizontal horopter is confined to a Vieth-Müller circle in the horizontal plane. To understand why this is so, consider a point P' above the point P on the horopter and to one side of the median plane. The angular separation of P and P' is larger to one eye than to the other because the points are nearer to one eye than to the other. Since point P is on the horopter, point P' cannot be on the horopter.

The same logic applies to all points outside the Vieth-Müller circle except for points within the median plane. Points within the median plane are an equal distance from each eye. The only sets of corresponding visual lines that intersect in the median plane are the sets contained in a corresponding pair of vertical planes which intersect in the median plane. Since the locus of intersection of

two vertical planes is a vertical line, the vertical optical horopter with eyes converged is a vertical line in the median plane that intersects the Vieth-Müller circle. The vertical horopter contains the fixation point only when the optic arrays converge symmetrically.

2.5.2 The theoretical point horopter

We defined the optic-array horopter by the criterion of congruence between corresponding visual lines. By this definition, points on two retinas on which corresponding visual lines project are corresponding points. It follows that the shapes and spatial dispositions of the retinas are irrelevant to the definition of the optic-array horopter—all retinas are projectively equivalent when corresponding points are defined this way. One retina could be a plane some distance from its nodal point, and the other could be a sphere near its nodal point, but the theoretical optic-array horopter with simple convergence will still be a Vieth-Müller circle plus a vertical line. When we define corresponding visual lines by the criterion of congruence, corresponding points on the retinas may or may not be congruent. The retinas are congruent (exactly superimposable) only when they have the same shape and the same positions with respect to the optic arrays.

Instead of defining correspondence in terms of congruence of visual lines, one can use the criterion of congruent retinal points. We refer to the horopter derived from this criterion as the **theoretical point horopter**. We now define the theoretical point horopter based on congruent retinal points with the following conditions fulfilled:

A. Corresponding retinal points are congruent when the two retinas are superimposed, which is ensured if the following conditions are fulfilled:

1. The two eyes have the same optical properties. The two retinas need not be spherical, but they must have the same shape and size.

2. When the two nodal points and the retinas are superimposed such that any two pairs of corresponding points are congruent, then all other pairs of corresponding points are also congruent. That is to say, there are no compressions, dilations, or shear distortions in the pattern of correspondence. These are the distortions that changes in eye position cannot correct. The pairs of points, as pairs, need not be homogeneously or isotropically distributed. For instance, there can be a greater density of corresponding points near the fovea or along certain meridians.

B. Certain assumptions must also be made about the movements and positions of the two eyes:

1. For each eye the optical nodal point and the centre of rotation coincide. This location may or may not be the centre of the eye but must be the same in the two eyes. In fact the optical nodal point is about 17 mm in front of the fovea and the centre of rotation is about 11 mm in front of the fovea. This means that when the eyes move into a position of asymmetrical convergence the nodal points, and hence the horopter, are deflected in that direction (Gulick and Lawson 1976).

2. The two visual axes intersect in whichever point is designated as the point of convergence within the normal range of convergence, that is; the eyes have normal mobility with no strabismus or vertical misalignment of the visual axes. This ensures that the foveas receive images from the same location in space.

3. The eyes are converged about parallel axes. Given that the other conditions are fulfilled, a sufficient condition for parallel convergence is that corresponding horizontal retinal meridians are coplanar. This ensures that the eyes are in torsional alignment and that the gaze is not elevated about non-parallel axes.

The theoretical point horopter and convergence

First, let the eyes be converged at infinity. When the eyes are in torsional alignment, the horopter is the surface of an infinitely large toroid containing the fixation point at infinity and hinged about the two nodal points. For practical purposes it may be regarded as a frontal plane at infinity. If the eyes are out of torsional alignment, the horopter at infinity is simply the fixation point plus a line in the median plane steeply inclined in depth. The reason for this will become clear later.

When the eyes are symmetrically converged within the horizon plane the horopter breaks down into two components: the horizontal horopter, or Vieth-Müller circle, passing through the fixation point and nodal points; and the vertical horopter, which is a vertical line passing through the fixation point. The proof is similar to that provided in the analysis of the optical horopter.

The theoretical vertical horopter

Prévost (1843) first pointed out that the theoretical vertical horopter is a line which, (a) lies in the median plane of the head and (b) is at right angles to the Vieth-Müller circle. It must pass through the Vieth-Müller circle for the given angle of convergence, since it would otherwise contain a disparate point as it traversed the plane of the horizontal

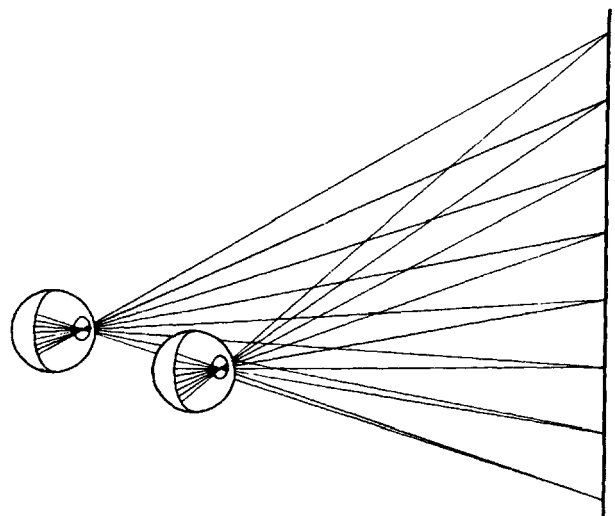


Figure 2.12. The theoretical vertical horopter.

Corresponding visual lines from the midvertical meridians of the two eyes intersect in a vertical line in the median plane of the head. With near convergence, visual lines from any other pair of corresponding vertical meridians do not intersect, since the image of any eccentric vertical line in one eye is larger than the image of that line in the other eye. With parallel convergence, the horopter is a plane at infinity, orthogonal to the visual axes.

horopter. It must also lie in the median plane, since we proved in the last paragraph that all points outside this plane, except those on the horizontal horopter or at infinity, produce vertically disparate images. Every point within the median plane has zero vertical disparity because each is at the same distance and has the same elevation to the two eyes. Thus, the locus of points in space with zero vertical disparity is the median plane of the head plus the plane containing the horizontal horopter. Within the plane containing the horizontal horopter, only points on the Vieth-Müller circle also have zero horizontal disparity. Within the median plane only one line also has zero horizontal disparity. This line is the intersection of the two planes containing the vertical retinal meridians, as shown in Figure 2.12. Therefore, within the median plane, only points on this line fall on corresponding vertical meridians, and therefore only these points have zero horizontal disparity. Any line in the median plane inclined to the plane of the horizontal horopter is the intersection of planes containing radial retinal meridians that are not parallel and therefore do not correspond geometrically.

We have thus proved that the theoretical vertical horopter is a line through the Vieth-Müller circle, in the median plane of the head and at right angles to the plane of regard. When the eyes are symmetrically converged, the vertical horopter

passes through the fixation point. When the eyes converge asymmetrically, the vertical horopter remains in the median plane of the head. Any point that is not on either the longitudinal horopter or the vertical horopter may have zero horizontal disparity or zero vertical disparity but cannot simultaneously have zero disparity in both horizontal and vertical directions.

Disparities in oblique quadrants

All points on a circle through any point on the vertical horopter and the nodal points of the eyes have the same binocular subtense and therefore have zero horizontal disparity. The locus of points with zero horizontal disparity is therefore a vertical cylinder. However, when the eyes converge, any point in space that is not in the median plane or in the plane containing the horizontal horopter produces images that are vertically disparate. Such points lie in the quadrants of the visual field. All such points project vertically disparate images because any vertical line off the midline lies at different distances from the two eyes and therefore subtends different angles to the two eyes. If one end of a such a line lies on the horizontal horopter, the other end will be vertically disparate.

Measuring vertical disparities with respect to horizontal lines of longitude introduces a second factor into vertical disparities in oblique quadrants. When the eyes converge, all corresponding longitudinal meridians in the two eyes, except the pair in the plane of regard, are relatively rotated. This introduces additional vertical disparities in the visual quadrants for this coordinate system. This factor is not evident when vertical disparities are measured with respect to horizontal lines of latitude, because all these lines remain parallel when the eyes converge. When a person converges at infinity, all points at infinity are in binocular correspondence because effects of eccentricity on relative angular size become vanishingly small and all pairs of corresponding horizontal meridians are coplanar, whichever coordinate system is used.

The theoretical horopter with cyclovergence

We have mentioned that if the eyes are out of torsional alignment when converged at infinity, the horopter is reduced to a line inclined in the median plane. When the eyes are symmetrically converged about parallel axes and then cycloverge inwards about the visual axes, the horizontal horopter remains a Vieth-Müller circle but becomes inclined far side up with respect to the horizontal plane of regard. At the same time, the vertical horopter becomes inclined top toward to viewer. When the

eyes cycloverge the other way, the Vieth-Müller circle becomes inclined far side down with respect to the plane of regard and the vertical horopter becomes inclined top away (see Figure 2.13).

The theoretical horopter with elevation of gaze

When one elevates the gaze by tilting the head back, keeping the angle of the eyes in the head constant, the whole space horopter moves upward in an arc. When the eyes converge symmetrically on a near point and each eye rotates upward in the head about an axis at right angles to the visual axis, the horizontal horopter remains in the horizon plane and the fixation point moves up along the vertical horopter, carrying the horizontal plane of regard with it. In this case the fixation point is no longer on the Vieth-Müller circle and the plane of regard is inclined to the horizontal Vieth-Müller circle. Since elevation of an eye about an axis at right angles to the visual axis does not cause a relative rotation of the principal vertical meridian, elevation of gaze does not affect the vertical horopter. This is explained in Figure 2.14. On the other hand, if the eyes tort inwards as they elevate, the horizontal horopter moves up and the vertical horopter becomes inclined top forward. Consequently, the location of the space horopter with elevated gaze depends on the cyclovergence accompanying gaze elevation in a particular person.

The theoretical horopter with oblique gaze

Finally, Helmholtz (1909) proved that when the eyes converge on a near point in an oblique direction, the horopter becomes a twisted cubic curve, as depicted in Figure 2.15 (see also Solomons 1975a, 1975b; Tyler 1983, 1989). The shape of the cubic curve depends on the amount of cyclovergence accompanying gaze elevation.

The theoretical horopter with relaxed assumptions

Now consider the consequences of violating condition A2, which stipulates that the sets of corresponding points in the two retinas are congruent.

Consider first a compression of corresponding points in the temporal retina of each eye relative to those in the nasal retina of the other eye. The resulting horopter can be determined by plotting the locus of intersections of visual lines from the corresponding points, as shown in Figure 2.16. For a given degree of compressive distortion of corresponding points, the shape of the horopter varies with the distance of convergence. For near convergence, the horopter is concave toward the viewer but is flatter than the Vieth-Müller circle (Figure 2.16a). At a certain distance of convergence, the

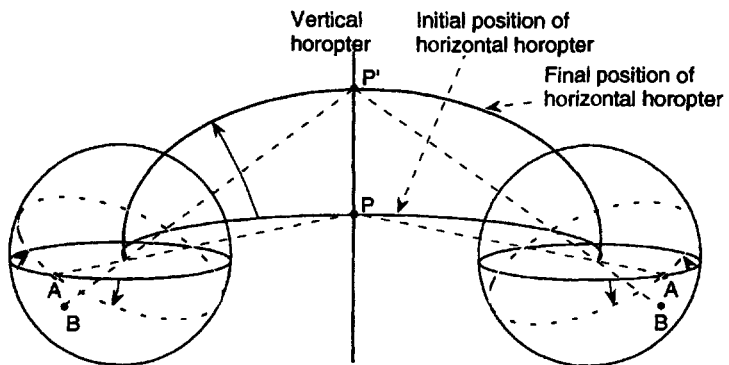


Figure 2.13. Effect of cyclovergence on the horopter.

When the eyes are symmetrically converged and cycloverge inwards, the horizontal horopter becomes inclined upwards with respect to the plane of regard and the vertical horopter becomes inclined top towards the eyes. After cyclovergence, the horizontal meridians through the foveas are no longer coplanar and therefore the only corresponding visual lines contained within them intersect the vertical horopter at P . The horizontal horopter through P' projects to coplanar meridians passing through points B which are below the meridians containing the foveas.

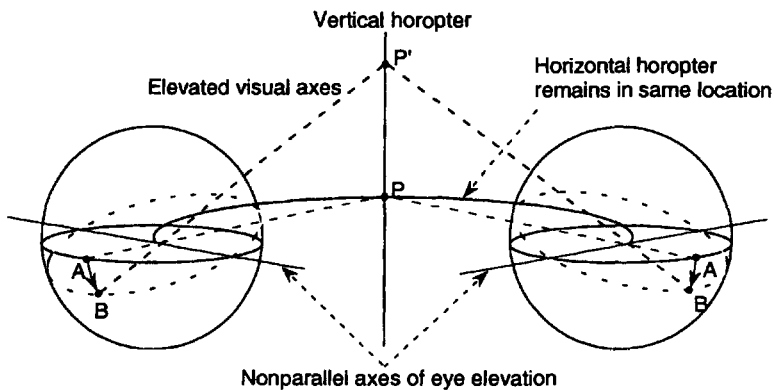


Figure 2.14. Effect of elevation of gaze on the horopter.

When the eyes are symmetrically converged and the gaze is elevated from P to P' , the horizontal horopter remains in the horizon plane and the vertical horopter remains in the same position. The fixation point moves up along the vertical horopter and the plane of regard is elevated with respect to the horizontal horopter. When the foveas are in position A , the main horizontal meridians (containing the foveas) are coplanar and lie in the same plane as the horopter. When the foveas are in position B , the main meridians are no longer coplanar and the only corresponding visual lines contained in them intersect the vertical meridian at P' . The horizontal horopter is now in the plane of two retinal meridians that moved into the position previously occupied by the main horizontal meridians.

horopter lies in a frontal plane (Figure 2.17b). With more divergence, the horopter becomes convex towards the viewer (Figure 2.16c).

An overall dilation of corresponding points in one eye relative to those in the other skews the horopter about a vertical axis, as shown in Figure 2.17. This case is discussed further in Section 2.8.

Consider, next, the effects of shearing vertical retinal meridians with respect to the horizontal meridians. Assume that the horizontal meridians remain parallel but the vertical meridians are rotated relative to each other. This has no effect on the horizontal horopter but the vertical horopter becomes inclined in the median plane. The geometry of this situation is discussed in Section 2.7.

2.5.3 Line horopters

The definition of a point horopter is that both horizontal and vertical disparities are zero. Helmholtz constructed a set of line horopters in which the requirement of conjoint horizontal and vertical zero disparities is relaxed. For a derivation of these horopters see Clement (1987). In line horopters, a line in one eye corresponds with a line in the other, but points within the lines need not be in correspondence.

The **horizontal-line horopter** (Figure 2.18a) consists of the plane containing the horizontal horopter and the median plane of the head, within which all points have zero vertical disparity but

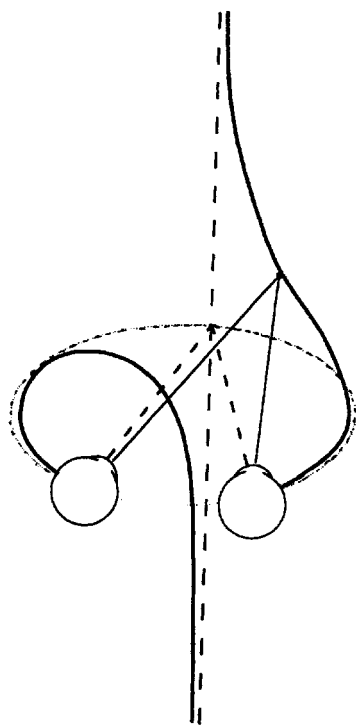


Figure 2.15. Horopter with oblique angle of gaze.
The space horopter becomes a twisted cubic curve when the eyes are converged in an oblique position.

variable horizontal disparity. Note that this horopter partitions space into quadrants, not into near and far zones.

The **vertical-line horopter** (Figure 2.18b) is a vertical cylindrical, passing through the fixation point, within which all points have zero vertical disparity but variable vertical disparity. The proof of this has already been provided. This horopter partitions space into near and far regions. The intersection of the horizontal- and vertical-line horopters defines the space horopter.

A **radial-line horopter** lying in the frontal plane through the fixation point, as shown in Figure 2.18c, is one in which corresponding retinal meridians are stimulated but horizontal and vertical disparities vary.

2.6 EMPIRICAL HORIZONTAL HOROPTER

In practice, none of the four assumptions underlying construction of the theoretical point horopter is perfectly satisfied in human vision, so that any empirically determined horopter deviates from the theoretical ideal. Before one can determine the horopter empirically one must establish a procedure for plotting corresponding points. To simplify matters, consider the horizontal horopter. In all

procedures the subject converges on a fixed point at a given distance and makes judgments about a test object exposed at each of several directions on either side of the fixation point. In dioptic procedures the observer moves a test object in depth along each of several cyclopean lines radiating out from a point between the eyes until it satisfies some specified visual criterion (see Figure 2.19). In dichoptic procedures the test object is a pair of stimuli presented in a stereoscope. Movement of the test object in depth is simulated by varying the horizontal disparity between the dichoptic stimuli relative to a fixated object. Several criteria have been used to determine when a test object is on the horopter. In each case it is assumed that the method maps corresponding points in the two retina. However, there is no absolute criterion by which the assumption can be checked, so that we cannot be sure that any method is valid. In particular, one cannot be sure that binocular correspondence, however measured, signifies zero disparity. As we will see there are grounds for suspecting that some methods are more valid than others. The types of horopter associated with the different criteria are listed here.

Investigators have attempted to deduce an appropriate geometry for mapping physical space onto subjective space. Data are derived from psycho-physical experiments in which subjects set isolated points of light to apparent equal separation at different depths (alley experiments) or to appear in frontal or other planes. The geometries turn out to be non-Euclidean, although their form depends on the type of task. These experiments are highly artificial, and the form of subjective geometry they reveal seems to have little practical or theoretical significance. Readers who wish to consult this literature should consult Luneburg (1947), Blank (1953), Foley (1964), Indow and Watanabe (1984), Rosar (1985), and Wagner (1985).

2.6.1 The fusion horopter

The fusion horopter is determined by the criterion of a fused image of a binocular test spot. Alhazen, in the eleventh century, showed that the locus of fused images is not in a frontal plane (see Section 1.2.2). Meissner (1854) first used this criterion systematically. Images fuse when they fall on corresponding points, but they also fuse when they fall near the point of exact correspondence. This range of disparities within which fusion occurs is known as Panum's fusional area (see Section 8.1). Thus, the horopter based on the criterion of fusion has a certain thickness, as depicted in Figure 2.20.

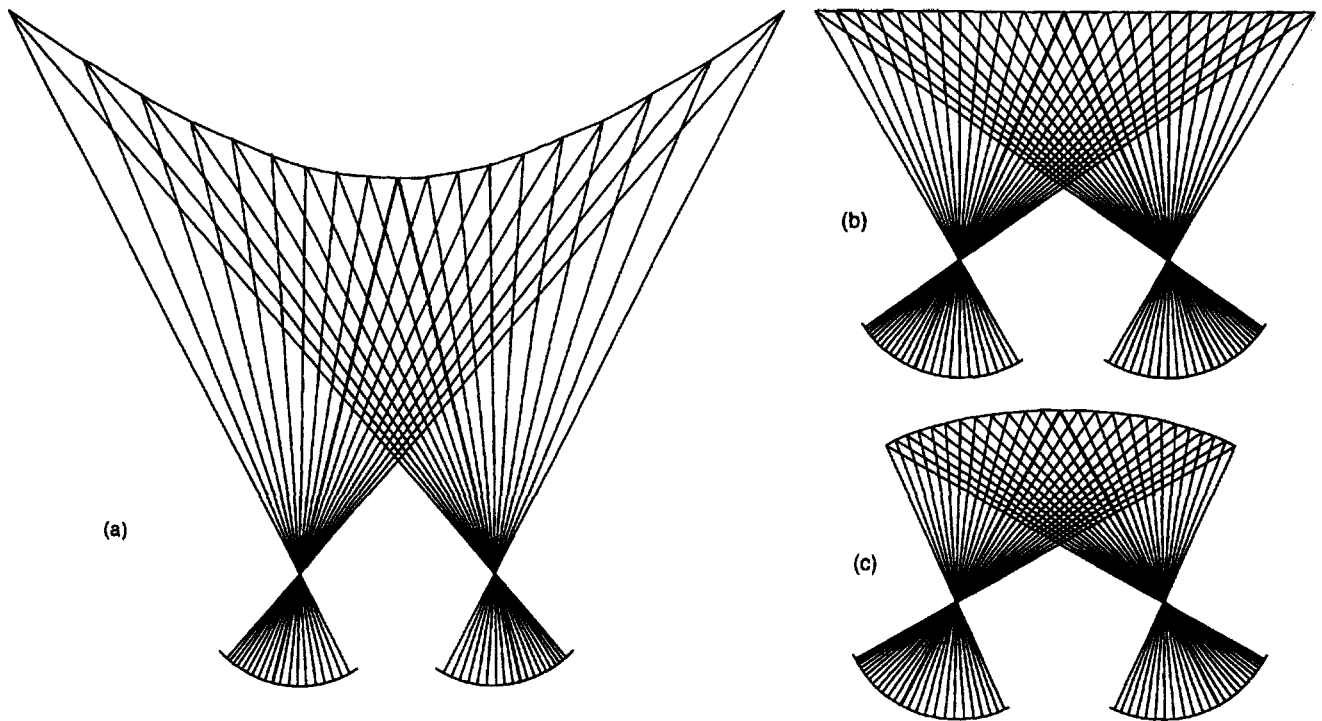


Figure 2.16. Horopters produced by compression of corresponding points in the temporal retinas relative to those in the nasal retinas.

Corresponding visual lines were first plotted for the straight-line horopter (b). The other horopters were constructed with the same relative spacing of corresponding points, with the visual axes (bold lines) converged on a more distant point (a) and on a nearer point (c).

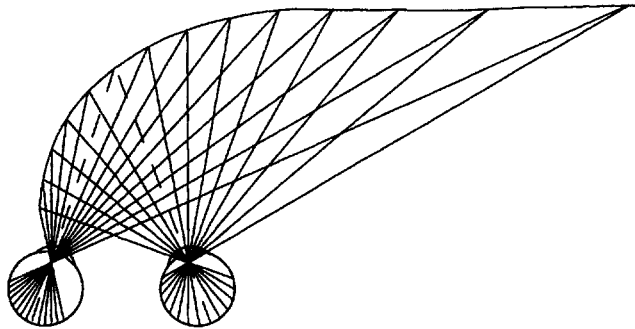


Figure 2.17. Dilation of corresponding points in one eye.
A dilation of corresponding points in one eye relative to those in the other causes the horizontal horopter to be skewed about a vertical axis. In this case the corresponding points in the right eye are more widely spaced than their partners in the left eye.

2.6.2 The midfusional-zone horopter

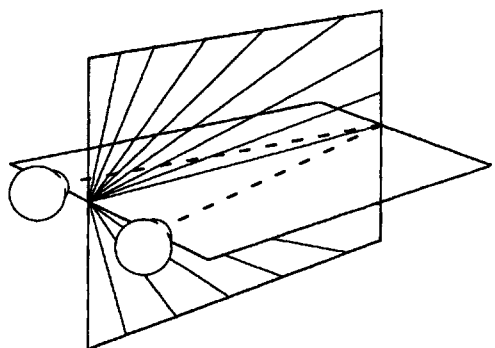
This horopter is determined by the midpoint between the limits of disparity within which the images of the test spot fuse (Panum's fusional limits). The horopter determined in this way has no thickness. This midpoint must be determined with care because the disparity at which two dichoptic

images first fuse when brought together is not the same as the disparity at which they first appear diplopic when separated (see Section 8.1.8).

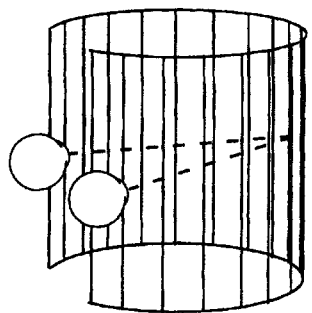
2.6.3 The maximum stereoscopic acuity horopter

The criterion for this horopter is the position in depth of two neighbouring test spots at which a change in depth of one relative to the other is detected most precisely (Tschermark 1900). This method relies on the assumption that the ability to detect a change in binocular disparity obeys Weber's law, according to which the minimum detectable change in depth between the test spots is least when the difference of disparity between them is least. Blakemore (1970d) made one of the few detailed measurements of the horopter defined by this criterion.

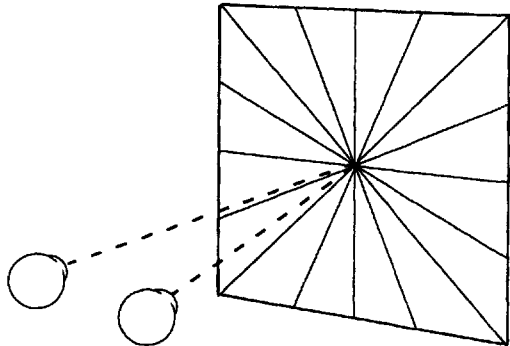
Stevenson et al. (1992) proposed a related criterion, according to which the horopter is the locus where the threshold for the detection of roughness due to random noise in a random-dot stereogram is lowest. The stereogram without noise appears as a smooth circular disc of dots in depth relative to a dark background. When added noise is detected the disc no longer appears smooth. This was called the



(a) Horizontal-line horopter. Only vertical disparities are zero.



(b) Vertical-line horopter. Only horizontal disparities are zero.



(c) Radial-line horopter. Only cyclodisparities are zero.
(Adapted from Clement 1987.)

Figure 2.18. Theoretical line horopters.

correlation horopter because the criterion is detection of a lack of perfect correlation between the images in the two eyes. It was found to lie within 2 to 3 arcmin of the nonius horopter, which is described next.

2.6.4 The nonius horopter

The criterion for the nonius horopter is the impression that a line presented to one eye is collinear with a neighbouring line presented to the other eye. To avoid problems of rivalry or fusion, the two

lines are positioned side by side or one above the other. Such pairs of lines are known as nonius lines, from the Latinized name of Pedro Nuñez, a sixteenth-century Portuguese mathematician who invented an early form of the Vernier scale. Tschermark (1900) was the first to use the nonius method to determine the horizontal horopter. The criterion of collinearity consists of two components: angular alignment, which signifies relative rotation of the images about the fixation point (orientation disparity), and lateral offset, which signifies horizontal or vertical disparity. Subjects must be instructed on which criterion to use.

In the **dioptic nonius procedure** the nonius lines are parts of the same vertical rod viewed with differently positioned masks in front of each eye, as shown in Figure 2.21. With the eyes fixated on an immobile target, the thin test rod is moved in depth until the segments of the rod appear aligned. The procedure is repeated for several azimuth positions of the test rod. Ames et al. (1932a) devised an efficient dioptic nonius display by screening several alternate sections of a vertical rod to the two eyes. The rod was then moved along a radial track until the subject saw the alternate sections as forming one line. This is known as the **grid nonius procedure**, although the interdigitated lines do not form a grid. One problem here is that any cyclovergence (opposite rotation of the eyes about the visual axes) disturbs alignment of the alternate sections of the line. Since cyclovergence varies with viewing distance, uncritical use of the grid nonius procedure may lead one to conclude that the coefficient of horopter deviation from the Vieth-Müller circle (H) is not constant. Indeed, Solomons (1975b) concluded that changes in cyclovergence could account for the inconstancy of H that Ogle (1964) reported.

In the **dichoptic nonius procedure** the nonius lines are presented in a stereoscope and their lateral separation and/or the angle between them is varied until they appear aligned. It is assumed that the alignment of vertical nonius lines indicates the locus of zero horizontal disparity. However, two vertical nonius lines do not appear parallel, because the corresponding vertical meridians are relatively rotated by about 2° (see Section 2.7). Strictly speaking, the nonius lines should be set to appear parallel before they are set to give zero lateral offset. Alignment of horizontal nonius lines indicates the locus of zero vertical disparity. The nonius method is suitable for a separate determination of horizontal- and vertical-line horopters. The full space horopter is the locus of points over the binocular field for which a pair of horizontal

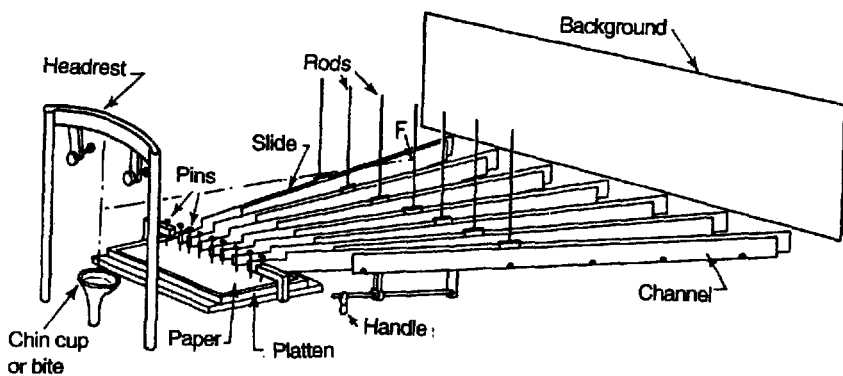


Figure 2.19. Ogle's horopter apparatus.

Each vertical test rod is moved in depth along a line radiating out from a point midway between the eyes until the observer reports that it satisfies some specified visual criterion. When all the rods have been set, the horizontal line at eye level through all the rods defines the horizontal horopter. (From Ogle 1964.)

nonius lines and a pair of vertical nonius lines are simultaneously in alignment. Since nonius lines do not come into binocular coincidence, they do not fall within Panum's fusional area, so that the nonius horopter is independent of the size of the fusional area. Theoretically, this is the purest measure of binocular correspondence since it equates the visual directions in the two eyes. The precision with which vertical nonius lines can be aligned in the centre of the visual field has been found to be about 0.7 arcmin when the gap between the lines is less than 1° (McKee and Levi 1987). This is less than the precision of Vernier acuity, probably because of the extra noise introduced into the nonius task by random vergence movements of the eyes. For targets presented in the peripheral retina, the precision of nonius settings declines, and the method becomes unreliable beyond an eccentricity of about 12° (Ogle 1964, p. 48). The judgments are easier if the test lines are kept in motion or flashed in rapid succession, as we shall see later.

The nonius method relies on the assumption that the alignment of nonius lines is not disturbed by extraneous factors such as the vergence state of the eyes, the apparent distance of the surface on which the lines are projected, or surrounding stimuli. In Sections 10.2.4 and 10.8.2 we discuss evidence that the apparent alignment of nonius lines can be perturbed by vergence and other stimulus factors. In spite of these problems, the nonius method is the most reliable way to plot the empirical horopter.

2.6.5 The zero-motion horopter

The criterion for this horopter is the impression of no motion between test spots, one in each eye,

flashed in alternation. Neighbouring test spots which appear fused when exposed simultaneously may appear to move when presented in alternation. This method therefore circumvents the problem of fusion within Panum's area. An analogous effect can be observed on the skin; two pointed rods about 2 cm apart applied to the skin of the back feel like one spot when applied at the same time, but like two spots in different locations when applied successively. Nakayama (1977) used two small dichoptic

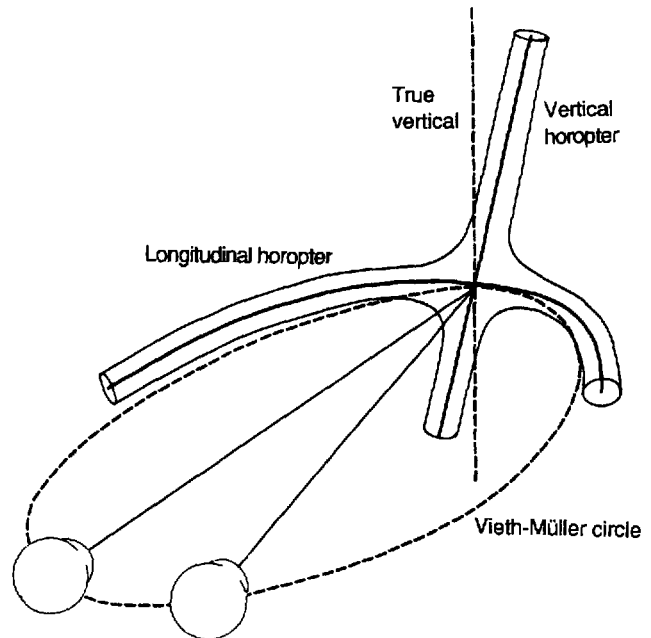


Figure 2.20. The space horopter.

The longitudinal horopter is shown as deviating from the Vieth-Müller circle—the Hering-Hillebrand deviation. The vertical horopter is inclined top away from the true vertical. The thickness of the horopter signifies Panum's fusional area.

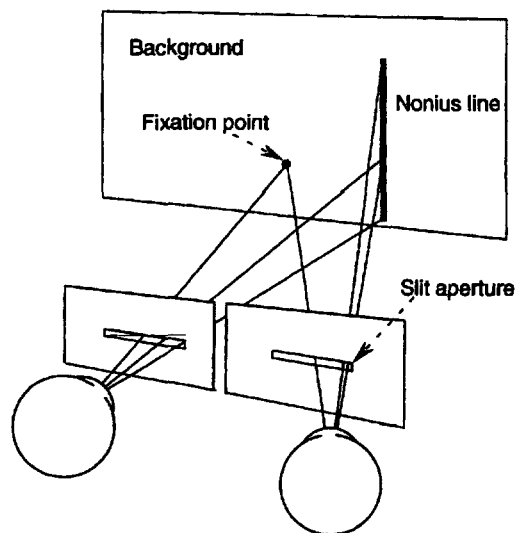


Figure 2.21. The dioptic nonius procedure.

The nonius lines are parts of the same vertical line viewed through horizontal masks in front of each eye with one mask vertically above the other. The subject fixates on a central point and the nonius line is moved radially out from a point between the eyes until it appears as one line. The procedure is repeated for several radial directions. (Adapted from Ogle 1964.)

lights, which flashed on in succession. Subjects adjusted the lateral separation of the lights until there was no apparent movement between them. This method is particularly good for peripheral viewing because in the periphery of the visual field motion between two points is relatively more visible than a stationary offset. Nakayama obtained measurements out to 30° of eccentricity with this method, which is far beyond the range of normal nonius measurements. However, he did not report the precision of his measurements.

2.6.6 The zero-vergence horopter

This horopter is the locus of points that do not evoke a change in vergence when the original fixation point is replaced by another point. This criterion was proposed by Ogle (1964) but has never been used.

2.6.7 Equal-distance and frontal-plane horopters

The equal-distance horopter is determined by the impression that the test object is at the same radial distance from the observer as the fixation spot. In other words, the spots are perceived as lying on the circumference of a circle concentric with the cyclopean eye of the observer. This horopter was first discussed by Hering. Only one or two points lying on this horopter have zero disparity defined in terms of optical or ideal retinal correspondence, while

the remainder have uncrossed disparities which increase with increasing eccentricity. Hence the empirically determined equal-distance horopter should be less concave than the Vieth-Müller circle except at infinity where the Vieth-Müller circle, the equal-distance horopter, and the frontal plane horopter all coincide.

In one study, the equal-distance horopter was found to be more concave than the Vieth-Müller circle (Shipley 1961) while in another it was less concave (Foley 1966). In a third study, observers judged whether a light source lying in the median plane at a distance of either 124 cm (3° convergence) or infinity (0° convergence) was closer to or farther away from the observer than a second light source positioned either -18 , -9 , $+9$ or $+18^\circ$ eccentrically (Foley 1970). For three out of the five observers, the locus of equal-distance settings was more concave than the Vieth-Müller circle while for the remaining two observers it was skewed closer on one side of the median plane and farther away on the other. With convergence at infinity, the locus of equal-distance settings was typically less concave, which is in the opposite direction to that predicted if the visual system had made allowance for the difference between the equal-distance horopter and the Vieth-Müller circle at different absolute distances. The effects are also opposite in direction to the changes in the shape of the apparent frontal-plane with changes in absolute distance found by Foley (1970) and Ogle (1964). *These experiments should be repeated using extended surfaces instead of isolated points and with displays which fill a larger part of the visual field.*

Instead of the criterion of equal distance some investigators have used the criterion of the frontal plane. An oculocentric frontal plane is orthogonal to the cyclopean axis—the line joining the point midway between the eyes and the intersection of the visual axes. A headcentric frontal plane is parallel to the plane of the face and is often referred to as the fontoparallel plane. The two frontal planes coincide when the cyclopean axis is orthogonal to the plane of the face and most determinations of the horopter have been done under these circumstances. Samples of the longitudinal horopter obtained by Ames et al. (1932b) using the frontal-plane criterion are shown in Figure 2.22. The subject set each of a set of vertical rods seen through a horizontal aperture to the apparent frontal plane. It can be seen that the frontal-plane horopter is less concave than the Vieth-Müller circle for near observation distances and becomes slightly convex at far distances. The viewing distance at which the apparent and objective frontal planes coincide has been

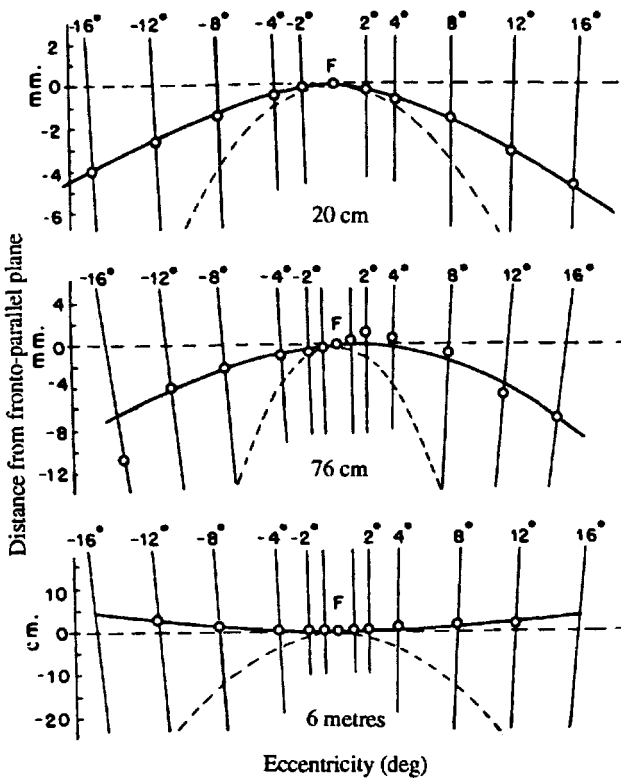


Figure 2.22. The apparent frontal plane horopter.

The plane is determined by setting vertical rods one at a time. The data are for one subject and three viewing distances, as indicated below each graph. Note that the apparent frontal plane is concave at viewing distances of 20 and 76 cm and convex at 6 m. The Vieth-Müller circle is indicated by the curved dotted lines. The vertical dimension is magnified relative to the horizontal dimension. (From Ames et al. 1932b.)

called the **abathic distance**. There are wide individual differences in the position of the frontal-plane horopter. Hering, Helmholtz, and Hillebrand noticed the deviation of the frontal plane horopter from the Vieth-Müller circle, now known as the **Hering-Hillebrand deviation**.

The apparent frontal plane does not coincide with the locus of zero disparity, and therefore does not indicate the distribution of corresponding points. Conversely, since the pattern of horizontal disparity created by a frontal surface varies with viewing distance, horizontal disparity alone cannot account for the accuracy of frontal-plane judgments. In normal viewing, we use monocular perspective cues when judging whether a plane is frontal and these are absent in the horopter apparatus. There is evidence that vertical disparities are involved in the perception of the frontal plane. The vertical-line stimulus used by Ames et al. contained no vertical disparities, which could account for the deviations of settings from the true values. Helmholtz (1909) showed

that the apparent and actual frontal planes closely coincide at any distance when the stimulus allows for the detection of vertical disparities (see Section 7.6.2).

It can be seen in Figure 2.17a that a variation in the shape of a zero-disparity horopter with viewing distance occurs when the separation of retinal elements increases toward the nasal sides of the each retina (Hillebrand 1929). More specifically, it has been argued that the Hering-Hillebrand deviation implies that the eccentricity of a point in the nasal hemiretina of either eye, ϕ_n , is greater than that of its corresponding point in the temporal retina of the other eye, ϕ_t and that, as eccentricity increases, the visual angle between corresponding points becomes progressively larger. It is assumed that the centres of the foveas are corresponding points.

In Section 7.6.7 we show that the horopter deviation derived in this way corresponds in direction but not in magnitude to the Hering-Hillebrand deviation. We will show that the deviation of the apparent frontal plane from the objective frontal plane, as determined by vertical rods, does not imply a differential compression of corresponding points but can be explained in terms of the absence of vertical disparities in the stimuli in the horopter apparatus used to obtain the frontal-plane horopter.

Ogle (1932) described the empirical horizontal horopter as a conic section containing the point of fixation and the two nodal points of the eyes. The conic section can be circular, elliptical, or hyperbolic. The general form of the horizontal horopter can be specified by the equation

$$\cot \phi_l - R_O \cot \phi_r = H \quad (2)$$

where ϕ_l and ϕ_r are the visual angles subtended at the left and right eyes, respectively, by the fixation point and any other point on the horopter. The constant H is the **horopter-deviation coefficient** and describes the curvature of the horopter at the fixation point relative to the curvature of the Vieth-Müller circle at that point. The constant R_O describes the degree to which the horopter is skewed with respect to the frontal plane. When $H = 0$ the horopter is circular and lies on the Vieth-Müller circle for all viewing distances. For other values of H it follows from equation (1) in Section 2.3.1 that, as viewing distance increases, a given angular difference between a pair of corresponding points signifies a greater deviation of the empirical horopter from the Vieth-Müller circle. For positive values of H , the empirical horopter is a

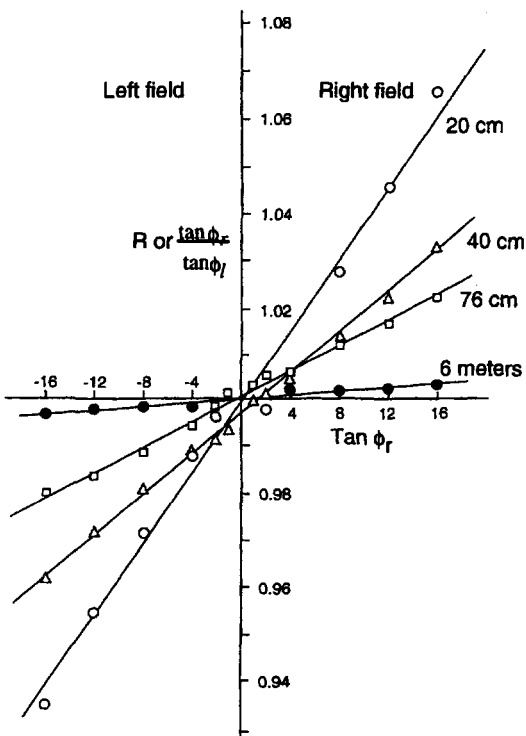


Figure 2.23. Plot of horopter data.

For the same data shown in Figure 2.22, the tangent of the angular subtense of the righteye image ($\tan \phi_r$) is plotted on the X axis and the tangent ratio of the angle of subtense of the two images (R) for each point along the empirical horopter is plotted on the Y axis. H is the slope of the resulting linear function, and R_0 is its Y-axis intercept. (From Ames et al. 1932b.)

concave ellipse with its long axis extending laterally beyond the Vieth-Müller circle at near viewing distances and, as viewing distance increases, it becomes flat and then convex to the viewer. Thus, for values of H greater than zero, there is a viewing distance, d , for which the horopter lies in the frontal plane. This is the abathic distance. This occurs when $d = a/H$, where a is the interpupillary distance. For negative values of H the horopter is an ellipse compressed laterally with respect to the Vieth-Müller circle and becomes a parabola with increasing viewing distance.

The constant, R_0 , is the ratio of magnification of the image of an object in one eye relative to the magnification of the image in the other eye. It indicates the degree to which the horopter is skewed with respect to the frontal plane. The skewing of the horopter by relative magnification of the images is illustrated in Figure 2.17. When $R_0 = 1$, the horizontal horopter is symmetrical about the median plane of the head.

Let R denote the ratio of the tangents of ϕ_l and ϕ_r for a given point on the horopter. Equation (2) can

be rewritten in the form

$$R = \frac{\tan \phi_r}{\tan \phi_l} = H \tan \phi_r + R_0 \quad (3)$$

If $\tan \phi_r$ is plotted on the X axis and the tangent ratio (R) of each point along the empirical horopter is plotted on the Y axis, then H is the slope of the resulting linear function and R_0 is its intercept on the Y axis, as illustrated in Figure 2.23.

There are three questions to be raised regarding the constancy of H : its constancy at different eccentricities of the stimulus, its constancy at different viewing distances, and its constancy in asymmetrical convergence. Ogle (1964) assumed that H was constant at different eccentricities and derived a single average value of H for each viewing distance. This average value was used to obtain linear plots of equation (3). Shipley and Rawlings (1970a) objected to this averaging procedure on the grounds that it hides potentially interesting fluctuations in the pattern of retinal correspondence evident in data from their own experiments (Rawlings and Shipley 1969).

Ogle (1964) showed that data from several investigators reveal that H is not constant as viewing distance changes. This suggests that there is some instability in the pattern of retinal correspondence. However, H could vary because of differential changes in the optics of the eyes resulting from changes in accommodation that accompany vergence changes, or because of changes in the positions of the nodal points with respect to the centres of rotation of the eyes. Another possible cause of the instability of H with viewing distance is that Ogle's criterion of setting points in a frontal plane changes with distance. We elaborate on this point in Section 7.6.

Flom and Eskridge (1968) found no appreciable change in the pattern of correspondence for changes in vergence between viewing distances of 10 cm and 6 m, using a nonius procedure in which the nonius lines were afterimages impressed on the two eyes. Wick (1990) estimated a 0.6° change in correspondence, as indicated by the change in alignment of dichoptic afterimages and Haidinger brushes, when the eyes were held in a maximally diverged position for several minutes, but their procedure was not free of artifacts.

Frontal horopter with asymmetrical convergence
With regard to the constancy of H with asymmetrical convergence, Ames et al. (1932b) reported that the shape of the frontal-plane horopter changed

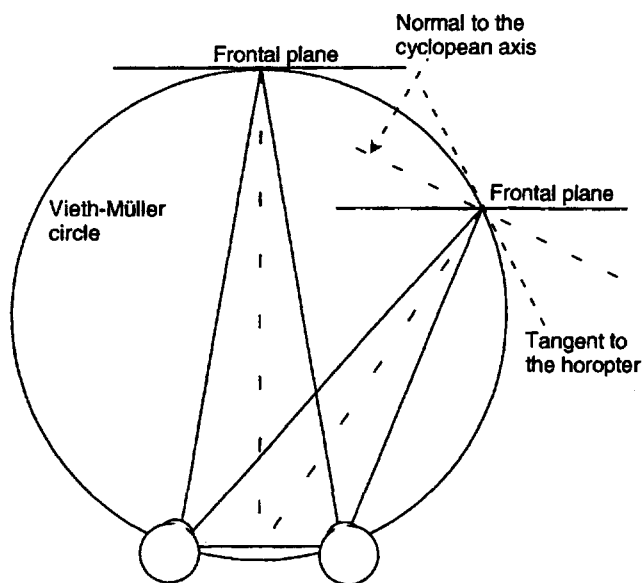


Figure 2.24. Frontal plane in asymmetrical convergence.
The frontal plane, the normal to the cyclopean axis, and the tangent to the Vieth-Müller circle coincide with symmetrical but not with asymmetrical convergence.

when the eyes were fixated on an eccentric target, although it changed in different ways for the two subjects. Herzau and Ogle (1937) and Lehnert (1941) investigated this question over a wide range of angles of eccentric gaze, using both the frontal-plane and the nonius criteria. In both studies, the frontal-plane horopter changed with changing angle of gaze but the nonius horopter remained constant. Flom and Eskridge (1968) also used a nonius method and found that correspondence is stable to within 6 arcmin for eccentric angles of gaze up to 12°. Lehnert (1941), Linksz (1952), and Shipley and Rawlings (1970a, 1970b) concluded that only the nonius method reveals the shape of the horopter. The nonius method equates visual directions in the two eyes, whereas the frontal-plane criterion has to do with placing points in a common plane, which may have little to do with whether or not those points have zero disparity.

At the beginning of this section an oculocentric frontal plane was defined as orthogonal to the cyclopean axis and a headcentric frontal plane was defined as parallel to the plane of the face. A third plane is one that is tangential to the Vieth-Müller circle at the fixation point. When the visual axes are horizontal and symmetrically converged the three planes coincide. With asymmetrical convergence or for a surface to one side of the median plane, these three planes do not coincide, as illustrated in Figure 2.24. Subjects asked to make frontal-plane judgments must be carefully instructed about which criterion to use (see Morrison 1977).

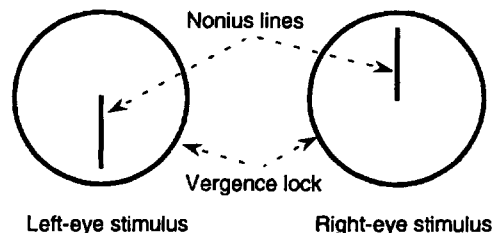


Figure 2.25. Volkmann discs.

The angular misalignment of the two nonius lines in the dichoptically combined image provides a measure of the declination of corresponding vertical meridians. In most people the corresponding vertical meridians are relatively extorted about 2°, and this reveals itself as a difference in the perceived orientation of vertical nonius lines, which should be visible when the displays are fused.

The perception of the frontal plane is discussed in more detail in Section 7.6.7.

2.7 EMPIRICAL VERTICAL HOROPTER

The geometrical vertical horopter is a single vertical line intersecting the horizontal horopter in the median plane, as shown in Figure 2.12. We will now see that the empirical vertical horopter is inclined top away in the median plane.

The nonius method is the best psychophysical procedure for determining the vertical horopter. In one form of the method, two dichoptic vertical lines or two horizontal lines are presented, one on each side of the fixation point. A binocularly viewed circle around the nonius lines holds horizontal and vertical vergence steady. These are known as **Volkmann discs** (see Figure 2.25). One of the lines is stationary and the other is rotated in a frontal plane about the point of fixation until the subject reports that the two lines appear aligned. It is assumed that dichoptic lines that appear aligned fall on corresponding meridians. Helmholtz (1909 vol. 3, p.408) first set horizontal nonius lines collinear to determine the alignment of the corresponding horizontal meridians. He then set vertical nonius lines collinear to determine the alignment of the corresponding vertical meridians. With the eyes symmetrically converged, the corresponding horizontal meridians were found to be almost parallel in his subject, but the corresponding vertical meridians were found to be extorted by about 2° relative to each other. Nakayama (1977) confirmed this relative tilt of the corresponding vertical meridians. Instead of using Volkmann discs, he plotted the horizontal disparity between diplopia pairs of points as a function of their distance above and below the fixation point. The points of lights

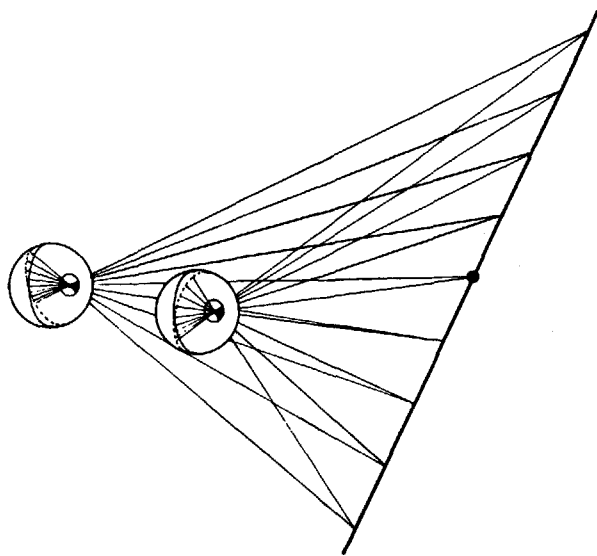


Figure 2.26. The empirical vertical horopter.

For near convergence, the vertical horopter is a straight line inclined top away in the median plane of the head. The dotted lines on the retinas indicate the corresponding vertical meridians. The solid lines indicate the true vertical meridians.

were flashed on in alternation and their lateral separation was adjusted until there was no apparent motion between them; at this point it was assumed that their images fell on corresponding vertical points.

Thus, when corresponding horizontal meridians are aligned, corresponding vertical meridians, measured by the nonius technique, are tilted about 1° on either side of the true vertical, with the top of each meridian tilted to the temporal side. This is known as the **angle of declination**. In other words, the binocular correspondence system is mapped by a horizontal shear distortion. The declination of the corresponding vertical meridians cannot be due to eye torsion since this would affect

horizontal meridians in the same way. For images of a line in the median plane of the head to fall on the extorted vertical meridians, the line must be inclined away from the observer, as shown in Figure 2.26. In Figure 2.27, θ is the angle of declination between the corresponding vertical meridians and i is the angle of inclination of the vertical horopter relative to the vertical. If a is the interocular distance and d the viewing distance, then

$$\tan \frac{\theta}{2} = \frac{a}{2x} \text{ and } \tan i = \frac{d}{x}$$

It follows that

$$\tan \frac{\theta}{2} = \frac{a \tan i}{2d} \quad (4)$$

For small values of θ

$$\theta = \frac{a \tan i}{d} \quad \text{or} \quad i = \tan^{-1} \frac{\theta d}{a} \text{ in radians} \quad (5)$$

Since the tangent of half the angle of convergence, $\phi/2$, equals $a/2d$, equation (4) can be written

$$\tan \frac{\theta}{2} = \tan \frac{\phi}{2} \tan i \quad (6)$$

For near viewing, the vertical horopter is nearly vertical and, as viewing distance increases, it becomes increasingly inclined until, for far viewing, it is parallel with the ground.

The shear of corresponding vertical meridians relative to corresponding horizontal meridians is probably a consequence of the fact that most horizontal surfaces are below eye level and inclined top away like ground-plane surfaces. Perhaps, in early development the pattern of correspondence is shaped by alignment of the vertical horopter with the ground plane (Krekling and Blika 1983). Cooper and Pettigrew (1979) showed electrophysiologically that the corresponding vertical meridians of

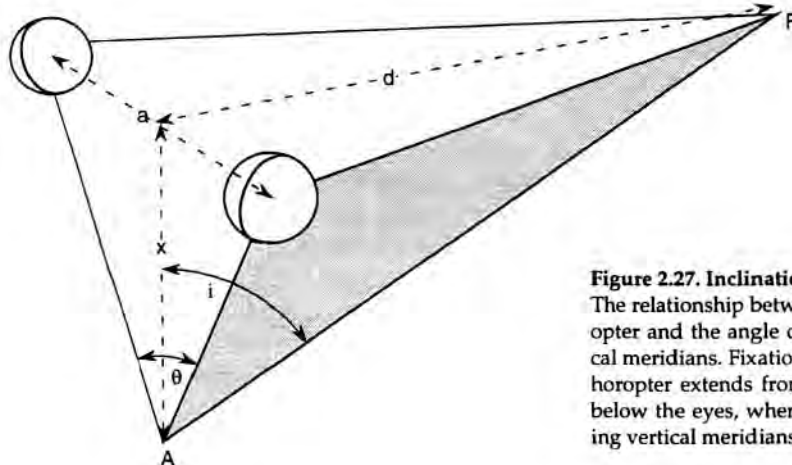


Figure 2.27. Inclination of the vertical horopter.

The relationship between the inclination, i , of the vertical horopter and the angle of declination, θ , of corresponding vertical meridians. Fixation is on point F at distance d . The vertical horopter extends from F to a point A at distance x vertically below the eyes, where the planes containing the corresponding vertical meridians intersect. Interocular distance is a .

owls and cats are rotated by an amount that places the vertical horopter along the ground for the eye height and viewing distance of these animals. Evidence reviewed in Section 15.2.4 suggests that the tuning of cortical cells to orientational misalignment of the images in the two eyes is modified in kittens exposed for some time after birth to prisms that rotate the images in opposite directions. Tyler (1991) reviewed the literature on the vertical horopter and the effects of cyclovergence.

2.8 ANISOMETROPIA AND ANISEIKONIA

2.8.1 Relation of anisometropia to aniseikonia

Types of anisometropia and aniseikonia

An ametropic eye is one in which the image is not brought to focus on the retina for some or all normal viewing distances. An emmetropic eye is one in which the image is in focus for all normal viewing distances. An ametropic eye can be myopic (short-sighted), in which case near objects but not far objects are in focus, or hypermetropic (long-sighted), in which case far but not near objects are in focus. Ametropia due to inadequate refractive power of the cornea or lens or to abnormal distance between cornea and lens is known as **refractive ametropia**. Uncorrected refractive ametropia has little if any effect on image size. However, correcting refractive ametropia with a spectacle lens alters the size of the image. Ametropia due to an abnormal axial length of the eyeball is known as **axial ametropia**. If the globe is shorter than the focal length, the eye is hypermetropic and the image is smaller than in an emmetropic eye. If the globe is longer than the focal length, the eye is myopic and the image is larger than in an emmetropic eye.

In **anisometropia** one eye is more myopic or more hypermetropic than the other. In **meridional anisometropia** the difference in refractive error is along only one meridian. This occurs when the two eyes have astigmatism of different magnitudes. Anisometropia due to refractive myopia or hypermetropia is known as **refractive anisometropia** and that due to axial ametropia is known as **axial anisometropia**.

The term “**aniseikonia**” was introduced by Lancaster (1938) to refer to a difference between the two eyes in the perceived size of an object. We use the term **optical aniseikonia** to denote aniseikonia due to a physically measured difference in the sizes of the retinal images that typically arises in uncorrected axial anisometropia or in corrected refractive anisometropia. Little if any difference in the

size of the image occurs with corrected axial anisometropia or with uncorrected refractive anisometropia. Aniseikonia can occur in people for whom the images in the two eyes are equal in size, in which case it must be due entirely to nonoptical causes (Carlton and Madigan 1937). We refer to this condition as **neural aniseikonia**. Small amounts of aniseikonia are common in emmetropes. For instance, Gillott (1957) found that 40 per cent of emmetropes showed aniseikonia of at least 0.8 per cent.

An objectively measured difference between the sizes of the retinal images does not necessarily produce aniseikonia, as measured psychophysically. For instance, a difference in image size can arise from axial anisometropia but this may not result in a perceived difference in image size. It is believed that in this case the effect of the difference in image size is cancelled by an opposite neural aniseikonia. Furthermore, neural aniseikonia may persist after a difference in image size has been corrected. These statements are explained in the following.

Aniseikonia of eccentric gaze occurs for objects displaced to one side of the median plane of the head. This is because such an object is nearer to one eye than to the other and therefore projects a larger image in that eye. Lancaster preferred not to use the term aniseikonia for this effect because it is present in all eyes and he applied the term to abnormal situations only. **Induced aniseikonia** is produced by wearing a magnifying lens in front of one eye. In this case, the eye with the larger image must move further than the eye with the smaller image when the gaze is directed to an eccentric visual object. This is because the eye moves with respect to the magnifying lens, which is fixed relative to the head. Thus, with induced aniseikonia, the eyes must adopt an unusual vergence angle when fixating an eccentric object. In other words, the locus of isovergence is disturbed by induced aniseikonia. This produces a differential effect on phoria (see Section 10.2.3)—an effect known as **optical anisophoria** (Remole 1989). Eye movements are not affected by aniseikonia due to intrinsic causes, nor by aniseikonia induced by contact lenses because the lenses move with the eyes.

Sorsby et al. (1962) measured anisometropias of between 2 and 15 dioptres in 68 patients. In 49 cases, more than 50 percent of the anisometropia was due to differences in axial length. A difference in axial length was the exclusive or predominant cause of anisometropias of over 2 dioptres. A difference in corneal curvature accounted for very little of the condition, and often reduced rather than increased the anisometropia due to other causes.

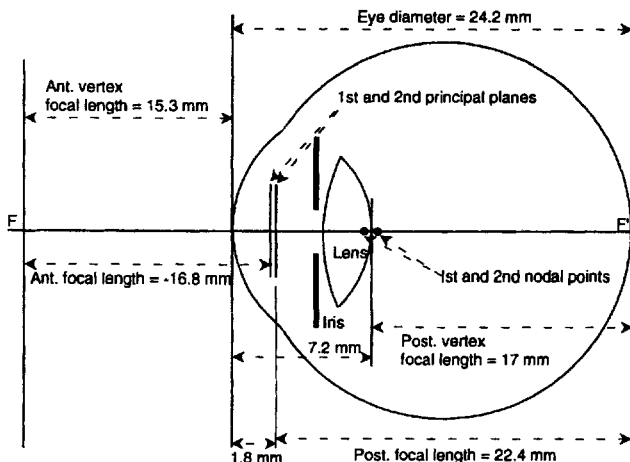


Figure 2.28. The Gullstrand schematic unaccommodated eye.

There has been considerable dispute about the clinical significance of aniseikonia.

Aniseikonia in axial ametropia

The refractive power of a lens in dioptres is the reciprocal of its focal length, f , in metres. The posterior focal length of the eye is the distance from the second principal point to the focused image of a distant object, as illustrated in Figure 2.28. In the emmetropic eye the focused image is on the retina. It follows that the linear size of the image of a distant object subtending angle θ at the second principal point of an eye, with refractive power D , is $f \tan \theta$, or $\tan \theta / D$. In other words, the size of the retinal image is inversely proportional to the refractive power of the eye's optical system. When an axially ametropic eye of refractive power D_1 is corrected by a lens of refractive power D_2 , the combined refractive power of eye and lens is given by

$$D_{1+2} = D_1 + D_2 - dD_1D_2$$

where d is the distance from the second principal point of the correcting lens to the first principal point of the eye. The anterior focal point of the eye is about 15 mm in front of the eye, which is about where a spectacle lens is worn. Thus, when an axial ametropia is corrected by a spectacle lens, $f = d$ and, since $D_1 = 1/f$, $D_{1+2} = D_1$. This means that when axial ametropia is corrected by a thin spectacle lens, the size of the optical image is the same as that in an emmetropic eye. This is known as Knapp's law. Note that the law applies only to axial ametropia corrected by a thin lens placed at the anterior focal plane of the eye. Consider the case of an axial myopia. The eyeball is elongated so that the in-focus image is formed in front of the retina. The out-of-focus image on the retina is larger than

the in-focus image. A thin corrective spectacle lens worn about 15 mm in front of the eye moves the in-focus image back onto the retina but does not affect its size. This means that the in-focus image which is now on the retina is the same size as that in an emmetropic eye but smaller than the out-of-focus image in the eye before it was corrected. When an axial hypermetropia is corrected, the image is magnified with respect to the image before correction. The vertex distance is the distance from the back surface of the lens to the cornea. For an axial ametropia corrected by a thin lens at a vertex distance of 18 mm, the image is changed in size by about 2 per cent for each dioptre of correction. This decreases to 1.25 per cent for a vertex distance of 12 mm. Thus the change in image size becomes smaller as the corrective lens is moved closer to the eye. There is no change in image size with contact lenses because these are worn on the eye. For a refractive ametropia of lenticular origin the image size is changed about 1 per cent per dioptre of correction (von Bahr 1993). These values apply to thin lenses. The effects are larger for prescription lenses and depend on their thickness and prescription power.

For people with uncorrected axial anisometropia, the image in one eye is larger than that in the other. We have just seen that a spectacle lens worn before an eye with axial ametropia causes the image to be the same size as that in an emmetropic eye. In spite of this, many patients complain that things appear larger or smaller with a corrected eye than with the normal eye. One possible reason for this is as follows. An eye with axial myopia is elongated. As a consequence, the retina is stretched and receptor density is reduced. Thus, although the out-of-focus retinal image of an object is enlarged in an eye with uncorrected axial myopia, it covers the same number of receptors as that of the image of a normal eye (Rose and Levinson 1972; Bradley et al. 1983). When the retinal image in an eye with axial myopia is brought into focus and made optically the same size as that in the other eye, the "neural" image becomes smaller than that in the other eye because it is spread over fewer receptors. In other words, the images in the two eyes are made equal but a residual neural aniseikonia remains. The differential magnification of the images produced by axial anisometropia need not be corrected optically, because it is at least partially corrected by the differential stretching of the retinas. Another problem with optical correction is that the retina may be stretched by different amounts in different locations. This issue does not seem to have been investigated. Relationships between anisometropia and aniseikonia are summarized in Table 2.2.

Table 2.2. Summary of the effects of anisometropia on aniseikonia.
The statements are generalizations which may not be true in every case.

Condition	Optical Aniseikonia	Neural Aniseikonia
Uncorrected axial anisometropia	Present	Present
Corrected axial anisometropia	Not present	Present
Uncorrected refractive anisometropia	Not present	Not present
Corrected refractive anisometropia	Present	Not present

Aniseikonia in aphakia

Adults with unilateral loss of a lens (aphakia) can have vision restored by a spectacle lens, a contact lens, or an intraocular lens implant. Clinical studies have revealed that correction with spectacles leads to an aniseikonia of 20 per cent or more, which severely disrupts binocular vision. Correction with a contact lens also produces aniseikonia because the replacement lens is some distance in front of the original lens. The aniseikonia is between 4 and 10 per cent, depending on whether the aphakic eye was originally hypermetropic or myopic respectively (Ogle et al. 1958). Stereopsis is possible with this magnitude of aniseikonia in most adult patients but not in children (Highman 1977). Correction with an intraocular implant produces only about 2 per cent of aniseikonia because the replacement lens is in essentially the same position as the original lens. This type of correction restores binocular stereopsis in most patients (Girard et al. 1962; Miyake et al. 1981). It has been estimated that over three million lens implant operations are performed every year (Lakshminarayanan et al. 1993). Even with this type of correction, the amount of aniseikonia varies with the state of accommodation of the normal eye relative to the fixed accommodation of the aphakic eye (Ivashina 1981) and also increases if a supplementary corrective spectacle lens has to be worn (Miyake et al. 1981). When intraocular lenses are implanted into both eyes aniseikonia will occur if the lenses are not in equivalent locations or are not parallel (Lakshminarayanan et al. 1993).

There has been some dispute over how much aniseikonia can be tolerated without loss of stereopsis. Ogle (1964) put the upper limit of tolerated aniseikonia in the space eikonometer at 5 per cent. Others have found that stereopsis in a normal visual environment is also impossible when aniseikonia exceeds between 5 and 8 per cent (Campos and

Enoch 1980). However, Highman (1977) reported that stereopsis is present with aniseikonias up to 19 per cent and Julesz (1960) reported that depth is still apparent in a random-dot stereogram when the images differ in size by 15 per cent (see Figure 12.4). Estimates of tolerated aniseikonia clearly depend on the test used to assess stereopsis.

Vertical aniseikonia, like horizontal aniseikonia, causes a frontal surface to appear slanted in depth. This is known as the induced effect. For instance, a vertical magnification of the image in the right eye causes a frontal surface to appear slanted to the same degree, but in the opposite direction, as the same horizontal magnification of the image. It is as if the images are isotropically scaled to make the vertical sizes the same, with transfer of the disparity into the horizontal dimension. This issue is discussed more fully in Section 7.6.5.

2.8.2 Measurement of aniseikonia

An instrument for measuring the magnitude and meridional direction of aniseikonia is known as an eikonometer. There are two basic types of eikonometer, the direct comparison eikonometer and the space eikonometer.

Direct comparison eikonometer

The direct comparison eikonometer presents dichoptic stimuli simultaneously in a stereoscope. The stimuli can be two identical patterns which appear side by side or they can be concentric displays like those shown in Figure 2.29. The difference in size of the two images that appear equal in size indicates the magnitude of aniseikonia (Barker 1936; Allen 1937). Subjects may have difficulty comparing the sizes of images in the visual periphery when fixating a central point. If subjects are allowed to move their gaze to the monocular images in succession, the images may become misaligned due to fixation

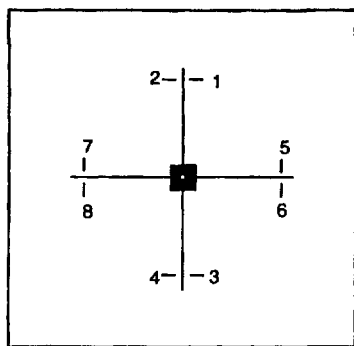


Figure 2.29. Display for direct comparison eikonometer.

Fixation is maintained on the binocular central square. The odd-numbered lines are presented to one eye and the even-numbered lines to the other. The magnification of an afocal lens in front of one eye is adjusted until the pairs of lines appear aligned. (From Ogle 1964.)

disparity or phoria and this would interfere with the measurement of aniseikonia.

In a related method, two parallel lines are presented to one eye in a stereoscope and a scale is presented to the other eye. The subject indicates the perceived distance between the lines by the numbers on the scale. The stimuli are interchanged between the eyes, and the measurement repeated. The mean of the readings indicates aniseikonia for the meridian extending between the parallel lines. Aniseikonia along other meridians is measured by setting the parallel lines in other directions.

Brecher (1951) designed a test in which one eye views two points of light directly and the other eye views them through Maddox rods which spread the points out into vertical streaks. Aniseikonia is indicated by the apparent separation of the two points relative to the apparent separation of the two streaks.

Dichoptic points and lines have the advantage that they provide only a weak fusional stimulus. If the subject has a phoria the points will be displaced relative to the streaks which would make the judgment of relative separation difficult. This problem may be overcome by nulling the phoria with a prism. Another way to reduce the tendency to fuse the dichoptic stimuli in the direct comparison eikonometer is to alternate them to the two eyes (Brecher et al. 1958). Aulhorn's phase-difference haploscope can be used to measure aniseikonia (Aulhorn 1966). Half circles are presented alternately to each eye in rapid succession to produce the impression of a whole circle. Horizontal aniseikonia is measured by projecting one half circle above the other and adjusting one half until it appears the same size as the other and the two appear as a circle. Vertical aniseikonia is measured by projecting the half circles side by side.

In all these methods the magnification of an afocal lens placed before one eye is changed until the image appears the same size as that in the other eye. Aniseikonia is then indicated by the setting of the afocal lens.

An ordinary ophthalmic lens changes the effective focal distance of the image relative to the object in addition to changing the magnification of the image. For purposes of measuring aniseikonia, only a change in image size is required. An afocal lens changes the size of the image but has no power, that is, it does not change the focal distance of distant objects. Lenses can be designed that magnify images of objects at different distances by the same amount. A lens unit available from the American Optical Company can be adjusted to produce a range of magnifications with little change in the optical distance of the image relative to the object (see Ogle 1964). A **meridional afocal lens** is cylindrical, and magnifies the image along only one meridian, the meridian at right angles to the axis of the lens.

Space eikonometer

Use of the space eikonometer involves the psycho-physical determination of distortions in stereoscopic vision induced by aniseikonia. The method can be used only with subjects with stereoscopic vision. People with severe aniseikonia are unable to fuse the images and are thus unable to make judgments about stereoscopic distortions. A vertically oriented meridional lens magnifies the image horizontally. Such a lens worn before one eye introduces horizontal disparity between the images in the two eyes, which causes a surface in a frontal plane to appear slanted about a vertical axis, as illustrated in Figure 2.30. The geometry of this type of disparity is discussed in Section 7.2. People with meridional aniseikonia should experience corresponding distortions of visual space. However, these distortions may not be noticed in a normal visual environment because of the many veridical monocular cues to depth. When monocular cues are eliminated or reduced, the distortions due to aniseikonia are apparent and the degree and meridional axis of aniseikonia is indicated by the magnitude and direction of apparent slant of a frontal surface. Between 1932 and 1947 Ames and his associates at the Dartmouth Eye Institute in Hanover, New Hampshire, devised tests of aniseikonia based on this principle (see Burian 1948 for a history of the institute).

Figure 2.31 shows the essential features of the space eikonometer (Ames 1945). The subject views a frame containing a pair of oblique threads from a distance of about 3 m. A pair of vertical threads is suspended about 60 cm in front of the frame and a

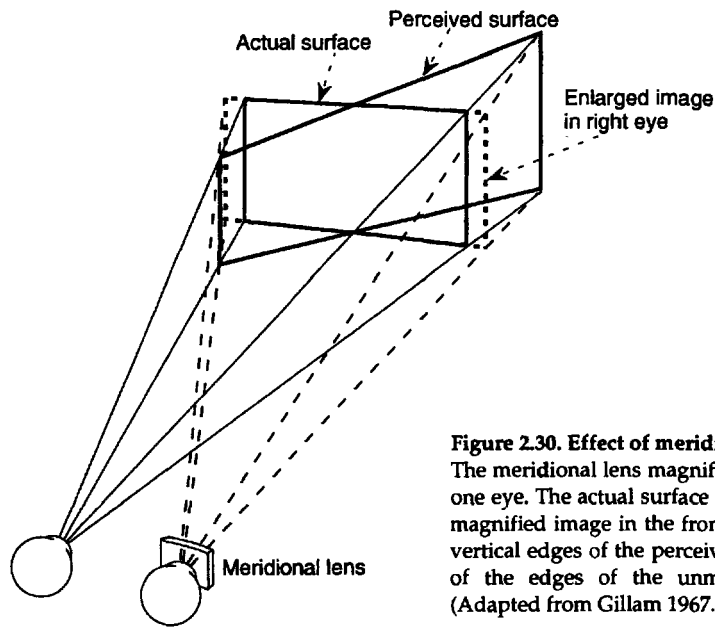


Figure 2.30. Effect of meridional lens on perceived slant.

The meridional lens magnifies the horizontal dimensions of the image in one eye. The actual surface lies in the frontal plane. The projection of the magnified image in the frontal plane is shown by bold dotted lines. The vertical edges of the perceived surface are located where the projections of the edges of the unmagnified and magnified images intersect. (Adapted from Gillam 1967.)

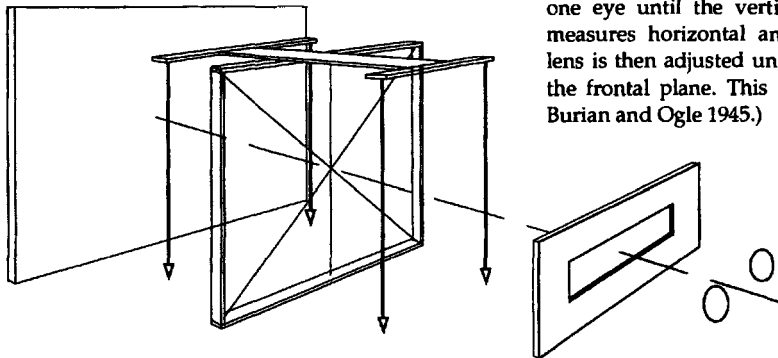


Figure 2.31. The space eikonometer.

The subject first adjusts a vertically oriented meridional lens in front of one eye until the vertical threads appear in the frontal plane. This measures horizontal aniseikonia. A horizontally oriented meridional lens is then adjusted until the crosswires in the square frame appear in the frontal plane. This measures vertical aniseikonia. (Adapted from Burian and Ogle 1945.)

second pair of threads is suspended 60 cm beyond the frame. The subject views the oblique and vertical threads through an aperture which hides their ends. A horizontal aniseikonia causes one of each pair of threads to appear nearer than the other member of the pair. The subject adjusts a vertical-axis meridional lens in front of one eye until the pairs of threads appear in frontal planes. This measures the horizontal component of aniseikonia.

Vertical aniseikonia does not affect the appearance of vertical threads because their ends are not in view. Once horizontal aniseikonia is cancelled by the setting of the vertical threads, any residual apparent slant or inclination of the oblique threads must be due to vertical aniseikonia. A vertical aniseikonia causes the cross to appear slanted out of the frontal plane because vertical magnification of an oblique cross is geometrically equivalent to horizontal minification, if the ends of the cross are

hidden. The subject adjusts a meridional lens with horizontal axis until the cross formed by the oblique threads appears in a frontal plane. This provides a measure of the vertical component of aniseikonia. Aniseikonia along an oblique axis induces a cyclodisparity into the images of the vertical lines which makes these lines appear inclined about a horizontal axis (Burian and Ogle 1945). The geometry of this effect is illustrated in Figure 2.32. The magnitude of an oblique aniseikonia is measured by rotating the images of the vertical lines until they appear in the frontal plane. Ogle (1964) provides more details on space eikonometers.

Remole (1983) has developed a simplified and easy to administer version of the space eikonometer in which the subject sets a display of rods to a frontal plane in each of several orientations (see also Remole 1992a, 1992b). This allows aniseikonia to be determined in oblique as well as horizontal

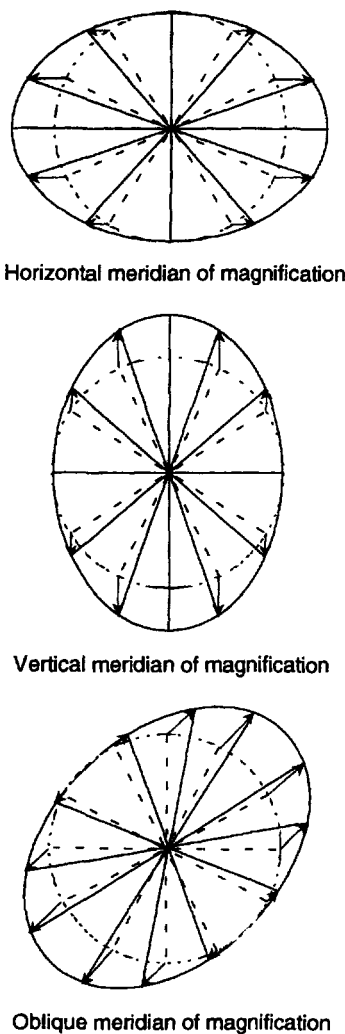


Figure 2.32. Disparities produced by aniseikonia.

The dotted lines represent the image in one eye and the solid lines represent the magnified image in the other eye. (Adapted from Burian and Ogle 1945.)

and vertical meridians. The use of featureless lines removes any contaminating effects due to the induced effect, described in Section 7.6.5 (Remole et al. 1993). The space eikonometer measures aniseikonia with a precision of about ± 0.2 per cent, although the precision achieved depends on the patient (Gillott 1956).

The Keystone View Company developed a set of stereograms (stereo-eikonograms) for use in an amblyoscope. The stereograms have varying degrees of disparity and replicate the targets seen in the eikonometer with varying degrees of depth. Instead of setting a meridional magnifying lens the subject selects the stereogram that appears frontal. See Ogle (1964), Berens and Bannon (1963), Halass (1966), and Rayner (1966) for reviews of aniseikonia and eikonometry.

2.8.3 Adaptation to aniseikonia

One can ask whether people adapt to prolonged exposure to meridional aniseikonia. Burian (1943) had three observers with normal vision wear a horizontal meridional lens in front of one eye for between 8 and 14 days. The lens magnified the image only in the horizontal direction. At first the subjects reported spatial distortions—table tops appeared inclined and walls appeared to slant at unusual angles. After 2 or 3 days these distortions were no longer noticed in normal visual surroundings but they reappeared in surroundings where monocular cues to depth were impoverished, such as a wide meadow. The space distortions were found to be undiminished when measured with a space eikonometer or horopter apparatus under conditions where monocular cues to depth were reduced to a minimum, even at the end of the exposure period. The results of this study suggest that the binocular stereoscopic system does not adapt to prolonged exposure to aniseikonia and that long-term adaptation to aniseikonia is due to an increased reliance on cues to distance other than binocular disparity. Similar results were reported by Miles (1948) in five subjects exposed to long-term adaptation to the induced effect produced by vertical magnification of the image in one eye. Morrison (1972) also produced similar results in eight subjects exposed for an average of 12 days to horizontal aniseikonia and in two subjects exposed to vertical aniseikonia. Remole (1991) also found adaptation of the perceptual effects of aniseikonia in a real-world setting but little reduction in eikonometer settings, even after 4 years.

Other evidence suggests that exposure to aniseikonia induces an adaptive recalibration of the disparity-detection system. Epstein and Morgan (1970) found that equidistance settings of two luminous vertical lines in dark surroundings changed after subjects walked about a building for one hour wearing a meridional lens that magnified the image in one eye horizontally by 5 per cent. The aftereffect represented about 37 per cent of full adaptation to the meridional lens. In a later study, Epstein and Morgan-Paap (1974) obtained a similar change in frontal-plane settings after inspection of a simple stimulus containing a conflict between disparity and perspective information. Lee and Ciuffreda (1983) conducted a similar experiment in which subjects wore a lens that vertically magnified the image in one eye. Changes in the calibration of horizontal disparity were measured by a Howard-Dolman apparatus. The lens produced an induced effect, which took some minutes to reach its

maximum value. The induced effect then diminished over a period of about 20 minutes of exposure to the lens. With further exposure over a 2-hour period, the induced effect partially returned. Perhaps, with even longer exposure, the induced effect would have returned to its full value. In the experiments of Burian and others, in which adaptation of the disparity system was not found, the meridional lens was worn for several days. Thus, differences in the exposure period may account for the differences in the results of different investigators. It is not clear, why adaptation of the disparity system to aniseikonia should wear off over an extended period.

Thus one group of investigators concluded that adaptation to a mismatch between disparity and

other cues to distance does not affect depth perception in a task that depends only on disparity, while a second group of investigators concluded that the coding of binocular disparity is altered by exposure to discordant depth cues. All the investigators used the task of setting stimuli to equidistance as their test procedure. Gogel and Szoc (1974) measured the effects of exposure a conflict between disparity and perspective by both a test involving equidistance settings and one involving the alignment of nonius lines. Only the former test was affected by the adaptation procedure. Since the nonius test is a more reliable indicator of binocular correspondence, these results suggest that the basic pattern of binocular correspondence is not affected by exposure to discordant visual cues.

Sensory Coding

3.1 Structure of sense organs	69
3.2 Types of sensory coding	70
3.2.1 Impulse codes	70
3.2.2 Monopolar and bipolar detectors	71
3.2.3 Primary coding	72
3.2.4 Secondary coding	74
3.2.5 Feature detectors	75
3.2.6 Metamerism	78
3.2.7 Sensory opponency	79
3.3 Temporal coding	80
3.3.1 Temporal coding in the single neurone	80
3.3.2 Temporal synchrony and sensory coding	81
3.4 Transfer functions	84
3.4.1 Linear systems	84
3.4.2 Coding spatial frequency and position	87
3.4.3 Nonlinear systems	91
3.5 Psychophysical procedures	92
3.5.1 Basic methods	92
3.5.2 Sensory detection and resolution	96
3.5.3 Sensory discrimination	98
3.5.4 Temporal thresholds	99
3.6 Psychoanatomical techniques	100
3.6.1 Threshold summation and masking	100
3.6.2 Adaptation and contrast effects	101
3.6.3 Interocular transfer	102
3.6.4 Tests of monocular independence	102
3.6.5 Dichoptic composite stimuli	103
3.6.6 Cyclopean stimuli	103
3.6.7 Trading functions	103
3.6.8 Effects of attention and stimulus familiarity	104

3.1. STRUCTURE OF SENSE ORGANS

Most human sense organs consist of receptors arranged on a sensory epithelium supported by a mechanical structure. The mechanical structure of the receptors, the sensory epithelium, and associated parts is intricately designed to serve the following three purposes.

- Filtering appropriate stimuli.* The receptors of a given sensory system are designed to respond preferentially to one type of stimulus energy, called the **adequate stimulus**. This does not mean that they are insensitive to other forms of stimulation. For instance, retinal receptors are sensitive to pressure applied to the side of the eyeball, changes in temperature, and electric currents. The eyeball and

surrounding tissues normally shield the eye from these forms of energy. Similarly, the receptors on the basilar membrane of the ear are protected from forms of energy other than sound by the mechanical properties of the skull and the fluid-filled cavity in which the membrane is suspended. To take another example, the semicircular canals respond preferentially to head rotation because their sensory hair cells project into a fluid-filled annulus, and the utricles respond preferentially to head tilt because their sensory hair cells have heavy crystals attached to them.

- Efficient collection of stimulus energy.* Mechanical structures within a receptor ensure that stimulus energy is efficiently collected. For example, the molecules of photopigment are arranged on a folded membrane within the retinal receptors and the whole structure forms a tube that acts as a wave

guide (see Section 4.1). The packing of receptors on the sensory membrane is also designed for efficient energy collection. For instance, the cones form a dense hexagonal mosaic in the central retina. Structures associated with sense organs are also designed for efficient transmission of energy to the sensory epithelium. For example, the three ossicles in the middle ear act as a lever that matches the mechanical impedance of air to that of the fluid in the inner ear. In vision, the cones are aligned with the centre of the pupil to ensure that the maximum amount of light enters the receptors.

3. *Ensuring the proper spatial distribution of stimuli.* The simplest sensory systems consist of a single detector that increases its rate of response monotonically as the strength of stimulation increases. The simple eye spots of some invertebrates are essentially of this type. More complex sensory systems, such as the skin, the eye, and the ear, have receptors distributed over a sensory membrane. In the skin, stimuli are applied directly to different locations so no special devices are required to ensure that the spatial distribution of receptors corresponds to the spatial distribution of stimuli. The ear has a frequency analyzer, in the form the response of the basilar membrane to travelling waves, which creates an ordered distribution of frequencies over the hair cells. The semicircular canals of the vestibular system are arranged in orthogonal planes so that different directions of head rotation are distinctly coded. The eye requires a lens to ensure a faithful distribution of light to an image. The fact that we have two eyes separated laterally enables us to form images which contain binocular disparities for the coding of depth. The vergence system allows the images of inspected objects to be brought into spatial correspondence.

3.2 Types of sensory coding

3.2.1 Impulse codes

The action potential, or nerve impulse, is the basic unit for long-range transmission of information in the nervous system. An action potential is a transitory change in the standing potential across the cell membrane of a neurone, which travels at a velocity of up to 15 metres per second along the axon. All action potentials in any neurone have the same amplitude and are said to obey the **all-or-none law**. All-or-none action potentials in the visual system are first formed at the level of ganglion cells. Receptors and bipolar cells respond in a graded or analogue fashion (see Section 4.1.1). Thus a receptor responds to stimulus energy by a graded change in membrane

potential, known as a **generator potential**. Because it has a fixed amplitude, an action potential is a **quantized signal**. A system that transmits signals as a temporal string of quantized impulses is as an **impulse-code system**. An impulse-code is used for long-range transmission in the nervous system, just as it is in the digital computer. An efficient impulse-code system has the following requirements:

1. It must use quantized signals of fixed amplitude. The reason is that such signals are relatively immune to the effects of noise within the system because they are stronger than all but the most severe noise.
2. Quantized signals must get neither weaker nor stronger during transmission. An axon with a diameter of 1 mm has a resistance of about 10^{10} ohm/cm, which is about 10^7 higher than metal. If any form of signal in an axon relied on passive electrical conduction, it would fade within a few millimetres. Nerve impulses are boosted to a fixed amplitude at the nodes of Ranvier, which occur about every millimetre along an axon.
3. Signals in an impulse code must not coalesce during transmission and they must arrive in the same temporal order in which they were sent. Two properties of nerve conduction ensure that these two requirements are met. First, although large-diameter axons conduct more rapidly than small-diameter axons, the velocity of conduction of impulses along a given axon is constant. Second, after an impulse has been transmitted, the cell is unresponsive, or refractory, for a few milliseconds. As a consequence, nerve impulses are discrete and cannot get out of order. A further consequence of the refractory period is that a nerve cell can transmit only up to a limiting frequency, which is about 500 impulses per second, allowing for a maximum rate of transmission of information of 500 bits per second.

Since signal amplitude is fixed, an impulse-code system cannot use amplitude modulation for transmitting information along a single axon. In the single axon, information can be transmitted only in terms of time of occurrence, temporal frequency, or as a modulation of temporal frequency.

An impulse code system can be used to construct a digital (number) code, as in computers. In a defined interval of time an impulse signifies the binary number 1 and the absence of an impulse signifies the binary number 0. In each case one bit of information is coded. A given message is conveyed as a string of binary numbers, each of defined length (a word). In a transmitted message a master clock defines the temporal position of each binary number in a word.

Hence time is quantized as well as signal strength in a digital code. In a stored message each number in a word is placed in a defined location.

Neural impulses generated by particular stimuli in a given neurone do not occur in discrete time intervals within well-defined "words", so there is no digital coding in the nervous system. Thus, a sensory nerve does not transmit information about whether an impulse occurred or did not occur in a predefined time interval. However, synchrony between signals in different neurones is an important attribute of neural signalling, as we will see in Section 3.3.2. A sensory neurone attached to a single receptor transmits information about the state of depolarization of the receptor, which is a function of stimulus magnitude. The efficient encoding of this information is ensured because a generator potential is lawfully related to the logarithm of stimulus intensity and the frequency of nerve impulses in a sensory neurone is a linear function of the generator potential.

The preceding statements refer to steady-state conditions within the normal operational range of a sensory system. The firing rate of most sensory neurones declines when a constant stimulus is applied. Thus, most sensory systems (including vision) are a-c coupled and transmit information about changes in stimulation rather than about the absolute level of stimulation. In vision, the matter is further complicated because a given ganglion cell axon receives inputs from several receptors through a complex cellular network—its receptive field. This implies that the frequency of firing of a ganglion cell is related to the spatial distribution or motion of stimuli within its receptive field and not merely to the total energy falling on the receptors. Another possibility, which we discuss later, is that the temporal pattern of firing of a ganglion cell, not merely its frequency, is related to the stimulus distribution.

The preceding discussion refers to long-range transmission of information in the nervous system. But the most important coding processes in the nervous system do not occur in axons but at synapses, where signal transmission obeys very different rules and information from many sources can be combined using operations such as addition, subtraction, multiplication, and mutual inhibition. These operations are typically local, nonlinear, and analogue. Synaptic transmission is graded rather than quantal and short interneurones transmit in an analogue fashion rather than by neural impulses. Glial cells, which outnumber neurones, may also take part in the transmission process (Nedergaard 1994). Local analogue processes occurring in parallel within a network can be performed much more rapidly than equivalent in-series digital processes executed in

computers (Koch et al. 1986). Analogue processes are dedicated to a particular task whereas digitally programmed processes in computers may be modified. Lack of flexibility is not a disadvantage in a system in which all inputs are subjected to the same limited range of transformations and in which speed of processing is important. However, we will see in the next chapter that parallel processes within neural networks possess some of flexibility, even in the primary visual cortex. Flexibility can also be achieved in slower serial processing at a later stage. Efficient artificial visual systems will almost certainly come to embody the same principles.

Stimulus-contingent changes at synapses allow for some short-term flexibility in processing and for long-term learning. Short feedforward and feedback interneurones that occur in clusters of synapses transmit information in an analogue fashion rather than by neural impulses. Thus, the real work of the nervous system is achieved by analogue processes within clusters of synapses. The basic computational unit of the nervous system is the individual synapse rather than the neurone as a whole. The axonal impulse-code system is simply a way to get information from one synaptic cluster to the next. Computers are digital throughout, both for transmission of signals and for signal processing.

3.2.2 Monopolar and bipolar detectors

Some stimulus dimensions have direction as well as magnitude and may be said to be **bipolar stimulus dimensions**. For example, visual motion along a given axis is a bipolar stimulus feature, since the motion can be in either of two directions. Some receptors are **bipolar detectors** because they have a monotonic bipolar response to bipolar stimuli. They are thus able to code both the magnitude and direction of bipolar stimuli. For instance, a hair cell in a semicircular canal of the vestibular system hyperpolarizes monotonically when the head rotates one way and depolarizes monotonically when it rotates the other way. At the level of nerve impulses, neurones cannot produce a bipolar response with respect to a zero-response resting state, since there are no negative nerve impulses. However, they can produce bipolar responses relative to a resting state of maintained discharge. For example, the afferent fibres from the semicircular canals maintain a steady discharge that declines when the head turns one way and increases when it turns the other way.

There seem to be no truly bipolar detectors at any stage of the visual system. Retinal receptors do not generate bipolar receptor potentials—they all hyperpolarize when stimulated. Consider for

example the simple bipolar stimulus feature of light-on as opposed to light-off. Light-on and light-off responses are achieved in distinct bipolar cells (called bipolar because of their structure, not because of their function). Each bipolar cell is a **monopolar detector**. A monopolar detector acts as a half-wave rectifier, since it responds to alternate half cycles of a bipolar stimulus as it oscillates through its full set of values. A cell that gave distinct signals for both light increase and light decrease would need to maintain a discharge when there was no change in illumination.

There are several reasons why it is more efficient to have two sets of oppositely tuned monopolar detectors than a single bipolar detector: (1) Monopolar detectors do not need a maintained discharge. (2) Any disturbance of the maintained discharge upsets the calibration of a bipolar system. For instance, alcohol upsets the maintained discharge of vestibular receptors, with well-known consequences. (3) Two monopolar detectors have double the dynamic range of a bipolar detector. (4) The outputs of monopolar detectors can be combined to produce a difference signal or ratio signal that is independent of changes in a stimulus feature to which both detectors are equally sensitive. For instance, if the output of a detector tuned to one orientation is subtracted from that of a detector tuned to another orientation, the resulting signal is independent of the overall luminance of the stimulus, since this affects both detectors in the same way. There is a price to pay for monopolar detectors; there must be twice as many monopolar detectors as bipolar detectors and there must be an additional opponency mechanism that combines the two rectified signals into a unitary signal (see Section 3.2.7). The detectors in the semi-circular canals of the vestibular system do not rectify the head-acceleration signal. Presumably, for them, the need to economize on the number of detectors and subsequent analysis outweighs the disadvantage of maintaining a discharge when the head is not moving. Also, these detectors respond to only one stimulus feature and have no need for a mechanism to discount the effect of stimulus intensity. Simplicity and the consequent speed of processing is important for vestibular detectors because they control eye-stabilizing reflexes and postural responses, which must be executed rapidly.

3.2.3 Primary coding

We refer to a coding process evident at the level of the individual receptor as a **primary coding process** and to a stimulus feature coded by a primary sensory process as a **primary feature**. A primary coding

process can involve changes in the frequency of firing in individual receptors or a specialization of different detectors for different stimulus values. Thus, in the eye, stimulus intensity is a primary feature because it involves frequency coding, and position and colour are primary features because they involve sets of differentially tuned receptors. Beyond the basic coding process, primary features become elaborated by interneuronal processing. The basic types of primary coding process are as follows:

Frequency coding

The physical intensity of a stimulus is the energy falling on unit area of a sensory surface in unit time. When an adequate stimulus varies in intensity but not in any other respect, the response of a receptor is some monotonic, saturating function of physical intensity, modified by effects of adaptation. The response of a receptor or of a detector at a higher level to a stimulus of a given area and duration depends on the total physical energy falling within the receptive field of the detector and within the time interval for which the energy is integrated over time. At the psychophysical level, the area relationship in vision manifests itself as **Ricco's law**, which states that for a stimulus of fixed short duration and below a certain area, the visual threshold is inversely proportional to the product of the area and intensity of the stimulus. The time relationship manifests itself as **Bloch's law**, which states that for a stimulus of a fixed area and below a certain duration, the threshold is inversely proportional to the product of time and intensity. It is a general feature of sensory receptors that their firing rate increases monotonically with increasing stimulus intensity, with a saturation of response at high intensity levels. For a given class of receptors, the steepness of the tuning function and the position of the tuning function along the stimulus-intensity axis may vary from receptor to receptor.

The effectiveness of a stimulus of a given intensity varies as a function of other attributes of the stimulus. For example, for a given physical intensity of light, the frequency of response of a retinal cone is a bell-shaped function of the frequency (wavelength) of the light, and the frequency of response of an auditory receptor is a bell-shaped function of the frequency of a sound of a given intensity. Finally, the effectiveness of a stimulus also varies as a function of its position with respect to the receptor or to the receptive field of a detector at a higher level. The variation in the response of a sensory detector as a function of changes in the position of a small stimulus within its receptive field is known as the **point-spread function**. The direction from which a

stimulus impinges on a receptor may also affect its power to evoke a response. For instance, a retinal cone is more sensitive to light that has passed through the centre of the pupil than to light arriving from other directions; a phenomenon known as the **Stiles-Crawford effect**.

The temporal features of the response of a single detector can code stimulus onset and offset, stimulus duration, and changes in stimulus intensity over time. It has been suggested that temporal modulation of the response train of a single receptor also plays a part in pattern recognition (see Section 3.3.1).

Labelled-line codes

A labelled-line code depends on the type of sensory cell stimulated. For instance, three types of cone preferentially code long, medium, and short wavelengths, and different types of receptors in the skin code pain, pressure, and temperature. In a general sense, the different sensory modalities such as vision and audition are labelled lines, in that each evokes distinct sensations. The detectors with similar stimulus selectivity in a labelled-line system are usually referred to as **sensory channels**. The concept of labelled line neurones is related to the concept of **specific nerve energies** associated with Johannes Müller (1843) although the idea originated before Müller (see Boring 1950, p. 80). It is a general rule that all labelled-line detectors have a bandpass tuning function in which the firing rate at first increases and then decreases as the stimulus is varied over the sensitivity range of the detector. This introduces an essential ambiguity into the response of any single labelled-line detector, in contrast to the unambiguous monotonic tuning functions of responses to stimulus intensity. The response of a detector in a labelled line system is also ambiguous because a change in response could be due to either a change in stimulus intensity or a change in the stimulus dimension to which the detector is tuned. There are two types of labelled-line coding.

Topographic coding.

In each sensory modality there is one topographic labelled-line system in which each detector is distinctly tuned to a particular position of the stimulus on the sensory epithelium, by virtue of its position. In vision, this is known as the **local-sign system**. A sensory system can devote its topographic system to only one sensory feature, which is the local sign, or topographic, feature for that sensory system. We refer to this as the **local-sign exclusion rule**. For both vision and touch, position is the local-sign, or topographic, feature, for audition it is frequency, and for the utricle it is direction of head acceleration.

The retinal image has a precise geometry which can be encoded only if the receptors maintain a fixed spatial order. Once the spatial attributes of an image have been coded into a set of nerve impulses in the optic nerve, a fixed spatial ordering of those nerves is no longer required, as long as the specific connections that each neurone makes are preserved as far as the stage where spatial information is encoded into some other form or evokes a response. The fact that the visual hemifields are represented in different hemispheres or that the mapping of the retina onto the cortex can be described as a conformal logarithmic function (see Section 4.2.1) has no significance for spatial coding. Within the nervous system it is only the connections that cells make with other cells that count; the geometry of the disposition of cells on the cortical surface is irrelevant for coding of spatial information, although it is important for economizing on the lengths of interconnections.

Nontopographic coding.

All labelled-line systems, other than the local-sign system, in a given sensory modality are nontopographic. In a nontopographic system the detectors differ in terms of their tuning to a stimulus attribute arising from their filter characteristics, rather than in terms of their position on the sensory epithelium. For instance, the three-cone colour system is a nontopographic labelled-line system in which the receptors act as differential filters for wavelength, which is not a position-dependent stimulus feature.

A complete set of colour channels must be present at each location of the local-sign system, which itself has only one complete set of channels. This puts a severe constraint on the number of colour channels. If a feature other than local sign were to be coded by many channels, only a subset of these channels would be activated at a given time. This degrades the spatial resolution of the local-sign system. Also, the sensory epithelium would have to be very large. For instance, if there were many colour channels the retina would become impossibly large. It was this logic that led Thomas Young (1802) to propose that there are only three types of receptor for coding colour and that they have widely overlapping tuning functions. The only way to escape this constraint is to have an eye with one part devoted to colour coding and a distinct part devoted to spatial resolution. One animal, the mantis shrimp, has this type of eye. One set of low-density ommatidia contains at least ten types of colour pigment which filter the incoming light, and which are thus capable of resolving the chromatic spectrum. Two sets of high-density achromatic ommatidia resolve the image spatially. The three sets of ommatidia

converge on the same location in space. See Section 16.3 for more details of these remarkable eyes.

All primary sensory features must be coded in terms of either temporal frequency, local sign, or receptors with distinct tuning functions for a nontopographic feature. In the visual system, this means that individual receptors can signal only intensity, temporal changes in intensity, oculocentric direction (local sign), and wavelength. Coding for other features must be deferred to a stage beyond the receptors. We now discuss deferred, or secondary coding.

3.2.4 Secondary coding

Coding processes that require the cooperative activity of several receptors or of neurones at a later stage of processing are **secondary coding processes**. Visual features such as motion, orientation, and disparity are **secondary features** because they are spatial, or spatiotemporal derivatives of the sensory input and are not represented in the activity of single receptors. Wavelength cannot be derived from the spatial or temporal properties of the local-sign system and therefore requires its own set of dedicated receptors. Colour has its own secondary features such as colour opponency and constancy. Neither motion nor disparity could be coded by a single receptor. Orientation could be coded by oriented receptors but this does not happen in practice, since all visual receptors have a circular cross section.

We are able to see the motion, orientation, and depth of stimuli at each location in the visual field. There must therefore be a complete set of detectors for each of these features represented at each location of the visual field. However, secondary features do not require dedicated receptors because the outputs from a given set of receptors can be configured in different ways to code different secondary features. The formation of distinct channels for secondary features can occur in the retina or can be deferred until inputs reach the visual cortex. In a complex visual system it helps to defer coding of secondary features because there is more room in the brain than in the eye for the neural processes required for channelling these features. All detectors for secondary features are labelled-line, multichannel systems.

Multiple-channel systems

Consider first the possibility that all the detectors sensitive to a given feature have the same broadband tuning function that spans the range of detectable stimuli. If the detectors are to distinguish between all values of the feature, their frequency of firing must change monotonically as the stimulus moves through its possible values. We have already seen

that only the response of detectors to changes in stimulus intensity is monotonic. The tuning functions of all primary or secondary labelled-line detectors to features of the stimulus other than intensity show a nonmonotonic, bandpass characteristic. For instance, a retinal cone shows a bandpass response when the wavelength of a light of fixed intensity is varied or when the position of the stimulus is varied, and a hair cell in the auditory cochlea shows a bandpass response as the frequency of a tone of fixed intensity varies. But for a bandpass tuning function, different values of the stimulus generate the same response, so the response is ambiguous.

The universal solution to this problem is to have different receptor tuned to a particular bandwidth of the feature continuum and with the different tuning functions overlapping. Receptors with the same bandwidth are often referred to as channels. Each single value of the stimulus evokes a unique combination of responses in the set of channels. However, different mixtures of stimulus values can evoke the same responses—the system is metameristic. The response of a detector in a multichannel system is also ambiguous because changes in stimulus intensity are confounded with changes in the stimulus feature to which the detector is tuned. A change in stimulus intensity can be distinguished from a change in the stimulus feature by using the difference in response of two neighbouring detectors.

For fine discrimination over a wide stimulus range it is better to have several sets of detectors, with those in each set tuned to a particular restricted range of the stimulus continuum. This is because the design characteristics of an efficient detector for one end of the continuum differ from those of a detector at the other end. For example, the design of a visual detector for high spatial frequency (fine patterns) is fundamentally different from that of a detector for low spatial frequency (coarse patterns). To take another example, a detector sensitive to vertical lines has a vertically oriented receptive field which renders it insensitive to horizontal lines.

For detectors of stimulus intensity, the stimulus range is typically partitioned out among several monotonically tuned detectors, with the tuning functions of the different detectors at different positions along the intensity continuum. Thus the intensity tuning functions of rods are shifted toward the low-intensity end of the intensity axis relative to those of cones. For labelled-line detectors with bandpass tuning functions, each type of detector devotes its bandwidth to only part of the stimulus continuum. In both cases, the response range of the system as a whole is increased. In the following discussion we are concerned with only multichannel

Table 3.1 Types of Sensory Code

Primary coding (evident in the single receptor)
Frequency code (monotonic tuning functions)
Examples Stimulus intensity Stimulus intermittency
Labelled-line code
<i>Topographic</i> Example: Local sign/ visual direction
<i>Nontopographic</i> Example: Colour
Secondary coding (distributed at receptor level but later channelled in labelled-lines)
Examples: Spatial scale Orientation Movement Disparity
Higher-order coding (mixed primary or secondary features in one modality)
Examples: Motion-in-depth Patterns of optic flow Size constancy
Intersensory coding (mixed features from different modalities)
Examples: Perception of the vertical, Headcentric visual direction

labelled-line systems in which each channel has a bandpass tuning function.

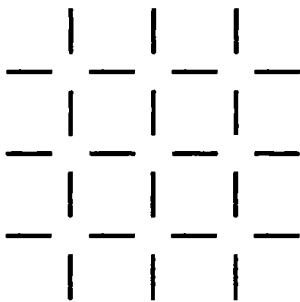
A single channel of a multichannel labelled-line system can determine the value of a stimulus with a precision no finer than the width of its tuning function. This presents no problem if there are many channels, as in the million-channel local-sign system of the eye. However, according to the local-sign exclusion rule, there can be no more than one multi-channel local-sign system in a given sense organ. Having many channels is not the only way to achieve good discrimination. The other way is to have few channels, with overlapping tuning functions. There is no theoretical limit to the precision with which the value of a stimulus can be detected by a two-channel system if the outputs of the two channels to the same stimulus are compared. The Germans made use of this fact during the Second World War. Their bombers navigated down the locus of intersection of two overlapping radio beams. Any departure from this locus was immediately detected by a change in the strength of the signal from one beam relative to that from the other. For this system to work, the tuning functions of the channels must overlap but the output of each channel must retain its identity. If the tuning

functions did not overlap there would be no continuity of fine discrimination across the sensory dimension. Any detector system with only a few overlapping tuning functions retains the power to detect a change in the value of a single stimulus but loses the capacity to resolve two or more stimuli presented at the same time to the same set of detectors. We refer to such systems as **metameric sensory systems**. Most sensory systems are metameric, including the system that codes binocular disparity. The properties of metameric systems are discussed in more detail in the following sections. Types of sensory coding are listed in Figure 2.1.

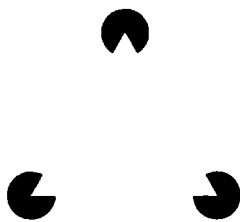
3.2.5 Feature detectors

A feature detector is a neurone whose firing rate varies as a function of a change in a well-defined stimulus feature. A stimulus feature is **channelled** at a specific level in the nervous system when detectors for that feature exist at that level. In other words, the feature is represented explicitly at that level (Marr 1982). Light intensity is channelled in the retina, since a change in light intensity changes the firing rate of ganglion cells. Other stimulus features channelled at the retina are contrast, position, flicker, stimulus duration, and wavelength. Motion is channelled in the retina of the frog and rabbit but in primates it is not channelled until the visual cortex. Orientation and disparity are also first channelled in the visual cortex—in the retina they are **unchannelled, or distributed**. It would be inefficient to have more than the minimum number of features channelled in the retina because, if many specific features were encoded there, most receptors would be inactive most of the time and this would degrade acuity and require a larger eye. It is better to have a set of receptors with more or less the same broad response characteristics in the retina so that light may be detected at all locations. Once the visual information is neurally coded there is no need for a densely packed array of similarly tuned detectors. Thus, in the central nervous system different types of cells can be specialized for detection of specific information concerning secondary or higher-order stimulus features.

The tuning function of a cell in the visual cortex to a particular stimulus feature is determined by recording the firing rate of the cell as that feature is varied for a stimulus presented in the cell's receptive field. The results of this type of investigation can give rise to the mistaken idea that cortical cells code a particular simple feature and that the outputs of such cells provide stable signals in response to particular stimuli. There are several problems with this view. Cortical cells, at least those in the striate



(a) Ehrenstein's figure. The gaps between the lines appear as white discs. This is modal contour completion. The lines seem to extend behind the discs. This is amodal contour completion.



(b) Kanizsa triangle. The figure is interpreted as a white triangle in front of three black discs. The sides of the triangle are seen even though there is no luminance contrast. This is modal contour completion. The edge of the missing part of each disc is not seen as a contour but the disc appears complete. This is amodal contour completion. (Adapted from Kanizsa 1979.)

Figure 3.1. Modal and amodal completion of contours.

and peristriate areas, are modulated by changes in more than one stimulus feature, and their responses vary as a function of the responses of other cells and as a function of attention and learning. For instance, a cell in the primary visual cortex may show selective tuning to changes in the contrast, length, colour, motion, and orientation of a stimulus. The cell cannot be said to code any one of these features unambiguously, since variations in firing rate may be due to a change in any one or any combination of them. It is believed that particular stimulus features are distinguished by the cooperative activity of populations of cells tuned to that particular feature. For example, the orientation of a line may be uniquely coded by the output of the set of orientation-sensitive cells that the given stimulus excites. The motion of the same line could be coded by the output of the set of motion-sensitive cells that it excites. Since the two sets of cells are at least partly different, each stimulus feature is coded distinctly, although not necessarily in the activity of individual cells.

Linkages between similar feature detectors

Evidence reviewed in Sections 4.2.2 and 15.1.5 shows that orientation detectors in the visual cortex that are

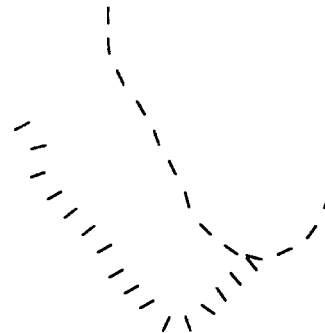
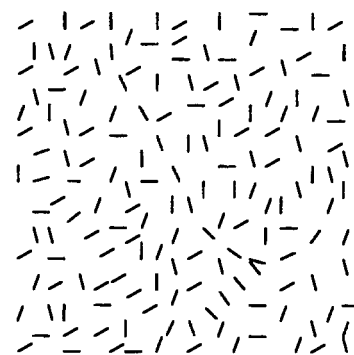


Figure 3.2. Detection of aligned sets of lines.

In the upper figure a set of elements aligned with the line through the set can be detected among a background of randomly oriented elements more easily than a set of elements orthogonal to the line through the set. The two sets of elements are shown in the bottom figure. (Adapted from Field et al. 1993.)

tuned to lines with the same orientation are linked by excitatory lateral connections. There is evidence from the cat that these linkages are particularly strong for orientation detectors that not only have the same orientation tuning but which have their preferred orientations aligned (Nelson and Frost 1985). Polat and Sagi (1994) have produced psycho-physical evidence that collinear stimuli show mutual facilitation to a greater degree than stimuli with the same orientation but which are not collinear. Morgan and Hotopf (1989) referred to these sets of connected orientation detectors as **collector units**, and Field et al. (1993) referred to them as **association fields**. Although this concept was developed in relation to orientation, one could generalize it to cover associations between other feature-detectors. For instance, an association field of motion detectors with similar direction sensitivities could underlie the perception of shape defined by motion (the gestalt phenomenon of common fate). A set of detectors of this type could be called a **motion coherence detector**. An association field of disparity detectors sensitive to the same binocular disparity could serve to unite points lying in a given depth plane and could be called a **surface-in-depth detector**.

A more specific name for an association field concerned with orientation is **alignment detector**. Alignment detectors could form the physiological basis for the following perceptual phenomena.

Basic to all perception is the ability to perceive a coherent object even when parts of it are occluded by other objects. The Gestalt psychologists proposed several principles of figural organization—namely, contiguity, continuity, similarity, good figure, and common motion—to explain how a set of isolated stimuli is perceived as a coherent pattern (see Koffka 1935). We experience an object as complete when part of it is hidden, an effect known as **amodal completion**. For instance, the cut-out corner pieces in Figure 3.1b appear as full discs partially occluded by the corners of a triangle. Sometimes we see an object as complete when parts of its boundary cannot be seen because they have the same luminance and texture as the background, in other words, when the boundaries are camouflaged. This phenomenon was first described by Schumann (1904). An example devised by Ehrenstein (1941) is shown in Figure 3.1a. Figure 3.1b shows one of the figures devised by Kanizsa (1979). We are conscious of the camouflaged edges of the triangle even though there is no physical contrast in those regions. This is known as **modal completion**. These types of display are known as **cognitive contours** or as subjective or illusory contours. The general rule is that modal completion occurs when the object to which the edge belongs is perceived in the foreground, and amodal completion occurs when the object is perceived in the background and occluded by a shape in the foreground. In both cases the activation of alignment detectors could be responsible for the strong tendency to see disconnected but aligned edges as belonging to the same object. We will see in Chapter 12 that cognitive contours have been useful in investigating the properties of stereoscopic vision. See Kanizsa (1979) and Parks (1984) for reviews of this general topic.

Psychophysical evidence supports the idea that we are particularly sensitive to collinear sets of points. For instance, patterns of collinear dots, known as Glass patterns stand out within an irregular array of dots, as can be seen in Figure 14.7. The stereoscopic implications of Glass patterns are discussed in Section 14.4. Morgan and Hotopf (1989) explained the diagonal lines seen running between the intersections of regular grid patterns as due to the activation of alignment detectors. Aligned line elements are easy to detect among randomly oriented elements, as can be seen in Figure 3.2 (Field et al. 1993). The line elements do not have to fall on a straight line but can form tangents to a curved line. Furthermore, the line elements may be a few degrees

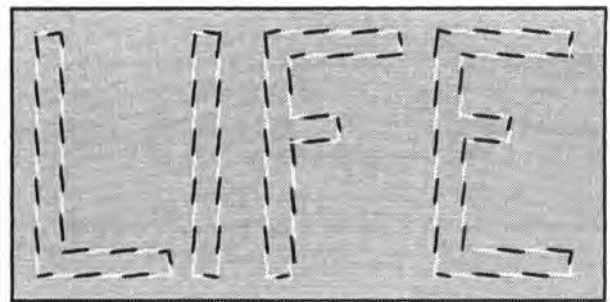


Figure 3.3. Conflict between local and global orientation.
The overall lines forming the letters are parallel to the edges of the page but the line elements are not aligned. The apparent orientation of the letters is biased in the direction of the line elements. (Adapted from Fraser 1908.)

out of alignment with the line joining them and still be interpreted as belonging to the same line. But in this case the perceived orientation of the line may be distorted in the direction of the line elements, as can be seen in the well-known “crazy letters” illusion shown in Figure 3.3 (Fraser 1908). We obviously perceive coherent three-dimensional objects but there have been very few studies of figural continuity in the third dimension (see Section 12.3).

It is believed that inhibitory linkages between similar feature detectors serve to enhance contrast. Mach bands are one manifestation of this type of process (Ratcliff 1965; Sagi and Hochstein 1985). These inhibitory linkages seem to operate over shorter distances than the excitatory linkages mentioned earlier. Matsubara et al. (1985) found lateral interconnections in area 18 of the cat, between cortical cells with orthogonal orientation preferences. These connections spanned only 2 mm and were inhibitory (see Section 4.2.2).

Higher-order features

In many cases it is an advantage to have cells that respond to a combination of features. For instance, cells in several visual areas are jointly tuned to disparity and direction of motion. These cells are selectively responsive to motion in different depth planes (see Sections 4.8 and 12.5.4) or to an approaching object (see Section 13.2). Thus, for purposes such as comparing the distances of different objects, the visual system seeks to isolate specific features, but, for other purposes it seeks to detect the conjoint variation between two features, as when one registers both motion and disparity information in judging whether an approaching object is likely to hit the head. An attribute of the visual world that is coded in terms of the conjunction of two or more simple features is a **higher-order feature**. A higher-order

feature is **intramodal** when it is derived from features in the same sense organ, and **intermodal** when it involves the conjunction of information from more than one sense organ. For instance, a decision about whether retinal-image motion is produced by a motion of the seen object or of the observer's eyes or head requires coordination of information from the retina and from the senses that detect motion of the eyes and the head.

Certain higher-order features, such as the direction of approach of an object, are coded by dedicated neural units with selective tuning functions for this composite feature. A system of dedicated hardware of this type is the most efficient and rapid way of coding vital types of information that recur frequently. The extension of this idea to ever more complex features has given rise to the concept of the **pontifical cell**, or grandmother cell—a cell specifically dedicated to the recognition of features as complex as one's grandmother. The notion of dedicated hardware at this level of complexity has severe limitations since it would require an explosively large number of dedicated cells, each of which would be dormant most of the time. A much more efficient procedure at the level of complex features is one analogous to programming in a computer in which complex forms are stored as descriptions using general components and rules of composition (algorithms). Language works this way, and the higher recognition processes of perception have language-like properties. For instance, when we recognize a face we may construct a type of description by combining features from different parts of the face, an ability reflected in the way a portrait is built up by police sketch artists (see Rolls 1994).

The processing of higher-level features is dominated by selective attention. Attention is the process of concentrating limited resources on the task of immediate importance. Eye movements that centre the fixation point on the object of interest constitute an attentive mechanism, as do vergence movements that bring the plane of zero binocular disparity into the plane containing objects of interest. There are also processes of selective attention within the central nervous system, because we can attend to objects not imaged on the fovea. Stereoscopic depth as an attention-getting stimulus is discussed in Section 6.1.6. Further discussion of attention is beyond the scope of this book (see Koch and Ullman 1985).

Recurrent feedback in the tuning of feature detectors

Inhibitory connections between cells seem to play as important a role as excitatory connections at all levels of the nervous system. These take two forms: inhibitory loops, which feed back to an earlier stage of

processing, and inhibitory loops which feed forward. A procedure called temporal slice analysis has been used to investigate this issue. The response of a feature detector unit is recorded electrophysiologically in 10-ms time intervals after the onset of a relevant stimulus and the temporal build-up of the cell's response is determined. Recurrent inhibitory loops reveal themselves as a delay in the achievement of the cell's steady-state response, whereas feedforward loops incur no such delay. Use of this procedure has shown that basic feature detectors in the visual system, such as those for orientation and binocular disparity, involve feedforward rather than feedback loops (see Sections 4.2.3 and 4.6.1). This has the advantage that feature detectors reach their steady-state response very soon after stimulus onset, allowing the animal to recognize briefly exposed or moving stimuli. It has also been argued that neural units responsive to complex features, such as cells in the inferotemporal cortex that respond selectively to faces, involve only feedforward loops (Oram and Perrett 1992). However, higher-order feedback systems must be involved when the response of cortical cells coding particular features is modified by attention or by the behavioural significance of the stimulus (see Section 4.2.7).

3.2.6 Metamerism

In abstract terms, a metameric sensory system produces an identical output for certain physically distinct mixtures of stimuli, but distinct outputs to the components of one of the mixtures compared with the components of the other mixture, when they are presented one at a time. For instance, the colour system cannot distinguish between mixtures of wavelengths that stimulate the three colour channels in the same proportions, but can discriminate between the same wavelength components when they are presented one at a time. In physiological terms, a metameric system is a set of detectors with mutually overlapping tuning functions along a particular stimulus continuum. All visual features, other than luminance, contrast, and perhaps flicker, are processed by sets of detectors that are, at least to some extent, metameric. The visual local-sign system contains one million channels in the form of one million ganglion cells. Thus the stimulus continuum of retinal position is covered by one million tuned receptors (receptive fields). This system is metameric only locally within each small region of the retina where a group of receptive fields forms a mutually overlapping set. Similarly, the frequency coding system in audition is metameric only locally within each critical band (a region along the basilar

membrane over which hair-cell tuning functions mutually overlap). By contrast, the receptor stage of the colour system is wholly metameristic, since it has only three overlapping channels over the whole stimulus continuum. Detectors for motion, orientation, and binocular disparity are also metameristic, although the number of channels and their degree of overlap in each case is not known with certainty.

The study of metamerically matched stimuli provides a powerful psychoanatomical technique. A metameristic stimulus is a combination of physical stimuli within a stimulus continuum that produces a sensation of a single value within that continuum, even though the stimuli produce distinct sensations when presented separately. For instance, a mixture of wavelengths produces a sensation of a single colour but the components of the mixture produce distinct colour sensations when displayed separately in space or in time. Two stimuli are said to be metamers when they consist of different combinations of physical stimuli from the same sensory continuum but create identical sensations. A set of metamers forms an equivalence class under the operation of resolution but not under the operation of discrimination.

Inferences from the use of metameristic stimuli are based on two assumptions. First, once stimuli have been combined metamerically, information about the component stimuli is lost. Second, two stimuli that produce identical sensations generate identical physiological activity at some location in the nervous system. It follows from these assumptions that the perceptual identity of two metamerically matched stimuli cannot be disturbed by any change applied equally to the neural signals from the two stimuli after each has been metamerically combined. If two metamerically matched stimuli remain matched for all possible changes of the stimuli applied equally to both, then the metameristic process must be at the initial site of processing of that sensory system. Conversely, if some change applied equally to two stimuli disturbs a metameristic match, the metameristic process must be preceded by a process that detects the applied sensory change, or there is a nonlinear feedback between later and earlier stages of processing. Thus, we infer that trichromacy is achieved at the front end of the visual system from the fact that metameristic colour matches continue to match for all states of adaptation of the eye (Grassmann's third law). For a more complete analysis of this logic, see Brindley (1957). Furthermore, the shape of the metameristic matching function for colour (the CIE colour chart) provides a basis for powerful inferences about the nature of the cone mechanisms responsible for trichromacy.

We show in Section 6.3 that similar binocular disparities within a local spatial region can average to produce an impression of one depth plane. This means that two different mixtures of disparities could average to give the same depth impression. These would be metameristic matches within the disparity system. Nobody has investigated the stability of such matches over different states of visual adaptation. However, they should change with adaptive changes occurring in the retina but not with changes occurring beyond the primary visual cortex.

Metameristic systems exhibit several related properties, which are discussed in subsequent sections of this chapter.

3.2.7 Sensory opponency

Strictly speaking an opponent system extracts the difference between inputs from two oppositely tuned detectors for a given bipolar sensory continuum. In the colour system inputs from red and green detectors are combined in an antagonistic or seesaw fashion as are those from blue and yellow (red plus green) detectors. Since a change in luminance affects members of each opponent pair equally, colour opponency produces signals that vary with hue, independently of changes in luminance. The luminance signal is derived by adding the inputs from the red and green cone types. Inputs from matching pairs of semicircular canals on opposite sides of the head are combined in a similar push-pull fashion to signal the direction of head rotation (see Howard 1982). The term "opponency" is often used to denote any sensory mechanism in which a difference signal is generated, even if the stimuli do not form a bipolar sensory continuum. For instance, opponency in this sense within the orientation domain makes orientation discrimination independent of contrast over a wide range of contrasts (Regan and Beverley 1985). Independence of contrast has been also been reported for spatial frequency discrimination (Regan 1982), speed discrimination (McKee et al. 1986) and temporal-frequency discrimination (Bowne 1990).

We will see in Section 5.6.1 that detection of binocular disparity is largely independent of luminance and contrast, suggesting that opponency also operates within the disparity-detection system, in the form of a signal representing the difference in local sign of the inputs from the two eyes. In Chapter 7 we will see that the extraction of other types of difference signals within the disparity system renders stereoscopic vision immune to the effects of misalignment, image misalignment, and unequal magnification of the images in the two eyes.

Binocular rivalry is a type of sensory opponency operating between the two eyes when they are presented with distinct stimuli. This topic is discussed in Chapter 8.

3.3 TEMPORAL CODING

3.3.1 Temporal coding in the single neurone

A radical idea of temporal sensory coding has been proposed in a series of publications by a group at the National Institute of Health in Bethesda (Richmond and Optican 1987, 1990; Richmond et al. 1990; Gawne et al. 1991). They recorded from complex cells in the visual cortex of an alert monkey as it fixated each of a set of small patterns of black and white squares and rectangles (Walsh patterns). The spike train of a cell's response to each stimulus was smoothed to produce a spike-density profile over the first 260 ms. Principal components, that accounted for successively smaller amounts of variance, were extracted from these profiles over the set of stimuli. The response of a cell to a particular stimulus could then be described as a weighted sum of these components. The first component was correlated with mean firing rate. Higher order components of the spike train presumably arose because of differential latencies of subregions of the receptive field or differential delays in recurrent inhibitory influences arising from different regions of the receptive field. The effect of varying one stimulus feature depended on the value of the other features so that the stimulus features interacted non-additively. The response was the same for many combinations of the three stimulus features used in the experiment, namely, pattern, duration, and contrast. However, theoretical analysis based on the principal components of the spike train allowed the investigators to extract some information about each stimulus feature as well as about combinations of features. In practice, this process requires additional neural machinery and, since there is no indication of what this would be, the approach leaves the problem of stimulus analysis in the nervous system unsolved. Furthermore, the analysis was based on only three stimulus features. A typical complex cell in the visual cortex is also influenced by stimulus motion, colour, flicker, disparity, and size. Thus, in practice, the job of disentangling the contribution of each feature to the principal components of the spike train of a single neurone becomes more difficult to perform.

The novel claims of the approach are (1) that temporal modulation of responses in single

neurones is a function of the spatial configuration of the stimulus and (2) that the central nervous system is capable of decoding this temporal information. The traditional view is that transmission of sensory information in the single axon is in terms of response frequency, with temporal modulation serving to indicate only temporal modulations of stimulus strength.

Tovée et al. (1993) applied a similar analysis of principal components to the responses of cells in the primate temporal cortex to faces. They also found that the first principal component of the spike train reflects the mean firing rate of the cell and accounts for about 70 per cent of the variance. Furthermore, they found that about 85 per cent of the information about firing rate available during a 400-ms period could be extracted during the first 50 ms of the cell's response and almost half of it was available in the first 20 ms. Signals passing from the visual cortex to the inferior temporal cortex pass through four stages, each of which adds about 20 ms to the total latency of response in the temporal cortex (Rolls 1992). This suggests that effective information about firing frequency is extracted in about 20 ms at each stage of processing. If we assume a firing rate of 100 Hz, this means that firing frequency estimates in a single neurone are based on up to five spikes. Tovée et al. found that only about 19 and 8.5 per cent of the information in a spike train was contained in the second and third principal components, respectively. Furthermore, a good part of this information was found to reflect the latency of the cell's response. They concluded that features of the response train other than the mean firing rate are probably not significant for cortical processing. Other aspects of temporal coding have been reviewed by Dinse et al. (1990a).

Higher-order components in the temporal wave form do not necessarily have to be analyzed to be useful. Unanalyzed temporal waveforms could serve the following two purposes.

1. Temporal waveforms could be used to identify surface discontinuities. An evenly textured surface has a consistent texture, colour, contrast, and motion, so that the set of detectors in that region respond with similar and synchronous response trains. The responses of the cells onto which the detectors converge would be enhanced by this stimulus synchrony because synchronous inputs summate at synapses. Hence, the postsynaptic cells would resonate to inputs from an evenly textured region. At the boundary of two textured regions would be a discontinuity in the pattern of resonance which could allow the visual system to identify and

locate the boundary even before any analysis of particular stimulus features had taken place. There is evidence from recordings of responses of single cells in the visual cortex that cells with similar responses to stimulus orientation fire in synchrony (see Section 4.2.2). Evidence of neuronal mass activity related to texture segregation has been revealed in the visual evoked potentials from the human scalp (Lamme et al. 1993). Fahle (1993) found that a temporal phase difference of only 5 ms between the temporal modulation of groups of spatially homogeneous points was sufficient to segregate perceptually one group of points from the background.

2 Temporal waveforms could serve to match binocular images. The tuning characteristics of the component monocular receptive fields of a binocular cell in the visual cortex tend to be similar. When the same image falls on corresponding points in the two retinas, the two temporal response trains arriving at a binocular cell are the same and in phase. They could serve to generate a cross-correlation function even though what is correlated is not analyzed. Thus, the similarity of temporally modulated signals arriving at a binocular cell could serve to indicate whether the eyes were properly converged on a given stimulus.

When a person looks at a textured surface, the mutual entrainment of the responses of a set of binocular cells provides an enhanced signal when the eyes are properly converged. Perhaps temporal waveforms also play a role in the detection of differential disparities and in binocular rivalry. A model of this type of process has been provided by Murata and Shimizu (1993). Tootell et al. (1988c) reported enhanced neural activity (as reflected in the uptake of deoxyglucose) along cortical loci corresponding to borders between differently textured regions of a stimulus display. This enhanced activity was evident only when the display was viewed binocularly.

Whether or not stimulus-evoked temporal features of the spike train carry information, cortical neurones show stereotyped differences in the waveforms and repetitive firing properties of their action potentials. Thus, there are "regular spiking", "fast spiking", and "bursting" cortical neurones (Connors and Gutnick 1990). These differences depend on the intrinsic properties of ion channels on the cell's soma and dendrites (Solomon et al. 1993). Similar differences exist in the response properties of motor neurones, such as those controlling movements of the eyes (see Section 10.7). Bursting neurones probably play a role in generating synchronized activity in populations of cortical cells, which we will now discuss.

3.3.2 Temporal synchrony and sensory coding

Improved stimulus tuning

Neighbouring cells in the visual cortex with similar tuning to stimulus orientation, often show correlated activity to the same single stimulus (Braitenberg 1985; Krüger and Aiple 1989). This correlated activity is believed to be mediated by lateral connections in the visual cortex (see Sections 4.2.2 and 15.1.5). Ghose et al. (1994) measured the strength of correlated discharge of nearby pairs of cells in the cat visual cortex and found that it was stimulus dependent and not a simple consequence of the unicellular responses. Although the optimal tuning of cell pairs to spatial and temporal frequency and velocity was similar to that of the component cells, the receptive fields of cell pairs were narrower and their responses were briefer. This suggests that correlated discharges of neighbouring cells achieve a higher degree of spatial and temporal resolution than is achieved by single cells. Correlated activity between cells with different tuning characteristics could help to resolve the ambiguity in the response of single cells. For example, cells which respond both to dark and light bars may fire in synchrony only in the presence of a dark bar (Ghose et al. 1994).

Hebbian synapses

Hebb (1949) speculated that learning depends on competitive reinforcement of synaptic contacts. He proposed that when activity in a presynaptic cell is temporally correlated with activity in a postsynaptic cell, the synaptic contacts between the cells are strengthened. When activity in the two cells is not correlated, the synaptic contacts are weakened. Synapses behaving in this way are known as **Hebbian synapses**. When two presynaptic cells converge on a postsynaptic membrane, the activity in either presynaptic cell is more highly correlated with that in the postsynaptic cell when the converging inputs are synchronous rather than asynchronous. This is because the postsynaptic membrane summates potentials from converging synchronous signals more effectively than those from asynchronous signals. The outcome is that correlated activity in two or more afferent pathways gains preferential access to the nervous system and, over time, leads to more efficient transmission along that neural pathway. When converging inputs are persistently uncorrelated the synaptic strength of the one most highly correlated with the postsynaptic potential increases at the expense of the synaptic strength of the other input. Computer simulations of cortical pyramidal cells have revealed that cortical cells could, in theory, detect coincidence between single

spikes in the submillisecond range (Softky 1994). We will see in Chapter 15 that Hebbian synapses are important in the development of the visual system, particularly in the development of binocular vision. For recent discussions of Hebbian synapses, see Clothiaux et al. (1991), Dan and Poo (1992), and Ahissar et al. (1992).

A Hebbian synapse strengthens synaptic connections when converging inputs covary, and can therefore be thought of as a covariance detector that responds to what is common between two inputs. Synaptic connections can be reversibly strengthened or weakened in brain slices of the cat visual cortex by correlating postsynaptic responses generated by stimulation of white matter with those generated by depolarization or hyperpolarization of the postsynaptic membrane by injection of current through the recording electrode (Frégnac et al. 1994).

Some sensory systems act as difference detectors since they respond to what is different between two inputs—they decorrelate the input. For instance, a ganglion cell does not fire when its receptive field is evenly illuminated but does fire when there is a change of luminance gradient across the receptive field. Ganglion cells work this way because of mutual inhibitory connections within the inner plexiform layer of the retina (see Section 4.1.1). The advantage of this system is that messages are transmitted to the brain only about spatial or temporal changes in the proximal stimulus—the regions that are most informative. Mutual inhibitory mechanisms are responsible for contrast processes at various levels in a variety of sensory systems. Contrast mechanisms reduce the response to regions of constant stimulation relative to regions of changing stimulation. Mutual inhibitory mechanisms are also responsible for opponent processes that occur at many levels in sensory systems. Opponent mechanisms detect one stimulus change in the presence of other changes, as we saw in Section 3.2.7. In Section 13.2 we discuss examples of opponent mechanisms in stereopsis. Barlow (1991) referred to mutual inhibitory mechanisms as anti-Hebbian interactions, because they detect differences rather than coincidence. He suggested that Hebbian and anti-Hebbian mechanisms work together at successive levels within the processing hierarchy of the visual system—the Hebbian mechanisms detect coincidences between inputs, the anti-Hebbian mechanisms sharpen the distinctions between sets of detected coincidences.

Stimulus binding

The presence of many visual areas, each devoted to coding specific features of a visual stimulus, raises the problem of how this distributed activity is

synthesized into a single percept. This has been dubbed the “binding problem” (Hinton et al. 1986). Different visual objects are juxtaposed and may overlap and move. Thus, a given pattern of neural activity is only fleetingly related to a given stimulus object—the same cells may code several complex objects in rapid succession. The problem has two aspects. In the first place, a similar visual feature occurring over many receptive fields must be recognized as belonging to a single object. This could be called **spatial binding for a given feature**. For instance, the boundary of a large object stimulates many orientation detectors and their outputs must be related to form a coherent percept of the object’s shape. In the second place, objects possess particular concatenations of distinct visual features which must be recognized as belonging to the same object. This could be called **feature binding for a given object**.

One solution to the binding problem is to suppose that the diverse activities evoked by a given object ultimately converge on a single cell devoted to recognition of that particular object. Such a mapping process requires an impossibly large number of dedicated cells and connections.

The other general solution to the binding problem is to suppose that objects are coded by the response of feature-extracting systems in different processing streams and at several levels of processing, and that these responses become bound into a particular spatiotemporal pattern of activity (Zeki and Shipp 1988). Each neurone participates in many different patterns, and only the spatiotemporal response of a particular cell assembly is unique to a particular object. Temporal synchrony of the pattern of neural activity evoked by a given stimulus, coupled with desynchronization between one pattern of activity and others, could allow the same network to code distinct stimuli in rapid succession and distinguish between several temporally or spatially overlapping stimuli (Milner 1974; Malsburg and Schneider 1986). Also, temporal synchrony between responses evoked by similar but spatially separated stimuli could serve to bind the responses into an integral whole, or Gestalt.

Visual stimulation causes groups of adjacent cells in the visual cortex of both the anaesthetized and alert cat to discharge in synchrony at frequencies of between 30 and 80 Hz, which is outside the range of spontaneous background activity responsible for the alpha rhythm or the 4 to 7 Hz theta waves that occur during sleep (Gray and Singer 1989). Cells in the lateral geniculate nucleus show no evidence of synchronous firing in this frequency range. Cortical cells were found to fire in high-frequency bursts of two to four spikes at intervals of 15 to 30 ms. A given visual

stimulus has been found to evoke synchronous and highly correlated responses in different parts of the primary visual cortex separated by up to 7 mm, between cells with non-overlapping receptive fields but similar tuning to orientation. Furthermore, two parallel bars falling on distinct receptive fields evoked widespread synchronous activity when they moved in a common direction (see Gray et al. 1991). Two differently oriented bars falling on overlapping receptive fields produced synchronous activity in two assemblies of cells, which could be distinguished according to their orientation tuning (Engel et al. 1991).

Such activity could serve to bind responses to a continuous edge spanning many receptive fields. It could thus be part of a mechanism for the representation of common figural properties of coherent objects. It has also been claimed that cells in different cortical areas and in different hemispheres respond in synchrony at between 35 and 85 Hz to a stimulus to which the cells are similarly tuned (Eckhorn et al. 1988; Jagadeesh et al. 1992). This type of synchronous activity was most pronounced in response to stimuli with continuous contours and common motion (Gray et al. 1991), as one would expect of a system that helps bind distinct features of a given object. The oscillations need not themselves code stimulus-specific information. They could serve to co-energize sets of feature detectors for the formation and consolidation of cell assemblies in the process of learning. Once a cell assembly has been consolidated, synchronous activity could activate it for the purpose of object recognition. Synchronous activity in a distributed set of cells can be evoked quickly enough to allow a familiar object to be recognized in a fraction of a second (Gray et al. 1991).

Sillito et al. (1994) have produced evidence that synchronized activity in the visual cortex induces synchronized activity in relay cells of the LGN and they suggest that this feedback mechanism concentrates neural circuitry onto the stimulus. We are still left with the problem of how the activity of cell assemblies is accessed by other neural processes (Engel et al. 1992).

Attentional processes are probably very important in organizing neural activity into unitary patterns. Crick and Koch (1990) proposed that visual attention based on stimulus position serves to bind neural activity arising from diverse features of a single object in a given location to form a unitary percept. They proposed that this process is facilitated by temporal synchronization of the responses of neural centres activated by the various features of the object. Niebur et al. (1993) have developed a neural model of this type of process which involves 40 Hz synchronized neural activity. This mechanism

serves to bind associated features in a given location. We will see in Section 4.2.7 that visual attention can be based on stimulus features rather than position alone. This calls for a process serving spatial binding for a given feature distributed over several locations.

One source of the synchronous activity in the visual cortex could be the inherent oscillation of the membrane potentials of cortical pyramidal cells in layer 5 of the visual cortex. In the absence of stimulation, these oscillations are in the 5- to 12-Hz range, but computer modelling indicates that during stimulation, and with appropriate synaptic coupling, much higher frequencies could be generated (Silva et al. 1991). A second source of synchronous activity could be oscillations generated by time delays in recurrent inhibitory loops in the cortical network (Freeman 1975), and a third could be neural oscillations arising in the lateral geniculate nucleus, or retina (Ariel et al. 1983; Ghose and Freeman 1992). Several investigators have developed neural networks which model synchronized activity in the visual cortex (Eckhorn et al. 1990; Schuster and Wagner 1990; Grossberg and Somers 1991; Sporns et al. 1991; Wilson and Bower 1991). Chawanya et al. (1993) developed a neural network model that simulates synchronized oscillations within and between orientation columns of the visual cortex and in which the strength of the phase correlations between different columns reflects the length and continuity of bar-shaped stimuli (see also König and Schillen 1991). Schillen and König (1994) described a neural network model which developed synchronized firing after temporal correlation between the activation of distributed assemblies responding to different features of an object. Christakos (1994) has provided a mathematical basis for analysis of synchrony in neural nets using the coherence function, which expresses the extent to which two processes covary as a function of frequency. It is the frequency-domain analogue of the squared cross-correlation coefficient.

Tempting as these speculations are, they must be treated with caution. Young et al. (1992) could find no evidence of stimulus-evoked synchronous activity in the 30- to 60-Hz range in the primary visual cortex or in the middle-temporal area (MT) of either the anaesthetized or alert monkey. Some signs of oscillation were found in the inferotemporal cortex, but only in the alert monkey. Ghose and Freeman (1992) could find no consistent relationship between oscillatory discharges in cortical cells and specific features of the stimulus, other than stimulus strength as reflected in the mean firing rate of cells. Engel et al. (1992) suggested that oscillatory responses may have been missed in these studies because the responses are not strictly periodic and

contain a broad band of frequencies. In spite of this doubt about whether widespread synchrony of neural activity is an important coding mechanism, there can be little doubt that the synchronous convergence of similar inputs at particular synapses plays a role in tuning the responses of cortical cells during development and in perceptual learning, as we see at various points in this chapter and Chapter 15 (see Trotter et al. 1992).

3.4 TRANSFER FUNCTIONS

3.4.1 Linear systems

A system is any device that transforms inputs into outputs in a lawful way to achieve some specified function. The aim of systems analysis is to determine experimentally and mathematically the function that transforms well-defined inputs into specified outputs. This function is known as a **transfer function**. One must first specify a set of inputs. In the visual system this could be a set of stationary black-white gratings, a set of coloured patches, a set of objects at different distances, or any other stimuli that can evoke responses. One must then specify the outputs. In the visual system these could be rates of detection, discriminations, recognitions, eye movements, or neural discharges at some specified site. For a given set of stimuli and well specified responses one may derive the transfer function of a system as a whole or of any of its components. A natural system, such as the eye, has an unspecifiably large number of components. Human-made systems usually have well-defined components, or modules, which function independently, and the transfer function of the whole system may be derived by linear combination of the transfer functions of the modules. The combined transfer function of in-series modules is derived by multiplication and that of parallel modules by addition. Modular systems are relatively easy to construct (or genetically programme) and errors in them are easy to trace and treat locally. Many physiological systems, such as the heart, kidney, and lungs can be considered as modular units that operate autonomously. However, no physiological system is strictly linear, and the performance of the whole system is not predictable from the responses of the components. The visual system has certain obvious structural-functional modules, such as the lens, the two eyes, and the extraocular muscles. Physiological and psychophysical investigations have revealed what look like modular structures in the neural processing of visual inputs, such as the various cell types in the retina, the LGN,

and the various in-series and parallel processing streams in the central nervous system.

One may say that the aim of visual science is to identify and characterize these functional modules and derive the rules governing their interactions. This is an ambitious enterprise. Just consider the bewildering array of potential modular components that one can choose to investigate. One can select a pigment molecule, any receptor cell, amacrine cell, bipolar cell, or ganglion cell, or any collection of these cells, or any synapse or collection of synapses, or the optic nerve or any of the large number of visual centres in the brain. For each component one must choose the stimuli used for testing and the responses deemed to be of interest. The visual system or any component of the system is sensitive to an unspecifiably large number of stimuli and responds in an unspecifiably large number of ways. For example, a retinal receptor is responsive to light, pressure, chemical changes, and electricity, and responds by changing its membrane potential, temperature, optical properties, oxygen consumption, and chemical composition. In addition, no two cells and no two eyes are exactly alike. The visual system changes over time, because of adaptation, learning, and aging. It is also an evolving system with a history and, we hope, a future. An investigator must decide which aspects of the system are to be studied and at what level of generality and abstraction; there is no such thing as a complete analysis of any natural system. The visual system is what it is. The descriptions and theories that we erect are human constructs based on an arbitrary selection of some aspect of the system derived for some specific purpose and based on certain assumptions. Even when a functional description has been found that successfully mimics some aspect of the visual system, it may not specify the physiological structures involved. The reason for this is that a given function can be instantiated in many different physical systems. A functional description is like defining the algorithm of a process that can be executed by distinct machines, or hardware. See Marr (1982) for a discussion of this issue.

Systems fall into two main classes, linear and nonlinear, each requiring very different experimental and mathematical procedures. In very general terms, a linear system is one in which the response to input *A* plus input *B* is equal to the sum of the responses to *A* and *B* separately. This is the **principle of superposition**. Also, in a linear system, the response to a given input is the same whenever it is applied. This is the **principle of time invariance**. In practice, any system is linear only over a certain range of stimulus values. A complex system such as the eye behaves as a linear system in some respects

and as a nonlinear system in other respects. Components of a system may be highly nonlinear and yet produce a linear response when working together. For example, an amplifier may be nonlinear and produce a distorted output but be linear when an error feedback signal is added. The following provides only a very general guide to systems analysis and indicates sources from which more detailed information can be obtained.

The spatial-frequency domain

The fundamental assumption underlying linear systems analysis is that the transfer function of a system is fully characterized when ones knows how the system responds to a set of sine-wave inputs. The reason sine waves are often used in systems analysis is explained in the next paragraph. In a linear system, a sine-wave input produces a sine-wave output with the same frequency. The signal can be shifted in phase and its amplitude either attenuated or amplified. Over the part of the frequency spectrum for which the change in amplitude is constant, the system is said to have a flat response. A low-pass system is one that attenuates responses above a specified frequency, and a high-pass system is one that attenuates responses below a specified frequency. A bandpass system is one that transmits inputs over only a limited band of frequencies. In practice, the response of any natural system begins to weaken and eventually stops as frequency is increased beyond a certain limit; thus, all natural systems are either low-pass or bandpass systems. Within the transmission range of a linear system, different frequencies may be attenuated by differing amounts.

In 1807 Fourier established a fundamental theorem which is used extensively in linear systems analysis (the paper he wrote at that time was rejected and not published until 165 years later). The core idea is that any waveform can be synthesized by combining a specified set of pure sine waves in appropriate phase relationships. Note that a pure sine wave in the temporal domain extends forever; it has no beginning or end. A pure sine wave in the spatial domain extends indefinitely in space. If the waveform is periodic and repeats at a frequency of F Hz, the component sine waves include one with a frequency of F Hz (the fundamental) plus sine waves with frequencies which are multiples of F . For example, a repetitive square wave is composed of a sine wave with a frequency, F , equal to that of the square wave, plus all odd harmonics ($3F, 5F, 7F, \dots$) with amplitudes decreasing in inverse proportion to frequency. Thus, the frequency components of a repetitive waveform are a series of discrete components described mathematically by a Fourier series.

If the waveform is aperiodic, the frequencies of the component sine waves vary continuously and are described mathematically by a Fourier integral. In either case the **Fourier transform** of a signal gives the amplitude and phase of each sine wave components of the original waveform. The amplitude of component sine waves as a function of their frequency is the **amplitude spectrum**, or modulation transfer function of the original waveform. The phase of component sine waves as a function of frequency is the **phase spectrum**, or phase transfer function. For example, the amplitude spectrum of a single impulse, such as a very brief burst of sound, consists of pure tones of all possible frequencies, all of equal amplitude. The set of pure tones coincide (are in phase) at only one moment in time; at all other moments they mutually cancel because they are out of phase. A transient signal is known as an **impulse**, or delta function. A narrow vertical line may be considered to be a spatial impulse composed of an infinite number of vertical spatial sine waves of equal amplitude which are in phase only at that particular location. At all other locations the sine waves cancel to a constant luminance level.

The modulation transfer function

The modulation amplitude of a grating is the difference in luminance between the peaks and troughs (see Figure 9.1). When a sinusoidal grating of a given spatial frequency is transmitted through an optical system, its amplitude is to some degree attenuated by the summed effects of light loss and dispersion. The attenuation of amplitude produced by an optical system is the reciprocal of the gain of the system, where gain is the ratio of the amplitude modulation of the image grating to that of the object grating. This definition can be generalized to cover both optical systems and image-processing systems.

In any practical system, the attenuation of modulation amplitude is complete for all spatial frequencies above a certain value. This simply means that the system cannot resolve gratings above a certain spatial frequency. The human visual system—the whole system, not only the optics—is also insensitive to gratings below a certain spatial frequency. The range of frequencies resolved by any system is its spatial bandwidth (or bandpass) at that contrast. Gratings with frequencies outside the spatial bandwidth appear as homogeneous patches of light.

The **modulation transfer function (MTF)** of a system is some measure of the transmission of signal amplitude (gain) plotted against the frequency of the input. In a system that transmits temporally modulated signals, such as the ear, the MTF is expressed in terms of temporal frequency. In a system that

transmits spatial information, such as the eye, the MTF is expressed in terms of spatial frequency. The spatial modulation transfer function of the eye is derived from responses to sinusoidal gratings, that is, black and white gratings in which luminance is modulated sinusoidally as a function of position. The spatial frequency of a sinusoidal grating is measured in cycles (black and white pairs of bars) per degree of visual angle. From Fourier's theorem it follows that a visual display, however complex, in which luminance is modulated in only one direction, can be synthesized by superimposing sets of aligned sinusoidal gratings, with suitable amplitudes, phases, and wavelengths. These sets of gratings constitute the spatial Fourier components of the display. In practice, luminance cannot be modulated about a value of zero since there is no negative light. All spatial patterns therefore contain a certain mean level of luminance which can be regarded as a d.c., or zero spatial-frequency component which must be added to the Fourier transform.

Any two-dimensional visual scene can be synthesized by superimposing sets of sine-wave gratings, with each set oriented at a different angle in the plane of the display. This fact makes spatial sine waves convenient components to work with. Another convenient property of spatial sine waves is that a sinewave grating is the only spatially extended pattern that is transmitted through a linear system unchanged in form. If a set of spatial sine waves is transmitted through an homogeneous linear system, the image consists of a set of sine waves with the same spatial frequencies. The modulation amplitudes of component spatial frequencies can change by different amounts in a linear system. A linear system may also displace, rotate, or invert the image, because such transformations do not affect spatial frequency. Strictly speaking, a linear system cannot magnify or minify the input with all frequencies scaled up or down proportionally. However, most optical systems either minify or magnify the image. This need not violate the assumption of linearity if the object and image are expressed in terms of the visual angles subtended at a common nodal point in the optical system. It is only the linear dimensions of the image that are minified or magnified, not the angles subtended at the nodal point.

By the superposition property of a linear system, the output produced by a set of superimposed pure sine waves can be predicted from the response to each sinewave taken singly. Thus, once the modulation transfer function of a linear system is known, one can calculate the amplitude of its response to any input by carrying out an inverse Fourier transform. One can combine two spatial dimensions and

time to produce a three-dimensional spatiotemporal Fourier transform which specifies the unique set of drifting sinewave gratings at each orientation that are required to synthesize a given moving display.

The spatial modulation transfer function of an optical system describes the gain of modulation amplitude as a function of the spatial frequency of a sinusoidal grating, for a constant mean luminance. In an optical system the transfer function is derived by using a photoelectric probe to measure the luminance modulation (contrast) of a sinusoidal grating and of the image of the grating at each spatial frequencies within the spatial bandwidth of the system. In the eye, one measures the variation in the contrast of the retinal image by an optical probe in association with an ophthalmoscope. The ratio of image contrast to stimulus contrast defines contrast transmission, or gain, which is plotted as a function of spatial frequency. This function indicates how efficiently the system transmits spatial sine waves. However, any visual display can be redescribed by Fourier analysis as a set of sine waves. If the spatial MTF of a linear system has been determined, one can predict the quality of the image of any pattern. A Fourier analysis of the pattern is first performed, then each sine-wave component is amplified or attenuated by an amount determined by the MTF. When the pattern is restored by Fourier synthesis, it defines the image produced by the system. The image can be regarded as the result of passing the visual display through a set of infinitely narrowly tuned sine-wave luminance filters. For a full specification of the image, one must also know how spatial phase is shifted as a function of spatial frequency. This is the phase transfer function. The optical transfer function is derived from the modulation transfer function and the phase transfer function and, when defined for all orientations of the image, it fully specifies the performance of an optical system for a given aperture and axis. Although a linear system as a whole can be formally described by this analysis, one need not assume that the system contains distinct components that actually carry out these operations.

Point-spread functions

The point-spread function provides an alternative measure of the optical quality of an image. Even if the image is perfectly focused, diffraction of light by the pupil, dispersion in the optical media of the eye, and scatter of light by the surface of the retina cause each point in the distal array to be represented by a blurred disc in the image. If the effects of dispersion and scatter are ignored, it is possible to calculate the diffraction-limited distribution of light in the image of a point of light. This turns out to be a central

bright disc, known as Airy's disc, surrounded by bright and dark rings arising from the way light waves alternately summate and cancel. This is the diffraction point-spread function. The diameter of the Airy's disc in radians of visual angle is given by $2.44l/a$, where l is the wavelength of the light and a is the diameter of the pupil, both expressed in the same units. For a 2.3 mm pupil and a wavelength of 550 nm, Airy's disc is 1 arcmin of visual angle in diameter. This corresponds to about three times the diameter of a foveal cone, so that the central disc produced by a bright point of light, however small, stimulates about seven cones.

A similar calculation can be done for a thin-line stimulus, in which case we have a line-spread function. A thin line in the spatial domain is analogous to a brief flash in the temporal domain. Both are impulses, or delta functions. Impulses are used widely in testing communication systems, both natural and man-made. The reason is that the Fourier transform of an impulse is a set of equal-amplitude sine waves extending evenly across the whole frequency spectrum. The crests of the waves coincide at a place which defines the position of the impulse, and at all other places, crests and troughs cancel. When the eye is exposed to a thin line, it is as if a complete set of spatial sine waves were simultaneously injected into the visual system. The modulation transfer function of the eye determines how each component is attenuated and the Fourier transform of the frequency response of a linear system measured with sine-wave gratings is its response to a spatial impulse (the line-spread function). This mathematical relationship forms the basis of many inferences about the performance of the eye, cortical cells, and the visual system as a whole. It has been assumed up to now that the spatial modulation transfer function is the same for all orientations of the test gratings. If this is so, the system is said to be isotropic; if not, it is anisotropic. Astigmatism is an example of anisotropy in the visual system. For an introduction to linear systems analysis, see Toates (1975). For more detailed treatments see Bracewell (1978), Cooper and McGillem (1967), and Brigham (1974).

The contrast-sensitivity function

When the concept of modulation transfer function is applied to an image-processing system, rather than an optical system, the method for determining the modulation amplitude of the output must be adapted to the type of output that the system produces. In a biological or manufactured optical system, the output is an image that can be measured with a physical instrument. A variety of responses is used to measure the transfer function of a visual

system beyond the optics of the eye. The modulation amplitude of the output can be derived from objective responses in the form of eye movements or the responses of a cell or of a set of cells in the visual system. On the other hand, it may be indicated by psychophysical judgments made by subjects under specified conditions. De Lange (1958) was the first to apply linear systems analysis to psychophysical data, in his investigations of visual flicker. Campbell and Robson (1968) first applied these methods to psychophysical data derived from the use of spatial patterns modulated in luminance. In this application the output of the visual system is defined as the luminance contrast required for detection of a sine-wave grating at some specified criterion for detection. The threshold contrast as a function of spatial frequency is known as the contrast sensitivity function, which may be regarded as the modulation transfer function of the contrast detection mechanism of the visual system as a whole at threshold. We will see in Chapter 5 that an analogous sensitivity function relates the threshold modulation of a corrugated surface in depth to the spatial frequency of the depth modulations of the surface. In general, we define the modulation transfer function of any system as a mapping of the output of the system onto sinusoidal inputs of varying frequency. At suprathreshold contrasts, the output of the visual system is assessed by asking observers to match the contrast of gratings at different spatial frequencies (Georges and Sullivan 1975).

3.4.2 Coding spatial frequency and position

For many purposes it is convenient to specify the spatial Fourier components of a visual display or of responses of the visual system. As we have seen, it is a particularly useful procedure when one is testing the linearity of some aspect of the visual system. Fourier analysis or any other type of mathematical analysis applied to input or output signals is known as signal analysis. In applying such methods one does not necessarily assume that the system is linear. The methods may be used simply as a convenient way to describe stimuli, summarize responses, or construct linear models of a system.

A linear system transmits signals of different frequencies without distortion or interactions. The lens of the eye is a reasonably linear transmission system. But a system that merely transmits different spatial frequencies does not detect the different frequency components in complex signals. For detection, the different frequencies must stimulate distinct detectors, so that the system carries out a Fourier analysis, or redescription, of the input to produce output signals that indicate the amplitude of each frequency

in the input. The human ear can be said to produce at least a crude Fourier analysis of sound patterns. This is because the ear has many distinct channels, each responding to a narrow range of sound frequencies. Campbell and Robson (1968) proposed that the human visual system has distinct channels, each tuned to a particular range of spatial frequencies and, as a consequence, achieves a spatial Fourier analysis of visual patterns.

Three psychophysical procedures have been used to determine the number and bandwidth of the spatial-frequency channels of the visual system. The first is the method of adaptation, in which the range of spatial frequencies over which an adapting grating elevates the threshold of a subsequently exposed test grating is determined (Blakemore and Campbell 1969). The second is the method of subthreshold summation, in which the range of spatial frequencies over which subthreshold gratings reduce the threshold of a superimposed test grating is determined (Graham and Nachmias 1971). The third is masking, in which one determines the range of frequencies over which suprathreshold masking gratings elevate the threshold of a superimposed test grating (Stromeyer and Julesz 1972). After allowing for differences in procedure, the results are reasonably consistent with the conclusion that there are at least six spatial-frequency channels with a half-amplitude bandwidth of about 2.2 octaves for the lowest spatial-frequency channel and about 1.3 octaves for the highest spatial-frequency channel (Wilson 1991).

The idea of spatial-frequency channels in the visual system can be misleading. In theory, any system capable of detecting the spatial Fourier components of complex patterns efficiently must fulfill three requirements; (1) it must possess a set of detectors each of infinite size and very narrow spatial-frequency bandwidth, (2) it must be spatially homogeneous, and (3) it must encode both amplitude and phase. In such a system, it is not just the detectors of low spatial frequency that must be large, but also those that detect high spatial frequency. This condition is not satisfied in the visual system, since receptive fields are comparatively small and not narrowly tuned to spatial frequency. The condition of spatial homogeneity is also not fulfilled, since receptive fields become larger and less dense in the peripheral retina. This issue is relevant to the question of whether spatial frequency and spatial position are coded by the same or by distinct mechanisms. At first glance this may appear to be an empirical issue, requiring an experimental approach. However, at least part of the answer can be arrived at by a theoretical analysis, once the general properties of a particular system are known. This analysis was initially

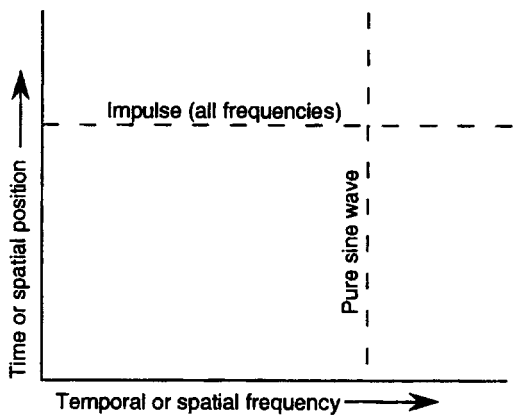


Figure 3.4. The impulse and pure sine wave.

A temporal impulse (delta function) occurs at a well-defined time, with its energy distributed evenly over the whole temporal-frequency spectrum. A pure tone contains only one frequency but extends over an infinite period of time. Similarly, a spatial impulse (fine line) occurs at a well-defined location, with its energy distributed over the spatial-frequency spectrum. A pure spatial sine wave has only one spatial frequency but extends over infinite space.

applied by Gabor (1946) to temporal signals in acoustic systems, rather than to spatial frequency and position. Nevertheless, the conclusions apply to both domains.

If the frequency dimension of a signal is represented on the X axis and the time dimension on the Y axis of Cartesian coordinates, we have what is known as a time-frequency diagram. Consider an impulse of sound (delta, or impulse function) occurring at a well-defined time but with energy distributed evenly over the whole frequency spectrum (an impulse contains all Fourier components, all with the same amplitude). The impulse is represented in the time-frequency diagram as a horizontal line (Figure 3.4). An impulse is a useful test stimulus to apply to linear systems because, if a linear system's response to a pulse is known, one can calculate the modulation transfer function of the system. This is because the response to the impulse of any linear system is the Fourier integral of its modulation transfer function. Consider, next, a pure tone of infinite duration which has a well-defined frequency but an undefined temporal epoch, and is therefore represented in the time-frequency diagram as a vertical line. Any finite signal may be regarded as intermediate between the pulse, which is determinate in time but not in frequency, and the infinite sine wave, which is determinate in frequency but indeterminate in time. A detector can be designed to extract information about the time of occurrence of events but disregard frequency, or to detect frequency and disregard time. For instance, an ideal oscillograph with uniform response over the whole

frequency range and a very short time constant (quick decay or response) is an instrument of the first type, and a bank of narrowly tuned oscillators, each with a long time constant, may be regarded as an example of the second type of instrument. One instrument cannot do both jobs with maximum efficiency because the design characteristics are incompatible.

The same argument applies if we substitute spatial frequency for temporal frequency and position for time. Note that the ideal spatial frequency detector is narrowly tuned to spatial frequency and has a long space constant (infinitely large receptive field), and the ideal position detector is broadly tuned to spatial frequency and has a small receptive field. Because of these opposed requirements, it is impossible to design an instrument that will extract both types of information with maximum efficiency. If both types of information are required from the same instrument, there must inevitably be a compromise, which is expressed by the fact that in any instrument

$$\text{Time constant} \times \text{bandwidth} > 1/2$$

A consequence of this relationship in the space domain is that, if we define the sensitivity of a detector to differences in position as D_s , and its sensitivity to spatial frequency as D_f , then the product of these uncertainties cannot be less than one-half, or

$$D_s \times D_f > 1/2$$

This reciprocity between two uncertainties is essentially the same as that expressed in Heisenberg's principle of uncertainty, which states that it is impossible to know both the position and frequency characteristics (mass) of a fundamental particle at the same time. The best compromise between the detection of position and that of spatial frequency is achieved when $D_s \times D_f$ is a minimum, which in the ideal case is 0.5. Gabor defined the characteristics of a detector for which this would be true. For a detector in the space domain, these requirements are that the sensitivity profile of each detector should be a Gaussian (normal) distribution and that at each location there should be pairs of detectors with sensitivity profiles in quadrature. A Gaussian distribution has the unique property that its Fourier transform is also a Gaussian function. Two sensitivity profiles are in quadrature when one is phase shifted 90° with respect to the other, like a sine wave and a cosine wave. A Gaussian profile multiplied by a cosine wave produces a symmetrical function and a Gaussian profile multiplied by a sine wave produces

an asymmetrical function. Cortical cells with symmetrical (cosine) and antisymmetrical (sine) sensitivity functions are in quadrature, with sensitivity profiles phase-shifted by 90°. There is evidence that these types of cells occur in pairs in the visual cortex, with different pairs tuned to different regions of the spatial-frequency spectrum (Pollen and Ronner 1981). These two requirements are summarized by the expression

$$S(x) = e^{\frac{-x^2}{2s^2}} \cos 2\pi Fx \text{ (or } \sin 2\pi Fx)$$

where $S(x)$ is the sensitivity profile across the X axis of a detector, s is the standard deviation of the sensitivity profile, F is the optimal spatial frequency to which the detector is tuned, and x is distance along the X axis (Kulikowski 1980).

Thus, it seems that the visual system is designed to achieve an optimal compromise between the detection of spatial frequency and the detection of position. This arrangement also seems to be ideally suited for optimally deblurring and reducing noise in the visual input.

The function formed by multiplying a sine or cosine function with a Gaussian function is known as a **Gabor function**. One can think of a Gabor function as the image produced by looking at a sine or cosine wave through a Gaussian window. The shape of the Gabor function varies according to the width of the Gaussian window, or envelope. With a very wide Gaussian envelope, the Gabor function is a sinewave (narrowband display) and with a very narrow envelope it becomes a delta function, (broadband display). An intermediate case is shown in Figure 3.5. There is thus a family of Gabor functions extending from a sinewave to a line (Graham 1989). At intermediate values, the Gabor function is a spatially localized patch of damped sine or cosine waves, known as a **Gabor patch**. For a given spatial frequency of the sine wave, the spatial-frequency bandwidth of the patch is inversely proportional to the size of the Gaussian window. Just as any visual scene can be decomposed into sinewaves it can also be decomposed into Gabor patches derived from a Gaussian function of specified width.

In physiological terms, the receptive field of a ganglion cell can be considered to be formed by the superimposition of an excitatory centre with a Gaussian sensitivity profile and an inhibitory surround with a somewhat wider Gaussian sensitivity profile. The composite sensitivity profile is known as a **difference of Gaussians (DOG)**. The DOG profile of a ganglion cell is circular symmetric. The receptive field of a cortical cell may be represented as an

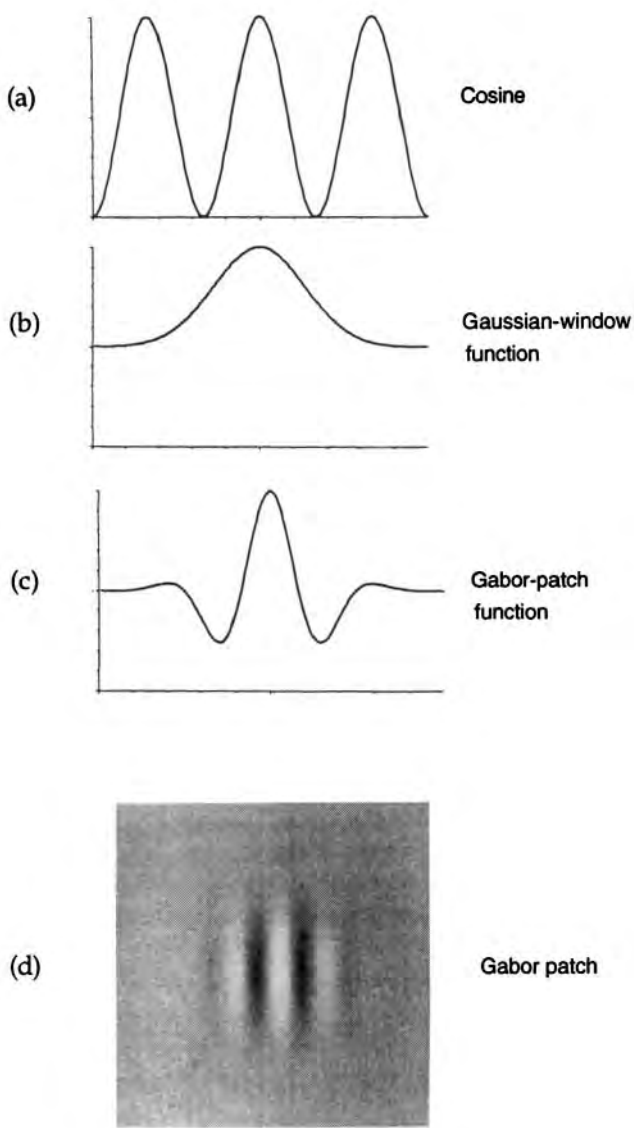


Figure 3.5. A Gabor patch.

A Gabor patch (c and d) results from viewing a patch with a sine or cosine luminance profile (a) through an aperture with a Gaussian (normal) luminance profile (b). (Adapted from Graham 1989.)

elongated DOG, which is either bilaterally symmetrical (cosine) when the excitatory and inhibitory components are in phase, or asymmetrical (sine), when they are 90° out of phase.

If, the receptive fields of the basic units of the visual system conform to these specifications, it would seem natural to use stimuli with these spatial characteristics since they are stimuli that should be most easily detected. Hugh Wilson and others have used DOGs extensively in the study of contrast sensitivity and stereoscopic vision, as we will see in later chapters. A DOG stimulus, unlike a sine-wave grating,

has a well-defined location. It also has a peak, or optimal spatial frequency, which can be varied by changing the width of the Gaussian distributions.

Since a Gaussian function is not a pure sine wave, it necessarily has a certain spatial bandwidth. By differentiating a Gaussian one obtains a Gaussian with a narrower spatial bandwidth. The sixth and tenth derivatives of a Gaussian function, known as D6 and D10, are often used in visual experiments, including those on stereopsis.

Alternatively, the sensitivity profiles of the receptive fields of the basic detector units of the visual system can be described as two-dimensional Gabor functions of different sizes, with symmetrical or asymmetrical profiles, and oriented at different angles. Each detector has an orientation bandwidth of about 15°, a half-amplitude spatial-frequency bandwidth of about 1.5 octaves, and a length-to-width ratio of about 2:1. Recently, a branch of mathematics known as **wavelet theory** developed for analyzing complex spatial patterns into wavelet functions has been applied in vision (see Daugman 1990, 1991). Wavelets, like receptive fields, are localized, self-similar, undulatory functions which differ with respect to size (dilation), position (translation), and phase. If the wavelets are anisotropic, like the elongated receptive fields of cortical cells, they also differ in orientation (rotation). Even with a sparse sampling of size and orientation one can construct any complex pattern from a defined set of wavelets, with a resolution limited by the smallest wavelets in the set.

Once the sensitivity profile of a linear detector is known its response to any stimulus can be derived by the process of **convolution**. The distribution of light intensity across the receptive field of the detector is plotted. At each spatial location the stimulus magnitude is multiplied (weighted) by the local value (height) of the sensitivity profile. This is repeated for each location across the receptive field of the detector and all the values are then added (integrated) to yield a single number, which represents the response of that detector to that stimulus.

Other types of mathematically defined filters have been borrowed from physics and used to characterize low-level visual processing. These include zero crossings (Marr 1982), Cauchy functions (Klein and Levi 1985), dipoles (Klein and Levi 1986; Klein et al. 1990), and cepstral filters (Yeshurun and Schwartz 1990 see Section 6.2.1). Although each formalism has advantages, it is unlikely that the visual system conforms exactly to any one of them.

Any set of coding primitives is complete when all stimuli that the system can discriminate can be represented by weighted sums of the primitives. For example, zero crossings (regions of maximum

change in luminance) do not form a complete set of primitives because there are textures that appear different but produce the same representations in terms of zero crossings (see Daugman 1990). In a complete coding system, the number of independent degrees of freedom in the code is at least as large as the dimensionality of the stimuli.

A second important attribute of coding primitives is their orthogonality, or linear independence. A coding process is optimally efficient when the primitives are independent, so that each captures a property of the input not captured by any other—there is no metamerism in the system. The components of biological sensory systems are nonorthogonal. For instance, the semicircular canals of the vestibular system are not at 90° to each other, and the tuning functions of motion detectors and orientation detectors in the visual system overlap. The advantages and disadvantages of overlapping tuning functions were described in Section 3.2.6.

3.4.3 Nonlinear systems

There are several types of nonlinearity in the visual system. For some types, the system is approximately linear over a limited range of amplitude modulation. An essential nonlinearity is one that does not approach linearity when input amplitude is reduced. Multiplication, division, and rectification are essential nonlinearities. Following is a list of common nonlinearities encountered in sensory systems.

1. *Thresholds.* In the region of the threshold output is not a linear function of input and the principle of superposition does not hold. One reason for this is that intrinsic noise in the system becomes larger in proportion to the signal as signal strength is reduced. Another reason is that sensory events become quantal near the threshold. For instance, whether or not light at threshold luminance is detected depends on the statistical probability of light quanta being absorbed by pigment molecules.

2. *Compressive nonlinearities.* In this type of nonlinearity the response fails to keep pace with the input as stimulus strength is increased. The logarithmic relationship between stimulus intensity and the generator potential of retinal receptors is a nonlinear property of this type. A ceiling effect is a saturation of response at high levels of stimulus intensity. The system may be linear over its operating range but as stimulus intensity is increased beyond a certain level the response levels off to an asymptotic value. In an accelerating nonlinearity the output increases more rapidly than the input. This typically occurs near the sensory threshold.

3. *Rectification.* Many cells act as half-wave rectifiers of the input; that is, they respond only to displacements of the stimulus in one direction along the stimulus continuum. For example, the retinal bipolar cells respond either only to stimulus onset or only to stimulus offset. Also, many motion detectors in the visual cortex respond only to motion in one direction. We will see that some detectors of binocular disparity are also half-wave rectifiers in that they respond only to crossed or only to uncrossed disparities (see Section 4.4). The combined output of two half-wave rectifiers, with signs ignored, constitutes a fully rectified signal. A fully rectified signal of binocular disparity would signal the amplitude of a disparity without indicating its sign. The combined output of two half-wave rectifiers, with signs intact, reconstitutes the original signal. The need for rectification arises because many natural stimuli, such as motion and binocular disparity, are bipolar; that is, they extend in both directions with respect to a norm. Thus, movement along a given axis can be in one direction or the other with respect to the norm of zero motion. Advantages of rectification in sensory processing were discussed in Section 3.2.2.

4. *Hysteresis.* This is a nonlinear property in which the response of a system to a particular stimulus value depends on the direction from which that stimulus value was approached. For instance, the binocular fusion mechanism shows hysteresis in that the disparity at which initially fused stimuli become diplopic is not the same as the disparity at which initially diplopic stimuli fuse to create the impression of one object (see Section 8.1.8).

5. *Nonlinear facilitation and inhibition.* These types of nonlinearity arise when the response of a cell to two inputs is higher or lower than the sum of the responses to each input acting alone. Ganglion cells, relay cells in the lateral geniculate nucleus, and simple cells in the visual cortex are reasonably linear in that their responses to complex stimuli can be predicted from the superimposition of their responses to simpler stimuli. Complex cells in the visual cortex and visually responsive cells in higher visual centres, such as the inferior temporal cortex and parietal cortex, respond in a highly nonlinear way to visual inputs. Detectors at all levels of the nervous system show inhibitory interactions which are believed to enhance the activity at boundaries between distinct regions relative to that within homogeneous regions. As we will see in Section 4.4, nonlinear facilitation occurs in the response of binocular cells in the visual cortex to inputs from the two eyes. This type of nonlinearity is extreme in so-called “and” cells which respond only when they receive inputs from the two eyes simultaneously.

6. *Responses to cross-modulation products.* The output of a linear system to two superimposed sine waves is two sine waves which have the same frequencies as the input. The output of a nonlinear system consists of the same two fundamentals plus harmonics of each input, plus sums and differences of these harmonics, such as $3F_1 + 2F_2$. These are known as cross-modulation products and are characteristic of nonlinear systems. Since each type of rectifying nonlinear system produces a characteristic pattern of cross-modulation products, it is possible to draw up a catalogue of these response patterns. One can then infer the type of rectifier in a given system by measuring its cross-modulation products and consulting the catalogue. Regan and Regan (1988) developed a more general mathematical treatment involving the zoom fast Fourier transform. This gives a very high resolution of the cross-modulation products produced by two sinewave inputs. When applied to the analysis of evoked potentials generated in the human visual cortex by two lights flashing at different frequencies, it produces a sharp separation between stimulus-related signals and signals arising from noise, as shown in Figure 4.20. Zhou and Baker (1993) recorded from cells in the visual cortical areas 17 and 18 of the cat, which responded to cross-modulation products (spatial beats) of three superimposed sinewave gratings, even though the spatial frequencies of the gratings were outside the tuning range of the cells. Cross-modulation products are not detected by a purely linear system, since they are not represented in the Fourier domain. Cells generating cross-modulation products must therefore operate through nonlinear processing.

7. *Adaptation and learning.* Sensory adaptation, or short-term modification of the response of a specific sensory system exposed to constant stimulation, is a nonlinearity because it violates the time-invariance assumption of linear systems; that is, the assumption that the response of the system to a given input remains constant. The long-term modification of a response to a given stimulus through learning is also a nonlinear property. Spontaneous changes in the interpretation of a visual stimulus, such as occur in reversible perspective and ambiguous figure-ground displays are also nonlinearities.

The analysis of nonlinearities

The response of a linear system to any input can be calculated when its frequency response (or equivalently, its response to an impulse) is known. Thus, the response of the system to a set of sine-wave inputs can be used to predict the response to any input. This follows from the principle of superposition and from the fact that any signal can be

represented in the frequency domain as a set of superimposed sine waves in appropriate phase. This is not true of a nonlinear system. There is no general method for characterizing nonlinear systems. The method of Wiener kernels can be used for systems that (1) do not change rapidly over time and (2) become linear as signal strength is reduced. One first measures the response of the system to Gaussian (white noise) stimuli and then calculates the Wiener kernels, which are essentially terms in a power series, with the zeroth-order term representing the response of the system to a static input, the first-order term the linear characteristics of the response, and higher terms representing nonlinearities. The details of this procedure are provided in Marmarelis and Marmarelis (1978).

Bennett (1933) introduced a variant of the Wiener kernel method, with improved signal-to-noise ratio, which involves testing a system with a small set of superimposed sinewave inputs rather than white noise. Victor (1979) used this procedure to analyze responses of single neurones in the visual pathway.

Nonlinear systems are studied by building an analogue computer from components with similar nonlinear features and allowing it to simply compute the output to defined inputs. Alternatively, a digital computer can be programmed to simulate a nonlinear system. Lehky et al. (1992) characterized the nonlinear receptive fields of complex cells of the monkey visual cortex by recording the responses of cells to a great variety of patterned stimuli. A neural network was then created for each neurone using an iterative optimization algorithm. The responses of the cell to some stimulus patterns defined the training set for the neural network. Lehky et al. predicted the cell's responses to patterns not used in the training set with a median correlation of 0.78. For discussions of neural-network methods, see Rumelhart et al. (1986), Hinton (1989), and Miller et al. (1991).

Neural network models of this type characterize the receptive field structure of a cell or set of cells but do not indicate the function of the cell or cells being modelled. For a discussion of nonlinear visual processes, see Pinter and Nabet (1992).

3.5 PSYCHOPHYSICAL PROCEDURES

3.5.1 Basic methods

This section briefly outlines psychophysical methods used to measure thresholds for the detection, resolution, and discrimination of stimuli.

The basic parameters of any human performance are accuracy and precision. Take the task of setting a

variable stimulus to appear equal to a standard stimulus, such as setting one object to appear at the same distance as another. The **point of objective equality** (POE) is the objective value of the standard, and the **point of subjective equality** (PSE) is the signed mean of a series of settings of the variable that appear equal to the standard. Accuracy is indicated by the difference between the POE and the PSE, that is, the mean of the signed deviation scores with respect to the POE. Where the POE is zero, accuracy is equal to the PSE. Accuracy is synonymous with **constant error** and bias. The **precision** of performance in a task is indicated by the mean of unsigned deviation scores with respect to the PSE. Related measures are the standard deviation, variance, and standard error of scores. Precision is synonymous with sensitivity, variability, and variable error. The term "accuracy" is often used where "precision" is meant. Accuracy is also often used inappropriately to signify the mean of unsigned deviation scores with respect to the POE. This measure confounds accuracy and precision, and should be avoided. Its use has generated a lot of confusion. Accuracy and precision, are independent, or orthogonal, measures.

In assessing human performance on detection or discrimination tasks, it is useful to have some idea of the theoretical limit that can be reached by any detector, living or manufactured. A detector that performs at this theoretical limit is known as an **ideal observer** for that task. For instance, it is possible to calculate the performance of an ideal observer for the detection of light, given the quantal nature of light and the "noise" within which the signal is presented. The ideal observer for a particular task provides a yardstick for assessing the performance of a human observer on that same task. An ideal observer for stereopsis is described in Section 5.3.3.

For an account of basic psychophysical methods readers are referred to Guilford (1954), Torgerson (1958), Swets (1964), Green and Swets (1966), and Gescheider (1976). All the standard psychophysical methods have been used in the study of binocular vision and stereopsis. In the **method of adjustment** the subject adjusts a variable stimulus until it matches a standard stimulus. In the **method of limits**; the experimenter increases or decreases the variable stimulus until the response of the subject changes. These methods are especially useful for measuring steady-state constant errors. For instance, to measure how a inclined surface affects the apparent inclination of a superimposed test line, subjects are asked to set the line to the apparent vertical, and the mean signed error indicates the extent of the induced inclination. Errors of anticipation and habituation are avoided by averaging settings from trials in

which the line starts at various angles on either side of the vertical.

The mean signed error of settings with respect to the true value (POE) is the **constant error** and is a measure of bias or accuracy. The standard deviation, or other measure of variability, of settings about the signed mean of the settings measures the precision of the judgments and reflects the sensitivity of the sensory system. Both the method of adjustment and the method of limits require the stimulus to be exposed for at least as long as it takes to make a setting or judgment.

The **method of constant stimuli** is used when the effect being measured is transient or when it is important to avoid the presentation of stimuli in an ordered sequence. Suppose we are using this procedure to measure the accuracy and precision of setting a variable stimulus to match a comparison stimulus. About seven values of the variable stimulus are selected that lie within the region of uncertainty on either side of the PSE. On each trial one of these stimuli and the comparison stimulus are presented briefly and the subject indicates which of the two is greater in magnitude. Subjects are asked to make a decision even when the two stimuli look alike. The order of presentations is randomized and each stimulus is presented many times. The percentage of trials in which the variable stimulus is judged to be greater than (or less than) the standard stimulus is plotted on the Y axis against stimulus magnitude on the X axis to yield a **psychometric function**. The function is usually an S-shaped curve in the form of a cumulative normal distribution, or normal ogive (an example is shown in Figure 9.2).

Thus the psychometric function defines the relationship between variations in some stimulus attribute and the probability of a particular psychophysical response. The value of the stimulus that yields 50 per cent "greater-than" judgments is the PSE. The difference between the PSE and the POE is the constant error. The difference between the 50 per cent point and the value of the stimulus that yields 75 per cent of "greater than" judgments is usually taken as a measure of the upper discrimination threshold. The difference between the 50 per cent point and the 25 per cent point defines the lower discrimination threshold. The method of constant stimuli may also be used to measure the detection threshold for a given stimulus attribute. In this case, a single stimulus is presented with various values close to the detection threshold, and subjects report whether or not they have detected it. The psychometric function is a plot of the percentage of times the stimulus was detected against the value of the stimulus on the X axis. The detection threshold is usually

defined as the value of the stimulus that yields 50 per cent detection, although the actual percentage chosen is arbitrary.

Probit analysis (Finney 1971) is used to improve the fit of a cumulative normal curve to a set of data and thus to derive more precise estimates of the parameters of the function. Both the ordinate (response probability) and abscissa (stimulus strength) are first transformed into standard scores, that is, into standard-deviation units (Z scores). This has the effect of linearizing the psychometric function. Weights are then assigned to each datum point in inverse proportion to its standard error, which means that greater weight is given to points in the upper part of the psychometric function. In addition, datum points near the centre of the psychometric curve are weighted more heavily because they contribute more to the determination of the position of the curve than do points at either end of the curve. The best fitting line is then determined by the process of weighted linear regression.

Staircase methods

Judgments about stimulus values that lie some distance from the PSE are less informative than stimuli near the PSE. It is therefore best to concentrate stimuli near the PSE. Stimuli should also be symmetrically arranged around the PSE so as to avoid biasing the results. A derivative of the method of limits, known as the **staircase method**, provides an efficient way of achieving these two goals. In this method stimuli are presented briefly in ascending or descending order, until the response of the subject changes. The order of the stimulus progression is then reversed until the subject's response changes again. In this way the stimulus values home-in on the PSE. The threshold is the mean of a criterion number of trials after the judgments have reached a constant level of fluctuation. The difficulty of deciding when a constant level has been reached can be avoided by defining the threshold as the stimulus value above which 50 per cent of the judgments are "yes". If the step size is too great, the subject merely alternates between "yes" and "no" judgments, and if it is too small, time is wasted. It is a useful strategy to start with a large step size and reduce the step size during the course of the experiment. A simple rule is to halve the step size when the response of the subject reverses and double it again if a criterion number of similar responses are made in succession.

With a simple staircase procedure the subject can begin to anticipate when to change the response. For instance, if several "yes" judgments have been made in succession the subject may guess that it is time to say "no" even though no change in the stimulus has

been detected. The **double-staircase method** reduces the effects of sequential dependencies. In this method two staircase sequences are run at the same time with stimuli from the two sequences presented in random order (Cornsweet 1962). Several variations of the staircase method have been devised (Taylor and Creelman 1967; Watson and Pelli 1983).

Signal detection procedures

When a stimulus is presented on every trial, subjects seemingly improve their performance by adopting a more lax criterion, that is, by being willing to report a stimulus although very unsure of its presence. On the other hand, subjects may seemingly perform less well by adopting a stricter criterion. Classical psychophysical methods do not distinguish between a change in the detectability of the stimulus and a change in the willingness of the subject to report its presence. **Signal detection theory** was developed to measure the separate contributions of these two factors (Green and Swets 1966). In this theory, a signal is a well-defined physical event which a sensory system, or receiver, is attempting to detect. The basic idea is that all neural discharges created by a signal are accompanied by noise, arising either from other stimuli or random events in the sensory system. It is assumed that the noise level fluctuates at random around a mean value with a given variance. The neural discharge, or sensory response, generated by a given signal is also assumed to vary at random around a mean value, with the same variance as for the noise alone. The **detectability** of the signal with respect to the noise is defined as the difference between the mean of the distribution of the sensory response generated by noise alone and the mean of the distribution of the sensory response generated by the noise plus the signal, divided by the variance of the distributions. Detectability is denoted by the symbol d' ("d prime").

Within the threshold region, a subject is necessarily uncertain about whether a weak sensation is due to a signal or spurious stimuli in the surroundings or in the sensory system. With sensory activity of a given strength the subject can be more or less willing to report the presence of the signal. The level of sensory activity above which the subject reports the presence of a signal is the **criterion level**, denoted by the symbol β . The subject's task is essentially that of estimating the likelihood that the sensory activity on a given trial arises from noise plus a signal relative to the likelihood that it arises from noise alone. The ratio of these two likelihoods is known as the likelihood ratio and forms the most efficient basis for a detection task. The variations of sensory response to noise and to signal plus noise are assumed to be

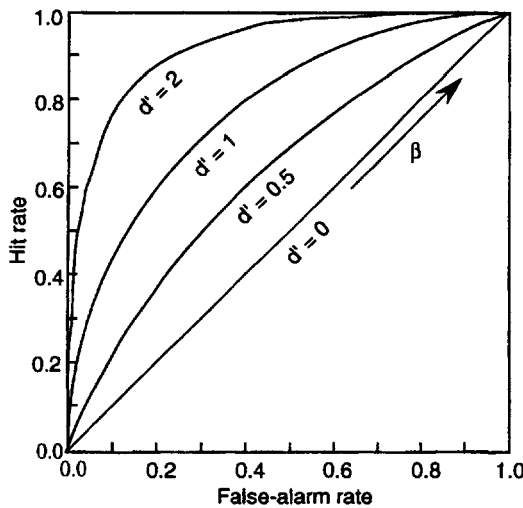


Figure 3.6. A hypothetical set of ROC curves.

The symbol d' signifies the detectability of the stimulus and each curve represents a locus of constant detectability. The position along each curve represents β , or the criterion at which the subject is operating.

normally distributed with the same variance, responses on different trials are assumed to be independent, and performance is assumed to be stable over a set of trials.

The method of signal detection separates out the effects of changes in the criterion from true changes in the detectability of the stimulus. A series of signals of varying strength in the region of the threshold are presented at random along with catch trials in which there is no signal but only internal noise in the sensory system. A record is kept of the rate at which targets are detected in a given number of trials (hit rate) and the rate at which targets are reported when none is present (false-positive rate). These data are plotted on a graph with hit rates along the Y axis and false-positive rates along the X axis. On this basis, a best-fitting curve is found for the data. This curve is known as the **receiver operating characteristic**, or ROC curve (see Figure 3.6). If the hit rate increases in simple proportion to the false positive rate (diagonal ROC curve) it signifies that the subject was merely guessing, since the hit rate is improved only by an equal increase in false positives. The detectability of the stimulus is indicated by the separation between the subject's ROC curve and the diagonal. The criterion is given by the point along the ROC curve at which the subject is operating. Signal-detection procedures can be used with physiological data derived from the responses of single neurones as well as with psychophysical data. Macmillan and Creelman (1991) have written a users guide for signal detection theory.

A simple procedure for ensuring that measurements of thresholds are not affected by changes in

criterion was proposed by Blackwell (1952). Subjects are presented with two stimulus windows, either at the same time or sequentially. Only one of the windows contains a stimulus. For each of many trials, in which stimulus strength and position are varied at random, subjects are forced to say which window contains the stimulus, hence the name **two-alternative forced-choice (2AFC) procedure**. McKee et al. (1985) have described this procedure. A two-alternative decision is independent of changes in criterion, since subjects are forced to choose on each trial. The percentage of correct responses is plotted on the ordinate against the value of the stimulus. This is the psychometric function, which normally conforms to a cumulative normal function (normal ogive). Since the chance level of performance is 50 percent, ordinate values run between 50 and 100 per cent. The stimulus value that a subject correctly identifies 75 per cent of the time is taken as the threshold. The 75 per cent point is the mean of the psychometric function based on the forced-choice procedure. The slope of the psychometric function indicates the rate at which performance improves as stimulus strength is increased. It is the reciprocal of the standard deviation of the distribution of responses. The standard error of judgments for each stimulus value is calculated by the equation for the standard error of a proportion. The standard error is largest when subjects are most uncertain in their judgments, which is when the test and comparison stimuli are most similar. As the percentage of correct responses increases, the standard error tends to decrease.

Scaling

In another class of psychophysical methods, known as **sensory scaling**, subjects make categorical judgments about the magnitudes or sensory qualities of stimuli. Readers are referred to Torgerson (1958) and Garner (1962) for a survey of these procedures.

Phenomenological analysis

Many perceptual phenomena can be investigated by simply asking subjects to describe what they see. The Gestalt psychologists pioneered this method. Most visual phenomena were discovered by chance observation or by an inspired guess that a given phenomenon may occur if stimuli are arranged in a particular configuration. For instance, Celeste McCollough, extrapolating from some work on chromatic aberration, anticipated that something of interest would be seen if alternating gratings were paired with alternating colours. That led to the discovery of one of the first contingent aftereffects (see Section 9.4.6). Wheatstone's discovery of the

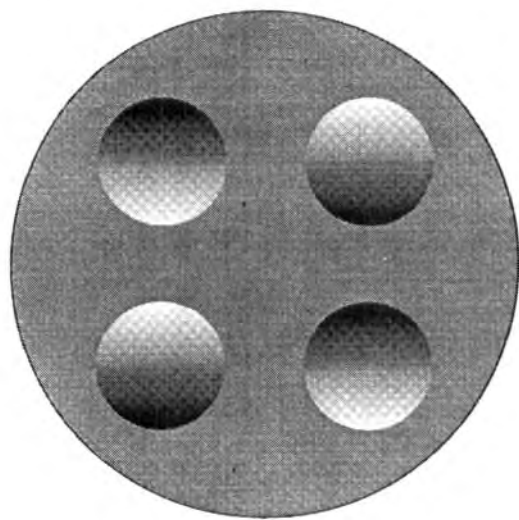


Figure 3.7. Frames of reference in shape from shading.
When the figure is inverted, the two discs that looked like mounds look like hollows and the two discs that looked like hollows look like mounds. When the figure is viewed with inverted head, it is revealed that the factor determining the apparent convexity or concavity of the discs is their orientation to the head rather than to gravity. When the figure is viewed below the chin almost parallel with the body, with head erect, the crucial factor turns out to be the orientation of the discs to the retina.

stereoscope and his subsequent observations with a variety of stereograms revealed the basic characteristics of the human stereoscopic system.

Once a visual phenomenon has been discovered, the stimulus conditions that give rise to it can be established by comparing the frequency of its appearance under different experimental conditions. Sometimes, powerful inferences can be made about mechanisms underlying visual processes from qualitative observations of effects under cleverly devised circumstances.

There are no general procedures for this type of investigation, but great care must be taken not to overgeneralize conclusions. For instance, two of the discs in Figure 3.6 look like mounds, and two look like hollows. When the figure is inverted, the two discs that looked like mounds look like hollows and the two that looked like hollows look like mounds. In most textbooks it is concluded that the convexity or concavity of a shaded region is interpreted in a way consistent with the light source being above with respect to the ground. However, when Figure 3.6 is viewed with the head upside-down, impressions of convexity and concavity are determined by the orientation of the dark and light areas relative to the head, rather than to gravity. But even this is not the correct account. When the figure is viewed with head upright but with the figure at a steep angle beneath the chin, so that the part of the picture that is "top" with respect to gravity and to the head is

upside-down on the retina, the convexities and concavities are interpreted in terms of retinal coordinates (Howard et al. 1990).

Stimulus dimensions are heavily confounded. One may think that a well-defined stimulus dimension has been isolated in a perceptual experiment and that one has uncovered the function relating a perceptual effect to variations in that dimension. But changes in the selected dimension may be incidental to changes in another crucial dimension that one has not considered. Only the vigilance and imagination of the investigator in designing control conditions can prevent one falling in to this trap; there are no foolproof rules. Perhaps half the literature in perception consists of investigators pointing out how other investigators have failed to take account of crucial stimulus dimensions, and of criticized investigators pointing out that they have not failed to take them into account. Even when a physical stimulus responsible for a given sensory effect has been properly identified there is still the question of how the stimulus is processed in the nervous system. Identical responses to identical stimuli can be mediated by many types of intervening processes.

3.5.2 Sensory detection and resolution

Sensory detection

A stimulus is detected when a sufficient number of quanta falling in unit time in one region of the retina is discriminably different from the mean number of quanta falling within the surrounding region. In a typical task, a light line of a given length and luminance, on a background of a different luminance, is varied in thickness until the line is detected. Because of diffraction, the image of a line is spread across several receptors so that detection reduces to the task of detecting a luminance gradient. For an illuminated line no line is so thin that it cannot be detected, because the luminance of the line can be increased to compensate for any reduction in width to generate a discriminable luminance gradient. One can talk about the minimum resolvable thickness of an illuminated line only if the contrast between line and surround is specified. It has been estimated from frequency-of-seeing curves that a short line of light seen against a dark background is detected at above chance level if two quanta of light are absorbed within a critical area and within a critical time period, estimated to be about 10 ms. Stimulus energy is completely summed within this critical area (Ricco's law) and critical time (Bloch's law). The critical area and time vary with the wavelength of light and with the retinal location stimulated (Bouman and van den Brink 1952; Schwarz 1993).

A black line seen against a bright background must be at least 0.5 arcmin wide to be detected, however bright the background (Hecht and Mintz 1939). The visual target can also be the boundary between two unequally illuminated regions. In all cases, performance depends on the ability to detect a luminance gradient—the subject is not required to respond to any other spatial attribute of the stimulus.

Sensory resolution

Two stimuli are resolved when they are detectable as two stimuli. The minimum condition for two stimuli to be spatially resolved is that they must excite two detectors at a discriminably higher level than they excite one detector in an intermediate location. Thus, a set of detectors in a square lattice can resolve a periodic stimulus such as a black-white grating only if the spatial period of the grating (distance between two black bars) is at least twice the spacing of the detectors. This is known as the **Nyquist limit**. A related statement is that two detectors with overlapping tuning functions, each with a standard deviation of s , can resolve two stimuli separated by a distance of between 2 and 3 s . This is known as the **Rayleigh criterion**. The colour system has only three channels, with very wide and overlapping tuning functions. Since neither the Nyquist limit nor the Rayleigh criterion is satisfied in this system, our capacity to resolve wavelengths is zero. No matter what wavelengths are present in a patch of light, we see only one colour. The colour we see depends on the relative extent to which the different colour receptors are excited, and if two lights with different wavelength components excite the three receptors in the same ratios, those lights appear identical, even though the wavelength components are discriminably different when presented one at a time. The lights are said to be metamerically matched.

Low resolution due to metamerism is particularly evident in the skin. Two or more points applied to a area of skin feel like one point at an intermediate position. The apparent position of the fused stimuli depends on their relative strengths. Békésy (1967) used the term "funneling" for this metamerically averaged process.

The visual local-sign system is metamerically matched only locally. It has about one million channels (ganglion cells) which, at the theoretical limit, allow it to resolve a black and white grating with bars as narrow as the diameter of receptors. In other words, resolution is limited by the ability of the neighbouring receptive fields to detect differences in luminance contrast. Two or more visual stimuli falling wholly within an area of the retina where the

excitatory regions of neighbouring receptive fields mutually overlap appear as one stimulus in a position that depends on their relative luminances. This occurs when two short parallel lines are seen together within an area of about 2 arcmin, which is about the size of the smallest receptive fields in the retina (Badcock and Westheimer 1985; Watt et al. 1983). This metamerically merged of stimuli occurs over larger distances in the peripheral retina because receptive fields are larger there. When the lines are presented separately (one above the other or successively) their distinct positions can be discriminated to much finer limits, just as wavelengths can be discriminated when presented in different spatial locations. Spatial discriminations beyond the Nyquist limit are referred to as hyperacuity, as we will see.

Width resolution

As two initially superimposed fine lines are separated, the first impression is of a line increasing in width. This is because the distribution of activity over the set of detectors becomes broader as the lines separate, but the two peaks of excitation are not distinct enough to be discriminated. Thus, two spatially separated lines can be distinguished from two perfectly superimposed lines before they are far enough apart to be seen as two distinct lines. This type of resolution is **width resolution**, and it exceeds the limits set by the Nyquist or Rayleigh criteria. In colour, width resolution shows itself as a loss of saturation as a monochromatic light is replaced by two monochromatic lights that produce the same hue as the monochromatic light. Snippe and Koenderink (1992) have developed an ideal observer for width discrimination and hyperacuity in metamerically sensory systems.

Metamerism in secondary features

Loss of resolution because of metamerism is difficult to investigate in secondary spatial or spatial-temporal features—features derived from the initial coding of local sign and time—because all such features can be also resolved by the million-channel, local-sign system for visual direction. Thus, even if orientation detectors could not resolve the angle between two intersecting lines, the lines would still be perceptibly distinct because they fall on distinct regions of the retina. Two neighbouring or intersecting short lines at slightly different orientations should metamerize their orientations (they should appear as one line at an intermediate orientation). There seem to be no experimental investigations of this possibility, but perhaps metamerically processes within excitatory regions of neighbouring orientation detectors can explain why closely spaced parallel lines appear wavy

and why the orientation of a short, briefly presented line is difficult to detect (Andrews 1967).

For similar reasons, metamerism should be evident in visual motion and we have evidence that it is. A display of short-lifetime dots moving in different directions in the same general direction appears as a set of dots moving in a common mean direction. The discriminability of a change in the mean direction of motion for a mixed display of dots was the same as for an array of dots all moving in the same direction (Watamaniuk et al. 1989). Furthermore, an array of short-lifetime dots moving in the same direction at different speeds resembles an array of dots moving at the mean speed of the set (Watamaniuk and Duchon 1992). Averaging of speed does not occur when the dots have a long lifetime because the differences between the speeds of the component dots are then discriminated on the basis of relative changes in position of identifiable dots. These results can be explained in terms of metameristic processes within the motion-detection system. Metamerism in the disparity system is discussed in Section 6.3.

3.5.3 Sensory discrimination

Two stimuli are discriminated if one is detectably different from the other, given that they have been resolved as two stimuli, either in space or in time. A metameristic system with poor resolution can have exquisite discrimination. For instance, even though the wavelength resolving power of the human eye is zero, it can discriminate between many hundreds of spectral colours (or their metamers), as long as they are presented sequentially (resolved in time) or to different regions of the retina (spatially resolved). *Resolution* requires the detection of a difference between the means of two overlapping and simultaneously present distributions of activity along the sensory continuum. Since the two distributions of activity are present at the same time, the detection of either mean is confounded by the presence of the other stimulus, so that performance is subject to the Nyquist limit. *Discrimination* depends on the detection of a difference in the mean response of a set of detectors responding to one stimulus and the mean response of a second set of detectors responding to the other stimulus, when the two sets of detectors are stimulated at different times or occur in different locations on the sensory surface. There is no theoretical limit to the precision with which the mean of a single distribution can be registered when no confounding stimuli are present. Precision depends on the square root of the number of photons and their spatial distribution. In neural terms, the precision with which the location of a single stimulus can be

registered by a set of detectors depends on the rate of change of response across the set. The discrimination of a difference of location of two resolved stimuli depends on the steepness of the tuning functions at the point where the inflection points of the two tuning function overlap. That is, it depends on the relative rate of change of the signal in the two detectors as the stimulus is moved over the stimulus continuum. This point is illustrated in Figure 3.7 for orientation discrimination. Resolution depends mainly on the signal-to-noise ratio and on the tuning width and density of sensory channels along the sensory continuum. The noisiness of the individual channels seems to be less important for discrimination than for resolution (Bowne 1990).

The fine discrimination in sensory systems, compared with resolution, explains hyperacuity. An example is the ability to detect a vernier offset between two lines which is several times smaller than the mean spacing of receptive fields. Another example is the task of setting a point midway between two other points, which has yielded thresholds of approximately 1 arcsec (Klein and Levi 1985). The distinction between resolution and discrimination (hyperacuity) in a locally metameristic spatial modality can be vividly illustrated on the skin. If the skin of the back is prodded simultaneously by two pencils about 1 cm apart, they metamerize; that is, they feel like one object at an intermediate position. But if the pencils are presented sequentially with the same separation, their distinct positions can be discriminated (Loomis and Carter 1978).

Discrimination functions

Discrimination sensitivity in a metameristic system should show local maxima at places where the tuning functions of detectors intersect, because this is where the difference signal changes most rapidly. The well-known hue-discrimination function is an example. The local sign system is locally metameristic and it, too, should show undulating discrimination functions. There has been some contention about whether sensitivity to changes in the separation of lines shows peaks and troughs as the distance between the lines is varied (Hirsch and Hylton 1982; Westheimer 1984a). Wilson (1986) interpreted some data from Klein and Levi (1985) as showing peaks and troughs analogous to those in the hue-discrimination function. Regan and Price (1986) found undulations in sensitivity to changes in line orientation as the line was varied in orientation. The highest sensitivity to changing orientation occurred at vertical and horizontal, which suggests that the tuning functions of orientation detectors intersect at these values. This means that the peaks of orientation tuning

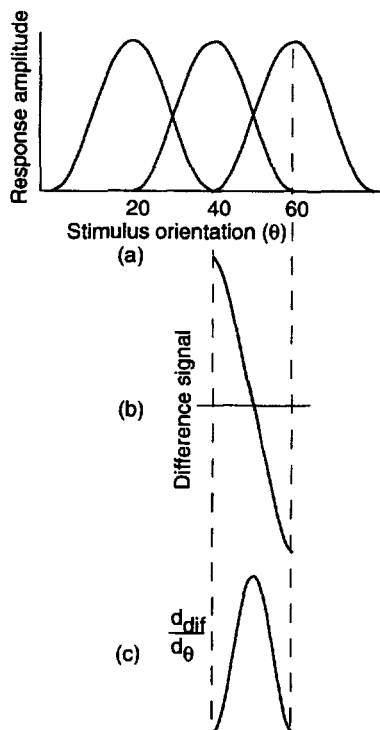


Figure 3.8. Detection and discrimination of orientation.

- (a) Hypothetical tuning functions of three orientation detectors.
- (b) Signed difference in firing rate of neighbouring orientation detectors as a stimulus is rotated from 40° to 60°.
- (c) The orientation discrimination function derived by differentiating the difference signal. The difference signal is strongest at the peaks of the tuning functions, but the discrimination signal is strongest at the point of intersection of the tuning functions.

functions are on either side of the main meridians. This raises the interesting possibility that in any sensory system, neighbouring detectors intersect where sensitivity to change is required to be highest. Another illustration of this point is that sensitivity to changes in binocular disparity (stereoscopic depth) is greatest about zero disparity, which is where the tuning functions of disparity detectors seem to overlap. This issue is discussed in Section 5.3.2.

All this suggests that a stimulus is detected most efficiently when it excites a detector at the peak of its tuning function but that a change in a stimulus along a feature continuum is discriminated best when the stimulus falls on the steep flanks of the tuning functions of neighbouring detectors. Snowden et al. (1992) produced physiological evidence supporting this conclusion. Motion-sensitive cells in V2 and the temporal lobe (MT) of the alert monkey had directional tuning functions with a half-width of 50° at half-height. Although a cell fired most vigorously when the stimulus excited the peak of its tuning function, different rates of firing occurred for directions differing by as little as 1.1° when the stimulus excited a cell on the flank of its tuning function.

3.5.4 Temporal thresholds

Temporal aspects of sensory processing have been studied with a great variety of procedures. Only a brief outline of methods used to study temporal aspects of stereopsis will be reviewed.

With a suprathreshold stimulus one can measure the time required to detect a stimulus. In a typical experiment, subjects press a key as quickly as possible at the first appearance of the stimulus, and the averaged response time is the reaction time. The reaction time includes the time taken for the stimulus to be processed and the time taken for the response to be prepared and executed. If the same response is used for different stimuli, differences between reaction times provide a measure of differences in sensory processing time. These procedures have been used to study effects of learning on the processing time for stereopsis, as we will see in Section 5.11.

In some cases the results of temporal processing of sensory inputs are reflected directly in a nontemporal percept. For instance, a difference in arrival of sounds to the two ears of a few milliseconds causes an apparent shift in the position of the sound source that subjects can identify by simply pointing in the appropriate direction, taking as long as they wish. Similarly, in the Pulfrich stereophenomenon, a target moving in a frontal plane appears to move in depth when image processing in one eye is delayed by introducing a dark filter in front of that eye. A very precise mapping of interocular time differences into disparities can be obtained by simply asking subjects to indicate the depth of the path of the moving target (see Section 13.1).

In another temporal procedure the duration of time for which the stimulus is presented increases gradually on succeeding trials until the subject reports either the presence of the stimulus or some defined change in the stimulus. The resulting measure is known as the temporal threshold. Subjects are not required to respond rapidly but are merely required to say on each trial whether or not the stimulus occurred. As the luminance intensity of a stimulus is increased, the temporal threshold becomes vanishingly small. As the stimulus is weakened the temporal threshold increases up to a limiting value that depends on the capacity of the sensory system to integrate stimulus energy over time. This threshold is the temporal integration time. The capacity of a sensory system to integrate stimuli over time can also be investigated by presenting brief stimuli in succession with variable inter-stimulus intervals. This topic is discussed in more detail in the next section.

3.6 PSYCHOANATOMICAL TECHNIQUES

Psychoanatomical procedures are based on psychophysical procedures and allow one to make inferences about where and in what order information is processed in the visual system. It has been established that certain visual processes, such as trichromacy and luminance contrast, occur within the retina. These procedures do not establish the precise site of a postretinal visual process. However, they have provided information about (a) the existence of processes devoted to the detection of certain features, (b) the number of channels involved in the processing of a feature, (c) the order in which visual processes occur, (d) the bandwidth of the channels processing given features, and (e) the linearity of processing and the characterization of nonlinearities, such as signal rectification and ceiling effects (compressive nonlinearity). Several psychoanatomical techniques are described in the following sections. The ways in which they have been used in the study of stereopsis are described in other parts of the book.

3.6.1 Threshold summation and masking

Two sensory channels are said to be independent when the probability that one of them will detect a given stimulus is unaffected by the simultaneous stimulation of the other, and when the internal noise associated with one detector is uncorrelated with the internal noise associated with the other. When the same weak stimulus is presented to each of two independent channels, the probability that the stimulus will be detected is greater than the probability of detection of the same stimulus presented to only one channel. This is because, when more detectors are stimulated, the signal in one or other of them is more likely to exceed the fluctuating noise level than when only one is stimulated. This is known as **probability summation**. Pirenne (1943) introduced this concept into visual science. For two detectors of equal sensitivity, the probability of detecting a stimulus using both (P_b), relative to that of detecting it with either one alone (P_1 and P_2) is given by

$$P_b = (P_1 + P_2) - P_1 P_2$$

Quick (1974) provided the following simplified formula for calculating the effect of probability summation on stimulus detection when there are several detectors with different sensitivities,

$$s = \left[\sum_{i=1}^N |s_i|^p \right]^{\frac{1}{p}}$$

where N is the number of independent receptors responding to a set of stimuli, s_i is the sensitivity of the i th detector, and p is the slope of the psychometric function at the point where a stimulus is detected 50 per cent of the time.

If the probability of detecting a stimulus presented to two channels is greater than that of detecting the same stimulus presented to only one channel by an amount that exceeds probability summation, then the two channels are not independent. This means that neural signals in the two channels converge at some point so that their signal strength is summed before a decision is made about the presence of a stimulus. If the noise in one channel is not correlated with that in the other channel the noise signals partially cancel out, so that the noise after convergence is less than the sum of the noise in the two channels. This improves the signal-to-noise ratio and increases the probability of detection above the level of probability summation.

Consider a sensory continuum detected by a multichannel sensory system. By definition, a cell within a subchannel responds to all stimuli that fall within the bandwidth of that subchannel and within the receptive field of that cell. In other words, signals from stimuli within this bandwidth converge on a common neural pathway. By varying the relative values of two simultaneously presented stimuli over the sensory continuum one can determine the stimulus range over which neural summation occurs. This reveals the bandwidth of subchannels within sensory systems. For example, the tuning bandwidth of orientation detectors has been inferred from the range of orientations over which subthreshold summation of two stimuli for the detection of orientation occurs (Thomas and Gille 1979). Similarly, the spatial-frequency bandwidth of detectors has been inferred from the range of spatial frequencies over which subthreshold summation of grating acuity occurs (Wilson and Gelb 1984). In audition, the range of tones affected by exposure to a particular tone—the critical band—is essentially the tuning width of receptors along the basilar membrane of the cochlea. The application of subthreshold summation to sensory processing of two-dimensional spatial contrast stimuli has been reviewed by Graham (1989). Applications of subthreshold summation to binocular vision are discussed in Section 9.2.

A briefly presented suprathreshold stimulus tends to elevate the threshold of a briefly presented test stimulus presented in the same location or in a neighbouring location, at the same time or in close temporal contiguity. This is known as **masking** and its applications to binocular vision are discussed in Section 9.3. In Section 8.3 we will see that the extent

to which an image in one eye suppresses a distinct image in the other eye (binocular suppression) depends on the relative spatial frequencies, orientations, and contrasts of the images in the two eyes. This suggests that visual inputs are processed for spatial frequency, orientation, and contrast before binocular suppression occurs.

3.6.2 Adaptation and contrast effects

Contrast and assimilation

In many instances the appearance, rather than the detection threshold, of a stimulus is affected by another stimulus presented at the same time or successively. It is assumed that these interactions occur because of overlap between the tuning functions of neighbouring detectors for a particular visual feature. For instance, the distance between two parallel lines is underestimated when they are separated by a gap slightly greater than is needed to resolve them. This is an assimilation effect. When parallel lines are slightly further apart than about 4 arcmin they appear to repel each other (Köhler and Wallach 1944; Badcock and Westheimer 1985). This is a simultaneous contrast effect. Successive contrast effects in visual location are known as **figural aftereffects**. Assimilation is probably due to spatial summation of signals in the particular mechanism. Contrast is probably due to spatial inhibition. The greater spatial range of contrast than of assimilation is presumably due to inhibitory interactions extending beyond summatory interactions.

There are contrast effects in motion (Nakayama and Tyler 1978) and in motion-in-depth (Regan and Beverley 1978b). In orientation, simultaneous contrast reveals itself as geometrical illusions, and successive contrast as tilt aftereffects, which can be as large as 5° when the test stimulus is presented for durations as short as 100 ms (Wolfe 1984). Contrast aftereffects also occur in the spatial-frequency domain (see Howard 1982). Contrast effects in depth are discussed in Section 12.1. Physiological correlates of simultaneous and successive contrast effects have been revealed in the responses of single cells in the visual cortex. See Saul and Cynader (1989) for references on this topic.

Contrast effects serve to enhance signals associated with changes in stimulation relative to signals associated with regions of steady stimulation. If it is assumed that contrast effects depend on the extent to which sensory channels overlap, they provide a powerful psychophysical procedure for measuring the physiological properties of metameristic systems, such as the number and bandwidth of channels coding a given feature.

If an effect in sensory dimension *A* occurs only for certain values of the stimulus dimension *B*, then it is reasonable to conclude that the stimulus is first processed within the *B* dimension before it is processed for *A*. For instance, certain visual effects, such as perspective illusions, occur with stimuli defined by luminance but not with chromatic stimuli. They must therefore occur after chromatic and achromatic channels are partitioned.

Oppositional sensory dimensions

In many sensory dimensions there are natural balance points, or **norms**. For instance "vertical" is a norm for orientation, "equidistance" is a norm for relative depth and "stationarity" is a norm in a scale of movement from one direction to the opposite. Such stimulus dimensions are known as **oppositional**. It seems to be a universal characteristic of oppositional stimulus dimensions that prolonged inspection of a stimulus displaced from the norm causes that stimulus to appear more like the norm and other stimulus values on the same dimension to be displaced accordingly. Thus, when one looks at a tilted line it gradually appears more vertical and a vertical line looks tilted in the opposite direction, a phenomenon known as the **tilt aftereffect**. When one looks at a moving display it appears to slow down and a subsequently presented stationary display appears to move in the opposite direction, a phenomenon known as the **motion aftereffect**. Curved lines come to look more straight and objects at different distances appear more equidistant.

A persistent asymmetry of stimulation with respect to a norm signifies that there is a systematic distortion of the visual input, and normalization adjusts the system to the disturbance. For example, on average, the natural world contains as many lines slanting or curving one way as lines slanting or curving another way. Even if a natural object in the world is slanted, the slant it creates in the eye balances out as the observer moves about and views it from different directions. A persistent slant or curvature over the whole visual field signifies that the visual system is wrongly calibrated and in need of correction. After a while, systems that detect orientation or curvature automatically adjust themselves. Thus, normalization can be regarded as an automatic calibration or error-correcting mechanism.

A plausible physiological explanation for normalization can be provided in terms of adaptation within opponent mechanisms. It is simply necessary to assume that the tuning functions of detectors tuned to opposite sides of the norm intersect at the position of the norm and that a stimulus appears at the norm when the distribution of activity in the set

of detectors is symmetrical about the norm. For instance, after a line just off the vertical has been inspected for some time, it should appear displaced toward the vertical because the detector on that side of vertical will have become adapted, or fatigued, relative to the one on the other side of vertical. Note that inspection of a vertical line has no effect because it falls in a region where it excites two detectors equally. Similarly, the opponent colours red and green normalize toward gray, whereas an equal mixture of red and green remains gray. We suggest that the tuning functions of systems in which normalization is an advantage have evolved or grown so that they intersect at the position of the natural norm. This has the added advantage that sensitivity to change in the stimulus feature is greatest at this position. Normalization is due to selective adaptation, but its effect on a particular stimulus depends on differential tuning widths or differing concentrations of detectors along a sensory continuum.

Contingent aftereffects

Sensory adaptation can result in an elevation of threshold, lasting a few minutes. There are also adaptation processes that can last days or even weeks. The best known of these are the **contingent aftereffects**. For example, a period of exposure to red vertical lines alternating with green horizontal lines produces a long-lasting aftereffect in which vertical lines look slightly green and horizontal lines look slightly red (McCollough 1965). These effects can be understood as mechanisms for correcting for cross-talk between feature-detection systems. The orientation-color contingent effect may be responsible for nulling the perceptual effects of chromatic aberration in the optical system of the eye, or in lenses that people habitually use. Long-lasting adaptation effects have also been reported for simple visual features, such as visual motion (Favreau 1979) and visual tilt (Wolfe and O'Connell 1986). Long-lasting effects occur when test trials do not immediately follow the induction stimulus. However, these seemingly simple effects may be specific to the induction stimulus that produced them and, if so, they may be best described as contingent aftereffects. The relevance of contingent aftereffects to binocular vision is reviewed in Section 9.4.6.

3.6.3 Interocular transfer

A visual effect is said to show interocular transfer if the stimulus inducing it is presented to one eye and the test stimulus in which the effect is induced is presented to the other eye. It is argued that an effect showing interocular transfer must arise in binocular

cells and, since true binocular cells are not present before the primary visual cortex, interocular transfer signifies that the processes responsible for the after-effect are cortical. This argument is not always valid. An afterimage shows interocular transfer, in the sense that an afterimage impressed on one eye is visible when that eye is closed and the other eye opened. This does not prove that afterimages are cortical in origin, it simply means that activity arising in a closed eye still reaches the visual cortex and can appear superimposed on whatever the open eye is seeing. This interpretation is confirmed by the fact that an afterimage is no longer visible when the eye in which it was formed is paralyzed by the application of pressure to the eyeball (Oswald 1957). To prove that an aftereffect is cortical, one must show that it survives paralysis of the eye.

Another problem with the test of interocular transfer concerns the state of adaptation of the eyes. In nontransfer trials the adapted eye is also the tested eye and therefore it has the same state of adaptation in both induction and test periods. In transfer trials the adapted eye is open during the adaptation period and closed during the test period and the tested eye is at first closed and then opened. The two types of trial are therefore not comparable for drawing inferences about the site of the aftereffect. This problem can be solved by keeping both eyes in the same state of adaptation.

Interocular transfer is reviewed in Section 9.4.

3.6.4 Tests of monocular independence

The test of monocular independence is related to that of interocular transfer. In the test of independence, opposite induction stimuli are presented to each eye and the aftereffect is tested in each eye separately. For instance, a leftward-moving textured display is presented to the right eye and a rightward-moving display is presented at the same time to the corresponding area of the left eye. A stationary test pattern is then presented to each eye in turn to reveal whether the direction of the aftereffect in each eye is appropriate to that eye's induction stimulus. If it is, then at least some aftereffect must have been generated in pathways specific to each eye. If the aftereffect in each eye is just as strong as when that eye alone is exposed to an induction stimulus, it is concluded that the processes responsible for the aftereffect are totally independent in the two eyes. If the aftereffect were generated wholly in a pathway common to both eyes, induction stimuli of equal magnitude but opposite sign should cancel when one is presented to each eye. Experiments involving this procedure are reviewed in Section 9.4.

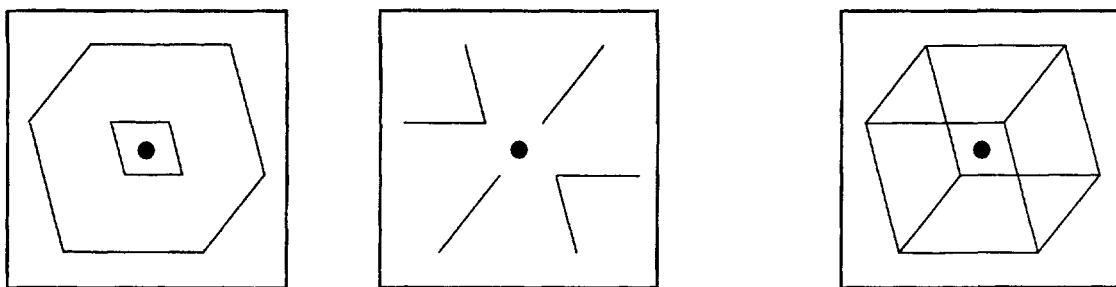


Figure 3.9. A dichoptic composite stimulus.

Dichoptic combination of the two displays on the left produces the shape on the right.

3.6.5 Dichoptic composite stimuli

We define a dichoptic composite stimulus as one in which part of the stimulus is presented to one eye and part to the other, where both parts are required for the composite percept. For instance, a display of lines presented to one eye can be combined dichoptically with a different display of lines in the other eye so that they combine into a composite shape not evident in either monocular image, as in Figure 3.8. The literature on dichoptic composite stimuli is reviewed in Section 9.4.2.

3.6.6 Cyclopean stimuli

Cyclopean procedures were defined in Section 1.1.4. In the most general sense a cyclopean visual process is one that occurs in the central nervous system rather than in the retina. In this sense the processes responsible for coding orientation, motion, and disparity are cyclopean. We use the term in a more restricted sense to describe a type of experimental procedure in which a stimulus is formed centrally but not on either retina. For instance, any visual impression surviving paralysis of the eyes must be cyclopean and so must any visual impression induced by direct stimulation of the visual cortex. In a dichoptic cyclopean procedure, stimuli presented to each eye generate a visual impression not evident in either eye. Creating an impression of depth from binocular disparity is a cyclopean procedure.

We explained in Section 3.2.3 that the local-sign system has one set of detectors, consisting of one million ganglion cells. Shape is represented by differential stimulation within this local-sign system. However, the retina is also paved with repeating sets of detectors for spatial frequency, motion, flicker, and colour. This means that shape can be coded in terms of patterns of stimulation over any of these features, even when there are no boundaries defined by luminance contrast. Thus, shape can be coded in terms of texture, motion, flicker, or colour

with mean luminance between different regions held constant. Each of these locally coded features can be synthesized as a dichoptic cyclopean stimulus.

A dichoptic cyclopean stimulus is one defined by a feature or features not present in either monocular image. The stimulus emerges only after dichoptic images have been combined. Any perceptual phenomenon visible in a cyclopean stimulus is a cyclopean phenomenon and must depend on cortical processes, since cyclopean stimuli are not formed before the cortex. A dichoptic cyclopean stimulus can be an area of binocular rivalry, disparity, dichoptic motion or flicker, or any combination of these features. Once synthesized, a cyclopean shape can be made to move by simply moving the dichoptic boundaries that define it. Different ways of synthesizing cyclopean images and experiments on cyclopean vision are reviewed in Chapter 14.

3.6.7 Trading functions

Two or more types of stimulus may generate the same perceptual effect. For instance, the sensation that a sound source is in a particular direction can be generated by a difference in time of arrival of sounds at the two ears or by an interaural difference in sound intensity. One of these cues can be used to generate an apparent offset of a sound source relative to the median plane. This offset can then be nulled by an opposite offset produced by the other cue. The set of null points for different values of each sensory cue defines a trading function. This process of titrating one cue against another allows one to investigate the degree of equivalence between cues and the relative efficacy of equivalent cue systems. An example of a trading function in stereoscopic vision is provided by the titration of binocular disparity against monocular parallax, as described in Section 13.5.5 and the titration of disparity against perspective described in Section 11.2.2. This procedure is applicable only when the two cues interact in a continuous fashion.

Some cues interact in an winner-take-all fashion so that, at any time, the percept is determined by only one of them. An example is provided by a conflict between binocular disparity and figural overlap, as discussed in Section 11.2.4.

3.6.8 Effects of attention and stimulus familiarity

Effects of practice and learning

Most investigations of the response properties of cortical cells are carried out on anaesthetized animals. With this procedure, effects due to changes of attention, motivation, or learning remain undetected during a particular recording session. There is a growing body of evidence from work on unanæsthetized animals that all these factors modify the responses of cortical neurones. The concept of sets of cortical cells tuned to specific and fixed stimulus features must give way to a view of the cortex as a highly flexible organ in which response characteristics of cells depend on neighbouring stimuli and the activity of other centres in the brain. Section 4.2.7 reviews some of the literature on this issue.

Practice leads to improvement in a variety of simple visual tasks, such as orientation discrimination, contrast detection, and Snellen acuity (see Bennett and Westheimer 1991). However, no significant effects of prolonged practice could be found for a gap bisection task (Klein and Levi 1985) or a three-point alignment task (Bennett and Westheimer 1991), both of which are hyperacuity tasks. Bennett and Westheimer could not find any practice effects with a grating discrimination task. It is not clear why practice helps in some cases and not in others.

Poggio et al. (1992) proposed that the nervous system sets up task-specific neural modules by a process of learning that leads to improved performance on a repeated visual task. This idea was illustrated by a computer simulation of a neural network that manifested improved performance in a vernier acuity task when provided with appropriate feedback. Naïve observers showed a similar task-specific improvement in vernier acuity over a few tens of trials when given knowledge of results. The model replicated several features of human performance, such as the dependence of vernier acuity on the length and relative orientation of the test lines. Fahle and Edelman (1993) obtained improvement on a vernier acuity task after prolonged practice, even without knowledge of results, and this effect was specific to the orientation of the test stimulus. The ability to see a shape defined by relative motion of line elements has been found to improve with practice but in this case the learning was not specific to the orientation of line elements or to the direction of motion

(Vidyasagar and Stuart 1993). We will see in Section 5.11 that stereoacuity also improves with practice.

In a real-life situation it is not clear what constitutes visual feedback in hyperacuity tasks. Perhaps visual feedback in the form of an error signal is not required. Improvement may occur because of an increase in response efficiency of a particular configuration of cortical cells due either to repetitive stimulation or attention-driven facilitatory processes from higher levels in the nervous system. An increase in response efficiency could involve a narrowing of the tuning functions of cortical detectors for the set of features involved in the task. It could also involve recruitment of detectors with neighbouring tuning functions, thus providing a better sampling of stimulus features. Learning, as ordinarily understood, need not be involved. It could simply be a matter of the nervous system recruiting its local resources for the performance of a repeated specific task. According to this view there would be a cost in terms of a performance decrement on similar tasks. It is difficult to see how any general learning-dependent improvement could occur in adult visual mechanisms responsible for basic tasks such as visual acuity, since we use our eyes all the time we are awake. However, it is possible that the system has evolved ways to concentrate those basic mechanisms when we repeatedly perform a specific task. Feature-detecting systems may have an inherent capacity to modify their tuning functions locally and temporarily to improve performance on specific tasks, either by error feedback or simply as a result of stimulus repetition. Attention is a process for concentrating limited resources on a selected task, as we will now see.

Preattentive and focal processing

In any complex information processing system a choice must be made between processing all information simultaneously or devoting specialized resources to the analysis of the item of greatest importance in a particular location. Parallel processing is faster than sequential scanning but it would be biologically expensive to repeat the complex neural circuits for in-depth analysis at each location of the visual field. It is better to have one complex mechanism that can be applied to any location of interest. The visual system uses both strategies. Inputs over the whole visual field are rapidly processed in parallel but only to a certain level, which has been called the preattentive level (Neisser 1967). Items of particular interest are then foveated or attended to and processed in greater detail at the level of focal attention which is limited to the location where attention is focused. This question is discussed in Section 6.1.6.

The physiology of binocular vision

4.1 The eye and visual pathways	105
4.1.1 The eye	105
4.1.2 Ganglion-cell receptive fields	109
4.1.3 Lateral geniculate nucleus	111
4.2 The visual cortex	114
4.2.1 Visual-cortical projections	114
4.2.2 Structure of primary visual cortex	115
4.2.3 Stimulus tuning of cortical cells	118
4.2.4 Ocular-dominance columns	120
4.2.5 Parvo-and magnocellular areas	123
4.2.6 Other visual areas	124
4.2.7 Effects of attention and learning	128
4.3 Midline Interactions	129
4.3.1 Partitioning of hemiretinas	130
4.3.2 Transcallosal connections	130
4.4 Disparity detectors	132
4.4.1 Disparity detectors in the cat	133
4.4.2 Disparity detectors in the monkey	134
4.5 Disparity tuning functions	136
4.5.1 Shape of disparity tuning functions	136
4.5.2 Receptive-field offset	140
4.6 Types of disparity coding	141
4.6.1 Disparity of spatial scale	141
4.6.2 Detectors for orientation disparity	142
4.6.3 Detectors for curvature disparity	142
4.6.4 Coding for disparity and motion	142
4.7 Disparity coding in parvo- and magnocellular channels	143
4.8 VEPs and binocular vision	144
4.8.1 Introduction	144
4.8.2 VEPs and binocular summation	144
4.8.3 VEPs and stereopsis	146

4.1 THE EYE AND VISUAL PATHWAYS

4.1.1 The eye

General structure of the eye

The cross-section of the human eye is illustrated in Figure 4.1. The human eyeball is approximately spherical with a diameter of about 24 mm. The cornea has a radius of curvature of about 8 mm, and its outer surface is the principal refractive element in the eye, accounting for about 80 per cent of the eye's total refraction. The pupil and associated iris muscles situated just in front of the lens act as an aperture stop to control the amount of light entering the eye. Changes in the size of the pupil also affect the

optical quality of the image. Thus, as the pupil enlarges, diffraction increases, spherical aberration decreases, and depth of focus decreases. For a given viewing distance and level of illumination, the pupil automatically adjusts in size to achieve the best compromise between these optical factors.

The lens has a diameter of about 9 mm and a thickness of about 4 mm. Its refractive index is about 1.4 at the centre and about 1.38 in the outer regions. The visual axis of the eye is the line joining the point of fixation and the centre of the fovea. The optic axis of the eye passes through the centres of the optical elements and intersects the retina about 1.5 mm on the nasal side of the fovea and about 0.5 mm above it. It thus makes an angle of about 5° to the visual

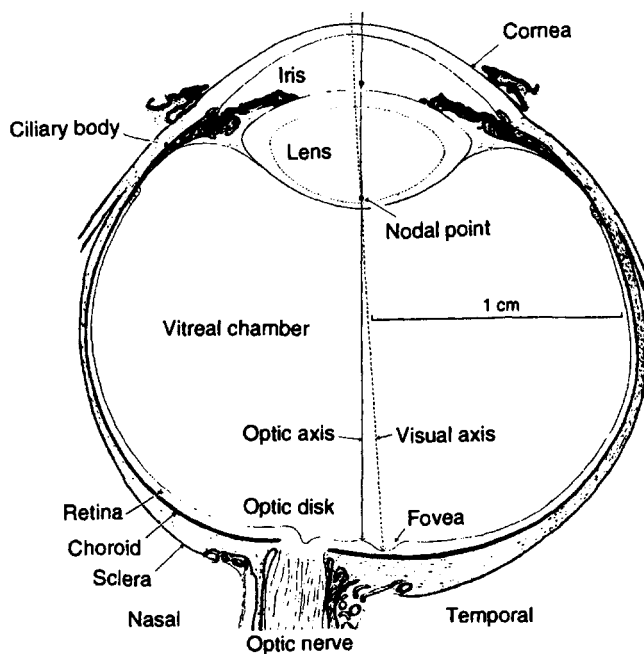


Figure 4.1. Horizontal section through the human eye.
(From figure 125 of *The vertebrate visual system*, by Polyak, 1957, published by University of Chicago Press.)

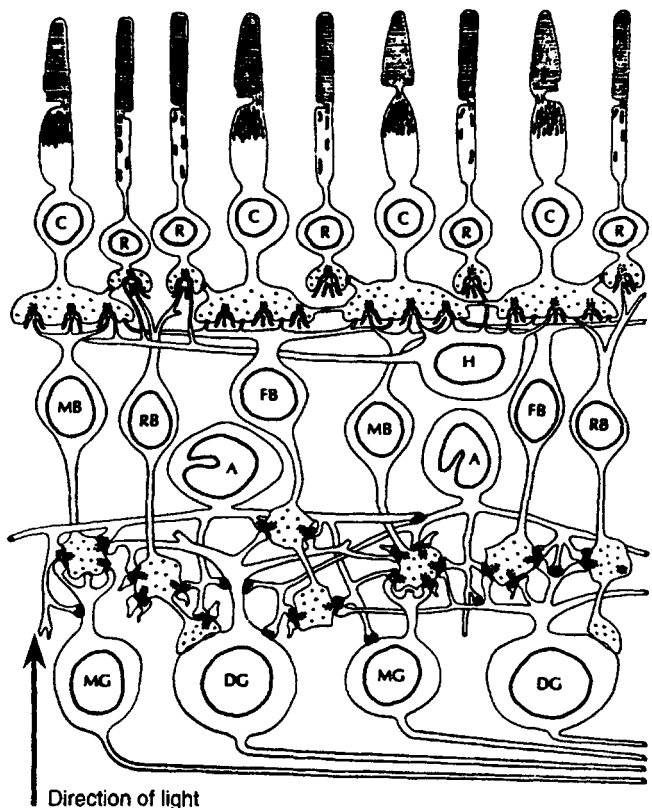


Figure 4.2. The general structure of the retina.
Rods and cones are signified by R and C. H signifies a horizontal cell in the outer plexiform layer and A signifies an amacrine cell in the inner plexiform layer. Cell bodies containing the letter B are various types of bipolar cells and those containing the letter G are various types of ganglion cells. (Adapted from Dowling and Boycott 1966.)

axis. This is known as the angle α . For details of the structure of the eye, see Polyak (1957), Davson, (1980), and Charman (1991). Section 15.1 deals with the development of the eye.

The retina

The structure of the retina is depicted in Figure 4.2. The detailed structure of the retina was first revealed by Ramón y Cajal using the Golgi staining method and described in a series of papers between 1888 and 1933 (see Polyak 1941). The retina is a multilayered membrane about 250 μm thick at the fovea and diminishing to about 100 μm in the periphery. The receptors are densely packed in the outer layer, furthest removed from the source of light. There are two main types of receptor—rods and cones. Rods have high sensitivity, an exclusively peripheral distribution, and broad spectral tuning. Cones have lower sensitivity, high concentration in the fovea, decreasing concentration in the peripheral retina, and three types of spectral tuning, peaking at around 450, 535, and 565 $\text{m}\mu$.

The shadows of the blood vessels of one's own retina become visible when one looks through an illuminated pinhole. As the pinhole is moved from side to side, the shadows undergo parallactic motion because they are some distance in front of the receptors. Müller (1854) measured the magnitude of this

parallactic motion and, by applying his results to retinal anatomy, deduced that light is absorbed in the outer segments of rods and cones.

Subsequent investigations have revealed that each receptor has an elongated outer segment, an inner segment, a cell body, and a synaptic terminal. The outer segment, about 50 μm long, consists of membrane folded into about 750 layers to form a stack of discs. About 10^8 molecules of photopigment are packed along the membrane so that light passing through the layers stands a good chance of being absorbed by one of the molecules. From time to time, discs are shed from the outer segment and absorbed by the pigment epithelium that lies between the retina and the choroidal layer of the eyeball (Young 1971).

The image plane of the eye's optical system is at the level of the inner segments but all the photopigments are in the outer segment. Light entering an inner segment of a receptor at the correct angle is

guided into and along the outer segment by internal reflection. The two segments therefore act as a waveguide. Their efficiency as waveguides is enhanced by the fact that the diameter of a receptor is similar to the wavelength of light. Most light enters the inner segment at the correct angle because the photoreceptors are aligned with the centre of the pupil which is the direction from which most light rays come. This alignment of the photoreceptors explains why we are more sensitive to light passing through the centre of the pupil than to light passing through its margin, an effect known as the **Stiles-Crawford effect**. This mechanism reduces the effects of light scatter and of aberrations in the light that passes through the margins of the eye's optical system (see Enoch and Tobey 1981).

Some alignment of receptors is present in the neonate and is presumably determined by the way receptors are packed together. However, the fine alignment must be controlled by an active process because it has been found to recover in local areas disturbed by retinal detachment (Campos et al. 1978). Furthermore, the magnitude of the Stiles-Crawford effect is reduced after an eye has been occluded for several days and subsequently returns to its normal value after the occluder is removed (Enoch et al. 1979).

The human retina has about 120 million rods and 6 million cones. The retinal magnification factor (RMF) is the linear distance on the retina corresponding to one degree of visual angle. The RMF in the human fovea is about 0.29 mm/deg (Williams 1988). The primate fovea is a centrally placed pit about 1.5 mm in diameter which contains a regular hexagonal mosaic of cones with a mean spacing of between 2 and 3 μm . Cone density in the human retina varies between 100,000 and 324,000 per mm^2 at the fovea and declines to about 6,000 per mm^2 at an eccentricity of 10° (Curcio et al. 1990). Rods are absent in the fovea and reach a peak density of about 160,000 per mm^2 at an eccentricity of about 20° (Osterberg 1935). In the fovea there is at least one ganglion cell for every cone so that, in this region, each cone can convey a distinct signal to the visual cortex whereas, in the peripheral retina, inputs from large groups of cones and rods converge. Thus, the capacity of the retina to sample the distribution of light over the image declines systematically with increasing eccentricity.

Image resolution

Like most optical systems, that of the eye suffers from diffraction, dispersion, and spherical aberration in addition to chromatic aberration. The net effect of these optical factors is that the image of a point of

light is spread over an area of at least seven receptors. The distribution of light in the image may also differ along different meridians because of the effects of astigmatism, and it may also be skewed by the effects of coma. The distribution of light in the image from a point source—the point-spread function defined in Section 3.4.1.—depends on the diameter of the pupil in a complex way (Campbell and Gubisch 1966). The wider the point-spread function the lower the ability of the eye to resolve a grating. However, a wider point-spread function may improve the detectability of changes in the spatial location of distinct images because more receptors are stimulated, which can provide an improved estimate of the mean position of the stimulus. With a pupil diameter of less than about 2 mm, most of the light dispersion is due to diffraction, and the optical system can be regarded as linear. The optical quality of the eye, like that of any linear optical system, is completely specified by its modulation transfer function (MTF). The MTF is obtained by measuring the contrast of the image of a fixed-contrast sinusoidal grating at each spatial frequency over the visible range of spatial frequencies. The contrast and spatial frequency of a sinusoidal grating are defined in Figure 9.1. The MTF of the optical system of an eye is the function that relates the proportional loss of contrast in the image to the spatial frequency of a grating. At spatial frequencies below about 5 c/deg, almost all the contrast in the stimulus is preserved in the image. At about 40 c/deg contrast is reduced about tenfold, and at above about 60 c/deg all contrast in the image is lost. The optical quality of the image is substantially constant out to an eccentricity of about 12°, beyond which it declines with increasing distance from the optic axis (Jennings and Charman 1981).

Aliasing

Two stimuli can be spatially resolved only if they excite two detectors at a discriminably higher level than they excite a detector in an intermediate location. Thus, a set of independent detectors arranged in a square lattice can resolve a periodic stimulus, such as a grating, only if the spatial period of the stimulus is at least twice the spacing of the detectors. This is the Nyquist limit and a stimulus that exceeds this limit is said to be undersampled. For a hexagonal lattice, like the cone mosaic, it is easy to prove that the Nyquist limit is $\sqrt{3}$ times the spacing of the detectors.

When the image of a grating finer than the Nyquist limit is projected on the retina, it forms an interference or moiré pattern with the receptor mosaic, as illustrated in Figure 4.3. Although the

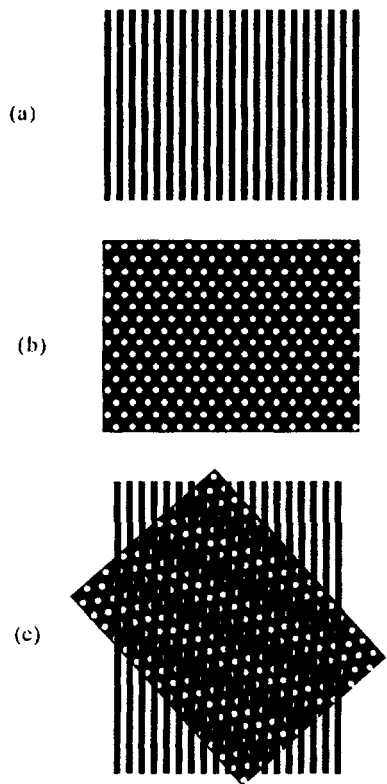


Figure 4.3. Aliasing.

A fine grating (a) projected onto the hexagonal retinal mosaic (b) produces an interference (moiré) pattern (c). The moiré pattern is most evident when the spatial frequency of the grating is slightly higher than that of the retinal mosaic. The pattern has a 60° periodicity because of the hexagonal packing of foveal receptors. (Reprinted with permission from Nature, Wässle and Boycott, Copyright, 1991, Macmillan Magazines Ltd.)

grating is not visible, the interference pattern is visible because the bars of the grating come into and out of phase with the receptors at a spatial frequency lower than that of the grating. If the spatial frequency of the receptor mosaic is f and that of the stimulus grating is $f + n$, then the interference pattern will have a spatial frequency of n . This process is known as **aliasing**. However, the effects of aliasing are not normally visible because the optics of the eye are not capable of forming images as fine as the Nyquist limit, at least not in the foveal region. Thus, the optics of the eye constitute an anti-aliasing filter.

There is a way to make the effects of aliasing visible. Two laser beams are converged on the retina to form a fine interference pattern. This pattern may be finer than the spacing of the retinal mosaic since it bypasses the optics of the eye. By comparing grating acuity for a normal grating with that for interference fringes, Campbell and Gubisch showed that visual performance in the fovea is limited by the eye's optics rather than by the density of receptors.

Because of the hexagonal packing of the receptors, the moiré pattern changes as the interference pattern is rotated through 60°. The period of the finest visible moiré pattern reveals that the mean spacing of receptors is about 0.5 arcmin, corresponding to a resolution limit of about 60 cycles/deg, a value that tallies with anatomical determinations of the spacing of foveal cones. Above the 60 c/deg limit, the interference pattern may be visible because of aliasing. The 60 c/deg resolution limit for an interference pattern is somewhat finer than the finest pattern that can be resolved using the eye's optics, which means that foveal performance is limited by the optical quality of the image rather than by the spacing of receptors (see also Williams 1988; Hirsch and Curcio 1989). Outside the fovea, the density of receptive fields seems to be the limiting factor in resolution.

Haig (1993) has suggested that, in addition to providing an anti-aliasing filter, the high density of receptors relative to the resolving power of the eye's optics compensates for the degradation of spatial sampling due to the presence of three types of wavelength-sensitive cones. However, his argument seems to be based on an overestimation of the resolving power of the retinal mosaic. The close correspondence between the resolving power of the fovea and the size of foveal cones implies that each cone provides an independent sampling of spatial information which is conveyed to the brain. This tallies with the fact that the ratio of ganglion cells to cones in the fovea is at least one-to-one.

An interference pattern bypasses the optics of the eye but is still subject to pre-neural factors such as quantal fluctuations in the stimulus, opacities of the ocular media, and the aperture, quantal efficiency, and density of receptors. Banks et al. (1987) compared the contrast sensitivity of the human observer with that of an ideal observer incorporating the pre-neural properties of the human visual system. They concluded that foveal performance is limited by pre-neural factors rather than by neural processing occurring beyond the receptor level.

The receptor potential

An electrode in the form of a glass capillary 0.1 μm in diameter filled with salt solution can be inserted into a retinal receptor, and the potential difference between this electrode and one outside the cell can be measured. In their unstimulated state, retinal receptors have a resting potential difference of about -40 millivolts across the cell membrane, due to an inflow of positive sodium and calcium ions through the membrane of the outer segment and an outflow through the membrane of the inner segment. When

light is absorbed in the outer segment, the pigment molecules isomerize (change their molecular shape). This initiates an amplifying cascade of chemical events within the cell that results in hydrolysis of guanocine monophosphate (GMP) molecules. This in turn closes the channels through which sodium and calcium ions enter the outer segment, resulting in a fall in the concentration of these ions within the cell and hyperpolarization of the cell membrane. The membrane of the inner segment contains a sodium-potassium ionic pump that modifies the voltage changes induced in the outer segment and initiates the release of a synaptic neurotransmitter (see Yau and Baylor 1989).

The degree of hyperpolarization of the cell membrane is proportional to the rate at which light quanta are absorbed by the photopigment. Within the linear range of the system this is proportional to the luminance of the light. One or two quanta of light are sufficient to cause a measurable change in the membrane potential. This represents an enormous degree of relatively noise-free amplification (Baylor et al. 1987). Thus, a **receptor potential** is a continuously graded signal, or analogue signal. Graded potentials also occur locally at synapses throughout the nervous system, where they are known as **postsynaptic potentials**.

Bipolar cells

The second main layer of the retina consists of bipolar cells. Each cone terminates in a flat synaptic pedicle. Dendritic fibres from bipolar cells contact the surface of the pedicle in flat synaptic boutons. In addition, the pedicle surface is pitted with several synaptic invaginations, each containing a single dendritic fibre from a bipolar cell and two fibres from horizontal cells. Each rod terminates in a synaptic pedicle with a single invagination containing a dendritic fibre from a bipolar cell and two from horizontal cells.

The boundary region between the receptors and the bipolar cells is known as the **outer plexiform layer**. Rod bipolars are fed by up to 45 rods. Some cone bipolars, known as midget bipolars, are fed by only one cone whereas diffuse cone bipolars are fed by several neighbouring cones. In the dark, a neurotransmitter is continuously released from receptors into bipolar cells. The neurotransmitter is L-glutamate or a similar substance (Dowling 1987). When a receptor absorbs light the rate of neurotransmitter release is reduced. This causes **on bipolar cells**, which make invaginating synapses with receptors, to become hyperpolarized and **off bipolar cells**, which make flat synaptic connections, to become depolarized.

Bipolar cells, like receptors, respond in a graded fashion to changes in stimulus strength. **Horizontal cells** run laterally in the outer plexiform layer over a distance of about 1 millimetre. They, also, respond in a graded fashion. Each horizontal cell receives inputs from all the cones within its dendritic field and also makes synaptic contact with several bipolar cells. Signals in horizontal cells are also believed to feed back to cones in the form of a delayed depolarization, but the extent and significance of this process has been a subject of debate (Burkhardt 1993).

Ganglion cells

Ganglion cells form the third and final main layer of the retina. The region between bipolar and ganglion cells is known as the **inner plexiform layer**. Each ganglion cell forms synaptic junctions with one or more bipolar cells in the inner plexiform layer. All-or-none **action potentials** are first formed at the level of the ganglion cells. An action potential is all-or-none because it occurs only at a fixed amplitude for that nerve cell. The implications of all-or-none coding are discussed in Section 3.2.1. Whereas a receptor potential is local, an action potential is a brief event that travels along an axon, sometimes for considerable distances. The speed of propagation of an action potential is proportional to axon diameter, which varies between 0.1 and 20 μm in vertebrates. In the largest axons, conduction speed reaches 120 m/s. Within the central retina, the ratio of receptors to ganglion cells is less than one-to-one, but becomes many-to-one in the periphery. **Amacrine cells** form lateral inhibitory connections with bipolar cells and ganglion cells within the inner plexiform layer, with dendritic fields of up to 1 mm in diameter. Amacrine cells, like ganglion cells, generate all-or-none action potentials. Thirty types of amacrine cells have been described, but the functional significance of the different types is obscure (see Rowe 1991).

4.1.2 Ganglion-cell receptive fields

The set of receptors that directly or indirectly affects the firing of a given ganglion cell is the **receptive field** of that ganglion cell, a term introduced by Hartline (1938). Kuffler (1953) showed that ganglion-cell receptive fields in the cat retina are circular, with a concentric organization of excitatory and inhibitory regions. Receptive fields with a central excitatory region and inhibitory surround are known as **on-centre receptive fields** and cause the ganglion cell to fire preferentially to the onset of a stimulus in the receptive-field centre. Those with an inhibitory central region and excitatory surround are known as

off-centre receptive fields and cause the ganglion cell to fire to stimulus offset. Ganglion cells have overlapping receptive fields. Those with overlapping receptive fields that are either both on-centre or both off-centre tend to fire at the same time, while those with opposite-sign centres tend not to fire at the same time (Mastronarde 1983). On-centre and off-centre receptive fields feed into pathways that remain distinct as far as the visual cortex (Schiller 1992). The centre of an on-centre receptive field receives direct signals from receptors through on-bipolar cells and indirect signals from horizontal cells that originate in off-bipolar cells. The centre of an off-centre receptive field receives direct signals from off-bipolar cells and indirect signals from horizontal cells that originate in on-bipolar cells. Thus, bipolar cells act on ganglion cells in a "push-pull" fashion and increase the dynamic range of these cells to changes in luminance (Sterling 1990). The organization of receptive fields into excitatory and inhibitory regions also ensures that the strongest signals come from a local region of changing luminance rather than from homogeneous areas of illumination. The most vigorous signals sent to the brain therefore arise from regions where luminance changes spatially or over time. These are the signals that contain useful information. The on-channel can be selectively blocked by applying aminophosphonobutyrate (APB) to an animal's retina. This impairs the animal's ability to detect light increments and reduces contrast sensitivity. However, responses to shape, colour, and movement are only mildly impaired (Schiller et al. 1986).

X and Y cells

In the cat, ganglion cells fall into three classes—X, Y, and W—each of which includes on and off types (Enroth-Cugell and Robson 1966). Type X cells have small receptive fields that are concentrated in the central retina, clearly organized into excitatory and inhibitory regions, and show linear summation of luminance distributions. Type Y cells are more widely distributed over the retina, have larger receptive fields that are not segregated into clearly defined regions, and show nonlinear summation of luminance distributions.

Achromatic and colour-opponent cells

In primates, ganglion cells are broadly classified into **colour-opponent cells** and **achromatic cells** rather than X and Y cells. Primates also have W cells.

Colour-opponent cells project to the **parvocellular laminae** of the LGN. They have small receptive fields, hence the prefix "parvo-", which is the Latin word for small. They constitute about 90 per

cent of the total number of ganglion cells. Lennie et al. (1991) suggested that, at least for eccentricities up to 10°, each colour opponent ganglion cell has a receptive field centre consisting of a single cone, sensitive to short, medium, or long wavelengths, that feeds directly through a bipolar cell to the ganglion cell. The receptive field surround contains all the cones in the immediate neighbourhood, which feed into bipolar cells through horizontal cells. Thus, the receptive field surround consists of a random mix of cone types. If this is how the receptive fields are organized, it would provide the cell with colour opponency.

Each cone probably drives at least two bipolar cells and two ganglion cells, one on-centre and one off-centre (Kolb 1970). A colour-opponent ganglion cell fires at its baseline rate when the two regions are stimulated equally. The firing rate increases above baseline when the excitatory region is stimulated most and decreases below the baseline rate when the inhibitory region is stimulated most. For example, a cell with a red-excitatory centre and green inhibitory surround produces an increased response to a stimulus within the long-wavelength end of the spectrum and a decreased response to a stimulus in the medium-wavelength region of the spectrum. Note that single opponent cells do not respond to chromatic changes over space.

Colour-opponent ganglion cells have small receptive fields, a high luminance threshold, produce a sustained response to continued stimulation, and conduct nerve impulses at medium velocity. Their small receptive fields enhance their spatial resolution, but their sustained characteristic reduces their temporal resolution. Thus, parvocellular cells in the monkey can resolve gratings up to 40 c/deg but are most sensitive to temporal frequencies of only 10 Hz (Derrington and Lennie 1984).

Achromatic cells have large receptive fields and project to the **magnocellular laminae** of the lateral geniculate nucleus. The prefix "magnō-" is derived from the Latin word for large. Achromatic cells have receptive field centres and receptive field surrounds made up of a variety of cone types or rods. They are thus broadly tuned to wavelength and do not show colour opponency. They are therefore referred to as **broad-band-cells**. However, for some of them, the receptive field centre and surround are not in spectral balance and colour opponency is revealed under certain conditions of stimulation (Shapley 1991). Some have excitatory centres and inhibitory surrounds (on-centre cells) and others have inhibitory centres and excitatory surrounds (off-centre cells). Their large receptive fields enhance their light-collecting efficiency, which renders them sensitive at

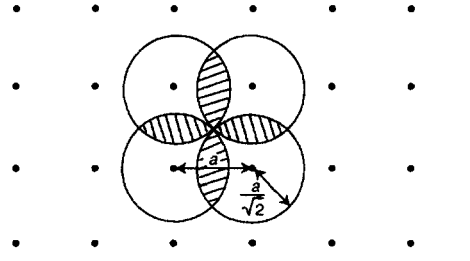
lower luminance levels. Cells with large receptive fields also have higher sensitivity because they have a higher signal-to-noise ratio. Noise is due to fluctuations in photon distribution and to spontaneous events at the photopigment and synaptic levels. When N receptors feed into one receptive field, the total noise is proportional to \sqrt{N} .

Broadband-cells have large-diameter axons and, since conduction velocity is proportional to axon diameter, they conduct nerve impulses rapidly. They show a transient rather than a sustained response to continued stimulation. Their large receptive fields reduce their spatial resolution but their transient characteristic improves their temporal resolution, that is, it makes them able to respond to higher rates of flicker than the sustained colour-opponent cells. Thus, in the monkey, broadband-cells can resolve gratings up to a spatial frequency of only about 10 c/deg but are most sensitive to temporal frequencies of 20 Hz (Derrington and Lennie 1984). Few if any broadband-cells projecting to the magnocellular laminae of the LGN are found in the fovea.

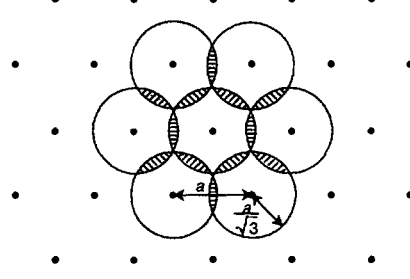
Ganglion cells are classified in several other ways according to the organization of their receptive fields, but a detailed discussion of this topic goes beyond the scope of this book. For more details on the structure and function of the retina, see Polyak (1941), Dowling (1987), and Wässle and Boycott (1991).

For each cone in the central fovea of the monkey retina there are three to four ganglion cells, decreasing to one ganglion cell per cone at an eccentricity of about 15°. In the peripheral retina there are many more cones than ganglion cells (Wässle et al. 1990). A single receptor typically contributes to the centre and surround of several ganglion-cell receptive fields. In other words, neighbouring receptive fields overlap. However, there is some evidence that the receptive fields of a given type of ganglion cell pave the retina efficiently without too much overlap or too many gaps.

For receptive field centres arranged in a square lattice and separated by distance a , as in Figure 4.4a, the minimum radius of the receptive fields required for complete coverage is $\frac{a}{\sqrt{2}}$. For receptive fields arranged in an hexagonal lattice, as in Figure 4.4b, the minimum radius for complete coverage is $\frac{a}{\sqrt{3}}$. Wässle et al. (1981) found that for a given type of ganglion cell the ratio of receptive field spacing to receptive field diameter was close to that predicted from the most efficient coverage for a hexagonal lattice. Thus, at every point the retinal image is efficiently sampled for the different visual features that each of the different types of receptive field detects.



(a) For receptive fields arranged in a square lattice with centres distance a apart, the minimum radius required for complete coverage is $\frac{a}{\sqrt{2}}$.



(b) For receptive fields arranged in an hexagonal lattice, the minimum radius is $\frac{a}{\sqrt{3}}$.

Figure 4.4. Coverage of ganglion-cell receptive fields.
(Adapted from Wässle et al. 1981.)

4.1.3 Lateral geniculate nucleus

In Section 2.2 we described how the axons of ganglion cells from each nasal hemiretina decussate in the chiasma to join corresponding axons from the contralateral temporal hemiretina. About 90 per cent of the axons then go to a part of the thalamus known as the lateral geniculate nucleus (LGN) where they segregate into distinct layers, or *laminae*. In the laminae they synapse with *relay cells*, the axons of which go to the primary visual cortex. The other 10 per cent of ganglion cell axons project to other subcortical structures (Schein and Monasterio 1987).

Methods for tracing connections of single cells in the nervous system fall into two classes – anatomical and physiological. In anatomical methods a chemical or radioactive tracer is injected at one site in the living animal and its subsequent distribution is detected at more peripheral sites (retrograde tracing) or more central sites (orthograde tracing) in histological preparations. In physiological methods the responses of a particular cell are detected by an electrode inserted into the living animal, while an electrical signal is applied at some other location or a natural stimulus is applied to the sense organ. While most electrophysiological experiments have been conducted on anaesthetized and paralyzed animals; it is also possible to record responses of single cells in the alert animal.

Recently, chemical and electrophysiological methods have been combined. A voltage-sensitive dye is applied to the exposed surface of the cerebral cortex in the living animal. A visual or electrical stimulus is administered to a given location and the changes in the dye induced by the neural activity are recorded optically. In this way the spatial and temporal distribution of activity is seen over a wide area (Orbach and Van Essen 1993).

The LGN of the cat contains four principal laminae—A, A1, C, and C1—and two others known as C2 and C3. Cells in laminae A and C receive their inputs from the contralateral eye and those in laminae A1 and C1 from the ipsilateral eye. The two A laminae contain similar types of cells but the cells in lamina C originating in the nasal hemiretina are considerably larger than those in layer C1 originating in the temporal hemiretina. The axons of most X and Y cells terminate in laminae A and A1 with about 62 per cent of all Y cells terminating in lamina A1. The C lamina receives a few X and Y cells but mainly W cells. W cells are a heterogeneous group of slowly conducting ganglion cells with large receptive fields having poorly defined excitatory and inhibitory regions and poor spatial and temporal resolution. In addition, the cat's LGN has two associated nuclei known as the medial interlaminar nucleus and the geniculate wing (Kaas et al. 1972).

Retinogeniculate pathways in the monkey have been investigated anatomically by tracing the retrograde transport of horseradish peroxidase from specific layers of the LGN to specific types of ganglion cell in the retina (Perry et al. 1984) and electrophysiologically by recording from cells in the LGN (Kaplan and Shapley 1986).

The axons of colour-opponent ganglion cells terminate in the four dorsal laminae in the primate LGN, where they synapse with relay cells (Figure 4.5). They are known as the parvocellular laminae, because the cells within them are small. Inputs from the ipsilateral eye go to laminae 3 and 5 and those from the contralateral eye go to laminae 4 and 6. The whole visual channel, including the colour-opponent cells, the relay cells in the LGN, and the cortical pathways to which they subsequently lead, is known as the **parvocellular system**.

The axons of achromatic ganglion cells terminate in the two ventral laminae of the LGN, known as the magnocellular laminae, because the cells within them are large. Inputs from the ipsilateral eye go to lamina 2 and those from the contralateral eye go to lamina 1, as shown in Figure 4.5. The achromatic cells, the magnocellular laminae, and the subsequent pathways into which they feed are known as the **magnocellular system**.

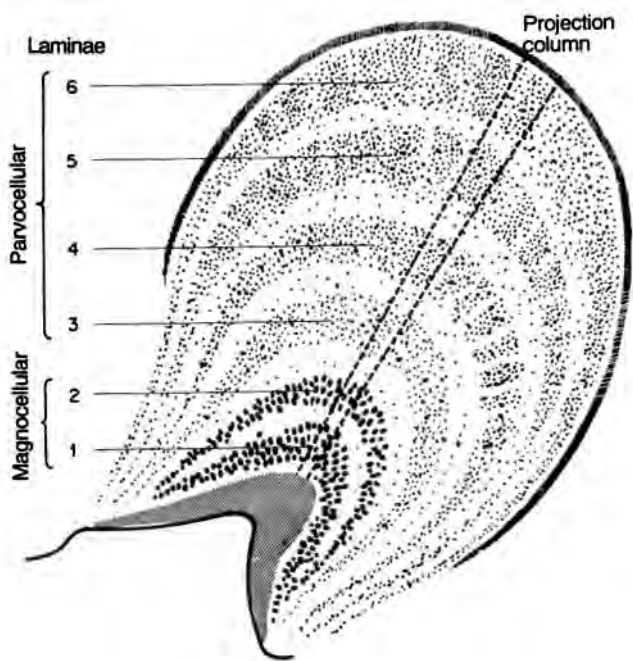


Figure 4.5. The lateral geniculate nucleus.

Illustration of lamination and projection columns in a coronal section of the lateral geniculate nucleus of a monkey. A projection column is defined as containing 90 per cent of the cells with a single visual direction. (From Szentágothai 1973.)

Hendry and Yoshioka (1994) recently identified a third population of geniculocortical neurones in the LGN of the monkey. They seem to be W-type cells occupying interlaminar regions and projecting to cytochrome-oxidase blobs (see Section 4.2.5) in layers 2 and 3 of the visual cortex.

The four parvocellular and two magnocellular laminae occur in part of the LGN devoted to the central retina. In parts devoted to the peripheral binocular visual field there are only four laminae, two parvocellular laminae and two magnocellular laminae. The blind spot is represented in the transition zone between the six-layered and four-layered regions (Lee and Malpeli 1994). The region devoted to the monocular temporal crescent of the visual field receive only crossed inputs and therefore contain only two laminae, one parvocellular and one magnocellular (Kaas et al. 1972). The inputs to each lamina in the LGN are projected in systematic retinotopic order. Inputs from corresponding areas of the two eyes lie in **projection columns** running at right angles to the laminae, as shown in Figure 4.5.

The receptive-field and response properties of each relay cell are fundamentally the same as those of the ganglion cell with which it is connected. Furthermore, there is the same number of relay cells as ganglion cells although there may be some

divergence and convergence of optic nerve fibres onto LGN relay cells (Schein and Monasterio 1987). Although neurones in the LGN receive a direct excitatory input from only one eye, there is evidence of extensive inhibitory and excitatory interactions in the LGN and of inputs from places other than the retina (Marrocco and McClurkin 1979; Kato et al. 1981; Ahlsén et al. 1985). It seems that all the interneurones in the LGN contain the inhibitory neurotransmitter gamma-aminobutyric acid (GABA) and all GABAergic cells in the LGN are interneurones. According to one estimate, only about 20 per cent of synaptic junctions found on geniculate relay neurones of the cat originate in the retina. About 50 per cent derive from the visual cortex and the other 30 per cent are inhibitory (GABAergic) inputs from interneurones or inputs from the perigeniculate nucleus, the brainstem reticular formation, the superior colliculus, and the locus coeruleus (Sherman and Koch 1986). According to Montero (1992) only 12 per cent of synaptic junctions on relay cells in the cat LGN are from the retina but 25 per cent of synapses on interneurones are of retinal origin, with 37 per cent of cortical origin. Many of the inputs to the LGN from sources other than the eye terminate in the interlaminar spaces, where they synapse with dendritic extensions from cells in the main laminae (see Casagrade and Brusco-Bechtold 1988).

In the alert monkey, rapid eye movements, blinks, and auditory and somaesthetic stimuli produce nonspecific responses in the LGN, even in the dark (Hotta and Kameda 1963; Feldman and Cohen 1968). It has been suggested that these non-retinal inputs serve attentional processes (Crick 1984; Sherman and Koch 1986) but their nonspecificity suggests a general arousal function rather than attentional gating of specific locations or stimuli. Electrical stimulation of the mesencephalic tegmentum, an arousal mechanism in the brain stem, increases the response of relay cells in the LGN (Livingstone and Hubel 1981). This increase is particularly evident for stimuli in the centres of the receptive fields of relay cells (Hartveit et al. 1993). The neuroanatomy of the LGN is reviewed in Garey et al. (1991).

Binocular responses in the LGN

In the cat, the response of many cells in the LGN is inhibited by stimulation of the eye from which they do not receive a direct excitatory input (Suzuki and Kato 1966; Xue et al. 1987). The direct excitatory and indirect inhibitory inputs arise from corresponding regions in the two eyes (Sanderson et al. 1969; Singer 1970). The inhibitory influences are postsynaptic and could be mediated by either intrageniculate connections or corticofugal influences from the visual

cortex. There is some dispute about the role of cortical influences. Some investigators have found that binocular interactions in the LGN of the cat require an intact visual cortex. Reports that interocular influences are greatest when the stimuli presented to the two eyes differ in position, orientation, contrast, and movement prompted the suggestions that cortical influences facilitate transmission of signals from stimuli lying on the horopter, and are involved in binocular fusion and rivalry (see Section 8.3) (Schmielau and Singer 1977; Varela and Singer 1987). Others have reported that binocular interactions in the LGN do not depend on corticofugal influences (Tumosa et al. 1989; Tong et al. 1992). Moore et al. (1992) found that responses of LGN cells to stimulation of the dominant eye of the cat are not much affected by changes in the orientation or direction of motion of stimuli presented to the non-dominant eye but are affected by changes in the spatial frequency of those stimuli. They suggested that these processes balance the responses to small interocular differences in stimulus contrast by adapting the relative contrast gains of inputs from the two eyes (see Section 5.6.4). Perhaps binocular rivalry and gain control are served by different processes in the LGN. McClurkin et al. (1993) suggested that cortical feedback to the LGN modulates the number and temporal waveform of spikes in parvocellular neurones so as to enhance differences in response to distinct stimuli.

There has been conflicting evidence on binocular responses in the primate LGN. Rodieck and Dreher (1979) reported some suppression of the response of LGN cells of the monkey to stimulation of the dominant eye by stimulation of the nondominant eye, but only in the magnocellular laminae. Marrocco and McClurkin (1979) found that about 13 per cent of cells in both the parvo- and magnocellular laminae of the LGN of the monkey responded only to binocular stimulation. These studies were conducted on anaesthetized and paralyzed monkeys. Schroeder et al. (1990) used multiple electrodes to record responses of cells in the LGN of the alert monkey to light flashes. They found four basic types of binocular interaction in both the parvo- and magnocellular laminae. For one type, stimulation of the nondominant eye reduced the response below the spontaneous level. For a second type, stimulation of the nondominant eye increased the response above the spontaneous level. For a third type, the response was less vigorous to binocular stimulation than to stimulation of only the dominant eye. For a fourth type, the response was more vigorous to binocular than to monocular stimulation. Since the researchers used multiple electrodes, they could not estimate the

proportion of cells showing these different responses. The latency of interactions was too short to involve corticofugal influences. However, the later response components could have been due to cortical influences. It is unfortunate that only featureless flashes were used, since binocular interactions revealed by psychophysical procedures depend on the presence of contours (see Section 8.3.2).

4.2 THE VISUAL CORTEX

4.2.1 Visual-cortical projections

Each optic radiation projects to the ipsilateral primary visual cortex in the occipital lobe at the caudal pole of the cerebral cortex. The primary visual cortex of subprimates is also known as Brodmann's **area 17**. In primates it is usually referred to as **V1**. It is also known as the **striate cortex** because of the prominent stripe of Gennari it contains. The primary visual cortex in each hemisphere is mainly on the banks of the calcarine sulcus, a deep horizontal fissure on the medial surface of the occipital lobe.

The magnification factor

The retinotopic order of incoming axons is topographically, but not metrically preserved in the primary visual cortex, with the central parts of the retina represented near the caudal pole of the occipital lobe and the monocular crescents represented more rostrally. The area of cortex devoted to the fovea is disproportionately greater than that devoted to the peripheral retina. The distance apart in millimetres of two points along the surface of the visual cortex that corresponds to one degree of visual angle in the visual field is known as the **magnification factor (M)** (Daniel and Whitteridge 1961). In primates, M decreases with increasing eccentricity from the centre of the visual field, but is similar for corresponding eccentricities on all meridians of the visual field. Cowey and Rolls (1974) estimated M for the human visual system using data from a study by Brindley and Lewin (1968) on the distribution of impressions of light (phosphenes) evoked by electrodes implanted at various locations in the visual cortex of a human subject. At an eccentricity of 2°, M was approximately 4 mm/deg and declined monotonically to 0.5 mm/deg at an eccentricity of 25°. A more recent estimate puts M at 11.5 mm/deg for the human fovea (Drasdo 1977). For all positions in the visual field, Hubel and Wiesel (1974b) found that a microelectrode must move between 2 and 3 mm over the surface of the monkey visual cortex before an entirely new region of the visual field is represented. It is reasonable to conclude from this that the

same number of millimetres of visual cortex is devoted to each ganglion-cell receptive field. One estimate is that 0.88 mm of human visual cortex is devoted to one receptive field (Ransom-Hogg and Spillmann 1980). It follows that the amount of cortex devoted to each degree of visual field is directly related to visual acuity and inversely related to the mean size of ganglion-cell receptive fields (Rolls and Cowey 1970; Rovamo and Virsu 1979).

These facts are briefly summarized by saying that ganglion-cell receptive fields, and hence areas of the retina that can just spatially resolve two stimuli, are represented by equal areas in the visual cortex. Because these spatial units are smaller and therefore more numerous in the fovea than in the periphery of the retina, the fovea claims proportionately more of the cortical surface (its magnification factor is greater) than does the retinal periphery. When allowance is made for the decrease in magnification factor with increasing eccentricity, visual functions such as vernier acuity are performed about as well at all eccentricities (Levi et al. 1985). Thus, visual hyperacuity depends on the number of processing units in the visual cortex that are devoted to the task irrespective of retinal location.

There has been some dispute about whether the variation in the cortical magnification factor arises simply from the differential density of ganglion cells over the retina or whether each ganglion cell from the fovea feeds into more cortical cells than each ganglion cell from the peripheral retina. Wässle et al. (1990) counted the cones and ganglion cells at different eccentricities in the eye of the monkey and concluded that the 1000-to-1 change in ganglion cell density with increasing eccentricity could account for the change in the magnification factor. On average, there are about three ganglion cells for each foveal cone. Azzopardi and Cowey (1993) came to the opposite conclusion. Using a retrograde tracer to determine directly the number of ganglion cells projecting to measured areas of the striate cortex of the macaque monkey, they found that foveal cones were allocated 3.3 times more cortical tissue than peripheral cones in one animal and 5.9 times more in a second animal.

It has also been claimed that for the magnocellular system the number of afferents per unit cortical area increases steeply with increasing eccentricity. Thus, each magnocellular axon from more central retinal regions has many more cortical cells devoted to it than each axon from the periphery (Schein and Monasterio 1987). There is a constant number of magnocellular afferents per point image, defined as the area of cortex activated by a stimulus at a point in space (equivalent to the number of receptive-field

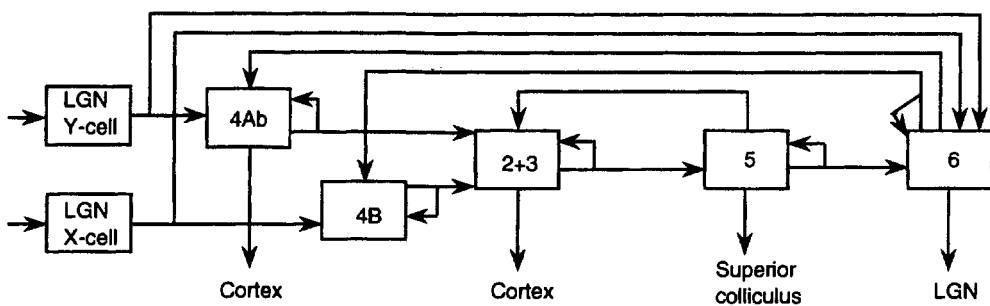


Figure 4.6. Intracortical connections of the cat's visual cortex.

The numbers refer to layers of the visual cortex. (Reprinted with permission from Gilbert and Wiesel, 1985, Vision Research, Pergamon Press.)

centres of ganglion cells that overlap a given point on the retina).

Topology of cortical mapping

The mapping of the retina onto the cortex can be described as the conformal logarithmic function,

$$\omega = \log(z + a)$$

where z is a complex number denoting the position of a point on the retina, ω is a complex number representing the position of the stimulus on the cortex, and a is a constant. A function is conformal if its first derivative (in this case the magnification factor) is isotropic (independent of orientation) and if the sizes of local angles are preserved.

Schwartz (1980) illustrated how, in a logarithmic mapping, the cortical images of squares of different sizes are transformed into images of the same size and shape, but in different locations. In a similar way, retinal images that are rotated with respect to each other are transformed into images differing in spatial phase. The recognition of size- and orientation-invariant features in the image formed by such a system reduces to the computationally simpler process of deriving translation-invariant properties. Schwartz argued that the logarithmic retinocortical mapping is a part of a process for extracting size- and orientation-invariant properties of visual objects.

One problem with this theory is that retinal images differing in position are transformed into images differing in size, and this complicates the problem of deriving position-invariant features. Schwartz's model of shape recognition is essentially a template-matching model and is adequate for the extraction of only very simple invariant features in a highly structured input. Furthermore, although this model may be computationally sound, it is not clear how it applies to the visual cortex. The geometrical layout of Schwartz's cortical "image" is not represented in the activity of cortical cells; thus, the

geometry of the image on the cortical surface cannot enter into spatial descriptions that the visual system constructs. Cortical cells code the local sign of their origin on the retina not their local sign in the cortex.

The form that retinotopic mapping takes has to do with devoting equal computational space in the cortex to equally discriminable regions of oculocentric space and has nothing to do with producing an image on the surface of the cortex that is then processed as such. The nervous system knows nothing about the spatial distribution of cells and synapses, only about patterns of connections. In contrast, the function of retinotopic mapping probably has to do with bringing into juxtaposition those cells that process similar features within a local region of oculocentric space, so that local neural processes, such as facilitation and inhibition, can be achieved economically. We will see in what follows that cells responsive to particular stimulus features are organized in distinct slabs of cortical tissue and that lateral interactions within the visual cortex are confined to fairly local regions.

4.2.2 Structure of primary visual cortex

Cortical layers

The mammalian visual cortex is a convoluted sheet of neural tissue about 2 mm thick consisting of six main layers designated layers 1 to 6, with layer 1 at the outer surface and layer 6 bordering the inner white matter. The white matter is made up of bundles of axons that project to and from other cortical regions and subcortical nuclei. Combined physiological and anatomical investigations in the monkey have revealed that inputs from the magnocellular laminae of the LGN terminate in spiny stellate cells in the upper half of layer 4C, known as layer 4C α , and those from the parvocellular laminae terminate in the lower half of layer 4C, known as layer 4C β , and in layer 4A (Hubel and Wiesel 1977; Tootell et al. 1988a). The predominant projection from cells in layer 4C α is to layer 4B in the same 1-mm-wide

vertical column of tissue, and then to cells in layers 2 and 3 in the same column and also in neighbouring columns (Katz et al. 1989). Cells in layer 4C β project to layers 4A and 3. Cells in layer 4C α also project sparsely to layer 5 and those in layers 4C α and 4C β project sparsely to layer 6. Cells in layers 2 and 3 project to cells in layers 5 and 6, which in turn project back into layer 4 (Gilbert and Wiesel 1979; Fitzpatrick et al. 1985). These relationships for the cat's visual cortex are illustrated in Figure 4.6. Layer 4B of the primary visual cortex contains a dense horizontal plexus of myelinated axons.

Types of cortical cell

There are two main histological classes of cell in the visual cortex: **circular stellate cells**, most of which radiate dendrites in all directions, and **pyramidal cells** that have triangular cell bodies with a single long apical dendrite and several shorter basal dendrites (see Figure 4.7). Figure 4.7c after page 310 is a stereogram of a pyramidal cell prepared from one of Ramón y Cajal's slides. Pyramidal cells form excitatory (glutaminergic) synapses. There are two types of stellate cell, spiny and smooth, so called because of the presence or absence of spines on their dendrites. All inputs to the visual cortex impinge on spiny stellate cells in layer 4. The spiny stellate cells project horizontally within layer 4, but their dendrites remain mainly within the same local column of cells (ocular-dominance column). Smooth stellate cells occur in other layers and are thought to be inhibitory (GABAergic) interneurons. Cells of the neocortex differ with respect to the types and distributions of ion channels on their somata and dendrites, which determine how the cells transform inputs into a spike-train output. Connors and Gutnick (1990) have distinguished "regular spiking" cortical neurones which are the type usually recorded from, "fast spiking neurones", and "bursting" neurones which generate a stereotyped pattern of neural spikes.

Collateral connections

Collaterals from the axons of pyramidal cells project horizontally for up to 8 mm within layers 2, 3, and 5. This represents several receptive field diameters. These horizontal projections are typically longer along one axis and produce spaced clusters of predominantly excitatory synapses (Rockland and Lund 1982; Gilbert and Wiesel 1985). Radioactive labelling has revealed that horizontal dendrites link cells with a similar preference for the orientation of the stimulus (Gilbert and Wiesel 1989; Hirsch and Gilbert 1991). Ts'o et al. (1986) showed this same type of linkage in the visual cortex of the cat as revealed in

patterns of correlated firing between cortical cells with similar orientation tuning that were within a few millimetres of each other. Grinvald et al. (1994) applied a voltage-sensitive dye to the visual cortex of the monkey and observed the real-time spread of activity evoked by a locally applied visual stimulus. Activity spread from its initial locus at a velocity of 100 to 250 $\mu\text{m}/\text{s}$ to cover an area with a radial space constant of 1.5 mm along ocular dominance columns and 3 mm orthogonal to the columns.

Cortical cells linked by horizontal fibres could serve to build large receptive field units that respond to lines in a particular orientation, as discussed in Section 3.2.5 (Mitchison and Crick 1982). For this purpose, the linkup should be between cells tuned to collinear stimuli rather than between cells with similar orientation preference but for which the preferred stimuli are orthogonal. Nelson and Frost (1985) revealed a highly specific form of facilitation in the cat visual cortex between neurones with aligned orientation tuning functions. Polat and Sagi (1994) have produced psychophysical evidence that collinear stimuli show mutual facilitation to a greater degree than stimuli with similar orientation but which are not collinear.

Lateral connections could also serve to modify the response of cells according to the nature of surrounding stimuli (Gilbert et al. 1991). There is considerable psychophysical evidence that visual acuity and discrimination are degraded when a test stimulus is flanked by other stimuli (see Section 9.3.5). The processes responsible must be cortical since the effects are present when the test and flanking stimuli are presented to different eyes (Westheimer and Hauske 1975). Furthermore, stimulus interactions are, like interactions between cortical cells, affected by how similar in shape and size the test stimulus is to the flanking stimuli (Kooi et al. 1994).

These pathways could also be involved in long-term stimulus-dependent changes in cortical responses. Long-term changes in synaptic conductivity along these lateral pathways in the cat's visual cortex have been induced by pairing synaptic responses with conditioning shocks of depolarizing current (Hirsch and Gilbert 1993).

Matsubara et al. (1985) found lateral interconnections in area 18 of the cat between cortical cells with orthogonal orientation preferences. The connections spanned only 2 mm and were inhibitory (GABAergic). Such connections may serve to increase contrast between neighbouring lines with different orientations. In the visual cortex of the monkey, Krüger and Aiple (1989) found mainly excitatory interconnections between cells up to 0.4 mm apart with orthogonal orientation tuning. There is a body

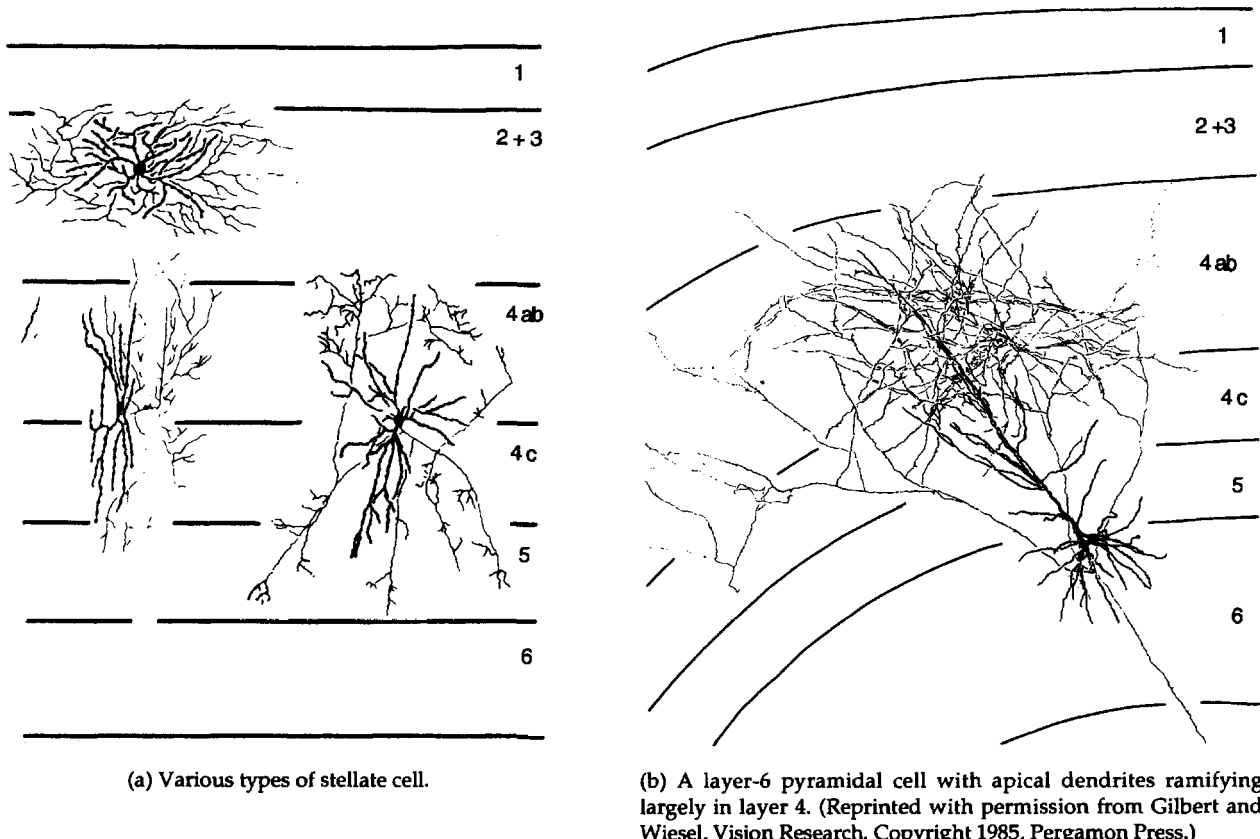


Figure 4.7. Classes of cell in the mammalian visual cortex.

of psychophysical evidence that neighbouring stimuli show mutual inhibition whereas stimuli further apart show mutual facilitation (see Polat and Sagi 1994).

Buhl et al. (1994) recently described three types of local inhibitory interneurones in the hippocampus of the rat. "Basket cells" synapse on the somata of hundreds of principal cells and cause rapid hyperpolarization followed by rebound. This type of cell could cause synchronous firing of large cell populations. "Axo-axonic cells" synapse only on the initial segment of the axon of the principal cells. This type seem well suited to control the discharge of principal cells. "Bistratified" cells synapse with the base and apical dendrites of principal cells and have properties like those of Hebbian synapses. There is thus a division of labour between different cell types in controlling the activity of cortical cells. Whether similar types of cell exist in the visual cortex has yet to be revealed. All outputs leave the visual cortex along pyramidal-cell axons. Those from layers 2 and 3 project to other cortical areas and those from layers 5 and 6 project to subcortical regions, as described later.

Receptive fields of cortical cells

A neurone within the visual cortex responds, or modifies an existing response, when an appropriate stimulus falls within a specific retinal area. That area is defined as the **receptive field of the cortical cell**, and its position is specified by the location of its centre. Receptive field centres are represented retinotopically within each layer of area 17, although this arrangement is perturbed by local random scattering of the same order of magnitude as the size of the receptive fields at each location (Hubel and Wiesel 1977). The response of a cortical cell can be modified by stimuli that fall well outside the receptive field as defined by simple stimuli (Hammond and McKay 1981; Nelson and Frost 1985).

Each spiny stellate cell in layers 4A and 4C receives a direct input from only one eye. These cells have circular-symmetric receptive fields resembling those of the parvocellular or magnocellular LGN cells that feed into them (Blasdel and Fitzpatrick 1984). Thus, they lack orientation specificity; that is, their response does depend on the orientation of the stimulus. Most of the other cells in the primary visual cortex have elongated receptive fields. They fall

into two classes, simple and complex, according to the organization of their receptive fields.

Simple cells have an excitatory on-centre and two flanking inhibitory off-zones, an off-centre with flanking on-zones, or an on-zone flanked by a single off-zone, as depicted in Figure 4.8. The frequency of response of a simple cell to a stimulus that fills its receptive field is a linear sum of the frequencies of its responses to spots of light falling in each part of words, simple cells integrate luminance in a linear fashion. However, simple cells show three types of the receptive field, when tested separately. In other nonlinearity—their response saturates at high stimulus contrasts, they respond more rapidly at high contrasts, and their response to superimposed orthogonal stimuli is less than their response to a stimulus in one orientation (cross-orientation inhibition). These nonlinearities could arise from a gain-control mechanism that depends on scaling (dividing) the cell's response by the pooled activity of neighbouring cells—a process called normalization (Carandini and Heeger 1994). Normalization makes it possible for a cell's response to critical features of the stimulus, such as motion, orientation, and disparity, to be independent of stimulus contrast.

The receptive fields of **complex cells** are not clearly segregated into excitatory and inhibitory zones. Moreover, these cells integrate luminance in a nonlinear fashion. Simple cells tend to be stellate cells and complex cells tend to be pyramidal cells but this correlation between structure and function is not perfect (Gilbert and Wiesel 1979). In Hubel and Wiesel's hierarchical model, simple cells feed into complex cells. However, Ghose et al. (1994) revealed only monosynaptic excitatory connections from complex to simple cells in the cat. According to this evidence, connections from simple to complex cells must be polysynaptic. The organization of the visual cortex is reviewed by Valverde (1991) and its development is discussed in Section 15.1.5.

4.2.3 Stimulus tuning of cortical cells

Orientation tuning

Both simple and complex cells respond best when a line or edge is oriented along the long axis of the cell's receptive field. The stimulus orientation that evokes the strongest response in a given cell is its **preferred orientation**. The function relating the firing rate of a cell to the orientation of a line centred within its receptive field is its **orientation tuning function**. An example is shown in Figure 4.9. The full tuning bandwidth of a cell is indicated by the width of the tuning function at half the height of its maximum response. The full bandwidths of

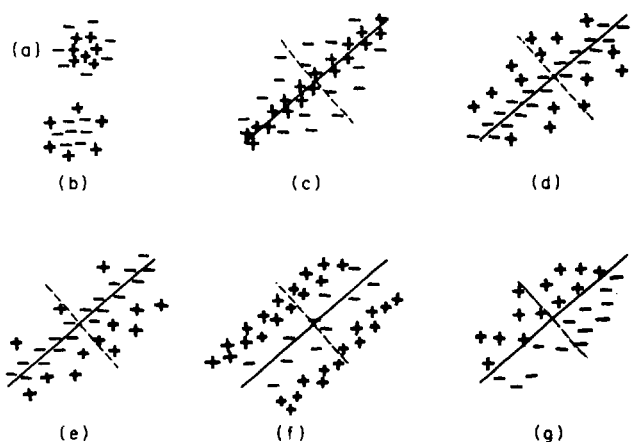


Figure 4.8. Types of receptive field.

(a) An on-centre receptive field of a ganglion cell.
 (b) An off-centre receptive field of a ganglion cell.
 (c)-(g) Receptive fields of simple cells in the cat visual cortex. These particular receptive fields have a preferred orientation of 45°. (From Hubel and Wiesel 1962. Reproduced by permission of the Journal of Physiology.)

orientation tuning functions of cells in the monkey striate cortex range from 6° (sharply peaked tuning) to 180° (flat tuning). The mean is about 40°, which covers about a quarter of the maximum range of 180° (DeValois et al. 1982a).

Hubel and Wiesel's original idea was that the orientation selectivity of a cortical cell derives from the way ganglion-cell receptive fields feeding into it are lined up on the retina. Recent confirmation of this idea has been provided by Ferster (1987), Stryker (1991), and Chapman et al. (1991). There is evidence that patterns of intracortical inhibition also play a role in determining the orientation selectivity of cortical cells (Sillito et al. 1980). One possibility is that intracortical inhibition sharpens the tuning of cortical cells for both spatial frequency and orientation by attenuating their response to low spatial frequencies (Vidyasaga and Mueller 1994).

Inhibitory mechanisms, at either a precortical or cortical level, that help to determine the orientation selectivity of a cortical cell could involve recurrent feedback loops or feedforward loops. Celebrini et al. (1993) demonstrated that the orientation selectivity of a cortical cell is present and fully formed in the first 10 ms of its response. Evidence suggesting a longer build-up time for orientation selectivity in some cortical cells has been provided by Shevelev et al. (1993). A short build-up time is inconsistent with the idea that feedback loops are involved in orientation tuning, since they would produce a relatively slow build up of orientation selectivity at stimulus onset. The faster, feedforward mechanism allows the animal to assess the orientation of a

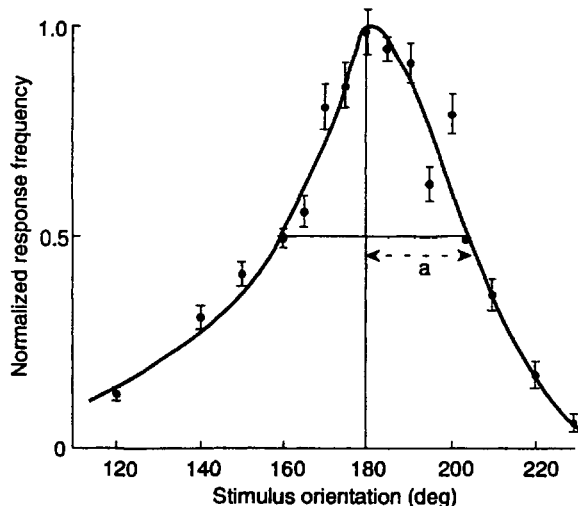


Figure 4.9. Orientation tuning function of a cortical cell.
The cell is a simple cell in the cat's visual cortex. Vertical bars are standard errors. Distance *a* is half the width of the tuning function at half amplitude, and represents the cell's orientation selectivity. The tuning function of this cell is asymmetrical. (Reproduced with permission from Heggelund and Albus, 1987, Vision Research, Pergamon Press.)

stimulus seen briefly. We will see later that the disparity selectivity of cortical cells is also rapidly developed after stimulus onset.

In the primary visual cortex of the alert monkey, the response of a cell to a particular stimulus tends to be suppressed by the addition of a textured surround. The degree of suppression increases with increasing density of the surround (Knierim and Van Essen 1992). Furthermore, the response of some cells in the cat's visual cortex to an optimal stimulus centred on the receptive field is larger when surrounding lines outside the normal receptive field of the cells have a contrasting, rather than the same, orientation or spatial frequency (Nelson and Frost 1978; DeAngelis et al. 1994). The orientation-specific surround effect was found to take 8 to 20 ms to develop (Knierim and Van Essen 1992). DeAngelis et al. found that for some cells the inhibitory effect of similarly oriented stimuli could be evoked dichoptically. This suggests that it depends on intracortical inhibitory connections. This mechanism could provide a physiological basis for the perceptual segregation of textured regions, since the response of cells of this type would be highest for texture boundaries (see Section 6.1.6).

Columnar organization

Lorente de Nò (1949) was the first to propose that the cerebral cortex is organized into columns containing cells with similar tuning properties. By studying patterns of synaptic linkages anatomically he showed that the connections run predominantly

vertically from layer to layer with fewer connections running horizontally. The first functional evidence of columnar organization was provided by Sperry et al. (1955). He found that vertical slicing of the visual cortex produced little or no effect on the ability of cats to perform fine visual discriminations. Mountcastle (1956) produced the first electrophysiological evidence of columnar organization in the cerebral cortex by recording from single cells in the somatosensory area of the cat. He wrote, "neurons which lie in narrow vertical columns, or cylinders, extending from layer II through layer IV make up an elementary unit of organization, for they are activated by stimulation of the same single class of peripheral receptors, from almost identical peripheral receptive fields." Columnar organization is a fundamental property of the whole cerebral cortex and we will see in Chapter 15 that the cortex develops by columnar growth from the cellular lining of the embryonic ventricles. This lining contains a protomap of the prospective cytoarchitectonic areas (Rakic 1988).

The cells in each small column of cortical tissue running at right angles to the surface have similar preferred orientations, although there is sometimes a reversal of orientation tuning at layer 4 (Dow 1991). These columns of similarly tuned cells are **orientation columns**. In the cat and monkey the orientation preference of cells rotates through its full range of 180°, as one traverses across the cortical surface through a distance of 0.5 to 1.0 mm. Cells with the same orientation preference form vertical columns extending through the various cortical layers. We will see in Section 4.2.5 that, over the surface of the cortex, cells tuned to different orientations are arranged like the spokes of a wheel around singularities containing cells with nonoriented receptive fields. Each cell in the visual cortex is also selectively tuned to a particular range of spatial frequencies of a grating that falls within its receptive field (see Section 3.4.2). There is some dispute about the columnar organization of cells with the same spatial-frequency tuning. We return to this question in the next section.

Spatiotemporal aspects of cortical cells

Cortical cells are also differentially tuned to the temporal aspects of stimuli falling within their receptive fields. Each cell has a characteristic latency for a defined stimulus, and many show a biphasic response to a brief stimulus. In addition, most cells in the visual cortex respond best when the stimulus moves in a particular direction, the **preferred direction**. The axis of the preferred direction of an orientationally tuned cell is at right angles to the long axis of its receptive field. Thus, the columnar

organization of the axes of preferred motion corresponds to the columnar organization of preferred orientation. Some cells respond to movement in either direction along a given axis of motion and are said to be bidirectional. Other aspects of spatiotemporal coding were discussed in Section 3.3.

One can think of a cortical cell as having a spatiotemporal tuning function and a spatiotemporal structure to its receptive field. Plotting the spatiotemporal structure of a receptive field using a single stimulus probe is a time-consuming procedure. The so-called reverse correlation algorithm provides a rapid procedure (DeAngelis et al. 1993a). A continuous series of briefly exposed bar-shaped stimuli is presented. The stimuli occur at different positions within the spatial confines of the receptive field and at different times within the temporal epoch over which the response of the cell persists. The responses of the cell are then cross-correlated backwards in time with the input to yield the spatiotemporal impulse response of the cell. The method works only if the cell behaves linearly, and can therefore be applied only to simple cortical cells.

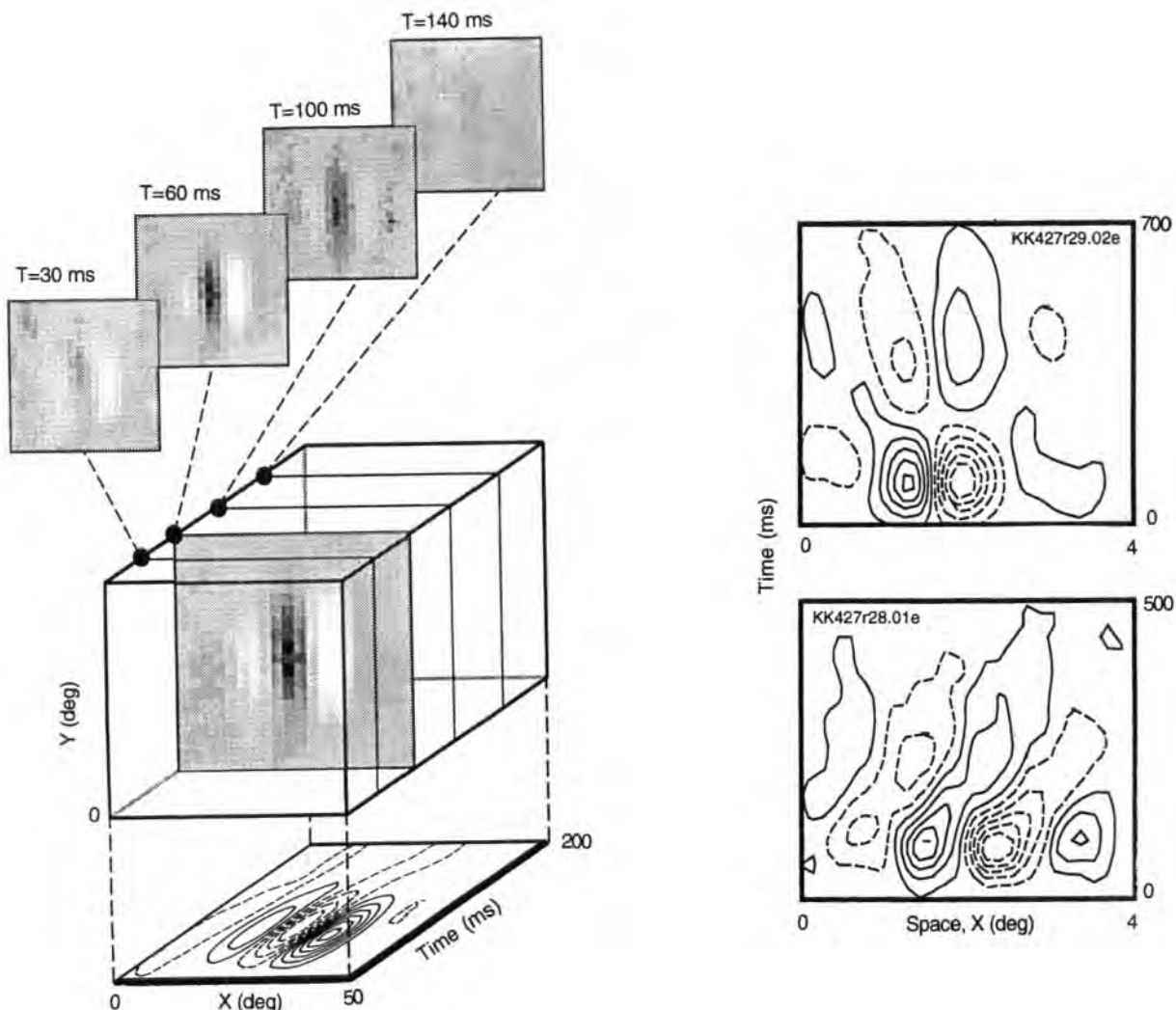
An example of the spatiotemporal structure of a simple cell receptive field is shown in Figure 4.10a. Each slice represents the momentary activity within the excitatory and inhibitory regions of the receptive field, and the sequence along the time dimension represents the temporal phasing of the response. Figure 4.10b shows the plot of the receptive field along one spatial dimension on the abscissa and over time on the ordinate. In the first example, the positions of the excitatory and inhibitory regions are constant over time, and the cell is said to show space-time separability. The response of the cell is the simple product of its spatial response and its temporal response. Note that the temporal response of this cell is biphasic. In the second example, there is a spatial shift of activity within the receptive field over time and the cell is said to show space-time inseparability (space and time interact). Cells of this type show a preference for stimuli moving in the direction in which their spatiotemporal tuning function is "tilted" in the space-time domain. Cells with space-time separable response profiles are generally not selective for a particular direction of motion. After making allowance for the nonlinearity of the response of simple cells to contrast, DeAngelis et al. (1993b) were able to predict the direction selectivity of simple cells from the spatiotemporal profiles of their receptive fields, indicating that simple cells embody a linear spatiotemporal filter. The direction sensitivity of simple cells has also been derived by linear summation of the membrane potential

fluctuations obtained from intracellular recordings in the visual cortex of the cat (Jagadeesh et al. 1993). Other aspects of the spatiotemporal properties of the receptive fields of cortical cells have been reviewed by Dinse et al. (1990a).

4.2.4 Ocular-dominance columns

The first direct physiological evidence of convergence of inputs from the two eyes onto the same cortical cells was provided by Hubel and Wiesel (1959), working with the cat. In the monkey, each local group of cells in layer 4C receives excitatory inputs from only one eye. These inputs are then relayed to cells in other layers in the same vertical column of cortical tissue and most of these cells also receive inputs from the other eye through cells in layer 4C in neighbouring columns. Cells receiving inputs from both eyes are known as **binocular cells**. The binocular cells in a given vertical column respond most strongly to stimulation of a particular eye. Columns receiving a excitatory input predominantly from one eye alternate with columns receiving an excitatory input predominantly from the other eye. These alternating bands of cortical tissue are known as **ocular-dominance columns**, but "ocular-dominance bands" is perhaps a better term.

Each binocular cell has two receptive fields, one in each eye, with similar oculocentric positions. The two receptive fields are similar in their tuning to orientation, spatial frequency, and direction-of-motion. They also have the same length-summation, end-stopping, and simple or complex characteristics (Hubel and Wiesel 1962, 1968; Maske et al. 1984; Skottun and Freeman 1984; Hammond and Fothergill 1991). Binocular cortical cells that respond to excitatory inputs from either of the two eyes do so with similar short latency, suggesting that they receive direct inputs from layer-4 cells of the ipsilateral eye and from layer-4 cells of the contralateral eye, rather than a direct input from one eye and an indirect input from the other (Ito et al. 1977). Not only is the latency of excitatory inputs to a binocular cell the same, but so is the complete pattern of synaptic inputs from the two eyes, involving monosynaptic excitatory inputs and polysynaptic excitatory and inhibitory inputs (Ferster 1990). The issue of differential response latencies is discussed in more detail in Section 13.1.1. This fundamental similarity in receptive fields allows the visual system to match the images in the two eyes, which is a prerequisite for the creation of a unified binocular field. Nevertheless, differences between the receptive fields of binocular cells do occur and, as we will see in later sections of this chapter, these differences form the



(a) Each panel shows the receptive field profile of the cell at a particular time after stimulus onset. White areas represent responses to a small flashed bright bar and dark areas represent responses to a flashed dark bar. The projection of the set of panels at the bottom of the figure produces a plot of the spatiotemporal profile of the cell for one spatial dimension. Solid contours are boundaries of bright-excitatory, on-response regions. Dashed lines are boundaries of dark-excitatory, off-response regions.

(b) Spatiotemporal response profiles of simple cells from an 8-week-old cat. The upper example is of a cell showing space-time separability in which the response profile is the product of the space and time profiles. The lower example is of a cell showing space-time inseparability. This type of cell is selectively responsive to motion in the direction of the "tilt" of spatiotemporal regions in the receptive field profile.

Figure 4.10. Spatiotemporal response profiles of simple cells in cat's visual cortex.
(From DeAngelis et al. 1993a.)

basis of disparity-detecting mechanisms and stereopsis. Ocular-dominance columns were first revealed by recording from a series of single cortical cells as the recording electrode was moved tangentially to the cortical surface. They were then revealed anatomically in the monkey by the Nauta degeneration method, which involves tracing areas of cell degeneration in the cortex produced by selective destruction of LGN cells arising from a

given eye (Hubel and Wiesel 1969). Grafstein and Laureno (1973) showed that a mixture of tritiated proline and tritiated fructose injected into the eye of a living mouse gradually travels up the axons of the optic nerve and becomes concentrated in cells in layer 4 of the contralateral visual cortex. The resulting patterns of radioactivity in thin sections of tissue from the visual cortex are recorded on film to produce autoradiographs. Wiesel et al. (1974) used

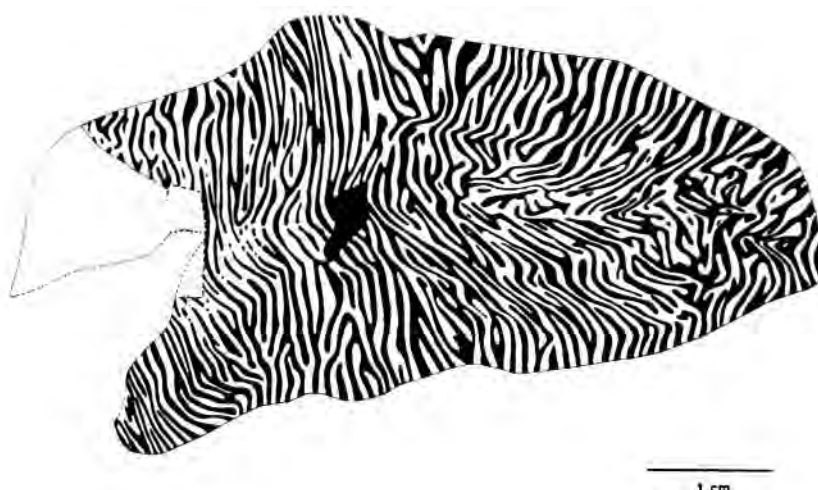


Figure 4.11. Ocular-dominance bands of the monkey visual cortex.
The pattern was derived from a series of autoradiographs and transposed onto a three-dimensional map of the visual cortex. (From LeVay et al. 1985.)

the same method to reveal the ocular-dominance columns in the *macaque* monkey. The macaque is an old world monkey but similar ocular-dominance columns have been found in *Cebus*, a new world monkey (Rosa et al. 1992). In a related procedure, deoxyglucose labelled with carbon 14 is injected into the animal which is then exposed to stimuli presented to one eye for an hour or more. The labelled glucose compound is taken up by metabolically active neurones in the visual cortex that respond to the stimulated eye and not by inactive neurones related to the closed eye (Sokoloff et al. 1977). An autoradiograph is produced from thin cortical sections.

Cells taking up radioactive tracer in the hemisphere contralateral to the injected eye are all those that normally receive a strong excitatory input from that eye. Since cells with balanced ocular dominance also receive excitatory inputs from the ipsilateral eye, the dark bands produced by injection of one eye must overlap those produced by injection of the other eye. The cells not taking up radioactive tracer injected into one eye receive either an indirect inhibitory input or no input from the contralateral eye.

The separate slices of an autoradiograph can be combined by computer reconstruction into a complete pattern of columns. Using data on the topography of the visual cortex, the pattern of ocular-dominance columns can be transposed onto a three-dimensional map of the visual cortex, as shown in Figure 4.11.

Recently it has become possible to image patterns of cortical activity *in vivo*. Dyes sensitive to voltage changes associated with neural impulses are infused into cortical tissue of the living animal. The animal is exposed to specific stimuli, and the differential

reflectivity of the cortical surface is recorded photographically. Dyes introduce side effects, but visually induced changes in cortical reflectivity can now be photographed without the use of dyes. An example of an *in vivo* photograph of ocular-dominance columns obtained in this way by Ts'o et al. (1990) is shown in Figure 4.12. Hitchcock and Hickey (1980) obtained evidence of ocular-dominance columns in postmortem sections of human striate cortex.

Columns with left-eye ocular dominance form into a series of parallel bands, each 0.25 to 0.5 mm wide, interspersed with similar bands with right-eye dominance. The bands extend through all the layers of the visual cortex (Tootell et al. 1988c). In each half of the visual cortex the whole visual hemifield is retinotopically mapped onto the ocular-dominance bands of the left eye, and again onto the ocular-dominance bands of the right eye. Along the bands this representation is continuous, but across them it is interrupted by the alternations between left- and right-eye bands. For details of how these interrupted retinotopic representations are organized see Hubel and Wiesel (1977). To some extent the bands follow isoeccentricity lines, but the major factor determining the pattern is the tendency of bands to run across the elliptical visual cortex rather than along its length (LeVay and Voigt 1988). This is the simplest way to combine two circular monocular retinotopic maps onto an elliptical surface.

Hubel and Wiesel (1962) introduced a seven-group ocular-dominance scale. Cells in group 1 respond only to inputs from the contralateral eye and those in group 7 only to inputs from the ipsilateral eye. The eye not evoking a response in a given cell is known as the silent eye. Cells in group 4 respond

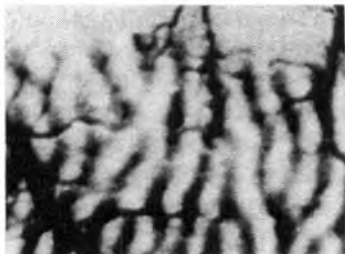


Figure 4.12. Photograph of ocular-dominance bands.
The image is from the visual cortex of the living monkey. Dark bands are columns dominated by the left eye. The boundary between V1 and V2 is across the top of the picture. Ocular-dominance bands do not cross this boundary. (From Ts'o 1990. Copyright, 1990 by the AAAS.)

equally well to inputs from either eye, and the cells in the other groups have a corresponding degree of ocular dominance. In the monkey, 72 per cent of cells in V1 fall into groups 2 to 6 (Schiller et al. 1976). This scale is based only on the excitatory effects of monocular stimulation from each eye separately. It takes no account of the few cells that fire only in response to binocular stimulation (Grüsser and Grüsser-Cornehls 1965). More important, it takes no account of the fact that practically all cells in groups 1 and 7 lying within the binocular field, and classified as exclusively monocular by Hubel and Wiesel's criterion, are affected by the simultaneous stimulation of the corresponding region in the silent eye. In fact, cells with strong ocular dominance show evidence of stronger binocular interactions of this type than do cells classified as having a balanced binocular input (Gardner and Raiten 1986). The effect produced by stimulation of the silent eye may be inhibitory and reduce the response evoked by the dominant eye or it may involve subthreshold facilitation and lower the threshold of response to stimuli applied to the dominant eye (Grüsser and Grüsser-Cornehls 1965; Henry et al. 1969; Bishop et al. 1971; Poggio and Fischer 1977; Kato et al. 1981). All the direct visual inputs to cortical cells in layers 4C and 4A are believed to be excitatory (Garey and Powell 1971).

One might suppose that cells that respond directly to stimulation of only one eye would not be concerned with coding binocular disparity. In fact it is now known that most cells serving the binocular field with a strong monocular dominance have indirect inputs from the other eye and are just the cells that code large binocular disparities. The classification of cortical cells into ocular-dominance columns is further complicated by the fact that the ocular dominance of some complex cells varies over time and depends on the spatial frequency and velocity of the stimulus (Hammond 1979, 1981).

The width of the region of visual cortex containing a full 180° cycle of orientation preferences is roughly the same as that of an ocular-dominance column. Regions containing a full set of orientation-tuned cells for each eye are called **hypercolumns**. In the monkey, hypercolumns have a diameter of 0.5 to 1.0 mm at all eccentricities, at least out to 15° . It is assumed that a hypercolumn contains all the cell types required for coding of a full range of visual features in the area of the visual field from which it derives its inputs (Hubel and Wiesel 1974). Neighbouring hypercolumns receive inputs from overlapping retinal regions, and each hypercolumn is fed by the same number of ganglion cells. We pointed out earlier in this section that cells in neighbouring columns interact through excitatory and inhibitory dendritic connections. The development of ocular-dominance columns is discussed in Section 15.2.

4.2.5 Parvo-and magnocellular areas

In 1978 Margaret Wong-Riley informed Hubel and Wiesel that she had found clusters of cells in the primary visual cortex of the monkey, with a high concentration of cytochrome oxidase. This is a metabolic enzyme found in the mitochondria of neurones and its concentration is a sensitive indicator of neuronal activity (Wong-Riley 1979a, 1989). Two years later Horton and Hubel (1981) investigated the physiological properties of regions with high levels of cytochrome oxidase and found that they are centred on the ocular-dominance columns and contain cells not tuned to orientation. These regions are called **blobs**. The spaces between the blobs have a lower concentration of cytochrome oxidase and are known as **interblobs**. The centres of the blobs are about 0.4 mm apart, making about 5 blobs per mm^2 and a total of about 15,500 in the binocular visual field of the macaque (Schein and Monasterio 1987). The density of blobs is about half this value in the monocular visual cortex. The number of parvocellular cells projecting to each blob remains constant at about 110 over the visual field of the monkey. Cells in the blobs and interblobs have the following properties:

1. Blob cells are not tuned to orientation; interblob cells are tuned to orientation.
2. Blob cells show strong colour opponency, some specializing in red/green opponency, and others in blue/yellow opponency. Only a few interblob cells show some colour opponency (Livingstone and Hubel 1984).
3. Blob cells respond best to gratings with low contrast and spatial frequency, interblob cells prefer higher spatial frequencies (Tootell et al. 1988b).

4. In the binocular cortex, cells in half the blobs respond most strongly to one eye, those in the other blobs respond most strongly to the other eye. This means that each blob occurs in the centre of an ocular-dominance column (Ts'o et al. 1990). The blobs occur in rows superimposed on the ocular-dominance columns (Horton 1984).

The functional properties of cells in the blob and interblob regions are not sharply segregated; border cells can show both colour and orientation specificity (Ts'o and Gilbert 1988). Subsequent investigations in the monkey have revealed that both the blobs and interblobs receive inputs from the parvocellular layers of the LGN. They therefore constitute two subdivisions of the parvocellular system. Cells in layer 4B of V1 receive inputs from the magnocellular layers of the LGN and are not part of the blob-interblob system (Livingstone and Hubel 1984, 1987).

There are two views about the significance of the blob-interblob division of the parvocellular system. According to Livingstone and Hubel they represent a dichotomy into a channel specialized for colour but not form and a channel specialized for colourless form. DeValois and DeValois (1988) proposed a different scheme in which the primary distinction between blobs and interblobs is in spatial-frequency tuning (see also DeValois 1991). This scheme is illustrated in Figure 4.13. Blobs contain cells tuned to low spatial-frequency stimuli (coarse detail) and the interblobs contain cells tuned to high spatial-frequency stimuli (fine detail), with a gradual transition between the two, rather than a dichotomy. They argued that the predominance of colour-coded cells in the blobs is a simple consequence of the fact that parvocellular cells operate as colour-opponent cells for low spatial frequency stimuli and as luminance-contrast cells for high spatial-frequency stimuli. This accords with the analysis provided by Ingling (see Section 4.7). They also argued that the finer tuning for orientation in the interblobs is a consequence of the fact that cells tuned to higher spatial frequencies also have narrower tuning for orientation. The two views both end up with a similar division of cell types, but the DeValois' scheme makes this division consequent on a fundamental segregation of cells according to spatial-frequency tuning.

It is widely believed that orientation bands are orthogonal to bands defined by eye of origin—the ocular-dominance bands. However, there was never any convincing evidence for this so-called “ice-cube” picture of orientation and ocular-dominance columns. In the DeValois' scheme, cells with a particular orientation preference are arranged radially out from the centre of a blob. The orientation

preference changes in an ordered sequence as one rotates round the centre of the blob, as shown in Figure 4.13. The orientation columns thus form pinwheel patterns. The cells in the centre have no orientation tuning and thus form singularities within the orientation column system. Proceeding out from the centre, the cells are tuned to progressively higher spatial frequencies. Different blobs have different chromatic properties.

This radial scheme of orientation tuning was first proposed by von Seelen (1970) and Braitenberg and Braitenberg (1979), who suggested that the centre of each radial unit is occupied by a giant Meynert cell that guides the development of the unit. Meynert cells are solitary giant pyramidal cells occurring in layer 5 of the primary visual cortex. They have a mean spacing of about 110 mm in the foveal cortex, and each cell sends a richly branched apical dendrite into cortical layers 1 and 2 and other dendrites into layers 5 and 6. These are the layers in which intracortical connections originate (Chan-Palay et al. 1974). Electrophysiological recording from single cells distributed in a grid over the visual cortex of the cat has provided evidence for the pinwheel organization (Swindale et al. 1987; Dow 1991). Single-cell recording is an exhausting procedure. Pinwheel patterns of orientation-selective cells have been revealed more directly by the optical imaging of light reflected from the cortical surface (Ts'o et al. 1990). Regions responding to a grating presented in a particular orientation have higher absorption of red light because of the presence of deoxyhaemoglobin. Bonhoeffer and Grinvald (1993) used this procedure to produce detailed maps of the pinwheel organization of area 18 of the cat. Since the preferred direction of motion of a cortical cell is orthogonal to its preferred orientation, motion selectivity is also organized in a radial fashion. However, for a set of cells tuned to a particular orientation, cells tune to motion in one direction do not seem to be spatially segregated from those tuned to motion in the opposite direction (Bonhoeffer and Grinvald 1993).

4.2.6 Other visual areas

Axons leaving the primary visual cortex emerge from pyramidal cells in layers above and below layer 4. Axons from layers 2 and 3 project retinotopically to a series of other visual areas of the occipital lobe that surround the striate cortex. These are known as the **prestriate cortex** or **circumstriate belt**. In primates this belt includes visual areas V2, V3, V3A, and V4. The circumstriate belt also includes areas MT (middle temporal, or V5), VP (ventral posterior), and VOP (ventral occipitotemporal) (Zeki

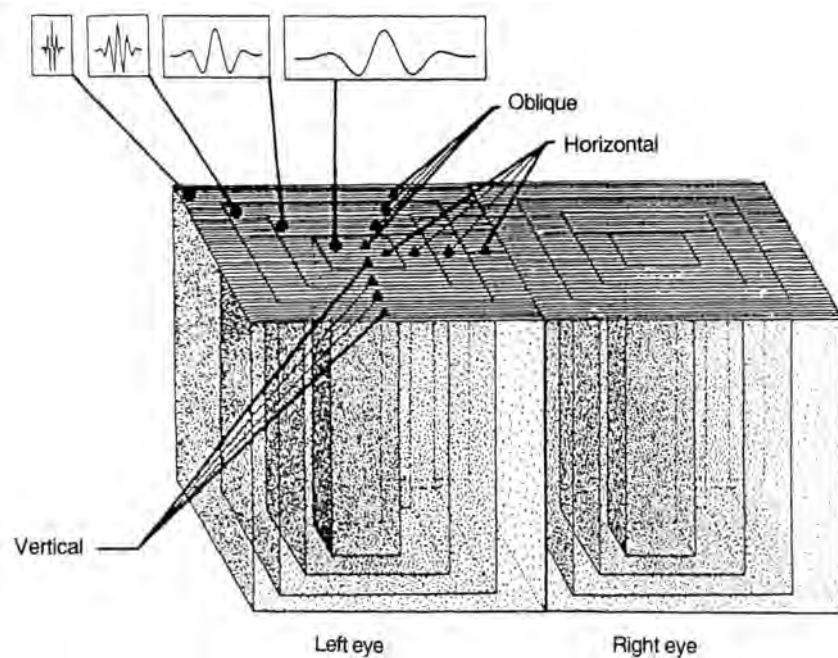


Figure 4.13. The pinwheel organization of the primate visual cortex.

Each module (blob plus interblob region) is devoted to one eye. Along each radius of a module, cells are tuned to progressively higher spatial frequencies but have the same orientation preference. Orientation preference changes in an ordered sequence as one rotates around the centre of the module. (From DeValois 1988.)

1974b; Wong-Riley 1979b; Maunsell and Van Essen 1983a). The prestriate cortex sends intracortical fibres to visual areas in the inferotemporal cortex (Gross 1973), the parietal lobe, and the frontal lobe. In the parietal lobe, at least ten visual areas have been identified, and these occupy most or all of Brodmann's area 7. One of these areas, which will be mentioned at various places in this book, occurs in the superior temporal sulcus and is known as area MST (medial superior temporal). The temporal lobe also contains many visual areas. Thirty-two distinct visual areas have been revealed in the brain of the monkey with over 300 pathways connecting them (Felleman and Van Essen 1991; Van Essen et al. 1992). No doubt other visual areas remain to be discovered.

The striate cortex (V1) contains a fine and well-ordered representation of the contralateral visual hemifield. The visual hemifield is represented in a much less orderly fashion in each extrastriate visual area. The representation is coarser because the receptive fields are larger and there are topographic irregularities in the mapping from one visual area to another. In some visual areas some parts of the visual field are exaggerated relative to their representation in V1 and other parts are diminished or absent. Areas V2, V3, and V3A contain a retinotopic mapping of the visual fields, although not all regions

of the visual field are necessarily represented in each area. Most of the cells in these three areas are orientation selective. In area V4 only the central 20° of the visual hemifield is represented, which seems to be related to the fact that this area contains many colour-coded cells, and that colour coding is confined to the central region of the retina. The so-called motion area in the temporal lobe has multiple representations of the visual hemifields but is nevertheless referred to as a single visual area because all the cells within it respond to similar features of the visual stimulus (Zeki 1978).

Outputs from pyramidal cells in layers 5 and 6 of the primary visual cortex project to ipsilateral and perhaps also to contralateral subcortical regions (Creutzfeldt 1977), including the pretectum, superior colliculus (Berman et al. 1975), pulvinar, LGN, and other areas of the thalamus (Gattas et al. 1979), the caudate nucleus, and the cerebellum by way of pontine nuclei (Brodal 1972). Details of cortical efferents are provided by Swadlow (1983).

The tuning characteristics of cells in V2 resemble those of cells in V1, except that cells in V2 have larger receptive fields, are more likely to be binocular, and are almost all complex cells. However, important differences between one visual area and another may not be revealed by the tuning characteristics of single cells but only by differences in the ways

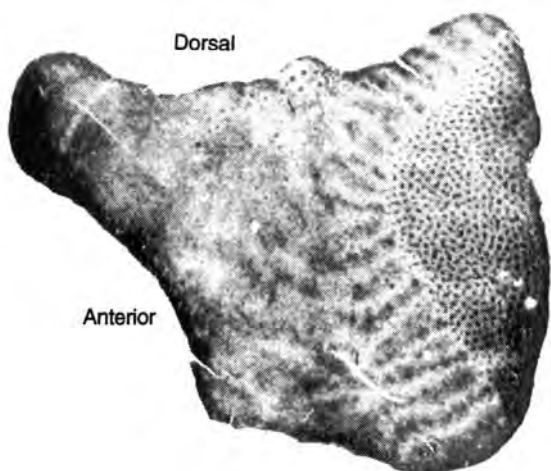


Figure 4.14. Cytochrome oxidase areas of visual cortex.
A section from layer 3 of the lateral surface of the visual cortex of the squirrel monkey, stained to reveal cytochrome oxidase. The spotted area is V1 and the adjoining striped area is V2. (From Tootell et al. 1983, Copyright 1983 by the AAAS.)

in which cells are linked into larger functional units. Present-day methods are not well suited to reveal such differences. Another problem in trying to understand the functions of higher visual centres is that patterns of connections between cortical cells that may be revealed are difficult to interpret without some theory about the functions the system is designed to accomplish.

In the monkey, V2 is not partitioned into ocular-dominance columns. However, it shows alternating stripes when stained to reveal the presence of cytochrome oxidase. The stripes run over the surface of V2 approximately perpendicular to the border with V1, as shown in Figure 4.14. They extend through all the layers with pairs of thick and thin dark stripes alternating with lighter staining interstripes (Tootell et al. 1983). It has been claimed that the blob regions of V1, containing mostly nonorientation-specific, colour-coded cells of the parvocellular system, project to the thin stripes. However, Nealey and Maunsell (1994) revealed a strong magnocellular input to the blobs. The interblob regions, containing the orientation-tuned cells of the parvocellular system, project to the nonstaining interstripes. Cells of the magnocellular system project from layer 4C α to layer 4B and then to the thick stripes (Blasdel et al. 1985; DeYoe and Van Essen 1985; Hubel and Livingstone 1987). This subdivision of cell types is not complete; there are cells tuned to both colour and depth, others tuned to colour and orientation, and some tuned to all three features (Ts'o et al. 1989; Levitt et al. 1994).

Beyond V2 the two parts of the parvocellular system project ventrally to distinct regions of area V4 and then to distinct regions of the inferotemporal

cortex. Neurones in the inferotemporal cortex tuned to similar complex stimulus features are aligned in columns normal to the cortical surface (Fujita et al. 1992). Evidence from the monkey suggests that the parvocellular system feeding into the inferotemporal cortex is specialized for colour vision, fine pattern vision, and fine stereopsis. These functions are associated with object recognition, including the recognition of complex objects such as faces (Perrett et al. 1989; Tanaka et al. 1991; Schiller and Lee 1991; Rolls 1994). Evidence that area V4 is specialized for colour in the human brain has been provided by positron emission tomography (PET), which revealed that blood flow to V4 increases when subjects view a coloured display (Zeki et al. 1991). However, stimulation of V4 following pharmacological blockade of parvo- or magnocellular layers in the LGN has revealed a strong input to V4 from both the parvo- and magnocellular systems (Ferrera et al. 1994).

The magnocellular system feeding into the posterior parietal cortex is specialized for coding low spatial frequency, fast flicker and motion, spatial location, and coarse stereopsis. These functions are associated with the analysis of the spatial positions and motions of objects (Ungerleider and Mishkin 1982; Schiller et al. 1990; Lagae et al. 1993). Magnocellular inputs project dorsally to areas V3 and V5, and to areas in the parietal lobe including the middle temporal area (MT) in the superior temporal sulcus, and the medial superior temporal area (MST) (Shipp and Zeki 1985; Krubitzer and Kaas 1990; Motter 1991). Figure 4.15 shows these relationships.

The middle temporal area (MT) of the owl monkey has recently been shown to have distinct bands (Born and Tootell 1992). The cells in one set of bands have centre-surround antagonistic receptive fields. The response to a central moving stimulus is inhibited by surround motion in the same direction and enhanced by surround motion in the opposite direction. These cells therefore respond best to relative motion. Cells in other bands respond best to motion in the same direction over a large area and are therefore sensitive to the type of visual motion produced by movements of the head. These cells seem to be designed to detect patterns of optic flow generated by self motion (Duffy and Wurtz 1991). Similar types of cell have been reported in the optic tectum of the pigeon (Frost et al. 1981) and in the suprasylvian cortex of the cat (Krüger et al. 1993). The PET scan has revealed that V5 (MT) in the human brain is specialized for motion (Zeki et al. 1991). The responses of cells in the posterior parietal cortex, are coded in retinocentric coordinates but are modified by eye movements (Andersen et al. 1990; Duhamel et al. 1992). Cells have been found in the anterior bank of

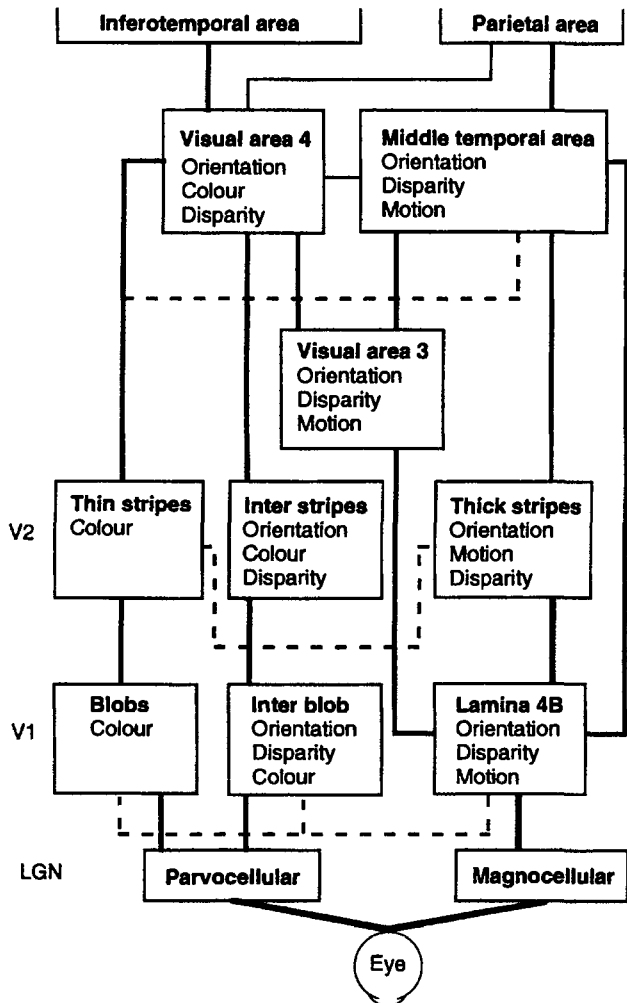


Figure 4.15. Pathways connecting visual areas.

Visual areas of the macaque monkey, with an indication of the functional specialization of each area. (Adapted from De Yoe and Van Essen 1988.)

the parietal lobe (V6) in the monkey with receptive fields defined in headcentric rather than retinocentric coordinates (Galletti et al. 1993).

Some studies on the effects of lesions within the parvo- and magnocellular systems of the monkey support the idea of two major processing streams. Within the parvocellular system, lesions in the parvocellular laminae of the LGN produce deficits in colour vision, fine pattern discrimination, and fine stereopsis (Schiller et al. 1990). Lesions in V4 also produce colour-vision defects, although they are less severe and less permanent than those produced by lesions in the LGN. Lesions in the inferior temporal lobe produce deficits in object recognition (Pohl 1973). Within the magnocellular system, lesions in the magnocellular laminae of the LGN produce deficits in motion perception, high-frequency flicker perception, and pursuit eye movements (Schiller et al. 1990) as well as reduced contrast sensitivity for

low spatial frequency gratings modulated at high temporal frequencies (Merigan and Maunsell 1990). Lesions in MT produce similar deficits (Dürsteler et al. 1987). Lesions in the posterior parietal cortex in man and other primates are associated with loss of spatial memory, disturbances of spatial attention, and defects in representing spatial relations (see Critchley 1953 and Andersen 1987 for reviews). Studies using fluorescent tracers have shown that the two major processing streams also have distinct projections to subcortical nuclei (Baizer et al. 1993).

The distinction between the processing stream for spatial localization and that for colour and object recognition extends into the prefrontal cortex. In the monkey the posterior parietal cortex projects to the principal sulcus and arcuate regions of the frontal cortex. Cells in these regions respond to spatially localized stimuli and maintain their response during intervals when the animal is required to remember the location of the stimulus after it has been removed (Funahashi et al. 1989). The inferotemporal cortex projects to the inferior prefrontal convexity. Lesions in this area in monkeys and humans produce deficits in the recognition of complex objects, such as faces and words. Cells in this region show a response to complex patterns that is relatively independent of the size, orientation, and colour of the pattern. They continue to respond to a pattern during intervals when the pattern must be remembered (Wilson et al. 1993).

Thus, the parvo- and magnocellular systems have different though overlapping functions. The anatomical distinction between the two streams is by no means complete. Although V4 receives a predominant input from the parvocellular system, cells in V4 showed markedly reduced activity when the magnocellular system in the LGN was blocked (Ferrera et al. 1994). Furthermore, although inputs to MT are mainly from the magnocellular system, a few sites showed evidence of receiving inputs from the parvocellular system (Ferrera et al. 1992). There is also evidence of partial convergence of parvo- and magnocellular inputs even in the primary visual cortex (see Schiller et al. 1990). In addition, there are extensive interconnections between all visual areas, especially between the temporal and parietal lobes (DeYoe and Van Essen 1988).

Ultimately, information from these interrelated parallel streams must be combined to form unitary percepts of objects and of spatiotemporal relationships. Boundaries in the visual field defined by colour, texture, motion, and disparity typically coincide. If each of these features were processed independently some means would have to be found to keep contours defined by different visual features

in register. Otherwise we would experience the world like a poorly printed photograph in which colour spills across edges. Another reason for interconnections between regions processing different features is that ambiguity in the location of contours defined by one feature can be resolved by reference to another feature. Thus, information flow between different systems allows one to exploit redundancies in the visual world.

It has been proposed that the magnocellular system is solely responsible for coding depth and that the parvocellular system is blind to binocular disparity (Livingstone and Hubel 1988). Cells sensitive to binocular disparity are certainly present in area V3 and in MT, which are considered part of the magnocellular system (Maunsell and Van Essen 1983b; Felleman and Van Essen 1987). But, as we will see in Section 4.7, the idea that disparity detection is confined to the magnocellular system must be rejected.

The cells within the boundaries between one visual area and another—for example, between V1 and V2—have receptive fields along either the vertical or horizontal retinal meridian. These boundary regions can therefore be recognized by a sudden change in retinotopic representation. One consequence of this juxtaposition of cells from the main retinal meridians is that retinotopic representations of visual hemifields in succeeding visual areas are mirror images of each other (Cowey 1979). Regions representing the vertical meridians are connected by fibres running through the corpus callosum.

The picture that emerges is of a series of retinotopically coded visual areas, each of which processes different visual features. The system is hierarchical in that each area receives its inputs from the striate cortex, sometimes by way of other areas. The system is parallel in that there is divergence into distinct areas that handle different visual features. At the same time, centres higher in the sequence send recurrent signals back to earlier stages and the parallel pathways interact and presumably ultimately converge into common processes that determine perception and action (see Grossberg 1990; Rockland and Van Hoesen 1994).

The retinotopic arrangement of cells within the various visual areas serves two purposes. In the first place, lateral inhibition occurs only between cells that are near neighbours. Inhibition is required only locally because one of its main functions seems to be to attenuate the response from regions of local homogeneous activity, thus accentuating the response from regions with high gradients of activity. This ensures that information regarding changes in stimulation passes to the next level of analysis, thereby economizing on information transmission

(Barlow 1961). Second, pooling of spatial and other information is required more often over small regions than over larger regions, so that keeping spatially contiguous regions together economizes on the lengths of dendritic connections. The coding of visual location and spatial pattern depends ultimately on which axons connect to which, rather than on the spatial disposition of the pathways in the central nervous system. The notion of a topographic code, in the sense of the spatial arrangement of cells over a surface, ceases to have any significance beyond the retina. All features are coded in the central nervous system in terms of cell connections and the simultaneous and successive patterns of cell firing, not in terms of the spatial dispositions of cells. Spatial maps demonstrate to an experimenter that spatial information is present but, for the perceiver, the spatial organization of the stimulus is represented by spatiotemporal patterns of neural connections.

4.2.7 Effects of attention and learning

Most investigations of the response properties of cortical cells have been carried out on anaesthetized animals. In such a procedure, any effects due to changes of attention, or motivation remain undetected. A growing body of evidence from work on unanaesthetized animals indicates that these factors modify the responses of cortical neurones. The concept of sets of cortical cells tuned to specific and fixed stimulus features must give way to a view of the cortex as a highly flexible organ in which the response characteristics of cells are conditional on influences arising from other centres in the brain. We discussed in Section 3.3.2 the possibility that neural activity in different parts of the brain that underlies a particular percept may be linked by response synchronization. We will describe four types of attention enhancement of the responses of cortical cells. The first results from general arousal, the second is location specific, the third is stimulus specific, and the fourth results from learning.

Effects of general arousal

It was mentioned in Section 4.1.3 that the activity of relay cells in the LGN is enhanced in states of general arousal. Livingstone and Hubel (1981) found that cells in the primary visual cortex of the awake cat generally show a reduced spontaneous firing rate and an enhanced response to visual stimuli compared with when the animal is asleep. Some cells in V1 and V2 respond more vigorously before saccadic eye movements but not specifically to eye movements to stimuli in their receptive field (Robinson et al. 1980; Moran and Desimone 1985). In other words,

the enhanced response is one of general arousal rather than being location- or feature-specific.

Location-specific attention enhancement

The responses of cortical cells to a given stimulus are influenced by the locus of attention. Thus, many cells in the parietal lobe of the monkey respond more vigorously to a stimulus when the animal is attending to it, reaching for it, or fixating it, whatever that stimulus may be (Lynch et al. 1977; Bushnell et al. 1981). Increased rates of response of cells to stimuli to which monkeys are redirecting their attention have also been noted in the temporal and frontal lobes (Fischer and Boch 1981; Wurtz et al. 1980). Many cells in the frontal eye fields and posterior parietal cortex of the monkey respond more vigorously to stimuli in their receptive field toward which the animal is just about to make a saccadic eye movement (Robinson et al. 1978). In all these cases the enhanced response is related to the location of the stimulus rather than to its identity.

The response of a single cortical cell to a given stimulus is influenced by stimuli outside the receptive field of the cell (Nelson and Frost 1978; Gilbert and Wiesel 1990). Furthermore, occlusion of the receptive field of a cortical cell accompanied by stimulation of the surrounding area over a period of 10 minutes has been found to cause a five-fold increase in the area of the occluded receptive field (Chino et al. 1992; Pettet and Gilbert 1992). A local artificial scotoma applied in one eye leads to an expansion of both monocular receptive fields of cortical cells serving that area (Volchan and Gilbert 1995). The expansion is thus due to cortical mechanisms. A small stimulus near the boundary of an artificial scotoma is perceptually displaced towards the centre of the scotoma (Kapadia et al. 1994).

Stimulus-specific attention enhancement

Attention-selective processes in V1 and V2 may be related to pattern discrimination rather than to the act of attending to a single stimulus to make an eye movement or reaching. When monkeys were required to select a test bar in a particular orientation from among bars in other orientations, the cells in V1 and V2 showed enhanced response to the bar (Motter 1993). Response enhancement did not occur when monkeys attended to an isolated bar.

A form of attentional gating related to the identity of the stimulus has also been revealed in area V4 (Moran and Desimone 1985). Cells in area V4 have receptive fields between 2 and 4° wide and respond to colour and spatial attributes of stimuli. When effective and ineffective stimuli were presented simultaneously within a cell's receptive field, the cell

responded only when the animal attended to the effective stimulus. When the animal attended to the ineffective stimulus, the response to the effective stimulus was suppressed. An ineffective stimulus presented outside the cell's receptive field had no power to inhibit responses. A similar process of attentional gating was revealed in the inferotemporal cortex and, since many cells in this area have receptive fields covering the whole retina, the response to an effective stimulus was inhibited when the animal attended to any ineffective stimulus.

Learning-specific enhancement

Receptive fields of cells in the somatosensory and auditory cortex have been shown to undergo considerable reorganization following either intracortical microstimulation or different types of sensory stimulation (Dinse et al. 1990b; Racanzone et al. 1993). Within the primary visual area of the cat, long-term changes in synaptic conductivity along lateral pathways have been induced by pairing synaptic responses with conditioning shocks of depolarizing current (Hirsch and Gilbert 1993). This suggests that these pathways are involved in stimulus-dependent changes in cortical responses.

Visual stimuli having behavioural relevance as a result of learning evoke stronger responses in cortical cells. Thus, about one-third of the cells in the visual cortex of the monkey increased their response about 20 per cent when the stimulus was one that the animal had been trained to recognize (Haenny and Schiller 1988). A similar response increment plus a narrowing of orientation tuning was shown by about three quarters of cells in area V4. Zohary et al. (1994a) found a 13 per cent increase in sensitivity of motion-sensitive cells in MT and MST of the monkey associated with a 19 per cent improvement in the ability to discriminate directions of visual motion. These feature-specific effects are presumably due to feedback from higher-order visual systems. Ablation of area V4 in monkeys produced severe deficits in their ability to select less prominent stimuli from an array, and in their ability to generalize discrimination learning to new stimuli (Schiller and Lee 1991). Some cells in the inferotemporal cortex of monkeys responded more vigorously when a feature of the stimulus, such as colour, was one to which the animal must attend in order to solve a discrimination task (Fuster and Jervey 1981).

4.3 MIDLINE INTERACTIONS

Suppose that inputs from the nasal and temporal hemiretinas are perfectly partitioned in the chiasma,

so that all axons from each nasal hemiretina go to the contralateral cerebral hemisphere and all those from the temporal hemiretina go to the ipsilateral hemisphere. Objects to the left of both visual axes (regions A and B in Figure 4.16) produce images that lie in the right visual cortex and objects to the right of both visual axes (regions C and D) produce images that lie in the left visual cortex. In each case, the images have uncrossed disparity when the object is beyond the point of fixation and crossed disparity when it is nearer than this point (see Section 2.3.1 for a definition of "crossed" and "uncrossed" disparities). Consider an object lying in the zone between the visual axes. The images of an object beyond the fixation point (region E) fall on the nasal halves of each retina and those of an object nearer than the fixation point (region F) fall on the temporal halves. In both cases, the images project to opposite cerebral hemispheres. Stereopsis based on differences between direct binocular inputs to cortical cells would be impossible for such objects. In fact, stereoscopic acuity is particularly good for objects lying on the midsagittal plane near the fixation point. Therefore, it seems that there must be cortical cells serving the midline region that have receptive fields in opposite hemiretinas in the two eyes. Evidence for this convergence of inputs has been provided from the cat. A strip of cortex at the boundary between areas 17 and 18 of each hemisphere contains binocular cells with receptive fields which overlap in the midline of the visual field (Stone 1966; Leicester 1968; Blakemore 1969). Cortical cells in this region have receptive field centres 2.5° into the ipsilateral visual field, along the horizontal meridian. Along more eccentric horizontal meridians, the receptive field centres extend up to 10° into the ipsilateral field (Payne 1990). Two mechanisms could underlie bilateral projection to midline cells; imperfect partitioning of inputs from the hemiretinas at the optic chiasma, and interhemispheric connections projected through the corpus callosum.

4.3.1 Partitioning of hemiretinas

Linksz (1952) suggested that the nasal and temporal hemiretinas are not perfectly partitioned. One reason for this could be that ganglion cells with large receptive fields in the midline region would necessarily receive inputs from receptors in both halves of the retina. It is also believed that, in a region extending about 1° on either side of the vertical retinal meridian in the cat, some ganglion cells project to the ipsilateral LGN and some project to the contralateral LGN (Nikara et al. 1968; Sanderson and Sherman 1971; Levick et al. 1981). By recording from

ganglion cell axons that crossed in the chiasma, Kirk et al. (1976a, 1976b) found that, although cells with a brisk sustained response (X cells) did not have receptive fields that encroached more than 0.5° across the retinal midline, cells with a brisk transient response (Y cells) and slowly conducting cells (W cells) had receptive fields that encroached 15° or more over the midline. W cells have large receptive fields and project mainly to subcortical nuclei such as the medial interlaminar nucleus and superior colliculus. This suggests that they are involved more with the control of vergence than with stereopsis. However, Pettigrew and Dreher (1987) found cells in cortical area 19 of the cat which received inputs from W-type ganglion cells and were tuned to zero or uncrossed disparities.

In the monkey, horseradish-peroxidase labelling techniques have revealed that within a 1° wide vertical strip around the midvertical meridian, which expands to 3° in the region of the fovea, there is a mixture of decussating and nondecussating ganglion cells (Bunt and Minckler 1977). In humans, bilateral projection from the foveal region has been used to explain foveal sparing, that is, the preservation of vision in an area around the fovea following unilateral occipital damage. Against the idea of direct bilateral projection in humans is a report that the reaction time for the response of a hand controlled by one half of the brain to a stimulus presented just in the nasal half of the monocular visual field is longer than to one presented just in the temporal visual field. This is what one would expect if the first reaction time involves a longer route through the corpus callosum (Lines and Milner 1983). We will now consider other evidence for transcallosal visual inputs.

4.3.2 Transcallosal connections

Bilateral projection to midline cortical cells could be carried by interhemispheric fibres in the corpus callosum even if inputs from the retinas are perfectly partitioned. Retinal areas near the vertical meridian project to the region between cortical areas 17 and 18 in the cat and to the region between V1 and V2 in the monkey. In both animals, this boundary region is well served by interhemispheric connections (Choudhury et al. 1965; Hubel and Wiesel 1967; Harvey 1980). In the monkey, 80 per cent of transcallosal inputs to the boundary region are from the foveal area and only 20 per cent are from the retinal periphery. In V1, the terminals of these neurones are confined to cortical layers 2, 3, 4B, and 5 whereas in V2 they occur in all layers (Kennedy et al. 1986). Regions representing the retinal vertical midline in other visual areas in the cerebral cortex also receive

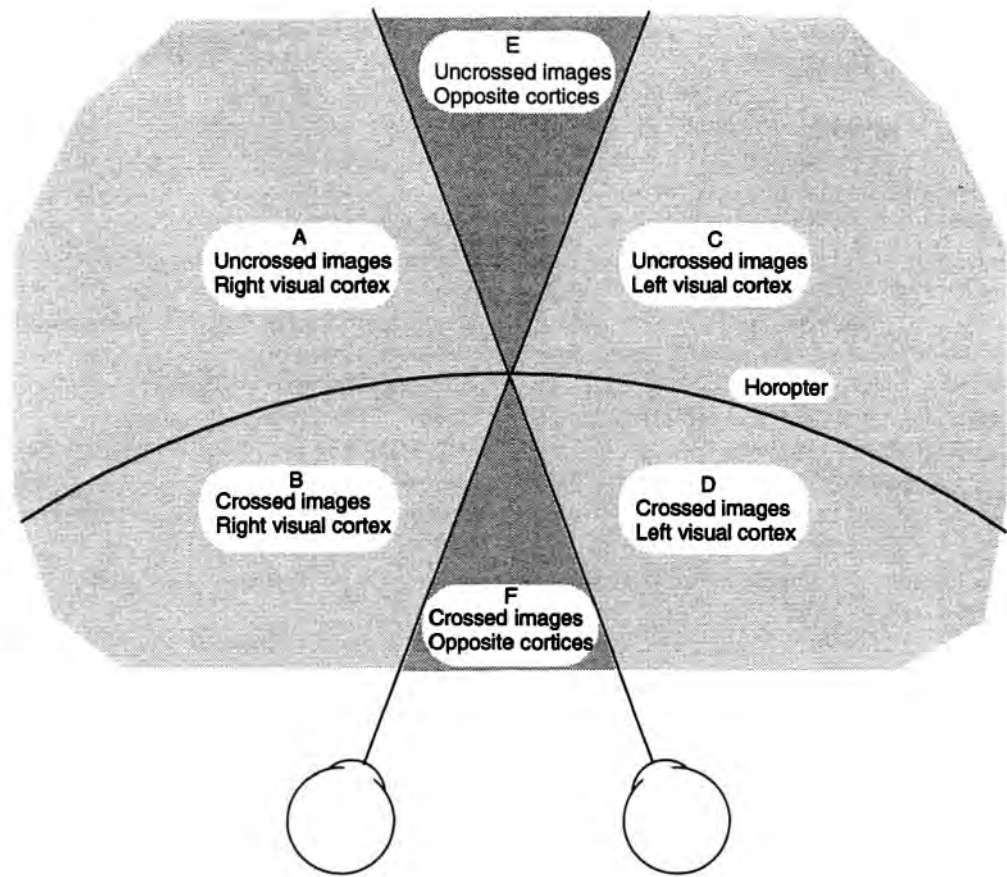


Figure 4.16. Divisions of the visual field.

The diagram shows regions where the images of an object project to the left visual cortex, the right visual cortex, or opposite visual cortices. Also indicated are regions in which the images are crossed (left eye's image to the right of right eye's image and vice versa) or uncrossed (left eye's image to the left of right eye's image).

transcortical inputs. Visual areas V4 and MT (middle temporal cortex) in the monkey receive extensive transcallosal inputs which, although most dense near the representation of the vertical meridian, are not confined to the midline region (Van Essen and Zeki 1978; Maunsell and Van Essen 1987). There is evidence from recordings made in V4 of the alert monkey that transcallosal influences extending more than a degree or two beyond the vertical midline are purely inhibitory. Desimone et al. (1993) speculated that these widespread inhibitory influences are concerned with colour constancy and figure-ground segregation rather than with stereopsis. Anatomical studies on human brains have revealed bands of transcallosal terminals along the boundary between areas 17 and 18 and in surrounding areas (Clarke and Miklossy 1990). Some of these transcallosal connections are present at birth, although their full development, at least in the cat, depends on normal binocular experience (Lund and Mitchell 1979). The functions of the corpus callosum have been

reviewed by Berlucchi (1972) and Kennedy et al. (1991).

One approach to the issue of midline stereopsis is to study the effects of midsagittal section of the optic chiasm. This procedure severs all direct inputs from the contralateral eye to each hemisphere, so that any remaining binocular cells in the visual cortex receive their contralateral input indirectly through the corpus callosum (Berlucchi and Rizzolatti 1968). There has been some dispute about how many binocular cells survive in split-chiasm cats. Estimates have varied from none (Milleret and Buser 1984), to 30 per cent (Lepore and Guillemot 1982), and up to 76 per cent (Cynader et al. 1986). In split-chiasm cats there is a complete loss of binocular cells responsive to uncrossed disparity arising from stimuli in the median plane (Lepore et al. 1992). This is what one would expect because the images of such objects fall on the nasal hemiretinas, the inputs from which are severed in the split-chiasm cat. Split-chiasm cats performed poorly on a random-dot stereo discrimination test

presented on a jumping stand, which constitutes a test of fine stereopsis (Lepore et al. 1986). On the other hand, Blakemore (1970a) reported the case of a boy in whom the decussating pathways in the optic chiasm were completely sectioned and who retained an ability to discriminate depth in the region of the midline, as revealed by a coarse test of stereopsis involving disparities of at least 3 arcmin.

A second approach to the issue of midline stereopsis is to study the effects of cutting transcallosal inputs. The physiological effects are discussed first. Cooling the border between areas 17 and 18 in one hemisphere of the cat produced a selective loss of binocularly in a significant number of midline cells in the other hemisphere (Blakemore et al. 1983). Transection of one optic tract also led to a loss of binocularly in the contralateral hemisphere (Lepore et al. 1983). Guillemot et al. (1993) found that almost all the disparity-tuned cells in area 19 of the cat lost their disparity tuning following section of the corpus callosum, suggesting that these cells receive their input from the contralateral eye by this route. Section of the corpus callosum in adult cats produced a long-term reduction in the proportion of binocularly driven cells with receptive fields extending 4° to either side of the retinal midline region (Payne et al. 1984). However, there is conflicting evidence on this point. For instance, Elberger and Smith (1985) reported that callosal section affected binocularly and visual acuity at all retinal eccentricities, when performed on cats before the age of about 3 weeks, and had no effect after that age (see also Elberger 1989, 1990). Minciachchi and Antonini (1984) also failed to find any loss of binocularly in areas 17 and 18 of unanaesthetized callossectomized adult cats. However, they did not test the cells for disparity sensitivity. Part of the effect of early callosectomy on binocularly may be due to eye misalignment which this procedure introduces (Elberger 1979). Binocular cells in visual areas beyond areas 17 and 18, such as the lateral suprasylvian area and the superior temporal sulcus, are not affected by neonatal callosectomy in the normal cat but are affected by this procedure in Siamese cats, in which the visual pathways fully decussate (Zeki and Fries 1980; Elberger and Smith 1983; Marzi et al. 1982).

A few studies have been conducted on the behavioural effects of callosectomy. In cats with neonatal section of the callosum, coarse stereopsis revealed in reactions to a visual cliff was adversely affected (Elberger 1980). Mitchell and Blakemore (1970) reported a clinical case in which section of the corpus callosum led to a disruption of midline stereopsis, also measured by a test sensitive to only coarse (large) disparities. In other studies fine stereopsis

was not affected by callosal section in the neonatal or adult cat (Timney et al. 1985; Lepore et al. 1986). The corpus callosum has several parts. Transection of the part known as the splenium did not affect midline stereopsis in the monkey (Cowey 1985) and section of all parts other than the anterior commissure was without effect in monkeys (LeDoux et al. 1977) and humans (Bridgman and Smith 1945). It looks as though the crucial fibres serving midline stereopsis cross in the anterior commissure.

Some fibres could cross from the lateral geniculate nucleus to the opposite visual cortex. The evidence for such connections is controversial (Glickstein et al. 1964; Wilson and Cragg 1967). In cats with unilateral removal of the visual cortex, midline cells tuned to fine disparity were still present in the remaining hemisphere but cells tuned to coarse disparity were lost (Gardner and Cynader 1987).

All these findings support a suggestion made by Bishop and Henry (1971) that the callosal pathway is responsible for midline bilateral integration only for coarse stereopsis, whereas fine stereopsis in the midline depends on overlap of direct visual inputs in the midline region. Linksz (1971) made the plausible suggestion that coarse disparities carried by the corpus callosum are used to initiate vergence and that impressions of depth from coarse disparities are a secondary phenomenon arising from the command centres controlling vergence. This idea is supported by the fact that a patient with section of the corpus callosum failed to produce vergence movements in response to targets in the visual midline but responded when images were in the same hemisphere (Westheimer and Mitchell 1969). Some observational support for this idea is provided in Section 6.2.6. Linksz also suggested that fine stereopsis depends on disparities between direct visual inputs from the two eyes and is concerned with the perception of relative distances, the solidity of objects, and the three-dimensional structure of surfaces.

4.4 DISPARITY DETECTORS

We explained in Section 1.2.2 that before the 1960's many leading visual scientists, including Helmholtz, believed that binocular stereopsis does not arise from the conjunction of visual inputs at an early stage of visual processing but from high-level cognitive processes. Ramón y Cajal (1911) proposed that inputs from corresponding regions of the two retinas converge on what he called "isodynamic cells" and that this mechanism forms the basis of unified

binocular vision. This idea received experimental verification when Hubel and Wiesel (1959, 1962) reported that the receptive fields of binocular cells occupy corresponding positions in the two eyes. If this were strictly true, and if each binocular cell had identical receptive fields in each eye, all binocular cells would respond optimally to stimuli lying along the horopter, and disparity could not be recovered from the output of such cells. The search for binocular cells that are selectively tuned to different disparities was beset with the problem of ensuring that the images in the two eyes are in binocular register. If the images are slightly out of register, a cell that is really tuned to zero disparity will appear to be tuned to a disparity equal to the extent of image misregistration. Also, any movement of the eyes during the recording introduces artifacts. Several procedures have been used to solve this problem. In the anaesthetized animal, eye movements are controlled by paralyzing the eye muscles and attaching the eyeball to a clamped ring. The direction of gaze is controlled by a rotating mirror or a prism of variable power. In the reference-cell procedure, the responses of two cells are recorded—a test cell and a reference binocular cell—with receptive fields in the central retinas. Changes in the response of the reference cell indicate when eye movements have occurred (Hubel and Wiesel 1970a). In a related procedure, the response of a reference cell to monocular stimulation is used to monitor eye drift (Maske et al. 1986a). Another specification of image stability is provided by the responses of two LGN cells of foveal origin, one from each eye (LeVay and Voigt 1988). These procedures indicate when eye drift has occurred, but they do not specify when test stimuli have zero disparity, since the reference cell may not be tuned to zero disparity. One solution to this problem is to use the mean response of several reference cells to define zero disparity (Nikara et al. 1968). Another procedure is to use an ophthalmoscope to project images of retinal blood vessels onto the screen on which the stimuli are presented (Bishop et al. 1962; Pettigrew et al. 1968). As we will see, the problem is simplified when testing is done on an alert monkey trained to converge on defined targets.

4.4.1 Disparity detectors in the cat

Barlow, Blakemore, and Pettigrew (1967) reported from Berkeley, California, that certain binocular cells in the visual cortex of the cat respond selectively to line and bar stimuli with a particular binocular disparity, that is, stimuli normally produced by an object at a given distance from the plane of fixation. Similar findings were reported about the same time

from Sydney, Australia, by Pettigrew, Nikara, and Bishop (1968).

Disparity-selective neurones are usually referred to as **disparity detectors**. The frequency of firing of a cortical cell as a function of the disparity of the stimulus is its **disparity tuning function**. The disparity to which a cell responds most vigorously is its **preferred disparity**. A preferred disparity also has a sign (crossed or uncrossed) and an axis (horizontal, vertical, or oblique). The **disparity selectivity** of a cell is indicated by the width of its disparity tuning function at half its height. The narrower the tuning function, the higher the cell's selectivity. The mean fluctuation in the firing rate of a binocular cell for a constant stimulus is the **response variability** of the cell (Crawford and Cool 1970). A binocular cell shows **facilitation**, **summation**, or **occlusion** depending on whether its response to a binocular stimulus is greater than, equal to, or less than the sum of responses to monocular stimuli.

The preferred disparity of a cell is measured by observing its response to stimuli presented simultaneously to the two eyes as a function of disparity. In a related procedure, the mean retinotopic position of the receptive field of a binocular cell is determined first in one eye and then in the other. The spatial separation in degrees of visual angle between the two separately determined monocular fields is the **receptive field offset**. It is often assumed that the preferred disparity of a given binocular cell is equal to the cell's receptive field offset. However, it is not easy to determine the relationship between these two measures. The receptive field offset can be measured only in cells that respond to each eye separately and perhaps not all disparity-sensitive cells are of this type. Furthermore, because many cells tuned to disparity give an excitatory response to stimulation of one of the eyes but not of the other (when tested separately) their receptive field offset cannot be determined. In any case, the disparity sensitivity of some or all binocular cells may depend on offsets of subunits within their receptive fields rather than on the offset of the fields as a whole (see Section 4.5.2).

Each retina projects retinotopically into the visual cortex so that as one progresses across the cortical surface within an ocular-dominance column a systematic change occurs in the retinal location of the receptive fields in the single eye. However, in each small region of the cortical surface there is a random scatter of receptive field locations. In the cat, the variance of this scatter has been estimated to be 0.12° (Albus 1975). If the monocular fields in a given small region are paired at random to form receptive fields of binocular cells, then the variance of the field

offsets should equal the sum of the variances of the monocular scatters. For the cat, this is approximately true (Bishop 1979).

The preferred disparities in the study by Barlow et al. were distributed horizontally over a 6.6° range and vertically over a 2.2° range. Other investigators have found that the preferred disparities for cells in the cat's visual cortex have a standard deviation of only about 0.5° for both horizontal and vertical disparities for eccentricities of up to 4°, increasing to 0.9° at an eccentricity of 12° (Nikara et al. 1968; Joshua and Bishop 1970; von der Heydt et al. 1978). These values suggest a range of disparities of only about 3°. Ferster (1981) found no cells sensitive to disparities over 1°. There are at least two reasons for these discrepancies. The first is that the apparent peak disparity to which a given cell is tuned is affected by the extent to which eye movements are controlled. The second is the accuracy with which the position of zero disparity is registered in testing.

Blakemore (1970c) found that disparity-selective cells in the visual cortex of the cat were arranged in distinct columns of tissue, which he called constant depth columns. Blakemore also described another type of columnar arrangement in which the binocular cells were driven by receptive fields in the contralateral eye that were all in the same region of the retina and by receptive fields in the ipsilateral eye that were scattered over several degrees. The cells in such a column therefore have a variety of preferred disparities, but they all respond to a stimulus lying on a given oculocentric visual line of one eye. The column "sees" along a tube of visual space lined up with an oculocentric visual direction of one eye. This finding should be replicated with more adequate control of receptive field mapping.

There are three main types of disparity-tuned cells in areas 17 and 18 of the cat. Cells of the first type have a narrow disparity tuning function centred at zero disparity and are known as **tuned excitatory cells**. Cells of the second type fire maximally to crossed disparities and are known as **near cells**. Cells of the third type respond to uncrossed disparities and are known as **far cells**. As we will see, similar types of cell have also been found in the monkey. The distinction between the physiological responses of these cell types was not always clear and the cells probably lie along a continuum. Some cells which could not be placed in any of these categories are described in later sections of this chapter. Tuned excitatory cells are ocularly balanced, that is, they respond equally well to stimulation of either eye.

The near and far cells show strong ocular dominance, that is, they respond more strongly to stimulation of one eye than of the other or only to

stimulation of one eye when each eye is tested separately (Fischer and Krüger 1979; Ferster 1981). Thus, most cells with high ocular dominance are sensitive to nonzero disparity and cells driven well through either eye are tuned to disparities close to zero or are nonselective for disparity (Maske et al. 1986a, 1986b; Gardner and Raiten 1986; LeVay and Voigt 1988). After ablation of areas 17 and 18, cats lost their ability to discriminate depth based on disparity although abilities such as vernier acuity and brightness discrimination survived (Ptito et al. 1992).

Disparity-tuned cells have also been found in area 19 of the cat. Pettigrew and Dreher (1987) found that such cells receive inputs from W-type ganglion cells and are tuned to zero or uncrossed disparities compared with the predominant crossed-disparity tuning of cells in area 17. Guillemot et al. (1993) found that only about 34 per cent of cells in area 19 of the cat were tuned to disparity compared with over 70 per cent in area 17. They also found that almost all disparity-tuned cells in area 19 lost their disparity tuning following section of the corpus callosum, suggesting that these cells receive their input from the contralateral eye by this route. W cells have large receptive fields and may be involved more with the control of vergence than with stereopsis.

Although there are binocular interactions in the LGN (see Section 4.1.3), disparity-tuned cells have not been found in the LGN of the cat (Xue et al. 1987). Disparity-tuned cells have been found in the superior colliculus of the cat (Berman et al. 1975) and opossum (Dias et al. 1991). The superior colliculus is a subcortical nucleus with multisensory inputs that is concerned with the direction of attention and the control of saccadic eye movements to designated regions in visual space. A directional map of space based on visual inputs overlays a directional map based on auditory inputs. Only further work will reveal whether this coordinated mapping extends to the third dimension. Such a mapping could help to initiate vergence eye movements.

4.4.2 Disparity detectors in the monkey

Hubel and Wiesel (1970a) were the first to look for disparity-tuned cells in the anaesthetized monkey. They found no evidence of disparity-tuned cells in V1 but found them in V2. Their inability to find them in V1 was probably due to inadequate control of eye alignment. More recent recordings from V1 and several other visual areas of the anaesthetized monkey have revealed the same three types of disparity-tuned cell found in the cat plus an infrequent type that is inhibited by zero disparity, known as **tuned inhibitory cells**. These four types of cell have

been found in V1 but are especially prevalent in V2, where at least 70 per cent of neurones have been found to be tuned to horizontal disparity in the monkey (Poggio 1984; Hubel and Livingstone 1987). Ablation of the foveal region of V2 in the monkey caused a severe elevation of stereo threshold (Cowey and Wilkinson 1991). According to one estimate, about 45 per cent of cells in V3, which borders V2, are disparity-tuned, about half of them being tuned excitatory cells and the others belonging to the other three classes (Felleman and Van Essen 1987). Similar types of disparity-tuned cell have also been found in area VP, which also borders V2 (Burkhalter and Van Essen 1986). About two-thirds of cells tested in the middle temporal visual area (MT) belong to the same four disparity-tuned types. Most of these cells were found to be as sensitive to vertical as to horizontal disparity (Maunsell and Van Essen 1983b).

Poggio and Fischer (1977) were the first to record from disparity-tuned cells in the cortex of an alert animal—the rhesus monkey. These findings were extended in subsequent papers from the laboratory of Gian Poggio in Johns Hopkins University in Baltimore (Poggio and Talbot 1981; Poggio et al. 1985, 1988a; Poggio 1991). The monkey was trained to fixate a small visual target while bar stimuli were presented in different depth planes relative to the fixation target. The problem of aligning the two visual fields was thus greatly simplified. Both bar stimuli and random-dot stereograms were used to determine the disparity tuning functions of the cells. In addition, the sensitivity of cells to changes in dichoptic correlation was determined with dynamic random-dot displays that changed from being correlated in the two eyes to being uncorrelated.

More than half the simple and complex cells in V1 were found to be disparity tuned and an increasing proportion of disparity-tuned cells was found as testing progressed into areas V2, V3, and V3A. About equal numbers of simple and complex cells were disparity-tuned, but complex cells were particularly sensitive to the depth in random-dot stereograms. The subfields within the receptive fields of complex cells presumably allow these cells to respond to the disparity between the microelements of the stereogram. The complex cells were also more sensitive than simple cells to changes in image correlation in a random-dot stereogram, probably for the same reason. Some cells sensitive to differences in image correlation were also sensitive to the sign and degree of disparity, while others were sensitive to differences in image correlation only when disparity was zero (Gonzalez et al. 1993).

The cells found in the alert monkey were classified into six types, the four already described

(excitatory cells tuned to zero disparity, tuned inhibitory cells, and near and far cells) plus tuned excitatory cells tuned to either crossed disparities or uncrossed disparities. Figure 4.17 shows sample tuning functions of the six types. Another type of cell responding to stimuli moving in opposite directions in the two eyes is described in Section 13.2.5. Tuned excitatory cells with a narrow tuning function peaking at zero disparity are the most common type. They are all inhibited by uncorrelated images and tend to have balanced ocular dominance. Tuned inhibitory neurones are suppressed by stimuli around zero disparity and most of them are excited by uncorrelated images. The tuning functions of these two types of cell are symmetrical and form reciprocal pairs. The near cells respond to crossed disparities and are inhibited by uncrossed disparities and the far cells have the opposite characteristics. The near and far cells do not have a well-defined preferred disparity and only about a third of them respond to changes in image correlation. Their tuning functions are asymmetrical and also form reciprocal pairs, as depicted in Figure 4.18. The tuned inhibitory and the near and far cells tend to have strong monocular dominance, suggesting that inputs from the weaker eye inhibit those from the dominant eye, except when the stimulus is at the appropriate depth relative to the horopter. The tuned near and tuned far cells have tuning functions with a well-defined preferred disparity peaking at crossed or uncrossed disparities of up to 0.5° and have an inhibitory flank on the zero disparity side of the tuning function. They also form a reciprocal pair.

The classification of disparity detectors into six classes and the scheme depicted in Figure 4.17 are abstractions in terms of standard prototypes and one should not regard them as a fixed number of exclusive types. Disparity detectors do not fall into exclusive categories and are not uniform over the visual field.

Poggio suggested that excitatory/inhibitory pairs of disparity detectors provide the physiological basis for fine stereopsis and that the near/far pairs provide the physiological basis for coarse stereopsis. This argument is based on the different widths of the tuning functions. However, we know that very fine discriminations can be achieved with a set of broadly tuned channels (see Section 3.5.3). For instance, the chromatic channels are broadly tuned but achieve fine discriminations of colour. On this basis the near/far disparity channels should provide good discrimination for differences in disparity around zero because their tuning functions are steepest and overlap just at zero. The relative change in signal strength in the two channels is therefore greatest at

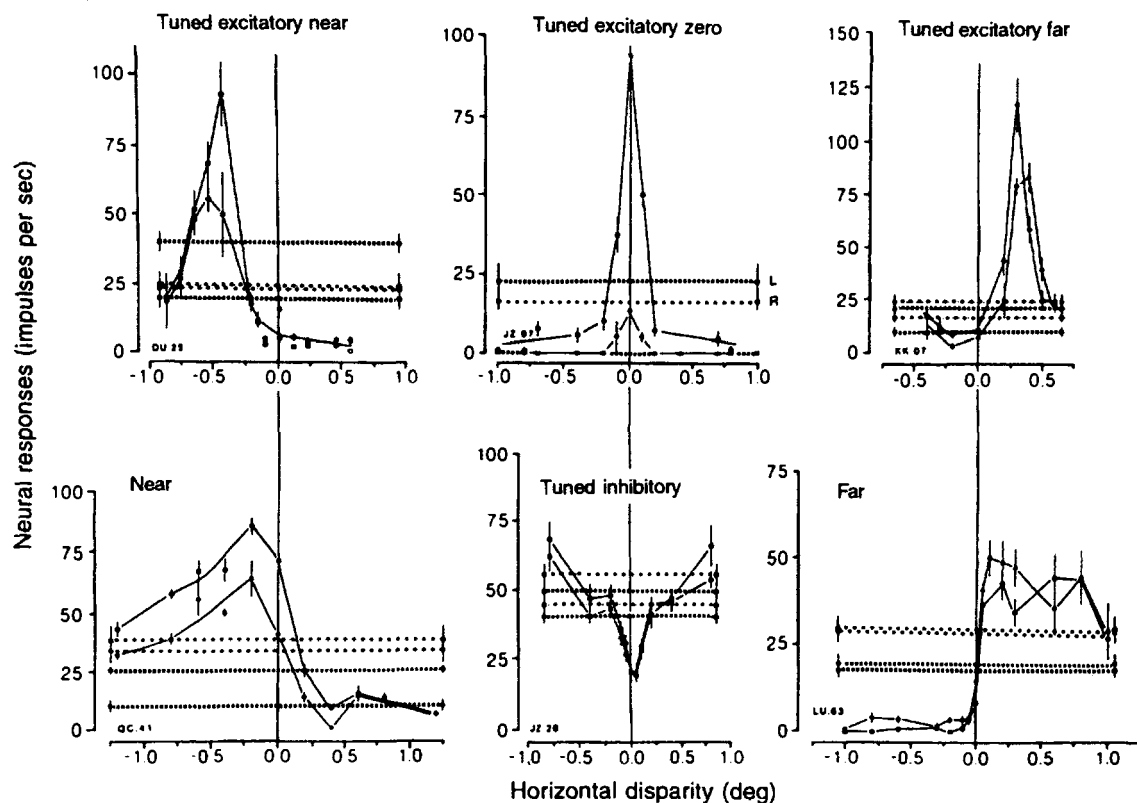


Figure 4.17. Six classes of disparity-tuned cells in monkey visual cortex.

For each function, the frequency of nerve impulses was plotted for different horizontal disparities of a bright bar moving in each of two opposed directions across the cell's receptive field. For each cell, the functions for the two directions of motion are plotted separately. Vertical bars are standard errors. The dotted horizontal lines are the responses of the right eye alone to the two directions of stimulus motion and the horizontal dashed lines are the responses of the left eye alone. (From Poggio 1991.)

this point, as can be seen in Figure 4.18. Fine discrimination around zero-disparity based on narrowly tuned detectors would require several detectors tuned to different disparities (see Lehky and Sejnowski 1990 for discussion of this issue).

Trotter et al. (1992) recorded from disparity-tuned cells in V1 of the alert monkey as the animal fixated on a visual target at distances of 20, 40, and 80 cm. At each distance an array of random dots was presented with various degrees of horizontal disparity relative to the fixation target. The size of the dots, the dot display, and the disparities were scaled for distance so that the retinal images were the same for each distance. The response of most cells was modulated by changes in viewing distance. For most cells, disparity selectivity emerged at only one distance or was sharper at one distance than at other distances. They concluded that the signals mediating these changes in response were derived from changes in vergence or accommodation. The investigators were convinced that the pattern of retinal stimulation was the same at the different distances. However, changes in cyclovergence are known to accompany

changes in vergence, and since no precautions were taken to prevent or compensate for cyclovergence the resulting changes in the alignment of the images may have caused the observed changes in the responses of cortical cells. Furthermore, the pattern of vertical disparities produced by a display in a frontal plane varies with distance (see Section 7.6.7) and this factor may have contributed to the observed changes in response of cortical cells.

4.5 DISPARITY TUNING FUNCTIONS

4.5.1 Shape of disparity tuning functions

The tuning function of a cortical cell for horizontal or vertical disparities defines the response of the cell, specified in impulses per second, as a function of the separation of two optimally oriented dichoptic bars or gratings. Zero separation is defined in terms of the averaged responses of several cells in the foveal region. Tuning functions for orientation disparities are discussed in Section 4.6.2. A disparity tuning

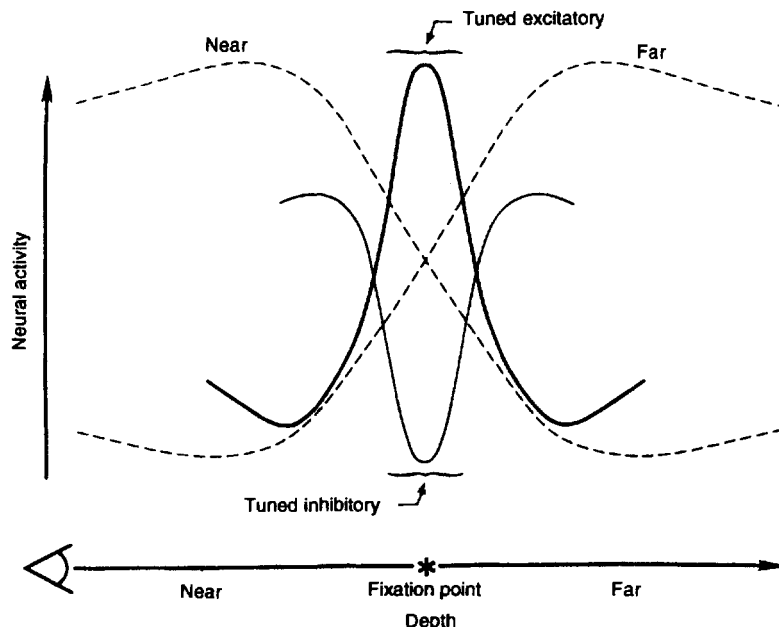


Figure 4.18. Idealized tuning functions of four types of cortical cell.

Tuned excitatory and tuned inhibitory cells are optimally tuned to zero disparity, and their tuning functions form a reciprocal pair. The tuning functions of "near" and "far" cells, represented by dotted lines, are asymmetrical and do not show a well-defined preferred disparity. They also form a reciprocal pair. (Reproduced with permission from Poggio et al., 1985, Vision Research, Pergamon Press.)

function, like any other sensory tuning function, has five basic features:

1. The peak amplitude of response.
2. The tuning width, specified as the width (sometimes half width) of the tuning function at half its peak amplitude.
3. The degree of symmetry of the tuning function about its peak amplitude.
4. The preferred disparity, that is, the size and sign of disparity that evokes the strongest response.
5. The polarity of the cell's response, that is, whether it is monopolar or bipolar (oppositional) with respect to its resting level of discharge. All disparity-sensitive cells are monopolar. For instance, there are none for which the rate of discharge increases above a resting level with, say, crossed disparities and decreases below the resting level with uncrossed disparities. Colour opponent cells and sensory cells in the vestibular apparatus are examples of bipolar, or oppositional, detectors.

The first three features define the shape of the tuning function, the fourth specifies its position along the disparity axis, and the fifth defines its position along the response axis. In this section we discuss the factors that determine the shape of a disparity tuning function.

It has been claimed that one can account for the shape of the disparity tuning functions of simple cortical cells in the cat in terms of the size and strength of the excitatory and inhibitory regions of the cell's receptive fields (Bishop et al. 1971; Ferster 1981). Ohzawa and Freeman (1986a) stimulated simple cells in the cat's visual cortex with dichoptic drifting sinusoidal gratings of optimal spatial frequency and orientation. Most cells responded most vigorously when the gratings in the two eyes were in a particular spatial phase and least when they were 180° away from the optimal phase (see Figure 4.19). Phase-specific interactions were no longer present when the gratings in the two eyes were orthogonal. The phase specificity of a cell's response did not depend on the degree of ocular dominance of the cell, except for a few strongly monocular cells that showed a purely inhibitory, phase-independent response to stimulation of the silent eye. Furthermore, the modulation of a cell's response was the same for dichoptic gratings with very different luminance contrasts as it was for those with equal contrasts (Freeman and Ohzawa 1990). There must be a gain-control mechanism that keeps the monocular inputs to disparity-tuned cells in balance.

The important point is that binocular interactions of most simple cells could be predicted from the linear summation of the excitatory and inhibitory

zones revealed by the cell's response to gratings presented to each eye separately. Linear summation of excitatory and inhibitory zones revealed when each eye was tested separately accounted for phase-specific binocular interactions in about 40 per cent of complex cells (Ohzawa and Freeman 1986b). About 40 per cent of complex cells exhibited nonphase-specific responses and about 8 per cent showed a purely inhibitory influence from one eye.

Hammond (1991) agreed that most simple cells show a phase-specific response but found that most complex cells do not. The excitatory and inhibitory zones of the receptive field of a simple cell are spatially segregated whereas, for a complex cell, the excitatory zones are coextensive for single bright and dark stimuli, and inhibition is revealed only as an interaction between two stimuli (Movshon et al. 1978). In either case, a phase-specific modulation of response implies that the spatial period of zones for a given cell is similar in the two eyes. The origin of excitatory and inhibitory zones within the receptive fields of cortical cells is not known. If they depend on cortical interactions after monocular inputs are combined, it is not surprising that they match in the two eyes.

Ohzawa et al. (1990) developed a model of the monocular receptive fields that feed into a complex binocular cell. The receptive field for each eye consists of four subunits, each with a distinct luminance profile. A luminance profile of a subunit is the function describing how the firing of the cell is modulated above or below its resting level as a stimulus is moved over the subunit. In each eye, the fields of one pair of subunits have symmetrical (cosine) luminance profiles of opposite polarity and those of the other pair have asymmetrical (sine) luminance profiles of opposite polarity, as shown in Figure 4.20 a and b. In each eye, the signals from the opposed symmetrical subunits mutually inhibit each other, as do those from the opposed asymmetrical subunits. Outputs from these two push-pull systems from the same eye combine through a nonlinear half-wave rectifier. The output of the symmetrical system is 90° out of spatial phase with respect to that of the asymmetrical system. The two are said to be in quadrature. A model complex cell with matching properties in the two eyes fires maximally when the stimulus occupies the same position in each eye. Such a cell has a symmetrical tuning function about zero disparity.

Ohzawa et al. modelled a binocular cell tuned to a nonzero disparity by providing receptive field subunits with a double quadrature organization, as shown in Figure 4.20c. In this case, the receptive field for the right eye is 90° phase shifted relative to

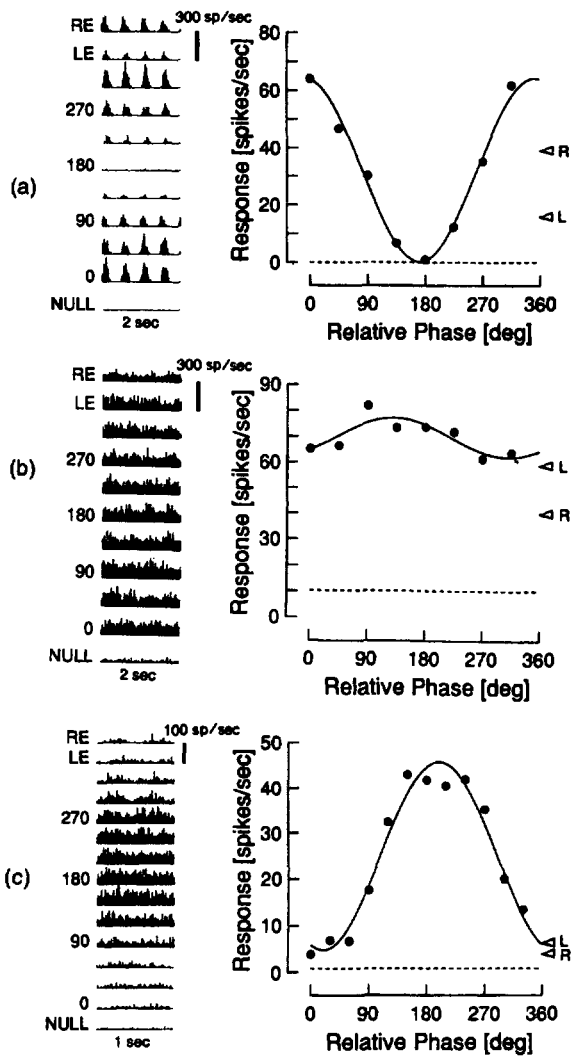
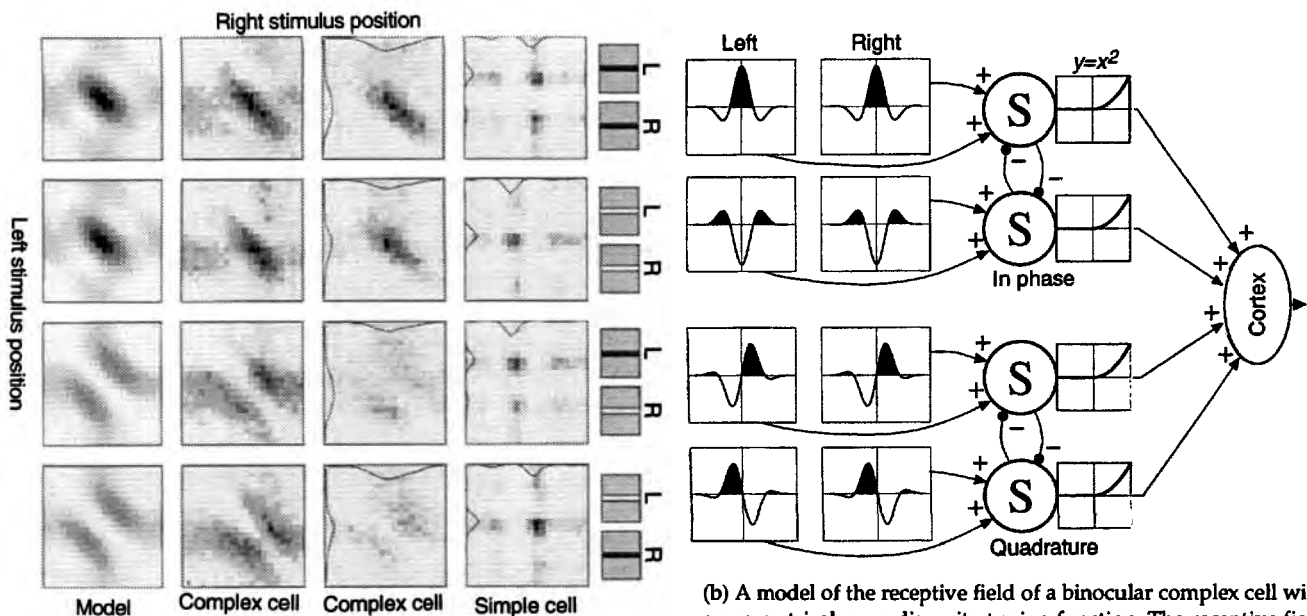


Figure 4.19. Cortical responses to dichoptic gratings.
Responses of a simple cell (a) and complex cells (b and c) in the visual cortex of a cat to a drifting grating presented dichoptically at various relative spatial phases. The time histogram of the cell's responses is shown to the left of each graph, first for each eye stimulated separately, and then for various relative phases of dichoptic stimulation. Dashed lines on the graphs represent the level of spontaneous activity. (Reproduced with permission from Freeman and Ohzawa, 1990, Vision Research, Pergamon Press.)

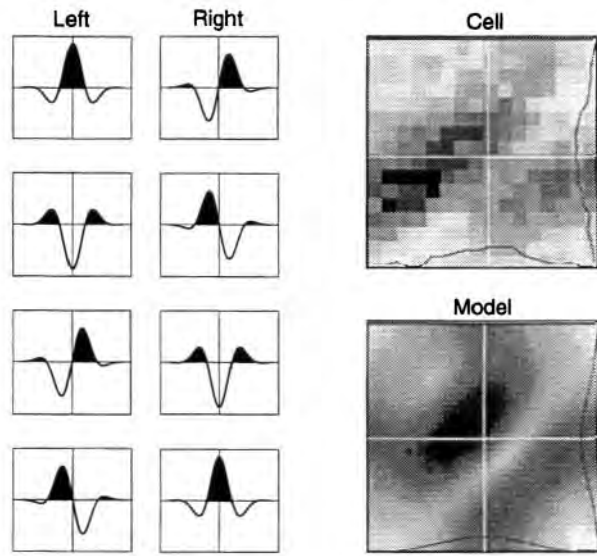
that for the left eye for all four subunits, which means that the cell fires maximally only when the stimulus in one eye is offset with respect to that in the other. A similar model has been developed by Nomura et al. (1990) and Nomura (1993).

If a cell has a periodic pattern of excitatory and inhibitory zones it could show several peaks of response as the relative phase of the images of a dichoptic bar stimulus is varied. This could account for the fact that many cortical cells have been found to have more than one peak in their disparity tuning function (Ferster 1981).



(a) Each square in the top three rows shows the firing rate (higher rate—darker) of a binocular cell in the cat visual cortex as a function of the lateral positions of optimally oriented bars in the left (abscissa) and right (ordinate) eyes. The different columns of squares show the responses to the bar stimuli indicated at the top. The two stimuli on the left have the same luminance polarity in the two eyes so that in the two columns on the left, the tuning functions have a single peak because the stimuli come into register at only one position. The two stimuli on the right have opposite polarity in the two eyes. This causes the tuning functions in the two columns on the right to have two peaks. The two peaks arise because there is one excitatory central region in the eye with a bright bar and two excitatory surround regions in the eye with a dark bar (off flanks of simple cells are excitatory for dark bars). The separation between the two peaks for opposite-polarity stimuli reveal the spatial period of the receptive-field subunits. The profiles along the edges of some of the squares represent the tuning functions of the cells to the stimulus in each eye, when presented alone. The bottom row of squares indicates the responses predicted from the theoretical model.

(b) A model of the receptive field of a binocular complex cell with a symmetrical, zero-disparity tuning function. The receptive field contains four subunits, marked S, arranged as two mutually inhibitory pairs, one pair operating in phase, the other operating in quadrature (90° phase). The nonlinear response characteristic of each subunit and the complex cell into which they feed are represented on the right. Each of the four subunits receives an input from both eyes. The profiles of the receptive fields in each eye are shown on the left, with dark areas representing excitatory regions and unfilled areas representing inhibitory regions. In each eye, the fields of one pair of subregions have symmetrical (cosine) luminance profiles of opposite polarity and those of the other pair have asymmetrical (sine) luminance profiles of opposite polarity.



(c) Hypothetical receptive-field subunits for a binocular complex cell tuned to nonzero disparity. This cell was modelled by providing receptive-field subregions with a double quadrature organization. (From Ohzawa et al. 1990. Copyright 1990 by the AAAS.)

Figure 4.20. Cortical cell responses to disparity offset.

Orientation and disparity tuning

It is reasonable to suppose that a disparity-tuned cell with a given preferred stimulus orientation would respond best to disparities at right angles to the receptive field axis. Maske et al. (1986a) found this to be true for cortical cells of the cat that lack inhibitory end zones in their receptive fields (non end-stopped cells). End-stopped cells responded to disparities along their common axis as well as, or almost as well as, to disparities at right angles to the axis, as long as the stimuli were shorter than the receptive field.

Assume that depth is signalled by disparities at right angles to the axis of the receptive field. It is generally assumed that relative depth is signalled by horizontal rather than vertical disparities. On this basis, one would expect more disparity-tuned cells with preferred orientations near the vertical than cells with preferred orientations near the horizontal. Ohzawa and Freeman (1986a) found the degree of binocular interaction for cells preferring horizontal stimuli, as a population, to be similar to that for cells tuned to vertical stimuli. Other investigators have found that disparity-tuned cells preferring vertical stimuli respond more strongly than those preferring horizontal stimuli (Maske et al. 1986a). We must reject the idea that stereopsis is based only on horizontal disparities. Vertical disparities play at least three roles in stereopsis. First, they control the vertical vergence movements of the eyes required to keep the images in vertical correspondence. Second, they are involved in the detection of absolute distance, as we will see in Section 7.6.7. Third, depth is signalled by the ratio of horizontal to vertical disparity rather than by horizontal disparity alone. This makes judgments of surface inclination independent of changes in cyclovergence and judgments of surface slant independent of aniseikonia (see Sections 7.5 and 7.6.5).

Dynamics of disparity detectors

The inhibitory processes involved in the creation of disparity selectivity of cortical cells could involve feedback or feedforward loops. Thorpe et al. (1991) found that the disparity tuning of cortical cells is fully developed in the first 10 ms of response, which suggests that only feedforward inhibitory loops are involved. Yeshurun and Schwartz (1990) have developed a model based on cepstral filters (see Section 6.2.1) of how stereoscopic disparity can be derived from feedforward processing.

4.5.2 Receptive-field offset

If the preferred disparity of a cortical cell depends on the relative offset of its receptive fields in the two eyes, one should be able correlate the two quantities.

There are two cases to consider, inter-receptive-field offset and intra-receptive-field offset.

Inter-receptive-field offset

In the first case the receptive fields of the binocular cell are the same in the two eyes, that is, they have the same preference for orientation, motion, and spatial frequency and, in particular, the same distribution of excitatory and inhibitory zones. Variations in the preferred disparity of this type of cortical cell is due to the difference in position between the receptive fields in the two eyes—their **inter-receptive-field offset**. In practice, the receptive-field offset cannot be determined for all disparity-tuned cells because many of them show a strong monocular dominance; that is, they respond to stimuli presented to one eye but not to those presented only to the other eye. Some disparity-selective cells, known as AND cells, do not respond to stimuli presented to either eye alone but only to the joint stimulation of both eyes. Furthermore, many of the cells in which a receptive field offset can be measured are not disparity selective (von der Heydt et al. 1978). There is no necessary linkage between the size of matching receptive fields and the preferred disparity of the cortical cell into which they feed. A binocular cell with small matching receptive fields could have a large receptive field offset and therefore be tuned to a large disparity, and a cell with large receptive fields could have a zero offset and therefore be tuned to zero disparity. For instance, Pettigrew et al. (1968) found complex cells with large receptive fields in the cat that were narrowly tuned to disparity.

Intra-receptive-field offset

In the second case, the positions of the two receptive fields in each retina are the same, and disparity preference is determined by relative offsets between excitatory and inhibitory zones within the monocular receptive fields. This is an **intra-receptive-field offset**. For instance, the receptive field of a cell in one eye could have a symmetric (cosine) sensitivity profile and that in the other an asymmetric (sine) profile, as illustrated in Figure 4.20c. Some cortical cells have been reported to have this type of intra-receptive-field offset (Freeman and Ohzawa 1990; DeAngelis et al. 1991). Other receptive fields of a binocular cell could differ in their preferred spatial periodicity. Such cells would be sensitive to differences in spatial width or frequency between the images in the two eyes and would be able to code the slant of a surface in depth (see Section 7.2). Hubel and Wiesel (1962) and Maske et al. (1984) failed to find cortical cells with different receptive-field

structures, but their methods seem not to have been refined enough to reveal the crucial differences. Other receptive fields could differ in their orientation selectivity and would be sensitive to orientation disparities generated by inclined surfaces. These two possibilities are discussed in the next section.

DeAngelis et al. (1991) mapped the receptive-field profiles of cortical cells of cats for each eye and, by fitting these profiles with Gabor functions, obtained the phase difference between the two eyes. Almost all cells tuned to stimuli oriented within 20° of the horizontal had receptive fields with matching or near matching phases, which suggests that these cells code depth in terms of inter- rather than intra-receptive field offset. Note that the crucial input for these cells is vertical disparity or a radial gradient of vertical disparity along horizontal meridians. Cells tuned to stimuli within 20° of the vertical had receptive fields with a wide variety of phase relationships, which suggests that these cells code depth in terms of intra-receptive-field offsets. Note that the crucial input for these cells is horizontal disparity or a radial gradient of horizontal disparity along vertical meridians. There is evidence that both horizontal and vertical orientation disparities are used to code the inclination of surfaces. However, we will see in Sections 7.6 and 7.6 that gradients of horizontal disparity are processed locally whereas gradients of vertical disparity are processed more globally over the whole visual field, for purposes of driving cyclovergence and scaling horizontal disparities for torsional misalignment of the eyes. The anisotropy in the cortical processing of inter- and intrareceptive-field disparities revealed by De Angeles et al. may underlie the psychophysically determined anisotropy.

Cells with small receptive fields with intra-receptive-field offsets, whether they are simple or complex cells, are necessarily tuned to small disparities, since a small receptive field cannot have a large intra-receptive-field offset. Simple cells with large receptive fields must be tuned to large disparities since a simple cell with a large receptive field is essentially a scaled-up version of one with a small receptive field. The receptive field of a complex cell has several subunits within each of which there are excitatory and inhibitory detectors. The disparity preference of a complex cell with a large receptive field would therefore depend on the size and spatial disposition of the offset subunits within the receptive field rather than on the size of the receptive field as a whole. A tendency for small receptive fields to have small offsets and for large receptive fields to have large offsets could account for why cells with greater retinal eccentricity are tuned to larger disparities.

Cells in V1 have smaller receptive fields than those in V2 and this could account for the fact that V1 contains more cells tuned to zero disparity than cells tuned to near or far disparities while V2 contains more near and far cells than zero-disparity cells (Ferster 1981). Psychophysical evidence on the relationship between disparity and spatial scale is reviewed in Section 5.7.

A binocular cell with intra-receptive-field offset could also have an intra-receptive-field offset. It is possible that the intra-receptive field offset of a binocular cell could be nulled by an opposite inter-receptive field offset. For any binocular cell, any uncertainty in the registration of the relative positions of its monocular receptive fields would produce a corresponding uncertainty in the calibration of intra-receptive field disparities by that cell. Therefore, the detection of intra-receptive field disparity is not independent of the detection of inter-receptive field disparity. The joint determination of the two types of disparity is subject to the same uncertainty associated with the determination of position and spatial frequency (see Section 3.4.2).

4.6 TYPES OF DISPARITY CODING

The disparity-tuned cells discussed so far have to do with the detection of point disparities, that is, disparities defined by displacement of a small image in one eye relative to a similar small image in the other eye. It is possible that some disparity detectors are specifically designed for the detection of other types of disparity. Three types of disparity are considered in this section: disparity defined by a difference in spatial periodicity (spatial scale) which could be related to the perception of surface slant about a vertical axis, disparity defined by a difference in stimulus orientation, which could be related to the perception of surface inclination about a horizontal axis, and disparity of curvature that could be related to the perception of surface curvature in depth.

4.6.1 Disparity of spatial scale

Hammond and Pomfrett (1991) reported that, for a majority of cells in the visual cortex of the cat, the spatial frequency evoking the best response from one eye is slightly different from that evoking the best response from the other eye. Most cells of this type were found to be tuned to a higher spatial frequency in the dominant eye than in the other eye. Furthermore, such cells were more likely to be tuned to orientations close to the vertical than were cells with matching spatial-frequency characteristics.

These cells could provide the physiological mechanism for the detection of depth in surfaces slanting about a vertical axis (see Section 7.2).

4.6.2 Detectors for orientation disparity

Blakemore et al. (1972) measured the orientation of a bar eliciting the maximum response in single binocular cells in the visual cortex of the cat for stimuli presented to each eye in turn. For many cells the optimal orientations for the two monocular receptive fields differed. These differences had a range of over 15°, with a standard deviation of over 6°. Hubel and Wiesel (1973) were unable to confirm these findings but the eyes may not have been in torsional alignment. Nelson et al. (1977) replicated Blakemore et al.'s finding after controlling for possible contaminations due to eye torsion induced by paralysis and anaesthesia. For each cell, the widths of the orientation tuning functions for the two receptive fields were very similar. Thus, cells sharply tuned to orientation in one eye were also sharply tuned in the other eye even though the preferred orientations in the two eyes could differ. The response of a binocular cell was facilitated above its monocular level when the stimulus in each eye was centred in the receptive field and oriented along its axis of preferred orientation. As the stimuli were rotated away from this relative orientation, the response of the cell declined to below its monocular level, although this inhibitory effect was not strong. However, the orientation tuning functions of the binocular cells to changes in orientation disparity were no narrower than the monocular orientation tuning functions. They argued that such broadly tuned orientation disparity detectors could not play a role in the fine discrimination of inclination about a horizontal axis. However, it was shown in Section 3.5.3, that fine discrimination does not require finely tuned channels.

Häny et al. (1980) found a small number of cells in V2 of the alert monkey that were sensitive to changes in the angle of inclination of small stimuli about a horizontal axis. A 45° change in the inclination of the stimulus in the median plane, corresponding to an orientation disparity of 2°, caused the response of these cells to drop to half its maximum. By comparison, the smallest tuning width of cells tuned to orientation of monocular stimuli is reported to be 6°, with a mean of 40° (DeValois et al. 1982a).

Orientation disparities produced by a line inclined in depth could be detected on the basis of gradients of point disparities rather than by cells specifically tuned to orientation disparities. Häny et al. (1982) devised a stimulus containing only orientation disparity. A dynamic random-dot display

created a cyclopean vertical grating with no horizontal disparities, because the dots were dichoptically uncorrelated. They found five cortical cells that responded to orientation disparities in this stimulus. It seems that the visual cortex of the monkey contains cells specifically tuned to orientation disparity.

Interocular differences in preferred orientation suggest that different cells are tuned to different orientation disparities. Such cells could be called **orientation disparity detectors** and could provide a physiological basis for the detection of depth in surfaces inclined about a horizontal axis (see Section 7.4). Inclined surfaces contain disparities between vertically oriented surface features, and such disparities would be detected by cells tuned to orientations near the vertical rather than near the horizontal.

Orientation disparity detectors tuned to orientations near the horizontal could be used to allow for orientational misalignment of the two images, as discussed in Section 7.5. They could also be used to detect the differential orientational disparities produced by surfaces slanted in depth about a vertical axis (see Section 7.2). They could also evoke cyclovergence, as discussed in Section 10.7.4. For this latter purpose the cells would need to be sensitive to only low spatial frequency stimuli.

Bishop (1979) suggested that, as for horizontal disparities, the range of preferred orientation disparities to which cortical cells are tuned arises from the random pairing of monocular receptive fields for which there is a random scatter of preferred orientations. It is of interest that the range of preferred orientation disparities to which binocular cells of the cat's visual cortex respond is about the same as the range of orientation disparities that the cat normally encounters.

4.6.3 Detectors for curvature disparity

Rogers and Cagenello (1989) showed that differences in curvature of dichoptic lines evoke a sensation of surface curvature. If the receptive fields in the two eyes feeding into a binocular cell were tuned to lines of different length, the cell would be sensitive to differential curvature in the two eyes. DeAngelis et al. (1994) found a few cells of this type in the visual cortex of the cat.

4.6.4 Coding for disparity and motion

Cells selectively responsive to both movement and binocular disparity occur in several visual areas of the cerebral cortex. Some cells in areas 17 and 18 of the monkey respond selectively to stimuli moving in a given direction in the two eyes, with some

responding to only crossed-disparity stimuli and others to only uncrossed-disparity stimuli (Poggio and Fischer 1977; Poggio and Talbot 1981). These disparity-tuned motion detectors exert a disparity-dependent control over pretectal centres controlling optokinetic nystagmus (see Section 12.5.6). Grasse (1994) obtained physiological evidence that the response of about half the cells of the NOT in the cat that respond to moving displays are also tuned to binocular disparity; some showing an excitatory response to a limited range of disparities and others an inhibitory response.

Cells selectively tuned to both motion and disparity have also been found in the medial temporal visual area (MT) of the monkey, together with cells that respond to both crossed and uncrossed disparities but not to zero disparity (Maunsell and Van Essen 1983b). The cells in MT that respond best to zero horizontal disparity also respond best to zero vertical disparity. Finally, some cells in the medial superior temporal cortex (MST) of the monkey are jointly tuned to direction of motion and to the sign of disparity (Komatsu et al. 1988). More of these jointly tuned cells were sensitive to crossed disparity than to uncrossed disparity. These cells have large receptive fields suggesting that they are more suitable for gating OKN than for coding depth. Saito et al. (1986) found cells in MST of the monkey that respond preferentially to patterns rotating in depth. Psychophysical evidence of a coupling between motion and stereopsis is reviewed in Section 12.5.

In Section 13.2.5 we review visual mechanisms sensitive to the direction of approaching objects.

4.7 DISPARITY CODING IN PARVO- AND MAGNOCELLULAR CHANNELS

Livingstone and Hubel (1988) proposed that the parvocellular system is blind to depth. They based their conclusion on the report by Lu and Fender (1972) that depth cannot be seen in an isoluminant random-dot stereogram. This argument relies on the false assumption that the parvocellular system is wholly chromatic. We saw in Section 4.2.5 that the parvocellular system is not merely a colour-opponent system; it also codes high spatial-frequency stimuli defined by luminance contrast. An isoluminant stimulus shuts off only the luminance-contrast component of the parvocellular system. In any case, stereopsis could not be confined to the magnocellular system, as Livingstone and Hubel argued, because that system does not have the high spatial resolution exhibited by the disparity-coding system (see Section 5.3). The more reasonable conclusion

from the Lu and Fender study is that the chromatic component of the parvocellular system does not code depth. Even this conclusion has to be modified, as we will see in the following and in Section 6.1.4.

The distinction between the chromatic and luminance channels is not the same as that between the parvocellular and magnocellular systems. While the magnocellular system is wholly or almost wholly achromatic, the parvocellular system is both chromatic and luminance based. The parvocellular system is structurally simple but functionally complex and can be considered to consist of four subchannels. Which subchannel is activated depends on the spatial and temporal characteristics of the stimulus (Ingling and Matinez-Ugieras 1985; Ingling 1991). Consider a ganglion cell in the red-green (r-g) opponent system. For a plain steady stimulus (low spatial and temporal frequency) the responses from the red and green zones of the cell's receptive field are subtracted to yield an opponent chromatic signal. This subtractive process manifests itself as a photometric subadditivity; that is, the threshold for detection of a mixture of green and red light is higher than one would predict from the thresholds of green and red lights tested separately. When the red-green stimulus is flickered, the red and green components begin to add to yield a luminance signal and the cell loses its spectral opponency and shows photometric additivity. When a high spatial-frequency pattern is added to a steady red-green stimulus the r-g components again begin to add and the cell again loses its spectral opponency and shows photometric additivity. In other words, the pure chromatic channel is a low spatial and low temporal frequency system. The r-g system is a colour-opponent system for low spatial and temporal frequencies, a pure luminance system for either high temporal or high spatial frequencies, and a mixed system in the middle range of spatial and temporal frequencies.

This means that one is not likely to find evidence of stereopsis with isoluminant stereograms consisting of high spatial-frequency patterns. We will see in Section 6.1.4 that there is some evidence that isoluminant stereopsis occurs with low spatial-frequency patterns but not with high spatial-frequency patterns. The magnocellular system has no colour opponency and cannot process high spatial frequencies. Therefore, this system will not see depth in any isoluminant stimuli nor in fine patterns defined by luminance contrast. The magnocellular or parvocellular layers in the LGN of the monkey can be destroyed selectively by injecting ibotenic acid. Lesions in the parvocellular layers produced major deficits in stereopsis with fine patterns but no deficit in stereopsis with coarse patterns. Lesions in the

magnocellular layers produced deficits in high temporal-frequency flicker and motion perception but no deficits in stereopsis (Schiller et al. 1990). Ingling and Grigsby (1990) reported depth in afterimages of a perspective illusion and a reversible perspective figure, and depth in disparate afterimages has been reported by others (see Section 5.8.2). They assumed that afterimages do not arise in the transient magnocellular system and concluded that these sensations must arise in the parvocellular system. Depth sensations in these illusions are absent at isoluminance, so that if we accept Ingling and Grigsby's assumption, the sensations they observed must have arisen in the luminance component of the parvocellular system. However, this argument is weakened by recent evidence that afterimages do arise in the magnocellular system (Schiller and Dolan 1994).

In summary, this evidence, and other evidence cited in Section 6.1.4, leads to the following conclusions. Only the parvocellular system processes disparity in fine patterns defined by luminance contrast or in coarse isoluminant patterns. Both the parvo- and magnocellular systems process disparity in coarse patterns defined by luminance contrast.

4.8 VEPs AND BINOCULAR VISION

4.8.1 Introduction

Because of their high level of interconnectivity, cortical neurones tend to fire in synchrony. Furthermore, subgroups of cells tend to fire at different frequencies. In addition to these spontaneous firing patterns, groups of cells tend to respond together in characteristic ways in response to particular stimuli. The synchronous firing of groups of cells generates fluctuating electrical fields that can be detected either at the surface of the brain or on the scalp. Electrical fields generated by the visual cortex are known as **visual evoked potentials**, (VEPs). Pyramidal cells are the most likely source of VEPs. A pyramidal cell runs at right angles to the cortical surface and forms an electrical dipole when it fires. A single electrode on the scalp is affected by the activity of thousands of pyramidal cells since the meninges, skull, and scalp diffuse and average the potentials arising from the underlying area of tissue. Records can be taken only from cortical tissue that runs parallel to the surface of the brain and not from tissue within the fissures. Prominent types of synchronous activity arising from the visual cortex include alpha waves at a frequency of between 8 and 13 Hz, evident in awake subjects, delta waves at between 0.5 to 4 Hz that

arise in the sleeping subject, and beta waves at between 14 Hz and 30 Hz that arise when the subject is engaged in an attentive task. Gamma waves at even higher frequencies are detected in single cells or small groups of cells but not at the scalp.

In a typical experiment, the location, magnitude, and form of VEPs are related to parameters of the visual stimulus. Usually a well-defined repetitive visual stimulus is applied. The response is then filtered and averaged over many cycles of stimulus repetition. The signal-averaging procedure emphasizes components in the VEP that are time-locked to the stimulus and attenuates components due to extraneous stimuli and intrinsic noise which, being unrelated to the stimulus, average out over several cycles. In a related procedure, responses of the same region to distinct stimuli are recorded or recordings are made of the responses of distinct cortical regions to the same stimulus. The degree of coherence (shared power) between these recordings as a function of stimulus frequency is then used to derive a coherence function. A coherence function is the frequency domain analogue of the (squared) cross-correlation coefficient, and its value varies between 0 and 1. In this way one can assess the extent to which distinct stimuli evoke the same response and distinct cortical regions respond to the same stimulus.

A commonly used procedure is to identify prominent peaks and troughs in the VEP and label them according to their amplitude, latency, and polarity. There are many sources of uncertainty in interpreting these components. For instance, Harter et al. (1973) reported that only the late (200-250 ms) component of the evoked response reflects the activity of binocular cells, as indicated in a greater response to identical stimulation to both eyes than to rivalrous inputs. Others have found that only the early component (100-150 ms) is correlated with stereoscopic vision (Regan and Spekreijse 1970). Results have also been found to depend on electrode position, stimulus contrast, and, as we will see below, the spatial and temporal properties of the stimulus. There is also a good deal of intersubject variability. A review of human brain electrophysiology has been provided by Regan (1989a).

The VEP has been used to reveal two properties of binocular mechanisms—summation and suppression between inputs from the two eyes on the one hand, and stereopsis on the other.

4.8.2 VEPs and binocular summation

In investigations of binocular summation and suppression using the VEP, two basic comparisons are made. First, the magnitude of the VEP evoked by

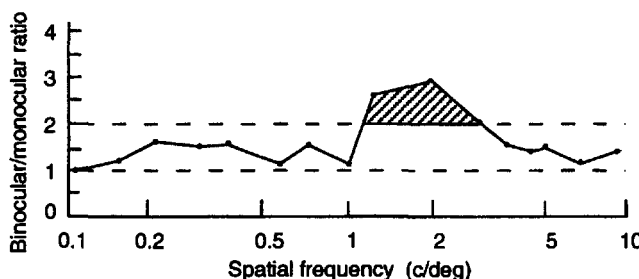


Figure 4.21. Evoked potentials and spatial frequency.
Ratio of the magnitude of the binocular VEP to that of the monocular VEP as a function of the spatial frequency of a vertical grating. The grating was counterphase modulated at a temporal frequency of 30 Hz. (From Apkarian et al. 1981.)

monocular stimulation of each eye is compared with that evoked by binocular stimulation. Second, the response when the two eyes receive identical stimuli is compared with that when the stimuli in the two eyes are uncorrelated. The idea is that only congruent stimuli summate their inputs whereas rivalrous stimuli compete for access to binocular cells. The results are used to assess the following outcomes.

1. *Summation.* A binocular VEP that is simply the sum of the monocular responses could signify that visual inputs are processed by independent mechanisms in the visual cortex. But it could also signify that the inputs from the two eyes are summed linearly by binocular cells. If summation is partial it signifies that some inputs converge and show less than full linear summation. A binocular response that equals the mean of the monocular responses (zero summation) signifies binocular rivalry in which the input from one eye suppresses that from the other when both are open or in which the two eyes gain alternate access to cortical cells. It could also arise from binocular cells that average the inputs from the two eyes.

2. *Inhibition.* A binocular response that is less than the mean of the monocular responses signifies strong mutual inhibition between left- and right-eye inputs. It could also occur in binocular rivalry when a strong stimulus in one eye is suppressed by a weak stimulus in the other eye.

3. *Imbalance.* A monocular response from one eye that is stronger than that from the other signifies a weakened input from one eye or suppression by one eye of the response to the other eye, even when the dominant eye is closed. This condition arises from anisometropia and strabismus (see Section 15.7).

4. *Facilitation.* A binocular response that is greater than the sum of the monocular responses indicates the presence of a facilitatory binocular

interaction that one might expect in a mechanism for detecting binocular disparity. The most extreme facilitation arises in binocular AND cells that respond only to excitation from both eyes and give no response to monocular inputs.

A thorough investigation of binocular facilitation of the VEP in adults was conducted by Apkarian et al. (1981). They presented normal adult subjects with vertical gratings of various spatial frequencies with luminance modulated in counterphase at various temporal frequencies. Binocular facilitation of the amplitude of the VEP as a function of spatial frequency for a fixed temporal frequency of 30 Hz is shown in Figure 4.21. It can be seen that for this subject binocular facilitation is limited to spatial frequencies in the region of 2 c/deg, which is not the region where the monocular response has its peak. Binocular facilitation was also found in a specific range of temporal frequencies of contrast modulation, generally between 40 and 50 Hz, and to be higher at higher contrasts. The range of spatial and temporal frequencies within which facilitation occurred varied from subject to subject.

The dependence of binocular facilitation on the spatial and temporal properties of the stimulus probably explains the wide variation in the degree of binocular facilitation reported in previous studies (Cigánek 1970; Harter et al. 1973; Srebro 1978). Furthermore, tests of binocular functioning that rely on the comparison of monocular and binocular VEPs are suspect if they are not based on appropriate stimulus parameters. One solution is to record evoked potentials while the stimulus is swept through a range of stimulus values. This sweep procedure was first used by Regan (1973). The amplitude of the evoked potential was recorded as the refractive power of a lens in front of an eye was varied for each of several astigmatic axes. This provided a rapid determination of the required refractive correction. In a second study, VEPs were recorded as a checkerboard pattern loomed in size, with brightness held constant (Regan 1977).

Norcia and Tyler (1985) recorded the VEP as the spatial and temporal frequencies of a grating were swept through a range of values. This gave a spatiotemporal VEP profile. This method is particularly useful with children too young to be tested by psychophysical procedures. In addition to providing a better basis for comparison of VEPs under a range of stimulus values, the sweep method is very much faster than the presentation of different stimulus values in discrete trials.

When a vertical grating is presented to one eye and a horizontal grating to the other, the subject

experiences binocular rivalry (see Section 8.3). It is believed that binocular rivalry is due to competition between uncorrelated inputs from the two eyes for access to binocular cells. Spekreijse et al. (1972) found that the amplitude of the VEP associated with a counterphase-modulated pattern was strongly reduced when it was perceptually suppressed by a steady pattern presented to the other eye compared with when it was presented with a blank field in the other eye. Since misaccommodation can cause a large reduction in the VEP, the reduced VEP from suppressed images could be due to the suppressed eye becoming misaccommodated. Spekreijse et al. showed that the rivalry effects are not due to misaccommodation by obtaining the same result when the rivalrous stimuli were presented in the context of correlated stimuli that served to keep both eyes properly accommodated. Apkarian et al. (1981), also, found evidence of binocular rivalry in the VEP showing that a vertical grating to one eye and a horizontal grating to the other produced a VEP that showed zero interocular summation.

Another approach to using VEPs for detecting binocular interactions is to look for evidence of nonlinear interactions in the response to dichoptic flicker. Suppose that the left eye views sinusoidal flicker of frequency F_1 and the right eye views sinusoidal flicker of frequency F_2 . Nonlinear processes produce harmonics of F_1 in the left monocular channel and harmonics of F_2 in the right monocular channel. Nonlinear processes occurring after the monocular signals are combined produce cross-modulation terms of the general form $nF_1 + mF_2$, for integral values of n and m . The relative amplitudes of these terms depend on the nature of the nonlinearities both before and after binocular convergence. Regan and Regan (1988, 1989) provided a mathematical analysis of these processes and showed that nonlinear processing occurring after binocular convergence can be isolated from that occurring before convergence. They pointed out that, in contrast with the random-dot techniques described later, this procedure allows one to explore binocular functions even when acuity is low in one or both eyes. Figure 4.22 shows a $(F_1 + F_2)$ component recorded by an ultrahigh resolution Fourier analysis, known as zoom-FFT. This component of the response must arise from nonlinear processes occurring after binocular convergence (Regan and Regan 1986). Baitch and Levi (1988) used the same technique to show that the $(F_1 + F_2)$ component is much weaker in stereoblind than in normally sighted subjects. Thus, only subjects with normal stereoscopic vision showed evidence of a nonlinear combination of monocular inputs, presumably arising from the

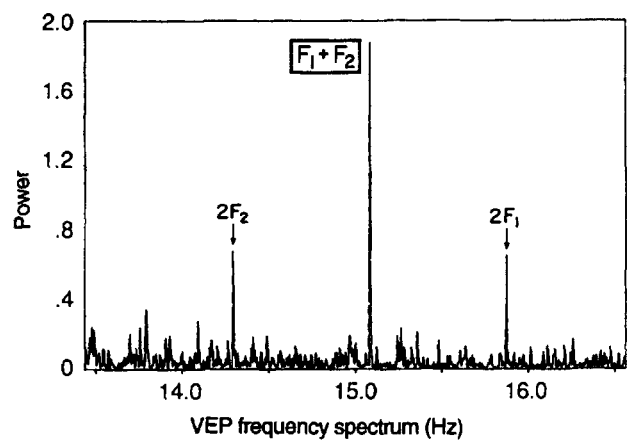


Figure 4.22. Nonlinear processing of dichoptic flicker.
 One eye viewed a homogeneous field flashing at 8 Hz (F_1) with 17 per cent amplitude modulation while the other viewed a light flashing at 7 Hz (F_2) with 12 per cent modulation. The VEP spectrum was recorded at a resolution of 0.004 Hz by zoom-FFT. The $F_1 + F_2$ component in the VEP indicates a nonlinear process sited after binocular convergence. (From Regan and Regan 1986.)

way in which binocular cells combine signals from the two eyes. The more linear addition of signals in the stereoblind subjects presumably arises from the two pools of monocularly driven cells.

4.8.3 VEPs and stereopsis

There are several problems to be solved in relating changes in the VEP specifically to changes in stereoscopic depth based on binocular disparity. It must first be demonstrated that the response is not due to stimulus-locked eye movements. The second problem is to ensure that monocular cues to depth do not intrude. This can be done by using random-dot stereograms. The third problem is to change the depth in the stereogram without introducing unwanted motion signals. This can be done by using a dynamic random-dot stereogram in which the microelements forming each monocular image are replaced at the frame rate of the display, so that there is no motion of monocular dots during the change of depth in the stereogram. Finally, one must ensure that the changes in the VEP are due to the perceived change in depth rather than to a change in the degree of correlation between the patterns of dots in the two eyes. This can be done by alternating the stereogram between equal and opposite disparities rather than between zero disparity and either crossed or uncrossed disparity. A second type of control is to compare the VEP evoked by a random-dot stereogram alternating in depth because of a change in horizontal disparity with that evoked by a similar change in vertical disparity. This control must be applied with caution because depth

sensations can arise from certain types of vertical disparity, as we will see in Section 7.6.

Fiorentini and Maffei (1970) found that periodically reversing the contrast of dichoptic vertical gratings produced a larger VEP when the spatial frequency of one grating was increased with respect to that of the other. The impression was of a surface slanted in depth about a vertical axis. The magnitude of the VEP increased as the apparent slant of the surface increased. When the dichoptic gratings fell on distinct regions of the visual field, differences in spatial frequency did not affect the VEP. They concluded that the magnitude of perceived depth determines the magnitude of the VEP. This conclusion is valid only if the VEP is unaffected by spatial-frequency differences between horizontal gratings which do not produce an impression of slant.

Regan and Spekreijse (1970) presented subjects with a static random-dot stereogram in which the horizontal disparity of the central square alternated between zero and 10, 20, or 40-arcmin. Every half-second the central square appeared to jump forward from the plane of the background and then jump back. A positive-going VEP occurred about 160 ms after each depth change and was followed by a negative-going response. The monocular stimulus produced an appearance of global motion (short-range apparent motion) for displacements less than 20 arcmin and an associated monocular VEP, but no global motion and no VEP for a 40 arcmin displacement. This same stimulus, however, produced a large VEP when viewed dichoptically. An equivalent change in vertical disparity produced a much smaller VEP and they concluded from this and from eye-movement controls that the changes in the VEP were related specifically to the changes in perceived depth and not to motion of parts of one of the monocular images, changes in disparity unrelated to depth, or eye movements.

Lehmann and Julesz (1978) used a dynamic random-dot stereogram in which a rectangular area appeared to move out from the background and then back every half-second. With a display confined to the left visual hemifield (right hemiretinas) each change in apparent depth was followed by a VEP in the right hemisphere, as one would expect from the fact that the right hemiretinas project to the right hemisphere. There was a smaller mirror-image echo of the response in the left hemisphere (see Figure 4.23). With a display confined to the left hemiretinas, the major VEP occurred in the left hemisphere with a smaller echo in the right hemisphere. They argued that both hemispheres process cyclopean stereopsis in a similar fashion, which runs counter to some evidence from the clinical literature that damage to the

right hemisphere produces a selective impairment of stereopsis (see Section 15.4). There were no controls for possible eye-movement artifacts in this study.

A **dynamic random-dot correlogram** is a display of randomly distributed dots alternating between any two of the following states: being in the same positions in the two eyes (+1 correlation), being uncorrelated in position in the two eyes (zero correlation), or being in the same positions but of opposite luminance polarity (-1 correlation) (Julesz and Tyler 1976). These changes between two states are cyclopean, since they are not evident in either monocular image. A much stronger VEP was evoked by a dynamic random-dot correlogram that involved a change in state than by a dynamic display of dots that remained either correlated or uncorrelated (Miezin et al. 1981). The evoked potentials from a dynamic random-dot correlogram therefore reflect the cyclopean features of the stimulus.

Julesz et al. (1980) measured the amplitude of the VEP evoked by a dynamic random-dot correlogram and compared it with that evoked by a dynamic random-dot stereogram in which alternate squares of a checkerboard pattern appeared to move in and out of the plane of the background squares. Both displays produced distinctive VEPs with a dominant latency of about 250 ms compared with when one eye was occluded (see Figure 4.24). However, the response to the random-dot stereogram had a larger amplitude than that to the correlogram and the waveforms generated by the two stimuli differed.

It was concluded that the greater response to the stereogram was specifically related to the appearance of depth as opposed to the change in the degree of interocular correlation of the dots. These responses occurred only in subjects with functional stereopsis and the authors suggested that they could be used as a simple nonverbal screening test for stereopsis. However, it is not clear whether or not the response was influenced by vergence eye movements, and there was no control for the effects of vertical disparities.

If binocular facilitation is related to stereopsis based on horizontal disparity, it should not occur for a horizontal grating because extended horizontal gratings do not create horizontal disparities. In conformity with this expectation, Apkarian et al. (1981) found that the binocular response to a horizontal grating was the sum of monocular responses, while that to a vertical grating showed facilitation.

Norcia et al. (1985) used a dynamic array of random-dots that alternated as a whole between a crossed disparity and an equal uncrossed disparity while the subject converged on a stationary fixation point. For disparity amplitudes up to about 15 arcmin, the

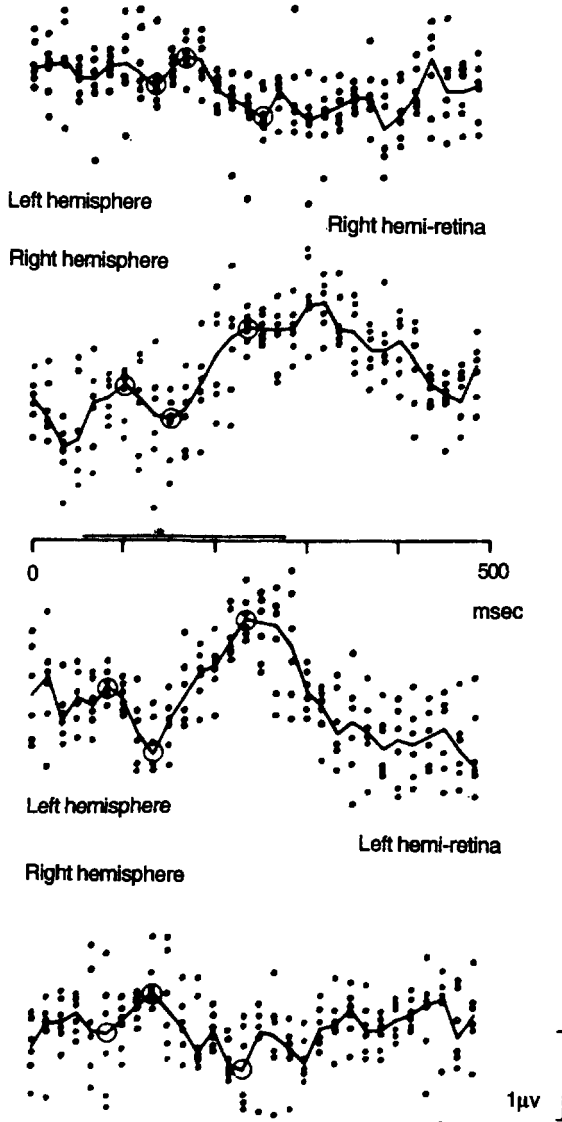


Figure 4.23. Evoked potentials and stereopsis.

Averaged evoked potentials in response to changes in depth of a random-dot stereogram presented to either the right or left hemifield and recorded from either the right or left cerebral hemisphere. With a display confined to the left visual hemifield (right hemiretinas), each change in apparent depth (indicated by circles) produced a VEP in the right hemisphere, as one would expect from the fact that the right hemiretinas project to the right hemisphere. A small mirror-image echo of the response is evident in the left hemisphere. (From Lehmann and Julesz 1978.)

amplitude of the VEP increased as a linear function of the amplitude of disparity modulation. Above this amplitude the response first declined and then rose to a second peak at a disparity of about 70 arcmin. The response to larger amplitudes of disparity alternation had a shorter latency but a greater phase lag than the response to smaller amplitudes of disparity.

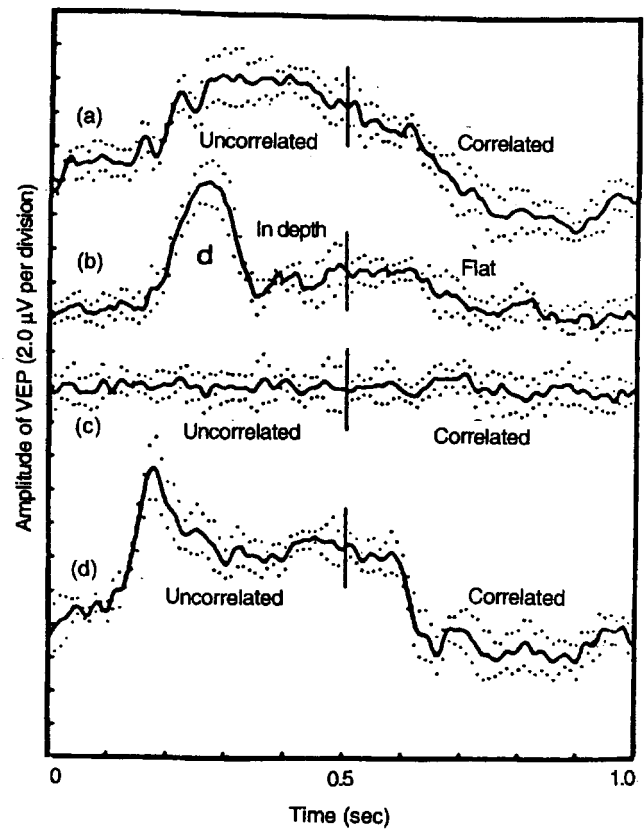


Figure 4.24. Evoked potentials and image correlation.

(a) VEP in response to a dynamic random-dot pattern alternately correlated and uncorrelated in the two eyes.
 (b) VEP in response to a cyclopean checkerboard alternating between being flat and in depth.
 (c) The same stimulus as in (a) but with one eye closed.
 (d) Same as in (a) but with the anaglyph spectacles removed. (c) and (d) were control conditions. Results for two subjects. (Reproduced with permission from Julesz et al., 1980, Vision Research, Pergamon Press.)

They argued that the two peaks in the VEP represent two disparity processing mechanisms, one for fine and one for coarse disparities (see Section 5.5.3).

Katsumi et al. (1986) investigated the effects of optically induced aniseikonia on the degree of binocular summation as revealed in the VEP recorded from the surface of the human head. The stimulus was a checkerboard pattern undergoing contrast reversal at 12 Hz. When the pattern was more than 5 per cent larger in one eye than in the other, there was no evidence of a greater VEP to binocular than to monocular stimulation. The tolerance of the stereoscopic system for aniseikonia is discussed in Section 2.8.

Other aspects of the VEP and stereopsis are discussed in Section 15.2.2 and the whole question of evoked potentials is reviewed by Regan (1989a).

The limits of stereoscopic vision

5.1 Basic terminology and tasks	149
5.2 Tests of stereoscopic vision	151
5.2.1 Howard-Dolman and related tests	151
5.2.2 Standard stereogram tests	151
5.2.3 Cyclopean stereogram tests	151
5.3 Stereoacuity— basic concepts	155
5.3.1 Stereoacuity	155
5.3.2 Depth discrimination thresholds	155
5.3.3 An ideal observer for stereoacuity	158
5.4 The upper disparity limit	159
5.5 Spatial factors in stereoacuity	159
5.5.1 Stimulus eccentricity	159
5.5.2 Stimulus spacing	160
5.5.3 Spatial frequency of disparity modulation	161
5.5.4 Comparison of Crossed-uncrossed disparity	166
5.5.5 Target orientation	167
5.6 Luminance contrast and stereopsis	168
5.6.1 Effects of luminance and contrast	168
5.6.2 Contrast-sensitivity and stereopsis	169
5.6.3 Thresholds for detection and depth	170
5.6.4 Effects of interocular differences	170
5.6.5 Stereoacuity and colour	172
5.7 Disparity and spatial scale	172
5.7.1 Introduction	172
5.7.2 Spatial scale and disparity	173
5.7.3 Spatial scale and stereoscopic gain	175
5.7.4 Spatial scale and stereopsis masking	176
5.8 Stereoacuity and eye movements	177
5.8.1 Eye movements between targets	177
5.8.2 Stereoacuity and stabilized images	177
5.8.3 Stereoacuity and vergence drift	178
5.8.4 Stereoacuity and head movements	179
5.9 Stereoacuity and other acuities	180
5.10 Temporal factors in stereopsis	183
5.10.1 Processing time for stereopsis	183
5.10.2 Effects of interocular delay	185
5.10.3 Effects of interstimulus delay	186
5.10.4 Effects of lateral stimulus motion	186
5.10.5 Temporal modulation of disparity	187
5.11 Experiential and practice effects	191

5.1 BASIC TERMINOLOGY AND TASKS

The **depth-discrimination threshold** is the smallest depth interval between two stimuli that a subject can reliably report. The mean unsigned error or the standard deviation of a set of equidistance settings is the traditional measure of the depth threshold. Some investigators use the method of constant stimuli and

define the depth-discrimination threshold as the separation in depth between two test stimuli that is discriminated on 75 per cent of trials. The double-staircase method further refines the measuring procedure (Blakemore 1970d). Criterion problems are eliminated by a two forced-choice procedure in which subjects decide which of two stimuli contains a depth interval (Blackwell 1952). The two stimuli

are either presented side by side or one after the other. In a related task, subjects decide whether a stimulus object is nearer than or beyond a comparison object, usually with fixation maintained on the comparison object. The statistical reliability of interpolation of the threshold point in the psychometric function is improved by curve-fitting procedures coupled with assignment of weights derived from probit analysis to data points (Section 3.5.1). The end result is a measure of the least separation in depth, Δd , between the test and comparison stimuli that evokes a sensation of depth for a given distance, d , of the comparison stimulus from the viewer.

Stereoacuity (η) is the depth-discrimination threshold expressed in angular terms. It is the difference between the binocular subtense of the standard stimulus and that of the variable stimulus in its threshold position, as illustrated in Figure 2.6. We showed in Section 2.3.1 that, to a first approximation, the depth difference (Δd) and the angular measure of stereoacuity (η) are related by

$$\eta = \frac{a\Delta d}{d^2} \text{ in radians} \quad (1)$$

where a is the interpupillary distance. These values can be converted into seconds of arc by multiplying by 206,000. This means that to a first approximation, stereoacuity is proportional to the stereo base (distance between the eyes) and inversely proportional to the square of the viewing distance.

In standard tests of stereoacuity the subject fixates one of the targets or is allowed to look from one to the other. Thus, at any instant one of the targets has zero disparity and the measure is referred to as stereoscopic acuity, or stereoacuity. In other tests the subject fixates a third target so that the test and comparison targets have a standing disparity, known as a **disparity pedestal**. In this case the **depth-discrimination threshold** is the just discriminable depth between the test and comparison targets with the subject converged on the fixation target. The **upper limit of disparity** is the largest disparity that can evoke an impression of depth.

Stereoscopic accuracy is the signed difference, or constant error, between perceived depth and actual depth. The smaller the error the higher the accuracy. There are three types of stereoscopic inaccuracy.

In the first type, zero disparity correctly signifies no depth between test and comparison stimuli but depth intervals on either side of zero are under- or over-estimated by a fixed ratio. Thus, the scale of perceived depth is expanded or contracted relative to that of actual depth. **Stereoscopic gain**, is the magnitude of perceived depth between two stimuli

one unit of depth apart. In more general terms, it is the ratio of perceived depth to actual depth. Usually one of the test stimuli is fixated and assumed to have zero disparity. Gain has a value of 1 when perceived depth and actual depth are equal. Perceived depth can be determined from subjects' estimates of the depth between two targets, or by asking subjects to place a probe at the same apparent depth as a test target. In the matching method the gain of the probe must be 1 and the probe and test targets should not interact. It is not easy to check these requirements, but even if they are not met the method may allow one to compare stereo gains of different test targets. A stereoscopic visual system is symmetrical when discrimination and efficiency are the same for crossed and uncrossed disparities. We will see that the normal human stereoscopic system has systematic asymmetries and some people have severe asymmetries, to the extent of being unable to process either crossed or uncrossed disparities.

The second type of stereoscopic inaccuracy is one in which the scale of perceived depth is shifted by a constant amount with respect to that of actual depth. The scaling of disparity in one part of the visual field could be disturbed relative to that in another part of the field. Thus, two objects with the same disparity would appear to lie in different depth planes, and all other depth intervals would be scaled accordingly. We saw in Section 2.8.1 that something like this occurs when the image in one eye is magnified horizontally with respect to that in the other eye. It can also occur when stereoscopic targets are seen against a slanting or inclined background (see Section 12.1).

In the third type of stereoscopic inaccuracy the signs of disparity are systematically reversed. A system that confused all crossed disparities with uncrossed disparities would have constant errors everywhere except at zero disparity. People seem to be incapable of adjusting to prisms which optically reverse the signs of disparities and there are no reports of people who see disparities in reverse. The disparity sign mechanism must be hard-wired.

However, it does not follow that a point with a crossed disparity will necessarily be seen as closer than a point with either zero or an uncrossed disparity. The disparity of a point specifies its location with respect to the Vieth-Müller circle and at large head-centric eccentricities uncrossed points can be closer than the fixation point and crossed points can be farther away (Figure 2.24). It is also true that an eccentrically positioned surface which is slanting with respect to the cyclopean direction (closer on the left and farther away on the right, or vice versa) can have a disparity gradient opposite in sign to that of a surface with the same slant positioned close to the

midline. In general, the visual system seems to be capable of interpreting both the relative distances of points and the slant of surfaces with respect to the cyclopean direction even when the surfaces are eccentric with respect to the head. However, observers may report slant reversals when information about the surface's eccentricity, derived from eye position and vertical disparities, is weak (Gillam 1967). Conflicting perspective information plays an important role in slant reversals (Gillam 1993).

5.2 TESTS OF STEREOSCOPIC VISION

5.2.1 Howard-Dolman and related tests

The best known test of stereoacuity, first used by Helmholtz, is to set a vertical rod to appear in the same frontal plane as two equidistant flanking rods. In the Howard-Dolman test adopted by the American Air Force during the 1914–18 war, the subject views two 1-cm diameter vertical rods at 6m through a horizontal aperture placed near the eyes that occludes the ends of the rods. (Howard 1919). The subject pulls a string attached to one rod until the two rods appear equidistant. Several monocular cues are present in this test, including the relative widths of the images of the rods and motion parallax due to head movements. Howard claimed that the binocular depth threshold was about 20 times lower than the monocular threshold, but Pierce and Benton (1975) found it to be only about 2.4 times lower. The Verhoeff (1942) stereopter uses three rods seen against a back-illuminated screen. The rods differ in thickness, thus eliminating the size cue to relative distance. But monocular cues to distance are best eliminated by creating rods in a stereoscope and varying the apparent distance of the variable rod by changing the binocular disparity of its images. There are several tests of this type, including the Bausch and Lomb Ortho-Rater used by the American Navy during the 1940–45 war (Fletcher and Ross 1953).

In Hering's falling bead test the subject fixates on a bead hanging on a vertical thread and the experimenter drops a second bead in front of or behind the first thread and slightly to one side (Hering 1865). The drop takes about 200 ms. The subject reports the relative depths of the two beads.

5.2.2 Standard stereogram tests

Titmus Stereo test

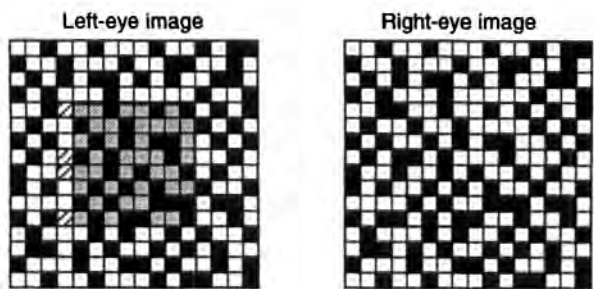
The Titmus stereo test is available from the Stereo Optical Co., Chicago, IL 60641. It consists of three types of stereogram: the Stereo Fly test, the Circle

test (derived from the Wirt test), and the Animal Stereo test. All the stereograms are viewed through polarizing spectacles. The Fly test is for young children. It is a stereogram of a house fly that appears in depth when properly fused. The child is asked to touch the wing of the fly, and stereopsis is indicated if the child reaches in front of the plane of the stereogram. The Circle test has nine numbered diamonds, each containing four circles. One of the circles in each diamond has a disparity, ranging from 40 to 400 arcsec, and the subject has to indicate which of the circles appears out of the plane of the other three. The Animal test consists of three rows of animals with one animal in each row having a disparity of 100, 200, or 300 arcsec. With the coarser disparities it is possible to pick out the correct stimulus in the Circle and Animal tests with only one eye open. This is done by observing the lateral displacement of the correct image relative to the other images (Cooper and Warshowsky 1977). Simons and Reinecke (1974) found that many amblyopes, who were presumed to lack stereopsis, could pick out the correct stimulus in the Circle and Animal tests, and assumed that they were using this monocular cue. True stereopsis is indicated if subjects can report the relative depth plane of the odd circle and not merely that it is odd.

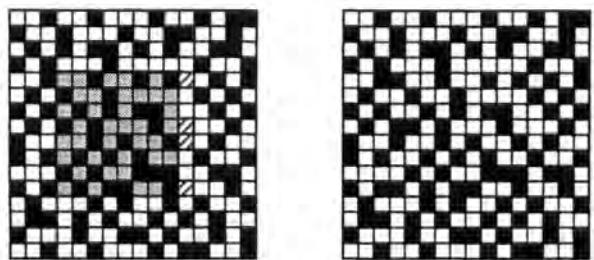
5.2.3 Cyclopean stereogram tests

In 1960 Bela Julesz introduced random-dot stereograms into the field of stereoscopic vision and this had a profound effect on subsequent research. The essential stages in creating a random-dot stereogram are illustrated in Figure 5.1. A similar process is easily programmed in a computer. Shapes visible only after monocular images are combined are cyclopean images. Julesz used the term global stereopsis to refer to stereopsis generated by cyclopean images. The elements comprising the stereogram can be lines, crosses, or other texture elements, rather than dots, as long as they are randomly arranged. Thus, random-dot stereograms are a subset of a broader class of cyclopean stereograms. Cyclopean stereograms are discussed further in Section 6.1.

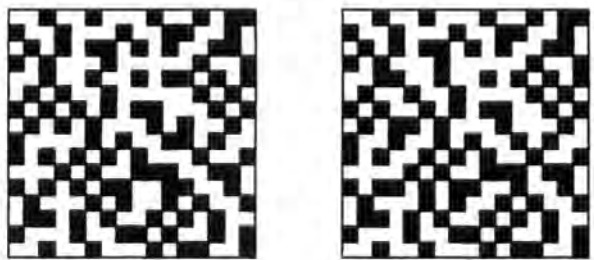
In a cyclopean stereogram there should be no monocular evidence about the shape or depth of the global form seen when the two images are fused. A global form is one larger than the individual elements making up each monocular image. However, one must not conclude that monocular cues to depth do not operate in cyclopean stereograms. The uniformity of texture and the absence of differential image blur in a random-dot stereogram constitute monocular cues that the display is flat. In other words, the monocular information about depth



(a) Black dots are arranged at random in about half the squares of a grid and the pattern is duplicated. A sub-set of dots is cut out of one of the patterns, with cuts along the sides of the squares so that dots are not dissected.



(b) The cut region is shifted an integral number of small squares. Overlapping dots on one side of the shifted region are transferred to the empty space on the other side.



(c) The grid is removed. When viewed in a stereoscope, the shifted region appears in front of or behind the background, depending on the way the shifted region was moved.

Figure 5.1. Creating a random-dot stereogram.

conflicts with disparity information. This point is vividly illustrated when one moves the head from side to side while viewing a random-dot stereogram containing a central square in depth. The zero motion parallax (a monocular cue that the display is flat) causes the square to appear to move with the head, rather than remain in a stable position.

The high dot density of random-dot stereograms is a disadvantage for some purposes. Monocular cues to relative displacement can be virtually eliminated in a display with low dot density by use of a ring of dots with zero disparity, surrounding a single dot with variable disparity. If the diameter of the ring is about 20 times the disparity of the central dot, the offset of the image of the dot is not

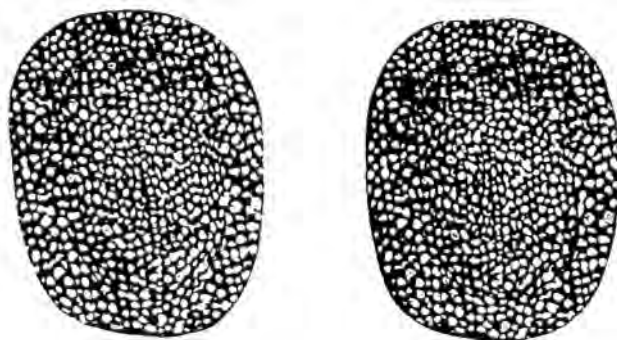
discernible when viewed with either eye alone (Westheimer and McKee 1980a).

Julesz was not the first person to make a cyclopean stereogram, but he was the first to realize its significance and to develop it as a research tool. In 1939 Boris Kompaneysky, a member of the Russian Academy of Fine Arts, published the cyclopean stereogram shown in Figure 5.2a. It portrays the face of Venus camouflaged in an array of white on black blobs. The cyclopean image is not perfectly hidden in the monocular images (Tyler 1994).

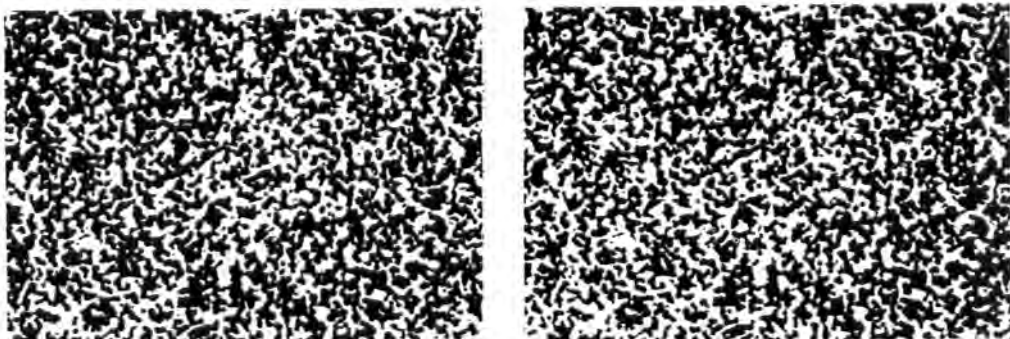
In 1954 Claus Aschenbrenner (1954) published the cyclopean stereogram shown in Figure 5.2b. When fused, the word "leak" appears in relief. Aschenbrenner worked on photographic reconnaissance and made the stereogram out of pieces of paper from a paper punch. This is not a perfect procedure because elements of the pattern are dissected along the borders of the shifted region and this could provide monocular information about these borders, although none is identifiable in this example. In computer-generated random-dot stereograms the disparate region is shifted an integral number of dots, so that it is not evident in either eye's image.

In his 1960 paper Julesz reported that the impression of depth in a random-dot stereogram survives a considerable addition of noise to one of the images (Figure 5.3a). The noise creates the impression of lacy depth superimposed on the depth planes defined by disparity. He also reported that depth is seen when every second point in alternate lines is made black in one eye and white in the other, so that no pair of corresponding points has identical neighbours. However, stereopsis fails when all pairs of dots have reversed luminance polarity (see Section 6.2.10). Julesz found that depth is difficult to see when the dots in the disparate region are isolated among dots that are uncorrelated in the two eyes, (Figure 5.3b). Uncorrelated dots thus destroy the impression of a coherent depth plane. However, we will see in Section 6.3 that depth is seen in random-dot stereograms that do not form coherent depth planes, as long as dot density is not too great. Stereopsis also survives considerable blurring of one of the images (Figure 6.1c).

Julesz found that depth in a random-dot stereogram takes longer to see than that in a normal stereogram and that the time needed to see cyclopean depth is shorter after repetitive trials (see Section 5.11). Placing an outline around the disparate region or making the region lighter in one eye than in the other makes the depth much easier to see. Julesz realized that corresponding points in the two images cannot be found by a simple cross-correlation process in which zones of defined size in the two

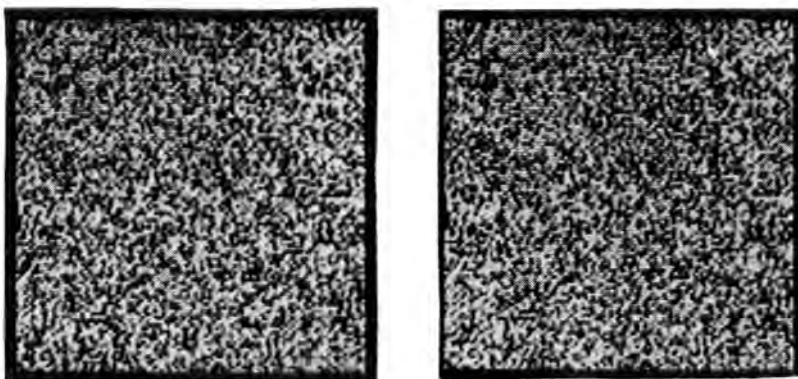


(a) A stereogram made by Boris Kompaneysky in 1939 reveals the face of Venus when fused by divergence.

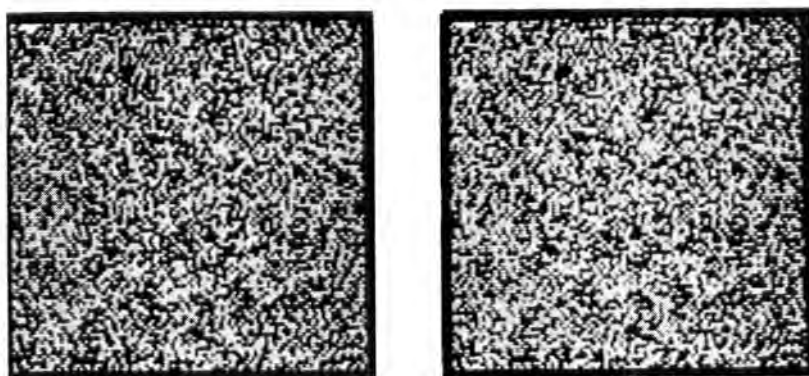


(b) A stereogram made by Aschenbrenner in 1954 contains the word "leak" when fused by divergence.

Figure 5.2. Early cyclopean stereograms.



(a) Depth is seen in a random-dot stereogram with considerable Gaussian noise.



(b) Depth is difficult to see after addition of uncorrelated dots. (From Julesz 1960.)

Figure 5.3. Effects of noise on random-dot stereograms.

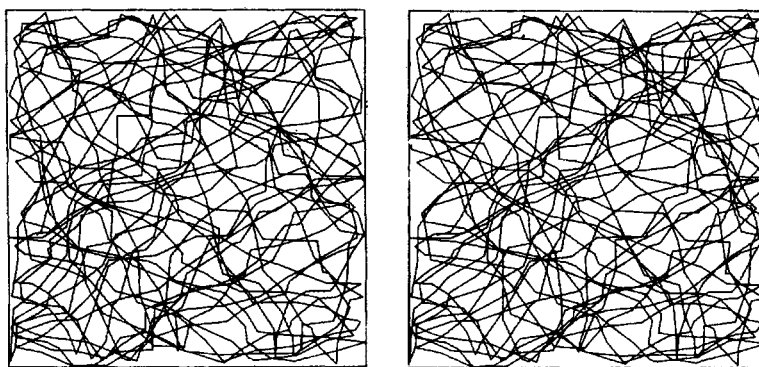


Figure 5.4. A random-line stereogram.

A stereogram formed from lines generated by a random walk. When fused by convergence it creates the impression of a crater. (From Ninio, Perception, 1981, 10, 403-10. Pion, London.)

eyes are compared. If the compared zones are small, one cannot account for the resistance of the impression of depth to perturbations of the dots and if the zones are large one cannot account for how very small regions of disparity can give rise to depth. We will see in Section 5.7 that the image-matching process is carried out at several levels of image size and with respect to a variety of visual tokens.

Ninio (1981) composed cyclopean stereograms from lines generated by a random walk and then deformed the lines presented to one eye according to the disparities in a three-dimensional shape. The example shown in Figure 5.4 creates the impression of a protruding annulus. This method is not suitable for creating disparity discontinuities since these show in the monocular image as breaks in the lines. In standard random-dot stereograms a region of dots in one eye is shifted by an integral number of dots to create a sharp discontinuity of disparity. Along vertical discontinuities a line of dots is visible to one eye but not to the other. These monocular occlusion zones play a crucial role in depth perception (see Section 12.4). When cyclopean stereograms are generated by continuous rather than discrete modulations of disparity, disparity can be a fraction of the interdot spacing and there need be no monocular zones. Tyler and Raibert (1975) devised a computer algorithm for generating random-dot stereoratings (see Figure 5.12).

The following clinical screening tests for stereoscopic vision are based on the random-dot stereogram. They have the great advantage over traditional tests of containing no monocular cues to indicate the correct response. Some care must be taken in interpreting the results since some people with otherwise normal stereoscopic vision have difficulty fusing random-dot stereograms, especially if they cannot correctly focus on the stimulus.

TNO Test

This test was developed by Walraven (1975) of the Institute for Perception at Soesterberg in the Netherlands and is available from Alfred Poll Inc., New York, NY 10019. It consists of six random-dot stereograms printed as red/green anaglyphs to be viewed through spectacles fitted with red and green filters. Three of the stereograms are designed for children and have a monocularly visible object in addition to a cyclopean object visible only when the pictures are properly fused. The monocularly visible object gives the children something to see and lets them believe they have passed when they do not see the cyclopean object. Each of the three plates designed for adults contains four cyclopean discs each with a missing sector in one of four positions. The disparities in the discs range from 15 to 480 arcsec. It has been claimed that the TNO test diagnoses stereoblindness in children more reliably than the traditional Titmus Stereo Test (Walraven 1975).

Random-Dot E test

This test was devised by Reinecke and Simons (1974) and is available from Stereo Optical Co., Chicago, IL 60641. The subject views a random-dot stereogram with polaroid spectacles. A capital letter E stands out from a background with a disparity that varies with viewing distance. The subject has to indicate the orientation of the letter or which of two cards has a letter.

Frisby Stereo test

The Frisby stereo test is available from Clement-Clark, Ltd., Airmed House, Edinburgh Way, Harlow, Essex, CM20 2ED, UK. It consists of three clear plastic plates of variable thickness. On each plate three circular discs of randomly arranged dots are placed on either the front or the back surface,

and a fourth disc is placed on the opposite surface. The actual depth between the two displays of dots creates a binocular disparity of between 15 and 340 arcsec, depending on the thickness of the glass and the viewing distance. For each plate, subjects identify the disc which differs in depth from that of the other three discs on the plate. A stereoscope is not required for this test, since the depth between the test patches is real. This overcomes the problem that some people have in fusing dichoptic images and makes the test easy to use with young children who resist wearing anaglyph or polaroid spectacles.

Care must be taken to ensure that subjects do not derive information from parallax arising from movements of the head or the plate. Out of 34 adult subjects only one could perform above chance when asked to select the odd patch with monocular viewing. This subject presumably used uncontrolled monocular cues, such as parallax, accommodation, or perspective. Only two subjects failed the test with binocular viewing (Cooper and Feldman 1979).

There have been several investigations of correlations between different tests of stereopsis. Warren (1940) found that, although both the Howard-Dolman and the Keystone tests showed good test-retest reliability, the correlation between them was not significant. This lack of correlation was confirmed by Hirsch (1947) who concluded that many people have difficulty fusing dichoptic images in a test like the Keystone test, whereas this is not a problem in the Howard-Dolman test. Simons (1981a) compared the efficiency of the Random-Dot E test, the Frisby test, and the TNO test in diagnosing stereo deficiencies. Laboratory and clinical tests differ in several ways. For instance, most laboratory tests involve discrimination between opposite disparities while clinical tests involve detection of a disparity with respect to zero (Fahle et al. 1994).

5.3 STEREOACUITY— BASIC CONCEPTS

5.3.1 Stereoacuity

There is general agreement that, under the best conditions, stereoacuity is in the range 2 to 6 arcsec. This is similar to the limits of vernier acuity (Howard 1919; Andersen and Weymouth 1923; Woodburne 1934; Tyler 1973). Monkeys have been found to have stereoacuities in the same range (Sarmiento 1975; Harwerth and Boltz 1979). When the offsets of the images in the two eyes are equal and opposite, disparity is the sum of the two monocular offsets. At stereo threshold the offset in the images in each eye is only half that required for the detection of vernier

offset. In other words, subthreshold monocular offsets are combined by the cortical stereoscopic system into a detectable disparity signal.

It has been reported that stereoacuity is better for crossed than for uncrossed disparities. Woo and Sillanpaa (1979) reported a mean value of 5.6 arcsec for crossed disparity and 14.5 arcsec for uncrossed disparity. Grabowska (1983) reported a similar difference. Differences between crossed and uncrossed disparities are reviewed in Section 5.5.4. The effects of stimulus variables on stereoacuity are discussed in later sections of this chapter. The development of stereoacuity is reviewed in Section 15.2.

5.3.2 Depth discrimination thresholds

Stereoacuity, as measured by standard tests, is with respect to the plane of zero disparity. One can also ask subjects to fixate on a point and make threshold judgments about the relative depth of two neighbouring stimuli, both away from the horopter. The two comparison stimuli are said to be on a **disparity pedestal** and the resulting threshold is referred to as the **depth-discrimination threshold**. These concepts are illustrated in Figure 5.5.

Ogle (1953) asked subjects to adjust a thin line until it had the same apparent depth as a comparison line set at various pedestal disparities with respect to the fixation point. The depth-discrimination threshold increased exponentially with increasing size of the pedestal. Blakemore (1970d) used a double staircase method to measure depth discrimination for two luminous slits, one above and one below a fixation point, and seen against a dark background as a function of the disparity in the images of both slits with respect to the fixation point; that is, as a function of the size of a disparity pedestal. Like Ogle, he found that the discrimination threshold increased exponentially with increasing size of the pedestal. Reliable relative depth judgments were made when the two slits were up to 2° of disparity away from the fixation point. Data were obtained for centrally placed stimuli and for stimuli at retinal eccentricities of 5 and 10°. The rate of increase of the relative disparity threshold on a logarithmic scale was steeper for centrally placed stimuli than for eccentric stimuli and for crossed than for uncrossed disparity pedestals (see Figure 5.6). Similar results were reported by Krekling (1974) and Westheimer and McKee (1978). Depth judgments have been reported in random-dot stereograms that are up to 2° out of binocular alignment (see Section 8.1.8).

Badcock and Schor (1985) used elongated DOG patches with centre spatial frequencies between 0.15 and 9.6 c/deg. The standard patch was presented

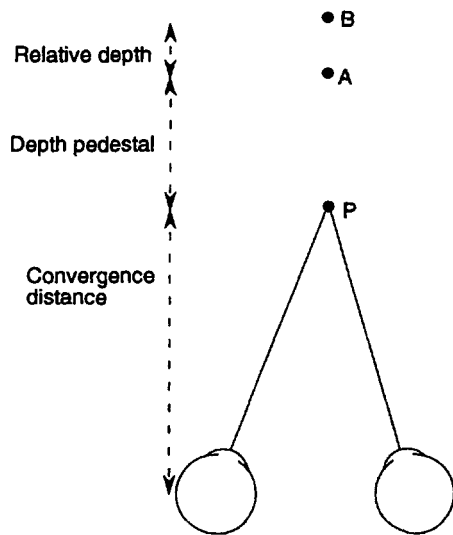


Figure 5.5. The concept of a depth pedestal.

With convergence on P , the disparity between A and B is on a disparity pedestal, defined as the disparity between P and A .

with a crossed or an uncrossed disparity pedestal of between 10 and 80 arcmin and the test patch was pulsed on for 750 ms at various neighbouring disparities, with fixation anchored on a point. Figure 5.7 shows that the stereo discrimination threshold increased exponentially with increasing size of the disparity pedestal. However, whereas Ogle (1953) and Blakemore (1970d) found that the threshold increased exponentially up to 2° of disparity, Badcock and Schor found that for disparities greater than about 20 arcmin, the threshold tended to level off.

The break in the continuity of the discrimination function reported by Badcock and Schor suggests that two processes are involved in disparity coding. One possibility is that fine disparities are processed by disparity detectors that rapidly lose sensitivity with increasing disparity, and large disparities are processed by detectors that have a more constant response with increasing disparity. Another possibility is that, as stimuli become diplopic with large disparities, subjects do not see depth but consciously use the relative separations of the diplopic images. Blakemore controlled for this factor by jittering the relative separations of the images from trial to trial. Siderov and Harwerth (1993b) found that after taking this precaution, discrimination functions were still discontinuous, as reported by Badcock and Schor, rather than continuous, as reported by Blakemore. When they took the extra precaution of randomly varying the crossed and uncrossed disparity of the stimuli, the discrimination functions became exponential and continuous. They concluded that the disparity detection mechanism shows a continuous exponential rise in the discrimination threshold

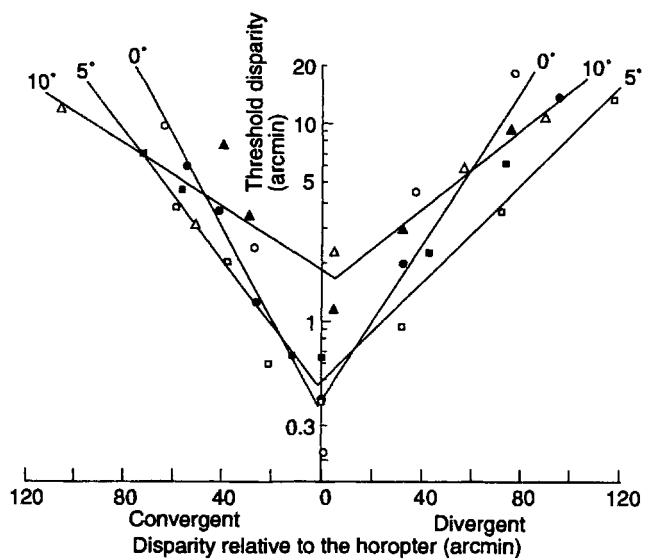


Figure 5.6. Stereoacuity and absolute disparity.

The disparity threshold for detecting relative depth between two vertical lines as a function of the absolute disparity in the images of the lines (depth pedestal). The three plots are for centrally placed stimuli (circles) and for stimuli at 5° (squares) and 10° (triangles) of eccentricity. Filled symbols for subject 1, closed symbols for subject 2. (Adapted from Blakemore 1970d.)

with increasing disparity and that the leveling off of the function at larger disparities reported by Badcock and Schor was due to the intrusion of judgments based on explicit width-matching.

The random-dot stereogram shown in Figure 12.4 creates a central square standing out from a background even though the whole image in one eye is magnified 10 per cent with respect to that in the other eye (Julesz 1963). One might expect that differential magnification of images would produce an impression of slant about a vertical axis (see Section 7.2). This expected impression is not evident in Figure 12.4, and in Section 7.2 we argue that this is because slant is coded in terms of the difference between horizontal and vertical magnification in the two eyes. In Figure 12.4 the visual system partials out the step disparity from the difference in overall magnification of the images. Superimposing a step disparity on a differential magnification of the images is equivalent to placing the step disparity on a disparity pedestal. Under these circumstances, one would expect stereoscopic acuity to be lower than for a step disparity presented alone. In line with this expectation, Reading and Tanlamai (1980) found that the stereoscopic threshold in random-dot stereograms and in several standard tests of stereoacuity was elevated in proportion to the degree of magnification of the image in one eye. *The whole question of how well people extract different components of*

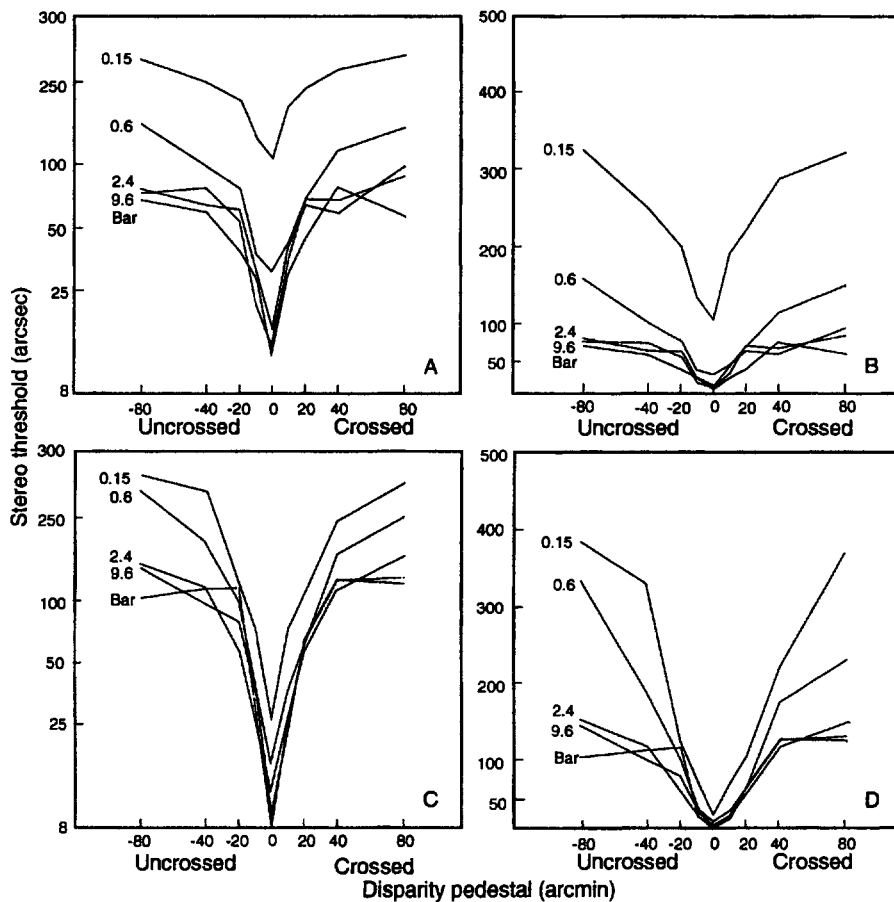


Figure 5.7. Depth discrimination as a function of disparity of comparison stimulus.

The threshold for discrimination of depth between a test stimulus and a comparison stimulus as a function of the disparity of the standard stimulus. Each curve shows the results for stimuli (DOG patches) of a specific centre spatial frequency (indicated by the number by the curve). Panels A and B show the results when test and comparison stimuli were DOGs. Panels C and D are results when the comparison stimulus was a thin bright bar and the test stimulus was a DOG. Panels B and D show the same data as panels A and C with the stereo thresholds plotted on linear scales. Results for one subject. (From Badcock and Schor 1985.)

disparity, such as horizontal, orientational, and differential magnification when they are present simultaneously, is one that has not been systematically explored.

Evidence is accumulating that a change in disparity applied equally to all images in view creates little or no impression of a change in depth. For instance, the threshold for the detection of a displacement in depth of a single line stepped from zero disparity to either a crossed or uncrossed disparity was found to be about 1 arcmin. When the stepped stimulus was flanked by parallel lines that remained in the fixation plane, the threshold was reduced to a few seconds of arc (Westheimer 1979a). This suggests that the visual system is especially sensitive to changes of disparity across local regions of the retina. The function relating depth sensitivity to the spatial frequency of depth modulation is discussed in Section 5.5.3. A system that responds to disparity gradients uncouples relative disparity signals from absolute

disparities over the whole field. The uncoupled signal is independent of fluctuations in vergence and provides a mechanism suited to detecting local depth gradients that indicate the shapes of three-dimensional objects. This issue is discussed in detail in Sections 7.8 and 12.1.1.

Local perturbations of depth applied to a smooth surface are detected more easily than when applied to a rough surface (Norman et al. 1991). Thus, subjects easily discriminated between a fully coherent random-dot surface with a low spatial-frequency depth modulation and the same surface with 4 per cent of incoherent dots. As more incoherent points were added, the threshold for detecting a difference in coherence increased. This is intuitively obvious with bolder stimuli. A single well-defined out-of-the-plane stimulus is easily detected among coplanar stimuli, but it is lost when added to a set of stimuli lying in different planes. We will see in Section 6.1.6

that simple depth features are processed in parallel and therefore pop out when presented in isolation or in the context of distinct depth features.

Duwaer and van den Brink (1982a) measured the threshold for discriminating between the vertical disparity of two horizontal test lines and that of two horizontal comparison lines. The threshold decreased by a factor of 2 as the disparity of the comparison lines increased from zero to 1.7 times above the threshold for detection of disparity, and decreased with larger disparities of the comparison lines.

The effects of the spatial frequency of depth modulation on depth discrimination is discussed in Section 5.5.3. Depth discrimination is compared with equivalent monocular tasks in Section 5.9.

5.3.3 An ideal observer for stereoacuity

Rose (1948) introduced the concept of the **quantal efficiency** of the human eye in detecting a visual stimulus at low light levels. Quantal efficiency is the ratio of the performance of a human observer to that of an ideal detector limited only by the statistical fluctuations in the arrival of quanta (quantal noise). Quantal efficiency provides an absolute reference for assessing human performance in this task. Visual performance is influenced by (1) quantal noise in the test stimulus, (2) the presence of extraneous stimuli, (3) the efficiency of the visual system in capturing and transducing light quanta, and (4) internal noise in the visual system. Barlow (1978) introduced the related concept of **statistical efficiency**. This measure is designed for tasks that involve detecting a suprathreshold patterned stimulus in the presence of extraneous stimuli. If the stimulus, presented alone, is well above threshold and is adequately resolved by the visual system, the ideal detector is not limited by quantal noise or optical factors, but only by noise due to extraneous stimuli. The method is applicable only to tasks defined with enough precision to allow one to specify the theoretical limit of performance.

Harris and Parker (1992) measured the statistical efficiency of two human subjects in detecting a vertical step of disparity in a random-dot pattern. The dichoptic pairs of dots on one side of the step were set at zero disparity relative to a surrounding pattern, and those on the other side were set at a disparity which varied from trial to trial. An extra horizontal disparity was imposed at random on each pair of dots, with a mean of zero and a standard deviation of s_{noise} across the set of dots. The value of s_{noise} varied from trial to trial. The ideal detector uses all the information present in the stimulus to detect the disparity step among the noise, given that it knows about where the step will be. For this purpose the

mean disparity of all the dot pairs on one side of the step was subtracted from the mean disparity of pairs on the other side, to yield the mean disparity difference, Δ . The addition of noise with standard deviation of s_{noise} caused the mean disparity of the n dots on each side of the step to vary from trial to trial with a standard error of the mean of

$$s = \frac{s_{noise}}{\sqrt{n}}$$

This is the standard error of the disparity signal. The mean disparity difference over the standard error of the disparity signal is the signal to noise ratio, or

$$d' \text{ ideal} = \frac{\Delta}{s}$$

This defines the ideal discriminability of the stimulus. The statistical efficiency of the human observer, F , is the square of the ratio of the discrimination performance of the observer, d' , to the ideal discriminability of the stimulus:

$$F = \left(\frac{d'}{d' \text{ ideal}} \right)^2$$

Harris and Parker found that stereoscopic efficiency was between 20 and 30 per cent when the display had fewer than 30 dots and declined to 2 per cent as the number of dots increased to about 200. Changes in dot density with number of dots held constant had little effect. Increasing the width of the stimulus, with dot density held constant, caused a drop in efficiency but only for high dot densities. It looks as though humans use only a limited set of dots from the total number available. Presumably, they use the dots closest to the disparity edge, since differential disparities in this region define a second-order disparity gradient that is not subject to adaptation. Noise makes it difficult to detect the second-order gradient because it injects second-order disparities over the whole display. We will see in Section 6.2.1 that observers use up to 10,000 elements when detecting interocular correlation in a zero-disparity random-dot display. In that case the crucial information is not confined to one region of the display. In a further study, Harris and Parker (1994a) found that stereoefficiency of human observers declined as the variance of the disparity noise increased. They explained this in terms of increased difficulty in matching the dots. When this factor was controlled by restricting the dots to two well-spaced columns, stereo efficiency remained constant as noise amplitude increased. They argued that efficiency is limited by processes beyond image matching under these circumstances (see also Harris and Parker 1994b).

5.4 THE UPPER DISPARITY LIMIT

Ogle (1952) used the method of adjustment to determine the maximum disparity between the images of a thin vertical line with respect to a fixation point that produced (a) the impression of depth with a fused image (Panum's fusional area), (b) an impression of depth with double images, and (c) a vague impression of depth combined with an impression of double images. He called the strong impression of depth created with fused or double images **patent stereopsis** and the vague impression of depth with more obvious diplopia **qualitative stereopsis**. In the foveal region, Panum's fusional area extended to about ± 5 arcmin, the region of patent stereopsis to about ± 10 arcmin, and that of qualitative stereopsis to about ± 15 arcmin. At an eccentricity of 6° , patent stereopsis extended to about 70 arcmin and qualitative stereopsis to about 2° . We will see that these estimates are lower than those found in recent studies.

Westheimer and Tanzman (1956) improved on Ogle's procedure by presenting the stereoscopic stimuli only briefly, which eliminated effects of changing vergence. They also used the constant stimulus method, which eliminated errors of anticipation. For disparities up to about 7° most subjects could detect whether the test target was stereoscopically nearer or further away than the fixation spot. Subjects detected the position of a stimulus with uncrossed disparity more reliably than that of a stimulus with crossed disparity. Using a similar procedure, Blakemore (1970d) found that subjects correctly categorized the depth of a midline dichoptic slit relative to a fixation point at well above chance levels for crossed disparities of between 4 and 7° and for uncrossed disparities of between 9 and 12° . Richards and Foley (1971) used a signal-detection paradigm and found even higher disparity limits. Although the ability to classify the depth of a 100 ms stimulus relative to a fixation stimulus at a distance of 170 cm began to deteriorate at a disparity of 1° or less, subjects still performed above chance with a crossed disparity of 16° . This degree of disparity corresponds to that produced by an object about 21 cm from the eyes with the eyes converged at 170 cm. Foley et al. (1975) asked subjects to point with unseen hand to the position in depth of briefly exposed visual targets with various degrees of disparity. Correct categorization of depth began to deteriorate at disparities of about 2° whereas pointing remained accurate for larger disparities. Pointing performance was still above chance for a disparity of 8° , the highest disparity tested.

These differences in the upper limit of disparity may reflect the fact that different investigators used

different luminance levels and contrasts. A reduction in luminance from mesopic to scotopic levels degraded the ability to discriminate depth arising from 0.5° of disparity but improved the ability from 4° of disparity. A reduction in luminance contrast at photopic levels of luminance had a similar differential effect (Richards and Foley 1974). Time of exposure is another important factor. Ogle (1952) noticed that the disparity limits for stereopsis were reduced with prolonged viewing of the target.

Both stereoscopic efficiency and the upper disparity limit for stereopsis increase if subjects look back and forth between the targets rather than hold the gaze on one of them (see Foley and Richards (1972) in Section 11.1.8).

In most experiments on the upper disparity threshold, the stimuli were presented for a shorter period than the latency of vergence. Therefore eye movements did not affect the stimulus. However, vergence may have had an effect because even briefly exposed stimuli with large disparities could evoke an appropriate vergence response that occurs after the stimulus has been shut off (see Section 10.5.5). Subjects' judgments may be prompted by the vergence movement rather than by a direct appreciation of the disparity. All investigators seem to have overlooked this possibility.

5.5 SPATIAL FACTORS IN STEREOACUITY

5.5.1 Stimulus eccentricity

Stereoacuity declines with increasing eccentricity of the compared targets. Rawlings and Shipley (1969) measured the threshold for the discrimination of the relative depth of two neighbouring points as a function of their horizontal distance from a fixation point in 2° steps out to 8° . The results are shown in Figure 5.8. Figure 5.6 shows that stereoacuity decreases less steeply with increasing size of the depth pedestal as the stimuli being compared are moved into the periphery (Blakemore 1970d). Krekling (1974) pointed out that this leads to the paradoxical result that stimuli on a depth pedestal of 80 arcmin have a higher stereo threshold when they are in the central visual field than when they are at an eccentricity of 5° .

An impression of stereoscopic depth produced by a small vertical bar oscillating in depth at 2 Hz between 0 and 0.4° , can be appreciated out to at least 20° of eccentricity (Richards and Regan 1973). Figure 5.9 shows the disparity threshold for detecting relative depth between vertical lines, 4 arcmin in length, presented at various angles of eccentricity above and below a fixation point (McKee 1983).

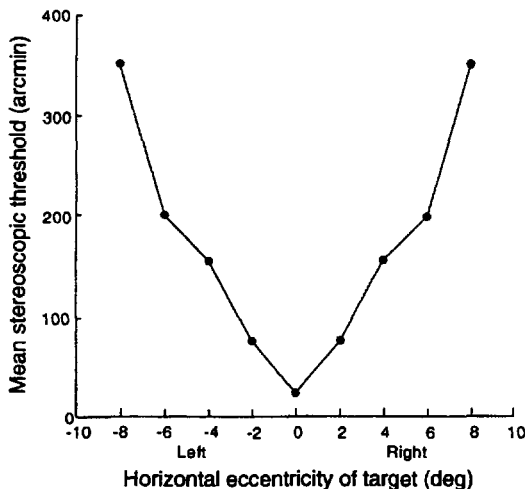


Figure 5.8. Stereoacuity and horizontal eccentricity.
The disparity threshold for discrimination of the relative depth of two neighbouring points as a function of their horizontal distance from the fixation point. Mean data from three subjects. (From Rawlings and Shipley 1969.)

5.5.2 Stimulus spacing

This section is concerned with the effects of the spacing of discrete stimuli on stereoacuity. The concepts of disparity gradient, disparity ramp, and ramp density relevant to this section were defined in Section 2.3.3. Stereoacuity improves as the length of vertical target lines increases up to about 20 arcmin, after which further increases in length produce little improvement (McKee 1983).

It seems that stereoacuity and vernier acuity are the same when the line targets are separated vertically by between 2 and 4 arcmin. For vertical separations less than this, the vernier threshold is two or three times lower than the stereo threshold (Berry 1948; Stigmar 1970). For vertical separations greater than 4 arcmin, Berry found stereo thresholds to be less than vernier thresholds but Stigmar found them to be similar.

Stereoacuity improved when the vertical distance between a comparison line and a test line was increased up to about 0.2° (Westheimer and McKee 1980a). With greater separations between comparison and test elements, the trend was reversed, that is, more disparity was required to reach threshold with increasing separation, slowly at first and then more steeply (Hirsch and Weymouth 1948a, 1948b). As a pair of stereo targets becomes more removed from the fovea, an even greater separation between comparison and test elements is required for optimal stereoacuity (Westheimer and Truong 1988). Similar crowding effects occur with monocular acuities.

The preceding experiments were conducted at threshold levels of disparity. Suprathreshold effects

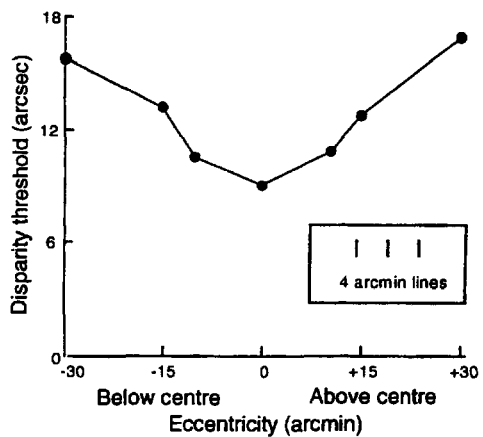


Figure 5.9. Stereoacuity and vertical eccentricity.

The horizontal disparity threshold for discrimination of depth between lines at vertical eccentricities of up to 30 arcmin. Data for one subject. (Reproduced with permission from McKee, 1983, Pergamon Press.)

are now considered. It is to be expected that under conditions favouring high stereoacuity (small JND for depth) a given suprathreshold disparity would produce an impression of greater depth than when stereoacuity is low. Bülthoff et al. (1991) asked subjects to scale the apparent depth between two stimuli with reference to a set of comparison stimuli. They found that, for a given disparity difference, the perceived depth difference between the test stimuli decreased as their lateral separation decreased, that is, as the disparity gradient increased. For example, for a disparity difference of 6 arcmin the perceived depth decreased as the lateral separation between the targets decreased from 20 to 3 arcmin, that is, as the disparity gradient increased from 0.3 to 2. In other words, as two stimuli approach each other horizontally, each within a different frontal plane, the depth between them appears to decrease. For a given disparity gradient, the depth between two stimuli became progressively underestimated as the disparity between the stimuli was increased (with a proportional increase in lateral separation). In other words, as the depth of a disparity ramp was increased the perceived depth as a fraction of actual depth became less. *These experiments need to be extended to a wider range of disparity gradients and lateral separations. It is to be expected from the results of Hirsch and Weymouth's experiment that the trends would be reversed with more gradual gradients and larger horizontal separations.*

The experiments reviewed so far used only two targets. It is therefore not clear whether the results were due to the increasing depth of the ramp or to the increasing separation between the stimuli (ramp density). The effects of varying ramp density (the number of stimulus points per unit distance along

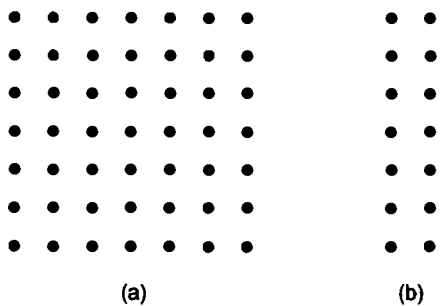


Figure 5.10. Stereoacuity and length of depth ramp.

(a) In a display with several columns of dots the threshold horizontal disparity between adjacent columns for the perception of slant about a vertical axis had a mean value of 127 arcsec. (b) The mean disparity for the perception of slant between an isolated pair of columns was only 11.7 arcsec. Thus the threshold for detecting depth was lower for a short ramp than for a long ramp of the same density and disparity gradient. (Reproduced with permission from Mitchison and Westheimer 1984, Vision Research, Pergamon Press.)

the ramp) are now considered. The disparity threshold for discriminating the depth between two fixed stereo targets increased when a third point was interpolated between them to form a linear depth ramp. The threshold continued to increase as more points were interpolated on the ramp (Fahle and Westheimer 1988). This was found for both horizontal and vertical arrays of points. The addition of points between two fixed points does not alter the disparity gradient. It was concluded that the depth between neighbouring points (disparity density) is the most important variable determining the depth threshold. It is not clear whether the crucial variable is the lateral separation between points (angular subtense) or their separation along the depth ramp (ramp density), since these factors covaried. In any case, this result suggests the operation of a local process akin to crowding. Fahle and Westheimer also found that, for a given lateral separation between the stimuli, the depth threshold was higher for a ramp 1° long than for one 0.1° long. Thus, a second factor is the length of the depth ramp, which suggests the operation of a global factor.

The importance of the length of a depth ramp was also revealed by Mitchison and Westheimer (1984), who found that the disparity threshold for detection of the slant between two columns of dots with a given lateral separation was lower than when the two columns were embedded in a long disparity ramp with the same dot density and disparity gradient (Figure 5.10). In other words, depth in a ramp of fixed gradient and density is harder to detect in a long ramp than in a short ramp.

The stereo threshold for a test line relative to a fixated line has been found to be elevated if the test

line is flanked by other lines in the plane of fixation (Butler and Westheimer 1978). This effect reached its peak value of a sixfold increase in stereo threshold when the distance between the test lines and flanking lines increased to about 2.5 arcmin, and declined with greater separations. The effect fell to zero as the flanking lines were moved from the fixation plane into the same plane as the test line. This is another instance of so-called disparity crowding (see also Kumar and Glaser 1992).

In these experiments the depth threshold was elevated both by increasing the density or the absolute number of disparate elements. This suggests that the crucial factor is the number of disparate elements falling within the range of some integrative mechanism. This could be either a disparity-averaging mechanism (see Section 6.3) or a lateral-inhibition mechanism. If lateral inhibition occurs only between detectors with similar disparity sensitivities, then the effects of crowding should be larger for linear disparity surfaces than for nonlinear disparity surfaces, such as a sinusoidal disparity corrugation. This issue is discussed in the following section. Another factor in these crowding effects may be vergence eye movements (see Section 6.2.11). The whole issue is an aspect of two broader questions; depth contrast, discussed in Chapter 12, and the relationship between stereoscopic vision and spatial frequency of disparity modulation, discussed in the next section.

5.5.3 Spatial frequency of disparity modulation

This section deals with the relationship between stereopsis and the amplitude and spatial frequency of continuous modulations of disparity. The basic quest is to derive a sensitivity function for disparity and compare it with the transfer function for detection of modulations of luminance.

Disparity modulation of a line

Tyler (1973, 1975a) conducted the first experiment on this topic and introduced the general concept of the scaling of stereoacuity by the spatial frequency of depth modulation. A straight vertical line subtending 15° was presented to one eye and a wavy vertical line to the other. Combined stereoscopically they produced the impression of a line curved sinusoidally in depth. The threshold amplitude of disparity modulation decreased with increasing frequency of disparity modulation, reaching a minimum at about 1 c/deg after which it rose to a limiting value at a frequency of about 3 c/deg. There was no stereopsis above this frequency of depth modulation. This function defines the sensitivity function for the detection of disparity modulation in

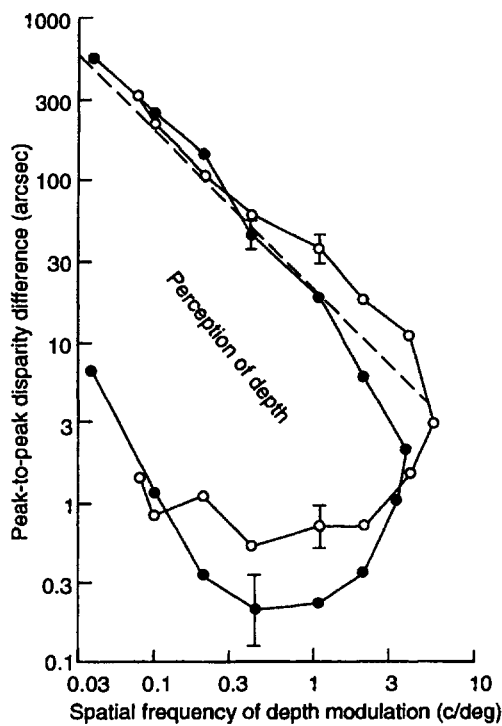


Figure 5.11. Stereopsis and depth modulation.

Disparity threshold and upper disparity limit of stereopsis as a function of spatial frequency of depth modulation in a vertical line. Filled circles—fixed size of aperture. Open circles—aperture varied in size so that one period of depth modulation was visible at each frequency. Data for one subject. (Reproduced with permission from Tyler 1975a, Vision Research, Pergamon Press.)

a line. The threshold for the monocular detection of the undulations in a line showed a similar dependency on the frequency of undulation at spatial frequencies below about 0.5 c/deg, but monocular undulations could be detected best at about 3c/deg and were visible up to about 12 c/deg. It looks as though the upper frequency limit of disparity modulation for stereopsis is determined by factors other than the capacity of each eye to detect undulations in a line. Tyler also showed with this stimulus that the longer the spatial period of each cycle of disparity modulation became, the larger was the upper limit of disparity that elicited depth. In other words, the upper disparity limit is scaled in proportion to the spatial period of disparity modulation; the greater the spatial period, the larger the disparity that can be processed. Tyler suggested that upper threshold performance was based on a disparity gradient limit.

Figure 5.11 shows both the lower and upper disparity limits of stereopsis combined into one graph for one of Tyler's subjects. One set of data was obtained with a constant size of display and hence a variable number of depth modulations, and the other set was obtained with a constant number of depth modulations and hence a variable size of

display. For higher frequencies of depth modulation both the lower and upper disparity limits were somewhat elevated when the number of cycles was held constant compared with when the size of the display was kept constant. Tyler concluded that disparity information is integrated over about two cycles of depth modulation. A related finding is that the larger the area of a region of constant disparity in a random-dot stereogram, the higher is the upper limit of disparity (Tyler and Julesz 1980).

Disparity modulation in random-dot stereograms

A wavy line is not ideal for studying spatial modulations of disparity because a change in the frequency of disparity modulation is accompanied by changes in the spatial frequency of position modulation in the monocular image. A better stimulus is provided by a random-dot stereogram, with a sinusoidally modulated disparity, which appears as a corrugated surface when fused. A surface with horizontal corrugations is created by sinusoidally shearing rows of dots in one member of an identical pair of random-dot displays in a horizontal direction; rows sheared sinusoidally in the direction of crossed disparity alternate with rows sheared sinusoidally in the direction of uncrossed disparity, as in Figure 5.12. The sheared rows, indicated in the figure by wavy edges, are not visible in the monocular image and therefore do not provide a cue to the spatial frequency or amplitude of the depth corrugations. A surface with vertical corrugations is created by oppositely compressing columns of dots in two stereograms. This is not always a useful stimulus because the columns can be seen in the monocular images as modulations in dot density, which introduce visible modulations of mean luminance if the disparity gradient is steep.

A threshold function for disparity-modulations can be obtained for corrugated random-dot stereograms. In this function, stereoscopic thresholds are plotted as a function of the spatial frequency of sinusoidal depth modulation. The stereogram shown in Figure 5.12 depicts a frequency-swept grating of disparity modulation, analogous to a frequency- and amplitude-swept grating of luminance modulation. By asking subjects to mark the boundary between the region to the left where the surface appears to be corrugated and the region to the right where it appears to be flat, Tyler (1974a) determined a threshold function. This showed a fall-off in sensitivity for corrugation frequencies above 1 c/deg. The upper limit of disparity modulation for stereopsis, found by asking subjects to mark the highest row of the frequency swept corrugation which still appeared to be corrugated, was about 4 c/deg—close to the value obtained with a depth-modulated line.

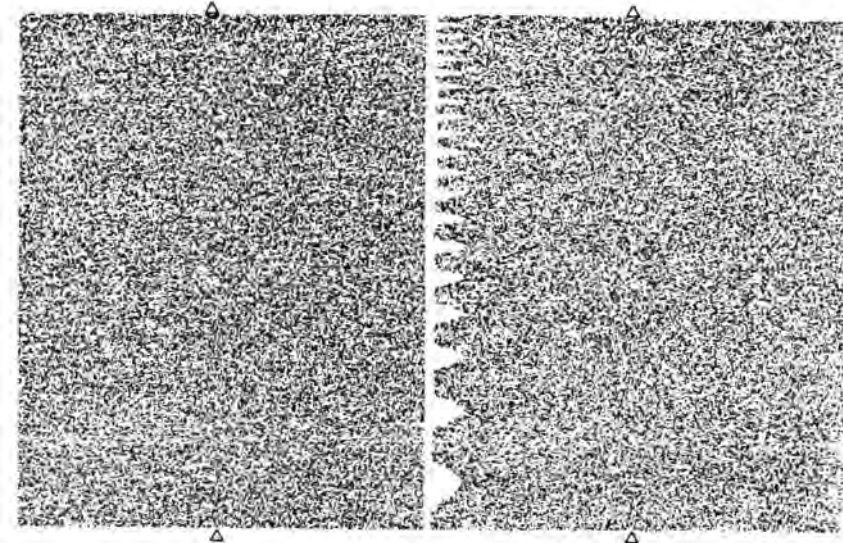


Figure 5.12. Frequency-swept grating of disparity modulation.

After the images are fused, the level above which depth modulations are not visible defines the upper limit of spatial frequency of disparity modulation for stereopsis. (From Tyler 1974a. Reprinted by permission of Nature, 251, 140-42. Copyright 1974 Macmillan Magazines Limited.)

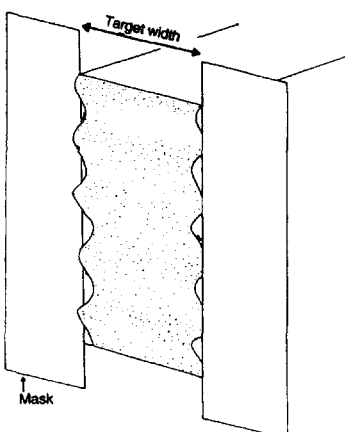
This upper limit was not due to the inability of subjects to resolve the dots in the monocular image. Nor was it much affected by a tenfold reduction in dot density. This latter finding does not accord with Fahle and Westheimer's report, discussed in Section 5.5.2, that stereoacuity is degraded as the number of elements defining a given depth gradient increases. The crucial difference between the experiments may be that the display used by Fahle and Westheimer was a single depth ramp (first-order disparity) and the effects may have been due to a tendency to see isolated inclined surfaces as lying in the frontal plane (see Section 12.1.2). In Tyler's display several depth undulations (second-order disparities) prevent normalization to the frontal plane.

The upper limit of frequency at which depth corrugations are seen is not the upper limit for perceived depth because, above the point where corrugations are seen, depth transparency is perceived; that is, one is aware of dots dispersed in several depth planes. The question of depth transparency is discussed in Section 6.3. Tyler showed with his stimulus that the upper disparity limit for stereopsis is also scaled in proportion to the spatial period of disparity modulation.

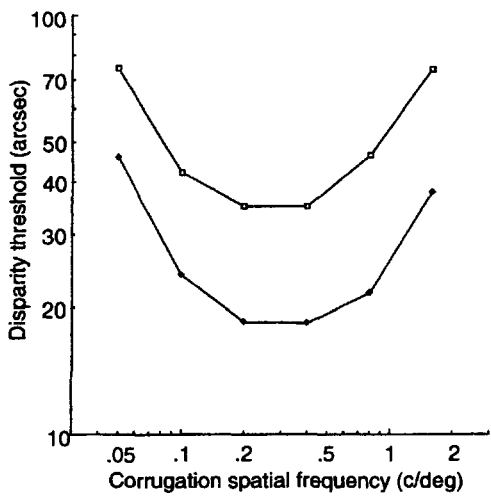
Figure 5.13b shows the threshold function for disparity modulations obtained by Rogers and Graham (1982) for a random-dot stereogram with horizontally modulated depth corrugations of between 0.1 and 1.6 c/deg. Note that the thresholds for perceiving depth modulations are lowest at around 0.3 to 0.5 c/deg and are higher for frequencies of

disparity modulation above and below this value. Rogers and Graham (1985) showed that the fall-off in sensitivity at low corrugation frequencies was not due to the small number of cycles present in their displays, since a similar fall-off was found with disparity surfaces which had a difference of Gaussians disparity profile. Bradshaw and Rogers (1993b) recently made observations over a wider range of corrugation frequencies from 0.0125 c/deg (80° period) to 3.2 c/deg, using three different sizes of display (10°, 20°, and 80°). Sensitivity for perceiving disparity modulations extended down to corrugation frequencies of at least 0.0125 c/deg. For several observers, thresholds for detecting peak-to-trough disparity corrugations were less than 3 arcsec at the optimal frequencies between 0.3 and 0.5 c/deg, when the peaks and troughs were separated by more than 1° of visual angle. Thresholds for vertically oriented corrugations of low spatial frequency are typically higher than for horizontally oriented corrugations (Figure 5.13c) but there are considerable individual differences in the magnitude of this anisotropy, which are discussed in Section 7.7.1.

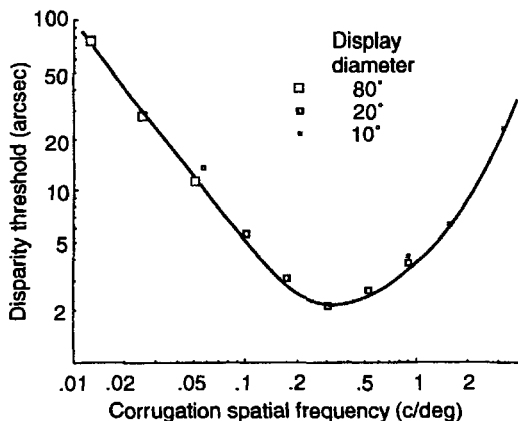
Figure 5.13d shows the disparity-corrugation sensitivity function (the reciprocal of the depth-modulation threshold) obtained by Schumer and Julesz (1984) for corrugated surfaces offset on 25- and 40-arcmin crossed and uncrossed disparity pedestals. With the pedestal corrugations, the corrugation frequency giving peak depth sensitivity is progressively reduced and the high-frequency loss becomes more severe. These results further support



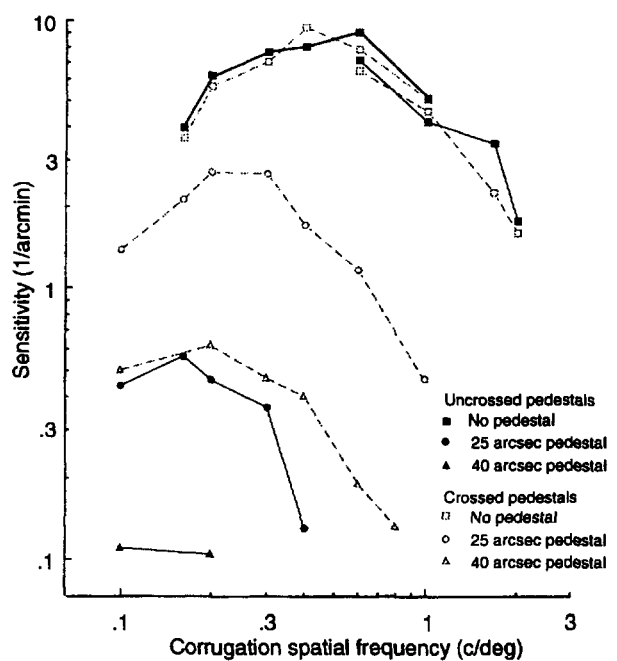
(a) Appearance of the display used by Schumer and Julesz, 1984.



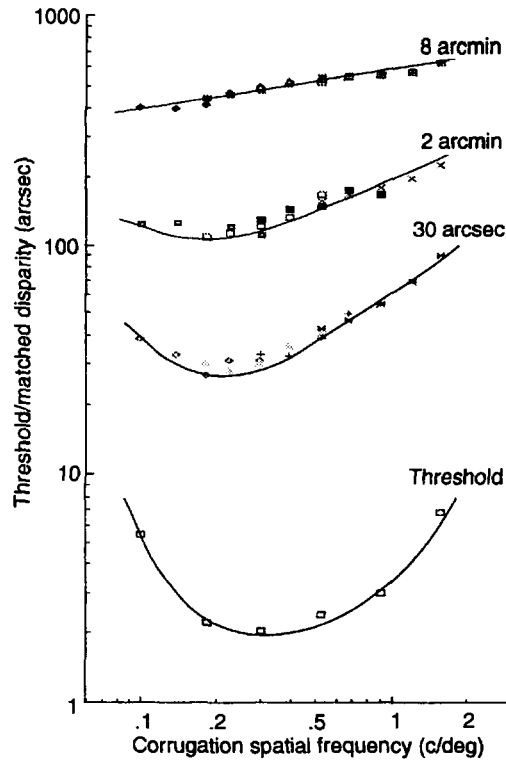
(b) Thresholds for detecting a corrugated random-dot surface as a function of the spatial frequency of the corrugations. Lowest thresholds of around 17 arcsec of peak-to-trough disparity occurred at a frequency of depth modulation of around 0.3 c/deg. Results for two observers using an ascending method of limits. (Adapted from Rogers and Graham 1982.)



(c) Thresholds for detecting corrugated surfaces as a function of corrugation spatial frequency from 0.0125 to 3.2 c/deg. Thresholds are slightly higher for the highest corrugation frequencies on the 80° display and for the lowest corrugation frequencies on the 20° display. Thresholds approximately double with each halving of corrugation frequency for low frequencies.



(d) Sensitivity for detecting disparity modulations as a function of frequency of modulation for displays superimposed on disparity pedestals. (Redrawn from Schumer and Julesz 1984.)



(e) Bottom curve; thresholds for detecting a corrugated surface as a function of corrugation frequency. Upper curves; subjects set disparity in a test surface to match depth in a reference surface with peak-to-trough disparity indicated on each curve. At supra-threshold disparities, the functions flatten out. This subject saw slightly less depth in high- than in low-frequency corrugations.

Figure 5.13. Disparity modulation sensitivity.

the conclusion that, as a depth-modulated display is removed further from the zero-disparity plane, the perception of depth occurs only with more gradual disparity gradients. Note also that sensitivity for displays on crossed pedestals is greater than for those on uncrossed pedestals, which also confirms evidence already cited. Schumer and Julesz suggested that this asymmetry between crossed and uncrossed disparities is due to subjects misconverging about 5 arcmin in front of the fixation target.

Supra-threshold matching functions

The threshold functions for disparity modulation show a bandpass characteristic with the lowest thresholds for detecting depth corrugations at frequencies of around 0.3 to 0.5 c/deg. These functions can be thought of as shifted down the spatial frequency axis by a factor of ten compared with the equivalent threshold functions for luminance modulation (Campbell and Robson 1968). At supra-threshold contrast levels in the luminance domain, Georgeson and Sullivan (1975) found that the contrast matching functions flattened out, so that the subjective contrast of gratings of all spatial frequencies with the same physical contrast appeared to be the same whenever the contrast was a factor of a hundred or more above threshold.

Ioannou et al. (1993) have reported a similar "contrast constancy" effect for disparity modulations. Observers were asked to match the amount of peak-to-trough depth seen in a fixed amplitude disparity corrugation at one of a number of corrugation frequencies between 0.1 and 1.6 c/deg to a variable amplitude reference corrugation. When the peak-to-trough depth in the corrugations was just above threshold, observers judged the low- and high-spatial-frequency corrugations to have less depth than the reference corrugation of intermediate corrugation frequency. However, when the peak-to-trough depth was a factor of a hundred or more above threshold (4 arcmin), the matching functions flattened out and corrugations of all spatial frequencies were perceived to have approximately the same amount depth (Figure 5.13e). As in the luminance domain, there appears to be a mechanism which compensates at supra-threshold levels of disparity modulation for the visual system's poorer sensitivity at threshold levels of disparity modulation for both low and high spatial frequency corrugations.

Visual channels for disparity modulation

The question now arises as to whether there is a single channel sensitive to the full range of disparity modulation or two or more independent channels. Evidence from single-cell recording in the visual

cortex, reviewed in Chapter 4, points to the existence of at least two populations of disparity-tuned cells, one tuned to small disparities and the other to large disparities. But this in itself does not establish that there are channels specifically tuned to the spatial modulation of disparity. Two methods have been used to measure the bandwidth of disparity-modulation channels—adaptation and masking.

Schumer and Ganz (1979) found that the disparity threshold for a random-dot stereogram with a given corrugation frequency, f , was not affected by the superimposition of another disparity grating of frequency $3f$. This is evidence that disparity is processed in independent channels with a maximum bandwidth of ± 1.6 octaves. They also measured the effect of prolonged exposure to a disparity grating of fixed corrugation frequency on the threshold of a test grating, as a function of the corrugation frequency of the test grating. The elevation of threshold was found to centre on the frequency of the adapting grating and to be confined to about two octaves within the visual system's total corrugation bandwidth (see also Section 12.1). This result also supports the notion of independent and broadly tuned disparity-modulation channels with overlapping tuning functions. There could be a multistage system involving low-level disparity-modulation detectors, each with a narrow disparity range, feeding into broadly tuned higher-level channels. But the final outcome is that the disparity-detection system is a metamer system, like colour, orientation, spatial frequency, and many other sensory systems (see discussion in Section 3.2.6). Two or more contiguous stimuli with disparity modulations falling well within the bandwidth of a single channel should be metamERICALLY combined by that channel into one signal. This is related to the topic of disparity averaging discussed in Section 6.3. Two stimuli processed by distinct channels could interact by mutual inhibition, or opponency, as in colour opponency. On the other hand, distinct channels could interact by mutual facilitation or a combination of inhibition and facilitation, depending on the relative frequencies of disparity modulation in the two stimuli.

Tyler (1983) used a masking paradigm to measure the bandwidth of disparity-modulation channels. The threshold for detection of a depth-modulated grating was determined in the presence of a masking grating of variable spatial frequency relative to the spatial frequency of the stimulus. The disparity-modulation channels were estimated to have a bandwidth of about one octave. This masking procedure underestimates the width of sensory channels because the mask affects the channel upon

which it is centred but leaves neighbouring overlapping channels relatively unaffected. This problem of "off-channel viewing" can be overcome by use of a notched mask consisting of two non-overlapping bandpass masks which are symmetrically positioned about the test stimulus. The threshold of the test stimulus is measured as a function of the width of the notch between the two masks. With this procedure Cobo-Lewis and Yeh (1994) obtained channel bandwidths for disparity modulation of about twice the value reported by Tyler and more in agreement with those reported by Schumer and Ganz. However, comparison between data derived from the various methods depends on certain assumptions, such as the linearity of the mechanisms involved and the symmetry of the tuning functions.

5.5.4 Comparison of Crossed-uncrossed disparity

Woo and Sillanpaa (1979) found that mean stereoacuity was 5.6 arcmin for crossed disparity targets and 14.5 arcsec for uncrossed disparity targets. A similar difference was reported by Grabowska (1983). However, Larson (1990) found that stereoacuity on the Frisby and TNO stereo tests was, on average, no better for crossed than for uncrossed crossed disparity. Schumer and Julesz (1984) found depth sensitivity for displays on crossed pedestals was greater than for those on uncrossed pedestals and suggested this asymmetry is due to a tendency of subjects to misconverge about 5 arcmin in front of the fixation target. Lasley et al. (1984) asked people to categorize the depth of a test stimulus with respect to a comparison stimulus for disparities between $\pm 4^\circ$ and derived estimates of d' from the percentage of correct scores. They found that some people performed better with crossed disparities and others with uncrossed disparities but that, on average, crossed disparities were more precisely categorized than uncrossed disparities. We will see in Section 15.3 that under certain circumstances some people cannot detect crossed disparities, while others cannot detect uncrossed disparities. Herring and Bechtoldt (1981) used a more discriminating five-category scale—"very far," "far," "equal," "near" and "very near"—in conjunction with Thurstone's method of successive intervals for which the maximum likelihood solution has been programmed (Schönemann and Tucker 1967). They found that crossed and uncrossed disparities up to 45 arcmin were categorized with equal precision.

Westheimer and Tanzman (1956) presented stereoscopic stimuli only briefly to eliminate monocular cues and effects of changing vergence. Subjects detected the position of a stimulus with uncrossed

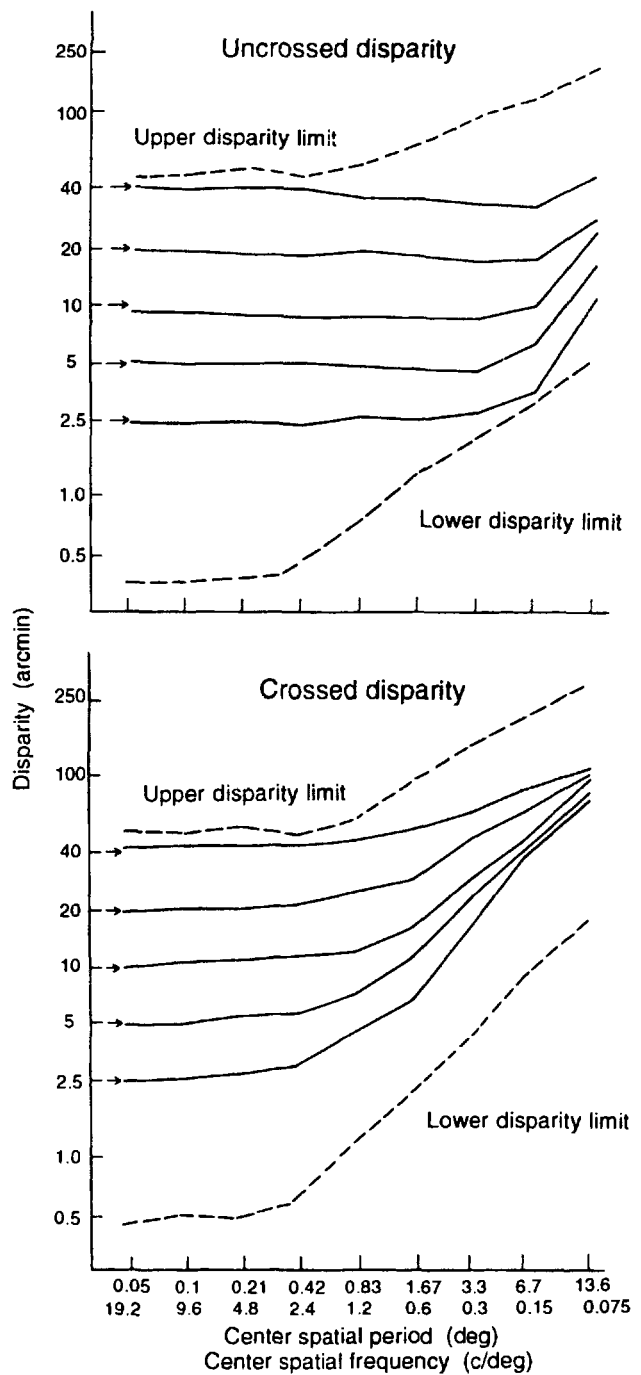


Figure 5.14. Stereopsis and spatial frequency.

The dotted curves indicate the upper and lower disparity limits for stereopsis as a function of the spatial frequency of DOG patches for uncrossed (upper figure) and crossed (lower figure) disparities. The solid lines indicate the efficiency with which disparity in a DOG patch is coded into depth. Depth efficiency is the disparity in a vertical-line depth probe required to match the disparity in the DOG patch. The disparities of the DOG patches for which efficiency was measured are indicated by the arrows on the Y axis. Results for one subject. (Reproduced with permission from Schor and Wood 1983, Vision Research, Pergamon Press.)

disparity more reliably than that of a stimulus with crossed disparity. However, these were large disparities between 1° and 10°. Using a similar procedure, Blakemore (1970d) found that subjects correctly categorized the depth of a centrally placed dichoptic slit relative to a fixation point at well above chance levels for crossed disparities of between 4 and 7° and for uncrossed disparities of between 9 and 12°.

Schor and Wood (1983) also investigated this question using small patches with difference-of-Gaussian luminance profiles. It can be seen in Figure 5.14 that stereoacuity deteriorated when luminance spatial frequency fell below 2.4 c/deg, for both crossed and uncrossed disparities. Figure 5.14 also shows that, for low spatial frequency displays, less depth was evoked by a given disparity when it was crossed than when it was uncrossed. These results are discussed more fully in Section 5.7.3. The whole question of differences between the responses of the visual system to crossed and uncrossed disparities has been reviewed by Mustillo (1985).

5.5.5 Target orientation in the frontal plane

Consider a Howard-Dolman display with featureless rods seen through an aperture that occludes the ends of the rods. Several investigators have reported that stereoacuity declines in proportion to the cosine of the angle of tilt of the rods in the frontal plane (see Ogle 1955 and Ebenholtz and Walchli 1965). There are at least five possible causes for this effect, which we now consider.

- When a vertical rod is tilted in the frontal plane through angle ϕ , the horizontal disparity between corresponding points of the two images remains the same but the orthogonal distance between the images becomes smaller in proportion to $\cos \phi$, as illustrated in Figure 5.15. The dependence of stereoacuity on $\cos \phi$ would follow if subjects used the disparity between orthogonal points rather than the horizontal disparity. When the rod is vertical ($\phi = 0^\circ$), the disparity is equal to the orthogonal distance between the images. But when the rod is tilted, the nearest-neighbour matches are between orthogonally opposite points rather than between horizontally opposite points. When the rod is horizontal ($\phi = 90^\circ$) the images are superimposed and if the rod is featureless and its ends are not in view, all stereo cues are eliminated.

Friedman et al. (1978) investigated this question using two 0.25°-diameter discs exposed for 100 ms, with a fixation cross midway between them. Subjects estimated the amount of depth for a fixed horizontal disparity of 1° as the axis of the discs was tilted at

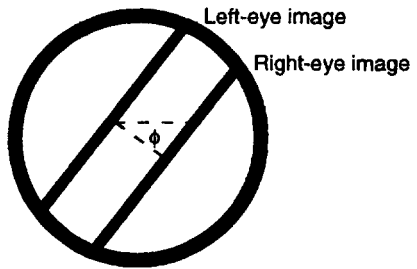


Figure 5.15. Stereopsis with tilted stimulus.

When a vertical rod is tilted in the frontal plane through angle ϕ the horizontal disparity between corresponding points of the two images remains the same but the orthogonal distance between the images becomes smaller in proportion to $\cos \phi$. Disparity between the ends of the rod is obscured when it is viewed through a circular aperture.

various angles. Perceived depth declined more rapidly than the cosine of the angle of tilt of the two discs relative to the horizontal. They concluded that a vertical disparity attenuates the impression of depth evoked by a given horizontal disparity.

- The reduction in stereoacuity with increasing tilt of test rods could also arise because a given horizontal disparity is more difficult to detect when there is a crowding of images. As a test rod becomes more tilted the horizontally matching points in the images become increasingly crowded by neighbouring points along the rods. There is no evidence on this point other than that reported in Section 5.5.2.

- Another factor might be that disparities between vertical lines are detected more efficiently than those between tilted lines. This would be the case if there were a preponderance of binocular cells tuned to vertically oriented lines. The evidence on this point is equivocal (see Section 4.3).

- Still another factor might be that monocular contrast sensitivity and vernier acuity are higher for vertical lines than for oblique lines (see Howard 1982) and, insofar as stereo disparity depends on monocular sensitivity and acuity, one might expect the same anisotropy for stereoacuity.

- Blake et al. (1976) proposed that the loss of stereoacuity with tilt is due to a reduction in the height of the test rods along the vertical retinal meridian as the angle of tilt increases. They cited a paper by Andersen and Weymouth (1923) to the effect that stereoacuity declines with a reduction in line length. This is most unlikely to be a factor with rods as long as those used in the experiments reported by Blake et al. Davis et al. (1992) found that the stereo acuity for oblique difference-of-Gaussian patches was not improved by an increase in the length of the patches, which also argues against the factor of line length.

A test between the orthogonal-matching factor and the other possible factors would be to measure stereoacuity using rods with distinguishable features along their lengths. With these stimuli the visual system would probably use regular horizontal disparities rather than orthogonal disparities, because the images would be matched on the basis of similarity rather than by the nearest-neighbour rule. Any crowding effect would remain and so would any effect due to a preference for vertical lines.

For a random-dot stereogram depicting a square-wave depth grating, stereoacuity was about twice as good when the grating was oriented vertically than when it was oriented horizontally (White and Odom 1985). This result is related to the anisotropy in the perception of horizontal and vertical depth modulations reported by Rogers and Graham (1983). The relation of stereopsis to the orientation of surface features is discussed in detail in Chapter 7. Stereopsis is also affected by whether lines comprising a stereogram have the same orientation in both eyes. This issue is discussed in Section 6.2.3.

5.6 LUMINANCE CONTRAST AND STEREOPSIS

5.6.1 Effects of luminance and contrast

Berry et al. (1950) reported that increasing the luminance of stereo targets up to 10 millilamberts improved stereoacuity at least threefold, after which a further increase in luminance had little effect. The function relating stereoacuity to luminance was steeper than that relating vernier acuity to luminance, but the two functions had a similar shape. A discontinuity in the function relating stereoacuity to luminance is evident as luminance is reduced from the mesopic into the scotopic range, at between 0.1 and 0.01 millilamberts (Mueller and Lloyd 1948; Lit and Hamm 1966).

For stereograms consisting of vertical sine-wave gratings, the stereo threshold was approximately inversely related to the square root of Michelson contrast, for contrasts between 0.01 to 1.0 (Legge and Gu 1989). Cormack et al. (1991) used a random-dot stereogram and found a cube-root dependency of stereoacuity on contrast at suprathreshold levels of contrast (see Figure 5.16). The difference is probably due to the different spatial-frequency content of the stimuli used in the experiments. At contrasts below about five times the threshold, Cormack et al. found stereoacuity to be proportional to the square of contrast. This is what one would expect in the threshold region, where performance is limited by a constant level of intrinsic noise. There is thus agreement that stereoacuity has a weak dependence on contrast at

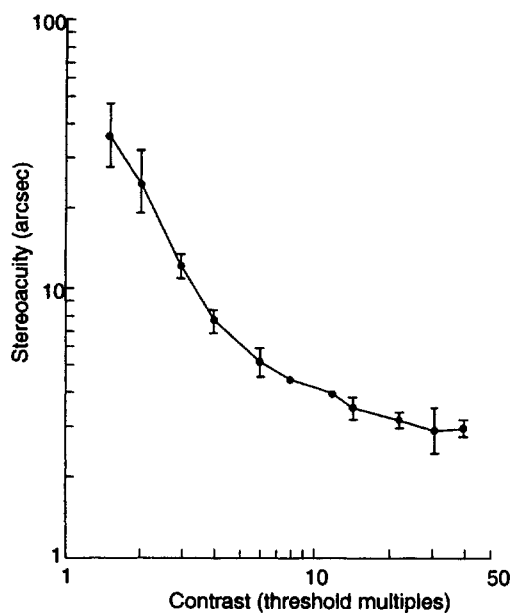


Figure 5.16. Stereoacuity and luminance contrast.

At suprathreshold contrasts, acuity is proportional to the cube-root of contrast over almost a log unit of contrast. Below a contrast of 10-times-above-threshold, acuity is proportional to the square of contrast. Data for one subject. (Reproduced with permission from Cormack et al. 1991, Vision Research, Pergamon Press.)

suprathreshold levels but declines rapidly as contrast approaches the contrast threshold.

Loss of the high spatial-frequency content of a stereo display degrades stereoacuity more than monocular acuity. As the image in one eye was optically blurred, the loss in Snellen acuity in that eye was proportional to the loss in stereoacuity, as assessed by the Titmus Fly test (Levy and Glick 1974). Stereoacuity was also degraded when the low spatial-frequency components of the target were removed (Westheimer and McKee 1980b). The contrast-sensitivity function for stereopsis is discussed in more detail in the next section.

Richards and Foley (1974) looked at the suprathreshold effects of changing luminance and contrast on the ability of subjects to discriminate between crossed and uncrossed disparities over a wide range of disparities. A reduction in luminance from mesopic to scotopic levels degraded depth discrimination for disparities up to 0.5°. However, for 4° of disparity, depth discrimination improved as luminance was reduced to the cone threshold, after which it declined with further reduction of luminance. A reduction in luminance contrast at photopic levels of luminance had a similar differential effect. They argued that there is less lateral inhibition, and therefore more neural summation, at low levels of luminance or contrast and that this increased summation facilitates the processing of large disparities.

5.6.2 Contrast-sensitivity and stereopsis

Frisby and Mayhew (1978a) derived a contrast-sensitivity function for stereopsis by measuring the luminance contrast required for detecting depth in random-dot stereograms in which the spatial frequency of the dot pattern varied between 2.5 ± 0.2 c/deg and 15 ± 0.2 c/deg. The disparity in the stereograms varied from 3 to 22 arcmin. Since the stereo thresholds did not vary as a function of the disparity of the stimulus, the results were averaged over the set of disparities. They also measured the contrast sensitivity for detection of the same dot patterns seen dioptically. The results for one subject are shown in Figure 5.17. It can be seen that the forms of the two functions are similar (correlation 0.96) and it was concluded that the mechanism for stereopsis is not sensitive to a particular spatial frequency as far as contrast thresholds are concerned. In Frisby and Mayhew's experiment the dot patterns were detected with dioptic viewing at a contrast between 0.3 and 0.4 log units below that required for the detection of depth. A similar high correlation between the contrast-sensitivity function for dot detection and the stereo contrast-sensitivity function was obtained by Legge and Gu (1989) and Smallman and MacLeod (1994a).

Legge and Gu (1989) used a stereogram consisting of two identical vertically oriented sine-wave gratings presented with variable horizontal disparity. Subjects judged the sign of the depth of the test grating with respect to a zero-disparity comparison grating just below it. The threshold disparity for detection of depth was thus determined as a function of the spatial frequency of the grating for each of several contrasts. This is a contrast sensitivity function for stereopsis (not to be confused with the corrugation, or disparity-modulation sensitivity function discussed in Section 5.5.3). For a given contrast, on a log/log plot, threshold disparity was inversely proportional to spatial frequency, reaching a minimum at about 3 c/deg, after which the threshold increased in an irregular fashion. As the spatial frequency of a regular grating increases, disparity becomes ambiguous, since it is unclear which bar should be paired with which. This is the wallpaper illusion discussed in Section 2.3.5. and may account for the irregularity of the stereo threshold above 3 c/deg. The binocular contrast-sensitivity function for detecting a luminance modulation also peaked at about 0.3 c/deg and fell off at lower spatial frequencies in a similar way to the falloff of the stereo threshold. This further supports the idea of a close link between the binocular detectability of a grating and the detectability of disparity in a grating.

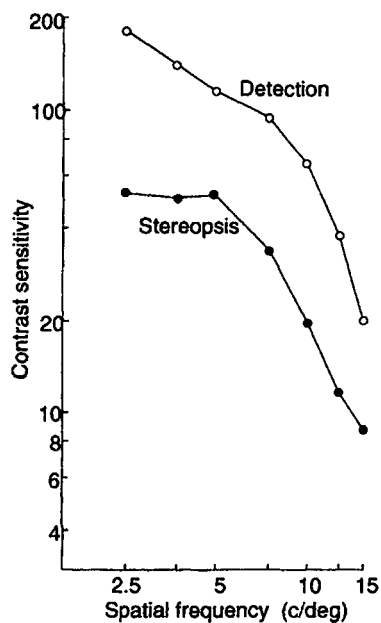


Figure 5.17. A contrast-sensitivity function for stereopsis. The upper curve shows the contrast required for detection of a binocularly viewed random-dot pattern as a function of the spatial frequency of the pattern. The lower curve shows the contrast required for detection of depth in a random-dot stereogram as a function of the spatial frequency of the dot pattern. Averaged values for one subject from stereograms with disparities between 3 and 22 arcmin. (From Frisby and Mayhew 1978a, Perception, 10, 403-10. Pion, London.)

Legge and Gu found that the spatial frequency for which the stereo threshold was minimum was about the same for all contrasts. However, the stereo threshold was approximately inversely related to the square root of Michelson contrast. This latter finding is consistent with the idea that, as contrast is reduced, the internal noise in the visual system becomes proportionately larger and adversely affects the signal-to-noise ratio. Halpern and Blake (1988) reported similar results using elongated D10 Gaussian patches, which resemble small patches of sine-wave grating. They used a wider range of spatial frequencies and found that stereoacuity is less affected by changes in contrast at higher spatial frequencies. This may explain why stereoacuity has been found to vary with the cube root of contrast in a random-dot stereogram (Cormack et al. 1991). Halpern and Blake concluded that disparity is processed by spatial-frequency tuned mechanisms with a compressive nonlinear dependence on contrast.

Heckmann and Schor (1989a) confirmed that spatial frequency and contrast are the crucial factors determining the stereo threshold. On the one hand, stereo thresholds were the same for sinusoidal-grating targets with the same spatial frequency and contrast but with different luminance gradients or

spatial phases. On the other hand, for targets differing in contrast but with the same luminance gradient, thresholds were lower for the target with higher contrast. Patterson (1990) found that stereo acuity for a grating with a spatial frequency of 8 c/deg was impaired when the stimulus was counterphase flickered at between 5 and 20 Hz but the same flicker had little effect at lower spatial frequencies.

It seems safe to conclude from this evidence that there is a close relationship between stereoacuity and the contrast and spatial frequency of a stimulus.

5.6.3 Thresholds for detection and depth

Frisby and Mayhew's data depicted in Figure 5.17 show that a dot pattern seen with both eyes was discriminated from an evenly illuminated area at a contrast of 0.3 to 0.4 log units below that required to detect depth in a random-dot stereogram. They concluded that the stereoscopic mechanism requires a stronger stimulus than the mechanism responsible for detecting the dots comprising the stereogram. Smallman and MacLeod (1994a) found a mean difference of only 0.25 log units between the contrast threshold for the detection of dots and that for the detection of depth in a random-dot display. Halpern and Blake (1988) found a similar small difference using D10 Gaussian patches. Mansfield and Simmons (1993) pointed out that binocular detection thresholds for dots should be lower than stereo thresholds, on the basis of probability summation. This is because binocular detection operates when the stimulus in either eye is above threshold whereas stereopsis requires both stimuli to be above threshold. When Mansfield and Simmons used random-dot stimuli, similar to those used by Frisby and Mayhew, they obtained a similar difference between binocular detection and stereo thresholds to that found by other investigators. However, they found very little difference between the contrast threshold for detection of a monocular patch of random dots and the contrast threshold for the detection of depth in a random-dot stereogram, at the disparity for which the contrast threshold for depth was lowest. They concluded that once the stimuli in both eyes are detected no extra stimulus strength is required to detect disparity and depth.

5.6.4 Effects of interocular differences

Stereoacuity is reduced when the level of illumination differs in the two eyes (Rady and Ishak 1955; Lit 1959a) and when the contrast is not the same in the two eyes (Simons 1984; Halpern and Blake 1988;

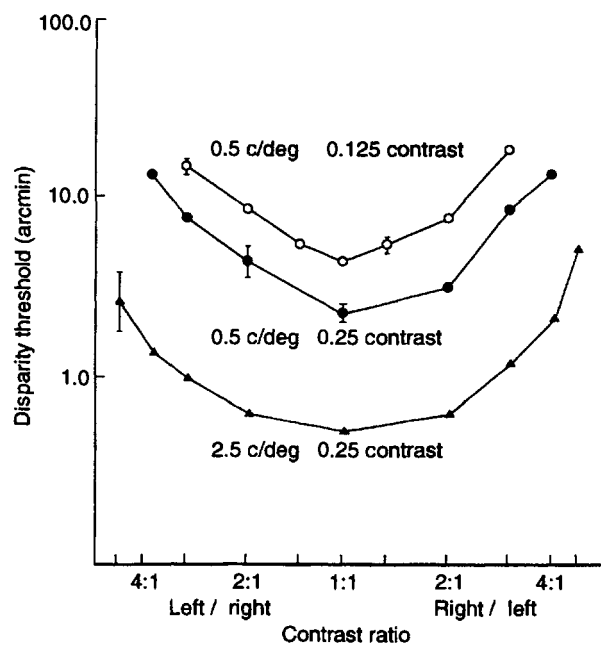


Figure 5.18. Stereoacuity and relative contrast.

Disparity threshold for discriminating depth in a grating relative to a zero-disparity comparison grating as a function of the relative contrast of the images in the two eyes. The contrast was 0.125 or 0.25 and the spatial frequency of the gratings was 0.5 or 2.5 c/deg. Results for one subject. (Reproduced with permission from Legge and Gu 1989, Vision Research, Pergamon Press.)

Legge and Gu 1989). This reduction in acuity cannot be ascribed simply to the loss in mean luminance or contrast, because a given reduction of contrast in one eye reduces stereoacuity about twice as much as the same reduction applied to both eyes. It can be seen in Figure 5.18 that the effect of unequal contrast on the threshold for detection of depth in a dichoptic grating is relatively the same for spatial frequencies of 0.5 c/deg and 2.5 c/deg (Legge and Gu 1989). However, Schor and Heckmann (1989) found that interocular differences in contrast produced a greater loss of stereoacuity for a 0.8-c/deg grating than for a 3.2-c/deg grating.

In spite of the effect of differing contrasts on stereoacuity, the impression of depth persists with quite large differences in contrast. This relative immunity of stereopsis to unbalanced inputs could be due to a binocular contrast-gain mechanism in the LGN. The response per unit change in contrast (contrast gain) of many cells in the LGN of the cat to stimulation of one eye has been found to be changed by simultaneous stimulation of the other eye. In the cat, this effect survives removal of the visual cortex (Tong et al. 1992).

Wilson (1977) revealed a hysteresis effect that depends on the relative contrast of the images in the two eyes. The stimuli were 4.5°-wide stereograms

consisting of vertical sinusoidal gratings. The spatial frequency of the grating in one eye was set at various values between 0.5 and 8 c/deg, and in each case the spatial frequency of the grating in the other eye was set 1.2 times higher. This created the impression of a surface slanted in depth about a vertical axis (see Section 7.2). The contrast of the image in one eye was held constant at 0.5 while that in the other was either increased from zero or decreased from 0.5 to zero. When contrast was increased from zero the impression of slant was delayed beyond the point where the impression of slant was lost when contrast was reduced from 0.5 (see Figure 5.19).

Wilson argued that this contrast-dependent hysteresis is independent of eye movements because the difference in spatial frequency between the images is not affected by eye movements. This argument is not conclusive. A high-contrast image in one eye and a low-contrast image in the other eye provide a weak stimulus for convergence. We argue in Section 7.2.6 that vergence allows one to scan effectively over a disparity gradient created by a difference in spatial frequency of the two images, and that these scanning movements aid stereopsis. Once an effective pattern of vergence movements has been formed, with images of equal contrast, it should be easy to maintain it after considerable loss of contrast in one eye. However, effective eye movements may be difficult to establish when the images differ initially in contrast. This interpretation explains why Wilson found no hysteresis when the gratings had a spatial frequency of only 0.5 Hz. At this spatial frequency there would be only eight cycles in the display which, with a frequency ratio of 1.2, would produce only two nodes where the displays are in phase (produce zero disparity). This should make it easy to see depth without vergence movements. The multiple zero-disparity nodes in high spatial-frequency depth ramps make it difficult to see a single slanted surface without the aid of vergence. Furthermore, a low spatial-frequency display is more visible in the peripheral retina than a high spatial-frequency display. For both these reasons scanning eye movements are not as necessary for the perception of depth in low spatial-frequency depth ramps as in high spatial-frequency depth ramps. Wilson modelled the hysteresis effect in terms of a neural network with positive feedback among disparity detectors generated by disinhibitory circuits.

The loss of stereoacuity with unequal contrast in the two eyes may be explained in terms of the signal-to-noise ratio. The disparity detection process involves the extraction of a difference signal from two signals, each with its own noise. Devices such as differential amplifiers, which combine signals in this

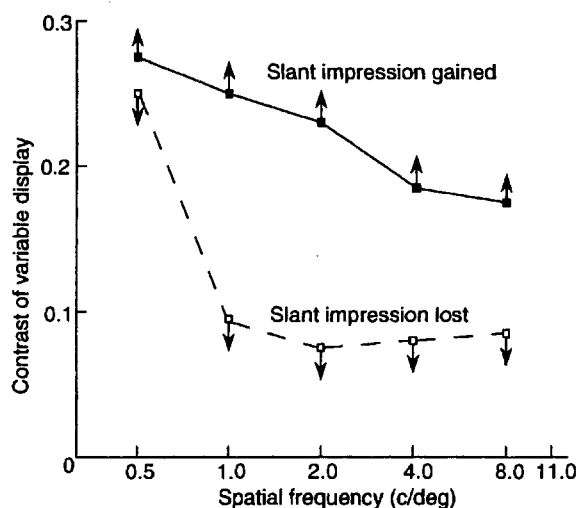


Figure 5.19. A contrast hysteresis effect in stereopsis.

The curve with upward pointing arrows indicates the contrast of a sinusoidal-grating stereogram at which slant was perceived as contrast increased. The curve with the downward pointing arrows indicates the contrast at which the impression of slant was lost, as contrast declined. Data for one subject. (Adapted with permission from Wilson 1977, Vision Research, Pergamon Press.)

way, produce a signal with an improved signal-to-noise ratio because the uncorrelated noise signals tend to cancel. When the signal from one eye is stronger than that from the other, the noise from the two eyes would not be cancelled as effectively and stereoacuity would therefore be degraded.

A factor in the loss of stereoacuity with unequal illumination may be the fact that the visual latency for a dim stimulus is longer than that for a bright stimulus. Thus, with unequal illumination, the signals from the two eyes arrive at the visual cortex at different times. This could degrade stereoacuity in either of the following two ways:

1. The stimulus asynchrony arising from differential illumination could directly interfere with the detection of disparity. For instance, it has been suggested that the response of a binocular cell to a stimulus from the nasal hemiretina is more rapid than its response to a matching stimulus from the temporal hemiretina and this difference allows the brain to identify the eye of origin of each signal and thus distinguish between crossed and uncrossed images (Bower 1966). Reading and Woo (1972) measured the elevation of stereo threshold due to unequal illumination of dichoptic stimuli presented for 40 ms or less and then tested whether this could be nulled by introducing an interocular time delay. They found no nulling of one effect by the other and concluded that the effect of unequal illumination on stereoacuity is not due to differential latency. They did not consider the second way in which differential latency may affect stereoacuity.

2. A differential latency of signals from the two eyes translates into a disparity if the two stimuli move together, as in the Pulfrich stereophenomenon (see Section 13.1 for a fuller discussion of this issue). Movement of the stimuli in a frontal plane in the direction of the eye receiving the weaker stimulus creates an uncrossed disparity, and movement the other way creates a crossed disparity. With a stationary stimulus, to-and-fro eye movements impose a variable disparity signal into the test disparity and reduce the signal-to-noise ratio. *The differential latencies in the Reading and Woo experiment did not translate into disparity because the stimuli were exposed for only 40 ms, and the effects of eye movements would not be significant with such short exposures. The experiment should be repeated with longer exposure times.*

5.6.5 Stereoacuity and colour

Pennington (1970) measured stereoacuity as a function of colour using the Howard-Dolman apparatus, with the vertical rods emitting a narrow band of wavelengths in the red, green, or blue parts of the spectrum. The differently coloured rods were equated for apparent luminance and viewed against a dark background. Stereoacuity for the red rods relative to that for the green rods varied from subject to subject, but all subjects had a lower acuity with blue rods. This could be due to the low density of blue cones in the retina and their relatively large receptive fields. In this stimulus, the rods varied in colour but their borders were also defined by luminance contrast. Stereopsis for targets defined entirely by colour is discussed in Section 6.1.4.

5.7 DISPARITY AND SPATIAL SCALE

5.7.1 Introduction

In two-dimensional vision, acuity and spatial scale are linked. For instance, for low spatial frequencies, vernier acuity is a constant fraction of the spatial period of the visual targets (Levi and Klein 1985). Also, vernier acuity is constant for different retinal eccentricities when scaled for the mean size of receptive fields (and the cortical magnification factor) (Levi and Klein 1985).

Felton et al. (1972) suggested that disparity is processed by distinct size channels in the visual system—small disparities by small (high spatial frequency) channels and coarse disparities by large (low spatial frequency) channels. This linkage between disparity and spatial scale is referred to as the **size-disparity correlation**. Marr and Poggio (1979)

and Frisby and Mayhew (1980a) proposed models of the stereoscopic system based on this idea.

With periodic visual patterns, there is a geometrical reason why disparity detection must be linked to spatial scale. For instance, the largest disparity over which the two images of a periodic grating can be matched in a particular way is one-half of the spatial period of the grating. If the disparity is greater than this, the images of the grating match up in a different way, as in the wallpaper illusion. Only low spatial-frequency elements allow the visual system to identify matches between the images at disparities greater than the periodicity of the high spatial-frequency component of the display. The distance between matching elements in a periodic pattern increases with increasing spatial scale. Furthermore, since there are necessarily fewer matching contours in low-frequency components of a display than in high-frequency components, there is less chance of finding the wrong match in the large spatial scale, coarse-disparity system than in the small spatial scale, fine-disparity system. It is therefore an efficient strategy to first find correspondences between the low spatial-frequency components of a display and use these to drive vergence eye movements to reduce these disparities to a minimum so that residual fine disparities can be detected by the small spatial scale system (Marr and Poggio 1979).

In stereograms consisting of isolated stimulus elements rather than periodic patterns there are other reasons for expecting the scale of disparity processing to be linked to spatial scale. First, assume that disparity coding depends only on the spatial offset of identical monocular receptive fields. Theoretically, a binocular cell with small receptive fields in the two eyes could code large disparities if the receptive fields of the cell were far apart, although such a system would be prone to register nonmatching images. On the other hand, a binocular cell with large receptive fields would have difficulty detecting small disparities because the positional tuning of such cells would be too coarse to produce a finely tuned disparity signal. Thus, when disparity detection is based on offsets of receptive fields, the lower limit, but not the upper limit, of disparity tuning is closely tied to the spatial scale of the stimulus.

Predictions are different if disparity tuning of binocular cells depends on offsets of subregions within the monocular receptive fields (intra-receptive-field disparity) rather than on offsets of the receptive fields as a whole (inter-receptive-field disparity). In this case, as we have already argued in Section 4.5.2, the diameter of the cell's receptive fields sets an upper limit to the disparity that a given cell can detect. However, a cell with large receptive

fields could be sensitive to disparities as small as excitatory and inhibitory subregions within its receptive fields. Thus, when disparity detection is based on offsets of regions within receptive fields, the upper limit but not the lower limit of disparity tuning is closely tied to the spatial scale of the stimulus elements.

There are also functional reasons for expecting different sizes of disparity to be processed in distinct spatial-scale channels. First, it would allow signals in each channel to be used for specific purposes. For instance, the large-size channel could control large transient vergence eye movements while the small-size channel could control the vergence locking mechanism (see Section 10.5.8) and pursuit eye movements (see Section 12.5.6). Second, Each channel could help to resolve ambiguities in the matching of images processed in the other channel.

Psychophysical evidence bearing on the linkage between disparity and the two-dimensional spatial frequency of the visual display is reviewed in the following three sections.

5.7.2 Spatial scale and disparity

If disparity detection and spatial scale are linked, stimuli with high spatial frequency should have a lower contrast threshold for detecting depth with small compared with large disparities, and stimuli with low spatial frequency should have a lower threshold with large compared with small disparities. These trends were not evident in the data from Frisby and Mayhew (1978a), presented in Section 5.6.2. However, Smallman and MacLeod (1994b) pointed out that in Frisby and Mayhew's experiment, subjects may have altered their vergence slightly to bring disparities into the most sensitive range for each spatial frequency. In their own experiment, subjects first stabilized convergence using two nonius lines before they were exposed to two random-dot patches for 160 ms. One patch had a crossed disparity and the other an uncrossed disparity. Subjects indicated in a forced-choice procedure whether the nearer patch was on the right or on the left. The contrast required for 75 per cent correct depth identification was determined for centre spatial frequencies between 1 and 15 c/deg and for disparities between 1 and 20 arcmin. Peak stereo sensitivity in the resulting stereo contrast-sensitivity function was at 3 c/deg, a value that agrees with that obtained by other investigators. However, unlike Frisby and Mayhew, they found that threshold disparities were linked to spatial scale. Thus, at a centre spatial frequency of 15 c/deg, the range of detectable disparities was confined to between 1 and

7 arcmin. At a centre spatial frequency of 1 c/deg, sensitivity was very low for 1 arcmin of disparity and best for 20 arcmin of disparity. As spatial frequency increased, coarser disparities became undetectable. Thus, above a frequency of 3 c/deg, disparities of more than 20 arcmin were undetected, and above 7 c/deg, disparities more than 15 arcmin were undetected. Over the range of centre spatial frequencies from 1 to 15 c/deg there was a fivefold change in the disparity that was most easily detected. The data were transformed into spatial phase. For instance, a disparity of 5 arcmin at a spatial frequency of 3 c/deg is equivalent to a binocular-phase disparity of 90°. The resulting functions provided some support for the quadrature model of disparity detection proposed by Freeman and Ohzawa (see Section 4.5.2). These data therefore provide strong support for the idea of size-disparity correlation.

If there is a linkage between the processing of disparity and spatial scale, both the stereoscopic threshold and the upper limit of stereopsis should be related to the spatial frequency of the stimulus. Schor and Wood (1983) investigated this question using small patches with difference-of-Gaussian (DOG) luminance profiles with centre spatial frequencies between 0.075 and 19.2 c/deg, each with a bandwidth at half-height of 1.75 octaves. Figure 5.14 shows that (1) the threshold for discriminating the depth between such a patch and a comparison stimulus and (2) the upper disparity limit for stereopsis were both constant for spatial frequencies above about 2.4 c/deg. Below this value, both quantities decreased as spatial frequency was increased. With increasing spatial frequency, the depth-discrimination threshold rose faster than the upper disparity limit, with the result that the range of disparities evoking depth sensations became narrower as spatial frequency increased.

If disparities are processed in distinct spatial-frequency channels, one would expect the decline of stereoscopic threshold with increasing size of a disparity pedestal to be steeper for high than for low spatial-frequency stimuli. Badcock and Schor (1985) investigated this question using DOG patches with centre spatial frequencies between 0.15 and 9.6 c/deg. Vergence was controlled with a fixation point and associated nonius lines. The results of this experiment are shown in Figure 5.7. The rate of increase of the depth-discrimination threshold with increasing disparity of the test and comparison stimuli was not much influenced by the spatial frequency of the display for spatial frequencies of 0.6 c/deg and above, but for the 0.15 c/deg patch the rate of increase was significantly steeper. The

authors concluded that these results do not support the idea that large disparities are most effectively processed by low spatial-frequency channels. But perhaps one should not compare different spatial-frequency channels on the basis of the angle of minimum discriminated disparity. It may be more meaningful to compare them on the basis of the minimum phase shift within each channel, that is, in terms of the minimum angle divided by the spatial period of the stimulus. Siderov and Harwerth (1993a) also found that depth-discrimination thresholds were not affected by a difference of 2 octaves between a 2-c/deg DOG test stimulus and a DOG comparison stimulus.

There is a feature of Badcock and Schor's results that supports the idea of a coupling between the visual channels tuned to different spatial frequencies of luminance modulation and those tuned to disparity. For spatial frequencies above 2.4 c/deg, stereopsis was absent when the disparity pedestal was greater than 20 arcmin and subjects had to base their discriminations of depth on sensations of diplopia. However, with the lowest spatial frequencies, stereopsis was experienced for all sizes of pedestal. Thus, it seems that the low spatial-frequency system is required for coding large disparities as depth. But this is not surprising since, with large disparities and high spatial frequency displays, corresponding elements become difficult to see.

In two-dimensional vision, the effect of spatial frequency on vernier acuity depends on the lateral separation between the stimuli being compared. Toet et al. (1987) measured the displacement threshold for patches with a Gaussian contrast profile at the contrast threshold as a function of the blur and spatial separation of the patches. For a constant ratio of blur to patch separation, the threshold increased linearly with increasing blur. It was concluded that the relative spatial position of stimuli at a given resolution is detected with an accuracy that is a constant fraction of the receptive-field width at that level of blur (resolution). When the separation between the stimuli was sufficient to allow them to be seen as two but less than 25 times the spread of the stimuli, the displacement threshold was independent of the distance between the stimuli. When the separation between the stimuli was more than 25 times the blur parameter, the displacement threshold increased as a linear function of separation for a given value of blur. It was concluded that there are two processing strategies; a linear process that provides a direct measure of relative position when the stimuli are close relative to their size and the a nonlinear process that involves indirect comparison of stimulus positions when the stimuli are further

apart than a critical value. This second process is adversely affected by increasing the separation between the stimuli.

Hess and Wilcox (1994) used stimuli similar to those used by Toet et al. but instead of the threshold for lateral offset they measured the disparity threshold for the perception of relative depth between a Gabor patch and similar patches above and below it presented for 0.5s. Each patch was a sinusoidal grating, in sine phase, confined within a window with a Gaussian luminance profile. The diameter of the window (indicated by its standard deviation) varied between 5 and about 100 arcmin. As the size of the window increased for a given spatial frequency the spatial-frequency bandwidth of the Gabor patch decreased (see Section 3.4.2). The disparity threshold was independent of the separation between the patches for targets with centre spatial frequencies of 0.66 and 5.24 c/deg and 1.13 octave bandwidth but increased rapidly with increasing separation for a target of 5.24 or 10.4 c/deg and 0.18 octave bandwidth. Thus, narrow-band stimuli (large patches) showed a strong dependence on the separation of the targets.

For a given separation of the targets and a fixed diameter of the Gaussian window, the stereo threshold decreased linearly as the spatial frequency of the Gabor patches increased from 0.1 to 10 c/deg. This dependence of acuity on spatial frequency was the same for different sizes of Gaussian window showing that it was a function of spatial frequency and not the number of sine waves in the window. These results differs from those for monocular vernier acuity which was found to be independent of the spatial frequency of fixed-diameter Gabor patches (Hess and Holiday 1992). For a given separation of the targets and a fixed spatial frequency, the stereo threshold increased steeply as the size of the Gaussian window increased from a value corresponding to a bandwidth of 0.5 octaves. For smaller Gaussian windows (broadband stimuli) the stereo threshold was independent of changes in the size of the window. Thus, for small Gaussian windows (broadband stimuli) the stereo threshold depended on the spatial frequency of the stimuli but not on the size of the window or the spatial separation of the stimuli and for large Gaussian windows (narrow band stimuli) the threshold depended on the size of the window and the separation of the stimuli but less on their spatial frequency.

Hess and Wilcox proposed that the dependence of stereoacuity on spatial frequency with broadband stimuli reflects the operation of a linear system, and its dependence on the size of the Gabor patch with narrowband stimuli reflects the operation of a

nonlinear (non Fourier) process analogous to Fourier and non-Fourier processes revealed in the coding of motion and texture. The crossover between the two processes occurred with a Gaussian envelope corresponding to a bandwidth of 0.5 octaves or about four cycles of the sinewave within the window. The dependence of stereoacuity on spatial frequency with broadband stimuli could reflect the operation of a phase-dependent disparity detection system (see Section 4.5.2).

Suppose that stimuli with low spatial frequency and coarse disparity are used for the preliminary matching of images to within the range of mechanisms sensitive to high spatial frequency and fine disparity. On this basis, Rohaly and Wilson (1993) argued that people should be better able to discriminate depth in a high spatial-frequency stimulus set on a depth pedestal in the presence of a low spatial-frequency surround than when only high spatial frequencies are present in the stimulus. They tested this prediction using elongated D6 Gaussian patches with spatial frequencies separated by 2 octaves. The low spatial-frequency surround was either in the same stereo depth plane as the high spatial-frequency test patch or in the plane of the zero-disparity comparison stimulus. The stereo discrimination threshold increased exponentially as the pedestal disparity of the test patch increased relative to the zero-disparity comparison stimulus, both when the low spatial-frequency stimulus was present and when it was absent. They concluded that disparity in low spatial frequency stimuli does not shift the scale of disparity processing within high spatial-frequency stimuli.

5.7.3 Spatial scale and stereoscopic gain

A linkage between disparity processing and spatial frequency would lead one to expect that stereoscopic gain is related to spatial frequency. The magnitude of perceived depth produced by a given disparity in a Julesz stereogram was found not to vary significantly when the spatial frequency of luminance modulation of the stereogram was varied between centre frequencies of 2.5 and 16.2 c/deg (Mayhew and Frisby 1979a). The disparity range of 2.6 to 20.8 arcmin used in this experiment may have been too small to reveal the effects of spatial-frequency tuning on stereoscopic gain. Schor and Wood (1983) also investigated this question using small patches with difference of Gaussian luminance profiles with a wider range of disparities. Stereo gain was measured by adjusting a depth probe, consisting of a thin black line, to match the perceived depth of a Gaussian patch. The stimulus was shown for as long as

required, and nonius targets were used to monitor the accuracy of convergence. It is unlikely that vergence was held perfectly steady by this procedure. The greater the disparity in the probe required to match the depth of the patch, the less was the gain with which disparity in the patch was translated into depth. Whereas stereoacuity, as indicated by the lower dotted line in Figure 5.14, began to deteriorate when spatial frequency fell below 2.4 c/deg, stereo efficiency, as indicated by the solid lines, did not begin to fall until spatial frequencies were much lower. The solid lines also indicate that stereo gain began to deteriorate at a lower spatial frequency for fine disparities than for coarse disparities. Gain deteriorated at a lower spatial frequency for uncrossed than for crossed disparities as well. This means that, for low spatial frequency displays, less depth was evoked by a given disparity when it was crossed than when it was uncrossed. Thus, the distance from the fixation plane of low spatial-frequency stimuli with crossed disparity was strongly underestimated. It looks as though stereo gain is higher for the high spatial-frequency/fine-disparity system than for the low spatial-frequency/coarse-disparity system. Furthermore, low spatial-frequency Gaussian patches with zero disparity appeared to lie behind the fixation plane defined by a fixation spot (Schor and Howarth 1986). Note that a low spatial-frequency stimulus has a lower apparent contrast than a high spatial frequency stimulus. When the apparent contrasts of the stimuli were made equal, the differential loss of stereo gain was much reduced. The different stereo channels therefore seem to be linked to different effective contrasts as much as to different spatial frequencies.

Note that the spatial frequency of the comparison stimulus in these experiments was constant while that of the test stimulus was varied. At least part of the effect of the spatial frequency of the test stimulus on perceived depth could be due to monocular perspective—a tendency to see larger objects as being further away than small objects. Such an effect has been reported by others. For instance, Brown and Weissstein (1988) reported that a high spatial-frequency grating appeared closer than an adjacent low spatial-frequency grating, even when disparity indicated the contrary. One must be cautious in drawing conclusions from experiments in which test and comparison stimuli differ, because the results may not reflect properties of the stereoscopic system alone. They may arise from the interplay between the disparity-based stereoscopic system and other cues to depth. The amount of perceived depth could be the outcome of a trading relationship between

distinct cues. This question is discussed in Section 11.2. There is no reason to expect that a trading relation between cue systems would affect the discrimination threshold for either of the cues presented alone. For instance, just because two lines in the Muller-Lyer illusion appear to differ in length does not mean there is any loss in the ability to discriminate a change in the relative lengths of the two lines. Discrimination reflects a person's ability to detect changes in a stimulus feature rather than the ability to compound different cue systems in assessing the magnitude of a sensory effect relative to some norm.

Watt (1987) proposed that the sequential processing of first the low and then the high spatial frequencies of the stimulus is characteristic of two-dimensional acuity processes, such as vernier acuity and orientation acuity, as well as of stereoacuity. If only high spatial frequencies are present in the stimulus, these are processed without delay. Watt found that, in each type of acuity with mixed high and low spatial frequencies, acuity improved as stimulus exposure time increased, up to about one second. He proposed that this improvement occurs because, when two stimuli are compared in a discrimination task, they are compared within the low spatial-frequency system before being compared within the high spatial-frequency system. Grating resolution was not found to be higher with longer stimulus durations. This may be because, in a resolution task, an inhomogeneity is detected in a stimulus but one stimulus is not compared with another, as it is in a discrimination task. In the stereoacuity test the subject detected the disparity-defined depth of a vertical test line relative to a comparison line placed beneath it. The results are shown in Figure 5.20. It can be seen that with short durations only large disparities evoked a sensation of depth but that, as stimulus duration increased, depth was evoked by finer disparities in the display. This result was interpreted as being due to an initial processing of only coarse disparity by low spatial-frequency visual filters followed by processing at a finer scale within a high spatial-frequency system. The theory does not predict that depth in a stereogram containing only low spatial frequencies is processed more rapidly than the same depth in a stereogram containing only high spatial frequencies. However, the time-dependent probability of detecting a disparity at a given spatial scale has not been determined. Although Watt provided stimuli that were designed to stabilize vergence, no measurements of vergence were made and nonius targets were not provided. *This experiment should be repeated with better control over vergence.* We will return to the question of the processing time for stereopsis in Section 5.10.1.

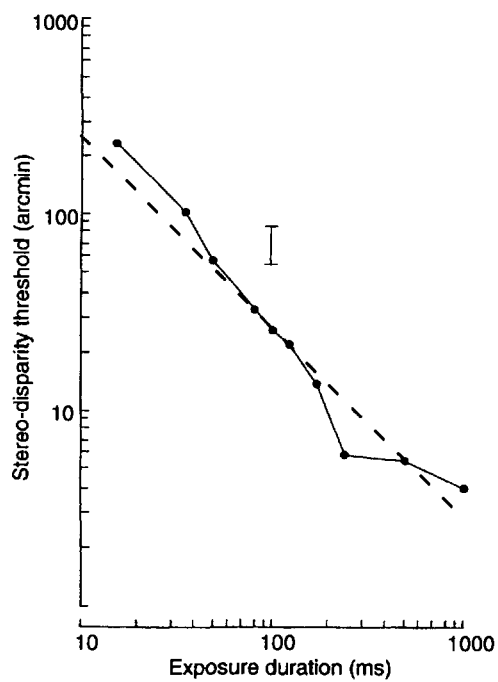


Figure 5.20. Stereoacuity and exposure time.
Disparity threshold for detecting depth in a line relative to a zero-disparity line, as a function of exposure time. With short durations, only large disparities evoked a sensation of depth. As stimulus duration increased, depth was evoked by finer disparities. The dashed line indicates the slope expected if stereo threshold varies linearly with duration. Results for one subject. The insert is a sample standard deviation. (From Watt 1987.)

5.7.4 Spatial scale and stereopsis masking

The spatial-frequency selectivity of stereoscopic vision may be investigated by measuring the effects of adding noise of specified spatial frequency content to stereograms composed of patterns confined to a specified spatial-frequency bandwidth. Random texture added to bandpass-filtered random-dot stereograms abolished stereopsis when the signal-to-noise ratio was less than 1:1.4 and the spatial frequency of the noise overlapped that of the stereogram. But stereopsis was not affected when signal and noise were two octaves or more apart (Julesz and Miller 1975). This transition is related to the fact that depth is not perceived in a random-dot stereogram when the spatial-frequency content of the dioptic images does not overlap (see Section 6.1.3).

Yang and Blake (1991) systematically investigated the question of masking noise by varying the spatial frequency content of the noise relative to that of the random-dot stereogram and, in each case, measuring the amount of noise required to bring the threshold of depth detection to a criterion level. They concluded from the form of the resulting masking functions that there are only two spatial-frequency

channels for crossed disparities and two for uncrossed disparities within the stereoscopic system, but that both crossed and uncrossed channels serve in the detection of both fine and coarse disparities. This conclusion runs counter to the idea of a coupling between fine disparities and high spatial frequency and coarse disparity and low spatial frequencies. The argument may not be conclusive because the noise may not have gained access to postfusion mechanisms responsible for the detection of disparity, and their stimulus may have induced luminance rivalry. Spatial-frequency interactions in binocular fusion are discussed in Section 8.1.4.

The orientation selectivity of masking noise can be investigated by measuring the effects of adding noise consisting of lines with specified orientation with respect to the orientation of lines that define depth in a random-line stereogram. The degree of masking should be some function of the orientation of the noise relative to that of the disparity-defining lines. This topic is discussed in Section 6.1.2.

5.8 STEREOACUITY AND EYE MOVEMENTS

5.8.1 Eye movements between targets

Consider the task of detecting a difference in depth between one target and a second target. A loss in stereoacuity occurs as the lateral separation between two stereo targets increases beyond about 0.2° (Section 5.5.2). However, the loss is not as great when the eyes are allowed to move from one target to the other compared with when the gaze is fixed on one of the targets (Hirsch and Weymouth 1948a, 1948b; Ogle 1939c). Some data on this point are shown in Figure 5.21 (Rady and Ishak 1955). There are four possible reasons for the improvement of stereoacuity with eye movements:

1. The change in vergence as the gaze is transferred from one target to the other could improve depth discrimination either because of information provided by motor efference or by sensory feedback from the extraocular muscles (Wright 1951). There is no evidence on this point.

2. Stereoacuity could be improved with eye movements because halfway through a movement from one target to the other the two images are both relatively near the fovea (Ogle 1956). This presupposes that one can sample disparities during saccadic eye movement, which is most unlikely.

3. Disparity information from one target, extracted when it is foveated, could be retained in memory and compared with that from the other

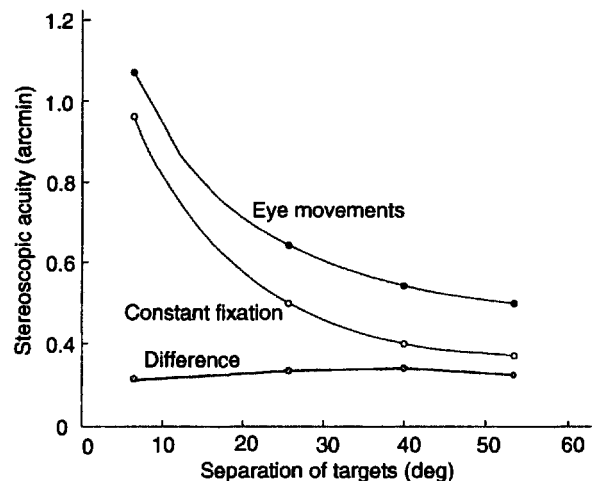


Figure 5.21. Stereoacuity and lateral separation.

Acuity for the perception of relative depth between two illuminated apertures as a function of their lateral separation. In the upper curve, subjects were allowed to look from one stimulus to the other. In the middle curve, subjects fixated one of the stimuli. The lower curve is the difference between the conditions. Mean results for 10 subjects. (From Rady and Ishak 1955.)

target once that target is foveated. This presupposes that the eyes do not converge, or converge incompletely, on the new target until it has been foveated. This is usually so because saccades are more rapid than vergence movements. Stereo depth perception is certainly possible with sequentially presented targets, as we will see in Section 5.10.2. Enright (1991a) supported this theory by showing that stereopsis is possible when the gaze is alternated between two targets positioned so that, when one of them is fixated, one of the images of the other target falls on the blind spot of one eye. Thus, the disparities produced by the two targets were never in view at the same time. Wright (1951) conducted a similar experiment.

4. If the eyes remain stationary, the disparities in the test objects remain constant. Under these circumstances perceived depth between the test objects adapts out and they come to appear nearer to the frontal plane (see Section 12.1.2). If the eyes move back and forth between the targets, disparity changes in both magnitude and position. This should prevent depth normalization to the frontal plane. There is no direct evidence on this point.

5.8.2 Stereoacuity and stabilized images

Vergence movements between different objects in a three-dimensional scene play a significant role in depth discrimination. However, vergence changes are not required for stereoscopic vision, since depth is apparent in stereograms presented for durations much shorter than the latency of vergence which

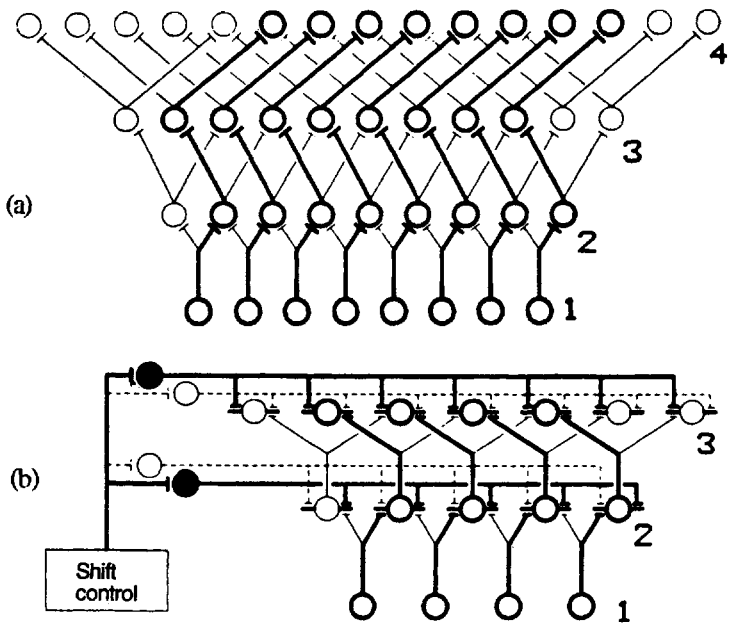


Figure 5.22. Shifter circuit.

The circuit was proposed by Anderson and Van Essen (1987) to account for the immunity of stereoscopic vision to fluctuation in disparity caused by instabilities in vergence.

(a) The cells in each layer bifurcate to contact a pair of cells at the next level. At each level, lateral fibres control which of the bifurcating inputs is active.

(b) A shift control alters the receptive-field boundaries of cells in the LGN or in the striate cortex nulling the effects of image motion due to ocular tremor.

is at least 150 ms (Dove 1841; Westheimer and Mitchell 1969). Depth can be seen in briefly exposed random-dot stereograms where the subject can have no prior knowledge of the stimulus (Julesz 1963; Mayhew and Frisby 1979a; Tyler and Julesz 1980). Furthermore, depth may be seen in afterimages of line stereograms (Ogle and Reiher 1962). Depth may also be seen in afterimages of random-dot stereograms but only when the dots are well spaced, since the texture of a closely spaced random-dot pattern is not visible in an afterimage (Evans and Clegg 1967). Ogle and Weil (1958) found that the mean stereo threshold rose from about 10 to 40 arcsec as exposure duration of the test object was reduced from 1 s to 7.5 ms. They concluded that, although small involuntary eye movements are not essential for stereopsis, they help because they keep the images in motion. Shortess and Krauskopf (1961) however, found a similar dependence of stereoacuity on stimulus duration when the images were retinally stabilized. It seems that small movements of the eyes during fixation neither aid nor hinder stereopsis, but that disparity is integrated over time in a manner analogous to integration of luminance over time as described by Bloch's law. This question is discussed further in Section 5.10.1. Section 5.10.4 reviews the effects of image motion on stereoacuity.

5.8.3 Stereoacuity and vergence drift

The small movements of an eye that occur when a small visual target is fixated are almost as large with binocular fixation as with monocular fixation (St. Cyr and Fender 1969). Uncorrelated movements of the two eyes produce a corresponding variation in the disparity between the images of a binocularly fixated object. Motter and Poggio (1984) found that the eyes of a monkey were misconverged by more than 7 arcmin in both the horizontal and vertical directions about 60 per cent of the time when the animal was fixating a small target. Fluctuations in disparity arising from these eye movements occur equally over the whole visual field. They suggested that a dynamic feedback process prevents drifts in vergence from interfering with stereoscopic vision. A specific neural model of this process, called a shifter circuit, was proposed by Anderson and van Essen (1987). The idea is that the receptive field boundaries of cells in the LGN or in the striate cortex are dynamically adjusted to null the effects of image motion in the manner described in Figure 5.22. In the shifter-circuit model, the relative topographic mapping changes, not the size of receptive fields. Motter and Poggio (1990) produced physiological evidence in favour of the shifter circuit hypothesis, although

this has been questioned on the grounds that eye movements were inadequately monitored and stimuli were inappropriately large (Gur and Snodderly 1987). There are three strong arguments against the shifter-circuit idea, as applied to nulling the effects of involuntary eye movements:

1. No visual feedback mechanism could respond quickly enough to null the effects of microsaccades, which constitute a major portion of involuntary eye movements.

2. The mechanism would have to operate locally rather than correct for whole-field image motion, since vernier acuity, and therefore probably stereoacuity also, is normal for targets oscillating simultaneously in opposite directions (Fahle 1991). But if it does act locally, it would be disadvantageous if such a mechanism were to null slowly changing local disparities since such changes usually signify real differences in depth.

3. Disparity changes too large to be accommodated by the proposed shifter circuit, when applied evenly over the whole visual field, do not give rise to sensations of changing depth (Erkelens and Collewijn 1985a; Regan et al. 1986a). Furthermore, stereoscopic vision is not disturbed by normally occurring fixation disparities (see Section 10.2.4) nor by experimentally imposed fixation disparities of over one degree (Fender and Julesz 1967). If shifter circuits nulled fixation disparities the disparities would no longer be visible; but they are visible when tested with nonius lines.

All that is required to account for the fact that stereoscopic vision is not disturbed by overall conjugate or disconjugate motions or displacements of retinal images is that the stereoscopic system registers only first or higher spatial derivatives of disparity, as discussed in Chapter 7. Such a mechanism simply responds to local disparity differences and discontinuities and therefore automatically rejects steady-state or temporally modulated disparities applied equally over a given region. Note that as we approach a three-dimensional visual scene, disparities are not changed by the same amount over the whole scene because the disparity per unit depth separation between a pair of objects is inversely proportional to the square of viewing distance (see Section 2.3.1). Disparities in different areas are not changed homogeneously even when we approach a flat, frontal-plane surface, because the gradients of vertical and horizontal disparities in such a surface vary with viewing distance and eccentricity (see Section 7.1.3). Homogeneous changes in disparity are produced only by horizontal or vertical

misconvergence or by inappropriate cyclovergence and are therefore best ignored by the depth perception system. However, even though homogeneous changes of disparity are ignored for purposes of stereopsis, they must be detected at some level because they evoke appropriate corrective vergence movements and can give rise to sensations of changing size (see Section 12.1.1).

Stereoacuity and vergence angle

Most investigators have found that stereoacuity is not affected significantly by changes in the distance of the visual target, that is, by changes in the angle of vergence required to fixate it (Ogle 1958; Brown et al. 1965), although some deterioration in stereoacuity has been reported at viewing distances of 50 cm or less (Amigo 1963; Lit and Finn 1976). For vertical rods at a fixed distance, depth discrimination thresholds were lower when subjects fixated the moving rod than when they fixated the stationary rod (Lit 1959b). Presumably, the change in vergence supplemented the change disparity.

5.8.4 Stereoacuity and head movements

When the head rotates in the dark about a given axis, the eyes execute compensatory movements in the opposite direction, interspersed with saccadic return movements. This response is known as the vestibuloocular response (VOR). Stimuli evoking VOR originate in the semicircular canals of the vestibular system. The gain of the response, indicated by the ratio of eye velocity to head velocity, is low for low frequencies of head oscillation but rises to about 1 at a frequency of about 2 Hz and remains about 1 up to a frequency of about 5 Hz. When the eyes are open, VOR is supplemented by optokinetic nystagmus (OKN), evoked by the motion of the image of the stationary scene over the retina. The gain of OKN is highest at low frequencies of scene motion so that when VOR and OKN occur together, as they do when we rotate the head, the gain of the combined response remains high over a wider range of frequencies than that of either response alone. With an overall gain of 1 the images remain stationary on the retinas as the head moves. Visual performance during head rotation is illustrated by the fact that one can read a stationary book while the head is oscillated at over 5 Hz. When a book is oscillated in front of a stationary observer, reading is impaired at 2 Hz, indicating that the VOR supplements OKN at high frequencies (Benson and Barnes 1978). Performance is intermediate when a person reads a book that moves with the head; in this case VOR is evoked but OKN is not (Barnes et al. 1978).

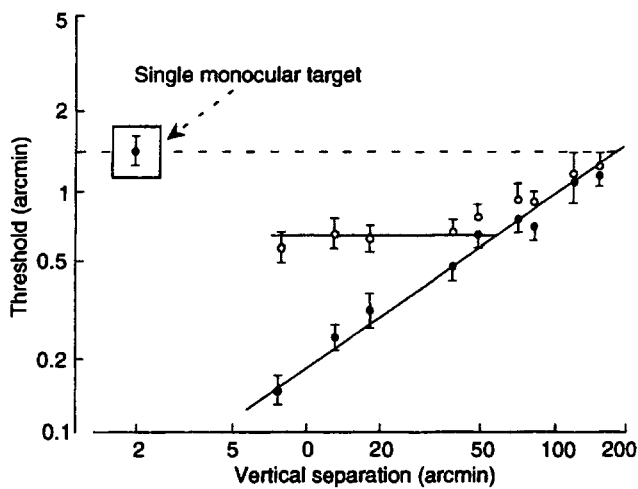


Figure 5.23. Vernier acuity and stereoacuity compared.

The empty symbols show the offset acuity for two monocularly viewed vertical lines (vernier acuity). The solid symbols show the offset acuity for dichoptic vertical lines (nonius acuity). Both are shown as a function of the vertical separation between the lines. The inset shows the threshold for detection of a change in the position of a monocular line in the absence of a reference line. Results for one subject. (From McKee and Levi 1987.)

People vary in the extent to which their images are stabilized during head rotation, and the two eyes do not always move by the same amount (Steinman et al. 1982). Steinman and Collewijn (1980) asked subjects to fixate a visual target while rotating the head from side-to-side at between 0.25 and 5 Hz. In one subject, the gain of eye movement relative to head movement was 0.87 in one eye but only 0.66 in the other. In spite of imperfect image stabilization and vergence control, all subjects reported that the scene appeared stable and binocularly fused. Furthermore, stereoacuity and the ability to fuse random-dot stereograms were not much disturbed by imperfections of image stability during head rotation up to 2 Hz (Patterson and Fox 1984a; Steinman et al. 1985). Instability of vergence introduces an overall, or zero-order, disparity into the visual scene. A mechanism that responds only to first or higher spatial derivatives of disparity would therefore be immune to changes of vergence and would account for visual performance under these conditions. Collewijn et al. (1991) reviewed literature on the effects of head movements on stereoacuity.

5.9 STEREOACUITY AND OTHER ACUITIES

It seems reasonable to suppose that visual processes involved in stereoacuity are similar to those involved in other forms of pattern acuity, such as vernier acuity. Indeed stereoacuity and vernier

acuity are very similar for targets in the foveal region, but it has been claimed that they are affected in different ways by changes in the eccentricity and the spatial disposition of test targets. Stigmar (1971) reported that when the test lines were brought closer together, increasing blur had more effect on vernier acuity than on stereoacuity. However, Westheimer (1979b) found that blur had more effect on stereoacuity than on vernier acuity, and Westheimer and Pettet (1990) found that a reduction of contrast or of exposure time also had a more adverse effect on stereoacuity than on vernier acuity.

Such comparisons between stereoacuity and vernier acuity are difficult to make because the two types of acuity are not comparable measures. We need comparable dichoptic and binocular or monocular tasks. For instance, in vernier acuity, one judges the offset between two parallel lines both seen by the two eyes (binocular acuity) or both seen by one eye (monocular acuity). The equivalent dichoptic task is the nonius task in which one eye sees one of the lines and the other eye sees the other. An unavoidable difference is that fluctuations in convergence disturb the alignment of nonius lines but not of binocularly viewed vernier targets. To take another example, in a typical stereoacuity task the separation between one pair of dichoptic targets is compared with that between a second pair of dichoptic targets. This is not comparable with a vernier acuity task in which the position of one target is compared with that of another target. The binocular task comparable to a stereoacuity task is one involving comparison of the separation between one pair of targets with that between a second pair of targets, viewed binocularly (McKee et al. 1990a). We now review the literature with these points in mind.

McKee and Levi (1987) compared binocular vernier acuity with dichoptic vernier acuity (nonius acuity) as a function of the vertical separation between the vertical target lines. In the nonius task, convergence was first stabilized by having the subject look at the aligned vertical nonius lines in the context of a binocular frame. The frame was then removed and the nonius lines were shown briefly in one of several offset positions. For small vertical separations of the target lines, binocular vernier acuity was higher than nonius acuity, but at separations greater than about 1°, both acuities were identical and increased as a power function of target separation (see Figure 5.23). When the vernier targets were oscillated from side to side at a frequency and amplitude which mimicked the effect produced by fluctuations in the vergence position of the eyes, dioptic vernier acuity matched nonius acuity even for small separations of the test lines. Thus, when

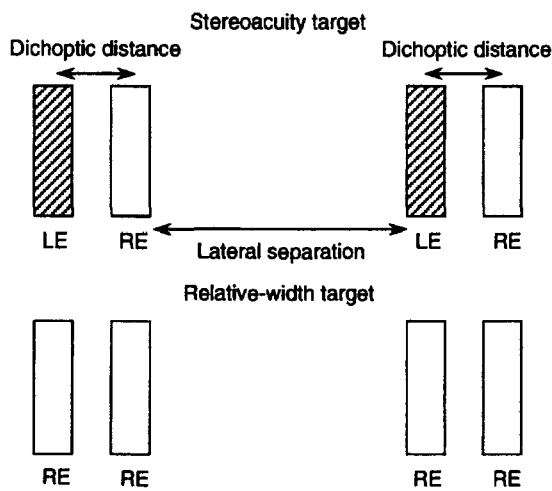


Figure 5.24. Stereoacuity and relative separation.

Stimuli used to compare stereoacuity with acuity for relative separation. In the stereoacuity task subjects detected the depth between one pair of dichoptic lines and a second pair of dichoptic lines. In the relative-width task subjects detected a difference in the distance between one pair of lines and the distance between a second pair of lines, seen by the same eye. Both tasks were performed for a range of lateral separations between the two pairs of lines. (Reproduced with permission from McKee et al. 1990a, Vision Research, Pergamon Press.)

effects of convergence jitter are taken into account, binocular and dichoptic versions of vernier acuity depend on the same limiting process in the nervous system, which is probably the positional uncertainty of position-detecting units in the visual cortex (see Section 3.5.3). Fahle (1991) has obtained similar results.

Schor and Badcock (1985) measured both stereoacuity and vernier acuity using elongated DOG (difference of Gaussians) patches placed one above the other. Although vernier acuity declined rapidly as the stimulus was moved eccentrically up to 40 arcmin from the fovea, stereoacuity remained reasonably constant. However, when the disparity of the stereo target was increased by an amount that brought the monocular images to lie 40 arcmin on either side of the fovea, stereoacuity was severely reduced. In other words, stereoacuity is high for targets slightly displaced from the fovea as long as they remain on the horopter. That must mean that cortical cells tuned to fine disparities are well represented in a reasonably wide area of the central visual field. Detectors for binocular vernier offset must have receptive fields that are more tightly clustered in the fovea. However, we have already pointed out that stereoacuity and vernier acuity are not comparable measures. Therefore, differences between them may not reflect a fundamental difference in the processing of dichoptic and binocular stimuli.

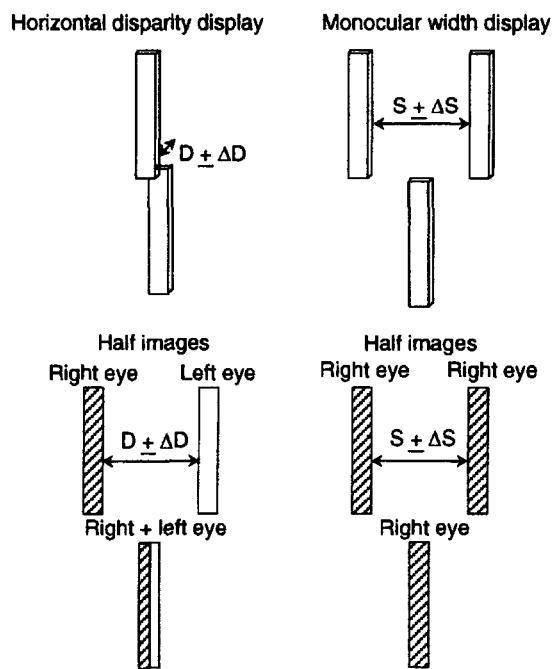


Figure 5.25. Stereoacuity and width discrimination.

Displays used to compare a stereo-increment task with a monocular width-increment task. In the stereo task subjects fixated a line and detected a change in depth of a second line placed above it, about each of several depth pedestals. In the monocular task subjects fixated a line and detected a change in the distance between two other lines about each of several initial separations. (Reproduced with permission from McKee et al. 1990b, Vision Research, Pergamon Press.)

Stereo and vernier acuities are affected to different extents by changes in target separation. Vernier acuity fell off more steeply than stereoacuity when the vertical distance between target lines increased (Berry 1948) or when the lateral separation between target lines increased (Westheimer and McKee 1979). But these results may not reflect fundamental differences between stereo and vernier acuities. McKee et al. (1990a) conducted a similar experiment using comparable dichoptic and monocular stimuli (Figure 5.24). In the stereo task, the least detectable change in depth was determined between one pair of dichoptic vertical lines and a second pair of lines. In the monocular task, the least detectable difference in lateral separation was determined between one pair of vertical lines and a second pair of lines. Performance on these two tasks was the same and remained the same as the lateral separation between the two pairs of lines increased to 4.8°. Thus, the ability to compare the distance between one set of lines with that between another set is the same, whether the lines are dichoptic pairs or visible to the same eye.

McKee et al. (1990b) designed a second set of comparable stereoscopic and monocular stimuli (Figure 5.25). In the stereo task the subject fixated a

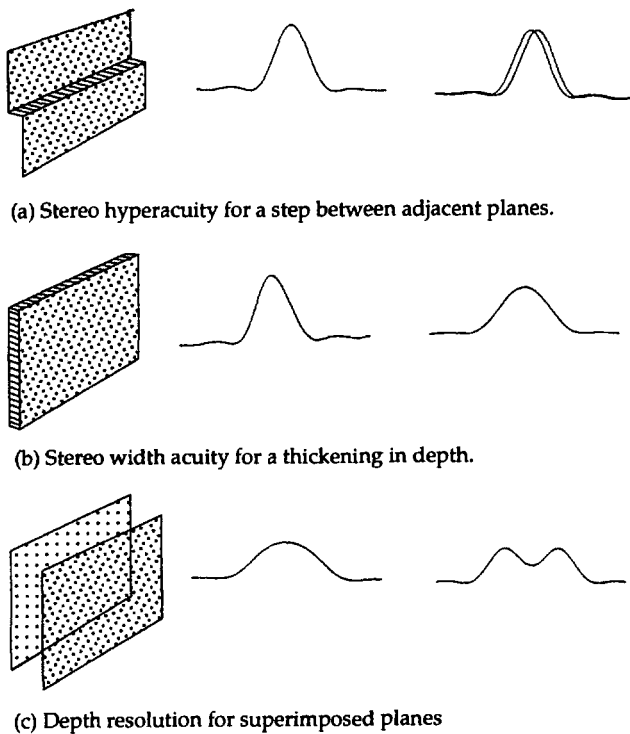


Figure 5.26. Three types of stereo acuity.

Hypothetical distributions of neural activity corresponding to zero-disparity and the threshold stimulus for each task are on the right. (Reproduced with permission from Stevenson et al. 1989, Vision Research, Pergamon Press.)

bar while the disparity in a pair of dichoptic bars varied from trial to trial about each of several disparity pedestals. In the monocular task subjects fixated a bar while the lateral distance between two other bars varied from trial to trial about each of several mean values. Since the nonfixated bars were not resolved as two, subjects detected the change in width of the apparently single bar. The Weber fraction for detection of depth change was several times higher than that for detection of width change in the pair of nonfixated bars. The depth threshold fell with longer viewing time but remained above the monocular threshold. Thus, while stereoacuity and lateral separation acuity are similar, disparity thresholds based on disparity pedestals are much higher than increment thresholds for lateral distance. This suggests that stereoscopic vision is most useful for small depth intervals centred on the horopter.

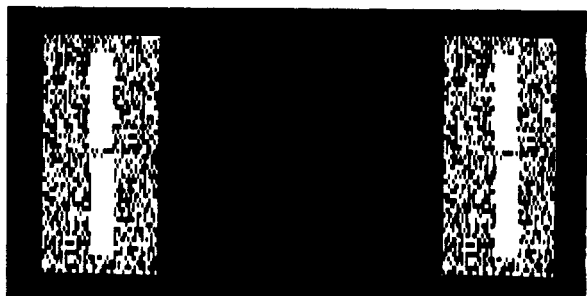
Types of stereoacuity:

Sections 3.2 showed that there are different types of monocular acuity, and they differ in the level of performance that they allow. One can ask whether analogous types of acuity exist in the stereo domain and, if so, whether the levels of performance they allow differ similarly. Stevenson et al. (1989) used

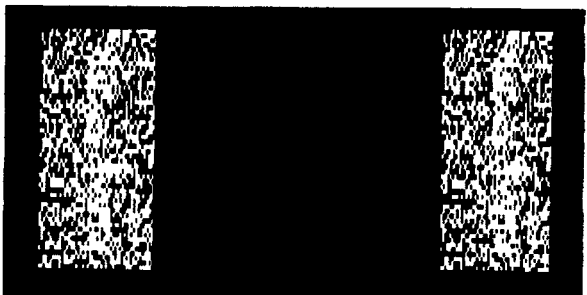
random-dot stereograms to create the three stereo tasks illustrated in Figure 5.26. In the first task, subjects detected a step between two adjacent depth planes. This is analogous to vernier acuity, although not strictly equivalent, as the preceding discussion shows. The threshold for this task was about 3 arcsec. The second task was a super-resolution task in which subjects discriminated between a flat stereo surface and one in which disparities were just sufficient to cause a visible increase in the thickness of the surface without creating the appearance of two surfaces. Tyler (1983) called this range of fused depth surfaces **pyknostereopsis**. Measuring the lower limit of pyknostereopsis is analogous to the monocular task of detecting a small separation of two parallel lines by the apparent thickening of the perceived single line (see Section 3.5.2). The threshold for this task was between 15 and 30 arcsec. The third task was to detect whether two overlapping depth surfaces had an empty gap between them. Tyler called the range within which two overlapping depth surfaces are seen **diastereopsis**. The lower bound of diastereopsis is the upper bound of pyknostereopsis. Overall, the order of performance on the three stereo tasks resembled the order of performance for the analogous monocular tasks.

Cyclopean vernier acuity

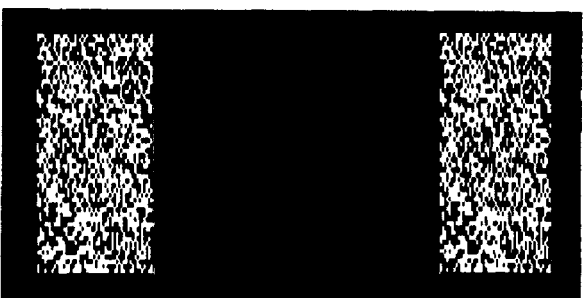
Vernier acuity is normally measured with two vertical black lines seen against a white background, that is, with lines defined by luminance contrast. Morgan (1986) measured vernier acuity with cyclopean lines defined by binocular disparity so that they were not visible in either monocular image. With nondisparate displays, vernier acuity fell off rapidly as dots were added to the white bars seen against a random-dot background and it fell to zero when the bars became indistinguishable from the background. This can be appreciated by looking down the set of stereograms in Figure 5.27 without fusing them. When the vertical bars were set in stereo relief (3.3 arcmin disparity) with respect to the background, vernier acuity fell off less rapidly from an initial value of about 18 arcsec as dots were added to the bars, and remained at a level of about 40 arcsec when the bars became cyclopean (not visible in either monocular image). This can be appreciated by looking down the set of stereograms in Figure 5.27 after fusing them. Thus, vernier acuity with lines defined by disparity is not as high as it is for lines defined by luminance. One problem is that the vertical border is jittered by spurious dot correspondences in the cyclopean case. *This experiment should be repeated with horizontal boundaries defined by shear disparity, which have no ambiguities.* This suggestion is from Christopher Tyler.



(a) Vernier bars well defined by luminance plus disparity.



(b) Bars defined poorly by luminance plus disparity.



(c) Bars defined by disparity alone.

Figure 5.27. Cyclopean vernier acuity.
 (From Morgan 1986, Perception, 15, 157–62. Pion, London.)

Cyclopean shape discrimination

Regan and Hamstra (1994) constructed a cyclopean rectangle in a random-dot stereogram and measured the just-discriminable difference between the height and width (aspect ratio) of the rectangle over a wide range of crossed and uncrossed disparities. Also, the perceived depth of the cyclopean rectangle was matched to that of a luminance-defined bar. The threshold for discriminating differences in aspect ratio remained high until disparity was well above the threshold for detecting the rectangle (indicated by the arrow in Figure 5.28a). The threshold then fell to a minimum at intermediate disparities and increased again at high disparities. However, matched depth was linearly proportional to disparity right up to the point at which fusion was lost for the rectangle. Regan and Hamstra concluded that this dissociation reveals a distinction between two classes of neural

mechanisms, one involving spatial interactions among local disparity-sensitive mechanisms.

Although the effect of disparity on aspect-ratio discrimination was different for crossed and uncrossed disparities, the lowest threshold (about 4 per cent) was similar for the two types of disparity. This value implies that each edge of the rectangle was localized with a precision of about 0.6 arcmin. This is much better than expected on the basis of the 3 to 5-c/deg maximum acuity for cyclopean gratings (Tyler 1974a). This distinction in the cyclopean domain parallels that between resolution (grating acuity) and discrimination (hyperacuity) in the luminance domain (see Section 3.5.2).

In Figure 5.28b, the dots surrounding the cyclopean rectangle were switched off, creating a luminance-defined grating with the same spatial sampling as the cyclopean grating. With these conditions, disparity had much less effect on aspect-ratio discrimination than with the cyclopean rectangle. The lowest discrimination threshold (3 per cent) was similar for crossed and uncrossed disparities and was only a little lower than in the cyclopean case. In Figure 5.28c the dots within the cyclopean rectangle were moved obliquely at a velocity equal and opposite to that of the dots outside the rectangle, creating a motion-defined rectangle. Again, the effect of disparity was minimal. The lowest discrimination threshold (1.9 per cent) was less than for the luminance-defined rectangle, possibly because the edges were defined by more dots during the presentation interval.

Cyclopean orientation discrimination

The effect of disparity on orientation discrimination is similar to its effect on aspect-ratio discrimination, as shown in Figure 5.28a (Hamstra and Regan 1994). The lowest orientation discrimination threshold is similar for crossed and uncrossed disparities and falls within the range found for orientation discrimination of luminance-defined bars or gratings.

5.10 TEMPORAL FACTORS IN STEREOPSIS

5.10.1 Processing time for stereopsis

Two related questions concern processing time for stereopsis. First, how long must a stimulus be exposed for depth to be detected? Second, how long does it take to process depth information after a brief stimulus has been switched off?

Stimulus duration and stereopsis

In Section 5.8.2 it was mentioned that Dove (1841) and several other investigators since, reported that

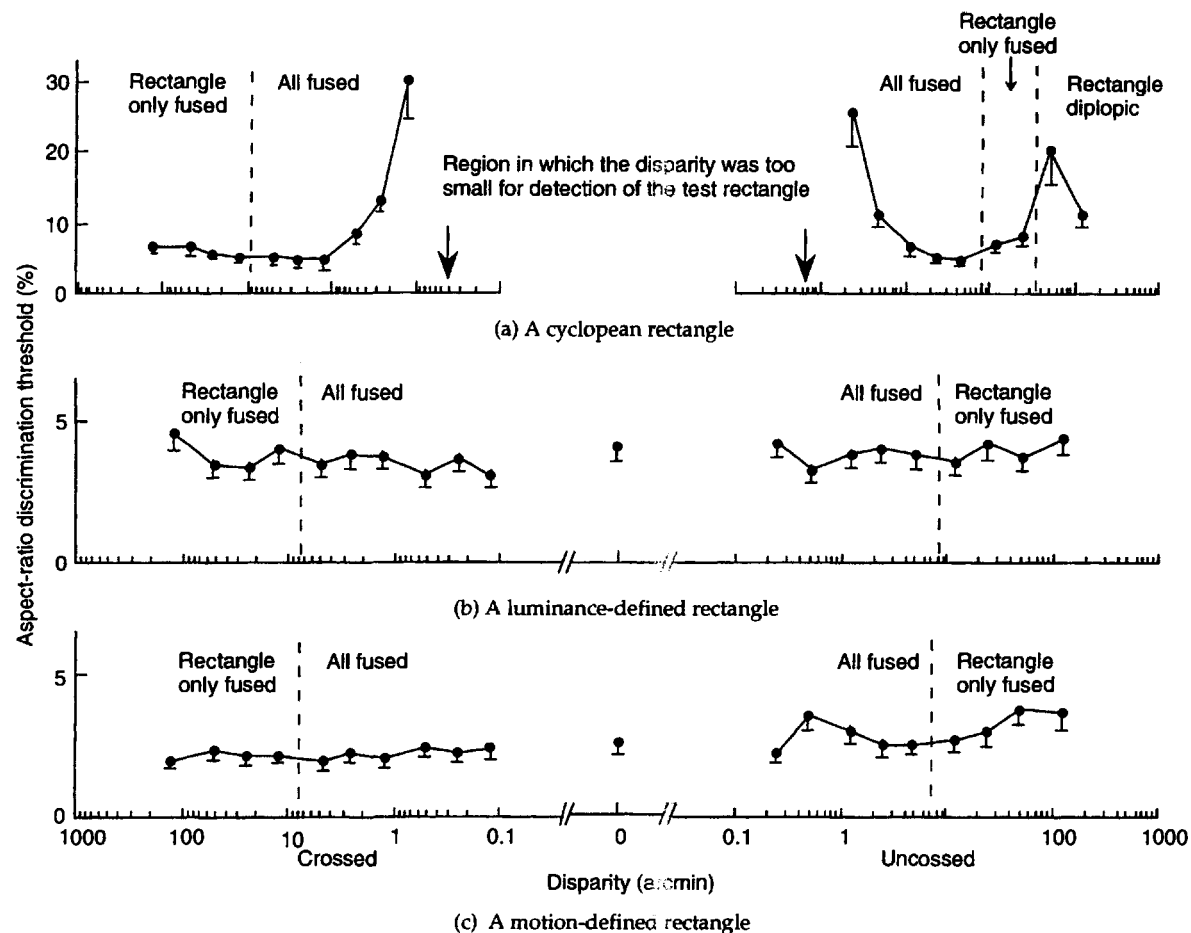


Figure 5.28. Aspect-ratio discrimination and disparity.

Aspect-ratio discrimination for a rectangle as a function of disparity for (a) a cyclopean rectangle, (b) a luminance-defined rectangle, and (c) a motion-defined rectangle. Each vertical finely dashed line is a boundary between disparities where all the dots of the stereogram were fused and those where only the dots comprising the test rectangle were fused. Error bars are standard errors. (Modified from Regan and Hamstra 1994, Vision Research, Pergamon Press.)

depth may be perceived in stereograms illuminated for a few milliseconds. Langlands (1926, 1929) was the first to measure stereo acuity as a function of stimulus duration. He found that the threshold disparity in a Howard-Dolman test was constant for exposures of up to 0.1 s and decreased for longer exposures up to 3 s, beyond which it again stayed constant. Hertel and Monjé (1947) found that the stereo threshold in a modified Howard-Dolman test decreased as exposure time was reduced from 500 to 40 ms. In these studies there was inadequate control of eye fixation, of luminance and contrast of the test objects, and of the state of light adaptation. Ogle and Weil (1958) controlled fixation, systematically varied the contrast between the test object and the background, and controlled the state of light adaptation by keeping the luminance of the background constant. Using the method of constant stimuli, subjects reported the relative depth between two vertical

lines placed 30 arcmin on either side of a central vertical fixation line. The mean stereo threshold, η , rose from about 10 to 50 arcsec as the duration of exposure, t , of the test lines was reduced from 1 s to 7.5 ms, in approximate conformity with the expression

$$\eta = -kt^a$$

where k is the threshold at one second and a is an exponent, which was about -0.3. A similar relationship was found with random-dot stereograms in humans (Harwerth and Rawlings 1977) and in monkeys (Harwerth and Boltz 1979). Shortess and Krauskopf (1961) found a similar dependence of stereoacuity on stimulus duration when the images of the target were stabilized on the retinas. It seems that disparity information is integrated over time in a manner analogous to the integration of luminance

over time as described by Bloch's law, although the exponent for luminance is 1 rather than -0.3.

In Section 5.7.3 we reported Watt's finding that stereoacuity for a line target improves as the duration of stimulus exposure is increased up to one second (see Figure 5.20). He suggested that this is due to the sequential recruitment of finer disparity-detecting mechanisms operating at increasing spatial frequency. Even if fine disparities are processed after coarse disparities, one could still ask whether the probability of detecting a given disparity at a given spatial scale increases with longer exposure time. Clearly, any stimulus must be exposed long enough to be detected but, according to Bloch's law, with a high-contrast, high-luminance stimulus this critical duration becomes vanishingly small. *No critical experiments on this question seem to have been done.*

Tyler (1991) measured the disparity required for detection of depth in a random-dot stereogram as a function of the magnitude of either crossed or uncrossed disparity. For both types of disparity the threshold was inversely proportional to stimulus duration, decreasing from about 50 arcmin at a duration of 7 ms to about 1 arcmin at 160 ms. In other words, fine disparities take longer to detect than coarse disparities and there is integration of disparity information up to a limiting time of about 180 ms. He cited evidence that integration of information from stimuli in the luminance domain occurs over only about 40 to 50 ms.

We review physiological data on processing time for stereopsis in Section 4.8.3.

Processing time for stereopsis

Depth can be seen in simple stereograms exposed for only 1 ms. Time of exposure of the stimulus is therefore not a crucial factor as long as the luminance is sufficient to ensure that the stimulus is seen. However, it takes time to process the information in a stereogram after a briefly exposed stimulus. Julesz (1964) obtained an estimate of stereoscopic processing time in the following way. A random-dot stereogram depicting a central square with unambiguous depth, biased the interpretation of an ambiguous stereogram in which the central square could be seen as either beyond or nearer than the surround (see Figure 6.26). The unambiguous stereogram was presented very briefly and followed by the ambiguous stereogram at various interstimulus intervals. When the interstimulus interval was less than about 50 ms the unambiguous stereogram did not bias the interpretation of the ambiguous stereogram and it was concluded that 50 ms is the time required to extract the depth information in the first stereogram. Uttal et al. (1975) measured the masking effect of an

uncorrelated random-dot display on the forced-choice detection of depth in a random-dot stereogram. Performance was degraded when the mask followed the test stimulus by less than about 50 ms. They also confirmed that the crucial time is not the exposure time of the stimulus but the time provided for unimpeded processing of the disparity information, either while the stimulus remains on or after it has been turned off. These conclusions refer to optimal conditions of viewing and to people who readily see depth in stereograms. Many people have difficulty seeing depth in random-dot stereograms and may require many seconds or minutes before they see depth. This topic is discussed in Section 5.11.

5.10.2 Effects of interocular delay

Several early investigators, starting with Exner in 1875, reported that stereoscopic vision is possible when there is a delay between the images presented to the two eyes (see Stevenson and Stanford 1908) but lack of precise timing devices did not allow the effect to be explored quantitatively. Ogle (1963) asked subjects to fixate a binocular target and judge the relative depth of a second target in another depth plane after it was exposed briefly to each eye in succession. For disparities between 30 and 150 arcsec, depth judgments were not affected by delays of up to about 25 ms between the offset of the left-eye and the onset of the right-eye image. With longer interocular delays, performance declined to chance levels at a limiting delay of about 100 ms. The limiting delay was increased to about 250 ms when the dichoptic targets were exposed repetitively, a result previously reported by Efron (1957).

Wist and Gogel (1966) asked subjects to adjust the depth of a disc to match that of one of a pair of continuously visible comparison targets separated in depth. The disc was seen alternately by each eye for 4 ms with various interocular delays and various intervals between pairs of flashes. With long intervals between pairs of flashes, depth settings remained accurate for interocular delays of up to 32 ms, beyond which they were more variable and indicated that less depth was perceived in the disc. With shorter intervals between pairs of flashes, performance was maintained with interocular delays up to 65 ms.

Thus, all investigators agree that longer interocular delays are tolerated when several stimuli are presented in rapid succession, indicating that information about depth is integrated over short time intervals. Part of the reason for this may be that afterimages of the alternately exposed images build up and remain more visible when the stimuli are presented in quick succession. When the duration of

exposure of the stimuli presented alternately to the two eyes was increased from 20 to 500 ms, the interstimulus interval within which depth was still evident decreased from over 150 ms to zero (Herzau 1976). Presumably, when each monocular image is presented for an appreciable period it becomes well registered as a distinct monocular image and does not fuse with an image presented sequentially to the other eye, even with zero time interval.

In the preceding studies the shapes of the disparate targets were visible monocularly. Ross and Hogben (1974) used random-dot stereograms in which the cyclopean shape was visible only after binocular fusion. The stimuli were presented once to each eye for 10 ms with various interocular delays. Subjects' ability to detect the depth of the cyclopean object was unaffected by interocular delays of between 36 and 72 ms and remained above chance level for delays of up to about 150 ms.

The most obvious explanation for stereopsis with an interocular delay is that signals from one eye persist long enough to interact with those from the other. Engel (1970a) has presented some evidence that monocular visual persistence times are similar to the tolerated interocular delays.

5.10.3 Effects of interstimulus delay

A related issue concerns the effects of introducing a delay between the presentation of a stereo test target, and a comparison target. As we have already seen, stereoacuity with simultaneously presented targets can be as fine as 3 arcsec. Stereoacuity with targets presented sequentially but with no interval of time between them has been found to be up to ten times coarser than with simultaneous presentation (Westheimer 1979a). This degradation of stereoacuity could be due mutual masking of adjacent sequential stimuli (see Section 9.3). The loss of stereoacuity with successive presentation was much less for targets separated 10° than for adjacent targets (Enright 1991b). The effect of increasing separation could also be explained by masking, since masking decreases with increasing separation of stimuli. Enright explained the difference between spatially adjacent and separated targets in terms of the greater instability of fixation with adjacent targets.

Kumar and Glaser (1994) used a vertical test line set at various disparities with respect to two comparison lines 13 arcmin on either side of the test line. The test line and the comparison lines were presented in alternation for periods of up to 50 ms. With a single presentation of each stimulus in the dark the stereo threshold exceeded 120 arcsec and was about 50 arcsec when the room lights were on, which is

similar to the value obtained by Westheimer under the same conditions. However, when the two alternating stimuli were presented repeatedly the stereo threshold declined rapidly as the number of repetitions increased. After five repetitions the threshold was similar to that obtained with simultaneous viewing. Subjects must have integrated information over this number of repetitions.

Stereoacuity also declines as the dark interval between two successively presented targets increases. Foley (1976b) presented a line in the plane of fixation for 2 s and then, after a dark interval of between 0 and 32 s, a second line for 100 ms in a different depth plane. For interstimulus intervals up to about 0.1 s the minimum detectable depth between the two lines increased slowly from an initial value of about 1 arcmin. With longer intervals the threshold increased more rapidly to a final value of about 30 arcmin. The threshold for vernier offset, although lower than that for depth in two of the three subjects, increased in a similar way with an increasing time interval between the presentation of the two lines. Foley explained this effect in terms of noise in the vergence system and a loss of memory for the position of the first stimulus.

5.10.4 Effects of lateral stimulus motion

Microsaccades and drifting motions of the eyes during fixation neither aid nor degrade visual acuity, since grating acuity and vernier acuity are the same when the target is optically stabilized on the retina as when it is viewed normally (Keesey 1960; Gilbert and Fender 1969). Furthermore, imposed motion of a vernier target up to a velocity of 2.5°/s did not degrade vernier acuity (Westheimer and McKee 1977). In Section 5.8.2 we noted that stereoacuity is also not affected when the target is optically stabilized on the retina. Like vernier acuity, stereoacuity was not affected when either the fixation target or the comparison target placed just below it moved at velocities of up to 2°/s (Westheimer and McKee 1978). The threshold for detection of the relative depth between two targets was adversely affected when both targets moved in depth at 2°/s. Lit (1960) increased the sideways motion of a comparison rod relative to a stationary fixation rod placed just below it from 1.5 to 40°/s. The variability of equidistance settings of the rods increased linearly with increasing velocity. The effects of increased velocity could be offset by an increase in the illumination of the rods (Lit and Hamm 1966). For apertures wider than about 10° the effects of velocities between 7 and 40°/s were independent of the width of the aperture across which the moving rod moved (Lit and Vicars 1970). For the

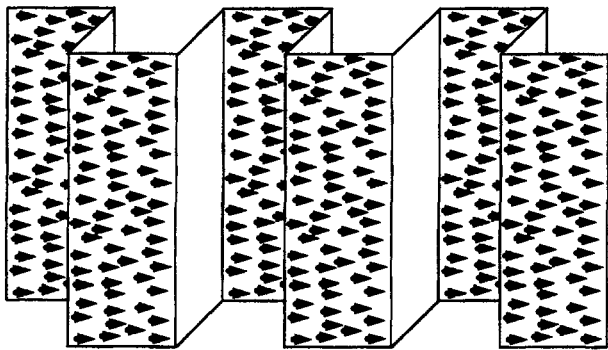


Figure 5.29. Stereoacuity and microtexture motion.

A random-dot stereogram defined a vertical squarewave depth grating with 1.8 arcmin of disparity. The grating was stationary but the dots defining it moved at various velocities over its surface, changing their disparity each time they crossed a disparity boundary. (Adapted from Hadani and Vardi 1987.)

40°/s rod this gave an exposure time of 0.25 s. Thus, as long as the stimulus was visible for 0.25 s, the total time of exposure was not a critical variable for this range of velocities. Presumably the critical variable was the dwell time of the stimulus in each retinal location. With apertures less than 10°, the variability of settings increased rapidly for all velocities, showing that for stimulus exposure times less than 0.25 s the crucial variable was the total time of exposure.

In the preceding experiments, the sideways motion of the visual display was tied to the depth of the display; that is, the objects that moved were the same objects that were seen in depth. Hadani and Vardi (1987) devised the display depicted in Figure 5.29. The vertical squarewave depth grating with a fixed 1.8 arcmin peak-to-trough disparity was stationary while the dots defining it moved at various velocities over its surface, changing their disparity each time they crossed a disparity boundary. The motion of the dots induced optokinetic nystagmus, causing the eyes to pursue the moving dots with periodic saccadic returns. Stereoacuity was impaired at dot velocities of between 1 and 3°/s. At higher velocities, performance improved until, at a velocity of 11°/s, it was equal to that with stationary dots. Records of the movements of the subjects' eyes revealed that optokinetic nystagmus was most evident at those velocities where the loss in stereoacuity was greatest. When the dots moved sinusoidally from side to side, stereoacuity was not affected by the motion of the dots. With this type of motion, saccadic phases of optokinetic nystagmus do not occur. This suggests that impairment of stereoacuity with continuous motion of texture over the surface of a stereogram is due to intrusion of saccades that disrupt the binocular fusion of the display.

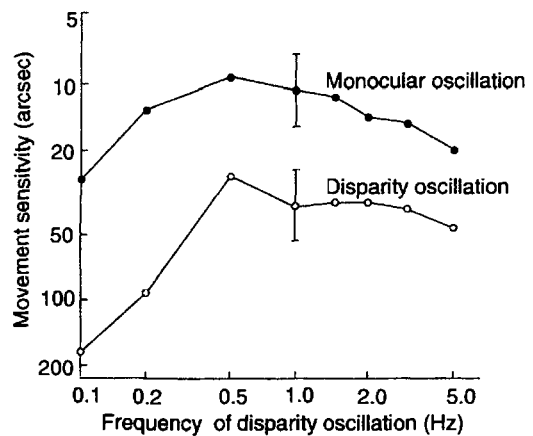


Figure 5.30. Sensitivity depth modulation.

Sensitivity to disparity-induced motion in depth as a function of frequency of sinusoidal oscillation of disparity (lower curve). The upper curve shows monocular sensitivity to oscillatory motion. Results for one subject. (Adapted from Tyler 1971.)

5.10.5 Temporal modulation of disparity

It was mentioned in Section 5.10.1 that stereoacuity deteriorates as the duration of exposure of the test object is reduced. In those studies, a single pair of targets was presented with fixed disparity. A related question concerns the effect of temporal modulations of depth on stereoacuity. Richards (1951) was the first to tackle this issue. He found that the disparity threshold for detecting stepwise depth oscillations of a vertical line with respect to two flanking lines rose rapidly as the frequency of oscillation increased above 1 Hz. Depth could not be seen at frequencies above about 4 Hz. He did not explore frequencies below 1 Hz. Tyler (1971) measured sensitivity to temporal modulation of disparity of a single line with respect to a stationary line for frequencies from 0.1 to 5 Hz. Figure 5.30 shows that depth sensitivity declined as modulation frequency increased above about 2 Hz or decreased below 1 Hz, but the form of the function for lateral motion was similar to that for motion in depth. Regan and Beverley (1973a) measured sensitivity to temporal disparity modulation of a vertical line superimposed on a fixed display of random dots. The attenuation of motion sensitivity at low frequencies of depth modulations centred on 5-arcmin depth pedestals was more severe than for modulations centred on zero disparity, especially for uncrossed-disparity pedestals (see Figure 5.31). It can also be seen that, for squarewave depth modulations, low-frequency attenuation is virtually absent for oscillations centred on zero disparity and is less for oscillations about 5 arcmin pedestals than for sinusoidal modulations of depth.

The loss of stereoacuity for temporal depth modulation frequencies higher than 1 Hz was more

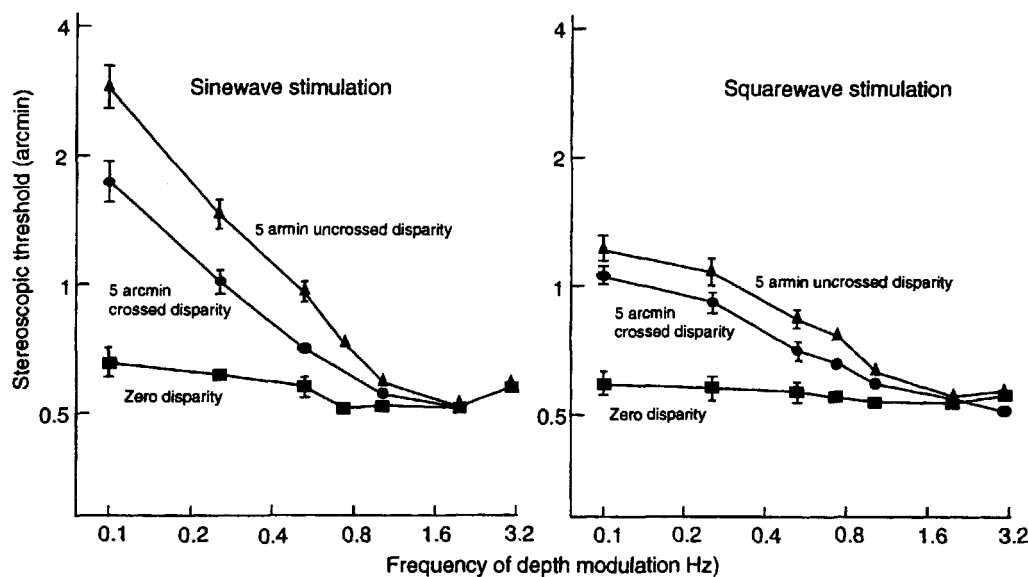


Figure 5.31. Sensitivity to depth modulation.

The curves on the left show the disparity modulation threshold for the detection of sinusoidal motion in depth as a function of the frequency of depth modulation. The legends on the curves indicate the disparity about which depth was modulated. The curves on the right show the same thresholds for detection of squarewave depth modulations. (Reproduced with permission from Regan and Beverley 1973a, Vision Research, Pergamon Press.)

severe for oscillations about a crossed disparity pedestal than for those about an uncrossed disparity pedestal. For both types of pedestal, high-frequency attenuation was more severe for stepped movements away from and then back toward the fixation plane than for stepped movements toward and then away from the fixation plane (Beverley and Regan 1974).

Suprathreshold depth perception is also affected by temporal depth modulations. Richards (1972) measured the magnitude of perceived depth by asking subjects to match the depth of a probe to the maximum apparent depth of a test bar as it moved either stepwise or sinusoidally through the fixation plane. The results for sinusoidal depth modulation are shown in Figure 5.32. For all amplitudes of depth oscillation, depth perception failed completely at a frequency of about 6 Hz. For sinusoidal disparity modulations of between 0.5 and 2°, depth efficiency peaked for temporal modulations of between about 0.5 and 1 Hz and decreased monotonically with increasing modulation rate above 1 Hz. The low-frequency attenuation of efficiency was, like the attenuation of stereoacuity, absent for squarewave depth modulations. This fits nicely with Regan and Beverley's finding that low-frequency attenuation of stereoacuity is virtually absent for squarewave modulations around zero disparity (Figure 5.31). Thus, suprathreshold sinusoidal changes in disparity of less than 0.5° generate more depth at low rates of depth oscillation whereas changes in disparity of between 0.5 and 2° generate more depth at higher

rates of temporal modulation. Richards used only crossed disparities in his display. Regan and Beverley (1973a) confirmed that suprathreshold depth efficiency declines monotonically for depth modulations of between 2.5 and 20 arcmin and found that the loss in efficiency began at lower temporal frequencies for crossed than for uncrossed disparities, providing more evidence that crossed and uncrossed disparities are processed in distinct channels.

If small disparities are processed by high spatial-frequency channels and large disparities by low spatial-frequency channels, as evidence reviewed in Section 5.7 suggests, then one would expect the differential effects of temporal modulation that Richards found for large and small disparities to show for stereo displays with low and high spatial frequency luminance patterns. In conformity with this expectation the stereo threshold for spatial-frequencies below about 2.5 c/deg was lower for a 1-Hz depth modulation than for the same static disparity, but the stereo threshold for patterns with high spatial frequency was the same for modulated as for static disparities (Schor et al. 1984a).

It looks as though the response of the low spatial-frequency/large disparity system is boosted by temporally changing disparity, at least up to 1 Hz, and that the high spatial-frequency/small disparity system is equally responsive to modulations of 1 Hz and steady-state disparities. Thus, over this range of sinusoidal temporal modulation, the low-frequency system has a transient characteristic and the high-

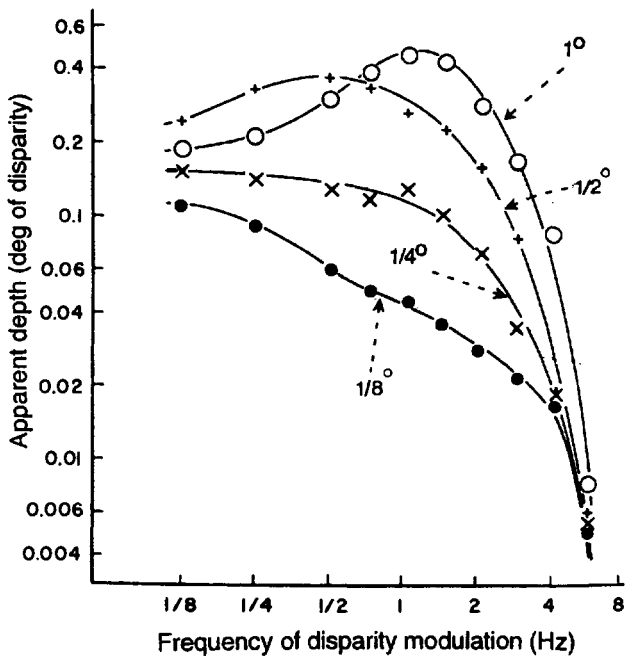


Figure 5.32. Apparent depth and depth modulation.
The apparent depth of a test bar, as it moved either stepwise or sinusoidally through the fixation plane, as a function of frequency of depth modulation. The curves are for four amplitudes of depth modulation, as indicated on each curve. (From Richards 1972.)

frequency system a sustained characteristic. Perhaps the low spatial-frequency, transient system is the magnocellular system and the high spatial frequency, sustained system is the parvocellular system (see Section 4.7).

In the preceding studies it was claimed that the acuity of both the fine and coarse stereo systems declines to zero at a frequency of depth oscillation of between 4 and 6 Hz. However, this conclusion must be qualified. Regan and Beverley (1973a) found that depth impressions ceased for a bar oscillating sinusoidally in depth at about 6 Hz. When the bar oscillated discretely in sudden jumps, however, the impression of depth diminished for temporal frequencies of up to about 3.2 Hz, but then the whole appearance of the display changed from a bar oscillating in depth to that of two bars at different distances. The magnitude of apparent depth between the two bars was unaffected by further increases in the frequency of disparity oscillation. A similar effect was noticed by Norcia and Tyler (1984). They found that a display of random dots filling a monitor screen appeared to move back and forth relative to the monitor frame as the disparity of the dots alternated between -1.25 and +1.25 arcmin. Above an oscillation frequency of 6 Hz the impression of one plane moving back and forth gave way to an impression of two pulsating depth planes, one seen through the other. Above 14 Hz the pulsation ceased and two

steady depth planes were seen. Thus, 6 Hz is the upper limit for the perception of alternating motion in depth but not for the perception of depth. It is not clear whether the pulsation noticed up to 14 Hz was a pulsation in depth or a residual cyclopean flicker in the display. The pulsation was not visible monocularly.

There is no upper temporal modulation limit for the perception of distinct static depth planes. The concept of integration time for each exposure does not apply when there is rapid alternation between two depth planes because, although each exposure of a depth plane is of very short duration, the information can be integrated over several exposures. To see motion in depth, the visual system must keep track of the sequence of rapidly alternating disparities and it is this ability that breaks down at 6 Hz.

Several investigators have compared the effects of to-and-fro sideways motion on the detection of lateral motion with the effects of to-and-fro motion in depth on the detection of motion in depth as a function of temporal frequency. Foley and Tyler (1976) found that the threshold for a briefly exposed fixed vernier offset was similar to the threshold for a briefly exposed fixed disparity between two lines and that both thresholds decreased in a similar way as exposure duration increased from 25 to 200 ms. Since a given angle of disparity is twice the angle of stimulus displacement in each eye, the offset detected in each eye at the stereo offset threshold is about half the vernier-offset threshold.

The relationship between the threshold for motion in depth and that for lateral motion is more complicated. Tyler (1971) found that the threshold for back and forth motion of a vertical line in stereoscopic depth relative to a fixation line was three or more times higher than the threshold for to-and-fro lateral displacement of a monocular line (see Figure 5.30). He called this **stereomovement suppression**. In a later study the possible contaminating effects of vergence were controlled by having two lines, 20 arcmin apart, move in depth in antiphase (Tyler 1975b). Stereoscopic movement suppression occurred at oscillation rates above 1 Hz. Below 1 Hz the threshold for movement in depth was, if anything, slightly lower than that for equivalent lateral movement. Tyler concluded that stereomovement suppression is due to inhibition between neurons sensitive to movement in one direction in one eye and those sensitive to movement in the opposite direction in the other eye. But the fact that rapid sequential opposed changes in depth are detected less well than a single depth offset suggests that sequential motion signals in the disparity domain inhibit each other. That is, detectors for motion-in-

depth in one direction are inhibited by detectors for motion-in-depth in the opposite direction, when the two detectors are stimulated in quick succession. Another way to think about this is to say that sequential changes in disparity metamerize to an average value. This interpretation is not supported by Tyler's finding of a similar suppression of antiphase motion between vertically disparate images. It seems that inhibition is characteristic of how disparity is used to process binocular fusion rather than depth.

Tyler et al. (1992) measured the threshold for the perception of changing depth of a vertical line that had sinusoidal depth modulations along its length. Both the spatial frequency and the temporal frequency of depth modulation were varied. The threshold for detecting lateral oscillation of a monocular wavy line was also determined. Thus, the stereo threshold and the lateral-motion threshold were determined as a function of temporal frequency up to 3 Hz, and of spatial-modulation frequencies between 0.05 and 1.5 c/deg. There were large individual differences but, in general, the threshold for detection of monocular oscillation was lowest at high spatial and high temporal frequencies (Figure 5.33). The disparity threshold for detection of stereo motion was best at low temporal frequencies, as the stereo motion effect had revealed, and at medium spatial frequencies, as revealed in experiments reported in Section 5.5.3 (see also White and Odom 1985). The difference functions for stereo and monocular motion thresholds are shown in Figure 5.33c.

With isoluminant red-green gratings, thresholds for oscillations of position were the same when the two gratings were viewed by the same eye or dichoptically so that position shifts produced oscillation of the grating in depth (Tyler and Cavanagh 1991). In other words, stereomovement suppression was not present in isoluminant gratings. Tyler and Cavanagh concluded that stereomovement is processed separately in luminance and chromatic channels.

In apparent contradiction to these findings Regan and Beverley (1973a) found that sensitivity to a 0.1 Hz sinusoidal to-and-fro motion in depth of a line relative to a random-dot background was up to twice that for binocular lateral motion, when depth modulations were no greater than ± 10 arcmin of disparity from the fixation plane (see Figure 5.34a). Tyler's test and comparison targets were separated by 20 arcmin whereas, Regan and Beverley's reference stimulus was a field of closely packed dots superimposed on the test stimulus. Tyler (1975a) suggested that sensitivity to motion in depth improves when compared stimuli are closer together, that is, when the disparity gradient is steeper or the spatial frequency of depth modulation is higher.

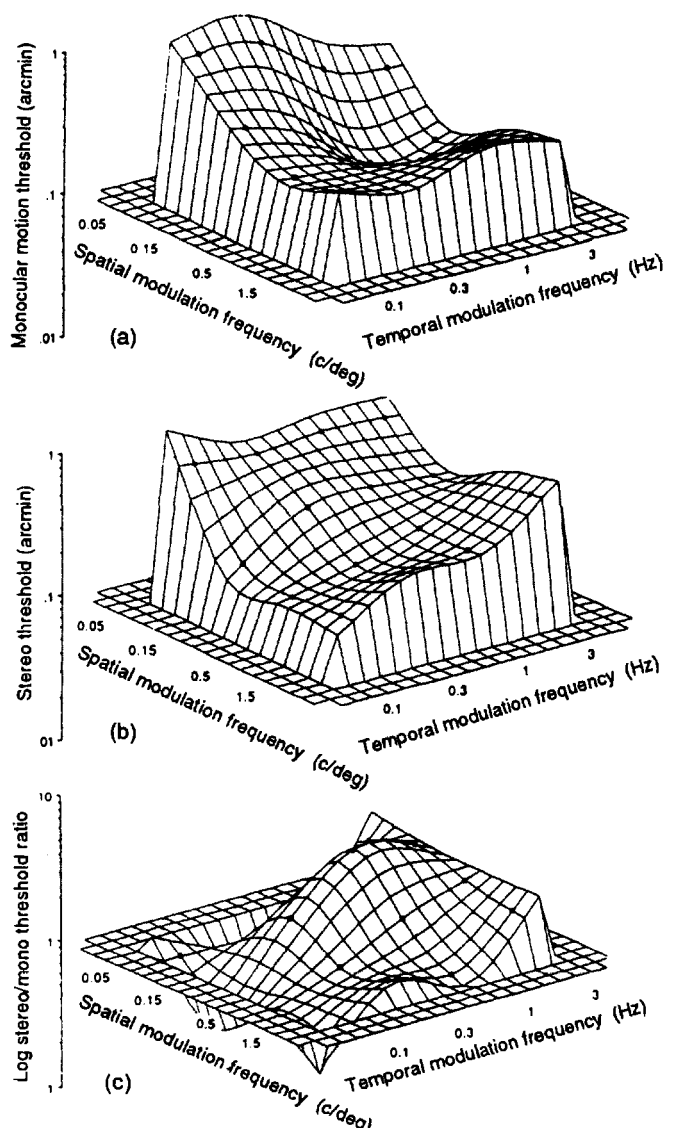


Figure 5.33. Spatiotemporal features of stereoacuity.

(a) The threshold for detection of sinusoidal perturbations of a monocularly viewed wavy line as a function of the spatial and temporal frequency of line oscillations.

(b) The disparity threshold for detection of peak-to-peak depth modulation in an oscillating wavy line as a function of the spatial and temporal frequency of line oscillation.

(c) The ratio of the stereo threshold to the monocular threshold for detection of oscillations of a line. Points below the base plane indicate stereo thresholds lower than monocular thresholds, those above indicate a stereo impairment. Dots are data points. Surfaces were fitted by cubic spline interpolation. (From Tyler et al. 1992.)

Regan and Beverley (1973b) dissociated the frequency of the movements of the image in each eye from the frequency of the motion in depth produced by these movements. They did this by oscillating the monocular images at a slightly different frequency so that the motion in depth changed as the monocular motions came in and out of phase; that is, the

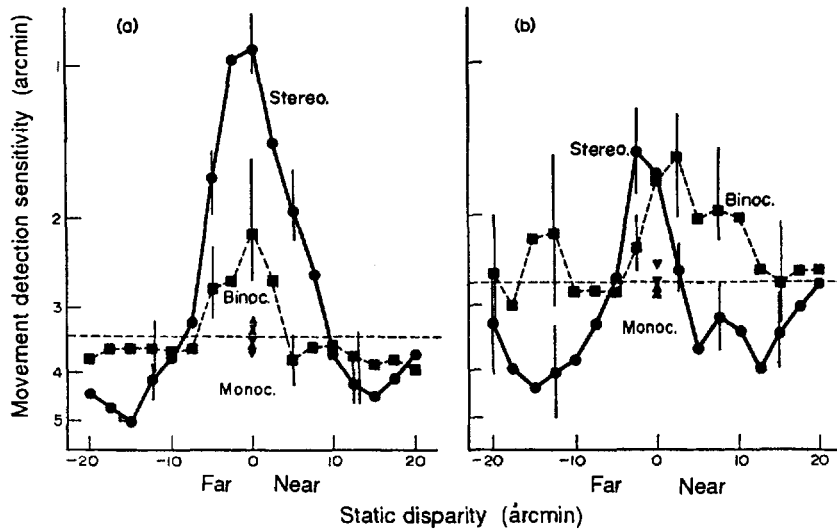


Figure 5.34. Stereoacuity and depth modulation.

(a) The solid line indicates the sensitivity (reciprocal of threshold) to oscillatory motion in depth of a vertical bar, as a function of the fixed disparity about which the oscillation occurred. The curve with dashes indicates the sensitivity to sideways oscillation of the bar as a function of the same variable.

(b) The same curves for a stereoanomalous subject. Results for one subject (Reproduced with permission from Regan and Beverley 1973a, Vision Research, Pergamon Press.)

motion in depth ran at the difference, or beat frequency of the two monocular oscillations. Although motion in depth was not detected at a beat frequency above about 5 Hz, the monocular motions remained visible up to a frequency of about 25 Hz.

Evidence already cited suggests that attenuation of stereoacuity at certain temporal frequencies of depth modulation is greater between alternating movements on a crossed-disparity pedestal than between those on an uncrossed pedestal, and that acuity attenuation is greater for movements stepped away from and back to the fixation plane than for movements toward and then away from the fixation plane. In all these cases a motion in depth one way is followed by a motion in depth the other way. There are more metamerism interactions between disparity detectors than between sequential motions in depth in the same direction, since the spatiotemporal tuning functions of the detectors of such motions are more likely to overlap. Low temporal-frequency attenuation may be more severe for sinusoidal than for square-wave depth modulations (see Figure 5.31) because, in sinusoidally modulated depth, inhibitory interactions occur between sequentially stimulated disparity detectors of the same sign whereas, in squarewave modulated depth about zero disparity, all the contiguous interactions are between detectors of opposite sign. The characteristics of the system can be derived from sinusoidal inputs only if the system is linear. This question needs further exploration. An experiment is needed in which the threshold

and efficiency of motion detection are measured for different temporal sequences of disparity change down or up linear or curved disparity ramps and compared with those for interlaced disparity changes of opposite sign.

5.11 EXPERIMENTAL AND PRACTICE EFFECTS

Effects of practice on stereo acuity

It was mentioned in Section 3.6.8 that vernier acuity improves with practice, even in the absence of feedback. There have been several reports that stereoacuity also improves with practice. Practice was found to improve stereoacuity in the Howard-Dolman test but only for one of the two subjects tested (Lit and Vicars 1966). Wittenberg et al. (1969) asked subjects to adjust repeatedly an object seen in a stereoscope to appear at the same distance as a second object. After 20 such training sessions spread over 2 weeks, subjects showed a significant improvement in stereoacuity compared with subjects in a control group who were tested and retested without intervening training. Foley and Richards (1974) trained a stereoanomalous subject over 12 one-hour sessions to discriminate between crossed disparities, uncrossed disparities, and zero disparity with stimuli presented for as long as the subject wished. After this training, the subject's stereoanomaly revealed with a flashed target was considerably reduced. Fendick and Westheimer (1983) had two subjects perform a criterion-free stereoacuity test in sessions of 900

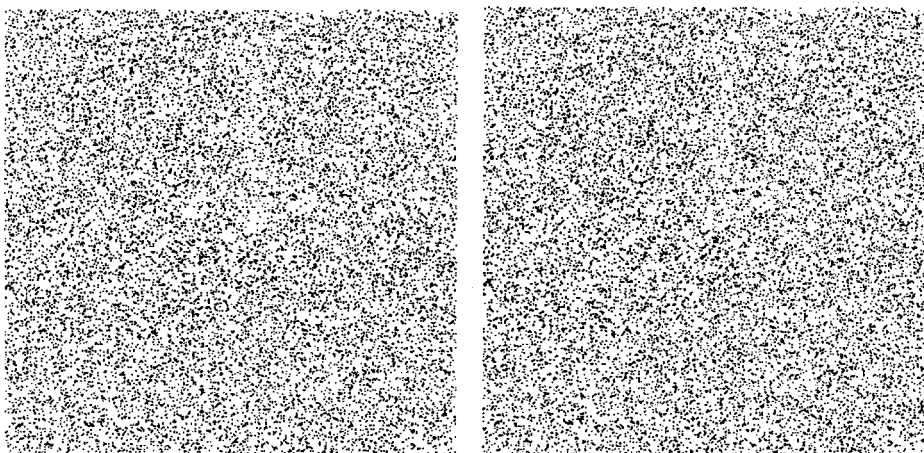


Figure 5.35. Stereogram of a complex spiral.

trials, each repeated over a period of 9 weeks. When the stereo targets were removed 5° from the fovea, performance improved over about the first 2,000 trials for both subjects. When the targets were imaged on the fovea, only one subject showed any improvement. Whatever the reason for improvement of stereoacuity with practice, the effect is clearly subject to large individual differences.

The stereo threshold declines with practice particularly for very brief stimuli. Even for practiced observers, some initial trials were required for stimulus durations of less than 100 ms before performance stabilized (Kumar and Glaser 1993). For stimuli exposed for only 5 ms the threshold declined about 10-fold during several hundred trials. There was little effect of practice for exposures of 1000 ms (Kumar and Glaser 1994). In these experiments, luminance was kept constant so that the effects of short stimulus duration could have been due to a reduction of total retinal flux. Westheimer et al. kept the total retinal flux constant.

It has been reported that stereoacuity is adversely affected when binocular vision is restored after one eye has been occluded for some time. Thus, Wallach and Karsh (1963) found a 40 per cent increase in variability in a depth-matching task after subjects had worn an eye patch alternately on the two eyes for 24-hours. Herman et al. (1974) exposed subjects to 8 hours of monocular patching and also obtained a large increase in variability in a stereo depth-matching task. The effect cannot be due to simple disuse since 8 hours of binocular occlusion had no effect. The time course for the buildup and decline of the effect of monocular occlusion was not studied, and the cause of the effect remains obscure. Monocular occlusion in young animals leads to permanent loss of stereoscopic vision, but not in mature animals (see Chapter 15).

Effects of practice on stereo latency

In his original paper on random-dot stereograms Julesz (1960) reported that it takes longer to see depth in a random-dot stereogram than in a normal stereogram or a random-dot stereogram in which the cyclopean form is outlined in the monocular images. Several authors have agreed that it can take several seconds or even minutes to see depth in a random-dot stereograms portraying a "complex" surface such as the spiral (Figure 5.35) or hyperbolic paraboloid surfaces presented in Julesz (1971) (Frisby and Clatworthy 1975; MacCracken and Hayes 1976; Ramachandran 1976; MacCracken, Bourne and Hayes 1977). It is not clear whether the long latencies are due to the large range of disparities present in these stereograms or to the complexity of the surfaces. A direct test would involve presenting the same complex surfaces with a range of disparities within Panum's fusional range.

Julesz (1960) also reported that the time to see cyclopean depth shortens after repetitive trials. The reduction of latency persisted during the same day but only partially from one day to another (MacCracken and Hayes 1976).

Learning to see random-dot stereograms is not due to subjects becoming familiar with the shape of the cyclopean object because telling them about what they can expect to see or showing them a model of the cyclopean object had no effect on how long it took them to see depth in the actual stereogram (Frisby and Clatworthy 1975).

Julesz (1971) suggested that depth in random-dot stereograms takes much longer to see than that in ordinary stereograms because, in a random-dot stereogram, there are no clear visual features to guide vergence eye movements and that it takes time to learn the sequence of vergence eye movements required to fuse the image. He wrote: "In order to obtain

fusion one has to shift areas in registration . . . If one proceeds in the wrong sequence it will take a very long time . . . However, if one learns the proper sequence of vergence movements . . . the step by step interlocking of areas follows rapidly." (page 217).

Some support for this **eye movement hypothesis** is provided by the fact that stereo latency can be much shorter when depth features in a random-dot stereogram are made monocularly conspicuous by drawing a line round them or by adding clearly visible shapes in the same depth plane (Sayre and Frisby 1975). Paradoxically, stereo latency was shortened by the introduction of a difference in dot density between the stereo regions, even when this difference was below the monocular threshold (Julesz and Oswald 1978;). The eye-movement theory also gains support from the finding that reduction in stereo latency does not transfer fully across a change in the sign of the disparity of the stereo pattern (O'Toole and Kersten 1992).

The eye-movement theory does not explain why the reduction in stereo latency with repeated exposure to a stereogram made up of randomly positioned oblique lines transferred to other stereograms made up of similarly oriented line elements but not to those with line elements oriented along the opposite oblique, even though they depicted the same shape (Ramachandran and Braddick 1973). This pattern-specific effect suggests a purely sensory process. For instance, if stereo processing proceeds independently in different orientation-tuned channels, learning could be confined to one stereo orientation channel. Ramachandran (1976) claimed that the reduction in stereo latency is fully preserved when the pattern of dots is changed in a random-dot stereogram without changing dot density or the macro-pattern. A more sensitive forced-choice discrimination procedure revealed that latency reduction did not transfer fully when 50 per cent of the dots were changed but did transfer fully when the luminance polarity of all the dots was changed (O'Toole and Kersten 1992). One would have to assume in this case that subjects learn the patterns of the local clusters of dots. However, changing the micropattern of a random-dot stereogram had less effect than changing the orientation of elements in a random-line stereogram. The drop in latency with repeated exposure does not transfer when the stereogram is moved from one retinal location to another (O'Toole and Kersten 1992), nor when the subject fixates on a different point in Julesz's hyperbolic paraboloid (Ramachandran 1976;). Blurring one image of a random-dot stereogram, keeping disparity constant, has also been found to disrupt transfer of latency reduction (Long 1982). All this evidence suggests

that reduction of response time with random-dot stereograms is due to local sensory factors rather than to eye movements or higher cognitive factors. *An experiment is needed in which transfer is tested across stereograms filtered to different size ranges. If disparity processing occurs in distinct size channels, one would expect little transfer under these conditions.*

The reduction in response times with complex stereograms may be due in part to a change in the criterion for seeing "the object in depth". Bradshaw et al. (1992) minimized criterion effects in two ways. First, they used the more objective criterion of whether the spiral shape unwound clockwise or counter-clockwise and second, they gave subjects a series of practice trials for discriminating clockwise and counterclockwise spirals defined by luminance. Response times averaged about 3 s even on the first presentation of the stereogram to naïve subjects. There was a practice effect but it was necessarily small, given the short latencies found on the first trial.

To test the eye movement hypothesis, Bradshaw et al. varied the peak-to-base disparity with the same complex spiral surface. Response times for 80 and 40 arcmin spirals were not significantly different. Contrary to the eye-movement hypothesis, latencies were slightly longer for 20 arcmin spirals in which the details of the shape were more difficult to see. Goryu and Kikuchi (1971) and Sayre and Frisby (1975) reported that latencies were longer for stereograms with larger disparities but their stereograms depicted a square rather than a spiral.

It seems likely that the more objective and well-learned criterion used in the Bradshaw et al. experiment was partly responsible for shorter response times but they also observed that the spiral stereogram and particularly the hyperbolic paraboloid stereogram in Julesz' (1971) book contain many uncorrelated elements (Figure 35). Frisby and Clatworthy (1975), Ramachandran (1976), and MacCracken and Hayes (1976) all used these stereograms to measure response times. Julesz (1971) drew attention to the importance of binocular correlation and devised a test of stereoscopic ability based on a set of stereograms with decreasing correlation.

The average time to identify the shape of their hyperbolic paraboloid was just 3 s compared with 9.1 s for the version in Julesz (1971) (Bradshaw et al. 1992). Christophers et al. (1993) measured response times for (1) discriminating the direction in which the spiral unwound and (2) detecting the presence of small discrete steps on the spiral surface while independently manipulating the binocular decorrelation. Latencies for discriminating the spiral direction increased 42 per cent for stereograms with a 30 per cent decorrelation and by almost 100 per cent

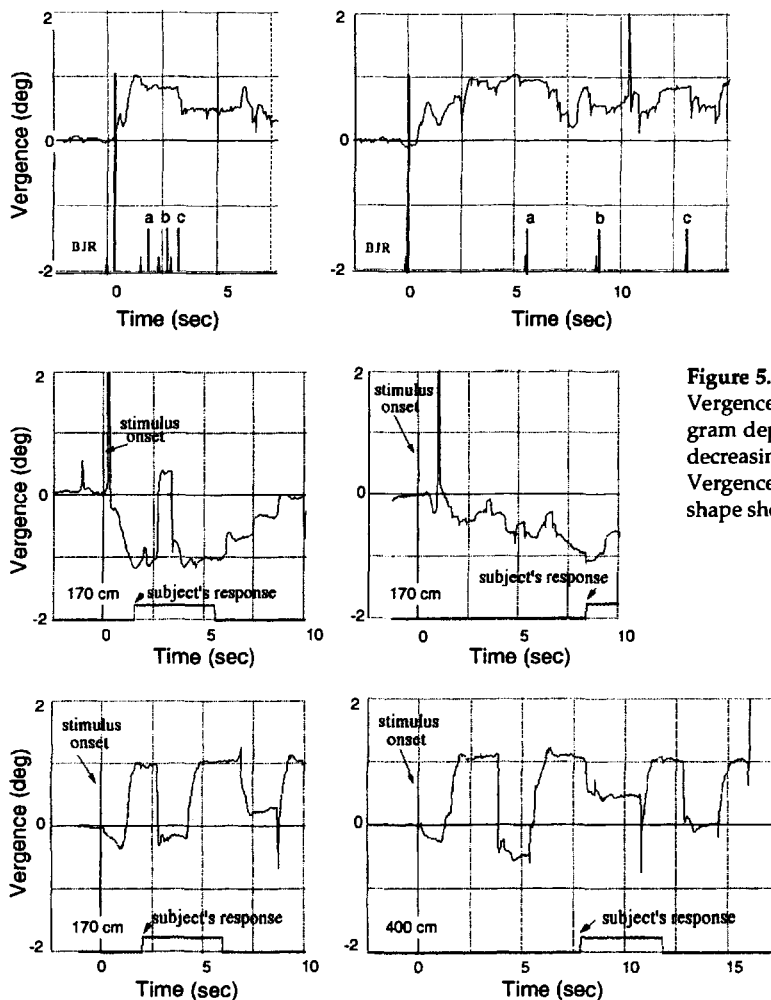


Figure 5.36. Vergence and decorrelation.

Vergence changes in response to a random-dot stereogram depicting a 60 arcmin spiral (1 arcmin dots, dot density 10 per cent, viewing distance 57 cm). Vergence was more rapid and complete for the 100 per cent correlated version (left) than for the 30 per cent decorrelated version (right). Latencies for identifying the direction of the spiral *a*, the complete three-dimensional shape *b*, and the discrete steps on the spiral surface *c* were shorter with the fully correlated stereogram.

Figure 5.37. Individual differences in vergence changes.

Vergence changes in response to viewing a random-dot stereogram depicting a 90 arcmin 'wedding cake' of concentric discs of decreasing size and increasing disparity, viewed at 170 cm. Vergence was more rapid and the latency for identifying the shape shorter for the experienced subject (left).

Figure 5.38. Vergence and viewing distance.

Vergence changes in response to a random-dot stereogram depicting a 90 arcmin 'wedding cake' of concentric discs of decreasing size and increasing disparity. Vergence changes were similar when the stereogram was displayed at 170 cm (left) and 400 cm (right) but response times for identifying the shape were much shorter at the closer distance. The two stereograms had the same angular size and disparity.

for detecting the small discrete steps. Christophers and Rogers (1994) also reported that viewing distance affected the time taken to identify the shape of a random dot surface. Mean latencies increased from 2.4 to 8.1 s when viewing distance increased from 57 cm to 400 cm, even though the visual angle and disparities of the stereogram remained the same.

These results show that the response criterion, the disparity range, the degree of correlation between the stereoscopic images, and the viewing distance all affect response times for seeing complex random-dot surfaces. However, they do not provide any further evidence for the role of eye movements in the perception of complex stereograms. Christophers et al. (1993) used scleral search coils to measure vergence movements to view the tip of the spiral surface and found them to be slower and less complete with a 30 per cent decorrelated stereogram (Figure 36).

Christophers and Rogers (1994) recorded the eye movements of one experienced and one naïve observer and found that vergence changes were slower for the naïve observer with the same stereogram (Figure 37). For both observers and stereograms with

large disparities, the shape of the surface was typically not reported until several seconds after the eyes had made the appropriate vergence movements to the most disparate part of the surface.

This effect was particularly evident with more distant surfaces. Figure 38 shows that at a viewing distance of 400 cm, the subject had converged close to the tip of the 90 arcmin "wedding cake" shape many seconds before the shape was reported. The amplitude and latency of vergence changes were similar for the two viewing distances. In extreme cases, the shape was never reported even though the eyes had converged to bring the disparate dots into the fusional range. Christophers and Rogers (1994) concluded that while subjects require vergence changes to see the shape of surfaces with a large disparity range, the vergence changes did not guarantee that the shape would be seen.

A clearer idea of the role of eye movements in the perception of complex random dot stereograms would be gained by making the vergence system open loop so that the subject's vergence movements have no effect on the disparities in the surface.

Matching corresponding images

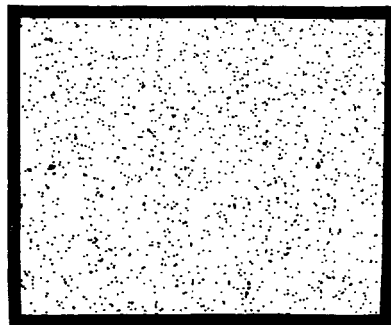
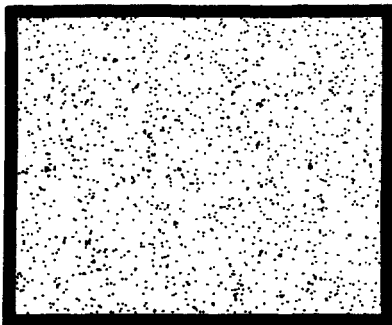
6.1 Tokens for disparity-based stereo	195
6.1.1 Luminance-defined edges and gradients	197
6.1.2 Oriented or nonoriented disparity detectors	200
6.1.3 Boundaries defined by spatial frequency	202
6.1.4 Colour-defined regions	206
6.1.5 Motion-defined regions	209
6.1.6 Stereopsis as a preattentive feature	209
6.2 Matching disparate images	212
6.2.1 Finding corresponding images	212
6.2.2 The unique-matching rule	216
6.2.3 Matching similar features	217
6.2.4 Minimizing unpaired images	219
6.2.5 Matching nearest-neighbour images	220
6.2.6 Matching adjacent images	220
6.2.7 Limiting disparity gradients	221
6.2.8 The relative order of images in the two eyes	222
6.2.9 Matches in disparity and size domains	223
6.2.10 The same-sign rule of luminance polarity	224
6.2.11 The surface smoothness constraint	226
6.2.12 Image matching and edge continuity	228
6.2.13 Stereo integration over vergence changes	229
6.2.14 Epipolar image matches	229
6.2.15 Extraction of relative disparities	229
6.3 Averaging and transparency	230

6.1 TOKENS FOR DISPARITY-BASED STEREO

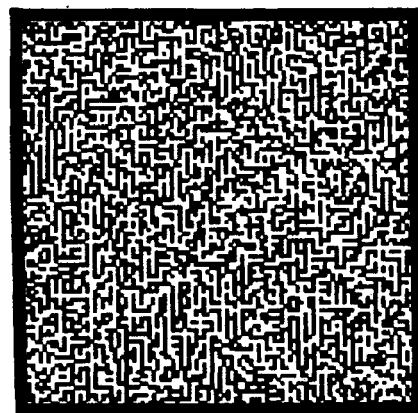
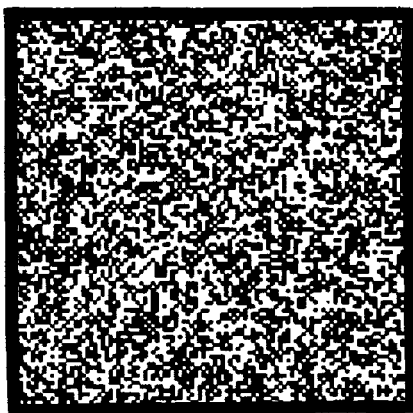
In all stereograms that give rise to an impression of depth based on binocular disparity, the essential disparity is between contours visible in each monocular image. It is often claimed that random-dot stereograms are devoid of such monocular images, but this is not true. The essential disparity in a random-dot stereogram is between the matching black/white dots visible in the monocular image. Depth is seen in a random-dot stereogram even when the pattern of disparities between the dots does not define a cyclopean shape, as in Figure 6.1a. A cyclopean shape not evident in the monocular images emerges only when the disparate dots are arranged in coherent regions that share the same disparity, as in the typical random-dot stereogram. However, the cyclopean shape is defined by the pattern of disparities in the microelements of the stereogram and is therefore not the primary stimulus for the detection of disparity. The cyclopean shape may act as a powerful confirmation that the correct

match has been found between the dichoptic displays. Julesz (1960) coined the term **global stereopsis** for this process. The dot patterns in the typical random-dot stereogram contain large clusters that are recognizably the same in the two eyes. These clusters must help in the binocular matching process. However, the addition of a small proportion of extra dots in one image can camouflage the appearance of similar dot clusters in the two eyes, as in Figure 6.1b. In spite of this, depth is still evident in the stereogram. Recognizable dot clusters are therefore not essential for the matching process, as long as there are sets of matching dots in the two images; that is, an overall correlation at some scale. The dot patterns may be matched in terms of their common low spatial-frequency components when the match between high spatial-frequency components is disrupted by blurring one image, as in Figure 6.1c.

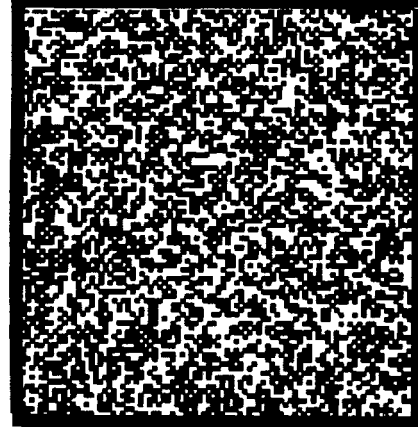
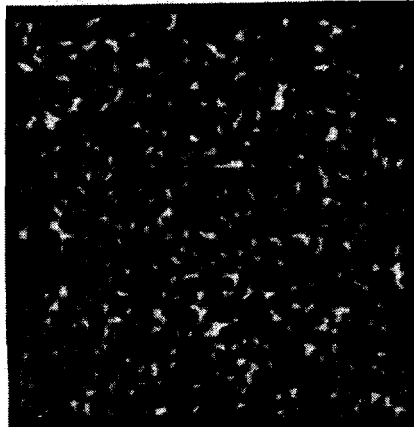
Depth may also be seen in a random-dot stereogram containing a disparity between the boundary of a region of dichoptically uncorrelated dots and a region in which the dots are correlated in position



(a) Depth is seen in a random-dot stereogram when the pattern of disparities between the dots does not define a cyclopean shape. (From Brookes and Stevens 1989. Copyright (1989) by the American Psychological Association. Reprinted by permission.)



(b) A few extra dots are added to the right-eye image so as to camouflage the dot clusters. In spite of this, depth is still evident in the fused stereogram.



(c) Stereopsis survives considerable blurring of one of the images. (From Julesz 1971. Copyright, 1971, by Bell Telephone Laboratories Incorporated.)

Figure 6.1. Properties of random-dot stereograms.

between the two eyes, as in Figure 6.9. But for this to work the two regions must be defined by differential dot density or spatial frequency to create regions visible in each eye. The rule still holds that all stereograms must have disparity-producing edges in

each monocular image—if not at the micropattern level, then at the macropattern level; if not in terms of edges defined by luminance contrast, then in terms of edges defined by motion, colour, or texture; if not at one spatial frequency, then at another. That

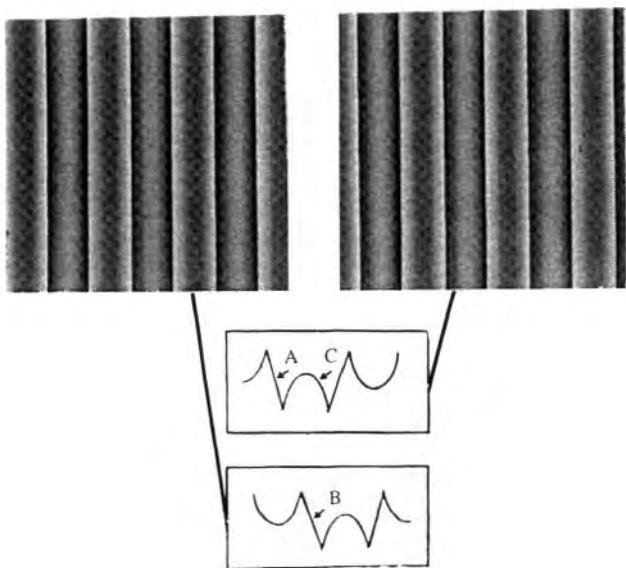


Figure 6.2. Pseudo-squarewave stereogram.

A stereogram composed of a squarewave grating with the fundamental missing. The luminance profiles for each image are shown below, with the luminance zero crossings in the images convoluted with a spatial-frequency channel centred on the 3rd harmonic of the grating indicated by arrows. The peaks of the luminance distributions are phase shifted 90° but the nearest zero crossings are phase shifted less than this. (Adapted from Mayhew and Frisby 1981.)

is not to say that one need be aware of the features that define disparate regions, nor that these features are perceptually analyzed before the stage of disparity detection. Furthermore, evidence reviewed in Section 5.9 suggests that sensations of depth may be elicited by lateral separations between dichoptic images that are too small to be detected when the images are presented to one eye.

The first purpose of this chapter is to define the stimulus tokens used to detect regions differing in binocular disparity. The different types of disparity—that is, point disparity, orientation disparity, and spatial-frequency disparity—are discussed in the next chapter. The second purpose of the present chapter is to describe the rules governing how the visual system combines binocularly disparate elements.

6.1.1 Luminance-defined edges and gradients

Luminance-defined edges

An edge defined by luminance contrast is the most prevalent token for detecting disparity. In the simplest case there are two well-defined objects, and the images of one object have a binocular disparity which differs from the disparity between the images of the other object. In a more complex case, disparity occurs between elements of textured regions, as in

the random-dot stereogram. Images with very different luminance contrast may be fused to yield stereopsis, although it was noted in Section 5.6 that stereoacuity is degraded when the images in the two eyes differ in contrast. It is not surprising that some difference in contrast is tolerated because the stereoscopic images of natural scenes sometimes differ locally in contrast because of the different vantage points of the two eyes. However, the contrast polarity of the images must be the same in the two eyes, as we will see in Section 6.2.10. Furthermore, the orientation of contrast defined edges must be similar in the two eyes (see Section 6.2.3).

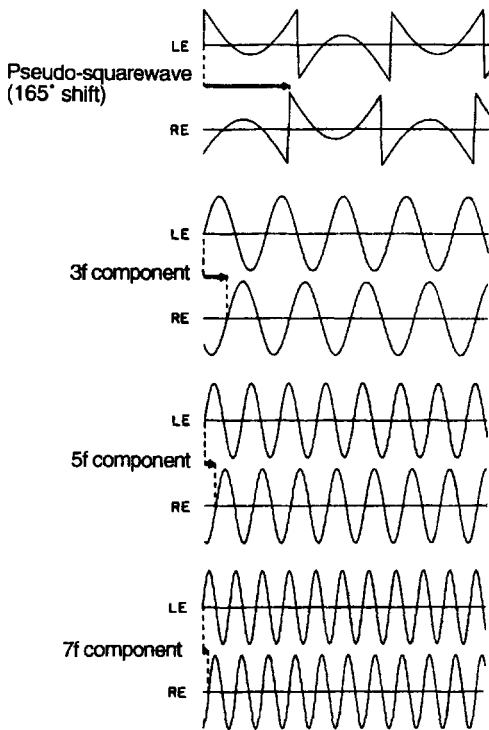
The question remains of what type of local discontinuity in luminance is selected for interocular matching. Marr and Poggio (1979) proposed that binocular matching occurs between regions where the second spatial derivative of luminance is zero, that is, at the inflection point. These regions are known as **luminance zero crossings**, and occur where the luminance gradient is steepest. In the Marr and Poggio model, matching of zero crossings is done separately on each output of four spatial filters, ranging from fine to coarse. This helps to minimize ambiguities in the matching process. Once achieved, matches are stored in a buffer memory, referred to as the $2^{1/2}$ -D sketch. The output of the low spatial-frequency filter is also used to control vergence. Grimson (1981) developed a computer implementation of this model and tested it on a variety of stereograms. Note that zero crossings occur, not at the peaks of luminance, but at the inflection points, in the zone between two different levels of luminance.

Mayhew and Frisby (1981) produced evidence against the view that disparities are derived exclusively from zero crossings. They showed that an impression of depth is evoked by stereograms with no disparity between zero crossings but only between luminance peaks. A matching process that relied only on zero crossings would fail in such a case, and Mayhew and Frisby concluded that the visual system uses peaks in the luminance distribution with the same contrast sign when these are valuable. The stimulus for their experiment was designed as follows. In Fourier terms, a squarewave grating of black and white bars consists of superimposed sinewave gratings of spatial frequencies of f , $3f$, $5f$, and succeeding odd harmonics, with contrasts in inverse proportion to their frequencies. In a pseudo-squarewave, or missing-fundamental grating the fundamental frequency, f , is omitted. Mayhew and Frisby found that the depth evoked by a stereogram consisting of two phase-shifted pseudo-squarewave gratings, as shown in Figure 6.2, corresponded to the

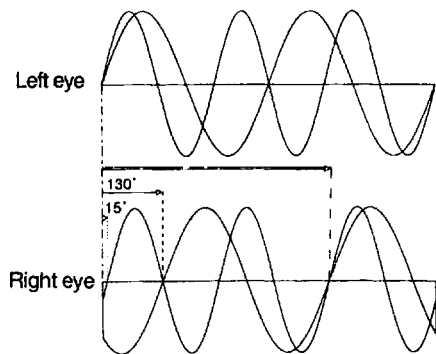
disparity between the clearly defined contrast edges corresponding to the original squarewave grating rather than to the disparity between the nearest-neighbour zero crossings, even though the latter disparity was smaller. This is probably because a match based on edges brings all features of the two images into correspondence whereas a match based on the nearest-neighbour match of zero crossings in the composite luminance profile brings only parts of the displays into correspondence. In addition, the nearest-neighbour match may not have been favoured because the luminance gradients of the nearest-neighbour zero crossings in the stimulus were very different in the two eyes. Boothroyd and Blake (1984) obtained the same result for a pseudo-squarewave grating of 1 c/deg but, as we will now see, they obtained different results with patterns of higher spatial frequency.

Rather than think about disparities between zero-crossings of the composite waveform of a compound grating one can think of the disparities between the component spatial frequencies. The component sine-waves of a pseudo-squarewave grating are shown in Figure 6.3a. Note that the disparity between the nearest neighbour zero-crossings of the composite luminance profile of the grating is approximately the same as that between the 3f components. With a pseudo-squarewave grating based on a 3-c/deg square grating Boothroyd and Blake found that most subjects saw depth corresponding to disparity between the 3f components. This may be because, with a fundamental spatial frequency of 3 c/deg, the luminance gradient of the nearest-neighbour zero crossing (determined by the 3f component) more closely resembles that of the main zero-crossing in the composite luminance profile than is the case with a fundamental spatial frequency of 1 c/deg.

A simpler approach to the question of stereopsis in compound gratings is to use gratings with only two spatial-frequency components, and variable phase and contrast. Boothroyd and Blake found that when each image consisted of a 3-c/deg sine wave grating plus a 9-c/deg grating the perceived depth corresponded to the disparity between the 3-c/deg components. Note that with this display both components are brought into register only when the 3-c/deg components are matched. Thus, with equal contrasts, a match was preferred that brought both components into register rather than one based on the 9-c/deg component, which provided a nearest-neighbour match. When the contrast of the 3-c/deg images was reduced, perceived depth changed to that corresponding to disparity between the 9-c/deg images, even though the contrast of the 3-c/deg images was still sufficient to evoke depth when they



(a) Disparities between the component spatial frequencies of a squarewave grating with missing fundamental and a 165° phase shift between the two eyes.

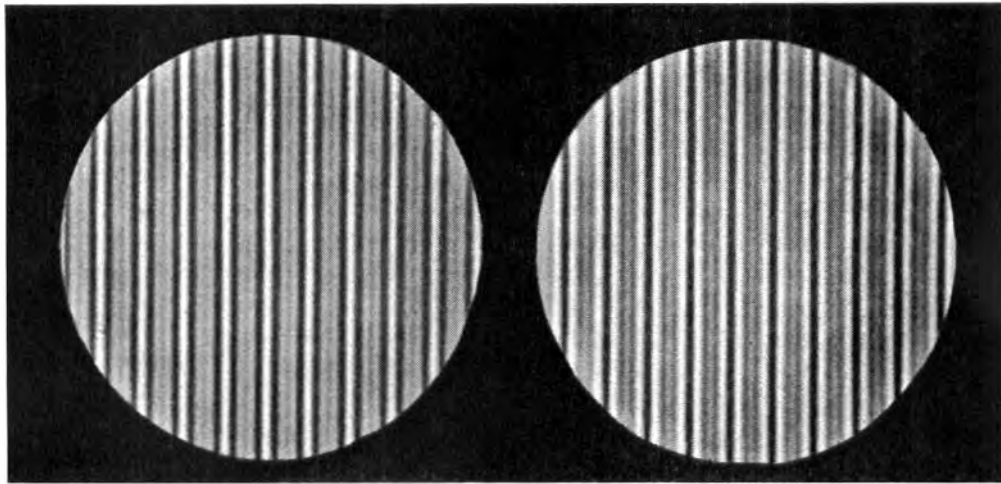


(b) A 6-c/deg grating and a 9-c/deg grating are presented to each eye with a 130° interocular phase shift. The binocular images can be matched to bring either of the sine-wave components into correspondence or to bring both into correspondence, as indicated by the arrows. (Reproduced with permission from Boothroyd and Blake 1984, Vision Research, Pergamon Press.)

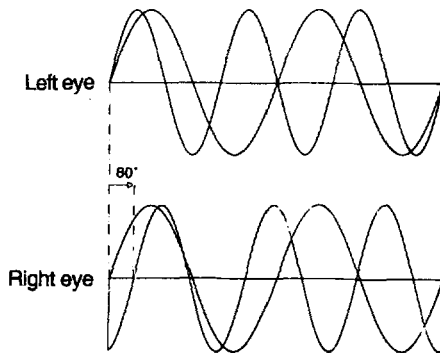
Figure 6.3. Types of phase-shifted disparity.

alone were present. In this case the nearest-neighbour match of the higher contrast components won out over the best overall pattern match.

When the component gratings are multiples of each other (harmonics), as in a 3-c/deg plus 9-c/deg grating, matching the lower component necessarily



(a) A stereogram composed of two sine-wave gratings of different spatial frequency in each eye, with the two gratings in one eye shifted by different amounts. Subjects report seeing two distinct depth planes. The disparities defining the two depth planes are formed from the high-contrast and low-contrast lines of the moiré patterns formed in each eye.



(b) The luminance profiles of the gratings in the stereogram. The components in one eye are shifted by different amounts with respect to those in the other eye, so they cannot be brought into binocular correspondence simultaneously. (Reproduced with permission from Boothroyd and Blake 1984, Vision Research, Pergamon Press.)

Figure 6.4. Stereogram with components shifted by different amounts in each eye.

brings all other components into register. With a 6-c/deg plus 9-c/deg grating this is no longer true, and subjects have three matching options, as can be seen in Figure 6.3b. When the contrasts of the component gratings were the same, perceived depth corresponded to the disparity in the compound grating, that is, to a disparity giving the best overall pattern match between the two images. Depth corresponding to the disparity between the component gratings was perceived only when the contrast of one or other of the components was reduced.

In the cases mentioned so far, all spatial-frequency components were shifted together, so that there was a way to match all components simultaneously. In the stereogram shown in Figure 6.4a the component gratings are shifted by different amounts

so that they cannot be simultaneously matched in the two eyes, as illustrated in Figure 6.4b. The pattern in each eye is a moiré pattern with high and low contrast bars in different locations in the two eyes, as in Figure 6.4a. The periodicity of these bars is not the same as that of either frequency component of the display. Boothroyd and Blake's subjects saw two depth planes, one produced by disparity between the high-contrast bars in the moiré pattern and the other by disparity between the low-contrast bars. Percepts associated with the disparities between the component spatial frequencies were not evident.

Luminance-defined gradients

Depth can be perceived in stereograms in which disparity is between smoothly graded changes in

luminance rather than between well-defined edges. Mallot (1993) devised stereograms consisting of elliptical patches with the three luminance profiles shown in Figure 6.5. The first luminance profile was an asymmetrical parabola which lacked zero crossings because the second derivative of a parabola is constant. However, there was disparity between the peaks of the two asymmetrical luminance distributions, as shown in Figure 6.5a. The second luminance profile was described as an asymmetric cubic profile. It also lacked zero crossings but in this case the peaks of the two asymmetrical functions in the two eyes were set at zero disparity. Thus, the only disparity was that between the local luminance gradients of the images in the two eyes, which can be thought of as a disparity between the centroids of the two images. The third luminance profile was derived from an asymmetrical hyperbola. In the binocular images there were no disparities of zero crossings, of peak luminance, or of centroids. Mallot described the disparity in terms of the mean square difference in intensity. In a control condition, the luminance gradients were identical in the two eyes. In a forced-choice procedure, subjects judged whether two stereograms were the same or different. They also described the kind of difference they perceived. In a second procedure subjects indicated which of two stereograms appeared nearer. Apart from an overall difference in depth, the stereograms appeared curved in depth, but this effect was due to shading rather than to disparity. Although discrimination from the comparison stimulus was easiest with the parabolic luminance profile, subjects reported depth in all three types of stereograms. It seems that stereopsis can be based on disparities between luminance peaks and centroids and between mean square differences of luminance.

Other stereoscopic effects produced by luminance gradients are described in Section 7.8.4.

Summary

It seems that binocular matches that optimize the overall pattern match between the images are preferred, whether these pattern matches are based on zero crossings or on luminance peaks. Matches between component spatial frequencies are used only when these are the most prominent features. When an overall match between the images is not possible, matches between subpatterns are often used to generate an impression of multiple depth planes or depth corrugations. Stereopsis can also be based on disparities between low spatial-frequency peaks of luminance distributions, luminance centroids and other derivatives of luminance gradients.

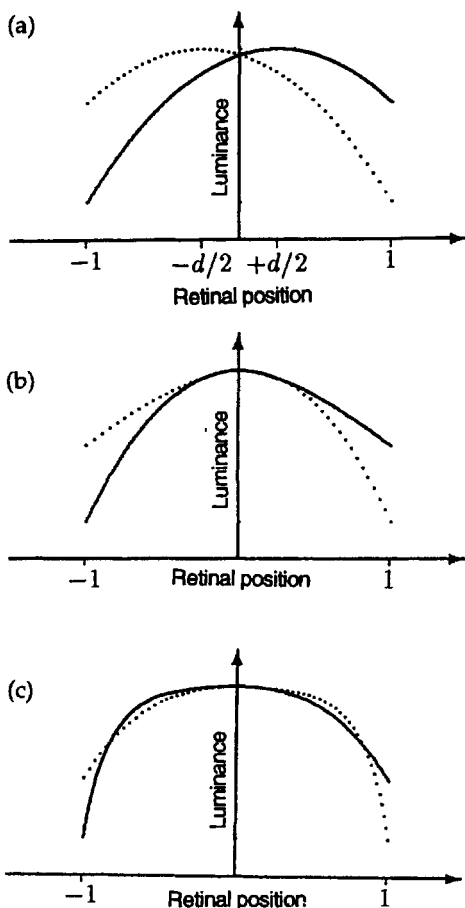


Figure 6.5. Luminance intensity profiles for stereograms.

The solid line represents the luminance profile for a circular patch presented to one eye and the dotted line represents the profile for a patch presented to the other eye.

(a) Parabolic profiles with no zero crossings but with a disparity between the peaks of the distributions.

(b) Profiles with no zero crossings, and no disparity between peaks. There is disparity between the centroids of the distributions.

(c) Profiles with no zero crossings, no disparity between peaks, and no disparity between centroids, which are balanced by the addition of an additional cubic term to the distribution. There is disparity between the mean square difference in the luminance distributions. (Adapted from Mallot 1994.)

6.1.2 Oriented or nonoriented disparity detectors

Stereopsis with orthogonally oriented features

It has been claimed that depth can be seen in a stereogram in which the only horizontal disparity is between regions in which lines in one eye are orthogonal to those in the other eye, as in Figure 6.6 (Ramachandran et al. 1973a; Kaufman 1974, p. 306). However, such displays have potential artifacts. In the figure used by Kaufman the lines in the centre squares were thicker than those in the surround, so there was a difference in space-average luminance.

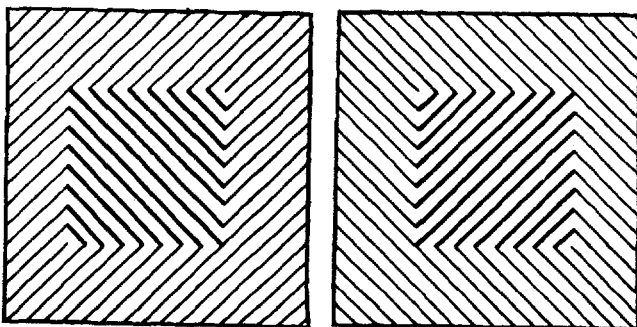


Figure 6.6. Stereogram with orthogonal lines. The impression of depth is unstable and could be due to nonrivalrous features of the display along the boundary between rivalrous regions. (From Kaufman 1974, p. 306.)

O'Shea (1989) did not obtain stereopsis when he eliminated this artifact and the effects of vergence. In the displays used by Kaufman and by Ramachandran, the ends of the lines of the inner squares abutted those of the surround to create a series of v-shapes, as in Figure 6.6. The tips of these v-shapes could serve as nonrivalrous stimuli. Furthermore, the region in which the v-shapes are formed does not have the same space-average luminance as the rest of the display. It would be unwise to draw strong conclusions from this type of display.

Mitchell and O'Hagen (1972) found that setting the lines in the left-eye image of a random-line stereogram at right angles to the lines in the right-eye image did not affect the stereo threshold if the lines were less than 3 arcmin long, but the threshold rose rapidly as the lines became longer. It seems that disparity between boundaries of regions containing oppositely oriented lines does not serve as a reliable cue to depth unless the lines are very short. Further discussion of this issue is provided in Section 6.2.3.

Orientation specificity of stereopsis

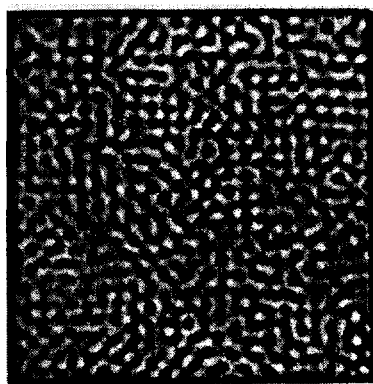
One approach to the question of orientation specificity of matches in stereopsis is to investigate the orientation specificity of stereoscopic aftereffects. Julesz (1971, p. 92) reported that a depth-contrast effect (see Section 12.1) produced by inspecting of a random-line stereogram with the lines in a particular orientation was not specific to the orientation of the line elements in the test stimulus. Mansfield and Parker (1993) pointed out that the terminations of the line elements in a random-line stereograms contain a broad band of contrast energy at all orientations and are therefore not appropriate for investigating orientation specificity.

A second approach to the question of orientation selectivity in stereopsis is to measure the effects of adding noise, consisting of line elements with

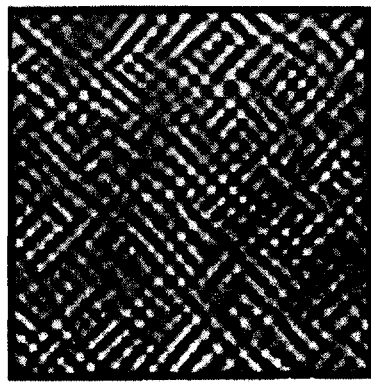
specified orientation, to a random-line stereogram. One might expect the degree of masking to be greatest when the orientation of the noise lines is similar to that of the disparity-defining lines. Mayhew and Frisby (1978) created a type of random-line stereogram by passing random-dot patterns through oriented Gaussian filters, as in Figure 6.7a. Masking noise consisting of line elements with the same orientation as that of the disparity-defining lines was added to one eye. When the signal-to-noise ratio was 1:1, as in Figure 6.7b, stereopsis was degraded but not eliminated. With a signal-to-noise ratio of 1:1.4, as in Figure 6.7c, stereopsis was eliminated. Subjects reported that the quality of stereopsis was the same when the noise elements were set an angle of 45° to the disparity-defining elements of the stereogram as when they had the same orientation. It was concluded that the masking of stereopsis by noise is not orientation specific.

From the preceding experiment, Mayhew and Frisby also drew the general conclusion that human disparity coding, at least for random-line stereograms, uses nonoriented visual channels. This is at variance with physiological evidence that most binocular cells are orientation selective with similar orientation tuning in the two eyes (see Section 4.4). Mayhew and Frisby's conclusion was challenged by Parker et al. (1991), who found that the effectiveness of masking noise, as indicated by a forced-choice depth-discrimination task, was clearly reduced as the angle between noise elements and the elements of a line stereogram was increased from 0° to 90° (see Frisby and Pollard 1991). Part of the masking was independent of the orientation of the mask and this isotropic component was more evident with low than with high spatial-frequency elements (Mansfield and Parker 1993).

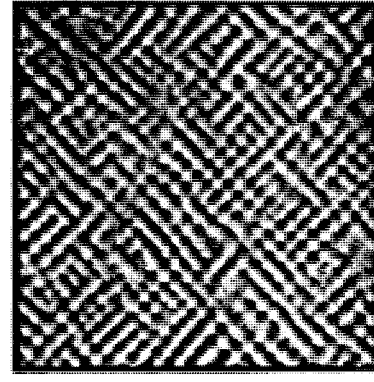
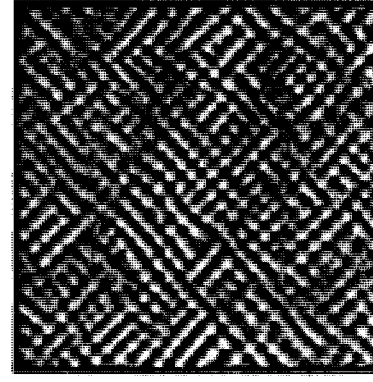
Mayhew and Frisby (1979b) supported their conclusion that disparity coding does not involve oriented detectors by pointing out that an orientation-tuned system would have difficulty detecting closely packed horizontal depth corrugations in a random-dot stereogram because the receptive fields suitable for detecting orientation would extend across several depth modulations. They supported this argument by showing that horizontal depth corrugations cannot be detected in random-line stereograms containing line elements within 45° of the vertical. This is not a conclusive argument because horizontal depth corrugations could be coded by horizontally oriented detectors. It was mentioned in Section 4.4 that horizontal disparity may be coded by end-stopped binocular cells tuned to horizontal lines. Mayhew and Frisby found that depth corrugations were visible in stereograms in which line elements



(a) A random-line stereogram formed by passing random-dot patterns through oriented Gaussian filters.



(b) The same stereogram with added uncorrelated lines with the same orientation as the lines defining the disparity, to give a signal-to-noise ratio of 1:1. Stereopsis is degraded but not eliminated.



(c) Stereogram with signal-to-noise ratio of 1:1.4. Stereopsis is eliminated. (From Mayhew and Frisby 1978. Perception, 7, 431-436, Pion, London.)

Figure 6.7. Effect of uncorrelated noise on stereopsis.

were oriented along the corrugations, but not as well as with a random-dot stereogram. They interpreted this difference as supporting their theory.

On balance, the physiological and psychophysical evidence suggests that detectors tuned to orientation are involved in disparity coding. They are certainly involved in the image-matching process, because similarly oriented lines fuse and orthogonal lines rival (see Section 6.2.3). Furthermore, disparity

between oriented visual features may serve to define disparity in its own right. This issue is discussed in Chapter 7.

6.1.3 Boundaries defined by spatial frequency

The texture of a homogeneously patterned surface may be defined in terms of the shapes, orientations, sizes, or spacing of the texture elements.

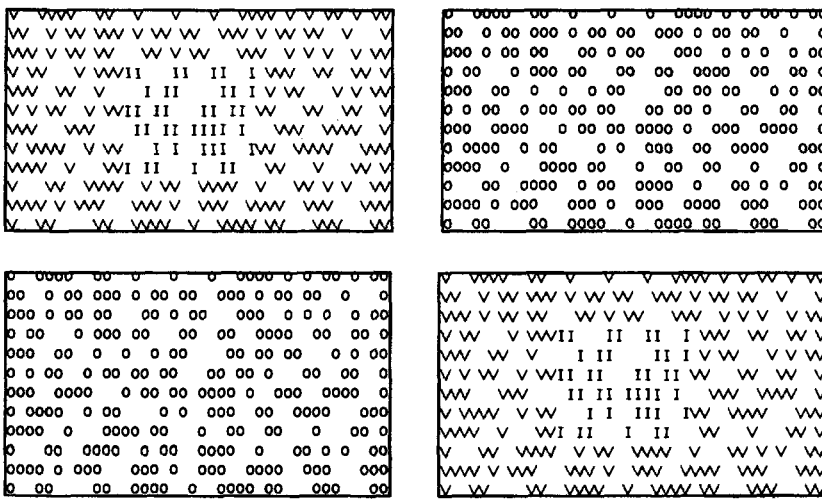


Figure 6.8. Stereogram formed from letters that differ in the two eyes.

The letters in the two eyes differ but the letter spacings are the same. The central region of I's in the left image are laterally offset relative to a similarly spaced region of o's in the right image. An impression of depth is produced in spite of the dissimilarity of the letters. (From Kaufman and Pitblado 1965.)

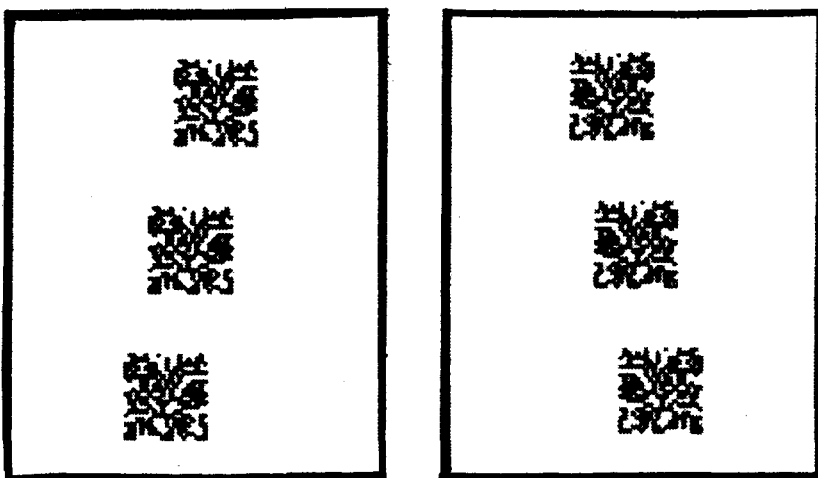
The boundaries of differently textured regions can define disparity change and create an impression of a step in depth as long as the texture is the same for each region, in the two eyes. In this section we are concerned with what happens when the position and mean size of texture elements in one or other region of a stereogram are not the same in the two eyes. The question of whether differences in size or spatial frequency may define disparity is discussed in Chapter 7.

Figure 6.7a demonstrates that depth is created in a random-dot stereogram in which the dot clusters are dissimilar in the two eyes. The stereogram in Figure 6.8 demonstrates that depth may also be created in a stereogram in which the disparity is carried by the boundaries between textured regions, even though the texture elements defining each region are dissimilar in the two eyes. The clustering of the letters is the same in the two images except that the boundary between the central region in one image is displaced with respect to the central region in the other image. The disparity is therefore defined in terms of the boundary between element clusters, which constitute a low spatial-frequency texture feature, rather than by the elements, which constitute a high spatial-frequency texture feature.

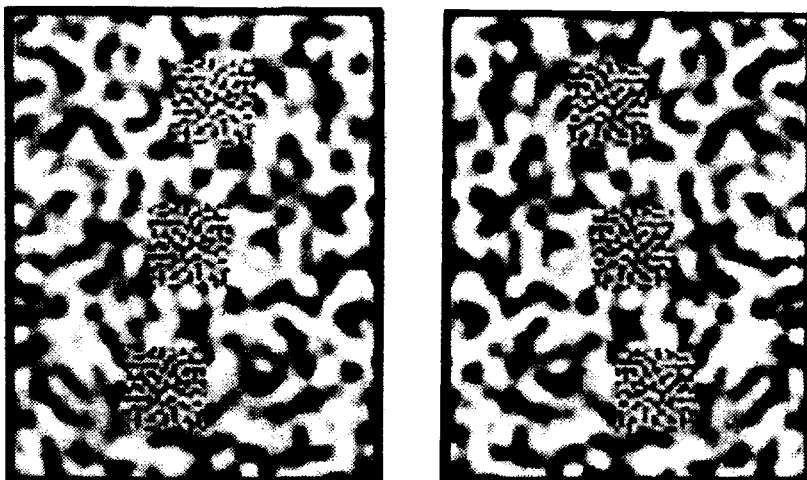
Mayhew and Frisby (1976) devised the random-dot stereograms shown in Figure 6.9. Figure 6.9a produces good stereopsis in spite of the mismatch of the high spatial-frequency elements within the squares. Mayhew and Frisby concluded that stereopsis is processed by a visual channel tuned to the boundaries of the squares, in the presence of pattern mismatches in the high-frequency channel tuned to the contents of the squares. Note that the spatial-

frequency content of the boundaries of the squares is not well defined. Stereopsis is also possible with the stereogram in Figure 6.9b which has texture rivalry in the background as well as within the squares. However, this works only when the spatial frequency of the texture in the background differs from that of the texture in the squares. In other words, the boundaries of the squares must be clearly visible in the monocular images. In a later paper, Mayhew et al. (1977) devised an algorithm capable of searching within rivalrous textured regions for a subset of points possessing point-for-point correspondences sufficient for the computation of disparity.

Ramachandran et al. (1973a) and Frisby and Mayhew (1978b) devised the stereograms shown in Figure 6.10. Figure 6.10a is a random-element stereogram with corresponding figure regions containing elements with a spatial frequency of 2.5 c/deg, which match in position, and corresponding surround regions containing elements with a spatial frequency of 10 c/deg, which also match in position. This produces good stereopsis for both crossed and uncrossed disparities. In Figure 6.10b, the spatial frequencies of corresponding regions match but the positions of elements do not. This produces an impression of depth but only for crossed disparities. This asymmetry would be explained if the impression of depth was due to a figure-on-ground effect, which causes a figure (the square) to appear in front of a background, rather than by disparity. In Figure 6.10c, corresponding regions differ in both spatial frequency and position of elements. This does not produce stereopsis, presumably because the spatial frequencies in the corresponding regions of each stereograms are very different.



(a) A random-dot stereogram in which the texture within the disparate squares is uncorrelated in the two eyes. Depth is easily perceived.



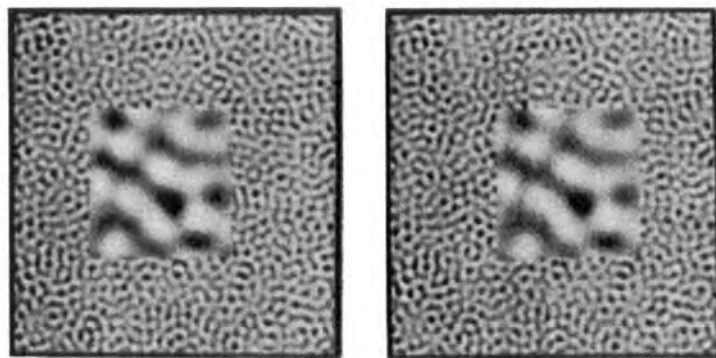
(b) A stereogram in which texture elements are uncorrelated in both the disparate squares and the background. Depth is perceived but only if, as in this case, the boundaries of the disparate regions are clearly visible in each eye. (From Mayhew and Frisby 1976. Reprinted by permission of Nature, 264, 53-56. Copyright, 1976. Macmillan Magazines Limited.)

Figure 6.9. Effects of uncorrelated texture on stereopsis.

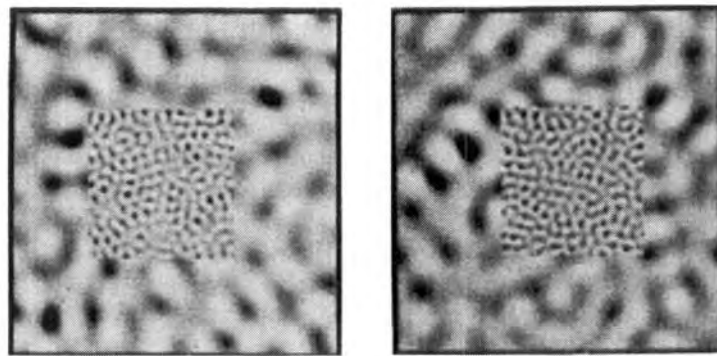
Rivalrous stereograms produce a variety of paradoxical depth effects, which defy simple analysis. For instance, depth sensations can be produced by the stereogram shown in Figure 6.11a, containing a figure region that occurs in only one eye (see also Ninio and Mizraji 1985). Depth in this case is not due to disparity but probably arises because a high spatial-frequency region tends to appear as a figure in front of a low spatial-frequency background. In a related effect (Figure 6.11b) a high-contrast patch appears nearer than a low-contrast patch when presented on the same background (O'Shea et al. 1994c).

Summary

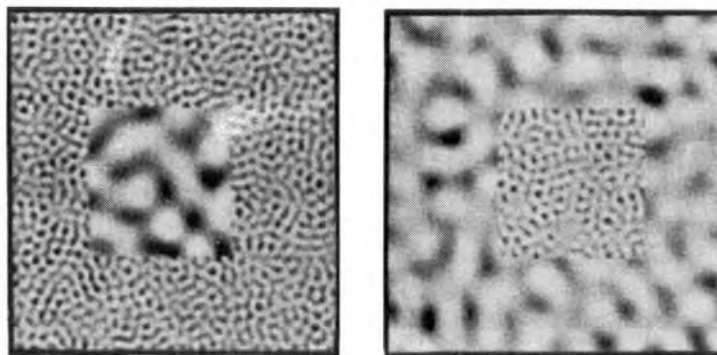
Stereopsis is best when corresponding regions of stereograms have matching pattern elements, as in a regular random-dot stereogram. In that case the texture characteristics of the disparate figure can be made the same as those of the zero-disparity background because stereopsis is based on point-for-point matching of microelements of the display and not on the boundaries of regions defined by differences in the size, density or shape of elements. If the micropattern elements do not match in the two eyes, stereopsis is still possible and is based on the



(a) A stereogram with inner regions containing matching elements with a spatial frequency of 2.5 c/deg, and surround regions containing matching elements with a spatial frequency of 10 c/deg. Viewing at 20 times picture height creates good depth.



(b) In this stereogram the spatial frequencies of corresponding regions match, but the positions of elements do not. This produces stereopsis, but only for crossed disparities. Stereopsis may be due to intrusion of a monocular figure-ground effect.

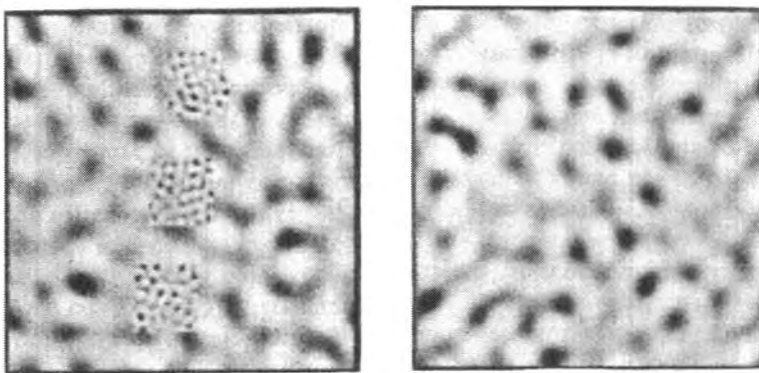


(c) In this stereogram both the inner and outer regions differ in spatial frequency. This does not support stereopsis. (From Frisby and Mayhew 1978b. Perception, 7, 661-678. Pion, London.)

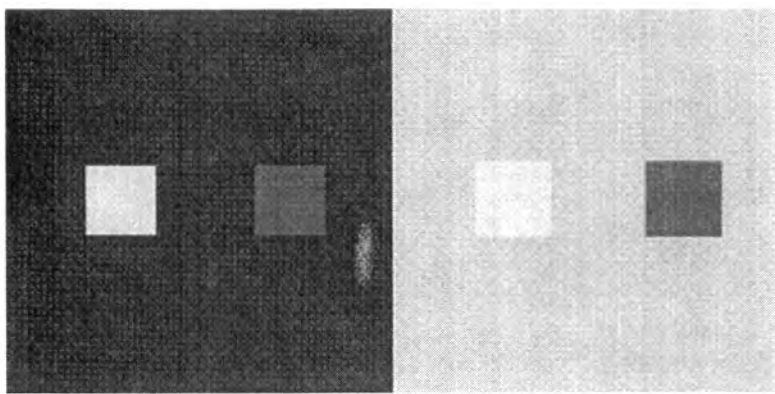
Figure 6.10. Disparities in position and spatial-frequency.

disparity between the boundaries of the discriminably different regions of the stereogram. But for this to work, these boundaries must be visible in each eye. Differences of spatial frequency (size and density of elements) can serve to make these boundaries visible. However, spatial-frequency

differences are useful only if (a) the corresponding regions in the two eyes are not too dissimilar in spatial frequency and (b) the parts of the stereogram within each eye have sufficiently distinct spatial frequencies. Put more simply, regions segregated in each eye on the basis of spatial frequency form



(a) An impression of depth is created by fusing these two images, even though the figure region occurs in only one eye and there is no disparity. The depth impression is probably due to a monocular figure-ground effect. (From Frisby and Mayhew 1978b. *Perception*, 7, 661-678, Pion, London.)



(b) In each display the high-contrast square appears nearer than the low-contrast square, even though the two squares on the left have the same luminance as the two on the right. (Adapted from O'Shea et al. 1994c.)

Figure 6.11. Depth from differences in spatial frequency and contrast.

the basis for disparity detection if the spatial frequency of corresponding regions are similar in the two eyes. Spatial frequency may not be the only texture feature that can form the basis for the perceptual segregation of regions in stereograms lacking point-for-point correspondence in the microelements that make up a pattern.

6.1.4 Colour-defined regions

The visual system has a set of chromatic channels designed to detect colour differences in the absence of luminance gradients, and achromatic channels designed to detect differences in luminance independently of colour. Several investigators have enquired whether disparity-based stereopsis is confined to the achromatic channels. The procedure has been to see whether depth is perceived in isoluminant stereograms, that is, stereograms with regions

differing in hue but not in luminance. A second question is whether colour, in the presence of luminance contrast, helps the image matching process.

Two differently coloured patches are isoluminant when they excite the luminance channel of the visual system to the same degree. There are two main criteria for deciding when two patches differing in hue are isoluminant: the point of minimum perceived flicker when the two patches are rapidly alternated, and the point where the border between two abutting patches is minimally distinct (Kaiser 1971). Even after two patches have been set to equiluminance by one of these criteria, luminance fringes may be introduced by chromatic aberrations in the optical components of the eye or apparatus. Rapid alternation of a display on a colour monitor may produce luminance fringes because of the differential rise time of phosphors. Another problem is that an isoluminant match under static conditions will not hold when the

display is moved, because the different colour channels have different dynamics. Eye movements may be sufficient to upset an isoluminant match. Equiluminance is also not the same for different regions of the retina. A final problem is that chromatic and achromatic borders cannot be compared unless their effective contrasts are equated, and we will see that there is no simple way to do this.

Lu and Fender (1972) presented random-dot stereograms with the dots in one colour and the background in another colour. There were 100 dots in the display, each subtending 0.1°. Various colour combinations were tried but in no case was depth reported when the dots and background differed in colour but not in luminance (see also Gregory 1979).

Comerford (1974) used the minimally distinct border criterion to equate the luminance of a red, green, or blue wheel-shaped object relative to that of a white or green background. The disparity of the object relative to the surrounding aperture was set at either 7 or 30 arcmin. The percentage of correct judgments of depth was better for the red-green stimulus than for the other colour combinations. However, performance was not reduced at the isoluminant point except for the red-on-white stimulus. The disparity in these displays was between low spatial-frequency patterns, namely, the disc and the surrounding aperture. Since the chromatic system operates most effectively at low spatial frequencies, the chromatic signal would be stronger in this stimulus than in the high spatial-frequency display used by Lu and Fender. This could account for the discrepant results. Comerford recorded percentage of correct scores for fixed disparities, not stereoscopic acuity. Therefore, he did not prove that stereoscopic acuity is as high under isoluminant conditions as under luminance-contrast conditions.

De Weert (1979) used a random-dot stereogram with the dots and background in various colour combinations. For all colour pairs the impression of depth disappeared in the neighbourhood of the isoluminant point defined by minimum perceived contrast, although not at the isoluminant point defined by minimum flicker. In a stereogram consisting of two large bars, depth was perceived for all values of relative luminance. However, this comparison was biased in favour of the bar stereogram since it had a disparity of 33 arcmin compared with a disparity of only 13 arcmin in the random-dot stereogram. In a later study, de Weert and Sadza (1983) reported that subjects could correctly identify the depth in both an isoluminant random-dot stereogram and an isoluminant stereogram consisting of a large monocularly defined shape when the disparity in both stereograms was +3.6 arcmin. Subjects rated the

sensation of depth to be very poor in both stereograms at isoluminance. There may be problems here. Both stereograms subtended only about 3° and were surrounded by a high-contrast border. Subjects may have responded to the disparity in the border created by changing convergence on the elements of the stereogram. They had ample opportunity to learn to do this since they were given 500 forced-choice presentations, each followed by a signal indicating whether the response was correct. Furthermore, the effects of luminance artifacts in the video display and of chromatic aberration were not assessed.

Monkeys were found capable of detecting depth in random-dot stereograms at isoluminance, but with a much reduced level of success. Recordings from microelectrodes showed that magnocellular cells in the LGN retained some response to isoluminant stimuli (Logothetis et al. 1990).

The following factors should be taken into account when comparing isoluminant stimuli with stimuli defined by luminance.

Relative efficiency of luminance and chromatic detectors
Because of the overlap in the spectral sensitivities of the red and green cones, the information available at the level of the receptors is reduced when an edge defined by luminance is replaced by one defined by colour. Scharff and Geisler (1992) used an ideal-observer analysis of the photoreceptor mosaic to calculate the equivalent contrasts of colour-defined and luminance-defined edges. They measured stereo discrimination for six subjects with an isoluminant red-green random-dot stereogram blurred to reduce the effects of chromatic aberration. Only three of the six subjects could fuse the stereogram. For the other three subjects, depth discrimination was worst at the point of isoluminance. However, these subjects used the information in the isoluminant display as efficiently as the equivalent contrast of the display would allow. Jordan et al. (1990) found that subjects used chromatic cues more efficiently than luminance cues in finding the correct match between the images of an ambiguous stereogram. Simmons and Kingdom (1994) found that disparity tuning for luminance and chromatic visual systems are similar, although chromatic stimuli require somewhat higher contrast relative to the detection threshold.

Relative density of cone types

The second factor to be taken into account when comparing chromatic and achromatic stimuli is the relative spacing of different types of cone. The blue cones are virtually absent in the central fovea and much less dense than red or green cones, in the rest of the retina. In the baboon, at eccentricities over 5°,

13 per cent of receptors are blue cones, 33 per cent are red cones, and 54 per cent are green cones (Marc and Sperling 1977). Blue cones also have larger receptive fields and poorer contrast sensitivity than red and green cones, and these factors could also contribute to the low stereoacuity in the blue system. It is not surprising that stereoacuity for isoluminant blue-on-yellow random-dot stereograms was 43 arcsec, about one-ninth of acuity for stimuli defined by luminance (Grinberg and Williams 1985).

Another factor that may be related to receptor density is the instability of gaze observed when a person attempts to fixate an isoluminant pattern (Tyler and Cavanagh 1991).

Temporal properties of luminance and chromatic systems
A third factor in comparing chromatic and achromatic stimuli is the relative sensitivity of chromatic and luminance channels to transient stimuli. The chromatic channel of the parvocellular system is relatively insensitive to transient stimuli and should therefore be most sensitive to depth oscillations at low temporal frequencies. The luminance channel, and especially the magnocellular channel, are sensitive to transient stimuli and are most sensitive to oscillations in depth at higher frequencies.

Tyler and Cavanagh (1991) investigated this question by measuring the amplitude of disparity modulation required for detecting depth in a red-green grating as a function of the temporal frequency of depth modulation. Figure 6.12 shows that with a grating of 10 per cent contrast the stereo threshold was lowest at a temporal frequency of about 3 Hz, and showed a steep increase below this frequency. With an isoluminant grating, the lowest threshold was at about 1 Hz and showed no significant increase at lower frequencies. Below 1 Hz, the depth threshold for the isoluminant grating was the same or less than for the luminance grating.

With luminance-defined stimuli, the threshold for monocularly viewed motion is lower than that for motion-in-depth defined by disparity. This is stereomovement suppression (see Section 5.10.4). Tyler and Cavanagh (1991) found that, with isoluminant red-green gratings, the threshold for oscillations of spatial phase was the same when the gratings were viewed by the same eye or viewed dichoptically to produce oscillation in depth. Thus, stereomovement suppression was not present in isoluminant gratings. They concluded that stereomovement is processed separately in luminance and chromatic channels.

Effects of chromatic and achromatic noise

Stuart et al. (1992) argued that if chromatic contours are not used in stereopsis, then stereopsis should not

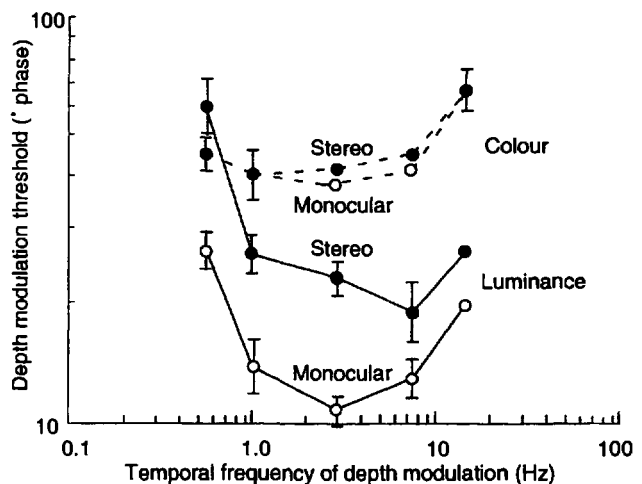


Figure 6.12. Chromatic and achromatic depth-modulation acuity. The curves with filled symbols show the amplitude of disparity modulation required for detection of depth in a red-green chromatic grating (upper curves) and a luminance grating (lower curves) as a function of temporal frequency of depth modulation. At higher temporal frequencies the luminance channel is more sensitive to depth modulations than is the chromatic channel. The curves with unfilled symbols show the threshold for monocular oscillatory motion in the chromatic (upper curve) and luminance channels (lower curve), as a function of temporal frequency. In the chromatic channel, the function for depth modulation is similar to that for oscillatory monocular motion. However, the depth modulation thresholds in the luminance channel are higher than those for monocular motion, an effect dubbed stereomovement suppression. (Adapted from Tyler and Cavanagh 1991.)

be disturbed by the addition of chromatic noise to a random-dot stereogram. They measured the time taken to discriminate two depth planes in a random-dot stereogram as a function of the percentage of added noise. They added luminance noise, chromatic noise, or both, with the effective contrast of the luminance and chromatic elements equated by the procedure used by Scharff and Geisler, mentioned earlier. At low levels of contrast (14.6 per cent) the addition of more than 20 per cent of chromatic noise increased the time taken to complete the task or made it impossible to see depth. On the other hand, subjects could discriminate depth when 50 per cent of the dots were mismatched in luminance and the only correlated dots were defined by colour. At luminance contrasts of 28 and 37 per cent, but with the effective chromatic contrast remaining at 14.6 per cent, the addition of chromatic noise had very little effect, and only a small percentage of luminance noise was tolerated. The researchers argued that this decline in the contribution of colour to stereopsis at high levels of luminance contrast is to be expected if both colour and luminance are processed within a "double duty" system, such as the parvocellular system, rather than by two independent systems.

Isoluminant stimuli do not reveal the full contribution of colour to visual performance. Gur and Akri (1992) showed that contrast sensitivity is enhanced when colour contrast is added to a grating defined by luminance contrast. They explained this in terms of the contribution of cells that respond to both the chromatic and luminance components of the stimuli.

Summary

We are presented with three interpretations of the presence of some stereopsis at isoluminance. Either the chromatic component of the parvocellular system is capable of some processing of disparity, or the magnocellular system is capable of responding weakly to isoluminant stimuli, or both possibilities may be true. In any case, we cannot assume that the parvo- and magnocellular systems are totally segregated and cannot draw firm conclusions about the site of disparity processing from stereo performance at isoluminance. Chromatic contrast may enhance the impression of depth induced by luminance contrast, so that isoluminant stimuli do not reveal the full contribution of the chromatic component. Isoluminance degrades stereoscopic vision, and the loss seems to be greater for disparities defined by small elements than for those defined by large elements. Stereoscopic acuity has usually not been measured with isoluminant displays, so little is known about the magnitude of the loss. The loss may be no more than one would predict from the loss in monocular resolution at isoluminance for the same type of pattern, because of the lower contrast sensitivity and the wider spacing of receptors. Artifacts such as chromatic aberration and the presence of luminance-contrast borders may have contributed to the depth sensations reported in isoluminant displays. There has been no systematic attempt to determine whether the loss in stereopsis at isoluminance is relatively greater for small than for large disparities. One cannot conclude from the weakness of stereopsis at isoluminance that stereopsis is confined to the magnocellular system.

Other aspects of colour and stereopsis are discussed in Sections 4.8, 5.6, and 8.2.

6.1.5 Motion-defined regions

The question addressed in this section is whether an impression of depth can be generated by disparate regions defined only by motion. Julesz (1971, p. 83) used a display in which each eye saw columns of short vertical lines with the lines moving in opposite horizontal directions in alternate columns. The motion of each line in one eye was out of phase with the

motion of the corresponding line in the other eye. This eliminated positional disparities from the stereogram. One square region of the display in one eye was horizontally shifted to produce a disparity. The motion in the two eyes was correlated in the shifted region, and uncorrelated in the surround region. The square was not seen in depth. It was concluded that motion is not a token for disparity-based stereopsis, and that motion is processed after disparity. However, Julesz was careful to point out that a negative result is not conclusive. Note that the motion signals had the same magnitude and direction in the two regions of the stereogram. Presumably, the visual system failed to detect the dichoptic correlation of the motion signals in the disparate region of the stereogram and hence failed to detect the disparity.

Halpern (1991) devised a stereogram with disparity between forms defined by motion alone. The two eyes were presented with a different display of random dots. In each display a central square of dots moved from side to side through 20 arcmin with respect to the surrounding dots, with deletion of dots along the leading edge of the square and accretion of dots along the trailing edge. The squares in the two eyes moved out of phase by amounts that generated 1, 3, or 5 arcmin of disparity. Subjects correctly identified depth produced by crossed and uncrossed disparities. However, settings with a depth probe revealed that, even with the largest disparity, very little depth was perceived for uncrossed disparities in the square. Halpern suggested that the cue of accretion and deletion of dots at the edges of the square served as a monocular cue that the square was in front of the background, and this detracted from the impression of depth created by uncrossed disparities. This conclusion was supported by a further experiment in which a cyclopean moving square was created by combining dynamic random-dot displays so that the factor of accretion and deletion of dots was removed. In this case, both crossed and uncrossed disparities produced impressions of depth commensurate with the imposed disparity. In these experiments, the motion signals in the two regions of the stereogram were different. The visual system had simply to detect this difference to detect the disparity in the moving region. The fact that it did so suggests that motion can be a token for disparity-based stereopsis.

6.1.6 Stereopsis as a preattentive feature

In pattern vision a distinction is drawn between preattentive features that are processed in parallel and immediately "pop out" in mixed displays and features that are identified only after a serial search

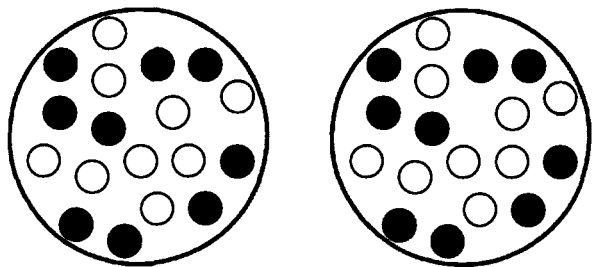
(Beck 1967, 1972). When the time taken to find an odd object is independent of the number of surrounding objects the defining feature is said to be preattentive. For instance, the time taken to find a vertical line set among horizontal lines is independent of the number of horizontal lines in the display. When the time taken to find an odd object increases with the number of other objects in the display, the defining feature is said to require a serial search (Treisman 1988). It seems that there is only a limited set of preattentive visual features, including orientation, colour, curvature, flicker, motion, size, and depth (Julesz and Bergen 1983). They correspond to those features served by dedicated feature detectors, either in the retina or in the primary visual cortex.

A difference in depth between objects is a preattentive feature because the time it takes to find a single object not at the same depth as a number of surrounding objects is independent of the number of objects. Depth defined by binocular disparity is also a preattentive feature, as can be seen in Figure 6.13a.

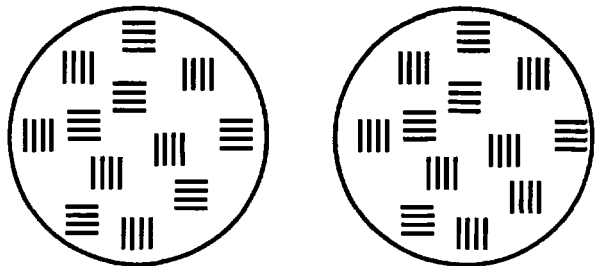
Holliday and Braddick (1991) asked whether the first spatial derivative of disparity (disparity gradient) is also a preattentive feature. Subjects were presented with an array of small squares slanted in depth by different amounts, and had to indicate whether one of the squares was slanted in a different direction from all the others. The time taken to make this decision was independent of the number of squares in the array, and Holliday and Braddick concluded that a disparity gradient is a preattentive or primitive visual feature. *It would be worth repeating the same experiment using disparity curvatures based on the second spatial derivative of disparity.*

Detection of a patch of rivalrous gratings placed within a display of non rivalrous gratings, as in Figure 6.13b, requires a serial search. A patch with reversed luminance polarity in the two eyes, exhibiting binocular lustre, pops out from a set of patches with the same luminance polarity in the two eyes, as can be seen in Figure 6.13c (Wolfe and Franzel 1988). However, a patch of rivalrous colour among patches of binocularly matching colour does not pop out, as can be seen in Figure 6.13d after page 310.

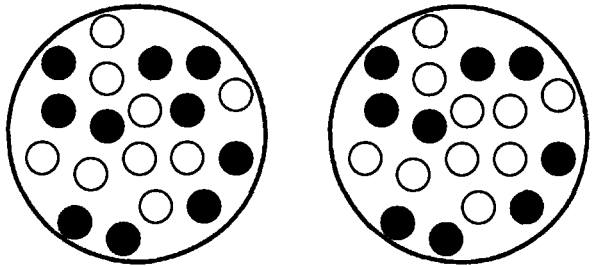
In monocular vision, textured regions defined by the shapes of texture elements immediately stand out, as shown in Figure 6.14a. Nothdurft (1985) claimed that cyclopean textured regions not visible in a monocular image perceptually segregate when they are in different depth planes (Figure 6.14b). When the cyclopean textured regions are all at the same depth relative to a random-dot background, as in Figure 6.14c, the different regions can be seen only after close scrutiny. He concluded that cyclopean textures can be segregated by depth but not by form.



(a) Stereoscopic depth is preattentive.



(b) Wolfe and Franzel (1988) claimed that detection of contour rivalry requires a serial search.

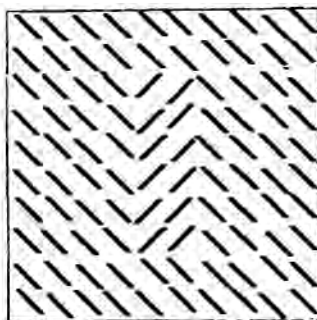


(c) Detection of a patch with rivalrous luminance polarity does not require a serial search.

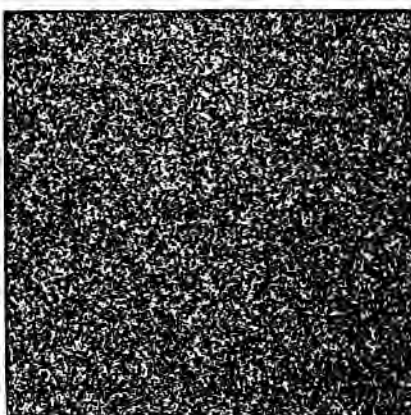
Figure 6.13. Testing for preattentive cyclopean features.

A feature is preattentive when the time taken to find a stimulus exhibiting it is independent of the number of other stimuli.

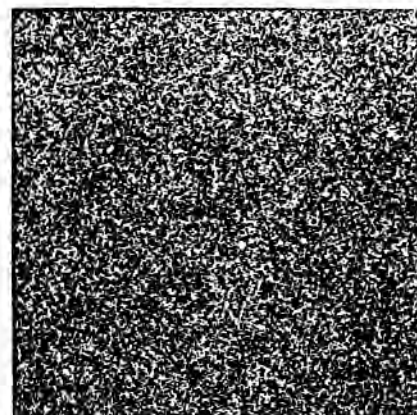
We agree that cyclopean textures can be segregated by depth. However, the conclusion that cyclopean textures cannot be segregated by form rests on the comparison between a display like that in part (a) of Figure 6.14 and that in part (c). This is not a fair comparison, since the monocularly viewed texture elements in (a) are seen against a featureless white background whereas the cyclopean texture elements in (c) are seen against a distracting background of dots. Monocular texture boundaries are also difficult to see when camouflaged by dots. Failure to



(a) Textured region defined by the shape of elements immediately stands out.



(b) Cyclopean textured regions in different depth planes perceptually segregate.



(c) Cyclopean textured regions in one depth plane do not readily segregate. (From Nothdurft 1985. Perception, 14, 527-537. Pion, London.)

Figure 6.14. Cyclopean texture segregation.

segregate cyclopean texture elements may not represent a failure within the cyclopean domain but an accidental consequence of the random dots used to generate cyclopean stimuli.

Detection of an object defined by the conjunction of two or more simple features has been reported to be serial (Treisman and Gelade 1980). For example, a line that is both red and vertical does not pop out of

a display of lines that can be either red and horizontal or blue and vertical. According to this evidence, visual processing at the preattentive level operates on separate features rather than on combinations of features. This is called the feature-integration theory. One problem in applying the theory is defining what is meant by a single preattentive feature. There are at least three ways to define a simple feature.

1. Preattentive features may be defined as those that are processed in parallel. But this definition renders the feature-integration theory circular.

2. A second approach is to define a preattentive feature as one involving only one sensory dimension, such as position, colour, movement, or orientation. There is then the problem of defining what is meant by one sensory dimension. For instance, all the so-called single features studied by Treisman are really conjunctive because the stimuli differed in position as well as in the feature being studied.

3. Finally, one can define a preattentive feature as one that has a dedicated feature detector at an early stage in visual processing. On this basis a conjunctive feature would be preattentive if it had a dedicated detector. At each location in the visual field there is a complete set of detectors for features other than position, such as colour, orientation, and movement. The position of the stimulus is also detected at each location by the local sign system. In this sense all feature detectors are conjunctive since they are spatially localized. This explains why people can attend to a region of a large display and conduct a parallel search for a second feature, such as colour, within that region (Treisman 1982). The same would be true for the conjunction of a visual feature and disparity-defined depth, if each depth plane possessed a complete set of feature detectors.

To test the last idea Nakayama and Silverman (1986) showed observers a set of objects moving up in a far depth plane defined by disparity and a set of objects moving down in a near depth plane. They were asked to find a target object that was either moving down in the far plane or up in the near plane. The time taken for this task was independent of the number of moving dots. This result implies that features such as motion and colour are independently processed in different depth planes. The depth planes were defined by disparity in this experiment. *Experiments are needed to discover whether the same independent processing occurs in depth planes defined by other cues to depth.*

In Nakayama and Silverman's experiment only two depth planes were used. *An experiment could be designed in which subjects have to find the depth plane containing an object that differs in colour or motion from the objects in the other depth planes. The question is whether the time for such a task is independent of the number of depth planes. In other words, is search across depth planes conducted in series or in parallel?*

Motion-in-depth is a conjunctive feature that is a strong candidate for parallel search, since it is known that dedicated detectors exist for this feature (see Section 13.2.5).

6.2 MATCHING DISPARATE IMAGES

6.2.1 Finding corresponding images

In Section 2.3.5 we described the Keplerian projection that defines all possible pairwise matches between the images in the two eyes for simple arrays of pointlike objects. It was shown that vergence eye movements, the nearest-neighbour rule, the unique-matching rule, and the similarity rule can prevent inappropriate matches. In a natural three-dimensional scene there are overlapping objects with complex shapes in several depth planes, complex disparity gradients and, occasionally, transparent textured surfaces that require additional rules and strategies for guiding the image-matching process. These rules are described in the following sections.

Vergence movements of the eyes are fundamental to image matching when there is a large initial disparity or several superimposed displays at different depths. People have tended to underestimate the role of vergence in stereopsis. The fact that depth can be seen in displays which are too brief to allow vergence changes (Dove 1841) does not mean that vergence does not play a role when sufficient time is allowed. The eyes are constantly changing their angle of convergence from one depth plane to another, guided by binocular disparity and several other cues to depth. The evidence reviewed in Section 10.5.7 suggests that large disparities provide a phasic signal which initiates a vergence response in the right direction but is unable to maintain steady vergence. As the eyes move, the large disparities in the target plane are reduced until they come within the tuning range of fine disparity detectors. A more or less steady state of vergence is maintained by error feedback from tonic disparity detectors operating on local detail within the selected plane. Large disparities in other depth planes are not allowed to initiate another vergence movement until the observer decides to change vergence. Once the eyes are converged on a given depth plane, the disparities in that plane are reduced to zero, or at least to within Panum's fusional range. Disparities arising from objects in other planes can then be used to code depth. To a first approximation, and for small areas, the images in the two eyes arising from each depth plane are similar, and the visual system must match the images in each pair for the disparities in the various depth planes to be extracted.

The problem of how the visual system finds these matching pairs of images to guide vergence and then to code relative depth is known as the **correspondence problem**. In the simplest case the solution is equivalent to sliding one image over the other and

finding the position that gives the highest cross-correlation between the images. Julesz (1971) referred to this as a "shift and subtract model" which was implemented in a computer program called "automap". Where the visual display consists of a collection of randomly arranged objects of different sizes or shapes within a single frontal plane, there is only one well-defined maximum in the correlation function defined over relative translations of the two images. The correlation can never be perfect except for a surface lying on an isodisparity circle with little vertical extent, or for an extended surface at an infinite distance. If the plane containing the objects is slanted or inclined in depth, the binocular images are relatively sheared, compressed, or rotated and therefore cannot be brought into congruence by translation alone. However, cross-correlation functions may be defined over shear, compression, or rotation. Note that matches over relative horizontal and vertical translations of the two images can be found by horizontal and vertical vergence, and matches over relative rotations can be found by cyclorvergence (see Section 10.7). Eye movements cannot find matches over transformations defined by shear or compression but, as we will see in Section 6.2.13, lateral scanning eye movements coupled with vergence can help even in these cases.

The process of image matching is complicated still further in natural scenes because objects are often distributed in distinct depth planes. In this case the translation cross-correlation function of the images has several peak values distributed over the visual field. The best strategy is to look for matching images within local areas of the visual field, rather than over the whole of it. But even this strategy does not work when objects occur in multiple overlapping planes, as when we look into the branches of a tree or through a set of textured transparent surfaces. There are now distinct peaks in the cross correlation function in each direction of the visual field. Another problem with deriving correlation functions on too local a scale is that the process becomes subject to effects of noise. A global correlation process has a better signal-to-noise ratio but fails to detect local variations in depth. We will see later that these conflicting requirements can be resolved if image correlations are performed independently within distinct ranges of disparity, image size, orientation, and direction and if the matching process is related to changes in vergence.

The correlation function defined over a given relative transformation of two images resembles a three-dimensional landscape, with local maxima occurring as depressions; the higher the correlation the deeper the depression (see Sperling 1970). Once

a depression is found, either by vergence eye movements or by a neural process, the visual system locks into that value because any departure from it increases mean disparity. Each depression can be thought of as a position of least energy representing a stable state in the matching process. Similar images that fall on corresponding points in the two retinas serve to lock vergence. Once vergence is locked, matches found between images of objects outside the plane of vergence serve as a basis for judging relative depth.

There is no unique match of images, even locally, for an extended array of dots arranged in a regular lattice in a frontal plane because there is an equally good match at any multiple of the interdot separation. We shall see in Section 12.2.3 that the apparent depth of a region with a repetitive texture is primed by unambiguous disparities that may be present at the edges of the region. When the dots are arranged randomly, as in a random-dot stereogram, each depth plane has a unique best solution because the dots form distinct local clusters and only relative position of the images gives the highest correlation between them. However, the best match may be hard to find because there could be several lesser maxima in the correlation function defined over translation. In other words, a spurious fit between a sizable subset of dots may be found, which prevents the system finding a better match for the whole surface. Noisy jitter would help to shake the system out of a shallow depression in the correlation landscape and into a more stable deeper depression. Jitter in vergence would serve this purpose, but processes of this kind also operate at the neural level. Once the best match has been found it is like being in a deep depression and the system is unlikely to be shaken out of it. This process may partly explain why it often takes a long time to see depth in a random-dot stereogram unless each image contains clearly identified matching features (see Section 5.11). The spontaneous alternations of perspective in the perception of the Necker cube and the alternations in ambiguous figures probably arise from a process akin to noisy jitter. Computer algorithms and neural-network models of this type of process have been developed (see Hopfield 1982 and Kienker et al. 1986).

Detection of interocular correlation

Several people have investigated the sensitivity of the visual system to the degree of cross-correlation between images in the two eyes. Mathematically, correlating two spatial displays involves assigning a signed normalized value to the luminance, or some derivative of the luminance, of each point in each eye, multiplying the values for the members of each

pair of corresponding points and averaging the products. In the simplest case, each display is paved with an equal number of black (-1) and white (+1) image points, or pixels. A correlation of 1 means that all interocular pairs of image points are identical and there is a unique match in luminance for every pixel. A correlation of zero means that 50 per cent of the pairs of image points have the same luminance polarity and 50 per cent the opposite polarity. A correlation of -1 implies that all pairs of image points have opposite luminance polarity; wherever one image point is dark the other image point is light. The same measure can be applied to dark and light points distributed over a gray background. The measure works only if the dots have the same distribution in both eyes and differ only in luminance polarity. If the dots are not identically distributed, some dots in one eye will fall in the spaces between the dots in the other eye rather than on other dots. This calls for a different measure of correlation because the way the visual system combines congruent or rivalrous edges is very different from the way it combines an edge in one eye with a region of homogeneous luminance in the other. In such a case, pairs of images falling on corresponding points could be assigned a value of +1, and each pair of unmatched images a value of -1. The degree of image correspondence could be defined as the mean of these values. No simple measure of image correspondence embodies both the criterion of matching luminance polarity and that based on fused and unfused points.

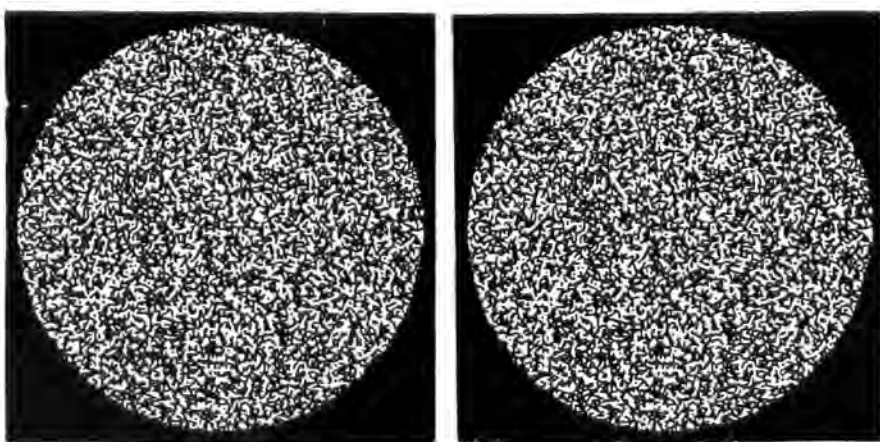
Tyler and Julesz (1978) measured peoples' ability to detect a change in the degree of correlation between dichoptic dynamic random-dot displays as a function of stimulus area and duration. All the dots fell on corresponding retinal points and correlation was defined in terms of their relative luminance polarity. The time taken to detect a change in correlation decreased as the area of the display increased to about 5 deg^2 , after which the duration threshold was independent of area. Because one dot density was used it is not clear whether the crucial factor was the number of dots or the area of the display. With larger displays adding extra area may have been ineffective because of the retinal eccentricity of the added dots. Tyler and Julesz found that subjects could detect changes of correlation of only 1 per cent and sometimes in only 3 ms, suggesting that correlation detection is done in parallel over the display, rather than serially. In other words, it suggests that dichoptic luminance polarity is a preattentive visual feature (see Section 6.1.6). The ease with which dots with reversed polarity can be found among a set of dots with the same polarity is illustrated in Figure

6.13d. Changes from a state of correlation to one of decorrelation were detected about 10 times faster than changes from decorrelation to correlation. This could be because all points must be checked to establish that a display is correlated whereas to establish that it is uncorrelated requires the detection of only one unmatched image.

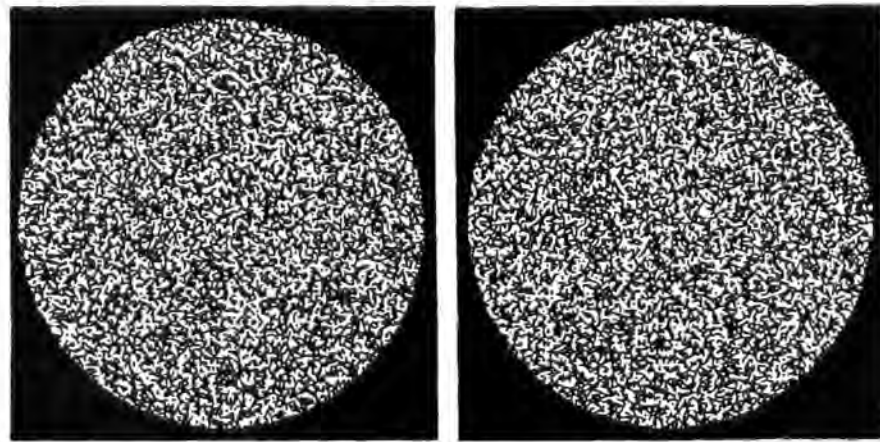
In an earlier paper Tyler and Julesz (1976) measured the time to detect a transition between an uncorrelated random-dot display (zero correlation) to a display with opposite luminance polarity (-1 correlation) and vice versa. These transitions involve the engagement or disengagement of the binocular rivalry mechanism. Both transitions took longer to detect than transitions between correlated and uncorrelated states or between states of +1 and -1 correlation. These latter transitions involve the engagement or disengagement of the binocular correspondence mechanism. Under the best conditions, a transition from correlation to decorrelation was detected in 2 ms. They explained their results by postulating that the rivalry mechanism is less efficient in detecting transitions than is the mechanism that detects binocular correspondence.

Cormack et al. (1991) presented a dynamic random-dot display to each eye. During one time interval the displays were correlated, and during another interval they had some degree of decorrelation, which varied from display to display, as shown in Figure 6.15. Subjects had to say which of the two displays was decorrelated. At above about 10 times the contrast threshold, subjects could identify a display with 1 per cent of decorrelation, and the correlation threshold was independent of changes in contrast. They explained this constancy of the correlation threshold on the basis of a model in which the signal (the peak in the correlation function) and the extrinsic noise (lesser peaks due to spurious matches in the display) both vary with the square of contrast, as shown in Figure 6.16. This similar dependence of signal and noise on contrast means that the signal-to-noise ratio remains constant as contrast is varied. As contrast was reduced below a value of 10-times-above-threshold, the correlation threshold increased rapidly. A similar rapid rise of stereoacluity occurs at low contrasts (see Figure 5.16). A rapid rise in threshold must occur near the threshold because intrinsic noise necessarily becomes stronger than the signal at low levels of stimulation.

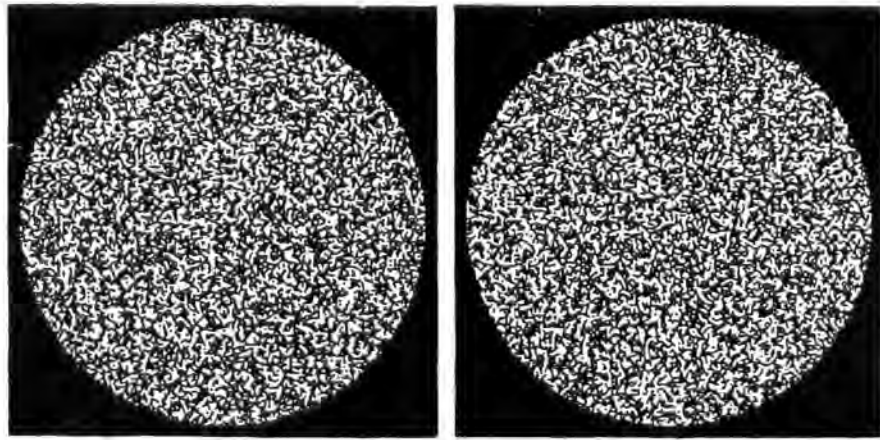
Cormack et al. (1994) varied the degree of interocular correlation of random dots in a dichoptic dynamic random-dot display. Subjects detected in which of two time intervals the correlation changed from a mean value of zero to some positive value. The area of the display varied between 0.14 and 7 deg^2 and



(a) The two images are correlated 100 per cent. They fuse to create a flat plane.



(b) The interocular correlation is 50 per cent. A flat plane is still perceived but with some dots out of the plane.



(c) The correlation is zero and a flat plane is not perceived. Subjects had to detect transitions between different states of correlation. (Reproduced with permission from Cormack et al. 1991, Vision Research, Pergamon Press.)

Figure 6.15. Stereograms with different degrees of interocular correlation.

its duration varied between 49 and 800 ms. With up to about 10,000 elements, the correlation threshold was inversely proportional to the total number of elements in the display, regardless of its size or duration. With more elements, performance levelled

off to a constant value of about 0.1. These results did not reveal well-defined integration areas or integration times but conformed to an ideal observer which detects the statistical attributes of the total number of elements in the display for up to 10,000 elements.

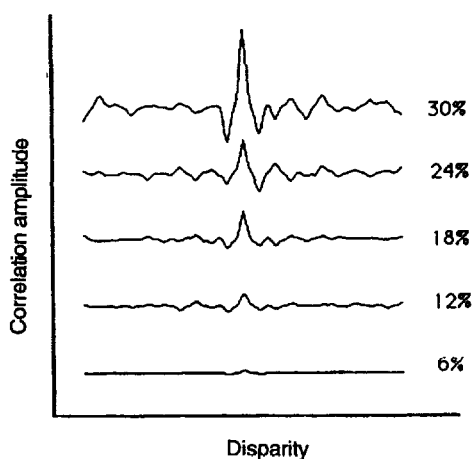


Figure 6.16. Cross-correlation functions.

A family of cross-correlation functions for a random-dot stereogram with 80 per cent interocular correlation but decreasing contrast (indicated by numbers on the right). The curves are vertically separated on the Y axis. The signal (peak in the correlation function) and the extrinsic noise (lesser peaks due to spurious matches in the display) both vary with the square of contrast. The functions are displaced vertically. (Reproduced with permission from Cormack et al. 1991. Vision Research, Pergamon Press.)

In Section 5.3.3 we described an experiment by Harris and Parker in which they found that subjects used the information in only about 20 elements of a random-dot stereogram in detecting a disparity-defined depth edge. But in this task the crucial information is contained in the region of the depth edge whereas in the task of detecting correlation in a zero-disparity display, the information is distributed over the whole display.

These experiments on correlation detection test the system under the most stringent stimulus conditions. Natural images do not consist of random-dot patterns but of lines, edges, and distinctly coloured surfaces, which simplify the task of finding matches between the images in the two eyes. These natural redundancies in the patterns of proximal stimulation impose constraints on the possible interpretations of particular stimuli. The algorithms, or matching rules, described in the following sections may explain how the visual system exploits these constraints in finding the best match between the binocular images.

Cepstral filters

A **cepstrum** is the power spectrum of the logarithm of the Fourier transform of a time-varying or space-varying signal. Cepstrum is an anagram of 'spectrum'. The concept was developed by Bogert et al. (1963) and was originally applied to the detection of echoes in seismic signals reflected from layers of the earth's crust. The method is suited to the characterization of repetitive structures such as echoes.

Each echo generates an easily located peak in the cepstrum. The location of this peak signifies the echo delay. The echo signal can then be removed by filtering and the original signal reconstituted by the inverse transform.

Yeshurun and Schwartz (1989, 1990) developed a model of disparity detection using cepstral filters. The unit visual input in the model consists of a patch of image about 5 arcmin in diameter spread across a left-eye and a right-eye ocular dominance column. Half the patch is derived from one eye and the other half from a corresponding region in the other eye. It is assumed that the disparity to be detected lies within this region. The Fourier transform of this pair of abutted images is derived and the power spectrum of the logarithm of the transform plotted to yield the cepstrum. Any horizontal disparity between the images shows as a localized peak, with a position on the x axis which signifies disparity magnitude. The non-linearity introduced by the logarithmic transformation renders this procedure specifically sensitive to repetitive structures in the input signal which, in this case, take the form of a binocular disparity. Furthermore, unlike correlation procedures, the disparity signal in cepstral analysis is not subject to interference from spatial frequency terms in the component images. For these reasons the signal-to-noise ratio is several times higher than that achieved by correlation of the two images. The method is highly resistant to blurring, rotations, and differential magnification of the images. Degradations of the input smear the disparity signal in the cepstrum but do not shift its mean position.

It is unreasonable to expect the visual system to derive a Fourier transform of the visual input. It was explained in Section 3.4.2 that this would require a large set of detectors of spatial frequency, each with very large receptive fields. However, an estimation of the spatial-frequency power spectrum of a local binocular image patch may be derived by a small set of detectors each with a 1.5 octave bandwidth. The output of this stage would then have to be transformed logarithmically to yield the cepstrum with its peak signal representing the disparity. This process would be carried out in parallel at each location of the visual field.

6.2.2 The unique-matching rule

It is a basic property of the world that a small well-defined object has a unique position in three-dimensional space at any one time and that there cannot be more than one object in any one place. This constraint makes it possible for the matching process to operate with the rule that each point in the image of

one eye matches, at most, one point in the image of the other eye at any one time. According to the unique-matching rule, once a pair of image points has been matched by the disparity-detection system, all other potential matches for those points are excluded.

Weinshall (1991) claimed that multiple depth planes seen in an ambiguous random-dot display are due to double-duty disparity matching. However, Pollard and Frisby (1990) pointed out that multiple planes may be seen in such displays without violating the unique-matching rule. Each point in one eye could be matched with only one point in the other eye but different matches could occur in different parts of the stereogram, creating the impression of two planes. If each dot is matched with only one dot then the number of dots perceived in all the depth planes should not exceed the number of dot pairs, whereas with multiple fusions the number of perceived dots would exceed the number of dot pairs. Recently, Weinshall (1993) herself showed that the perceived density of dots in the depth planes was consistent with each dot having been matched with only one other dot. Thus, the unique-matching rule is not violated in this type of display in which each element in one eye has at least one matching element in the other eye.

Current physiological theories of disparity detection allow multiple matches insofar as several binocular cells share inputs from the same monocular receptive fields. Perhaps multiple matches are made initially and the unique-matching rule is applied at a later stage in which the best set of unique matches is retained by the application of other criteria described in the following (Grimson 1981).

Panum's limiting case presents a special problem for the unique-matching rule. The eyes are converged on a vertical line seen by both eyes and a second vertical line is presented to only one eye, slightly to the temporal side of the fused line (see Figure 12.63). The second monocular line appears to lie in a depth plane beyond the binocular fused line. Hering (1865) proposed that the impression of depth in Panum's limiting case can be explained if the image in the eye that sees only one line is matched with each of the two images in the other eye, one match signifying one depth plane and the other match a second depth plane. If true, this would violate the unique-matching rule. However, Panum's limiting case can be explained without assuming double-duty matching of this type (see Section 12.4.6).

McKee et al. (1994a) has produced evidence that a single visual target in one eye can simultaneously mask two targets presented to the other eye. The stimulus display is shown in Figure 6.17. Each visual

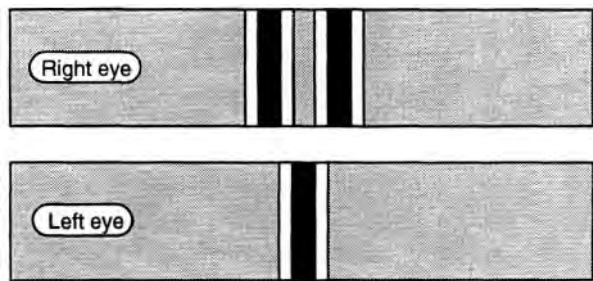


Figure 6.17. Display used to study double-duty matching.
The display in each eye was 1.5° long by 0.8° high. Each of the three targets consisted of a black line 2.75 arcmin wide flanked by white lines 1.35 arcmin wide. The background had the same mean luminance as the targets, so the targets were not visible from a distance. (Adapted from McKee et al. 1994.)

target consisted of a vertical black line flanked with white lines. They were presented on a gray background with the same mean luminance. This had the effect of eliminating low spatial frequencies. Two targets were presented to the right eye 7 arcmin apart. The contrast-increment threshold for each of the targets in the right eye was elevated by the presence of a similar target in the left eye placed in an intermediate position. The threshold elevation was as great as when only one target was presented to the right eye, suggesting that the single target in the left eye was capable of simultaneously masking both targets in the right eye. Furthermore, the perceived depth between the two targets, as indicated by a depth probe, also indicated that the single target in the left eye was matched at the same time with both targets in the right eye. Vergence was controlled in all conditions by having subjects align nonius lines before the stimulus was presented and presentation time was only 200 ms.

One possible problem here is that each target consisted of three lines. The single target in the left eye was thus not really a single stimulus. Perhaps the two white lines of the target in the left eye independently masked or stereoscopically combined with white lines in the right eye. This would not violate the unique-matching rule.

6.2.3 Matching similar features

A corollary of the rule that each object has a unique position in space is that the images of an object in the two eyes are fundamentally similar in size, shape, colour, and motion. Images that differ markedly in any of these respects most likely arise from different objects. The image-matching process makes good use of this constraint. With several objects in view, the more they differ in shape the less ambiguity there is in the way their images can be matched.

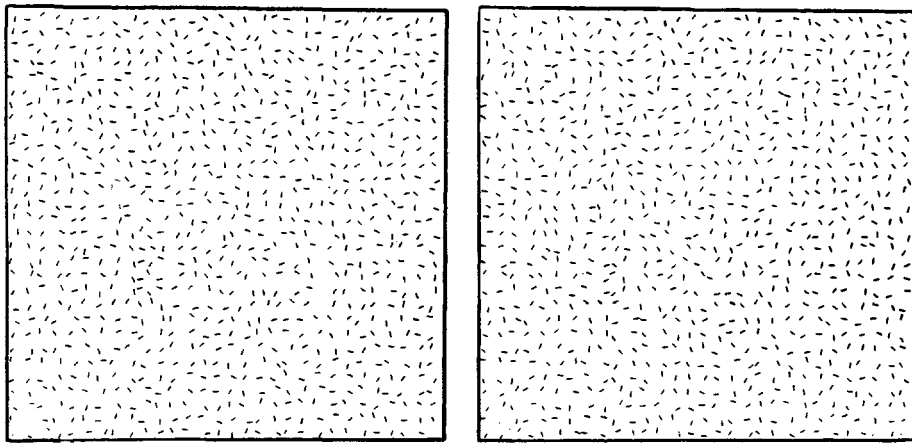


Figure 6.18. Stereopsis with orthogonal line elements.

Some depth is still evident in a random-line stereogram with orthogonal line elements, as long as the lines are short. (From Frisby and Julesz 1976. Perception, 4, 151-158. Pion, London.)

In the typical random-dot stereogram the pattern of dots in each image has an overall similarity of texture and this may partly explain why it takes some time to see depth in these stereograms. Depth latency is reduced when clearly discriminable elements, such as corners and blobs, are added to random-dot stereograms with large disparity steps (Saye and Frisby 1975).

When the images falling on corresponding retinal points differ in shape they tend to rival rather than fuse (see Chapter 8). In this section we ask about the degree of similarity between the shapes of images that is required for stereopsis. We consider just two attributes of shape, namely, spatial frequency (size and texture density) and orientation.

As noted in Section 6.1.2, it has been claimed that depth can be seen in a stereogram consisting of lines that are orthogonal in the two eyes, as in Figure 6.6. However, it was also noted that there are several artifacts in this type of display. Stereoacuity is severely reduced when the orthogonal lines are more than 3 arcmin long (Mitchell and O'Hagen 1972). It seems that disparity between boundaries of regions containing oppositely oriented lines does not serve as a cue to depth. The question addressed in this section is what degree of orientational mismatch the disparity-detection process tolerates.

Mitchell (1969) reported that depth could be discriminated in a stereogram consisting of a horizontal line to one eye and a vertical line to the other, as long as the disparity between them was sufficient to ensure that they were imaged on distinct regions of the retinas. In this case, depth judgments may have been based on the vergence movements of the eyes that the disparate stimuli induced rather than directly on the disparity itself. Even briefly exposed

disparate images induce vergence, which then occurs after the stimulus is switched off. In other words, one cannot argue that vergence plays no part in depth perception with briefly exposed stimuli.

One pair of lines cannot be used to investigate the effects of small angles of image misalignment on stereopsis because small differences in orientation are the natural cue for apparent inclination in depth, as we will see in Section 7.4. Frisby and Roth (1971) overcame this problem by using a random-line stereogram consisting of many randomly oriented line elements in which the depth of the cyclopean image was created by the horizontal disparity of a region of the display. The lines were about 12 arcmin long and the central square region had either a crossed or uncrossed disparity of 18 arcmin. When the lines had the same orientation in the two eyes the depth of the central square was clearly visible. The impression of depth began to deteriorate when the orientations of the lines differed by 10° and virtually no depth was reported when they differed by more than 45°.

Frisby and Julesz (1975a, 1975b, 1976) also found that the amount of perceived depth in a random-line stereogram decreased as the difference in orientation of line elements in the two eyes increased and, like Mitchell and O'Hagen, they found that increasing the length of the lines increased the disruptive effects of orientation differences (see Figure 6.18). One can explain these effects by supposing that stereopsis with differently oriented images depends on the registration of disparities between the low spatial-frequency components of the stimuli, and that when the lines become too long the large point-disparities between the ends of the lines begin to obtrude. The disruptive effects of differences in orientation of line

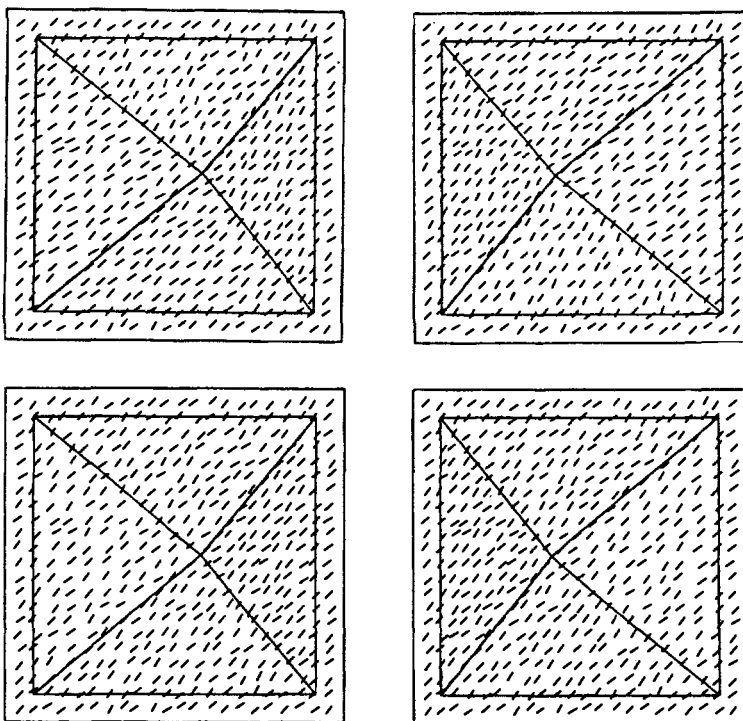


Figure 6.19. Orientation disparities conforming to a surface.

In the upper stereogram the relative orientations of the line elements produce disparities appropriate to the slope of the pyramid produced by disparities in the continuous lines. This creates a smooth-sided pyramid. In the lower stereogram there are no disparities between the line elements. This creates a stepped pyramid. (From Ninio 1985, Perception, 14, 305-34, Pion, London.)

elements in a random-line stereogram are probably due to the inability of binocular cells to detect horizontal disparity between stimuli that differ in orientation by more than a critical amount. It was shown in Section 4.4 that the receptive fields of binocular cells have similar orientation tuning in the two eyes.

In the random-line stereograms just described, the difference in orientation between the lines in the two eyes bore no relation to the depth in the stereogram. The pairs of corresponding lines in the upper stereogram in Figure 6.19 have orientation disparities appropriate to the inclinations of the sides of the pyramid that is defined in terms of horizontal disparities between the lines. In this case the lines appear to lie smoothly on the sides of the receding pyramid (Ninio 1985). In the figure's lower stereogram the lines in each pair have the same orientation in the two eyes and the fused images appear to lie on steps on the sides of the pyramid (see Section 7.4.2).

Ninio and Herlin (1988) and Herbomel and Ninio (1993) created stereograms from different types of textured surface. In each case the texture was the same in the two eyes and subjects had to identify whether each of five protuberances was convex or concave. The main factors that shortened the time taken to complete the task were discontinuities of

texture and diversity in the positions and orientations of texture elements. These factors presumably helped because they increased the information about the correct match of corresponding elements. Correct depth percepts were evoked more readily by vertical than by horizontal line elements, but only when there was some irregularity in the orientation or spacing of the elements. Monocular cues to the location of the protuberances played a minor role.

The effect of differences in spatial frequency between the images in the two eyes on stereoacuity was investigated by Schor et al. (1984a). They used spatially filtered barlike patterns (DOGs) and found an elevation of stereo threshold as the difference in the centre spatial frequency of the displays in the two eyes was increased.

A computer algorithm that uses the similarity constraint to solve the binocular correspondence problem is described by Reimann and Haken (1994).

6.2.4 Minimizing unpaired images

This rule states that the best match between the images in the two eyes is the one producing the minimum number of unpaired images. None of the matching rules states that each point in the binocular



Figure 6.20. Stereogram of dots with only one disparity node.

When the gaze is held at the left end of the row by fusing the bold lines, a slanted surface is seen extending over the first few dots, beyond which depth impressions become vague. A continuous depth ramp is seen when the gaze moves across the display. As the gaze moves, vergence changes, as indicated by the fact that the fine nonius lines are out of alignment when the gaze is at the left end of the row but are in alignment when the gaze is at the right end.

field of one eye must be matched with a point in the other eye. It is explained in Section 12.4 that in the neighbourhood of a non horizontal step in depth there is a region seen by one eye that cannot be seen by the other eye. We refer to these regions as **monocular zones**. Monocular occlusion indicates the presence of a depth edge. The matching process is helped by the fact that monocular zones occur in coherent patches near disparity discontinuities and obey other rules described in Section 12.4.1. Monocular zones confirm that a correct match has been found, since coherent regions of unmatched images are not likely to arise by chance. Under certain circumstances a compelling impression of depth arises from monocular zones in the absence of disparity. This topic is discussed in Sections 7.9 and 12.4.5. Unpaired images arising from incorrect matching tend to be distributed at random and act like noise to degrade stereoacuity, as described in Section 5.2.3.

6.2.5 Matching nearest-neighbour images

Consider an image in one eye between two similar images in the other eye. According to the nearest-neighbour rule the visual system will match the image in one eye with a similar image in the other eye, with respect to which it has the least disparity for a particular state of convergence. The images of objects in or near the horopter are automatically fused and matched when the disparity is less than the monocular resolution limit. The farther an object is from the plane of the horopter, the less likely it is that its images will be matched. It is a good strategy to give priority to nearest-neighbour images because images with a large disparity necessarily arise from objects well away from the plane of convergence and are therefore likely to be of less interest.

In one part of the scene there may be a surface covered with a repetitive texture. The nearest-neighbour matching rule produces the wrong match when the disparity between corresponding images is more than half the spacing of the textural elements. The surface will then be seen in an anomalous depth

plane. The **wallpaper illusion** illustrates this point (see Section 2.3.5). However, if the surface also contains well-spaced lines or edges, each with a distinct contrast, length, or shape, the matching process should have no difficulty in finding the correct match for these features by the nearest-neighbour rule. Once the well-spaced features have been matched, the same disparity could be applied to any finer repetitive features. The images of particular elements on a textured surface may be constrained to match non-nearest neighbours to optimize the match of the whole surface. This strategy would work when it is correctly assumed that the sparse features and the repetitive features belong to the same surface. Usually, the communality of different textural elements on a surface is apparent because of the coherence of the overall pattern they make. Mallot et al. (1994) found that well-spaced features provide a more efficient basis for finding the correct match in stereograms, then do high spatial frequency features. However, they found that people do not always process images this way but sometimes use fine detail to disambiguate the matching of coarse detail. Several stereograms have been devised to illustrate the point that the matching of finely spaced texture elements is primed by the matching of widely-spaced or non-repetitive features. Section 12.2.3 provides examples.

6.2.6 Matching adjacent images

Consider an image in one eye to one side of two images in the other eye. If the single image is matched with the image in the other eye that is not its closest neighbour, the matched images would have another image between them. This violates the nearest-neighbour rule in a stronger sense because the match is now between elements that are not even neighbours. The rule is that, other things being equal, adjacent images are matched in preference to non-adjacent images.

A conflict between adjacent images and nearest-neighbour images arises in the stereogram shown in Figure 6.20. When the first dots in each row are

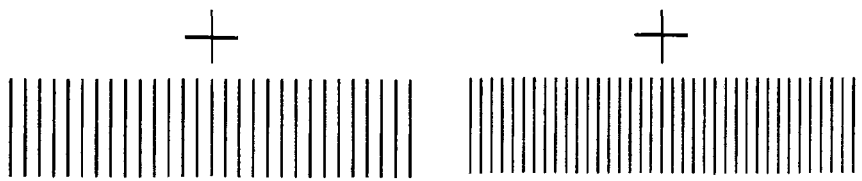


Figure 6.21. The Venetian-blind effect.

A stereogram of dense vertical lines that produces closely spaced nodes of zero disparity to create the impression of a Venetian blind. Short ramps between nodes, which occur every three lines, are interspersed with step returns.

fused, the fifth dot in the left eye's image coincides with the sixth dot in the right eye's image. By the nearest-neighbour rule, the fifth and sixth dots should be matched. But if these dots are matched, the sixth dot in the left eye and one of the dots in the right eye would remain unmatched. Ramachandran et al. (1973b) claimed that this stereogram produces the impression of a continuous depth ramp and concluded that matching occurs between dots that are not neighbours. This means that the process that minimizes the number of unpaired images wins out over the process that seeks the nearest-neighbour match and forces non-adjacent images to be matched.

This evidence is not conclusive. We have found that when fixation is held on the two leftmost dots in Figure 6.20, only the first few dots appear slanted—the others appear to lie on a frontal plane. This is because the disparities become ambiguous and hard to detect in the periphery. When the gaze is allowed to wander over the whole row, an impression of a coherent slanted configuration of dots emerges. By inserting pairs of nonius lines above the dots one can show that the eyes change their angle of vergence as they scan over the row of dots. This brings successive pairs of dots into correspondence and allows one to build up an integral impression of a slanted surface, by storing successive partial impressions of slant in a buffer store. At each stage of this process the nearest-neighbour rule is maintained, and unpaired images some distance from the point of convergence are simply ignored.

This process of sequential scanning can be further explored by using vertical lines instead of dots and varying their number and spacing. Let the number of lines per degree of visual angle be f in the left eye and $f + x$ in the right eye. With the eyes held stationary, the lines in the two eyes fall on corresponding points x times per degree of visual angle. Let each of these positions be called a node. When nodes occur frequently, as in Figure 6.21, fusion of the images creates the impression of a Venetian blind in which short ramps between nodes are interspersed

with step returns to a frontal plane at each node. This is what one would expect from the pattern of nearest-neighbour disparities over the array. When the nodes are far apart, as in Figure 6.20, and when the gaze is held in one position, a slanted surface is seen extending over the first few dots, beyond which depth impressions become vague.

A similar effect occurs when one inspects a surface covered with a regular pattern of dots inclined in depth about a horizontal axis, as in Figure 2.9. The surface breaks up into a set of horizontal planes with a step between each plane. Within each plane the dots in one eye fuse with their nearest neighbours in the other eye to create the impression of an inclined surface but at the boundary between one plane and the next the nearest-neighbour match shifts to dots relatively shifted one interdot spacing. There seems to be no convincing evidence that the rule of matching adjacent images is ever broken in favour of non-adjacent images when all the images are similar.

Nonadjacent images arise when the disparity gradient is greater than two (see Section 2.3.3). We shall see in the next Section that disparate images arising from a disparity gradient of more than one do not fuse. However, even images with a disparity gradient of 2 may evoke a sensation of depth. This suggests that nonadjacent images are matched when there are no other alternatives. This issue is discussed more fully in the next two Sections.

6.2.7 Limiting disparity gradients

Marks on a straight line slanted about a vertical axis generate a horizontal gradient of horizontal disparity, defined as the difference between the disparities of any two points on the line divided by their angular lateral separation (see Section 2.3.3 for definitions of relevant terms). Marks lying on a line inclined about a horizontal axis generate a vertical gradient of horizontal disparity. Points lying on either the horizontal or vertical horopter produce a disparity gradient of zero. Points lying along a visual line of one eye have a horizontal gradient of disparity of 2

because, as explained in Section 2.3.3, the difference in disparity between any two pairs of corresponding images on a visual line is twice the lateral separation between them (Burt and Julesz 1980; Trivedi and Lloyd 1985). The horizontal gradient of disparity of collinear points on an opaque surface cannot exceed a value of 2, because beyond that value the surface is not visible to one eye. It follows that points producing a horizontal disparity gradient greater than 2 cannot belong to an opaque surface. Distinct objects at different distances and marks on transparent surfaces can produce disparity gradients greater than 2. The geometrical constraint on the size of the disparity gradient does not apply to vertical gradients of disparity between points on surfaces inclined about a horizontal axis, since all points on such a surface remain visible to both eyes until the surface becomes aligned with the plane of regard. The vertical gradient of horizontal disparity along such a surface approaches a value of infinity.

In addition to the geometrical limit on the disparity gradient, Burt and Julesz (1980) found that, with two objects having a disparity gradient greater than 1, the images of only one of the objects can be fused. The fusional limit is scaled to the gradient of disparity (see Section 8.1.5 for details on this point). However, the relevance of stimulus spacing to stereopsis is open to several interpretations, as we saw in Section 5.5.2. The unfused images could still code depth, since disparity may be detected between unfused images. However, the depth between objects on a steep disparity gradient is underestimated compared with that between objects on a less steep gradient (see Section 5.5.2). The problem of how depth is perceived between objects lying between the visual axes, or indeed between any pair of visual lines, is discussed in the next section and in Section 4.3. Pollard et al. (1985) developed a computer algorithm incorporating the constraint of not allowing matches between images with disparity gradients greater than 1. In addition, their algorithm uses the epipolar constraint and the unique-match constraint.

6.2.8 The relative order of images in the two eyes

A visual line is any straight line passing through the nodal point of an eye and the pupil. Corresponding visual lines are any pair consisting of one from each eye, that intersect in either the horizontal or vertical horopter. The region between a pair of corresponding visual lines is an intervisual-line region and that between the visual axes is the intervisual-axis region. Consider a line intersecting a point, A on the horopter and lying between the two corresponding visual lines that meet at A , as in Figure 6.22. Any

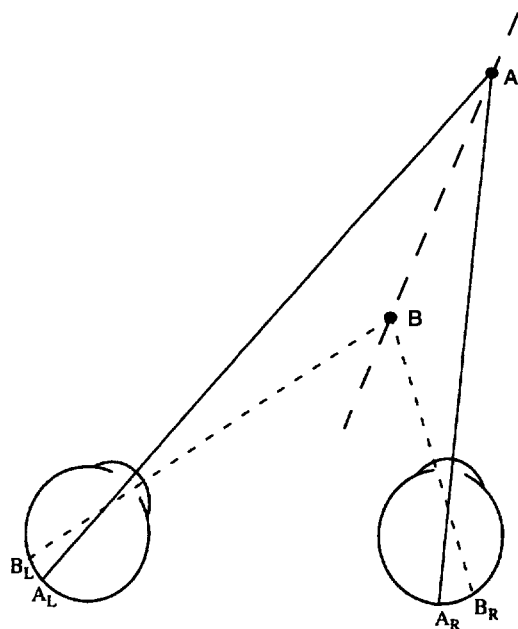


Figure 6.22. Disparity with loss of topological continuity.

(a) Objects A and B lie on a line lying between the two corresponding visual lines that intersect at A . The relative order of the images of A and B is not the same in the two eyes, and the images of B are separated by those of A .

pair of objects, A and B , lying on such a line have a horizontal disparity gradient greater than 2.

There are three problems in matching the images of objects with a horizontal disparity gradient greater than 2:

1. *Topological discontinuity.* The images of the two objects in the left eye, are in reversed left-right order with respect to the images of the same objects in the right eye. In other words, the relative order, or topological continuity of corresponding images is not preserved for horizontal disparity gradients greater than 2. Note that this rule applies to objects with a disparity gradient greater than 2 that lie within the region between any pair of corresponding visual lines and not only to objects between the visual axes. For two objects with a horizontal disparity gradient less than 2, the image of A is to the left of the image of B in one eye and also to the left of the image of B in the other eye, and the topology is preserved.

2. *Intercalated images.* A related problem with objects having a horizontal disparity gradient greater than 2 is that the images with the greater disparity are separated by the images with the smaller disparity, as Figure 6.22 shows. This should severely complicate the problem of matching these disparate images. For an inter-receptive field disparity mechanism that relies on the offset of subregions within corresponding monocular receptive fields (see Section 4.5.2), matching would become

impossible, since it is difficult to see how a binocular cell could operate when a fused pair of images is inserted between the disparate images.

3. *Opposite-hemisphere projection.* Corresponding images from any object within an intervisual-axis region, other than those arising from the fixated object, present a further problem for the image-matching process. They fall in opposite retinal hemifields and hence project to opposite cerebral hemispheres (see Section 4.3). The disparate images of any object lying outside the intervisual-axis region are both projected to the same side of the brain.

Perhaps disparity gradients greater than 2 do not code depth directly but only through the mediation of vergence. When the two displays of dots and lines in Figure 6.23 are fused with convergence and with the gaze held firmly on the dots, the images of the vertical lines in the lefthand column appear on each side of the fused dot in the same depth plane. As soon as the eyes are allowed to converge on the vertical lines the lines appear in front of the dots. The depth of the vertical lines relative to the dots is more apparent in the righthand column when vergence is held firmly on the dots, although even here the lines and dots may appear coplanar after a while. In the lefthand column the disparity gradient is 2 and the disparate vertical lines are separated by the fused image of the dots. In the righthand column the disparities are the same but the disparity gradient is less than two and the images of the lines fall to one side of the fused image of the dots. We suggest that the steep disparity gradient with out-of-order images in the lefthand column does not code depth directly but only as a result of a vergence change. Vergence could help in two ways. First, when the eyes remain converged on the dot, the disparity of the low spatial-frequency content of the images in the two eyes induces a fixation disparity into the fused image of the dot which causes it to appear nearer than the monocular lines. Second, when the eyes change convergence from the dot to the line, the vergence movement and the resulting change in the pattern of disparity create an impression of depth.

6.2.9 Matches in disparity and size domains

The disparity between the images of an object increases to a first approximation as a linear function of the distance of the object from the plane of convergence. The process of matching images in each of several depth planes is simplified if it is performed within channels tuned to different magnitudes of disparity. To a first approximation, a match found between a pair of images with a given disparity

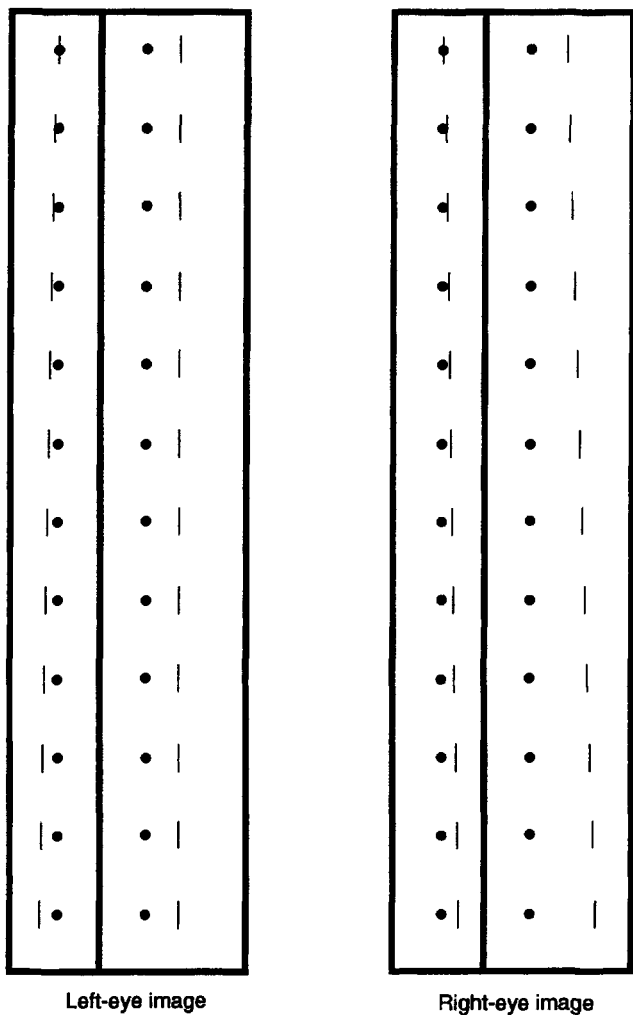


Figure 6.23. Depth from high and low disparity gradients. The vertical lines in each column of the fused image appear in front of the dots with convergent fusion and behind them with divergent fusion. The depth increases down each column. When convergence is held firmly on the dots, the vertical lines in the left column appear diplopic and in the same plane as the dots. The lines in the right column tend to remain fused and in depth. Disparities in the two columns are the same but images in the left column form a steeper disparity gradient and are topologically out of order.

applies to all image pairs within a local area in the same depth plane. There is also a natural correlation between disparity magnitude and image blur, since images of objects farther from the plane of zero disparity are correspondingly more out of focus. Images of out-of-focus objects lack fine detail (steep luminance gradients) and cannot be detected by small receptive fields. This natural constraint could be used to advantage by the image-matching system. Matching of fine disparities could be done within the high luminance-gradient, or fine-scale system (by small receptive fields in the central retina) and matching of coarse disparities could be done within

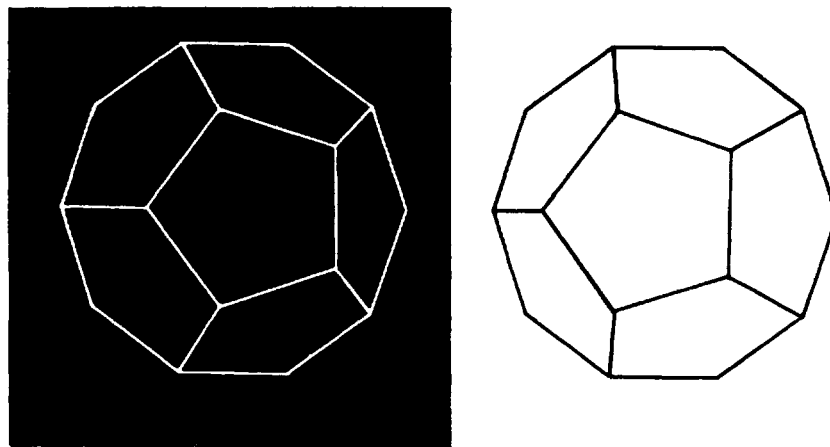


Figure 6.24. Stereogram with lines of opposite luminance polarity.
This can create an impression of depth. (From Helmholtz 1909.)

the low luminance-gradient, or coarse-scale system. Such a coupling of two correlated stimulus features would help in segregating distinct depth planes and minimize cross talk between the two component processes. Evidence that disparity processing is carried out in distinct disparity-tuned and size-tuned channels is reviewed in Sections 5.5.3 and 5.7.

Within a given depth plane, luminance gradients differ in width, amplitude, shape, and the regularity of their spatial distribution. Matches between well-spaced and pronounced luminance gradients in a surface are the easiest to detect and, once detected, could propagate along connected edges and lines. Furthermore, matches between well-spaced edges and lines could propagate to other edges and lines in the same depth plane. In particular, matches between well-spaced and pronounced features could help to guide the matching of closely spaced and less distinct features in a given depth plane. This hierarchical, coarse-to-fine search has been used as an algorithm in computer vision (Rosenfeld and Vanderbrug 1977). The cooperativity between spatial scale and disparity channels can work only as long as the various types of visual feature belong to the same surface. Mayhew and Frisby (1980, 1981) implemented a computer algorithm based on cross-channel cooperativity. They called it "stereoedge". The process could be reiterative in that it could start by selecting all feature pairs that, by the nearest-neighbour rule, have the same disparity and then retain only those conforming to a well-formed surface by criteria such as figural continuity or meaningfulness and, finally, look for non nearest-neighbour matches that conform to the same surface. Where there are several depth planes, the logical procedure is to look first for matching images in the plane of convergence with zero disparity. By using

disparity detectors narrowly tuned about zero disparity, most of the spurious matches between neighbouring image features are eliminated. Once the zero-disparity plane is well defined, the system can explore matches sharing other disparities.

The whole process is greatly simplified if the eyes converge on each depth plane in turn. Vergence eye movements to a given plane could be evoked by disparities between well-spaced and prominent features, leaving the matching of finer and less well-pronounced features until after the eyes have moved. Once the images in one depth plane have been matched, the unique-matching rule forbids those same images from being used in other matches. All other image points, except those in monocular zones, are disparate and further matches will be sought and vergence movements evoked only from this pool of images. As the eyes converge from one plane to another, the sets of matched images and the depth information extracted from them could be retained in a buffer memory, leading to a progressive reduction in the pool of unmatched points.

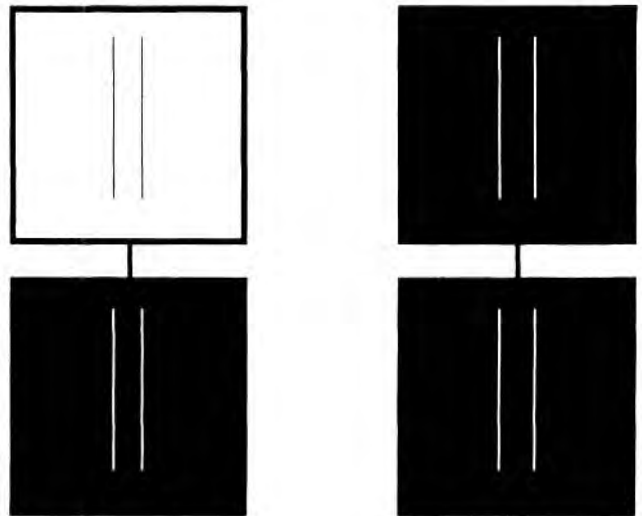
6.2.10 The same-sign rule of luminance polarity

The same-sign rule of binocular fusion states that edges of reversed-contrast polarity in the two eyes do not fuse and are not used by the disparity-detecting system. Evidence on the use of this rule by the visual system is conflicting. Helmholtz (1909, Vol. 3, p. 512) produced the stereogram shown in Figure 6.24. White lines on a black background are presented to one eye and black lines on a white background to the other eye. Depth is seen in the fused image and Helmholtz concluded that disparity between contours of opposite luminance contrast may be used to code depth. But depth in a reversed-

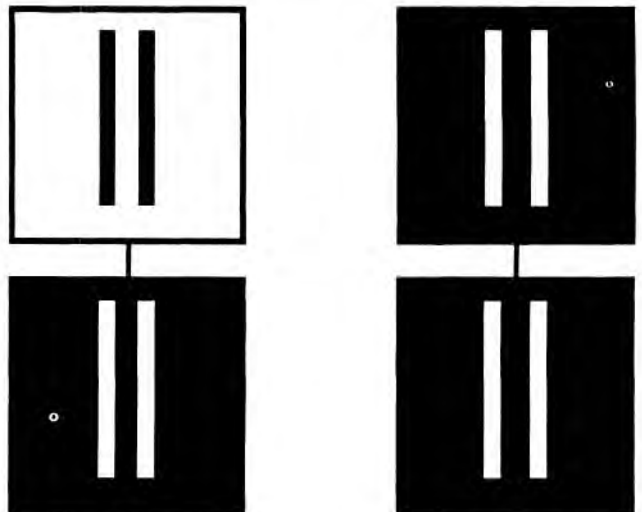
contrast stereogram consisting of thin lines may be due to the binocular fusion of opposite edges of the lines in the two eyes, since these edges have the same contrast polarity (Kaufman and Pitblado 1965). According to this hypothesis, depth should not be seen when the lines in the reversed-contrast stereogram are so wide that edges with similar contrast polarity are too far apart to fuse, as illustrated in Figure 6.25. Treisman (1962) failed to find stereopsis under these conditions. However, Kaufman and Pitblado (1969) reported that some subjects saw depth at a fully reversed-contrast border in spite of not being able to fuse the images. Lateral inhibition at a high-contrast edge generates Mach bands, that is, a darker region on the dark side of the border and a lighter region of the light side. Kaufman and Pitblado suggested that depth at a wide reversed-contrast border is due to disparity between edges of similar polarity selected from these Mach bands.

Krol and van de Grind (1983) obtained depth at a reversed-contrast border when contrast was too low to generate Mach bands and suggested a different explanation to that proposed by Kaufman and Pitblado. They found that the eyes misconverged on the reversed-contrast border, and this has two effects. First, the two diplopic contrast boundaries are treated as unpaired monocular images and are defaulted to the plane of zero disparity. Second, the lateral edges of the display (with similar-contrast polarity) acquire a disparity. The monocular boundary lines are therefore seen in depth relative to the disparity induced into the lateral edges of the display by vergence. The sign of the depth depended on whether the eyes over- or underconverged on the reversed-contrast border. This is the same default rule for unpaired images that is discussed in connection with the unique-matching rule (Section 12.4.6). This explanation preserves the same-polarity matching rule. Levy and Lawson (1978) obtained valid stereopsis when the contrast at a wide dichoptic border was only partially reversed, with gray-on-white in one eye and gray-on-black in the other.

Stereopsis does not occur in a densely textured random-dot stereogram in which the two images have reversed luminance polarity (see Figure 6.26a). However, Julesz (1971, p. 157) observed stereopsis in reversed-polarity stereograms in which the density of the dots was reduced or when correlated colour was added. Cogan et al. (1993) also obtained depth in low-density reversed-polarity stereograms, like that shown in Figure 6.26b, although the stereo threshold was higher than with same-polarity stereograms and the dots did not fuse. We wondered whether depth would be obtained in a high-density stereogram when dots are replaced by thin lines, as



(a) Fusion of the luminance-reversed fine lines in the upper stereogram produces depth, like that produced by the same-polarity images in the lower stereogram.



(b) Luminance-reversed broad lines in the upper stereogram do not produce depth. The same-polarity images in the lower stereogram do produce depth. (From Krol and van de Grind 1983, Perception, 12, 425-438. Pion, London.)

Figure 6.25. Reversed luminance polarity and line width.

in Figure 6.26c. We could not get depth unless the density was considerably reduced, as in Figure 6.26d. Most likely, the visual system detects the disparity between the same-sign edges in this type of stereogram. Depth is seen even in a dense polarity-reversed random-dot stereogram when the briefly exposed images to the two eyes are presented with a delay of about 75 ms (Cogan et al. 1993). With such a delay the negative component of the biphasic temporal response of the visual system to the first stimulus coincides with the positive initial component of the second stimulus. The two simultaneous images therefore have the same contrast polarity.

When one eye views a white letter on a black ground superimposed on a slightly shifted black letter on a white ground, and the other eye sees only the white letter on a black ground (as in Figure 6.32), the apparent depth is in the opposite direction to that corresponding to the disparity between the two letters (Anstis and Rogers 1975; Rogers and Anstis 1975). This is because the visual system registers the disparity between edges of similar contrast rather than between edges of opposite contrast. It can be seen in Figure 6.27 that when the edges with opposite contrast have a crossed disparity, those with the same contrast have an uncrossed disparity. This accounts for the reversal in apparent depth.

In spite of these complexities there seems to be no good basis for rejecting the same-sign rule of fusion and disparity matching of luminance-defined edges. However, rivalry between regions of unfused reversed luminance polarity can be a stereoscopic cue in its own right, as we will see in Section 7.8.3.

A related question is whether stereopsis requires the images in the two eyes to be the same colour. Treisman (1962) obtained stereo depth from the stereogram shown in Figure 6.28 (see after page 310) and concluded that colour rivalry can occur while the disparity between the coloured regions evokes a sensation of depth. A random-dot stereogram with a red filter in front of one eye and a green filter in front of the other eye appeared to alternate in colour by binocular rivalry while the central square appeared to stand out in depth (Ramachandran and Sriram 1972). It was concluded that information from the suppressed image remains available for stereopsis. Depth seen in anaglyphs provides another example of the simultaneous occurrence of colour rivalry and depth.

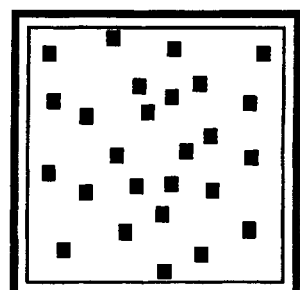
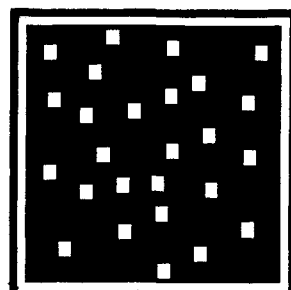
One cannot conclude that just because the coloured background of a stereogram undergoes rivalry the stereoscopic matching of the dots is also subject to rivalry. Rivalry is a spatially local process and could be occurring between coloured regions within or between the dots without affecting the disparity process based on luminance-defined edges of the dots. Rivalry could also be specific to different chromatic channels; rivalry in the channel processing information from contour-free coloured regions may occur independently of that in the channel-processing information from luminance-defined contours (see Section 4.7).

6.2.11 The surface smoothness constraint

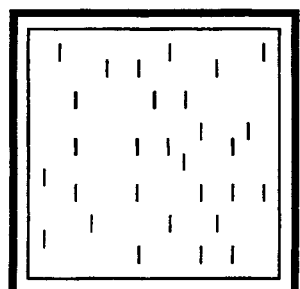
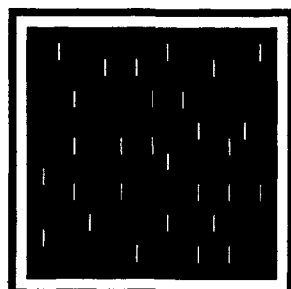
A smooth textured surface lying outside the horopter produces a disparity field that is continuous and smooth over each local neighbourhood. Such



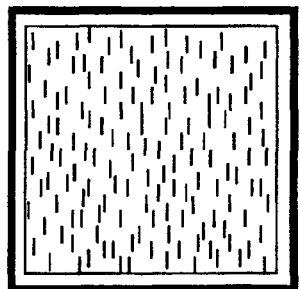
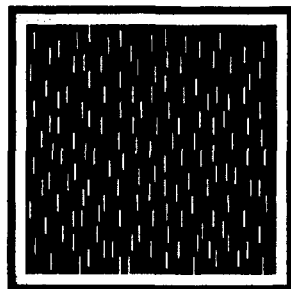
(a) Depth is not seen in a random-dot stereogram in which the images in the two eyes have reversed luminance polarity, even though the central region has a horizontal disparity.



(b) A weak impression of depth is evident in a low-density random-dot stereogram with reversed luminance polarity. (After Cogan et al. 1993.).



(c) Depth is evident in a low-density stereogram with thin lines.



(d) We do not see depth in a high-density stereogram with lines.

Figure 6.26. Stereopsis and reversed luminance polarity.

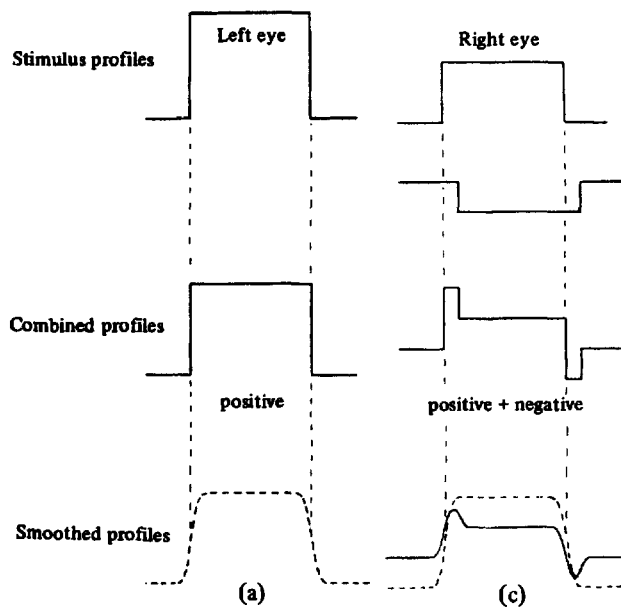


Figure 6.27. Misconvergence on reversed contrast border.
The luminance profiles of one bar presented to the left eye and two reverse-contrast bars presented to the right eye are shown at the top. The combined luminance profiles in each eye are shown in the middle and the smoothed combined luminance profiles are shown at the bottom. (From Rogers and Anstis 1975.)

a disparity field is said to be differentiable. The disparity field produced by a textured transparent surface with other objects visible through it, is not continuous. However, there is continuity within the set of elements that define the transparent surface, that is, continuity over a particular plane in three-dimensional space. A dense three-dimensional array of random dots, like a swarm of gnats, can be said to contain all possible disparity surfaces, since any plane cutting such a display contains a set of points with a constant or continuously varying disparity. We might fleetingly see these planes, just as we fleetingly see coherent patterns of motion in a field of randomly moving dots but the general impression is of a three-dimensional array of dots. Most of the time the natural world is sparsely populated with objects and most of the space we live in is empty. Furthermore, the natural visual environment tends to be bounded by opaque surfaces, such as the ground, walls, and clouds. Thus, natural surfaces tend to occur in isolation, that is, with no other surfaces in the same three-dimensional neighbourhood. It follows from these ecological constraints that, when a coherent disparity surface is detected in the process of image matching it provides strong confirmation that the correct match has been found for the set of features that conform to

that surface. On simple statistical grounds, an incorrect match of the features in the two eyes is unlikely to create coherent gradients. A smooth surface constrains and therefore simplifies the matching process because, as soon as it is found, the image points constituting it become matched, and the unique-matching rule forbids other matches for these points.

In their computational model of the stereoscopic system, Marr and Poggio (1976) postulated a surface continuity constraint in conjunction with the unique-matching rule and the similarity constraint (see also Marr et al. 1978). The continuity principle is based on an assumption that most surfaces are smooth. But this assumption is not required. Even if most surfaces were highly convoluted or discontinuous, detection of a surface with constant or gradually changing disparity would be taken as evidence that a correct image match had been made. The only assumption required is simply that any highly structured, or low-entropy, sensory signal is more likely to arise from a structure in the world than from chance events in the sensory system. An array of points arranged in a regular three-dimensional lattice, even though they do not define a surface, may also confirm that a proper match has been made. In other words, the crucial factor may not be the smoothness of a two-dimensional surface but the regularity of the disparity field, whether in two dimensions or three. Of course, the visual system must possess a mechanism for distinguishing between continuous (differentiable) disparity fields as opposed to discontinuous disparity fields. In fact the world contains more continuous and smooth surfaces than highly irregular surfaces so that, through experience, this will add to the probability that a match that yields a smooth surface is the correct one.

Marr and Poggio also argued that all image pairs in a given region tend to conform to the same smooth surface and concluded that mismatched images are pulled into conformity by a cooperative process in which neighbouring binocular cortical cells with similar disparity tuning are mutually facilitatory and those with different tuning are mutually inhibitory. It has been demonstrated that a few images with an unambiguous disparity can bias the interpretation of a larger array of images with ambiguous disparity (Julesz and Chang 1976).

Figure 6.29 is an example of an ambiguous stereogram. But the biasing process does not involve a perceived change in the disparity between a given set of matched points but rather a change in which sets of images are matched. Only one of the sets of matches creates the impression of a smooth surface and therefore that is the one preferred.

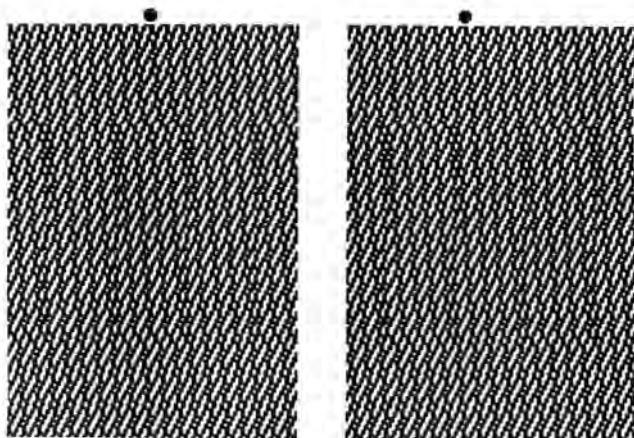


Figure 6.29. Stereograms with ambiguous depth.

The central square contains images with both uncrossed and crossed disparity. The percept alternates between a rectangle nearer than or beyond the background and a series of vertical bars. The rectangle is seen when the dots at the top are fused and the bars are seen when the dots at the bottom are fused.

Any change in perceived disparities in the direction of creating an impression of a smoother surface occurs only for pairs of images with very similar disparities, as the disparity-averaging process described in Section 6.3 suggests. Larger differences in disparity are, if anything, perceptually enhanced, as described also in Section 6.3. The idea that smooth disparity gradients have precedence over disparity discontinuities is an unwarranted extension of the continuity principle. The continuity principle does not forbid us from seeing disparity discontinuities, when they exist. The world is full of disparity discontinuities and we have no difficulty seeing them. In fact, Section 6.2.15 proposes that depth discontinuities produce stronger signals than smooth disparity gradients because discontinuities are more informative, just as luminance discontinuities are more informative than luminance gradients.

The idea that smooth disparity gradients have precedence has led to the proposition that disparity detectors with similar disparity tuning are mutually facilitatory while those differing in disparity tuning mutually inhibit each other (Nelson 1975). Mutual facilitation is required in the sense that a set of matched images conforming to a disparity gradient confirms that the correct match has been found. Other matches are then preempted for that set of image points. Mutual inhibition is not required. When a coherent surface is transparent and there is another surface beyond it, image pairs with other disparities are interspersed among those defining the transparent surface. We have no difficulty seeing



Figure 6.30. Disparity interpolation.

With divergent fusion, the lefthand edge of the inner square appears continuous and concave, and the righthand edge appears convex. Subjective diagonal ridges appear between opposite sides of the square. Depth is reversed with convergent fusion. (From Harris and Gregory 1973, Perception, 2, 235-247, Pion, London.)

superimposed transparent surfaces under these conditions, as long as the density of dots is not too great. This shows, as Prazdny (1985a) pointed out, that the disparity in interspersed image points is not suppressed by the disparity in adjacent image pairs that have already been matched. Indeed, the phenomenon of depth contrast discussed in Section 12.1 suggests that closely neighbouring disparities combine rather than inhibit each other. The second surface becomes visible once an appropriate match has been found for the interspersed features and other matches for that set of features are then preempted. In each local region in the area of overlap of two surfaces there is severe disparity discontinuity but each surface is continuous within itself.

The surface continuity principle does not apply to the two-dimensional visual field but only to particular depth regions within three-dimensional space. If there are no coherent disparity surfaces or other regularities in the scene, as for instance in a swarm of gnats or a cloud of snowflakes, we must use constraints other than surface continuity in three-dimensional space to guide the search for correct image matches.

6.2.12 Image matching and edge continuity

Continuity of edges also provides strong evidence that images have been correctly matched. Matching is facilitated when each monocular image contains continuous edges or contours. For instance, depth in a random-dot stereogram is seen more rapidly when the monocular images that define the disparate region are surrounded by a continuous line (Julesz 1960). Depth discontinuities in the world normally occur along the edges of objects and are often accompanied by discontinuities of texture, colour,

and motion. Even in the absence of accompanying monocular discontinuities, a continuous step of disparity confirms that the correct match has been found, since a continuous step of disparity is most unlikely to occur by chance.

Disconnected depth edges are not suppressed, it is only that, when a continuous depth edge is found, it preempts other interpretations for the set of matched points that define that edge. Discovery of a depth edge prompts a search for its continuation, especially when the edge is interpreted as belonging to an identifiable object. Thus continuous depth edges are perceived across gaps when the resulting percept is one of a complete figure in depth (Harris and Gregory 1973). This process is illustrated in Figure 6.30. With divergent fusion or use of the stereoscope, the left edge of the inner square appears continuous and concave, and the right edge appears convex. In addition, subjective diagonal ridges appear between the opposite sides of the square. This constraint is exploited by the "stereoedge" algorithm developed by Mayhew and Frisby (1980). The effects of continuity constraints on depth judgments are discussed in Section 12.3.

6.2.13 Stereo integration over vergence changes

By changing vergence, a depth plane seen by only the coarse-disparity, large-scale system can be brought within range of the fine-disparity, small-scale system. In other words, the vergence system provides a disparity and spatial-resolution zoom mechanism. Marr and Poggio (1979) proposed that the distinct analyses done at each vergence angle are integrated and stored in a buffer memory, which they called the $2^{1/2}$ -D sketch. In this way the viewer builds up an internal representation of the three-dimensional scene, which can be used to direct further exploratory eye movements and other types of behaviour. Evidence favouring this view is reviewed in Section 6.2.6, and the importance of vergence in stereopsis is mentioned in Sections 6.2.8, 11.1, 11.3, and 12.4.6.

6.2.14 Epipolar image matches

For any visual system with intersecting visual axes, the point of convergence, the two nodal points of the eyes, and the two visual axes lie in the horizontal plane of regard, as shown in Figure 2.5a. The plane containing the two nodal points and any object, whether or not it is in the plane of regard, can be called a **binocular plane**. The plane of regard is the binocular plane which passing through the centres of the two foveas. Any other binocular plane cuts the

two retinas in horizontal meridians of longitude an equal distance above or below the foveas. These are known as **epipolar meridians**. In these definitions it is assumed that the visual axes lie in the same plane: that is, that the angle of vertical vergence is zero. Note that the elevation of binocular planes is defined in retinocentric coordinates, with the foveas as origin, whereas the orientation of binocular planes and of the meridians they intersect is defined in headcentric coordinates. Epipolar meridians are corresponding retinal meridians only when the eyes are in torsional alignment. But whatever the alignment of the eyes, all objects in a given binocular plane produce images lying in a pair of epipolar meridians, and all objects in other planes necessarily produce images lying in other pairs of epipolar meridians. Thus, for a given image point in one eye, one need look for a matching image only in the epipolar meridian of the other eye. Note also that there are never any vertical disparities between points on a pair of epipolar lines. The horizontal disparity of the images lying in a pair of epipolar meridians is zero only for an object lying on the horizontal or vertical horopter (see Section 2.3.2). For all other objects, the disparities of images on a given pair of epipolar meridians are not zero. This epipolar constraint reduces the search for matching images from two dimensions to one, if the visual system is able to keep track of which pairs of meridians are epipolar. This constraint is probably not useful in a biological system because of the difficulty of knowing which meridians lie in a given binocular plane (see Section 7.1.3). However, the constraint may be exploited in a machine vision system. Prazdny (1983) devised a purely visual algorithm for assigning images to epipolar meridians.

6.2.15 Extraction of relative disparities

When disparity is coded in terms of the relative, rather than absolute, activity in a local set of distinct disparity channels, the problem of finding the uniquely correct match between the image features in the two eyes is eased, since the same pattern of relative disparities is present for different matches of the images as a whole. For instance, if the vergence angle were to change, some disparities would be increased but others would be decreased thus keeping relative disparities the same. Tyler and Julesz (1980) pointed out that spurious disparity signals due to fluctuations of vergence or to noise in the visual system are randomly distributed about some mean value and therefore cancel when combined by a disparity pooling mechanism (see Section 6.3). A related point is that disparity modulations of more than 5 c/deg are not registered by the visual system

(see Section 5.5.3), and because visual noise tends to be of high spatial frequency, this helps in the rejection of spurious signals. Relative disparity is discussed in more detail in Chapter 7.

6.3 AVERAGING AND TRANSPARENCY

It was argued in Section 3.2.6 that sensory systems devoted to the detection of a particular stimulus attribute usually consist of sets of detectors with overlapping tuning functions. Distinct stimuli falling within the Nyquist limit of such a system are not resolved, but typically produce a signal that is a weighted average of the activity in the set of stimulated detectors. In other words, the stimuli are combined metamerically to produce the impression of one stimulus. Physiological and psychophysical evidence reviewed in other sections suggests that disparity is detected by a limited number channels with overlapping tuning functions. Evidence reviewed in this section shows that when two stimuli with sufficiently similar disparities are presented within the same location of the visual field their disparities average, or metamerize, to produce an impression of one stimulus at an intermediate depth.

A random-dot display with two overlapping sets of disparate images can produce an impression of one surface seen through another, an effect known as **depth transparency** (Julesz and Johnson 1968), an impression of one plane at an intermediate depth, an effect known as **disparity averaging**, or an impression of a hazy display of dots at different depths, sometimes referred to as **lacy depth**. Consider the simplest case of a display of random dots with disparity d_1 superimposed on a second display with disparity d_2 . Six variables are likely to affect the occurrence of disparity averaging as opposed to the perception of distinct depth planes in such a display:

1. The disparity between the image points within each component display.

2. The difference in disparity between the component displays ($d_1 - d_2$), or Δd . As Δd increases, the component disparities should begin to excite detectors with non-overlapping tuning functions and be seen as distinct depth planes. If there were only three types of disparity detector with broadly overlapping tuning functions, as in the colour system, then, for all detectable values of Δd , the components would not be resolved when they fall on the same location in the visual field.

3. The mean of the two disparities, $(d_1 + d_2)/2$.

4. The density of the points in the monocular image of each component display.

5. The mean distance between the pairs of disparate images in one display and the pairs of disparate images in the other. In a random-dot stereogram with superimposed depth planes, variables 4 and 5 are confounded. One would predict that a region of mixed disparities is more easily resolved into distinct depth planes when the pairs of disparate elements in one display are well separated laterally from those of disparate elements in the other.

6. The separation in time between stimuli with different disparities should facilitate their perceptual separation into distinct depth planes. This factor is discussed in Section 13.1.

Kaufman et al. (1973) presented both halves of a random-dot stereogram to both eyes. The disparity in the central region of the stereogram was set at various values between 4 and 10 arcmin. In each case, a central region of random dots with a given crossed disparity was superimposed on a region with an equal uncrossed disparity. When the combined images were equally bright the central region appeared to be in the same depth plane as the surrounding zero-disparity region. Kaufman et al. concluded that the two oppositely signed disparities combined, or metamerized, into an average value of zero. When the brightness of the two crossed images was made unequal, the central region appeared to move in depth in the direction of the uncrossed images, and *visa versa*. In other words, more weight was given to the disparity components with the same brightness in the two eyes. It is not clear whether this effect was due to the fact that one pair of images differed in brightness and one pair did not or to an image in one of the pairs being dim. Another problem with this procedure is that when one of the images of a pair is made very dim, a bright monocular image remains in the other eye, which adds uncorrelated noise. *It would be interesting to know what would happen if the brightness of both the crossed images were varied relative to that of both the uncrossed images.* If the brightness of one pair of images is reduced, there must come a point where the perceived depth conforms to the disparity of the brighter pair of images. The only uncertainty concerns the slope of the function relating perceived depth to the relative brightness of images with competing disparities. We saw in Section 3.2.6 that metamic poolig in other sensory systems depends on the relative strengths of component stimuli.

A further problem with this procedure is that the effect may be due to averaging of luminance in the two halves of each monocular image rather than to averaging at the binocular level. Rogers and Anstis (1975) favoured this interpretation. In their own

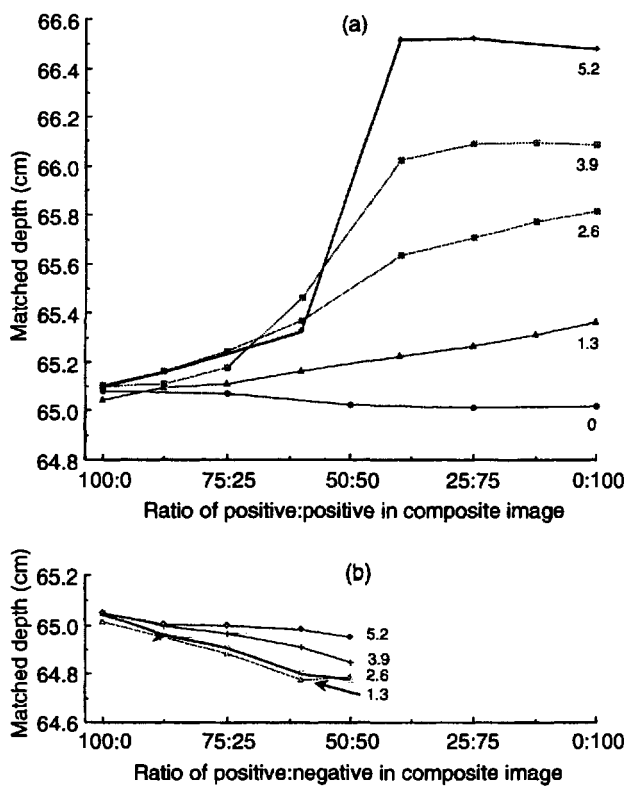


Figure 6.31. Perceived depth with composite images.

The left eye saw a 50-percent-density random-dot pattern; the right eye saw the same pattern plus a version with slight uncrossed disparity. The contrast ratio of patterns in the right eye is given on the abscissa and the displacement (arcmin) is the parameter of each curve. In (a) the two patterns seen by the right eye had the same contrast and as the contrast ratio changed, the matched depth shifted *towards* the disparity of the displaced positive pattern. In (b) the displaced pattern seen by the right eye was contrast reversed (negative) and the matched depth shifted *away* from the disparity of the displaced negative pattern. (Redrawn from Rogers and Anstis 1975.)

experiments the image to one eye was a random-dot pattern with dots subtending 25 arcmin while the image to the other eye was a composite of two identical but slightly displaced images. When the separation between the images in the composite was less than 2 arcmin, the perceived depth of the surface changed smoothly as the balance between the two images in the composite was varied from 100:0 per cent to 0:100 per cent. With larger separations the depth changed abruptly near the 50:50 per cent balance point, from being determined principally by the (zero) disparity of one of the images in the composite to the nonzero disparity of the other (Figure 6.31a).

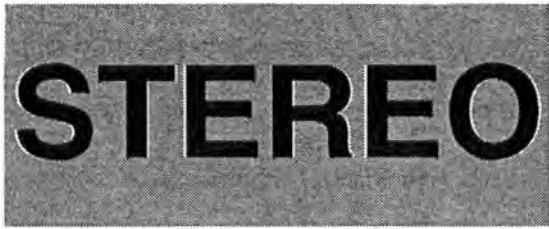
This result by itself does not prove that luminance averaging in the composite image to one eye was responsible for the change in perceived depth rather than disparity averaging between the separate

pairs of matched images in the two eyes. In their second experiment, Rogers and Anstis presented a single (positive) random dot pattern to one eye and a composite of two slightly displaced images to the other, one of which was contrast reversed (negative) (Figure 6.32). Whenever the balance between the two images in the composite was less than 50:50 per cent, so that more of the contrast-reversed image was present in the composite, rivalry rather than depth was seen, as might be expected given previously reported findings on stereopsis with opposite contrast stimuli (Section 6.2.10). However, when the balance was changed between 100:0 and 50:50 per cent, so that the positive image remained dominant in the composite, the perceived depth changed smoothly but in the opposite direction to that predicted by the disparity of the negative image in the composite (Figure 6.31b).

It is unlikely that the observed depth change is due to the disparity averaging between the paired positive-positive and positive-negative images for three reasons. First, it would require the single image in one eye to be paired with both the positive and negative images in the other eye, thereby violating the unique-matching rule (Section 6.2.2). Second, it would require that opposite contrast images in the two eyes be matched, which was shown to be impossible when the negative picture dominated in the composite image. Third, even if a match had been made between the positive and negative images, the predicted depth would be in the direction of displacement of the negative image and thus the predicted depth from disparity averaging should have been in the direction of the disparate negative image rather than in the opposite direction.

Rogers and Anstis modelled the consequences of simple spatial summation or averaging of the luminance contours of the composite positive-positive and positive-negative images, before they are compared by the stereoscopic system, and found a good agreement with their empirical results. In addition, they argued that the existence of comparable reversed effects in the perception of moving patterns (reversed apparent motion) and in the vernier alignment of positive-negative composite contours was accounted for more parsimoniously by a single averaging mechanism which modifies the positions of contours before they are used by the separate stereoscopic, motion, and vernier alignment mechanisms (Anstis and Rogers 1975; Rogers 1976).

Foley and Richards (1978) combined two disparate vertical lines, which by themselves created the impression of a single line beyond a fixation point, with two other lines, which by themselves



STEREO

Figure 6.32. Reversed depth with positive and negative stereograms.

The right eye's image consists of black letters on white background. The left eye's image consists of a 60:40 composite picture of black letters on a white surround and disparate white letters on a dark surround. The reversed contrast letters S, E, and E are displaced to the left (uncrossed disparity) and letters T, R, and O to the right (crossed disparity). When fused with divergent viewing, letters S, T, and E appear in front; in the opposite direction to their disparities.

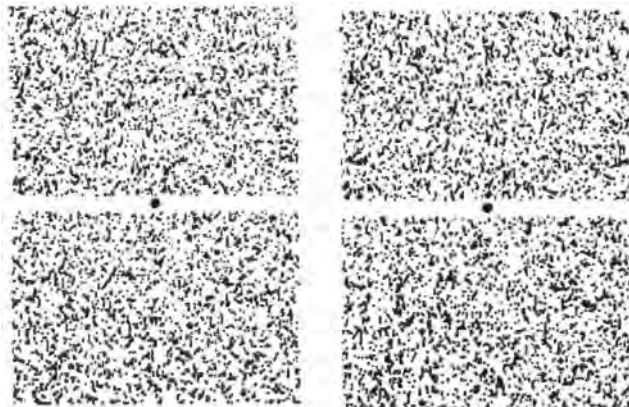
appeared as a line in front of the fixation point. When the two pairs of images were equally bright, subjects saw two lines in the plane of a fixation point placed midway between them, or four lines if fixation was nearer one or the other component line. When one pair of images was dimmed, the brighter pair appeared closer to the position in which it appeared when presented alone. They concluded that perceived depth in this display represented the mean of the two component disparities, weighted for luminance. The difference between the two disparities was 2° (see also Foley 1976a).

Krol and van de Grind (1986) suggested that the effect reported by Foley and Richards is an artifact of changing vergence. They found that vergence is pulled away from the fixation point toward fusing the brighter images and concluded that this, not disparity averaging, causes the images to appear displaced in the same direction. This interpretation is supported by evidence, cited later, that true disparity averaging occurs only over disparity differences of a few minutes of arc and not over the 2° of disparity difference used in the Foley and Richards study. Birch and Foley (1979) obtained similar results when vergence was controlled by nonius lines. However, Tam and Ono (1987) spotted another artifact in Foley and Richard's display. When fixation is held at a point midway between the component lines, the two pairs of images fall on corresponding points, as shown in Figure 2.10. It is meaningless to talk about disparity averaging in this case, since there are no disparities. When fixation is slightly nearer or farther than the midpoint, the left-left and the right-right images, which signify lines near the plane of fixation, are closer to each other than the left-right and right-left images, which signify two lines in different depth planes. As a left image in one eye and a right image in the other eye are dimmed, the left-left and right-right matches become less probable and the left-right, right-left

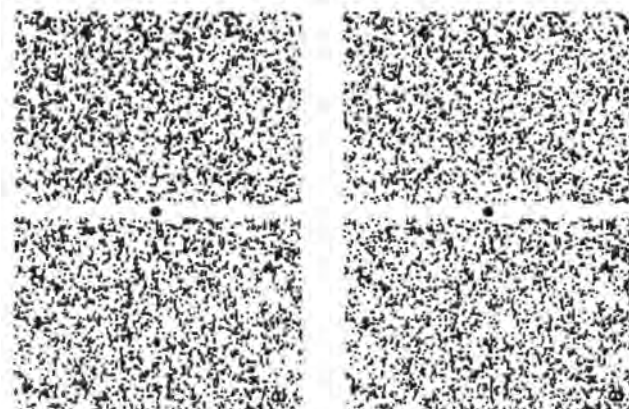
matches more probable, and a shift will occur from seeing two coplanar lines to seeing two lines separated in depth. This has nothing to do with depth averaging; it is simply a question of changing the way pairs of images are combined. A sudden shift in image matching should cause the lines to appear to flip from one position to the other. Tam and Ono observed a sudden flip rather than the gradual transition reported by Foley and Richards.

Akerstrom and Todd (1988) showed subjects either two superimposed depth planes, which created an impression of transparent depth (as in Figure 6.33a), or two side-by-side depth planes (as in Figure 6.33b). Fixation was maintained on the dot at an intermediate depth between the displays. Various combinations of crossed and uncrossed disparities were used ranging from -14, +28 arcmin to -49, +63 arcmin. As the difference in disparity between the component surfaces increased, it became more difficult to see depth transparency but not more difficult to see a depth step. The simplest way to interpret the increased difficulty with transparent surfaces is to say that, as the disparate images in each depth plane were moved further apart, it became more likely that image elements belonging to one depth plane would be paired with nearest-neighbour elements belonging to the other depth plane. As the disparities became very large the superimposed display degenerated into a mishmash of randomly matched images, creating an impression of lacy depth. *To get at the question of the effect on depth segregation of increasing the depth between the planes, one should use displays in which the effects of increasing depth are not contaminated with the increased likelihood of spurious disparity matches.* We will see later that, when the experiment is done this way, depth segregation improves with increasing depth separation between the planes.

Akerstrom and Todd also found that depth transparency became less likely as dot density increased.



(a) Stereogram with superimposed depth planes.



(b) Stereogram with side-by-side depth planes. (From Akerstrom and Todd 1988. Perception and Psychophysics. Reprinted by permission of Psychonomic Society, Inc.)

Figure 6.33. Superimposed and adjacent depth planes.

A simple explanation of this effect is that, as dots become tightly packed relative to the disparities, the chance of spurious matches increases, leading to an impression of lacy depth. Making the dots in the component depth planes different in colour facilitated the perception of depth transparency. Images differing in color are probably less likely to form spurious matches. Depth transparency was not facilitated by differences in orientation of line elements in the two depth planes. These results can also be explained by factors other than disparity averaging.

The evidence reported so far does not provide good evidence for disparity averaging. Parker and Yang (1989) designed a better display for studying disparity averaging and transparency. In this display, horizontal rows of dots with disparity d_1 alternate with rows of dots with disparity d_2 , as shown in Figure 6.34. The patch containing the alternating rows is set in a surrounding region in which all dots have zero disparity. The difference in disparity between the rows is Δd and the average disparity is $(d_1 + d_2)/2$. Note that in this display, $\Delta d = (d_1 + d_2)/2$,

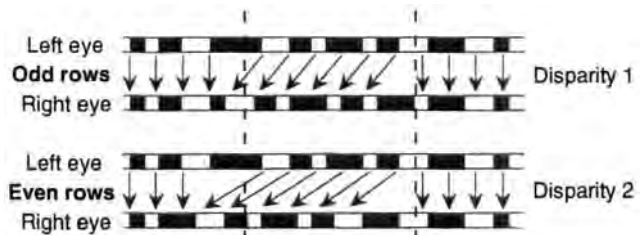


Figure 6.34. Display used to study disparity averaging. Rows of dots with 1 unit of disparity alternate with rows with 2 units of disparity. Flanking regions contain zero disparity. (From Parker and Yang 1989). Reproduced with permission from Vision Research, Pergamon Press.)

and the lateral separation between the component rows can be varied independently. Subjects set the depth of a comparison patch placed in the zero-disparity surround to equal the depth of the mixed-disparity test patch. For values of Δd up to about 114 arcsec, the apparent depth of the test patch was equal to the average disparity, showing that disparity averaging had occurred within this range. Disparity averaging occurred at values of Δd of up to about 200 arcsec, but only when the average disparity of the test display was displaced from zero, that is, when the fixation point was not midway between the two depth planes. With larger Δd values subjects saw two depth planes with depth transparency. Within the range where averaging occurred, changes in the stereoscopic appearance of the display contingent on changes in Δd could still be discriminated. These results support the view that what was taken for disparity averaging in the previous experiments was really the result of competition between conflicting disparity matches within the displays.

Parker and Yang did not vary the vertical separation between the component rows of their display; thus, they did not determine the spatial range of disparity averaging, as opposed to its disparity range. Rohaly and Wilson (1994) approached this question using a dichoptic pair of cosine gratings of one spatial frequency superimposed on a second pair with a different spatial frequency. One of the fused pairs had the same zero disparity as the fixation point and the other had a disparity of 112 arcsec. Subjects compared the perceived depth in the test display with that in a comparison display in which the disparity of the two cosine gratings was always equal. The test gratings appeared as a single display at an intermediate depth with respect to the fixation point (disparity averaging) when the spatial frequencies of the gratings differed by less than 3.5 octaves. No thickening of the display in depth was noticed. With greater differences the two gratings appeared in different depth planes, one seen

through the other. When the contrast of one grating was increased relative to that of the other, perceived depth moved in the direction of the grating with the higher contrast. They proposed a multi-channel model of disparity averaging in which the stimulus components are processed at different spatial scales. They posited a small amount of cross-channel inhibition to account for the data at high contrasts.

The dichoptic combination of two vertical gratings with different spatial frequencies creates an impression of a surface slanted about a vertical axis (see Section 7.2). Superimposition of two disparity ramps composed of similar gratings but with different slants created an impression of a slanted surface at an intermediate angle in one subject and a surface that slanted at a greater angle than either ramp in the other subject (Richards and Foley 1981). The increase in perceived slant was explained in terms of inhibitory side bands in the monocular spatial-frequency channels. But these different impressions, and others mentioned in the paper, could arise out of confusion over which of the pair of gratings in one eye to match with which of the two gratings in the other eye. When the spatial frequency of the gratings comprising one of the ramps differed from that comprising the other by more than 2 octaves, an impression of two slanted surfaces was created. It was concluded that the bandwidth of the monocular spatial-frequency channels feeding into the mechanism responsible for the perception of slant is about 2 octaves.

Anderson (1992) constructed a random-dot stereogram in which half the dots had 12.5 arcmin of crossed disparity and half had 12.5 arcmin of uncrossed disparity. This appeared as two superimposed planes, one beyond and one nearer than a surrounding display of random dots with zero disparity. In a second stereogram half of each set of dots were given random values of disparity between plus and minus 12.5 arcmin, with the other half of each set remaining in the nearer or farther plane. This appeared as a volume of dots rather than two planes. As the two-plane display was replaced by the volume display, the depth appeared to shrink, and during the opposite transition the depth appeared to expand. This apparent change in perceived depth was nulled when the range of disparities in the volume display was increased by about 50 per cent and each display was exposed for 140 ms. With longer durations of exposure, subjects could detect this transition because they had time to notice whether

or not some of the dots were at an intermediate depth. Anderson explained the contraction of apparent depth during the transition between the two displays in terms of depth averaging in the volume display.

The magnitude of depth averaging revealed by this procedure is about three times greater than that reported by Parker and Yang. However, there may be an artifact in Anderson's measure. During the transition from the volume display to the two-plane display half the dots migrated from an intermediate position to one or other of the limiting surfaces. This motion should generate an impression of expansion in depth. The opposite transition should generate an impression of contraction in depth. These impressions would add to any effect due to disparity averaging. Control measurements are required in which the depth of a constantly visible two-plane display is nulled against that of a constantly visible volume display. In fact, Stevenson et al. (1991) did an experiment of this type. They superimposed a random-dot surface with a disparity of between zero and 15 arcmin and a zero disparity random-dot surface, as shown in Figure 11.17. Subjects adjusted the disparity of a comparison random-dot surface until it appeared at the same depth as the zero-disparity surface. This procedure revealed that when the superimposed surfaces were less than about 4 arcmin apart, they appeared as one surface at an intermediate depth. The degree of disparity averaging was about one-third that reported by Anderson and was therefore in line with that reported by Parker and Yang.

So far, in this section, we have assumed that disparity averaging is a process within the disparity-coding mechanism that is akin to color metamerism. Neighbouring stimuli with similar disparities evoke distributions of activity within the set of disparity detectors. When these distributions are not sufficiently distinct, they coalesce into a single distribution of activity with a peak at an intermediate position. Such a process would have to occur beyond the point where monocular images are combined. But what is claimed to be disparity averaging could also be due to spatial interactions between the elements in each monocular image. Spatial attraction and repulsion between monocular images are well-known phenomena (see Section 12.1). It is not known which of these processes is responsible for disparity averaging, but they probably both contribute.

Types of disparity

7.1 Theoretical considerations	235
7.1.1 Monocular coordinate systems	236
7.1.2 Binocular coordinate systems	240
7.1.3 Projection surfaces and camera calibration	243
7.1.4 The concept of disparity	246
7.1.5 Information provided by disparities	249
7.2 Disparities on slanted surfaces	254
7.2.1 Dif-size or width disparity	254
7.2.2 Horizontal size ratio (HSR)	255
7.2.3 Dif-frequency disparity	255
7.2.4 Cumulative horizontal disparity	256
7.2.5 Beat patterns of horizontal disparity	256
7.2.6 Sequentially scanned local disparities	256
7.2.7 Orientation disparity	257
7.2.8 Deformation and angular disparity	257
7.2.9 Polar disparity	258
7.3 Perception of slant	258
7.3.1 Dif-frequency and width disparities	259
7.3.2 Deformation and slanted surfaces	265
7.4 Disparities on inclined surfaces	268
7.4.1 Horizontal point or positional disparity	269
7.4.2 Orientation disparity	269
7.4.3 Deformation and angular disparity	271
7.4.4 Cumulative horizontal disparity	271
7.4.5 Polar disparity	271
7.5 Perception of inclination	271
7.5.1 Orientation disparity and inclination	271
7.5.2 Deformation disparity and inclination	275
7.6 Vertical disparity	280
7.6.1 Causes of vertical disparity	280
7.6.2 Absolute vertical disparities	281
7.6.3 Relative vertical disparities and size ratios	281
7.6.4 Computational theory of vertical disparities	283
7.6.5 The induced effect	285
7.6.6 Predictions and empirical evidence	288
7.6.7 The perception of frontal surfaces	292
7.7 Disparity-defined shape	295
7.7.1 Theoretical considerations	295
7.7.2 Shape perception in disparity surfaces	298
7.8 Miscellaneous types of disparity	305
7.8.1 Stereopsis from geometrical illusions	305
7.8.2 Chromostereopsis	306
7.8.3 Luminance rivalry as a depth cue	307
7.8.4 Stereopsis due to unequal image illumination	310
7.8.5 Specularity disparity	312

7.1 THEORETICAL CONSIDERATIONS

Binocular disparity is the general term that refers to the differences between retinal images created by viewing the world from two slightly different positions or vantage points. These differences can be

specified and measured with respect to either the optic arrays subtended at the two vantage points (Section 2.1) or the images projected on retinas or camera planes. The metric properties of an image produced by a given optical array depend on the shape of the projection surface and its position with

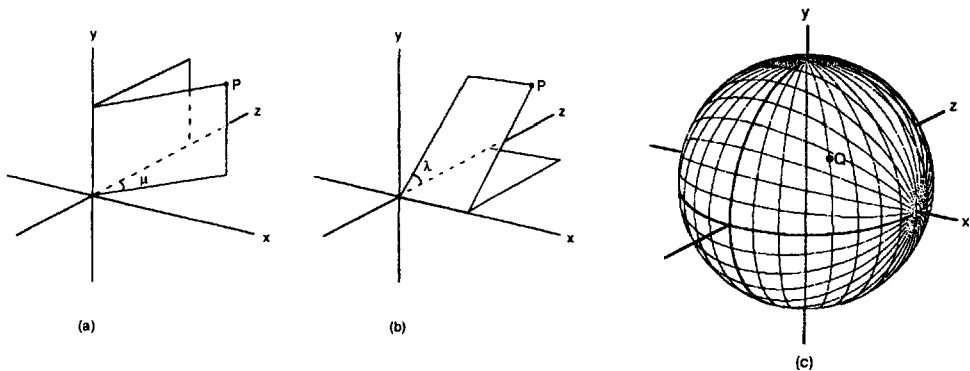


Figure 7.1. Longitudinal-azimuth/longitudinal-elevation axes.

- (a) The azimuth of point P is the dihedral angle μ between a vertical plane passing through P and the zero azimuth (y - z) plane.
- (b) The elevation of point P is the dihedral angle λ between an elevated plane passing through P and the zero elevation (x - z) plane.
- (c) Points with the same azimuth project to lines of longitude passing through north-south poles. Points with the same elevation project to lines of longitude passing through east-west poles.

respect to the vantage point. The nature and extent of binocular disparities also depend on the coordinate system used to measure the images. It is important to distinguish between disparities due to viewing the world from two vantage points and those due to the coordinate system. The former disparities provide a basis for the **computational theory** of binocular stereopsis, which identifies the nature of information about the structure and layout of the visual world. To evaluate mechanisms used to extract this information in a visual system we must consider projection surfaces, coordinate systems, and image properties as well as the computational theory.

These issues are considered in the first section of this chapter. We start by describing coordinate systems that can be used to measure visual directions from a single eye. Next we consider how interocular differences in direction of a single point can be measured when the coordinate axes of the eyes are either aligned or not aligned. We then show how the shape of the projection surface affects the pattern of binocular disparities and we distinguish between the **absolute disparity** of a single point and the **relative disparity** of two or more points. **Horizontal** and **vertical disparity** are defined and we examine the information that each provides. We also consider the effects of eye movements on the measurement of disparity. Finally, we define and discuss higher-order disparities as an alternative basis for describing differences between binocular images.

7.1.1 Monocular coordinate systems

The optic array specifies directions from which light reaches a given vantage point and is consequently

expressed in terms of angles of elevation and azimuth within a **spherical coordinate system**. Five spherical coordinate systems are now described.

1. Longitudinal-azimuth/longitudinal-elevation axes

In this coordinate system the azimuth of a point is defined as the dihedral angle between a vertical plane passing through the point and the zero azimuth plane (Figure 7.1a). The elevation of a point is the dihedral angle between an elevated plane passing through the point and the zero elevation plane (Figure 7.1b). The consequences of measuring azimuth and elevation in this way can be appreciated by considering the projection onto a spherical surface of all points in space having the same angles of either azimuth or elevation. A plane of equally eccentric or **isoazimuth** points projects to a **great circle** passing through north-south poles, along the y axis of the coordinate frame. A plane of **isoelevation** points projects to a great circle with east-west poles, along the x axis of the coordinate frame (see Figure 7.1c). **Lines of longitude** on a globe are great circles passing through the poles and we thus refer to this coordinate system as having **longitudinal-azimuth/longitudinal-elevation axes** (see also Table 2.1).

2. Longitudinal-azimuth/latitudinal-elevation axes

In the longitudinal-azimuth/latitudinal-elevation system, azimuth is measured as the dihedral angle between a vertical plane passing through the point in space and the zero azimuth plane (as with the longitudinal/longitudinal system), but elevation is measured in the azimuth plane containing the point (Figure 7.2a). This is equivalent to rotating the longitudinal/longitudinal coordinate system around the y axis for each point in the scene, before measuring

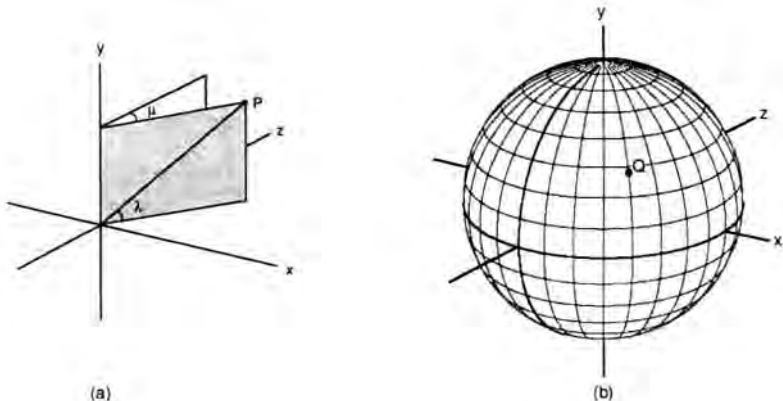


Figure 7.2. Longitudinal-azimuth/latitudinal-elevation axes.

- (a) Azimuth is the dihedral angle μ between a vertical plane passing through point P and the zero azimuth plane. Elevation λ is measured within the azimuth plane containing the point.
- (b) Points with the same azimuth project to lines of longitude passing through north-south poles on the y axis. Points with the same elevation project to parallel circles or lines of latitude around the y axis.

its elevation. Note that there appears to be an implicit order in carrying out the measurements—azimuth is measured first, then elevation within the azimuth plane. However, this was done for the purposes of exposition and is not an inherent property of the coordinate system.

Points in space with the same azimuth project onto a great circle joining the north-south poles, as for the longitude/longitude system. Points with the same elevation project onto a line of latitude around the vertical axis of the projection sphere. Lines of latitude form a set of parallel circles like lines of latitude on a terrestrial globe (see Figure 7.2b). We refer to this coordinate system as having **longitudinal-azimuth/latitudinal-elevation axes**. This way of measuring azimuth and elevation corresponds to the gun-turret model, so-called because a fixed gun is first rotated to the correct azimuth, and then elevated appropriately.

If we compare measurements of visual direction using these two coordinate systems, two features emerge. First, the values of azimuth and elevation are typically not the same. A point Q with an azimuth of 45° and an elevation of 40° , in a longitude/longitude system, has azimuth/elevation coordinates of $45^\circ/30.7^\circ$ in a longitudinal-azimuth/latitudinal-elevation system. Second, what is regarded as horizontal or vertical also differs in different coordinate systems. Two points are regarded as “horizontal” when they have the same elevation. This means that they must lie along the same isoelevation line in the projected image. These lines are different for different coordinate systems.

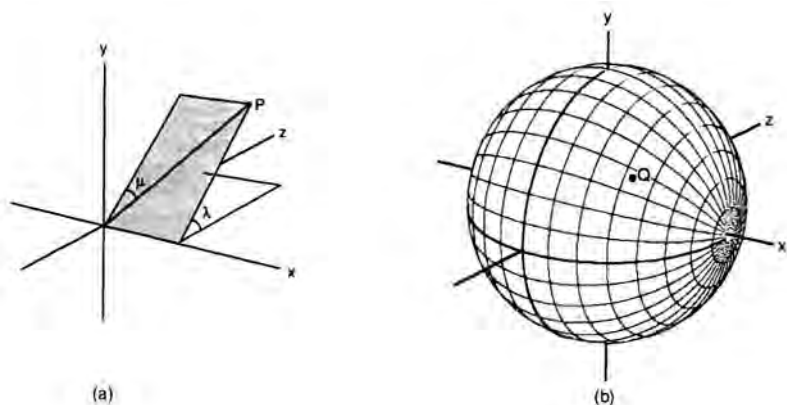
There is a similarity between the longitudinal-

azimuth/latitudinal-elevation axes just described and the **Fick system**, used to specify positions of the eyes (see Section 10.1.2). In the Fick system, azimuth is assessed first with reference to the sagittal plane of the head rather than of the eye and the eyes are assumed to rotate gimbal fashion. There is thus an inherent order in defining elevation and azimuth, which does not apply when we use this coordinate system to measure the oculocentric position of a point in space.

3. Latitudinal-azimuth/longitudinal-elevation axes

In the third spherical coordinate system, elevation is the dihedral angle between an elevated plane passing through the point in space and the zero elevation plane. Azimuth is then measured within the elevated plane containing the point (Figure 7.3a). This is equivalent to rotating the longitudinal/longitudinal coordinate system around the horizontal (x) axis for each point in the scene before measuring its azimuth. Points in space with the same elevation project onto a great circle joining the east-west poles on the x axis of the spherical projection surface, as for the longitude/longitude system, but points with the same azimuth now project onto a line of latitude with respect to the x axis of the projection sphere (Figure 7.3b). We can refer to the coordinate framework as having **latitudinal-azimuth/longitudinal-elevation axes**.

What is regarded as horizontal in this scheme is the same as for longitude/longitude measurements but differs from longitude/latitude measurements. Verticals, on the other hand, are different from those measured under either of these schemes. The azimuth/eccentricity coordinates of our point Q in

**Figure 7.3. Latitudinal-azimuth/longitudinal-elevation axes.**

- (a) Elevation is the dihedral angle λ between an elevated plane passing through point P and the zero elevation plane. Azimuth μ is measured within the elevation plane containing the point.
 (b) Points with the same elevation project to lines of longitude passing through east-west poles on the x axis. Points with the same azimuth project to parallel circles or lines of latitude around the x axis.

space under this system are $37.4^\circ/40^\circ$. Note that the azimuth and elevation planes passing through a point are always orthogonal in both this and the previous scheme, which means that what is defined as horizontal is always orthogonal to what is defined as vertical. This is not true when azimuth and elevation are measured in a longitude/longitude system.

The latitudinal-azimuth/longitudinal-elevation coordinate system resembles the Helmholtz system for specifying eye movements. In the Helmholtz system, elevation is assessed first with reference to the transverse plane of the head and azimuth is assessed with respect to an axis orthogonal to that plane.

4. Latitudinal-azimuth/latitudinal-elevation axes

The fourth system for measuring the oculocentric position of a point can be thought of as a longitudinal/longitudinal coordinate system rotated around both x and y axes. Elevation is measured within the azimuth plane containing the point and azimuth is measured within the elevated plane containing the point (Figures 7.4a and b). As for the longitude/longitude system, the azimuth and elevation planes that pass through the point are typically not orthogonal. Points in space with the same azimuth project onto a circle of latitude around the x axis of the spherical projection surface, and points with the same elevation project onto a circle of latitude around the y axis of the coordinate framework (Figure 7.4c). We refer to the coordinate framework as having latitudinal-azimuth/latitudinal-elevation axes. Horizontals under this scheme are the same as those under the longitudinal/latitudinal scheme and verticals are the same as those measured with latitudinal-azimuth/longitudinal-elevation. The azimuth/eccentricity coordinates of our point Q in space are $37.4^\circ/30.7^\circ$ under this system.

5. Polar coordinates

The fifth way of measuring the visual direction of a point in space is in terms of a polar coordinate or perimetric scheme in which the position of a point is expressed in terms of a polar or meridional direction (φ) and an angle of eccentricity (θ) in the radial direction (see Figure 7.5a). If measurements of polar position are made on a spherical projection surface, this will correspond to the point's direction in terms of a polar angle from an arbitrary zero, such as the 3 o'clock position, and its eccentricity in the meridional or radial direction. This is equivalent to putting the pole along the z axis and measuring polar direction in terms of lines of longitude through this pole and eccentricity in terms of lines of latitude around the z axis (see Figure 7.5b).

Coordinate transformations

Two important points emerge from considering these five ways of specifying the direction of a point—the values of azimuth and elevation differ and what is regarded as horizontal or vertical also changes. The differing values are related by a simple coordinate transformation. In the human visual system, this is equivalent to saying that a given receptor in the retina could be labelled with the values of any or, indeed, all of the different coordinate systems. Similarly, the orientation of a line on the retina—horizontal, vertical, or in between—could be measured according to any or all of the coordinate schemes, although the answers would be different.

If the values of azimuth and elevation and what is regarded as horizontal and vertical can be transformed from one coordinate system to another, is there any reason to prefer one particular system? To answer this question we need to consider that when

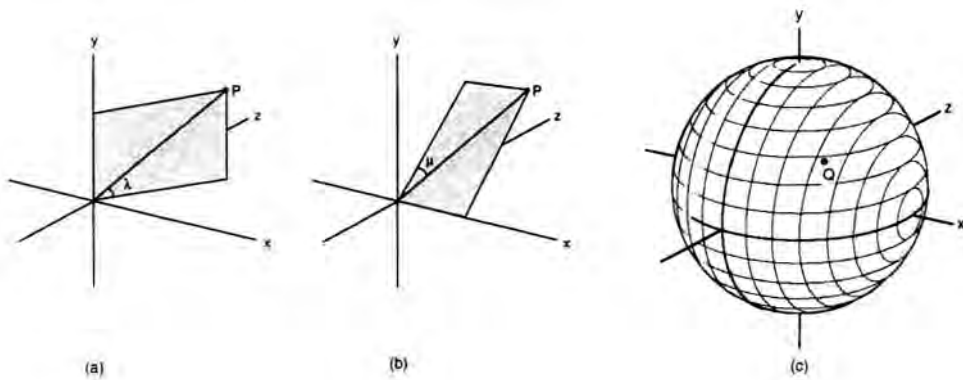


Figure 7.4. Latitudinal-azimuth/latitudinal-elevation axes.

- (a) Elevation λ is measured within the vertical azimuth plane through point P .
- (b) Azimuth is measured within the elevated plane passing through point P .
- (c) Points with the same azimuth project to lines of latitude around the x axis.
Points with the same elevation project to lines of latitude around the y axis.

the eyes move, the coordinate system necessarily moves with them. The eyes also move with respect to each other so that the coordinate axes of the eyes are not usually aligned. This means that, with any coordinate system, it is impossible to perceive the visual direction of an object with respect to the head without knowing the positions of the eyes.

As we will see in the next section, stereopsis is not based on the absolute position of a point in space from two vantage points—absolute disparity—but rather on differences in direction of two or more points in space—relative disparity or simply disparity. Hence we can reformulate the question and ask which coordinate system is best for describing relative disparity. Relative disparity depends on the measurement of angular differences between pairs of points in the same eye (Section 7.1.2). The separation of a pair of points projected on a spherical surface does not change when that surface is rotated around its centre, but the measurement of that separation and its attribution as a horizontal or vertical separation depends on the coordinate system used to measure it. Hence the correct choice of coordinate system is important.

Consider first the measurement of the separation of a pair of points in a single eye using longitudinal-azimuth/latitudinal-elevation coordinates. Since the coordinate framework is rotationally symmetric around the y axis (Figure 7.2), such a rotation (a horizontal eye movement) does not affect the azimuth and elevation separations of a pair of points. This can be appreciated visually by noticing that the spacing of the lines of longitude and latitude which constitute the “ruler” is not affected when the sphere is rotated around the y axis. What is regarded

as horizontal or vertical is similarly unaffected by horizontal eye movements. The same is not true for rotations of the coordinate frame around the x axis. Measurements of azimuth and elevation differences and what is regarded as horizontal or vertical are all modified by vertical eye movements.

A complementary pattern of invariances and variances holds when disparity is measured using latitudinal-azimuth/longitudinal-elevation axes because the coordinate framework is rotationally symmetric around the x axis (Figure 7.3). Vertical eye movements do not affect the measurement of azimuth and elevation differences or what is regarded as horizontal or vertical; horizontal movements do.

With latitudinal-azimuth/latitudinal-elevation axes (Figure 7.4), the set of latitudes for measuring azimuth are rotationally symmetric about the x axis and the set of latitudes for measuring elevation are rotationally symmetric about the y axis. This means that azimuth differences used in calculating horizontal disparities are unaffected by vertical eye movements and elevation differences used in calculating vertical disparities are unaffected by horizontal eye movements.

A complementary pattern of invariances and variances holds when disparity is measured using longitudinal-azimuth/longitudinal-elevation axes (Figure 7.1). Azimuth differences are unaffected by horizontal eye movements and elevation differences are unaffected by vertical eye movements. The polar system for measuring visual direction (Figure 7.5) is not rotationally symmetric about either the x or y axes and, as a consequence, measurements of differences in polar direction and eccentricity are altered by both vertical and horizontal eye movements.

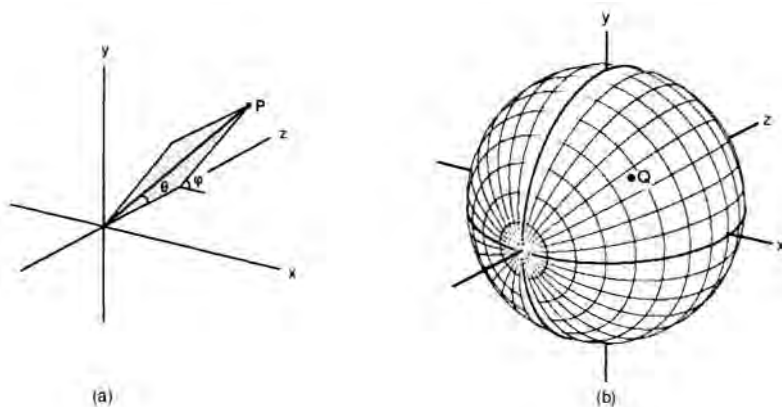


Figure 7.5. Polar coordinate or perimeter scheme.

(a) Polar direction φ is the dihedral angle between a plane passing through point P and the zero meridional plane (x - z). Polar eccentricity θ is measured within the meridional plane passing through P .
(b) Points with the same polar direction project to lines of longitude passing through poles on the z axis. Points with the same polar eccentricity project to parallel circles or lines of latitude around the z axis.

Summary

The preceding discussion suggests that there is no good reason for preferring one coordinate system over another for measuring the direction of a single point from a single vantage point. However, important differences between the coordinate systems emerge if we consider specifying the difference in direction (separation) between a pair of points when the coordinate axes can rotate. In none of the five coordinate systems are both azimuth and elevation differences invariant with both horizontal and vertical eye movements. As a consequence, it is somewhat arbitrary which of the five systems is used to define binocular disparities. In the human visual system, it could be argued that it is particularly important that measurements of horizontal and vertical disparities remain unaffected by horizontal vergence. The only coordinate scheme that satisfies this requirement has longitudinal-azimuth and latitudinal elevation axes—the gun-turret model. For this reason it is the best choice for describing and measuring disparities. This system has the related advantage that a “horizontal” separation between a pair of points always remains horizontal and a “vertical” separation remains vertical with both horizontal vergence and version movements of the eyes. In subsequent sections we will use the gun turret coordinate system to define horizontal and vertical disparities. However, binocular disparities can be described using the other coordinate systems and there may be other reasons for preferring one system over another. The preceding discussion makes it clear that the measurement of azimuth and elevation and the assessment of what is vertical and horizontal are not trivial problems for any visual system to solve. An alternative solution is to restrict

measurements of visual directions to regions close to the origin of the coordinate framework (close to the fovea). For small angles, the measurement of azimuth and elevation differences are unaffected by the choice of coordinate system. If this is done, however, it is necessary to have precise information about the positions of the eyes with respect to the head to interpret the visual information correctly.

7.1.2 Binocular coordinate systems

To discuss the concept of binocular disparity, we need to consider how the direction of a point in space can be measured with respect to a pair of coordinate systems which are separated horizontally but not necessarily aligned with respect to each other.

Aligned coordinate axes

For a binocular system in which the coordinate axes for determining elevation and azimuth are fixed and aligned, but separated horizontally by the interocular distance, the bipolar coordinates of a single point (Section 2.3.2) can be calculated from the separate elevation and azimuth at the two vantage points, irrespective of the coordinate system used. The bipolar coordinates define the visual or *cyclopean* direction of the point from a hypothetical cyclopean eye located midway between the two eyes. The location of a point in space is fully specified under these conditions, since it is always possible to project the visual directions back out of the optic arrays so that the rays converge at a particular point in space. However, while every point in space is fully specified by the azimuth and elevation angles at each of the two eyes or vantage points, particular pairs of elevation and azimuth values correspond to a single

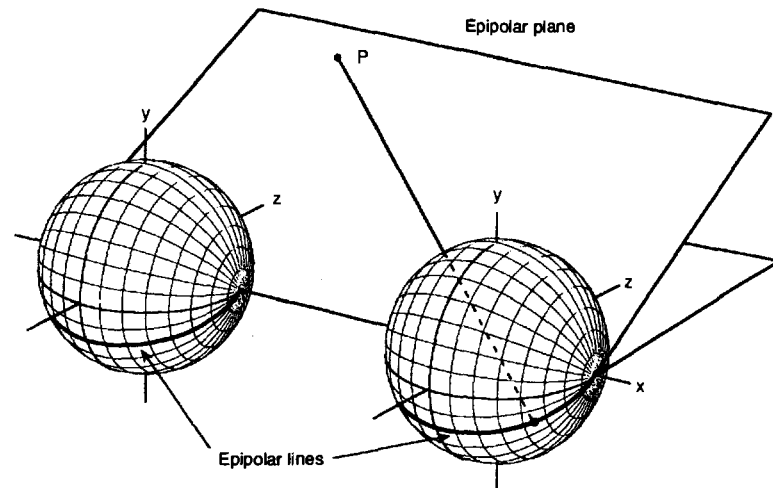


Figure 7.6. Epipolar planes and epipolar lines.

An epipolar plane passes through a point P in the visual scene and the optical centres of the two eyes. Once the visual direction of the point is established in one eye (right eye), the only possible location of the corresponding point in the other eye is along an epipolar line, which is the projection of the epipolar plane. Epipoles are great circles passing through poles on the interocular axis. Consequently, the location of epipoles on the retina is not fixed if the eye rotates.

point in space only if the projected visual directions from the two eyes intersect.

If the coordinate frameworks of the two eyes are aligned, there is a single plane which passes through the point in space and the optic centres of the eyes. This is known as the **epipolar plane**. This fact restricts the search space for finding the correct binocular match once the direction of the point in one eye has been established (Section 6.2.14). In other words, the **correspondence problem** is eased. That search space is the common or epipolar plane that projects to a single line on the other retina—the **epipolar line** (Figure 7.6). All epipolar planes pass through the axis joining the optical centres of the two eyes and, if the eyes are fixed and aligned, the epipoles have fixed and constant loci on the retinas; they correspond to great circles between poles on the interocular axis. If the eyes are free to move, the location of the epipoles on the retinas changes—the retinas rotate under the epipoles which remain fixed with respect to the interocular axis. Hence it is impossible to know the loci of epipolar lines on the retina of a moveable eye without knowing eye position. For this reason it seems unlikely that the human visual system could exploit a strict epipolar constraint in finding correct binocular matches.

If the interocular separation of the two eyes is known, the absolute distance to a point in space is specified by the angles of elevation and azimuth, provided that the coordinate frameworks are aligned. The visual directions of a single point in space from two separated vantage points are always different (unless the point lies at infinity), and that

point is regarded as disparate if either its elevation or its azimuth from the two eyes differs. A binocular difference in the azimuth of a point is a measure of its **absolute horizontal disparity**, and a difference in its elevation is a measure of its **absolute vertical disparity**.

$$\text{Absolute horizontal disparity} = \alpha_L - \alpha_R \quad (1)$$

$$\text{Absolute vertical disparity} = \beta_L - \beta_R \quad (2)$$

Four points are worth noting.

1. Simple geometry shows that the binocular difference in azimuth of a point—the absolute horizontal disparity—equals its binocular subtense (Figure 2.6).

2. Absolute horizontal and vertical disparities of a point in space depend on the coordinate system (see earlier) but, just as monocular measurements of a point's azimuth and elevation can be transformed from one coordinate system to another, so too can a point's absolute horizontal and vertical disparities, if the coordinate axes are fixed and aligned.

3. The absolute disparity of a point provides only limited information about its position with respect to an isodisparity circle (see below). The azimuth and elevation from each eye are needed to locate the point in space and determine its absolute distance.

4. The information provided by the azimuth and elevation of a single point with binocular viewing is available only if (1) the coordinate frames in the two eyes or cameras are fixed and aligned or (2) there is

additional information about the precise positions of the eyes or cameras, if they are free to move. If neither of these conditions holds, there is no reliable information about the point's position in space. The first condition holds in machine vision systems when the cameras are set up and calibrated very precisely, and it also may be relevant for species such as the owl whose eyes can move through only a very small angle (see Section 16.7). Under these circumstances the absolute distance to a point is specified by the elevation and azimuth values, whatever coordinate system is used to measure those values.

Independent coordinate axes

If the eyes or cameras of a binocular system are free to move independently, the absolute location of a point in space can be determined only with additional information about the precise positions of the eyes or cameras. This information may be available from proprioception (feedback) or efference copy (feedforward) from the eye or camera control system. Alternatively, as we will see, the binocular images themselves contain information about the vergence and version angles of the eyes which can be used to locate eye positions (see Section 7.2).

If the optic axes of the eyes or cameras are able to move so as to position the image of a point at the origins of the coordinate axes, the absolute horizontal and vertical disparities of the point are necessarily zero. The absolute position of the point is then completely specified by the orientations of the optic axes. In the human visual system, this corresponds to fixating the point so that its images fall on the foveas of the two eyes. Under these conditions, the visual system is acting as a **range-finder** and, if the separation of the two eyes and the orientations of the optic axes are known, absolute distance can be calculated. Evidence that the human visual system is able to make judgments about the absolute distance of a single point in space from eye position information alone is reviewed in Section 11.1.

Although the absolute position of a point and its distance from the observer cannot be determined without knowledge of eye position, absolute disparities do provide some information about the position of the point with respect to where the eyes or cameras are "looking". As long as the optic axes of the eyes or cameras intersect in a forward direction, the magnitude and sign of the absolute horizontal disparity of a single point provide information about the location of the point with respect to the Vieth-Müller circle (Section 2.5), even if the "fixation point" is not visible. If the optic axes of the eyes or cameras do not intersect, the absolute horizontal disparity of a point provides no reliable information.

Binocular disparity detectors

The preceding discussion is relevant to the physiological finding that some binocularly driven cells in the primate visual system have receptive fields in either the same or slightly different equivalent positions in the two retinas (see Sections 4.4 and 4.5). These cells can be thought of as **absolute disparity detectors** capable of specifying the disparity of a point with respect to the visual axes of the two eyes. As we have seen, absolute disparities provide information about the location of a point with respect to the Vieth-Müller circle passing through the convergence point. Does the human visual system have access to that information? As far as we are aware, the critical experiment has not been done, but it would involve monitoring the vergence positions of the two eyes, in the absence of a fixation point. A single point close to the convergence point would then be flashed on and the observer would report whether the point was in front of or behind where he or she was looking. Absolute disparity detectors should be able to provide this information. It is likely that observers can do this task if the value of the absolute disparity is sufficiently large, but we predict that thresholds will be much higher than those found previously for discriminating a difference in depth of a pair of points in the visual field (Section 5.3).

Experiments of Erkelens and Collewijn (1985a) and Regan et al. (1986a) provide evidence that our ability to use absolute horizontal disparities is very limited. They presented a pair of identical random dot patterns to the two eyes. The two patterns moved sinusoidally in a horizontal direction, but in antiphase, thereby simulating (to a first approximation) the motion of a surface toward and away from the observer. At a temporal frequency of 0.2 Hz, observers reported that the fused pattern did not give any impression of motion in depth. If the observers tracked the antiphase movements of the binocular pattern with vergence eye movements the images would not have moved across the retinas and the results would indicate that we do not have access to reliable vergence signals. In fact, Erkelens and Collewijn monitored eye movements and found that observers did make vergence movements in response to the stimulus, but the gain of the vergence was less than 100 per cent. This indicates that vergence changes did not completely compensate for the movement of the images across the retinas so that the disparity of all points in the pattern would have changed. The absolute disparity-detecting cells found in the primate visual system ought to have responded to this changing stimulus, but the psychophysical evidence suggests that we do not have

access to this information for judging location in depth with respect to the convergence point. However, subjects did notice a change in the apparent size of the display that could have been due to either changing vergence or changing disparity.

7.1.3 Projection surfaces and camera calibration

There has been debate in the past about the differences between the projection of images onto curved surfaces, such as the mammalian retinas, or onto flat planes as in film and TV cameras. Clearly, the location, size, and shape of an image projected onto different surfaces, change with the location and shape of the surface. However, the measurement of visual direction from a single vantage point, as well as angular size and shape, are not affected as long as the projection surface is appropriately calibrated. In other words, all that is needed is a look-up table that specifies the angular coordinates of all positions on the projection surface. Furthermore, angular coordinates may be transformed and specified according to any one of the five coordinate systems described in Section 7.1.1. The particular receptor (or pixel) stimulated provides the complete information about the direction of the point with respect to the axes of any or all of the coordinate systems.

In machine vision, it has generally been assumed that it is necessary to know precisely the axes of the cameras in a stereo rig and other **camera calibration parameters** to interpret differences between stereoscopic images. As was indicated earlier, this information may be derived from sensors monitoring the camera positions or, alternatively, from the visual information provided by vertical disparities (Mayhew and Longuet-Higgins 1982). Once the axes of the two cameras are known, the entire metric structure of a three-dimensional scene can be recovered. For those working in biological vision, it has generally been assumed that **viewing-system parameters** such as the vergence angle of the eyes or the degree of eccentric fixation are not known precisely. Consequently, the emphasis in most biological research has been on exploiting the characteristics of binocular images which do not depend on knowledge of eye position, at least explicitly. This strategy has often resulted in proposals for determining the three-dimensional scene properties, which are valid in only a few very restricted situations, such as with symmetric gaze or for small fields of view close to the point of fixation, as we will see.

Shape of the retina

There are two main types of image disparity in a binocular viewing system. The first is an **overall**

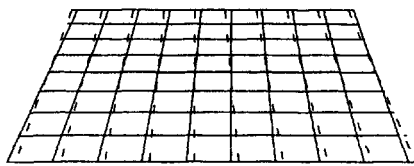
disparity due to a horizontal, vertical, or rotary offset of one image relative to the other. The second is the pattern of **relative disparities** that remains when overall disparity has been reduced to a minimum. Overall disparities may be nulled by appropriate vergence movements. A vergence movement may be defined as an **opposed movement of two retinas, each within the plane of a stationary image, which affects overall disparity without changing relative disparities**. Overall disparities are determined wholly by the vergence state of the eyes and do not convey useful information about the structure of the visual scene. The pattern of relative disparities that a given visual display produces in a binocular viewing system is determined wholly by the relation between the geometrical perspective in one eye relative to that in the other eye. Binocular disparity may therefore be called **binocular perspective**.

There are two basic types of retina or camera plane, flat and spherical. For simplicity we shall refer to both as retinas. For each type there is a type of vergence that satisfies the definition given above. Flat retinas should remain coplanar and vergence should involve a horizontal, vertical, or rotary motion of the retinas, each within the flat image plane. The lens of each eye should remain fixed so that each retina moves with respect to a stationary image, and the stereobase remains constant. It is usual to achieve convergence in binocular video cameras by rotating each camera like a eye. But this is not a true convergence, since each camera plane does not move within the image plane and therefore the movement changes the perspective in the image. The changes in perspective change the relative disparities in the images in addition to changing the overall disparity. These changes in disparity then have to be computed out by registering the vergence movement. Spherical retinas should converge by rotation about the nodal point of each eye, which is approximately what our own eyes do. This ensures that each retina moves within the plane of the stationary spherical image and that no changes in perspective are introduced into the image and that the stereobase remains constant.

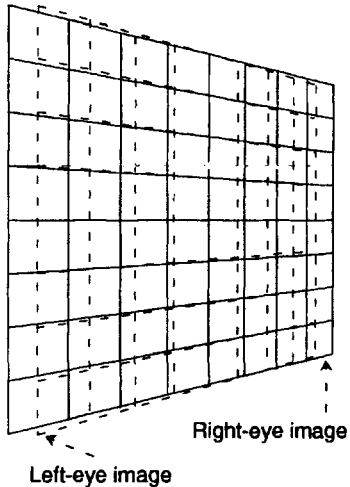
We shall now consider the patterns of disparity and the horopters produced by flat parallel retinas with linear and rotary convergence and by spherical retinas with rotary convergence.

Patterns of disparity on flat coplanar retinas

A display in a frontal plane projects onto a flat retina undistorted by perspective; parallel lines remain parallel and angles remain unchanged. Therefore, a frontal plane display produces no relative disparities between the images on two coplanar retinas. In other



(a) A surface inclined top away causes the images of vertical lines on the left retina to be tilted to the left with respect to those on the right retina. There are no vertical disparities.



(b) A surface slanted about a vertical axis causes the image on one retina to be compressed horizontally relative to that on the other retina. There are no vertical disparities.

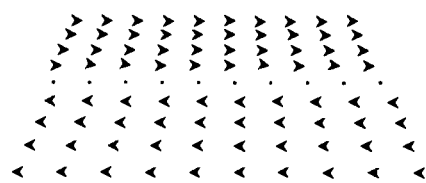


Figure 7.7. Patterns of disparity produced on flat coplanar retinas.

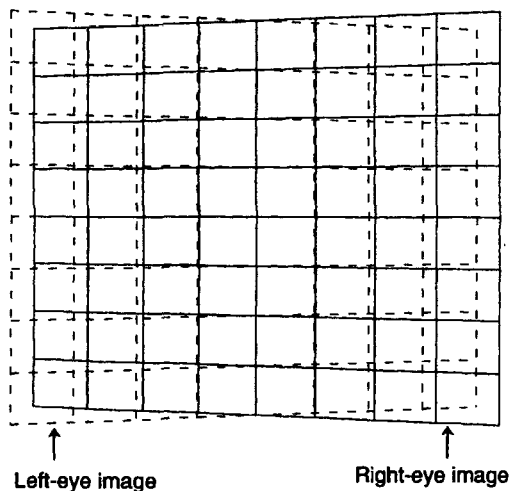
words, the space horopter for two coplanar retinas is the frontal plane upon which the retinas are converged. Convergence is achieved by an opposed horizontal translation of the retinas to the point where images from the same point in space are projected onto corresponding points in the two retinas. We assume that the retinas are rotationally aligned.

In a robotic stereo system the required convergence of images from coplanar camera planes could be achieved by a translation of the digital images within a computer. This arrangement has the advantage that vertical disparities are eliminated, which simplifies computation. However, there are three disadvantages to translating digital images produced by coplanar retinas. The first is that, after convergence, all disparities are of one sign because the cameras are converged at infinity. This reduces the sensitivity of the system. The second is that the detectors must have a uniform density, which would prevent the exploitation of the system used in the human visual system of having a high concentration of receptors in the part of the retina used for fine discriminations. Thirdly, the visual fields of coplanar retinas have little binocular overlap at near

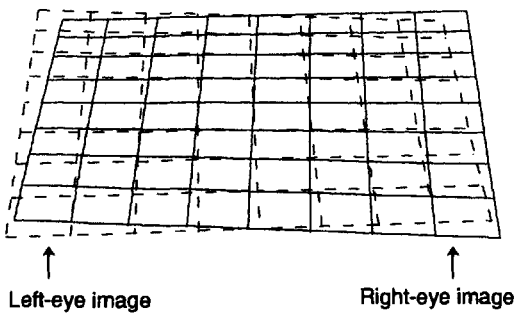
distances. In practice therefore, the video cameras of robotic systems use rotational convergence. The disadvantages of linear convergence can be reduced or eliminated by using a physical translation of the camera image plane rather than of the digital image.

The patterns of disparity produced by slanted and inclined surfaces on coplanar retinas are shown in Figure 7.7. An inclined surface produces gradients of horizontal disparity above and below the horizon. There are no vertical disparities. A slanted surface produces a single gradient of horizontal disparity in which one image is compressed horizontally with respect to the other. Again, there are no vertical disparities although horizontal lines in one eye are rotated with respect to those in the other, with one sign of rotation above the horizon and the opposite sign below the horizon.

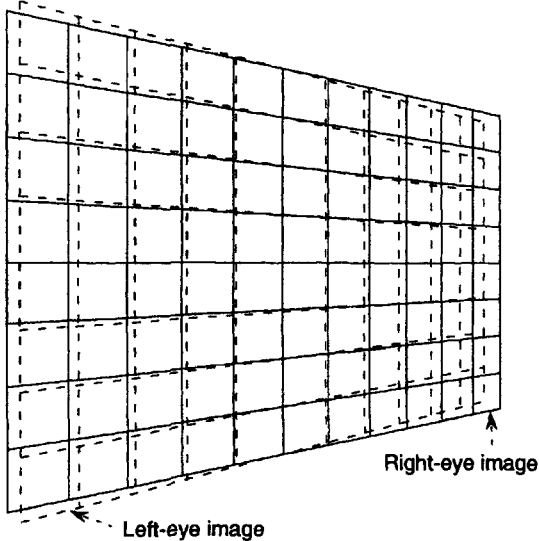
Disparity on flat retinas with converged visual axes
 Assume that the retinas are symmetrically converged by rotation so that the visual axes converge on a point, as in Figure 7.8. A rectangular display in a frontal plane projects onto each retina as a trapezoid with a horizontal taper because the object plane is not parallel to the image plane. The taper is



(a) A surface in a frontal plane produces a gradient of horizontal disparity on either side of the median plane. Images of points in the visual quadrants acquire a gradient of vertical disparity. Images of horizontal lines in the upper visual field acquire a gradient of orientation disparity with one sign and images of lines in the lower visual field acquire a gradient of orientation disparity with the opposite sign.



(b) A surface inclined top away causes the images of vertical lines on the left retina to be tilted to the left with respect to those on the right retina. Vertical disparities similar to those produced by a frontal surface are also present.



(c) A surface slanted about a vertical axis causes the images of vertical lines on one retina to be compressed relative to those on the other retina. Vertical disparities similar to those produced by a frontal surface are also present.

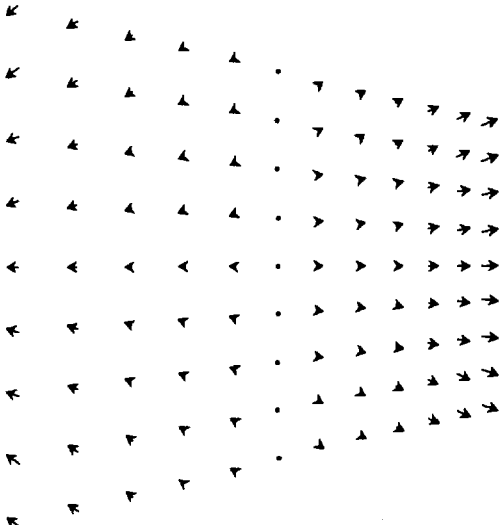
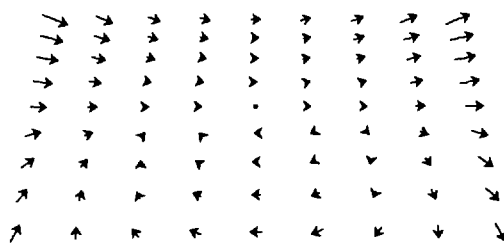
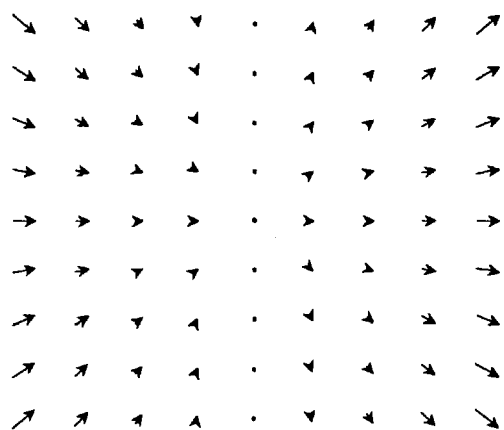


Figure 7.8. Disparities produced on flat retinas orthogonal to converged visual axes.

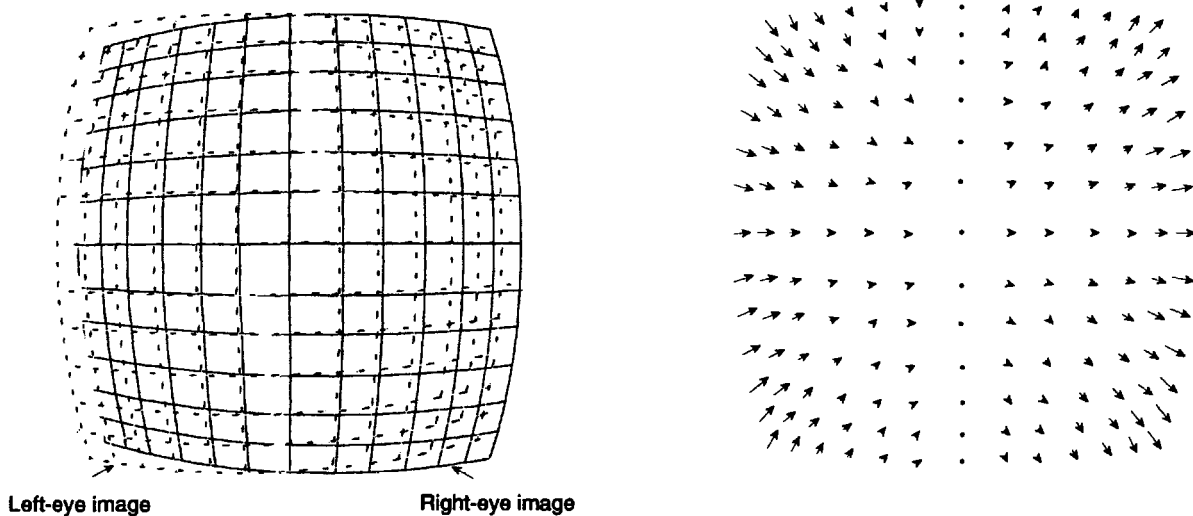


Figure 7.9. A representation of disparities produced on spherical retinas by a frontal surface.

opposite in sign in the two retinas and produces the pattern of disparities shown in Figure 7.8a. Note that there are both horizontal and vertical disparities. For a given angle of vergence, horizontal disparity is proportional to horizontal eccentricity and vertical disparity is also proportional to horizontal eccentricity with a secondary dependence on vertical eccentricity. Both types of disparity reduce to zero along horizontal and vertical lines passing through the point of convergence. These lines therefore constitute the horopter for this system. Disparities reduce everywhere to zero as the frontal display is moved to infinity and the vergence angle reduces to zero.

The patterns of disparity produced by inclined and slanted surfaces on flat retinas converged by rotation are shown in Figures 7.8b and c. An inclined surface produces a pattern of horizontal disparities similar to that produced on coplanar retinas but, whereas coplanar retinas produce no vertical disparities, converged retinas produce gradients of vertical disparities in the four quadrants of the combined image. A slanted surface produces images which are relatively compressed horizontally in one image, like those produced on coplanar retinas, but there are also vertical disparities gradients in the quadrants.

Patterns of disparity on spherical retinas cannot be represented accurately on a flat drawing. We have made an attempt to represent the disparities produced by a frontal plane surface on spherical retinas in Figure 7.9. The disparities produced on spherical retinas by frontal, inclined, and slanted surfaces are similar to those produced on converged flat retinas. The main difference is that on spherical retinas horizontal disparities are larger relative to

vertical disparities than they are on converged flat retinas. This is because the distance from the nodal point to the retina is constant for a spherical retina but not for a flat retina. Note, however, that the magnitudes of the disparities depend on the choice of coordinate system used to measure disparity. Figure 7.9 depicts the patterns of disparity on a spherical retina measured according to the longitudinal-azimuth/latitudinal elevation or gun turret system.

7.1.4 The concept of disparity

It was shown earlier that if the precise positions of the eyes or cameras are known, the entire structure of the three-dimensional scene can be recovered (see Longuet-Higgins 1982). In this section, we consider what information can be recovered from binocular images when the eyes or cameras are free to move independently and their positions are not known precisely. It is assumed that the optic axes of the eyes converge on a single point in space. If this is true, the optic axes of the eyes lie in a plane passing through the point and the optical centres of the two eyes—the plane of regard. If the eyes are torsionally aligned, the y axis of the coordinate frame in each eye is orthogonal to the plane of regard and passes through its optic centre. We will assume that visual direction in each eye is measured using longitudinal azimuth/latitudinal elevation coordinates—the gun-turret model—since measurements of azimuth and elevation differences using this model are invariant, with horizontal eye movements (Section 7.1.2). Under this system, vertical azimuth planes in each of the eyes radiate out from the y axes (Figure 7.10).

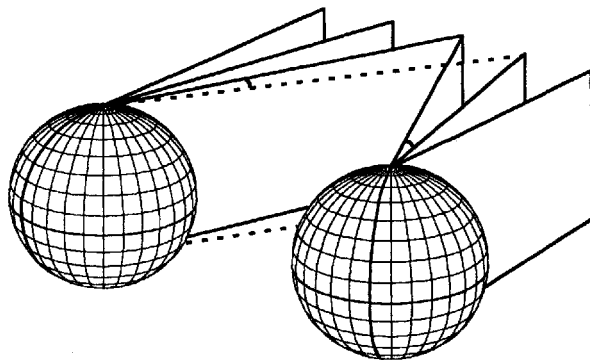


Figure 7.10. Azimuth planes.

In a longitudinal-azimuth/latitudinal-elevation system, all points which lie in a vertical plane through the y axis have the same azimuth. Points which lie in different vertical planes radiating from the eye have different azimuths. The horizontal separation between a pair of points in the same eye (used in the calculation of width disparity) is given by the angular difference between the azimuth planes in which they lie.

The vertical plane projecting to the fixation point in each eye is the plane from which the azimuth angle in that eye is measured.

The **relative horizontal disparity**, or simply the **horizontal disparity** of a pair of points, is defined as the difference between the absolute horizontal disparities of the two points:

$$\text{Horizontal disparity} = (\alpha_{1L} - \alpha_{1R}) - (\alpha_{2L} - \alpha_{2R}) \quad (3)$$

Alternatively, and mathematically equivalent, the horizontal disparity can be expressed as the binocular difference in the horizontal separation of the points measured separately for each eye. This involves rearranging the terms in equation (3):

$$\text{Width disparity} = (\alpha_{1L} - \alpha_{2L}) - (\alpha_{1R} - \alpha_{2R}) \quad (4)$$

Equation (4) represents a difference in angular width—a **horizontal width disparity** (or **horizontal dif-size disparity**). Width disparity can be measured for any pair of points and not just those aligned in a horizontal direction. It corresponds to the binocular difference of the separate angles between the azimuth planes containing the two points in each eye (Figure 7.10). Expressing the horizontal disparity as a width disparity makes it clear that only the angular separation of the points has to be measured (separately in the two eyes) rather than the absolute directions of the image points on the retina, which vary according to the positions of the eyes.

The **relative vertical disparity**, or simply the **vertical disparity** of a pair of points, can be defined similarly as the difference in the absolute vertical disparities of the two points:

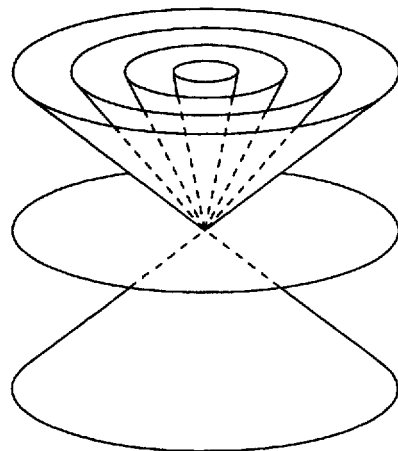


Figure 7.11. Elevation cones.

In a longitudinal-azimuth/latitudinal-elevation system, all points which lie in a cone rotated around the y axis have the same elevation, including the zero elevation disc. Points which lie in different cones have different elevations. The vertical separation between a pair of points in the same eye (used in the calculation of height disparity) is given by the difference between the elevation cones in which they lie.

$$\text{Vertical disparity} = (\beta_{1L} - \beta_{1R}) - (\beta_{2L} - \beta_{2R}) \quad (5)$$

As for horizontal disparity, vertical disparity can also be expressed as the binocular difference in the vertical separation between the points measured separately in each eye:

$$\text{Height disparity} = (\beta_{1L} - \beta_{2L}) - (\beta_{1R} - \beta_{2R}) \quad (6)$$

The **vertical height disparity** (or **vertical dif-size disparity**) represented by equation (6) makes it clear that only the angular separation has to be measured (separately in the two eyes), rather than the absolute directions of the image points in the two eyes.

To measure a horizontal width disparity or a vertical height disparity we also need to define "horizontal" and "vertical" for a binocular system in which the eyes move. As indicated earlier, a line joining two points may be regarded as vertical if the points have the same azimuth. In a gun-turret system, this means that the points must lie in the same vertical azimuth plane that passes through the optic centre in that eye and is orthogonal to the plane of regard (Figure 7.10). A line joining a pair of points is horizontal if the points have the same elevation. In the gun-turret model, elevation is measured within the vertical plane passing through the point, so that points are horizontal if they lie on the same cone rotated around the y axis (Figure 7.11).

Although this is not the only way to define vertical and horizontal, the gun turret system has the advantage that (1) measurements of height (elevation)

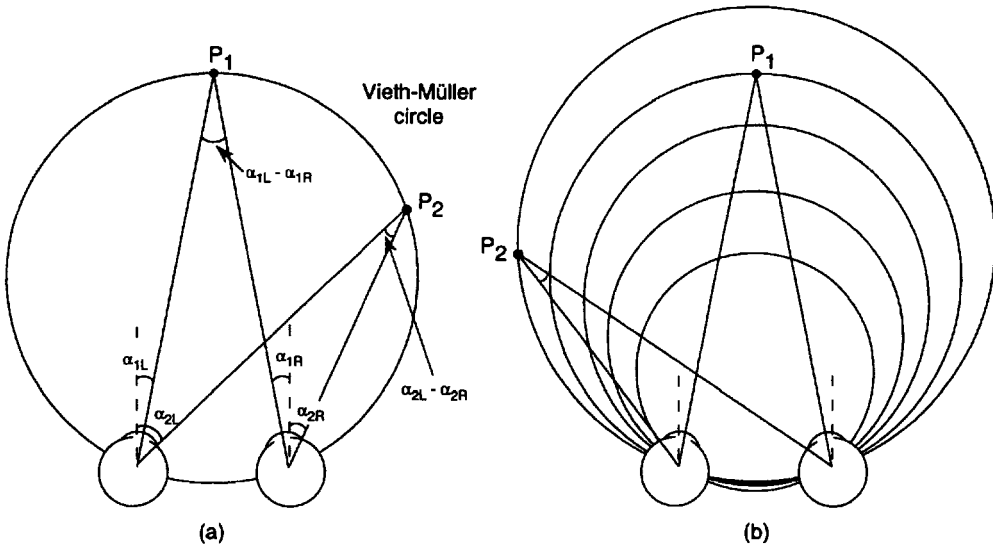


Figure 7.12. The Vieth-Müller and isodisparity circles.

The absolute azimuths of two points P_1 and P_2 are specified with respect to aligned axes in the two eyes. The binocular subtense of each point corresponds to the difference between their absolute azimuths— $(\alpha_{1L} - \alpha_{1R})$ and $(\alpha_{2L} - \alpha_{2R})$. The locus of all points with the same binocular subtense is a circle passing through the optic centres of the two eyes—an isodisparity circle. When the eyes are converged on a point as in (a), that isodisparity circle is the Vieth-Müller circle. Points lying on different isodisparity circles, as in (b), are disparate.

and width (azimuth) differences between points and (2) what is regarded as vertical or horizontal are unaffected by changes of gaze or vergence (horizontal eye movements) within the plane of regard. This is equivalent to saying that horizontal width disparities and vertical height disparities are assessed with respect to the plane of regard.

A corollary of this last statement is that the horizontal width disparities and the vertical height disparities of a pair of points typically will have different values if the eyes are elevated to a new plane of regard. The angular separation of the points cannot change, nor indeed their physical separation when projected onto a spherical surface, but the coordinate axes used to define what is vertical or horizontal will have rotated and hence the measurements of horizontal and vertical separation will be different.

For the measurement of binocular disparity, both horizontal and vertical are defined with respect to the plane of regard, that is, they are defined in oculocentric rather than headcentric coordinates. Accordingly, an oculocentric frontal surface is defined as perpendicular to the plane of regard and changes with the elevation of gaze. The principal oculocentric frontal plane is the plane containing the interocular axis which is orthogonal to the plane containing the visual axes (the plane of regard). The term "frontoparallel plane" has been used to denote any plane parallel to the principal frontal plane, but we use the simple term "frontal plane" to refer to any frontal plane.

Isodisparity circles

Equation (4) shows that the horizontal disparity of a pair of points can be expressed as a horizontal width disparity. Simple geometry shows that this is also equivalent to the difference between the binocular subtenses of the two points (Figure 7.12a). From this it can be seen that the locus of all points that have the same relative horizontal disparity with respect to a given point P_1 is a circle which passes through that point and the optic centres of the two eyes. These circles are referred to as isodisparity circles (Figure 7.12b). In the special case where the eyes are fixated on one of the points, the isodisparity circle is the Vieth-Müller circle (see Section 2.5).

You will notice that if the eyes are elevated to a new position, the isodisparity circles lie in the plane of elevation, because horizontal disparity is registered in the plane of regard. This observation has led previous authors to suggest that the complete locus of isodisparity points is a toroidal surface formed by revolving the horizontal horopter round the interocular axis. This is incorrect when horizontal disparity is defined as a difference in the azimuth of points measured in the plane of regard. The locus of isodisparity points for horizontal disparity is a cylinder extended upwards and downwards from the isodisparity circle in the plane of regard. An isodisparity cylinder is formed by the intersections of pairs of azimuth planes radiating from the two eyes which have the same binocular subtense at the two eyes (Figure 7.13).

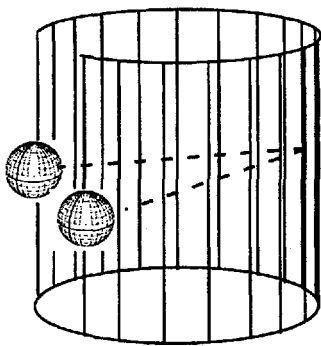


Figure 7.13. Isodisparity cylinder.

Vertical azimuth planes from the two eyes intersect as a vertical line when the eyes are torsionally aligned. The angle between any binocular pair of azimuth planes is the binocular subtense. The locus of intersection of binocular pairs of azimuth planes which have the same binocular subtense is a cylinder. All points on an isodisparity cylinder have the same horizontal disparity.

The vertical disparities of points lying in the plane of regard are all zero because points in the plane of regard have a zero angle of elevation, by definition. The vertical disparities of points lying in the median plane of the head are also zero because the loci of intersections between binocular cones of elevation all lie in the median plane (Figure 7.14). The only points which have both zero horizontal and zero vertical disparity are those which are common to the zero disparity cylinder and either the median plane of the head or the plane of regard. These common points consist of the Vieth-Müller circle in the plane of regard plus the (oculo-centrally defined) vertical line through the fixation point. In the preceding analysis, it is assumed that the eyes are torsionally aligned in the plane of regard. See Section 2.5.2 for discussion of the effects of torsional misalignment on the horopter.

7.1.5 Information provided by disparities

Horizontal disparities

What information do relative (horizontal width) disparities provide? The sign (positive or negative), of the horizontal disparity between two points provides limited information about the relative positions of the two points in space. Measuring azimuth in a clockwise direction from above, a positive value of $(\alpha_{1L} - \alpha_{1R}) - (\alpha_{2L} - \alpha_{2R})$ specifies that point 2 is outside the isodisparity circle passing through point 1 (Figure 7.12b); a negative value specifies that it lies inside of that circle (see Section 2.5.2). For a pair of points close to the median plane of the head, this is equivalent to saying that point 2 is farther away than point 1 in the first case and closer in the second. However, this statement is true only under the

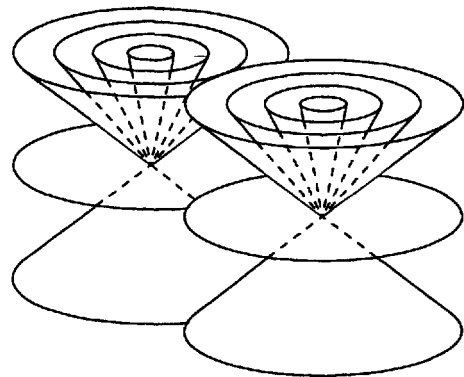


Figure 7.14. Intersection of binocular elevation cones.

The loci of intersecting pairs of elevation cones with the same elevation in the two eyes all lie in the median plane of the head. Hence, all points in the median plane have zero vertical disparity.

special condition of a pair of points close to the median plane of the head. In general, the sign of a horizontal disparity specifies only the relative locations of the two points with respect to isodisparity circles (Figure 7.12b).

What information does the magnitude of a horizontal disparity provide? A larger disparity corresponds to a larger depth difference but the magnitude of the depth difference is not specified by the magnitude of the horizontal disparity because horizontal disparities also depend on the absolute distance of the two points. The same horizontal disparity is created by a pair of points with a small depth difference which is close to the observer as is created by a pair of points with a large depth difference far away from the observer. Put another way, the spacing between a pair of isodisparity circles with a constant disparity difference becomes larger as the diameter of the circles increases. The spacing between a pair of isodisparity circles also varies with eccentricity. Thus, horizontal disparity in a binocular system with convergence provides information about relative position at a particular eccentricity and at a specified distance. The precise locations of the points in space cannot be recovered unless there is additional information about the absolute distance and the headcentric eccentricity of points.

Vertical disparities

What information do vertical disparities provide? Longuet-Higgins (1982) showed that the positions in space of three or more points which do not all lie on the same meridian are fully determined by the horizontal and vertical coordinates of their images on the two retinas as long as the planes of the horizontal meridians of the two eyes coincide—that

is, the eyes are vertically and torsionally aligned (Section 7.6). Is any information available if the eyes are not torsionally aligned? To answer this question, it is useful to consider the binocular ratio of the vertical sizes—the **vertical size ratio** or **VSR**—of a pair of points rather than their differences, as expressed in Equation 6.

$$\text{VSR} = (\beta_{1L} - \beta_{2L}) / (\beta_{1R} - \beta_{2R}) \quad (7)$$

VSRs are unaffected by small amounts of vertical and torsional misalignment. The sign and magnitude of the VSRs clearly provide some information about the eccentricity of the two points with respect to the median plane of the head. In general, the VSR of two points increases with increasing eccentricity from the median plane because the points become closer to one eye than to the other. But the magnitude of the VSR also depends on the absolute distance to the points. The same VSR can be created by a pair of points at a small (headcentric) eccentricity which are close to the observer as is created by a pair of points at a large eccentricity and far way. Hence, the VSR of a pair of points provides information about **eccentricity** at a specified **distance**. The locus of all points with the same VSR in the plane of regard is shown in Figure 7.15. In Section 7.6.6, we show that the VSR and the local horizontal gradient of VSR specify the absolute distance to a surface when the points are close to the plane of regard.

First-order disparities

The absolute disparity of a single point can be referred to as a zero-order disparity. The complete disparity characteristics of a scene can be described in terms of the zero-order disparities in different visual directions. The two-dimensional distribution of zero-order horizontal disparities created by a visual scene is referred to as a **disparity vector field** (see Figures 7.7 and 7.8). It should be emphasized that a disparity vector field alone does not provide a complete description of the structure and layout of the scene—referred to as a **depth or range map**—for two reasons. First, a disparity vector field is a description of disparities with respect to a particular fixation point. Second, the disparity of a pair of points with a given physical separation in depth varies with absolute distance and headcentric eccentricity (see Section 7.1.4).

The construction of a disparity vector field, which makes explicit the disparity values of scene points as a function of visual direction, can be likened to the formation of a retinal image or **gray-level representation**, which makes explicit the luminance values of all scene points (Marr 1982). Since the function of the

visual system is to interpret images rather than merely reproduce them, it follows that the visual processing after the formation of a gray-level representation or disparity vector field must involve calculating changes of luminance and changes of disparity. Spatial changes of disparity are particularly important for representing three-dimensional shape and layout, but temporal changes of disparity also need to be considered (Sections 13.3 and 13.4).

First-order spatial changes of disparity are referred to as **disparity gradients** and expressed in angular terms (Burt and Julesz 1980). There are two different horizontal disparity gradients: one in the horizontal (azimuth) direction and one in the vertical (elevation) direction. Similarly, there are two vertical disparity gradients. The horizontal disparity gradient between two points is usually expressed as the difference in absolute disparity ($\Delta\alpha$) divided by the average or cyclopean separation in a horizontal direction ($\Delta\phi$):

$$\frac{\Delta\alpha}{\Delta\phi} = \frac{(\alpha_{1L} - \alpha_{1R}) - (\alpha_{2L} - \alpha_{2R})}{\{(\alpha_{1L} - \alpha_{1R}) + (\alpha_{2L} - \alpha_{2R})\}/2} \quad (8)$$

In the limit as $\Delta\phi \Rightarrow 0$, the disparity gradient becomes $\partial\alpha/\partial\phi$. The disparity gradients in the horizontal and vertical directions can be expressed as $\partial\alpha/\partial\phi_h$ and $\partial\alpha/\partial\phi_v$, and the vertical disparity gradients in the horizontal and vertical directions as $\partial\beta/\partial\phi_h$ and $\partial\beta/\partial\phi_v$. Although expressed in angular terms, disparity gradients can be measured in projected images, as long as the projection surfaces have been appropriately calibrated.

In Section 7.1.3 the relative disparity of a pair of points was defined as the difference between the absolute disparities of the points (top line of equation 8). This means that relative disparity has some of the properties of a first-order disparity, including its sign, but is unrelated in magnitude because the angular separation of the two points is not taken into account.

It is often assumed that a horizontal gradient of horizontal disparity— $\partial\alpha/\partial\phi_h$ —specifies the slant of a surface (up to a scaling factor) with respect to the cyclopean direction. This is true, however, only for surfaces that lie close to the median plane. In general, the horizontal gradient of horizontal disparity specifies the slant of the surface with respect to an isodisparity cylinder at the point of intersection (Figure 7.13). Knowledge of the distance of the surface and its headcentric eccentricity is needed to convert this slant estimate into one that can be expressed with respect to the cyclopean direction. The vertical gradient of horizontal disparity— $\partial\alpha/\partial\phi_v$ —

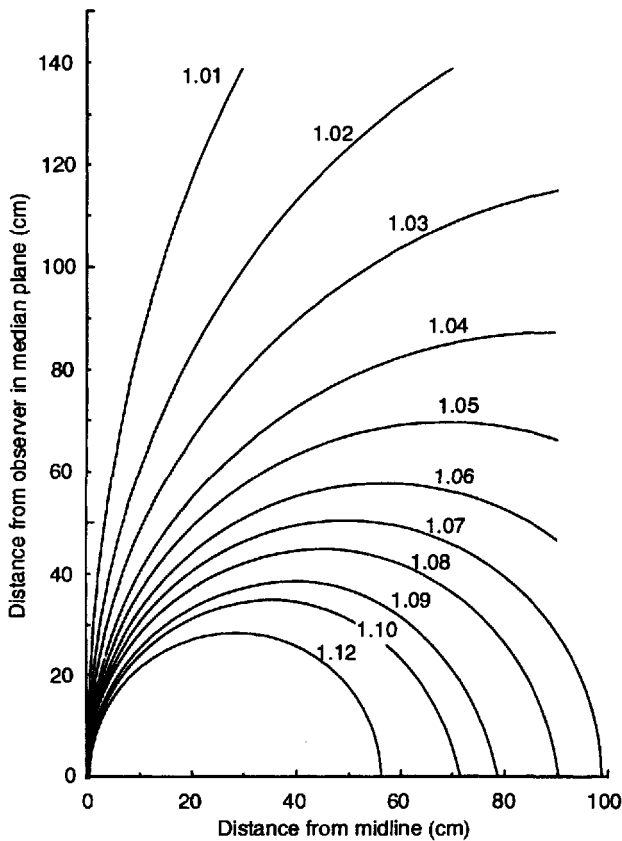


Figure 7.15. VSRs as a function of eccentricity and distance.

Each curve connects the points in the scene which have a particular vertical size ratio (VSR) given by its parameter. VSRs increase with increasing eccentricity (for a constant distance). The VSR created by an object close to the observer and close to the median plane of the head can be the same as that of an object farther away and at a greater eccentricity. (Adapted from Gillam and Lawergren 1983.)

specifies the inclination of a surface (up to a scaling factor) with respect to the vertical horopter.

Differential invariants

Koenderink and van Doorn (1976a) have drawn attention to a useful decomposition of the first-order disparity fields created by binocular viewing. Instead of describing the four horizontal and vertical disparity gradients in the horizontal and vertical directions ($\partial\alpha/\partial\theta_h$; $\partial\alpha/\partial\theta_v$; $\partial\beta/\partial\theta_h$; $\partial\beta/\partial\theta_v$), they described the disparity field in terms of the four differential components: **expansion or dilatation**; **curl or rotation**; and two components of **deformation**, or **shear** needed to map one eye's image onto the other (Figure 7.16). These are mathematically equivalent descriptions, and one can be transformed into the other by the appropriate algebra. Koenderink and van Doorn suggested that there are advantages in

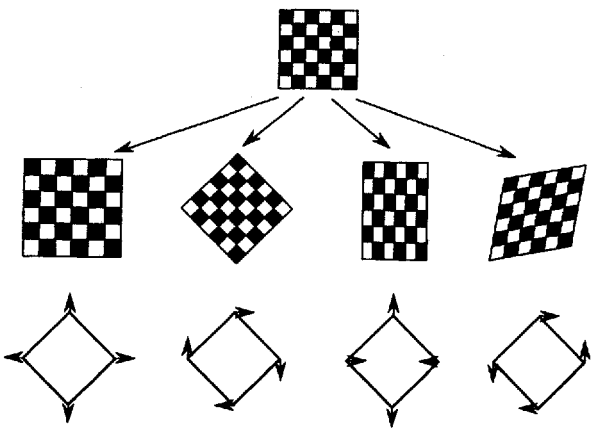


Figure 7.16. Differential transformations.

The four differential invariants—expansion, rotation, and two components of deformation or shear—are represented as transformations of a chequerboard gauge figure. Koenderink (1985) pointed out that the differential characteristics of the disparity field (in mapping one eye's image on to the other) can be fully described in terms of these invariant transformations.

expressing the disparity field in terms of differential components. First, like all descriptions of the first-order or disparity gradient field, they eliminate any contribution of absolute disparity. In practical terms this means that a spatially unchanging disparity field, as might be created by misalignments of the eyes or the cameras, is not represented. Second, the components of deformation capture information about the slant and inclination of a stereoscopic surface even when the images are not the same size or are misaligned. The invariance to dilatation is useful for discounting the slant of eccentric surfaces or disparities created by anisometropia. The invariance to rotation is useful to offset effects of torsional misalignment between the two eyes.

A surface which is eccentric with respect to the head, whether it is fixated or falls in peripheral vision, is necessarily closer to one eye than to the other and will therefore be larger in angular extent. If the surface is close to the plane of regard and normal to the cyclopean direction, it will be uniformly larger in both horizontal and vertical directions in one eye. Consequently, the mapping of one eye's image onto the other can be expressed uniquely in terms of the dilatation component; there is no component of deformation (Figure 7.17). This is also true if the eccentric surface lies in an elevated direction, but only if azimuth and elevation angles are measured in the direction of the elevated surface. It follows that if a stereoscopic surface has zero deformation, it must lie in a plane normal to the cyclopean direction.

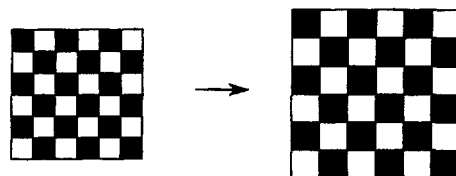


Figure 7.17. Isotropic magnification of one eye's image.

When a surface lies in an eccentric position with respect to the head, its vertical size will be larger. If the surface is normal to the cyclopean direction, it will be larger in a horizontal direction by the same amount that it is larger in a vertical direction. The binocular images are related by a dilatation (isotropic magnification) only; there is no deformation.

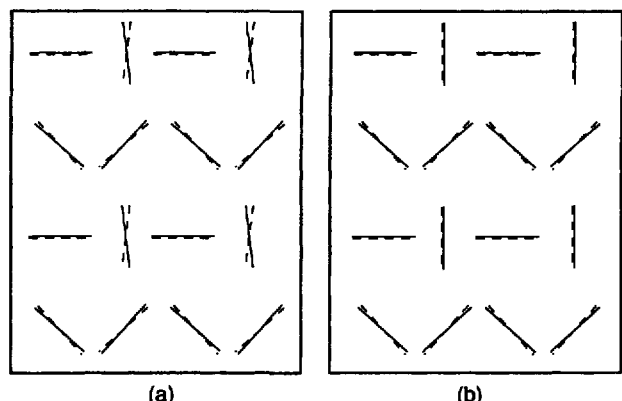


Figure 7.18. Inclination, slant and orientation disparities.

(a) For a small surface inclined around a horizontal axis the orientation disparities of vertical line elements are maximal and those of horizontal elements are zero. The orientation disparities of 45° elements are half those of the verticals and they are in the same direction for both $+45^\circ$ and -45° elements.

(b) For a small surface slanted around a vertical axis the orientation disparities of both vertical and horizontal elements are zero. $\pm 45^\circ$ elements have orientation disparities which are in opposite directions.

Disparity deformation captures information about the slant of a surface with respect to the cyclopean direction irrespective of where the surface lies in the visual field and irrespective of where the observer's eyes are pointing. This is a potentially very useful invariance that any visual system might exploit. In contrast, the gradient of horizontal disparity in a horizontal direction ($\partial\alpha/\partial\theta_h$) specifies the slant of the surface (up to a scaling factor) with respect to an isodisparity circle rather than the cyclopean direction. Additional information about the eccentricity of the surface and its distance from the observer is needed to correct the slant estimate from the horizontal gradient alone. This observation is relevant to explanations of the induced effect (see Section 7.6.7).

The invariance of stereoscopic deformation to a rotational misalignment of the coordinate axes is also very important in any practical visual system. Torsional misalignment of the two eyes or cameras introduces disparity gradients into the binocular images which have nothing to do with the three-dimensional scene characteristics. In particular, torsional misalignment creates a gradient of horizontal disparity in the vertical direction ($\partial\alpha/\partial\theta_v$) and a gradient of vertical disparity in the horizontal direction ($\partial\beta/\partial\theta_h$). The former gradient is similar to that produced by a surface that is inclined with respect to the frontal plane (see Section 7.3). Torsional misalignment does not alter the amount of deformation between binocular images, so that surface slant (up to a scaling factor) can be calculated directly without needing to estimate the degree of torsional misalignment.

In describing the idea of differential invariants, nothing has been said about how they might be extracted from the binocular images. Koenderink (1986) suggested that deformation could be computed by monitoring the binocular differences in the orientation of local line elements at different absolute orientations. For example, if there are orientation

disparities of vertically oriented line elements but not of horizontally oriented elements, this is the signature of a surface inclined about a horizontal axis (Figure 7.18a). Orientation disparities of $+45^\circ$ line elements in one direction and orientation disparities of -45° line elements in the opposite direction, is the signature of a surface slanted about a vertical axis (Figure 7.18b). Binocular images with orientation differences of the same direction and magnitude for line elements of all orientations is the signature of torsional misalignment of the eyes or cameras.

The two components of disparity deformation can be expressed in terms of the disparity gradients. The first component—**Def₁**—corresponds to the ratio of $\partial\alpha/\partial\theta_h$ to $\partial\beta/\partial\theta_v$, and is immune to the effects of an isotropic size difference between the eyes. The second component—**Def₂**—corresponds to the ratio of $\partial\alpha/\partial\theta_v$ to $\partial\beta/\partial\theta_h$ and is immune to the effects of a rotation of one eye's image with respect to the other.

Scaling with distance

In considering zero-order disparities, it was pointed out that a horizontal disparity does not, by itself, specify the depth difference between two points because disparities are inversely related to the square of absolute distance from the observer (Section 2.3.1). Doubling the distance for a given separation in depth reduces the disparity to one-quarter. How does absolute distance affect first-order disparities, including the two components of deformation? Consider two points on a 45° slanted surface close to the median plane (Figure 7.20b).

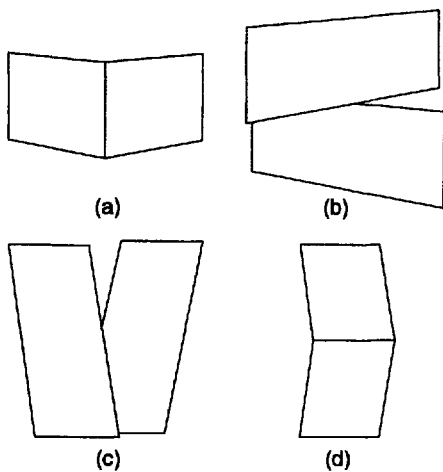


Figure 7.19. Changes of disparity gradient.

Second-order disparities describe the change of disparity gradient over visual angle. The four components are: (a) a change of slant in a horizontal direction, (b) a change of slant in a vertical direction, (c) a change of inclination in a horizontal direction, and (d) a change of inclination in a vertical direction.

Doubling the distance of the surface reduces the disparity between the points to one quarter but the angular separation of the points (ϕ) is halved. To a first approximation, the disparity gradient is an inverse function of distance rather than of distance squared. The same is true of the disparity deformation components. Consequently, both disparity gradients and disparity deformation need to be scaled by absolute distance to calculate the physical slant or inclination of a surface or a pair of points.

There are many advantages in expressing the disparity field in terms of the local deformation between image features but for some purposes this description might not be appropriate. Torsional misalignment of the eyes introduces a particular pattern of horizontal and vertical disparities which affects all features. In other words, there is a single viewing-system parameter corresponding to the degree of torsional misalignment. This means that calculation of deformation for each local patch in the scene is redundant; a single correction could be applied to all surfaces in the visual field if the viewing-system parameter were known. Similarly, the overall binocular size difference created by a surface to one side of the median plane is just one part of an overall gradient of binocular size differences across the whole visual field. Thus, it need not be corrected locally; a single correction could be applied to all surfaces in the visual field.

Second-order disparities

First-order disparities, or disparity gradients, describe the change of disparity over visual angle.

Second-order disparities describe the change of disparity gradient over visual angle and can be referred to as the **second spatial derivatives** of the disparity field or, by analogy with the idea of a disparity gradient, **disparity curvatures**. In the case of horizontal disparities, there are four components or partial derivatives: $\partial^2\alpha/\partial\theta_h^2$ —the horizontal change of horizontal disparity gradient in a horizontal direction; $\partial\alpha/\partial\theta_h\partial\theta_v$ —the vertical change of horizontal disparity gradient in a horizontal direction; $\partial^2\alpha/\partial\theta_v^2$ —the vertical change of horizontal disparity gradient in a vertical direction; and $\partial\alpha/\partial\theta_v\partial\theta_h$ —the horizontal change of horizontal disparity gradient in a vertical direction. The four partial derivatives are best illustrated diagrammatically in terms of the surfaces that would generate them as in Figure 7.19. Similarly, there are four second-order partial derivatives of the vertical disparity field.

What are the advantages of describing disparities in terms of the second spatial derivatives? Like disparity gradients, second spatial derivatives are not affected by horizontal or vertical misalignments of the coordinate axes at the two vantage points. In addition, the second spatial derivatives of projected images are unaffected by small torsional misalignments of the coordinate axes. The lack of variation of second-order measurements to misalignments of the eyes or cameras is a useful feature that any visual system could potentially exploit.

Moreover, the local value of the second spatial derivative remains roughly constant with changes in viewing distance. This can be seen most easily by considering the plan view of a surface curved about a vertical axis, as shown in Figure 7.20. The disparity gradients of the two sections of the surface will both be halved (approximately) with a doubling of the viewing distance, as shown previously, but the distance between the two sections will also be halved, making the change of disparity gradient roughly constant. This means that unlike the zero- and first-order disparities, second-order disparities do not have to be scaled in the visual system by viewing distance (Rogers and Cagenello 1989). However, this is true only for surfaces close to the median plane of the head. In general, second-order disparities have to be scaled by some estimate of headcentric eccentricity.

Section 7.1 has been concerned with the availability of information in both the optic arrays at two vantage points and in the projection of binocular images. The following sections examine the disparities created by slanted and inclined surfaces and provide a review of the psychophysical evidence for the use of particular types of retinal disparity in the human visual system.

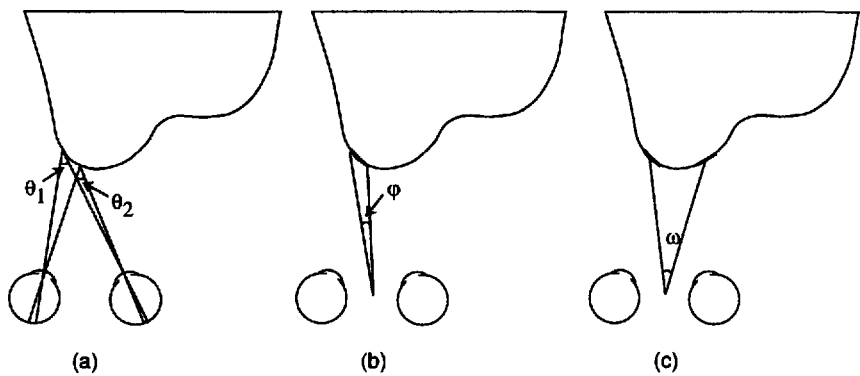


Figure 7.20. Disparity Curvature.
 (a) The disparity between a pair of points corresponds to the difference in their binocular subtenses ($\theta_1 - \theta_2$).
 (b) Disparity gradient corresponds to the difference in disparity between two points divided by their separation (ϕ).
 (c) Disparity curvature is the difference in disparity gradient of two surface patches divided by their separation (ω). Local disparity curvature remains constant with changes in viewing distance.

7.2 DISPARITIES ON SLANTED SURFACES

We distinguish nine related types of disparity produced by a surface slanted about a vertical axis.

7.2.1 Dif-size or width disparity

The simplest description of the horizontal disparities created by a slanted surface is given by the binocular difference in angular separation of two points at the two eyes—($\alpha_{1L} - \alpha_{2L}$) - ($\alpha_{1R} - \alpha_{2R}$)—which is referred to as a **horizontal width disparity**, or a **dif-size disparity** (equation 4). As was shown in Section 7.1.4, horizontal width disparity is mathematically equivalent both to the relative disparity of the two points and to the difference in the absolute horizontal disparities of the two points (equation 3).

It has often been assumed that relative or dif-size disparity specifies the relative depth of two horizontally separated points on a slanted surface, with respect to either the frontal plane or the direction of gaze. This is incorrect. Dif-size disparity provides information about the slant of the surface with respect to the tangent plane of an isodisparity cylinder at the point where the surface cuts the cylinder (Section 7.1.4) but only up to a scale factor of distance. It is only when the two points are close to the median plane of the head that dif-size disparity can be said to indicate the slant of the surface with respect to the frontal plane. Three factors affect the dif-size disparity of horizontally separated points measured at the two eyes: (1) the slant of the surface, (2) the eccentricity of the surface with respect to the median plane of the head, and (3) the distance of the surface.

Consider a short horizontal line, AB , viewed by one eye, as in Figure 7.21. The visual angle subtended by the line decreases as the line moves horizontally within a frontal plane into an eccentric position, ϵ . Two factors are responsible for this. The first factor operates alone when the line maintains a

constant angle to the line of sight, as in Figure 7.21. The distance of the line from the eye increases in inverse proportion to $\cos \epsilon$. Since the angular subtense of AB is also inversely proportional to the distance, it is proportional to $\cos \epsilon$. The second factor is that, as the line AB moves into an eccentric position while remaining in a frontal plane, the visual axis intersects the line at a sharper angle (Figure 7.22). This effect is also proportional to $\cos \epsilon$. Together, these two factors cause the image of line AB to decrease in proportion to $\cos^2 \epsilon$. The image of AB also changes in the other eye but because of the lateral separation of the eyes, the perspective changes in the two eyes are out of phase when both eyes view the same line.

When the line lies across the median plane of the head, its ends have an equal and opposite angle of eccentricity to the two eyes. The two cosine functions therefore have the same absolute value and the images in the two eyes are equal in size. As the line moves within a frontal plane to a horizontally eccentric position, the two angles of eccentricity change by different amounts. There is thus a phase difference between the two $\cos^2 \epsilon$ functions, and the image in one eye is larger than that in the other. Disparity between images of a line thus varies with eccentricity.

At infinity, the difference between the two angles of eccentricity reduces to zero, whatever the angle of eccentricity, as does the difference between the cosine functions. There are therefore no size differences between the images of objects at infinity. As the line comes nearer to the eyes along an eccentric hyperbola of Hillebrand the two angles of eccentricity increase by equal and opposite amounts, as does the effect of the phase difference between the cosine functions. Thus, the disparity in the images of an eccentric line depends on both the eccentricity of the line and the distance from the principal frontal plane containing the interocular axis to the frontal

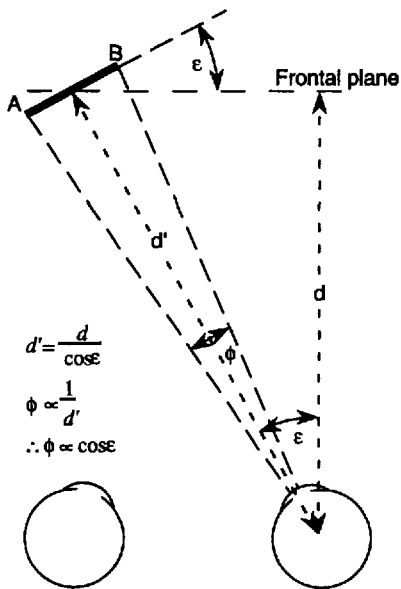


Figure 7.21. Angular subtense in the frontal plane I.
(a) The angular subtense, ϕ , of line AB decreases as it moves along a frontal plane into azimuth position, ϵ , while maintaining a constant angle to the line of sight. This is because the distance of the line from the eye, d , increases in proportion to $\cos \epsilon$.

plane within which the line lies. Figure 7.66 is a three-dimensional plot of the joint effects of eccentricity and viewing distance on the size difference between the images in the two eyes of a frontal-plane horizontal line.

A horizontal line which remains tangential to the horizontal horopter projects equal images in the two eyes at all eccentricities, and therefore creates zero dif-size disparity. For such a line the change in image size due to the changing angle of the line to the lines of sight cancels the change in image size due to the changing eccentricity of the line. The images of a vertical line moved into an eccentric position along the horizontal horopter acquire a dif-size disparity proportional to the difference between two $\cos \epsilon$ functions.

7.2.2 Horizontal size ratio (HSR)

Dif-size or width disparity is defined as the binocular difference in angular size. The **horizontal size ratio** (HSR) is defined as the ratio of the angular sizes in the two eyes.

$$\frac{(\alpha_{1L} - \alpha_{2L})}{(\alpha_{1R} - \alpha_{2R})} \quad (8)$$

The size difference and the size ratio have similar properties, but there are also important differences. The same three factors affect the value of the HSR—

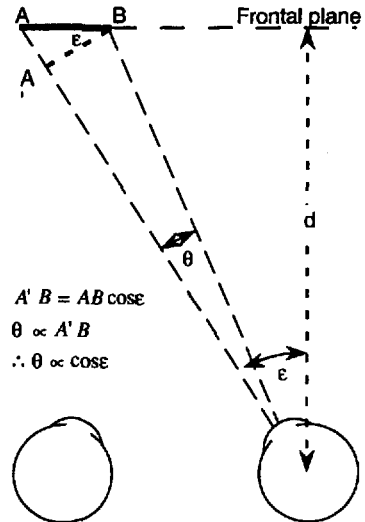


Figure 7.22. Angular subtense in the frontal plane II.
If the line AB remains in the frontal plane as it is moved into an eccentric position, its angular subtense decreases because it becomes inclined to the line of sight by angle ϵ . This effect is also proportional to $\cos \epsilon$. Therefore, the angular subtense of a line in the frontal plane ϵ decreases in proportion to $\cos^2 \epsilon$.

the slant of the line, its eccentricity, and its distance. The HSR always has the same sign as the dif-size disparity, but its magnitude depends on the angular separation of the two points. The HSR is a first-order disparity description which provides information about the disparity gradient, whereas dif-size is a zero-order difference measure. Consider two closely spaced and horizontally separated points whose angular subtense to the two eyes is $\alpha_{1L} - \alpha_{2L}$ and $\alpha_{1R} - \alpha_{2R}$ respectively. The dif-size disparity is defined as $(\alpha_{1L} - \alpha_{2L}) - (\alpha_{1R} - \alpha_{2R})$ (equation 4). Dividing the disparity difference by the angular separation in the right eye ($\alpha_{1R} - \alpha_{2R}$) yields the disparity gradient:

$$\text{Disparity gradient} = \frac{(\alpha_{1L} - \alpha_{2L}) - (\alpha_{1R} - \alpha_{2R})}{(\alpha_{1R} - \alpha_{2R})} \quad (9)$$

$$\text{Disparity gradient} = \text{HSR} - 1 \quad (10)$$

Thus, the HSR of a pair of closely spaced points corresponds to the disparity gradient plus 1. One consequence of measuring size ratios rather than the size differences is that for a surface with a given degree of physical slant, HSR varies inversely with distance rather than with distance squared.

7.2.3 Dif-frequency disparity

It follows from the preceding analysis that a vertical grating in a frontal plane, when viewed with one eye, produces a perspective texture gradient

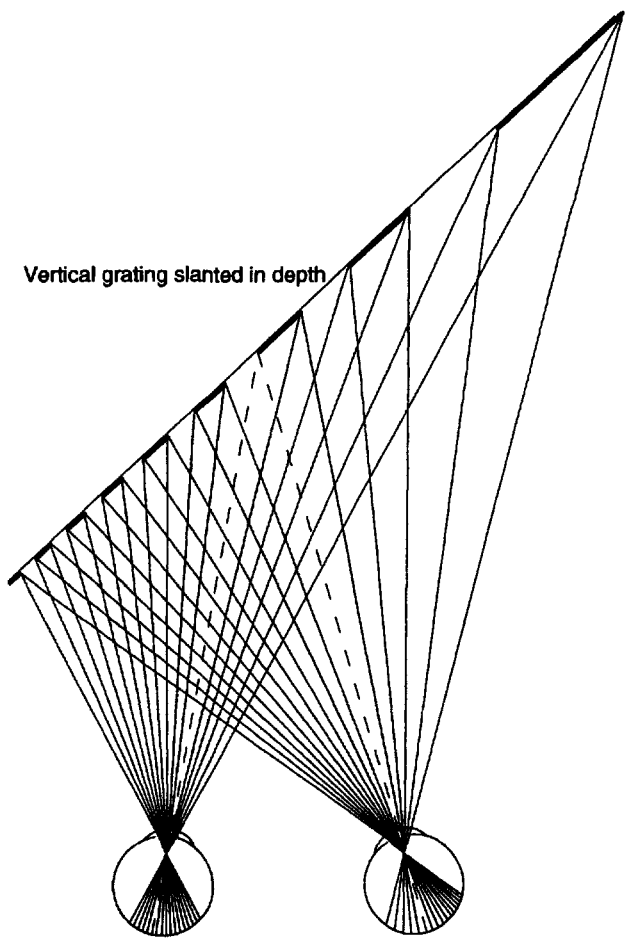


Figure 7.23. Disparity for a surface slanted about the vertical. The bars on the slanted vertical grating are spaced so as to subtend equal angles in the left eye. The image of the grating in the right eye has a lower mean spatial frequency and shows a gradation of spatial frequency across the image. For a grating subtending a small visual angle, the difference in mean spatial frequency of the images is the main effect and is known a dif-frequency disparity. The dashed lines are the visual axes.

extending in both directions from the position straight ahead of the eye. A similar perspective gradient is produced in the other eye. Because these two gradients are out of phase, a vertical grating in a frontal plane produces a gradient of horizontal disparity extending in both directions out from the midline. This gradient of horizontal disparity also increases as the grating is slanted in depth about a vertical axis in the median plane. Consider a vertical grating slanted about a vertical axis with the lines spaced so as to cancel the perspective texture gradient in the left eye, as in Figure 7.23. The left-eye image has a regular periodicity. The image of the same grating in the right eye has a lower mean spatial frequency. After Tyler and Sutter (1979) we refer to a dichoptic ratio of spatial frequency as dif-frequency disparity. Note, also, that the right-eye

image has a gradient of spatial frequency as well as a mean difference. This is a second-order effect for displays subtending small angles. A slanted, evenly textured surface produces an image with a perspective gradient in each eye. Because the two visual axes cut the surface at different angles, the texture gradient is slightly steeper in one eye than in the other, as shown in Figure 7.23. Thus, dif-frequency disparities are usually superimposed on monocular perspective gradients. In a stereoscope, a pure dif-frequency disparity may be introduced into displays with no perspective gradient. This introduces a conflict because the dif-frequency disparity signifies that the surface is slanted while a zero-perspective gradient signifies that it is in a frontal plane.

7.2.4 Cumulative horizontal disparity

A surface slanted about a vertical axis also produces a pattern of conventional horizontal disparities in the two images. If the eyes remain converged on the near edge of the surface, the horizontal disparity of matching features in the two eyes is zero at that position and increases linearly across the slanted surface to the far edge. We will refer to this as the cumulative horizontal disparity.

7.2.5 Beat patterns of horizontal disparity

A slanted surface covered with a regular periodic pattern, such as a vertical grating, produces images in which similar pattern elements periodically fall on corresponding retinal regions. The result is a periodic modulation of horizontal disparity rather than a steady accumulation of disparity across the whole surface. Consider a slanted surface covered with a pattern of similar closely spaced elements interspersed with a distinct set of similar widely spaced elements, as in Figure 7.24. The closely spaced elements show a disparity modulation and the widely spaced elements a cumulative disparity. In other words, high spatial-frequency components signify slant only in each local region, whereas low spatial-frequency components, in principle, could signify slant over a large surface. At more eccentric regions of the retina only large disparities between coarse surface features can be detected. Note, however, that the slant is with respect to the isodisparity circle and has to be scaled with distance.

7.2.6 Sequentially scanned local disparities

In the cases considered so far it was assumed that the eyes remained converged in one location on the slanted surface. People normally scan the gaze over



Figure 7.24. Dif-frequency disparity with closely and widely spaced elements.

When the dots are fused the dif-frequency disparity in the closely spaced dots creates slant only locally. The same dif-frequency disparity in the widely spaced lines creates an impression of slant over a longer distance.

a slanted surface and as the gaze moves toward the far edge, the eyes diverge so as to keep matching features on the two foveas. The coarse disparities in the surface provide the initial signal for the change in vergence as the gaze shifts from one position to the next and the fine disparities provide the final fine control for vergence. We showed in Section 5.3.2 that smaller differences in disparity can be detected with respect to zero disparity than when they are presented on a disparity pedestal. Therefore the disparity information in the neighbourhood of the fixation point, whether it be dif-size, dif-frequency, or horizontal disparity, provides the most precise indication of the slant of the surface in that region. The coarser the pattern, the larger the radius within which disparities are effectively detected. The sequentially acquired samples of local slant information provide a basis for building an internal representation of the slant of the surface. This internal representation facilitates the control of subsequent sweeps of gaze, and these confirm and refine the impression of slant.

7.2.7 Orientation disparity

Orientation disparities are more usually associated with inclined surfaces, but they are also present in slanted surfaces. Vertical lines on a slanted surface do not create orientation disparities and neither do horizontal lines close to the horizontal meridian, assuming that the eyes are torsionally aligned. Lines of all other orientations do create orientation disparities with the maximum values created by $\pm 45^\circ$ lines for a given degree of slant. The relationship between orientation disparity and line orientation is shown in Figure 7.25. The orientation disparity created by a line of a single orientation is inherently ambiguous. Orientation disparities are also generated by torsional misalignments of the eye and by surfaces inclined around a horizontal axis. Surfaces slanted around a vertical axis create a pattern of orientation disparities in which the amplitude of the orientation disparity ϕ is modulated by the orientation of the line element approximately according to a $\sin(2t)$ function where t is the projected orientation of the

line with respect to the horizontal (Figure 7.25). Orientation disparities on the major diagonals are not only maximal in magnitude but they are also opposite in sign. The spatial pattern of orientation disparities created by a slanted surface is similar to the spatial pattern of polar direction disparities described in Section 7.2.9.

The preceding analysis is based on line elements within a small field of view. With larger fields of view, there will be small orientation disparities of horizontal line elements close to the median plane, which increase with increasing elevation from the horizon plane, as a consequence of perspective viewing from slightly different vantage points. These orientation disparities are of opposite sign above and below the horizon plane and may play a role in signalling the absolute distance of the surface (Section 7.6). Note that an isotropic magnification of one eye's image with respect to the other, as would be created by a surface which is eccentric with respect to the head, has no effect on the orientation disparity field. The orientation disparity field of all radial line elements on any surface which is normal to the cyclopean direction is everywhere zero, whatever its distance from the observer.

7.2.8 Deformation and angular disparity

The most useful description of the binocular differences created by a slanted surface would be one which was both unique to slanted surfaces and invariant to location of the surface in the visual field, direction of gaze, and distance from the observer. None of the types of disparity we have discussed so far satisfies all these requirements. The characteristic that comes closest is **deformation disparity**, defined as the amount of deformation needed to map one eye's image onto the other. Deformation disparity specifies the amount of slant with respect to the cyclopean direction and is invariant up to a scale factor of absolute distance—that is, it provides information about cyclopean slant at a distance. Slant around a vertical axis is specified by the Def_1 component identified earlier (Section 7.1.5) and is equivalent to the ratio of HSR (horizontal size ratio) to the VSR

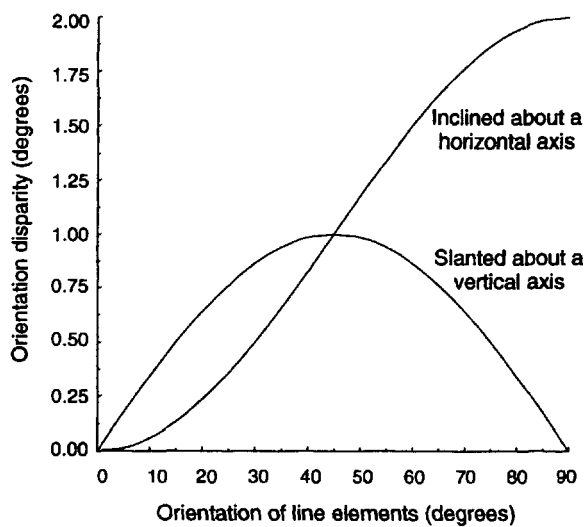


Figure 7.25. Orientation disparity and line orientation.
The orientation disparity of line elements covering either a 17° inclined or a 17° slanted surface as a function of the orientation of the line element. Vertical line elements (90°) create the largest orientation disparities on inclined surfaces whereas +45° line elements create the largest orientation disparities on slanted surfaces. The largest orientation disparity on a slanted surface is just half that on an inclined surface, for a given slant or inclination.

(vertical size ratio), where the HSR equals $\partial\alpha/\partial\theta_h$ (the gradient of horizontal disparity in a horizontal direction) plus one, and the VSR is equal to $\partial\beta/\partial\theta_v$ (the gradient of vertical disparity in a vertical direction) plus one.

The invariance of deformation disparity to location in the visual field arises because deformation is immune to the effects of an isotropic size difference between the images characteristic of eccentric surfaces. Koenderink (1986) suggested that deformation disparity can be measured to a good approximation by monitoring the orientation disparities created by line elements at several different absolute orientations. Figure 7.25 shows that for a slanted surface, orientation disparity ϕ is modulated by the orientation of the line element in the projected image approximately according to a $\sin(2t)$ function. Hence there is a binocular disparity in the angular difference between pairs of lines in the separate monocular images, which can be referred to as an **angular disparity**. For a slanted surface, the angular disparity is maximal for pairs of lines in the projected image which are close to +45° and -45°. In contrast, the angular disparity between pairs of lines in the projected image which are close to 0° and 90° is zero. The modulation of angular disparities of orthogonal line elements as a function of their absolute orientations in the projected image provides the signature of a slanted surface (Figure 7.42).

7.2.9 Polar disparity

The disparity of a single point can be represented in polar coordinates in terms of a meridional direction (ϕ) and an angle of eccentricity (θ) in the radial direction (Section 7.1.1). Liu et al. (1994a) have recently proposed that the binocular differences in the directional component (ϕ) could be used to judge the slant and inclination of surfaces. Consider, for example, the pattern of polar direction disparities created by a planar surface slanting about a vertical axis (Figure 7.26). Clearly, the individual values of polar direction disparity provide no information about local surface slant, but Liu et al. claim that the radial pattern of polar direction disparities could be matched against a template to derive both the direction and magnitude of slant, although the latter would have to be scaled by viewing distance in the same way as other types of disparity.

This is an interesting new possibility, but it is not without problems as Liu et al. acknowledge. First, the pattern of polar direction disparities is not invariant over changes of vertical and horizontal eye position, including small vergence changes (Section 7.1.1). Polar direction disparities provide a method of calculating the slant and inclination of the particular surface patch that is fixated. With fixation, the pattern of polar direction disparities created by a slanting surface resembles the pattern of orientation disparities created by the same surface. But there is an important difference. Polar disparities are expressed in terms of a binocular difference in the direction of a point from the origins of the two coordinate frames—that is, a difference in the implicit radial orientations. Elements used to measure orientation disparity need not pass through the origin.

Second, polar direction disparities are necessarily zero along the horizontal meridian (assuming the eyes are torsionally aligned) and, as a consequence, it would be impossible to determine the slant of a row of dots along the horizontal meridian if polar direction disparities were the only mechanism available. Third, absolute polar direction disparities are affected by torsional misalignment of the two eyes which causes the pattern of polar direction disparities to be rotated around the z axis.

7.3 Perception of slant

We now discuss the use of these different types of disparity in the perception of slant. The issue is inherently complicated but a general reluctance of investigators to consider alternative interpretations of their data has caused further complications.

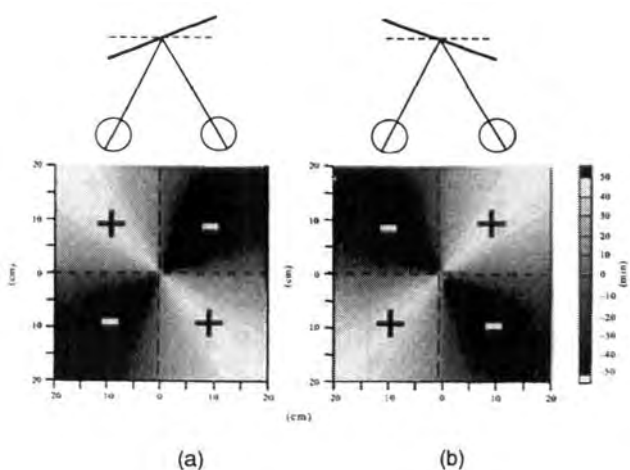


Figure 7.26. Polar angle disparity map of a slanted surface.
The grayscale value indicates the polar angle disparity of each point on a surface slanted 10° away to the right (a) or 10° away to the left (b) as a function of its two-dimensional location in the visual field. Surface subtended 40 × 40 cm at a distance of 40 cm. (Reproduced with permission from Liu et al. 1994a, Vision Research, Pergamon Press.)

7.3.1 Dif-frequency and width disparities

Magnification of one image relative to the other in a horizontal direction produced, for instance, by placing a meridional lens before one eye causes frontal surfaces to appear slanted in depth (Ogle 1964). Blakemore (1970b) proposed that dif-frequency disparity is detected by specialized disparity detectors, distinct from those that detect point and orientation disparities. Campbell and Robson (1968) introduced the idea of visual channels tuned to specific spatial frequencies. This led to the idea that the visual system carries out a Fourier analysis of the visual scene into component sine and cosine luminance modulations. This cannot be true in anything but a trivial sense because detectors for Fourier components of a signal must have infinite extent, in time for a time-varying signal or in space for a space-varying signal, and must sample the frequency spectrum at an infinite number of points in both sine and cosine phase (Gabor 1946). The visual system could therefore not even approximate a spatial Fourier analyzer unless all receptive fields were as large as the retina and there were a very large number of them, each tuned to a narrow range of spatial frequencies (see Section 3.4.2). A typical ganglion cell has a receptive field of concentric excitatory and inhibitory zones. A receptive field of this type is most sensitive to a local periodic pattern of luminance that matches both the position and periodicity of its excitatory and inhibitory zones. Each ganglion cell has a spatial-frequency bandwidth of around 2 octaves. It therefore acts as a

spatial filter tuned, not to spatial frequency, but to the local spatial periodicity of luminance, that is, to the size, position, and periodicity of a local area of luminance modulation. Most investigators still talk about spatial-frequency tuned disparity detectors. It is better to talk about local spatial-periodicity disparity detectors, or dif-size disparity detectors.

Psychophysical evidence suggests that at each retinal location there are at least four channels with distinct but overlapping spatial-periodicity tuning functions (Wilson and Bergen 1979; Georgeson and Harris 1984). Physiological evidence from cats (Movshon et al. 1978) and monkeys (DeValois et al. 1982b) supports this conclusion. Each has a half-amplitude bandwidth of between 1 and 2 octaves of spatial periodicity. The mean size of the receptive fields of ganglion cells increases with increasing retinal eccentricity. Excitatory regions of receptive fields subtend about 6 arcmin at the fovea and about 12 arcmin at an eccentricity of 4° (Wilson and Giese 1977). If the size tuning of the receptive field of a binocular cell in one eye differs from that of its receptive field in the other eye, the cell responds best to a specific difference in spatial period in the images of a slanted surface. Blakemore proposed that such cells are also orientation selective, responding best to vertically oriented lines, since horizontal gratings do not produce differential spatial frequencies in the two eyes when slanted. This argument is misleading. The images of horizontal line elements on a slanted surface differ in length in the two eyes and are detected by cortical cells with horizontally tuned receptive fields. The correct rule is that dichoptic differences in spatial periodicity (image size) along horizontal meridians signify slant; those along vertical meridians do not signify slant. Differences in horizontal spatial periodicity occur as differences in the horizontal extent of texture elements or of the intervals between them. Unless the texture elements are long featureless lines, their orientation is immaterial.

Dichoptic vertical gratings differing in spatial frequency can create the impression of a slanted surface even when there is no monocular texture gradient. This can be confirmed by fusing the upper stereogram in Figure 7.27, although it usually takes some time before the impression of depth emerges. The fused rectangular images look trapezoidal because of size-distance scaling. A slanted surface would have to be trapezoidal to produce rectangular images. When the difference in spatial frequency is too high, as in the lower stereogram of Figure 7.27, an impression of steps or of several slanted surfaces like a Venetian blind replaces that of a single slanted surface (Blakemore 1970b). The Venetian blind effect is particularly evident when the mean spatial

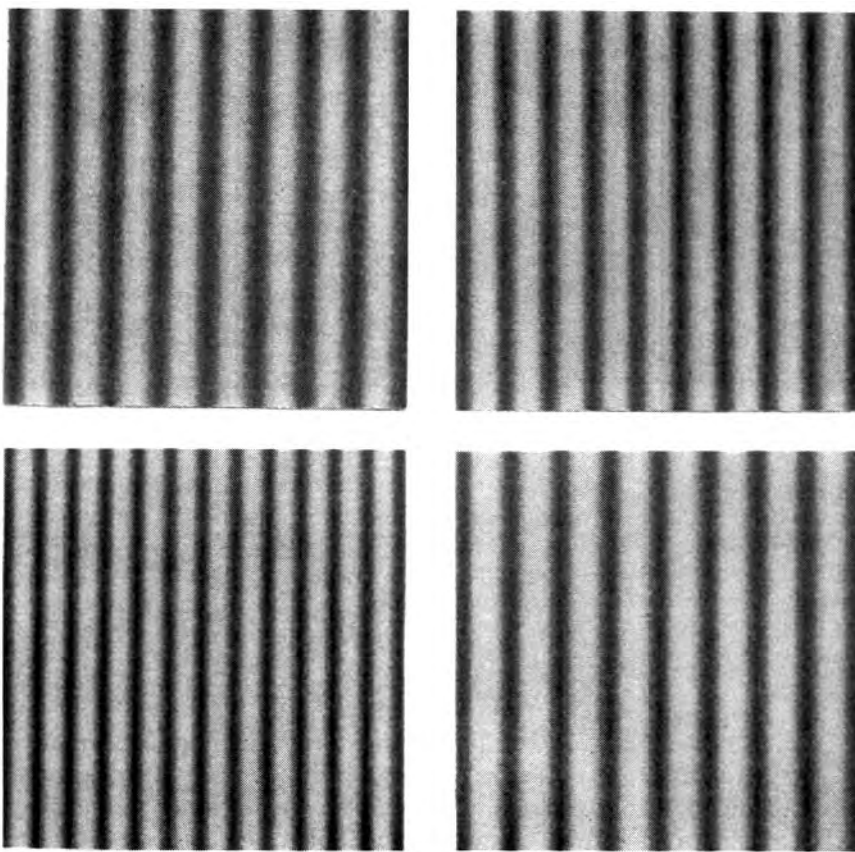


Figure 7.27. Dif-frequency disparity.

Stereograms with vertical gratings that differ in spatial frequency in the two eyes. When the disparity is not too great, as in the upper stereogram, fusion creates a slanted surface, even with no monocular texture gradient. When the disparity is large, as in the lower stereogram, the impression of a slanted surface is replaced by that of a series of steps. (Reproduced with permission from Blakemore 1970c, Vision Research, Pergamon Press.)

frequency is high and the display is wide. This is what one would expect because, under these circumstances, there is a periodic modulation of disparity over the surface, corresponding to the beat frequency of the two gratings ($f_1 - f_2$). An illusory difference in spatial frequency produced by pre-adapting one eye to a grating of a different frequency does not generate an impression of depth (Sloane and Blake 1987). For gratings between 2 and 6 c/deg, a spatial-frequency difference of about 10 per cent produces the largest slant, as can be seen in Figure 7.28. Fiorentini and Maffei (1971) claimed that an impression of depth is created by presenting gratings of the same spatial frequency to the two eyes and reducing the contrast of one of them, but Blake and Cormack (1979c) failed to replicate this effect.

Blakemore (1970b) asked subjects to increase or decrease the spatial frequency of a vertical grating presented to one eye relative to that of a fixed grating presented to the other eye until the impression of slant broke down. This was done for a range of spatial frequencies of the fixed grating. Note that the

gratings in the two eyes remained the same width. Figure 7.29 shows that the range of spatial frequency ratios (expressed as ratios of spatial period—HSRs) over which the impression of slant persisted was greatest for a grating with a spatial frequency of about 3 c/deg and fell off for smaller and larger frequencies. Blakemore argued that if slant were coded in terms of the cumulative horizontal disparity across the grating, the impression of depth would be independent of the spatial frequency of the grating and the curves in Figure 7.29 would have been flat. He wrote, "If the computation is really a point-for-point affair I can see no reason why it should depend on the spatial frequency of the pattern, as long as it can be distinctly resolved." It is now known that thresholds for horizontal disparity vary with spatial frequency in just the way Blakemore's results revealed (see Section 5.7). Thus, the results of this experiment did not justify Blakemore's conclusion that dif-frequency disparity codes slant. In any case, the same evidence could support the idea that local size or width disparities code slant because

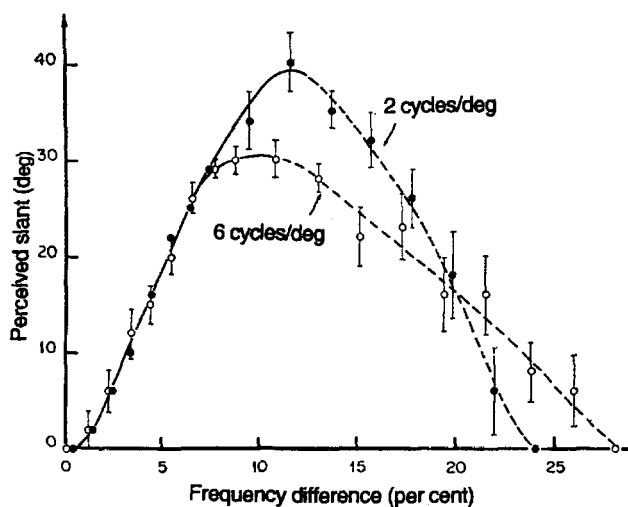


Figure 7.28. Dif-frequency and magnitude of slant.

Perceived slant about a vertical axis of a dichoptic vertical grating as a function of the percentage difference in spatial frequency between the images. Vertical bars are standard deviations. The left-eye grating had a fixed spatial frequency of either 2 or 6 c/deg, as indicated on the curves. For both gratings, a spatial-frequency difference of about 10 per cent produced the largest apparent slant. (Reproduced with permission from Fiorentini and Maffei 1971, Vision Research, Pergamon Press.)

saying that the visual system is most sensitive to spatial frequency of about 3 c/deg is equivalent to saying it is most sensitive to a spatial period of about 0.3°.

Another point is that the two images in Blakemore's stereogram had the same width in the two eyes. This biases the system against using the cumulative horizontal disparity because a true cumulative disparity results in a narrower overall display in one eye than in the other, with the number of pattern elements remaining the same in the two eyes. Van der Meer (1978) compared the apparent slant produced by vertical gratings of various spatial frequencies, first with gratings with the same width in each eye, but a different number of bars, like those used by Blakemore, and then with gratings with the same number of bars in each eye, but different widths. With the first type of grating he found the drop off in perceived slant at higher spatial frequencies that Blakemore found, but there was no drop off with the differential-width gratings. This suggests that people use the overall horizontal disparity produced by a slanted surface when it is properly presented. Further evidence for this conclusion is now reviewed.

One of the original stereograms devised by Wheatstone (see Figure 1.5) contained a dif-frequency disparity, so the concept is not new. The

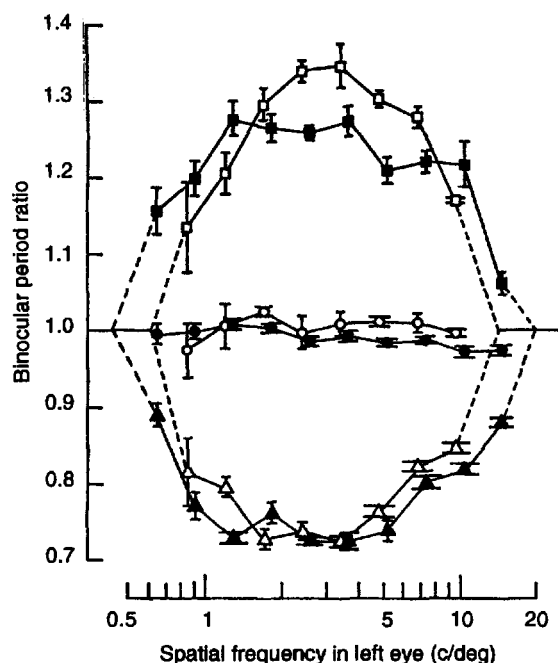
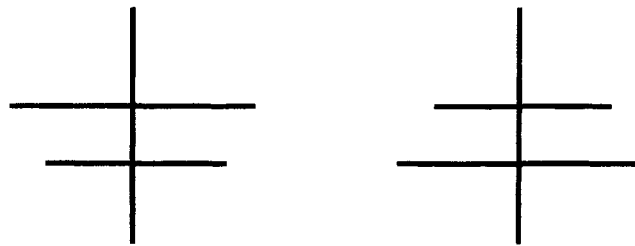


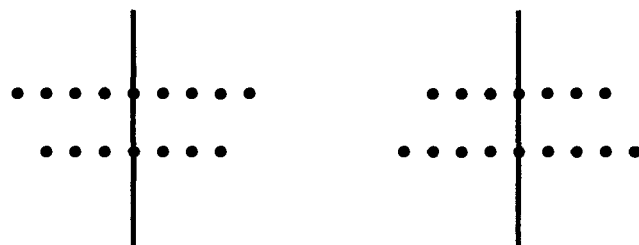
Figure 7.29. The limits of dif-frequency disparity.

The maximum ratio of spatial periods of dichoptic vertical gratings that generates the impression of a slanted surface, as a function of the spatial frequency of the grating presented to the left eye. For the square datum points, the spatial frequency of the right-eye image was less than that of the left-eye image. For the triangular datum points, the spatial frequency of the left-eye image was least. The round datum points indicate settings of the stimulus to the apparent frontal plane. The results for two subjects are plotted separately. The vertical bars represent standard errors. (Reproduced with permission from Blakemore 1970b, Vision Research, Pergamon Press.)

stereogram shown in Figure 7.30a produces impressions of two lines slanting in opposite directions (Wilde 1950). The lines appear to slant even though there is no disparity information along the lines. This is an example of the principle enunciated in Section 12.4 that, in the absence of information to the contrary, depth impressions are interpolated into figural areas bounded by disparity discontinuities. In the stereogram shown in Figure 7.30b the spacing of the dots is the same in the two eyes, but there are two extra dots in one eye. This gives rise to an impression of slant, especially if the gaze moves across the display. The impression of depth cannot be due to dif-frequency disparity. It could be due to the overall dif-size disparity, but another possibility is that the conditions for Panum's limiting case are present at each end of the display (see Section 12.6.6). One should avoid drawing firm conclusions from this display because the impression of slant is very unstable. For instance, when the gaze is fixed in the centre of the row of dots the two end dots appear to float out in depth leaving the central dots in a frontal plane.



(a) When fused the two lines appear to slant in opposite directions, even though information about the relative spatial frequency of the images is reduced to a minimum.



(b) The rows of dots have the same spacing in the two eyes but each row in one eye has two extra dots. Fusion of the images produces a fluctuating impression of slant. (From Wilde 1950.)

Figure 7.30. Depth from differences in line length.

Ramachandran and Nelson (1976) devised the stereogram shown in Figure 7.31. When the images are properly fused, they create the impression of a slanted row of dots because one row is longer than the other. The corresponding pairs of dots within the rows have slight disparities that cause each pair to appear independently slanted in the opposite direction to the slant of the whole row. The horizontal disparity between the pairs signifies slant of the whole row while the disparities within the pairs signify independent slant of the pairs. Note, however, that when the gaze is held in one location, especially at one end of the row, the impression of overall slant of the row is lost and the slant of only the pair of dots being fixated is apparent. This may be interpreted as evidence that overall depth is signalled by the accumulation of information from several local areas as the gaze is allowed to wander over the row (see Section 6.2.13 for more discussion of this point).

Blakemore also found that perceived slant remained constant when he increased the width of his vertical-grating display. He argued that this is what one would expect from the constant difference in frequency but not what one would expect from the increasing cumulative horizontal disparity. It would be an inefficient system that registered slant in terms of the accumulated horizontal disparity across a surface without regard for the relative lengths of the images of the surface in the two eyes. A system that sequentially scans horizontal disparities would also

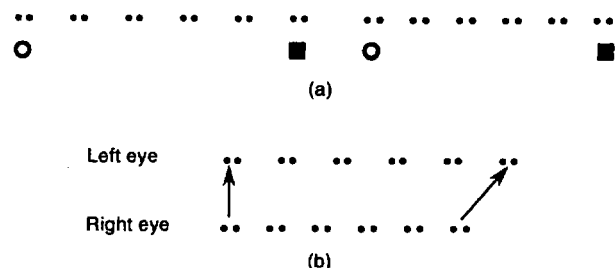


Figure 7.31. Global and local slant.

Fusion of the images in (a) creates the impression of a slanted row of dots because one row is more widely spaced than the other, as shown in (b). The corresponding pairs of dots within the rows have slight disparities that cause each pair to appear independently slanted in the opposite direction to the slant of the whole row. (After Ramachandran and Nelson 1976.)

be independent of the length of the surface. Furthermore, as Tyler and Sutter (1979) pointed out, wider displays extend into the peripheral retina where depth impressions require larger disparities, and it may be this factor that accounts for Blakemore's flat function.

Tyler and Sutter produced their own evidence in favour of the dif-frequency theory of slant perception. They presented a luminance-modulated grating of 1.5 c/deg to each eye, in which the fine texture consisted of random dynamic vertical lines. The gratings were caused to drift from side to side at 4°/s (1 Hz) either in phase or in antiphase. Both cases produced a good impression of static slant. They argued that the point-for-point disparity mechanism was inactive in the opposed-movement condition because the impression of back-and-forth movement in depth that it should have produced was not present, only the impression of slant. The argument collapses with the evidence cited in Section 12.1.1 that overall changes in horizontal disparity do not produce impressions of changing depth.

Tyler and Sutter also obtained an impression of slant, albeit only for large differences in spatial-frequency, when the dynamic lines in the dichoptic images were uncorrelated. They argued that this impression arises from a primitive pure dif-frequency mechanism, which they called protostereopsis. None of this evidence supports the idea that the perception of slant is based on global dif-frequency disparities, as opposed to local dif-size disparities, and it all ignores the possible contribution of sequentially scanned local disparities.

Wilson (1976) objected to the view that the perception of slant relies on dif-frequency disparities. He pointed out that Blakemore's stimuli omitted the texture gradients that occur in actual surfaces. A

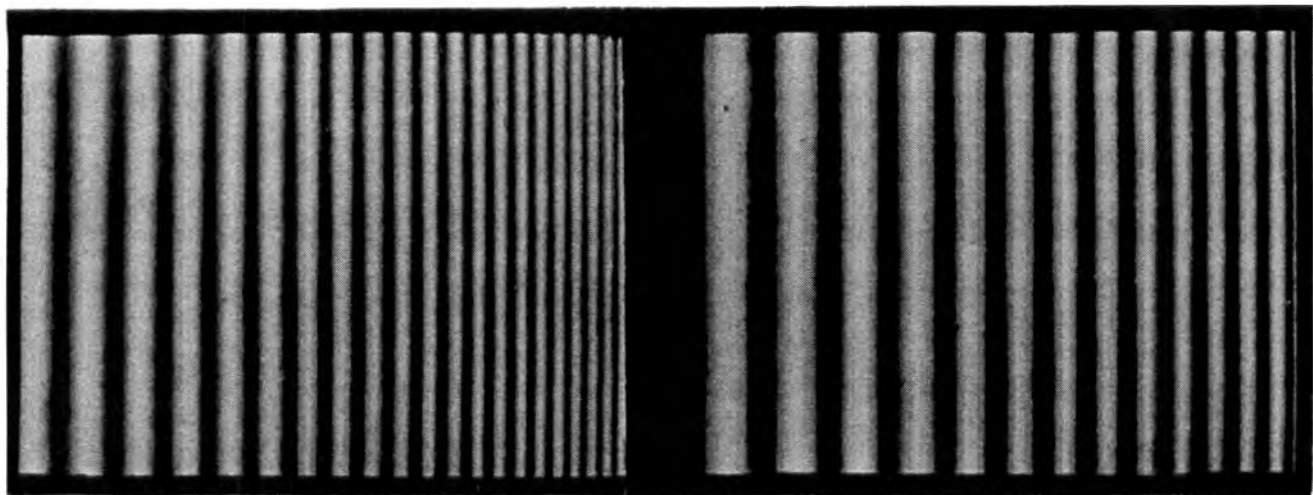


Figure 7.32. Stereogram with monocular texture gradients plus a dif-frequency disparity.
(Reproduced with permission from Wilson 1976, Vision Research, Pergamon Press.)

natural texture gradient has a wide range of spatial frequencies that should disrupt the visual system's ability to compare spatial frequencies by narrowly tuned spatial-frequency detectors. However, he found that surfaces with monocular texture gradients, such as those shown in Figure 7.32, were more easily detected as slanting than were surfaces with only dichoptic size differences and no texture gradients. He argued that this cannot be due to supplementary depth information provided by the texture gradients because a texture gradient by itself is ambiguous with regard to the direction of slant. This is not a convincing argument because the texture gradient does provide extra information, even though it is unsigned. He proposed that we use local dif-size disparity detectors. Since the size of receptive fields increases in a more or less linear fashion with increasing retinal eccentricity, the position on the retina best suited to detect a dif-size disparity depends on the absolute size of the images along the texture gradient. Wilson proposed that people optimize their ability to detect dif-size disparities by moving the eyes to bring the texture gradients into correspondence with the retinal gradient of receptive field size. The slant of a surface covered with a regular fine pattern would be difficult to detect by a pure dif-frequency mechanism because the ability to detect a fine pattern declines rapidly with increasing eccentricity. More to the point, the ability to discriminate between two high spatial-frequency patterns declines even faster with increasing eccentricity, as can be seen in Figure 7.33 (Greenlee 1992).

It has been argued that the size-matching strategy has some advantages over the point-for-point

system for coding slant. The point-for-point system requires a precise matching of specific texture elements in the two eyes. In a long slanted surface covered with a repetitive texture containing a mixture of spatial frequencies, the images may be difficult to match because corresponding elements become increasingly separated at locations on the surface more remote from the point of fixation. The size-matching process works even if the correct matching elements are not found because the mean size difference between elements can be detected between nonmatching elements. However, this advantage applies only if the viewer holds fixation constant, which is most unnatural. When the gaze wanders, the slant can be sampled at several locations along the surface and disparities outside the foveal region can be ignored while each sample is being registered. It has also been argued that moving one image relative to the other should perturb the point-for-point system whereas the size-matching process should be relatively immune to this procedure. Blakemore (1970b) confirmed that motion of one image at $1^{\circ}/s$ does not seriously degrade slant perception. This is not a very convincing argument since the horizontal point-for-point system is probably capable of registering horizontal disparities within short periods.

Levinson and Blake (1979) reported that monocular gratings with similar harmonic content and different cycle width produce an impression of slant. They concluded from this that dif-frequency disparity codes slant. However, a group, including Blake, pointed out that both these monocular stimuli produce similar responses in size-tuned channels and that the impression of slant could arise from dif-size disparity or from horizontal disparity derived from

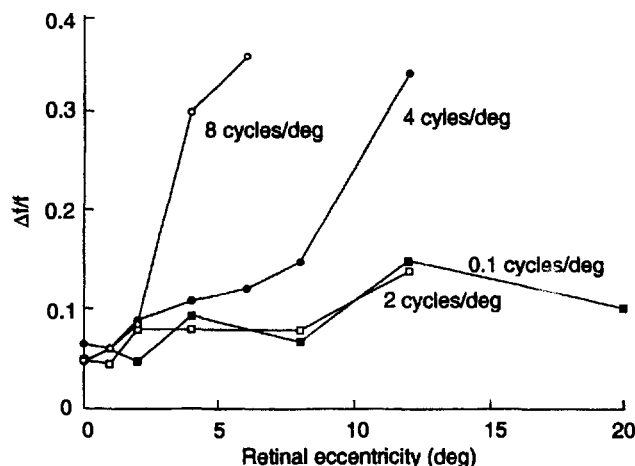


Figure 7.33. Spatial-frequency discrimination.

Spatial-frequency discrimination thresholds as a function of retinal eccentricity, for four baseline spatial frequencies. Stimuli were Gaussian-truncated sinewave gratings with a spatial-frequency bandwidth of 0.5 octaves, at five times the contrast threshold. (Reproduced with permission from Greenlee 1992, Vision Research, Pergamon Press.)

the output of these size-tuned channels (Halpern et al. 1987). In their own experiment Halpern et al. used the stereogram shown in Figure 7.34. The degree of apparent slant created by a difference of spatial frequency between two vertical gratings decreased when they introduced an overall horizontal disparity into the grating with respect to the edges of the circular aperture. The whole display was presented briefly with convergence held in the plane of the aperture. They argued that this decrement of perceived slant would not occur if slant were coded in terms of dif-frequency disparity but would occur if it were coded in terms of horizontal disparity. This is not a well-founded argument. Adding a horizontal disparity made the grating appear beyond the circular frame. The disparity within the grating was thus placed on a disparity pedestal with respect to the circular frame, which was in the plane of convergence. Disparities on disparity pedestals are registered less efficiently than those on a base of zero-disparity, as we saw in Section 5.3.2.

Summary

What conclusions can be drawn about the mechanisms underlying the perception of surface slant when the binocular stimulus consists of a grating pattern of slightly different frequency in the two eyes? Although several authors have suggested that dif-frequency disparity may underlie this ability, the arguments are not convincing. First, no physiological evidence exists that there are spatially extended receptive fields that could measure spatial frequency rather than the local spatial period.

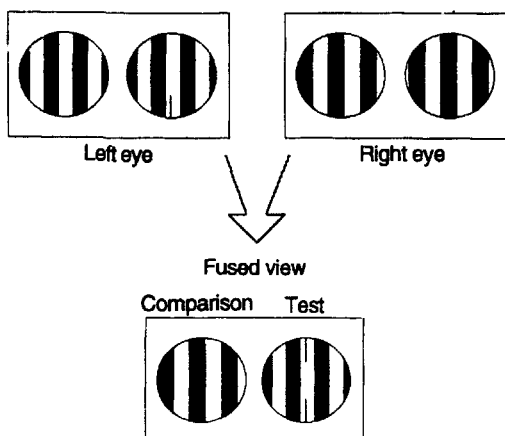


Figure 7.34. Dif-frequency plus horizontal disparity.

The stereogram used by Halpern et al. (1987) to investigate the effect of an overall horizontal disparity on the apparent slant produced by a dif-frequency disparity. The apparent slant created by a difference of spatial frequency between two vertical gratings was reduced when an overall horizontal disparity with respect to edges of the circular aperture was introduced. (Reproduced with permission from Vision Research, Pergamon Press.)

Second, the fact that dichoptic grating patterns of slightly different spatial frequency are typically seen as a Venetian blind surface (with periodic modulation in depth) when the eyes are prevented from scanning the grating is evidence in favour of local size differences rather than dif-frequencies. Third, the fact that slant can still be seen when (1) the grating pattern to one eye is drifted, (2) the patterns to the two eyes oscillate either in phase or in antiphase, or (3) binocularly uncorrelated random noise gratings are presented, shows only that the underlying mechanisms can extract width or size differences rapidly. There is no convincing evidence favouring the idea of dif-frequency disparity over dif-size disparity. On the other hand, evidence suggests that scanning eye movements do play a role in slant perception by building up a representation based on local slant estimates.

It should be added that the use of grating patterns to investigate slant perception is potentially misleading because extended one-dimensional grating patterns provide no information about the relative vertical sizes of binocular images. As we have shown in Section 7.1.5, horizontal size differences or dif-frequency disparities vary as a function of both the slant of the surface and its eccentricity. Therefore, a difference in spatial frequency between binocular gratings is not sufficient to specify whether the grating is slanting or the eyes are viewing the patterns eccentrically. Rogers and Bradshaw (1994) showed that the relative vertical size of binocular gratings plays an important role in judgments of

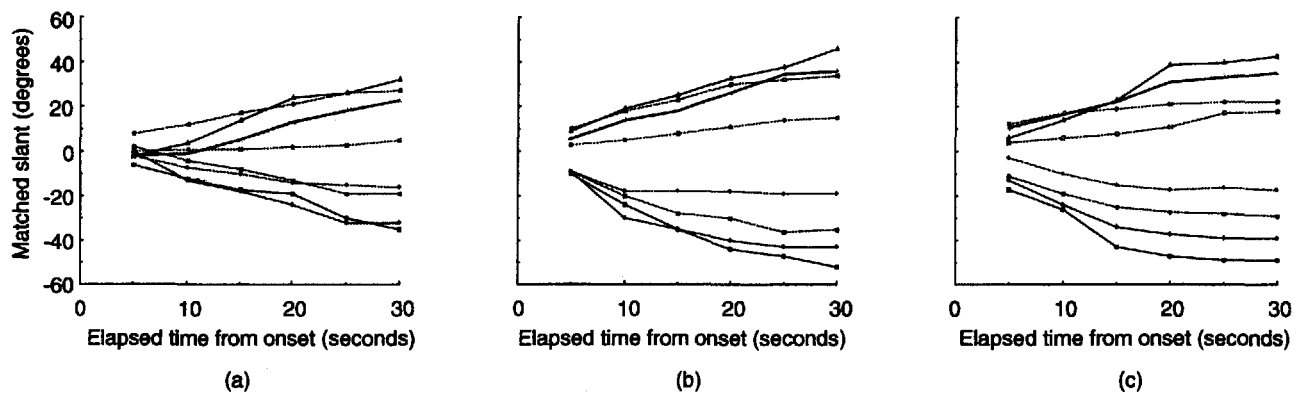


Figure 7.35. The build-up of perceived slant over time.

Three different slanted surfaces were presented to observers: (a) a pure dif-frequency sine wave; (b) a dif-frequency sine wave plus superimposed random dots; and (c) random dots. Slant angles were: $\pm 15^\circ$, $\pm 30^\circ$, $\pm 45^\circ$ and $\pm 60^\circ$. Observers matched the perceived slant using a tactile paddle. Settings were monitored every 5 s. The results showed that perceived slant in dif-frequency gratings builds up more slowly and is less veridical even after 30 s than for gratings with superimposed random dots (b). Perceived slant built up most rapidly and was largest with surfaces covered with random-dots (c). (From Rogers and Bradshaw 1994.)

surface slant. The same frequency difference in binocular gratings can produce an impression of slant in one direction when the vertical extents to the two eyes are the same and in the opposite direction when the vertical magnification of the lower frequency grating is larger than its horizontal magnification. This is a variant of Ogle's induced effect (Section 7.6.5).

In addition, the impression of slant from gratings of different frequencies is often more difficult to see, takes longer to build up, and never reaches the same magnitude compared to when the same gratings are covered with random noise (Figure 7.35). These results suggest that one-dimensional gratings are not an ideal stimulus for investigating slant perception.

7.3.2 Deformation and slanted surfaces

The images of an eccentrically placed surface which is normal to the cyclopean direction differ uniformly in magnification because the surface is closer to one eye than to the other (Figure 7.17). Notice that this is true whether or not the surface is fixated—it is a property of all surfaces which are eccentric with respect to the head. Within limits, we are able to judge whether a surface is normal to the cyclopean direction, suggesting that the human visual system is capable of taking the eccentricity of the surface into account. The reader can verify this point by maintaining fixation on a point on a flat surface which is normal to the direction of gaze while rotating the head about the vertical axis. The apparent slant of the surface does not appear to change even though the relative sizes of the binocular images

change. Moreover, this constancy is not restricted to surfaces which are normal to the cyclopean direction.

To achieve constancy in the perception of eccentric surfaces, the visual system needs to correct the width and dif-frequency disparities created by an eccentric surface with some estimate of the surface's eccentricity. Two pieces of information are needed to determine headcentric eccentricity: the oculocentric location of the image and the average gaze angle of the eyes. For a fixated surface, only the latter is needed. If information about gaze angle were obtained from the oculomotor system alone, we would expect that the uniform (isotropic) expansion of one eye's image with respect to the other to give the impression of slant when the images are presented across the median plane of the head since dif-frequency and width disparities are present. The stereogram shown in Figure 12.3a shows that this does not happen. The surface appears to lie in a frontal plane even though it contains a gradient of horizontal disparity.

This result suggests that the visual information provided by the difference in the vertical sizes of binocular images is used to rescale horizontal width and dif-frequency disparities. In Section 7.1.5 it was suggested that this could be achieved in two ways.

1. Local differential characteristics of binocular images could be extracted directly (Koenderink and van Doorn 1976a). The amount of deformation needed to map one eye's image onto the other is affected by both horizontal and vertical size differences and is zero for eccentric surfaces which are

normal to the cyclopean direction because the binocular images are related by a uniform expansion.

2. Vertical disparities created by all surfaces in the scene could provide an estimate of a whole-field viewing parameter—the angle of eccentric gaze. This estimate could then be used to rescale horizontal width and dif-frequency disparities of each local surface (Mayhew and Longuet-Higgins 1982).

Is there any evidence that the visual system adopts one or other of these strategies? In Section 7.1.5 we pointed out that the measurement of deformation is necessarily a **local operation** while the alternative strategy involves calculating a single **whole-field parameter** from all features in the visual scene. This suggests that the two hypotheses can be distinguished using a display in which local deformation is different in different parts of the scene. In particular, if local deformation is calculated by comparing the relative horizontal size (HSR) of a surface patch to its relative vertical size (VSR) (Section 7.2.8), it should be possible to see different slants in two or more surface patches with the same horizontal sizes (HSRs) but different vertical sizes (VSRs) because they create different amounts of deformation. On the other hand, if slant perception is based on calculating a single whole field parameter, the same slant should be perceived because there can only be one estimate of the angle of eccentric fixation, which is used to correct the (identical) width disparities of all surface patches.

In support of the deformation hypothesis, Rogers and Koenderink (1986) found that different slants could be seen in two patches within the same stereogram which had different relative vertical sizes but the same relative horizontal size. The effect may be observed in Figure 7.36 (see also Figure 12.7). However, differential slant between surfaces can be seen only when the number of patches with different vertical magnifications is small and the amount of slant is much less than would be predicted by the deformation differences present.

These results are incompatible with the idea of a single whole-field parameter but they are also incompatible with the calculation of disparity deformation for each separate surface. It is not surprising that deformation is not calculated for each separate surface since, as we pointed out in Section 7.1.5, the idea of calculating deformation disparity is inherently redundant. In normal viewing, the vertical sizes of separate surfaces in the scene are not independent. They are necessarily related by their relative eccentricities in the visual field. The independent manipulation of vertical size differences can be achieved only in the laboratory.

When there is only one surface in view, the two hypotheses make the same predictions. Ogle's induced effect (Ogle 1938, 1939a, 1939b) provides good evidence that a binocular vertical size difference over the whole visual field creates an impression of slant. When there are many surfaces in view it may not be necessary to calculate whole-field parameters, because the second spatial derivatives of the horizontal disparity field may be sufficient to specify relative slant or curvature.

This raises a further point about the perception of slanted surfaces. The stereoscopic displays used in most experiments on slant perception were presented in the context of a monitor screen or other surrounding objects, rather than in isolation. Observers may have responded to the relative slant between the stimulus and its surround rather than to the absolute slant of the stimulus.

Slant thresholds

Thresholds for discriminating the direction of slant (left wall versus right wall) have been measured in semidarkness with minimal stereo cues from surrounding surfaces. Cagenello and Rogers (1988, 1993) obtained thresholds of around $\pm 2.1^\circ$ from a frontal plane using random-dot displays subtending 20° by 20° and a forced-choice procedure. At their 57-cm viewing distance, this corresponds to a disparity gradient of about $0.17 \text{ arcmin}/\text{deg}$. Thresholds for discriminating the direction of inclination of surfaces of the same visual extent were significantly lower, at around $\pm 1.3^\circ$ from the vertical for their two observers. The anisotropy in thresholds for slanted and inclined surfaces is also evident in surfaces with suprathreshold slant or inclination (Rogers and Graham 1983) (Figure 7.37). A single slanted surface is typically seen as less slanting than a single inclined surface is seen inclined when both have the same angle to the frontal plane. Latencies for the perception of slant are typically longer than those for the perception of inclination (Gillam et al. 1984).

Using surfaces of a smaller angular extent (0.5° to 2°), Mitchison and McKee (1990) reported slant thresholds for 10 observers which were higher by a factor of ten when expressed in terms of disparity gradient but the thresholds of the best observers were more similar to those reported by Cagenello and Rogers. Four out the 10 observers in Mitchison and McKee's study showed a marked anisotropy as a function of the surface orientation and were unable to detect any slant in surfaces several tens of degrees away from the frontal plane.

Characteristics of the monocular images also affect slant discrimination thresholds. Ardit (1982) found that thresholds for slant detection were

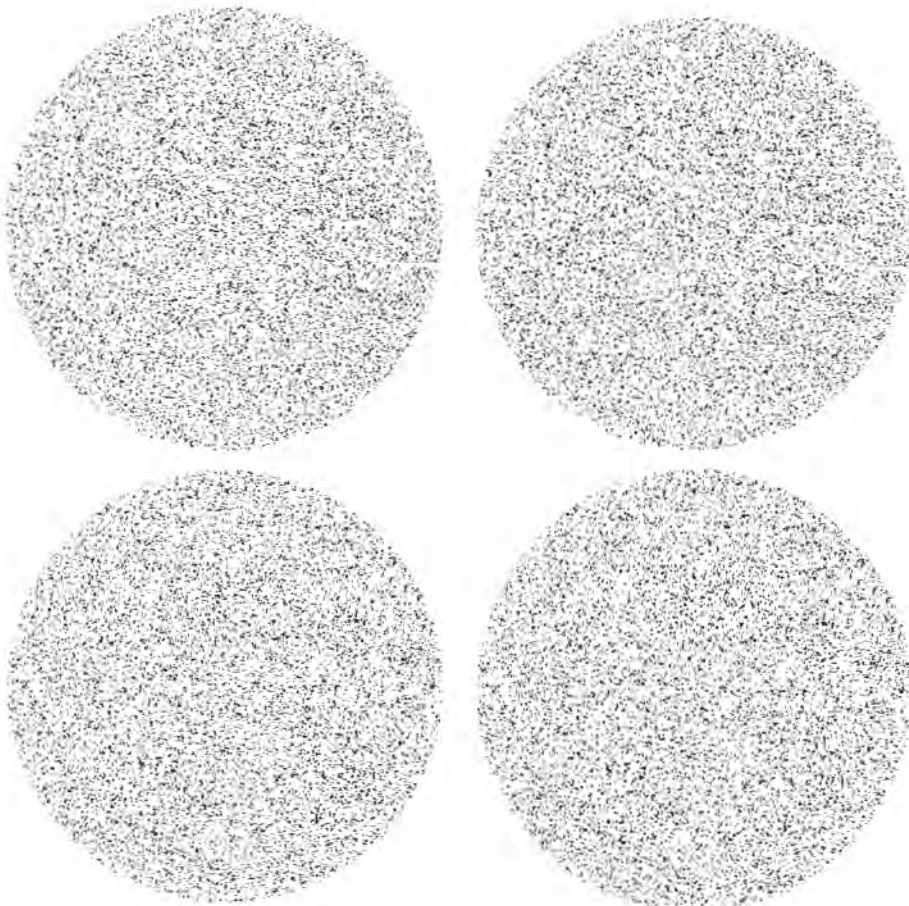


Figure 7.36. Opposite induced effects in the upper and lower fields.

In the upper stereogram, the random-dot pattern seen by the right eye is vertically magnified; in the lower stereogram, the random-dot pattern seen by the left eye is vertically magnified (with divergent viewing). The two pairs of images have no horizontal disparities. If the perception of slant is based on calculating the amount of local deformation, separate slants should be seen in the two stereograms. If a whole field parameter is calculated, corresponding to the angle of eccentric gaze, and a correction applied to all disparity gradients in scene, there should be no difference in slant in the two halves of the stereogram.

lower for a $\pm 45^\circ$ cross hair pattern than for a $0/90^\circ$ cross hair pattern. Cagenello and Rogers (1988, 1993) found a similar pattern of results with gridline stimuli. Thresholds for discriminating direction of slant were much higher— ± 3.0 to 4.0° from the frontal plane—when the stereo images consisted of a grid of 0° and 90° lines instead of random dots. On the other hand, when the stereo images consisted of a grid of $\pm 45^\circ$ lines, thresholds for slant discrimination were similar to those for random dots, at around $\pm 1.5^\circ$ from a frontal plane (Figure 7.38). Cagenello and Rogers interpreted these results as providing evidence for the use of either orientation or angular disparity in slant perception (see Section 7.2.8). A different explanation was suggested by Gillam and

Ryan (1992). They argued that the smaller amount of slant perceived in suprathreshold surfaces covered with a grid of 0° and 90° lines was the result of conflicting monocular perspective information. The magnitude of the conflicting perspective information would be very small in the case of threshold measurements of slant, but it is still possible that observers were influenced by its presence in the Cagenello and Rogers study.

Vertical/horizontal anisotropy

Although orientation disparities may contribute to differences in the perception of slanted and inclined surfaces they are not sufficient since the anisotropy is evident in random-dot surfaces which do not have

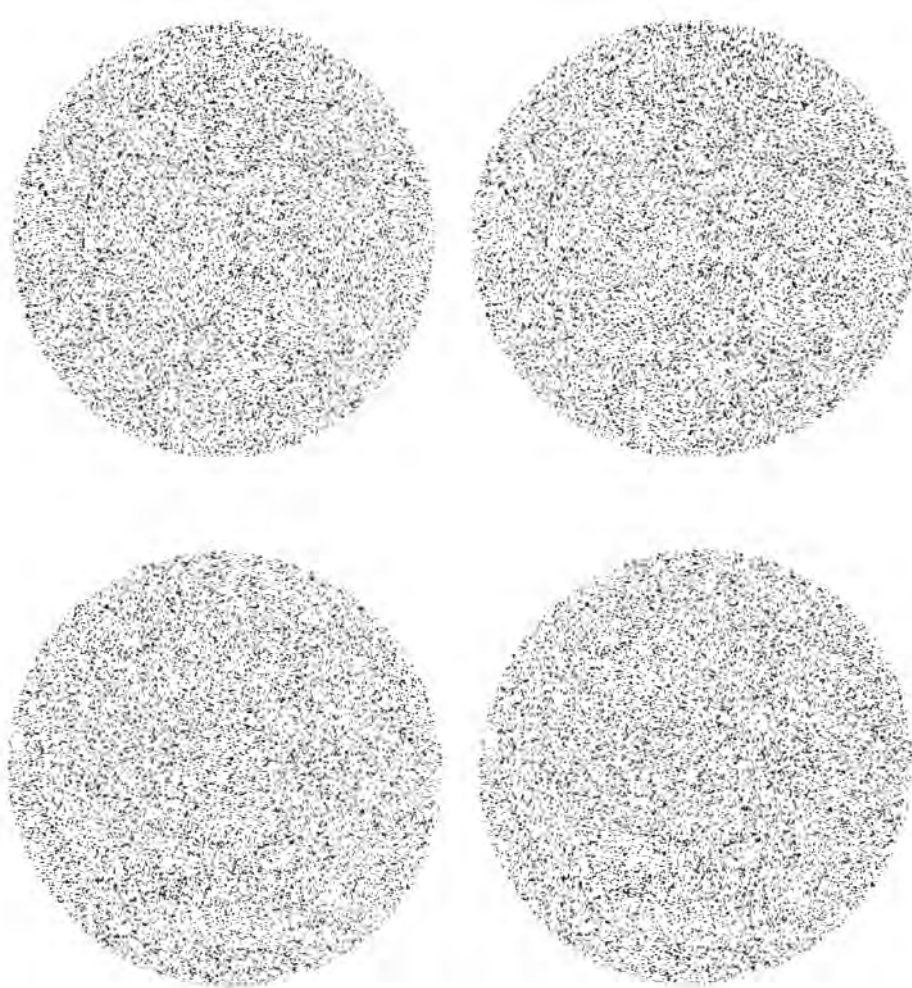


Figure 7.37. Perception of slant and inclination in planar surfaces.

The upper stereogram depicts a planar surface with a uniform disparity gradient which is slanted around a vertical axis. In the lower stereogram the planar surface is inclined around a horizontal axis. When there is only a single planar surface in the visual field, most observers perceive the amount of slant to be less than the amount of inclination. Gillam et al. (1984) reported that the perceived slant builds up over several seconds.

oriented features (Figure 7.37). Moreover, thresholds for detecting vertically oriented corrugations are higher than for horizontally oriented corrugations (Rogers and Graham 1983; Bradshaw and Rogers 1993b) and the amount of perceived depth in vertically oriented suprathreshold corrugations is less than for horizontally oriented corrugations.

Threshold and suprathreshold anisotropies are evident in the stereograms with swept corrugation frequency and swept amplitude depicted in Figures 7.39 and 7.40. The range of corrugation frequencies and the depth modulation changes are the same in the two stereograms but most observers perceive (1) less depth in the low frequency vertical corrugations and (2) that the boundary for detecting low-

frequency vertical corrugations extends a shorter distance across the stereogram than that for detecting horizontal corrugations. For most observers the anisotropy is especially evident with low corrugation frequencies and planar surfaces and may not be evident for all readers in Figures 7.39 and 7.40 which only subtend a small visual angle.

7.4 DISPARITIES ON INCLINED SURFACES

We distinguish five types of disparity produced by a surface inclined about a horizontal axis. Empirical evidence for the effectiveness of these different types of disparity is reviewed in Section 7.5.

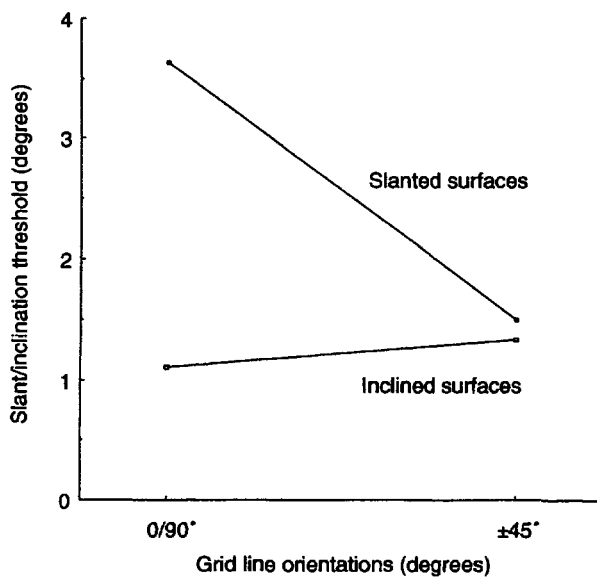


Figure 7.38. Slant/inclination thresholds with grid patterns.
Thresholds were measured for both slanted and inclined planar surfaces as a function of the orientation of grid lines on the surface—either 0° and 90° or ±45°. For slanted surfaces, thresholds for the ±45° grids were a factor of two smaller than for the 0/90° grids. For inclined surfaces, thresholds were similar for the two grids. (Redrawn from Cagenello and Rogers 1993.)

7.4.1 Horizontal point or positional disparity

A surface inclined about a horizontal axis has, by definition, a gradient of horizontal disparity in a vertical direction— $\partial\alpha/\partial\theta_v$ (Section 7.1.5). Consequently, there is a disparity difference between any pair of points which varies with the spatial separation of the points and the orientation of the axis joining the two points. Horizontal disparities on a surface inclined about a horizontal axis are maximal for two vertically separated points and zero for two horizontally separated points.

7.4.2 Orientation disparity

A straight line inclined in the median plane through an angle i with respect to the frontal plane produces images in the two eyes that differ in orientation by angle θ . If a is the interocular distance and d the viewing distance then for small values of θ

$$\theta = \frac{a \tan i}{d} \quad \text{or} \quad i = \tan^{-1} \frac{\theta d}{a} \quad \text{in radians} \quad (11)$$

as shown in Figure 2.19. A family of curves showing θ for different values of i and d , for an interocular distance of 6.5 cm, is shown in Figure 7.41. The correct estimation of the three-dimensional angle of inclination from the 2-D angle of tilt of the images requires a nonlinear scaling of both the angle of

inclination and the viewing distance. If the corresponding vertical meridians of the eyes were congruent and always in correct orientational alignment, the angle of declination would be unambiguously given by the orientation disparity between the images in the two eyes. But the corresponding vertical meridians are not congruent and the eyes change their orientational alignment, that is, they undergo cyclovergence (see Section 10.7). The noncongruence of corresponding vertical meridians is revealed by the fact that when the horizontal meridians are aligned, the corresponding vertical meridians are inclined top outward by about 2° with respect to the true vertical. Thus, according to the preceding formula, the line that projects images onto these inclined meridians (the vertical horopter) is inclined top away by an amount that varies with distance (see Section 2.7). The inclination of the vertical horopter must also be allowed for when one estimates the inclination of objects at different distances. The issue is complicated further by the fact that cyclovergence accompanies horizontal vergence and changes with the elevation of gaze (see Section 10.7). The effects of these two factors are discussed later.

The most distinctive parts of a visual scene consist of oriented edges and lines. Consider a frontal surface covered with vertical and horizontal lines. For a small, centrally placed surface the images of the lines in the two eyes will be approximately parallel. When the surface is inclined top away the images of horizontal lines remain approximately congruent but the images of vertical lines in the left eye tilt to the left and those in the right eye tilt to the right, as shown in Figure 7.8b. Thus, the images of vertical lines are sheared with respect to the images of horizontal lines (see Section 2.7 for details). The images of horizontal lines in the upper visual field acquire a gradient of cyclorotation with one sign, and those in the lower visual field acquire a gradient of cyclorotation with the opposite sign, as shown in Figure 7.8b. These patterns of cyclorotation create equivalent patterns of disparity if we assume that corresponding vertical meridians are parallel and corresponding horizontal meridians are parallel.

For present purposes, ignore the anisotropy of vertical and horizontal corresponding meridians discussed in Section 2.7. The geometry of orientation disparities on inclined and slanted surfaces has an important consequence. Cyclovergence can null the orientation disparity of vertical lines on an inclined surface since the angular disparity of vertical lines is the same all over the surface, but it cannot null the orientation disparity of horizontal lines on a slanted surface since the disparity is not constant and is opposite in sign above and below the horizon plane.

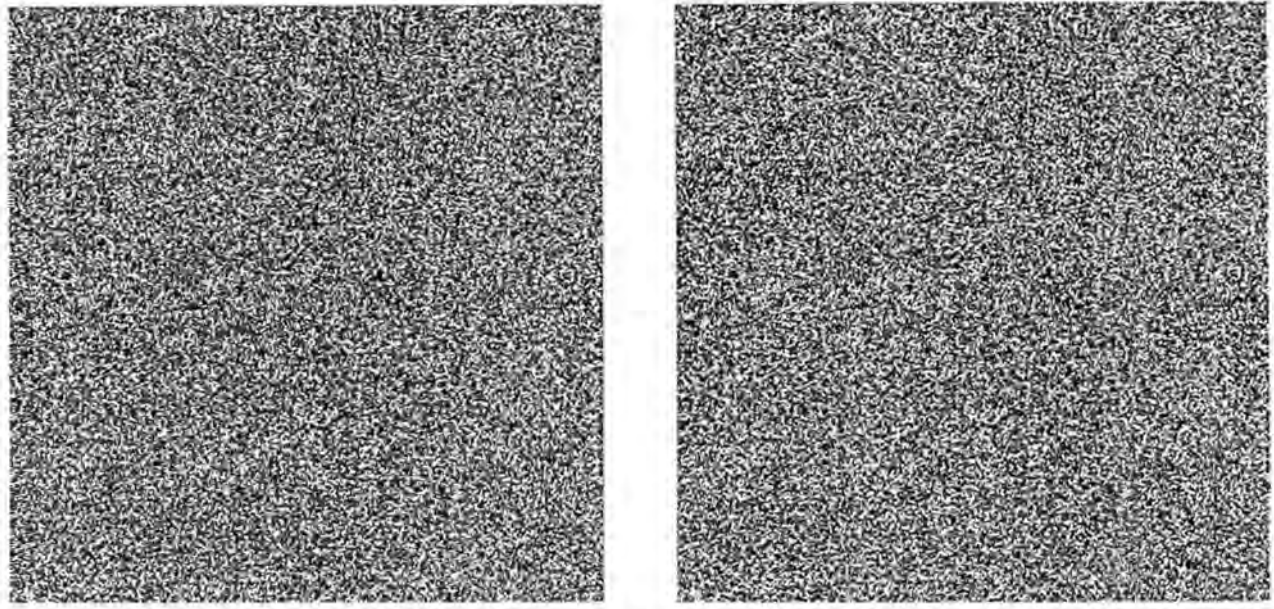


Figure 7.39. Swept corrugation frequency/swept amplitude horizontal corrugations.

The horizontally oriented corrugations are swept in spatial frequency from low (at the bottom) to high (at the top). The peak-to-trough amplitude is swept from maximal (on the left) to zero (on the right) for all the corrugations. The depth modulations of medium frequency corrugations (0.3-0.5 c/deg) can be seen farther to the right than either low or high frequency corrugations which is consistent with the sensitivity functions shown in Figure 5.31.

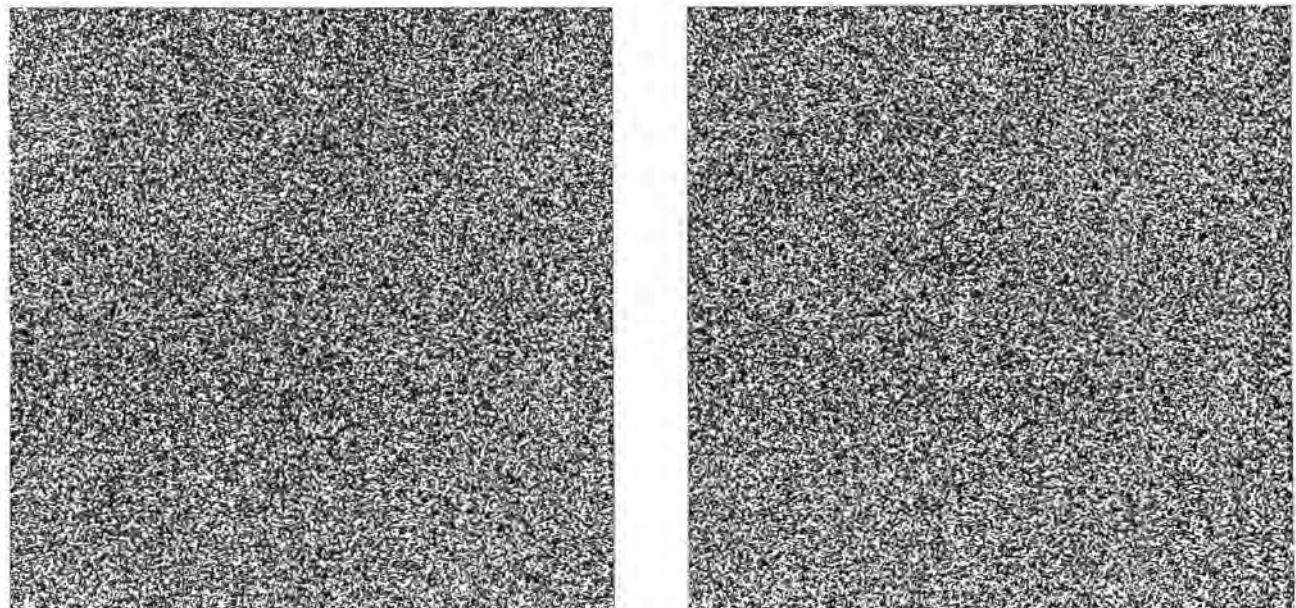


Figure 7.40. Swept corrugation frequency/swept amplitude vertical corrugations.

The vertically oriented corrugations are swept in spatial frequency from low (on the left) to high (on the right). The peak-to-trough amplitude is swept from maximal (at the bottom) to zero (at the top) for all the corrugations. Most observers report that the vertical corrugations have less depth and they can be seen less far up the stereogram than the horizontal corrugations shown in Figure 7.39.

Both these patterns of orientation disparity should be preserved since they contain essential information for stereo inclination and slant. A disparity between images along the horizontal meridian can be due only to misalignment of the eyes, not to depth. These disparities are best not preserved since they do not contain information about the world. It would therefore be a good strategy to evoke cyclovergence by cyclodisparities between points along the horizontal meridian of the visual field. Once these cyclodisparities are nulled, any residual cyclodisparities can be used to code depth. Apart from providing a good matching rule, this strategy reduces the absolute value of the residual disparities and thus brings them within range of finer disparity detectors. We will see in Section 10.7.4 that cyclovergence is indeed evoked more effectively by cyclo-rotation of horizontals than of verticals. This could also be true of the image-matching process; that is, the matching process could initially pay most attention to matching the images of horizontal lines and edges along the central horizontal meridians and seek corresponding images in other orientations only when these are found.

Orientation disparities could be detected in terms of gradients of point disparities or by cells with elongated receptive fields tuned to dichoptic differences in the orientation of line elements. The physiological evidence for the existence of cells specifically tuned to orientation disparities was reviewed in Section 4.6.2.

7.4.3 Deformation and angular disparity

Koenderink (1986) suggested that a good approximation of deformation disparity can be obtained from orientation disparities created by line elements at several absolute orientations (see Section 7.2.8). For inclined surfaces, Figure 7.25 shows that orientation disparity θ is modulated by the orientation of the line element approximately according to a $\sin^2(t)$ function, where t is the absolute orientation of the line element. Hence there is a disparity in the angular difference between pairs of lines in the separate monocular images, which is referred to as an angular disparity. For an inclined surface, the angular disparity is maximal for pairs of lines close to 0° and 90° . In contrast, the angular disparity between pairs of lines close to $+45^\circ$ and -45° is zero. The modulation of angular disparities of orthogonal line elements as a function of their absolute orientations provides the signature of an inclined surface. The patterns of angular disparity created by slanted and inclined surfaces are complementary (Figure 7.42).

7.4.4 Cumulative horizontal disparity

A surface inclined about a horizontal axis also produces a pattern of conventional horizontal disparities. If the eyes converge on the bottom of the surface, the horizontal disparity of matching features is zero at that position and increases linearly over the inclined surface to the top. We refer to this as cumulative horizontal disparity in a vertical direction.

7.4.5 Polar disparity

In Section 7.1.1 it was shown that the disparity of a single point can be represented in polar coordinates in terms of meridional direction (ϕ) and angle of eccentricity (θ) in the radial direction. As for slanted surfaces, Liu et al. (1994a) proposed that binocular differences in the directional component (ϕ) could be used to judge the inclination of a surface. A planar surface inclined about a horizontal axis creates the polar direction disparities shown in Figure 7.43. Liu et al. claimed that the spatial pattern of polar direction disparities generated by an inclined surface could be matched against this template to derive the inclination. However, as we pointed out in Section 7.2.9., polar direction disparities are not invariant with vertical, horizontal, and torsional misalignments of the eyes. It is therefore appropriate to think of polar disparities as providing a basis for measuring the slant and inclination of the fixated surface.

7.5 PERCEPTION OF INCLINATION

There are two major issues in the perception of inclination: first, whether there is a separate orientation-disparity mechanism, and second, whether the visual system calculates the amount of deformation needed to map one eye's image onto the other.

7.5.1 Orientation disparity and inclination

Blakemore et al. (1972) identified binocular cells in cat visual cortex in which the optimal orientations of the separate monocular receptive fields were different (Section 4.6.2). The optimal orientation disparity for different cells varied between plus and minus 15° . These cells would respond to the binocular differences in the orientation of line elements lying on an inclined surface, although the orientation disparities created by the majority of inclined surfaces are much smaller than 15° . Although the binocular cells studied by Blakemore et al. were sensitive to orientation differences, they were also sensitive to

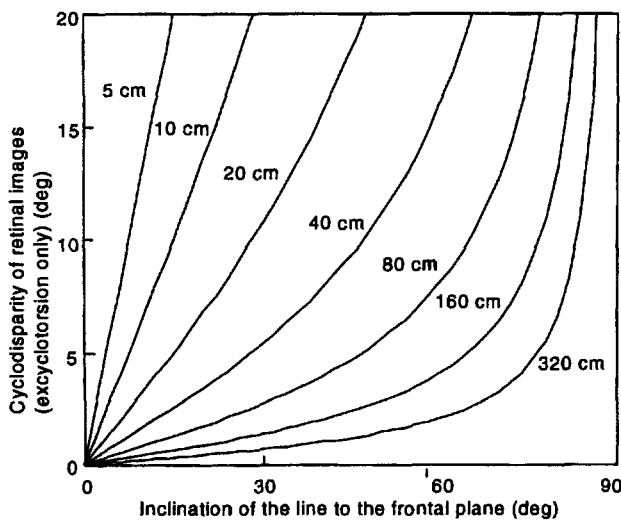


Figure 7.41. Cyclodisparity and inclination.

A family of curves showing the cyclodisparity in the images of a line inclined at various angles and at various distances in the median plane, for an inter-ocular distance of 6.5 cm. It is assumed that the eyes do not undergo cyclovergence.

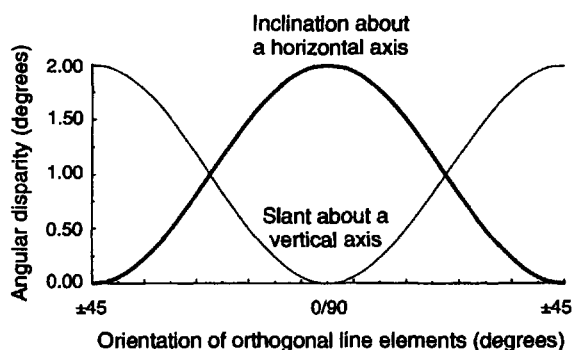


Figure 7.42. Angular disparity and line orientation.

Angular disparity is calculated by measuring the difference in angle between a pair of differently oriented line elements in each monocular image. Angular disparity is the difference between these separate monocular differences. For a pairs of lines which are approximately orthogonal in each eye's image, angular disparities are maximal when the lines are oriented at 0° and 90° and zero for ±45°, for inclined surfaces. Angular disparities for slanted surfaces are maximal for ±45° lines and zero for 0° and 90° lines.

positions of the images on the two retinas. In other words, they were influenced by both positional and orientation disparity. To make the case that the function of these cells is to signal orientation disparity, it is necessary to show that they are more sensitive to orientation differences than to position differences, which was not done (Nelson et al. 1977). In addition to these practical considerations, one should remember that orientation disparities are also created by torsional misalignments of the two eyes and by slanted as well as inclined surfaces; thus, the idea that orientation disparity codes for inclination is, at best, incomplete (Section 7.3.2).

Two strategies have been used to investigate whether people use orientation disparities in the perception of surface inclination. In the first, the binocular stimuli contain orientation disparities between corresponding line elements but the horizontal disparities of individual points are either zero or average to zero in a local area. An unfortunate consequence of this strategy is that information provided by orientation and point disparities is in conflict, at least at some spatial scales. In the second strategy, the stimuli contain point and orientation disparities which are both consistent with the inclination of the depicted surface. The image characteristics, and in particular the presence of oriented features, are then adjusted to maximize or minimize orientation disparities. The second strategy has the advantage that there is never a conflict between point and orientation disparities.

Conflicting orientation and positional disparities

Von der Heydt et al. (1978) exploited the first strategy. Their stimuli consisted of one-dimensional noise gratings which were uncorrelated in the two eyes. The lack of binocular correlation between individual bars meant that the responses of all point disparity mechanisms (based on nearest-neighbour matching) were distributed symmetrically around zero disparity. The orientation difference between the bars of the uncorrelated noise grating was varied and inclination was perceived for orientation disparities between 0.3° and 20°. Consistent with these psychophysical findings, Häny et al. (1977) found five cells in monkey striate cortex that responded to the one dimensional noise gratings which were uncorrelated in the two eyes.

Although these results appear to be good evidence for the use of orientation disparity, the argument is not conclusive. Assume that binocular units with a different optimal orientation preference in the two eyes are stimulated by the nearest-neighbour matching of uncorrelated bars of the same luminance polarity in the two eyes. The binocularly pairings at any moment will differ randomly in their relative image positions creating a distribution of positional disparity centred on zero. Because the bars in the one-dimensional noise vary in width, the random binocular pairings also create a distribution of width disparity centred on zero width difference.

At any moment, however, a pair of uncorrelated bars which stimulate an orientation disparity unit also creates a vertical gradient of horizontal

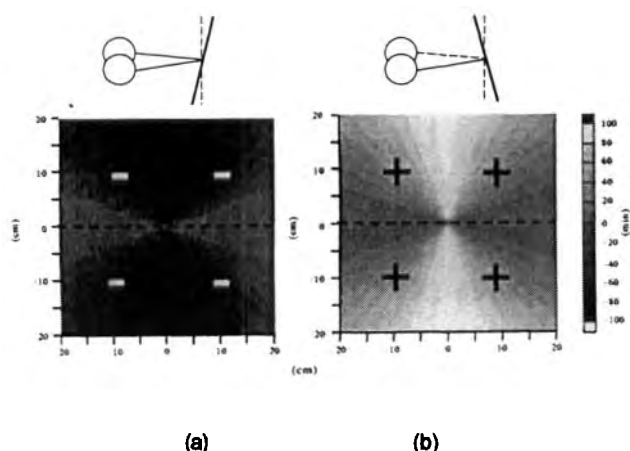


Figure 7.43. Polar angle disparity map of an inclined surface.
The grayscale value indicates the magnitude of the polar angle disparity of each point on a surface inclined 10° top away (a) or 10° top towards (b) as a function of its 2-dimensional location in the visual field. Surface subtended 40 × 40 cm at a distance of 40 cm. (Reproduced with permission from Liu et al. 1994a, Vision Research, Pergamon Press.)

positional disparities. The perception of inclination could be based on this gradient rather than on orientation disparity. A slightly different technique for investigating orientation disparities was adopted by Ninio (1985). He used a static and dense array of short line elements or needles distributed over a four-sided pyramid. The needles were binocularly correlated and the positional disparity of each of the needle centres was always appropriate to its location on the surface of the pyramid. Not surprisingly, when there was an appropriate disparity between the ends of the needles and the needles themselves had orientation disparities appropriate for line elements covering the faces of the pyramid, observers judged the surfaces of the pyramid to be smooth. When there was zero disparity between ends of the needles and needles had identical orientations in the two eyes (signalling a frontal orientation), the surfaces were judged to be "bristly" with the needles protruding out of the pyramid faces.

In the two experimental conditions, the needles had either (1) orientation disparities appropriate for the slant of the pyramid faces but no appropriate horizontal disparities between the tips of the needles or (2) appropriate horizontal disparities between the tips of the needles but no orientation disparities. These manipulations were achieved by independently varying the orientation and length of the needles in one eye's image. Initially, all of the needles were approximately the same orientation (either +45° or -45°). Under these circumstances, observers

judged the surfaces of the pyramids to be slightly smoother in the first condition than the second.

Ninio interpreted these results in terms of an orientation-disparity mechanism that is at least as important as the positional disparity mechanism in the visual system. The problem with this interpretation is that it makes two assumptions. First, that positional disparities are derived only from the tips of the needles, and second, that the presence of inappropriate vertical disparities does not disrupt the horizontal disparity mechanism. There is a further consideration. The orientation disparity information provided by lines of roughly the same orientation is necessarily ambiguous as to whether it arises from a slanted or inclined surface or is the result of torsional misalignment between the two eyes (see Section 7.2.7).

In a subsequent experiment, the same judgments were made using pyramids covered with both +45° and -45° needles. In this case, angular disparities between pairs of oriented elements provide unambiguous information about the direction of surface slant and rule out torsional misalignment as a possible cause. As a result, this stimulus provides a better test for the use of orientation and angular disparities, but the opposite pattern of results was reported. The surfaces of the pyramid appeared to be more bristly when the orientation disparities were appropriate and the positional disparities were inappropriate than vice versa (Ninio 1985).

Consistent orientation and positional disparities

DeValois et al. (1975) looked at the aftereffects produced by prolonged viewing of an inclined surface as a technique for investigating the role of orientation disparities. Their inclined adapting surface was covered with a triangular pattern which created orientation disparities between corresponding lines in the two eyes. The existence of an inclination aftereffect following prolonged viewing of this surface does not, by itself, constitute evidence in favour of the orientation disparity hypothesis. DeValois et al., however, found that the aftereffect was still seen when it was superimposed on a surface that was disparate with respect to the fixation point. In their second experiment, the inclined surface was moved vertically during the adaptation period so that each retinal region was exposed to the entire range of crossed and uncrossed disparities.

Together these two results suggest that the depth aftereffects derive from mechanisms that code gradients of disparity rather than the disparities of individual points (see Section 12.3.3), but they do not provide conclusive evidence for the role of orientation disparities. Rogers and Graham (1985) and Lee

and Rogers (1992), for example, reported that the depth aftereffects produced by adaptation to a sinusoidally corrugated random-dot-covered surface generalized to test surfaces in other depth planes but in neither case were orientation disparities involved.

Cagenello and Rogers (1988, 1993) pursued the alternative strategy of manipulating image characteristics to avoid a conflict between inclination signalled by positional and orientation disparities. They showed that thresholds for detecting the slant of a surface covered with a grid of $\pm 45^\circ$ lines were considerably lower ($\pm 1.5^\circ$ from a frontal plane) than for a surface covered with a grid of vertical and horizontal lines ($\pm 3.5^\circ$); (see Section 7.2.7). This result is consistent with the use of orientation disparities since there are no orientation disparities between either 0° or 90° elements on a slanted surface.

For inclined surfaces, on the other hand, thresholds were approximately the same (1.25° from a frontal plane) whether the surface was covered with a grid of $\pm 45^\circ$ or vertical and horizontal lines (Figure 7.38). Given that the magnitude of the orientation disparities created by the vertical lines in the vertical and horizontal line grid is twice as large as the orientation disparity created by the 45° lines in the $\pm 45^\circ$ grid (Figure 7.25), this result is inconsistent with the use of orientation disparities, at least for the detection of inclination at threshold.

By manipulating the angular extent of the surface, Braddick (1968, 1979) sought to provide evidence consistent with the use of orientation disparity in the perception of inclined surfaces. He reasoned that if the perception of inclination were based on orientation disparity, the onset of diplopia with large angles of inclination would be unaffected by the angular extent of the surface since the magnitude of the orientation disparity remains constant. On the other hand, if the onset of diplopia depended on the magnitude of the disparity difference between the upper and lower edges of the inclined surface, diplopia would occur sooner with the larger surfaces. His stimuli were line gratings close to vertical in the two eyes. The results showed that the onset of diplopia was unaffected by the extent of the surface but instead depended on a critical value of the orientation disparity. Unfortunately, this interpretation is confounded by the fact that the larger surfaces stimulate more peripheral regions of the retinas, where the thresholds for diplopia are likely to be higher than in foveal regions.

A similar criticism can be made against other studies which have looked at thresholds for perceiving inclination as a function of surface size. If inclination thresholds depend only on orientation disparity, they should be affected by the size of the surface

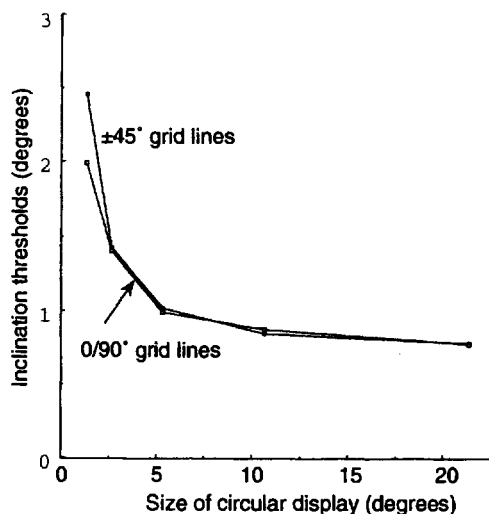


Figure 7.44. Inclination thresholds as function of display size. Thresholds for discriminating the direction of three-dimensional inclination (ground/sky plane) as a function of the size of display. The stimulus was a grid of white lines on a dark background with either $\pm 45^\circ$ or $0^\circ/90^\circ$ orientations. Thresholds decreased sharply with increasing display size up to 5° and then remained more constant for larger displays. Average of 2 observers. (Adapted from Cagenello and Rogers 1989)

only to the extent that there are more samples of orientation disparity in larger surfaces. On the other hand, if inclination thresholds are based only on the magnitude of the disparity difference between the upper and lower edges of the surface, inclination thresholds should decrease substantially with increasing size of the surface, but only if disparity thresholds are unaffected by retinal eccentricity. If disparity thresholds increased with retinal eccentricity, inclination thresholds would remain relatively unaffected by surface size.

Cagenello and Rogers (1989, 1993) found that thresholds for discriminating the direction of inclination (ground plane or sky plane) in stereoscopic surfaces close to the frontal plane decreased sharply as the size of the surface patch increased from 1° to 5° in diameter, but remained fairly constant at around 0.8° of inclination for larger surfaces of up to 21° in diameter (Figure 7.44). The fact that thresholds remained constant for surfaces larger than 5° led these authors to conclude that orientation disparity rather than positional disparities provided the limitation at threshold. The maximum orientation disparity was less than 0.1° at the threshold inclination. However, thresholds for discriminating surface inclination would also stay roughly constant if disparity thresholds increased with retinal eccentricity.

Cagenello and Rogers also reported that inclination thresholds were similar for a surface covered with a grid of horizontal and vertical lines as for a

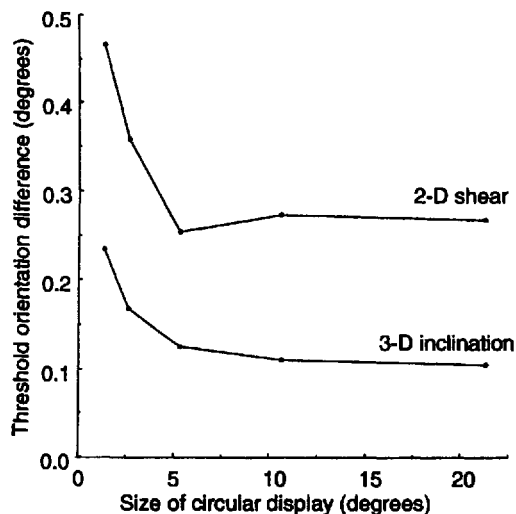


Figure 7.45. Inclination and shear thresholds.

Thresholds for discriminating the direction of stereo inclination (ground/sky plane) or frontal-plane tilt of binocular shear (clockwise/counterclockwise) as a function of display size. The stimulus was a grid of white lines on a dark background with 0° and 90° orientations. Stereo thresholds are expressed as an orientation difference between the eyes; tilt thresholds as tilt from the vertical. Average of 3 subjects. (Redrawn from Cagenello and Rogers 1989.)

surface covered with a grid of $\pm 45^\circ$ lines (Figure 7.44). If the maximum orientation disparity present were the limiting factor, inclination thresholds should have been lower by a factor of 2 for the 0/90° stimuli (see Section 7.2.7).

If inclination discrimination is limited by the threshold of orientation disparity, we should expect the orientation disparity present at the threshold for discriminating inclination to be similar to the threshold orientation for discriminating binocular (non-stereoscopic) tilt. In other words, at the point where observers can just discriminate that a surface covered with vertical and horizontal lines is inclined away from a frontal plane (a ground-plane or sky-plane surface), they should be able to discriminate whether an identical grid of vertical and horizontal lines presented to the two eyes (a dioptic stimulus) is sheared clockwise or counterclockwise. In addition, three-dimensional inclination thresholds and frontal-plane shear thresholds should vary in the same way as a function of stimulus size.

Cagenello and Rogers (1989) found evidence to support the second prediction. Three-dimensional inclination thresholds and frontal-plane shear thresholds decreased with increasing stimulus size in a similar manner (Figure 7.45). However, at the point when observers could reliably judge the direction of inclination ($\pm 1^\circ$ from a frontal plane), the binocular orientation differences (~6 arcmin) were 2

to 3 times smaller than those that could be discriminated in the nonstereoscopic shear task (~15 arcmin). These results suggest that three-dimensional inclination thresholds are not limited by the same factors that limit tilt judgments, and thus it is unlikely that orientation disparities are responsible for the limit of inclination discrimination at threshold.

7.5.2 Deformation disparity and inclination

The idea of orientation disparity as the basis of slant and inclination judgments is, at best, incomplete. The orientation disparity of any line element is affected by the state of torsional alignment of the eyes so that the only reliable information indicating the slant or inclination of a surface is contained in the pattern of orientation disparities as a function of line orientation (see Section 7.2.7). This point is rarely acknowledged. In most studies on the perception of slant and inclination, however, investigators have used stimuli containing lines of more than one orientation which therefore provide an unambiguous pattern of orientation disparities. In other experiments, a binocularly correlated surround has provided the necessary reference for interpreting the ambiguous disparities of oriented features within the surround.

As a consequence, it is inappropriate to claim that these experiments have investigated the role of orientation disparity per se. Rather, they have looked at the role of relative orientation disparity or angular disparity, which is the binocular difference in the angular separation of pairs of oriented elements in each of the monocular images. Angular disparities have the additional advantage over orientation disparities that they are unaffected by torsional misalignment of the two eyes.

The deformation needed to map one eye's image on to the other—deformation disparity—also shares the property of being invariant with respect to the cyclovergence (Section 7.1.5). In addition, deformation disparity is invariant to a uniform magnification of the image in one eye. Is there any evidence that the visual system computes deformation disparity? In the case of slanted surfaces, Rogers and Koenderink (1986) argued that Ogle's induced effect (Ogle 1938, 1939a, 1939b) is evidence that the visual system computes deformation disparity since a vertical magnification of one eye's image can independently create the impression of surface slant (Gillam et al. 1988a). Note that a horizontal magnification of one eye's image produces a gradient of horizontal disparity in a horizontal direction ($\partial\alpha/\partial\theta_h$) while a vertical magnification produces a gradient of vertical disparity in a vertical direction ($\partial\beta/\partial\theta_v$).

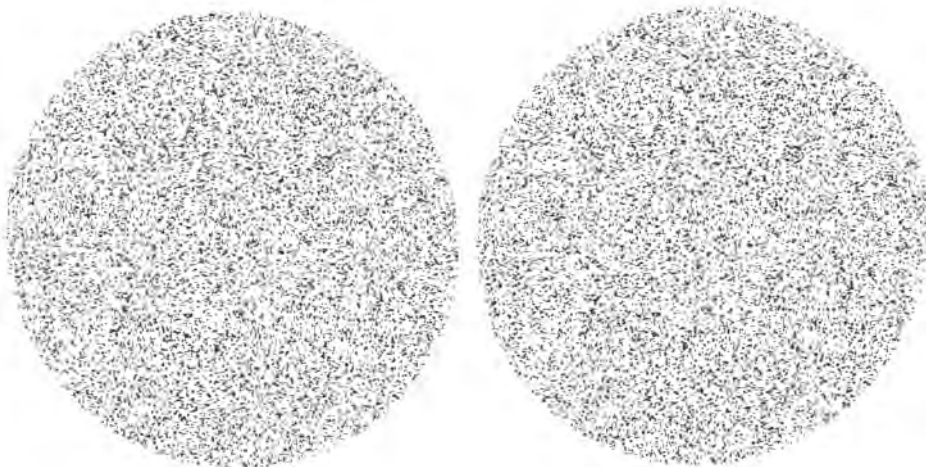


Figure 7.46. Binocular images related by a vertical shear.

The images in this stereogram are related by a vertical shear. There are no horizontal disparities between corresponding points but instead, there is a horizontal gradient of vertical disparity. If the visual system measures the amount of deformation between binocular images to determine surface inclination, the fused surface should appear to be inclined in depth.

To determine surface inclination, it is not sufficient to measure the gradient of horizontal disparities in a vertical direction ($\partial\alpha/\partial\theta_v$) because a similar gradient is also created by torsional misalignment of the two eyes. Surface inclination (up to a scale factor of distance) is specified by the ratio of $\partial\alpha/\partial\theta_v$ to $\partial\beta/\partial\theta_h$ (Section 7.1.5). The calculation of deformation can be thought of as the normalization of the gradient of horizontal disparities in the vertical direction with the gradient of vertical disparities in the horizontal direction. When the eyes are torsionally aligned along the horizontal meridian, the gradient of vertical disparities in a horizontal direction ($\partial\beta/\partial\theta_h$) is zero and the degree of inclination is signalled by the gradient of horizontal disparities in a vertical direction ($\partial\alpha/\partial\theta_v$).

It follows that a test for the use of deformation disparity in the perception of surface inclination is provided by a pair of stereo images in which the usual indicator of inclination, a gradient of horizontal disparities in a vertical direction ($\partial\alpha/\partial\theta_v$), is zero, but instead there is a gradient of vertical disparities in a horizontal direction ($\partial\beta/\partial\theta_h$). This corresponds to the situation in which the binocular images are related by a vertical shear (Figure 7.46). The use of vertically sheared images to study inclination is analogous to the use of vertically magnified images (Ogle's induced effect) to study slant (Gillam and Rogers 1991). If observers perceive inclination in stereoscopic images related by a vertical shear, this would provide evidence that the human visual system calculates the amount of deformation disparity.

Cagenello and Rogers (1990) reported that a stereogram consisting of a pair of 20°-diameter random-dot patterns related by a vertical shear was perceived to be inclined, as predicted by the deformation hypothesis. The amount of perceived inclination was about 75 per cent of that predicted by the deformation hypothesis when observers inspected the surface for several seconds. Although this result appears to be good evidence for the deformation hypothesis, the authors noticed that when exposure time was increased from 1 to 6.5 s, perceived inclination increased from about 30 per cent to 75 per cent of that predicted. They argued that the increase in perceived inclination was probably due to a change in cyclovergence, which would convert the vertically sheared stimulus pattern into a horizontally sheared image pattern (Figure 7.47). No similar increase in perceived inclination occurred with a pair of 20°-diameter random-dot patterns related by a horizontal shear, suggesting that the increase was not the result of a generalized buildup in the perception of inclination.

Cagenello and Rogers also reported that inclination could be seen initially in a stereogram consisting of 20°-diameter random-dot patterns related by a rotation but that the amount of perceived inclination decreased as the exposure time was increased from 1 to 6.5 seconds. The appearance of inclination in a pair of stereo images related by a rotation is not predicted by the deformation hypothesis because the gradient of horizontal disparities in a vertical direction is the same as the gradient of vertical disparities in a horizontal direction. Indeed, the calculation of

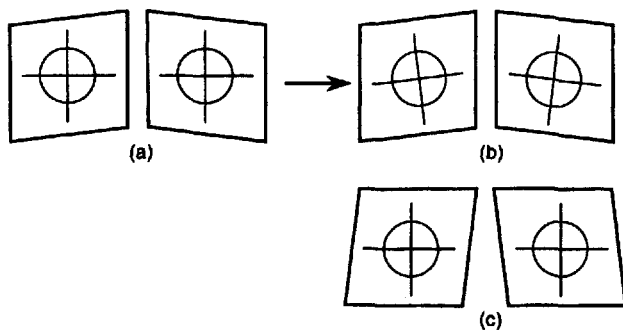


Figure 7.47. The effect of cyclovergence on vertical shear.
 (a) The torsionally aligned eyes are presented with stereoscopic images related by a vertical shear with no horizontal disparities.
 (b) If the eyes extort, the horizontal gradient of vertical disparities in the original images is converted into a vertical gradient of horizontal disparities, which is the same as that produced by an inclined surface, as shown in (c). (Adapted from Rogers 1992.)

deformation is specifically designed to be invariant to the effects of torsional misalignment between the eyes.

These two results suggest that the visual system does not normalize the gradient of horizontal disparities in the vertical direction with the gradient of vertical disparities in the horizontal direction, as would be expected by the deformation hypothesis. Rogers (1992) has argued that there is no need for the human visual system to explicitly calculate the amount of deformation with binocular viewing. Instead, it could use the gradient of vertical disparities in a horizontal direction ($\partial\beta/\partial\theta_h$) as a signal to drive the cyclovergence system, and thereby align the binocular images along the horizontal meridian. An estimate of the degree of surface inclination could then be obtained by monitoring the gradient of horizontal disparities in a vertical direction ($\partial\alpha/\partial\theta_v$). In support of this idea, Rogers and Howard (1991) have shown that a gradient of vertical disparities in a horizontal direction is a much more effective stimulus for driving cyclovergence than a gradient of horizontal disparities in a vertical direction (see Section 10.7).

Further evidence against the deformation hypothesis is provided by the results of experiments in which equal and opposite deformations were presented in spatially separated regions of the same stereogram. The stereoscopic images consisted of a dumbbell-shaped figure in which the dots in the left half were related by a vertical shear in one direction and the dots in the right half were related by a vertical shear in the opposite direction (Figure 7.48). If perceived inclination is based on the amount of local deformation, opposite inclinations should be seen in the two halves of the dumbbell figure. On the other

hand, if perceived inclination is based only on the gradient of horizontal disparities in a vertical direction, no inclination should be seen.

Notice that cyclovergence, if it occurs, introduces a similar gradient of horizontal disparities in a vertical direction to both sides of the dumbbell stimulus. Cagenello and Rogers (1990) reported that only a very small differential slant was perceived between the two halves of the dumbbell figure and it was in the opposite direction to that predicted by the deformation hypothesis (see Figure 7.48). We shall see that this result is consistent with the use of relative vertical and horizontal disparity by the visual system.

Gillam and Rogers (1991), also, obtained results inconsistent with the idea that the stereopsis uses deformation disparity. Subjects matched the perceived inclination of a probe to that of 10°-diameter stereoscopic display. They reported little apparent inclination with a vertical-shear disparity, which contained deformation, but cyclorotated images, which contained no deformation, appeared inclined.

Overall, these results suggest that the inclination perceived in binocular images related by a vertical shear is either less than predicted by the deformation disparity (Cagenello and Rogers 1990) or almost absent (Gillam and Rogers 1991). But this is not the whole story.

Howard and Kaneko (1994) used a random-dot stereoscopic display 75° in diameter with a totally black surround. Subjects judged the perceived inclination of the fused image by setting a tactile paddle. A visual comparison stimulus was not used because it introduces unwanted disparities. The four types of disparity used in the experiment are illustrated in Figure 7.49. The results in Figure 7.50a show that, for disparities of up to about 4°, the magnitude of perceived inclination of a display containing only vertical-shear disparities was almost as large as that produced by only horizontal disparities. Moreover, for all disparities, there was no perceived inclination when the image in one eye was rotated with respect to that in the other eye. With images related by opposite vertical and horizontal shear (true deformation) of up to about 4°, the perceived inclination was almost twice that produced by horizontal or vertical shear alone. With disparities greater than about 4°, the displays became disparate and inclination became difficult to judge. These results provide strong support the idea that the visual system uses the difference between the gradients of vertical and horizontal disparities (deformation) in coding inclination. However, the results would be explained if the eyes underwent cyclovergence so as to transfer vertical disparities into horizontal disparity. Howard

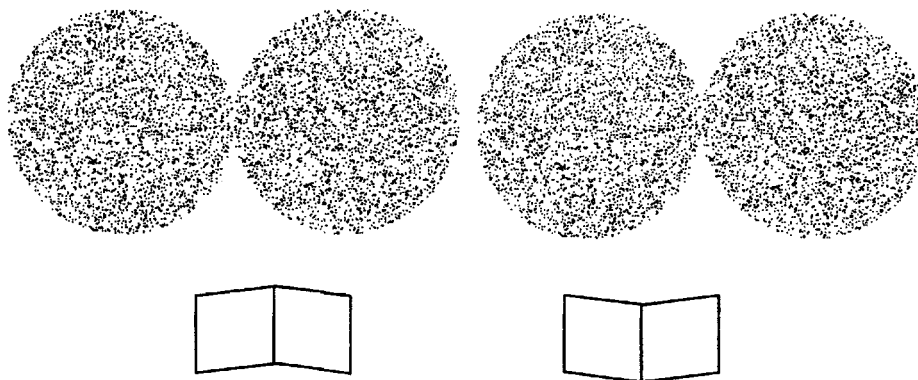


Figure 7.48. Equal and opposite vertical shear in the half-fields.

The dots in the left half-fields are related by vertical shear in one direction and the dots in the right half-fields are related by vertical shear in the opposite direction. If perceived inclination is based on local deformation, opposite inclinations should be seen in the left and right half-fields. In fact, a small relative inclination can be seen, but in the opposite direction to that predicted by the deformation hypothesis. (Adapted from Rogers 1992.)

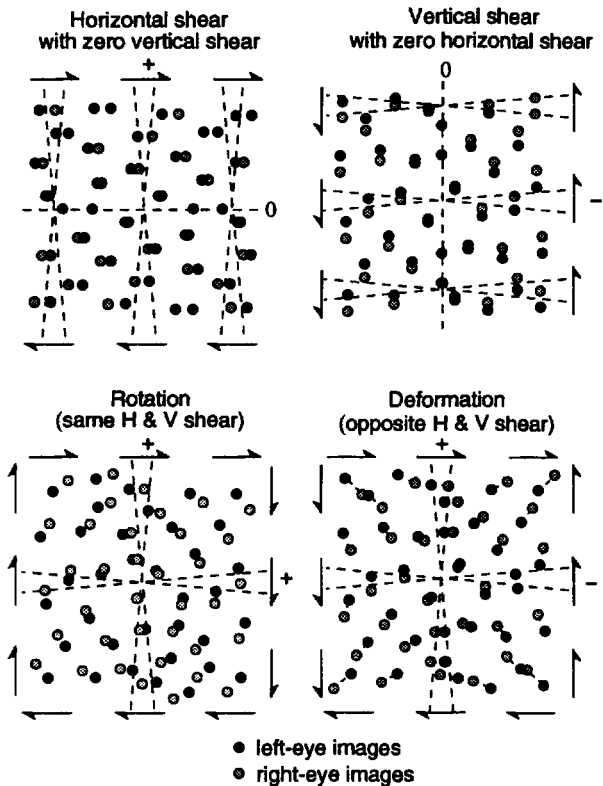


Figure 7.49. Four types of shear disparity.

(Reprinted with permission from Howard and Kaneko 1994, Vision Research, Pergamon Press.)

and Kaneko checked on this possibility by using four subjects in whom incyclovergence was much stronger than excyclovergence. If cyclovergence were the only factor in the inclination judgments the same asymmetry should have occurred in the psychophysical results. But no such asymmetry was present. The visual system must possess a neural

mechanism for deriving the deformation disparity in these large, whole-field stimuli. *This experiment needs to be repeated with objective recording of cyclovergence at the same time as settings of the tactile paddle.*

The opposite result obtained by Cagnello and Rogers with the dumbbell display was probably due to the presence of two surface patches with opposite vertical disparities which made the average vertical disparity zero. In other words, deformation is calculated for the whole visual scene and not for separate parts. The opposite results obtained by Gillam and Rogers were probably due to the fact that the test display was only 10° in diameter and was seen in the context of a dimly lit room. The zero vertical disparities in the dimly lit surround would serve as the reference for assessing the horizontal disparity in the small display. Thus, the vertical-shear disparity in the small test display would have little effect.

Howard and Kaneko repeated their experiment with test displays of various sizes displayed either on a totally black background or within a zero disparity annulus. With a display 10° in diameter or with displays of any size seen with a zero-disparity surround the results agreed with those obtained by Gillam and Rogers (see Figure 7.51).

This is an important point. It means that vertical-shear disparity is not used locally to scale horizontal-shear disparity in the presence of a large surrounding display in which vertical disparity is zero. The vertical-shear disparity signal used to scale horizontal shear disparity is derived, not locally, but from the display as a whole. This is what one would expect if the use of relative-shear disparities is designed to protect against torsional misalignment of the eyes that occurs in cyclophoria and oblique gaze.

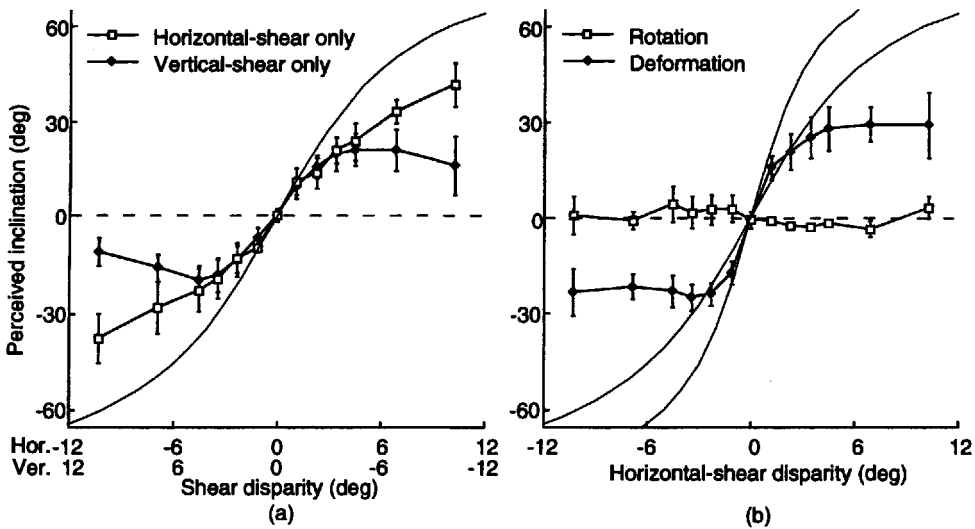


Figure 7.50. Perceived inclination and shear disparity.

(a) For horizontal-shear only and vertical-shear only. The dotted line is the zero inclination for the vertical-shear stimulus predicted from the horizontal disparity. The sigmoid line is the inclination for both shear conditions predicted from deformation disparity.

(b) For stimulus rotation and deformation. The dotted line is the zero inclination for stimulus rotation predicted from deformation disparity. The shallow sigmoid curve is the inclination for stimulus rotation and deformation predicted from the horizontal disparity. The steep sigmoid curve is the inclination for stimulus deformation predicted from the deformation disparity. Mean results of four subjects. Error bars are standard errors of the mean. (Adapted from Howard and Kaneko 1994.)

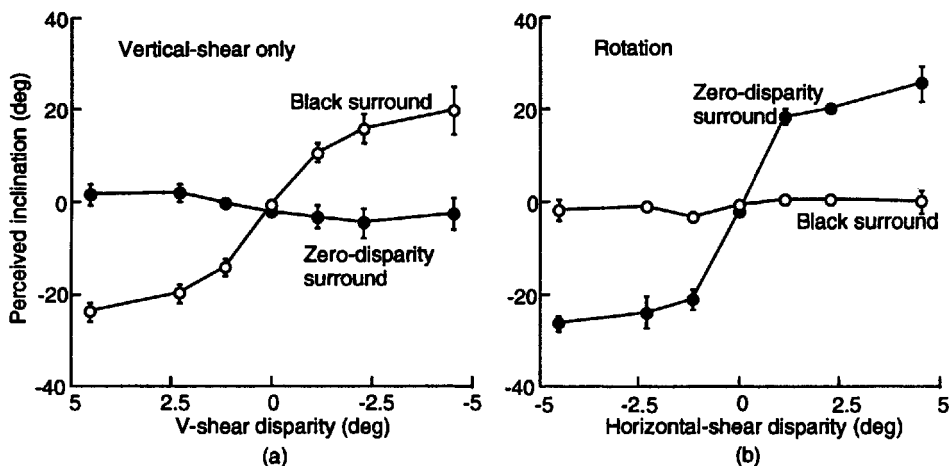


Figure 7.51. Perceived inclination and shear disparity with zero-disparity surround.

The perceived inclination of a 30° diameter random-dot display as a function of stimulus vertical shear (a) and rotation (b). In one condition the test display was within a zero-disparity annulus extending out to 60° and in a second condition the surround was black. Mean results of three subjects. (Adapted from Howard and Kaneko 1994.)

Such misalignments affect the whole visual image and are therefore most reliably detected by vertical-shear disparity over the whole field. Vertical-shear disparity over the whole visual field does not usually arise from any cause other than misalignment of the eyes. Any difference between the overall vertical disparity in the scene and a horizontal shear disparity in the images of a particular surface must be due to inclination of the surface.

Local gradients of vertical-shear disparity are also produced on a slanted surface; the disparities above eye level have one sign and those below eye level have the opposite sign. Local vertical-shear disparity is therefore not a reliable indication that the eyes are out of alignment. Horizontal-shear disparities are extracted locally, because surfaces inclined to different extents can be in view at the same time. But each horizontal disparity should be scaled with reference

to the mean vertical-shear disparity over the whole field because it is this that signifies how far out of alignment the eyes are. In other words, the state of torsional alignment of the two eyes is a single viewing-system parameter (see Section 7.1.5) which has consequences for all visible surfaces.

Howard and Kaneko's results show that this viewing-system parameter is registered and influences our perception of whole-field surface inclination. The situation may differ when there are several surfaces with different inclinations in the scene. Our perception of the absolute inclination of a surface can be substantially modified by the inclination of neighbouring surfaces—simultaneous depth contrast (see Section 12.2.4). This suggests that the relative vertical gradients of horizontal disparity (horizontal shear disparities) may be sufficient to account for our perception of three-dimensional shape. Information about the absolute inclination of surfaces is either not registered or simply ignored.

7.6 VERTICAL DISPARITY

The fact that the eyes are separated horizontally means that the principal disparities are horizontal or, strictly speaking, parallel to the interocular axis. However, there are also vertical differences between binocular images and the purpose of this section is to outline the circumstances under which they arise, to determine the information they contain, and to evaluate the empirical evidence that human observers use the available information.

7.6.1 Causes of vertical disparity

It is useful to distinguish between three situations which create vertical disparities. First, vertical disparities are created in the optic arrays at two vantage points as a result of viewing the world from two slightly different positions. Second, vertical disparities are created (or eliminated) as a consequence of the particular coordinate system chosen to measure disparity (Section 7.1) and third, vertical disparities are created by the vertical or torsional misalignment of the coordinate axes in the two eyes.

Consider the last category first. If the optic arrays at the two eyes are identical but the eyes or cameras used for measuring the optic arrays are misaligned either horizontally, vertically, or torsionally, the images of objects in the scene will fall on noncorresponding retinal regions. With a vertical misalignment, the vertical disparities are the same for all features along a particular vertical meridian and they decrease with eccentricity along any horizontal

meridian. Their magnitudes are equivalent to the spacing between the isoelevation great circles in the longitudinal/longitudinal coordinate system (Figure 7.1) This pattern of vertical disparities is the stimulus for compensatory vertical vergence, which eliminates those disparities. Notice that a horizontal misalignment of the eyes (a vergence shift) does not change the pattern of relative horizontal disparities when these are measured within a longitudinal-azimuth/latitudinal-elevation coordinate system.

With a torsional misalignment of the eyes, an identical gradient of vertical disparity is created along all horizontal meridians and this is the stimulus for compensatory cyclovergence, as Rogers and Howard (1991) and De Bruyn, Rogers, Bradshaw, and Howard (1992) have shown. These two patterns of vertical disparities, which result from the misalignment of the eyes, are quite different from the patterns of vertical disparities created by characteristics of the visual scene, as we will see.

Vertical disparities are also created (or eliminated) by the particular coordinate system chosen to measure vertical direction. As we saw in Section 7.1.1, two points which have the same elevation in one coordinate system may have different elevations in another coordinate system. For binocular viewing with either aligned coordinate axes or where there is precise information about the relative orientations of the misaligned axes, the choice of coordinate system is of little consequence because the coordinates can be mapped from one system to another. However, it is important that the choice of coordinate system is made explicit when describing the characteristics of the disparity field in order to avoid confusion. For example, there are no vertical disparities (whatever the scene structure), when vertical position (elevation) is measured with respect to lines of longitude passing through poles on the interocular axis, since these are the epipolar lines (Figure 7.6).

The situation is more complicated when vertical disparities are measured from two vantage points but the precise positions of the coordinate axes (positions of the eyes) are not known. We will assume that this is true of the human visual system. If the positions of the coordinate axes are not known, the difference in elevation of a point from the two vantage points—its absolute vertical disparity—provides no useful information, as we show in the next section. The relative vertical disparities of two or more points, on the other hand, can provide information about the headcentric eccentricity of those points at a distance. The choice of coordinate system for describing vertical disparities is relevant because it affects whether measurements vary with changes in vergence and version (Section 7.1.1).

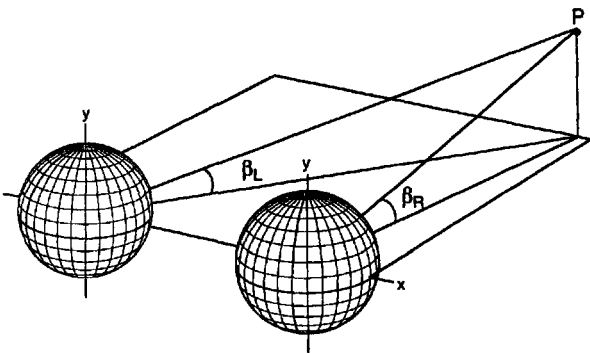


Figure 7.52. Absolute vertical disparity.

The absolute vertical disparity of a point corresponds to the difference between the angles of elevation measured separately in the two eyes— $\beta_L - \beta_R$. In the longitudinal-azimuth/latitudinal-elevation system, elevation is measured within the azimuth plane containing the point.

In the subsequent sections we consider the patterns of vertical disparities created by the scene characteristics, although one should bear in mind that it may not be a simple matter to differentiate between the different causes of vertical disparities in a particular pair of binocular images.

7.6.2 Absolute vertical disparities

Consider first the differences in the optic arrays at two horizontally separated vantage points measured with respect to identical spherical coordinate frames with their origins at each of the two vantage points (Figure 7.52). The location of any point in space can be expressed in terms of its (vertical) elevation and (horizontal) azimuth. The **absolute vertical disparity** of any point in space is the difference in the vertical elevations of that point in the two eyes:

$$\beta_L - \beta_R$$

Since vertical elevation is defined with respect to a particular plane passing through the two vantage points and the fixation point (the plane of regard), the vertical disparities of all points lying in the plane of regard will be zero. An elevated point may or may not have a vertical disparity depending on its eccentricity with respect to the median plane of the head. Using a gun turret coordinate system (longitudinal-azimuth/latitudinal-elevation), the azimuth of a point is measured in the plane of regard, irrespective of elevation, and elevation is measured within the azimuth plane containing the point (Figure 7.2). The angle of elevation from one eye (β_L) is equal to that from the other (β_R) when the point is equidistant from the eyes, assuming that the eyes are vertically and torsionally aligned. This is true (1) for

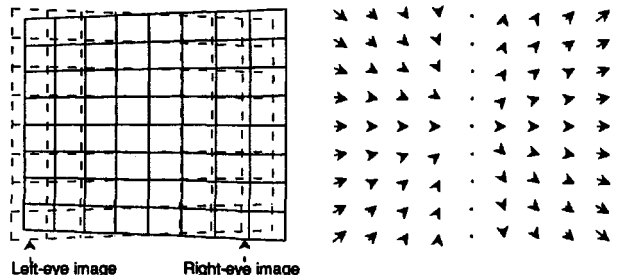


Figure 7.53. Pattern of disparity created by a frontal surface.

The pattern of disparities created by a frontal surface close to the observer when projected onto converged planar retinas. There are no vertical disparities for points which lie in either the median plane of the head or the plane of regard.

all points in the median plane of the head and (2) for all eccentric points as the distance from the two eyes approaches infinity (Figure 7.52), irrespective of horizontal convergence. The disparity vector field created by a frontal surface located close to the observer shows the absence of vertical disparities of all points lying in either the median plane of the head or the plane of regard of the disparity field (Figure 7.53; Tyler 1991).

The vertical components of the disparity vectors created by a frontal surface at infinity are zero. Figure 7.53 also shows that vertical disparities created by an extended surface can be seen as arising from the difference in perspective from two slightly different vantage points. Rogers and Bradshaw (1992, 1993) referred to the vertical-disparity field as a consequence of differential perspective. Notice that there is both a linear perspective component, evident in the differential horizontal gradient of vertical height, and a compression or foreshortening component, which is evident in the differential horizontal gradient of horizontal size.

7.6.3 Relative vertical disparities and size ratios

Relative vertical disparity

As we indicated in Section 7.6.1, absolute vertical disparities are affected by the state of vertical and torsional alignment of the two eyes as well as by the scene structure. Hence it may be more useful to consider the **relative vertical disparity** of pairs of points. The distinction between absolute and relative vertical disparities is the same as that between absolute and relative horizontal disparities described in Section 7.1. The relative vertical disparity (or simply vertical disparity) between a pair of points separated in a vertical direction is shown in Figure 7.54 and corresponds to the difference of their absolute vertical disparities (equations 5 and 6):

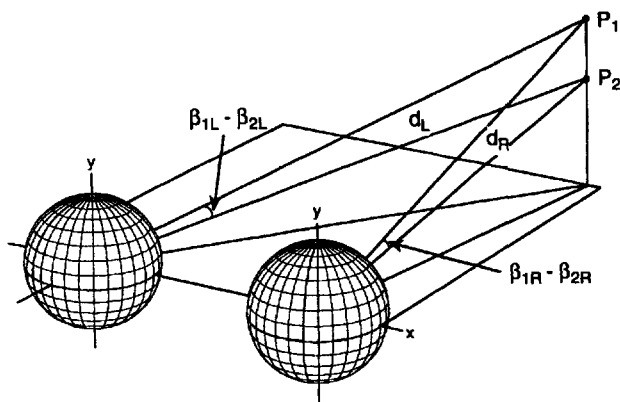


Figure 7.54. Relative vertical disparity of a pair of points. The relative vertical disparity of points P_1 and P_2 corresponds to the difference between their absolute disparities: $\beta_{1L} - \beta_{1R}$ and $\beta_{2L} - \beta_{2R}$. This is equivalent to the difference between $\beta_{1L} - \beta_{2L}$ and $\beta_{1R} - \beta_{2R}$ measured separately in the two eyes. d_L and d_R represent the distances to the points from the two eyes.

$$\text{Relative vertical disparity} = (\beta_{1L} - \beta_{1R}) - (\beta_{2L} - \beta_{2R})$$

A small vertical misalignment of the eyes produced by a vertical phoria, introduces a particular pattern of vertical disparities to all points, as indicated in Section 7.6.1, but the relative vertical disparities of pairs of points (expressed in angular terms) is unaffected by either horizontal or small vertical misalignments of the eyes. The relative vertical disparity of a closely-spaced pair of vertically separated points is also unaffected by small torsional misalignment.

The question of whether vertical disparities are the result of scene characteristics or eye misalignment is therefore easy to solve—the relative vertical disparities of vertically separated points are affected only by scene characteristics and not by eye misalignment. This observation is analogous to the fact that a change in the vergence state of the eyes changes the horizontal disparity of a single point but not the relative horizontal disparity of a pair of points (see Section 7.1.4).

By measuring the relative vertical disparities of pairs of vertically separated points, the visual system renders itself immune to the effects of small eye misalignments. Describing vertical disparities according to a gun turret coordinate system also means that their measurement is unaffected by changes of vergence and version within the plane of regard.

The terms of equation 5 can be rearranged to express relative vertical disparity as a difference between the angular size differences subtended at the two eyes (equation 6):

$$\text{Vertical height disparity} = (\beta_{1L} - \beta_{2L}) - (\beta_{1R} - \beta_{2R})$$

If the two points are close together, then dividing by $(\beta_{1R} - \beta_{2R})$, the vertical separation of the points in the right eye, yields the **vertical disparity gradient** of the two points in the vertical direction:

$$\text{Disparity gradient} = \frac{(\beta_{1L} - \beta_{2L}) - (\beta_{1R} - \beta_{2R})}{(\beta_{1R} - \beta_{2R})} \quad (12)$$

$$= \frac{(\beta_{1L} - \beta_{2L})}{(\beta_{1R} - \beta_{2R})} - 1 \quad (13)$$

The expression $(\beta_{1L} - \beta_{2L}) - (\beta_{1R} - \beta_{2R})$ can be referred to as the **vertical size ratio** (VSR)—the ratio of the angular separations of the two points in a vertical direction measured separately in the two eyes. For a pair of closely spaced points, it follows that

$$\text{VSR} = 1 + \text{vertical disparity gradient}$$

This formulation highlights the fact that the VSR of a pair of closely spaced points is a function only of the disparity gradient and hence is unaffected by a vertical misalignment of the eyes. In addition, VSRs are unaffected by either the vergence state of the eyes or their state of eccentric gaze within the plane of regard when elevation is measured according to the gun turret coordinate system, since the coordinate system is rotationally symmetric about the y axis—a point we return to later.

Vertical size ratios (VSRs)

The description and measurement of the vertical-disparity field in terms of VSRs turns out to be very useful (see also Bishop 1989). As we showed in the previous section, the VSR of a pair of closely spaced points is unaffected by small vertical and torsional misalignments of the eyes and, instead, depends on just one factor: the relative distance of the points from the two eyes.

For a pair of closely spaced points on a surface ($<5^\circ$ such that $\tan \alpha = \alpha$ in radians), the ratio of the vertical separation of the points in the two eyes (VSR) is the ratio of their inverse distances from the two eyes (d_R/d_L) (Figure 7.54). The VSR is also unaffected (by definition) by the slant (around a vertical axis) of the surface on which the points lie. Moreover, Gillam and Lawergren (1983) have shown that the VSR is also relatively unaffected by the inclination of the surface (around a horizontal axis) on which the points lie.

VSRs depend only on the relative distances of the points from the two eyes. The next step is to determine how relative distance from the two eyes is affected by headcentric eccentricity, absolute distance, and elevation of the points from the plane of regard.

Consider first a pair of points close to the plane of regard. In general, VSRs increase with increasing eccentricity from the median plane and reach a maximum at an eccentricity of 90° when the difference in distance from the eyes is maximal, as can be seen in Figure 7.55. However, VSRs by themselves do not specify eccentricity since they also vary as a function of absolute distance. As absolute distance increases, the distance of the points from two eyes approaches the same value and the VSR tends towards one. Ogle (1939c) calculated that at an eccentricity of 30°, the VSR varies from 1.004 for an object at 6 m to 1.18 for an object at 20 cm. Hence a given VSR specifies the eccentricity at a distance. Howard (1970) turned the argument around and observed that (if eccentricity is known), the VSR "could form the basis for judgments of absolute distance".

The changes in VSR with headcentric eccentricity and absolute distance described in the previous paragraph apply to points which lie close to the plane of regard. What is the effect of elevation on VSRs? Unfortunately, the answer depends in part on the choice of coordinate system used to define visual direction. If azimuth and elevation are measured with the coordinate axes converged in the direction of the points, that is, according to a latitudinal/latitudinal system, VSRs are unaffected by elevation. Measured according to the other coordinate systems, VSRs vary with elevation. Hence the graph shown in Figure 7.55 has a general applicability only when the points are close to the plane of regard.

7.6.4 Computational theory of vertical disparities

Mayhew and Longuet-Higgins (1982)

A computational theory of vertical disparities was elaborated by Mayhew and Longuet-Higgins (1982), Mayhew (1982), and Longuet-Higgins (1982). Extending a proof from the optic flow situation, Longuet-Higgins (1982) showed that the positions in space of just three or more points which do not all lie on the same meridian are fully determined by the horizontal and vertical coordinates of their images on the two retinas *as long as the planes of the horizontal meridians of the two eyes coincide*. Moreover, if only two nonmeridional points are visible, the retinal images generally admit, only two distinct three-dimensional interpretations, one of which is usually unrealistic. Having proved that the information for recovering the entire three-dimensional structure of the scene is potentially available from just two views, Mayhew (1982) suggested a way of extracting the information in which vertical disparities are used to provide an estimate of the viewing-system

parameters of convergence distance (d) and the angle of eccentric gaze (g). This idea is particularly attractive because it shows that there is a source of visual information to specify the vergence state of the eyes and the extent of asymmetric fixation—information previously thought to be available only from the oculomotor system. Mayhew showed that the absolute vertical disparity, V , of a single point depends on both its absolute distance and its eccentricity. Specifically,

$$V = \frac{I_{cr}}{d} + \frac{I_{rg}}{d} \quad (14)$$

where I is the interocular distance, c and r are the horizontal and vertical eccentricities respectively, d is the viewing distance from the cyclopean point and g is the gaze angle (Mayhew 1982). The quantities, d and g , are unknown but if the vertical disparities can be measured for a pair of points, the equations for the two vertical disparities can be solved and the viewing distance and direction of gaze can be determined. This method is based on the use of absolute vertical disparities (rather than relative disparities or VSRs) and will work only if the eyes are perfectly aligned, both vertically and torsionally.

Clement (1992) argued that the requirement that the eyes be torsionally aligned makes the theory an unlikely model of the visual system. Instead, he suggested that Petrov's (1980) fusional scheme, which first checks whether the disparities of a number of points correspond to a possible object and gaze angle, provided a more likely solution (but see Porrill and Mayhew 1994).

An alternative theory

A different method for determining the three-dimensional scene structure was suggested by Gillam and Lawergren (1983). Their analysis was based on the idea of vertical magnifications or vertical size ratios described earlier. In particular, they suggested that the gradient of the VSR-eccentricity function could be used to compute the absolute distance to a surface since (1) there is an approximately constant gradient of VSRs across a surface as a function of horizontal angular eccentricity, and (2) that gradient varies with the distance from the cyclopean point to a surface. Moreover, they showed that the gradient of the VSR-eccentricity function does not change substantially if the surface is slanted or inclined by up to 40° around the vertical and horizontal axes, respectively. They also made the important point that their analysis does not depend on where the eyes are converged or on their direction of eccentric gaze. VSRs are solely a function of the headcentric

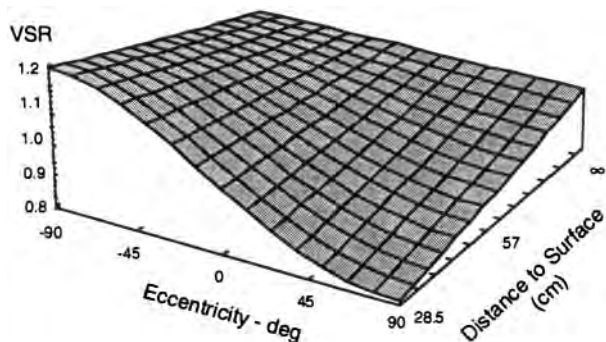


Figure 7.55. Vertical size ratios as a function of distance.

A vertical size ratio (VSR) of a feature is the ratio of its vertical angular extents at the two eyes. All features in the median plane of the head (eccentricity = 0) have VSRs of 1.0. For a particular distance of the feature from the observer, VSRs increase (to the left) and decrease (to the right) with increasing eccentricity. VSRs tend towards 1.0 with increasing distance for features at all eccentricities as the distances from the two eyes become more similar. (Redrawn from Rogers and Bradshaw 1994b.)

eccentricity and absolute distance to the surface and are therefore quite independent of how the eyes are positioned, as we showed in Section 7.6.3.

The two analyses can be partially reconciled in the following way. If the eyes are fixated on an eccentrically located surface, the gradient of the VSR-eccentricity function described by Gillam and Lawergren specifies the absolute distance and headcentric eccentricity of that surface. Hence it is still possible, although not strictly necessary, to derive the viewing-system parameters of convergence distance (d) and the angle of eccentric gaze (g) which form the basis of Mayhew's implementation. The difference in Gillam and Lawergren's implementation is that the information about the viewing-system parameters may be seen as a consequence of the absolute distance and headcentric eccentricity of the fixated surface, rather than of the positions of the eyes. Conversely, it is also possible within Mayhew's implementation to provide information about the absolute distance and headcentric eccentricity of any nonfixated surface in the visual scene, but it is achieved by first computing the viewing-system parameters of convergence distance and angle of eccentric gaze and then using the relative disparity and retinal eccentricity of the particular surface to scale the horizontal disparities and calculate the system independent parameters.

There are, however, significant differences between the two analyses. In Mayhew and Longuet-Higgins' analysis, all points in the scene could, in theory, contribute to the calculation of two global viewing-system parameters and there is no

requirement that the points lie on continuous surfaces. For Gillam and Lawergren, the gradient of the VSRs over a surface provide a purely local estimate of the distance to the surface.

Gillam and Lawergren's analysis can be extended to take into account the effects of larger eccentricities and different elevations. Figure 7.55 shows how the VSR of a small ($<5^\circ$) surface patch (oriented normally to the cyclopean direction) varies as a function of its horizontal eccentricity and absolute distance. The VSR is 1.0 for a patch which lies across the median plane (0° eccentricity), and increases with eccentricity reaching a maximum at $\pm 90^\circ$ eccentricity (since the ratio of the distances from the two eyes is maximal at this point). For a surface patch at a very large distance from the observer, the VSR is 1.0 for all eccentricities, because the distances from the two eyes approach the same value. The centre portion of this graph, where the VSR-eccentricity function is approximately linear, represents the situation described by Gillam and Lawergren. The gradient in this centre portion is a simple function of the absolute distance to the surface.

In the general case, the absolute distance to the surface can be calculated from the VSR of a surface patch together with the local horizontal gradient of the VSR at that point. Together, these two quantities uniquely determine the absolute distance to the surface patch and its headcentric eccentricity, for surfaces which lie close to the plane of regard.

It is important to note that for a scene containing a number of surfaces at different absolute distances from the observer, the magnitude of the VSR and the local horizontal gradient of the VSR will be different for each different surface. In other words, a computational theory based on VSRs does not yield a single viewing-system parameter which applies to all parts of the visual scene, but instead provides local information to specify the absolute distance and headcentric eccentricity of each individual surface.

It should be noted that there is an inherent redundancy to the computational theory based on VSRs. The VSR of a surface patch together with the local gradient of the VSR uniquely determine the absolute distance to the surface and its headcentric eccentricity and this will be true for all surface patches in the scene. But the eccentricity of separate surface patches in the scene is not independent of their spatial layout and the absolute distances are not independent of the horizontal disparities between patches. It is therefore unnecessary and indeed wasteful to determine these quantities separately for each separate surface. It would be more economical to derive a single headcentric eccentricity parameter—which could be the angle of eccentric gaze of the

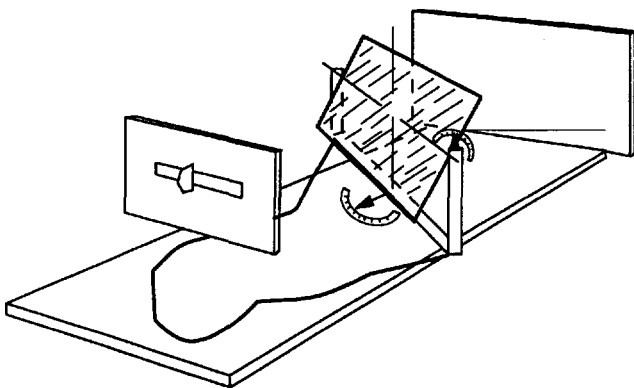


Figure 7.56. Apparatus used to measure the induced effect. Subjects viewed the textured transparent surface through a slit and set it to the apparent frontal plane. Aniseikonia in the horizontal and vertical meridians was indicated by errors about each of the two axes. (Adapted from Ogle 1939.)

eyes—and a single distance parameter of the fixated surface based on the pooled information from the entire visual image.

Michaels (1986) provided an ecological and non-mathematical analysis of binocular vision which revealed the importance of the vertical component of the disparity field in specifying the absolute distances of surfaces. She also presented evidence that manipulations of vertical disparities in stereograms simulating the viewing of wall surfaces influenced judgments of apparent slant and where the surface would intersect the observer's midfrontal plane.

7.6.5 The induced effect

A surface lying in a frontal plane appears slanted about a vertical axis when the image in one eye is horizontally magnified relative to the image in the other eye. The surface appears to slant away from the eye with the smaller image. The geometry of this situation is shown in Figure 2.28. The same surface appears to slant in the opposite direction when the image that was previously smaller along the horizontal meridian is now made smaller along the vertical meridian. Ogle (1938) called this the **induced effect**. The effect was first reported by Lippincott (1889) and by Green (1889) but the first systematic experiments on the induced effect were conducted by Ogle (1938) in the Dartmouth Eye Institute.

Ogle measured the induced effect by asking the subject to set a 30 by 30 cm glass plate covered with random dots to the apparent frontal plane while viewing the plate through a lens which magnified the image in one eye. The plate was 40 cm from the eyes and was viewed through a horizontal slit which restricted the visual field to the plate, as shown in

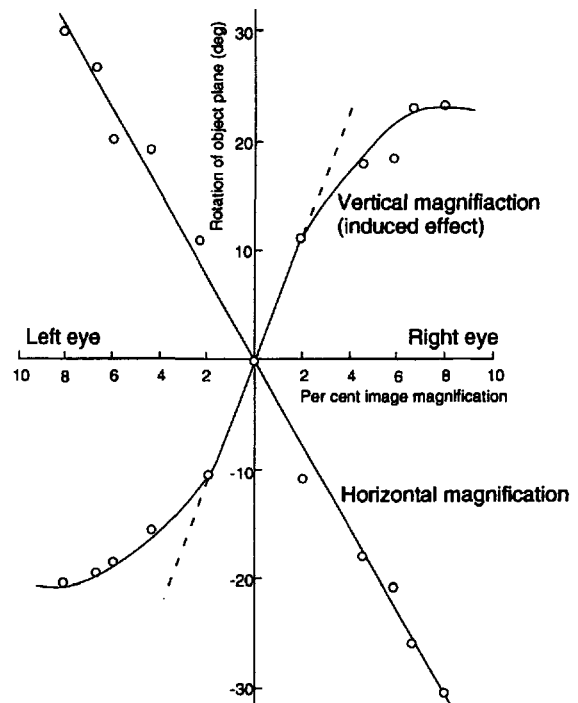


Figure 7.57. Differential magnification and apparent slant. Errors in setting a textured surface to the frontal plane as a function of the per cent horizontal or vertical magnification of the left- or right-eye image. The stimulus filled the binocular field at a distance of 40 cm. Data for one subject. (Adapted from Ogle 1938.)

Figure 7.56. Most monocular cues to the slant of the surface were thus eliminated. A sample set of results for one subject is shown in Figure 7.57. The dashed diagonal line shows the predicted slant of the test surface as a function of horizontal magnification of the image in one eye. The function was derived from the equation:

$$\tan y = -\frac{d(M-1)}{a(M+1)}$$

in which y is the angle of surface slant, M is the proportional horizontal magnification of the image in one eye, d is distance of the point of fixation, and a is half the interpupillary distance.

It can be seen that perceived slant increased in proportion to the magnification of one image with respect to the other. The induced effect has three characteristics, (1) **gain**, or magnitude of perceived slant produced by 1° of image magnification, (2) the **linear range** over which the effect is proportional to image magnification, and (3) **peak value**. The gain in Ogle's data was between 3 and 3.5° of apparent slant per degree of magnification. It can be seen in Figure 7.57 that the gain was the same for slant induced by horizontal magnification as for that induced by

vertical magnification. Thus, a given vertical disparity produced an impression of slant similar to that produced by the same degree of horizontal disparity. Westheimer (1984b) found that subjects were much less sensitive to a given percentage of differential vertical magnification than to the same percentage of horizontal magnification, as reflected in the proportion of trials for which slant was reported. The magnitude of perceived slant was not measured so that a direct comparison with Ogle's data is not possible.

It can also be seen in Figure 7.57 that the linear range for horizontal magnification extended over 10 per cent of magnification but only over about 3 per cent for vertical magnification. The peak value was also greater for horizontal than for vertical magnification. Ogle noted that differences in image magnification due to anisometropia rarely exceed 6 per cent. Magnification of one eye's image induced little or no apparent slant of the test surface.

Ogle concluded that "... some mechanism compensates for the difference in the sizes of the images in the vertical meridian but can only do so by an overall change in the relative sizes of the ocular images." He conjectured that the induced effect may be related to the fact that the relative size of the images changes as a stimulus is moved into the periphery of the visual field.

Ogle (1939a) obtained an induced effect when the stimulus consisted of two black bars in the median plane symmetrically arranged above and below a horizontal row of dots, with fixation on the centre dot. The vertical eccentricity of each bar varied between 1 and 11.4°. Geometrically, the magnitude of vertical disparity in the images of the bars was proportional to the magnification of the lens and the eccentricity of the bars. The results showed that for a 10 per cent difference in image size, the gain of the induced effect increased slightly as the eccentricity of the test bars increased. Ogle argued that the increasing vertical disparity with increasing image separation was largely offset by the decrease in sensitivity of the peripheral retina to vertical disparity. The other possibility is that the visual system derives a measure of image magnification by scaling disparity with eccentricity.

In a third paper Ogle (1939b) found that the induced effect decreased as the inclination of the surface increased. The maximum effect occurred when the test surface was inclined slightly backwards to conform with the inclined vertical horopter. It was also found that the induced effect produced by a horizontal row of dots and two vertically oriented test bars decreased as the test bars were stereoscopically removed from the plane of the

row of dots. Thus, in both cases, the induced effect was greatest when the test display contained zero horizontal disparities.

Westheimer (1978) could not obtain an induced effect with vertical lines or a square subtending 24 arcmin and exposed for 500 ms although horizontal magnification of the image in one eye produced the expected slant. Perhaps vertical disparities in such small displays are not used, since they do not normally arise.

Mayhew and Longuet-Higgins (1982) and Gillam and Lawergren (1983) cited the induced effect as the principal evidence that the visual system uses vertical disparities in coding depth. Localized induced effects (within a larger visual display) can be created mechanically (Williams 1970), photographically, or electronically (Rogers and Koenderink 1986) while global induced effects across the whole visual scene are most easily created using an aniseikonic lens in front of one eye (Ogle 1938; Gillam et al. 1988a). A vertical magnification creates perceived slant around a vertical axis, such that a frontal surface seen with a vertical magnification to the right eye is seen with the right-hand edge closer to the observer than the left-hand edge. The opposite slant is perceived if the axis of the aniseikonic lens is rotated through 90° to produce a horizontal magnification of the right eye's image.

Ogle called the latter the **geometric effect** because it is predicted from the geometry of the situation—a near-left, far-right surface will create binocular images that have a larger horizontal extent in the right eye than in the left. The induced effect, on the other hand, creates no horizontal disparities, and hence any theory of binocular stereopsis which considers only horizontal disparities would not predict the perceived slant of the surface.

Ogle realized that any surface away from the median plane of the head subtends a larger vertical angle in one eye than the other. He therefore reasoned that for correct registration of the slant of the surface, the retinal images must be scaled (isotropically) to the same height. If this were the case, a vertical magnification of one eye's image should be interpreted as a consequence of eccentric viewing. The resulting scaling to bring the vertical sizes of the binocular images into congruence induces a horizontal disparity difference, which is interpreted as slant with respect to the direction of gaze. An alternative way of thinking about the induced effect is that the only real-world surface that creates a vertical size difference but no horizontal size difference is an eccentric surface slanting with respect to the cyclopean normal (see Figure 7.58; Gillam and Lawergren 1983).

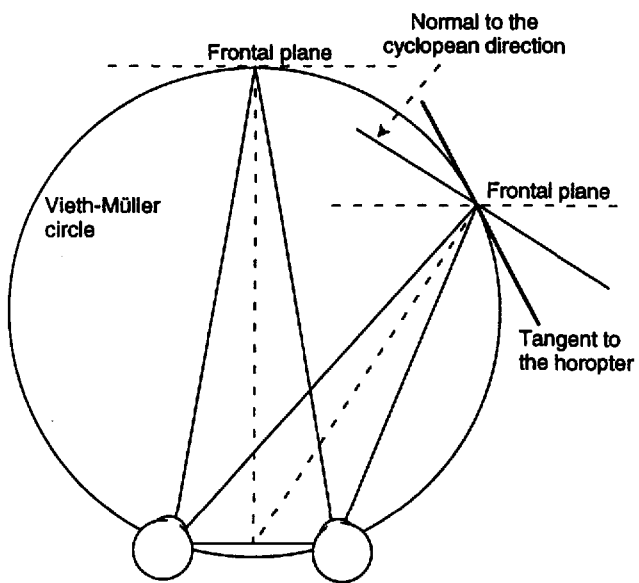


Figure 7.58. Geometry of the induced effect.

All points on the Vieth-Müller circle have zero disparity. Any local planar surface which is tangential to the V-M circle will have a zero gradient of horizontal disparity. However, because the surface is closer to the right eye than to the left, it will have a larger angular extent in the right eye. The stimulus situation is identical to that of Ogle's induced effect in which the image is magnified vertically (but not horizontally) in one eye.

Mayhew and Longuet-Higgins based their conclusion that the induced effect is evidence for the use of vertical disparities on the following argument. The vertical size difference created by the aniseikonic lens would be interpreted as information that the gaze was eccentric. Since horizontal disparities are a function of gaze angle and distance as well as scene structure (Mayhew 1982), the computed slant of all surfaces in the scene would be affected by the nonzero gaze angle term. Their theory predicts that the induced effect should be the same as the geometric effect for the same magnification. For small magnifications (<3 per cent) the induced effect has been found to be about the same as the geometric effect, but at larger magnifications (>8 per cent) the induced effect decreases rather than increases (Figure 7.57). At first sight, this result appears to be inconsistent with the predictions of the vertical disparity hypothesis, but Mayhew and Longuet-Higgins (1982) and Frisby (1984) have argued that vertical magnifications larger than 5 per cent would be created only by impossibly large gaze angles together with very close viewing distances. The falloff in the induced effect beyond this 5 per cent value is therefore consistent with the characteristics of binocular images within the normal working range of distances and angles of gaze.

More recently, Gillam et al. (1988a) measured the induced and geometric effects with a matching technique rather than the nulling procedure used in many previous experiments. They found that induced slant was greater than that created by the geometric effect for a magnification difference of under 1 per cent and reached an asymptote at approximately 2 per cent magnification. They attributed the small effect to conflicting indicators of eccentricity given by the eye movement system. They also found that the induced effect did not vary with observation distance, although Frisby (1984) has questioned whether this is true when the results for distance and gaze angle combinations that could not occur in natural viewing are excluded.

Alternative explanations

Does the induced effect constitute evidence for the use of vertical disparities by the human visual system? It is certainly consistent with the use of the vertical component of the overall disparity field, but it does not follow that the vertical disparities are used to compute the viewing-system parameters of distance (d) and gaze angle (g) explicitly, prior to the interpretation of horizontal disparities, in the way suggested by Mayhew (1982) and Frisby (1984).

An alternative explanation, proposed by Koenderink and van Doorn (1976a), is that the visual system computes the amount of deformation needed to map one eye's image onto the other (see Section 7.1.5). According to this analysis, the deformation produced by a vertical expansion of one eye's image is equivalent to, and should be indistinguishable from, the deformation produced by the horizontal expansion of the other eye's image. The perceived slant in the induced effect is therefore consistent with the deformation hypothesis. The advantage of the deformation hypothesis is that the system could simply ignore any isotropic expansion of one eye's image compared to the other to compute surface slant. Quite independently, the difference in overall size (amount of dilatation) could be used to indicate the eccentric location of the surface.

It is not clear whether the accounts are completely distinguishable. Mayhew and Frisby emphasized extraction of the whole-field viewing-system parameters (d) and (g), while the Koenderink and van Doorn emphasized the local differential characteristics of the disparity field. If vertical disparities are used to provide a single viewing-system parameter, the visual system would be expected to pool or average the vertical disparities over the entire visual scene, even if they are of different magnitudes.

Stenton et al. (1984) reported that pooling did indeed occur in a 7.2 by 7.2° display of 16 points with a

range of vertical disparities. Moreover, computing a single viewing-system parameter rules out obtaining two or more induced effects in different parts of the visual field since this requires different local specifications of the viewing-system parameters. Rogers and Koenderink (1986) reported that opposite induced effects are seen simultaneously under certain conditions. In one situation, they found that an induced effect which signalled an eccentric gaze angle to the left was seen in the right half of the display at the same time that an opposite induced effect which signalled an eccentric gaze angle to the right was seen in the left half of the display.

Rogers and Koenderink's result seems inconsistent with the idea of computing a single viewing-system parameter of gaze angle. On the other hand, it is not possible to induce a large number of local surface slants in different directions, as a theory based on the amount of local deformation disparity predicts. The inherent redundancy of calculations based on local operations discussed in Section 7.6.4 is relevant here. A possible compromise is that viewing-system parameters are calculated but the calculations are based on local measurements over a part rather than the whole of the visual field. Gårding et al. (1994) have made a similar proposal.

A different explanation of the induced effect has been proposed by Ardidt et al. (1981a) and Ardit (1982). These authors argued that, if one considers a vertical expansion of one eye's image of a pair of crossed oblique lines at $\pm 45^\circ$, there is a set of possible matches between the lines which have horizontal disparities consistent with a surface slanted about a vertical axis. For this stimulus, the induced effect can be explained in terms of horizontal disparities. Ardit et al. were apparently unaware that Ogle had allowed for this possibility (1964, p. 248).

The induced effect occurs for stimuli in which this explanation is impossible, such as a pattern of vertical lines. Furthermore, although a single pair of crossed oblique lines provides a pattern of horizontal disparities consistent with slant about a vertical axis, multiple oblique lines which maintain their horizontal separation with vertical magnification are more consistent with inclination about a horizontal axis than with the slant about a vertical axis seen in the induced effect (Gillam and Lawergren 1983; Mayhew and Frisby 1982).

7.6.6 Predictions and empirical evidence

Predictions of the vertical-disparity hypothesis

The analysis presented in Sections 7.6.3 and 7.6.4 shows that the vertical-disparity field created by either a minimum of three noncollinear points or a

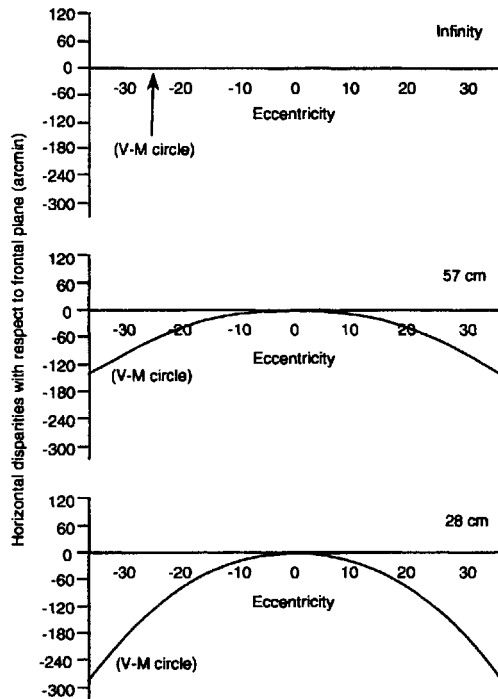


Figure 7.59. Frontal planes and Vieth-Müller circles.

At infinity, a frontal plane coincides with the Vieth-Müller circle—all points on the plane have zero disparity. At closer distances (57 and 28 cm), all eccentric points on a frontal plane are disparate with respect to the circle or (as illustrated) the Vieth-Müller circle can be thought of as disparate with respect to a frontal plane. The pattern of horizontal disparities varies with distance to the frontal plane. Thus, horizontal disparities alone do not specify whether a surface is frontal.

surface patch is capable of providing information about the absolute distances to points and surfaces in the visual scene. Apart from the induced effect discussed in the previous section, is there any evidence that the human visual system is able to use vertical disparities? To answer this question, consider an experiment in which the vertical-disparity field is manipulated to simulate surfaces at different absolute distances. At least four different predictions can be made:

1. The simulated surface should appear either closer to or farther away from the observer.
2. The perceived depth and shape of stereoscopic surfaces should be affected.
3. The perceived size of objects and texture elements should be affected.
4. The overall shape of a surface along horizontal meridians should appear to change.

The first prediction follows naturally if the visual system uses the characteristics of the vertical-disparity field as information about the absolute distance to the surface. A simulated surface containing

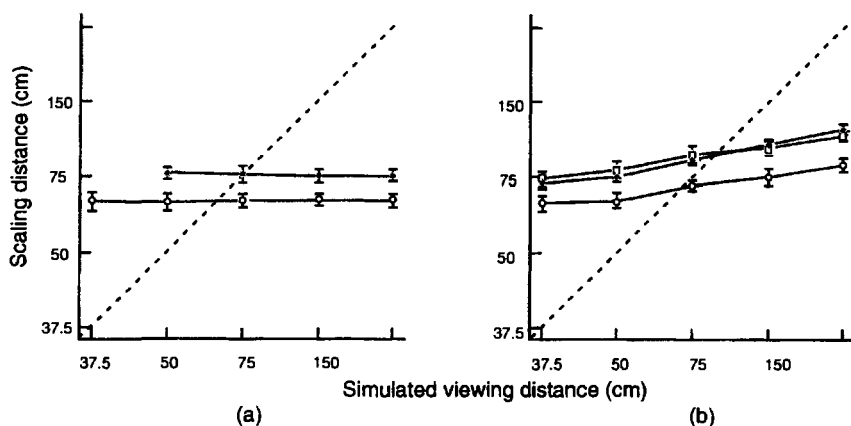


Figure 7.60. Effects of vertical disparity and vergence on perceived shape from disparity. Observers judged whether a horizontal cylindrical surface appeared more, or less, elongated than an semi-circular cylinder at three viewing distance: 50 cm (open circles); 75 cm (solid circles); 150 cm (squares). Manipulations of vertical disparity had no effect on perceived shape (a) but vergence angle manipulations (b) had an effect equivalent to 25 per cent of that required for complete constancy (dotted diagonal line). Results for one subject are expressed in terms of an equivalent scaling distance. (Redrawn from Cumming, Johnston, and Parker 1991.)

vertical disparities appropriate to a distant surface should be seen as farther away than a surface containing vertical disparities appropriate to a close surface.

The second prediction follows if it is assumed that the absolute distance estimate derived from the vertical-disparity field is used to scale horizontal disparities in a similar way to the scaling of horizontal disparities by vergence or other distance cues. More depth should be seen in a stereogram with vertical disparities appropriate for a far surface than for a simulated near surface.

The third prediction follows if it is assumed that the absolute distance estimate derived from the vertical-disparity field is used to scale the size of objects and the texture elements covering a surface. Objects should appear larger and the surface texture of objects should appear coarser when the vertical disparities are appropriate for a far surface. The fourth prediction can be understood by considering the particular case of a frontal surface, although similar effects are predicted for all stereoscopic surfaces. The pattern of horizontal disparities created by a frontal surface varies with the absolute distance to the surface. When the eyes are fixated on a frontal surface at infinity, all points on the surface have zero disparity (top row, Figure 7.59).

At close viewing distances, a frontal surface creates uncrossed horizontal disparities in all directions except where the surface cuts the median plane, because the surface deviates significantly from the Vieth-Müller circle (see Figure 7.59). To judge whether a surface is flat it is therefore necessary to have additional information about the absolute distance to the surface. Although a frontal

surface is used to illustrate this point, it applies to all surfaces—to correctly judge the shape of a surface along a horizontal meridian from horizontal disparities, additional information is required. This information could be provided by vergence signals from the eyes or by the pattern of vertical disparities. If vertical disparities are used as a source of information about absolute distance, we should predict that the perceived shape of a surface containing a particular and fixed pattern of horizontal disparities will be affected by manipulations of the vertical-disparity field (prediction 4).

Empirical evidence

Until recently, nobody has claimed that either the perceived absolute distance or the perceived size of objects and texture elements—predictions (1) and (3)—is affected by vertical disparity manipulations. In 1991, Sobell and Collett and Cumming et al. reported that vertical disparity manipulations had no effect on the perceived depth or the local shape of stereoscopic surfaces—prediction (2) (Figure 7.60a). In contrast, Cumming et al. showed that the alternative source of information about absolute distance—vergence angle—had a significant effect on the perceived shape of stereoscopic surfaces (Figure 7.60b).

With respect to the fourth prediction, Helmholtz (1909) provided evidence and several clear demonstrations that vertical disparity manipulations can affect the perceived shape of stereoscopic surfaces. This evidence has either been discounted or forgotten, as Bishop (1989) pointed out (Figure 7.61).

Why are vertical disparities so ineffective? Westheimer (1978, 1984b) has argued on the basis of his own experimental evidence that the visual

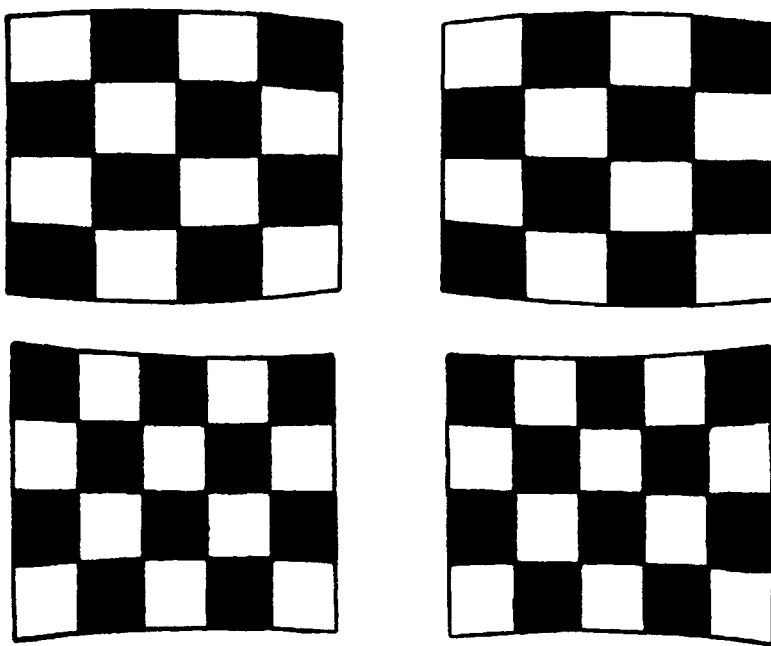


Figure 7.61. Helmholtz's stereograms to illustrate the effects of vertical disparities.
The two chequerboard stereograms have vertical distortions which create vertical disparities between the two halves. With divergent fusion, the upper chequerboard pattern (mimicking a surface at a large distance) is seen as convex in depth in a horizontal direction from left to right. The lower stereogram has the opposite vertical distortion (mimicking a surface at a close distance) and the fused chequerboard pattern is seen as concave in a horizontal direction from left to right.

system does not have the necessary sensitivity to extract vertical disparities. Using a display consisting of either a square or vertical line elements which subtended less than $1^\circ \times 1^\circ$, he found that vertical disparity detection (based on the slant created by vertical magnification) had at most only one-tenth of the sensitivity of horizontal disparity detection (based on the slant created by horizontal magnification). In a later study using an inverted V configuration of five dots, Westheimer (1984b) found that sensitivity to vertical disparities was at least an order of magnitude less than for horizontal differences (threshold for vertical magnification = 11.9 per cent; threshold for horizontal magnification = 1.6 per cent). Note, however, that in both these studies the total size of the stimulus was less than $1^\circ \times 1^\circ$.

The recent results of Rogers and Bradshaw (1992, 1993) demonstrate that vertical disparity manipulations can have a significant effect on the perceived depth, size, and shape of stereoscopic surfaces. First, they showed that manipulations of the vertical-disparity field do affect the perceived depth in sinusoidal disparity corrugations—prediction (2). When the vertical-disparity field was appropriate to a surface located at infinity, the depth in the corrugations specified by a fixed peak-to-trough

horizontal disparity was approximately twice that perceived when the vertical-disparity field was appropriate to a surface at 28 cm from the observer (Figure 7.62). The authors pointed out that the depth scaling is much less than that required for complete depth constancy but the result provided the first clear evidence that vertical disparity manipulations do affect perceived depth in stereoscopic surfaces. Rogers and Bradshaw (1993) also reported that when the vertical-disparity field was appropriate to a surface at infinity, the surface was perceived to lie at a greater distance (prediction 1), and that the size of the texture elements covering the surface appeared to be larger (prediction 3) than when the vertical-disparity field was appropriate to a surface at 28 cm.

Display size

How is it possible to resolve the inconsistency of Rogers and Bradshaw's positive results and the negative findings of Cumming et al. and Sobell and Collett? The answer appears to lie in the size of the display. Figure 7.63 shows that the VSRs of elements on a frontal surface increase with horizontal eccentricity, reaching a maximum at around $\pm 45^\circ$. The overall size of the display used by Cumming et al. was about 11° ($\pm 5.5^\circ$) so that the maximum VSR for

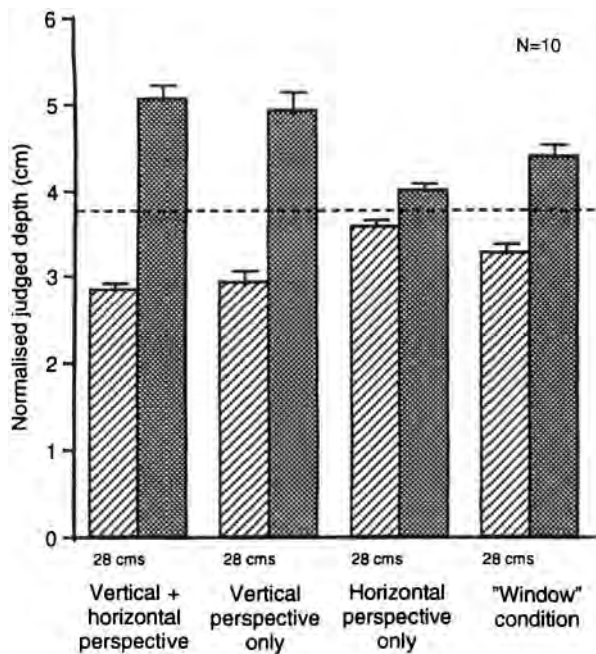


Figure 7.62. Effects of vertical disparity on perceived depth. Observers estimated the peak-to-trough depth in horizontal corrugations occupying the central ($25^\circ \times 20^\circ$) region of the $75^\circ \times 75^\circ$ display. When the vertical and horizontal perspective components were appropriate for a surface at infinity, the depth was judged to be approximately double that when the cues were appropriate for 28 cm. Most of this effect was due to manipulations of the vertical component. Depth scaling was still found when the perspective cues were limited to the area surrounding the corrugations in the "window" condition. (Redrawn from Rogers and Bradshaw 1993.)

their closest distance (37.5 cm) was less than 1.015 (a 1.5 per cent size difference). This may be below the detection threshold or at least the threshold for the depth scaling process. Rogers and Bradshaw's displays, on the other hand, extended to 75° ($\pm 37.5^\circ$) and the maximum VSR for their closest distance (28 cm) was around 1.12 (a 12 per cent size difference). To test this possibility directly, Bradshaw and Rogers (1994) measured the amount of depth scaling as a function of display size. Observers used adjustable calipers to indicate the amount of perceived depth. They found that the amount of depth scaling declined to zero when the display was masked down to just 10° in diameter (Figure 7.64). To see the effects of vertical disparities on depth scaling requires that the displays subtend at least 10° in diameter.

Contradictory cues

A second factor may have reduced the amount of depth scaling in Bradshaw and Rogers' experiment and helped eliminate the effect in Cumming et al. and Sobell and Collett's experiments. In each of these studies, vergence and accommodation were

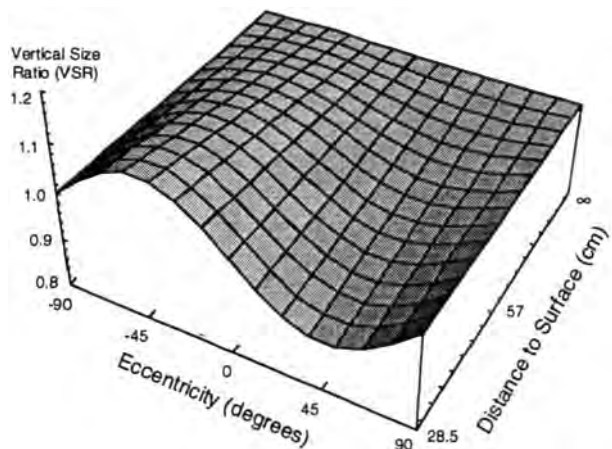


Figure 7.63. Vertical size ratios (VSRs) for a frontal surface. The three-dimensional graph shows how VSRs of a frontal surface vary with headcentric eccentricity and the distance to the surface in the median plane. The pattern of VSRs is different from that shown in Figure 7.55 because the distance to eccentric parts of a frontal surface increases with increasing eccentricity. For a frontal surface, VSRs are maximal at an eccentricities of $\pm 45^\circ$ and decrease back to 1.0 at eccentricities of either $+90^\circ$ or -90° , as the distance to the surface approaches infinity.

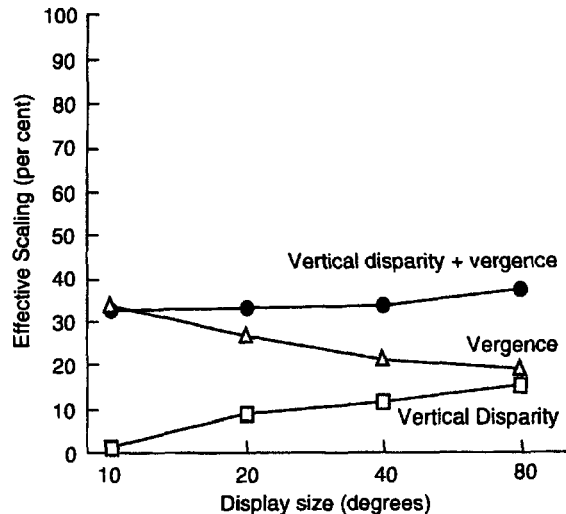


Figure 7.64. Disparity scaling and display size. Disparity scaling is expressed as a percentage of that needed for perfect constancy at different distances. When both vertical disparities and the vergence angle indicated the viewing distance, constancy was about 35 per cent for all sizes of display. When vertical disparities alone specified viewing distance and vergence was held constant, constancy was about 15 per cent for the largest (80° diameter) displays and decreased to zero for 10° displays. Constancy was around 35 per cent with vergence manipulations with the smallest (10°) display. The effectiveness of vergence decreased with increasing display size. Average of 3 observers (redrawn from Rogers and Bradshaw 1994b).

held constant and, as a consequence, provided the visual system with contradictory information about the absolute distance to the surface. To assess the effect of contradictory information on depth scaling, Bradshaw and Rogers compared the amount of depth scaling produced by manipulations of either (1) the vertical-disparity field (keeping vergence constant) or (2) the vergence state (keeping vertical disparities constant), or (3) both cues together. The pattern of results was clear. With large (75° diameter) displays, vergence angle and vertical disparity manipulations both had similar quantitative effects on depth scaling, which were equivalent to ~20 per cent of that required for complete constancy (Figure 7.64). When both cues signalled the changes in simulated viewing distance, the combined effect of the two cues rose to over 30 per cent. This result strongly suggests that the presence of the contradictory vergence angle information in Rogers and Bradshaw's (1993) and other previous experiments was responsible, at least in part, for the small amount of depth constancy.

The pattern of results for small (10° diameter) displays was quite different. The effect of manipulating the vertical-disparity field on depth scaling was negligible (as Cumming et al. found), while the effect of vergence angle manipulations, which were now free of the contradictory influence of the vertical-disparity field, rose to over 30 per cent of that required for complete scaling (see Figure 7.64). *Unfortunately, it does not appear to be possible to contrive the converse situation where the effects of vergence state are eliminated or minimized in order to assess the true role of the vertical disparity cues.*

7.6.7 The perception of frontal surfaces

Rogers et al. (1993) and Rogers and Bradshaw (1994b) also investigated the effects of vertical disparity manipulations on the perceived shape of frontal surfaces (prediction 4). As was indicated earlier, frontal surfaces at different absolute distances create different patterns of horizontal disparities according to the extent to which the frontal surface deviates from the Vieth-Müller circle (see Figure 7.59). It is clear from the results of experiments on the apparent frontal plane by Helmholtz (1909), Ames et al. (1932b), Ogle (1964), Foley (1980), and others that we are able to compensate, at least in part, for these changes (Bishop 1989). Their results show that there are often small deviations in settings of a horizontal row of vertical rods to the apparent frontal plane (a concave locus is chosen at close viewing distances and a convex locus at far viewing distances). However, the direction of these deviations does not

match those predicted by the disparities of frontal surfaces with respect to corresponding retinal points (Figure 7.59). If frontal judgments were made on the basis of these disparities alone, we would expect close frontal surfaces to be seen as convex and far frontal surfaces as flat. If we assume that the nasal eccentricity of corresponding points is larger than the temporal eccentricity, the predicted direction of the deviations in observers' judgments is correct but the magnitude of the deviations is too small (see Figure 2.1.6; Tyler 1991). This suggests that the pattern of horizontal disparities alone does not constitute a sufficient basis for making frontal-plane judgments either in theory or in practice.

In principle, either the vergence state of the eyes or information in the vertical-disparity field could provide the necessary scaling signal. Three factors may have lessened the effectiveness of vertical-disparity cues in the experiments of Helmholtz and Ogle. First, the displays were generally quite small with the consequence that the vertical disparities were below the detection threshold (see Westheimer 1978, 1984b). Second, the displays were often masked by fixed screens above and below the display, which would have eliminated any vertical-disparity cues from the boundaries of the stimuli. Third, the stimuli were often vertical rods which lacked the features necessary to provide vertical disparity information. Indeed, Helmholtz noted that the introduction of beads on the vertical rods, which provided better vertical disparity information, had a significant effect on frontal-plane judgments. Ogle repeated Helmholtz's experiment with beads and obtained a negative result but he placed the beads on the central fixation rod which could not, in principle, provide information about the absolute distance of the rods (Bishop 1989).

Rogers and Bradshaw's (1994b) experiments on the shape of frontal surfaces used large, densely textured patterns which extended over 75° ($\pm 37.5^\circ$) in both horizontal and vertical directions. The patterns were rear projected, using a Wheatstone stereoscope configuration of mirrors at $\pm 45^\circ$ to the lines of sight. The distance information was provided by either (a) vertical disparity manipulations alone, (b) vergence angle alone, or (c) both cues together. In each case, the patterns were carefully synthesized to create images appropriate to a range of viewing distances between 28 cm and infinity. In reality, the patterns were always presented on screens at a distance of 57 cm from the observer's eyes so that accommodation and other potential cues to absolute distance were held constant.

The results from their experiments were clearcut. When both vertical disparities and vergence

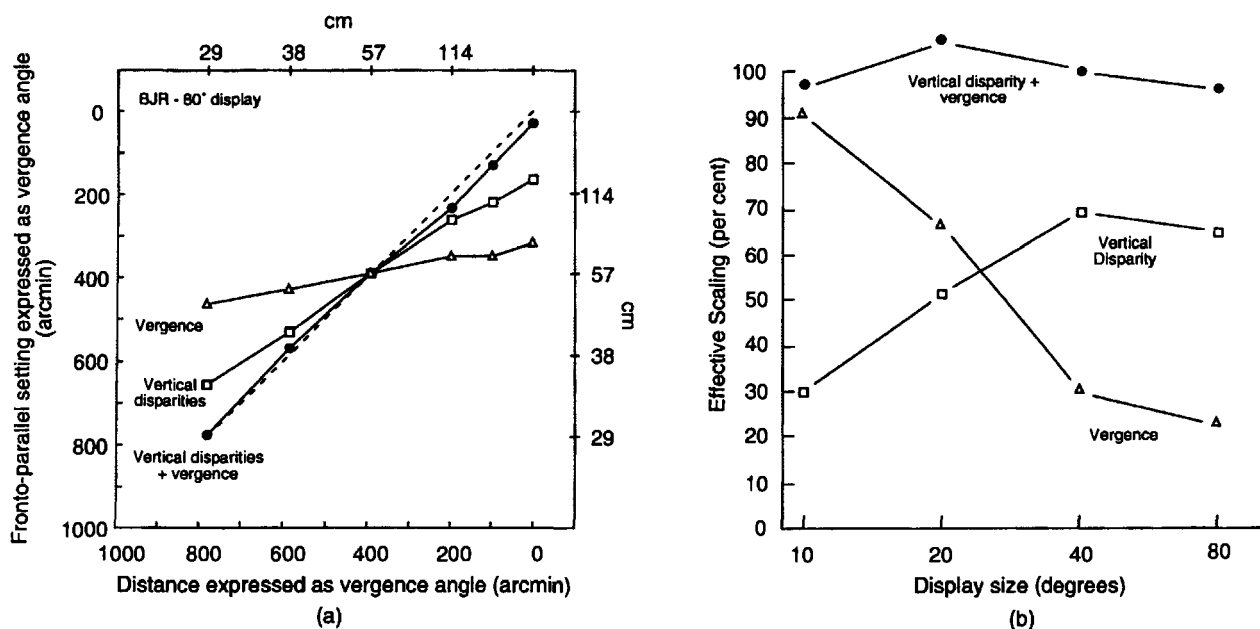


Figure 7.65. Frontal surface scaling and display size.

Observers adjusted the pattern of horizontal disparities across the surface until it appeared to be flat. The distance, expressed here as a vergence angle, was specified by either vertical disparities, vergence angle or both cues together.

(a) When both cues specified the distance, the pattern of horizontal disparities chosen was close to that created by a physical surface at that distance (dashed line). Constancy was poorer when only one cue specified the distance. Results for one observer with an 80° display.

(b) Frontal surface scaling expressed as a percentage of that needed for perfect constancy at different distances, as a function of display size. When both vertical disparities and the vergence angle indicated the viewing distance, constancy was close to 100 per cent for all display sizes. When vertical disparities alone specified the viewing distance and vergence was held constant, constancy was nearly 70 per cent for the largest displays and decreased for smaller displays. Vergence manipulations had large effect (~90 per cent scaling) on the shape of frontal surfaces when the display was small but the effect diminished with increasing display size. Average of 3 observers (redrawn from Rogers and Bradshaw 1994b).

signalled the viewing distance, the scaling was close to 100 per cent of that required for perfect frontal-surface judgments at different distances (Figure 7.65a). With the 80° display, there was not even the slightest tendency to see close frontal surfaces as convex and far frontal surfaces as concave as found in earlier experiments (Figure 2.22). When vertical-disparity cues signalled the viewing distance and vergence cues were held constant for a distance of 57 cm, the scaling was reduced to around 70 per cent of that required for complete constancy. When vergence cues signalled the viewing distance and vertical-disparity cues were held constant for a distance of 57 cm, the scaling was less than 30 per cent of that required for complete constancy, indicating that vertical-disparity cues are much more effective (in the presence of contradictory information) than vergence cues in these large displays.

Rogers and Bradshaw repeated their observations for several different-sized displays ranging from 10° to 80° (Figure 7.65b). With a small display which

subtended only 10° of visual angle, the pattern of results reversed; vertical-disparity cues now had only a small effect (as might be predicted from their small magnitude) while vergence cues (now largely released from the contradictory influence of the vertical disparities) provided more than 70 per cent of the scaling required for complete constancy.

Visual sensitivity to patterns of horizontal and vertical disparity was investigated by Rogers et al. (1993). With vergence fixed at 57 cm (6.5°), they measured thresholds for discriminating whether an 80° diameter surface was curved in a convex or concave direction with respect to the frontal plane. With the vertical disparities fixed for a viewing distance of 57 cm, observers were presented with a sequence of surfaces each containing a pattern of horizontal disparities that would be created by a frontal surface either slightly closer or farther than 57 cm. The slope of the psychometric function characterizes the observer's ability to discriminate surface curvature along the horizontal meridian.

The results can be expressed in terms of the difference in equivalent vergence angle of the surface that an observer can reliably discriminate as curved in a concave or convex direction. For surfaces at 57 cm, the best threshold was 6 arcmin (0.1°), meaning that the observer could reliably discriminate the curvature of a surface which had the pattern of horizontal disparities appropriate to a surface 6 arcmin (< 1 cm) in front of or behind a 57 cm surface.

Sensitivity to changes in vertical disparity was measured with the pattern of horizontal disparities fixed and appropriate to the 57 cm viewing distance. Observers were presented with a sequence of surfaces, each containing the pattern of vertical disparities that would be created by a surface either slightly closer or farther than 57 cm. The best threshold was 8 arcmin (0.13°), meaning that the observer could reliably discriminate the curvature of a surface which had vertical disparities appropriate to a surface 8 arcmin (1.2 cm) in front of or behind a 57 cm surface.

Expressing the sensitivity to changes in horizontal surface curvature in terms of the vergence angle difference of surfaces at different distances allows a direct comparison of the visual system's sensitivity to horizontal and vertical disparity manipulations. For large surfaces subtending 80° visual angle, sensitivity to gradients of vertical disparity is about 70 per cent of that to gradients of horizontal disparity. For smaller surfaces, sensitivity to gradients of vertical disparity falls off more rapidly than sensitivity to gradients of horizontal disparity for judgments of surface curvature in a horizontal direction.

The 70 per cent effectiveness of vertical disparities compared with horizontal disparities for frontal plane curvature discriminations with large surfaces closely matches the 70 per cent figure obtained when observers adjusted the pattern of horizontal disparities until a surface appeared flat (Figure 7.65). This is not coincidental. Discrimination performance reveals the trading function between vertical and horizontal disparities when both cues are close to the actual viewing distance of 57 cm. The adjustment data reveal the effects of setting one cue (vertical disparities) to simulate a quite different viewing distance (28 cm or ∞) and then determining which pattern of horizontal disparities is needed to make the surface appear flat.

Rogers and Bradshaw (1994b) noted one significant difference between the effects of vertical disparities on depth and size scaling and their effect on the apparent shape of frontal surfaces. For displays which subtended less than 10° , they found no effect of vertical disparity manipulations on perceived depth (Figure 7.64). On the other hand, the same

manipulations did affect the perceived curvature of frontal surfaces even when the display consisted of a 1° high horizontal strip, which is consistent with Helmholtz's original observations. This suggests that while vertical disparities are used in both depth scaling and for frontal plane shape judgments, different processes and mechanisms may be involved.

Rogers and Bradshaw's results with small (10°) displays are also compatible with those of a study by Westheimer and Pettet (1992). They used a stereoscopic display consisting of just five points, and the observer's task was to adjust the horizontal disparity of the centre dot until it appeared to be in the plane of the surrounding four dots positioned at the corners of a square subtending $7^\circ \times 7^\circ$. Vertical disparities were introduced into the surrounding four dots which were appropriate to the viewing of either (a) a very close surface (by magnifying the vertical distance between the left-hand pair of dots and minifying it between the right-hand pair of dots in the left image, and vice versa for the right image) or (b) a physically impossible surface lying beyond infinity with the opposite characteristics. They found that the amount of horizontal disparity that had to be added to the centre dot for the dot configuration to appear coplanar (in a frontal plane) was only 25 per cent of the magnitude of the vertical disparities of the surrounding dots. As can be seen in Figure 7.53, a real frontal surface creates vertical disparities with the same value as the horizontal disparities along the major ($\pm 45^\circ$) diagonals of the surface.

Westheimer and Pettet interpreted their results as showing that vertical disparities are weighted less than horizontal disparities in the computation of surface slant. It should be pointed out, however, that the magnitudes of the vertical disparities used by Westheimer and Pettet correspond to the viewing of a surface just 6.5 cm in front of the eyes—a convergence angle of 50° —or of an impossible surface beyond infinity with a divergence angle of -50° ! Hence the 25 per cent effectiveness of the vertical disparities they found under these conditions may simply be due to the physical impossibility of the chosen stimuli. Alternatively, the relatively small size of their displays ($7^\circ \times 7^\circ$) may have been responsible. Our own results suggest that it was the small size of Westheimer and Pettet's displays that was responsible for the incomplete scaling rather than the impossibility of the vertical disparity magnitudes. Using a 10° -diameter densely textured field, Rogers and Bradshaw (1994b) found a similar (30 per cent) effectiveness of the vertical disparities needed for veridical frontal-plane judgments (Figure 7.65), which corresponds closely to Westheimer and Pettet's results.

Direct assessment of the frontal plane

We have already remarked on the similarity in the pattern of results obtained in the depth scaling experiments (Figure 7.64) and the scaling for the perception of frontal surfaces (Figure 7.65): (1) scaling is maximal when both vertical disparities and vergence angle specify the viewing distance, (2) the effectiveness of vertical disparities increases with increasing display size, and (3) the effectiveness of vergence angle decreases with increasing display size. There was also a significant difference. The presence of both vergence and vertical-disparity cues yielded scaling that was close to 100 per cent of that required for complete constancy of frontal-plane judgments. The effectiveness of depth scaling, on the other hand, was never greater than 40 per cent. Why should this be so? The presence of other cues (such as accommodation and vergence) provided contradictory information about absolute distance but there is no reason why the contradictory information should have a greater influence in the depth scaling situation, given that the experimental displays and stimulus characteristics were similar in the two cases. One possibility is that while the depth scaling task requires an explicit estimation of viewing distance prior to the scaling process, the frontal-plane task relies on a direct computation which does not involve the explicit estimate of distance.

A direct strategy for determining whether a frontal surface is flat has been suggested by Rogers and Bradshaw (1993). They derived an expression relating the VSRs of elements lying on frontal surfaces to their horizontal eccentricity and the distance to the surface (Figure 7.55). They also derived an expression for the horizontal size ratio (HSR) of elements lying on the same frontal surface (Figure 7.66) and found that the two expressions were related by a simple square relationship. If a surface is a flat and frontal surface, the value of the HSR for each local patch is simply the value of the VSR squared:

$$\text{HSR} = \text{VSR}^2$$

In addition, the gradient of the HSR function is exactly twice that of the VSR function. To determine whether a surface in a frontal plane is flat, the visual system does not need to compute the distance to the surface directly—it would only have to measure the VSR and the HSR (or their spatial gradients) to test whether the particular relationship holds.

This is an attractive possibility, and it is possible that the human visual system makes use of these simple invariants. However, the direct computation of whether a surface is flat and frontal cannot account for the differing patterns of results for the

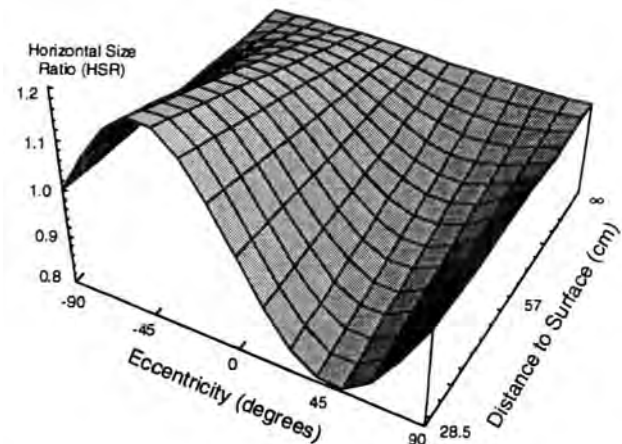


Figure 7.66. Horizontal size ratios (HSRs) for a frontal surface. The three-dimensional graph shows how HSRs of a frontal surface vary with headcentric eccentricity and distance to the surface in the median plane. The pattern of HSRs is very similar to the pattern of VSRs created by a frontal surface (Figure 7.63) except for the magnitude. At any particular eccentricity and absolute distance, the value of the HSR is precisely that of the VSR².

depth scaling and the frontal-plane judgments described earlier. While it is true that the scaling from vertical disparities is much higher for the frontal-plane task which does not require an explicit computation of distance, Rogers and Bradshaw's results show that the scaling of frontal surfaces is also higher when only vergence cues are available to make the judgment (Figure 7.65). Frontal plane judgments cannot be based on image invariants when vergence is manipulated.

7.7 DISPARITY-DEFINED SHAPE

7.7.1 Theoretical considerations

In laboratory situations, experimenters present single planar surfaces which are slanted or inclined with respect to a frontal plane. In the natural world, we more often see several surfaces in which there are both disparity differences between the surfaces and disparity changes within each surface. The purpose of this section is to consider what information is available for characterizing the shapes of disparity-defined surfaces and the invariance of that information to changes in the location of the surface within the visual field. The following section (7.7.2) will consider the results of experimental studies on shape perception from disparity cues.

In discussing the perception of slant and inclination, it was emphasized that quite different results obtain when more than a single surface is visible. These differences may be a consequence of the way

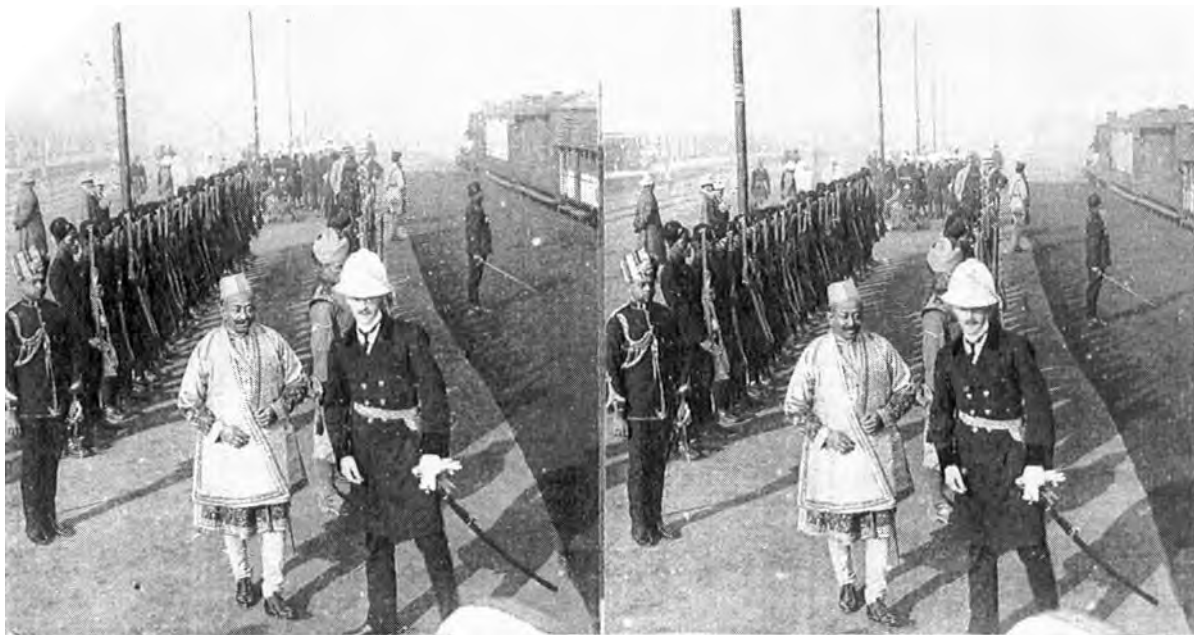


Figure 7.67. The "cardboard cut-out" phenomenon.

People and objects in pictorial stereograms often appear as cardboard cut-outs even when the visual angle and the disparities of the original scene are reproduced correctly. The phenomenon is a consequence of the fact that size scales with $1/d$ whereas disparity scales with $1/d^2$, where d is the distance to the object. Size and depth scaling are often inappropriate in a stereoscope because vergence and vertical disparities cues signal a closer viewing distance than in the original scene.

the disparity field is affected by eye movements and the distances of surfaces from the observer. Horizontal, vertical, and torsional eye movements all affect the absolute disparity of a single point and therefore absolute disparities provide only limited information when the precise positions of the eyes are not known (Section 7.1.2). Relative horizontal disparities, including width disparities, size ratios, and the orientation disparities between pairs of points do not change with either horizontal or vertical eye movements but they do not provide unambiguous information about the slant and inclination of a surface because they are affected by the absolute distance and the headcentric eccentricity of the points, and by the cyclovergence state of the eyes.

The deformation needed to map one eye's image onto the other remains invariant with cyclovergence and with the eccentricity of the surface with respect to the head. However, because the deformation disparity of a particular surface varies with its absolute distance, it must still be scaled to determine the slant or inclination of the surface (Section 7.1.5). When there are two or more surfaces in the visual scene, the computation of deformation disparity becomes redundant because the state of torsional alignment and the relative locations of the surfaces with respect to the head are whole-field parameters which affect all visible surfaces.

The existence and role of whole-field parameters suggests that the situation may be simpler rather than more complicated when there is more than one slanted or inclined surface in the visual field. The changes of disparity or the changes of disparity gradient over a surface may contain sufficient information to specify surface shape which is relatively unaffected by the location of the surface, its distance from the observer, and the alignment of the eyes. In this first section, we consider the higher-order properties of the disparity field and the link between these properties and our perception of surface shape.

The variant and invariant properties of curved surfaces
In section 7.1.5 we saw that for smoothly curved surfaces, the second spatial derivative of the disparity field—the **disparity curvature**—remains invariant to changes in the absolute distance to the surface. This is an interesting invariant property but unfortunately it does not tell us much about the shape of a surface. First of all, the disparity curvature of a given surface varies with its eccentricity with respect to the head (Section 7.1.5). Second, the local disparity curvature of a curved surface with a particular radius of curvature depends on the average gradient of the surface to the line of sight. The disparity curvature of a surface patch with a particular radius of curvature varies with the gradient of the surface normal.

The easiest way to appreciate this point is to consider the surface for which the local disparity curvature is the same for all points on a surface. It is not a sphere or a cylinder of constant diameter. Instead, it is a surface with a parabolic disparity profile since the second derivative of the equation for a parabola is a constant. This means that unless the disparity gradient as well as the disparity curvature is known, the local radius of curvature of the surface patch cannot be calculated.

Third, the invariance of disparity curvature to changes of absolute distance applies only to **local disparity curvature**. Consider a sinusoidally corrugated surface seen at different distances. The disparity curvature of either the peaks or the troughs of the corrugations (or any other part of the surface) is the same at different absolute distances, but the change of disparity curvature over space changes with distance because the angular separation of a peak and a trough varies as a function of distance. In general, we use the term **surface shape** to describe the changes of curvature over a surface rather than the local curvature at a particular point.

Hence, while local disparity curvature is invariant with viewing distance, shape estimates based on changes of disparity curvature must be affected. In particular, the third spatial derivatives of the disparity field increase directly with absolute distance and therefore need to be scaled in order to achieve shape constancy. Higher-order spatial derivatives of the disparity field are also not invariant to changes in viewing distance. Consequently, if the estimates of the absolute distance to the surface are inaccurate or inappropriate we should expect judgments of surface shape to be affected by changes in the viewing distance. This is a consequence of the geometry of binocular stereopsis and is true whether shape estimates are based on disparities, disparity gradients, or disparity curvatures.

Cardboard cut-out phenomenon

The fact that third spatial derivative descriptions of the disparity field vary as a function of viewing distance can probably account for the so-called **cardboard cut-out phenomenon** seen in pictorial stereograms. Many readers will have noticed that objects and people in stereograms typically appear much flatter, like cardboard cut-outs, than when viewed in the real scene (Figure 7.67). This is still true when the angular size of objects in the stereogram is the same as their angular size in the original scene and the stereo pictures are taken from two positions separated by the interocular distance, so that the images reaching the eyes are identical to those created by the original scene.

We can explain the cardboard cut-out phenomenon in the following way. To a first approximation the disparities created by a given object or surface vary inversely with the square of the distance. The angular size of an object varies inversely with distance, again to a first approximation ($\text{size} \propto 1/d$). This means that if the visual system has an incorrect estimate of distance and uses it to scale disparities and angular sizes, the perceived shape in terms of the depth to size ratio will be incorrect. In particular, if distance is underestimated, the depth from disparity scaling will be too small compared with the perceived size from size scaling. Thus, if distance is underestimated, objects and surfaces should look flattened (Foley 1980; Johnston 1991).

In most stereoscopes, the distance indicated by accommodation, convergence, and any other cues is typically much smaller than that of the surfaces in the original scene. Under these circumstances, we predict that objects and surfaces look flattened, as they do in most stereoscopes. If this explanation is correct, we should also expect the opposite effect; objects and surfaces should look more elongated in depth and more sharply curved when the cues to distance in the stereoscope signal a greater distance than that of the objects in the original scene. As indicated earlier, it is not necessary to assume that the particular strategy adopted by the visual system is one in which the distance estimate is used to scale disparities and visual angles. The same predictions are made if the visual system scales disparity gradients or any other order of disparity which varies with viewing distance.

The invariant properties of frontal surfaces

There is a second property of disparity-defined surfaces which is unaffected by the viewing distance. In Section 7.6.7 we showed that the binocular horizontal size ratios (HSRs) across a frontal surface vary with headcentric eccentricity approximately according to a $\sin(2\epsilon)$ relationship where ϵ is the headcentric eccentricity (see Figure 7.66). The vertical size ratios (VSRs) across a frontal surface also vary with headcentric eccentricity approximately according to a $\sin(2\epsilon)$ function (see Figure 7.63), but the amplitude of the VSR-eccentricity function is exactly half that of the HSR-eccentricity function for a particular distance. In addition, the gradient of the HSR-eccentricity function across the midline will be exactly double that of the VSR-eccentricity function. What information do these properties of the disparity field provide?

When there is just a single patch in the visual scene, and the HSR of the patch is the square of the VSR, the patch must lie in a frontal plane whatever

its distance from the observer. For a pair of patches which both satisfy the HSR=VSR² requirement, they must both lie in frontal planes but not necessarily the same frontal plane. When the HSR-eccentricity function created by an extended surface is smooth (lacking disparity discontinuities) and the gradient of that function is exactly double that of the VSR-eccentricity function, the surface must be flat as well as lying in a frontal plane. As yet, there is no empirical evidence that the visual system uses these properties as a basis for judgments about the orientation and flatness of a surface irrespective of its distance. Moreover, it should be borne in mind that the relationship between HSRs and VSRs holds only for surfaces close to the plane of regard.

7.7.2 Shape perception in disparity surfaces

Relative slant and inclination

Gillam et al. (1984) have shown that differences in perceived slant or inclination of two or more surfaces are seen more rapidly and more veridically than the absolute slant or inclination of a single surface. Two factors probably contributed to the better performance: (1) the presence of disparity discontinuities in their "twisted" surfaces and (2) the presence of disparity gradient discontinuities in their "twisted" and "hinged" surfaces. These results should not surprise us given the ambiguity of both vertical and horizontal gradients of horizontal disparity referred to earlier (Section 7.7.1). Information about the absolute slant or absolute inclination of a single planar surface is not provided by horizontal disparities alone because they are also affected by the absolute distance to the surface and its eccentricity with respect to the median plane of the head.

We are not aware of any studies which have measured the veridicality of relative slant judgments but informal observations suggest that the perceived difference of slant in a pair of surfaces does not change when there is an isotropic difference in the sizes of the binocular images (as would be produced by eccentric viewing). If this result survives systematic investigation, there are at least two possible explanations. The visual system may calculate the appropriate whole-field parameter and use it to correct the slant estimates of all surfaces in the scene or, alternatively, judgments of relative slant may be based on the relative disparity gradients of the different surfaces. *This issue needs to be investigated*

A similar analysis applies to inclined surfaces. The rotation of one image of a stereopair around its centre introduces a vertical gradient of horizontal disparity but this does not create an impression of inclination. If the stereogram depicts two or more

surfaces with different inclinations, the perceived difference of inclination does not vary when one image of the stereopair is rotated. The visual system may calculate a whole-field parameter indicating the cyclovergence state and uses it to correct the inclination estimates of all surfaces in the scene. Alternatively, judgments of relative inclination may be based on the relative disparity gradients of the different surfaces. The evidence presented in Section 12.2.4 suggests that the larger of two inclined surfaces may also normalize towards the frontal plane.

The existence of contrast effects in the perception of slanted and inclined surfaces suggest that relative slant and relative inclination play important roles in surface perception (Section 12.2). In general, differences of slant or inclination are more readily perceived than the absolute slant or inclination of individual surfaces. Graham and Rogers (1982a), for example, reported that the centre strip in a display of three horizontal strips had to have up to 60 per cent of the inclination of the surrounding strips before it appeared to lie in a frontal plane (Section 12.2.4). Mitchison and Westheimer (1984) found that a pair of vertical lines appeared to be at the same distance from the observer only when they had close to 100 per cent of the disparity gradient of the surrounding slanted surface.

Surface curvature and shape

In the previous section we looked at the perception of surfaces with either disparity discontinuities or disparity gradient discontinuities. How good are we at detecting surface curvature and how veridical are our perceptions of shape in surfaces which lack zero- and first-order discontinuities? Only a few studies have addressed this issue. Thresholds for discriminating the direction of curvature (convex or concave), in random-dot-covered cylindrical surfaces with a parabolic profile are very small. For a 20° diameter display depicting a horizontally oriented cylinder, the direction of surface curvature could be reliably discriminated when the radius of curvature at the peak of the cylinder was greater than 400 cm, corresponding to a disparity curvature of less than 0.02 arcmin/deg² (Cagenello and Rogers 1989, Rogers and Cagenello 1989). Thresholds varied as a function of the display size and were a factor of ten higher when the display subtended only 2.66° in diameter (Figure 7.68a). Thresholds for vertically oriented cylinders were typically 1.5 times those for horizontally oriented cylinders, and were also influenced by the orientation of gridlines (0/90° or ±45°) across the surface, although to a lesser extent than thresholds for discriminating slanting surfaces (Section 7.5.1).

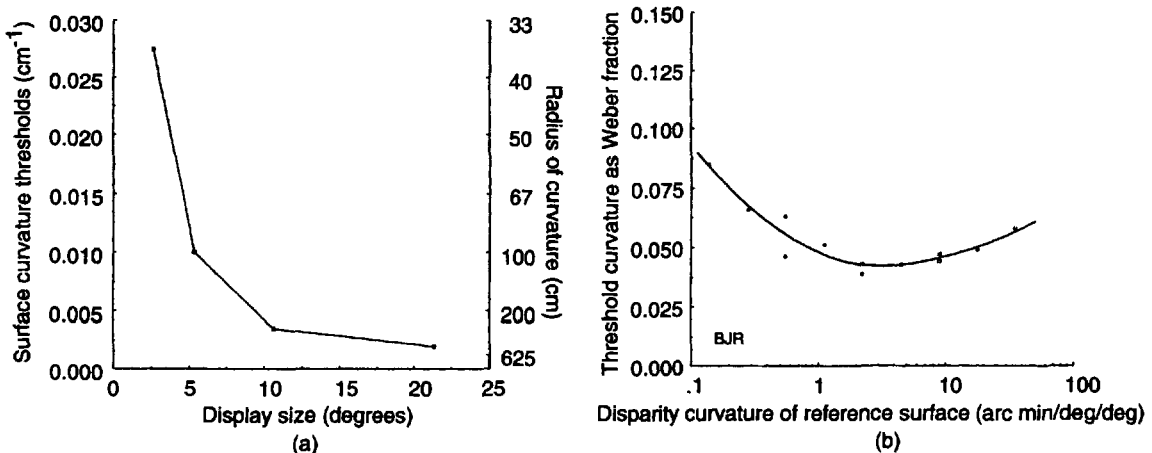


Figure 7.68. Discrimination thresholds for surface curvature.

(a) Thresholds for discriminating between convex and concave curvature in horizontally oriented parabolic corrugations as a function of display size. Thresholds decreased with increasing display size reaching a minimum of less than 0.002 cm^{-1} (500 cm radius of curvature) for the largest display (21.6°). Average of two observers.

(b) Thresholds for discriminating one suprathreshold parabolic curved surface from another, expressed as a fraction of the reference curvature. Weber fractions were smallest (<5 per cent) for curved surfaces with a 3 arc min/deg/deg disparity curvature (2.25 cm radius).

Suprathreshold curvature discrimination thresholds have also been determined for cylindrical surfaces with a parabolic disparity profile. At the optimal curvature of around 3 arcmin/deg², Rogers and Cagenello (1989) reported that the curvature of two random-dot covered surfaces could be reliably discriminated when the curvature difference was less than 5 per cent of the reference disparity curvature (Figure 7.68b). In another experiment, Rogers (1986) found that observers could accurately match the perceived curvature of two parabolic surfaces at different distances (57 and 114 cm).

Apart from the depth matching study, the results described so far have dealt with thresholds for detecting and discriminating curved surfaces rather than the veridicality of shape perception from disparity. To assess the veridicality of shape perception we need to define an appropriate task that observers can perform using some internal standard. Johnston (1991) suggested the criterion of an apparent semicircular cylinder—a cylinder in which the depth of the half cylinder appears equal to its half width or half height.

How good are we at judging whether a cylinder with a semicircular profile has this property? According to the results of Johnston (1991), our perception of disparity-defined shape is very poor. The disparity-defined cylinder, covered with a dense but even texture, which was perceived to be semicircular at 53 cm actually had a depth which was 67 per cent of its radius. The cylinder perceived to be semicircular at 214 cm actually had a depth which was 175 per cent of the radius (Figure 7.69). Johnston

attributed this poor performance to use of an incorrect estimate of absolute distance to the surface in the depth- and size-scaling processes with the consequence that there was only one distance (between 75 cm and 1 m) at which performance was veridical.

The analysis presented in Section 7.7.1 showed that the change of disparity curvature over a curved surface, which is related to the surface shape, changes with the viewing distance to the surface. As a consequence, some estimate of distance is needed to achieve shape constancy. This is easy to see in the case of a semicircular cylinder because the angular radius of the cylinder will approximately halve with each doubling of the viewing distance, whereas the base-to-peak disparity of the cylinder will reduce to approximately one-quarter, with each doubling of the viewing distance. When viewing distance is underestimated, surface curvature from disparity cues should be underestimated and when distance is overestimated, surface curvature should be overestimated, which is exactly the pattern of results found by Johnston.

Why should performance be so bad on this task when observers perform so well on judgments of the flatness of frontal surfaces, as we will see in the next section? There are several possibilities. First, one could argue that the task was not really concerned with surface shape because observers matched only the perceived depth of the cylinder until it appeared to be equal to the radius. But this would not account for the fact that depth/height judgments varied as a function of viewing distance. The apparent depth to height of a surface is an aspect of shape perception.

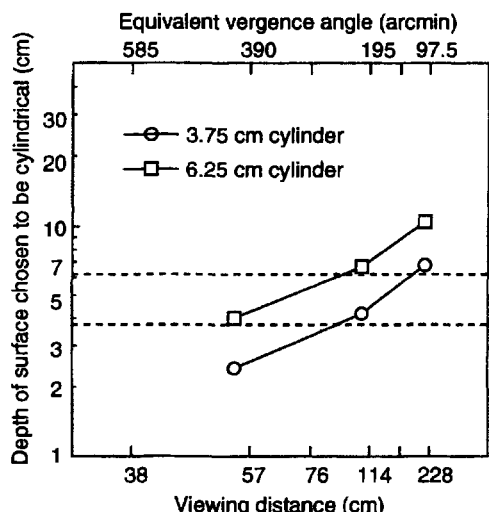


Figure 7.69. Apparent depth of semicircular cylinders.

Forced-choice judgments about the shape of cylindrical surfaces with different depth:height ratios as a function of viewing distance. Perfect constancy is indicated by the dashed lines. At the near distance, a cylinder with less depth than its radius was judged semicircular. At the far distance, a cylinder with more depth than its radius was judged semicircular. Results for one subject. (Adapted from Johnston 1991.)

A second possible reason why the chosen task yielded poor constancy comes from the use of a semicircular cylinder. It is a good choice because observers do have an internal (cognitive) standard for judging depth to height, but it is less satisfactory because the disparity gradient becomes infinitely large at the boundaries of the cylinder surface. Disparities cannot, in principle, provide complete information about the three-dimensional shape of a cylinder.

The third possible reason for the systematic distortions in shape observed in Johnston's study concerns the availability of information about the distance to the cylindrical surface and the presence of conflicting depth cues. The display screen was positioned at different physical distances from the observer, so that both vergence and accommodation were appropriate. However, vertical disparities were not varied and, because of the diverging optical pathways to the screen, were probably appropriate to a hypothetical distance beyond infinity. This factor may not be important in this study because the angular size of display was small and vertical disparities have been shown to be ineffective in depth scaling for displays smaller than 10° (Section 7.6.6).

More important, the displays were viewed in darkness, which eliminated many potential distance cues from the layout of the room and any receding surfaces. The recent experiments of Glennerster et al. (1994) have addressed these issues. First, they measured the amount of constancy in the task of matching the apparent depth in horizontally oriented

stereoscopic corrugations for two surfaces at different distances. Their results confirmed and extended Rogers' (1986) finding that constancy was close to 100 per cent on this task for surfaces between 28 cm and 228 cm when there are many cues which indicate the distance of the surfaces from the observer. (Figure 7.70). To do the matching task, however, we do not need accurate information about the absolute distance to each of the two surfaces. Relative distance information is all that is required. Nevertheless, these results clearly show that depth constancy can be close to perfect when observers are able to make relative judgments.

Glennerster et al. also investigated depth constancy when observers made absolute judgments about the shape of a single surface (Figure 7.71). Overall, they found constancy to be much higher (~70 per cent) than that reported by Johnston (<30 per cent), although never as high as when observers made relative rather than absolute judgments. Constancy was slightly higher for judgments of the apparent "squareness" (90° difference in inclination) of horizontally oriented "roof" surfaces compared with apparent semicircular cylinder judgments. The choice of psychophysical procedure, constant stimuli as in Johnston's study versus method of adjustment in Rogers' (1986) study, did not affect the results. Eliminating information about the ground plane surface by occluding all of the scene apart from the display screens or making the vertical disparity or vergence cues inconsistent both reduced constancy but never to values below 60 per cent. Similar results were obtained by Glennerster et al. with naïve observers.

How can the remaining differences between the two studies be resolved? It is possible that order effects may play a role. In our experiments, observers were always tested in the reduced-cue situations after they had seen the layout of the displays in the full-cue conditions. Testing naïve observers in the opposite order reduced constancy further, but their performance returned to that of the experienced observers as soon as they were tested in the full-cue situation.

Durgin et al. (1994) have provided additional evidence on the veridicality of shape judgments at different distances. Instead of using simulated three-dimensional surfaces displayed on computer screens, they used real objects seen in a brightly lit, fully structured visual environment. Their stimuli consisted of wooden cones with the apex pointing towards the observer. The cones had depths which varied from 50 per cent to 200 per cent of the diameter of the base and were positioned at one of five viewing distances between 1 and 3 m from the

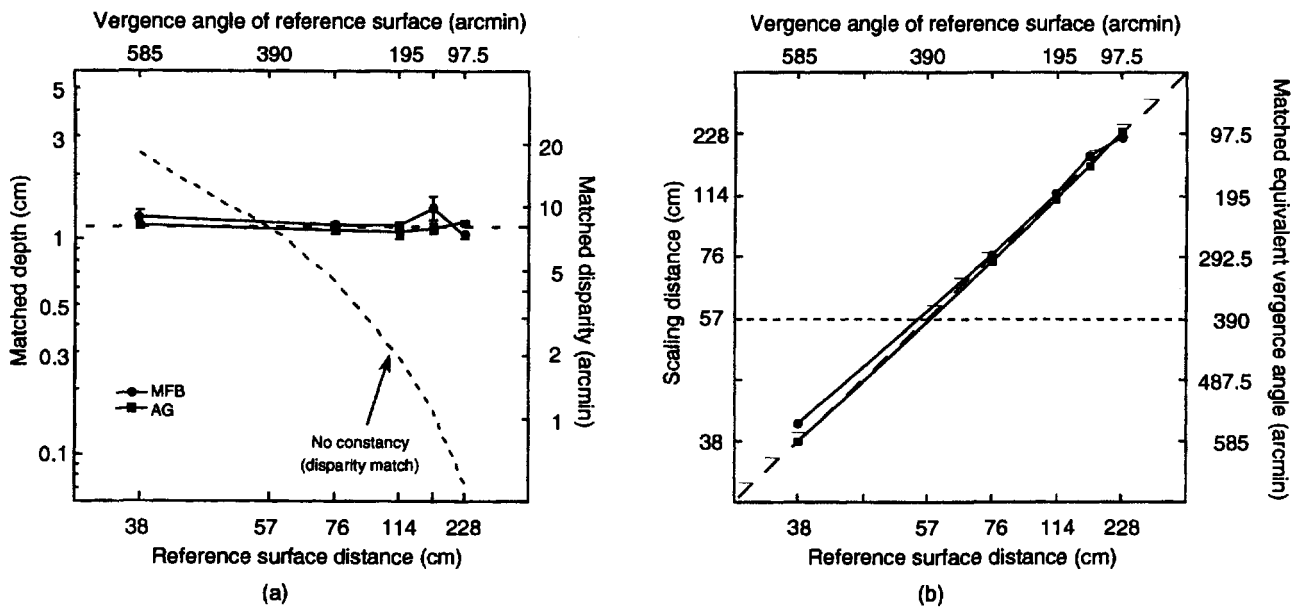


Figure 7.70. Depth constancy: matching perceived depth in corrugations at different distances.

(a) Observers adjusted the peak-to-trough depth of sine-wave corrugations at 57 cm to match the perceived depth of reference corrugations at distances between 38 and 228 cm. The settings are close to the horizontal dashed line indicating perfect constancy.

(b) The same data replotted in terms of the scaling distance—that is, the distance the reference corrugations would have to be for them to have the same depth as the adjustable surface. Perfect constancy is the dashed positive diagonal. The extent of constancy was estimated from the slope of the best-fitting straight line through the data points. (Adapted from Glennerster et al. 1994.)

observer. Observers adjusted a two-dimensional icon on a computer screen to match the perceived angle of the apex of the cone.

The results indicate no underestimation of the depth-to-width ratio of the cones even at the viewing distance of 3 metres. At closer viewing distances their subjects tended to overestimate the depth in relation to the width of the base but, overall, stereoscopic constancy was very high. Durnin et al. argued that the differences between their own and Johnston's (1991) results (showing very poor constancy) can be explained by two factors: (1) the presence of additional depth cues in their structured visual environment and (2) the unreliability of the cues that were available (vergence and accommodation) in the dim illumination conditions used by Johnston.

Further work is needed to clarify these issues but as a general conclusion it can be said that relative depth and shape constancy can be close to veridical for distances up to 3 metres when information about depth and distance is abundant. The geometry of binocular viewing shows that accurate estimation of distance is the key to veridical shape judgments. For distances beyond a metre, oculomotor cues alone do not provide the necessary scaling information.

Shape index

Koenderink (1990) has proposed a radically different approach to understanding and investigating three-dimensional shape perception which involves a new definition of what we mean by shape. Shape is an intrinsic property of a surface which does not depend on the observer's viewing position. Koenderink showed that smooth quadratic surfaces can be characterized along two dimensions—their shape and their curvedness. Shape, according to this definition, is a scale-independent quantity (size of the surface or units used to measure size does not matter). It is related to the so-called principal curvatures of the surface by the following expression:

$$S = -\frac{2}{\pi} \arctan \left(\frac{K_{\max} + K_{\min}}{K_{\max} - K_{\min}} \right)$$

where K_{\max} and K_{\min} are the principal curvatures. Different shaped surfaces have different shape indices. A sphere, for example, which has the same curvature in all directions, has a shape index of 1 (Figure 7.72). A cylinder, which has no curvature along its axis and maximum curvature in the orthogonal direction, has a shape index of 0.5.

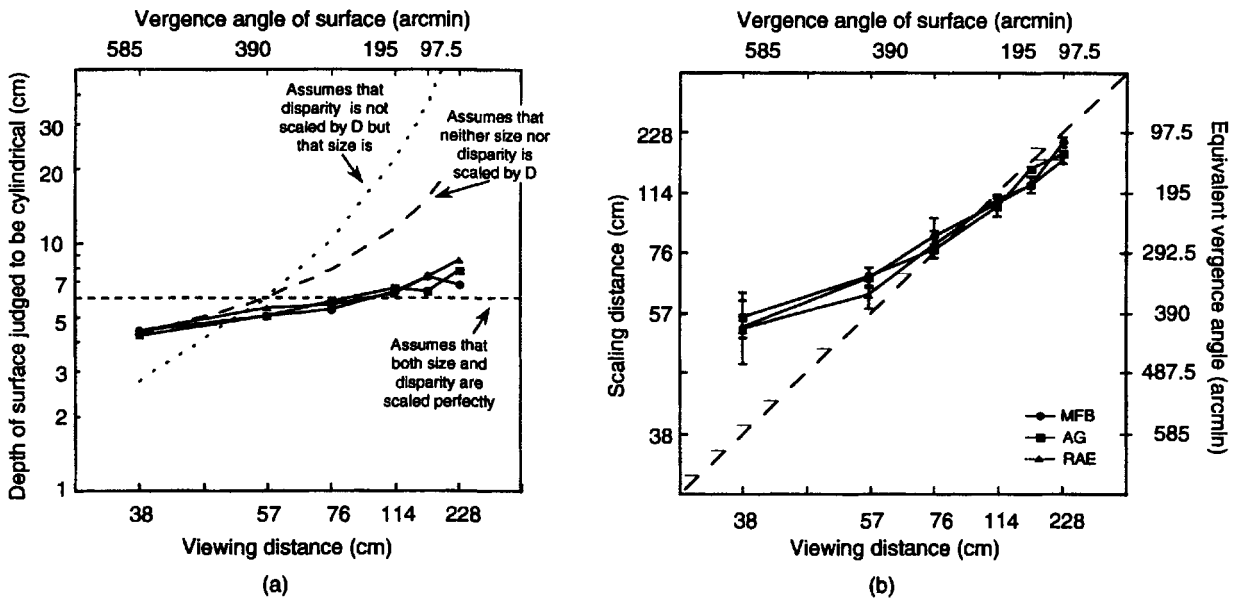


Figure 7.71. Depth constancy: absolute judgement of the apparently semi-circular cylinder.

(a) Observers adjusted the peak-to-trough depth of an horizontal elliptical cylinder until its depth appeared to be equal to its radius for cylinders at distances between 38 and 228 cm. The chosen depth increased slightly with increasing viewing distance indicating a departure from perfect constancy (horizontal dashed line).

(b) The same data replotted in terms of the scaling distance—that is, the distance the cylinder would have to be for that disparity to height ratio to be truly semicircular. Perfect constancy is the dashed positive diagonal. The extent of constancy was estimated from the slope of the best-fitting straight line through the data points. Overall constancy was better than 70 per cent for cylinders at distances between 57 and 228 cm (adapted from Glennerster et al. 1994).

A saddle shape, which is convex in one direction and concave in the orthogonal direction, has a shape index of 0. Two surfaces which have shape indices of the opposite sign have the opposite shapes like a stamp and a mould (De Vries et al. 1993). The curvedness of a surface is a measure of how curved the surface is. It depends on scale (size of the surface and the units used to measure size) and is calculated using the following expression:

$$C = \sqrt{\frac{K_{\max}^2 + K_{\min}^2}{2}}$$

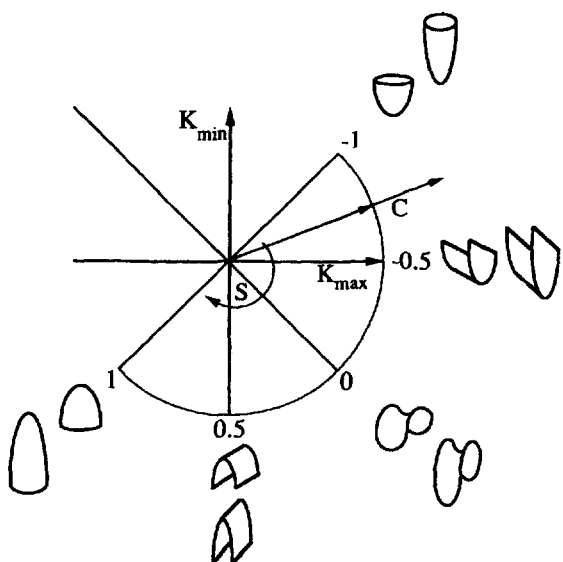
The shape index and curvedness are independent characteristics and together they uniquely define the shape of a smooth surface patch. Moreover, it is important to stress that they are local descriptions of a surface patch rather than overall descriptions of the surface. Normally, a particular surface has different shape indices and different curvednesses in different locations. Only a sphere has the same shape index and curvedness over all its surface.

Koenderink's classification of surfaces according to their shape and curvedness allows us to investigate shape perception more systematically. For example, it provides a criterion for distinguishing

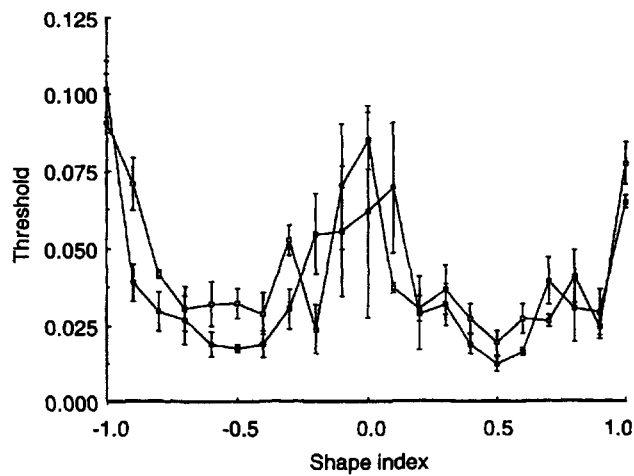
between "simple" and "complex" random-dot surfaces (Julesz 1971; see Section 5.11) and allows us to investigate whether response times for discriminating simple and complex shapes differ. (Uttal 1987; Uttal et al. 1988).

De Vries et al. (1993) investigated the discriminability of surfaces with different shape indices and different curvednesses. Observers assigned surfaces covered with random-dots into one of eight categories corresponding to equal intervals along the shape index scale. Before the experiment, observers were presented with wire-frame pictures of surfaces with different shape indices to familiarize them with the scale. The curvedness of the surfaces varied between blocks of trials and corresponded to one of four different values.

Between 70 and 90 per cent of the categorizations were correct. The best performance was found towards the ends of the shape index scale (± 1) and the poorest performance for discriminating saddle shapes with an index close to zero. Shape discriminations were better for surfaces with larger curvednesses, when the trials were blocked according to curvedness, but showed a more random pattern in the second experiment in which curvedness was completely randomized over all trials.



(a) Shape and curvedness indices. Koenderink (1990) has shown that the local curvature of surface patch can be characterized by its shape index (angular coordinate) and its curvedness (radial coordinate). Convex spheres have a shape index of 1 and concave spheres (hollows) have a shape index of -1. Cylinders with convex and concave curvature have shape indices of 0.5 and -0.5 respectively while saddles have a shape index of 0. The degree of curvature—curvedness—increases radially from the centre in this representation. (Reproduced with permission from de Vries et al. 1994, Vision Research, Pergamon Press.)



(b) Shape discrimination thresholds for 21 reference shapes with shape indices between -1.0 and +1.0. Curvedness was fixed at either 0.5 cm^{-1} (open squares) or 1.0 cm^{-1} (filled squares). Thresholds were lowest for cylinders (shape index = ± 0.5) and highest for saddle shapes (index = 0.0) and symmetrical ellipsoids (index = ± 1.0). (Redrawn from de Vries et al. 1994.)

Figure 7.72. Thresholds for discriminating shape differences.

When observers were asked to assign a shape index number to the presented shape (rather than assign the shape to one of eight categories), an almost perfect linear relationship was found with little influence of the curvedness of the surfaces. De Vries et

al. (1994) have extended these findings further. Rather than categorizing or labelling surfaces with different shape indices, observers made forced-choice discriminations between surfaces with similar shape indices.

Discrimination performance was best for cylindrical surfaces with shape indices of either -0.5 or +0.5 and all observers found saddle-shaped surfaces (shape index 0) and symmetrical ellipsoids (shape index ± 1) more difficult to discriminate. Performance was very impressive. The best observer could discriminate a shape-index difference of 0.01 which corresponds to one two hundredths of the entire shape index scale from -1.0 to +1.0. Discrimination thresholds did not vary significantly for surfaces with curvedness values of between 0.5 and 1.0 cm^{-1} (see Figure 7.72b).

De Vries et al. (1994) also reported the surprising result that shape discrimination thresholds were not raised when either (1) the curvedness of the different shaped surfaces was varied from trial to trial with values between 0.3 and 1.25 cm^{-1} or (2) the slant of the different shaped surfaces was randomly varied with values between $\pm 30^\circ$, or (3) both curvedness and slant were varied.

The shape index has provided a useful metric for classifying and creating surfaces and, in addition, these results show that observers are able to learn and use the shape index to discriminate between different surfaces. Although the results provide no evidence that the visual system classifies local surface patches according to their shape index and curvedness, the use of the shape index allows shape discrimination performance to be compared for different depth cues (Erens et al. 1991).

The apparent frontal plane

The third situation that has been used to study the veridicality of our perception of disparity-defined surfaces is the apparent frontal plane. Helmholtz (1909) reported that three vertical threads which were physically aligned in a frontal plane did not always appear to lie in a frontal plane. When the threads were close to the observer, the centre thread was seen to lie closer than the outer two, as if on a convex surface, but when the threads were far away from the observer, the centre thread was seen by some observers to lie slightly farther away than the outer two, as if on a concave surface. Helmholtz appreciated the fact that the outer threads have an uncrossed disparity (they lie outside the Vieth-Müller circle) with respect to the central thread when the threads lie in a frontal plane that is close. When the threads lie in a frontal plane that is far away there are no disparity differences since they all lie on the

Vieth-Müller circle. Consequently, observers need additional information about absolute distance to judge whether the threads lie in a frontal plane.

Helmholtz attributed the lack of veridicality in observers' judgments to the poor information about distance available from convergence (p 319). However, he was also aware that there is a second source of information about the absolute distance to objects in the visual scene. The information is given by the binocular differences in the vertical size of an object when it is to one side of the median plane of the head (Figure 7.61). These differences arise because the object is closer to one eye than to the other and, as we showed in Section 7.6.3, they can be used to estimate the distance of a surface.

To test whether vertical size differences affect our perception of frontal surface alignment, Helmholtz fastened gilt beads on to the three threads used in his alignment task. The angular differences in the vertical separation of the beads provide information about the absolute distance to the threads. He wrote: "Thereupon the illusion described (that the threads appeared to be misaligned) disappears almost entirely" (p. 322). In other words, when binocular images of the three threads contain both horizontal and appropriate vertical disparities, the perception of their frontal alignment at different distances is close to veridical. Helmholtz made similar observations through diverging or converging prisms, and concluded that the vergence state of the two eyes also affects judgments of frontal alignment. He noted, that the effect is diminished when the plane surface is covered with visible figures or letters.

Many subsequent experiments have attempted to measure the locus of points or vertical lines which appear to lie in a frontal plane (for example, Ames et al. 1932b). Ogle (1932, 1964) obtained the most extensive results, which reveal that at close distances observers perceived the rods in his horopter apparatus to lie in a frontal plane when their physical locus was slightly concave. At far distances (>6 m), observers perceived the rods in the horopter apparatus to lie in a frontal plane when their physical locus was slightly convex (see Section 2.6.7). These results have been referred to extensively and used to support the idea that judgments of frontal planes are not veridical. This pattern of results was obtained, however, with uniform and untextured rods which had their upper and lower ends masked by an aperture close to the observer. Under these conditions, there is no information about the differences in the vertical sizes of the rods, that Helmholtz had shown previously to be crucial for correct judgments of frontal plane alignment. In other words, the lack of veridicality in these subsequent experiments merely

shows how performance on this task is degraded when distance information is inadequate.

We have recently repeated Helmholtz's original experiment but with a densely textured field instead of just three threads (Rogers and Bradshaw 1994b). When both vergence and vertical disparity information was available and appropriate to a surface between 28 cm and infinity, judgments of whether the surface that appeared flat and frontal showed no systematic deviation from an actual frontal surface at the specified distance (Figure 7.65a). Like Helmholtz, we found that both vergence and vertical disparity information contributed to the veridicality of the judgment and for large displays, vertical disparities had the larger effect. When either source of information was held constant or made incompatible, judgments were nonveridical.

Disparity correction and normalization

The striking difference between the veridicality of frontal plane judgments and the poorer constancy of shape and depth judgments led Gårding et al. (1994) to propose that two separate processes are involved. The first they refer to as **disparity correction**, uses the horizontal and vertical components of the disparity field to compute **scaled relative nearness**. This does not give the precise metric structure of objects and their layout but instead a description of the shapes of the surfaces up to a scaling factor, or **relief transformation** (Koenderink and van Doorn 1991). In this respect, scaled relative nearness is similar to the calculation of deformation disparity which provides information about the slant and inclination of surface patches up to a scale factor of distance (Koenderink and van Doorn's 1976a; see Section 7.1.4.). However, they are not identical. Deformation provides information about surface shape with respect to the cyclopean direction whereas scaled relative nearness (like horizontal disparities) provides information about shape with respect to isodisparity circles. Consequently, it does not specify the actual shape of the surface since the curvatures of isodisparity circles vary with the absolute distance to the surface (Figure 7.12).

Gårding et al. suggest that many judgments, including that of the flatness of frontal planes, can be made on the basis of scaled-relative-nearness without the need for the second-stage process—**disparity normalization**—in which the complete metric structure of the scene is calculated. Disparity normalization would allow observers to judge the amount of depth in surfaces. The disparity correction process, like the calculation of deformation, uses the vertical component of the disparity field but while the calculation of deformation is carried out locally,

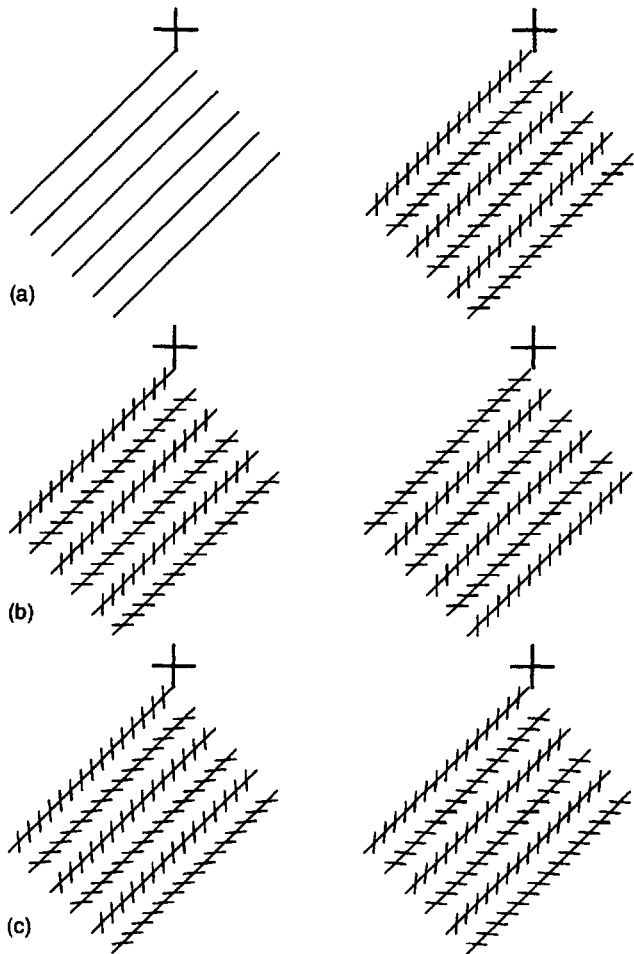


Figure 7.73. Stereopsis from the Zöllner illusion.

Lau (1922) could not obtain a convincing impression of depth by combining the Zöllner illusion in one eye with parallel lines in the other eye, as in (a), nor by dichoptically combining oppositely oriented Zöllner illusions, as in (b). He claimed to see depth in combined Zöllner illusions in which the angle of cross hatching was slightly different in the two eyes, as in (c).

disparity correction uses vertical disparities over a region which is smaller than the entire visual field. Hence, the regional disparity correction model of Gårding et al. can be thought of as a compromise between the use of vertical disparities on a local basis and the global calculation of viewing-system parameters, as proposed by Mayhew and Longuet-Higgins (1982).

To support their model, Gårding et al. cited empirical evidence that the manipulation of the vertical disparity field to simulate the viewing of surfaces at different distances affects the perceived curvature of vertical cylinders but not of horizontal cylinders. However, a similar result is also predicted by the viewing-system parameter model of Mayhew and Longuet-Higgins and the deformation model.

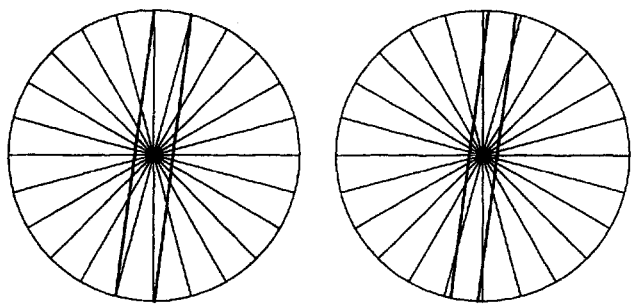


Figure 7.74. Stereopsis from the Hering illusion.

Lau (1922) claimed that straight lines made to appear curved by different amounts in the two eyes because of the Hering illusion may generate an impression of curvature in depth when combined stereoscopically.

All three models predict that vertical size changes will affect the perceived slant but not the inclination of surfaces (Ogle's induced effect). Consequently all three models predict that introducing a horizontal gradient of vertical disparities to simulate surfaces at different distances will affect perceived curvature in a horizontal but not in a vertical direction.

7.8 MISCELLANEOUS TYPES OF DISPARITY

7.8.1 Stereopsis from geometrical illusions

One may ask whether an impression of depth can be created by dichoptic lines that are equal but appear different in shape or length. Lau (1922) presented a set of oblique parallel lines to one eye and the same set of parallel lines with cross-hatching to the other eye, as in Figure 7.73a. The parallel lines with cross-hatching appear nonparallel, an effect known as the Zöllner illusion. Lau did not obtain a consistent impression of depth with this display. When he combined two oppositely oriented Zöllner illusions, as in Figure 7.73b, the predominant impression was of rivalry rather than of depth. He did obtain consistent impressions of differential inclination of the parallel lines when the cross-hatching was only slightly different in the two eyes. He concluded that the visual system uses the pseudodisparity between the parallel lines induced by the configurational properties of the two monocular images. However, the slight difference in orientation of the cross-hatching constitutes a real disparity, and it is not clear what effect this has on the appearance of the parallel lines. Lau (1925) presented the stereogram shown in Figure 7.74, which he claimed produced an impression of curvature in depth in the two intersecting straight lines. Squires (1956) experienced stereoscopic depth in the dichoptic Zöllner and



Figure 7.75. Dichoptic combination of Müller-Lyer illusions.
Disparity between the low spatial-frequency components creates an impression of slant in depth. (After Glennerster and Rogers 1993.)

Poggendorf illusions. Others have not been able to replicate these effects (Ogle 1962; Julesz 1971).

Glennerster and Rogers (1993) designed the stereogram shown in Figure 7.75, which creates two lines inclined in depth. The perceived depth was commensurate with the disparity predicted from the two-dimensional Müller-Lyer illusion in each eye. In terms of the low spatial-frequency components of the images, the line with outgoing fins is objectively longer than the line with ingoing fins. The depth could be due to the disparity between the two lines in terms of the low spatial-frequency components of the images. Thus, there is no reason to suppose that the difference in perceived length of the horizontal lines in the Müller-Lyer illusion is registered before the disparity between the images is detected.

7.8.2 Chromostereopsis

For most people a red patch appears to stand out in depth when viewed with both eyes on a blue background. This effect is known as **chromostereopsis** and was known to Goethe (1810) and Brewster (1851). It is believed to be due to chromatic aberration. The refractive index of the eye's optic system for short wavelengths (blue light) is about one dioptrē greater than that for long wavelengths (red light). This means that blue light is brought to focus in a plane nearer to the lens than the plane in which red light is brought into focus. This effect is known as **longitudinal chromatic aberration**.

Chromostereopsis could be due to the greater degree of accommodation required to focus blue objects compared with that required to focus red objects. There seems to be no evidence on this point. Any effect due to this cause would be evident with both monocular and binocular viewing. It cannot be the only cause of binocular chromostereopsis since depth is seen with very small artificial pupils, which eliminate the effects of differential image blur due to longitudinal chromatic aberration.

For most people the retinal intercept of the eye's optic axis (the line passing through the centres of the eye's four refractive surfaces) is on the nasal side of the fovea. The angle between the optic and visual

axes is the **angle alpha**. This nasal offset of the optic axis creates a parallactic displacement of the images of red objects toward the temporal retina relative to those of blue objects. The visual angle between the image of a point object in blue light and the image of the same object in red light defines the magnitude of the **transverse chromatic aberration**. An object illuminated by both red and blue light produces **chromatic diplopia** in each eye. Consider a small blue object and a neighbouring red object placed vertically above it in the same frontal plane. The opposite transverse chromatic aberration in the two eyes induces a crossed disparity in the image of the red object with respect to that of the blue object (Hartridge 1918). This causes the red object to appear nearer than the blue object. We will refer to this as **red-in-front-of-blue chromostereopsis**. A red object acquires an uncrossed disparity relative to a blue object in those people for whom the angle alpha has the opposite sign. They therefore experience **blue-in-front-of-red chromostereopsis**.

The direction of chromostereopsis can be reversed by moving artificial pupils both in a nasal direction or both in a temporal direction with respect to the centres of the natural pupils (Vos 1960). Moving the artificial pupils nasally induces blue-in-front-of red stereopsis and moving them the other way has the opposite effect. This is because moving a pupil changes the position of the optic axis but not of the visual axis, thus changing the sign of transverse chromatic aberration. Thus, changes in the magnitude and sign of transverse chromatic aberration brought about by changing the lateral distance between small artificial pupils are accompanied by equivalent changes in chromostereopsis (Owens and Leibowitz 1975; Simonet and Campbell 1990a; Ye et al. 1991). Thus, it is well established that chromostereopsis can be explained in terms of transverse chromatic aberration for small pupils.

Chromostereopsis is often enhanced by spectacles containing chromatically uncorrected lenses. Viewing a display through prisms also increases the chromatic aberration in the retinal images. Thus, if blue and red patches are viewed through base-in prisms of about 5 dioptres the blue patch appears

closer than the red patch. When the prisms are placed base-out, the depth order of the colours is reversed. Covering the temporal half of each pupil produces the same effect as looking through converging prisms (Kishto 1965).

The red-in-front-of-blue stereopsis experienced by most people reverses to blue-in-front-of-red stereopsis at low levels of illumination (Kishto 1965). Four explanations of this effect have been proposed.

The first possibility is that it is due to an increased sensitivity of the eye to blue light relative to red light in low illumination (the Purkinje shift). Sundet (1972) disproved this theory by showing that chromostereopsis still reverses when pupil size is varied without a change in retinal illumination.

The second possibility is that reversal of chromostereopsis is due to the pupils moving in a nasal direction when they dilate in response to reduced illumination. Changes of pupil centration of about 0.2 mm occur during pupil dilation or constriction but they are very variable from person to person, tend to be the same in both eyes, and are not related to the direction of pupil change (Walsh 1988). Sundet (1976) found that chromostereopsis reversed when the diameters of artificial pupils were changed without a change in position. Thus, although lateral shifts of the pupils may affect chromostereopsis, the reversal of chromostereopsis with decreasing illumination occurs when such shifts are not present.

The third possibility is that, when the pupils dilate, the effective centre of each pupil shifts in a nasal direction with respect to its geometrical centre (Vos 1960, 1966). In the human eye, light passing through the centre of the pupil is transmitted to the retina with less loss than light passing through peripheral parts of the pupil. This is the well-known **Stiles-Crawford effect**. The exact point in the pupil through which light is transmitted most efficiently is known as the effective centre of the pupil. This can be determined by observing a flashed pattern of concentric rings reflected from the corneal surface. The foveal cones automatically align themselves with this point of maximum luminance. If we define the optic axis in terms of the effective centre of the pupil, a shift of this centre is equivalent to a shift in the optic axis. The nasalward shift of the effective centres of the pupils reverses the sign of the angle alpha for most people and thus reverses the sign of chromostereopsis. Simonet and Campbell (1990b) reported that not all changes in chromostereopsis with changing illumination level were accompanied by changes in monocular transverse chromatic aberration. However, Ye et al. (1992) found that changes in chromostereopsis with changes in pupil size were closely matched by changes in chromatic diplopia,

and chromostereopsis could be predicted accurately from transverse chromatic aberration.

A fourth possible factor is the border contrast between the coloured stimuli and the background. Verhoeff (1928) observed blue-in-front-of-red chromostereopsis when the letters were printed on white paper and a red-in-front-of-blue effect when they were printed on black paper. Dengler and Nitschke (1993) found the same transition when the colour of the background was changed. They suggested that changes in border contrast were not properly controlled by Kishto when he reduced the overall luminance of the stimuli.

The chromatic fringes seen when prisms are first put on gradually fade because of neural adaptation. However, the increased chromostereopsis remains, showing that the adaptation to the colour fringes has no effect on the optical dispersion produced by the prisms (Hajos 1962). Colourblind people experience chromostereopsis since the effect is optical in origin and has nothing to do with whether colour is correctly coded in the retina (Kishto 1965).

7.8.3 Luminance rivalry as a depth cue

An interesting phenomenon occurs with a stereogram consisting of a set of black circular rims filled with white in one eye and the same set of black rims filled with black (equivalent to black discs) in the other eye, as in Figure 7.76 (Howard 1994). The black rims fuse to form a set of holes through which are seen the rivalrous contents. This creates the impression of a black-and-white dotted surface seen through the holes. The only disparity is one that is implied between the rivalrous contents of the circles. In other words, luminance rivalry is serving as a disparity cue in its own right. This was dubbed the **sieve effect**. There are three depth effects, already described in the literature, to which the sieve effect could be related.

1. Depth can be produced by disparity between thin lines with opposite luminance polarity (see Section 6.2.10). But this works only when the opposite-polarity stereograms have a conventional horizontal disparity. Since none of the stereograms of Figure 7.76 has a disparity, the impression of depth in the sieve effect is created by the rivalry alone.

2. A random-dot stereogram with a surround region with the same dot pattern in the two eyes and a central square filled with similar dot patterns that are uncorrelated in the two eyes produces an impression of fluctuating depth, even though there is no disparity between the uncorrelated regions. O'Shea and Blake (1987) dubbed this **rivaldepth** and

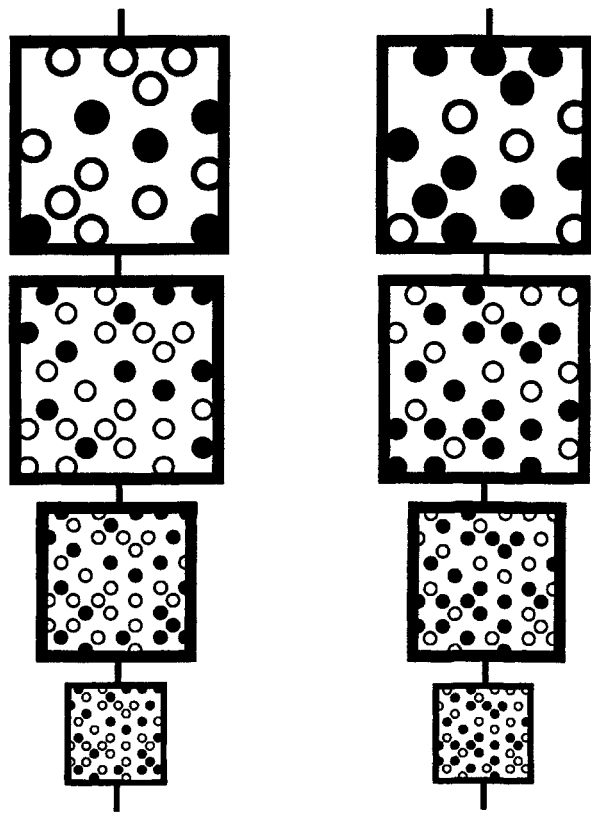


Figure 7.76. The sieve effect.

For most people, fusion of each of these displays creates an impression of a surface with holes, with a black and white surface seen through the holes. (From Howard 1994.)

found that its direction is a function of the direction of fixation disparity. This suggests that the effect is due to disparity in the nonrivalrous surround induced relative to an indeterminate disparity in the inner square. This effect cannot account for the perceived depth in the sieve effect because the sieve effect has a definite and consistent depth, even without misconvergence. Rivaldepth is described in more detail in Section 12.2.3.

3. The sieve effect could be related to Panum's limiting case. On the side of each fused disc in which the edge of the monocular white disc is on the temporal side of the adjacent binocular black rim, the stimulus configuration is similar to Panum's limiting case, in which a monocular line on the temporal side of an adjacent binocular line appears to lie beyond the binocular line (see Section 12.6.6).

However, the other lateral edge of the white disc is on the nasal side of the black rim, and this should create the impression that the monocular edge is in front of the binocular edge. According to all theories of Panum's limiting case, the inner disc should appear slanted in depth about a vertical axis. Indeed, Panum designed the stereogram shown in Figure

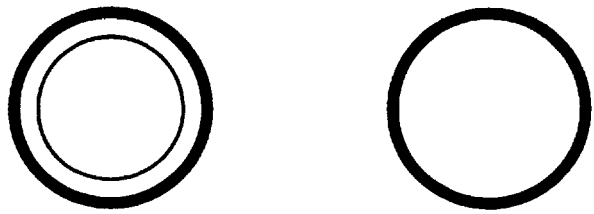


Figure 7.77. The display used by Panum (1858).

With crossed fusion of the outer circles the inner circle appears to slant about a vertical axis, right side forward. Uncrossed fusion should create the opposite effect. There is no binocular rivalry in this display.

7.77 which creates this impression, but with discs much larger than those producing the sieve effect. The sieve effect is clearly not the same as Panum's limiting case.

The sieve effect can be explained as follows. It is noted in Section 8.4.2 that rivalry within a small area shows exclusive dominance, that is, either one or another image is seen exclusively at any one time. Therefore, at any one time the contents of each fused element are seen as either white or black. Over the whole pattern, the contents of some elements will appear black and some white. A dotted surface seen through holes in a near surface creates this same proximal stimulus, as illustrated in Figure 7.78.

When the discs subtend more than about 1°, as in Figure 7.79, the rivalrous contents appear as a fluctuating silvery sheen at an indeterminate depth, an effect known as binocular lustre. This is probably because luminance rivalry in large areas does not show exclusive dominance but rather mosaic dominance or, in this case, the peculiar sensation of binocular sheen at an intermediate level of silvery gray (see Section 8.4.2).

Figure 7.80 shows that the sieve effect is replaced by indeterminate depth when the rivalrous discs are the same size in the two eyes, so that there are no binocular rims (the gray background keeps the white discs visible). This is probably because there is no longer an impression of a rimmed porthole through which the rivalrous surface is seen.

When the thickness of the black rims is increased, the sieve effect gives way to a very different impression. This is seen most clearly in Figure 7.80, in which the white discs are reduced to small spots. After a period of viewing, the white spots appear to float in depth, sometimes in front of the background and sometimes beyond it. The white spots remain in view and show dominance rivalry, rather than exclusive alternating rivalry or lustre. The spots remain visible because there are no nearby contours in the other eye to compete with them. They appear

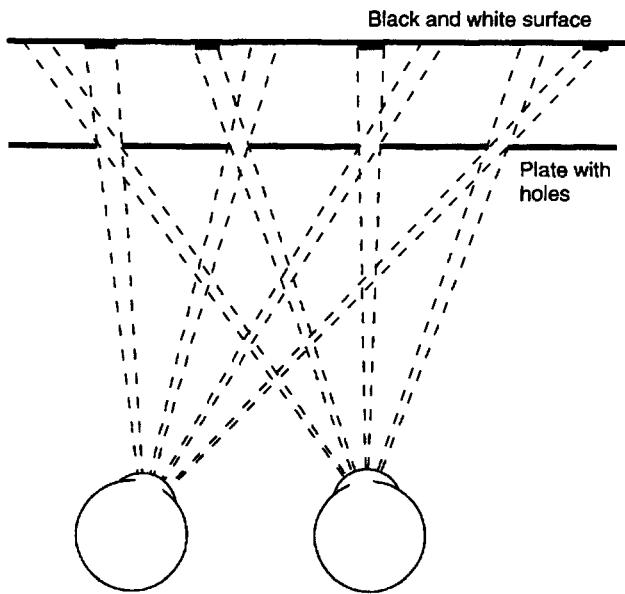


Figure 7.78. A sieve creates rivalry without disparity.
Illustrating how a black and white surface seen through holes in a near surface creates a pattern of binocular rivalry without disparity. (From Howard 1994.)

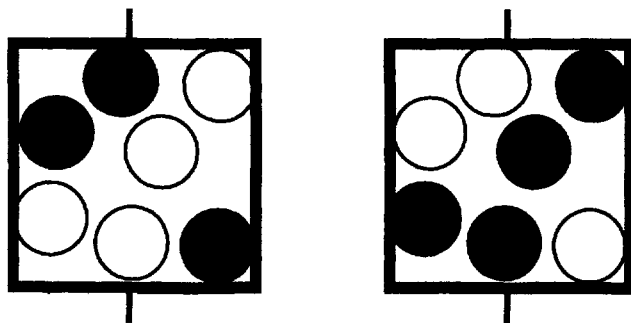
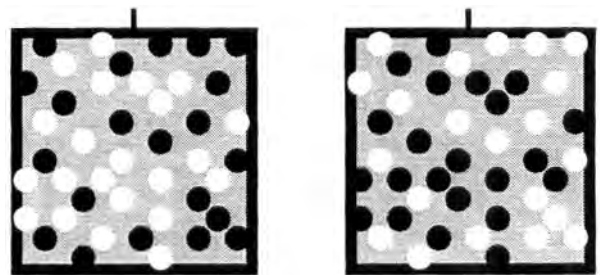


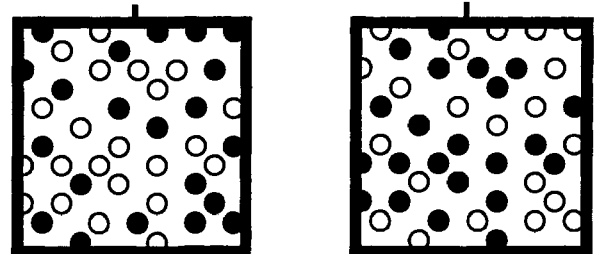
Figure 7.79. Rivalrous large discs create lustre.
Discs subtending more than about 1° create binocular lustre, rather than the sieve effect. (From Howard 1994.)

to float in space probably because of vergence instability due to the white spots having no corresponding stimulus in the other eye. The lack of a good fusion lock produces instability of vergence which causes each dot to sometimes come closer to that edge of the black disc with which it has an uncrossed disparity and at other times to come closer to the edge with which it has a crossed disparity. These disparities could account for the fluctuations in depth of the dots relative to the surround. The depth effect with small dots is not due to rivalry but to disparities induced by vergence.

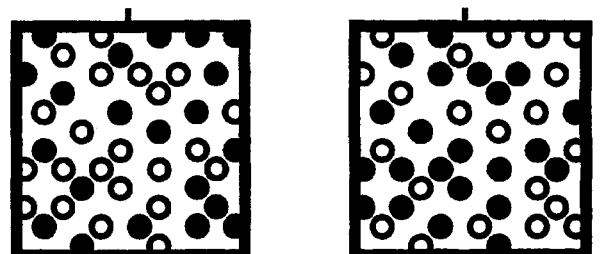
When the contrast between the rivalrous discs is decreased, as in Figure 7.81, the sieve effect is reduced or absent. This could be because, for small rivalrous regions of low contrast, exclusive rivalry is replaced by luminance mixture (Liu et al. 1992).



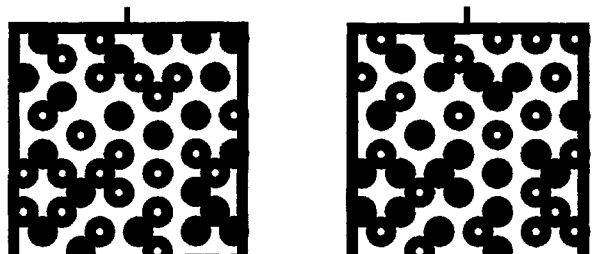
(a) With black and white discs the same size, the sieve effect is not seen clearly.



(b) White discs slightly smaller than the black discs create the sieve effect.



(c) As the white discs are reduced in size, the sieve effect is replaced by an impression of white dots in front of or behind the black discs.



(d) White discs reduced to dots no longer rival with the black discs but appear as a set of white dots in front of or behind the surrounding display. (From Howard 1994.)

Figure 7.80. Effect of relative disc size on the sieve effect.

Summary

The sieve effect occurs when monocular discs are superimposed on slightly larger binocular discs of opposite luminance polarity. The monocular discs must be within the range of sizes and contrasts for exclusive rivalry. With large discs, the sieve effect gives way to binocular lustre. If the monocular discs

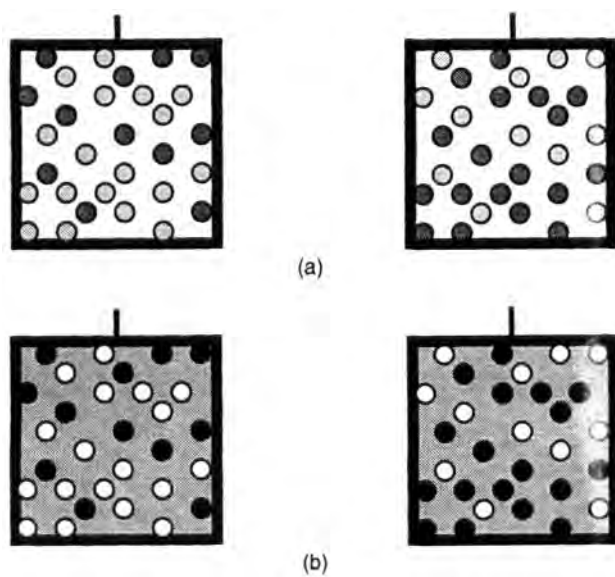


Figure 7.81. Sieve effect with reduced contrast.

The sieve effect is less impressive when luminance contrast between the rivalrous discs is reduced. The sieve effect remains strong when contrast between the discs and the background is reduced. (From Howard 1994.)

are small relative to the binocular discs, there is permanent dominance of the monocular discs, and the sieve effect is replaced by a variable-depth effect that probably depends on vergence instability.

7.8.4 Stereopsis due to unequal image illumination

When an illuminated square in dark surroundings is viewed with a neutral filter in front of one eye, the square appears slanted about a vertical axis. Münster (1941) first reported this effect and Ogle (1962) gave it the name **irradiation stereoscopy**. It can be explained in terms of irradiation, in which the brighter image is larger than the dim image (Békésy 1970). The difference in horizontal size of the images is equivalent to the horizontal disparity produced by a square slanting in depth about a vertical axis.

While irradiation stereoscopy is due to unequal image sizes which are local to each object, aniseikonia results from an overall difference in image size. In irradiation stereoscopy each illuminated area appears to slant about its own vertical axis, whereas in aniseikonia the contents of the visual field appear to slant as a whole. When a set of alternating black and white bars, like those shown in Figure 7.82, is viewed with a neutral filter in front of one eye, each white bar appears to slant about its own vertical axis making the set of bars appear like a Venetian blind. If the black bars are seen as objects, they too appear to slant but in the opposite direction, so the set of black and white bars appears like a folded screen.

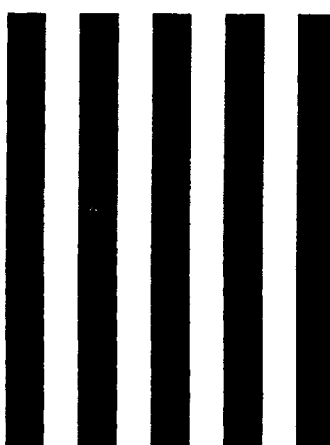


Figure 7.82. Irradiation stereoscopy.

If the display is viewed with a neutral density filter in front of one eye the images of the white bars in the well illuminated eye are enlarged relative to the images in the dimmed eye. This causes each white bar to appear slanted in depth and creates a Venetian blind or a folded screen. When the filter is placed in front of the other eye the white bars appear to slant in the opposite direction.

The direction of the folds reverses when the filter is moved to the other eye. The effect persists when the gaze moves over the display. The effect that occurs with magnification of one image of a grating requires stable fixation, and each flute of the Venetian blind involves several bars of the grating, not individual bars (see Section 7.2). Some people experience the irradiation type of Venetian-blind effect in a vertical grating with no filter. Cibis and Haber (1951) suggested that this is due to a natural difference in the illumination or focus of the eyes. They called this condition **anisopia** (see also Miles 1953). The irradiation effect should be enhanced by confining the difference in luminance to the horizontal because differences in overall image size produce little slant. This can be done by using long vertical bars rather than squares, as in the figure.

The apparent slant of a differentially illuminated square can be nulled by a change in the width of one of the images. Cibis and Haber used this procedure and found that the apparent slant of a square was approximately linear up to a filter density of 1.25, and saturated at a density of about 2.5. When a textured disc rotating in a frontal plane is viewed with a neutral filter over one eye, it appears inclined about a horizontal axis. This is a manifestation of the Pulfrich effect (see Section 13.1). At the same time, the disc appears slanted about a vertical axis because of irradiation stereoscopy (Walker 1976).

Kumar (1995) reported the effect shown in Figure 7.83 in which the left white panel appears in front of the right panel when the stereogram is fused by crossed fusion at a viewing distance of 2 m. He

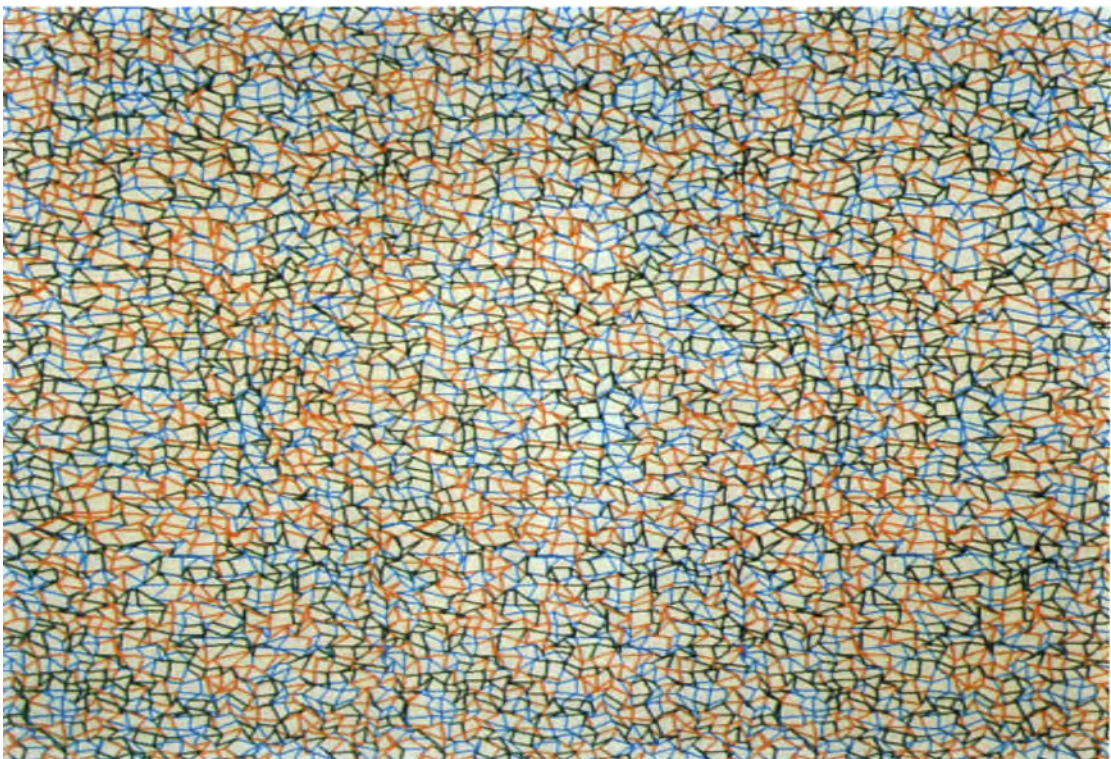


Figure 1.20. An autostereogram designed by J. Ninio.
It creates an annulus-shaped valley or ridge, according to whether it is viewed with convergence or divergence.

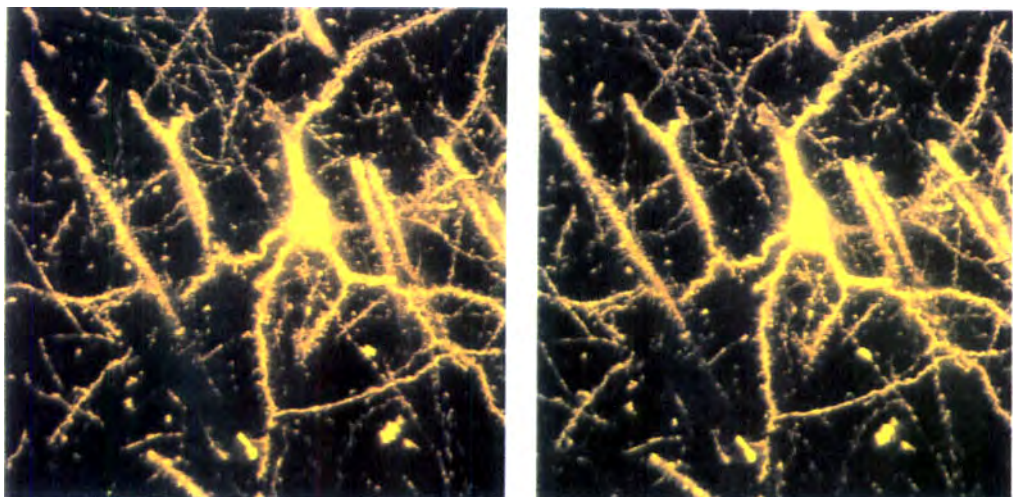


Figure 4.7c. Stereogram of a cortical pyramidal cell.
This stereogram was prepared from one of Ramón y Cajal's slides. With divergent fusion, the three-dimensional cell body and part of the apical dendrite can be seen. (From Boyde 1992.)

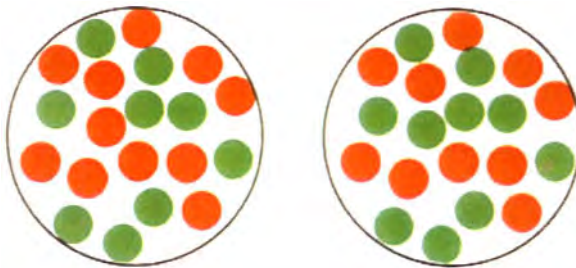


Figure 6.13d. Colour rivalry requires a serial search.
When the displays are binocularly fused, detection of the pair of discs containing rivalrous colours requires a serial search.



Figure 6.28. Stereopsis accompanied by colour rivalry.
Colour rivalry occurs between the coloured circles while disparity evokes a sensation of depth. (Adapted from Treisman 1962.)

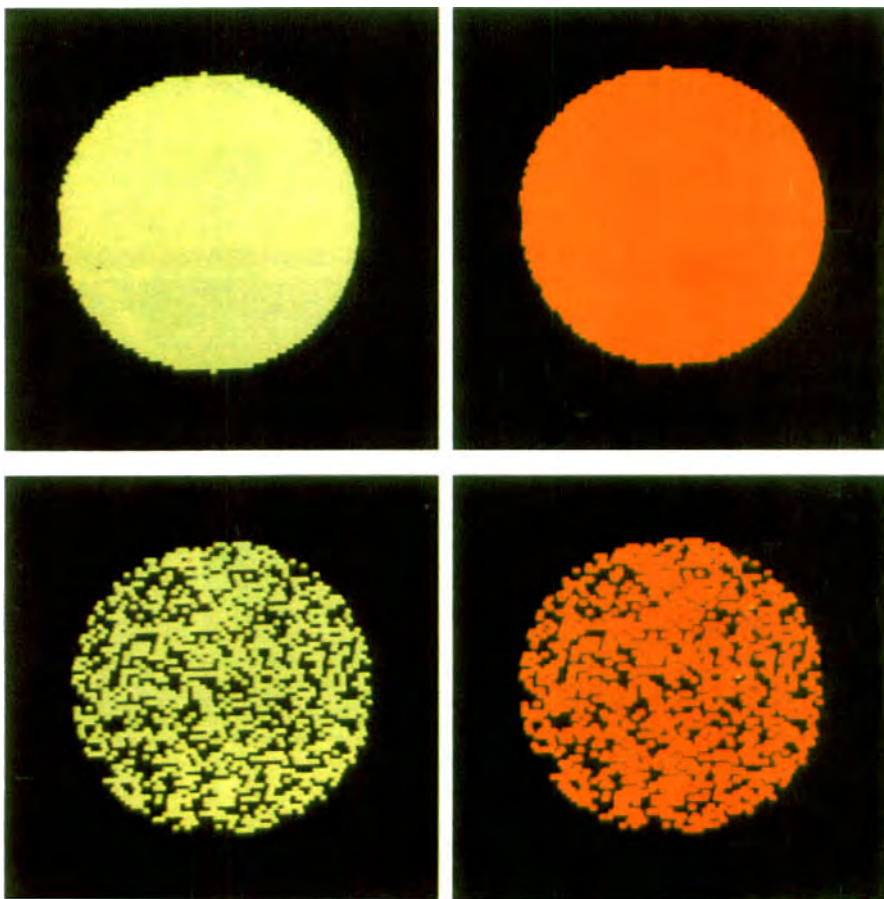


Figure 8.11. The effect of texture on colour rivalry.
The solid discs produce colour rivalry. The textured discs produce stable colour mixing.
(Reproduced with permission from de Weert and Wade 1988, Vision Research, Pergamon Press.)

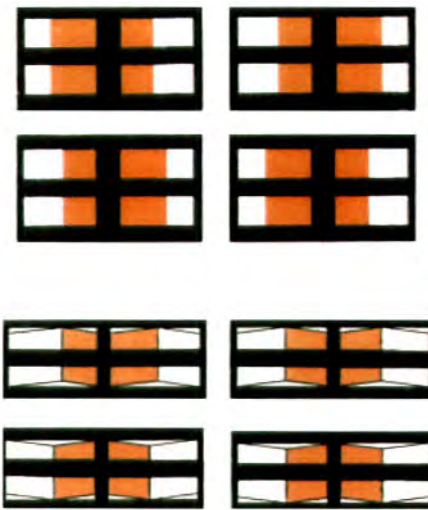


Figure 12.48. Stereopsis and surface transparency.
 (a) A stereogram producing the impression of a near transparent red square or of a far opaque red square, depending on whether the edges of the red region are seen in crossed or uncrossed disparity. In both cases the red square appears flat even though the disparity information is compatible with the perception of a corrugated surface, as depicted in (b). (From Nakayama and Shimojo 1992. Copyright, 1992, by the AAAS.)

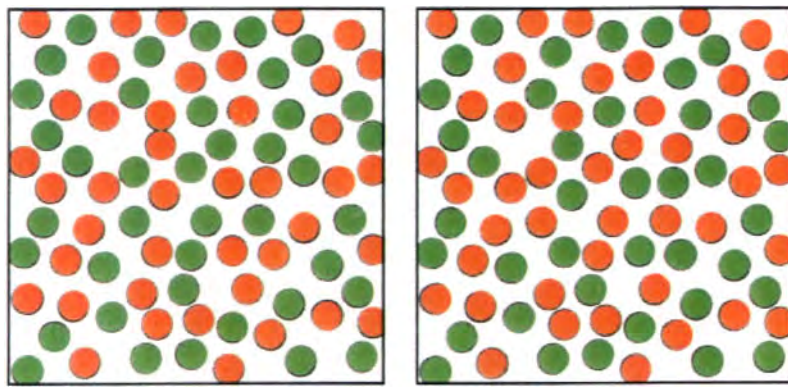


Figure 14.2a. A cyclopean shape defined by colour rivalry.
 The coloured dots are distributed randomly in each eye, with the colours in the two eyes matching in the surround but not in the central region.

This page intentionally left blank

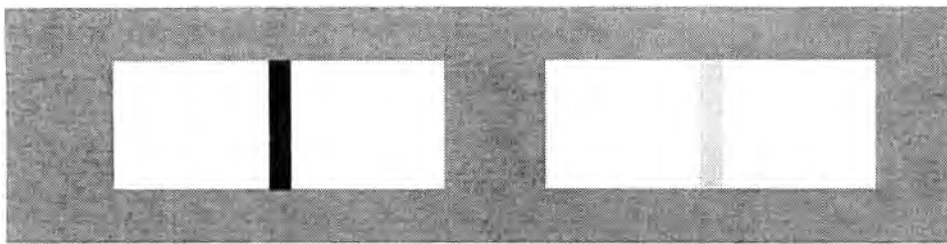


Figure 7.83. Stereopsis due to a difference in illumination.

Kumar claimed that when the stereogram is crossed fused at a viewing distance of 2 m, the left panel appears closer than the right panel. There are no disparities in the stereogram, only a difference in luminance between the images of the vertical bar. (Adapted from Kumar 1995)

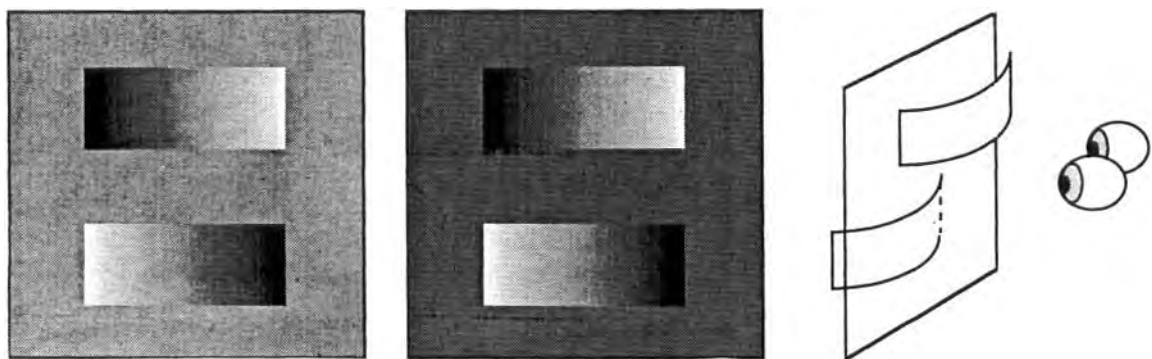


Figure 7.84. Stereopsis from contrast gradients.

The same luminance gradients are set in surroundings with different luminance to create dichoptic differences in contrasts at the ends of the gradients. After fusion, the upper and lower gradients appear displaced in depth, as depicted on the right. They may also appear curved in depth.

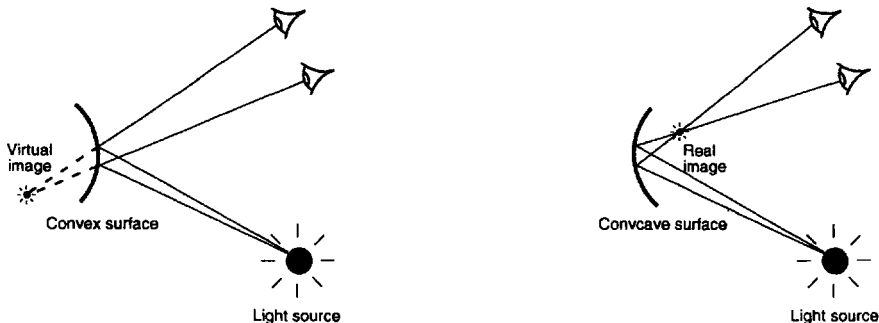


Figure 7.85. Specular disparity.

Reflection of light off a convex mirror surface (left) creates a virtual image of the light source behind the surface. Reflection of light off a concave mirror surface (right) usually creates a real image of the light source in front of the surface. (Redrawn from Blake and Bültlhoff 1990).

claimed that this effect is not due to irradiadiation but did not offer an alternative explanation.

Stereopsis from dichoptic contrast gradients

Ho and Howard recently found that depth can be created from the fusion of two luminance gradients that differ in contrast with their surroundings, as in Figure 7.84. It is suggested that the apparent centre of each gradient is shifted toward its high-contrast

end. Since the high-contrast end of the gradient in one eye is opposite that in the other, the opposite offsets of the apparent centres produces a horizontal pseudodisparity. The disparity is crossed in one pair of images relative to that in the other pair. In addition to appearing offset in depth, the centre regions appear curved in depth because of the shading.

Other aspects of stereopsis from gradients of luminance are discussed in Section 6.1.1.

7.8.5 Specularity disparity

The geometry of binocular disparity viewing means that features on a surface may be imaged in different relative positions in the two eyes. But not all luminance changes in an image are due to surface features. Gradients of luminance (shading) are created when an undulating matt surface with Lambertian reflectance properties intersects the principal direction of illumination at different angles. Moreover, the gradients of luminance will change when the angle of illumination changes. When the surface has specular properties and reflects light more in one direction than others, flat as well as undulating surfaces create gradients of luminance and the location of these gradients referred to as specularities also change their position when the angle of illumination changes. In the limit of specularity, the surface is a mirror and the angle of reflection is equal to the angle of incidence. If a specular surface is convex to the observer, the reflected light forms a virtual image behind the surface. If the surface is concave, the reflected light forms a real image which is generally (but not always) in front of the surface (Figure 7.85). Koenderink and van Doorn (1980) have analyzed the properties of specularities during the movement of the observer. Blake and Bültlhoff (1991) have extended this model to binocular viewing situations. Their analysis showed that specular relative disparities provide information about the direction and amount of curvature in a surface which any visual system could, in principle, exploit.

To test whether human observers are able to use specularity disparity, Blake and Bültlhoff (1990) conducted two experiments. In the first, the test surfaces were stereoscopic textured convex and concave ellipsoids and a convex sphere and observers adjusted the disparity of specularity to maximize the perceived glossiness of the surface. All seven observers judged the convex sphere to be most glossy when the specularity disparity was uncrossed (placing it behind the surface), as the specular stereo model would predict, and the average value of the

disparity was only slightly less than that predicted by the model.

Maximum glossiness was also reported when the specularity was positioned behind the surface for most of the trials involving the convex ellipsoids. The results for the concave surfaces, however, were not consistent with the model. Four of the observers judged the surface to be most glossy when the specularity had zero disparity (placing it on the surface) and two when it had an uncrossed disparity—in the opposite direction to the model predictions.

In their second experiment, Blake and Bültlhoff showed observers a shaded and textured surface in which all the texture elements had zero disparity. The shading and texture information was ambiguous as to whether it was generated by a convex or a concave surface. Five observers viewed a sequence of stereograms in which the specularity was either in front of or behind the surface by 5 arcmin in a random sequence and made a forced-choice decision whether the surface appeared convex or concave. At first, observers gave responses which were not consistent with the direction of the specularity but after about 20 exposures, all observers could reliably report the direction of surface curvature.

These results provide some limited evidence that the human visual system is able to use the disparity of specular reflections to judge the direction of surface curvature. However, the fact that none of the observers gave appropriate responses to the concave surfaces weakens the claim that the visual system uses the location of the specularity to signal the direction of surface curvature. Moreover, there is no evidence at present that observers are able to use the magnitude of the specularity disparity as a source of information about the degree of curvature of the surface, as the model predicts. The forced choice experiment certainly shows that observers can learn to discriminate between stereoscopic stimuli which have opposite directions of specularity disparity but this does mean that these differences actually create an impression of convexity or concavity. *Further experimentation is needed to clarify this issue.*

Binocular fusion and rivalry

8.1 Binocular fusion	313
8.1.1 Introduction	313
8.1.2 Procedures for measuring the limits of fusion	315
8.1.3 The fusion limit and eccentricity	316
8.1.4 Effects of spatial frequency and contrast	316
8.1.5 The fusion limit and stimulus interactions	317
8.1.6 Temporal factors in the limits of fusion	320
8.1.7 Vertical and orientation fusion limits	320
8.1.8 Hysteresis and plasticity of fusion limits	322
8.2 Dichoptic colour mixture	325
8.3 Stimulus determinants of rivalry	328
8.3.1 Basic phenomena of binocular rivalry	328
8.3.2 Luminance, contrast, and contour density	328
8.3.3 Relative velocity	332
8.3.4 Position on the retina	332
8.3.5 Relative orientation	332
8.3.6 Effects of eye movements	333
8.3.7 Effects of duration and temporal frequency	333
8.3.8 Monocular rivalry	334
8.4 Binocular suppression selectivity	335
8.4.1 The generality of suppression	335
8.4.2 Spatial zones of binocular rivalry	335
8.4.3 Penetration of suppressed images	337
8.4.4 Suppression and eye dominance	337
8.5 Rivalry and stereopsis	338
8.5.1 The suppression theory of binocular fusion	339
8.5.2 Two-channel and dual-response accounts	340
8.6 The site of binocular suppression	341
8.6.1 Suppression and spatial-frequency	341
8.6.2 Suppression and visual motion	343
8.7 Models of binocular rivalry	344
8.8 Neurology of binocular rivalry	345
8.9 Cognition and binocular rivalry	347
8.9.1 Voluntary control of rivalry	347
8.9.2 Binocular rivalry and meaning	347

8.1 BINOCULAR FUSION

8.1.1 Introduction

Since the time of the Greeks there has been a long history of speculation and argument about how the inputs from the two eyes combine to form a unified impression of the visual world. Before 1838, the year Wheatstone demonstrated that binocular disparity plays a crucial role in depth perception, the dominant problem associated with binocular vision was that of explaining how a single unified visual

percept is formed from the inputs from two eyes. It had been realized since the time of Aristotle and Euclid that the two eyes have slightly different views of the world and a few people had suggested that this contributes to the perception of depth (See Section 1.2.2). However, this aspect of binocular vision was generally ignored and discussion centred on the problem of how the images from two eyes combine to produce the impression of a single percept. There were two types of explanation. According to the **fusion theory** of binocular combination, dissimilar images engage in alternating suppression

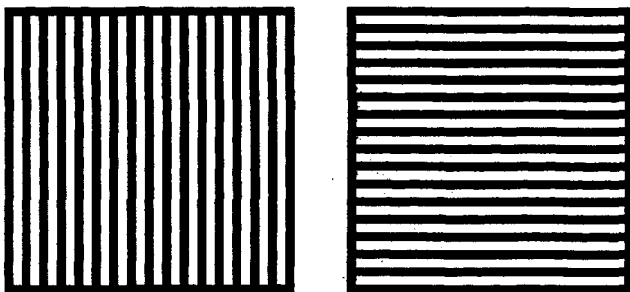


Figure 8.1. Rivalry from orthogonal gratings.

Orthogonal gratings, stereoscopically combined, exhibit mosaic rivalry. The horizontal lines dominate in one location, the vertical lines in another. Areas of dominance constantly fluctuate.

but similar images falling on corresponding retinal locations gain access to the visual system at the same time and form a unitary visual impression. According to the **suppression theory**, both similar and dissimilar images from the two eyes engage in alternating suppression at a low level of visual processing.

In the fusion theory the two images are said to fuse, although it is not always clear what this term implies. Except under special circumstances the two inputs are not simply summed, since that would mean objects would look twice as bright when viewed with two eyes as when viewed with one. Nor is the identity of each signal lost in the fusion process, since that would mean images with crossed disparity could not be distinguished from those with uncrossed disparity. We will take the term **fusion** to mean that similar images presented to the two eyes appear as one and are processed simultaneously rather than successively. Even if we admitted that similar images are fused and processed simultaneously, the following two questions remain. Where in the nervous system does fusion occur? What rules of combination are involved in the fusion process? Many investigators, including Helmholtz, believed that fusion is a mental, or psychic, act. In modern terms we would say that it occurs at a higher, or cognitive, level of processing. Since 1959, when Hubel and Wiesel discovered binocular cells in the primary visual cortex, most investigators believe that the experiential fusion of similar images and the processes by which binocular differences between them are extracted occur at this level. We will see that rivalry between nonsimilar images may not be confined to this level. Most recent work on this topic has been concerned with the stimulus conditions that produce fusion.

According to the suppression theory of binocular vision, superimposed images from the two eyes always rival by mutual inhibition, even when they are identical. It is claimed that, in any location in the

visual field, only one eye's input is seen at any one time, but the eye that dominates varies from place to place and alternates over time, resulting in a mosaic of alternating dominance and suppression. Both the fusion and suppression theories agree that images in the two eyes tend to rival when they are very different in spatial or temporal characteristics. Thus, when one eye views a horizontal grating while the other eye views a vertical grating, as in Figure 8.1, only one grating is seen at any one time in a given region. The two images compete for access to higher levels of visual processing by a process of alternating inhibition. This is the phenomenon of **binocular rivalry**. We will see later that that two rivalrous stimuli are both processed up to a certain stage. Binocular rivalry is visible when the two images differ; the fusion and suppression theories make the same predictions under these circumstances. The predictions differ only when the images are similar. However, one cannot apply a direct test of the suppression theory when the images are the same, since any rivalry that may occur would not be visible.

In spite of this difficulty it has now been established by an indirect test that similar images do not inhibit each other in the manner required by the suppression theory (see Section 8.5.1). When the images from corresponding regions in the two eyes are identical, information from both, albeit in altered forms, is passed on to higher visual processes to give rise to an impression of a fused image. When the images from corresponding regions differ in an appropriate way, they fuse but the disparities are registered and produce an impression of depth. When the images from corresponding regions are very different, they rival so that only one of them gains access to higher stages of visual processing at any one time in any one location. Thus, similar and dissimilar binocular images are processed in fundamentally different ways. This difference in processing does not occur immediately.

Several investigators have noticed that rivalrous stimuli form a combined percept when presented for less than 200 ms. This suggests that both similar and dissimilar stimuli are initially processed simultaneously and then segregate into those that remain fused and are processed simultaneously, and those that rival and are processed sequentially. We will also see that low-contrast dissimilar stimuli do not rival, even when exposed for some time. Furthermore, the segregation between stimuli that fuse and those that rival is not complete, even for long-duration and high-contrast stimuli. Thus, some low-level features of a suppressed image can affect the processing of the dominant image and, on the other hand, the fusion process involves both inhibitory

and excitatory processes. Thus, the actual processes underlying binocular vision are more complex than either the fusion theory or suppression theory suggest. The evidence for these statements is now reviewed.

8.1.2 Procedures for measuring the limits of fusion

In the eleventh century Alhazen noticed that images of an object continue to appear single when they do not fall exactly on corresponding visual lines. In his *Treatise of Optics*, written in 1775, Harris wrote, "An object that is a little out of the plane of the horopter, may yet appear single." (p. 113). Wheatstone (1838) also noticed that images in a stereoscope fuse even though they do not fall exactly on corresponding points. Thus, when a small point of light is presented to a given location in one eye, it fuses with a similar point of light presented to the other eye as long as one point falls within a certain area centred on the other. This area is known as **Panum's fusional area**, after Peter Ludvigh Panum, Professor of physiology at Kiel, who described the first systematic experiments on the effect in 1858 (see Section 1.2.2). The fusional range is larger for stimuli separated horizontally than for stimuli separated vertically, thus making fusional areas elliptical (Panum 1858; Ogle and Prangen 1953). However, at least part of this difference may be due to asymmetries in vergence eye movements (Mitchell 1966b).

The terms **diplopia threshold** or **fusion limit** denote the largest retinal disparity between two images for which the impression of a single fused image can be maintained. For a given direction of image separation, the diameter of Panum's fusional area is the sum of the diplopia threshold for crossed disparity and that for uncrossed disparity. The diplopia threshold is not always symmetrical; for some subjects it is greater for uncrossed images while for others it is greater for crossed images. An asymmetry would result if the subject were not correctly converged on the fixation target. Therefore, these asymmetries must, at least in part, reflect the effects of fixation disparity. The relationship between the fusion limit and fixation disparity is discussed in Section 10.2.4. Richards (1971a) concluded that asymmetries of the fusion limit are not due only to fixation disparity but also reflect the independent processing of crossed and uncrossed images. The size of the fusional area depends on many factors such as retinal eccentricity, stimulus duration, the presence of surrounding stimuli, and the criterion for single vision adopted by the subject. Reported values have ranged from a few minutes of arc to several degrees.

The most commonly used procedures for measuring fusion limits are the method of adjustment and the method of limits. The subject or experimenter gradually increases the disparity in fused dichoptic stimuli until the subject reports diplopia. Then, starting with the stimuli well separated, disparity is decreased until the subject reports fusion. As we will see, there is a hysteresis effect so that the disparity at which two images appear double when initially fused is greater than the disparity at which they fuse when initially seen as double. It is difficult to control vergence eye movements with the method of adjustment. Nonius lines indicate changes in vergence but introduce extra stimuli that may contaminate the measurements, since fusion limits are known to be affected by neighbouring stimuli. In the method of constant stimuli, the subject aligns nonius lines just before the disparate stimuli are presented briefly. Stimuli with different disparities are presented in random order, and a psychometric function of percentage of "single stimulus" judgments against disparity is plotted. The diplopia threshold is conventionally defined as the point on the psychometric function where 50 per cent of the judgments are "single stimulus" judgments. This method has the advantage that stimuli can be presented for a duration too short to evoke vergence eye movements. However, brief exposure introduces a temporal transient into the stimuli and, as we will see later, Panum's area is increased when stimuli are rapidly alternated in disparity. In a criterion-free, forced-choice procedure subjects are asked to discriminate between a pair of disparate stimuli and a spatially adjacent or subsequently presented pair of stimuli with zero disparity. The disparity giving 75 per cent accuracy is generally taken as the threshold.

Finally, there is the problem of the criterion used in judging diplopia. When the horizontal limits of fusion are being measured, one must ensure that subjects are judging fusion rather than apparent depth between the disparate stimuli. This is a severe problem with the forced-choice procedure because subjects tend to rely on apparent depth if that is the only difference they see. However, apparent depth is not a problem when the vertical limits of fusion are being measured. In monocular resolution, as two lines are moved further apart, the first sensation is of a single line becoming thicker. Similarly, a thickening of dichoptic stimuli may be noticed before fusion is lost (Heckmann and Schor 1989b). Also, as dichoptic stimuli are separated, there comes a point where edges of opposite luminance polarity are superimposed. This may evoke a sensation of binocular lustre or rivalry. If the two stimuli rival, an apparent change in position may occur. Generally,

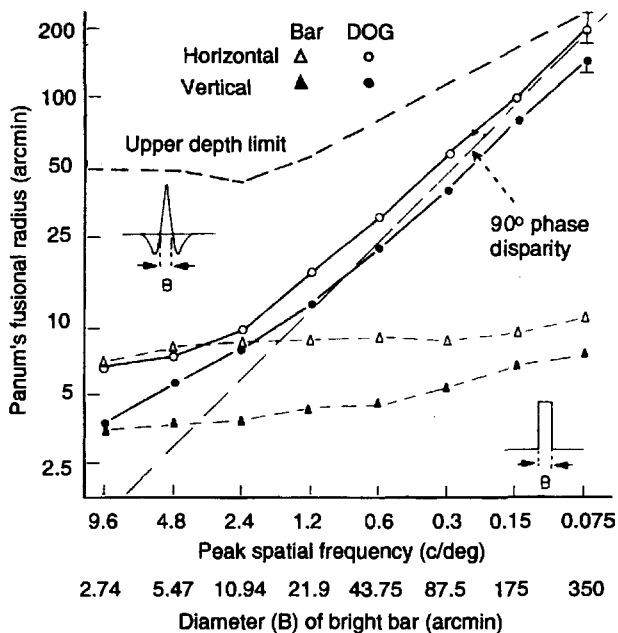


Figure 8.2. Fusion limits and spatial frequency.

The diplopia threshold (radius of the fusional area) as a function of the peak spatial frequency of two Gaussian patches (spatial bandwidth 1.75 octaves) and of the width of two bright bars. For patches with a spatial frequency below about 1.5 c/deg, the diplopia threshold corresponds to a 90° phase shift of the stimulus, indicated by the dotted line. The fusion limit for the bars remains the same as that of the high spatial frequency patch. (Reproduced with permission from Schor et al. 1984, Vision Research, Pergamon Press.)

experimenters who allowed subjects to use criteria other than diplopia obtained smaller fusion limits than those obtained by experimenters who insisted on the criterion of diplopia.

8.1.3 The fusion limit and eccentricity

It is difficult to measure the diplopia threshold when the stimulus is more than about 10° away from the fovea. Nevertheless, all investigators agree that the threshold increases with increasing eccentricity. In studies reviewed by Mitchell (1966b), there were wide variations in the rate of increase and the shape of the function. In an experiment by Palmer (1961), the subject fixated between two marks 40 arcmin apart. A test spot 1.5 arcmin in diameter was presented for 10 ms with various disparities. The fusion limit was about 10 arcmin in the fovea and increased to about 30 arcmin at an eccentricity of 6°. Mitchell (1966a) reported a similar dependence on eccentricity.

Crone and Leuridan (1973) found that beyond an eccentricity of 10°, the diplopia threshold increased in proportion to horizontal eccentricity and was on average about 7 per cent of the angle of eccentricity.

This means that, on average, a person can tolerate a 7 per cent aniseikonia without experiencing diplopia. Ogle (1964) reported a value of 6 per cent. Hampton and Kertesz (1983b) found that the diameter of the fusional area increased linearly with horizontal eccentricity with a slope of approximately 0.13° per degree of eccentricity. This rate of increase with increasing eccentricity is similar to the rate of increase of the magnification factor, as determined by Rovamo and Virsu (1979) in the human visual cortex. There is evidence that the diameter of the fusional area increases less rapidly along the vertical meridian than along the horizontal meridian (Ogle and Prangen 1953).

We will see later that the fusion limit for a pair of images is smaller when other images are nearby. In studying the fusion limit as a function of eccentricity, the subject fixates a binocular stimulus to hold vergence constant while the test stimulus is moved into more peripheral positions. The increase in the fusion limit with increasing eccentricity may therefore be at least partly due to the increasing distance between the fixation stimulus and the test stimulus. Levi and Klein (1990) described a procedure for unconfounding the effects of eccentricity and separation in the measurement of vernier acuity. The procedure could be adapted for measurement of stereo acuity. *The independent effect of increasing eccentricity could be measured by placing a zero-disparity stimulus at a fixed distance from the test stimulus as the test stimulus is moved into the periphery. The zero-disparity stimulus could be an annulus around the test stimulus. The independent effect of changing image proximity could be measured by changing the separation between two stimuli on the circumference of a circle centred on the fixation point.*

8.1.4 Effects of spatial frequency and contrast

Several investigators have reported that the fusion limit is greater for gratings of low spatial frequency than for those of high spatial frequency.

Schor et al. (1984b) used vertical bars with a difference of Gaussian (DOG) luminance profile, with a spatial-frequency bandwidth of 1.75 octaves at half height, superimposed on a small fixation spot. Nonius lines were used to check for changes in vergence, which were claimed to be less than 1 arcmin. Subjects adjusted the disparity between two patches until they noticed an increase in width, a lateral displacement, or a doubling. The results are shown in Figure 8.2, where it can be seen that the fusion limit (radius of the fusional area) increased as the spatial frequency of the stimulus decreased. The fusion limit in the vertical direction was consistently smaller than in the horizontal direction. Below a

spatial frequency of about 1.5 c/deg, the limit of fusion corresponded closely to a 90° phase shift of the stimulus, indicated by the diagonal line. When the measurements were repeated with both Gaussian bars presented to one eye, the results also fell on the diagonal line. This is not surprising, because a 90° phase shift is the Rayleigh limit for monocular resolution (see Section 3.5.2). They concluded that, at low spatial frequencies the limit of binocular fusion is determined by the same factors that determine monocular grating resolution.

Both these limits are much coarser than acuity for vernier offset (Heckmann and Schor 1989b). Note that Schor et al. used a liberal criterion for the limit of fusion; even a slight thickening or displacement of the stimulus counted as diplopia. Perhaps the binocular and monocular limits would not match with a stricter criterion for diplopia. For spatial frequencies over about 2.4 c/deg, the horizontal fusion limit levelled off to a value between 5 and 10 arcmin. Thus, for high spatial frequencies, the Rayleigh limit of 90° phase-shift detection ceases to be the limiting factor for diplopia resolution but not for monocular resolution. In fact, in this study and that of Schor et al. (1989), the fusion limit at the highest spatial frequencies was between three and six times the width of the centre of the DOG, as depicted in Figure 8.2. Presumably the spatial resolution of dichoptic stimuli is determined by some factor other than the limit for monocular resolution.

These results emphasize the special properties of the fusion process at high spatial frequencies and pose a challenge for current theories of the underlying neural mechanism. The experiment was repeated with sharp-edged bars with widths and luminances equal to those of the bright central component of the DOG patterns. It can be seen from Figure 8.2 that the fusion limits for the bars resembled those for the narrowest Gaussian pattern, suggesting that subjects were using the edges of the bars (the highest spatial-frequency component) to make their judgments. On the other hand, Woo and Reading (1978) found diplopia thresholds for single bars were lower than monocular resolution thresholds for the same bars.

The dependence of the fusion limit on the highest visible spatial-frequency component of a stimulus might arise because, for a given contrast, high spatial-frequency stimuli have a steeper luminance gradient than low spatial-frequency stimuli. Schor et al. (1989) investigated this issue using a criterion-free, forced-choice procedure in which subjects had to decide which of two horizontal sine-wave gratings contained a vertical disparity. Note that this procedure forced subjects to use any available cue, including thickening and displacement of lines, as

well as diplopia. However, they could not use stereo depth because the gratings were horizontal. The fusion limit was measured for each of several spatial frequencies at each of several contrasts. The logic was that if spatial frequency is the crucial factor rather than the luminance gradient, then changing the contrast for a fixed spatial frequency should have no effect. But if contrast or the luminance gradient are crucial factors, then changing contrast should have an effect, since halving the contrast halves the luminance gradient for a sinusoidal grating of fixed spatial frequency. The results showed almost no effect of changing contrast across a range of spatial frequencies from 0.4 to 3.2 c/deg, a result confirmed by Heckmann and Schor (1989b). Furthermore, the fusion limit was not affected by a change in luminance gradient produced by adding a low spatial-frequency component to the sine-wave gratings, even when the added component had the higher contrast. They concluded that binocular fusion is based on information in independent spatial-frequency channels rather than on the overall luminance distribution. We saw in Section 6.1.1 that matching of disparate images for the detection of stereo depth can involve the overall luminance distribution of the images under certain circumstances and spatial-frequency components under other circumstances. Schor et al. argued that the fusion limit is not affected by changes in contrast because a change in contrast has the same effect on binocular cells that register fused images as on monocular cells that register diplopic images. The effect of contrast thus cancels out. We saw in Section 5.6 that stereoacuity is adversely affected by a reduction in contrast. This is presumably because the detection of disparity upon which stereoacuity is based depends only on binocular cells. Certainly, the effects of contrast and spatial frequency on diplopia detection are not the same as their effects on disparity detection.

Changes in stimulus luminance of up to 3 log units above the value at which the stimuli are difficult to see also have little effect on the fusion limit (Siegel and Duncan 1960; Mitchell 1966a).

8.1.5 The fusion limit and stimulus interactions

Helmholtz (1909) had noticed that disparate points are less likely to fuse with other objects nearby. The two lines in Figure 8.3a readily fuse when convergence is held on the surrounding circle. At a viewing distance of 50 cm the lines have a disparity of about 10 arcmin. When a second pair of lines with the same magnitude of disparity is added, as in Figure 8.3b, the lines no longer fuse. By independently varying the distance between the pairs of lines in

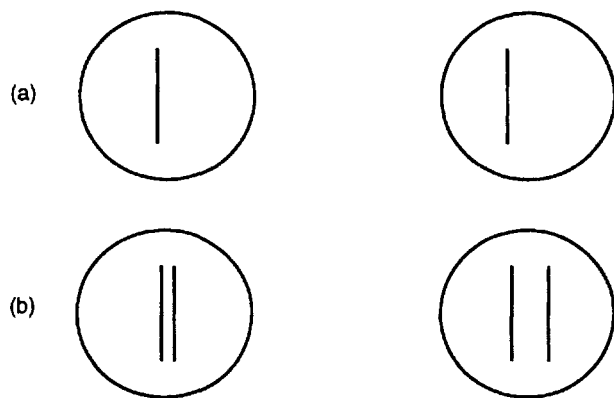


Figure 8.3. Effects of lateral spacing on fusion.

(a) The vertical lines fuse when the eyes converge on the circle.
 (b) When a second pair of lines with the same disparity with respect to the circles is added, the lines no longer fuse. At a viewing distance of 30 cm, the lines have a disparity of 18 arcmin.
 (Adapted from Braddick 1979.)

one eye and the distance between disparate images in the two eyes, Braddick (1979) demonstrated that the crucial factor limiting fusion for a given disparity is the monocular spacing of the images rather than the presence of competing disparate images. Contaminating effects of changing vergence were avoided by having subjects align nonius lines before the displays were exposed for only 80 ms—too short a time for vergence movements to occur.

Braddick also showed that the reduction in the fusion limit is most evident when the closely spaced monocular images are parallel, vertically aligned, and equal in length. It is as if two closely spaced lines in one eye evoke responses in detectors of smaller spatial scale than those evoked by a single line. Thus, diplopia detection proceeds within a system of higher spatial resolution when this finer system is recruited.

Tyler (1973) quantified the limits of spatial interactions for fusion and first established a gradient limit for fusion. The difference in disparity between two points divided by the mean angular separation of the images is the disparity gradient. The geometry of disparity gradients was discussed in Section 2.3.3. Points lying on a visual line of one eye have a disparity gradient of 2, and those lying on a line that passes through the point midway between the eyes have a disparity gradient of infinity. Burt and Julesz (1980) found that the disparity limit for maintained fusion of two points decreased as the angular separation between that pair and a fused pair of points decreased. This phenomenon is illustrated in Figure 8.4. Two dichoptic images do not fuse when the disparity gradient with respect to a neighbouring fused pair of images exceeds a value of about 1. Thus, in the bottom rows in Figure 8.4a, the

disparity gradient is steeper than 1 and, although the members of the fixated pair of dots fuse, those of the other pair remain separate.

Note that, in Figure 8.4a, the fused pair of dots in the bottom rows lie more or less between the unfused dots, as illustrated in the two columns of dots on the left. Perhaps this spatial intrusion of the fused pair between the unfused pair prevents the flanking pair from fusing. This factor is absent in Figure 8.4b because the two disparate points are both to one side of the fused points. Burt and Julesz referred to the orientation of the disparity gradient as the dipole angle. In Figure 8.4a the dipole angle is 90° and in Figure 8.4b it is close to 0°. The largest disparity gradient for which the nonfixated images could be fused was found to be independent of the dipole angle. Given that the disparity gradient limit for fusion is 1, it follows that each fused object in the visual field creates a surrounding forbidden zone, as illustrated in Figure 8.5. Within this zone, the disparity gradient is greater than 1 and fusion of disparate images does not occur, unless the disparity is vanishingly small. Prazdny (1985b) confirmed that the limiting disparity gradient is 1 for similar stimulus elements but found that the largest disparity gradient for fusion increased to 1.4 when the objects differed in size and to over 2 when the objects also differed in luminance polarity. Thus, more interaction occurs between similar objects than between less similar objects.

Wilson et al. (1991) measured the effects of a background grating of one spatial frequency on the fusion limit of small vertically elongated D6 Gaussian patches, as shown in Figure 8.6. Each Gaussian patch had a spatial bandwidth of 1 octave with a centre spatial frequency that varied between 0.5 and 12 c/deg. The righthand patches had zero disparity and the lefthand patches were presented with variable disparity. Subjects fixated between the patches and the stimuli were presented for 165 ms. Subjects reported whether or not the lefthand patches were fused. The diplopia threshold decreased about 3.9 times when the patches were superimposed on a grating with a spatial frequency twice that of the Gaussian patches but was not affected by a grating with a spatial frequency four times that of the patches. Further tests revealed that coarse spatial scales constrained disparity processing in fine scales, but fine scales did not constrain processing in coarse scales. These effects cannot be due to changes in vergence since the stimuli were presented only briefly. They were found not to depend on the spatial phase of the test patches relative to that of the background grating but did depend on the test and background stimuli having the same orientation. Wilson et al.

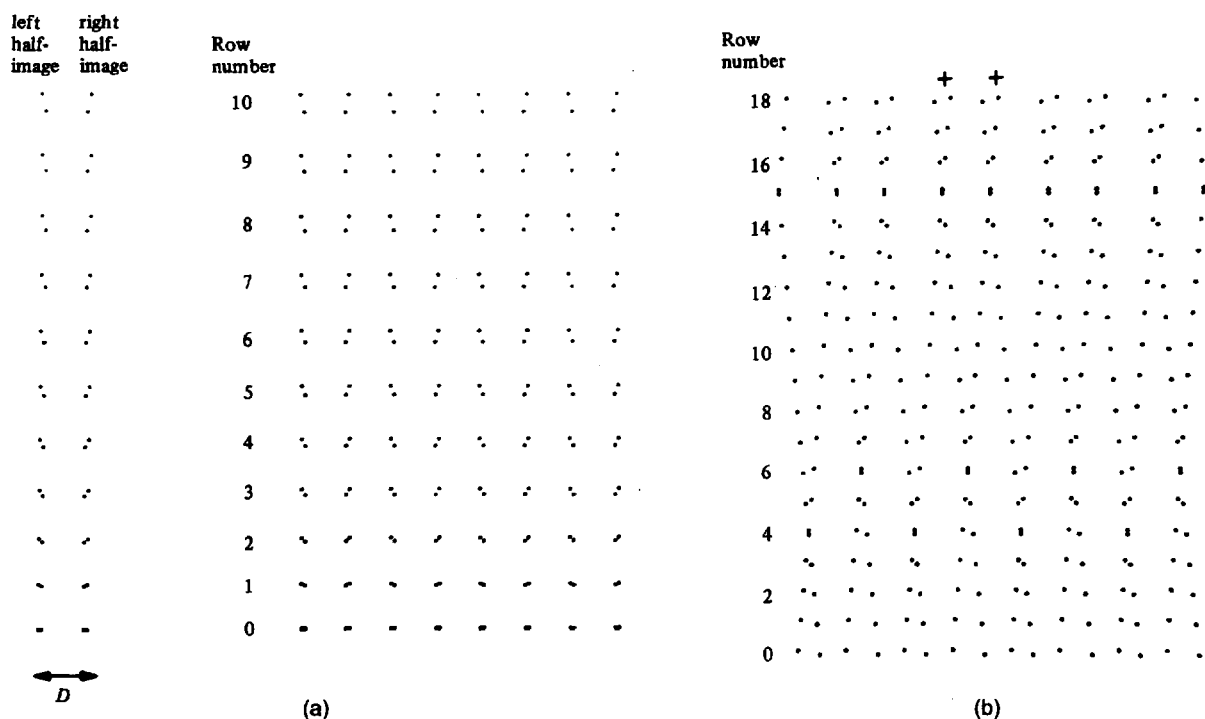


Figure 8.4. The disparity-gradient limit for binocular fusion.

(a) Diverge or converge to fuse neighbouring columns of dots, as shown in the inset on the left. If the lower pair of dots is fused in each set of four dots, the upper pair fuses only if the disparity gradient is not higher than about 1. The disparity gradient increases down the rows and may be calibrated for a given viewing distance. The disparity-gradient limit for fusion can then be determined by reading off the row number at which fusion of the upper pair of dots fails.

(b) The disparity gradient is horizontal rather than vertical. (From Burt and Julesz 1980, Perception, 9, 671-682, Pion, London.)

concluded that binocular disparities are processed in at least three distinct spatial-frequency channels, each with subchannels for near (crossed), zero, and far (uncrossed) disparities. To account for their data, they postulated that far and near cells inhibit far and near cells, respectively, in the next higher spatial-frequency channel and that zero-disparity cells inhibit both near and far cells in the next higher spatial-frequency channel. They argued that these effects could be accomplished by inhibitory feedback suppressing an appropriate subset of monocular inputs.

Scheidt and Kertesz (1993) conducted a similar experiment with an induction stimulus consisting of D10 Gaussian patterns in a 5° circular area around a central fixation point and a similar test pattern in a larger annulus around the induction stimulus. The inner area and the surrounding annulus were separated by a 0.5° ring. Both sets of patterns had a peak spatial frequency of 0.75 c/deg, but the disparity of the induction stimulus varied from trial to trial between ±15 arcmin. When the stimuli were exposed

simultaneously for 167 ms, the fusional range of the test stimuli was reduced relative to a condition in which the induction stimulus was an evenly illuminated area. These results essentially confirm those obtained by Wilson et al. for this spatial frequency. However, when the stimuli were exposed continuously, the fusional range of the test stimulus was reduced only in the presence of an induction stimulus with uncrossed disparity. Scheidt and Kertesz proposed that interactions between fusional stimuli have a fast, wholly inhibitory, component and a slow component that is inhibitory or facilitatory, depending on whether the disparities in the interacting stimuli have the same or opposite signs.

The effects of the disparity gradient and of the spatial frequency of superimposed gratings are presumably aspects of the same underlying mechanism. The mechanism ensures that when stimuli of different spatial scale are crowded together, detectors of small spatial scale are devoted to the analysis of disparity between finer elements of the stimulus. This ensures that the fusion mechanism does not

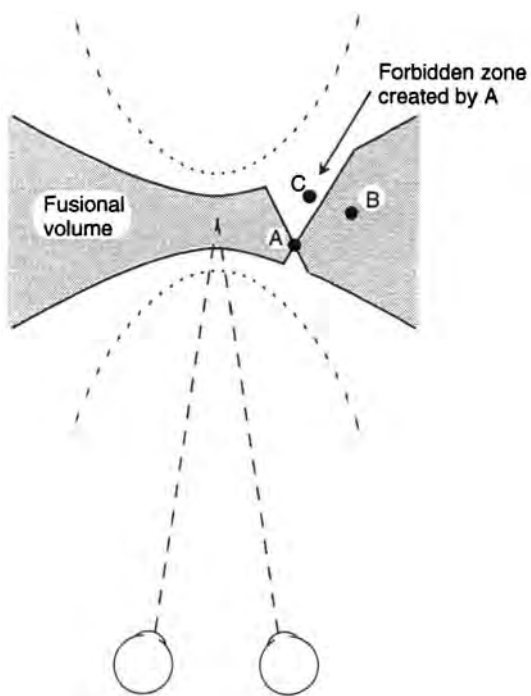


Figure 8.5. Disparity-gradient limit for fusion.

Given that the disparity-gradient limit for fusion is 1, a fused object in the visual field, such as object *A*, creates a surrounding zone within which the disparate images of a second object, such as *C*, will not fuse. The images of object *B* fuse in the presence of *A*, since *B* is outside the "forbidden" zone created by *A*. The dotted lines represent the disparity limits for stereopsis. (Adapted from Burt and Julesz 1980, Perception, 9, 671-682. Pion, London.)

combine distinct parts of a complex stimulus pattern. We discuss spatial-frequency interactions in stereoscopic acuity in Sections 5.7 and 8.6.1.

8.1.6 Temporal factors in the limits of fusion

There has been some dispute about the effects of stimulus duration on the fusion limit. Mitchell (1966a) found that the fusion limit for horizontal disparity was unaffected by increasing exposure time from 10 to 120 ms. Palmer (1961) reported similar findings. Duwaer and van den Brink (1982b) found that the diplopia threshold for vertical disparity in one subject decreased from about 10 arcmin to about 6 arcmin as exposure time was increased from 20 to 200 ms. Woo (1974a) found that the mean horizontal diameter of the fusional area of three subjects for a short vertical line increased from about 2 to 4 arcmin when the duration of exposure increased from 5 to 100 ms. The reasons for these contradictory findings remain obscure.

Woo (1974b) presented two 10-ms dichoptic stimuli sequentially with various intervals of time

between them. The diplopia threshold was not affected until the delay was between 30 and 40 ms. With longer delays the stimuli began to be seen as discrete temporal events.

Schor and Tyler (1981) explored the dependence of fusional limits on the spatiotemporal properties of the stimuli. In investigating horizontal fusion limits, they presented two vertical wavy lines dichoptically with opposite phases of the waves in the two eyes. From trial to trial they changed the horizontal disparity between the aligned peaks of the waves by changing the amplitude of the waves. Two sets of these lines were placed 0.5° on either side of a fixation cross (Figure 8.7). To measure vertical fusion limits the lines were horizontal. The spatial frequency of the waviness of the lines varied between 0.125 and 2.0 c/deg. The sign of the disparity of the dichoptic lines reversed at temporal frequencies between 0.1 and 5 Hz. At any instant, the disparity of the lines on one side of the fixation cross was opposite to that in the lines on the other side. This reduced any tendency to change convergence. They determined the amplitude of disparity modulation at which diplopia became apparent for each spatial and temporal frequency of disparity modulation. The results are shown in Figure 8.8. The horizontal width and vertical height of the fusional area increased as the spatial frequency of the waviness of the stimulus decreased. With low spatial-frequency lines the horizontal fusion limit, but not the vertical fusion limit, decreased with increasing temporal frequency. This effect was very small with high spatial-frequency stimuli.

8.1.7 Vertical and orientation fusion limits

Nielsen and Poggio (1984) measured the degree of vertical disparity that subjects could tolerate before being unable to detect depth in a random-dot stereogram. Subjects fixated a point which was switched off just before the stereogram was exposed for 117 ms. Vertical disparities of up to about 3.5 arcmin could be tolerated in the central region of the stereogram and of up to about 6.5 arcmin in the stereogram as a whole. The tolerance for vertical disparity was slightly extended when monocular cues to the horizontal disparity within the stereogram were visible. It is not clear from this report whether subjects experienced diplopia at the point where depth discrimination broke down.

When superimposed dichoptic lines are tilted in the frontal plane in opposite directions about their point of intersection, they are eventually seen as double. The angle at which they appear double can be called the fusion limit for orientation disparity.

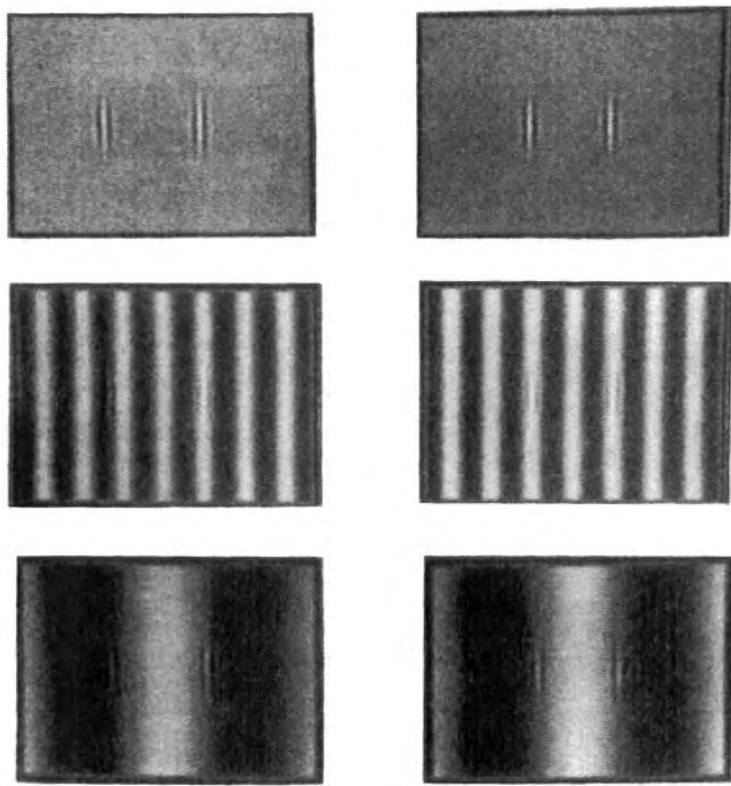


Figure 8.6. Fusion limit and superimposed spatial frequencies.

The top stereogram is a pair of D6 patches with a horizontal disparity. When fused, one patch appears in front of the other. In the middle stereogram the D6 patches are superimposed on a grating 2 octaves lower in spatial frequency. The left-hand D6 can no longer be fused. In the lower stereogram the D6 patches are superimposed on a grating 4 octaves lower in spatial frequency. The D6 patches fuse and appear in transparent depth. (From Wilson et al. 1991.)

If orientation disparities and linear disparities are processed by distinct mechanisms, one would expect the fusion limit for orientation disparity to be independent of the length of the lines. However, the fusion limit for cyclodisparity could also be independent of line length if the limit depends on point disparities, because the point-disparity fusion limit increases with eccentricity.

Kertesz (1973) found that a larger orientation disparity was required to induce diplopia in lines subtending 2° than in lines subtending 9°. It appears that point disparities rather than orientation disparities determine the cyclofusional limit and that the fusion limit for point disparity does not increase linearly with eccentricity for eccentricities of under 10°. The fusion limit of orientation disparity was smaller for a set of parallel lines than for single lines. This could be because the fusion limit for crowded stimuli is smaller than for single stimuli, or because gratings induce more cyclovergence than single lines (see Section 10.8.4). Kertesz did not control for the effects of cyclovergence because, at the time, he did not believe it occurred.

It has been reported that the fusion limit for orientation disparity is about 2° for horizontal lines and 8° for vertical lines (Ames 1926; Beasley and Peckham 1936). This is consistent with the fact that the fusion limit for horizontal point disparity is larger than that for vertical point disparity. However, cyclovergence is evoked with greater magnitude by cyclorotated horizontal lines than by cyclorotated vertical lines (see Section 10.8.4), and unless this is taken into account, comparison between the fusion limits for horizontal and vertical orientation disparities is not valid.

We have noticed, as did O'Shea and Crassini (1982), that when a grid of horizontal and vertical lines is rotated in opposite directions in the two eyes, the horizontal lines appear diplopic before the vertical lines. This confirms that the fusion limit is greater for vertical lines (horizontal-shear disparity) than for horizontal lines (vertical-shear disparity) because cyclovergence affects both lines equally. To control for effects of cyclovergence, these experiments should be repeated with opposite directions of disparity on either side of the fixation point.

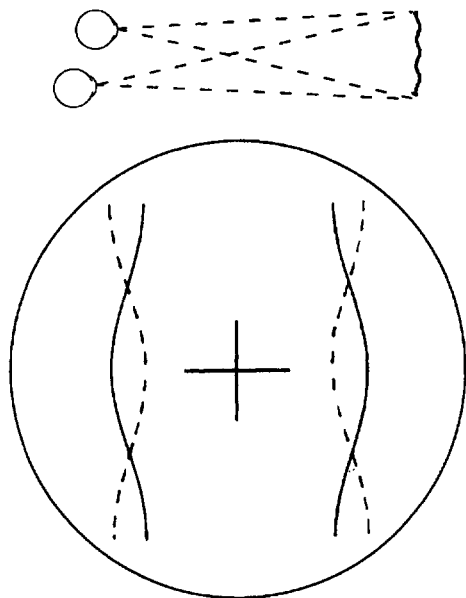


Figure 8.7. Spatiotemporal aspects of the fusion limit.

The solid wavy lines represent the images in one eye, and the dashed wavy lines represent the images in the other eye. The images in the two eyes were alternated at a frequency of between 0.1 and 5 Hz to create a pair of lines undulating in depth, as shown in the upper figure, with the sign of the undulation alternating over time. The sets of lines were 0.5° on either side of a fixation cross. (Reproduced with permission from Schor and Tyler 1981, Vision Research, Pergamon Press.)

8.1.8 Hysteresis and plasticity of fusion limits

The fusion limit has been found to be smaller when diplopic stimuli are moved together until they fuse (the refusion threshold) than when fused stimuli are moved apart until they appear diplopic (the diplopia threshold). Fusional hysteresis has led to a good deal of theorizing about the neural mechanisms that might be responsible for this cooperative property of binocular combination. However, hysteresis is not peculiar to binocular fusion; all psychophysical thresholds exhibit hysteresis according to the direction from which they are approached. Fusional hysteresis may be a manifestation of this general property of sensory systems, rather than a special property of the binocular fusion mechanism.

Fender and Julesz (1967) measured the diplopia threshold and the refusion threshold when the images in the two eyes were optically stabilized so that the images did not move as the eyes moved. The stimulus to each eye was a single black line viewed on a 6°-wide white surround that was also stabilized. As the images of dichoptic vertical lines were moved apart horizontally, diplopia became apparent at an uncrossed disparity of 65 arcmin, and when the images were moved toward each other they fused at a disparity of 42 arcmin. When the images of

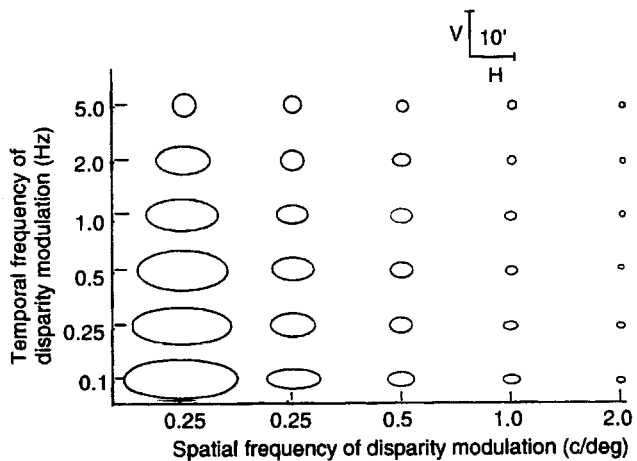


Figure 8.8. Fusional areas and spatial frequency.

The axes of the ellipses represent the horizontal and vertical diameters of Panum's fusional area. Both diameters of the fusional area increase as the spatial frequency of the waviness of the stimulus lines shown in Figure 8.7 decreases. The horizontal but not the vertical diameter of the fusional area decreases as the temporal frequency of depth modulation increases, especially at low spatial frequencies. (Reproduced with permission from Schor and Tyler 1981, Vision Research, Pergamon Press.)

dichoptic horizontal lines were moved apart or towards each other vertically, diplopia thresholds were about 19 and 12 arcmin, respectively. Thus, there was a hysteresis effect in both cases. Fusion limits with stabilized images were at least 20 arcmin smaller than with normal viewing. Fender and Julesz measured changes of vergence during fixation and claimed that these could account for the greater fusion limits in normal viewing than in stabilized viewing. These fusion limits are larger than those reported by other investigators, but the line was 13 arcmin wide, which may have inflated the values.

These measurements were repeated for both crossed and uncrossed disparities of a retinally stabilized black line, but with the border of the surrounding 3° white disc unstabilized (Diner and Fender 1987). The diplopia threshold for increasing disparity, either crossed or uncrossed, was about 20 arcmin, and the refusion limit was about 10 arcmin. When an unstabilized fixation cross was added just above the line, these limits were reduced by about 5 arcmin. Fender and Julesz's study thus showed a larger range of fusion with the disparities occurring over the entire contents of the visual field, than Diner and Fender's study, where only some of the elements were disparate. This is what one would expect based on the disparity gradients in the two types of display. With an overall disparity, the disparity gradient is zero, but with a disparity applied to only one element of the display it is not zero. Put another way, the diplopia limit is greater when there is not a zero-disparity comparison stimulus in view.

Fender and his associates argued on the basis of the hysteresis effect that the fusional area becomes elongated in the direction of a gradually increasing disparity. Diner and Fender (1988) asked whether this elongation represents an overall expansion of the fusional area in both directions or an extension of the leading edge of the fusional area in the direction of movement, accompanied by a contraction of the lagging edge. In other words, does the area expand or merely shift its mean disparity. To answer this question, they presented a fixed vertical line to the fovea of one eye and gradually moved a test line in the other eye in the direction of increasing crossed or increasing uncrossed disparity. Both lines were optically stabilized on the retina. The moving test line was replaced periodically for 2 ms by a probe line that was placed at each of several locations on either side of the fixed stimulus line. Subjects reported whether the probe line and stimulus line were fused or diplopic. When the disparity of the test stimuli was near zero, the disparity limits for the probe were approximately symmetrical about zero (Figure 8.9a). When the moving test line had an uncrossed disparity of 12 arcmin, both the left and right boundaries of the fusional area shifted in the uncrossed direction (Figure 8.9b), and when the test line had a crossed disparity of 16 arcmin the boundaries of the fusional area shifted in the crossed direction (Figure 8.9c). It was concluded that the boundaries of the fusional area move in the direction of the overall disparity in a visual display and do not expand. In fact, the data suggest that the fusional areas may contract rather than expand.

In a second experiment, Fender and Julesz (1967) used 3.4°-wide retinally stabilized random-dot stereograms consisting of 100 × 100 dots, each subtending about 2 arcmin. A central square of dots stood out in depth by a fixed disparity, and the disparity of the whole display in one eye was increased or decreased with respect to that in the other eye at a rate of 2 arcmin/s. Since the square did not exist in either monocular image it was not perceived until the images were binocularly combined. Fender and Julesz argued that "for random-dot stereoscopic images there is no difference between fusion thresholds and the thresholds for stereopsis." This is a strange conclusion since it is well known that stereoscopic depth can be perceived with diplopic images. A nonfused array of dots has a hazy rivalrous appearance compared with the planar appearance of a fused array. The fusion limit for random-dot displays is ill defined. Oddly, the stereogram in the published paper consists of two uncorrelated random-dot displays. One subject saw depth in retinally stabilized stereograms when the images were separated

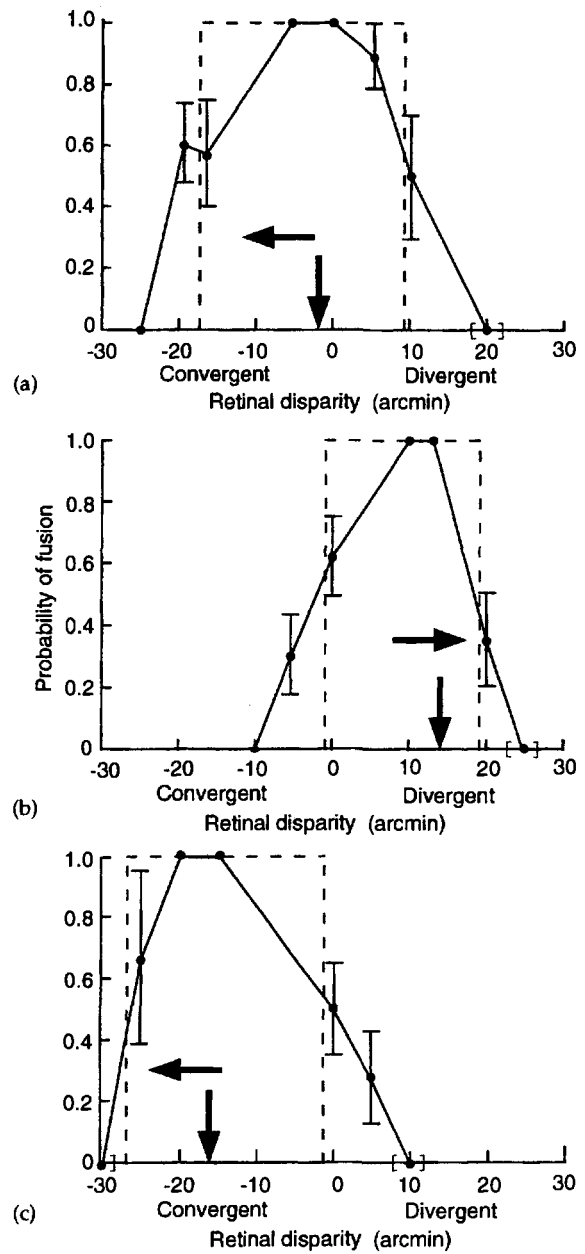


Figure 8.9. Displacement of Panum's fusional area.
A line in one eye was moved slowly into an eccentric position with respect to a fixed line in the other eye, in the direction indicated by the horizontal arrows. At a disparity indicated by the vertical arrows, a briefly exposed probe was used to reveal the fusional limits on either side of the fixed line. The dashed lines represent the rectangular approximations to the curves. It can be seen that the fusional area as a whole moves in the direction of changing disparity. (From Diner and Fender 1988.)

horizontally up to 2° and vertically up to about 20 arcmin. We are not told whether the planes in depth still appeared smooth or whether they took on a hazy rivalrous appearance. Depth was not seen in initially unfused images until they were within 6 arcmin of each other horizontally and 1 arcmin

vertically. Thus, a larger horizontal disparity limit and a larger hysteresis effect were obtained with the criterion of perceived depth using a random-dot stereogram than with the criterion of diplopia using the line target. It is not clear from this comparison whether the crucial factor is the criterion or the type of display.

Using a similar procedure, Piantanida (1986) measured both crossed and uncrossed disparity limits for the whole of a retinally stabilized random-dot stereogram. The criterion was the perception of a cyclopean figure of fixed relative disparity. The range (sum of crossed and uncrossed limits) for increasing disparity was between 68 and 150 arcmin, and the range for decreasing disparity was between 46 and 96 arcmin. A small hysteresis effect was thus replicated although the impression of a cyclopean form was regained at a much larger disparity than in the Fender and Julesz study. Piantanida reported that the stereograms still appeared fused after the cyclopean shape could no longer be seen. However, the criterion for fusion was the elongated appearance of the square outline of the stereogram. It was not reported whether the surface of the stereogram appeared as a flat plane or as hazy depth. Loss of fusion of the matching set of dots may have occurred before, not after, the loss of the cyclopean shape.

Hyson et al. (1983) approached the issue of fusion hysteresis with a different procedure. They measured the overall disparity limit for the perception of a spiral in depth with fixed relative disparity in normally viewed 9.8°-wide random-dot stereograms (1,000 x 1,000 dots). The subject was free to change convergence to different depth planes within the stereogram. The vergence movements of the eyes were measured as the displays were slowly separated. The extent to which the mean position of vergence failed to keep up with the imposed disparity gave a measure of the overall disparity between the images. Depth could be seen and maintained for up to 10 s with up to 3° of image disparity. As soon as depth was lost, the eyes returned to their original converged position. The displays were then brought slowly together until the impression of depth returned, which was, on average, 2.6° in from the point where the depth had been lost. Thus, the disparity limit for maintained depth and the hysteresis effect were even larger than with the smaller disparity stereogram used by Fender and Julesz.

These large tolerated disparities need not be regarded as extensions of Panum's fusional area, since the criterion was perceived depth, not diplopia. The subjects saw depth produced by a fixed relative disparity in a random-dot stereogram with up to 3° of overall disparity. This is equivalent to the task of

registering a disparity superimposed on a disparity pedestal, as discussed in Section 5.3.2. For instance, reliable relative depth judgments were made between two lines when they were up to 2° of disparity away from the fixation point (Blakemore 1970d). Hyson et al. argued that, although random-dot images must fall on nearly corresponding retinal regions before depth is registered when first viewing a stereogram, the visual system is capable of retaining a record of matching dot clusters over large disparities well outside the normal limits of fusion once depth in the stereogram has been perceived. This process would be aided if the visual system registered large dot clusters or used the edges of the stereogram. Hyson et al. called this process "neural remapping." This term is misleading because it suggests that the pattern of neural correspondence has been remapped. But this is not established by these results. The relative disparity that defined the depth in the stereograms remained constant; only the overall disparity changed. Evidence reviewed in several places in this book suggests that depth is coded in terms of relative disparity not absolute disparity. It is not necessary to assume that corresponding points are remapped but only that, up to a point, overall disparities are disregarded in favour of relative disparities.

In the last section we mentioned that Diner and Fender found that the fusional area for lines shifted in the direction of a slowly moving disparity. Erkelens (1988) investigated the same issue using a 30°-wide random-dot stereogram. The images were retinally stabilized for vergence movements but not for version. The subjects could thus look towards different parts of the stereogram but could not change convergence appropriate to the disparity in these areas. The disparity limits for slowly increasing crossed and uncrossed pedestal disparities were measured with the criterion of perceived depth. The same limits were also measured for randomly presented pedestal disparities. The limits for increasing disparity were similar to those for static disparities, but the limits for regaining the impression of depth were less than for either increasing or static disparities. Erkelens concluded that a history of perceiving fused images does not shift the disparity limit for the perception of depth, but a history of perceiving images of a given disparity contracts the limit for that same disparity. These results confirm the hysteresis effect, and Piantanida's claim that limits for regaining the impression of depth are higher than those reported by Fender and Julesz. But the results contradict Diner and Fender's claim that the disparity range for stereopsis with an increasing disparity is shifted relative to that for a static

disparity. However, Diner and Fender did not investigate the refusion limit relative to the static disparity limit.

Duwaer (1983) pointed out that the disparity limit measured by the criterion of detected depth within a random-dot stereogram is a limit of stereo depth rather than of fusion. He found that the diplopia limit for a fixation square superimposed on a random-dot stereogram was within normal limits of about 0.3° , while depth was seen in the stereogram up to a limiting disparity of about 1.3° . He argued that the major hysteresis effect observed with random-dot stereograms does not represent a change in the fusional limits, as Fender and Julesz believed, but is due to the difficulty of regaining the correct binocular match once images have become disparate. However, Piantanida (1986) and Erkelens (1988) both claimed that random-dot stereograms remain fused even after the impression of depth is lost. This is difficult to reconcile with the small fusional limits reported for displays with high spatial-frequency content, as reported in Section 8.1.4.

Summary

However this debate is resolved, to perceive depth in a random-dot stereogram the two images must first be matched. Fender and Julesz claim that this initial matching does not occur unless the images are within a few arcminutes of being in binocular register, but Erkelens claims that it can occur with more than over 1° of disparity between the images. In any case, once the disparity that defines the pattern in depth has been detected, up to 2° of overall disparity between the two images is tolerated before the sensation of depth is lost. The visual system detects the disparity discontinuity within the stereogram despite the disparity present over the stereogram as a whole. It is generally agreed that, when disparity is reduced from a state of diplopia and no depth, depth in a random-dot stereogram is not perceived until the disparity has reached a lower level than that at which depth disappears when disparity is increased. Some investigators interpret this hysteresis effect as a shift in the limits of stereoscopic fusion as disparity is slowly increased, but Erkelens interprets it as a contraction of the limits of fusion due to previous exposure to unfused images.

In all the experiments on the diplopia threshold reviewed here the stimuli were lines, bars, or dots. As the images of such stimuli are separated the contours with the same luminance polarity move further apart and contours of opposite polarity move closer together and eventually coincide. With further separation the opposite polarity contours separate. The diplopia threshold is therefore a threshold for diplopia between contours of opposite

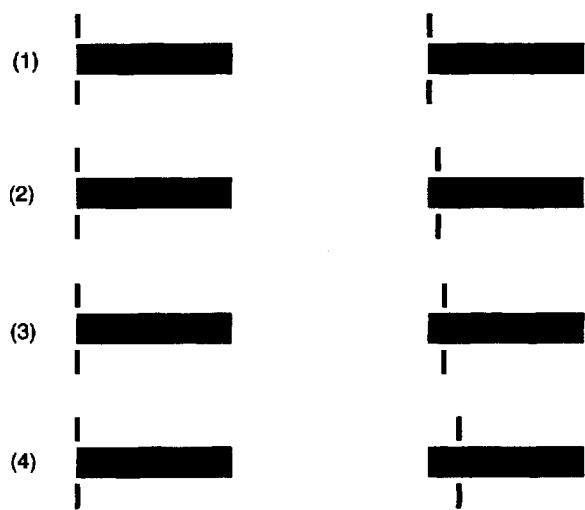


Figure 8.10. Diplopia threshold for single contours.

A display to investigate the diplopia threshold for contours of the same polarity. Each pair of patterns is fused with vergence maintained on the vertical bars. In successive rows, disparity between the horizontal rectangles increases. At a certain disparity the left-hand edges of the rectangles become diplopic and rival.

luminance polarity. To investigate the diplopia threshold for contours of the same polarity, one would have to use the stimuli shown in Figure 8.10.

8.2 Dichoptic colour mixture

Under some circumstances, an illuminated area of one colour presented to one eye appears to rival a similar area of another colour presented to the other eye. This is known as **colour rivalry**. Under other circumstances, two different colours combine to create the impression of a third colour. This is known as **binocular colour mixing**. There has been some dispute about whether binocular colour mixing ever occurs, and even those who believe that it occurs disagree about the necessary conditions.

The earliest reference to binocular colour mixing seems to be a study by Haldat (1806) in which he reported that dichoptically combined images of glass prisms containing coloured liquid appeared in an intermediate hue. Later in the nineteenth century there was a controversy between those who adopted the Young-Helmholtz theory, which stipulated that all colours can be formed from mixtures of red, green, and blue light, and those who adopted the Hering or Ladd-Franklin theories, which stipulated that the sensation of yellow arises from a distinct process in the retina. It was argued that the Young-Helmholtz theory predicts a sensation of yellow arising from the dichoptic combination of red and

green whereas the latter two theories do not. It is ironic that for Helmholtz (1909) binocular yellow was an artifact due to colour adaptation, binocular suppression, and unconscious inference, whereas Hering (1879) regarded it as due to interaction of visual inputs at a central location (for a bibliography of early studies see Johannsen 1930). Helmholtz's reluctance to regard binocular yellow as due to a central combination of inputs arose from his belief that inputs from the two eyes are not combined physiologically. We know now that the trichromatic stage of colour processing is followed by two retinal opponent processes, one between red and green receptors and one between blue and yellow. Yellow does not arise from a distinct cone type but is formed by inputs from red and green receptors (see Boynton 1979). The theoretical significance of binocular colour mixture is still not clear.

Many early investigators claimed to see binocular yellow. For instance, Hecht (1928) saw yellow when he combined a red illuminated patch with a green illuminated patch. Murray (1939) pointed out that the Wratten filters used by Hecht extended into the yellow region of the spectrum. Dunlap (1944) argued that binocular yellow is an artifact of adaptation of the eye to the red light and claimed to see yellow when both eyes looked at red patches for some time. He concluded that "binocular color mixture can be laid away in the museum of curious superstitions." But the problem lives on. Prentice (1948) claimed to have overcome Murray's objection by using narrow-band Farrand interference filters centred on 530 m μ (green) and 680 m μ (red), neither of which extends into the yellow region of the spectrum. He obtained good binocular yellow even with short exposure, and the fused image became more yellow with longer exposure. Others have also reported binocular yellow with narrow-band filters and appropriate controls for colour adaptation. However, Hurvich and Jameson (1951) pointed out that the spectral purity of the red and green filters is irrelevant. The crucial factor is the chromatic bandwidth of the receptors, since a receptor cannot distinguish between one wavelength and another within its tuning range—the principle of univariance. The wavelengths selected by Prentice and others evoked sensations of yellowish red and yellowish green and it was therefore not surprising that they produced binocular yellow. When Hurvich and Jameson used unique red and green, which evoke the purest sensations of red and green, the dichoptic mixture was not yellow but white. This still represents a form of binocular colour mixing that needs to be explained. The colours used by Hurvich and Jameson were close to being opponent colours that produce white

when mixed monocularly. As ordinarily understood, the opponent mechanism resides in the retina, so that the occurrence of binocular white must depend on a distinct cortical process.

Colour matches obtained under dichoptic viewing differ from those obtained with monocular viewing. Lights combined monocularly obey Abney's law; that is, the luminances of differently coloured lights add linearly. Lights combined dichoptically, whether of the same or different colours, do not obey Abney's law of linear luminance summation but produce an intermediate brightness, especially when they are similar in luminance (see Section 9.2.2). Dichoptic colour matches are less saturated and more variable than similar matches made monocularly. The proportion of green to red required to match a spectral yellow and the proportion of yellow required to cancel blue were found to be less with dichoptic than with monocular viewing (Hoffman 1962; Hovis and Guth 1989). De Weert and Levelt (1976) presented a dichoptic mixture of equiluminous lights of different wavelength in a small area and asked subjects to adjust the relative luminances of two lights of the same two wavelengths presented to both eyes in an adjacent small area until the two areas appeared most similar in hue. They did this for many pairs of wavelengths and derived a set of hue-efficiency functions for the dichoptic mixtures. Reasonably good matches of hue were obtained between the dichoptic and dioptic stimuli with the same wavelength components. In general, a smaller amount of the wavelength component nearer the middle of the spectrum was required in the dichoptic mixture than in the dioptic mixture. When a grid of black lines was superimposed on a coloured patch in one eye the colour in that eye became strongly dominant over the untextured coloured patch in the other eye. A coloured patch presented to an amblyopic eye contributed less to the dichoptic colour than a patch presented to the nonamblyopic eye (Lange-Malecki et al. 1985).

Hering (1861) observed that dichoptic colour mixtures are more stable with small than with large stimuli and this has been confirmed more recently (Thomas et al. 1961; Ikeda and Sagawa 1979). With large stimuli, people experience colour rivalry rather than colour mixture. With stimuli subtending less than 2°, most subjects reported stable colour mixture (Grimsley 1943; Gunter 1951). With a display subtending 3.5°, the impression of binocular colour mixture was unstable but became stable when a fusible micropattern was superimposed on the display, (de Weert and Wade 1988), as in Figure 8.11 (see after page 310). One could think of the textured pattern as breaking up the display into small regions and thus

preventing rivalry. Binocular colour mixture is difficult to see in the presence of rivalrous patterns (Dawson 1915).

Hering (1861) observed that prolonged inspection of a dichoptic mixture produces more stable colour mixtures. Johannsen (1930) suggested that prolonged inspection causes the colour in each eye to become desaturated through adaptation and this, rather than duration, is responsible for the increased stability of colour mixtures. However, dichoptic colour mixtures also seem to be more stable with very short exposure times. Thus, synchronous flicker of red and green dichoptic stimuli increased the apparent saturation and stability of binocular yellow and the best results were obtained with flash durations of less than 100 ms and interflash durations of more than 100 ms (Gunter 1951). We will see in Section 8.3.7 that binocular rivalry of contours does not occur with brief stimuli. Stimulus asynchrony of more than 25 ms disrupts the impression of binocular yellow (Ono et al. 1971a).

Dichoptic colour mixtures are more stable (1) at lower than at higher luminance levels and (2) when the luminance in the two eyes is the same. These effects were observed by Hering and confirmed by Dawson (1915) and Johannsen (1930). Colour mixtures become more stable as the saturation of the colours decreases (Dawson 1915). Matches between dichoptic and dioptic mixtures are most stable when the components of the dichoptic mixture are presented on a dark rather than a light background (Thomas et al. 1961).

The periods of colour rivalry that occur with larger visual fields are more pronounced the greater the colour difference presented to the two eyes. Ikeda and Nakashima (1980) gradually increased the dichoptic difference in the wavelength of a 10° test patch until the subject reported colour rivalry. The threshold difference for the occurrence of rivalry varied as a function of wavelength in a manner closely resembling the hue-discrimination curve. In other words, threshold colour differences for the production of rivalry were equally discriminable. Sagawa (1982) asked whether the threshold for discriminating between two patches of wavelength λ and $\lambda + \Delta\lambda$ presented to one eye was affected when patches of wavelength λ were superimposed in the other eye. The idea was that if colour processing is independent in the two eyes, the addition of the dichoptic masking patches would not affect the discrimination threshold. Wavelength discrimination deteriorated in the presence of the masking stimulus, but the extent of the deterioration was largely independent of the luminance of the masking stimuli. This suggests that dichoptic masking between

chromatic signals is independent of the luminance component of the visual stimulus.

Summary

We conclude that dichoptic colour mixing is a genuine phenomenon but differs in several respects from monocular colour mixing. Dichoptic colour mixing is more stable with small or textured patches than with large homogeneous patches, with flickering stimuli than with steady stimuli, and with patches of low luminance and saturation and equal luminance and chromaticity than with bright and saturated patches or patches of unequal luminance. Its occurrence implies that there must be colour mechanisms in the cortex in addition to those in the retina. The literature on binocular colour mixing has been reviewed by Hovis (1989).

8.3 STIMULUS DETERMINANTS OF RIVALRY

8.3.1 Basic phenomena of binocular rivalry

When corresponding regions of the two eyes are stimulated by very different patterns, the stimuli rival in terms of our conscious perception, rather than fuse into a composite pattern. This perceptual alternation between nonfusible dichoptic stimuli is known as binocular rivalry. The stimulus seen at a given time is the **dominant stimulus** and the stimulus that cannot be seen is the **suppressed stimulus**. When both stimuli are small one tends to see all of one image or all of the other in alternation. This is known as **exclusive dominance**.

With large patterns of equal area, a part of one pattern is dominant in one area and a part of the other in another area, with these areas of dominance fluctuating over time. This is known as **mosaic dominance**. Thus, when a patch of vertical lines is presented to one eye and a patch of horizontal lines to the other, as in Figure 8.1, one sees vertical lines in one area and horizontal lines in another, with the areas constantly shifting about. For short periods, only vertical lines or only horizontal lines may be seen.

A patterned stimulus is generally dominant over a blank field in the other eye. For example, a small black disc on a white ground remains visible when superimposed on a larger black disc presented to the other eye, as shown in Figure 8.12a. The edge of the small black disc suppresses the surrounding homogeneous region in the larger disc so that the edge of the small disc remains visible. The same contour-preserving process is seen when a vertical bar in one eye is superimposed on a horizontal bar in the other

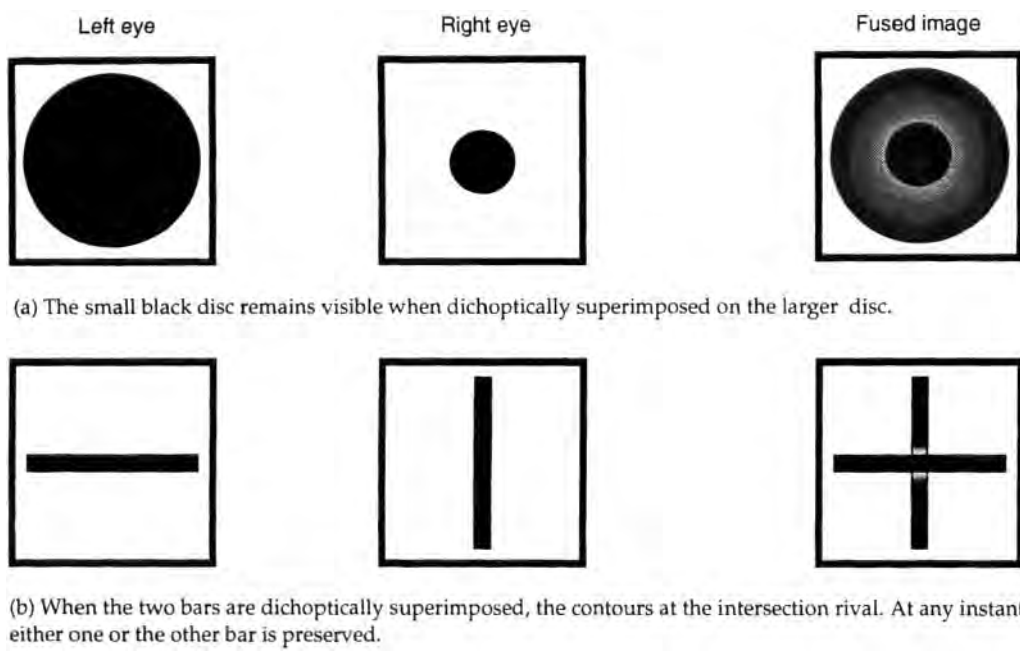


Figure 8.12. Preservation of contours in binocular rivalry.

eye, as shown in Figure 8.12b. The zone of suppression surrounding a contour presented to only one eye presumably results from the inhibitory surrounds of the receptive fields of the cells excited by the contour. A model of this process has been proposed by Welpe et al. (1980).

We will see in the following sections that, under certain circumstances such as with brief exposure or at low contrast, rivalrous patterns may appear superimposed. A pattern with higher spatial frequency in one eye may appear to stand out in depth relative to a pattern with lower spatial frequency in the other eye (Yang et al. 1992). The question arises as to whether dissimilar dichoptic images that appear superimposed should be regarded as fused. Note that the perceived direction of fused similar images is midway between the directions of the two monocular images (see Section 14.5.3), and disparity between fused similar images codes depth. Dissimilar images that appear superimposed rather than rivalrous have neither of these properties, and the processes responsible for their apparent superimposition may differ from those responsible for fusion of similar images. We therefore refer to the simultaneous appearance of dissimilar images as **image superimposition** rather than image fusion. Fox (1991) reviewed the literature on binocular rivalry.

8.3.2 Luminance, contrast, and contour density

Interocular differences in luminance and contrast

Levelt (1965b 1966) reported evidence that the strength of a rivalrous stimulus is proportional to

the amount of contour per unit area and that the radius of action of a given contour increases as the contrast of the contour is increased. He proposed that an increase in the strength of an image decreases the duration of the period for which that image is suppressed, but the duration for which an image of a given strength is suppressed does not depend on the strength of the image suppressing it (Whittle 1965; Levelt 1965b; Fox and Rasche 1969). In words, a strong stimulus is suppressed for shorter periods than a weak stimulus. An image with no contours is regarded as having zero strength and is believed to remain suppressed indefinitely by a patterned stimulus in the other eye. As we will see, this is not always true.

Bossink et al. (1993) recently challenged Levelt's proposition. They varied stimulus strength by varying luminance contrast, colour contrast, and the velocity of a moving dot pattern. Levelt's proposition was only partially confirmed. They agreed that the strength of a suppressed image had more effect on suppression duration than did the strength of a dominant image. However, the strength of the dominant image had a significant affect on the duration for which it was dominant. Mueller and Blake (1989) found that the overall rate of alternation of rivalrous patterns depended mainly on the contrast of the patterns in their depressed phase but that the contrast of the patterns in their dominant phase had some effect.

A grating near the contrast threshold can rival an orthogonal high-contrast grating in the other eye, but the low-contrast grating is visible for only short

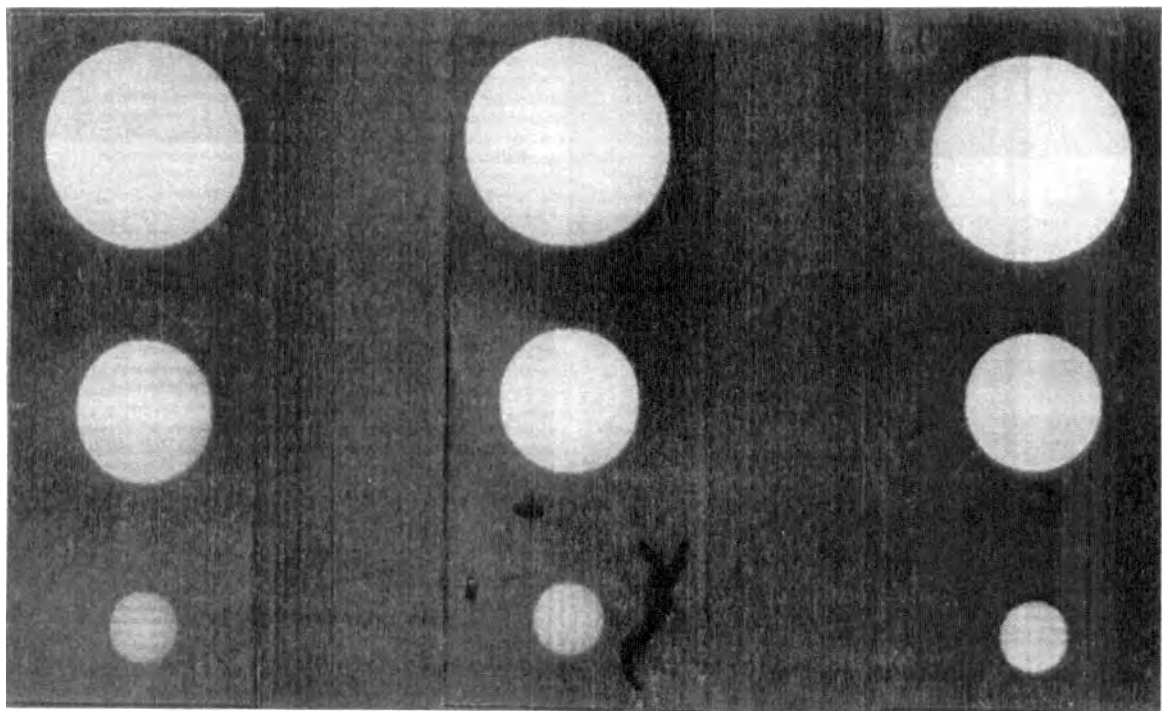


Figure 8.13. Dichoptic superimposition of low-contrast edges.

Fusion of the images in the two lefthand columns results in superimposition of orthogonal edges. At high contrast these edges rival but at low contrast they appear superimposed for several seconds and create the impression of plaids, as depicted in the righthand column. (Reproduced with permission from Liu et al. 1992, Vision Research, Pergamon Press.)

periods. The least contrast in an image that will instigate rivalry is the **rivalry contrast threshold**. The rivalry contrast threshold as a function of the spatial frequency of rivalrous gratings has been found to be similar to the contrast-sensitivity function of monocularly viewed gratings (Blake 1977). Thus, a spatial frequency of about 4 c/deg, requires the least contrast to initiate rivalry. This is the spatial frequency for which contrast sensitivity is highest. However, a stimulus consisting of a sine-wave grating of 4 c/deg is not as dominant as a stimulus consisting of a broad mixture of spatial frequencies (Fahle 1982a). This supports the idea that rivalry occurs between distinct spatial-scale channels in the visual system. When the pattern in one eye is blurred it is suppressed for longer periods than when it is sharply focused. This could be due to the reduction of contrast in the blurred stimulus and also to the narrowed range of spatial frequencies, which means that fewer channels are stimulated by the rivalrous stimulus (Fahle 1982b).

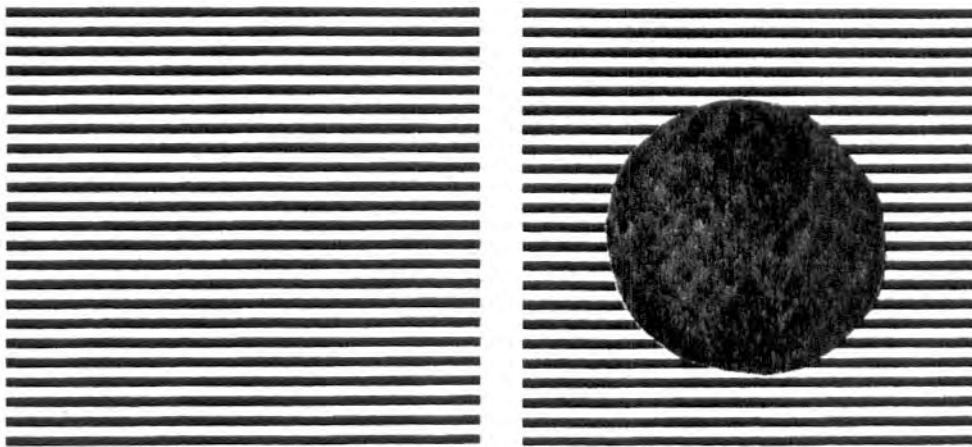
The threshold for detection of a flash is elevated when the flash is presented at about the same time as a sudden change in brightness in the other eye (Bouman 1955). Presumably the change in the non-tested eye causes that eye to become dominant and this suppresses the response to the test flash. Blake

and Camisa (1979) found the elevation of threshold of a test flash presented to an eye when it was suppressed by the other eye to be independent of the relative contrasts of the two stimuli. They concluded that, once a stimulus is suppressed, the degree, as opposed to the duration, of suppression is independent of its contrast. Makous and Sanders (1978) reported that dimming one of the images has no effect on the degree of suppression, a result confirmed by Hollins and Bailey (1981).

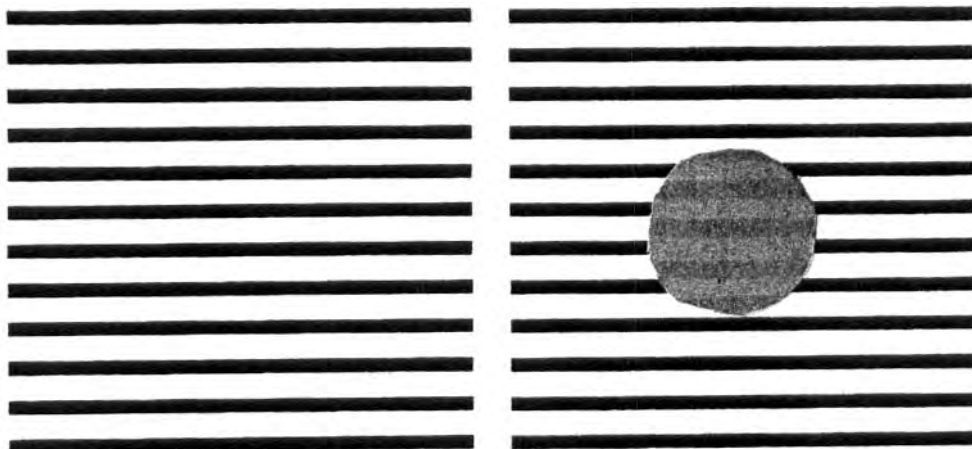
Blake and Camisa (1979) reported that the lower the contrast of the suppressed stimulus the more time it needs before becoming dominant. Hollins and Bailey found that lowering the luminance of the suppressed image has the same effect. We must distinguish between the extent of suppression, which is not affected by the contrast or luminance of the suppressed image, and the length of the period for which an image is suppressed, which is affected by these attributes of the suppressed image.

Dichoptic gratings differing in colour show longer periods of exclusive dominance than those of the same colour (Wade 1975b; Hollins and Leung 1978).

The fact that stimuli with high contrast or high spatial frequency tend to suppress stimuli with low contrast or low spatial frequency helps people who wear a contact lens for hyperopia on one eye and a



(a) When the fine grating is oscillated slowly up and down while viewed with the nondominant eye, the dark field of the closed eye occasionally blots out the centre of the grating. The dark field appears as a gray diagonal meshwork, as depicted on the right.



(b) When one eye fixates the stationary coarse grating, the dark field of the closed eye occasionally blots out the centre of the grating and contains a low-contrast counterphase grating of the same spatial frequency, as depicted on the right. (From Howard 1959.)

Figure 8.14. Binocular dominance of the closed-eye.

lens for myopia on the other eye. For near viewing, the image in one eye is in sharper focus than that in the other and for far viewing the image in the other eye is in sharper focus. Patients nevertheless see in sharp focus at all distances because the sharply focused image suppresses the less well focused image. Under scotopic conditions the less well focused image is not suppressed (Schor et al. 1987).

Effects of the luminance and contrast of both images

High-contrast orthogonal gratings alternate more rapidly than low-contrast gratings, and continuous lines alternate more rapidly than broken lines (Alexander 1951). Alternations of rivalry occur much less frequently and suppression spreads over wider

areas when both images are at scotopic rather than photopic light levels (Breese 1909; Kaplan and Metlay 1964; O'Shea et al. 1994a). Two low-contrast gratings show longer periods of exclusive dominance than do two high-contrast gratings. For a given contrast, gratings with a spatial frequency of 3 c/deg show longer periods of exclusive dominance than do gratings with higher or lower spatial frequencies (Hollins 1980). Rivalry between random-dot patterns showed a similar dependence on spatial frequency (de Weert and Wade 1988).

Orthogonal dichoptic gratings with the contrast of both set just above the threshold do not begin to rival for many seconds after exposure, but appear superimposed as a plaid pattern (Liu et al. 1992). As

the contrast of the gratings increases, the time before rivalry is experienced becomes shorter. For a given contrast, gratings with higher spatial frequency appear as plaids longer than those with lower spatial frequency (see Figure 8.13)—probably because higher spatial-frequency gratings have higher contrast thresholds.

One way to think about these effects is that when both members of a dichoptic display have low contrast, neither of them has sufficient stimulus strength to suppress the other. Liu et al. showed that a nonrivalrous aperture surrounding the stimulus significantly enhanced combination of dichoptic images.

It would be worthwhile to study rivalry in large low-contrast gratings in which any possible contribution of an aperture is minimized.

Dominance of homogeneous fields

It is generally believed that a featureless visual field never rivals a patterned stimulus. However, a closed eye, which may be said to contain a featureless black field, can suppress a highly textured stimulus. When the dominant eye is closed while the other eye views the black and white grating of Figure 8.14a as it is oscillated up and down at about 2 Hz, a gray patch containing a diagonal meshwork pattern appears to spread out from the centre of the grating and blot it out (Howard 1959). The meshwork pattern periodically spreads and then recedes. The effect is not Troxler fading of the grating, because Troxler fading does not occur with moving stimuli. People with only one eye did not experience this effect, supporting the idea that the occluding patch is the dark field of the closed eye. When a coarse grating, like that of Figure 8.14b, is held still, the dark field of the closed eye may still occlude the lines but, instead of a meshwork pattern, the occluded region contains a faint phase-reversed image of the grating that is confined to a small central patch, as depicted in Figure 8.14c. Not everyone sees this image. Dynamic visual noise viewed by one eye may be suppressed by a blank field in the other eye (Tyler personal communication). All these effects are strong violations of Levelt's proposition that the more highly patterned stimulus is dominant in binocular rivalry.

An homogeneous luminous field (Ganzfeld) tends to fade from view after it has been inspected for some time. Bolanowski and Doty (1987) found that fading did not occur when the Ganzfeld was viewed with both eyes, and concluded that fading with a monocular stimulus is due to suppression of the luminous field by the dark field of the closed eye. Gur (1991) agreed that sudden blackout in a Ganzfeld occurs only when one eye is closed and

that it is due to binocular rivalry, but found that the gradual fading associated with adaptation of a stationary patterned image occurs with both monocular and binocular viewing. Rozhkova et al. (1982) found the same to be true of large textured displays optically stabilized on the retina. From a review of the literature on fading of afterimages, Wade (1978) concluded that one of the major factors in the fading of monocular afterimages is rivalry between the afterimage and the dark field of the closed eye.

8.3.3 Relative velocity

A moving stimulus presented to one eye is dominant for longer periods than a similar stationary stimulus presented simultaneously to the other eye (Breese 1899). The duration of dominance of a moving grating over a stationary grating was found to increase with its speed (Wade et al. 1984). However, a clear advantage of one speed over another was not observed when dichoptic displays moved at different speeds in the same direction (Blake et al. 1985).

Rivalry also occurs between dichoptic displays of random dots moving at the same speed but in directions that differ by more than 30° (Blake et al. 1985; Wade et al. 1984). Fusion of stimuli moving in different directions that differ by only a few degrees results in the appearance of a display moving on an inclined depth plane. For both monocular and binocular stimuli visual thresholds are generally lower for vertical and horizontal lines or gratings than for oblique stimuli—the so-called oblique effect. By analogy, one might expect that dot patterns moving vertically or horizontally would be dominant over dot patterns moving in an oblique direction, but this question has not been investigated.

8.3.4 Position on the retina

Each visual hemisphere of the monkey has more binocular cells with a dominant input from the contralateral eye (the nasal hemiretina) than binocular cells with a dominant input from the ipsilateral eye (temporal hemiretina) (LeVay et al. 1985). One might therefore expect a stimulus presented to the nasal half of the retina of one eye to dominate that presented to the temporal half of the retina of the other eye.

In conformity with this expectation, Köllner (1914) found that when a homogeneous green field was presented to the left eye and a similar red field to the right eye for about 100 msec, the green field dominated in the left visual field (nasal half of the left eye) and the red field in the right visual field (nasal half of the right eye). In other words, with

both eyes open, the left eye dominated in the left visual field and the right eye dominated in the right visual field. With longer viewing, the coloured fields began to rival. Crovitz and Lipscomb (1963a, 1963b) found that when the displays presented to the nasal and temporal visual fields are separated by a vertical black band, the colour projected to the nasal half of each eye remained dominant for prolonged periods.

Fahle (1987) also showed that the pattern of alternation of rivalrous stimuli varies as a function of the position of rivalrous stimuli in the visual field. A vertical grating subtending 10° was presented to the left eye and a similar horizontal grating to a corresponding region of the right eye. The grating in the right eye was dominant for slightly longer than that in the left eye when they were presented within a 20° radius around the fixation point. This was attributed to the fact that most people have a dominant right eye, but it could also be due to horizontal gratings tending to dominate vertical gratings. When the stimuli were presented more than 20° to the left of the fixation point, the left eye was dominant for about twice as long as the right eye, and when they were presented more than 20° to the right, the right eye became about twice as dominant as the left eye. Thus, in both cases, the temporal visual field (nasal hemiretina) of one eye tended to dominate the nasal visual field (temporal hemiretina) of the other eye. This asymmetry of hemifield dominance is presumably related to the asymmetry of projections of nasal and temporal hemifields onto the visual cortex. This issue is discussed in Sections 15.1.5.

Fahle pointed out that, in people with convergent strabismus, the fovea of the deviating eye has to compete with the dominant temporal hemifield of the other eye whereas the fovea of divergent strabismus competes with the nondominant nasal hemifield of the other eye. This could account for why convergent strabismus develop amblyopia in the deviating eye whereas divergent strabismus do not (see Section 15.7.1).

8.3.5 Relative orientation

Abadi (1976) found that the contrast of a grating presented to one eye required to suppress a grating presented to the other eye was independent of the relative orientation of the gratings, when the angle between the gratings was larger than 20°. However, as the difference in orientation was reduced below 20°, progressively less contrast was required for suppression. From this, Abadi concluded that suppression is greatest between lines with similar orientations. He speculated that suppression is due to inhibitory connections between orientation columns in

the visual cortex and that these connections are strongest between columns tuned to similar orientations. There is disagreement about the role of inhibitory or excitatory lateral connections in the visual cortex in binocular rivalry, as we will see in Section 8.8. Abadi's stimuli were at near-threshold contrasts where rivalry tends not to occur, and his results may have reflected a threshold-elevating effect due to contrast adaptation rather than binocular rivalry (see Section 9.3.6). In any case, Blake and Lema (1978) pointed out that Abadi's data could also support the conclusion that inhibitory influences are weaker between lines with similar orientation, since only a low-contrast stimulus in one eye was required to overcome the inhibitory influence of the image in the other eye. Using a detection-threshold procedure with suprathreshold stimuli, Blake and Lema could find no evidence that the strength of suppression varied as a function of the relative orientation of the stimuli.

8.3.6 Effects of eye movements

The rate of alternation of rivalrous images is partly under stimulus control and partly determined by autonomous neural processes. A sudden motion or increase in luminance contrast of a suppressed image tends to terminate the suppression. The eyes constantly execute small saccadic movements and Levelt (1967) proposed that the sudden movements of the suppressed retinal image trigger reversals of binocular dominance. However, the rate of dominance reversal of rivalrous images has been found to be the same for retinally stabilized as for normal images (Blake et al. 1971). This shows that eye movements are not necessary for rivalry but it does not exclude a possible role for eye movements when they are allowed. Sabrin and Kertesz (1983) applied a more critical test of the eye-movement theory by stabilizing the image in only one eye. Rivalry still occurred but the stabilized image was suppressed for longer periods than the unstabilized eye. When a motion simulating the effects of microsaccades was imposed on the stabilized image the periods for which it was suppressed returned to their normal value. Thus, eye movements do affect the rate of binocular rivalry when their effects are unequal in the two eyes.

The spread of suppression around a contour into an uncontoured region in the other eye was found to be more extensive when the eyes executed vergence movements (Kaufman 1963). This effect was explained in terms of a time lag in recovery from suppression, which causes the moving eyes to leave a wake of suppression in their path.

8.3.7 Effects of duration and temporal frequency

Dawson (1913) noticed that rivalry ceased when he rapidly blinked his eyes. Hering (1920) reported that when rivalrous stimuli are presented for a brief period they do not rival but appear as two complete superimposed stimuli. Several investigators have since noticed the same phenomenon. For instance, high-contrast dichoptic vertical and horizontal gratings appeared to combine or partially combine into a grid pattern when shown for less than about 200 ms but appeared to rival in the normal way when presented for more than 400 ms (Anderson et al. 1978). High-contrast dichoptic orthogonal gratings did not rival when flashed on for 50 msec at a rate of 2 flashes per second (Kaufman 1963). Similarly, afterimages of orthogonal gratings did not rival when presented on a background illuminated at 2 flashes per second (Wade 1973). Thus, the inhibitory processes responsible for suppression take time to develop. Before these processes are developed, dichoptic stimuli can slip past the suppression mechanism and reach consciousness. Another way to think about these effects is that the rivalry mechanism is less evident in the transient channel of the visual system than in the sustained channel.

Subjects who continuously suppressed the input from one eye in a rivalrous situation experienced the combined image of dichoptic gratings when the stimuli were presented for 150 ms (Wolfe 1986a). Leonards and Sireteanu (1993) found that the time course for the development of rivalry in some amblyopes was the same as in normal subjects but other amblyopes showed partial or complete dominance of the image in the good eye during the initial period of exposure, giving way to rivalry or continued dominance of the good eye with longer exposure. Each amblyope behaved like a normal subject when the image in the good eye was attenuated appropriately.

Although orthogonal gratings combined into a plaid when exposed dichoptically for 10 ms, they appeared to rival when presented in an intermittent sequence with interstimulus intervals of less than 150 ms, just as they would if presented continuously (Wolfe 1983a, 1983b). Thus, the rivalry mechanism integrates over short time intervals and, once switched on, stays on for at least 150 ms, briefly affecting the appearance of subsequently exposed stimuli.

Even though briefly exposed dissimilar patterns presented dichoptically for brief periods appear as a combined image, Blake et al. (1991a) found that subjects could distinguish between such a dichoptic image and the same pair of images briefly presented to one eye.

O'Shea and Blake (1986) presented an unkontoured field flickering at 4 Hz to one eye and a similar field flickering at between 0.5 and 16 Hz to the other eye. These stimuli produced very few reports of rivalry, and instead subjects reported a single field flickering at an intermediate frequency. A small probe superimposed on the flickering field of one eye remained visible. They concluded that rivalry does not occur within the transient channel of the visual system, which is most effectively engaged by flickering, uncontoured stimuli. Orthogonal dichoptic gratings counterphase modulated at different frequencies were found to rival in the usual way, but the grating flickering at the lower frequency created longer dominance phases than the one flickering at a higher frequency.

We mentioned in Section 5.10.2 that stereopsis occurs when disparate stimuli are presented to the two eyes in close succession. Rivalry also occurs between stimuli presented briefly to the two eyes in succession, as long as the interval between them is not too great. Thus, binocular rivalry between orthogonal gratings presented in alternation to the two eyes at rates above about 20 Hz was indistinguishable from that between simultaneously presented stimuli (O'Shea and Crassini 1984). Some rivalry was apparent in stimuli alternating at 3 Hz, but below this frequency both stimuli were seen in alternation, often with apparent motion from one to the other. Rivalry also occurred between stimuli presented alternately for 5 ms to each eye, with up to 100-ms intervals between stimuli. This is the same interval of time over which stereoscopic depth occurs with alternating stimuli to the two eyes (see Section 5.10.2).

Summary

It can be stated that the strength of a suppressed image has more effect on the duration of suppression than does the strength of the dominant image. The strength of an image is determined by the amount of contour it contains, its contrast, spatial frequency, and motion. However, we have already seen that the dark field of a closed eye can suppress an oscillating grating, so that the dark field of a closed eye must be regarded as having some strength. A stimulus presented to the nasal retina of one eye tends to dominate that presented to the temporal retina of the other eye. Low-contrast stimuli and stimuli presented for less than 200 ms do not rival but appear superimposed, which suggests that rivalry does not occur in the transient channel of the visual system. For certain time parameters, rivalry still occurs between stimuli presented successively to the two eyes.

8.3.8 Monocular rivalry

Breese (1899) noticed rivalry between a diagonal grid of black lines on a red ground optically superimposed in the same eye on an oppositely oriented grid of lines on a green ground. Sometimes only one or the other set of lines was seen, and sometimes parts of each. The colours associated with each set of lines fluctuated accordingly. Breese introduced the term "monocular rivalry" to refer to rivalry between images in one eye. Monocular rivalry between differently coloured gratings was most pronounced when they were superimposed at right angles. When the angle between them was less than about 20°, the colours and lines combined into a stable percept (Campbell et al. 1973). The alternation of orthogonal coloured gratings presented to the same eye was more frequent and more complete when the colours were complementary rather than noncomplementary or black and white (Rauschecker et al. 1973; Wade 1975b). The rate of alternation of crossed-gratings decreased with increasing spatial frequency but did not change significantly with changes in contrast (Atkinson et al. 1973).

The rate of alternation of crossed gratings presented to one eye was considerably lower than that of rivalrous dichoptic gratings, suggesting that monocular and binocular rivalry are different mechanisms (Wade 1975b; Kitterle and Thomas 1980).

It has been suggested that monocular rivalry is due to eye movements that cause afterimages to reinforce or attenuate components of the pattern (Georges and Phillips 1980). But this cannot explain how Breese sometimes observed parts of each rivalrous grating. Furthermore, effects of eye movements cannot be the only factor, since monocular rivalry may be observed in afterimages, which are not affected by eye movements. Two bar-shaped afterimages within 1° of each other were more visible when they were parallel than when they were orthogonal (Atkinson 1972). Successive presentation to one eye of a white horizontal bar and a white vertical bar, both on black backgrounds, produced an afterimage in which the vertical and horizontal bars showed rivalry, complete with white halos at the intersections of black bars. Monocular rivalry was particularly impressive between an afterimage and a real bar. This rivalry appeared similar to that between orthogonal afterimages impressed separately in the two eyes (Sindermann and Lüddeke 1972).

When afterimages of a vertical and a horizontal bar are formed successively, there is some retention of the neural activity in each eye associated with the contours within the region where the afterimages in-

tersect. The competition between these persisting monocular neural processes is presumably responsible for the rivalry seen with afterimages.

In monocular diplopia a stimulus presented to one eye appears double, with the image in its normal oculocentric position appearing normally bright and the anomalous image appearing dim. Bielschowsky (1898) superimposed in one eye the normal bright image of a diplopic red patch on the dim image of a diplopic green patch. Instead of producing the hue formed when two normal images of different hue are combined, the coloured patches rivalled in the manner of two patches presented dichoptically.

Ramachandran et al. (1994a and b) made a similar observation on a patient with intermittent exotropia. A patch of vertical lines was superimposed in the same eye on the dim diplopic image of a patch of horizontal lines. The subject experienced mosaic rivalry rather than the checkerboard pattern obtained when two orthogonal gratings of the same contrast are superimposed in the same eye.

The response of a cell in the visual cortex to an optimally oriented bar or grating is suppressed by the superimposition of an orthogonal bar or grating (see Section 8.8). This is known as **cross-orientation inhibition**. It is largely independent of the relative spatial phases of superimposed gratings and operates over a wide difference in spatial frequency between the superimposed stimuli. This process does not operate between gratings presented dichoptically and is therefore not the cause of binocular rivalry, but it could be a factor in monocular rivalry, as Campbell et al. (1973) suggested.

Monocular rivalry may belong to a broader class of phenomena that fall under the heading of perceptual ambiguity. These include ambiguities of figure-ground organization, as in the Rubin cross and the face-vase figure; ambiguities of figural organization, as in Boring's mother-in-law/daughter figure; and reversible perspective, as in the Necker cube. These effects probably operate at many levels in the nervous system and are therefore unlikely to vary in the same way with changes in stimulus conditions.

A patterned stimulus presented to one eye appears to fade when steadily fixated for some time. The effect is particularly evident with blurred edges and is enhanced if the image is optically stabilized on the retina. This is known as **Troxler fading** and is believed to be due to local adaptation. Like binocular rivalry, Troxler fading in a complex pattern is piecemeal and fluctuates. There has been dispute about what role Troxler fading plays in binocular rivalry (Crovitz and Lockhead 1967). Liu et al. (1992) suggested that it is particularly important in rivalry at near-threshold contrasts but not at high contrasts.

8.4 BINOCULAR SUPPRESSION SELECTIVITY

8.4.1 The generality of suppression

Binocular suppression is a nonselective inhibitory process that removes all stimuli within the suppressed region from consciousness (Fox and Check 1966a). Thus, suppression affects a given region of the visual field of one eye and not a particular stimulus or stimulus feature within that region.

Inspection of a moving visual display evokes an automatic movement of the eyes, known as optokinetic nystagmus. When a visual display presented to one eye moves in one direction and that presented to the other eye moves in the opposite direction the eyes follow whichever stimulus is dominant. Whenever a change in image dominance occurs there is a corresponding change in the direction of eye movement (Enoksson 1963; Fox et al. 1975). This procedure has been used to investigate binocular rivalry in the monkey (Logothetis and Schall 1990).

It has been reported that a light flash presented to an eye in its suppressed phase of binocular rivalry evokes a weaker pupillary response than one presented to the eye in its dominant phase (Bárány and Halldén 1948; Richards 1966). Lowe and Ogle (1966) could not replicate this effect, but they did find that, when rivalrous fields differ in luminance, a small constriction of the pupil occurs as the brighter field comes into dominance. This process must involve centrifugal pathways from the visual cortex to the subcortical centres controlling the pupil.

Although nothing within a suppressed region is visible, in the sense of being available to consciousness, we will see in the following two sections that certain features of the suppressed visual input influence the duration for which the image is suppressed.

8.4.2 Spatial zones of binocular rivalry

The evidence reviewed in this section suggests that rivalry occurs within discrete areal units of the visual system and that these units increase in size with increasing eccentricity. Blake et al. (1992) referred to these units as **spatial zones of binocular rivalry**. The following two procedures have been used to measure zones of rivalry.

Zones of exclusive dominance

With large rivalrous displays, like those shown at the top of Figure 8.15, the whole image in one eye is totally suppressed only infrequently by that in the other eye; usually the two displays rival in a piece-meal fashion to produce a shifting mosaic of monocular images. Small rivalrous displays, like those at

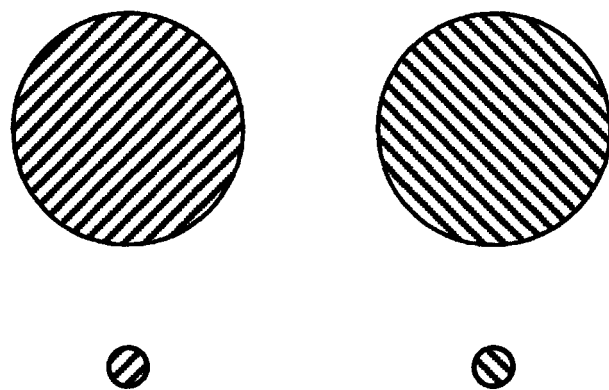


Figure 8.15. Effect of area on rivalry.

With large rivalrous displays, the whole of one image is totally suppressed by the other image only infrequently. Small displays tend to rival as a whole. (Adapted from Blake et al. 1992.)

the bottom of Figure 8.15, tend to rival as a whole. Blake et al. (1992) measured the percentage of viewing time that a pair of orthogonal gratings (6 c/deg) in a circular patch showed exclusive dominance rather than mosaic dominance as a function of the size and eccentricity of the patch. At the fovea the mean diameter of the largest patch that exhibited exclusive dominance 95 per cent of the time was 8.1 arcmin. According to Schein and Monasterio (1987), this is close to the estimated size of a cortical hypercolumn in the monkey visual cortex (the region containing one complete set of ocular-dominance columns).

Blake et al. noted the similarity between the area within which rivalry is exclusive and the area over which suppression from a contour in one eye encroaches on a noncontoured area in the other eye or on neighbouring contours in the other eye. The size of the patch, with appropriately scaled spatial frequency, that generated only exclusive rivalry increased with eccentricity in a manner similar to the increasing size of receptive fields and of the cortical magnification factor (the diameter of cortical tissue devoted to each degree of visual angle).

Spread of the spatial zone of rivalry

The spread of the zone of rivalry around a dominant contour was measured by Kaufman (1963). He presented a pair of parallel thin lines to one eye and a single orthogonal line to the other. In dichoptic viewing the single line cut across the two parallel lines and subjects reported when the part of the single line between the two parallel lines was totally suppressed. As the distance between the parallel lines increased from 7 arcmin to 3.8° the proportion of time for which the single line was visible

increased exponentially from about 3 per cent to about 45 per cent with the increase being most rapid for separations of less than 15 arcmin. The zone of suppression in a vertical direction was smaller than that in a horizontal direction.

Liu and Schor (1994) used Kaufman's procedure with elongated DOG patches which had a spatial-frequency bandwidth of 1.75 octaves and a variable mean spatial frequency. Two parallel patches in one eye were superimposed for one second on a continuously visible single orthogonal patch in the other eye. In any trial the spatial frequency of all the lines was the same but was varied from trial to trial. Liu and Schor were thus able to measure the zone of rivalry as a function of the spatial frequency of the stimuli. Subjects reported whether they saw a single patch between the two parallel patches. The size of the suppression zone decreased linearly with increasing spatial frequency from about 150 arcmin at a spatial frequency of 1 c/deg to about 15 arcmin at a spatial frequency of 10 c/deg. At low spatial frequencies the rivalry zone was about twice as wide vertically as horizontally, at 4 c/deg it was circular, and at high spatial frequencies it became a horizontal ellipse.

Schor et al. (1984) had previously found that Panum's fusional area also decreased with increasing spatial frequency (see Section 8.1.4) but Panum's fusion area was much smaller than the zone of rivalry at all spatial frequencies.

Liu and Schor also found that the zone of rivalry increased rapidly with increasing contrast of the Gaussian patches up to a contrast of about 30 per cent, after which it increased less rapidly. The small zone of rivalry with low contrast, high spatial frequency stimuli could explain why orthogonal gratings fuse rather than rival when they have low contrast and high spatial frequency (see Section 8.3.2).

At scotopic levels of illumination, suppression was found to spread over larger areas of rivalrous gratings than at photopic levels (O'Shea et al. 1988). Furthermore, the size of Panum's fusional area was larger at scotopic levels. Both these effects could be due to the fact that, at scotopic levels, the excitatory regions of the receptive fields of ganglion cells become larger because inhibitory effects from the surround become weaker (Barlow et al. 1957).

Independence of zones of suppression

As a general rule, when the two eyes are exposed to several distinct pairs of rivalrous stimuli, the members of each pair rival independently rather than in synchrony. But there are exceptions to this rule. Connected patterns tended to appear and disappear as units, and dichoptic contour segments forming a

continuous cyclopean line tended to rival in synchrony, even though the two segments were in different eyes (Whittle et al. 1968). A textured annulus placed around one of two small rivalrous gratings was found to increase the duration of exclusive dominance of that grating. Also, the monocular annulus was more clearly visible when the grating it surrounded was fused with a similar grating in the other eye than when it was in rivalry with an orthogonal grating in the other eye (Fukuda and Blake 1992). The boundaries of rivalrous subregions were not determined by physically disconnected meaningful units such as words (Blake and Overton 1979)

8.4.3 Penetration of suppressed images

When a suppressed image is changed in certain ways, the suppressed phase is rapidly terminated. The change therefore must have penetrated the suppression process. Blake and Fox (1974a) presented a horizontal grating to the right eye and a vertical grating to the left eye. The horizontal grating had high contrast and was counterphase modulated at 4 Hz whereas the vertical grating had low contrast and was not modulated. The horizontal grating suppressed the vertical grating. The suppressed phase was terminated by an increase in the contrast of the suppressed image but not by a decrease in its contrast. Changes in the spatial frequency or orientation of the suppressed image did not terminate the suppressed phase. It was concluded that only energy increments penetrate the suppressive process.

This evidence is not conclusive because the imposed changes may have been insufficient to overcome the flicker and larger contrast in the dominant image. In any case, changes in spatial frequency and orientation involve local changes in contrast, even if there is no mean change in contrast.

Walker and Powell (1979) repeated the experiment with the left and right images equally dominant and found that changes in the contrast, spatial phase, or spatial frequency of the suppressed image terminated the suppressed phase. Changes in spatial frequency and orientation involve local changes in stimulus energy and transient signals. O'Shea and Crassini (1981a) found that suppression was rapidly terminated when the orientation of a suppressed image was changed by more than 20°, but not when it was changed by less than 20°. Larger changes in orientation could involve stronger transient signals than small changes in orientation. It may not be necessary to conclude that spatial frequency or orientation are analyzed as such in the suppressed image or that suppression acts selectively with respect to orientation and spatial frequency.

The suppressed phase was not terminated when horizontal and vertical rivalrous patterns in the two eyes were interchanged (Blake et al. 1980a). Alternating the images changes both to the same extent, and it is therefore not surprising that the change in the suppressed eye did not penetrate suppression.

A small near-threshold test flash superimposed on a grating presented to only one eye was detected less frequently than when it was accompanied by a similar test flash presented to a corresponding region in the dark field of the other eye (Westendorf et al. 1982). It was concluded that a stimulus in a suppressed eye can summate binocularly with one presented in a dominant eye. But the test flash on the dark ground may not have been suppressed continuously by the grating in the other eye and may therefore have increased the probability of detection even if the two flashes did not summate.

Inspection of any pattern for a period of time leads to a loss of apparent contrast and, if a pattern is inspected with fixed gaze, parts and sometimes the whole of the pattern periodically fade completely. This is the Troxler effect. When an image is retinally stabilized by optical means, it fades for as long as the image is stabilized. It is therefore not surprising that prior inspection of a patterned stimulus by one eye decreased the duration of dominance of that stimulus when it was dichoptically paired with a rivalrous stimulus (Wade and de Weert 1986).

8.4.4 Suppression and eye dominance

Eye dominance is defined in a general way as a preference for the use of one eye over the other. Most people are right-handed and right-eyed, but there are conflicting claims about whether eye dominance is correlated with handedness such that those who are left-handed tend also to be left-eyed (Miles 1930; Eyre and Schmeeckle 1933; Gronwall and Sampson 1971). In animals with hemidecussating visual inputs, eye dominance has nothing to do with cerebral dominance, because each eye projects to both cerebral hemispheres.

The following three criteria have been used to define eye dominance:

1. The dominant eye is the one with better visual acuity or other measure of visual functioning. When there is an imbalance of function between the two eyes, as when one eye has better acuity or contrast sensitivity, the better eye tends to suppress the weaker eye. In severe cases, the weaker eye is amblyopic and is permanently suppressed when both eyes are open (see Section 15.7.3).

2. The dominant eye is the one used for sighting when, for instance, one looks at a distance object through a ring held in both hands at arm's length with both eyes open.

3. The dominant eye is the one seeing a rivalrous stimulus for a longer period than the other eye.

There are many tests of eye dominance based on these definitions, and a good deal of controversy exists about whether the different tests correlate. For instance, rivalry tests of ocular dominance have been found to be poorly correlated with sighting tests (Washburn et al. 1934). This literature has been reviewed by Coren and Kaplan (1973), who conducted a factor analysis on the results of 13 tests of eye dominance given to 57 normal subjects. The results revealed three principal factors, acuity dominance, sighting dominance, and rivalry dominance, with most of the variance being accounted for by sighting dominance. The subjects in this study had normal vision. In amblyopes, the principal factor in eye dominance is the amblyopia.

8.5 RIVALRY AND STEREOPSIS

The view of Galen that the two images fuse in the optic chiasma held sway for about 1,500 years and was replaced in the seventeenth century by the view that fusion occurs in the brain (see Section 1.2.1). After 1838, when Wheatstone proved that binocular disparity formed the basis of stereoscopic vision, the need arose to reconcile the fusion of images with the processing of disparity. Four basic accounts of the relationship between fusion and disparity detection have been proposed. We have named them the mental theory, the suppression theory, the two-channel theory, and the dual-response theory.

1. *The mental theory.* Helmholtz (1909) objected to idea of fusion of images at an early stage of visual processing. He wrote that "*The content of each separate field comes to consciousness without being fused with that of the other eye by means of organic mechanisms; and therefore, the fusion of the two fields in one common image, when it does occur, is a psychic act.*" (p. 499). His argument was based on the fact that black in one eye and white in the other do not produce gray, as the fusion theory would predict, but binocular lustre. This objection does not hold if only similar images fuse. He also pointed out that with very short exposures we can distinguish between depth based on crossed images and that based on uncrossed images. This means that we must register which eye receives which image, and he argued that this would not be possible if the two images fused. This

objection to the fusion theory does not hold for a mechanism containing some binocular cells tuned to crossed disparities and others tuned to uncrossed disparities. Such cells create a unified set of signals from the two inputs but preserve all the information required to code depth. In talking about a "psychic act" Helmholtz was motivated by the observation that we do not normally notice the many diplopia images arising from objects out of the plane of the horopter. This must be an attentional process, since the diplopia images become visible when we make a special effort to see them. On the other hand, Helmholtz did not support the suppression theory in which the images are processed in alternation, although his only argument against the theory was that, "*the perception of solidity given by the two eyes depends upon our being at the same time conscious of the two different images.*" (Helmholtz 1893, p. 262).

Sherrington (1904) also believed that binocular fusion results from "*a psychical synthesis that works with already elaborated sensations contemporaneously proceeding.*" From his experiments on binocular flicker (see Section 9.2.3) he concluded that fusion is not based on a physiological mechanism like the convergence of nerve impulses in the final common path of the motor system.

2. *The suppression theory.* According to the suppression theory of binocular vision there is only one form of binocular interaction, namely, rivalry, which operates for both similar and dissimilar images. According to one account, the position of each image is sampled intermittently and disparity is detected by a subsequent comparison process. According to the second view, information from the suppressed image is processed for purposes of disparity detection (Kaufman 1964). In this form, the suppression theory is equivalent to the two-channel account.

3. *The two-channel theory.* According to this theory, rivalry and fusion with stereopsis are distinct processes that occur in separate neural channels. Thus, a given dichoptic stimulus may engage both processes. For instance, similar but not identical dichoptic images may elicit alternating suppression in one channel and at the same time engage the disparity-detecting mechanism through the other channel. Therefore, these neural channels can be activated simultaneously in the same location of the visual field (Wolfe 1986b).

4. *The dual-response theory.* According to this theory, rivalry is a state of gross alternating suppression occurring between dissimilar dichoptic stimuli. Similar images do not alternate, but fuse to produce a stable signal that engages the disparity detection system. Rivalry and fusion are distinct processing modes of the same neural circuits and

therefore may occur at the same time in different parts of the visual field, but not simultaneously in the same location. Another view is that they may occur in the same location but with one occurring in the chromatic channel and the other in the achromatic channel. The disparity-detection mechanism may involve inhibitory processes in the ocular dominance columns but not a gross alternation between the images in the two eyes.

8.5.1 The suppression theory of binocular fusion

The suppression theory of binocular fusion states that binocular rivalry occurs even when the stimuli presented to the two eyes are the same. According to Duke-Elder (1968b, p. 684) the earliest references to the suppression theory were made by Porta (1593), Gassendi (1658), and du Tour (1760). Washburn (1933) and Verhoeff (1935) gave fuller accounts of the suppression theory, although they produced no evidence other than general observations about binocular rivalry. A lively account of the suppression theory was provided by Asher (1953).

One cannot test the suppression theory by observing binocular rivalry since it is not possible to tell which eye is seeing the stimulus when the stimuli are alike. The theory can be tested by measuring the effects of suppression on a test stimulus presented to an eye both when the eye is in its suppressed phase and when it is in its dominant phase. Three indicators of suppression are available, (1) the luminance or duration threshold of a test flash (Wales and Fox 1970), (2) the reaction time of a response made to a test flash, and (3) success in recognizing a flashed patterned stimulus such as a letter.

When a vertical grating was presented to one eye and a horizontal grating to the other, it took observers longer to respond to a flash superimposed on the suppressed image than to one superimposed on the dominant image. When the orientation of the grating was the same for both eyes, the reaction time to the flash was the same for either eye and the same as when the flash was superimposed on a monocularly viewed grating (Fox and Check 1966a). This suggests that neither image is suppressed when the images in the two eyes are identical. A flash was also detected equally well by either eye when the two gratings had a disparity that produced a slanted surface (Blake and Camisa 1978). Thus, superimposed dichoptic images do not suppress each other when they differ enough to yield an impression of depth.

In another study, subjects recognized a letter superimposed on a dominant image but not one superimposed on a suppressed image (Fox and

Check 1966b). A letter superimposed on either one of a pair of fused images was consistently recognized just as well as when it was superimposed on a stimulus presented to only one eye.

On the other hand, Makous and Sanders (1978) reported that a test flash presented to one eye when the two eyes viewed identical patterns was not detected as frequently as when the eyes viewed different patterns with the flash presented to the eye in its dominant phase of rivalry. This does not prove that the eyes engage in alternating rivalry when viewing identical patterns; it may simply reflect some degree of constant mutual inhibition between identical stimuli.

When a vertical grating was presented to one eye and superimposed vertical and horizontal gratings to the other eye, reaction time to a decrement in contrast in any one of the gratings was the same for all three gratings. In other words, neither of the vertical gratings was suppressed, nor was the horizontal grating that was superimposed on one of the vertical gratings. The vertical grating, being fused with the vertical grating in the other eye, kept the superimposed horizontal lines dominant (Blake and Boothroyd 1985). This demonstrates that fusion takes precedence over rivalry. Presumably a fused image supports a nonfused image only over a certain distance.

According to the suppression theory, reaction times to a monocular flash superimposed on a binocularly viewed stimulus should show a skewed distribution because the image on which the flash is superimposed is sometimes in its suppressed phase and sometimes in its dominant phase. O'Shea (1987) found the expected skewed distribution when the stimuli were rivalrous but not when they were similar and fused.

Summary

Most of the evidence just cited supports the view that alternate suppression of one image by the other does not occur when congruent or near-congruent patterns are fused. We must therefore reject this form of the suppression theory of binocular fusion. That is not to deny that mutual inhibition of images is involved in the fusion of similar images. The physiological evidence reviewed in Section 4.5 shows that some binocular cells are strongly dominated by excitatory inputs from only one eye and are inhibited by inputs from the other eye. The psychophysical evidence suggests that any mutual inhibition between the two eyes when they view similar images is the same for both eyes and does not result in the alternation of suppression seen when the images are dissimilar.

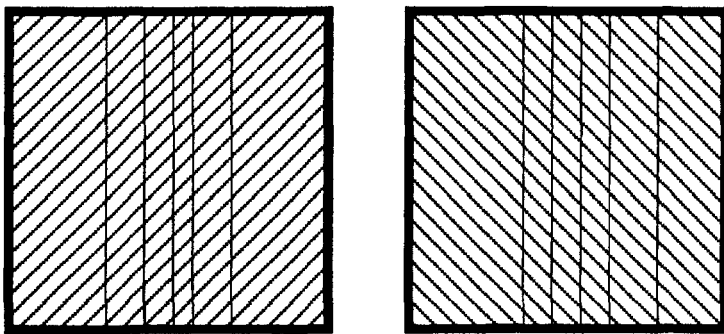
8.5.2 Two-channel and dual-response accounts

According to the dual-channel account, fusion and rivalry are distinct processes that can coexist in the same location in the visual field and be evoked by the same stimulus. According to the dual-response account, rivalry occurs only when images have failed to fuse. Furthermore, fusion and rivalry are not evoked by the same stimulus and do not occur simultaneously in the same location in the visual field. We will now review the evidence on the question of whether fusion and rivalry can occur simultaneously in the same location.

Kaufman (1964) prepared a random-dot stereogram with a green background in one eye and a red background in the other. The disparate patterns of black dots generated a cyclopean form in depth while the colours of the background produced binocular colour rivalry. Kaufman argued that colour rivalry and fusion stereopsis occur simultaneously in the same location. The same point is illustrated by the fact that depth is evident in anaglyph stereograms in which the two eyes are presented with differently coloured images. However, we do not have to conclude that the dots engaged in both rivalry and fusion-stereopsis but only that, while rivalry occurs in the chromatic channel, fusion stereopsis can occur in the achromatic pattern channel. This would be a weak version of the dual-channel theory. A stronger version, espoused by Tyler and Sutter (1979) and Wolfe (1986b), is that rivalry and fusion stereopsis occur simultaneously for the same patterned stimuli. We will look at some of the evidence for this strong version of the dual-channel theory. Other literature on the coincidence of rivalry and stereopsis is reviewed in Section 6.1.2.

An impression of depth is apparent in disparate non-rivalrous lines superimposed on a background of rivalrous lines, as in Figure 8.16 (Ogle and Wakefield 1967). This could be regarded as supporting the view that rivalry and fusion can coexist in the same location, but it could also be interpreted as another example of fusion taking precedence over rivalry in regions where corresponding images are located.

Julesz and Miller (1975) found that depth was still apparent in a random-dot stereogram when random-dot noise with a spatial-frequency 2 octaves higher than that of the stereogram was added to the stimulus in one eye. They argued that, in a given spatial region, stimuli of one spatial frequency can generate stereopsis while stimuli of another spatial frequency can generate rivalry. Blake et al. (1991b) used a similar stimulus but concluded that impressions of stereopsis and rivalry are generated in

**Figure 8.16. Stereopsis with rivalry.**

Depth is apparent in the nonrivalrous vertical lines superimposed on the background of rivalrous lines. (Reproduced with permission from Ogle and Wakefield 1967, *Vision Research*, Pergamon Press.)

distinct regions of the stereogram rather than in the same region. Subjects viewed a random-dot stereogram that yielded depth. Random-dot noise was added to one eye. When the noise had low contrast, subjects saw depth and a single stable display including the noise. At intermediate contrast levels, regions of rivalry and regions of depth were seen but not in the same place. At high contrast levels, the noisy display was dominant and there was not much evidence of depth.

It has been claimed that suppressed images may contribute to stereoscopic depth. Blake et al. (1980a) presented a vertical grating in one eye and a horizontal grating in the other. A vertical grating was presented for 1 s to the same eye as the horizontal grating during periods when only the horizontal grating was visible. During these periods, subjects reported seeing a vertical grating slanted in depth according to the disparity between the two vertical gratings, one of which was in the suppressed eye. They concluded that information for stereopsis is extracted before the suppression stage or it survives suppression because it is processed in a parallel channel. However, they admitted that the presence of similarly oriented lines in the two eyes during the 1 s test period may have temporarily suspended the suppression process, at least in those parts of the display containing near-congruent images. In view of this possibility this evidence does not provide strong support for the idea of parallel channels for rivalry and stereopsis arising in the same location.

Tyler and Sutter (1979) obtained an impression of slant from stereograms consisting of randomly changing vertical bars filtered to give slightly different spatial-frequency bands in the two eyes (dif-frequency disparity discussed in Section 7.2.3). The impression of slant persisted even when the lines were uncorrelated in the two eyes and drifted at 4°/s in opposite directions. Rivalry thus existed both between the uncorrelated lines and the two directions of motion. They argued that this impression of slant arises from a primitive dif-frequency mechanism in

which width disparity is detected at the same time as the uncorrelated bars engage in rivalry. However, in the uncorrelated displays only a subset of bars rivalled at any instant, and perhaps the disparity signal was carried by bars that were not in rivalry.

If rivalry and disparity are processed by the same neural machinery operating in different ways, then it should take time to switch from the rivalry-processing mode to the disparity-processing mode.

Harrad et al. (1994) investigated this question. They presented half of a stereo target to the left eye and a grid of oblique lines to the right eye and asked the subject to press a button when the stereo target was suppressed by the grid. At this point the grid was replaced by the other half of the stereo target for a variable period of time and the subject judged the relative depth of the two vertical lines of the stereo target. Stereoacuity was elevated for 150 to 200 ms after the grid was removed. A control condition showed that the effect was not due to monocular masking. These are shorter intervals than the mean period for which the stereo half target would have remained suppressed if the grid had not been replaced by the other half target. They concluded, in agreement with Wolfe (1986b), that the onset of a fusible target terminates suppression but that the fusion and disparity detection mechanism takes time to become fully operational.

Summary

The view that fusion and rivalry occur simultaneously in the same location and in distinct channels has been championed by Wolfe (1986b) and contested by Blake and O'Shea (1988) and by Timney et al. (1989). Readers are referred to these sources for a detailed assessment of the evidence bearing on the two theories. On balance, we believe the evidence favours the dual-response account, namely, that rivalry and stereopsis are mutually exclusive outcomes of visual processing in any given location of the visual field. At least this seems to be the case for visual processing of patterned stimuli. However, it is

possible that rivalry within the purely chromatic channel can proceed simultaneously with stereopsis based on disparity between patterned images in the same location. Evidence reviewed in Section 4.2.5 shows that chromatic and patterned stimuli are processed in channels that are partially distinct, even at the level of the retina and geniculate nucleus. Evidence reviewed in Section 6.1.4 suggests that stereoscopic processing is very weak or absent in the purely chromatic channel.

8.6 THE SITE OF BINOCULAR SUPPRESSION

Presumably, the processing of complex visual features occurs only for images that have survived binocular suppression, since suppression eliminates all conscious awareness of suppressed visual stimuli. Since binocular suppression depends on the relative position, orientation, and contrast of the images in the two eyes, it is to be expected that some processing of these features precedes suppression. The evidence reviewed here shows that certain visual induction effects that depend on the spatial frequency, orientation, and motion of stimuli are evident while the induction stimulus is suppressed.

8.6.1 Suppression and spatial-frequency

Blake and Fox (1974b) found that a binocularly suppressed stimulus created a threshold-elevation after-effect and concluded that suppression occurs after the site where this effect is generated. They used the stimulus shown in Figure 8.17. An adaptation grating was presented continuously or intermittently to one eye for 30 s, after which the subject adjusted the contrast of a newly exposed comparison grating in a neighbouring position in the same eye to match the apparent contrast of the adaptation grating. The adaptation grating showed the familiar loss of apparent contrast, which was greater for continuous exposure than for intermittent exposure, in conformity with results of previous investigations. The experiment was then repeated, but with the adaptation grating suppressed for at least half the 30-s adaptation period by a rivalrous grating present in the other eye. In two strabismic subjects capable of alternating suppression, the adaptation grating was suppressed for the full 30 s (Blake and Lehmkuhle 1976). In spite of this suppression, the adaptation effect was as strong as when the adapting grating was visible for the whole 30-s period.

In a second experiment, Blake and Fox (1974b) used a similar procedure to show that the spatial-frequency aftereffect (a perceived shift in spatial

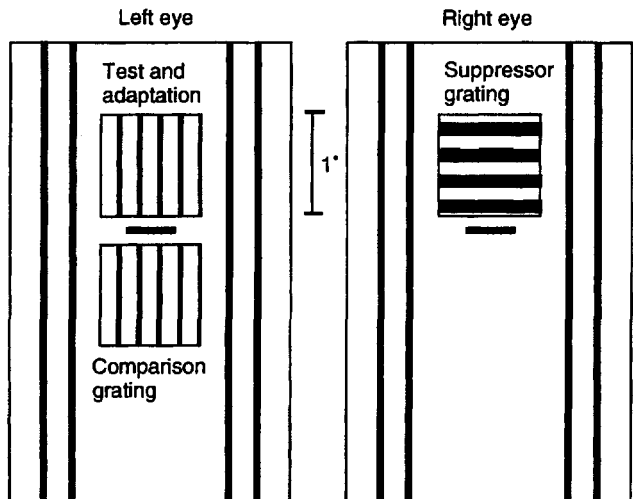


Figure 8.17. Threshold elevation from suppressed image. Stimuli used by Blake and Fox (1974b) to reveal that adaptation to a suppressed grating may generate a threshold-elevation effect. During the adaptation period, subjects fixated within the horizontal bar and the adaptation grating in the left eye was suppressed by the grating in the right eye. In the test period the right-eye grating was removed and subjects matched the contrast of a newly exposed comparison grating in the left eye to that of the test grating. (Reprinted by permission of Nature, 249, 488-490; Copyright, 1974, Macmillan Magazines Limited.)

frequency away from that of an induction stimulus) was also at full strength when the induction grating was suppressed for a good part of the induction period. Blake and Fox concluded that binocular suppression occurs at a site after that responsible for the contrast adaptation effect and the spatial-frequency aftereffect. However, they measured these aftereffects only in the previously suppressed eye, and the results could be due to adaptation of monocular neurones that are unaffected by suppression (but unavailable to consciousness). Perhaps the contrast of the adaptation grating was reduced by the afterimage of the suppressor grating in the other eye.

Blake and Overton (1979) overcame the problem of unsuppressed monocular neurones by showing that the threshold-elevation aftereffect tested in the eye opposite to that exposed to the induction stimulus was also not weakened when the induction stimulus was suppressed for a substantial part of the induction period. They also found that adaptation to a grating presented to one eye lessened the subsequent dominance of that grating when it was pitted against an orthogonal grating in the other eye. Wade and Wenderoth (1978) reported that the tilt aftereffect was also not weakened when the induction stimulus was suppressed for a good part of the induction period.

These results strengthen the conclusion that the processes responsible for contrast adaptation, the spatial-frequency aftereffect, and the tilt aftereffect occur before those responsible for binocular suppression. Blake and Overton were convinced that contrast adaptation and the spatial-frequency aftereffect are cortical and therefore occur at least in area V1. Since the aftereffects preceded binocular suppression, they concluded that binocular suppression occurs beyond V1. They agreed that it must be processed fairly early, because it is not a cognitive process and does not occur in meaningful units (see Section 8.9.2). We now look critically at the claim that binocular suppression occurs beyond V1.

Both contrast and spatial frequency are, at least to some extent, coded at the retinal level—contrast by lateral inhibitory processes and spatial frequency in terms of receptive fields of different sizes. The processes responsible for the two aftereffects may therefore arise in the retina or LGN and, if they do, the argument for placing binocular suppression beyond V1 collapses. The belief that spatial-frequency aftereffects are cortical is based on the fact that they show interocular transfer. This, in itself, is not a convincing argument. An afterimage shows interocular transfer, in the sense that an afterimage impressed on one eye is visible when that eye is closed and the other eye opened. This does not prove that afterimages are cortical in origin, but simply that activity arising in a closed eye still reaches the visual cortex.

An afterimage is no longer visible when the eye in which it was formed is inactivated by the application of pressure to the eyeball (Oswald 1957). Thus, to prove that any aftereffect is cortical, one must show that it survives pressure blinding of the eye to which the induction stimulus was presented. An eye may be rapidly rendered temporarily blind by applying pressure to the eyeball. Blake and Fox (1972) found that the threshold-elevation effect survived retinal paralysis, but this still leaves open the possibility of LGN involvement. The conclusion that spatial-frequency aftereffects are cortical is supported by the finding that exposure to a grating of a given spatial frequency and orientation reduces the firing rates of neurones in the visual cortex but not of those in the LGN (Movshon and Lennie 1979).

Even if contrast and spatial-frequency aftereffects are cortical and precede binocular suppression we still do not have to conclude that the site of suppression is beyond V1. The processes responsible for contrast and spatial-frequency coding and those responsible for the combination of binocular inputs could occur sequentially within V1.

The "square-wave illusion" is an example of spatial-phase adaptation (Leguire et al. 1982). When a

grating with a triangular luminance profile is viewed for some time it begins to look like a square-wave grating, that is, a grating with the same frequency components but with the component spatial frequencies in antiphase rather than in phase. Binocular suppression of the induction stimulus severely reduces the illusion (Blake and Bravo 1985). It looks as though more complex effects that depend on interactions between several spatial frequencies occur after suppression.

Vertical lines covering a disc appear tilted clockwise when the disc is surrounded by an annulus of lines tilted counter-clockwise. This is simultaneous tilt contrast. There is conflicting evidence as to whether tilt contrast persists when the lines of the induction annulus are suppressed by an annulus of horizontal lines in the other eye. Wade (1980) found that it did survive suppression, but Rao (1977) found that it did not.

Vertical lines appear tilted clockwise after inspection of counterclockwise tilted lines presented in the same location. This is the tilt aftereffect. Wade found that the magnitude of the tilt aftereffect was not reduced when the inspection stimulus was suppressed by a rivalrous horizontal grating presented to the other eye. These effects must be cortical because precortical sites have no orientation tuning (see Section 4.1.2).

Summary

We conclude that processes responsible for the threshold-elevation effect, the spatial-frequency aftereffect, the tilt aftereffect, and perhaps tilt contrast occur before those responsible for binocular suppression. It is difficult to draw firm conclusions about the site where binocular suppression occurs.

8.6.2 Suppression and visual motion

When an image is suppressed, all visual attributes of the image, including its motion, are removed from conscious awareness. It takes a person longer to react to a motion signal that has its onset while the stimulus is suppressed than to one that has its onset in a non-suppressed period. Presumably, the suppressed image must become dominant before its motion can be detected (Fox and Check 1968).

The motion aftereffect from a suppressed image

Even though motion remains unavailable to consciousness during suppression, some processing of motion signals occurs before the stage of suppression. When a moving textured display is viewed for some time, a stationary display seen in the same location appears to move in the opposite direction.

This is the motion aftereffect. The duration of the monocularly observed motion aftereffect increases with the duration of the inspection stimulus. Lehmkuhle and Fox (1975) found that the duration of the motion aftereffect when the test and adapting gratings were viewed by the same eye was not reduced when the adapting stimulus was suppressed for a substantial fraction of the inspection period by a stimulus presented to the other eye. Also, the amount of interocular transfer of the motion aftereffect was the same when the induction stimulus was suppressed by binocular rivalry as when it was visible for the whole inspection period (O'Shea and Crassini 1981b). Thus, some processing of visual motion must precede suppression. On the other hand, the motion aftereffect produced by a rotating display or by a rotating spiral was attenuated when the induction stimulus was suppressed (Lack 1978; Wiesenfelder and Blake 1990). The visual processes responsible for detecting rotary and spiral motions are more complex than those responsible for detecting simple linear motion. Binocular suppression seems to occur after the site of simple motion detection but before that of complex motion detection. One cannot argue from this that suppression occurs beyond V1, because several stages of visual processing may occur in V1.

Apparent movement from a suppressed image

There has been some dispute about whether rivalry suppresses the generation of apparent movement. Ramachandran (1975) found that a spot superimposed on a suppressed pattern did not generate apparent motion with respect to a nearby spot presented sequentially on the dominant pattern in the other eye. On the other hand, Wiesenfelder and Blake (1991) found that apparent motion between two sequentially presented spots could be detected when the first spot was suppressed by a rivalrous stimulus. The apparent motion with a suppressed image was not as clear as that seen with both spots in view, and they concluded that the motion signal is weakened by suppression.

Shadlen and Carney (1986) obtained dichoptic apparent movement by presenting a flickering grating in one eye and the same grating to the other eye but with a 90° spatial phase shift and a 90° temporal phase shift (see Section 13.4.1). Carney et al. (1987) had one eye view a yellow and black grating while the other eye viewed an isoluminant red and green grating. When the two gratings flickered with a 90° spatial and temporal phase shift, apparent motion was seen in a direction consistent with the luminance component of the alternating gratings. But colour rivalry was seen at the same time. They

concluded that rivalry can occur in the colour channel of the visual system while motion is seen in the luminance channel. This is similar to the argument used by Ramachandran and Sriram (1972) to account for the simultaneous occurrence of stereopsis and colour rivalry in a random-dot stereogram (see Section 6.2.10).

To account for these effects, it may not be necessary to assume that two channels are simultaneously activated at the same spatial location. Colour rivalry may have occurred locally within areas between the contours that defined the apparent movement. In other words, the two effects may have been segregated spatially rather than by virtue of parallel visual channels serving the same spatial location.

8.7 MODELS OF BINOCULAR RIVALRY

The simplest way to think about binocular rivalry is to suppose that it is due to mutual inhibition between competing stimuli arising in the two eyes. This can be called the **mutual suppression mechanism**. If the two images mutually suppressed each other, like red and green cone inputs to the colour-opponent mechanism, the outcome would be a steady response weaker than that to either input alone. The mutual inhibition must be time dependent in the manner of a bistable oscillator (Matsuoka 1984; Sugie 1982). To account for the alternation between rivalrous images, one must suppose that the *potency* of the dominant image to inhibit the suppressed image gradually weakens but without affecting the *visibility* of the dominant image. At the same time the suppressed image recovers its potency to inhibit the dominant image without affecting the visibility of the suppressed image. At a certain threshold point the suppressed image becomes visible and the dominant image becomes suppressed. The two images then reverse their roles. The rule is that a visible image gradually loses its inhibitory potency while the nonvisible image gains in inhibitory potency. The rate of alternation depends on the time constants of these processes and the relative visual *strengths* of the two images. The strength of an image is determined by its luminance, contrast, and figural complexity. The inhibitory potency of an image depends on its strength and its changing value in the duty cycle. Whether an image is visible or suppressed depends on its strength and inhibitory potency relative to the image in the other eye. Any change in the relative strengths of the two images results in a corresponding change in the relative durations of their dominance and suppression phases.

An alternative view is that an image does not compete when it is suppressed. The duration of dominance of an image depends only on the strength of the dominant image and not on its strength relative to the suppressed image. This can be called the **dominant suppression mechanism**. A third alternative is to suppose that the duration of the dominance and suppression phases depend only on the strength of the suppressed image. This view conforms with Levelt's proposition, which was presented in Section 8.3.2. We refer to this as the **suppression recovery mechanism**.

These three views lead to different predictions when the contrast of the image in one eye (say the left eye) is increased while that in the other eye is kept the same. According to the mutual inhibition account, the duration of left-eye dominance should increase and that of right-eye dominance should decrease by a proportional amount, leaving the overall rate of alternation the same. According to the dominant inhibition account, the periods when the strengthened stimulus is seen should increase but the periods when the constant stimulus is seen should remain unchanged. According to the suppression recovery account, periods when the strengthened stimulus is seen should remain constant and periods when the constant stimulus is seen should be shortened. There is evidence in favour of the latter prediction and hence of the suppression recovery account of binocular rivalry (Levelt 1966; Fox and Rasche 1969). However, Mueller and Blake (1989) found that the contrast of a pattern in its dominant phases exerts some influence on the rate of alternation. Bossink et al. (1993) cited evidence that the strength of the dominant image has some effect on the duration of the dominant phase, although they agreed that the influence of a dominant image is less than that of a suppressed image. Mueller and Blake suggested that a mutual suppression mechanism is responsible for rivalry but that it contains an element that makes frequency of rivalry increase with contrast and a nonlinear element sensitive to unbalanced contrast in the two eyes.

Fox and Check (1972) measured the magnitude of suppression by the elevation of the threshold for detecting a test flash superimposed on the suppressed image. The magnitude of suppression tested at several times during the suppression period was found to be constant. They argued that this contradicts the mutual suppression account of rivalry. But the mutual-inhibition theory as we have formulated it does not predict that the visibility of the suppressed image increases but only that its potency to inhibit the dominant image increases.

The converse of this finding is that a dominant image does not become visibly weaker during its dominance phase even though its inhibitory potency weakens. It is only at the point when the images change dominance-suppression roles that there is a change in visibility. In other words, the gradual change in relative inhibitory potential finally results in a saltatory, or winner-take-all, change in visibility. One must distinguish between the visibility of an image (whether it is dominant or suppressed), the strength of an image, and the inhibitory potency of an image.

The dominant suppression and suppression recovery mechanisms make the duration of the dominance phases of the two images independent, since each depends only on its own strength and not on its relation to the other stimulus. Autocorrelation procedures have revealed that the durations of succeeding dominance phases vary randomly and independently of each other (Fox and Herrmann 1967; Walker 1975). Furthermore, the independence and random variation of succeeding phases was the same when the images on each retina were stabilized or viewed as afterimages as when they were viewed normally (Blake et al. 1971; Wade 1975a). This seems to exclude eye movements as a cause of the random variation of dominance phases in binocular rivalry. However, Blake et al. were not justified in concluding from their data that the cause must be central.

Since the duration of suppression depends on the features of the suppressed image, Walker (1978b) argued that these features must somehow evade suppression. But this would follow only if high-level features were involved, and the evidence for this is not very convincing (see Section 8.9.2). Several of the features affecting suppression such as contrast, spatial frequency, and flicker are already coded in the retina. One could explain their effect on recovery from suppression by supposing that inputs from the suppressed eye charge a buffer mechanism and that when the accumulated charge reaches a threshold value it breaks through the inhibitory barrier of the other eye's image. The rate of charging of the buffer depends on the firing frequency of the inputs from the suppressed eye, which in turn depends on features such as contrast, spatial frequency, and flicker. These features would not have to be processed separately, since each contributes to the undifferentiated mean rate of afferent discharge.

A simple reciprocal suppression process cannot account for all the facts of binocular rivalry. However, a type of mutual inhibition which gives greater weight to the suppressed image and is sensitive to contrast imbalance may provide an adequate account. Neural models of binocular rivalry based

on oscillation in recurrent inhibitory connections have been proposed by Lehky (1988), Blake (1989), and Mueller (1990). Readers are referred to these sources for details.

8.8 NEUROLOGY OF BINOCULAR RIVALRY

Little is known about the neural processes mediating binocular rivalry. The lateral geniculate nucleus (LGN) is the earliest stage where these processes could occur. Each cell in the LGN receives a direct input from only one eye and does not respond when only the other eye is stimulated. Nevertheless, for many cells, the response is modified by stimulation of the eye from which the cell does not receive a direct input. This modification could be mediated either by intrageniculate inhibitory connections or by descending influences from the visual cortex. There is some dispute about the role of cortical influences. Some investigators found that binocular interactions in the LGN of the cat require an intact visual cortex (Varela and Singer 1987) while others found that they do not (Tumosa et al. 1989; Tong et al. 1992). A report that interocular influences in the LGN are greatest when the stimuli presented to the two eyes differ in orientation, contrast, and movement prompted the suggestion that these visual features are involved in binocular rivalry, since binocular rivalry is affected by interocular differences between the same features (Varela and Singer 1987).

Others have found that interocular influences in the LGN of the cat are not much affected by changes in stimulus orientation or direction of motion but are affected by changes in spatial frequency (Moore et al. 1992; Sengpiel et al. 1995). This suggests that interocular influences in the LGN serve to balance the responses to small interocular differences in stimulus contrast by adapting the relative contrast gains of the inputs from the two eyes. Interocular influences in the LGN could control both rivalry and contrast gain or the two functions could be served by different classes of interactive processes in the LGN. Even if the inhibitory interactions responsible for binocular rivalry do occur in the LGN, they must depend, at least in part, on signals descending from higher centres, where visual features such as orientation and motion are detected.

At the level of the visual cortex, Lansing (1964) reported that binocular rivalry is accompanied by changes in the cortically evoked potentials recorded from the human head above the visual cortex. A 50°-wide illuminated area flashing at 8 Hz was presented continuously to the left eye, and a steady striped pattern was presented for periods of 5 s to

the right eye. When the striped pattern was present, subjects reported that it dominated the flickering field, and when this happened there was an 82 per cent reduction in the evoked potential fluctuations that were synchronized with the flickering field.

The response of a cell in the visual cortex to an optimally oriented bar or grating is suppressed by the superimposition of an orthogonal bar or grating in the same eye (Bishop et al. 1973; Morrone et al. 1982; Bonds 1989). This is known as cross-orientation inhibition. It is largely independent of the relative spatial phases of the superimposed gratings and operates over a wide difference in spatial frequency between the gratings. Ferster (1987) suggested that the effect originates in the lateral geniculate nucleus, but DeAngelis et al. (1992) list several arguments favouring the view that it results from intracortical inhibition. This is a likely candidate for the mechanism of binocular rivalry and dichoptic masking (Legge 1984a). However, cross-orientation inhibition could not be elicited in cortical cells when orthogonal bars or gratings were presented to different eyes of the anaesthetized cat, even though it was evident when both stimuli were presented to the same eye (Burns and Pritchard 1968; Ferster 1981; DeAngelis et al. 1992). This suggests that the effect is generated before the signals from the two eyes are combined and is not the basis for binocular rivalry.

However, Sengpiel and Blakemore (1994) recently found that the ongoing response of binocular cells in area 17 of the cat to a grating presented in its preferred orientation to the dominant eye diminished when they suddenly presented an orthogonal grating to the other eye. This suppression was not seen when the gratings in the two eyes had the same orientation, except in strabismic cats for which interocular suppression was independent of orientation (see also Sengpiel et al. 1995). It was also not evident in monocular cells in layer 4 of the visual cortex, before the level of binocular cells.

Collaterals from the axons of pyramidal cells in area 17 project horizontally for up to 8 mm within layers 2, 3, and 5. This represents several receptive-field diameters. These horizontal dendrites produce spaced clusters of predominantly excitatory synapses (Gilbert and Wiesel 1985), and radioactive labelling in the cat has revealed that they link cells with a similar preference for the orientation of the stimulus (Gilbert and Wiesel 1989; Hirsch and Gilbert 1991). These dendrites are therefore unlikely to serve as a basis for binocular rivalry, which occurs between stimuli differing in orientation. They could serve to build large receptive-field units that respond to lines in a particular orientation, or they could serve to modify the response of cells according

to the nature of surrounding stimuli (Gilbert et al. 1991). Binocular rivalry is presumably served by shorter inhibitory connections between cortical cells (see Section 4.2.2).

A high-contrast grating presented to one eye, permanently suppresses the response to a low-contrast grating presented to the other eye, when the two gratings are set at a small angle to each other. Binocular cells in areas 17 and 18 of the cat modulated their firing rate in response to a 4.8-Hz phase reversal in the luminance of a low-contrast grating presented to one eye when a homogeneous field was present in the other eye. When a high-contrast grating was added to the other eye, however, the response modulation due to the low-contrast grating was no longer present (Berardi et al. 1986). These effects may have more to do with dichoptic contrast masking that occurs between similar patterns than with binocular rivalry that occurs between distinct patterns in the two eyes.

Logothetis and Schall (1989) trained monkeys to press one key when viewing a display moving to the left and another key when viewing a display moving to the right. When shown dichoptic displays moving in opposite directions, the monkeys changed their response, as first one and then the other display became dominant. While monkeys were making these responses, the experimenters recorded the activity of motion-sensitive binocular cells in the superior temporal sulcus, probably in MT. Some cells that normally responded to a given direction of motion responded only when the monkey indicated that the stimulus moving in that direction was dominant. However, most cells did not exhibit this behaviour.

This evidence places the site of binocular suppression for this type of stimulus in or before MT. A few cells in MT responded to the suppressed stimulus. This could be because some inputs reached this part of the brain from a suppressed image, but it could also be due to the possibility that not all of one image was suppressed.

No firm conclusions can yet be drawn about the physiological mechanisms underlying binocular rivalry.

8.9 COGNITION AND BINOCULAR RIVALRY

So far, binocular rivalry has been discussed as if it were determined by low-level features of the stimulus plus a low-level process that causes a periodic alternation in suppression. We now ask whether binocular rivalry is determined wholly by these "bottom-up" processes or is affected by influences

descending from higher levels in the nervous system, so-called "top-down" processes.

During the 1950s and 1960s there was a lot of interest in the effects of high-level cognitive variables on what had been regarded as low-level visual and perceptual functions. There are two types of cognitive variables. The first type refers to the characteristics and temporary state of the observer, and includes such variables as the observer's attention, expectations, and emotional state. The second type refers to high-level attributes of the stimulus, such as its familiarity, meaning, and emotional significance. Binocular rivalry was selected as a convenient tool for studying the effects of both types of cognitive factor. We deal with each type of variable in turn.

8.9.1 Voluntary control of rivalry

Several investigators have enquired whether the rate of alternation of rivalrous stimuli is under voluntary control. Breese (1899) reported that subjects could influence the duration for which one or the other of two rivalrous stimuli was seen, but he noticed that the eyes moved whenever subjects exercised this control. The more the eyes moved over a dominant stimulus, the longer that stimulus remained in view. Furthermore, a moving stimulus was dominant over a stationary stimulus. Voluntary control over rivalry may therefore have been mediated by eye movements.

Others have agreed that one can exercise some degree of voluntary control over the rate of binocular rivalry (Meredith and Meredith 1962; Lack 1969). However, eye movements and blink rate were not controlled and there was no objective verification of subjects' reports of the relative dominance of rivalrous stimuli in these studies. Reports of rivalry may be checked by superimposing a test stimulus either on the stimulus reported as dominant or on the one reported as suppressed. It has been established that a test stimulus is not visible when superimposed on a suppressed image (Fox and Check 1966b). The ability of the subject to report the test stimulus can thus be used to confirm that the stimulus reported as dominant is indeed dominant. Using this procedure, Collyer and Bevan (1970) found that subjects showed a 10 per cent improvement in their ability to detect a test flash superimposed on a given image after they were given three seconds to bring that image into dominance over a rivalrous image in the other eye. However, voluntary control of dominance was not always achieved, was not continuous, and may have involved only part of the stimulus in one eye.

8.9.2 Binocular rivalry and meaning

In Section 8.4.3 we discussed how a suppressed image may influence certain visual effects such as binocular summation and interocular aftereffects. These processes involve only low-level features of the stimulus such as luminance, contrast, and motion. What is the evidence that high-level, or semantic, features of a suppressed stimulus are processed? Zimba and Blake (1983) addressed this question by making use of the semantic priming effect. In this effect, prior presentation of a word shortens the time needed to decide whether a subsequently presented stimulus is a random letter string or a word semantically related to the priming word. The priming effect was found to operate only when the priming word was presented to an eye in its dominant phase of interocular rivalry. A priming word presented to an eye in its suppression phase had no effect on subsequently presented stimuli. According to this evidence, binocular rivalry occurs at a lower level of visual processing than the level where semantic content is analyzed.

The opposite conclusion was drawn from a study of rivalry in word strings (Rommetveit et al. 1968). They presented a word such as "wine" to one eye and a typographically similar word such as "nine" to the same location in the other eye. These rivalrous words were presented next to a binocularly viewed word, such as "red", that made a meaningful phrase, such as "red wine", with one of the rivalrous pairs but not with the other. In a brief exposure the semantically relevant word was more frequently reported than the irrelevant word. However, a person may be less likely to read "red nine" than "red wine" when both words are presented side by side to the same eye. Since there was no control for this possibility, the results cannot be accepted as evidence for semantic penetration of rivalry suppression. Furthermore, the stimulus exposure may have been too brief to allow rivalry to develop.

A person can follow a verbal message presented to one ear when a different verbal message is presented to the other ear (Cherry 1953; Lewis 1970). Blake (1988) found that subjects could not read a message presented to one eye when a different message was presented to the other eye, even when the messages were in distinct fonts or when the message to be read started 5 seconds before the other.

An erect face has been found to be seen more frequently than the same face inverted, when the two are combined dichoptically (Engel 1956; Hastorf and Myro 1959). But this may not mean that the basic rivalry process is affected by meaning. For much of the time, dominance was incomplete and parts of

each face were visible. Parts of an erect face are more familiar than parts of an inverted face and are therefore more likely to form the basis of the decision about whether the face is erect or inverted. Furthermore, certain features of a face are less affected by inversion than others. For instance, an erect eye and an inverted eye are more alike than an erect and inverted nose. These factors could bias judgments in favour of an erect face quite apart from any influence of binocular rivalry. *This idea could be tested by seeing whether a binocularly viewed face consisting of an equal mixture of erect and inverted regions is more often reported to be erect or inverted.*

Ono et al. (1966) presented subjects with pairs of photographs of faces combined dichoptically. More rivalry was reported between the faces that had been rated as less similar on a variety of criteria, such as pleasant and unpleasant, than between those that had been rated as more similar. But it is not clear from this whether the crucial variable was similarity in terms of the semantic criteria or similarity in terms of low-level features such as the relative positions of contours.

There are also reports that the relative dominance of dichoptically combined words matched for number of letters and frequency of usage depends on the emotional impact of the words as determined by their sexual or aggressive significance (Kohn 1960; Van de Castle 1960). Such results may reflect the willingness of subjects to report that they saw a certain word rather than a greater visual dominance of one type of word over another.

Several studies have reported that the personal significance of the contents of a picture affects which picture predominates when two different pictures are combined dichoptically. For example, Bagby (1957) presented a picture with North American content, such as a boy playing baseball or an American landscape, to one eye and a picture with Mexican content, such as a matador or a Mexican landscape, to the other eye. For North American subjects North American pictures were most often seen while for Mexican subjects, the Mexican pictures were most often seen.

Several problems are associated with these studies of cognitive and personal variables. The frequency with which one stimulus is reported rather than the other may reflect the greater salience of local features of one of the stimuli during those periods when parts of each stimulus are visible. Because of this greater salience of partial features, one stimulus is more likely to be reported than the other during the periods of mixed dominance. This will extend the time during which one stimulus is reported but will not necessarily reflect any basic effect of

meaning on the rivalry process itself. Another problem is that recognition will be more rapid when the more familiar picture is totally dominant than when the unfamiliar picture is totally dominant.

Yu and Blake (1992) attempted to overcome these problems. They found that a face showed longer periods of exclusive dominance over a geometrical comparison pattern than did a control stimulus with the same spatial-frequency content and mean contrast as the face. They obtained the same result when the relative dominance of the patterns was assessed by the reaction time for detection of a probe flashed on the geometrical pattern. The control face may have been more dominant than the control stimulus because it was a face or because it had a coherent shape. They investigated this issue by comparing the duration of exclusive dominance of a hidden

'Dalmatian-dog' figure before it was seen as a dog and again after it was seen as a dog. The dog pattern became more dominant after subjects had been shown that it was a dog by placing a tracing of a dog over it. However, a scrambled version of the dog pattern also became more dominant after subjects had seen the same tracing placed over it. This effect must have been due to suggestion since it was not based on any objective feature of the stimuli. An upright version of the dog pattern was more dominant than an inverted version even though subjects were not aware of the dog. Whatever effects of stimulus configuration are revealed by this set of experiments, they are small compared with effects of stimulus variables such as contrast, spatial frequency, colour, motion, and orientation.

Binocular masking and transfer

9.1 Interocular effects	349
9.2 Binocular summation.....	349
9.2.1 Binocular summation of contrast detection	349
9.2.2 Binocular summation of brightness	356
9.2.3 Dichoptic critical flicker fusion	359
9.2.4 Dichoptic sensitivity to pulsed stimuli	361
9.3 Dichoptic visual masking	363
9.3.1 Introduction	363
9.3.2 Types of visual masking	364
9.3.3 Masking with homogeneous illumination.....	364
9.3.4 Masking with superimposed patterns	365
9.3.5 Visual crowding	368
9.3.6 The threshold-elevation effect	369
9.3.7 Metacontrast.....	369
9.4 Transfer of figural effects	370
9.4.1 Introduction	370
9.4.2 Figural effects with dichoptic composites	371
9.4.3 Interocular transfer of tilt contrast.....	373
9.4.4 Interocular transfer of the motion aftereffect	375
9.4.5 The spatial-frequency shift	378
9.4.6 Interocular transfer of contingent aftereffects.....	378

9.1 INTEROCULAR EFFECTS

In a visual induction effect, one stimulus (the conditioning, or induction stimulus) has an effect on another stimulus (the test stimulus). There are three types of induction effect. The first is **subthreshold summation**, in which the detection threshold of a test stimulus is lowered in the presence of the induction stimulus. The second type is **visual masking** in which the induction stimulus reduces the visibility of the test stimulus. When the induction and test stimuli are presented at the same time it is simultaneous masking, and when they are presented successively it is successive masking. Further subdivisions of masking are set out in Table 9.1. In the third type of induction effect, the figural properties of the test stimulus are affected rather than its visibility. For instance, an induction stimulus may cause an apparent change in the orientation, size, or movement of the test stimulus. These are **figural induction effects**. As with masking, the induction and test stimuli can be presented simultaneously or successively. Geometrical illusions are simultaneous figural effects, and the tilt aftereffect and motion aftereffect are successive effects.

Interocular transfer occurs when a visual effect produced by an induction stimulus applied to one eye is revealed in a test stimulus applied only to the other eye. Interocular transfer of visual effects has been studied for three purposes: (1) to reveal the site of processes responsible for a particular effect, (2) to investigate how inputs from the two eyes are combined, and (3) to reveal the effects of visual pathology on the combination of inputs from the two eyes. The first two purposes are discussed in the following sections and the third is discussed in Section 15.9.

9.2 BINOCULAR SUMMATION

9.2.1 Binocular summation of contrast detection

There is said to be **binocular summation** when visual detection or discrimination is performed better with two eyes than with one eye. The reasons that have been suggested for binocular summation fall into three categories: (1) peripheral factors such as a monocular-binocular difference in fixation, accommodation, pupil size, or rivalry, (2) probability summation, and (3) neural summation of signals from

the two eyes. The literature has been concerned with measuring and understanding the contribution of each of these factors to binocular summation. Blake and Fox (1973) thoroughly reviewed the work on binocular summation up to 1972 and Blake et al. (1981a) extended the review up to 1980.

Peripheral factors

Visual resolution measured with the Landolt C or a with a high-contrast grating is slightly higher with binocular than with monocular viewing (Blake and Fox 1973). Possible peripheral factors are as follows.

1. For a given luminance the diameter of the pupil of an eye increases when the other eye is in darkness and this may degrade acuity. Horowitz (1949) found that the monocular-binocular difference in acuity was reduced when the effects of changing pupil size were removed by an artificial pupil. Another way to eliminate effects of changes of pupil size is to illuminate the nontested eye at the same mean luminance as the eye being tested.

2. Fixation may be better with binocular vision than with monocular vision.

3. If the axis of astigmatism is different in the two eyes, their combined action may be superior to either one. There does not seem to be any systematic evidence on this and the previous possibility.

4. The blank field of the closed eye may rival a patterned image in the seeing eye (see Section 8.3.2). However, rivalry may not affect acuity when the test display is dominant. Acuity is reduced when a monocular test pattern in the dominant phase of rivalry is accompanied by a distinct stimulus in the other eye but not when the stimulus in the other eye is a blank field (Freeman and Jolly 1994).

5. Finally, there may be some form of neural facilitation between the signals from the two eyes. Before this latter possibility can be considered, one must discount the effects of probability summation.

Probability summation

Pirenne (1943) pointed out that at least part of the monocular-binocular difference in acuity may be explained by the statistical advantage of having two detectors. The probability of detecting a stimulus using both eyes (P_b) relative to that of detecting it with either eye alone (P_l and P_r) is given by

$$P_b = (P_l + P_r) - P_l P_r \quad (1)$$

For example, if the probabilities P_l and P_r are 0.5, P_b = 0.75—an improvement of 50 per cent. For the same reason, one is more likely to get at least one head by throwing two coins rather than one. This is classical

probability summation. Bárány (1946) independently proposed the same idea.

There has been considerable debate about the form of the probability function most appropriate for understanding binocular summation. Eriksen (1966) pointed out that formula (1) does not make proper allowance for guessing behaviour and Eriksen et al. (1966) proposed a version to take this factor into account. Another problem is that the calculation is invalid if judgments made with one eye are not independent of those made with the other. For instance, if the thresholds in the two eyes fluctuate together because of some central process, such as fatigue or inattention, then the assumption of independence is violated. If the correlation between noise-related activity were 1 then there would be no statistical advantage in having two eyes. Even a weak correlation between noise-related activity of different neurones can restrict the statistical advantage of probability summation (Zohary et al. 1994b).

In this analysis, we assumed that signals from the two eyes do not combine before a signal denoting the presence or absence of each monocular stimulus has been generated, and that a central decision process has access only to these independently processed signals. Now consider what might happen if the neural signals are combined before a decision about the presence of the stimulus is made.

Empirical determination of probability summation

Theoretical complications implicit in defining probability summation can be side-stepped by measuring the contribution of probability summation empirically and then using this measure as a basis from which to assess the contribution of other factors contributing to binocular summation. This is done by measuring the effect of one stimulus on another stimulus when they are separated spatially or in time. The logic here is that true neural summation does not occur for stimuli well separated in space or in time but that probability summation does occur when the stimuli are separated. We will now see that stimuli separated spatially or in time do not summate beyond the level of probability summation.

Empirically, binocular summation is reduced to the level of probability summation when the time interval between two brief stimuli is increased to more than about 100 ms (Matin 1962; Thorn and Boynton 1974). Temporal aspects of binocular summation are discussed in more detail in Section 9.2.4.

Linear summation of dichoptic inputs

Assume a simple linear summation of neural signals and internal noise independent of stimulus strength. Combining two weak stimuli in the same area of one

eye doubles the probability of detection because the signal strength doubles at the level of the generator potential within the linear range, while internal noise stays the same. The signal-to-noise ratio is doubled (see Section 3.5.2). When signals from two eyes are combined in the brain, trains of discrete nerve impulses combine, not generator potentials. Suppose that two stimuli are presented dichoptically and the neural signals sum linearly at a central site. If the noise in the two eyes is perfectly correlated, neural summation confers no advantage because, although signals due to the stimuli add, so do those due to noise, leaving the signal-to-noise ratio the same. If the noise in the two eyes is uncorrelated, neural summation provides an advantage because two uncorrelated noise sources partially cancel when combined. The combined noise level of two sources of uncorrelated noise is $\sqrt{2}$ times that of each source, but the strength of the signal arising from the stimuli is doubled. If neural signals combine this way, then binocular sensitivity should be $\sqrt{2}$ times the monocular sensitivity (Campbell and Green 1965). With neural summation of monocular signals no classical probability summation occurs, because there are no independent decision processes.

Campbell and Green realized that their analysis rests on the assumption that noise does not arise from a closed or evenly illuminated eye. If it did, binocular performance would be twice as good as monocular performance, since the same binocular noise would be present in both cases, with the signal arising from the binocular stimulus being twice as strong as that from the monocular stimulus. Evidence reviewed in the last chapter suggests that a contour in one eye suppresses activity arising from a corresponding area of even illumination in the other eye. If this is true then noise from an eye lacking contoured stimuli should be either attenuated or completely switched off. However, the only way to be sure that an unstimulated eye has no effect is to pressure blind it. Makous et al. (1976) found that the sensitivity of a single eye improved when the other eye was pressure blinded rather than closed. It was also assumed in Campbell and Green's analysis that there is no internal noise peculiar to the channel in which the signals from the two eyes are summed.

A mechanism that sums the inputs from the two eyes can gain an advantage greater than $\sqrt{2}$ over the single-eye performance in the following three ways.

1. The binocular advantage would be 2 if there were no internal noise before the summation of signals and no severe saturation effects.

2. The binocular advantage would be greater than $\sqrt{2}$ if nerve impulses below the sensation

threshold summed to a suprathreshold value at a central site. Light quanta are summed at the receptor level before nerve impulses are generated, that is, at the level of the generator potential. Under ideal experimental conditions, noise-free stimuli are summed completely within the limits set by Bloch's law of temporal summation and Ricco's law of spatial summation (Schwarz 1993). But for this process to operate at a central site one would have to assume that a stimulus strong enough to generate nerve impulses in one eye would be subthreshold for detection at a higher level when only one eye is open.

3. There could be a facilitatory nonlinear summation of inputs from the two eyes. A binocular AND-gate mechanism must work this way since it is a device that responds only when receiving signals simultaneously from both eyes. If all binocular cells were AND-gates we would see nothing unless both eyes were open. This would be superadditivity with a vengeance. Some binocular cells respond only when both eyes are stimulated (Grüsser and Grüsser-Cornehls 1965), and it may be these cells that determine the level of binocular summation. On the other hand, there are binocular cells that are excited by inputs from one eye and inhibited by inputs from the other. These cells would counteract the influence of the AND cells. There are reasons for believing that AND cells respond best to similar inputs from the two eyes and that inhibitory influences are strongest when the inputs differ. We will see that the advantage of binocular vision over monocular vision is greatest when the stimuli presented to the eyes are similar in shape, size, and contrast.

Signal-detection theory and binocular summation

An account of the processing of summed signals has also been provided in terms of signal-detection theory. In signal-detection theory d' is the criterion-free measure of the detectability of a stimulus, defined as the mean of the fluctuation in the strength of the noise plus neural signal, minus the mean of the fluctuation in the strength of the noise, divided by the common standard deviation of the two fluctuations. When two independent detectors with the same variance of signal and noise are exposed to the same stimulus, the joint detectability of the summed stimulus d'_b is related to the detectabilities of the stimulus in each detector acting alone, d'_l and d'_r , by

$$d'_b = [(d'_l)^2 + (d'_r)^2]^{1/2} \quad (2)$$

This is equivalent to saying that the precision with which the mean of a population is estimated increases in proportion to the square root of the number of observations. Under optimal conditions

this formulation gives the same $\sqrt{2}$ advantage of two eyes over one eye predicted by Campbell and Green's formulation. Green and Swets (1966) referred to this formulation as the **integration model** because it is based on the idea that signals are perfectly summed before a detection decision is made. It is a model of neural summation rather than of probability summation because, in probability summation, all signal-to-noise processing is done in each eye and only "yes" or "no" signals are finally combined. Guth (1971) argued that when the probability of correct detection for each eye (P_m), is the same, the probability of correct detection with both eyes, (P_b) is

$$P_b = P_m + d(P_m - 0.5) \quad (3)$$

where d is the difference between the miss rate and the false-alarm rate. With $P_m > 0.5$, it follows from this equation that when the false-alarm rate is smaller than the miss rate, $P_b > P_m$, but when the miss rate is smaller than the false alarm rate $P_b < P_m$. Guth also argued that whether two eyes perform better than one eye depends on the relative performance of the two eyes and on the relative frequencies of no-signal catch trials to signal trials.

In this discussion we have assumed that neural signals from each eye reach the brain along a single channel and that signal and noise sum algebraically, at least from spatially congruent contoured stimuli. There is some support for the idea that uncorrelated external noise in the two eyes sums algebraically (Braccini et al. 1980). However, visual inputs are grouped into different size-scaled channels, each with its own source of noise, and inputs combine by both summation and inhibition into partially distinct mechanisms in visual cortex. We will see that several models of these processes have been proposed.

Empirical studies of binocular summation

Campbell and Green (1965) measured the contrast sensitivity (reciprocal of threshold contrast) for a sinusoidal grating of various spatial frequencies. The pupils were atropinized and stimuli were viewed through artificial pupils. In monocular testing, the nontested eye viewed a diffuse field with the same mean luminance as the display in the tested eye. Binocular sensitivity was $\sqrt{2}$ higher than monocular sensitivity, in conformity with the idea of simple summation of signals from the two eyes, as mentioned previously. With spatial frequency the same in the two eyes, the ratio of monocular to binocular contrast sensitivity was constant over the visible range of spatial frequencies, a result confirmed by Blake and Levinson (1977). In these experiments, and in others mentioned later, contrast is Michelson

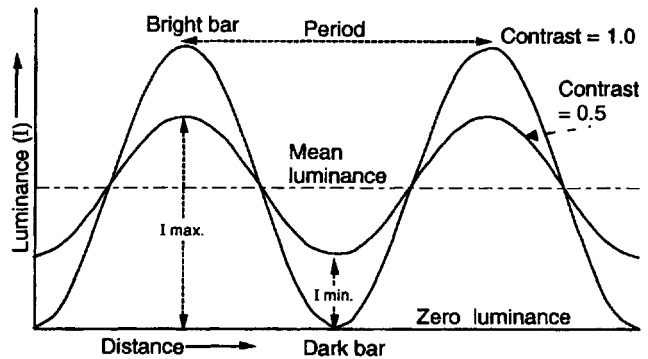


Figure 9.1. Characteristics of a sine-wave grating.

An illustration of the concepts of spatial frequency, luminance modulation, mean luminance, and Michelson contrast of a grating with a sinusoidally modulated luminance profile. Spatial frequency is the number of modulations per degree of visual angle—the reciprocal of the period. Two levels of contrast are illustrated.

$$\text{Mean luminance} = \frac{I_{\max} + I_{\min}}{2}$$

$$\text{Luminance modulation} = I_{\max} - I_{\min}$$

$$\text{Luminance contrast} = \frac{I_{\max} - I_{\min}}{I_{\max} + I_{\min}}$$

contrast, as defined in Figure 9.1. As Michelson contrast is varied, the mean luminance of the grating remains constant. When the mean luminance of a monocular grating was doubled, Campbell and Green found that contrast sensitivity increased by a ratio of only 1.17. We can explain this low ratio by saying that, although the rate of neural firing increases when luminance increases, sensitivity to a difference in luminance (contrast) does not increase in proportion, because the differential threshold increases with increasing level of stimulation. Thus, in experiments on binocular summation of contrast it must be assumed that what is summed is not the signals representing luminance in the two eyes, because summation of these signals would not produce the observed improvement in contrast sensitivity; rather, signals representing contrast are derived in each eye, and it is these signals that sum. The processes of lateral inhibition in the retina generate signals related to contrast which are relatively unaffected by changes in the level of illumination. The binocular advantage can be explained if it is assumed that the contrast signals sum and that noise sums only by $\sqrt{2}$. We will see in the next section that there is other evidence that signals representing luminance do not sum binocularly.

Binocular summation is reduced when the stimuli in the two eyes are spatially separated. Thus, the detectability of a small flashed target fell to the level of summation defined by Green and Swets'

integration model when the disparity of a flashed dichoptic target relative to a fused binocular stimulus was larger than about 20 arcmin, a disparity at about the limit of binocular fusion (Westendorf and Fox 1977). Binocular summation of low-contrast gratings, as reflected in the reaction time for detection, fell to the level of probability summation as disparity increased beyond the limits of Panum's fusional area (Harwerth et al. 1980). The disparity limit of binocular fusion increases as the spatial frequency of the stimulus is reduced (see Section 8.1.4). The range of disparities over which binocular summation occurred showed a similar dependence on spatial frequency (Rose et al. 1988). It appears that binocular summation above the level of probability summation occurs only between dichoptic stimuli that are close enough to fuse.

The tuning characteristics of a binocular cell are fundamentally the same for stimuli presented to one eye as for those presented to the other eye. It is therefore not surprising that interocular summation of contrast sensitivity occurs only when the stimuli presented to the two eyes have similar orientations and spatial frequencies (Julesz and Miller 1975; Westendorf and Fox 1975; Blake and Levinson 1977), directions of motion and temporal properties (Blake and Rush 1980), clarity of focus (Harwerth and Smith 1985), and wavelength (Trick and Guth 1980).

Wolf and Zigler (1963, 1965) measured the detectability of a 1° test patch at various positions on a circle with a radius of 10° around the fovea. Detectability was greater for binocular than for monocular viewing except when the test patch fell on the midvertical meridian of the visual field. They argued that the two halves of a test patch on the midvertical meridian project to opposite cerebral hemispheres so that, although each hemisphere receives inputs from both eyes, it receives only half the total area.

In summary, it can be stated that binocular summation of contrast is greater for stimuli that are close together in space and in time, have similar stimulus characteristics, and stimulate the same hemisphere.

Legge (1984a) found that the monocular contrast-detection threshold for a 0.5 c/deg sine-wave grating was about 1.5 times the binocular threshold, which is similar to the value reported by Campbell and Green. In other words, the contrast of a monocular grating must be increased about 50 per cent to be equally visible as a binocular grating. The slopes of the inflection points of monocular and binocular psychometric functions for this task had the same value of about 2, as shown in Figure 9.2a. The horizontal separation of the monocular and binocular psychometric functions indicates the difference in threshold for a given percentage of

signal detection. In this example, for a detection rate of 75 per cent, the monocular threshold is 1.4 times the binocular threshold. The vertical separation between the two functions indicates the difference in percent detection for a given contrast. In Figure 9.2b the psychometric functions are plotted on log-log coordinates, and percent detection is converted into the detectability measure, d' . This reveals that when the two curves have a slope of 2, the difference between binocular and monocular detectability for a given contrast, as indicated by the vertical separation of the functions, has a ratio of 2 to 1. For functions with a slope of 1, the ratio of thresholds is the same as the ratio of detectabilities. In general, the detectability (d') for a grating of contrast C presented to one eye is given by the relationship

$$d' = \left(\frac{C}{C'} \right)^n \quad (4)$$

where C' is the threshold contrast (at a criterion of $d' = 1$, or approximately 76 per cent correct detection), and n is the slope of the psychometric function, which in Legge's experiment was 2.

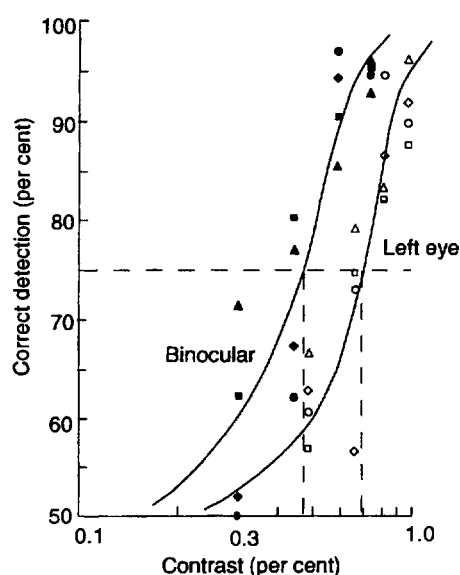
Thus, when the psychometric function for detection has a slope of 2, the monocular contrast threshold is 1.4 times the binocular threshold, as predicted by neural summation of contrast, but the detectability of a binocularly viewed grating at the binocular threshold is twice that of a monocularly viewed grating at the monocular threshold. According to equation (2), neural summation predicts that binocular and monocular detectabilities should have a ratio of 1.4 to 1. The difference between the ratio of contrast-detection thresholds and the ratio of detectabilities arises because the detectability of a stimulus is not a linear function of its contrast.

Legge (1984b) proposed that the effective binocular contrast of a grating (C_b) is the quadratic sum of the monocular contrasts (C_l and C_r) or

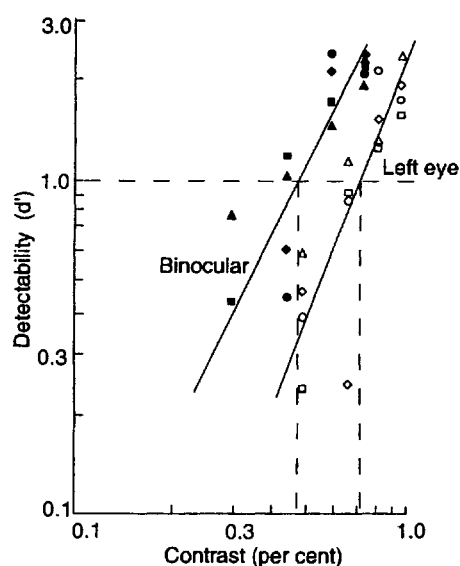
$$C_b = \sqrt{(C_l)^2 + (C_r)^2} \quad (5)$$

When dichoptic stimuli have the same contrast and the eyes have the same threshold, the binocular contrast threshold is $\sqrt{2}$ times the monocular threshold. The quadratic summation rule assumes that the stimuli in the two eyes are the same except in contrast. Presumably the model could be generalized to accommodate other differences between the stimuli in the two eyes by adding weighting functions to the two monocular contrasts.

When the luminance of a grating was made very different in the two eyes by placing a neutral-density



(a) Psychometric functions showing percent correct detection of a 0.5 c/deg grating as a function of its contrast, for monocular and binocular viewing. For 75 per cent detection, the monocular contrast threshold is about 1.5 times the binocular threshold, as indicated by the separation between the vertical lines. At the inflection points both functions have a slope of about 2.



(b) The same psychometric functions plotted on log-log coordinates with percent detection converted into the detectability measure, d' . For a d' of 1.0 (about 76 per cent detection) the horizontal distance between the functions indicates that the monocular contrast threshold is about 1.5 times the binocular threshold. The vertical distance between the functions indicates that, for a given contrast, the detectability of a binocular grating is about twice that of a monocular grating. (Reproduced with permission from Legge 1984a, Vision Research, Pergamon Press.)

Figure 9.2. Monocular and binocular grating detection as a function of contrast.

filter over one eye, the grating became less detectable than when the eye with the neutral filter was closed. This effect was constant across the visible range of spatial frequencies (Pardhan et al. 1989) and is related to Fechner's paradox, which is discussed later in this section.

Anderson and Movshon (1989) used vertical sinusoidal gratings with the same luminance, phase, and spatial frequency in the two eyes. In each trial the interocular contrast ratio was set at some value and the subject adjusted the contrast of both stimuli until the grating was visible. Data for one subject are shown in Figure 9.3. The threshold contrasts of the two monocular gratings for each interocular contrast ratio define a **binocular summation contour**. For perfect linear summation of binocular signals, the contour should fall on a diagonal line, and for complete independence, with no probability summation, it should fall along lines parallel to each axis, as shown in Figure 9.3. In fact, the data fell between these two limits. The data were fitted with the following power equation:

$$\left(\frac{m_l}{\alpha_l}\right)^\sigma + \left(\frac{m_r}{\alpha_r}\right)^\sigma = 1 \quad (6)$$

where m_l and m_r are the threshold contrasts of the

left- and right-eye gratings when presented as a dichoptic pair, α_l and α_r , are the contrast thresholds of each grating measured separately, and σ is a parameter inversely related to the magnitude of binocular summation. When the monocular contrasts are equal and $\sigma = 2$, the formula becomes equivalent to Legge's quadratic summation formula and the ratio of binocular to monocular thresholds is $\sqrt{2}$. The mean value of σ was close to 2.

Anderson and Movshon argued that, if binocular summation represents the combined action of several visual mechanisms, it should be possible to probe the contribution of each mechanism by selective masking or by adaptation. They measured the binocular summation contour when noise was added to the two dichoptic gratings. In one condition the noise was the same in both eyes (correlated) and in another condition it was uncorrelated in the two eyes. When contrast was similar in the two eyes, the threshold with uncorrelated noise was about $\sqrt{2}$ better than that with correlated noise, as one would predict from Campbell and Green's formula. However, as the contrasts in the two eyes became more different, the difference between correlated and uncorrelated noise became smaller.

These results can be explained in the following way. When the contrasts in the two eyes are similar,

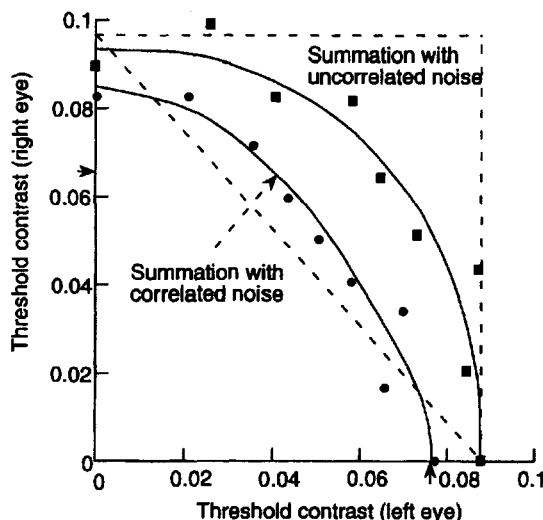


Figure 9.3. Binocular summation contours.

Detection of a dichoptic grating in the presence of uncorrelated and correlated noise. For each datum point the interocular contrast ratio was fixed and subjects adjusted the contrast of both dichoptic gratings until the fused grating was visible. Arrows indicate thresholds for monocular stimuli masked by monocular noise. The diagonal dashed line indicates where data should fall with perfect linear summation of binocular signals with uncorrelated noise. Dashed lines parallel to the axes indicate loci of zero neural or probability summation. Data for one subject. (Reproduced with permission from Anderson and Movshon 1989, Vision Research, Pergamon Press.)

binocular cells that summate inputs from the two eyes are maximally stimulated, and signals and noise summate to give an advantage to inputs with uncorrelated noise. But when the interocular contrasts differ, the summation mechanism is turned off and mutual inhibition responsible for binocular rivalry is turned on. The eye with the stronger signal suppresses inputs from the other eye so that, in the extreme case, signal and noise from only one eye are available. Under these circumstances it makes no difference whether the noise in the two eyes is correlated or uncorrelated. Actually, as we have already argued, some such mechanism must be assumed in the Campbell and Green model to account for why noise from a closed eye does not reduce the monocular contrast threshold. Anderson and Movshon assumed that there are several ocular-dominance channels, each of which can be selectively adapted, and they produced evidence to this effect. They dubbed this the distribution model of binocular summation. The general form of the binocular summation contour represents the summed response of several ocular-dominance channels.

Another manifestation of binocular summation is that visually evoked potentials recorded from the surface of the head are greater when a grating moving in one direction is presented to one eye and a

grating moving in the opposite direction is presented to the other eye compared with when either moving grating is presented alone (Ohzawa and Freeman 1988).

Binocular summation for suprathreshold discrimination

Legge (1984a) used a forced-choice procedure to measure the threshold for detection of an increment of contrast in a suprathreshold pedestal grating set at various levels of contrast. Both the binocular and the monocular psychometric functions for suprathreshold discrimination had a slope of 1. As the contrast of the pedestal grating contrast rose from zero to 0.25 the advantage of binocular over monocular discrimination was reduced to zero. Thus, the amount of binocular summation of contrast decreased as the initial contrast of the grating on which the increment was imposed increased. The smaller level of binocular summation for suprathreshold discrimination than for detection can be explained if one assumes that at low levels of contrast the neural effect of a stimulus is a positively accelerating function of contrast, and at higher levels of contrast a saturation of response occurs. There is evidence for this assumption. For a monocularly viewed grating with a contrast of up to about 0.25, the contrast-difference threshold is much smaller than the absolute level of contrast required for detection (Nachmias and Sansbury 1974).

Bearse and Freeman (1994) obtained further evidence for this conclusion. They measured orientation discrimination for one-dimensional Gaussian patches as a function of stimulus contrast and duration. Binocular performance was 66 per cent better than monocular performance for stimuli that were both brief (50 ms) and of low contrast (8 per cent). When either duration or contrast was increased beyond a certain level, binocular and monocular performances became equal. These results are consistent with the results of earlier experiments in which discrimination of the orientation of high-contrast gratings was found to be similar for monocular and binocular viewing (Andrews 1967). It seems that binocular energy summation occurs in the contrast or temporal threshold region, where the response of the visual system is an accelerating function of stimulus energy, and that response saturation limits binocular summation for discrimination between stimuli which are well above detection threshold.

Binocular summation has been found to be very small or absent for more complex visual tasks performed at a suprathreshold level of contrast, such as recognition of letters on a noisy background (Townsend 1968; Frisén and Lindblom 1988). The crucial factor, however, was probably the fact that

the stimuli were suprathreshold rather than that they were complex. There is evidence that the accuracy with which a briefly exposed letter is recognized is greater with binocular than with monocular presentation. The advantage of binocular viewing fell to the level of probability summation when letters presented to the two eyes were separated by intervals of more than 50 ms or when the letters were presented to noncorresponding areas (Eriksen et al. 1966; Eriksen and Greenspon 1968). As one would expect, the ability to recognize either of two letters was reduced when they were superimposed dichoptically but not when they were presented to noncorresponding areas or successively (Greenspon and Eriksen 1968).

Summary

It can be concluded from the evidence just presented that, in people with normal binocular vision, binocular thresholds for luminance increments in discrete stimuli and for contrast detection in gratings are lower than monocular thresholds to a greater extent than predicted by either classical or signal-detection probability summation. Binocular summation is greatest when the stimuli have similar shapes, sizes, and locations. In other words, summation is greatest when the visual mechanisms responsible for fusion are engaged rather than those responsible for rivalry. Binocular summation is not evident with discrimination tasks between stimuli well above the detection threshold, presumably because of response saturation. In stereoblind people, binocular summation is no more than one would predict from probability summation (see Section 15.9.1). This further supports the idea that in people with normal vision, near-threshold excitatory signals from the two eyes are at least partially summed when they impinge on cortical binocular cells.

9.2.2 Binocular summation of brightness

If the inputs from the two eyes sum in a simple fashion, one would expect an illuminated area to appear about twice as bright when viewed with two eyes than when viewed with only one eye. In fact, Jurin in 1755 and Fechner, in 1860 (see Sherrington 1904), observed that an illuminated area appears only slightly brighter when viewed with two eyes. A bright light presented to one eye may actually appear less bright when a dim light is shone into the other eye, an effect known as **Fechner's paradox**.

Levelt's experiments on brightness summation

To investigate binocular brightness summation, Levelt (1965a) presented a 3° luminous disc on a

dark ground to corresponding regions in each eye. With one of the discs at a fixed luminance, the subject adjusted the luminance of the disc in the other eye until the combined image appeared to have the same brightness as a similar dioptic stimulus with the same fixed luminance in the two eyes. The dioptic and dichoptic stimuli were presented sequentially in the centre of the visual field. The results for one subject for a dioptic stimulus with a luminance of 20 cd/m² are shown in Figure 9.4. It can be seen that over the straight part of the curve, the brightness of the dioptic comparison stimulus was equal to the mean brightness of the dichoptic test stimuli. When both eyes were stimulated at the same luminance, the dichoptic and dioptic stimuli were, necessarily, identical. As the luminance of the stimulus was increased in one eye, it had to be decreased in the other eye by a proportionate amount to maintain the match with the dioptic stimulus. Some subjects gave a greater weighting to one of the dichoptic images than to the other.

The slope of the linear function reversed when the luminance of the disc in one eye was set at or near zero, as indicated by the dashed lines in Figure 9.4. Under these circumstances more luminance was required in the brighter disc to match the dioptic stimulus when the dimmer disc was visible than when there was no stimulus in the other eye. This is Fechner's paradox. For the data in Figure 9.4, a luminance of about 32 cd/m² was required to match a monocular disc with a dioptic stimulus of 20 cd/m², whereas a higher luminance was required when a dimly illuminated disc was visible in the other eye. Fechner's paradox can be explained by assuming that the processes underlying dichoptic brightness averaging involve both summation and inhibition. When border contrast is similar in the two eyes, summation predominates, with greater weight being given to the stimulus with the greater contrast, but when the contours in the two eyes differ greatly in contrast, inhibition outweighs summation. When the contrasts are opposite in sign, inhibition becomes evident as binocular rivalry (Fry and Bartley 1933). Inputs from a totally uncontoured region in one eye are usually suppressed by inputs from a contoured region in the other eye.

One cannot be sure that a closed eye makes no contribution to a binocular match. Zero contribution from an eye can be guaranteed only if the eye is pressure blinded. It was noted in the last section that an eye's sensitivity is increased when the other eye is pressure blinded rather than just closed. The magnitude of the visual potential evoked from the human scalp by monocular stimulation was found to be lower when the other eye was closed and dark

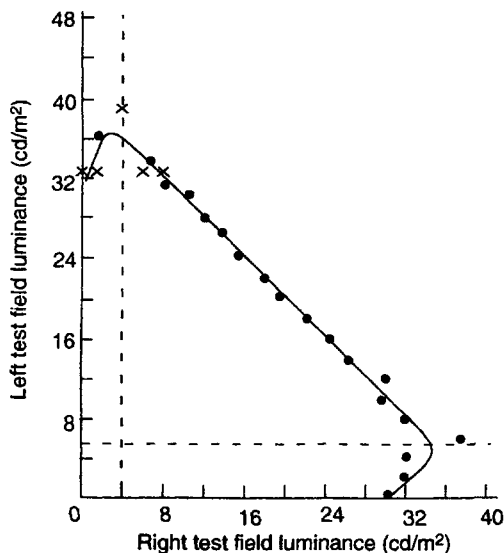


Figure 9.4. Dichoptic equal-brightness curve.

Equal-brightness curve for a 3° luminous disc presented to both eyes at a luminance of 20 cd/m² with respect to a fused pair of dichoptic discs set at various luminance ratios. The dashed lines indicate the boundaries of the near zero-disparity region within which dichoptic summation fails and Fechner's paradox is evident. Data for one subject. (From Levelt 1965b.)

adapted than when it was adapted to a dim homogeneous light (Eysteinsson et al. 1993). It seems that a fully dark-adapted eye exerts an inhibitory influence on the other eye.

When Levelt (1965b) superimposed a 2°-diameter black ring on one of the dichoptic discs, the contribution of that disc to the brightness match increased. Furthermore, in the immediate neighbourhood of a contour presented to only one eye, binocular brightness was determined wholly by the luminance in that eye. This effect of an added contour can also be understood in terms of Fechner's paradox.

Levelt explained his results by stating that the binocular impression of brightness (B) depends on a weighted sum of the luminances of the monocular stimuli (E_l and E_r). The weights (w_l and w_r) sum to 1 and depend on the relative dominance of the two eyes and the relative strengths of the two stimuli, determined mainly by contours they contain. Thus

$$B = w_l E_l + w_r E_r \quad (7)$$

This is a purely formal theory since it can describe many results if appropriate weights are selected, and there is no independent procedure for deciding the weights. Furthermore, it assumes a linear transduction of stimulus luminance and contrast into neural signals signifying brightness. Since the weights sum to 1 the formula cannot account for binocular brightness in excess of the average of the monocular

luminances. De Weert and Levelt (1974) added a parameter to the simple luminance-averaging formula to account for the fact that brightness summation is slightly better than predicted by averaging and to account for Fechner's paradox.

Levelt assumed that dichoptic luminances rather than dichoptic brightnesses were averaged. Teller and Galanter (1967) held the luminance of monocular patches constant while varying their brightness, either by changing the adaptive state of the eye or by changing the contrast between the patches and their background. In both cases the brightness of dichoptically viewed patches varied with the imposed change in monocular brightness. In particular, the level of luminance of the stimulus in one eye at which Fechner's paradox was evident did not depend on the absolute luminance of the stimulus but on its luminance relative to the luminance threshold.

Other models of brightness summation

Erwin Schrödinger (1926), as a change from his work on fundamental physics, proposed an equation in which the weight assigned to each monocular input (f_l and f_r) was the ratio of the signal strength from that eye to the sum of the strengths of the signals from the two eyes.

$$B = f_l \frac{f_l}{f_l + f_r} + f_r \frac{f_r}{f_l + f_r} \quad (8)$$

MacLeod (1972) added to this account by proposing that the strength of a neural signal, f , is a logarithmic transform of the stimulus contrast, as specified by

$$f = f_0 + \log\left(\frac{l}{l_0}\right) \quad (9)$$

where f_0 is the internal noise, l is the difference in luminance across the contour, and l_0 is the threshold luminance difference. A good fit to Levelt's data in Figure 9.4 was obtained by setting $B = 1.36$, $f_0 = 0.34$, and $l_0 = 2 \text{ cd/m}^2$ for each eye.

Several other models of binocular brightness summation have been proposed. Engel (1967, 1969, 1970b) used a weighted quadratic sum model to account for the binocular summation of brightness. In this formulation, the brightness of a binocular stimulus derived from magnitude estimation (ψ_b) is related to the brightness of monocular stimuli (ψ_l and ψ_r) by the expression

$$\psi_b = \sqrt{\left(w_r \psi_r\right)^2 + \left(w_l \psi_l\right)^2} \quad (10)$$

The weighting functions were derived from normalized autocorrelation functions of the image in each eye, and reflected the amounts of contour and contrast in each image. They thus served the same function as the weights in Levelt's formula except that Engel provided a definite process for determining their values.

Engel's function resembles the quadratic summation model used by Legge to describe binocular summation of contrast sensitivity (equation 5), and which Legge and Rubin (1981) used to describe summation of contrast in suprathreshold gratings. Legge and Rubin used the same procedure as Levelt. They presented a standard binocular grating, identical in the two eyes, and a fixed test grating in the right eye. Subjects adjusted the contrast of a test grating in the left eye until the fused test gratings appeared to have the same contrast as the standard grating, for different values of the fixed test grating. All the gratings had the same phase and spatial frequency. An example of an equal-contrast curve for 8 c/deg gratings and three contrasts of the standard grating is shown in Figure 9.5. The results for gratings of 1 c/deg were similar except that the departure from averaging was more severe at low contrast. The results lie close to the curve representing a summation index of 2 but well inside the diagonal, which represents an index of 1 (contrast averaging). This means that disproportionate weight is given to the grating with the higher contrast.

In Levelt's averaging formula, the gratings are simply weighted in proportion to their contrasts. Perhaps the extra weight to the dominant contrast arises because Legge's stimulus was a grating with many contrast borders, whereas Levelt used simple luminance discs with contours only around the edges. There is a hint of Fechner's paradox in Figure 9.5, which shows in the way some of the data points turn in toward the origin as they approach the axes. Quadratic summation implies that the contrast signal is squared in each eye before the two signals are combined with a compressive nonlinearity.

Curtis and Rule (1978) proposed that monocular contrasts sum like vectors to produce binocular contrast. When vectors of length C_l and C_r , at an angle of θ are summed, the resultant vector, C_b is given by

$$(C_b)^2 = (C_l)^2 + (C_r)^2 + 2C_l C_r \cos\theta \quad (11)$$

When the angle θ is set to 120° the function reduces to averaging, when it is set at 90° it reduces to Legge's quadratic sum formulation, and when it is set at 0° it reduces to a simple sum. Curtis and Rule did not propose a physiological representation of their vector-addition process. This formula contains

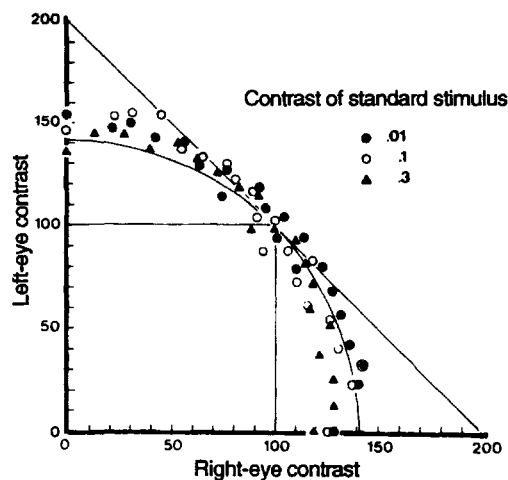


Figure 9.5. Dichoptic equal-contrast function.

An example of an equal-contrast curve for 8 c/deg gratings. For each contrast of the right-eye grating the contrast of a left-eye grating was varied until the fused image appeared equal in contrast to a binocular standard grating. Both test contrasts are expressed as a percentage of that of the standard stimulus. Results are presented for one subject for three contrasts of the standard grating. The diagonal line represents the results expected on the basis of averaging the contrasts in the two eyes. The circle represents the results expected from a quadratic summation rule. The horizontal and vertical lines indicate the results expected when the match is determined solely by the image with the higher contrast. (From Legge and Rubin 1981, Perception and Psychophysics, 30, 49-61. Reprinted by permission of Psychonomic Society, Inc.)

no weightings to allow for differences between the images in the two eyes but could easily be modified to do so.

In other models of binocular brightness summation, there are assumed to be binocular processes that extract differences between stimulation in the two eyes and other processes that extract sums of binocular inputs. For instance, in a model proposed by Lehky (1983), dichoptic stimuli with matching contours are processed in the summing channel while those with opposite luminance polarity are processed in the differencing, or rivalry, channel. Lehky also used a vector-sum formula and interpreted the angle between the vectors as the relative contributions of the summing and differencing channels. Cohn et al. (1981) found that stimuli in the summing channel, such as binocular increments of luminance, were selectively masked by noisy fluctuations of luminance that were correlated in the two eyes. On the other hand, signals in the differencing channel, such as a luminance increment in one eye and a decrement in the other, were selectively masked by uncorrelated noise. It was argued that this evidence supports a two-process model of binocular combination. Cogan (1987) proposed that the

differencing channel consists of binocular cells receiving an excitatory input from one eye and an inhibitory input from the other, and that the summing channel consists of binocular cells receiving only an excitatory input from both eyes. He assumed that there are no purely monocular cells in the binocular field. The net binocular response is the pooled output of the two channels. Sugie (1982) developed a neural network model of these processes.

Although the models proposed by Fry and Bartley, Levelt, and Engel stress the importance of contour as a factor determining the amount of binocular brightness summation, the factor was not systematically explored. Leibowitz and Walker (1956) found that the amount of binocular summation of brightness decreased as the size of the stimulus was reduced from 1° to 15 arcmin. They attributed this effect to the reduction in the proportion of contour to area, as area was increased.

Bolanowski (1987) obtained estimates of binocular summation when all contours were removed from the visual field. He used a Ganzfeld produced by illuminating table tennis balls trimmed to fit over the eyes. Subjects rated the apparent brightness of the Ganzfeld presented for 1 s either to one eye or to both eyes. The results for different levels of illumination are shown in Figure 9.6. The apparent brightness of the binocular Ganzfeld was about twice that of the monocular Ganzfeld. Binocular summation of brightness was thus complete. When the diameter of the stimulus was reduced to 2°, binocular brightness was about the same as monocular brightness, as found by Levelt. The various models of brightness summation can accommodate this result if appropriate weights are assigned to visual contours.

The reaction time for a button-pressing response to a flashed stimulus becomes shorter with increasing luminance. One manifestation of binocular summation is that the reaction time to a flashed binocular stimulus is shorter than the mean of the reaction times to monocular flashes (Minucci and Connors 1964). Haines (1977) reported that the reaction time to a flashed binocular stimulus was about 35 ms shorter than that to a monocular stimulus.

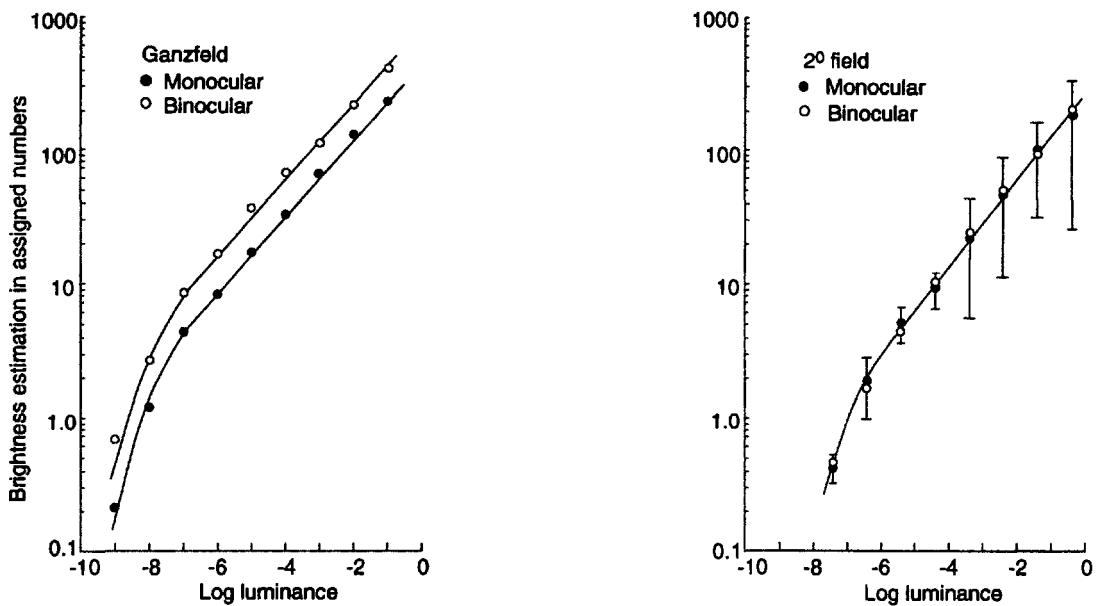
Another manifestation of suprathreshold binocular summation is that the visual evoked potential recorded from the scalp over the visual cortex is of greater magnitude when a grid pattern is flashed to both eyes than when it is flashed to only one eye. Binocular facilitation did not occur when the grid patterns to the two eyes were different in size nor when one eye was exposed to flashed diffuse light rather than to a grid (Harter et al. 1974). This latter finding is puzzling in view Bolanowski's finding of

the complete brightness summation of a Ganzfeld. Perhaps the crucial difference is that Bolanowski used a 1-s exposure rather than a flash; the temporal boundaries of a flash may have the same effect as spatial contours.

9.2.3 Dichoptic critical flicker fusion

The frequency at which a flickering light appears to fuse into the impression of a continuous light is known as the **critical fusion frequency (CFF)**. With increasing luminance the CFF increases up to a limit of about 50 Hz (Crozier and Wolf 1941). Sherrington (1904) hypothesized that, if inputs from the two eyes converge on the same cells in the same way that motor efferents converge in a final common path, then the CFF should be higher for a flickering light viewed binocularly than for one viewed monocularly. He also hypothesized that the CFF should be higher for flickering lights presented in phase to the two eyes than for lights presented in antiphase. Sherrington found the CFF to be only about 3 per cent higher for in-phase than for antiphase dichoptic flicker and concluded that there is very little convergence of binocular inputs. He wrote, "The binocular sensation attained seems combined from right and left unisensory sensations elaborated independently." If flicker fusion occurred in the retina, the neural discharge in the optic nerve produced by a light flickering just above the CFF would be indistinguishable from that produced by a steady light of the same mean luminance. When two such signals are combined at a later stage, no amount of binocular summation can restore the sensation of flicker. In other words, the absence of augmentation of binocular flicker does not prove that the inputs from the two eyes remain distinct.

Sherrington underestimated the difference between in-phase and antiphase binocular CFF. More recently, the CFF for in-phase flicker was found to be between 4.5 and 10 per cent higher than for antiphase flicker (Ireland 1950; Baker 1970). This is due to neural summation in binocular cells, since it is higher than predicted by probability summation (Peckham and Hart 1960) and no significant difference between inphase and antiphase flicker sensitivity was found in subjects lacking stereoscopic vision (Levi et al. 1982). We now know that many inputs from the two eyes do converge on common cells. Nevertheless, Sherrington's main conclusion still stands, namely, that lights flickering in phase do not simply sum to produce a flicker sensation of twice the amplitude of each component. But this probably reflects the fact that the processes responsible for limits on flicker fusion are largely in



(a) Magnitude estimations of apparent brightness of a Ganzfeld presented to both eyes (upper curve) and to one eye (lower curve) as a function of log luminance.

(b) Magnitude estimations of the apparent brightness of a 2° spot presented to both eyes (empty symbols) and to one eye (solid symbols). Vertical bars are standard errors. Means of eight subjects. (Reproduced with permission from Bolanowski 1987, Vision Research, Pergamon Press)

Figure 9.6. Dichoptic apparent brightness.

the retina. On the other hand, the partial elevation of in-phase over antiphase flicker could be due to sensations of flicker arising from monocular cells. Even a few monocular cells would retain a signal of flicker after all binocular cells have ceased to register it. Thus, the CFF is not a sensitive measure of binocular summation. Furthermore, Sherrington worked at suprathreshold levels, where inhibitory as well as excitatory interactions occur between inputs to binocular cells. Interocular summation of flicker sensitivity is more likely to be revealed at threshold levels of luminance.

Another factor could be the presence of contours in the stimuli. We have already noted that dichoptic brightness summation is increased when the images contain no contours. Thomas (1956) found that the CFF with in-phase dichoptic flicker is increased by the addition of parallel lines to each image, even when the lines in one eye are orthogonal to those in the other.

Dichoptic interactions of flicker can also be investigated by determining the magnitude of luminance modulation of a flickering light required for the detection of flicker. This measure, expressed as a percentage of luminance modulation of a sinusoidally flickering light, when plotted over a range of temporal frequencies, is the **temporal contrast-sensitivity function**, also known as a De Lange function

(De Lange 1954). It is the temporal analogue of the spatial contrast-sensitivity function and has a similar bandpass shape. For an homogeneous foveal field, flicker sensitivity increases with increasing flicker rate up to a peak value of about 2 per cent luminance modulation at about 10 Hz, above which it falls rapidly to zero at a frequency of about 50 Hz. For flicker rates above about 10 Hz, sensitivity for in-phase dichoptic flicker was found to be about 40 per cent higher than for antiphase dichoptic flicker or for monocular flicker (see Figure 9.7).

At low flicker rates, sensitivity for in-phase dichoptic flicker was up to four times higher than that for antiphase flicker (Cavonius 1979). This could be because of summation of neural signals arising from lights flickering in phase in the two eyes, which is **dichoptic summation of in-phase signals**, or because of summation of opposite-sign signals from lights flickering in antiphase, which is **dichoptic summation of antiphase flicker**. The summation of in-phase signals seems to be the crucial factor, because sensitivity to antiphase dichoptic flicker was about the same as sensitivity to monocular flicker with the other eye exposed to a steady field (van der Tweel and Estévez 1974; Cavonius 1979). Other evidence reviewed in the following section supports the idea of dichoptic summation of in-phase flicker but not of antiphase flicker.

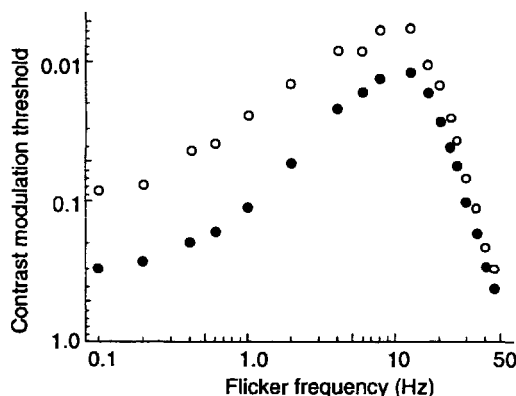


Figure 9.7. Detection of dichoptic flicker.

Threshold contrast modulation for detection of flicker of a 1° illuminated spot as a function of flicker frequency. The solid symbols are for in-phase dichoptic flicker. The open symbols are for counterphase dichoptic flicker. Results for one subject. (Adapted from Cavonius 1979. Copyright The Experimental Psychology Society.)

9.2.4 Dichoptic sensitivity to pulsed stimuli

Temporal sensitivity can also be explored with single flashes. The stimulus can be a light spot that is momentarily extinguished (negative polarity) or a dark spot that is momentarily increased in luminance (positive polarity). The threshold for detection of flashed test spots that either both increased or both decreased in luminance in the two eyes was lower than the threshold for detection of a flashed increase of luminance in one eye coupled with a decrease in the other (Westendorf and Fox 1974). The same-sign flashes were detected at a level above that of probability summation, whereas the opposite-sign flashes were detected at about the level of probability summation, thus providing further support for summation of dichoptic in-phase signals and independence of dichoptic antiphase signals. When one of the flashed targets was a vertical bar and the other was a horizontal bar, flash detection was at the level of probability summation for both same- and opposite-sign flashes (Westendorf and Fox 1975).

One can think of the receptive field of a ganglion cell as having a spatial sensitivity profile; an on-centre receptive field has an excitatory centre with a Gaussian profile and an inhibitory surround with a wider Gaussian profile. One can also think of a receptive field as having a temporal-sensitivity profile. An on-centre receptive field responds with an excitatory discharge to a flash of light in the centre followed by an inhibitory phase. An off-centre field responds in the same way to a briefly darkened spot. An estimate of the durations of these phasic responses to light pulses can be obtained by measuring either the probability of seeing or the threshold

for detection of a pair of flashes as the interstimulus interval is increased. The procedure is analogous to Westheimer's procedure for measuring the spatial properties of receptive fields (see Section 9.3.3).

Bloch's law under monocular and dichoptic conditions

Under the most favourable conditions, the visibility of a single flash is proportional to its duration up to about 100 ms. In this period, visibility depends on the product of intensity and duration, a relationship known as **Bloch's law**. The limiting period of temporal integration is decreased by increasing the area of the stimulus, keeping luminance constant, or by increasing the luminance of the background (Barlow 1958). Two flashed stimuli with the same size and luminance polarity presented to one eye physically sum their stimulus energy. The increased probability of seeing two simultaneous flashes relative to the probability of seeing one flash depends on the slope of the psychometric function. In one study the probability of seeing two 10-ms flashes superimposed in the same eye within 50 ms of each other was about 0.75, relative to a probability of 0.32 for detection of each flash alone (Bouman and van den Brink 1952).

Similarly, within the limits of Bloch's law, the visibility of dichoptic flashes depends on the total energy in each flash, that is, on the product of the duration and intensity of each flash (Westendorf et al. 1972). Cogan et al. (1982) found that the detectability of low-contrast dichoptic flashes set within fused binocular contours was at least twice that of a monocular flash. The binocular advantage was not as large for high-contrast flashes. Binocular detectability, even for low-contrast flashes, was only 41 per cent better than monocular detectability when the background contours were omitted from one eye. It was suggested that binocularly fused contours engage the binocular cells of the mechanisms responsible for binocular fusion, which fully sum low-contrast stimulus energy. Contours in only one eye engage the monocular mechanisms or the binocular rivalry system, which reduces the degree of binocular summation.

Monocular detection of flashes separated in time

When two flashes presented to the same eye are separated in time by more than about 100 ms, the probability of detecting at least one of them is no longer influenced by neural interactions between them, but only by probability summation. This is the zero level of neural interaction. As the interflash interval is increased from zero, the mutual facilitation of the stimuli decreases to zero at about 35 ms, when the inhibitory phase of one flash coincides with the

excitatory phase of the other. With a longer interval, the stimuli show mutual inhibition as the two inhibitory phases come into coincidence. When the interval reaches 100 ms there is zero interaction because the responses no longer overlap. Flashes with opposite luminance polarity physically cancel when presented at the same time. When presented with a short interstimulus interval they show inhibitory interactions, and with longer interstimulus intervals they show facilitatory interactions (Ikeda 1965; Rashbass 1970; Watson and Nachmias 1977). These results can be explained by assuming that a flash generates an initial response of one sign and a secondary response of the opposite sign. The sign of the responses depends of the polarity of the flash, and the interactions between successive flashes depends on how the excitatory and inhibitory phases interact.

Dichoptic detection of flashed stimuli separated in time

Matin (1962) measured the probability of detecting dichoptic flashes 35 arcmin in diameter and 2 ms duration as a function of the time interval between them. Binocular summation was greater than that predicted by classical probability summation only for interstimulus intervals less than about 100 ms. Similar results were obtained by Thorn and Boynton (1974). Note that inhibitory effects found with monocular flashes were not reported with these dichoptic stimuli. These experiments provide evidence that similar signals falling simultaneously on corresponding points are processed by a mechanism involving real neural summation. Blake and Fox (1973) review other early experiments on this topic.

More recently, the study of interactions between flashed stimuli has been extended to flashed gratings. With such stimuli, the alternation may involve a spatiotemporal displacement, not merely a temporal displacement. This is because two gratings of opposite luminance polarity presented in succession can be regarded as having been displaced spatially by one-half period of the grating. When presented to the same eye in two 5 ms flashes twice in quick succession, a sine-wave grating with a spatial frequency of 0.75 c/deg showed summation up to an interstimulus interval of about 50 ms, followed by a small inhibitory effect. A similar but weaker facilitatory effect occurred when the gratings were presented dichoptically, but the inhibitory phase was absent (Figure 9.8). Gratings with opposite luminance polarity (180° spatial phase shift) presented to the same eye showed an initial inhibitory phase followed by a facilitatory phase, as shown in the figure. Opposite-polarity gratings presented dichoptically showed no evidence of either facilitation or inhibition (Green

and Blake 1981). A similar result was reported for two light flashes with the same and opposite polarity (Cogan et al. 1990). Blake and Levinson (1977) did find dichoptic interactions between gratings of opposite polarity (180° phase shift), but these were high spatial-frequency gratings, and a slight misvergence may have brought them into phase. Rose (1978) found that the contrast threshold for detection of apparent movement in a sinusoidal grating between 0.5 and 7 c/deg, which reversed in spatial phase at 3.5 Hz, was 1.9 times lower with binocular than with monocular viewing, a result difficult to reconcile with the preceding findings.

Responses to light onset and light offset are processed in visual channels that remain distinct at least up to the visual cortex (see Section 4.1.1). Nevertheless, these channels must interact to account for the inhibitory interactions that occur when opposite-sign flashes are presented to the same eye with a small interflash interval. From the preceding evidence it seems that dichoptic interactions between transient signals of opposite sign in the two eyes do not occur at any level.

Investigators have concluded from this result that opposite-polarity stimuli arising from the two eyes are processed independently. But this is the wrong way to look at it. Think of two steady square-wave gratings presented 180° out of spatial phase to one eye. Clearly, the gratings are invisible because they physically cancel to a homogeneous gray. When the same gratings are presented dichoptically they do not physically cancel, but rival. At any instant, the dominant grating is seen just as well as when there is no grating in the other eye; that is, the suppressed grating does not weaken the visibility of the dominant grating (Bacon 1976). From the point of view of visibility, the two gratings are processed independently, but only one of them is processed at any one time in a given location. However, although opposite polarity dichoptic stimuli do not engage in simultaneous mutual inhibition, they do engage in alternating suppression, or rivalry.

The same argument can be applied to superimposed flashes of opposite polarity. They physically cancel when presented simultaneously to the same eye, and the excitatory and inhibitory phases of their neural responses interact when the flashes are presented successively to one eye. When presented dichoptically, opposite-polarity flashes rival but during the dominant phase of either one, the stimulus remains just as visible as a flash presented to only one eye. As the interstimulus interval is increased, rivalry ceases and both stimuli become visible as independent events; they do not, as with monocular viewing, engage in mutual inhibition.

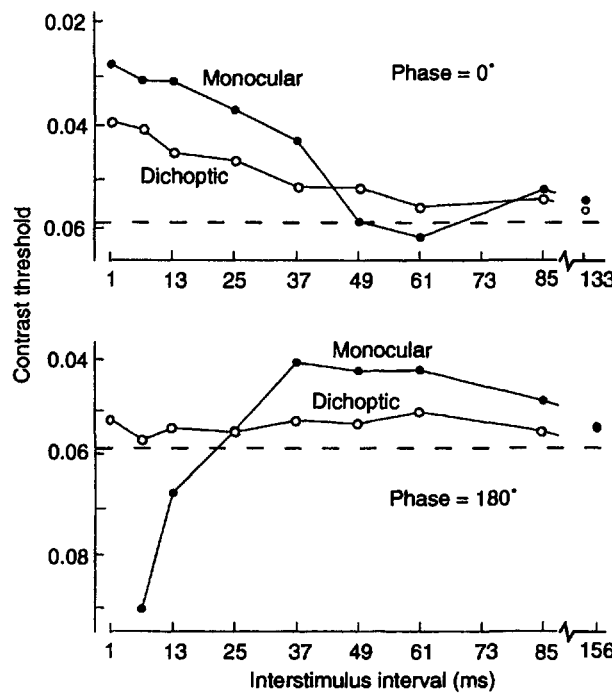


Figure 9.8. Dichoptic masking and spatial phase.

The top graph shows the contrast threshold for detection of two spatially in-phase, 0.75-c/deg gratings presented for 5 ms each, as a function of interstimulus interval. The gratings were presented to opposite eyes (empty symbols) or to the same eye (solid symbols). The bottom graph shows the same functions, but with the two gratings in spatial counterphase. The dashed lines indicate the thresholds for the first grating alone. Results for one subject. (Reproduced with permission from Green and Blake 1981, Vision Research, Pergamon Press.)

It is interesting to note in this context that the threshold for detecting a low-contrast grating was lowered when it was presented just after a similar grating with a spatial phase offset of 90°, but this facilitation was not evident when the two gratings were presented dichoptically (Georgeson 1988). The facilitation occurred between sequentially presented dichoptic gratings when they were in spatial register. According to this evidence, although the binocular detection mechanism combines dichoptically superimposed stimuli, it does not combine dichoptic stimuli in spatiotemporal quadrature.

Summary

We can conclude that there is considerable interaction between inputs from the two eyes in response to flicker, especially for low frequencies and within the modulation threshold region. In-phase flicker with similarly shaped stimuli is detected above the level predicted by probability summation, whereas antiphase flicker is detected at or below the level of probability summation. Binocular summation of

stimulus energy occurs under conditions that foster binocular fusion but not under conditions that foster binocular rivalry. Light flashes or gratings with similar luminance polarity show summation when presented in quick succession either to the same eye or to opposite eyes. Flashes or gratings with opposite polarity show summatory and inhibitory phases when presented to the same eye but not when presented dichoptically. However, opposite-polarity dichoptic flashes do engage in alternating suppression. As far as visibility is concerned, they are processed in distinct channels, but these channels engage in suppressive rivalry.

9.3 DICOPTIC VISUAL MASKING

9.3.1 Introduction

A basic problem in all studies of interocular effects is that merely closing an eye does not stop inputs from that eye reaching the cortex. For instance, an afterimage impressed on one eye is visible when that eye is closed and the other eye opened, a fact first noted by Isaac Newton (see Walls 1953). This does not prove, as was once thought, that afterimages are cortical in origin; it simply means that activity arising in a closed eye still reaches the visual cortex (Day 1958). We now know that an afterimage is no longer visible when the eye in which it was formed is pressure blinded (Oswald 1957). Pressure blinding is achieved by pressing the finger against the side of the eye for about 30 s. This cuts off the blood supply to the retina and the eye remains blind until the pressure is relieved. It is dangerous to keep the pressure on for more than about one minute.

Another problem in studies of interocular transfer of successive induction effects is that in nontransfer trials the same eye is used in both induction and test periods, whereas in transfer trials the adapted eye is open during the adaptation period and closed during the test period, and the tested eye is at first closed and then opened. The sudden transition in the state of adaptation of the eyes in transfer trials could cause a spurious weakening of the aftereffect being tested. This problem can be solved by keeping both eyes in the same state of adaptation at all times. As we will see, this precaution has been applied in only one study.

There are three procedures for proving that an effect is cortical in origin.

- 1 The first procedure is to show that the effect survives pressure blinding of the eye to which the induction stimulus was presented.

2 A second procedure is to demonstrate that the effect depends on visual features that are known to be processed only in the visual cortex. For instance, it is believed on the basis of physiological evidence that the orientation of visual stimuli is first processed in the visual cortex; thus an induction effect that is specific to the orientation of the stimulus should be cortical in origin.

3 A third procedure is to show directly by electrophysiological recording that the first signs of changes in the response of cells resulting from the presence of an induction stimulus in retina, lateral geniculate nucleus, and visual cortex arise at the level of the cortex. Other general problems associated with drawing conclusions from studies of interocular transfer were discussed by Long (1979).

Next we review the literature on the interocular transfer of visual induction effects, starting with visual masking.

9.3.2 Types of visual masking

We saw in Section 9.2.1 that when an induction stimulus is near the threshold contrast for detection it lowers the detection threshold of a test stimulus. In visual masking, a suprathreshold induction stimulus, or mask, reduces the visibility of a briefly exposed test stimulus. The mask is usually presented briefly and the test stimulus is presented either at the same time as the mask, slightly before it, or slightly after it. In one class of experiments, the mask is a disc of uniform luminance. In other experiments the mask is an edge with defined contrast polarity or a grating with sinusoidal luminance profile. In dioptic masking, the mask and test stimulus are presented to both eyes, while in dichoptic masking, the mask is presented to one eye and the test stimulus to the other. The main types of masking paradigm are listed in Table 9.1.

Dichoptic masking differs from binocular rivalry in two ways. First, in dichoptic masking the test stimulus is usually presented for less than 200 ms, which is too short a time for binocular rivalry to manifest itself (see Section 8.3.7). Second, dichoptic masking is maximal when the test and masking stimuli have similar visual features, whereas binocular rivalry is most evident between stimuli that differ widely in shape, orientation, spatial frequency, or colour. Dichoptic masking probably occurs at an early stage in the combination of binocular signals whereas rivalry occurs later, at a stage when patterned inputs are compared (see Section 9.3). They could both occur at different stages of processing within V1.

Table 9.1. Types of visual masking

Simultaneous masking

Induction and test stimuli superimposed
Test and induction stimuli adjacent – crowding

Successive masking

Induction and test stimuli superimposed
Forward masking – first stimulus masks second
Backward masking—second masks first
Induction and test stimuli spatially adjacent
Paracontrast – first stimulus masks second
Metacontrast – second stimulus masks first

9.3.3 Masking with homogeneous illumination

The visibility of a flash of a given luminance varies with the state of light adaptation of the eye to which it has been presented. However, most investigators have found that the overall state of light adaptation of one eye does not affect the threshold sensitivity of the other eye for a featureless stimulus (Crawford 1940a; Mitchell and Liaudansky 1955; Cogan 1989). Wolf and Zigler (1955) found some evidence of interocular effects but their adapting stimulus was not devoid of visual texture.

Crawford (1940b) and Westheimer (1965) introduced the paradigm of exposing a test spot briefly on the centre of a featureless disc-shaped conditioning stimulus. The luminance threshold of the test spot was measured as a function of the duration, luminance, size, and eccentricity of the conditioning stimulus.

Battersby and Wagman (1962) measured the detection threshold for a small test flash presented at various intervals of time before or after the offset of a larger illuminated disc. The 5-ms test flash, 40 arcmin in diameter, was presented to one eye and the 500-ms conditioning disc to the other eye. The results for one subject are shown in Figure 9.9. The threshold was elevated when the test flash was presented between 100 ms before and 100 ms after the onset of the 500-ms conditioning disc, and was maximal when the two events occurred at the same time. The threshold elevation was greater with smaller conditioning stimuli. When a conditioning stimulus of 5° diameter was on for more than 100 ms before the test flash appeared, the threshold for detecting the test flash was not significantly above the monocular threshold. As the conditioning stimulus was reduced in size, bringing its border closer to the test flash, the threshold for seeing the test flash became increasingly elevated during the whole period of the conditioning stimulus.

Markoff and Sturr (1971) conducted a similar experiment to investigate the effects of changing the

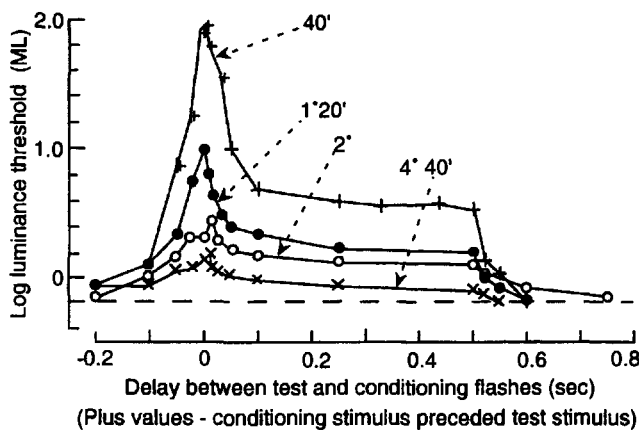


Figure 9.9. Dichoptic masking and interstimulus delay.

The luminance threshold for detection of a 40-arcmin, 5-ms test flash as a function of time before or after a 500-ms dichoptic conditioning stimulus. The four curves are for different diameters of the conditioning stimulus, indicated by a number on each curve. The dotted line is the threshold without the conditioning flash. Results for one subject. (From Battersby and Wagman 1962.)

size of the conditioning stimulus, with the test and conditioning stimuli presented simultaneously. A 5-ms test flash, 3.5 arcmin in diameter, was presented at the same time as a conditioning stimulus that was exposed for 50 ms, 200 ms, or continuously. The two stimuli were presented either monocularly or dichoptically. The two top graphs of Figure 9.10 show that, with both monocular and dichoptic viewing, the luminance threshold for detection of a foveal test flash rose as the diameter of the conditioning patch increased from 10 to about 21 arcmin, after which it declined to a steady value that depended on the luminance of the conditioning spot. This can be explained in terms of the structure of the on-centre receptive fields of ganglion cells. A small conditioning stimulus adds to the stimulation of the on-centre and elevates the differential threshold, but, as its area increases, its edge encroaches on the inhibitory surround. When it gets larger still, its edge extends beyond the inhibitory surround, and masking declines to a level that depends on the luminance of the mask. The stimulus that produces peak masking is larger at scotopic than at photopic levels of luminance, presumably because the inhibitory surround is weaker at scotopic levels. Peak masking size is also larger with peripheral than with foveal viewing, presumably because receptive fields get larger in the periphery (see bottom two graphs in Figure 9.10).

It can be seen in Figures 9.9 and 9.10 that detection of a test spot in one eye is not affected by a conditioning disc wider than about 3° presented to the other eye. Therefore, pure luminance masking

within homogeneous areas does not occur between the eyes. One can infer that both monocular and dichoptic masking are due to interactions between the contiguous edges of the conditioning and test stimuli. We return to this topic shortly. It can also be seen in Figures 9.9 and 9.10 that a small conditioning disc, presented foveally, most effectively masks a test flash in the other eye when the conditioning disc is presented briefly—there is very little masking when it is visible continuously. One can infer that dichoptic masking is due to rivalrous interactions between stimulus onsets or offsets of contiguous edges. Chromatically selective dichoptic masking occurs with large masking flashes but only within the blue-cone system (Boynton and Wisowaty 1984).

An eye was found to be locally more sensitive to light when the test flash was just within the boundary of a light-adapted region in the other eye than when the other eye was dark adapted (Lansford and Baker 1969; Paris and Prestrude 1975). This result is difficult to understand since the stimulus conditions were complex. (see also Makous et al. 1976).

Summary

The general conclusion to be drawn from these experiments is that a large area of steady illumination in one eye does not affect the visibility of a stimulus presented to the other eye, but the visibility of a test flash in one eye is reduced if it occurs close in time to a change in luminance in the other eye or is spatially adjacent to a contour in the other eye. In all the following experiments, both the induction and test stimuli are patterned and are usually presented for brief periods so that there are contiguous edges and temporal transients.

9.3.4 Masking with superimposed patterns

Effects of contrast and spatial frequency

In a typical masking experiment a subject is shown a sinusoidal masking grating twice in succession. A test grating is superimposed on one of the masking gratings and the subject has to say which this is. The contrast of the test grating required for 75 per cent success in this forced-choice task is the threshold contrast. When the masking and test gratings have the same spatial frequency and phase, and when the contrast of the mask is low, the threshold contrast of the test grating is lower than when the mask is not present. In other words, the induction stimulus facilitates detection of the test grating. As the contrast of the mask increases above about 0.3, the threshold contrast of the test grating increases linearly, as shown in Figure 9.11a. In effect, this function expresses Weber's law for incremental contrast.

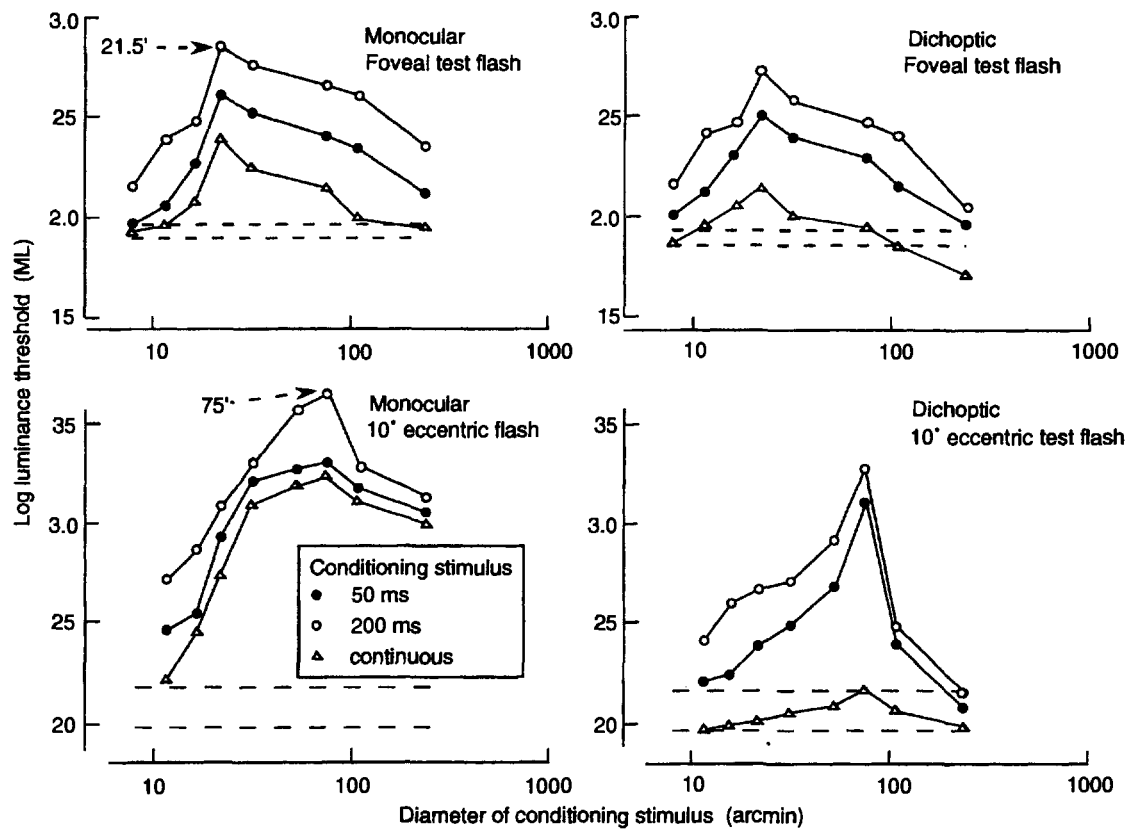


Figure 9.10. Dichoptic masking as function of stimulus size and duration.

The luminance threshold for detection of a 5-ms test flash presented at the same time as a conditioning stimulus, either to the same eye (left two graphs) or to the opposite eye (right two graphs). The three curves in each graph are for three durations of the conditioning stimulus. The top two graphs are for a foveal test flash, the bottom two for a test flash at 10° eccentricity. The dashed lines indicate the semi-interquartile range of the resting threshold for that position for monocular and binocular conditions. Results for one subject. (From Markoff and Sturr 1971.)

In dichoptic masking the test grating is presented to one eye and the masking grating to the other eye. It can be seen in Figure 9.11b that, for dichoptic viewing, with 200-ms exposures of the stimuli, the initial facilitatory effect is weaker but the masking effect is stronger than in monocular viewing (Legge 1979). The weak facilitatory effect represents binocular summation, discussed in Section 9.2.1, and the increased masking at higher contrast must represent interocular inhibition.

A high-contrast pattern in one eye and a low-contrast test pattern in the other is a similar condition to that which produces Fechner's paradox—a lowering of binocular brightness relative to monocular brightness (see Section 9.2.2). This inhibitory effect is not the same as binocular suppression, which occurs in binocular rivalry, because suppression is greatest when the patterns in the two eyes are dissimilar whereas, as we will now see, masking is greatest when the patterns in the two eyes are similar.

Like binocular summation of simultaneously presented threshold stimuli, the masking effect of a

grating is greatest when the spatial frequency and orientation of the test and mask are the same (Gilinsky and Doherty 1969). The threshold elevation as a function of the spatial frequency of a masking grating for a given spatial frequency of a test grating is the **spatial-frequency masking function**. Spatial-frequency tuning functions give an indication of the bandwidth of channels tuned to different spatial frequencies (Legge 1979). However, it is difficult to compare the spatial-frequency bandwidth of dichoptic and monocular masking functions since the two functions have very different slopes (Figure 9.12).

Masking as a function of relative disparity

A tone embedded in noise is easier to detect with two ears than with one ear, especially when the tone is presented in antiphase to the two ears. This phenomenon is known as **binaural unmasking** and the difference between masking with inphase and antiphase tones is known as the **binaural masking-level difference**. Henning and Hertz (1973) revealed a visual analogue of these effects. A visual noise

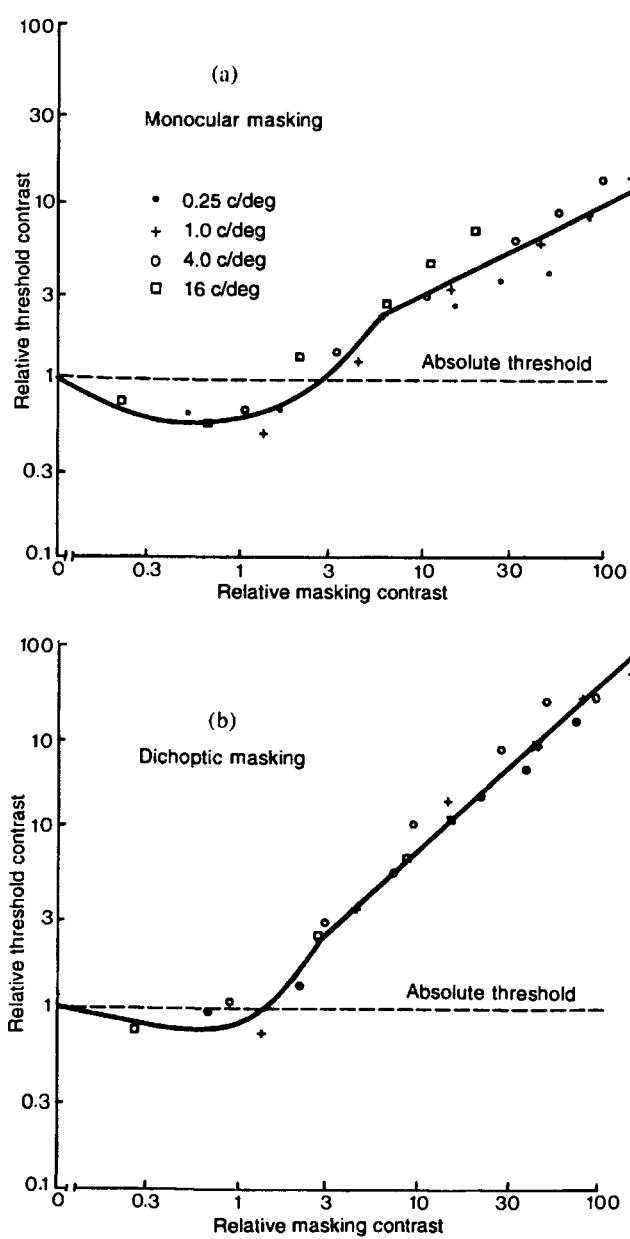


Figure 9.11. Monocular and dichoptic contrast masking.
 (a) The contrast threshold for detection of a grating as a function of contrast of a masking grating in the same eye.
 (b) The contrast threshold for detection of a grating presented to one eye as a function of the contrast of a masking grating presented to the other eye. The gratings were spatially in-phase and presented together for 200 ms. Data for the different spatial frequencies of the gratings are scaled according to the unmasked threshold contrast. Data from two subjects. (From Legge 1979.)

stimulus consisting of a mixture of vertical gratings within a narrow band of spatial frequencies, and slowly varying in contrast and phase, was presented to both eyes. A sinusoidal test grating of fixed contrast and phase and at the mean spatial frequency of the noise was superimposed on the noise.

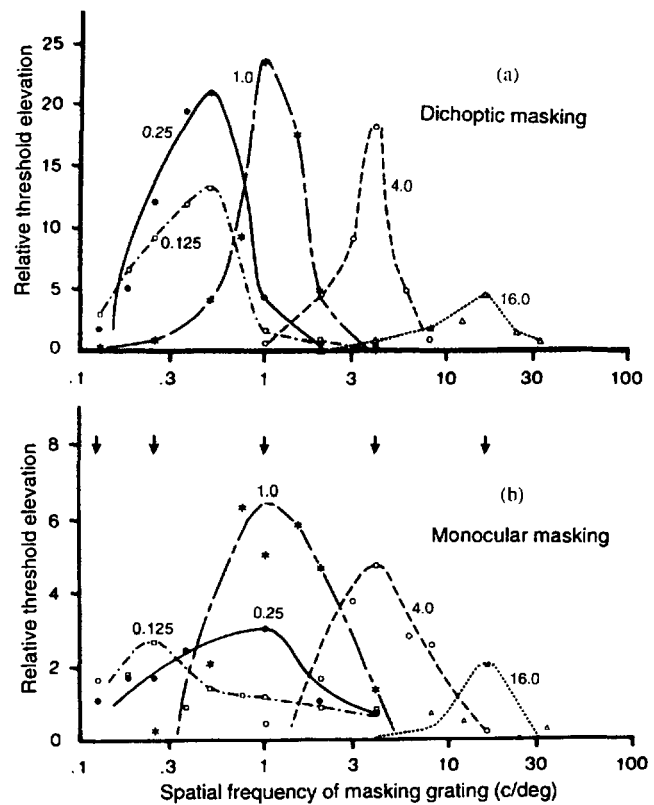


Figure 9.12. Dichoptic spatial-frequency masking.
 (a) Each curve shows the elevation of the contrast threshold of a test grating of a particular spatial frequency presented to the right eye, as a function of the spatial frequency of a masking grating presented to the left eye. The arrows indicate the spatial frequencies of the test gratings. The masking grating had a contrast of 0.19. The two gratings were presented together for 200 ms. Threshold elevation is the ratio of the threshold with the mask to that without the mask. Numbers on the curves signify the spatial frequencies of the test grating. Mean results from two subjects.
 (b) Monocular spatial-frequency masking functions with mask and test gratings presented to the same eye. (From Legge 1979.)

The test grating was either spatially in phase in the two eyes or spatially in antiphase. As with auditory stimuli, the test grating was detected at much lower contrasts when in antiphase than when in phase in the two eyes, but only for spatial frequencies of less than about 6 c/deg. This **binocular masking-level difference** did not depend on the temporal modulation of signal and noise (Henning and Hertz 1977).

Since vergence was not controlled, one cannot be sure whether the signal or the noise was in antiphase. In other words, we do not know whether antiphase noise is a less effective mask or whether an antiphase test stimulus is more resistant to masking. Also, Henning and Hertz did not mention whether the antiphase signal and the noise appeared in different depth planes; any misconvergence on the antiphase grating would induce either a crossed or uncrossed disparity into the noise display.

Moraglia and Schneider (1990) controlled for vergence and investigated the role of perceived depth in masking. They used a luminance-modulated Gabor patch as the test stimulus and a background area of broadband Gaussian noise as the mask. With convergence held on the background the visibility of the superimposed test patch was augmented when it had a horizontal disparity of 13.5 arcmin. It was augmented to a lesser extent when its disparity was 40.5 arcmin. In both cases the test patch appeared out of the plane of the noise. However, the appearance of depth was not required for augmentation of visibility because 13.5 arcmin of vertical disparity also augmented the visibility of the test patch (Moraglia and Schneider 1991). Visibility of a patch with a horizontal or vertical disparity of 67.5 arcmin was no better than with zero disparity, and the augmentation effect was absent when the test patch and noise were oriented at 90° to each other (see also Schneider et al. 1989). These results and others reported by Schneider and Moraglia (1992) suggest that dichoptic masking occurs at the cyclopean level within the disparity-detecting mechanism and that a stimulus is released from masking when its disparity differs from that of the mask.

We will see in Section 9.3.7 that backward masking is also reduced when the mask and the test stimulus are in different depth planes. A depth-dependent effect has also been found for simultaneous masking of a pattern by a surrounding annulus (Fox and Patterson 1981). In a related experiment McKee et al. (1994b) found that a test bar in one eye is masked to a lesser degree by a superimposed mask in the other eye when a second bar, similar to the mask, is placed adjacent to the test bar. They argued that the mask becomes stereoscopically matched with the adjacent bar rather than with the test bar, which releases the test bar from masking. This suggests that the process of stereo matching occurs before the site of dichoptic contrast discrimination.

Masking between suppressed and dominant images

Instead of asking how a stimulus in one eye masks a stimulus in the other eye, one can ask how a stimulus in the suppressed phase of binocular rivalry masks another stimulus that is in either the suppressed phase or the dominant phase. Westendorf (1989) measured the reaction time to the onset of a monocular probe superimposed on one of a pair of rivalrous dichoptic patterns, both when that member of the pair was in its dominant phase and when it was in its suppressed phase. When the probe was presented in the dominant phase the suppressed image in the other eye had no effect on the visibility of the probe. When the probe was presented during the

suppressed phase, however, its detection was delayed, and the delay was greater when the probe and suppressed image were identical rather than different. The greater effect with identical stimuli was ascribed to masking, since masking is greatest between identical stimuli and rivalry suppression is maximum between dissimilar stimuli. Thus, a suppressed image does not mask a probe on a dominant image but does mask a suppressed probe. It was concluded that dichoptic pattern masking occurs at a more central site than binocular suppression.

9.3.5 Visual crowding

A stimulus is more easily detected and its features more easily discriminated when it is presented in isolation than when it is flanked or surrounded by other similar stimuli. This effect is known as **crowding** or **contour interaction**.

The contrast threshold for detecting a 2° diameter counterphase-modulated vertical grating was elevated by an annular radial grating extending out to 20° in the same eye. Threshold elevation was larger when the radial grating was moving rather than stationary (Marrocco et al. 1985). Significant threshold elevations for both stationary and moving annular gratings were also found for dichoptic viewing.

The orientation of the letter T was more easily recognized for an isolated letter than for one flanked by two other letters (Toet and Levi 1992). Changes in the tilt of an isolated line were more easily discriminated than changes in the tilt of the same line flanked on both sides by other lines, even when the flanking lines had the same orientation as the test line (Westheimer et al. 1976). Also, vernier acuity was better for an isolated visual target (Levi et al. 1985). Crowding effects are more severe when the test and flanking stimuli are similar in size and shape (Kooi et al. 1994). This suggests that the effect is cortical in origin. This idea is further supported by the fact that crowding effects occur when the test stimulus is presented to one eye and the flanking stimuli to the other (Flom et al. 1963; Westheimer and Hauske 1975; Westheimer et al. 1976).

Crowding could be mediated by the lateral cortical connections discussed in Section 4.2.2. The angular range of crowding is similar to the angular range of cortical lateral connections, and both processes show a similar dependence on stimulus eccentricity (Tripathy and Levi 1994). Tripathy and Levi presented a test letter T to the monocular region in the left eye corresponding to the blind spot in the right eye. Subjects reported the orientation of the test letter less accurately when the three Ts were placed in the region surrounding the blind spot in the right eye.

This suggests that lateral cortical connections run from the region surrounding the blind spot in one eye into the monocular region corresponding to the blind spot in the other eye. The cortical area corresponding to the blind spot contains only monocular cells in the sense that each cell receives direct inputs from only one eye (LeVay et al. 1985). Nevertheless, if lateral connections run into the monocular area, this area is not strictly monocular.

9.3.6 The threshold-elevation effect

In the threshold-elevation effect a period of inspection of a suprathreshold masking grating elevates the contrast threshold of a subsequently exposed test grating. The threshold-elevation effect shows interocular transfer of about 65 per cent of its monocular value (Blakemore and Campbell 1969; Hess 1978). The effect is observed only when the adaptation and test gratings have a similar spatial frequency and orientation. The degree of interocular transfer of the threshold-elevation effect remained the same when the eye seeing the induction grating was pressure blinded in the interval between the induction and the test periods showing the effect to be cortical in origin (Blake and Fox 1972). The functions relating the threshold-elevation effect to the contrast and duration of the induction stimulus were the same for the monocular aftereffect as for the transferred after-effect (Bjorklund and Magnussen 1981).

The elevation of contrast threshold produced by an induction grating on a test stimulus presented to the same eye was reduced when the induction grating was accompanied by a grating of a different spatial frequency presented to the other eye. This interocular effect operated only when the gratings were vertical which suggests that it is related to stereopsis (Ruddock and Wigley 1976; Ruddock et al. 1979).

All this evidence suggests that the contrast-elevation effect occurs at a site more central than that at which visual inputs are combined. The threshold-elevation effect measured binocularly was the same whether the induction stimulus was presented to one eye or the other or alternately to the two eyes, as long as the total duration was the same (Sloane and Blake 1984). This suggests that the binocular aftereffect represents the pooled effect from binocular cells differing in ocular dominance.

9.3.7 Metacontrast

In another form of successive masking, the induction and test stimuli are presented only briefly and in adjacent locations rather than the same location. For instance, a visual pattern presented for a small

fraction of a second is not seen when followed by a stimulus in a nearby location when the interstimulus interval (ISI) is between 40 and 80 ms. This is known as **metacontrast** (Alpren 1952). Under certain circumstances the first stimulus masks the second stimulus. This is known as **paracontrast**. Metacontrast seems to have been first observed by Exner (1868), but was first explored systematically by Werner (1935, 1940) who used the disc-ring configuration in which a test disc is not seen when followed by a masking annulus. It is as if the new edge desensitizes the system for subsequent processing in the same location. The outer contour of the disc coincides with the inner contour of the annulus and these two contours have opposite luminance polarity. The superimposition or close proximity of similar contours of opposite polarity seems to be a general feature of stimuli that generate metacontrast. Various theories of the effect have been proposed and are reviewed by Weisstein (1972).

The degree of masking of a 0.25° test disc, flashed on just before a slightly larger disc presented briefly to the same eye, was greatly reduced when the larger disc was immediately followed by a surrounding annulus, also in the same eye (Schiller and Greenfield 1969). Presumably the outer annulus masked the larger disc, which was then less able to mask the inner test disc. When the conditioning and test stimuli were presented to one eye and the outer annulus to the other, the effect of the conditioning stimulus on the test stimulus was not weakened (Robinson 1968). Any postchiasmal effect of the annulus on the conditioning stimulus did not relieve the prechiasmal inhibitory effect of the conditioning stimulus on the test stimulus. This suggests that metacontrast does not show interocular transfer. However, the following evidence suggests that it does.

Metacontrast can affect the perception of depth in a random-dot stereogram. The accuracy with which depth in a random-dot stereogram was detected, as revealed by a forced-choice procedure, was reduced by a mask consisting of a random-dot display that depicted a noisy three-dimensional array of dots. Masking was greatest when the interstimulus interval was less than 50 ms (Uttal et al. 1975). It is not clear from this result whether the masking effect depends on disparity in the mask—the same effect may also be produced by a two-dimensional mask. The results were interpreted in terms of the time it takes to perceive depth in a random-dot stereogram.

Metacontrast with cyclopean images

Metacontrast can occur between a cyclopean shape and a binocular shape defined by luminance contrast, although this interdomain masking is less than

when induction and test stimuli are either both cyclopean or both binocular (Patterson and Fox 1990). Lehmkuhle and Fox (1980) constructed a dynamic random-dot stereogram depicting an annular mask and a disc-shaped test stimulus. Metacontrast occurred when the mask was presented just before the test disc. Metacontrast weakened as the test stimulus moved nearer to the viewer than the mask, but stayed constant when the test stimulus was moved beyond the mask (see Section 12.5.2).

Dichoptic metacontrast

Dichoptic metacontrast can be studied by presenting the test stimulus and mask to different eyes. Werner found that dichoptic metacontrast was the same as when the stimuli were seen by the same eye (see also Kahneman 1968). Kokers and Rosner (1960) also reported dichoptic metacontrast with a variety of stimuli. However, there are differences between dichoptic and dioptic metacontrast. For small inter-stimulus intervals, dichoptic masking is more pronounced than dioptic masking (Schiller and Smith 1968), perhaps because of binocular rivalry. Dichoptic, but not dioptic, metacontrast decreases with repetition of the stimuli (Schiller and Wiener 1963).

One way to think about dichoptic metacontrast is to assume that the newly delivered stimulus switches dominance to the eye seeing the new stimulus before the processing of the first stimulus is complete in the other eye. Oppositely polarized luminance edges rival, even when presented simultaneously. Werner (1940) argued against explaining dichoptic metacontrast in terms of binocular rivalry on the grounds that masking should occur when the mask precedes the test stimulus as well as when it follows it. This is not a strong argument. When the test stimulus follows the mask, it causes a switch of dominance to the eye containing the test stimulus. This should remove the contribution that rivalry makes to forward masking, leaving only the contribution of other factors.

9.4 TRANSFER OF FIGURAL EFFECTS

9.4.1 Introduction

Physiological studies reviewed in Chapter 4 revealed the following types of cell in the visual cortex:

1. Binocular OR cells, which respond to excitatory inputs from either eye but no more strongly to both eyes than to either alone, some responding equally to either eye and others more vigorously to one eye than to the other.

2. Binocular AND cells, which respond only when excited by inputs from both eyes simultaneously.

3. Excitatory/inhibitory cells, which receive an excitatory input from one eye and an inhibitory input from the other.

4. Purely monocular cells, which receive an input from only one eye.

These types of cell probably form a continuum of types and their response properties may not be fixed; for instance, their response to fusible stimuli may differ from their response to rivalrous stimuli, and the excitatory/inhibitory ratio may vary as a function of stimulus strength.

Psychophysical experiments on interocular transfer of figural induction effects have been conducted to explore the role of the various types of cell in binocular processing. A major issue in this literature is concerned with the types of cortical cell that are required to account for the results of interocular transfer experiments. Wolfe and Held (1981, 1983) championed the view that AND cells are required in addition to OR cells and monocular cells. Moulden (1980) developed an account based on monocular cells and three types of OR cell that differ in their degree of ocular dominance, but no AND cells. Cogan (1987) proposed a model of binocular processing in which only binocular cells are involved. There is something arbitrary about such accounts because each explains a different set of data and could probably accommodate new data by adjusting parameters or by adding extra assumptions.

Table 9.2 summarizes the five basic experimental paradigms used in studies of interocular transfer of figural induction effects.

1. *Interocular transfer paradigm.* In this procedure one first measures the figural induction effect with the induction and test stimuli in the same eye then with the two stimuli in different eyes. The transferred effect is expressed as a percentage of the same-eye effect. The following logic is then applied. The percentage transfer should (a) increase according to the extent to which the induction and test stimuli excite the same binocular OR cells, (b) diminish according to the extent to which the test stimulus excites unadapted monocular cells, (c) be influenced by the extent to which the different classes of cortical cells inhibit each other, (d) be influenced by the presence of post-induction effects in the closed eye during the test period, and (e) not be affected by the presence of binocular AND cells, since such cells do not contribute to the strength of either the monocular effect or the transferred effect.

Table 9.2 Paradigms used to study interocular transfer of figural effects

Paradigm	Induction stimulus	Test stimulus
1. Interocular transfer	monocular	monocular, same or other eye
2. Monocular vs. binocular test	monocular	monocular, same or both eyes
3. Binocular recruitment	monocular or binocular	binocular
4. Alternating monocular	alternating eyes	monocular or binocular
5. Cyclopean stimuli	cyclopean or noncyclopean	cyclopean or noncyclopean

2. *Monocular versus binocular test.* In this procedure the induction stimulus is presented monocularly and the test stimulus either monocularly to the same eye or to both eyes. For example, Wolfe and Held (1981) argued that unadapted AND cells, which are activated only when both eyes are open, cause the tilt aftereffect to be less with binocular testing than that with monocular testing. The aftereffect with binocular testing after monocular induction would also be reduced through the activation of unadapted monocular cells associated with the unadapted eye. Wolf and Held determined the reduction of the aftereffect due to this factor by measuring the amount of interocular transfer. The degree of transfer was insufficient to account for the reduction from one eye to two eyes. The extra reduction in the aftereffect was put down to the effect of recruitment of unadapted AND cells in binocular testing.

3. *Binocular recruitment.* In this procedure the aftereffect is first measured with both the induction and test stimuli viewed binocularly and then with a monocular induction stimulus and a binocular test stimulus. The presence of AND cells should make the aftereffect with binocular induction larger than with monocular induction. Wilcox et al. (1990) pointed out that this argument cannot be used to infer the presence of binocular AND cells. While it is true that binocular testing after monocular induction brings unadapted AND cells into play, which reduce the aftereffect, it also brings the monocular cells of the adapted eye into play, which increase the aftereffect. Since there is no way of knowing the relative contributions of these opposed influences, it is not possible to draw conclusions about what types of cortical cell are involved in the aftereffect.

4. *Alternating monocular induction.* In this procedure the induction stimulus is presented alternately to each eye for a period of time, and the test stimulus is then presented to either one eye or both simultaneously (Blake et al. 1981b). The following logic is then applied. The alternating induction

sequence adapts binocular OR cells and monocular cells for both eyes. Therefore, for these types of cells, the aftereffect should be the same for monocular and binocular testing. Since the alternating induction sequence does not adapt AND cells, the aftereffect is diluted by the activation of these unadapted cells during binocular testing. With monocular testing, the AND cells are not excited and therefore do not dilute the aftereffect. Thus, any reduction in the aftereffect with binocular testing relative to monocular testing indicates the presence of AND cells. This logic is not subject to the ambiguity present in the binocular-recruitment paradigm.

5. *Cyclopean stimuli.* A cyclopean induction or test stimulus is defined by disparities in a random-dot stereogram. Such cyclopean stimuli do not excite purely monocular cells. Both induction and test stimuli can be cyclopean or either one can be cyclopean and the other a conventional contrast-defined stimulus. The logic underlying the use of cyclopean stimuli in interocular transfer experiments becomes apparent in what follows.

Any asymmetry in ocular dominance should result in more interocular transfer from one eye than from the other. A person lacking binocular cells should show neither interocular transfer nor binocular recruitment of cortically mediated aftereffects (see Section 15.9.3).

There are many pitfalls in applying these arguments. Most investigators have ignored the contaminating effects of sudden changes in adaptation of the eyes, and all have ignored the possibility that inputs arising from a closed eye may interact with what is seen with the open eye. The literature has become complex and rather contentious.

9.4.2 Figural effects with dichoptic composites

A dichoptic composite stimulus is one in which part of a patterned stimulus is presented to one eye and part to the other, where both parts are required for a

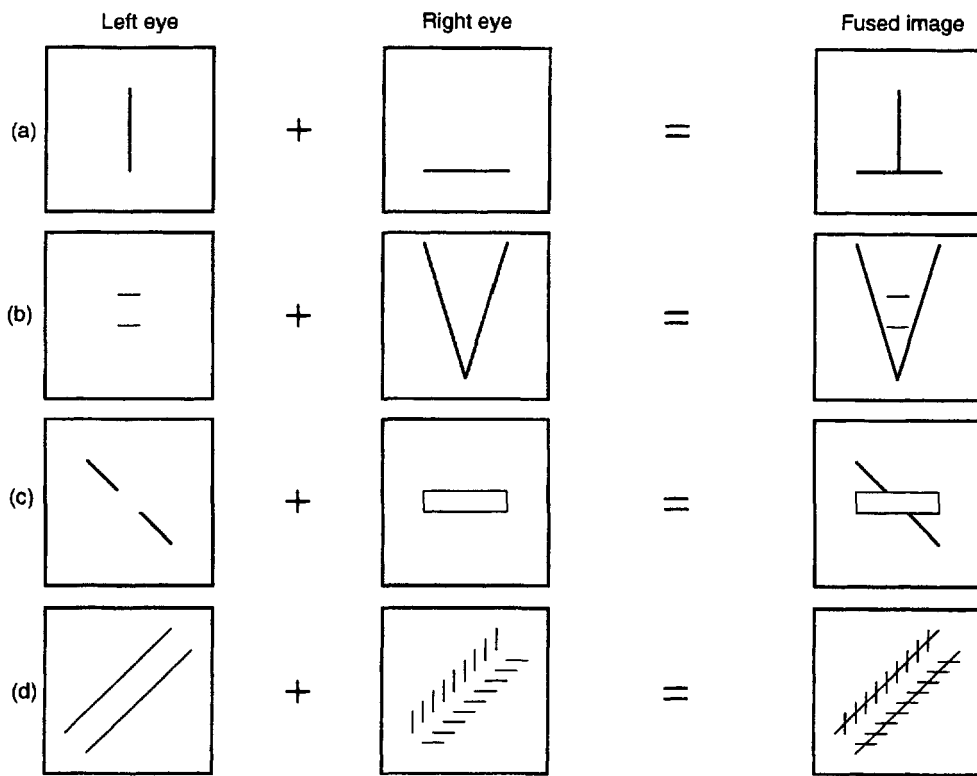


Figure 9.13. Dichoptic composite visual illusions.

Fusion of the left-eye and right-eye patterns produces the complete pattern shown on the right. Binocular rivalry occurs in the bottom figure, which makes it difficult to decide whether the illusion occurs in the dichoptic image.

given visual effect. The effect produced by a dichoptic composite display is cyclopean only in a weak sense because a similar effect is produced when the two parts of the stimulus are combined in one eye. Witazek (1899) was apparently the first person to use dichoptic composite stimuli. He created a dichoptic composite of the Zöllner illusion shown in Figure 9.13d. Inspection of this display produces severe rivalry, but Witazek claimed that the illusion was evident after a period of practice. Ohwaki (1960) found that dichoptic composite illusions are much reduced in magnitude compared with normally viewed versions, and concluded that the illusions are largely retinal in origin. Day (1961) obtained similar results but concluded that the decrement of the illusions with dichoptic viewing is due to binocular rivalry. Springbett (1961) did not see the Zöllner and Hering illusions in dichoptic composites even in the brief moments of the rivalry sequence when both components were clearly visible. The problem is that in these illusions the lines in the two eyes overlap and thus rival. Springbett did see the Müller-Lyer illusion when the fins were presented to one eye and the connecting lines to the other. Rivalry is less of a problem in this case because the component lines do

not overlap. He concluded that this illusion depends on processes occurring after binocular fusion. This is not a convincing argument because a Müller-Lyer illusion is evident in a figure consisting only of fins, as in Figure 9.14.

The vertical-horizontal illusion, in which a vertical line appears longer than an equal horizontal line, also survives when the two lines are dichoptic, and in this case there is no rivalry and no intruding monocular effect (Harris et al. 1974).

The most thorough investigation of dichoptic composite illusions was conducted by Schiller and Wiener (1962). For the first three displays in Figure 9.13 the dichoptic components do not overlap and, when these were presented briefly to further minimize binocular rivalry, the illusory effects were almost as strong as with normal viewing. Very little illusion was evident in the last display, in which the component lines overlap. Schiller and Wiener concluded that these illusions depend primarily on central processes, but that the illusion is not seen in Figure 9.13d because of binocular rivalry.

Several of the geometrical illusions occur in fully cyclopean shapes generated in random-dot stereograms (see Section 14.2).

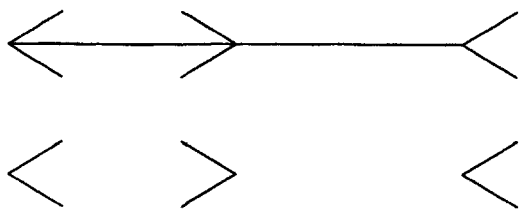


Figure 9.14. The Müller-Lyer illusion.

The illusion is evident in a figure consisting only of fins.

9.4.3 Interocular transfer of tilt contrast

In tilt contrast the apparent orientation of a test line changes when a second line at a slightly different orientation in the frontal plane intersects the test line or is placed next to it. In a commonly used form of tilt contrast, inspection of an off-vertical line induces an apparent tilt of a vertical line in the opposite direction. When the two stimuli are presented at the same time, the effect is known as **simultaneous tilt contrast**, and when the test stimulus is presented after the induction stimulus the effect is known as successive tilt contrast or the **tilt aftereffect**. It is generally believed that simultaneous tilt contrast is due to inhibitory interactions between orientation detectors in the visual cortex. A similar mechanism is probably involved in the tilt aftereffect, but an added factor is believed to be the selective adaptation of the orientation detectors responding to the induction stimulus, leading to a bias in the activity of the population of orientation detectors responding to the test stimulus (see Howard 1982 for a review of this topic). In both cases it has been proposed that interocular transfer of tilt contrast is mediated by binocular cells tuned to orientation in the visual cortex (Coltheart 1973).

There seems to be general agreement that tilt contrast does not occur when the induction stimulus and the test stimulus are presented to different eyes simultaneously, with the angle between the lines less than about 10° (Virsu and Taskinen 1975; Walker 1978a). One reason for this may be that lines close together tend to rival. For larger angles between induction and test stimuli, Walker obtained a small amount of interocular effect and Virsu and Taskinen obtained transfer equal to about 60 per cent of the amount obtained with monocular viewing of both the induction and test stimuli. Virsu and Taskinen used intersecting lines 3° long, which were subject to binocular rivalry and fusion, whereas the display used by Walker was free from these defects since it consisted of an annular induction grating with an outer diameter of 4.8° which surrounded a 1.6° diameter test grating.

A textured surface rotating in the frontal plane about the visual axis causes a superimposed vertical line to appear tilted in a direction opposite to the background motion. When the rotating surface was presented to one eye and the line to the other, this effect remained at full strength in subjects with normal binocular vision but was significantly reduced in stereoblind subjects (Marzi et al. 1986). Motion-induced tilt seems to be a more strongly binocular effect than static tilt contrast.

The tilt aftereffect shows interocular transfer when the induction line or grating is presented to one eye and the test line to the other. Estimates of the extent of transfer have varied between 40 and 100 per cent (Gibson 1937; Campbell and Maffei 1971). In this case binocular rivalry is not a factor because the induction and test displays are presented successively. Interocular transfer of the tilt aftereffect is positively correlated with stereoacuity and is absent in people lacking stereoscopic vision (see Section 15.9.3).

When the world is viewed through prisms, straight lines appear convex toward the base of the prism. After some time the lines appear straight again, and for a while after the prisms are removed straight lines appear curved in the opposite direction. This curvature aftereffect has been reported to show between 60 and 100 per cent interocular transfer (Gibson 1933; Hajos and Ritter 1965).

Wolfe and Held (1981) used an induction stimulus consisting of vertical lines in the frontal plane tilted one way in the top half and the other way in the bottom half, to form a chevron pattern. Inspection of such a pattern causes a subsequently seen set of straight lines to appear as a chevron bent in the opposite direction. In the test period, subjects adjusted a chevron pattern until it appeared as a set of parallel lines. Wolfe and Held applied paradigm 2 (see preceding) and found that after monocular inspection the aftereffect transferred about 70 per cent when testing was done on the other eye, but was only 40 per cent when the testing was binocular. They concluded that unadapted monocular cells were responsible for the dilution of the aftereffect in going from one eye to the other, and the recruitment of unadapted binocular AND cells was responsible for the extra dilution in going from one eye to two. Moulden (1980) did a similar experiment using a single set of parallel tilted lines rather than the chevron pattern and obtained the opposite result. However, Wolfe and Held pointed out that higher-level normalization processes may be involved in the stimulus used by Moulden. Wilcox et al. (1990) used both the chevron and tilted-lines stimuli and obtained the same result as Moulden. They

concluded that because of the uncertain role of unadapted monocular cells, the existence of binocular AND cells cannot be established by this procedure.

In addition, Wolfe and Held applied paradigm 4 and found that after alternating monocular adaptation the binocular aftereffect was less than either monocular aftereffect. They argued that unadapted AND cells were also responsible for this result. The argument is more convincing in this case since there were no unadapted monocular cells. Wilcox et al. (1990) obtained a similar result and agreed with Wolfe and Held that this supports the idea of there being binocular AND cells. Blake et al. (1981b) found that gratings presented in alternation to the two eyes produced equal threshold elevations in monocular and binocular test stimuli. This argues against the existence of AND cells but, as Wolfe and Held pointed out, the threshold-elevation effect may fall below the luminance threshold of AND cells.

Wolfe and Held (1982) provided further support for the existence of AND cells. The induction stimulus was a chevron pattern defined by binocular disparities in a random-dot stereogram so that the pattern was not visible to either eye. The test stimulus was a noncyclopean chevron pattern defined by luminance, which subjects set into alignment. The aftereffect showed only when the test pattern was viewed binocularly. Wolfe and Held argued that the effect would have been visible with a monocularly viewed test stimulus if the cyclopean induction pattern had stimulated binocular OR cells. A cyclopean induction stimulus does not adapt monocular cells. They concluded that a cyclopean image involves the stimulation of mainly AND cells that require a simultaneous input from both eyes. They admitted that the procedure may have been insensitive to the response of a small percentage of OR cells to the cyclopean image. Binocular viewing of a noncyclopean induction stimulus produced equal monocular and binocular aftereffects. Although monocular cells and binocular OR cells were adapted in this case, there should have been some advantage of binocular viewing, since it alone brought in AND cells. They suggested that the absence of a binocular advantage was due to a ceiling effect.

Wolfe and Held did not examine the case in which the induction stimulus is monocular and therefore noncyclopean, and the test stimulus is cyclopean. According to their theory there should be no aftereffect because monocular stimulation cannot adapt binocular AND cells, and only AND cells are excited by a cyclopean image. Burke and Wenderoth (1989) conducted this experiment with the stimuli shown in Figure 9.15. They found that all subjects saw an aftereffect in the vertical line defined by

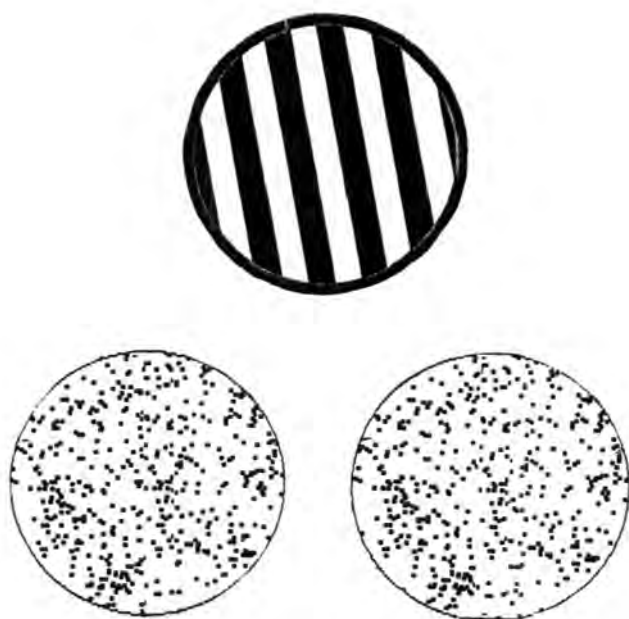


Figure 9.15. A cyclopean tilt aftereffect.

Monocular inspection of the upper grating for about 3 minutes causes the cyclopean bar in the stereogram to appear tilted to the right. (From Burke and Wenderoth 1989, Perception, 18, 471-482. Pion, London.)

disparity in the random-dot stereogram after monocular inspection of tilted lines defined by luminance. Binocular inspection of the tilted lines produced a similar result. They used an induction stimulus with a single set of tilted lines whereas Wolfe and Held used a chevron pattern. Adaptation to a single set of tilted lines brings in tilt normalization—the high-level process that causes a tilted display to appear vertical. The chevron-pattern effect depends on interaction between the two halves of the pattern rather than tilt normalization. Whether or not this makes a difference remains to be investigated.

From another series of experiments on the diminution of the tilt aftereffect when going from monocular adaptation to binocular testing Wolfe and Held (1983) concluded that binocular AND cells are more sensitive to low than to high spatial frequencies and are not responsive to near-threshold stimuli or to stimuli that are blurred in one eye. They pointed out that stereopsis is sensitive to the same stimulus features and concluded that AND cells are involved in stereopsis.

Binocular AND cells are known to exist from physiological evidence (see Section 4.4), but they seem to be few in number. Perhaps the role of binocular AND cells in binocular vision will never be resolved by psychophysical means, because there are so many factors to be taken into account and the same data can be explained by making different assumptions about the types of cell present, their

inhibitory or facilitatory interactions, their differential luminance thresholds, their differential dependence on stimulus features such as spatial frequency, and the degree of binocular congruence of the images.

Paradiso et al. (1989) obtained 92 per cent interocular transfer of the tilt aftereffect when the test stimulus was composed of subjective contours but only 46 per cent when it was a real bar. The same difference was found whether the induction stimulus consisted of a subjective bar or a real bar. They related this finding to the fact that von der Heydt et al. (1984) had found cells responding to subjective contours only in V2 of the alert monkey, an area in which there are more binocular cells than in V1.

The response of a cell in the visual cortex to an optimally oriented bar or grating is suppressed by a superimposed orthogonal bar or grating (Bishop et al. 1973; Bonds 1989). This is known as **cross-orientation inhibition**. It is largely independent of the relative spatial phases of the gratings and operates over a wide difference in spatial frequency. Cross-orientation inhibition was not elicited when the test and orthogonal gratings were presented to different eyes (DeAngelis et al. 1992), which suggests that crossorientation inhibition is generated in the visual cortex before signals from the two eyes are combined, and is not responsible for interocular transfer of orientation aftereffects.

The response of a cell in the cat's visual cortex to an optimal stimulus centred on the receptive field is larger when surrounding lines outside the cell's normal receptive field have a contrasting orientation than when they have the same orientation (see Section 4.2.2). DeAngelis et al. (1994) found that, for some cells, the inhibitory effect of similarly oriented lines could be evoked dichoptically. This suggests that it depends on intracortical inhibitory connections. This could provide a physiological basis for interocular transfer of orientation aftereffects.

9.4.4 Interocular transfer of the motion aftereffect

In the motion aftereffect, inspection of a textured display moving in one direction causes a stationary display seen subsequently to appear to move in the opposite direction. Aristotle (trans. 1931) saw the effect after looking at a flowing river, and mentioned it in his *Book of Dreams*. Purkinje (1825) noticed that after looking at a cavalry parade the houses appeared to move in the opposite direction. Addams (1834) rediscovered the effect when he saw the landscape appear to move after he had been looking at the falls of Foyers in Scotland. Purkinje and Addams believed that the effect was due to continuation of

nystagmic eye movements. The early work on the effect was reviewed by Wohlgemuth (1911). Holland (1965) provided a more recent review.

The motion aftereffect can be conveniently observed by inspecting the centre of a rotating spiral for about a minute and then transferring the gaze to a stationary pattern. An inwardly rotating spiral causes an apparent expansion of a subsequently viewed stationary pattern and an outwardly rotating spiral causes an apparent contraction (Plateau 1950). The spiral aftereffect cannot be due to eye movements since it occurs in all radial directions simultaneously. The magnitude of the motion aftereffect has been measured by recording its duration (Pinckney 1964), estimating its apparent velocity (Wright 1986), nulling it with a real motion in the opposite direction (Taylor 1963), and measuring its effect on the threshold for detection of motion in the adapted and unadapted directions (Levinson and Sekuler 1975). In a variant of the latter procedure, Raymond (1993) measured the motion aftereffect in terms of the elevation in the motion-coherence threshold. The motion-coherence threshold is the percentage of coherently moving dots in a dynamic random-dot display required for detecting unidirectional motion.

A large part of the motion aftereffect shows when the inspection display is presented to one eye and the test display to the other. The interocular transfer of the motion aftereffect was first noted by Dvorak (1870) and has been confirmed by several investigators (Ehrenstein 1925; Freud 1964; Lehmkuhle and Fox 1976). In the literature reviewed by Wade et al. (1993), estimates of the magnitude of the transferred aftereffect relative to that elicited in the same eye varied between zero and 78 per cent, with a mean of about 50 per cent. All the zero-transfer results were obtained using moving square-wave gratings and the rather insensitive criterion of duration of the aftereffect. For all other stimuli and criteria, interocular transfer was at least 40 per cent. The estimate of 78 per cent was obtained by Lehmkuhle and Fox after they had prevented sudden changes in the state of light adaptation in the transition from induction period to test period. When they did not control this factor, the aftereffect showed only 52 per cent interocular transfer. Other investigators do not seem to have controlled for this factor.

Raymond (1993) obtained 96 per cent transfer of the aftereffect of motion of a random-dot display when assessed by elevation of motion-coherence thresholds. There would be no sudden changes of luminance with stimuli of this kind, which may account for the high interocular transfer. Raymond favoured the view that the detection of motion coherence depends on extrastriate areas such as MT,

which are known to consist wholly of binocular cells and to be sensitive to the degree of coherent motion (Murasugi et al. 1993).

Nishida et al. (1994) cited evidence that the motion aftereffect tested with a static grating reflects activity at a lower level in the nervous system than the motion aftereffect tested with a directionally ambiguous grating flickering in counterphase. In conformity with this evidence, they found that the aftereffect induced by a drifting grating defined by luminance showed between 30 and 50 per cent interocular transfer when tested with a static grating but almost 100 per cent transfer when tested with a flickering pattern. A flickering test pattern also showed almost complete transfer of a motion aftereffect produced by inspection of a drifting grating defined by texture rather than by luminance. The motion coherence test used by Raymond and the counterphase flicker test used by Nishida et al. both involve dynamic rather than static displays and the greater amount of transfer obtained with them probably reflects the fact that dynamic displays are processed at a higher level in the nervous system. Steiner et al. (1994) found less interocular transfer of the motion aftereffect from translatory motion than from expansion or rotation and argued that this is because the latter types of motion involve processing at higher levels of the visual system.

If motion detectors were in the retina, one might expect some interocular transfer of the effect, since closing the eye in which the induction stimulus was presented would not prevent inputs from the adapted detectors from reaching the visual cortex. However, the motion aftereffect transferred from one eye to the other when the retina of the eye exposed to the induction stimulus was pressure blinded just after the exposure period (Barlow and Brindley 1963; Scott and Wood 1966). This proves that at least some of the motion detectors responsible for motion aftereffects in humans are at a higher level than the retina. We now consider the physiological evidence for interocular transfer of the motion aftereffect.

Physiological evidence has accumulated that motion detectors in primates are not located in the retina or LGN, but occur in the primary visual cortex and other visual areas in the central nervous system. Substantial evidence exists that motion detection is mediated by a set of cortical detectors, each optimally sensitive to a particular direction and speed of motion, but with overlapping tuning functions at each location of the visual field (see Sekuler et al. 1978). The motion aftereffect is believed to be due to selective adaptation of the motion detectors responding to the inspection stimulus, which causes an imbalance in the response of the set of motion

detectors to a stationary stimulus. It has been reported that the motion aftereffect is not induced by inspection of a moving display that fills the visual field (Wohlgemuth 1911). This is perhaps not surprising, since the optokinetic response of the eyes would tend to null the motion of the image over the retina. Retinal motion is preserved when there is relative motion in the visual field. In any case, relative motion is a more potent visual stimulus than absolute motion (Snowden 1992).

It is reasonable to suppose that interocular transfer of the motion aftereffect is mediated by motion-sensitive binocular cells in V1 or at a higher level. Recent experiments on the visual cortex of the cat have provided direct evidence for this idea. Motion-sensitive cells in the visual cortex of the unanaesthetized and lightly anaesthetized cat showed a decline in their rate of firing after the cat was exposed to a moving grating for 30 s. For about 30 s after the stimulus was turned off, the same cells remained less sensitive to motion in the adapted direction and more sensitive to motion in the opposite direction (Vautin and Berkley 1977; Hammond et al. 1988). Cells that had been adapted to a moving grating presented to one eye showed similar but weaker aftereffects when tested with stimuli presented to the other eye. This interocular transfer in a given cell was stronger when the induction stimulus was presented to the eye that provided the dominant input to that cell than when it was presented to the non-dominant eye. No transfer of the aftereffect occurred for cells classified as monocular (Hammond and Mouat 1988). Interocular transfer of direction-specific motion adaptation was most evident in simple cortical cells and showed only when the cells were adapted to motion in the preferred direction (Cynader et al. 1993). The interocular motion aftereffect, like the monocular aftereffect, is specific to the direction of motion of the induction stimulus. Thus, the directional tuning of binocular cortical cells must be the same for both eyes. This explains why binocular contrast sensitivity for moving gratings presented dichoptically is better than monocular contrast sensitivity only when the gratings move in the same direction (Arditi et al. 1981b).

Exposure of one eye to a stimulus moving in one direction while the other eye was exposed to a stimulus moving in the opposite direction produced no aftereffect when both eyes viewed a stationary test stimulus. But when only one eye viewed the test stimulus, the aftereffect was in a direction opposite to that of the induction stimulus to which that eye had been exposed (Wohlgemuth 1911; Anstis and Moulden 1970). When oppositely oriented gratings were viewed dichoptically after opposite motion

was viewed in the two eyes, the rivalry of the gratings was accompanied by a rivalry of apparent motion (Ramachandran 1991).

These phenomena could be due to the existence of monocular motion-sensitive cells in the visual cortex, which selectively adapt to inputs only from one eye. But each monocular aftereffect could also represent adaptation in that subset of binocular cells for which that eye forms the dominant input. Anstis and Duncan (1983) extended this paradigm as follows. A rotating spiral was seen rotating clockwise for 5 seconds by the left eye, and then for 5 s by the right eye, and finally rotating counterclockwise for 5 s by both eyes. The sequence was repeated 40 times. In the test period a stationary spiral appeared to rotate counterclockwise when viewed by either eye alone and clockwise when viewed by both eyes. Similar eye-specific aftereffects were reported by Jiao et al. (1984). The binocular aftereffect must have arisen in binocular cells.

The monocular effects in Anstis and Duncan's study could not have been induced in monocular cells in a straightforward way, since each eye was exposed to equal clockwise and counterclockwise motion. Three processes have been proposed to account for these monocular aftereffects:

1. Anstis and Duncan suggested that the response of the set of monocular cells responding to clockwise motion was inhibited by the activation of binocular cells responding to clockwise motion.

2. Tyler suggested to us that these effects can be explained by the results of his (1971) experiment in which binocular motion signals suppressed monocular motion signals (see Section 5.10.5). Thus, the counterclockwise binocular motion signals do not excite monocular cells and therefore do not cancel effects of monocular exposure to clockwise motion.

3. Van Kruysbergen and de Weert (1993) distinguished between a pure monocular system, a simple binocular system, and a pure binocular system. In Anstis and Duncan's experiment, the pure monocular system for each eye was exposed to equal amounts of clockwise and counterclockwise motion and therefore did not exhibit an aftereffect. The simple binocular system received 5 s of clockwise motion from each eye separately and 5 s counterclockwise motion from the two eyes simultaneously. Overall, it was exposed to clockwise motion for a longer period than to counterclockwise motion and therefore generated a counterclockwise aftereffect with monocular testing. The pure binocular system was activated by only counterclockwise motion and therefore exhibited a clockwise aftereffect with binocular testing. It must be assumed that the pure binocular system gives a stronger aftereffect than the

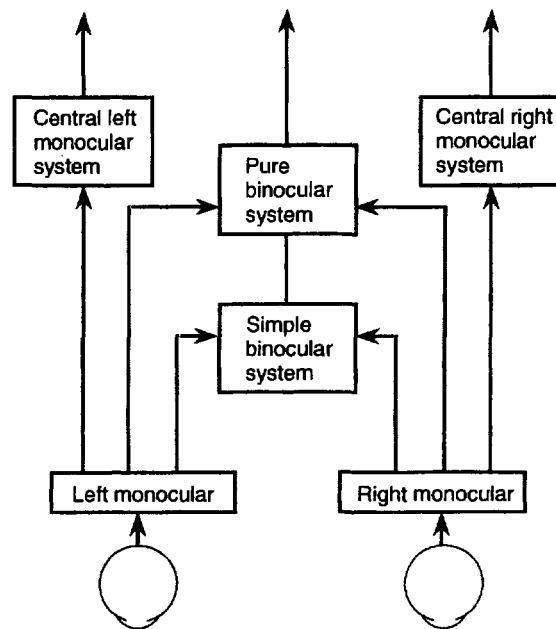


Figure 9.16. Monocular and dichoptic motion detection.

Set of motion-detection systems proposed by Kruysbergen and de Weert to account for monocular and binocular motion after-effects. (After Kruysbergen and de Weert 1993.)

simple binocular system; otherwise the two would cancel with binocular testing. van Kruysbergen and de Weert repeated Anstis and Duncan's experiment with a modification in which subjects were unaware of which condition they were exposed to. They produced further evidence for the pure monocular system and the two types of binocular system. In addition, their results suggest the existence of a central monocular system for each eye. These various systems are depicted in Figure 9.16 (see also van Kruysbergen and de Weert 1994).

One could imagine inducing a leftward aftereffect in one eye, a rightward aftereffect in the other eye, and, say, an upward aftereffect in both eyes.

A motion aftereffect can also be created by the motion of cyclopean contours which are not present in either monocular image (Papert 1964; Anstis and Moulden 1970). This aftereffect must depend on binocular cells since only binocular cells register a cyclopean image.

A stationary object superimposed on a moving background appears to move in the opposite direction, an effect known as **induced visual motion**. Swanston and Wade (1985) presented a stationary test line to one eye and a symmetrically expanding background to the other. Induced visual motion evident with ordinary binocular viewing was not present in the dichoptic condition, although binocular rivalry complicated the dichoptic judgments.

The effects of rivalry were eliminated by confining the moving display to an annulus surrounding a stationary disc. With this display, dichoptic induced motion occurred at about 30 per cent of its normal value (Day and Wade 1988). It is possible, however, that part of the dichoptic effect resulted from cyclo-rotation of the eyes induced by the moving annulus.

9.4.5 The spatial-frequency shift

After inspection of a grating of a given spatial frequency, a grating of lower spatial frequency appears coarser than it normally appears and a grating of higher spatial frequency appears finer (Blakemore and Sutton 1969). This is known as the **spatial-frequency shift**. The aftereffect shows interocular transfer when the inspection grating is presented to one eye and the test grating to the other, although the size of the transferred effect relative to the ordinary shift aftereffect does not seem to have been measured (Murch 1972). The spatial-frequency shift aftereffect can also be produced by cyclopean shapes generated in a random-dot stereogram (see Section 14.2).

Favreau and Cavanagh (1983, 1984) obtained interocular transfer of the spatial-frequency aftereffect with isoluminant coloured gratings, but only when the test grating was exposed for less than 400 ms or was flickering. They argued that the interocular transfer reflected the activity of colour-coded binocular cells with transient characteristics that have been found in V4 of the monkey. Transfer of other effects involving colour is discussed in the next section and the question of stereopsis with isoluminant stimuli is discussed in Section 6.1.4.

9.4.6 Interocular transfer of contingent aftereffects

A contingent aftereffect is one that depends on a particular combination of two stimulus features. The first contingent aftereffect to be reported involved colour and orientation. The human eye is not corrected for chromatic aberration, which means that red light is brought into focus nearer the lens than blue light. This produces colour fringes along black-white borders away from the optic axis. However, we do not see these colour fringes, presumably because the visual system applies a correction at a neural level. Colour fringes that are specific to the luminance polarity of edges appear when we view the world through prisms, because prisms increase the degree of chromatic aberration above its normal level. For instance, base-left prisms produce blue fringes on the right of light regions and red fringes on the left. These fringes disappear after the prisms

have been worn for a few days, which reinforces the idea that the neural system can compensate for them. In a footnote to a paper on adaptation to prismatically induced curvature, Gibson (1933) reported that colour fringes of opposite sign were seen for several hours after removal of prisms that had been worn for 3 days. These so-called **phantom fringes** must be neural rather than optical in origin since they show in monochromatic light (Hay et al. 1963). Phantom fringes represent the first-known example of a contingent aftereffect, because the colours were contingent on the polarity of the edge.

Celeste McCollough (1965) discovered a type of orientation-contingent colour aftereffect that can be induced in a few minutes. Subjects viewed an orange and black vertical grating for 10 s then a blue and black horizontal grating for 10 s. After several minutes of exposure to these alternating stimuli, a vertical achromatic grating appeared black and blue-green (the complementary colour of the vertical induction grating) and a horizontal grating appeared black and orange (the complementary colour of the horizontal induction grating). This type of contingent aftereffect is known as the **McCollough effect**. The McCollough effect is not an ordinary colour aftereffect obtained by gazing steadily at a coloured grating, since all regions of the retina are stimulated by both colours when the eyes scan the inspection stimuli. Also, the effect lasts for several hours, days, or even months, unlike aftereffects produced by single stimulus features, which last only minutes. See Stromeier (1978) for a review of this topic.

McCollough noted that there was no colour-contingent aftereffect when the inspection stimuli were presented to only one eye and the test stimuli to the other eye, except for one subject who reported an aftereffect in which the same rather than the complementary colours appeared in the test stimuli. This is the **positive contingent aftereffect**. Several other investigators have confirmed that the negative McCollough effect does not transfer to a nonadapted eye (Murch 1974; Stromeier 1978). Adaptation to prism-induced chromatic fringes has also been found not to transfer from one eye to the other (Hajos and Ritter 1965). Nine out of 27 subjects tested by Mikaelian (1975) observed a weak positive McCollough aftereffect in an eye that was not exposed to the induction stimulus, and 15 of the subjects observed the positive aftereffect in the unstimulated eye after scanning the achromatic test stimulus with both eyes for some time.

White et al. (1978) argued that keeping one eye closed during the induction period does not provide a fair test of interocular transfer, since the two eyes receive different levels of luminance and colour.

They overcame this problem by presenting the pattern component of the inspection stimulus to one eye while both eyes saw the colour component. Thus, one eye was exposed to red vertical and green horizontal gratings, as in the regular McCollough effect, while the other eye saw only the alternating colours, without the patterns. White et al. obtained a negative aftereffect when the eye seeing only the colour was tested. The positive aftereffect was seen when the eye that had been exposed to the patterned stimulus was pressure blinded during testing. This provides strong evidence that the figural processes responsible for the McCollough effect occur, at least partially, in binocular cells. *The conclusion would be strengthened if the experiment were also done the other way around—exposing one eye to the regular McCollough induction stimuli and the other eye only to alternating achromatic gratings.*

MacKay and MacKay (1975) fully partitioned the two stimulus components between the two eyes during the 20-minute inspection period. One eye saw only black and white gratings alternating in orientation while the other eye saw only a uniform green field alternating with a uniform red field. A black-white test grating presented to the eye that had been exposed to only uniform colour appeared in the colour complementary to that of the inspection stimulus with the same orientation. However, a test grating presented to the eye that had been exposed only to achromatic gratings appeared in the same colour as its matching inspection stimulus, that is, it was a positive aftereffect. Both these transferred effects were less than one third the strength of a normal McCollough aftereffect. Over et al. (1973) failed to observe any interocular transfer of the McCollough effect when they used a similar method with a 20-minutes of induction. However, the rate of alternation between the pairs of right and left eye stimuli was higher than in the MacKay and MacKay experiment. Potts and Harris (1979) used a similar procedure and obtained the negative aftereffect when the test grating was presented to the eye previously exposed to colour, but no aftereffect, when the eye exposed to colour was closed. Thus, interocular transfer of the McCollough effect is not always observed and, when observed, is much weaker than the direct effect, suggesting that the aftereffect depends mainly on processes before binocular fusion.

White et al. (1978) induced equal McCollough effects in the two eyes simultaneously, either in phase or out of phase. Each eye was exposed to a conventional McCollough inspection stimulus with the gratings and colours changing either in phase in the two eyes or in antiphase in the two eyes. After in-phase inspection the binocular aftereffect was

greater than either of the separate monocular aftereffects. After antiphase inspection the binocular aftereffect was weaker than either of the monocular aftereffects. It is surprising that there was any binocular aftereffect following antiphase inspection. These results provide evidence of binocular facilitation and cancellation of the McCollough effect, since only the binocular stimulus varied between the in-phase and antiphase induction conditions. However, the binocular facilitation was not large, suggesting that the major part of the McCollough effect is induced before the site of binocular convergence. On the basis of binocular facilitation, one would expect monocular aftereffects to be greater after in-phase than after antiphase induction, since only in-phase induction provides an effective stimulus for either binocular OR cells or AND cells. White et al. did not mention this point but a scrutiny of their data reveals no difference of this type. Kavadellas and Held (1977) also failed to find that monocular aftereffects after binocular induction with identical stimuli are greater than those after binocular induction with opposed stimuli. They did not compare monocular and binocular aftereffects and used a colour-contingent tilt aftereffect rather than a McCollough effect.

White et al. also demonstrated that aftereffects specific to each eye can be induced at the same time. Furthermore, when a black and white stimulus was presented to only one eye after a binocular induction period, the extinction of the aftereffect was largely confined to that eye (Savoy 1984). This evidence strengthens the conclusion that the McCollough effect depends mainly on processes occurring before the site of binocular convergence. This conclusion is also supported by the fact that White et al. found the aftereffect to be at full strength when, for much of the induction period, the induction stimulus presented to one eye was perceptually suppressed by a rivalrous stimulus presented to the other eye.

A coloured aftereffect contingent on the direction of motion of a black and white grating was created by combining particular colours with particular directions of motion (Hepler 1968). Inspection of a red disc rotating clockwise alternating with a green disc rotating counterclockwise produced a motion aftereffect in a stationary patterned disc, which varied in direction according to the colour of the disc (Mayhew and Anstis 1972). Stromeyer and Mansfield (1970) found that the colour-contingent motion aftereffect did not transfer to an eye that was closed during the induction period. Favreau (1978) found a positive colour-specific motion aftereffect, in its regular negative form does not transfer when the previously unstimulated eye was tested, but she did find a transferred positive contingent aftereffect.

In these studies a stationary test stimulus appeared to move in one direction when shown in one colour and in the opposite direction when shown in another colour. Smith (1983) found that the threshold for detecting motion of a rotating coloured spiral was elevated by prior inspection of a spiral moving in the same direction and with the same colour. This colour- and direction-specific threshold-elevation effect showed significant interocular transfer. This suggests that there are double-duty binocular cells jointly tuned to motion and colour revealed only when both the induction and test stimulus are moving, presumably because the cells do not respond to stationary stimuli.

Positive contingent aftereffects accord with a well-known property of afterimages. An ordinary coloured afterimage is in the complementary hue when it is projected on a light background and in the same hue when projected on a dark background or seen in the dark field of a closed eye (Sumner and Watts 1936; Robertson and Fry 1937). This dependence of the hue of an afterimage on the luminance of the background has nothing to do with binocular interactions (Howard 1960). Thus, it is not surprising that the contingent aftereffect is positive when the eye exposed to colour in the induction period is

closed during the test period. Note that MacKay obtained the ordinary negative aftereffect when the eye exposed to colour in the induction period was open during the test period. *We predict that transferred contingent aftereffects will be in their negative rather than their positive form if, during the inspection and test periods, the unstimulated eye is evenly illuminated rather than being closed.*

Summary

The complex series of experiments and theoretical arguments reviewed in this section yield the following conclusions. (1) Some aftereffects show more interocular transfer than others. (2) The magnitude of an aftereffect is determined by some pooling of activity from different types of cortical cells, including monocular cells, binocular OR cells, and possibly also binocular AND cells. (3) There is some evidence favouring the presence of both binocular OR cells and binocular AND cells. (4) Contingent aftereffects are due largely to processes occurring before binocular fusion. Evidence reviewed in Section 15.9.3 shows that people with defective binocular vision show less interocular transfer than do those with normal vision.

Vergence eye movements

10.1 Eye movements in general	381
10.1.1 Types of eye movement	381
10.1.2 Coordinate systems for eye movements	383
10.1.3 General features of vergence	385
10.2 Tonic vergence	386
10.2.1 Dark vergence	386
10.2.2 Strabismus	387
10.2.3 Phoria	387
10.2.4 Fixation disparity	388
10.2.5 Vergence adaptation	390
10.2.6 Adaptation to noncomitant vergence demand	392
10.3 Accommodation and vergence	393
10.4 Proximal vergence	398
10.5 Disparity vergence	399
10.5.1 The range of vergence	400
10.5.2 Disparity threshold for vergence	401
10.5.3 The stability of vergence	401
10.5.4 Vergence to peripheral stimuli	401
10.5.5 Vergence latency	402
10.5.6 Vergence velocity and gain	402
10.5.7 Trigger and fusion-lock components	404
10.5.8 Modelling the vergence system	407
10.6 Vergence-version interactions	408
10.6.1 Hering's law of equal innervation	408
10.6.2 Additivity of vergence and version	411
10.6.3 Oculomotor adaptation to aniseikonia	413
10.6.4 Oculomotor adaptation to monocular paresis	414
10.6.5 Vergence and the gain of the VOR	415
10.7 Cyclovergence	417
10.7.1 Types of torsional response	417
10.7.2 The measurement of cyclovergence	418
10.7.3 The dynamics of cyclovergence	419
10.7.4 The stimulus for cyclovergence	421
10.8 The neurology of vergence	424

10.1 EYE MOVEMENTS IN GENERAL

10.1.1 Types of eye movement

Eye movements serve three basic functions: stabilization of the retina with respect to the image as the head moves, fixation and pursuit of particular objects, and convergence of the visual axes on a particular object. Image stabilization is achieved by the **vestibuloocular response** (VOR), which is a conjugate eye movement evoked by stimuli arising in the vestibular organs (semicircular canals, utricle, and saccule) as the head moves (see Howard 1986).

The VOR occurs even when the eyes are closed, but when the eyes are open it is supplemented by **optokinetic nystagmus** (OKN) evoked by the motion of the image of the visual scene (see Howard 1993a). Both these responses are involuntary and were the first types of eye movement to evolve.

Eye movements for the fixation and voluntary pursuit of particular objects evolved in animals with foveas. Voluntary rapid eye movements (saccades) allow the gaze to move quickly from one part of the visual scene to another. Voluntarily pursuit movements maintain the image of a particular moving object on the fovea.

Table 10.1. Terminology for horizontal, vertical, and torsional vergence.

Type of vergence movement	Name of vergence movement
Opposed horizontal rotation	Horizontal vergence
Visual axes moving in	Convergence
Axes moving out toward parallel	Divergence
Opposed vertical rotation	Vertical vergence
Right visual axis up, left axis down	Right supravergence (left infravergence)
Left visual axis up, right axis down	Left supravergence (right infravergence)
Opposed torsional rotation	Cyclovergence
Vertical meridians rotate top in	Incyclovergence
Vertical meridians rotate top out	Excyclovergence

The third basic type of eye movement, namely, convergence of the visual axes on a particular object, is well developed in animals with frontal vision such as primates. Coordinated movements of the eyes in opposite directions occur in a horizontal plane, a vertical plane, or around the visual axes. Until recently it was believed that primates were the only animals with vergence eye movements. Hughes (1972) recorded vergence in cats, but found a good deal of individual variation. Some lateral-eyed animals, such as the chameleon, the pigeon, and the rabbit are capable of converging the eyes (see Chapter 16).

During fixation, the eyes exhibit so-called **physiological nystagmus**, consisting of a mixture of slow drifts and microsaccades with a mean standard deviation of about 0.1° (Steinman et al. 1973; Ott et al. 1992). The amplitude of these movements can be reduced by voluntary effort (Steinman et al. 1967). Marshall and Talbot (1942) suggested that the constant motion of the retinal image produced by fixation tremor improves visual acuity. It is well known that if image motion is stopped, all objects fade from view after a short time. Eye movements are clearly needed for vision, but acuity and contrast sensitivity are not adversely affected by image stabilization before the image fades (Tulunay Keesey 1960; Gilbert and Fender 1969). Furthermore, imposed image motions at velocities up to $2.5^\circ/\text{s}$ have been found to have no effect on acuity (Westheimer and McKee 1975, 1977). A person makes fewer microsaccades when detecting fine detail, which would be a counterproductive if microsaccades improved acuity (Winterson and Collewijn 1976; Bridgeman and Palca 1980). It seems therefore that physiological nystagmus has not evolved to improve acuity.

A movement of an eye considered singly is known as a **duction**—abduction when the eye moves temporally, adduction when it moves nasally, and torsion when it rotates about the visual axis.

A combined movement of the two eyes in the same direction is known as a conjugate movement, or **version**. The eyes can move together laterally, vertically, or in an oblique direction. A conjugate rotation of the eyes around each visual axis is known as **ocular torsion** or **cycloversion**.

A movement of both eyes in opposite directions is a disjunctive movement, or **vergence**. In horizontal vergence, the visual axes move within a plane containing the interocular axis, and in vertical vergence they move in planes orthogonal to this axis. The eyes also move in opposite directions about the two visual axes, a response known as **cyclovergence**. Combined rotations of the eyes about two or three axes are also possible. Table 10.1 presents the terminology used to describe the three types of vergence. For a discussion of the anatomy and mode of action of the extraocular muscles see Carpenter (1988).

The centre of rotation of an eye is not at the centre of the eye and is not fixed with reference to the orbit (Park and Park 1933). In other words, the eye translates a little as it rotates. For most purposes, however, it can be assumed that the human eye rotates about a fixed centre 13.5 mm behind the front surface of the cornea. The direction of gaze is specified with respect to the median and transverse planes of the head. The straight-ahead, or **primary position**, of an eye is not easy to define precisely, because the head and the eye lack clear landmarks. For most purposes the primary position of an eye may be defined as the direction of gaze when the visual axis is at right angles to the plane of the face and the **interocular axis**, which is the line joining the centres of rotation of the two eyes. An eye moves from the primary position into a **secondary position** when the visual axis moves from the primary position within either a sagittal or a transverse plane of the head. An eye moves into a **tertiary position** when the visual axis moves into an oblique position.

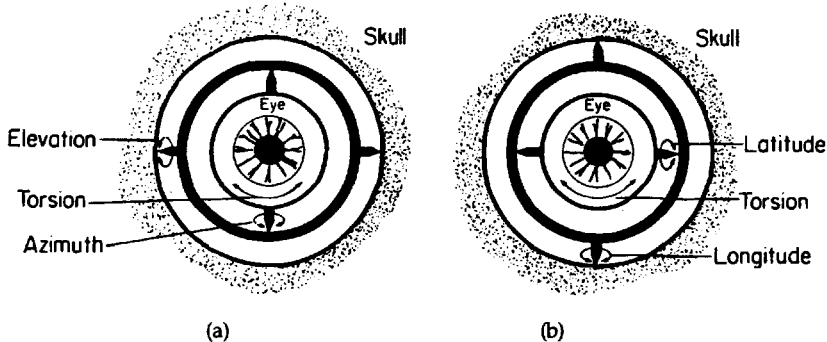


Figure 10.1. Axis systems used to specify eye movements.

(a) In the Helmholtz system the horizontal axis is fixed to the skull, and the vertical axis rotates gimbal fashion about the horizontal axis.

(b) In the Fick system the vertical axis is fixed to the skull.

Procedures for measuring eye position are reviewed by Collewijn et al. (1975), Young and Sheena (1975), and Eizenman et al. (1984).

10.1.2 Coordinate systems for eye movements

We assume that all eye movements involve pure rotations about a fixed centre. We thus ignore small translations. The position or rotation of an eye may be specified using any of four coordinate systems. The choice is arbitrary although for a given purpose one system may have practical advantages.

Helmholtz system.

In the Helmholtz coordinate system the horizontal axis, about which vertical eye movements occur, is assumed to be fixed to the skull. The vertical axis rotates gimbal fashion about the horizontal axis and does not retain a fixed angle to the skull. The direction of the visual axis is expressed in terms of elevation (λ) and azimuth (μ) (see Figure 10.1a). Torsion is a rotation of the eye about the visual axis with respect to the vertical axis of eye rotation.

Fick system.

In this system the vertical axis is assumed to be fixed to the skull, and the angular position of the visual axis is expressed in terms of latitude (θ) and longitude (ϕ). Torsion is rotation of an eye about the visual axis with respect to the horizontal axis of eye rotation. The Fick system is the Helmholtz system turned to the side through 90° (see Figure 10.1b).

Perimeter system.

This system is a polar coordinate system in which an axis straight out from the eye socket is assumed to be fixed to the head. Movements of an eye are expressed in terms of the angle of eccentricity (π) and

of meridional direction (κ) of the visual axis in relation to a spherical scale fixed with reference to the head and with its zero point on the visual axis when the eye is in its primary position.

These three systems are the same spherical coordinate system, simply anchored to the head in different ways (Fry et al. 1945). A specification of eye position can be transformed between the three systems by the following equations:

$$\tan \lambda = \frac{\tan \theta}{\cos \phi} = \sin \kappa \tan \pi$$

$$\sin \mu = \sin \phi \cos \theta = \sin \pi \cos \kappa$$

Listing's system.

Listing proposed that any rotation of an eye may be regarded as occurring about an axis in a plane known as **Listing's plane**. Helmholtz called this **Listing's law**. Listing's system is a two-parameter system and cannot specify torsional rotations of the eye. Listing's plane is fixed with respect to the head and coincides with the midfrontal or equatorial plane of the eye when the eye is in its primary position (plane HD'D in Figure 10.2). For elevations and depressions of the eye, the axis in Listing's plane is the horizontal axis, for lateral movements it is the vertical axis, and for oblique movements it is between the horizontal and vertical axes. More precisely, the axis of rotation in Listing's plane is at right angles to the plane containing the visual axis in both its initial and final positions (plane OPB). Thus, in any given movement of an eye, only one axis is assumed to exist; it always lies in Listing's plane, but its orientation in that plane depends on the meridian along which the movement occurs. The extent of an eye movement is the angle between the initial and final directions of gaze (the angle of eccentricity π). The direction of an eye movement is specified by the

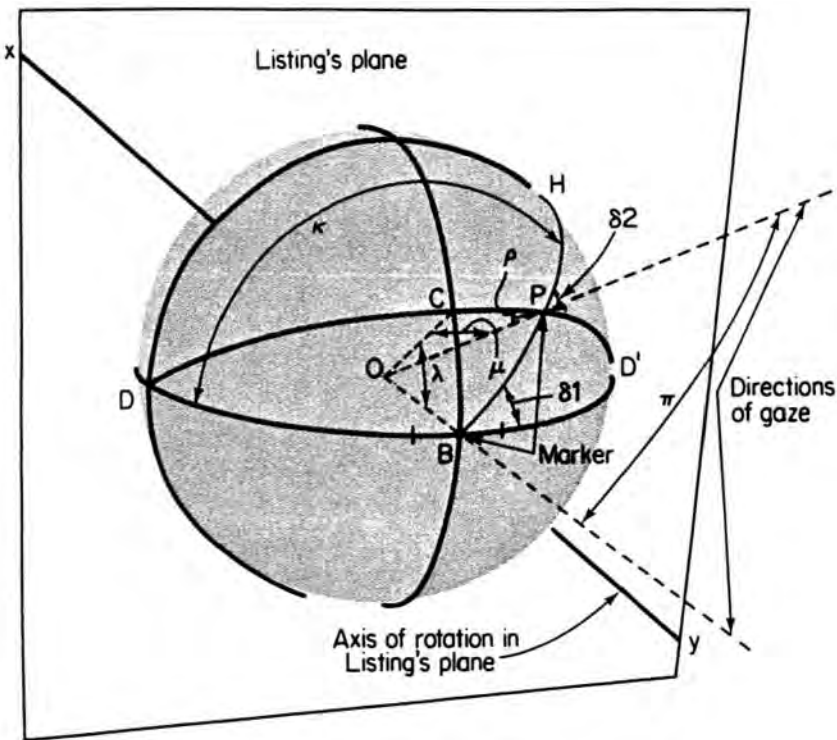


Figure 10.2. The geometry of eye movements.

The direction of gaze is assumed to have moved from the primary position OB to an oblique position, OP , through an angle of eccentricity π , along the meridian BH , which is at an angle κ to the horizontal meridian DBD' . This is equivalent to it having occurred about axis xy in the equatorial frontal plane (Listing's plane). The horizontal marker between the small vertical bars initially makes an angle δ_1 with the meridian along which the eye moves. According to Listing's law, this angle remains constant ($\delta_1 = \delta_2$). The eye can also be regarded as having moved on Helmholtz axes, through an angle of elevation λ and an angle of azimuth μ . In the Helmholtz system, for angle δ to remain constant, the eye and marker must undergo torsion through angle ρ relative to the final plane of regard DCD' .

angle between the meridian along which the visual axis moves and a horizontal line in Listing's plane (δ or its supplement κ).

Listing's law may be tested by impressing a short horizontal reference line on the eyeball in its primary position and seeing whether the angle between the line and the meridian along which the eye moves (angle δ_2) remains constant. The law appears to be correct for conjugate eye movements (Quereau 1954; Fry 1968; Ferman et al. 1987a), but when the angle of convergence changes, the law does not hold and torsion, as defined by a change in the angle δ_2 , does occur (Allen and Carter 1967). Furthermore, when the eyes are converged they undergo extorsion during downward gaze shifts and intorsion during upward gaze shifts. Mok et al. (1992) suggested that these movements can be accounted for if one assumes that Listing's plane in each eye is rotated temporally when the eyes are converged. Thus, for a given degree of convergence, Listing's law holds for changes in version with respect to rotated Listing's

planes. The effects of eye torsion on the vertical horopter were discussed in Section 2.7. Listing's law, even in this modified sense, does not hold in certain other circumstances, (see Section 10.7).

Torsion in the Helmholtz system is the angle between a horizontal marker on the eye and the plane within which the visual axis moves ($D'PD$), that is, angle ρ in Figure 10.2. In Fick's system, torsion is the complement of angle ρ . These angles are a function of angle δ and the angle of eccentricity, π , and are not constant, even when the eyes obey Listing's law. Thus, when an eye moves into a tertiary position, it normally shows no torsion in Listing's coordinate system, but it does show torsion in the Fick or Helmholtz systems. Any torsion occurring when the eye is in a primary or secondary position of gaze has the same angular value in all coordinate systems. The Helmholtz and Fick systems, being three-axis systems, can be used to specify torsion whereas Listing's system was not designed for this purpose, because it is only a two-parameter system.

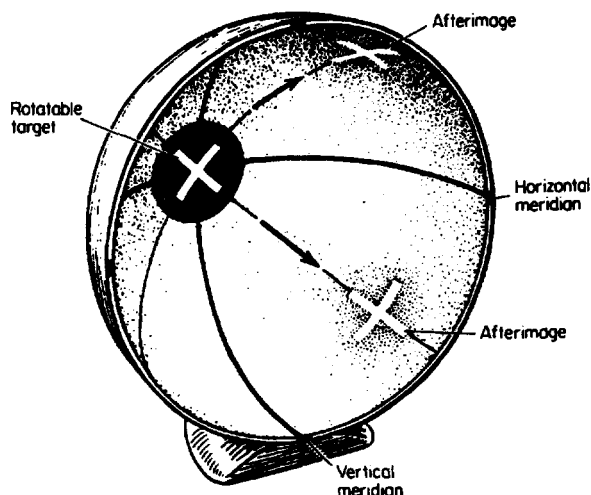


Figure 10.3. Demonstration of Listing's law.

The eye, in its primary position of gaze, is placed at the centre of curvature of a hemisphere and an afterimage of a cross is impressed on it. The afterimage retains the same orientation with respect to the meridian along which the gaze moves. This indicates the validity of Listing's law. (From Noorden, 1990.)

The eyes do not obey Listing's law during sleep, showing that they are not mechanically constrained to move this way. However, they obey the law when they move in the dark, so visual feedback is not required. Therefore, movements obeying Listing's law must be due to neural programmes (Nakayama 1975). Since Listing's plane is fixed to the head, eye-movement commands are referred to the head rather than to a coordinate system fixed to the eye.

Listing's law has the important consequence that, as the gaze travels along any line in the visual field, the retinal image of the line remains self congruent, and continues to stimulate cortical orientation detectors tuned to the same orientation. This fact should be clear from Figure 10.3. It follows that an afterimage of a line imposed on the normally vertical meridian of an eye remains congruent with a circle parallel to the midvertical meridian of a sphere centred on the eye. These circles project as hyperbolic arcs in a frontal plane. This fact enables one to construct a more precise definition of the primary position of gaze than that given at the beginning of this section. The primary position of gaze may be defined as the centre of the set of hyperbolic arcs that have just been described (Nakayama 1978).

10.1.3 General features of vergence

Horizontal vergence is under voluntary control and occurs when fixation is changed from one depth plane to another or when a visual target is pursued as it moves in depth. The angle between the visual

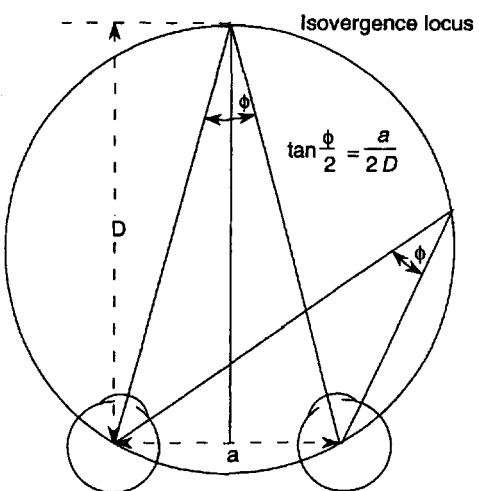


Figure 10.4. The angle of vergence.

Relationship between the angle of horizontal vergence, ϕ , the interocular distance, a , and the distance, D , between the interocular axis and the point where the isovergence locus cuts the median plane. With symmetrical convergence, D is the distance of the fixation point.

axes at the point where they intersect is the **vergence angle**. When a person fixates a point at infinity the visual axes are parallel and the vergence angle is zero. The eyes converge when the vergence angle increases and diverge when it decreases.

It can be seen from Figure 10.4 that for symmetrical convergence the angle of horizontal vergence, ϕ , is related to the interocular distance, a , and the distance of the point of fixation from a point midway between the eyes, D , by the expression

$$\tan \frac{\phi}{2} = \frac{a}{2D} \quad (1)$$

It follows from this equation that the change in vergence per unit change in viewing distance is much greater at near than at far viewing distances. About 70 per cent of a person's normal range of vergence is used for viewing distances of up to 1 metre.

An **isovergence locus** is the path traced by the point of fixation when version changes with vergence held constant. For a fixed elevation of gaze, the isovergence locus is a circle passing through the fixation point and the centre of rotation of each eye. This follows from the fact that a chord of a circle subtends the same angle at all points on the circumference. Note that the Vieth-Müller circle, or theoretical horopter, described in Section 2.5, intersects the nodal points of the eyes rather than their centres of rotation. If the eyes change their elevation, the isovergence locus becomes a toroidal surface formed by rotation of an isovergence circle round the line joining the centres of rotation of the two eyes.

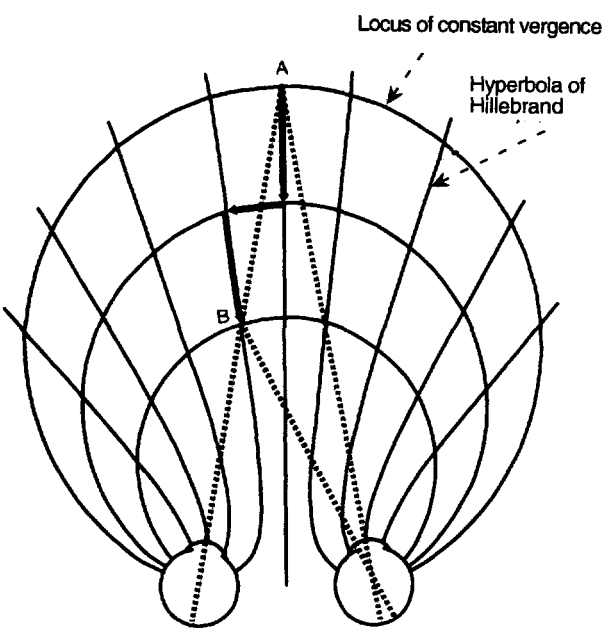


Figure 10.5. Loci of isovergence and isoversion.

Loci of constant vergence for changing version are circles through the centres of rotation of the two eyes. Loci of constant version for changing vergence are the hyperbolae of Hillebrand. As the gaze moves from A to B, both vergence and version change.

The loci of constant version for changing vergence are known as **hyperbolae of Hillebrand**, as shown in Figure 10.5. Equation (1) holds for asymmetrical convergence if D is defined as the distance to the point where the locus of isovergence cuts the median plane, rather than the distance to the point of fixation.

It was commonly believed until the early 1950s that only convergence required the active contraction of the extraocular muscles and that divergence resulted from passive elastic tension in the muscles. Electromyographic studies have revealed that the lateral recti contract when the eyes diverge, and all muscles are in a state of active contraction even when the eyes are in the primary position of gaze (Breinin and Moldaver 1955). Distinct neural mechanisms for convergence and divergence have now been identified (see Section 10.8).

Horizontal vergence changes with viewing distance and is therefore closely associated with voluntary shifts of gaze. Many people find it difficult to change their vergence state without the aid of a visual target. However, with some practice, people can readily gain voluntary control over horizontal vergence in the absence of a visual stimulus.

Vertical vergence and cyclovergence need not change for different viewing distances and these responses are not normally under voluntary control. There is a weak coupling between viewing distance

and cyclovergence, and changes in vertical vergence and cyclovergence occur with changes in the direction of gaze. Vertical vergence and cyclovergence are controlled by visual error signals which allow these responses to ensure that similar images fall on corresponding meridians of the eyes. The discussion that follows mainly concerns horizontal vergence. Cyclovergence is discussed in Section 10.7.

Just before, during, and just after a vergence response to a large disparity step there is a decrement in the ability to detect a visual target or the displacement or change in disparity of a target (Manning and Riggs 1984; Hung et al. 1989, 1990). This suppression of visual sensitivity associated with vergence is analogous to that associated with saccades (Volkmann et al. 1978; Matin 1974). Suppression probably helps the viewer to disregard the instability of the retinal images during vergence and may also help eliminate the effects of spurious disparity signals during the execution of large vergence movements.

Reviews of vergence have been provided by Alpern (1969), Schor and Ciuffreda (1983), Carpenter (1988), Collewijn and Erkelenz (1990), and Judge (1991). The development of vergence in the child is discussed in Section 15.2.3.

Maddox (1893) identified four types of horizontal vergence: tonic, accommodative, fusional (disparity), and voluntary vergence, often referred to as proximal vergence. These various forms of vergence are now described.

10.2 TONIC VERGENCE

10.2.1 Dark vergence

Tonic vergence is the tendency of the eyes to return to the state of vergence that they assume in the dark. This state is known as **dark vergence**. Astronomers have noticed that the eyes also become myopic in dim light and pilots have noticed that they become myopic when viewing the empty sky (Campbell and Primrose 1953). It is believed that dark vergence depends partly on tonic efferent discharge. The distance of the point of dark vergence varies between 0.62 and 5 m for different observers, with an average value of about 1.2 m and is consistent over time for the same individual if the conditions of testing are constant (Owens and Leibowitz 1980; Fisher et al. 1988). However, dark vergence can be altered temporarily. Maddox noted that it increases after a period of increased convergence demand induced by looking at fusible visual targets through base-out prisms. This effect has been confirmed many times.

In the dark, the eyes diverge from the position of dark vergence when the gaze is elevated and converge from that position when the gaze is depressed (Heuer and Owens 1987). After the eyes have been held in an elevated or depressed posture for a few minutes, the position of dark vergence with horizontal gaze is temporarily biased toward the previously maintained state (Heuer et al. 1988).

In deep sleep, anaesthesia, or death the eyes assume a posture known as the **anatomic position of rest** that represents the relaxed state of the muscles when lacking tonic innervation. The anatomic position of rest is more divergent than dark vergence, although there is no agreed value for this position (see Owens and Leibowitz 1983).

10.2.2 Strabismus

A person who cannot converge the eyes on the intended object is said to have a squint, also known as **strabismus** or **heterotropia**. Properly aligned eyes are **orthotropic**. Strabismus occurs in about 7 per cent of the population, and about 65 per cent of cases develop before the age of three years, with a mean age of onset of about 30 months (Graham 1974). There are many types of strabismus. In divergent strabismus, or **exotropia**, the visual axes are directed outward from the intended point. When the angle of deviation of an exotropic eye is the same for near as for far viewing, it is known as a basic exotropia. When the exotropia is combined with convergence insufficiency the angle of exotropia is larger with near than with far viewing, and when combined with divergence excess it is larger with far than with near viewing. In convergent strabismus, or **esotropia**, the visual axes are directed inward, and in vertical strabismus the two axes do not lie in the same horizontal plane. In **unilateral strabismus** one eye is consistently used for fixation when both eyes are open and the other eye always deviates. This type of strabismus is often accompanied by some loss of visual function in the deviating eye, a condition known as **amblyopia** (see Section 15.7). In a less common condition, known as **alternating strabismus** the person sometimes uses one eye and sometimes the other for fixation.

In **comitant strabismus** the deviation is the same in all directions of gaze, although it may vary according to the angle of convergence and from day to day. Comitant strabismus is due to a defect of the vergence mechanism rather than a defect of particular extraocular muscles and is sometimes reduced when refractive errors are optically corrected. In **noncomitant strabismus** the deviation varies with the angle of gaze. It is due to a paresis in one or

more extraocular muscle arising from damage to the muscle or to the oculomotor nerves. Noncomitant strabismus arising from paresis is also known as **paralytic strabismus**. The noncomitance is particularly evident when the patient attempts to move the eyes in the direction of action of the paretic muscles. Comitant strabismus and noncomitant strabismus of muscular origin may be partially or completely corrected by surgically adjusting the extraocular muscles or by injection of a neurotoxin into selected extraocular muscles (Scott 1981). It has also been claimed that strabismus may be cured by wearing prisms for a period of up to 6 months (see Noorden 1990). Estimates of the success of these methods in restoring some binocular vision have varied from 5 per cent (Flom 1963) to 50 per cent (Wick and Cook 1987). Corrective treatments have a cosmetic value even if binocular vision is not restored. The etiology of strabismus is unclear. It is often associated with uncorrected refractive errors and there is evidence of a genetic factor (Graham 1974).

More information on strabismus is provided by Lennerstrand et al. (1988) and Noorden (1990).

10.2.3 Phoria

Most people have a latent strabismus, or **phoria**, which does not show when both eyes are open and provided with a fusible stimulus. A phoria shows itself when the eyes are **dissociated**, that is, when no fusible stimuli are in view. It may therefore be regarded as the open-loop vergence error. **Orthophoria** is the condition of zero phoria. There are several ways to dissociate the eyes: by closing or covering one eye, by presenting nonoverlapping dichoptic stimuli, or by presenting overlapping but rivalrous stimuli. A horizontal phoria may be observed as a deviation of a covered eye either inward (**esophoria**) or outward (**exophoria**) from its position when it is uncovered. Horizontal phoria is conventionally measured while the open eye of the subject is accommodated on a distant object, because it is believed that effects of accommodation on vergence are least with far accommodation. Horizontal phorias of up to 4 prism dioptres (about 2°) are considered normal. A deviation of the left eye upward or downward is a left hyperphoria or left hypophoria, respectively, and similar deviations of the right eye are either a right hyperphoria or a right hypophoria. A torsional deviation of an eye is a **cyclophoria**: top-inward is an **incyclophoria** and top-outward, an **excyclophoria**. It takes about 20 seconds for an eye to come to rest in its position of phoria after it has been covered (Schor 1979a). When the magnitude of phoria varies with the

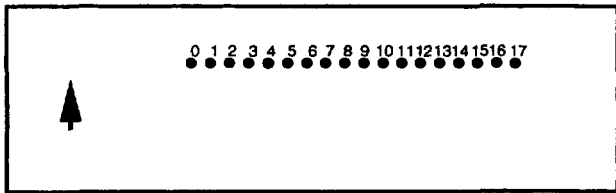


Figure 10.6. A simple phorometer.

The display is placed in a stereoscope, one eye viewing the arrow and the other eye the scale. The subject indicates which numbered dot is aligned with the arrow.

eccentricity of gaze, it is known as **anisophoria** (Friedenwald 1936). An essential anisophoria is due to paresis of one or other extraocular muscle in one eye and optical anisophoria is due to optical magnification of the image in one eye by a spectacle lens.

If phoria represents the tonic state of an eye when relieved from fusional demand it should be highly correlated with dark vergence. The two measures are correlated, but horizontal phoria is typically more divergent than dark vergence (O'Shea et al. 1988). The difference could be due to the fact that the accommodative state of an eye is different in dark vergence and in phoria. We will see in the next section that changes in accommodation evoke changes in vergence. In dark vergence the eyes are probably accommodated at a near distance whereas phoria is measured with the subject accommodated on a distant object (Owens and Tyrrell 1992). Rosenfield and Ciuffreda (1990) found that, for most subjects, phoria and dark vergence were highly correlated for measurements with open-loop accommodation produced by viewing through 0.5 mm pupils. The difference between phoria and tonic vergence could also be due to differing states of proximal vergence in the two conditions of measurement and Rosenfield and Ciuffreda obtained evidence that this was a factor in a few of their subjects. The tonic state, and hence the direction and magnitude of a phoria, can be changed temporarily by holding the eyes in an extreme position of divergence or convergence, as we will see later.

Phoria may be measured objectively by monitoring the change in position of the deviating eye as a cover is placed in front of it. In the simplest procedure the clinician increases the power of a prism placed before the deviating eye until a change in position of that eye is no longer observed when the eye is alternately covered and uncovered. The power of the prism indicates the degree of phoria in prism dioptres and the orientation of the prism indicates the direction of phoria. This method depends on the ability of the clinician to observe small deviations of the eye. An instrument for measuring the position of the eye is used when greater precision is required.

In so-called subjective tests of phoria the subject is required to align visual targets. Given that the subject is able to make the judgments, subjective methods are as precise as, if not more precise than, objective methods. In the first type of subjective procedure a single visual target is introduced to both eyes in such a way that the fusional response is disengaged. For instance, in the **Maddox-rod test** the subject views a point of light directly with one eye and the same point through a set of high-power cylindrical prisms with the other eye. Depending on which way the prisms are oriented, they spread the point of light out into either a horizontal or a vertical line. The prism power required to bring the point and line back into superimposition, as indicated by the subject, indicates the degree of phoria—horizontal phoria when the line is vertical and vertical phoria when it is horizontal.

In the second type of subjective measure of phoria, dichoptic stimuli are presented in a stereoscope. Again, the targets must be designed so that the fusional response is disengaged. In one procedure the subject reads off the position of a small marker seen by one eye relative to a calibrated horizontal scale seen by the other eye (see Figure 10.6). Vertical phoria is measured with a vertical scale, and cyclophoria with an annular scale. There must be nothing else in view that could serve to lock vergence. Such a device is known as a **phorometer**.

Various stereoscopic devices are used in orthoptic practice to measure phoria, but they all derive from Hering's haploscope, the essential features of which are shown in Figure 10.7. The subject's head is fixed so that the centre of rotation of each eye is above the centre of rotation of one of the horizontal arms of the instrument. The visual targets are mounted on the ends of arms and reflected into the eye by mirrors set at 45°. The accommodative distance of each target is adjusted by moving it along the arm. Horizontal phoria is indicated by the angular position of the arm required to bring dissociated targets into alignment. There is also a control for varying the vertical position of each target. In the clinic, haploscopes are known as amblyoscopes, synoptophores or troposcopes, depending on the manufacturer. For a review of orthoptic procedures used in the diagnosis and treatment of anomalies of binocular eye movements see Griffin (1976) and Pickwell (1984).

10.2.4 Fixation disparity

The tendency of the eyes to drift in the direction of a phoria may manifest itself as a slight deviation from the intended state of vergence when both eyes are open. This condition is known as **fixation disparity**.

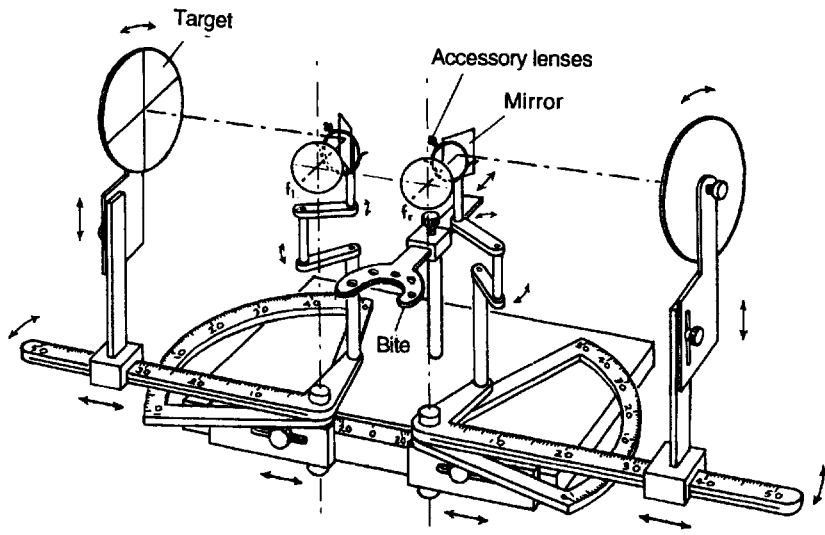


Figure 10.7. The essential components of a haploscope.
(From Noorden 1990.)

Fixation disparity is also referred to as **associated phoria**, that is, phoria measured when the fusional reflexes are engaged. Most people have some fixation disparity whether or not they have a measurable dissociated phoria. It is usually less than 6 arcmin with foveal fixation but can be as great as 20 arcmin with peripheral visual targets (Wick 1985). The phenomenon was first mentioned by Hofmann and Bielschowsky (1900), who referred to it as fixation lag. In 1937 Bielschowsky emigrated from Europe to the United States where he was director of the Dartmouth Eye Institute, until his death in 1940. Kenneth Ogle, who worked in the same institute, first used the term "fixation disparity".

The simplest view of fixation disparity is that the images of an object a person is attempting to fixate do not fall exactly on corresponding points. In other words, the horopter does not pass through the fixation target when there is a fixation disparity. A fixation disparity is not noticed by the viewer because the offset of the visual axes is too small to disrupt fusion of the images of the fixated object. The disparate images fall within Panum's fusional area. A fixation disparity may be seen in the offset of a pair of nonius lines placed near a fixated object. The visual angle through which nonius lines must be displaced to bring them into alignment provides the conventional measure of fixation disparity (Mallett 1964; Sheedy 1980). Fixation disparity may be measured by this procedure with a precision of about 1 arcmin. There is a danger that attention on the nonius lines may increase or even induce the error in fixation, since nonius lines do not provide a stimulus for bifoveate fixation (Verhoeff 1959).

Hebbard (1962) proposed an objective method for measuring fixation disparity. He measured the positions of each eye by reflecting a beam of light off a mirror mounted on a contact lens. He assumed that with one eye occluded the open eye accurately fixes a target, and the change in position of an eye which occurs when the other eye is opened is the contribution of that eye to fixation disparity. The combined shift in fixation for the two eyes, which we call the **fixation shift**, was assumed to equal the fixation disparity. He concluded from tests on one subject that the nonius and objective methods give essentially the same result. But the logic of this method is open to doubt, since a monocular target may not be accurately foveated.

The width of the contrast bands (Mach bands) that occur along a black-white border increase with increasing distance of the border from the fovea. Remole (1984, 1985) measured the width of the contrast band in a vertical border as a function of the eccentricity of the border for each eye separately. Similar measurements made with dichoptic viewing provided a measure of the fixation shift as a function of the magnitude of forced vergence. The fixation shift was found to be much larger than fixation disparity measured by nonius alignment. It was suggested that the nonius offset arises from two effects; fixation shift and a subjective displacement of the relative directions of the two nonius lines which reduces the effects of the fixation shift. Furthermore, the relation between fixation shift and fixation disparity was found to change with changes in forced vergence. The two measures were correlated between subjects only for forced vergence of over 5

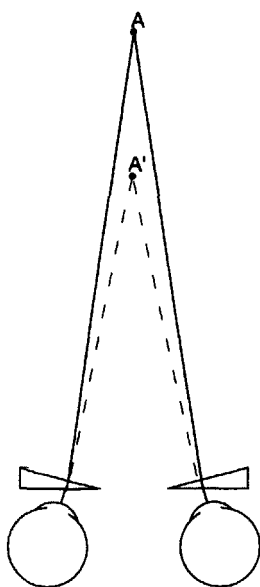


Figure 10.8. The effect of base-out prisms on vergence.

Base-out prisms cause object *A* to appear at position *A'* with a consequent increase in the degree of convergence needed to fixate it. Base-in prisms have the opposite effect.

dioptries (Remole et al. 1986). It seems that corresponding points defined by nonius alignment (equal visual directions) are not the same as those defined with respect to the central fovea, as used in monocular fixation. Kertesz and Lee (1987) also found considerable differences between fixation disparity measured with nonius lines and an objective measure of the fixation shift, and concluded that fixation disparity cannot be derived from uniocular changes in fixation. They also concluded that the nonius method is an unreliable measure of fixation disparity, but the basis for this conclusion is not clear. Measurements of fixation disparity do not seem to vary significantly when the eyes move into positions of eccentric gaze (McKee et al. 1987).

Fixation disparity (associated phoria) is typically smaller than phoria (measured with the eyes dissociated) but the two effects are generally correlated in magnitude and direction (Ogle et al. 1949; Ogle and Prangen 1951, 1953;). Jampolsky et al. (1957) reported that, for far fixation, fixation disparity was correlated with esophoria but did not increase with increasing exophoria. For near fixation, fixation disparity was a function of both esophoria and exophoria. It has been suggested that lack of correlation between fixation disparity and phoria is due to fixation disparity being influenced by tonic imbalance in the accommodative vergence system, in addition to imbalance in the vergence system. When accommodation was made open-loop by viewing through a pinhole, fixation disparity and phoria became more closely related (Semmlow and

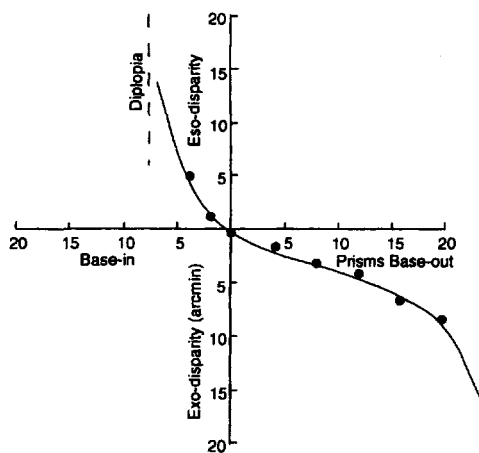
Hung 1979). Since phoria is related to the position of dark vergence (tonic balance) one would also expect fixation disparity to be related to dark vergence. In conformity with this expectation it has been reported that, as the distance of fixation deviates from the position of tonic balance, fixation disparity increases in the direction of the position of tonic balance (Owens and Leibowitz 1983; Jaschinski-Kruza 1994). In general, when a person converges or diverges outside the position of tonic balance, the eyes are pulled back toward it within the limits of Panum's fusional area. However, we will now see that the tonic state of vergence changes when vergence is maintained outside the tonic state for some time and takes time to return to its normal value.

10.2.5 Vergence adaptation

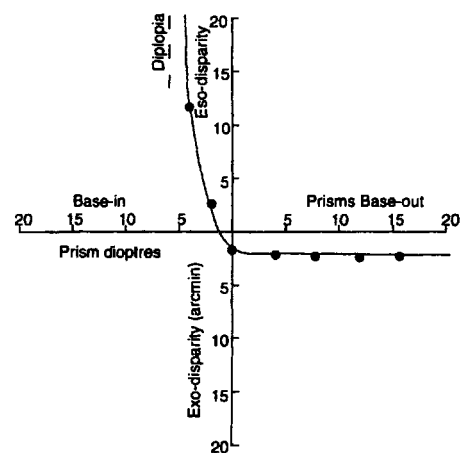
Forced-vergence curves

When base-out prisms are placed before the eyes, as shown in Figure 10.8, the amount of convergence required to fixate a given object is increased. Vergence demand is said to be increased. Base-in prisms have the opposite effect. The function relating fixation disparity on the *y* axis to the degree of vergence demand (prism power) on the *x* axis is known as the **forced-vergence curve** (Ogle et al. 1967). The *y*-intercept of the curve indicates the amount of fixation disparity in the absence of prisms and the *x*-intercept indicates the prism power required to reduce fixation disparity to zero. People vary widely in the form of the forced-vergence curve; Ogle described four basic types of curve, as illustrated in Figure 10.9. Type I is sigmoid in shape, showing an accelerating degree of fixation disparity as the prism power is increased from zero, one way or the other. Type II shows an accelerating change of fixation disparity to decreased vergence demand induced by base-in prisms, but no change to increased vergence demand induced by base-out prisms. Type III shows changes in response to increased vergence demand, but not to decreased demand. Type IV shows little change to either increased or decreased vergence demand. People showing this type of curve are said to have a flat forced-vergence curve. Beyond a certain prism power the images no longer fuse. The forced-vergence curve for a given person is reasonably consistent over time, but small changes occur as fixation is changed from near to far.

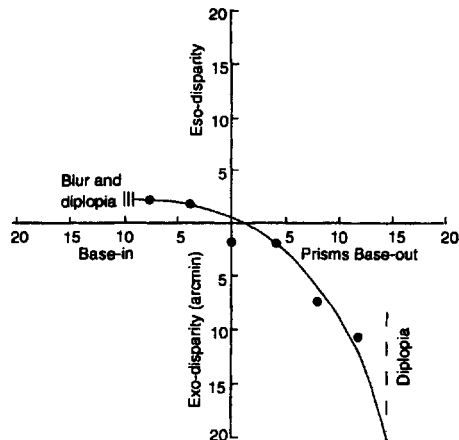
The state of tonic vergence is said to adapt to the vergence demand in those parts of a forced-vergence curve that do not change with changed demand. The adaptation is confined to base-out prisms for type II subjects and to base-in prisms for type III subjects. With full adaptation, preexposure fixation disparity



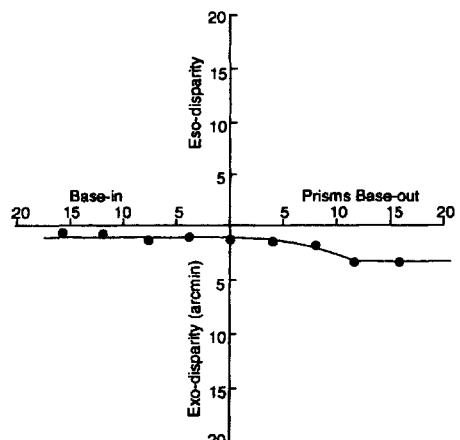
Type I is sigmoid, showing an accelerating fixation disparity as prism power increases from zero, either way.



Type II shows accelerating fixation disparity to decreased vergence demand, induced by base-in prisms, but no change to increased vergence demand.



Type III shows changes in response to increased vergence demand but not to decreased vergence demand.



Type IV shows little change to either increased or decreased vergence demand.

Figure 10.9. Basic types of forced-vergence curves.

(Adapted from K. Ogle, T. Martens, and J. Dyer, *Oculomotor imbalance in binocular vision*. Copyright Lea & Febiger, 1967.)

is maintained when measured with the prisms in place for both base-out and base-in prisms (Ogle and Prangen 1953; Schor 1979b). The longer the exposure to a given vergence demand, the flatter the forced-vergence curve becomes (Mitchell and Ellerbrock 1955). Thus, in people with a flat vergence curve, fixation disparity measured with the prisms still in place remains constant because the subject has adapted to the increased vergence demand—they are said to “eat the prism”. For such people it is pointless to use prisms for the correction of fixation disparity or phoria.

It has been known since the time of Maddox that viewing the world through base-in or base-out prisms, even for a few minutes, leads to a shift of

tonic vergence lasting minutes or hours, as revealed in the position of dark vergence, phoria, or fixation disparity after the prisms are removed (Alpern 1946). Fixation disparity and phoria, as measured just after prisms are removed, can begin to change within the first minute of exposure to base-out or base-in prisms (Schor 1979a, 1979b). One must allow adequate intervals between tests of phoria to avoid aftereffects from previous tests. Vergence adaptation has also been demonstrated in the monkey (Morley et al. 1988).

Ogle et al. (1967) reported that about 25 per cent of the patients tested in their clinic had a forced-vergence curve that varied according to whether vergence was near or far. This same phenomenon

occurred in about 40 percent of a sample of normal adults (Wick 1985). The most frequent change was from a type I curve with far convergence to a type II curve with near convergence.

Adaptation of the vergence system has been demonstrated with increased vergence demand of up to 3 prism dioptres vertically and 10 dioptres horizontally (Carter 1963, 1965; Henson and North 1980). People adapt to larger vergence demands more easily when the prismatic displacement is introduced gradually (Sethi and North 1987). Vergence adaptation is more complete when the stimulus is in the centre of the visual field rather than the periphery (Carter 1965; McCormack et al. 1991).

Fixation disparity also changes when positive or negative lenses are placed before the eyes, because such lenses change accommodation, which in turn induces a corresponding change in the resting state of vergence. Furthermore, prolonged exposure to a particular state of accommodation produces changes in the resting state of accommodation, the resting state of vergence, and phoria (Schor 1983). This reciprocal coupling between accommodation and vergence is discussed in Section 10.3. Vergence demand may also be increased by viewing the world through a telestereoscope that, effectively, increases or decreases the interocular distance. The effects are not quite the same as those produced by prisms. Prisms add a constant amount to required vergence over the whole range of distance, whereas increased vergence demand produced by a telestereoscope is inversely related to distance (see Figure 10.11).

When prism power is increased beyond a certain limit in either direction, diplopia becomes apparent. The diplopia limit varies with the state of tonic adaptation of the extraocular muscles. For instance, diplopia occurred when a visual target was viewed through 3-dioptre prisms, which forced vertical divergence. However, after viewing a visual target for between 3 and 10 minutes through 6-dioptre prisms the diplopia seen with 3-dioptre prisms was overcome and vertical fixation disparity sometimes returned to its normal value (Ogle and Prangen 1953). While fusional limits change with an imposed change in vergence demand, the difference between the upper and lower fusional limits (fusional amplitude) remains constant (Stephens and Jones 1990). The tonic state of the eyes is clearly not fixed but adapts to the current level of vergence, more rapidly and completely in some people than in others.

Fixation disparity and Panum's fusional area

When the magnitude of fixation disparity is increased by forced convergence or divergence, the maximum fixation disparity before diplopia is seen

corresponds to the radius of Panum's fusional area. Under normal viewing conditions, fixation disparity does not usually extend as far as the radius of Panum's fusional area (Duwaer and van den Brink 1981a). Panum's fusional area is enlarged when the high spatial frequencies are removed from the stimulus by optical blurring. Normally, when this is done, fixation disparity also increases (Hebbard 1964). However, people with a flat forced-vergance curve, that is, a very adaptable state of tonic vergence, do not show this dependency of fixation disparity on Panum's fusional area (Schor et al. 1986a). Panum's fusional area also increases with eccentricity. Ogle et al. (1967) found that fixation disparity did not increase as a square serving as the fused stimulus became larger, that is, as its edges became more eccentric in the visual field. Other investigators have reported that fixation disparity does increase with the eccentricity of the fusional stimulus (Francis and Owens 1983). The answer to this apparent conflict of evidence seems to be that some people show a dependence on eccentricity and some do not. Thus, for people with an adaptable state of tonic vergence, fixation disparity and the forced-vergance function are independent of the eccentricity of the fusional stimulus (Saladin and Carr 1983; Schor et al. 1986a).

For detailed reviews of fixation disparity, see Ogle et al. (1967), Schor (1983), and Sethi (1986). The literature of the neurology of vergence adaptation is reviewed later in this chapter.

10.2.6 Adaptation to noncomitant vergence demand

When a person views the world through base-in or base-out prisms the change in vergence demand is said to be comitant, that is, the same for all directions of gaze. A change in vergence demand that varies with the angle of gaze is said to be noncomitant. For instance, a noncomitant vergence demand is induced by spectacle lenses which create unequal magnification of the images in the two eyes, a condition known as optical aniseikonia (see Section 2.8). This happens when the two eyes require different amounts of optical correction. When the gaze is directed away from the optic axes of a spectacle lens, the lens acts like a prism which increases in power as a function of the angle of gaze. If the lenses do not have the same power the eyes must move different amounts to maintain fusion. A person can compensate for the effects of spectacles by turning the head so that the eyes look through the centres of the lenses, and lenses can be made that optically correct for aniseikonia. However, most people do not need to compensate in either of these ways because they

adapt to the noncomitant vergence demand by a noncomitant change in the vergence movements of the eyes. Thus, a person used to reading with unequal lenses learns to elevate the visual axis of one eye relative to that of the other to bring images of the same object onto the fovea. The change in vergence is noncomitant; that is, it varies according to the eccentricity of gaze. A person who has made such an adjustment of vergence shows a phoria that depends on the direction of gaze when tested with dissociated viewing. This type of phoria is known as noncomitant phoria, or anisophoria (Ellerbrock and Fry 1941, 1942; Ellerbrock 1948; Allen 1974).

The adaptive field

When a person holds the gaze in one direction while adapting the state of vergence to a fixed prism-induced disparity, the resulting change in phoria occurs in about 30 minutes. Although the change in vergence is maximal for that direction of gaze, it also shows when the eyes look in neighbouring directions along the same meridian. The eye positions over which a locally applied change in vergence spreads is called the **adaptive field** (Henson and Dharamshi 1982). Schor et al. (1993a) found that changes in phoria after adaptation to a fixed direction of gaze were constant over an 18°-wide field, showing that the adaptive field is at least this wide.

Noncomitant adaptation to a gradient of disparity, such as that produced by spectacles, takes much longer than comitant adaptation to constant disparity (Sethi and Henson 1984). With noncomitant adaptation, a specific degree of adaptation must be applied at each direction of gaze along a given meridian, so an interaction must occur between the adaptive fields associated with each eye position. Schor et al. (1993a) investigated this interaction by having subjects adapt to two separated targets with opposite prism-induced vertical disparities. They used vertical rather than horizontal vergence because it is not affected by accommodation. Adaptation of vergence was greater with greater lateral separations of the targets or with smaller imposed disparities. Thus, the steeper the disparity gradient between targets, the more difficult it became to acquire differential adaptation of vergence.

Schor et al. proposed a two-mechanism model of vergence adaptation. The first is a global mechanism of rapid onset, which generalizes to all eye positions along a given meridian. The second is a slower, local mechanism, responsible for position-dependent adaptation that allows one to adapt to distinct disparities in the visual field. The local mechanism shows some spread, so adaptation to distinct disparities does not occur when they are too close together.

Meridional specificity of noncomitant phoria adaptation
It seems that noncomitant adaptation of phoria is specific to the meridian along which the disparity gradient is presented. Thus, Maxwell and Schor (1994) adapted subjects to two different vertical disparities at different locations along either the horizontal or the vertical meridian. Phoria adaptation was noncomitant only for the meridian along which the different disparities had been displayed and was comitant (independent of eye position) along the orthogonal meridian. The noncomitant component built up more slowly than the comitant component.

Schor et al. (1993b) adapted subjects by having them converge on stationary targets at different positions along an optically induced disparity gradient. This resulted in a position-dependent phoria and a differential movement of the eyes during visual pursuit, but it did not produce disjunctive saccades. The mechanism responsible for the independent adaptation of saccadic amplitude in the two eyes (see Section 10.6.2) must be independent of that responsible for the adaptation of static vergence and visual pursuit. Gleason et al. (1992) developed a model of the processes responsible for adaptation of static vergence and disjunctive pursuit.

It was explained in Chapter 2 that when the eyes are converged on a near point directly ahead, all points in an oblique position on a frontal surface have a vertical disparity. Thus, when a person moves the gaze from a straight-ahead position to an oblique point on a frontal surface, the eyes must execute a vertical vergence movement to bring the newly fixated object into vertical correspondence (see Figure 10.10). They must also execute movements with different azimuth angles along a frontal plane. For instance, a vertical vergence of three prism dioptres is required to fixate a point 24° up and 24° to one side on a frontal plane, at a distance of 33 cm (Ogle and Prangen 1953). Furthermore, the required vergence for a given direction of gaze varies with the distance of the surface. In other words, the human visual system, in its normal functioning, is adept at changing vergence as a function of the direction as well as the distance of gaze.

10.3 ACCOMMODATION AND VERGENCE

Horizontal vergence and accommodation normally occur together. The two responses are accompanied by an appropriate change in pupil diameter; the pupil constricts with near vergence/accommodation to compensate for the narrowed depth of field and increased spherical aberration caused by near

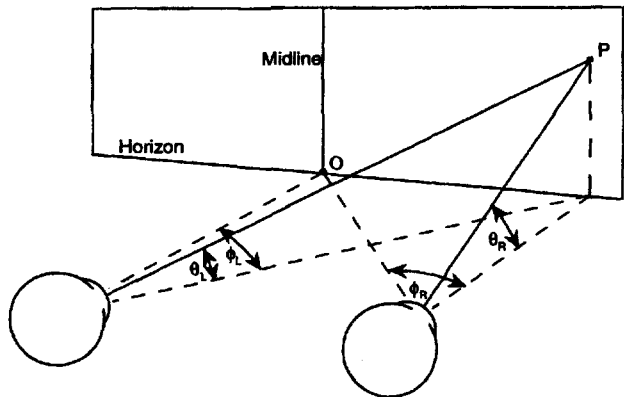


Figure 10.10. Unequal versions needed for oblique gaze.

When the gaze moves from a straight-ahead position, O , to an oblique position, P , on a frontal surface the eyes must execute a vertical vergence movement to bring the images of the newly fixated object into vertical correspondence. This is because the height of P above the horizon subtends a larger angle, θ , to one eye than to the other eye. The eyes must also execute unequal horizontal movements, since angle ϕ_R is larger than angle ϕ_L .

accommodation, and dilates with far vergence to reduce diffraction and improve retinal illumination. The three concomitant changes are known as the **near-triad** response. The literature on this topic is reviewed in Semmlow and Hung (1983) and Kotulak and Schor (1986). The following account concentrates on the coupling between horizontal vergence and accommodation.

Basic features of accommodation

About two-thirds of the refractive power of a human eye is in the surface of the cornea, since this surface separates two media of very different optical density. This fixed focal length system brings the images of objects at any distance onto a plane not far from the retina. The ciliary muscles, under the control of the parasympathetic pathway of the third cranial nerve, adjust the curvature of the lens, and hence the refraction of the eye, to bring the images of objects at a particular distance into clear focus. This response is known as **accommodation**.

An optometrist can measure the accommodative capacity of the eye by standard eye charts with a precision of up to 0.25 dioptres. There are four objective procedures for measuring dynamic changes of accommodation. In the first method, changes in the shape of the front surface of the lens are indicated by changes in the size of the third Purkinje image of a point of light reflected from the lens surface. In the second method, the sharpness of the retinal image is observed through an ophthalmoscope. In a related technique, two narrow slits imaged by infrared light are made to coincide in the retina when the eye is

accommodated at infinity. A reflected image of the images of the slits is then formed on a photocell and the separation of the images as a function of accommodative distance is measured objectively. This instrument is known as the infrared optometer and is the most precise method of measuring the accommodative state of the eye (Campbell 1956). The third method depends on the use of a retinoscope to observe motion parallax of the reflected retinal image. A retinoscope consists essentially of a small mirror which reflects the image of a point source into the subject's eye. The ophthalmologist observes this image through a hole in the centre of the mirror. As the mirror is rotated from side to side the image of the point of light can be seen sweeping from side to side in the patient's pupil. The parallactic motion of the image is nulled when the point source is brought to the anterior focal point of the eye by the addition of appropriate lenses. The assumption is that the patient's lens is relaxed to its far point of accommodation, that is, the most distant point to which the eye can accommodate. In the fourth method, neural activity is recorded in or near the ciliary muscles. Methods of measuring accommodation are reviewed by Howland (1991).

When the gaze is fixed on a small target, the accommodative state of the eye shows a prominent fluctuation of about 0.3 dioptres at a frequency of between 1 and 2 Hz (Campbell et al. 1959). These fluctuations become less regular when the pupil is constricted. Pupil constriction increases the depth of focus and thereby reduces the extent to which an image becomes blurred as the lens changes its focal length. The fluctuations cannot be understood as an excursion between the limits of detectable blur because, on this basis, they should increase with increasing depth of focus. The fluctuations were found to increase in frequency when the stimulus was oscillated in depth at above 1 Hz. This shows that fluctuations of accommodation are under feedback control from the retina. Blur of the retinal image must be the crucial stimulus for accommodation.

Averaged blur signals from the retina are transmitted to the visual cortex and parietotemporal areas and then to the Edinger-Westphal nucleus in the midbrain. Motor commands are sent through the oculomotor nerve (IIIrd cranial nerve) to the ciliary ganglion and ciliary muscles (see Ciuffreda 1991).

Accommodation occurs with a mean latency of about 370 ms and takes about 1 s to reach a steady-state value (Campbell and Westheimer 1960; Tucker and Charman 1979). Note that an image out of the eye's plane of focus produces **defocus blur** whereas a poorly focused photograph produces **target blur**. Defocus blur is under feedback control since it is

removed when the eyes accommodate; but target blur is not under feedback control and therefore remains blurred as the eyes accommodate. A sudden change in target blur induces a transient accommodative response, but the eyes soon return to their previous state (Phillips and Stark 1977). Presumably, the way the image changes during fluctuations in accommodation provides the visual system with a means to distinguish between the two types blur.

Since an out-of-focus image is blurred by an equal amount on either side of the plane of focus, static blur does not indicate the desired direction of a response. Under natural viewing conditions, a variety of cues, such as perspective, overlap, parallax, and disparity indicate the depth of an out-of-focus object relative to an in-focus object. In the absence of such cues, the visual system could use either dynamic or static information inherent in the misaccommodated image to detect the sign of misaccommodation, that is, to distinguish between a stimulus beyond the plane of accommodation and one nearer than the plane of accommodation. Whatever cues are used, they are not available to conscious control, since subjects cannot, without training, manually bring a stimulus into focus when the ciliary muscles are paralyzed with homatropine (Campbell and Westheimer 1959; Troelstra et al. 1964).

The sign of dynamic error feedback is the first type of cue that could signify the direction of accommodative responses. An initial response could be made at random and corrected if it is in the wrong direction. Campbell and Westheimer (1959) found that subjects made many initial errors in their responses to an out-of-focus image when cues to the direction of misaccommodation were eliminated. Troelstra et al. (1964) measured the initial accommodative response to 400 ms random steps of a horizontal line in depth after trying to eliminate all cues to the direction of misaccommodation. Two of three subjects still responded in the correct direction and the third made 50 per cent errors, indicating that he was hunting. Presumably, the two accurate subjects were using some cue that had not been successfully eliminated. Hunting is therefore a possible mode of operation when other cues are not available. The changing size of the image also contributes to control of accommodation, although it has not been proved that it plays a crucial role in controlling the direction of the response (Kruger and Pola 1986).

The other possibility is that the visual system relies on some static asymmetrical feature in the defocused image. Chromatic aberration of the lens is one candidate feature. Longitudinal chromatic aberration is due to shorter wavelengths being more strongly refracted than longer wavelengths, up to a

difference of about 2 dioptres. Transverse chromatic aberration is due to the axial misalignment of the pupil, lens, and fovea and causes red light to fall more temporally than blue light. The colour fringes produced by both these effects vary according to whether the image is under- or over-accommodated. What is the evidence that we make use of this asymmetry?

About 60 per cent of people were found to be unable to accommodate in monochromatic light, for which there is no chromatic aberration (Fincham 1951). Campbell and Westheimer (1959) had subjects view a high-contrast test object through a lens placed with its second principal focus in the pupil. This eliminated changes in image size and illumination as the distance of the test object was varied. The accommodative mechanism of the eye was paralyzed by homatropine. The target was suddenly displaced by 0.5 or 1.0 dioptre and subjects adjusted the target manually to restore it to focus. Once they became familiar with the control they were able to make an initial movement in the correct direction on every trial. When the chromatic and spherical aberrations of the eye were corrected, subjects could not perform above chance (see also Kruger and Pola 1986). An isoluminant red-green border or an isoluminant red-green grating did not elicit appropriate accommodative responses (Wolfe and Owens 1981) even though subjects could see that the grating was out of focus (Switkes et al. 1990). Perhaps the chromatic-aberration fringes are distorted or not detectable with isoluminant stimuli. Changes in the magnitude or direction of either form of chromatic aberration did not affect static accommodation (Bobier et al. 1992). This indicates that there is no preferential focusing on a particular wavelength.

Whatever the mechanism used to sign the direction of accommodation, there is evidence that it fails for images more than 2 dioptres out of focus (Fincham 1951).

Measures of accommodation and vergence

Accommodation is measured in dioptres. Accommodation in dioptres is the reciprocal of the viewing distance in metres. Thus, 2 dioptres of accommodation are required to bring an object at a distance of 0.5 metres into clear focus. To make horizontal vergence commensurate with accommodation, vergence can be specified in metre angles. One metre angle of convergence is the convergence required for the binocular fixation of an object at a distance of 1 metre in the median plane. The vergence angle in metre angles is the reciprocal of the distance of the fixation point in metres. The vergence angle in degrees corresponding to a metre angle of M , for an

interpupillary distance a in metres, is $2 \tan^{-1} a/M/2$. Thus, the convergence in degrees corresponding to 1 metre angle varies with interpupillary distance.

In clinical practice convergence is specified by a third measure known as **prism dioptres**. A prism with a power of 1 prism dioptre displaces the visual axis by 1 cm at a distance of 1 m. It follows that the angle of convergence in dioptres is the interocular distance in centimetres divided by the viewing distance in metres. Thus, a person with an interocular distance of 6.5 cm must exert 6.5 dioptres of convergence when fixating an object in the midline at a distance of 1 m. Measurements of vergence in either metre angles or prism dioptres are not applicable at near viewing distances.

Accommodative convergence

A change in accommodation is normally accompanied by a change in vergence; an increase in accommodation evokes convergence and a decrease evokes divergence. This coupling of responses is known as **accommodative convergence (AC)**. Accommodative horizontal vergence may be evoked by a binocularly fused stimulus that is out of the plane of accommodation. Since accommodative convergence does not depend on disparity, it can be evoked by a stimulus presented to only one eye. In fact Müller (1843) first discovered accommodative convergence by noting the convergence of the eyes as a stimulus was moved along the line of sight of one eye with the other eye closed. He realized that the link between the two responses is not immutable, since he observed that one can learn to change accommodation without changing vergence. The two responses are linearly related over a 5-dioptre range of accommodation. Vertical vergence and cyclovergence are not evoked by misaccommodation since there is no natural linkage between image blur and vertical or torsional misalignment of images.

The amplitude of accommodative convergence (AC) evoked by a 1 dioptre change of accommodation (A) is known as the **AC/A ratio**. Accommodative convergence can be measured by recording the change in alignment of a covered eye produced by placing negative lenses in front of the viewing eye. If vergence is measured in metre angles and accommodation in dioptres, the AC/A ratio is typically about 0.8 to 0.9 in young subjects (Alpern and Larson 1960). Ogle et al. (1967) proposed that a more valid procedure is to measure the change in fixation disparity with binocular viewing as a function of lens-induced changes in accommodation for each of several states of prism-induced vergence. The two methods do not necessarily produce the same result, but the reason for this has not been determined (see

Judge 1985). The accommodative response is difficult to measure in routine clinical practice and under these circumstances the AC/A ratio is measured with reference to the stimulus to accommodation, it being assumed that the accommodative response is proportional to the stimulus. This is known as the **stimulus AC/A ratio**, as opposed to the **response AC/A ratio** obtained when accommodation is measured. The two measures do not always give the same result (Ripps et al. 1962).

The gain of accommodative convergence can be expressed as the ratio of the actual vergence change to the ideal vergence change required to fuse the target (Judge and Miles 1985; Judge 1987). This measure has the advantage that it allows one to make direct comparisons between subjects with different interocular distances.

Convergence is more effectively evoked by disparity than by misaccommodation. For instance, the dynamics of the initial portion of a vergence response were not improved when a pure disparity stimulus was supplemented by an accommodation stimulus, although an accommodation stimulus did improve the velocity and precision of the final stages of the vergence response (Semmlow and Wetzel 1979). Furthermore, when vergence was evoked in the monkey by disparity alone, its phase lag was smaller and its velocity higher than when it was evoked by misaccommodation alone (Cumming and Judge 1986). Accommodation seems to provide a moderate contribution to vergence for stimuli that are only slightly out of focus in a large vergence movement, accommodation contributes only when the movement is nearly complete (Hung et al. 1983).

When objects are viewed through a telestereoscope, like that shown in Figure 10.11, it is as if the eyes are further apart. This increases the required change in vergence per unit change in accommodation. Thirty minutes of exposure to a telestereoscope increased the AC/A ratio in response to the increased demand (Judge and Miles 1985). Note that base-in or base-out prisms do not alter the change of vergence required per unit change in accommodation, they simply add a constant amount to the degree of vergence at all accommodation distances.

People with strabismus and some people with amblyopia without accompanying strabismus show vergence responses similar to those in people with normal vision but with one eye closed (Kenyon et al. 1980a). In other words, strabismics show accommodative vergence but not disparity vergence.

Convergence accommodation

A change in horizontal vergence, however it is evoked, is accompanied by an appropriate change in

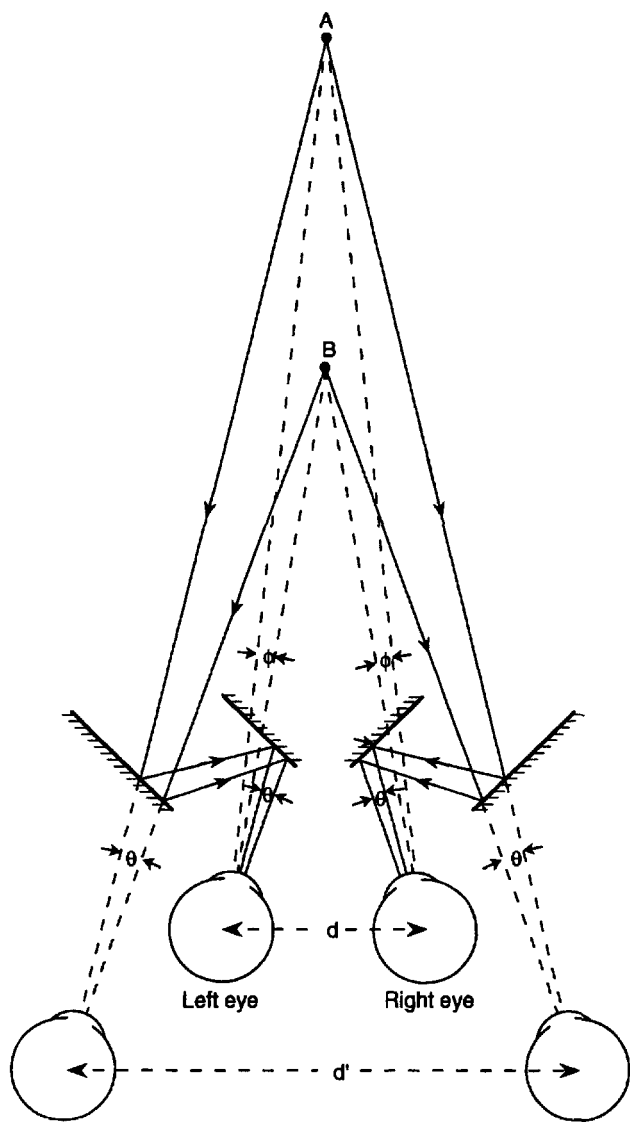


Figure 10.11. A telestereoscopic device.

The effective interocular distance is increased from d to d' . This increases the convergence required when changing fixation between two near objects, such as A and B (angle θ is larger than angle ϕ). The device also increases the path length of the light rays, which decreases the amount of accommodation. The ratio of convergence to accommodation is therefore increased.

the accommodative state of the eyes, a response known as **convergence accommodation (CA)**. The change in convergence accommodation per unit change in convergence is known as the **CA/C ratio**. Convergence accommodation is measured when vergence is changed in the absence of the blur cue to changing accommodation. The blur cue can be removed by converging on objects at different distances while viewing through pinholes. An object seen through a pinhole remains in clear focus whatever its distance and whatever the accommodative state of the eye. However, some blur remains with

pinholes of a practical size. Use of this method has revealed that accommodation is a linear function of convergence. For young adults, accommodation in dioptres is approximately equal to vergence in metre angles, so that the gain of the response can be said to be 1. The gain has been found to be smaller in older and more presbyopic subjects (Fincham 1955; Fincham and Walton 1957).

A speckle interference pattern formed on the retina by two laser beams provides a more effective stimulus for studying convergence accommodation, since such a pattern is independent of the state of accommodation. Using this procedure, Kersten and Legge (1983) also found that the average accommodation of the two eyes is linearly related to vergence angle over the accommodative range of the eye, with a mean CA/C ratio of 0.91. The CA/C ratio was reduced very little when the luminance of the stimulus was reduced to scotopic levels. Accommodation was found not to vary with changes in the angle of gaze. The gain of convergence accommodation may also be conveniently measured by the ratio of the actual change in accommodation to the ideal change required to accommodate the new visual target.

Horizontal convergence also increases the horizontal radius of curvature of the cornea, especially in young people (Löpping and Weale 1965). This effect is believed to be due to tension induced in the cornea by contraction of the medial rectus muscle.

Relation between convergence accommodation and accommodative vergence

Convergence accommodation and accommodative convergence are two aspects of the same underlying functional unity of vergence and accommodation. It is believed that the commands for the two responses are issued concurrently and interact reciprocally. However, the eyes begin to verge before they begin to accommodate, since the skeletal rectus muscles respond more rapidly than the autonomic ciliary muscles (Allen 1953). In spite of this functional unity, accommodation and vergence assume independent resting states in the dark (Owens and Leibowitz 1980). There is conflicting evidence about whether the resting states of vergence and accommodation, although different, are correlated (see Gray et al. 1993). However, when allowance is made for differences in the AC/A ratio between subjects, dark accommodation may be predicted from tonic vergence (Wolf et al. 1990). There is probably also some uncorrelated noise in the two systems. People with an unusually high AC/A ratio tend to have a lower than normal CA/C ratio. Abnormally high AC/A or CA/C ratios are accompanied by low adaptability of the resting state of accommodation and high

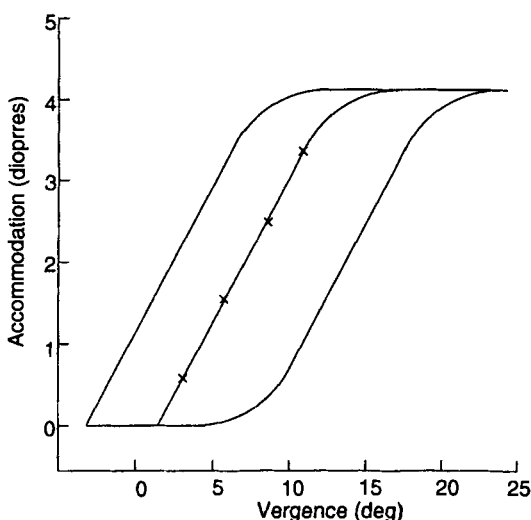


Figure 10.12. The zone of clear single binocular vision.

The width of the zone represents the range of vergence within which accommodation remains tolerably precise. Phoria is represented by a line running parallel to the sides of the zone. The slope of the edges of the zone indicates the accommodative-convergence relationship (AC/A ratio). (Adapted from Fry 1939.)

adaptability of tonic vergence. Unusually low ratios are accompanied by high adaptability of accommodation and low adaptability of tonic vergence (Schor and Horner 1989; Polak and Jones 1990).

At frequencies of stimulus oscillation below about 0.1 Hz, accommodation does not respond to changes in vergence and vergence does not respond to changes in accommodation. As stimulus frequency is increased to about Hz, the CA/C and AC/A ratios increase in a nonlinear fashion (Schor and Kotulak 1986). The values of both ratios are subject to fatigue (Schor and Tsuetaki 1987).

The range of accommodation and the range of vergence possible without excessive error in either is known as the **zone of clear single binocular vision**. Figure 10.12 shows a representation of this zone (Fry 1939). The width of the zone represents the range of vergence within which accommodation remains tolerably precise, and is approximately constant at all levels of accommodation. The right-hand boundary represents the limit of convergence, and the slope of this boundary indicates that higher degrees of convergence can be achieved when aided by near accommodation. This supports the idea that accommodative convergence adds to other stimuli that evoke convergence to produce an enhanced motor response. The situation is complicated by the fact that strong convergence evokes an excessive accommodative response through the mediation of convergence accommodation (Semmlow and Heerema 1979). Phoria (error of vergence for each value of accommodation) is represented by a line

running parallel to the sides of the zone of clear vision. With training, people can learn to dissociate vergence and accommodation, which broadens the zone of clear vision (Hofstetter 1945; Heath and Hofstetter 1952). The slope of the edges of the zone of clear vision indicates the accommodative-convergence relationship (AC/A ratio) for that person.

A telestereoscope, such as that shown in Figure 10.11, increases the effective interocular separation, and therefore the required change in convergence per unit change in accommodation. This decreases the required gain of AC/A and increases the required gain of CA/C. On the other hand, periscopic spectacles that bring the two visual axes to the midline, reduce the effective interocular separation and reduce to zero the change in vergence involved in accommodating at different distances. Miles et al. (1987) found that after 30 minutes of exposure to a telestereoscope, subjects revealed a mean shift of 37 per cent in their AC/A gain, which returned to normal over a period of about 4 hours with normal viewing. Exposure to periscopic spectacles had very little effect on AC/A gain. Exposure to base-out prisms that increase required convergence by a constant amount at all distances caused a predicted downward shift in the AC/A curve and an upward shift in the CA/C curve, rather than changes in gain. Base-in prisms that reduce required vergence by a constant amount caused a downward shift in the CA/C curve but had no effect on the AC/A curve. Thus, the reciprocal coupling between accommodation and convergence are subject to adaptive changes, although the effects are asymmetrical. These changes could be due to the operation of error-sensing feedback in the reciprocal control loops, but muscular fatigue could also contribute.

Reviews of accommodative vergence and vergence accommodation are provided by Alpern (1969), Morgan (1968), Ciuffreda and Kenyon (1983), and Fry (1983). Semmlow and Venkiteswaran (1976) have dealt with the dynamic aspects of accommodative vergence, and models of the interactions between accommodation and vergence have been developed (Schor and Kotulak 1986; Polak and Jones 1990; Schor et al. 1992; Schor 1992). The Schor and Kotulak model is shown in Figure 10.19.

10.4 PROXIMAL VERGENCE

The type of vergence that Maddox called voluntary vergence is usually referred to as proximal vergence. It is evoked by stimuli that give the impression of being nearer or further in the absence of disparity or accommodation cues. For instance, increasing the

size of the projected image of a playing card has been found to evoke a change in vergence (Ittleson and Ames 1950; Alpern 1958). Predebon (1994) also obtained an effect of the familiar size of a monocularly viewed object on vergence. Transient vergence was evoked by an isolated square changing sinusoidally in size at a fixed distance (Erkelens and Regan 1986). Vergence was also induced when the images of the square varied in disparity but not in size. The vergence response to a combined change in size and disparity was the linear sum of the two component responses. Accommodation induced by changes in the apparent distance of an object without any actual change in distance is known as proximal accommodation. Perhaps depth cues driving proximal vergence do so indirectly by evoking a change in accommodation, which then evokes vergence. Evidence for this view has been provided by McLin et al. (1988). They found that the ratio of vergence to changing size resembled the ratio of vergence to changing accommodation (AC/A ratio) and concluded that size changes evoke accommodation directly and vergence indirectly.

A change in disparity could contribute to the divergence produced when the size of an object increases. The edges of an object lying in the frontal plane acquire an uncrossed disparity as they get further from the fovea, because they become progressively more distant from the concave horopter. An experiment should be conducted with an object changing size within the same curved plane of the horopter or within a frontal plane at the abathic distance, that is, the distance at which the horopter lies in the frontal plane (see Section 2.6). Furthermore, according to this explanation, an object at a far distance where the horopter is convex should induce divergence when it is made larger.

Subjects made large and rapid changes in vergence when they looked back and forth between two horizontal fluorescent rods seen at different distances in dark surroundings (Wick and Bedell 1989). It was claimed that because the rods were horizontal the only cues to depth were the relative thickness and height of the rods in the field, but accommodation cues were not eliminated. Enright (1987a) found that subjects converged when an apparently near part of the drawing of a cube was monocularly fixated, and diverged when an apparently far part was fixated. In this case the cue to depth was provided only by perspective and the display was free from artifacts present in the displays used by other investigators. Vergence movements were also elicited in the closed eye when subjects changed the direction of gaze of the other eye from those parts of a painting that depicted near objects to those parts that depicted far objects (Enright 1987b).

Rosenfield et al. (1991) measured the proximal vergence evoked with accommodation cues eliminated by having subjects view the display through pinholes, and with disparity cues to depth eliminated by inducing a vertical disparity between the images in the two eyes. A letter chart viewed in the laboratory was the target for distances up to 6 metres and objects such as buildings seen out of the window were targets for distances of up to 1,500 metres. Vergence and accommodation changed linearly with increasing distance of the target, up to about 3 metres, after which vergence remained constant.

Vergence induced by an attempt to fixate one's unseen finger in the dark would also be proximal vergence, although people seem not to be very accurate in performing this task and changes in vergence seem to be independent of changes in accommodation in the dark (Fincham 1962). Voluntary changes in vergence to imagined objects in the dark also fall under the heading of proximal vergence (McLin and Schor 1988). Such vergence movements are unreliable and poorly correlated with the distance of the imagined object (Erkelens et al. 1989b).

The mechanism that signs the direction of accommodation does not work for images out of focus more than 2 dioptres (Fincham 1951). Furthermore, disparities of more than about 4° do not evoke vergence (see Section 10.5.1). Other depth cues, such as perspective and motion parallax, operate at distances outside these limits. Thus, vergence movements to objects at a distance far removed from the plane of convergence are, by definition, proximal vergence. Proximal vergence and proximal accommodation bring the accommodative and disparity cues to within a range in which they can help converge the visual axes accurately onto the desired depth plane. Schor et al. (1992) have devised a feedback control model of these processes.

10.5 DISPARITY VERGENCE

The type of vergence that Maddox called fusional vergence is evoked by binocular disparity, and is therefore usually referred to as disparity vergence. Horizontal disparity induces horizontal vergence, vertical disparity induces vertical vergence, and cyclodisparity induces cyclovergence. In each case the stimulus for vergence (the vergence error) is the absolute disparity of the to-be-fixated object, that is, its disparity with respect to the horopter. We saw in Chapter 7 that stereoscopic depth is derived from relative disparities and is largely immune to changes in absolute disparity. Thus, the disparity signal for vergence is not the same as that for stereopsis.

10.5.1 The range of vergence

The change in vergence required when the gaze is moved from infinity to a distance of 25 cm is approximately 14°. About 70 per cent of the total occurs for distances of up to 1 metre. A person's range of fusional vergence is tested clinically by using Risley prisms which change the lateral alignment of dichoptic targets without changing their optical distance. The prisms are first set so that the dichoptic images are easily fused. The prisms are then slowly adjusted so that the angular separation between the images is increased or decreased. To maintain a fused image, the subject is forced to increase or decrease vergence gradually without changing accommodation. The limits to which vergence can be forced before fusion is lost defines the range of vergence, which is, on average, is about 10° comprised of 3.5° of divergence and 6.5° of convergence relative to the state of dark vergence (Jones and Stevens 1989). The range is similar in humans and monkeys (Boltz and Harwerth 1979). A range of 7.5° has been reported for vertical vergence with a stimulus subtending 2° (Ellerbrock 1949) but values up to 11° (5.5° in either direction) have been reported with a patterned display subtending 57° (Duwaer 1982). The amplitude of vertical vergence is reduced by induced aniseikonia; that is, when the image in one eye is made larger than that in the other (Ellerbrock 1952).

Strictly speaking, in deriving the range of vergence from the maximum stimulus disparity for which fusion is maintained, allowance should be made for the contribution of the radius of Panum's fusional area. As horizontal vergence is forced further from the position of dark vergence, the eyes tend to return to that position. This tendency manifests itself as an increasing fixation disparity, although this does not show in people who adapt their tonic vergence to changed vergence demand (see Section 10.2.5).

A disparity in a vertical sine-wave grating cannot induce vergence movements larger than one half-cycle of the grating. In a random-dot display the visual system has difficulty finding matching images when disparity exceeds the mean separation of the dots, unless there are well-defined dot clusters. Nevertheless, Frisby and Mayhew (1980b) and Mowforth et al. (1981) claimed that vergence is initiated by disparities that exceed the dot separation in random-dot displays, when low spatial-frequency clusters are not present. Each eye was shown a 5° by 5° patch of texture formed by spatially filtering random-dot displays with circular Gaussian filters that had centre spatial frequencies of 1.75, 3.5, or 7.0 c/deg,

with a centre spatial frequency to bandwidth ratio of 1:5. The patches had a crossed or uncrossed disparity of either 28 or 56 arcmin. In response to 28 arcmin of disparity, appropriate vergence movements were induced with all three spatial frequencies. Frisby and Mayhew claimed that appropriate vergence movements are made when the disparity far exceeds the mean spacing of texture elements. However, inspection of their 7-c/deg texture, shown in Figure 10.13, reveals the presence of identifiable clusters of texture elements extending over at least 1 degree of visual angle. This must be due to an inadequacy of the filtering process that they used. A disparity of 56 arcmin induced only oscillations of vergence with the 7 c/deg texture. In this case, the disparity was too large in terms of the texture clusters and the vergence system relapsed into an oscillation.

Erkelens and Collewijn (1985b) presented subjects with a random-dot stereogram with a fixed disparity of 36 arcmin between different regions. Vergence was recorded as the experimenter moved the whole image in one eye laterally with respect to that in the other eye. The eyes accurately followed the increasing separation of the images to begin with, but with an increasing lag as the separation increased beyond a certain point. When the disparity between the retinal images reached between 1 and 2°, the images no longer fused and depth in the stereogram was no longer seen, though some vergence was still evident. When the physical separation of the images reached about 4°, vergence suddenly returned to a value that was independent of the stimulus. When the movement of the stimulus was reversed, vergence was reactivated at a smaller angle of stimulus separation than that at which it broke down. Note that in this experiment the stimulus contained a wide range of spatial frequencies and the disparity was introduced gradually. Erkelens and Collewijn explained the hysteresis effect by the fact that the eyes returned to a more convergent position after vergence broke down, which shifted the disparity of the images in the convergent direction.

It is not surprising that random-dot displays with a disparity of over 4° do not evoke vergence. *The upper disparity limit for the initiation and maintenance of vergence should be determined using stimuli with well-separated elements, both as the disparity is increased gradually to the break point of vergence and for disparate stimuli that are suddenly exposed.* In the natural world, vergence movements are made between near and distant stimuli where the initial disparity of the target stimulus exceeds 4°. In making such movements, we are presumably aided by cues to depth other than disparity, such as perspective.

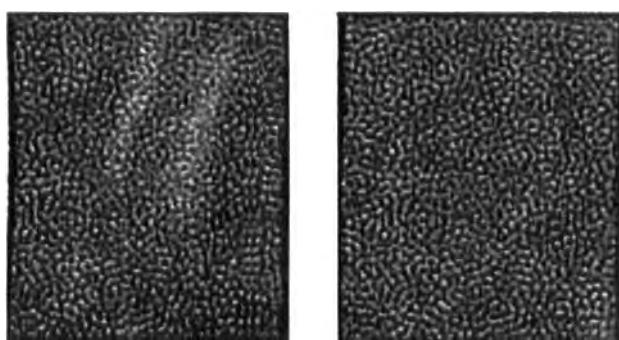


Figure 10.13. Stimulus used by Frisby and Mayhew (1980b).
Clusters of texture elements, similar in the two eyes, can be seen extending over at least 1° of visual angle. (Reproduced with permission from Vision Research, Pergamon Press.)

10.5.2 Disparity threshold for vergence

Duwaer and van den Brink (1981b) determined the smallest disparity required to initiate vertical vergence, as indicated by displacement of nonius lines. Since vertical vergence is not under voluntary control it provides a clean measure of the disparity/vergence threshold. For stimuli presented for 2 s at eccentricities of up to 4°, vergence was initiated by a disparity of about 1 arcmin. The vergence-initiation threshold was higher for stimuli presented for only 160 ms at eccentricities greater than 4°. These disparity thresholds were much smaller than the disparities at which singleness of vision was lost. *The disparity/vergence threshold should be determined with an objective method of recording eye movements, and compared with that used for coding of depth.*

The essential information used by the disparity-detection system could be the cross correlation between local regions of the images in the two eyes. Experiments supporting this view were reviewed in Section 6.2.1, where it was shown that the ability to detect a correlation between the images of a dynamic random-dot display is affected by the proportion of uncorrelated dots and by luminance contrast.

Stevenson et al. (1994) enquired whether the same information is used to evoke vergence eye movements. Their stimulus was a dynamic random-dot display set at various disparities within a zero-disparity circular aperture. This stimulus contained no monocular stimuli to vergence. A vertical line anchored vertical vergence and cyclovergence. Subjects aligned two vertical nonius lines and tried to keep them aligned for 60 s after the display of dots was introduced, either with a constant disparity or with a 15-arcmin sinusoidal modulation of disparity. In spite of the subjects' effort to keep the

nonius lines aligned, the eyes showed vergence responses to the dot pattern. The velocity of these responses for a given disparity, although low compared with uninhibited vergence, showed a similar dependence on interocular correlation and stimulus contrast as did the psychophysical detection of correlation (see Section 6.2.1). Stevenson et al. concluded that vergence uses the same stimulus information as that used for detecting image correlation. In a random-dot display, cross-correlation provides the only information about disparity. Other sources of information, such as contour matching or colour matching, are available in real-life visual scenes and no doubt also contribute to the control of vergence.

10.5.3 The stability of vergence

The small movements of an eye that occur when fixation is held on a small visual target are almost as large with binocular fixation as with monocular fixation (St. Cyr and Fender 1969). The combined variation in the visual axes of the two eyes produces a corresponding variation of disparity in the images of a binocularly fixated object. Motter and Poggio (1984) found that for about 60 per cent of the time the eyes of a monkey were misconverged by more than 7 arcmin in both the horizontal and vertical directions when the animal was fixating a small target. Fluctuations in disparity arising from these eye movements occurred equally over the whole visual field. They suggested that a dynamic feedback process insulates stereoscopic vision from the effects of fixation tremor. A neural model of this process, called a shifter circuit, was proposed by Anderson and van Essen (1987). We argued in Section 5.8.3 that such a mechanism is not required because even large disparity changes applied evenly over the visual field do not produce sensations of changing depth (Erkelens and Collewijn 1985a, 1985c; Regan et al. 1986a). All that is required is that the stereo system registers only first or second spatial derivatives of disparity (see Section 7.1.5). For the same reason, stereopsis is not disturbed by naturally occurring fixation disparities or by experimentally imposed fixation disparities (Fender and Julesz 1967).

10.5.4 Vergence to peripheral stimuli

The velocity and magnitude of vergence induced by disparity steps or ramps was greater for stimuli presented in the centre of the visual field than for those presented 3° into the periphery (Hung et al. 1991). Also, a stimulus with a given disparity became less effective in maintaining an accurate state of vergence

as it moved into the peripheral visual field (Francis and Owens 1983; Hampton and Kertesz 1983a). Furthermore, a large disparate stimulus was more effective in evoking vergence than was the same stimulus with the central 10°-wide region occluded by an artificial scotoma (Boman and Kertesz 1985). One reason for these differences between centrally and peripherally evoked vergence is that Panum's fusional area increases in the periphery so that, with more eccentric stimuli, the tendency of the eyes to return to the position of dark vergence induces a larger fixation disparity without loss of fusion (Ludvigh and McKinnon 1966). In other words, the peripheral retina tolerates larger disparities without triggering vergence than does the central retina. Another reason may be that peripheral disparity detectors have a smaller internal-loop gain (vergence signal per unit steady-state disparity) than do those serving the central retina. A third factor could be the increasingly transient character of disparity detectors as one moves into the peripheral retina.

Large, bold, disparate images presented suddenly to the parafoveal region can induce temporary diplopia in a small centrally fixated object (Burian 1939; Winkelman 1951). However, people have no difficulty fusing the images of a central object in the continued presence of disparities in the peripheral retina (Ludvigh et al. 1965). Disparate visual images placed near a centrally fixated visual object can induce a fixation disparity (see Section 10.5.3).

The range of vergence within which a centrally placed stimulus can be held in a fused state is increased slightly by the addition of more peripheral stimuli, but only if the added stimuli are in a nearby depth plane; peripheral stimuli with disparities above about 0.5° did not contribute to the maintenance of extreme positions of vergence in fixating a central stimulus (Jones and Stevens 1989).

The greater effectiveness of central stimuli in evoking vergence is behaviourally advantageous because vergence is designed to bring the images of objects of greatest interest to lie on corresponding retinal points so that residual disparities can be coded as depth. We will see in Section 10.7.4 that cyclovergence is evoked just as effectively by peripheral stimuli as by central stimuli. But the purpose of cyclovergence is to bring the whole visual scene into register, not particular images.

10.5.5 Vergence latency

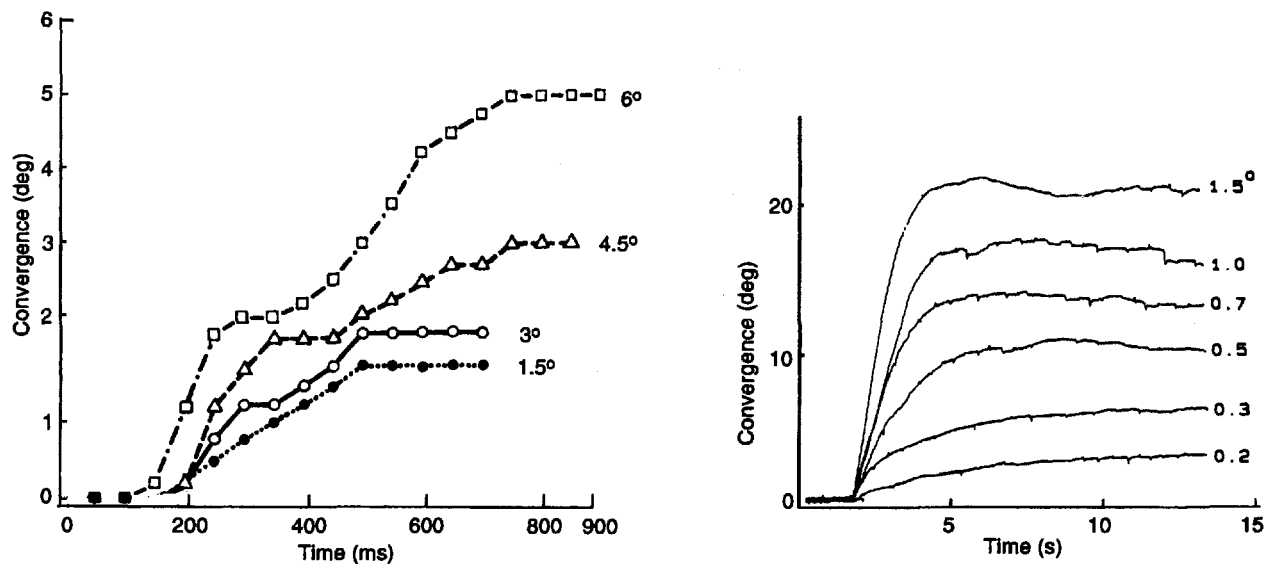
Vergence eye movements made in response to, for instance, a 2° step change in stimulus disparity have a mean latency of between 130 and 250 ms, a mean velocity of about 10°/s, and they take about 1 s to

complete (Rashbass and Westheimer 1961). There is thus plenty of time during the execution of a vergence movement for visual information to be used to guide the response to its goal state. This is in contrast to a conjugate saccadic eye movement which is not affected by new sensory information arriving between 80 ms before the saccade starts and its completion (Becker and Jürgens 1975). Although convergence movements have a shorter rise time than divergence movements once they have begun (Zuber and Stark 1968; Mitchell 1970; Krishnan et al. 1973a) they take longer to get started, that is, they have a longer latency (Krishnan et al. 1973b).

Several investigators have commented on the fact that the phase lag of vergence in response to a sinusoidal modulation of disparity is much smaller than one would predict from the 160 ms latency to a step stimulus. This difference cannot be due to the temporal regularity, and hence predictability, of the sinusoidal stimulus compared with a step, because a series of regularly spaced steps have just as long a latency as a series of steps occurring at irregular intervals (Rashbass and Westheimer 1961). Although responses to uniform sinusoidal stimuli have a shorter latency than those to unpredictable combinations of sinusoidal stimuli, the difference is not large enough to account for the difference in the responses evoked by sinusoidal and step stimuli (Zuber and Stark 1968; Krishnan et al. 1973a). But this mystery arises only if one believes that vergence is controlled by a single-channel linear system. In a nonlinear system there is no justification for predicting the phase lag to a smoothly varying stimulus from that to a discretely varying stimulus. To solve the mystery, one need only suppose that the visual system takes longer to code a large step in disparity than each small increment or decrement in a smoothly varying stimulus. As we saw in Section 4.5.1, large and small disparities tap distinct channels in the disparity-coding system and there is no reason to suppose that the latencies of the different channels are the same. When subjects initiate and therefore anticipate the motion of a visual target, the vergence movement starts even before the stimulus moves (Erkelens et al. 1989a). However, when subjects manually tracked a visual target moving sinusoidally in depth at various frequencies, vergence lag was no smaller than when the target was tracked by vergence alone (Koken and Erkelens 1993).

10.5.6 Vergence velocity and gain

Figure 10.14a shows the time course of symmetrical convergence eye movements to step changes of disparity from an initial vergence angle of 1.6°. The



(a) Time course of symmetrical closed-loop vergence evoked by step changes of disparity of up to 6°. (From Westheimer and Mitchell 1956. Copyright 1956, American Medical Association.)

(b) Time course of symmetrical open-loop vergence in response to step changes in disparity of up to 1.5°. (From Pobuda ad Erkelens 1993.)

Figure 10.14. The time course of vergence.

responses to steps larger than 1.5° were biphasic, and Westheimer and Mitchell (1956) suggested that the second, slower, component represents accommodative vergence. Figure 10.14b shows convergence to open-loop steps in disparity from an initial value of about 2.5° obtained by Pobuda and Erkelens (1993). The velocity of vergence to each step was initially constant and then declined to produce a constant, maintained angle of vergence. Both the initial velocity and maintained vergence increased with increasing size of the disparity step.

Pobuda and Erkelens explored the relationship between vergence velocity and stimulus velocity by comparing closed-loop responses to a stimulus that changed in disparity through 8° in 1 s, either smoothly or in two, four, or eight steps. The pattern of changing vergence was approximately a low-pass filtered version of the change in disparity with a lag of one reaction time. Vergence was not sensitive to the velocity of changing disparity as such, since the time course of the overall response was similar in the smooth and stepped conditions. A model of the vergence system based on these features of the response will be discussed in Section 10.5.8.

Symmetrical vergence movements made in response to a target moving along the midline in natural visual surroundings kept up with the stimulus with an accuracy of about 98 per cent for stimulus velocities up to about 40°/s (Erkelens et al. 1989a). At higher stimulus velocities, vergence progressively failed to keep up with the stimulus, but performance was better when the subject controlled the

movement of the stimulus than with when the experimenter controlled it. Vergence velocity kept to within about 10 per cent of stimulus velocity up to a velocity of 100°/s when vergence was evoked by a voluntary to-and-fro motion of the subject's torso with respect to a stationary target. These vergence velocities are very much higher than those reported by Ludvigh and McKinnon (1968), but in their study the stimulus was an isolated bar under the control of the experimenter.

The peak velocity of voluntary changes of vergence between two fixed stimuli within the median plane of the head increased from about 50°/s for vergence changes of 5° to about 200°/s for vergence changes of 34° (Erkelens et al. 1989b).

The gain and phase lag of vergence movements of one young subject made in response to both predictable and unpredictable sinusoidally changing disparity in a pair of dichoptic vertical lines are shown in Figure 10.15. It can be seen that the gain was close to 1 (zero decibel loss) for frequencies up to about 1 Hz and fell off above a frequency of 1.5 Hz (Krishnan et al. 1973a).

The dependence of vergence amplitude on the initial disparity of the stimulus can be investigated by presenting the stimulus for a duration less than the latency of the response. In this way, the response is not affected by the change in disparity that occurs as soon as the response commences. In effect, the response is open-loop during this initial period. The peak amplitude of vergence in response to a 200-ms flashed stimulus increased nonlinearly with

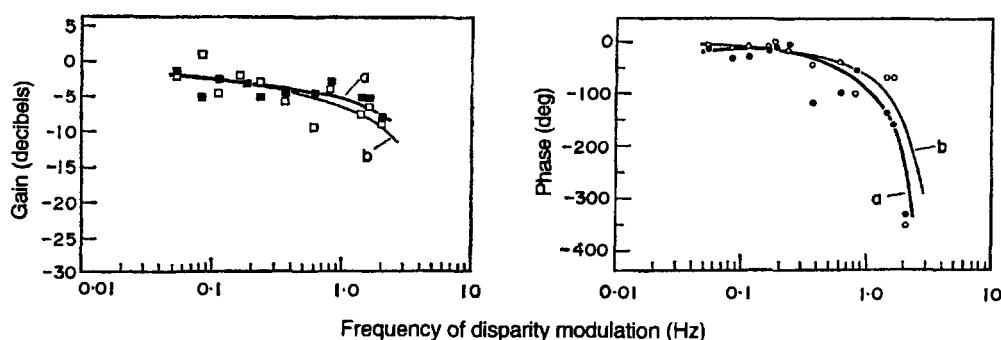


Figure 10.15. Gain and phase lag of vergence.

Gain and phase lag of vergence movements to predictable (lines marked *a*) and unpredictable (lines marked *b*) sinusoidal changes in disparity as a function of the spatial frequency of disparity modulation. The amplitude of the vergence stimulus was 1.75 metre angles. Results for one subject. (Reproduced with permission from Krishnan et al. 1973a, Vision Research, Pergamon Press.)

increasing stimulus disparity, reaching a maximum for a disparity of between 2 and 3°, as shown in Figure 10.16 (Jones 1980). Also shown in the figure is the vergence amplitude/disparity profile of a person who responded only to a stimulus with uncrossed disparity. Other subjects responded only to a crossed disparity. With longer stimulus durations, the asymmetrical responses showed only as slight differences in latency and velocity. Jones (1977) found that about 20 per cent of his subjects had marked asymmetries in their vergence to flashed stimuli.

The dependence of vergence velocity on the initial disparity of the stimulus can also be investigated by presenting a step disparity in the open-loop condition, that is, with the stimulus coupled to the output of the eye monitor so that, whenever there is a change in vergence, the lateral offset of the stimulus is changed, keeping disparity constant. Rashbass and Westheimer (1961) used open-loop steps of disparity and found that, with steps of up to about 1°, the velocity of vergence was approximately proportional to the size of the disparity. One subject showed a 10°/s increase in velocity for each 1° increase in disparity. Vergence velocity was approximately proportional to disparity up to a value of about 4° in the initial phase of a normal closed-loop response before feedback had time to be effective. This suggests that the open-loop transfer function of the vergence system involves the conversion of the initial disparity signal into a velocity signal. Mays et al. (1986) have suggested that, as the response proceeds, the velocity signal is integrated into the position signal required to maintain the eyes in their new state of vergence. The greater the eccentricity of the targets between which vergence movements are made, the lower the velocity of vergence in the initial phase of the response (Schor et al. 1986b).

Erkelens (1987) used open-loop crossed-disparity steps of from 0.25 to 10° between the images of three stimuli: a vertical bar, a cluster of random dots, and the inner region of a random-dot stereogram. It can be seen in Figure 10.17 that, on average, the maximum velocity of vergence increased more or less linearly with increasing disparity up to about 3° and continued to increase up to a disparity of about 4°, after which it declined to zero at about 9°. The three types of stimulus gave similar results and, although the velocity of vergence differed widely between subjects, velocity as a function of disparity was much the same for all subjects. Convergence was more rapid than divergence. The peak velocity of vergence has been found to be the same under a variety of viewing conditions (Hung et al. 1994).

Appropriate vergence movements were evoked when the stimuli presented to the two eyes differed in luminance by up to 1.6 log units, although the velocity of the response decreased as the difference in luminance was increased (Mitchell 1970).

10.5.7 Trigger and fusion-lock components

There is abundant evidence that vergence can be triggered by large disparities, even when the disparate stimuli are dissimilar in shape and occur on opposite sides of the midline and hence on opposite cerebral hemispheres (Winkelmann 1953). However, vergence is maintained on a particular object to within about 2 arcmin, only by similar images falling within Panum's fusional area (Riggs and Niehl 1960). These two types of response are referred to as the transient and sustained components of vergence, but the terms **trigger component** and **fusion-lock component** better describe their functions. The components of vergence are seen most clearly in

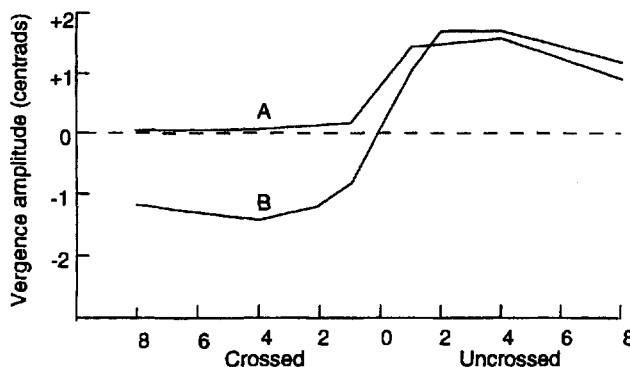


Figure 10.16. Vergence amplitude and disparity.

The peak amplitude of vergence in response to a 200-ms flashed stimulus as a function of binocular disparity. Curve B is from a subject showing a symmetrical response to crossed and uncrossed stimuli and curve A is from a subject who responded only to uncrossed disparities. (Adapted from Jones 1980.)

vergence responses to open-loop disparity. For instance, Erkelens (1987) found that open-loop disparities of up to 2° caused the eyes to converge between 15 and 25° and then to remain in the converged position for as long as the stimulus lasted. Thus, for open-loop disparities up to 2° the response was sustained. Open-loop disparities of 2 to 5° drove the eyes to a convergence of up to 35°, but the eyes drifted back to a vergence of less than 5°; that is, the initial response was transient. For disparities larger than 5° the eyes were driven to a less extreme position and the response was also transient and sometimes did not occur. The disparity at which the response became transient was found to be the same as that at which the images were no longer fused. Thus, vergence is initiated by disparities well outside the fusional range and sustained by disparities that are small enough to provide a fusional lock.

Erkelens also found that a transient response to a large open-loop disparity reduced response velocity to other stimuli presented subsequently, but only when they had similar disparities. Thus, the short-term adaptive process underlying the transience of the trigger component to a given disparity is localized to a given range of disparities.

The distinction between a transient response and a sustained response is not only a question of whether the stimulus is within the spatial range of the fusion-lock mechanism. Stimuli within range of the fusion-lock mechanism, which normally evoke a sustained response, evoke a transient response when the images are too dissimilar for binocular fusion. For instance, dichoptic vertical lines with 2° of horizontal disparity evoked a sustained vergence response, but the response was not maintained when one of the lines was horizontal. The response to a briefly exposed pair of similar stimuli is the same as

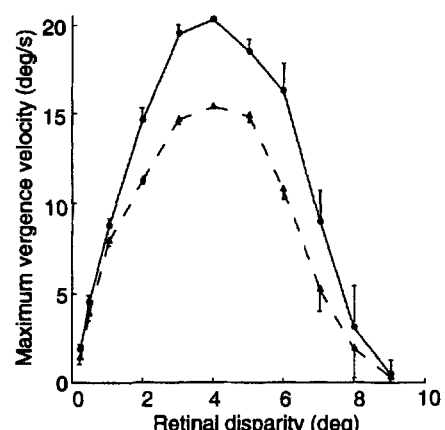


Figure 10.17. Vergence velocity and binocular disparity.

Peak vergence velocity as a function of disparity between images of a vertical bar (dotted line) and a random-dot stimulus (continuous line). Bars are standard deviations. Means of five subjects. (Adapted from Erkelens 1987.)

that to long exposure to a dissimilar pair of stimuli. Both pairs of stimuli evoke the same transient trigger response which is not maintained because neither pair of stimuli is fusible. The similar stimuli do not fuse because of the brief exposure, and the pair with long exposure do not fuse because they are dissimilar. When a pair of similar and a pair of dissimilar dichoptic images are presented briefly at the same time, a transient response is just as likely to be triggered by the disparity in the matching pair as by that in the nonmatching pair (Jones 1980; Jones and Kerr 1972; Semmlow et al. 1986).

Thus, vergence can be triggered by disparate stimuli that do not have the same shape but is not maintained in the absence of matching features that provide a fusional lock, that is, an error signal for fine vergence control (Westheimer and Mitchell 1969; Jones 1980). Transient horizontal vergence is also evoked when dichoptic stimuli are up to about 3° out of vertical alignment (Mitchell 1970). In this case the constant vertical misalignment does not allow the images to get within range of the horizontal fusion-lock mechanism.

Jones (1980) found that about 20 per cent of subjects with otherwise normal binocular vision responded asymmetrically to briefly exposed disparities; some did not respond to crossed disparities while others did not respond to uncrossed disparities with respect to the resting state of vergence. An example is shown in Figure 10.16. The anomaly was not evident with long exposure of disparate stimuli.

The dynamics of trigger and fusion-lock vergence

The transient component of vergence to a given disparity can be isolated from the sustained component by presenting the stimulus for less than 200 ms.

Results shown in Figure 10.16 reveal that the peak amplitude of transient vergence evoked by a 200-ms stimulus is proportional to the initial disparity up to about 2° of crossed or uncrossed disparity and reaches its peak value at about 4° of disparity (Jones 1980). These values are similar to those reported in the previous section for open-loop stimuli.

The transient and sustained components of vergence were investigated quantitatively by Semmlow et al. (1986). They varied the disparity between two vertical-line targets by up to 4°, either in one step or in a ramp of constant velocity from 0.7 to 36°/s. Up to a ramp velocity of 1.4°/s, subjects tracked the changing disparity smoothly, which was taken as evidence that vergence was controlled by the sustained component of vergence. The smooth response exhibited proportional control; that is, the velocity of vergence was proportional to stimulus velocity. At higher velocities the smooth response was interspersed with rapid responses (see Figure 10.18). The ratio of peak velocity to amplitude of these rapid interludes was the same as that of the transient response to a 4° disparity step (they fell on the same main sequence). This suggests that the rapid interludes are transient responses. Their constant main-sequence characteristics persuaded Semmlow et al. that they are preprogrammed, or ballistic, movements based on a sampling of accumulated disparity in the ramping stimulus, in contrast to the proportional control of sustained responses.

Hung et al. (1986) designed a model of the vergence system, simulating these features of the response. In the preceding section we reported that Erkelens found a continuous change in vergence velocity as a function of disparity and argued against the idea of there being two distinct feedback dynamics in the sustained and transient systems.

The steplike responses to rapid disparity ramps reported by Semmlow et al. could be due to an irregularity in the vergence error signal resulting from failure of vergence to keep up with the stimulus. The stimulus for vergence is disparity, or stimulus separation minus vergence. With rapidly changing disparity ramps, vergence lags the stimulus and the disparity error accumulates to a level that triggers a transient response, which in turn restores the disparity error to within range of the sustained mechanism. With gradual ramps, disparity error does not accumulate to the level required to trigger a transient response. Analogously, voluntary pursuit of a target moving in the frontal plane is interrupted by catch-up saccades when the target moves too rapidly. Alternating fast and slow vergence does not occur when the stimulus ramp is presented in open-loop mode (Erkelens 1987;

Pobuda and Erkelens 1993). Under these conditions the disparity error is constant, since the movement of the stimulus is coupled to that of the eyes.

Functions of trigger and fusion-lock vergence

The transient response to large disparities serves a useful function. When a person changes convergence from one plane to another, the large disparities in the target plane trigger an appropriate response. Once the images from the target plane have been fused, the large disparities arising from other depth planes should be ignored, at least until a decision has been made to converge on some other plane. If large disparities in nontarget depth planes were not ignored, the vergence system would never be able to settle down into a desired state. The only study of the role of target selection in initiating vergence was conducted by Erkelens and Collewijn (1991). Subjects had no difficulty in making appropriate vergence movements to voluntarily selected parts of line or random-dot stereograms as the stimuli were stepped in depth in random sequence, even though this caused nonselected elements to become disparate. Subjects could also track a chosen part of a stereogram when the selected disparity was coupled to their eye movements in open-loop control.

The vergence system should continue to respond to small disparities after vergence has homed in on the target because they indicate whether vergence is adequately maintained at the desired distance. That is presumably why vergence responses to small disparities are sustained rather than transient. This continued responsiveness to small disparities should make it difficult to maintain a precise state of vergence on an object in a given depth plane when there are objects in nearby depth planes, especially when they project images on the same retinal region. This should not matter because, (1) If vergence were controlled by the averaged disparity in the region of the target plane rather than by only the disparity in one pair of images, the images of a particular object would still be within Panum's area, and depth perception would not be disturbed. (2) If vergence oscillated within the region of the target plane, the relative disparities in the visual scene would be preserved. (3) Scanning vergence movements should help build up a representation of the 3-dimensional structure of the local region. Vergence stability in regions containing fine disparity gradients has not been explored, but is mentioned in Section 10.5.2.

Summary

Vergence can be triggered by nonfusible stimuli or by stimuli outside the fusional range, but it cannot be maintained in a given state unless the fusion-lock

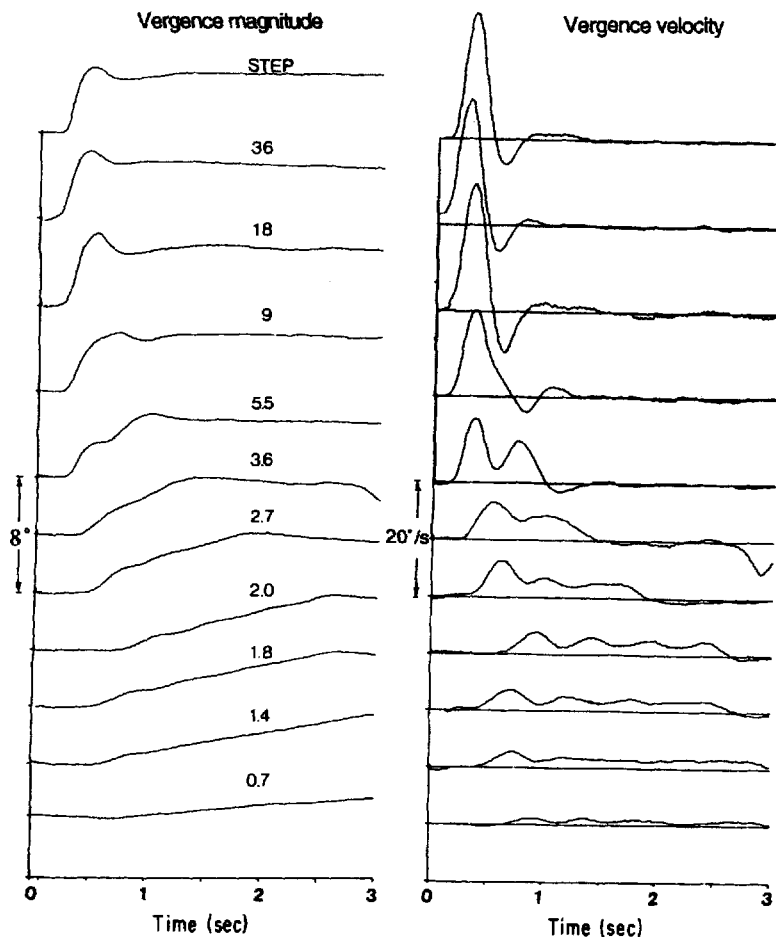


Figure 10.18. Vergence as a function of size and velocity of disparity change. The curves on the left are the time courses of vergence as a function of the velocity of a 4° change in disparity of two vertical lines. The velocity of the change in disparity in degrees per second is indicated above each curve. The curves on the right are the velocity profiles of the responses. The top curves are responses to a 4° step change in disparity. Data are based on the mean responses of two subjects. (From Semmlow et al. 1986. Reprinted with permission of J. B. Lippincott Co., Philadelphia.)

mechanism is engaged. In a normal environment we see a multitude of disparate stimuli, each capable of triggering a vergence movement. We decide which stimulus to respond to. When we change fixation from one distance to another we must disengage the fusion-lock mechanism, allow the new visual object to trigger an appropriate vergence response, and re-engage the fusion-lock process. One can think of the trigger component of vergence as being the one engaged whenever we decide to change convergence. If a new fusible stimulus does not materialize after the trigger response, vergence is not maintained in the new position and the response is transient. If a fusible stimulus does come into view, the fusion-lock mechanism is engaged and the response is sustained. There is some debate about the different dynamics of the two types of vergence.

The neurological evidence bearing on this question is reviewed in Section 10.8. *Sustained and transient responses have not been studied in vertical vergence or cyclovergence.*

10.5.8 Modelling the vergence system

A linear model of the vergence system has been proposed by Krishnan and Stark (1983). The system was assumed to be under continuous sensory control, unlike the ballistic saccadic system. It was also assumed that the eyes maintain a reasonably accurate state of vergence in the presence of a steady-state disparity. This could be achieved in two ways. A neural integrator could derive the final state of vergence from the integral of response velocity. Alternatively, the system could have a high internal-

loop gain, defined as eye velocity per unit disparity, which would allow it to sustain the required steady-state contraction of muscles from a small steady-state disparity error signal. Krishnan and Stark's model incorporates two parallel controllers. The first controller has fast, transient (derivative) dynamics with an eye-velocity output proportional to the instantaneous magnitude of disparity one reaction time earlier. The other has slow, tonic dynamics with a leaky output related to the integral of eye velocity. The leaky output accounts for the slow drift of the eyes back to a resting state in the dark. Each controller has its own internal-loop gain, and the two are combined with a pure delay of 160 ms.

One weakness of the model is that it produces too slow a response to step inputs when the internal-loop gain of the integral controller is set low, and oscillations when it is set high. Performance could be improved by making the controller responsive to the predicted position of the visual target, but this would work only for predictable movements and, as has already been pointed out, vergence stability does not depend on whether the stimulus is predictable. Perhaps the phase lag of one of the control elements, when operating in a continuous tracking mode, is less than one would predict from the latency of vergence in response to disparity steps, and this may account for the otherwise puzzling stability of the real vergence system (Rashbass 1981).

Krishnan and Stark's model deals with the nonlinear asymmetry between divergence and convergence by an appropriate asymmetry in the internal-loop gains. The compressive nonlinearities of the vergence system in the form of saturating levels of velocity and amplitude and nonlinear interactions between vergence and version are not incorporated into the model. Nonlinearities arising from high-level control of vergence, as when a person decides to respond to one of several disparities, are also not incorporated into the model.

A model which incorporates interactions between the vergence and accommodation systems and an integrator which accounts for adaptive changes in tonic vergence has been proposed by Schor and Kotulak (1986) (see Figure 10.19). Zee and Levi (1989) have proposed the model shown in Figure 10.20, which incorporates the contribution of the saccadic system to vergence and the adaptive plasticity of the vergence system (see Section 10.2.5).

Pobuda and Erkelens (1993) proposed that vergence signals are processed through several parallel channels with low-pass characteristics. The gain of each channel is specific to a particular range of disparity amplitudes. As an eye movement in response to a given disparity progresses, control passes from

the channel sensitive to large disparities to that sensitive to small disparities. The channels are insensitive to the rate of change of disparity. Pobuda and Erkelens also proposed that the overall lag of the system is comprised of a delay of between 80 and 120 ms in the vergence-processing loop plus a lag in the mechanical plant. The lag in the processing loop is less than the 160 ms assumed in the other models and accounts for the small phase lag in response to sinusoidal stimuli which other models could not explain (see Section 10.5.5). The model also incorporates a slow integrator, like that proposed by Schor (1979a), to account for adaptation of tonic vergence. Although each channel is linear, their combined action introduces a nonlinearity, since the gain of the response varies with the stimulus amplitude.

Semmlow et al. (1986) and Hung et al. (1986) proposed a "dual-mode" model of disparity control. A fast initial preprogrammed response is followed by a slower late component under feedback control. In this model the dynamics of the initial response are always the same, since the response does not depend on error feedback. For an open-loop disparity signal, the theory predicts a series of step-like responses, as a series of vergence movements are triggered by the persistent disparity signal. Semmlow et al. (1994) found the step-like response to an open-loop signal, which they claimed supports their model.

10.6 VERGENCE - VERSION INTERACTIONS

10.6.1 Hering's law of equal innervation

When binocular fixation changes between two points differing in both depth and direction, the eyes execute both vergence and version movements. When the eyes track a spot as it moves slowly from one point to the other, vergence is combined with slow voluntary pursuit. When the gaze moves rapidly from one point to the other, vergence is combined with a saccade. The following discussion is about how vergence is combined with these two types of version.

Hering (1868) proposed that the movement of one eye is accompanied by a movement of the other eye of equal amplitude and velocity, either in the same or in the opposite direction. This has come to be known as Hering's law of equal innervation. Movements of a single eye, or ductions, are specified in terms of magnitude, direction, and velocity. Coordinated movements of the two eyes are specified in terms of version and vergence components. Version is a movement of the two eyes of equal magnitude and direction, and vergence is a movement of

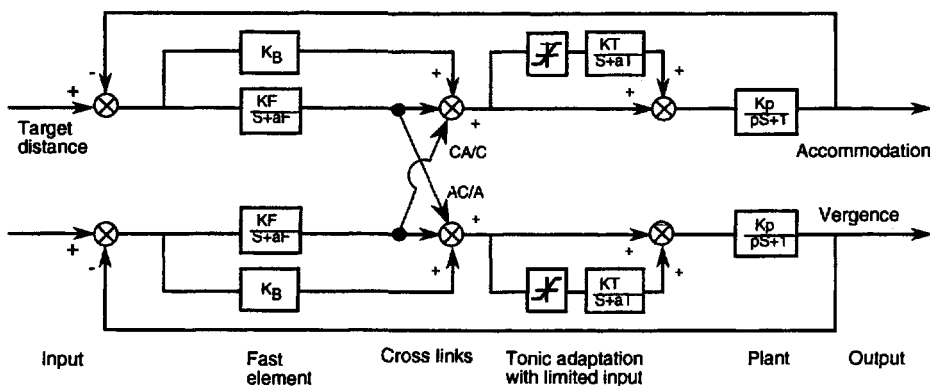


Figure 10.19. Model of vergence accommodation.

The mutual interactions between the vergence and accommodation systems occur between the phasic and tonic neural integrators in the feedforward paths. The inputs to the tonic integrators have a saturation limit which could produce amplitude-dependent nonlinearities of the AC/A and CA/C ratios. The transfer function of each module is indicated by a Laplace transform. (From Schor and Kotulak 1986. Reproduced with permission from Vision Research, Pergamon Press.)

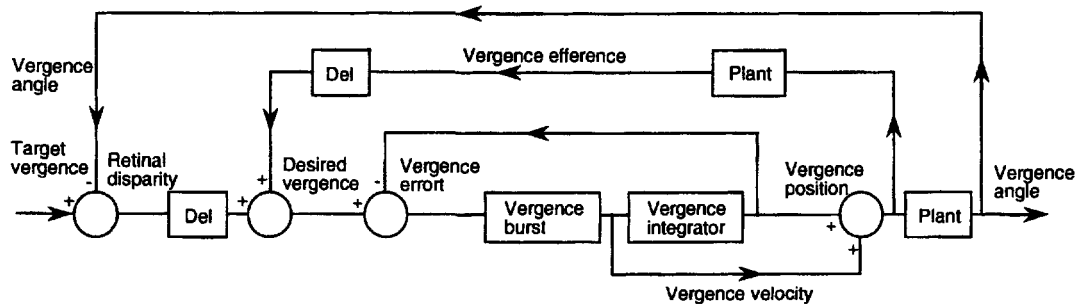


Figure 10.20. Outline of a model of the vergence mechanism.

The desired angle of vergence is derived by adding retinal disparity to the present vergence angle. A feedback signal derived from cells that carry velocity and position signals (burst-tonic neurones) passes through an internal model of the oculomotor plant and a compensating time delay (Del). The difference between the desired vergence state and the feedback signal provides a vergence-error signal, which drives vergence-burst neurones. The output of the burst neurones provides a velocity signal to the oculomotor nuclei and, by integration, a vergence position signal which maintains the eyes in the desired final state. (From Zee and Levi 1989.)

the two eyes of equal magnitude but opposite direction. A circle passing through the centres of rotation of the two eyes and the fixation point is the path traced by the fixation point as vergence is held constant while version changes. A hyperbola of Hillebrand is the path traced when version is held constant while vergence changes (see Figure 10.5). Mathematically, any movement of the two eyes may be described as the sum of a version and a vergence. Let θ be the version component with movements toward the right signed positive and let μ be the vergence component with convergence signed positive. For a pure vergence, the movement of each eye equals $\mu/2$. In general (after Ono 1980)

$$\theta + \left(\frac{\mu}{2}\right) = \text{rotation of the left eye} \quad (2)$$

$$\theta - \left(\frac{\mu}{2}\right) = \text{rotation of the right eye} \quad (3)$$

Hering's law would be a tautology if it merely stated that all binocular movements may be described as the sum of a version and a vergence component, and that each component may be regarded as the sum or difference of two equal movements in the two eyes. It is clear from Hering's use of the phrase "equal innervation" that he was thinking of component neural processes not merely mathematical components.

A stronger expression of the law is that the velocity of the two eyes is always equal. Many people have interpreted Hering's law in this way, and Hering himself wrote, "The two eyes are so related to one another that one cannot be moved independently of the other: rather, the musculature of both eyes reacts simultaneously to one and the same impulse of will." (Hering 1868, p. 152). But this is not what Hering really meant, for he went on to write, "it is possible for us to move both eyes

simultaneously about different angles and with different speeds . . . and even to move one eye outward or inward while the other remains still." Consider the idealized case, in which the gaze shifts from point *A* to point *B*, both lying on the visual axis of the left eye. This movement may be decomposed into an equal version signal for both eyes of θ and an equal vergence signal, which in this case must move the right eye through angle $-\mu/2$ and the left eye through angle $\mu/2$. When these values are put into equations (2) and (3) they cancel for the left eye and add for the right eye. The right eye therefore does all the moving and the left eye remains stationary. It is in this way that Hering's law is compatible with the occurrence of unequal movements of the two eyes.

It is clearly not the amplitude or velocity of the movements of the two eyes that are equal in Hering's law, but the amplitude and velocity of the vergence component in each eye and the version component in each eye. One can erect the hypothesis that, when version and vergence are executed simultaneously, eye velocity is a linear sum of the velocities of each component movement acting alone. The empirical evidence bearing on this version of Hering's law is discussed in Section 10.6.2. Hering's law should perhaps be called the **law of equal component innervations**. The actual movement that these two components produce in a given eye may be zero because they may be directed in opposite directions and therefore cancel.

The neurology of Hering's law

Hering's law implies that there are two centres in the nervous system, one for vergence and one for version, and the innervation to one eye is always the same as to the other from each of these centres. The simplest assumption is that these innervations are combined linearly in the final common path so that the movement of each eye is the algebraic sum of the innervations from the two centres. Strictly speaking, Hering's law does not require a linear combination of version and vergence signals; it only requires that the version signals remain equal and the vergence signals remain equal. For instance, it does not forbid the two version signals from being attenuated when combined with vergence signals.

Each motoneurone pool in the brainstem innervates almost exclusively one extraocular muscle in one eye; the trochlear nucleus innervates the contralateral superior oblique muscle, the abducens nucleus the ipsilateral lateral rectus, and the motoneurone pools in the oculomotor nucleus innervate the ipsilateral medial rectus, inferior oblique, and inferior rectus, as well as the contralateral superior rectus (Evinger 1988). Moschovakis et al. (1990),

recording from premotoneurones responsible for vertical saccades, found that they branch to innervate all the motoneurone pools that move both eyes conjugately. This provides a basis for Hering's law at least for conjugate vertical saccades.

Hering believed that there are distinct motoneurones for version and vergence movements, and the effects of the two types of innervation combine in the muscles themselves. The distinct motoneurones could either converge on the same muscle fibres, or different muscle fibres could be devoted to each component. Hering believed in the second possibility and thought he detected opposed contractions in the muscles of the stationary eye during a change of fixation along that eye's visual axis. More recently, investigators claim to have detected them electromyographically (Tamler et al. 1958). But this response may have resulted from slight saccadic movements when vergence is changed rapidly along the line of sight of one eye, or to torsional movements that accompany a change in vergence (see Allen and Carter 1967). Others found no changes in electrical activity of muscles of a stationary eye under these conditions (Breinin 1955; Blodi and Van Allen 1957).

Enright (1980) has revealed that there is also a slight lateral translation of an eye when vergence changes along its visual axis. But these torsional and translatory movements of the eyes are probably incidental to the version and vergence components and have no functional significance.

O'Keefe and Berkley (1991) produced evidence of a coupling of the movements of the two eyes mediated by proprioception. Infusion of a paralytic agent into the muscle capsule of one eye in the anaesthetized cat reduced the spontaneous changes in position of both eyes. Without the paralytic agent neither passive movement of one eye nor application of a local anaesthetic into the muscles of one eye had any effect on the other eye. It was suggested that the eyes are coupled by signals arising in proprioceptors in the extraocular muscles and that these signals are gated by efferent signals.

Vergence and saccadic intrusions

There is the related question of crosstalk between version and vergence. Is the response to a stimulus requiring a pure version devoid of a vergence component, and is a required pure vergence devoid of a version component? Bahill et al. (1976) noted that subjects with normal vision sometimes execute unequal saccades in the two eyes, but they regarded these events as anomalous. Collewijn et al. (1988b) found that vertical saccades to targets in the upper half of the visual field were associated with a small but definite transient divergence and those to targets

in the lower half of the field with a transient convergence. The stimuli were positioned so that, as each target was fixated, the angle between the visual axes remained constant. This ensured that a vergence change was not required as the gaze moved from one stimulus to another. It was suggested that vergence intrusions are due to the general tendency for objects below eye level to be near and objects above eye level to be far away. However, the situation is complicated by the fact that the vertical horopter is inclined top away, which means that the targets in the upper half of the visual field had a crossed disparity and those in the lower half an uncrossed disparity. The vergence movements associated with vertical saccades may simply be induced by these disparities. Zee et al. (1992) also observed intrusions of vergence into vertical saccades.

Colleijn et al. (1988a) found that in horizontal saccades to stimuli lying on the locus of isovergence the motion of the abducting eye had a larger amplitude, higher peak velocity, and shorter duration than that of the adducting eye (toward the nose). As a result the eyes diverged transiently by up to 3° and a postsaccadic drift of the eyes was required to bring the gaze onto the target. These vergence movements could be due to the intrusion of a phoria when the fusional lock is lost temporarily during a saccade (Kapoula et al. 1987). They could also be due to the fact that the elastic resistance of an eye to nasalward motion is greater than to temporalward motion (Collins et al. 1981). Zee et al. (1992) confirmed the existence of intrusions of vergence into horizontal saccades and also ascribed them to asymmetries in the mechanical properties of the lateral and medial recti muscles. The whole issue is complicated by the fact that the horizontal horopter, defined as a circle through the nodal points of the two eyes, does not coincide with the locus of isovergence, defined as a circle through the centres of rotation of the two eyes. This means that a target on the locus of isovergence should have a crossed disparity when the eyes are in the straight-ahead position. This would induce convergence rather than divergence, but perhaps the horizontal horopter is closer than the isovergence locus at the viewing distance used in these experiments.

In spite of all these complexities and qualifications Hering's law remains as a fundamental statement of how frontal-eyed animals, such as cats and primates, move their eyes. They do not generally move the eyes independently like a chameleon; the two visual axes intersect at the point of fixation, and a closed eye moves along with the open eye. Intrusions of saccades into vergence eye movements are discussed in the next section.

10.6.2 Additivity of vergence and version

Hering's law does not stipulate that version and vergence components are combined linearly but only that any nonlinearity applies equally to the two eyes. However, one can erect the hypothesis that, when version and vergence are executed simultaneously, eye velocity is a linear sum of the velocities of each component movement acting alone. This could be called the strong version of Hering's law. This hypothesis can be tested under two conditions: when vergence is combined with slow voluntary pursuit, and when it is combined with conjugate saccades.

Additivity of slow version and vergence was investigated by introducing step changes in the disparity of a target that subjects were pursuing slowly along a horizontal track in the frontal plane (Miller et al. 1980). The velocity of an eye for which the version and vergence signals were opposite in direction was the linear sum of the component velocities. Note that in this case the component innervations were delivered to distinct extraocular muscles. When the version and vergence signals drove the eyes in the same direction, an 11 per cent loss in additivity occurred. In this case the combined innervations impinged on the same muscles, and one could explain the loss in additivity in terms of a compressive non-linearity at the neuromuscular junction. In both cases, the innervations themselves may well have been combined linearly in the oculomotor nuclei from independent command centres.

Additivity of saccadic version and vergence was investigated by recording the response to a target that was stepped to a new position, differing in both direction and depth. According to the traditional account, a version made in response to a stepped stimulus is normally saccadic and occurs with a latency of about 200 ms and a velocity of up to 600°/s, while vergence has a latency of about 150 ms and a peak velocity of about 20°/s. Therefore, in a rapid eye movement involving both vergence and version, vergence should start before version, then the required version should be achieved quickly, leaving the rest of the slow vergence to be completed. If we assume for the sake of simplicity that the stimulus is stepped along the visual axis of the left eye and vergence is inhibited during the time that version is occurring, the resulting eye movements should be as depicted in Figure 10.21. A pure vergence occurs at the start, that is, the eyes track along a hyperbola of Hillebrand. Then the version kicks in and moves the gaze for both eyes along an isovergence locus. Finally, the residue of the vergence occurs, again carrying the gaze along a hyperbola of Hillebrand back onto the visual axis of the left eye. Note that the

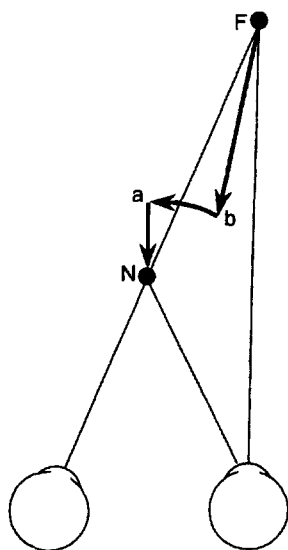


Figure 10.21. Hypothetical path of vergence-version.
The arrows indicated the hypothetical path traversed by the point of fixation as the gaze moves from point F to point N. The eyes first converge to point b, then execute a conjugate saccade to point a, and finally complete the vergence movement to point N.

law of equal component innervations holds throughout this sequence. With a sequential programming of version and vergence, the amplitudes and velocities of the eyes are always equal, not merely the amplitudes and velocities of the component commands.

Several investigators have obtained records of eye movements during a rapid change in gaze, involving both vergence and version components, which showed the two components occurring sequentially in the general manner just described (Alpren and Ellen 1956; Westheimer and Mitchell 1956; Yarbus 1967). Ono and Nakamizo (1978) found this pattern only when vergence and accommodation were dissociated or when the target moved down the visual axis of one eye. In other cases Ono and Tam (1981) found multiple saccades, especially for large vergence changes. Pickwell (1972) also found that the relative magnitudes of version and vergence components depended on whether the stimulus was aligned with the left or right visual axis. This was explained in terms of a displacement of the cyclopean eye (see Section 14.5.2) toward the dominant eye. Others found no evidence of a clear temporal separation between vergence and version components (Erkelens et al. 1989b). Recent evidence, which we now review, suggests that the control of vergence, especially asymmetrical vergence, is more complex than a simple sequential combination of rapid version and slow vergence components.

In the first place, the saccadic component is not switched off while vergence is occurring. There is thus the question whether the saccadic and vergence

components combine additively when they occur together. Ono et al. (1978) found that during the convergence phase of an eye movement evoked by a target that stepped in both lateral direction and depth, the differences of amplitude and velocity between the two eyes were much greater than predicted from a linear addition of component velocities. A similar supra-additivity of components was found when a step change in the lateral direction of gaze was superimposed on a tracking vergence made in response to a target moving slowly in depth (Saida and Ono 1984). Similarly, it has been reported that when accidental microsaccades occurred during a vergence movement, the difference in velocity between the two eyes was greater than that predicted on the basis of a simple addition and subtraction of the vergence movements from the saccadic movement (Kenyon et al. 1980b).

In line with this evidence, Enright (1984, 1986) reported that when subjects made rapid changes in fixation, involving both vergence and version, they made short-latency saccadic movements, which were unequal in magnitude in the two eyes. Between 40 and 70 per cent of the required vergence was achieved by these asymmetrical saccadic movements. However, there was no quantitative determination of whether the velocity-magnitude characteristics of these rapid eye movements conformed to the "main-sequence" properties of regular saccades. Furthermore, it is not clear whether these unequal saccades were confined to asymmetrical vergence, since Enright did not look for them in symmetrical vergence movements within the median plane. Levi et al. (1987) did find saccades of unequal amplitude and, in a few cases, saccades in opposite directions in symmetrical vergence, especially in the early part of divergence movements. Corrective conjugate saccades often occurred at the end of vergence movements. Similar movement patterns have been found in the monkey (Maxwell and King 1992).

Erkelens and Collewijn (1985b) found no evidence of eye movements with saccadic velocities in rapid symmetrical vergence movements. In a more recent study, however, symmetrical vergence movements between two fixed stimuli were found to contain some small disjunctive saccades (Erkelens et al. 1989b). Asymmetrical vergence was achieved largely by asymmetrical saccades, as Enright had found. The equal-direction displacement of binocular saccades is the version, or conjunctive, component and the opposite-direction displacement is the vergence, or disjunctive, component of the saccade. The effect of a disjunctive component in a saccade is to make the movements of the two eyes unequal in velocity and magnitude. Approximately 95 per cent

of a divergence of 11° when combined with a version of 45° was accomplished by unequal saccades. Only 75 per cent of a similar convergence movement was accomplished by unequal saccades. Unequal saccades had the same duration in the two eyes, but one was slower than the other and neither had the same main-sequence dynamics (ratio of amplitude to peak velocity) as a regular conjugate saccade. Enright (1992a) reported evidence that, although the pulse of innervation for the saccades in the two eyes is the same, the step component that determines the final position is generated independently in the two eyes.

Unequal saccades have been found to occur particularly frequently in accommodative vergence with monocular viewing and with binocular viewing in strabismic patients who lack disparity vergence (Kenyon et al. 1980b).

Unequal saccades during vergence could perhaps be due to nonlinear interactions between vergence and version signals in motoneurones or in the oculomotor muscles. Zee et al. (1992) have devised three models of these interactions. Whatever the cause, the effect is equivalent to a saccadic vergence, which means that the saccadic system makes its own contribution to rapid changes in asymmetrical vergence and to a lesser extent to symmetrical vergence. Saccades made between visual targets in different depth planes have a longer latency than those between targets in the same depth plane, although it is not known whether this effect is due to increased time for stimulus processing or to increased time for organization of the response (Honda and Findlay 1992). The combination of version and vergence is discussed in detail by Ono (1983).

10.6.3 Oculomotor adaptation to aniseikonia

Adaptation to saccadic dysmetria

When a saccade misses the intended target it is said to be **dysmetric**; it is hypometric if it undershoots the target and hypermetric if it overshoots the target. It has been known for some time that the saccadic system adapts itself to an imposed dysmetria. Dysmetria may be imposed by triggering a saccade to an eccentric target and then, when the saccade is in midflight, displacing the target to a different position along the path of the eye's movement. The displacement of the target is not visible and so the subject overshoots or undershoots the target and a secondary saccade is required. After a few trials the amplitude of the first saccade becomes modified so as to bring the gaze close to the position of the displaced target (McLaughlin 1967; Henson 1978). It is easier to correct for hypometria than for hypermetria (Miller et al. 1981; Deubel et al. 1986).

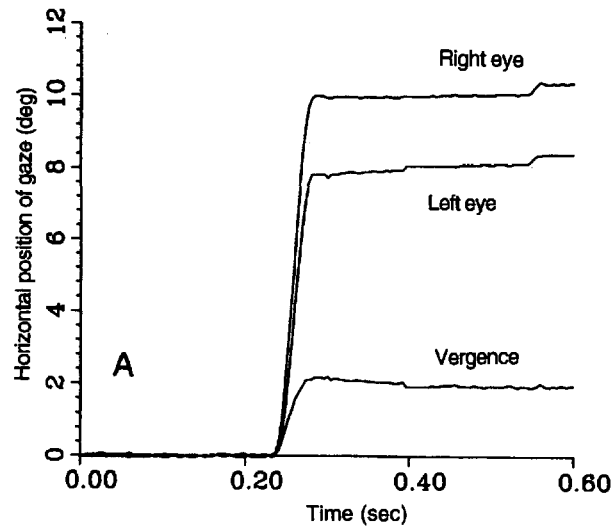


Figure 10.22. Unequal saccades in anisometropia.

Record of unequal saccades made by a 12-year-old boy adapted to anisometropic spectacles, after the spectacles were removed. The visual target was 10° to the right of the initial fixation point. The unequal magnitude of the saccades in the two eyes created a spurious vergence. (From Oohira et al. 1991. Reprinted with permission of J. B. Lippincott Co., Philadelphia.)

The induced change in saccadic gain is limited to saccades within $\pm 30^\circ$ of the direction of the saccade used in training (Deubel 1987).

Saccadic adaptation to aniseikonia

In all the preceding studies the saccadic gain of both eyes changed in the same way, and only recently has it been shown that the saccadic system of one eye can adapt independently of that of the other. More recently, the saccadic systems of the two eyes have been shown to be able to adapt simultaneously to dysmetrias of opposite sign.

Spectacles worn to correct unilateral myopia of refractive origin produce aniseikonia—they enlarge the image in one eye relative to that in the other (see Section 2.8 for definitions of terms). This is because the spectacle lenses are offset from the cornea and do not move with the eyes; contact lenses do not produce this effect. An off-axis object produces images which have different angles of eccentricity in the two eyes. To make an accurate binocular saccade to such an object from the straight-ahead position, the two eyes must move through unequal angles, thus disobeying Hering's law of equal innervation. People who wear spectacles to correct for refractive anisometropia develop compensatory asymmetries in saccadic eye movements (Erkelens et al. 1989c; Lemij and Collewijn 1991a). Monkeys show the same adaptive response (Oohira and Zee 1992). Figure 10.22 shows a record of unequal saccades made by a

12-year old boy who had worn spectacles for 7 years to correct for an 11-dioptre myopia in one eye. The acquired saccadic asymmetry compensated for almost all the optical aniseikonia. After 3 months of wearing corrective contact lenses, which do not produce aniseikonia, the saccadic eye movements became almost completely equal in size (Oohira et al. 1991).

Even short periods of exposure to aniseikonia can produce appropriate changes in relative saccadic amplitudes in the two eyes. For instance, Lemij and Collewijn (1991b) found that after only 1 hour of adaptation to a 2-dioptre lens in front of one eye, the amplitudes of saccades in the two eyes differed by the amount required for accurate binocular acquisition of eccentric targets along the horizontal and vertical meridians. More powerful lenses caused larger adaptive effects up to a limit of 6 dioptres. Six hours of adaptation to 6-dioptre lens, which caused one image to be magnified 12 per cent, produced appropriate saccadic asymmetries. Bush et al. (1993) projected random-dot patterns to the two eyes with an 8 per cent difference in size. Saccades to a superimposed target shown to one eye immediately produced saccades of unequal magnitude of between 4 and 7.5 per cent. This suggests that disparity can signal unequal saccades without a period of adaptation or learning. It was mentioned earlier that adaptation of conjugate saccades to imposed dysmetria is specific to the visual meridian along which training occurred. Nonconjugate saccadic adaptation to anisometropia has also been found to be directionally specific, at least with respect to the main orthogonal and oblique directions within which anisometric training was applied (Lemij and Collewijn 1992).

Adaptation of pursuit to aniseikonia

The above studies involved the adaptation of the saccadic system to optically induced aniseikonia. Schor et al. (1990) enquired whether aniseikonia also induces unequal voluntary pursuit in the two eyes and, if so, whether adaptations of the saccadic and pursuit systems are independent. In the pursuit condition, subjects maintained vergence on a pair of horizontal dichoptic lines as the lines moved up and down at 10°/s through an amplitude of 20°, giving a frequency of 0.25 Hz, over a period of 2 hours. In the saccade condition, subjects followed step displacements of the same horizontal lines, which occurred every half-second for 2 hours. In both cases, horizontal vergence was maintained on a fixed vertical line as the eyes followed the vertically moving target. The image in one eye was magnified 10 per cent so that the horizontal line in one eye moved further

than that in the other. The training produced a 7.3 per cent asymmetry of pursuit amplitude between the two eyes but only about 1 per cent of saccadic asymmetry. Saccadic training produced a 6 per cent asymmetry of saccadic amplitude but only about 2.5 per cent of pursuit asymmetry. In other words, the adaptation effects were largely specific to the type of eye movement used in training. No adaptation occurred when visual error feedback was withheld during and just after each eye movement.

10.6.4 Oculomotor adaptation to monocular paresis

An adaptive response of the saccadic and voluntary pursuit systems occurs when one eye is partially paralyzed (paretic) (Optican et al. 1985). In one study, a man with sudden onset of paralysis of the left abducens nerve developed saccadic undershooting of desired targets (hypometria) in his left eye; his other eye happened to be strabismic. Saccadic accuracy (orthometria) recovered after a while, but lapsed when the paretic eye was patched (Kommerell et al. 1976). A similar recovery of saccadic orthometria was reported in a patient with sudden onset of right third-nerve palsy. During the 6-day recovery period, the left eye was patched (Abel et al. 1978). Experimentally induced paresis in the horizontal recti of monkeys causes the affected eye to be hypometric. With the good eye patched for 6 days, the paretic eyes of monkeys regained orthometria but became hypometric again when the patch was switched (Optican and Robinson 1980). This capacity to recover from the effects of paresis seems to depend on the integrity of the cerebellum, since lesions of the cerebellum induced permanent saccadic hypermetria (Optican 1982).

In these studies of saccadic adaptation to monocular paresis, the normal eye was kept patched during the recovery period, and whatever adaptation occurred for the viewing eye was also found in the patched eye. In other words, the adaptation was conjugate. The visual system apparently treats both eyes alike if there is no visual information to indicate that they should be treated differentially. The first indication that the saccadic system can adapt to paresis differentially in the two eyes was provided by Snow et al. (1985). They weakened the tendon insertions of the medial and lateral recti in one eye of six monkeys, causing saccades for this eye to be hypometric to a greater or lesser extent. After 30 days of binocular viewing, the ratio of saccadic amplitudes in the two eyes returned to normal in all the animals, although recovery was faster in those animals with less initial hypometria. After recovery of balance in the amplitudes of saccades, saccadic

durations were longer and peak velocities smaller in both eyes. Furthermore, when the recovered operated eye was patched, its hypometria returned. It was concluded from these two facts that recovery of saccadic balance depends on changes in neural control and not merely on recovery of strength in the operated eye. Viirre et al. (1988) disturbed the normal balance of saccades in monkeys by recession (surgical reinsertion) of one of the rectus muscles in one eye. After a period of binocular viewing, the deviation of the operated eye disappeared and saccades in both eyes became orthometric. This adaptation did not occur in all the animals tested.

The experiments described in this and the previous section demonstrate that, as long as there is appropriate visual feedback, the saccadic system can compensate for aniseikonia or for an unbalanced muscular system by changing the balance of innervations to the two eyes. Binocular visual inputs also seem to be required just for the regular maintenance of binocular coordination of saccades, since simply patching one eye in normal monkeys for 6 days produced hypermetria and postsaccadic drift in that eye, which rapidly cleared up when both eyes were open (Vilis et al. 1985; Viirre et al. 1987).

The key to understanding unequal saccades in asymmetrical vergence may lie in the way people adapt the saccadic system to naturally occurring disparities in the visual field. None of the investigators mentioned that the images in the two eyes have a built-in pattern of aniseikonia. It can be seen in Figure 10.10, for instance, that the angle of both azimuth and of elevation through which the right eye must move from a midline point *O* to acquire the visual target *P* in the upper righthand quadrant of the headcentric visual field is larger than that through which the left eye must move. Saccadic asymmetry varies as a function of the position of the target in the visual field and the distance from the observer of the plane containing the visual targets. *An experiment is needed to discover whether saccades have the required asymmetry. If they do, it means that saccadic adaptations to induced aniseikonia and the presence of asymmetrical saccades in asymmetrical vergence are natural extensions of the same mechanism.*

10.6.5 Vergence and the gain of the VOR

When a person is rotated in the dark, the eyes execute the rhythmic, conjugate, reflex movement known as the vestibuloocular response (VOR). Movements in the opposite direction to the head at about the same velocity (the slow phases) alternate with rapid return movements (the quick phases). The stimuli for VOR arise in the semicircular canals

of the vestibular system, and the response can be elicited in a horizontal or vertical direction or about the visual axis (torsional nystagmus), depending on which pair of canals is in the plane of body rotation. The VOR is present in neonates and is basically under the control of centres in the vestibular nucleus and cerebellum (see Howard 1986 for a review). The VOR occurs in the dark but usually occurs when the eyes are open when it is supplemented by optokinetic nystagmus (OKN) evoked by relative motion of the visual scene (see Section 12.5.6). In addition a vestibuloocular response is evoked by linear motion of the body in the dark (Baloh et al. 1988). This is referred to as **linear VOR**. The stimulus in this case arises in the utricles and saccules—vestibular organs sensitive to linear acceleration. This response is also supplemented by OKN. The VOR and OKN responses stabilize the retinal image of stationary surroundings as the head rotates or translates.

Linear VOR and viewing distance

Image stability is perfect when the slow phases of compensatory eye movements have the same velocity relative to the head as the angular motion of the surroundings relative to the head. With linear self-motion, the angular velocity of the compensatory eye movements required for image stability is zero for viewing at infinity because the images of objects at infinity do not move relative to the head. For perfect image stability at viewing distance *D*, the angular eye velocity, θ , for a linear displacement (*L*) of the head is given by $\theta = \tan^{-1} L/D$. With eyes open, any inadequacy in the linear VOR could be compensated by OKN, which is naturally scaled for viewing distance because the angular velocity of the stationary scene relative to the head, which provides the drive to OKN, is inversely related to viewing distance. Paige (1989) found that eye velocity increased as the visual stimulus was brought nearer, but not rapidly enough to compensate for the reduction in distance. The scaling of linear VOR could be achieved in the dark if the response was coupled to the vergence state of the eyes. Several procedures have been used to reveal whether linear VOR is intrinsically scaled for viewing distance without the help of the optokinetic system. One procedure is to use imaginary visual targets. Gresty et al. (1987) found that the velocity of the VOR in the dark increased when a linear component was added to a rotation of the head about a vertical axis, and increased still further when subjects imagined that they were looking at a near visual object.

Another procedure is to observe the response under conditions where visual inputs cannot operate. Viirre et al. (1986) found that in the monkey the

velocity of eye movements increased as the linear component of the head motion was increased and as the distance of a stationary visual target was decreased. They concluded that this modulation of linear VOR is not visually mediated because it occurred in the first 20 ms of the start of head movement, which is below the latency of OKN, and at frequencies of head rotation beyond the range of OKN. Presumably, the distance of the visual target was assessed before the start of the head motion.

A third procedure for measuring linear VOR without intrusion of OKN is to record the initial response after the visual target has been switched off. Schwarz et al. (1989) measured the velocity of linear VOR in monkeys in response to linear sideways acceleration of the body during the initial period in the dark after the monkeys had fixated for some time on an LED at one of several distances between 6 and 150 cm. The velocity of linear VOR was inversely proportional to viewing distance. At the longest distance the mean gain (the ratio of eye velocity to eye velocity required for image stability) was 1.5 but fell to 0.7 at the nearest distance. The velocity of OKN evoked by linear motion of a textured display past the stationary animal was also inversely related to the distance of the display, but the gain of OKN remained constant. It was suggested that the increase in the velocity of linear VOR with near viewing helps offset the saturation of OKN with increasing velocity.

It seems from this evidence that the linear VOR is inversely scaled for viewing distance even without help from optokinetic nystagmus. The scaling could arise from visual cues to distance seen before the movement starts or from the state of vergence during the movement. Paige (1991) asked human subjects to fixate visual targets at various distances while they oscillated their bodies up and down. The gain of vertical VOR continued to be related to viewing distance for some time after the target was switched off. The coupling between VOR gain and viewing distance was affected when subjects viewed the visual targets through prisms which increased the required vergence, but not when they viewed the targets through lenses which changed the required accommodation.

Rotary VOR and viewing distance

The velocity of eye movements required to stabilize the image of a stationary object when the head rotates about the midbody axis varies inversely with viewing distance. This is because the eyes undergo a translatory motion when the head rotates. The translatory motion is due to the offset of the eyes from the axis of head rotation. For a head rotation of θ , the

rotation of an eye, ϕ , required to stabilize the image of a stationary object at distance D is

$$\phi = \theta + \tan^{-1} \frac{d \sin \theta}{D} \quad (4)$$

where d is the distance from the axis of head rotation to the centre of rotation of the eye. For a distant object the effects of translation are negligible, but for an object at the near point, the velocity of eye movements required for image stability is about double that required at infinity. Thus, the gain of the VOR (eye velocity divided by head velocity) required for image stability increases from 1 at infinity to 2 for near vision. This scaling of the gain of the VOR with distance could be achieved if the VOR were supplemented by OKN. But this could happen only in illuminated surroundings. The scaling could be achieved in the dark if VOR were linked to vergence.

Biguer and Prablanc (1981) measured the gain of the VOR during coordinated movements of the eyes and head to an eccentric visual target. When the target was near, the VOR component of the eye movement had a higher gain than when the target was far. This was still true when the target was switched off just before the head started to move, showing that visual error signals during the movement are not necessary for modulation of VOR gain. Biguer and Prablanc concluded that the modulation depends on visual distance cues seen before the movement started. Hine and Thorn (1987) measured the gain of the VOR while subjects rotated the head from side to side through 30° and converged on an LED at various distances. The gain of VOR was modulated by distance according to theoretical predictions when the target was visible. The modulation continued, but less adequately, after the target was extinguished. VOR gain was not affected by lenses which changed accommodation but was affected by prisms which changed vergence. They concluded that vergence can provide the signal for modulation of VOR.

Snyder et al. (1992) rotated monkeys at velocities between 30 and 500°/s for 40 ms at various times just before or during vergence eye movements between targets at different distances. The gain of VOR increased linearly with increasing vergence angle. The latency of the VOR was shorter than the latency of vergence, and the VOR showed evidence of modulation of gain appropriate to the visual target on which the gaze was not yet directed. This suggests that the signal for modulation of VOR is derived from the central motor command related to the shift of attention to the new vergence target rather than from proprioceptive feedback from the extraocular muscles.

10.7 CYCLOVERGENCE

10.7.1 Types of torsional response

Conjunctive torsion of the two eyes is known as **cycloversion**. Cycloversion occurs under the following circumstances. (1) Nystagmic cycloversional movements of the eyes are evoked by rotating a frontal plane display around the fixation point (Brecher 1934; Cheung and Howard 1991). This is optokinetic cycloversion. (2) A small cycloversional displacement of the eyes is evoked by visually inspecting a large stationary display of lines tilted from the vertical in the frontal plane (Goodenough et al. 1979). (3) Vertical vergence induced by vertical disparity is accompanied by cycloversion. Left-over-right vertical vergence evokes a top-to-left cycloversion and vice versa (Enright 1992; van Rijn and Collewijn 1994). (4) Rotation of the head about the roll axis in the dark induces cycloversion in the opposite direction with a velocity gain of about 0.6 up to a limiting amplitude of about 8° (Collewijn et al. 1985; Ferman et al. 1987b). This counterrolling response is evoked by stimulation of the vestibular system. When the head is tilted with eyes open the optokinetic and vestibular signals combine to increase the velocity gain of counterrolling to about 0.7 (Leigh et al. 1989).

Disjunctive torsion, or **cyclovergence**, is evoked by cyclodisparities in the images in the two eyes (Kertesz and Sullivan 1978) and as a component of horizontal vergence (Allen and Carter 1967) and vertical vergence (Enright 1992b). **Cyclophoria** is a torsional misalignment of the eyes in the absence of cyclofusional stimuli. Although normally torsion is neither produced nor inhibited by voluntary effort, it can be evoked voluntarily after an extended period of practice (Balliet and Nakayama 1978).

The terminology for torsion has been confused and the following definitions are used here. **Cyclorotation** refers to the rotation of a visual object or its retinal image about the visual axis of an eye with respect to head coordinates. It is signed positive if the top of the object rotates toward the median plane of the head (incyclorotation) and negative if it rotates in the other direction (excyclorotation). A common rotation of two dichoptic stimuli or their images is conjunctive cyclorotation, and any difference in their rotations is disjunctive cyclorotation. The term **declination** refers to the total signed angle of disjunctive cyclorotation of a pair of dichoptic stimuli or of their retinal images (Ogle and Ellerbrock 1946) and the term **inclination** refers to the slant in depth of an object about a horizontal axis with respect to the vertical, signed positive top away. If a is the interpupillary distance and d the

observation distance, then a line with an inclination i projects as a pair of retinal images with a declination angle θ . It was shown in Section 2.7 that the angle of declination is related to the angle of inclination by the following expression:

$$\tan \frac{\theta}{2} = \frac{a \tan i}{2d} \quad (5)$$

For small values of θ

$$\theta = \frac{a \tan i}{d} \text{ or } i = \tan^{-1} \frac{\theta d}{a} \text{ in radians}$$

The **cyclodisparity** of a specified pair of dichoptic images is their relative orientation in retinal coordinates, designated positive or negative according to whether the images are rotated top toward or top away from each other. Two dichoptic images have zero cyclodisparity if they appear parallel. If, in addition, they lie on corresponding vertical retinal meridians, they also have zero horizontal disparity.

Cycloduction is the torsional state of a single eye indicated by the dihedral angle between the median plane of the head and the plane containing a specified meridian of the eye and the visual axis. The usual reference meridian is the normally vertical meridian as indicated by selected landmarks on the eyeball or the afterimage of a vertical line. Cycloduction is designated incycloduction or excycloduction, depending on whether the eye is rotated top toward or top away from the median plane. Cycloversion is the equal component of the eyes' cycloductions; levocycloversion when the eyes rotate top to the subject's left and dextrocycloversion when they rotate top to the subject's right.

Cyclovergence is the difference between the eyes' cycloductions, designated incyclovergence or exocy clovergence depending on whether there is a top-in or top-out relative rotation. Cyclovergence is zero when two horizontal nonius lines on opposite radii of a dichoptic display in the frontal plane appear parallel. It is best to use horizontal rather than vertical nonius lines as reference because, under normal circumstances, corresponding horizontal meridians are parallel while corresponding vertical meridians have a positive declination of about 2° (Helmholtz 1909, vol. 3, p. 408). The declination of vertical corresponding meridians causes the vertical horopter (the locus of points in space that stimulate corresponding vertical retinal meridians) to be inclined, top away, out of the frontal plane by an amount that varies with viewing distance (see Section 2.7). The inclination of the vertical horopter may also be affected by cyclovergence that

accompanies a change in horizontal vergence (Amigo 1974). It follows from these definitions that, for horizontal lines, cyclodisparity equals disjunctive cyclorotation minus cyclovergence.

Various investigators over the last 100 years, including Hering (see Ogle and Ellerbrock 1946), Verhoeff (1934), Kertesz (1972) and Krekling (1973a), denied that cyclovergence occurred and in almost all textbooks the response is not mentioned. In some cases investigators changed their minds when they used more effective stimuli, particularly stimuli subtending a visual angle in excess of 25° and containing many horizontal and vertical elements.

10.7.2 The measurement of cyclovergence

The following psychophysical methods have been used to measure cyclovergence in response to static cyclodisparities.

Setting a line or points in the median plane to vertical

In this method the observer rotates a test line in the median plane of the head until it appears vertical. The method is based on the assumption that a line seen binocularly appears vertical if and only if its images fall on corresponding vertical retinal meridians, and any error in the vertical setting is due to cyclovergence, according to formula (4). However, this assumption is faulty. The phenomena of slant contrast and normalization discussed in Section 12.1 demonstrate that a line does not necessarily appear vertical when its images fall on corresponding meridians. Also, the slanting-line method gives different results depending on whether or not a reference plane was provided in the form of a circle round the test line (Harker 1960). Another problem with the method is that a slanted line is a stimulus for cyclovergence and may therefore contaminate the results. This problem is at least partially overcome by presenting the test stimulus briefly, after the stimulus for cyclovergence has been removed. Ellerbrock (1954) further minimized the effect of the test stimulus by setting two points rather than a line into the apparent frontal plane. Amigo (1974) used a similar procedure to investigate the vertical horopter. Hampton and Kertesz (1982) compared the settings of a sequentially presented test line with an objective measure of cyclovergence and showed that even with this precaution the perceived slant of the test line was less than that corresponding to the residual cyclodisparity in the line and therefore did not indicate the degree of cyclotorsion. A sequential test stimulus may overcome one problem, but does not overcome the problems of slant contrast and normalization.

Nulling cyclodisparity in dichoptic stimuli

In one form of this method dichoptic lines are rotated in opposite directions in the frontal plane until the images fuse into one, or appear collinear. This method was first used by Meissner in about 1854 (Le Conte 1881) and was also used by Volkmann (see Helmholtz 1909). Cogan (1979) pointed out that this measure of cyclovergence does not agree with that based on judgments of apparent vertical, since a line does not necessarily appear vertical when the images in the two eyes appear collinear. His experimental results revealed that, on average, a line was set within 3° of true vertical in the median plane whereas two dichoptic images in the frontal plane, one red and one green, had to be incyclorotated by an amount corresponding to an inclination of 31° to fuse into a single image. Although setting two dichoptic images into collinearity may be the better procedure, it has its own problems. Superimposed dichoptic images tend to exhibit binocular rivalry and it is difficult to detect cyclodisparity once the images lie within Panum's fusional area. Here, too, a slanted line is a stimulus for cyclovergence and may therefore contaminate the results.

The nonius method

In the nonius method cyclovergence is indicated by the angle through which a horizontal line presented to one side of the fixation point in one eye has to be rotated to appear parallel to a horizontal line presented in the opposite field of the other eye. Horizontal and vertical vergence are held steady by a binocular circle surrounding the lines. This stimulus display is known as Volkmann discs. This method is the torsional equivalent of nonius methods used to measure horizontal and vertical vergence. Hofmann and Bielschowsky (1900) were the first to use this procedure systematically. With it they recorded cyclovergence of about 5°, induced by disjunctive cyclorotation of a dichoptic textured display through 8°. Verhoeff (1934) also used a nonius method and found cyclovergence to be a slow response with magnitudes of up to 6° induced by an 8° disjunctive cyclorotation of textured patterns. He also found that a greater amplitude of cyclovergence is induced by textured patterns than by simple line patterns, and more by cyclorotation of horizontal lines than of vertical lines. Hermans (1943) used a nonius method to determine the position of the vertical horopter. Although subject to artifacts, the nonius method is the only satisfactory psychophysical method for measuring cyclovergence.

Howard et al. (1993) superimposed a pair of nonius lines on the centre of a 75° dichoptic textured display, (see Figure 10.23.) The two images had a

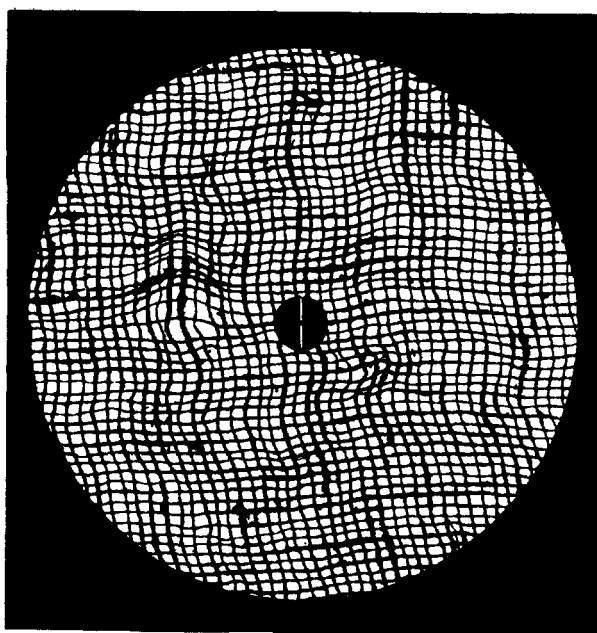


Figure 10.23. Objective and nonius cyclovergence.
A dichoptic textured display subtending 75° was disjunctively cyclorotated through 12° at various frequencies. Cyclovergence was measured objectively and by aligning nonius lines at the centre. (From Howard 1992.)

static cyclorotation of 12° or were rotated sinusoidally in antiphase through an amplitude of 12°, at frequencies between 0.05 and 2 Hz. Subject nulled the apparent offset of the nonius lines in the static disparity condition and nulled their rocking motion in the dynamic conditions. Results shown in Figure 10.24 reveal that, for static cyclodisparity, the nonius setting was slightly higher than the magnitude of the cyclovergence measured objectively, using scleral coils, as described later. When the display rotated back and forth, the nonius lines appeared to rock through a greater amplitude than predicted from the magnitude of cyclovergence. With one eye closed, the nonius line appeared to move in a direction opposite to that of the rotating surround. This is the well-known phenomenon of induced visual motion. When both eyes were open, the two monocularly induced motion effects combined with the effects of cyclovergence to create the large apparent rocking motion of the nonius lines. Thus, the nonius method is a reasonably valid measure of cyclovergence, but only for static or slowly changing disparities.

Objective recording of cyclovergence

Methods for recording eye movements, such as the corneal reflex method, electrooculography, and the use of Purkinje images, do not record eye torsion. Methods that rely on photographing the iris or episcleral blood vessels do not provide a continuous

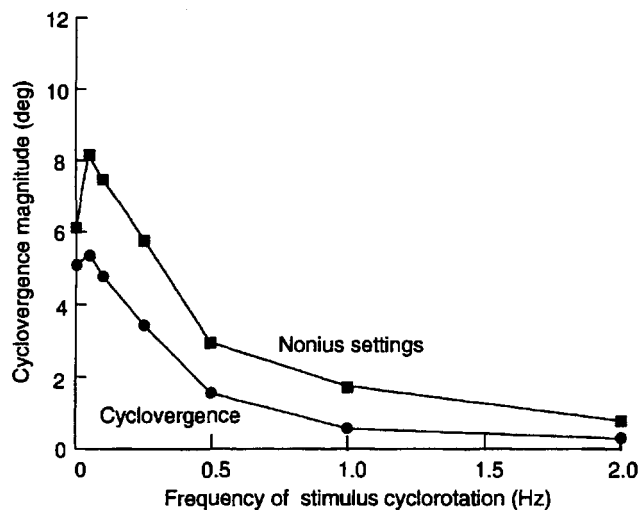


Figure 10.24. Measures of cyclovergence.
Objectively measured cyclovergence and nonius-line settings as a function of the frequency of cyclorotation of the dichoptic display shown in Figure 10.23. Mean data from three subjects. (Adapted from Howard et al. 1992.)

record of torsion. The photographs must be analyzed frame by frame or subjected to optical autocorrelation procedures (Howard and Evans 1963). Kertesz (1972) used the photographic method but failed to find cyclovergence. It is now known that his stimulus was too small. Crone and Everhard-Halm (1975) and Hooton et al. (1979) used the photographic procedure with a more adequate stimulus and obtained clear evidence of cyclovergence.

A scleral search coil mounted on an annular contact lens has been developed (Collewijn et al. 1985), and is available from Skalar Medical in Delft. When the coil is placed on an eye within an oscillating magnetic field, a voltage proportional to the sine of the torsional position of the eye is generated (Robinson 1963; Collewijn et al. 1975; Ferman et al. 1987b). With this method one obtains a low-noise signal that continuously registers the torsional position of an eye to within a few minutes of arc. The only drawback of the method is that the contact lenses can be worn for only about 30 minutes at one time. Kertesz and Sullivan (1978) used the scleral-coil procedure and obtained a cyclovergence response of 3.5° to a ±5° step of cyclodisparity in dichoptically presented patterned displays subtending 50°.

10.7.3 The dynamics of cyclovergence

Howard and Zacher (1991) used scleral search coils to measure the gain and phase lag of cyclovergence as a function of the frequency and amplitude of disjunctive cyclorotation of the 75° dichoptic textured display shown in Figure 10.24. This stimulus was chosen because it contains a broad range of

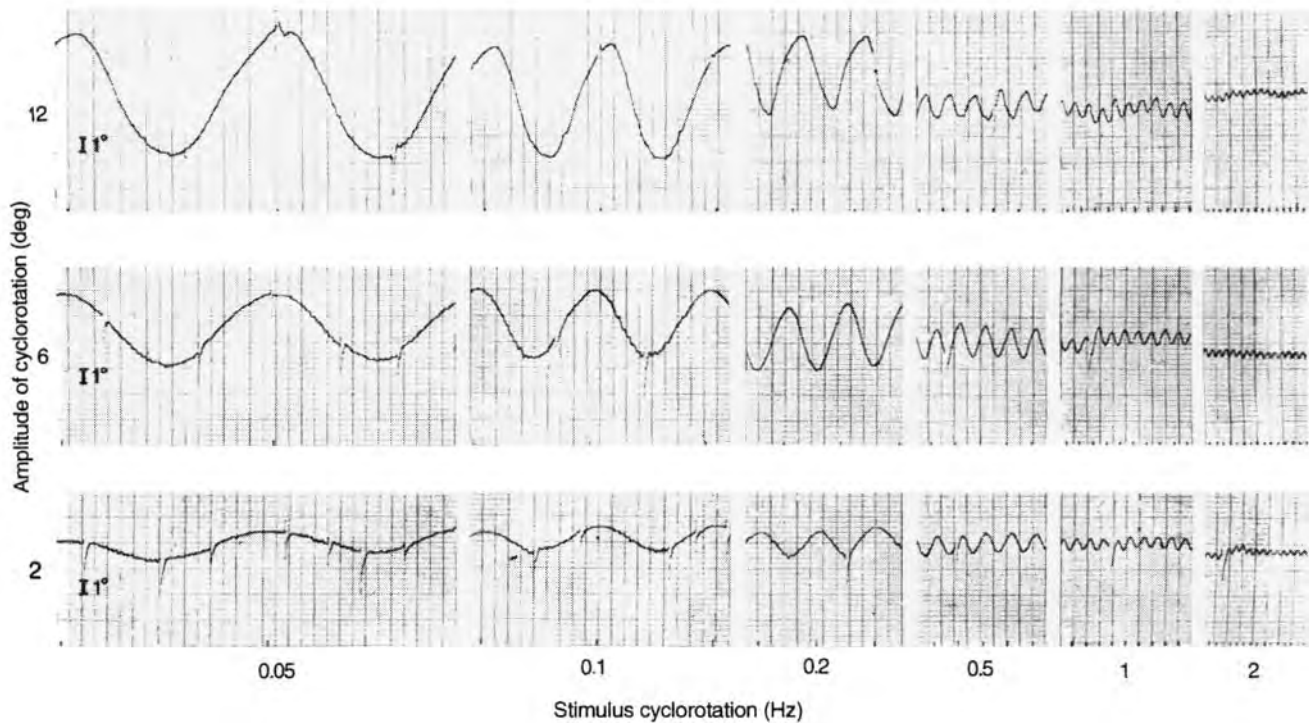


Figure 10.25. Chart recordings of cyclovergence.

Cylorvergence responses for different frequencies and amplitudes of disjunctive cyclorotation of the stimulus shown in Figure 10.24. The traces represent the difference between the opposed cyclorotations of the two eyes. The sharp impulses are blinks. (From Howard and Zacher 1991. Reprinted with permission of Springer-Verlag, Heidelberg.)

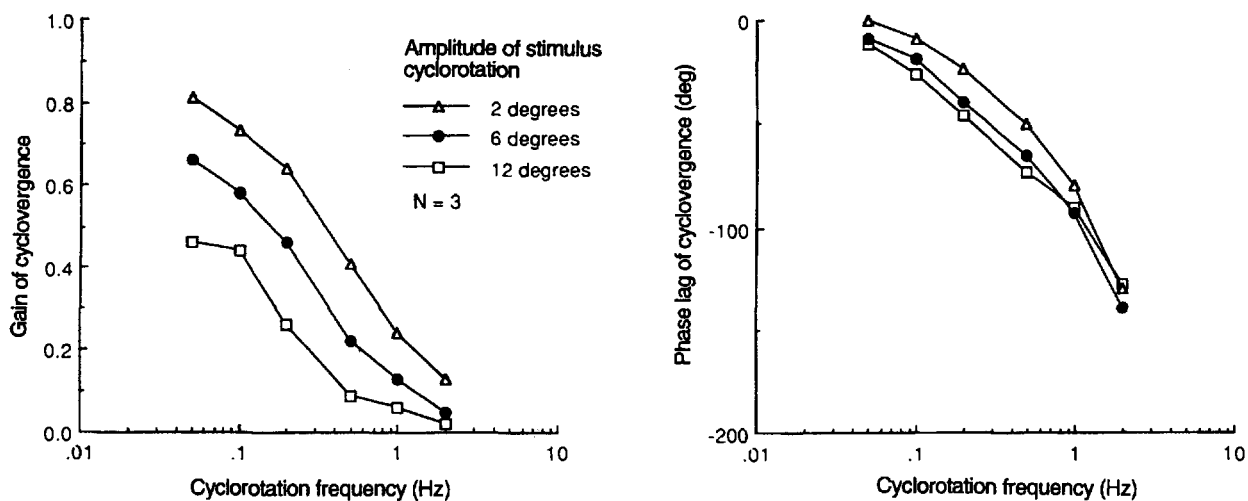


Figure 10.26. Gain and phase lag of cyclovergence.

Gain and phase lag of cyclovergence as a function of frequency of cyclorotation for three amplitudes of cyclorotation. Each curve is derived from the data of three subjects. (From Howard and Zacher 1991. Reprinted with permission of Springer-Verlag, Heidelberg.)

spatial frequencies, has both vertical and horizontal elements to act as cyclofusional stimuli and is a good stimulus for keeping horizontal and vertical vergence constant. A regular grid pattern is not suitable because the eyes tend to misconverge on such stimuli. Since the display was circular and the

surroundings black, there were no stationary lines to provide a cyclofusional anchor. The dichoptic displays were rotated in counterphase about the fixation point to give peak-to-peak amplitudes of disjunctive cyclorotation of 2, 6, or 12°, at frequencies of from 0.05 to 2 Hz. The gain of cyclovergence was

defined as the mean peak-to-peak amplitude of cyclovergence divided by the peak-to-peak amplitude of disjunctive cyclorotation of the stimulus. A set of recordings of cyclovergence from one subject is shown in Figure 10.25. It can be seen in Figure 10.26a that the gain of the response declined with increasing stimulus frequency. Figure 10.26b shows that phase lag was imperceptible at a frequency of 0.05 Hz, and increased with increasing frequency of cyclorotation, reaching values of over 100° at a frequency of 2 Hz.

The main feature of cyclovergence is that it is designed to cope with cyclorotations of low frequency and amplitude, as indicated by the fact that the mean gain is highest and the associated phase lag lowest at a cyclorotation frequency of 0.05 Hz and amplitude of 1°. For one young adult, the gain of cyclovergence reached 0.91 at this frequency and amplitude. Van Rijn et al. (1992) obtained a gain of only 0.2, but they used only one frequency of stimulus rotation of 0.2 Hz and a stimulus diameter of only 28°. In a recent paper they obtained a mean gain of over 0.4 when they used a 48°-wide display oscillating at 0.15 Hz (van Rijn et al. 1994a). We will see in the next section that the gain of cyclovergence declines rapidly as stimulus area is reduced.

The dependence of cyclovergence gain on the amplitude of cyclorotation demonstrates that the cyclovergence system is nonlinear, because the gain of a linear system is independent of stimulus amplitude for a given frequency. The function relating gain in decibels to frequency for a stimulus amplitude of 6°, has a slope of 20 db/decade for the five highest frequencies (gain in decibels is 20 times the log of response amplitude divided by the log of stimulus amplitude). This is the value one would expect of a first-order system. However, the phase lag at the corner frequency corresponding to a gain of -3 db was much smaller than expected from a first-order or a second-order system.

The high gain and low phase lag for low stimulus frequencies and small amplitudes is what one would expect of a system designed to correct for slight rotary misalignments of binocular images produced by cyclophoria or by torsional drifts of the eyes that occur as the gaze moves over a three-dimensional scene. Cyclovergence does not have to deal with rapid external events. Disjunctive cyclorotations of the distal visual stimulus as a whole occur only under very special circumstances as, for instance, when one observes an isolated vertical line changing its inclination. Under normal circumstances, orientation disparities produced by inclined lines or surfaces, occur in the context of other objects which are either upright or inclined in another way.

Spontaneous variation in cyclovergence during fixation has been found to have a standard deviation of about 0.2°, which is higher than the standard deviation of between 6 and 8 arcmin for conjugate horizontal and vertical movements of the eyes during fixation (Ferman et al. 1987b; Ott et al. 1992). Spontaneous changes in cyclovergence had a standard deviation of about 6 arcmin with fixation on an isolated point in the dark and only about half this value when a textured background was present (Enright 1990; van Rijn et al. 1994a).

10.7.4 The stimulus for cyclovergence

An orientation disparity between the images of lines in the horizontal plane of regard can be due only to eye misalignment, whereas an orientation disparity from a vertical line may be due to inclination of the line in depth. It would therefore be adaptive if cyclovergence were evoked only by disparities in horizontal elements, leaving residual disparities in vertical elements intact as cues for inclination. This strategy prevents diplopia in horizontals and reduces useful disparities to their lowest amplitudes where disparity gradients are most effectively detected.

Ogle and Ellerbrock (1946) claimed that more cyclovergence is evoked by cyclorotated verticals than by cyclorotated horizontals. However, they measured cyclovergence by setting a line to the vertical, which we have already seen is subject to artifacts. The more reliable nonius method revealed cyclorotation of horizontals is the more effective stimulus (Nagel 1868; Verhoeff 1934; Crone and Everhard-Halm 1975). Rogers and Howard (1991) used scleral search coils to measure the gain of cyclovergence to 80° diameter textured patterns which were subjected to either (1) an equal and opposite rotation between the two eyes, or (2) an equal and opposite vertical shear, or (3) an equal and opposite horizontal shear, or (4) an equal and opposite deformation. The vertically shearing patterns created cyclodisparities along the horizontal meridians but not along vertical meridians and the horizontally shearing patterns created the opposite pattern of cyclodisparities.

Figure 10.27 shows the eye movement records for one subject for patterns subjected to an equal and opposite rotation. The difference between the left and right eyes' torsional signals (third trace) shows a gain of over 90 per cent for a densely textured pattern oscillating at a frequency of 0.1 Hz. The difference signal is reproduced in Figure 10.28a together with the difference signals for shearing and deforming patterns. The gain of cyclovergence for a vertical shearing pattern (Figure 10.28b), which created the same magnitude of cyclodisparities along horizontal

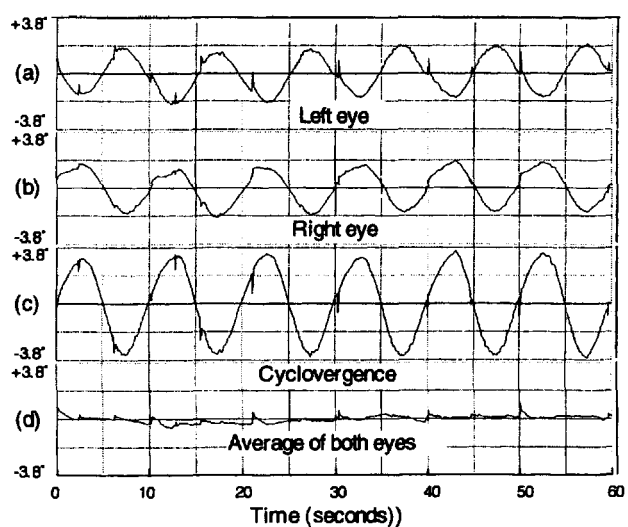


Figure 10.27. Cyclovergence to counter-rotating patterns.

Records of torsional movements of the left eye (a) and right eye (b) evoked by identical textured 80° patterns which rotated in opposite directions in the two eyes through $\pm 1.9^\circ$ at a frequency of 0.1 Hz. The difference signal (c) shows that the gain of cyclovergence for this subject was over 90 per cent. The mean signal (d) shows no trace of cycloversion. (Adapted from Rogers 1992.)

meridians, was only slightly lower even though there were no cyclodisparities along vertical meridians. In contrast, the gain of cyclovergence for a horizontally shearing pattern (Figure 10.28c) was negligible. Figure 10.28d shows a gain of over 60 per cent to a deforming pattern which created the same magnitude and direction of cyclodisparities along horizontal meridians as the rotating pattern but the opposite direction of cyclodisparities along vertical meridians. Seen together, these results provide convincing evidence that cyclovergence is driven primarily by vertical disparities along the horizontal meridians and minimally by horizontal disparities along the vertical meridians. This means that any residual horizontal disparities of elements along vertical meridians are more likely to be due to the inclination of surfaces in the visual scene rather than a state of torsional misalignment of the eyes (Rogers 1992). Figure 10.29 shows that the gain of cyclovergence is much higher in response to vertical shear disparity than to horizontal shear disparity over a range of frequencies of cycolorotation of the stimuli. This result was confirmed by van Rijn et al. (1994b).

Frisby et al. (1993) questioned whether the greater effectiveness of vertical disparities along the horizontal meridians in driving cyclovergence is true when real rather than stereoscopic surfaces are used. They measured cyclovergence using vertical nonius lines while the subject viewed an steeply inclined surface. Differences in the orientation of the nonius lines occurred which were equivalent to 50 per cent

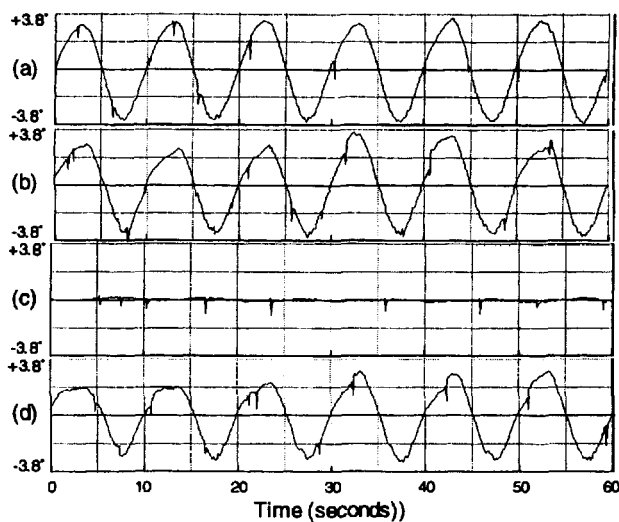


Figure 10.28. Cyclovergence to shearing and rotating patterns.
Cyclovergence recorded using scleral coils. Trace (a) shows the response to counter-rotating patterns, as illustrated in Figure 10.27c., in which the gain of cyclovergence is over 90 per cent. The gain of the response to patterns which sheared vertically (b) is over 80 per cent while that to horizontally shearing patterns (c) is negligible. The gain of cyclovergence to deforming patterns (d) is over 65 per cent. (Redrawn from Rogers 1992.)

of the orientation disparities created by the inclined surface. Since an inclined surface does not create a net cyclodisparity along horizontal meridians, it ought not to evoke cyclovergence, according to the results of Rogers and Howard and van Rijn et al.

Bradshaw and Rogers (1994) repeated the experiment of Frisby et al. using both 20 and 80° surfaces which changed their inclination at 0.1 Hz. They monitored cyclovergence objectively using scleral search coils and with vertical and horizontal nonius lines. The results for one observer in Figure 10.30 show no significant cyclovergence and provide additional evidence that cyclovergence is not driven by horizontal disparities along vertical meridians even when these are created by a real inclined surface.

Bradshaw and Rogers found no misalignment of nonius lines when they were oriented horizontally, as would be expected if the eyes do not change their cyclovergence to an inclined surface, but they did find significant misalignments when the nonius lines were oriented vertically. They suggested that this result would be predicted if the nonius lines tended to be seen as part of the surface. An inclined line in the plane of a surface creates an orientation disparity between the eyes, but we do not see the orientation difference, only its inclination in depth. If the top half of the line is seen by only one eye and the bottom half by the other and each halves is seen in the plane of the surface, the two lines will have an orientation difference—a nonius misalignment—even though they are seen as aligned on the surface.

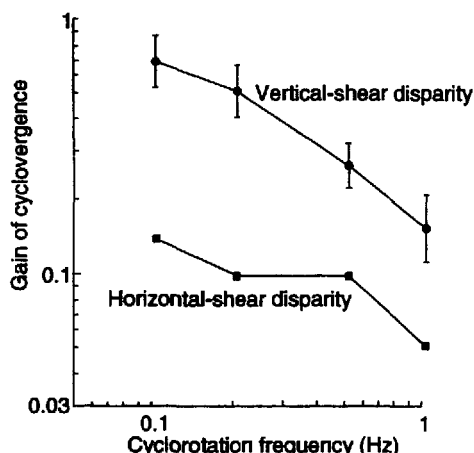


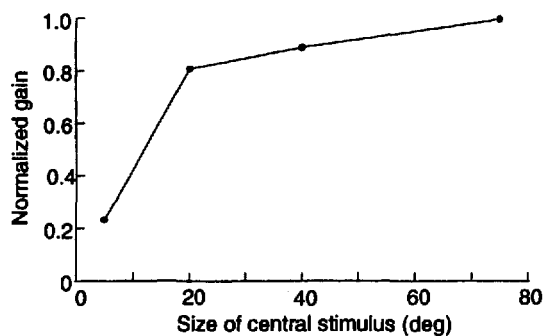
Figure 10.29. Cyclovergence anisotropy.

Gain of cyclovergence as a function of the frequency of disjunctive cyclorotation of vertical lines and of horizontal lines. Mean of four subjects. (From Rogers and Howard 1991.)

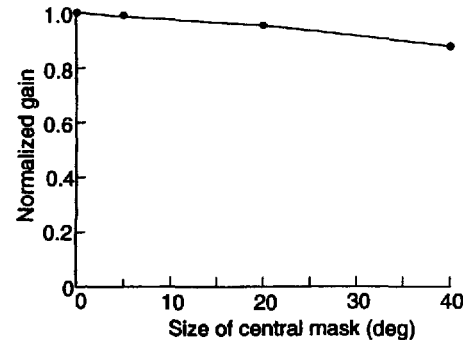
If this explanation is correct, the misalignment of the vertical nonius lines reported by Frisby et al. to inclined surfaces may be an artifact of the nonius method when vertical nonius lines are surrounded by an inclined surface, rather than evidence for cyclovergence. Ono and Mapp (1994) have used a similar argument to suggest that nonius lines may not always be a reliable indicator of the vergence state of the eyes when the lines are seen to lie in the surrounding disparate surface.

Torsional misalignment of the eyes creates a horizontal gradient of vertical disparities between corresponding points along horizontal meridians. The largest vertical disparities are created by the most eccentric points which explains why the gain of cyclovergence is larger for larger cyclorotating patterns. Torsional misalignment also creates orientation disparities between horizontally oriented elements which are of the same magnitude at all eccentricities. These orientation disparities are a potential stimulus for driving cyclovergence.

DeBruyn et al. (1992) tested this possibility with a display consisting of dynamic, horizontally oriented random-noise gratings which were either correlated or uncorrelated between the two eyes. The gratings were cyclorotated at 0.1 Hz in opposite directions in the two eyes and torsional eye movements recorded objectively using scleral search coils. Correlated noise gratings which created both orientation disparities and a horizontal gradient of vertical disparities were an effective stimulus for driving cyclovergence but uncorrelated noise gratings produced no cyclovergence, even though the change in orientation of the bars could be clearly seen in either monocular image.



(a) Normalized gain of cyclovergence as a function of the diameter of a central display.



(b) Gain of cyclovergence as a function of the diameter of a central black occluder superimposed on the display.

Figure 10.30. Cyclovergence and display area.

The full stimulus subtended 75° and cyclorotated at 0.05 Hz. The gain for the largest display was 0.64. Mean results of four subjects. (Adapted from Howard and Sun 1994.)

Howard et al. (1994) used scleral search coils to measure the gain of cyclovergence as a function of the area and position of the stimulus. In one set of conditions, circular textured displays with diameters of 5, 20, 40, and 75° were used and in a second set of conditions, black discs occluded the central 5, 20, or 40° of the 75° display. Each display was cyclorotated through a peak-to-peak amplitude of 12° at 0.05 and 0.2 Hz. It can be seen from Figure 10.30a that a 5° display evoked weak cyclovergence, and the gain of the response improved as the diameter of the display increased from 20 to 75°. Kertesz and Sullivan (1978) also reported an increase in the gain of cyclovergence for one subject as the stimulus diameter was increased from 10° to 50°. On the other hand, it can be seen in Figure 10.30b that the gain of cyclovergence was not reduced when the central 40° of the stimulus was occluded. The gain of optokinetic torsional nystagmus induced by conjugate rotation of the display was severely reduced by occlusion of the central 40°, and previous studies have shown that the same is true of horizontal optokinetic nystagmus (Howard and Ohmi 1984).

One may conclude that cyclovergence requires a large stimulus, but this does not have to be in the

centre of the visual field. If cyclovergence is driven by point disparities, then this might explain the need for a large stimulus and the indifference to occlusion of the central retina, since point disparities in a display rotating about the visual axis increase linearly with stimulus eccentricity. If cyclovergence is driven by orientation disparity detectors, the preceding results demonstrate that it is driven only by those with large receptive fields. This makes sense since the only purpose of cyclovergence is to keep the images of the main horizontal features of the visual field orientationally aligned so that residual disparities in vertical elements can be used to code differential inclinations of particular objects, especially those in the centre of the visual field.

10.8 THE NEUROLOGY OF VERGENCE

The oculomotor nerves and nuclei

The three pairs of extraocular muscles are shown in Figure 10.31. They receive their innervation from three cranial nerves: the third (oculomotor), the fourth (trochlear nerve), and the sixth (abducens) nerve. Each nerve originates in a brainstem nucleus of the same name. The three nuclei are called the oculomotor nuclei, which is confusing because it is also the name of one of them. Each extraocular muscle has an outer **orbital layer** and an inner **global layer**. Each layer has two main types of muscle fibres. The first consists of singly innervated fibres each receiving one motor axon that ends in a cluster of neuromuscular junctions at a restricted locus on the nerve fibre (*en plaque* endings). These fibres are fast-acting. The second type consists of smaller, multiply innervated fibres with many neuromuscular junctions distributed over the whole length of the fibre (*en grappe* endings). These fibres are slow-acting but capable of maintaining constant states of tonic contraction. It is not known whether these multiple endings derive from one or several motor axons. The two types of muscle fibres form distinctive subtypes within both the orbital and global layers (see Spencer and Porter 1988; Porter and Baker 1992). Sensory cells in specialized muscle fibres (muscle spindles) and in Golgi tendon organs are innervated by afferent nerve fibres. There are also distinct types of efferent nerve fibres, some have a mean diameter of $2.5 \mu\text{m}$ and are unmyelinated and others have a mean diameter of about $9 \mu\text{m}$ and are myelinated (Alpern and Wolter 1956). Many of the smaller axons are either sensory or motor and innervate blood vessels.

In the oculomotor nuclei, cells projecting to the rectus muscles are segregated into three groups: A,

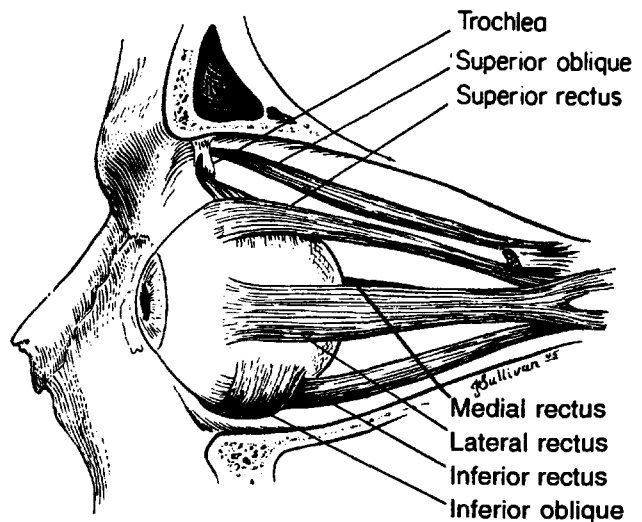


Figure 10.31. The extraocular muscles of the left eye.

(From Cogan 1956 *Neurology of the ocular muscles*, Courtesy of Charles C. Thomas, Publisher, Springfield, Illinois.)

B, and C. The cells in group C have smaller cell bodies and thinner axons than those in the other two groups and project to smaller and slower muscle fibres (Porter et al. 1983). It has been suggested that the small-diameter nerves innervating slow muscle fibres form a distinct pathway for vergence (Jampel 1967; Büttner-Ennever and Akert 1981). However, Keller and Robinson (1972) recorded the activity of cells in the abducens nucleus of the monkey and showed that no type of eye movement was the exclusive product of a particular set of oculomotor neurones. By their own admission, their electrode may have failed to record the activity of small cells exclusively devoted to vergence. We cannot be sure that integration of version and vergence signals is achieved in the oculomotor nuclei rather than involving distinct efferent fibres.

A disparity of about 4° generates the most rapid vergence movements, and vergence is evoked even by disparities of up to 9° . These are larger disparities than those to which cortical cells have so far been found to respond (see Section 4.4). Symmetrical vergence movements within the midsagittal plane are instigated by stimuli that project images to opposite cerebral hemispheres. Evidence reviewed in Section 4.3.2 suggests that the detection of large disparities between such images depends on interhemispheric connections routed through the corpus callosum. This idea is supported by the fact that a patient with section of the corpus callosum failed to produce vergence movements in response to targets in the visual midline but responded when the images were projected to the same hemisphere (Westheimer and Mitchell 1969). The importance of the callosal

pathway for the control of vergence is also indicated by the misalignment of the eyes in callossectomized cats (Payne et al. 1981).

The generation of signals for vergence

Conjugate horizontal pursuit movements require the simultaneous contraction of the lateral rectus muscle of one eye and the medial rectus muscle of the other. These movements are organized in the pons from where signals pass to the ipsilateral abducens nucleus. This nucleus contains lateral rectus motoneurones that innervate the ipsilateral lateral rectus muscle, and abducens internuclear neurones from which axons arise that cross the midline, ascend in the medial longitudinal fasciculus (MLF), and terminate in the medial rectus subdivision of the contralateral oculomotor nucleus. This internuclear circuit is specific to conjugate eye movements, since damage to the MLF creates a defect in conjugate movements while leaving vergence movements intact, a defect known clinically as internuclear ophthalmoplegia (Evinger et al. 1977).

Horizontal vergence eye movements require the simultaneous activation of either both medial recti or both lateral recti, and therefore require a different neural circuit. Until recently, nothing was known about the specific neural processes controlling vergence. Some earlier studies had failed to find cells in the oculomotor nuclei of the monkey that discharge only in association with vergence eye movements (Keller and Robinson 1972; Keller 1973). Mays and Porter (1984) agreed that most cells in the oculomotor nuclei of the monkey carry signals for both conjugate and disjunctive eye movements, although not all neurones participated equally in the two types of eye movement.

Schiller (1970) reported a few cells specifically related to vergence in the caudal region of the monkey's oculomotor nuclear complex. During vergence movements, medial rectus motoneurones in the oculomotor nucleus displayed signals related to both the position and the velocity of the eye, just as they do for conjugate eye movements (Gamlin and Mays 1992). Motoneurones of the superior oblique muscles in the trochlear oculomotor nucleus also discharge during vergence movements (Mays et al. 1991). Their discharge is presumably related to cyclovergence, which is known to accompany vergence.

In a more detailed study, Mays (1984) found that the firing rate of cells in the mesencephalic reticular formation of the monkey just dorsal and lateral to the oculomotor nuclei, was related to vergence angle in an approximately linear manner and was not affected by conjugate eye movements. These cells are

referred to as **vergence-angle cells**. Most of the cells increased their firing rate specifically during convergence and a few during divergence. Most of them responded during a change in vergence or during a change in accommodation, but some responded only to changes in vergence and some only to changes in accommodation (Zhang et al. 1992). Vergence-angle cells responded with monosynaptic latencies to antidromic stimulation of medial rectus motoneurones in the ipsilateral but not in the contralateral oculomotor nucleus (Zhang et al. 1991). Thus, convergence does not involve efferent pathways that cross the midline.

Vergence-angle cells have also been found in alert monkeys trained to track a visual target as it moved sinusoidally to-and-fro along the visual axis of one eye or the other at frequencies of 0.1 or 0.2 Hz (Judge and Cumming 1986). On average, the firing rate of these cells increased or decreased by 16 spikes/s for each degree of change in vergence and, like the cells described by Mays, most of them increased their firing rate during convergence rather than during divergence. The typical cell responded in the same way when the stimulus moved along the visual axis of one eye as it did when it moved along that of the other eye. There was no response when the eyes moved in the same direction, and most cells responded in the same way with both eyes open as with only one eye open. The cells had a mean phase lag of 34° relative to the stimulus, which is significantly greater than the value of 16.8° reported for cells in the oculomotor nuclei (Robinson 1981). The delay between the firing of a cell and the start of a vergence movement response to a visual stimulus was found to vary between 35 and 70 ms. When a cell was electrically stimulated, a vergence response was initiated with a mean delay of about 30 ms.

More recently Mays et al. (1986) discovered a new class of vergence-related cells in the same area, just dorsal and lateral to the oculomotor nucleus, and in a more dorsal area extending into the pretectum. These cells responded with a burst of activity just before and during vergence movements that alert monkeys had been trained to make in response to stimuli that stepped in depth or moved along a depth ramp. The firing-rate profile of these cells was related to the velocity profile of the vergence movement, and the total number of spikes in a burst was related to the size of the vergence movement. These are referred to as **vergence-burst cells**. The burst cells responded in the same way when the animal tracked a depth ramp, thus maintaining the stimulus in a state of near zero disparity, from which it was argued that the response of these cells is related to eye velocity and not to the velocity of changing

disparity. On average, the response of a cell preceded the eye movement by 22 ms.

Some cells showed a burst of activity related to response velocity and a tonic response proportional to the maintained vergence angle. The tonic response showed only for larger vergence movements, presumably because only a large movement brought the eyes to a position of gaze for which a sizable tonic innervation was needed to prevent them from drifting back to their resting state. These are **vergence burst-tonic cells**. Most of the burst and burst-tonic cells responded only to convergence movements, but a small number of divergence burst and burst-tonic cells were found. The burst cells presumably form the neural substrate of transient vergence (see Section 10.5.7). It is not known which areas of the brain provide the input to the vergence-related cells in the midbrain.

In many people the state of tonic imbalance between the eyes returns to its pre-exposure value during a period of exposure to base-in or base-out prisms (see Section 10.2.5). Morley et al. (1992) recorded from cells in the region dorsal to the oculomotor nucleus in the alert monkey, before and after the animal had been exposed for some time to visual targets at one of various accommodation and

vergence distances. Only a few of the cells retained the same relationship between firing rate and vergence angle, so whatever mechanism is responsible for the adaptation of phoria to changed vergence demand must lie outside this region.

Neurology of cyclovergence

Almost nothing is known about the neurology of cyclovergence. In the monkey, conjugate torsional movements of the eyes induced by tilting the head are accompanied by the firing of burst neurones in the interstitial nucleus of Cajal, which lies near the rostral tip of the oculomotor nucleus. Neurones in the right nucleus respond when the eyes rotate clockwise from the point of view of the animal and those in the left nucleus respond when the eyes rotate counterclockwise. Cells in the same nucleus respond when the eyes execute vertical saccades, with both up and down movements being represented in both left and right nuclei (Vilis et al. 1989). Furthermore, microstimulation of cells in the interstitial nucleus of Cajal induces conjugate saccadic torsional eye movements, which obey the same clockwise-counterclockwise rule (Crawford et al. 1991).

Stereo constancy and depth cue interactions

11.1	Vergence and perceived distance	427
11.1.1	Stimulus conditions	427
11.1.2	Visual distance and visual size	428
11.1.3	Visual distance estimated by pointing	429
11.1.4	Verbal estimation of distance	429
11.1.5	Illusory motion parallax	429
11.1.6	Micropsia and macropsia	431
11.1.7	Perceptual effects of maintained vergence	431
11.1.8	Vergence and judgments of relative depth	434
11.2	Interactions between binocular stereopsis and other depth cues	435
11.2.1	Types of cue interaction	435
11.2.2	Disparity and structure-from-motion	438
11.2.3	Disparity - perspective interactions	448
11.2.4	Interactions between disparity and overlap	450
11.2.5	Interactions between stereo and shading	455
11.2.6	Cognition and depth cue interactions	456
11.3	Stereoscopic depth constancy	456
11.3.1	Depth constancy for disparity steps	456
11.3.2	Depth constancy for gradients and curvature	459
11.3.3	Speed constancy	459

11.1 VERGENCE AND PERCEIVED DISTANCE

11.1.1 Stimulus conditions

The horizontal disparity between the images of an object is a linear function of the distance of the object from the horopter. Although the steepness of this linear function varies with the distance of fixation, horizontal disparity alone does not provide information about the egocentric distance of an object. There is evidence that the pattern of horizontal and vertical disparities across a large surface in the frontal plane can be used to code egocentric distance (see Section 7.6.7). If an object lies on an inclined or slanted textured surface its distance can be appreciated from perspective cues, especially when the observer is moving so as to generate a parallactic flow pattern (see Section 13.5). The distance of a familiar object can also be appreciated by the size of its retinal image. When all these cues are eliminated, the only potential source of information about absolute distance comes from accommodation and vergence.

Descartes, in his *La Dioptrique* (1637), described the eyes as "feeling out" a distance by a convergence of their optic axes, just as a blind man might feel out a distance with two staves, one in each hand. In his *Essay Towards a New Theory of Vision* (1709), Berkeley

argued that the perceived distance of an isolated object from the viewer depends on muscular sensations of convergence and, at near distances, on visual blur and eye strain arising from accommodation (Boring 1942). Early but inconclusive experiments on vergence cues to distance were conducted by Hillebrand (1894) and Bourdon (1902).

Accommodation as a cue to distance

The role of accommodation in judgments of distance is controversial. The results of several experiments are invalid because of the use of poor accommodative stimuli. There is conflicting evidence about whether accommodation affects judgments of distance when it conflicts with vergence (Richards and Miller 1969; von Holst 1973). The issue is complicated by the fact that vergence and accommodation are linked responses, so it is difficult to control one while varying the other. There is also conflicting evidence about whether accommodation has any effect when it conflicts with perspective (Wallach and Norris 1963; Gogel and Sturm 1972). In most studies, the state of accommodation was not measured objectively, it was simply assumed that subjects accommodated on the required target, which is something that most people fail to do with any accuracy. Fisher and Ciuffreda (1988) used both a good

accommodative stimulus, consisting of high contrast patterns, and a poor accommodative stimulus in the form of a fuzzy disc. Accommodation was measured with an optometer that provided no intruding stimuli. Subjects estimated the distance of the monocular targets by pointing to them with a hidden hand. With high-contrast targets, apparent distance decreased linearly with increasing accommodation, but there were large individual differences. Subjects tended to overestimate distances less than about 3.2 dioptres (31 cm) and underestimate larger distances. Each dioptre change in accommodation resulted in about a 0.25-dioptre change in apparent distance. With the poor accommodation stimulus, perceived distance did not vary with accommodation.

Joint control of accommodation and vergence

When effects of joint changes in vergence and accommodation are being investigated, accommodation distance is made equal to vergence distance. We use the term **accommodation/vergence distance** to refer to the optical distance of the target determined by both accommodation and vergence. On the other hand, the accommodation distance may be varied while vergence is held constant, or vergence distance may be varied while accommodation is held constant. There are two ways to vary vergence while holding other cues to distance constant or ineffective. The first is to present dichoptic targets in a stereoscope with variable offset between the images, and the second is to view the target through base-in or base-out wedge prisms. However, constant accommodation and constant size signify that distance is not changing and may therefore detract from a person's ability to base judgments of distance on vergence. This problem can be overcome by randomly varying accommodation and target size so that these cues are dissociated from the distance of the target, as specified by convergence. An even better solution is to eliminate accommodation as a cue by viewing the stimulus through pinholes which increase the depth of focus. Size as a cue to distance can be eliminated by using a point source of light. The luminance of the target should also be kept constant or varied at random.

The range of distances over which testing is conducted is a crucial variable because, as has already been mentioned, the change of vergence per unit change in distance is an inverse logarithmic function of distance. Since vergence changes very little beyond 2 m, it is unlikely to serve as a cue to distance beyond 2 m.

Finally, one must select a psychophysical procedure for measuring the perceived distance of the target. The following procedures have been used.

11.1.2 Visual distance and visual size

The joint effects of vergence and accommodation on perceived distance can be studied by comparing the apparent distance of a test object seen through prisms and lenses so that it is at one accommodation/vergence distance, with the apparent distance of a second object seen directly so that it is at another accommodation/vergence distance. The subject alternates between viewing the test object and the comparison object so that only one of them is seen at one time. The retinal images of the two objects are made the same size, to neutralize size cues to distance. In a related procedure subjects judge the relative sizes of the test and comparison objects rather than their relative distances; the idea being that perceived relative size is proportional to perceived relative distance, according to the size-distance invariance principle. We will refer to these two procedures as the visual-distance and visual-size procedures, respectively. In one of the first studies of the roles of vergence and accommodation in judgments of absolute depth, estimates of the distances of monocularly viewed luminous discs presented in dark surroundings were very poor at distances between 16 and 100 cm when their retinal images remained equal in size (Bappert 1923). However, since the targets were viewed monocularly, any change in vergence was conditional on a change of accommodation and the actual vergence changes were not recorded. Crannell and Peters (1970) conducted a similar experiment using a point of light in dark surroundings at distances between 2 and 50 feet. They used binocular viewing, taking care to eliminate cues of relative size and brightness. Judgments were so variable that it was not possible to discern any significant correlation between actual and judged distances.

More recently, binocular judgments based on the visual-size procedure have been found to correspond to the relative accommodation/vergence distances of the test objects, but only for viewing distances below 1 m (Leibowitz and Moore 1966; Wallach and Floor 1971). Individuals varied widely in their ability to use accommodation/vergence as a cue to absolute distance (Richards and Miller 1969). Thus, the results of experiments involving the visual-distance and visual-size procedures support the idea that accommodation/vergence is used to scale the egocentric distance of a visual object, but only at near distances. However, procedures that involve comparing the distances of two visual objects are basically unsatisfactory. When used with binocular viewing, disparity cues could be introduced into the images of one object as the gaze is suddenly transferred from the other, before the required vergence

movement has occurred. Moreover, there is a tendency for two isolated objects to appear in the same depth plane.

11.1.3 Visual distance estimated by pointing

The apparent distance of an object can be determined by asking subjects to set an unseen marker to the apparent distance of the visual target. This method can be used only when the object is within reaching distance. Thus, Swenson (1932) asked subjects to move an unseen marker to the perceived distance of a single binocularly viewed luminous disc offering no cues of relative size or luminance. Errors of less than 1 cm were obtained in the range 25 to 40 cm. When accommodation was optically adjusted to one distance by lenses, and vergence to another distance by prisms, judgments of distance were a compromise between the two but with more weight given to the vergence cue. Foley and Held (1972) used the same method but eliminated accommodation as a variable by using a dichoptic pair of lights with variable disparity. Judged distance increased as the disparity-distance of the target increased from 10 to 40 cm, but subjects consistently overreached with a median error of 25 cm, which was independent of distance. The precision of pointing, as indicated by the standard deviation, was +2°.

A related procedure is to have subjects match the perceived visual size of a single test target presented at various accommodation/vergence distances with the length of a subsequently presented rod seen with full depth cues. Wallach and Floor (1971) used this procedure and found that egocentric distance was perceived with 95 per cent accuracy for distances up to 120 cm.

11.1.4 Verbal estimation of distance

People can be trained to give verbal estimates of the distance of a single visual object at different accommodation/vergence distances. Subjects made reasonably accurate verbal estimates of the distance of a point source of light viewed binocularly in dark surroundings at accommodation/vergence distances of between 0.5 and 9 m (Morrison and Whiteside 1984). Accuracy was still good when the target was exposed for only 200 ms, so that the eyes did not have time to converge on the stimulus. This suggests that the relevant information was supplied by combining information from the disparity of the flashed target with information about the resting state of vergence. Accuracy was not as good when only the accommodation distance was varied as when only the vergence distance was varied.

Gogel (1972) reported that when two objects at different distance are seen in dark surroundings, the apparent distance of the more distant object remains the same as when it alone is present but the distance of the nearer object is underestimated compared with when it is presented alone. Mershon et al. (1993) found the same **far-anchor effect** in the context of motion in depth. They presented two small illuminated rectangles stereoscopically separated in depth, with one of them stereoscopically moving to and fro in depth. Subjects more often judged correctly which of the two targets was moving in depth when the nearer target moved than when the more distant target moved. In other words, subjects were predisposed to see the more distant target as stationary. A similar predisposition to see more distant objects as stationary is reported in Section 12.7.7.

11.1.5 Illusory motion parallax

Normally the visual world does not appear to move when one moves one's head along a straight path from side to side. Lateral movements of the head produce two kinds of parallax. In the first place they produce parallactic movement between objects at different distances, which provides information about the relative distances of the objects confounded by their absolute distance (see Section 13.5). Movements of the head also produce relative motion between a given object and the head of the observer. Consider the case of a person moving the head from side to side along a linear path while fixating a stationary point of light in dark surroundings. For a linear motion of the head at a given velocity, the velocity of eye rotation required to keep fixation on the point of point is inversely related to the distance of the light, and becomes zero at infinity. Therefore, the rotation of the eyes, as indicated by efference or by proprioceptive feedback, could provide accurate information about the distance of a fixated stationary target. Note that for this to be possible the viewer must correctly register three attributes of the motion of the head: its direction with respect to the direction of gaze, its velocity, and that it is a purely translatory motion. If the movements of either the eyes or the head are misregistered, the motion of the object relative to the observer will be misperceived if its distance is correctly perceived, or its distance from the observer will be misperceived if its motion relative to the observer is correctly perceived. Rotations of the head produce headcentric visual motion, which is approximately independent of distance. It is not totally independent of distance because the eyes are offset from the axis of head rotation, which causes them to translate when the head rotates.

If, during sideways motion of the head, the distance of an accurately tracked stationary target is underestimated, the eyes move more slowly than they should for that perceived distance. The stationary target therefore appears to move in the same direction as the head. When the distance of the target is overestimated, the eyes move faster than they should for that perceived distance and the target appears to move in the opposite direction to the head (Hay and Sawyer 1969; Wallach et al. 1972b). We refer to these misperceptions of motion as **illusory motion parallax**. The motion of a stationary object relative to the moving self is correctly interpreted as due to motion of the self only when the distance of the object is correctly perceived and the motions of the eyes and the head are correctly registered. This **motion-distance invariance principle** is a special case of the size-distance invariance principle.

This invariance principle is illustrated by the common observation that a face on a poster seems to follow one as one walks past it. This effect is particularly evident when a stereogram is viewed with the head moving from side to side (Tyler 1974b). The motion parallax between the near and far features of a real object is ascribed to motion of the self rather than of the object. In the picture of a face or in a stereogram the expected motion parallax is not present even though the object appears to have depth. An object with depth can be seen without motion parallax only if it moves with the viewer. It is as if the visual system has a natural appreciation of the degree of motion parallax of parts of an object relative to each other or of motion of an object relative to the self generated by motion of the head. As long as this natural scaling of relative motion and distance holds, the object is perceived to be stationary, but any departure from this natural scaling is interpreted as a rotation or translation of the object.

Another illustration of the motion-distance invariance principle can be obtained by placing two identical coins side by side on a uniform surface. If the head moves while the two coins are fused by convergence, the coins appear to move with the head, and if they are fused by divergence they appear to move against the head (Hay and Sawyer 1969).

Scaling between motion and distance need not depend on a high-level inferential process and it is not under conscious control. However, as we will see in Section 11.1.7, the perceived distance of an isolated object can be modified, at least temporarily, by exposure to an unusual association between distance and vergence such as is produced by wearing base-out or base-in prisms.

Gogel and Tietz (1973) varied the actual distance of a point of light seen in dark surroundings until it

appeared not to move when the subject moved the head linearly from side to side. According to the motion-distance invariance principle this is the distance at which the subject correctly perceives the distance of the stimulus, assuming that the movements of the eyes and head are correctly registered. When the stimulus was placed further away than this neutral distance it appeared to move with the head, indicating that its distance was underestimated, and when it was placed nearer than the neutral distance it appeared to move against the head, indicating that its distance was overestimated. In other words, in the absence of depth cues other than convergence, an isolated object appears to lie at a specific distance, which, generally, is about 2 m. Gogel called this the **specific-distance tendency**. Gogel did not enquire whether the apparent distance of an isolated object is related to dark accommodation or dark vergence.

Owens and Leibowitz (1976) found that the distance at which the distance of a monocularly viewed point of light is correctly perceived, as indicated by the head-parallax test, is not related to dark accommodation but to the position of vergence assumed by the eyes in the dark. Gogel (1982) argued that an explanation in terms of the resting state of vergence does not work when both eyes are fixated on the test object.

In this analysis it was assumed that the movements of the eyes and the head are correctly registered but the distance of the point of light is not. Suppose it was the other way around. Assume that a person underestimates the movements of the eyes when fixating a distant point while moving the head from side to side. By the motion-distance invariance principle this causes the point to appear to move with the observer. Assume also that a person overestimates the movement of the eyes when fixating a near point of light. This should cause the point to appear to move against the motion of the observer. In other words, the same illusory movements of an isolated point can be explained in terms of misjudgments of the movements of the eyes or misjudgments of the distance of the point. The parallax phenomenon could be due to the specific distance tendency, that is, a tendency to underestimate far distances and overestimate near distances, or to a **specific eye-velocity tendency**, that is, a tendency to under register slow version movements and over register fast version movements.

Just such a theory of illusory parallax motion has been proposed by Post and Leibowitz (1982). When the head moves from side to side, stimuli arising in the utricles of the vestibular system evoke a reflex compensatory movement of the eyes, known as the

linear vestibuloocular reflex (LVOR). For objects at infinity, the required gain of LVOR is zero and the response is inhibited by visual fixation. They proposed that these inhibitory signals are interpreted as a movement of the eyes in the direction opposite to the LVOR signal. This causes the point of light to appear to move with the head. For objects close to the observer the natural gain of LVOR is supplemented by extra innervation generated by visual fixation of the stationary target, and this is interpreted as extra movement of the eyes in the direction of the LVOR signal. This causes the light to appear to move against the head. At a certain distance the natural gain of the LVOR is appropriate to hold fixation on the target without the help of inhibitory or supplementary inputs from visually evoked eye movements. This is the distance at which the point of light appears to be stationary as the head is moved.

There is evidence that the gain of the LVOR in the dark varies with vergence angle (see Section 10.6.5). However, there is no direct evidence that eye movements are misregistered in the manner required to explain illusory parallax motion. Evidence cited previously, based on static judgments of distance, independently support the specific distance tendency. Perhaps illusory parallax motion is due to misregistration of both distance and eye velocity. *The other possibility, which nobody seems to have considered, is that illusory motion parallax is due to misregistration of motion of the head. Nothing is known about people's ability to register the velocity of the head when it is moved actively from side to side in the dark.* When the body is moved passively at a constant velocity there are no nonvisual sensory inputs and the relative motion between the self and the visual surroundings is totally ambiguous, as illustrated by the phenomenon of illusory self-motion, or linearvection (see Howard 1982).

11.1.6 Micropsia and macropsia

When the ciliary muscles are paralyzed by atropine, objects appear smaller and nearer in spite of the image remaining the same size. This effect, known as atropine micropsia, was first described by Aubert (1865). Koster (1896) proposed that it is due to induction of accommodative convergence by the effort to accommodate in spite of the atropine paralysis. The induced vergence acts as a signal that the visual object is nearer than it really is, and this leads to underestimation of its size by the principle of size-distance invariance. Eserine contracts the ciliary muscles and has been reported to induce macropsia. In this case, there is an attempt to relax accommodation. Base-out prisms increase the

convergence required to fixate an object (see Figure 10.8) and decrease the perceived size of the object. The telestereoscope (see Figure 10.11) has the same effect. Base-in prisms have the opposite effect.

The dependence of perceived size and distance on vergence and accommodation is vividly illustrated by the **wallpaper effect**. When a regularly repeating pattern, such as that shown in Figure 2.9, is viewed with the eyes overconverged by a multiple of the period of the pattern, the images of the pattern remain fused, but the angle of vergence corresponds to a distance nearer than the true distance. As a result, the pattern appears nearer and therefore smaller than it is, an effect known as **vergence micropsia**. When the eyes are underconverged on the pattern it appears further and larger than it is, an effect known as **vergence macropsia**. When the pattern is in a frontal plane there is a gradient of horizontal and vertical disparities across it, because, with increasing eccentricity, the elements of the pattern lie further from the horizontal and vertical horopters. Furthermore, these disparity gradients vary as a function of viewing distance (see Section 7.6.7). Ittleson (1960) believed that vergence micropsia and macropsia result from these changes in disparity and claimed that there are no vergence-induced changes in perceived size when the repeating pattern is placed in the horizontal horopter.

Ono et al. (1971b) checked this claim by asking subjects to set an unseen pointer to the apparent distance of a wire-mesh surface for different amounts of misconvergence. In one condition the surface was a vertical cylinder containing the horizontal horopter defined by the Vieth-Müller circle, and in another condition the surface was in a frontal plane. Distance estimates in the frontal-plane condition conformed more closely to those predicted from vergence-distance scaling than did estimates in the horopter-plane condition, but some vergence-distance scaling was evident in the horopter-plane condition, especially when subjects saw the surface for the first time. The horopter-plane condition did not eliminate all disparity gradient cues since there would still be a gradient of vertical disparity in the quadrants of the display. *This problem could be resolved by using a repeating pattern consisting only of vertical lines. or of a row of dots confined to the horizontal horopter.*

11.1.7 Perceptual effects of maintained vergence

It was shown in Section 10.2.5 that viewing the world through base-in or base-out prisms, even for a few minutes, leads to a shift of tonic vergence lasting minutes or hours, as revealed by the position of dark vergence, phoria, or fixation disparity.

Postural aftereffects

Tonus aftereffects known as postcontraction, or postural persistence, occur in all muscular systems. A dramatic illustration of postcontraction is the involuntary elevation of the arm after it has been pressed with some force against a wall. Distortions of head-centric space are produced when the eyes are held in an off-centre position for a short time. For instance, after the eyes have been held in an eccentric position of gaze for a minute or two and the observer attempts to return the gaze to the straight-ahead position the eyes are displaced in the direction of previous deviation. Furthermore, a person attempting to point to a visual target with unseen hand misses in the direction of previous eye deviation. The aftereffects of asymmetrical eye posture on egocentric localization seem to have been first reported by MacDougall (1903) and confirmed by Park (1969) and Craske et al. (1975). The change in apparent straight ahead after holding the eyes in an eccentric position increases with both the eccentricity and the duration of the previous eye position and has a maximum value of about 8° (Paap and Ebenholtz 1976). The preceding effects are due to the asymmetrical posture of the eyes rather than the asymmetrical position of the visual target (Hill 1972; Morgan 1978). It has also been known for some time that an object seen in dark surroundings appears to drift in the opposite direction to that of a previous deviation of the eyes (Gregory and Zangwill 1963; Levy 1973). An asymmetrical posture of the head leads to similar effects on the apparent straight-ahead (Howard and Anstis 1974; Ebenholtz 1976).

The aftereffects of asymmetrical eye posture are also revealed in physiological studies. Eckmiller (1974) recorded from single units in the region of the oculomotor nuclei of the monkey. The firing rate of each unit was related to the position of the eyes in their orbits. However, the firing rate of a given cell was higher after the eyes had approached a given position from a less eccentric direction than after they had approached the same position from a more eccentric direction. Thus, the cells manifested hysteresis. The difference between ingoing and outgoing impulse rates was between 5 and 22 impulses/sec, corresponding to a difference in eye position of several degrees. These physiological data are compatible with the psychophysical findings, and both types of effect could be due to any of the following interrelated sources of hysteresis:

1. Muscles become more responsive to a given level of innervation after a period of active contraction. This effect is known as posttetanic potentiation (Hughes 1958; Olson and Swett 1971). It is

counterbalanced by the fact that the elastic tension in the antagonist muscle is increased by prestretching (Bosco and Komi 1979).

2. There is a persistent sensory discharge from muscle-spindle receptors after the contraction of a muscle, which is probably due to an alteration in the contractile state of extrafusal (ordinary muscle fibres) and intrafusal muscle fibres (muscle fibres within sensory muscle spindles) (Hutton et al. 1973).

3. The discharge from Golgi tendon organs and ligament receptors adapts when these structures are subjected to steady tension (Houck 1967; Ferrell 1980). There are muscle spindles, Golgi tendon organs, and palisade endings in human eye muscles (Cooper et al. 1955; Richmond et al. 1984). Stimulation of proprioceptors in the extraocular muscles by vibration causes a point of light to appear to move (see Velay et al. 1994).

Perceived distance and changes in the tonic vergence

Several investigators have reported that viewing the world for a few minutes through base-out prisms or through a telestereoscope, both of which increase vergence demand, leads to an overestimation of perceived distance when the device is removed, and viewing the world through base-in prisms, which decrease vergence demand, leads to underestimation of perceived distance. These effects are what one would expect if the state vergence serves as a cue to absolute distance. A dispute has arisen about whether these aftereffects are due to (a) changes in the tonic state of vergence, (b) a recalibration of the vergence/apparent distance system arising from the disturbed relation between vergence and disparity on the one hand and other cues to distance, such as familiar size, motion parallax, and perspective on the other, or (c) a recalibration of the vergence/apparent distance system arising from the interaction between the observer and the visual environment.

The first experiment of this kind was conducted by Wallach et al. (1963). Subjects viewed rotating wire forms for 10 minutes through a telestereoscope that increased the effective interocular distance by 117 per cent. Subsequently, with normal viewing, the perceived depth in a wire form was reduced by 20 per cent, although its perceived size was unchanged. A similar increase in perceived depth was induced when the telestereoscope was arranged so as to reduce the interocular distance. Wallach et al. interpreted these results in terms of the conflict between binocular disparity and other cues to depth that were not changed by the telestereoscope, in particular, motion parallax and perspective.

Viewing the world through a telestereoscope or prisms may have produced a tonic change in the eye

muscles, and this may have contributed to the effect reported by Wallach and his collaborators. Wallach and Halperin (1977) produced evidence that muscular aftereffects do not account for the whole of the effects of adaptation to prisms (see also von Hofsten 1979). On the other hand, Fisher and Ebenholtz (1986) used a similar procedure to that used by Wallach et al. (1963) and obtained similar aftereffects even when there was no conflict between disparity and monocular cues to depth during the induction period. They concluded that the aftereffects of viewing through a telestereoscope are due to a change in the tonic state of the extraocular muscles, which causes a change in the apparent distances of objects. Even a small change in apparent distance would have a large effect on perceived relative depth in an object, because the disparity produced by a given depth interval is inversely proportional to the square of the viewing distance. In comparison, changes in the apparent size of objects would be small because the angular size of an object is inversely related to distance, not to the square of distance. Fisher and Ciuffreda (1990) obtained direct evidence of a change in tonic vergence and perceived distance as well as of a change in perceived depth after subjects moved about in a building and performed simple tasks for 30 minutes while wearing a telestereoscopic device. The distance and depth aftereffects were opposite to those predicted from a conflict between disparity cues and monocular cues but were consistent with the causal factor being a change in the tonic state of vergence.

Several other lines of evidence support the idea that changes in perceived distance arise from changes in the tonic state of vergence. In one experiment, a 6-minute period of fixation of a visual target in a stereoscope at a near distance, defined by disparity, produced a subsequent overestimation in the perceived distance of a test object. Six minutes of fixation of an object at a far distance produced an underestimation in perceived distance. Maintained fixation at an intermediate distance of about 32 cm produced no aftereffects, presumably because this was the distance corresponding to dark vergence (Ebenholtz and Wolfson 1975). In a related experiment, subjects fixated an isolated visual target at a distance of 41 cm for 6 minutes through prisms ranging from 20 dioptre base-out, requiring 32° of convergence, to 8 dioptre base-in, requiring 0.1° of divergence. The size of the aftereffect was approximately proportional to the depth interval between the position of maintained vergence during the induction period and the position of the test object, which happened to be near the position of dark vergence (Paap and Ebenholtz 1977). In both these

experiments other depth cues were either held constant or reduced to a minimum and the experimenters concluded that changes in apparent distance resulting from maintained vergence are due simply to changes in muscle tone rather than to conflicting depth cues. Maintained near vergence increases tonus in the medial rectus muscles, so that less innervation is required to hold the gaze on an object. This creates the impression that the object is further away than it normally appears to be. Maintained far vergence has the opposite effect. The evidence cited at the beginning of this section establishes that such changes in muscle tone in extraocular muscles do occur.

Changing the relationship between vergence and other cues to distance

Even though the primary effect of maintained vergence is probably a change in the tonic state of the extraocular muscles, the way this affects judgments of depth depends on the presence of other cues to distance.

Wallach et al. (1972a) showed that the scaling of perceived depth can be changed by having subjects walk about for 20 minutes wearing 1.5-dioptre base-in prisms, which decreased the convergence required to fixate an object, or base-out prisms, which had the opposite effect. The prisms altered the relationship between convergence and other cues to depth such as perspective, disparity, and familiar size. After adaptation, subjects matched the length of a rod they could feel but not see to the depth between the back and front of a wire pyramid. The absolute distance of the pyramid could be detected only on the basis of accommodation and vergence. The estimates of depth within the pyramid changed after subjects had adapted to the prisms, although not by as much as would have been predicted if the visual system had fully adapted to the altered state of vergence. Subjects also estimated the apparent distance of a test object before and after adaptation, by pointing to the position of the object with the unseen hand. The change in apparent distance was the same percentage of full adaptation that was evident in the rod-matching test. It was concluded that pairing an unusual state of vergence with a veridical depth cue leads to a recalibration of the vergence cue to distance and to a corresponding change in depth constancy.

O'Leary and Wallach (1980) conducted an experiment to test whether perceptual scaling of depth can be induced by an apparent change in distance induced by a false familiar-size cue. A normal dollar bill and one reduced to 0.72 of normal size were presented at the same distance in dark surroundings.

A 1-cm disc was suspended in front of each bill. Subjects set a pair of calipers by touch to match the depth interval between each disc and its dollar bill. If the perceived distances of the bills had been determined by their angular sizes the smaller bill should have appeared 1.39 times as far away as the normal bill, and the depth interval for the smaller bill should have appeared larger than that for the normal bill by a factor of $(1.39)^2$, or 1.93. In fact it appeared to be larger by a factor of 1.7. This result demonstrates that an unusual relationship between convergence and familiar size can affect the scaling of perceived depth, but it is not clear what the scaling factor was since the perceived distances of the test objects were not determined. A change in perceived distances of objects, as revealed by pointing with an unseen hand, has been produced in subjects who inspected their own feet for 3 minutes through base-out prisms (Craske and Crawshaw 1974).

Heuer and Lüscher (1983) obtained an aftereffect when cues to distance other than vergence were absent during the induction period, demonstrating that adaptation of the oculomotor system is sufficient to generate the perceptual aftereffect. However, the aftereffect was stronger when conflicting cues to distance were present during the induction period, demonstrating that cue conflict also contributes to the aftereffect. When unaffected cues were present only during the test period, the aftereffect of maintained vergence, as revealed in the error of placing the unseen finger under a test target, was reduced compared with when only vergence cues were available in the test period.

Effects of visual-motor experience

There is some evidence that at least part of the effect of wearing prisms is due to recalibration of central processes arising from active visual-motor experience. For instance, it has been reported that the effects of wearing 4-dioptre base-out prisms on perceived distance were greater for subjects who moved actively or passively through a building during the 20-minute induction period than for subjects who read a magazine (Owens and Leibowitz 1980). It is not clear whether the smaller effect in the second set of subjects was due to the fact that they did not move or to the fact that they maintained a fairly constant angle of vergence. Ebenholtz (1981) obtained a greater effect on perceived distance in subjects who wore 5-dioptre base-out prisms for 15 minutes while moving about in a normal visual environment than in subjects who maintained an equivalent convergence on an object for the same length of time. But this difference may have been due to the fact that the subjects in the second group

were exposed to an impoverished visual stimulus with fixed vergence while those in the first group observed a natural scene containing many objects and monocular cues to distance.

11.1.8 Vergence and judgments of relative depth

In Section 5.8.1 it was shown that, although eye movements are not required for stereopsis, smaller differences in depth between two targets separated by a large lateral distance can be detected when the eyes are allowed to move between them. The present section deals with whether the depth between two objects in the same visual direction but separated by a large distance in depth is more accurately perceived when the eyes converge from one to the other than when the gaze is locked on one of them.

Foley and Richards (1972) placed a test object at various distances in front of a screen. The screen was at an optical distance of either 250 or 24 cm. In the eye-movement condition, subjects were asked to look back and forth between object and screen and set the object to a specified distance relative to the screen. In the no-eye-movement condition, subjects fixated a point on the screen and estimated the relative distance of a disparate test object, flashed on for 80 ms. Incidental differences between the two conditions, such as the difference in exposure time, were allowed for in control conditions. The results for one subject are shown in Figure 11.1. When vergence eye movements were allowed, subjects gave reasonably accurate estimates of the distance of the test target from the screen, relative to the distance of the screen to the eye, for all distances of the target. Over the middle range of distances of the test object the perceived relative distance was overestimated by about 10 per cent. When eye movements were not allowed, the perceived relative depth between target and screen was accurate only when the target was near the screen, that is, when disparity was small. As the test object came nearer to the subject and disparity increased, relative distance was grossly underestimated; that is, the test object appeared much closer to the screen than it actually was.

One could say that the test object and screen normalized to the same depth plane when vergence eye movements were not allowed (see Section 12.1). Thus, small disparities are accurately registered without vergence eye movements but large disparities are not. Improved performance with eye movements could be due to information provided by vergence in the form of either motor efference or kinesthetic inputs from the extraocular muscles, or it could be due to the changes in disparity that eye movements produce.

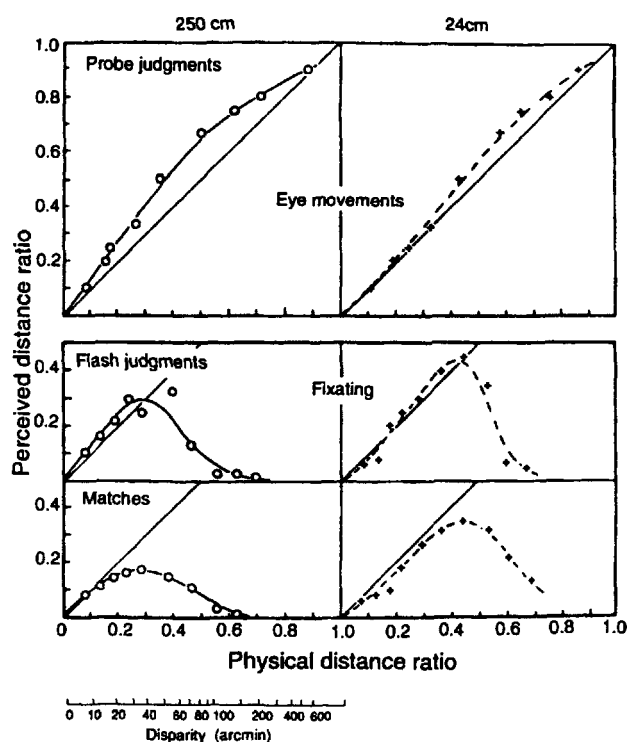


Figure 11.1. Perceived distance and relative distance.

The perceived distance of a test object relative to a screen as a function of the ratio between the two distances, with the screen at a fixation distance of 250 and 24 cm. The top curves show the results when the subject was allowed to look between the test object and the screen. The middle curves are for when the subject remained fixated on a point on the screen and the test object was flashed on for 80 ms. The bottom curves are for when the subject set a depth probe to match the perceived depth of the flashed target. Results for one subject. (From Foley and Richards 1972, Perception and Psychophysics, 11, 423-427. Reprinted by permission of Psychonomic Society, Inc.)

11.2 INTERACTIONS BETWEEN BINOCULAR STEREOPSIS AND OTHER DEPTH CUES

11.2.1 Types of cue interaction

Many perceptual judgments are based on spatial information derived from different detectors, either in the same sense organ or in different sense organs. The distinct types of information are called cues. Judgments along a single dimension may be based on cues arranged in parallel or in series. In a parallel system, any one cue is sufficient for the defined judgment. In an in-series system, all cues are needed for the judgment. Compound spatial judgments may be based on a simple conjunction of cues, as when we judge both the size and position of an object.

An example of a system of parallel spatial cues is provided by the task of judging the direction of a sound source either by the difference of sound intensity in the two ears or by the relative time of

arrival of sounds at the two ears. It is to be expected that the variance of a judgment made on the basis of two or more parallel cues will be less than the variance of a judgment made on the basis of only one cue. According to one formulation, the reciprocal of the variance of the composite judgment equals the sum of the reciprocals of the variances of the component judgments.

An example of an in-series system of spatial cues is provided by the task of judging the visual direction of an object relative to the head. For this judgment we must register the retinal position of the image of the object and the position of the eye in the head. An in-series cue system is involved in the task of judging the three-dimensional relief of a surface from the motion parallax produced by sideways motion of the head, as discussed in Section 13.5. Other examples are presented in Section 11.2.2. The constant error of the judgment should be the algebraic sum of the constant errors of the two component tasks, and the variance of the judgment should equal the sum of the variances of the component tasks (see Howard 1982).

In this section we are concerned with parallel cues for the perception of relative depth. In a parallel cue system, information from one cue may conflict with that from another. Such conflicts can be resolved in several ways, as indicated in what follows.

1. *Cue averaging and summation.* Consider a parallel cue system in which a judgment may be based on either of two sensory cues. For nonintensive sensory dimensions, such as direction and orientation, the most efficient way to combine sensory cues is to take the weighted mean, with weights determined by some estimate of the reliability of each cue. Theoretically, the variance of the judgment based on both cues is lower than that based on either cue alone, and constant errors add. For example, the direction of a sound source may be detected on the basis of the intensity difference at the two ears or of the difference in time of arrival of sound at the two ears. When the two cues agree, judgments are more precise and accurate than with either cue acting alone. When they conflict, the sound is judged to be in an intermediate direction. An apparent offset of a sound source produced by one cue may be cancelled by an opposite offset produced by the other cue. The set of null points for different values of each sensory cue defines a **cue trading function**. The titration of one cue against another allows one to investigate the equivalence and relative efficiency of cue systems.

The situation is more complex for intensive sensory dimensions such as distance. If judgments based on each cue tend to be underestimations, the

mean will be no more accurate than the most accurate cue acting alone. If the cues are summed, accuracy can be increased. However, if each cue provides a reasonably accurate estimate of depth, it is better to take the mean than the sum, because the sum provides a large overestimation.

A trading function arises when two cues interact continuously producing either the weighted algebraic sum or mean. Examples of a trading function in stereoscopic vision are provided by the titration of binocular disparity against monocular parallax, as described in Section 11.2.2; the titration of disparity against monocular cues to motion in depth, as described in Section 13.2; and the titration of disparity against perspective, as described in Section 11.2.3. Some in-parallel cues interact discontinuously, in which case a conflict is resolved in one of the following three ways.

2. *Cue dominance*. Judgments may be based on only one cue, with the other cue being suppressed when in conflict. For instance, when the sound of a ringing bell does not arise from the seen bell, the sound seems to come from the seen bell and the conflicting auditory information is ignored.

3. *Cue dissociation*. Each cue may be interpreted as arising from a distinct object. For instance, when the spatial separation between a seen bell and a heard bell is too great, two bells are perceived.

4. *Cue reinterpretation*. One of the cues may be reinterpreted in a way that renders it compatible with the other. An example of this type of cue interaction is the resolution of conflict between binocular disparity and figural overlap, as discussed in Section 11.2.4.

5. *Cue disambiguation*. The sign of a particular cue may be ambiguous unless supplemented by another. For instance, the same input from the otolith organs can arise from head acceleration or head tilt. The ambiguity is resolved either by inputs from the semicircular canals or the eyes. Image blur provides information about the distance of an object from a fixated object but does not indicate which object is nearer. The cue of overlap indicates nothing about the distance between two objects but does indicate which is nearer.

Bülthoff and Mallot (1987, 1988) suggested a different classification of cue interactions based on five categories: *Accumulation*; *Veto*; *Cooperation*; *Disambiguation* and *Hierarchy*. *Disambiguation* is common to both classifications while *veto* is an alternative name for *cue dominance*, in *hierarchy* information from one cue is used as raw data for a second. *Accumulation* and *cooperation* in Bülthoff and Mallot's scheme are different forms of *cue averaging* or *summation*. The

difference between the two is a function of the extent and level at which the interaction is assumed to take place. *Accumulation* refers to the interactions between the outputs of essentially independent mechanisms whereas in *cooperation* the interaction is more substantial and occurs at an earlier stage. Bülthoff and Mallot use the example of the cooperative synergistic interaction between modules dealing with detection of poor or noisy cues. Most empirical studies on depth cue integration have focused on cue averaging and summation. Models of interactions between depth cues have also been developed.

Models of cue interactions

Dosher et al. (1986) carried out one of the first empirical studies on the interactions between disparity, motion, and luminance cues. Their results could be modelled in terms of a weighted linear combination of the individual depth cues. Maloney and Landy (1989) developed this idea and proposed a simple statistical framework for modelling the combination of multiple depth estimates from different cue systems. It was assumed that the different sources of depth information are processed independently (modularity) and that the final representation is in the form of a depth map which describes the depth of points in different visual directions. In the model, the outputs of the different modules are "fused" into a single depth estimate at each point in the scene. Their model also assumes a linear combination of depth estimates and was not designed to account for severe conflict of depth cues.

Maloney and Landy made the important point that different cues provide different sorts of information. Whereas motion parallax and binocular disparities can, in principle, provide complete information to create a depth map of points in different visual directions, texture gradients and linear perspective provide information only up to an unknown scaling factor. In the third class of cues identified by Maloney and Landy (which includes the kinetic depth effect) there is an additional uncertainty about the sign of depth and the direction of rotation of the moving object. Consequently, the first requirement of any model of cue combination is to transform the information provided by the different cues into a common form. Maloney and Landy suggested that cues which provide the missing parameters "promote" the information signalled by the other cues so that all depth cues provide comparable absolute depth estimates. The ideal-observer model then produces a weighted linear combination of the outputs of different modules.

To test the model, Landy et al. (1991a) looked at the accuracy of observers' judgments of the depth-

to-width ratio of vertically oriented cylindrical surfaces specified by the kinetic depth effect (KDE) and texture cues. They found that the interactions between the two sources of information were adequately described by a simple averaging model in which the texture cue was weighted more heavily (0.62) than the motion cue. In the experiments of Young et al. (1993), observers judged the depth-to-width ratio of a vertically oriented cylinder (as in their previous experiment) but the motion of the cylinder was around a horizontal rather than a vertical axis. The interactions between the two cues were again well-modelled by a simple linear combination in which the motion cue was weighted more heavily than texture for one out of the three observers and more similarly weighted for the other two. Not surprisingly, when the texture cue was weakened by introducing nonisotropic texture elements, the weighting for the texture cue diminished.

Clark and Yuille (1990) distinguished between "weak fusion" and "strong fusion" models. Weak fusion occurs between the outputs of independent mechanisms and is similar to Bülthoff and Mallot's idea of *accumulation*. In strong fusion, which is related to Bülthoff and Mallot's idea of *cooperation*, information from the different cues is processed cooperatively to derive a depth estimate. Strong fusion models predict nonlinear interactions between the different cues whereas weak fusion models preclude such interactions (Young et al. 1993). As we noted earlier, different cues provide different sorts of information about the absolute depth in a particular visual direction which may need scaling or "promoting" using a parameter obtained from another depth cue. Cue promotion implies more than the accumulation of evidence from independent modules and is therefore not a characteristic of weak fusion models. To accommodate cue promotion, Landy et al. (1991b) have suggested the idea of "modified weak fusion" which limits the form of interaction between the cues specifically to cue promotion. Other forms of cooperative interaction characteristic of strong fusion are not allowed in "modified weak fusion". In some situations, the same parameter may be missing and the unscaled estimates may be averaged prior to the scaling process. This would be regarded as weak fusion.

In the experiments of Landy et al. (1991b) and Young et al. (1993), the inconsistency between cues was kept to a minimum, using a procedure known as **perturbation analysis**. Under these conditions, the accuracy of judgments based on motion and texture cue interactions can be modelled by a simple weighted linear combination of estimates derived from the individual cues. Linearity of combination is

consistent with the idea of weak fusion and unlikely according to a strong fusion model. The ideal-observer model of Landy et al. also predicts that the weights given to the different depth cues should alter with changes in the reliability of a particular cue. The relevant experimental results also support this prediction.

The weak fusion and modified weak fusion models described so far all assume that the desired depth representation is in terms of a depth map and, as a consequence, those cues which do not provide complete depth information have to be "promoted" using information and parameters supplied by the richer cues. In contrast, Bülthoff (1991) has emphasized the differences between the information provided by different cues and suggested that quite different experimental probes are needed to investigate cue interactions depending on the assumed level of representation. Based on his own experiments on the interactions between edge-based and intensity-based disparities which are described in Section 11.2.5, Bülthoff (1991) proposed a Bayesian framework to model the integration of different depth cues (see also Bülthoff and Yuille 1991). Under this scheme different cues are weighted according to their robustness and smoothing is applied to improve the accuracy of the depth estimates. For example, little smoothing is needed to improve the reliability of depth cues such as the edge disparities since these provide accurate depth estimates. On the other hand, binocular differences in the shape of the luminance profile—intensity-based disparities—are less reliable and require more smoothing. Bülthoff has argued that the predictions of the Bayesian model are consistent with the results of his own experiments in which observers adjusted a depth probe to appear on the surface of ellipsoid shapes of rotation (Section 11.2.5). In general, models of cue combination based on energy minimization or regularization predict that in the absence of reliable information, surfaces will regress towards the frontal plane. An alternative to the Bayesian framework has been proposed by Poggio et al. (1988b) based on Markov Random Fields (MRFs).

The differences between the modified weak fusion model of Landy et al. (1991b) and Bülthoff's (1991) Bayesian model may owe more to the different sorts of interactions that the two models have attempted to explain. Non-linear interactions such as dominance or vetoing have been observed experimentally, particularly when the cues differ in the kind of information they provide. On the other hand, when the cues provide similar information and the quantitative discrepancies between the cues are small, both models predict the linear averaging

that has been observed experimentally. Bülthoff and Yuille (1991) argue that the Bayesian approach provides a more general framework for thinking about both low- and high-level vision by incorporating general assumptions and constraints (see also Yuille et al. 1991). This strategy may be contrasted with the view that there is no real theory of vision but only a "bag of tricks" which provides particular solutions in particular situations (Ramachandran and Anstis 1986). The problem with the Bayesian approach is that it can predict the patterns of cue interaction in novel situations only in rather general terms. As a general point, we may also question the wisdom of designing models to account for interactions between discrepant or contradictory sources of depth information which never occur in normal viewing.

11.2.2 Disparity and structure-from motion

Cross-cue biasing between disparity and shape-from-motion

Evidence for an interaction between binocular disparity and monocular motion parallax information was provided by Graham and Rogers (1982b). Their first experiment was designed to test whether the prior inspection of a corrugated surface specified by either disparities or motion parallax could bias the direction of perceived depth in ambiguous corrugations specified by the other cue. The horizontal rows in the ambiguous test stereogram contained repeating patterns of random dots (as in an autostereogram) which allowed the dots to be matched either in front of or behind the fixation point by an amount which depended on the period of repetition (Rogers and Graham 1984). The ambiguous motion parallax corrugations consisted of the same pattern of horizontal shearing motion normally created by horizontal corrugations during side-to-side movements of the observer's head. In the absence of an associated head movement, the shearing pattern is still perceived as horizontal corrugations but the perceived depth of the corrugations and the perceived direction of oscillation about a vertical axis becomes ambiguous like a kinetic depth effect (KDE) display (Rogers and Graham 1979). After 15 s of adaptation to an unambiguous motion parallax surface, the ambiguous stereo corrugations were overwhelmingly biased towards a phase in the opposite direction to that seen during adaptation. Similarly, following 15 s of adaptation to an unambiguous disparity surface, the ambiguous motion corrugations were overwhelmingly biased towards a phase in the opposite direction to that seen during adaptation (see also Rogers and Graham 1984). These are both examples of cue disambiguation.

Nawrot and Blake (1989) reported a similar result. The direction of apparent rotation of a sphere covered with random dots under parallel projection (kinetic depth effect) is necessarily ambiguous. Following 90 s of binocular inspection of a rotating sphere in which the disparities of the moving dots provided unambiguous information about the depth and direction of rotation (Braunstein et al. 1986; Dosher et al. 1986), an ambiguous rotating sphere in which all dots had zero disparities was seen to rotate in the opposite direction. The aftereffect lasted for up to 30 s. Nawrot and Blake concluded that extended exposure to structure from stereopsis subsequently influences the perception of structure from motion and this provides evidence of an interaction between the two sources of information. However, the site of the interaction may be different in Nawrot and Blake's and Graham and Rogers' experiments. In the latter case, prior adaptation to a disparate surface affected the direction of perceived depth in an ambiguous parallax surface whereas in Nawrot and Blake's experiment, it was the direction of three-dimensional rotation that was affected by adaptation to a rotating three-dimensional structure. Both are examples of cue disambiguation but the site of the disambiguation is likely to be different as a subsequent experiment by Nawrot and Blake shows.

Nawrot and Blake (1991a) reported that adaptation to a rotating sphere with unambiguous disparity also biased the perceived direction of rotation of a monocularly viewed rotating sphere, showing that cue disambiguation can operate between binocular and monocular processes as well as between disparity and structure from motion. On the other hand, they found that prolonged viewing of a KDE rotating sphere disambiguated by disparity cues did not create an impression of three-dimensional rotation in the opposite direction when the test stimulus was a stationary sphere. This suggests that their effect was not a disparity-contingent motion aftereffect like that reported by Anstis and Harris (1974) but rather a motion-contingent disparity aftereffect.

Nawrot and Blake (1991a) suggested that there is a special link between disparity and structure-from-motion processes. They found that although the presence of several other nonstereoscopic sources of information, such as perspective (Braunstein 1966), occlusion (Braunstein et al. 1982; Anderson and Braunstein 1983) and luminance proximity (Dosher et al. 1986), could disambiguate the direction of perceived rotation in an ambiguous KDE display when presented at the same time, adaptation to unambiguous KDE displays was not sufficient to bias the direction of rotation in an ambiguous KDE display

viewed subsequently. For example, prolonged inspection of rotating KDE sphere under polar projection, in which there were few reversals in the perceived direction of rotation, failed to bias the perceived direction of rotation of a rotating sphere seen under parallel projection. Although consistent with the idea of a special link between disparity and structure-from-motion processes, these results may be a consequence of the fact that disparity is a more powerful source of disambiguating information.

In a later paper Nawrot and Blake (1993a) report that a brief 1000 ms exposure to two sheets of random dots moving in opposite (left-right) directions, one with 1 arcmin of crossed disparity and the other with 1 arcmin of uncrossed disparity, was sufficient to bias the impression of rotation in an ambiguous KDE sphere rotating about the 'y' axis. In this case, however, the biasing effect was in the same direction as the brief priming display rather than in the opposite direction following an extended inspection period. They also reported the converse effect that viewing an ambiguous KDE display can bias the direction of perceived rotation of a display containing unambiguous disparity cues. In these priming effects, a weak or ambiguous stimulus takes on the same characteristic as the priming stimulus in contrast to the previous adaptation effects reported by Smith (1976), Rogers and Graham (1984) and Nawrot and Blake (1989) in which an ambiguous stimulus takes on an appearance which is complementary to the adapting display.

Nawrot and Blake also noted that ambiguous kinetic depth displays can be indistinguishable from displays with unambiguous disparity information, which they argue is more consistent with "strong fusion" between the motion and disparity processing systems. Nawrot and Blake (1991b) have proposed a neural-network model of interactions between disparity and structure from motion which is consistent with many of these results. Further evidence of links between the motion and disparity systems was reported by Nawrot and Blake (1993b). They used a dynamic visual noise stimulus in which the dots survived for only one frame before being replaced. With a small interocular delay between the presentations of the same dynamic noise pattern, observers perceived the dots swirling around the fixation point, clockwise or counterclockwise depending on which eye received the delayed presentation (Ross 1974; Tyler 1974c; see Section 13.1.10). Nawrot and Blake found that 15 s of adaptation to a stereoscopic display consisting of frontal planes of dots moving in opposite directions at different depths was sufficient to bias the appearance of rotation in depth of an ambiguous dynamic visual

noise in the opposite direction. Moreover, the biasing was still effective when there was an interocular delay between the presentation of the dynamic visual noise dots, which provided unambiguous information for the opposite direction of rotation. These results show that depth aftereffects following adaptation to moving disparate surfaces interact quantitatively with depth from interocular delay.

Between-cue cancellation of aftereffects

Graham and Rogers (1982a) reported that prolonged viewing of a sinusoidally corrugated surface, defined by either disparity or motion parallax, created a depth aftereffect such that a physically flat test surface appeared corrugated in the opposite direction (Section 12.3.2). The strength of these aftereffects was measured with a nulling technique in which either disparity or parallax depth was introduced into the test surface until the surface appeared flat. In some cases, up to 80 per cent of the depth in the inspection surface had to be introduced into the test surface for it to appear flat. Graham and Rogers (1982b) subsequently reported that the depth aftereffects created by prolonged inspection of sinusoidal corrugations specified by either binocular disparities or monocular motion parallax could be nulled or cancelled with depth from the other cue. Specifically, the aftereffect created by adaptation to a binocular corrugated surface in which the corrugations were specified by disparities could be nulled with motion parallax depth when the observer viewed a single random-dot test pattern and made side-to-side head movements. Likewise, the aftereffect created by adaptation to a monocular corrugated surface, in which the corrugations were specified by motion parallax during side-to-side movements of the observer's head, could be nulled with disparities when the observer remained stationary and viewed a pair of random dot patterns binocularly. Graham and Rogers (1982b) reported that the amount of depth needed to null the aftereffects in the between-cue situation was always much less than in the within-cue situation and that more motion parallax was needed to null the effects of adaptation to disparity surfaces than vice versa.

These results provide evidence of quantitative cue averaging between the depth aftereffects created by one cue and physical depth provided by a different cue. In addition, they show that an aftereffect from a binocular cyclopean stimulus can be seen in a monocular test pattern.

Subthreshold summation

If the mechanisms responsible for our perception of three-dimensional structure from binocular

disparities and motion parallax do interact in terms of cue averaging or summation at some stage in the processing hierarchy, we would predict that thresholds for detecting depth in surfaces which are specified by both cues will be lower than thresholds for detecting depth in surfaces specified by either cue alone. In other words there should be subthreshold summation. Bradshaw and Rogers (1992) looked for evidence of subthreshold summation in the detection of sinusoidal corrugations of different corrugation frequencies (0.1, 0.2, and 0.4 c/deg). Thresholds for discriminating the phase of the corrugations (0° or 180°) were first measured separately for binocular disparity- and motion parallax-specified surfaces while the observer made side-to-side head movements. Thresholds were then measured for depth corrugations specified by both cues in which the relative amplitudes of the two cues were scaled or normalized according to their respective individual thresholds. Bradshaw and Rogers reported that thresholds for discriminating the combined cue corrugations were almost a factor of two lower than the normalized thresholds for the separate cue surfaces. The size of this subthreshold summation effect is greater than that predicted by most models of probability summation (Graham 1989) and the authors concluded that the mechanisms involved in processing disparity and motion parallax must interact at a relatively early stage before the point where threshold judgments are made.

Cornilleau-Peres and Droulez (1993) measured thresholds for the detection of curvature from either binocular disparities, motion parallax, or the two cues together. In addition, they looked for evidence that the visual system uses the small differences between the patterns of optic flow reaching the two eyes—motion disparity—as a source of information about surface curvature. Their theoretical work suggested that motion disparity is a potential cue to surface shape (Cornilleau-Peres and Droulez (1990, 1994). Motion disparities are created only by surfaces which translate parallel to the interocular axis and hence there should be a difference in curvature detection thresholds for horizontally and vertically translating surfaces, if the visual system uses motion disparities.

In all the experiments, observers made a forced-choice discrimination between planar and curved surfaces. Thresholds for surfaces specified by motion cues were generally lower than for disparity surfaces and lowest for surfaces specified by both cues but the amount of facilitation was no greater than predicted by probability summation. No systematic differences were found for the different directions of motion. In an additional experiment, the right and

left eyes' images were decorrelated but the patterns of optic flow were made slightly different to create motion disparities. Observers were unable to make a discrimination between planar and curved surfaces even with the maximal degree of surface curvature.

Rogers and Graham (1982) and Bradshaw and Rogers (1992) both reported that thresholds were lower for disparity corrugations than motion parallax corrugations whereas Cornilleau-Peres and Droulez (1993) reported a small difference in the opposite direction. Cornilleau-Peres and Droulez pointed out that the thresholds for detecting surface curvature from motion cues are similar in the two experiments and the difference in the pattern of results is a consequence of the lower disparity thresholds obtained by Rogers and Graham.

Between-cue threshold elevation

Depth aftereffects are created after inspection of the pattern of disparities created by a three-dimensional surface which is stabilized on the retina (Section 12.3.4). If the eyes are allowed to scan vertically over horizontal depth corrugations, rather than tracking along a contour parallel to the corrugations, no depth aftereffect is seen. Instead, thresholds are temporally raised for detecting corrugations of the same or similar frequencies (Schumer and Ganz 1979). Bradshaw and Rogers (1993a) investigated whether the elevation of thresholds for perceiving three-dimensional corrugations following adaptation to a supra-threshold corrugated surface defined by one depth cue transferred to a surface specified by the other depth cue. Separate thresholds were first measured for discriminating the phase of disparity and parallax corrugations of 0.2 c/deg prior to adaptation. For their two observers, the average threshold was 4.9 arcsec for the disparity condition and 6.5 arcsec for the parallax condition. After more than 3 minutes of adaptation to a 4.5 arcmin disparity-defined corrugation (60 times above threshold) which reversed in phase every 2 s, thresholds for discriminating the phase of disparity corrugations of the same spatial frequency had increased by an average of 112 per cent (within-cue threshold elevation). Thresholds for discriminating the phase of motion parallax corrugations following adaptation to parallax-defined corrugations increased by an average of 76 per cent (within-cue threshold elevation).

Thresholds for discriminating the phase of disparity corrugations after adaptation to parallax corrugations were raised by 50 per cent while thresholds for discriminating the phase of parallax corrugations after adaptation to disparity corrugations rose by 45 per cent (between-cue threshold

elevation). Bradshaw and Rogers concluded that the disparity and motion parallax mechanisms are not independent and must interact quantitatively at an early stage in the processing hierarchy.

Depth in surfaces defined by disparity and parallax.

The underlying similarity of the computational theory of binocular disparity and monocular motion parallax is outlined in Section 13.5. In essence, binocular disparity can be thought of as the special, discrete case of the continuous parallax transformation created by translation of the vantage point. The discreteness of binocular images necessarily leads to a potential problem in identifying which parts of one eye's image correspond to which parts in the other eye's image—the correspondence problem. However, if the matching process is appropriately constrained by (1) typical scene characteristics, (2) the geometry of the viewing situation, and (3) the characteristics of the matching primitive, the correspondence problem can be solved (see Section 6.2).

The correspondence problem is less severe in the continuous sequence of images created when an observer makes side-to-side head movements, which we refer to as motion parallax. In general, Richards (1985) has shown that the information for depth from binocular disparity is less determinate than the information from structure from motion. There are several additional problems, however, in the interpretation of continuous parallax transformations and structure-from-motion transformations in general. First, any differences between the relative positions of corresponding features in the two simultaneous binocular images must be the result of their relative positions in space (assuming that the eyes are vertically, horizontally, and torsionally aligned). In motion parallax, any relative motion of image features may be due to either a difference in depth or to relative movement of the features themselves. This means that it is necessary to make assumptions about either the global or local rigidity of the features in order to interpret structure-from-motion transformations correctly (Johansson 1973; Todd 1981; Koenderink 1986; see Section 13.5). There is a fundamental ambiguity in the interpretation of structure-from-motion transformations which cannot be solved unless rigidity is assumed.

Consider a monocular observer who makes a small horizontal head movement while viewing a three-dimensional surface (Helmholtz 1909). Let us assume that the extent of movement is small compared with the distance between the observer and the surface so that this distance remains approximately constant. If the extent of movement equals the interocular distance, the two views of the surface

at the limits of the head movement are identical to the two simultaneous views of the binocular observer. To put it another way, the information for motion parallax, like binocular stereopsis, arises as a consequence of viewing the surface from slightly different angular directions (see also Durgin et al. 1994). Hence, we can refer to these two sources of information as **motion perspective** and **binocular perspective** respectively.

In addition, it can be seen that the optic array transformation of the surface during observer movement around the surface is essentially equivalent to that produced when the observer remains stationary and the surface rotates around a vertical axis. This suggests that there is a second potential ambiguity in the interpretation of motion parallax as to whether the pattern of relative motion is due to observer motion or object rotation. In principle, several sources of information could be used to solve this ambiguity including: (1) kinaesthetic and vestibular signals and (2) the relative optic flow between the surface and other parts of the visible scene. Note that this ambiguity exists even if we assume the surface is rigid.

For the purpose of determining the three-dimensional structure of a surface, it does not matter whether the observer has moved or the surface has rotated with respect to the observer, although in both cases the direction and amount of change in the angular viewing direction must be correctly registered. If it is not, the amount of depth in the surface will be incorrectly calculated. For example, the same pattern of relative motion between the peaks and troughs of the corrugations is created by a surface with a large peak-to-trough depth which rotates through a small angle as by a surface with a small peak-to-trough depth which rotates through a larger angle, to a first approximation (Rogers and Collett 1989; Durgin et al. 1994).

This suggests the existence of a third source of ambiguity in the interpretation of structure-from-motion transformations which arises whenever the change in viewing direction is not known precisely. There is an equivalent ambiguity in the interpretation of binocular disparities. To calculate the correct metric properties of the scene from binocular disparities, the difference in the angular viewing directions from the two vantage points has to be known, as well as their interocular separation. For binocular vision, there are two possible sources of this information: (1) the proprioceptive or efference copy signals indicating the vergence state of the eyes and (ii) the pattern of vertical disparities (Section 7.6). The empirical evidence suggests that we use both sources of information.

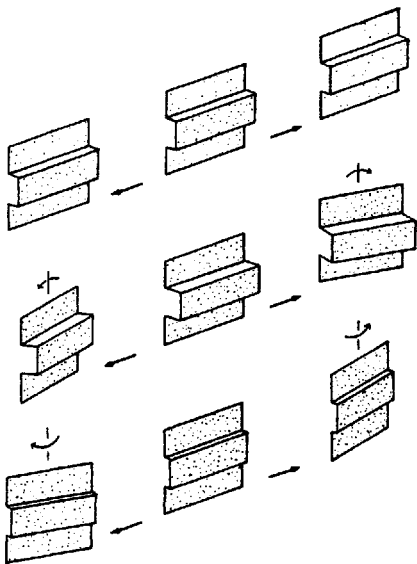


Figure 11.2. The ambiguity of motion parallax.

When a corrugated surface translates to and fro in a frontal plane (upper trace), there is relative motion between points on the surface with different depths. To a first approximation, the same amount of relative motion is created by a surface with more depth which simultaneously rotates in a concave direction as it translates (middle trace), or a surface with less depth which simultaneously rotates in a convex direction as it translates (bottom trace). (Adapted from Rogers and Collett 1989.)

In the case of motion parallax, there are two equivalent sources of information about the change of viewing direction: (1) absolute motion parallax and (2) the perspective changes of objects and surfaces close to the observer. The latter are directly analogous to the vertical disparities created by binocular viewing. In principle, it should be possible to register the change in the viewing direction of an object or surface created by observer movement—absolute motion parallax—but in practice it seems unlikely since the visual system would have to monitor not only the rotation of the eye in the head but also the rotation of the head on the shoulders and of the body with respect to the ground. Rogers and Rogers (1992) have shown that proprioceptive and vestibular information is partially effective in disambiguating the direction of rotation and the relative order of the depth structure in an ambiguous KDE stimulus, but there is no evidence that proprioceptive information alone is capable of specifying the change in viewing direction. Evidence that we are able to use perspective information to specify the change of viewing direction in the KDE and motion parallax situations is reviewed below.

For displays which subtend less than about 5°, the perspective information specifying the change of viewing direction both between the eyes and over

time is too small to be detected. However, the continuous transformation in the motion case provides additional information about the change of viewing direction as a consequence of the acceleration component of the flow field, which is not available in binocular viewing or motion sequences consisting of just two frames (Richards 1985). If the visual system uses this information, the shape of the three-dimensional surface will be completely specified. If not, the shape of a surface is only defined up to a scale factor (see also Todd and Bressan 1990; Todd and Norman 1991). Durgin et al. (1994) have shown that the size of the foreshortening component for rotations of 15° from the frontal plane is very small and unlikely to be a reliable source of information. Support for this conclusion was provided by Caudek and Proffitt (1993) who showed that information about the angle of rotation in shape-from-motion displays is not recovered for small angles of rotation and, by Eagle and Blake (1994) who showed that a large angle of rotation is necessary to extract metric shape from motion reliably.

Depth and rotation trade-off

Rogers and Collett (1989) investigated interactions between motion parallax and binocular disparity as sources of information about the depth of three-dimensional surfaces. Indirectly, their experiments also provide evidence about the effectiveness of perspective changes and the acceleration component of the flow field as sources of information about the change in angular viewing direction in the motion parallax situation. The motion parallax simulated in their experiments was equivalent to that produced by a three-dimensional corrugated surface which translates to and fro in a frontal plane (object-produced parallax). To achieve this, a pair of display oscilloscopes was mounted on a platform which was swung in a frontal plane in front of the observer (Figure 13.28). The fixed mirrors in front of the eyes allowed each screen to be viewed by only one eye.

Consider first the translation of a real corrugated surface in front of an observer. If the extent of translation is small compared with the distance from the observer to the surface, the same pattern of relative motion between the peaks and troughs of the corrugations would be created by (1) a surface with a particular depth, which translated (without rotating) along a path in the frontal plane, (2) a surface with a larger peak-to-trough depth which simultaneously rotated towards the observer at the ends of its translation (concave path), and (3) a surface with a smaller peak-to-trough depth which simultaneously rotated away from the observer at the ends of its translation (convex path) (Figure 11.2).

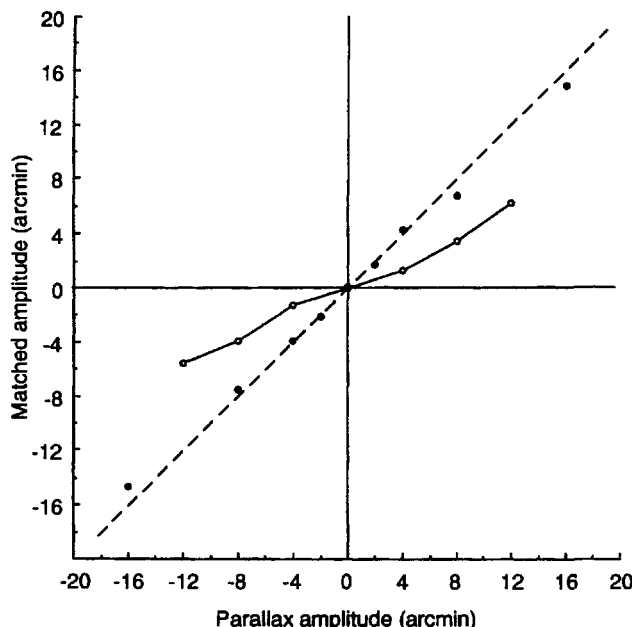


Figure 11.3. Perceived depth in motion parallax surfaces. Observers matched the depth seen in parallax corrugations which translated to and fro in a frontal plane to a variable amplitude disparity-plus-parallax surface. With monocular viewing (filled circles), matched depth was close to veridical. With binocular viewing (open circles), matched depth was about 50 per cent of the depth specified. (Adapted from Rogers and Collett 1989.)

How does the visual system deal with this ambiguity? To answer this question, Rogers and Collett asked observers to match the perceived depth in a sinusoidally corrugated surface specified by monocular parallax to a separate, variable amplitude corrugated surface specified by binocular disparities. The perceived depth was similar to that predicted on the assumption that the corrugated surface translated along a straight path within a frontal plane (Figure 11.3). In addition, observers reported that it did not appear to rotate as it translated to and fro. This result suggests that the visual system does have access to additional information which signals the change in slant of the surface as it translated along its frontal path.

In their second experiment, Rogers and Collett independently manipulated (1) the amount of motion parallax and (2) the disparity between the peaks and troughs of the corrugations. If parallax alone is intrinsically ambiguous with respect to the trade-off between depth and rotation (as suggested previously), the presence of disparity information to specify the "correct" depth should allow a unique solution. If the visual system uses disparity to determine the depth in the corrugations, changing the amount of parallax motion should have no effect on the perceived depth but should affect the amount of perceived rotation.

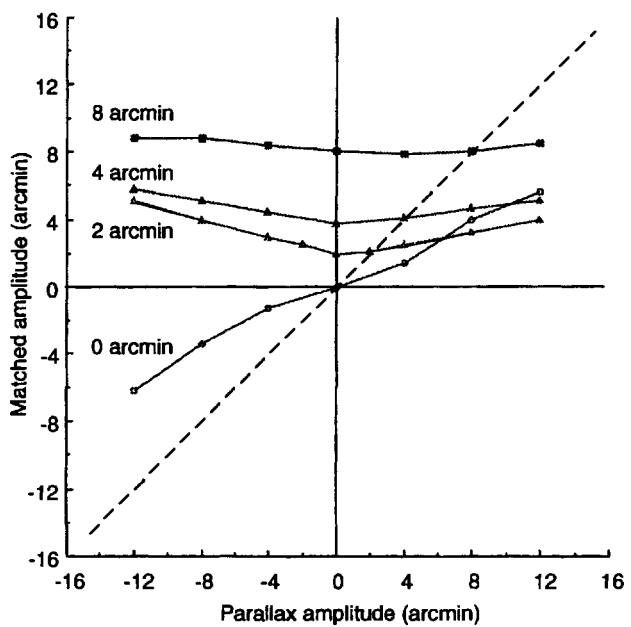


Figure 11.4. Perceived depth in disparity plus parallax surfaces. Observers matched the amount of depth seen in a translating corrugations specified by different amounts of motion parallax (abscissa) and disparity (parameter of different curves). The amount of parallax depth had little effect on perceived depth when the disparity of the corrugations was large (8 arcmin). For small amplitude disparity corrugations (including zero amplitude), perceived depth increased with increasing parallax. (Adapted from Rogers and Collett 1989.)

The results presented in Figure 11.4 show the perceived depth (measured using a variable amplitude matching surface) as a function of the amplitude of motion parallax. For large amplitudes of peak-to-trough disparity (> 8 arcmin), the best-fitting functions have only a very shallow slope, indicating that the amount of parallax had little effect on perceived depth. Under these conditions, observers reported that the surface appeared to rotate as it translated across the median plane, with a "concave" rotation when the parallax amplitude was smaller than the disparity amplitude and a "convex" rotation when the parallax amplitude was larger than the disparity amplitude.

With small peak-to-trough disparities, the slopes of the best-fitting functions were significantly different from zero, indicating that the perceived peak-to-trough depth increased with increasing amplitude of motion parallax. For the particular case in which the disparity amplitude was zero (signalling a flat surface) the perceived depth increased linearly with parallax amplitude and was approximately 50 per cent of that found with monocular viewing (Figure 11.4). The perceived rotation of the surface was always convex and increased in magnitude with increasing amplitude of the parallax signal.

Overall, the results show that motion parallax and binocular disparity do interact quantitatively in determining the perceived depth of these simulated translating surfaces—cue averaging or weak fusion does occur. One interpretation of the data is that the weighting given to disparity increases with disparity amplitude so that a high weighting is given to large disparities, and this principally determines the perceived depth, while a low weighting is given when the disparity amplitude is small or zero (specifying flatness). Rogers and Collett (1989) suggested an alternative explanation in which the interpretation of the "ambiguous" motion parallax information is affected both by the presence of disparity cues and by the presence of additional perspective information which signals the extent of rotation of the surface as it translates.

To understand this proposal we need to return to the statement made previously that motion parallax created by a translating three-dimensional surface is ambiguous with respect to the depth and the amount of convex or concave rotation as it translates. This statement is true only for a surface of small angular extent or one which rotates through a small angle. For a larger three-dimensional surface, there are changes in its angular width and height as it translates and these perspective changes provide unambiguous information about the amount of rotation of the surface with respect to the line of sight. Hence the change in perspective of an extended surface as it translates across the frontal plane provides information about the amount by which it has rotated, just as the difference in perspective present in two simultaneous binocular views provides information about the angular difference of the lines of sight from the two vantage points to the surface (Section 7.6). Consequently, the perspective changes in the image of a translating three-dimensional surface could be used to determine the amount of rotation and thereby disambiguate the "ambiguous" parallax motion. Rogers and Collett did not consider the additional information available from the acceleration component of the flow field which also allows the amount of rotation to be calculated.

As we indicated previously, the fact that depth is seen veridically in monocular translating parallax surfaces suggests that the people use either the changing perspective in transforming images or the acceleration component of the flow field to determine the extent of rotation of translating three-dimensional surfaces. When both motion parallax and disparities are present, there are two constraints on the interpretation of the parallax information—perspective and flow-field acceleration provide a constraint on the amount of perceived rotation of the

surface with respect to the line of sight and disparities provide a constraint on the amount of perceived depth. If the interpretation of the motion parallax involved setting the depth to that specified by the disparities, the amount of predicted rotation would be incompatible with that specified by the perspective changes and the flow-field acceleration. If the interpretation of the motion parallax was based on the amount of rotation specified by the perspective changes and flow-field acceleration, the perceived depth would be incompatible with that specified by the disparities.

With the large amplitude disparity surfaces used by Rogers and Collett, the predicted rotation if motion parallax is inconsistent with disparity is necessarily small and not necessarily incompatible with the perspective and flow-field information. With small amplitude disparity surfaces, on the other hand, the predicted rotation is large and therefore incompatible with the perspective and flow-field information. Under these circumstances, we should expect the perceived depth to be influenced by the amount of parallax as well as the disparity. This was precisely the pattern of results found empirically.

Williams (1994) measured perceived rotation and perceived depth in translating surfaces. His results were consistent with the idea that the interpretation of parallax information is constrained by both the amount of depth specified by disparities and the amount of rotation specified by either the change of perspective or the acceleration component of the flow field. He also reported that manipulations of the perspective component of the flow field affected both the perceived depth and the perceived rotation of the translating parallax surfaces (see also Rogers and Bradshaw (1991)). This shows that the visual system does use the change of perspective provided by large displays as a source of information about the change of slant. *For a particular amount of rotation, the change in perspective of a surface which subtends only a small visual angle becomes vanishingly small, and therefore we predict that the pattern of results observed by Rogers and Collett (1989) should be significantly affected by the size of the display.*

Perceived shape of surfaces defined by disparity and structure-from-motion

Important evidence of accumulation, veto, and cooperation in the interactions between binocular disparity and structure from motion (SFM) has been provided by Braunstein et al. (1986), Dosher et al. (1986), and Tittle and Braunstein (1991, 1993). Braunstein et al. (1986) showed that disparities can disambiguate the sign of depth for computer-generated

orthographic projections of texture elements on the surface of a rotating sphere. Dosher et al. (1986) obtained a similar result for the perspective projection of rotating wire-frame Necker cubes. These are both cooperative interactions. On the other hand, the presence of dynamic occlusion provided by opaque structure-from-motion stimuli was sufficient to veto the conflicting disparity information (Braunstein et al. 1986).

Further evidence of cooperativity was found by Braunstein et al. (1986) and Rouse et al. (1989). They reported that observers who could not detect the depth of disparate targets in a static stereo test were able to judge the direction of rotation correctly in structure-from-motion displays with additional disparity cues. This facilitative interaction between disparities and structure-from-motion is not confined to stereo-deficient observers. Tittle and Braunstein (1989) reported that the perceived depth-to-height ratio of a transparent cylinder rotating about a horizontal axis with unchanging structure-from-motion information was affected by the presence of binocular disparities. This result is inconsistent with Richards' (1985) suggestion that under these conditions disparities should provide information only about the sign of depth and the perceived shape should depend solely on structure from motion.

In the experiments of Tittle and Braunstein (1993), observers viewed stereograms of horizontal transparent cylinders which either rotated about a horizontal axis or translated along a horizontal path. The judged depth-to-height ratio of the cylinders was always greater than for static cylinders and the ratio increased as the depth specified by disparity increased. In fact the depth-to-height judgments were reasonably consistent with the magnitude of the disparities present, suggesting that disparity is weighted more heavily than structure from motion in this situation. This pattern of results was also found in Rogers and Collett's (1989) study. The trading function between disparity and structure from motion is characteristic of an accumulation or weak fusion interaction while the disambiguation of the direction of rotation suggests a cooperative interaction between the two cues.

Tittle and Braunstein (1993) considered the possibility that the facilitative effect of motion in the presence of disparity cues is due to the fact that matches between corresponding points are easier to establish when the points are moving. If this were true then shortening the presentation time should make the correspondence problem more difficult to solve. The results did not confirm this prediction. However, they did find that the disruptive effect of high density patterns in the perception of transparent

cylinders (Akerstrom and Todd 1988) was reduced when the dots were moving. This is consistent with the hypothesis that motion facilitates disparity processing by helping to resolve the correspondence problem.

Four conclusions about the relationship between disparities and structure from motion were drawn by Tittle and Braunstein (1993). First, the interactions can be cooperative and facilitative as evidenced by the fact that the depth from a display containing both cues could be more than the sum of the depths from displays containing only one cue. Second, depth from displays containing both disparity and structure from motion does not depend solely on the depth specified by structure from motion, whereas Richards' (1985) model predicts that it does. Third, the facilitation provided by structure-from-motion displays increases as the matching of binocular images is made more difficult by increasing the density of texture element. Fourth, the facilitation is not just due to the presence of opposite directions of motion but rather to the presence of structure from motion in the displays. Seen together, these results suggest that the processing of structure from motion and binocular disparity is not strictly modular with the outputs combined on the basis of a weighted averaging but that cooperative and facilitative interactions are also operating.

Depth-to-size invariance

When a surface translates along a frontal path across the median plane of the head the slant of the surface with respect to the cyclopean direction changes. In the previous section it was shown that there are two potential sources of information to specify the change of slant with respect to the cyclopean direction. First, for a surface which subtends more than about 5°, there are perspective changes in the vertical size and horizontal width. The same perspective changes occur for a surface which rotates to and fro through a small angle about a vertical axis (without translating) and again the perspective changes provide information about the change of slant of the surface. Notice that in both cases, the amount of perspective change is a function only of the change of slant angle and is independent of distance, for surfaces of a given angular extent.

The second source of information to specify the change of slant comes from the acceleration component of the flow field. If the surface has depth there will be relative motion between parts of the surface at different distances as it rotates—structure from motion. The magnitude of the relative motion depends both on the depth difference and the degree of slant change. For a surface which is twice as far

away, but of the same angular size, the same amount of relative motion (in angular terms) is created by a surface which has twice the depth difference (to a first approximation). Turning the argument around, it follows that all surfaces which have the same ratio of depth to their physical size will create the same amount of relative motion for a given change of slant. Hence if information about the change of slant is available from either the perspective changes or the acceleration component of the flow field, the ratio of the amount of relative motion to the angular size in the optic array specifies the depth-to-size ratio of the surface irrespective of its distance from the observer (Richards 1985).

Johnston et al. (1994) have proposed that this invariant characteristic allows the visual system to determine the shape of moving surfaces irrespective of the distance from the observer to the surface, where shape is defined in terms of a depth-to-height or depth-to-width ratio. The same invariant property is also characteristic of the parallax produced by a surface which translates across the observer's line of sight (object-produced parallax) and the parallax produced when an observer makes side-to-side head movements whilst viewing a three-dimensional surface (observer-produced parallax). For a given change of slant of the surface with respect to the line of sight, the ratio of the parallax motion to the angular size is the same for all surfaces which have the same depth-to-size ratio.

The same is also true of disparity surfaces. For the same difference in slant of a surface seen from two vantage points, the ratio of the disparity to the angular size is unaffected by the distance to the surface. But the difference in slant from the two eyes stays the same only if the vergence angle is kept constant for surfaces at different distances. If vergence is changed, the invariant relationship no longer holds and the shape of surfaces can be correctly determined only if there is additional information about the vergence angle of the eyes. *If vergence is kept constant, shape constancy (in terms of the depth-to-size ratio), should be perfect for surfaces at different distances.* In situations where vergence is not held constant, Johnston et al. (1994) make the interesting suggestion that the visual system could use this invariant property of moving surfaces to facilitate the interpretation of binocular disparities.

To test this idea, Johnston et al. presented observers with horizontally oriented and textured cylindrical surfaces which were either (1) stationary and specified by disparities, or (2) oscillating about a vertical axis and specified by relative motion (viewed monocularly) or, (3) oscillating about a vertical axis and specified by both relative motion and

disparities. Their results clearly demonstrate an interaction between the two sources of information—binocular disparities and relative motion. In particular, they found that semicircular cylinders defined by disparities alone appeared significantly flattened by a factor of two when the cylinders were displayed at a 200 cm viewing distance. They attributed the flattening to an underestimation of the viewing distance from vergence signals (see also Johnston 1991 and Section 7.7.2). In contrast, the same semicircular cylinders defined by relative motion (rocking to and fro about a vertical axis) were perceived veridically.

When both cues were available, the shape of the cylinders was also perceived veridically. This pattern of results is consistent with a veto model in which the relative motion to angular size ratio, which unambiguously specifies the shape (depth-to-size ratio) of the surface, determines the perceived shape. According to this model, disparity information is simply ignored for judgments of perceived shape. However, the predictions of the simple veto model are inconsistent with the results of the second experiment carried out by Johnston et al. In this experiment, relative motion and binocular disparity specified different depth-to-size ratios of the cylinder. If the shape of the cylinder is determined by the ratio of relative motion to the angular size alone, variations in the depth-to-size ratio from disparity cues should have no effect on perceived shape. On the contrary, the results show that a cylinder with a depth-to-height ratio specified by disparities of less than one (that is, flattened) was judged as circular only when the depth-to-height ratio specified by relative motion was greater than one. In other words, there is a trading relation between the two sources of information. Johnston et al. argue that the interaction between disparity and structure-from-motion cues evident in the results cannot be described by a linear combination rule characteristic of weak fusion models. Instead they suggest that results are more compatible with the idea of modified weak fusion involving an initial stage of cooperative interaction to determine the missing distance parameter followed by a stage of weighted linear summation in which the weights applied to the different cues can change depending on the viewing distance and the number of frames present in the motion sequence.

The invariance of relative motion to the angular size ratio with changes in the absolute distance of moving surfaces predicts a high degree of constancy for depth-to-width judgments. The displays used by Johnston et al. tested this hypothesis with a structure-from-motion stimulus which oscillated around a vertical axis but a similar constancy is also

predicted for observer- and object-produced parallax situations. Ono et al (1986) and Rivest et al. (1989) measured depth constancy in corrugated surfaces at different distances when the motion parallax was linked to active movements of the observer's head. They found poor constancy for judgments of the depth in corrugated surfaces more than 1 m away. *To test the depth-to-size invariance hypothesis, this experiment should be repeated with judgments of perceived shape (depth-to-width ratios) for surfaces of different shapes presented at different distances.*

The invariance of relative motion to the angular size in motion parallax displays is not sufficient to explain the veridicality (rather than the constancy) of depth-to-size judgments in the experiments of Johnston et al. (1994). The visual system must also be capable of deriving an accurate estimate of the change of slant of the surface from either the perspective or acceleration components of the flow field as the surface changes its orientation with respect to the line of sight. As we indicated earlier, the fact that the perceived depth of monocular motion parallax surfaces was close to veridical in Rogers and Collett's (1989) study suggests that the visual system is able to extract the change of perspective, at least with their 20° diameter displays. Further evidence is provided by Williams (1994) who reported that manipulations of the vertical perspective component affected both the amount of perceived depth and the amount of perceived rotation in translating parallax surfaces. In the experiments of Johnston et al., however, the angular size of the surface defined by structure from motion was only 1.72° at the 200 cm viewing distance which means that the perspective changes created by the rotation of the surface through ±15° were negligible. Indeed, Johnston et al. (1994) concluded that the visual system does not use changes of perspective provided by moving surfaces. Their own interpretation was that the acceleration component of the flow field is responsible for the veridicality of shape judgments. The lack of veridicality in shape judgments when only two frames were presented in the structure-from-motion condition is consistent with this conclusion.

Temporal factors

Uomori and Nishida (1994) have noted temporal changes in the perceived depth of surfaces which provide conflicting disparity and SFM information. The SFM information depicted an opaque vertical cylinder which rotated continuously around its vertical axis. The binocular disparities depicted a horizontal cylinder. A preadaptation stimulus depicting either the disparity-defined horizontal cylinder or the vertical cylinder defined by shape

from motion was sometimes presented for 10 s before the conflicting-cue display. In the absence of the pre-adapting stimulus, the conflicting-cue display was typically seen as a vertically-oriented cylinder at the start of the 60 s inspection period and subsequently as a combination of the two cylinders (a barrel shape) or, in some cases, as a horizontally-oriented cylinder. There were large individual differences between the patterns of results for the 4 observers. The effect of the preadapting stimulus was to bias the reports away from shape depicted in that the preadapting period, which is consistent with the results of Rogers and Graham (1984) and Nawrot and Blake (1989), but an overall temporal change from depth defined by shape-from-motion to depth defined by disparity was still evident. The authors attributed the temporal changes seen in the conflicting-cue display to adaptation of the shape-from-motion mechanism. *It would be interesting to see if there is a similar change with displays in which the disparity and shape-from-motion cues provided more similar shape information.*

Disparity between motion boundaries

Evidence of a different kind of interaction between the motion and disparity systems is provided in an experiment by Lee (1970c). In a stereoscopic display, each eye saw a vertical strip of random dots which oscillated sinusoidally from side-to-side occluding and exposing a background of similar random dots. The boundaries of the vertical strip were not visible in any snapshot of the display. The dot patterns of both strip and background were uncorrelated between the two eyes so that there were never any corresponding points. However, the locations of the contours between the moving strip and the stationary background were correlated binocularly and when a binocular phase difference was introduced between the sinusoidal motions of the oscillating strips seen by the two eyes, the vertical strip was seen to rotate in an elliptical path in depth similar to that seen in the Pulfrich effect (Section 13.1). This shows that kinetic boundaries constitute a token which can be matched by the stereoscopic system (Section 6.1.5).

Rogers (1987) showed that a binocular phase difference between standing wave patterns of shearing motion can also be detected by the visual system. Each eye saw a similar pattern of shearing motion in which the dots moved up and down along vertical paths with sinusoidal motion. The amplitude of vertical motion varied sinusoidally with horizontal position to create a standing wave pattern of shearing motion. Seen monocularly, the standing wave pattern was seen as a three-dimensional vertical

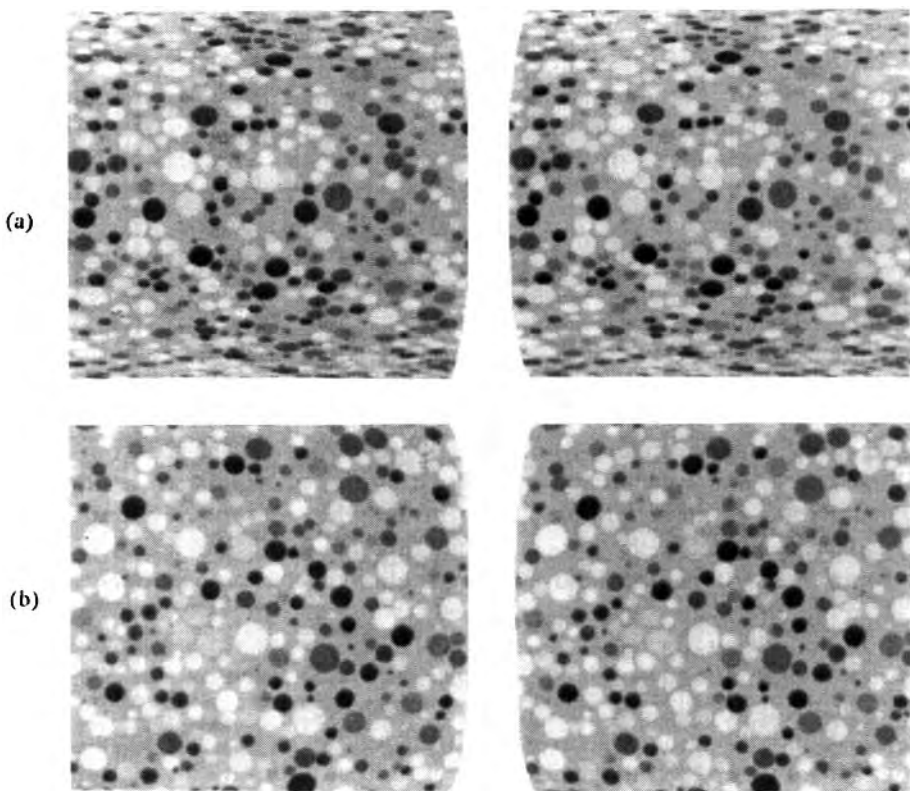


Figure 11.5. Stereograms with compatible and incompatible texture gradients.

(a) Divergent fusion creates a cylinder in depth with compatible disparity and texture gradient .

(b) In this case, disparity is the same as in (a) but the texture gradient signifies a flat surface.
(Reproduced with permission from Cumming et al. 1993. Vision Research, Pergamon Press.)

corrugation which rocked to and fro about a horizontal axis through the centre of the pattern, like a kinetic depth effect stimulus. The dot patterns seen by the two eyes were uncorrelated but there was a correlation between the positions of the nodes and antinodes of the standing wave motion. The vertical corrugations appeared to rock to and fro in front of the fixation point when the nodes and antinodes had a crossed disparity, and beyond the fixation point when they had an uncrossed disparity.

There are two possible explanations of this effect. The visual system might detect the phase difference between the correlated vertical motions in the two eyes. If so, the use of standing-wave patterns of motion in this experiment suggests that binocular matching can occur between the smooth (low frequency) as well as the sharp (high frequency) kinetic boundaries used in Lee's (1970c) experiment. Alternatively, the structure-from-motion could be interpreted separately in the two eyes before the disparity between the three-dimensional structures is derived. That is, the visual system could use—**structure-from-motion disparity**—rather than **kinetic boundary disparity**. No evidence was provided to distinguish between these two possibilities.

11.2.3 Disparity - perspective interactions.

Perspective in all its forms arises from the reduction in the size of the retinal image of an object in the frontal plane as its distance from the eye increases. Although the cause is always the same, perspective takes many forms depending on the type of visual display. The image of an object orthogonal to a visual line shrinks as the object is taken further away. This is the **size-distance law**. As the object recedes, the images of parts below the visual axis rise up toward the fixation point and the images of parts above the visual axis fall toward the fixation point. This is referred to as the cue of **image elevation**. The images of vertical lines on a surface inclined about a horizontal axis or of horizontal lines on a surface slanted about a vertical axis become shorter as the inclination or slant of the surface increases. This is known as **foreshortening**. The images of parallel vertical lines on a surface inclined about a horizontal axis or of horizontal lines on a surface slanted about a vertical axis become tapered toward the more distant side of the surface. This is known as **linear perspective**. The images of the elements of an inclined or slanted textured surface become smaller

and more tightly packed towards the more distant side of a surface. This is a **texture gradient**. The images of texture elements on a surface curved in depth also become smaller and more dense, but in addition, they change their aspect ratio. For example the images of circles on a convex cylindrical surface become increasingly elliptical round the curve of the cylinder. This may be called **aspect-ratio perspective**. A simple texture gradient, defined by decreasing size and increasing density of texture elements, provides information about how planes recede into the distance, whereas aspect-ratio perspective provides the most effective information about surface curvature (Cutting and Millard 1984; Todd and Akerstrom 1987).

Youngs (1976) had subjects judge the angle of inclination of a featureless 2° high by 4° wide rectangle seen in a stereoscope. In one condition the rectangle was tapered to simulate an inclination about a horizontal axis of 45° and disparity information corresponding to the same angle of inclination was either present or absent. The rectangle appeared to slant about 25° when perspective was present but judgments were not affected by disparity, either in the presence or absence of perspective. This suggests that linear perspective is a more powerful cue to distance than disparity. However, we are not told whether an outer frame was visible surrounding the test rectangle. Disparity is ineffective when relative disparities are kept to a minimum.

Gillam (1968) found that the accuracy of slant judgments for a monocularly viewed surface slanted 18° about a vertical axis was high when the surface was covered with horizontal lines or a grid, but that slant was severely underestimated when the surface was covered with vertical lines or random dots. In other words, the accuracy of slant judgments based on linear perspective was higher than those based on foreshortening, and adding linear perspective to foreshortening did not improve accuracy. In a second condition, the marked surfaces were in the frontal plane and the image in one eye was magnified horizontally relative to that in the other eye to simulate disparities corresponding to slants of up to 30°. The slant of the surface with horizontal lines was severely underestimated for stereoscopic slants greater than 15° but the slant of the surface with vertical lines was accurately perceived for all angles of slant up to 30°. Thus the strong monocular cue of linear perspective at a value of zero slant reduced the impression of slant produced by disparity but the weak monocular cue of foreshortening set at zero had no effect on disparity-induced slant.

Cumming et al. (1993) investigated effects of different types of texture perspective on the perceived

depth of a horizontal half cylinder viewed in a stereoscope. Two of their stereograms are shown in Figure 11.5. The depth portrayed by perspective was held constant while disparity-defined depth was varied to determine the value for which the subject judged the depth of the half cylinder to be equal to its width. In the first experiment, texture elements were circles and three components of perspective were manipulated independently; texture element size, density, and aspect ratio. Thus, the contribution of each texture component to perceived depth was assessed by the degree of disparity required to make the stimulus appear cylindrical. Aspect-ratio was the only component of perspective that contributed significantly to perceived depth, confirming Cutting and Millard (1984). Todd and Akerstrom (1987) found an effect of element size only in combination with changing aspect ratio. In a second experiment, Cumming et al. used randomly mixed horizontal ellipses as texture elements. With these stimuli, subjects could not estimate local curvature from local aspect ratio but could derive an estimate of curvature from the change in mean ellipticity. Perceived depth was little affected by a moderate degree of variation in ellipticity of the elements, as in Figure 11.6a, but fell off severely when the variation was large, as in Figure 11.6b. This could be because of the large variation in element ellipticity or the anisotropy introduced by elongation of the elements in only one direction. Use of the stimulus depicted in Figure 11.6c revealed that texture anisotropy was the main factor. The authors concluded that people accurately perceive the three-dimensional shapes of isotropic surfaces on the basis of the overall gradient of aspect ratio. Perhaps they neglect changes in texture density because it is not necessarily constant in a frontal surface.

Johnston et al. (1993) used textured stereograms of half cylinders, triangular ridges, and spheres. Combinations of texture gradients and disparity were found which yielded judgments of shapes that were as deep as they were wide. At a viewing distance of 200 cm, depth generated by disparity was underestimated 50 per cent when the texture was flat and significantly less when the texture gradient was in accord with disparity. At a distance of 50 cm, depth generated by disparity was only slightly underestimated when texture was flat and was slightly overestimated when the texture gradient was correct. A given disparity is more effective at near than at far distances. Adding the correct texture gradient had a stronger effect for vertical cylinders than for horizontal cylinders. This suggests that relative compression disparity produced on surfaces slanted about a vertical axis is a weaker cue to depth than

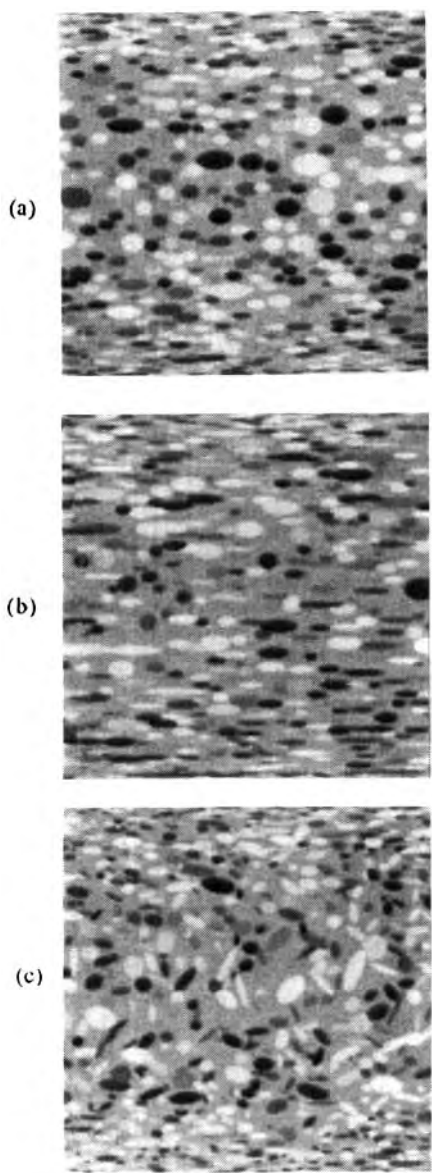


Figure 11.6. Types of texture gradient.

- (a) Texture gradient with elliptical texture elements.
- (b) Texture gradient with very elongated texture elements
- (c) Texture gradient with randomly oriented elliptical texture elements. (Reproduced with permission from Cumming et al. 1993. Vision Research, Pergamon Press.)

shear disparity produced on surfaces inclined about a horizontal axis. A similar anisotropy was noted by Rogers and Graham (Section 12.2.4) and Gillam et al. (Section 12.1.1). Some subjects reported that texture elements did not always appear to lie in the plane of the stereo surface, like the texture elements in Figure 6.18. Perspective in a texture element may therefore be interpreted locally rather than affect the appearance of the surface on which it lies.

Buckley and Frisby (1993) used stereograms depicting vertical and horizontal cylindrical ridges in

which perspective and disparity specified a depth of the ridge of between 3 and 9 cm. The perspective cue was specified mainly by the changing aspect ratio of ellipses. The perspective and disparity cues were consistent in one set of conditions and inconsistent in another set (see Figure 11.7). Subjects matched the perceived depth of the ridge to one of a set of numbered ridge profiles. The results are shown in Figure 11.8. The depth of ridges was judged with reasonable accuracy when the stereo and perspective cues were consistent, as shown by the points linked by a dotted line. Furthermore, depth with only the monocular cue present was underestimated by about one-third compared with when both cues were present and consistent. The vertical ridges showed a large interaction between the two cues; as the depth specified by the perspective cue was reduced, variations in disparity had less effect, and had no effect when perspective depth was only 3 cm. This effect was very much less with horizontal ridges. Thus, disparity arising from a vertically oriented cylinder does not supplement perspective, defined by changing aspect ratio, unless the perspective specifies a large depth. For horizontal cylinders, disparity supplements perspective for all values of both cues. Similar results were obtained with triangular ridges with linear perspective rather than perspective defined by changing aspect ratio. The anisotropy was absent when real three-dimensional cylinders were used. The only difference between the stereograms and the real cylinders seems to have been the absence of accommodation cues to distance in the stereograms. It seems that with the stereogram of the vertical cylinder, disparity was not sufficiently strong to add to the depth created by the perspective cue in the absence of the accommodation cue.

Schriever (1924) presented stereoscopic photographs of three-dimensional objects, such as a cone and tunnel, with disparity reversed. He found that depth in the photographs was judged in terms of the perspective rather than disparity.

11.2.4 Interactions between disparity and overlap

An example of a conflict between disparity and the overlap cue to relative distance is provided by the stereogram in Figure 11.9a. An uncrossed disparity in the vertical stick causes it to appear beyond the horizontal stick. In this case stereoscopic depth and the figural continuity of the vertical stick are in agreement. With a crossed disparity, the two sticks do not appear to separate in depth because this would contradict the monocular information that the horizontal stick is nearer than the vertical bar (Schriever 1924). This is an example of cue

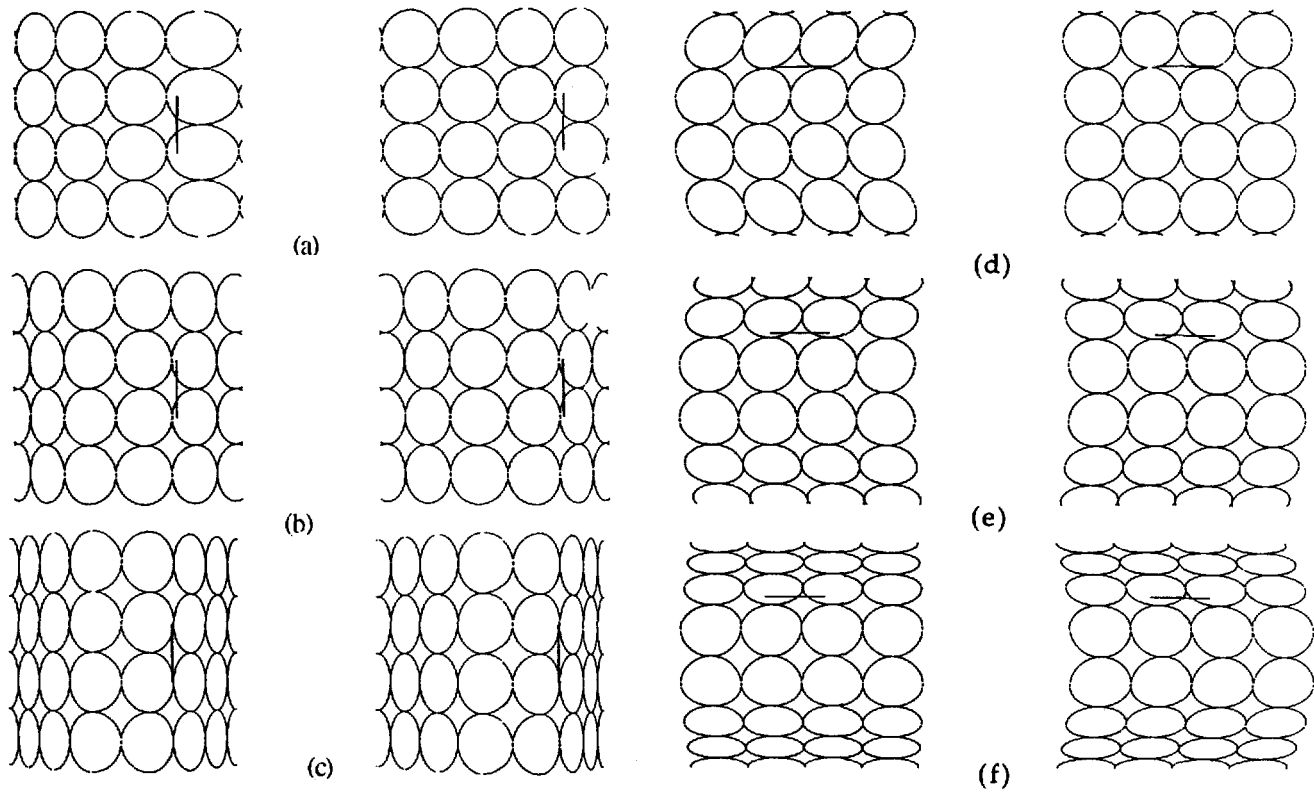


Figure 11.7. Stereograms used to study cue interactions.

Convergent fusion of each stereogram at a distance of 57 cm produces a vertical or horizontal parabolic ridge. Disparity is the same in all stereograms. In (b) and (e) disparity and perspective cues are consistent. In (a) and (d) perspective indicates less depth than disparity. In (c) and (f) perspective indicates more depth than disparity. Perspective had a greater effect on perceived depth for the vertical ridges than for the horizontal ridges. For some observers this differential effect wore off with practice. (Adapted from Buckley and Frisby 1993.)

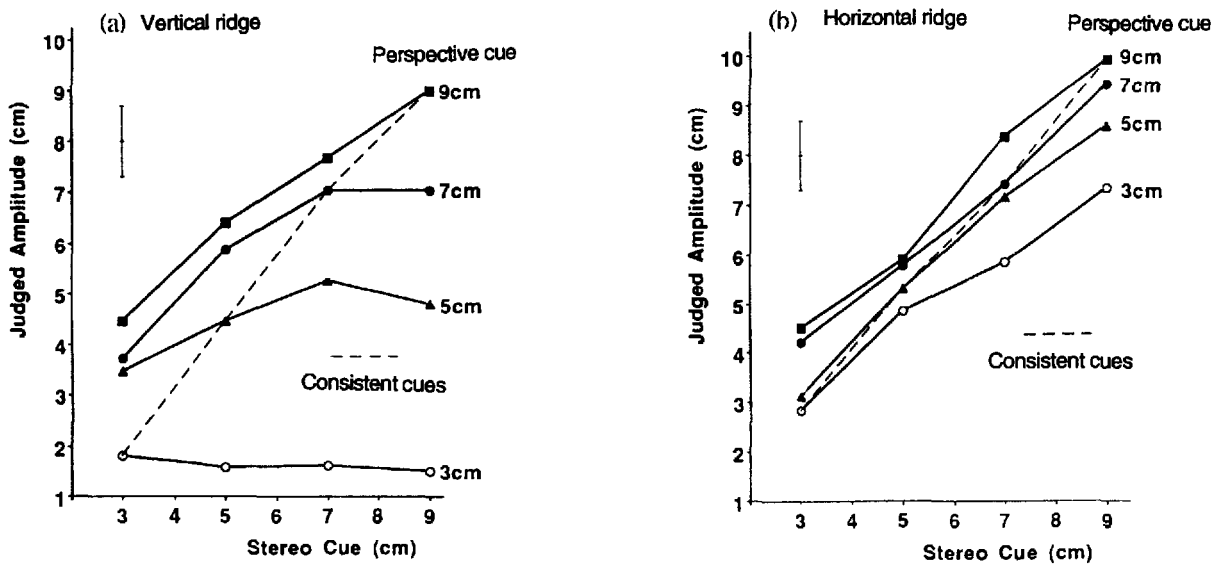
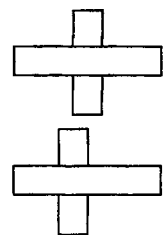
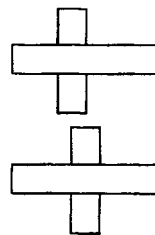
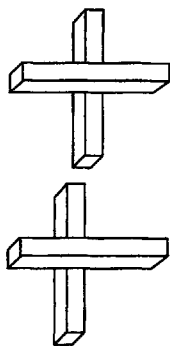
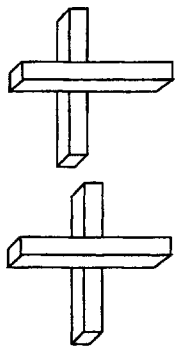


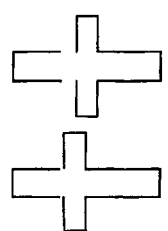
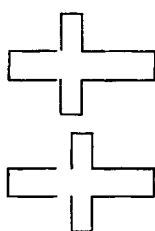
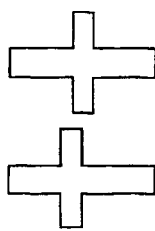
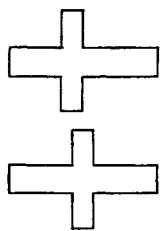
Figure 11.8. Interaction between perspective and disparity.

Judged amplitude of depth in vertical and horizontal ridges as a function of the depth specified by disparity for four depths specified by perspective. The dotted line joins points where disparity and perspective cues were consistent. Error bar is the mean standard error. Means of six subjects. (Adapted from Buckley and Frisby 1993.)



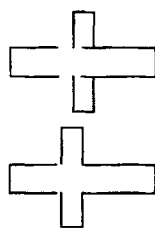
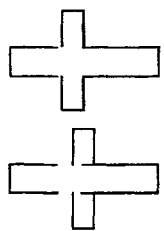
(a) With uncrossed disparity (*top*), the vertical stick appears beyond the horizontal stick. With crossed disparity (*bottom*), the figural information that the horizontal stick is nearer overrides the conflicting disparity information. (Adapted from Schriever 1924.)

(b) With uncrossed disparity (*bottom*), the ends of the horizontal rectangle sometimes appear curved away from the viewer.



(c) The ends of the horizontal wings appear curved away with uncrossed disparity (*top*) and toward the viewer with crossed disparity (*bottom*). (Adapted from Zanforlin 1982.)

(d) The left wing is disconnected and its perceived depth is governed by disparity. The right wing remains attached and disparity is disregarded or interpreted as bending.



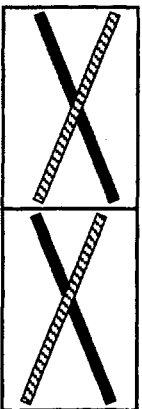
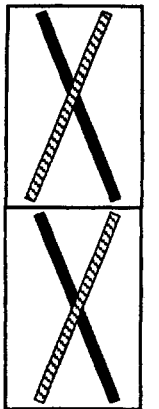
(e) Both horizontal wings are disconnected from the vertical wings, and the depth of both is interpreted according to disparity.

Figure 11.9. Effects of figural continuity on stereopsis.

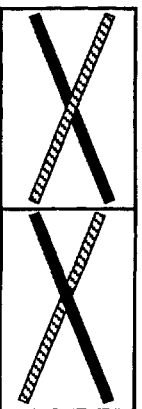
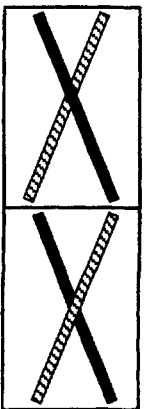
dominance. When the sticks are replaced by flat bars, as in Figure 11.9b, the ends of the horizontal bar sometimes appear to bend away from the viewer when disparity and overlap cues conflict. In this case, the overlap cue dominates at the intersection and the disparity cue dominates at the ends of the horizontal bar. In Figure 11.9c the cross remains connected, but the horizontal wings appear to bend toward the viewer with an uncrossed disparity and away from the viewer with a crossed disparity (Zanforlin 1982). In Figure 11.9d one horizontal wing is disconnected from the disparate vertical lines. This removes the restraining influence of figural continuity and allows that wing to appear in depth relative to the vertical wings. The left wing remains attached and is therefore not seen in depth, although

it may appear to bend. In Figure 11.9e both wings are figurally disconnected from the verticals and both therefore appear in depth relative to the vertical wings.

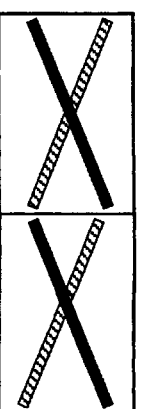
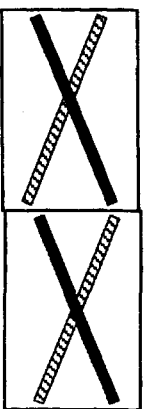
In the stereograms in Figure 11.9b there is disparity at the ends of the horizontal bar but not along its length. There is therefore no conflict between disparity and overlap where the bars intersect. When the disparity at the ends of the horizontal bar is compatible with the overlap cue, the whole bar is displaced in depth relative to the vertical bar by depth interpolation. When the end disparity and overlap cue are incompatible, only the ends of the horizontal bar are seen displaced in depth because the overlap cue prevents interpolation of depth into the centre. This causes the horizontal bar to appear bent.



(a) Overlap and disparity are compatible when the shaded bar is near but incompatible when the black bar is near. In the incompatible pair the black bar appears as two pieces in front of the shaded bar.



(b) The overlap cue is compatible for one eye but incompatible for the other eye. In the pair in which the shaded bar is nearer, it appears transparent and for some of the time both bars are seen simultaneously at the intersection. In the pair in which the black bar appears nearer it appears broken into two pieces and the shaded bar dominates the rivalry process.



(c) Overlap and disparity are compatible when the black bar is near but incompatible when the shaded bar is near. In the incompatible pair the shaded bar is interpreted as transparent.

Figure 11.10. Stereograms illustrating interpretations of conflict between overlap and disparity.

The situation is different when both bars are set at an oblique angle, as in Figure 11.10 (Howard 1993b). There is now disparity information along the whole length of the bars. In Figure 11.10a the overlap cue and disparity are compatible when the shaded bar has a crossed disparity (stereoscopically nearer) but are incompatible when the black bar has a crossed disparity. In the incompatible pair the black bar does not appear bent forward, as it did in Figure 11.9b, but appears as two pieces in front of the shaded bar, with a gap where the two bars intersect. We refer to this as figural segmentation. This is an example of cue reinterpretation because the overlap cue is reinterpreted as a broken bar. This interpretation occurs because it is the only way to resolve the conflict between disparity and the overlap. Figural continuity of the black bar is sacrificed so that the disparity depth cue can be preserved without contradicting the overlap cue. In Figure 11.10b the overlap cue is compatible for one eye in both the crossed and uncrossed-disparity pairs but incompatible for the other eye in both pairs. In the pair in which the shaded bar is stereoscopically nearer, it appears transparent and for some of the time both bars are seen simultaneously at the intersection. In the pair in which the dark bar is stereoscopically nearer, it appears broken into two pieces and the shaded bar dominates in binocular rivalry. In Figure 11.10c the overlap and disparity are compatible when the black bar is stereoscopically nearer, but incompatible when the shaded bar is stereoscopically nearer. In the incompatible pair the shaded bar is interpreted as continuing across the black bar as a transparent object with subjective edges. Figural continuity is preserved for both bars, and the conflict between disparity and overlap is resolved by inferring the presence of a continuous transparent object. This is another example of cue reinterpretation.

There are thus four ways in which an incompatibility between disparity and an overlap cue to depth can be resolved: (1) Dominance of overlap over disparity, in which the overlap cue is preserved and conflicting disparity information is ignored. This is a case of cue dominance. (2) Phenomenal bending, in which both cues are preserved but in different locations. This is a case of cue dissociation. (3) Figure segmentation, in which occlusion is reinterpreted as figural discontinuity. (4) Transparency, in which occlusion is reinterpreted as one surface seen through another. The last two are cases of cue reinterpretation. In none of these cases is the overlap cue and conflicting disparity preserved in the same location. In other words, there is no trading relationship between disparity and overlap, as there is, for instance, between disparity and monocular parallax (see

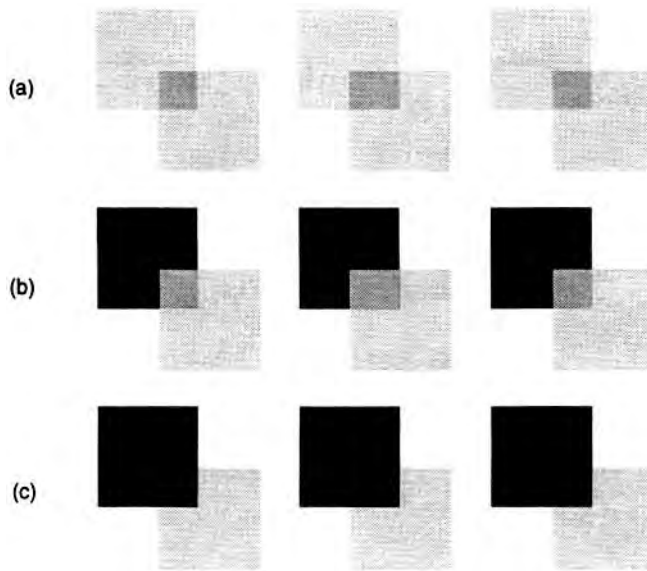


Figure 11.11. The effects of transparency on stereopsis.

(a) The transparency cue is ambiguous and is compatible with both crossed and uncrossed disparity.

(b) Depth is seen more readily when disparity is consistent with the gray square nearer than the black square than the other way round. However, as soon as the black square looks like transparent frosted glass, depth in the two cases appears equal.

(c) Depth is seen more readily for a black square in front of a gray square than the other way round. As soon as the gray square is interpreted as transparent, depth in the two cases appears equal.

Section 13.5.5). Evidence that there is a trading relationship between disparity and overlap is now considered.

With a display like that shown in Figure 11.11a the cue of surface transparency is ambiguous, so that one is free to interpret either surface as being in front. The two surfaces are therefore seen in depth, whatever the sign of the disparity. In Figure 11.11b the black square appears to occlude the textured square, and there is thus a conflict of cues when the black square has an uncrossed disparity relative to the textured square. Trueswell and Hayhoe (1993) claimed that more disparity was required to evoke an impression of relative depth when the transparency cue and disparity were in conflict than when they were in agreement. They implied that the conflicting overlap cue is ignored if there is sufficient disparity, which would amount to a trading relationship between these two cues. However, these results can be interpreted in another way. Howard (1993b) noticed that after some time the black square in the cue conflict configuration in Figure 11.11b appears as a piece of dark transparent glass through which the gray square can be seen. Before this percept emerges, the black and gray

squares appear coplanar, but after it emerges the apparent depth between the black and gray squares appears the same as that between black and gray squares in a non conflict configuration. Thus, when the set of stereograms in Figure 11.11 is free fused and the black squares have been interpreted as transparent, all the squares will appear to lie in the same two depth planes. In other words, disparity information is completely suppressed when the two cues are in conflict but no loss of stereoscopic efficiency occurs once the transparency of the squares has been reinterpreted. There is no evidence of a trading relationship between the two cues. Trueswell and Hayhoe used the probability of seeing depth as their measure of stereoacuity. Reports of depth when the black square appeared transparent and of no depth when it appeared opaque would generate a spurious measure of stereoacuity. Probability of seeing is an invalid measure of acuity under conditions of unstable criteria.

Figure 11.11c provides another illustration of how disparity can force one to reinterpret transparency cues. Depth is seen readily on the side in which the black square has a crossed disparity, since this is compatible with the occlusion of the gray square by

the black square. At first, depth is not seen on the side in which the black square has an uncrossed disparity, but after a while the gray square appears complete and pops out in front of the black square. When this happens the physically missing corner of the gray square is subjectively filled in as part of a transparent gray square (Howard 1993b). This same effect has also been reported by Watanabe and Cavanagh (1993).

11.2.5 Interactions between stereo and shading

The interpretation of a gradient of shading as surface curvature requires assumptions about the uniformity of incident illumination and the reflectance of the surface.

Shipley (1971) drew attention to the following translation of a passage from a paper by Ernst Mach (1866), which shows that he had the concept of making a stereogram with weak monocular cues:

The plastic monocular effect of the rotating discs has led me to construct binocular situations of this type using rotating cylinders and to observe them under a stereoscope. If I move a vertical straight line as directrix through a sinusoid, a wavy cylinder surface results. This I illuminate from the side and provide for the two eyes two such illuminated surfaces next to one another on the same rotating cylinder. In this case all light intensities are continuous from one level to another. Each image alone gives the impression of the plastic cylindrical surface referred to above. They appear even more plastic when I superimpose the two images by crossing my eyes. In this way, the stereoscopic images can be constructed without any contours.

Bülthoff and Mallot (1987, 1988) investigated the interaction between disparity and shading cues in the perception of smooth-shaded ellipsoids of rotation. The effect of different cue combinations on the perceived shape of the ellipsoids was measured with a stereoscopic probe which observers placed so that it appeared to lie on the surface of the ellipsoid. Four cue combinations were examined: (1) Flat-shaded polyhedral ellipsoids with discrete facets with disparities between both the boundaries of the polyhedral edges (E^+) and the shading patterns (D^+); (2) Smooth-shaded ellipsoids with disparate shading patterns (D^+) but no edge disparities because the shading was smooth (E^-); (3) Flat-shaded polyhedral ellipsoids with zero disparities between the polyhedral edge boundaries (E^+) and identical shading patterns (D^-); and (4) Smooth-shaded ellipsoids with identical shading patterns (D^-) but no edge disparities because the shading was smooth (E^-).

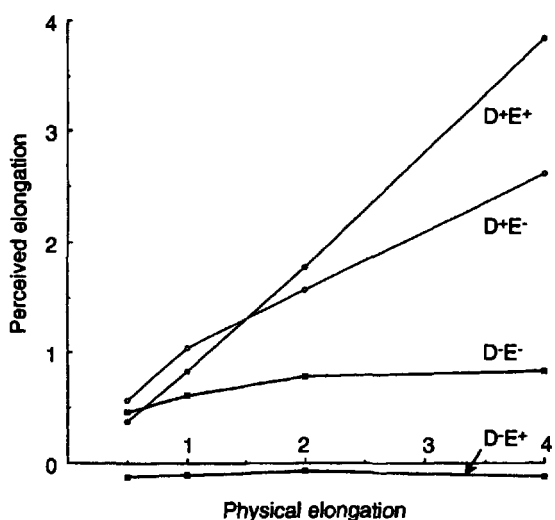


Figure 11.12. Shape from edge- and intensity-based disparity. Smooth-shaded and flat-shaded ellipsoids of rotation were presented to observers and perceived depth was measured with a stereoscopic probe. The shading patterns were either disparate or identical. Perceived elongation was close to veridical when both edge and intensity-based cues were present ($D+E^+$). Removing edge-based information reduced the perceived depth to ~70 per cent ($D+E^-$). No depth was seen when there was contradictory shading and edge information ($D-E^+$). (Redrawn from Bülthoff and Mallot 1987.)

The ellipsoids appeared to contain the most depth when both shading and edge disparities were appropriate to the ellipsoid shape. The elimination of edge-based disparities in the smoothly-shaded ellipses (condition 2) reduced perceived depth to about 70 per cent. The surfaces appeared almost flat in condition 3 when the edge disparities signalled no depth in the surface. Bülthoff and Mallot argued that the large difference between perceived depth for the smoothly-shaded ellipses which either provided disparate shading (condition 2) or did not (condition 4) reveals the importance of shading disparities (Figure 11.12). They point to the advantage of an intensity-based disparity mechanism which detects the disparity between changes of image intensity over an edge-based disparity mechanism for which the inputs are necessarily discrete and often sparse.

To account for their results, Bülthoff and Mallot favour an accumulation model in which the contributions of different depth cues are summed to create the amount of perceived depth, but they suggest that vetoing may also be involved. In particular, the results of experiment 3 suggest that the presence of edge-based stereo disparities effectively vetoes any impression of depth derived from either shape from shading or shape from disparate shading. In practice, however, it is difficult to distinguish between

the predictions of a vetoing operation and averaging with a very high weight attached to one of the cues.

11.2.6 Cognition and depth-cue interactions

Wheatstone (1838) noticed that simple stereograms viewed in a pseudostereoscope appear in reverse depth, but that stereograms of familiar objects still appear in their correct depth. He attributed this resistance of real objects to reversal of disparity to familiarity. However, real objects, unlike simple line stereograms contain monocular cues to depth, such as texture perspective, which is not affected by viewing in a pseudostereoscope. Georgeson (1979) created a random-dot stereogram of a face in which there was no texture perspective. Under these circumstances, a concave face appeared concave. Van den Enden and Spekreijse (1989) replaced the natural texture in a photographic stereogram of a face by projecting texture onto the stereogram in such a way that the texture density was uniform over the face. After a period of viewing, a pseudoscopically viewed face appeared concave.

This evidence suggests that familiarity is not the key factor in causing faces to resist the effects of pseudoscopic viewing. However, Deutsch et al. (1990) pointed out that the texture that Van den Enden and Spekreijse added to their stereogram provided enhanced disparity information and that this, rather than the removal of texture perspective, may have accounted for the tendency of subjects to see the pseudoscopic face as concave.

These issues remain unresolved, but the following evidence suggests that familiarity does affect depth reversal when depth cues are in conflict.

Simple drawings representing three-dimensional shapes, or monocularly viewed three-dimensional objects, such as a wire cube, spontaneously reverse in apparent depth. Even with binocular viewing, a rotating three-dimensional wire cube reverses in apparent depth for brief periods when viewed for a few minutes (Howard 1961). Each reversal in apparent depth is accompanied by an apparent reversal in the direction of rotation. Klopfer (1991) asked subjects to view a face mask binocularly as it rotated about its midvertical axis. When the concave side of the mask turned toward the subject it appeared convex and the direction of rotation of the mask appeared to reverse. A rotating upside down face mask or an unfamiliar object reversed in apparent depth and direction of rotation less readily. These observations suggest that binocularly viewed unfamiliar objects are less likely to show spontaneous depth reversals than familiar objects. The concave unfamiliar objects still tended to be seen as convex,

probably because there are more convex objects than concave objects. This can be regarded as another aspect of familiarity.

A static face mask viewed from the concave side appears convex and this has been taken as evidence that familiarity overrides conflicting information from binocular disparity (Gregory 1970). The shading on a concave mask seen as convex is also inappropriate, since a concave mask illuminated from above appears to be illuminated from below when seen as convex. A translucent concave mask transilluminated from above appears to be illuminated from above when seen as convex. This probably explains an observation of the authors that a translucent concave mask reverses more readily than an opaque mask. Hill and Bruce (1993) found that a concave opaque mask more readily appeared convex when it was illuminated from below; thus appearing to be illuminated from above when seen as concave. They also found that an inverted concave mask was less readily seen as convex than an upright mask.

There is no good evidence that the apparent reversal of images seen in a pseudostereoscope results from an inversion of the sign of disparity coding in the visual system. Some evidence on this question was reviewed in Section 12.3.2. Yellott and Kaiwi (1979) projected a random-dot stereogram onto the concave surface of a face mask and found that, although the face appeared convex, the apparent depth in the stereogram was normal. This demonstrates that the apparent reversal of a concave mask is not due to reversal of disparity sign because any such reversal would affect the random-dot stereogram as well as the mask. It also demonstrates that reversal of a mask is not due to neglect of disparity information because the disparity in the stereogram was processed even when the mask was seen in reverse.

11.3 STEREOSCOPIC DEPTH CONSTANCY

11.3.1 Depth constancy for disparity steps

To a first approximation, the binocular disparity in radians, μ , produced by an object at distance d in front of or behind a fixation point is given by

$$\mu = \frac{ad}{D^2}$$

where D is the distance of the fixation point from the observer and a is the interpupillary distance. Thus, for a given distance of convergence, the disparity between the images of an object is proportional to the

interocular distance and to the distance in depth between the object and the point of convergence. Also, the disparity produced by an object at a given distance from the fixation point is inversely proportional to the square of the fixation distance. Thus, the depth between two objects required to produce a given disparity increases rapidly as the distance of the objects increases. This means that disparity provides accurate coding of depth between two objects only if allowance is made for this inverse square law. The ability to make accurate judgments of relative depth at different absolute distances is known as **depth constancy**. The earlier literature on depth constancy is reviewed in Ono and Comerford (1977).

Even casual observation reveals that we have at least some depth constancy. For instance, the apparent depth of a box does not seem to vary when it is placed at different distances. Depth constancy causes a scene viewed through binoculars to appear flattened. Thus, familiar objects seen through binoculars tend to look their normal size but appear nearer because of the magnification produced by the binoculars. The linear magnification causes a linear increase in binocular disparity rather than a squared increase in disparity that results when objects are actually brought nearer. This shortfall in disparity scaling relative to that expected by depth constancy causes scenes viewed through binoculars to appear flattened (Wallach and Zuckerman 1963). A similar argument applies to the depth seen in stereograms viewed from different distances. With increasing distance, disparities decrease linearly rather than by distance squared and, as a result, perceived depth increases linearly as the distance of the stereogram increases (Wallach et al. 1979).

Depth constancy can be achieved only if the viewer registers the absolute distance of an object correctly. Information about distance could be derived from sensory or motor signals associated with vergence (see Section 11.1), from other cues to depth such as familiar size and linear perspective, or from vertical disparities, as explained in Section 7.6.7. The literature on the perception of absolute distance from monocular cues is complex, and will not be reviewed here. Fairly recent reviews have been provided by Foley (1980) and by Sedgewick (1986).

Procedures for measuring depth constancy fall into three classes according to whether they involve the use of a depth probe, a comparison stimulus held at a fixed distance, or the matching of a distance in depth with a distance in the frontal plane.

Use of a depth probe

In this procedure subjects adjust the distance of a visual comparison object, or probe, until it appears to

be at the same distance as the near edge of the test object and then at the same distance as the far edge. There is a logical problem in using a probe in this way. The perceived distance of the probe may also be based on disparity. It would therefore be subject to the same perceptual scaling for distance as the test objects. Even if the apparent depth of the probe was based on other depth cues, these cues could also be subject to depth scaling. One simply cannot use a probe that is subject to any kind of perceptual scaling for distance to measure distance scaling in a test object. The fact that subjects accurately match the distance of the probe to that of the test object does not allow any conclusions to be made about the perceived distance of the test object. It is like concluding that a person judges the length of a stick accurately simply because he can set another stick to appear the same length. Instead of a visual depth probe some investigators asked subjects to point with an unseen hand to each visual test object. It must be independently determined that the felt position of the hand is accurately related to depth.

Use of a comparison depth interval

In this procedure subjects set a comparison depth interval presented at a fixed absolute distance to match the depth dimension of a test object presented at various distances. This is a reasonable procedure but it requires the subject to change convergence in looking from the comparison stimulus to the test stimulus. The effects of vergence movements can be avoided if the test stimulus is presented for less than 150 ms and the comparison stimulus is set to the remembered depth of the test stimulus. Otherwise the comparison object could be a pair of calipers, which the subject sets by touch. Verbal estimates of the depth interval in the test object have been used but produce very variable data.

Apparently nobody has used the most straightforward version of this procedure in which a depth interval between two objects at one distance is matched with the depth interval between an identical pair of objects seen at each of several other distances, with all cues to the distance of one member of each pair of targets present, but no cues except disparity to indicate the distance of the other member of each pair (but see Rogers 1986 and Glennerster et al. 1994). This is the best procedure because it gets directly at the main question, namely, given that the depth intervals between two identical sets of objects appear the same when they are at the same distance, do they continue to appear the same when one set of objects is taken further away?

Use of a comparison distance in the frontal plane

In this procedure for measuring depth constancy,

subjects set the depth dimension of the test stimulus to appear equal to one of its lateral dimensions. This may not give a precise measure of depth constancy, because the lateral dimension of the object may also be perceptually scaled for distance. However, it does address an important related question about whether the relative proportions of an object remain perceptually constant at different viewing distances.

Experiments on depth constancy

Gogel (1960) proposed that perceived depth resulting from a given disparity is scaled by the perceived lateral size per unit angular size of objects in the same depth plane. More specifically, he proposed that disparity is scaled by the perceived lateral size of an object divided by its angle of subtense. If the linear dimensions of an object are correctly perceived, the ratio of perceived lateral size to the angle of subtense increases linearly with distance. This follows from the fact that when the distance of an object is doubled, the visual angle it subtends is halved. Notice that the visual angle subtended by a familiar object provides reliable information about its distance. Gogel's hypothesis could therefore be restated as a claim that the perceived depth induced by a given disparity is a linear function of the perceived absolute distance from the viewer. He asked subjects to set a test spot beyond a rectangle to a distance equal to the width of the rectangle, which was 10 cm. There were some rather weak perspective cues to the distance of the rectangle but not to that of the spot. As the distance of the rectangle was increased from 1.6 to 4.8 m the distance of the spot required to match the perceived width of the rectangle increased in linear proportion. The same result was obtained when the test object remained at the same physical distance but was made to appear at different distances (Gogel 1964). According to depth constancy the perceived distance of the spot from the rectangle should have been constant. The breakdown in depth constancy may have been due to the fact that the vertical edges of the featureless rectangle were over 1° of visual angle away from the test spot at the near distance and may therefore have provided only weak disparity information. Furthermore, a separate test revealed that subjects grossly underestimated the distance to the rectangle. The procedure of matching the depth interval to the lateral size of the test object measures depth constancy only if the perceived lateral size of the rectangle remains constant. A separate test revealed that subjects' judgments of the lateral size of the rectangle remained reasonably constant.

Ritter (1979) asked subjects to fixate a target while a test object was presented for 100 ms at a constant

crossed disparity of 20 arcmin. The fixation and test objects were then removed, and subjects set a depth probe to the remembered position of each object. Subjects set the probe accurately and it was concluded that people have almost perfect depth constancy over the 60- to 180-cm range of absolute distance used. These conclusions are invalidated by the fact that they were based on the use of a depth probe. In an earlier experiment Ritter (1977) asked subjects to match a comparison depth interval at a given absolute distance with the depth dimension of a three-dimensional wire object. This is a better procedure because the comparison stimulus was immune to changes in depth scaling, assuming that it was perceived as remaining at the same distance. Although there was no significant effect of distance on perceived relative depth, results were very variable and the distance range was only 60 to 180 cm.

Collett et al. (1991) asked subjects to estimate the depth between two textured surfaces which abutted along the horizontal meridian. Depth was created by a colour anaglyph method on a computer screen. The display was between 2 and 10 ° wide and was viewed from a distance of between 45 and 130 cm. Estimates of a constant depth interval dropped with increasing viewing distance when the display had a constant angular size, but were nearly independent of viewing distance when the linear size of the display was constant. At any distance, depth appeared greater as the angular size of the display was reduced and this effect became more pronounced with increasing viewing distance. Collett et al. concluded that there are two components to depth scaling operating in the conditions of their experiment. The first is viewing distance, as indicated by oculomotor cues and the second is the change in angular size with changing distance. The second factor becomes the dominant factor as viewing distance increases.

In studying depth constancy at large viewing distances it is difficult to keep disparity constant and eliminate the effects of other depth cues such as accommodation. Cormack (1984) overcame these problems by using a pair of disparate afterimages as the test object. Good stereo depth can be obtained from afterimages, and their use has the advantage that a given disparity between two afterimages remains the same over changes in vergence or accommodation (Wheatstone 1838; Ogle and Reiher 1962). Subjects either matched the perceived depth of the afterimage with a variable depth probe or gave verbal estimates of its absolute distance and its depth relative to a fixation point set at each of several distances. Afterimages with disparities of 16.3 or 4.5 arcmin were viewed with reference to a fixation point at various distances up to 27 m in a corridor or

up to 6 km outside at night. In both cases, surrounding objects were sufficiently visible to provide perspective information about distance. The only results reported were derived from the use of the depth probe. Therefore, the fact that they revealed almost perfect depth constancy up to 27 m must be regarded with suspicion.

In view of the many conflicting results and the great variety of testing procedures, some of which are suspect, it is difficult to draw firm conclusions about depth constancy. We need a well-designed experiment directed towards answering the main question under conditions approximating those of normal viewing. A severe lack of depth constancy is not evident when one observes a natural scene.

11.3.2 Depth constancy for gradients and curvature

A theoretical analysis of the relationship between disparity and distance has been provided by Rogers and Cagenello (1989). For two objects, A and B , separated by a fixed depth, the difference in disparity between them, $m_A - m_B$ is inversely proportional to the square of their distance from the viewer, or $m_A - m_B = k/D^2$. The change in disparity per unit of visual angle is the disparity gradient, or $(m_A - m_B)/\theta$. Now the visual angle subtended by a pair of objects is inversely proportional to their distance from the viewer along a fixed visual direction, or $\theta = k/D$. Therefore, $(m_A - m_B)/\theta$ is proportional to $1/D$. In other words, the disparity gradient between two objects is an inverse linear function of their distance along a given visual direction. Put another way, the disparity gradient is the first spatial derivative of the absolute difference in disparity between two points, and any first derivative of a squared function based on disparity is a linear function. The rate of change of a disparity gradient (the second spatial derivative of disparity) defines the curvature in depth of a surface. It follows that the second derivative of depth, defined as the rate of change of disparity gradient per unit of visual angle, or $(m_A - m_B)/\theta^2$, is totally independent of changes in distance.

This means that when a person judges the slant or inclination of a surface at different distances, only a simple allowance for distance need be made. When a person judges the local curvature of a surface in depth no account need be taken of changes in distance.

Johnston (1991) presented subjects with convex cylindrical surfaces defined solely by disparity in a random-dot stereogram. The width/depth ratio of the cylinder was varied and the subject had to decide whether it was flatter or more peaked in depth

than a circular cylinder. This was done at viewing distances of 53, 107, and 214 cm with the only cue to distance being provided by a binocular fixation target superimposed on the centre of the stereogram. At the nearer distance the cylinder had to be flatter than a circle to appear circular, and at the larger distance it had to be deeper to appear circular. Judgments were approximately correct at the intermediate distance. Similar distortions of curvature as a function of distance occur in measurements of the horizontal horopter (see Sections 2.6.7 and 7.6.7). At first sight, these are not the results one would expect if subjects were basing their judgments on the second derivative of depth. Instead they would be explained if they were judging the depth differences in the display and applying an incorrect scaling for distance. On this basis, the results would be explained if the subjects overestimated short distances and underestimated longer distances. This pattern of errors in judging distance has often been reported (Foley 1980; Gogel 1977) but never explained.

The poor shape constancy reported by Johnston is not incompatible with the possibility that human observers use the second spatial derivative of disparity as a basis for judging surface curvature. As we explained in Section 7.7.2, the invariance of disparity curvature to changes in distance is only true of the local surface curvature. The overall shape of a surface is specified by the changes of local disparity curvature over space (the third spatial derivative of disparity) which does not remain invariant with changes in distance. This is a geometric fact and hence all theories of shape perception from disparity predict that perceived surface shape will vary if the distance of the surface is judged incorrectly.

The recent results of Glennerster et al. (1994) and Durgin et al. (1994) show that depth constancy is not always poor. In both these studies, depth constancy was almost perfect when measured in more naturalistic experimental situations where there was abundant information about the three-dimensional layout of objects and surfaces (see Section 7.7.2). As a general conclusion, shape constancy from disparity cues appears to be poor whenever the information about the absolute distance to the disparate objects or surfaces is limited or ambiguous.

11.3.3 Speed constancy

An object moving at a given angular velocity appears to have a higher linear velocity when it is perceived as being in the distance rather than near. This is known a speed scaling. In the presence of adequate cues to depth, objects travelling at the same linear speed in frontal planes at different distances

appear to have the same speed, in spite of the fact that their angular velocities vary with their distance. This effect is called **speed constancy** and is related to the well-known scaling of perceived size with apparent depth. Rock et al. (1968) found that, with binocular viewing, subjects could accurately adjust the linear speed of one luminous circle to match that of a second circle at a different distance when cues to distance such as accommodation and relative size were eliminated. Subjects also matched the linear sizes of the circles. The speed matches and size matches were similar, and it was concluded that perceived linear speed is a function of perceived linear extent traversed in unit time.

In Rock's experiment, the moving stimulus was not seen against a frame of reference. Brown (1931) found that if all the linear dimensions of a moving display are doubled without any change in distance, then speed has to be doubled to remain perceptually the same. This is known as the transposition principle. Speed constancy has been found to be particularly good when the moving object is seen against a background which is size scaled for depth (Wallach 1959; Epstein 1978).

McKee and Welch (1989) asked subjects to estimate the velocity of a bar moving at 10 or 26 cm/s presented at various disparities relative to a fixation target for a mean duration of 150 ms. Estimates of velocity conformed to angular velocity and there was no evidence of speed constancy. McKee and Welch also found that the Weber fraction for the discrimination of linear velocity was higher than that for the discrimination of angular velocity. The Weber fractions for discrimination of linear size and angular size for a stationary object at different distances were similar. According to this evidence, speed constancy is not controlled by the same process as size constancy.

There are several possible reasons for the lack of speed constancy in this display. Disparity was the only cue to depth and the bar remained the same angular size. We will see later that speed constancy shows only when size is also scaled for distance. The brief exposure time may have interfered with the judgment of depth—evidence reviewed in Section 5.10.3 shows that stereoacuity for moving targets is particularly degraded for short exposures. Finally, there were no objects or texture in the plane of the moving bar to provide a relative scaling of speed. The following evidence suggests that perceived

speed of a textured display is scaled by the density of the texture.

Mowafy (1991) found that a monocular target moving horizontally over a stereoscopically defined textured surface slanted about a vertical axis appeared to roll along the slanted surface and increase in speed in relation to the increase in its perceived distance, even though the target actually moved at constant velocity in the frontal plane.

Zohary and Sittig (1993) asked subjects to match the perceived velocity of a random-dot kinematogram at a distance of 1 m with that of a second kinematogram at 2 m. They matched the linear velocities of the stimuli when the sizes of the dots in the two displays were also scaled to distance. Settings of a probe to the distance of the displays were related to distance but not by the same function that related speed estimates to distance. When the dots in the two stimuli had the same retinal size, subjects tended to match angular velocities, and speed constancy broke down, as in the experiment by McKee and Welch. It was concluded that estimates of relative speed are based on relative size judgments rather than on judgments of distance. Since only one set of distances was used, these results tell us nothing about the relation between relative speed estimates and disparity scaling as a function of distance. Rock used a single visual object and found that speed scaling is achieved when size is not scaled for depth. Perhaps with many dots the absence of size scaling outweighs the binocular cues to depth. The threshold for the detection of linear motion in random-dot displays has been found to be relatively independent of viewing distance for velocities up to about 400 mm/s. This suggests that motion sensitivity for a textured display is scaled for the spatial density of the display (van de Grind et al. 1992). This would follow from the assumption that low velocities are detected by motion detectors with small receptive fields (stimulated by dense patterns) and high velocities are detected by motion detectors with large receptive fields (stimulated by coarse patterns).

Wallach (1976) reviewed speed constancy. There is an extensive literature on size constancy but most of it is not directly related to binocular stereopsis. See Foley (1980) and Sedgewick (1986) for reviews. The topic of optic flow and depth perception is discussed further in Section 13.5. Reviews of the topic of optic flow are provided by Lee (1980), Cutting (1986), and Simpson (1993).

Depth contrast and interactive processes

12.1 Stereopsis and absolute disparity	461
12.1.1 Normalization of disparity ramps	462
12.2 Simultaneous depth contrast	465
12.2.1 Depth contrast with lines and points	466
12.2.2 Long-range depth contrast	467
12.2.3 Short-range depth contrast	469
12.2.4 Depth contrast in surfaces	473
12.2.5 Disparity contrast mechanisms	481
12.3 Successive depth contrast	484
12.3.1 Depth aftereffects	484
12.3.2 Disparity aftereffects	486
12.3.3 Models of depth aftereffects	490
12.3.4 Phase-independent adaptation	495
12.3.5 Hypercyclopean aftereffects	497
12.4 Stereoscopic interpolation	497
12.4.1 Depth interpolation over blank areas	497
12.4.2 Depth interpolation over monocular areas	500
12.4.3 Interpolation into ambiguous regions	501
12.5 Stereo and figural organization	505
12.5.1 Stereopsis and texture segregation	505
12.5.2 Stereopsis and figure-ground organization	507
12.5.3 Stereopsis and subjective contours	508
12.6 Monocular occlusion	512
12.6.1 Basic rules	512
12.6.2 Monocular occlusion and depth continuity	513
12.6.3 Occlusion, camouflage, and rivalry	514
12.6.4 Monocular occlusion and surface opacity	514
12.6.5 Monocular occlusion and stereopsis	515
12.6.6 Occlusion and Panum's limiting case	518
12.7 Depth-specific visual processes	523
12.7.1 Apparent brightness and relative depth	523
12.7.2 Threshold-elevation effect and relative depth	524
12.7.3 Depth-specific figural effects	524
12.7.4 Stereopsis and segregation of motion	525
12.7.5 Apparent motion between depth planes	527
12.7.6 Stereopsis and pursuit eye movements	529
12.7.7 Stereopsis and induced visual motion	532

12.1 STEREOPSIS AND ABSOLUTE DISPARITY

There is considerable evidence that a change in depth is not perceived when horizontal disparity is changed equally over the whole of the visual field (Gogel 1965; Nelson 1977; Erkelens and Collewijn 1985a; Regan et al. 1986a). In Erkelens and Collewijn's experiment subjects observed a random-dot stereogram while the whole image in one eye moved from side to side in antiphase with the whole

image in the other eye, at frequencies up to 0.5 Hz and amplitudes up to 3°. The rest of the visual field was black. The whole display appeared stationary, even though the relative depths within the stereogram were perceived at all times. The antiphase motion of the images of the stereogram induced a corresponding change in vergence which cancelled some but, it was claimed, not all of the changing disparity. When a stationary vertical grating was superimposed on the stereogram the whole

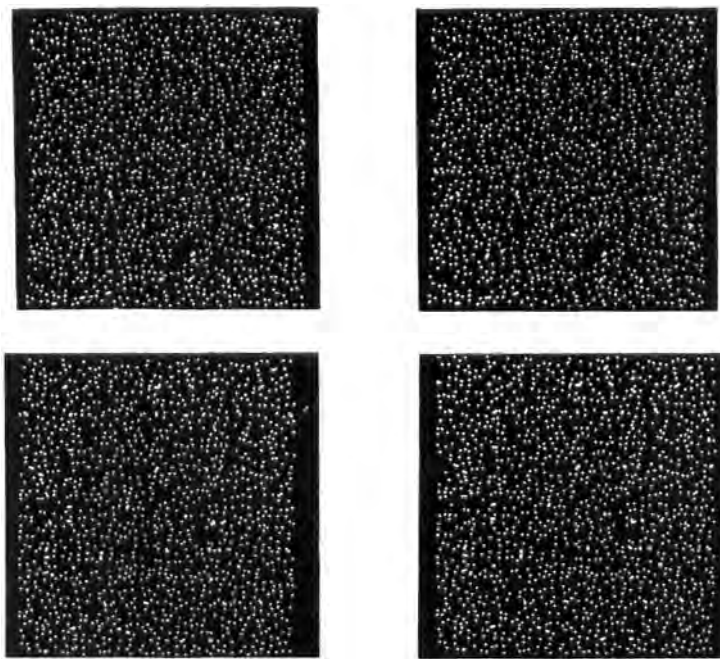


Figure 12.1. Perceived depth in single and double slanting surfaces.
Depth in a random-dot stereogram of a single slanted surface, as in the upper figure, takes longer to see than depth in a stereogram of two surfaces slanted in opposite directions, as in the lower figure. (From Gillam et al. 1988b. Copyright by the American Psychological Association. Reprinted by permission.)

stereogram appeared to move in depth relative to the grating. When an in-phase component of motion was added to the antiphase motion, subjects could see the mean side-to-side motion but not motion in depth. The perception of depth induced by counterphase dichoptic motion is discussed in more detail in Section 13.2.4.

In normal viewing, a constant static disparity over a surface on which one has attempted to converge is due to an offset error of convergence, so-called fixation disparity (Ogle 1964). Changes in absolute disparity in extended displays are most likely due to unintended changes in vergence, which can be quite large (Steinman and Collewijn 1980). In either case it is best to ignore such disparities as signals for depth. Relative disparities within the visual field are immune to the effects of vergence and, as we will see, it is these that are used for coding depth.

12.1.1 Normalization of disparity ramps

A flat surface slanted in depth around a vertical axis creates a ramp of horizontal disparities over the whole surface (see Section 7.2). The image in one eye is laterally compressed with respect to that in the other eye; there is a compression-expansion disparity. A surface inclined in depth around a horizontal

axis creates a vertical gradient of horizontal shear disparities (see Section 7.4). Both are first-order or first-derivative disparities since the rate of change of horizontal disparity along any meridian is constant. Several lines of evidence suggest that first-derivative disparities induce only a weak impression of depth.

Depth in a random-dot stereogram representing a single surface slanted or inclined in depth takes longer to see than depth in a stereogram representing two adjacent surfaces slanted or inclined in opposite directions (Figure 12.1; Gillam et al. 1988b). It can be concluded that disparity discontinuities are more readily detected than simple disparity gradients. Gillam et al. also found that the depth of a single surface inclined about a horizontal axis was seen more quickly than that of a surface slanted about a vertical axis, suggesting that depth involving shear disparity is detected more easily than that involving compression disparity (see also Rogers and Graham 1983). Other instances of this anisotropy are described in what follows and in Section 11.2.2.

In the Gillam et al. study, the edges of the monitor screen were visible, so that the single-surface stereograms were not devoid of disparity discontinuities. To study how disparity ramps are perceived, it is essential that all disparity discontinuities be removed from the visual field.

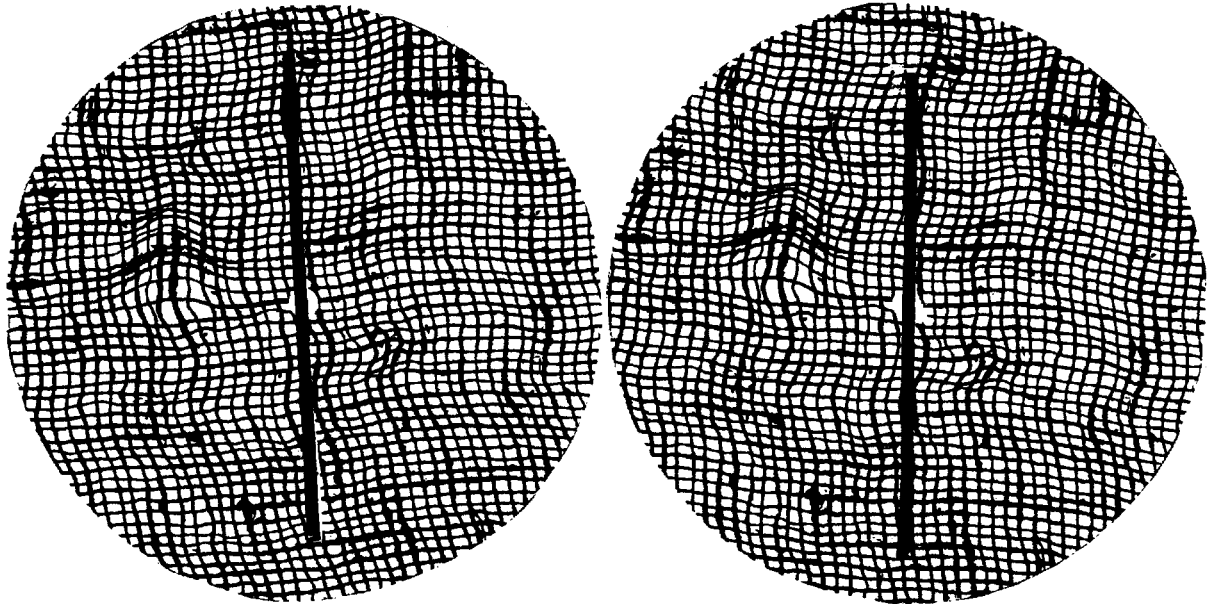


Figure 12.2. Inclination induced in a line by a cyclorotated background.

A textured stereogram with 10° of cyclodisparity produces little or no apparent inclination about a horizontal axis. A vertical line with zero disparity appears inclined by an amount corresponding to the disparity in the background, but in the opposite direction. The effect is not very evident in a small display but is complete with a large display seen in dark surroundings.

Surfaces or lines inclined about a horizontal axis appear less inclined than they are (Gogel 1956, 1965; Harker 1962; Enright 1990). This is one instance of what Gogel refers to as the **equidistance tendency**. The equidistance tendency is an example of a broader class of phenomena known as normalization. In normalization a stimulus which is to one side of a norm in a sensory dimension, appears more similar to the norm than it is. Thus, a tilted line appears more vertical than it is, a moving display appears to slow down, and a point to one side of the median plane appears to be more centrally placed than it is. In depth normalization one can say that unbounded depth plateaus and depth ramps normalize to the norm of either equidistance or zero disparity gradient. Examples of depth normalization are now described.

A constant orientation disparity over the whole visual field creates only a weak impression of inclination in depth or none at all. Thus, stereograms differing in orientation by as much as 7°, although binocularly fused, did not appear to be inclined in depth (Julesz 1964). Similarly, the stereogram shown in Figure 12.2 appears to remain in the frontal plane even though the images differ in orientation by 10°, corresponding to an inclination in depth of over 60°. A vertical line superimposed on the fused image appears to slant by almost the full 60°. A similar slant contrast effect was reported by Nelson (1977), and is discussed in more detail later. Related depth

contrast effects have been known for some time and are described in Section 12.2.

A constant orientation disparity over the whole field is normally due to changes in cyclovergence and, like constant horizontal disparities, are best ignored as signals for depth. This explains why normal fluctuations in cyclovergence do not interfere with the ability to detect relative differences in inclination between different objects (Enright 1990). We saw in Section 7.5.2 that inclination is coded in terms of the difference between horizontal and vertical orientation disparities.

In an analogous way, if we assume that slant is coded by the difference between the horizontal and vertical magnifications of images, an equal magnification along both axes should not produce slant. Thus the overall magnification of one image in Figure 12.3a does not produce slant, even though the fused image contains the same gradient of horizontal disparity as that produced by a surface slanted in depth about a vertical axis (Figure 12.3b). Vertical magnification of the image in one eye creates an impression of slant in a direction opposite to that created by horizontal magnification (Figure 12.3c). This is the induced effect discussed in Section 7.6.5. A vertical magnification in one eye creates the same difference between vertical and horizontal disparities as a horizontal magnification of the image in the other eye. The induced effect is most pronounced in a display that fills the binocular field. A pair of

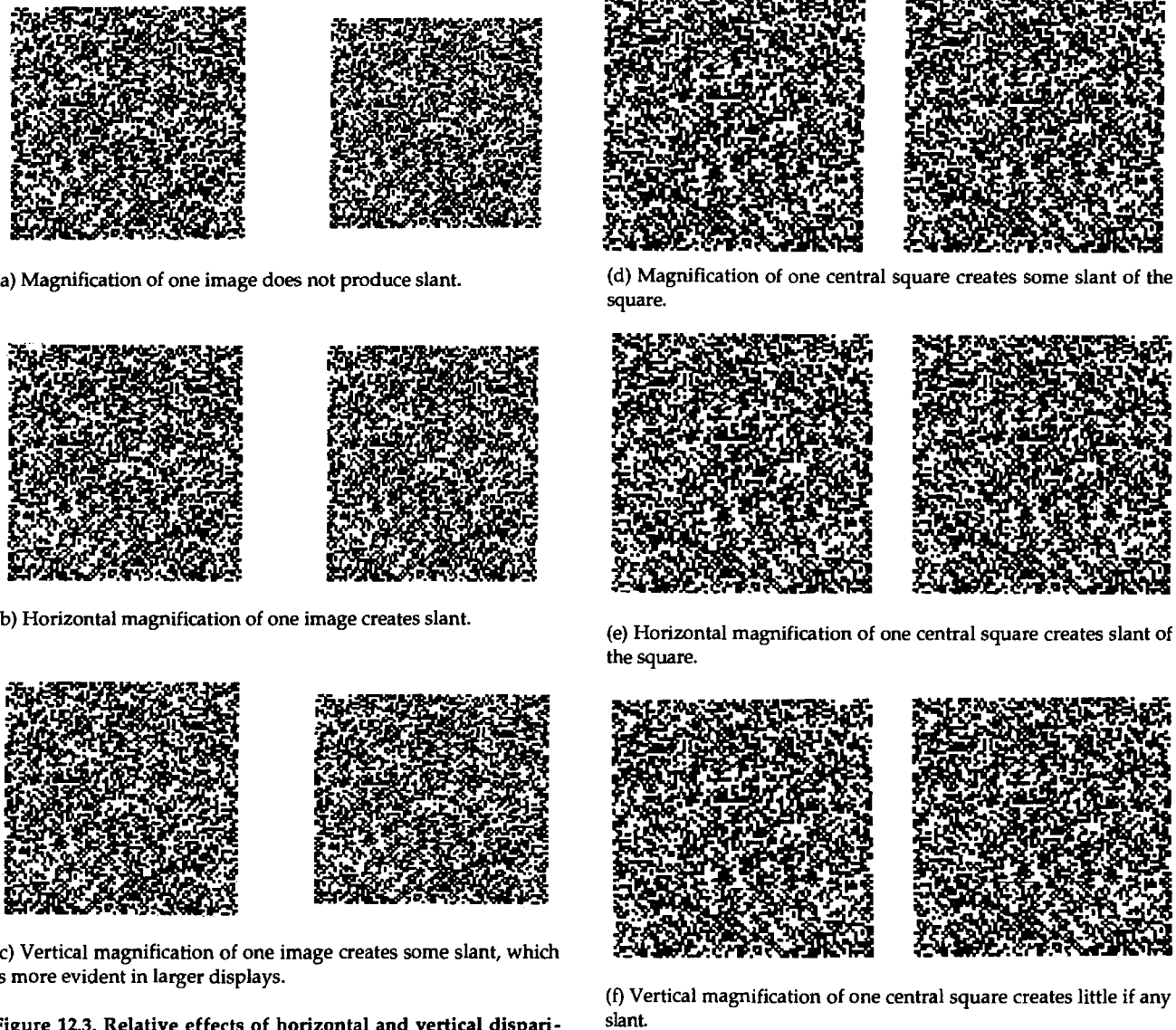


Figure 12.3. Relative effects of horizontal and vertical disparities on perceived slant about a vertical axis.

equal-sized horizontal lines superimposed on images that differ in size, creates the impression of a line slanted by an amount corresponding to the horizontal disparities in the surrounding images (Nelson 1977). Eye movements cannot explain this effect since they cannot change the relative magnification of the images. The enclosed test line should appear to slant because there is a difference between its zero-horizontal disparity and the vertical disparity in the surround.

When a region which differs in overall magnification in the two eyes is set in a zero-disparity surround, as in Figure 12.3c, it creates an impression of slant in a direction corresponding to the horizontal-disparity component. This is because the horizontal-disparity component is assessed with reference to the mean vertical disparity over the whole display

rather than to that in only the central region. A region with a vertical disparity produces little or no slant (induced effect) when set in a zero-disparity surround (see Figure 12.3e). This is because the vertical disparity of the central region is averaged in with the zero vertical disparity of the surround.

Depth plateaus, or regions of constant (zero-derivative) disparity, and depth ramps, where disparity changes at a constant rate (first-derivative disparity), are poorly registered by the visual system when seen in isolation. In the absence of evidence to the contrary such stimuli may appear to lie in the frontal plane. The visual system is most sensitive to regions in which there is a second-derivative component of disparity, such as a depth step, a gradient discontinuity, or a curvature of depth. We will see in Section 12.2 that regions of constant or ambiguous

disparity or regions of constant disparity gradient are scaled with respect to bordering disparity discontinuities. Zero- or first-order disparities occurring over the whole visual field or over most of it are disregarded because these are the disparities that could arise from changes in convergence or cyclovergence. The preceding evidence supports the following set of propositions:

1. There is a hierarchy of disparity detectors. At the first level, simple local disparities are detected. At the second stage, differences in the output of neighbouring simple detectors are detected by local disparity-gradient detectors. Gradient detectors operating along vertical meridians detect gradients of disparity shear which code inclination and those operating along horizontal meridians detect gradients of disparity compression-rarefaction which code slant. At the third stage, differences between disparity-gradient detectors are registered by second-derivative detectors. The second-derivative detectors operate over wider areas than the others.

2. Zero- and first-order disparities unbounded by disparity discontinuities normalize to zero disparity, completely or partially, depending on the stimulus conditions. There are two types of unbounded zero- and first-order disparities. First, are those common to the whole field which, by definition, have no boundaries. These occur naturally when the eyes are not properly converged or cycloerged. Second, there are those occurring within a local region and set on a featureless white background, like a drawing on white paper.

The simplest way to account for normalization is to say that the outputs of zero- and first-order detectors, although used for the control of vergence, cyclovergence and for extraction of second-order disparities, are disregarded for coding depth. In the absence of evidence to the contrary, such regions are set to a default value of zero.

The mechanism responsible for normalization could involve mutual inhibition between disparity detectors for the same or similar disparities. In the luminance domain, lateral mutual inhibition reduces the output from regions of equal or slowly changing luminance and, by comparison, preserves the output from regions of rapidly changing luminance. By analogy, in the stereo domain, lateral inhibition would preserve regions where disparity changes more rapidly than in regions where disparity changes less rapidly (see Section 12.2.5). Evidence for lateral inhibition between disparity detectors is reviewed in Section 5.5.3.

3. Second-order disparities are detected with short latency, do not normalize, and are used for

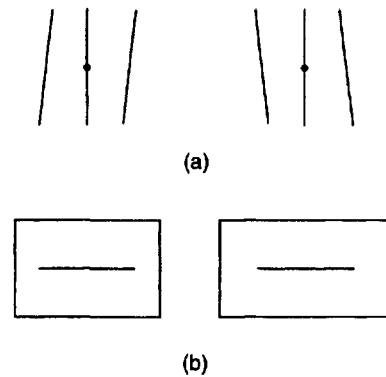


Figure 12.4. Depth contrast stimuli from Werner (1938).
The centre line in (a) has no orientation disparity and should appear to lie in a frontal plane. In the presence of the outer flanking lines which have an orientation disparity, the centre line appears inclined in depth. The horizontal line in (b) is of the same length in the two images but in the presence of the surrounding frames which have different widths, the horizontal line appears slanted in depth.

coding depth changes and boundaries. Zero- or first-order disparities occurring within areas bounded by second-order disparities are used to interpolate depth between these boundaries.

4. It follows that a second-order disparity between an object and a normalized surrounding region is preserved. This relative disparity is seen with respect to the normalized surrounding region, rather than with respect to a true zero disparity. This causes the central object to appear displaced in depth relative to when it is presented in a region which is truly in the frontal-plane. This apparent displacement in depth is one of the phenomena referred to as depth contrast, which is the topic of the next section.

12.2 SIMULTANEOUS DEPTH CONTRAST

Simultaneous contrast effects or induced effects are defined as the perceptual effects arising from the spatial configuration of different stimulus values from a particular sensory dimension. They include induced motion (Duncker 1929), induced colour (Kirschmann 1890), spatial-frequency contrast (MacKay 1973), figural contrast and curvature contrast (Gibson 1933) and tilt contrast (Gibson 1937).

Successive contrast effects or aftereffects are defined as perceptual effects of prolonged stimulation of the visual system by a given stimulus value from a specified sensory dimension. They include motion aftereffects (Wohlgemuth 1911), colour aftereffects (Hering 1861), spatial frequency aftereffects

(Blakemore and Sutton 1969), figural aftereffects (Köhler and Wallach 1944), curvature aftereffects (Gibson 1933), and tilt (orientation) aftereffects (Gibson and Radner 1937).

Both classes of effects are interesting because they represent distortions or illusions in the way we perceive the world (Gregory 1980) but more importantly because they reveal properties of mechanisms of sensory coding (Sutherland 1961; Mollon 1974; Anstis 1975; Frisby 1979). In addition, it has been argued that both classes of effects are manifestations of the visual system's strategy of coding the temporal and spatial changes of sensory stimuli in preference to steady values (von Bekesy 1967; Over 1971; Anstis 1975). Successive and simultaneous contrast effects may also interact. For example, Anstis and Reinhardt-Rutland (1976) found that an object manifesting induced movement can generate a motion aftereffect and that an object manifesting a motion aftereffect may induce motion into a neighbouring object. Analogous interactions have also been reported between colour aftereffects and colour contrast (Anstis et al. 1978).

12.2.1 Depth contrast with lines and points

Werner (1937, 1938) provided one of the earliest reports of depth contrast. His stereograms were based on line stimuli like those shown in Figure 12.4. In Figure 12.4a, the two flanking lines have an orientation disparity which causes them to appear inclined in the direction of a sky plane with divergent viewing. The central line has no orientation disparity. It appears in a frontal plane when presented alone but inclined in depth in the direction of a ground plane when presented with the flanking lines. In Figure 12.4b, the vertical edges of the surrounding frame have a width disparity and therefore give the impression of a frame slanted around a vertical axis, as if lying on a left wall surface. The horizontal line is the same length in the two eyes. When presented by itself, it appears in a frontal plane but in the presence of the disparate outer frame, it appears to slant with its right side closer to the observer, as if lying on a right wall surface (Werner 1937). Werner (1938) related the apparent inclination of the test line to the inclination of the surrounding, inducing lines. With up to 7° of orientation disparity in the flanking lines (corresponding to an inclination in depth of more than 60° at a viewing distance of 60 cm) his four observers introduced between 40 and 100 per cent of the orientation disparity present in the outer lines into the test line before it appeared to lie in a frontal plane. Werner claimed that these very powerful contrast effects cannot be explained in terms of

"induction" from the "visible depth of the outer lines" because the empirical functions which related the visible depth in the flanking lines to their orientation disparity have a significantly different shape. In particular, he noted that when the flanking lines had an orientation disparity of only 30 arcmin, they appeared in a frontal plane but the test line appeared inclined in depth. Instead, Werner argued that depth contrast "is the outcome of a change of correspondence within the binocular field". According to this idea, the labels for disparate points are modified by the contrast configuration.

Ogle (1946) extended Werner's findings, using multiple flanking induction lines and a single test line (or vice versa), and reported powerful contrast effects in the former case but little or no effect in the latter case. However, he rejected Werner's idea of a change of correspondence and claimed instead that the surrounding lines change the cyclovergence state of the eyes thus creating a true orientation disparity of the centre line. To test this hypothesis, he attempted to measure cyclovergence using a pair of vertically separated pearl beads (seen by both eyes) which were mounted on an adjustable inclined surface. Observers set the beads to appear in a frontal plane. Ogle found that the beads had to be inclined by about 90 per cent of the inclination of the surrounding inducing lines to appear in a frontal plane. Ogle concluded that cyclovergence had taken place. His argument, however, overlooks the fact that the beads used to test cyclovergence are subject to similar depth contrast effects as is the original test line and, consequently, this method is invalid (Section 10.7.2). We (Howard et al. 1993) measured cyclovergence by an objective method and showed that the amount of induced inclination in a vertical line superimposed on a cyclorotated background is independent of the amplitude of cyclovergence (Figure 12.5). In other words, induced depth corresponds to the total disparity between the images of the background and those of the line and not to the disparity transferred into the images of the line by cyclovergence. Furthermore, the cyclorotated background appeared to lie in a frontal plane and all the apparent inclination was in the line. This supports the normalization theory of depth contrast; the larger display normalizes to the frontal plane, and the relative orientation disparity between it and a vertical test line is accounted for by the perceived inclination of the test line. The normalization of the cyclorotated background may be partially due to cyclovergence, but this is not the main cause because we found that the background appeared to lie in the frontal plane even for people with little cyclovergence. The subject of cyclovergence is dealt with in Section 10.7.

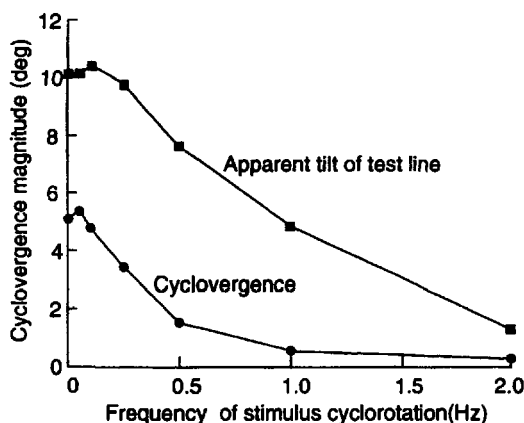


Figure 12.5. Cyclovergence and induced tilt.

The upper curve shows the apparent slant of a vertical line superimposed on a textured background, as a function of the frequency of cyclorotation of the background through an amplitude of 6°. The lower curve shows cyclovergence in response to cyclorotation of the textured background. (From Howard et al. 1993.)

Even if cyclovergence does play a role in the contrast seen in this stimulus configuration, it cannot explain the powerful depth contrast seen in Werner's other configuration involving an outer inducing frame slanted, rather than inclined in depth (Figure 12.4b), which is not a stimulus for cyclovergence. To reconcile this inconsistency, Ogle claimed (without providing data), that if an inducing rectangle is drawn to conform to the images of an actual rectangle slanted out of the frontal plane, depth contrast does not occur. This post hoc explanation is not very plausible and, as we shall see, depth-contrast effects are just as large for configurations in which there is no stimulus for cyclovergence.

Pastore (1964) investigated a variant of Werner's slant-contrast effect with a display consisting of a pair of lines of equal length seen by the two eyes (Figure 12.6a). The inducing stimulus was a pair of dots with an uncrossed disparity (with respect to the test line) at one end of the test line and a pair of dots with crossed disparity at the other end. Of his 20 subjects, 16 saw depth contrast in the test line. Clearly, this effect cannot be attributed to cyclovergence. In a subsequent paper, Pastore and Terwilliger (1966) obtained depth-contrast effects when an identical test square shown to both eyes was surrounded by just four points close to the corners, which had either crossed or uncrossed disparities. When the points at the bottom of the square had an uncrossed disparity and those at the top a crossed disparity, the square appeared inclined in the direction of a ground plane. When the points on the left of the square had a crossed disparity and those on the right an uncrossed disparity, the square

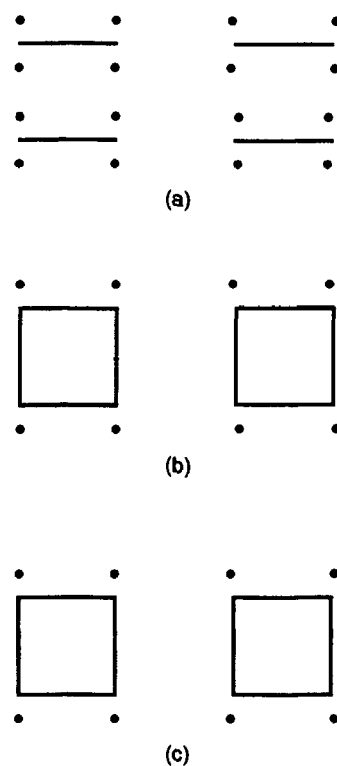


Figure 12.6. Depth contrast effect with lines and points.

- (a) The horizontal lines are the same length but appear slanted in depth when pairs of dots with opposite disparities are positioned at the ends. (Redrawn from Pastore 1964.)
- (b) Identical squares appear inclined with disparate dots at the corners.
- (c) Identical squares appear slanted with disparate dots at the corners. (Redrawn from Pastore and Terwilliger 1966.)

appeared slanted, as if lying on a right wall surface. Pastore and Terwilliger noted that the wall-surface contrast effect was seen by more observers than the sky/ground plane effect. Ogle's cyclovergence explanation predicts the opposite because cyclovergence is induced only by cyclodisparity.

12.2.2 Long-range depth contrast

Contrast, as normally understood, operates between adjacent stimuli—it is a local effect. The phenomena demonstrated by Werner operate over large separations between induction and the test stimuli. For this and other reasons explained later we classify this type of effect as long-range depth contrast. Werner noticed that the line appeared slanted only to the extent that the frame appeared not to slant and argued that the inclined square rescales correspondence in the contained region. The effect is analogous to the well-known rod-and-frame effect in perceived verticality in which a tilted frame appears vertical, causing a vertical line contained within it to appear tilted in the opposite direction. In the stereoscopic

case the slant of the square is normalized, or underestimated because it has only a first-order disparity and is not bounded by a disparity discontinuity. When this display is viewed as a drawing there are depth discontinuities in the surrounding visual field but the effect works because the region immediately surrounding the square is devoid of texture. Since the relative disparity between the square and line is preserved, the zero disparity in the line has to be rescaled by the amount of normalization in the square. The line therefore appears to slant in the opposite direction.

Giving a phenomenon a name does not explain it. We suggest that normalization is a default judgment which occurs because the visual system disregards zero- and first-order spatial stimuli.

A test of the role of depth normalization in the long-range depth contrast effect shown in Figure 12.4 is to surround the rectangle with another rectangle slanted in the opposite direction. (Figure 12.7). If the outer rectangle normalizes, it should carry the inner rectangle with it to preserve the strong disparity signal generated by the relative slant of the rectangles. This in turn should cause the line to appear to slant in the direction of the inner rectangle which surrounds it. On the other hand, if depth normalization is a local rather than a global phenomenon, the apparent slant of the line should be determined by the slant of the immediately surrounding rectangle. Figure 12.7a shows the normal induced slant effect. The line in Figure 12.7b appears to slant in the opposite direction which is consistent with the induced slant from the additional rectangle immediately surrounding it. The stereogram in Figure 12.7c provides additional evidence that depth contrast is a local phenomenon. Opposite directions of depth contrast can be seen simultaneously in displays separated by only 1 or 2°.

Kumar and Glaser (1991) measured the simultaneous depth contrast induced into a pair of test dots by a surrounding disparate frame up to 25° away. Depth contrast was influenced by (1) the disparity of the inducing frame, (2) the size of the inducing frame, (3) the separation of the test dots, and (4) the vertical separation between the test dots and the inducing frame. Depth contrast was measured by finding the disparity between the test dots (separated laterally by 21 arcmin) needed for them to appear in a frontal plane. For a 12°-wide rectangular frame, contrast increased from 1.5 to 3-6 arcmin as the disparity of the surrounding frame increased from 0.25 to 2°. For larger disparities, it remained approximately constant. Kumar and Glaser noted that thresholds for discriminating which dot was closer (sensitivity) also increased by a factor of five or more with increasing frame disparity.

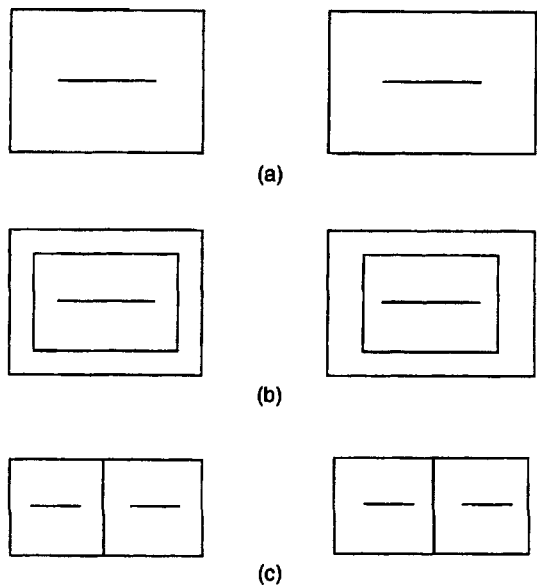


Figure 12.7. Global versus local normalization.

- The horizontal line appears to slant right side closer as a result of depth contrast from the surrounding slanted rectangle.
- The outer rectangle and the horizontal line are identical to (a) but the line appears to slant in the opposite direction (left side closer) due to the slant contrast from the additional, immediately surrounding rectangle.
- The two horizontal lines appear to slant in opposite directions as a result of local, rather than global, normalization.

Second, more depth contrast (up to 8 arcmin) was obtained when the horizontal width of the surrounding frame was reduced from 12° to 1° and third, for a given frame size, induced depth increased with increasing separation of the test dots from 21 to 240 arcmin. This third result is reminiscent of Ryan and Gillam's (1993) finding that the aftereffects of prolonged viewing of a pair of disparate lines were greater when tested on a pair of lines with greater separation (see Section 12.3.3). Both results suggest that disparity gradient mechanisms are involved. Fourth, depth contrast was maximal when the disparate inducing features lay along the same horizontal line as the test dots and was abolished when the two inducing features were laterally separated by 9° and vertically separated by more than 8°.

Kumar and Glaser (1991) also investigated simultaneous depth contrast when the images of the surrounding frame had a vertical rather than horizontal size difference. The frame appears to slant, which is Ogle's induced effect (see Section 7.6.5). Depth contrast, however, was much smaller than for a horizontal size difference and never exceeded 1 arcmin. For all three observers, depth contrast increased with an increase of the vertical disparity from 0.5° to 1° and decreased with a further increase. It would be interesting to see whether the inverted 'U'-

shaped function Kumar and Glaser obtained for depth contrast covaries with the inverted 'U'-shaped function which describes the induced effect as a function of vertical disparity (Ogle 1964; Gillam et al. 1988a).

Temporal properties

In a subsequent paper, Kumar and Glaser (1993) investigated the temporal aspects of depth contrast with the same simple configuration of a pair of test dots within a surrounding frame. The largest depth contrast occurred with the shortest exposure of 10 ms, as Werner (1937) had originally noted, and the effect was reduced by a factor of two or more for presentation times longer than 0.5 s. For exposures of many seconds, depth contrast almost completely disappeared. This was also true when the inducing frame oscillated horizontally. The largest depth contrast occurred when the surrounding frame was exposed for 10 ms between 200 and 500 ms before the test dots appeared, and there was little or no depth contrast when the frame was exposed 500 ms or more after the test dots had been presented. Kumar and Glaser pointed out that the strong depth contrast obtained with 10 ms exposures rules out Ogle's explanation of the effect in terms of cyclovergence. Note that there are no comparable reports of a weakening of depth contrast effects in surfaces with increasing exposure duration (Section 12.2.4).

Depth contrast of a quite different kind has been reported by Richards (1972) when the test and inducing targets lie in the median plane. The test target was a vertical 2° line which had either a crossed or uncrossed disparity with respect to a fixation point. Observers matched the perceived depth of the test line with a probe several degrees to one side. The inducing stimulus was a pair of short vertical bars just above and below the test line. When the test line had a disparity of plus or minus 1° and the inducing bars had disparities of the same sign as the test lines, the depth of the test line was typically underestimated by an essentially constant amount over a disparity range of 0.2° to 8°. When the inducing bars had a disparity opposite in sign to that of the test line, the depth of the test line was greatly underestimated. Richards referred to the effect as **disparity masking**. Smaller amounts of disparity masking were created when the test lines had either small disparity pedestals of either 0.25° or 0.5°, or large pedestals of 2° or 4°. In addition, the presence of monocular inducing features significantly reduced the apparent depth of the test lines with crossed (but not uncrossed) disparity.

To account for these results, Richards (1972) proposed that: (1) there are two independent mechanisms which selectively encode crossed and

uncrossed disparities, (2) the disparities of targets which stimulate the same disparity mechanism are pooled and (3) there is inhibition between the crossed and uncrossed pools of disparity detectors. A similar pattern of results was found when the stimuli were presented 5° to the right of the fixation point, suggesting that these effects are not simply a consequence of using midline stimuli.

12.2.3 Short-range depth contrast

In the depth-contrast effects described so far, the test and inducing stimuli were spatially separated by between several tens of minutes and a few tens of degrees. Other experiments have shown that the disparity values of inducing features separated by just a few minutes of arc can also affect the apparent depth of test targets. Westheimer (1986b), for example, studied the effect of a pair of vertical flanking lines on the apparent coplanarity of a central triplet of vertical lines (12 arcmin apart) which were initially aligned in a frontal plane (Figure 12.8). Two main parameters were investigated: (1) the disparity of the flanking lines with respect to the central triplet and (2) the angular separation between the flanking lines and the inner triplet. When the flanking lines were just 2 arcmin to the left and right of the central triplet and they had an uncrossed disparity, the centre line of the triplet needed to be displaced in an uncrossed (the same) direction to appear coplanar with the outer lines of the triplet. It is as if the uncrossed disparity of the flanking lines is averaged with the disparity of the outer lines of the triplet. Westheimer referred to the effect as "depth attraction" or "depth pooling" of neighbouring disparate stimuli. Moreover, the displacement varied linearly with the disparity of the flanking lines for disparities of up to 100 arcsec. The slope of the function relating the disparity of the centre line to the disparity of the flanking lines at the point of apparent coplanarity was termed the "induction coefficient". Disparity averaging is discussed further in Section 6.3.

When the flanking lines were separated by more than 4-6 arcmin from the outer lines of the triplet, the centre line had to be displaced in the opposite direction to the flanking lines to appear coplanar with the outer lines of the triplet. Westheimer referred to this effect as "depth repulsion".

Westheimer found that the critical separation between the triplet and the flanking lines at which depth attraction changed to repulsion varied between 4 and 6 arcmin for different observers. Effects of a similar type and magnitude occurred when the elements of the inducing stimulus (dots in this case) were separated vertically rather than horizontally.

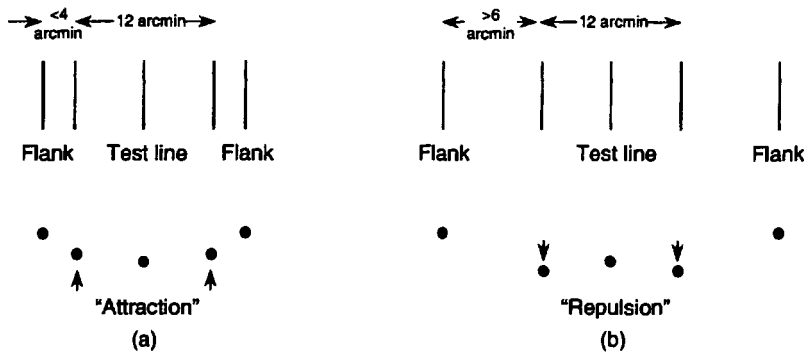


Figure 12.8. Depth "attraction" and "repulsion".

Westheimer (1986b) used a configuration of five lines to measure depth contrast. The plan view of the lines is shown underneath. On any given trial, disparity of the test line was varied and the observer's task was to judge if the inner triplet of lines was coplanar. When the flanking lines were spatially separated by less than 4–6 arcmin away from the inner triplet (a), the test line appeared to lie in front of its immediate neighbours—the result of depth pooling. With a greater separation, the test line appeared to lie behind (b), which Westheimer attributed to depth “repulsion”.

Contrast effects were also found for a configuration in which a short horizontal line was placed between a pair of vertically separated points, both with the same disparity with respect to the line (Westheimer and Levi 1987). Observers judged the depth between this horizontal line and a comparison line which was displaced laterally by 10 arcmin. As with the earlier results, the test line appeared displaced in the direction of the disparate flanking dots when their vertical separation was less than about 5 arcmin but in the opposite direction when the separation was greater (Figure 12.9).

Westheimer and Levi (1987) pointed out that both the attraction and repulsion effects could be due to shifts of the target lines within each of the monocular images rather than to interactions in the processing of disparity. To control for this possibility, they created a display in which the luminance polarity of the flanking dots and the test line was either the same or different. If the attraction and repulsion effects occur in disparity processing, the luminance polarity of the flanking dots should have no effect, while if the effect is in the luminance domain within each monocular image, the pattern of results might be reversed. For two of their three observers, there was a characteristic reversal from attraction to repulsion at 6 to 8 arcmin separation of the test line and the flanking dots, although the attraction effect was smaller. Westheimer and Levi attributed the smaller attraction effect to the monocular luminance-based interactions. As a consequence, the authors claimed to have a “persuasive argument that disparity interaction is a separate phenomenon”.

The labelling of this effect as depth “repulsion” is not justified by their results because they did not test

the apparent depth of the induction spots. The effect could just as well be a depth scaling effect, like that revealed in Figure 12.7 in which the apparent depth of the induction stimulus normalizes toward zero and the apparent depth of the zero-disparity stimulus is rescaled accordingly. In other words, the apparent distance between the induction and test stimuli may not increase, as the term “depth repulsion” suggests, but both stimuli may move together in a direction which normalizes the depth of the induction stimulus. Even if it were shown that there is a repulsion component to this effect, this could be due to figural aftereffects between the monocular images. The induction effect was still present for a separation of 36 arcmin between induction and test stimuli, beyond which the experimenters did not test. Another problem here is that convergence was not controlled and the effect could simply be due to vergence cancelling some of the disparity in the induction stimulus, and thereby conveying an opposite disparity into the test stimulus. Note that vergence cannot be responsible for the depth induction effect in Figure 12.7 because the slant of the induction stimulus is not affected by changes of convergence.

Stevenson et al. (1991) claimed to confirm the presence of depth attraction and repulsion, using stimuli in which monocular effects could not occur. The induction stimulus was a random-dot surface with a disparity of between zero and 15 arcmin and the test stimulus was a superimposed zero-disparity random-dot surface, as shown in Figure 12.10. Subjects adjusted the disparity of a comparison surface until it appeared at the same depth as the test surface. The results were very similar to those

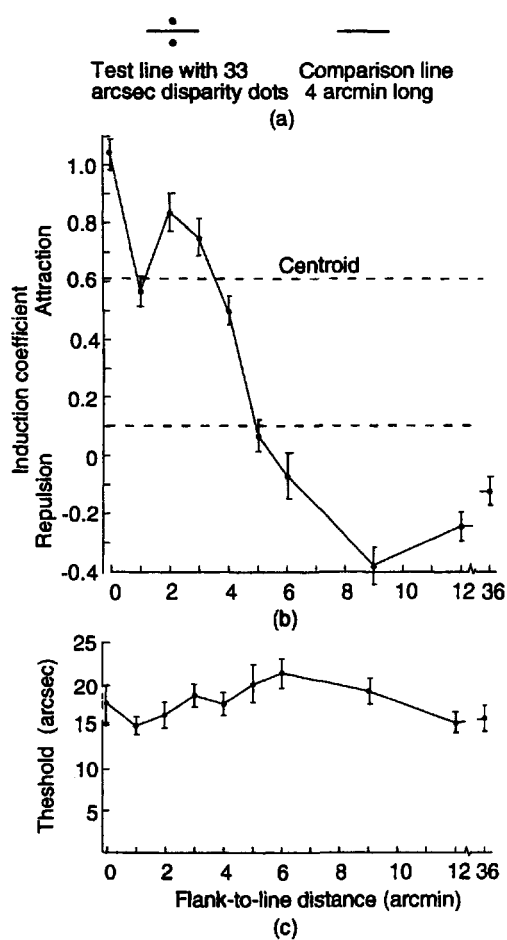


Figure 12.9. Stereopsis and stimulus adjacency.

(a) Visual display. The horizontal test line had zero disparity. The two dots had a horizontal disparity of 33 arcsec, either crossed or uncrossed. The horizontal disparity of the comparison line was adjusted until the line appeared at the same depth as the test line. (b) Apparent depth of the test line as a function of the spatial separation between the test line and the dots. Positive values on the Y axis signify that the test line appeared displaced toward the depth plane of the dots. The line marked "centroid" indicates the attraction predicted from interaction between monocular images. (c) Disparity thresholds for the same conditions. Results for one subject. (Adapted from Westheimer and Levi 1987.)

reported by Westheimer and Levi. When the induction and test surfaces were less than about 4 arcmin apart they appeared as one surface at an intermediate depth, an effect which can be thought of as depth averaging (see Section 6.3). For larger separations the surfaces were said to repel each other. But again, this description is not justified because the apparent depth of the induction surface was not measured. Here also, changes in vergence may account for the effect. Another problem is that the three random-dot surfaces were viewed through an 11° circular aperture which would introduce contaminating step disparities.

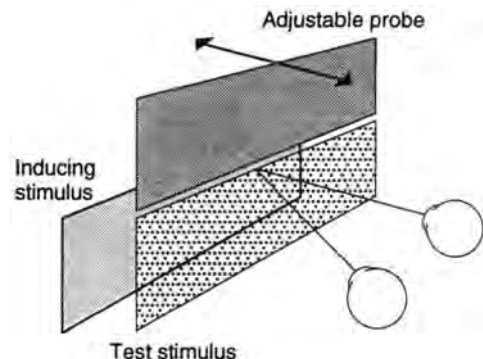


Figure 12.10. Depth attraction and repulsion.

The induction stimulus was a random-dot surface with a disparity of between zero and 15 arcmin and the test stimulus was a superimposed zero-disparity random-dot surface. Subjects adjusted the depth of the probe surface until it appeared at the same depth as the test surface. (From Stevenson et al. 1991. Reproduced with permission from Vision Research, Pergamon Press.)

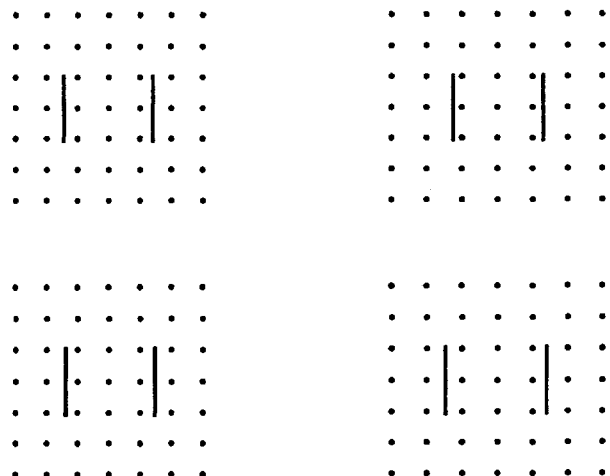


Figure 12.11. Depth contrast and salience.

The vertical lines in the upper stereogram are equally spaced in the two images and when seen in isolation appear equidistant. When seen against a 7x7 grid of dots with a disparity gradient, the righthand line appears closer, with divergent viewing. In the lower stereogram, the horizontal magnification of the lines in the right eye's image is the same as that of the grid of dots. Mitchison and Westheimer (1984) found that the lines appeared equidistant when they had a similar magnification as the background.

In summary, short-range contrast in stereopsis is not firmly established. Apparent attraction between elements with similar disparities occurs but is probably due to disparity averaging. So-called repulsion effects that are claimed to exist between elements with somewhat greater disparity differences are partially due to monocular interactions, and any binocular contribution may not be a repulsion of two elements but a rescaling of both toward zerodisparity. Some or all of this effect may be due to vergence.

The depth-contrast effect with closely spaced lines was also studied by Mitchison and Westheimer

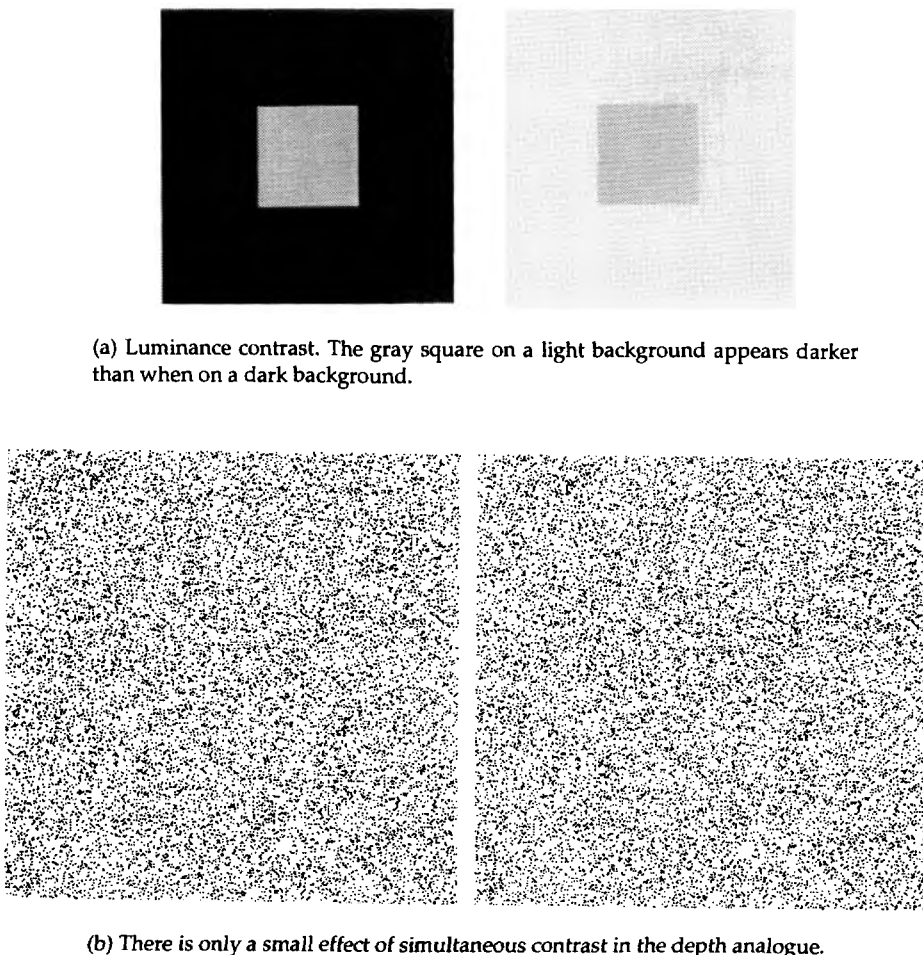


Figure 12.12. Luminance contrast and depth contrast compared.

(1984), although the effects were interpreted somewhat differently. In the simplest configuration, they showed that a single disparate line positioned either to the left or right of a pair of zero-disparity test lines, caused the test lines to appear at different distances in the direction of depth repulsion. When the three lines were each separated by 12 arcmin, the test lines had to be offset by 30% of the disparity of the inducing line to appear at the same distance. Mitchison and Westheimer argued that this and a number of similar demonstrations are compatible with the idea that judgments of equidistance and coplanarity are made with reference to a local norm, defined by the local disparity values. This reference effect was demonstrated most dramatically in judgments of the equidistance of a pair of horizontally-separated vertical lines seen against the background of a 7×7 lattice of dots with a horizontal disparity gradient (Figure 12.11). The vertical lines were perceived at the same distance only when they had a disparity gradient similar to that of the background lattice. This result is consistent with the idea that the slanting lattice of dots provides a reference plane

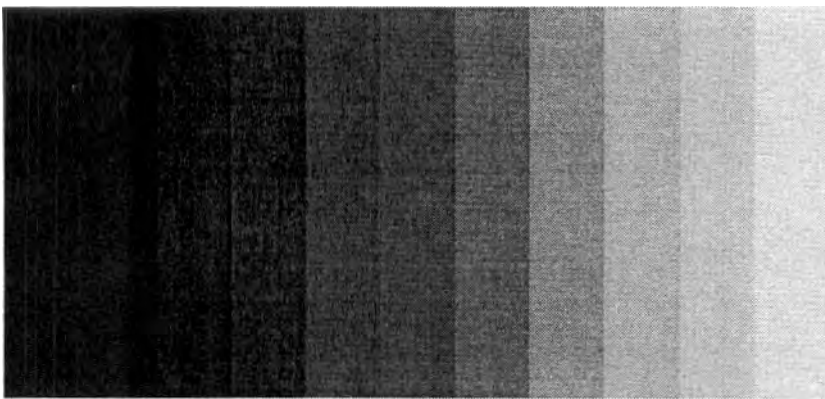
which is then used to make judgments of relative distance and coplanarity.

Salience

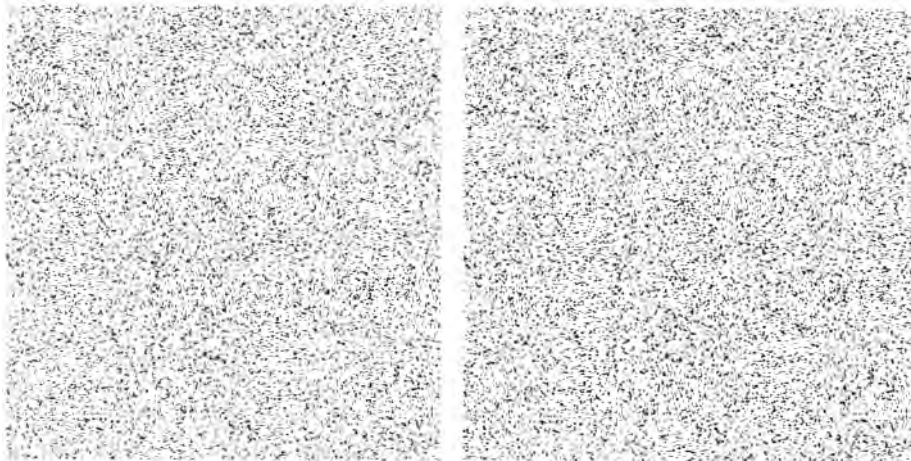
In order to explain their effects, Mitchison and Westheimer (1984) developed the idea of the **salience** of objects, derived from the disparity values of neighbouring points. The idea has its origins in Gogel's **adjacency principle** which states that the effectiveness of relative cues between objects varies inversely with their perceived separation, either in a frontal plane or in depth (Gogel 1963; Gogel and Mershon 1977; Richards 1972). Mitchison and Westheimer, calculated salience L by summing weighted relative disparities (d) of neighbouring points:

$$L = \sum w_i \cdot (d_i - d)$$

It follows that the test lines shown in the lower part of Figure 12.11 have equal salience (and thus appear at the same distance) when the two lines have the same disparity with respect to their local backgrounds. For one of the five observers, the data fitted



(a) Luminance contrast. Each vertical strip is homogeneous in luminance but appears graded in luminance because of contrast between neighbouring strips.



(b) A random-dot stereogram producing a series of vertical steps. The steps do not exhibit contrast bands in depth analogous to those seen in luminance.

Figure 12.13. Contrast bands in luminance and depth compared.

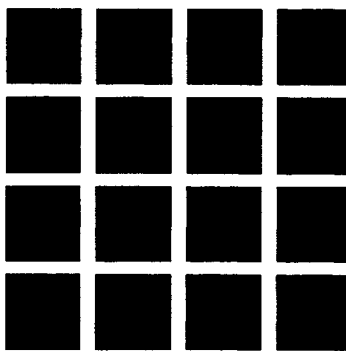
the predictions from this simple model when the weighting factor (scaled inversely with distance) was applied to all neighbouring features. For two other observers, the results were better modelled by assuming that only the nearest-neighbouring points influence salience. For the other two subjects, results were intermediate. Mitchison and Westheimer suggested that the visual system calculates salience to determine which points in the scene are coplanar and to assess the boundaries (gradient discontinuities) between planar surfaces.

12.2.4 Depth contrast in surfaces

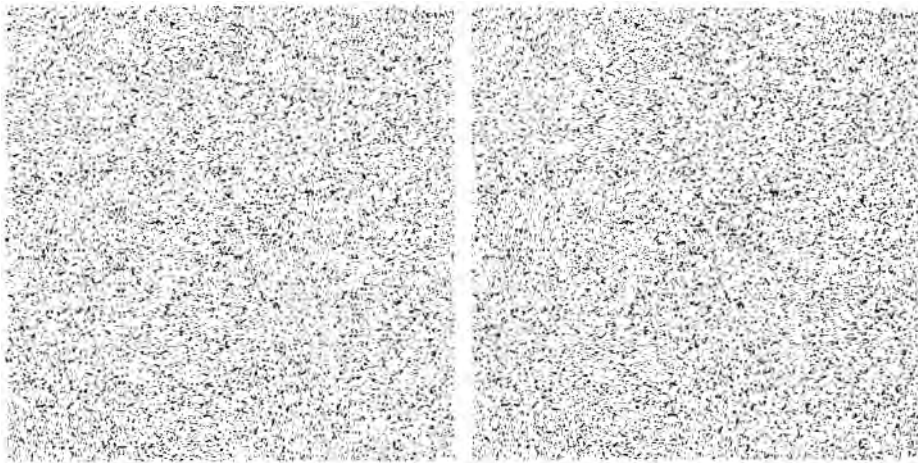
Contrast between areas of constant disparity

Anstis (1975) provided one of the first demonstrations of simultaneous depth contrast which can be attributed unambiguously to spatial interactions

between disparity mechanisms. The stereogram depicted a pair of vertically separated discs with the same disparity (Figure 12.12b). The upper disc was surrounded by a surface with uncrossed disparity and the lower disc by a surface with crossed disparity. The upper disc appears slightly closer than the lower disc (Graham and Rogers 1982a), although Brookes and Stevens (1989b) could not see this effect in a similar display. The effect is analogous to simultaneous contrast in the luminance domain in which a gray square appears lighter on a dark background than on a light background (Figure 12.12a; Cornsweet, 1970). Graham and Rogers (1982a) observed that a pair of disparate planes on either side of a horizontal step edge appear to be inclined in depth instead of lying in frontal planes. The effect is similar to the disparity analogue of the Chevreul illusion which was reported by Brookes and Stevens (1989b).



(a) The Herman grid. Dark patches are seen at the intersections of the white lines.



(b). The fused images produce a grid of squares standing out from the background. There is no evidence of a depth effect analogous to the luminance-contrast of the Herman grid.

Figure 12.14. The Herman grid in luminance and in depth compared.

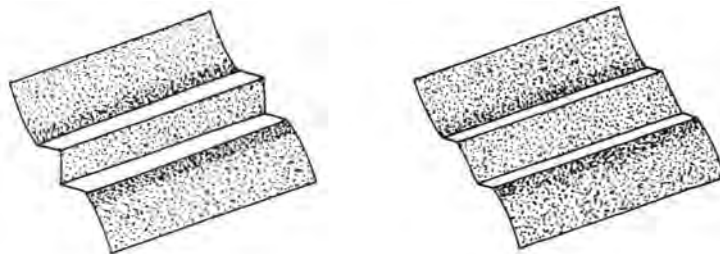
They noted that the individual steps are not seen as curved in depth, as in the luminance Chevreul illusion shown in Figure 12.13a, but rather as planar with a slight slant, as in Figure 12.13b.

Julesz (1971) created the disparity analogue of the Herman grid in which there is a disparity between the grid and the squares lying between the grid lines (Figure 12.14b). In the luminance Herman grid (Figure 12.14a), the intersections appear darker than the remainder of the grid but in the disparity analogue there is no apparent depth change at the intersections (see also Brookes and Stevens 1989b). Similarly, there does not appear to be a disparity analogue of Mach bands for a surface consisting of two outer flanking planes at different distances which are smoothly connected by a horizontal or a vertical disparity ramp (Brookes and Stevens 1989b). While there are no local bands of greater or less depth, equivalent to luminance Mach bands, the depth gradients of the three regions are often misper-

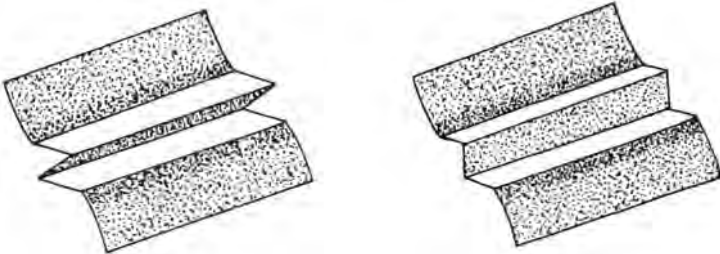
ceived, as we will see later. Apart from the disparity analogue of the Chevreul illusion, contrast effects between regions of constant disparity are weak if present at all. The depth analogue of the Chevreul illusion may not really be an exception to this rule because the staircase has an underlying disparity gradient.

Gradient contrast

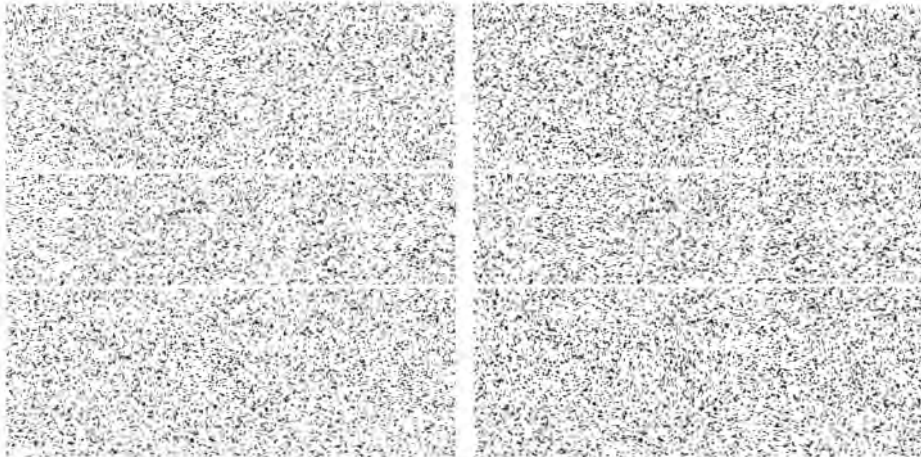
In general, surfaces with a gradual change in depth tend to normalize to the frontal plane whereas depth discontinuities are preserved. Some of the most convincing simultaneous contrast effects in the disparity domain are created by configurations of different disparity gradients (Graham and Rogers 1982a). For example, the stereogram in Figure 12.15c depicts a steep ground plane cut across by a horizontal strip of dots lying in a frontal plane, as shown on the left of Figure 12.15a. The inclined surround causes the horizontal strip to appear inclined top forwards,



(a) Perspective drawings of the surfaces used by Graham and Rogers (1982a) to measure depth contrast.



(b) A representation of the perceived shape of the surfaces, due to depth contrast



(c) The surrounding surface has a sinusoidal inclination profile as shown in (a). The horizontal strip across the centre has no gradient of inclination but when seen against the inclined surround it appears inclined in depth in the opposite direction.

Figure 12.15. Depth contrast with inclined surfaces.

as depicted in Figure 12.15b. Graham and Rogers (1982a) measured the induced inclination using a nulling technique. Subjects introduced a vertical gradient of disparity into a horizontal strip until it appeared to lie in a frontal plane. The inclination of the surrounding surfaces to the vertical varied between 9° and 33°. Between 4° and 9° of inclination had to be introduced into the horizontal strip to make it appear frontal, corresponding to between 20 and 60 per cent of the inclination of the surround.

There are at least two possible explanations of the depth-contrast shown in Figure 12.15c. First, there might be inhibitory interactions between disparity gradient detectors on either side of the depth discontinuities.

If the effect of the inhibition is to enhance the size of the discontinuity, the upper and lower edges of the horizontal strip should appear displaced in depth in opposite directions and thereby generate the appearance of inclination. Alternatively, there might be inhibitory interactions between disparity gradient detectors on either side of the discontinuities. These would induce an inclination into the horizontal strip, opposite in direction to that of the surround. According to this view, the effect would be due to disparity gradient contrast rather than disparity contrast.

To decide between these two possibilities, Rogers et al. (1988) used the same stimulus and nulling technique as Graham and Rogers (1982a) but they

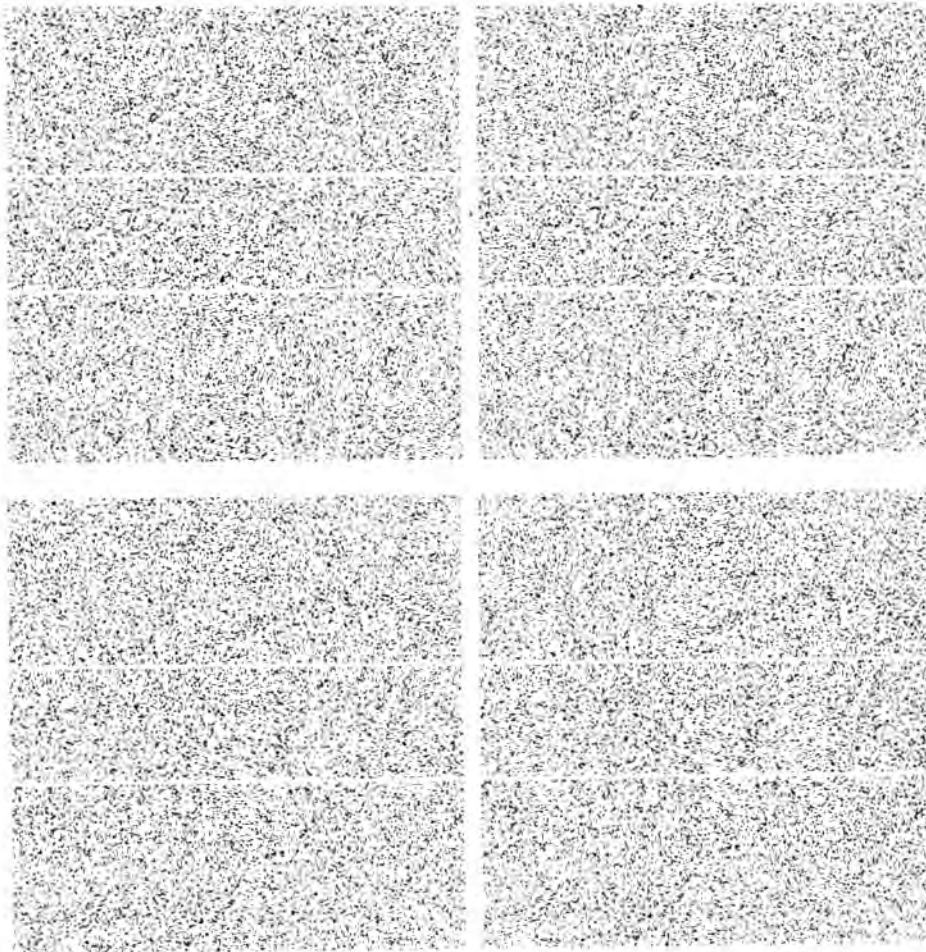


Figure 12.16. Depth contrast with disparity and disparity gradient discontinuities.

The horizontal strip in both stereograms has no disparity gradients and presented by itself would appear to lie in a frontal plane. The upper stereogram has a disparity discontinuity between the flanking regions and the centre strip, but no gradient discontinuity—only a small contrast effect is seen. The lower stereogram has a gradient (inclination) discontinuity but no disparity discontinuity and the contrast effect is much larger.

independently varied (1) the size of the disparity discontinuity between the horizontal strip and the surround and (2) the disparity gradient in the surround. Figure 12.16 shows that depth contrast is much larger when there is a change in disparity gradient than when there is only a disparity discontinuity. This result suggests that gradient contrast is more powerful than disparity contrast in binocular stereopsis.

Disparity gradients and partial derivatives

The stereogram used by Graham and Rogers contains just one of four possible spatial configurations of disparity gradients. In their display, there was a change in a vertical direction of a vertical gradient of (horizontal) disparity, corresponding to the partial derivative— $\partial^2\alpha/\partial\theta_v\partial\theta_h$ (see Section 7.1.5). In a second configuration (Figure 12.18a), the change of gradient is in the same direction as the gradients themselves

but this time they are both in a horizontal direction, corresponding to the partial derivative— $\partial^2\alpha/\partial\theta_h\partial\theta_h$. Stevens and Brookes (1987) demonstrated depth contrast using a configuration in which an annular target presented against a slanting surface appears to slant the other way (Figure 12.17a; Brookes and Stevens 1989b). It is the disparity analogue of Koffka's ring (Koffka 1935).

In the remaining configurations, the direction of change of disparity gradient is orthogonal to the disparity gradients. In Figure 12.18b, the horizontal gradient of disparity (slant) changes in a vertical direction— $\partial^2\alpha/\partial\theta_v\partial\theta_h$. In Figure 12.18c, the vertical gradient of disparity changes in a horizontal direction— $\partial^2\alpha/\partial\theta_h\partial\theta_v$. Note that the latter configuration is the surface analogue of Werner's (1938) depth-contrast effect using just three lines with orientation disparities. The configuration in Figure

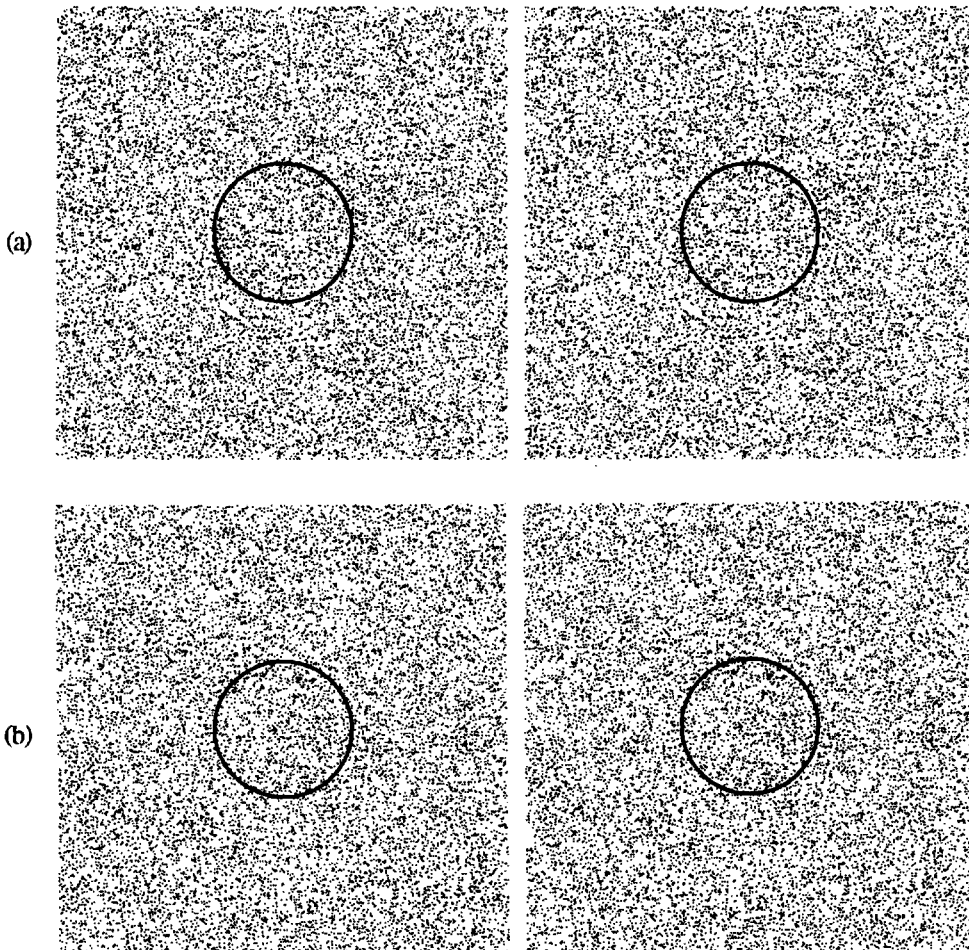


Figure 12.17. Slant and inclination contrast between a line target and a random-dot background.

(a) The background has a relative-compression disparity that creates a slanted surface. The zero-disparity ring appears slanted in the opposite direction. (Redrawn from Brookes and Stevens 1989b.)
 (b) The background has a horizontal-shear disparity which creates an inclined surface. The zero-disparity ring appears inclined in the opposite direction.

12.18a is the surface analogue of Werner's contrast effect based on the binocular difference in width of the surrounding rectangle (see Section 12.2.1).

The stereograms shown Figures 12.17 and 12.18 demonstrate that the magnitude of gradient contrast depends on the direction of the disparity gradients—more contrast is seen in slanting than inclined surfaces. Gradient contrast depends less on whether the change of disparity gradient is in a direction parallel or orthogonal to the disparity gradients—a similar amount of contrast is seen when the change is in the same direction as the disparity gradient as when it is orthogonal. Moreover, we have observed that the slant or inclination of the test strip, which has no disparity gradient, can appear as large as that of the inducing flanking regions, which contain the disparity gradient. These contrast effects can be measured using a nulling technique. When the change of slant

was in a vertical direction (Figure 12.18b), the test strip appeared to lie in a frontal plane only when it contained between 85 and 95 per cent of the disparity gradient of the flanking regions, for a 20° diameter random-dot display. When the change of inclination was in a horizontal direction (Figure 12.18c), the test strip appeared in a frontal plane when it contained between 70 and 85 per cent of the disparity gradient of the flanking regions. The strength of the contrast effects with these different configurations mirrors the visibility of double slanting and inclined surfaces reported by Gillam et al. (1988b) (see Section 12.1.1). Single slanted surfaces are more difficult to see than single inclined surfaces and changes of slant or inclination in the same direction as the disparity gradient (hinges) are more difficult to see than changes of slant or inclination in an orthogonal direction (twists).

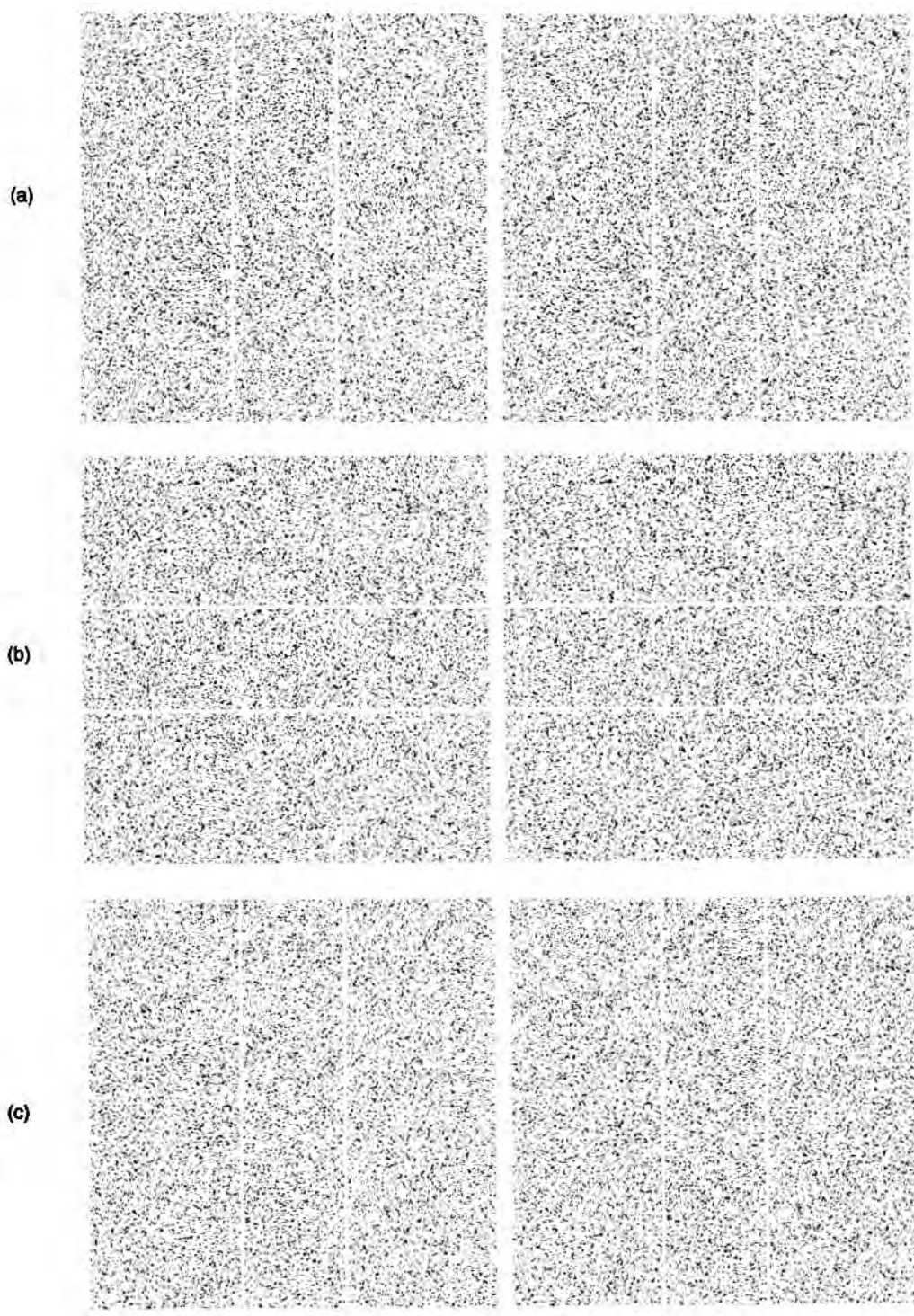


Figure 12.18. Depth contrast with inclined and slanted surfaces.

In each of the three stereograms the centre strip has no disparity gradient in either a vertical or horizontal direction and, presented by itself, would appear to lie in a frontal plane.

(a) The regions on both sides of the vertical central strip have a disparity gradient in a horizontal direction. The central strip appears to slant in the opposite direction to the flanking regions as a result of contrast.

(b) The regions above and below the horizontal central strip have a disparity gradient in a horizontal direction. The central strip appears to slant in the opposite direction.

(c) The regions on either side of the vertical central strip have a disparity gradient in a vertical direction. The central strip appears to be inclined in the opposite direction.

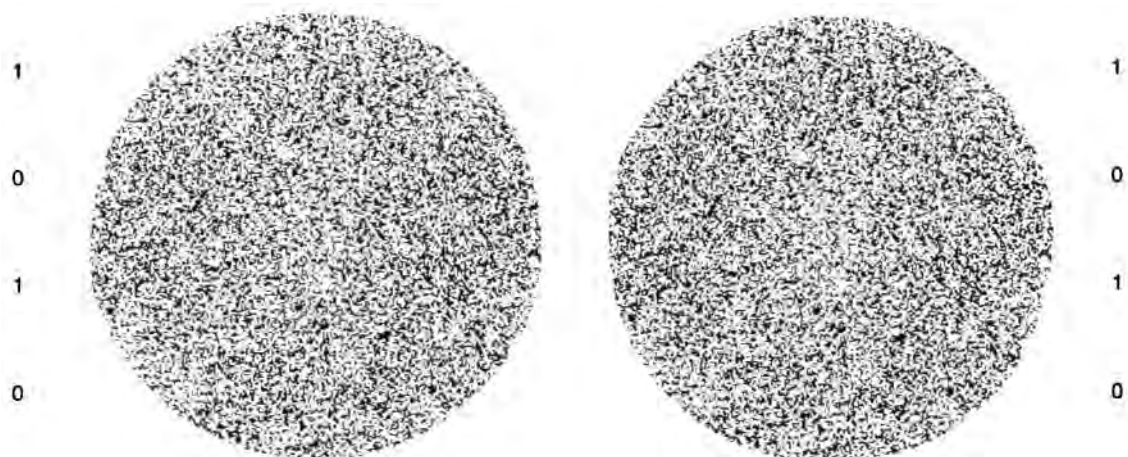


Figure 12.19. Depth contrast in a surface with no discontinuities.

The surface depicted in this stereogram is a smoothed version of Figure 12.18b. The rows between the "0" markers have no disparity gradient while those between the "1" markers have a disparity gradient in a horizontal direction. Perceptually, the amount of slant between the two sets of markers appears to be approximately equal but opposite in direction. The change of slant is readily perceived but information about slant appears to be lost.

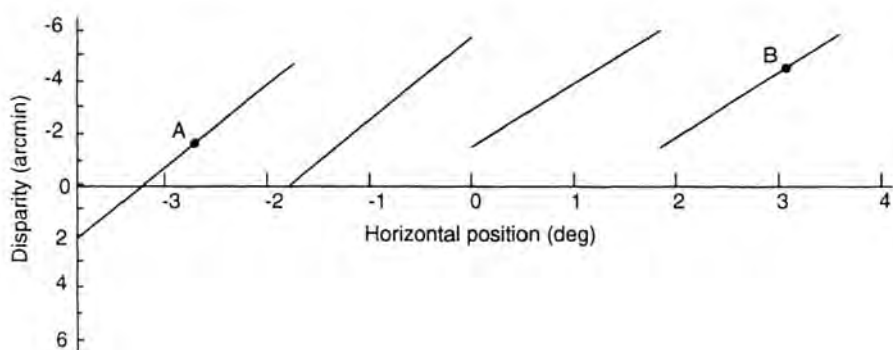
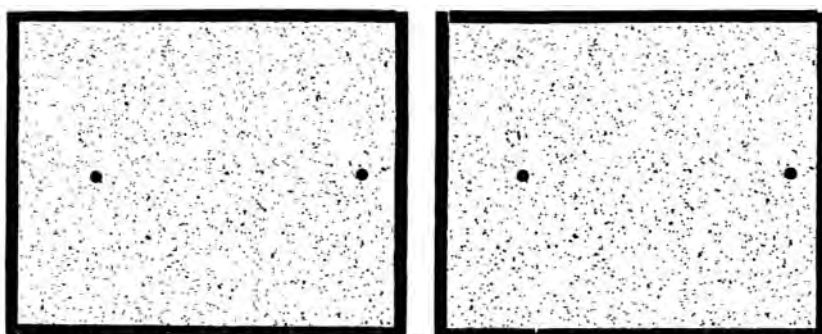
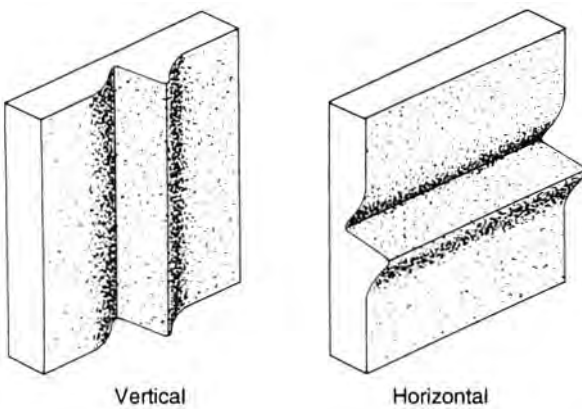
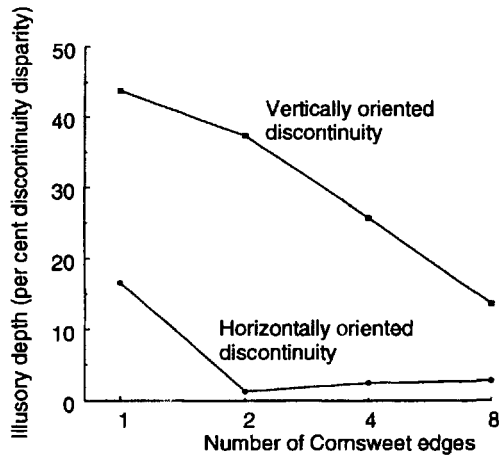


Figure 12.20. Effect of underestimation of gradual disparity ramp.

Stereogram containing a set of disparity ramps, depicted in the lower figure. When fused by divergence, the dot A appears nearer than the dot B, even though B is nearer than A in terms of disparity. This is because the depth in the gradual ramps is underestimated relative to the depth in the steps. Negative disparities are crossed. (From Brookes and Stevens 1989b. Copyright, 1989, by the American Psychological Association. Reprinted by permission.)



(a) In the display shown on the left, depth is defined by relative compression of images and the planar surface on the side of the peaked ridge appears nearer than the surface on the side of the groove. (From Rogers and Graham 1983. Copyright 1983 by the AAAS.)



(b) The size of the disparity analogue of the Craik-O'Brien-Cornsweet illusion as a function of (1) the orientation of the disparity discontinuity and (2) the number of Cornsweet edges across the 20° display. A single Cornsweet edge (Figure 12.21a) can be thought of as half a cycle of a "missing fundamental" stimulus with a spatial period of 20°. The illusion was larger when the discontinuity was oriented vertically and the number of Cornsweet edges was smaller. Mean results of 2 subjects.

Figure 12.21. Craik-O'Brien-Cornsweet illusion in depth.

The stereogram in Figure 12.19 demonstrates that a substantial contrast effect occurs in the absence of a disparity discontinuity. The dots making up the horizontal strips between the outer "0" markers have no disparity gradient whereas the dots between the outer "1" markers have a disparity gradient from far left to near right. However, the slant in the rows between the two sets of markers appears approximately equal and opposite in direction.

Another significant misperception of the shape of random-dot disparity gradients was reported by Brookes and Stevens (1989a). A left-to-right sawtooth disparity profile created the impression of a

cumulative series of depth steps (a staircase), each of which displayed only a slight depth gradient (Figure 12.20). Thus, the shallow disparity gradients are either not registered or significantly underestimated compared with the sharp disparity discontinuities. Brookes and Stevens showed that the misperception of the surface shape affected the apparent depth of a pair of horizontally-separated dots that lay in same relative positions of the sawtooth disparity profile and therefore had the same disparity values. The appearance of the sawtooth profile as a staircase caused the two dots to appear at different distances. When the dots were placed in different relative positions on the sawtooth disparity profile so that dot B had 3 arcmin of crossed disparity compared to A, dot A was seen as closer in 66 per cent of the trials.

Craik-O'Brien-Cornsweet illusion

A further disparity analogue of a luminance-contrast effect—the Craik-O'Brien-Cornsweet illusion—was reported by Anstis et al. (1978). In the luminance domain, the illusion is created when two regions of the same luminance are separated by a double spur-shaped profile consisting of a sharp discontinuity with gradual luminance gradients leading towards the equiluminous flanking regions. A similar luminance profile—the so-called missing fundamental—can be created by subtracting the fundamental frequency from a square wave. Most observers report that the flanking region connected to the light side of the discontinuity appears brighter than the flanking region connected to the dark side of the discontinuity (Craik 1966; O'Brien 1958; Cornsweet 1970).

In the disparity analogue, the outer flanking regions have identical disparities but appear to lie at different distances from the observer (Figure 12.21a). With a depth discontinuity of 2.5 cm, about 0.5 cm of depth had to be introduced into the flanking regions for them to appear equidistant for viewing distances between 72 and 290 cm (Anstis et al. 1978).

Rogers and Graham (1983) investigated the depth analogue of the Craik-O'Brien-Cornsweet illusion using random-dot stereograms rather than real surfaces. The flanking regions appeared equidistant when they had a disparity difference of up to 40 per cent of the disparity of the discontinuity and the effect was larger when there were fewer Cornsweet edges and the disparity gradients were shallower. Also, the illusion was considerably larger with a vertical depth discontinuity involving a relative compression disparity than with a horizontal discontinuity involving a shear disparity (Figure 12.22). Like Anstis et al., they concluded that the stereo system is relatively insensitive to gradual, low spatial frequency, changes of disparity, in the

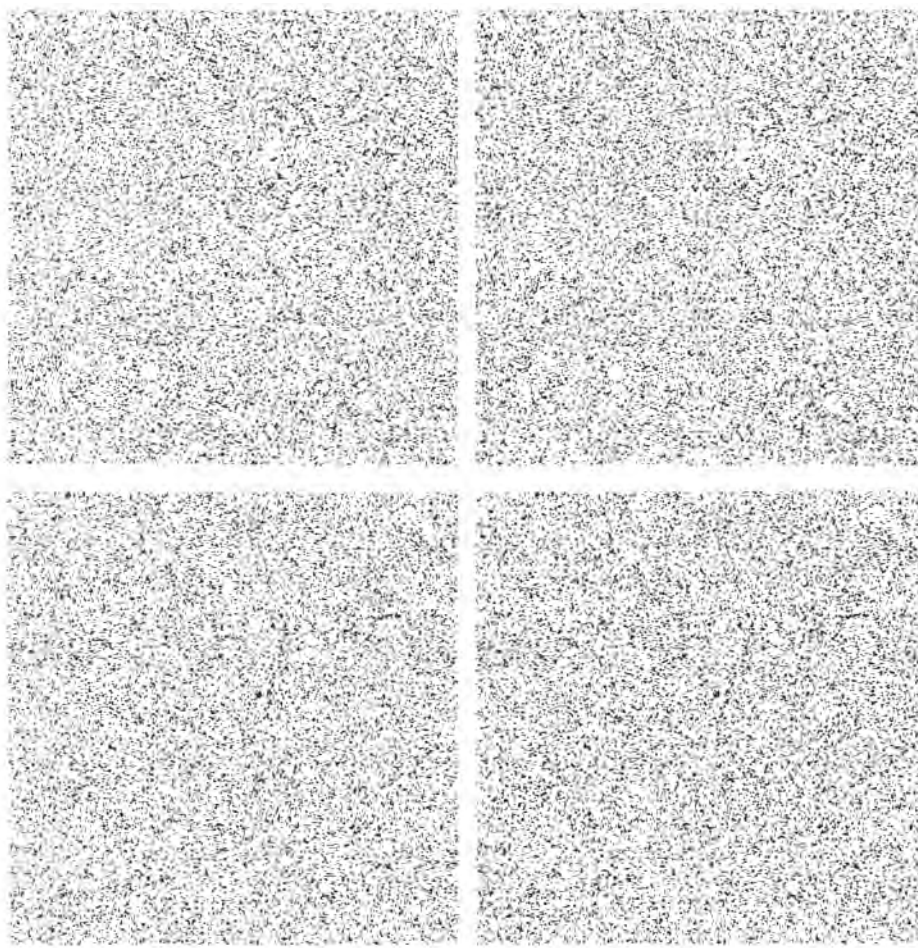


Figure 12.22. Craik-O'Brien-Cornsweet illusion in depth.

In the upper stereogram, the discontinuity is vertical. The outer flanking region on the left side typically appears closer although it has the same disparities as the outer flanking region on the right. In the lower stereogram, the discontinuity is horizontal and most observers report that the upper and lower flanking regions appear at the same distance.

regions on either side of the disparity discontinuity, compared with the sharp, high spatial frequency changes of the discontinuity itself. The anisotropy of this effect as a function of the orientation of the depth discontinuity is consistent with the greater fall-off in sensitivity to low spatial frequency vertical corrugations than to horizontal corrugations (Rogers and Graham 1983; Bradshaw and Rogers 1993b).

12.2.5 Disparity contrast mechanisms

Disparity receptive fields

Several authors have suggested that many of the depth-contrast effects described so far can be explained in terms of lateral excitatory and inhibitory interconnections between neurones which signal similar disparities (Anstis et al. 1978; Schumer and Ganz 1979; Schumer and Julesz 1984; Westheimer

1986b). The idea of a centre-surround disparity receptive field with a differential weighting of disparity signals as a function of spatial position is the disparity analogue to the receptive fields of retinal ganglion cells which show a selectivity to spatial changes of luminance. Brookes and Stevens (1989b), in particular, have drawn an explicit comparison between the coding of depth and brightness. The typical model involves facilitation from neighbouring detectors signalling similar disparities and lateral inhibition from more distant detectors which also signal similar disparities (model A) (Figure 12.23). Such a mechanism would give little response to a planar surface with either unchanging or slowly changing disparity values.

It is often not appreciated that while on-centre/off-surround and off-centre/on-surround receptive fields in the luminance domain are selective to a

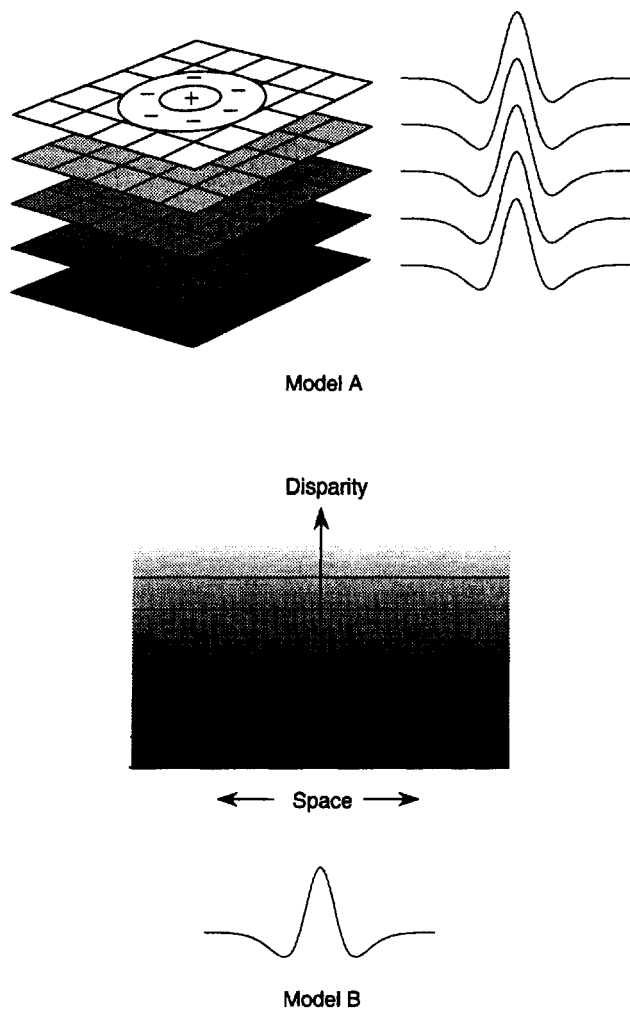


Figure 12.23. Disparity receptive fields.

In Model A, the convolution of the stimulus with the weighting function (receptive field) is assumed to take place within each disparity plane. Features in other disparity planes have no effect on receptive field outputs. The "strength" of the stimulus used in the convolution is assumed to vary with the density and contrast of disparity features within the particular disparity plane.

In Mitchison's (1993) model (Model B), the "strength" of the stimulus in each spatial location corresponds to the disparity value in that location measured on a unipolar scale. Hence the largest output of a receptive field will be produced when the disparity profile surrounding that location has the same shape as the receptive field profile.

local increment or decrement in luminance respectively (the sign of the second spatial derivative of luminance), centre-surround disparity receptive fields of the type proposed (model A) respond well to both local maxima and local minima in disparity as well as to local disparity gradients in any direction. In other words, receptive fields which operate only within particular a disparity plane function as nonspecific spatial-change-of-disparity mechanisms which do not detect constant-disparity regions.

Asymmetric disparity receptive fields with lateral inhibition between neighbouring detectors in the same disparity plane would suffer the same fate of providing a nonspecific spatial-change-of-disparity signal, in contrast to the equivalent luminance receptive fields which are selective to a particular spatial direction of luminance change .

Why do the selectivities of these disparity receptive fields differ from those of luminance receptive fields? In a luminance domain, a receptive field convolves the luminance distribution with a weighting function described by the shape of the receptive field profile. The operation of convolution involves summing the products of the amount of light falling on a particular region of the receptive field with the value of the weighting function in that region (see Section 3.4.2). In the disparity domain it is not obvious what corresponds to the "amount of light" in the convolution operation. It could be a measure of the strength of the disparity features, and as such would depend on the density and contrast of features in each part of the receptive field. Alternatively, it could be the disparity values in different spatial positions. This question has never been adequately discussed. In model A, this problem is dealt with by assuming that a separate convolution takes place in each disparity plane so that different features with different disparities never interact.

Mitchison (1993) has proposed that a closer analogue to a luminance receptive field is one in which disparity (measured on a unipolar scale) is weighted according to the shape of the receptive field (Model B) (Figure 12.23). In this case, a disparity centre-surround receptive field can signal local maxima or minima of disparity just as luminance receptive fields signal local maxima or minima of luminance. Mitchison (1993) has developed a simple neural network based on this model which can account for many aspects of depth contrast. The model has three stages. In the first stage, there is disparity pooling over each local region implemented by mutual facilitation between similar disparity-tuned mechanisms. The second stage involves interpolation of a depth map between separate disparity features in the scene (see Section 12.4). These first two stages are regarded as preprocessing prior to the crucial third stage involving a "Laplacian like" differential weighting of rate-coded disparities in neighbouring locations.

While this model has many advantages it also has several problems. Luminance is represented at all locations in the visual field whereas disparity is represented only where there is a change of luminance. Disparity information is necessarily sparse. Disparity is not alone in this respect. Orientation and

texture are represented only where there is a change of luminance because they are secondary features of the image derived from the primary luminance distribution. As a consequence, Mitchison's model will work only if the density and contrast (or other measure of the strength of signal) of disparate points is similar in different spatial regions. The absence or scarcity of changes of luminance in a given region has the same effect as features which have the arbitrary disparity corresponding to the origin of the unipolar scale and this confounds the measurement of disparity. To offset this problem, Mitchison suggested that two smoothing operations—disparity pooling and spatial interpolation—are carried out before the calculation of salience, to create a continuous and even spatial distribution of disparity.

The second problem with the model is practical rather than conceptual. According to Mitchison, disparity is rate coded on a unipolar scale. If the scale were truly unipolar, no special significance would be attached to zero disparity, which does not fit easily with the psychophysical evidence from both disparity aftereffects and disparity contrast effects. Moreover, physiological evidence is more compatible with the coding of disparity in disparity-tuned cells rather than with rate coding. However, rate-coded disparity signals could be computed from the outputs of disparity-tuned mechanisms (Mitchison 1993).

The second problem can be overcome by a simple modification of the original model. In the modified scheme, the disparity signals are measured on a signed bipolar scale (see Section 3.2.2) by taking the difference between the outputs of broadly-tuned crossed and uncrossed disparity detectors before being differentially weighted according to the receptive field profile. These receptive fields produce a maximum output when disparities falling in the centre and surround are maximally different, enabling the receptive field to signal an approximation to the second spatial derivative of disparity.

A signed bipolar scale of disparity does not eliminate problems caused by the discreteness and non-homogeneity of disparity signals, but these factors would affect the receptive field output less than with a unipolar scale. The corollary of this point is that zero-disparity features have little effect on the receptive field's output—a prediction which could be tested experimentally. In addition, the model predicts that a greater density or contrast of features with a particular, non-zero disparity will bias the overall firing rate of these receptive fields and thereby affect perceived depth. Note that a receptive field elongated in one direction has different second-derivative tuning characteristics in orthogonal

directions. Abolishing the inhibitory surround in a particular direction creates a receptive field with a second-derivative characteristic which is orientationally selective.

A model B asymmetric receptive field, producing maximum output when disparities falling on the two sides are maximally different, would be sensitive to the first spatial derivative of disparity (disparity gradient). Note also that although the symmetrical receptive fields proposed above for the measurement of second spatial derivatives are isotropic they signal only changes of disparity gradient in the direction of the disparity gradient—the partial derivatives: $\partial^2\alpha/\partial\theta_v^2$ and $\partial^2\alpha/\partial\theta_h^2$ (Section 12.2.4). However, changes in disparity gradient orthogonal to a disparity gradient could be calculated by taking the difference between the outputs of neighbouring asymmetric receptive fields tuned to different disparity gradients.

Modelling the empirical evidence

It is often assumed that a successful model of depth contrast creates a depth or range map that matches the perceived depth of features and surfaces. The enterprise is analogous to explanations of Mach bands or the Herman grid illusion in which the outputs of hypothetical receptive fields are compared with distortions of perceived brightness (see Baumgartner 1964). The success of the modelling is judged by the extent to which the outputs of hypothetical receptive fields signalling either brightness or depth match the perceived brightness or apparent depth assessed psychophysically. But concentric receptive fields in the cat or monkey retina do not signal brightness as such but rather an approximation to the local second spatial derivative of luminance. There is no reason to expect a correlation between the strength of signals from hypothetical receptive fields and perceived brightness in different local regions—the receptive field output indicates how rapidly the luminance gradient is changing, not the luminance magnitude.

The same point is relevant to the modelling of disparity receptive fields in the depth domain. If the function of disparity receptive fields is to signal an approximation to the second spatial derivative of disparity, there is no reason to expect a correlation between the receptive field's output in a given spatial location and the perceived depth in the same location.

In proposing the idea of salience, Mitchison (1993) resisted the temptation of equating the output of disparity receptive fields directly to perceived depth. Salience is not a measure of depth but of a local difference in depth between a feature and its

surrounding features. Consequently, salience indicates whether a feature is coplanar with, in front of, or behind its neighbours and is independent of the disparities of the features (zero-order properties) or their disparity gradient (first-order properties). This is quite different from the idea of facilitation or inhibition between disparity detectors distorting the resulting depth map as implied by the words "attraction" and "facilitation". The advantages of computing second-order descriptions of the disparity field have also been considered by Rogers (1986), Stevens and Brookes (1987), Gillam et al. (1988b), Brookes and Stevens (1989b), and Rogers and Cagenello (1989).

How compatible is the idea of taking second-order measurements of the disparity field with the depth-contrast effects described earlier? In the classic depth-contrast demonstrations of Werner (1937, 1938) and Ogle (1946) the depth gradient of the test feature is seen in the opposite direction to that of the inducing features. This suggests that the visual system has access to the difference between the spatial gradients of test and inducing features and (conversely) has little access to their absolute disparity gradients (Section 12.2.1). The depth-contrast effects seen in surfaces with different disparity gradients (Anstis et al. 1978; Graham and Rogers 1982a; Rogers and Graham 1983; Stevens and Brookes 1987; Brookes and Stevens 1989b) are also consistent with the idea that spatial changes in disparity gradients are adequately coded but that the absolute disparity gradients of the inducing and test surfaces tend to be ignored (Section 12.2.4). The finding that disparity gradients are more effective than disparity discontinuities in creating depth contrast provides further evidence in support of these proposals (Rogers et al. 1988). Note also that disparity analogues of the Herman grid and simultaneous contrast which involve surfaces with different disparities but no disparity gradients, do not produce significant contrast effects (Section 12.2.4).

Can the short-range contrast effects involving a small number of closely spaced discrete targets be accounted for by the same processes as the long-range contrast effects with either discrete targets or surfaces? The size of the contrast effects and the ranges over which they operate are often quite different in the two situations. Mitchison's (1993) idea of calculating the local salience between features seems better able to account for depth contrast involving discrete targets whereas the idea of calculating the partial derivatives seems more plausible for densely textured surfaces. However, both ideas involve deriving a representation based on the second spatial derivative of disparity.

An analogy between depth and brightness?

How similar are the contrast effects created by disparate stimuli to those found in the luminance domain and to what extent are the explanations of the two classes of effects comparable? Brookes and Stevens (1989b) have argued that processing in both cases involves the reconstruction of a brightness or depth map from higher-order spatial derivatives of the original signal. However, they also noted some significant differences in the existence and magnitude of depth contrast in the two domains. To account for these differences, they suggest three hypotheses: (1) contrast in the depth domain may be more subtle and therefore difficult to detect; (2) disparity and luminance processing differ in that there is only limited access to the original (absolute) signal in the latter case; and (3) disparity receptive fields which summate over a small neighbourhood are unlikely because they would cause problems for depth segregation and transparency. Hence although in favour of the use of second spatial derivatives in the disparity domain, Brookes and Stevens suggest that these may be derived from two consecutive first-order differences—by a process of shifting or remapping—rather than by convolving the stimulus with receptive fields. It is not clear, however, that this would account for the empirical differences between contrast effects in the two domains. Mitchison and Westheimer (1990), on the other hand, suggest that differences in the way we perceive luminance and depth result from the fact that there is no need to integrate the second spatial derivative description of disparities to provide a depth map, as there is in the luminance case.

12.3 SUCCESSIVE DEPTH CONTRAST

The evidence presented in Section 12.2 shows how simultaneous contrast effects in the depth domain can provide important clues about the spatial properties of disparity mechanisms. In the present section we consider successive contrast effects or aftereffects in the depth domain as a source of evidence of the temporal, adaptive properties of those mechanisms.

12.3.1 Depth aftereffects

Disparate and inclined lines

Köhler and Emery (1947) first reported "figural aftereffects in the third dimension" following the classic study of two-dimensional figural aftereffects by Köhler and Wallach (1944). After prolonged inspection of a line either inclined or slanted with respect to the frontal plane, a frontal test line appeared

inclined or slanted in the opposite direction. They noted that the test line always appeared displaced away from the inspection line, just as a vertical line in the frontal plane appears tilted clockwise after inspection of a line tilted counterclockwise. Moreover, they found that the three-dimensional figural aftereffect was more pronounced for inspection and test lines inclined around a horizontal axis than for those slanted around a vertical axis. Adaptation to three-dimensional chevron or curved inspection lines produced negative aftereffects similar to the two-dimensional aftereffects reported by Gibson (1933). These results led Köhler and Emery to suggest a common basis for the two- and three-dimensional aftereffects. They also claimed, however, that following the alternating presentation of monocular inspection stimuli to the two eyes, such that the inspection lines were not seen in depth, there was never "the faintest indication" of a three-dimensional aftereffect. From this they concluded that aftereffects in the third dimension cannot be attributed to separate monocular two-dimensional tilt aftereffects and that "visual depth is a sensory fact."

In an attempt to identify the cause of depth aftereffects, Howard and Templeton (1964) asked observers to inspect a pair of horizontally-separated, vertical contours positioned at different distances from the observer. The test contours were disparate by varying amounts and subjects judged which of the two test contours was closer. Steady fixation on a point in between the disparate inspection contours caused the point of subjective equality (when the two test contours appeared to be at an equal distance) to be displaced in the direction of the inspection distances by amounts which ranged from 25 per cent to over 150 per cent of the inspection disparity. Howard and Templeton concluded that the results supported the idea of a "norm of equidistance" analogous to the normalization processes in two dimensional tilt perception described by Gibson (1937), but acknowledged that two dimensional figural shifts in the positions of the monocular contours may have contributed to the depth aftereffect in their situation.

Mitchell and Baker (1973) measured a three-dimensional aftereffect created by prolonged viewing of a single disparate line. After 3 minutes of inspection of a 2° vertical line, which had a disparity of between -25 and +25 arcmin with respect to the fixation point on different trials, a zero-disparity test line appeared displaced in the opposite direction. The aftereffect was measured by a nulling technique in which the briefly exposed test line was displaced in the direction of the adapting line until it appeared equidistant with the fixation point. The aftereffects

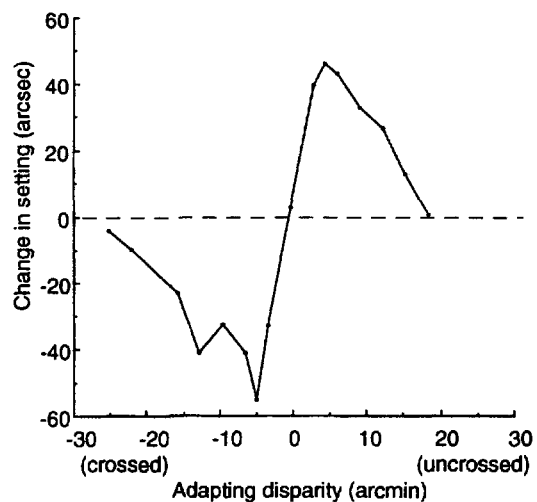


Figure 12.24 Depth aftereffects from line stimuli.

Depth aftereffect magnitude following inspection of a 2° high line with a disparity indicated by the abscissa. The aftereffect was maximal when the line had about 6 arcmin of either crossed or uncrossed disparity with respect to the fixation point. (Redrawn from Mitchell and Baker 1973.)

were largest when the inspection line had between 5 and 10 arcmin of either crossed or uncrossed disparity and declined to zero when the disparity was increased to ± 25 arcmin (Figure 12.24). Mitchell and Baker obtained depth aftereffects with inspection periods as short as 15 s and the aftereffect magnitude became asymptotic with periods greater than 2 min. Aftereffects were seen only when the inspection and test lines stimulated similar retinal regions—a lateral shift of only 10 arcmin abolished them. They pointed out that their aftereffects were larger (up to 90 arcsec) than many previously reported, which they attributed to their use of a very brief test interval. However, their aftereffects are not atypical when expressed as a percentage of the disparity of the adapting stimulus (25%).

Although two-dimensional tilt aftereffects and three-dimensional inclination aftereffects share common features (Wenderoth 1971), Köhler and Emery (1947) reported that the successive dichoptic presentation of oppositely tilted lines to the two eyes failed to create an depth aftereffect. This suggests that different mechanisms are involved. Milewski and Yonas (1977) argued that if two-dimensional tilt and three-dimensional inclination aftereffects with line stimuli are mediated by a common contour orientation mechanism, they would expect the variables which affect one aftereffect to also affect the other. They tested whether the three-dimensional inclination aftereffect was tuned to the spatial frequency of the adapting stimulus in a similar way to the tuning of tilt aftereffect (Ware and Mitchell 1974b). Their results showed little transfer of the

inclination aftereffect from inspection gratings of 3.7 c/deg to test gratings of 1.2 c/deg or vice versa. This result is consistent with the idea of a common mechanism but they made no measurements of the transfer of the tilt aftereffect with the same patterns for comparison. Even if such a similarity does exist, it does not mean that a common mechanism is involved.

Mack and Chitayat (1970) had subjects move about for 40 minutes while wearing binocular prisms that produced 5° opposite rotations of the images about the visual axes in the two eyes. After the prisms were removed, subjects showed a mean change of about 12° in the apparent inclination of a test line in a direction opposite to the anomalous inclination induced by the prisms. The torsional positions of the eyes were found not to have changed during exposure to the prisms.

Textured surfaces

Bergman and Gibson (1959) measured depth aftereffects following a four-minute exposure to an inclined textured surface which "lacked visible contours". The perceived inclination of the frontal test surface was opposite to that of the inspection surface. After viewing inspection surfaces inclined either 15°, 30°, or 45°, the aftereffect had a similar value of around 2.7°, when measured with a nulling procedure. The magnitude of the aftereffect was similar following either monocular or binocular inspection and it did not matter whether the inspection surface was fixated or scanned. The strong three-dimensional aftereffect from monocular inspection (presumably due to the texture gradient) means that one cannot conclude that the aftereffects following binocular inspection were due to adaptation of disparity mechanisms. Gibson and Bergman concluded that the monocular and binocular processes responsible for the aftereffects "are alike in being susceptible to adaptation". They also argued that use of a textured inspection surface precluded the generation of monocular figural aftereffects.

Wenderoth (1970) questioned this claim and, in his own experiments, used a high-contrast lattice which covered a 30° inclined inspection surface. He found aftereffects corresponding to just over 3.5° of inclination after only two minutes of adaptation and an exponential dissipation of the aftereffect over the following five minutes.

These early experiments leave unresolved the original question of whether three-dimensional aftereffects result from figural satiation processes (Köhler and Emery 1947) or normalization (Bergman and Gibson 1959). Moreover, they provide no

unequivocal evidence that aftereffects in the third dimension are due to the adaptation of disparity mechanisms rather than either (1) adaptation of mechanisms sensitive to other depth cues or (2) adaptation of separate monocular figural processes occurring before binocular comparison.

12.3.2 Disparity aftereffects

Disparate patches

To show that depth aftereffects are due to adaptation of disparity mechanisms, one must use inspection and test stimuli in which (1) there are no monocular cues to the relative depth or slant of the surface, (2) the position, orientation, and curvature statistics of the inspection pattern are evenly distributed, and (3) the inspection and test patterns are different. Blakemore and Julesz (1971) used random-dot stereograms as the inspection and test stimuli, which satisfied all three criteria. The inspection stereogram portrayed a pair of vertically-separated, disparate squares with disparities of +2 and -2 arcmin with respect to the fixation bar. The squares lay in front of a random-dot field which had an uncrossed disparity of 6.7 arcmin. Observers scanned along a fixation bar placed midway, both laterally and in depth, between the squares (upper Figure 12.25). In the test stereogram, both squares had zero disparity with respect to the fixation bar and the surrounding field had the same uncrossed disparity as that in the adaptation stereogram (lower Figure 12.25).

The authors did not provide detailed results but claimed that the squares in the test stereogram had to have disparities of -30 and +30 arcsec with respect to the fixation point to null the effects of adapting to the -2 and +2 arcmin disparities of the inspection squares for 2 minutes. Moreover, the persistence of the aftereffect (but not its magnitude) increased with increasing adaptation time up to the maximum time used of 5 minutes. Long and Over (1973) extended Blakemore and Julesz' study by measuring the depth aftereffect created by prolonged viewing of a stereogram depicting a single square either in front of or behind the surround. The disparity of the square varied between ± 20 arcmin and the aftereffect was measured by a nulling procedure which altered the disparity of the test square according to the observer's previous response. The aftereffect was zero when the adapting square was coplanar with the surround and it reached a maximum when the adapting square had between 4 and 8 arcmin of either crossed or uncrossed disparity, corresponding to around 25 per cent of the depth in the adapting surface. It declined to zero when the disparity of the adapting square was greater than 20 arcmin (Figure

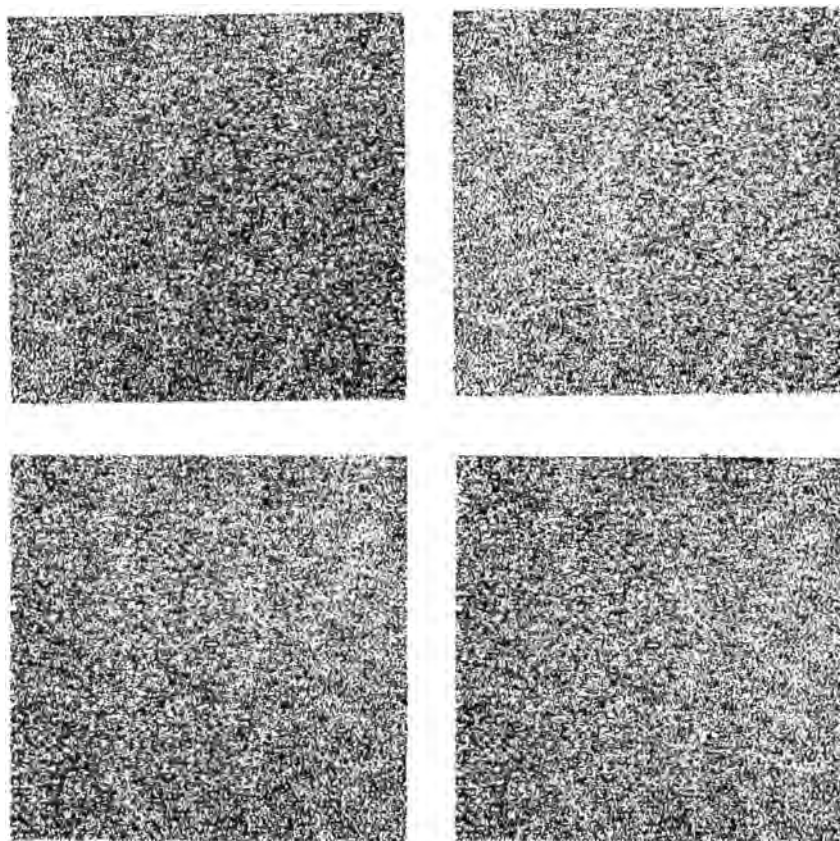


Figure 12.25. A depth aftereffect.

Fusion of the images in the upper stereogram by convergence or divergence produces two squares at different distances. Fixate the small rectangle for about 1 minute and transfer the gaze to the lower stereogram. For a short while the two equidistant squares will appear to lie in different depth planes. (From Blakemore and Julesz 1971. Copyright 1971 by the AAAS.)

12.26). Note the similarity between the results of this study and those of Mitchell and Baker who used line stimuli (Figure 12.24). The authors interpreted their results as being consistent with the selective adaptation of two pools of disparity detectors, one sensitive to crossed disparities and the other to uncrossed disparities (Richards 1970; 71b), each with an upper limit of around 16 arcmin of disparity.

Very similar results were obtained with single dichoptic bars as induction and test stimuli. Such stimuli have the advantage that they allow one to explore the spatial range of the depth aftereffect. The depth aftereffect occurred only for test and induction stimuli separated laterally by less than about 16 arcmin. In other words, the depth aftereffect is spatially localized (Mitchell and Baker 1973). The aftereffects in these studies were between 15 and 25 per cent of the disparity in the inspection stimulus.

Depth adaptation in random-dot stereograms also manifests itself in the effect it produces in a stereogram with ambiguous depth. Thus, when a

random-dot stereogram depicting a square in front of a background was inspected, a subsequently seen stereogram in which the disparity of the central square was ambiguous was seen as a square behind the background (Long and Over 1974b).

Possible reversal of sign of disparity

In stereopsis, crossed images produce the impression of an object in front of a zero-disparity background, and uncrossed images produce the impression of an object beyond the background. In 1852 Wheatstone constructed a pseudoscope consisting of a Dove prism before each eye with the reflecting surface vertical. This reversed the disparities between the images and also the sign of vergence required to fixate at different distances. Objects such as the inside of a cup, an embossed medal, a globe, and a skeletal cube appeared in reversed depth when viewed in the pseudoscope. However, the majority of familiar objects appeared in their normal relief, which Wheatstone proposed was due to strong monocular cues to depth. Evidence cited in Sections

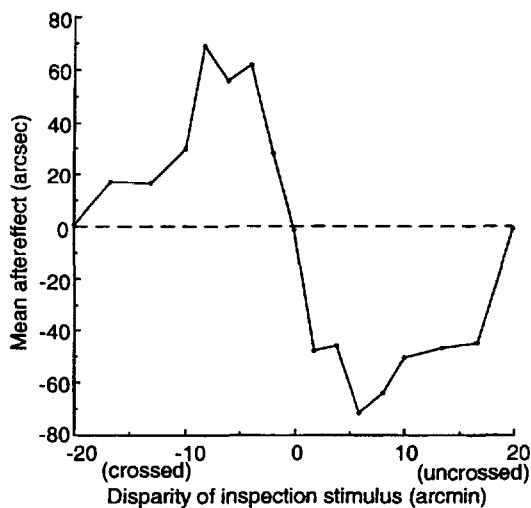


Figure 12.26 Aftereffects from a disparate random-dot figure. Depth aftereffect, measured using a nulling technique, following inspection of a centre square with a disparity indicated by the abscissa. The aftereffect was maximal when the square had about 6 arcmin of either crossed or uncrossed disparity with respect to the surround. (Redrawn from Long and Over 1973.)

11.2.2 and 11.2.6 indicates that he was at least partly correct in this supposition. He also noted that some three-dimensional objects, such as an intaglio or a salt crystal, may appear in reverse relief even when viewed normally with two eyes. However, he did not believe that there was a inversion of disparity coding in such cases. Monocular cues such as perspective are inherently ambiguous and prone to spontaneous reversal, as evidenced in the wellknown Necker cube. Perspective spontaneously reverses even with three-dimensional objects, such as a skeletal cube, if the object is viewed steadily for several minutes. The reversal of perspective overrides conflicting disparity information (Howard 1961).

Shimojo and Nakayama (1981) had an observer wear pseudoscopic prisms for 9 days. This experience had no effect on the perceived depth in random-dot stereograms. However, line stereograms that depicted objects such as a pyramid were often seen in reverse depth or in unstable depth after the 9 days. But this type of stereogram contains perspective cues, and these, rather than the disparity, may have become more unstable. We have already noted that a few minutes of normal viewing of three-dimensional skeletal shapes, such as pyramids and cubes, causes them to reverse in depth spontaneously, and the longer viewing is continued, the more unstable the perceived depth becomes. Ichikawa and Egusa (1993) repeated Shimojo and Nakayama's experiment with five subjects wearing reversing prisms for 10 days. After the first few days, three of the subjects reported reversed depth in a random-dot stereogram but the effect usually

wore off towards the end of the ten-day period. The reversed depth was most evident when subjects did not fixate and it is possible that misconvergence produced anomalous disparities. Changes in convergence induced by the prisms were not measured. This is the only evidence that the sign of disparity can be reversed in the nervous system by prolonged exposure to anomalous visual inputs.

Adaptation of distinct channels

Stevenson et al. (1992) used a depth-adaptation procedure to estimate the number of distinct disparity-detection channels in the visual system. Subjects inspected a 9° array of random dots for 60 s, with 0.5-s toppling-up exposures. The arrays had different degrees of crossed or uncrossed disparity with respect to a surrounding aperture. Between exposures, subjects were tested for 100 ms with the same display with uncorrelated dots added. Their task was to detect the presence of the uncorrelated dots that added an impression of fuzzy depth to an otherwise smooth surface. The percentage of uncorrelated dots required for detection was about twice as high after adaptation as before, when the disparity in the test and adaptation stimuli was the same. When the disparity of the two stimuli differed by between 5 and 10 arcmin, the effect of adaptation declined to zero. Stevenson et al. concluded that the visual mechanisms that process interocular correlation are sharply tuned for disparity. This suggests that there are many distinct channels in this mechanism, although whether these are all present in one location or are spread out over the 9° area of their stimulus is unclear from their results.

Corrugation aftereffects

The results of different studies may be compared by expressing depth aftereffects as a percentage of the depth in the inspection surface. The aftereffects described so far were around 25 per cent, with the exception of one condition in Howard and Templeton's experiment. In contrast, Graham and Rogers (1982a) reported much larger aftereffects. Their inspection stereogram depicted a sinusoidally corrugated surface with horizontal ridges. The corrugation frequency was 0.1 c/deg and the peak-to-trough amplitudes of disparity were 2.5, 5, 10, and 20 arcmin (Figure 12.27). Observers tracked a fixation point which oscillated horizontally along a constant disparity contour midway between a peak and a trough of the corrugations to prevent the build-up of afterimages. After an initial 30 s inspection period, a test surface was displayed for 1 s. In a top-up procedure, the adapting surface was displayed for a further 8 s followed by a 1 s view of the

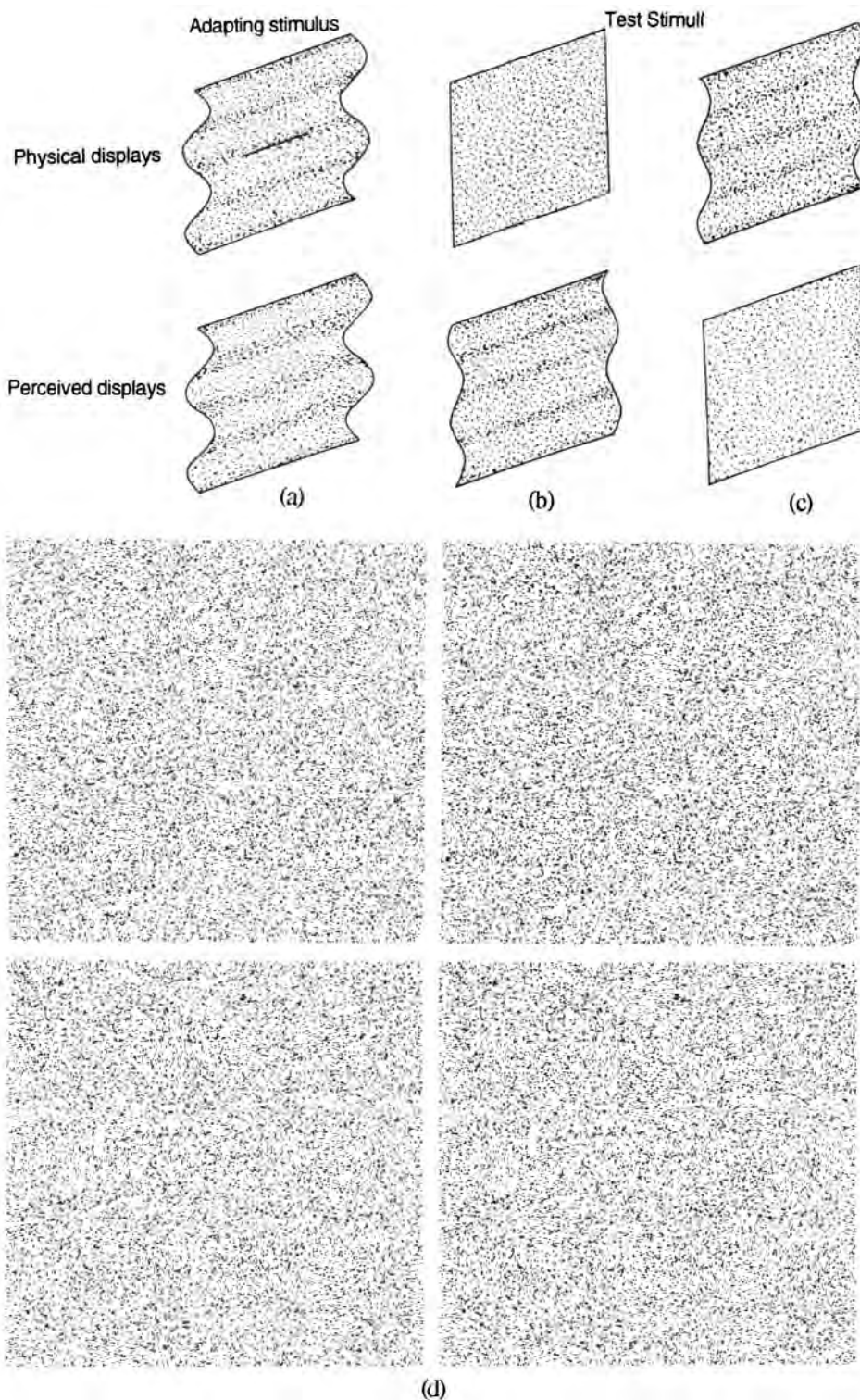


Figure 12.27. A depth aftereffect produced by depth corrugation.

- (a) Subjects viewed a surface with sinusoidal depth corrugations while tracking a fixation point moving along a horizontal line in the centre of the display.
- (b) Subsequently, a flat test surface appeared to be corrugated in depth with opposite phase to that of the adapting surface.
- (c) The magnitude of the aftereffect was measured by asking subjects to adjust the depth modulation of a test surface until the surface appeared flat. (From Graham and Rogers 1982, Perception, 11, 247-262, Pion, London.)
- (d) Inspection and test stereograms.

test surface, and the cycle repeated for 2 minutes. After viewing the inspection surface, the physically flat test surface appeared corrugated in the opposite direction to the adapting surface. The aftereffect was measured by adjusting the peak-to-trough disparity of the test surface until it appeared flat during its 1 s presentation (Figure 12.27c). The largest aftereffects (10–12 arcmin peak-to-trough disparity), were created by the 20 arcmin adapting surface but the largest proportional or percentage aftereffects (70–85 per cent) were created by the smallest amplitude of the adapting surface (2.5 arcmin).

Graham (1983) reported that aftereffects created by prolonged viewing of 8 arcmin sinusoidally corrugated surfaces of different corrugation frequencies remained at about 60 per cent of the adapting surface amplitude between 0.05 c/deg and 0.4 c/deg, but decreased sharply with higher corrugation frequencies. Lee (1994), on the other hand, found that the aftereffects created by prolonged viewing of a 10 arcmin sinusoidally corrugated surface fell off sharply when the corrugation frequency was increased from 0.06 to 0.5 c/deg. The sizes of the aftereffects in his study, however, were typically much smaller than those reported by Graham (1983). Note that unless tracking along the fixation bar is very precise, the depth profile will be "smeared" across different retinal regions and consequently reduce the strength of the measured aftereffect. High-frequency corrugations will be more affected by poor tracking.

Why were the depth aftereffects found by Graham and Rogers so much larger than those reported previously? Informal observations suggest that surfaces with continuously-varying disparity profiles generate larger aftereffects than the discrete depth planes or inclined planar surfaces used in previous studies. In the luminance domain, Georgeson and Turner (1985) reported that square wave luminance gratings produce weaker afterimages than sinusoidal gratings.

Graham and Rogers suggested that a second reason for their large depth aftereffects was the use of a topping-up procedure coupled with the brief presentations of the test stereograms (Mitchell and Baker 1973). Informal observations suggest that corrugation aftereffects decline with a time constant of just a few seconds. Depth aftereffects of up to 50 per cent have been reported by Wenderoth et al. (1968) after adaptation to real inclined surfaces with both disparity and monocular depth cues. The main result of their experiment was that the starting position of the inclined test surface affected subsequent measurements which they attributed to the rapid dissipation of the aftereffect. Thus, when the starting point of the test surface was closest to the "true"

final setting, the aftereffect was up to 50 per cent of the inclination present in the adapting surface. It follows that the optimal procedure for measuring depth aftereffects is one in which (1) the time spent viewing the test surface is minimized (Mitchell and Baker 1973) and (2) the starting position of the test surface is as close as possible to the final setting. The topping-up procedure used by Graham and Rogers was clearly optimal in both these respects and probably contributed to their large aftereffects.

12.3.3 Models of depth aftereffects

Satiation versus normalization

What can these disparity aftereffects tell us about the coding of binocular disparity? Consider first the two models that have been proposed to explain 2-dimensional tilt aftereffects. In the first, a "satiation" process causes a reduction in the sensitivity of particular cortical mechanisms as a result of prolonged viewing of a tilted line (Köhler and Emery 1947). In the second, a "normalization" process shifts the norm of the vertical or horizontal after the viewing of a line close to the vertical or horizontal (Bergman and Gibson 1959). Coltheart (1971) proposed a satiation model based on the properties of cortical receptive fields in the cat visual cortex to account for the tilt aftereffect. According to this model, orientation-selective mechanisms are selectively adapted by prolonged viewing of a tilted inspection stimulus. Unlike the normalization model, Coltheart's model can account for a tilt aftereffect following adaptation to an inspection figure which coincides with the norm (vertical or horizontal) (Köhler and Wallach 1944; Templeton et al. 1965). However, the fact that the apparent tilt of a line oriented slightly off the vertical decreases with prolonged inspection suggests that normalization is also involved (Taylor 1962; Morant and Harris 1965). Coltheart (1971) has suggested that the three-dimensional (median plane tilt) aftereffects reported by Köhler and Emery (1947) and Bergman and Gibson (1959) can be explained in a similar way by postulating multiple mechanisms selectively sensitive to different inclinations ("median plane orientations"). The observation that the apparent inclination of an off-vertical line decreases with prolonged viewing (Bergman and Gibson 1959) suggests that a normalization process may also be involved in the perception of three-dimensional inclination based on disparity.

Two channel versus multichannel models

Long and Over (1973) suggested that their own aftereffects from viewing a disparate square are consistent with the idea of two separate pools of crossed

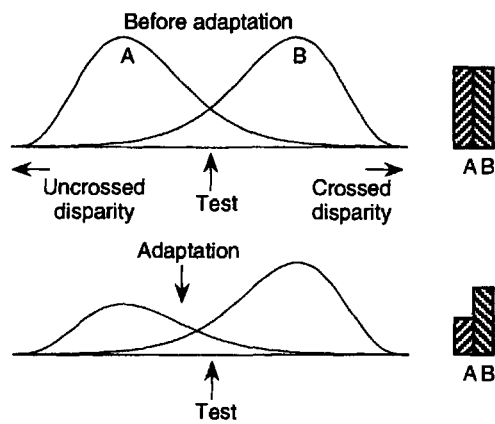


Figure 12.28. Two-channel model of depth aftereffects.

Model of disparity coding based on two broadly tuned mechanisms with peak sensitivities to uncrossed (A) and crossed (B) disparities. Disparity is signalled by the balance of activity in the two channels. Before adaptation, a zero-disparity test stimulus creates equal activity in the two channels (upper right). After adaptation to an uncrossed disparity stimulus, the test stimulus creates more activity in the crossed channel (lower right).

and uncrossed disparity detectors which are selectively adapted by prolonged viewing of a disparate surface. According to this model, the depth of a three-dimensional point is signalled by the balance or ratio of activity in the two pools. Prolonged viewing of an inspection surface with either crossed or uncrossed disparities adapts one pool more than the other. As a result, a zero-disparity test stimulus creates unequal activity in the two pools and signals a disparity which is displaced away from the adapting disparity (Figure 12.28).

Alternatively, the coding of disparity might involve many pools of disparity detectors each tuned to a particular range of disparity values. In a multichannel model, disparity is coded by the central tendency of the activity over several channels (Figure 12.29). In general, the larger the number of channels involved, the less the coding of that sensory dimension will be subject to metamerism (see Section 3.2.6).

Köhler and Wallach (1944) and Over (1971) suggested that particular significance attaches to a "balanced" output of opponent channels in a two-channel system. In disparity coding, this is produced by a zero-disparity stimulus and, in motion, by a stationary stimulus. In a multi-channel system, as has been suggested for the coding of orientation (Coltheart 1971) and spatial frequency (Wilson and Bergen 1979), no particular significance is attached to any particular response profile. Over (1971) has argued that negative aftereffects occur for nontopographic stimulus features, such as motion, wavelength, luminous intensity and skin temperature, which are coded by an opponent-process organized

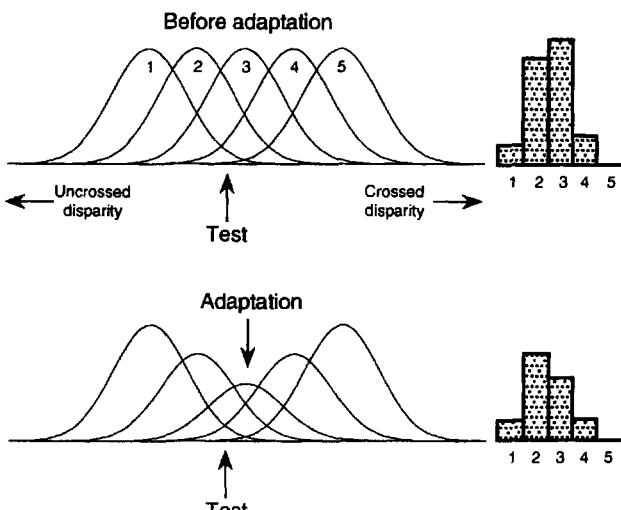


Figure 12.29. Multichannel model of depth aftereffects.

Model of disparity coding based on five selectively tuned mechanisms with different peak sensitivities (1–5). Disparity is signalled by the central tendency of the activity of separate mechanisms. Before adaptation, an uncrossed small disparity test stimulus creates the profile of activity indicated on the right. After adaptation to a zero-disparity stimulus, the profile of activity created by the same test stimulus is shifted farther to the left and away from the adapting stimulus.

around a norm or neutral point. Figural aftereffects, on the other hand, occur when topographic coding in a multichannel system is involved. However, with a suitable choice of parameters, both topographic and non-topographic models can predict the disparity aftereffects described so far.

A further piece of evidence relevant to the number of disparity channels has emerged from the study of depth aftereffects. Both two-channel and multichannel models of disparity coding predict that following prolonged viewing of a crossed or uncrossed disparity, a zero-disparity test stimulus generates an output in the opposite direction to the adapting stimulus. A multichannel model, such as that proposed to explain Blakemore and Sutton's spatial-frequency-shift predicts that the shift in the central tendency of the channels' outputs is always *away* from the adapting stimulus whatever its value on that dimension. This is referred to as the **distance paradox** (Figure 12.29). A two-channel model predicts that the balance of activity will always be shifted in the direction of the less adapted channel, even when the test stimulus is in the same direction as the adapting stimulus but larger (Figure 12.30).

Rogers and Graham (1985) designed an experiment to distinguish between these different predictions. Observers adapted to a sinusoidally corrugated surface which had a peak-to-trough amplitude of either 4, 8, or 12 arcmin of disparity. The aftereffect was then "superimposed" on a sinusoidally

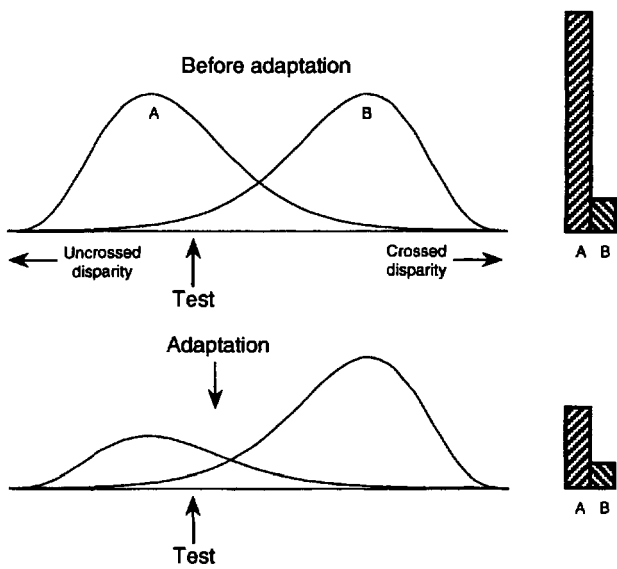


Figure 12.30. Predictions of a two channel model.

Both two-channel and multichannel models of depth aftereffects predict a negative aftereffect when the test stimulus is a zero disparity surface. Only a two-channel model predicts a shift in the balance of activity towards the less adapted channel (B) when the test stimulus is in the same direction as the adapting stimulus (uncrossed disparity) but has a greater magnitude.

corrugated test surface with a peak-to-trough disparity either less than or greater than that of the original adapting surface. The perceived amplitude of the test surface was measured using a variable amplitude comparison surface seen on an unaffected area of the retina. Their results show that the perceived depth of the test surface was always less than its physical amplitude, even when the amplitude of the test surface was greater than that of the adapting surface (Figure 12.31).

Second, the reduction in the perceived amplitude was approximately the same whatever the amplitude of the test corrugation, as long as it had the same phase. Third, the effects of prolonged viewing were noticeable only when the test surface had either the same phase as the adapting surface or zero-disparity modulation. Smallman and McLeod (1994b) have reported a similar pattern of results. Rogers and Graham interpreted these findings as evidence in favour of a two-channel rather than a multichannel model of disparity coding. It is not clear, however, whether these results allow one to distinguish between the two-channel coding of local disparity, as Long and Over originally proposed, and a two-channel model based on disparity gradients or disparity curvatures (see the following).

Note that the critical prediction of a two-channel model—that the response activity will always be displaced towards the unadapted channel even when the value of test stimulus is in the same

direction but larger than the adapting stimulus—will also be true for the last channel in a multichannel coding system. Hence, it can be used as a test for location of the lowest and highest channels in a multichannel coding system.

Zero- first- or second-order disparities

In both two-channel and multichannel models of disparity coding, it is assumed that disparities are measured locally in a particular retinal region—i.e. as zero-order disparities. As a consequence, the possible interactions between disparate features are restricted to those which have different disparities in the same retinal region. It seems plausible that coding of binocular disparity might also involve the local spatial configuration of disparities (see Sections 12.2.5 and 7.1). For example, there might be detectors for spatial changes of disparity which show adaptive properties as a result of prolonged stimulation. The spatial changes might be either disparity gradients (1st spatial derivatives of disparity) or changes of disparity gradient (2nd spatial derivatives). Channels selective for disparity gradients or disparity curvatures might be organized in opponent pairs on either side of a norm—corresponding to inclination and declination gradients or concave and convex curvatures, for example—or they might have a multichannel organization with each channel tuned to a particular value of disparity gradient or disparity curvature, as Coltheart (1971) suggested (Table 12.1). The observation that depth aftereffects are larger following prolonged viewing of sinusoidal corrugations than of square wave corrugations may be thought to be more consistent with the class of models which codes disparity gradients.

Rogers and Graham (1985) cite other evidence of disparity gradient coding. For example, they claimed that the prolonged viewing of a sinusoidal corrugated surface lying entirely in front or behind the fixation point still produced a negative depth aftereffect when “superimposed” on a zero-disparity test surface. This suggests that the relevant factor for the creation of a corrugation aftereffect is the spatial change of disparity in the adapting surface rather than the disparities of individual points on the surface. The argument is not conclusive however since a negative corrugation aftereffect is also predicted by a model based on the adaptation of local disparity detectors, with the appropriate choice of parameters. Moreover, the claim that aftereffects can still be seen following the prolonged viewing of a corrugated surface which lies entirely in front of or behind the fixation point needs to be qualified. Lee and Rogers (1992) found that depth aftereffects were maximal when a 10 arcmin peak-to-trough adapting

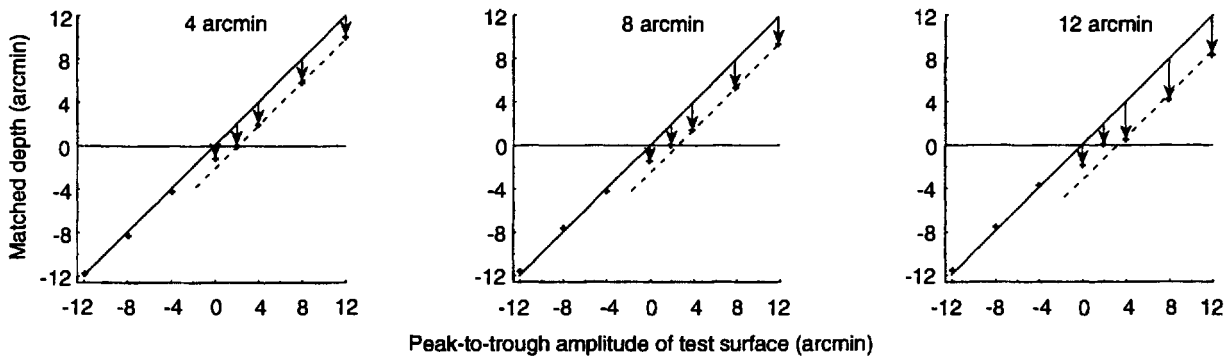


Figure 12.31. Superimposing depth aftereffects on corrugated test surfaces.

Observers adapted to a sinusoidally corrugated surface with peak-to-trough amplitude indicated on each graph. After adaptation, the aftereffect was "superimposed" on a test surface with a peak-to-trough amplitude given by the abscissa. The perceived depth was matched to a variable amplitude matching surface alongside. The effect of adaptation—the downward pointing arrows—was always to reduce the amount of perceived depth in the test surface, whether its amplitude was greater or less than the adapting surface. When the test surface was of opposite corrogation phase, the perceived depth was generally unaffected. (Redrawn from Rogers and Graham 1985.)

surface was in the plane of fixation and decreased by a factor of two or more when the corrugated adapting surface was superimposed on a disparity pedestal greater than ± 16 arcmin. The complete tuning curve for superimposing depth aftereffects on a zero-disparity test surface following adaptation to corrugated surfaces with different disparity pedestals had a half-height, full bandwidth of around 30 arcmin (Figure 12.32).

Lee and Rogers also investigated the converse situation, in which aftereffects of viewing of a corrugated surface in the zero-disparity plane were superimposed on test surfaces with different disparity pedestals. The aftereffects were largest when the test surface was also in the zero-disparity plane and decreased with the increasing pedestal (either crossed or uncrossed) of the test plane. The full bandwidth at half amplitude of the aftereffect was also found to be around 30 arcmin. Further studies show that corrugation aftereffects are maximal when the adapting and test surfaces lie in the same disparity plane. In other words, they are tuned to the pedestal of the adapting surface (Figure 12.33). One unexpected finding was that depth aftereffects created by adaptation to a corrugated surface lying in either a crossed or uncrossed disparity plane and superimposed on a test surface in the same depth plane were considerably larger than when the adaptation and test surfaces were both in the zero-disparity plane (Lee and Rogers 1992). This suggests a greater adaptability of mechanisms sensitive to larger disparities. If mechanisms sensitive to larger disparities exhibit greater adaptability, this would also predict a normalization effect in which the apparent

inclination of a stereoscopic surface decreases with prolonged viewing, as Bergman and Gibson (1959) observed in the perception of inclined lines. In addition, Lee and Rogers found that the peaks of the aftereffect tuning functions following adaptation to corrugations lying in either a crossed or uncrossed disparity plane were typically displaced away from the zero-disparity plane (Figure 12.33).

Disparity-gradient adaptation

Ryan and Gillam (1993) provided further evidence that three-dimensional aftereffects can result from disparity gradient adaptation. Observers adapted to a pair of horizontally separated vertical lines with a fixed disparity of 6.9 arcmin. The lateral separation of the lines varied between 25 and 43 arcmin so that the disparity gradient changed from 17 to 9 arcmin/deg. A pair of vertical lines separated by 34 arcmin served as the test probe. These had a variable disparity which could be adjusted to cancel any aftereffect. Ryan and Gillam found that the aftereffect measured by this nulling technique decreased with increasing lateral separation of the adapting lines. In other words, the size of the aftereffect varied with the disparity gradient of the adapting lines. Conversely, when the lateral separation of the inspection lines was held constant, but the separation of the test lines varied between 25 and 43 arcmin, the aftereffect increased with increasing lateral separation of the test lines. The most striking result was found when the adapting lines had a disparity of 8.5 arcmin and a separation of 21 arcmin (corresponding to a disparity gradient of 24 arcmin/deg). Under these circumstances, the mean

Table 12.1. Models of disparity coding

Order of representation	Two-channel organization	Multichannel organization
Zero-order (Absolute disparities)	Broadly tuned Crossed and uncrossed disparity detectors	Narrowly tuned Disparity detectors (tuned to particular disparity)
First-order (Disparity gradients)	Broadly tuned Ground-sky plane inclination detectors Broadly tuned Left- and right-wall slant detectors	Narrowly tuned Inclination detectors Narrowly tuned Slant detectors (tuned to particular disparity gradient)
Second-order (Disparity curvatures)	Broadly tuned Convex and concave curvature detectors	Narrowly tuned Disparity curvature detectors (tuned to particular disparity curvature)

aftereffect with test lines laterally separated by 213 arcmin was 12 arcmin—larger than the disparity between the adapting lines. The disparity gradient of the test stimulus which appeared equidistant was 3.3 arcmin/deg or 14 per cent of the gradient of the adapting lines. Ryan and Gillam argued that these results could not be accounted for by the adaptive properties of either absolute disparity detectors with receptive field properties similar to those identified by Barlow et al. (1967) or relative disparity detectors which do not take the lateral separation between the disparate points into account. Instead, the results are consistent with mechanisms which code disparity gradients and show adaptive properties.

The use of line stimuli in Ryan and Gillam's (1993) study raises the possibility that monocular positional shifts might also have played a part (cf. Howard and Templeton 1964), but this seems unlikely since observers scanned continually over the inspection stimuli in the adaptation phase. Two interesting questions arise from this study. *First, if the pair of test lines has a steeper disparity gradient than that of the adapting lines, does the depth gradient of the test lines appear to be larger or smaller compared with that of a pair of control lines?* The latter result was found following adaptation to the sinusoidally-corrugated surfaces used by Rogers and Graham (1985) and suggests that disparity gradients are coded in terms of a two-channel opponent mechanism ('left slant' versus 'right slant'). The former result, on the other hand, suggests a multi-channel model of disparity-gradient coding. *Second, is the same pattern of results found when the disparate stimuli are separated vertically rather than horizontally?* The significant anisotropy in the way we perceive disparity surfaces (Rogers and Graham 1983) suggests that aftereffects from inclined and slanted surfaces may also be different.

In all the studies of three-dimensional aftereffects described so far, the three-dimensional depth profile of the inspection pattern remained constant with respect to the observer's fixation. In Graham and Rogers' (1982a) experiments, for example, the observer tracked a fixation point which oscillated horizontally across the surface along a constant-disparity contour midway between a peak and a trough of the corrugation. Even in the experiments of Bergman and Gibson (1959) and Ryan and Gillam (1993) in which observers were allowed to scan over the slanting stereoscopic surface, the same disparity gradient was present at the eyes during all fixations. Under these circumstances, the statistics of the adapting stimuli form a selected set out of the total possible sets. The attribution of an aftereffect to a mechanism sensitive to a particular characteristic, such as absolute disparity, relative disparity, disparity gradient, or disparity curvature, depends on the particular choice of stimuli and viewing conditions. For example, prolonged viewing of the pair of disparate squares in Blakemore and Julesz' (1971) experiment would selectively stimulate crossed and uncrossed absolute disparity detectors in regions above and below the fixation point. However, the depth profile would also selectively stimulate disparity-gradient and curvature mechanisms in those regions and hence it is difficult to attribute the aftereffect to one particular mechanism in this case. On the other hand, an experiment involving adaptation to a slanted or inclined surface which oscillates in depth with respect to the fixation point is easier to interpret because the adaptation selectively stimulates a selected set of disparity-gradient mechanisms and absolute disparity mechanisms are stimulated by the entire set of possible disparity values (DeValois et al. 1975; see Section 7.5.1).

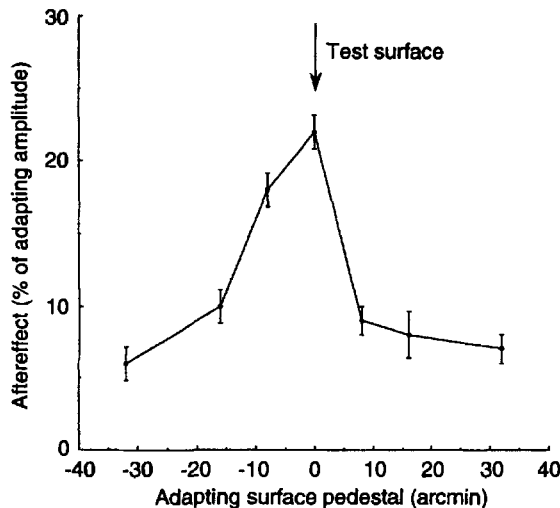


Figure 12.32. Tuning function for depth aftereffects—1.

Prolonged viewing of a 10 arcmin sinusoidal adapting surface modulated around zero disparity caused a flat test surface in the zero-disparity plane to appear corrugated in the opposite direction. Aftereffects were largest when the adapting surface lay in the zero-disparity plane and fell off when the adapting surface had either a crossed or uncrossed disparity pedestal. The tuning of aftereffect strength as a function of the adapt-surface pedestal had a half-height bandwidth of around 30 arcmin. (Redrawn from Lee and Rogers 1992.)

12.3.4 Phase-independent adaptation

Manipulating the characteristics of the stimuli may help to differentiate between mechanisms selective to different orders of disparity, but there is a further consideration. The site of adaptation may be in low-level mechanisms sensitive to local disparities or disparity gradients or at a higher-level stage in which the activity from a number of localized detectors is pooled. In the former case, the mechanisms are said to be position-, or phase-dependent. The depth aftereffects described so far are generally thought to be due to adaptation of phase-dependent mechanisms. They are analogous to negative afterimages in the luminance domain. In Graham and Rogers' (1982a) experiments, it was necessary to keep the disparity profile of the adaptation surface fixed with respect to the fixation point to present a selective set of disparities, disparity gradients, and curvatures to a given retinal region. If observers had been allowed to scan over the corrugated surface, the entire set of disparity-, disparity gradient-, and curvature-detectors would be stimulated and hence no depth aftereffect would be seen.

On the other hand, free inspection of a corrugated disparity surface may adapt higher-level mechanisms sensitive to spatial changes of disparity which are not tied to a particular retinal location. Such mechanisms are said to be position- or phase-

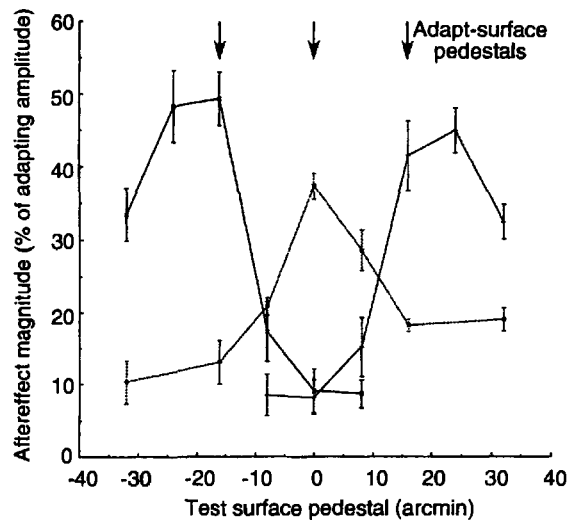


Figure 12.33. Tuning function for depth aftereffects—2.

Aftereffects following viewing of a 10 arcmin sinusoidal surface modulated around zero disparity were largest when the test surface lay in the zero-disparity plane and fell off when the test surface had either a crossed or uncrossed disparity pedestal (centre curve). The tuning of the effect as a function of the test-surface pedestal had a half-height bandwidth of around 30 arcmin. Depth aftereffects when the adaptation surface was superimposed on a disparity pedestal of either -16 or +16 arcmin were typically larger. The maxima of the tuning functions were close to the value of the adapt-surface pedestal. (Redrawn from Lee and Rogers 1992.)

independent. Contrast threshold elevation (Blakemore and Campbell 1969) is thought to provide evidence for (adaptable) phase-independent mechanisms in the luminance domain. Blakemore and Sutton's (1969) study of the shift in perceived spatial frequency of a grating following inspection of a high-contrast grating of a neighbouring spatial frequency is also regarded as providing evidence of a phase-independent mechanism. The tuning functions of contrast threshold elevation and the spatial-frequency shift have been used as a measure of the frequency bandwidth of the underlying phase-independent mechanisms.

Is there any evidence of phase-independent adaptation effects in the disparity domain? Schumer and Ganz (1979) required observers to move their gaze slowly up and down over a disparity corrugation with horizontal peaks and troughs of either 0.52 or 1.57 c/deg for 5 minutes. The sinusoidal corrugations were defined by dynamic visual noise. The peak-to-trough amplitude of the corrugations was not given. Since any given retinal region was stimulated by both crossed and uncrossed disparities, positive and negative disparity gradients, and positive and negative disparity curvatures, no negative aftereffects were seen upon inspection of a flat test surface. Instead, Schumer and Ganz looked at how

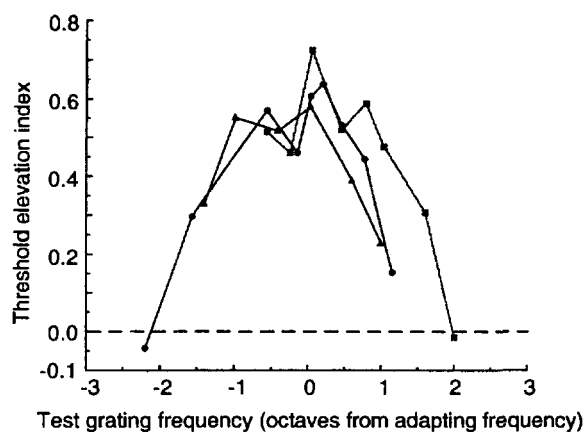


Figure 12.34. Bandwidth of stereoscopic channels.

Threshold elevation for detecting disparity gratings following adaptation to corrugated inspection surfaces of 0.52 (circles), 1.4 (triangles) and 1.57 (squares) c/deg. The three curves are normalized to show threshold elevation as a function of the difference between the inspection and test gratings in octaves. (Redrawn from Schumer and Ganz 1979.)

adaptation affected thresholds for perceiving corrugated surfaces. They measured thresholds for detecting disparity corrugations from 0.4 to 3.5 c/deg by a method of limits before and after adaptation. Threshold elevation was expressed as the ratio of post- to preadaptation thresholds minus one. An index of 0 indicates zero threshold elevation and an index of 1 indicates a doubling of thresholds.

Schumer and Ganz found that thresholds for perceiving disparity corrugations were elevated up to 60 per cent when the test surface had the same corrugation frequency as the adapting surface (Figure 12.34). Thresholds were elevated to a lesser degree for test corrugations with frequencies less or greater than the adapting surface. The full bandwidth of the threshold-elevation effect at half amplitude was 2-3 octaves. The authors pointed out that this bandwidth is somewhat larger than that for contrast threshold elevation in the luminance domain, reported by Blakemore and Campbell (1969). Schumer and Ganz interpreted their results as evidence for a set of broadly-tuned disparity-corrugation channels, each maximally sensitive to a different corrugation frequency. Additional evidence for this idea comes from a second, subthreshold summation experiment. In this case, thresholds for detecting depth modulations of compound corrugation surfaces consisting of $f + 3f$ corrugation frequencies were principally determined by the thresholds of the individual components and were unaffected by the phase relationship (peaks-add or peaks-subtract) of the components (Schumer and Ganz 1979).

While it is likely that conventional depth aftereffects result from adaptation of localized (phase-

dependent) disparity mechanisms, it does not follow that threshold elevation-effects, which do not depend on stabilization of the disparity changes with respect to fixation, result from adaptation of phase-independent mechanisms. If the eyes are allowed to scan over a disparity profile, so that each retinal location is stimulated by a variety of disparities, disparity gradients, and disparity curvatures, there will be no net aftereffect visible on a flat test surface because all phase-dependent detectors are equally adapted. On the other hand, adaptation of localized mechanisms coding disparity, disparity gradient, or disparity curvature may be revealed in threshold-elevation measurements. Hence, to predict threshold-elevation effects in the depth (or any other domain), it is not necessary to postulate higher-level, phase-independent mechanisms which receive inputs from localized phase-dependent mechanisms.

Jones and Tulaney-Keesey (1980) suggested a paradigm to test for a separate phase-independent mechanism in the luminance domain. Observers fixated and adapted to a grating which alternated in counterphase at 1 or 10 Hz. Following adaptation, no afterimage was visible on a uniform test patch but thresholds for detecting a low-contrast grating of the same spatial frequency were raised, as might be expected. However, for adaptation occurring only in phase-independent (non-localized) luminance mechanisms, threshold elevation should be the same for all gratings of that spatial frequency whatever their phase. If at least some of the adaptation is due to phase-dependent mechanisms, threshold elevation should be less for gratings with either 90 or 270° phase not present during the adaptation period.

In the luminance domain, Jones and Tulaney-Keesey found that threshold elevation was the same for gratings of all phases and concluded that the channels involved are not selectively tuned for spatial phase. Graham and Rogers (1983) carried out a similar experiment in the disparity domain using a corrugated adapting stimulus which reversed in depth every few seconds. The perceived depth of supra-threshold disparity corrugations with 0° or 180° phase was subsequently reduced to a greater extent than that of test corrugations with 90° or 270° phase not seen during adaptation (Figure 12.35). This suggests that at least part of the threshold-elevation effects reported by Schumer and Ganz (1979) can be attributed to adaptation of localized or phase-dependent disparity mechanisms.

It might be thought that effects of adapting to random-dot (cyclopean) surfaces which stimulate either "simple binocular processes" or "purely binocular mechanisms" (Wolfe and Held 1981, 1982, 1983) would be visible only when the visual system

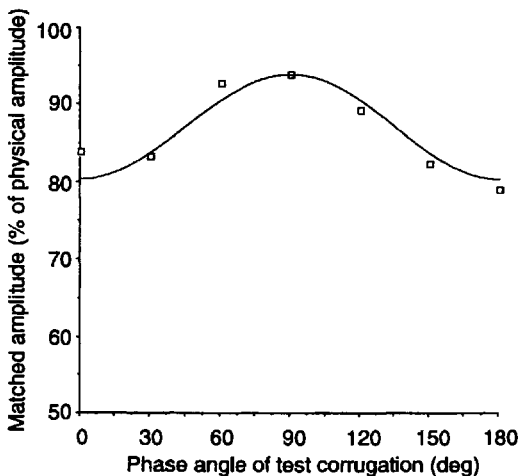


Figure 12.35. Phase dependency of depth aftereffects.

The perceived depth of a sinusoidally-corrugated surface is reduced following adaptation to a phase-alternating corrugated surface. Mean data for 2 subjects. Depth reduction is greatest for 0° and 180° phase test corrugations and least for 90° phase corrugations. The line is the best-fitting cosine curve.

is stimulated binocularly. This turns out not to be the case. Rogers and Graham (1985) reported that after adapting to disparity-defined random-dot corrugations, a weak aftereffect is visible on presentation of a single, monocular test field. If the reader adapts to the sinusoidal corrugations depicted in Figure 12.27d, by running the eyes to and fro along the horizontal fixation line (to prevent the build-up of conventional afterimages), a small negative corrugation aftereffect can be seen when one eye is covered up.

12.3.5 Hypercyclopean aftereffects

Tyler (1975c) introduced the concept of a **hypercyclopean level of analysis** to apply to processes "beyond the basic analysis of disparity" (see also Section 14.2). According to this idea, there are hypothetical mechanisms which extract or filter different spatial configurations of disparity (surface shapes) in an analogous way to mechanisms in the luminance domain which extract or filter different spatial configurations of luminance such as orientation, curvature, size, and spatial frequency. According to Tyler, the essential characteristic of a hypercyclopean effect is that it must be independent of the particular disparities stimulating a particular retinal region. Hence, while the previously described phase-dependent disparity aftereffects are classified as cyclopean aftereffects, the phase-independent contrast-elevation effects described by Schumer and Ganz are classified as hypercyclopean aftereffects (Tyler 1991). If the argument in the previous section is correct, the

so-called phase-independent threshold-elevation effects in the disparity domain are not necessarily the consequence of adaptation in hypercyclopean mechanisms.

Hypercyclopean tilt aftereffects were first demonstrated by Tyler (1975c). After prolonged inspection of a stereo grating at one of several different orientations, the perceived orientation of a horizontally oriented stereo grating was displaced away from the inspection stereo grating by up to 2° (Figure 12.36). The effect was maximal when the inspection stereo grating was about 30° from the horizontal and declined to zero when it was 60° from the horizontal. In addition, Tyler showed that the effects of adapting to noncyclopean, luminance-defined gratings transferred to a cyclopean test grating although with only half the magnitude of that following hypercyclopean adaptation.

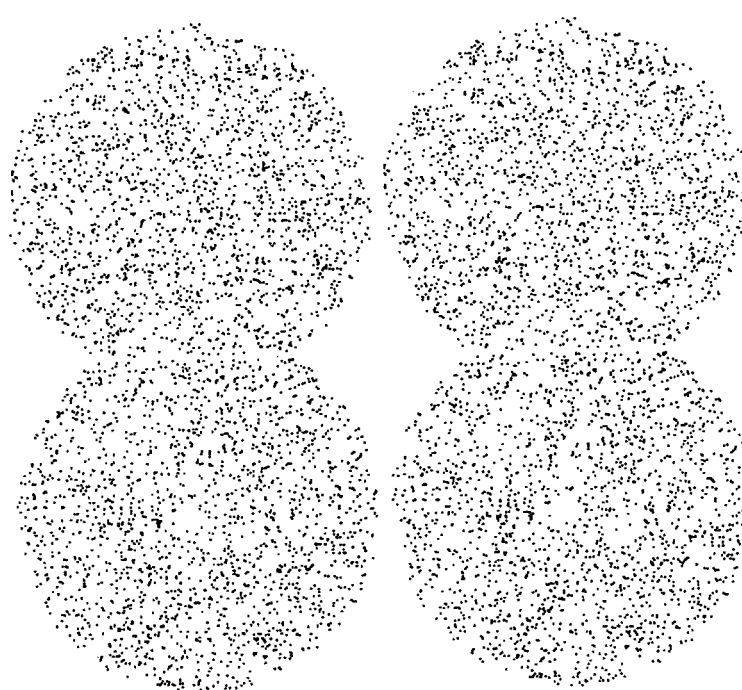
Tyler (1975c) also reported a hypercyclopean spatial-frequency shift. During adaptation, observers scanned a horizontal bar positioned midway between two disparity gratings with different corrugation frequencies (Figure 12.37). After adaptation, identical disparity gratings above and below the fixation point were perceived to have different corrugation frequencies. No data were given on the magnitude or frequency tuning of the effect but Tyler suggested that the hypercyclopean spatial-frequency shift does not transfer to disparity gratings of different orientations.

12.4 STEREOSCOPIC INTERPOLATION

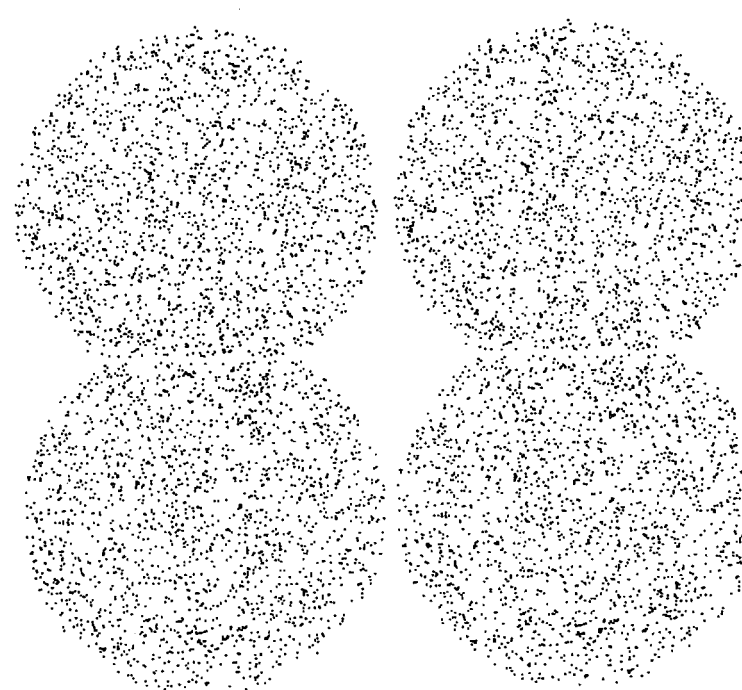
The basic question discussed in this section is how depth is perceived in an area carrying ambiguous disparity information when the area is adjacent to regions carrying well-defined disparity information. In other words, how is depth interpolated or extrapolated from a region of unambiguous disparity to a region of no disparity or ambiguous disparity? There are three cases of depth interpolation or extrapolation to be considered: (1) over a blank area, (2) over an area containing only monocular texture, and (3) over an area with ambiguous disparity information.

12.4.1 Depth interpolation over blank areas

A blank area flanked by well-defined steps of depth with respect to a textured background can appear as an opaque surface in depth even though the surface itself contains no disparity information. Thus, the blank area in the stereogram shown in Figure 12.38a appears as an opaque surface in depth rather than as



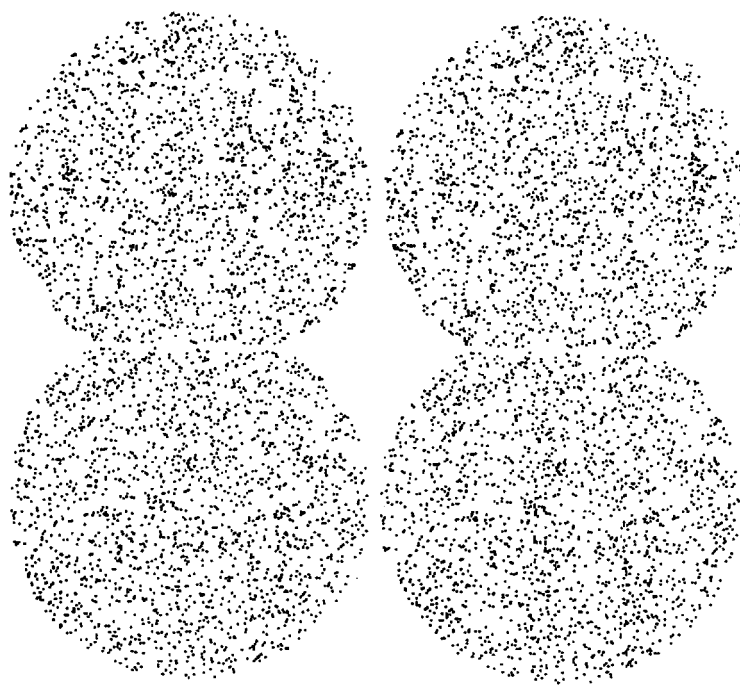
Adaptation stereogram



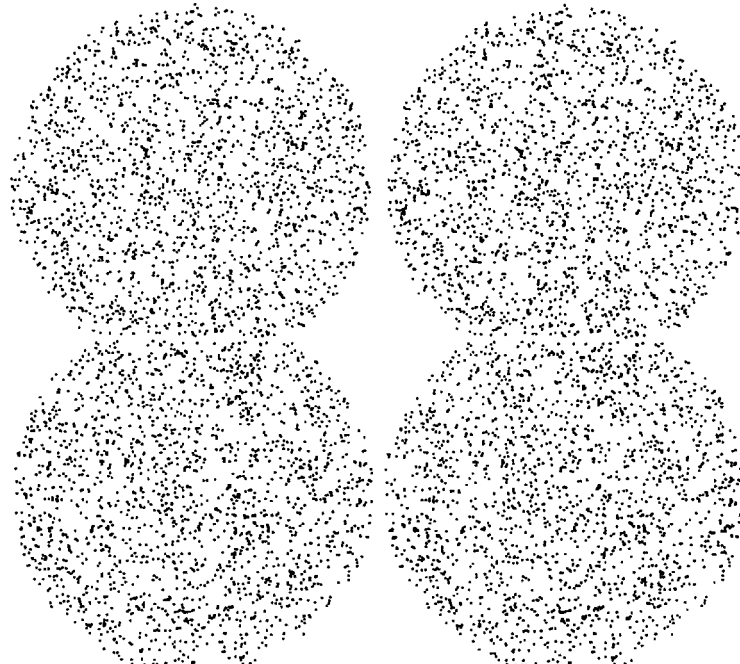
Test Stereogram

Figure 12.36. Hypercyclopean tilt aftereffect.

The sinusoidal corrugations in the upper and lower halves of the *adaptation stereogram* are oriented counterclockwise and clockwise respectively with respect to the vertical. Together they form a cyclopean chevron stimulus pointing to the right. The upper and lower corrugations in the *test stereogram* are both oriented vertically. After 30s viewing of the adaptation stereogram (allowing the eyes to track along the boundary between the upper and lower corrugations), the corrugations in the upper and lower halves of the test stereogram should appear to form a chevron in the opposite direction. This is a hypercyclopean tilt aftereffect first demonstrated by Tyler (1975c).



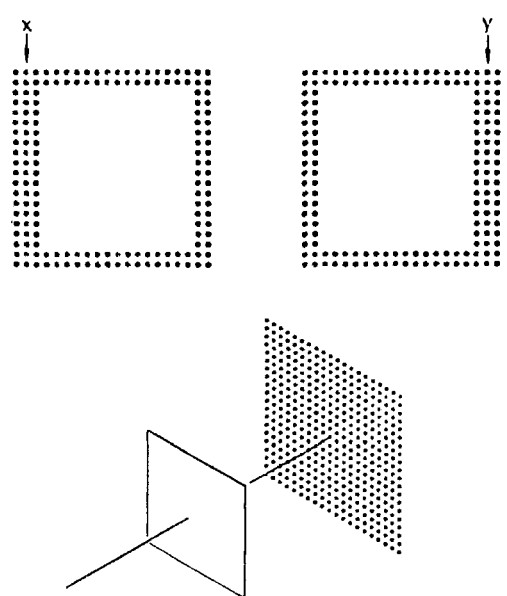
Adaptation stereogram



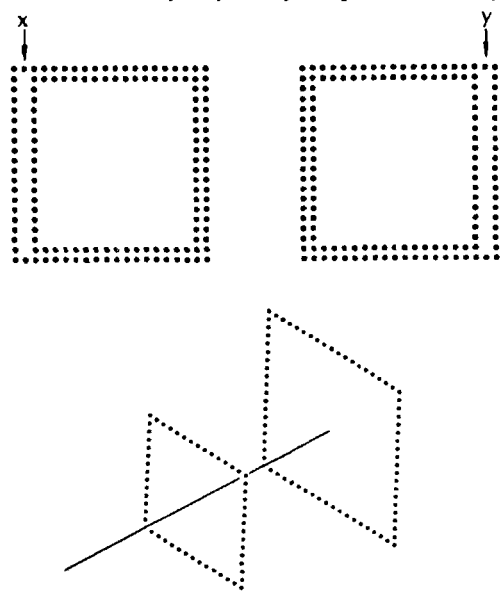
Test stereogram

Figure 12.37. Hypercyclopean spatial-frequency aftereffect.

The vertically oriented sinusoidal corrugations in the upper and lower halves of the *adaptation* stereogram have different spatial frequencies. The upper and lower corrugations in the *test* stereogram both have the same spatial frequency. After 30s viewing of the *adaptation* stereogram (allowing the eyes to track along the boundary between the upper and lower corrugations), the corrugations in the upper and lower halves of the *test* stereogram should appear to be of different spatial frequencies. This is a hypercyclopean spatial-frequency aftereffect first demonstrated by Tyler (1975c).



(a) The blank area in the stereogram appears as an opaque white surface in depth hiding a background surface covered with dots. This interpretation is due to the presence of monocular occlusion zones (lines of dots seen by only one eye) at positions *x* and *y*.



(b) The blank area in this stereogram appears as an outline square seen in front of another outline square. The monocular zones are blank. (From Lawson and Mount 1967. Copyright, 1977, by the AAAS.)

Figure 12.38. Monocular occlusion and surface continuity.

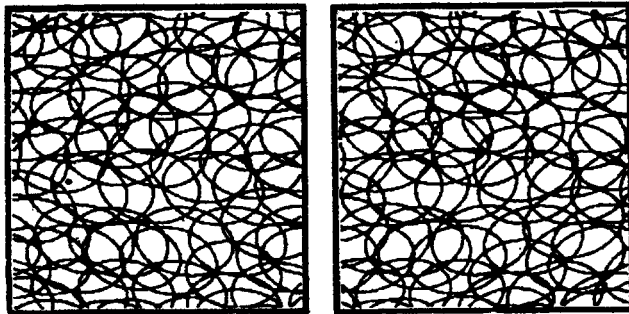
a frame in depth. Note that the blank square is flanked by two monocular zones, one on the left, seen only by the left eye, and one on the right, seen only by the right eye. The discussion in Section 12.4.4 shows how these monocular zones trigger the impression of an opaque square occluding a part of

each eye's view of the underlying textured background as well as the impression that the textured background extends beneath the square. Note also that there is no disparity information along the upper and lower edges of the blank area. In one study, the apparent depth of the blank area relative to the surround increased as the luminance contrast between the two regions was increased (Würger and Landy 1989). The apparent depth of the blank area also increased as the disparity at the edges increased, but not at the same rate. Depth interpolation was destroyed when the blank region was filled with binocularly uncorrelated low-frequency texture, but survived the addition of high-frequency texture. Further examples of depth interpolation over blank areas are given in Section 12.4.3.

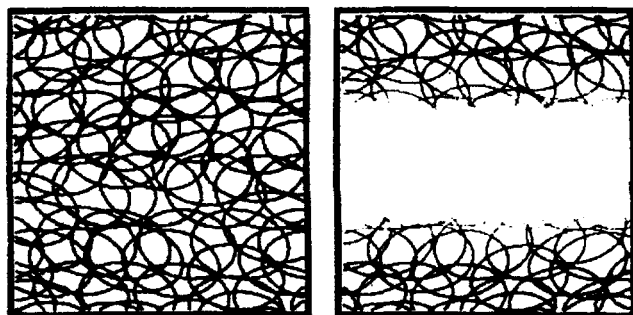
The importance of monocular zones in prompting the impression of surface continuity across a blank area is revealed by Figure 12.38b. Here, a disparate outline square with the occlusion zones left blank appears as a frame in depth, since the absence of appropriate occlusion zones indicates that there is no occluded surface. Thus, a disparity along a vertical edge gives rise to the impression of a surface in depth only when the monocular flanks that such a disparity produces are present (see Section 12.6.2).

12.4.2 Depth interpolation over monocular areas

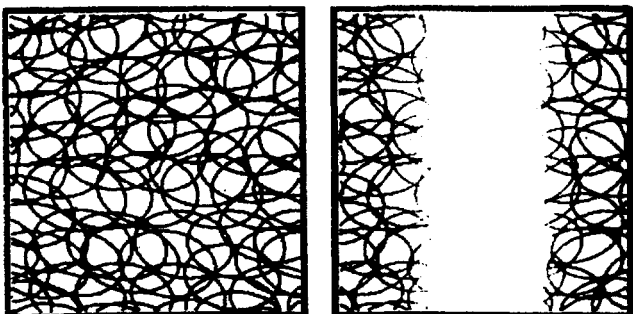
Collett (1985) placed a rectangle of random dots seen by only one eye between two rectangular random-dot regions in which disparities produced the impression of two surfaces inclined in depth toward each other, like two halves of a roof or two sides of a valley. The monocular surface appeared to extend the slope of the adjacent binocular regions, producing the appearance of a roof with a rounded top or a valley with a rounded bottom. The apparent depth of the interpolated monocular region was determined by setting a small depth probe to match the depth of different points along the surface. A monocular region placed between two frontal planes at different depths also appeared to join the two planes with a smooth curve, in this case a smooth S-shaped ramp conforming to a geodesic of least mean rate of change of curvature. The impression of a smooth ramp remained when a discontinuity in dot density was inserted into the centre of the monocular zone. When the dots in the monocular region moved at a different speed but in the same direction as those in the binocular regions, however, the monocular region sometimes appeared to separate from the flanks and occupy a distinct depth plane. This is not surprising since monocular parallax can generate an impression of depth (see Section 13.5).



(a) A stereogram portraying two inclined planes meeting in a horizontal ridge when fused by convergence, or two surfaces meeting in a groove when fused by divergence.



(b) The same stereogram with the ridge region omitted in one image. This creates a rounded ridge or groove.



(c) The same stereogram with the central region missing in one eye. This creates a continuous ridge or groove. (From Buckley et al. 1989, Perception, 18, 563–588, Pion, London.)

Figure 12.39. Depth interpolation.

Buckley et al. (1989) used similar displays, but removed the sharp boundaries between binocular and monocular regions. Since sharp boundaries are a cue to surface discontinuity their removal strengthens the impression of surface interpolation between the binocular regions. The stereogram in Figure 12.39a appears as two inclined planes meeting in a horizontal ridge when the images are fused by convergence. In the stereogram in Figure 12.39b the ridge of the roof is seen by only one eye and the fused image appears like a roof with a smoothly curved ridge. The visual system interpolates a curve

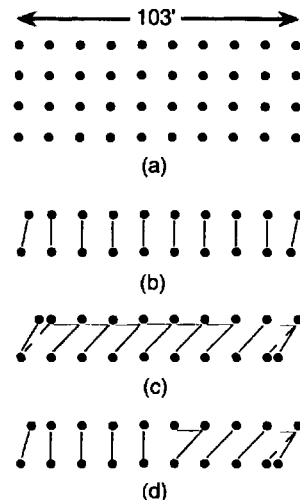


Figure 12.40. Disparity interpolation.

(a) Regular dot lattice used to investigate disparity interpolation.
 (b) A disparity of less than the interdot spacing is introduced into the end columns of dots. The dots in the centre of the lattice are matched to their nearest neighbours.

(c) A disparity of more than the interdot spacing is introduced in the end columns of dots. This forces the dots in the centre of the lattice to match with dots which are not their nearest neighbours.

(d) A small disparity is introduced in the righthand column of dots and a large disparity in the lefthand column. Dots inside the lattice are matched in two ways, creating a step in depth in the centre of the lattice. (From Mitchison and McKee 1987a. Reproduced with permission from Vision Research, Pergamon Press.)

of minimum curvature (a geodesic) in the absence of precise stereoscopic information. In Figure 12.39c a portion across the ridge is missing in one eye. Nevertheless, a complete ridge is seen in the fused image. Note that the ellipses seen in the monocular images appear as circles on inclined planes when the images are fused. This is an instance of shape constancy triggered by stereopsis.

12.4.3 Interpolation into ambiguous regions

When the same regular array of dots is seen by both eyes, the viewer can change which pairs of dots fall on corresponding points by changing the convergence of the eyes. This is the well-known wallpaper effect discussed in Section 2.3.5. Mitchison and McKee (1987a) started with a regular lattice of dots spaced at intervals of 5 arcmin, as shown in Figure 12.40a. When a disparity of less than half the interdot spacing was introduced in the end columns (Figure 12.40b), the other dots in the lattice appeared to lie in depth behind the end columns, which is what one would expect if each dot in one eye was binocularly matched to its nearest neighbour in the other eye. But when the dots in the end columns had a disparity greater than half the interdot spacing (Figure 12.40c), the other dots in the lattice appeared

to come in front, indicating that dots in one eye were paired, not with their original nearest neighbours, but with dots in the direction of the disparity of the end dots. In other words, the disparity in the end dots determined the binocular matches made in the centre of the lattice.

Since subjects were allowed some time to make judgments, changes of vergence could be responsible for these changes in binocular matches. The eyes simply had to change their convergence to match the disparity in the end dots and thus alter the nearest dichoptic neighbours of all the other points in the lattice. However, this cannot be the whole story because the effects of end-dot disparities were found not to propagate to distinct nearby lattices in which the end dots were not disparate. In other words, the effects of edge disparities were confined to the display to which the edges belonged. For lattices up to about 5° wide, disparities on the edges affected the depth seen in the centre. Furthermore, when the disparity at one side of a lattice was less than the interdot spacing and that at the other side was greater than the interdot spacing, as depicted in Figure 12.40d, subjects saw a depth step halfway across the lattice.

Thus, two matching rules were operating at the same time, which could not happen by a simple nearest-neighbour rule. The rule must be that *dichoptic matching of points within a region of constant disparity is determined by the nearest region within the same figure where there is a sharp disparity gradient, even when this runs counter to the nearest-neighbour rule.*

When the effects of convergence were avoided, by having subjects fixate a point in the plane of the dots before the display was shown for only 150 ms, the whole lattice appeared to be in the plane of the end dots or to slope between the end rows when they had different disparities. In other words, under these circumstances, the depth of the end rows was interpolated over the whole display. It is as if there were no competing disparities in the centre of the lattice. Perhaps this is a default impression due to lack of time for processing the pattern of disparities within the figure. When the interpoint spacing was increased beyond about 20 arcmin, depth interpolation did not occur even with short exposures (Mitchison and McKee 1987b; McKee and Mitchison 1988). Presumably, disparities are easier to process in displays with larger interdot separations (less steep disparity gradients).

Interpolation between subjective contours

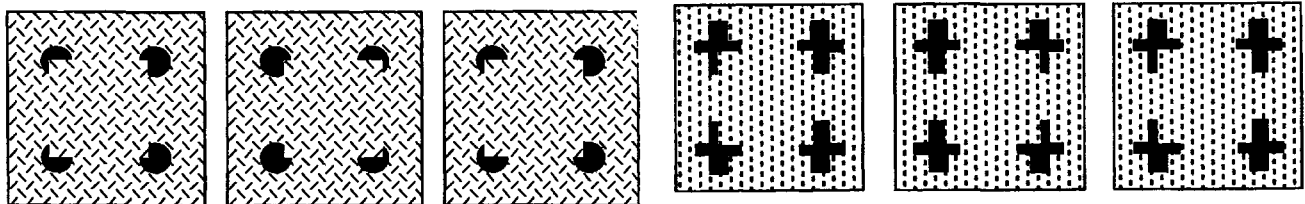
Depth interpolation can occur in an area defined by subjective contours, as demonstrated in Figure 12.41a. When the left and middle patterns are fused

by convergence, a textured square appears to stand out (Ramachandran and Cavanagh 1985; Ramachandran 1986). The only physical disparity is that between the cutout sectors in the black discs. The set of sectored discs (pacmen) create a subjective square in each eye by modal completion, and the disparity between these squares prompts the visual system to find a corresponding set of matching disparities between the dots of the regular lattice within the squares. Ramachandran called this interpolation process **disparity capture**. As one would expect, disparity capture is strongest when the disparity in the corner discs is equal to the interdot spacing.

When the disparity in the corner elements is crossed, the central square appears to stand out and disparity capture is restricted to the texture elements within the subjective square. This confirms the evidence cited previously that interpolation of crossed disparity is confined to the area bounded by a steep disparity gradient, although subjective patterns are bounded by a disparity step only within the corner regions. When the middle and right patterns of Figure 2.41a or b are fused by convergence, the disparity is uncrossed and the central square appears to lie beyond the outer frame of the background. Under these circumstances, only the texture elements in each of the four cut out sectors appear to lie in a more distant plane as if seen through four port holes. The four pieces of texture link up by amodal completion to create the impression of a square mostly hidden by the foreground. In this case an interpretation involving amodal completion of the sides of the inner square (occluded edges) is more compatible with the perceived depth relationships than modal completion (cognitive contours).

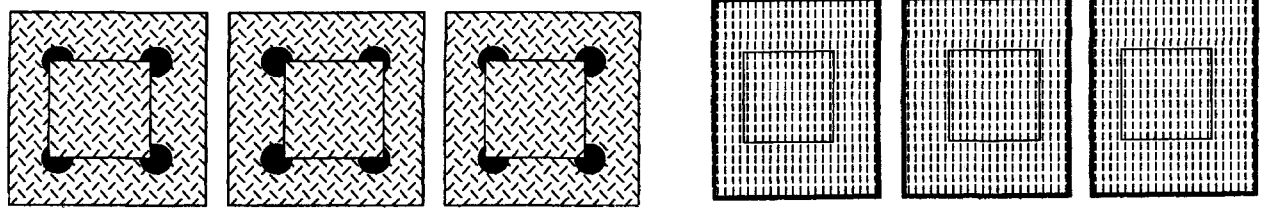
Disparity capture occurs when the sides of the cognitive square are replaced by lines (Figure 12.41b), showing that cognitive contours are not essential. But there is little if any capture when the pacmen are removed, leaving only the disparate squares (Figure 12.41c). This suggests that disparity is not sufficient to produce disparity capture. The key element for vivid capture seems to be the implicit differential occlusion of the corner elements; that is, the presence of monocular occlusion zones in the corner elements. Capture occurs when the inner square is placed on a black rectangle (Figure 12.4d) because this provides differential occlusion of the rectangle by the inner square.

According to Ishigushi and Wolfe (1993), disparity capture occurs when the disparate parts of the stereogram consist of complete squares, as when the left and middle patterns of Figure 2.41g are fused by convergence. This creates a crossed disparity of the inner square which appears to stand out, carrying

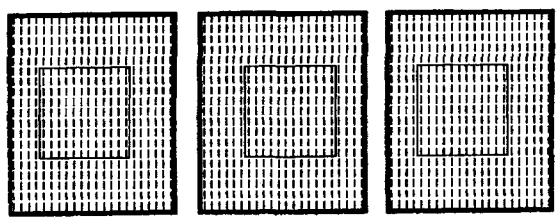


(a) Convergent fusion of left and middle patterns creates a textured square standing out. The middle and right patterns create a textured square visible through four holes. (From Ramachandran 1986. Perception and Psychophysics, 39, 361-373. Reprinted by permission of Psychonomic Society Inc.)

(f) This stereogram creates a square in depth even though subjective squares are not evident monocularly. (Adapted from Mather 1989.)

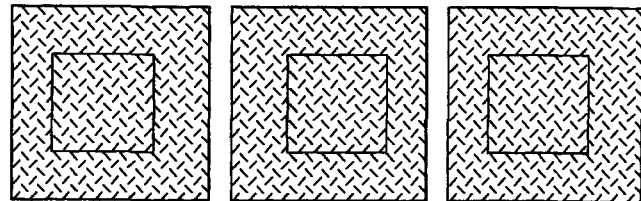


(b) Disparity capture persists with convergent fusion of left and middle patterns when lines replace subjective contours. Fusion of middle and right patterns creates an unstable impression of the whole textured surface lying beyond the corner elements.

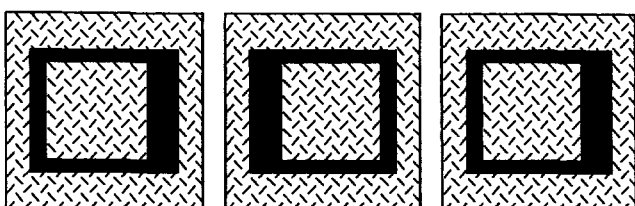


(g) Ishigushi and Wolfe claimed that convergent fusion of the left and middle patterns creates disparity capture of the texture in the inner square. Fusion of the middle and right patterns creates an unstable transparent textured surface with the inner square beyond, a textured surface beyond the outer frame, or a hole in a textured surface. (Adapted from Ishigushi and Wolfe 1993.)

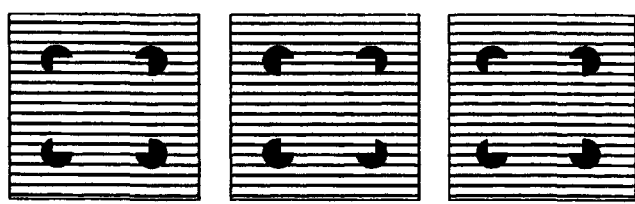
Figure 12.41. Interpolation into areas of ambiguous disparity.



(c) Disparity capture is weak or absent when the corner elements are removed.



(d) Capture occurs when disparity is supplemented by occlusion of a background



(e) Only the top and bottom few lines are carried forward with the square, because continuity of the centre lines with those in the background creates one surface. (Adapted from Ramachandran 1986. Perception and Psychophysics, 39, 361-373. Reprinted by permission of Psychonomic Society Inc.)

the enclosed texture elements with it. We find this effect to be weak compared with when there are occluded corner elements, as in Figure 12.41b. They argued that this impression is stable because the sign of disparity is compatible with the assumption that the small square is a figure on a ground. In other words, it is reasonable to interpolate the crossed disparity of a figure into a region of ambiguous disparity within the figure. Convergent fusion of the middle and right patterns of Figure 12.41g creates an uncrossed disparity of the inner frame which appears beyond the outer frame of the fused patterns. Ishigushi and Wolfe reported that in this case subjects interpreted the depth of the texture elements in several ways. First, a hole was seen in the foreground. This interpretation was rarely seen because other information, such as the absence of shadows, contradicted this impression. Second, the texture appeared in the foreground as a transparent surface through which could be seen the inner frame. Third, the whole textured surface appeared to lie beyond the outer frame of the stereogram in the plane of the inner square. All these impressions were unstable.

Ramachandran (1986) found that disparity capture works when the texture elements are vertical

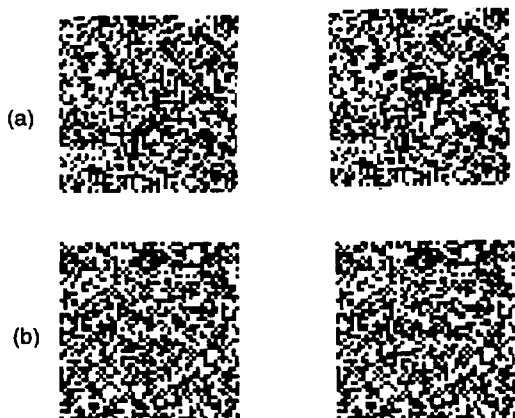


Figure 12.42. Rivaldepth.

Stereograms similar to those used by O'Shea and Blake (1987). The dots in the inner square of (a) are uncorrelated. Those in the inner square of (b) have reversed luminance. Each stereogram creates a sensation of depth but with indeterminate sign.

lines. When they are horizontal lines, as in Figure 12.41e, only two or three lines at the top and bottom of the inner square come forward, the rest stay in the plane of the background. The lines ending in the pacmen prompt the impression that they occlude the pacmen and are thus part of a figure on a ground. The continuity of the lines across the boundary of the subjective square prompts the impression that the lines form one surface. These effects do not require subjective squares to be apparent in the monocular images; similar effects to those in Figure 12.41a are also produced by Figure 12.41f (Mather 1989). But in this case, as in Figure 12.41a, there is an implied occlusion of the corner elements by the inner square when the inner square appears in front.

We conclude that disparity capture occurs within a region bounded by crossed-disparity edges or by subjective edges which are modal extensions of crossed-disparity edges, but only when other contour elements exist that prompt the impression of being occluded by the foreground pattern. Disparity alone creates little if any disparity capture. Modally completed edges define a figure in front of a ground and therefore foster disparity capture. Disparity capture occurs within an area bounded by uncrossed disparity edges but does not extend into the region bounded by amodally completed edges. Amodally completed edges define a shape occluded by a foreground surface which is therefore hidden from view. This does not foster disparity capture within the foreground region.

Interpolation into regions of uncorrelated texture

When the surround region of a stereogram containing correlated textures is made visibly distinct from a central region containing uncorrelated textures—

for instance, by a difference in dot density—the central uncorrelated region is seen in a depth plane consistent with the disparity along its lateral edges (see Section 6.1.3). In other words, a clearly seen disparity defined in terms of the boundaries between monocularly distinct regions of rivalrous texture is interpolated into the rivalrous region, which itself contains no disparity information.

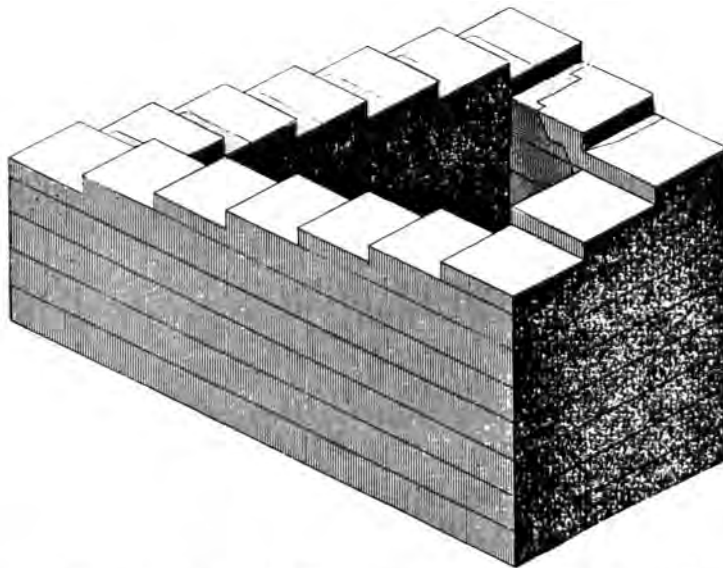
Rivaldepth

A random-dot stereogram consisting of a surround region with the same dot pattern in the two eyes and a central square filled with dot patterns that are uncorrelated in the two eyes produces an impression of fluctuating depth, even though there is no disparity between the uncorrelated regions (Julesz 1960; Frisby and Mayhew 1978b). O'Shea and Blake (1987) dubbed this **rivaldepth** and used the stereograms shown in Figure 12.42. In the top stereogram the central region consists of uncorrelated dots and in the bottom stereogram the dots in the central region have opposite luminance polarity. In each case, subjects reported that the central region appeared in depth, either in front of or beyond the surround.

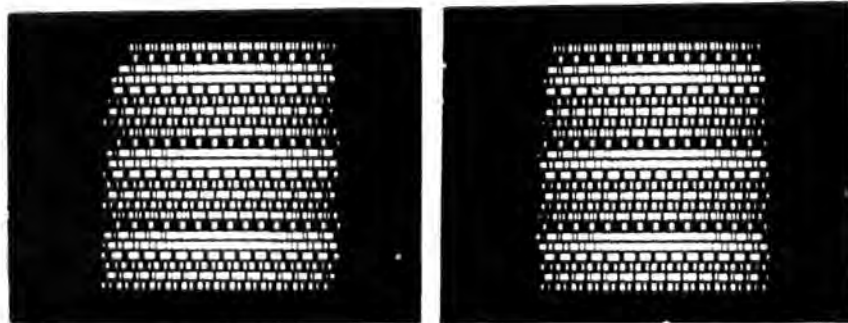
O'Shea and Blake argued that rivaldepth is related to the vague impression of depth that arises in random-dot stereograms in which the disparity is too large to detect. The direction of perceived depth in the inner square was found to be related to fixation disparity. This suggests that subjects were responding to the disparity between the nonrivalrous regions induced by the fixation disparity relative to an indeterminate disparity in the inner square. Misconvergence would not induce a detectable disparity into the uncorrelated region since this region has no defined disparity to begin with. It was shown in Section 7.8.3 that under the correct stimulus conditions an impression of depth with unambiguous sign can be created by rivalry alone.

An ever-ascending stereoscopic staircase

Figure 12.43a shows an ever-ascending staircase produced by misleading perspective cues (Penrose and Penrose 1958). The rule that binocular matching in a region of constant disparity is done to minimize the perceived difference in depth between that region and a neighbouring region, can be used to construct a stereo version of this illusion, as in Figure 12.43b (Papathomas and Julesz 1989). Most people see a continuously ascending set of steps in depth as they slowly move their gaze from the top of the stereogram to the bottom, in spite of the fact that the disparity periodically jumps back to its previous value. Part of the reason for this is probably that the eyes change convergence as they scan the display.



a) An ever-ascending staircase created by illusory perspective. (From Penrose and Penrose 1958.)



(b) A stereo version of the ever-ascending staircase. When the images are fused, one sees a continuously ascending set of steps in depth as the gaze moves slowly from top to bottom, in spite of the fact that the disparity jumps back periodically to its previous value. (From Papathomas and Julesz 1989, Perception, 18, 589-594. Pion, London.)

Figure 12.43. Ever ascending staircases in perspective and stereoscopic depth.

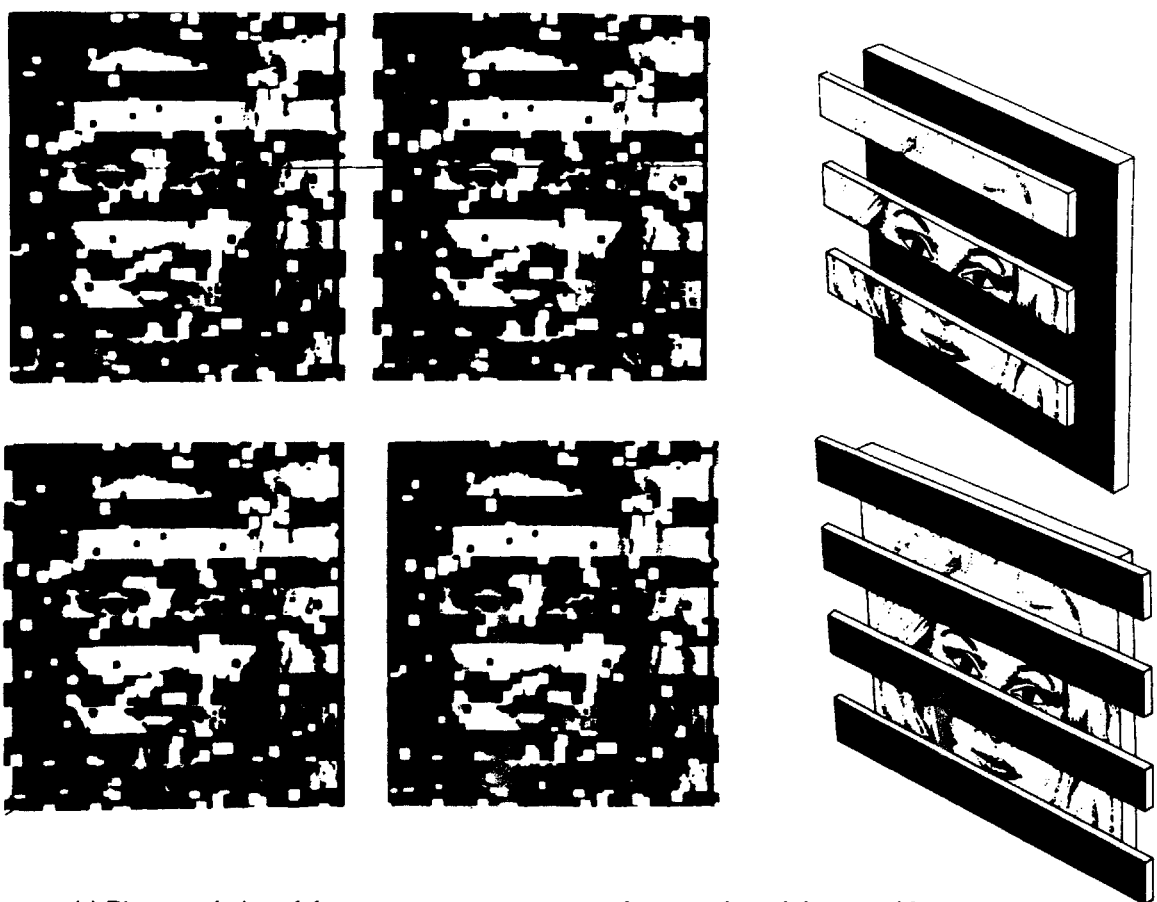
12.5 STEREO AND FIGURAL ORGANIZATION

The Gestalt psychologists described how ambiguous patterns are interpreted according to certain basic principles of figural organization (Koffka 1935). These principles include similarity of form, proximity, continuity, common fate, and *Pregnanz*, or good form. The influence of similarity of form and of proximity in determining the ways in which images in the two eyes are matched was discussed in Section 6.2. The influence of common fate is discussed in Section 13.4. The influence of figural continuity, figure-ground organization, and good figure are discussed in the following two sections.

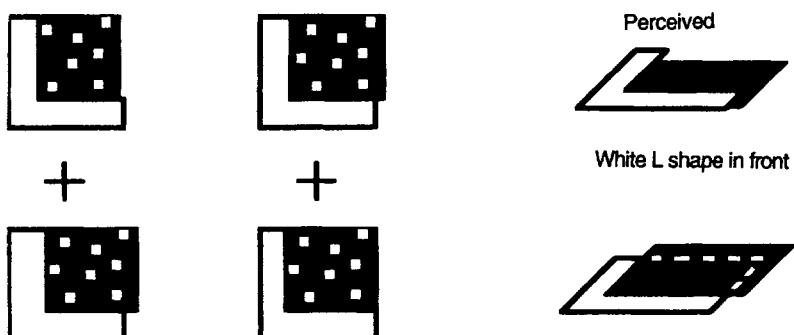
12.5.1 Stereopsis and texture segregation

Stereopsis can affect the appearance of surface continuity. For instance, when we view an object

through a picket fence it appears as a continuous object even though parts of it are occluded by the fence. When the spaces and bars are a certain width, the whole object is seen as alternating monocular strips. With a fence of horizontal bars there are no monocular occlusion zones but, instead, alternate regions of a far object are occluded to both eyes. When the sign of the disparity in the far surface is reversed, the visible strips appear in front of the occluding bars. The object now appears fractionated and the bars look like parts of a continuous far surface (Nakayama et al. 1989). These relationships are illustrated in the stereograms in Figure 12.44a. In the example shown in Figure 12.44b the white region appears as a letter L when disparity indicates that it is in front of the black square and as an occluded square when the disparity is reversed. The time required for detection of a reversed L among normal L's was shorter when the shapes were seen as



(a) Divergent fusion of the upper stereogram creates a face seen through horizontal bars, as shown on the right. Divergent fusion of the lower stereogram creates strips of a face in front of a continuous black surface. (From Nakayama et al. 1989, Perception, 18, 55-68, Pion, London.)



(b) Divergent fusion of the upper stereogram causes an L to appear in front of a black square. In the lower stereogram the L is seen as a partially occluded white square (From He and Nakayama 1992, Nature. Copyright, 1992, Macmillan Magazines Limited.)

Figure 12.44. Effects of stereopsis on figural continuity.

complete in the foreground than when they were seen as parts of occluded squares in the background (He and Nakayama 1992). In other words, the feature-matching process in a pop-up task (see Section 6.1.6) occurs after shapes are segregated in different depth planes.

He and Nakayama (1993) applied this idea to the problem of texture segregation. In Figure 12.45 the top stereogram, when fused by convergence, creates the impression of a region of white bars in a surrounding region of white L's, with an array of twenty dotted squares in the background. Texture

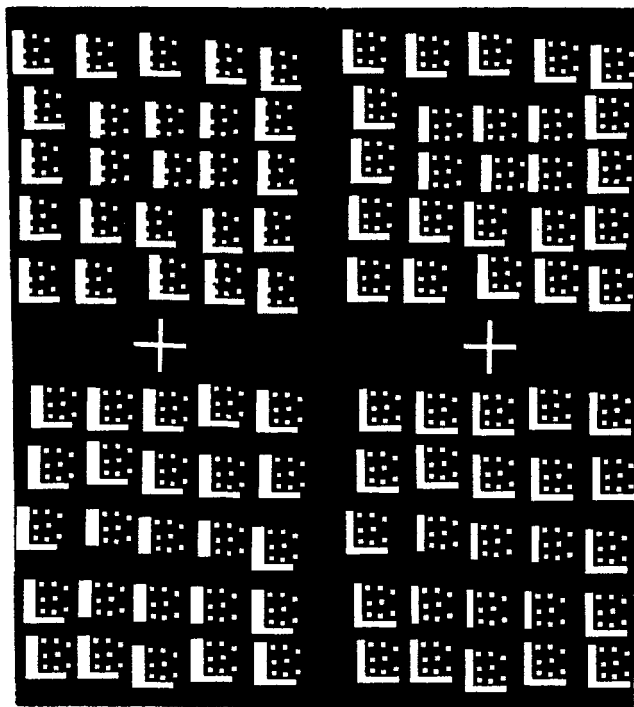


Figure 12.45. Effects of stereopsis on texture segregation.
Divergent fusion of the upper stereogram creates white L's and I's which segregate into distinct regions. The lower stereogram creates partially occluded white squares and the L's and I's do not easily segregate. (Reprinted from He and Nakayama 1993, with kind permission from Elsevier Science Ltd.)

segregation between the bars and L's is readily achieved. The bottom stereogram creates the impression of amodally completed white squares partially occluded by dotted squares seen in the foreground. Texture segregation of the bars and L's is now difficult to achieve. In a control condition in which the white elements did not abut the dotted squares there was no difference between the two depth conditions in the segregation of the L's and I's. This demonstrates that depth segregation plus amodal completion are required for the difference in texture segregation evident in Figure 12.45. The generally accepted theory of texture segregation is that it occurs at an early stage of visual processing and depends on a set of filters selectively responsive to simple features such as orientation, colour, motion, and size. In terms of these features, the two stereograms of Figure 12.45 are equivalent. They become distinct only after the stage at which the displays are segregated into distinct depth planes and formed into shape elements by the operation of occlusion and amodal completion. Thus, these higher-order features must be added to the list of features that determine texture segregation.

Just as stereoscopic depth may affect the impression of surface continuity, surface continuity may prime or inhibit stereoscopic depth. This issue is discussed in Section 11.2.3.

12.5.2 Stereopsis and figure-ground organization

In certain patterns, such as the well-known Rubin's cross, there is an ambiguity about which part is seen as figure and which part as ground. The figure-ground organization of such patterns alternates spontaneously. A spontaneous change in figure-ground organization can prime or inhibit stereoscopic depth. For instance, the stereogram in Figure 12.46a creates the impression of two bars at different distances. But the same disparity between the bar images in Figure 12.46b creates the impression of a slanted white rectangle, because the addition of the horizontal lines converts the white regions into figures and the dark bars into background (Wilde 1950). Thus, depth induced by disparity between parts of a pattern seen as figure has precedence over depth induced by disparity between parts seen as background. The stereogram in Figure 12.46c provides another illustration of the same principle. When the images are fused and the dark bars are seen as figures on a white ground, the dark bars appear as planes slanted in depth, but when the white bars are seen as figures, the white bars appear as slanted planes, as illustrated in Figures 12.46d and e. It is not possible to see both sets of slanted planes at the same time (Metzger 1975).

The Gestalt principle of *Pregnanz*, or good figure, is not easy to define. In general it states that when a pattern is compatible with more than one interpretation, the simplest interpretation is most likely to be perceived. If the principle is to have explanatory value the notion of "simplest interpretation" must be defined by criteria that are independent of the way ambiguous figures are interpreted. Several criteria have been proposed, three of which are discussed—symmetry, minimum number of figural discontinuities, and independence of changes in vantage point (generic viewpoint).

The influence of symmetry on the perception of three-dimensional form is illustrated by Figure 12.47. The pattern on the left appears flat even though it could be interpreted as the projection of a cube seen end-on. One explanation of this is that the two-dimensional shape has complete radial symmetry. The pattern on the right is easily seen as a cube. In this case, the cube has more perfect symmetry than its two-dimensional projection.

The stereogram in Figure 12.48a (see after page 310) is seen as a red transparent square nearer than



(a) Fusion of the two pairs of vertical bars creates the impression of two bars at different distances.



(b) Fusion of the same black bars creates the impression of a slanted white rectangle, because the addition of the horizontal lines converts the white region into a figure and the dark bars into background. (Adapted from Wilde 1950.)

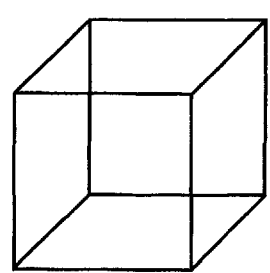
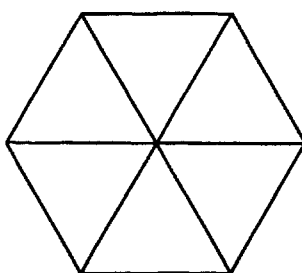


(c) When the dark bars are seen as figures on a white ground, they appear as slanted planes, as in (d). When the white bars are seen as figures, they appear as slanted planes, as in (e). The crossed and uncrossed versions alternate independently. These effects may take time to develop. (Adapted from Metzger 1975.)



Figure 12.46. Figure-ground reversals and stereopsis.

the black frame or as an opaque red square behind the frame, depending on whether the red square is seen with crossed or uncrossed disparity. The same pattern of disparity is compatible with a surface with a double ramp, as depicted in Figure 12.48b. The preference for the square could be due to its lack of surface discontinuities compared with the corrugated surface. Nakayama and Shimojo (1992) explained the preference for the square in terms of the relative likelihood of each interpretation. This particular proximal stimulus of a corrugated surface is unlikely because it arises only when the surface is seen from one vantage point. From any other



(a)

(b)

Figure 12.47. Influence of symmetry on depth perception.

(a) The pattern could be an end-on projection of a cube but is seen as a flat figure because it forms a radially symmetrical pattern in two dimensions.

(b) The pattern is easily seen as a three-dimensional cube because a cube from this vantage point has more perfect symmetry than its two-dimensional projection.

vantage point the top and bottom edges of the corrugated surface would be visible as disparate stimuli, as depicted in Figure 12.48b. The square is a more likely proximal stimulus because it remains fundamentally the same when the vantage point changes. The general principle is that we prefer interpretations that arise from a generic viewpoint; that is, interpretations that do not arise merely as a result of viewing an object from a particular vantage point.

12.5.3 Stereopsis and subjective contours

Depth from subjective contours

In Figure 3.1a a complete triangle is visible even though its presence is indicated only by the apparently occluded sectors of three black circles. The apparently completed edges of the triangle are known as subjective contours, or cognitive contours, and the white triangle is a subjective shape. The corner shapes are known as inducing elements. Because of its shape, this particular type of inducing element is often referred to as a "pacman". In the original Ehrenstein figure the inducing elements were lines, as shown in Figure 3.1b. Subjective contours arise because the figure-ground relationships of the display are most simply interpreted if it is assumed that an opaque white surface occludes part of each inducing element. In other words, a subjective contour is the edge of a subjective plane which would have to be present to account for the coherent set of partial occlusions (Ehrenstein 1941; Kanizsa 1979; Coren and Porac 1983). A subjective shape appears to overlap the inducing elements and, on that account, appears nearer than the inducing elements. However, the impression of depth is vague and not quantitatively defined.

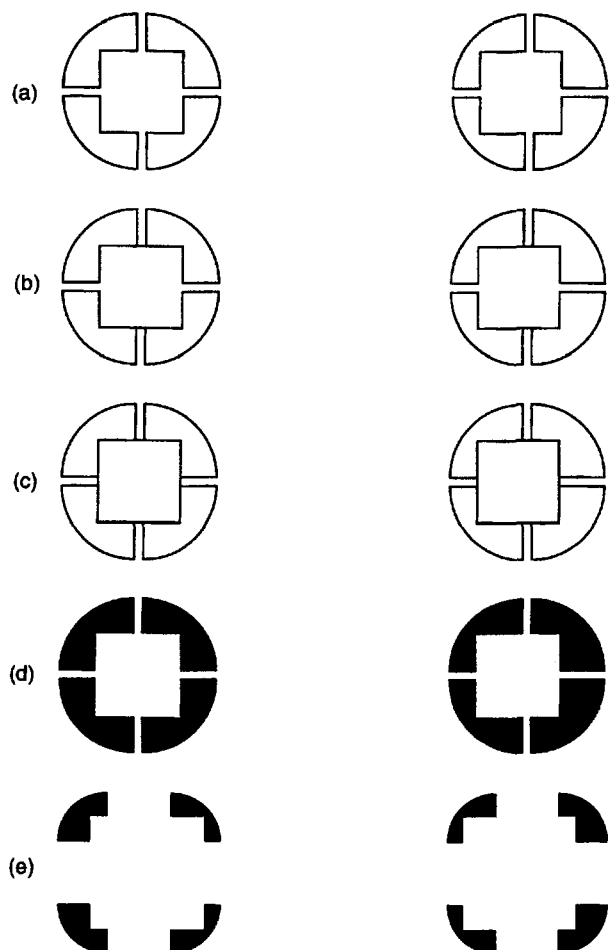


Figure 12.49. Subjective contours and stereopsis.

- (a) Disparity in the vertical edges creates a square in depth connected to the circle by horizontal and vertical ramps.
- (b) Continuous horizontal edges sever upper and lower ramps.
- (c) Square completely separated from the background.
- (d) Continuous edges to the square are not required for its segregation from the surround when evidence of occlusion is provided at the corners.
- (e) Evidence of occlusion at the corners can generate the impression of edges where none exist.

The apparent depth of a subjective shape relative to the inducing elements is enhanced and becomes well defined when two slightly different subjective shapes are combined stereoscopically. For example, when the stereogram in Figure 12.49a is fused, the disparity in the vertical edge creates an impression of a square in depth connected by horizontal and vertical ramps to the outer segments. In Figure 12.49b, evidence of occluding horizontal edges severs the connection of the square to the upper and lower segments, and these ramps are no longer seen. In Figure 12.49c, all sides of the square seem to occlude the outer segments and all the ramps disappear. In Figure 12.49d, evidence of occlusion at the

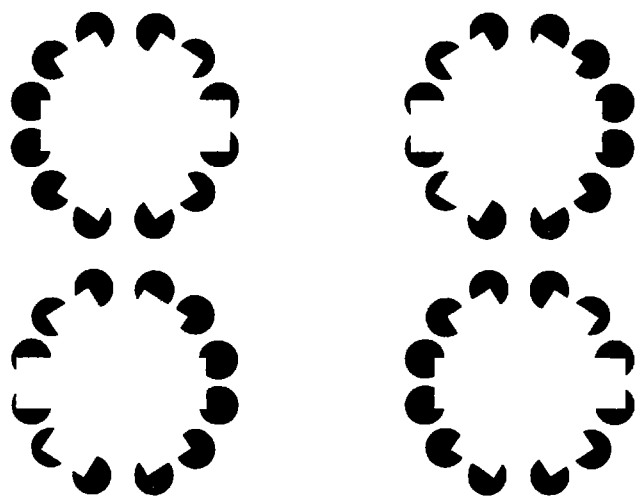
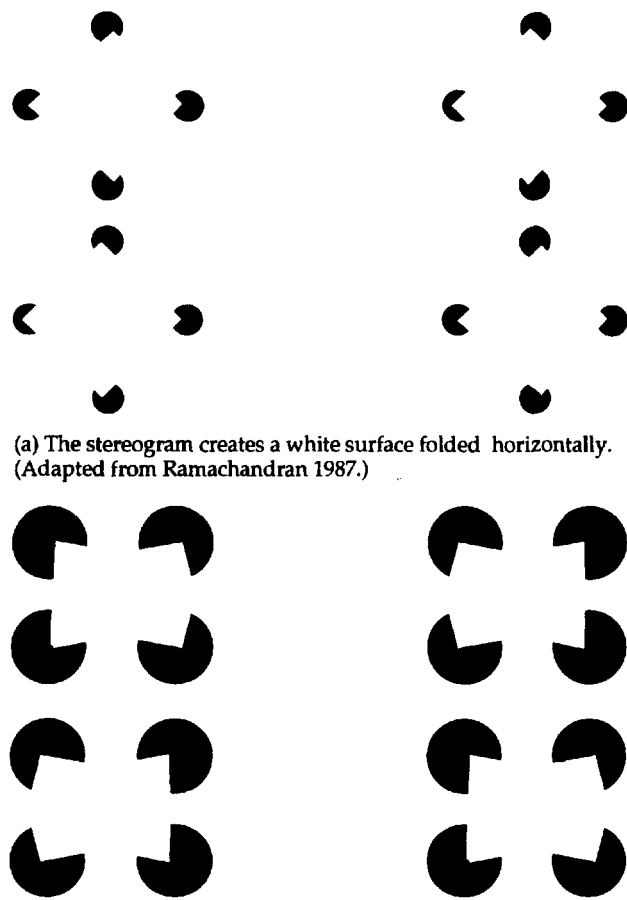


Figure 12.50. Subjective rectangles in multiple planes.

The stereograms create three rectangles overlapping in depth either in front of or beyond the ring of black discs. (Adapted from Ramachandran 1987.)

corners of the inner square is sufficient to segregate the square from the outer segments. In Figure 12.49e, evidence of occlusion at the corners supports the percept of edges across large gaps (Blomfield 1973; Ramachandran 1986). The disparity between these squares relative to the outer boundary of the four circles generates an impression of depth. We thus have a four-tiered process: occlusion, subjective contour, disparity, and depth. As one would expect from this account, the clarity of the subjective contour is enhanced when the direction of disparity reinforces the monocular cues that the subjective surface is in front, and attenuates its clarity when disparity and monocular occlusion cues conflict (Gregory and Harris 1974; Lawson et al. 1974). In these experiments the subjective shapes were visible in each monocular display. But they do not have to be. A white square is seen in depth in the stereogram shown in Figure 12.49f even though the subjective contours are not seen in the monocular images. The stereogram in Figure 12.50 produces the impression of three overlapping rectangles above or below the plane of the corner elements. The stereogram shown in Figure 12.51a produces a square folded in depth (Ramachandran 1987) and that shown in Figure 12.51b shows a saddle-shaped surface (Carman and Welch 1992).

A transparent textured surface held in front of a subjective shape formed by line terminations, as in the Ehrenstein figure shown in Figure 3.1b, causes the subjective shape to appear in the plane of the textured surface rather than in the plane of the inducing elements (Spillmann and Redies 1981). Watanabe and Cavanagh (1994) found that this



(a) The stereogram creates a white surface folded horizontally.
(Adapted from Ramachandran 1987.)

(b) The stereogram creates a saddle-shaped white surface.
(Adapted from Carman and Welch 1992.)

Figure 12.51. Subjective surfaces folded in depth.

effect does not work for the Kanizsa figure in which subjective shapes are defined by sectored discs, as in Figure 3.1a. They concluded that stereoscopic information is much weaker in the Ehrenstein figure, in which the subjective shape is defined only by line terminations than in the Kanizsa figure, in which the subjective shape is defined by edges.

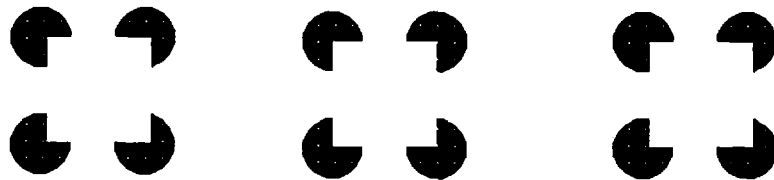
Depth from cyclopean subjective contours

In the preceding displays the corner elements were defined by luminance. Prazdny (1985c) made random-dot stereograms with cyclopean inducing elements defined by disparity, that were not visible in either monocular image, as in Figure 12.52a. None of the subjects reported subjective contours in these displays. Subjective contours were reported for black inducing elements superimposed on a background of random dots that were uncorrelated in the two eyes, as in Figure 12.52b. Prazdny's subjects saw subjective contours with luminance-defined corner elements possessing an uncrossed disparity with respect to a random-dot background, but not with

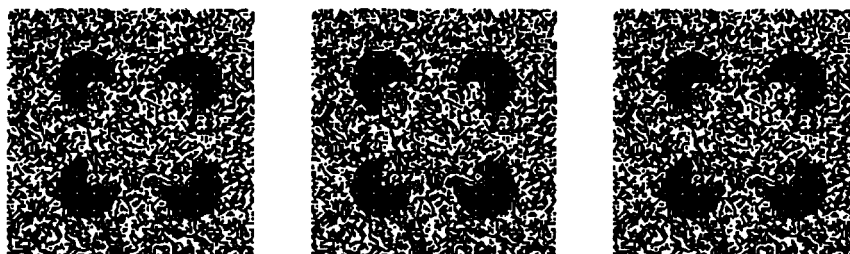
elements with a crossed disparity, as illustrated in Figure 12.52c. Prazdny concluded that subjective contours are formed only from inducing elements defined by luminance. However, Mustillo and Fox (1986) claimed that subjective contours are visible with cyclopean pacmen defined by uncrossed disparity, as in one half of Figure 12.52a but not with crossed disparity, as in the other half of the figure. They concluded that subjective contours can be induced by cyclopean inducing elements. This may be a pseudo issue because the subjective contours seen against a textured background may differ from those seen against a plane background. With a textured background, one may select the dot clusters between the pacmen that suggest a connecting contour. In other words, the contour is not subjective because it contains luminance-defined edges. All investigators agreed that subjective contours are not seen when the luminance or disparity-defined pacmen are stereoscopically in front of the textured background. This is not surprising because the disparity of the random dots is unambiguous and the textured disparity is therefore seen as a coherent surface beyond the corner elements. The textured background comes forward with the pacmen in Figure 12.41a because the disparity of the repetitive texture is ambiguous. The question as to whether cyclopean elements can induce subjective contours must remain unanswered until someone has thought of a way to construct a random-dot display with cyclopean inducing elements and ambiguous disparity but with no monocular cues.

Depth from transparent subjective shapes

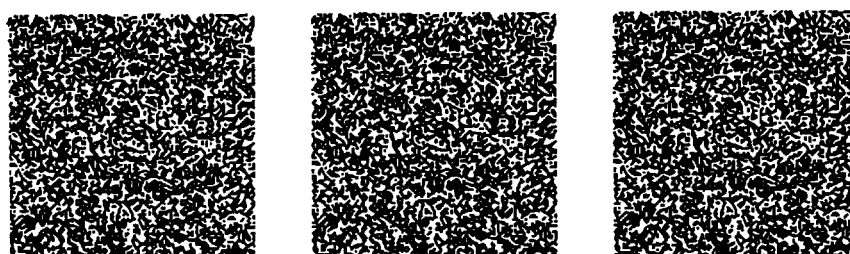
Transparency can also affect how disparity between subjective contours is interpreted. With crossed disparity in the stereogram shown in Figure 12.53a the gray sectors on the white circles create the impression of a transparent square. The square appears in front of the striped background, which can be seen through the square. When the disparity places the square beyond the white circles, the subjective contours along the sides of the square disappear and so does the impression of transparency. Instead, one has the impression of four circular windows, each containing one corner of a more distant gray square. When the gray sectors are replaced by the lines of the background, as in Figure 12.53b, the square with crossed disparity is interpreted as opaque, forcing the interpretation that the lines within the square are on the surface of the square and come forward with it (Nakayama et al. 1990). With uncrossed disparity the corners of a square with lines is seen through four portholes. The surface depicted in the stereogram Figure 12.54 is paradoxical since one end



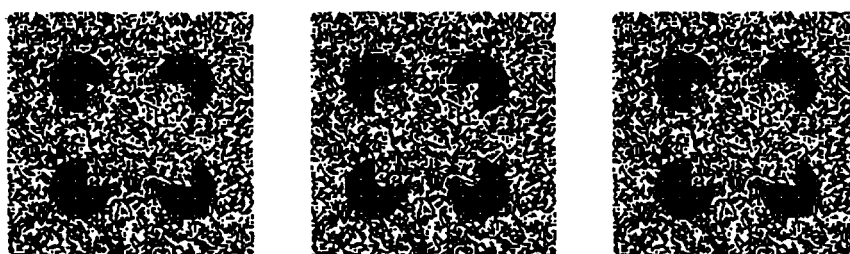
(a) The crossed-disparity stereogram creates a subjective square standing out in depth. The uncrossed-disparity stereogram creates a square seen through four port holes.



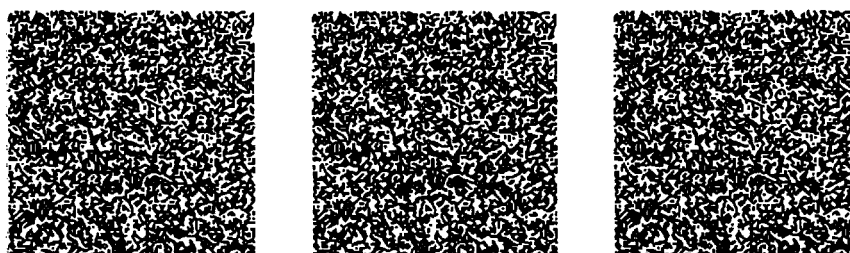
(b) Four pacmen do not create a subjective square when superimposed on a textured background.



(c) Cyclopean pacmen do not create a subjective square.

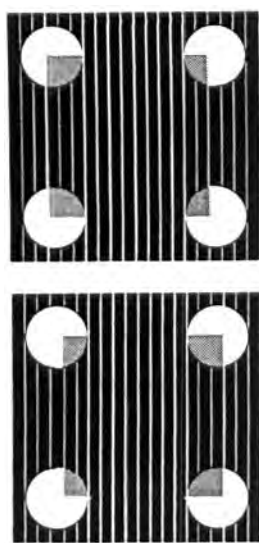


(d) Pacmen with a secondary disparity, as in (a) do not produce a subjective square.

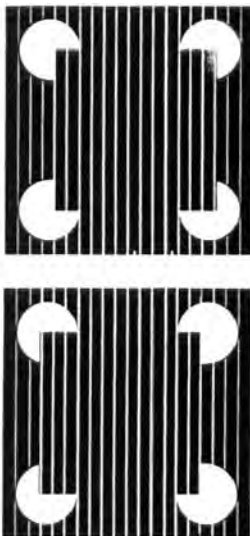


(e) Cyclopean pacmen with a secondary disparity also do not produce a subjective square.

Figure 12.52. Stereopsis and subjective contours.



(a) With crossed disparity, a transparent square stands out from the background and the lines remain with the background. With uncrossed disparity, a gray square is seen through port holes.



(b) With crossed disparity, the square appears opaque and carries the lines forward with it. With uncrossed disparity, the square is seen through portholes. (Adapted from Nakayama et al. 1990.)

Figure 12.53. Effect of transparency on stereopsis.

appears beyond the pacmen and the other in front. Even a single dot seen in depth can trigger a sensation of transparency, as can be seen in Figure 12.55.

12.6 MONOCULAR OCCLUSION

12.6.1 Basic rules

Next to the vertical edges of an opaque object, as in Figure 12.56, there are regions of a far surface visible to only one eye. This is **monocular occlusion**. The

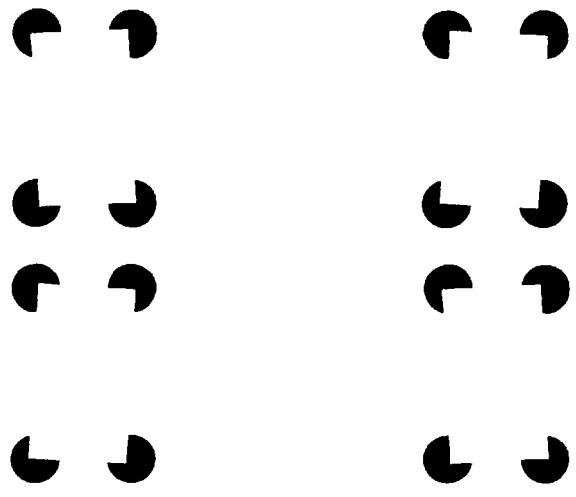


Figure 12.54. Paradoxical surfaces inclined in depth.

occluded regions will be referred to as **monocular zones**. A region of space visible only to the left eye is a **left monocular zone** and a region visible only to the right eye is a **right monocular zone**. Note that an occlusion zone is defined with respect to the eye that sees. A region visible to both eyes is a **binocular zone** and a region not visible to either eye is a **binocular occlusion zone**.

An object lying in front of a surface is visible if the object and the surface have very similar textures and luminances, that is, if the object is camouflaged against the surface. In Figure 12.57, the near object is camouflaged to the left eye because its image is superimposed on a matching far surface, but it can be seen by the right eye because this eye sees it against a different surface. This is **monocular camouflage**.

Monocular occlusion and camouflage obey the following simple geometrical rules:

1. The monocular zone of the left eye is to the left of the occluding object and that of the right eye is to the right of the occluding object (see Figure 12.56a). The rule is that monocular zones due to occlusion in each eye are on the temporal side of the binocular object. A near object camouflaged to one eye is seen by the other eye on the nasal side of the far object. Therefore monocular zones due to camouflage are on the nasal side of the binocular object.

2. A monocular zone due to occlusion is more distant than the binocular object and may contain an object or part of a surface. A monocular zone due to camouflage is nearer than the binocular object and usually contains an isolated object.

3. The physical size of a monocular zone due to either occlusion or camouflage is affected only slightly by changing accommodation, version, or

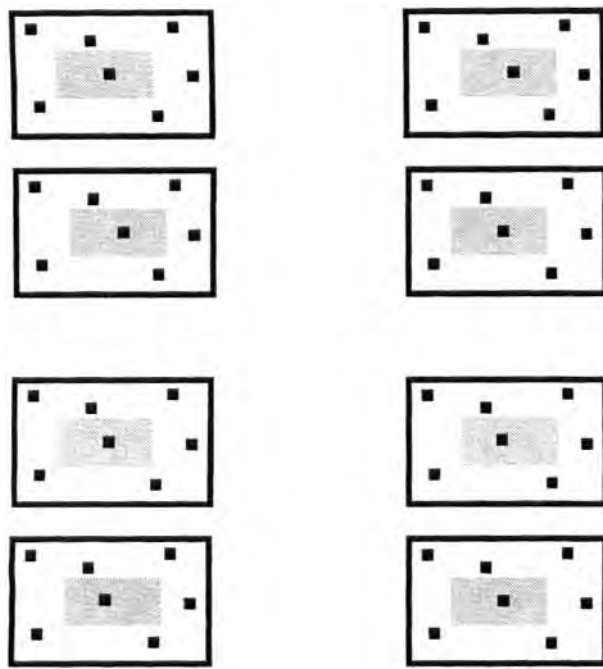
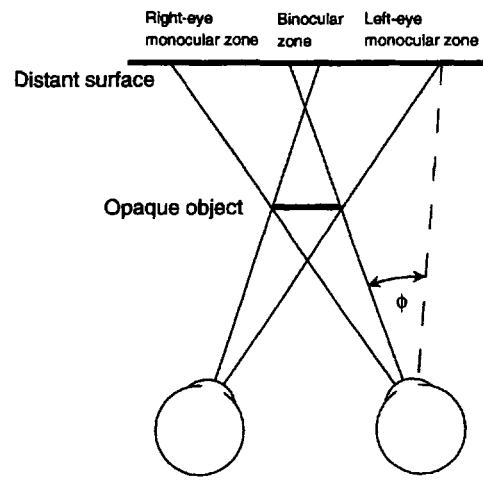


Figure 12.55. Opacity or transparency triggered by a dot.
A dot seen in depth appears coplanar with an opaque surface in the two top stereograms or appears through a transparent surface in one of the lower stereograms. (From Nakayama et al. 1990, Perception, 19, 497-513, Pion, London.)

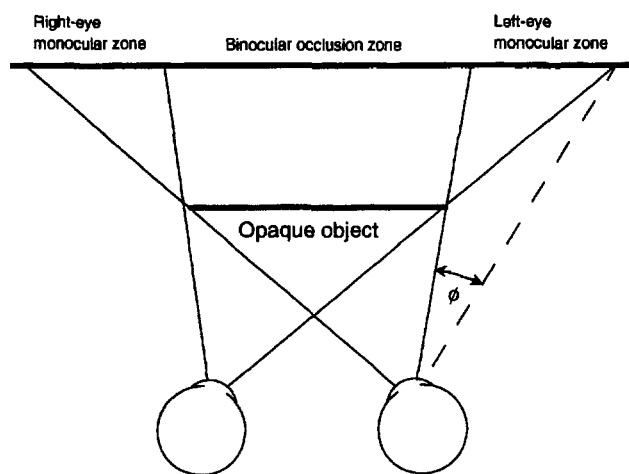
vergence. There is a slight change because the centre of rotation of the eye and the nodal point are not in the same position.

4. The angular subtense of a monocular zone (angle ϕ in Figure 12.56) is inversely proportional to the distance of the occluding object from the viewer. For a binocular object at a given distance, angle ϕ increases as the distance of the occluded surface increases. An occlusion zone becomes vanishingly small as the binocular object approaches the far surface, as the far surface approaches the near object, or as both objects are moved further away from the viewer. A viewer who sees a monocular zone changing in angular size knows only that one or some combination of these three things is happening. The size, or a change in the size, of a monocular occlusion zone is a potential source of unambiguous information about distance only if the viewer knows either the distance of the occluder or the distance of the occluded surface.

5. An object narrower than the interocular distance produces two monocular zones which, beyond a certain distance, are separated by a binocular zone, as shown in Figure 12.56a. An object wider than the interocular distance produces monocular zones separated by a zone within which neither eye can see, as in Figure 12.56b.



(a) When the occluding object is shorter than the interocular distance, both eyes see the region between the occlusion zones.



(b) When the occluding object is longer than the interocular distance, neither eye sees the region between the monocular zones.

Figure 12.56. Monocular occlusion zones.

When an opaque object is held in front of the eyes, each eye sees a region of a far surface not visible to the other eye. The angular subtense of a monocular occlusion zone is indicated by ϕ .

The following discussion is concerned with how the visual system makes use of monocular occlusion or camouflage in judging depth.

12.6.2 Monocular occlusion and depth continuity

Monocular occlusion occurs wherever two surfaces are separated by a steep depth discontinuity which is not horizontal. It could therefore be used by the visual system to indicate the presence of a depth discontinuity as opposed to a gradual depth ramp with a disparity gradient of less than 2 (see Section 2.3.3). Gillam and Borsting (1988) argued that a monocular occlusion zone is more visible and therefore more

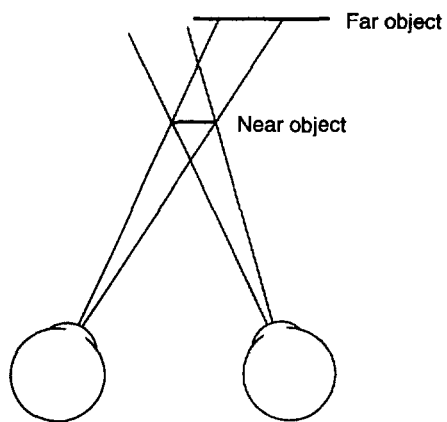


Figure 12.57. Monocular camouflage zone.

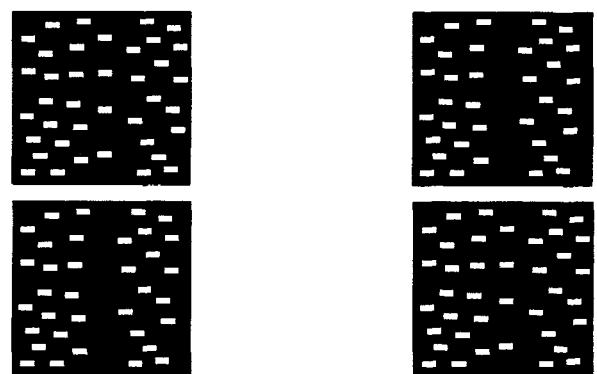
An object in front of another object on the same line of sight of an eye will not be visible to that eye if the two objects have similar surfaces. One is camouflaged against the other. The near object may be visible to the other eye on the nasal side of the far object.

effective as a cue for depth discontinuity if it is textured rather than blank. In support of this idea they found that it took less time to recognize a depth edge in a random-dot stereogram when the monocular zone was filled with dots, like those in the background, rather than left blank. The crucial factor, however, may be the similarity between the texture in the occluded zone and that in the rest of the far surface rather than the absence of texture in the occluded zone. *A control is needed in which the texture in the occluded zone differs from that in the rest of the far surface.*

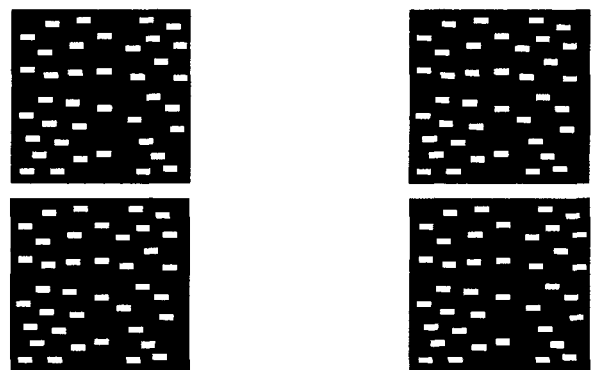
Nakayama and Shimojo (1990) devised the stereograms shown in Figure 12.58 to illustrate the role of monocular zones in creating the impression of a sharp depth edge. In the upper stereogram, the disparity between the left and right halves is accompanied by a monocular zone of three dots. This creates the impression of a depth step with a straight edge. The lower stereogram has the same disparities, but all the dots are seen by both eyes and there is no impression of a straight edge.

12.6.3 Occlusion, camouflage, and rivalry

According to the rule for monocular occlusion already mentioned, a left monocular zone occurs on a left-facing occluding edge and a right monocular zone on a right-facing occluding edge. Shimojo and Nakayama (1990) devised the display shown in Figure 12.59, which violates this rule. The left eye's image has a monocular crescent of horizontal lines on both sides of the black disc. But only the crescent on the left occur in the left-eye's image of a black disc standing in front of a textured background. This crescent therefore survives binocular rivalry with the



(a) Divergent fusion of the top stereogram creates a vertical step with a straight edge, which appears to abut the three rectangles that are visible to only one eye. In the bottom stereogram the monocular rectangles are seen by the inappropriate eye and do not create an edge.



b) These stereograms create a step with a jagged edge, since there are no monocular elements to define the sharp edge of the step.

Figure 12.58. Monocular zone creates sharp depth edge.

(Adapted with permission from Nakayama and Shimojo 1990, Vision Research, Pergamon Press.)

dots and appears to be part of the far textured surface rather than of the black disc, as proposed by Julesz (1964). The monocular crescent on the right is on the wrong side to be interpreted as a monocular zone due to occlusion. Its image is therefore suppressed by the rivalrous textured image in the right eye. Thus, the rivalry mechanism is coupled to the mechanism that interprets monocular occlusion, giving precedence to ecologically valid images.

12.6.4 Monocular occlusion and surface opacity

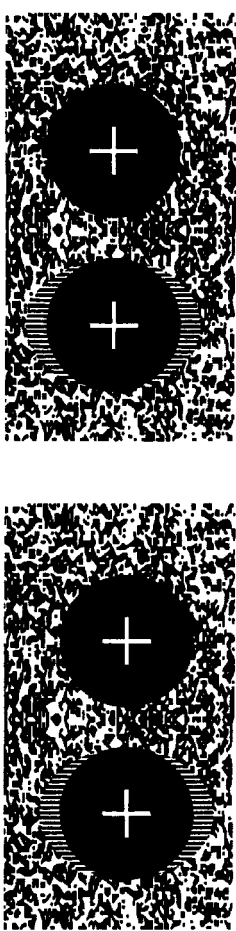
Lawson and Mount (1967) described the stereogram shown in Figure 12.38a. When the two images are fused, an apparently opaque white square stands out in front of a background of dots, which seem to extend behind the white square. A monocular column of dots occurs along each vertical edge of the fused image. The two vertical edges are linked by



Figure 12.59. Normal and anomalous occlusion zones.
When the fused image is seen as a black disc in front of the background, the occlusion zone on the appropriate (temporal) side is suppressed, whereas that on the inappropriate (nasal) side remains visible. When the fused image is seen as a disc beyond the background, both occlusion zones are inappropriate, and both are visible. (Adapted from Shimojo and Nakayama 1990.)

top and bottom rows of dots seen by both eyes. The foreground square appears opaque, which is what it would have to be to create occlusion zones. The occluded far surface appears to continue behind the white square. This is the most parsimonious conclusion. Kaufman (1965) had produced similar displays using rows of letters instead of dots, as in Figure 12.60. The stereogram in Figure 12.38b produces the impression of a frame of dots in front of another frame of dots. Here the impression of an opaque square and a continuous surface of dots is not evoked because each column of dots has a matching set in the other eye; there are no monocular zones. Thus, monocular zones provide effective information about the opacity of foreground objects and about texture continuity in background surfaces.

One cannot conclude that the information provided by monocular zones in Figure 12.38a



p f j v n b l r p e r u h j e
k y i e r h g l k j r f l o j h
m o w e i k t u h r b f j v
b f v f k i w j l b h k r i g
t r h g n i u h i m p o u w

i a j f g j f f k u v c u w q
f j v n b l r p e r u h j e
y i e r h g l k j r f l o j h
o w e i k t u h r b f j v
f v f k i w j l b h k r i g
t r h g n i u h i m p o u w

p f j v n b l r p e r u h j e
k y i e r h g l k j r f l o j h
m o w e i k t u h r b f j v
b f v f k i w j l b h k r i g
t r h g n i u h i m p o u w

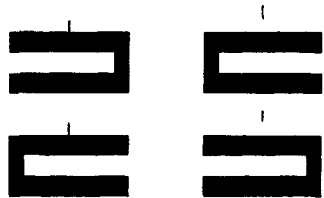
Figure 12.60. Stereopsis from nonmatching letters.
The central region of letters appears to be in front of or behind the unpaired upper and lower rows. The disparity is defined with respect to unpaired columns of letters on the left- and righthand edges of the images. (Adapted from Kaufman 1965.)

contributes to the impression of depth, as opposed to opacity, because a type of disparity is present. The images in the two eyes extend by different amounts on either side of the fixation point. Thus, a disparity exists between the whole image (inner square plus monocular flank) in one eye and that in the other, relative to the images of the square. This, rather than monocular occlusion, could be responsible for the impression of depth. This question is now considered in more detail.

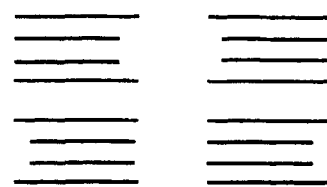
12.6.5 Monocular occlusion and stereopsis

Euclid noticed in 300 BC that one eye sees a part of a sphere not seen by the other eye. Galen, in the second century AD, described how part of a more distant surface is seen by only one eye. Leonardo da Vinci noticed the same thing in the fifteenth century and commented on its role in creating an impression of depth (see Section 1.2.2). Thus the possibility that monocular occlusion plays a role in depth perception was mentioned before anyone suggested that disparity between corresponding images had anything to do with depth perception. After Wheatstone's conclusive demonstration of the role of disparity, people forgot about the possible role of monocular occlusion and interest in this factor has only recently been revived.

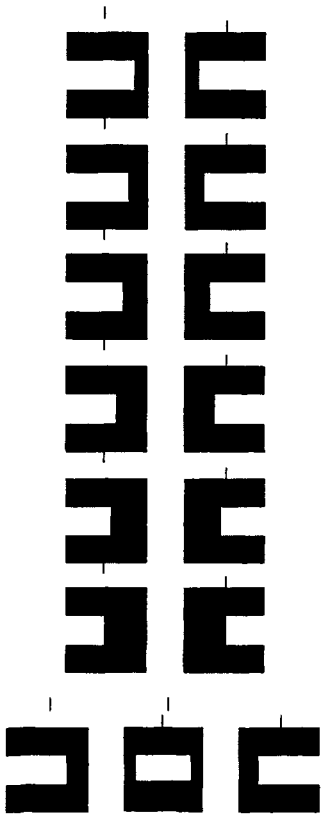
The impression of depth in Panum's limiting case after the effects of misvergence have been allowed for, provides an example of stereopsis from monocular occlusion. The sieve effect described in



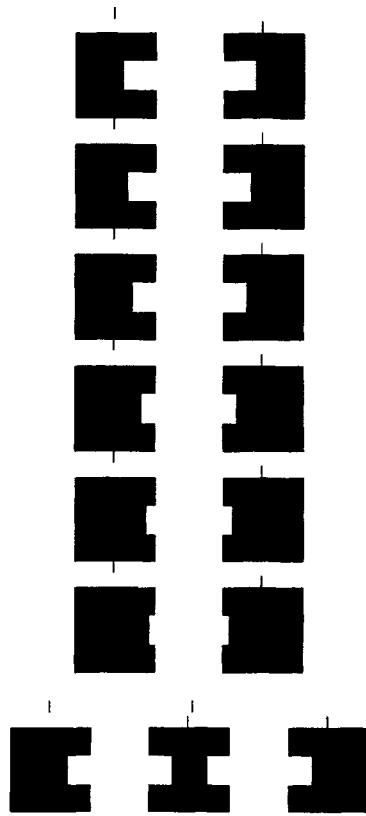
(a) The cross-fused stereogram appears as a white rectangle in front of a black rectangle. The other appears as a white rectangle seen through a black rectangle. The nonius lines are offset in opposite directions in the two cases, showing that the eyes are misconverged. (Adapted from Liu et al. 1994.)



(b) The horizontal boundaries in (a) contain disparities that create the same depth impressions. (From Gillam 1995.)



(c) Convergent fusion of the six stereograms creates the display at the bottom, in which a white rectangle appears to stand out. The depth and nonius offset increase down the set.



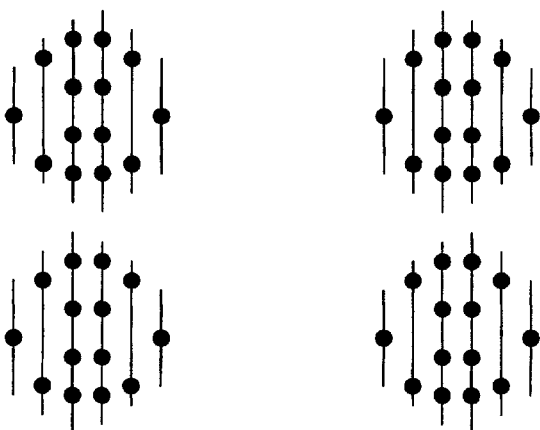
(d) Convergent fusion of the six stereograms creates the display at the bottom, in which two white rectangles appear to stand out. The depth and nonius offset increase up the sets.

Figure 12.61. Stereopsis from shapes lacking corresponding vertical edges.

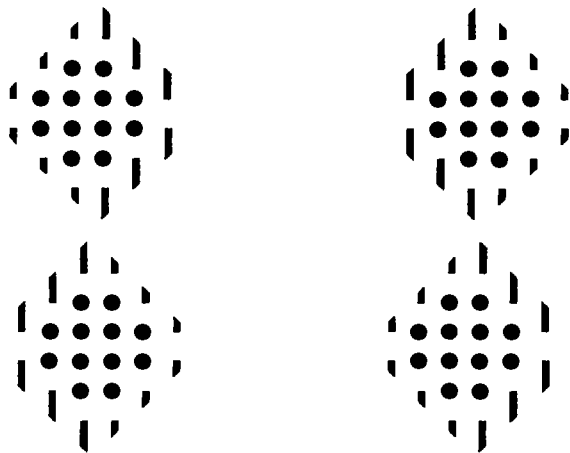
Section 7.8.3 can also be regarded as an example of stereopsis from monocular occlusion. In each rivalrous disc of the display, one eye sees a black disc in a ring where the other eye sees a white disc in the ring. This creates the same impression as that created by viewing a dotted surface through a small black-rimmed hole, as illustrated in Figure 7.75. Note that there are no disparities in the display shown in Figure 7.3.

Liu et al. (1994b) recently produced another demonstration of stereopsis from monocular occlusion, using a stereogram like that shown in Figure

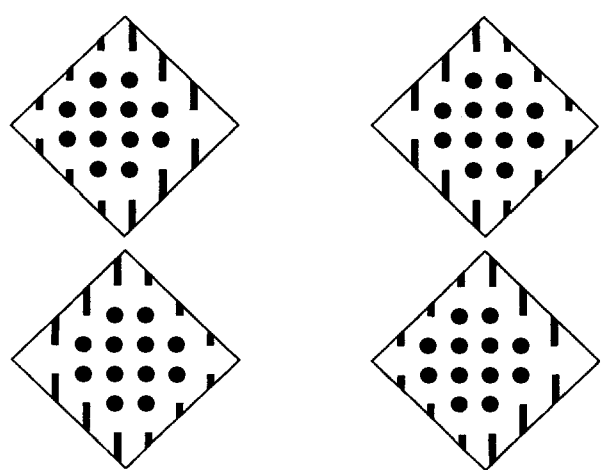
12.61a. When the images are fused with divergence, a white rectangle stands out from a black rectangle, and when viewed with convergence, the white rectangle appears through a hole in the black rectangle. There are no corresponding lateral edges in the white rectangle by which horizontal disparity can be generated, and Liu et al. argue that the effects arise from the black monocular zones that occur at each end of the white rectangle in the fused image. The proximal stimulus is equivalent to that produced by a white rectangle partially occluding or seen beyond a larger black rectangle. However, there are possible



(a) Fused by divergence, the upper stereogram creates a display seen through a diamond-shaped aperture. Edges of the aperture appear as a subjective contour. The lower stereogram creates an ambiguous impression of depth. (Adapted from Anderson 1994.)



(b) The edges of the subjective aperture are straighter when the line elements have slanting ends.



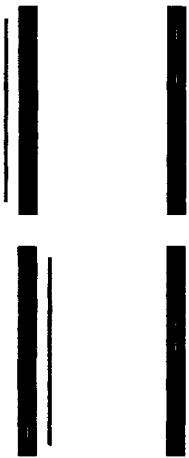
(c) Addition of outlines illustrates the disparity between the images of the subjective aperture.

Figure 12.62. Stereopsis and monocular occlusion.

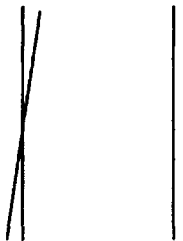
artifacts here. Gillam (1995) pointed out that disparities between the horizontal boundaries create the same relative depth as that created by the Liu et al. figure. (see Figure 12.61b) Furthermore, when nonius lines are placed on the images with the attention focused on the illusory depth of the white rectangle, the nonius lines can be seen to separate horizontally. This shows that a disparity is induced into the images of the black rectangle—a crossed disparity when the black rectangle appears nearer than the white rectangle and an uncrossed disparity when it appears beyond the white rectangle. The images of the white rectangle do not acquire a disparity since they have no overlapping vertical edges. The illusory depth in this figure could therefore arise from an illusory depth of the black rectangle relative to the white rectangle. The white rectangle defaults to the plane of convergence (zero disparity). To prove that occlusion zones create depth in their own right, one would have to show that the depth effect survives when the eyes are correctly converged on the black rectangle. Misconvergence on the black rectangles must be due to the asymmetry of the images. It is as if the edges with opposite luminance polarity repel each other.

When the white element in each image is shorter than half the width of the black element, as in Figure 12.61d, the white rectangle in the fused image breaks into two and the depth relations are reversed from when the white element is wider than half the black rectangle (Figure 12.61c). Note that the white elements are on the inside of the black rectangles in the first set and on the outside in the other set. If the two sets of stereograms are viewed with convergent fusion, the perceived depth relations are the same in the two sets. Perceived depth increases as the length of the white elements in Figure 12.61d is increased and the length of the white elements in Figure 12.61c is decreased. In both cases, the offset of the nonius lines above each stereogram increases with the increasing apparent depth of the white rectangles, as one would expect if the effects were due to vergence-induced disparity in the black elements. To prove that the effect is due to monocular occlusion, as suggested by Liu et al., requires vergence control.

Anderson (1994) recently demonstrated another example of how monocular occlusion can serve as a cue to depth in the absence of disparity. The effect is demonstrated in Figure 12.62a. The black dots are identical in the two eyes but the lines in one eye are longer than those in the other. This difference in length could perhaps induce apparent slant, as discussed in Section 7.6.5. But instead of slant one sees the lines and dots in a frontal plane through an aperture. One end of each line is seen only by one



(a) When fused by divergence, the top stereogram is in the occlusion configuration and the bottom stereogram is in the camouflage configuration. The thin vertical line appears beyond the wide bar in the occlusion configuration and nearer than the black bar in the camouflage configuration. The white nonius lines are aligned when the eyes are accurately converged on the black bar. Note that there is a tendency for the nonius lines to drift apart in opposite directions in the two stereograms.



(b) Fusion of the vertical lines creates two lines inclined in depth.

Figure 12.63.. Panum's limiting case.

eye and this creates the impression of a contour occluding the image of one eye. These impressions of an occluding contour become integrated into a continuous edge of an aperture. The impression of a straight occluding edge is enhanced when the ends of the lines are cut at an angle, as in Figure 12.62b. This depth effect produced by occlusion seems to be free of vergence artifacts.

In Figure 12.62c the subjective aperture has been replaced by a real frame. There is now a horizontal disparity between the frame and the contents of the frame. In Figure 12.62a there is a disparity between a subjective frame created by the monocular occlusions and the contents of the subjective frame. Anderson and Nakayama (1994) have reviewed the role of monocular occlusion in stereoscopic vision.

12.6.6 Occlusion and Panum's limiting case

In Panum's limiting case one eye views a single vertical bar and the other eye views the same vertical

bar flanked on the temporal side by a vertical line, as in the upper part of Figure 12.63a. This is the occlusion configuration. When the two images of the bar are fused by divergence or in a stereoscope, the monocular line appears to lie beyond the bar, in accordance with the rules mentioned in Section 12.6.1. The white lines in the bars are nonius lines aligned in the fused image when the eyes are properly converged on the bar. In the lower part of Figure 12.63a the monocular line is on the nasal side of the binocular bar when the images are fused with divergence. This is the camouflage configuration. For many people this causes the line to appear in front of the bar, also in accordance with the rule mentioned in Section 12.6.1. Figure 12.64 is a random-dot stereogram version of Panum's limiting case (Allik 1992). For each dot in one eye there is a matching dot in the other eye plus a neighbouring unmatched dot. When fused, the stereogram creates two planes of dots, one containing the binocular dots and the other containing the monocular dots. Panum's limiting case has been regarded as a puzzle because there are no obvious disparities in the display; the binocularly fused bar has zero disparity, and the monocular line has no corresponding image in the other eye.

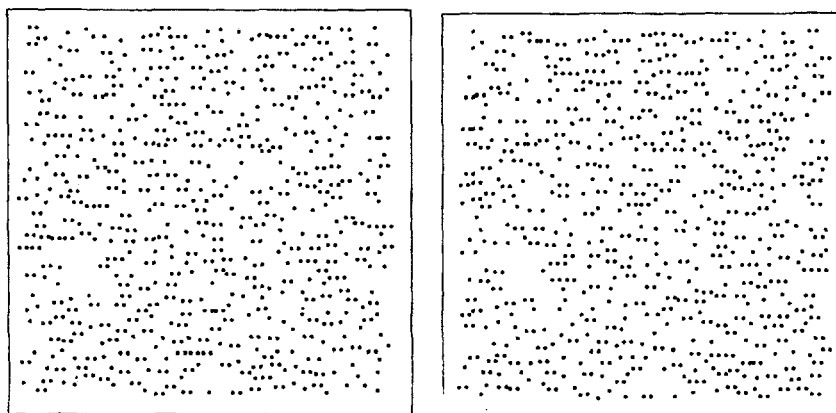
The following five theories have been proposed to account for the impression of depth in Panum's limiting case. Each theory can be extended to account for depth in the camouflage configuration.

The stimulus configuration theory

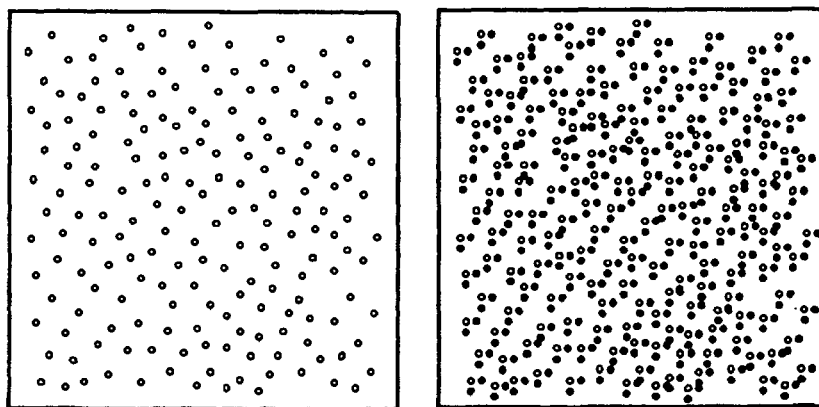
According to this theory, monocular occlusion and camouflage create impressions of relative depth in the absence of disparity information. The visual system interprets the depth of monocularly occluded or camouflaged objects according to the rules listed in Section 12.6.1. This is not to say that the process is conscious, or even that it involves high-level cognitive processes.

Double-duty image matching

Many investigators have agreed with Hering (1879) that Panum's limiting case may be explained in terms of an ordinary disparity-detecting process without recourse to inferential processes. He proposed that one of the images of the binocular bar is paired with the image of the bar in the other eye and at the same time with the monocular image of the line in the other eye. It is assumed that the eyes are accurately converged on the bar so that its images fall on corresponding points, and that the bar appears in the plane of convergence. The uncrossed disparity between one image of the bar and a monocular line on the temporal side creates the impression that the line is beyond the bar, and the crossed



(a) For each dot in one eye there is a matching dot in the other eye plus a neighbouring unmatched dot. The single and double dots are distributed between the eyes so the total number of dots is the same in the two eyes. When fused, the stereogram creates two depth planes. (From Allick 1992, Perception, 21, 731-746, Pion, London.)



(b) A random-dot stereogram version of Panum's limiting case with additional monocular dots placed vertically below each binocular element.

Figure 12.64. Random-dot stereograms of Panum's limiting case.

disparity between one image of the bar and a monocular line on the nasal side creates the impression that the line is nearer than the bar. If this is the correct explanation, it provides the only exception to the unique-matching rule, which states that an image in one eye is matched with only one image in the other eye at any one time (see Section 6.2.2). Note that Hering's theory does not imply that the image in one eye fuses with two images in the other eye, but only that disparities are detected between an image in one eye and two images in the other.

Disparity between distinct spatial-frequency components
The images of the bar and the line in one eye can be considered to form one low spatial-frequency image with its centroid between the bar and the line. The disparity between this low spatial-frequency image and the single image in the other eye could be compared with the zero disparity between the images of

the bar. This would involve a type of double-duty matching of images, but the two matches would occur within distinct spatial-scale channels and therefore could be regarded as occurring between distinct pairs of stimuli. Double-duty matching in different spatial scales can be tolerated, since it does not seriously disrupt the image-matching process.

Vergence-induced disparity account

Perceived depth in Panum's limiting case could be due to disparity induced into the images of the binocular bar by vergence eye movements. This idea was first stated by Lau (1925) and reiterated by Kaufman (1976). Suppose that the eyes are accurately converged on a single vertical bar with nothing else in view. When a monocular line is placed on the temporal side of the binocular bar, as in Panum's limiting case, the symmetry of the images in the two eyes is disturbed. The bar and the line in one eye

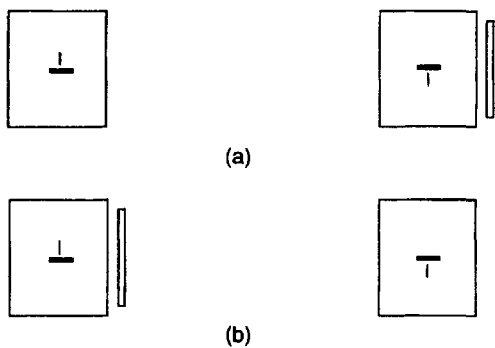


Figure 12.65. Stereograms from Nakayama and Shimojo (1990).
 (a) A monocular line on the temporal side of a binocular rectangle produced the occlusion configuration.
 (b) A monocular line on the nasal side of the rectangle produced the camouflage configuration. The rectangle subtended 137 X 417 arcmin at 70 cm. The nonius lines within the rectangles indicated when the eyes were converged on the rectangle.

form one low spatial-frequency image with its centroid shifted towards the monocular line. The disparity between this image and the single image in the other eye evokes divergence which injects a crossed disparity (fixation disparity) into the images of the bar. At the same time, the two images of the bar provide a high spatial-frequency disparity signal to the vergence lock system, which prevents the fixation disparity from exceeding the limits of Panum's fusional area. The induced disparity in the images of the bar cause it to appear nearer than the monocular line. When the monocular line is placed on the nasal side of the bar, the resulting image asymmetry induces convergence, which injects an uncrossed disparity into the images of the bar. This causes the bar to appear beyond the monocular line. In both cases the unpaired image of the line conveys no disparity information to the stereoscopic system and is therefore treated like a binocular image with zero disparity and, like a zero-disparity image, appears in the horopter (the plane of convergence). In this account it is assumed that the low-frequency disparity induces vergence but does not play a direct role in perceived depth, but the theory would not be substantially altered if this assumption were relaxed.

Fusion of the stereogram shown in Figure 12.63b creates the impression of two lines inclined in depth. In this case, one can argue that the cyclodisparity between the vertical line in one eye and the centroid of the two lines in the other eye induces cyclovergence, which injects cyclodisparity between the images of the vertical lines. The fused vertical line therefore appears inclined in depth relative to the monocular tilted line. The monocular tilted line also appeared inclined in depth, probably because of depth contrast.

In Hering's double-duty disparity theory the binocular bar has a zero disparity and appears in the plane of convergence, and the monocular line appears displaced in depth because of disparity between it and one of the images of the bar. According to the vergence theory, the monocular line appears in the plane of convergence and the binocular bar is displaced in depth because of a disparity induced in its images.

The rule that unpaired monocular images are defaulted to the horopter was proposed by Aguilonius in 1613 and has wide application. Because of its importance we call it the **horopter default rule** for unpaired images. This rule does not apply if the monocular images are seen as belonging to a textured surface. In that case, monocular images in the occlusion configuration are seen as part of a surface behind an occluding object, and those in the camouflage configuration are seen as part of a transparent textured surface lying in front of an object. In both cases the images are defaulted to the depth of those surfaces, whether or not they lie in the horopter. We call this the **similar-surface default rule** for unpaired images.

The vergence theory of Panum's limiting case has two bonuses. It does not violate the unique-matching rule for images of similar spatial scale and it avoids the problem of having to explain how disparities far beyond the fusion limit can code depth.

Monocular figural repulsion

In the figural aftereffect a line causes a neighbouring line in the same frontal plane to appear displaced from the inspection line. In this effect both lines are seen by the same eye or by both eyes. If this effect operates in Panum's limiting case, the monocular line would repulse the image of the bar in the same eye and thus create a disparity between the two images of the bar. Westheimer (1986a) found the figural repulsion effect to be too small to account for Panum's limiting case. The evidence for these theories of Panum's limiting case is now considered.

Empirical studies of Panum's limiting case

Nakayama and Shimojo (1990) presented evidence which favours the configuration theory of Panum's limiting case. Stereograms such as those shown in Figure 12.65 created an impression of depth only if the monocular line was on the temporal side of the binocular rectangle. When the monocular line was on the nasal side—the camouflage configuration—only one of the three subjects saw the line nearer than the bar, which is where it should appear according to all theories. In the quantitative part of the experiment, subjects maintained their vergence

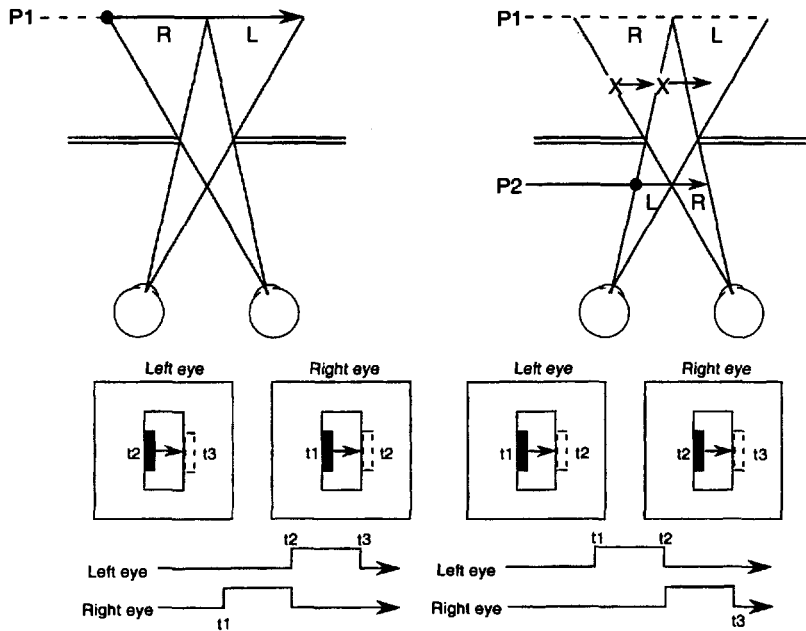


Figure 12.66. Spatiotemporal aspects of motion past a slit.

The top figures are the plan views, the middle figures are the front views as seen by the subject, and the bottom figures show the temporal relationships of the monocular bars passing behind the apertures. In the three figures on the left the moving bar appears in the left eye just as it disappears from the right eye. This created the impression of smooth motion of the bar behind the aperture. In the three figures on the right the bar appears in the eyes in reversed order. This created the impression of two bars moving side by side behind the slit. The bars were 1.7° apart and the aperture was 20 arcmin wide at a viewing distance of 80 cm. (Adapted from Shimojo et al. 1988.)

on the binocular rectangle, as indicated by the alignment of nonius lines. The magnitude of perceived depth between the rectangle and the line, as indicated by the settings of a depth probe, was found to be a function of the distance between the line and the edge of the rectangle for distances of up to about 30 arcmin. This result is compatible with the configuration theory and with Hering's theory. It is not compatible with the vergence theory if vergence was truly held on the binocular rectangle.

Shimojo et al. (1988) created a stereoscopic display simulating an object moving from left to right behind a screen containing a binocular aperture, as in Figure 12.66. As the object moved, it was seen first by only the right eye and then by only the left eye. This created an impression that the moving object was behind the aperture. If the observers were using the sequentially perceived disparity between the moving images, they would have continued to see depth when the time order of the two images was reversed, leaving the direction of motion and the sequential disparity the same. However, under these circumstances, the impression of depth gave way to an impression of two objects moving just behind the aperture. Thus, it was argued that an impression of depth requires a correctly ordered sequence of

monocular images moving in an appropriate direction and signed with respect to eye of origin. This phenomenon does not uniquely support the theory that elevates monocular occlusion to the rank of an independent depth cue.

Howard and Ohmi (1992) recently demonstrated that misconvergence accounts for much of the depth in Panum's limiting. It was first established that a monocular image induces fixation disparity in a neighbouring binocular line. The subject fused the dichoptic images of a black vertical bar. A white nonius line was superimposed on each image of the bar, as shown in Figure 12.63. A black vertical line was added about 0.5° to the right of the bar. This line was visible either only to the right eye (temporal line) or only to the left eye (nasal line). All subjects reported that the line on the temporal side induced a crossed disparity, as indicated by the displacement of the nonius lines. Not all the subjects saw depth, but those who did saw the binocular bar nearer than the monocular line. This is monocular occlusion, or the classic Panum effect. The line on the nasal side induced an uncrossed disparity, which showed as an uncrossed displacement of the two nonius lines. The binocular bar now appeared to be beyond the monocular line. This is monocular camouflage.

Thus, the expected fixation disparities predicted by the vergence account certainly occur and in directions appropriate to the resulting depth impressions. However, this in itself does not disprove the other two theories. Both the configuration theory and Hering's theory state that the direction of perceived depth in Panum's limiting case depends on whether the monocular line is on the temporal or the nasal side of the binocular bar. The vergence theory states that the direction of perceived depth depends on the sign of the disparity induced into the binocular bar. Thus, according to this theory, reversing the sign of fixation disparity will reverse the sign of perceived depth, whether the monocular line is on the temporal or the nasal side of the binocular bar.

To test these conflicting predictions, Howard and Ohmi used the stereogram shown in Figure 12.67. A vertical line was presented on both sides of the bar in one eye. The line on the temporal side was in the occlusion configuration and that on the nasal side was in the camouflage configuration. A white fixation spot was presented dichoptically on the bar with various crossed or uncrossed disparities so that the dot appeared to be in various positions in depth. The offset of two nonius lines was tied to the disparity in the fixation dot so that when the subject converged on the spot, the nonius lines appeared to be aligned. In this way vergence was controlled. For each setting of the dot the subject fixated the dot and reported the relative positions in depth of the bar and each monocular line and also the depth of one monocular line relative to the other. When the white dot forced subjects to converge nearer than the bar, they reported that both monocular lines appeared closer than the bar and when they converged beyond the bar, they reported that both monocular lines appeared beyond the bar.

It was concluded that the apparent depth of a monocular object relative to an adjacent binocular object is determined mainly by disparity induced into the images of the binocular object by vergence. Monocular objects simply default to the plane of zero disparity (the plane of convergence). Only the vergence theory can account for the fact that both the temporal and nasal monocular lines appeared nearer or beyond the binocular bar, depending on the state of convergence. The contour repulsion effect would not operate with the display used in this experiment because a monocular line was on both sides of the image of the bar in one eye, so contour repulsion effects cancel.

Jaensch (1911) had also noticed that depth in Panum's limiting case is reversed when the eyes are unnaturally converged. He concluded that convergence causes the monocular image to fuse with the



(a) When the white spot is fixated and the nonius lines are aligned, the images of the black bar have zero disparity. Most observers report that the line on the left appears beyond the bar and that on the right nearer than the bar.



(b) Fixation of the offset white spot and nonius lines creates a crossed disparity in the black bar, which makes both monocular lines appear beyond the bar.



(c) Fixation of the offset white spot and nonius lines creates an uncrossed disparity in the black bar, which makes both monocular lines appear nearer than the bar.

Figure 12.67. Panum's limiting case and misconvergence.
A monocular line is presented on both sides of one image of the binocular bar. With divergent fusion, the line to the left of the bar is in the occlusion configuration and that to the right is in the camouflage configuration. (From Howard and Ohmi 1992.)

other image in the other eye, bringing the unfused image onto the nasal side and hence into the camouflage configuration. He argued that an unfused image on the temporal side, evokes a "convergence impulse" which causes it to appear behind. When the unfused image is on the nasal side, it evokes a "divergence impulse" which causes it to appear in front. He did not mention the disparity in the fused images produced by these vergence impulses.

We conclude that the apparent depth of a monocular line relative to a binocular bar in Panum's limiting case with relaxed vergence is mainly due to the effects of vergence induced by the dichoptic asymmetry of the images. The vergence induces a disparity into the binocular bar, which

appears displaced in depth relative to the monocular line. Since the monocular line has no matching image in the other eye, it defaults to the plane of zero disparity. Perhaps stereoscopic depth induced by disparities of more than about 30 arcmin is also due to vergence-induced disparities of much smaller magnitude. This issue is discussed in Section 6.2.9.

When subjects in Howard and Ohmi's experiment converged in the plane of the bar, the line in the occlusion position still appeared beyond the occluding bar and the line in the camouflage configuration appeared nearer than the bar. Thus, occlusion and camouflage create an impression of depth after one allows for the effects of misvergence. Nakayama and Shimojo (1990) also controlled vergence and found that apparent depth in the occlusion configuration is a function of lateral separation between line and bar.

This effect could be explained either by the stimulus configuration theory or the theory that assumes that the bar and line images in one eye are treated as a single low spatial-frequency stimulus. Ono et al. (1992) found an occlusion effect when vergence was held constant in the plane of a binocular bar but only when the monocular object was one that could be occluded by the binocular object. In other words, the display had to be ecologically valid. This supports the stimulus-configuration account rather than the low spatial-frequency disparity account, since the registration of low spatial-frequency disparity should not depend on ecological factors.

There is no reason to assume that depth in Panum's limiting case is due to double-duty matching of retinal images. Therefore, Panum's limiting case does not provide an exception to the unique-matching rule. Gettys and Harker (1967) found that perceived depth in Panum's limiting case was proportional to the lateral separation between the binocular and monocular stimuli up to a limiting value, which was as high as 55 arcmin when free eye movements were allowed. Westheimer (1986) found that the apparent depth in Panum's limiting case declined to zero when the lateral separation between the monocular and binocular images was increased to 30 arcmin. It was concluded in both of these studies that binocular and monocular images engage in double-duty matching. But vergence was not controlled in these experiments. We would say that the tendency for the monocular line to induce vergence increases as its distance from the binocular bar increases up to a certain point.

Weinshall (1991) claimed that multiple depth planes seen in an ambiguous random-dot display were due to double-duty disparity matching. However, she has recently produced evidence that

this is not the case (Weinshall 1993). The double-nail illusion (Krol and van de Grind 1980) has also been interpreted as being due to double-duty disparity matching. But it was shown in Section 2.3.5 that this effect is due simply to convergence slipping into a plane midway between the rods, which causes the image of the near rod in the left eye to fuse with the image of the far rod in the right eye and vice versa. Since there are no unfused images, and hence no disparities with respect to the plane of convergence, the stimulus is identical to that produced by two rods in the plane of convergence (Ono 1984).

Other evidence reviewed in Section 6.2.2 provides no conclusive support for the idea of double-duty disparity matching. We can abandon the idea that depth sensations in Panum's limiting case arise from the large disparity between the monocular line and the binocular bar. However, there may be a contribution from the disparity between the two stimuli in one eye considered as a one low spatial-frequency stimulus and the single stimulus in the other eye.

12.7 DEPTH-SPECIFIC VISUAL PROCESSES

It would be a great advantage to an animal with stereoscopic vision to be able to process information in the depth plane on which the eyes are converged, without interference from stimuli arising from other depth planes. One obvious advantage would be that widely disparate images outside the plane of convergence and the illusory direction signals arising from them could be more easily ignored. There is a growing body of evidence for this type of selective visual processing. The rule governing depth specificity is not always the same. For instance, pursuit eye movements are induced by the display in the plane of convergence, but illusory self-motion (vection) is evoked by the more distant of two moving visual displays, even when the eyes are converged on the nearer display.

12.7.1 Apparent brightness and relative depth

The apparent brightness of an achromatic surface depends on the luminance of other surfaces that the viewer assumes are illuminated by the same light source and oriented to the light source at the same angle. Two coplanar surfaces with the same reflectance appear the same brightness. If the perspective in boundaries or in the texture of one surface is adjusted to make the surface appear inclined, its apparent brightness relative to a coplanar surface changes (Gilchrist 1980). Similarly, the perceived brightness of a constant-luminance test patch varies

with the luminance of the surface with which it is coplanar. Schirillo and Shevell (1993) adjusted the disparity of a constant-luminance test patch so that the patch appeared in the same depth plane as a nearer brightly illuminated or a more distant dimly illuminated checkered display. The change in apparent depth did not affect the physical contrasts of the three displays. When in the plane of the highly illuminated display, the test patch appeared 15 per cent brighter relative to a constant comparison patch than when it was in the plane of the less well illuminated display. Judgments of the lightness (shade of gray) of the test patch were similarly affected. Thus local contrast in the monocular image is not sufficient to account for perceived lightness of adjacent patches when the relative distances of the patches changes.

In whiteness contrast, a gray patch on a dark ground appears whiter than a gray patch on a light ground, as in Figure 12.2a. For objects in the same frontal plane, the magnitude of whiteness contrast decreases with increasing lateral separation between the two patches (Freeman 1967). Mershon and Gogel (1970) asked subjects to scale the perceived whiteness of a gray test patch as it was moved stereoscopically out of the plane of a dark background patch. Whiteness contrast decreased with increasing depth between the two patches. Gibbs and Lawson (1974) found that depth contrast remained the same when the gray test patches were stereoscopically nearer or further away than the inducing patches.

12.7.2 Threshold-elevation effect and relative depth

The contrast threshold for detecting a luminance grating is elevated for some time after exposure to a grating with a similar spatial frequency (see Section 9.3.6). Felton et al. (1972) found the threshold-elevation effect to be maximum when induction and test gratings were in the same disparity depth plane and to be reduced when they were in distinct depth planes, after allowing for effects of changed relative phases and eccentricities of the two gratings. They used gratings with spatial frequencies of between 0.2 and 7.6 c/deg and disparities of up to 1.25°. Blakemore and Hague (1972) obtained similar results and concluded that disparity tuning functions have a half-width at half-amplitude of less than 10 arcmin. Long and Over (1974a) measured disparity-selective masking using a random-dot stereogram containing a central square offset from a background. The contrast threshold for the detection of depth in the stereogram was elevated maximally after exposure to an adaptation stereogram with the same disparity. The disparity tuning functions inferred from their data have a half-width at half-amplitude of about 2

arcmin, which they suggested is the tuning width of fine disparity detectors used in the perception of depth in random-dot stereograms. The threshold-elevation effect for stereopsis is related to depth aftereffects, which are discussed in Section 12.2.

12.7.3 Depth-specific figural effects

Visual sensitivity and apparent depth

An apparent change in depth associated with figure-ground reversal is sufficient to induce changes in visual sensitivity. A test spot superimposed on a reversible figure-ground display, such as Rubin's cross, is detected at a lower luminance when the region it is superimposed on is seen as a foreground figure than when the same region is seen as ground (Frank 1923; Wong and Weisstein 1982).

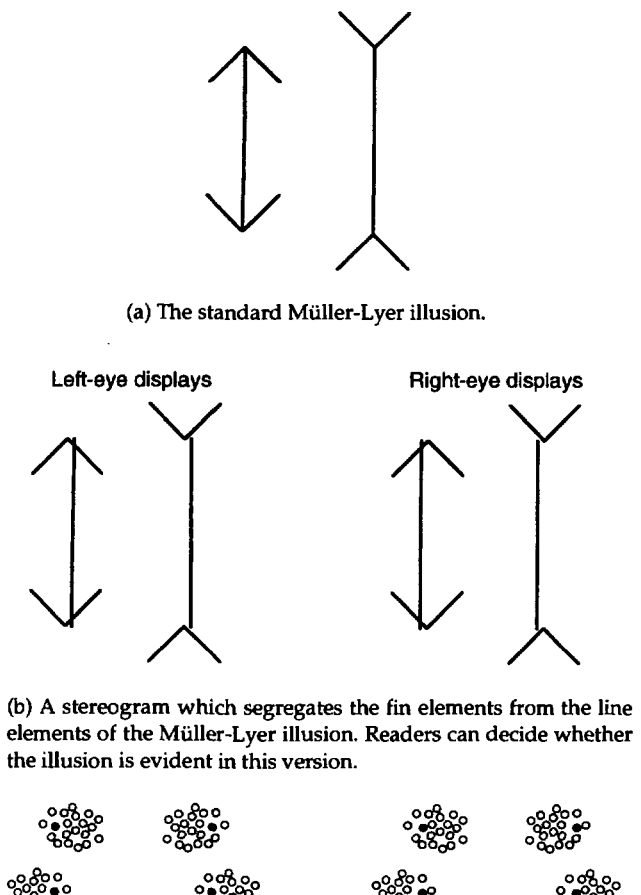
Metacontrast and relative depth

A briefly presented visual pattern is not seen when followed by a stimulus (mask) in a nearby location with an interstimulus interval (ISI) of between 40 and 80 ms. This is known as metacontrast. Lehmkuhle and Fox (1980) constructed a dynamic random-dot stereogram containing an annular mask and a disc-shaped test stimulus. Metacontrast was reduced when the test stimulus was nearer than the mask but not when it was beyond the mask. Thus, the strength of metacontrast varies as a function of the depth between the mask and the test stimulus. It seems that greater weight is given to an object in the foreground than to one in the background. A similar depth-dependent effect has been found for simultaneous masking of a patterned area by a surrounding annulus (Fox and Patterson 1981).

Geometrical illusions and relative depth

The distortion induced into a test figure in the Ponzo illusion (see Figure 9.13b) was reduced when the test lines were placed stereoscopically out of the depth plane of the V-shaped inducing stimulus (Greene et al. 1972; Gogel 1975). Similarly, the apparent tilt of a vertical line induced by a tilted frame (the rod-and-frame effect) was reduced when the rod was brought closer to the viewer than the frame (Gogel and Newton 1975). Gogel subsumed such effects under the term "adjacency principle".

The Müller-Lyer illusion, shown in Figure 12.68a, and related illusions can be described as a tendency to judge the separation of two clusters of stimuli in terms of the separation between the centroids of the clusters. The illusion is perhaps less evident when the fins and the enclosed lines are stereoscopically separated in depth (Figure 12.68b). The black dots in Figure 12.68c seem further apart when embedded in



(c) The type of stimulus used by Harris and Morgan (1993). The two-dimensional illusion is seen by comparing the separations of the upper and lower pairs of black dots in one half of the stereogram, and the three-dimensional version is seen by making the same comparison after the two halves are fused.

Figure 12.68. Stereopsis in the Müller-Lyer illusion.

dot clusters that are relatively nearer to each other. It is as if we are pulled in the direction of judging the separation between the dot clusters rather than that between the isolated dots within the clusters. Harris and Morgan (1993) stereoscopically separated the black dots and the dots in the clusters into two depth planes, as in Figure 12.68c, and found that the illusion was no longer evident for most of their subjects.

12.7.4 Stereopsis and segregation of motion

Stereopsis and the barber-pole illusion

There is an essential ambiguity in the perceived direction of motion of a grating seen through an aperture. For instance, a grating moving diagonally within a circular frame, as in Figure 12.69a, is physically equivalent to one moving in any direction between straight down and straight across. The reason

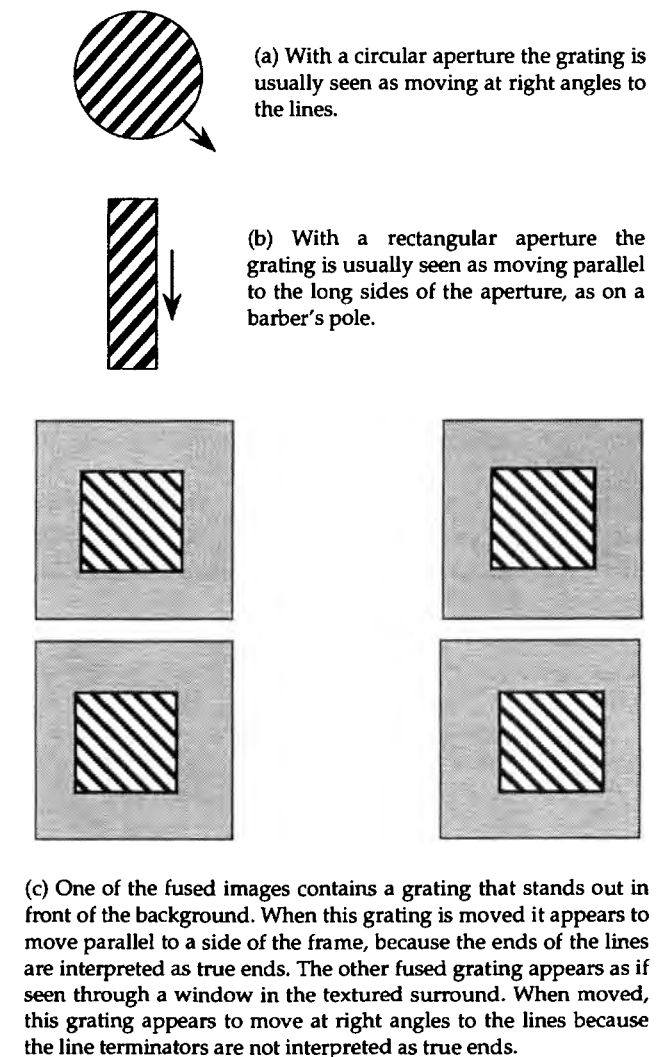


Figure 12.69. Ambiguous direction of aperture motion.

for this ambiguity is that featureless lines provide no information about whether they are moving along their length. Motion of lines within a circular frame is usually interpreted as occurring at right angles to the lines because, on average, the ends of the lines move in this direction. With a rectangular frame, obliquely moving lines appear to move parallel to the long sides of the frame, as in the barber-pole illusion (Figure 12.69b) because the ends of the lines move predominantly in this direction. These biases occur because the line ends are regarded as true (intrinsic) ends and not as extrinsic ends due to occlusion by the frame. When a moving grating stereoscopically stands in front of a stationary surround, as indicated in one of the fused images of Figure 12.69c, the ends of the lines are unambiguously true ends and the motion is seen in the direction of motion of the ends, that is, parallel to one or other side

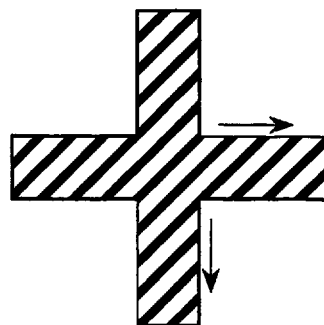
of the frame. When the grating is seen through a stereo aperture, as in the other part of Figure 12.69c, the line ends become occlusion boundaries of an extended grating, and the motion is seen at right angles to the lines rather than parallel to the edges of the aperture (Shimojo et al. 1989). Thus, the perception of motion depends on the way line ends are interpreted, which can depend on stereo cues.

It is fashionable to argue that because one percept depends on another it must be processed at a later stage. According to this logic the way line ends are interpreted must precede the interpretation of motion. But the logic is flawed. There is no reason why the outcome of a perceptual process should not feed back to an earlier stage or to a parallel stage and affect what is occurring there. Without supporting anatomical or physiological evidence, one cannot draw firm conclusions about the order in which sensory qualities are processed merely from the way one perceptual phenomenon depends on another.

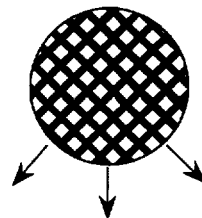
Ho and Berkley (1991) devised an interesting variant of the barber-pole illusion. Two barber poles were superimposed in the form of a cross-over, in which the lines moved diagonally, as in Figure 12.70a. The initial impression is of coherent diagonal motion but this gives way to the impression of lines moving vertically down in the vertical frame, together with a set of lines moving horizontally within the horizontal frame. Figure-ground rivalry occurs at the intersection; at any time one of the coexisting displays appears to stand out and occlude the other. A subjective boundary is created along the edges of the grating which appears in front. When one of the barber poles is made stereoscopically in front of the other, it dominates as the figure most of the time.

Stereopsis and perception of superimposed motions

When a textured surface is seen through a transparent textured surface the independent motion of the two surfaces is clearly perceived. The perceptual coherence of each surface is preserved in spite of the fact that stimuli moving in opposite directions are present in each location. Perhaps depth cues, including disparity, help in this process of perceptual segregation. However, depth cues are not necessary because two random-dot patterns moving in opposite directions on a computer screen are perceived as two distinct surfaces. At any instant one is seen as nearer than the other but the perceived depth relationship changes spontaneously. The coherence of motion of each set of moving dots must be responsible for the successful segregation of the two moving displays. The Gestalt psychologists referred to this figural coherence of elements sharing a common motion as the "principle of common fate".



(a) The moving grating breaks up into two orthogonal gratings, each moving parallel to one arm of the cross and with one appearing in front of the other. This impression is fostered when the lines in one arm are stereoscopically separated in depth relative to those in the other arm. (Ho and Berkley 1991.)



(b) Two gratings moving orthogonally are seen as two segregated gratings or as a coherent plaid moving in an intermediate direction. When the gratings are seen in different depth planes the impression of two segregated gratings predominates.

Figure 12.70. Patterns of motion segregation.

Two superimposed parallel gratings moving at the same speed in opposite directions create the impression of a stationary grating flickering in counterphase. This is not surprising because the two stimuli are physically equivalent. Two oblique, orthogonal square-wave gratings moving in opposite directions past an aperture (Figure 12.70b) can be seen as a coherent plaid moving in an intermediate direction or as two independent gratings sliding over each other, each moving in a direction orthogonal to the lines of the grating. The ambiguity arises, as in the barber-pole illusion, because the lines provide no information about motion along their length. This is known as a plaid display. It has been proposed that component motion of each grating is first detected in the visual cortex and these motion signals are synthesized into coherent plaid motion at a higher level, possibly in the middle temporal area (MT) (Movshon et al. 1985). Coherent motion is most likely when the two gratings are similar in contrast and spatial frequency. Component motion tends to be seen when the gratings differ in either of these ways, and it has been concluded that there are distinct motion processes for each of these sensory

attributes (Adelson and Movshon 1982). Most relevant in the present context is the finding that the plaid display is interpreted as two gratings sliding over each other when they are separated in depth defined by disparity (Adelson and Movshon 1984). In both these studies the eyes remained fixated on a stationary point. This is important because if the eyes are allowed to move they could track one or the other grating and null its retinal motion. For orthogonal gratings, the coherent plaid pattern moves faster than either component grating. Simpson and Swanston (1992) found that, when the fixation point was removed and the gratings were in the same depth plane, the eyes tracked at a velocity approaching that of the coherent plaid motion. When the gratings were separated in depth, the eyes tracked at the slower velocity of one or other component grating (see Section 12.7.6). Thus, the motion signals responsible for motion perception are the same as those responsible for evoking pursuit eye movements. Two gratings sliding over each other are more likely to be perceived than coherent motion when luminance relations between the gratings create the impression that one of the gratings is transparent (Stoner et al. 1990). Trueswell and Hayhoe (1993) constructed a plaid display with both transparency and disparity as cues to depth between the component gratings. When the two cues were consistent, only a small disparity was required to create component motion; but when the two cues were inconsistent, much greater disparity was required before coherent motion broke down into component motion. Von Grünau et al. (1993) reported similar results.

Two superimposed dot patterns moving in opposite directions do not generate a motion aftereffect when they are in the same depth plane but do so when they are in distinct depth planes defined by disparity (see Section 13.3.2).

Depth from motion-defined shapes

A shape may be defined by a region of moving random dots within a surround of stationary random dots. As soon as the motion ceases, the shape is invisible. This is known as structure from motion, or **motion-defined shape**. The sensitivity to vernier offset of two motion-defined bars is almost as good as that for two bars defined by luminance contrast (Regan 1986a). The pattern of motion within a motion-defined shape can be graded in velocity to simulate a surface curved in depth, even when disparity indicates that the surface is flat. Richards and Lieberman (1985) reported that subjects accurately perceived a motion-defined solid shape when the region of moving dots was presented with a fixed crossed disparity with respect to the stationary sur-

rounding dots, but not when the moving dots were presented with an uncrossed disparity. Thus, motion-defined shapes nearer than the plane of convergence were more accurately perceived than those beyond the plane of convergence. However, Bradshaw et al. (1987) found that the threshold for discrimination between a flat and a three-dimensional motion-defined shape was the same for crossed as for uncrossed disparities.

The silhouette of a rotating object, such as a bent piece of wire, appears as a three-dimensional object even without disparity cues. As soon as rotation stops, the silhouette appears two-dimensional. This is known as the **kinetic depth effect** and is another instance of structure from motion. A kinetic depth effect is created by an appropriate cyclic transformation of a motion-defined shape. Thus, the kinetic depth effect, like shape, can be independent of luminance-defined contours. Prazdny (1986) formed a motion-defined shape undergoing a kinetic depth transformation and then introduced a disparity into the moving dots so that the shape appeared to lie in a depth plane either in front of or beyond the surrounding plane of stationary dots. The solid shape defined by the kinetic depth effect appeared in a plane defined by the disparity offset of the dots.

An aftereffect of motion is specific to the plane in depth of the moving stimulus that induces it (see Sections 12.7.6 and 13.3.2).

12.7.5 Apparent motion between depth planes

A series of static pictures presented sequentially in adjacent positions generates a compelling impression of motion. To see motion the visual system must relate the elements in one picture to the corresponding elements in the next picture. This correspondence problem in motion is analogous to that in stereoscopic vision, and some of the same stimulus tokens are used in the two cases. For instance, matches between displaced images, like matches between disparate images, are established on the basis of shape, size, orientation (Ullman 1980), luminance polarity, colour (Green 1986, 1989), and proximity (Ullman 1979; Burt and Sperling 1981).

As the distance between two successively presented lights in a frontal plane is increased, a longer time interval is required to create the optimal sensation of apparent motion. Corbin (1942) measured the time interval for optimal apparent motion for two lights in a frontal plane and for two lights lying on an inclined plane, one further away than the other. He found that the distance between the lights in three-dimensional space rather than the angular separation of the lights was the crucial variable

determining the optimal time interval. There were two problems with the display; the surrounding frame changed in angular size and shape when it was inclined, and the stimulus lights were seen obliquely and therefore with smaller retinal area when the display was inclined. Attneave and Block (1973) obtained a similar result when these problems were rectified. Disparity was the principal depth cue in these two studies, although Attneave and Block obtained some effect of perceived depth when the only cue to depth was provided by perspective cues in a surrounding textured surface.

When a stimulus is followed rapidly by two identical flanking stimuli in the same frontal plane, apparent motion occurs in the direction of the flanking stimuli which is closer to the initial stimulus. Ullman (1978) found that the lateral separation of two lights rather than their separation in depth determined which way a stimulus appeared to move. However, his result lacks generality since the only depth cue in the display was the position of line elements in an isometric drawing of a rectangular block.

Mutch et al. (1983) reinvestigated this question using an initial central point of light followed by similar points, one above and one below at different lateral separations and at different depths relative to the initial point. The results confirmed Ullman's finding that the strength of apparent motion is determined by the lateral separation between successive stimuli rather than by their actual or perceived separation in depth. However, when the light point appeared to move in depth it appeared to move at a greater velocity than when it moved through the same visual angle in a frontal plane. It thus covered the greater apparent distance in the same time. Corbin and Attneave and Block measured the quality of motion as it depended on the time interval, rather than the direction of motion, which may explain why their results seem to conflict with the results of Ullman and Mutch et al.

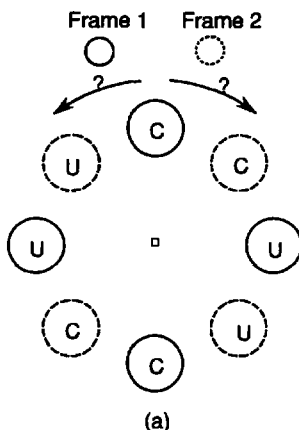
Green and Odom (1986) also produced evidence that apparent motion occurs preferentially between successive stimuli that are in the same depth plane. They concluded that similarity of depth is a token for forming correspondence matches for motion. They constructed a random-dot stereogram consisting of eight 1.3°-diameter discs surrounding a central fixation point. The four discs in the main quadrants were in alternate crossed and uncrossed disparity depth planes and were succeeded by the four diagonal discs, which were also in alternate depth planes relative to the fixation point. One such frame sequence is shown in Figure 12.71. The subject had to say which way the discs appeared to rotate. When the discs were equally spaced, each disc in the first

frame was equally near to a disc in the same plane as it was to a disc in a different plane. With a 24 arcmin disparity difference, subjects saw the discs rotate in a direction corresponding to same-plane image matching. When the difference in depth between the discs was reduced, subjects began to see rotation in the other direction on some trials, and the direction of motion was ambiguous when there was no disparity difference. When the lateral distance between the same-plane discs was made larger than the lateral separation between the different-plane discs, subjects saw the discs rotate in the direction of different-plane matches and the discs appeared to move in depth. It was concluded that although stereo depth can serve as a token for the disambiguation of visual motion, it is secondary to the token of proximity in the same depth plane. But there is another way to interpret these results, as we will now see.

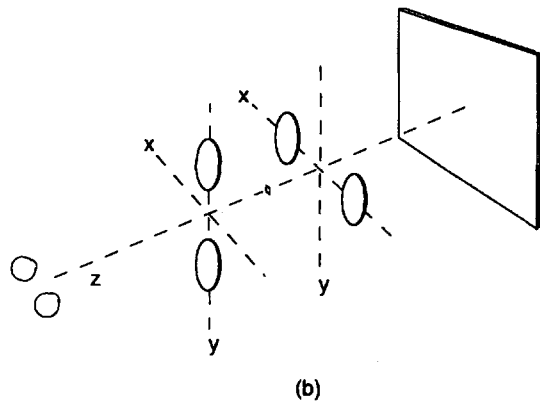
The frontal-plane discs in Green and Odum's display were coplanar but the discs in one depth plane were not coplanar with respect to those in the other depth plane. The same was true of the LEDs used by Mutch et al. Perhaps apparent motion occurs preferentially between stimuli that lie in the same plane, whether this plane is a frontal plane or a plane inclined in depth. He and Nakayama (1994a) arranged four squares in a square configuration, flashing in alternation so that they were as likely to be seen as two squares moving horizontally or as two squares moving vertically. When the whole display was stereoscopically inclined about a horizontal axis, the two horizontal motions were in the same depth plane and the two vertical motions were between different depth planes. All the motions were between squares in the same plane of the motion. Under these circumstances there was no preference for motions within the same depth plane over those in different depth planes. Thus, the important factor governing the ease of seeing apparent motion is the coplanarity of the moving elements rather than whether the motion is in a frontal plane or in depth. He and Nakayama (1994b) produced further evidence that apparent motion occurs preferentially between shapes that lie on a common surface even when the shapes have a different orientation. This suggests that the perception of surfaces upon which objects lie is achieved early in visual processing.

Configurational factors in stereo apparent motion

Apparent motion occurs out of the plane containing the shape when the configurational properties of the stimulus render the impression of motion within the plane improbable (Wertheimer 1912). Thus, a rapid alternation of the two triangles in Figure 12.72a produces an impression of a triangle rotating out of



(a) The four patches marked C were in a crossed-disparity depth plane, and the four marked U were in an uncrossed-disparity depth plane relative to the central fixation point. The set of patches outlined with solid lines alternated with the set outlined with dotted lines. Subjects indicated which way the patches appeared to rotate.



(b) The display, as seen by the subject. (From Green and Odom 1986. Copyright 1986, by the AAAS.)

Figure 12.71. Disparity as a token for apparent motion.

the plane whereas an alternation of the squares in Figure 12.72b produces an impression of a square moving in a frontal plane. An impression of motion out of the plane occurs when triangles are presented in sequence dichoptically, although not as readily as with monocular viewing (Gerbino 1984).

Summary

The many complicating factors in the experiments just reviewed make it difficult to draw firm conclusions. It seems that, other things being equal, apparent motion is seen preferentially between stimuli that appear to lie in the same plane, even though this plane is inclined in depth. However, when configurational cues forbid a good pattern match within the same plane, apparent motion occurs out of the plane containing the moving shape. The issue of whether apparent motion occurs between stimuli presented alternately to the eyes is discussed in Section 13.4.

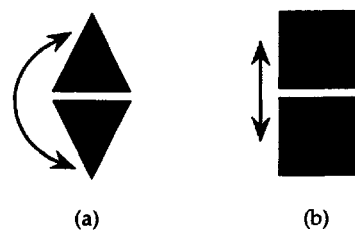


Figure 12.72. Three-dimensional apparent motion.

- (a) Apparent motion occurs in three dimensions when the pyramids are alternated in rapid succession, because their configurational properties prompt a three-dimensional interpretation.
- (b) Alternation of squares produces motion within a plane.

12.7.6 Stereopsis and pursuit eye movements

Optokinetic nystagmus

A textured display moving across the field of view induces a series of eye movements in the direction of stimulus motion interspersed with quick return movements, a response known as *optokinetic nystagmus* (OKN). The response is present in all vertebrates with mobile eyes and is designed to stabilize the retinal image as a whole as the animal moves about. Under normal circumstances, OKN occurs at the same time as the vestibuloocular response (VOR) induced by rotation of the head (see Howard 1993a for a review).

Two neural systems are believed to control OKN, a subcortical system with primary processing in the nucleus of the optic tract (NOT) but with inputs from the visual cortex in higher mammals, and a more recently evolved system related to voluntary smooth-pursuit eye movements.

In mammals, visual signals to subcortical nuclei controlling OKN are conveyed from each retina along the accessory optic tract, which terminates in the contralateral accessory optic system (Simpson 1984). This system has three subnuclei: the lateral, medial, and dorsal terminal nuclei. The lateral and medial nuclei seem to be mostly concerned with vertical OKN. The dorsal terminal nucleus and the nucleus of the optic tract (NOT) in the pretectum form one functional unit concerned with horizontal OKN (Grasse and Cynader 1990). Signals from the NOT are conveyed to the vestibular nucleus, which receives inputs from the horizontal semicircular canals. Separate or combined rotations of the visual surroundings and of the body result in neural activity in these cells proportional to the velocity of the visual stimulus relative to the body (Waespe and Henn 1979). From the vestibular nucleus, signals responsible for OKN and VOR ascend to the oculomotor nuclei along the medial longitudinal fasciculus and the tract of Deiters.

In most afoveate animals, such as the rabbit, horizontal OKN is controlled by the subcortical system just described, with little or no input from higher visual centres. In the rabbit the cells in the right NOT respond only to stimuli moving nasally presented to the left eye, and cells in the left NOT only to stimuli moving nasally presented to the right eye (Collewijn 1975). This asymmetry of directional tuning provides an explanation for the fact that rabbits and other lateral-eyed animals with one eye open show OKN only if the visual stimulus moves in a temporonasal direction, a feature of OKN known as **directional preponderance**. When both eyes are open, OKN occurs to both directions of motion, since an adequate stimulus is present in one of the eyes and the two eyes respond as a pair.

In cats, about half the cells in each NOT receive inputs from binocular cells in the visual cortex and therefore respond to stimuli presented to either eye, but only to stimuli moving in the same direction in space—to the right for cells in the right NOT and to the left for cells in the left NOT. Thus, in a normal cat with one eye open, signals reach both nuclei of the optic tract—the contralateral nucleus by the direct pathway and the ipsilateral nucleus by the cortical pathway. Since the cells in the two nuclei have opposite directional preferences, OKN occurs for both directions of stimulus motion, even when only one eye is open (Hoffmann and Stone 1985; Hoffmann and Distler 1986). The direct retinal component may be selectively removed by injection of tetrodotoxin (a suppresser of neural activity) into the vitreus of one eye. After this procedure, responses of the cat's NOT to direct inputs from the contralateral eye were severely reduced while its responses to cortically mediated stimulation of the ipsilateral eye were intact (Grasse 1991).

Recently, evidence has been accumulating about the role of the NOT in primates. A lesion in one NOT in the monkey reduces the gain of OKN toward the side of the lesion and reduces or abolishes afternystagmus in the same direction, leaving smooth pursuit of visual objects and saccadic eye movements intact (Schiff et al. 1988). Cells in each NOT of the intact monkey respond to stimuli presented to either eye moving ipsilaterally with velocities of between $0.1^\circ/\text{s}$ and $400^\circ/\text{s}$. Whereas cells in the NOT of the rabbit and cat respond only to large moving stimuli, those in the monkey also to stimuli less than 1° in diameter. Most NOT cells have large receptive fields which include the fovea. All the cells in the monkey NOT are driven binocularly, and it is concluded that the directly innervated monocular cells are poorly represented in primates (Mustari and Fuchs 1990).

One may conclude that the subcortical NOT system in the rabbit, cat, and monkey serves as the initial afferent mechanism for OKN. In foveate mammals many cells in the NOT receive inputs from directionally tuned binocular cells in the ipsilateral visual cortex. These inputs cause NOT cells to respond to (a) stimuli in either eye, which makes OKN in either eye bidirectional, (b) stimulus velocities higher than $100^\circ/\text{s}$, and c) small moving stimuli as well as large textured stimuli, at least in the monkey.

The smooth-pursuit component of OKN

Smooth-pursuit eye movements serve primarily to maintain the image of an object of interest on the fovea and therefore occur only in foveate animals. It is believed that the smooth-pursuit mechanism contributes to optokinetic nystagmus induced by whole-field motion, especially in primates. The motion signals serving smooth-pursuit eye movements are conveyed to the visual cortex from where they are relayed to higher visual centres specialized for the analysis of motion, notably the middle temporal (MT) and medial superior temporal (MST) cortices (Komatsu and Wurtz 1988) and the posterior parietal cortex, an area also known to be associated with visual attention (Kawano et al. 1984). These centres also contain cells that respond to eye movements (Newsome et al. 1988). The dorsolateral pontine nucleus receives inputs from all these centres and from the superior colliculus and conveys signals to the vermis and flocculus of the cerebellum which has a modulating effect on smooth pursuit, OKN, and VOR (Suzuki and Keller 1984; Noda 1986; Mustari et al. 1988). The smooth-pursuit pathway is finally relayed to the vestibular nucleus and on to the oculomotor nuclei along a pathway distinct from that carrying signals for VOR and the NOT component of OKN (Langer et al. 1985).

Complete removal of the visual cortex in the monkey leads to severe reduction in the gain of OKN, especially in response to high-velocity stimuli, and induces a temporonasal preponderance in monocularly evoked OKN. Optokinetic afternystagmus is still intact. In other words, OKN in the monkey lacking a visual cortex resembles OKN in afoveate animals (Zee et al. 1987). Lesions in MT and MST of the monkey cause a reduction in OKN gain toward the side of the lesion and result in an inability to match the velocity of pursuit to the velocity of a moving target (Dürsteler and Wurtz 1988).

OKN and stereopsis

Geometrically, a rotation of an eye compensates for a head rotation because the centre of rotation of the eye is not far from that of the head. However,

rotation of an eye cannot compensate for a linear motion of the head. This is because the images of objects at different distances move at different angular velocities when an animal moves along a linear path. In animals with laterally placed eyes, such as the rabbit, OKN is evoked in each eye only by stimuli moving temporonasally; they show directional preponderance (Collewijn 1975). When a rabbit rotates the head about a vertical axis, the leading eye registers the temporonasal motion of the visual scene, which induces OKN in both eyes. This response, together with VOR, helps stabilize the retinal image of the visual scene. When a rabbit moves forward, OKN does not occur because both eyes receive an ineffective nasotemporal motion of the image. No useful purpose would be served by OKN under such circumstances since the rabbit has no stereoscopic mechanism that would allow it to select a particular plane of motion within the parallactic motion of the visual scene, and the response would destabilize the images of objects straight ahead.

In animals with stereoscopic vision, the visual inputs feeding directly to the pretectum are supplemented by inputs routed through the visual cortex and by the cortically controlled smooth pursuit mechanism. These cortical systems render OKN bidirectional in each eye. Thus, a person moving forward while looking sideways at a stationary three-dimensional scene is able to move the eyes at the velocity required to stabilize the images of objects in the plane of convergence, while ignoring distracting motion signals arising from objects at other distances. Howard and Ohmi (1984) suggested that this ability arises because the cortical system augments OKN only if the cortical motion detectors are stimulated by moving images with zero binocular disparity. This idea is supported by the fact that all the cells in the visual cortex of the cat that project to the pretectum receive inputs from both eyes (Hoffmann 1982), a prerequisite for cells involved in the registration of binocular disparity. Furthermore, neonate human infants in whom the visual cortex has not yet acquired mature binocular cells, and adults with defective binocular vision, manifest a directional preponderance of OKN like that found in the rabbit (Hine 1985; Mehdorn 1982; Schor and Levi 1980; Van Hof-van Duin and Mohn 1982; Tychsen and Lisberger 1986; Reed et al. 1991). Thus, the main reason for the evolution of a cortical component to OKN is to allow animals with foveate eyes and stereoscopic vision to deal with complex motion signals generated by linear motion through a three-dimensional world.

It has been known for some time that OKN is disrupted when convergence is not within the plane of

the moving display (Mackensen 1953), although this effect had not been attributed to disparity. Howard and Gonzalez (1987) showed that horizontal OKN is slowed or absent when a moving display is made binocularly disparate by voluntary misvergence, and that misvergence, itself, is not the cause of this effect. They also showed that when there are two overlapping displays, one moving and one stationary, the occurrence of OKN depends on which display is in the plane of convergence.

With horizontal OKN a stationary stimulus for the control of vergence cannot be provided, since it inhibits horizontal OKN. These limitations were overcome by moving the visual display vertically and anchoring the subject's vergence on a central vertical line (Howard and Simpson 1989). This line provided a good stimulus for vergence but did not affect OKN, because it was parallel to the direction in which the eyes moved. Also, the disparity of the moving display could be changed without changing vergence or accommodation. The scleral search coil procedure was used to record the gain of OKN while the subject looked at the vertical line superimposed on the display shown in Figure 12.73 as it moved vertically at 12.5 or 24°/s. The disparity of the moving display was varied between -2.5° and +2.5°.

The functions relating the mean gain of OKN to the disparity of the moving display for each subject for a stimulus velocity of 24°/s are shown in Figure 12.74. The mean functions for the four subjects are also plotted. For all subjects, OKN gain had a maximum value when the disparity of the display was zero. For both stimulus velocities and both directions of motion, the gain of OKN was reduced by an amount related to the degree of binocular disparity in the moving display. The tuning functions relating OKN gain to disparity were narrower and more symmetrical for a stimulus velocity of 24°/s than for one of 12°/s. The mean decline in the gain of OKN with uncrossed disparities was not significantly different from the decline with crossed disparities.

Disparity could modulate OKN in two ways. In the first way, cells in the primary visual cortex tuned to zero disparity could send facilitatory inputs directly to the pretectal centres controlling OKN. The second possibility is that, within the fast OKN system (the smooth-pursuit component feeding through the pontine nuclei and cerebellum), signals for eye movements arise only from detectors that respond to moving stimuli with zero disparity. If all the stimuli in the visual field are disparate, OKN is left under the control of the low-gain, slow system, the one fed by direct visual inputs to the pretectum. It is unlikely that cortical cells responding to disparate inputs play an inhibitory role, either at the level of the

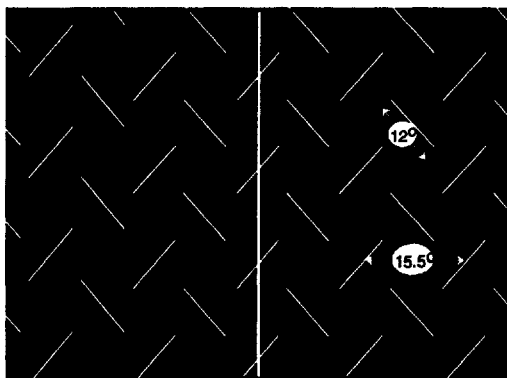


Figure 12.73. The effect of disparity on vertical OKN.
The display was 57° high by 70° wide and moved vertically up or down at 12 or 24°/s with various crossed and uncrossed disparities. To avoid spurious matches, the horizontal distance between the oblique lines was more than twice the maximum disparity. Subjects converged on the vertical white line at a distance of 0.92 m. (Reprinted by permission of Springer-Verlag, Heidelberg.)

prectectum or within the smooth-pursuit system. If they did, OKN would not operate in a normal three-dimensional scene because there are usually more disparate inputs than nondisparate inputs. These effects cannot be due to a simple change of attention, because subjects were asked to attend to the vertical line in all conditions and the elements of the moving display were at a constant distance from the fovea at all times. This coupling between OKN and stereopsis enables a person to stabilize the images of those parts of the scene within a selected depth plane. Although the gain of OKN is related to the disparity of the moving stimulus, it is still an open question whether other cues to depth, such as accommodation, also play a role in allowing humans to stabilize images in one selected depth plane.

Pursuit in and out of the plane of a textured surface

The coupling between eye movements and disparity could also serve a second function—that of allowing a person to pursue a moving object seen against a background of stationary objects at another distance. Howard and Marton (1992) found that smooth eye movements in pursuit of an object moving over a textured background are less disrupted by saccades when the pursued object and the background are in distinct depth planes than when they are in the same depth plane. This result has been confirmed by Neary (1992) and in the monkey by Kimmig et al. (1992). See also Kawano et al. (1994b).

Physiology of link between eye movements and disparity

Grasse (1994) found that in the cat the response of about half the cells of the NOT that respond to moving displays are also tuned to binocular disparity; some show an excitatory response to a limited range

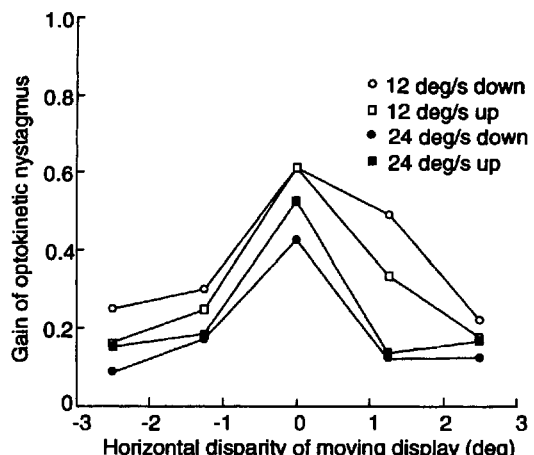


Figure 12.74. Optokinetic gain as a function of disparity.
The gain of optokinetic nystagmus as a function of disparity in a vertically moving display. Results are shown for two velocities and two directions of vertical motion. Means of four subjects. (Adapted from Howard and Simpson 1989.)

of disparities and others show an inhibitory response to disparity.

Cells selectively responsive to both movement and binocular disparity occur in several visual areas of the cerebral cortex (see Section 4.6.4). For instance, some cells in areas 17 and 18 of the monkey respond selectively to stimuli moving in a given direction in the two eyes, with some responding only to crossed-disparity stimuli and others only to uncrossed-disparity stimuli (Poggio and Fischer 1977; Poggio and Talbot 1981). Similar cells have been found in the monkey, in MT (Maunsell and Van Essen 1983b) and MST (Komatsu et al. 1988). In MST more of the jointly tuned cells were sensitive to crossed disparity than to uncrossed disparity. A hint of this type of asymmetry was found in the Howard and Simpson experiment. These cells have large receptive fields, suggesting that they are more suitable for gating OKN than for coding depth. Psychophysical evidence of a coupling between motion and stereopsis is reviewed in Section 12.7.

12.7.7 Stereopsis and induced visual motion

A stationary object seen against a moving background typically appears to move in the opposite direction. This effect, first described in detail by Duncker (1929), is known as **induced visual motion**. Wallach et al. (1978) devised a useful procedure for measuring induced motion. The subject visually pursues a small test spot superimposed on a large textured display moving horizontally. The spot moves slowly along a vertical track through about 10° and then returns quickly to its initial position before starting another vertical movement. The

apparent tilt of the path of motion of the test spot reflects the vector sum of its real vertical motion and its horizontal induced motion. The subject estimates the slant of the motion path by setting a tactile rod to the same apparent slant and thus provides a measure of induced visual motion. This will be referred to as the *tilt test*.

Induced motion has at least three distinct components: retinotopic induced motion due to motion contrast, oculomotor induced motion due to misregistration of movements of the eyes, andvection-entrained (exocentric) induced motion due to misregistration of movements of the head and body.

Retinotopic induced motion

Induced motion with respect to a retinal frame of reference is presumably caused by lateral interactions between motion detectors in the visual system, in a manner analogous to colour contrast and tilt contrast.

The retinotopic component of induced motion was isolated by having two abutting displays, one above the other, moving horizontally at 5°/s in opposite directions, with a test stimulus moving vertically at 1.4°/s on each (Ohmi and Howard 1991). Any perceived relative tilt in the paths of motion of the test spots, as the subject looked at the boundary between the displays, reflected only retinotopic induced motion, since induced motion due to misregistration of movements of the eyes or of the head cannot occur in two directions at the same time. The effect was at most 0.1°/s, or 2 per cent of the velocity of the induction stimulus. Nakayama and Tyler (1978) reported that a pair of parallel lines pulsing in and out in opposite directions induced an apparent pulsation of a pair of parallel stationary lines placed between them. The apparent velocity of this effect was also low.

Oculomotor induced motion

Oculomotor induced motion is due to misregistration of the way the eyes are moving in the head. Headcentric induced motion is the sum of the retinotopic and oculomotor components, since both cause an apparent motion of the stationary test spot relative to the head. Roelofs and van der Waals (1935) proposed a theory to account for the oculomotor component. When a person fixates a stationary object seen against a moving background, the involuntary optokinetic motion of the eyes (OKN) is held in check by voluntary fixation. Suppose that the efference signal required to hold OKN in check is registered by the perceptual mechanism responsible for judging the motion of the eyes but that the efference signal generated by the OKN mechanism is

not perceptually registered. The fixated object should appear to move at the same velocity as the moving background but in the opposite direction. If both efferent signals are properly registered, the eyes and the fixated object should be judged to be stationary. In other words, incomplete perceptual registration of the inhibited OKN signal relative to the voluntary efference signal should cause a corresponding impression that a stationary object is moving in the opposite direction to the motion of the background. In support of this "nystagmus-suppression theory" Heckmann and Post (1988) showed that changes in the induction stimulus that increase OKN gain also increase the vigor of induced motion.

A stimulus was designed to evoke only oculomotor induced motion, in addition to the small retinotopic component (Heckmann and Howard 1991). The eyes converged on a test spot in the plane of a large textured display moving horizontally at 20°/s, thus providing the conditions for OKN and hence for oculomotor induced motion. A similar more distant stationary display seen through the moving display suppressedvection and vection-entrained induced motion for reasons that are explained later. Under these circumstances induced motion of the test spot measured by the tilt test was about 1.5°/s. This was largely oculomotor induced motion, because the retinotopic component is very small. It could not be vection-entrained induced motion because vection was suppressed. When the test spot was in the plane of the more distant stationary display, no induced motion occurred. With only one moving display, induced motion was severely reduced when the test spot and fixation were out of the plane of the moving display. Gogel and MacCracken (1979) reported a similar depth-adjacency effect. In a supplementary experiment, Heckmann and Howard showed that the crucial factor is not the depth adjacency of the test spot and the induction stimulus but rather the depth adjacency of the induction stimulus and the point of fixation. In other words, the crucial factor is whether or not the stimulus conditions are those that generate OKN.

When fixation was in the plane of the moving display in Howard and Heckmann's experiment, induced motion had a velocity of about 1.5°/s and was thus about 7.5 per cent of the velocity of the induction stimulus. Only a small part of this effect was due to the retinotopic component. Thus, OKN efference was perceptually misregistered by at most 7.5 per cent relative to the voluntary efference that inhibited it. In other words, 92.5 per cent of the OKN efference was correctly registered. Other evidence confirms that OKN efference is well registered (Howard et al. 1989; Bedell et al. 1989).

Exocentric (vection-entrained) induced motion

Viewing a large moving display evokes a compelling sensation of self-motion in the opposite direction. This is known as **vection**. The literature onvection is reviewed in Dichgans and Brandt (1978) and Howard (1982). Vection is experienced in the wide-screen cinema or when one looks at a moving train while sitting in a stationary train. Movement of the whole visual scene rarely occurs unless the observer is moving. Furthermore, the semicircular canals and utricles cease to signal motion of the body at constant velocity. So it is not surprising that whole-scene motion is interpreted as due to self motion.

During vection, all stationary foreground objects also appear to move in the opposite direction to the moving background—they appear to move with the head, not relative to the head. Brandt et al. (1975) showed that a stationary object inhibits circularvection if it is seen stereoscopically beyond the moving display, but has no effect if the subject sees it nearer than the moving display. Ohmi and Howard (1987) confirmed the dominant role of background motion and showed that the dominance of the more distant display does not depend on depth cues, because an apparent reversal of the background-foreground relationships of two coplanar displays moving in opposite directions is sufficient to reverse vection.

It has been reported that circularvection is much more effectively induced by a moving scene confined to the peripheral retina than by one confined to the central retina (Brandt et al. 1973). In these studies, when the stimulus was confined to the periphery, the central retina was occluded by a dark disc, which would predispose subjects to see the peripheral display as background, and it may have been this rather than its peripheral position that caused it to induce strongvection. Similarly, when the stimulus was in the central retina, subjects may have seen it as a figure against a ground, which could account for the small amount ofvection evoked by it.

Howard and Heckmann (1989) showed that when one allows for the relative distances and areas of two displays, displays in the central visual field are just as effective as those in the periphery in evokingvection. The display perceived to be more distant dominatesvection, whether it is in the centre or periphery of the visual field. This is what one might expect, because near objects often move independently of the self and therefore provide unreliable evidence for self motion. The more distant scene

rarely moves, so motion of its retinal image is a reliable indicator of self-motion. Vection is determined by the motion of the more distant of two superimposed displays even when the eyes are converged on the near display. When the near display is stationary,vection still occurs and carries the near display along with it. There is novection when the far display is stationary, even when the near display is moving and the eyes are converged on it.

The rule thatvection is evoked by a more distant display even in the presence of a stationary near display was used to devise a stimulus that produced onlyvection-entrained induced visual motion. The eyes converged on a stationary textured surface, which eliminated OKN and oculomotor induced motion, while a moving display seen through the stationary display evoked strongvection and equally strongvection-entrained induced motion of the test spot and of the whole stationary display. Vection was often saturated, that is, the background appeared stationary and the subject felt the body and the test spot were moving in the opposite direction at the velocity of the moving display, namely, $20^\circ/\text{s}$. However, the path of motion of the test spot always appeared vertical, and therefore the tilt test did not reveal the presence of the very strongvection-entrained induced visual motion. Thus, the tilt test is not responsive tovection-entrained induced motion because, duringvection, the frame of reference for judging verticality is carried along with the apparent motion of the self.

Finally, oculocentric andvection-entrained induced motion were evoked in opposite directions at the same time by presenting subjects with two superimposed displays at different distances, one moving to the left and the other to the right. Subjects converged on the nearer display, which evokedOKN and oculomotor induced motion of a test spot as revealed by the tilt test. At the same time, the test spot appeared to move along with the self because ofvection induced by the far display. The two forms of induced visual motion were in opposite directions.

People readily experience 100 per centvection andvection-entrained induced motion at velocities of up to $60^\circ/\text{s}$. Headcentric (oculomotor) induced motion, which includes retinotopic and oculomotor components, was about $1.5^\circ/\text{s}$, and retinotopic induced motion was only about $0.1^\circ/\text{s}$. Thus, the three forms of induced visual motion differ in magnitude.

Spatiotemporal aspects of stereopsis

13.1 The Purfrich effect	535
13.1.1 Visual-latency spatial-disparity hypothesis	536
13.1.2 Alternative explanations	539
13.1.3 The Mach-Dvorak effect	540
13.1.4 Stroboscopic Pulfrich effect	541
13.1.5 Spatiotemporal averaging	542
13.1.6 Luminance and visual latencies	545
13.1.7 Light and dark adaptation	545
13.1.8 Role of contrast	548
13.1.9 Eye movements and the Pulfrich effect	549
13.1.10 Dynamic visual noise Pulfrich effect	551
13.1.11 Pulfrich effect and stereoblindness	554
13.2 Stereopsis and motion in depth	554
13.2.1 Judging time to collision	554
13.2.2 Impact direction for a monocular point	555
13.2.3 Relative motion cues to impact direction	557
13.2.4 Binocular cues to impact direction	559
13.2.5 Physiology of motion in depth	563
13.3 Aftereffects of motion in depth	565
13.3.1 Aftereffects of rotation in depth	565
13.3.2 Aftereffects from disparity-specific motion	566
13.3.3 Aftereffects from changing-disparity	567
13.4 Dichoptic motion	567
13.4.1 Dichoptic apparent motion	567
13.4.2 The dichoptic motion aftereffect	570
13.5 Stereopsis and motion parallax	571
13.5.1 Theoretical considerations	572
13.5.2 Perspective information	575
13.5.3 Spatial derivatives of disparity and parallax	577
13.5.4 Disparity and motion parallax compared	577
13.5.5 Quantitative studies	579
13.5.6 Disparity and parallax induced effects	581
13.5.7 Additional similarities and differences	581
13.5.8 Individual differences	583

13.1 THE PULFRICH EFFECT

The most widely known and thoroughly researched stereophenomenon involving moving targets is the **Pulfrich effect**, but it was not the first to be reported. In a lecture given to the Bohemian Academy of Sciences in Prague in 1872, Ernst Mach described an experiment by Dvorak in which a sinusoidally moving object seen with an interocular delay appeared displaced in depth. This is known as the **Mach-Dvorak effect**. The observer fixated a stationary point while the object moved horizontally along

a path within the fixation plane. An interocular delay was introduced by exposing the moving target intermittently—first to one eye and then to the other (see Section 13.1.3).

In 1922 Carl Pulfrich reported a second spatiotemporal stereophenomenon in which a pendulum is swung in a frontal plane at right angles to the line of sight and observed with both eyes but with a neutral density or coloured filter over one eye. A bob at the end of the pendulum appears to move in depth in an elliptical path with the major axis approximately coincident with the true path of motion.

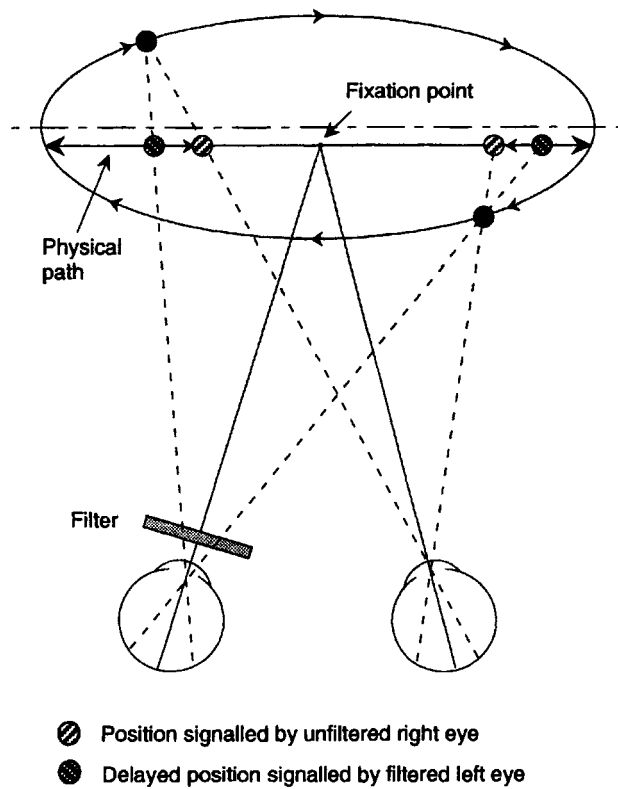


Figure 13.1. The Pulfrich pendulum illusion. The path of the pendulum bob predicted by the visual latency hypothesis. With the filter over the left eye, the pendulum appears to rotate in a clockwise elliptical path in depth, as seen from above. Note that the physical path of the pendulum bob (continuous line) does not coincide with the major axis (dashed line) of the perceived elliptical path.

The motion is clockwise (as seen from above) when the filter covers the left eye and counterclockwise when it covers the right eye (Figure 13.1). This effect is now known as the **Pulfrich effect**.

Pulfrich (1858–1927) designed optical instruments for the Carl Zeiss Company in Jena. He developed various surveying instruments including a stereoscopic rangefinder and a stereocomparator, which detected changes in the positions of astronomical objects. In the stereocomparator, two pictures of astronomical objects, taken sequentially, are combined in a stereoscope so that moving objects acquire a disparity and appear displaced in depth. He founded stereo-photogrammetry and in 1920 became interested in physiological optics and colorimetry.

Although Pulfrich produced the first full account of the Pulfrich effect, the phenomenon was first noticed by the astronomer Max Wolf in 1920 while measuring the positions of stars recorded on stereoscopic plates. As he moved the plates, the stars seemed to move in depth relative to a fixed marker (see historical note in Morgan and Thompson 1975). Fertsch, Pulfrich's associate at the Zeiss laboratories,

showed that this effect was due to unequal illumination of the eyes produced by the unequal density of the plates. Ironically, Pulfrich was blind in one eye and could not observe the effect named after him.

If the density of the filter in front of one eye is increased, the pendulum bob moves in a deeper ellipse and, if the density is sufficiently great, the excursion of the bob in depth can exceed the amplitude of its side-to-side movement. However, when the density of the filter exceeds 2.5 log units, the depth excursion declines to zero since the filtered eye is effectively occluded (Pulfrich 1922; Krekling 1973b). An increase in the speed of the pendulum bob, as would be produced by a larger amplitude of swing or a shorter pendulum, also increases the amount of illusory depth. The Pulfrich effect can be seen if the eyes fixate a stationary point close to the path of the swinging pendulum bob, but it can also be seen when the observer actively tracks the pendulum bob, providing there is some stationary reference point in the field of view (Kahn 1931; Rogers et al. 1974) (see Section 13.1.9).

13.1.1 Visual-latency spatial-disparity hypothesis

Pulfrich's explanation of the effect, which he attributed to Fertsch, is that the dimmer stimulus in the filtered eye is registered with a longer latency than the unfiltered image in the other eye. Thus, the signals about the object's position are relayed to the visual cortex with a temporal offset. The filtered eye is effectively "seeing in the past" compared with the unfiltered eye (Gregory 1966). For a stationary object, the interocular difference in latency is of little consequence, but for any moving object, the filtered eye sees the object in a slightly earlier spatial position than the unfiltered eye. This creates a binocular disparity between the two images of the moving object at any given moment. On the basis of this hypothesis, Lit (1949) and Weale (1954) showed mathematically that for a pendulum swinging in simple harmonic motion, the apparent path of a pendulum bob will be elliptical in depth. There is an apparent contradiction here because one would expect the displacement toward the observer to be smaller than that away from the observer, since the depth created by a given disparity varies inversely with the square of the viewing distance (Ogle 1962; Lit 1968). This asymmetry can be demonstrated by extending corresponding visual lines from the two eyes to the points where they intersect (Liang and Pieron 1947). Weale (1954) and Levick et al. (1972) have shown, however, that the apparent path is a true ellipse, but its major axis lies slightly beyond the physical path of the pendulum (Figure 13.1). This shift can be seen with

careful observation, and is evident in the differences between the near and far pointer settings for some of the observers in Lit's careful studies (Lit 1949, 1960). On the other hand, Trincker (1953), Katz and Schwartz (1955), Harker and O'Neal (1967), and Landrigan and Bader (1981) reported significant departures in the perceived path from the expected elliptical shape that are not predicted by the latency hypothesis. Emerson and Pesta (1992) suggested that some of these departures are predicted by the latency hypothesis if it is generalized appropriately.

The latency hypothesis correctly predicts that the Pulfrich effect increases with either a denser filter or greater speed of the pendulum bob (Lit 1949, 1960). In addition, the size of the Pulfrich effect depends on the observation distance (Lit and Hyman 1951) and the contrast and luminance of the target and background (Lit 1968). In support of the latency hypothesis, Brauner and Lit (1976) compared visual latencies derived from the Pulfrich effect with simple reaction times using comparable visual targets and the same range of luminance. While the shapes of the two luminance-latency functions were similar, reaction times increased more rapidly than latencies derived from the Pulfrich effect at low luminances. They attributed this to the additional motor component involved in reaction times.

Alpern (1954) measured the temporal offset between two 12 ms flashes of light of unequal intensity needed for them to appear exposed simultaneously. As the intensity difference between the flashes increased, the temporal offset between the dim and bright flashes had to be increased, but the magnitude of the offset was typically much smaller than the estimates of visual latency derived from the Pulfrich effect. Further evidence consistent with the visual latency explanation of the Pulfrich effect comes from Kolehmainen and Keskinen (1974) who noted that the effect is abolished when the pendulum swings in a vertical direction in a frontal plane, perpendicular to the interocular axis. The authors point out that under these conditions, the filter creates a vertical disparity between the positions of the pendulum bob signalled by the two eyes which should not produce an apparent displacement in depth (see Section 7.6). The hypothesized dependency of latency on brightness led Pulfrich to propose that his phenomenon could be used to assess the relative brightnesses of different colours. As a result, he entitled his paper "*Die Stereoskopie im Dienste der isochromen und heterochromen Photometrie*." However, as Lit (1949) correctly pointed out, this would require that retinal latency be a function of perceived brightness only, independent of wavelength, which is not the case.

Nickalls (1986) has drawn attention to a closely related variant of the Pulfrich illusion, which was originally described by Pulfrich. The observer views a vertical rod mounted eccentrically on a horizontal turntable. Viewed from the same height as the turntable, the rod oscillates to and fro horizontally, like a swinging pendulum bob, but because of its circular path in depth, there is a physical phase lag in the positions of the images projected to the two eyes in the absence of differential filtering. This phase lag provides the physical basis for the observer's judgment of the direction of rotation. Pulfrich noted that when the turntable display was viewed with a filter over one eye the direction of apparent rotation in depth depended on the speed of rotation. For example, with clockwise rotation of the turntable (as seen from above) and a filter in front of the right eye, the apparent rotation was counterclockwise at fast speeds and reversed in direction as the turntable slowed down. With the turntable rotating at constant speed, Nickalls observed that the apparent direction of rotation of the rod on the turntable reversed with a change in viewing distance.

Pulfrich's turntable effect can be thought of as "pitting" the physical circular motion of the rod in one direction against the filter-induced elliptical motion in the opposite direction. At very low turntable speeds, the depth effect created by the filter is minimal and hence the phase lag created by the turntable's physical rotation determines the rod's perceived path. At higher turntable speeds, the filter-induced depth effect is dominant and it determines the perceived path. However, this is merely a redescription of what is seen. In order to explain the interaction between the physical path and the effects of the filter we need to consider the situation more carefully. Simple geometry shows that the physical path of the rotating rod creates a constant phase difference between the sinusoidal motions reaching the two eyes. If we assume that the effect of the filter is to increase the latency for signalling the moving target's position in the filtered eye, a second binocular phase lag will be created between the sinusoidal motions signalled to the cortex. If the magnitude of these two phase lags is equal but opposite in direction, the target should appear to describe a path which is close to a frontal plane (Nickalls 1986). The fact that the physically based and physiologically based phase lags cancel each other out at a particular turntable speed provides good evidence, which has been ignored previously, to support the visual latency hypothesis. Note also that the turntable effect is equivalent to the nulling technique used by Rogers and Anstis (1972) to measure the size of the Pulfrich effect. In this technique a physical phase

offset in the sinusoidal motions of the dichoptic targets presented to the two eyes was used to cancel the filter-induced phase lag (see Section 13.1.6).

A further test of the visual latency hypothesis was provided by Julesz and White (1969). They prepared a computer-generated film loop in which each frame was a random-dot stereogram portraying a centre square with a crossed disparity. Successive frames of the film portrayed a similar disparate square but the dots making up each stereogram were uncorrelated from one frame to the next. Although the movie sequences appeared as dynamic random noise when viewed monocularly, the disparate centre square was clearly visible when the sequence was seen binocularly (Julesz and Payne 1968). In order to test the latency hypothesis, all the right eye's images were displaced by one frame in the movie sequence producing a delay of one frame between the times that the correlated frames were presented to the two eyes. Observers viewed the movie with an adjustable neutral-density filter over the eye receiving the leading frame. When the frames were presented at a rate of 12 per second (80 ms interframe interval), observers saw only a scintillating field of dots, but as filter density increased, they saw the centre square standing in front of the surround. This percept can occur only if the neutral density filter increased latency into the left eye's visual pathway, which conveys the sequence of leading frames to the cortex.

At lower overall luminances (0.01 compared with 0.1 foot lamberts), Julesz and White found that less filtering was required to cancel the effect of temporal displacement of frames, which is consistent with the often reported finding that a given differential filtering produces a larger Pulfrich effect at lower luminance (Lit 1949; Alpern 1968; Rogers and Anstis 1972). For frame rates above 12 per second, Julesz and White found that while the best stereopsis occurred with a small amount of filtering to the leading eye, the centre square was still seen with no filtering. They suggested that two or more frames of the movie sequence might be visually averaged through "temporal inertia" and thereby allow a proportion of the binocular frames within the averaging period to be correlated (see Section 13.1.5).

The additional visual latency introduced by a filter of a given density was measured by Ross and Hogben (1975). They used Julesz and White's technique of delaying the sequence of images to one eye. The delay could be adjusted in 20 ms steps between 0 and 80 ms. For each delay, they measured the number of correct identifications of the orientation of a stereoscopic target—a horizontal or a vertical strip—with either no filter, a 1 log unit filter over the left eye, or the same filter over the right eye. At the

luminance level used by Ross and Hogben, a delay of up to 40 ms between the presentation of the stereoscopic images was tolerated without affecting discrimination performance (see Ross and Hogben 1974). The psychometric function of the number of correct identifications against lag was shifted to the right by about 20 ms when the filter covered the left (leading) eye, and by 25 ms to the left when it covered the right (lagging) eye.

In a display which was described as having "two bobs each way on the Pulfrich effect" (Ross and Hogben 1975), two dots were displaced in apparent motion in opposite directions along the same horizontal path. With a neutral density filter over one eye, one dot appeared to translate in front of the reference plane and the other behind. Ross and Hogben found that the displacement in depth produced by covering one eye with a filter could be cancelled completely by introducing a physical delay to the presentation of dots in the other eye.

A technique for creating three-dimensional movies

The visual latency hypothesis predicts that the disparity between the images of a moving target seen with a filter over one eye increases in proportion to the velocity of movement. Consequently, observers should perceive a gradient of depth while viewing a two-dimensional display of moving targets which have a gradient of velocities, with the fastest moving targets appearing displaced most from their two-dimensional paths. To test this prediction, Rogers and Anstis (1972) created a movie film with the camera pointing out of the side window of a car and a train. When displayed on a screen, those parts of the scene closest to the camera during filming moved most rapidly across the screen while more distant parts of the scene remained virtually stationary. If the overall direction of motion across the screen is to the right, then by covering the right eye with a neutral density filter, the most rapidly moving objects create the largest crossed disparities and the entire scene is perceived as three dimensional. This effect was demonstrated on BBC TV in 1970. Enright (1970) reported the converse effect, in which the apparent speed of objects viewed from the side window of a moving car is increased or reduced by covering one eye with a neutral-density filter. In this case, the increased latency creates a change in the apparent distance of objects, which affects their apparent speed through constancy processes (see Section 11.3.3).

Nonstereoscopic versions of the Pulfrich effect

The visual-latency explanation of the Pulfrich effect is also supported by several related demonstrations

using nonstereoscopic targets. One of the earliest of these demonstrations was by Hess (1904) who noted that the dimmer of two illuminated moving targets appeared to lag behind the brighter. He was also the first to measure the size of the differential lag by introducing a physical lead into the dimmer target's movement until the targets appeared to move in alignment. In a variant of the Hess effect, Prestrude (1971) and Prestrude and Baker (1968) presented observers with a dichoptic pair of concentric rotating discs, each with a radial line inscribed on it. With equal illumination of the two discs, the radial lines appeared aligned as the discs rotated, but with a filter over one eye, one line appeared to lag behind the other. The delay was measured by nulling it with a phase lead to the disc seen through the filtered eye, until the lines again appeared to be aligned.

Wilson and Anstis (1969) created a monocular display similar to that used by Hess consisting of a pair of vertical lines, one above the other, both of which oscillated at the same frequency along horizontal sinusoidal paths. The observer fixated a point midway between the paths of the two targets so that the images of the targets fell on different regions of the same retina. When the luminance of one line was reduced, that line appeared to lag behind the other. The size of the delay was again measured by introducing a phase lead to the oscillation of the dimmer line until the lines appeared to be aligned. This demonstration shows that the effect of luminance on visual latencies is localized and can be different for different parts of the same retina. Williams and Lit (1983) measured the magnitude of both the Hess effect and the Pulfrich effect using comparable targets and found them to be similar, at least under photopic conditions of illumination.

13.1.2 Alternative explanations

Although Fertsch's visual-latency spatial-disparity hypothesis is consistent with both the original Pulfrich effect and the nonstereoscopic versions such as the Hess effect just described, two alternative explanations of the Pulfrich effect have been proposed. The first, suggested by Harker (1967), is based on the idea of saccadic suppression which accompanies both voluntary eye movements and microsaccades (Dodge 1900; Zuber and Stark 1966). Since the period of suppression is a function of target illumination, saccadic suppression becomes a candidate for explaining the Pulfrich effect. Harker claimed that, for a moving target which appears and disappears, suppression would occur first in the filtered eye and then in the unfiltered eye, and both eyes would recover simultaneously. He further suggested that

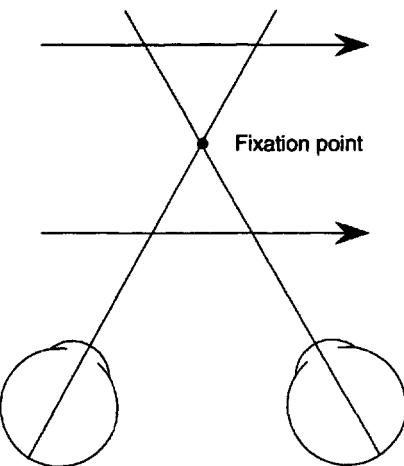


Figure 13.2. Contiguous temporal disparity.

A target which moves in front of the fixation point from left to right will stimulate a given retinal area (e.g. fovea) in the left eye before it stimulates the corresponding retinal area in the right eye. The temporal disparity is in the opposite direction for a rightward moving point beyond the fixation point.

asymmetries in the perceived path of the Pulfrich pendulum bob, referred to in 13.1.1, are more consistent with the suppression explanation, although he provided no evidence for this. While saccadic suppression may play a role in the viewing of a moving object under conditions of intermittent illumination, there seems to be no need to invoke it to explain the Pulfrich effect. On the contrary, Kirkwood et al. (1969) reported that the Pulfrich effect is equally apparent whether the observer tracks the pendulum bob or fixates on a stationary point, and their eye-movement recordings showed no evidence of macro- or microsaccades in either condition.

The second and more plausible alternative explanation is based on the assumption that visual latencies vary with the luminance of the stimulus (the latency hypothesis) but the perceived elliptical path of the pendulum bob is due to temporal rather than spatial disparity mechanisms. The visual-latency spatial-disparity explanation assumes that the visual system monitors the difference in the signalled spatial position of a moving point at each moment in time—**simultaneous spatial disparity**. However, it is also possible that the visual system monitors the temporal difference in the stimulation of corresponding points on the two retinas—**contiguous temporal disparity** (Ross 1974; Burr and Ross 1979). A temporal disparity, by itself, provides no information about the relative depth of the point but, this can be computed with additional information about the speed and direction of movement of the point (Figure 13.2).

The receptive fields of some binocular cells in area 18 of the cat visual cortex were found to be selectively tuned to both the spatial and temporal disparity of their binocular inputs (Cynader et al. 1978; Gardner et al. 1985). However, it was not established whether the temporal-disparity tuning was also tied to the direction of movement, which is essential if these cells are to signal the direction of relative depth. Carney et al. (1989) recorded responses from simple cells in the cat visual cortex to drifting sinewave gratings. They noted that the responses were modulated by the interocular phase difference of the moving gratings, thereby providing selective disparity tuning. The data from a typical cell showed a maximal response to an interocular phase difference of around 50° with a half-amplitude bandwidth of ±45°. The average phase shift created by 1 and 2 log unit filters placed over one eye was determined for 67 cells. A 1 log unit filter over one eye shifted the peak response by over 40° and a 2 log unit filter shifted it by around 100°. For the frequency and velocity of the grating used in the experiment, these phase shifts correspond to temporal shifts of 11.3 and 29.1 ms respectively. The authors pointed out that these values are very close to psychophysical estimates obtained by Rogers and Anstis (1972) in their study of the Pulfrich effect. The phase shift in the response created by a given filter varied with the drift rate of the grating which is consistent with the psychophysical observation that the size of the Pulfrich effect varies with the speed of the pendulum bob. The data of Carney et al. provide powerful support for the idea that a neutral-density filter increases visual latency. However, as the authors note, these data do not indicate whether the selective tuning of the cells is for the spatial or temporal disparity of moving targets, since the two are necessarily confounded when using continuously illuminated targets.

One might think that Julesz and White's (1969) demonstration that the centre square is not perceived with a one-frame delay in the dichoptic presentation of random-dot patterns is inconsistent with the temporal-disparity hypothesis. However, there is no inconsistency because the random dots themselves do not have a coherent speed and direction of movement.

Wist (1968, 1970) suggested that the visual system is sensitive to contiguous temporal disparities. He showed that when a single flashed target is presented first to one eye and then to the other, with a temporal offset greater than 60 ms, observers typically report that the target appears beyond the simultaneously visible fixation point and that the effect increases with increasing temporal offset.

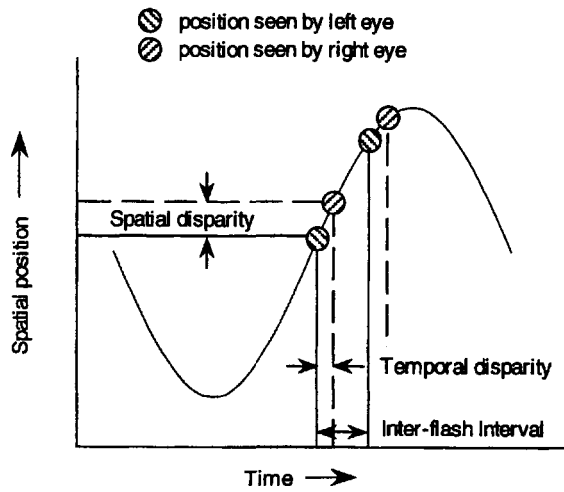


Figure 13.3. The Mach-Dvorak effect.

Space-time representation of the Mach-Dvorak effect. The sinusoidally-oscillating pendulum bob is seen only intermittently and at an earlier spatial location and earlier time by the left eye than by the right eye.

Bower (1966) similarly reported that small temporal offsets (<5 ms) in the dichoptic presentation of a disparate line can affect judgments of the line's position in depth. He found that the latency effect interacted with the location of the target to the left or right of the fixation point, which he attributed to different transmission times of signals from the nasal and temporal hemiretinas. It is not clear how the depth shifts found by Wist and Bower relate to the effects reported by Ross (1974) and Burr and Ross (1979), since the targets were stationary in the former experiments and, as a consequence, one cannot make an unambiguous prediction of where the targets should lie in depth in relation to the fixation point.

13.1.3 The Mach-Dvorak effect

In the classical Pulfrich situation with a swinging pendulum bob, the spatial- and temporal-disparity explanations yield similar predictions, but Morgan and Thompson (1975) have suggested that the Pulfrich effect, seen with stroboscopic illumination and long interflash intervals is more consistent with the idea of contiguous temporal disparity. To examine this idea one must distinguish between several illusory effects observed when moving targets are illuminated stroboscopically. The first is the Mach-Dvorak effect, in which a target oscillating along a horizontal path is illuminated intermittently, with the exposures at slightly different times to the two eyes. Observers report that the moving target describes an elliptical path in depth, as in the Pulfrich effect, although in the Mach-Dvorak effect there is no differential filtering of the target to the

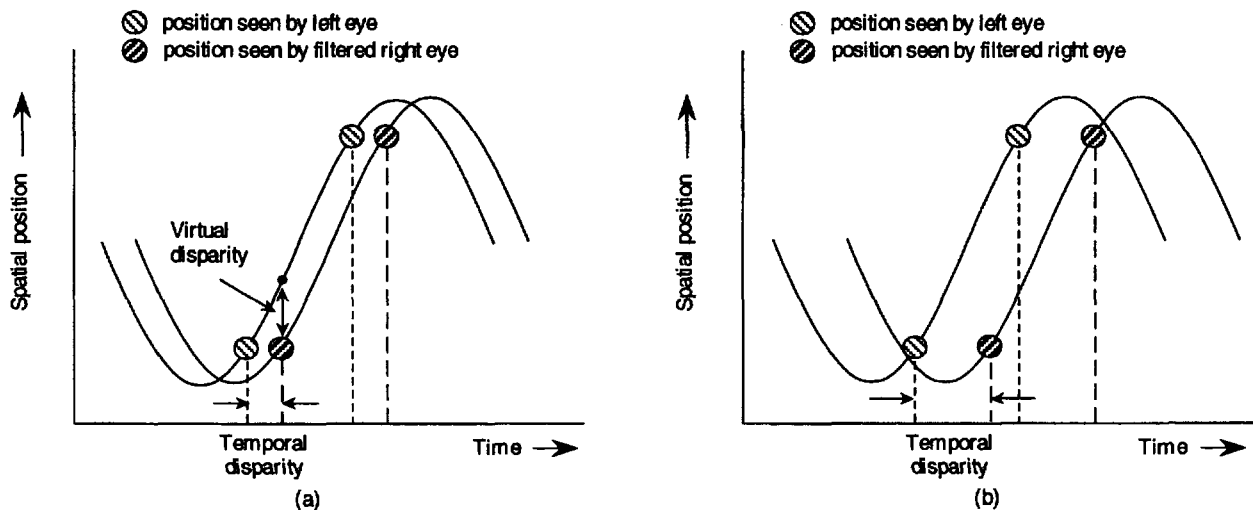


Figure 13.4. The stroboscopic Pulfrich pendulum illusion.

- (a) The sinusoidally-oscillating target is illuminated at the same spatial position to the two eyes but with a temporal delay to the right eye due to the filter-induced latency.
- (b) If the latency created by the filter is greater than half the inter-flash interval, the position signalled by flash 1 in the right eye is temporally closer to the disparate position signalled by flash 2 in the left eye. With perfect spatio-temporal averaging in each eye, there would be a "virtual disparity" between the target positions in the two eyes at any instant in time.

two eyes (Harker 1967). Note that, under these conditions, there are no simultaneous spatial disparities—the target is never seen at the same time in different positions, and no contiguous temporal disparities—the target is never seen at different times in the same position (Figure 13.3).

Lee (1970a) noted that when the rate of stroboscopic illumination was 20 Hz (50 ms between flashes) and the left eye viewed the target 0 to 25 ms *after* the right eye, the target appeared to describe a counter-clockwise path in depth. When the left eye viewed the target 0 to 25 ms *before* the right eye, the apparent path was clockwise. He concluded that binocular pairing occurs between pairs of neural signals which have the smaller temporal disparity, and that the illusory depth is due to the spatial disparity between the closest temporally paired flashes in the two eyes (Figure 13.3). In support of this idea, Lee noted that the introduction of a filter-induced temporal delay in one eye changed the point at which the observer's responses switched from clockwise to counterclockwise. Lee argued that the visual system tolerates differences in arrival time of spatially disparate signals from the two eyes, because such differences arise naturally from interocular luminance differences. Note that according to Lee's interpretation, the visual system does not use temporally disparate inputs from the two eyes as a signal for relative depth, it merely tolerates their existence. Indeed, one could argue that the Mach-Dvorak effect provides clear evidence that the visual system is unable to offset the spatial disparity of the noncontiguous inputs to

the two eyes against the temporal disparity of the spatially disparate inputs, as an ideal system should (see Section 13.1.5).

13.1.4 Stroboscopic Pulfrich effect

In a second experimental situation investigated by Lee (1970b), the oscillating target was illuminated intermittently at 20 Hz (50 ms between flashes), as with the Mach-Dvorak effect, but the flashes occurred at the same instant for both eyes. The stroboscopically illuminated target was viewed with a neutral-density filter over one eye. Under these conditions, the two eyes signalled the same spatial position at slightly different times and thereby created a contiguous temporal disparity (Figure 13.4a). Observers reported that the target described an elliptical path in depth similar to the Pulfrich effect seen under conditions of continuous illumination. Lee reported that the ellipticity of the perceived path could be reduced to zero by introducing an appropriate temporal and spatial offset between the exposures to the two eyes, of the sort used to create the Mach-Dvorak effect. Put another way, this shows that the Mach-Dvorak effect can be nulled by viewing the intermittently illuminated target with a filter over one eye.

At first sight, it appears that the stroboscopic Pulfrich effect cannot be explained in terms of a filter-induced spatial disparity, since the same spatial position is signalled by the two eyes (assuming that the filter-induced delay is less than half the time

between flashes). Moreover, the effect would not be predicted if the Mach-Dvorak effect were due solely to the spatial disparity between temporally disparate signals from the two eyes. The stroboscopic version of the Pulfrich effect shows that a temporal disparity between the binocular signals of moving targets alone is capable of producing a depth effect, either through a mechanism directly sensitive to temporal disparities or indirectly through the conversion of temporal disparities into spatial disparities (see later).

Morgan and Thompson (1975) investigated Lee's stroboscopic version of the Pulfrich effect in more detail. First, they found that the effect can be seen with intermittent target presentation, provided the time between flashes is less than 100 ms. Second, they showed that longer interflash intervals can be tolerated with greater densities of the monocular filter. Third, they investigated whether the effect can still be explained in terms of spatial disparities, even though there are no spatial disparities between the positions of the images reaching the two eyes. One possibility is that the visual system makes an incorrect pairing between the target in the filtered eye with the previously exposed (and therefore spatially disparate) target in the unfiltered eye. If the visual system does not "know" about the filter-induced delay, it would be susceptible to such incorrect pairings. Hence, when the delay induced by the filter is greater than half the time between flashes, a depth effect is predicted on the basis of the spatial disparity of the binocular images which are closest together in time (Figure 13.4b). If spatial disparities were the only factor responsible for the stroboscopic Pulfrich effect under these conditions, one would expect the phase shift needed to null the effect to be an integral multiple of the time between flashes. Morgan and Thompson showed that this is not so, and therefore suggested that temporal disparities may also be involved. Curiously, they paid little attention to those conditions in which the filter-induced delay was much shorter than the time between flashes, so that the dichoptic signals most closely spaced in time had zero spatial disparity. These circumstances provide the best evidence for the independent detection of temporal disparities.

There is a potential artifact in the interpretation of the Pulfrich effect seen under stroboscopic conditions. When the eyes track the pendulum bob, rather than fixate a stationary marker, the image of the marker moves across the retinas. When the marker is illuminated continuously, but attenuated in one eye, the temporal delay in the filtered eye introduces a spatial disparity of the marker with respect to the tracked bob (Rogers et al. 1974). Morgan and

Thompson considered this an unlikely explanation of their results because 1) their observers were instructed not to move their eyes and 2) eye movements do not predict the observed dependency of the effect on the interflash interval.

Morgan (1975) introduced a new variant of the stroboscopic Pulfrich effect. The stroboscopically illuminated target oscillated horizontally in a frontal plane, with flashes occurring at the same instant in both eyes, as in Lee's (1970b) original demonstration. One eye, however, was presented with a pair of target bars, one in a position corresponding to that of the single bar seen by the other eye, and the other in a position corresponding to the previous position of the single bar. Observers saw two or more bars (as in a picket fence) moving in an elliptical path around the fixation point. The targets moved clockwise when the extra bar was seen by the left eye, and counterclockwise when it was seen by the right eye. The depth effect could be cancelled by covering the eye seeing the single bar with an appropriate filter. Morgan suggested that the effect could be explained by either 1) the pairing of the single bar seen by one eye with the second (disparate) bar seen by the other eye or 2) the pairing of the single bar with a spatially averaged representation of the two bars seen by the other eye. These two possibilities could have been distinguished by the size of the effect, but no data are given.

13.1.5 Spatiotemporal averaging

The idea that "filling-in", or spatiotemporal averaging, might play a role in Lee's (1970b) stroboscopic Pulfrich effect and Morgan's (1975) variant was explored by Morgan (1976, 1980). He presented a pair of moving stroboscopically illuminated targets to the same eye (interflash interval, 80 ms), in vertical alignment (one above the other) but with a temporal delay in their respective exposures. This is the stroboscopic equivalent of the Hess effect (Section 13.1.2). Observers perceived a vernier offset in the targets; the delayed target appeared to lag behind the undelayed target. Morgan concluded that perceived spatial position is derived from spatiotemporal averaging of the target's discrete trajectory. Acuity for detecting the vernier offset of targets moving stroboscopically is comparable to that found for continuously illuminated vernier targets (Morgan 1981; Burr 1979). As with the stroboscopic Pulfrich effect, it is possible that the result is an artifact of tracking eye movements that cause the temporally disparate target positions to stimulate spatially disparate retinal regions. However, eye movement recordings revealed that the eyes did not track the targets.

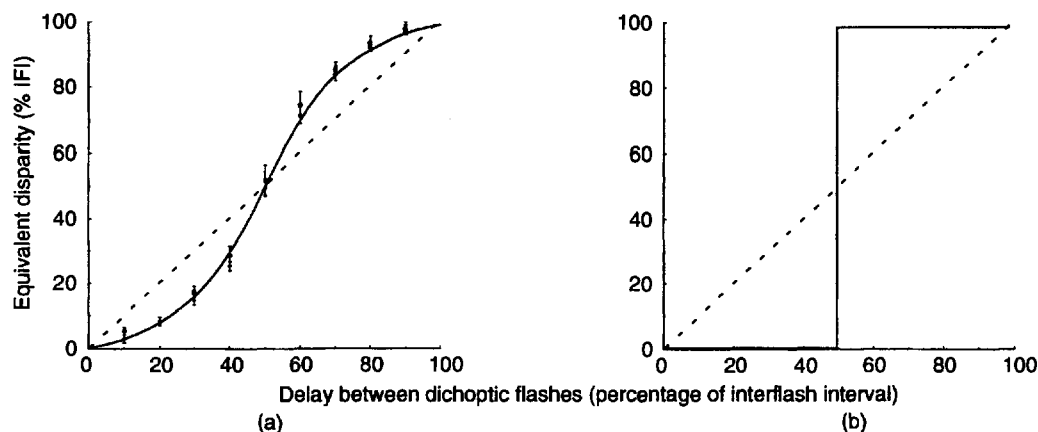


Figure 13.5. Results with the stroboscopic Pulfrich illusion.

(a) Morgan (1979) found that the spatial disparity needed to cancel the apparent elliptical path of the stroboscopic Pulfrich effect varied in a sigmoid fashion as a function of the delay between the flashes (expressed as a percentage of the interflash interval).

(b) If the temporally disparate targets signalled by the two eyes were paired together on the basis of those which occurred closest in time, the function should show a discontinuity when the delay is 50% of the interflash interval. Perfect spatiotemporal averaging of the target's position predicts a straight line indicating a complete trade-off between temporal and spatial disparities (dashed line).

(Adapted from Morgan 1979.)

In a further study of spatiotemporal averaging in the stroboscopic Pulfrich effect, Morgan (1979) showed that when the delay between exposure of a stroboscopically illuminated moving target (50 ms interflash interval) was varied between 0 and 50 ms (0 to 100 per cent of the interflash interval), the physical disparity needed to cancel the apparent elliptical path in depth showed a sigmoid-shaped function (Figure 13.5a). If the temporally disparate target bars seen by the two eyes were paired on the basis of those occurring closest in time (and temporal disparity was simply ignored), the function should have shown a break at half the interflash interval. At this point, the binocular pairings should switch from those with zero spatial disparity to those with a spatial disparity corresponding to the distance travelled between flashes (Figure 13.5b). Perfect spatiotemporal averaging, on the other hand, predicts a linear function, indicative of a complete trade-off between the temporal and spatial characteristics. A linear function means that the target has an effective disparity corresponding to that produced by a continuously illuminated target. Burr and Ross (1979) refer to the spatial disparity arising from perfect spatiotemporal averaging as the **virtual disparity** of a stroboscopically illuminated target (Figure 13.4a). Morgan also found that the same targets which produced the sigmoid function, produced a linear function when the level of illumination was lower, suggesting that spatiotemporal averaging increases with decreasing illumination.

Instead of using filters to create binocular temporal disparity between stroboscopically illuminated

targets, Burr and Ross (1979) manipulated the temporal offset directly. When the stroboscopically illuminated target was seen to move smoothly, they reported that virtual disparity behaves "exactly like true disparity" and consequently suggested that the temporal disparity is converted into a spatial disparity rather than being detected by a separate mechanism. Burr and Ross allowed their observers to track the moving target in most of their experiments, and hence there is a possibility that eye movements converted the temporal disparities into spatial disparities. They rejected this possibility however, since depth was still seen when observers fixated a stationary marker. While this control shows that some component of the target's virtual disparity is detected, it does not prove that virtual disparities and real spatial disparities show a perfect trade-off under conditions of fixation.

The results from Mach and Dvorak (1872), Lee (1970a) and Morgan and Thompson (1975) described previously all show little evidence of a trade-off between spatial and temporal disparities, while those of Burr and Ross (1979) apparently show an almost perfect trade-off. To resolve these inconsistencies, Morgan (1979) suggested that spatiotemporal averaging is effectively complete when the interflash interval is small (<10 ms), but for interflash intervals greater than 50 ms, there is little spatiotemporal averaging and the appearance of the stroboscopically illuminated Pulfrich target is predominantly (but not exclusively) based on the spatial disparity between the target positions occurring closest together in time. In apparent contradiction, Burr and

Ross reported a good trade-off between spatial and temporal disparities when the interflash interval was as long as 50 ms. However, subjects were allowed to track the stroboscopically illuminated targets, so that temporal disparities could be converted into spatial disparities. The two sets of results can be reconciled if it is assumed that some spatiotemporal averaging occurs when the interval between stroboscopic flashes is as long as 50 ms, but that the averaging is not necessarily complete.

The near perfect trade-off between spatial and temporal disparities with short interflash intervals is consistent with a single mechanism which extracts the simultaneous spatial disparities between binocular images after some sort of spatiotemporal averaging. However, the evidence presented so far does not preclude a separate mechanism sensitive to temporal disparities of moving targets when they stimulate corresponding retinal regions. The issue of temporal disparity is examined further in Section 13.1.10.

Further evidence for spatiotemporal averaging was provided by Morgan (1977). He distinguished between two possible consequences of placing a neutral density filter over one eye: 1) an increase in latency which would shift the signalled position of the leading edge of a moving target and 2) an increase in the amount of spatiotemporal integration or smoothing. This would blur and shift the position of the leading edge of a moving target and also widen its apparent width (Figure 13.6e). To distinguish between these two possibilities, Morgan presented a dichoptic pair of continuously illuminated oscillating bars with different widths. Observers adjusted the phase between the motions of the bars until the fused target appeared to oscillate in a frontal plane. This occurred when the mean visual directions of the targets were aligned, rather than either their leading or trailing edges (Figure 13.6a-c). This suggests that spatiotemporal averaging does occur and is approximately linear over the range of target widths used. In addition, the depth effects due to differences in target width interacted with those produced by differential filtering. From this, Morgan concluded that one reason for the depth effect in the normal Pulfrich effect is that the filter "smears out the target in that eye backward in the direction of motion." This conclusion does not follow from the results. While the results indicate a role for spatiotemporal averaging in the absence of differential filtering, they do not provide any evidence that averaging is increased by the filter. If the filter increases the amount of averaging, the filtered target should appear more blurred and wider, as well as to lag behind in the vernier alignment task used by Morgan (1976).

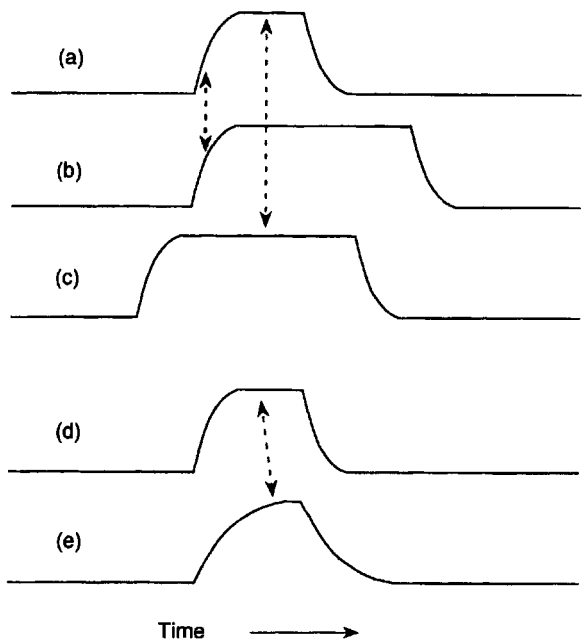


Figure 13.6. Increased persistence or latency difference?

When moving dichoptic bars of the same luminance but different widths were presented to the two eyes with their leading edges aligned, as in (a) and (b), Morgan (1977) observed a Pulfrich-like rotation in depth. The effect was abolished when the geometrical centres of the two bars were aligned, as in (a) and (c). Morgan argued that the effect of a filter over one eye is to increase the persistence and thereby introduce an offset between the geometric centres of the bars in the two eyes, as in (d) and (e).

In 1977 Wist et al. reported that the magnitude of the depth shift created by a moving grating depends on the spatial frequency of the grating. Observers viewed a continuously drifting grating binocularly with a neutral-density filter over one eye. The filter displaced the drifting pattern in a convergent direction and the observers adjusted the speed of motion until the pattern appeared to lie at the same distance as a stationary marker disc positioned in front of the display. The visual-latency hypothesis predicts that the magnitude of the depth shift is independent of the spatial frequency of the drifting pattern. But Wist et al. found that the displacement in depth was smaller for low spatial-frequency patterns. Hence, a low spatial-frequency pattern had to move faster than a high spatial-frequency pattern to create the same displacement in depth. For each halving of spatial frequency, a 1.6 fold increase in angular speed was needed to produce the same displacement in depth. They found a similar relationship between the width of a single stripe and the magnitude of depth displacement. Diener et al. (1976) showed previously that the perceived speed of moving gratings increases linearly with increasing spatial frequency. Wist et al. claimed that this effect and the

effect of spatial frequency on depth displacement are quantitatively similar, and concluded that the Pulfrich effect depends on the perceived rather than the actual speed of the moving stimulus.

13.1.6 Luminance and visual latencies

Early measurements of the Pulfrich effect and its dependence on luminance level were made by Pulfrich (1922), Engelking and Poos (1924), Bannister (1932), and Lythgoe (1938). However, Lit (1949) carried out the first comprehensive study of the dependence of visual latencies on luminance using the Pulfrich effect. He used a black vertical rod (10 arcmin wide) which oscillated with simple harmonic motion along a linear path in a frontal plane against a uniformly illuminated background of 610 millilamberts. Observers fixated a similar but stationary rod just below the moving rod and adjusted its position until it appeared to lie under the moving rod, on either its apparent forward or its apparent backward excursion (Figure 13.1). Absolute visual latencies cannot be determined directly using the Pulfrich effect, but latency differences (Δt) between the eyes can be measured as a function of (1) the degree of filtering of one eye's image with respect to the other ($\Delta \log I$) and (2) the overall level of illumination (I). Lit reported that the latency difference increased with increasing difference in luminance between the two eyes ($\Delta \log I$) and that for a given luminance difference, the latency difference was greater at lower overall luminance levels. However, he did not speculate on the exact mathematical relationship between luminance and visual latency. Previously, Lythgoe (1938) had proposed a logarithmic relationship between the latency difference and the ratio of retinal illuminations, while Rock and Fox (1949) claimed that the magnitude of the Pulfrich effect was a compound logarithmic function of filter density.

In an important theoretical paper, Alpern (1968) reanalyzed Lit's data and devised the technique of cascading the separate graphs—which relate the latency difference (Δt) to the binocular luminance difference ($\Delta \log I$) at different overall luminance levels (I)—into a single cumulative function. He showed that the cascaded plot of $\log(T_0 - \Delta t)$ against $\log I$ (retinal illuminance) in trolands was well fitted by a straight line, suggesting a power-law relationship of the form

$$T = T_0 - \Delta t = kI^{-p}$$

where T is the visual latency, T_0 and k are arbitrary constants and p is the power law exponent. Lit's data were fitted best with a power-law exponent of

around -0.2. This means that every 1 log unit decrease in luminance level ($\Delta \log I$) lengthens the visual latency by around 60 per cent. In contrast, Standing et al. (1968) suggested that perceptual latency varies approximately with the logarithm of the stimulus intensity:

$$T = -a \log I + c$$

but their data were collected only over a 3 log unit range of intensities. As mentioned previously, Wilson and Anstis (1969) developed a monocular, nonstereoscopic method for measuring visual latencies as a function of luminance for moving targets projected on different parts of the same retina. Using Alpern's technique of cascading the data curves to create a single cumulative delay function, they showed that the results were well fitted by a power-law expression with exponents of between -0.29 and -0.50 for their three observers. They suggested that the slightly higher values of their exponent than that obtained by Lit might have been due to the fact that artificial pupils were not used in their experiment.

Rogers and Anstis (1972) reverted to a binocular, stereoscopic task for measuring visual latencies but, in contrast with previous studies, they used a nulling technique to measure the Pulfrich effect, on the grounds that it is easier to judge whether a target is oscillating in a frontal plane than to set a pointer to the position of maximum excursion. To this end, a phase lead was progressively added to the motion of the oscillating target seen by the filtered eye until the target appeared to move along a frontal path. They measured latencies over a 6 log unit range of luminances and found that the results were well described by a power-law relationship with exponents of -0.20 and -0.22 for their two observers (Figure 13.7)—very close to the values obtained by Alpern in his reanalysis of Lit's data. Rogers and Anstis also replotted the results from the experiments of Lit (1949), Standing et al. (1968), Wilson and Anstis (1969), and Prestrude (1971), and in each case a good fit was found to a power-law relationship between visual latencies and luminance level (Figure 13.8).

13.1.7 Light and dark adaptation

In the studies of the Pulfrich effect described so far, both eyes were always fully adapted to their respective light intensities. Hence, while one can conclude that visual latencies vary with luminance, it is not clear whether the effect is a direct consequence of the differential luminance levels or the differential state of adaptation resulting from the different luminance levels. It has often been assumed that the

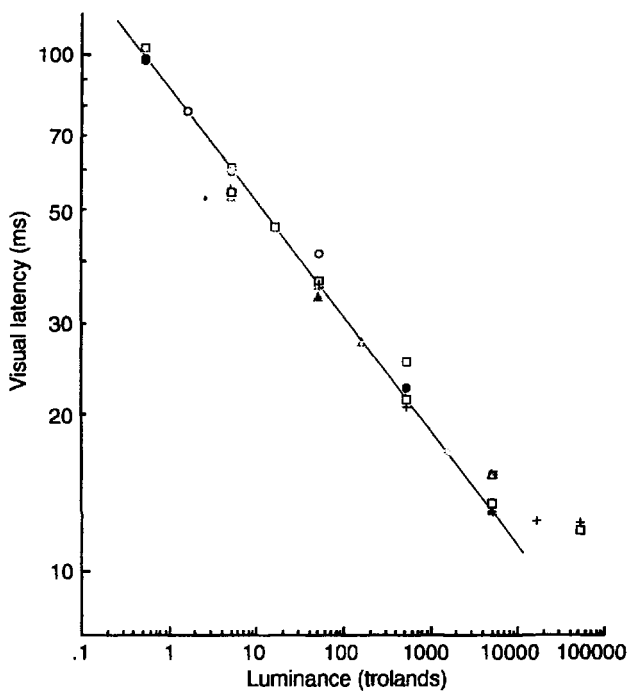


Figure 13.7. Visual latencies as a function of luminance.

Latency differences between the two eyes for one observer measured using the Pulfrich effect. The separate relative latency curves were cascaded by shifting each vertically. The linear fit of the data on log-log co-ordinates indicates that visual latencies are a power law function of luminance and can be expressed as: $T=kl^p$ where p is the power-law exponent and k is a constant. (Redrawn from Rogers and Anstis 1972.)

increased delays are due to the dark adapted state of the filtered eye (Gregory 1966). Lythgoe (1938) claimed that changing the adaptation state alone affects visual latencies. The evidence for this claim came from observations of a swinging pendulum bob viewed without filters but with one eye illuminated with an additional glare source. The direction of the resultant Pulfrich effect was consistent with shorter visual latencies in the light-adapted eye. A similar result was also reported by Diamond (1958). The argument is not conclusive, however, because the light from the glare source would have added to the luminance of the pendulum bob in addition to its effect on the adaptation state of that eye.

Subsequent experiments have looked at the effects of prior adaptation on the subsequent viewing of a pendulum bob either with or without differential filtering. Rock and Fox (1949) reported that 15 minutes of prior dark adaptation of one eye produced a small Pulfrich effect equivalent to a weak filter (about 0.1 log units), when the pendulum was viewed without filters. The effect decayed away over 60 seconds, confirming the earlier observations of

Engelking and Poos (1924). Lythgoe (1938) looked for a similar effect after 5 minutes of prior dark adaptation but found that the pendulum appeared to swing in an almost straight path and thus concluded that "the retinal interaction is largely confined to the mechanism of photopic vision." The effects of prior light adaptation are more clearcut. Crawford (1938) found that a Pulfrich effect could be seen after prior light adaptation of one eye, and suggested that the latent period of vision varies with the concentration of photopigment in the receptors. Using artificial pupils to control for the effects of changing pupil size, Standing et al. (1968) recorded the observer's setting of an adjustable pointer beneath the near point of the apparent path of a moving target. They found that the size of the Pulfrich effect increased over the 20-minute period following the introduction of a filter over one eye, which had a density of between 0.3 and 3.0 log units. The increase in the size of the effect was considerable and accounted for 60 per cent of the effect obtained in the fully adapted situation. They pointed out that this figure is likely to be an underestimation of the effects of adaptation, since the initial phase of dark adaptation is extremely brief and probably occurred before the first measurements were made.

Rogers and Anstis (1972) studied effects of prior adaptation on visual latency. Subjects adjusted the phase between a pair of oscillating rods, which were viewed dichoptically, until the fused image appeared to move in a frontal plane. The targets in the two eyes were unequally illuminated during an initial adaptation period, but were equally illuminated while settings were made. This contrasts with the procedure used by Standing et al. in which the eyes were equally illuminated during adaptation and unequally illuminated during testing. After cascading the separate $\Delta t / \Delta \log I$ graphs at different overall luminance levels during testing into a single cumulative function using a technique similar to that used by Alpern (1968), Rogers and Anstis presented their results as a three-dimensional graph. The height of the surface indicated the magnitude of visual latencies as a function of the luminance level of the target and the prior state of visual adaptation (Figure 13.9). The positive diagonal crossing the surface connects the data points of all conditions in which the observer was fully adapted to the luminance seen by the eye (adaptation state = luminance of target). This curve is well described by the power-law expression described earlier.

The shape of the surface shows that the major effect on visual latencies is due to the luminance of the target, and the effects of the prior adaptation level are much smaller. Specifically, when one eye of the

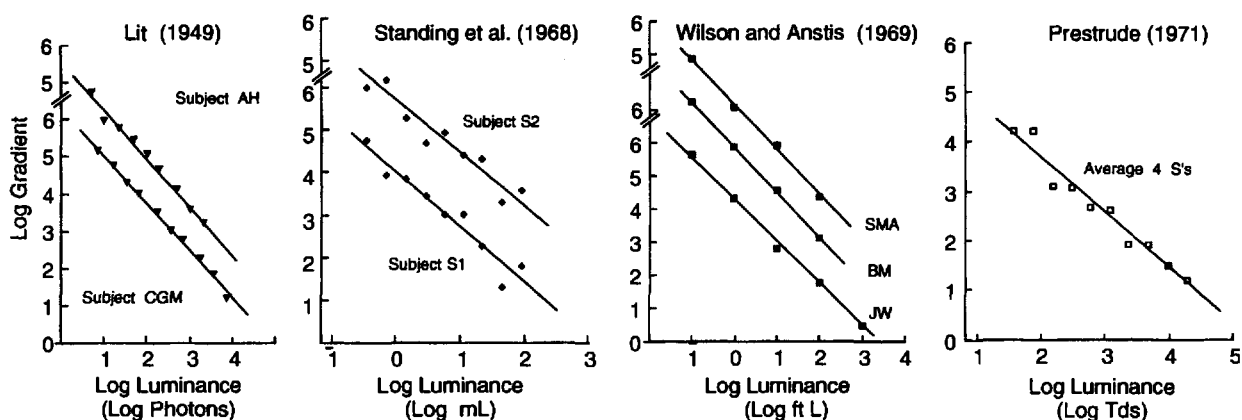


Figure 13.8. Results from four studies of the Pulfrich effect.

The data of Lit (1949), Standing et al. (1968), Wilson and Anstis (1969), and Prestrude (1971) have been cascaded using Lit's technique and the gradients of the best-fitting functions replotted on log-log coordinates. (Redrawn from Rogers and Anstis 1972.)

observer is dark adapted before viewing the oscillating target (points to the left of the positive diagonal), there is almost no effect of prior adaptation. This finding is consistent with the earlier results of Lythgoe (1938) and Rock and Fox (1949).

On the other hand, when one eye of the observer is light adapted before viewing the oscillating target (points to the right of the positive diagonal), there is a small and consistent effect such that latencies were initially shorter and increased as the eye adapted to the prevailing illumination. The time courses of these two effects are shown in Figure 13.10. It should be noted, however, that the changes in latency with prior light adaptation were small in comparison to the effect of luminance level and were limited to the first minute of exposure to the new luminance level, unlike the results reported by Standing et al.

Rogers and Anstis (1972) also reported two paradoxical effects which occurred only at very high luminance levels (>4.0 log trolands). First, when one eye was adapted to a fairly intense light and the intensity was suddenly increased, the latency of that eye paradoxically became longer by up to 12 ms and decreased only over the subsequent 60 s of viewing (the hump on the lower left of the positive diagonal in Figure 13.9). Second, when one eye was adapted to an intense light of >4.0 log trolands and the intensity was suddenly reduced by 1 or 2 log units, the visual latency of that eye became longer (as might be expected), but as the eye dark adapted down to the new level, the latency became significantly shorter over a period of about 60 s (the hump on the lower right of the positive diagonal in Figure 13.9). Rogers and Anstis offered no explanation for these paradoxical effects which occurred only at very high luminance levels when most of the pigment in the receptors would have been bleached.

In conclusion, there is good evidence that prior light adaptation of one eye produces a Pulfrich effect when the luminance of the target to the two eyes is equal. It remains unclear, however, why the time course of the adaptation effect on visual latencies was so rapid in Rogers and Anstis's experiment (<60s) and much slower in Standing et al.'s study (15 - 20 min), although the contrast relationship of the moving target may be a factor. Prestrude and Baker (1971) observed changes in visual latency over the first 100 s after adapting to an intense bleaching source in one eye. The moving target was a dark line on a light background, as in the Rogers and Anstis study. On the other hand, Prestrude and Baker found longer lasting changes (over 5 min) when the

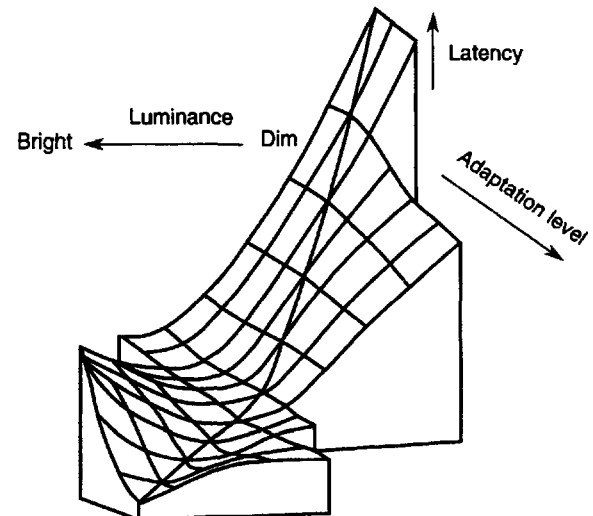


Figure 13.9. Latencies as a function of luminance & adaptation. Visual latencies, on a linear scale as a function of the luminance of the target during testing and the prior state of adaptation of the eye. (Redrawn from Rogers and Anstis 1972.)

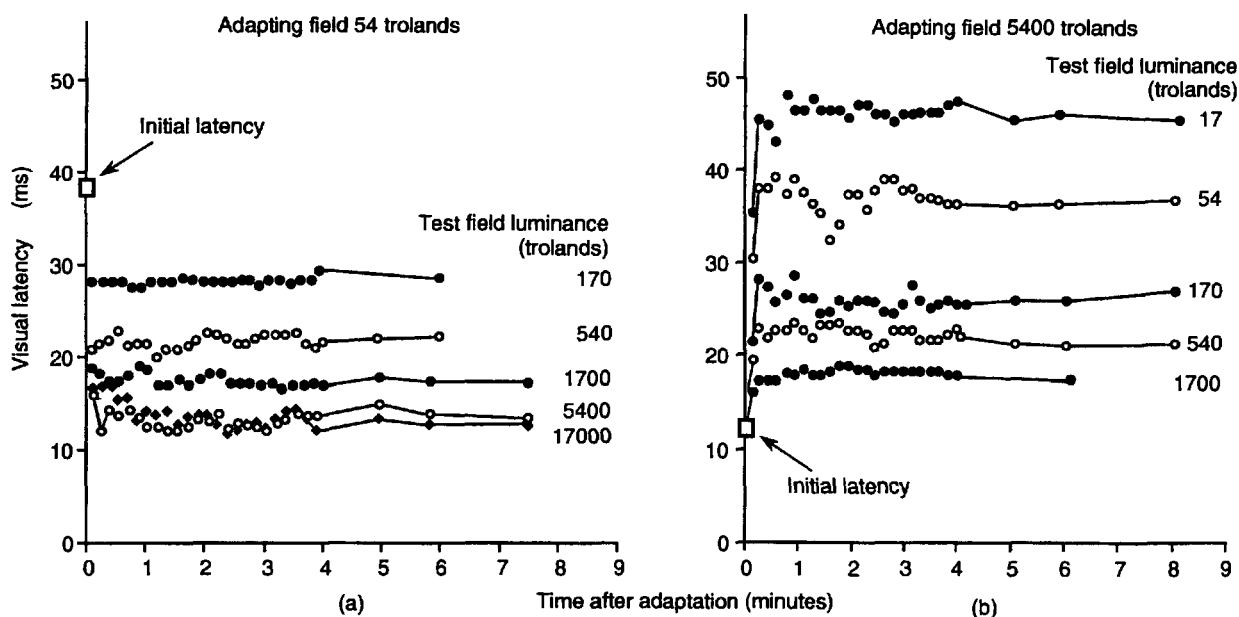


Figure 13.10. Visual latencies as a function of time following prior dark or light adaptation.
Time course of visual latency following prior adaptation to either a dark field of 54 trolands (a) or a light field of 5400 trolands (b). Prior dark adaptation had little effect on latencies whereas prior light adaptation resulted in shorter latencies for the first 30 s. (Redrawn from Rogers and Anstis 1972.)

moving target was a light line on a dark background, as in the Standing et al. study.

The virtual absence of an effect of prior dark adaptation found in most studies is consistent with the shorter time course of light than of dark adaptation. It is also important to stress that it has been impossible to measure changes in visual latency that might occur within the first few hundred milliseconds of adaptation to a different intensity level using the Pulfrich effect. Hence, all that can be concluded is that changes in latency occurring after the first second are generally much smaller than those found under steady-state conditions.

Long-term adaptation effects

There have been several reports of a long-term adaptation to visual latency differences created by differential illumination of the two eyes. Douthwaite and Morrison (1975) found that the magnitude of the Pulfrich effect decreased by 25-50 per cent over a 5-day period of wearing a 0.7 log unit tinted lens (80 per cent attenuation) in one eye. Wolpert et al. (1993) confirmed these results using two observers, and showed that the computed interocular delay decreased approximately linearly over a 9-day period of wearing a 0.6 log unit filter (75 per cent attenuation) to reach a value less than half that measured on the first day. The rate of adaptation for the particular conditions used by Wolpert et al. was estimated to be around 1 ms per day. Upon removal of the filter after 9 days, so that the target illumination in the

two eyes was equal, there was a small Pulfrich effect in the opposite direction, calculated to be equivalent to a 4 - 5 ms reduction in the latency of the previously filtered eye. This effect decreased to less than half over the first 24 hours and to zero over the following 3 days. Douthwaite and Morrison, on the other hand, reported that the reversed Pulfrich effect disappeared within a few minutes. Heard and Papakostopoulos (1993) also reported a slight decline in the magnitude of the Pulfrich effect during the wearing of an 1.8 log unit filter over one eye for seven days and a subsequent aftereffect on removal of the filter which lasted for several further days. Wolpert et al. suggested that the most likely site of the long-term adaptation effect is in the retina rather than in the cortex, and that it does not result from changes in pupil diameter. The fact that the course of the initial long-term adaptation effect and the subsequent recovery both have time constants of several days suggests that these effects have a different origin from those responsible for the changes of sensitivity found during dark and light adaptation.

13.1.8 Role of contrast

Dodwell et al. (1968) attempted to measure the effect of the target contrast on the Pulfrich effect with minimal differential adaptation of the two eyes. Four reference rectangles of the same luminance in the two eyes surrounded the differentially filtered moving targets, consisting of a series of bright bars

moving across a very dark background. A Pulfrich effect was seen, but the experiment does not provide clear evidence for the role of target contrast. Neither does it rule out the possibility that target luminance or adaptation level was responsible, since the adaptive state of the retinal receptors may have been differentially affected by the differently illuminated bars.

A better test for the role of contrast in the Pulfrich effect is to use dark target bars of unequal luminance which move over a light background of the same luminance in the two eyes. If peak luminance in the binocular displays is crucial, there should be no effect, but if space-average luminance is crucial there should be a Pulfrich effect with the eye seeing the darker bars subject to a longer latency. On the other hand, if contrast is crucial, there should be a Pulfrich effect with the eye seeing the darker target bars (with higher contrast) subject to a shorter latency.

The results of Prestrude and Baker (1971) suggest that there is more to the visual latencies than target contrast alone. They measured the phase difference between dichoptic target discs rotating about the same centre, each with a superimposed radial line. There were two conditions: 1) white radii (3.8 log trolands) on a dark background (2.3 log trolands) and 2) dark radii on a white background, keeping the luminance levels of the dark and white areas and the target contrast the same in the two situations. When the targets were viewed with a filter covering one eye, a greater latency difference was found for the white targets on a dark background (which had the lower space-average luminance) suggesting that the space-average luminance is the critical variable. This conclusion is further supported by the finding that the latency difference was the same when the background in the dark target/light background configuration was reduced to the same retinal luminance as the dark background in the light target/dark background configuration. This result strongly suggests that peak luminance is not the crucial variable, and neither is the direction or magnitude of target contrast. The single variable that appears to account for all these results is the space-average luminance level. Note that these results were obtained using a nonstereoscopic alignment task and the experiment needs to be repeated in a Pulfrich situation.

13.1.9 Eye movements and the Pulfrich effect

In the introduction to this section 13.1, we pointed out that the Pulfrich effect is readily seen whether the observer fixates a stationary point or visually tracks the pendulum bob, as long as some other reference point is in the field of view (Kahn 1931;

Kirkwood et al. 1969). According to the latency hypothesis, in the fixation condition, the increased latency in the filtered eye creates a binocular disparity in the signalled position of the moving bob (Figure 13.11a). However, when the observer tracks the pendulum bob the images of the target remain close to the foveas and hence the latency difference cannot be translated into a spatial disparity (Figure 13.11b). If the bob is well tracked, the Pulfrich effect should not be seen. However, the eyes may track the apparent elliptical path in depth predicted by the visual-latency spatial-disparity hypothesis, rather than the physical path of the bob (Figure 13.11c). In this case, there would be a continuous change in depth signalled by the vergence system, but it would always be accompanied by a corresponding change in binocular disparity between the images of the pendulum bob. No Pulfrich effect should occur in this situation, either. Even if tracking were poor, the speed of the target over the retinas would be considerably less than under fixation conditions and hence, at best, a very small Pulfrich effect should be observed. As Kirkwood et al. (1969) and others reported, however, the magnitude of the effect is typically similar whether subjects fixate or track.

Rogers et al. (1974) suggested that the Pulfrich effect seen when the observer tracks the moving target is due to the effects of the filter on stationary objects in the field of view. As the eyes track the moving bob, the images of any stationary object are displaced across the retinas, and the increased latency of the filtered eye creates a binocular disparity in the position of the stationary object with respect to that of the moving bob. To test this hypothesis, observers were instructed to track a moving target of unequal luminance in the two eyes, but with the background maintained at the same luminance. No Pulfrich effect was seen. In the converse situation in which the moving target was of equal luminance in the two eyes and the background was differentially filtered, a Pulfrich effect was seen, but only while the eyes tracked the target; it disappeared as soon as the stationary background was fixated. These findings provide clear evidence that the Pulfrich effect seen when observers track the pendulum bob results from the differential filtering of the stationary background rather than the differential filtering of the moving target.

An apparently contradictory result was obtained by Wallach and Goldberg (1977). They claimed that a Pulfrich effect was seen when observers tracked an oscillating target viewed against a differentially-illuminated but featureless background. Subjects estimated the depth of the apparent elliptical path. The estimated depth was significantly smaller with

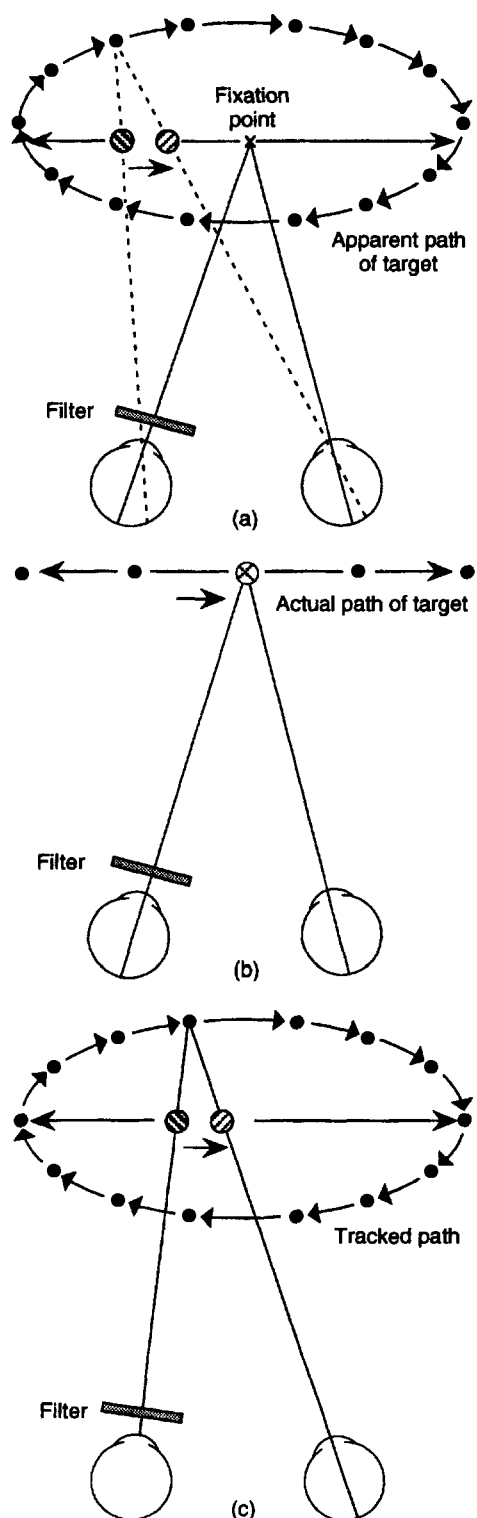


Figure 13.11. Fixating and tracking the Pulfrich pendulum.
 (a) The latency hypothesis predicts an elliptical path when the subject fixates on a stationary point.
 (b) No illusion is predicted with perfect tracking of the pendulum bob.
 (c) No illusion is predicted when the eyes track the bob in depth, because corresponding changes in disparity accompany the changes in vergence. (Redrawn from Rogers et al. 1974.)

a featureless than with a featured background. In addition, four of their 24 observers "had trouble getting a clear effect" in the latter situation. It is possible that the authors' prior expectations of the likely perceptual outcome influenced their results since in those cases where the observer's description of the path "was faulty", "the correct motion path was suggested to the subject and the exposure was repeated" (Wallach and Goldberg 1977). The presence of the differentially-illuminated edges of the aperture surrounding the moving target may also have provided a stereoscopic reference frame.

What movements do the eyes make when tracking a moving target which is differentially filtered in the two eyes? In two brief accounts, Reading (1973, 1975) claimed that vergence eye movements occurred when observers tracked a differentially filtered target, and she speculated that the Pulfrich effect under these conditions was a consequence of proprioceptive feedback from the extraocular muscles. Rogers et al. (1974) also recorded eye movements while observers tracked either 1) a differentially filtered oscillating target, with the background luminance equal in the two eyes, or 2) a target moving around a true elliptical path in depth. The latter condition verified that observers were capable of making the appropriate changes in vergence needed to track a target which described an elliptical path in depth. In the former condition, they found no changes in vergence, which suggests that observers simply tracked the physical path of the moving target, as would be expected from theoretical considerations. It was also noted that the Pulfrich effect disappeared as soon as the observer started to track, which is consistent with the fact that the background was of equal luminance in the two eyes.

In a later experiment, Ono and Steinbach (1983) reported that there were no vergence changes when an observer tracked a pendulum bob with both the background and target filtered. In this case, a Pulfrich effect could be seen. They suggested that the electrooculogram used by Reading to record eye position was incapable of resolving small vergence movements, and therefore her results were artifactual.

Enright (1985) confirmed the findings of Rogers et al. (1974) and Ono and Steinbach (1983) that continuous changes of vergence are not elicited when an observer tracks a differentially filtered pendulum bob, except during the first few hundred milliseconds of tracking. Although no continuous changes of vergence (consistent with following an elliptical path) occurred after the first second of tracking, Enright did report systematic errors of vergence such that his observers' eyes maintained

constant divergence of between 34 to 55 arcmin. These vergence errors were several times larger than those seen under conditions of steady fixation and seemed to be a consequence of interocular differences in illumination (Enright 1985).

13.1.10 Dynamic visual noise Pulfrich effect

The experiments of Julesz and White (1969) and Ross and Hogben (1974) show that the stereoscopic system can tolerate a temporal mismatch in the arrival times of binocularly correlated random-dot frames of up to 50 ms. Ross (1974) reported a new finding that under certain circumstances a temporal mismatch between binocular signals is not merely tolerated but can itself produce a stereoscopic effect. The display consisted of a central square region of dynamic noise seen at the same time by the two eyes. In the surround, the dynamic noise was physically delayed to one eye. When the temporal delay was longer than 70 ms, Ross (1974) observed that the temporally mismatched dots in the surround appeared to lie in a plane behind that of a central square containing temporally correlated dots. The depth effect could be cancelled by introducing a spatial disparity between the spatially correlated but temporally mismatched frames and was abolished when the surround dots were completely uncorrelated between the two eyes. In a later paper, Ross (1976) described the dots as appearing to lie on an upright cylinder rotating around its vertical axis, but other investigators have supported the original description and stressed the appearance of discrete planes of moving dots which lie predominantly (for some observers) behind the fixation point (Falk and Williams 1980; Neill 1981; Zeevi and Geri 1985). Ross interpreted his results as showing that the visual system could extract temporal as well as spatial disparities between images reaching the two eyes—a **temporal disparity hypothesis** (see Section 13.1.4).

A closely related effect was reported by Tyler (1974c). If a display of random dynamic noise, such as that created on a detuned TV receiver, is viewed with a neutral-density filter over, say, the left eye, the dynamic noise is seen in depth, with the dots seen in front appearing to stream to the left and the dots seen behind appearing to stream to the right. Overall, the dots appear to swirl in a clockwise direction as a dense cloud around the fixation point, with each dot's apparent velocity linked to its apparent displacement in depth from the TV screen. With the filter over the right eye, the dots swirl around the fixation point in a counterclockwise direction. The only difference between the Ross effect and the Tyler effect is that the temporal mismatch

was created by a physical delay in Ross' display and by a filter-induced delay in Tyler's. Zeevi and Geri (1985) showed that when dynamic visual noise is viewed with a filter over one eye, the apparent movement of the dots in an uncrossed disparity plane is a sufficient stimulus to create a movement aftereffect (see Section 13.4.2).

Three hypotheses have been proposed to explain the Pulfrich effect with dynamic visual noise:

1. *Temporal disparities* Ross (1974, 1976) suggested that the visual system is capable of detecting the temporal disparity of images which stimulate corresponding spatial locations on the two retinas (see Section 13.1.2). The rationale for a separate temporal disparity mechanism is that temporal disparities are created in the normal viewing of a three-dimensional scene when the eyes move. During an eye movement to the right, an uncrossed point stimulates corresponding retinal regions in the right eye earlier than in the left, and vice versa for a crossed point.

One problem with this hypothesis, as Neill (1981) pointed out, is that when the eyes move in a given direction, the direction of movement of crossed and uncrossed points is the same but the temporal disparities are in opposite directions. In the dynamic-noise Pulfrich effect, the temporal disparity is the same for crossed and uncrossed points, but the direction of perceived motion is opposite. Therefore, the two situations are not necessarily equivalent. In addition, the temporal disparity hypothesis predicts no depth effect when the eyes are stationary, and yet the dynamic-noise Pulfrich effect can still be seen during fixation (Tyler 1977). However, the temporal-disparity hypothesis can be reformulated in terms of temporal disparities of moving objects rather than of those created by eye movements. For example, an object with uncrossed disparity moving from right to left stimulates a region in the right retina before the corresponding region in the left retina, as will an object with crossed disparity moving left to right (Figure 13.2). This emphasizes the fact that for correct interpretation of temporal disparities, the direction of movement of the image must also be registered.

2. *Random spatial disparities* Tyler (1974c) chose to interpret his results in terms of spatial disparities. He argued that at any instant, uncorrelated dots seen by the two eyes are paired according to a nearest-neighbour principle (see Section 6.2.5). These random pairings generate both crossed and uncrossed disparities with a range of magnitudes, and should give rise to a cloud of dots at different distances in front of and beyond the fixation plane (Figure 13.12).

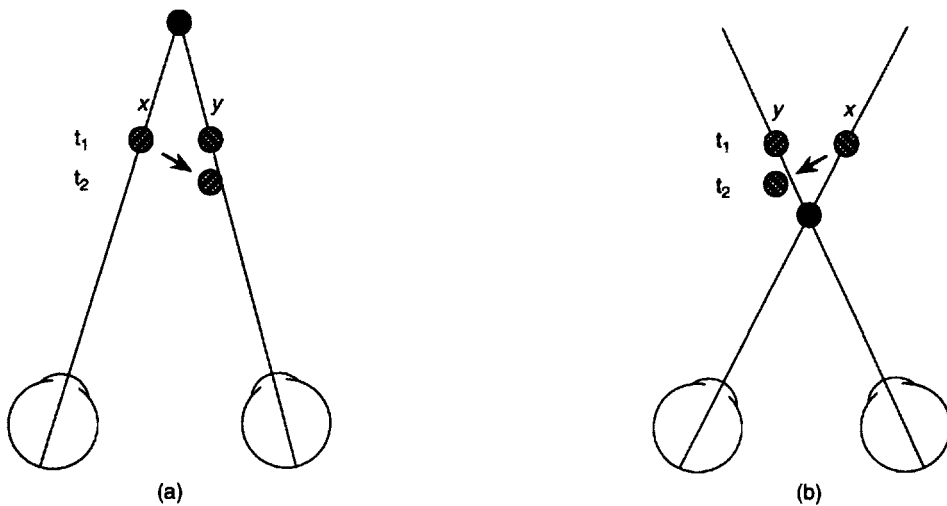


Figure 13.12. Tyler's random spatial disparity hypothesis.

At time t_1 , the random pairing of two closest spaced dots (x and y) creates either an uncrossed disparity (a) or a crossed disparity (b). At time t_2 , the left eye sees the delayed image of dot y which is to the right of x in (a) and to the left of x in (b). Hence, there is a necessary link between uncrossed disparity and motion to the right and crossed disparity and motion to the left.

Random correspondences between dots in different frames to the same eye would also give rise to apparent motion in all directions and with different velocities, according to the dot separations between frames. Tyler showed that there is a necessary geometric link between the predicted disparity of randomly paired dots between the eyes and the direction and velocity of apparent motion between dots in the same eye (Figure 13.12). For example, if a dot seen by the left eye is paired with a dot displaced to the right in the right eye (on a nearest-neighbour basis) it creates an uncrossed disparity. If the left eye is subsequently stimulated by the right eye's temporally delayed dot, the nearest dot for apparent motion must be to the right. Tyler argued that this association is consistent with the appearance of dots rotating or shearing in depth around the fixation point. He termed this explanation the **random spatial-disparity hypothesis**.

One problem with this explanation is that stereopsis should also be possible between uncorrelated patterns of random dots presented to the two eyes, either dynamically or statically. The random pairing of dots seen by the eyes should be sufficient for observers to see a dense cloud of dots lying at different depths. The only difference between the appearance of binocularly uncorrelated patterns and the dynamic-noise Pulfrich effect is that the dots should not appear to swirl in a consistent direction round the fixation point in the former case. Unfortunately, there is dispute as to what is seen when binocularly uncorrelated dot patterns are presented to the eyes. Tyler (1977) claims that depth is seen

"after some initial confusion" and that the appearance is enhanced when seen alongside a binocularly correlated noise field which appears as a single depth plane. MacDonald (1977) and Neill (1981), on the other hand, claim that only rivalry and no depth is seen under these conditions.

A crucial test between the temporal-disparity and random spatial-disparity hypotheses was carried out by Tyler (1977) using a display consisting of a sequence of uncorrelated random-dot frames presented with opposite contrasts to the two eyes. With a neutral-density filter over one eye, observers reported that the dots appeared to swirl in depth around the fixation point, as with the original effect, but in the opposite direction. According to the temporal-disparity hypothesis, depth would be expected only if the stereo system could correlate the temporally displaced dots of opposite contrast to the two eyes. Results obtained with static opposite contrast random-dot stereograms suggest that this is unlikely (see Section 6.2.10) but, even if it were possible, the hypothesis would still fail because it would predict the same direction of three-dimensional swirling with complementary as with correlated noise. Falk and Williams (1980), however, claimed that the reversed direction of swirling seen with opposite contrast dynamic-noise patterns to the two eyes is compatible with the apparent-motion hypothesis described below.

3. *Apparent movement cascades* The third hypothesis invoked to explain the dynamic noise Pulfrich effect was proposed by Mezrich and Rose (1977) and Ward and Morgan (1978). According to this

hypothesis, the effect depends on the apparent motion in "cascades" of dots in the noise and is therefore equivalent to the apparent-motion version of the Pulfrich effect (see Section 13.1.4). The essential difference between this hypothesis and Tyler's random spatial-disparity hypothesis is that for Tyler the apparent motion merely accompanies, or coexists with, the retinal disparity between points, whereas according to the apparent-motion hypothesis, a disparity is created between the spatiotemporal interpolated positions of the moving dots. To test the two hypotheses, Morgan and Ward (1980) created a sequence of random-dot frames in which each dot survived for a limited number of frames (between two and 30) instead of disappearing after a single frame appearance. In addition, each dot was displaced 3.6 arcmin to the right between each pair of frames during its lifetime. Instead of the Brownian motion seen in a sequence of uncorrelated random-dot frames, observers were able to perceive the direction of drift under both monocular and binocular viewing, even when the dot lifetime was as short as 2 frames. The time between frames was 25 ms, and there was an interocular delay of 12 ms. If dots in the leading eye's image had been paired with dots in the same image in the lagging eye, no depth should have been seen, but if dots in the leading eye's image had been paired with dots in the preceding image seen by the lagging eye, the depth should have corresponded to a disparity of 3.6 arcmin. In fact, the disparity corresponding to the matched depth varied between 0.5 and 1.7 arcmin and increased with increasing dot lifetime.

Tyler (1977) suggested that the compromise judgments between 0 and 3.6 arcmin could result from disparity averaging, but Morgan and Ward pointed out that this would not account for the fact that the depth effect increased with the lifetime of the dots in the sequence. Instead, they suggested that the results are more consistent with spatial interpolation of a target undergoing apparent motion, which has been demonstrated for both binocular and monocular moving targets (Burr and Ross 1979; Morgan 1979). In other words, their hypothesis suggests that a simultaneous spatial disparity exists between the interpolated positions of the discretely moving targets in the two eyes. Apart from containing the additional idea of interpolation or spatiotemporal averaging, this hypothesis is equivalent to Fertsch's explanation of the normal Pulfrich effect.

Overall, it would appear that Morgan and Ward's explanation is adequate to account for the effects seen with displays containing apparent-motion cascades, but it is not clear that it is superior to

Tyler's random spatial-disparity hypothesis in accounting for the original dynamic-noise effect in which there are no explicit motion cascades. In order to distinguish between the predictions of the three hypotheses, Falk and Williams (1980) carried out a careful study of the effects of changes in filter density, viewing distance, and dot rate. As evidence against the temporal-disparity hypothesis, they noted that the predicted velocity of disparate points calculated from the magnitude of the filter-induced delay is an order of magnitude larger than any velocity observed in their own or previous studies of the effect. Second, the apparent velocity of the streaming dots increases with the density of the filter covering one eye. According to the random spatial-disparity hypothesis, the speed of the streaming dots should be influenced only by the distance to the nearest-neighbour dot with which it is paired in apparent motion. Yet another problem for the random spatial-disparity hypothesis is that it makes no prediction of a depth effect when the filter-induced delay is significantly less than the interframe interval, while observations suggest an effect is still seen under these circumstances (Falk and Williams 1980).

Neill (1981) provided additional evidence of spatiotemporal averaging by varying the frame rate of the uncorrelated noise patterns. If spatiotemporal averaging is important, the apparent velocity of the streaming dots should be independent of the frame rate as long as the frequency is high enough to allow averaging over several frames. According to the random spatial-disparity hypothesis, the apparent velocity should increase, since each random dot is displaced to its nearest neighbour in a shorter period of time. In Neill's experiment, most observers opted to match the velocity of the uncrossed coherent sheet of dots which lay closest to the display screen. Varying the frame rate between 20 and 120 Hz had little effect on the matched velocity. Also, Neill pointed out that, according to the random spatial-disparity hypothesis, the effect should collapse if the filter-induced lag exceeds the interframe interval. Random disparities are still created between nearest corresponding dots in the simultaneously occurring uncorrelated dot frames, but because of the intervening frame, the direction of apparent motion is no longer systematically related to disparity. Neill's finding that the frame rate has little effect on the appearance of the dynamic-noise Pulfrich illusion is therefore not consistent with this prediction from the random spatial-disparity model.

Morgan and Tyler (1993) reported that the dynamic-noise Pulfrich effect is abolished when the individual noise frames are horizontally filtered to minimize horizontal apparent motion between

frames. In addition, they suggested that all three explanations of the effect can be combined into a more general model in which there are disparity detectors tuned both to a particular direction of horizontal motion and a direction of disparity.

13.1.11 Pulfrich effect and stereoblindness

The fact that a swinging pendulum bob is seen displaced in depth when viewed with a filter over one eye shows that the Pulfrich effect is a stereoscopic effect involving comparison of the spatiotemporal characteristics of the images in the two eyes. It is frequently remarked that Pulfrich could not have experienced the effect himself because he was blind in one eye (Gregory 1966). It is therefore of considerable interest that Thompson and Wood (1993) found that four stereoblind subjects saw a Pulfrich effect under certain conditions. In particular, all four could set a marker under the forward path of the pendulum bob when the dominant eye was filtered with a 1 log unit filter and the bob was tracked with the eyes. Only one stereoblind subject could set the marker when the nondominant eye was filtered and she was the only subject who could set the marker when fixating a stationary point.

The most obvious explanation of these results is that the stereoblind subjects were not completely stereoblind but instead stereo anomalous or simply poor at seeing depth in random-dot stereograms. Thompson and Wood's criterion for stereoblindness was the fusion of a simple random-dot stereogram depicting a central square standing in front of the surround—which all four subjects failed to achieve. In addition, three out of the four subjects showed no interocular transfer of the movement aftereffect. It is possible, however, that their subjects are able to see depth in simple line stereograms, which are more similar in their spatial characteristics to the pendulum bob, but not in random-dot stereograms which have a poorer signal-to-noise ratio.

13.2 STEREOPSIS AND MOTION IN DEPTH

13.2.1 Judging time to collision

The size of the image produced by an object is inversely proportional to the distance of the object from the eye. For a small spherical object moving toward an eye at a constant speed, the rate at which its image increases in size is proportional to the velocity of its approach and inversely proportional to the time to impact. The time to impact from the end of a time interval, t , is the time interval times the

original size divided by the change in size during that interval. Thus,

$$\text{Time to contact} = \frac{i_1}{i_2 - i_1} \quad (1)$$

where i_1 is the image size at the start of the time interval and i_2 is the image size at the end of the time interval. For unit observation time, time to impact is the original image size divided by the change in image size. For example, if the size of the image of an approaching object has doubled in 1 s it must have travelled half the distance from its starting point to the observer in 1 s, and will therefore hit the observer in another second. This idea was first proposed by Fred Hoyle (1957) in a science fiction novel about an asteroid approaching the earth. Note that information about the absolute size of the object or the distance of the object is not required for judgments about time to impact. An approaching distant bullet or a nearby insect will both hit in 1 s if their images double in size in that period. A rapidly looming image produced by an object at any distance is alarming because it signifies impact is imminent. Another way of expressing this is to say that the time to impact of an object moving at constant velocity is equal to the angular size of its image, θ , at a given time divided by the rate of change of image size at that time, $d\theta/dt$.

$$\text{Time to contact} = \frac{\theta}{d\theta/dt} \quad (2)$$

Lee (1976) called this ratio tau τ

Knowles and Carel (1958) seem to have been the first to measure people's ability to judge time to collision. Subjects were shown a looming grid pattern for some time and estimated how long it would take to hit them after it was switched off. They were reasonably accurate when the time to impact was less than 4 s but made progressively larger underestimations of time to contact as the time was increased beyond 4 s. Baker and Steedman (1962) asked subjects to judge when an approaching luminous disc, viewed monocularly in dark surroundings, had moved halfway from its starting position. Its speed was 10 or 20 in/s, its starting positions varied between 10 and 45 ft, and its initial angular size varied between 4 and 36 arcmin. Subjects responded too soon for the largest stimulus but too late for the smallest stimulus. This may be related to the fact that the threshold for detecting motion in depth was lower for objects subtending larger visual angles (Steedman and Baker 1962). Subjects reduced these systematic errors to about 6 per cent after several

hours of training with knowledge of results. In a similar study by Schiff and Detwiler (1979), subjects saw a movie of a black square subtending 0.75 or 3° moving toward them at various velocities, either on a white background or over a textured groundplane. After a variable period of time the screen went blank and subjects pressed a key when they thought the object would have reached them. Times to contact of up to 10 s were underestimated by a constant fraction of about 0.35, which was similar to the proportional underestimation found by Knowles and Carel. The proportional error increased when the actual time to contact was 16 s (see also McLeod and Ross 1983). Todd (1981) asked subjects to judge which of two looming squares on an oscilloscope screen would reach them first. The responses were 90 per cent accurate for a time-to-contact difference of 150 ms and did not reach chance level until the time difference was reduced to 10 ms. Estimates have been found to be more accurate for trajectories in the midline than for oblique trajectories (Schiff and Oldak 1990).

If the starting size of an object is held constant, the ratio $\frac{\theta}{d\theta/dt}$ is confounded with the rate of angular expansion, θ . In other words, a person could use either one or the other of these sources of information to discriminate between the times to contact of two objects. Interleaving two or three starting sizes does not provide a demonstration of which cue a subject is using. Regan and Hamstra (1993) used an 8 × 8 matrix of stimuli in which time to contact varied along the rows and rate of expansion ($d\theta/dt$) varied down the columns. Thresholds for both time to contact and rate of expansion could be obtained from a single data set. When subjects were instructed to indicate whether the time to contact of an expanding bright solid square was greater or less than the mean of the stimulus set, the threshold for time to contact was between 7 and 13 per cent over a range of times to contact of 1 to 4 s. This was about 100 times lower than the threshold for rate of expansion. Regan and Hamstra concluded that the human visual system contains a mechanism specifically sensitive to time to contact and which is independent of changes in either the angular size or the rate of change of angular size of the approaching object.

Equation 2 is satisfied by any stimulus variable, in addition to image size, that approximately varies inversely with distance, such as accommodation, vergence angle, and binocular disparity. Heuer (1993a) found that time-to-contact judgments were influenced by both changing size and changing disparity between dichoptic images of a small circle. When the two cues were in conflict, the changing-

size cue was dominant for objects larger than about 1°, but changing disparity (and/or vergence) was the dominant cue for objects smaller than 0.5°.

Several animals judge time to contact. For instance, diving birds, such as the gannet, accurately judge the time when they should fold their wings as they dive into water at high speed (Lee and Reddish 1981). Neurones have been found in the nucleus rotundus of the pigeon that respond at a constant time before an approaching object makes contact with the head, even when the size or velocity of the object varies widely. These cells could therefore control avoidance behaviour (Wang and Frost 1992). Locusts avoid collisions with other locusts when flying in a swarm (Robertson and Johnson 1993). In this case, all the objects are the same size and avoidance could be based on the size of the looming image rather than on tau. Lee (1976) and Cavallo and Laurent (1988) investigated the application of time-to-contact judgments to collision avoidance in automobiles. The theoretical issues in research on time to contact have been reviewed by Tresilian (1991, 1993).

13.2.2 Impact direction for a monocular point

As an object at a given distance approaches, its image expands at a rate proportional to the object's rate of approach. Whether the object appears to approach depends on whether the observer interprets the changing image size as due to motion in depth or to a change in the size of the object. For discussion of this topic readers are referred to Johansson (1964), Marmolin (1973), and Swanston and Gogel (1986).

At a given instant, the direction of motion of an object approaching an eye along a straight trajectory within a horizontal plane can be decomposed into two components, as illustrated in Figure 13.13. The first component is the **headcentric direction** of the object at a given instant. This indicates the direction of the point from which the object is approaching at a given instant. Headcentric direction is best specified in terms of meridional angle and eccentricity (polar coordinates). For simplicity we consider only trajectories in a horizontal plane, which will be specified in terms of the azimuth of the trajectory relative to the median plane of the head. The second component is the angle that the object's trajectory makes with the visual line which the object is traversing at that instant. This is the **impact direction** of the trajectory. When the trajectory lies along a visual line the impact direction is 0° and the object will hit the nodal point of the eye—the object is on a direct-impact trajectory. When the trajectory is not along a visual line, both the azimuth and impact direction change from moment to moment. If the trajectory of

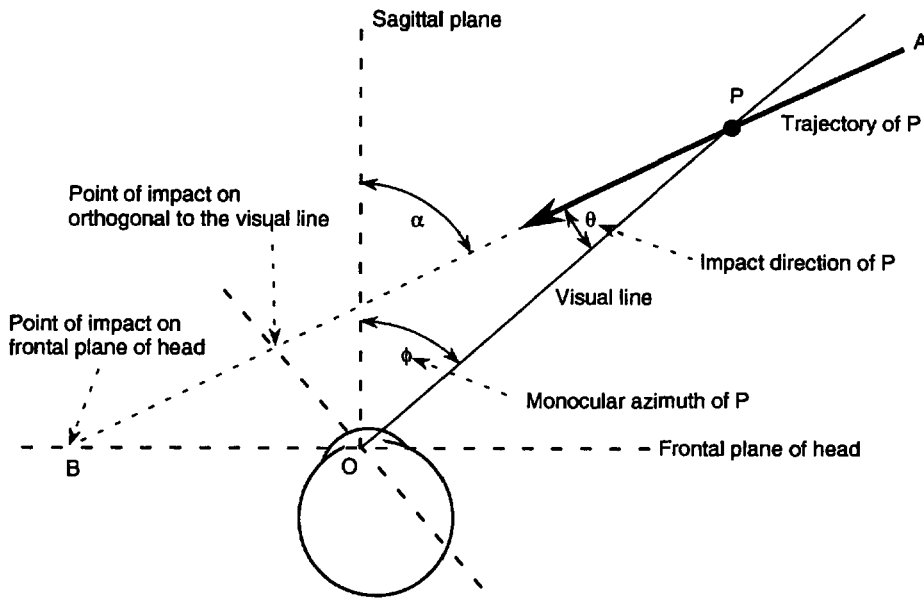


Figure 13.13. Motion in depth of a monocularly viewed object.

The monocular azimuth of an object P at a given instant, as it approaches an eye along trajectory AB , is the angle ϕ between the visual line, PO , on which P lies and a sagittal plane of the head. The monocular impact direction of P at a given instant is the angle θ between the trajectory and the visual line which P is traversing. Whatever the value of ϕ , for a specified distance of P from the eye, θ specifies the point of impact of P on a plane orthogonal to the visual line. For a given value of ϕ and distance of P , θ specifies the point of impact on the frontal plane of the head. The angle α , between P 's trajectory and a sagittal plane, equals $\theta + \phi$.

an object at distance D traverses a visual line at an angle θ , it will cut the plane containing the nodal point of the eye and orthogonal to the visual line at distance $D \tan \theta$ from the nodal point. Thus, the distance by which an approaching object will miss the eye depends only on its impact direction and distance. An object at azimuth ϕ and impact direction θ will impact the frontal plane of the head at distance $D \tan \theta \tan \alpha$ from the nodal point, where $\alpha = \theta + \phi$, as shown in Figure 13.13. Thus, for an object approaching within a horizontal plane, the distance within the frontal plane of the head by which it will miss the eye depends on the object's azimuth, its impact direction, and its distance from the eye.

Consider a monocularly viewed object of no discernible size, such as a point of light viewed in dark surroundings. Suppose that the headcentric direction of the point of light relative to the head is judged correctly. As such an object moves, the observer can detect only the component of its motion projected into the frontal plane. For an object moving at constant velocity, a change in its impact direction causes a change in the direction or velocity of the motion of the retinal image or, if the object is pursued by the eye, a change in the direction or velocity of the eye. In the absence of any other information, these cues to impact direction are

ambiguous because the retinal image motion produced by an object moving at a certain velocity within a frontal plane may be the same as that produced by an object traveling at an angle toward or away from the observer at some other velocity. If the object moves directly toward or away from an eye, its motion will be undetected when viewed monocularly. It is therefore not possible on this basis alone to judge whether the object is approaching or receding.

If the observer knows that a point source is moving, a judgment can be made about whether it is moving along a line of sight or along some other trajectory. Similarly, a moving observer can tell whether he or she is heading in the direction of an isolated point of light viewed monocularly. Suppose, for instance, that a pilot is flying a plane on a dark night toward a lighthouse or in pursuit of a light on another plane. Any perceived movement of the light relative to the head of the pilot indicates that the plane is not flying directly toward the light. The pilot will not know whether the plane is getting nearer to the target, since the target could be a light on a receding aircraft. If the motion of the light is seen against a part of the cockpit, the task reduces to that of vernier acuity and can be performed with great precision, as in aiming a gun with a gun sight. Llewellyn (1971) found that the precision and

accuracy of judgments about heading based solely on the apparent sideways drift of a small identifiable target were far better than the precision and accuracy of judgments based the focus of expansion of an array of objects, which we describe next.

13.2.3 Relative motion cues to impact direction

The point of impact

Consider a textured surface lying in a frontal plane. As it approaches the observer or as the observer approaches its image expands, or looms. If the observer knows that the surface is not actually varying in size, looming provides unambiguous information about the rate of approach and the location on the surface where impact will occur—the **point of impact** (Gibson 1950, 1958). The point of impact is often referred to as the **heading direction**. But if heading direction is defined as the direction along which the observer is moving relative to bodycentric coordinates, it is not fully specified by the point of impact. Heading direction in this sense requires information about the position of the eye in the head and of the head on the body. With monocular viewing, looming has three important features; its rate, focus, and symmetry. We considered rate of looming in the last section.

Assume that an observer is approaching a large textured surface, with the gaze fixed on the focus of expansion of the looming image. Under these circumstances, the focus of expansion indicates where on the surface impact will occur. James Gibson stressed the importance of looming for a pilot landing an aircraft (Gibson et al. 1955). The centre of a looming pattern is defined by relative motion and not by a particular object. It is therefore quite different from the case described in the last section. This difference becomes evident when the eye fixates and pursues a part of the expanding pattern that is not on the path of approach. The image of the pursued stimulus remains stationary on the retina and therefore forms the centre of the looming image of the approaching surface. The focus of expansion of the optic array moves over the retina. One can say that a translatory component due to the tracking motion of the eye has been added to the looming component of the forward self-motion, resulting in a shift of the focus of expansion to one side of the image of the point of impact or even the removal of the focus of expansion from the field of view (Regan and Beverley 1982). In other words, the focus of expansion of the retinal image no longer indicates the point of impact. A person would be able to recover the true point of impact if the motion of the eyes were taken into account. The translatory and

expansion components of the flow pattern could then be decomposed and the focus of expansion of the optic array recovered. Estimates of this ability have been produced, but this topic goes beyond the scope of this book (see Warren 1988; van den Berg 1992).

The task of detecting the point of impact is simplified when the observer moves through an array of objects at different depths. The path of self motion (a set of points of impact in depth) is specified by the locus of that set of objects that do not show parallax, that is, the set of objects remaining in alignment. This so-called **locus of zero parallax** is not affected by eye movements and, under the best conditions, reduces to a vernier acuity task (Regan and Beverley 1984; Cutting 1986). If the observer knows the direction of gaze, the locus of zero parallax indicates the headcentric heading.

Symmetry of looming

Finally, consider the symmetry of looming of a monocularly viewed object. A spherical object approaching the eye along the visual axis, or any other visual line, produces an image that expands symmetrically, and this signifies that the object will ultimately hit the observer if no avoidance response is made. If the object approaches an eye along any path other than a visual line, its image expands asymmetrically, and if this asymmetry is large enough it indicates that the object is destined to miss the head. Note that this cue depends only on the direction of the path of the approaching object relative to a visual line; it is not substantially affected by rotations of the eye. Furthermore, it does not indicate the azimuth direction of the approaching object, only its impact direction.

Avoidance behaviour in response to looming of shadows cast on a screen has been demonstrated in a variety of species, including crabs, chicks, monkeys, and humans (Schiff et al. 1962; Schiff 1965). There was some indication that animals could detect the impact direction of the simulated approach from the degree of asymmetry in the looming pattern. It is not known whether these avoidance responses to looming are innate or develop only after the experiential coupling of looming and impact. It has been claimed that avoidance responses to symmetrically expanding shadows occur in human infants only 2 weeks old (Ball and Tronick 1971; Bower et al. 1971). The avoidance responses were not observed when the shadows expanded asymmetrically or contracted. Yonas et al. (1977) found no evidence of avoidance responses to symmetrically looming shadows, or even to real approaching objects, in infants under about four months of age. However, they did find

that infants under 4 months of age followed a visual target that rose in the visual field. They suggested that the responses observed by Ball and Tronick were due to the attempt of the infant to keep the gaze fixed on the top of the approaching object as it rose higher in the visual field, and not to the movement of the object in depth. Dunkeld and Bower (1980) challenged this assertion and produced evidence that infants between 3 and 4 weeks of age show avoidance responses triggered specifically by the approach of an object, under conditions where responses to rising edges are controlled for. The avoidance response to a real approaching object in the human infant has been said to emerge between the second and fourth month (Peiper 1963). Yonas et al. (1978) found that infants began to respond to an approaching object in a stereoscope somewhere between the third and fifth month. Whether responses to looming are innate or learned, adult animals showing avoidance responses to an approaching object seen with one eye must possess a mechanism for the detection of the degree of symmetry in the looming image.

Regan and Kaushal (1993) have provided a mathematical analysis of monocular cues to the impact direction of an approaching object. The two cues are;

$$\text{the ratio } \frac{(d\phi / dt)}{(d\theta / dt)} \text{ and the ratio } \frac{(d\alpha_L / dt)}{(d\alpha_R / dt)}$$

where $d\phi/dt$ is the translational speed of the object's retinal image, $d\theta/dt$ is its rate of expansion, and $d\alpha_L/dt$ and $d\alpha_R/dt$ are the speeds of its opposite edges. They showed that the number of object radii by which the object will miss the eye within a plane orthogonal to the visual line the object is traversing is given by either cue. In psychophysical experiments they dissociated both the direction and speed of the frontal plane component of motion from the impact direction. Even in this situation, subjects could discriminate the impact direction to better than 0.1° . Regan and Kaushal concluded that the visual system contains a monocular mechanism sensitive to one of the two ratios described above, independent of the frontal plane component of the motion. The discrimination threshold for impact direction of an approaching object was similar for trajectories lying in horizontal, vertical, and oblique planes, which project onto horizontal, vertical, and oblique retinal meridians, respectively. The form of the discrimination threshold did not vary significantly as a function of the impact direction within a given plane and therefore provided no evidence of multiple channels tuned to impact direction. We will

see in the following that multiple channels have been revealed in the binocular detection of impact direction.

Adaptation of looming detectors

Looming detectors might be expected to manifest aftereffects due to adaptation, like those shown by detectors for other visual attributes, such as lateral motion and orientation. Regan and Beverley (1978a) reported evidence of this kind. They asked subjects to fixate a point between two flanking 0.5° black squares on a 15° by 10° white background. The small squares either pulsated sinusoidally in size or oscillated from side to side with a frequency of 2 Hz. Inspection of a square pulsating in size for 25 minutes specifically elevated the threshold for detection of pulsation in a test square but had very little effect on the threshold for detection of sideways motion. This suggests that looming is processed by specialized motion detectors distinct from those devoted to the detection of local unidirectional motion. When the pulsations and oscillations were slow one way (with a quick return ramp waveform) the threshold elevation was evident only when the ramp motions of the test and inspection squares were in the same direction.

In another experiment, subjects fixated a point at the centre of a 1° -wide bright square that loomed symmetrically at 24 arcmin/s for repeated periods of 0.1 s over a total period of 20 min. The square appeared to move continuously in depth and produced a strong aftereffect of receding motion in a stationary stimulus, which could be nulled by a real movement in the opposite direction. This aftereffect was restricted to the region of the retina stimulated by the inspection square, but showed at about 40 per cent of its normal strength when the test square was presented to an eye that had not been exposed to the inspection square (Regan and Beverley 1978b).

Regan and Beverley drew the following theoretical conclusions from their experiments. There are visual channels in specifically tuned to looming images, which are built up from detectors that analyze relative motion within different meridians. Each relative-motion detector linearly and accurately subtracts the output of local detectors that encode motion at two retinal locations within a given meridian (Regan and Beverley 1980; Regan 1986b). The two locations must be no more than 1.5° of visual angle apart, since adaptation to oscillating squares larger than this did not produce the type of aftereffect just described Beverley and Regan (1979a). They further proposed that a looming detector combines signals from orthogonal relative-motion detectors in a non-linear fashion. The nonlinearity is such that looming

signals are accepted only if the image is characteristic of a rigid nonrotating object (Beverley and Regan 1979b; 1980a). Thus, an image whose rate of expansion is not isotropic does not effectively drive the motion-in-depth system.

In a subsequent experiment Regan and Beverley (1979a) measured the reduction in sensitivity to size oscillations of a test square after adaptation to a radially expanding and contracting optic flow pattern of short lines. Threshold elevation was large only when the test square was exactly where the centre of the flow pattern had been. This was so even when the focus of the flow pattern was not on the fixation point (Regan et al. 1979). It was concluded that local looming detectors sample the optic flow pattern caused by self-motion through a three-dimensional world, and "light up" in the immediate vicinity of the focus of the flow pattern. For the flow pattern used, the divergence of velocity ($\text{div } V$) was large only at the focus of expansion, so that the looming detectors were acting as $\text{div } V$ detectors (Regan and Beverley 1979a; Regan 1986b). The significance of this point is that, by definition, $\text{div } V$ is not affected by eye movements. The aftereffect of adapting to a square pulsating in size was also specific to a range of frequencies of pulsation of the test square centred on the frequency of the adapting stimulus. Within a frequency band of 0.25 to 16 Hz there was evidence of three broadly tuned channels, each with a different preferred frequency (Beverley and Regan 1980b). In other words, in addition to being tuned to impact direction, looming detectors are tuned to the velocity of an approaching object.

Looming detection as a preattentive process

A stimulus moving in the frontal plane in one direction immediately pops out when set among stimuli moving in the opposite direction, and the time taken to detect the odd stimulus is independent of the number of stimuli. It has been suggested that this is evidence of cortical units at an early stage of processing tuned to the direction of lateral motion (see Section 6.1.5). If there are such cortical units dedicated to detecting looming, one would expect an expanding stimulus to pop out when set among contracting stimuli. However, Braddick and Holliday (1991) found that an expanding stimulus patch that periodically returned rapidly to its starting size, when set among stimuli that changed size in the same way but in counterphase, took longer to be detected when the number of distracting stimuli was increased. The distracting stimuli had staggered starting times so that the cue of relative size was not available. This suggests that detectors tuned to the direction of motion in depth do not occur at the

preattentive level of sensory processing. Sekuler (1992) also argued against there being specific detectors for motion in depth on the grounds that speed discrimination for looming, lateral motion, and rotation were similar, and performance with a variety of looming stimuli could be accounted by linear summation of lateral motion signals. Sekuler's suggestion, however, conflicts with psychophysical evidence that, although relative motion detectors are constructed by linear summation of detectors for oppositely directed retinal motion in any given direction (Regan 1986b), two-dimensional changing-size detectors are based on strongly nonlinear summation of orthogonal relative motion detectors (Beverley and Regan 1980a). Beverley and Regan suggest that nonlinear summation blocks access to the motion-in-depth system when the rate of image magnification is not characteristic of a rigid, nonrotating object (Beverley and Regan 1979b).

13.2.4 Binocular cues to impact direction

Theoretical analysis

The lines and angles used in specifying the direction of approach of an object P with respect to the two eyes are shown in Figure 13.14. The object lies on a cyclopean line passing through a point midway between the eyes and its cyclopean azimuth, ϕ , is the angle between the cyclopean line and the median plane of the head. The impact direction, β , of the point is the angle between the cyclopean line and the trajectory of the point (line AB).

Consider a pointlike object devoid of monocular cues to its distance approaching the head within the horizontal plane of regard at constant velocity. When the eyes remain perfectly converged on the approaching object, its distance is indicated by the angle of vergence, and its azimuth by the cyclopean azimuth of gaze. The impact direction of the object is indicated by the ratio of the vergence and version components of the tracking eye movement. The eye movement is a pure vergence when the tracked object moves along a hyperbola of Hillenbrand. Beyond a viewing distance of about 20 cm and for trajectories not too far from the median plane of the head, the hyperbolas of Hillebrand may be regarded as straight lines converging on a point midway between the eyes. The eye movement is a pure version when the object moves along an isovergence locus which is roughly equivalent to the horizontal horopter (see Figure 10.5). The role of tracking eye movements in judging the trajectories of approaching objects does not seem to have been investigated.

When the gaze is fixed on a stationary object while a second object moves toward the head, the

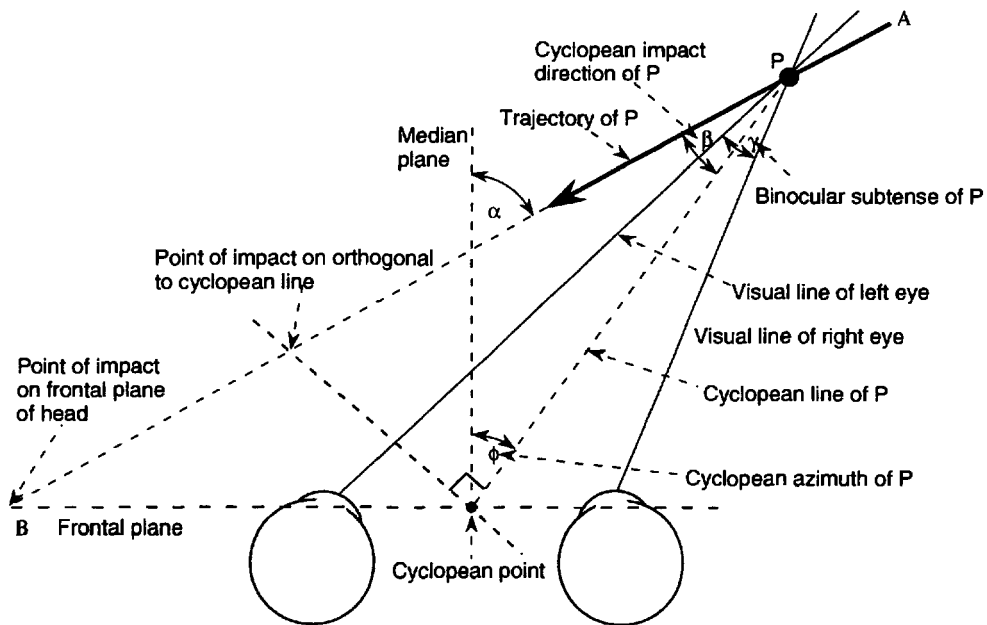


Figure 13.14. Motion in depth of a binocularly viewed object.

The cyclopean azimuth of point P as it approaches along trajectory AB is the angle ϕ between the cyclopean line on which P lies and the median plane of the head. The cyclopean impact direction of P at a given instant is the angle, β , between the trajectory and the cyclopean line which P is traversing. Whatever the value of ϕ , for a specified distance of P from the cyclopean point, β specifies the point of impact of P on a plane orthogonal to the cyclopean line. For a given value of ϕ and distance of P , β specifies the point of impact on the frontal plane of the head. The angle α , which P 's trajectory makes with the median plane, equals $\beta + \phi$.

relative motion of the images of the moving object in the two eyes varies with the impact direction of the object. Consider an object moving within the horizontal plane of regard. When it moves along a hyperbola of Hillebrand, the images in the two eyes move symmetrically outwards when the object approaches and symmetrically inwards when it recedes. The ratio of velocities is 1:1 in antiphase. Regan and Beverley pointed out that when the object moves along a visual line of one or the other eye, the image in only one eye moves and the ratio of velocities is 1:0. The visual line may be the visual axis or any other visual line. If the object moves along a path that misses the head to one side, the images move in the same direction, that is, in phase. The limiting case for in-phase motion is motion of the object along the horizontal horopter, when the ratio of movements is 1:1 in phase.

These relationships hold wherever the eyes are converged. Thus, at any instant, the relative motion of the images of an approaching object provides unambiguous information about an object's impact direction relative to both the hyperbola of Hillebrand and the visual lines it is traversing at that instant. These relationships are depicted in Figure 13.15. The direction, β , of an object's trajectory relative to the cyclopean line of sight on which the

object lies is given by

$$\tan \beta = \frac{I[(d\phi_R / dt) / (d\phi_L / dt)] + 1}{2D[(d\phi_R / dt) - 1]} \quad (3)$$

where $d\phi_R/dt$ and $d\phi_L/dt$ are the angular velocities of the left and right images, D is the distance of the object, and I is the interocular distance (Regan 1993).

Note that relative image motion does not indicate the headcentric azimuth of an object, since the same relative motion is produced whichever visual line the object traverses. In other words, relative image motion does not indicate the headcentric direction from which an object is approaching, it indicates only the angle of approach relative to a line of sight—the impact direction. Azimuth information is provided by the mean eccentricity of the images when the eyes are symmetrically converged on a stationary point in the midline or the mean angle of gaze when the eyes are converged on the approaching object. The direction of an object's approach in terms of headcentric elevation is indicated by the vertical eccentricity of the image or of the gaze.

The impact direction of an approaching object is also indicated by the ratio between the translational image velocity and the rate of change of disparity between the images of the object. When an object

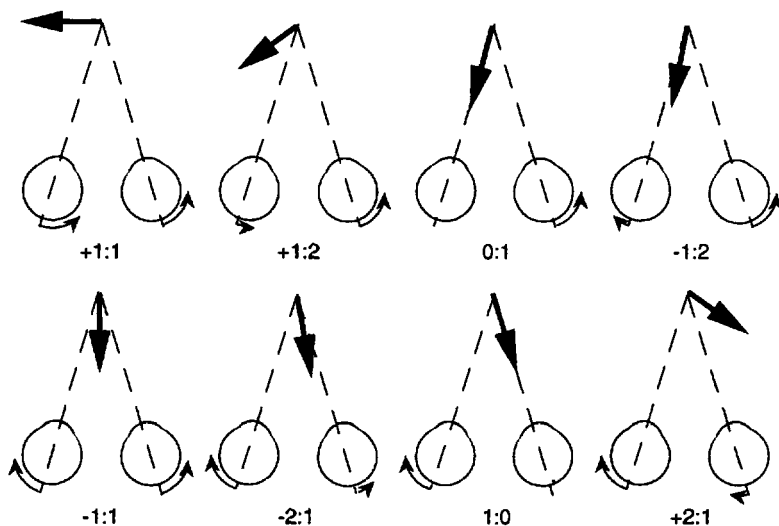


Figure 13.15. Impact direction and relative image velocity.

The relative speeds and directions of image motion in the two eyes are related to the impact direction of an object approaching in the plane of regard. The ratio of image velocity in the left eye to that in the right eye is given below each figure. Positive signs indicate that the images move in the same direction in the two eyes. Negative signs indicate they move in opposite directions and that the object will impact between the eyes. (Adapted from Beverley and Regan 1975.)

moves along the horopter there is no change in disparity, and when it approaches along a hyperbola of Hillebrand there is maximum change of disparity.

The angle of approach, β , relative to the cyclopean line of sight on which the object lies is given by

$$\tan \beta = \frac{I(d\phi/dt)}{D(dy/dt)} \quad (4)$$

where $d\phi/dt$ is the translational speed of the fused image and dy/dt is the rate of change of disparity (Regan 1993).

Equations (3) and (4) are mathematically equivalent. Furthermore, in natural conditions the cue of changing disparity covaries with relative image motion, so it is not possible to say which is being used. However, the two cues have distinct physiological implications: equation (3) implies that impact direction is derived from relative motion while equation (4) implies that it is derived from changing disparity. Regan (1993) provided evidence that changing disparity is a sufficient cue for impact direction. He created a dynamic random-dot stereogram of a square standing out in depth from a background. In a dynamic random-dot stereogram the dots are changed on every frame, so monocular cues to image motion are not present. When the disparity of the square was alternated continuously through 8 arcmin at 0.5 Hz, the square appeared to oscillate in depth—an effect noticed by Julesz (1971). The square was also oscillated at 0.5 Hz from side to side, in the

same direction in both eyes. When the ratio of disparity oscillation to lateral oscillation was varied, the angle of the square's motion in depth varied accordingly. Since the motion was cyclopean, subjects were not using relative motion of the monocular images as a cue to motion in depth—they must have been using the ratio of lateral motion to changing disparity. Cumming and Parker (1994) use a similar stimulus with similar results. They also devised a stimulus with visible monocular motion, opposite in each eye, but in which disparity changes were beyond the temporal resolution of stereopsis. This stimulus did not produce motion in depth. In another experiment, Cumming (1994) found that stereomotion thresholds correlated well with stereoacluity but poorly with detection of motion in a frontal plane. They concluded that stereomotion is detected mainly by temporal changes in binocular disparity.

In the experiments reviewed next, the two modes of binocular processing were not dissociated; thus, when reference is made to changing disparity it does not necessarily imply that subjects were using this information rather than relative image motion.

Sensitivity to binocular cues to motion in depth

The sensitivity to motion in depth of a small luminous target in dark surroundings was measured by Baker and Steedman (1961). The image size of the target increased or decreased at rates of between 0.25 and 2 arcmin/s. Detection of motion improved

with increasing luminance and increasing velocity and was higher with binocular than with monocular viewing. Under optimal conditions 75 percent correct detection was achieved when the visual angle of the target increased or decreased by 2 percent. In these experiments, the changing-disparity cue was not isolated from the monocular cue of changing size.

Data on the sensitivity of the changing-disparity cue for detecting motion in depth and discriminating changes in impact direction have been provided by Beverley and Regan (1975). Subjects converged in the plane of a textured surface containing nonius lines. A pair of dichoptically superimposed vertical bars was placed slightly to one side of the fixation point. Oscillation of the bars in antiphase from side to side created the impression of a single bar oscillating in depth. When the amplitude of oscillation was the same in the two eyes, the bar appeared to move in the median plane and the apparent impact direction of movement in depth could be changed by altering the relative amplitudes of side-to-side motion. A motion-in-depth sensitivity curve was obtained by measuring the threshold amplitude of stimulus oscillation required for the detection of motion in depth (Figure 13.16b). A direction discrimination curve was obtained by measuring the threshold change in relative amplitude of oscillation required for detecting a change in the direction of motion in depth (Figure 13.16a). There are three peaks in the discrimination curve—for trajectories directed to each eye and at a point midway between the eyes. This suggests that the tuning functions of distinct motion-in-depth channels overlap at these points (see Section 3.5.3). Figure 13.16c shows a hypothetical set of tuning functions derived from experiments on adaptation of motion in depth.

Heuer (1993b) also obtained an impression of motion in depth when the disparity between the images of an isolated object was changed, and reported that impact directions for such a stimulus were discriminated best for motions aimed at a point midway between the eyes. He did not find the peaks of direction discrimination for trajectories toward each eye that Beverley and Regan (1975) reported for a stimulus in which subjects fixated on a stationary object.

Impact direction and convergence

When the eyes remain converged on an approaching object there are no changing disparities in the images of that object. However, the images of stationary objects have a changing disparity which obeys the same rules as those governing the changing disparity in an approaching object that is not visually

tracked. In theory, the impact direction of the moving object could be detected from this information. This question has not been investigated. If the eyes converge in response to an approaching object but at too slow a rate, the images of both the object and stationary objects have changing disparities. In other words, the changing disparity is partitioned between the moving object and the stationary background according to the gain of the vergence response. However, the total relative change of disparity between object and background is constant and therefore provides accurate information about the impact direction and speed of approach.

If an approaching object is seen in dark surroundings and the eyes remain converged on it, then all changing disparity and relative image motion is lost. Suppose the cue of changing image size is not present. Under these circumstances, judgments of impact direction would have to be based on the convergence movements of the eyes. Regan et al. (1986a) found that some motion in depth was perceived when the disparity between the images of an isolated object was changed. The perceived motion of an isolated object was less than when a stationary reference point was in view. There was no changing size cue in this stimulus, so any perceived change in depth must have arisen either from changing convergence or from relative image motion or changing disparity resulting from a failure of vergence to keep the images in binocular register. In a control condition, involving the use of open-loop vergence, the cue of changing vergence in the absence of changing disparity was ineffective in producing sensations of motion in depth of an isolated object. Presumably, therefore, the perceived motion in the closed-loop condition was due to relative motion of the retinal images. With an array of dots in the frontal plane, an overall change in disparity did not give rise to a sensation of motion in depth. Regan et al. explained this difference between an isolated dot and an array of dots in evoking a sensation of motion in depth in terms of inhibitory interactions between the points of the multidot array.

However, this effect could be explained in another way. The sensation of motion of the multidot display would be inhibited by the absence of looming. In an actual display of moving dots the separation of the dots increases. With a single dot the absence of the expected looming would be less noticeable. A single dot surrounded by other dots some distance from it appeared to move in depth when the disparity of the whole array was changed. In this case the single dot would perhaps not be seen as belonging to the surrounding dots and, in any

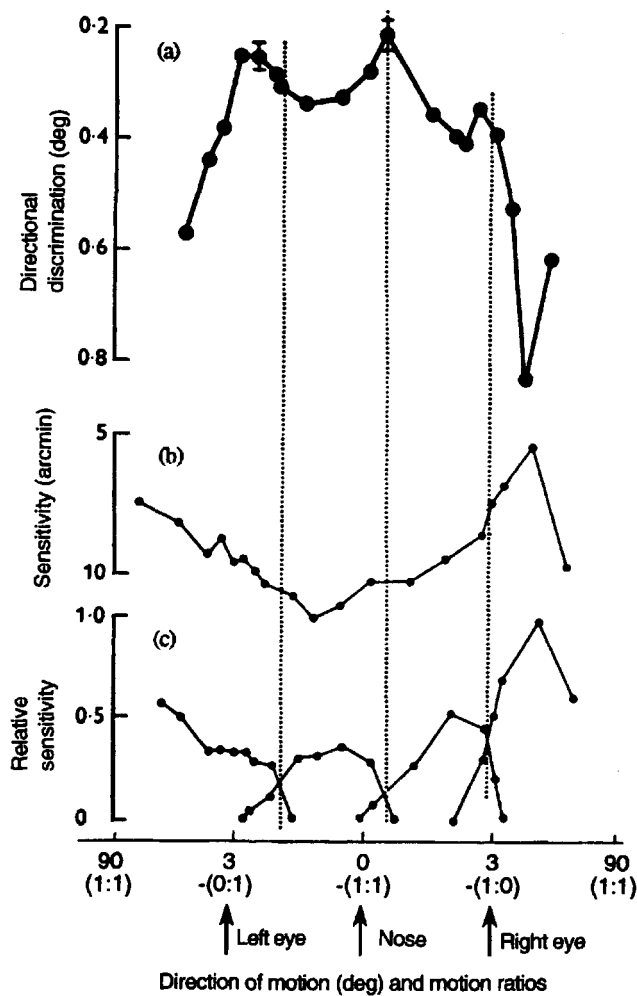


Figure 13.16. Sensitivity for motion in depth.

(a) Sensitivity to changes in the impact direction of a bar, as a function of the direction of motion relative to the median plane of the head.
 (b) The smallest amplitude motion in depth required for detection of motion as a function of direction of motion.
 (c) Sensitivity functions for four hypothetical binocular mechanisms, each tuned to a different range of impact directions. Results for one subject. Bars are standard deviations. (From Beverley and Regan 1975.)

case, the greater separation between it and the other dots would make it more difficult to detect whether the expected looming was occurring.

Interactions between monocular and binocular cues

Since the monocular cue of changing size and binocular cues evoke the same sensation of an approaching object, one can ask how they interact. Regan and Beverley (1979b) proposed that the two cues combine according to a simple weighted-sum model. They reported that a motion-in-depth sensation produced by changing size may be cancelled by an opposed change in relative disparity.

Furthermore, they found that a motion-in-depth aftereffect induced by inspection of a changing size stimulus may be nulled by a change in disparity. The changing disparity cue became more effective relative to the changing size cue as stimulus velocity or exposure time increased. The relative effectiveness of the two cues varied widely between subjects. Heuer (1987) confirmed that when the two cues have the same sign they combine by simple summation. However, when one cue signalled an approaching object and the other a receding object, they rivalled rather than combined, with now one and then the other cue dominating.

Stereomotion scotomata

The visual fields of many subjects with otherwise normal vision contain areas specifically blind to motion in depth, defined by changing disparity (Richards and Regan 1973). These have been called stereomotion scotomata. Sensitivity to static disparity and to sideways motion is normal in such areas. The stereomotion scotomata may be a few degrees in diameter or extend over a quadrant or most of the visual field. The defect in a given area may be specific for either crossed or uncrossed disparities, that is, for an object moving along a trajectory nearer than or beyond the plane of convergence. Furthermore, for some subjects the defect was specific to the direction of motion, that is, to motion toward or away from the person (Hong and Regan 1989). The defect takes several forms. In one form, motion in depth is seen initially but rapidly fades away. In a second form, the moving object appears diplopic, and in a third form the target appears stationary or appears to move from side to side rather than in depth. Stimuli within a stereomotion scotoma evoke only weak vergence movements when they move in depth but normal conjugate eye movements when they move from side to side (Regan et al. 1986b).

13.2.5 Physiology of motion in depth

The detection of monocular cues

There is physiological evidence for a visual mechanism specifically tuned to the impact direction of approaching objects, as defined by the symmetry of looming of monocular images. Updyke (1974) recorded from the superior colliculus of the monkey and found cells that responded best to objects approaching the animal's head, although it was not clear whether the crucial stimulus was the symmetry of monocular looming or the relative movements of binocular images. Zeki (1974a) found cells in the superior temporal sulcus of the monkey, an area including the middle temporal area (MT), that

responded specifically to two parallel bars moving in opposite directions within the receptive field of one eye. Some cells responded only to motion of bars toward each other and other cells responded only to motion of bars away from each other. One problem is that these cells may respond to increasing or decreasing amounts of light rather than specifically to motion. Regan and Cynader (1979) found 56 cells in area 18 of the cat that responded to changing size, and 19 of these cells responded to changing size independently of changes in light level. However, the response of almost all these 19 cells to changing size varied as a function of the location of the stimulus in the cell's receptive field. Some cells preferred an expanding stimulus in one part of the receptive field and a contracting stimulus in another part. It was pointed out that any cell that prefers the same direction of motion for a leading as for a trailing edge would respond more strongly to expansion in one part of its receptive field and to contraction in another part. Only one cell qualified as detector of expansion. However, the population response of the other cells could code expansion or contraction independently of position.

Area MT of the superior temporal sulcus projects to the ventral intraparietal sulcus (VIP). Cells in VIP of the monkey have response properties similar to those in MT (Colby et al. 1993). They are highly selective for direction and speed of retinal motion, and some respond best to a stimulus moving from any azimuth direction toward a particular point on the face of the animal. In other words, they are selective to impact direction. Cells tuned to the impact direction and velocity of an approaching object have also been found in the visual system of the locust. These cells responded to a monocular object, showing that their effective stimulus is looming rather than changing binocular disparity (Rind and Simmons 1992).

The detection of binocular cues

There is also physiological evidence for the presence of binocular visual mechanisms specifically tuned to impact direction, as defined by the opposite movement of images in the two eyes. Zeki (1974a) recorded from cells in the superior temporal sulcus of the monkey and found cells that responded to motion in one direction in one eye and to motion in the opposite direction in the other eye. However, Zeki did not stimulate both eyes simultaneously. Pettigrew (1973) did stimulate both eyes simultaneously, and found a few cells that responded best to oppositely directed movements in the two eyes.

Regan and Spekreijse (1970) recorded evoked potentials from the scalp over the visual cortex in human subjects as they watched a stereoscopic

display of simulated motion in depth, and obtained responses specifically related to the appearance of motion in depth. Responses for approaching motion differed from those for receding motion (Regan and Beverley 1973d). Cynader and Regan (1978) recorded from single cells in area 18 of the cat's visual cortex as the animal viewed a stereoscopically simulated display of a bar oscillating in depth along various impact directions within a horizontal plane. They found three types of cell. Cells of the first type were tuned to impact direction, with a directional range of 2 to 3°, which included trajectories that would hit or narrowly miss the cat's head. These "hitting-the-head" cells responded to opposite motion in the two eyes and were inhibited when both images moved in the same direction. Some of them did not respond to monocular motion while others responded to motion in the same direction in the two eyes when tested monocularly (Regan and Cynader 1982). Cells of the second type were tuned to trajectories that missed the head. These "missing-the-head" cells responded to stimuli moving in the same direction in the two eyes, but at different speeds. Cells of the third type were tuned to movements within a frontal plane, that is, to movements of the images in the same direction and at the same speed. The tuning functions of cells responding to an approaching object were largely unaffected by changes in the horizontal disparity of the moving images (Cynader and Regan 1982). Most hitting-the-head cells showed the same directional tuning and response amplitude when the velocity of the stimulus was increased from 10 to 40°/s, but some of these cells responded less vigorously to higher velocities (see Figure 13.17). Spileers et al. (1990) also found cells in area 18 of the cat's visual cortex that were selectively responsive to motion in depth independently of their response to either disparity or velocity, but they found more cells also selectively responsive to stimulus speed. They suggested that, as a set, these cells produce a three-dimensional map of the optic-flow field.

Cells responsive to opposed motion in the two eyes have also been reported in the lateral suprasylvian cortex (Claire-Bishop area) of the cat (Toyama et al. 1985). Other cells in this area responded to changing image size, and some of them were sensitive to both stimulus features.

Cells selectively responsive to opposed motion in the two eyes have also been reported in areas 17 and 18 of the monkey (Poggio and Talbot 1981). Unlike those described by Cynader and Regan in the cat, the cells in the monkey received excitatory and inhibitory inputs from both eyes and had opposite directional sensitivity to the inputs from the two eyes.

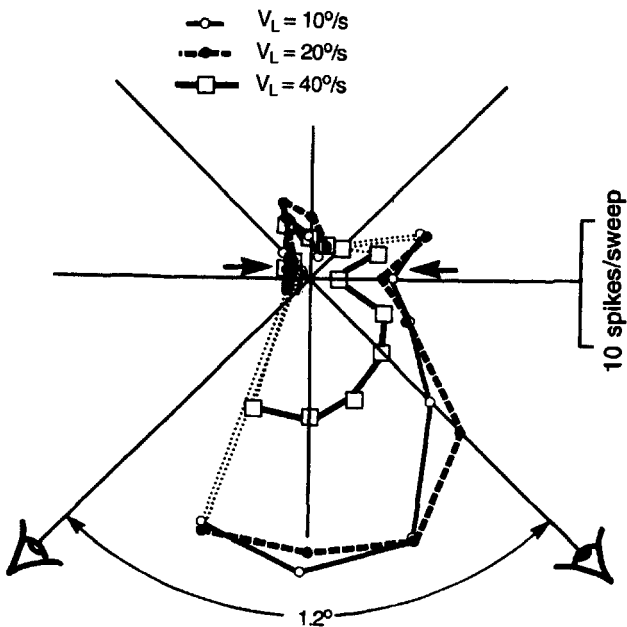


Figure 13.17. Cortical cell tuned to motion-in-depth.
A polar plot of response frequency of a cell in the visual cortex of the cat as a function of the impact direction of a stimulus approaching within the plane of regard. Response frequencies are indicated as radial distances and impact direction is indicated by direction with respect to the two eyes. The angular scale is distorted to emphasize the angle between the eyes. The three curves are for three velocities of stimulus motion, as indicated in the insert. (From Cynader and Regan 1982. Reprinted with permission of J. B. Lippincott Co., Philadelphia.)

However, the stimuli traversed the horopter in the study with monkeys, but not in the study with the cat. Cells in the posterior parietal cortex of the monkey have been found to respond specifically to stimuli rotating in depth, some to rotation about a horizontal axis and others to rotation about a vertical axis (Sakata et al. 1986).

Summary

One may conclude that the mammalian visual system contains cells specifically tuned to the symmetry of looming. Other cells are specifically tuned to binocular cues to motion in depth, but it is not known definitely whether the crucial cue is changing disparity or interocular differences in image motion. The binocular motion-in-depth mechanism is distinct from mechanisms coding static disparity or frontal plane motion, but it is not known whether the motion-in-depth mechanism is a distinct and parallel channel or is organized in series with the other coding processes. These monocular and binocular motion-in-depth mechanisms presumably pool their outputs into a system that directs the animal to make appropriate responses.

13.3 AFTEREFFECTS OF MOTION IN DEPTH

13.3.1 Aftereffects of rotation in depth

Aftereffects may be produced by inspecting objects rotating in depth. A drawing of a cube (Necker cube) periodically reverses in apparent depth, an effect known as reversal of perspective. A three-dimensional cube made from wire reverses in apparent depth every few seconds when viewed monocularly. It appears cubic in correct perspective and tapered in reverse perspective. This change in apparent shape is a simple consequence of size-distance scaling. A three-dimensional cube also reverses in depth when viewed binocularly for several minutes. Depth reversals occur when the cube rotates slowly around a grand diagonal, and an apparent reversal in the direction of motion accompanies each reversal. This must be so, because if the far side of the cube is moving to the right when it is seen in correct perspective, it will appear as the near side moving to the right in reversed perspective. If the rotating cube is viewed with both eyes until it reverses, which takes about 2 minutes, and is then rotated objectively in the other direction, it takes about 4 minutes before it reverses again (Howard 1961). In the induction period, the detectors sensitive to the specific direction of rotation in depth must become adapted to the point that the alternative interpretation of the stimulus takes precedence. The adaptation process must be specific to the direction of rotation in depth. The adapted state of the detectors for motion in depth has to unwind before becoming adapted in the other direction. The effect cannot be due to adaptation of simple motion detectors because at all positions there is as much motion in one direction as in the opposite direction. The integral effect over time is therefore zero. The effect is specific to the retinal location of the induction stimulus.

Any aftereffect from a real object rotating in depth could be due to adaptation of monocular or binocular cues to the direction of rotation. Monocular cues to changing depth are sufficient to induce aftereffects. We have already mentioned that Regan and Beverley (1978a) obtained an aftereffect from inspection of a looming square (see Section 13.2.3). Several minutes of inspection of a polar projection of a square rotating in depth has been found to cause a square in a parallel projection rotating in the same direction to appear to be rotating in the opposite direction (Petersik et al. 1984). A square in polar projection contains perspective information about the direction of rotation whereas a square in parallel projection contains no such information. Attentional factors enter into this type of aftereffect because

when two inspection figures moving in opposite directions were inspected simultaneously, the direction of the aftereffect depended on which of the inspection stimuli had been attended to (Shulman 1991).

Regan and Beverley (1973c) reported an aftereffect of rotation in depth defined only by disparity. Each eye saw a spot moving sinusoidally from side to side at 0.8 Hz. When the spots moved in phase in the two eyes, the fused image appeared to move in a frontal plane. When they moved 180° out of phase, the image appeared to move along a straight path in and out of the plane of the screen. A 90° phase difference created an impression of rotation around a circular orbit in depth in one direction, and a 270° phase shift created an impression of circular rotation in depth in the opposite direction. Other phase angles produced apparent motion around elliptical orbits in one direction or the other, as shown in Figure 13.18. The depth threshold for each of these stimuli was first established by adjusting the amplitude of target oscillation until depth was detected. When subjects had viewed a stimulus that appeared to rotate in depth in one direction for 10 minutes, the display no longer appeared to rotate in depth and the depth threshold for other stimuli rotating in the same direction was elevated. The depth threshold for stimuli rotating in the nonadapted direction was either unaffected or reduced.

A dynamic Lissajous figure produced on an oscilloscope appears like a sine wave pattern rotating in depth. Since its direction of rotation is ambiguous it appears to change periodically. When the figure is viewed with a dark filter in front of one eye, a pattern of disparities is produced and the direction of rotation is no longer ambiguous. This is the Pulfrich effect described in Section 13.1. Inspecting the stereo image for some minutes caused a subsequently seen ambiguous figure to appear to rotate in the opposite direction (Smith 1976). Similarly, inspection of the stereoscopic image of a rotating sphere caused a two-dimensional representation of a rotating sphere to appear to rotate in the opposite direction (Nawrot and Blake 1989, 1991a). Inspection of an array of dots moving in one direction with crossed disparity superimposed on uncrossed-disparity dots moving in the opposite direction caused an incoherently moving array of dots to appear as a structure moving in depth (Nawrot and Blake 1993b). The Lissajous-figure aftereffect was found to require the induction and test stimuli to have the same spatial frequency, suggesting the presence of visual channels tuned jointly to direction of motion, disparity, and spatial frequency (Chase and Smith 1981).

There are two ways to account for aftereffects of rotation in depth, when the depth is specified only

by disparity. The first possibility, proposed by Regan and Beverley (1973c), is that there are distinct sets of detectors, each jointly tuned to a specific direction of sideways motion and a specific sign of disparity. These **disparity-specific motion detectors** can be understood by referring to Figure 13.19. There must be at least four members to the set: left-motion crossed-disparity and left-motion uncrossed-disparity detectors, and right-motion crossed-disparity and right-motion uncrossed-disparity detectors. Physiological evidence for the existence of these detectors was reviewed in Section 13.2.5. The second possibility is that distinct sets of detectors are each tuned to a specific direction of changing disparity. These are the **changing-disparity detectors** discussed in the previous sections. There must be at least two sets of detectors to account for motion-in-depth aftereffects, one sensitive to the changing disparity produced by an approaching object and one sensitive to the changing disparity produced by a receding object. The experiments described in the following sections were designed to investigate aftereffects produced by each of these types of detector.

13.3.2 Aftereffects from disparity-specific motion

There is physiological evidence for disparity-specific motion detectors in several visual areas of the cerebral cortex, although there is no direct evidence of adaptation effects in these detectors. For instance, some cells in V1 and V2 of the monkey respond selectively to stimuli moving in a given direction in the two eyes; some responding only to crossed-disparity stimuli and others only to uncrossed-disparity stimuli (Poggio and Fischer 1977; Poggio and Talbot 1981). Similar cells have been found in the medial temporal visual area (MT) (Maunsell and Van Essen 1983b) and medial superior temporal area (MST) of the monkey (Komatsu et al. 1988).

There is psychophysical evidence of aftereffects induced specifically by disparity-specific motion detectors. After subjects alternately adapted to a patterned disc with crossed-disparity, rotating clockwise, and to a disc with uncrossed-disparity, rotating counterclockwise, a motion aftereffect in a stationary stimulus changed direction depending on the depth plane it was placed in (Anstis and Harris 1974). In another study, a motion aftereffect induced by a moving display was found to be weaker when the induction and test displays did not have the same sign of binocular disparity (Fox et al. 1982). Verstraten et al. (1994) found that oppositely moving dot patterns produced an aftereffect of opposed transparent motion only when the induction motions were in distinct disparity depth planes.

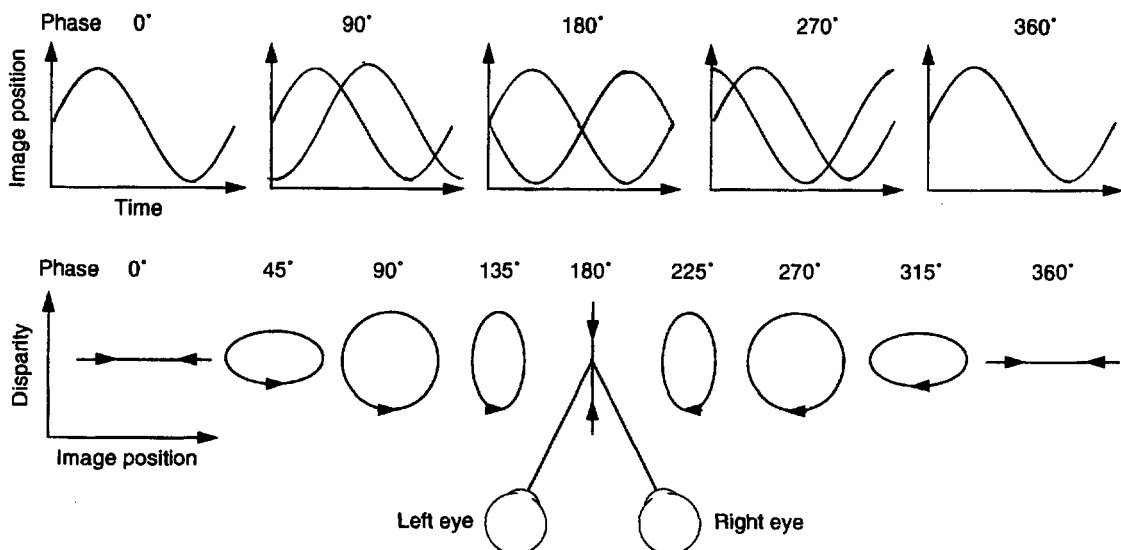


Figure 13.18. Motion in depth and phases of binocular image motion.

Phase relationships of the motion of dichoptic images of a spot (top row) and the orbits of apparent motion in depth that each creates (bottom row). When the images move in phase, the spot appears to move in a frontal plane, and when they move 180° out of phase, the spot appears to move along a straight path in and out. Intermediate phase angles create circular or elliptical orbits of motion within the plane of regard. (From Regan and Beverley 1973c. Copyright, 1973, by the AAAS.)

13.3.3 Aftereffects from changing-disparity

Psychophysical and physiological evidence for changing-disparity detectors was reviewed in Sections 13.3.2 and 13.3.3. Beverley and Regan (1973a) provided psychophysical evidence for after-effects produced specifically by visual channels tuned to changing disparity. Subjects viewed an irregular pattern of dots with the left eye and a matching pattern of dots with the right eye. The central 2° areas of the two patterns were sinusoidally oscillated from side to side. When the two displays were fused stereoscopically, the central area appeared to oscillate back and forth in depth along a linear path. Note that in this display there was no opposed motion in far and near planes, so disparity-specific motion detectors were not stimulated. The direction of motion in depth was varied by changing the phase and relative amplitudes (symmetry) of the movements of the central discs. After subjects viewed the display moving along a particular trajectory for 10 minutes, the amplitude of relative image motions required to evoke movement in depth in a test stimulus increased. Figure 13.20 shows that the change in sensitivity was greatest when the test movement was along a trajectory similar to that of the inspection movement, and fell to zero when the directions of the two movements differed by more than a certain amount. The data suggest that there are four visual channels for detecting impact direction, each tuned to a different range of directions: one for directions

aimed between the nose and the left eye, one for those aimed between the nose and the right eye, and one each for those aimed on either side of the head. Another four channels were postulated for motion away from the head.

13.4 DICOPTIC MOTION

13.4.1 Dichoptic apparent motion

Stationary stimuli presented in rapid succession in neighbouring locations appear as one stimulus in continuous motion. This phenomenon is known as apparent motion. There is a vast literature on the dependence of apparent motion on the spatial and temporal properties of the stimuli (see Anstis 1986). In Section 12.5.5 it was shown that apparent motion occurs within a plane inclined in depth as readily as within a frontal plane. The present section is concerned with whether apparent motion occurs between stimuli presented dichoptically between a stimulus presented to one eye and a succeeding stimulus presented in a neighbouring location to the other eye. Several investigators have reported apparent motion between isolated stimuli presented dichoptically (Shipley et al. 1945; Pantle and Picciano 1976; Braddick and Adlard 1978). However, it has been claimed that apparent motion does not occur with dichoptic random-dot patterns (Braddick 1974) or dichoptic sinusoidal gratings (Green and Blake 1981).

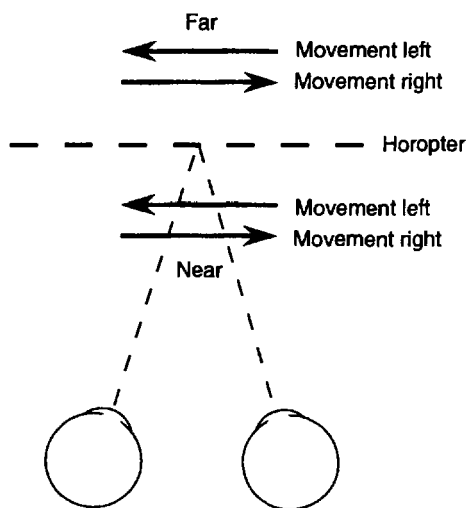


Figure 13.19. Coupling motion direction and disparity.

It is assumed that some cells sensitive to leftward motion are also tuned to crossed disparity while others are tuned to uncrossed disparity. Cells sensitive to rightward motion are also assumed to be selectively tuned to disparity. (Adapted from Regan 1989.)

Braddick (1974) proposed that there are two types of apparent motion—**short-range motion** and **long-range motion**. Detection of short-range motion involves motion detectors that respond to local spatiotemporal distributions of luminance, and detection of long-range motion operates after the shape of the stimuli has been extracted. In particular, it was proposed that the short-range process is responsible for the apparent motion of a displaced region of dots within a larger display of randomly flickering dots, when all the dots are seen by both eyes. This type of stimulus is known as a **random-dot kinematogram**. Using the criterion of perceptual segregation of the displaced region of dots, Braddick found that apparent motion is seen for displacements of successive images of only up to about 15 arcmin; with large displacements it becomes difficult to find the correct pairing of dots in successive images. Long-range apparent motion between well-defined stimuli can occur over several degrees. In a random-dot display the region of random dots seen in motion is not discriminable until motion occurs, and therefore shape discrimination occurs after rather than before motion detection. Using the same criterion of perceptual segregation of the displaced region of dots, Braddick found that apparent motion was not seen with dichoptic random-dot patterns, that is, when the successive images of the displaced central region of dots were seen alternately by the two eyes. They concluded that the short-range process does not operate with dichoptic stimuli. Perhaps, in the dichoptic domain, processes that seek correspondences between closely spaced successive

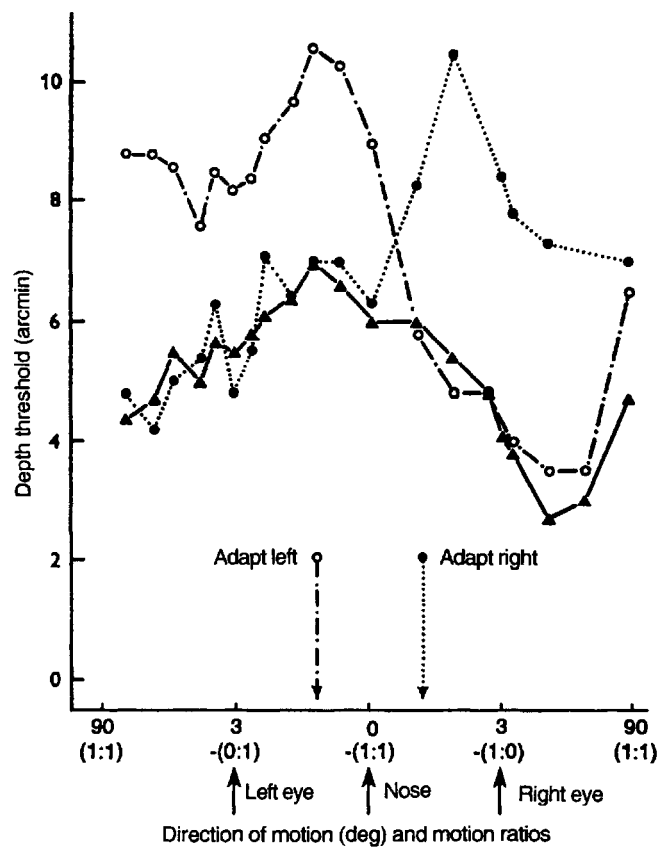


Figure 13.20. Adaptation to motion in depth.

The solid line shows the preadaptation threshold for motion in depth within the plane of regard as a function of the impact direction relative to the nose of the subject. The dashed line shows the threshold after the subject adapted to a stimulus moving toward a point between the nose and the left eye. The dotted line shows the threshold after adaptation to a stimulus moving toward a point between the nose and the right eye. (Adapted from Beverley and Regan 1973b.)

images are concerned with detection of disparity rather than motion. Apparent motion occurs with well-spaced and well-defined dichoptic stimuli, showing that the long-range system works with dichoptic stimuli. Cavanagh and Mather (1989) questioned whether there are distinct channels for short- and long-range motion. They suggested, instead, that all motion is detected by the same initial detectors and then processed in different ways

In contradiction to Braddick and to Green and Blake, Shadlen and Carney (1986) obtained apparent movement with dichoptic sinusoidal gratings flickering in alternation with a 90° temporal phase lag and a 90° spatial offset (in spatiotemporal quadrature). They concluded that the short-range motion system operates on dichoptic inputs. This result was confirmed by Georgeson and Shackleton (1989), but further experiments led them to conclude that this type of dichoptic apparent motion is long-range, not short-range. Their experiments are now described.

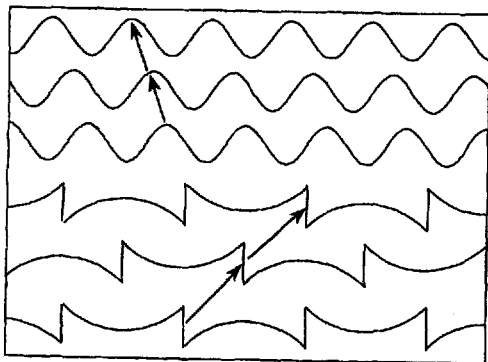


Figure 13.21. Spatial frequency and dichoptic motion.

A grating with a square luminance profile can be considered to possess a fundamental sine-wave component superimposed on odd-harmonic components. If the fundamental component is removed the luminance profile resembles that shown in the three bottom rows. A motion of a missing-fundamental grating to the right, as signified by the bottom two arrows, carries the peaked luminance bands of the grating to the right. The peaks of the third harmonic component also move to the right but appear to move the left because of the relative proximity of luminance peaks in that direction, as indicated in the top three rows. By noting which way the grating appears to move, one can reveal which aspect of the grating carries the motion signal in the visual system. (Reproduced with permission from Georgeson and Shackleton 1989, Vision Research, Pergamon Press.)

Dichoptic motion with missing fundamental displays

A square-wave grating can be considered to be composed of a sine-wave grating of the same spatial frequency (the fundamental) plus sine-wave gratings at odd multiples of the fundamental frequency (odd harmonics). The luminance modulation of the harmonics decreases in proportion to their spatial frequency. A square-wave grating appears to move in the direction of a repeated 90° phase shift of the fundamental spatial frequency. However, when the fundamental spatial frequency is removed, the phase-shifted grating appears to move in the opposite direction (Adelson 1982). This is because the third harmonic of a square wave moves 270° for a 90° shift of the fundamental, equivalent to a 90° shift in the opposite direction. It is believed that, in the absence of the fundamental, the short-range motion system is engaged by displacement of the third harmonic, and the visual system ignores the long-range displacement of the pattern of the grating as a whole, which is in the direction of the missing fundamental (see Figure 13.21). When Georgeson and Shackleton presented alternating missing-fundamental gratings dichoptically, the apparent motion was in the direction of the long-range displacement of the pattern as a whole, rather than in the direction of the third harmonic. They concluded that only the long-range

motion system operates dichoptically. When the contrast of the grating was low the dichoptic motion was in the direction of the third harmonic. This is because, at low contrast, the higher spatial-frequency components that define the shape of the grating as whole are below threshold.

It was noted in Section 6.1.1 that the binocular system detects the disparity between the overall shapes of missing-fundamental gratings, rather than that between the main spatial-frequency components, even when the latter disparity is smaller. Perhaps the preference for seeing dichoptic motion in terms of the displacement of the overall pattern rather than in terms of the displacement of the main spatial-frequency component is a property of the disparity mechanism. It may not reflect a basic inability of the binocular system to see short-range apparent motion. Debate on this issue continues Carney and Shadlen (1992; Georgeson and Shackleton 1992).

Dichoptic motion in spatiotemporal quadrature

More recently, Carney and Shadlen (1993) designed a dichoptic motion stimulus which they claimed taps the short-range motion system. A random-dot display with temporal sine-wave modulation of contrast was combined with the same pattern shifted vertically 90° in spatial phase and 90° in temporal phase. Since two stationary patterns in spatiotemporal quadrature are mathematically equivalent to a travelling wave, these stimuli combined in the same eye are equivalent to a vertically moving grating. An impression of a vertically moving grating was also created when the stimuli were combined dichoptically. The dichoptic motion had all the characteristics of short-range apparent motion, as defined by Braddick. Carney and Shadlen proposed that others had failed to obtain short-range motion in dynamic random-dot stereograms because of the following problems with their displays.

A dynamic random-dot kinematogram has motion signals in each monocular image. The other investigators overcame this problem by reversing the direction of motion after every two frames (Braddick 1974), by using only two frames (Green and Blake 1981), or by employing spatial displacements too large for monocular detection of motion (Georgeson and Shackleton 1989). The display used by Carney and Shadlen overcomes the problem of monocular motion by making the motion signals in their monocular images directionally ambiguous. Another problem with the earlier displays is that they required the detection of a moving figural region within a nonmoving surround rather than discrimination of a direction of motion. Thus, figure-



Figure 13.22. Ambiguous apparent motion.

The two rows of vertical lines, A and B, are shown in succession with two lines superimposed. With an interstimulus interval longer than 80 ms the group of lines appears to move from side to side as a whole. When the interval is short, the outer lines appear to jump over the two stationary inner lines.

ground discrimination was the criterion for detection of dichoptic motion, rather than discrimination of the direction of motion. These criteria are not equivalent. Chang and Julesz (1983) had found that direction discrimination for apparent motion in a random-dot kinematogram operates over larger distances than pattern discrimination. Also, Carney and Shadlen found that, when their dichoptic display contained a familiar figure, it was not recognized even though the direction of motion was detected. Figure-ground perception is perhaps disrupted by rivalry between microelements of the display. Whatever the reason for the disruption of figure perception in dichoptic kinetic displays, evidence about dichoptic motion based on the criterion of figure-ground segregation is not reliable. When the criterion of directional discrimination is used, the binocular system is shown to be capable of supporting apparent motion, both long-range and short-range.

Dichoptic motion with the Ternus display

It has been claimed that the distinction between short-range and long-range apparent motion can be illustrated by the ambiguous apparent motion evoked by the display shown in Figure 13.22, and first described by Ternus (1926). The two rows of vertical lines are shown in succession with the two centre lines superimposed. When the interstimulus interval is long (80 ms), the group of lines appears to move from side to side as a whole (group movement), but when the interval is short (20 ms), the outer line appears to jump over the two stationary inner lines (element motion). Several investigators have identified group movement with long-range apparent motion and single-line movement with short-range apparent motion. If one assumes that short-range apparent motion is not generated in cyclopean stimuli, one would expect only group motion to be seen when the two sets of lines of the Ternus display are presented dichoptically. This result was obtained by Pantle and Picciano (1976). However, Ritter and Breitmeyer (1989) obtained both group motion and element motion in a

dichoptic Ternus display. For both ordinary and dichoptic viewing, group motion became more likely as frame duration and the size of the stimulus elements were increased. Patterson et al. (1991) constructed a Ternus display with lines defined by disparity in a random-dot stereogram. Thus, both the lines and the apparent motion between them were cyclopean. They, too, obtained both group and element motion, with element motion predominating at short interstimulus intervals. It seems, therefore, that one cannot identify group motion with the long-range motion system and element motion with the short-range system, unless one abandons the notion that the short-range system does not operate in the cyclopean domain.

Dichoptic interpolation of flashes

Another approach to the question of dichoptic apparent motion is to ask whether dichoptic interpolation of a sequence occurs with flashed images presented out of phase to the two eyes. Green (1992) set up the three stimuli shown in Figure 13.23. In the first two displays each eye receives the same spatial sequence of bars presented in succession at a frequency f Hz or $2f$ Hz. Thus, in the second display a bar moving at the same effective velocity is sampled by both eyes at twice the temporal and spatial frequency as a bar in the first display. In the third display each eye sees the bar displacing at a frequency of f Hz but, since the displays in the two eyes are out of phase, the moving bar is sampled at a frequency of $2f$ Hz when the images are combined. Subjects reported that the smoothness of the apparent motion produced by the dichoptic display resembled that of the first display rather than the second. In other words, the impression of apparent movement depended on the sampling rate in each monocular image rather than the sampling rate in the cyclopean image. It was concluded that apparent movement interpolation is not achieved dichoptically.

13.4.2 The dichoptic motion aftereffect

A motion aftereffect can be induced by dichoptic motion. Anstis and Moulden (1970) presented a ring of six lights flashing in synchrony to one eye and an interleaved ring of six lights to the other eye, flashing in counterphase with respect to the first set. The display in each eye appeared as a set of flashing lights, but the binocular display appeared to rotate. After 30 s of exposure to the binocular display, a stationary ring of lights appeared to rotate in the opposite direction. This aftereffect must depend on binocular cells since only binocular cells registered the cyclopean motion.

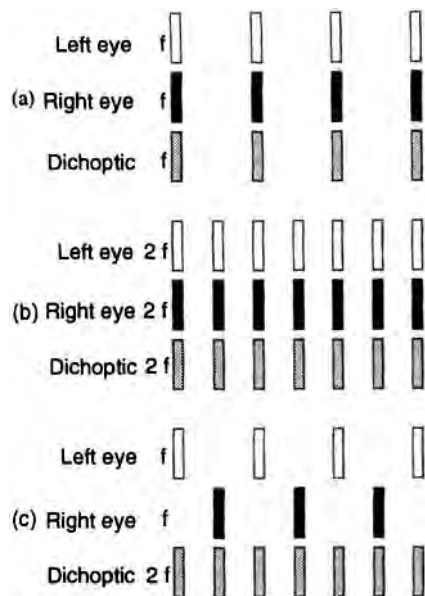


Figure 13.23. Stimulus displays used by Green (1992).

- (a) Each eye sees the same spatial sequence of bars presented in succession at frequency f Hz.
- (b) Each eye sees the same sequence presented at $2f$ Hz.
- (c) Each eye sees a sequence presented at f Hz but out of spatial and temporal phase in the two eyes. Dichoptically, the stimuli are seen at a rate of 2 Hz. However, the sensation of apparent motion produced by display (c) resembles that produced by display (a) rather than that produced by display (b).

Zeevi and Geri (1985) showed that the apparent movement of the dots in an uncrossed disparity plane when dynamic visual noise is viewed with a filter over one eye is sufficient to create a motion aftereffect. Observers were asked to fixate a point in the recessed plane of dots during an adaptation period of 20 s before the filter was removed. To guard against the obvious artifact that the observers might track the apparent motion of the noise pattern, Zeevi and Geri recorded eye movements and found that the aftereffect was still created when subjects fixated. The aftereffect typically lasted 1–3 s. In addition, they showed that the aftereffect was not the result of the dark adapted state of the filtered eye.

Carney and Shadlen (1993) produced dichoptic motion by presenting a counterphase-modulated horizontal sine-wave grating to each eye with successive left- and right-eye gratings displaced one-quarter of a spatial period and one-quarter of a temporal period (in spatiotemporal quadrature). This produced vertical cyclopean motion. Five minutes of inspection of this stimulus produced a motion aftereffect only slightly weaker than that produced by real motion. It was suggested that the difference was due to differential effects of eye movements in the two conditions and the presence of unadapted monocular cells in the dichoptic condition.

Patterson et al. (1994) produced a motion aftereffect from the motion of a cyclopean grating in a dynamic random-dot display. The induction time required to produce the cyclopean aftereffect was longer than that required to produce a regular motion aftereffect. The motion aftereffect induced by motion of a cyclopean pattern defined by disparity was evident in a moving test pattern defined by luminance, confirming an earlier report by Fox et al. (1982). This suggests that cyclopean motion and luminance-defined motion share a common substrate.

When a stimulus moving in one direction is presented to one eye and a similar stimulus moving in the opposite direction is presented to the other eye the two opposed motion aftereffects cancel when both eyes view a stationary display. However, when only one eye views the stationary test display, an aftereffect appropriate to that eye is seen (Wohlgemuth 1911). Thus, opposite motion aftereffects may be induced simultaneously into the two eyes. Each aftereffect could be built up in cortical monocular cells or in binocular cells dominated by one eye. Anstis and Moulden (1970) set up a dichoptic circular display of lights which appeared to rotate one way when viewed with either eye, but the other way when viewed with both. The direction of the aftereffect was opposite to that of the binocular motion. Thus, dichoptic motion induced in binocular cells dominated that induced in monocular cells.

13.5 STEREOPSIS AND MOTION PARALLAX

Motion parallax refers to the relative motion of the images of objects at different distances caused by the motion of the observer with respect to the objects. For an object at a given distance and a given motion of the observer, the extent of motion parallax between the object and a second object is proportional to the depth between the objects. The sign of the parallax depends on which object is nearer the viewer. For two objects separated by a fixed depth, the parallax produced by a given motion of the observer is inversely proportional to the square of the absolute distance of the two objects from the observer. These geometrical relationships are analogous to those for binocular disparity (Section 2.3), and monocular motion parallax, like binocular disparity can serve as a cue to depth.

Binocular disparity and motion parallax are very different sorts of information about the three-dimensional structure of objects and their layout: disparity is a binocular cue whereas motion parallax is essentially monocular; motion parallax is a dynamic cue whereas disparity is essentially static;

disparity-based stereopsis relies on discrete differences between the optic arrays created at two different vantage points at the same moment, while motion parallax is based on continuous changes in a single optic array occurring over time. The purpose of this section is to examine the similarities and differences between disparity-based stereopsis and stereopsis based on motion parallax. This is done with respect to 1) the computational theory of the underlying information and 2) empirical studies in which the two cue systems have been compared. Interactions between disparity and motion parallax cues are reviewed in Section 13.2.

13.5.1 Theoretical considerations

On the first page of his book *An Essay Toward a New Theory of Vision*, the empiricist philosopher George Berkeley (1709) asserted that "It is, I think, agreed by all that distance, of itself and immediately, cannot be seen" because two points lying along the same visual line would project to the same point on the retina "whether the distance be longer or shorter" (Figure 13.24a). This is a correct statement about the optics and geometry of a world of isolated, infinitely small points observed from a single vantage point at a single instant but is incorrect, when we consider opaque textured surfaces, since these constrain the characteristics of the optic array and thus limit the number of three-dimensional interpretations. The perception of depth in photographs provides sufficient evidence that there is information about the three dimensional shape and layout of objects in the instantaneous image from a single vantage point.

Optic array properties

The assertion that "distance cannot be seen" is also incorrect when we consider the optic arrays at two spatially separated vantage points. Simple geometry shows that the position of a point in space can be recovered completely and without ambiguity from the visual directions of the point from the two vantage points, together with knowledge of the distance between the vantage points (Figure 13.24b). Exploiting the advantages of two separated vantage points—binocular stereopsis—is the most obvious solution to Berkeley's problem of the "lost" information about distance. Moreover it provides a solution even in an impoverished environment of isolated points. A single visual point has an **absolute disparity** or binocular subtense which corresponds to the difference in the visual directions from the two vantage points (see Section 7.1.5). Distance can be recovered if the absolute disparity and the separation of the vantage points is known. Relative disparities, or

simply disparities, exist between two or more points at different distances and are based on the differences in visual direction from the two vantage points. Relative distance, or depth, up to a scaling factor can be calculated from the relative disparity and the distance between the vantage points.

A different but related solution is to consider the changes in a single optic array which occur over time. When an eye moves at right angles to the line of sight, as it does with side-to-side movements of the head or body, the visual direction of a stationary object changes continuously (unless the object lies at infinity). Again, simple geometry shows that the distance of a stationary object can be recovered from the change in visual direction of the object, plus knowledge of the distance and direction through which the vantage point has moved (Figure 13.24c). This assumes that the frame of reference for measuring visual direction translates but does not rotate. A single visible point creates an **absolute parallax** which corresponds to the change in visual direction with displacement of the vantage point. Absolute parallax is analogous to vergence information in binocular stereopsis. With two or more points at different distances, there is relative motion, or motion parallax, within the optic array. Relative distance, up to a scaling factor, can be derived from the magnitude of motion parallax and the displacement of the vantage point.

Image properties

These geometrical considerations show how differences between two optic arrays in binocular stereopsis and changes in a single optic array in monocular motion parallax can, in principle, be used to determine absolute and relative distance. The issue becomes more complicated when we go beyond the optic arrays to consider how the information might be extracted in a particular visual system. For animals like humans with moveable eyes, in which the frames of reference for visual direction rotate with the eyes, the task of specifying the difference in visual direction of an object from the two eyes—absolute disparity—involves knowing two things: 1) the angle of vergence between the eyes and 2) the local signs of the images on the two retinas.

The situation is more complex for monocular motion parallax, because the frame of reference for specifying the change of visual direction rotates with both the body, the head, and with the eye. Consequently, to measure the change of visual direction of a single point arising from observer movement, the visual system requires information about 1) the change in the retinal local sign of the image, 2) the rotation of the eye with respect to the head, 3) the

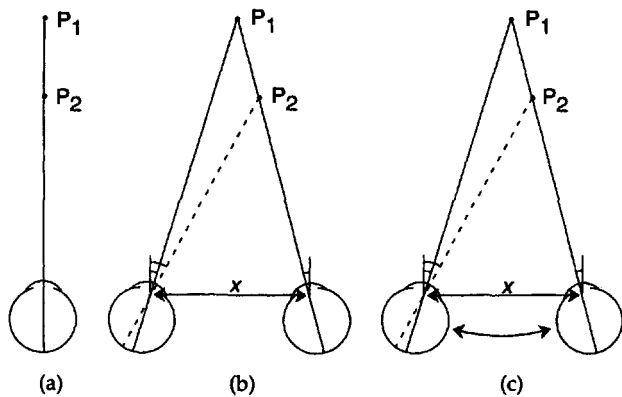


Figure 13.24. Information about the distance of isolated points.
 (a) All information about the distances of two isolated and infinitely small points P_1 and P_2 is lost when they are viewed from a single vantage point.
 (b) Knowing the visual directions of the points and the separation between two simultaneous vantage points (x) provides complete information about their positions in space.
 (c) The same information is available from one moving vantage point. (Redrawn from Rogers 1993.)

direction and amount of head translation, 4) the rotation of the head on body, and 5) the rotation of the head and body with respect to the ground. Not surprisingly, absolute parallax as a source of information about absolute distance is very ineffective (Gogel and Tietz 1973; see Section 11.1.5).

Fortunately, the situation is more straightforward if 1) there are several points in view and 2) there are three or more views of those points. Ullman (1979) has shown that the complete three-dimensional metric structure of the scene can be recovered from just three views of four noncoplanar points. Longuet-Higgins (1981) has similarly shown that three-dimensional structure and layout can be recovered from just two views of eight points.

It is worthwhile asking why more points or views allow the three-dimensional layout of the points to be determined. The answer is that with more points or frames there is often sufficient visual information to specify the locations of the coordinate frames used to measure visual direction. Thus, the visual system does not have to rely on nonvisual information to specify where the eyes are looking.

Consider first the situation in which a set of visible points is within a small part of the total visual field close to the median plane of the head. Under these circumstances, there are no vertical disparities (see Section 7.1.4). If the eye positions are not known, there is an ambiguity as to whether the cluster of points is close to the observer or far away. This can be appreciated by considering the set of corresponding visual lines from the points as the eyes converge horizontally. The bundle of corresponding rays can intersect at an infinite number of

distances from the observer, depending on where the eyes are converged. We can say that the relative locations of the points in space are known only up to a scaling factor of distance. Moreover, there is no visual information under these circumstances to specify eye positions.

There are two potential sources of visual information about eye position. The first arises when there are three or more views of an array of points. This can occur with motion-parallax when the observer makes side-to-side head movements and also when an object moves with respect to the observer. With three or more views, the "acceleration" component of the flow field—the rate of change of angular velocity—can be calculated. If the angular accelerations and velocities of the points are known, the absolute locations of the points in space can be calculated. This can be appreciated intuitively by considering a stereo system with three eyes or cameras. The projection out of the third eye of an extra bundle of light rays removes the remaining ambiguity about the scale factor of distance (Ullman 1979).

Unlike the trinocular stereo system, the optic flow case is not fully constrained even with three or more views because the separations of the three views is not known. The same ambiguity would arise if the interocular separations of the cameras were not known. However, the depth-to-width ratio of a particular surface is specified since both the amount of relative motion and the angular size of a surface scale inversely with distance. Richards (1985) has suggested that the invariance of the depth-to-width ratio in continuous optic flow sequences could be used to calibrate binocular disparities and thereby provide the missing parameter of viewing distance. Hence, integration of stereoscopic and motion parallax information allows the complete metric structure to be recovered from the motion of just three points in two binocular views seen under orthographic projection (Richards 1985; see Section 11.2).

So far we have assumed that all the points are clustered within a small part of the visual field so that vertical disparities are negligible. Ullman's structure-from-motion algorithm does not rely on the perspective projection of images. The second solution to the problem of knowing where the eyes are looking comes from the perspective effects of wide-angle viewing. With perspective information from four or more noncoplanar points, there is complete information about the locations of the points from just two views if the separation of the two vantage points and the interocular distance are known (Longuet-Higgins 1982). The role of perspective in binocular stereopsis and motion parallax is considered in more detail in the following section.

These observations make explicit the underlying similarity of disparity and motion parallax as cues to three-dimensional structure and layout. There is, however, one important difference. The differences in the visual directions of a number of points from two simultaneous binocular views are a necessary consequence of the three-dimensional layout of those points and the viewing geometry. The changes in visual direction of a number of points which occur over time when the observer moves may be a consequence of the three-dimensional layout of those points, but they may also be the result of the points themselves moving. Every demonstration of structure-from-motion using computer graphics on a flat screen provides proof of this assertion. The pattern of optic flow generated by a rigid solid object which moves with respect to the observer can always be re-created by an infinite number of alternative motion configurations, including one in which all points move across a flat surface. The number of possible alternatives can be reduced substantially, and often to one or two, if it can be assumed that each object and the array of objects are rigid (Johansson 1977; Ullman 1979). It has been proposed that the visual system uses a **rigidity constraint** in the interpretation of optic flow to limit the number of possible interpretations. For our visual world, which contains moveable animate objects, it would be inappropriate, and often impossible, to apply the rigidity constraint to the entire optic-flow field. Todd (1982) and Koenderink (1986) have therefore proposed solutions to the structure-from-motion problem based on the weaker assumption of **local rigidity**.

If we consider the different perspective views of an extended textured surface, rather than those of a world of isolated points, several additional properties of the disparity and parallax fields become evident. For a surface slanting around a vertical axis, the size, spatial frequency, and shape of images differ in the two eyes (Section 7.2). The same features of the monocular image change as the head moves horizontally. For a surface inclined around a horizontal axis, the orientation and shape of binocular images differ and the same features of the monocular image also change as the head moves horizontally (Section 7.4). For a surface which is curved around a horizontal axis, there may also be curvature differences between corresponding features in binocular images and curvature changes of the same features with observer movement. Evidence that the human visual system is able to make use of these binocular differences is discussed in Chapter 7.

All the differences between binocular images or changes over time in a monocular image described so far are consequences of the local structure of the

three-dimensional scene and the viewing geometry. If we consider vision to be a problem of **inverse optics**, these differences and changes may, in principle, be used to recover information about the relative distances and local three-dimensional structure in a visual scene.

The correspondence problem

In the discussion so far, the visual input to the parallax system has been considered to be a series of discrete frames in which the motions of points between frames can be expressed as velocities by dividing the displacement by the interframe interval or sampling time (Ullman 1979). According to this view, the visual system must first establish the correct match between visual features in succeeding frames before computing the motion of matched points. In other words, it must solve the correspondence problem for visual motion. Again this is analogous to the correspondence problem in matching images in binocular stereopsis (see Section 6.2.1). However, given that the input to the human visual system is usually continuous, rather than a series of discrete frames, it is not clear that the correspondence problem for motion must be solved explicitly before optic flow can be measured. The fact that the visual system can recover the three-dimensional structure from a sequence of discrete views of a scene does not mean that the visual input is coded as a series of discrete frames. This confuses the characteristics of the stimulus with the characteristics of the visual processes used to extract the information.

Differential invariants

So far we have shown that complete information about the three-dimensional structure and layout of an array of isolated points is available for both the binocular observer and the moving monocular observer, if we can assume rigidity. The world we live in, however, is typically composed of opaque textured surfaces rather than isolated points. An obvious property of surfaces is that depth modulations are usually gradual, rather than abrupt. Indeed, the local smoothness of surfaces has been proposed as a constraint to limit the number of possible matches and thereby aid the solution of the stereo correspondence problem (Marr and Poggio 1976, see also Section 6.2.11). A related consequence of living in a world of surfaces is that the optic-flow field generated by movements of the observer is spatially differentiable over local areas. Koenderink and van Doorn (1975, 1976b) have argued that it may be more appropriate to describe the optic-flow field created by observer movement in terms of the local

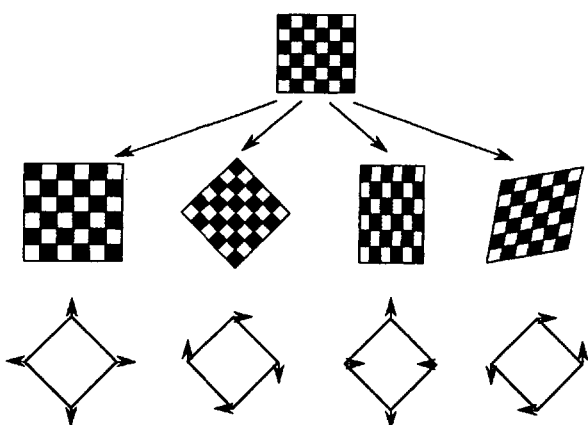


Figure 13.25. Differential invariant transformations.

The four differential invariants—expansion, rotation, and two components of deformation, or shear—are represented as transformations of a chequerboard. Koenderink (1985) pointed out that the differential characteristics of the optic flow field over time and of the disparity field can be described in terms of these differential invariants.

changes of angular velocity over space, which they referred to as **differential invariants**. The invariance in this case is with respect to overall translations of the flow field. The formal equivalence of binocular disparities and motion parallax is brought out again by the fact that the binocular disparity field created by a surface can also be described in terms of local changes in disparity over space (Koenderink and van Doorn 1976a).

In the optic flow case, the velocity field can be described using just four differential characteristics: 1) the amount of expansion or dilatation; 2) the amount of rotation or curl; and 3) and 4) two components of deformation or shear (Figure 13.25). Of particular interest with respect to the motion parallax transformation are the two components of deformation. Koenderink and van Doorn (1975) and Longuet-Higgins and Prazdny (1980) have shown that these two components provide information about the local slant and inclination of a surface up to a scaling factor of viewing distance. The similarity between disparity-stereopsis and motion-parallax stereopsis is revealed again by the fact that information about the local slant and inclination of a surface patch in the disparity case is specified by the amount of deformation needed to map one eye's image onto the other (Koenderink and van Doorn 1976a). Koenderink (1986) has argued that the differential properties of the optic flow and disparity fields provide useful information about the characteristics of the visual scene and the movements of the observer which are essential for guiding action. Moreover, Koenderink suggested that differential

properties are not merely mathematical abstractions, which are difficult or impossible to compute, but could be detected by simple biological mechanisms. In particular, the amount of local deformation in both the motion-parallax flow field and the binocular-disparity field can be determined by monitoring changes (or differences) in the orientation of local line elements at a number of orientations (Koenderink 1986). Several empirical studies, reviewed in Sections 7.2 and 7.3, suggest that the stereoscopic system may be able to detect the deformation needed to map one eye's image onto the other.

13.5.2 Perspective information

The word “perspective” refers to the fact that the geometric properties of optic arrays and projected images change with the viewing distance. For instance, doubling the distance to an object halves the angle subtended at the eye. Stereopsis based on disparity relies on differences in the simultaneous perspective views from two spatially separated eyes. That is why this source of information is referred to as binocular perspective. Stereopsis based on motion parallax relies on the successive perspective views that are created when an eye translates. It could be called successive or sequential perspective. Analysis of the geometry shows that the major differences between the perspective of simultaneous images lie along the axis separating the two eyes and those of successive images lie along the direction of displacement of the single eye. Hence most binocular disparities are horizontal or, strictly speaking, parallel to the interocular axis. Similarly, the motion parallax generated by horizontal head movements is mainly in a horizontal direction and that generated by vertical head movements is mainly in a vertical direction. However, we will now see that there are secondary effects which occur in the orthogonal directions in both cases when the angular size of the field of view is more than a few degrees.

A stationary monocular perspective view of a scene of unfamiliar objects cannot provide information about the *absolute distance* to any part of the scene, even if it contains textured surfaces. There will always be “equivalent configurations” which generate the same optic array (Ames 1955). The same is not true of the perspective views from two or more vantage points. Mayhew and Longuet-Higgins (1982) showed that just four noncoplanar points seen from two vantage points provide sufficient information to recover the complete three-dimensional structure of the points (see Section 7.5).

The additional information about absolute distance present in the perspective views from two

vantage points can be appreciated by considering a chequerboard surface lying in a frontal plane straight ahead of the observer. If the surface is close to the observer, the righthand edge subtends a larger angle to the right eye than to the left eye because it is closer to the right eye. The opposite is true of the lefthand edge (Figure 13.26a). However, if the surface is far away but subtends the same visual angle, the angular subtense of the lefthand and righthand edges approach the same value, since the distances from the two eyes become similar (Figure 13.26b).

The vertical angular separation of a pair of points at one eye divided by their vertical separation at the other eye is the binocular vertical-size ratio. For an extended surface there is a horizontal gradient of vertical-size ratios as a function of lateral eccentricity. For a given interocular distance, the horizontal gradient of the vertical-size ratios over a surface fully specifies the difference in the obliqueness of the surface from the two eyes (see Section 7.5). It follows that if the separation between the eyes is known, the absolute distance to the surface can be calculated (Figure 7.55). Rogers and Bradshaw (1992, 1993) have shown that the human visual system is able to exploit this particular consequence of binocular perspective viewing and use the information as a basis for judging absolute distance and size and for the scaling of horizontal disparities as a function of absolute distance (see Section 7.6.6).

The situation is similar in the motion parallax domain. Consider the same chequerboard surface lying in a frontal plane and centred on the median plane of the observer. As the observer moves from side to side in a plane parallel to that of the surface, the vertical angular subtense of both the right and left-hand edges changes, but in opposite directions, as the eye moves closer to one edge or the other. In other words there is a spatial gradient of vertical size which changes as the eye moves from side to side. This changing gradient of vertical size is analogous to the opposite gradients of vertical size created by binocular viewing. For a given movement of the head the change in the gradient of vertical size specifies the change in the obliqueness of the surface relative to the observer. When the surface is at infinity, there is no change in the gradient of vertical size because there is no change in the obliqueness of the surface from the different eye positions. For both binocular and monocular stereopsis, the difference or change in perspective provides information about the difference or change in the obliqueness of the surface. If the separation of the vantage points or the displacement of the single vantage point is known, the absolute distance to the surface can be calculated.

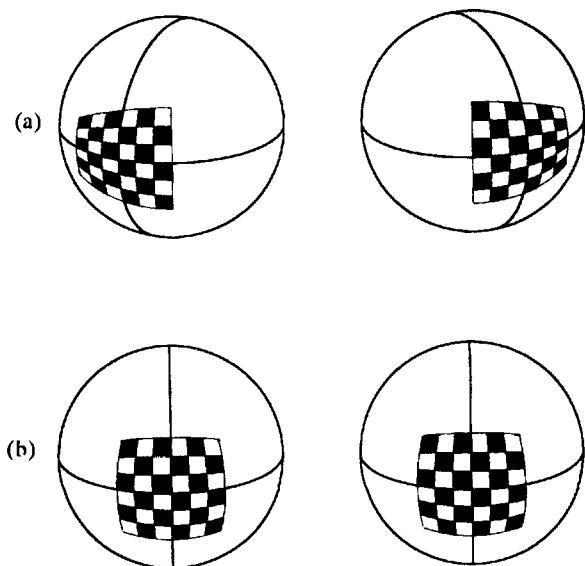


Figure 13.26. Perspective images from two vantage points.
The perspective images created by viewing a frontal chequerboard of the same angular extent from either a close distance (a) or far away (b). When the surface is close, there is an equal and opposite horizontal gradient of vertical size in the two images because the each vertical edge of the surface lies at different distances and therefore subtends different angles at each eye (a). When the surface is far away, the two images are identical (b). (Adapted from Rogers and Bradshaw 1993.)

As yet there does not seem to be any direct evidence that the human visual system makes use of the change in the gradient of vertical size that accompanies head movement in order to judge the absolute distance to a surface. However, Rogers and Collett's (1989) model of the interactions between parallax and disparity cues (see Section 11.2), predicts that a parallax surface would appear to rotate by a greater or lesser amount around a vertical axis as a consequence of manipulating the spatial gradient of vertical size. We have observed that there are indeed changes in the amount of perceived rotation when these perspective cues are manipulated and that the amount of perceived depth in a simulated corrugated surface can also be affected (Rogers and Bradshaw 1991, 1992).

In summary, there is clear evidence that the human visual system is capable of exploiting these particular consequences of perspective viewing for making judgments about absolute distance and size and for disparity scaling. Evidence that the visual system uses the equivalent information in the extraction of three dimensional structure from motion parallax is more limited and needs further investigation.

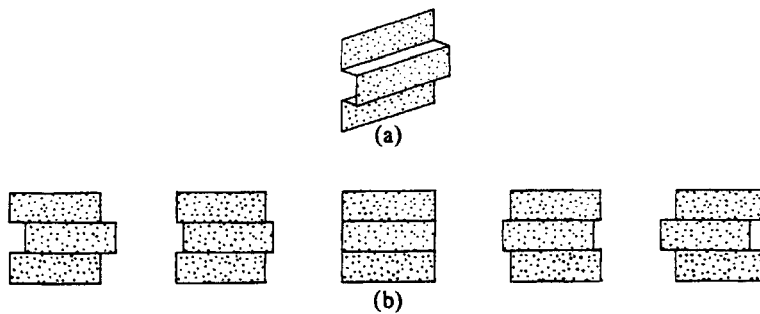


Figure 13.27. Motion parallax transformations.

When the square-wave surface depicted in (a) is viewed by a moving observer, relative motion is created between the surface features at different distances. This is motion parallax. The lower figure shows how the random-dot pattern on the screen was transformed with side-to-side head movements in order to simulate motion parallax. In the experiment, the transformation was continuous rather than discrete and the edges of the transforming pattern, which provide information about the surface shape, were not visible. (Redrawn from Rogers and Graham 1979.)

13.5.3 Spatial derivatives of disparity and parallax

There is another similarity between disparity and motion parallax as sources of depth information. The disparity between two points separated in depth by a given distance varies (approximately) inversely with the square of viewing distance—doubling the absolute distance to the points reduces the angular disparity to one-quarter of its previous value (see Section 2.3.1). Exactly the same relationship holds in the case of motion parallax. For a given extent of head movement, the amount of relative displacement between two points separated in depth by a given physical distance varies according to an inverse square law. For this reason, it is usually assumed that both disparity and motion parallax must be scaled by some estimate of the viewing distance for the depth separation between two points to be perceived (Section 13.5.5).

The disparity gradient between a pair of points, as defined in Section 2.3.3, or across a planar surface, also varies with viewing distance but according to an inverse, rather than an inverse square, relationship—doubling the absolute distance to the points halves the disparity gradient. (see Section 7.7). Thus, disparity gradients, which correspond to the first spatial derivatives of the disparity field, must also be scaled by some estimate of the viewing distance in order to calculate the slant or inclination of surfaces.

Rogers and Cagenello (1989) showed that for a smoothly curved surface, the local second spatial derivative of the disparity field—the **disparity curvature**—remains approximately constant with changes in viewing distance. This suggests that local curvature of a surface could be recovered from disparity curvature without scaling for distance.

The same properties also hold for motion parallax. The spatial gradient of relative velocities created by a planar surface patch varies inversely with viewing distance, while the second spatial derivative of the parallax field created by a curved surface patch—**parallax curvature**—remains approximately constant with changing viewing distance. At present, there is no clear evidence that the visual system makes use of these interesting invariants of the disparity and parallax fields.

Summary

To summarize the theoretical considerations, it has been shown that there are considerable similarities in the underlying computational theory of stereopsis based on disparity and that based on motion parallax. Given this fact, it seems likely that mechanisms which have evolved to detect disparity and motion parallax in the human visual system have much in common, and this is likely to be reflected in the results of empirical studies of performance in the two cases. These are considered in the following section.

13.5.4 Disparity and motion parallax compared

The similar appearance of the three-dimensional world from disparity and motion-parallax cues was first suggested by Helmholtz (1909). He wrote:

Suppose, for instance, that a person is standing still in a thick woods, where it is impossible for him to distinguish, except vaguely and roughly, in the mass of foliage and branches all around him what belongs to one tree and what to another. But the moment he begins to move forward, everything disentangles itself, and immediately he gets an apperception of the material contents of the woods

and their relations to each other in space, just as if he were looking at a good stereoscopic view of it. (p. 295-96)

While subsequent experimental studies have emphasized the precision and accuracy of the stereoscopic system (Chapter 5) and have demonstrated the effectiveness of disparity information when it is the only source of information available (Chapter 14), results from studies of motion parallax as a depth cue have been more equivocal. Early experiments revealed that observers are able to use motion parallax cues to distinguish the depth order and, in some cases, the depth separation of a small number of isolated points (Bourdon 1902; Cords 1913; Tschermak 1939; Graham et al. 1948; Zegers 1948). On the other hand, the perceived inclination of planar parallax surfaces was underestimated in several experiments (Gibson and Carel 1952; Gibson et al. 1959; Braunstein 1968; Degelman and Rosinski 1979). In addition, both the perceived depth order and the perceived inclination of parallax-defined surfaces has been found to be ambiguous in some situations (Gibson and Carel 1952; Gibson et al. 1959; Eriksson 1973; Farber and McKonkie 1979).

More recently Rock (1984) reported that observers were not able to make reliable judgments about the relative depth of a small number of discs at different absolute distances while making side-to-side head movements with only one eye open. Like Epstein and Park (1964) and Gogel (1977) before, Rock concluded that, "motion parallax does not by itself seem to be a cue to distance or depth."

To discover what factors influence the effectiveness of motion parallax as a source of information, we need to distinguish between two parallax situations. First, there is the situation described by Helmholtz in which relative motion on the retina is created by movement of the observer (observer-produced parallax). Second, there is relative motion created by movement of an object or surface with respect to a stationary observer (object-produced parallax). Many of the early studies which gave equivocal results, for example, Gibson and Carel (1952) and Gibson et al. (1959), simulated object-produced parallax. Several of the others, for example Graham et al (1948) and Eriksson (1973, 1974), simulated observer-produced parallax but with only a small number of objects in view. Neglect of either or both of these factors might account for the equivocal results.

In an attempt to answer these questions, Rogers and Graham (1979) investigated the effectiveness of motion parallax cues in both observer and object-produced parallax situations. In the former case, observers monocularly viewed a single random-dot

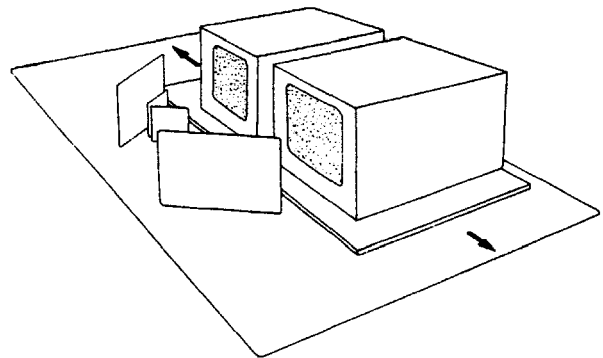


Figure 13.28. Simulating object-produced motion parallax.
Apparatus used by Rogers and Graham (1979) to simulate object-produced motion parallax. The screens were translated together and random-dot patterns on the screens were transformed in step with the movement to simulate the motion parallax produced by a three-dimensional surface translating across the observer's line of sight. The screens could be independently blanked to provide monocular parallax or both patterns could be made visible to study interactions between motion parallax and binocular disparity. (Rogers and Collett 1989.)

pattern displayed on an oscilloscope screen while making side-to-side head movements limited to an amplitude of 13 cm. When the observer's head was stationary, there were no cues to the shape or form of the simulated three-dimensional surface. Indeed, the available cues of accommodation and texture gradients indicated that the depicted surface was flat. As the observer moved his or her head from side to side, the pattern of random dots was transformed to mimic the motion parallax produced by a real three-dimensional surface with horizontal corrugations of different depth amplitudes and depth profiles (Figure 13.27). Observers had no problem differentiating between the different depth profiles and could match the amount of perceived depth to that in a static, disparity surface with reasonable accuracy.

The results were similar when the observer remained stationary and the parallactic motion in the display was coupled to sideways movements of the whole oscilloscope, thereby simulating the object-produced motion parallax created by a translating corrugated surface (Figure 13.28). In contrast to several earlier studies, Rogers and Graham found no ambiguities in judgments about the direction of the depth effects—rows of dots which moved in the opposite direction to the observer's movement (or in the same direction as the translating oscilloscope screen) appeared in front, as the geometry predicts (see Section 13.5.1). There was a marked similarity between the impression of depth created by motion

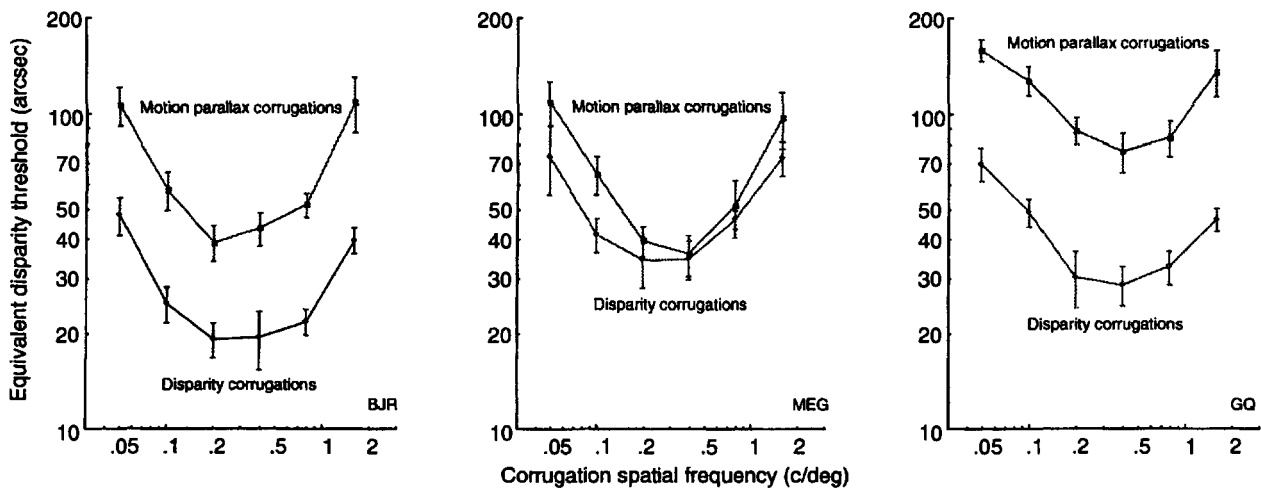


Figure 13.29. Comparison of disparity and parallax threshold functions.

Thresholds for detecting disparity- and motion-parallax corrugations as a function of corrugation frequency using a method of limits. The shapes of the disparity and parallax functions are similar for each of the three observers, with lowest thresholds at 0.3 c/deg and higher thresholds for both low and high corrugation frequencies. Disparity thresholds were, on average, half the parallax thresholds for these observers. (Redrawn from Rogers and Graham 1982.)

parallax and disparity-based stereopsis. Rogers and Graham claimed that the simulated parallax displays produced "a compelling impression of three-dimensionality not unlike that found with binocular stereopsis."

13.5.5 Quantitative studies

Thresholds

Quantitative similarities between disparity and motion parallax as sources of depth information have been reported by Rogers and Graham (1982) and Graham and Rogers (1982a). In the former study, thresholds for perceiving the three-dimensional structure of sinusoidal depth corrugations were measured as a function of the spatial frequency of the corrugations. Their results with disparity surfaces replicated Tyler's (1974a) finding of an increase in threshold for detecting disparity corrugations of high spatial frequency. In addition, they found that there was a fall-off in sensitivity for corrugations with a spatial frequency below 0.3 c/deg (Figure 5.13b). In a later study which used corrugations with a difference-of-Gaussians depth profile, Rogers and Graham (1985) showed that the fall-off in sensitivity at low spatial frequencies was not an artifact of the smaller number of cycles visible on the screen. Sensitivity also declined for surfaces which had a single cycle DOG profile of large spatial extent.

Rogers and Graham also measured thresholds for perceiving the three-dimensional structure of sinusoidal depth corrugations defined by motion

parallax. Peak sensitivity for perceiving the three-dimensional structure of horizontal corrugations occurred at corrugation frequencies of between 0.3 and 0.5 c/deg and the fall-off at low and high frequencies was similar to that for disparity corrugations (Figure 13.29). Thresholds for detecting disparity corrugations were typically half those for parallax corrugations, but some of this difference might have been due to the fact that parallax thresholds were measured under the more difficult conditions of monocular viewing and while the observer moved the head from side-to-side.

In their original study, Rogers and Graham (1979) used an increasing method of limits to determine the thresholds for perceiving three-dimensional structure. It is interesting to compare the results of a more recent study using a forced-choice procedure in which the observer had to judge whether the curvature of the central corrugation was concave or convex (Bradshaw and Rogers 1993b). Thresholds in this case were considerably lower than in the original study, at around 2 to 4 arcsec of peak-to-trough depth for the disparity corrugations (Figure 5.13c) and around 8 to 10 arcsec of equivalent peak-to-trough depth for the motion-parallax corrugations. The overall similarity of the shape of the sensitivity functions and the slightly lower thresholds for detecting disparity corrugations were not affected by the choice of psychophysical procedure.

Cornilleau-Peres and Droulez (1993) compared thresholds for detection of curvature in surfaces defined either by binocular disparities or motion

parallax. The parallax simulated a $\pm 12.45^\circ$ rotation of the surface around either a vertical or horizontal axis. Observers made a forced-choice discrimination between planar and curved surfaces. There was no significant anisotropy between motion around a horizontal or vertical axis but for five of the six observers, thresholds were lower for motion than for disparity-defined surfaces. Lowest thresholds were obtained when both disparity and motion cues were present (see Section 11.2). The 75 per cent points on the psychometric functions indicate that observers could discriminate a planar from a curved surface when its radius of curvature was around 1 m.

The slight advantage for surfaces defined by motion over those defined by disparity is in the opposite direction to the pattern of results obtained by Rogers and Graham (1982). Cornilleau-Peres and Droulez calculated the equivalent disparities of their curved surfaces at threshold and found that while the thresholds for moving surfaces were comparable to those of Rogers and Graham, those for the disparity-defined surfaces were at least four times higher. Figure 7.68 shows that the lowest thresholds for discriminating the direction of curvature in parabolic corrugations were equivalent to a radius of curvature of 5 m (Cagenello and Rogers 1989).

Cornilleau-Peres and Droulez suggested that the higher thresholds were probably due to the lower dot density of their images (400 dots compared with 32,000 dots over a similar area). The pixel size in their displays was 2 arc min, but disparities smaller than this value were simulated by a temporal interpolation procedure. The limitations of this temporal interpolation procedure compared with the (theoretically) infinite resolution of Rogers and Graham's (1982) analogue technique may also have contributed to the higher disparity thresholds obtained by Cornilleau-Peres and Droulez.

Contrast effects

Graham and Rogers (1982a) obtained further evidence of a similarity between disparity and motion parallax by finding similar successive and simultaneous contrast effects in the two domains. For example, after prolonged viewing of a sinusoidally corrugated surface defined by disparity or parallax, a flat test surface appeared corrugated in antiphase to the adapting surface (see Section 12.1). These depth aftereffects were measured with a nulling procedure and were similar whether the surface was defined by disparities or motion parallax. In Section 11.2 we described experiments which show that three-dimensional aftereffects created by prolonged inspection of a disparity surface can be nulled with monocular motion parallax cues and vice versa.

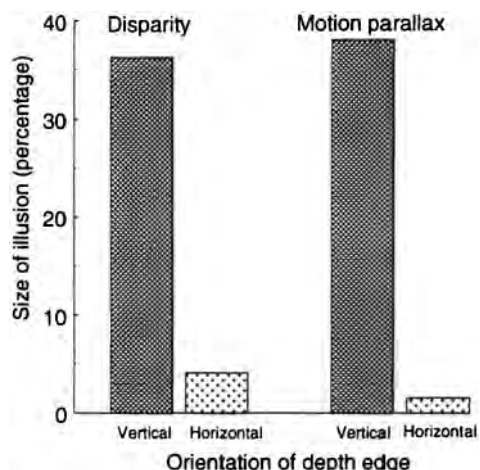


Figure 13.30. Craik-O'Brien-Cornsweet illusion in depth.

The size of the Craik-O'Brien-Cornsweet illusion in depth for surfaces defined by disparity and motion parallax, expressed as a percentage of the 8 arcmin depth discontinuity. In both cases the effect was much larger for a vertical than for a horizontal depth discontinuity. (Redrawn from Rogers and Graham 1983.)

Simultaneous contrast effects can be seen when a truly frontal surface is surrounded by flanking regions which are either inclined or slanted in depth (see Section 12.1). The effect of the flanking region is to make a frontal surface appear inclined or slanted in depth in the opposite direction to the inclination or slant of the surround (Figure 12.15). Graham and Rogers measured the strength of these simultaneous contrast effects using a nulling procedure, and again found that the magnitude and other characteristics were similar whether the surface was defined by disparities or by motion parallax.

Anstis, Howard, and Rogers (1978) reported a simultaneous contrast effect in the disparity domain. The outer flanking regions of a disparity surface with a Craik-O'Brien-Cornsweet scallop-shaped profile in depth appeared to lie in different depth planes (see Section 12.2.4). Rogers and Graham (1983a) reported a similar effect for surfaces specified by motion parallax, and the magnitudes of the effects in the two domains were very similar (Figure 13.30).

They also found that the illusion varied with the orientation of the depth discontinuity in the Craik-O'Brien-Cornsweet surface. The flanking regions appeared to lie in different depth planes when the depth discontinuity was vertical (flanking regions to the left and right) but when the depth discontinuity was horizontal (flanking regions above and below), there was little effect and the flanking regions appeared in the same depth plane (Figure 13.30). Moreover, and relevant to the present discussion, this anisotropy in the illusion was found whether the three-dimensional surface was defined by disparity or observer-produced motion parallax.

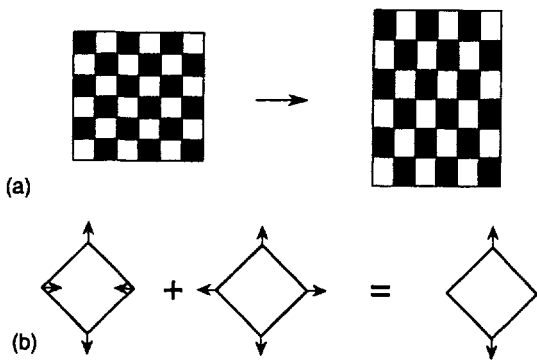


Figure 13.31. The induced effect transformation.

In Ogle's induced effect, the image seen by one eye is magnified vertically but not horizontally (a). The vertical expansion can be decomposed into a deformation component and an expansion component (b). (Adapted from Rogers and Koenderink 1986.)

13.5.6 Disparity and parallax induced effects

In the discussion of the computational theory of disparity-based stereopsis and motion parallax, it was pointed out that both cues are a consequence of perspective. The simultaneous difference in perspective is the basis of binocular stereopsis and the change of perspective over time is the basis of motion parallax. While perspective viewing offers a source of information about the relative depth and three-dimensional structure of objects and surfaces (Section 13.5.3), Mayhew and Longuet-Higgins (1982) have shown that it also provides information about the absolute distance to the surface (Section 7.6.4). They suggested that Ogle's induced effect, in which there is a vertical size difference between binocular images but no difference in their horizontal size, provides evidence that the human visual system uses vertical disparity.

Rogers and Koenderink (1986) provided further evidence of a similarity in the use of disparity and motion parallax by finding an analogous induced effect for surfaces defined by motion parallax. In the motion parallax case, observers viewed a random-dot pattern monocularly while making side-to-side head movements. The vertical size of the random-dot pattern increased as the head moved in one direction and decreased as it moved in the opposite direction. The two momentary images created at the outer limits of the head movement were identical to the stereoscopic images used by Ogle in his induced effect. In the induced effect based on disparities, observers reported that a random-dot pattern vertically magnified to the right eye appears slanted in depth, with the right edge appearing closer than the left edge. When the left eye's image was vertically magnified, the opposite slant was seen. In the motion parallax case, the righthand edge of the surface

appeared closer when vertical magnification increased with a rightward head movement and further away when magnification increases with a leftward head movement. Thus, the direction of the effect was the same in both domains. Perceived slant also increased with increasing vertical size difference up to a limit of 5–10 per cent, and with a similar change of vertical size.

One interpretation of these results is that the disparity and motion-parallax systems use the binocular vertical size differences and the vertical size changes over time, to compute the viewing system parameter of the angle of eccentric gaze, as was suggested by Mayhew and Longuet-Higgins (1982). Rogers and Koenderink (1986) pointed out that the existence of comparable induced effects in the two domains is also consistent with the visual system extracting the amount of deformation in the disparity and motion flow fields as a basis for judging surface slant (see Section 13.5.2). If the visual system decomposes the binocular disparity field into the differential invariants, as suggested by Koenderink and van Doorn (1976b), the vertical magnification of one image in Ogle's induced effect would yield both a deformation component and a dilatation component (Figure 13.31). Perceived slant in the disparity induced effect is consistent with the use of the deformation component. The dilatation component could signal the direction and extent of asymmetric gaze.

In the motion-parallax analogue of the induced effect, the perceived slant is again consistent with the use of the deformation component, and the dilatation component could signal the eccentricity of the surface. Alternatively, and formally equivalent, the dilatation component could signal the change in distance of the surface with each side-to-side head movement. Rogers and Koenderink reported that the plane of dots in the motion-parallax induced effect appears both to slant with respect to the frontal plane and to approach and recede with each sideways head movement. Whether these two interpretations are significantly different remains to be determined, but the existence of similar induced effects in the two domains provides further evidence of similarities between disparity and motion parallax as cues for three-dimensional shape and layout.

13.5.7 Additional similarities and differences

Shape index and curvedness discriminations

In Section 7.7.2 we described Koenderink's (1990) classification of smooth surfaces according to the shape index and the curvedness of local surface patches. De Vries et al. (1993) showed that observers can categorize and label surfaces with different

shape indices independently of the curvedness of the surface. van Damme et al. (1994) investigated shape identification and discrimination of smooth surfaces specified by motion parallax during active movements of the observer's head. In their first experiment, observers discriminated between the shape of a test image and that of a reference surface. The reference surface had one of eleven shape-index values between -1.0 and +1.0. Curvedness was kept constant within one series of eleven different reference-shape discriminations.

Shape discrimination thresholds, expressed as JNDs, were lowest for cylindrical surfaces with shape indices of ± 0.5 . Thresholds were higher for saddle shapes which were also the most difficult to categorize when defined by disparities (De Vries et al. 1993). Symmetrical elliptical shapes were also harder to discriminate when specified by motion parallax cues although they were the easiest to categorize when specified by disparities.

In their second experiment, curvedness discrimination thresholds were found to increase with increasing curvedness but when expressed as Weber fractions the lowest fractions (~15 per cent) were obtained for the least curved surfaces. In comparison, Rogers and Cagenello (1989) reported curvature discrimination thresholds for parabolic cylinders as low as 5 per cent for disparity-defined surfaces (Figure 7.68).

De Vries et al. (1994) repeated the shape discrimination experiments for surfaces defined by binocular disparities. They found a similar "W" shaped pattern of discrimination thresholds with best discrimination for cylindrical surfaces with shape indices close to either -0.5 or +0.5 and poorer performance for discriminating saddle shapes and symmetrical ellipsoids. The lowest JNDs for motion parallax-defined cylinders were around 0.025 on a shape index scale between -1.0 and +1.0, in comparison to the best observer's JNDs for disparity-defined cylinders which were around 0.015 on the same scale. Once again, the pattern of discrimination was very similar in the two domains with overall discrimination abilities slightly better in the disparity domain. These results mirror the differences in thresholds for detecting depth in disparity compared with motion parallax corrugations (Section 13.5.5).

Absolute shape judgments

In Section 7.7.2 we described the experiments of Durgin et al. (1994) which showed that judgments of the shape of both real and simulated three-dimensional surfaces from disparity can be close to perfect for distances up to 3 m. The same authors compared shape judgments when depth information was

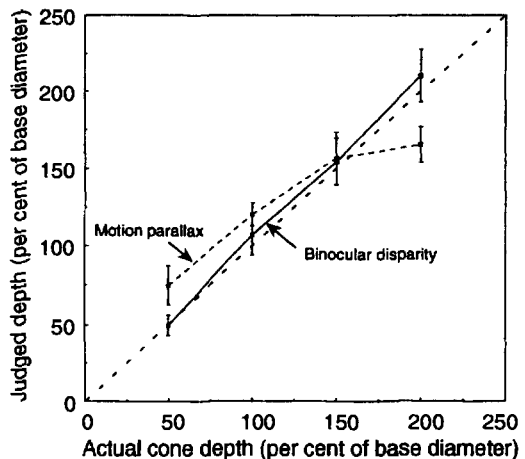


Figure 13.32. Perceived shape of disparity and parallax cones. Observers adjusted an icon on a monitor screen to match the perceived apex angle of cones of different heights specified either by binocular disparity or motion parallax. The judged depth was close to the actual depth for cones specified by disparities. The judged depth for motion parallax cones was overestimated for short cones and underestimated for tall cones. (Redrawn from Durgin et al. 1994.)

provided by motion parallax. The three-dimensional shapes were cones of nine different depths which moved continuously from left to right at constant speed creating object-produced motion parallax. The amplitude of travel was such that the change of angle of viewing the cones as they translated in front of the observer (4.92°) was the same as the vergence angle when observers viewed a stationary cone binocularly at a distance of 72 cm. Observers used a mouse-adjustable icon on a computer screen to indicate the perceived apex angle of the cone.

The results showed that while judgments of depth of the cone (as a percentage of the base diameter) from disparities closely matched the depth of the simulated cone, the depth from motion parallax only increased slightly with increasing simulated depth. Three-dimensional shape judgments under these conditions were very poor and quite different from the pattern of results reported by Rogers and Graham (1979) when observers were asked to match the perceived depth in sinusoidal corrugations.

Quite different results were obtained when real cones were seen in a brightly lit and structured environment and the observer made side-to-side head movements through 25 cm. Under these conditions, judgments of the heights of the cones were close to the actual heights, at least for cones with a height no greater than 150 per cent of the diameter of the base (Figure 13.32). Durgin et al. suggested that the improved performance was due, at least in part, to the superior information about the change in the angle

of viewing. The greater change in that angle (7.2° compared with 4.92°) together with the increased information about the change of angle from the surroundings, may have been responsible.

Absolute distance perception

Dees (1966) investigated the accuracy and precision of absolute distance estimates from binocular disparity and motion parallax cues. Observers were taught to use a scale of 1 to 20 for describing the perceived distance of a single ping-pong ball target subtending a visual angle of 2° against the background of a star field. Distance information was provided by either binocular disparities, or the motion parallax that would be created by a 2 foot side-to-side head movement, or both cues combined. Not surprisingly, the precision of observers' judgments decreased with increasing viewing distance. To compare the effectiveness of disparity and motion parallax cues, Dees used the variability of observers' judgments to calculate the amount of information transmitted to the observer. For disparity-based judgments, the information transmitted was 2.04 bits; for motion parallax-based judgments it was 2.415; and for the two cues combined it was 2.06. Although the difference is slight, Dees concluded that the combination of motion parallax and disparity is better than disparity alone but that motion parallax was "easily the most accurate". However, the superior performance with motion parallax may have been due to the fact that motion parallax was created by a displacement of the eye through 2 feet whereas in the binocular case the separation of the eyes is only $2\frac{1}{2}$ inches.

13.5.8 Individual differences

All the experimental evidence presented so far suggests a very close similarity in the way disparity and motion parallax information is extracted by the human visual system, but some differences have also been reported. According to Richards (1970), some 4 per cent of his sample of MIT undergraduates were unable to use the information provided by disparity and 10 per cent had great difficulty in seeing depth in Julesz random-dot stereograms. From his own observations, Julesz (1971) suggested that 2 per cent of observers are stereoblind and a further 15 per cent have particular difficulties in seeing depth in complex random-dot stereograms. Are there similar inabilities and deficiencies in the perception of depth from motion parallax? We know of no reports of people who cannot see the three-dimensional structure of surfaces in motion-parallax displays. Of the several hundred subjects tested we have not found one who did not see depth from parallax in our

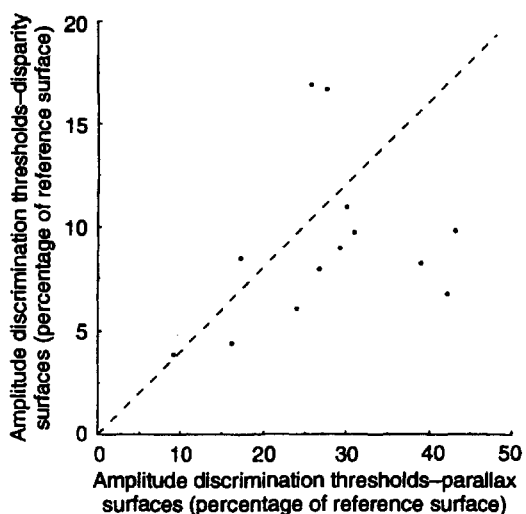


Figure 13.33. Disparity and parallax discrimination thresholds. Thresholds for discriminating differences in the peak-to-trough amplitude of sinusoidal corrugations for twelve naïve and one practiced observer. There is a weak correlation between disparity and parallax performance—observers who had lower thresholds for discriminating the amplitude of disparity corrugations tended to have lower thresholds for discriminating parallax corrugations. The dashed line shows where parallax thresholds are 2.5 times higher than disparity thresholds.

own observer-produced parallax displays. This is not surprising because motion parallax does not depend on the precise alignment of the two eyes and the development of appropriate binocular cells to the same extent as does disparity-based stereopsis.

While there are no reports of comparable "parallax-blind" observers, Richards and Lieberman (1985), reported that some observers were unable to see structure-from-motion in the kinetic depth effect when the figure was presented either in front of or behind the fixation point. They also presented evidence of a link between the ability to use stereoscopic information in either crossed or uncrossed disparity fields and the inability to see structure-from-motion in the same location although subsequent work by Bradshaw et al. (1987) has failed to replicate this finding.

In theory, there are three possible relationships between the ability to use disparity and the ability to use motion parallax. There might be "good" and "bad" observers, so that the correlation between performances on stereoscopic and parallax tasks is positive, as suggested by Richards and Lieberman's study. A compensation hypothesis predicts that observers would compensate for poor ability in using one cue by being better in using the other. In this case, the correlation between performance on the two tasks would be negative. In the limit, one might expect that stereoblind observers would show the

best motion-parallax performance. In a third scenario, there might be no relation between performance on disparity and motion-parallax tasks, and the correlation would be zero. Rogers (1984) used a task in which observers discriminated between the depths of sinusoidally corrugated surfaces of

different amplitudes. The surfaces were presented either binocularly with disparity cues or in an observer-produced parallax situation. The results for 13 observers are shown in Figure 13.33. They show only a weak relationship between the ability to use disparity and the ability to use motion parallax.

Vision in the cyclopean domain

14.1 The cyclopean domain	585
14.2 Cyclopean figural effects	587
14.3 Cyclopean motion and flicker	589
14.4 Inverse cyclopean phenomena	590
14.5 Binocular visual direction	591
14.5.1 Introduction	591
14.5.2 Laws of visual direction and the egocentre	591
14.5.3 The visual direction of disparate images	597
14.5.4 Determining the position of the egocentre	597
14.5.5 The position of the egocentre	598
14.5.6 Effects of phoria and strabismus	599
14.6 Utrocular discrimination	600

14.1 THE CYCLOPEAN DOMAIN

The three procedures for producing cyclopean effects were described in Section 1.1.2. We are concerned here only with the dichoptic cyclopean procedure in which distinct images in the two eye are superimposed or juxtaposed to produce an effect in the brain not evident in either monocular image.

Cyclopean effects that are not exclusively cyclopean

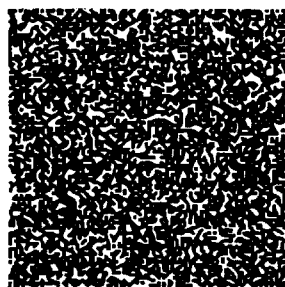
Sometimes the same visual effect can be produced by combining stimuli dichoptically as is produced when the same stimuli are combined in one eye. The dichoptic effect can be said to be cyclopean because the separate monocular images do not produce it, but it is not exclusively cyclopean because it can also be produced by combining the stimuli in the same eye. For instance, a display of lines presented to one eye can be combined dichoptically with a different display of lines in the other eye to form a composite image of a cube and this cube resembles the cube formed when the same lines are combined in one eye, as in Figure 3.3. The two effects are not identical; for instance, the cyclopean cube is disrupted by vergence eye movements whereas the monocular cube is unaffected. However, even when dichoptic and monocular effects are similar in appearance, one cannot be sure that the neural processes responsible for them are the same. Thus, exclusively cyclopean neural processes may be involved even when the dichoptic and monocular effects appear similar.

Dichoptic motion may be created by dichoptically combining moving stimuli so that the two stimuli

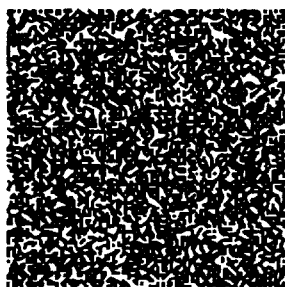
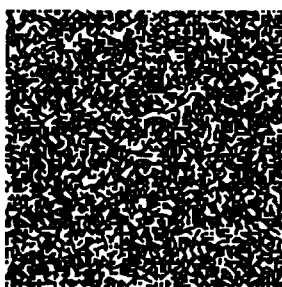
form a defined motion path not evident in either one. Dichoptic apparent motion can be formed by dichoptic alternation of two flashing lights with a spatial offset between them. Each eye sees only a stationary flashing light, and motion is not perceived until the images are combined. These motion effects, at the level of initial appearance, are not exclusively cyclopean because the same effects are produced by alternating the same stimuli to one eye. However, this does not prove that the neural processes are identical in the two cases. Careful study of the two effects is required to reveal possible effects of differences in neural processing. Colours formed by superimposing different colours in the two eyes would not be exclusively cyclopean if they obeyed the same laws of colour mixing as colours combined in the same eye. In fact dichoptic colour mixing does not obey these rules, so in these respects it is an exclusively cyclopean process (see Section 8.2).

Exclusively cyclopean effects

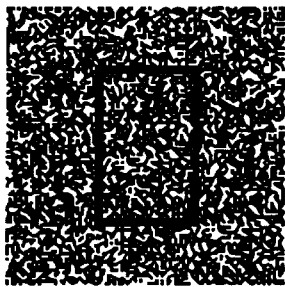
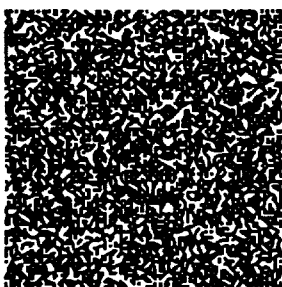
An exclusively cyclopean effect is one that arises when two stimuli are viewed dichoptically and which is not evident in either monocular image or when the same stimuli are combined in the same eye. An exclusively cyclopean effect arising from dichoptic stimulation depends on exclusively binocular processing. Binocular rivalry is exclusively cyclopean, since it is not the same as monocular rivalry (see Section 8.3). Binocular lustre formed by a dichoptic difference in luminance is an exclusively cyclopean effect, since the monocular combination of the same stimuli produces only a gray patch.



(a) The displays contain an annular region of uncorrelated dots. The dots in the inner square and surround are correlated. When the displays are fused the annulus is visible.



(b) A central rectangle contains uncorrelated dots and has a horizontal disparity. When the displays are fused, the rectangle is visible but has an indeterminate depth.



(c) Adding monocularly visible outlines to the disparate regions of uncorrelated dots produces unambiguous depth for the outline but not for the dots inside the outline.

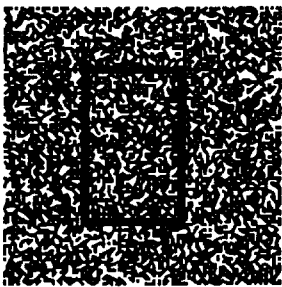


Figure 14.1. Cyclopean shapes defined by rivalry.

Whether the detection of disparity is regarded as exclusively cyclopean depends on which aspect of the task is considered. Thus, the disparate area in a random-dot stereogram is evident when the two halves of the stereogram are superimposed in one eye so that, in this sense, disparity detection is not exclusively binocular. On the other hand, although disparity detection is based on mechanisms of monocular spatial resolution, it has many features unique to the binocular process, and physiological evidence has revealed that disparity detection involves specialized cortical cells. The sense of depth arising from static disparity is exclusively cyclopean, although a perceptually identical effect can be produced by monocular motion parallax (see Section

13.5). The disparity in both standard stereograms and random-dot stereograms is cyclopean. The hallmark of a random-dot stereogram is that the shape defined by a region of disparity is also cyclopean whereas, in a pictorial stereogram, disparity discontinuities are usually evident as luminance boundaries in each monocular image. A luminance boundary cannot be taken as evidence of a disparity discontinuity in either type of stereogram.

Most of this book is devoted to the processing of binocular disparity. In this section we are concerned only with the perception of cyclopean shapes defined by disparity or other cyclopean features. A **cyclopean shape** can be constructed by confining a given cyclopean stimulus to one region of a larger display. Many random-dot stereograms contain a cyclopean shape defined by disparity. A related procedure is to present a region of pattern elements with random horizontal or vertical disparities, or both, within a region of dichoptically matching dots. Once synthesized, a cyclopean shape can be made to move by simply moving the cyclopean boundaries that define it. A cyclopean shape not defined in terms of disparity can also have disparity imposed on it, and displays of this type are mentioned in Section 6.1.3.

One can form cyclopean shapes defined by binocular rivalry by surrounding a region of dichoptically congruent elements by dichoptically dissimilar elements, as in Figure 14.1a. When the images are combined, the uncorrelated region appears to float at an indeterminate depth with respect to the correlated region. This has been called *rivaldepth* (O'Shea and Blake 1987). Some people have a consistent impression of depth as either in front or behind with this stimulus but, as was pointed out in Section 7.8.3, this is probably due to fixation disparity.

A horizontal disparity can be imposed on the boundaries of an uncorrelated region in a random-dot stereogram to determine whether boundaries defined by rivalry can generate stereoscopic depth. But inspection of Figure 14.1b reveals that the uncorrelated region still has an indeterminate depth. When the disparate boundaries of uncorrelated regions are outlined (Figure 14.1c), the outline appears in depth but the texture within the outline still appears at an indeterminate depth. There seem to have been no experiments on the perception of shapes defined by binocular rivalry. A consistent impression of stereoscopic depth occurs when a region of dichoptically uncorrelated dots has a different spatial frequency with respect to an uncorrelated surround. But in this case the disparate region is not cyclopean, since it is visible in both monocular images (see Figure 6.10). This question was discussed in Section 6.1.3.

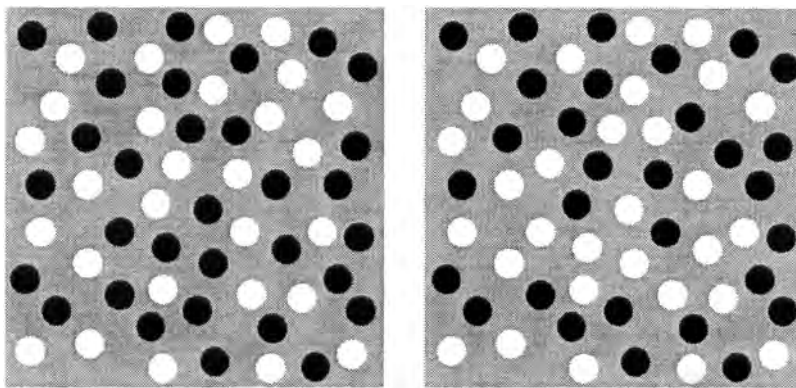


Figure 14.2b . A cyclopean shape defined by contrast rivalry.
The dots are distributed randomly in each eye, with the contrast in the two eyes matching in the surround but not in the central region.

An interesting phenomenon occurs when black annuli filled with white in one eye are combined with black discs in the other eye, as in Figure 7.11. The outer rims fuse to form a set of holes through each of which one sees a rivalrous region of black and white. This creates the impression of a black and white dotted surface seen through holes, which Howard (1994) dubbed the sieve effect (See Section 7.8.3). Here is a case in which opposite luminance polarity in the two eyes creates an impression of depth in its own right. This is an essentially cyclopean phenomenon.

The dichoptic combination of different coloured patches results either in colour rivalry or colour mixing. Binocular yellow, formed by presenting red to one eye and green to the other, may be regarded as a cyclopean colour (see Section 8.2). Cyclopean shapes defined by colour rivalry can be formed from dichoptic arrays of different coloured discs, with the colours matching between the two eyes in one region and not matching in another region, as in Figure 14.2a (see after page 310). The cyclopean shape defined in this way is not as clear as that defined by reversed luminance polarity, as shown in Figure 14.2b. This is probably because colour rivalry is not a preattentive feature, whereas reversed luminance polarity is (see Section 6.1.6). We failed to obtain stereopsis by imposing a disparity on a region of colour rivalry. Note that not all cyclopean shapes are exclusively binocular, since in many cases the same shape is evident when the two displays are combined in the same eye.

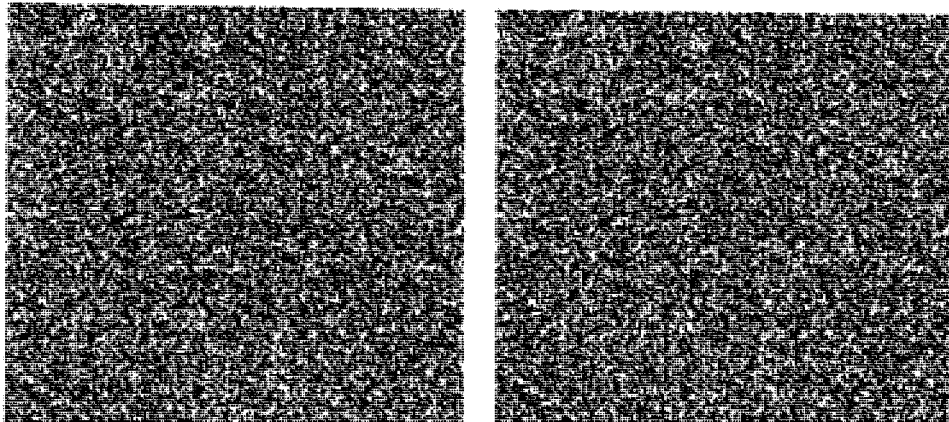
Any cyclopean effect not visible in either eye must depend on neural processes occurring at or beyond the lateral geniculate nucleus, but that does not prove that the effect is exclusively binocular, since the same effect may arise when the stimuli are combined in one eye. Any cyclopean effect that is

not visible when the same images are combined in one eye is the exclusive product of central binocular processes. The present section is a review of ways of synthesizing cyclopean stimuli and of the literature on the perception of cyclopean shapes.

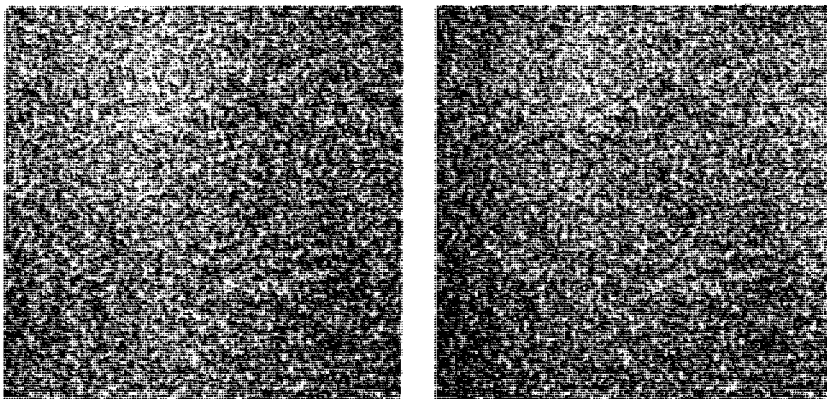
14.2 CYCLOPEAN FIGURAL EFFECTS

Several visual illusions, such as the Müller-Lyer illusion (Figure 14.3a), and reversible perspective (Figure 14.3b) are present in disparity-defined cyclopean shapes, showing that cortical processes are capable of generating them (Papert 1961, 1964; Julesz 1971). A beautiful collection of random-dot stereograms depicting a wide variety of cyclopean geometrical illusions is presented in Chapter 7 of Julesz's *Foundations of Cyclopean Perception* (1971). These include the Müller-Lyer, Poggendorff, vertical-horizontal, Ebbinghaus, Ponzo, and Zöllner illusions. Julesz observed that all but the Zöllner illusion were evident in the cyclopean form. This does not exclude the possibility that precortical processes may also contribute to these illusions.

The apparent lateral displacement of a bar away from the position of a previously inspected bar in a neighbouring location (the figural aftereffect) occurs between cyclopean bars defined by disparity (Walker and Kruger 1972). Tyler (1975c) generated a cyclopean stereo grating tilted in the frontal plane at 20° to the horizontal. After the gaze scanned across this grating for 30 s a subsequently seen horizontal cyclopean grating appeared tilted in the opposite direction. The aftereffect transferred 50 per cent to a noncyclopean test grating defined by luminance. Tyler also described a spatial-frequency aftereffect in the cyclopean domain. Inspection of a cyclopean stereo grating of one spatial frequency caused an



(a) The cyclopean Müller-Lyer illusion.



(b) The cyclopean reversible perspective illusion.

Figure 14.3. Cyclopean illusions.

These illusions work when the stereograms are fused with divergent gaze so that the forms stand out above the background. (From Julesz 1971. Copyright 1971, by Bell Telephone Laboratories Incorporated.)

apparent shift in the spatial frequency of a subsequently seen test grating with a different spatial frequency (see Figure 12.37).

Several visual tasks, including grating acuity, grating detection, orientation discrimination, and vernier acuity, are performed more precisely with stimuli oriented vertically or horizontally than with obliquely oriented stimuli (see Howard 1982). This anisotropy is referred to as the oblique effect. Mustillo et al. (1988) used a temporal two-alternative forced-choice procedure to measure subjects' ability to discriminate differences in the orientation of a cyclopean bar presented in vertical, horizontal, or oblique orientations. The bar was defined by a region of either crossed or uncrossed disparity in a random-dot stereogram. The mean discrimination threshold for vertical or horizontal bars was about 1.13° and that for oblique bars was about 2.3° . These

differences are similar to those reported for bars defined by luminance contrast. Targets with a crossed disparity yielded lower orientation-discrimination thresholds than targets with an uncrossed disparity.

It takes longer to identify familiar shapes, such as letters, when they are presented in an unusual orientation (see Howard 1982; Shepard and Cooper 1982). The function relating recognition time to the orientation of letters was found to be the same for letters defined by luminance contrast as for letters defined only by colour, motion, or binocular disparity (Jolicoeur and Cavanagh 1992). This task therefore depends on mental processes that are independent of low-level visual processing.

The effects reviewed in this section occur between shapes defined by disparity but do not necessarily involve interactions between disparity detectors after the point at which the disparate shape has been

detected. Contrast effects in the cyclopean domain that do involve interactions between different disparities are reviewed in Chapter 12.

14.3 CYCLOPEAN MOTION AND FLICKER

Several lines of evidence suggest that, in primates, motion detectors are situated in the visual cortex, not in the retina. For instance, the motion aftereffect is still visible after the eye exposed to the induction stimulus has been pressure blinded (Barlow and Brindley 1963). Furthermore, a movement aftereffect is not seen when the eye exposed to the inspection stimulus is paralyzed during the induction period (Pickersgill and Jeeves 1964). Given that motion detection is a cortical process, one would expect motion sensations to arise in the cyclopean domain. There are basically three types of cyclopean motion.

The first type of cyclopean motion, which is not exclusively cyclopean, is created by presenting a stimulus such as a white spot on a dark background to one eye followed by a similar stimulus to the other eye in a neighbouring position. When the stimuli are presented repeatedly, an impression of to-and-fro movement is created. Each monocular image appears as a flickering stimulus, but when the images are combined in a stereoscope they appear to move. In this case the motion is a dichoptic composite effect, since the same effect is produced by combining the stimuli in one eye. This is **dichoptic motion**, which was discussed in Section 13.4.

The second type of cyclopean motion, which we refer to as **motion of cyclopean stimuli**, is created by moving a cyclopean shape defined by rivalry, disparity, or colour in a random-dot stereogram. The random dots are correlated between the two eyes at any moment, but a new set of random dots is presented on every frame. This ensures that there are no monocular cues to the motion of the cyclopean form. In other words, the motion signal is not carried by the microelements of the stereogram but by the cyclopean macropattern, and is therefore not visible in either eye. Only random, Brownian motion is seen in each monocular image.

The third type of cyclopean motion is **stereoscopic motion in depth**, created by changing the disparity of a stimulus relative to an unchanging surround. In this case each image moves laterally so that the sensation of motion in the dichoptic image is not cyclopean. However, the sensation of motion in depth created by combining the images is cyclopean. This topic was discussed in Section 13.2.

The visual properties of motion-defined shapes viewed binocularly have been investigated by Regan

(1986a, 1989b). Motion may also be defined only by a cyclopean shape, as we see next.

Our main concern here is with motion of cyclopean stimuli created when a cyclopean shape defined by rivalry, disparity, or colour is moved. A motion aftereffect is created by prolonged viewing of a moving cyclopean image. Papert (1964) generated a disparity-defined cyclopean bar in a random-dot stereogram and caused it to move down over the background, taking care to remove all monocular cues to motion. After a period of inspection, a stationary cyclopean bar appeared to move in the opposite direction.

Julesz and Payne (1968) used a dynamic random-dot stereogram depicting a disparity-defined vertical grating, in which the binocularly correlated dots in the two images were replaced every 25 ms. This procedure removes coherent motion signals from the dots and confines coherent motion to the cyclopean boundaries of the grating. The temporal conditions for optimal apparent motion with a cyclopean stimulus differed from those for a binocularly viewed luminance grating, but this could have been due to the difference in effective contrast of the boundaries between the two types of display. At low temporal frequencies, the cyclopean and luminance displays appeared to oscillate from side to side, and at high temporal frequencies both displays appeared as two superimposed stationary gratings. At an intermediate frequency, the cyclopean grating appeared as a single stationary grating, an effect not evident with the luminance grating. The cause of this difference between the two types of motion remains obscure but must have had something to do with the apparent motion being carried only by the boundaries of the stripes and not by the texture within the stripes. The stationary effect was not seen when the dots were not renewed on every frame, but in this case the motion was no longer exclusively cyclopean.

Cyclopean motion has been shown to induce the involuntary pursuit motion of the eyes known as optokinetic nystagmus (Fox et al. 1978). The stimulus was a dynamic random-dot stereogram in which each image was replaced every 16 ms. A vertical grating in depth was created with 30 arcmin peak-to-trough disparity. The grating drifted across the display at a velocity of 9.3°/s. Stereoblind subjects do not respond to motion of cyclopean shapes, presumably because they do not see the shape (Archer et al. 1987). However, stereoblind subjects showed optokinetic nystagmus in response to dichoptic motion, which does not require prior detection of a cyclopean shape (Wolfe et al. 1981). Other aspects of the relation between pursuit eye movements and stereoscopic vision are discussed in Section 12.5.6.

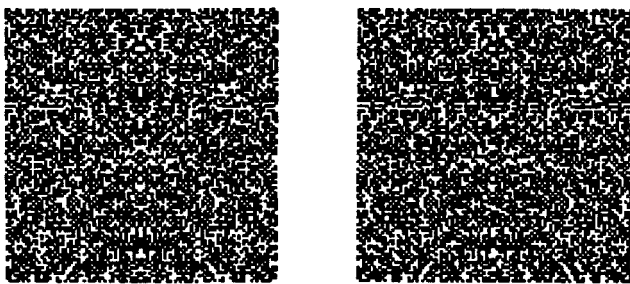


Figure 14.4. Inverse cyclopean effect.

Symmetry evident in the monocular images becomes difficult to detect when the images are fused. (Adapted from Julesz 1966.)

Patterson et al. (1992) generated moving depth gratings in dynamic random-dot stereograms and measured the duration threshold for detecting the direction of motion. The threshold decreased with increasing velocity and was therefore not based on a constant displacement threshold. It was concluded that dichoptic motion is processed by velocity-sensitive motion detectors rather than in terms of change in position. The duration threshold increased as the disparity in the moving grating was increased, in both the crossed and uncrossed direction. This could be because there are fewer detectors of large disparities than of small disparities.

Chang (1990) generated a horizontal grating defined by disparity in a random-dot stereogram and caused it to move upwards or downwards. The dots within the grating were either stationary, moved in the same direction as the grating, moved in the opposite direction, moved in an orthogonal direction, or were dynamic (replaced by a new array of dots on every frame). The motion of the grating was most pronounced and smooth when the grating and the dots moved together. When the dots and grating moved in different directions, the predominant motion was of the dots rather than of the grating. With dynamic random dots, the grating appeared to move but the motion was not smooth, and the addition of a small percentage of coherently moving dots was sufficient to bias the overall perceived direction of motion. When the dots were stationary, the grating appeared to undulate in depth, with only a weak sensation of vertical motion within the frontal plane. Note that, although the dots within the grating were stationary, there were opposite motion signals in the two eyes along the disparity boundaries of the moving grating. It was concluded that luminance-defined motion is required for cyclopean motion and that cyclopean motion within the frontal plane is processed by interactions between modulations in disparity and luminance-defined motion. Another way to summarize these results is to say that signals

from moving disparity contours are not sufficiently strong to override conflicting luminance-defined motion signals arising at the disparity boundaries.

14.4 INVERSE CYCLOPEAN PHENOMENA

In a random-dot stereogram a pattern visible to one eye can become invisible when the two images are fused. Julesz referred to this effect as **inverse cyclopean stimulation** (Julesz 1971). This can happen because parts of the pattern become scattered in different depth planes. For instance, the symmetry evident in one image of the stereogram in Figure 14.4 is lost when the images are fused. Regions visible in each monocular image of a random-dot stereogram may also disappear after fusion because their boundaries form complementary pairs, as in Figure 14.5 (Frisby and Mayhew 1979). In this case the regions are in the same depth plane. Frisby and Mayhew concluded from this that texture discrimination does not occur before monocular images are combined. But even if the textured regions were segregated before fusion they would surely combine into an homogeneously textured pattern at the cyclopean level.

A nice illustration of how monocular structure may be disguised in dichoptically combined images is provided by the dichoptic combination of Glass patterns. A Glass pattern is formed by taking a random array of dots and superimposing on it a second transformed copy of the same array, seen with the same eye. When the transformation is a radial expansion, a radial Glass pattern emerges; when it is a rotation, a concentric pattern emerges (Glass and Perez 1973). The Glass pattern is defined by aligned clusters of dots in the combined pattern. The displays in the stereogram of Figure 14.6a were made from the same random-dot array. A radially expanded copy of the array was added to the display in each eye and this second copy was displaced laterally in the right-eye display. Fusion of these displays creates the impression of two depth planes with no evidence of the Glass pattern in either. We can conclude that the pairing of the dots by disparity has gained precedence over the pairings in each eye that created the Glass pattern (Earle 1985). In Figure 14.6b, one set of dots is the same in the two images. In the left image the second set of dots is an expanded version of the first set. In the right image, the second set of dots is a different set of random dots. The images fuse to give an impression of dots dispersed at random in depth, again with the Glass pattern disguised. The perception of depth supersedes the perception of aligned dot pairs. When

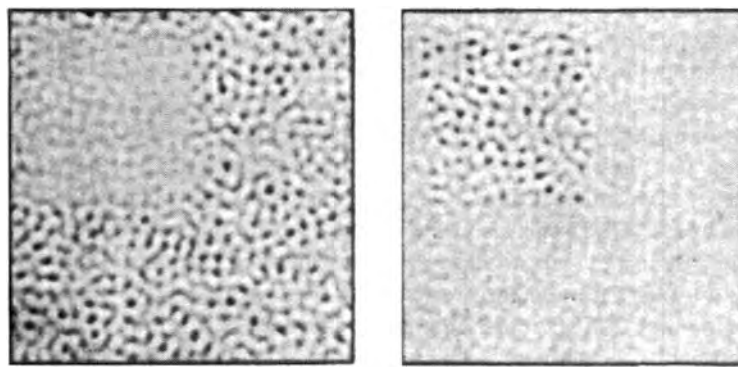


Figure 14.5. Inverse cyclopean effect in complementary patterns.
Boundaries between the textured regions in each monocular image disappear after fusion because the boundaries form complementary pairs and the bold patterns suppress the less bold patterns. (From Frisby and Mayhew 1979, Perception, 8, 153-156, Pion, London.)

pairs of dots defining the Glass pattern are shifted as a pair relative to matching pairs in the other eye (Figure 14.6c), the Glass pattern is preserved in the fused image. A Glass pattern not evident in either monocular image may be created in the cyclopean domain, as can be seen in Figure 14.6d. Adjusting the disparity between pairs of dots in monocular Glass patterns creates a cyclopean Glass pattern in depth (Figure 14.6e).

14.5 BINOCULAR VISUAL DIRECTION

14.5.1 Introduction

People find it easy to judge the lateral visual direction of an object in terms of its position to the left or right of the apparent median plane of the head or body. These planes constitute norms for these judgments. A judgment about the direction of a visual object with respect to the head requires the observer to register the position of the images in the eyes (the oculocentric component) and the angular position of the eyes in the head (the eye-position component). When the observer fixates the object, its images can be expected to fall precisely on the foveas, so that uncertainty about the oculocentric position of images contributes very little to the variance of judgments of the headcentric direction of the object. Under these circumstances, a headcentric directional judgment reduces to the task of registering the angular position of the eyes in the head. The position of the eyes in the head could be provided by proprioceptors in the extraocular muscles or by the efference to those muscles. It could also be provided visually by the position of the images of the orbital ridges and tip of the nose. However, the variability of judgments of straight ahead was not affected by

whether or not these structures were in view. It seems that the nose is too eccentric in each monocular visual field to be effective, since an external object fixed with respect to the head did reduce the variability of judgments when it was reasonably close to the target (Shebilske and Nice 1976; Wetherick 1977).

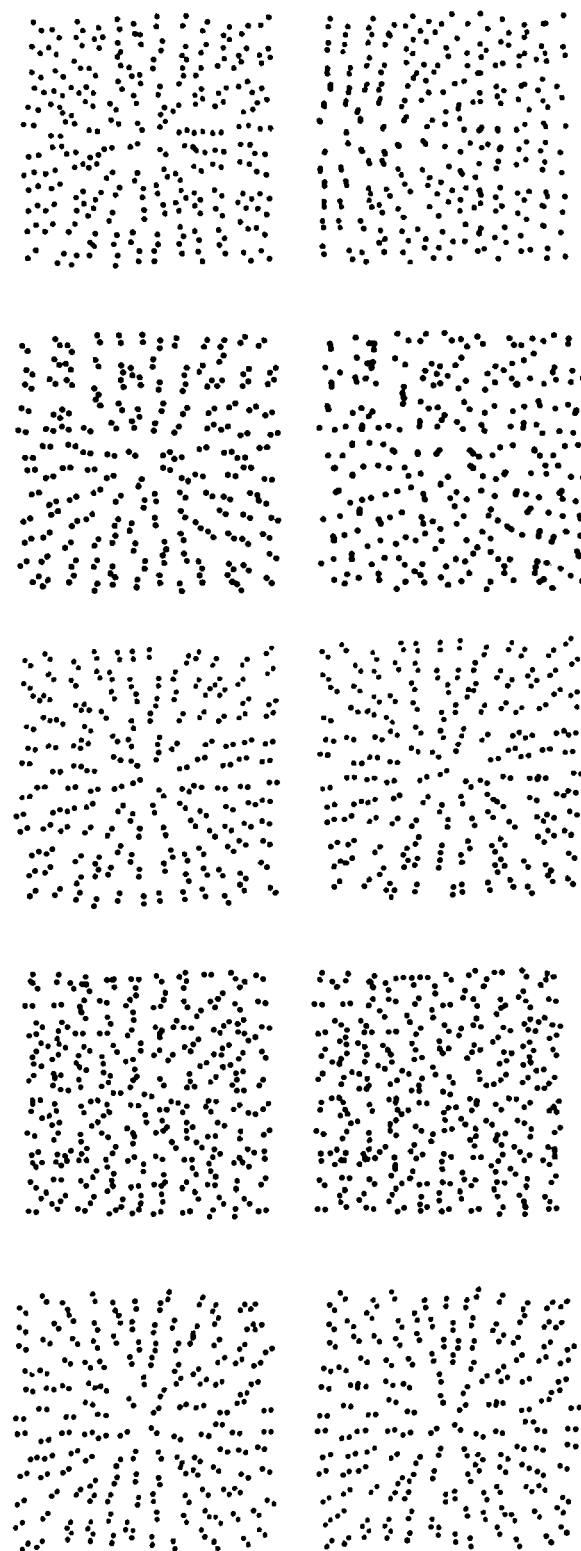
When an object is fixated with both eyes, the eyes point in different directions with respect to the median plane of the head, and yet, the visual object is judged to have a single direction in space. Somehow directional information from the two eyes combines to produce a unitary sense of visual direction.

One is then confronted with the question of which location in the head serves as the origin for such directional judgments. One possibility is that it is the dominant eye, but the evidence to be reviewed next suggests that directional judgments are referred to a point midway between the eyes, known as the **visual egocentre, or cyclopean eye**. Therefore, the directional information from each eye must somehow be transferred to this common egocentre. The next section is concerned with how this is done, both when the eyes fixate the target, so that the positions of the two images correspond, and when directional information is derived from disparate images.

14.5.2 Laws of visual direction and the egocentre

The law of oculocentric direction

The analysis of headcentric visual direction starts with the basic unit of oculocentric direction, namely, the visual line. In Section 2.1, a visual line was defined as any straight line passing through the pupil and the nodal point of an eye. A visual line is the locus of all points, fixed relative to the eye, which stimulate a given point on the retina. The visual line through the centre of the fovea is the visual axis. Any other visual line may be specified in terms of



(a) The left-eye image is a random-dot pattern plus a radially expanded copy. The right-eye image is the same but with one pattern displaced laterally. After fusion, two depth planes emerge and the radial pattern is lost.

(b) The left image is a random-dot pattern plus an expanded copy. The right image is the same plus another random-dot pattern. The images fuse to form an array of dots dispersed in depth with the Glass pattern not visible.

(c) The pairs of dots defining the Glass pattern in the left image are shifted laterally in the right image. The Glass pattern is now preserved in the fused image.

(d) The dots in the left image relative to those in the right image are adjusted to create a Glass pattern in the fused image that is not visible in either monocular image.

(e) The disparity between pairs of dots in the left image relative to pairs of dots in the right image is adjusted to create a three-dimensional cyclopean Glass pattern. (From Earle 1985, Perception, 114, 545-552, Pion, London.)

Figure 14.6. Inverse cyclopean effects in Glass patterns.

its angle of azimuth with respect to the eye's median plane, and of its angle of elevation with respect to the eye's midtransverse plane. The oculocentric direction of a visual line may also be specified in terms of its angle of eccentricity and meridional angle, as described in Section 2.3.1. For a given position of the eye, each fixed visual object has only one visual direction, which it shares with all objects on the same visual line. This means that objects on a visual line appear visually superimposed.

Monocular diplopia or polyopia in which single objects appear double or multiple, is an exception to this rule. This issue is discussed in Section 2.4.3. Objects on different visual lines appear in distinct locations. This rule does not apply to objects which are closer together than the resolution threshold of the visual system.

The preceding statements are summed up by the **law of oculocentric direction**, which states that *all objects on the same visual line are judged to be in the same oculocentric direction, which is unique to that set of objects.*

Laws of headcentric direction

For a given angular position of an eye, points in the same oculocentric direction are also judged to be in the same headcentric direction. Thus, the **law of headcentric direction** states that, *for a given position of the eye in the head, objects lying on the same visual line are judged to be in the same headcentric direction, which is unique to that visual line.*

When a person sights with one eye along a rod held about 30 cm from the eye, the rod lies along the visual axis and is experienced as pointing directly at the self. One may also align a rod with another visual line by maintaining fixation on a point in the median plane, while aligning an eccentrically placed rod. In this case, too, the rod appears to point directly at the self. Note that a rod aligned with a visual line for one position of the eye will not be aligned with any visual line, after the eye has rotated to another position. This is because the centre of rotation of the eye is behind the nodal point, so rotating the eye displaces the nodal point in the same direction as the eye movement (Figure 14.7). Brewster (1844b) referred to this as **ocular parallax**.

The lack of coincidence between the nodal point and the centre of rotation is revealed in a phenomenon in which an object near the nasal limit of the visual field can not be seen when the eye is turned sharply in toward the nose (Mapp and Ono 1986).

The visual **egocentre** is the location in the head toward which visually aligned objects appear to point. A more precise definition is given in what follows. Note that the egocentre is not necessarily the

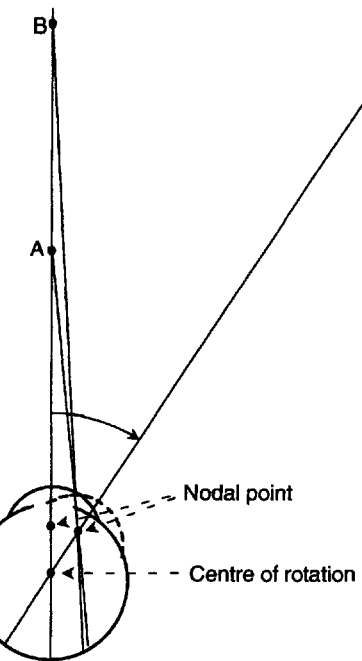


Figure 14.7. Loss of alignment with motion of an eye.

Two points, A and B, aligned when the eyes are in the primary position of gaze, are no longer aligned when the eye rotates to another position. This is because the nodal point is in front of the centre of rotation.

point towards which monocularly aligned objects actually point, which is, of course, the nodal point of the eye. In fact, as we will see, the egocentre is normally in the median plane of the head.

The **law of common monocular directions** states that, *in monocular viewing, all visual lines appear to be directed toward a common visual egocentre.* Any line that actually passes through the egocentre is referred to as a **cyclopean line**. If the egocentre coincides with the nodal point of an eye, visual lines and cyclopean lines coincide, but for other positions of the egocentre they do not coincide.

The next stage in the analysis is to assume that, in the binocular field, every retinal point in one eye has a corresponding point in the retina of the other eye, such that the images falling on the two points have a common visual direction. This is the principle of corresponding points. Each pair of corresponding points is associated with a pair of corresponding visual lines. It follows from the law of oculocentric direction and the principle of corresponding points that all objects on either of a pair of corresponding visual lines will appear spatially superimposed. This is the law of identical oculocentric visual directions applied to corresponding lines. In itself this does not prove that objects lying along corresponding visual lines will appear to be in the same headcentric direction for the two eyes. For instance, if each eye served

as its own centre of reference for headcentric direction, an object seen by one eye would seem to be in a different headcentric direction from that of an object on a corresponding line in the other eye, even though the two objects appear to occupy the same position in space. In fact, we will show that corresponding visual lines are referred to a common egocentre that is normally midway between the eyes. These principles can be summed up by the **law of common binocular directions**, which states that *in binocular viewing, all visual lines of either eye appear to point to a common egocentre midway between the eyes.*

To say that a visual line appears to point to the egocentre does not specify the apparent direction of that line relative to the midline of the head, since the direction of a line cannot be specified by reference to only one point. For any visual line we need to specify a point in space, the direction of which is judged correctly under normal circumstances. Assume that the headcentric direction of the point of fixation is correctly judged. This is a point on the horopter where the two visual axes intersect. We then generalize this idea and state that the headcentric directions of all points on the horopter (points where corresponding lines intersect) are judged correctly.

Thus, the apparent direction of lines within the horizontal plane of regard may be specified if (1) the directions of points on the horizontal horopter are judged correctly and (2) points lying on the same visual line are perceived as collinear. From the law of common binocular directions and from these assumptions one can derive the **law of cyclopean projection**, which states that *points lying along any visual line appear to be aligned with the egocentre and the physically defined point where the visual line intersects the horopter.* This can be regarded as a corollary to the law of common binocular directions.

With symmetrical convergence, points lying on the visual axis of an eye appear to lie in the median plane of the head. The visual axis makes an angle θ with the median plane and this angle is half the angle of convergence, as shown in Figure 14.8. If it is assumed that the horopter conforms to the Vieth-Müller circle and the egocentre lies on this circle, midway between the eyes, then θ is the angle between any visual line and the cyclopean line on which objects on the visual line appear to lie. Thus, for a given convergence distance, a line lying along any visual line will appear displaced by half the vergence angle with respect to that visual line.

Demonstrations of the laws of headcentric direction

Hering stated the law of common binocular directions in the following words: "For any given two corresponding lines of direction, or visual lines, there is in

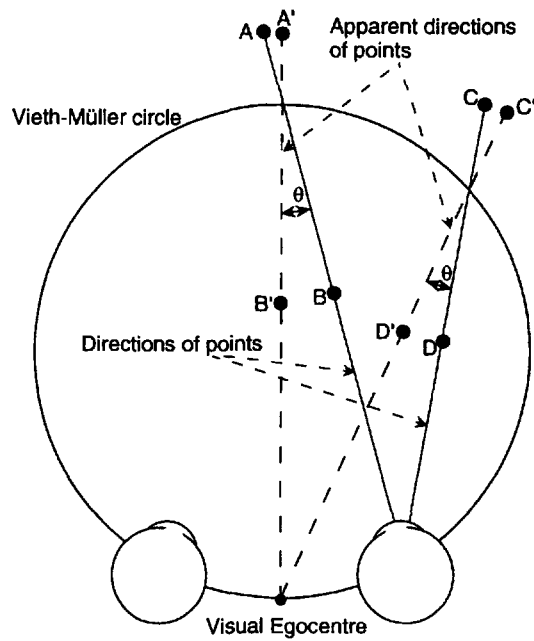


Figure 14.8. The egocentre and perceived direction.

Assume that the visual egocentre lies midway between the eyes on the Vieth-Müller circle and that the headcentric directions of points on the horopter are correctly judged. It follows that points, such as A and B, lying on a visual axis will appear to be aligned with the egocentre and the point where the visual axis intersects the horopter. The angle θ between the visual axis and the line on which the objects appear to lie is half the vergence angle. For a given angle of vergence, objects such as C and D, on any other visual line, will also appear to be displaced by this same angle.

visual space a single visual direction line upon which appears everything which actually lies in the pair of visual lines." (Hering 1879, p. 41). The truth of this statement was demonstrated in the following way:

Let the observer stand about half a metre from a window which affords a view of outdoors, hold his head very steady, close the right eye, and direct the left to an object located somewhat to the right. Let us suppose it is a tree which is well set off from its surroundings. While fixing the tree with the left eye a black mark is made on the window pane at a spot in line with the tree. Now the left eye is closed and the right opened and directed at the spot on the window, and beyond that to some object in line with it, for example, a chimney. Then with both eyes open and directed at the spot, this latter will appear to cover parts of the tree and chimney. Both will be seen simultaneously, now the tree more distinctly, now the chimney, and sometimes both equally well, according to which eye's image is victor in the conflict. One sees therefore, the spot on the pane, the tree and the chimney in the same direction. (Hering 1879, p. 38)

Hering used Figure 14.9 to illustrate this situation. Another way to illustrate the law of common

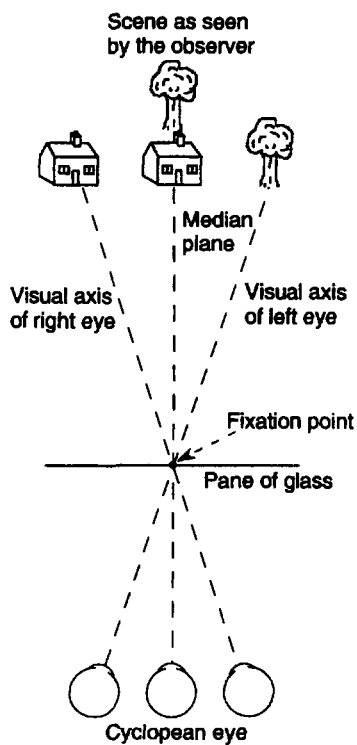


Figure 14.9. Hering's illustration of cyclopean direction.

While fixing a distant object (tree) with only the left eye open, a black spot on the pane of glass is aligned with the tree. When both eyes fixate the spot, a distant object (a house) in line with the spot for the right eye, and the object aligned with the left eye, appear superimposed.

binocular directions is to draw two lines on a card so that when the card is held in front of the eyes, the lines extend from the centre of each pupil to an apex, as in Figure 14.10. A thin vertical separator down the centre of the card ensures that each eye sees only its own line. If the two lines are visually distinct—for instance in different colours—and if fixation is maintained on the point where they intersect, the two lines appear as one line extending out from a point between the eyes. This display was first used by Alhazen in about 1040 AD to demonstrate binocular diplopia and the egocentre (see Section 1.2.2).

There is a problem when we judge the direction of an object with both eyes open, because the two eyes are not in the same place. To produce a unified sense of visual direction, the impressions derived from these two vantage points must be reconciled. The observations just described demonstrate that, at least for symmetrical convergence, we judge visual directions with reference to a point midway between the eyes. This common point of reference for the two eyes is the cyclopean eye, or egocentre. The directions of objects on any pair of corresponding visual lines are judged as though the objects are seen by the cyclopean eye, as shown in Figures 14.10 and 14.11.

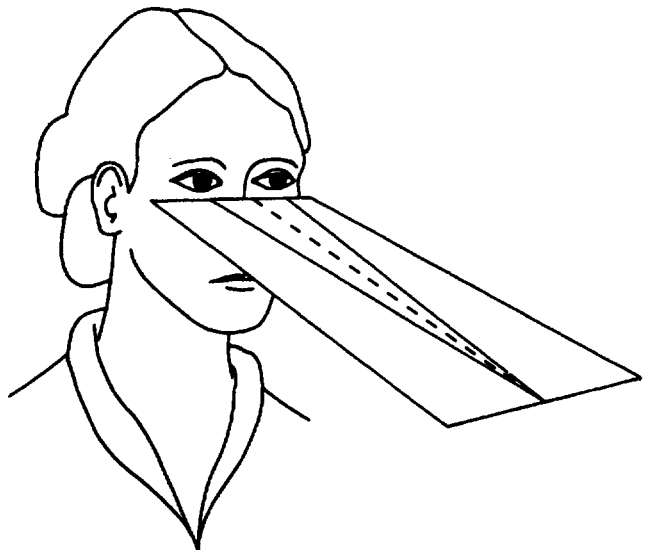


Figure 14.10. Illustration of the egocentre.

A simple way to demonstrate that visual directions are referred to an egocentre. Each line must point to the pupil of an eye, and fixation should be on the point where the lines meet. The two lines appear superimposed in the median plane of the head.

Church (1966) noticed that when 2-year-old children are asked to sight an object through a tube, they place the tube midway between the eyes. This was called the *cyclops effect*. Barbeito (1983) found that about one-third of a group of 3-year-olds behaved this way but only about one in ten of 4-year-olds. The cyclops effect has also been reported in young strabismic children and in children under 4 years of age, 2 years after they had one eye removed (Dengis et al. 1993a). Thus, young children behave as if they see out of the cyclopean eye and they must learn to bring a tube to one or the other eye to see through it. That is not to say that they consciously believe that their eyes are in the centre of the head.

A corollary of the law of common binocular directions is that two objects at different distances, which appear aligned when viewed with one eye, will not appear aligned when viewed with the other eye. This follows from the fact that two objects at different depths cannot fall simultaneously on corresponding visual lines in the two eyes. Corresponding visual lines intersect in only one point. This is demonstrated when one sights a distant object through a ring with one eye and then transfers the gaze to the other eye. When both eyes are open, there is conflicting information about the alignment of the ring and the object. In this situation there is a very large binocular disparity, and most people accept the information in one eye—their sighting eye—and ignore what they see with the other eye.

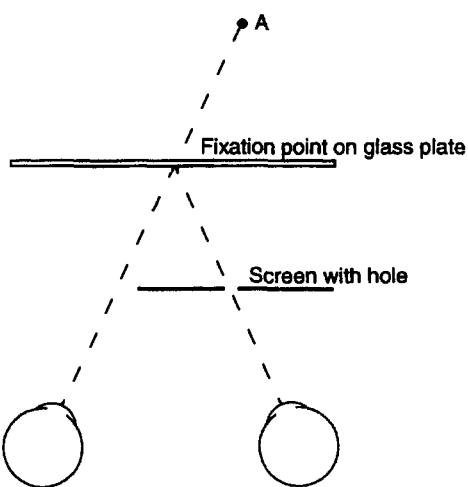


Figure 14.11. Illustrating Hering's law of visual direction. A card with a pinhole at its centre is held several centimetres in front of the right eye. A black dot on a pane of glass is fixated directly by the left eye and through the pinhole by the right eye. Object, A, on the visual axis of the left eye appears in the median plane behind the fixation point, even when the right eye is closed.

The sighting eye is therefore the eye one uses preferentially in making judgments about the alignment of objects well separated in depth.

A horizontal line extending away from the observer in the median plane of the head stimulates noncorresponding points in the two retinas, except where the line intersects the horopter. When the line is just below eye level it appears as a cross with its intersection point on the horopter. This cross is easily observed by taking a card with a line drawn on it and holding it horizontally just below eye level so that one end of the line touches the bridge of the nose. It is as if the space before one eye had rotated scissors-fashion about the fixation point over the space before the other eye, apparently transferring the objects on each visual axis to the median plane and, for each eye, objects in the objective median plane of the head to the visual axis of the opposite eye. This effect was also first described by Alhazen in the eleventh century.

With symmetrical convergence, all visible objects imaged on the foveas are judged to have the same headcentric direction, which lies approximately in the median plane of the head. This is true even when only one eye is open or when, because of an obstruction, the object can be seen by only one eye. This was demonstrated by Hering in the following manner. A card with a pin-hole at its centre is held several centimetres in front of the right eye. A black dot, F, on a pane of glass is fixated directly by the left eye and by the right eye through the pinhole, as illustrated in Figure 14.11. A small object, A, is

placed beyond the glass on the visual axis of the left eye. Although A is seen by only the left eye and is to the right of the median plane, it appears in the median plane behind the point F. If the right eye is closed, the impression remains the same. The apparent position of A changes only if the eyes change their positions.

Summary

Here are five laws or principles of visual direction:

1. The law of oculocentric direction states that objects on a given visual line appear to be aligned, or superimposed; that is, they appear to have the same oculocentric direction. A corollary of this law is that noncoincident retinal images give rise to a judgment of spatial separateness.

2. The law of headcentric direction states that, for a given position of the eye in the head, objects lying on the same visual line are judged to be in the same headcentric direction, which is unique to that visual line.

3. The law of common monocular directions states that all visual lines of an eye appear to point to the same visual egocentre.

4. The law of common binocular directions states that in binocular viewing, all visual lines of either eye appear to point to a common egocentre midway between the eyes.

5. The law of cyclopean projection states that points on a visual line appear to lie on the cyclopean line that intersects the visual line on the horopter. It follows from this law that objects on the visual axes of the two eyes when in symmetrical convergence are judged to be in the median plane of the head. In general, for asymmetrical stimuli and asymmetrical convergence, objects on any pair of corresponding visual lines are judged to be on a cyclopean line passing through the egocentre and the point in the horopter contained in both visual lines. It follows that an object seen and fixated by only one eye is judged to be in the direction of a line that intersects the egocentre and the point of binocular convergence. Complications due to phoria and strabismus are discussed in Section 14.5.6.

Ono (1979) described a similar set of principles. Although Hering is usually credited with first formulating principles of visual direction, an account of cyclopean projection was first provided by Alhazen in the eleventh century (see Section 1.2.2). Principles of cyclopean projection were also described by Wells in his book *Essay upon Single Vision with Two Eyes*, written in 1792, 87 years before Hering wrote his account (Ono 1981; Ono and Mapp 1994).

14.5.3 The visual direction of disparate images

The preceding analysis of visual direction accounts for how directional judgments are made about objects at different distances. The fact that the directions of objects at different distances along visual lines are judged in relation to a common egocentre means that the directions of all objects other than those in the horopter are misjudged (see Ono and Angus 1974). This seems intolerable from a behavioural point of view. However, one usually fixates an object to which one is attending, so the illusory directions of other objects are of little consequence.

We can think of the visual fields of the two eyes as uniting to form a single cyclopean field. The oculocentric directions of points within this cyclopean visual field are formed by the superimposition of the sets of corresponding lines from each retina. However, slightly disparate images also fused in the cyclopean field. One may then ask what determines the cyclopean direction of two fused but disparate images. The cyclopean oculocentric direction of a fused image could be that of the image from one or the other eye, or it could be the average of the oculocentric directions of the two monocular images, as originally proposed by Hering (1865). Ono et al. (1977) investigated this question by presenting subjects with the stereogram shown in Figure 14.12. When the eyes were converged so as to fuse the two outer circles, the fused image of the enclosed dots appeared centred in the fused image of the circle. This indicates that the cyclopean oculocentric direction of fused disparate images is the average of the oculocentric directions of the two monocular images. With large disparities, the experience of fusion gave way to an impression of two images in rivalry, with one dot being suppressed by the other. When this happened, the apparent direction of the dot was determined by whichever of the two disparate images was dominant at the time. When disparity between the monocular images was very large, the images neither fused nor rivalled, but appeared as two images. Sheedy and Fry (1979) also found that the cyclopean headcentric direction of fused disparate images is essentially an equally weighted compromise between the headcentric directions of the two monocular images. The perceived orientation of the fused image of stereograms consisting of gratings with a cyclodisparity is also the mean orientation of the disparate images (Kertesz 1980). Rose and Blake (1988) found that dichoptic vertical lines with a horizontal disparity of up to 1° appeared displaced toward each other. Thus, a tendency to average the oculocentric directions of dichoptic images is evident even in unfused images.

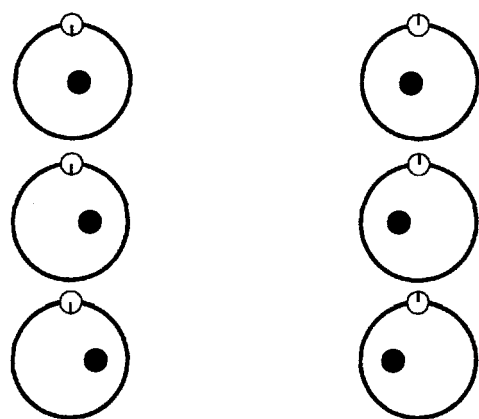


Figure 14.12. The visual direction of disparate images.

When the top two circles are fused, the black dots fuse into a single dot at the centre of the circle. The visual directions of the monocular images are averaged. When the second or third pair of circles is fused, the black dots do not fuse and their visual directions are not averaged. Nonius lines in the small circles indicate correct convergence. (Adapted from Ono et al. 1977.)

Erkelens and van de Grind (1994) have produced evidence that the rules governing the apparent visual direction of binocular and monocular images must be modified for monocular images within an occlusion zone bordering a vertical step of disparity.

14.5.4 Determining the position of the egocentre

Three procedures have been used to determine the location of the egocentre. In the method proposed by Howard and Templeton (1966), the subject fixates the near end of a rod lying in a horizontal plane at eye level and swings it within the horizontal plane until it appears to point directly at the self. This is repeated for different positions of the rod. The egocentre is defined as the intersection of the projections of the rod in its various positions. Mitson et al. (1976) modified this method by removing the distracting double images of the nonfixated parts of the rod. In this version, the rod is replaced by two stimuli at different distances from the subject. The subject switches on the near and far stimulus in alternation and moves the near stimulus until the imaginary axis joining the two stimuli is judged to be pointing directly at the self. The procedure is repeated for different directions, and the intersection of the projected axes is taken to be the egocentre.

In the method devised by Funaishi (1926) the subject fixates a point in the median plane at a distance of 2 metres and is shown other nonfixated targets in the same frontal plane. The subject aligns an unseen finger with each of the nonfixated targets, with the finger first in a frontal plane at one distance and then in a frontal plane at another distance.

The lines joining each pair of finger positions are extended back toward the subject, and their intersection defines the egocentre.

In the method devised by Roelofs (1959), the subject sights down a tube with one eye and indicates the place on the face where the tube appears to be aimed. This is repeated for different positions of the tube, and the egocentre is the intersection of the set of lines joining the front of the tube to each location on the face to which it appears to point. Barbeito and Ono (1979) tested the success of each method in predicting a subject's performance on other spatial tasks that depend on the location of the egocentre. These criterion tasks were judging the straight ahead, setting a point at one distance to be midway between two other points at another distance, and judging the extent of apparent movement of visual targets during accommodative vergence. Only the first method, involving the multiple alignment of targets with the egocentre, successfully predicted performance on these tasks. This is the only purely visual method, which may be why it relates best to other purely visual tasks. The Howard and Templeton method, as modified by Mitson et al., was also the most precise method, probably because it does not involve highly variable pointing responses.

14.5.5 The position of the egocentre

Consider two points, F and P , on the horizontal horopter, which we will assume conforms to the Vieth-Müller circle, as in Figure 2.11. The angle subtended by F and P at the nodal point of one eye is the same as the angle subtended by these points at the nodal point of the other eye—they have the same binocular subtense. This follows from the fact that a chord of a circle subtends equal angles at any point on the circumference of a circle. Furthermore, F and P subtend this same angle at the point between the eyes where the Vieth-Müller circle cuts the median plane. According to Hering's law of cyclopean projection, the direction of P with respect to F is judged as if both eyes were in the median plane of the head. If the cyclopean eye is on the Vieth-Müller circle, midway between the eyes, then the relative directions of any two points on the Vieth-Müller circle with respect to the egocentre is the same as their relative directions with respect to either eye. This provides a convenient theoretical definition of the egocentre. However, we will see in the following that the actual egocentre may lie further back in the head.

The headcentric azimuth direction of any point with respect to the egocentre is the dihedral angle between the median plane of the head and the

vertical plane containing the line joining the point to the egocentre. The headcentric elevation of any point with respect to the egocentre is the dihedral angle between the horizon plane and the line joining the point to the egocentre. If the egocentre is assumed to be the midpoint of the line joining the nodal points of the eyes, these two angles become the headcentric cyclopean azimuth and elevation, as defined in Section 2.3.2.

By the law of cyclopean projection, objects on corresponding visual lines appear on a line through the egocentre and the point where the two visual lines intersect. When the eyes are symmetrically converged and the objects lie on the two visual axes, all the objects appear to be in the median plane of the head. When the eyes are asymmetrically converged, the law applies only if the centre of rotation of each eye is at the same location as the nodal point. In fact, the nodal point is in front of the eye's centre of rotation, so the geometry of visual direction for asymmetrical convergence is more complex than indicated here.

If the eyes move into a tertiary position, the geometry of the headcentric directions of visual targets becomes even more complicated by the changed shape of the horopter with oblique gaze and by the fact that the eyes obey Listing's law (see Section 10.1.2). It also follows from the law of cyclopean projection that any object not on the horopter has two visual directions, one for each eye.

The fact that most people consistently use the same eye for sighting or aligning objects led Walls (1951) to suggest that the dominant eye is the egocentre. But most people judge directions as if both their eyes are located in the median plane of the head, no matter which eye they use in a sighting task (Ono and Barbeito 1982).

Barbeito and Simpson (1991) investigated this question quantitatively by asking subjects to point to a visual target seen by only one eye, for different angles of gaze of the other eye. The angle of gaze of the occluded eye was varied by having subjects fixate with both eyes on spots at different distances along the line of sight of the eye seeing the monocular target, as shown in Figure 14.13. The apparent direction of the monocular target closely coincided with that predicted from the principle that the visual direction of any point along the visual axis of one eye is specified by the line passing through the point of binocular convergence and the egocentre. The predicted locations are illustrated in Figure 14.13. For all subjects there was a linear relationship between changes in the angular position of the occluded eye and the apparent direction of the target seen by the other eye. However, for some subjects, the

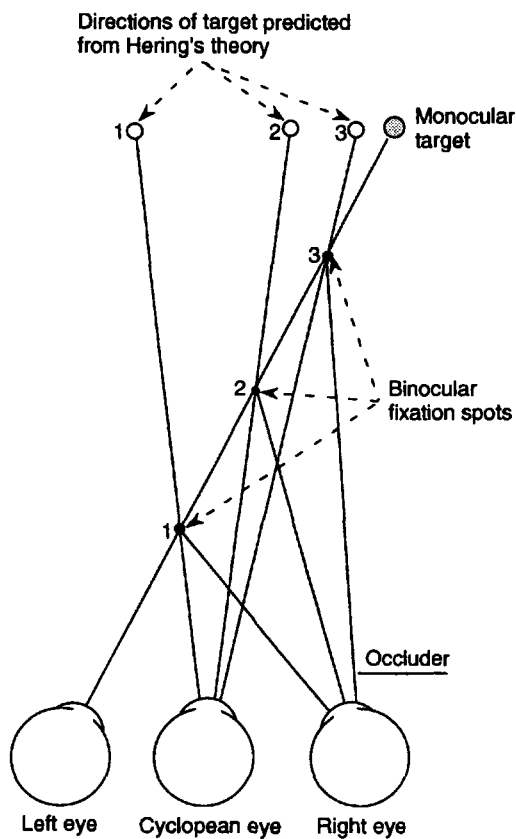


Figure 14.13. Testing Hering's laws of visual direction.
Subjects pointed to the monocular target, which was occluded to the right eye. The empty dots indicate the apparent position of the target for each of the three points of convergence, indicated by the black dots. (Adapted from Barbeito and Simpson 1991.)

slope of this function was not the same for both eyes. This could be because the egocentre was slightly off-centre for these subjects or because they gave more weight to one eye than the other, a tendency that may be related to eye dominance (Porac and Coren 1986).

We argued earlier that the egocentre can be defined as the point in the median plane of the head to which the relative visual directions of objects are projected unchanged. This definition places the egocentre just behind the corneal plane of the eyes. On the other hand, one might have predicted, on other theoretical grounds, that the egocentre is on the axis of rotation of the head. Directional judgments made in relation to such a centre would not be affected by rotations of the head on a vertical axis, as they would be if the egocentre were situated outside this axis.

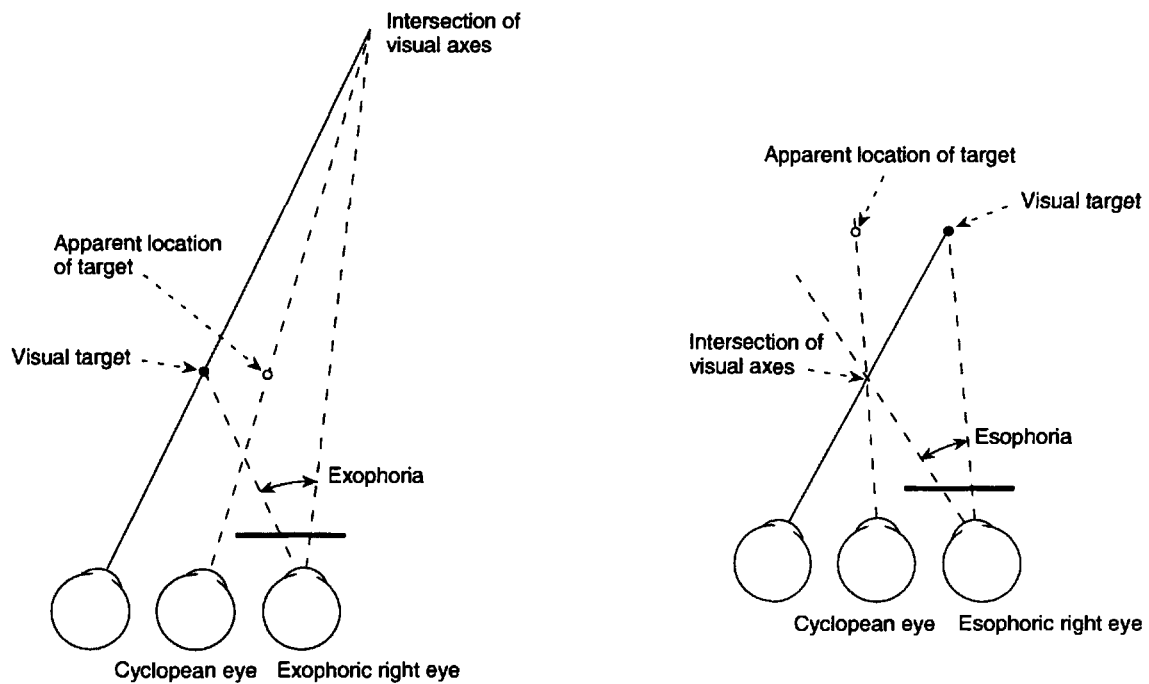
Funaishi (1927) and Roelofs (1959) reported that the egocentre lies on the centre of rotation of the head. On the other hand, Fry (1950) placed it several centimetres in front of the corneal plane. Barbeito

and Ono (1979) found that all methods of determining the position of the egocentre are critically dependent on accurate control of fixation. In the earlier methods, fixation was difficult to control, and this was probably why such divergent results were reported. Barbeito and Ono controlled fixation and found that, on average, the egocentre was very close to a point in the corneal plane midway between the eyes.

14.5.6 Effects of phoria and strabismus

The law of cyclopean projection states that objects on a corresponding pair of visual lines appear on a line through the egocentre and the point in the horopter contained in both visual lines. It is assumed that the eyes are correctly converged on a defined visual object. This situation is complicated by two conditions. One of these is phoria, which is a deviation of a closed eye inwards (esophoria) or outwards (exophoria) from the intended point of convergence. The other condition is a deviation of one or the other eye from the intended point of convergence when both eyes can see the same visual stimulus. This is a fixation disparity when the deviation is within Panum's fusional area and a tropia, or strabismus, when the deviation is larger.

Consider, first, the effects of phoria on egocentric localization. As long as convergence is maintained on a visual target, its direction is judged correctly, assuming that its distance is accurately judged. However, if one eye is esophoric, that eye will deviate inwards when it is occluded, and according to the law of cyclopean projection the perceived location of the target should shift away from the occluded eye (Figure 14.14a). For a person with an occluded exophoric eye, the perceived location of the target should shift toward the occluded eye through half the angle of changed convergence (Figure 14.14b). In both cases, the subject should experience an apparent movement of the target, in the direction of the phoria, as the phoric eye is occluded, and in the opposite direction as the phoric eye is uncovered. These predictions were confirmed by Ono et al. (1972), Ono and Gonda (1978), and Park and Shebilske (1991). Furthermore, when pointing to monocular visual targets, subjects made constant errors related to the direction of phoria, although they made some corrective adjustments when provided with visual feedback about their pointing errors (Ono and Weber 1981). These findings confirm that egocentric directions are judged in terms of pooled information about the positions of the two eyes and not merely the position of the dominant eye or the eye that happens to be seeing the target.



(a) An exophoric eye deviates outwards when occluded. The target appears displaced from the seeing eye, onto a line through the cyclopean eye and the intersection of the visual axes. (From Ono and Gonda 1978, *Perception*, 7, 75-83, Pion, London.)

(b) An esophoric eye deviates inwards when occluded. The target appears shifted toward the seeing eye, onto a line through the cyclopean eye and the intersection of the visual axes.

Figure 14.14. Visual direction and phoria.

A similar shift of a monocularly fixated object may be observed by a person with no phoria when the eyes change convergence while one eye is occluded. It has been reported that this shift does not occur if the fixated object is replaced by an afterimage, but the reason for this is not clear (Enright 1988).

A person with a constant strabismus of long standing learns to suppress the visual input from the deviating eye when both eyes are open. When only the deviating eye is open, that eye is able to fixate on an object and see it, although the covered normal eye will not be converged on the object being inspected. The question arises as to whether, under these circumstances, the direction of the object fixated by the strabismic eye is judged in terms of the position of that eye, the position of the covered normal eye, or their combined positions. Mann et al. (1979) showed that the second possibility is correct; constant strabismics learn to use the direction of their normal eye whether or not that eye is viewing the visual target. Alternating strabismics, on the other hand, judge the direction of a visual target in terms of whichever eye is open. These subjects learn to dissociate the two eyes in making directional judgments. People who have undergone surgery for correction of strabismus show shifts in pointing with the unseen hand to visual targets, although the

direction and magnitude of these shifts are not related in a simple way to the type of surgical correction (Steinbach et al. 1988). However, the location of the egocentre in strabismic children was found to be no different from that of children with normal vision. Furthermore, pre- and postsurgical measurements of the egocentre revealed that children showed no change in the egocentre after they underwent surgery for strabismus (Dengis et al. 1993b). Thus, the pointing errors manifest in strabismics must be due to a change in the registered position of the eye rather than to a shift of the egocentre. In children who had lost one eye at an early age, the visual egocentre was shifted toward the remaining eye. Normal children tested with only one eye open showed no such shift (Moidell et al. 1988).

14.6 UTROCLULAR DISCRIMINATION

Helmholtz (1909) asked whether one can tell which eye is stimulated by a monocular stimulus when there is no information, apart from the ocular site of the stimulus. Successful performance on this task is referred to as utrocular discrimination and the information on which it is based is called "eye-of-origin information" or "eye signature". Helmholtz did

not doubt that eye-of-origin information is available to the stereoscopic system since, if it were not, one would not be able to distinguish between depth based on crossed disparities and that based on uncrossed disparities. This information must also be available to the vergence system, since the eyes make appropriate vergence responses to crossed and uncrossed disparities, even in an open-loop situation (Howard 1970). The question is whether eye-of-origin information is available to consciousness when all extraneous cues are eliminated.

Helmholtz concluded that eye-of-origin information is not available to consciousness, but people have continued to investigate the question. It is not easy to design a test possessing no give-away cues. If the eyes differ in any way, a person will be able to distinguish between a stimulus presented to one eye and the same stimulus presented to the other eye. For instance, a person who is colour blind in one eye will make consistent judgments about which eye is stimulated by a coloured stimulus. If the person is confused about which eye is colour blind, all the answers may be wrong (invalid) even though discrimination is perfect (reliable). Even if all the answers are correct it does not mean that there is access to eye-of-origin information, but only that the person happens to know which eye is colour blind. A difference in contrast sensitivity between the two eyes can also serve as an extraneous cue to utrocular discrimination (Porac and Coren 1984; Steinbach et al. 1985).

Oculomotor cues and associated cues of binocular parallax may also serve as extraneous cues to utrocular discrimination. For instance, if the stimulus extends to the boundaries of the visual field, one may readily identify the stimulated eye by noting how far the stimulus extends to the left or to the right. Blinking an eye immediately reveals which eye is seeing. One group of investigators, including Pickersgill (1961), placed an occluder in front of one eye and asked subjects to report which eye saw a small flash of light. Some subjects performed at above chance level, but Templeton and Green (1968) pointed out that, for any subject with a phoria, the apparent direction of the stimulus would vary depending on which eye was occluded. A person using such a cue would be able to give consistent answers even if they were not the correct answers.

Smith (1945) overcame the problem of phoria by presenting an identical grid of lines to each eye. The subject fused the lines and reported which eye was stimulated by a flash presented on the fovea of one eye. Some subjects performed above chance level, which Smith explained in terms of differential eye-movement tendencies. However, Smith overlooked

the possibility that a subject with a fixation disparity (see Section 10.2.4) would see the flashed stimulus displaced with respect to the fused fixation target and could use this as an extraneous visual cue for utrocular discrimination. This interpretation is supported by the fact that performance fell to chance when the position of the test flash was varied. Performance also fell to chance when the experiment was repeated with fixation disparity controlled (Templeton and Green 1968; Ono and Barbeito 1985).

Blake and Cormack (1979a, 1979b) reasoned that, because stereoblind subjects have a preponderance of monocular cortical cells, they should have better utrocular discrimination than people with normal vision. Both eyes were exposed to the same homogeneously illuminated region on which a grating was superimposed in one eye. Subjects had to report which eye saw the grating. Subjects with normal vision performed well when the spatial frequency of the grating was low but performed at chance level when it was high. Stereoblind subjects performed well at all spatial frequencies. If valid, this test could be used to diagnose stereodeficiency. However, Barbeito et al. (1985) interpreted these results in a different way. They pointed out that many stereodeficient people are amblyopic in one eye and some have local scotomata. The appearance of the test grating would therefore vary according to whether it was presented to the good eye or the deficient eye and this could have served as an extraneous cue for utrocular discrimination. In Blake and Cormack's procedure, the addition of a grating to one eye involved a sudden change of luminance to that eye, and it may have been this rather than the grating that was detected. Barbeito et al. investigated this question by adding a condition in which the intensity of the illuminated patch in one eye was changed at the same time that a grating was added to the patch in the other eye. Subjects chose the eye in which the largest change in luminance occurred, rather than the eye to which the test grating was presented, even though they were asked to select the eye seeing the grating. The subjects reported a "feeling" in the eye receiving the change in luminance. Similar reports can be found in the older literature (Enoch et al. 1969). Martens et al. (1981) provided further evidence supporting the role of transient stimuli in utrocular discrimination.

Summary

It can be stated that eye-of-origin information is used by the stereoscopic system and by the vergence system. Attempts to show that people are aware of which eye is stimulated have been beset with many difficulties. There are several extraneous cues, such

as differences in sensitivity between the eyes and visual parallax due to oculomotor imbalance, that could allow people to make consistent judgments, even if those judgments are not necessarily correct. It seems that whatever genuine ability people have to

make accurate utrocular discriminations is based on the occurrence of a stimulus transient in one eye. It may turn out that this also provides a spurious cue in the form of reflex movements of the eye or pupil.

Development and pathology of binocular vision

15.1 Development of the visual system	603
15.1.1 Development of the eye	604
15.1.2 Development of the retina	605
15.1.3 Growth of the optic nerve and tract	606
15.1.4 Development of the LGN	608
15.1.5 Development of the visual cortex	609
15.1.6 Development of visual functions	615
15.2 Development of binocular vision	617
15.2.1 Behavioural procedures	617
15.2.2 VEPs and stereoscopic development	620
15.2.3 Development of vergence eye movements	620
15.2.4 Development of binocular correspondence	621
15.3 Stereoanomalies	622
15.4 Brain damage and stereopsis	624
15.5 Effects of dark rearing	625
15.6 Monocular deprivation	626
15.6.1 Subcortical effects of monocular deprivation	626
15.6.2 Cortical effects of monocular deprivation	627
15.6.3 Effects of binocular dissociation	630
15.7 Amblyopia	631
15.7.1 Symptoms and types of amblyopia	631
15.7.2 Development of amblyopia	633
15.7.3 Amblyopia and binocular vision	634
15.8 The critical period	635
15.8.1 The critical period in the cat	635
15.8.2 The critical period in the monkey	636
15.8.3 The critical period in humans	637
15.9 Binocularity in the stereoblind	637
15.9.1 Binocular summation in the stereoblind	637
15.9.2 Dichoptic masking in the stereoblind	638
15.9.3 Interocular figural effects in the stereoblind	639
15.10 Binocularity and proprioception	640
15.11 Albinism	642
15.11.1 Basic characteristics of albinism	642
15.11.2 Abnormal routing of the visual pathways	642
15.11.3 Congenital nystagmus	643

15.1 DEVELOPMENT OF THE VISUAL SYSTEM

The basic structures and mechanisms responsible for disparity-based stereoscopic vision begin to develop in the early embryo and become fully functional several months after birth. Initially development occurs through the action of genetically programmed processes that are independent of sensory stimulation. However, even before birth, spontaneous discharges in sensory nerves affect the formation of appropriate neural connections in the visual pathways. After birth, activity in sensory nerves arising

from the interaction of the developing organism with its environment determines the fine tuning of the visual system and the precise combination of pathways from the two eyes. Growth processes extending throughout childhood modify the stereoscopic mechanism. These growth processes involve: (1) changes in the size and shape of the eyes and their setting in the head, (2) modifications of accommodation and vergence, (3) changes in the size of the retina, (4) myelination of the visual pathways and visual cortex, and (5) changes in the distribution of dendrites and a reduction in the density of synaptic

contacts. The study of these various factors in the development of the visual system involves a variety of anatomical, physiological, clinical, and behavioural procedures.

Hebb (1949) proposed that synaptic contacts strengthen when the activity in pre- and postsynaptic cells is correlated, and weaken when activity in the two cells is uncorrelated. Synapses behaving in this way are **Hebbian synapses** (see Section 3.3.2). When activity in two presynaptic cells converging on a single cell is synchronous, it is more highly correlated with that in the postsynaptic cell than when it is asynchronous. This is because the postsynaptic membrane summates potentials from converging synchronous inputs more effectively than from asynchronous inputs. The outcome is that correlated activity in two or more afferent pathways increases the transmission efficiency of that pathway. When converging inputs are persistently uncorrelated, the synaptic strength of the one more highly correlated with the postsynaptic potential eventually increases at the expense of the synaptic strength of the other. We will see that Hebbian synapses play an important part in the fine tuning of synaptic connections in the developing visual system, even in the prenatal period.

The development of the visual system has been reviewed in a book edited by Simons (1993).

15.1.1 Development of the eye

The diameter of the adult eyeball is about 45 per cent larger than that of the newborn infant and its volume three times larger. The eye grows proportionately less than the body as a whole, which increases in volume about 20-fold. As the eye grows, the corneal surface increases about 50 per cent while the area of the retina approximately doubles from 590 mm² to 1250 mm² (Scammon and Wilmer 1950). The axial length of the human eye increases from about 15.5 mm at birth to its adult value of 24.5 mm, which is reached at about the age of 13 years, with about half the increase occurring in the first 2 years (Larson 1971). This means that the infant eye requires about 85 dioptres of refraction to focus an image compared with about 60 dioptres required by the adult eye (Lotmar 1976). Another consequence of the small size of an infant's eye is that 1° of visual angle corresponds to between 0.18 and 0.2 mm on the retina, compared with 0.29 mm on the adult retina (Hamer and Schneck 1984). Thus, for a given distal stimulus, the area of the retinal image in the infant eye is about half that in the adult eye.

As the eye grows, the curvature of the cornea changes to keep the image in proper focus. These

changes seem to be under visual feedback control. There is evidence that the axial length of the eyes of young cats and chickens increases to compensate for an experimentally induced refractive error (Wallman and Adams 1987; Schaeffel et al. 1988). This process is called **emmetropization**. (See Young and Leary 1991 for a review of this topic). When the eyelids of a young monkey are sutured so that only diffuse light can enter the pupil, or when the cornea is made semi-opaque, the eye develops an increased axial length and a consequent myopia (Wiesel and Raviola 1979). Of eight monkeys reared with a 9-dioptre contact lens on one eye, one showed no effect, one developed 3 dioptres of axial myopia, and five developed axial hyperopia of up to 3.5 dioptres in that eye. After the lens was removed, both types of refractive error diminished (Smith et al. 1994). This suggests that primates have a visually controlled emmetropization mechanism that can compensate for refractive errors of up to 3.5 dioptres. The visual control process is not understood but there is some evidence that the loss of contrast in the image over long periods increases the axial length of the eye (Bartmann and Schaeffel 1994).

The development of accommodation in infants has been studied by measuring the refractive state of the eye with a retinoscope, with the ciliary muscles paralyzed by a cycloplegic drug (see Section 10.3). Several investigators have reported that the human infant is about 2 dioptres hypermetropic relative to the average adult. Retinoscopy in young infants is unreliable, however, so the reported hypermetropia may be an artifact (Banks 1980).

The second way to study the development of accommodation is to measure the accommodative state of the eye as a large pattern is moved to different distances. The infrared optometer is the most precise method for measuring changes in accommodation (see Section 10.3) but cannot be used in infants because the subject must maintain fixation. With infants, refraction is measured with dynamic retinoscopy, which gives the sign of the refractive error but takes time to operate; or by photorefraction, which gives an accurate measure of the instantaneous magnitude of the refractive state of both eyes (Howland and Howland 1974). It is important to keep the size of the retinal image of the display constant to ensure that any lack of accommodation is not due to the stimulus falling below the resolution threshold. Infants at 1 month of age begin to show signs of changing accommodation and by 2 months they show a range of accommodation similar to that of the adult (Braddick et al. 1979; Banks 1980).

The eyes of children up to about the age of 4 years tend to be astigmatic, with a vertical axis of

astigmatism. Ophthalmologists call this an "against the rule" astigmatism. If children above that age, or adults, have astigmatism it tends to be along a horizontal axis—a "with the rule astigmatism" (Dobson et al. 1984; Gwiazda et al. 1984; Howland and Sayles 1984).

The depth of field of an eye is the range of distances within which an object is in focus for a given state of accommodation. Depth of field is inversely proportional to pupil diameter. Since the pupils of infants under 2 months of age are, on average, between 1 and 2 mm smaller than those of adults, depth of field is greater in the infant than in the adult (see Boothe et al. 1985). Thus, image quality is less affected by misaccommodation in the infant eye than in the adult eye. In any case, image quality is not as important for the infant retina because its ability to resolve high spatial-frequencies is poor. Accommodative convergence is present in 2-month-old infants; younger infants have not been tested (Aslin and Jackson 1979).

The distance between the eyes of the newborn infant is only about two-thirds that in the adult. Other things being equal, the minimum discriminable binocular disparity is directly proportional to interocular separation (see Section 5.3.1), so this factor alone accounts for a 50 per cent improvement of stereoacuity with age. Also, as the child grows, there must be a gradual recalibration of the system that maps disparity onto the perception of relative depth.

15.1.2 Development of the retina

The retina develops from an outgrowth of the forebrain, known as the optic vesicle. After making contact with the overlying ectoderm, the vesicle invaginates to form the optic cup. The lining of the optic cup forms the retina and the overlying ectoderm forms the lens and cornea. The precursors of retinal cells develop from the inner layer of the optic cup. Ganglion cells differentiate first, followed by cones, horizontal cells, bipolar cells, and lastly rods. In all cases, cells develop first in the central retina. By about the thirtieth embryonic day in the cat, the axons of ganglion cells begin to grow into the optic stalk and segregate into distinct bundles, or fascicles, separated by glial cells (Shatz and Sretavan 1986; Okada et al. 1994).

The development of the human retina has been recorded from 13 weeks of gestation to adulthood. The mosaic of foveal cones is identifiable at 13 weeks of gestation by the presence of a region containing only cones with a density of about 14,000 per mm^2 (Hendrickson and Yuodelis 1984; Hendrickson and Drucker 1992; Diaz-Araya and Provis 1992). By 24

weeks of gestation the foveal cones have a density of approximately 38,000 per mm^2 , compared with an adult value of over 100,000 per mm^2 . Cone density is inversely related to cell-soma diameter. The increase in cone density seems to be due to migration of cells toward the fovea from a circumferential region of undifferentiated cells rather than cell division within the central region (Diaz-Araya and Provis 1992).

One week after birth the human peripheral retina resembles that of the adult but the macular region covering about 5° of the central retina is very immature. There is a foveal depression, but all cell layers extend across it rather than being parted as in the adult retina. The principal mechanism for formation of the foveal depression seems to be migration of ganglion-cell bodies in the inner retinal layers away from the centre (Kirby and Steineke 1992). At 26 weeks of gestation the inner segments of rods and cones are rudimentary and there are no outer segments until 36 weeks of gestation. The cones in the foveal region of the one-week-old infant have inner and outer segments, but they are only about one sixteenth the length of adult segments. In the neonate peripheral retina, the inner and outer segments of rods and cones are 30 to 50 percent of adult length. The outer segments of cones continue to elongate for up to 5 years. Foveal cones become narrower with age, from 5 to 7.5 microns wide at birth to 1.8 to 2.2 microns in the adult (Yuodelis and Hendrickson 1986). This decrease in diameter means that a foveal cone subtends between 1.5 and 2.2 arcmin at the nodal point in the neonate eye and about 0.5 arcmin in the adult eye. The larger receptor aperture in the infant eye severely reduces the effective contrast of images of high spatial-frequency stimuli (Banks 1988). The retina of an 11-month-old infant is similar to that of the adult in both the periphery and the fovea (Abramov et al. 1982).

The retina of the monkey shows a similar development, but the fovea is more advanced at birth than in the human (Samorajski et al. 1965; Hendrickson and Kupfer 1976). The size of the visual field is smaller in human infants under 8 weeks of age than in the adult but to what extent this is due to optical factors rather than maturation of the retina is not known (Schwartz et al. 1987).

The adult human retina has between 4 and 6 million cones, with a peak density at the fovea that is highly variable from person to person (100,000 to 320,000 cones/ mm^2). The range of grating acuity predicted from these cone densities is 47 to 86 c/deg. Thus, on average, the retinal mosaic is well suited to deal with the highest spatial frequency (60 c/deg) transmitted by the optics of the eye (Campbell and Gubisch 1966). Cone density falls steeply with

increasing eccentricity, being ten times lower 4° away from the fovea than at the fovea. The human retina has 100 million or more rods and a central rod-free area about 1.25° in diameter. The two eyes have similar numbers of cones and rods and similar photoreceptor topography (Curcio et al. 1990).

The embryonic development of the eye is reviewed in Mann (1964) and in Lam and Shatz (1991). Robinson (1991) has reviewed the development of the retina, and the evolution of the visual system has been reviewed in Cronly-Dillon and Gregory (1991).

15.1.3 Growth of the optic nerve and tract

Axonal growth

The axons of ganglion cells grow out from the eye to the chiasma and then to the LGN and other subcortical centres. Secondary axons grow from the LGN along the optic radiations to layer 4 of the visual cortex. Substances required for growth are transported in intracellular vesicles along cytoskeletal fibres to the tip of a growing axon (Martenson et al. 1993). The tip of the axon forms a **growth cone** from which filopodia containing contractile actin fibres extend. The filopodia sense out the surroundings and determine the direction in which the axon grows.

Three main agents guide, accelerate, or retard the growth of axons. The first is the physical properties of the environment of the growing axon. Cartilage and other tissue form physical barriers, and extracellular spaces in the embryonic neural tissue form channels through which neurones migrate.

The second agent guiding axonal growth is molecules of glycoprotein, such as laminin, tenascin, and N-cadherin, secreted by astrocytes (a type of glial cell) in the epithelium surrounding growing axons. These molecules attach to the neural epithelium or organize into a fibrous complex known as the **extracellular matrix** (Sanes 1989). The extracellular matrix is substantially reduced after growth is complete. Glycoproteins attract growth cones and help axons adhere to the substrate. They probably also generate signals within the growing neurone, which alter gene expression of proteins involved in morphogenesis. Antibodies of these glycoproteins inhibit axonal growth (Cohen et al. 1986). Glycoproteins may also have enzymatic or proteolytic properties enabling them to modify the extracellular medium through which the growth cone develops (Pittman 1985). Some glycoproteins act as chemical repellents and create exclusion zones from which axons are deflected (Pini 1993). The filopodia of a growth cone observed under the microscope *in vitro* collapse completely when chemical repellents are applied (Fawcett 1993). Some types of glycoproteins

act specifically on different types of neurones by virtue of proteins on the surface of the growth cone, known as integrins, which act as specific receptor molecules (Reichardt 1992). The specific receptors convey signals to the contractile actin fibres of the growth cone and thereby control the rate and direction of growth of the axon. As an axon grows from one cellular environment into another, the type of glycoprotein to which it responds changes (see Dodd and Jessell 1988). Also, the type of glycoprotein most active in a given location may change over time (Cohen et al. 1986). Thus, growth cones encounter a complex spatiotemporal pattern of chemical influences as they migrate through the extracellular matrix (see Letourneau et al. 1994).

The third agent guiding axonal growth is the attraction of the axon by growth factors secreted by the target cell. As the axon approaches within about 300 µm of its target cell the action of glycoproteins is switched off and the growth cone comes under the control of **neurotrophins** secreted by the target cell (see Korschning 1993). These are a family of proteins which includes the **neurotrophic growth factor** (NGF). There is some evidence that neurotransmitters secreted by target cells also attract growth cones (Zheng et al. 1994). In addition to their role in attracting growth cones, neurotrophins may affect cell differentiation and synaptogenesis (see Allendoerfer et al. 1994). They also determine which neurones survive, as we will now see.

Competitive survival of ganglion cells

Ganglion-cell axons grow toward their target areas in subcortical nuclei such as the superior colliculus and lateral geniculate nucleus. The destination of a given axon seems to be determined by the retinal region from which it originates, since ganglion cells from a transplanted area of the protoretina in the toad still grow toward the destination appropriate to the original site (Fraser 1991). We will see later that other factors determine the precise way in which ganglion cells synapse with target cells in the LGN.

The number of axons in the optic nerve and tract increases up to the time of birth. In the rat and cat, about 60 per cent of these axons are lost during the first one or two postnatal weeks (Lam et al. 1982; Ng and Stone 1982). By the 95th embryonic day the optic nerve of the monkey contains about 2.85 million axons compared with 1.6 million in the adult. Axons are lost most rapidly between the 95th and 120th embryonic day, which is just when retinal terminals segregate into distinct layers in the LGN (Rakic and Riley 1983). The surplus of optic nerve axons could be due to axonal branching or to overproduction of ganglion cells. Recent evidence suggests that

ganglion cells are overproduced (Perry et al. 1983; Sefton 1986). In both normal cats and cats with one eye removed there is close agreement between the number of ganglion cells and the number of optic nerve fibres at each stage of development (Chalupa et al. 1984). A similar loss of motor axons innervating muscles has been noted during early development (Cowan 1973).

Competition for the neurotrophic growth factor secreted by target cells with which ganglion cells make synaptic contacts determines which optic-nerve axons survive and which die. The growth factor binds to receptor molecules on the surface of the growing axon (see Allendoerfer et al. 1994). It is then transported rapidly down the axon to the cell soma, where it regulates the expression of genes that control the production of proteins required for cell growth and survival (Spencer and Willard 1992). In the absence of the growth factor the neurone dies. Death of ganglion cells in tissue culture is prevented when the culture contains target cells or a growth factor derived from target cells, and death is promoted by blockage of synaptic activity (see Bray et al. 1992) or when the growth factor is removed in the growing visual system (see Raff et al. 1993). Some growth factors are highly specific, and thus ensure that only appropriate synaptic contacts survive (Korschning 1993).

Removal of one eye reduces the number of cells competing for central connections. Thus, when hamsters and rats had one eye removed *in utero*, the optic nerve from the remaining eye had about 20 per cent more axons than that of an eye of a normal animal (Jeffery and Perry 1982; Sengelaub and Finlay 1981). In cats with one eye removed prenatally, the remaining eye had about 180,000 ganglion cells compared with 150,000 in an eye of a normal cat, and the receptive fields of cortical cells were smaller in monocularly enucleated cats than in normal cats (Chalupa et al. 1984; Stone and Rapaport 1986).

In the developed retina of the monkey, the density of ganglion cells has been reported to be 300 times higher in the foveal region than in the far periphery (Perry and Cowey 1985) but more recently the density of ganglion cells has been estimated to be 1,000 higher in the fovea (Wässle et al. 1990). The processes responsible for the development of this differential density are not fully known. The loss of ganglion cells and their segregation into areas of different density is accompanied by differential growth of the retinal surface.

Myelin is a fatty substance secreted as an insulating sheath around each axon by cells formed from a type of glial cell, known as oligodendrocytes. Ganglion-cell axons begin to myelinate after the

period of axonal loss and the process mostly occurs postnatally (Garey 1984). Axon diameter and conduction velocity are correlated with the thickness of the myelin sheath. When myelination is prevented by x-ray irradiation, the axons do not increase in diameter, showing that growth of axon diameter depends on some factor derived from the myelin sheath (Colello et al. 1994). In humans, axons from the fovea myelinate before those from the peripheral retina, and myelination of subcortical visual pathways is complete by the third postnatal month (Yakovlev and Lecours 1967) and of the geniculocortical pathways by the sixth month (Magoon and Robb 1981). The myelination of the central nervous system is not complete until early adulthood.

Segregation of axons at the chiasma

When ganglion-cell axons reach the chiasma, they segregate into those that remain on the same side and those that decussate to the contralateral side. Axons from the nasal hemiretina decussate while those from the temporal hemiretina remain on the ipsilateral side. Two mechanisms have been proposed to account for this segregation. In the first, growing axons respond to structural or chemical signals as they approach the chiasma. In the second, axons from the temporal retina grow at random to one side or the other, and those taking the wrong route are subsequently eliminated.

Sretavan (1990) injected a fluorescent dye into the optic tract (postchiasma) of embryonic mice, which retrogradely labelled the axons in the optic nerve (prechiasma) according to whether they were destined to cross over in the chiasma or remain on the same side. This procedure revealed that ganglion-cell axons have an initial retinotopic order as they leave the retina, although axons from different classes of ganglion cell intermingle. When the axons reach the chiasma they lose their retinotopic order so that axons from the nasal retina, destined to remain undecussated, are intermingled with those from the temporal hemiretina destined to decussate. Thus, the partition mechanism that decides whether a given axon decussates or not has nothing to do with the position of the two types of fibres in the optic nerve. During development, the two types of axons arrive at the chiasma at the same time, so the partition mechanism has nothing to do with the relative time of arrival of fibres at the chiasma. Also during development, axons from the temporal retina at first follow the same route as those from the nasal retina as they approach the midline of the chiasma, but at this point the temporal fibres develop complex and ramified growth cones, which seem to sense out their environment. The temporal fibres

then bend sharply toward the ipsilateral side. It looks as though they are deflected from a tendency to decussate by a chemical or structural signal in the chiasma, which forbids them from crossing the chiasma midline and directs them into an ipsilateral route (Godement et al. 1990). Sretavan claimed that in mice very few axons follow the wrong route.

In ferrets, it has been reported that many axons from the temporal retina take the wrong route at the chiasma and are subsequently eliminated (Jeffery 1990). This provides a second mechanism whereby growing ganglion cells are prohibited from entering the inappropriate channel. In cats, ganglion-cell axons from the temporal retina that reach the chiasma at a later stage of development decussate and remain decussated. This could be because the chemical signal fades or because late-arriving axons are insensitive to that signal (see Reese and Baker 1992). The decussated axons are of a specific type, but their function remains obscure. In primates, all decussating axons from the temporal retina are eliminated. In mammals, all axons from the nasal retinas decussate, leaving none on the ipsilateral side.

After the chiasma, axons enter the optic tracts where they segregate according to the type of ganglion cell (parvocellular, magnocellular, W-cells) from which they originate. Axons of each type acquire a retinotopic order by a mechanism that is not understood. Thus, three transformations of axons occur in the chiasma: they form into crossed and uncrossed pairs, they become segregated according to cell type, and they re-establish a retinotopic order within each cell type. They then enter the lateral geniculate nuclei where they become segregated into distinct laminae, as we will now see.

Williams et al. (1991, 1994) have identified a recessive mutation in sheepdogs that causes all retinal axons to project to the ipsilateral LGN. The optic chiasm is thus eliminated—the animals are achiasmatic and manifest spontaneous nystagmus. The nasal retinal fibres terminate in ipsilateral layer A with the same topographic arrangement as that in the contralateral LGN in the normal dog. The temporal fibres project normally to the superimposed ipsilateral layer A1. Since the nasal fibres have not crossed the midline the nasal projection is mirror-image reversed with respect to the temporal projection and the two maps are congruent only along the vertical midline. Williams et al. argued that this reversed mapping can be explained if it is assumed that there is a fixed position-dependent chemoaffinity between retinal axons and LGN cells and layers. Thus, the selection of target cells in the LGN is controlled by the retinal position from which the axons originate rather than by their eye of origin.

Apkarian et al. (1994) described two achiasmatic children. Each optic nerve projected fully to the ipsilateral visual cortex as revealed by the absence of a VEP from the contralateral cortex in response to visual stimulation. The VEP results were confirmed by magnetic resonance imaging (MRI). The children, like the achiasmatic dogs, exhibited congenital nystagmus. A similar case in a 35-year old man has been reported by McCarty et al. (1992). Albinism, involves the opposite type of defect in which temporal retinal axons decussate instead of projecting to the ipsilateral cortex (see Section 15.11.2).

15.1.4 Development of the LGN

The structure of the lateral geniculate nucleus (LGN) was described in Section 4.1.3. In the cat, retinal afferents from the contralateral eye invade the LGN by the 32nd day of gestation, which is about 10 days after the first ganglion cells develop and about 5 weeks before birth. Afferents from the ipsilateral eye invade the LGN about 3 days later than those from the contralateral eye (Shatz 1983). This may be a consequence of the recent evolution of the non-decussating pathway. The visual consequences of this asymmetrical development are discussed in Sections 15.1.6. and 15.7.3. Inputs from the two eyes are at first intermingled and, in the cat, become almost fully segregated into distinct layers by about the 54th day of the 64-day gestation period. Dendrites in the LGN of the neonate cat bear large numbers of spines and growth cones. After about 4 months postnatally, the number of spines decreases and the growth cones disappear as the dendritic fields acquire their adult form (De Courten and Garey 1982).

Injection of radioactive tracers into the eyes of monkey foetuses has revealed that all LGN cells are formed by the 64th day of gestation and their segregation into six laminae takes place between the 64th and 110th day (Rakic 1976). The LGN of the neonate monkey has the same general morphology and laminar structure as that of the adult. Magnocellular and parvocellular neurones are clearly distinguishable on the basis of their responses to visual stimulation, although they have a low spontaneous rate of firing and long latencies compared with adult cells. In a study of 53 human brains, geniculate cells were found to increase rapidly in size during the first 6 to 12 months of postnatal life and then more slowly before reaching their full size at the age of 2 years. Cells in parvocellular layers develop faster than those in magnocellular layers (Hickey 1977).

The prenatal process of segregating visual inputs into eye-specific layers in the LGN seems to involve elimination of axonal side branches rather than a

loss of cells. In each layer, inputs from one eye competitively eliminate all inappropriate synaptic contacts from the other eye (Shatz 1990). There is a growing body of evidence that this process depends on bursts of synchronized nerve impulses arising in the prenatal retina (Meister et al. 1991). By the operation of Hebbian synapses, a majority of synapses firing in synchrony in a given region reinforce each other and suppress a minority of synapses which fire out of phase with the dominant input. It is unclear how this competitive process propagates to form well-defined layers. Some of the evidence for the dependence of cell segregation on bursts of synchronized impulses will now be reviewed.

When sodium-mediated action potentials in ganglion cells of the cat were unilaterally blocked by infusion of tetrodotoxin between embryonic day 45 and birth, the development of eye-specific layers in the LGN was severely disrupted by the proliferation of inappropriate dendritic growth (Shatz and Stryker 1988). Bilateral blockage of action potentials had less effect on dendritic morphology in the LGN than monocular blockage (Dalva et al. 1994). Ganglion cells in the cat retina become capable of generating action potentials by embryonic day 30 and the subsequent increase in sodium-mediated action potentials coincides with the period of innervation of the LGN by ganglion cell axons (Skaliora et al. 1993). Ganglion-cell action potentials are also required for the postnatal maturation of LGN synapses but, at that stage, inputs arising from visual experience are more effective than electrically evoked potentials in nonseeing kittens (Kalil 1990).

In the ferret, an animal with well-developed stereoscopic vision, the projections to the LGN are mapped retinotopically at birth but their segregation into distinct laminae is not complete until a week or two after birth (Jeffery 1989). In the neonate ferret the ipsilateral projection to the LGN arises only from the temporal hemiretina, as in the adult animal, but the contralateral projection arises from the whole retina and only later becomes confined to the nasal hemiretina (Jeffery 1990). The same developmental sequence is also evident in the cat and is disturbed when one optic tract is sectioned (Leventhal et al. 1988). The nerve fibres carrying the projections from the temporal retina to the contralateral LGN die off when they fail to find matching inputs from the other eye. In primates, this developmental process seems not to depend on visual experience since monkeys deprived of vision in one eye from birth to 27 weeks develop a substantially normal LGN, even though this type of deprivation leads to a reduction in the number of binocular cells in the visual cortex (Blakemore and Vital-Durand 1986a).

Competitive synaptic interactions generated by spontaneous neural discharges are probably also responsible for the fact that ganglion cells with on-centre and off-centre receptive fields segregate in the LGN and establish distinct connections with relay cells (Hahm et al. 1991). Early monocular deprivation permanently reduces the efficiency of synaptic transfer in the LGN (see Section 15.6.1).

Within the first 24 days after birth, cells in the LGN of kittens showed low rates of maintained discharge to general illumination, weak and long-latency responses to flashed stimuli, and absence of surround inhibition. Cells of the X-type showed mature response properties before Y-type cells (Daniels et al. 1978). The spatial resolution of a cell in the LGN is indicated by the highest spatial frequency of a drifting high-contrast grating that evokes a response in the cell. The spatial resolution of LGN cells with receptive fields at an eccentricity of more than 10° is much the same in the neonate monkey as in the adult. However, for the foveal region, LGN cells in the neonate monkey could resolve only up to about 5 c/deg compared with 35 c/deg in the adult (Blakemore and Vital-Durand 1986b).

The development of the LGN has been reviewed by Casagrade and Brusco-Bechtold (1988). The evolution of the mammalian visual pathways has been reviewed by Henry and Vidyasagar (1991).

15.1.5 Development of the visual cortex

General development of the visual cortex

The visual cortex, which was described in Section 4.2, is part of the convoluted surface of the mammalian forebrain, or neocortex. The neocortex contains areas for each sensory modality as well as motor areas and areas associated with a variety of cognitive and emotive functions. All areas have a sixlayered structure in which neurones in layer 6 project to the thalamus, those in layer 5 project to subcortical nuclei other than the thalamus, and those in layers 2 and 3 project to other cortical areas. All areas have the same basic cellular constituents and show evidence of a radial columnar organization.

In the first half of the gestation period the human cerebral cortex has very few gyri (convolutions) or sulci (grooves). Among the first sulci to appear are the parieto-occipital and calcarine sulci (Polyak 1957). As the cerebral cortex grows, the cerebral convolutions become increasingly complex. Before birth, the visual cortex grows more rapidly than other parts of the brain. At birth the human visual cortex is about half its mature volume, which it reaches about 4 months after birth. The brain as a whole at birth is only one-quarter of its mature volume,

which is not reached until the age of about 2 years (Sauer et al. 1983). The adult visual cortex occupies about one-thirtieth of the cortical surface. The visual cortex of the human neonate is between 1.4 and 1.7 mm thick, compared with a value of between 2.1 and 2.5 mm in the adult (Wong-Riley et al. 1993).

Cell density in the human visual cortex is over 1 million per mm³ at 2 weeks of gestation. It decreases to about 90,000 per mm³ at birth and then to about 40,000 per mm³ at 4 months postnatally, after which it remains stable (Leuba and Garey 1987). This is due to overall growth, since there seems to be no loss of neurones in the visual cortex with aging.

Formation of cortical layers

In humans, the first cortical neurones develop at about 40 days after conception and neurogenesis is complete by about the 125th day, that is, about halfway through gestation (Rakic 1988). Neurones destined for the cerebral cortex arise by mitosis in a neuroepithelium, known as the **ventricular zone**, which lines the lateral ventricles. The first generation of cells originating in the ventricular zone form the preplate. The preplate develops into the cortical plate, the cortical subplate, and the intermediate zone. After this, about 80 per cent of newly generated neurones from the ventricular zone migrate radially along fibres of glial cells through the **intermediate zone** and **cortical subplate** until they reach the **cortical plate** just below the enclosing pial membrane of the brain, next to the skull. The other cells migrate laterally or at an oblique angle, sometimes changing their direction of movement (O'Rourke et al. 1992). The cortical plate forms the six layers of the mature cortex. The other zones and plates disappear after neurogenesis is complete. Cortical zones of the 17-week human foetus are shown in Figure 15.1a.

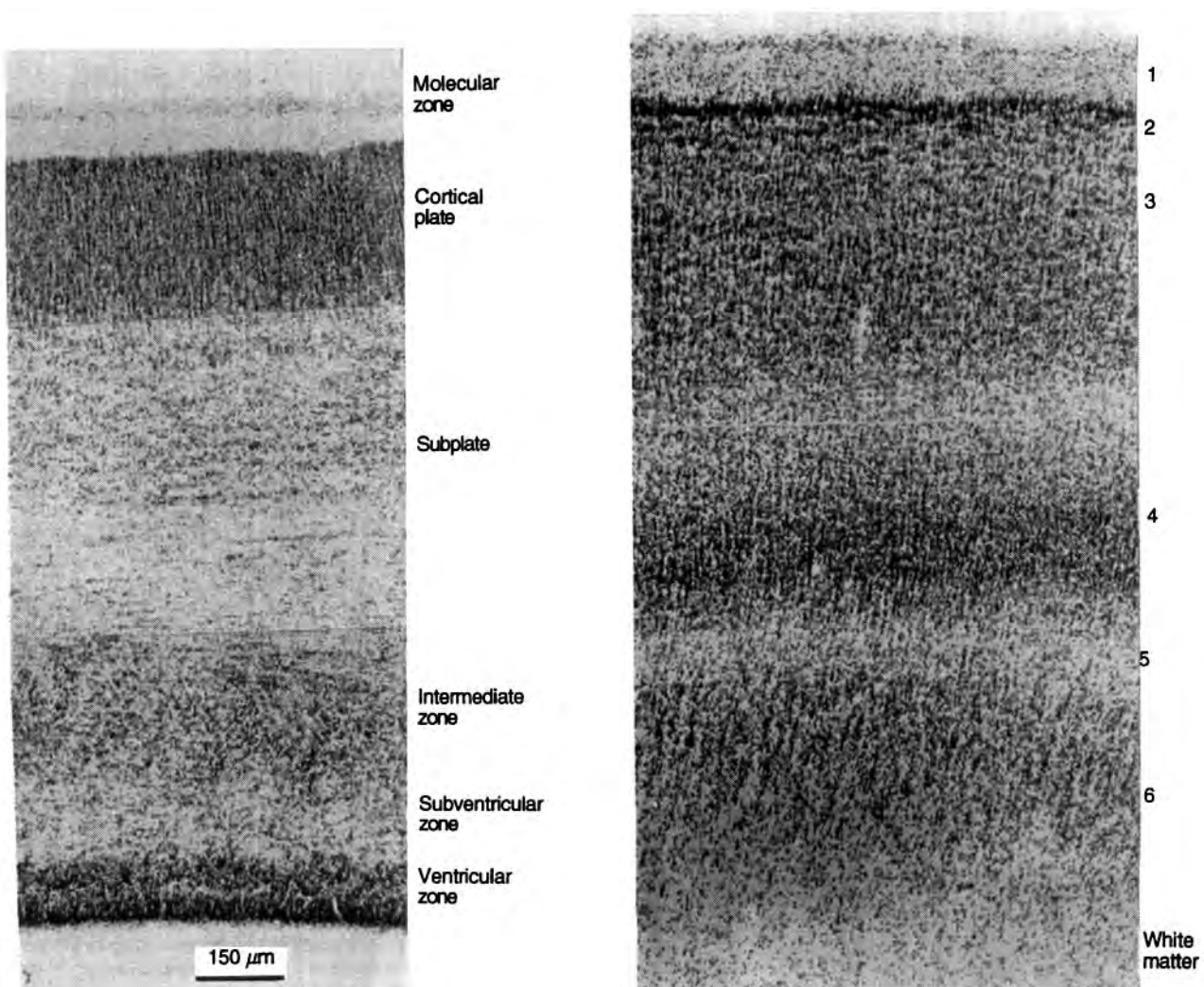
Signs of lamination begin to show in the cortical plate in V1 at about 140 days after conception and in V2 at about 160 days. In all mammalian species, the deepest layer, layer 6, develops first and the other layers develop from cells that migrate from the subplate toward the outer surface of the brain through layer 6 in successive waves (Rakic 1974; Luskin and Shatz 1985). The stripe of Gennari in layer 4B of V1 and the six layers of V1 and V2 are evident at about 185 days. In the human this inside-out development of V1 takes about 45 days. When cells first reach the cortical plate they have a simple structure. By the 30th week of gestation most cortical neurones have complex dendritic fields (Yan et al. 1992). A section of the visual cortex at birth is shown in Figure 15.1b. When the lamination of the visual cortex is complete, the intermediate zone and subplate form the virtually neurone-free white matter.

The layer into which a given neurone migrates from the subplate is predetermined, presumably by regulatory genes (homeobox genes). The fate of particular cells is followed by labelling them with tritiated thymidine. Cells developing first go to layer 6, and those developing later go to successively more superficial layers. A progenitor cell destined to migrate to layer 6 continued to do so when transplanted into the visual cortex of another animal at the stage when cells were migrating into layers 2 and 3 (McConnell and Kaznowski 1991). However, the particular area of neocortex that a given set of migrating cells forms does not seem to be predetermined, since a set of cells destined to form part of the visual cortex of the rat forms the afferent connections and architectonic features characteristic of the somatosensory cortex when transplanted into the developing somatosensory area (Schlagger and O'Leary 1991). Thus, different areas of the neocortex are determined by the identity of cells that migrate into them from other areas. In the visual cortex, the migrating cells are geniculocortical afferents.

Although the geniculocortical afferents reach the cortical plate well before their target cells in layer 4 are formed, they do not begin to migrate toward layer 4 until well after all the cortical layers have formed (Rakic 1988). This is known as the waiting period. At about the time this migration occurs, most of the subplate cells begin to die off (see Shatz et al. 1991). As we will see later, it has been suggested that subplate neurones guide afferent fibres to their proper destination in cortical layer 4. After the layers have formed, the cells in the various layers develop at a uniform rate (Lund et al. 1977).

Just before and after birth there is a rapid increase in the density and total number of synapses and in the thickness of layers in the primate visual cortex and the cortex as a whole (Rakic et al. 1986). In humans, this increase is most rapid between the ages of 2 and 4 months but continues to the postnatal age of about 8 months, when the mean synaptic density reaches about 25,000 per neurone. After about 8 months a massive but slow loss of synapses occurs to the adult level of about 10,000 synapses per neurone, which is reached by about the age of 11 years.

In the visual cortex of the macaque, synaptic density increases exponentially to the third postnatal month, after which it decreases, at first slowly and then more rapidly to reach its adult value after about 5 years (Bourgeois and Rakic 1993). There is no evidence of neurone loss during this process, but the cortical layers become thinner, in both humans and monkeys (O'Kusky and Colonnier 1982; Garey and de Courten 1983; Huttenlocher and de Courten 1987; Zielinski and Hendrickson 1992). Loss of synapses is



(a) A photomicrograph of a Nissl-stained section through the visual cortex of a 17-week human foetus. Neurones develop in the ventricular zone which lines the cerebral ventricle and migrate through the intermediate zone and cortical subplate to the cortical plate, just below the pial surface of the brain. The six layers of the visual cortex are not yet visible, but develop in the cortical plate.

(b) Photomicrograph of the visual cortex of the human neonate. The six layers of the visual cortex are formed and the subplate has become transformed into largely neurone-free white matter. (From Yan et al. 1992.)

Figure 15.1. The development of the human visual cortex..

related to the development of cortical dominance columns in which inputs compete for synaptic access to binocular cells. It is thus part of the process by which neural networks develop in response to maturational and environmental demands.

The projection of transcortical axons from area 17 to area 18 is established before birth in the cat. However, these axons are evenly distributed between the various cortical layers before the age of about 20 weeks, after which they arise mainly in layers 2 and 3. This maturational change does not depend on visual experience, since binocular deprivation up to 28 weeks of age did not stop it (Price and Blakemore 1985). During the same period, cells projecting to

area 18 form into clusters by elimination of projections from intercluster zones. Also, the projections from area 17 to area 18 become more localized during the first postnatal month (Price et al. 1994).

Development of lateral connections

We noted in Section 4.2.2 that cortical cells with similar orientation tuning are linked by fibres of pyramidal cells running parallel to the cortical surface in layers 2, 3, 4, 5, and 6. Long-range fibres extend up to 6 mm and form fine branches distributed in repeating clusters corresponding to the repeating orientation-selective columns (Gilbert and Wiesel 1979; Rockland and Lund 1982; Luhmann et al. 1986).

Hata et al. (1993) investigated the development of horizontal connections by a correlational analysis of spike trains recorded simultaneously at different lateral locations in the visual cortex of kittens, a procedure developed by Perkel et al. (1967). During the first 2 postnatal weeks, these connections were wholly excitatory; inhibitory linkages developed by the fourth week. Also, the connections were widespread, between cells with very different orientation preferences, and did not show the clustered distribution evident in the adult. By the seventh week the connections became confined to a radius of about 600 µm and to cells with similar orientation tuning. At the same time, the clustering pattern emerged. The process involves the growth and elimination of synaptic connections rather than cell death (Callaway and Katz 1990). Hata et al. also found that correlated firings developed first in layer IV but by the seventh postnatal week the frequency of firing in layer IV declined to the low level typical of the adult and was overtaken by firing rates in other layers.

Burkhalter et al. (1993) used a fluorescent dye to observe the development of lateral connections in a series of postmortem human visual cortices from 24 weeks of gestation to 5 years postnatal. Lateral connections first emerged at 37 weeks of gestation, after the development of radial connections at right angles to the cortical surface. As in the cat, lateral connections showed first in layer 4B, but also in layer 5 and then in layer 6. Fibre density increased rapidly, leading to the formation of a uniform plexus at 7 weeks postnatal. The patchiness typical of the adult emerged after the 8th postnatal week. Longer-range lateral connections in layers 2 and 3 did not emerge until the 16th postnatal week and reached their adult form by the 15th month. These long-range connections were patchy to begin with and remained patchy. Layer 4B is associated with the magnocellular system and layers 2 and 3 with the parvocellular system. This evidence suggests that the magnocellular system develops before the parvocellular system.

Dalva and Katz (1994) studied the development of connections in *in vitro* slices of the visual cortex of the ferret. The slices were perfused with a form of glutamate that remains inactive (caged) until photolyzed by ultraviolet light. By recording from a given cell as neighbouring cells were activated by the laser they were able to map out patterns of lateral connections. They confirmed that local connections are overproduced before birth and subsequently decline as long-range connections develop.

The long-range lateral connections could serve to code the presence of long contours belonging to a connected figure, which stimulate aligned receptive fields, as discussed in Section 4.2.2 (Mitchison and

Crick 1982; Nelson and Frost 1985). They could also serve to sharpen the selectivity of orientation detectors (Matsubara et al. 1985). Long-term changes in synaptic conductivity along these lateral pathways in the cat's visual cortex have been induced by pairing synaptic responses with conditioning shocks of depolarizing current (Hirsch and Gilbert 1993). This suggests that these pathways are involved in stimulus-dependent changes in cortical responses.

Development of cortical cell specificity

The metabolic enzyme cytochrome oxidase—a sensitive indicator of neural activity (see Section 4.2.2)—is present in the cortical plate of the human brain by the 26th week of gestation. Cytochrome-oxidase blobs are not evident in the visual cortex of the human until the 24th postnatal day and are well organized by the fourth month. Cytochrome-oxidase stripes in V2 are weakly evident in the human neonate (Wong-Riley et al. 1993). In contrast, both blobs and stripes are clearly evident in the visual cortex of the neonate macaque, although the distribution of the enzyme is not the same as in the adult animal (Horton 1984; Kennedy et al. 1985).

Braastad and Heggelund (1985) recorded from cells in area 17 of kittens between the ages of 8 days and 3 months. At 8 days the cells had receptive fields of both the X and Y type, spatially organized into excitatory and inhibitory zones. The receptive fields were large, and only about 40 per cent of them showed tuning to stimulus orientation, compared with more than 90 per cent at 4 weeks.

Pettigrew (1974) could not find cells with stimulus specificity in the visual cortex of visually inexperienced kittens in the first few weeks after birth. Freeman and Ohzawa (1992) recently reinvestigated this question using grating stimuli. Even in 2-week-old kittens, they found many simple and complex cells in area 17 which responded to stimulation of either eye and which were tuned to orientation and spatial frequency, although the responses were weak and unstable. Some of the cells were tuned to binocular disparity, although the proportion of such cells was lower than in the adult cat. The cells showed evidence of both excitatory and inhibitory binocular interactions. Freeman and Ohzawa could not determine what proportion of cortical cells was responsive, because unresponsive cells could not be detected. Between the second and third week, the vigour of the responses increased and there was a substantial increase in the proportion of binocular cells. By the fourth week, the tuning of cortical cells was similar to that of the adult cat. They concluded that the development of the basic physiological apparatus for stereopsis predates visual experience and

must therefore be genetically determined. Nevertheless, we will see in what follows that the maintenance and fine tuning of the stereoscopic system does depend on visual experience during early infancy.

Development of ocular-dominance columns

The organization of ocular-dominance columns in the visual cortex was described in Section 4.2.4. Hubel and Wiesel (1963) found most cells in the visual cortex of visually inexperienced kittens between the ages of 1 and 3 weeks were responsive to inputs from either eye but could be grouped into ocular-dominance columns in much the same way as in the adult cat. LeVay et al. (1978) found no evidence of ocular-dominance columns in the neonate cat, but they became evident 3 weeks after birth and resembled the adult pattern of columns by 6 weeks. Others have found some signs of ocular-dominance columns in visual areas 17 and 18 in the neonate cat (Albus and Wolf 1984; Blakemore and Price 1987a).

In the monkey, segregation of ocular-dominance columns begins during the second half of gestation, although the projections from the two eyes overlap extensively in layer 4C during the first 3 postnatal weeks (Wiesel and Hubel 1974; Rakic 1976). Ocular-dominance columns can be seen in the autoradiograph of the neonate monkey brain (Des Rosiers et al. 1978). The adult pattern of ocular dominance in the monkey is established by the age of six weeks (LeVay et al. 1980).

We noted in Section 4.2.4 that in adult cats and primates the geniculocortical afferents from the two eyes project to distinct cells in layer 4C, and from there inputs from both eyes project to binocular cells in other layers. In cats under 3 weeks of postnatal age, inputs from the two eyes are completely mixed in layer 4 and segregation into distinct cells is not complete until between 8 and 10 weeks of age (LeVay et al. 1978). This transition from a state of uniform binocular innervation to one of monocular dominance is believed to involve a phase of exuberant proliferation and homogeneous distribution of synaptic terminals followed by selective pruning or withdrawal of inappropriately connected dendrites. It has also been suggested that this pruning process is accompanied by expansion and maturation of appropriately connected dendrites. The process could also involve development of inhibitory connections.

Antonini and Stryker (1993) used immunohistochemical procedures to trace these growth processes at the cellular level and revealed that widely extending but immature branches of geniculocortical afferents are eliminated at the same time that other

branches grow in length and complexity and segregate into patches according to their eye of origin. The crucial mechanism seems to be competition between afferents from the two eyes for access to cortical cells. If one eye is closed during the critical period of cortical development in the first few months of life, the bands corresponding to the open eye expand at the expense of those corresponding to the closed eye (see Section 15.6.2). The development of cortical layers and columns is guided by the following processes.

Mechanical and chemical factors in cortical development

The factors which guide growing axons through the chiasma and LGN were described in Section 15.1.3. As ingrowing axons approach their destination in the visual cortex they are guided by gradients of diffusing neurotrophic growth factors, and molecular labels on the surfaces of target cells (Katz and Callaway 1992). These processes are probably also responsible for the collateral connections that cortical input cells (spiny stellate cells in layer 4) make with cells in layers 3 and 5 and that cortical output cells (pyramidal cells) make with layers 2, 3, and 5. These processes guide the radial growth of afferent axons into appropriate layers and dendritic growth between appropriate layers well before birth in both cats and primates.

Astrocytes, a type of glial cell, are also involved in guiding dendritic growth within the cortex. Astrocytes provide contact surfaces and act as phagocytes that dispose of cellular debris. During the critical period, astrocytes produce a variety of growth factors which seem to be required for cortical plasticity. Müller and Best (1989) transplanted living astrocytes from neonate kittens into the visual cortex of one hemisphere of adult cats and dead astrocytes into the other hemisphere. After 4 to 8 weeks of monocular deprivation, a change occurred in the ocular dominance of cells in the hemisphere with living neonate astrocytes but not in the other hemisphere.

Oligodendrocytes, the second type of glial cell, form myelin sheaths that insulate neurones from each another, except at synapses. The initial growth of afferent and laminar connections seems to be preprogrammed and does not depend on neural activity in the growing neurones (Lund et al. 1977). However, selective survival of synaptic connections guided by neural activity is required for the growth of specific patterns of synaptic arborizations within the cortical layers (see Katz and Callaway 1991). We will see later that neural activity arising from visual experience is involved in the formation of ocular-dominance columns.

The role of subplate neurones

Columnar organization seems to be influenced by subplate neurones. These neurones are located in the cortical subplate below cortical layer 6 and are present only in the developing cortex. Even before lamination is evident in the embryonic cortex, the subplate neurones send pioneer axons down through the internal capsule to the LGN, superior colliculus, and other areas of the developing cortex (McConnell et al. 1989; Allendoerfer and Shatz 1994). They also send axons into the cortical plate (the developing cortex), primarily into layers 1 and 4. There is evidence that subplate neurones of the visual cortex receive excitatory inputs from afferent fibres ascending from the LGN and transmit these signals to cells in the cortical plate (Friauf and Shatz 1991). Ghosh and Shatz (1992, 1994) disabled the subplate neurones in a particular region of the visual cortex of 1-week-old kittens by local application of kainic acid. The cortex above the affected region failed to develop ocular-dominance columns. The effect seems to have been specifically related to the loss of subplate neurones because application of kainic acid directly to layer 4 did not lead to this deficit. In the early postnatal period most of the subplate cells die. Subplate neurones and their axons can thus be regarded as a temporary scaffold for the development of geniculocortical connections. Ablation of subplate neurones in cat foetuses disrupted the development of axons from the visual cortex to the LGN (McConnell et al. 1994). The subplate therefore aids in the development of geniculocortical and corticothalamic pathways.

The role of spontaneous activity

Mammalian ganglion cells generate spontaneous neural activity well before birth. Bursts of neural activity are generated in the rat retina by at least embryonic day 17 (Galli and Maffei 1988) and in the cat retina by embryonic day 30 (Skaliora et al. 1993).

Goldfish developed ocular-dominance columns in the tectum when optic fibres from both eyes were forced to grow into one tectum. These columns did not develop when all optic nerve impulses in both eyes were blocked by intraocular injection of tetrodotoxin, a highly specific inhibitor of the sodium channel involved in neural conduction (Meyer 1982). Autoradiography failed to reveal any ocular-dominance columns in the visual cortex of kittens after both eyes had been injected with tetrodotoxin between the ages of 14 days and 8 weeks, and nearly all cortical cells were found to be well driven by stimuli in either eye (Stryker and Harris 1986). Simply rearing kittens in the dark does not have this effect. Antonini and Stryker (1993) found that

tetrodotoxin does not arrest general growth of dendrites or produce nonspecific growth but, instead, interferes with segregation of afferents into eye specific clusters. It looks as though ocular-dominance segregation depends on there being inputs from the eyes, but these inputs can be the spontaneous firing of ganglion cells and need not arise from visual stimulation.

Miller (1994) has developed a model of the development of simple-cell receptive fields and of cortical columns from activity-dependent competition between on- and off-centre visual inputs.

The role of the neurotransmitter NMDA

Several lines of evidence suggest that the segregation of distinct ocular-dominance columns depends on the presence of cortical cells which respond to the excitatory neurotransmitter, glutamate, acting through a type of synaptic receptor involving release of N-methyl-D-aspartate (NMDA) (Constantine-Paton et al. 1990). The density of NMDA-glutamate synapses increases abruptly in all layers of the visual cortex of the kitten during the period when inputs from the two eyes segregate into ocular-dominance columns. Toward the end of the critical period, the density of NMDA receptors declines to the adult level (Bode-Greuel and Singer 1989; Fox et al. 1989). Also, NMDA-mediated postsynaptic activity in the visual cortex is more pronounced in young than in adult rats (Carmignoto and Vicini 1992). Monocularly deprived kittens failed to show an ocular-dominance shift when NMDA was inhibited by a specific antagonist (Bear et al. 1990). Dark-rearing of the cat arrested the loss of NMDA receptors and thereby extended the period during which visual experience influenced the formation of ocular-dominance columns (Fox et al. 1991; see Section 15.5). Finally, infusion of a specific antagonist of NMDA receptors into one cerebral hemisphere of kittens reared with monocular occlusion prevented a switch of dominance of cells in that hemisphere after the occluder was moved to the other eye. Cells in the visual cortex of the untreated hemisphere showed the usual transfer of dominance after reversal of occlusion (Gu et al. 1989).

In excitatory synaptic transmission not mediated by NMDA, synaptic conductance depends only on presynaptic activity. By contrast, transmission mediated by NMDA also depends on depolarization of the postsynaptic membrane. The correlation between pre- and postsynaptic activity triggers a voltage-dependent response in the NMDA-mediated synapse which in turn produces a graded release of postsynaptic calcium ions. When the level of calcium ions exceeds a critical level it triggers a persisting

increase in synaptic conductance known as **long-term potentiation (LTP)**. Ionic concentrations below the critical level trigger a **long-term depression (LTD)** of synaptic conductance (Kirkwood and Bear 1994a). Thus, transmission in this type of synapse depends on an increase in the permeability of the cell membrane to calcium ions which occurs only when NMDA is present and when the membrane of the postsynaptic neurone is sufficiently depolarized (Mayer et al. 1984). The release of NMDA and glutamate within a local volume of neural tissue seems to be mediated by the production and diffusion of the membrane-permeable gas nitrous oxide (Montague et al. 1994; Wu et al. 1994).

The dependence of the release of NMDA on both the pre- and postsynaptic membrane potentials is just the property required of a mechanism for detecting coincident activity in inputs converging on a common cell. In other words, it is the property required of a Hebbian synapse, as described in Section 3.3.2. Singer (1990) has proposed that an excitatory input not strong enough to activate NMDA receptors above a critical level decreases the efficiency of the activated synapse and has no effect on other synapses on the same neurone. When the excitatory input reaches the threshold activation of NMDA, the efficiency of the activated synapse and of other simultaneously activated synapses is enhanced and that of simultaneously inactive synapses on the same neurone is weakened. We thus have a mechanism for establishing use-dependent neural networks.

Most investigations of the role of NMDA in neural plasticity have been conducted on *in vitro* preparations of cells from the hippocampus, a region of the old cortex, or palaeocortex, implicated in spatial memory (Sherry et al. 1992). Activation of NMDA synapses in the hippocampus in the adult brain leads to long-term potentiation of synaptic conductance (Fazeli 1992). Repeated activation of NMDA synapses in *in vitro* slices of cells from the visual cortices of rats and mice yields persistent changes in permeability to calcium ions similar to those found in slices of hippocampus, suggesting that the mechanism is common to both the old and new cortex (Kirkwood et al. 1993; Kirkwood and Bear 1994b; Weiss et al. 1993). Furthermore, low-frequency electric shocks delivered to the white matter underlying the hippocampus produce long-term potentiation, except when NMDA receptors are inhibited by an antagonist. The same has been found for shocks delivered to the white matter underlying the visual cortex in rats (Kimura et al. 1989). The precise role of NMDA receptors in cortical plasticity in the visual cortex is still a subject of debate and many details remain to be worked out (Fox and Daw 1993).

Neurotrophins and the neurotransmitters γ -aminobutyric acid (GABA) and norepinephrine have also been implicated in the development of the visual cortex. This topic is discussed in Section 15.6.2.

The role of patterned visual inputs

Evidence discussed in Section 15.6.2 reveals that the fine tuning and maintenance of binocular cells in the visual cortex depends on exposure of the two eyes to similarly patterned stimuli. The crucial factor may be synchrony of firing of inputs from the two eyes as they converge on binocular cells. Synchronous activity of inputs converging on a Hebbian synapse improves synaptic conductance.

Bienenstock et al. (1982) developed a mathematical model of the development of ocular dominance based on the idea of competition between inputs from the two eyes. A computer simulation of the interplay of several of the preceding factors revealed the conditions that could lead to the generation of ocular-dominance bands (Miller et al. 1989). The development of neuronal plasticity in the visual cortex has been reviewed by Frégnac and Imbert (1984) and by Rauschecker (1991).

15.1.6 Development of visual functions

Development of acuity and contrast sensitivity

The visual performance of human neonates could be limited by the immaturity of preneural structures. These factors include the optical quality of the eye and the image sampling of the retina, that is, the aperture, efficiency, and spacing of the photoreceptors. On the other hand, postreceptor mechanisms, such as the size and tuning characteristics of the receptive fields of ganglion cells and cortical cells could be a limiting factor.

Banks and Bennett (1988) estimated the contrast sensitivity and grating acuity for two ideal observers, one based on the preneural characteristics of the neonate human fovea and one with the characteristics of the adult fovea. This analysis yielded a predicted difference in the grating acuities of the infant and adult of 2 octaves compared with an actual difference of 3.5 to 4.5 octaves. They concluded that immaturity of preneural structures does not fully account for the visual performance of the neonate (see also Jacobs and Blakemore 1988). Wilson (1988) carried out a similar analysis from which he concluded that preneural factors play a greater role in limiting visual performance in neonates than was found in the Banks and Bennett study. Such analyses are valuable but can be no better than the set of assumptions and the data on which they are based.

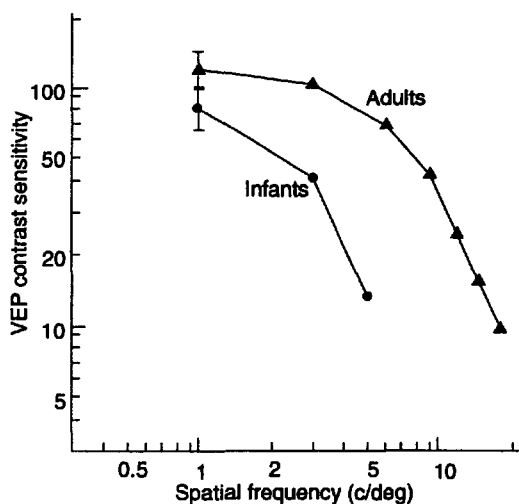


Figure 15.2. Contrast sensitivity and evoked potentials.
Mean contrast-sensitivity function of six adults (top curve) and of four 25- to 28-week-old infants. Contrast sensitivity was measured by the amplitude of the visual evoked potential recorded with surface electrodes, in response to gratings of various spatial frequencies counterphase modulated at 12 Hz for the infants and at 15 Hz for the adults. (Adapted from Norcia et al. 1986.)

The development of the retina, LGN, and visual cortex is coupled with an increase in visual resolution, defined as the angular subtense of one period of a grating with the highest detectable spatial frequency. Three behavioural criteria have been used to test grating resolution in young infants: the occurrence of optokinetic nystagmus in response to a moving grating, the pupil response to a grating presented against an equiluminant background, and the child's tendency to look at a patterned stimulus. Although these procedures do not always produce the same results, it is agreed that resolution for high-contrast gratings improves from approximately 50 arcmin at 1 month, to 10 arcmin at 3 months, and to 5 arcmin at 12 months of age (Dobson and Teller 1978; Jacobson et al. 1982; Cocker et al. 1994).

Norcia and Tyler (1985) recorded the evoked potentials from the infant's scalp in response to a frequency-swept, counterphase-modulated grating and obtained estimates of grating acuities of 13 arcmin at 1 month and 3 arcmin at about 12 months, which is about the adult level. These acuities are two to three times better than those reported from behavioural studies or other evoked-potential studies referenced in their paper. Their swept-frequency procedure provides a finer determination because it is fast and therefore immune to adaptation effects. It is also immune to the effects of probability summation (see Section 9.2.1). Grating acuity obtained by this method was only slightly better with binocular viewing than with monocular viewing, and was similar in the two eyes (Hamer et al. 1989).

There is also a developmental change in the contrast-sensitivity function, where sensitivity is defined as the reciprocal of contrast threshold and is plotted as a function of the spatial frequency of a grating with a sinusoidal modulation of luminance. In the monkey, contrast sensitivity to spatial frequencies below 5 c/deg was found to approach adult levels by the twentieth week, and sensitivity to higher spatial frequencies continued to improve until the twenty-eighth week, when the contrast-sensitivity function acquired its adult form (Boothe et al. 1980). The contrast-sensitivity function of human infants has been measured by both behavioural procedures and by use of visual evoked potentials (Atkinson et al. 1977; Banks and Salapatek 1978; Pirchio et al. 1978; Norcia et al. 1986). Norcia et al. obtained higher contrast sensitivities in infants than the other investigators. By 10 weeks the contrast sensitivity determined by the frequency-swept VEP reached adult levels for spatial frequencies below 1 c/deg (Norcia et al. 1988). However, the shapes of the functions were similar in all these studies, and so was the developmental trend toward greater contrast sensitivity and the extension of sensitivity to higher spatial frequencies, as shown in Figure 15.2.

Development of orientation sensitivity

Braddick et al. (1986) found no evidence of cortical cells tuned to orientation in the human neonate, as indicated by electrical potentials (VEP) evoked on the surface of the head by changes in the orientation of a grating. Evidence of orientation tuning in the cortex showed at the age of 6 weeks. Behavioural tests have revealed that 6-week-old human infants can discriminate between lines in opposite oblique orientations (Maurer and Martello 1980; Held 1981). More recently, discrimination between oblique gratings has been shown in human neonates. When newborn infants were shown two opposite oblique static gratings side by side they preferred looking at the one to which they had not been previously exposed (Atkinson et al. 1988; Slater et al. 1988). In other studies, 3-month-old infants could discriminate between gratings tilted 45° and 15°, and 4-month-old infants could discriminate between gratings tilted 45° and 22° (Bomba 1984; Borstein et al. 1986). The literature on the development of the ability to categorize orientations is reviewed in Howard (1982).

Development of motion sensitivity

To establish that infants are sensitive to visual motion one must demonstrate that they are responding specifically to motion rather than to flicker or change of position. Aslin and Shea (1990) found that at 6 weeks of age infants could distinguish between

stationary stripes and stripes moving at 9°/s relative to a stationary surround and at 12 weeks they could distinguish stripes moving at 4°/s. The velocity threshold did not vary with the width of the stripes, which indicates that the infants were judging motion rather than simple flicker. Dannemiller and Freedland (1993) showed that 14-week-old infants detect motion in standing-wave line stimuli, which allow sensitivity to motion to be distinguished from sensitivity to changes in position. The visual-evoked response in neonatal infants is much stronger for stimuli moving in a nasal direction than for stimuli moving in a temporal direction (Norcia et al. 1991). This directional asymmetry is also revealed in an asymmetry in optokinetic eye movements in the neonate (see Section 12.5.6). Wattam-Bell (1992) used a preferential-looking procedure to measure the maximum displacement (d_{max}) of a random-dot pattern for discrimination of the direction of motion and for discrimination between coherent and incoherent motion. Between 8 and 15 weeks of age, the oldest age tested, d_{max} increased for both tasks, but the increase was greater for slow than for rapid movements. These same developmental trends were evident in the magnitude of visual evoked potentials triggered by motion of checkerboard patterns (Wattam-Bell 1991). Directional sensitivity to motion develops for low velocities before it develops for high velocities. Hamer and Norcia (1994) used evoked potentials to measure displacement thresholds for a high-contrast, 1 c/deg grating oscillating from side to side at 6 Hz. In 12-week-old infants the oscillation threshold was ten times the adult value, even though contrast sensitivity was already half the adult value. The oscillation threshold was still over four times that of the adult in 1-year-old infants. Voluntary pursuit eye movements seem not to be present before 6 to 8 weeks of age (Aslin 1987).

Development of colour sensitivity

In the first month or two, infants are very poor at discriminating between different colours or between achromatic and chromatic stimuli, especially at the blue end of the spectrum (Varner et al. 1985; Adams et al. 1991). By 12 weeks, most infants can discriminate hues involving cones sensitive to short, medium, and long wavelengths. Banks and Bennett (1988) proposed that the poor colour discrimination in infants is due to poor general visual sensitivity rather than to a lack of different cone types. Allen et al. (1993) produced evidence for this idea by showing that the ratio between luminance and chromatic sensitivities, as indicated by visual-evoked potentials, is the same for 2- to 8-week-old infants as for adults.

Asymmetry of temporal and nasal hemiretinas

It was mentioned in Section 15.1.2 that the crossed visual pathways from the nasal hemiretinas develop before the uncrossed pathways. As a result, visual functions in the temporal half of the monocular visual field (nasal hemiretina) develop before those in the nasal hemifield (temporal hemiretina). For example, visual acuity revealed by preferential looking was found to be higher in the temporal than in the nasal visual field of infants between 2 and 11 months of age (Sireteanu et al. 1994). For some time after first opening their eyes, kittens oriented toward stimuli in the temporal visual field of an eye, but ignored stimuli in the nasal field (Sireteanu and Maurer 1982). Similarly, human infants below 2 months of age oriented their gaze toward an isolated light presented 30° into the temporal monocular field but failed to orient toward a light only 15° into the nasal field (Lewis and Maurer 1992). A similar procedure revealed that after the age of 2 months both hemifields and the binocular field expand rapidly until the age of 8 months and then more slowly until 12 months, the oldest age tested (Mohn and Van Hof-van Duin 1986).

Although the nasal hemifield remains smaller than the temporal hemifield, the two hemifields become more similar in size with increasing age. However, even in each visual hemisphere of the adult monkey there are more binocular cells with a dominant input from the contralateral eye (the nasal hemiretina) than cells with a dominant ipsilateral input (temporal hemiretina) (LeVay et al. 1985). The mature nasal hemiretina also remains more sensitive than the temporal hemiretina. Thus, the decrease in vernier acuity with increasing eccentricity of the stimulus is steeper in the nasal than in the temporal hemifield (Fahle and Schmid 1988). The nasal hemiretina has a higher density of receptors (Curcio et al. 1990) and the cortical magnification factor (the linear extent of cortical tissue devoted to each visual angle) is higher for the nasal than for the temporal hemiretina (Rovamo and Virsu 1979). Other aspects of hemifield asymmetry are discussed in Section 8.3.4.

The development of spatial vision has been reviewed by Mohn and Van Hof-van Duin (1991).

15.2 DEVELOPMENT OF BINOCULAR VISION

15.2.1 Behavioural procedures

Several behavioural procedures are used to trace the development of stereoscopic vision in human infants. The principal methods are listed with examples of experiments in which they have been used.

Cliff avoidance

Most young mammals show a natural avoidance response when confronted with a visible cliff (Gibson and Walk 1960). In one study, kittens used binocular cues in selecting the shallower of two steps by the age of 5 weeks (Timney 1981). In another study, human infants at the age of 2 months discriminated between the shallow and deep sides of a visual cliff, as indicated by the heart rate (Campos et al. 1970). However, several monocular cues to depth were available in these displays, so one cannot conclude anything about the development of binocular stereopsis in humans.

Visually guided reaching

The earliest identifiable responses of the infant's arm are the neck-tonic reflex evoked by rotation of the head, the traction reflex evoked by pulling the arm, and the grasp reflex evoked by touching the palm (Twitchell 1970). None of these innate reflexes is evoked by visual stimulation. White et al. (1964) outlined a normative developmental sequence of visually guided reaching in human infants. In the first month, infants do not attend to objects within arm's reach, and arm movements are unrelated to vision. In the second month, infants attend to near objects and become interested in their own arms. The first visually directed swiping movements of the arm develop, but the child grasps an object only if the hand touches it. In the third month, swiping gives way to directed arm movements, and the child looks back and forth between object and hand. By the fourth and fifth months the combined action of the arms comes under visual control and gives way to the ability to reach for and grasp an object. Bower et al. (1970) claimed to have observed infants only a few days old reaching toward visual objects and occasionally grasping them, but these observations have not been confirmed (Dodwell et al. 1976).

Reaching movements toward a visual object, without visual control once initiated, are called **visually triggered movements**. Responses that are modified during execution by visually perceived error are called **visually guided movements**. Visually triggered movements are studied with the hand kept out of view. A successful reaching movement to an isolated object without the sight of the hand requires information about the absolute distance of the object, which can be provided only by accommodation or vergence. A seen hand can be guided to an object by the use of binocular disparity and lateral offset between hand and object; absolute estimates of distance and direction are not required for visual guidance.

Several studies have been done on the development of the reaching response in infants and

conclusions have been drawn about the extent to which reaching and grasping movements signify that the infant has depth perception. For instance, 5-month-old infants moved the arm forward and made grasping movements with the hand when a virtual object was within reach but not when it was out of reach (Gordon and Yonas 1976; Bechtoldt and Hutz 1979). Granrud (1986) found that 4-month-old infants reached for a nearer object more consistently when looking with two eyes than with one. Furthermore, the superiority of binocular over monocular reaching was correlated with a preference for looking at a random-dot stereogram with relative depth rather than at one without. In another study, 5-month-old infants reached for an approaching object specified only by binocular information whereas 3½-month-old infants failed this test (Yonas et al. 1978).

It is not clear in any of these studies that performance depended only on disparity cues to depth as opposed to accommodation, vergence, and monocular cues. Nor is it clear to what extent the infants were judging the absolute distance of an object or the relative distance between the object and the hand.

Preferential looking

Some stimuli have a natural attraction for human infants. For instance, when presented with two stimuli with a minimum of other distractions, infants spend more time looking at the more brightly coloured stimulus or the one which moves, flashes, or has higher contrast. They also prefer a three-dimensional display rather than a flat display. In the preferential-looking procedure introduced by Fantz (1965), the infant is presented with two stimuli side by side, and a record is kept of the time the infant spends gazing at each. In a refinement of the method, the person watching the infant's eyes does not know which stimulus has been presented and follows a forced-choice, bias-free procedure in deciding whether the infant is looking at one stimulus or the other (Teller 1979).

Held et al. (1980) used the preferential-looking procedure in which infants viewed line stereograms through crosspolarizing filters. Displays in a two- and three-dimensional form were placed side by side. By 4 months of age, infants could distinguish a display with zero disparity from one with 1° of disparity and, by 5 months, stereoacuity had reached 1 arcmin, which was the limit of the apparatus.

Infants below the age of about 3½ months preferred to look at dichoptically combined orthogonal gratings rather than gratings with the same orientation in the two eyes. Shimojo et al. (1986) concluded

that the infants saw the orthogonal grating as a fused grid because they found that infants of this age prefer grids to gratings. They suggested that prestereoscopic infants see a grid because they lack the binocular suppression mechanism responsible for binocular rivalry. But their results could also be explained as a preference for rivalrous stimuli in infants because they are known to prefer changing stimuli over steady stimuli. This suggests that prestereoscopic infants do have binocular rivalry.

Dishabituation

In a variant of the preferential-looking procedure known as dishabituation, the infant is shown a given stimulus for some minutes or until signs of interest are no longer evident. The stimulus is then changed in a defined way, and the extent to which interest is reinstated is determined by observing movements of the infant's eyes or by recording indications of arousal such as increased heart rate. The stimulus is then changed in the reverse direction and, as a final control, each stimulus is flashed off and on again. Using the dishabituation procedure, Appel and Campos (1977) found that 2-month-old human infants showed a heartbeat arousal response when a flat random-dot display was changed into one having depth defined by disparity. The infants may have responded to changes in the monocular image rather than to changes in disparity or perceived depth. Atkinson and Braddick (1976) overcame this problem by using a random-dot stereogram that contained no monocular forms. Two out of four 2-month-old infants showed evidence of discriminating between a two- and three-dimensional display.

Birch et al. (1982) tested 128 human infants between the ages of 2 and 12 months using three vertical bars, the two outer ones had either crossed or uncrossed disparity relative to the central one. Stereoacuity was defined as the smallest disparity for which an infant showed at least 75 per cent preferential looking at a disparate stimulus rather than at a similar stimulus with bars aligned. Stereopsis began to show by the age of 3 months. The preferential looking revealed that three-quarters of the infants had discriminated a 1 arcmin of crossed disparity in the outer bars by the age of 5 months, but only a third of them discriminated an uncrossed disparity by this age. It was concluded that crossed-disparity detectors develop before uncrossed-disparity detectors. This conclusion is valid only if the infants remained converged on the central rod in both cases. Infants showed a similar sequence in the development of a preference for looking at binocularly identical stimuli rather than binocularly rivalrous stimuli (Birch et al. 1985).

Pursuit eye movements

The ability of an infant to detect a stimulus may also be revealed by moving the stimulus and observing whether the infant's eyes track it. Involuntary tracking movements of the eyes in response to large moving stimuli are present in the neonate. The first systematic study of the development of stereopsis in infants was carried out by Fox et al. (1980), using this method. They tested 40 infants between 2 $\frac{1}{2}$ and 6 months of age using a dynamic random-dot stereogram in which the cyclopean pattern moved left or right. An infant was deemed to have stereoscopic vision if its eyes followed the moving pattern. The motion of the cyclopean pattern was not visible to either eye alone, and no monocular cues to depth were present in the stimulus. According to this criterion, stereopsis was found to emerge between the ages of 3 $\frac{1}{2}$ and 6 months.

Operant conditioning

All the preceding procedures make use of a built-in response and therefore require a minimum of preliminary training. In operant conditioning the subject is first trained to make a response toward a designated stimulus. The presentation of one stimulus is coupled with reinforcement, and the presentation of another stimulus differing in some crucial respect is not reinforced. If the animal learns to make differential responses to the two stimuli one concludes that it has the sensory capacity to discriminate them. It is notoriously difficult to design stimuli that differ in the factor being studied and not in irrelevant factors. Ciner et al. (1989) developed an operant procedure for testing stereopsis in children aged 18 months and above. The child was first rewarded with a food object for pointing to a black ring which appeared on either the left or the right side. A random-dot stereogram depicting a ring in depth was then presented on either the left or the right, and a zero-disparity random-dot display was presented on the other side. The disparity in the test stereogram was increased until the child pointed consistently to it. Ciner et al. (1991) used this procedure with 180 children and found a steady improvement in stereoacuity from a mean of 250 arcsec at 18 months to 60 arcsec at 5 years of age. Improvement was most rapid around the age of 30 months, and was accompanied by a large decrease in intra- and intersubject variability. Birch and Hale (1989) used a similar procedure with a group of 76 normal infants between the ages of 19 and 60 months. They reported a mean stereoacuity of 77 arcsec at 19 to 24 months and 40 msec at 31 to 36 months. For more discussion of operant procedures in studies of the development of depth perception in animals see Mitchell and Timney (1982).

Standard stereo tests

Standard tests of stereoscopic vision can be applied once the child can speak. Stereoacuity norms for several standard tests have been reported for children between the ages of 3 and 6 years, by which age performance has been reported to be still below adult levels (Simons 1981b). Romano et al. (1975) used the Titmus stereotest to trace the progress of stereoacuity in 321 children between the ages of 1.5 and 13 years. Stereoacuity increased with age until it reached the value of 40 arcsec (the best the instrument could measure) by the age of 9 years. Cooper and Feldman (1978a) obtained better scores for children between 2 and 5 years of age when they were tested with a random-dot stereogram than with the traditional Titmus fly test or TNO test. The random-dot test was administered with an operant training procedure in which the children were rewarded for correctly reporting whether or not there was depth in the display. It is not clear whether the superior performance on the random-dot test was due to the test itself or to the increased attention and motivation provided by the training and rewards. Fox et al. (1986) tested children between the ages of 3 and 5 years on the Howard-Dolman test set up in the form of a game with rewards. The performance of the 5-year-olds was higher than previously reported and close to the adult level. However, measurements were not taken without the rewards and attentional aids, so we cannot tell whether these were responsible for the better performance of these children. None of the results produced by these behavioural procedures allow one to distinguish between the use of binocular disparities and the monitoring of vergence changes. This could be done with brief stimulus presentations.

15.2.2 VEPs and stereoscopic development

The logic for using visual evoked potentials (VEPs) from the surface of the scalp to investigate binocular functions was outlined in Section 4.8. Amigo et al. (1978) reported that binocular facilitation of the VEP first shows in normal infants at about the age of 2 months but is still below adult levels at 5 months, from which they concluded that the VEP can be used as a test of cortical binocularly. However, they tested each of their subjects at only one spatial frequency, which was 3 c/deg for adults and for infants varied between 1 and 3 c/deg, according to age. This makes it difficult to compare across ages, and they may have missed the spatial frequency that evokes the best response (see Section 5.5.3). Shea et al. (1987) recorded the VEP in response to temporally modulated checkerboard patterns with low and high

spatial frequencies and found that in most infants below the age of 10 months the binocular VEP was almost twice as strong as the mean monocular response, and the binocular response was even higher in infants below 5 months. The enhanced binocular VEP in infants may represent the summed response of two monocular pools of neurones rather than the activity of binocular neurones (Nuzzi and Franchi 1983). As the child gets older the neurones from the two eyes develop inhibitory interactions as part of the growth of binocularity. These inhibitory interactions reduce the level of binocular facilitation of the VEP. Many people with abnormal binocularity have an unusually large degree of interocular suppression, and it is argued that lack of binocular facilitation of the VEP is due to abnormal interocular suppression rather than to loss of binocular cells.

Most infants by the age of 4 $\frac{1}{2}$ months show VEPs specifically related to the presentation of random-dot stereograms (Petrig et al. 1981). In a test of general binocularity but not specifically stereopsis, VEPs were recorded from the scalps of infants between the ages of 4 and 36 weeks while they were shown random-dot patterns alternating at a rate of 1.9 Hz between being correlated and uncorrelated in the two eyes, and a control pattern which alternated between two uncorrelated states. The VEPs of most infants under 2 months of age showed the same response to the test as to the control stimulus, but by the third month all infants, except one with a strabismus, showed a distinct time-locked response to the test stimulus but not to the control stimulus (Braddick et al. 1980). A similar procedure was used in a longitudinal study, in which the median age for the first evidence of binocularity was 91 days (Braddick et al. 1983).

15.2.3 Development of vergence eye movements

Using ultrasound imaging it is possible to observe eye movements in the human foetus between 16 and 42 weeks of gestational age. A variety of slow and fast eye movements has been observed. After 30 weeks, bursts of synchronous and conjugate rapid eye movements were seen in several foetuses (Birnholz 1981). Vergence eye movements in human infants have been investigated by the corneal reflex method, in which the position of the image of a light reflected by the cornea is measured with respect to the centre of the pupil (Wickelgren 1967). The method is accurate to only about 5°, and indicates the position of the eye's optic axis rather than of the visual axis—the two can be several degrees apart (Slater and Findlay 1975a). Even allowing for this factor, one cannot obtain an accurate calibration of

the instrument since an infant cannot be asked to converge on targets at known distances. However, the method is suitable for detecting changes in convergence as a visual target is moved in depth. Slater and Findlay (1975b) found evidence of visually evoked changes in vergence in human neonates, but the responses were unstable and occurred only within a limited range of target distance.

Aslin (1977) used a photographic method to record vergence movements to a luminous cross as it approached or receded along the midline between 15 and 57 cm from the infant. One-month-old infants showed evidence of vergence in the appropriate direction, but in 3-month-old infants vergence was more likely to occur and was more closely matched to the speed of the target. The ability to correct for a prism placed before one eye was not consistently present until 6 months of age. The position of dark vergence, which represents the position to which the eyes return when not subject to vergence demand, is more convergent in infants than in adults. Thus, the position of dark vergence of infants between 5 and 20 weeks of age was, on average, at a fixation distance of 35 cm, compared with 120 cm for adults (Aslin et al. 1982).

Thorn et al. (1994) measured the development of binocularly in human infants between 2 and 21 weeks of age. Ocular alignment was determined by observing the deviation of the first Purkinje image of a light reflected from the cornea (the Hirschberg test). Prism and cover tests of strabismus cannot be used with young infants. Convergence was determined by visual examination, and binocular fusion by a test of preferential looking between a fusible pair of gratings and a rivalrous pair of gratings. The few infants that were not orthotropic during the first month were exotropic, and almost all infants were orthotropic by the fourth month. Convergence began to show at 6 weeks of age but full convergence did not occur until between the thirteenth and seventeenth week. Infants showed evidence of binocular fusion between the twelfth and sixteenth week, and there was a high correlation between the age of onset of convergence and that of binocular fusion.

The accuracy of accommodation is poor in young infants, largely because of the poor resolution of the infant visual system (Banks 1980). Accommodative vergence has been observed in 2-month-old infants but the magnitude of the response was not measured (Aslin and Jackson 1979). Only a weak contribution of accommodative vergence to vergence in the young infant is to be expected.

Although vergence movements are designed to bring images with large disparities into the range where fine disparities can be detected, infants do not

need to move their eyes to detect coarse disparities. Birch et al. (1983) found that infants over 6 months of age, with fully developed stereoacuity, are insensitive to errors of vergence of up to 1.4°. Children had to reach an average age of 4.1 months before they could distinguish depth in stereograms in which the disparity was allowed to reach 1.4°. From this it was concluded that the development of stereoacuity is limited by the maturation of disparity-detecting neurones and not by maturation of the vergence system. The argument depends on the assumption that the younger children would also tolerate vergence errors of up to 1.4° if the neural system were mature.

In normal adults the pupils constrict more with binocular illumination than with monocular illumination (ten Doesschate and Alpern 1967). Birch and Held (1983) used this fact to investigate the development of binocularly in infants. They found that the pupil responded more to binocular than monocular illumination by the age of 4 months, and the differential response was adult-like by the age of 6 months. However, Shea et al. (1985) found significant levels of binocular luminance summation in the pupillary response of 2-month-old infants and in stereoblind adults. Their data suggest that the development of the pupillary response is independent of the development of stereopsis.

15.2.4 Development of binocular correspondence

The basic pattern of binocular correspondence is laid down before birth. However, long-term experience with small-angle misalignment of the visual axes due to strabismus leads to an adaptive shift in the pattern of correspondence. This so-called anomalous correspondence is discussed in Section 2.4.2. But even when there is no obvious strabismus or anisometropia some flexibility in the pattern of binocular correspondence will be needed to compensate for subclinical differences between the eyes. Even with a stable pattern of binocular correspondence the growing child must constantly recalibrate the way in which disparities are coded into relative depth. This is because the interocular distance increases about 60 per cent from birth to adulthood, with 36 per cent of this increase occurring in the first 6 years (Aslin 1988). A linear rescaling is required since the disparity produced by a given depth interval at a given distance is proportional to the interocular distance (see Section 2.3.1).

The first experimental study of flexibility in binocular correspondence was conducted by Shlaer (1971). He raised kittens with prisms that introduced 2 or 4 prism dioptres of vertical disparity into the

images of the two eyes. At 4 months, binocular cells of the visual cortex were found to have developed a compensatory shift in the vertical alignment of their receptive fields in the two eyes.

The normal visual environment presents us with a persistent asymmetry of the disparity field. We see more outwardly sheared images (top outwards) than inwardly sheared images, since there are more ground surfaces than ceiling surfaces. In adults the vertical corresponding meridians are extorted about 2° with respect to each other when the horizontal meridians are aligned. This relative shearing of the vertical corresponding meridians causes the vertical horopter to be inclined top away (see Section 2.7). It is reasonable to suppose that the shear of the vertical meridians is a developmental adaptation to the predominance of outwardly sheared images. Two lines of evidence favour this hypothesis.

When kittens are exposed to prisms that disjunctively rotate the images in the two eyes through a small angle, the visual system adjusts by altering the orientation tuning of receptive fields so that they correspond with the imposed cyclorotation of the images. Shinkman and Bruce (1977) fitted 1-month-old dark-reared kittens with goggles that produced a total of 16° of torsional misalignment of the two images. After 12 weeks a full complement of cortical binocular cells was found and the preferred orientations of these cells for stimuli presented to each eye in turn were found to be relatively rotated by the amount of the induced optical rotation. Kittens showed incomplete adaptation of orientational selectivity to 24° of torsional misalignment of images (Bruce et al. 1981). Kittens exposed to 32° of misalignment showed a permanent disruption of binocularly and stereopsis (Shinkman et al. 1992). The capacity of cortical cells to accommodate their orientation tuning to imposed image cyclorotation was still present in kittens exposed to prisms after being reared in the dark until the age of 3 months but not in those dark-reared until the age of 4 months. The cortical cells of the latter group of kittens resembled those of visually deprived animals (Shinkman et al. 1983).

Crewther et al. (1980) found very little evidence of compensation of orientation tuning in binocular cells of kittens in which one or both eyes had been surgically rotated about the visual axis soon after birth. However, in most cases, the eyes were rotated more than 16° and surgical modification of the extraocular muscles may be more disruptive than optical rotation of images (see Section 15.10).

Häny and von der Heydt (1982) reared one set of normal kittens in an environment in which visible contours were confined to a floor plane below eye

level and which therefore produced only outwardly sheared images, and another set of kittens in an environment in which contours were confined to a ceiling plane above eye level and which therefore produced only inwardly sheared images. At 4 months of age the binocular cortical cells of the kittens had preferred orientations that differed in the two eyes in accordance with the type of disparity that the kittens had experienced. In another study from the same laboratory, kittens were reared with lenses that magnified each image by 9° along a particular axis. The axes of magnification were set at an angle of ±45° in the left and right eyes. This created gradients of both positional and orientational disparity, which could not be corrected by vergence. At 4 months, the cortical binocular cells of these animals were found to have adjusted the relative positions and orientations of their receptive fields in the two eyes in directions that compensated for the imposed disparities (Dürsteler and von der Heydt 1983).

A normal environment has stimuli with a variety of orientational disparities and these may be detected by binocular cortical cells whose receptive fields in the two eyes vary in their orientational selectivity (see Section 4.6). The results described here could be explained by a preferential survival during development of cortical cells tuned to the average orientational disparity in the visual environment. The other possibility is that the interocular orientation preferences of cortical cells shift to accommodate asymmetrical inputs. In either case it seems that early visual experience helps to shape the pattern of binocular orientational correspondence.

The literature on the development of binocular vision has been reviewed by Aslin and Dumais (1980), Yonas and Owsley (1987), Timney (1988), and Held (1991).

15.3 STEREOANOMALIES

Stereoanomalies with briefly exposed stimuli

Richards (1971b) asked subjects to report whether lines on each side of a fixation cross were in front of, behind, or coplanar with the cross. The lines were presented for 80 ms with disparities of between zero and 4°, while the subject fixated the cross. Some sample results are shown in Figure 15.3. The top figure is the result for a normal observer, the middle figure for a subject who failed to identify uncrossed disparities at above chance, and the bottom figure for one who failed to identify crossed disparities. Subjects also matched the perceived depth of the flashed target with a continuously visible

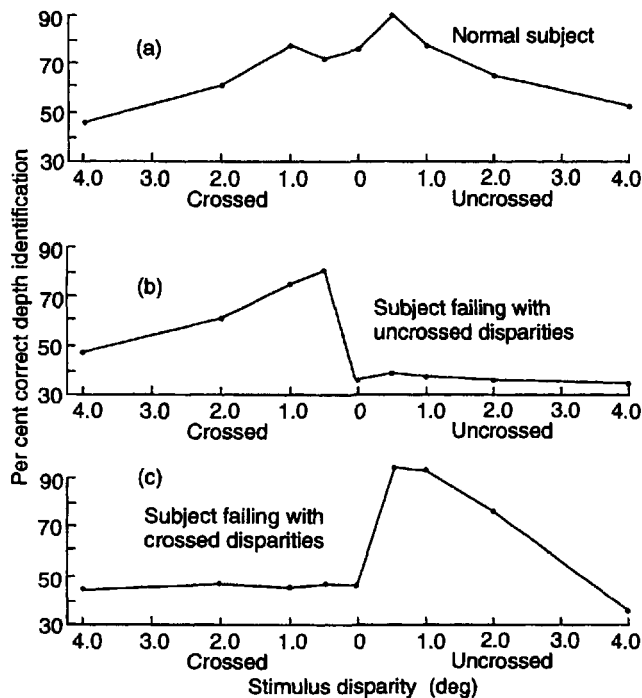


Figure 15.3. Depth judgments and disparity magnitude.
Per-cent correct identification of the depth of two lines relative to a fixation cross as a function of disparity in the lines. The lines were flashed on for 80 ms.
(a) For a normal observer.
(b) For a subject who failed to identify uncrossed disparities.
(c) For a subject who failed to identify crossed disparities. (From Richards 1971.)

stereoscopic probe seen subsequently. For subjects with normal stereoscopic vision, matched depth at first increased with increasing crossed or uncrossed disparity and then decreased as disparity increased toward 4°. The stereoanomalous subjects perceived either all crossed or all uncrossed disparities at the same depth as they perceived the zero-disparity stimulus. Thus, although the stereoanomalous subjects reported depth in their anomalous disparity region, they had the same sensation from a stimulus with zero disparity, presumably by contrast with the stimuli that they could detect normally.

Richards concluded that perceived depth depends on the pooling of inputs from three classes of broadly tuned disparity detectors, one class tuned to crossed disparities, one to uncrossed disparities, and one to zero disparities. He also concluded that some people lack either the crossed or uncrossed detectors and consequently fail to detect either crossed or uncrossed disparities or, having detected them, fail to distinguish between them. Richards estimated that up to about 30 per cent of the population have a stereoanomaly of this type (Richards 1970). We will see in what follows that the idea that

stereoanomalous subjects lack one or other class of disparity detector must be modified, since it has been found that the anomaly depends on the test used to diagnose it.

Luminance contrast and stereoanomalies

Stereoanomalies can be specific to the sign of luminance contrast in the visual target. Thus, observers who confuse either crossed- or uncrossed disparity stimuli with zero-disparity stimuli, reverse the sign of their confusion when the stimulus is changed from dark bars on a light background to light bars on a dark background (Richards 1973). This is hard to reconcile with the idea of a simple loss of either crossed or uncrossed disparity detectors.

Location- and motion-specific stereoanomalies

Stereoanomalies can also be specific to particular locations in the visual field. Richards and Regan (1973) developed stereo perimeter tests to investigate this question. In one test, a luminous vertical bar oscillating in depth at 2 Hz between 0 and 0.4° of crossed or uncrossed disparity was slowly moved into different positions in the visual field while the subject fixated a stationary point. The subject was deemed to have stereoscopic vision in a given region if the target was seen to move in depth rather than from side to side. In a second test, a target with $\pm 0.4^\circ$ of disparity was flashed on for 100 ms at different positions. A subject with apparently normal vision and stereopsis was studied in detail. With the moving target he had large areas in the visual field within which uncrossed disparities could not be detected and other regions in which crossed disparities could not be detected. However, the flashed target revealed almost no visual aberrations and neither did the moving target when it was made to flash on and off. Other subjects were found to behave in a similar fashion.

It looks as though the stereo anomalies with the moving target were due to differential suppression of one or other image rather than to the absence of one or other pool of disparity-detectors. But the main conclusion of the study was that crossed and uncrossed disparities are processed by distinct visual mechanisms. We saw in Section 4.4 that recent physiological evidence confirms this idea.

We have just seen that people with normal stereoscopic acuity for stationary targets may be blind to motion in depth (see also Section 13.2.4). The opposite seems also to be true. About half of a group of people classified as stereoanomalous with static displays could judge depth in moving displays, such as a rotating cylinder, in which depth was defined by disparity (Rouse et al. 1989).

Stereoanomalies with short and long exposures

Other investigators have reported that people classified as stereoanomalous when tested with brief exposure perform normally when tested with a longer exposure. For instance, Patterson and Fox (1984b) found that about 30 per cent of subjects could not detect 1° of crossed- or uncrossed disparity-depth in a dynamic random-dot stereogram exposed for 167 ms. However, all but one of the subjects performed perfectly when allowed to look at the stereograms for as long as they wished. Newhouse and Uttal (1982) obtained similar results. The stereoanomalous subjects may have succeeded with long exposure by simply converging or diverging the eyes and thus converting a disparity that they could not detect into one that they could detect. However, the subjects also performed perfectly when a stereo target was impressed on the eyes as an afterimage. It was concluded that the stereoanomalies revealed with flashed random-dot stereograms arise because subjects require longer to process disparity information, and not because they lack a basic stereo mechanism. Foley and Richards (1974) trained a stereoanomalous subject to discriminate between crossed disparities, uncrossed disparities, and zero disparity with stimuli presented for as long as the subject wished. After this training, the subject's stereoanomaly revealed with a flashed target was considerably reduced. The role of learning in the perception of depth in random-dot stereograms was discussed in Section 5.11.

15.4 BRAIN DAMAGE AND STEREOPSIS

Complete loss of stereoscopic vision and depth perception is not a common symptom of brain damage, but there have been several reports of patients for whom the world appeared to lie in a single frontal plane, like a picture (Riddoch 1917; Homes and Horrax 1919; Critchley 1953). Lesions of the right parietal lobe have been implicated in this disorder. Many patients with focal lesions of the cerebral hemispheres have some impairment of stereopsis although they do not notice the defect in their ordinary lives. Stereoscopic defects are commonly associated with other visual defects (Danta et al. 1978).

Cowey (1985) trained monkeys to discriminate the relative depths of two black rods. A tenfold increase in the stereoscopic threshold occurred after the part of V1 corresponding to the central 5° of the visual field was removed, and a variable but smaller increase occurred after removal of a similar region in V2. This effect of damage to the central visual field is to be expected since the test was one of fine stereopsis. A 50 per cent increase in the stereo threshold

after removal of the inferotemporal cortex was unexpected. Performance on a test of stereopsis that involved detecting a depth plane with a large disparity in a random-dot stereogram was found to be unaffected by removal of the central 5° of V1. Foveal vision is clearly not essential for this task. Removal of the central area of V2 or of most of the inferotemporal cortex slightly impaired performance on this test. Monkeys were unable to perform the task at all after extensive damage to the rostral superior colliculus and pretectum, which are subcortical regions associated with the control of eye movements. Subsequent tests revealed that these monkeys suffered from diplopia, which suggests that they were unable to control vergence. After removal of areas 17 and 18, cats lost their ability to discriminate depth based on disparity even though other abilities such as offset acuity and brightness discrimination survived (Ptito et al. 1992).

It is generally believed that the right hemisphere, which processes inputs from the left hemifield, is specialized for visuospatial tasks, such as visual localization, judgments of orientation, and depth perception, whereas the left hemisphere is specialized for language (Kimura and Durnford 1974; P. Milner 1974; Gazzaniga and LeDoux 1978). However, Birkmayer (1951) reported that of 70 brain-injured patients with impaired depth perception, 76 per cent had left-sided damage, and Rothstein and Sacks (1972) reported that patients with left parietal lobe lesions showed a greater stereoscopic deficit on a standard Titmus test than those with lesions in the right parietal lobe. Lehmann and Wälchli (1975) also used the Titmus test but failed to find differential effects of left and right hemisphere damage in neurological patients. The Titmus test does not test for disparities of less than about 40 arcsec.

More recently, Danta et al. (1978) found that stereoscopic defects in a sample of 54 patients were more likely to be associated with damage to the right temporal, parietal, and occipital lobes than with damage to these regions in the left hemisphere (see also Ross 1983). Lesions in the left hemisphere associated with stereoscopic deficits were found to lie preferentially in the frontal and temporal lobes. The question of the lateralization of stereoscopic defects as assessed by standard tests of stereopsis is far from settled. We now consider the lateralization of defects assessed by random-dot stereograms.

Several investigators have reported that patients with disease of the right cerebral hemisphere (serving the left visual field) more often fail to perceive depth in random-dot stereograms than do normal subjects or patients with disease of the left

hemisphere (Carmon and Bechtoldt 1969; Benton and Hécaen 1970; Hamsher 1978). In the last two studies it was found that patients with right and left hemisphere disease performed at the same level on standard stereoscopic tests in which the forms were visible monocularly. However, Ross (1983) found both types of stereopsis to be equally affected by right hemisphere damage, and Lehmann and Julesz (1978) found no difference between the visual evoked potentials recorded from the left hemisphere and those recorded from the right hemisphere when subjects were presented with random-dot stereograms (see Section 4.8.3).

It has been reported that normal subjects are better able to identify a cyclopean form in a random-dot stereogram when it is presented for 120 ms in the left visual field (right hemisphere) than when it is presented in the right visual field (Durnford and Kimura 1971). However, several cyclopean shapes were presented, and shape identification rather than stereoscopic vision may have been the factor responsible for the field asymmetry. Julesz et al. (1976a) used only one cyclopean shape in a dynamic random-dot stereogram and found no hemifield differences in the stimulus-duration threshold for detection of depth or in the limiting eccentricity at which a stereo target could be detected. Pitblado (1979) obtained a left-field (right hemisphere) superiority in the recognition of cyclopean shapes when the dots comprising the stereogram were small, but with large dots, performance was better in the right visual field projecting to the left hemisphere.

It has been proposed that stereopsis based on cyclopean forms in random-dot stereograms is more localized in the right hemisphere and stereopsis based on regular stereograms, in which the forms are visible in the monocular field, are more localized in the left hemisphere. Even if this were true, the crucial factor may be the relative spatial frequencies of the stimuli rather than whether or not they are cyclopean. Another possibility is that hemisphere-specific deficits reported with random-dot stereograms are due to aspects of the task other than stereopsis, such as form perception or reaction time. One way to test this would be to see whether such patients can see cyclopean shapes that are not defined by horizontal disparities (they could be defined by texture rivalry or vertical disparities) and whether they can see depth in random-dot stereograms in which the outlines of the forms are provided in the monocular images. The clinical category of hemisphere damage does not allow one to draw conclusions about the specific site of a deficit, and there is the problem of being sure that clinical samples are matched for potentially important factors such as age, intelligence, and motivation.

15.5 EFFECTS OF DARK REARING

Cats and monkeys reared in total darkness show no obvious changes in the number, size, or staining characteristics of cells in either the retina or LGN (Chow 1973; Hendrickson and Boothe 1976). However, dark rearing disrupts the normal development of cells in the visual cortex. During the first 3 or 4 weeks after birth, normal and dark-reared kittens have a similar number of cortical cells tuned to orientation and movement, and both possess binocular cells, of which some are tuned to disparity. After that time, cells tuned to orientation, motion, and disparity increase in number and stimulus specificity in normal animals, whereas, in dark-reared animals, the number of tuned cells decreases and the number of cells with nonspecific tuning increases (Pettigrew et al. 1968; Pettigrew 1974; Buisseret and Imbert 1976; Braastad and Heggelund 1985).

It thus seems that cortical cells of cats develop some stimulus specificity in the first few weeks of life in the absence of visual experience, but visual experience is required for the maintenance and further development of stimulus specificity, especially of specificity to high spatial frequencies and fine binocular disparity. Cells in area 18 also lose their stimulus specificity with dark rearing (Singer and Tretter 1976) and there are far fewer complex cells in area 18 of dark-reared cats than of normal animals (Blakemore and Price 1987b). A substantial number of cortical cells in the binocularly deprived kitten become unresponsive, weakly responsive, or respond erratically. The cells apparently do not die or lose their synaptic connections, since they recover their responsiveness when an excitatory amino acid is applied locally (Ramoa et al. 1987).

Cats dark reared for the first 6 months retained some cortical cells that responded to stimulation in either eye. However, the cats were permanently stereoblind. The cortical cells of kittens dark reared until 5 weeks of age rapidly regained some stimulus specificity when sight was restored (Imbert and Buisseret 1975) and they recovered some stimulus specificity for orientation, although not for direction of motion, even after 12 months of dark rearing (Cynader et al. 1976).

Monkeys raised for 7 weeks with both eyelids sutured had reduced contrast sensitivity in both eyes, but the deficit was much less than that produced in the occluded eye of a monkey raised with only one eye closed. Sensitivity to visual flicker and spectral sensitivity were not much affected by bilateral eye sutures. None of the binocularly deprived monkeys had binocular vision as assessed by

binocular summation of grating detection and detection of depth in a random-dot stereogram (Harwerth et al. 1991). Similar symptoms have been noted in humans after removal of bilateral cataracts at an early age (Mioche and Perenin 1986).

Dark-reared cats have profound deficits in visually guided behaviour, including obstacle avoidance, paw placing, directed jumping, depth perception, and visually elicited blinking. After the eyes have been opened, visually mediated behaviour gradually recovers (Van Hof-van Duin 1976a; Timney et al. 1978; Mitchell and Timney 1982). However, dark-reared cats remain deficient in learning complex visual discriminations, and their visual acuity does not return to a normal level (Smith et al. 1980). Dark-reared monkeys showed very rapid recovery in a forced-choice preferential looking task, but recovery was much slower in tasks requiring visually coordinated behaviour, such as paw placement or obstacle avoidance (Regal et al. 1976). The initial blindness may reflect a general unresponsiveness to visual stimulation rather than a complete loss of visual sensitivity.

Cats raised with bilateral suture of the eyelids show a more severe disruption of behaviour and less evidence of recovery after sight is restored than cats raised in darkness (Mower et al. 1982). Lid suturing allows diffuse light to enter the eyes and this must be responsible for the greater severity and permanence of deficits. We will see in the following that dark-reared cats have a prolonged period of cortical plasticity compared with normally reared cats. Visual inputs must accelerate the termination of the phase of cortical plasticity in the young animal, even when the visual inputs consist only of diffuse light. Children with congenital cataract in both eyes fail standard clinical tests of stereopsis after the cataracts have been removed, even when they are removed after only a few months. However, some of these children show evidence of coarse stereopsis when allowance is made for their amblyopia by testing with large stimuli and when allowance is made for strabismus by optically aligning the images (Tytla et al. 1993).

15.6 MONOCULAR DEPRIVATION

When cats or primates are subjected to a disruption of normal visual experience in one eye during a critical period in early life, the binocular cells of the visual cortex develop abnormal patterns of ocular dominance, and stereopsis is deficient or lost. Monocular deprivation may be experimentally induced by any of the following means:

1. Occlusion of one eye by placing an occluder over the cornea or suturing the eyelids. With lid suturing the retina is illuminated by diffuse light.
2. Creation of an artificial strabismus by surgically deviating an eye.
3. Optical deviation of the input to one or both eyes by prisms.
4. Optical induction of aniseikonia by securing a magnifying lens in front of one eye.
5. Immobilization of an eye by induction of muscle paralysis.

These experimental procedures are designed to mimic naturally occurring visual amblyopia in humans caused by disorders such as strabismus, anisometropia, aphakia, and cataracts.

15.6.1 Subcortical effects of monocular deprivation

Retinal effects

Retinal ganglion cells seem to be anatomically and functionally normal in eyes of cats that have been monocularly occluded or subjected to induced strabismus for as long as 18 months (Sherman and Stone 1973; Cleland et al. 1980; Cleland et al. 1982). Long-term deprivation does not affect the electroretinogram, that is, the flash- or pattern-evoked electrical response from the retina (Baro et al. 1990).

Physiological effects in the LGN

The effects of postnatal monocular occlusion or imposed strabismus are evident in the lateral geniculate nucleus, although not in such a severe form as in the visual cortex. The laminae into which inputs from the two eyes segregate are present in the LGN at birth (see Section 15.1.4). Their development depends on competitive interactions between retinogeniculate projections from the two eyes before birth. Rakic (1981) removed one eye from monkey foetuses in the second and third month of gestation. One year after birth the LGN lacked the normal laminar structure and the visual cortex lacked ocular-dominance columns.

In the cat, the somata of relay cells in laminae of the LGN serving an eye that has been occluded for some months after birth are considerably smaller than those serving the normal eye (Wiesel and Hubel 1963b; Hickey et al. 1977). Similar effects occur in monocularly deprived monkeys (Noorden and Middleditch 1975) and have been shown in the postmortem analysis of the LGN of a human strabismic amblyope (Noorden and Crawford 1992). In addition, relay cells in the LGN show evidence of reduced metabolic activity, as reflected in the decreased level of the metabolic enzyme, cytochrome

oxidase (Wong-Riley 1979b). The reduction in cell size has been reported to be about 20 per cent for LGN relay cells projecting to area 17 of the cat and up to 60 per cent for those projecting to area 18 (Garey and Blakemore 1977).

These effects are postsynaptic because there is no change in the size of presynaptic terminals. Relay cells in the LGN that receive inputs from the monocular crescent of the deprived eye retain their normal size and metabolic activity, as do relay cells for which the corresponding retinal region of the nonoccluded eye has been lesioned (Guillery 1972; Wong-Riley 1979b). Cats and monkeys reared with both eyes in total darkness show no obvious changes in the number, size, or staining characteristics of LGN cells (Chow 1973; Hendrickson and Boothe 1976). These facts demonstrate that the reduced size of LGN relay cells in monocularly deprived animals is due to competitive interactions with inputs from the normal eye. Changes in the size of cells in the LGN are closely correlated with changes in the ocular-dominance columns of the visual cortex when these are measured in the same animals (Vital-Durand et al. 1978). As long as the eye has not been occluded for more than about 6 weeks, the cells in the LGN recover to full size soon after the occlusion is switched to the other eye (Dürsteler et al. 1976). Cells in LGN laminae receiving inputs from an eye with strabismus-induced amblyopia are also reduced in size in proportion to the degree of amblyopia (Tremain and Ikeda 1982). Action potentials still arise in the retina of an occluded eye, and it seems that these play a part in maintaining some normality of function in the LGN, since LGN development in the cat is severely disturbed when these action potentials are abolished for several weeks by the application of tetrodotoxin (Archer et al. 1982).

Functional effects in the LGN

There is some controversy regarding the effects of monocular deprivation on the functional properties of cells in the LGN. The spatial contrast sensitivity of X cells in layers of the LGN receiving inputs from the strabismic eye of a cat has been found to be lowered, but only for gratings with high spatial frequency (Jones et al. 1984a; Chino et al. 1994). A similar defect was reported in cats raised with monocular occlusion (Maffei and Fiorentini 1976; Lehmkuhle et al. 1980). The spatial and temporal sensitivities of Y cells have been found to be normal in deprived laminae of the cat LGN, although several investigators have found a reduced number of Y cells or a reduction in Y-cell synapses in LGN laminae serving the deprived eye (Sireteanu and Hoffmann 1979; Mangel et al. 1983; Garraghty et al.

1989). Other investigators have found that the relative numbers and spatial properties of both X and Y cells are unaffected by monocular occlusion in the cat (Shapley and So 1980; Derrington and Hawken 1981) and in the monkey (Blakemore and Vital-Durand 1986a).

Effects on the superior colliculus

In mammals, the superior colliculus is a paired structure in the midbrain involved in coding the location of visual objects for the purpose of guiding saccadic eye movements. It is the homologue of the optic tectum of lower vertebrates. The cells in the superior colliculus receive direct visual inputs as well as inputs routed through the visual cortex. They have large, nonspecific receptive fields and many are binocular. Unlike cells in the visual cortex many cells in the superior colliculus retain their binocularity in cats reared with artificial strabismus or alternating occlusion of the eyes. In strabismic cats, however, the cells in the superior colliculus contralateral to the normal eye are heavily dominated by that eye. But this dominance of the normal eye was not apparent in cats that had been forced to use the deviating eye (Gordon and Presson 1977).

15.6.2 Cortical effects of monocular deprivation

In one of the first experimental studies of the effects of abnormal visual experience on the development of the visual cortex, Hubel and Wiesel (1965) reared kittens from birth to the age of 3 months or more with a surgically induced divergent deviation of one eye. This permanently reduced the number of binocular cortical cells responding to the strabismic eye to 20 per cent compared with 80 per cent for a normal eye. The binocular cells that would have responded to the strabismic eye were functionally converted to monocular cells driven only by the normal eye. Thus the ocular-dominance columns of the normal eye expand at the expense of those of the deprived eye. Essentially the same results have been noted in monkeys subjected to early surgically induced strabismus (Baker et al. 1974). Similar results also occurred in cats reared with prisms that disrupted the alignment of the visual axes (Bennett et al. 1980). Most cells in area 18 of strabismic cats also lose their binocularity, although binocular cells sensitive to motion in depth have been found to survive in area 18 (Cynader et al. 1984). In cats, convergent strabismus has been reported to have a greater effect on cortical cells than divergent strabismus (Yinon et al. 1975).

Rearing kittens for 3 months with one eye occluded rather than deviated also severely reduces

the number of cortical cells responding to the occluded eye and renders the cat virtually blind in that eye although, as we will see later, complete or partial recovery may occur if sight is restored at an early enough stage (Wiesel and Hubel 1963a; Blakemore 1976). The binocularity of cells in the cat's suprasylvian visual area was also disrupted (Spear and Tong 1980) and cortical inputs to the superior colliculus from the deprived eye were absent (Hoffmann and Sherman 1974). Stimulation of a deprived eye failed to evoke potentials in electrodes applied to the surface of the scalp (Baro et al. 1990). Surviving cells driven by the deviating eye of strabismic cats showed reduced sensitivity to high spatial frequencies, loss of contrast sensitivity, broadened orientation tuning, and loss of temporal resolution. However, cells driven by the normal eye also showed some loss in contrast sensitivity, which may have been due to persistent blur of the retinal image arising from the instability of gaze (Chino et al. 1983). Behavioural tests revealed some loss of contrast sensitivity in the nondeviating eye of strabismic cats (Holopigian and Blake 1983) and strabismic humans (Levi and Klein 1985).

Kittens raised with one eye occluded and the other exposed to only vertical lines possess binocular cells with an orientation preference for vertical lines. Cells preferring other orientations are driven by only the eye that was occluded (Rauschecker and Singer 1981).

Monkeys raised with one eye occluded for 3 weeks after birth also show a contraction of ocular-dominance columns for the deprived eye and an expansion of those for the seeing eye (LeVay et al. 1980). The change in relative sizes of the ocular-dominance columns can be seen in the autoradiograph of the visual cortex of a monocularly deprived monkey (Des Rosiers et al. 1978). The change in ocular dominance does not involve any significant change in the overall density of neurones or of synapses within cortical layers (O'Kusky and Colonnier 1982). In the striate cortex of the monkey, monocular deprivation also produces a severe reduction in the size of cytochrome-oxidase blobs dominated by the deprived eye (Trusk et al. 1990).

The following lines of evidence suggest that the normal development of binocular cells depends on balanced competitive interactions between simultaneous inputs from the two eyes and that effective binocularity is disrupted if this interaction is unduly weighted in favour of one eye. The evidence also suggests that changes in ocular dominance of cortical cells involve the balance between pre- and post-synaptic activity, that is, activity occurring before and after binocular axons have synapsed onto

cortical cells in layer 4. Inputs from an eye receiving patterned visual inputs gain a competitive advantage in innervating binocular cells over those from a closed or deviated eye. Finally, the following evidence suggests that intracortical inhibition plays a crucial, although not exclusive, role in this process.

Binocular and monocular deprivation compared

Cats reared in complete darkness retain a substantial number of cortical cells responsive to stimulation of either eye (Wiesel and Hubel 1965a, 1965b; Blakemore and Van Sluyters 1975; Kaye et al. 1982). This demonstrates that the strong shift of ocular dominance produced by monocular occlusion is not due simply to disuse but rather to competitive suppression of inputs from the deprived eye by inputs from the normal eye. However, it does not indicate where that competitive interaction occurs.

Removal of the nondeprived eye aids recovery

After a period of monocular deprivation, recovery of function in the occluded eye is more rapid if the good eye is removed rather than simply occluded. This recovery of function in the previously occluded eye involves an increase in the number of cortical cells responding to stimulation of that eye and some restoration of tuning functions of their receptive fields. It does not involve a restoration of binocular cells. Thus, in kittens after 4 weeks of monocular occlusion, the proportion of cortical cells responding to stimulation of the occluded eye increased to near normal levels within a few hours after enucleation of the nonoccluded eye. However, the properties of the receptive fields of these binocular cells remained abnormal. Even after 92 weeks of monocular occlusion, 22 to 40 per cent of cortical cells began to respond to the occluded eye after removal of the good eye (Kratz et al. 1976; Smith et al. 1978; Spear et al. 1980). Blakemore and Hawken (1982) confirmed this effect but found it only if the kitten had a period of binocular vision before one eye was occluded.

Recovery of a previously occluded eye after enucleation of the good eye takes only hours whereas recovery after switching the occluder to the other eye takes days, as we will see later. It seems that removing the eye removes its inhibitory influences on cortical cells and allows dormant excitatory inputs from the deprived eye to recover. However, recovery for most cells is not immediate, as it would be if it involved only a simple removal of inhibitory impulses from the good eye. Furthermore, temporarily pressure blinding the good eye restored input to only a few cortical cells (Blakemore et al. 1982), although it has been claimed that this procedure works only when afferents from the extraocular

muscles are also paralyzed (Crewther et al. 1978). Removal of all inputs from the good eye must allow some restorative processes to occur in the weakened, but still present, excitatory inputs from the deprived eye. Some of these restorative processes occur almost immediately; others take some time. We will see later that restoration of physiological functions in a deprived eye after removal of the good eye is accompanied by some restoration of visual function.

Inhibition from a deprived eye

Singer (1977) found that most cortical cells of a monocularly deprived cat did not respond to electrical stimulation of the optic nerve of the deprived eye, except for some responses with unusually long latency. However, when both eyes were stimulated, most cells showed short-latency inhibitory effects that were shown to depend on intracortical circuits. Freeman and Ohzawa (1988) found that, although there is a drastic reduction in the number of cortical cells responding to direct stimulation of a deprived eye after 8 weeks of monocular deprivation, a substantial proportion of cortical cells displayed evidence of both excitatory and suppressive inputs from the deprived eye when both eyes were stimulated simultaneously by a large phase-varying grating. Animals deprived of vision in one eye for more than a year had very few cortical cells that betrayed any evidence of inputs from the deprived eye.

Intracortical inhibition and cortical plasticity

Intracortical inhibition is mediated by the neurotransmitter GABA, the effects of which can be removed by application of its antagonist, bicuculline. When bicuculline was applied to the visual cortex of a monocularly deprived cat, about 40 per cent of cortical cells tested began to respond again to stimulation of the deprived eye although not to the point of gaining dominance over binocular cells (Burchfiel and Duffy 1981; Sillito et al. 1981). Blakemore et al. (1982) argued that part but not all of this effect could be due to the fact that bicuculline raises the general level of excitability of cortical cells to weak excitatory inputs. Thus, GABAergic intracortical inhibition contributes to adaptive responses of binocular cells to monocular deprivation, but perhaps changes in excitatory inputs or forms of intracortical inhibition mediated by other neurotransmitters are also involved. We saw in Section 15.1.5 that the neurotransmitter NMDA is also involved in the development of binocular cells and in neural plasticity in general.

Plasticity after blockage of postsynaptic activity

A shift in ocular dominance to the open eye during monocular deprivation does not occur for regions of

the visual cortex in which postsynaptic activity has been blocked by agents such as glutamate, tetrodotoxin, or muscimol (Shaw and Cynader 1984; Reiter et al. 1986). Reiter and Stryker (1988) found that cortical cells become more responsive to inputs from the closed eye than to those from the open eye when postsynaptic activity is blocked. Thus, the crucial changes during monocular deprivation are cortical and depend on the balance between pre- and postsynaptic activity (Hata and Stryker 1994). No shift in ocular dominance in monocularly deprived young rats occurred when deprivation was accompanied by intraventricular injections of one of the neurotrophins, known as the nerve growth factor (NGF) (Berardi et al. 1993). For a review of NGF receptors, see Meakin and Shooter (1992).

It is believed that NGF is produced in postsynaptic cells of the visual system during the critical period. The neurones from the two eyes compete for a limited amount of growth factor, and only those receiving a sufficient amount are maintained. Injection of extra growth factor allows all synapses to be maintained in the monocularly deprived animal. Furthermore, injection of NGF facilitates recovery of binocularity following a period of monocular deprivation (Carmignoto et al. 1993).

Noradrenaline and cortical plasticity

Catecholamines, particularly noradrenaline, have also been implicated in the control of neural plasticity in the developing cortex. Noradrenergic axons are among the first to innervate the cerebral cortex, and reach peak levels in the second postnatal month. In the adult brain, noradrenergic axons originating in the locus coeruleus seem to provide a diffuse, nonspecific innervation of the central nervous system (Levitt and Moore 1979). After the cortex was depleted of catecholamines by intraventricular injection of 6-hydroxydopamine, monocularly deprived kittens retained the normal proportion of binocular cells in area 17 and the cells of the seeing eye did not become dominant (Kasamatsu and Pettigrew 1979). This suggests that catecholamines are required for cortical plasticity during the critical developmental period. However, intraventricular injection of 6-hydroxydopamine produces severe side effects, including epileptic seizures. The locus coeruleus is a major source of catecholamines, and injection of 6-hydroxydopamine into this structure also caused a depletion of cortical noradrenaline and an associated loss of cortical plasticity. Electrical stimulation of the locus coeruleus in combination with deprivation led to a loss of binocular cells in adult cats. In other words, induced release of noradrenaline restored plasticity in the visual cortex of cats after the critical

period (Kasamatsu et al. 1985). Intracortical perfusion of noradrenaline had the same effect (Kasamatsu et al. 1979). Cortical cells showed a shift in ocular dominance in anaesthetized kittens exposed to monocular stimulation for 20 hours, but only when the cortex was directly infused with noradrenaline (Imamura and Kasamatsu 1988).

Others failed to find any loss of cortical plasticity in monocularly deprived kittens after depletion of cortical noradrenaline (Bear and Daniels 1983; Frégnac and Imbert 1984; Daw et al. 1985). In these experiments, noradrenaline was depleted by lesions of the locus coeruleus or by neonatal injection of 6-hydroxydopamine, rather than by injection at the time of monocular deprivation. In another experiment, no differences occurred in the short-term effects of noradrenaline on responses in the visual cortices of kittens and adult cats (Videen et al. 1984).

Bear and Singer (1986) seem to have resolved this conflicting evidence. They found that depletion of both noradrenaline and acetylcholine led to a loss of cortical plasticity, even though loss of either neurotransmitter alone had no effect. They also cited other evidence which suggests that the loss of cortical plasticity reported in the earlier studies occurred because local application of 6-hydroxydopamine depletes both norepinephrine and acetylcholine, rather than because of a specific depletion of noradrenaline.

All this evidence suggests that changes in patterns of postsynaptic intracortical excitation and inhibition play a dominant role in cortical plasticity. There is also evidence of a loss of geniculocortical afferents from a deprived eye (Thorpe and Blakemore 1975) and attenuation of responses of LGN relay cells serving the deprived eye presumably has some effect on the changes in ocular dominance.

15.6.3 Effects of binocular dissociation

Continued exposure of kittens to prisms that completely dissociate the images in the two eyes also leads to loss of binocular cells (Blakemore et al. 1975; Smith et al. 1979). Similar effects have been reported in the monkey (Crawford and Noorden 1979). Rearing cats with both eyes occluded but with one receiving modulated light through the closed lid did not induce a shift of ocular dominance to the stimulated eye (Singer et al. 1977). It seems that only binocular differences in exposure to patterned stimuli induce changes in ocular dominance. When both eyes receive patterned inputs that are temporally or spatially dissociated, there is no change in ocular dominance but there is a loss of binocular cells and stereopsis fails to develop.

Temporal dissociation of visual inputs

One way to dissociate visual inputs is to reverse the occluder between the eyes of the kitten on alternate days so that the two eyes see the same stimulus but not at the same time (Hubel and Wiesel 1965; Blakemore 1976). These procedures affect both eyes equally and, although they induce stereoblindness, they do not lead to loss of visual acuity in either eye or to an imbalance in the number of cells responding to each eye (Blake and Hirsch 1975).

Tieman et al. (1983) occluded each eye of kittens for a variable proportion of each day until they were 4 months old. In one group of animals the occluder was placed on each eye for the same length of time each day. In another group, one eye was occluded for twice as long as the other and in a third group one eye was occluded for eight times as long as the other. All groups showed a severe loss of binocular cortical cells. The greater the imbalance of eye exposure the higher the percentage of cells in the visual cortex that responded only to the more experienced eye. The cortical cells of kittens with a balanced input had relatively normal receptive fields. Cells responding to the less experienced eye showed a poorer response to visual motion, were more poorly tuned to orientation, and had smaller receptive fields than cells responding to the more experienced eye. The deficits were most pronounced in the hemisphere ipsilateral to the less experienced eye, that is, for inputs from the temporal hemiretina.

Visual inputs from the two eyes do not have to be precisely synchronous for normal development. Blasdel and Pettigrew (1979) found that cats developed normally if stimuli to the two eyes were alternated more frequently than 10 Hz. In this experiment, the animals were restrained during visual exposure. When kittens were allowed to move about while wearing shutters which alternately occluded the eyes, exposure periods in excess of 0.5 s disrupted the development of depth discrimination and led to a reduction in the number of binocular cells in the visual cortex (Altmann et al. 1987).

Spatial dissociation of visual inputs

Monkeys seeing through base-in prisms that completely dissociate the images in the two eyes from age 30 to 60 days lost almost all binocular cells in the visual cortex and had no stereopsis (Crawford and Noorden 1980; Crawford et al. 1983). These deficits were still present 3 years after the prisms were removed (Crawford et al. 1984). Since this treatment affected both eyes equally, there was no amblyopia nor strabismus. Three monkeys were raised with 27-dioptre (30°) base-in prisms (13.5 dioptres on each eye) in a cylinder lined with vertical stripes

(Noorden and Crawford 1981). Disruption of cortical binocular vision was as severe in these monkeys as in those raised with the same prisms but in a normal visual environment. It was expected that the repetitive pattern of stripes would have provided sufficient fusible stimuli to allow binocular cells to develop. However, a 13.5 dioptre prism introduces a nonlinear prismatic displacement and severe curvature of vertical lines and of horizontal lines above and below the horizon. These secondary distortions would have been opposite in the two eyes and would have prevented fusion. Cats reared with binocular lid closure but with temporally modulated diffuse light presented through the closed lid of one eye did not develop greater ocular dominance for that eye (Wilson and Sherman 1977a).

All these forms of deprivation have one thing in common; they reduce the frequency with which binocular cells are activated simultaneously by similarly patterned inputs. Hebb (1949) proposed that the efficiency of synaptic transmission is increased when subsets of presynaptic inputs are correlated (see Section 3.3.2). A corollary of this rule is that synaptic efficiency is lessened when subsets of presynaptic inputs are persistently uncorrelated. Binocular cells in the visual cortex seem to be good examples of the Hebbian model (Clothiaux et al. 1991).

Malach and Van Sluyters (1989) challenged this simple view. They exposed 4-week-old kittens to a 2-day period of monocular deprivation and then allowed them binocular vision, but with the previously deprived eye deviated. These animals showed some recovery of the number of cells driven by the deprived eye, although not to the level attained by animals allowed normal binocular vision. To reconcile these results with the Hebbian model, one would have to say that the degree of correlation between the inputs from misaligned eyes is higher than that between inputs from a closed eye and an open eye. The fact remains that normal binocular vision is required to maintain or restore the full complement of binocular cells.

15.7 AMBLYOPIA

15.7.1 Symptoms and types of amblyopia

Symptoms of amblyopia

When monocular deprivation is maintained for an extended period, the deprived eye manifests a combination of symptoms known as **amblyopia**, literally "blunt vision". This defect has been known for at least 200 years. For instance, Thomas Reid, Professor of Moral Philosophy in Glasgow, reported in 1764

that 20 people with strabismus all had a defect in the sight of one eye. The symptoms of amblyopia include loss of spatial vision as reflected in impaired performance on vernier and other hyperacuity tasks (Levi and Klein 1982a; Bradley and Freeman 1985a; Bedell et al. 1985), reduction in contrast sensitivity, sometimes for all spatial frequencies and sometimes for high spatial frequencies only (Hess and Howell 1977), and loss of grating acuity (Harwerth et al. 1983; Kratz and Lehmkuhle 1983). This set of symptoms may be explained in terms of a loss in contrast sensitivity. Levi and Klein (1985) proposed that the central visual field of strabismic amblyopes, although having the same density of ganglion cells, has fewer cortical processing units devoted to it, so it is spatially undersampled. For some amblyopes the deficit involves visual functions most dependent on the resolution of fine detail. However, when effects of spatial scale are allowed for, amblyopia is not primarily related to retinal locus (Bradley et al. 1985).

There has been some dispute about whether sensitivity to flicker and movement is reduced in amblyopia. Some subjects show normal flicker sensitivity, some show reduced sensitivity, and some show enhanced sensitivity in the amblyopic eye (Manny and Levi 1982). Bradley and Freeman (1985b) concluded that flicker sensitivity can be severely deficient in the amblyopic eye but can appear normal if the stimulus includes those spatial frequencies that are detected normally by the subject. However, they found contrast sensitivity in amblyopia to be highly dependent on spatial frequency, with high spatial frequencies being most affected, but largely independent of temporal frequency. They concluded that losses in temporal sensitivity are a consequence of losses in spatial contrast sensitivity.

Another class of symptoms seems to require a different explanation. These symptoms include confusion between neighbouring stimuli (Pugh 1958), and visual distortions of length and direction (Hess et al. 1978; Bedell and Flom 1981; Fronius and Sireteanu 1989; Lagreze and Sireteanu 1991). Spatial phase discrimination is also defective in amblyopia (see Bennett and Banks 1987; Kiper 1994). For instance, strabismic amblyopes need higher than normal contrasts to discriminate the relative phases of a grating composed of a fundamental and its third harmonic (Lawden et al. 1982). Hess and Field (1994) found evidence of spatial distortions in human strabismic amblyopes. Perhaps the local sign mechanism is spatially scrambled in the amblyopic eye, rather than being undersampled. Thus, in the amblyopic eye there may be uncertainty about both the position of each receptive field and the positions of receptive fields relative to their neighbours.

Eye movements evoked by stimuli presented to an amblyopic eye are also affected. People with strabismic and anisometropic amblyopia show instability of gaze when fixating an object with the affected eye, although gaze is stable for fixation with the normal eye or both eyes (Ciuffreda et al. 1980). Amblyopic eyes show saccadic hypometria, deficits in voluntary pursuit (Schor 1975), and disturbances of optokinetic nystagmus (Schor and Levi 1980; Sparks et al. 1986). Disparity-induced vergence is absent in amblyopia, even though vergence in response to changes in accommodation is normal (Kenyon et al. 1981). Strabismic amblyopes show systematic errors in pointing to visual targets when using their amblyopic eye (Fronius and Sireteanu 1994). Deficits due to monocular deprivation are similar in cats, monkeys, and humans.

These symptoms may be present in mild form in the nondeprived eye (Levi and Klein 1985). Acuity in an amblyopic eye becomes worse in proportion to the illumination level of the good eye (Noorden and Leffler 1966) and vision in an amblyopic eye may be totally suppressed when the other eye is open.

Types of amblyopia

Different types of deprivation give rise to different clinical types of amblyopia. **Deprivation amblyopia** is due to loss of form vision due to a cataract, ptosis, or retinal disorders. **Anisometropic amblyopia** is due to unequal refraction in the two eyes resulting from unequal eye growth (axial anisometropia) or corneal defects. **Strabismic amblyopia** is due to early strabismic misalignment of one eye. Amblyopia is more prevalent among esotropes (inward deviated eye) than among exotropes (outward deviated eye). Three reasons for this have been suggested: (1) exotropia develops more slowly than esotropia, (2) amblyopia does not occur in alternating strabismics and exotropia is more likely to be alternating than unilateral, and (3) in esotropes, the fovea of the deviating eye competes with the dominant temporal hemifield of the other eye whereas in exotropes the fovea competes with the nondominant nasal hemifield of the other eye (Buckley and Seaber 1982; Fahle 1987). This must be reconciled with a report that within the central 20° of the visual field of esotropic amblyopes, acuity in the nasal retina is more reduced than that in the temporal retina (Sireteanu and Fronius 1981). Hemifield differences are discussed in Sections 8.3.4 and 15.1.6. **Meridional amblyopia** is due to an uncorrected astigmatism and affects vision only for line images oriented along the astigmatic axis.

In some forms of amblyopia, hyperacuities, such as vernier acuity, are more severely affected than

resolution acuity or contrast sensitivity. This is true in monocularly deprived cats (Murphy and Mitchell 1991), strabismic monkeys (Kiorpis 1992), and strabismic humans (Levi and Klein 1982b; Levi et al. 1994). In many strabismic children, contrast sensitivity is almost the same in both eyes, but the deviating eye has a severe deficit in hyperacuity tasks and in tasks requiring the recognition of letters presented closely together (Howell et al. 1983). It seems that people with this form of amblyopia have difficulty with tasks requiring the isolation of spatial relationships for pattern identification. They are able to perform tasks in which a stimulus is simply distinguished from its background. In the normal eye, vernier acuity develops more slowly than resolution acuity, and the decline of vernier acuity with increasing eccentricity is much steeper than the decline of resolution acuity. Thus, the centre of an eye with strabismic amblyopia resembles that of the immature normal eye and the periphery that of the normal eye. Note that in strabismics, the image displacement is the same over the whole visual field but affects peripheral vision less because the periphery has larger receptive fields. This might explain why hyperacuity, which is a function of the centra retina, is affected more than resolution acuity in strabismic amblyopes.

In humans with anisometropic amblyopia, deficits on hyperacuity tasks are proportional to losses in resolution and contrast sensitivity (Levi and Klein 1982b; 1983). However, there is conflicting evidence on this point (Kiorpis et al. 1993). In anisometropes with aniseikonia, the differential magnification of the two images increases with eccentricity, so that the foveal region is affected less and the peripheral retina more. In strabismic amblyopia the two regions of the retina are affected equally. This could account for the more balanced loss of hyperacuity and resolution acuity in anisometropes.

When early disruption is applied equally to both eyes, by alternate occlusion or by optical dissociation of the visual inputs by prisms, both eyes develop with normal or near-normal acuity, but there is still a reduced number of binocularly driven cells and loss of stereopsis (Blake and Hirsch 1975).

An extended period of monocular deprivation in the kitten also produces deficits in visually guided paw placement and pattern discrimination and these deficits are more severe the longer the deprivation (Dews and Wiesel 1970). Early monocular occlusion also leads to misalignment of the occluded eye which becomes a permanent strabismus when both eyes are allowed to see (Quick et al. 1989). Strabismus also develops in human infants with congenital monocular cataracts (Robb et al. 1987).

Summary

It can be stated that the spatial distribution of visual defects over the visual field of an affected eye depends on the spatial frequency of the stimulus, the severity of the visual deprivation, and whether the amblyopia is due to strabismus or to anisometropia (Hess and Pointer 1985). It also depends on which half of the visual field is tested. The nasal hemifield (uncrossed cortical inputs) is more susceptible to the effects of deprivation than the temporal hemifield (crossed cortical inputs) in both cats (Sherman 1973; Ikeda and Jacobson 1977; Singer 1978; Bisti and Carmignoto 1986) and humans (Moran and Gordon 1982; Sireteanu and Fronius 1990). This could be a consequence of the fact that nasal hemiretinas develop more rapidly than temporal hemiretinas (see Sections 8.4.4 and 15.1.6 for other evidence of hemifield differences).

Spatial vision in amblyopia has been reviewed by Levi (1991).

15.7.2 Development of amblyopia

Amblyopia and neural competition

We saw in previous sections of this chapter that the loss of binocularity in monocularly deprived animals can be understood as a result of inputs from the two eyes competing for access to cortical cells. Several lines of evidence suggest that the development of amblyopia can be understood in the same way.

1. Visual performance is more severely degraded by monocular deprivation than by binocular deprivation. In the cat, both forms of early deprivation have more severe effects on temporal and spatial resolution than does ablation of area 17 in a normally reared adult cat (Lehmkuhle et al. 1982). At least part of the adverse effect of deprivation in the cat must therefore involve the extrastriate area and possibly other areas. The extrastriate area of the cat receives direct visual inputs (LeVay and Gilbert 1976). Area 17 is involved in the visual performance of dark-reared cats since contrast sensitivity is degraded by ablation of this area in dark-reared cats (Lehmkuhle et al. 1984).

2. A high proportion of cells in the monocular region of the visual cortex have normal receptive-field properties in monocularly deprived animals (Wilson and Sherman 1977b). Inputs to these cells do not have to compete with inputs from the other eye.

3. In the Siamese cat almost all cortical cells are driven only by the contralateral eye, and monocular deprivation has little if any effect on the receptive field properties of cortical cells in these animals (Berman and Payne 1982; Berman et al. 1989).

4. Smith et al. (1992) reared monkeys for between 30 and 90 days with base-in prisms. This caused a severe loss of binocular cells but did not produce a shift in ocular dominance, since cells responsive to either the left or the right eye were retained. This procedure did not induce amblyopia. Also, amblyopia was not produced in a subsequent period in which one eye was sutured, even though amblyopia was produced by monocular suturing applied at the same time in monkeys reared with normal vision. Thus, amblyopia is a result of a shift in ocular dominance, which excludes one eye from access to cortical cells. If an eye retains access to a substantial number of cortical cells, that eye is not amblyopic even though all binocular cells are absent.

5. An accelerated restoration of visual acuity in a previously occluded eye occurs after enucleation of the good eye in the cat (Smith and Holdefer 1985). Monkeys raised for 4 years with induced strabismus showed some recovery of visual function in the deviated eye after the normal eye had been removed. In the deviated eye of one monkey, visual acuity improved from 0.28 to 6.3 c/deg and the sensitivity to flicker increased by 25 Hz over an 11-month period after removal of the non-deviating eye (Harwerth et al. 1986a). The same type of recovery has been noticed in amblyopic humans after the nonamblyopic eye was lost (Vereecken and Brabant 1984).

We can conclude that as a binocular cell develops, the receptive fields in the two eyes become matched in their orientation and motion selectivity, and this matching process depends on visual experience. To allow this to happen, binocular cells must retain a higher degree of plasticity than monocular cells. With monocular deprivation, the matching process is disrupted and inputs from the deprived eye fail to guide the tuning properties of cortical cells.

Recovery from amblyopia

Some recovery from amblyopia in a strabismic eye can be achieved in children after the strabismus is surgically corrected. A traditional treatment for helping an eye recover from amblyopia is to patch the good eye. This is known as reverse patching. The idea is that the weak eye will have more chance to recover when it is not suppressed by the good eye. Evidence from animal studies cited earlier shows that a previously deprived eye recovers to a greater extent when the good eye is covered. However, the evidence from reverse patching in cats suggests that the deprived eye recovers only at the expense of visual deterioration in the good eye (Murphy and Mitchell 1987). A similar reciprocal effect has been observed in children with one eye

patched and there is some risk of children developing a double amblyopia if the good eye is occluded continuously for too long (Odom et al. 1981). Furthermore, recovery of an amblyopic eye when the good eye is patched is unstable. When both eyes of a cat were finally opened after a period of reverse occlusion, the relative performance of the eyes tended to revert to the prepatching state (Mitchell 1988b).

In a recent study, 90 per cent of a group of 64 human strabismic and anisometropic amblyopes under 7 years of age showed some improvement of acuity after various regimes of patching the good eye over a period of about 4 months. About 70 per cent of them showed a doubling of acuity in the amblyopic eye. Children older than 7 years showed less improvement after therapy. However, 67 per cent of all those that improved showed some subsequent loss of acuity in the year following cessation of the therapy (Rutstein and Fuhr 1992). The best regimen for optimal performance of both eyes seems to be one in which the good eye is patched for about half the time, with binocular vision allowed for the other half (Mitchell et al. 1986). In another regimen, known as penalization, the image in the good eye is optically blurred so as to reduce its power to suppress the image in the amblyopic eye (see Fahle 1983).

Strabismic amblyopia has been reviewed by Mitchell (1988c) and the effects of different regimens of occlusion on recovery from early monocular deprivation in kittens and their relevance to humans has been reviewed by Mitchell (1991). Literature on the efficacy of vision therapies for human amblyopia has been reviewed by Garzia (1987).

15.7.3 Amblyopia and binocular vision

Amblyopia and stereopsis

Humans with early strabismus, anisometropia, or uniocular cataract also suffer permanent amblyopia in one eye and partial or complete loss of binocularity (Levi et al. 1979a; Hess et al. 1981). People with severe strabismus fail tests of stereopsis whether or not their strabismus is accompanied by amblyopia (Cooper and Feldman 1978b). Thus, the crucial factor in loss of stereopsis is the strabismus rather than the amblyopia. However, amblyopes with stereoscopic vision show raised contrast thresholds for the detection of depth in random-dot stereograms (Wood et al. 1978). There is usually only a partial loss of binocular cells with anisometropic amblyopia and with strabismus of less than 3°. In these conditions, loss of stereopsis and binocular summation of threshold stimuli is confined to high spatial-frequency stimuli and is thus most evident in the foveal region. Thus for strabismic amblyopes,

stereopsis and binocular summation can be normal for low spatial-frequency stimuli, and the loss is therefore not evident in the visual periphery (Holopigian et al. 1986). The same is true of people with alternating strabismus (Sireteanu 1982).

It was shown in Section 13.2 that stereopsis is not a unitary ability; a person can be blind for motion in depth while possessing normal stereoscopic acuity for static objects, and selective loss of one type of stereopsis can be confined to one area of the retina. Static and motion-in-depth stereopsis are also differentially affected by early strabismus. Kitaoji and Toyama (1987) found that many strabismic subjects in whom the angle of strabismus was between 2 and 5° showed a loss of both static and motion-in-depth stereopsis in the central field but not in the peripheral field. Subjects with squint angles between 6 and 10° had lost static stereoscopic vision in the whole field although many of them had motion-in-depth stereopsis in the peripheral field.

Amblyopia and binocular suppression

People with strabismus do not fuse corresponding images and therefore experience diplopia. They also suffer from a symptom called **confusion** in which the dissimilar images falling on corresponding regions in the two eyes undergo rivalry. Many people with strabismus of early onset overcome these symptoms by suppressing vision in the deviating eye, although they can see with the deviating eye when it alone is open. This is known as **strabismic suppression**. With both eyes open, amblyopes have better access to information presented to their normal eye than to that presented to the amblyopic eye. Also, stimuli presented to the normal eye are not affected by competing stimuli presented to the amblyopic eye. For subjects with normal vision, vernier acuity for a target presented to one eye was found to be degraded by the presence of a similar target with a fixed horizontal offset presented to the other eye. For amblyopes, vernier acuity was not affected when the target was presented to the good eye and the competing target was presented to the amblyopic eye (McKee and Harrad 1993).

It is commonly assumed that strabismic suppression is an extreme form of the suppression observed in normal observers during binocular rivalry (Dale 1982). However, the two forms of suppression differ in several respects. In normal subjects, suppression occurs only between very dissimilar images whereas strabismic suppression also occurs between similar images (Schor 1977). For instance, when normal observers view dichoptic vertical gratings rotated out of alignment by a few degrees they see a fused image of a slanting surface. The gratings appear to

rival only when they are misaligned in the two eyes by many degrees. Strabismics suppress the image in the deviating eye even when the gratings in the two eyes have a very similar orientation. Thus, people with normal vision have a suppression mechanism for strongly dissimilar images and a fusion mechanism for similar images, whereas strabismics have only a rivalry mechanism for both similar and dissimilar images.

Suppression occurring during binocular rivalry causes a greater reduction in the sensitivity of the chromatic mechanism than of the achromatic mechanism (Smith et al. 1982). By comparison, strabismic suppression involves an equal reduction of sensitivity in the two mechanisms (Smith et al. 1985a). Suppression is stronger in normal rivalry suppression than in strabismic suppression (Holopigian et al. 1988).

Amblyopia and dichoptic masking

In people with normal vision, a low-contrast grating in one eye is masked by a similar high-contrast grating in the other eye (see Section 9.3.4). This is called dichoptic masking rather than rivalry because, unlike rivalry, it occurs optimally between matching dichoptic stimuli. The magnitude of masking increases as the dichoptic gratings are made more dissimilar in contrast (Legge 1979). Since the contrast of signals in an amblyopic eye is attenuated relative to that of signals in the good eye, one could argue that suppression of an amblyopic eye is an expression of the same mechanism that causes interocular masking in normal eyes.

Harrad and Hess (1992) tested this idea by measuring dichoptic masking with sinusoidal gratings in subjects with various kinds of amblyopia, after allowing for the difference in contrast sensitivity between the eyes. Most of the amblyopic subjects showed abnormal masking as a function of spatial frequency and as a function of interocular differences in contrast, when normalized to their deficit. The different types of amblyope showed specific types of masking abnormality. Only anisotropic amblyopes showed normal masking functions after allowance was made for interocular differences in contrast sensitivity. We have already mentioned that anisotropic amblyopia differs from other types of amblyopia in other respects. It was concluded that most types of amblyopia cannot be understood in terms of the normal mechanism of dichoptic masking, and they must involve more than a simple loss of contrast in the signals from the affected eye.

The subject of amblyopia has been reviewed recently by Ciuffreda et al. (1992).

15.8 THE CRITICAL PERIOD

The effects of monocular occlusion or other types of visual deprivation are permanent if they are applied early in life and maintained beyond a critical age. The interval of time during which visual deprivation has irreversible effects is known as the critical period. The critical period may not be the same for different types of visual deprivation or for different visual functions and it is not the same for different animals (Berman and Daw 1977; Harwerth et al. 1986b).

15.8.1 The critical period in the cat

The eyes of the cat are closed until about 10 days after birth. The period during which cortical cells are susceptible to the effects of monocular occlusion begins in the fourth week, remains high until the eighth week, and ends at about the twelfth week (Hubel and Wiesel 1970b; Dews and Wiesel 1970). During the period of peak susceptibility, around the age of 40 days, eye closure for 3 or 4 days is sufficient to induce permanent changes in the number of binocular cells and a deficit in depth discrimination (Timney 1990). In addition, allowing a kitten reared in darkness to see with one eye for a few hours during the peak period produced a distinct shift in ocular dominance to the open eye. The shift became evident two days after the eye had been opened (Peck and Blakemore 1975; Olson and Freeman 1980). In other studies, some effects of monocular occlusion on ocular dominance were found when applied between the fifth and seventh months (Cynader and Mitchell 1980; Cynader et al. 1980). Daw et al. (1992) agreed that the critical period for cortical cells in layer 4 of the visual cortex of the cat extends to the seventh month but found significant shifts in ocular dominance in other layers after monocular deprivation applied in the eleventh month. The critical period lasts longer for binocular cells in area 17 than for those in the extrastriate cortex (the lateral suprasylvian area) (Jones et al. 1984b).

For kittens reared in the dark for up to 10 months, subsequent monocular occlusion still caused a marked shift in ocular dominance of cortical cells toward the seeing eye. Thus, the critical period of cortical flexibility is extended if the animal is kept in the dark (Timney et al. 1980; Mitchell and Timney 1982). The processes responsible for the termination of the critical period must depend on visual stimulation.

The visual acuity of a deprived eye shows some recovery after sight has been restored but, as can be seen in Figure 15.4, the extent to which it does so declines exponentially as the period of deprivation is increased (Mitchell 1988a). When occlusion is

switched to the other eye at an early enough stage, the processes leading to the dominance of the first eye are reversed, and the longer the reverse occlusion is maintained the greater the shift in dominance to the previously occluded eye (Van Sluyters 1978). The evidence suggests that the same cells that were dominated by the previously open eye become dominated by the newly open eye (Olson and Freeman 1978). If the reversal of occlusion is delayed for too long, the reversal of ocular dominance does not occur and behaviour mediated by the previously occluded eye, such as visually guided reaching, cliff avoidance, and jumping across gaps, remains permanently impaired (Van Hof-van Duin 1976b).

In another study, reverse suturing of the eyes in a kitten at 5 weeks produced a complete switch in ocular dominance after a period of a few weeks, and the orientation specificity of receptive fields in the initially deprived eye improved while the specificity of receptive fields in the newly deprived eye decreased (Movshon 1976). Reverse occlusion also leads to recovery of orientation tuning as revealed in optical imaging of cortical activity (Kim and Bonhoeffer 1994). At the same time, the visual performance of the previously deprived eye improved from an initial state of functional blindness and the newly sutured eye became functionally blind (Movshon 1976). However, reverse sutured animals lacked binocular cells and were stereoblind. Reverse suturing after 14 weeks of monocular deprivation did not reverse the pattern of ocular dominance (Blakemore and Van Sluyters 1974).

A given period of reverse occlusion in the cat has been found to be more effective in promoting recovery when distributed over several sessions than when provided continuously in one session (Crewther et al. 1983). Simply allowing an animal to see with both eyes after a period of monocular occlusion may lead to some recovery but is not as effective as reverse suturing, which forces the animal to use its deprived eye (Mitchell et al. 1977; Mitchell 1988a).

Although reverse occlusion leads to some recovery of a previously deprived eye this recovery is at the expense of a loss of visual capacity in the other eye. When sight is restored to both eyes after a period of reverse suturing, the reverse-sutured eye loses its newly gained capacity and the other eye recovers. Thus, the gain achieved by reverse suturing is not permanent (Mitchell 1988b).

15.8.2 The critical period in the monkey

Monocular occlusion in the infant monkey from the second week of life causes a strong shift in ocular dominance of cortical cells from the closed to the

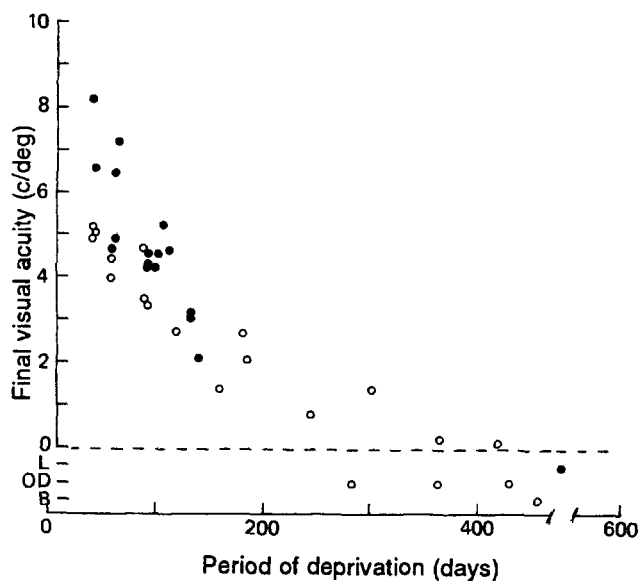


Figure 15.4. Restoration of visual acuity.

Visual acuity achieved by a deprived eye of a cat after restoration of sight as a function of duration of monocular deprivation. Each point is for one cat. Filled symbols are for cats reverse occluded during the recovery period, open symbols for cats with both eyes open during recovery. (From Mitchell 1988a.)

open eye. Monocular occlusion from an age of between 7 and 14 months had no influence on ocular-dominance columns in cortical layer 4C, but there was still some shift of ocular dominance in cells of the upper cortical layers (Blakemore et al. 1978; LeVay et al. 1980). Monocular deprivation in the adult monkey does not affect ocular dominance. Reverse suturing after monocular occlusion for the first 24 days led to a reversal of dominance to the other eye (Swindale et al. 1981). A reversal of ocular dominance was found even after 90 days of monocular occlusion (Crawford et al. 1989).

The critical period for monkeys seems to be longer than for cats. Anisometropia induced in the monkey by securing a minus 10-dioptral lens in front of one eye for 30 days produced little effect in the defocused eye. When continued for 60 days or more it produced persistent amblyopia in the defocused eye as revealed by a loss of contrast sensitivity for high spatial frequencies (Smith et al. 1985b).

The critical period in the monkey has been found to depend on the type of visual function. Thus, loss of scotopic sensitivity occurred only when monocular deprivation was initiated before 2 months of age. Spectral and contrast sensitivities were affected only when deprivation was initiated before 5 months of age. Loss of binocular vision occurred even when deprivation was initiated as late as 25 months (Harwerth et al. 1990).

15.8.3 The critical period in humans

Monocular deprivation in humans occurs as a consequence of unilateral cataracts, strabismus, and anisometropia in which the two eyes have differing refractive errors. Many people with strabismus have the condition surgically corrected. If the eyes of cats or monkeys remain in a deviated position over the critical period in the first few months of life, normal binocular vision is never recovered. Similarly, human infants with severe strabismus over several years never recover stereoscopic vision, even when the strabismus is corrected by surgery. Monocular vision or strabismus which develops in an older child or adult does not produce any loss of binocular functioning when the condition is corrected.

Banks et al. (1975) obtained an estimate of the critical period for normal visual development in humans by testing binocular functioning in 24 adults in whom strabismus in excess of 10° had been surgically corrected at various ages. Congenital esotropes who had corrective surgery before the age of 3 years tended to develop more normal binocular functions than those having the correction performed at a later age. However, stereoscopic vision is frequently poor even when surgery is performed at an early age (Atkinson et al. 1991). Surgery is justified by the amelioration of amblyopia and by the cosmetic improvement. For those subjects in whom the strabismus developed after the age of 4 years, corrective surgery produced complete restoration of binocular functioning no matter when it was performed. Banks et al. concluded that the sensitive period during which normal binocular inputs are required in humans is between the ages of 1 and 3 years.

Clinical studies support this conclusion (Robb and Rodier 1987; Dellar 1988; Smith et al. 1991). Kitaoji and Toyama (1987) found tests for crude stereopsis were performed better by subjects with corrected strabismus than by those with uncorrected strabismus. However, they did not provide data on the age at which the correction was performed. Even if surgery is applied too late to restore fine stereopsis it may help a person with a moderate degree of strabismic deviation to use any residual coarse stereopsis by bringing corresponding regions of the visual fields into register.

15.9 BINOCULARITY IN THE STEREOBLIND

An induction stimulus may have three basic types of effect on a test stimulus. The test stimulus can have its threshold reduced (threshold summation), or increased (threshold elevation), or some feature of

the test stimulus, such as its orientation, motion, or spatial frequency, may be apparently changed. Each of these effects can be induced in a test stimulus presented at the same time as or just after the induction stimulus. Most of these effects are manifested, although in reduced degree, when the induction stimulus is presented to one eye and the test stimulus to the other. In other words, they show interocular transfer.

Binocular summation and masking were discussed in Chapter 9 and interocular transfer of figural effects was discussed in Sections 3.3.3 and 9.4. This section is concerned with the extent to which people with defective binocular vision show binocular summation and masking and interocular transfer of aftereffects. The extent to which an induction effect shows interocular transfer has been taken as a measure of binocular interaction in the visual cortex. Given that an induction effect is cortical, any interocular transfer of the effect is assumed to reflect the extent to which the induction and test stimuli excite the same binocular cells in the visual cortex.

In normal subjects, the extent to which the transferred effect is less than that produced in the same eye is assumed to be due to dilution of the effect by unadapted monocular cells fed from the unadapted eye or by binocular AND cells that require simultaneous inputs from both eyes. If this logic is correct, a person lacking binocular cells should show no interocular transfer effects or binocular recruitment of cortically mediated induction effects. In practice there are many pitfalls in applying this logic, and the literature has become complex and rather contentious.

15.9.1 Binocular summation in the stereoblind

A near-threshold stimulus is more likely to be detected when it is presented to two eyes than when it is presented to one eye. This is **binocular summation**. Binocular summation can be due to either neural summation or probability summation. Neural summation is the process whereby subthreshold excitatory signals from the two eyes are summed when they impinge on cortical binocular cells. In measuring neural summation allowance must be made for the fact that detection based on the pooled output from two independent detectors shows a $\sqrt{2}$ advantage over that based on the output of a single detector. This is probability summation. We saw in Section 9.2.1 that there are different ways to calculate the effects of probability summation, and the safest procedure is to determine these effects empirically. This is done by measuring interocular effects under conditions in which neural summation is unlikely to

occur, for instance, when the stimuli in the two eyes are separated spatially or presented at slightly different times. In people with normal binocular vision, binocular luminance-increment and contrast-detection thresholds for overlapping and simultaneous stimuli are lower than monocular thresholds to a greater extent than predicted from probability summation (see Section 9.2.1). It is therefore believed that true neural summation occurs. Neural summation, like the response of cortical cells, is greatest for stimuli with the same orientation and spatial frequency (Blake and Levinson 1977). In people with severe loss of binocularity, binocular thresholds are simply what one would predict from probability summation, even with well-matched stimuli (Lema and Blake 1977; Westendorf et al. 1978; Levi et al. 1980; Blake et al. 1980b).

Dichoptic interactions of flicker are investigated by determining the magnitude of luminance modulation of a flickering light required for detecting flicker. This measure, plotted as a function of temporal frequency is the temporal contrast sensitivity function (see Section 9.2.4). For subjects with normal binocular vision, sensitivity for in-phase binocular flicker is about 40 per cent higher than for antiphase flicker (see Figure 9.7). At low flicker rates, sensitivity for in-phase flicker is up to four times higher than for antiphase flicker (van der Tweel and Estévez 1974; Cavonius 1979). No significant difference between in-phase and antiphase flicker sensitivity occurred in stereoblind subjects (Levi et al. 1982).

A spatially uniform, dichoptic patch flickering in the two eyes at slightly different frequencies creates the appearance of a rhythmic modulation of luminance at a frequency equal to the difference in frequency between the two patches. This visual beat phenomenon is a simple consequence of nonlinear binocular luminance summation as the two flickering patches come into and out of phase. Three subjects with alternating strabismus and normal visual acuity and three stereoblind strabismic amblyopes, failed to see dichoptic visual beats, thus providing more evidence that binocular neural summation is absent in stereoblind people (Baitch and Levi 1989).

15.9.2 Dichoptic masking in the stereoblind

It is generally more difficult to detect a briefly exposed suprathreshold test stimulus, such as a black and white grating, either when (1) it is superimposed on a similar suprathreshold stimulus than when it is presented alone (simultaneous masking) or (2) just before or just after the eye has been

exposed to a similar grating (successive masking, or the threshold-elevation effect) (Campbell and Kulikowski 1966). The test stimulus is masked by the adapting stimulus. In dichoptic masking, the mask is presented to one eye and the test stimulus to the other. Masking is said to show interocular transfer when it occurs dichoptically. In normal subjects, and at high contrasts, simultaneous dichoptic masking has been reported to be stronger than monocular masking (Legge 1979). Successive dichoptic masking was about 65 per cent as strong as monocular masking and the effect showed 65 per cent interocular transfer (Blakemore and Campbell 1969; Hess 1978).

There has been some dispute about whether dichoptic masking is present in stereoblind people with an early history of strabismus. Ware and Mitchell (1974a) found no interocular transfer of masking in two stereoblind subjects, whereas Lema and Blake (1977) found some transfer in three of their four stereoblind subjects. Anderson et al. (1980) also found interocular transfer of the threshold-elevation effect in seven stereoblind subjects, especially from a nonamblyopic eye to a normal eye, although to a lesser extent than in normal subjects. Hess (1978) tested one strabismic amblyope, with some residual stereopsis, who showed no interocular transfer of the threshold-elevation effect and another, with no stereopsis, who showed full transfer. In a later study he found that amblyopes show no threshold-elevation in the amblyopic eye after binocular adaptation, and concluded that threshold-elevation and amblyopic suppression occur at the same cortical level (Hess 1991). Levi et al. (1979b) found that subjects with abnormal binocular vision and amblyopia showed a normal level of interocular masking at suprathreshold levels of contrast (Figure 15.5). These same subjects failed to show interocular subthreshold summation. This suggests that in people with defective binocular vision, inhibitory interactions responsible for masking still occur between the left- and right-eye inputs to binocular cells but excitatory interactions responsible for subthreshold summation are absent. This is in accord with the evidence reviewed in Section 15.6.2.

An important factor that may help resolve some of the conflicting evidence about interocular transfer of the threshold-elevation effect, and of other aftereffects that we mention later, is the spatial frequency of the stimulus. It is well known that amblyopes tend to show a selective loss of contrast sensitivity for high spatial frequencies. Selby and Woodhouse (1981) found that amblyopes showed almost normal interocular transfer of the threshold-elevation effect with low spatial-frequency stimuli to which the normal and amblyopic eye were equally sensitive,

but little or no transfer with high spatial-frequency stimuli for which there was a difference in sensitivity in the two eyes. Some of these amblyopes had stereo vision, as tested on the Titmus test, and some did not, but their stereoscopic performance was not related to their degree of interocular transfer. It was concluded that stereopsis and interocular transfer of the threshold-elevation effect are not mediated by the same mechanism. However, the Titmus test involves high spatial-frequency stimuli, and it is not high spatial-frequency stereoacuity that one would expect to be related to interocular transfer of an aftereffect tested at a low spatial frequency. *Perhaps a relation between the two functions would be found if subjects were tested for stereoscopic vision with low spatial-frequency stimuli.*

A second but related factor in interocular transfer is the position of the stimulus. It was pointed out in Section 15.7.3 that even though stereoscopic vision may be lost in the central retina where both fine and coarse disparities are processed, it may be retained in the peripheral retina where only coarse disparities are processed. Binocular subthreshold summation and interocular transfer of the threshold-elevation effect were reduced or absent in strabismic and anisotropic amblyopes for stimuli confined to the central visual field. These effects were also absent in the visual periphery for anisometropes, but strabismics showed considerable interocular summation and transfer of the threshold-elevation effect in the peripheral field (Sireteanu et al. 1981). One would expect binocular vision in anisometropes to be disturbed more in the periphery than in the fovea because a differential magnification of the two images produces disparities that increase with eccentricity. In strabismics, the image displacement is the same over the whole visual field but affects peripheral vision less than foveal vision because the periphery has larger receptive fields.

15.9.3 Interocular figural effects in the stereoblind

The tilt aftereffect and the motion aftereffect were described in Section 9.4. For normal subjects these aftereffects transfer to an eye that was not exposed to the induction stimulus. The question to be discussed now is whether stereodeficient people show the same amount of interocular transfer of these effects as normal people. Before interocular transfer of a particular aftereffect can be accepted as evidence of normal binocular functioning, one must establish that the effect in question is entirely cortical in origin, rather than arising in the retina or LGN. In primates, it is generally believed that orientation and motion are first coded in the visual cortex. The

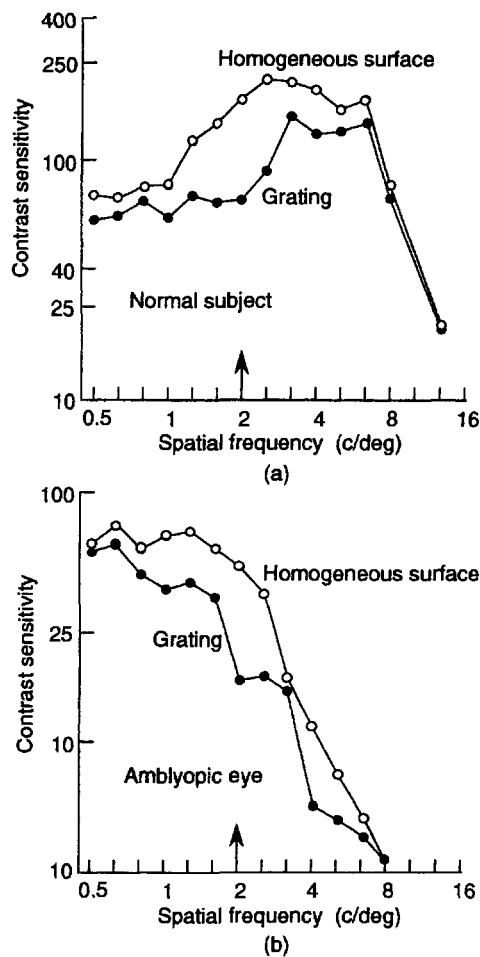


Figure 15.5. Dichoptic masking in an amblyopic eye.

(a) The contrast sensitivity for a grating presented to the right eye of a normal subject, with the left eye viewing a homogeneous surface (upper curve), or a 2 c/deg grating, 0.5 log units above threshold (lower curve).

(b) Contrast sensitivity of an amblyopic eye. The non-amblyopic eye views a homogeneous surface (upper curve), or a 2 c/deg grating (lower curve). Arrows show the spatial frequency of the mask. (From Levi et al. 1979b. Copyright 1979 by the AAAS.)

interocular transfer of orientation and motion after-effects have therefore been used as tests of normal binocular functioning. These after-effects are discussed in turn.

Inspection of an off-vertical line or grating induces an apparent tilt of a vertical line in the opposite direction. When the induction and test lines are presented at the same time, the effect is known as tilt contrast, and when the test line is presented after the induction stimulus, it is known as the tilt aftereffect. The tilt aftereffect shows interocular transfer when the induction line is presented to one eye and the test line to the other. Estimates of the extent of interocular transfer have varied between 40 and 100 per cent (Gibson 1937; Campbell and Maffei 1971). Some investigators found the extent of transfer to be

positively correlated with stereoacuity (Mitchell and Ware 1974) while others found no such correlation (Mohn and Van Hof-van Duin 1983). Subjects with strabismus acquired before the age of 3 years or with loss of stereopsis for other reasons have been found to show little or no interocular transfer of the tilt aftereffect (Movshon et al 1972; Ware and Mitchell 1974a Banks et al. 1975; Hohmann and Creutzfeldt 1975; Mann 1978).

The induction stimuli used in these experiments were gratings with a spatial frequency of about 7 c/deg, which tilted about 10° to the vertical and subtended 3° or less. Maraini and Porta (1978), used a 20°-wide grating stimulus with a spatial frequency of only 0.5 c/deg, and obtained a high level of interocular transfer of the tilt aftereffect in alternating strabismics. Moreover, although consistent strabismics (esotropes) showed no transfer from the dominant to the nondominant eye, they showed good transfer in the opposite direction, albeit less than in normal subjects. Inspection of a textured surface rotating in the frontal plane about the visual axis causes a superimposed vertical line to appear tilted in a direction opposite to the background motion. When the rotating surface was presented to one eye and the vertical line to the other, this effect remained at full strength in subjects with normal binocular vision but was significantly reduced in stereoblind subjects (Marzi et al. 1986).

Wade (1976) found no interocular transfer of the motion aftereffect produced by a rotating sectored disc, in six stereoblind adults who had strabismus in early childhood, and a little transfer in 11 subjects whose strabismus had been surgically corrected. Six subjects with mild strabismus and some stereoscopic vision showed some transfer of the aftereffect. Using a 10°-diameter rotating sectored disc, Mitchell et al. (1975) also found no interocular transfer of the motion aftereffect for subjects who were stereoblind either because of childhood strabismus or anisometropic amblyopia. For those subjects with some stereoscopic vision there was a positive correlation of 0.75 between the amount of transfer and stereoacuity. Mohn and van Hof-van Duin (1983) used a similar 10°-diameter sectored disc and found no interocular transfer of the aftereffect in stereoblind subjects but they found no correlation between the amount of transfer and stereoacuity in subjects with some stereo vision.

Keck and Price (1982) used an 8°-wide moving grating to test three groups of subjects (1) those who had central scotomata but some peripheral stereoscopic vision, (2) those with alternating strabismus but no stereoscopic vision, and (3) those with a consistent strabismus, anomalous correspondence,

and no stereoscopic vision. The subjects in all groups showed less transfer of the motion aftereffect than subjects with normal vision, but transfer was absent only in the third group. O'Shea et al. (1994b) found that interocular transfer of the motion aftereffect was significantly reduced in 10 strabismics of early onset with a stimulus confined to the central 2.8° of the visual field but not with a stimulus confined to an annular region between 20 and 40° of eccentricity.

Summary

There thus seems to be general agreement that little or no interocular transfer of aftereffects occurs in stereoblind subjects. However, some transfer has been found in certain types of stereoblind subjects, and there is considerable controversy about the correlation between the degree of transfer and stereoacuity. The conflicting findings from different laboratories could be due to different clinical samples, different diagnostic tests, or different stimuli used to measure interocular transfer. One potentially important factor is the size of the stimulus. There is more interocular transfer of the threshold-elevation effect when the stimulus is presented to the peripheral retina than when it is presented to the central retina, and it is known that some stereo vision is retained in the peripheral retina when it is lost in the central retina (Sireteanu et al. 1981). A related factor is the spatial frequency of the stimuli. Amblyopes show more interocular transfer of the threshold-elevation effect for low spatial-frequency stimuli to which both eyes are equally sensitive than for high spatial-frequency stimuli to which the amblyopic eye is relatively insensitive (Selby and Woodhouse 1981). *In future studies of interocular transfer of the motion and tilt aftereffects in people with visual defects, special attention should be given to the spatial frequency and area of stimuli used to test stereoscopic vision and interocular transfer.*

15.10 BINOCULARITY AND PROPRIOCEPTION

Sensory receptors exist in the extraocular muscles and/or in the muscle tendons in a variety of animals, including humans (Bach-y-Rita 1975; Richmond et al. 1984). Proprioceptive inputs from these receptors enter the brain along the ophthalmic branch of the trigeminal nerve (fifth cranial nerve). Responses to stretching of extraocular muscles have been recorded in cells of the superior colliculus (Donaldson and Long 1980), the vermis of the cerebellum (Tomlinson et al. 1978), the visual cortex (Buisseret and Maffei 1977), and the frontal eye fields (Dubrovsky and Barbas 1977).

Kittens with unilateral or bilateral section of proprioceptive afferents suffer permanent deficits in visual-motor coordination (Hein and Diamond 1983). One manifestation of this deficit is a loss of depth discrimination as revealed in a jumping-stand test (Graves et al. 1987). Fiorentini et al. (1985) reported that depth discrimination is affected by unilateral section of the ophthalmic nerve in adult cats, but Graves et al. found this to be true in only some cats. In a recent study, significant changes in depth discrimination in cats occurred only when a unilateral section of proprioceptive afferents was performed between the ages of 3 and 13 weeks or bilateral section between the ages of 3 and 10 weeks (Trotter et al. 1993).

Trotter et al. (1987) severed the proprioceptive afferents of kittens either unilaterally or bilaterally at various times in the first few months after birth. This did not cause strabismus or interfere with the movements of the eyes. After the operation some of the kittens were reared with normal binocular experience and some in darkness. One month after unilateral section of proprioceptive afferents during the critical period, both the seeing cats and the dark-reared cats showed a severe reduction in the number of binocular cortical cells, which was still present 2^{1/2} years later. Unilateral section of the nerve had no effect when performed during the first month after birth or in the adult cat. Bilateral section of the nerve had no effect on binocular cells no matter when it was performed.

In a more recent experiment Trotter et al. (1993) recorded from cells in the visual cortex of adult cats in which proprioceptive afferents had been severed unilaterally when the animals were between 5 and 12 weeks of age. The stimuli were moving sine-wave gratings with dichoptic phase (disparity) set at various values. In the cells of operated cats, the range and stability of disparity tuning and the degree of binocular suppression were reduced below the level of cells in normal cats.

Maffei and Bisti (1976) surgically deviated one eye of kittens soon after birth and at the same time occluded both eyes. The reduction in the number of cortical binocular cells was about the same as that produced by induced strabismus when both eyes were allowed to see. They concluded that asymmetrical movements of the two eyes, even in the absence of vision, is sufficient to disrupt binocularity in cortical cells. Others have failed to replicate this effect (Van Sluyters and Levitt 1980). Maffei and Bisti's conclusion was also challenged on the ground that monocular paralysis leads to a reduction in X cells in the LGN and the apparent loss of binocular cells was secondary to this (Berman et al. 1979). But this claim

has also been challenged by those who found no loss of X cells in the LGN after monocular paralysis (Winterkorn et al. 1981). This issue remains to be resolved. A report that surgical deviation of one eye in the adult cat leads to a loss of binocular cells (Fiorentini and Maffei 1974) could not be replicated (Yinon 1978).

Others have concluded that eye motility plays a role in cortical plasticity but only in combination with abnormal visual inputs. Thus, many cortical cells recovered their response to stimulation of a deprived eye only when the normal eye was both pressure blinded and had its extraocular muscles paralyzed (Crewther et al. 1978). Freeman and Bonds (1979) found that monocular presentation of a patterned display to anaesthetized kittens over a period of 12 hours did not reduce the number of binocularly activated cortical cells when the eye muscles were paralyzed during this same period. However, monocular exposure did reduce the number of binocular cells when the eyes were not paralyzed or were moved mechanically by the experimenter while they were paralyzed. Merely moving the eyes mechanically in darkness for 12 hours had no effect. It was concluded that cortical plasticity depends on a combination of nonmatching visual inputs and eye-movement information, apparently arising in proprioceptors in the extraocular muscles.

Buisseret and Singer (1983) came to the same conclusion after finding that neither monocular occlusion nor induced strabismus led to a change in the binocularity of cortical cells in the kitten when the proprioceptive afferents were abolished by bilateral section of the ophthalmic nerve carrying proprioceptive afferents.

Cortical cells that had lost their capacity to respond to an occluded eye responded to stimuli from that eye within minutes after the good eye was blinded by application of pressure, and an anaesthetic block was applied to the extraocular muscle afferents of the good eye. Neither procedure was effective when applied alone (Crewther et al. 1978). Thus, both proprioceptive and visual afference seem to play a role in maintaining a normal eye's suppression of a deprived eye.

Recovery of visual functions after a period of binocular deprivation is aided by ocular motility. Thus, Buisseret et al. (1978) found that 6-week-old dark-reared kittens showed some recovery of orientation selectivity of cortical cells when allowed to see, but not when their eye muscles were paralyzed.

On balance, this evidence suggests that eye proprioception plays a key role in cortical plasticity and in the development of depth perception, but just how this is accomplished remains a mystery.

15.11 ALBINISM

15.11.1 Basic characteristics of albinism

Albinism is a group of genetically determined disorders affecting the synthesis of melanin pigment. It occurs in all mammalian species. There are two main types of the disorder: **oculocutaneous albinism**, characterized by absence of pigment throughout the body, and **ocular albinism**, in which hypopigmentation is restricted to the eye. There are many subtypes, and the severity of the pigment deficit depends on at least eight different genes (see Kinnear et al. 1985 and Abadi and Pascal 1989 for reviews). About 1 in 17,000 people have oculocutaneous albinism and about 1 in 50,000 have ocular albinism, one form of which is linked to the X chromosome and occurs only in males (Jay et al. 1982). Several structural defects occur in all forms of albinism, including absence of ocular pigmentation, disorders in retinal structure, and disorders of the visual pathways. These defects are accompanied by strabismus, congenital nystagmus, and a variety of visual defects including reduced visual acuity and impaired or absent binocular fusion and stereopsis. The severity of these visual defects is correlated with the degree of pigment deficit (Sanderson et al. 1974).

The absence of melanin in the pigment epithelium behind the retina causes the ocular fundus, or concave interior of the eye, to appear orange-red and renders the choroidal blood vessels visible through the ophthalmoscope. Many albinos also have loss of pigmentation in the iris, which gives the eyes a characteristic pink appearance. Lack of pigment allows light to enter the eye through the sclera and iris and to reflect from the eye's internal surfaces, causing excessive illumination and glare. Albinos typically avoid the resulting visual discomfort and exposure to excessive doses of ultraviolet light by keeping away from bright lights, a response known as **photophobia**. The yellow macular pigment which reduces the effects of chromatic aberration is also absent in albinos. Albinos also tend to have astigmatism and high refractive errors, especially myopia.

Stereoscopic vision is either absent or deficient in albinos. In a mixed group of 18 human albinos, 9 showed some evidence of stereopsis when tested with a variety of stereo tests, including a random-dot stereogram, although only a simple pass-fail criterion was used (Apkarian and Reits 1989).

15.11.2 Abnormal routing of the visual pathways

The albinotic visual system shows characteristic defects. The most significant visual defect in the

present context is the unusual structure of the visual pathways. It was mentioned in Section 15.1.3 that in some neonate mammals the ipsilateral projection to the LGN arises only from the temporal hemiretina, as in the adult animal, but the contralateral projection arises from the whole retina and only later becomes confined to the nasal hemiretina (Jeffery 1990). Normally, the nerve fibres carrying the projections from the temporal retina to the contralateral LGN die off when they fail to find matching inputs from the other eye. In embryonic albino animals, whatever the cause of the albinism, these decussating fibres from the temporal retina are retained and disrupt the normal development of distinct layers in the LGN. Thus, many fibres from the temporal hemiretinas are misrouted. The part of the nasal retina closest to the midline also gives rise to some misrouted ganglion cells, but the most nasal parts of the retina have been found to be normal in several species of albino animals.

In albinos, cells in the LGN receiving normal uncrossed inputs form into distinct layers according to the eye of origin, as do those in normal animals, but cells receiving an abnormal contralateral input tend to group with cells in adjacent layers (Sanderson et al. 1974). A postmortem study of the LGN of a human albino revealed abnormal fusions of the four parvocellular layers and of the two magnocellular layers in the region of the LGN, which is normally six layered (see Section 4.1.3). In the normal LGN there is a small two-layered region devoted to the crossed inputs from the monocular crescent in the far periphery of the visual field. In the albinotic LGN this two-layered region is greatly extended because of the unusual number of crossed inputs (Guillery et al. 1975; Guillery 1986).

The terminals of the unusually routed visual inputs are arranged in a normal retinotopic order in the visual cortex but on the wrong side of the brain. They thus map a part of the ipsilateral rather than contralateral visual field and in mirror-reversed order (Kaas and Guillery 1973). This produces an unusual location of evoked potentials recorded from the scalp (Creel et al. 1978). In some Siamese cats, this mirror-reversed projection corrects itself to produce an essentially continuous representation of the visual field in each hemisphere (Hubel and Wiesel 1971). This is known as the Boston pattern. In other Siamese cats the reversed projection is not corrected but there is intracortical suppression of the anomalous inputs along with all other inputs from the same LGN lamina (Kaas and Guillery 1973). This is known as the Wisconsin pattern. These abnormally routed projections also disturb inputs to the oculomotor systems controlling vergence, which probably

explains why albinos and Siamese cats have strabismus and nystagmus. There is also a complete disruption of mechanisms for detecting disparity, so that albinos have little or no stereoscopic vision.

15.11.3 Congenital nystagmus

In normal vision the eyes show involuntary pursuit movements in the same direction as a moving visual display, interspersed with saccadic return movements. This reflex response is optokinetic nystagmus or OKN (see Howard 1993a for a review). In normal vision the subcortical nuclei controlling OKN receive direct inputs only from the nasal hemiretina of the contralateral eye, that is, from axons that decussate in the optic chiasma. Outputs from the visual cortex descend to the subcortical nuclei and counterbalance the inherent directional asymmetry of the subcortical mechanism (see Section 12.5.6). These cortical outputs derive from binocular cortical cells that normally receive both decussated and undecussated axons. The normal OKN system is held in symmetrical balance by the interplay of these two systems. In the albino, the excessive number of decussating axons upsets both the subcortical and cortical components of OKN and the balance between them, and this results in spontaneous nystagmus.

Spontaneous nystagmus consisting of a conjugate, involuntary oscillation of the eyes, usually in the horizontal direction, is a universal feature of albinism. Other types of spontaneous nystagmus of genetic origin, are known as congenital nystagmus. Nystagmus associated with albinism is due to a misrouting of the visual pathways which reveals itself in an asymmetry in the visual evoked potentials from the two sides of the brain. But visual evoked potentials do not show this asymmetry with congenital nystagmus not due to albinism (Apkarian and Shallo-Hoffmann 1991). An interesting feature of all forms of congenital nystagmus is that, unlike acquired nystagmus, it is not accompanied by oscillopsia. In other words, the patient does not perceive any oscillation of the visual world. People with congenital nystagmus learn to suppress or ignore the retinal motion signals that arise during nystagmus. They assess the stability of the visual world on the basis of information taken in when the eyes momentarily come to rest between nystagmic sweeps. A person with congenital nystagmus experiences

oscillopsia if the retinal image is artificially stabilized (Leigh et al. 1988). In congenital nystagmus there is usually a position of gaze for which nystagmus is minimal or absent. This so-called null position typically shifts in a direction opposite to the motion of a moving display. Also, congenital nystagmus is typically reduced when the patient converges on a near object (Dickinson 1986). Thus, patients may reduce their nystagmus either by looking at an object with the head directed to one side, so as to bring the gaze into the null position, or by voluntary convergence. Prisms or surgical rotation of the eyes may help by bringing the null angle of gaze into the primary, or straight-ahead position.

Patients with congenital nystagmus may show no OKN in response to visual motion, a response with unusually low gain, or so-called reversed OKN. In reversed OKN the slow phases, which normally compensate for the motion of the stimulus, occur in the opposite direction to that of the stimulus and often have an accelerating velocity profile instead of the constant velocity profile typical of normal slow phases (Dichgans and Jung 1975; Halmagyi et al. 1980; Yee et al. 1980). Reversed OKN occurs only in response to stimuli moving along the meridian in which the congenital nystagmus occurs (Abadi and Dickinson 1985). The reversal of OKN is presumably caused by the mirror-reversed projection of the abnormally routed cortical and pretectal inputs.

The vestibuloocular response (VOR) in albinos with congenital nystagmus has an unusually low gain when the head is oscillated at a low frequency although its gain may be normal at high frequencies. Albinos show weak or no VOR in response to caloric stimulation of the vestibular organs since this is equivalent to a low-frequency rotation of the head. Furthermore, optokinetic afternystagmus (OKAN) is absent and postrotatory nystagmus is unusually brief in people with congenital nystagmus (Demer and Zee 1984). This suggests that congenital nystagmus involves a defect in the velocity-storage mechanism common to OKN and VOR.

In conclusion, albinos suffer from optic glare, poorly developed retinas and visual pathways, instability of gaze, refractive error, and astigmatism. These factors contribute to loss of visual acuity and stereopsis, which is so severe in some albinos that they are classified as partially or completely blind.

This page intentionally left blank

Binocular and stereoscopic vision in animals

16.1 Introduction	645
16.2 Stereopsis in insects and spiders	646
16.3 Stereopsis in crustacea	649
16.4 Binocular vision in fish	649
16.5 Stereopsis in amphibia	651
16.6 Binocular vision in reptiles	653
16.7 Stereopsis in birds	653
16.8 Stereopsis in mammals	656
16.9 Final word	657

16.1 INTRODUCTION

Stereoscopic vision is particularly well developed in mammals with foveas, frontal vision, hemidecussating visual pathways, and vergence eye movements, such as felines (Fox and Blake 1971; Mitchell et al. 1979) and primates (Bough 1970; Cowey et al. 1975 Sarmiento 1975; Julesz et al. 1976b; Harwerth and Boltz 1979). In these animals, visual inputs from corresponding regions in the two retinas converge on cortical cells tuned to disparity (see Chapter 4). Stereoscopic vision in cats and primates forms the subject matter of the other chapters in this book. This chapter is concerned with stereoscopic vision in other animals.

The binocular field is that part of the total visual field within which the monocular fields overlap. A visual axis is a line passing through the nodal point of an eye and the centre of a fovea. Some eyes have more than one fovea and hence more than one visual axis. We define **frontal vision** as that in which visual axes (perhaps not the principal visual axes) converge on a common point. We define **true frontal eyes** as having only one pair of visual axes that typically intersect. In **lateral eyes**, the principal visual axes are normally directed in opposite directions and never intersect. Some animals, such as the chameleon, are able to direct their visual axes both to lateral positions, when they do not intersect, and frontally, when they do intersect. They thus have some frontal vision even though they don't have true frontal eyes. Some animals, such as the pigeon, are bifoveate and have two visual axes in each eye—a principal axis

that lies close to the optic axis and projects to a central fovea, and a second visual axis that projects to a fovea lying in the temporal retina (see Figure 16.1). The **angle alpha** between the two visual axes can be as large as 50°. Animals like this are classified as lateral eyed, because their principal visual axes point laterally and never intersect. However, they have frontal vision with respect to their secondary visual axes, because these axes do intersect. Many animals do not have foveas. For instance, the rabbit has a horizontal region in each retina where acuity is higher than in the rest of the retina, a region known as the visual streak. In such animals, frontality is indicated by the extent to which the two visual fields overlap. When threatened, many lateral-eyed animals, such as the pigeon, rabbit, and horse, turn their eyes outward to gain panoramic vision at the expense of losing binocular overlap. When they wish to get a better view of something ahead of them they converge their eyes to increase binocular overlap at the expense of some loss of panoramic vision.

Animals with overlapping visual fields do not necessarily have stereoscopic vision. Even the possession of frontal vision (intersecting visual axes) probably does not guarantee stereopsis. True frontal eyes are not required for stereopsis although, as far as we know, all animals with true frontal eyes have stereopsis. We will see that some form of stereopsis based on binocular vision is found in a variety of submammalian phyla, including insects, amphibians, and birds as well as in lateral-eyed mammals such as the rabbit and goat. Several reasons have been proposed to account for the evolution of true

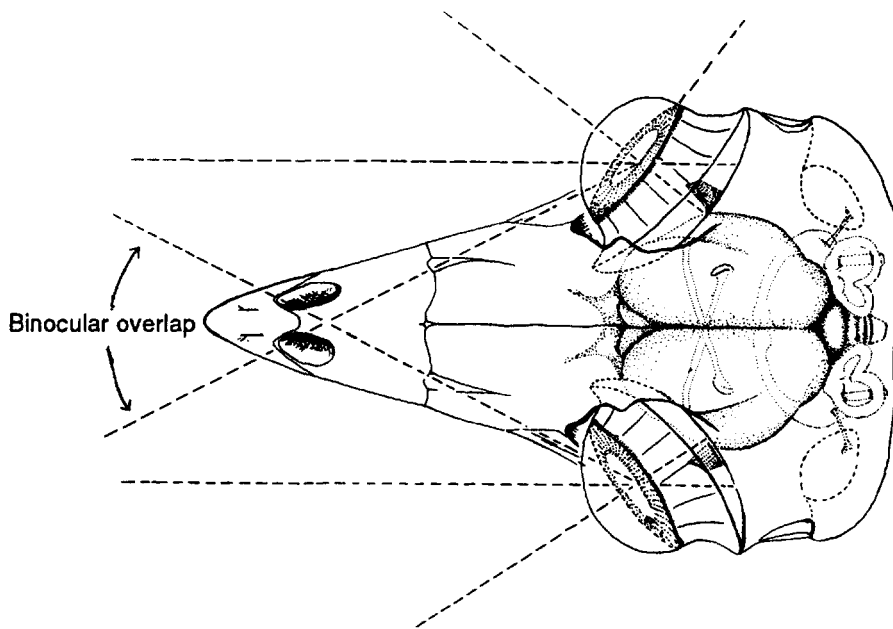


Figure 16.1. Diagram of the head of a bifoveate bird.

The lateral visual axis of each eye projects to the central fovea, and the frontal visual axis of each eye projects to a fovea in the temporal retina. (From Pettigrew 1986. Reprinted with permission of Cambridge University Press.)

frontal eyes, hemidecussation, and fully developed stereopsis, with the consequent loss of panoramic vision. Collins (1922) and Le Gros Clark (1970) suggested that it was an adaptation to arboreal life in which accurate judgments of distance are required to enable the animal to leap from branch to branch. However, many arboreal mammals, such as opossums, tree shrews, and squirrels, do not have frontal eyes. The squirrel, for instance, has only about 20 per cent binocular overlap. In small mammals, binocular overlap correlates with length of skull rather than with arboreality (Cartmill 1974). The second possibility is that frontal eyes evolved in predators to enable them to judge the distance of prey and to detect camouflaged prey (Cartmill 1974; Julesz 1971). Binocular stereopsis is very effective at revealing the presence of objects which are camouflaged by having similar luminance, colour, and texture to the surroundings. Motion parallax can also serve this function although at the cost of the predator having to move. Visually controlled predation is characteristic of many living prosimians and small marsupials, and these animals show primate-like specialization of the visual system. In a review of this question, Hughes (1977) proposed that the degree of binocular overlap is correlated with the evolution of visual-motor control of the forelimbs. In primates, all these factors probably created selective pressure for the evolution of frontal eyes and stereopsis.

16.2 STEREOPSIS IN INSECTS AND SPIDERS

The praying mantis

In many insects the visual fields of the two compound eyes overlap (Horridge 1978) so the possibility of binocular stereopsis exists in these animals. It has been reported that predatory insects such as dragonfly larvae, tiger beetles, praying mantis, and water scorpions rarely catch prey when one eye has been removed (Cloarec 1978). This suggests that they use binocular cues to relate their prey-catching activity to the distance of the target. This question has been investigated in the praying mantis (genera *Tenodera* and *Sphodromantis*). These insects have compound eyes about 4 mm apart with a central forward-looking region of high-density ommatidia and a 70°-wide binocular field. When a mantis with one eye occluded is presented with a fly, it centres the prey in its visual field by a saccadic movement of the head. When both eyes are open the head moves to a compromise position so that the images of the prey are equally displaced horizontally from the centre of vision in each eye (Rossel 1986). The mantis cannot centre a fly in both eyes simultaneously because the eyes cannot converge. When a vertical disparity between the images of an object was introduced by prisms, the head also took up an intermediate position in the vertical plane (Rossel et al. 1992). The mantis is also capable of

pursuing moving prey with visually guided smooth movements of the head (Rossel 1980).

When the prey is within a critical distance, the mantis strikes at it with its forelegs with an accompanying lunging motion of the middle and hind legs. The movements of the forelegs are adjusted to the distance of the prey and the attack is successful when the prey is within 15° of the midline of the head (Corrette 1989). When base-out prisms were placed in front of the eyes the distance of strike initiation was modified accordingly. A strike occurred when the binocular disparity of the target reached the same value as without the prisms (Rossel 1983). This suggests that the mantis uses binocular disparity rather than monocular cues to distance, such as motion parallax and image size, since monocular cues are not affected by prisms. There is other evidence that the mantis does not judge the distance of a prey object on the basis of image size (Rossel 1991). Accommodation is not a cue since compound eyes do not accommodate.

The fact that the compound eyes of the mantis do not move relative to the head means that a given image disparity is uniquely related to a given absolute distance of the visual object. The extraction of binocular disparities need not involve the elaborate image-matching process that occurs in higher mammals. Presumably, each eye is selectively tuned to detect moving prey with a given image size. If only one prey is within range at any one time, all that is required is that a central mechanism registers the direction of the prey by taking the mean of the local-sign information from the two eyes, and the distance of the prey by taking the difference between the horizontal positions of the two images. Rossel et al. (1992) found that the mantis still responded accurately to the distance of a target when the images were prismatically separated vertically by up to 15°, which suggests that the horizontal disparity is registered more or less independently of vertical separation. Such a mechanism would fail if several targets were in view at the same time. The mantis therefore uses disparity as a range-finding mechanism rather than a relative distance mechanism. Very little is known about the anatomy or physiology of the mantis brain.

Jumping spiders

Jumping spiders (family Salticidae) have four pairs of simple eyes; one principal anterior-median pair, a small median pair with no known function, an anterior-lateral pair, and a posterior-lateral pair. Their coverage of the visual field is depicted in Figure 16.2. The retinas of the principal median pair of eyes move sideways behind the stationary lenses. This

enables the animal to move the small nonoverlapping visual fields of its median eyes across most of the larger visual fields of the anterior-lateral pair of eyes, which partially overlap in the midline. These movements can be saccadic movements toward an object presented in the larger visual fields of the other eyes, slow movements in pursuit of a moving object, or regular side-to-side scanning movements across an object of between 0.5 and 1 Hz, combined with a slower 50° rotation of the retinas about the visual axes. All these movements are conjugate, so the two visual axes remain approximately parallel as they sweep across an object. (Land 1969). This system presumably provides a mobile region of high-resolution which helps the animal distinguish between prey, other jumping spiders, and other objects.

When a prey object enters the visual field, the spider first orients its body to centre the prey. Then the spider adopts one of two strategies. It either chases the prey and catches it on the run or, in some species, it stalks the prey and jumps on it from a distance of 3 cm or more. During stalking, the spider reduces its speed of approach as it gets near the prey. In this way it does not exceed the prey's threshold for detection of an approaching object (Dill 1975). Just before jumping, it attaches a web filament to the substrate. Removal of the median eyes does not affect orienting behaviour, showing that this is under the control of the lateral eyes, but a spider with only one median eye ignores stationary prey and jumps short of the target. Animals with both anterior-lateral eyes removed still swivel but no longer chase moving prey. It seems that the principal median eyes with scanning retinas are mainly responsible for judging the distance of the prey, especially for short distances. These eyes do not accommodate and do not use disparity since the visual fields do not overlap. Distance could be signalled by the temporal disparity between detection of the prey by one median eye and its detection by the other as the eyes scan from side to side. For a fixed velocity of scanning with parallel axes, this delay is approximately inversely proportional to the distance of the scanned object. It seems that in *Trie planiceps* the fixed anterior-lateral eyes contribute to judgments of distances greater than about 3 cm, since their removal has an effect on jumping accuracy at these distances (Forster 1979). Since the visual fields of these eyes overlap it is possible that binocular disparity is used. These eyes do not move so that any disparity would signal absolute distance.

Scanning eyes and motion parallax

The only other known animals with scanning retinas are certain copepods, such as *Copilia* (Gregory et al.

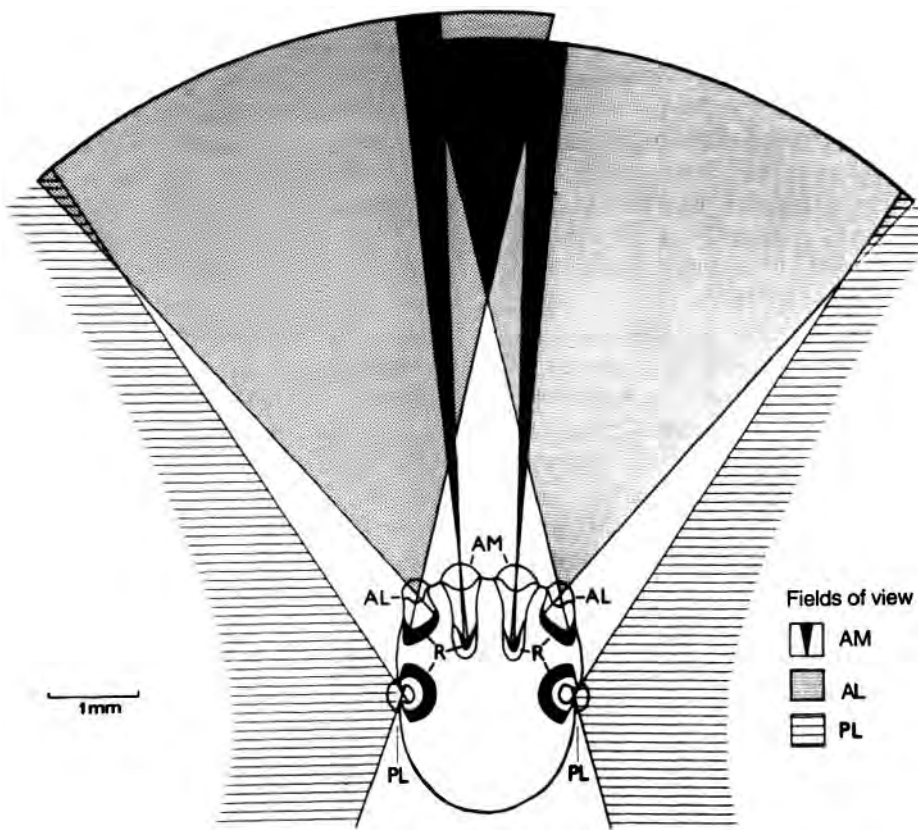


Figure 16.2. Visual fields of a jumping spider (family Salticidae).

The jumping spider has four pairs of simple eyes; one principal anterior median pair (AM), a small median pair of unknown function (not shown), an anterior-lateral pair (AL), and a posterior-lateral pair (PL). The retinas of the AM eyes move conjugately, sweeping their visual fields from side to side within the fields of the AL eyes. The fields of the AL eyes overlap in front. (From Forster 1979.)

1964; Downing 1972) and *Labidocera* (Land 1988). Certain crustacea, such as the mantis shrimp and some molluscs, such as the carnivorous sea snail (*Oxygyrus*), execute scanning movements of the whole eye. Scanning movements enable the animal to economize on the number of receptors or ommatidia, and it is characteristic of animals with scanning retinas or eyes that they have very few light detectors. Scanning eye movements in which visual information is coded during the movement must be slow enough to allow an image to dwell on each receptor or ommatidium long enough to be detected. The larger the angle of acceptance of the receptors (the coarser the resolution), the faster the eye can scan over a stationary scene before the dwell time for each detector falls below an acceptable limit of between 15 and 25 ms (Land et al. 1990). If the centre of rotation of an eye is some distance from the optical nodal point, scanning movements entail a translation of the vantage point which in turn creates differential motion parallax. This motion parallax could be used to code absolute and relative distances.

There is evidence that, when jumping across a gap, locust nymphs obtain distance information from parallax generated by lateral displacements of the anterior part of the body (Wallace 1959; Collett 1978). The locust adjusts the length of its jump as a function of the magnitude of image motion resulting from body motion, suggesting the use of absolute parallax information (see Section 13.5). However, the adjustment is the same for image motion against the head as for image motion of the same relative speed in the same direction as the head, showing that the sign of the motion is ignored (Sobel 1990). The sign can be ignored because, with no eye rotation, images always move against the head under natural circumstances, and taking the sign of the motion into account would unnecessarily complicate the control process. Locusts possess visual movement detectors that also encode the velocity and direction of an object's approach (Rind and Simmons 1992).

Bees use motion parallax generated by flight to judge the distances of objects (Lehrer et al. 1988; Egelhaaf and Borst 1992). It seems that bees are able to fly straight down a tunnel by balancing the speeds

of the motion signals arising from textures on the two sides of the tunnel, independently of the relative spatial periodicities of the patterns (Srinivasan and Zhang 1993). The motion detectors responsible for registering image speed have small receptive fields and are insensitive to the direction of motion. As in the parallax-detecting system of the locust, the detection of direction is unnecessary since images always move counter to the body during flight.

Bees have a second motion-detection system with large receptive fields that is concerned with optokinetic responses that stabilize yaw, pitch, and roll of the body. These detectors are designed to detect the null point of rotary motion that occurs when the body is stable. They are therefore not required to produce a well-calibrated speed signal.

There is thus a distinction between a motion-detecting system designed to control linear motions of the body which produces a directionally unsigned speed signal unconfounded by spatiotemporal frequency, and a motion-detecting system designed to null rotations of the body which produces a good directional signal but confounds speed and spatiotemporal frequency. It would be worthwhile to investigate the generality of this distinction throughout the animal kingdom.

Stalk-eyed flies (family Diopsidae) have long eye stalks. The increased interocular separation could serve to improve binocular stereopsis, but the eye stalks also provide a large translational component when the eyes scan and thus the potential for sensing motion parallax. Long eye stalks may also serve as a sexual attractant in males (Collett 1987).

16.3 STEREOPSIS IN CRUSTACEA

Mantis shrimps, are predatory marine crustaceans (order Stomatopoda) that inhabit shallow tropical waters. They live in burrows from which they emerge to stalk other small animals which they aggressively strike or spear with two large limbs. Their large mobile compound eyes possess many remarkable features. Each eye has a central horizontal band of six rows of ommatidia flanked by dorsal and ventral hemispherical regions containing several thousand ommatidia, as can be seen in Figure 16.3. Within each of the three regions, there is a group of ommatidia that are all directed to the same location in space. These "pseudopupils" show as three dark region in the figure. Exner (1891) suggested that this arrangement may allow range-finding stereoscopic vision to be achieved within each eye. The upper and lower converging regions of each eye are separated vertically, so that stereopsis would be

based on vertical disparities between the images in the two regions. If this is true, these animals are unique in two respects; in having monocular disparity-based stereopsis and in having stereopsis based on vertical rather than horizontal disparities.

The central band of ommatidia has a visual field a few degrees high and about 180° wide and seems to be involved in colour vision and the analysis of light polarization. In these central bands there are at least 10 types of ommatidia, each with either a distinct type of filter pigment or a distinct type of photopigment with distinct spectral absorption ranges. The rest of the eye is monochromatic (Marshall et al. 1991; Goldsmith and Cronin 1993). Colour is detected over a wide region because the eyes execute slow vertical and torsional movements through an angle of at least 60°. These movements are slow enough to allow the image to dwell on each ommatidium for at least 25 ms, which is estimated to be long enough for stimulus detection (Land et al. 1990). In addition, the eyes execute tracking movements in response to movements of a visual target. The two eyes move independently, as can be seen in Figure 16.3; note that conjugate eye movements are not required if stereopsis is achieved in each eye.

16.4 BINOCULAR VISION IN FISH

In bony fish (teleosts) the majority of optic nerve fibres project to the optic tectum—the homologue of the superior colliculus of mammals (Guthrie 1990). From the tectum, pathways project to the tegmentum, to three centres in the diencephalon (the thalamus, preoptic area, and pretectum), and to visual centres in the telencephalon. There are also direct visual inputs to mesencephalic nuclei, the pretectum, and the thalamus (Schellart 1990).

Bony fish have a small binocular field but most if not all inputs from the eyes project contralaterally to the optic tectum. Springer and Gaffney (1981) found a few uncrossed inputs to the optic tectum of the goldfish. Ipsilateral inputs may also reach the tectum by way of the tectal commissure. Recordings from single nerve fibres in the tectal commissure revealed only large, poorly defined monocular receptive fields (Mark and Davidson 1966). Some investigators found no binocular cells in the optic tectum of fish (Schwassmann 1968; Sutterlin and Prosser 1970; Fernald 1985). However, a few binocular cells with large monocular receptive fields and low sensitivity have been found in the tectum of the goldfish (see Guthrie 1990) and trout (Galand and Liege 1974).

The larvae of some deep sea fish, such as *Idiacanthus fasciola*, have eyes on the ends of long

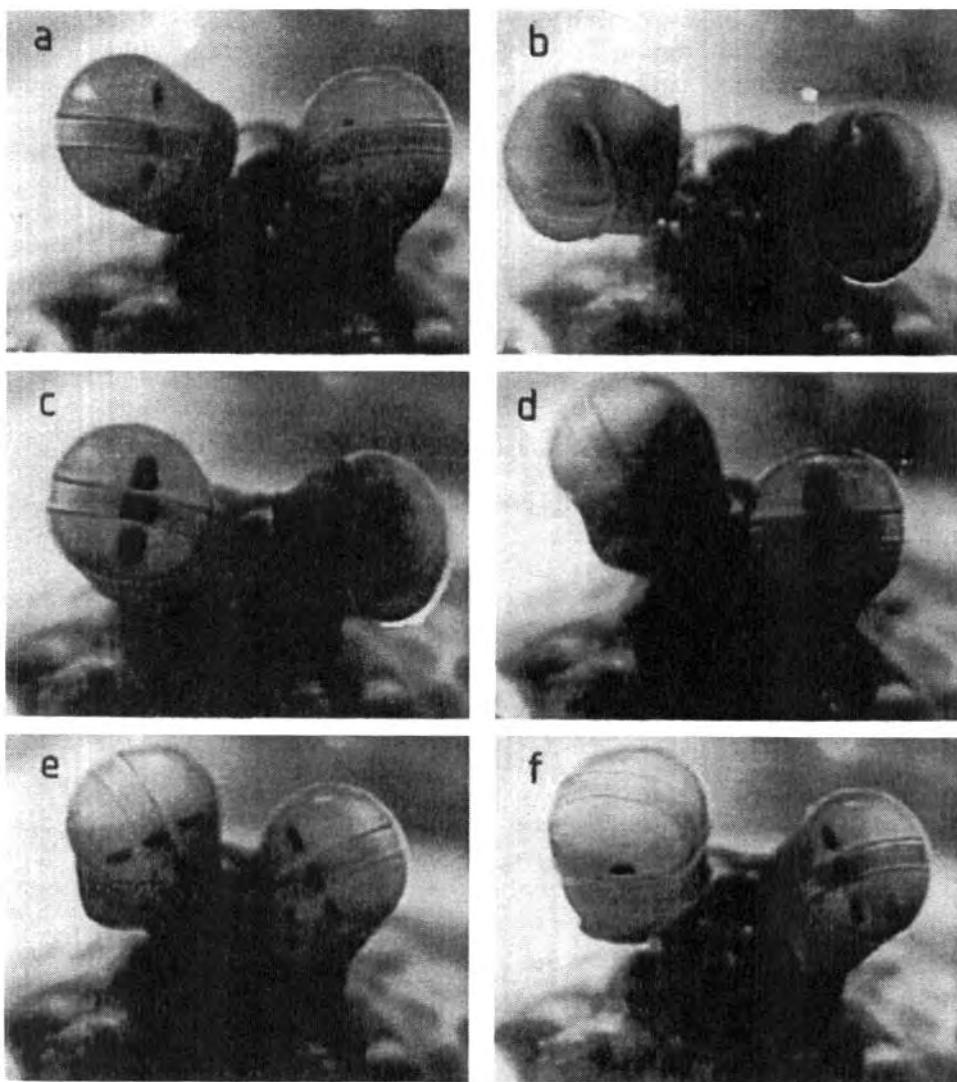


Figure 16.3. Compound eyes of the mantis shrimp (*Odontodactylus scyllarus*).
The central band of ommatidia are flanked by upper and lower hemispheres. Six frames of a videotape show how the eyes move independently through large angles, horizontally, vertically, and torsionally. The dark regions in each eye contain ommatidia directed to the same point in space, which could therefore serve as a basis for monocular stereopsis. (From Land et al. 1990.)

rods which are absorbed when the fish mature (Walls 1963). The rods hinge about their base and probably serve as a scanning mechanism rather than binocular vision. Hammerhead sharks also have eyes very far apart but this too seems unconnected with binocular vision, since their eyes are lateral.

Visual resolution of fish for a grating stimulus varies between 4 and 20 arcmin, according to species, compared with about 1 arcmin for humans (Douglas and Hawryshyn 1990; Nicol 1989). Fish have the involuntary nystagmic eye movements found in all animals with mobile eyes. Some teleost fish have foveas (Walls 1963) and some, such as the African cichlid fish (*Haplochromis burtoni*) move their

eyes independently to foveate particular objects. It has been observed that some of these voluntary saccadic movements involve a coordinated change in vergence when the visual object is in the binocular visual field (Schwassmann 1968; Fernald 1985). Insofar as vergence movements are evoked by image disparity, binocular cells must be involved. It is not clear what function these movements serve.

Douglas et al. (1988) trained goldfish (*Carassius auratus*) to distinguish a 5cm-diameter disc from a 10cm-diameter disc at a fixed viewing distance. The animals could still distinguish discs that were separated in depth so that they subtended the same visual angle. The fish thus exhibited size constancy

which implies that they take distance into account when judging the size of an object. They still showed size constancy when one eye was occluded so that monocular cues to depth are sufficient. Nobody has produced evidence of binocular stereopsis in fish.

16.5 STEREOPSIS IN AMPHIBIA

Binocular vision has been explored in amphibia, particularly in the anurans (frogs and toads). The visual system of anurans has been reviewed by Grüsser and Grüsser-Cornehls (1976). Frogs belonging to the family Ranidae, such as *Rana pipiens*, live both in water and on land and have laterally placed eyes with a visual field of almost 360° and a frontal binocular field up to 100° wide. It has been claimed that the binocular field widens to about 160° above the head (Fite 1973) but other investigators have revised this value down to 60° (Grobstein et al. 1980). If prey is seen within a range of 1 or 2 metres the frog moves forward in a series of jumps, making detours around objects if necessary. Once the prey is within a distance of about 5 cm it is captured by a flick of the tongue. Frogs usually bring the prey close to the body midline but can catch prey without first orienting the eyes or head, even when the prey is 45° or more from the midline. Within a distance of about 15 cm frogs have been found to select from several prey items on the basis of their linear sizes rather than their angular size. This suggests that within this range they have size constancy (Ingle and Cook 1977).

The dorsal anterior thalamus of the frog contains binocular cells that receive direct inputs from both ipsilateral and contralateral corresponding regions of the binocular field (Keating and Kennard 1976). The optic tectum on each side of the midbrain (mesencephalon) also contains binocularly driven cells that derive direct inputs from the contralateral eye and ipsilateral inputs from the contralateral tectum by way of the nucleus isthmi and the postoptic commissures (Fite 1969; Keating and Gaze 1970; Raybourn 1975; Gruberg and Lettvin 1980). It has been claimed that inputs from only the central region of the binocular field project to binocular cells in both optic tecta; the left flank was said to project to binocular cells in only the right optic tectum and the right flank only to binocular cells in the left optic tectum (Gaze and Jacobson 1962). However, subsequent investigations revealed that the whole binocular field of the frog projects to binocular cells in each tectum (Keating and Gaze 1970). Thus, there is a complete representation of the binocular field in each tectum. Note that in mammals the two halves

of the binocular field project to different cortical hemispheres. All binocular cells in the frog receive their inputs from corresponding regions in the visual field. Binocular cells are also found in diencephalic visual centres of the frog (Székely 1971). Visual inputs also go from the dorsal thalamus and diencephalon to the forebrain (telencephalon), an area that also receives somatosensory inputs (Kicliter and Northcutt 1975). Some of the cells in the telencephalon are also binocular (Liege and Galand 1972) but little is known about their function.

Finch and Collett (1983) recorded from binocular cells in the optic tectum of *Rana pipiens* and found that some cells had small receptive fields and responded best to spots that were dark below and light above. Other cells had very large receptive fields and responded to horizontal boundaries, dark below and light above. The cells with small receptive fields were tuned to zero vertical disparity and, on average, to 1.7° of horizontal disparity. The eyes of the frog do not change their vergence and are about 1.5 cm apart. Putting these values in formula (1) in Section 2.3.1 shows that cells registering 1.7° of disparity are maximally stimulated by an object at a distance of 50 cm. The largest disparity tuning was 3.4°, which corresponds to a distance of 25 cm. This suggests that the binocular cells of the tectum are not responsible for the estimation of distance within the 25-cm snapping zone. Gaillard (1985) conducted a similar study in *Rana esculenta* and agreed that tectal cells with the smallest receptive fields are not tuned to disparities within the snapping zone. However, they found a group of cells with receptive fields about 5° in diameter tuned to disparities of between 0.25° and 12°, corresponding to distances between 5 and 300 cm. These neurones could therefore serve to detect distances in the snapping zone.

Frogs of the family Pipidae, such as *Xenopus laevis*, are adapted to a completely aquatic life and feed on prey swimming above them. Because of this, their eyes migrate to the top of the head during metamorphosis. Each eye migrates 55° nasally and 50° dorsally with respect to the major body axes and, as a result, the lateral extent of the binocular field increases from 30° to 162°. At the same time, the proportion of each tectum devoted to the binocular visual field increases from 11 to 77 per cent and there is a corresponding increase in the intertectal commissures responsible for the ipsilateral retinotectal projection (Grant and Keating 1989a). These adaptive changes depend on visual experience, since they are impaired in animals deprived of early vision. In Pipid frogs reared in the dark, the contralateral retinotectal projections develop normally, but the mapping of the intertectal system shows signs of

disorder (Grant and Keating 1989b). However, a normal intertectal mapping is restored when sight is restored, even in frogs deprived of vision for 2 years after metamorphosis (Keating et al. 1992). Thus, there is no critical period for visual experience in the development of normal binocular vision in *Xenopus*, like that found in mammals (see Section 15.8).

When one eye of *Xenopus* at the tadpole stage was rotated through 90° or 180°, a new set of intertectal connections developed that brought the retinas back into spatial correspondence, but only when the developing animal was allowed to see (Keating and Feldman 1975; Grant and Keating 1992). Thus, in these animals, interactions between visual signals from the two eyes guide the development of intertectal connections so that neurones in the tecta receive inputs from corresponding visual directions. When the frog *Rana pipiens* was reared from the tadpole stage with one eye rotated 180°, there was no evidence of remapping of central connections even after both eyes were opened (Jacobson and Hirsch 1973; Skarf 1973). It appears that Pipid frogs compensate for eye rotation while Ranids do not. Visually guided plasticity in Pipids presumably arises because they must adapt their visual functions to the migration of their eyes to the top of the head. When one eye of *Xenopus* at the tadpole stage was replaced by an opposite eye from another tadpole, about half the animals developed intertectal connections with proper spatial correspondence, but the other animals developed abnormal intertectal connections (Beazley 1975). We saw in Section 15.8 that visual experience is required for the development of normal binocular vision in mammals.

Toads (*Bufo bufo*) also have panoramic vision with a large binocular field extending above the head. Unlike frogs, toads first orient themselves so as to centre their prey in the midline and then capture it with only a flick of the tongue (Fite 1973). Like frogs, toads do not converge their eyes, so their ability to snap at prey is not derived from vergence movements (Grüsser and Grüsser-Cornehls 1976; Grobstein et al. 1980). As in frogs, inputs from corresponding areas of the two retinas converge in the thalamic and midbrain visual areas.

Frogs and toads have good depth discrimination, as revealed by their ability to avoid objects and jump through apertures, over gaps, down steps, and onto objects (Ingle 1976). Toads make a detour around a fence when the prey is too far away to be caught through the fence. They make for gaps formed by overlapping barriers at different distances only if the gap is sufficiently wide—a task that can be performed only if they detect the depth separation between the barriers (Lock and Collett 1979).

A frog's ability to catch prey is not much affected by severing the optic tract of one eye, so monocular cues to distance are sufficient for this purpose (Ingle 1972). Stereoscopic vision based on disparity has not been demonstrated in frogs, but there is evidence of disparity-based stereopsis in toads, as we will now see.

When a negative lens was placed in front of one eye of a toad, with the other eye closed, the animal undershot the prey by an amount predictable from the assumption that it was using accommodation for judging distance. However, when both eyes were open, negative lenses had no effect, which suggests that toads use disparity cues when both eyes are open. This conclusion is strengthened by the fact that base-out prisms in front of the eyes caused toads to undershoot the target (Collett 1977; Collett et al. 1987). Thus, toads rely on accommodation when one eye is closed and on binocular disparity when both eyes are open. Since the vergence position of the eyes of toads does not change, the magnitude and sign of binocular disparity between the images of an object signifies the absolute distance of that object from the animal. This is the information that a toad needs when catching its prey.

Tongue-projecting salamanders (*Bolitoglossini*) catch prey by extending the tongue by up to two-thirds of their body length within 10 ms. Salamanders wait in ambush until a prey object appears and then project the tongue with great accuracy both in direction and distance. They can catch flies on the wing which implies that they take account of the temporal as well as the spatial characteristics of the stimulus. Tongue-projecting salamanders have frontal eyes with a 90° binocular field.

In most amphibians, each optic tectum receives a direct input from the contralateral eye and an indirect input from the ipsilateral eye through the nucleus isthmi. This relayed ipsilateral input involves a delay of at least 30 ms. Tongue-projecting salamanders are unique among amphibians in having a large direct ipsilateral projection to the tectum in addition to the indirect input relayed through the nucleus isthmi (Roth 1987). Since the direct pathway is more rapid than the indirect pathway they are able to process binocular inputs more rapidly than other amphibians. Each tectal hemisphere receives a complete projection from both eyes within the binocular visual field. The ipsilateral and contralateral projections in each hemisphere are in topographical correspondence and project onto binocular cells. The eyes have a fixed convergence and the monocular receptive fields are in closest correspondence for stimuli at about the maximum distance over which the tongue projects (Wiggers et al. 1994).

All this suggests that tongue-projecting salamanders judge distance by a range-finding disparity mechanism, but the details of disparity coding in the tectum remain to be discovered.

16.6 BINOCULAR VISION IN REPTILES

Chameleons live in shrubs and catch small insects with their sticky tongues. Chameleons have an all-cone retina and a well-developed fovea. Their laterally placed eyes are mounted in turret-like enclosures and can move over a range of 180° horizontally and 80° vertically (Walls 1963). Optokinetic nystagmus and the vestibulo-ocular response together achieve image stability with a gain of about 0.8 as the body moves (Gioanni et al. 1993). Spontaneous saccadic movements of large amplitude occur independently in the two eyes at random intervals (Mates 1978). When a chameleon has located a prey object it rotates its head to centre the prey, converges its eyes to achieve binocular fixation, and shoots its tongue out at great speed up to 1.5 times the length of its body.

Harkness (1977) filmed the motion of the tongue and found that the distance moved was related to the distance of the prey. Convergent prisms placed before the eyes did not cause the animals to undershoot the target, which suggests that chameleons do not use the vergence of the eyes as a range finder. However, when a negative lens was placed in front of one eye with the other eye closed the animals undershot the prey. When a positive lens was used they overshot the prey. It therefore seems that chameleons use accommodation for judging distance. They dilate the pupil when aiming at prey. This is an adaptive strategy since pupil dilation reduces the depth of field and therefore makes it easier to detect when an object is not in the focal plane. It is possible that they also use binocular disparity.

16.7 STEREOPSIS IN BIRDS

Binocular vision in the pigeon

The domestic pigeon (*Columba livia*) has laterally placed eyes with the optic axes set at an angle of about 120°. It has a total visual field of about 340° and a frontal binocular region with a maximum width of about 27°, which extends from 90° above the beak to about 40° below it (Martin and Young 1983). In the sample of birds tested by Martin and Young the visual field was widest 20° above the plane of the beak whereas in the sample tested by

Martinoya et al. (1981) it was 45° below the beak (see also McFadden and Reymond 1985). These differences may reflect differences in the convergence state of the eyes. In any case the binocular field is well placed to help the bird peck at seeds on the ground and locate a landing site. The binocular region is served by a specialized area in the temporal retina containing a high density of receptors, known as the *area dorsalis*. The *area dorsalis* projects 10 to 15° below the eye-beak plane and is distinct from the more laterally placed fovea used for lateral monocular viewing. The cones in the region of the *area dorsalis* contain red oil droplets whereas those in the region of the lateral fovea contain yellow pigment. The threshold for the resolution of a high-contrast grating presented to the lateral fovea has been reported to be between 1.16 and 4.0 arcmin, compared with a value of about 0.8 arcmin for human observers (Blough 1971). Peak contrast sensitivity was found at a spatial frequency of about 4 c/deg (Nye 1968). The acuity of the frontal fovea was found to be only slightly higher (Hahmann and Güntürkün 1993).

When the head of the pigeon is restrained, each eye is capable of executing saccades of up to 7° amplitude in response to stimuli presented in the lateral field, with each eye moving independently of the other. These movements bring the image of a laterally placed object onto the lateral fovea of one eye. Both eyes execute coordinated vergence movements to stimuli presented at near distances in the frontal visual field. These movements bring the images onto the *area dorsalis* in each eye. Vergence is most effectively evoked by stimuli 25° below the beak, which is the position occupied by objects on the ground at which the pigeon pecks. Before the head makes a pecking motion it moves forward in two successive movements, with the eyes converging on the ground (Goodale 1983; Bloch et al. 1984). Just before the final ballistic movement the grain is centred on the *area dorsalis* about 10° below the eye-beak axis. The eyes close during the final ballistic peck.

Like all birds, the pigeon has two main visual channels in the brain. One channel leads to the contralateral pretectum and optic tectum (the analogue of the superior colliculus in mammals), then to the ipsilateral nucleus rotundus and nucleus triangularis in the thalamus, and on to the ectostriatal complex and surrounding extrinsic recipient areas in the telencephalon. This is probably the phylogenetically older system since it is fully decussated and is fully developed by the time of hatching. Different regions of the nucleus rotundus of the pigeon are specialized for different functions. Cells in one region respond to changes in illumination over the whole visual

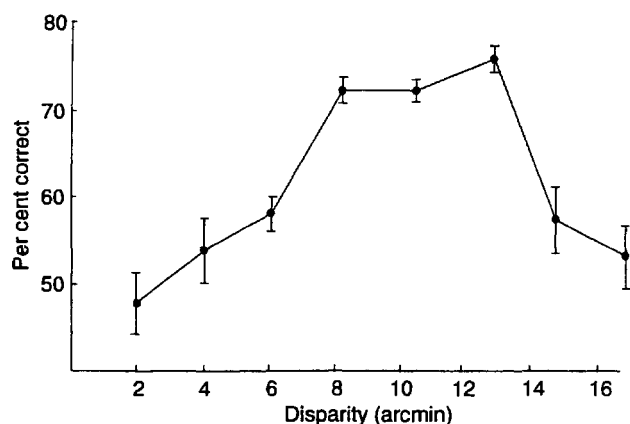


Figure 16.4. Stereoacuity in a sparrow hawk.

A sparrow hawk's percent correct detection of a stereogram containing depth, as a function of binocular disparity. Each point is based on between 50 and 350 trials. Vertical bars are standard errors. (From Fox et al. 1977. Copyright 1977, by the AAAS.)

field, those in another region are colour coded, those in a third region respond to differential motion, and those in a fourth region respond to motion in depth signalled by monocular looming, and are particularly sensitive to objects on a collision course with the head (Wang et al. 1993).

The second channel of the avian visual system consists of a fully decussated pathway to the optic thalamus (the homologue of the mammalian lateral geniculate nucleus) and, from there, a hemidecussated pathway to a centre on the dorsum of the diencephalon known as the *wulst* (German for "bulge"). This system is not fully developed in the pigeon until about 17 days after hatching, suggesting that visual inputs are required for its maturation (Karten et al. 1973). It has been suggested that this system contains small receptive fields that code the shapes and positions of stimuli (see Emmerson 1983).

Very few binocular cells have been found in either the pigeon's optic tectum or the *wulst* (Frost et al. 1983). However, binocular cells in the *wulst* may have been missed because of misalignment of the eyes. As we will see, binocular cells have been found in the *wulst* of other birds. There is conflicting evidence about stereoscopic vision in the pigeon. Martinoya et al. (1988) found that pigeons could discriminate between points of light presented one at a time at different distances. However, pigeons failed to discriminate between a pair of simultaneously presented stimuli set at different depths from a subsequently presented pair in the same depth plane. This suggests that they use a range-finding mechanism based on vergence rather than binocular disparity. It has been found possible to train pigeons to peck at one of two simultaneously presented panels that vary in relative depth. This procedure has revealed

that pigeons have a depth acuity of between 0.8 and 1.8 arcmin (McFadden 1987). Further experiments are required to prove that this ability is based on detection of disparities rather than on a vergence range-finding mechanism or monocular parallax.

Binocular vision in hawks

Hawks, like many predatory birds, have two foveas in each eye, a central fovea for sideways looking and a temporal fovea serving the binocular region of the visual field. They have an impressively large number of receptors per degree of visual angle. For instance, the American kestrel, or falcon (*Falco sparverius*) has about 8,000 receptors per degree and the red-tailed hawk (*Buteo jamaicensis*) about 15,000 per degree, compared with about 7,000 in the rhesus monkey (Fite and Rosenfield-Wessels 1975). Schlaer (1972) found that image quality in the live African eagle (*Dryotriorchis spectabilis*) is up to 2.4 times greater than in the human eye. The American kestrel can detect a grating with a spatial frequency of 160 c/deg compared with 60 c/deg in humans (Fox et al. 1976). However, the cone density and focal length of the kestrel's eye are not sufficiently greater than those of the human eye to account for its greater acuity. Snyder and Miller (1978) suggested a third way in which falconiform birds may achieve high acuity. They proposed that the highly concave surface of the foveal pit acts as a negative lens which, together with the positive lens of the eye, constitutes a telephoto lens system which effectively increases the focal length of the eye. Another possibility is that the effective density of receptors is increased when they lie on an oblique surface as opposed to a surface normal to the incident light.

Fox et al. (1977) trained a sparrow hawk to fly from a perch to a panel containing a dynamic random-dot stereogram in preference to one containing a similar two-dimensional random-dot pattern. The stereogram was created by the colour-anaglyph method, with the falcon wearing red and green filters. The percent correct response of the trained animal was recorded as the disparity in the stereogram was varied. It can be seen from Figure 16.4 that performance peaked for a disparity of about 12 arcmin. This suggests that the sparrow hawk has fully fledged stereoscopic vision enabling it to detect the three-dimensional shapes of objects, and not merely a range-finding mechanism serving the detection of absolute distance.

Binocular vision in owls

The owl uses auditory signals to locate the direction of prey. The head is rapidly turned to face the direction of the sound and, even in total darkness, the

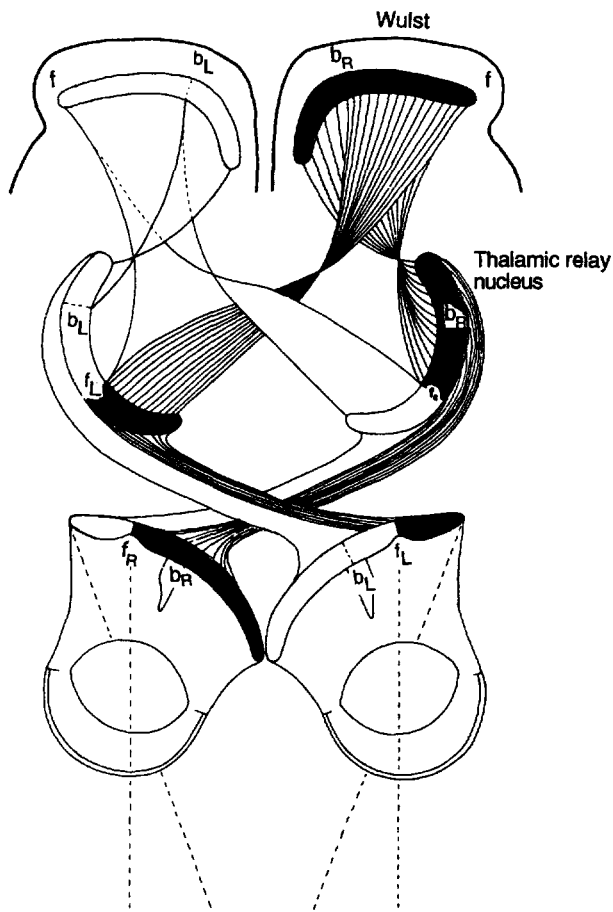


Figure 16.5. The visual pathways of the owl.

The optic nerves decussate fully as they project to the optic tectum and optic nucleus in the thalamus. The pathways from the thalamus to the wulst hemidecussate so that corresponding inputs from the binocular visual field are brought to the same destination in the wulst. The fovea for the frontal field is denoted by *f*, and the limits of the binocular field by *b*. (From Pettigrew 1986. Reprinted with permission of Cambridge University Press.)

owl can then swoop down and capture the prey. The auditory mechanism that signals the direction of sounds has been investigated in some detail (Konishi 1993) but it is not clear how the distance of the prey is derived from auditory signals. Perhaps the owl relies on its acquired knowledge of surfaces in its surroundings. There is evidence that owls use their eyes for judging distance when there is some light.

The tawny owl (*Strix aluco*) has a binocular visual field with a maximum width of 48° and a total visual field of 201° (Martin 1984). The retina has a single, temporally placed fovea which, in the great horned owl (*Bubo Virginianus*), has about 13,000 receptors per degree of visual angle (Fite and Rosenfield-Wessels 1975). The visual pathways of owls decussate totally at the chiasma and project retinotopically to the optic tectum. Each cell in the optic tectum responds both when a visual stimulus falls within its

receptive field and when a sound is heard from the same direction in space (Knudsen 1982). Since the eyes are virtually immobile in the head the spatial correspondence of the visual and auditory projections is constant. The full decussation of the visual inputs to the thalamus and tectum suggests that this system is concerned with directional aspects of behaviour rather than with distance. Figure 16.5 shows the hemidecussated bilateral projection from the optic nucleus in the thalamus to the wulst, which is particularly well developed in the owl. The physiological properties of cells in the wulst of the owl are very similar to those of cells in the mammalian visual cortex. Many binocular cells are tuned to binocular disparity, and their component receptive fields in the two eyes are similarly tuned for orientation and motion. The cells are also arranged in ocular dominance columns (Pettigrew and Konishi 1976; Pettigrew 1979).

Wagner and Frost (1993) measured the disparity tuning functions of cells in the wulst of the barn owl (*Tyto alba*) to sine wave gratings and to one-dimensional visual noise. Although the lesser peaks in the disparity tuning function varied as a function of the spatial frequency of the gratings, the main peak occurred at a characteristic disparity for that cell which was independent of spatial frequency. The characteristic disparity sensitivity of different cells ranged between 0 and 2.5°. Furthermore, the one-dimensional noise also produced a peak response at a disparity of 2°. A disparity-detection mechanism based on spatial-phase differences between cells with no lateral offset, as described in Section 4.5.2, produces tuning functions that vary with spatial frequency, whereas a mechanism based on positional offset produces tuning functions like those reported by Wagner and Frost. In the owl, the peak response of most cells tuned to disparities of less than about 3 arcmin did vary with spatial frequency. It looks as though an offset mechanism operates with large disparities and a phase-difference mechanism operates with small disparities.

It seems that the close similarity between the disparity-detecting mechanism of the wulst and that of the mammalian visual cortex is the product of a remarkable process of parallel evolution. Further work is needed to reveal how general this mechanism is among birds.

The eyes of the owl are very large in proportion to its head and move, at most, about 1° (Steinbach and Monev 1973). It is not known whether any of these eye movements involve vergence. On the other hand, the owl can rotate its head at high velocity through at least 180°. Since the eyes are locked in a more or less fixed position of vergence, binocular

disparity could code absolute depth as well as relative depth. In the young bird the eyes are diverged and take up their adult positions in the second month of life. When binocular vision is disrupted during this developmental phase the eyes fail to become properly aligned. Microelectrode recordings from binocular cells in the optic tectum of strabismic owls revealed that the monocular receptive fields were also misaligned (Knudsen 1989). Thus, the neural pattern of binocular correspondence is innate and presumably guides the alignment of the eyes in the young bird.

It is not known whether the owl is capable of discriminating absolute or relative depth by disparity, but the accuracy with which it catches its prey suggests that it has some form of visual or auditory capacity to judge depth. The barn owl apparently uses accommodative effort for judging near distances. When wearing a plus or minus lens in front of one eye and an occluder over the other, the animal made corresponding errors in pecking at a nearby object (Wagner and Schaeffer 1991).

16.8 STEREOPSIS IN MAMMALS

Many mammals, including rats, dogs, cats, pigs, and sheep avoid a cliff even when they are very young, thus showing that they are able to detect depth (Walk and Gibson 1961). But this ability probably depends on monocular depth cues such as perspective and motion parallax. Stereoscopic vision is well developed in frontal-eyed mammals such as cats and primates, and most of this book is devoted to stereopsis in these animals.

The meerkat (*Suricata suricatta*) is a frontal-eyed social carnivore of the mongoose family. Nothing is known about its visual pathways or visual cortex. However, it has been shown to possess stereoscopic vision that seems to depend on binocular disparity. One of the animals was trained to jump to the closer of two visual displays and with both eyes open it discriminated relative depths corresponding to disparities of about 10 arcmin (Moran et al. 1983). Thus, binocular stereoscopic vision has been demonstrated in the monkey, cat, and meerkat among frontal-eyed mammals. However, the visual fields of all mammals, except the Cetaceae (whales and dolphins) overlap to some degree. As we will now see there is some suggestive evidence that binocular stereopsis may also be present in some lateral-eyed mammals.

The rabbit has laterally placed eyes and, when crouched in the "freeze" position, has 360° panoramic vision with a frontal binocular area of about 24°. At least 90 per cent of optic-nerve fibres decussate in

the chiasma (Giolli and Guthrie 1969). The retina does not have a fovea but there is a relatively high concentration of receptors along an extended horizontal region known as the visual streak which receives the image of the visual horizon. There is also a high concentration of receptors in the posterior part of the retina, corresponding to the binocular region of the visual field, which is about 30° wide and extends from about 35° below eye level to about 160° above eye level. The rabbit uses this part of the retina when performing visual discrimination tasks (Hughes 1971). When the animal is in the freeze position, corresponding parts of the two retinas have a horizontal disparity of about 18°. By converging the eyes, the rabbit is able to match corresponding images in the two eyes but, when it does so, its visual fields no longer meet behind the head (Hughes and Vaney 1982). Convergence eye movements of up to about 18° have been recorded when the rabbit approaches a visual display (Zuidam and Collewijn 1979). Thus, the rabbit has two modes of viewing, one in which it preserves panoramic vision but loses all binocular correspondence, and one in which it achieves binocular correspondence within the binocular field at the expense of some loss in panoramic coverage.

The region of the rabbit's visual cortex corresponding to the binocular part of the visual field contains binocular neurones tuned to binocular disparity. At first it was reported that the component receptive fields in the two eyes were not similarly tuned for stimulus size and orientation (Van Sluyters and Stewart 1974a). However, when allowance was made for the fact that the eyes must converge 18° to bring corresponding images into register, binocular cells were found to have matching tuning functions in the two eyes (Hughes and Vaney 1982). The binocular cells of the rabbit showed very little evidence of the developmental plasticity found in the binocular cells of cats and primates (Van Sluyters and Stewart 1974b).

The rabbit can perform visual discrimination tasks in which binocular information must be integrated (Van Hof and Steele Russell 1977) and it has been observed to perform voluntary eye movements (Hughes 1971). However, there do not seem to have been any direct tests of stereopsis in the rabbit.

Cortical cells sensitive to binocular disparity have been found in ungulates. For instance, cells tuned to up to 6° of disparity have been found in the visual cortex of sheep, especially in area 18 (Clarke et al. 1976). Disparity-selective cells were found in the newborn lamb, although with broader tuning than in the adult animal (Clarke et al. 1979). Sheep have good depth judgment, but it is not known to what

extent this depends on binocular stereopsis. Cells sensitive to binocular disparity have also been found in the goat (Clarke and Whitteridge 1976). The goat is a lateral-eyed mammal with a 60°-wide binocular field and great agility, suggesting the possession of stereoscopic vision.

An autoradiographic study of projections to the visual cortex failed to reveal evidence of ocular dominance columns in sheep and goats (Pettigrew et al. 1984). Neonatal lambs and goats are much more advanced than neonatal cats and monkeys and are able to follow the mother and avoid obstacles and cliffs a few hours after birth. Nevertheless, brief periods of monocular deprivation in the lamb cause marked shifts in ocular dominance of binocular cortical cells (Martin et al. 1979).

Although there is no behavioural evidence of stereopsis in sheep or goats, such evidence exists for the horse. Timney and Keil (1994) trained two horses to select a display containing a square in real depth. After training they were shown random-dot stereograms viewed through red-green anaglyph filters. On most trials they selected the stereogram that depicted a square in depth. The mean disparity threshold for detection of depth was 14 arcmin.

The topic of depth vision in animals has been reviewed by Walls (1963), Hughes (1977), Collett and Harkness (1982), and Pettigrew (1991).

16.9 FINAL WORD

This is the end of our review of stereoscopic vision. Our understanding of this aspect of vision has advanced at an accelerating rate since the time of Euclid. It was only about 160 years ago that Wheatstone revealed the crucial role of binocular disparity. We are only now beginning to appreciate the extent to which depth perception relies on vertical as well as horizontal disparity and on complex patterns and spatial derivatives of disparity. We are

also beginning to understand how disparity is coupled to other types of visual information such as motion, figure-ground perception, and the perception of surfaces. Since 1968 there has been a steady accumulation of knowledge about the neural machinery involved in disparity processing but these mechanisms are also turning out to be more complex than at first believed. We have an ever growing repertoire of psychophysical, physiological, and computational techniques and there is an ever growing population of psychologists, physiologists, physicists, engineers, and computer scientists investigating stereoscopic vision.

Three new applications of stereopsis are opening up. The first is three-dimensional virtual reality systems used for entertainment, and for simulators for learning skills, such as flying, athletics, and surgery, where practice in a real environment is dangerous or costly. The second application is in telepresence systems in which a real-world scene is registered by a video camera and conveyed to an observer at a remote site. This allows people to operate mechanical devices in dangerous or inaccessible environments such as mines, nuclear reactors, fires, and inside human bodies. The third application of stereopsis is the design of artificial visual systems, especially those attached to robots operating in a three-dimensional environment in industry and in the extraterrestrial environment.

With all our advances in understanding, the sheer wonder of the appearance of solidity we experience when viewing a stereogram remains. In our attempts to understand visual consciousness we refer to neural networks, synchronous oscillations, cell assemblies, impulse trains, and quantum physics, but we are only groping in the dark. The astounding mystery of our conscious perception of a three-dimensional visual world, that confronts us whenever we open our eyes, continues to intrigue and baffle us and remind us of the wonderful piece of machinery that each of us carries in our head.

References

- Abadi, R. V. (1976). Induction masking—a study of some inhibitory interactions during dichoptic viewing. *Vision Research*, 16, 269–75. [332]
- Abadi, R. V. and Dickinson, C. M. (1985). The influence of pre-existing oscillations on the binocular optokinetic response. *Annals of Neurology*, 17, 578–86. [643]
- Abadi, R. V. and Pascal, E. (1989). The recognition and management of albinism. *Ophthalmology and Physiological Optics*, 9, 3–15. [642]
- Abel, L. A., Schmidt, D., Dell'Osso, L. F., and Daroff, R. B. (1978). Saccadic system plasticity in humans. *Annals of Neurology*, 4, 313–18. [414]
- Abramov, I., Gordon, J., Hendrickson, A., Hainline, L., Dobson, V., and LaBossiere, E. (1982). The retina of the newborn human infant. *Science*, 217, 265–7. [605]
- Adams, R. J., Courage, M. L., and Mercer, M. E. (1991). Deficiencies in human neonates' color vision: Photoreceptor and neural explanations. *Behavioural Brain Research*, 43, 109–14. [617]
- Addams, R. (1834). An account of a peculiar optical phenomenon seen after having looked at a moving body. *London and Edinburgh Philosophical Magazine and Journal of Science*, 5, 373–4. [375]
- Adelson, E. H. (1982). Some new illusions and some old ones analyzed in terms of their Fourier components. *Investigative Ophthalmology and Visual Science*, 22 (Abstracts), 144. [569]
- Adelson, E. H. and Movshon, J. A. (1982). Phenomenal coherence of moving visual patterns. *Nature*, 300, 523–5. [527]
- Adelson, E. H. and Movshon, J. A. (1984). Binocular disparity and the computation of two-dimensional motion. *Journal of the Optical Society of America*, 1A, 1266. [527]
- Aguilonius, F. (1613). *Opticorum libri sex*. Plantin, Antwerp. [14]
- Ahissar, E., Vaadia, E., Ahissar, M., Bergman, H., Arieli, A., and Abeles, M. (1992). Dependence of cortical plasticity on correlated activity of single neurons and on behavioral context. *Science*, 257, 1412–15. [82]
- Ahlsén, G., Lindström, S., and Lo, F-S. (1985). Interaction between inhibitory pathways to principal cells in the lateral geniculate nucleus of the cat. *Experimental Brain Research*, 58, 134–43. [113]
- Akerstrom, R. A. and Todd, J. T. (1988). The perception of stereoscopic transparency. *Perception and Psychophysics*, 44, 421–32. [232, 445]
- Albus, K. (1975). A quantitative study of the projection area of the central and paracentral visual field in area 17 of the cat. I. The precision of the topography. *Experimental Brain Research*, 24, 159–79. [133]
- Albus, K. and Wolf, W. (1984). Early postnatal development of neuronal function in the kitten's visual cortex: A laminar analysis. *Journal of Physiology*, 348, 153–85. [613]
- Alexander, L. T. (1951). The influence of figure-ground relationships on binocular rivalry. *Journal of Experimental Psychology*, 41, 376–81. [330]
- Alhazen, I. Book of optics. In *The optics of Ibn Al-Haytham* 2 volumes. Trans. by A. I. Sabra. Warburg Institute, University of London, 1989. [4]
- Allen, D., Banks, M. S., and Norcia, A. M. (1993). Does chromatic sensitivity develop more slowly than luminance sensitivity? *Vision Research*, 33, 2553–62. [617]
- Allen, D. C. (1974). Vertical prism adaptation in anisometropes. *American Journal of Optometry and Physiological Optics*, 51, 252–9. [393]
- Allen, D. G. (1937). A test for aniseikonia by the use of central fixation and fusion. *AMA Archives of Ophthalmology*, 17, 320–7. [64–65]
- Allen, M. J. (1953). An investigation of the time characteristics of accommodation and convergence of the eyes. *American Journal of Optometry and Archives of American Academy of Optometry*, 30, 393–402. [397]
- Allen, M. J. and Carter, J. H. (1967). The torsional components of the near reflex. *American Journal of Optometry and Archives of the American Academy of Optometry*, 44, 343–9. [384, 410, 417]
- Allendoerfer, K. L. and Shatz, C. J. (1994). The subplate, a transient neocortical structure: Its role in the development of connections between thalamus and cortex. *Annual Review of Neuroscience*, 17, 185–218. [614]
- Allendoerfer, K. L., Cabelli, R. J., Escandón, E., Kaplan, D. R., Nikolic, K., and Shatz, C. J. (1994). Regulation of neurotrophin receptors during the maturation of the mammalian visual system. *Journal of Neuroscience*, 14, 1795–811. [606]
- Allik, J. (1992). Resolving ambiguities in orientation, motion, and depth domains. *Perception*, 21, 731–46. [518]
- Alpern, M. (1946). The after-effect of lateral duction testing on subsequent phoria measurements. *American Journal of Optometry*, 23, 442–7. [391]
- Alpern, M. (1952). Metacontrast: Historical introduction. *American Journal of Optometry*, 29, 631–46. [369]
- Alpern, M. (1954). Relation of visual latency to intensity. *AMA Archives of Ophthalmology*, 51, 369–74. [537]
- Alpern, M. (1958). Vergence and accommodation: Can change in size induce vergence movements? *AMA Archives of Ophthalmology*, 60, 355–7. [399]
- Alpern, M. (1968). A note on visual latency. *Psychological Review*, 75, 260–4. [538, 545–6]
- Alpern, M. (1969). Types of eye movement. In *The eye*. Vol. 3, (ed. H. Davson), pp. 65–174. Academic Press, New York. [386, 398]
- Alpern, M. and Ellen, P. (1956). A quantitative analysis of the horizontal movements of the eyes in the experiment of Johannes Müller. *American Journal of Ophthalmology*, 42, 289–96. [412]
- Alpern, M. and Larson, B. F. (1960). Vergence and accommodation, IV. Effect of luminance quantity on the AC/A. *American Journal of Ophthalmology*, 49, 1140–9. [396]
- Alpern, M. and Wolter, J. R. (1956). The relation of horizontal saccadic and vergence movements. *AMA Archives of Ophthalmology*, 56, 685–90. [424]
- Altmann, L., Luhmann, H. J., Creuel, J. M., and Singer, W. (1987). Functional and neuronal binocularly in kittens raised with rapidly alternating monocular occlusion. *Journal of Neurophysiology*, 58, 965–80. [630]
- Ames, A. (1926). Cyclophoria. *American Journal of Physiological Optics*, 7, 3–38. [321]
- Ames, A. (1945). The space-eikonometer test for aniseikonia. *American Journal of Ophthalmology*, 28, 248–62. [65–6]
- Ames, A. (1955). *The nature of our perceptions, prehensions and behavior*. Princeton University Press, Princeton, N.J. [576]
- Ames, A., Glidden, G. H., and Ogle, K. N. (1932a). Size and shape of ocular images. I. Methods of determination and physiologic significance. *AMA Archives of Ophthalmology*, 7, 576–97. [55]

- Ames, A., Ogle, K. N., and Glidden, G. H. (1932b). Corresponding retinal points, the horopter and size and shape of ocular images. *Journal of the Optical Society of America*, **22**, 538–574; 575–631. [57-9, 60, 292, 304]
- Amigo, G. (1963). Variation of stereoscopic acuity with observation distance. *Journal of the Optical Society of America*, **53**, 630–5. [179]
- Amigo, G. (1974). A vertical horopter. *Optica Acta*, **21**, 277–92. [418]
- Amigo, G., Fiorentini, A., Pirchio, M., and Spinelli, D. (1978). Binocular vision tested with visual evoked potentials in children and infants. *Investigative Ophthalmology and Visual Science*, **17**, 910–15. [620]
- Andersen, E. E. and Weymouth, F. W. (1923). Visual perception and the retinal mosaic. I. Retinal mean local sign: An explanation of the fineness of binocular perception of distance. *American Journal of Physiology*, **64**, 561–94. [155, 167]
- Andersen, R. A. (1987). The role of the inferior parietal lobule in spatial perception and visual–vestibular integration. In *The handbook of physiology*, Sect. 1, *The nervous system*, Vol. IV, (ed. F. Plum, V. B. Mountcastle, and S. T. Geiger), pp. 483–58. American Physiological Society, Bethesda, MD. [127]
- Andersen, R. A., Bracewell, R. M., Barash, S., Gnadt, J. W., and Fogassi, L. (1990). Eye-position effects on visual memory and saccade-related activity in areas LIP and 7a of macaque. *Journal of Neuroscience*, **10**, 11776–96. [126]
- Anderson, B. L. (1992). Hysteresis, cooperativity, and depth averaging in dynamic random-dot stereograms. *Perception and Psychophysics*, **51**, 511–28. [234]
- Anderson, B. L. (1994). The role of partial occlusion in stereopsis. *Nature*, **367**, 365–7. [517]
- Anderson, B. L. and Nakayama, K. (1994). Towards a general theory of stereopsis: Binocular matching, occluding contours, and fusion. *Psychological Review*, **101**, 414–45. [518]
- Anderson, C. H. and Van Essen, D. C. (1987). Shifter circuits: A computational strategy for dynamic aspects of visual processing. *Proceedings of the National Academy of Science*, **84**, 6297–301. [178, 401]
- Anderson, G. J. and Braunstein, M. L. (1983). Dynamic occlusion in the perception of rotation in depth. *Perception and Psychophysics*, **34**, 356–62. [438]
- Anderson, J. D., Bechtoldt, H. P., and Dunlap, G. L. (1978). Binocular integration in line rivalry. *Bulletin of the Psychonomic Society*, **11**, 399–402. [333]
- Anderson, P. A. and Movshon, J. A. (1989). Binocular combination of contrast signals. *Vision Research*, **29**, 1115–32. [354]
- Anderson, P., Mitchell, D. E., and Timney, B. (1980). Residual binocular interaction in stereoblind humans. *Vision Research*, **20**, 603–11. [638]
- Andrews, D. P. (1967). Perception of contour orientation in the central fovea. Part I: Short lines. *Vision Research*, **7**, 975–7. [98, 355]
- Anstis, S. M. (1975). What does visual perception tell us about visual coding. In *Handbook of psychobiology*, (ed. C. Blakemore and M. S. Gazzaniga), pp. 269–323. Academic Press, New York. [466, 473]
- Anstis, S. M. (1986). Motion perception in the frontal plane. In *Handbook of human perception and performance*. Vol. 1, (ed. K. R. Boff, L. Kaufman, and J. P. Thomas), Chap. 16. Wiley, New York. [567]
- Anstis, S. M. and Duncan, K. (1983). Separate motion aftereffects from each eye and from both eyes. *Vision Research*, **23**, 161–9. [376]
- Anstis, S. M. and Harris, J. P. (1974). Movement aftereffects contingent on binocular disparity. *Perception*, **3**, 153–68. [438, 566]
- Anstis, S. M. and Moulden, B. P. (1970). After-effect of seen movement: Evidence for peripheral and central components. *Quarterly Journal of Experimental Psychology*, **22**, 222–9. [376–7, 570]
- Anstis, S. M. and Reinhardt-Rutland, A. H. (1976). Interactions between motion aftereffects and induced movement. *Vision Research*, **16**, 1391–4. [466]
- Anstis, S. M. and Rogers, B. J. (1975). Illusory reversal of visual depth and movement during changes of contrast. *Vision Research*, **15**, 957–61. [226, 232]
- Anstis, S. M., Howard, I. P., and Rogers, B. (1978). A Craik-Cornsweet illusion for visual depth. *Vision Research*, **18**, 213–17. [446, 480-1, 484, 581]
- Antonini, A. and Stryker, M. P. (1993). Development of individual geniculocortical arbors in cat striate cortex and effects of binocular impulse blockade. *Journal of Neuroscience*, **13**, 3549–73. [613]
- Apkarian, P. A. and Reits, D. (1989). Global stereopsis in human albinos. *Vision Research*, **29**, 1359–70. [642]
- Apkarian, P. A. and Shallo-Hoffmann, J. (1991). VEP projections in congenital nystagmus; VEP asymmetry in albinism: A comparison. *Investigative Ophthalmology and Visual Science*, **32**, 2653–6. [643]
- Apkarian, P. A., Nakayama, K., and Tyler, C. W. (1981). Binocularity in the human visual evoked potentials: Facilitation, summation and suppression. *Electroencephalography and Clinical Neurophysiology*, **51**, 32–48. [145–147]
- Apkarian, P. A., Bour, L., and Barth, P. G. (1994). A unique achiasmatic anomaly detected in non-albinos with misrouted retino-fugal projections. *European Journal of Neuroscience*, **6**, 501–7. [608]
- Appel, M. A. and Campos, J. J. (1977). Binocular disparity as a discriminable stimulus parameter for young infants. *Journal of Experimental Psychology*, **23**, 47–56. [619]
- Archer, S. M., Dubin, M. W., and Stark, L. A. (1982). Abnormal development of kitten retino-geniculate connectivity in the absence of action potentials. *Science*, **217**, 743–5. [627]
- Archer, S. M., Miller, K. K., and Helveston, E. M. (1987). Stereoscopic contours and optokinetic nystagmus in normal and stereoblind subjects. *Vision Research*, **27**, 841–4. [589]
- Arditi, A. (1982). The dependence of the induced effect on orientation and a hypothesis concerning disparity computations in general. *Vision Research*, **22**, 247–56. [266, 288]
- Arditi, A. (1986). Binocular vision. In *Handbook of perception and human performance*, Vol. 1, *Sensory processes and perception*, (ed. K. R. Boff, L. Kaufman and J. P. Thomas), Chap. 23. Wiley, New York. [1]
- Arditi, A., Anderson, P. A., and Movshon, J. A. (1981a). A simple explanation of the induced size effect. *Vision Research*, **21**, 755–64. [288]
- Arditi, A., Anderson, P. A., and Movshon, J. A. (1981b). Monocular and binocular detection of moving sinusoidal gratings. *Vision Research*, **21**, 329–36. [376]
- Ariel, M., Daw, N. W., and Rader, R. K. (1983). Rhythmicity in rabbit retinal ganglion cell responses. *Vision Research*, **23**, 1485–93. [83]
- Aristotle (1931). *Parva naturalia. De somni*. In *The works of Aristotle translated into English*. Vol. III. Oxford University Press, London. [375]
- Aschenbrenner, C. M. (1954). Problems in getting information into and out of air photographs. *Photogrammetric Engineering*, **20**, 398–401. [152]
- Asher, H. (1953). Suppression theory of binocular vision. *British Journal of Ophthalmology*, **37**, 37–49. [338]

- Aslin, R. N. (1977). Development of binocular fixation in human infants. *Journal of Experimental Child Psychology*, 23, 133–50. [621]
- Aslin, R. N. (1987). Motor aspects of visual development in infancy. In *Handbook of infant perception*. Vol. 1. *From sensation to perception*, (ed. P. Salapatek and L. B. Cohen), pp. 43–113. Academic Press, Orlando, FL. [617]
- Aslin, R. N. (1988). Anatomical constraints on oculomotor development: Implications for infant perception. In *Perceptual development in infancy* (ed. A. Yonas), pp. 67–104. Erlbaum, Hillsdale, NJ. [621]
- Aslin, R. N. and Dumais, S. T. (1980). Binocular vision in infants: A review and a theoretical framework. *Advances in Child Development*, 15, 53–94. [622]
- Aslin, R. N. and Jackson, R. W. (1979). Accommodative-convergence in young infants: Development of a synergistic sensory-motor system. *Canadian Journal of Psychology*, 33, 222–31. [605, 621]
- Aslin, R. N. and Shea, S. L. (1990). Velocity thresholds in human infants: Implications for the perception of motion. *Developmental Psychology*, 26, 589–98. [616]
- Aslin, R. N., Dobson, V., and Jackson, R. W. (1982). Dark vergence and dark focus in human infants. *Investigative Ophthalmology and Visual Science*, 22 (ARVO Abstracts), 105. [621]
- Atkinson, J. (1972). Visibility of an afterimage in the presence of a second afterimage. *Perception and Psychophysics*, 12, 257–62. [334]
- Atkinson, J. and Braddick, O. (1976). Stereoscopic discrimination in infants. *Perception*, 5, 29–38. [619]
- Atkinson, J., Braddick, O., and Moar, K. (1977). Development of contrast sensitivity over the first three months of life in the human infant. *Vision Research*, 17, 1037–44. [616]
- Atkinson, J., Campbell, F. W., Fiorentini, A., and Maffei, L. (1973). The dependence of monocular rivalry on spatial frequency. *Perception*, 2, 127–33. [334]
- Atkinson, J., Hood, B., Wattam-Bell, J., Anker, S., and Tricklebank, J. (1988). Development of orientation discrimination in infancy. *Perception*, 17, 587–95. [616]
- Atkinson, J., Smith, J., Anker, S., Wattam-Bell, J., Braddick, O. J., and Moore, A. T. (1991). Binocular and amblyopia before and after early strabismus surgery. *Investigative Ophthalmology and Visual Science*, 32, 820. [637]
- Attneave, F. and Block, G. (1973). Apparent movement in tridimensional space. *Perception and Psychophysics*, 13, 301–7. [528]
- Aubert, H. (1865). *Physiologie der Netzhaut*. E. Morgenstern, Breslau. [431]
- Aulhorn, E. (1966). Phasen Differenz-Haploskopie. *Klinische Monatsblätter für Augenheilkunde*, 148, 540. [65–6]
- Azar, R. F. (1965). Postoperative paradoxical diplopia. *American Orthoptic Journal*, 15, 64–71. [47]
- Azzopardi, P. and Cowey, A. (1993). Preferential representation of the fovea in the visual cortex. *Nature*, 361, 719–21. [114]
- Bach-y-Rita, P. (1975). Structural functional correlations in eye muscle fibres. Eye muscle proprioception. In *Basic mechanisms of ocular motility and their clinical implications*, (ed. G. Lennerstrand and P. Bach-y-Rita), pp. 91–108. Pergamon, New York. [640]
- Bacon, J. H. (1976). The interaction of dichoptically presented spatial gratings. *Vision Research*, 16, 337–44. [362]
- Badcock, D. R. and Schor, C. M. (1985). Depth-increment detection function for individual spatial channels. *Journal of the Optical Society of America*, 2A, 1211–15. [155, 173]
- Badcock, D. R. and Westheimer, G. (1985). Spatial location and hyperacuity: The centre/surround location contribution function has two substrates. *Vision Research*, 25, 1259–67. [97, 101]
- Bagby, J. W. (1957). A cross-cultural study of perceptual predominance in binocular rivalry. *Journal of Abnormal and Social Psychology*, 54, 331–4. [347]
- Bagolini, B. (1967). Anomalous correspondence: Definition and diagnostic methods. *Documenta Ophthalmologica*, 23, 346–98. [47]
- Bahill, A. T., Ciuffreda, K. J., Kenyon, R., and Stark, L. (1976). Dynamic and static violations of Hering's law of equal innervation. *American Journal of Optometry and Physiological Optics*, 53, 786–96. [410]
- Baitch, L. W. and Levi, D. M. (1988). Evidence for nonlinear binocular interactions in human visual cortex. *Vision Research*, 28, 1139–43. [146]
- Baitch, L. W. and Levi, D. M. (1989). Binocular beats: Psychophysical studies of binocular interaction in normal and stereoblind humans. *Vision Research*, 29, 27–37. [638]
- Baizer, J. S., Desimone, R., and Ungerleider, L. G. (1993). Comparison of subcortical connections of inferior temporal and posterior parietal cortex in monkeys. *Visual Neuroscience*, 10, 59–72. [127]
- Baker, C. A. and Steedman, W. C. (1961). Perceived movement in depth as function of luminance and velocity. *Human Factors*, 3, 166–73. [561]
- Baker, C. A. and Steedman, W. C. (1962). Estimation of visually perceived closure rates. *Human Factors*, 4, 343–7. [554]
- Baker, C. H. (1970). A study of the Sherrington effect. *Perception and Psychophysics*, 8, 406–10. [359]
- Baker, F. H., Grigg, P., and Noorden, G. K. von (1974). Effects of visual deprivation and strabismus on the response of neurons in the visual cortex of the monkey, including studies on the striate and prestriate cortex in the normal animal. *Brain Research*, 66, 185–208. [627]
- Ball, W. A. and Tronick, E. (1971). Infant responses to impending collision: Optical and real. *Science*, 171, 818–20. [557]
- Balliet, R. and Nakayama, K. (1978). Training of voluntary torsion. *Investigative Ophthalmology and Visual Science*, 17, 303–14. [417]
- Baloh, R. W., Beykirch, K., and Honrubia, V. (1988). Eye movements induced by linear acceleration on a parallel swing. *Journal of Neurophysiology*, 60, 2000–13. [415]
- Banks, M. S. (1980). The development of visual accommodation during early infancy. *Child Development*, 51, 646–66. [604, 621]
- Banks, M. S. (1988). Visual recalibration and the development of contrast and optic flow perception. In *Perceptual development in infancy*, (ed. A. Yonas), pp. 145–96. Erlbaum, Hillsdale, NJ. [605]
- Banks, M. S. and Bennett, P. J. (1988). Optical and photoreceptor immaturities limit the spatial and chromatic vision of human neonates. *Journal of the Optical Society of America*, A5, 2059–79. [617]
- Banks, M. S. and Salapatek, P. (1978). Acuity and contrast sensitivity in 1, 2, and 3-month-old human infants. *Investigative Ophthalmology and Visual Science*, 17, 361–5. [616]
- Banks, M. S., Aslin, R. N., and Letson, R. D. (1975). Sensitive period for the development of human binocular vision. *Science*, 190, 675–7. [637, 640]
- Banks, M. S., Geisler, W. S., and Bennett, P. J. (1987). The physical limits of grating visibility. *Vision Research*, 27, 1915–24. [108]
- Bannister, H. (1932). *Retinal reaction time*. Physical and Optical Societies report of a joint discussion on vision. pp. 227–34. The Physical Society, London. [545]
- Bappert, J. (1923). Neue Untersuchungen zum Problem des Verhältnisses von Akkommodation und Konvergenz zur Wahrnehmung der Tiefe. *Psychologische Studien (Leipzig)*, 7, 78–114. [428]

- Bárány, E. (1946). A theory of binocular visual acuity and an analysis of the variability of visual acuity. *Acta Ophthalmologica*, 24, 63–92. [350]
- Bárány, E. and Halldén, U. (1948). Phasic inhibition of the light reflex of the pupil during retinal rivalry. *Journal of Neurophysiology*, 11, 25–30. [335]
- Barbeito, R. (1983). Sighting from the cyclopean eye: The cyclops effect in preschool children. *Perception and Psychophysics*, 33, 561–4. [595]
- Barbeito, R. and Ono, H. (1979). Four methods of locating the egocentre: A comparison of their predictive validities and reliabilities. *Behavior Research Methods and Instrumentation*, 11, 31–6. [598–9]
- Barbeito, R. and Simpson, T. L. (1991). The relationship between eye position and egocentric visual direction. *Perception and Psychophysics*, 50, 373–82. [598]
- Barbeito, R., Levi, D., Klein, S., Loshin, D., and Ono, H. (1985). Stereo-deficients and stereoblinds cannot make utrocular discriminations. *Vision Research*, 25, 1345–8. [601]
- Barker, W. B. (1936). Binocular vision. *British Journal of Physiological Optics*, 10, 64–72. [64]
- Barlow, H. B. (1958). Temporal and spatial summation in human vision at different background intensities. *Journal of Physiology*, 141, 337–50. [361]
- Barlow, H. B. (1961). Possible principles underlying the transformations of sensory messages. In *Sensory communication*. (ed. W. A. Rosenblith), pp. 217–34. MIT Press, Cambridge, MA. [82]
- Barlow, H. B. (1978). The efficiency of detecting changes of density in random dot patterns. *Vision Research*, 18, 637–50. [158]
- Barlow, H. B. (1991). Vision tells you more than "what is there". In *Representations of vision*, (ed. A. Gorea), pp. 319–29. Cambridge University Press, New York. [32]
- Barlow, H. B. and Brindley, G. S. (1963). Inter-ocular transfer of movement aftereffects during pressure blinding of the stimulated eye. *Nature*, 200, 1349–50. [376, 589]
- Barlow, H. B., Blakemore, C., and Pettigrew, J. D. (1967). The neural mechanism of binocular depth discrimination. *Journal of Physiology*, 193, 327–42. [24, 133, 494]
- Barlow, H. B., Fitzhugh, R., and Kuffler, S. W. (1957). Change of organization in the receptive fields of the cat's retina during dark adaptation. *Journal of Physiology*, 137, 338–54. [337]
- Barnes, G. R., Benson, A. J., and Prior, A. R. J. (1978). Visual vestibular interaction in the control of eye movement. *Aviation Space and Environmental Medicine*, 49, 557–64. [179]
- Baro, J. A., Lehmkuhle, S., and Kratz, K. E. (1990). Electrotetrograms and visual evoked potentials in long-term monocularly deprived cats. *Investigative Ophthalmology and Visual Science*, 31, 1405–9. [626, 628]
- Bartmann, M. and Schaeffel, F. (1994). A simple mechanism for emmetropization without cues from accommodation or colour. *Vision Research*, 34, 873–6. [604]
- Battersby, W. S. and Wagman, I. H. (1962). Neural limitations of visual excitability. IV: Spatial determinants of retrochiasmal interaction. *American Journal of Physiology*, 203, 359–65. [364]
- Baumgartner, G. (1964). Neuronale Mechanismen des Kontrast- und Bewegungssehens. *Bericht der Deutschen Ophthalmologischen Gesellschaft*, 66, 111–25. [483]
- Baylor, D. A., Nunn, B. J., and Schnapf, J. L. (1987). Spectral sensitivities of cones of the monkey *Macaca fascicularis*. *Journal of Physiology*, 390, 145–60. [109]
- Bear, M. F. and Daniels, J. D. (1983). The plastic response to monocular deprivation persists in kitten visual cortex after chronic depletion of norepinephrine. *Journal of Neuroscience*, 3, 407–16. [630]
- Bear, M. F. and Singer, W. (1986). Modulation of visual cortical plasticity by acetylcholine and noradrenaline. *Nature*, 320, 172–6. [630]
- Bear, M. F., Kleinschmidt, A., Gu, Q., and Singer, W. (1990). Disruption of experience-dependent synaptic modification in striate cortex by infusion of an NMDA receptor antagonist. *Journal of Neuroscience*, 10, 909–25. [614]
- Beare, J. I. (1906). *Greek theories of elementary cognition from Alcmaeon to Aristotle*. Clarendon Press, Oxford. [4]
- Beare, J. I. (1931). Parva naturalia. De Somniis. In *The works of Aristotle*. Translated into English. (ed. W. D. Ross), Vol. 3, pp. 461b–462a. Oxford University Press, London. [4]
- Bearse, M. A. and Freeman, R. D. (1994). Binocular summation in orientation discrimination depends on stimulus contrast and duration. *Vision Research*, 34, 19–29. [355]
- Beasley, W. C. and Peckham, R. H. (1936). An objective study of "cyclotorsion". *Psychological Bulletin*, 33, 741–2. [321]
- Beazley, L. D. (1975). Development of intertectal neuronal connections in *Xenopus*: The effects of contralateral transposition of the eye and eye removal. *Experimental Brain Research*, 23, 505–18. [652]
- Bechtoldt, H. P. and Hutz, C. S. (1979). Stereopsis in young infants and stereopsis in an infant with congenital esotropia. *Journal of Pediatric Ophthalmology and Strabismus*, 16, 49–54. [618]
- Beck, J. (1967). Perceptual grouping produced by line figures. *Perception and Psychophysics*, 2, 491–5. [210]
- Beck, J. (1972). Similarity grouping and peripheral discrimination under uncertainty. *American Journal of Psychology*, 85, 1–19. [210]
- Becker, W. and Jürgens, R. (1975). Saccadic reactions to double step stimuli: Evidence for model feedback and continuous information uptake. In *Basic mechanisms of ocular motility and their clinical implications*. (ed. G. Lennerstrand and P. Bach-y-Rita), pp. 519–24. Pergamon, Oxford. [402]
- Bedell, H. E. and Flom, M. C. (1981). Monocular spatial distortion in strabismic amblyopia. *Investigative Ophthalmology and Visual Science*, 20, 263–8. [631]
- Bedell, H. E., Flom, M. C., and Barbeito, R. (1985). Spatial aberrations and acuity in strabismus and amblyopia. *Investigative Ophthalmology and Visual Science*, 26, 909–16. [631]
- Bedell, H. E., Klopferstein, J. F., and Yuan, N. (1989). Extraretinal information about eye position during involuntary eye movement: Optokinetic afternystagmus. *Perception and Psychophysics*, 46, 579–86. [533]
- Békésy, G. von (1967). *Sensory inhibition*. Princeton, N. J., Princeton University Press. [97, 466]
- Békésy, G. von (1970). Apparent image rotation in stereoscopic vision: The unbalance of the pupils. *Perception and Psychophysics*, 8, 343–7. [309]
- Bennett, M. J., Smith, E. L., Harwerth, R. S., and Crawford, M. L. J. (1980). Ocular dominance, eye alignment and visual acuity in kittens reared with an optically induced squint. *Brain Research*, 193, 33–45. [627]
- Bennett, P. J. and Banks, M. S. (1987). Sensitivity loss in odd-symmetric mechanisms underlies phase anomalies in peripheral vision. *Nature*, 326, 873–6. [631]
- Bennett, R. G. and Westheimer, G. (1991). The effect of training on visual alignment discrimination and grating resolution. *Perception and Psychophysics*, 49, 541–6. [104]
- Bennett, W. R. (1933). New results in the calculation of modulation products. *Bell Systems Technical Journal*, 228–43. [92]
- Benson, A. J. and Barnes, G. R. (1978). Vision during angular oscillation; the dynamic interaction of visual and vestibular mechanisms. *Aviation, Space and Environmental Medicine*, 49, 340–5. [179]

- Benton, A. L. and Hécaen, H. (1970). Stereoscopic vision in patients with unilateral cerebral disease. *Neurology*, **20**, 1084-8. [625]
- Berardi, N., Domenici, L., Parisi, V., Pizzorusso, T., Cellerino, A., and Maffei, L. (1993). Monocular deprivation effects in the rat visual cortex and lateral geniculate nucleus are prevented by nerve growth factor (NGF). I. Visual cortex. *Proceedings of the Royal Society, London*, **251**, 17-23. [629]
- Berardi, N., Galli, L., Maffei, L., and Siliprandi, R. (1986). Binocular suppression in cortical neurons. *Experimental Brain Research*, **63**, 581-4. [346]
- Berens, C. and Bannon, R. E. (1963). Aniseikonia. *AMA Archives of Ophthalmology*, **70**, 181-8. [67]
- Bergman, R. and Gibson, J. J. (1959). The negative aftereffect of the perception of a surface slanted in the third dimension. *American Journal of Psychology*, **72**, 364-74. [486, 490, 493-4]
- Berkeley, G. (1709). *An essay towards a new theory of vision*. Dublin, Jeremy Pepys. Reprinted 1922. New York, Dutton. [11, 572]
- Berlucchi, G. (1972). Anatomical and physiological aspects of visual functions of corpus callosum. *Brain Research*, **37**, 371-92. [131]
- Berlucchi, G. and Rizzolatti, G. (1968). Binocularly driven neurons in visual cortex of split-chiasm cats. *Science*, **159**, 308-10. [131]
- Berman, N. and Daw, N. W. (1977). Comparison of the critical periods for monocular and directional deprivation in cats. *Journal of Physiology*, **265**, 249-59. [635]
- Berman, N. and Payne, B. R. (1982). Monocular deprivation in the Siamese cat: Development of cortical orientation and direction sensitivity without visual experience. *Experimental Brain Research*, **46**, 147-50. [633]
- Berman, N., Blakemore, C., and Cynader, M. (1975). Binocular interaction in the cat's superior colliculus. *Journal of Physiology*, **246**, 595-615. [125, 134]
- Berman, N., Murphy, E. H., and Salinger, W. L. (1979). Monocular paralysis in the adult cat does not change cortical ocular dominance. *Brain Research*, **164**, 290-3. [641]
- Berman, N., Pearson, H. E., and Payne, B. R. (1989). Consequences of visual deprivation in the absence of binocular competitive mechanisms in Siamese cat area 17. *Developmental Brain Research*, **50**, 69-87. [633]
- Berry, R. N. (1948). Quantitative relations among vernier, real depth, and stereoscopic depth acuities. *Journal of Experimental Psychology*, **38**, 708-21. [160, 181]
- Berry, R. N., Riggs, L. A., and Duncan, C. P. (1950). The relation of vernier and depth discriminations to field brightness. *Journal of Experimental Psychology*, **40**, 349-54. [168]
- Beverley, K. I. and Regan, D. (1973a). Evidence for the existence of neural mechanisms selectively sensitive to the direction of movement in space. *Journal of Physiology*, **235**, 17-29. [567]
- Beverley, K. I. and Regan, D. (1973b). Selective adaptation in stereoscopic depth perception. *Journal of Physiology*, **232**, 40P. [567]
- Beverley, K. I. and Regan, D. (1974). Visual sensitivity to disparity pulses: Evidence for directional selectivity. *Vision Research*, **14**, 357-61. [188]
- Beverley, K. I. and Regan, D. (1975). The relation between discrimination and sensitivity in the perception of motion in depth. *Journal of Physiology*, **249**, 387-98. [562]
- Beverley, K. I. and Regan, D. (1979a). Visual perception of changing size: The effect of object size. *Vision Research*, **19**, 1093-104. [558]
- Beverley, K. I. and Regan, D. (1979b). Separable effects of changing size and motion in depth: Different neural mechanisms. *Vision Research*, **19**, 727-32. [559]
- Beverley, K. I. and Regan, D. (1980a). Visual sensitivity to the shape and size of a moving object: Implications for models of object perception. *Perception*, **9**, 151-60. [559]
- Beverley, K. I. and Regan, D. (1980b). Temporal selectivity of changing-size channels. *Journal of the Optical Society of America*, **70**, 1375-7. [559]
- Bielschowsky, A. (1898). Über monokulare Diplopia ohne physikalische Grundlage nebst Bemerkungen über das Sehen Schlielender. *Albrecht v. Graefes Archiv für Ophthalmologie*, **46**, 143-8. [47-8, 335]
- Bienstock, E. L., Cooper, L. N., and Munro, P. W. (1982). Theory for the development of neuron selectivity: Orientation specificity and binocular interaction in visual cortex. *Journal of Neuroscience*, **2**, 32-48. [615]
- Biguer, B. and Prablanc, C. (1981). Modulation of the vestibulo-ocular reflex in eye-head orientation as a function of target distance in man. In *Progress in oculomotor research*, (ed. A. F. Fuchs and W. Brecher), pp. 525-30. Elsevier, Amsterdam. [416]
- Birch, E. E. and Foley, J. M. (1979). The effects of duration and luminance on binocular depth mixture. *Perception*, **8**, 263-7. [232]
- Birch, E. E. and Hale, L. A. (1989). Operant assessment of stereoacluity. *Clinical Vision Science*, **4**, 295-300. [619]
- Birch, E. E. and Held, R. (1983). The development of binocular summation in human infants. *Investigative Ophthalmology and Visual Science*, **24**, 1103-7. [621]
- Birch, E. E., Gwiazda, J., and Held, R. (1982). Stereoacuity development for crossed and uncrossed disparities in human infants. *Vision Research*, **22**, 507-13. [619]
- Birch, E. E., Gwiazda, J., and Held, R. (1983). The development of vergence does not account for the onset of stereopsis. *Perception*, **12**, 331-6. [621]
- Birch, E. E., Shimojo, S., and Held, R. (1985). Preferential-looking assessment of fusion and stereopsis in infants aged 1-6 months. *Investigative Ophthalmology and Visual Science*, **26**, 366-70. [619]
- Birkmayer, W. (1951). *Hirnverletzungen*. Springer-Verlag, Vienna. [624]
- Birnholz, J. C. (1981). The development of human fetal eye movement patterns. *Science*, **213**, 679-80. [620]
- Bishop, P. O. (1979). Stereopsis and the random element in the organization of the striate cortex. *Proceedings of the Royal Society, London*, **B204**, 415-44. [134, 142]
- Bishop, P. O. (1989). Vertical disparity, egocentric distance and stereoscopic depth constancy: a new interpretation. *Proceedings of the Royal Society, London*, **B237**, 445-69. [283, 289, 292]
- Bishop, P. O. and Henry, G. H. (1971). Spatial vision. *Annual Review of Psychology*, **22**, 119-60. [132]
- Bishop, P. O. and Pettigrew, J. D. (1986). Neural mechanisms of binocular vision. *Vision Research*, **26**, 1587-600. [24]
- Bishop, P. O., Coombs, J. S., and Henry, G. H. (1973). Receptive fields of simple cells in the cat striate cortex. *Journal of Physiology*, **231**, 31-60. [345, 375]
- Bishop, P. O., Henry, G. H., and Smith, C. J. (1971). Binocular interaction fields of single units in the cat's striate cortex. *Journal of Physiology*, **216**, 39-68. [123, 137]
- Bishop, P. O., Kozak, W., and Vakkur, G. K. (1962). Some quantitative aspects of the cat's eye: Axis and plane of reference, visual field coordinates and optics. *Journal of Physiology*, **163**, 466-502. [133]
- Bisti, S. and Carmignoto, G. (1986). Monocular deprivation in kittens differentially affects crossed and uncrossed visual pathways. *Vision Research*, **26**, 875-84. [633]
- Bjorklund, R. A. and Magnussen, S. (1981). A study of interocular transfer of spatial adaptation. *Perception*, **10**, 511-18. [369]

- Blackwell, H. R. (1952). Studies of psychophysical methods for measuring thresholds. *Journal of the Optical Society of America*, *42*, 606–16. [95, 149]
- Blake, R. (1977). Threshold conditions for binocular rivalry. *Journal of Experimental Psychology: Human Perception and Performance*, *3*, 251–7. [329]
- Blake, R. (1988). Dichoptic reading: The role of meaning in binocular rivalry. *Perception and Psychophysics*, *44*, 133–41. [347]
- Blake, R. (1989). A neural theory of binocular rivalry. *Psychological Review*, *96*, 145–67. [345]
- Blake, R. and Boothroyd, K. (1985). The precedence of binocular fusion over binocular rivalry. *Perception and Psychophysics*, *37*, 114–24. [339]
- Blake, R. and Bravo, M. (1985). Binocular rivalry suppression interferes with phase adaptation. *Perception and Psychophysics*, *38*, 277–80. [343]
- Blake, A. and Bülthoff, H. (1991). Shape from specularities: computation and psychophysics. *Philosophical Transactions of the Royal Society*, *331*, 237–52. [311]
- Blake, R. and Camisa, J. (1978). Is binocular vision always monocular? *Science*, *200*, 1497–99. [338]
- Blake, R. and Camisa, J. (1979). On the inhibitory nature of binocular rivalry suppression. *Journal of Experimental Psychology: Human Perception and Performance*, *5*, 315–23. [329]
- Blake, R. and Cormack, R. H. (1979a). On utricular discrimination. *Perception and Psychophysics*, *26*, 53–68. [601]
- Blake, R. and Cormack, R. H. (1979b). Psychophysical evidence for a monocular visual cortex in stereoblind humans. *Science*, *203*, 274–5. [601]
- Blake, R. and Cormack, R. H. (1979c). Does contrast disparity alone generate stereopsis? *Vision Research*, *19*, 913–15. [260]
- Blake, R. and Fox, R. (1972). Interocular transfer of adaptation to spatial frequency during retinal ischaemia. *Nature New Biology*, *240*, 76–7. [342, 369]
- Blake, R. and Fox, R. (1973). The psychophysical inquiry into binocular summation. *Perception and Psychophysics*, *14*, 161–85. [349–50, 362]
- Blake, R. and Fox, R. (1974a). Binocular rivalry suppression: Insensitive to spatial frequency and orientation change. *Vision Research*, *14*, 687–92. [336]
- Blake, R. and Fox, R. (1974b). Adaptation to invisible gratings and the site of binocular rivalry suppression. *Nature*, *249*, 488–90. [341]
- Blake, R. and Hirsch, H. V. B. (1975). Deficits in binocular depth perception in cats after alternating monocular deprivation. *Science*, *190*, 1114–16. [630, 632]
- Blake, R. and Lehmkuhle, S. W. (1976). On the site of strabismic suppression. *Investigative Ophthalmology*, *15*, 660–3. [341]
- Blake, R. and Lema, S. A. (1978). Inhibitory effect of binocular rivalry suppression is independent of orientation. *Vision Research*, *18*, 541–4. [332]
- Blake, R. and Levinson, E. (1977). Spatial properties of binocular neurons in the human visual system. *Experimental Brain Research*, *27*, 221–32. [352–3, 362, 368]
- Blake, R. and O'Shea, R. P. (1988). "Abnormal fusion" of stereopsis and binocular rivalry. *Psychological Review*, *95*, 151–4. [340]
- Blake, R. and Overton, R. (1979). The site of binocular rivalry suppression. *Perception*, *8*, 143–52. [336, 341]
- Blake, R. and Rush, C. (1980). Temporal properties of binocular mechanisms in the human visual system. *Experimental Brain Research*, *38*, 333–40. [353]
- Blake, R., Camisa, J. M., and Antoinetti, D. N. (1976). Binocular depth discrimination depends on orientation. *Perception and Psychophysics*, *20*, 113–18. [167]
- Blake, R., Fox, R., and McIntyre, C. (1971). Stochastic properties of stabilized-image binocular rivalry alternations. *Journal of Experimental Psychology*, *88*, 327–32. [332, 344]
- Blake, R., Martens, W., and Di Gianfilippo, A. (1980b). Reaction time as a measure of binocular interaction in human vision. *Investigative Ophthalmology and Visual Science*, *19*, 930–41. [638]
- Blake, R., O'Shea, R. P., and Mueller, T. J. (1992). Spatial zones of binocular rivalry in central and peripheral vision. *Visual Neuroscience*, *8*, 469–78. [335]
- Blake, R., Overton, R., and Lema-Stern, S. (1981b). Interocular transfer of visual aftereffects. *Journal of Experimental Psychology: Human Perception and Performance*, *7*, 367–81. [371, 374]
- Blake, R., Sloane, M., and Fox, R. (1981a). Further developments in binocular summation. *Perception and Psychophysics*, *30*, 266–76. [350]
- Blake, R., Westendorf, D. H., and Overton, R. (1980a). What is suppressed during binocular rivalry? *Perception*, *9*, 223–31. [337, 340]
- Blake, R., Yang, Y., and Westendorf, D. (1991a). Discriminating binocular fusion from false fusion. *Investigative Ophthalmology and Visual Science*, *32*, 2821–25. [333]
- Blake, R., Yang, Y., and Wilson, H. R. (1991b). On the coexistence of stereopsis and binocular rivalry. *Vision Research*, *31*, 1191–203. [340]
- Blake, R., Zimba, L., and Williams, D. (1985). Visual motion, binocular correspondence and binocular rivalry. *Biological Cybernetics*, *52*, 391–7. [331]
- Blakemore, C. (1969). Binocular depth discrimination and the nasotemporal division. *Journal of Physiology*, *205*, 471–9. [130]
- Blakemore, C. (1970a). Binocular depth perception and the optic chiasm. *Vision Research*, *10*, 43–7. [132]
- Blakemore, C. (1970b). A new kind of stereoscopic vision. *Vision Research*, *10*, 1181–99. [259, 260, 263]
- Blakemore, C. (1970c). The representation of three-dimensional visual space in the cat's striate cortex. *Journal of Physiology*, *209*, 155–78. [134]
- Blakemore, C. (1970d). The range and scope of binocular depth discrimination in man. *Journal of Physiology*, *211*, 599–622. [54, 149, 155, 159, 167, 324]
- Blakemore, C. (1976). The conditions required for the maintenance of binocularity in the kitten's visual cortex. *Journal of Physiology*, *261*, 423–44. [628, 630]
- Blakemore, C. and Campbell, F. W. (1969). On the existence of neurones in the human visual system selectively sensitive to the orientation and size of retinal images. *Journal of Physiology*, *203*, 237–60. [88, 369, 495–6, 638]
- Blakemore, C. and Hague, B. (1972). Evidence for disparity detecting neurones in the human visual system. *Journal of Physiology*, *225*, 437–55. [524]
- Blakemore, C. and Hawken, M. J. (1982). Rapid restoration of functional input to the visual cortex of the cat after brief monocular deprivation. *Journal of Physiology*, *327*, 463–87. [628]
- Blakemore, C. and Julesz, B. (1971). Stereoscopic depth aftereffect produced without monocular cues. *Science*, *171*, 286–8. [486, 494]
- Blakemore, C. and Price, D. J. (1987a). The organization and postnatal development of area 18 of the cat's visual cortex. *Journal of Physiology*, *384*, 263–92. [613]
- Blakemore, C. and Price, D. J. (1987b). Effects of dark rearing on the development of area 18 of the cat's visual cortex. *Journal of Physiology*, *384*, 293–309. [625]
- Blakemore, C. and Sutton, P. (1969). Size adaptation: A new after-effect. *Science*, *166*, 245–7. [378, 465]

- Blakemore, C. and Van Sluyters, R. C. (1974). Reversal of the physioloogical effects of monocular deprivation in kittens: Further evidence for a sensitive period. *Journal of Physiology*, **237**, 195–216. [636]
- Blakemore, C. and Van Sluyters, R. C. (1975). Innate and environmental factors in the development of the kitten's visual cortex. *Journal of Physiology*, **482**, 663–716. [628]
- Blakemore, C. and Vital-Durand, F. (1986a). Effects of visual deprivation on the development of the monkey's lateral geniculate nucleus. *Journal of Physiology*, **380**, 493–511. [609, 627]
- Blakemore, C. and Vital-Durand, F. (1986b). Organization and post-natal development of the monkey's lateral geniculate nucleus. *Journal of Physiology*, **380**, 453–91. [609]
- Blakemore, C., Diao, Y., Pu, M., Wang, Y., and Xiao, Y. (1983). Possible functions of the interhemispheric connections between visual cortical areas in the cat. *Journal of Physiology*, **337**, 331–49. [132]
- Blakemore, C., Fiorentini, A., and Maffei, L. (1972). A second neural mechanism of binocular depth discrimination. *Journal of Physiology*, **226**, 725–49. [142, 271]
- Blakemore, C., Garey, L. J., and Vital-Durand, F. (1978). The physiological effects of monocular deprivation and their reversal in the monkey's visual cortex. *Journal of Physiology*, **283**, 223–62. [636]
- Blakemore, C., Hawken, M. J., and Mark, R. F. (1982). Brief monocular deprivation leaves subthreshold synaptic input on neurones of the cat's visual cortex. *Journal of Physiology*, **327**, 489–505. [628–9]
- Blakemore, C., van Sluyters, R. C., Peck, C. K., and Hein, A. (1975). Development of cat visual cortex following rotation of one eye. *Nature*, **B257**, 584–7. [630]
- Blank, A. A. (1953). Luneburg theory of binocular visual space. *Journal of the Optical Society of America*, **43**, 717–27. [53]
- Blasdel, G. G. and Fitzpatrick, D. (1984). Physiological organization of layer 4 in macaque striate cortex. *Journal of Neuroscience*, **4**, 880–95. [117]
- Blasdel, G. G. and Pettigrew, J. D. (1979). Degree of interocular synchrony required for maintenance of binocularity in kitten's visual cortex. *Journal of Neurophysiology*, **42**, 1692–710. [630]
- Blasdel, G. G., Lund, J. S., and Fitzpatrick, D. (1985). Intrinsic connections of macaque striate cortex: Axonal projections of cells outside lamina 4C. *Journal of Neuroscience*, **5**, 3350–69. [126]
- Bloch, S., Rivaud, S., and Martinoya, C. (1984). Comparing frontal and lateral viewing in the pigeon. III. Different patterns of eye movements for binocular and monocular fixation. *Behavioral Brain Research*, **13**, 173–82. [653]
- Blodi, F. C. and Van Allen, M. W. (1957). Electromyography of the extraocular muscles in fusional movements. *American Journal of Ophthalmology*, **44**, 136–44. [410]
- Blomfield, S. (1973). Implicit features and stereoscopy. *Nature*, **B245**, 256. [509]
- Blough, P. M. (1971). The visual acuity of the pigeon for distant targets. *Journal of the Experimental Analysis of Behavior*, **15**, 57–67. [653]
- Blunt, W. (1970). *The dream king*. Hamish Hamilton, London. [12]
- Bobier, W. R., Campbell, M. C. W., and Hinch, M. (1992). The influence of chromatic aberration on the static accommodative response. *Vision Research*, **32**, 823–32. [395]
- Bode-Greuel, K. M. and Singer, W. (1989). The development of N-methyl-D-aspartate receptors in cat visual cortex. *Developmental Brain Research*, **46**, 197–204. [614]
- Bogert, B. P., Healy, W. J. R., and Tukey, J. W. (1963). The frequency analysis of time series for echoes: Cepstrum, pseudoauto-covariance, cross cepstrum and saphe cracking. In *Proceedings of Symposium on Time Series Analysis* (ed. M. Rosenblatt), pp. 209–43. Wiley, New York. [216]
- Bolanowski, S. J. (1987). Contourless stimuli produce binocular brightness summation. *Vision Research*, **27**, 1943–51. [359]
- Bolanowski, S. J. and Doty, R. W. (1987). Perceptual "blankout" of monocular homogeneous fields (Ganzfelder) is prevented with binocular viewing. *Vision Research*, **27**, 967–82. [331]
- Boltz, R. L. and Harwerth, R. S. (1979). Fusional vergence ranges of the monkey: A behavioural study. *Experimental Brain Research*, **37**, 87–91. [400]
- Boman, D. K. and Kertesz, A. E. (1985). Horizontal fusional responses to stimuli containing artificial scotomas. *Investigative Ophthalmology and Visual Science*, **26**, 1051–6. [402]
- Bomba, P. C. (1984). The development of orientation categories between 2 and 4 months of age. *Journal of Experimental Child Psychology*, **37**, 609–36. [616]
- Bonds, A. B. (1989). Role of inhibition in the specification of orientation selectivity of cells in the cat striate cortex. *Visual Neuroscience*, **2**, 41–55. [345, 375]
- Bonhoeffer, T. and Grinvald, A. (1993). The layout of iso-orientation domains in area 18 of cat visual cortex: Optical imaging reveals a pinwheel organization. *Journal of Neuroscience*, **13**, 4157–80. [124]
- Boothe, R. G., Dobson, V., and Teller, D. Y. (1985). Postnatal development of vision in human and nonhuman primates. *Annual Review of Neuroscience*, **8**, 495–545. [605]
- Boothe, R. G., Williams, R. A., Kiorpes, L., and Teller, D. Y. (1980). Development of contrast sensitivity in infant Macaca nemestrina monkeys. *Science*, **208**, 1290–2. [616]
- Boothroyd, K. and Blake, R. (1984). Stereopsis from disparity of complex grating patterns. *Vision Research*, **24**, 1205–22. [198]
- Boring, E. G. (1942). *Sensation and perception in the history of experimental psychology*. Appleton-Century-Crofts, New York. [427]
- Boring, E. G. (1950). *A history of experimental psychology*. Appleton-Century-Crofts, New York. [73]
- Born, R. T. and Tootell, B. H. (1992). Segregation of global and local motion processing in primate middle temporal visual area. *Nature*, **357**, 497–9. [126]
- Bornstein, M. H., Krinsky, S. J., and Benasich, A. A. (1986). Fine orientation discrimination and shape constancy in young infants. *Journal of Experimental Child Psychology*, **41**, 49–60. [616]
- Bosco, C. and Komi, P. V. (1979). Potentiation of the mechanical behaviour of the human skeletal muscle through prestretching. *Acta Physiologica*, **106**, 467–72. [432]
- Bossink, C. J. H., Stalmeyer, P. F. M., and de Weert, C. M. M. (1993). A test of Levelt's second proposition for binocular rivalry. *Vision Research*, **33**, 1413–9. [328, 344]
- Bough, E. W. (1970). Stereoscopic vision in the macaque monkey. *Nature*, **225**, 41–2. [645]
- Bouman, M. A. (1955). On foveal and peripheral interactions in binocular vision. *Optica Acta*, **1**, 177–83. [329]
- Bouman, M. A. and van den Brink, G. (1952). On the integrate capacity in time and space of the human peripheral retina. *Journal of the Optical Society of America*, **42**, 617–20. [96, 361]
- Bourdon, B. (1902). *La perception visuelle de l'espace*. Reinwald, Paris. [427, 578]
- Bourgeois, J. P. and Rakic, P. (1993). Changes of synaptic density in the primary visual cortex of the macaque monkey from fetal to adult stage. *Journal of Neuroscience*, **13**, 2801–20. [610]
- Bower, T. G. R. (1966). A local sign for depth. *Nature*, **210**, 1081–2. [171]
- Bower, T. G. R., Broughton, J. M., and Moore, M. K. (1970). Demonstrations of intention in the reaching behavior of neonate humans. *Nature*, **228**, 679–81. [618]

- Bower, T. G. R., Broughton, J. M., and Moore, M. K. (1971). Infant responses to approaching objects: An indicator of response to distal variables. *Perception and Psychophysics*, 9, 193–6. [557]
- Bowne, S. F. (1990). Contrast discrimination cannot explain spatial frequency, orientation or temporal frequency discrimination. *Vision Research*, 30, 449–61. [79, 98]
- Boyde, A. (1992). Three-dimensional images of Ramón y Cajal's original preparations, as viewed by confocal microscopy. *Trends in Neuroscience*, 15, 246–8. [117]
- Boyle, R. (1688). *A disquisition about the final causes of natural things*. J. Taylor, London. See *Robert Boyle, the works*. Vol. 5, (ed. T. Birch). Olms, Hildesheim. [17]
- Boynton, R. M. (1979). *Human color vision*. Holt, Rinehart and Winston, New York. [326]
- Boynton, R. M. and Wisowaty, J. J. (1984). Selective color effects in dichoptic masking. *Vision Research*, 24, 667–75. [365]
- Braastad, B. O. and Heggelund, P. (1985). Development of spatial receptive-field organization and orientation selectivity in kitten striate cortex. *Journal of Neurophysiology*, 53, 1158–78. [612, 625]
- Braccini, C., Gambardella, G., and Suetta, G. (1980). A noise masking experiment in grating perception at threshold: The implications for binocular summation. *Vision Research*, 20, 373–6. [352]
- Bracewell, R. N. (1978). *The Fourier transform and its applications*. McGraw-Hill, New York. [87]
- Braddick, O. J. (1968). Binocular fusion and perceptual analysis. (Unpublished Ph.D., University of Cambridge). [274]
- Braddick, O. J. (1974). A short-range process in apparent movement. *Vision Research*, 14, 519–27. [567, 568]
- Braddick, O. J. (1979). Binocular single vision and perceptual processing. *Proceedings of the Royal Society, London, B*204, 503–12. [274, 318]
- Braddick, O. J. and Adlard, A. (1978). Apparent motion and the motion detector. In *Visual psychophysics and physiology*, (ed. J. C. Armington, J. Krauskopf, and B. R. Wooten), pp. 417–26. Academic Press, New York. [567]
- Braddick, O. J. and Holiday, J. E. (1991). Serial search for targets defined by divergence or deformation of optic flow. *Perception*, 20, 345–54. [559]
- Braddick, O. J., Atkinson, J., French, J., and Howland, H. C. (1979). A photorefractive study of infant accommodation. *Vision Research*, 19, 1319–30. [604]
- Braddick, O. J., Atkinson, J., Julesz, B., Kropfl, W., Bodis-Wollner, I., and Raab, E. (1980). Cortical binocularity in infants. *Nature*, 288, 363–5. [620]
- Braddick, O. J., Wattam-Bell, J., Day, J., and Atkinson, J. (1983). The onset of binocular function in human infants. *Human Neurobiology*, 2, 65–9. [620]
- Braddick, O. J., Wattam-Bell, J., and Atkinson, J. (1986). Orientation-specific responses develop in early infancy. *Nature*, 320, 617–19. [616]
- Bradley, A. and Freeman, R. D. (1985a). Is reduced vernier acuity in amblyopia due to position, contrast or fixation deficits? *Vision Research*, 25, 55–66. [631]
- Bradley, A. and Freeman, R. D. (1985b). Temporal sensitivity in amblyopia: An explanation of conflicting reports. *Vision Research*, 25, 39–46. [631]
- Bradley, A., Freeman, R. D., and Applegate, R. (1985). Is amblyopia spatial frequency or retinal locus specific? *Vision Research*, 25, 47–54. [631]
- Bradley, A., Rabin, J., and Freeman, R. D. (1983). Nonoptical determinants of aniseikonia. *Investigative Ophthalmology and Visual Science*, 24, 507–12. [64]
- Bradshaw, M. F., and Rogers, B. J. (1992). Subthreshold interactions between binocular stereopsis and motion parallax cues. *Investigative Ophthalmology and Visual Science*, 33 (ARVO Abstracts), 1332. [440]
- Bradshaw, M. F. and Rogers, B. J. (1993a). Elevation of depth thresholds following within and between cue adaptation of stereo and motion. *Investigative Ophthalmology and Visual Science*, 34 (ARVO Abstracts), 1036. [440, 579]
- Bradshaw, M. F. and Rogers, B. J. (1993b). Sensitivity to horizontally and vertically oriented stereoscopic corrugations as a function of corrugation frequency. *Perception*, 22 (Abstract Supplement), 117. [163, 268, 481]
- Bradshaw, M. F. and Rogers, B. J. (1994). Is cyclovergence state affected by the inclination of stereoscopic surfaces? *Investigative Ophthalmology and Visual Science*, 35 (ARVO Abstracts), 1316. [291, 422]
- Bradshaw, M. F., Frisby, J. P., and Mayhew, J. E. W. (1987). The recovery of structure from motion: no evidence for a special link with the convergent disparity mechanism. *Perception*, 16, 351–7. [527, 584]
- Bradshaw, M. F., Rogers, B. J., and DeBruyn, B. (1992). Perceptual latency and complex random-dot stereograms. *Perception*, 21 (Abstract Supplement), 84. [193]
- Braitenberg, V. (1985). An isotropic network which implicitly defines orientation columns: Discussion of an hypothesis. In *Models of the visual cortex*, (ed. D. Rose and V. G. Dobson), pp. 479–84. Wiley, New York. [81]
- Braitenberg, V. and Braitenberg, C. (1979). Geometry of orientation columns in visual cortex. *Biological Cybernetics*, 33, 179–86. [124]
- Brandt, T., Dichgans, J., and Koenig, E. (1973). Differential effects of central versus peripheral vision on egocentric motion perception. *Experimental Brain Research*, 16, 476–91. [534]
- Brandt, T., Wist, E. R., and Dichgans, J. (1975). Foreground and background in dynamic spatial orientation. *Perception and Psychophysics*, 17, 497–503. [534]
- Brauner, J. D. and Lit, A. (1976). The Pulfrich effect, simple reaction time, and intensity discrimination. *American Journal of Psychology*, 89, 105–14. [537]
- Braunstein, M. L. (1966). Sensitivity of the observer to transformations of the visual field. *Journal of Experimental Psychology*, 72, 683–9. [438]
- Braunstein, M. L. (1968). Motion and texture as sources of slant information. *Journal of Experimental Psychology*, 78, 247–53. [578]
- Braunstein, M. L., Anderson, G. J., and Riefer, D. M. (1982). The use of occlusion to resolve ambiguity in parallel projections. *Perception and Psychophysics*, 31, 261–7. [438]
- Braunstein, M. L., Anderson, G. J., Rouse, M. W., and Tittle, J. S. (1986). Recovering viewer-centred depth from disparity, occlusion, and velocity gradients. *Perception and Psychophysics*, 40, 216–24. [438, 444–5]
- Bray, G. M., Villegas-Pérez, M.-P., Vidal-Sanz, M., and Aguayo, A. J. (1992). Death and survival of axotomized retinal ganglion cells. In *Regeneration and plasticity in the mammalian visual system*, (ed. D. M-K. Lam and G. M. Garth), pp. 29–43. MIT Press, Cambridge, MA. [607]
- Brecher, G. A. (1934). Die optokinetische Auslösung von Augenrollung und rotatorischem Nystagmus. *Pflügers Archiv für die gesamte Physiologie*, 234, 13–28. [417]
- Brecher, G. A. (1951). A new method for measuring aniseikonia. *American Journal of Ophthalmology*, 34, 1016–21. [65]
- Brecher, G. A., Winters, D. M., and Townsend, C. A. (1958). Image alternation for aniseikonia determination. *American Journal of Ophthalmology*, 45, 253–8. [65]

- Breese, B. B. (1899). On inhibition. *Psychological Review, Monograph Supplements*, 3, (whole number 11). [331, 334, 347]
- Breese, B. B. (1909). Binocular rivalry. *Psychological Review*, 16, 410–15. [330]
- Breinin, G. M. (1955). The nature of vergence revealed by electromyography. *AMA Archives of Ophthalmology*, 54, 407–12. [410]
- Breinin, G. M. and Moldaver, J. (1955). Electromyography of the human extraocular muscles. I. Normal kinesiology; divergence mechanism. *AMA Archives of Ophthalmology*, 54, 200–10. [386]
- Brewster, D. (1844a). On the knowledge of distance given by binocular vision. *Transactions of the Royal Society of Edinburgh*, 15, 663–74. [28]
- Brewster, D. (1844b). On the law of visible position in single and binocular vision, and on the representation of solid figures by the union of dissimilar plane pictures on the retina. *Transactions of the Royal Society of Edinburgh*, 15, 349–68. [28, 593]
- Brewster, D. (1851). Notice of a chromatic stereoscope. *Philosophical Magazine*, 4th series, 3, 31. [306]
- Brewster, D. (1856). *The stereoscope, its history, theory and construction*. John Murray, London. [21]
- Bridgeman, B. and Palca, J. (1980). Role of microsaccades in high acuity observational tasks. *Vision Research*, 20, 813–17. [382]
- Bridgman, C. S. and Smith, K. U. (1945). Bilateral neural integration in visual perception after section of the corpus callosum. *Journal of Comparative Neurology*, 83, 57–68. [132]
- Brigham, E. O. (1974). *The fast Fourier transform*. Prentice-Hall, Englewood Cliffs, NJ. [87]
- Brindley, G. S. (1957). Two theorems in colour vision. *Quarterly Journal of Experimental Psychology*, 9, 101–4. [79]
- Brindley, G. S. and Lewin, W. S. (1968). The sensations produced by electrical stimulation of the visual cortex. *Journal of Physiology*, 196, 479–93. [114]
- Brodal, P. (1972). The corticopontine projection from the visual cortex of the cat. I. The total projection and the projection from area 17. *Brain Research*, 39, 297–317. [125]
- Brookes, A. and Stevens, K. A. (1989a). Binocular depth from surfaces versus volumes. *Journal of Experimental Psychology: Human Perception and Performance*, 15, 479–84. [480]
- Brookes, A. and Stevens, K. A. (1989b). The analogy between stereo depth and brightness. *Perception*, 18, 601–14. [473–6, 481–4]
- Brown, J. F. (1931). The visual perception of velocity. *Psychologische Forschung*, 14, 199–232. [459]
- Brown, J. M. and Weisstein, N. (1988). A spatial frequency effect on perceived depth. *Perception and Psychophysics*, 44, 157–66. [175]
- Brown, J. P., Ogle, K. N., and Reiher, L. (1965). Stereoscopic acuity and observation distance. *Investigative Ophthalmology*, 4, 894–900. [179]
- Bruce, C. J., Isley, M. R., and Shinkman, P. G. (1981). Visual experience and development of interocular orientation disparity in visual cortex. *Journal of Neurophysiology*, 46, 215–28. [622]
- Buckley, D. and Frisby, J. P. (1993). Interaction of stereo, texture and outline cues in the shape perception of three-dimensional ridges. *Vision Research*, 33, 919–33. [450]
- Buckley, D., Frisby, J. P., and Mayhew, J. E. W. (1989). Integration of stereo and texture cues in the formation of discontinuities during three-dimensional surface interpolation. *Perception*, 18, 563–88. [501]
- Buckley, E. G. and Seaber, J. H. (1982). The incidence of strabismic amblyopia. *Investigative Ophthalmology and Visual Science*, 22 (ARVO Abstracts), 162. [632]
- Buhl, E. H., Halasy, K., and Somogyi, P. (1994). Diverse sources of hippocampal unitary inhibitory postsynaptic potentials and the number of synaptic release sites. *Nature*, 368, 823–8. [117]
- Buisseret, P. and Imbert, M. (1976). Visual cortical cells: Their developmental properties in normal and dark reared kittens. *Journal of Physiology*, 255, 511–25. [625]
- Buisseret, P. and Maffei, L. (1977). Extraocular proprioceptive projections to the visual cortex. *Experimental Brain Research*, 28, 421–5. [540]
- Buisseret, P. and Singer, W. (1983). Proprioceptive signals from extraocular muscles gate experience-dependent modifications of receptive fields in the kitten visual cortex. *Experimental Brain Research*, 51, 443–50. [641]
- Buisseret, P., Gary-Bobo, E., and Imbert, M. (1978). Ocular motility and recovery of orientational properties of visual cortical neurones in dark-reared kittens. *Nature*, 272, 816–7. [641]
- Bülthoff, H. H. (1991). Shape from X: Psychophysics and computation. In *Computational models of visual processing*. (ed. M. S. Landy and J. A. Movshon), pp. 305–30, M.I.T. Press, Cambridge, MA. [437]
- Bülthoff, H. H. and Mallot, H. A. (1987). Interaction of different modules in depth perception. *Proceedings of 1st International Conference on Computer Vision*, 295–305. [436, 455]
- Bülthoff, H. H. and Mallot, H. A. (1988). Interaction of depth modules: stereo and shading. *Journal of Optical Society of America*, 5, 1749–57. [436, 455]
- Bülthoff, H. H. and Yuille, A. L. (1991). Bayesian models for seeing shapes and depth. *Comments Theoretical Biology*, 2, 283–314. [437–8]
- Bülthoff, H. H., Fahle, M., and Wegmann, M. (1991). Perceived depth scales with disparity gradient. *Perception*, 20, 145–53. [160]
- Bunt, A. H. and Minckler, D. S. (1977). Foveal sparing. New anatomical evidence for bilateral representation of central retina. *AMA Archives of Ophthalmology*, 95, 1445–7. [130]
- Burchfiel, J. L. and Duffy, F. H. (1981). Role of intracortical inhibition in deprivation amblyopia: Reversal by microiontophoretic bicuculline. *Brain Research*, 206, 479–84. [629]
- Burdea, G. and Coiffet, P. (1994). *Virtual reality technology*. Wiley, New York. [30]
- Burian, H. M. (1939). Fusional movements. *AMA Archives of Ophthalmology*, 21, 486–91. [402]
- Burian, H. M. (1943). Influence of prolonged wearing of meridional size lenses on spatial localization. *AMA Archives of Ophthalmology*, 30, 645–68. [67]
- Burian, H. M. (1948). History of the Dartmouth eye institute. *AMA Archives of Ophthalmology*, 40, 163–75. [65]
- Burian, H. M. (1951). Anomalous retinal correspondence. *American Journal of Ophthalmology*, 34, 237–53. [47]
- Burian, H. M. and Ogle, K. N. (1945). Meridional aniseikonia at oblique axes. *AMA Archives of Ophthalmology*, 33, 293–310. [66]
- Burke, D. and Wenderoth, P. (1989). Cyclopean tilt aftereffects can be induced monocularly: Is there a purely binocular process? *Perception*, 18, 471–82. [374]
- Burkhalter, A. and Van Essen, D. C. (1986). Processing of color, form and disparity information in visual areas VP and V2 of ventral extrastriate cortex in the macaque monkey. *Journal of Neuroscience*, 6, 2327–51. [135]
- Burkhalter, A., Bernardo, K. L., and Charles, V. (1993). Development of local circuits in human visual cortex. *Journal of Neuroscience*, 13, 1916–31. [612]
- Burkhardt, D. A. (1993). Synaptic feedback, depolarization, and color opponency in cone photoreceptors. *Visual Neuroscience*, 10, 981–9. [109]
- Burns, B. D. and Prichard, R. (1968). Cortical conditions for fused binocular vision. *Journal of Physiology*, 197, 149–71. [345]
- Burr, D. C. (1979). Acuity for apparent vernier offset. *Vision Research*, 19, 835–38. [542]

- Burr, D. C. and Ross, J. (1979). How does binocular delay give information about depth? *Vision Research*, **19**, 523–32. [539-40, 543, 553]
- Burt, P. and Julesz, B. (1980). Modifications of the classical notion of Panum's fusional area. *Perception*, **9**, 671–82. [222, 250, 318]
- Burt, P. and Sperling, G. (1981). Time, distance, and feature trade-offs in visual apparent motion. *Psychological Review*, **88**, 171–95. [527]
- Burton, H. E. (1945). The optics of Euclid. *Journal of the Optical Society of America*, **35**, 357–72. [4]
- Bush, G. A., van der Steen, J., and Miles, F. A. (1993). When two eyes see patterns of unequal size they produce saccades of unequal amplitude. *Society for Neuroscience Abstracts*, **19**, 785. [414]
- Bushnell, M. C., Goldberg, M. E., and Robinson, D. L. (1981). Behavioral enhancement of visual responses in monkey cerebral cortex. I. Modulation in posterior parietal cortex related to selective visual attention. *Journal of Neurophysiology*, **46**, 755–72. [129]
- Butler, T. W. and Westheimer, G. (1978). Interference with stereoscopic acuity: Spatial temporal, and disparity tuning. *Vision Research*, **18**, 1387–92. [161]
- Büttner-Ennever, J. A. and Akert, K. (1981). Medial rectus subgroups of the oculomotor nucleus and their abducens internuclear input in the monkey. *Journal of Comparative Neurology*, **197**, 17–27. [424]
- Cagenello, R. and Rogers, B. J. (1988). Local orientation differences affect the perceived slant of stereoscopic surfaces. *Investigative Ophthalmology and Visual Science*, **29** (ARVO Abstracts), 399. [266-7, 274]
- Cagenello, R. and Rogers, B. J. (1989). Binocular discrimination of line orientation and curvature and the stereoscopic discrimination of surface slant and curvature. *Investigative Ophthalmology and Visual Science*, **30** (ARVO Abstracts), 252. [275, 298]
- Cagenello, R. and Rogers, B. J. (1990). Orientation disparity, cyclo-torsion, and the perception of surface slant. *Investigative Ophthalmology and Visual Science*, **31** (ARVO Abstracts), 97. [276-7]
- Cagenello, R. and Rogers, B. R. (1993). Anisotropies in the perception of stereoscopic surfaces: The role of orientation disparity. *Vision Research*, **33**, 2189–201. [267, 274]
- Callaway, E. M. and Katz, L. C. (1990). Emergence and refinement of clustered horizontal connections in cat striate cortex. *Journal of Neuroscience*, **10**, 1134–53. [612]
- Campbell, F. W. (1956). A high-speed infra-red recording optometer. *Journal of Physiology*, **133**, 31P. [394]
- Campbell, F. W. and Green, D. G. (1965). Monocular versus binocular visual acuity. *Nature*, **208**, 191–2. [351-2]
- Campbell, F. W. and Gubisch, R. W. (1966). Optical quality of the human eye. *Journal of Physiology*, **186**, 558–78. [107, 605]
- Campbell, F. W. and Kulikowski, J. J. (1966). Orientational selectivity of the human visual system. *Journal of Physiology*, **187**, 437–45. [638]
- Campbell, F. W. and Maffei, L. (1971). The tilt aftereffect: A fresh look. *Vision Research*, **11**, 833–40. [373, 639]
- Campbell, F. W. and Primrose, J. A. E. (1953). The state of accommodation of the human eye in darkness. *Transactions of the Ophthalmology Society, UK*, **73**, 353. [386]
- Campbell, F. W. and Robson, J. G. (1968). Application of Fourier analysis to the visibility of gratings. *Journal of Physiology*, **197**, 551–66. [87, 165, 259]
- Campbell, F. W. and Westheimer, G. (1959). Factors influencing accommodation responses of the human eye. *Journal of the Optical Society of America*, **49**, 568–71. [395]
- Campbell, F. W. and Westheimer, G. (1960). Dynamics of accommodation responses of the human eye. *Journal of Physiology*, **151**, 285–95. [394]
- Campbell, F. W., Robson, J. G., and Westheimer, G. (1959). Fluctuations of accommodation under steady viewing conditions. *Journal of Physiology*, **145**, 579–94. [394]
- Campbell, F. W., Gilinsky, A. S., Howell, E. R., Riggs, L. A., and Atkinson, J. (1973). The dependence of monocular rivalry on orientation. *Perception*, **2**, 123–5. [334]
- Campos, E. C. and Enoch, J. M. (1980). Amount of aniseikonia compatible with fine binocular vision: Some old and new concepts. *Journal of Pediatrics, Ophthalmology and Strabismus*, **17**, 44–7. [64]
- Campos, E. C., Bedell, H. E., Enoch, J. M., and Fitzgerald, C. R. (1978). Retinal receptive field-like properties and Stiles-Crawford effect in a patient with a traumatic choroidal rupture. *Documenta Ophthalmologica*, **45**, 381–95. [107]
- Campos, J. J., Langer, A., and Crowitz, A. (1970). Cardiac responses on the visual cliff in prelocomotor human infants. *Science*, **170**, 196–7. [618]
- Carandini, M. and Heeger, D. J. (1994). Summation and division by neurons in primate visual cortex. *Science*, **264**, 1333–6. [118]
- Carlton, E. H. and Madigan, L. F. (1937). Relationship between aniseikonia and ametropia. *AMA Archives of Ophthalmology*, **18**, 237–47. [62]
- Carman, G. J. and Welch, L. (1992). Three-dimensional illusory contours and surfaces. *Nature*, **360**, 585–7. [509]
- Carmignoto, G. and Vicini, S. (1992). Activity-dependent decrease in NMDA receptor responses during development of the visual cortex. *Science*, **258**, 1007–11. [614]
- Carmignoto, G., Canella, R., Candeo, P., Comelli, M. C., and Maffei, L. (1993). Effects of nerve growth factor on neuronal plasticity of the kitten visual cortex. *Journal of Physiology*, **464**, 343–60. [629]
- Carmon, A. and Bechtoldt, H. P. (1969). Dominance of the right cerebral hemisphere for stereopsis. *Neuropsychologia*, **7**, 29–39. [625]
- Carney, T. and Shadlen, M. N. (1992). Binocularity of early motion mechanisms: Comments on Georgeson and Shackleton. *Vision Research*, **32**, 187–91. [569]
- Carney, T. and Shadlen, M. N. (1993). Dichoptic activation of the early motion system. *Vision Research*, **33**, 1977–95. [569, 571]
- Carney, T., Paradiso, M. A., and Freeman, R. D. (1989). A physiological correlate of the Pulfrich effect in cortical neurons of the cat. *Vision Research*, **29**, 155–65. [540]
- Carney, T., Shadlen, M., and Switkes, E. (1987). Parallel processing of motion and colour information. *Nature*, **328**, 647–9. [343]
- Carpenter, R. H. S. (1988). *Movements of the eyes*. Pion, London. [382, 386]
- Carter, D. B. (1963). Effects of prolonged wearing of prism. *American Journal of Optometry and Physiological Optics*, **40**, 265–73. [392]
- Carter, D. B. (1965). Fixation disparity and heterophoria following prolonged wearing of prisms. *American Journal of Optometry*, **42**, 141–52. [392]
- Cartmill, M. (1974). Rethinking primate origins. *Science*, **184**, 436–43. [646]
- Casagrade, V. A. and Brusco-Bechtold, J. K. (1988). Development of lamination in lateral geniculate nucleus: Critical factors. In *Advances in neural and behavioral development*. Vol. 3, (ed. P. G. Shinkman), pp. 33–78. Ablex, Norwood, NJ. [113, 609]
- Cass, E. E. (1941). Monocular diplopia occurring in cases of squint. *British Journal of Ophthalmology*, **25**, 565–77. [47]
- Caudek, C. and Proffitt, D. R. (1993). Depth perception in motion parallax and stereopsis. *Journal of Experimental Psychology: Human Perception and Performance*, **19**, 32–47. [442]

- Cavallo, V. and Laurent, M. (1988). Visual information and skill level in time-to-collision estimation. *Perception*, 17, 623–32. [555]
- Cavanagh, P and Mather, G. (1989). Motion: The long and short of it. *Spatial Vision*, 4, 103–29. [568]
- Cavonius, C. R. (1979). Binocular interactions in flicker. *Quarterly Journal of Experimental Psychology*, 31, 273–80. [360, 638]
- Celebrini, S., Thorpe, S., Trotter, Y., and Imbert, M. (1993). Dynamics of orientation coding in area V1 of the awake primate. *Visual Neuroscience*, 10, 811–25. [118]
- Chalupa, L. M., Williams, R. W., and Henderson, Z. (1984). Binocular interaction in the fetal cat regulates the size of the ganglion cell population. *Neuroscience*, 12, 1139–46. [607]
- Chan-Palay, V., Palay, S. L., Billings-Gagliardi, S. M. (1974). Meynert cells in the primate visual cortex. *Journal of Neurocytology*, 3, 631–58. [124]
- Chang, J. J. (1990). New phenomena linking depth and luminance in stereoscopic motion. *Vision Research*, 30, 137–47. [590]
- Chang, J. J. and Julesz, B. (1983). Displacement limits, direction anisotropy and direction versus form discrimination in random-dot cinematograms. *Vision Research*, 23, 639–46. [570]
- Chapman, B., Zahs, K. R., and Stryker, M. P. (1991). Relation of cortical cell orientation selectivity to alignment of receptive fields of the geniculocortical afferents that arborize within a single orientation column in ferret visual cortex. *Journal of Neuroscience*, 11, 1347–58. [118]
- Charman, W. N. (1991). Optics of the human eye. In *Vision and visual dysfunction*. Vol. 1, *Visual optics and instrumentation*. (ed. W. N. Charman), pp. 1–26. Macmillan, London. [106]
- Chase, W. and Smith, R. (1981). Spatial frequency channels tuned for depth and motion. *Vision Research*, 21, 621–5. [566]
- Chawanya, T., Aoyagi, T., Nishikawa, I., Okuda, K., and Kuramoto, Y. (1993). A model for feature linking via collective oscillations in the primary visual cortex. *Biological Cybernetics*, 68, 483–90. [83]
- Cherry, E. C. (1953). Some experiments on the recognition of speech with one and two ears. *Journal of the Acoustical Society of America*, 25, 975–9. [347]
- Chérubin d'Orléans, P. (1661). *La dioptique oculaire, ou la théorie, la positive, et la mécanique, de l'oculaire dioptique en toutes ses espèces*. Jolly et Bernard, Paris. [19]
- Chérubin d'Orléans, P. (1667). *La vision parfaite, ou les concours des deux axes de la vision, en un seul point de l'objet*. Marbre-Cramoisy, Paris. [19]
- Cheung, B. S. K. and Howard, I. P. (1991). Optokinetic torsion: Dynamics and relation to circularvection. *Vision Research*, 31, 1327–36. [417]
- Chino, Y. M., Shansky, M. S., Jankowski, W. L., and Banser, F. A. (1983). Effects of rearing kittens with convergent strabismus on the development of receptive field properties in striate cortex neurons. *Journal of Neurophysiology*, 50, 265–86. [628]
- Chino, Y. M., Cheng, H., Smith, E. L., Garraghty, P. E., Roe, A. W., and Sur, M. (1994). Early discordant binocular vision disrupts signal transfer in the lateral geniculate nucleus. *Proceedings of the National Academy of Science*, 91, 6938–42. [627]
- Chino, Y. M., Kaas, J. H., Smith, E. L., Langton, A. L., and Cheng, H. (1992). Rapid reorganization of cortical maps in adult cats following restricted deafferentation in retina. *Vision Research*, 32, 789–96. [129]
- Choudhury, B. P., Whitteridge, D., and Wilson, M. E. (1965). The function of the callosal connections of the visual cortex. *Quarterly Journal of Experimental Physiology*, 50, 215–19. [130]
- Chow, K. L. (1973). Neuronal changes in the visual system following visual deprivation. In *Handbook of sensory physiology*, Vol. VII/3A, (ed. R. Jung), pp. 599–630. Springer, New York. [625, 627]
- Christakos, C. N. (1994). Analysis of synchrony (correlations) in neural populations by means of unit-to-aggregate coherence computations. *Neuroscience*, 58, 43–57. [83]
- Christophers, R. A. and Rogers, B. J. (1994). The effect of viewing distance on the perception of random dot stereograms. *Investigative Ophthalmology and Visual Science*, 35 (ARVO Abstracts), 1624. [194]
- Christophers, R. A., Rogers, B. J., and Bradshaw M. F. (1993). Perceptual latencies, vergence eye movements and random-dot stereograms. *Investigative Ophthalmology and Visual Science*, 34 (ARVO Abstracts), 1438. [193–4]
- Church, J. (1966). *Language and the discovery of reality*. Vintage, New York. [595]
- Cibis, P. A. and Harris, H. (1951). Anisopia and perception of space. *Journal of the Optical Society of America*, 41, 676–83. [310]
- Cigánek, L. (1970). Binocular addition of the visually evoked response with different stimulus intensities in man. *Vision Research*, 10, 479–87. [145]
- Ciner, E. B., Scheiman, M. M., and Schanel-Klitsch, E. (1989). Stereopsis testing in 18- to 35-month-old children using operant preferential looking. *Optometry and Visual Science*, 66, 782–7. [619]
- Ciner, E. B., Schanel-Klitsch, E., and Scheiman, M. M. (1991). Stereoaquity development in young children. *Optometry and Vision Science*, 68, 533–6. [619]
- Ciuffreda, K. J. (1991). Accommodation and its anomalies. In *Vision and visual dysfunction*. Vol. 1, *Visual optics and instrumentation*. (ed. W. N. Charman), pp. 231–79. Macmillan, London. [394]
- Ciuffreda, K. J. and Kenyon, R. V. (1983). Accommodative vergence and accommodation in normals, amblyopes and strabismics. In *Vergence eye movements: Basic and clinical aspects*, (ed. M. C. Schor, K. J. Ciuffreda), pp. 99–162. Butterworth, Boston. [398]
- Ciuffreda, K. J., Kenyon, R. V., and Stark, L. (1980). Increased drift in amblyopic eyes. *British Journal of Ophthalmology*, 64, 7–14. [632]
- Ciuffreda, K. J., Levi, D. M., and Selenow, A. (1992). *Amblyopia: Basic and clinical aspects*. Butterworth, Boston. [635]
- Clark, J. J. and Yuille, A. L. (1990). *Data fusion for sensory information processing systems*. Kluwer, Boston. [437]
- Clarke, P. G. H. and Whitteridge, D. (1976). The cortical visual areas of the sheep. *Journal of Physiology*, 256, 497–508. [657]
- Clarke, P. G. H., Donaldson, I. M. L., and Whitteridge, D. (1976). Binocular visual mechanism in cortical areas I and II of the sheep. *Journal of Physiology*, 256, 509–26. [656]
- Clarke, P. G. H., Ramachandran, V. S., and Whitteridge, D. (1979). The development of the binocular depth cells in the secondary visual cortex of the lamb. *Proceedings of the Royal Society, London*, B204, 455–65. [656]
- Clarke, S. and Miklossy, J. (1990). Occipital cortex in man: Organization of callosal connections, related myelo- and cytoarchitecture, and putative boundaries of functional visual areas. *Journal of Comparative Neurology*, 298, 188–214. [131]
- Claudet, A. (1856). On various phenomena of refraction through semi-lenses or prisms, producing anomalies in the illusion of stereoscopic images. *Proceedings of the Royal Society*, 8, 104–111. [24]
- Clelend, B. G., Crewther, D. P., Crewther, S. G., and Mitchell, D. E. (1982). Normality of spatial resolution of retinal ganglion cells in cat with strabismus amblyopia. *Journal of Physiology*, 326, 235–49. [626]

- Cleland, B. G., Mitchell, D. E., Crewther, S. G., and Crewther, D. P. (1980). Visual resolution of retinal ganglion cells in monocularly-deprived cats. *Brain Research*, **192**, 261–66. [626]
- Clement, R. A. (1987). Line correspondence in binocular vision. *Perception*, **16**, 193–9. [52]
- Clement, R. A. (1992). Gaze angle explanations of the induced effect. *Perception*, **21**, 355–7. [283]
- Cloarec, A. (1978). Estimation of hit distance by *Ranatra*. *Biology and Behaviour*, **4**, 173–91. [646]
- Clothiaux, E. E., Bear, M. F., and Cooper, L. N. (1991). Synaptic plasticity in visual cortex: Comparison of theory with experiment. *Journal of Neurophysiology*, **66**, 1785–804. [81, 631]
- Cobo-Lewis, A. B. and Yeh, Y. Y. (1994). Selectivity of cyclopean masking for the spatial frequency of binocular disparity modulation. *Vision Research*, **34**, 607–20. [166]
- Cocker, K. D., Moseley, M. J., Bissenden, J. G., and Fielder, A. R. (1994). Visual acuity and pupillary responses to spatial structure in infants. *Investigative Ophthalmology and Visual Science*, **35**, 2620–5. [616]
- Cogan, A. I. (1978). Fusion at the site of the "ghosts". *Vision Research*, **18**, 657–64. [45]
- Cogan, A. I. (1979). The relationship between the apparent vertical and the vertical horopter. *Vision Research*, **19**, 655–65. [418]
- Cogan, A. I. (1987). Human binocular interaction: Towards a neural model. *Vision Research*, **27**, 2125–39. [358, 370]
- Cogan, A. I. (1989). Do background luminances interact during binocular fusion? *Perception and Psychophysics*, **46**, 560–6. [364]
- Cogan, A. I., Silverman, G., and Sekuler, R. (1982). Binocular summation in detection of contrast flashes. *Perception and Psychophysics*, **31**, 330–8. [361]
- Cogan, A. I., Lomakin, A. J., and Rossi, A. F. (1993). Depth in anticorrelated stereograms: Effects of spatial density and interocular delay. *Vision Research*, **33**, 1959–75. [225]
- Cogan, A. I., Clarke, M., Chan, H., and Rossi, A. (1990). Two-pulse monocular and binocular interactions at the differential luminance threshold. *Vision Research*, **30**, 1617–30. [362]
- Cogan, D. G. (1956). *Neurology of the ocular muscles*. Thomas, Springfield, Illinois. [424]
- Cohen, J., Burne, J. F., Winter, J., and Bartlett, P. (1986). Retinal ganglion cells lose response to laminin with maturation. *Nature*, **322**, 465–67. [606]
- Cohn, T. E., Leong, H., and Lasley, D. J. (1981). Binocular luminance detection: Availability of more than one central interaction. *Vision Research*, **21**, 1017–23. [358]
- Colby, C. L., Duhamel, J.-R., Goldberg, M. E. (1993). Ventral intraparietal area of the macaque: Anatomic location and visual response properties. *Journal of Neurophysiology*, **69**, 902–14. [564]
- Colello, R. J., Pott, U., and Schwab, M. E. (1994). The role of oligodendrocytes and myelin on axon maturation in the developing rat retinofugal pathway. *Journal of Neuroscience*, **14**, 2594–605. [607]
- Collett, T. S. (1977). Stereopsis in toads. *Nature*, **267**, 349–51. [652]
- Collett, T. S. (1978). Peering – a locust behaviour pattern for obtaining motion parallax information. *Journal of Experimental Biology*, **76**, 237–41. [648]
- Collett, T. S. (1985). Extrapolating and interpolating surfaces in depth. *Proceedings of the Royal Society, London*, **B224**, 43–56. [500]
- Collett, T. S. (1987). Binocular depth vision in arthropods. *Trends in Neuroscience*, **10**, 1–2. [649]
- Collett, T. S. and Harkness, L. I. K. (1982). Depth vision in animals. In *Analysis of visual behavior*, (ed. D. J. Ingle, M. A. Goodale, and R. J. W. Mansfield), pp. 111–76. MIT Press, Cambridge, MA. [657]
- Collett, T. S., Udin, S. B., and Finch, D. J. (1987). A possible mechanism for binocular depth judgments in anurans. *Experimental Brain Research*, **66**, 35–40. [652]
- Collett, T. S., Schwarz, U., and Sobel, E. C. (1991). The interaction of oculomotor cues and stimulus size in stereoscopic depth constancy. *Perception*, **20**, 733–54. [458]
- Collewijn, H. (1975). Direction-selective units in the rabbit's nucleus of the optic tract. *Brain Research*, **100**, 489–508. [530-1]
- Collewijn, H., and Erkelens, C. J. (1990). Binocular eye movements and the perception of depth. In *Eye movements and their role in visual and cognitive processes: Review of oculomotor research*, (ed. E. Kowler), pp. 213–61. Elsevier, Amsterdam. [386]
- Collewijn, H., Erkelens, C. J., and Steinman, R. M. (1988a). Binocular co-ordination of human horizontal saccadic eye movements. *Journal of Physiology*, **404**, 157–82. [411]
- Collewijn, H., Erkelens, C. J., and Steinman, R. M. (1988b). Binocular co-ordination of human vertical saccadic eye movements. *Journal of Physiology*, **404**, 183–97. [410]
- Collewijn, H., Steinman, R. M., Erkelens, C. J., and Regan, D. (1991). Binocular fusion, stereopsis and stereoacuity with a moving head. In *Vision and visual dysfunction*. Vol. 9, (ed. D. Regan), pp. 121–36. Macmillan, London. [180]
- Collewijn, H., van der Steen, J., Ferman, L., and Jansen, T. C. (1985). Human ocular counterroll, assessment of static and dynamic properties from electromagnetic scleral coil recordings. *Experimental Brain Research*, **59**, 185–96. [417, 419]
- Collewijn, H., van der Mark, F., and Jansen, T. C. (1975). Precise recording of human eye movements. *Vision Research*, **15**, 447–50. [383, 419]
- Collins, C. C., Carlson, M. R., Scott, A. B., and Jampolsky, A. (1981). Extraocular muscle forces in normal human subjects. *Investigative Ophthalmology and Visual Science*, **20**, 652–64. [411]
- Collins, E. T. (1922). *Arboreal life and the evolution of the human eye*. Lea and Febinger, New York. [646]
- Collyer, S. C. and Bevan, W. (1970). Objective measurement of dominance control in binocular rivalry. *Perception and Psychophysics*, **8**, 437–9. [346]
- Coltheart, M. (1971). Visual feature-analyzers and after-effects of tilt and curvature. *Psychological Review*, **78**, 114–21. [490-2]
- Coltheart, M. (1973). Colour-specificity and monocularity in the visual cortex. *Vision Research*, **13**, 2595–8. [373]
- Comerford, J. P. (1974). Stereopsis with chromatic contours. *Vision Research*, **14**, 975–82. [207]
- Connors, B. W. and Gutnick, M. J. (1990). Intrinsic firing patterns of diverse neocortical neurons. *Trends in Neuroscience*, **13**, 99–104. [81, 116]
- Constantine-Paton, M., Cline, H. T., and Debski, E. (1990). Patterned activity, synaptic convergence, and the NMDA receptor in developing visual pathways. *Annual Review of Neuroscience*, **13**, 129–54. [614]
- Cooper, G. R. and McGilllem, C. D. (1967). *Methods of signal and system analysis*. Holt, Rinehart and Winston, New York. [87]
- Cooper, J. and Feldman, J. (1978a). Operant conditioning and assessment of stereopsis in young children. *American Journal of Optometry and Physiological Optics*, **55**, 532–42. [620]
- Cooper, J. and Feldman, J. (1978b). Random-dot stereogram performance by strabismic, amblyopic and ocular-pathology patients in an operant-discrimination task. *American Journal of Optometry and Physiological Optics*, **55**, 599–609. [634]
- Cooper, J. and Feldman, J. (1979). Assessing the Frisby stereo test under monocular viewing conditions. *Journal of the American Optometry Association*, **50**, 807–9. [155]
- Cooper, J. and Warshowsky, J. (1977). Lateral displacement as a response cue in the Titmus stereo Test. *American Journal of Physiological Optics*, **54**, 537–41. [151]

- Cooper, M. L. and Pettigrew, J. D. (1979). A neurophysiological determination of the vertical horopter in the cat and owl. *Journal of Comparative Neurology*, 184, 1-26. [61]
- Cooper, S., Daniel, P. M., and Whitteridge, D. (1955). Muscle spindles and other sensory endings in the extrinsic eye muscles; The physiology and anatomy of these receptors and their connections with the brain-stem. *Brain*, 78, 564-83. [432]
- Corbin, H. H. (1942). The perception of grouping and apparent movement in visual depth. *Archives of Psychology*, No. 273. [527]
- Cords, R. (1913). Der Einfluss der parallaktischen Verschiebung auf die Tiefenwahrnehmung. *Klinische Monatsblätter für Augenheilkunde*, 51, 421. [578]
- Coren, S. and Kaplan, C. P. (1973). Patterns of ocular dominance. *American Journal of Optometry and Archives of American Academy of Optometry*, 50, 283-92. [337]
- Coren, S. and Porac, C. (1983). Subjective contours and apparent depth: A direct test. *Perception and Psychophysics*, 33, 197-200. [508]
- Cormack, L. K., Stevenson, S. B., and Schor, C. M. (1991). Interocular correlation, luminance contrast and cyclopean processing. *Vision Research*, 31, 2195-207. [168-9, 214]
- Cormack, L. K., Stevenson, S. B., and Schor, C. M. (1994). An upper limit to the binocular combination of stimuli. *Vision Research*, 34, 2599-608. [214]
- Cormack, R. H. (1984). Stereoscopic depth perception at far viewing distances. *Perception and Psychophysics*, 35, 423-28. [458]
- Cornilleau-Peres, V. and Droulez, J. (1990). Stereo-correspondence from optic flow. In *Proceedings of the first European conference on computer vision* (ed. O. Faugeras), pp. 326-30. Springer-Verlag, Berlin. [440]
- Cornilleau-Peres, V. and Droulez, J. (1993). Stereo-motion cooperation and the use of motion disparity in the visual perception of 3D structure. *Perception and Psychophysics*, 54, 223-39. [440, 580]
- Cornilleau-Peres, V. and Droulez, J. (1994). Velocity correspondence in stereokinetic images. *Computer Vision, Graphics and Image Processing, Image Understanding*, in press.
- Cornsweet, T. N. (1962). The staircase method in psychophysics. *American Journal of Psychology*, 75, 485-91. [94]
- Cornsweet, T. N. (1970). *Visual perception* Academic Press, New York. [473, 480]
- Corrette, B. J. (1989). Prey capture in the praying mantis *Tenodera aridifolia sinensis*: Coordination of the capture sequence and strike movements. *Journal of Experimental Biology*, 148, 147-80. [647]
- Cowan, W. M. (1973). *Neuronal death as a regulative mechanism in the control of cell number in the nervous system*. Academic Press, New York. [607]
- Cowey, A. (1979). Cortical maps and visual perception: The Grindley Memorial Lecture. *Quarterly Journal of Experimental Psychology*, 31, 1-17. [128]
- Cowey, A. (1985). Disturbances of stereopsis by brain damage. In *Brain mechanisms and spatial vision* (ed. D. J. Ingle, M. Jeannerod, and N. Lee), pp. 259-78. Nijhoff, Dordrecht. [132, 624]
- Cowey, A. and Rolls, E. T. (1974). Human cortical magnification factor and its relation to visual acuity. *Experimental Brain Research*, 21, 447-54. [114]
- Cowey, A. and Wilkinson, F. (1991). The role of the corpus callosum and extrastriate visual areas in stereoacuity in macaque monkeys. *Neuropsychologia*, 29, 465-79. [135]
- Cowey, A., Parkinson, A. M., and Warnick, L. (1975). Global stereopsis in monkeys. *Quarterly Journal of Experimental Psychology*, 27, 93-109. [645]
- Craik, K. J. W. (1966). *The nature of psychology* Cambridge University Press, Cambridge. [480]
- Crannell, C. W. and Peters, G. (1970). Monocular and binocular estimations of distance when knowledge of the relevant space is absent. *Journal of Psychology*, 76, 157-67. [428]
- Craske, B. and Crawshaw, M. (1974). Adaptive changes of opposite sign in the oculomotor systems of the two eyes. *Quarterly Journal of Experimental Psychology*, 26, 106-13. [434]
- Craske, B., Crawshaw, M., and Heron, P. (1975). Disturbance of the oculomotor system due to lateral fixation. *Quarterly Journal of Experimental Psychology*, 27, 459-65. [432]
- Crawford, B. H. (1938). Some observations on the rotating pendulum. *Nature*, 141, 792-3. [546]
- Crawford, B. H. (1940a). Ocular interaction in its relation to measurements of brightness threshold. *Proceedings of the Royal Society, London*, B128, 552-9. [364]
- Crawford, B. H. (1940b). The effect of field size and pattern on the change of visual sensitivity with time. *Proceedings of the Royal Society, London*, B129, 94-106. [364]
- Crawford, J. D., Cadena, W., and Vilis, T. (1991). Generation of torsional and vertical eye position signals by the interstitial nucleus of Cajal. *Science*, 252, 1551-3. [426]
- Crawford, M. L. J. and Cool, S. J. (1970). Binocular stimulation and response variability of striate cortex units in the cat. *Vision Research*, 10, 1145-53. [133]
- Crawford, M. L. J. and Noorden, G. K. von (1979). Concomitant strabismus and cortical eye dominance in young rhesus monkeys. *Transactions of the Ophthalmology Society, U. K.*, 99, 369-74. [630]
- Crawford, M. L. J. and Noorden, G. K. von (1980). Optically induced concomitant strabismus in monkeys. *Investigative Ophthalmology and Visual Science*, 19, 1105-9. [630]
- Crawford, M. L. J., De Faber, J. T., Harwerth, R. S., Smith, E. L., and Noorden, G. K. von (1989). The effects of reverse monocular deprivation in monkeys. II. Electrophysiological and anatomical studies. *Experimental Brain Research*, 74, 338-47. [636]
- Crawford, M. L. J., Smith, E. L., Harwerth, R. S., and Noorden, G. K. von (1984). Stereoblind monkeys have few binocular neurons. *Investigative Ophthalmology and Visual Science*, 25, 779-81. [630]
- Crawford, M. L. J., Noorden, G. K. von, Meharg, L. S., Rhodes, J. W., Harwerth, R. S., Smith, E. L., and Miller, D. D. (1983). Binocular neurons and binocular function in monkeys and children. *Investigative Ophthalmology and Visual Science*, 24, 491-5. [630]
- Creel, D., O'Donnell, F. E., and Witkop C. J. (1978). Visual system anomalies in human ocular albinos. *Science*, 201, 931-3. [642]
- Creutzfeldt, O. D. (1977). Generality of the functional structure of the neocortex. *Naturwissenschaften*, 64, 507-17. [125]
- Crewther, D. P., Crewther, S. G., and Pettigrew, J. D. (1978). A role for extraocular afferents in post-critical period reversal of monocular deprivation. *Journal of Physiology*, 282, 181-95. [629, 641]
- Crewther, S. G., Grewther, D. P., and Mitchell, D. E. (1983). The effects of short-term occlusion therapy on reversal of the anatomical and physiological effects of monocular deprivation in the lateral geniculate nucleus and visual cortex of kittens. *Experimental Brain Research*, 51, 206-16. [636]
- Crewther, S. G., Grewther, D. P., Peck, C. K., and Pettigrew, J. D. (1980). Visual cortical effects of rearing cats with monocular or binocular cyclotorsion. *Journal of Neurophysiology*, 44, 97-118. [622]
- Crick, F. (1984). The functions of the thalamic reticular complex: The searchlight hypothesis. *Proceedings of the National Academy of Science*, 81, 4586-90. [113]

- Crick, F. and Koch, C. (1990). Towards a neurobiological theory of consciousness. *Seminars in the Neurosciences*, 2, 263–75. [83]
- Critchley, M. (1953). *The parietal lobes*. Arnold, London. [127]
- Crone, R. A. and Everhard-Halm, Y. (1975). Optically induced eye torsion. I. Fusional cyclovergence. *Albrecht v. Graefes Archiv für Ophthalmologie*, 195, 231–9. [419, 421]
- Crone, R. A. and Leuridan, O. M. A. (1973). Tolerance for aniseikonia. I. Diplopia thresholds in the vertical and horizontal meridians of the visual field. *Albrecht v. Graefes Archiv für Ophthalmologie*, 188, 1–16. [316]
- Cronly-Dillon, J. R. and Gregory, R. L. (1991). *The evolution of the eye and visual system*. CRC Press, Boca Raton, Ann Arbor. [606]
- Crovitz, H. F. and Lipscomb, D. B. (1963a). Binasal hemianopia as an early stage in binocular color rivalry. *Science*, 139, 596–7. [332]
- Crovitz, H. F. and Lipscomb, D. B. (1963b). Dominance of the temporal visual fields at a short duration of stimulation. *American Journal of Psychology*, 76, 631–7. [332]
- Crovitz, H. F. and Lockhead, G. R. (1967). Possible monocular predictors of binocular rivalry of contours. *Perception and Psychophysics*, 2, 83–5. [334]
- Crozier, W. J. and Wolf, E. (1941). Theory and measurement of visual mechanisms: IV. Critical intensities for visual flicker, monocular and binocular. *Journal of General Physiology*, 24, 505–35. [359]
- Cumming, B. G. (1994). The relationship between stereoacuity and stereomotion thresholds. *Perception*, in press. [561]
- Cumming, B. G. and Judge, S. J. (1986). Disparity-induced and blur-induced convergence eye movement and accommodation in monkey. *Journal of Neurophysiology*, 55, 896–914. [396]
- Cumming, B. G. and Parker, A. J. (1994). Binocular mechanisms for detecting motion-in-depth. *Vision Research*, 34, 483–95. [561]
- Cumming, B. G., Johnston, E. B., and Parker, A. J. (1991). Vertical disparities and the perception of three-dimensional shape. *Nature*, 349, 411–13. [289]
- Cumming, B. G., Johnston, E. B., and Parker, A. J. (1993). Effects of different texture cues on curved surfaces viewed stereoscopically. *Vision Research*, 33, 827–38. [449]
- Curcio, C. A., Sloan, K. R., Kalina, R. E., and Hendrickson, A. E. (1990). Human photoreceptor topography. *Journal of Comparative Neurology*, 292, 497–523. [107, 606, 617]
- Curtis, D. W. and Rule, S. J. (1978). Binocular processing of brightness information: A vector-sum model. *Journal of Experimental Psychology*, 4, 132–43. [358]
- Cutting, J. E. (1986). *Perception with an eye to motion*. MIT Press, Cambridge, MA. [460, 557]
- Cutting, J. E. and Millard, R. T. (1984). Three gradients and the perception of flat and curved surfaces. *Journal of Experimental Psychology: General*, 113, 198–216. [449]
- Cynader, M. and Mitchell, D. E. (1980). Prolonged sensitivity to monocular deprivation in dark-reared cats. *Journal of Neurophysiology*, 43, 1026–40. [635]
- Cynader, M. and Regan, D. (1978). Neurons in cat parastriate cortex selective to the direction of motion in three-dimensional space. *Journal of Physiology*, 274, 549–69. [564]
- Cynader, M. and Regan, D. (1982). Neurons in cat visual cortex tuned to the direction of motion in depth: Effect of positional disparity. *Vision Research*, 22, 967–82. [564]
- Cynader, M., Berman, N., and Hein, A. (1976). Recovery of function in cat visual cortex following prolonged deprivation. *Experimental Brain Research*, 25, 139–56. [625]
- Cynader, M., Gardner, J., and Douglas, R. (1978). Neural mechanisms underlying stereoscopic depth perception in cat visual cortex. In *Frontiers in visual science* (ed. S. J. Cool and E. L. Smith), pp. 373–86. Springer, Berlin. [540]
- Cynader, M., Gardner, J. C., and Mustari, M. (1984). Effects of neonatally induced strabismus on binocular responses in cat area 18. *Experimental Brain Research*, 53, 384–99. [627]
- Cynader, M., Gardner, J. C., Dobbins, A., Lepore, F., Guillemot, J. P. (1986). Interhemispheric communication and binocular vision: Functional and developmental aspects. In *Two hemispheres – one brain: Functions of the corpus callosum*, (ed. F. Lepore, M. Ptito, and H. H. Jasper), pp. 198–209. Liss, New York. [131]
- Cynader, M., Giaschi, D. E., and Douglas, R. M. (1993). Interocular transfer of direction-specific adaptation to motion in cat striate cortex. *Investigative Ophthalmology and Visual Science*, 34, (ARVO Abstracts), 1188. [376]
- Cynader, M., Timney, B. N., and Mitchell, D. E. (1980). Period of susceptibility of kitten visual cortex to the effect of monocular deprivation extends beyond 6 months of age. *Brain Research*, 191, 545–50. []
- da Vinci, L. (1452). *Trattato della pittura*. Translated as *A treatise on painting* by J. E. Rigaud. London, 1802. [14]
- Dale, R. T. (1982). *Fundamentals of ocular motility and strabismus*. Grune and Stratton, New York. [634]
- Dalva, M. B. and Katz, L. C. (1994). Rearrangements of synaptic cortical connections in visual cortex revealed by laser photo-stimulation. *Science*, 265, 255–8. [612]
- Dalva, M. B., Ghosh, A., and Shatz, C. J. (1994). Independent control of dendritic and axonal form in the developing lateral geniculate nucleus. *Journal of Neuroscience*, 14, 3588–602. [609]
- Dan, Y. and Poo, M. (1992). Hebbian depression of isolated neuromuscular synapses in vitro. *Science*, 256, 1570–3. [82]
- Daniel, P. M. and Whitteridge, D. (1961). The representation of the visual field on the cerebral cortex in monkeys. *Journal of Physiology*, 159, 203–21. [114]
- Daniels, J. D., Pettigrew, J. D., and Norman, J. L. (1978). Development of single-neuron responses in kitten's lateral geniculate nucleus. *Journal of Neurophysiology*, 41, 1373–93. [609]
- Dannemiller, J. L. and Freedland, R. L. (1993). Motion-based detection by 14-week-old infants. *Vision Research*, 33, 657–64. [617]
- Danta, G., Hilton, R. C., and O'Boyle, D. J. (1978). Hemisphere function and binocular depth perception. *Brain*, 101, 569–89. [624]
- Darrah, W. C. (1964). *Stereo views. A history of stereographs in America and their collection*. Times and News Publishing Co., Gettysburg, PA. [22]
- Daugman, J. G. (1990). An information-theoretic view of analog representation in striate cortex. In *Computational neuroscience*, (ed. E. L. Schwartz), pp. 401–23. MIT Press, Cambridge, MA. [90-1]
- Daugman, J. G. (1991). Self-similar oriented wavelet pyramids: Conjectures about neural non-orthogonality. In *Representations of vision*, (ed. A. Gorea), pp. 27–46. Cambridge University Press, New York. [90]
- Davis, E. T., King, R. A., and Anoskey, A. (1992). Oblique effect in stereopsis. *Proceedings of the Society of Photo and Illumination Engineering*, 166, 465–75. [167]
- Davson, H. (1980). *Physiology of the eye*. Churchill Livingstone, Edinburgh. [106]
- Daw, N. W., Fox, K., Sato, H., and Czepita, D. (1992). Critical period for monocular deprivation in the cat visual cortex. *Journal of Neurophysiology*, 67, 197–202. [635]
- Daw, N. W., Videen, T. O., Rader, R. K., Robertson, T. W., and Coscia, C. J. (1985). Substantial reduction of noradrenaline in kitten visual cortex by intraventricular injections of 6-hydroxydopamine does not always prevent ocular dominance shifts after monocular deprivation. *Experimental Brain research*, 59, 30–5. [630]

- Dawson, S. (1913). Binocular and unocular discrimination of brightness. *British Journal of Psychology*, 6, 78–108. [333]
- Dawson, S. (1915). The experimental study of binocular colour mixture. I. *British Journal of Psychology*, 7, 510–51. [327]
- Day, R. H. (1958). On interocular transfer and the central origin of visual after-effects. *American Journal of Psychology*, 71, 784–9. [363]
- Day, R. H. (1961). On the stereoscopic observation of geometrical illusions. *Perceptual and Motor Skills*, 13, 247–58. [372]
- Day, R. H. and Wade, N. J. (1988). Binocular interaction in induced rotary motion. *Australian Journal of Psychology*, 40, 159–64. [378]
- De Bryun, B., Rogers, B. R., Howard, I. P., and Bradshaw, M. F. (1992). Role of positional and orientational disparities in controlling cyclovertical eye movements. *Investigative Ophthalmology and Visual Science* 33 (ARVO Abstracts), 1149. [280]
- De Lange, H. (1954). Relationship between critical flicker frequency and a set of low-frequency characteristics of the eye. *Journal of the Optical Society of America*, 44, 380–9. [360]
- De Lange, H. (1958). Research into the dynamic nature of the fovea–cortex system with intermittent and modulated light. *Journal of the Optical Society of America*, 48, 777–84. [87]
- de Courten, C. and Garey, L. J. (1982). Morphology of the neurons in the human lateral geniculate nucleus and their normal development. *Experimental Brain Research*, 47, 159–171. [608]
- de Vries, S. C., Kappers, A. M. L., and Koenderink, J. J. (1993). Shape from stereo: A systematic approach using quadratic surfaces. *Perception and Psychophysics*, 53, 71–80. [303, 582]
- de Vries, S. C., Kappers, A. M. L., and Koenderink, J. J. (1994). Influence of surface attitude and curvature scaling on discrimination of binocularly presented surfaces. *Vision Research*, 34, 2409–23. [304, 582]
- de Weert, C. M. M. (1979). Colour contours and stereopsis. *Vision Research*, 19, 555–64. [207]
- de Weert, C. M. M. and Levelt, W. J. M. (1974). Binocular brightness combinations: Additive and nonadditive aspects. *Perception and Psychophysics*, 15, 551–62. [357]
- de Weert, C. M. M. and Levelt, W. J. M. (1976). Comparison of normal and dichoptic color mixing. *Vision Research*, 16, 59–70. [326]
- de Weert, C. M. M. and Sadza, K. J. (1983). New data concerning the contribution of colour differences to stereopsis. In *Colour vision*, (ed. J. D. Mollon and L. T. Sharpe), pp. 553–62. Academic Press, New York. [207]
- de Weert, C. M. M. and Wade, N. J. (1988). Compound binocular rivalry. *Vision Research*, 28, 1031–40. [326, 330]
- DeAngelis, G. C., Ohzawa, I., and Freeman, R. D. (1991). Depth is encoded in the visual cortex by a specialized receptive field structure. *Nature*, 352, 156–9. [141]
- DeAngelis, G. C., Ohzawa, I., and Freeman, R. D. (1993a). Spatiotemporal organization of simple-cell receptive fields in the cat's striate cortex. I. General characteristics and postnatal development. *Journal of Neurophysiology*, 69, 1091–117. [120]
- DeAngelis, G. C., Ohzawa, I., and Freeman, R. D. (1993b). Spatiotemporal organization of simple-cell receptive fields in the cat's striate cortex. II. Linearity of temporal and spatial summation. *Journal of Neurophysiology*, 69, 1118–35. [120]
- DeAngelis, G. C., Robson, J. G., Ohzawa, I., and Freeman, R. D. (1992). Organization of suppression in receptive fields of neurons in cat cortex. *Journal of Neurophysiology*, 68, 144–163. [345, 375]
- DeAngelis, G. C., Freeman, R. D., and Ohzawa, I. (1994). Length and width tuning of neurones in the cat's primary visual cortex. *Journal of Neurophysiology*, 71, 347–74. [119, 142, 375]
- Dees, J. W. (1966). Accuracy of absolute visual distance and size estimation in space as a function of stereopsis and motion parallax. *Journal of Experimental Psychology*, 72, 466–76. [583]
- Degelman, D. and Rosinski, R. (1979). Motion parallax and children's distance perception. *Developmental Psychology*, 15, 147–52. [578]
- Dellar, M. (1988). Why should surgery for early-onset strabismus be postponed. *British Journal of Ophthalmology*, 72, 110–15. [637]
- Demer, J. L. and Zee, D. S. (1984). Vestibulo-ocular and optokinetic deficits in albinos with congenital nystagmus. *Investigative Ophthalmology and Visual Science*, 25, 739–45. [643]
- Dengis, C. A., Steinbach, M. J., Goltz, H. C., and Stager, C. (1993a). Visual alignment from the midline: A declining developmental trend in normal, strabismic and monocularly enucleated children. *Journal of Pediatric Ophthalmology and Strabismus*. in press. [595]
- Dengis, C. A., Steinbach, M. J., Ono, H., Kraft, S. P., Smith, D. R., and Graham, E. (1993b). Egocenter location in children with strabismus: In the median plane and unchanged by surgery. *Investigative Ophthalmology and Visual Science*, 34, 2990–5. [600]
- Dengler, M. and Nitschke, W. (1993). Color stereopsis: A model for depth reversals based on border contrast. *Perception and Psychophysics*, 53, 150–6. [307]
- Derrington, A. M. and Hawken, M. J. (1981). Spatial and temporal properties of cat geniculate neurones after prolonged deprivation. *Journal of Physiology*, 314, 107–20. [627]
- Derrington, A. M. and Lennie, P. (1984). Spatial and temporal contrast sensitivities of neurones in lateral geniculate nucleus of macaque. *Journal of Physiology*, 357, 219–40. [110–11]
- Des Rosiers, M. H., Sakurada, O., Jehle, Shinohara, J. J. M., Kennedy, C., and Sokoloff, L. (1978). Functional plasticity in the immature striate cortex of the monkey shown by the [¹⁴C]deoxyglucose method. *Science*, 200, 447–9. [613, 628]
- Descartes, R. (1664). Traité de l'homme. In *Oeuvres de Descartes* volume XI, (ed. C. Adam and P. Tannery), 1909, pp. 119–215. Cerf, Paris. [11]
- Desimone, R., Moran, J., Schein, S. J., and Mishkin, M. (1993). A role for the corpus callosum in visual area V4 of the alert monkey. *Visual Neuroscience*, 10, 159–71. [131]
- Deubel, H. (1987). Adaptivity of gain and direction in oblique saccades. In *Eye movements: From physiology to cognition*, (ed. J. K. O'Regan and A. Levy-Schoen), pp. 181–90. Elsevier, Amsterdam. [413]
- Deubel, H., Wolf, W., and Hauske, G. (1986). Adaptive gain control of saccadic eye movements. *Human Neurobiology*, 5, 245–53. [413]
- Deutsch, J. A., Ramachandran, V. S., and Peli, E. (1990). Binocular reversals despite familiarity cues: An artifact? *Science*, 249, 565–6. [456]
- DeValois, R. L. (1991). Orientation and spatial frequency selectivity. In *From pigments to perception*, (ed. A. Valberg and B. B. Lee), pp. 261–7. Plenum Press, New York. [124]
- DeValois, R. L. and DeValois, K. K. (1988). *Spatial vision*. Oxford University Press, New York. [124]
- DeValois, K. K., Heydt, R. von. der., Adorjani, C. S., and DeValois, R. L. (1975). A tilt aftereffect in depth. *Investigative Ophthalmology and Visual Science*, 15 (ARVO Abstracts), 90. [273]
- DeValois, R. L., Yund, E. W., and Hepler, N. (1982a). The orientation and direction selectivity of cells in macaque visual cortex. *Vision Research*, 22, 531–44. [118, 142]
- DeValois, R. L., Albrecht, D. G., and Thorell, L. G. (1982b). Spatial frequency selectivity of cells in macaque visual cortex. *Vision Research*, 22, 545–59. [259]

- Dews, P. B. and Wiesel, T. N. (1970). Consequences of monocular deprivation on visual behaviour in kittens. *Journal of Physiology*, **206**, 437–55. [632, 635]
- DeYoe, E. A. and Van Essen, D. C. (1985). Segregation of efferent connections and receptive field properties in visual area V2 of the macaque. *Nature*, **317**, 58–61. [126]
- DeYoe, E. A. and Van Essen, D. C. (1988). Concurrent processing streams in monkey visual cortex. *Trends in Neuroscience*, **11**, 219–26. [127]
- Diamond, A. L. (1958). Simultaneous brightness contrast and the Pulfrich phenomenon. *Journal of the Optical Society of America*, **48**, 887–90. [546]
- Dias, E. C., Rocha-Miranda, C. E., Bernardes, R. F., and Schmidt, S. L. (1991). Disparity selective units in superior colliculus of the opossum. *Experimental Brain Research*, **87**, 546–52. [134]
- Díaz-Araya, C. and Provis, J. M. (1992). Evidence of photoreceptor migration during early foveal development: A quantitative analysis of human fetal retinae. *Visual Neuroscience*, **8**, 505–14. [605]
- Dichgans, J. and Brandt, T. (1978). Visual–vestibular interaction: Effects on self motion perception and postural control. In *Handbook of sensory physiology*, Vol. VII, (ed. R. Held, W. Leibowitz, and H. L. Teuber), pp. 755–804. New York, Springer. [534]
- Dichgans, J. and Jung, R. (1975). Oculomotor abnormalities due to cerebellar lesions. In *Basic mechanisms of ocular motility and their clinical implications*, (ed. G. Lennerstrand and P. Bach-y-Rita), pp. 281–98. Pergamon, Oxford. [643]
- Dickinson, C. M. (1986). The elucidation and use of the effect of near fixation in congenital nystagmus. *Ophthalmology and Physiological Optics*, **6**, 303–11. [643]
- Diener, H. C., Wist, E. R., Dichgans, J., and Brandt, T. (1976). The spatial-frequency effect on perceived velocity. *Vision Research*, **16**, 169–76. [544]
- Dill, L. M. (1975). Predatory behaviour of the zebra spider, *Salticus Scenicus* (Araneae: Salticidae). *Canadian Journal of Zoology*, **53**, 1284–9. [647]
- Diner, D. B. and Fender, D. H. (1987). Hysteresis in human binocular fusion: Temporalward and nasalward ranges. *Journal of the Optical Society of America*, **4**, 1814–19. [322]
- Diner, D. B. and Fender, D. H. (1988). Dependence of Panum's fusional area on local retinal stimulation. *Journal of the Optical Society of America*, **5**, 1163–9. [323]
- Diner, D. B. and Fender, D. H. (1993). *Human engineering in stereoscopic viewing devices*. Plenum Press, New York. [30]
- Dinse, H. R., Krüger, K., and Best, J. (1990a). A temporal structure of cortical information processing. *Concepts in Neuroscience*, **1**, 199–238. [80, 120]
- Dinse, H. R., Racanzone, G. H., and Merzenich, M. M. (1990b). Direct observation of neural assemblies during neocortical representational reorganization. In *Parallel processing in neural systems and computers*, (ed. R. Eckmiller, G. Hartmann, and G. Hauske), pp. 65–69. Elsevier, Amsterdam. [129]
- Dobson, V. and Teller, D. Y. (1978). Visual acuity in human infants: A review and comparison of behavioral and electrophysiological studies. *Vision Research*, **18**, 1469–83. [616]
- Dobson, V., Fulton, A. B., and Sebris, S. L. (1984). Cycloplegic refractions of infants and young children: The axis of astigmatism. *Investigative Ophthalmology and Visual Science*, **25**, 83–7. [605]
- Dodd, J. and Jessell, T. M. (1988). Axon guidance and the patterning of neuronal projections in vertebrates. *Science*, **242**, 692–99. [606]
- Dodge, R. (1900). Visual perception during eye movements. *Psychological Review*, **7**, 454–65. [539]
- Dodwell, P. C., Harker, G. S., and Behar, I. (1968). Pulfrich effect with minimal differential adaptation of the eyes. *Vision Research*, **8**, 1431–43. [548]
- Dodwell, P. C., Muir, D., and Di Franco, D. (1976). Responses of infants to visually presented objects. *Science*, **194**, 209–11. [618]
- Donaldson, I. M. L. and Long, A. C. (1980). Interactions between extraocular proprioceptive and visual signals in the superior colliculus of the cat. *Journal of Physiology*, **298**, 85–110. [640]
- Dosher, B. A., Sperling, G., and Wurst, S. A. (1986). Tradeoffs between stereopsis and proximity luminance covariance as determinants of perceived 3D structure. *Vision Research*, **26**, 973–90. [436, 438, 444–5]
- Douglas, R. H. and Hawryshyn, C. W. (1990). Behavioural studies of fish vision: An analysis of visual capabilities. In *The visual system of fish*, (ed. R. H. Douglas and M. B. A. Djagoz), pp. 373–48. Chapman Hall, London. [650]
- Douglas, R. H., Eva, J., and Guttridge, N. (1988). Size constancy in goldfish (*Carassius auratus*). *Behavioural Brain Research*, **30**, 37–42. [650]
- Douthwaite, W. and Morrison, L. (1975). Flicker frequency and the Pulfrich phenomenon. *American Journal of Optometry and Physiological Optics*, **52**, 745–49. [548]
- Dove, H. W. (1841). Die Combination der Eindrücker beider Ohren und beider Augen zu einem Eindruck. *Monatsberichte der Berliner Akademie*, 251–2. [178, 212]
- Dow, B. M. (1991). Orientation and color columns in monkey striate cortex. In *From pigments to perception*, (ed. A. Valberg and B. B. Lee), pp. 269–74. Plenum Press, New York. [119]
- Dowling, J. E. (1987). *The retina: An approachable part of the brain*. Harvard University Press, Cambridge, MA. [109, 111]
- Dowling, J. E. and Boycott, B. B. (1966). Organization of the primate retina. *Proceedings of the Royal Society*, **B166**, 80–111. [106]
- Downing, A. C. (1972). Optical scanning in the lateral eyes of the copepod *Copilia*. *Perception*, **1**, 247–61. [648]
- Drasdo, N. (1977). The neurological representation of visual space. *Nature*, **266**, 554–6. [114]
- du Tour, E. F. (1760). Discussion d'un question d'optique. *Mémoires de Mathématique et de Physique présentés à l'Académie Royale des Sciences*, **3**, 514–30. [338]
- Dubrovsky, B. O. and Barbas, H. (1977). Frontal projections to dorsal neck and extraocular muscles. *Experimental Neurology*, **55**, 680–93. [640]
- Duffy, C. J. and Wurtz, R. H. (1991). Sensitivity of MST neurons to optic flow stimuli. II. Mechanisms of response selectivity revealed by small-field stimuli. *Journal of Neurophysiology*, **65**, 1346–59. [126]
- Duhamel, J.-R., Colby, C. L., and Goldberg, M. E. (1992). The updating of the representation of visual space in parietal cortex by intended eye movements. *Science*, **255**, 90–95. [126]
- Duke-Elder, S. (1968a). *System of ophthalmology*, Vol. II. *The anatomy of the visual system*. Kimpton, London. [12]
- Duke-Elder, S. (1968b). *System of ophthalmology*, Vol. IV. *The physiology of the eye and of vision*. Kimpton, London. [338]
- Duncker, K. (1929). Über induzierte Bewegung. *Psychologische Forschung*, **22**, 180–259. [465, 532]
- Dunkeld, J. and Bower, T. G. R. (1980). Infant response to impending collision. *Perception*, **9**, 549–54. [558]
- Dunlap, K. (1944). Alleged binocular mixing. *American Journal of Psychology*, **57**, 559–63. [326]
- Durgin, F. H., Proffitt, D. R., Olson, T. J., and Reinke, K. S. (1994). Comparing depth from binocular disparity to depth from motion. *Journal of Experimental Psychology: Human Perception and Performance*, in press. [459, 582]
- Durnford, M. and Kimura, D. (1971). Right hemisphere specialization for depth perception reflected in visual field differences. *Nature*, **231**, 394–5. [625]

- Dürsteler, M. R. and von der Heydt, R. (1983). Plasticity in the binocular correspondence of striate cortical receptive fields in kittens. *Journal of Physiology*, **345**, 87–105. [622]
- Dürsteler, M. R. and Wurtz, R. H. (1988). Pursuit and optokinetic deficits following chemical lesions of cortical areas MT and MST. *Journal of Neurophysiology*, **60**, 940–65. [530]
- Dürsteler, M. R., Garey, L. J., and Movshon, J. A. (1976). Reversal of the morphological effects of monocular deprivation in the kitten's lateral geniculate nucleus. *Journal of Physiology*, **261**, 189–210. [627]
- Dürsteler, M. R., Wurtz, R. H., and Newsome, W. T. (1987). Directional pursuit deficits following lesions of the foveal representation within the superior temporal sulcus of the macaque monkey. *Journal of Neurophysiology*, **57**, 1262–87. [127]
- Duwaer, A. L. (1982). Nonmotor component of fusional response to vertical disparity: A second look using an afterimage method. *Journal of the Optical Society of America*, **72**, 871–7. [400]
- Duwaer, A. L. (1983). Patent stereopsis with diplopia in random-dot stereograms. *Perception and Psychophysics*, **33**, 443–54. [325]
- Duwaer, A. L. and van den Brink, G. (1981a). Foveal diplopia thresholds and fixation disparities. *Perception and Psychophysics*, **30**, 321–9. [392]
- Duwaer, A. L. and van den Brink, G. (1981b). Diplopia thresholds and the initiation of vergence eye-movements. *Vision Research*, **21**, 1727–37. [401]
- Duwaer, A. L. and van den Brink, G. (1982a). Detection of vertical disparities. *Vision Research*, **22**, 467–78. [158]
- Duwaer, A. L. and van den Brink, G. (1982b). The effect of presentation time on detection and diplopia thresholds for vertical disparities. *Vision Research*, **22**, 183–9. [320]
- Dvorák, V. von (1870). Versuche über Nachbilder von Reizveränderungen. *Sitzungsberichte der Österreichischen Akademie der Wissenschaften*, **61**, 257–62. [375]
- Eagle, R. A. and Blake, A. (1994). 2-D limits on 3-D structure-from-motion tasks. *Investigative Ophthalmology and Visual Science*, **35** (ARVO Abstracts), 1277. [442]
- Earle, D. C. (1985). Perception of Glass pattern structure with stereopsis. *Perception*, **14**, 545–52. [590]
- Earnshaw, R. A., Gigante, M. A., and Jones, H. (1993). *Virtual reality systems*. Academic Press, London. [30]
- Ebenholtz, S. M. (1976). Additivity of aftereffects of maintained head and eye rotations: An alternative to recalibration. *Perception and Psychophysics*, **19**, 113–16. [432]
- Ebenholtz, S. M. (1981). Hysteresis effects in the vergence control system: Perceptual implications. In *Eye movements: Cognition and visual perception*, (ed. D. F. Fisher, R. A. Monty and J. W. Senders), pp. 83–94. Erlbaum, Hillsdale, N. J. [434]
- Ebenholtz, S. M. and Walchli, R. M. (1965). Stereoscopic thresholds as a function of head- and object-orientation. *Vision Research*, **5**, 455–61. [167]
- Ebenholtz, S. M. and Wolfson, D. M. (1975). Perceptual after-effects of sustained convergence. *Perception and Psychophysics*, **17**, 485–91. [433]
- Eckhorn, R., Bauer, R., Jordan, W., Brosch, M., Kruse, W., Munk, M., and Reitboeck, H. J. (1988). Coherent oscillations: A mechanism for feature linking in the visual cortex? *Biological Cybernetics*, **60**, 121–30. [83]
- Eckhorn, R., Reitboeck, H. J., Arndt, M., and Dicke, P. (1990). Feature linking via synchronization among distributed assemblies: Simulations of results from cat visual cortex. *Neural Computation*, **2**, 293–307. [83]
- Eckmiller, R. (1974). Hysteresis in the static characteristics of eye position coded neurons in the alert monkey. *Pflügers Archiv für die gesamte Physiologie*, **350**, 249–58. [432]
- Edgerton, S. Y. (1975). *The renaissance rediscovery of linear perspective*. Basic Books, New York. [9]
- Efron, R. (1957). Stereoscopic vision. I. Effects of binocular temporal summation. *British Journal of Ophthalmology*, **41**, 709–30. [185]
- Egelhaaf, M. and Borst, A. (1992). Is there a separate control system mediating a "centering response" in honeybees? *Naturwissenschaften*, **79**, 221–3. [648]
- Ehrenstein, W. (1925). *Probleme der ganzheitspsychologischen Wahrnehmungslehre*. Barth, Leipzig. [375]
- Ehrenstein, W. (1941). Über abwandlungen der L. Hermannschen helligkeitserscheinung. *Zeitschrift für Psychologie*, **150**, 83–91. [77, 508]
- Eizenman, M., Frecker, R. C., and Hallett, P. E. (1984). Precise non-contacting measurement of eye movements using the corneal reflex. *Vision Research*, **24**, 167–74. [383]
- Elberger, A. J. (1979). The role of the corpus callosum in the development of interocular eye alignment and the organization of the visual field in the cat. *Experimental Brain Research*, **36**, 71–85. [132]
- Elberger, A. J. (1980). The effect of neonatal section of the corpus callosum on the development of depth perception in young cats. *Vision Research*, **20**, 177–87. [132]
- Elberger, A. J. (1989). Binocularity and single cell acuity are related in striate cortex of corpus callosum sectioned and normal cats. *Experimental Brain Research*, **77**, 213–16. [132]
- Elberger, A. J. (1990). Spatial frequency thresholds of single striate cortical cells in neonatal corpus callosum sectioned cats. *Experimental Brain Research*, **82**, 617–27. [132]
- Elberger, A. J. and Smith, E. L. (1983). Binocular properties of lateral suprasylvian cortex are not affected by neonatal corpus callosum section. *Brain Research*, **278**, 259–98. [132]
- Elberger, A. J. and Smith, E. L. (1985). The critical period for corpus callosum section to affect cortical binocularity. *Experimental Brain Research*, **57**, 213–23. [132]
- Ellerbrock, V. J. (1948). Further study of effects induced by anisotropic corrections. *American Journal of Optometry, Archives of the American Academy of Optometry*, **25**, 430–7. [393]
- Ellerbrock, V. J. (1949). Experimental investigation of vertical fusional movements. *American Journal of Optometry*, **26**, 327–32. [400]
- Ellerbrock, V. J. (1952). Effect of aniseikonia on the amplitude of vertical divergence. *American Journal of Optometry and Archives of American Academy of Optometry*, **29**, 403–15. [400]
- Ellerbrock, V. J. (1954). Inducement of cyclofusional movements. *American Journal of Optometry and Archives of the American Academy of Optometry*, **31**, 553–66. [418]
- Ellerbrock, V. J. and Fry, G. A. (1941). The after-effect induced by vertical divergence. *American Journal of Optometry*, **18**, 450–4. [393]
- Ellerbrock, V. J. and Fry, G. A. (1942). Effects induced by anisotropic corrections. *American Journal of Optometry and Archives of the American Academy of Optometry*, **19**, 444–59. [393]
- Emerson, P. L. and Pesta, B. J. (1992). A generalized visual latency explanation of the Pulfrich phenomenon. *Perception and Psychophysics*, **51**, 319–27. [537]
- Emmerton, J. (1983). Functional morphology of the visual system. In *Physiology and behaviour of the pigeon*, (ed. M. Abs), pp. 221–66. London, Academic Press. [654]
- Engel, A. K., König, P., and Singer, W. (1991). Direct physiological evidence for scene segmentation by temporal coding. *Proceedings of the National Academy of Science*, **88**, 9136–40. [83]
- Engel, A. K., König, P., Kreiter, A. K., Schillen, T. B., and Singer, W. (1992). Temporal coding in the visual cortex: New vistas on integration in the nervous system. *Trends in Neuroscience*, **15**, 218–26. [83]

- Engel, E. (1956). The role of content in binocular resolution. *American Journal of Psychology*, 69, 87–91. [347]
- Engel, G. R. (1967). The visual processes underlying binocular brightness summation. *Vision Research*, 7, 753–67. [357]
- Engel, G. R. (1969). The autocorrelation function and binocular brightness mixing. *Vision Research*, 9, 1111–30. [357]
- Engel, G. R. (1970a). An investigation of visual responses to brief stereoscopic stimuli. *Quarterly Journal of Experimental Psychology*, 22, 148–66. [186]
- Engel, G. R. (1970b). Tests of a model of binocular brightness. *Canadian Journal of Psychology*, 24, 335–52. [357]
- Engelking, E. and Poos, F. (1924). Über die Bedeutung des Stereo-phaenomens für die isochrome und heterochrome Helligkeitsvergleichung. *von Graefes Archiv für Ophthalmologie*, 114, 340–79. [545–46]
- Enoch, J. M. and Tobey, F. L. (eds.) (1981). *Retinal photoreceptor optics*. Springer Verlag, Berlin. [107]
- Enoch, J. M., Birch, D. G., and Birch, E. E. (1979). Monocular light exclusion for a period of days reduces directional sensitivity of the human retina. *Science*, 206, 705–7. [107]
- Enoch, J., Goldmann, H., and Sunga, R. (1969). The ability to distinguish which eye was stimulated by light. *Investigative Ophthalmology and Visual Science*, 8, 317–31. [601]
- Enoksson, P. (1963). Binocular rivalry and monocular dominance studied with optokinetic nystagmus. *Acta Ophthalmologica*, 41, 544–63. [335]
- Enright, J. T. (1970). Distortions of apparent velocity: A new optical illusion. *Science*, 168, 464–7. [538]
- Enright, J. T. (1980). Ocular translation and cyclotorsion due to changes in fixation distance. *Vision Research*, 20, 595–601. [410]
- Enright, J. T. (1984). Changes in vergence mediated by saccades. *Journal of Physiology*, 350, 9–31. [412]
- Enright, J. T. (1985). On Pulfrich-illusion eye movements and accommodation vergence during visual pursuit. *Vision Research*, 25, 1613–22. [550–1]
- Enright, J. T. (1986). Facilitation of vergence changes by saccades: Influences of misfocused images and of disparity stimuli in man. *Journal of Physiology*, 371, 69–87. [412]
- Enright, J. T. (1987a). Perspective vergence: Oculomotor responses to line drawings. *Vision Research*, 27, 1513–26. [399]
- Enright, J. T. (1987b). Art and the oculomotor system: Perspective illustrations evoke vergence changes. *Perception*, 16, 731–46. [399]
- Enright, J. T. (1988). The cyclopean eye and its implications: Vergence state and visual direction. *Vision Research*, 28, 925–30. [600]
- Enright, J. T. (1990). Stereopsis, cyclotorsional "noise" and the apparent vertical. *Vision Research*, 30, 1487–97. [421, 463]
- Enright, J. T. (1991a). Exploring the third dimension with eye movements: Better than stereopsis. *Vision Research*, 31, 1549–62. [177]
- Enright, J. T. (1991b). Stereo-thresholds: Simultaneity, target proximity and eye movements. *Vision Research*, 31, 2093–100. [186]
- Enright, J. T. (1992a). The remarkable saccades of asymmetrical vergence. *Vision Research*, 32, 2261–76. [413]
- Enright, J. T. (1992b). Unexpected role of the oblique muscles in the human vertical fusional reflex. *Journal of Physiology*, 451, 279–93. [417]
- Enroth-Cugell, C. and Robson, J. G. (1966). The contrast sensitivity of ganglion cells of the cat. *Journal of Physiology*, 187, 517–52. [110]
- Epstein, W. (1978). Two factors in the perception of velocity at a distance. *Perception and Psychophysics*, 24, 105–14. [460]
- Epstein, W. and Morgan, C. L. (1970). Adaptation to unioocular image magnification: Modification of the disparity-depth relationship. *American Journal of Psychology*, 83, 322–9. [67]
- Epstein, W. and Morgan-Paap, C. L. (1970). The effect of level of depth processing and degree of informational discrepancy on adaptation to unioocular image magnification. *Journal of Experimental Psychology*, 102, 585–94. [67]
- Epstein, W. and Park, J. (1964). Examination of Gibson's psycho-physical hypothesis. *Psychological Bulletin*, 62, 180–96. [578]
- Erens, R., Kappers, A. M. L., and Koenderink, J. J. (1991). Limits on the perception of local shape from shading. In *Studies in perception and action*, (ed. P. J. Beek, R. J. Bootsma, and P. C. W. van Wieringen), pp. 72–5. Rodopi, Amsterdam. [303]
- Eriksen, C. W. (1966). Independence of successive inputs and uncorrelated error in visual form perception. *Journal of Experimental Psychology*, 72, 26–35. [350]
- Eriksen, C. W. and Greenspon, T. S. (1968). Binocular summation over time in the perception of form at brief durations. *Journal of Experimental Psychology*, 76, 331–6. [356]
- Eriksen, C. W., Greenspon, T. S., Lappin, J., and Carlson, W. A. (1966). Binocular summation in the perception of form at brief durations. *Perception and Psychophysics*, 1, 415–9. [350, 356]
- Eriksson, E. S. (1972). Motion parallax and distance perception. *Report 117. Department of Psychology*, University of Uppsala, Sweden. [578]
- Eriksson, E. S. (1973). Movement parallax during locomotion. *Report 144. Department of Psychology*, University of Uppsala, Sweden. [578]
- Eriksson, E. S. (1974). Movement parallax during locomotion. *Perception and Psychophysics*, 16, 197–200. [578]
- Erkelens, C. J. (1987). Adaptation of ocular vergence to stimulation with large disparities. *Experimental Brain Research*, 66, 507–16. [404, 406]
- Erkelens, C. J. (1988). Fusional limits for a large random-dot stereogram. *Vision Research*, 28, 345–53. [324–5]
- Erkelens, C. J. and Collewijn, H. (1985a). Motion perception during dichoptic viewing of moving random-dot stereograms. *Vision Research*, 25, 583–8. [179, 242, 401, 461]
- Erkelens, C. J. and Collewijn, H. (1985b). Eye movements in relation to loss and regaining of fusion of disjunctively moving random-dot stereograms. *Human Neurobiology*, 4, 181–8. [400, 412]
- Erkelens, C. J. and Collewijn, H. (1985c). Eye movements and stereopsis during dichoptic viewing of moving random-dot stereograms. *Vision Research*, 25, 1689–700. [401]
- Erkelens, C. J. and Collewijn, H. (1991). Control of vergence: Gating among disparity inputs by voluntary target selection. *Experimental Brain Research*, 87, 671–78. [406]
- Erkelens, C. J. and Regan, D. (1986). Human ocular vergence movements induced by changing size and disparity. *Journal of Physiology*, 379, 145–69. [399]
- Erkelens, C. J. and van de Grind, W. A. (1994). Binocular visual direction. *Vision Research*, 34, 2963–9. [597]
- Erkelens, C. J., Van der Steen, J., Steinman, R. M., and Collewijn, H. (1989a). Ocular vergence under natural conditions. I. Continuous changes of target distance along the median plane. *Proceedings of the Royal Society*, B236, 417–40. [402–3]
- Erkelens, C. J., Steinman, R. M., and Collewijn, H. (1989b). Ocular vergence under natural conditions. II. Gaze shifts between real targets differing in distance and direction. *Proceedings of the Royal Society*, B236, 441–65. [399, 403, 412]
- Erkelens, C. J., Collewijn, H., and Steinman, R. M. (1989c). Asymmetrical adaptation of human saccades to anisometropic spectacles. *Investigative Ophthalmology and Visual Science*, 30, 1132–45. [413]
- Euclid (300 BC/1945). *Optics*. Translated by H. E. Burton. *Journal of the Optical Society of America*, 35, 357–72. [4]

- Evans, C. R. and Clegg, J. M. (1967). Binocular depth perception of "Julesz patterns" viewed as perfectly stabilized retinal images. *Nature*, **215**, 893–5. [178]
- Evinger, C. (1988). Extraocular motor nuclei: Location, morphology and afferents. In *Neuroanatomy of the oculomotor system*, (ed. J. A. Büttner-Ennever), pp. 81–118. New York, Elsevier. [410]
- Evinger, L. C., Fuchs, A. F., and Baker, R. (1977). Bilateral lesions of the medial longitudinal fasciculus in monkeys: Effects on the horizontal and vertical components of voluntary and vestibular induced eye movements. *Experimental Brain Research*, **28**, 1–20. [425]
- Exner, S. (1868). Über die zu einer Gesichtswahrnehmung Nötige Zeit. *S. B. Akademie Wissenschaft. Wein*, **58**, 601–32. [369]
- Exner, S. (1891). *Die Physiologie der facettirten Augen von Krebsen und Insecten*. Deuticke, Wien. English translation (1989) by R. Hardie. Springer, New York. [649]
- Eyre, M. B. and Schmeckle, M. M. (1933). A study of handedness, eyedness and footedness. *Child Development*, **4**, 73–8. [337]
- Eysteinsson, T., Barris, M. C., Denny, N., and Frumkes, T. E. (1993). Tonic interocular suppression, binocular summation, and the evoked potential. *Investigative Ophthalmology and Visual Science*, **34**, 2443–8. [357]
- Fahle, M. (1982a). Cooperation between different spatial frequencies in binocular rivalry. *Biological Cybernetics*, **44**, 27–9. [329]
- Fahle, M. (1982b). Binocular rivalry: Suppression depends on orientation and spatial frequency. *Vision Research*, **22**, 787–800. [329]
- Fahle, M. (1983). Non-fusible stimuli and the role of binocular inhibition in normal and pathologic vision, especially strabismus. *Documenta Ophthalmologica*, **55**, 323–40. [634]
- Fahle, M. (1987). Naso-temporal asymmetry of binocular inhibition. *Investigative Ophthalmology and Visual Science*, **28**, 1016–17. [332, 632]
- Fahle, M. (1991). Psychophysical measurement of eye drifts and tremor by dichoptic or monocular vernier acuity. *Vision Research*, **31**, 209–22. [179, 181]
- Fahle, M. (1993). Figure-ground discrimination from temporal information. *Proceedings of the Royal Society*, **B254**, 199–203. [81]
- Fahle, M. and Edelman, S. (1993). Long-term learning in vernier acuity: Effects of stimulus orientation, range and of feedback. *Vision Research*, **33**, 397–412. [104]
- Fahle, M. and Schmid, M. (1988). Naso-temporal asymmetry of visual perception and of the visual cortex. *Vision Research*, **28**, 293–300. [617]
- Fahle, M. and Westheimer, G. (1988). Local and global factors in disparity detection of rows of points. *Vision Research*, **28**, 171–8. [161]
- Fahle, M., Fahle, S. H., and Harris, J. (1994). Definition of thresholds for stereoscopic depth. *British Journal of Ophthalmology*, **78**, 572–6. [155]
- Falk, D. S. and Williams, R. (1980). Dynamic visual noise and the stereophenomenon: Interocular time delays, depth, and coherent velocities. *Perception and Psychophysics*, **28**, 19–27. [551–53]
- Fantz, R. (1965). Visual perception from birth as shown by pattern selectivity. *Annals of the New York Academy of Science*, **118**, 793–814. [618]
- Farber, J. M. and McConkie, A. B. (1979). Optical motions as information for unsigned depth. *Journal of Experimental Psychology: Human Perception and Performance*, **5**, 494–500. [578]
- Favreau, O. E. (1978). Interocular transfer of color-contingent motion aftereffects; positive aftereffects. *Vision Research*, **18**, 841–4. [379]
- Favreau, O. E. (1979). Persistence of simple and contingent motion aftereffects. *Perception and Psychophysics*, **26**, 187–94. [102]
- Favreau, O. E. and Cavanagh, P. (1983). Interocular transfer of a chromatic frequency shift. *Vision Research*, **23**, 951–7. [378]
- Favreau, O. E. and Cavanagh, P. (1984). Interocular transfer of a chromatic frequency shift: Temporal constraints. *Vision Research*, **24**, 1799–804. [378]
- Fawcett, J. W. (1993). Growth-cone collapse: Too much of a good thing? *Trends in Neuroscience*, **16**, 165–7. [606]
- Fazeli, M. S. (1992). Synaptic plasticity: On the trail of the retrograde messenger. *Trends in Neuroscience*, **15**, 115–17. [615]
- Feldman, M. and Cohen, B. (1968). Electrical activity in the geniculocalate body of the alert monkey associated with eye movements. *Journal of Neurophysiology*, **31**, 455–66. [113]
- Felleman, D. J. and Van Essen, D. C. (1987). Receptive field properties of neurons in area V3 of macaque monkey extrastriate cortex. *Journal of Neurophysiology*, **57**, 889–920. [128, 135]
- Felleman, D. J. and Van Essen, D. C. (1991). Distributed hierarchical processing in the primate cerebral cortex. *Cerebral Cortex*, **1**, 1–47. [125]
- Felton, T. B., Richards, W., and Smith, R. A. (1972). Disparity processing of spatial frequencies in man. *Journal of Physiology*, **225**, 349–62. [524]
- Fender, D. and Julesz, B. (1967). Extension of Panum's fusional area in binocularly stabilized vision. *Journal of the Optical Society of America*, **57**, 819–30. [179, 322–3, 401]
- Fendick, M. and Westheimer, G. (1983). Effects of practice and the separation of test targets on foveal and peripheral stereoacluity. *Vision Research*, **23**, 145–50. [191]
- Ferman, L., Collewijn, H., and Van den Berg, A. V. (1987a). A direct test of Listing's law – I. Human ocular torsion measured in static tertiary positions. *Vision Research*, **27**, 929–38. [384]
- Ferman, L., Collewijn, H., Jansen, T. C., and van den Berg, A. V. (1987b). Human gaze stability in horizontal, vertical and torsional direction during voluntary head movements, evaluated with a three-dimensional scleral induction coil technique. *Vision Research*, **27**, 811–28. [417, 419, 421]
- Fernald, R. D. (1985). Eye movements in the African cichlid fish, *Haplochromis burtoni*. *Comparative Physiology*, **156**, 199–208. [649–50]
- Ferrell, W. R. (1980). The adequacy of stretch receptors in the cat kneejoint for signalling joint angle throughout a full range of movement. *Journal of Physiology*, **299**, 85–100. [432]
- Ferrera, V. P., Nealey, T. A., and Maunsell, J. H. R. (1992). Mixed parvocellular and magnocellular geniculocalate signals in visual area V4. *Nature*, **358**, 756–8. [127]
- Ferrera, V. P., Nealey, T. A., and Maunsell, J. H. R. (1994). Responses in macaque visual area V4 following inactivation of the parvocellular and magnocellular LGN pathways. *Journal of Neuroscience*, **14**, 2080–88. [126–7]
- Ferster, D. (1981). A comparison of binocular depth mechanisms in areas 17 and 18 of the cat visual cortex. *Journal of Physiology*, **311**, 623–55. [134, 137–8, 141, 345]
- Ferster, D. (1987). Origin of orientation selective EPSP's in simple cells of cat visual cortex. *Journal of Neuroscience*, **7**, 1780–91. [118, 345]
- Ferster, D. (1990). Binocular convergence of excitatory and inhibitory synaptic pathways onto neurons of cat visual cortex. *Visual Neuroscience*, **4**, 625–9. [120]
- Field, D. J., Hayes, A., and Hess, R. F. (1993). Contour integration by the human visual system: Evidence for a local "association field". *Vision Research*, **33**, 173–93. [76–7]

- Finch, D. J. and Collett, T. S. (1983). Small-field, binocular neurons in the superficial layers of the frog optic tectum. *Proceedings of the Royal Society, London*, **B217**, 491–7. [651]
- Fincham, E. F. (1951). The accommodation reflex and its stimulus. *British Journal of Ophthalmology*, **35**, 381–93. [395, 399]
- Fincham, E. F. (1955). The proportion of ciliary muscular force required for accommodation and convergence. *Journal of Physiology*, **128**, 99–112. [397]
- Fincham, E. F. (1962). Accommodation and convergence in the absence of retinal images. *Vision Research*, **1**, 425–40. [399]
- Fincham, E. F. and Walton, J. (1957). The reciprocal actions of accommodation and convergence. *Journal of Physiology*, **137**, 488–508. [397]
- Finlay, D., Quinn, K., and Ivinskis, A. (1982). Detection of moving stimuli in the binocular and nasal visual fields by infants three and four months old. *Perception*, **11**, 685–90. [32]
- Finney, D. J. (1971). *Probit analysis*. Cambridge University Press, London. [94]
- Fiorentini, A. and Maffei, L. (1970). Electrophysiological evidence for disparity detectors in human visual system. *Science*, **169**, 208–9. [147]
- Fiorentini, A. and Maffei, L. (1971). Binocular depth perception without geometrical cues. *Vision Research*, **11**, 1299–1305. [260]
- Fiorentini, A. and Maffei, L. (1974). Change of binocular properties of the simple cells of the cortex in adult cats following immobilization of one eye. *Vision Research*, **14**, 217–8. [641]
- Fiorentini, A., Maffei, L., Cenni, M. C., and Tacchi, A. (1985). Deafferentation of oculomotor proprioception affects depth discrimination in adult cats. *Experimental Brain Research*, **59**, 296–301. [641]
- Fischer, B. and Boch, R. (1981). Enhanced activation of neurones in prelunate cortex before visually guided saccades of trained rhesus monkeys. *Experimental Brain Research*, **44**, 129–37. [129]
- Fischer, B. and Krüger, J. (1979). Disparity tuning and binocularity of single neurons in cat visual cortex. *Experimental Brain Research*, **35**, 1–8. [134]
- Fischer, F. P. and Wagenaar, J. W. (1954). Binocular vision and fusion movements. *Documenta Ophthalmologica*, **7**, 359–91. [32]
- Fisher, S. K. and Ciuffreda, K. J. (1988). Accommodation and apparent distance. *Perception*, **17**, 609–21. [427]
- Fisher, S. K. and Ciuffreda, K. J. (1990). Adaptation to optically-increased interocular separation under naturalistic viewing conditions. *Perception*, **19**, 171–80. [433]
- Fisher, S. K. and Ebenholtz, S. M. (1986). Does perceptual adaptation to telescopically enhanced depth depend on the recalibration of binocular disparity? *Perception and Psychophysics*, **40**, 101–9. [433]
- Fisher, S. K., Ciuffreda, K. J., Tannen, B., and Super, P. (1988). Stability of tonic vergence. *Investigative Ophthalmology and Visual Science*, **29**, 1577–81. [386]
- Fite, K. V. (1969). Single unit analysis of binocular neurons in the frog optic tectum. *Experimental Neurology*, **24**, 475–86. [651]
- Fite, K. V. (1973). The visual fields of the frog and toad: A comparative study. *Behavioural Biology*, **9**, 707–18. [651–2]
- Fite, K. V. and Rosenfield-Wessels, S. (1975). A comparative study of deep avian foveas. *Brain, Behaviour and Evolution*, **12**, 97–115. [654–5]
- Fitzpatrick, D., Lund, J. S., and Blasdel, G. G. (1985). Intrinsic connections of macaque striate cortex: Afferent and efferent connections of lamina 4C. *Journal of Neuroscience*, **5**, 3329–49. [116]
- Fletcher, J. L. and Ross, S. (1953). Tests of stereoscopic vision: A review. *International Record of Medicine and Quarterly Review of Ophthalmology*, **166**, 551–62. [151]
- Flom, M. C. (1963). Treatment of binocular anomalies in children. In *Vision of children, an optometric symposium*, (ed. M. J. Hirsch, R. E. Wick), pp. 197–228. Chilton, Philadelphia. [387]
- Flom, M. C. (1980). Corresponding and disparate retinal points in normal and anomalous correspondence. *American Journal of Optometry and Physiological Optics*, **57**, 656–65. [46]
- Flom, M. C. and Eskridge, J. B. (1968). Change in retinal correspondence with viewing distance. *Journal of the American Optometry Association*, **39**, 1094–7. [59]
- Flom, M. C. and Weymouth, F. W. (1961). Centricity of Maxwell's spot in strabismus and amblyopia. *AMA Archives of Ophthalmology*, **66**, 260–8. [47]
- Flom, M. C., Heath, G. G., and Takahashi, E. (1963). Contour interaction and visual resolution: Contralateral effects. *Science*, **142**, 979–89. [368]
- Foley, J. M. (1964). Desarguesian property in visual space. *Journal of the Optical Society of America*, **54**, 684–92. [53]
- Foley, J. M. (1966). Locus of perceived equidistance as a function of viewing distance. *Journal of the Optical Society of America*, **56**, 822–7. [57]
- Foley, J. M. (1970). Loci of perceived, equi-, half- and double-distance in stereoscopic vision. *Vision Research*, **10**, 1201–9. [57]
- Foley, J. M. (1976a). Binocular depth mixture. *Vision Research*, **16**, 1263–7. [232]
- Foley, J. M. (1976b). Successive stereo and vernier position discrimination as a function of dark interval duration. *Vision Research*, **16**, 1269–73. [186]
- Foley, J. M. (1980). Binocular distance perception. *Psychological Review*, **87**, 411–34. [292, 297, 456, 458–9]
- Foley, J. M. and Held, R. (1972). Visually directed pointing as a function of target distance, direction, and available cues. *Perception and Psychophysics*, **12**, 263–8. [429]
- Foley, J. M. and Richards, W. (1972). Effects of voluntary eye movement and convergence on the binocular appreciation of depth. *Perception and Psychophysics*, **11**, 423–27. [159, 434]
- Foley, J. M. and Richards, W. (1974). Improvement in stereoaanomaly with practice. *American Journal of Optometry and Physiological Optics*, **51**, 935–8. [191, 624]
- Foley, J. M. and Richards, W. (1978). Binocular depth mixture with non-symmetric disparities. *Vision Research*, **18**, 251–6. [231]
- Foley, J. M. and Tyler, C. W. (1976). Effect of stimulus duration on stereo and vernier displacement thresholds. *Perception and Psychophysics*, **20**, 125–8. [189]
- Foley, J. M., Applebaum, T. H., and Richards, W. A. (1975). Stereopsis with large disparities: Discrimination and depth magnitude. *Vision Research*, **15**, 417–21. [159]
- Forster, L. M. (1979). Visual mechanisms of hunting behaviour in *Trite planiceps*, a jumping spider (Araneae: Salticidae). *New Zealand Journal of Zoology*, **6**, 79–93. [647]
- Fox, K. and Daw, N. W. (1993). Do NMDA receptors have a critical function in visual cortical plasticity? *Trends in Neuroscience*, **16**, 116–22. [615]
- Fox, K., Daw, N., Sato, H., and Czeplita, D. (1991). Dark-rearing delays the loss of NMDA-receptor function in kitten visual cortex. *Nature*, **350**, 3623–7. [614]
- Fox, K., Sato, H., and Daw, N. (1989). The location and function of NMDA receptors in cat and kitten visual cortex. *Journal of Neuroscience*, **9**, 2443–54. [614]
- Fox, R. (1991). Binocular rivalry. In *Vision and visual dysfunction*. Vol. 9. *Binocular vision*, (ed. D. Regan), pp. 93–110. Macmillan, London. [328]
- Fox, R. and Blake, R. R. (1971). Stereoscopic vision in the cat. *Nature*, **233**, 55–6. [645]

- Fox, R. and Check, R. (1966a). Binocular fusion: A test of the suppression theory. *Perception and Psychophysics*, 1, 331–4. [335, 338]
- Fox, R. and Check, R. (1966b). Forced-choice form recognition during binocular rivalry. *Psychonomic Science*, 6, 471–2. [339]
- Fox, R. and Check, R. (1968). Detection of motion during binocular rivalry suppression. *Journal of Experimental Psychology*, 78, 388–95. [342]
- Fox, R. and Check, R. (1972). Independence between binocular rivalry suppression duration and magnitude of suppression. *Journal of Experimental Psychology*, 93, 283–9. [344]
- Fox, R. and Herrmann, J. (1967). Stochastic properties of binocular rivalry alternations. *Perception and Psychophysics*, 2, 432–6. [344]
- Fox, R. and Patterson, R. (1981). Depth separation and lateral interference. *Perception and Psychophysics*, 30, 513–20. [368, 524]
- Fox, R. and Rasche, F. (1969). Binocular rivalry and reciprocal inhibition. *Perception and Psychophysics*, 5, 215–17. [328, 344]
- Fox, R., Aslin, R. N., Shea, S. L., and Dumais, S. T. (1980). Stereopsis in human infants. *Science*, 207, 323–4. [619]
- Fox, R., Lehmkuhle, S. W., and Westendorf, D. H. (1976). Falcon visual acuity. *Science*, 192, 263–5. [654]
- Fox, R., Lehmkuhle, S. W., and Bush, R. C. (1977). Stereopsis in the falcon. *Science*, 197, 79–81. [654]
- Fox, R., Lehmkuhle, S. W., and Leguire, L. E. (1978). Stereoscopic contours induce optokinetic nystagmus. *Vision Research*, 18, 1189–92. [589]
- Fox, R., Patterson, R., and Francis, E. L. (1986). Stereoacuity in young children. *Investigative Ophthalmology and Visual Science*, 27, 598–609. [620]
- Fox, R., Patterson, R., and Lehmkuhle, S. (1982). Effect of depth position on the motion aftereffect. *Investigative Ophthalmology and Visual Science*, 22 (ARVO Abstracts), 144. [566, 571]
- Fox, R., Todd, S., and Bettinger, L. A. (1975). Optokinetic nystagmus as an objective indicator of binocular rivalry. *Vision Research*, 15, 849–53. [335]
- Francis, E. L. and Owens, D. A. (1983). The accuracy of binocular vergence for peripheral stimuli. *Vision Research*, 23, 13–19. [392, 401]
- Frank, H. (1923). Über die Beeinflussung von Nachbildern durch die gestalteigenschaften der projektionsfläche. *Psychologische Forschung*, 3, 33–7. [524]
- Fraser, J. (1908). A new visual illusion of direction. *British Journal of Psychology*, 2, 307–20. [77]
- Fraser, S. E. (1991). Relative roles of positional cues and activity-based cues in the patterning of the retinotectal projection. In *Development of the visual system* (ed. D. M-K. Lam and C. J. Shatz), pp. 123–32. MIT Press, Cambridge, MA. [606]
- Freeman, A. W. and Jolly, N. (1994). Visual loss during interocular suppression in normal and strabismic subjects. *Vision Research*, 34, 2043–50. [350]
- Freeman, R. B. (1967). Contrast interpretations of brightness constancy. *Psychological Bulletin*, 67, 165–87. [524]
- Freeman, R. D. and Bonds, A. (1979). Cortical plasticity in monocularly deprived immobilized kittens depends on eye movement. *Science*, 206, 1093–5. [641]
- Freeman, R. D. and Ohzawa, I. (1988). Monocularly deprived cats: Binocular tests of cortical cells reveal functional connections from the deprived eye. *Journal of Neuroscience*, 8, 2491–506. [629]
- Freeman, R. D. and Ohzawa, I. (1990). On the neurophysiological organization of binocular vision. *Vision Research*, 30, 1661–76. [137, 140]
- Freeman, R. D. and Ohzawa, I. (1992). Development of binocular vision in the kitten's striate cortex. *Journal of Neuroscience*, 12, 4721–36. [612]
- Freeman, W. J. (1975). *Mass action in the nervous system*. Academic Press, New York. [83]
- Frégnac, Y. and Imbert, M. (1984). Development of neuronal selectivity in the primary visual cortex of the cat. *Physiological Reviews*, 64, 325–434. [615, 630]
- Frégnac, Y., Burke, J. P., Smith, D., and Friedlander, M. J. (1994). Temporal covariance of pre- and postsynaptic activity regulates functional connectivity in the visual cortex. *Journal of Neurophysiology*, 71, 1403–21. [82]
- Freud, S. L. (1964). The physiological locus of the spiral aftereffect. *American Journal of Psychology*, 77, 422–8. [375]
- Friauf, E. and Shatz, C. J. (1991). Changing patterns of synaptic input to subplate and cortical plate during development of visual cortex. *Journal of Neurophysiology*, 66, 2059–71. [614]
- Friedenwald, J. S. (1936). Diagnosis and treatment of anisophoria. *AMA Archives of Ophthalmology*, 15, 283–307. [388]
- Friedman, R. B., Kaye, M. G., and Richards, W. (1978). Effect of vertical disparity upon stereoscopic depth. *Vision Research*, 18, 351–2. [167]
- Frisby, J. P. (1979). *Seeing*. Houghton Mifflin, London. [466]
- Frisby, J. P. (1984). An old illusion and a new theory of stereoscopic depth perception. *Nature*, 307, 592–3. [287]
- Frisby, J. P. and Clatworthy, J. L. (1975). Learning to see complex random-dot stereograms. *Perception*, 4, 173–8. [192–3]
- Frisby, J. P. and Julesz, B. (1975a). Depth reduction effects in random-line stereograms. *Perception*, 4, 151–8. [218]
- Frisby, J. P. and Julesz, B. (1975b). The effect of orientation difference on stereopsis as a function of line length. *Perception*, 4, 179–86. [218]
- Frisby, J. P. and Julesz, B. (1976). The effect of length differences between corresponding lines on stereopsis from single and multi-line stimuli. *Vision Research*, 16, 83–7. [218]
- Frisby, J. P. and Mayhew, J. E. W. (1978a). Contrast sensitivity function for stereopsis. *Perception*, 7, 423–9. [169, 173]
- Frisby, J. P. and Mayhew, J. E. W. (1978b). The relationship between apparent depth and disparity in rivalrous texture stereograms. *Perception*, 7, 661–78. [203, 504]
- Frisby, J. P. and Mayhew, J. E. W. (1979). Does visual texture discrimination precede binocular fusion. *Perception*, 8, 153–6. [590]
- Frisby, J. P. and Mayhew, J. E. W. (1980a). Spatial frequency tuned channels: Implications for structure and function from psychophysical and computational studies of stereopsis. *Philosophical Transactions of the Royal Society*, 290, 95–116. [172]
- Frisby, J. P. and Mayhew, J. E. W. (1980b). The role of spatial frequency tuned channels in vergence control. *Vision Research*, 20, 727–32. [400]
- Frisby, J. P. and Pollard, S. B. (1991). Computational issues in solving the stereo correspondence problem. In *Computational models of visual processing*, (ed. M. S. Landy and J. A. Movshon), pp. 331–57. MIT Press, Cambridge, MA. [201]
- Frisby, J. P. and Roth, B. (1971). Orientation of stimuli and binocular disparity coding. *Quarterly Journal of Experimental Psychology*, 23, 367–72. [218]
- Frisby, J. P., Buckley, D., Bergin, L., and Hill, L. (1993). Cyclo-torsion to slanted surfaces with consistent and conflicting stereo and texture slant cues. *Perception*, 22 (ECVP Abstracts), 115. [422]
- Frisén, L. and Lindblom, B. (1988). Binocular summation in humans: Evidence for a hierarchical model. *Journal of Physiology*, 402, 773–82. [355]
- Fronius, M. and Sireteanu, R. (1989). Monocular geometry is selectively distorted in the central visual field of strabismic amblyopes. *Investigative Ophthalmology and Visual Science*, 30, 2034–44. [631]

- Fronius, M. and Sireteanu, R. (1994). Pointing errors in strabismics: Complex patterns of distorted visuomotor coordination. *Vision Research*, 34, 689–707. [632]
- Frost, B. J., Scilley, P. L., and Wong, S. C. P. (1981). Moving background patterns reveal double-opponency of directionally specific pigeon tectal neurons. *Experimental Brain Research*, 43, 173–85. [126]
- Frost, B. J., Goodale, M. A., and Pettigrew, J. D. (1983). A search for functional binocularly in the pigeon. *Proceedings of the Society for Neuroscience*, 9, 823. [654]
- Fry, G. A. (1939). Further experiments on the accommodation-convergence relationship. *American Journal of Optometry*, 16, 325–34. [398]
- Fry, G. A. (1950). Visual perception of space. *American Journal of Optometry*, 27, 531–53. [599]
- Fry, G. A. (1968). Nomograms for torsion and direction of regard. *American Journal of Optometry and Archives of American Academy of Optometry*, 45, 631–41. [384]
- Fry, G. A. (1983). Basic concepts underlying graphical analysis. In *Vergence eye movements: Basic and clinical aspects*, (ed. M. C. Schor, K. J. Ciuffreda), pp. 403–38. Butterworth, Boston. [398]
- Fry, G. A. and Bartley, S. H. (1933). The brightness of an object seen binocularly. *American Journal of Ophthalmology*, 16, 687–93. [356]
- Fry, G. A., Treleaven, C. L., and Baxter, R. C. (1945). Specification of the direction of regard. *American Journal of Optometry*, 22, 351–60. [383]
- Fujita, I., Tanaka, K., Ito, M., and Cheng, K. (1992). Columns for visual features of objects in monkey inferotemporal cortex. *Nature*, 360, 343–6. [126]
- Fukuda, H. and Blake, R. (1992). Spatial interactions in binocular rivalry. *Journal of Experimental Psychology: Human Perception and Performance*, 18, 362–70. [336]
- Funahashi, S., Bruce, C. J., and Goldman-Rakic, P. S. (1989). Mnemonic coding of visual space in the monkey's dorsolateral prefrontal cortex. *Journal of Neurophysiology*, 61, 331–49. [127]
- Funaishi, S. (1926). Weiteres über das Zentrum des Sehrichtungen. *von Graefes Archiv Ophthalmologie*, 117, 296–303. [597]
- Funaishi, S. (1927). Über die falsche Lichtlokalisierung bei geschlossenen Lidern sowie über das subjektive Zyklopäneuge. *von Graefes Archiv für Ophthalmologie*, 119, 227–34. [599]
- Fuster, J. M. and Jervey, J. P. (1981). Inferotemporal neurons distinguish and retain behaviorally relevant features of visual stimuli. *Science*, 212, 952–5. [129]
- Gabor, D. (1946). Theory of communication. *Journal of the Institute of Electrical Engineers*, (London), 93, 429–57. [88, 259]
- Gaillard, F. (1985). Binocularly driven neurons in the rostral part of the frog optic tectum. *Journal of Comparative Physiology*, A157, 47–55. [651]
- Galand, G. and Liege, B. (1974). Réponses visuelle unitaires chez la truite. In *Vision in fishes, new approaches in research*, (ed. M. A. Ali), pp. 127–36. Plenum, New York. [649]
- Galen, C. (175). *De usa partium croppers humani*. Trans. M. T. May, 1968, Cornell University Press, Ithaca, NY. [5]
- Galletti, C., Battaglini, P. P., and Fattori, P. (1993). Parietal neurons encoding spatial locations in craniotopic coordinates. *Experimental Brain Research*, 96, 221–9. [127]
- Galli, L. and Maffei, L. (1988). Spontaneous impulse activity of rat retinal ganglion cells in prenatal life. *Science*, 242, 90–1. [614]
- Garnlin, P. D. R. and Mays, L. E. (1992). Dynamic properties of medial rectus motoneurons during vergence eye movements. *Journal of Neurophysiology*, 67, 64–74. [425]
- Gårding, J., Porrill, J., Mayhew, J. E. W., and Frisby, J. P. (1994). Binocular stereopsis, vertical disparity and relief transformations. *Vision Research*, 34, (in press). [288, 304]
- Gardner, J. C. and Cynader, M. S. (1987). Mechanisms for binocular depth sensitivity along the vertical meridian of the visual field. *Brain Research*, 413, 60–74. [132]
- Gardner, J. C. and Raiten, E. J. (1986). Ocular dominance and disparity-sensitivity: Why there are cells in the visual cortex driven unequally by the two eyes. *Experimental Brain Research*, 64, 505–14. [123, 134]
- Gardner, J. C., Douglas, R. M., and Cynader, M. S. (1985). A time-based stereoscopic depth mechanism in the visual cortex. *Brain Research*, 328, 154–57. [540]
- Garey, L. J. (1984). Structural development of the lateral geniculate nucleus and visual cortex in monkey and man. *Human Neurobiology*, 3, 75–80. [607]
- Garey, L. J. and Blakemore, C. (1977). The effects of monocular deprivation on different neuronal classes in the lateral geniculate nucleus of the cat. *Experimental Brain Research*, 28, 259–78. [627]
- Garey, L. J. and de Courten, C. (1983). Structural development of the lateral geniculate nucleus and cortex in monkey and man. *Behavioural Brain Research*, 10, 3–13. [610]
- Garey, L. J. and Powell, T. P. S. (1971). An experimental study of the termination of the lateral geniculo-cortical pathway in the cat and monkey. *Proceedings of the Royal Society, London*, B179, 41–63. [123]
- Garey, L. J., Dreher, B., and Robinson, S. R. (1991). The organization of the visual thalamus. In *Neuroanatomy of the visual pathways and their development*, (ed. B. Dreher and S. R. Robinson), pp. 176–234. Boston, CRC Press. [113]
- Garner, W. R. (1962). *Uncertainty and structure as psychological concepts*. Wiley, New York. [95]
- Garraghty, P. E., Roe, A. W., Chino, Y. M., and Sur, M. (1989). Effect of convergent strabismus on the development of physiologically identified retinogeniculate axons in cats. *Journal of Comparative Neurology*, 289, 202–12. [627]
- Garzia, R. P. (1987). Efficacy of vision therapy in amblyopia: A literature review. *American Journal of Optometry and Physiological Optics*, 64, 393–404. [634]
- Gassendi, P. (1658). *Gassendi: opera omnia*. Vol. 2, p. 395. Lyon. [338]
- Gattass, R., Oswaldo-Cruz, E., and Sousa, A. P. B. (1979). Visual receptive fields of units in the pulvinar of cebus monkey. *Brain Research*, 160, 413–30. [125]
- Gawne, T. J., Richmond, B. J., and Optican, L. M. (1991). Interactive effects among several stimulus parameters on the responses of striate cortical complex cells. *Journal of Neurophysiology*, 66, 379–89. [80]
- Gaze, R. M. and Jacobson, M. (1962). The projection of the binocular visual field on the optic tecta of the frog. *Quarterly Journal of Experimental Physiology*, 47, 273–80. [651]
- Gazzaniga, M. S. and LeDoux, J. E. (1978). *The integrated mind*. Plenum, New York. [624]
- Georges, M. A. (1979). Random-dot stereograms of real objects: Observations on stereo faces and moulds. *Perception*, 8, 585–8. [456]
- Georges, M. A. (1988). Spatial phase dependence and the role of motion detection in monocular and dichoptic forward masking. *Vision Research*, 28, 1193–1205. [363]
- Georges, M. A. and Harris, M. G. (1984). Spatial selectivity of contrast adaptation: Models and data. *Vision Research*, 24, 729–41. [259]
- Georges, M. A. and Phillips, R. (1980). Angular selectivity of monocular rivalry: Experiment and computer simulation. *Vision Research*, 20, 1007–13. [334]
- Georges, M. A. and Shackleton, T. M. (1989). Monocular motion sensing, binocular motion perception. *Vision Research*, 29, 1511–23. [568]

- Georgeson, M. A. and Shackleton, T. M. (1992). No evidence for dichoptic motion sensing: A reply to Carney and Shadlen. *Vision Research*, 32, 193-8. [569]
- Georgeson, M. A. and Sullivan, G. D. (1975). Contrast constancy: Deblurring in human vision by spatial frequency. *Journal of Physiology*, 252, 627-56. [87, 165]
- Georgeson, M. A. and Turner, R. S. E. (1985). Afterimages of sinusoidal, square-wave and compound gratings. *Vision Research*, 25, 1709-20. [490]
- Gerbino, W. (1984). Low-level and high-level processes in the perceptual organization of three-dimensional apparent motion. *Perception*, 13, 417-28. [529]
- Gernsheim, H. (1969). *History of photography*. McGraw-Hill, New York. [9, 19, 22, 26]
- Gerstmann, J. and Kestenbaum, A. (1930). Monokuläres Doppelzsehen bei cerebralen Erkrankungen. *Zeitschrift für Neurologie und Psychiatrie*, 128, 42-56. [47]
- Gescheider, G. A. (1976). *Psychophysics: Method and theory*. Erlbaum, Hillsdale, NJ. [93]
- Gettys, C. F. and Harker, G. S. (1967). Some observations and measurements of the Panum phenomenon. *Perception and Psychophysics*, 2, 387-95. [523]
- Ghose, G. M. and Freeman, R. D. (1992). Oscillatory discharge in the visual system: Does it have a functional role? *Journal of Neurophysiology*, 68, 1558-74. [83]
- Ghose, G. M., Freeman, R. D., and Ohzawa, I. (1994). Local intracortical connections in the cat's visual cortex: Postnatal development and plasticity. *Journal of Neurophysiology*, 72, 1290-303. [118]
- Ghose, G. M., Ohzawa, I., and Freeman, R. D. (1994). Receptive-field maps of correlated discharge between pairs of neurons in the cat's visual cortex. *Journal of Neurophysiology*, 71, 330-46. [81]
- Ghosh, A. and Shatz, C. J. (1992). Involvement of subplate neurons in the formation of ocular dominance columns. *Science*, 255, 1441-3. [614]
- Ghosh, A. and Shatz, C. J. (1994). Segregation of geniculocortical afferents during the critical period: A role for subplate neurons. *Journal of Neurophysiology*, 71, 3862-80. [614]
- Gibbs, T. and Lawson, R. B. (1974). Simultaneous brightness contrast in stereoscopic space. *Vision Research*, 14, 983-7. [524]
- Gibson, E. J. and Walk, R. D. (1960). The visual cliff. *Scientific American*, 202, 64-71. [618]
- Gibson, E. J., Gibson, J. J., Smith, O. W., and Flock, A. (1959). Motion parallax as a determinant of perceived depth. *Journal of Experimental Psychology*, 54, 40-51. [578]
- Gibson, J. J. (1933). Adaptation, after-effect and contrast in the perception of curved lines. *Journal of Experimental Psychology*, 16, 1-31. [373, 378, 465-6, 485]
- Gibson, J. J. (1937). Adaptation, aftereffect, and contrast in the perception of tilted lines. II. Simultaneous contrast and the areal restriction of the aftereffect. *Journal of Experimental Psychology*, 20, 553-69. [373, 465, 639]
- Gibson, J. J. (1950). *The perception of the visual world*. Houghton Mifflin, Boston. [557]
- Gibson, J. J. (1958). Visually controlled locomotion and visual orientation in animals. *British Journal of Psychology*, 49, 182-94. [557]
- Gibson, J. J. and Carel, W. (1952). Does motion perspective independently produce the impression of a receding surface? *Journal of Experimental Psychology*, 44, 16-8. [578]
- Gibson, J. J. and Radner, M. (1937). Adaptation, aftereffect, and contrast in the perception of tilted lines. I. Quantitative studies. *Journal of Experimental Psychology*, 20, 453-67. [466]
- Gibson, J. J., Olum, P., and Rosenblatt, F. (1955). Parallax and perspective during aircraft landings. *American Journal of Psychology*, 68, 373-85. [557]
- Gilbert, C. D. and Wiesel, T. N. (1979). Morphology and intracortical projections of functionally characterized neurones in the cat visual cortex. *Nature*, 280, 120-5. [116, 118, 611]
- Gilbert, C. D. and Wiesel, T. N. (1985). Intrinsic connectivity and receptive field properties in visual cortex. *Vision Research*, 25, 365-74. [116, 345]
- Gilbert, C. D. and Wiesel, T. N. (1989). Columnar specificity of intrinsic horizontal and connections in cat visual cortex. *Journal of Neurophysiology*, 61, 2432-42. [116, 346]
- Gilbert, C. D. and Wiesel, T. N. (1990). The influence of intrinsic horizontal and corticocortical connections in the primary visual cortex of the cat. *Vision Research*, 30, 1689-1701. [129]
- Gilbert, C. D., Ts'o, D. Y., and Wiesel, T. N. (1991). Lateral interactions in visual cortex. In *From pigments to perception*, (ed. A. Valberg and B. B. Lee), pp. 239-47. Plenum Press, New York. [116, 346]
- Gilbert, D. S. and Fender, D. H. (1969). Contrast thresholds measured with stabilized and non-stabilized sine-wave gratings. *Optica Acta*, 16, 191-204. [186, 382]
- Gilchrist, A. L. (1980). When does perceived lightness depend on perceived spatial arrangement? *Perception and Psychophysics*, 28, 527-38. [523]
- Gilinsky, A. S. and Doherty, R. S. (1969). Interocular transfer of orientational effects. *Science*, 164, 454-5. [366]
- Gillam, B. (1967). Changes in the direction of induced aniseikonic slant as a function of distance. *Vision Research*, 7, 777-83. [151]
- Gillam, B. J. (1968). Perception of slant when perspective and stereopsis conflict: Experiments with aniseikonic lenses. *Journal of Experimental Psychology*, 78, 299-305. [449]
- Gillam, B. (1993). Stereoscopic slant reversals: a new kind of 'induced' effect. *Perception*, 22, 1025-36. [151]
- Gillam, B. (1995). Quantitative depth without binocular correspondence not yet demonstrated. *Nature*, in press. [517]
- Gillam, B. and Borsting, E. (1988). The role of monocular regions in stereoscopic displays. *Perception*, 17, 603-8. [513]
- Gillam, B. and Lawergren, B. (1983). The induced effect, vertical disparity, and stereoscopic theory. *Perception and Psychophysics*, 34, 121-30. [282-3, 286, 288]
- Gillam, B. and Rogers, B. (1991). Orientation disparity, deformation, and stereoscopic slant perception. *Perception*, 20, 441-8. [276]
- Gillam, B. and Ryan, C. (1992). Perspective, orientation disparity, and anisotropy in stereoscopic slant perception. *Perception*, 21, 427-39. [267]
- Gillam, B., Flagg, T., and Finlay, D. (1984). Evidence for disparity change as the primary stimulus for stereoscopic processing. *Perception and Psychophysics*, 36, 559-64. [266, 298]
- Gillam, B., Chambers, D., and Lawergren, B. (1988a). The role of vertical disparity in the scaling of stereoscopic depth perception: An empirical and theoretical study. *Perception and Psychophysics*, 40, 477-83. [275, 286-7, 469]
- Gillam, B., Chambers, D., and Russo, T. (1988b). Postfusional latency in slant perception and the primitives of stereopsis. *Journal of Experimental Psychology: Human Perception and Performance*, 14, 163-75. [462, 477, 484]
- Gillott, H. F. (1956). The effect on binocular vision of variations in the relative sizes and levels of illumination of the images. *British Journal of Physiological Optics*, 13, 122-46, 218-34. [67]
- Gillott, H. F. (1957). The effect on binocular vision of variations in the relative sizes and levels of illumination of the images. Part III. *British Journal of Physiological Optics*, 14, 43-58. [62]
- Gioanni, H., Bennis, M., and Sansonetti, A. (1993). Visual and vestibular reflexes that stabilize gaze in the chameleon. *Visual Neuroscience*, 10, 947-56. [653]

- Giolli, R. A. and Guthrie, M. D. (1969). The primary optic projections in the rabbit. An experimental degeneration study. *Journal of Comparative Neurology*, **136**, 99–126. [656]
- Girard, L. J., Friedman, B., Moore, C. D., Blau, R. I., Binkhorst, C. D., and Gobin, M. H. (1962). Intraocular implants and contact lenses. *AMA Archives of Ophthalmology*, **68**, 762–75. [64]
- Glass, L. and Perez, R. (1973). Perception of random-dot interference patterns. *Nature*, **246**, 360–2. [590]
- Gleason, G., Schor, C., Lunn, R., and Maxwell, J. (1992). Directionally selective short-term nonconjugate adaptation of vertical pursuits. *Vision Research*, **33**, 33–46. [393]
- Glennerster, A., and Rogers, B. J. (1993). New depth to the Müller-Lyer illusion. *Perception*, **22**, 691–704. [306]
- Glennerster, A., Rogers, B. J., and Bradshaw, M. F. (1994). The effects of (i) different cues and (ii) the observer's task in stereoscopic depth constancy. *Investigative Ophthalmology and Visual Science*, **35** (ARVO Abstracts), 2112. [300, 459]
- Glickstein, M., Miller, J., and Smith, O. A. (1964). Lateral geniculate nucleus and cerebral cortex: Evidence for a crossed pathway. *Science*, **145**, 159–61. [132]
- Godement, P., Salaun, J., and Mason, C. A. (1990). Retinal axon pathfinding in the optic chiasma. *Neuron*, **5**, 173–86. [608]
- Goethe, J. W. von (1810). *Zur Farbenlehre*. Tübingen. [306]
- Gogel, W. C. (1956). The tendency to see objects as equidistant and its inverse relation to lateral separation. *Psychological Monographs*, **70** (Whole No. 411). [463]
- Gogel, W. C. (1960). The perception of shape from binocular disparity cues. *Journal of Psychology*, **50**, 179–92. [458]
- Gogel, W. C. (1963). The visual perception of size and distance. *Vision Research*, **3**, 101–20. [472]
- Gogel, W. C. (1964). Perception of depth from binocular disparity. *Journal of Experimental Psychology*, **67**, 379–86. [458]
- Gogel, W. C. (1965). Equidistance tendency and its consequences. *Psychological Bulletin*, **64**, 153–63. [461, 463]
- Gogel, W. C. (1972). Scalar perceptions with binocular cues to distance. *American Journal of Psychology*, **85**, 477–97. [429]
- Gogel, W. C. (1975). Depth adjacency and the Ponzo illusion. *Perception and Psychophysics*, **17**, 125–32. [524]
- Gogel, W. C. (1977). An indirect measure of perceived distance from oculomotor cues. *Perception and Psychophysics*, **21**, 3–11. [459, 578]
- Gogel, W. C. (1982). Analysis of the perception of motion concomitant with a lateral motion of the head. *Perception and Psychophysics*, **32**, 241–50. [430]
- Gogel, W. C. and MacCracken, P. J. (1979). Depth adjacency and induced motion. *Perception and Motor Skills*, **48**, 343–50. [533]
- Gogel, W. C. and Mershon, D. H. (1977). Local autonomy in visual space. *Scandinavian Journal of Psychology*, **18**, 237–50. [472]
- Gogel, W. C. and Newton, R. E. (1975). Depth adjacency and the rod-and-frame illusion. *Perception and Psychophysics*, **18**, 163–71. [524]
- Gogel, W. C. and Sturm, R. D. (1972). A comparison of accommodation and fusional convergence as cues to distance. *Perception and Psychophysics*, **11**, 166–8. [427]
- Gogel, W. C. and Szoc, R. (1974). Differential modification of the equidistance and nonius horopter. *Vision Research*, **14**, 1441–9. [68]
- Gogel, W. C. and Tietz, J. D. (1973). Absolute motion parallax and the specific distance tendency. *Perception and Psychophysics*, **13**, 284–92. [430, 573]
- Goldsmith, T. H. and Cronin, T. W. (1993). Retinoids of seven species of mantis shrimp. *Visual Neuroscience*, **10**, 915–20. [649]
- Gonzalez, F., Krause, F., Perez, R., Alonso, J. M., and Acuna, C. (1993). Binocular matching in monkey visual cortex: Single cell responses to correlated and uncorrelated dynamic random dot stereograms. *Neuroscience*, **52**, 933–9. [135]
- Goodale, M. A. (1983). Visually guided pecking in the pigeon (*Columba livia*). *Brain Behavior and Evolution*, **22**, 22–40. [653]
- Goodenough, D. R., Sigmund, E., Oltman, P. K., Rosso, J., and Mertz, H. (1979). Eye torsion in response to a tilted visual stimulus. *Vision Research*, **19**, 1177–9. [417]
- Gordon, B. and Presson, J. (1977). Effects of alternating occlusion on receptive fields in cat superior colliculus. *Journal of Neurophysiology*, **40**, 1406–14. [627]
- Gordon, F. R. and Yonas, A. (1976). Sensitivity to binocular depth information in infants. *Journal of Experimental Child Psychology*, **22**, 413–22. [618]
- Goryu, K. and Kikuchi, T. (1971). Disparity and training in stereopsis. *Japanese Psychological Research*, **13**, 148–152. [197]
- Grabowska, A. (1983). Lateral differences in the detection of stereoscopic depth. *Neuropsychologia*, **21**, 249–57. [155, 166]
- Grafstein, B. and Laureno, R. (1973). Transport of radioactivity from eye to visual cortex in the mouse. *Experimental Neurology*, **39**, 44–57. [121]
- Graham, C. H., Baker, K. E., Hecht, M., and Lloyd, V. V. (1948). Factors influencing thresholds for monocular movement parallax. *Journal of Experimental Psychology*, **38**, 205–23. [578]
- Graham, M. E. (1983). Motion parallax and the perception of three-dimensional surfaces. Ph.D. thesis, University of St Andrews. [490]
- Graham, M. E. and Rogers, B. J. (1982a). Simultaneous and successive contrast effects in the perception of depth from motion-parallax and stereoscopic information. *Perception*, **11**, 247–62. [298, 439, 473–5, 484, 488, 494–5, 579–80]
- Graham, M. E. and Rogers, B. J. (1982b). Interactions between monocular and binocular depth aftereffects. *Investigative Ophthalmology and Visual Science*, **22** (ARVO Abstracts), 272. [438–9]
- Graham, M. E. and Rogers, B. J. (1983). Phase-dependent and phase-independent depth aftereffects. *Perception*, **12**, (Abstract Supplement), A16. [496]
- Graham, N. and Nachmias, J. (1971). Detection of grating patterns containing two spatial frequencies: A comparison of single-channel and multiple-channel models. *Vision Research*, **11**, 251–9. [88]
- Graham, N. V. S. (1989). *Visual pattern analyzers*. New York, Oxford University Press. [89, 100, 440]
- Graham, P. A. (1974). The epidemiology of strabismus. *British Journal of Ophthalmology*, **58**, 224–31. [387]
- Granrud, C. E. (1986). Binocular vision and spatial perception in 4- and 5-month-old infants. *Journal of Experimental Psychology: Human Perception and Performance*, **12**, 36–49. [618]
- Grant, S. and Berman, N. E. J. (1991). Mechanisms of anomalous retinal correspondence: Maintenance of binocularity with alteration of receptive-field position in the lateral suprasylvian (LS) visual area of strabismic cats. *Visual Neuroscience*, **7**, 259–81. [47]
- Grant, S. and Keating, M. J. (1989a). Changing patterns of binocular visual connections in the intertectal system during development of the frog, *Xenopus laevis*. I. Normal maturational changes in response to changing binocular geometry. *Experimental Brain Research*, **75**, 99–116. [651]
- Grant, S. and Keating, M. J. (1989b). Changing patterns of binocular visual connections in the intertectal system during development of the frog, *Xenopus laevis*. II. Abnormalities following early visual deprivation. *Experimental Brain Research*, **75**, 117–32. [652]
- Grant, S. and Keating, M. J. (1992). Changing patterns of binocular visual connections in the intertectal system during development of the frog, *Xenopus laevis*. III. Modifications following early eye rotation. *Experimental Brain Research*, **89**, 383–96. [652]

- Grasse, K. L. (1991). Pharmacological isolation of visual cortical input to the cat accessory optic system: Effects of intravitreal tetrodotoxin on DTN unit responses. *Visual Neuroscience*, 6, 175–183. [530]
- Grasse, K. L. (1994). Positional disparity sensitivity of neurons in the cat accessory optic system. *Vision Research*, 13, 1673–89. [143, 532]
- Grasse, K. L. and Cynader, M. S. (1990). The accessory optic system in frontal-eyed animals. In *Vision and visual dysfunction*. Vol. IV. (ed. A. L. Leventhal), pp. 111–39. Macmillan, London. [529]
- Graves, A. L., Trotter, Y., and Frégnac, Y. (1987). Role of extraocular muscle proprioception in the development of depth perception in cats. *Journal of Neurophysiology*, 58, 816–31. [641]
- Gray, C. M. and Singer, W. (1989). Stimulus-specific neuronal oscillations in orientation columns of cat visual cortex. *Proceedings of the National Academy of Science*, 86, 1698–1702. [82]
- Gray, C. M., Engel, A. K., König, P., and Singer, W. (1991). Synchronous neuronal oscillations in cat visual cortex: Functional implications. In *Representations of vision* (ed. A. Górea), pp. 83–96. Cambridge University Press, New York. [83]
- Gray, L. S., Winn, B., Gilmartin, B., Eadie, A. S. (1993). Objective concurrent measures of open-loop accommodation under photopic conditions. *Investigative Ophthalmology and Visual Science*, 34, 2996–3003. [397]
- Green, D. M. and Swets, J. A. (1966). *Signal detection theory and psychophysics*. Wiley, New York. [93–4, 352]
- Green, J. (1889). On certain stereoscopic illusions evoked by prismatic and cylindrical spectacle-glasses. *Transactions of the American Ophthalmology Society*, 449–56. [285]
- Green, M. (1986). What determines correspondence strength in apparent motion. *Vision Research*, 26, 599–607. [527]
- Green, M. (1989). Color correspondence in apparent motion. *Perception and Psychophysics*, 45, 15–20. [527]
- Green, M. (1992). Temporal sampling requirements for stereoscopic displays. In *Stereoscopic displays and applications*. *Proceedings of the Society of Photo and Illumination Engineering*, 1665, 101–11. [570]
- Green, M. and Blake, R. (1981). Phase effects in monoptic and dichoptic temporal integration: Flicker and motion detection. *Vision Research*, 21, 365–72. [362, 567]
- Green, M. and Odom, J. V. (1986). Correspondence matching in apparent motion: Evidence for three-dimensional spatial representation. *Science*, 233, 1427–29. [528]
- Greene, R. T., Lawson, R. B., and Godek, C. L. (1972). The Ponzo illusion in stereoscopic space. *Journal of Experimental Psychology*, 95, 358–64. [524]
- Greenlee, M. W. (1992). Spatial frequency discrimination of band-limited periodic targets: Effects of stimulus contrast, bandwidth and retinal eccentricity. *Vision Research*, 32, 275–83. [263]
- Greenspon, T. S. and Eriksen, C. W. (1968). Interocular nonindependence. *Perception and Psychophysics*, 3, 93–6. [356]
- Gregory, R. L. (1966). *Eye and brain*. World University Library, London. [536, 546, 554]
- Gregory, R. L. (1970). *The intelligent eye*. McGraw-Hill, New York. [456]
- Gregory, R. L. (1979). Stereo vision and isoluminance. *Proceedings of the Royal Society, London*, B204, 467–76. [207]
- Gregory, R. L. (1980). Perceptions as hypotheses. *Philosophical Transactions of the Royal Society London*, B290, 181–97. [466]
- Gregory, R. L. and Harris, J. P. (1974). Illusory contours and stereo depth. *Perception and Psychophysics*, 15, 411–16. [509]
- Gregory, R. L. and Zangwill, O. L. (1963). The origin of the auto-kinetic effect. *Quarterly Journal of Experimental Psychology*, 15, 252–61. [432]
- Gregory, R. L., Ross, H. E., and Moray, N. (1964). The curious eye of *Copilia*. *Nature*, 201, 1166–8. [647]
- Gresty, M. A., Bronstein, A. M., and Barratt, H. (1987). Eye movement responses to combined linear and angular head movement. *Experimental Brain Research*, 65, 377–84. [415]
- Griffin, J. R. (1976). *Binocular anomalies. Procedures for vision therapy*. Professional Press, Chicago. [46, 388]
- Grimsley, G. (1943). A study of individual differences in binocular color fusion. *Journal of Experimental Psychology*, 32, 82–7. [326]
- Grimson, W. E. L. (1981). A computer implementation of a theory of human stereo vision. *Philosophical Transactions of the Royal Society*, B292, 217–53. [197, 217]
- Grinberg, D. L. and Williams, D. R. (1985). Stereopsis with chromatic signals from the blue-sensitive mechanism. *Vision Research*, 25, 531–7. [208]
- Grinvald, A., Lieke, E. E., Frostig, R. D., and Hildesheim, R. (1994). Cortical point-spread function and range lateral interactions revealed by real-time optical imaging of macaque monkey primary visual cortex. *Journal of Neuroscience*, 14, 2545–68. [116]
- Grobstein, P., Comer, C., and Kostyk, S. (1980). The potential binocular field and its tectal representation in *Rana pipiens*. *Journal of Comparative Neurology*, 190, 175–85. [651–2]
- Gronwall, D. M. A. and Sampson, H. (1971). Ocular dominance: A test of two hypotheses. *British Journal of Psychology*, 62, 175–85. [337]
- Gross, C. G. (1973). Visual functions of inferotemporal cortex. In *Handbook of sensory physiology*. Vol. VII/3B, (ed. R. Jung), pp. 451–82. Springer, New York. [125]
- Grossberg, S. (1990). A model cortical architecture for the preattentive perception of 3-D form. In *Computational neuroscience*, (ed. E. R. Schwartz), pp. 117–38. MIT Press, Cambridge, MA. [128]
- Grossberg, S. and Somers, D. (1991). Synchronized oscillations during cooperative feature linking in a cortical model of visual perception. *Neural Networks*, 4, 453–66. [83]
- Gruberg, E. R. and Lettvin, J. Y. (1980). Anatomy and physiology of a binocular system in the frog *Rana pipiens*. *Brain Research*, 192, 313–25. [651]
- Grüsser, O. J. and Grüsser-Cornehlis, U. (1965). Neurophysiological Grundlagen des Binocularsehens. *Archiv für Psychiatrie und Zeitschrift für die gesamte Neurologie*, 207, 296–317. [123, 351]
- Grüsser, O. J. and Grüsser-Cornehlis, U. (1976). Neurophysiology of the anuran visual system. In *Frog neurobiology*, (ed. R. Llinás and W. Precht), pp. 297–385. New York, Springer. [651]
- Gu, Q., Bear, M. F., and Singer, W. (1989). Blockade of NMDA-receptors prevents ocularity changes in kitten cortex after reversed monocular deprivation. *Development Brain Research*, 47, 281–88. [614]
- Guilford, J. P. (1954). *Psychometric methods*. McGraw-Hill, New York. [93]
- Guillemot, J. P., Paradis, M. C., Samson, A., Ptito, M., Richer, L., and Lepore, F. (1993). Binocular interaction and disparity coding in area 19 of visual cortex in normal and split-chiasm cats. *Experimental Brain Research*, 94, 405–17. [132, 134]
- Guillery, R. W. (1972). Binocular competition in the control of geniculate cell growth. *Journal of Comparative Neurology*, 144, 117–30. [627]
- Guillery, R. W. (1986). Neural abnormalities in albinos. *Trends in Neuroscience*, 9, 364–7. [642]
- Guillery, R. W., Okoro, A. N., and Witkop, C. J. (1975). Abnormal visual pathways in the brain of a human albino. *Brain Research*, 96, 373–7. [642]

- Gulick, W. L. and Lawson, R. B. (1976). *Human stereopsis*. Oxford University Press, New York. [1, 24, 50]
- Gunter, R. (1951). Binocular fusion of colours. *British Journal of Psychology*, **42**, 363–72. [326-7]
- Gur, M. (1991). Perceptual fade-out occurs in the binocularly viewed Ganzfeld. *Perception*, **20**, 645–54. [331]
- Gur, M. and Akri, V. (1992). Isoluminant stimuli may not expose the full contribution of color to visual functioning: Spatial contrast sensitivity measurements indicate interaction between color and luminance processing. *Vision Research*, **32**, 1253–62. [209]
- Gur, M. and Snodderly, D. M. (1987). Studying striate cortex neurons in behaving monkeys: Benefits of image stabilization. *Vision Research*, **27**, 2081–7. [179]
- Guth, S. L. (1971). On probability summation. *Vision Research*, **11**, 747–50. [352]
- Guthrie, D. M. (1990). The physiology of the optic tectum. In *The visual system of fish*, (ed. R. H. Douglas and M. B. A. Djamgoz), pp. 300–42. Chapman Hall, London. [649]
- Gwiadza, J., Scheiman, M., Mohindra, I., and Held, R. (1984). Astigmatism in children: Changes in axis and amount from birth to six years. *Investigative Ophthalmology and Visual Science*, **25**, 88–92. [605]
- Hadani, I. and Vardi, N. (1987). Stereopsis impairment in apparently moving random dot patterns. *Perception and Psychophysics*, **42**, 158–65. [187]
- Haenny, P. E. and Schiller, P. H. (1988). State dependent activity in monkey visual cortex. I. Single cell activity in V1 and V4 on visual tasks. *Experimental Brain Research*, **69**, 225–44. [129]
- Hahm, J. O., Langdon, R. B., and Sur, M. (1991). Disruption of retinogeniculate afferent segregation by antagonists to NMDA receptors. *Nature*, **351**, 568–70. [609]
- Hahmann, U. and Güntürkün, O. (1993). The visual acuity for the lateral visual field of the pigeon. *Vision Research*, **33**, 1659–64. [653]
- Haig, N. D. (1993). Why is the retina capable of resolving finer detail than the eye's optical or neural systems? *Spatial Vision*, **7**, 257–73. [108]
- Haines, R. F. (1977). Visual response time to colored stimuli in peripheral retina: Evidence for binocular summation. *American Journal of Optometry and Physiological Optics*, **54**, 387–98. [359]
- Hajos, A. (1962). Farbunterscheidung ohne "Farbigsehen". *Naturwissenschaften*, **49**, 93–7. [307]
- Hajos, A. and Ritter, M. (1965). Experiments to the problem of interocular transfer. *Acta Psychologica*, **24**, 81–90. [373, 378]
- Halaas, S. (1966). Aniseikonia – a survey of the literature. *American Journal of Optometry and Archives of the American Academy of Optometry*, **43**, 505–24. [67]
- Haldat, C. (1806). Expériences sur la double vision. *Journal de Physique*, **63**, 387–401. [325]
- Halmagyi, G. M., Gresty, M. A., and Leech, J. (1980). Reversed optokinetic nystagmus (OKN): Mechanism and clinical significance. *Annals of Neurology*, **7**, 429–35. [643]
- Halpern, D. L. (1991). Stereopsis from motion-defined contours. *Vision Research*, **31**, 1611–17. [209]
- Halpern, D. L. and Blake, R. (1988). How contrast affects stereoacluity. *Perception*, **17**, 483–95. [169-70]
- Halpern, D. L., Patterson, R., and Blake, R. (1987). What causes stereoscopic tilt from spatial frequency disparity. *Vision Research*, **27**, 1619–29. [264]
- Hamer, R. D. and Norcia, A. M. (1994). The development of motion sensitivity during the first year of life. *Vision Research*, **34**, 2387–402. [617]
- Hamer, R. D. and Schneck, M. E. (1984). Spatial summation in dark-adapted human infants. *Vision Research*, **24**, 77–85. [604]
- Hamer, R. D., Norcia, A. M., Tyler, C. W., and Hsu-Winges, C. (1989). The development of monocular and binocular VEP acuity. *Vision Research*, **29**, 397–408. [616]
- Hammond, J. H. (1981). *The camera obscura. A chronicle*. Hilkger, Bristol. [7, 9]
- Hammond, P. (1979). Stimulus dependence of ocular dominance of complex cells in area 17 of the feline visual cortex. *Experimental Brain Research*, **35**, 583–9. [123]
- Hammond, P. (1981). Non-stationarity of ocular dominance in cat striate cortex. *Experimental Brain Research*, **42**, 189–95. [123]
- Hammond, P. (1991). Binocular phase specificity of striate cortico-tectal neurones. *Experimental Brain Research*, **87**, 615–23. [138]
- Hammond, P. and Fothergill, L. K. (1991). Interocular comparison of length summation and end-inhibition in striate cortical neurones of the anaesthetized cat. *Proceedings of the Physiological Society*, **446**, 232P. [120]
- Hammond, P. and MacKay, D. M. (1981). Modulatory influences of moving textured backgrounds on responsiveness of simple cells in feline striate cortex. *Journal of Physiology*, **319**, 431–42. [117]
- Hammond, P. and Mouat, G. S. V. (1988). Neural correlates of motion after-effects in cat striate cortical neurones: Interocular transfer. *Experimental Brain Research*, **72**, 21–8. [376]
- Hammond, P. and Pomfrett, C. J. D. (1991). Interocular mismatch in spatial frequency and directionality characteristics of striate cortical neurones. *Experimental Brain Research*, **85**, 631–40. [141]
- Hammond, P., Mouat, G. S. V., and Smith, A. T. (1988). Neural correlates of motion after-effects in cat striate cortical neurones: Monocular adaptation. *Experimental Brain Research*, **72**, 1–20. [376]
- Hampton, D. R. and Kertesz, A. E. (1982). Human response to cyclofusional stimuli containing depth cues. *American Journal of Optometry and Physiological Optics*, **59**, 21–7. [418]
- Hampton, D. R. and Kertesz, A. E. (1983a). Fusional vergence response to local peripheral stimulation. *Journal of the Optical Society of America*, **73**, 7–10. [402]
- Hampton, D. R. and Kertesz, A. E. (1983b). The extent of Panum's area and the human cortical magnification factor. *Perception*, **12**, 161–65. [316]
- Hamsher, K. de S. (1978). Stereopsis and unilateral brain disease. *Investigative Ophthalmology and Visual Science*, **17**, 336–43. [625]
- Hamstra, S. J. and Regan, D. (1994). Orientation discrimination in cycloptic vision. *Vision Research*, in press. [183]
- Hänni, P. and von der Heydt, R. (1982). The effect of horizontal-plane environment on the development of binocular receptive fields of cells in cat visual cortex. *Journal of Physiology*, **329**, 75–92. [622]
- Hänni, P., von der Heydt, R., and Poggio, G. F. (1977). Binocular neuron responses to tilt in depth in the monkey visual cortex: evidence for orientation disparity processing. *Union of Swiss Societies of Experimental Biology Abstracts*, **A26**. [272]
- Hänni, P., von der Heydt, R., and Poggio, G. F. (1980). Binocular neuron responses to tilt in the monkey visual cortex. Evidence for orientation disparity processing. *Experimental Brain Research*, **41**, A26. [142]
- Harker, G. S. (1960). Two stereoscopic measures of cyclorotation of the eyes. *American Journal of Optometry and Archives of the American Academy of Optometry*, **37**, 461–73. [418]
- Harker, G. S. (1962). Apparent frontoparallel plane, stereoscopic correspondence, and induced cyclorotation of the eyes. *Perceptual and Motor Skills*, **14**, 75–87. [463]
- Harker, G. S. (1967). A saccadic suppression explanation of the Pulfrich phenomenon. *Perception and Psychophysics*, **2**, 423–6. [539, 541]

- Harker, G. S. and O'Neal, O. L. Jr. (1967). Some observations and measurements of the Pulfrich phenomenon. *Perception and Psychophysics*, 2, 438–40. [537]
- Harkness, L. (1977). Chameleons use accommodation cues to judge distance. *Nature*, 267, 346–9. [653]
- Harrad, R. A. and Hess, R. F. (1992). Binocular integration of contrast information in amblyopia. *Vision Research*, 32, 2135–50. [635]
- Harrad, R. A., McKee, S. P., Blake, R., and Yang, Y. (1994). Binocular rivalry disrupts stereopsis. *Perception*, 23, 15–28. [340]
- Harris, J. (1775). *A treatise of optics*. B. White, London. p. 171. [12, 17]
- Harris, J. M. and Morgan, M. J. (1993). Stereo and motion disparities interfere with positioning averaging. *Vision Research*, 33, 309–12. [525]
- Harris, J. M. and Parker, A. J. (1994a). Constraints on human stereo dot matching. *Vision Research*, 34, 2761–72. [158]
- Harris, J. M. and Parker, A. J. (1994b). Objective evaluation of human and computational stereoscopic visual systems. *Vision Research*, 34, 2773–85. [158]
- Harris, J. M. and Parker, A. J. (1992). Efficiency of stereopsis in random-dot stereograms. *Journal of the Optical Society of America*, 9, 1–12. [158]
- Harris, J. P. and Gregory, R. L. (1973). Fusion and rivalry of illusory contours. *Perception*, 2, 235–47. [229]
- Harris, L. and Jenkin, M. (1993). *Spatial vision in humans and robots*. Cambridge University Press, Cambridge. [30]
- Harris, V. A., Hayes, W., and Gleason, J. M. (1974). The horizontal–vertical illusion: Binocular and dichoptic investigations of bisection and verticality components. *Vision Research*, 14, 1323–6. [372]
- Harter, M. R., Seiple, W. H., and Musso, M. (1974). Binocular summation and suppression: Visually evoked cortical responses to dichoptically presented patterns of different spatial frequency. *Vision Research*, 14, 1169–80. [359]
- Harter, M. R., Seiple, W. H., and Salmon, L. (1973). Binocular summation of visually evoked responses to pattern stimuli in humans. *Vision Research*, 13, 1433–46. [144–5]
- Hartline, H. K. (1938). The responses of single optic nerve fibres of the vertebrate eye. *American Journal of Physiology*, 121, 400–15. [109]
- Hartridge, H. (1918). Chromatic aberration and the resolving power of the eye. *Journal of Physiology*, 52, 175–246. [306]
- Hartveit, E., Ramberg, S. I., and Heggelund, P. (1993). Brain stem modulation of spatial receptive field properties of single cells in the dorsal lateral geniculate nucleus of the cat. *Journal of Neurophysiology*, 70, 1644–55. [113]
- Harvey, A. R. (1980). A physiological analysis of subcortical and commissural projections of areas 17 and 18 of the cat. *Journal of Physiology*, 302, 507–34. [130]
- Harwerth, R. S. and Boltz, R. L. (1979). Stereopsis in monkeys using random dot stereograms: The effect of viewing duration. *Vision Research*, 19, 985–91. [155, 184, 645]
- Harwerth, R. S. and Rawlings, S. C. (1977). Viewing time and stereoscopic threshold with random-dot stereograms. *American Journal of Optometry and Physiological Optics*, 54, 452–7. [184]
- Harwerth, R. S. and Smith, E. L. (1985). Binocular summation in man and monkey. *American Journal of Optometry and Physiological Optics*, 62, 439–46. [353]
- Harwerth, R. S., Smith, E. L., and Levi, D. M. (1980). Suprathreshold binocular interactions for grating patterns. *Perception and Psychophysics*, 27, 43. [353]
- Harwerth, R. S., Smith, E. L., Boltz, R. L., Crawford, M. L. J., and Noorden, G. K. von (1983). Behavioral studies on the effect of abnormal early visual experience in monkeys: Spatial modulation sensitivity. *Vision Research*, 23, 1501–10. [631]
- Harwerth, R. S., Smith, E. L., Crawford, M. L. J., and Noorden, G. K. von (1990). Behavioral studies of the sensitive period of development of visual functions in monkeys. *Behavioural Brain Research*, 41, 179–98. [636]
- Harwerth, R. S., Smith, E. L., Duncan, G. C., Crawford, M. L. J., and Noorden, G. K. von (1986a). Effects of enucleation of the fixating eye on strabismic amblyopia in monkey. *Investigative Ophthalmology and Visual Science*, 27, 246–54. [633]
- Harwerth, R. S., Smith, E. L., Duncan, G. C., Crawford, M. L. J., and Noorden, G. K. von (1986b). Multiple sensitive periods in the development of the primate visual system. *Science*, 232, 235–8. [635]
- Harwerth, R. S., Smith, E. L., Paul, A. D., Crawford, M. L. J., and Noorden, G. K. von (1991). Functional effects of bilateral form deprivation in monkeys. *Investigative Ophthalmology and Visual Science*, 32, 2311–27. [626]
- Hastorf, A. H. and Myro, G. (1959). The effect of meaning on binocular rivalry. *American Journal of Psychology*, 72, 393–400. [347]
- Hata, Y. and Stryker, M. P. (1994). Control of thalamocortical afferent rearrangement by postsynaptic activity in developing visual cortex. *Science*, 265, 1732–5. [615]
- Hata, Y., Tsumoto, T., Sato, H., Hagiwara, K., and Tamura, H. (1993). Development of local interactions in cat visual cortex studied by cross-correlation analysis. *Journal of Neurophysiology*, 69, 40–56. [612]
- Hay, J. C. and Sawyer, S. (1969). Position constancy and binocular convergence. *Perception and Psychophysics*, 5, 310–12. [430]
- Hay, J. C., Pick, H. L., and Rosser, E. (1963). Adaptation to chromatic aberration by the human visual system. *Science*, 141, 167–9. [378]
- He, Z. J. and Nakayama, K. (1992). Surface versus features in visual search. *Nature*, 359, 231–3. [506]
- He, Z. J. and Nakayama, K. (1993). Perceiving textures: Beyond filtering. *Vision Research*, 34, 151–62. [506]
- He, Z. J. and Nakayama, K. (1994a). Apparent motion determined by surface layout not by disparity or 3-dimensional distance. *Nature*, 367, 173–4. [528]
- He, Z. J. and Nakayama, K. (1994b). Perceived surface shape not features determines correspondence strength in apparent motion. *Vision Research*, 34, 2125–35. [528]
- Heard, P. F. and Papakostopoulos, D. (1993). Long term adaptation of the Pulfrich illusion. *Investigative Ophthalmology and Visual Science* 34 (ARVO Abstracts), 1053. [548]
- Heath, G. and Hofstetter, H. W. (1952). The effect of orthoptics on the zone of binocular vision in intermittent exotropia – a case study. *American Journal of Optometry and Archives of American Academy of Optometry*, 29, 12–31. [398]
- Hebb, D. O. (1949). *The organization of behavior*. Wiley, New York. [81, 604, 631]
- Hebbard, F. W. (1962). Comparison of subjective and objective measurements of fixation disparity. *Journal of the Optical Society of America*, 52, 706–12. [389]
- Hebbard, F. W. (1964). Effect of blur on fixation disparity. *American Journal of Optometry and Archives of the American Academy of Optometry*, 41, 540–48. [392]
- Hecht, S. (1928). On the binocular fusion of colors and its relation to theories of color vision. *Proceedings of the National Academy of Science*, 14, 237–41. [326]
- Hecht, S. and Mintz, E. U. (1939). The visibility of single lines at various illuminations and the retinal basis of visual resolution. *Journal of General Physiology*, 22, 593–612. [97]
- Heckmann, T. and Howard, I. P. (1991). Induced motion: Isolation and dissociation of egocentric andvection–entrained components. *Perception*, 20, 285–305. [533]

- Heckmann, T. and Post, R. B. (1988). Induced motion and optokinetic afternystagmus; parallel response dynamics with prolonged stimulation. *Vision Research*, 28, 681–94. [533]
- Heckmann, T. and Schor, C. M. (1989a). Is edge information for stereoacuity spatially channelled. *Vision Research*, 29, 593–607. [169]
- Heckmann, T. and Schor, C. M. (1989b). Panum's fusional area estimated with a criterion-free technique. *Perception and Psychophysics*, 45, 297–306. [315, 317]
- Heggelund, P. and Albus, K. (1978). Orientation selectivity of single cells in striate cortex of cat: The shape of orientation tuning curves. *Vision Research*, 18, 1067–71. [119]
- Hein, A. and Diamond, R. (1983). Contributions of eye movement to the representation of space. In *Spatially oriented behavior*, (ed. M. Jeannerod), pp. 119–33. Springer, Berlin. [641]
- Held, (1981). Acuity in infants with normal and anomalous visual experience. In *The development of perception: Psychobiological perspectives*. Vol. 2, (ed. R. N. Aslin, J. R. Roberts, M. R. Petersen). Academic Press, New York. [616]
- Held, R. (1991). Development of binocular vision and stereopsis. *Vision and visual dysfunction*. Vol. 9. *Binocular vision*, (ed. D. Regan), pp. 170–8. Macmillan, London. [622]
- Held, R., Birch, E. E., and Gwiazda, J. (1980). Stereoacuity of human infants. *Proceedings of the National Academy of Science*, 77, 5572–4. [618]
- Helmholtz, H. von. (1893). *Popular lectures on scientific subjects*. (Trans. by E. Atkinson). Longmans Green, London. [22, 338]
- Helmholtz, H. von. (1909). *Physiological Optics*. Dover, New York. 1962 English translation by J. P. C. Southall from the 3rd German edition of *Handbuch der Physiologischen Optik*. Vos, Hamburg. [18, 51, 60, 224, 292, 303, 317, 417–18, 441, 578, 600]
- Hendrickson, A. and Boothe, R. (1976). Morphology of the retina and dorsal lateral geniculate nucleus in dark-reared monkeys (*Macaca nemestrina*). *Vision Research*, 16, 517–21. [625, 627]
- Hendrickson, A. and Drucker, D. (1992). The development of parafoveal and mid-peripheral human retina. *Behavioural Brain Research*, 49, 21–31. [605]
- Hendrickson, A. and Kupfer, C. (1976). The histogenesis of the fovea in the macaque monkey. *Investigative Ophthalmology and Visual Science*, 15, 746–56. [605]
- Hendrickson, A. and Yuodelis, C. (1984). The morphological development of the human fovea. *Ophthalmology*, 91, 603–12. [605]
- Hendry, S. H. C. and Yoshioka, T. (1994). A neurochemically distinct third channel in the macaque dorsal lateral geniculate nucleus. *Science*, 264, 575–7. [112]
- Henning, G. B. and Hertz, B. G. (1973). Binocular masking level differences in sinusoidal grating detection. *Vision Research*, 13, 2455–63. [366]
- Henning, G. B. and Hertz, B. G. (1977). The influence of bandwidth and temporal properties of spatial noise on binocular masking-level differences. *Vision Research*, 17, 399–402. [367]
- Henry, G. H. and Vidyasagar, T. R. (1991). The evolution of visual pathways. In *The evolution of the eye and visual system*, (ed. J. R. Cronly-Dillon and R. L. Gregory), pp. 442–65. CRC Press, Boca Raton, Ann Arbor. [609]
- Henry, G. H., Bishop, P. O., and Coombs, J. S. (1969). Inhibitory and sub-liminal excitatory receptive fields of simple units in cat striate cortex. *Vision Research*, 9, 1289–96. [123]
- Henson, D. B. (1978). Corrective saccades: Effects of altering visual feedback. *Vision Research*, 18, 63–7. [413]
- Henson, D. B. and Dharamshi, B. G. (1982). Oculomotor adaptation to induced heterophoria and anisometropia. *Investigative Ophthalmology and Visual Science*, 22, 234–40. [393]
- Henson, D. B. and North, R. E. (1980). Adaptation to prism-induced heterophoria. *American Journal of Optometry and Physiological Optics*, 57, 129–37. [392]
- Hepler, N. (1968). Color: A motion-contingent aftereffect. *Science*, 162, 376–7. [379]
- Herbomel, P. and Ninio, J. (1993). Processing of linear elements in stereopsis: Effects of positional and orientational distinctiveness. *Vision Research*, 33, 1813–25. [219]
- Hering, E. (1861). *Beiträge zur Physiologie*. Vol. 5. Engelmann, Leipzig. [326, 465]
- Hering, E. (1865). Die Gesetze der binocularen Tiefenwahrnehmung. *Archiv für Anatomie, Physiologie und Wissenschaftliche Medicin*, 152–165. [151, 217, 597]
- Hering, E. (1868). *Die Lehre vom Binocularen Sehen*. Engelmann, Leipzig. [408–9]
- Hering, E. (1879). *Spatial sense and movements of the eye*. (English Trans. by C. A. Radde). American Academy of Optometry, Baltimore, 1942. [518, 594]
- Hering, E. (1920). *Outlines of a theory of the light sense*. (English translation by L. Hurvich and D. Jameson). Harvard University Press, Cambridge, MA, 1964. [333]
- Herman, J. H., Tauber, E. S., and Roffwarg, H. P. (1974). Monocular occlusion impairs stereoscopic acuity, but total visual deprivation does not. *Perception and Psychophysics*, 16, 225–8. [192]
- Hermans, T. G. (1943). Torsion in persons with no known eye defect. *Journal of Experimental Psychology*, 32, 307–24. [418]
- Herring, R. D. and Bechtoldt, H. P. (1981). Categorical perception of stereoscopic stimuli. *Perception and Psychophysics*, 29, 129–37. [166]
- Hertel, K. and Monjé, M. (1947). Über den Einfluss des Zeitfactors auf das räumliche Sehen. *Pflügers Archiv für die gesamte Physiologie*, 249, 295–306. [184]
- Herzau, V. (1976). Stereosehen bei alternierender Bildarbeit. *Albrecht v. Graefes Archiv für Ophthalmologie*, 200, 85–91. [168]
- Herzau, W. and Ogle, K. N. (1937). Über den Größenunterschied der Bilder beider Augen bei asymmetrischer Konvergenz und seine Bedeutung für das Zweiäugige Sehen. *Albrecht v. Graefes Archiv für Ophthalmologie*, 137, 327–63. [60]
- Hess, C. (1904). Untersuchungen über den Erregungsvorgang im Sehorgan bei kurz- und bei länger dauernder Reizung. *Pflügers Archiv für die gesamte Physiologie*, 101, 226–62. [539]
- Hess, R. F. (1978). Interocular transfer in individuals with strabismic amblyopia: A cautionary note. *Perception*, 7, 201–5. [369, 638]
- Hess, R. F. (1991). The site and nature of suppression in squint amblyopia. *Vision Research*, 31, 111–17. [638]
- Hess, R. F. and Field, D. J. (1994). Is the spatial deficit in strabismic amblyopia due to loss of cells or an uncalibrated disarray of cells. *Vision Research*, 34, 3397–406. [631]
- Hess, R. F. and Holliday, I. (1992). The coding of spatial position by the human visual system. *Vision Research*, 32, 1085–97. [174]
- Hess, R. F. and Howell, E. R. (1977). The threshold contrast sensitivity function in strabismic amblyopia: Evidence for a two type classification. *Vision Research*, 17, 1049–55. [631]
- Hess, R. F. and Pointer, J. S. (1985). Differences in the neural basis of human amblyopia: The distribution of the anomaly across the visual field. *Vision Research*, 25, 1577–94. [633]
- Hess, R. F. and Wilcox, L. M. (1994). Linear and non-linear filtering in stereopsis. *Vision Research*, 34, 2431–8. [174]
- Hess, R. F., Campbell, F. W., and Greenhalgh, T. (1978). On the nature of the neural abnormality in human amblyopia; neural aberrations and neural sensitivity loss. *Pflügers Archiv für die gesamte Physiologie*, 377, 201–7. [631]
- Hess, R. F., France, T. D., and Tulunay-Keesey, U. (1981). Residual vision in humans who have been monocularly deprived of pattern stimulation in early life. *Experimental Brain Research*, 44, 295–311. [634]

- Heuer, H. (1987). Apparent motion in depth resulting from changing size and changing vergence. *Perception*, 6, 337–50. [563]
- Heuer, H. (1993a). Estimates of time to contact based on changing size and changing target vergence. *Perception*, 22, 549–63. [555]
- Heuer, H. (1993b). Direction discrimination of motion in depth based on changing target vergence. *Vision Research*, 33, 253–6. [562]
- Heuer, H. and Lüschow, U. (1983). Aftereffects of sustained convergence: Some implications of the eye muscle potentiation hypothesis. *Perception*, 12, 337–46. [434]
- Heuer, H. and Owens, D. A. (1987). Variations of dark vergence as a function of vertical gaze deviation. *Investigative Ophthalmology and Visual Science*, 28 (ARVO Abstracts), 315. [387]
- Heuer, H., Dunkel-Abels, G., Brüwer, M., Kröger, H., Römer, T., and Wischmeier, E. (1988). The effects of sustained vertical gaze deviation on the resting state of the vergence system. *Vision Research*, 28, 1337–44. [387]
- Hickey, T. L. (1977). Postnatal development of the human lateral geniculate nucleus: Relationship to a critical period for the visual system. *Science*, 198, 836–8. [608]
- Hickey, T. L., Spear, P. D., and Kratz, A. E. (1977). Quantitative studies of cell size in the cat's dorsal lateral geniculate nucleus following visual deprivation. *Journal of Comparative Neurology*, 172, 265–82. [626]
- Highman, V. N. (1977). Stereopsis and aniseikonia in unisocular aphakia. *British Journal of Ophthalmology*, 61, 30–3. [64]
- Hill, A. L. (1972). Direction constancy. *Perception and Psychophysics*, 11, 175–8. [432]
- Hill, H. and Bruce, V. (1993). Independent effects of lighting, orientation, and stereopsis on the hollow-face illusion. *Perception*, 22, 887–97. [456]
- Hillebrand, F. (1894). Das Verhältnis von Akkommodation und Konvergenz zur Tiefenlokalisierung. *Zeitschrift für Psychologie*, 7, 97–151. [427]
- Hillebrand, F. (1929). *Lehre von den Gesichtsempfindungen auf Grund hinterlassener*. Springer, Vienna. [58]
- Hine, T. (1985). The binocular contribution to monocular optokinetic nystagmus and after nystagmus asymmetries in humans. *Vision Research*, 25, 589–98. [531]
- Hine, T. and Thorn, F. (1987). Compensatory eye movements during active head rotation for near targets: Effects of imagination, rapid head oscillation and vergence. *Vision Research*, 27, 1639–57. [416]
- Hinton, G. E. (1989). Connectionist learning procedures. *Artificial Intelligence*, 40, 185–234. [92]
- Hinton, G. E., McClelland, J. L., and Rumelhart, D. E. (1986). Distributed representations. In *Parallel distributed processing*, Vol. 1, (ed. D. E. Rumelhart and J. L. McClelland), pp. 77–109. MIT Press, Boston. [82]
- Hirsch, J. A. and Gilbert, C. D. (1991). Synaptic physiology of horizontal connections in the cat's visual cortex. *Journal of Neuroscience*, 11, 1800–9. [116, 345]
- Hirsch, J. A. and Gilbert, C. D. (1993). Long-term changes in synaptic strength along specific intrinsic pathways in the cat visual cortex. *Journal of Physiology*, 461, 247–62. [116, 129, 612]
- Hirsch, J. and Curcio, C. A. (1989). The spatial resolution capacity of the human foveal retina. *Vision Research*, 29, 1095–101. [108]
- Hirsch, J. and Hylton, R. (1982). Limits of spatial-frequency discrimination as evidence of neural interpolation. *Journal of the Optical Society of America*, 72, 1367–74. [98]
- Hirsch, M. J. (1947). The stereoscope as a means of measuring distance discrimination. *American Journal of Optometry*, 24, 442–6. [155]
- Hirsch, M. J. and Weymouth, F. W. (1948a). Distance discrimination. I. Theoretical consideration. *AMA Archives of Ophthalmology*, 39, 210–23. [160, 177]
- Hirsch, M. J. and Weymouth, F. W. (1948b). Distance discrimination. II. Effect on threshold of lateral separation of the test objects. *AMA Archives of Ophthalmology*, 39, 224–31. [160, 177]
- Hitchcock, P. F. and Hickey, T. L. (1980). Ocular dominance columns: Evidence for their presence in humans. *Brain Research*, 82, 176–9. [122]
- Ho, W. A. and Berkley, M. A. (1991). Interactions between channels as revealed by ambiguous motion stimuli. *Investigative Ophthalmology and Visual Science*, 32 (Abstracts), 829. [526]
- Ho, W. A. and Howard, I. P. (1994). Depth perception from contrast-gradient disparity. Presented at the *Conference on Stereopsis*, Tübingen. [310]
- Hoffman, C. S. (1962). Comparison of monocular and binocular color matching. *Journal of the Optical Society of America*, 52, 75–80. [326]
- Hoffmann, K. P. (1982). Cortical versus subcortical contributions to the optokinetic reflex in the cat. In *Functional basis of ocular motility disorders*, (ed. G. Lennerstrand, D. S. Zee, and E. L. Keller), pp. 303–11. Pergamon Press, New York. [531]
- Hoffmann, K. P. and Distler, C. (1986). The role of direction selective cells of the nucleus of the optic tract of cat and monkey during optokinetic nystagmus. In *Adaptive processes in vision and oculomotor systems*, (ed. E. L. Keller and D. S. Zee), pp. 261–7. Pergamon, New York. [530]
- Hoffmann, K. P. and Sherman, S. M. (1974). Effects of early monocular deprivation on visual input to cat superior colliculus. *Journal of Neurophysiology*, 37, 1276–86. [628]
- Hoffmann, K. P. and Stone, J. (1985). Retinal input to the nucleus of the optic tract of the cat assessed by antidromic activation of ganglion cells. *Experimental Brain Research*, 59, 395–403. [530]
- Hofmann, F. B. and Bielschowsky, A. (1900). Über die der Willkür entzogenen Fusionsbewegungen der Augen. *Pflügers Archiv für die gesamte Physiologie*, 80, 1–40. [389, 418]
- Hofstetter, H. W. (1945). The zone of clear single binocular vision. *American Journal of Optometry and Archives of American Academy of Optometry*, 22, 301–33 and 361–84. [398]
- Hohmann, A. and Creutzfeldt, O. D. (1975). Squint and the development of binocularity in humans. *Nature*, 254, 613–14. [640]
- Holland, H. C. (1965). *The spiral after-effect*. Pergamon, Oxford. [375]
- Holliday, I. E. and Braddick, O. J. (1991). Pre-attentive detection of a target defined by stereoscopic slant. *Perception*, 20, 355–62. [210]
- Hollins, M. (1980). The effect of contrast on the completeness of binocular rivalry suppression. *Perception and Psychophysics*, 27, 550–6. [330]
- Hollins, M. and Bailey, G. W. (1981). Rivalry target luminance does not affect suppression depth. *Perception and Psychophysics*, 30, 201–3. [329]
- Hollins, M. and Leung, E. H. L. (1978). The influence of color on binocular rivalry. In *Visual psychophysics and physiology*, (ed. J. C. Armington, J. Krausfopf, and B. R. Wooten), pp. 181–90. Academic Press, New York. [329]
- Holopigian, K. and Blake, R. (1983). Spatial vision in strabismic cats. *Journal of Neurophysiology*, 50, 287–96. [628]
- Holopigian, K., Blake, R., and Greenwald, M. (1986). Selective losses in binocular vision in anisometropic amblyopes. *Vision Research*, 26, 621–30. [634]
- Holopigian, K., Blake, R., and Greenwald, M. J. (1988). Clinical suppression and amblyopia. *Investigative Ophthalmology and Visual Science*, 29, 444–51. [635]

- Homes, G. and Horrax, G. (1919). Disturbances of spatial orientation and visual attention, with loss of stereoscopic vision. *Archives of Neurology and Psychiatry*, 1, 385–407. [624]
- Honda, H. and Findlay, J. M. (1992). Saccades to targets in three-dimensional space: Dependence of saccadic latency on target location. *Perception and Psychophysics*, 52, 167–74. [413]
- Hong, X. and Regan, D. (1989). Visual field defects for unidirectional and oscillatory motion in depth. *Vision Research*, 29, 809–19. [563]
- Hooten, K., Myers, E., Worall, R., and Stark, L. (1979). Cyclovergence: The motor response to cyclodisparity. *Albrecht v. Graefes Archiv für Ophthalmologie*, 210, 65–8. [419]
- Hopfield, J. J. (1982). Neural networks and physical systems with emergent collective computational abilities. *Proceedings of the National Academy of Sciences*, 79, 2554–8. [213]
- Horowitz, M. W. (1949). An analysis of the superiority of binocular over monocular visual acuity. *Journal of Experimental Psychology*, 39, 581–96. [350]
- Horridge, G. A. (1978). The separation of visual axes in apposition compound eyes. *Philosophical Transactions of the Royal Society*, B258, 1–59. [646]
- Horton, J. C. (1984). Cytochrome oxidase patches: A new cytoarchitectonic feature of monkey visual cortex. *Philosophical Transactions of the Royal Society*, B304, 199–253. [124, 612]
- Horton, J. C. and Hubel, D. H. (1981). Regular patchy distribution of cytochrome oxidase staining in primary visual cortex of the macaque monkey. *Nature*, 292, 762–4. [123]
- Hotta, T. and Kamena, K. (1963). Interactions between somatic and visual or auditory responses in the thalamus of the cat. *Experimental Neurology*, 8, 1–13. [113]
- Houck, J. (1967). A viscoelastic interaction which produces one component of adaptation in responses of Golgi tendon organs. *Journal of Neurophysiology*, 30, 1482–93. [432]
- Hovis, J. K. (1989). Review of dichoptic color mixing. *Optometry and Vision Science*, 66, 181–90. [327]
- Hovis, J. K. and Guth, S. L. (1989). Dichoptic opponent hue cancellations. *Optometry and Vision Science*, 66, 304–19. [326]
- Howard, H. J. (1919). A test for the judgment of distance. *American Journal of Psychology*, 2, 656–75. [151, 155]
- Howard, I. P. (1959). Some new subjective phenomena apparently due to interocular transfer. *Nature*, 184, 1516–17. [330]
- Howard, I. P. (1960). Attneave's interocular color-effect. *American Journal of Psychology*, 73, 151–2. [379]
- Howard, I. P. (1961). An investigation of a satiation process in the reversible perspective of a revolving skeletal cube. *Quarterly Journal of Experimental Psychology*, 13, 19–33. [488, 565]
- Howard, I. P. (1970). Vergence, eye signature, and stereopsis. *Psychonomic Monograph Supplements*, 3, 201–4. [283, 601]
- Howard, I. P. (1982). *Human visual orientation*. Wiley, Chichester. [11, 101, 167, 373, 431, 435, 534, 588, 616]
- Howard, I. P. (1986). The vestibular system. In *Handbook of Perception and Performance*, (ed. K. R. Boff, L. Kaufman and J. P. Thomas), Chap. 11. Wiley, New York. [381]
- Howard, I. P. (1993a). The optokinetic system. In *The vestibulo-ocular reflex, nystagmus and vertigo*, (ed. J. A. Sharpe and H. O. Barber), pp. 163–84. Raven Press, New York. [381, 529, 643]
- Howard, I. P. (1993b). The resolution of conflict between disparity and overlap cues to depth. *NATO Advanced Research Workshop*, Toronto, June. [453–5]
- Howard, I. P. (1994). Depth from binocular rivalry without spatial disparity. *Perception*, in press. [307]
- Howard, I. P. and Anstis, T. (1974). Muscular and joint-receptor components in postural persistence. *Journal of Experimental Psychology*, 103, 167–70. [432]
- Howard, I. P. and Evans, J. (1963). The measurement of eye torsion. *Vision Research*, 3, 447–55. [419]
- Howard, I. P. and Gonzalez, E. G. (1987). Optokinetic nystagmus in response to moving binocularly disparate stimuli. *Vision Research*, 27, 1807–17. [531]
- Howard, I. P. and Heckmann, T. (1989). Circularvection as a function of the relative sizes, distances and positions of two competing visual displays. *Perception*, 18, 657–67. [534]
- Howard, I. P. and Kaneko, H. (1994). Relative shear disparities and the perception of surface inclination. *Vision Research*, 34, 2505–17. [277]
- Howard, I. P. and Marton, C. (1992). Visual pursuit over textured backgrounds in different depth planes. *Experimental Brain Research*, 90, 625–9. [532]
- Howard, I. P. and Ohmi, M. (1984). The efficiency of the central and peripheral retina in driving human optokinetic nystagmus. *Vision Research*, 24, 969–76. [423, 531]
- Howard, I. P. and Ohmi, M. (1992). A new interpretation of the role of dichoptic occlusion in stereopsis. *Investigative Ophthalmology and Visual Science*, 33 (ARVO Abstracts), 1370. [521]
- Howard, I. P. and Simpson, W. S. (1989). Human optokinetic nystagmus is linked to the stereoscopic system. *Experimental Brain Research*, 78, 309–14. [531]
- Howard, I. P. and Templeton, W. B. (1964). The effect of steady fixation on the judgment of relative depth. *Quarterly Journal of Experimental Psychology*, 16, 193–203. [485, 494]
- Howard, I. P. and Templeton, W. B. (1966). *Human spatial orientation*. Wiley, London. [597]
- Howard, I. P. and Zacher, J. E. (1991). Human cyclovergence as a function of stimulus frequency and amplitude. *Experimental Brain Research*, 85, 445–50. [419]
- Howard, I. P., Sun, L., and Shen, X. (1994). Cycloversion and cyclovergence: The effects of the area and position of the visual display. *Experimental Brain Research*, in press. [423]
- Howard, I. P., Bergström, S. S., and Ohmi, M. (1990). Shape from shading in different frames of reference. *Perception*, 19, 523–30. [96]
- Howard, I. P., Giaschi, D., and Murasugi, C. M. (1989). Suppression of OKN and VOR by afterimages and imaginary objects. *Experimental Brain Research*, 75, 139–45. [533]
- Howard, I. P., Ohmi, M., and Sun, L. (1993). Cyclovergence: A comparison of objective and psychophysical measurements. *Experimental Brain Research*, 97, 349–55. [418, 466]
- Howell, E. R., Mitchell, D. E., and Keith, C. G. (1983). Contrast thresholds for sign gratings of children with amblyopia. *Investigative Ophthalmology and Visual Science*, 24, 782–7. [632]
- Howland, H. C. (1991). Determination of ocular refraction. In *Vision and visual dysfunction*. Vol. 1, *Visual optics and instrumentation*, (ed. W. N. Charman), pp. 399–414. Macmillan, London. [394]
- Howland, H. C. and Howland, B. (1974). Phoptorefraction: A technique for the study of refractive state at a distance. *Journal of the Optical Society of America*, 64, 240–9. [604]
- Howland, H. C. and Sayles, N. (1984). Photorefractive measurements of astigmatism in infants and young children. *Investigative Ophthalmology and Visual Science*, 25, 93–102. [605]
- Hoyle, F. (1957). *The black cloud*. pp. 26–7. Penguin Books, London. [554]
- Hubel, D. H. and Livingstone, M. S. (1987). Segregation of form, color and stereopsis in primate area 18. *Journal of Neuroscience*, 7, 3378–415. [126, 135]
- Hubel, D. H. and Wiesel, T. N. (1959). Receptive fields of single neurones in the cat's visual cortex. *Journal of Physiology*, 148, 574–91. [22, 120, 133]

- Hubel, D. H. and Wiesel, T. N. (1962). Receptive fields, binocular interaction and functional architecture in the cat's visual cortex. *Journal of Physiology*, **160**, 106–54. [22, 120, 122, 133, 140]
- Hubel, D. H. and Wiesel, T. N. (1963). Receptive fields of cells in striate cortex of very young, visually inexperienced kittens. *Journal of Neurophysiology*, **26**, 994–1002. [613]
- Hubel, D. H. and Wiesel, T. N. (1965). Binocular interaction in striate cortex of kittens reared with artificial squint. *Journal of Neurophysiology*, **28**, 1041–59. [627, 630]
- Hubel, D. H. and Wiesel, T. N. (1967). Cortical and callosal connections concerned with the vertical meridian in the cat. *Journal of Neurophysiology*, **30**, 1561–73. [130]
- Hubel, D. H. and Wiesel, T. N. (1968). Receptive fields and functional architecture of monkey striate cortex. *Journal of Physiology*, **195**, 215–43. [120]
- Hubel, D. H. and Wiesel, T. N. (1969). Anatomical demonstration of columns in the monkey striate cortex. *Nature*, **221**, 747–50. [121]
- Hubel, D. H. and Wiesel, T. N. (1970a). Stereoscopic vision in macaque monkey. *Nature*, **225**, 41–2. [133–4]
- Hubel, D. H. and Wiesel, T. N. (1970b). The period of susceptibility to the physiological effects of unilateral eye closure in kittens. *Journal of Physiology*, **206**, 419–36. [635]
- Hubel, D. H. and Wiesel, T. N. (1971). Aberrant visual projections in the Siamese cat. *Journal of Physiology*, **218**, 33–62. [642]
- Hubel, D. H. and Wiesel, T. N. (1974). Uniformity of monkey striate cortex: A parallel relationship between field size, scatter, and magnification factor. *Journal of Comparative Neurology*, **158**, 295–306. [123]
- Hubel, D. H. and Wiesel, T. N. (1977). Functional architecture of macaque monkey visual cortex. *Proceedings of the Royal Society, London*, **B198**, 1–59. [115, 117, 122]
- Hughes, A. (1971). Topographical relationships between the anatomy and physiology of the rabbit visual system. *Documenta Ophthalmologica*, **30**, 33–159. [656]
- Hughes, A. (1972). Vergence in the cat. *Vision Research*, **12**, 1961–94. [382]
- Hughes, A. (1977). The topography of vision in mammals of contrasting life style: Comparative optics and retinal organization. In *Handbook of sensory physiology*. Vol. VII/5. *The visual system in vertebrates*. (ed. F. Crescitelli), pp. 615–756. Springer, New York. [32, 646, 657]
- Hughes, A. and Vaney, D. I. (1982). The organization of binocular cortex in the primary visual area of the rabbit. *Journal of Comparative Neurology*, **294**, 151–64. [656]
- Hughes, J. R. (1958). Post-tetanic potentiation. *Physiological Review*, **38**, 91–113. [432]
- Hung, G. K., Semmlow, J. L., and Ciuffreda, K. J. (1983). Identification of accommodative vergence contribution to the near response using response variance. *Investigative Ophthalmology and Visual Science*, **24**, 772–7. [396]
- Hung, G. K., Semmlow, J. L., and Ciuffreda, K. J. (1986). A dual-mode dynamic model of the vergence eye movement system. *IEEE Transactions on Biomedical Engineering*, **BME-33**, 1021–36. [406, 408]
- Hung, G. K., Semmlow, J. L., Sun, L., and Ciuffreda, K. J. (1991). Vergence control of central and peripheral disparities. *Experimental Neurology*, **113**, 202–11. [401]
- Hung, G. K., Sun, L., Semmlow, J. L., and Ciuffreda, K. J. (1990). Suppression of sensitivity to change in target disparity during vergence eye movements. *Experimental Neurology*, **110**, 291–7. [386]
- Hung, G. K., Wang, T., Semmlow, J. L., and Ciuffreda, K. J. (1989). Suppression of sensitivity to surround displacement during vergence eye movements. *Experimental Neurology*, **105**, 300–5. [386]
- Hung, G. K., Ciuffreda, K. J., Semmlow, J. L., and Horng, J. L. (1994). Vergence eye movements under natural viewing conditions. *Investigative Ophthalmology and Visual Science*, **35**, 3486–92. [404]
- Hurvich, L. M. and Jameson, D. (1951). The binocular fusion of yellow in relation to color theories. *Science*, **114**, 199–202. [326]
- Huttenlocher, P. R. and de Courten, C. (1987). The development of synapses in striate cortex of man. *Human Neurobiology*, **6**, 1–9. [610]
- Hutton, R. S., Smith, J. L., and Eldred, E. (1973). Postcontraction sensory discharge from muscle and its source. *Journal of Neurophysiology*, **36**, 1090–103. [432]
- Hyson, M. T., Julesz, B., and Fender, D. H. (1983). Eye movements and neural remapping during fusion of misaligned random-dot stereograms. *Journal of the Optical Society of America*, **73**, 1665–73. [324]
- Ichikawa, M. and Egusa, H. (1993). How is depth perception affected by long-term wearing of left-right reversing spectacles. *Perception*, **22**, 971–84. [488]
- Ikeda, H. and Jacobson, S. G. (1977). Nasal field loss in cats reared with convergent squint: Behavioural studies. *Journal of Physiology*, **270**, 367–81. [633]
- Ikeda, M. (1965). Temporal summation of positive and negative flashes in the visual system. *Journal of the Optical Society of America*, **55**, 1527–34. [362]
- Ikeda, M. and Nakashima, Y. (1980). Wavelength difference limit for binocular color fusion. *Vision Research*, **20**, 693–7. [327]
- Ikeda, M. and Sagawa, K. (1979). Binocular color fusion limit. *Journal of the Optical Society of America*, **69**, 316–20. [326]
- Imamura, K. and Kasamatsu, T. (1988). Acutely induced shift in ocular dominance during brief monocular exposure: Effects of cortical noradrenaline infusion. *Neuroscience Letters*, **88**, 57–62. [630]
- Imbert, M. and Buisseret, P. (1975). Receptive field characteristics and phasic properties of visual cortical cells in kittens reared with or without visual experience. *Experimental Brain Research*, **22**, 25–36. [625]
- Indow, T. and Watanabe, T. (1984). Parallel-alleys and distance-alleys on horopter plane in the dark. *Perception*, **13**, 165–82. [53]
- Ingle, D. (1972). Depth vision in monocular frogs. *Psychonomic Science*, **29**, 37–38. [652]
- Ingle, D. (1976). Spatial vision in anurans. In *The amphibian visual system – a multidisciplinary approach*, (ed. K. Fite). Academic Press, New York. [652]
- Ingle, D. and Cook, J. (1977). The effect of viewing distance upon size preference of frogs for prey. *Vision Research*, **17**, 1009–13. [651]
- Ingling, C. R. (1991). Psychophysical correlates of parvo channel function. In *From pigments to perception*, (ed. A. Valberg and B. B. Lee), pp. 413–24. Plenum Press, New York. [143]
- Ingling, C. R. and Grigsby, S. S. (1990). Perceptual correlates of magnocellular and parvocellular channels: Seeing form and depth in afterimages. *Vision Research*, **30**, 823–8. [144]
- Ingling, C. R. and Martinez-Uriegas, E. (1985). The spatiotemporal properties of the r-g X-cell channel. *Vision Research*, **25**, 33–8. [143]
- Ioannou, G. L., Rogers, B. J., Bradshaw, M. F., and Glennerster, A. (1993). Threshold and supra-threshold sensitivity functions for stereoscopic surfaces. *Investigative Ophthalmology and Visual Science*, **34** (ARVO Abstracts), 1186. [165]
- Ireland, F. H. (1950). A comparison of critical flicker frequencies under conditions of monocular and binocular stimulation. *Journal of Experimental Psychology*, **40**, 282–6. [359]

- Ishigushi, A. and Wolfe, J. M. (1993). Asymmetrical effect of crossed and uncrossed disparity on stereoscopic capture. *Perception*, 22, 1403-13. [502]
- Ito, M., Sanides, D., and Creutzfeldt, O. D. (1977). A study of binocular convergence in cat visual cortex neurons. *Experimental Brain Research*, 28, 21-35. [120]
- Ittleson, W. H. (1960). *Visual space perception*. Springer, New York, pp. 123-27. [431]
- Ittleson, W. H. and Ames, A. (1950). Accommodation, convergence and their relation to apparent distance. *Journal of Psychology*, 30, 43-62. [399]
- Ivashina, A. I. (1981). Aniseikonia for near vision with unilateral aphakia corrected by intraocular lenses. *Annals of Ophthalmology*, 13, 1309-11. [64]
- Ivins, W. M. (1973). *On the rationalization of sight*. Da Capo Press, New York. [9]
- Jacobs, D. S. and Blakemore, C. (1988). Factors limiting the postnatal development of visual acuity in the monkey. *Vision Research*, 28, 947-58. [615]
- Jacobson, M. and Hirsch, H. V. B. (1973). Development and maintenance of connectivity in the visual system of the frog. I. The effects of eye rotation and visual deprivation. *Brain Research*, 49, 47-65. [652]
- Jacobson, S. G., Mohindra, I., and Held, R. (1982). Visual acuity in infants with ocular diseases. *American Journal of Ophthalmology*, 93, 198-209. [616]
- Jaensch, E. R. (1911). Über die Wahrnehmung des Raumes. Eine experimentell-psychologische Untersuchung nebst Anwendung auf Ästhetik und Erkenntnislehre. *Zeitschrift für Psychologie und Physiologie der Sinnesorgane*, 6 (Supplement), 1-448. [522]
- Jagadeesh, B., Gray, C. M., and Ferster, D. (1992). Visually evoked oscillations of membrane potential in cells of visual cortex. *Science*, 257, 552-4. [82]
- Jagadeesh, B., Wheat, H. S., and Ferster, D. (1993). Linearity of summation of synaptic potentials underlying selectivity in simple cells of the cat visual cortex. *Science*, 262, 1901-4. [120]
- Jampel, R. S. (1967). Multiple motor systems in the extraocular muscles of man. *Investigative Ophthalmology*, 6, 288-93. [424]
- Jampolsky, A., Flom, B. C., and Freid, A. N. (1957). Fixation disparity in relation to heterophoria. *American Journal of Ophthalmology*, 43, 97-106. [390]
- Jaschinski-Kruza, W. (1994). Dark vergence in relation to fixation disparity at different luminance and blur levels. *Vision Research*, 34, 1197-204. [390]
- Javal, E. (1865). De la neutralisation dans l'acte de la vision. *Annals Oculist*, Paris, 54, 5-16. [427]
- Jay, B., Witkop, C. J., and King, R. A. (1982). Albinism in England. *Birth Defects*, 18, 319-25. [642]
- Jeffery, G. (1989). Shifting retinal maps in the development of the lateral geniculate nucleus. *Developmental Brain Research*, 46, 187-96. [609]
- Jeffery, G. (1990). The topographic relationship between shifting binocular maps in the developing dorsal lateral geniculate nucleus. *Experimental Brain Research*, 82, 408-16. [608-9, 642]
- Jeffery, G. and Perry, V. H. (1982). Evidence for ganglion cell death during development of the ipsilateral retinal projection in the rat. *Developmental Brain Research*, 2, 176-80. [607]
- Jennings, J. A. M. and Charman, W. N. (1981). Off-axis image quality in the human eye. *Vision Research*, 21, 445-55. [107]
- Jiao, S. L., Han, C., Jing, Q. C., and Over, R. (1984). Monocular-contingent and binocular-contingent aftereffects. *Perception and Psychophysics*, 35, 105-10. [376]
- Johannsen, D. E. (1930). A quantitative study of binocular color vision. *Journal of General Psychology*, 4, 282-308. [326-7]
- Johansson, G. (1964). Perception of motion and changing form. *Scandinavian Journal of Psychology*, 5, 181-208. [555]
- Johansson, G. (1973). Visual perception of biological motion and a model for its analysis. *Perception and Psychophysics*, 14, 201-11. [441]
- Johansson, G. (1977). Studies on visual perception of locomotion. *Perception*, 6, 365-76. [574]
- Johnston, E. B. (1991). Systematic distortions of shape from stereopsis. *Vision Research*, 31, 1351-60. [297, 299, 446, 459]
- Johnston, E. B., Cumming, B. G., and Parker, A. J. (1993). Integration of depth modules: Stereopsis and texture. *Vision Research*, 33, 813-26. [449]
- Johnston, E. B., Cumming, B. G., and Landy, M. S. (1994). Integration of stereopsis and motion shape cues. *Vision Research*, 34, 2259-75. [446-7]
- Jolicoeur, P. and Cavanagh, P. (1992). Mental rotation, physical rotation, and surface media. *Journal of Experimental Psychology: Human Perception and Performance*, 18, 371-84. [588]
- Jones, K. R., Kalil, R. E., and Spear, P. D. (1984a). Effects of strabismus on responsivity, spatial resolution, and contrast sensitivity of cat lateral geniculate neurons. *Journal of Neurophysiology*, 52, 538-52. [627]
- Jones, K. R., Spear, P. D., and Tong, L. (1984b). Critical periods for effects of monocular deprivation: Differences between striate and extrastriate cortex. *Journal of Neuroscience*, 4, 2543-52. [635]
- Jones, P. F. and Aitken, G. J. M. (1994). Comparison of three-dimensional imaging systems. *Journal of the Optical Society of America*, 11, 2613-21. [26]
- Jones, R. (1977). Anomalies of disparity detection in the human visual system. *Journal of Physiology*, 264, 621-40. [404]
- Jones, R. (1980). Fusional vergence: Sustained and transient components. *American Journal of Optometry and Physiological Optics*, 57, 640-4. [404-6]
- Jones, R. and Kerr, K. E. (1972). Vergence eye movements to pairs of disparity stimuli with shape selection cues. *Vision Research*, 12, 1425-30. [405]
- Jones, R. and Stevens, G. L. (1989). Horizontal fusional amplitudes. *Investigative Ophthalmology and Visual Science*, 30, 1638-42. [400, 402]
- Jones, R. K. and Lee, D. N. (1981). Why two eyes are better than one: The two views of binocular vision. *Journal of Experimental Psychology: Human Perception and Performance*, 7, 30-40. [2]
- Jones, R. M. and Tulunay-Keesey, U. (1980). Phase selectivity of spatial frequency channels. *Journal of the Optical Society of America*, 70, 66-70. [496]
- Jordan, J. R., Geisler, W. S., and Bovik, A. C. (1990). Color as a source of information in the stereo correspondence process. *Vision Research*, 30, 1955-70. [207]
- Joshua, D. E. and Bishop, P. O. (1970). Binocular single vision and depth discrimination. Receptive field disparities for central and peripheral vision and binocular interaction on peripheral single units in cat striate cortex. *Experimental Brain Research*, 10, 389-416. [134]
- Judge, S. J. (1985). Can current models of accommodation and vergence control account for the discrepancies between AC/A measurements made by the fixation disparity and phoria methods. *Vision Research*, 25, 1999-2001. [396]
- Judge, S. J. (1987). Optically-induced changes in tonic vergence and AC/A ratio in normal monkeys and monkeys with lesions of the flocculus and ventral paraflocculus. *Experimental Brain Research*, 66, 1-9. [396]
- Judge, S. J. (1991). Vergence. In *Vision and visual dysfunction*. Vol. 8, *Eye movements*, (ed. R. H. S. Carpenter), pp. 157-72. Macmillan, London. [386]

- Judge, S. J. and Cumming, B. G. (1986). Neurons in monkey midbrain with activity related to vergence eye movement and accommodation. *Journal of Neurophysiology*, 55, 915–30. [425]
- Judge, S. J. and Miles, F. A. (1985). Changes in the coupling between accommodation and vergence eye movements induced in human subjects by altering the effective interocular distance. *Perception*, 14, 617–29. [396]
- Julesz, B. (1960). Binocular depth perception of computer generated patterns. *Bell System Technical Journal*, 39, 1125–62. [64, 151, 192, 195, 228, 504]
- Julesz, B. (1963). Stereopsis and binocular rivalry of contours. *Journal of the Optical Society of America*, 53, 994–9. [156, 178]
- Julesz, B. (1964). Binocular depth perception without familiarity cues. *Science*, 145, 356–62. [185, 463, 514]
- Julesz, B. (1971). *Foundations of cyclopean perception*. University of Chicago Press, Chicago. [1, 192–3, 22, 5, 303, 474, 561, 584, 590]
- Julesz, B. and Bergen, J. R. (1983). Textons, the fundamental elements on preattentive vision and perception of texture. *Bell Systems Technical Journal*, 62, 1619–45. [210]
- Julesz, B. and Chang, J.-J. (1976). Interaction between pools of binocular disparity detectors tuned to different disparities. *Biological Cybernetics*, 22, 107–19. [228]
- Julesz, B. and Johnson, S. C. (1968). Stereograms portraying ambiguous perceivable surfaces. *Proceedings of the National Society*, 61, 437–41. [230]
- Julesz, B. and Miller, J. E. (1975). Independent spatial frequency tuned channels in binocular fusion and rivalry. *Perception*, 4, 125–43. [176, 339, 353]
- Julesz, B. and Oswald, H. P. (1978). Binocular utilization of monocular cues that are undetectable monocularly. *Perception*, 7, 315–22. [193]
- Julesz, B. and Payne, R. A. (1968). Differences between monocular and binocular stroboscopic movement perception. *Vision Research*, 8, 433–44. [538, 589]
- Julesz, B. and Tyler, C. W. (1976). Neuronropy, an entropy-like measure of neural correlation in binocular fusion and rivalry. *Biological Cybernetics*, 22, 107–19. [147]
- Julesz, B. and White, B. (1969). Short term visual memory and the Pulfrich phenomenon. *Nature*, 222, 639–41. [538, 540, 551]
- Julesz, B., Breitmeyer, B., and Kropfl, W. (1976a). Binocular-disparity-dependent upper-lower hemifield anisotropy and left-right hemifield isotropy as revealed by dynamic random-dot stereograms. *Perception*, 5, 129–41. [625]
- Julesz, B., Kropfl, W., and Petrig, B. (1980). Large evoked potentials to dynamic random-dot correlograms permit quick determination of stereopsis. *Proceedings of the National Academy of Science*, 77, 2348–51. [147]
- Julesz, B., Petrig, B., and Buttner, U. (1976b). Fast determination of stereopsis in rhesus monkey using dynamic random dot stereograms. *Journal of the Optical Society of America*, 66, 1090. [645]
- Kaas, J. H. and Guillory, R. W. (1973). The transfer of abnormal visual field representations from the dorsal lateral geniculate nucleus to the visual cortex in Siamese cats. *Brain Research*, 59, 61–95. [642]
- Kaas, J. H., Guillory, R. W., and Allman, J. M. (1972). Some principles of organization in the dorsal lateral geniculate nucleus. *Brain, Behaviour and Evolution*, 6, 253–99. [112]
- Kahn, R. H. (1931). Über den Stereoeffekt von Pulfrich. *Pflügers Archiv für die gesamte Physiologie*, 227, 213–24. [536, 549]
- Kahneman, D. (1968). Methods, findings, and theory in studies of visual masking. *Psychological Bulletin*, 70, 693–7. [370]
- Kaiser, P. (1971). Minimally distinct border as a preferred psychophysical criterion in visual heterochromatic photometry. *Journal of the Optical Society of America*, 61, 966–71. [206]
- Kalil, R. E. (1990). The influence of action potentials on the development of the central visual pathway in mammals. *Journal of Experimental Biology*, 153, 261–76. [609]
- Kanizsa, G. (1979). *Organization in vision: Essays on Gestalt perception*. Praeger, New York. [77, 508]
- Kapardia, M. K., Gilbert, C. D., and Westheimer, G. (1994). A quantitative measure for short-term cortical plasticity in human vision. *Journal of Neuroscience*, 14, 451–7. [129]
- Kaplan, E. and Shapley, R. M. (1986). The primate retina contains two types of ganglion cells, with high and low contrast sensitivity. *Proceedings of the National Academy of Science*, 83, 2755–7. [112]
- Kaplan, I. T. and Metlay, W. (1964). Light intensity and binocular rivalry. *Journal of Experimental Psychology*, 67, 22–6. [330]
- Kapoula, Z., Hain, T. C., Zee, D. S., and Robinson, D. A. (1987). Adaptive changes in post-saccadic drift induced by patching one eye. *Vision Research*, 27, 1299–307. [411]
- Karten, H. J., Hodos, W., Nauta, W. J. H., and Revzin, A. M. (1973). Neural connections of the “visual Wulst” of the avian telencephalon. Experimental studies in the pigeon (*Columba livia*) and owl (*Speotyto cunicularia*). *Journal of Comparative Neurology*, 150, 253–77. [654]
- Kasamatsu, T. and Pettigrew, J. D. (1979). Preservation of binocularity after monocular deprivation in the striate cortex of kittens treated with 6-hydroxydopamine. *Journal of Comparative Neurology*, 185, 139–61. [629]
- Kasamatsu, T., Pettigrew, J. D., and Ary, M. (1979). Restoration of visual cortical plasticity by local microperfusion of norepinephrine. *Journal of Comparative Neurology*, 185, 163–82. [630]
- Kasamatsu, T., Watabe, K., Heggelund, P., and Schöller, E. (1985). Plasticity in cat visual cortex restored by electrical stimulation of the locus coeruleus. *Neuroscience Research*, 2, 365–86. [630]
- Kato, H., Bishop, P. O., and Orban, G. A. (1981). Binocular interaction on monocularly discharged lateral geniculate and striate neurons in the cat. *Journal of Neurophysiology*, 46, 932–51. [113, 123]
- Katsumi, O., Tsuyoshi, T., and Hirose, T. (1986). Effect of aniseikonia on binocular function. *Investigative Ophthalmology and Visual Science*, 27, 601–4. [148]
- Katz, L. C. and Callaway, E. M. (1991). Emergence and refinement of local circuits in cat striate cortex. In *Development of the visual system*, (ed. D. M-K. Lam and C. J. and Shatz), pp. 197–215. MIT Press, Cambridge, MA. [613]
- Katz, L. C. and Callaway, E. M. (1992). Development of local circuits in mammalian visual cortex. *Annual Review of Neuroscience*, 15, 31–56. [613]
- Katz, L. C., Gilbert, C. D., and Wiesel, T. N. (1989). Local circuits and ocular dominance columns in monkey striate cortex. *Journal of Neuroscience*, 9, 1389–99. [116]
- Katz, M. S. and Schwartz, I. (1955). New observation of the Pulfrich effect. *Journal of the Optical Society of America*, 45, 523–24. [537]
- Kaufman, L. (1963). On the spread of suppression and binocular rivalry. *Vision Research*, 3, 401–15. [332, 335]
- Kaufman, L. (1964). Suppression and fusion in viewing complex stereograms. *American Journal of Psychology*, 77, 193–205. [338, 339]
- Kaufman, L. (1965). Some new stereoscopic phenomena and their implications for theories of stereopsis. *American Journal of Psychology*, 78, 1–20. [515]
- Kaufman, L. (1974). *Sight and mind. An introduction to visual perception*. Oxford University Press, London. [200]
- Kaufman, L. (1976). On stereopsis with double images. *Psychologia*, 19, 224–33. [519]

- Kaufman, L. and Pitblado, C. (1965). Further observations on the nature of effective binocular disparities. *American Journal of Psychology*, 78, 379–91. [225]
- Kaufman, L. and Pitblado, C. B. (1969). Stereopsis with opposite contrast conditions. *Perception and Psychophysics*, 6, 10–12. [225]
- Kaufman, L., Bacon, J., and Barroso, F. (1973). Stereopsis without image segregation. *Vision Research*, 13, 137–47. [230]
- Kavadellias, A. and Held, R. (1977). Monocularity of color-contingent tilt aftereffects. *Perception and Psychophysics*, 21, 12–14. [379]
- Kawano, K., Sasaki, M., and Yamashita, M. (1984). Response properties of neurons in posterior parietal cortex of monkey during visual–vestibular stimulation. I. Visual tracking neurons. *Journal of Neurophysiology*, 51, 340–51. [530]
- Kawano, K., Inoue, Y., Takemura, A., and Miles, F. A. (1994). Effect of disparity in the peripheral field on short-latency ocular following responses. *Visual Neuroscience*, 11, 833–7. [532]
- Kaye, M., Mitchell, D. E., and Cynader, M. (1982). Depth perception, eye alignment and cortical ocular dominance of dark-reared cats. *Developmental Brain Research*, 2, 37–53. [628]
- Keating, M. J. and Feldman, J. D. (1975). Visual deprivation and intertectal neuronal connexions in *Xenopus laevis*. *Proceedings of the Royal Society, London*, B191, 467–74. [652]
- Keating, M. J. and Gaze, R. M. (1970). The ipsilateral retinotectal pathway in the frog. *Quarterly Journal of Experimental Physiology*, 55, 284–92. [651]
- Keating, M. J. and Kennard, C. (1976). Binocular visual neurones in the frog thalamus. *Proceedings of the Physiological Society*, 258, 69P. [651]
- Keating, M. J., Dawes, E. A., and Grant, S. (1992). Plasticity of binocular visual connections in the frog, *Xenopus Laevis*: Reversibility of effects of early visual deprivation. *Experimental Brain Research*, 90, 121–8. [652]
- Keck, M. J. and Price, R. L. (1982). Interocular transfer of the motion aftereffect in strabismus. *Vision Research*, 22, 55–60. [640]
- Keele, K. D. (1955). Leonardo da Vinci on vision. *Proceedings of the Royal Society of Medicine*, 48, 384–90. [9–10, 14]
- Keesey, U. T. (1960). Effects of involuntary eye movements on visual acuity. *Journal of the Optical Society of America*, 50, 769–74. [186]
- Keller, E. L. (1973). Accommodative vergence in the alert monkey. *Vision Research*, 13, 1565–75. [425]
- Keller, E. L. and Robinson, D. A. (1972). Abducens unit behaviour in the monkey during vergence eye movements. *Vision Research*, 12, 369–82. [424–5]
- Kennedy, H., Bullier, J., and Dehay, C. (1985). Cytochrome oxidase activity in the striate cortex and lateral geniculate nucleus of the newborn and adult macaque monkey. *Experimental Brain Research*, 61, 204–9. [612]
- Kennedy, H., Dehay, C., and Bullier, J. (1986). Organization of the callosal connections of visual areas V1 and V2 in the macaque monkey. *Journal of Comparative Neurology*, 247, 398–415. [130]
- Kennedy, H., Meissirel, C., and Dehay, C. (1991). Callosal pathways and their compliancy to general rules governing the organization of corticocortical connectivity. In *Neuroanatomy of the visual pathways and their development*, (ed. B. Dreher and S. R. Robinson), pp. 324–59. CRC Press, Boston. [131]
- Kenyon, R. V., Ciuffreda, K. J., and Stark, L. (1980a). Dynamic vergence eye movements in strabismus and amblyopia: Symmetric vergence. *Investigative Ophthalmology and Visual Science*, 19, 60–74. [396]
- Kenyon, R. V., Ciuffreda, K. J., and Stark, L. (1980b). Unequal saccades during vergence. *American Journal of Optometry and Physiological Optics*, 57, 586–94. [412–3]
- Kenyon, R. V., Ciuffreda, K. J., and Stark, L. (1981). Dynamic vergence eye movements in strabismus and amblyopia: Asymmetric vergence. *British Journal of Ophthalmology*, 65, 167–76. [632]
- Kepler, J. (1604). *Ad vitellionem paralipomena*. Marnium and Haer, Frankfurt. [11]
- Kepler, J. (1611). *Dioprice*. Vindelicorum, Augsburg. [11]
- Kersten, D. and Legge, G. E. (1983). Convergence accommodation. *Journal of the Optical Society of America*, 73, 332–8. [397]
- Kertesz, A. E. (1972). The effect of stimulus complexity on human cyclofusional response. *Vision Research*, 12, 699–704. [418–9]
- Kertesz, A. E. (1973). Disparity detection within Panum's fusional areas. *Vision Research*, 13, 1537–43. [321]
- Kertesz, A. E. (1980). Human fusional vergence. *Proceedings of the Eye Movement Conference*. (OMS 80), California Institute of Technology, Pasadena. [597]
- Kertesz, A. E. and Lee, H. J. (1987). Comparison of simultaneously obtained objective and subjective measurements of fixation disparity. *American Journal of Optometry and Physiological Optics*, 64, 734–8. [390]
- Kertesz, A. E. and Sullivan, M. J. (1978). The effect of stimulus size on human cyclofusional response. *Vision Research*, 18, 567–71. [417, 423]
- Kicliter, E. and Northcutt, R. G. (1975). Ascending afferents to telencephalon of ranid frogs: An anterograde degeneration study. *Journal of Comparative Neurology*, 161, 239–54. [651]
- Kienker, P. K., Sejnowski, T. J., Hinton, G. E., and Schumacher, L. E. (1986). Separating figure from ground with a parallel network. *Perception*, 15, 197–216. [213]
- Kim, D. S. and Bonhoeffer, T. (1994). Reverse occlusion leads to a precise restoration of orientation preference maps in visual cortex. *Nature*, 370, 370–2. [636]
- Kimmig, H. G., Miles, F. A., and Schwarz, U. (1992). Effects of stationary textured backgrounds on the initiation of pursuit eye movements in monkeys. *Journal of Neurophysiology*, 68, 2147–64. [532]
- Kimura, D. and Durnford, M. (1974). Normal studies on the function of the right hemisphere in vision. In *Hemisphere function in the human brain*, (ed. S. J. Dimond and J. G. Beaumont), pp. 25–47. Paul Elek Ltd., London. [624]
- Kimura, F., Nishigori, A., Shirokawa, T., and Tsumoto, T. (1989). Long-term potentiation and N-methyl-D-aspartate receptors in the visual cortex of young rats. *Journal of Physiology*, 414, 125–44. [615]
- Kinnear, P. E., Jay, B., and Witcop, C. J. (1985). Albinism. *Survey of Ophthalmology*, 30, 75–101. [642]
- Kiorpes, L. (1992). Effect of strabismus on the development of vernier acuity and grating acuity in monkeys. *Visual Neuroscience*, 9, 253–9. [632]
- Kiorpes, L., Kipper, D. C., and Movshon, J. A. (1993). Contrast sensitivity and vernier acuity in amblyopic monkeys. *Vision Research*, 33, 2301–11. [632]
- Kiper, D. C. (1994). Spatial phase discrimination in monkeys with experimental strabismus. *Vision Research*, 34, 437–47. [631]
- Kirby, M. A. and Steineke, T. C. (1992). Morphogenesis of retinal ganglion cells during formation of the fovea in the Rhesus macaque. *Visual Neuroscience*, 9, 603–16. [605]
- Kirk, D. L., Levick, W. R., Cleland, B. G., and Wässle, H. (1976a). Crossed and uncrossed representation of the visual field by brisk-sustained and brisk-transient cat retinal ganglion cells. *Vision Research*, 16, 225–31. [130]
- Kirk, D. L., Levick, W. R., and Cleland, B. G. (1976b). The crossed or uncrossed destination of axons of sluggish-concentric and non-concentric cat retinal ganglion cells, with an overall synthesis of the visual field representation. *Vision Research*, 16, 233–6. [130]

- Kirkwood, A. and Bear, M. F. (1994a). Homosynaptic long-term depression in the visual cortex. *Journal of Neuroscience*, 14, 3404-12. [615]
- Kirkwood, A. and Bear, M. F. (1994b). Hebbian synapses in visual cortex. *Journal of Neuroscience*, 14, 1634-45. [615]
- Kirkwood, A., Dudek, S. M., Gold, J. T., Aizenman, C. D., and Bear, M. F. (1993). Common forms of synaptic plasticity in the hippocampus and neocortex in vitro. *Science*, 260, 1518-21. [615]
- Kirkwood, B., Ellis, A., and Nicol, B. (1969). Eye movement and the Pulfrich effect. *Perception and Psychophysics*, 5, 206-8. [539, 549]
- Kirschmann, A. (1890). Über die quantitativen Verhältnisse des simultanen Helligkeits- und Farbenkontrastes. *Philosophische Studien*, 6, 417-491. [465]
- Kishto, B. N. (1965). The colour stereoscopic effect. *Vision Research*, 5, 313-30. [307]
- Kitaoji, H. and Toyama, K. (1987). Preservation of position and motion stereopsis in strabismic subjects. *Investigative Ophthalmology and Visual Science*, 28, 1260-67. [634, 637]
- Kitterle, F. L. and Thomas, J. (1980). The effects of spatial frequency, orientation, and color upon binocular rivalry and monocular pattern alternation. *Bulletin Psychonomic Society*, 16, 405-7. [334]
- Klein, R. (1977). Stereopsis and the representation of space. *Perception*, 6, 327-32. [2]
- Klein, R. and Stein, R. (1934). Über einem Tumor des Kleinhirns mit anfallsweise auftretendem Tonverlust und monokulärer Diplopie bzw. binokulärer Triplopie. *Archiv für Psychiatrie und Nervenkrank*, 102, 478-92. [47]
- Klein, S. A. and Levi, D. M. (1985). Hyperacuity thresholds of 1.0 second: Theoretical predictions and empirical validation. *Journal of the Optical Society of America*, A2, 1170-90. [90, 98]
- Klein, S. A. and Levi, D. M. (1986). Local multipoles for measuring contrast and phase sensitivity. *Investigative Ophthalmology and Visual Science*, 27 (ARVO Abstracts), 225. [90]
- Klein, S. A., Casson, E., and Carney, T. (1990). Vernier acuity as line and dipole detection. *Vision Research*, 30, 1703-19. [90]
- Klopfer, D. S. (1991). Apparent reversals of a rotating mask. A new demonstration of cognition in perception. *Perception and Psychophysics*, 49, 522-30. [456]
- Knierim, J. J. and Van Essen, D. C. (1992). Neuronal responses to static texture patterns in area V1 of the alert monkey. *Journal of Neurophysiology*, 67, 961-80. [119]
- Knowles, W. B. and Carel, W. L. (1958). Estimating time-to-collision. *American Psychologist*, 13, 405-6. [554]
- Knudsen, E. I. (1982). Auditory and visual maps of space in the optic tectum of the owl. *Journal of Neuroscience*, 2, 1177-94. [655]
- Knudsen, E. I. (1989). Fused binocular vision is required for development of proper eye alignment in barn owls. *Visual Neuroscience*, 2, 35-40. [656]
- Koch, C. and Ullman, S. (1985). Shifts in selective visual attention: Towards the underlying neural circuitry. *Human Neurobiology*, 4, 219-27. [78]
- Koch, C., Marroquin, J., and Yuille, A. (1986). Analog "neuronal" networks in early vision. *Proceedings of the National Academy of Science*, 83, 4263-7. [71]
- Koenderink, J. J. (1985). Space, form and optical deformations. In *Brain mechanisms and spatial vision*. (ed. D. Ingle, M. Jeannerod, and D. Lee), pp. 31-58. Martinus Nijhoff, The Hague. [575]
- Koenderink, J. J. (1986). Optic flow. *Vision Research*, 26, 161-80. [252, 258, 271, 441, 574-5]
- Koenderink, J. J. (1990). *Solid shape*. MIT Press, Cambridge. [301, 303, 582]
- Koenderink, J. J. and van Doorn, A. J. (1975). Invariant properties of the motion parallax field due to movement of rigid bodies relative to an observer. *Optica Acta*, 22, 773-91. [575]
- Koenderink, J. J. and van Doorn, A. J. (1976a). Geometry of binocular vision and a model for stereopsis. *Biological Cybernetics*, 21, 29-35. [251, 265, 287, 304]
- Koenderink, J. J. and van Doorn, A. J. (1976b). Local structure of movement parallax of the plane. *Journal of the Optical Society of America*, 66, 717-23. [575, 582]
- Koenderink, J. J. and van Doorn, A. J. (1980). Photometric invariants related to solid shape. *Optica Acta*, 27, 981-96. [311]
- Koenderink, J. J. and van Doorn, A. J. (1991). Affine structure from motion. *Journal of the Optical Society of America*, 8A, 377-85. [304]
- Koffka, K. (1935). *Principles of Gestalt psychology*. Harcourt Brace, New York. [77, 476, 505]
- Köhler, W. and Emery, D. A. (1947). Figural aftereffects in the third dimension of visual space. *American Journal of Psychology*, 60, 159-201. [484-6, 490]
- Köhler, W. and Wallach, H. (1944). Figural aftereffects: An investigation of visual processes. *Proceedings of the American Philosophical Society*, 88, 269-357. [100, 466, 484, 490-1]
- Kohn, H. (1960). Some personality variables associated with binocular rivalry. *Psychological Record*, 10, 9-13. [348]
- Koken, P. W. and Erkelens, C. J. (1993). Simultaneous hand tracking does not affect human vergence pursuit. *Experimental Brain Research*, 96, 494-500. [402]
- Kolb, H. (1970). Organization of the outer plexiform layer of the primate retina: Electron microscopy of Golgi-impregnated cells. *Philosophical Transactions of the Royal Society*, B258, 261-83. [110]
- Kolehmainen, K. and Keskinen, E. (1974). Evidence for the latency-time explanation of the Pulfrich phenomenon. *Scandinavian Journal of Psychology*, 15, 320-21. [537]
- Kolers, P. A. and Rosner, B. S. (1960). On visual masking (meta-contrast): Dichoptic observation. *American Journal of Psychology*, 73, 2-21. [370]
- Köllner, H. (1914). Das funktionelle Überwiegen der nasalen Netzhauthälften im gemeinschaftlichen Sehfeld. *Archiv Augenheilkunde*, 76, 153-64. [331]
- Komatsu, H. and Wurtz, R. H. (1988). Relation of cortical areas MT and MST to pursuit eye movements. I. Localization and visual properties of neurons. *Journal of Neurophysiology*, 60, 580-603. [530]
- Komatsu, H., Roy, J. P., and Wurtz, R. H. (1988). Binocular disparity sensitivity of cells in area MST of the monkey. *Society for Neuroscience Abstracts*, 14, 202. [143, 532, 566]
- Kommerell, G., Oliver, D., and Theopold, H. (1976). Adaptive programming of phasic and tonic components in saccadic eye movements. *Investigative Ophthalmology*, 15, 657-60. [414]
- König, P. and Schillen, T. B. (1991). Stimulus-dependent assembly formation of oscillatory responses: I. Synchronization. *Neural Computation*, 3, 155-66. [83]
- Konishi, M. (1993). Listening with two ears. *Scientific American*, 268, 66-73. [655]
- Kooi, F. L., Toet, A., Tripathy, S. P., and Levi, D. M. (1994). The effect of similarity and attention on contour interaction in peripheral vision. *Spatial Vision*, in press [116, 368]
- Korschning, S. (1993). The neurotrophic factor: A reexamination. *Journal of Neuroscience*, 13, 2739-48. [606-7]
- Koster, W. (1896). Zur Kenntnis der Mikropie und Makropie. *Archiv für Ophthalmologie*, 42, 35-45. [431]
- Kotulak, J. C. and Schor, C. M. (1986). The dissociability of accommodation from vergence in the dark. *Investigative Ophthalmology and Visual Science*, 27, 544-51. [394]

- Kratz, K. E. and Lehmkuhle, S. (1983). Spatial contrast sensitivity of monocularly deprived cats after removal of the non-deprived eye. *Behavioural Brain Research*, 7, 261–6. [631]
- Kratz, K. E., Spear, P. D., and Smith, D. C. (1976). Postcritical-period reversal of effects of monocular deprivation on striate cortex cells of the cat. *Journal of Neurophysiology*, 39, 501–11. [628]
- Krekling, S. (1973a). Comments on cyclofusional eye movements. *Albrecht v. Graefes Archiv für Ophthalmologie*, 188, 231–8. [418]
- Krekling, S. (1973b). Some aspects of the Pulfrich effect. *Scandinavian Journal of Psychology*, 14, 87–90. [536]
- Krekling, S. (1974). Stereoscopic threshold within the stereoscopic range in central vision. *American Journal of Physiological Optics*, 51, 626–34. [155, 159]
- Krekling, S. and Blika, S. (1983). Development of the tilted vertical horopter. *Perception and Psychophysics*, 34, 491–3. [61]
- Krishnan, V. V. and Stark, L. (1983). Model of the disparity vergence system. In *Vergence eye movements: Basic and clinical aspects*, (ed. M. C Schor and K. J. Ciuffreda), pp. 349–72. Butterworth, Boston. [407]
- Krishnan, V. V., Farazian, F., and Stark, L. (1973b). An analysis of latencies and prediction in the fusional vergence system. *International Journal of Optometry*, 50, 933–9. [402]
- Krishnan, V. V., Phillips, S., and Stark, L. (1973a). Frequency analysis of accommodation, accommodative vergence and disparity vergence. *Vision Research*, 13, 1545–54. [402-3]
- Krol, J. D. and van de Grind, W. A. (1980). The double-nail illusion: Experiments on binocular vision with nails, needles, and pins. *Perception*, 9, 651–69. [45, 523]
- Krol, J. D. and van de Grind, W. A. (1983). Depth from dichoptic edges depends on vergence tuning. *Perception*, 12, 425–38. [225]
- Krol, J. D. and van de Grind, W. A. (1986). Binocular depth mixture: An artifact of eye vergence? *Vision Research*, 26, 1289–98. [232]
- Krubitzer, L. A. and Kaas, J. H. (1990). Cortical connections of MT in four species of primates: Areal, modular, and retinotopic patterns. *Visual Neuroscience*, 5, 165–204. [126]
- Krüger, J. and Aiple, F. (1989). The connectivity underlying the orientation selectivity in the infragranular layers of monkey striate cortex. *Brain Research*, 447, 56–65. [81, 116]
- Krüger, K., Kiefer, W., Groh, A., Dinse, H. R., and von Seelen, W. (1993). The role of the lateral suprasylvian visual cortex of the cat in object–background interactions: Permanent deficits following lesions. *Experimental Brain Research*, 97, 40–60. [126]
- Kruger, P. B. and Pola, J. (1986). Stimuli for accommodation: Blur, chromatic aberration and size. *Vision Research*, 26, 957–71. [395]
- Kubie, L. S. and Beckmann, J. W. (1929). Diplopia without extraocular palsies, caused by heteronymous defects in the visual fields associated with defective macular vision. *Brain*, 52, 317–33. [427]
- Kubovy, M. (1986). *The psychology of perspective and Renaissance art*. Cambridge University Press, Cambridge. [9]
- Kuffler, S. W. (1953). Discharge patterns and functional organization of mammalian retina. *Journal of Neurophysiology*, 16, 37–68. [109]
- Kulikowski, J. J. (1980). Processing of patterns by simple cells in the cat visual cortex. *Neuroscience Letters*, Suppl. 53. [89]
- Kumar, T. (1995). Stereopsis due to luminance difference in the two eyes. *Vision Research*, 35, 255–62. [310]
- Kumar, T. and Glaser, D. A. (1991). Influence of remote objects on local depth perception. *Vision Research*, 31, 1687–99. [468]
- Kumar, T. and Glaser, D. A. (1992). Depth discrimination of a line is improved by adding other nearby lines. *Vision Research*, 32, 1667–76. [161]
- Kumar, T. and Glaser, D. A. (1993). Initial performance, learning and observer variability for hyperacuity tasks. *Vision Research*, 33, 2287–300. [192, 469]
- Kumar, T. and Glaser, D. A. (1994). Some temporal aspects of stereoacuity. *Vision Research*, 34, 913–25. [192]
- Lack, L. C. (1969). The effect of practice on binocular rivalry control. *Perception and Psychophysics*, 6, 397–400. [346]
- Lack, L. C. (1978). *Selective attention and the control of binocular rivalry*. Mouton, New York. [343]
- Lagae, L., Raiguel, S., and Orban, G. A. (1993). Speed and direction selectivity of macaque middle temporal neurons. *Journal of Neurophysiology*, 69, 19–39. [126]
- Lagreze, W. D. and Sireteanu, R. (1991). Two-dimensional spatial distortions in human strabismic amblyopia. *Vision Research*, 31, 1271–88. [631]
- Lakshminarayanan, V., Enoch, J. M., and Knowles, R. A. (1993). Residual aniseikonia among patients fitted with one or two intraocular lenses (pseudophakic corrections). *Optometry and Vision Science*, 70, 107–10. [64]
- Lam, D. M-K. and Shatz, C. J. (1991). *Development of the visual system*. MIT Press, Cambridge, MA. [606]
- Lam, K., Sefton, A. J., and Bennett, M. R. (1982). Loss of axons from the optic nerve of the rat during early postnatal development. *Developmental Brain Research*, 3, 487–91. [606]
- Lamme, V. A. F., van Dijk, B. W., and Spekreijse, H. (1993). Organization of texture segregation processing in primate visual cortex. *Visual Neuroscience*, 10, 781–90. [81]
- Lancaster, W. B. (1938). Aniseikonia. *AMA Archives of Ophthalmology*, 20, 907–12. [62]
- Land, M. F. (1969). Movements of the retinæ of jumping spiders (Salticidae: Dendryphantinae) in response to visual stimuli. *Journal of Experimental Biology*, 51, 471–93. [647]
- Land, M. F. (1988). The functions of eye and body movements in *Labidocera* and other copepods. *Journal of Experimental Biology*, 140, 381–91. [648]
- Land, M. F., Marshall, J. N., Brownless, D., and Cronin, T. W. (1990). The eye-movements of the mantis shrimp *Odontodactylus scyllarus* (Crustacea: Stomatopoda). *Journal of Comparative Physiology*, 167, 155–66. [648-9]
- Landrigan, D. T. and Bader, I. A. (1981). The Pulfrich effect: Filtering portions of both eyes. *Journal of Psychology*, 109, 165–72. [537]
- Landy, M. S., Maloney, L. T., and Young, M. J. (1991a). Psychophysical estimation of the human depth combination rule. *Sensor fusion III: 3-D Perception and Recognition. Proceedings of the SPIE*, 1383, 247–54. [436]
- Landy, M. S., Maloney, L. T., Johnston, E. B., and Young, M. J. (1991b). In defense of weak fusion: Measurement and modelling of depth cue combination. *Mathematical studies in perception and cognition*, pp. 91–3. New York University, New York. [437]
- Lange-Malecki, B., Creutzfeldt, O. D., and Hinse, P. (1985). Haploscopic colour mixture with and without contours in subjects with normal and disturbed binocular vision. *Perception*, 14, 587–600. [326]
- Langer, T., Fuchs, A. F., Chubb, M. C., Scudder, C. A., and Lisberger, S. C. (1985). Floccular efferents in the rhesus macaque as revealed by autoradiography and horseradish peroxidase. *Journal of Comparative Neurology*, 235, 26–37. [530]
- Langlands, N. M. S. (1926). Experiments on binocular vision. *Transactions of the Optical Society (London)*, 28, 45–82. [184]

- Langlands, N. M. S. (1929). Experiments on binocular vision. *Medical Research Council, Special Report Series*, No. 133. His Majesty's Stationery Office, London. [184]
- Lansford, T. G. and Baker, H. D. (1969). Dark adaptation: An interocular light-adaptation effect. *Science*, **164**, 1307–9. [365]
- Lansing, R. W. (1964). Electroencephalographic correlates of binocular rivalry in man. *Science*, **146**, 1325–7. [346]
- Larsen, J. S. (1971). The sagittal growth of the eye. IV. Ultrasonic measurement of the axial length of the eye from birth to puberty. *Acta Ophthalmologica*, **49**, 873–86. [604]
- Larson, W. L. (1990). An investigation of the difference in stereoacluity between crossed and uncrossed disparities using Frisby and TNO tests. *Optometry and Vision Science*, **67**, 157–61. [166]
- Lasley, D. J., Kivlin, J., Rich, L., and Flynn, J. T. (1984). Stereo-discrimination between diplopic images in clinically normal observers. *Investigative Ophthalmology and Visual Science*, **25**, 1316–20. [166]
- Lau, E. (1922). Versuche über das stereoskopische Sehen. *Psychologische Forschung*, **2**, 1–4. [305]
- Lau, E. (1925). Über das stereoskopische Sehen. *Psychologische Forschung*, **6**, 121–6. [305, 519]
- Lawden, M. C., Hess, R. F., and Campbell, F. W. (1982). The discrimination of spatial phase relationships in amblyopia. *Vision Research*, **22**, 1005–16. [631]
- Lawson, R. B. and Mount, D. C. (1967). Minimum conditions for stereopsis and anomalous contour. *Science*, **158**, 804–6. [514]
- Lawson, R. B., Cowen, E., Gibbs, T. D., and Whitmore, C. G. (1974). Stereoscopic enhancement and erasure of subjective contours. *Journal of Experimental Psychology*, **103**, 1142–6. [509]
- Le Clerc, S. (1679). *Discours touchant de point de vue, dans lequel il est prouvé que les chose qu'on voit distinctement, ne sont vues que d'un œil*. Jolly, Paris. [17]
- Le Conte, J. (1881). *Sight*. London, Kegan Paul. [418]
- Le Gros Clark, W. E. (1970). *History of the primates*. British Museum (Natural History), London. [646]
- LeDoux, J. E., Deutsch, G., Wilson, D. H., and Gazzaniga, M. S. (1977). Binocular stereopsis and the anterior commissure in man. *The Physiologist*, **20**, 55. [132]
- Lee, B. (1994). Aftereffects and the representation of stereoscopic surfaces (Unpublished D.Phil. thesis, Oxford University). [490]
- Lee, B. and Rogers, B. R. (1992). Aftereffects of stereoscopic surfaces are selectively tuned to the plane of the adapting surface. *Investigative Ophthalmology and Visual Science*, **33** (ARVO Abstracts), 1372. [273, 492-3]
- Lee, D. and Malpeli, J. G. (1994). Global form and singularity: Modeling the blind spot's role in lateral geniculate morphogenesis. *Science*, **263**, 1292–4. [112]
- Lee, D. N. (1970a). A stroboscopic stereophenomenon. *Vision Research*, **10**, 587–93. [541, 543]
- Lee, D. N. (1970b). Spatio-temporal integration in binocular-kinetic space perception. *Vision Research*, **10**, 65–78. [541]
- Lee, D. N. (1970c). Binocular stereopsis with spatial disparity. *Perception and Psychophysics*, **9**, 216–8. [447-8]
- Lee, D. N. (1976). A theory of visual control of braking based on information about time-to-collision. *Perception*, **5**, 437–59. [554, 555]
- Lee, D. N. (1980). The optic flow field: The foundation of vision. *Philosophical Transactions of the Royal Society*, **290**, 169–79. [460]
- Lee, D. N. and Reddish, P. E. (1981). Plummeting gannets: A paradigm of ecological optics. *Nature*, **293**, 293–4. [555]
- Lee, D. Y. and Ciuffreda, K. J. (1983). Short-term adaptation to the induced effect. *Ophthalmology and Physiological Optics*, **3**, 129–35. [67]
- Legge, G. E. (1979). Spatial frequency masking in human vision: Binocular interactions. *Journal of the Optical Society of America*, **69**, 838–47. [366, 635, 638]
- Legge, G. E. (1984a). Binocular contrast summation. I. Detection and discrimination. *Vision Research*, **24**, 373–83. [345, 353, 355]
- Legge, G. E. (1984b). Binocular contrast summation. II. Quadratic summation. *Vision Research*, **24**, 385–94. [353]
- Legge, G. E. and Gu, Y. (1989). Stereopsis and contrast. *Vision Research*, **29**, 989–1004. [168–70]
- Legge, G. E. and Rubin G. S. (1981). Binocular interactions in suprathreshold contrast perception. *Perception and Psychophysics*, **30**, 49–61. [358]
- Leguire, L. E., Blake, R., and Sloane, M. (1982). The square-wave illusion and phase anisotropy of the human visual system. *Perception*, **11**, 547–56. [342]
- Lehky, S. R. (1983). A model of binocular brightness and binocular loudness perception in humans with general applications to nonlinear summation of sensory inputs. *Biological Cybernetics*, **49**, 89–97. [358]
- Lehky, S. R. (1988). An astable multivibrator model of binocular rivalry. *Perception*, **17**, 215–28. [345]
- Lehky, S. R. and Sejnowski, T. J. (1990). Neural model of stereoacluity and depth interpolation based on a distributed representation of stereo disparity. *Journal of Neuroscience*, **10**, 2281–99. [136]
- Lehky, S. R., Sejnowski, T. J., and Desimone, R. (1992). Predicting responses of nonlinear neurons in monkey striate cortex to complex patterns. *Journal of Neuroscience*, **12**, 3568–81. [92]
- Lehmann, D. and Julesz, B. (1978). Lateralized cortical potentials evoked in humans by dynamic random-dot stereograms. *Vision Research*, **18**, 1265–71. [147, 625]
- Lehmann, D. and Wälchli, P. (1975). Depth perception and localization of brain lesions. *Journal of Neurology*, **209**, 157–64. [624]
- Lehmkuhle, S. W. and Fox, R. (1975). Effect of binocular rivalry suppression on the motion aftereffect. *Vision Research*, **15**, 855–9. [343]
- Lehmkuhle, S. W. and Fox, R. (1976). On measuring interocular transfer. *Vision Research*, **16**, 428–30. [375]
- Lehmkuhle, S. W. and Fox, R. (1980). Effect of depth separation on metaccontrast masking. *Journal of Experimental Psychology: Human Perception and Performance*, **6**, 605–21. [524]
- Lehmkuhle, S. W., Kratz, K. E., and Sherman, S. M. (1982). Spatial and temporal sensitivity of normal and amblyopic cats. *Journal of Neurophysiology*, **48**, 372–87. [633]
- Lehmkuhle, S. W., Kratz, K. E., Mangel, S. C., and Sherman, S. M. (1980). Effects of early monocular lid suture on spatial and temporal sensitivity of neurons in dorsal lateral geniculate nucleus of the cat. *Journal of Neurophysiology*, **43**, 542–56. [627]
- Lehmkuhle, S. W., Sherman, S. M., and Kratz, K. E., (1984). Spatial contrast sensitivity of dark-reared cats with striate cortex lesions. *Journal of Neuroscience*, **4**, 2419–24. [633]
- Lehnert, K. (1941). Über wahre und Scheinhörpteren. *Pflügers Archiv für die gesamte Physiologie*, **245**, 112–20. [60]
- Lehrer, M., Srinivasan, M. V., and Zhang, S. W. (1988). Motion cues provide the bee's visual world with a third dimension. *Nature*, **332**, 356–7. [648]
- Leibowitz, H. and Moore, D. (1966). Role of accommodation and convergence in the perception of size. *Journal of the Optical Society of America*, **56**, 1120–23. [428]
- Leibowitz, H. and Walker, L. (1956). Effect of field size and luminance on the binocular summation of suprathreshold stimuli. *Journal of the Optical Society of America*, **46**, 171–2. [359]
- Leicester, J. (1968). Projection of the vertical meridian to cerebral cortex of the cat. *Journal of Neurophysiology*, **31**, 371–82. [130]

- Leigh, R. J., Maas, E. F., Grossman, G. E., and Robinson, D. A. (1989). Visual cancellation of the torsional vestibulo-ocular reflex in humans. *Experimental Brain Research*, 75, 221-6. [417]
- Leigh, R. J., Rushton, D. N., Thurston, S. E., Hertle, R. W., and Yaniglos, S. S. (1988). Effects of retinal image stabilization in acquired nystagmus due to neurologic disease. *Neurology*, 38, 122-7. [643]
- Lema, S. A. and Blake, R. (1977). Binocular summation in normal and stereoblind humans. *Vision Research*, 17, 691-5. [638]
- Lemij, H. G. and Collewijn, H. (1991a). Long-term nonconjugate adaptation of human saccades to anisotropic spectacles. *Vision Research*, 31, 1939-54. [413]
- Lemij, H. G. and Collewijn, H. (1991b). Short-term nonconjugate adaptation of human saccades to anisotropic spectacles. *Vision Research*, 31, 1955-66. [414]
- Lemij, H. G. and Collewijn, H. (1992). Nonconjugate adaptation of human saccades to anisotropic spectacles: Meridian-specificity. *Vision Research*, 32, 453-64. [414]
- Lennstrand, G., Noorden, G. K., and von and Campos, E. C. (1988). *Strabismus and amblyopia*. Plenum, New York. [387]
- Lennie, P., Haake, P. W., and Williams, D. R. (1991). The design of chromatically opponent receptive fields. In *Computational models of visual processing*, (ed. M. S. Landy and J. A. Movshon), pp. 71-82. MIT Press, Cambridge, MA. [110]
- Leonards, U. and Sireteanu, R. (1993). Interocular suppression in normal and amblyopic subjects: The effect of unilateral attenuation with neutral density filters. *Perception and Psychophysics*, 54, 65-74. [333]
- Lepore, F. and Guillemot, J. P. (1982). Visual receptive field properties of cells innervated through the corpus callosum in the cat. *Experimental Brain Research*, 46, 413-24. [131]
- Lepore, F., Ptito, M., and Lassonde, M. (1986). Stereoperception in cats following section of the corpus callosum and/or the optic chiasma. *Experimental Brain Research*, 61, 258-64. [132]
- Lepore, F., Samson, A., and Molotchnikoff, S. (1983). Effects on binocular activation of cells in visual cortex of the cat following the transection of the optic tract. *Experimental Brain Research*, 50, 392-6. [132]
- Lepore, F., Samson, A., Paradis, M-C., and Ptito, M. (1992). Binocular interaction and disparity coding at the 17-18 border: Contribution of the corpus callosum. *Experimental Brain Research*, 90, 129-40. [131]
- Letourneau, P. C., Condic, M. L., and Snow, D. M. (1994). Interactions of developing neurons with the extracellular matrix. *Journal of Neuroscience*, 14, 915-28. [606]
- Leuba, G. and Garey, L. J. (1987). Evolution of neuronal numerical density in the developing and aging human visual cortex. *Human Neurobiology*, 6, 11-18. [610]
- LeVay, S. and Gilbert (1976). Laminar patterns of geniculocortical projection in the cat. *Brain Research*, 113, 1-19. [633]
- LeVay, S. and Voigt, T. (1988). Ocular dominance and disparity coding in cat visual cortex. *Visual Neuroscience*, 1, 395-414. [122, 133-4]
- LeVay, S., Connolly, M., Houde, J., and Van Essen, D. C. (1985). The complete pattern of ocular dominance stripes in the striate cortex and visual field of the macaque monkey. *Journal of Neuroscience*, 5, 486-501. [331, 369, 617]
- LeVay, S., Stryker, M. P., and Shatz, C. J. (1978). Ocular dominance columns and their development in layer IV of the cat's visual cortex: A quantitative study. *Journal of Comparative Neurology*, 179, 223-44. [613]
- LeVay, S., Wiesel, T. N., and Hubel, D. H. (1980). The development of ocular dominance columns in normal and visually deprived monkeys. *Journal Comparative Neurology*, 191, 1-51. [613, 628, 636]
- Levelt, W. J. M. (1965a). Binocular brightness averaging and contour information. *British Journal of Psychology*, 56, 1-13. [356]
- Levelt, W. J. M. (1965b). *On binocular rivalry*. Institute for Perception, Soesterberg, The Netherlands. [328]
- Levelt, W. J. M. (1966). The alternation process in binocular rivalry. *British Journal of Psychology*, 57, 225-38. [344]
- Levelt, W. J. M. (1967). Note on the distribution of dominance times in binocular rivalry. *British Journal of Psychology*, 58, 143-5. [332]
- Leventhal, A. G., Schall, J. D., Ault, S. J., Provis, J. M., and Vitek, D. J. (1988). Class-specific cell death shapes the distribution and pattern of central projection of cat retinal ganglion cells. *Journal of Neuroscience*, 8, 2011-27. [34, 609]
- Levi, D. M. (1991). Spatial vision in amblyopia. In *Spatial vision*, (ed. D. Regan), pp. 212-38. CRC Press, Boca Raton, FL. [633]
- Levi, D. M. and Klein, S. (1982a). Hyperacuity and amblyopia. *Nature*, 298, 268-9. [631]
- Levi, D. M. and Klein, S. (1982b). Differences in vernier discrimination for gratings between strabismic and anisotropic amblyopes. *Investigative Ophthalmology and Visual Science*, 23, 389-407. [632]
- Levi, D. M. and Klein, S. (1983). Spatial localization in normal and amblyopic vision. *Vision Research*, 23, 1005-17. [632]
- Levi, D. M. and Klein, S. (1985). Vernier acuity, crowding and amblyopia. *Vision Research*, 25, 979-91. [172, 628, 631-2]
- Levi, D. M. and Klein, S. A. (1990). The role of separation and eccentricity in encoding position. *Vision Research*, 30, 557-85. [316]
- Levi, D. M., Harwerth, R. S., and Manny, R. E. (1979a). Suprathreshold spatial frequency detection and binocular interaction in strabismic and anisotropic amblyopia. *Investigative Ophthalmology and Visual Science*, 18, 714-25. [634]
- Levi, D. M., Harwerth, R. S., and Smith, E. L. (1979b). Humans deprived of normal binocular vision have binocular interactions tuned to size and orientation. *Science*, 206, 852-3. [638]
- Levi, D. M., Harwerth, R. S., and Smith, E. L. (1980). Binocular interactions in normal and anomalous binocular vision. *Documenta Ophthalmologica*, 49, 303-24. [638]
- Levi, D. M., Klein, S. A., and Aitsebaomo, A. P. (1985). Vernier acuity, crowding and cortical magnification. *Vision Research*, 25, 963-77. [114, 368]
- Levi, D. M., Klein, S. A., and Wang, H. (1994). Discrimination of position and contrast in amblyopic and peripheral vision. *Vision Research*, 34, 3293-313. [632]
- Levi, D. M., Pass, A. F., and Manny, R. E. (1982). Binocular interactions in normal and anomalous binocular vision: Effects of flicker. *British Journal of Ophthalmology*, 66, 57-63. [359, 638]
- Levi, L., Zee, D. S., and Hain, T. C. (1987). Disjunctive and disconjugate saccades during symmetrical vergence. *Investigative Ophthalmology and Visual Science*, 28 (ARVO Abstracts), 332. [412]
- Levick, W. R., Cleland, B. G., and Coombs, J. S. (1972). On the apparent orbit of the Pulfrich pendulum. *Vision Research*, 12, 1381-8. [536]
- Levick, W. R., Kirk, D. L., and Wagner, H. G. (1981). Neurophysiological tracing of a projection from temporal retina to contralateral visual cortex of cat. *Vision Research*, 21, 1677-9. [130]
- Levinson, E. and Blake, R. (1979). Stereopsis by harmonic analysis. *Vision Research*, 19, 73-8. [263]
- Levinson, E. and Sekuler, R. (1975). The independence of channels in human vision selective for direction of movement. *Journal of Physiology*, 250, 347-66. [375]

- Levitt, J. B., Kiper, D. C., and Movshon, A. (1994). Receptive fields and functional architecture of macaque V2. *Journal of Neurophysiology*, **71**, 2517-42. [126]
- Levitt, P. and Moore, R. Y. (1979). Development of the noradrenergic innervation of neocortex. *Brain Research*, **162**, 243-59. [629]
- Levy, J. (1973). Autokinesis direction during and after eye turn. *Perception and Psychophysics*, **13**, 337-42. [432]
- Levy, M. M. and Lawson, R. B. (1978). Stereopsis and binocular rivalry from dichoptic stereograms. *Vision Research*, **18**, 239-46. [225]
- Levy, N. S. and Glick, E. B. (1974). Stereoscopic perception and Snellen visual acuity. *American Journal of Ophthalmology*, **78**, 722-4. [168]
- Lewis, J. L. (1970). Semantic processing of unattended messages using dichotic listening. *Journal of Experimental Psychology*, **85**, 225-8. [347]
- Lewis, P. (1944). Bilateral monocular diplopia with amblyopia. *American Journal of Ophthalmology*, **27**, 1026-7. [47]
- Lewis, T. L. and Maurer, D. (1992). The development of the temporal and nasal visual fields during infancy. *Vision Research*, **32**, 903-11. [617]
- Liang, T. and Pieron, H. (1947). Recherches sur la latence de la sensation lumineuse par la méthode de l'effet chronostéréoscopique. *Année Psychologique*, **48**, 1-51. [536]
- Liège, B. and Galand, G. (1972). Single-unit visual responses in the frog's brain. *Vision Research*, **12**, 609-22. [651]
- Lindberg, D. C. (1976). *Theories of vision from Al-Kindi to Kepler*. University of Chicago Press, Chicago. [6, 24]
- Lines, C. R. and Milner, A. D. (1983). Nasotemporal overlap in the human retina investigated by means of simple reaction time to lateral light flash. *Experimental Brain Research*, **50**, 166-72. [130]
- Linksz, A. (1952). *Physiology of the eye*. Vol. II. Vision. Grune and Stratton, New York. [60, 130]
- Linksz, A. (1971). Comments on the papers by C. Blakemore (1969, 1970) and D. E. Mitchell and C. Blakemore (1970). *Survey of Ophthalmology*, **15**, 348-53. [132]
- Lippincott, J. A. (1889). On the binocular metamorphopsia produced by correcting glasses. *AMA Archives of Ophthalmology*, **18**, 18-30. [285]
- Lit, A. (1949). The magnitude of the Pulfrich stereophenomenon as a function of binocular differences in intensity at various levels of illumination. *American Journal of Psychology*, **62**, 159-81. [536-8, 545]
- Lit, A. (1959a). Depth-discrimination thresholds as a function of binocular differences of retinal illumination at scotopic and photopic levels. *Journal of the Optical Society of America*, **49**, 746-52. [170]
- Lit, A. (1959b). The effect of fixation conditions on depth discrimination thresholds at scotopic and photopic illumination levels. *Journal of Experimental Psychology*, **58**, 476-81. [179]
- Lit, A. (1960). Effect of target velocity in a frontal plane on binocular spatial localization at photopic retinal illuminance levels. *Journal of the Optical Society of America*, **50**, 970-3. [186, 537]
- Lit, A. (1968). Illumination effects on depth discrimination. *The Optometric Weekly*, **59**, 42-54. [536-7]
- Lit, A. and Finn, J. P. (1976). Variability of depth-discrimination thresholds as a function of observation distance. *Journal of the Optical Society of America*, **66**, 740-2. [179]
- Lit, A. and Hamm, H. D. (1966). Depth-discrimination for stationary and oscillating targets at various levels of illumination. *Journal of the Optical Society of America*, **56**, 510-16. [168, 186]
- Lit, A. and Hyman, A. (1951). The magnitude of the Pulfrich stereophenomenon as a function of distance of observation. *American Journal of Optometry and Physiological Optics*, **28**, 564-80. [537]
- Lit, A. and Vicars, W. M. (1966). The effect of practice on the speed and accuracy of equidistance-settings. *American Journal of Psychology*, **72**, 464-9. [191]
- Lit, A. and Vicars, W. M. (1970). Stereoacuity for oscillating targets exposed through apertures of various horizontal extents. *Perception and Psychophysics*, **8**, 348-52. [186]
- Little, A. M. G. (1971). *Roman perspective painting and the ancient stage*. Star Press, Kennebunk, Maine. [9]
- Liu, L. and Schor, C. M. (1994). The spatial properties of binocular suppression zone. *Vision Research*, **34**, 937-47. [336]
- Liu, L., Stevenson, S. B., and Schor, C. M. (1994a). A polar coordinate system for describing disparity. *Vision Research*, **34**, 1205-22. [258, 271]
- Liu, L., Stevenson, S. B., and Schor, C. M. (1994b). Quantitative stereoscopic depth without binocular correspondence. *Nature*, **367**, 66-9. [516]
- Liu, L., Tyler, C. W., and Schor, C. M. (1992). Failure of rivalry at low contrast: Evidence of a suprathreshold binocular summation process. *Vision Research*, **32**, 1471-9. [309, 329, 334]
- Livingstone, M. S. and Hubel, D. H. (1981). Effects of sleep and arousal on the processing of visual information. *Nature*, **291**, 554-61. [113, 128]
- Livingstone, M. S. and Hubel, D. H. (1984). Anatomy and physiology of a color system in the primate visual cortex. *Journal of Neuroscience*, **4**, 309-56. [123]
- Livingstone, M. S. and Hubel, D. H. (1987). Connections between layer 4B of area 17 and the thick cytochrome oxidase stripes of area 18 in the squirrel monkey. *Journal of Neuroscience*, **7**, 3371-7. [124]
- Livingstone, M. S. and Hubel, D. H. (1988). Segregation of form, color, movement, and depth: Anatomy, physiology, and perception. *Science*, **240**, 740-9. [128, 143]
- Llewellyn, K. R. (1971). Visual guidance of locomotion. *Journal of Experimental Psychology*, **91**, 245-61. [556]
- Lock, A. and Collett, T. (1979). A toad's devious approach to its prey: A study of some complex uses of depth vision. *Journal of Comparative Physiology*, **131**, 179-89. [652]
- Logothetis, N. K. and Schall, J. D. (1989). Neuronal correlates of subjective visual perception. *Science*, **245**, 761-3. [346]
- Logothetis, N. K. and Schall, J. D. (1990). Binocular motion rivalry in macaque monkeys: Eye dominance and tracking eye movements. *Vision Research*, **30**, 1409-19. [335]
- Logothetis, N. K., Schiller, P. H., Charles, E. R., and Hurl Bert, A. C. (1990). Perceptual deficits and the activity of the color-opponent and broad-band pathways at isoluminance. *Science*, **247**, 214-17. [207]
- Long, G. M. (1979). The dichoptic viewing paradigm: Do the eyes have it? *Psychological Bulletin*, **86**, 391-403. [364]
- Long, N. R. (1982). Transfer of learning in transformed random-dot stereostimuli. *Perception*, **11**, 409-14. [193]
- Long, N. R. and Over, R. (1973). Stereoscopic depth aftereffects with random-dot patterns. *Vision Research*, **13**, 1283-7. [486, 490]
- Long, N. R. and Over, R. (1974a). Stereospatial masking and aftereffect with normal and transformed random-dot patterns. *Perception and Psychophysics*, **15**, 243-8. [524]
- Long, N. R. and Over, R. (1974b). Disparity masking with ambiguous random-dot stereograms. *Vision Research*, **14**, 31-4. [487]
- Longuet-Higgins, H. C. (1981). A computer algorithm for reconstructing a scene from two projections. *Nature*, **293**, 133-5. [573]

- Longuet-Higgins, H. C. (1982). The role of the vertical dimension in stereoscopic vision. *Perception*, 11, 371-6. [246, 249, 283, 574]
- Longuet-Higgins, H. C. and Prazdny, K. (1980). The interpretation of a moving retinal image. *Proceedings of the Royal Society, London*, B208, 385-97. [575]
- Loomis, J. M. and Collins, C. C. (1978). Sensitivity to shifts of a point stimulus: An instance of tactile hyperacuity. *Perception and Psychophysics*, 24, 487-92. [98]
- Löpping, B. and Weale, R. A. (1965). Changes in corneal curvature following ocular convergence. *Vision Research*, 5, 207-15. [397]
- Lorente de Nò, R. (1949). Cerebral cortex: Architecture, intracortical connections, motor projections. In *Physiology of the nervous system*. 3rd edn, (ed. J. F. Fulton), Chap. 15. Oxford University Press, London. [119]
- Lotmar, W. (1976). A theoretical model for the eye of new-born infants. *Albrecht von Graefes Archive für klinische und experimentelle Ophthalmologie*, 198, 179-85. [604]
- Lowe, K. N. and Ogle, K. N. (1966). Dynamics of the pupil during binocular rivalry. *AMA Archives of Ophthalmology*, 75, 395-403. [335]
- Lu, C. and Fender, D. H. (1972). The interaction of color and luminance in stereoscopic vision. *Investigative Ophthalmology*, 11, 482-90. [143, 207]
- Ludvigh, E. and McKinnon, P. (1966). Relative effectiveness of foveal and parafoveal stimuli in eliciting fusion movements of small amplitude. *AMA Archives of Ophthalmology*, 76, 443-9. [402]
- Ludvigh, E. and McKinnon, P. (1968). Dependence of the amplitude of fusional convergence movements on the velocity of the eliciting stimulus. *Investigative Ophthalmology*, 7, 347-52. [403]
- Ludvigh, E., McKinnon, P., and Zaitzeff, L. (1965). Relative effectiveness of foveal and parafoveal stimuli in eliciting fusion movements. *AMA Archives of Ophthalmology*, 73, 115-21. [402]
- Luhmann, H. J., Millán, L. M., and Singer, W. (1986). Development of horizontal intrinsic connections in the cat striate cortex. *Experimental Brain Research*, 63, 443-8. [611]
- Lund, J. S., Boothe, R. G., and Lund, R. D. (1977). Development of neurons in the visual cortex of the monkey (*Macaca nemestrina*): A Golgi study from fetal day 127 to postnatal maturity. *Journal of Comparative Neurology*, 176, 149-88. [610, 613]
- Lund, R. D. and Mitchell, D. E. (1979). Plasticity of visual callosal projections. *Society of Neuroscience Symposium*, 4, 142-52. [131]
- Luneburg, R. K. (1947). *Mathematical analysis of binocular vision*. Ann Arbor, Michigan, Edwards. [53]
- Luskin, M. B. and Shatz, C. J. (1985). Neurogenesis of the cat's primary visual cortex. *Journal of Comparative Neurology*, 242, 611-31. [610]
- Lynch, J. C., Mountcastle, V. B., Talbot, W. H., and Yin, T. C. T. (1977). Parietal lobe mechanisms for directed visual attention. *Journal of Neurophysiology*, 40, 362-89. [129]
- Lynes, J. A. (1980). Brunelleschi's perspectives reconsidered. *Perception*, 9, 87-99. [9]
- Lythgoe, R. J. (1938). Some observations on the rotating pendulum. *Nature*, 141, 474. [545-7]
- MacCracken, P. J. and Hayes, W. N. (1976). Experience and latency to achieve stereopsis. *Perception and Motor Skills*, 43, 1227-31. [192]
- MacCracken, P. J., Bourne, J. A., and Hayes, W. N. (1977). Experience and latency to achieve stereopsis: a replication. *Perceptual and Motor Skills*, 45, 261-262. [192]
- MacDonald, R. I. (1977). Temporal stereopsis and dynamic visual noise. (Letter to the editor). *Vision Research*, 17, 1127-8. [552]
- MacDougall, R. (1903). The subjective horizon. *Psychological Review*, Monograph Supplement 4. [432]
- Mach, E. (1866). Über die physiologische Wirkung räumlich vertheilter Lichtreize (Dritte Abhandlung). *Sitzungsberichte der Österreichischen Akademie der Wissenschaften*, 54, 393-408. Trans. in F. Ratcliff, *Mach bands*. pp. 285-98. Holden-Day, San Francisco, 1965. [455]
- Mach, E. and Dvorak, V. (1872). Über Analoga der persönlichen Differenz zwischen beiden Augen und den Netzhautstellen desselben Auges. *Sitzungsberichte der königlichen böhmischen Gesellschaft der Wissenschaft*, Prague, 65-74. [543]
- Mack, A. and Chitayat, D. (1970). Eye-dependent and disparity adaptation to opposite visual-field rotation. *American Journal of Psychology*, 83, 352-69. [486]
- MacKay, D. M. (1973). Lateral interaction between neural channels sensitive to texture density. *Nature*, 245, 159-61. [465]
- MacKay, D. M. and MacKay, V. (1975). Dichoptic induction of McCollough-type effects. *Quarterly Journal of Experimental Psychology*, 27, 225-33. [379]
- Mackensen, G. (1953). Untersuchungen zur Physiologie des optokinetischen Nystagmus. *Klinische Monatsblätter für Augenheilkunde*, 123, 133-43. [531]
- MacLeod, D. I. A. (1972). The Schrödinger equation in binocular brightness combination. *Perception*, 1, 321-4. [357]
- Macmillan, N. A. and Creelman, C. D. (1991). *Detection theory: A users guide*. Cambridge University Press, New York. [95]
- Maddox, E. E. (1893). *The clinical use of prisms and the decentring of lenses*. John Wright & Sons, Bristol, England. [386]
- Maffei, L. and Bisti, S. (1976). Binocular interaction in strabismic kittens deprived of vision. *Science*, 191, 279-80. [641]
- Maffei, L. and Fiorentini, A. (1976). Monocular deprivation in kittens impairs the spatial resolution of geniculate neurones. *Nature*, 264, 754-5. [627]
- Magoon, E. H. and Robb, R. M. (1981). Development of myelin in human optic nerve and tract. *AMA Archives of Ophthalmology*, 99, 655-9. [607]
- Makous, W. and Sanders, R. K. (1978). Suppressive interactions between fused patterns. In *Visual psychophysics and physiology*. (ed. J. C. Armington, J. Krausopf, and B. R. Wooten), pp. 167-79. Academic Press, New York. [329, 339]
- Makous, W., Teller, D., and Boothe, R. (1976). Binocular interaction in the dark. *Vision Research*, 16, 473-6. [351, 365]
- Malach, R. and Van Sluyters, R. C. (1989). Strabismus does not prevent recovery from monocular deprivation: A challenge for simple Hebbian models of synaptic modification. *Vision Neuroscience*, 3, 267-73. [631]
- Malebranche, N. (1674). *De la recherche de la vérité*. Preland, Paris. [17]
- Mallett, R. F. J. (1964). The investigation of heterophoria at near and a new fixation disparity technique. *The Optician*, 148, 547-551, 574-81. [389]
- Mallot, H. A. (1993). Computational psychophysics of stereoscopic depth perception. In *Grundlagen und Anwendungen der Künstlichen Intelligenz*. (ed. O. Herzog, T. Christaller, and D. Schütt), pp. 60-73. Springer Verlag, Berlin. [200]
- Mallot, H. A. and Bideau, H. (1990). Binocular convergence influences the assignment of stereo correspondences. *Vision Research*, 30, 1521-3. [45]
- Mallot, H. P., Dartsch, S., and Arndt, P. A. (1994). Is correspondence search in human stereo vision a coarse-to-fine process? *Cognitive Science Memo No. 6*, Max Planck Institute for Biological Cybernetics, Tübingen. [220]
- Maloney, L. T. and Landy, M. S. (1989). A statistical framework for robust fusion of depth information. *Visual communication and image processing IV. Proceedings of the SPIE*, 1199, 1154-63. [436]
- Malsburg, C. von der and Schneider, W. (1986). A neural cocktail-party processor. *Biological Cybernetics*, 54, 29-40. [82]

- Mangel, S. C., Wilson, J. R., and Sherman, S. M. (1983). Development of neuronal response properties in the cat dorsal lateral geniculate nucleus during monocular deprivation. *Journal of Neurophysiology*, 50, 240–64. [627]
- Mann, I. (1964). *The development of the human eye*. Grune and Stratton, New York. [606]
- Mann, V. A. (1978). Different loci suggested to mediate tilt and spiral motion aftereffects. *Investigative Ophthalmology and Visual Science*, 17, 903–9. [640]
- Mann, V. A., Hein, A., and Diamond, R. (1979). Localization of targets by strabismic subjects: Contrasting patterns in constant and alternating suppressors. *Perception and Psychophysics*, 25, 29–34. [600]
- Manning, K. A. and Riggs, L. A. (1984). Vergence eye movements and visual suppression. *Vision Research*, 24, 521–26. [386]
- Manny, R. E. and Levi, D. M. (1982). Psychophysical investigations of the temporal modulation sensitivity function in amblyopia: Spatiotemporal interactions. *Investigative Ophthalmology and Visual Science*, 22, 525–34. [631]
- Mansfield, J. S. and Parker, A. J. (1993). An orientation-tuned component in the contrast masking of stereopsis. *Vision Research*, 33, 1535–44. [201]
- Mansfield, J. S. and Simmons, D. R. (1993). Contrast thresholds for the identification of depth in bandpass-filtered stereograms. *Perception and Psychophysics*, In press [170]
- Mapp, A. P. and Ono, H. (1986). The rhino-optical phenomenon: Ocular parallax and the visible field beyond the nose. *Vision Research*, 26, 1163–5. [593]
- Maraini, G. and Porta, R. (1978). Interocular transfer of a visual aftereffect in early-onset esotropia. *AMA Archives of Ophthalmology*, 96, 1853–6. [640]
- Marc, R. E. and Sperling, H. G. (1977). Chromatic organization of primate cones. *Science*, 196, 454–6. [207]
- Mark, R. F. and Davidson, T. M. (1966). Unit responses from commissural fibres of optic lobes of fish. *Science*, 152, 797–9. [649]
- Markoff, J. I. and Sturr, J. F. (1971). Spatial and luminance determinants of the increment threshold under monoptic and dichoptic viewing. *Journal of the Optical Society of America*, 61, 1530–7. [364]
- Marmarelis, P. Z. and Marmarelis, V. Z. (1978). *Analysis of physiological systems: the white noise approach*. Plenum, New York. [92]
- Marmolin, H. (1973). Visually perceived motion in depth resulting from proximal changes. I. *Perception and Psychophysics*, 14, 133–42. [555]
- Marr, D. (1982). *Vision*. Freeman, San Francisco. [75, 84, 90, 250]
- Marr, D. and Poggio, T. (1976). Cooperative computation of stereo disparity. *Science*, 194, 283–7. [575]
- Marr, D. and Poggio, T. (1979). A computational theory of human stereo vision. *Proceedings of the Royal Society, London*, B204, 301–28. [172, 197, 229]
- Marr, D., Palm, G., and Poggio, T. (1978). Analysis of a cooperative stereo algorithm. *Biological Cybernetics*, 28, 223–39. [227]
- Marrocco, R. T. and McClurkin, J. W. (1979). Binocular interaction in the lateral geniculate nucleus of the monkey. *Brain Research*, 168, 633–7. [113]
- Marrocco, R. T., Carpenter, M. A., and Wright, S. E. (1985). Spatial contrast sensitivity: Effects of peripheral field stimulation during monocular and dichoptic viewing. *Vision Research*, 25, 917–24. [368]
- Marshall, N. J., Land, M. F., King, C. A., and Cronin, T. W. (1991). The compound eyes of mantis shrimps (Crustacea, Hoplocarida, Stomatopoda). II. Colour pigments in the eyes of stomatopod crustaceans: Polychromatic vision by serial and lateral filtering. *Philosophical Transactions of the Royal Society, B334*, 57–84. [649]
- Marshall, W. H. and Talbot, S. A. (1942). Recent evidence for neurological mechanisms in vision leading to a general theory of sensory acuity. *Biological Symposium*, 7, 117–64. [382]
- Martens, W., Blake, R., Sloane, M., and Cormack, R. H. (1981). What masks utricular discrimination. *Perception and Psychophysics*, 30, 521–32. [601]
- Martenson, C., Stone, K., Reedy, M., and Sheetz, M. (1993). Fast axonal transport is required for growth cone advance. *Nature*, 366, 66–9. [606]
- Martin, G. R. (1984). The visual fields of the tawny owl, *Strix aluco*. *L. Vision Research*, 24, 1739–51. [655]
- Martin, G. R. and Young, S. R. (1983). The retinal binocular field of the pigeon (*Columba livia*: English racing homer). *Vision Research*, 23, 911–15. [653]
- Martin, K. A. C., Ramachandran, V. S., Rao, V. M., and Whitteridge, D. (1979). Changes in ocular dominance induced in monocularly deprived lambs by stimulation with rotation gratings. *Nature*, 277, 391–3. [657]
- Martinoya, C., Le Houezec, J., and Bloch, S. (1988). Depth resolution in the pigeon. *Journal of Comparative Physiology, A163*, 33–42. [654]
- Martinoya, C., Rey, J., and Bloch, S. (1981). Limits of the pigeon's binocular field and direction for best binocular viewing. *Vision Research*, 21, 1197–200. [653]
- Marzi, C. A., Antonini, A., Di Stefano, M., and Legg, C. R. (1982). The contribution of the corpus callosum to receptive fields in the lateral suprasylvian visual areas of the cat. *Behavioural Brain Research*, 4, 155–76. [132]
- Marzi, C. A., Antonucci, G., Pizzamiglio, L., and Santillo, C. (1986). Simultaneous binocular integration of the visual tilt effect in normal and stereoblind observers. *Vision Research*, 26, 477–83. [373, 640]
- Maske, R., Yamane, S., and Bishop, P. O. (1984). Binocular simple cells for local stereopsis: Comparison of receptive field organizations for the two eyes. *Vision Research*, 24, 1921–9. [120, 140]
- Maske, R., Yamane, S., and Bishop, P. O. (1986a). End-stopped and binocular depth discrimination in the striate cortex of cats. *Proceedings of the Royal Society, London*, B229, 257–76. [133–4, 140]
- Maske, R., Yamane, S., and Bishop, P. O. (1986b). Stereoscopic mechanisms: Binocular responses of the striate cells of cats to moving light and dark bars. *Proceedings of the Royal Society, London*, B229, 227–56. [134]
- Mastronarde, D. N. (1983). Correlated firing of cat retinal ganglion cells. I. Spontaneously active inputs to X- and Y-cells. *Journal of Neurophysiology*, 49, 303–24. [110]
- Mates, J. W. B. (1978). Eye movements of African chameleons: Spontaneous saccadic timing. *Science*, 199, 1087–9. [653]
- Mather, G. (1989). The role of subjective contours in capture of stereopsis. *Vision Research*, 29, 143–6. [504]
- Matlin, E. (1974). Saccadic suppression: A review and an analysis. *Psychological Bulletin*, 81, 899–917. [386]
- Matlin, L. (1962). Binocular summation at the absolute threshold for peripheral vision. *Journal of the Optical Society of America*, 52, 1276–86. [350, 362]
- Matsubara, J., Cynader, M., Swindale, N. V., and Stryker, M. P. (1985). Intrinsic projections within visual cortex: Evidence for orientation-specific local connections. *Proceedings of the National Academy of Science*, 82, 935–9. [77, 116, 612]
- Matsuoka, K. (1984). The dynamic model of binocular rivalry. *Biological Cybernetics*, 49, 201–8. [343]
- Maunsell, J. H. R. and Van Essen, D. C. (1983a). The connections of the middle temporal visual area (MT) and their relationship to a cortical hierarchy in the macaque monkey. *Journal of Neuroscience*, 3, 2563–86. [125]

- Maunsell, J. H. R. and Van Essen, D. C. (1983b). Functional properties of neurons in middle temporal visual area of the macaque monkey. II. Binocular interactions and sensitivity to binocular disparity. *Journal of Neurophysiology*, **49**, 1148–67. [128, 135, 143, 532, 566]
- Maunsell, J. H. R. and Van Essen, D. C. (1987). Topographic organization of the middle temporal visual area (MT) in the macaque monkey: Representational biases and the relationships to callosal connections and myeloarchitectonic boundaries. *Journal of Comparative Neurology*, **266**, 535–55. [131]
- Maurer, D. and Martello, M. (1980). The discrimination of orientation by young infants. *Vision Research*, **20**, 201–4. [616]
- Maxwell, J. S. and King, W. M. (1992). Dynamics and efficacy of saccade-facilitated vergence eye movements in monkeys. *Journal of Neurophysiology*, **68**, 1248–59. [412]
- Maxwell, J. S. and Schor, C. M. (1994). Mechanisms of vertical phoria adaptation revealed by time-course and two-dimensional spatiotopic maps. *Vision Research*, **34**, 2441–51. [393]
- Mayer, M. L., Westbrook, G. L., and Guthrie, P. B. (1984). Voltage-dependent block by Mg²⁺ of NMDA responses in spinal cord neurones. *Nature*, **309**, 261–3. [615]
- Mayhew, J. E. W. (1982). The interpretation of stereo-disparity information: The computation of surface orientation and depth. *Perception*, **11**, 387–404. [283–4, 287–8]
- Mayhew, J. E. W. and Anstis, S. M. (1972). Movement aftereffects contingent on color, intensity, and pattern. *Perception and Psychophysics*, **12**, 77–85. [379]
- Mayhew, J. E. W. and Frisby, J. P. (1976). Rivalrous texture stereograms. *Nature*, **264**, 53–6. [203]
- Mayhew, J. E. W. and Frisby, J. P. (1978). Stereopsis masking in humans is not orientationally tuned. *Perception*, **7**, 431–6. [201]
- Mayhew, J. E. W. and Frisby, J. P. (1979a). Convergent disparity discriminations in narrow-band-filtered random-dot stereograms. *Vision Research*, **19**, 63–71. [175, 178]
- Mayhew, J. E. W. and Frisby, J. P. (1979b). Surfaces with steep variations in depth pose difficulties for orientationally tuned disparity filters. *Perception*, **8**, 691–8. [201]
- Mayhew, J. E. W. and Frisby, J. P. (1980). The computation of binocular edges. *Perception*, **9**, 69–86. [224, 229]
- Mayhew, J. E. W. and Frisby, J. P. (1981). Psychophysical and computational studies towards a theory of human stereopsis. *Artificial Intelligence*, **17**, 349–85. [197, 224]
- Mayhew, J. E. W. and Frisby, J. P. (1982). The induced effect: arguments against the theory of Ardid, Kaufman and Movshon. *Vision Research*, **22**, 1225–8. [288]
- Mayhew, J. E. W. and Longuet-Higgins, H. C. (1982). A computational model of binocular depth perception. *Nature*, **297**, 376–8. [243, 266, 283, 287, 304, 576, 581]
- Mayhew, J. E. W., Frisby, J. P., and Gale, P. (1977). Computation of stereodisparity from rivalrous texture stereograms. *Perception*, **6**, 207–8. [203]
- Mays, L. E. (1984). Neural control of vergence eye movements: Convergence and divergence neurons in mid-brain. *Journal of Neurophysiology*, **51**, 1091–108. [425]
- Mays, L. E. and Porter, J. D. (1984). Neural control of vergence eye movements: Activity of abducens and oculomotor neurons. *Journal of Neurophysiology*, **52**, 743–61. [425]
- Mays, L. E., Porter, J. D., Gamlin, P. D. R., and Tello, C. A. (1986). Neural control of vergence eye movements: Neurons encoding vergence velocity. *Journal of Neurophysiology*, **56**, 1007–21. [404, 425]
- Mays, L. E., Zhang, Y., Thorstad, M. H., and Gamlin, P. D. R. (1991). Trochlear unit activity during ocular convergence. *Journal of Neurophysiology*, **65**, 1484–91. [425]
- McAllister, D. F. and Robbins, W. E. (1987). Three-dimensional imaging techniques and display technologies. *Proceedings of the International Society for Optical Engineering*, **761**, 35–43. [27]
- McCarty, J. A., Demer, J. L., Hovis, L. A., and Nuwer, M. R. (1992). Ocular motility anomalies in developmental misdirection of the optic chiasma. *American Journal of Ophthalmology*, **113**, 86–95. [608]
- McClurkin, J. W., Optican, L. M., and Richmond, B. J. (1994). Cortical feedback increases visual information transmitted by monkey parvocellular lateral geniculate nucleus neurons. *Visual Neuroscience*, **11**, 601–17. [113]
- McCollough, C. (1965). Colour adaptation of edge-detectors in the human visual system. *Science*, **149**, 1115–16. [102, 378]
- McConnell, S. K. and Kaznowski, C. E. (1991). Cell cycle dependence of laminar determination in developing neocortex. *Science*, **254**, 282–5. [610]
- McConnell, S. K., Ghosh, A., and Shatz, C. J. (1989). Subplate neurons pioneer the first axon pathway from the cerebral cortex. *Science*, **245**, 978–2. [614]
- McConnell, S. K., Ghosh, A., and Shatz, C. J. (1994). Subplate pioneers and the formation of descending connections from cerebral cortex. *Journal of Neuroscience*, **14**, 1892–1907. [614]
- McCormack, G. (1990). Normal retinotopic mapping in human strabismus with anomalous retinal correspondence. *Investigative Ophthalmology and Visual Science*, **31**, 559–68. [47]
- McCormack, G., Fisher, S. K., and Wolf, K. (1991). Retinal eccentricity of fusion detail affects vergence adaptation. *Optometry and Vision Science*, **68**, 711–17. [392]
- McFadden, S. A. (1987). The binocular depth stereoacuity of the pigeon and its relation to the anatomical resolving power of the eye. *Vision Research*, **27**, 1967–80. [654]
- McFadden, S. A. and Reymond, L. (1985). A further look at the binocular visual field of the pigeon (*Columba livia*). *Vision Research*, **25**, 1741–6. [653]
- McKee, M. C., Young, D. A., Kohl, P., Reinke, R., and Yolton, R. L. (1987). Effect of head and eye positions on fixation disparities, phoria, and ductions at near. *American Journal of Optometry and Physiological Optics*, **64**, 909–15. [390]
- McKee, S. P. (1983). The spatial requirements for fine stereoacuity. *Vision Research*, **23**, 191–8. [159–60]
- McKee, S. P. and Harrad, R. A. (1993). Fusional suppression in normal and stere anomalously observers. *Vision Research*, **33**, 1645–58. [634]
- McKee, S. P. and Levi, D. M. (1987). Dichoptic hyperacuity: The precision of nonius alignment. *Journal of the Optical Society of America*, **4A**, 1104–8. [56, 180]
- McKee, S. P. and Mitchison, G. J. (1988). The role of retinal correspondence in stereoscopic matching. *Vision Research*, **28**, 1001–12. [502]
- McKee, S. P. and Welch, L. (1989). Is there a constancy for velocity? *Vision Research*, **29**, 553–61. [460]
- McKee, S. P., Bravo, M. J., Smallman, H. S., and Legge, G. E. (1994a). The "uniqueness constraint" and binocular masking. *Perception*, in press [217]
- McKee, S. P., Bravo, M. J., Taylor, D. G., and Legge, G. E. (1994b). Stereo matching precedes dichoptic masking. *Vision Research*, **34**, 1047–60. [368]
- McKee, S. P., Klein, S. A., and Teller, D. Y. (1985). Statistical properties of forced-choice psychometric functions: Implications of probit analysis. *Perception and Psychophysics*, **37**, 286–98. [95]
- McKee, S. P., Levi, D. M., and Bowne, S. F. (1990b). The imprecision of stereopsis. *Vision Research*, **30**, 1763–79. [181]
- McKee, S. P., Silverman, G. H., and Nakayama, K. (1986). Precise velocity discrimination despite random variations in temporal frequency and contrast. *Vision Research*, **26**, 609–19. [79]

- McKee, S. P., Welch L., Taylor, D. G., and Bowne, S. F. (1990a). Finding the common bond: Stereoacuity and the other hyper-acuities. *Vision Research*, 30, 879–91. [180-1]
- McKenna, M and Zeltzer, D. (1992). Three dimensional visual display systems for virtual environments. *Presence*, 1, 421–58. [28]
- McLaughlin, S. C. (1967). Parametric adjustment in saccadic eye movements. *Perception and Psychophysics*, 2, 359–62. [413]
- McLeod, R. W. and Ross, H. E. (1983). Optic-flow and cognitive factors in time-to-collision estimates. *Perception*, 12, 417–23. [555]
- McLin, L. N. and Schor, C. M. (1988). Voluntary effort as a stimulus to accommodation and vergence. *Investigative Ophthalmology and Visual Science*, 29, 1739–46. [399]
- McLin, L. N., Schor, C. M., and Kruger, P. B. (1988). Changing size (looming) as a stimulus to accommodation and vergence. *Vision Research*, 28, 883–98. [399]
- Meakin, S. O. and Shooter, E. M. (1992). The nerve growth factor family of receptors. *Trends in Neuroscience*, 15, 323–31. [69]
- Mehdorn, E. (1982). Nasal-temporal asymmetry of the optokinetic nystagmus after bilateral occipital infarction in man. In *Functional basis of ocular motility disorders*, (ed. G. Lennerstrand, D. S. Zee, and E. L. Keller), pp. 321–4. Pergamon Press, New York. [531]
- Meissner, G. (1854). *Beiträge zur Physiologie des Sehorganes*. W. Engleman, Leipzig. [53]
- Meister, M., Wong, R. O. L., Baylor, D. A., and Shatz, C. J. (1991). Synchronous bursts of action potentials in ganglion cells of the developing mammalian retina. *Science*, 252, 939–43. [609]
- Meredith, G. M., and Meredith, C. G. W. (1962). Effect of instructional conditions on rate of binocular rivalry. *Perceptual and Motor Skills*, 15, 655–64. [346p]
- Merigan, W. H. and Maunsell, J. H. R. (1990). Macaque vision after magnocellular lateral geniculate lesions. *Visual Neuroscience*, 5, 347–52. [127]
- Mershon, D. H. and Gogel, W. C. (1970). Effect of stereoscopic cues on perceived brightness. *American Journal of Psychology*, 83, 55–67. [524]
- Mershon, D. H., Jones, T. A., and Taylor, M. E. (1993). Organizational factors and the perception of motion in depth. *Perception and Psychophysics*, 54, 240–9. [429]
- Metzger, W. (1975). *Gesetze des Sehens*. Woldemar Kramer Verlag, Frankfurt. [507]
- Meyer, R. L. (1982). Tetrodotoxin blocks the formation of ocular dominance columns in goldfish. *Science*, 218, 589–91. [614]
- Mezrich, J. J. and Rose, A. (1977). Coherent motion and stereopsis in dynamic visual noise. *Vision Research*, 17, 903–10. [552]
- Michaels, C. F. (1986). An ecological analysis of binocular vision. *Psychological Research*, 48, 1–22. [285]
- Miezin, F. M., Myerson, J., Julesz, B., and Allman, J. M. (1981). Evoked potentials to dynamic random-dot correlograms in monkey and man: A test for cyclopean perception. *Vision Research*, 21, 177–9. [147]
- Mikaelian, H. H. (1975). Interocular generalization of orientation specific color aftereffects. *Vision Research*, 15, 661–3. [378]
- Miles, P. W. (1948). A comparison of aniseikonic test instruments and prolonged induction of artificial aniseikonia. *American Journal of Ophthalmology*, 36, 687–96. [67]
- Miles, P. W. (1953). Anomalous binocular depth perception due to unequal image brightness. *AMA Archives of Ophthalmology*, 50, 475–8. [310]
- Miles, W. R. (1930). Ocular dominance in human adults. *Journal of General Psychology*, 3, 412–30. [337]
- Miles, F. A., Judge, S. J., and Optican, L. M. (1987). Optically induced changes in the couplings between vergence and accommodation. *Journal of Neuroscience*, 7, 2576–89. [398]
- Milewski, A. and Yonas, A. (1977). Texture size specificity in the slant aftereffect. *Perception and Psychophysics*, 21, 47–9. [485]
- Miller, J. M., Anstis, T., and Templeton, W. B. (1981). Saccadic plasticity: Parametric adaptive control by retinal feedback. *Journal of Experimental Psychology: Human Perception and Performance*, 7, 356–66. [413]
- Miller, J. M., Ono, H., and Steinbach, M. J. (1980). Additivity of fusional vergence and pursuit eye movements. *Vision Research*, 20, 43–8. [411]
- Miller, K. D. (1994). A model for the development of simple cell receptive fields and the ordered arrangement of orientation columns through activity-dependent competition between on- and off-center inputs. *Journal of Neuroscience*, 14, 409–41. [614]
- Miller, K. D., Keller, J. B., and Stryker, M. P. (1989). Ocular dominance column development: Analysis and simulation. *Science*, 245, 605–15. [615]
- Miller, W. T., Sutton, R. S., and Werbos, P. J. (1991). *Neural networks for control*. MIT Press, Cambridge, MA. [92]
- Milleret, C. and Buser, P. (1984). Receptive field sizes and responsiveness to light in area 18 of the adult cat after chiasmotomy. Post-operative evolution; role of visual experience. *Experimental Brain Research*, 57, 73–81. [131]
- Milner, B. (1974). Hemispheric specialization: Scope and limits. In *The neurosciences: Third study programme*, (ed. F. O. Schmitt and F. G. Worden), pp. 75–89. MIT Press, Cambridge, MA. [82]
- Milner, P. M. (1974). A model for visual shape recognition. *Psychological Review*, 81, 521–35. [624]
- Minciachchi, D. and Antonini, A. (1984). Binocularly in the visual cortex of the adult cat does not depend on the integrity of the corpus callosum. *Behavioural Brain Research*, 13, 183–92. [132]
- Minucci, P. K. and Connors, M. M. (1964). Reaction time under three viewing conditions: Binocular, dominant eye, and nondominant eye. *Journal of Experimental Psychology*, 67, 268–75. [359]
- Mioche, L. and Perenin, M. T. (1986). Central and peripheral residual vision in humans with bilateral deprivation amblyopia. *Experimental Brain Research*, 62, 259–72. [626]
- Mitchell, A. M. and Ellerbrock, V. J. (1955). Fixation disparity and the maintenance of fusion in the horizontal meridian. *American Journal of Optometry*, 32, 520–34. [391]
- Mitchell, D. E. (1966a). Retinal disparity and diplopia. *Vision Research*, 6, 441–51. [317, 320]
- Mitchell, D. E. (1966b). A review of the concept of "Panum's fusional areas". *American Journal of Optometry*, 43, 387–401. [315–6]
- Mitchell, D. E. (1969). Qualitative depth localization with diplopic images of dissimilar shape. *Vision Research*, 9, 991–4. [218]
- Mitchell, D. E. (1970). Properties of stimuli eliciting vergence eye movements and stereopsis. *Vision Research*, 10, 145–62. [402, 404–5]
- Mitchell, D. E. (1988a). The extent of visual recovery from early monocular or binocular visual deprivation in kittens. *Journal of Physiology*, 395, 639–60. [635–6]
- Mitchell, D. E. (1988b). The recovery from early monocular visual deprivation in kittens. In *Perceptual development in infancy*, (ed. A. Yonas), pp. 1–34. Erlbaum, Hillsdale, N. J. [634, 636]
- Mitchell, D. E. (1988c). Animal models of human strabismic amblyopia. In *Advances in neural and behavioral development*. Vol. 3, (ed. P. G. Shinkman), pp. 209–69. Ablex, Norwood, NJ. [634]
- Mitchell, D. E. (1991). The long-term effectiveness of different regimens of occlusion on recovery from early monocular deprivation in kittens. *Philosophical Transactions of the Royal Society*, B333, 51–79. [634]

- Mitchell, D. E. and Baker, A. G. (1973). Stereoscopic aftereffects: Evidence for disparity-specific neurones in the human visual system. *Vision Research*, 13, 2273-88. [485, 487, 490]
- Mitchell, D. E. and Blakemore, C. (1970). Binocular depth perception and the corpus callosum. *Vision Research*, 10, 49-54. [132]
- Mitchell, D. E. and O'Hagan, S. (1972). Accuracy of stereoscopic localization of small line segments that differ in size or orientation for the two eyes. *Vision Research*, 12, 437-54. [201, 218]
- Mitchell, D. E. and Timney, B. (1982). Behavioural measurement of normal and abnormal development of vision in the cat. In *Analysis of visual behavior* (ed. D. J. Ingle, M. A. Goodale, and R. J. W. Mansfield), pp. 483-523. MIT Press, Cambridge, MA. [619, 626, 635]
- Mitchell, D. E. and Ware, C. (1974). Interocular transfer of visual after-effect in normal and stereoblind humans. *Journal of Physiology*, 236, 707-21. [640]
- Mitchell, D. E., Cynader, M., and Movshon, J. A. (1977). Recovery from the effects of monocular deprivation. *Journal of Comparative Neurology*, 176, 53-63. [636]
- Mitchell, D. E., Kaye, M., and Timney, B. (1979). Assessment of depth perception in cats. *Perception*, 8, 389-96. [645]
- Mitchell, D. E., Murphy, K. M., Dzioba, H. A., and Horne, J. A. (1986). Optimization of visual recovery from early monocular deprivation in kittens: Implications for occlusion therapy in the treatment of amblyopia. *Clinical Vision Science*, 1, 173-7. [634]
- Mitchell, D. E., Reardon, J., and Muir, D. W. (1975). Interocular transfer of the motion aftereffect in normal and stereoblind observers. *Experimental Brain Research*, 22, 163-75. [640]
- Mitchell, R. T. and Liaudansky, L. H. (1955). Effect of differential adaptation of the eyes upon threshold sensitivity. *Journal of the Optical Society of America*, 45, 831-4. [364]
- Mitchison, G. (1993). The neural representation of stereoscopic depth contrast. *Perception*, 22, 1415-26. [482-4]
- Mitchison, G. and Crick, F. (1982). Long axons within the striate cortex: Their distribution, orientation, and patterns of connection. *Proceedings of the National Academy of Science*, 79, 3661-5. [116, 612]
- Mitchison, G. J. and McKee, S. P. (1987a). The resolution of ambiguous stereoscopic matches by interpolation. *Vision Research*, 27, 285-94. [501]
- Mitchison, G. J. and McKee, S. P. (1987b). Interpolation and the detection of fine structure in stereoscopic matching. *Vision Research*, 27, 295-302. [502]
- Mitchison, G. J. and McKee, S. P. (1990). Mechanisms underlying the anisotropy of stereoscopic tilt perception. *Vision Research*, 30, 1781-91. [266]
- Mitchison, G. J. and Westheimer, G. (1984). The perception of depth in simple figures. *Vision Research*, 24, 1063-73. [161, 298, 471-2]
- Mitchison, G. J. and Westheimer, G. (1990). Viewing geometry and gradients of horizontal disparity. In *Vision: coding and efficiency* (ed. C. Blakemore), pp. 302-9. Cambridge University Press, Cambridge. [484]
- Mitson, L., Ono, H., and Barbeito, R. (1976). Three methods of measuring the location of the egocentre: Their reliability, comparative locations and intercorrelations. *Canadian Journal of Psychology*, 30, 1-8. [597]
- Miyake, S., Awaya, S., and Miyake, K. (1981). Aniseikonia in patients with a unilateral artificial lens, measured with Aulhorn's phase difference haploscope. *American Intraocular Implant Society Journal*, 7, 36-9. [64]
- Mohn, G. and Van Hof-van Duin, J. (1983). On the relation of stereoacuity to interocular transfer of the motion and the tilt aftereffects. *Vision Research*, 23, 1087-96. [640]
- Mohn, G. and Van Hof-van Duin, J. (1986). Development of the binocular and monocular visual fields of human infants during the first year of life. *Clinical Vision Science*, 1, 51-64. [617]
- Mohn, G. and Van Hof-van Duin, J. (1991). Development of spatial vision. In *Spatial vision* (ed. D. Regan), pp. 179-211. CRC Press, Boca Raton, FL. [617]
- Moidell, B., Steinbach, M. J., and Ono, H. (1988). Egocenter location in children enucleated at an early age. *Investigative Ophthalmology and Visual Science*, 29, 1348-51. [600]
- Mok, D., Ro, A., Cadena, W., Crawford, J. D., and Vilis, T. (1992). Rotation of Listing's plane during vergence. *Vision Research*, 32, 2055-64. [384]
- Mollon, J. (1974). Aftereffects and the brain. *New Scientist*, 61, 479-82. [466]
- Molyneux, W. (1692). *A treatise of Dioptricks*. B. Tooke, London. [11]
- Montague, P. R., Gancayco, C. D., Winn, M. J., Marchase, R. B., and Friedlander, M. J. (1994). Role of NO production in NMDA receptor-mediated neurotransmitter release in cerebral cortex. *Science*, 263, 973-7. [615]
- Montero, V. M. (1992). A quantitative study of synaptic contacts on interneurons and relay cells of the cat lateral geniculate nucleus. *Experimental Brain Research*, 86, 257-70. [113]
- Moore, R. J., Spear, P. D., Kim, C. B. Y., and Xue, J. T. (1992). Binocular processing in the cat's dorsal lateral geniculate nucleus III. Spatial frequency, orientation, and direction sensitivity of nondominant-eye influences. *Experimental Brain Research*, 89, 588-98. [113, 345]
- Moraglia, G. and Schneider, B. (1990). Effects of direction and magnitude of horizontal disparities on binocular unmasking. *Perception*, 19, 581-93. [368]
- Moraglia, G. and Schneider, B. (1991). Binocular unmasking with vertical disparity. *Canadian Journal of Psychology*, 45, 353-66. [368]
- Moran, G., Timney, B., Sorenson, L., and Desrochers, B. (1983). Binocular depth perception in the Meerkat (*Suricata suricatta*). *Vision Research*, 23, 965-9. [656]
- Moran, J. and Desimone, R. (1985). Selective attention gates visual processing in the extrastriate cortex. *Science*, 229, 782-4. [128]
- Moran, J. and Gordon, B. (1982). Long term visual deprivation in a human. *Vision Research*, 22, 27-36. [633]
- Morant, R. B. and Harris, J. R. (1965). Two different aftereffects of exposure to visual tilts. *American Journal of Psychology*, 78, 218-26. [490]
- Morgan, C. L. (1978). Constancy of egocentric visual direction. *Perception and Psychophysics*, 23, 61-8. [432]
- Morgan, M. J. (1975). Stereoillusion based on visual persistence. *Nature*, 256, 639-40. [542]
- Morgan, M. J. (1976). Pulfrich effect and the filling in of apparent motion. *Perception*, 5, 187-95. [542, 544]
- Morgan, M. J. (1977). Differential visual persistence between the two eyes: A model for the Fertsch-Pulfrich effect. *Journal of Experimental Psychology: Human Perception and Performance*, 3, 484-95. [544]
- Morgan, M. J. (1979). Perception of continuity in stroboscopic motion: A temporal frequency analysis. *Vision Research*, 19, 491-500. [543, 553]
- Morgan, M. J. (1980). Spatiotemporal filtering and the interpolation effect in apparent motion. *Perception*, 9, 161-74. [542]
- Morgan, M. J. (1981). Vernier acuity and stereopsis with discontinuously moving stimuli. *Acta Psychologica*, 48, 57-67. [542]
- Morgan, M. J. (1986). Positional acuity without monocular cues. *Perception*, 15, 157-62. [182]

- Morgan, M. J. and Hotopf, W. H. N. (1989). Perceived diagonals in grids and lattices. *Vision Research*, **29**, 1005–15. [76-7]
- Morgan, M. J. and Thompson, P. (1975). Apparent motion and the Pulfrich effect. *Perception*, **4**, 3–18. [536, 540, 542-3]
- Morgan, M. J. and Tyler, C. W. (1993). Dynamic visual noise stereophenomenon revisited. *Investigative Ophthalmology and Visual Science*, **34** (ARVO Abstracts), 708. [553]
- Morgan, M. J. and Ward, R. (1980). Interocular delay produces depth in subjectively moving noise patterns. *Quarterly Journal of Experimental Psychology*, **32**, 387–95. [553]
- Morgan, M. W. (1955). A unique case of double monocular diplopia. *American Journal of Optometry*, **32**, 70–87. [47]
- Morgan, M. W. (1968). Accommodation and vergence. *American Journal of Optometry and Archives of American Academy of Optometry*, **45**, 417–53. [398]
- Morley, J. W., Judge, S. J., and Lindsey, J. W. (1992). Role of monkey midbrain near-response neurons in phoria adaptation. *Journal of Neurophysiology*, **67**, 1475–92. [426]
- Morley, J. W., Lindsey, J. W., and Judge, S. J. (1988). Prism-adaptation in a strabismic monkey. *Clinical Vision Science*, **3**, 1–8. [391]
- Morrison, J. D. and Whiteside, T. C. D. (1984). Binocular cues in the perception of distance of a point source of light. *Perception*, **13**, 555–66. [429]
- Morrison, L. C. (1972). Further studies on the adaptation to artificially-produced aniseikonia. *British Journal of Physiological Optics*, **27**, 84–101. [67]
- Morrison, L. C. (1977). Stereoscopic localization with the eyes asymmetrically converged. *American Journal of Optometry and Physiological Optics*, **54**, 556–66. [60]
- Morrone, M. C., Burr, D. C., and Maffei, L. (1982). Functional complications of cross-orientation inhibition of cortical visual cells. I. Neurophysiological evidence. *Proceedings of the Royal Society London*, **B216**, 335–54. [345]
- Moschovakis, A. K., Scudder, C. A., and Highstein, S. M. (1990). A structural basis for Hering's law: Projections to extraocular motoneurons. *Science*, **248**, 1118–19. [410]
- Motter, B. C. (1991). Beyond extrastriate cortex: The parietal visual system. In *Vision and visual dysfunction*. Vol. IV, (ed. A. L. Leventhal), pp. 371–87. Macmillan, London. [126]
- Motter, B. C. (1993). Focal attention produces spatially selective processing in visual cortical areas V1, V2, and V4 in the presence of competing stimuli. *Journal of Neurophysiology*, **70**, 909–19. [129]
- Motter, B. C. and Poggio, G. F. (1984). Binocular fixation in the rhesus monkey: Spatial and temporal characteristics. *Experimental Brain Research*, **54**, 304–14. [178, 401]
- Motter, B. C. and Poggio, G. F. (1990). Dynamic stabilization of receptive fields of cortical neurons during fixation of gaze in the macaque. *Experimental Brain Research*, **83**, 37–43. [178]
- Moulden, B. P. (1980). After-effects and the integration of patterns of neural activity within a channel. *Philosophical Transactions of the Royal Society of London*, **B290**, 39–55. [370, 373]
- Mountcastle, V. B. (1956). Modality and topographic properties of single neurons of cat's somatic sensory cortex. *Journal of Neurophysiology*, **19**, 408–34. [119]
- Movshon, J. A. (1976). Reversal of the behavioural effects of monocular deprivation in the kitten. *Journal of Physiology*, **261**, 175–87. [636]
- Movshon, J. A. and Lennie, P. (1979). Pattern-selective adaptation in visual cortical neurones. *Nature New Biology*, **278**, 850–2. [342]
- Movshon, J. A., Thompson, I. D., and Tolhurst, D. J. (1978). Spatial and temporal contrast sensitivity of neurones in areas 17 and 18 of the cat's visual cortex. *Journal of Physiology*, **283**, 101–20. [138, 259]
- Movshon, J. A., Adelson, E. H., Gizzi, M. S., and Newsome, W. T. (1985). The analysis of moving visual patterns. In *Pattern recognition mechanisms*, (ed. C. Chigas, R. Gattas, and C. Gross), pp. 117–51. Springer, New York. [526]
- Movshon, J. A., Chambers, B. E. I., and Blakemore, C. (1972). Interocular transfer in normal humans, and those who lack stereopsis. *Perception*, **1**, 483–90. [640]
- Mowafy, L. (1991). Static depth cues do affect the perceived direction of motion. *Perception*, **19**, 595–609. [460]
- Mower, G. D., Caplan, C. J., and Letsou, G. (1982). Behavioral recovery from binocular deprivation in the cat. *Behavioural Brain Research*, **4**, 209–15. [626]
- Mowforth, P., Mayhew, J. E. W., and Frisby, J. P. (1981). Vergence eye movements made in response to spatial-frequency-filtered random-dot stereograms. *Perception*, **10**, 299–304. [400]
- Mueller, C. G. and Lloyd, V. V. (1948). Stereoscopic acuity for various levels of illumination. *Proceedings of the National Academy of Science*, Washington, **34**, 223–7. [168]
- Mueller, T. J. (1990). A physiological model of binocular rivalry. *Visual Neuroscience*, **4**, 63–73. [345]
- Mueller, T. J. and Blake, R. (1989). A fresh look at the temporal dynamics of binocular rivalry. *Biological Cybernetics*, **61**, 223–32. [328, 344]
- Müller, C. M. and Best, J. (1989). Ocular dominance plasticity in adult cat visual cortex after transplantation of cultured astrocytes. *Nature*, **342**, 427–30. [613]
- Müller, H. (1854). Über die entopische Wahrnehmung der Netzhautgefäße, insbesondere als Beweismittel für die Lichtperception durch die nach hinten gelegenen Netzhautelemente. *Verhandlungen der Physiologischen Medizin Gesellschaft Würzburg*, **5**, 411. [12, 106]
- Müller, J. (1826). *Zur Vergleichenden Physiologie des Gesichtssinnes des Menschen und der Thiere*. Cnobloch, Leipzig. [18]
- Müller, J. (1843). *Elements of physiology*. Vol. 2, pp. 1147–8. Trans. by W. Baly. Taylor and Walton, London. [73, 396]
- Münster, C. (1941). Über den Einfluss von Helligkeits Unterscheiden in Beiden Augen auf die stereoscopische Wahrnehmung. *Zeitschrift für Sinnesphysiologie*, **69**, 245–60. [310]
- Murasugi, C. M., Salzman, C. D., and Newsome, W. T. (1993). Microstimulation in visual area MT: Effects of varying pulse amplitude and frequency. *Journal of Neuroscience*, **13**, 1719–29. [376]
- Murata, T. and Shimizu, H. (1993). Oscillatory binocular system and temporal segmentation of stereoscopic depth surfaces. *Biological Cybernetics*, **68**, 381–91. [81]
- Murch, G. M. (1972). Binocular relationships in a size and color orientation specific aftereffect. *Journal of Experimental Psychology*, **93**, 30–4. [378]
- Murch, G. M. (1974). Color contingent motion aftereffects: Single or multiple levels of processing. *Vision Research*, **14**, 1181–4. [378]
- Murphy, K. M. and Mitchell, D. E. (1987). Reduced visual acuity in both eyes of monocularly deprived kittens following a short or long period of reverse occlusion. *The Journal of Neuroscience*, **7**, 1526–36. [633]
- Murphy, K. M. and Mitchell, D. E. (1991). Vernier acuity of normal and visually deprived cats. *Vision Research*, **31**, 253–66. [632]
- Murray, E. (1939). Binocular fusion and the locus of 'yellow'. *American Journal of Psychology*, **52**, 117–21. [326]
- Mustari, M. J. and Fuchs, A. F. (1990). Discharge patterns of neurons in the pretectal nucleus of the optic tract NOT in the behaving primate. *Journal of Neurophysiology*, **64**, 77–90. [530]

- Mustari, M. J., Fuchs A. F., and Wallman, J. (1988). Response properties of dorsolateral pontine units during smooth pursuit in the Rhesus macaque. *Journal of Neurophysiology*, 60, 664–86. [530]
- Mustillo, P. (1985). Binocular mechanisms mediating crossed and uncrossed stereopsis. *Psychological Bulletin*, 97, 187–201. [167]
- Mustillo, P. and Fox, R. (1986). The perception of illusory contours in the hypercyclopean domain. *Perception and Psychophysics*, 40, 362–3. [510]
- Mustillo, P., Francis, E., Oross, S., Fox, R., and Orban, G. A. (1988). Anisotropies in global stereoscopic orientation discrimination. *Vision Research*, 28, 1315–21. [588]
- Mutch, K., Smith, I. M., and Yonas, A. (1983). The effect of two-dimensional and three-dimensional distance on apparent motion. *Perception*, 12, 305–12. [528]
- Nachmias, J. and Sansbury, R. V. (1974). Grating contrast: Discrimination may be better than detection. *Vision Research*, 14, 1039–42. [355]
- Nagel, A. (1868). Über das Vorkommen von wahren Rollungen des Auge um die Gesichtslinie. *Archiv für Ophthalmologie*, 14, 228–46. [421]
- Nakayama, K. (1975). Coordination of extraocular muscles. In *Basic mechanisms of ocular motility and their clinical implications* (ed. B. Lennerstrand and P. Bach-y-Rita), pp. 193–208. Pergamon, New York. [385]
- Nakayama, K. (1977). Geometric and physiological aspects of depth perception. *Proceedings of Society of Photo-Optical Instrument Engineers*, 120, 2–9. [56, 60]
- Nakayama, K. (1978). A new method of determining the primary position of the eye using Listing's law. *American Journal of Optometry*, 55, 331–6. [385]
- Nakayama, K. and Shimojo, S. (1990). Da Vinci stereopsis: Depth and subjective occluding contours from unpaired image points. *Vision Research*, 30, 1811–25. [514, 520, 523]
- Nakayama, K. and Shimojo, S. (1992). Experiencing and perceiving visual surfaces. *Science*, 257, 1357–63. [508]
- Nakayama, K. and Silverman, G. H. (1986). Serial and parallel processing of visual feature conjunctions. *Nature*, 320, 264–5. [212]
- Nakayama, K. and Tyler, C. W. (1978). Relative motion induced between stationary lines. *Vision Research*, 18, 1663–8. [101, 533]
- Nakayama, K., Shimojo, S., and Ramachandran, V. S. (1990). Transparency: Relation to depth, subjective contours, luminance, and neon color spreading. *Perception*, 19, 497–513. [510]
- Nakayama, K., Shimojo, S., and Silverman, G. H. (1989). Stereoscopic depth: Its relation to image segmentation, grouping, and the recognition of occluded objects. *Perception*, 18, 55–8. [505]
- Nawrot, M. and Blake, R. (1989). Neural integration of information specifying structure from stereopsis and motion. *Science*, 244, 716–18. [438–9, 447, 566]
- Nawrot, M. and Blake, R. (1991a). The interplay between stereopsis and structure from motion. *Perception and Psychophysics*, 49, 230–44. [438, 566]
- Nawrot, M. and Blake, R. (1991b). A neural network model of kinetic depth. *Visual Neuroscience*, 6, 219–27. [439]
- Nawrot, M. and Blake, R. (1993a). On the perceptual identity of dynamic stereopsis and kinetic depth. *Vision Research*, 33, 1561–71. [439]
- Nawrot, M. and Blake, R. (1993b). Visual alchemy: stereoscopic adaptation produces kinetic depth from random noise. *Perception*, 22, 635–42. [439, 566]
- Nealey, T. A. and Maunsell, J. H. R. (1994). Magnocellular and parvocellular contributions to the responses of neurons in macaque striate cortex. *Journal of Neuroscience*, 14, 2069–79. [126]
- Neary, C. (1992). The effect of a binocular disparate background on smooth pursuit eye movements. *Perception*, 21 (Supplement 2), 52. [532]
- Nedergaard, M. (1994). Direct signaling from astrocytes to neurons in cultures of mammalian brain cells. *Science*, 263, 1768–71. [71]
- Needham, J. (1962). *Science and civilization in China*. Vol 4, Part 1. Cambridge University Press, London. [6, 9]
- Neill, R. A. (1981). Spatio-temporal averaging and the dynamic visual noise stereophenomenon. *Vision Research*, 21, 673–82. [551–3]
- Neisser, U. (1967). *Cognitive psychology*. Appleton-Century-Crofts, New York. [104]
- Nelson, J. I. (1975). Globality and stereoscopic fusion in binocular vision. *Journal of Theoretical Biology*, 49, 1–88. [228]
- Nelson, J. I. (1977). The plasticity of correspondence: After-effects, illusions and horopter shifts in depth perception. *Journal of Theoretical Biology*, 66, 203–66. [461, 463–4]
- Nelson, J. I. and Frost, B. J. (1978). Orientation selective inhibition from beyond the classic visual receptive field. *Brain Research*, 139, 359–65. [119, 129]
- Nelson, J. I. and Frost, B. J. (1985). Intracortical facilitation among co-oriented, co-axially aligned simple cells in cat striate cortex. *Experimental Brain Research*, 61, 54–61. [76, 116–7, 612]
- Nelson, J. I., Kato, H., and Bishop, P. O. (1977). Discrimination of orientation and position disparities by binocularly activated neurons in cat striate cortex. *Journal of Neurophysiology*, 40, 260–83. [142, 272]
- Newhouse, M. and Uttal, W. R. (1982). Distribution of stereoanomalies in the general population. *Bulletin of the Psychonomic Society*, 20, 48–50. [624]
- Newsome, W. T., Wurtz, R. H., and Komatsu, H. (1988). Relation of cortical areas MT and MST to pursuit eye movements. II. Differentiation of retinal from extraretinal inputs. *Journal of Neurophysiology*, 60, 604–20. [530]
- Newton, I. (1704). *Opticks*. Smith and Walford, London. 1799 printing based on the 4th edition. New York, Dover. [12]
- Ng, A. Y. K. and Stone, J. (1982). The optic nerve of the cat: Appearance and loss of axons during normal development. *Developmental Brain Research*, 5, 263–71. [606]
- Nickalls, R. W. D. (1986). The rotating Pulfrich effect, and a new method of determining visual latency differences. *Vision Research*, 26, 367–72. [537]
- Nicol, J. A. C. (1989). *The eyes of fishes*. Clarendon Press, Oxford. [650]
- Niebur, E., Koch, C., and Rosen, C. (1993). An oscillation-based model for the neuronal basis of attention. *Vision Research*, 33, 2798–802. [83]
- Nielsen, K. R. K. and Poggio, T. (1984). Vertical image registration in stereopsis. *Vision Research*, 24, 1133–40. [320]
- Nikara, T., Bishop, P. O., and Pettigrew, J. D. (1968). Analysis of retinal correspondence by studying receptive fields of binocular single units in cat striate cortex. *Experimental Brain Research*, 6, 353–72. [130, 133–4]
- Ninio, J. (1981). Random-curve stereograms: A flexible tool for the study of binocular vision. *Perception*, 10, 403–10. [154]
- Ninio, J. (1985). Orientational versus horizontal disparity in the stereoscopic appreciation of slant. *Perception*, 14, 305–14. [219, 273–4]
- Ninio, J. and Herlin, I. (1988). Speed and accuracy of 3D interpretation of linear stereograms. *Vision Research*, 28, 1223–33. [219]
- Ninio, J. and Mizraji, E. (1985). Errors in the stereoscopic separation of surfaces represented with regular textures. *Perception*, 14, 315–28. [204]

- Nishida, S., Ashida, H., and Sato, T. (1994). Complete transfer of motion aftereffect with flickering test. *Vision Research*, 34, 2707-16. [376]
- Noda, H. (1986). Mossy fibres sending retinal slip, eye, and head velocity signals to the flocculus of the monkey. *Journal of Physiology*, 379, 39-60. [530]
- Nomura, M. (1993). A model for neural representation of binocular disparity in striate cortex: Distributed representation and veto mechanism. *Biological Cybernetics*, 69, 165-71. [138]
- Nomura, M., Matsumoto, G., and Fugiwara, S. (1990). A binocular model for the simple cell. *Biological Cybernetics*, 63, 237-42. [138]
- Noorden, G. K. von (1990). *Binocular vision and ocular motility*. Mosby, St Louis, MO. [1, 387]
- Noorden, G. K. von and Crawford, M. L. J. (1981). Failure to preserve cortical binocularity in strabismic monkeys raised in a unidirectional visual environment. *Investigative Ophthalmology and Visual Science*, 20, 665-70. [631]
- Noorden, G. K. von and Crawford, M. L. J. (1992). The lateral geniculate nucleus in human strabismic amblyopia. *Investigative Ophthalmology and Visual Science*, 33, 2729-32. [626]
- Noorden, G. K. von and Leffler, M. B. (1966). Visual acuity in strabismic amblyopia under monocular and binocular conditions. *AMA Archives of Ophthalmology*, 76, 172-7. [632]
- Noorden, G. K. von and Middleditch, P. R. (1975). Histology of the monkey lateral geniculate nucleus after unilateral lid closure and experimental strabismus: Further observations. *Investigative Ophthalmology*, 14, 674-83. [626]
- Norcia, A. M. and Tyler, C. W. (1984). Temporal frequency limits for stereoscopic apparent motion processes. *Vision Research*, 24, 395-401. [189]
- Norcia, A. M. and Tyler, C. W. (1985). Spatial frequency sweep VEP: Visual acuity during the first year of life. *Vision Research*, 25, 1399-408. [616]
- Norcia, A. M., Sutter, E. E., and Tyler, C. W. (1985). Electrophysiological evidence for the existence of coarse and fine disparity mechanisms in human. *Vision Research*, 25, 1603-11. [147]
- Norcia, A. M., Tyler, C. W., and Allen, D. (1986). Electrophysiological assessment of contrast sensitivity in human infants. *American Journal of Optometry and Physiological Optics*, 63, 12-15. [616]
- Norcia, A. M., Tyler, C. W., and Hamer, R. D. (1988). High visual contrast sensitivity in the young human infant. *Investigative Ophthalmology and Visual Science*, 29, 44-9. [616]
- Norcia, A. M., Garcia, H., Humphry, R., Holmes, A., Hamer, R. D., and Orel-Bixler, D. (1991). Anomalous motion VEPs in infants and in infantile esotropia. *Investigative Ophthalmology and Visual Science*, 32, 436-9. [617]
- Norman, J. F., Lappin, J. S., and Zucker, S. W. (1991). The discriminability of smooth stereoscopic surfaces. *Perception*, 20, 789-807. [157]
- Nothdurft, H. C. (1985). Texture discrimination does not occur at the cyclopean retina. *Perception*, 14, 527-37. [210]
- Nuzzi, G. and Franchi, A. (1983). Binocular interaction in visual-evoked responses: Summation, facilitation and inhibition in a clinical study of binocular vision. *Ophthalmic Research*, 15, 261-82. [620]
- Nye, P. W. (1968). The binocular acuity of the pigeon measured in terms of the modulation transfer function. *Vision Research*, 8, 1041-53. [653]
- O'Brien, V. (1958). Contour perception, illusion and reality. *Journal of the Optical Society of America*, 48, 112-19. [480]
- Odom, J. V. and Chao, G. M. (1987). A stereo illusion induced by binocularly presented gratings: Effects of number of eyes stimulated, spatial frequency, orientation, field size, and viewing distance. *Perception and Psychophysics*, 42, 140-9. [43]
- Odom, J. V., Hoyt, C. S., and Marg, E. (1981). Effects of natural deprivation and unilateral eye patching on visual acuity of infants and children. *AMA Archives of Ophthalmology*, 99, 1412-16. [634]
- Ogle, K. N. (1932). An analytical treatment of the longitudinal horopter; its measurement and application to related phenomena, especially to the relative size and shape of the ocular images. *Journal of the Optical Society of America*, 22, 665-728. [58, 304]
- Ogle, K. N. (1938). Induced size effect. I. A new phenomenon in binocular space-perception associated with the relative sizes of the images of the two eyes. *AMA Archives of Ophthalmology*, 20, 604-23. [266, 275, 285-6]
- Ogle, K. N. (1939a). Induced size effect. II. An experimental study of the phenomenon with restricted fusion stimuli. *AMA Archives of Ophthalmology*, 21, 604-25. [266, 275, 286]
- Ogle, K. N. (1939b). Induced size effect. III. A study of the phenomenon as influenced by horizontal disparity of the fusion contours. *AMA Archives of Ophthalmology*, 22, 613-35. [266, 275, 286]
- Ogle, K. N. (1939c). Relative sizes of ocular images of the two eyes in asymmetrical convergence. *AMA Archives of Ophthalmology*, 22, 1046-67. [177, 283]
- Ogle, K. N. (1946). The binocular depth contrast phenomenon. *American Journal of Psychology*, 59, 111-26. [466, 484]
- Ogle, K. N. (1952). On the limits of stereoscopic vision. *Journal of Experimental Psychology*, 44, 253-9. [159]
- Ogle, K. N. (1953). Precision and validity of stereoscopic depth perception from double images. *Journal of the Optical Society of America*, 43, 906-13. [155]
- Ogle, K. N. (1955). Stereopsis and vertical disparity. *AMA Archives of Ophthalmology*, 53, 495-504. [167]
- Ogle, K. N. (1956). Stereoscopic acuity and the role of convergence. *Journal of the Optical Society of America*, 46, 269-73. [177]
- Ogle, K. N. (1958). Note on stereoscopic acuity and viewing distance. *Journal of the Optical Society of America*, 48, 794-8. [179]
- Ogle, K. N. (1962). The optical space sense. In *The eye*. Vol. 4, (ed. H. Davson), pp. 211-432. Academic Press, New York. [306, 310, 536]
- Ogle, K. N. (1963). Stereoscopic depth perception and exposure delay between images to the two eyes. *Journal of the Optical Society of America*, 53, 1296-304. [185]
- Ogle, K. N. (1964). *Researches in binocular vision*. Hafner, New York. [1, 55, 57, 59, 64-6, 259, 292, 304, 316, 462, 469]
- Ogle, K. N. and Ellerbrock, V. J. (1946). Cyclofusional movements. *AMA Archives of Ophthalmology*, 36, 700-35. [417-8, 421]
- Ogle, K. N. and Prangen, A. de H. (1951). Further considerations of fixation disparity and the binocular fusional processes. *American Journal of Ophthalmology*, 34, 57-72. [390]
- Ogle, K. N. and Prangen, A. de H. (1953). Observations on vertical divergences and hyperphorias. *AMA Archives of Ophthalmology*, 49, 313-34. [390-3]
- Ogle, K. N. and Reiher, L. (1962). Stereoscopic depth perception from after-images. *Vision Research*, 2, 439-47. [178, 458]
- Ogle, K. N. and Wakefield, J. M. (1967). Stereoscopic depth and binocular rivalry. *Vision Research*, 7, 89-98. [339]
- Ogle, K. N. and Weil, M. P. (1958). Stereoscopic vision and the duration of the stimulus. *AMA Archives of Ophthalmology*, 59, 4-17. [178, 184]
- Ogle, K. N., Burian, H. M., and Bannon, R. E. (1958). On the correction of unilateral aphakia with contact lenses. *AMA Archives of Ophthalmology*, 59, 639-52. [64]

- Ogle, K. N., Martens, T. G., and Dyer, J. A. (1967). *Oculomotor imbalance in binocular vision and fixation disparity*. Lea and Febiger, Philadelphia. [1, 390-2, 396]
- Ogle, K. N., Mussey, F., and Prangen, A. de H. (1949). Fixation disparity and the fusional processes in binocular single vision. *American Journal of Ophthalmology*, **32**, 1069-87. [390]
- Ohmi, M. and Howard, I. P. (1991). Induced visual motion; dissociation of oculocentric and headcentric (oculomotor) components. *Investigative Ophthalmology and Visual Science*, **32** (ARVO Abstracts), 1272. [533]
- Ohmi, M., Howard, I. P., and Landolt, J. (1987). Circularvection as a function of foreground-background relationships. *Perception*, **16**, 17-22. [534]
- Ohwaki, S. (1960). On the destruction of geometrical illusions in stereoscopic observation. *Tohoku Psychological Folia*, **29**, 24-36. [372]
- Ohzawa, I. and Freeman, R. D. (1986a). The binocular organization of simple cells in the cat's visual cortex. *Journal of Neurophysiology*, **56**, 221-42. [137, 140]
- Ohzawa, I. and Freeman, R. D. (1986b). The binocular organization of complex cells in the cat's visual cortex. *Journal of Neurophysiology*, **56**, 243-60. [138]
- Ohzawa, I. and Freeman, R. D. (1988). Cyclopean visual evoked potentials: A new test of binocular vision. *Vision Research*, **28**, 1167-70. [355]
- Ohzawa, I., DeAngelis, G. C., and Freeman, R. D. (1990). Stereoscopic depth discrimination in the visual cortex: Neurons ideally suited as disparity detectors. *Science*, **249**, 1037-41. [138]
- Okada, M., Erickson, A., and Hendrickson, (1994). Light and electron microscopic analysis of synaptic development in Macaca monkey retina as described by immunocytochemical labeling for the synaptic vesicle protein. *Journal of Comparative Neurology*, **339**, 535-58. [605]
- O'Keefe, L. P. and Berkley, M. A. (1991). Binocular immobilization induced by paralysis of the extraocular muscles of one eye: Evidence for an interocular proprioceptive mechanism. *Journal of Neurophysiology*, **66**, 2022-33. [410]
- Okoshi, T. (1976). *Three-dimensional imaging techniques*. Academic Press, New York. [26, 28]
- O'Kusky, J. and Colonnier, M. (1982). Postnatal changes in the number of neurons and analysis in normal and monocularly deprived animals. *Journal of Comparative Neurology*, **210**, 291-306. [610, 628]
- O'Leary, A. and Wallach, H. (1980). Familiar size and linear perspective as distance cues in stereoscopic depth constancy. *Perception and Psychophysics*, **27**, 131-5. [433]
- Olson, C. B. and Swett, C. P. (1971). Effect of prior activity on properties of different types of motor units. *Journal of Neurophysiology*, **34**, 1-16. [432]
- Olson, C. R. and Freeman, R. D. (1978). Monocular deprivation and recovery during sensitive period in kittens. *Journal of Neurophysiology*, **41**, 65-74. [636]
- Olson, C. R. and Freeman, R. D. (1980). Cumulative effect of brief daily periods of monocular vision on kittens striate cortex. *Experimental Brain Research*, **38**, 53-6. [635]
- O'Malley, C. D. (1964). *Andreas Vesalius of Brussels*. Cambridge University Press, London. [10]
- Ono, H. (1979). Axiomatic summary and deductions from Hering's principles of visual direction. *Perception and Psychophysics*, **25**, 473-7. [596]
- Ono, H. (1980). Hering's law of equal innervation and vergence eye movement. *American Journal of Optometry and Physiological Optics*, **57**, 578-85. [409]
- Ono, H. (1981). On Well's (1792) law of visual direction. *Perception and Psychophysics*, **30**, 403-6. [597]
- Ono, H. (1983). The combination of version and vergence. In *Vergence eye movements: Basic and clinical aspects*, (ed. M. C. Schor, K. J. Ciuffreda), pp. 373-400. Butterworth, Boston. [413]
- Ono, H. (1984). Exorcising the double-nail illusion: Giving up the ghost. *Perception*, **13**, 763-8. [45, 523]
- Ono, H. and Angus, R. (1974). Adaptation to sensory-motor conflict produced by the visual direction of the hand specified from the cyclopean eye. *Journal of Experimental Psychology*, **103**, 1-9. [597]
- Ono, H. and Barbeito, R. (1982). The cyclopean eye vs. the sighting-dominant eye as the center of visual direction. *Perception and Psychophysics*, **32**, 201-10. [598]
- Ono, H. and Barbeito, R. (1985). Utrocular discrimination is not sufficient for utrocular identification. *Vision Research*, **25**, 289-99. [601]
- Ono, H. and Comerford, J. (1977). Stereoscopic depth constancy. In *Stability and constancy in visual perception*, (ed. W. Epstein), pp. 91-128. Wiley, Toronto. [457]
- Ono, H. and Gonda, G. (1978). Apparent movement, eye movements and phoria when two eyes alternate in viewing a stimulus. *Perception*, **7**, 75-83. [599]
- Ono, H. and Mapp, A. P. (1994). A restatement and modification of Wells-Hering's laws of visual direction. *Perception*, in press. [423, 597]
- Ono, H. and Nakamizo, S. (1978). Changing fixation in the transverse plane at eye level and Hering's law of equal innervation. *Vision Research*, **18**, 511-19. [412]
- Ono, H. and Steinbach, M. J. (1983). The Pulfrich phenomenon with eye movement. *Vision Research*, **23**, 1735-7. [550]
- Ono, H. and Tam, W. J. (1981). Asymmetrical vergence and multiple saccades. *Vision Research*, **21**, 739-43. [412]
- Ono, H. and Wade, N. J. (1985). Resolving discrepant results of the Wheatstone experiment. *Psychological Research*, **47**, 135-42. [21]
- Ono, H. and Weber, E. U. (1981). Nonveridical visual direction produced by monocular viewing. *Journal of Experimental Psychology: Human Perception and Performance*, **7**, 937-47. [599]
- Ono, H., Angus, R., and Gregor, P. (1977). Binocular single vision achieved by fusion and suppression. *Perception and Psychophysics*, **21**, 513-21. [597]
- Ono, H., Hasdorff, A. H., and Osgood, C. E. (1966). Binocular rivalry as a function of incongruity in meaning. *Scandinavian Journal of Psychology*, **7**, 225-33. [348]
- Ono, H., Komoda, M., and Mueller, E. R. (1971a). Intermittent stimulation of binocular disparate colors and central fusion. *Perception and Psychophysics*, **9**, 343-7. [327]
- Ono, H., Mitson, L., and Seabrook, K. (1971b). Change in convergence and retinal disparities as an explanation for the wallpaper phenomenon. *Journal of Experimental Psychology*, **91**, 1-10. [431]
- Ono, H., Nakamizo, S., and Steinbach, M. J. (1978). Nonadditivity of vergence and saccadic eye movement. *Vision Research*, **18**, 735-39. [412]
- Ono, H., Shimono, K., and Shibuta, K. (1992). Occlusion as a depth cue in the Wheatstone-Panum limiting case. *Perception and Psychophysics*, **51**, 3-13. [523]
- Ono, H., Wilkinson, A., Muter, P., and Mitson, L. (1972). Apparent movement and change in perceived location of a stimulus produced by a change in accommodative vergence. *Perception and Psychophysics*, **12**, 187-92. [599]
- Ono, M. E., Rivest, J., and Ono, H. (1986). Depth perception as a function of motion parallax and absolute-distance information. *Journal of Experimental Psychology: Human Perception and Performance*, **12**, 331-7. [447]

- Oohira, A. and Zee, D. S. (1992). Disconjugate ocular motor adaptation in rhesus monkey. *Vision Research*, 32, 489–97. [413]
- Oohira, A., Zee, D. S., and Guyton, D. L. (1991). Disconjugate adaptation to long-standing, large-amplitude spectacle-corrected anisometropia. *Investigative Ophthalmology and Visual Science*, 32, 1693–703. [414]
- Optican, L. M. (1982). Saccadic dysmetria. In *Functional basis of ocular motility disorders* (ed. G. Lennerstrand, D. S. Zee, and E. L. Keller), pp. 441–51. Pergamon Press, New York. [414]
- Optican, L. M. and Robinson, D. A. (1980). Cerebellar-dependent adaptive control of primate saccadic system. *Journal of Neurophysiology*, 44, 1058–76. [414]
- Optican, L. M., Zee, D. S., and Chu, F. C. (1985). Adaptive response to ocular muscle weakness in human pursuit and saccadic eye movements. *Journal of Neurophysiology*, 54, 110–22. [414]
- Oram, M. W. and Perrett, D. I. (1992). Time course of neural responses discriminating different views of the face and head. *Journal of Neurophysiology*, 68, 70–84. [78]
- Orbach, H. S. and Van Essen, D. C. (1993). *In vivo* tracing of pathways and spatio-temporal activity patterns in rat visual cortex using voltage sensitive dyes. *Experimental Brain Research*, 94, 371–92. [110]
- O'Rourke, N. A., Dailey, M. E., Smith, S. J., and McConnell, S. K. (1992). Diverse migratory pathways in the developing cerebral cortex. *Science*, 258, 299–302. [610]
- O'Shea, R. P. (1987). Chronometric analysis supports fusion rather than suppression theory of binocular vision. *Vision Research*, 27, 781–91. [339]
- O'Shea, R. P. (1989). Depth with rival, Kaufman-type stereograms. *Investigative Ophthalmology and Visual Science*, 30 (ARVO Abstracts), 389. [201]
- O'Shea, R. P. and Blake, R. (1986). Dichoptic temporal frequency differences do not lead to binocular rivalry. *Perception and Psychophysics*, 39, 59–63. [333]
- O'Shea, R. P. and Blake, R. (1987). Depth without disparity in random-dot stereograms. *Perception and Psychophysics*, 42, 205–14. [308, 504, 586]
- O'Shea, R. P. and Crassini, B. (1981a). The sensitivity of binocular rivalry suppression to changes in orientation assessed by reaction-time and forced-choice techniques. *Perception*, 10, 283–93. [336]
- O'Shea, R. P. and Crassini, B. (1981b). Interocular transfer of the motion after-effect is not reduced by binocular rivalry. *Vision Research*, 21, 801–4. [343]
- O'Shea, R. P. and Crassini, B. (1982). The dependence of cyclofusion on orientation. *Perception and Psychophysics*, 32, 195–6. [321]
- O'Shea, R. P. and Crassini, B. (1984). Binocular rivalry occurs without simultaneous presentation of rival stimuli. *Perception and Psychophysics*, 36, 266–76. [333]
- O'Shea, R. P., Blake, R., and Wolfe, J. M. (1994a). Binocular rivalry and fusion under scotopic luminances. *Perception*, 23, 771–84 [330]
- O'Shea, R. P., McDonald, A. A., Cumming, A., Peart, D., Sanderson, G., and Moltenov, C. B. (1994b). Interocular transfer of the movement aftereffect in central and peripheral vision of people with strabismus. *Investigative Ophthalmology and Visual Science*, 35, 313–17. [640]
- O'Shea, R. P., Blackburn, S. G., and Ono, H. (1994c). Contrast as a depth cue. *Vision Research*, 34, 1595–604. [204]
- O'Shea, W. F., Ciuffreda, K. J., Fisher, S. K., Tannen, B., and Super, P. (1988). Relation between distance heterophoria and tonic vergence. *American Journal of Optometry and Physiological Optics*, 65, 787–93. [336, 388]
- Osterberg, G. (1935). Topography of the layer of rods and cones in the human retina. *Acta Ophthalmologica*, Supplement 6, 1–103. [107]
- Oswald, I. (1957). After-images from retina and brain. *Quarterly Journal of Experimental Psychology*, 9, 88–100. [102, 342, 363]
- O'Toole, A. J. and Kersten, D. J. (1992). Learning to see random-dot stereograms. *Perception*, 21, 227–43. [193]
- Ott, D., Seidman, S. H., and Leigh, R. J. (1992). The stability of human eye orientation during visual fixation. *Neuroscience Letters*, 142, 183–6. [382, 421]
- Over, R. (1971). Comparison of normalization theory and neural enhancement explanation of negative aftereffects. *Psychological Bulletin*, 75, 225–43. [466, 491]
- Over, R., Long, N., and Lovegrove, W. (1973). Absence of binocular interaction between spatial and color attributes of visual stimuli. *Perception and Psychophysics*, 13, 534–40. [379]
- Owens, D. A. and Leibowitz, H. W. (1975). Chromostereopsis with small pupils. *Journal of the Optical Society of America*, 65, 358–9. [306]
- Owens, D. A. and Leibowitz, H. W. (1976). Oculomotor adjustments in darkness and the specific distance tendency. *Perception and Psychophysics*, 20, 2–9. [430]
- Owens, D. A. and Leibowitz, H. W. (1980). Accommodation convergence and distance perception in low illumination. *American Journal of Physiological Optics*, 57, 540–50. [386, 397, 434]
- Owens, D. A. and Leibowitz, H. W. (1983). Perceptual and motor consequences of tonic vergence. In *Vergence eye movements: Basic and clinical aspects* (ed. M. C. Schor, K. J. Ciuffreda), pp. 25–98. Butterworth, Boston. [387, 390]
- Owens, D. A. and Tyrrell, R. A. (1992). Lateral phoria at distance: Contributions of accommodation. *Investigative Ophthalmology and Visual Science*, 33, 2733–43. [388]
- Paap, K. R. and Ebenholtz, S. M. (1976). Perceptual consequences of potentiation in the extraocular muscles: An alternative explanation for adaptation to wedge prisms. *Journal of Experimental Psychology*, 2, 457–68. [432]
- Paap, K. R. and Ebenholtz, S. M. (1977). Concomitant direction and distance aftereffects of sustained convergence: A muscle potentiation explanation for eye-specific adaptation. *Perception and Psychophysics*, 21, 307–14. [433]
- Paige, G. D. (1989). The influence of target distance on eye movement responses during vertical linear motion. *Experimental Brain Research*, 77, 585–93. [415]
- Paige, G. D. (1991). Linear vestibulo-ocular (LVOR) and modulation by vergence. *Acta Otolaryngologica*, 48, 282–6. [416]
- Palmer, D. A. (1961). Measurement of the horizontal extent of Panum's area by a method of constant stimuli. *Optical Acta*, 8, 151–9. [316, 320]
- Pantle, A. and Picciano, L. (1976). A multistable movement display: Evidence for two separate motion systems in human vision. *Science*, 193, 500–2. [567, 570]
- Panum, P. L. (1858). *Physiologische Untersuchungen über das Sehen mit zwei Augen*. Schwets, Keil. [42, 315]
- Papathomas, T. V. and Julesz, B. (1989). Stereoscopic illusion based on the proximity principle. *Perception*, 18, 589–94. [504]
- Papert, S. (1961). Centrally produced geometrical illusions. *Nature*, 191, 733. [587]
- Papert, S. (1964). Stereoscopic synthesis as a technique for locating visual mechanisms. *MIT Quarterly Progress Report*, 73, 239–43. [377, 587, 589]
- Paradiso, M. A., Shimojo, S., and Nakayama, K. (1989). Subjective contours, tilt aftereffects, and visual cortical organization. *Vision Research*, 29, 1205–13. [375]
- Pardhan, S., Gilchrist, J., and Douthwaite, W. (1989). The effect of spatial frequency on binocular contrast inhibition. *Ophthalmology and Physiological Optics*, 9, 46–9. [354]

- Paris, J. and Prestrude, A. M. (1975). On the mechanism of the interocular light adaptation effect. *Vision Research*, **15**, 595–603. [365]
- Park, J. N. (1969). Displacement of apparent straight ahead as an aftereffect of deviation of the eyes from normal position. *Perception and Motor Skills*, **28**, 591–7. [432]
- Park, K. and Shebilske, W. L. (1991). Phoria, Hering's Laws, and monocular perception of direction. *Journal of Experimental Psychology: Human Perception and Performance*, **17**, 219–31. [599]
- Parker, A. J. and Yang, Y. (1989). Spatial properties of disparity pooling in human stereo vision. *Vision Research*, **29**, 1525–38. [233]
- Parker, A. J., Johnston, E. B., Mansfield, J. S., and Yang, Y. (1991). Stereo, surfaces, and shape. In *Computational models of visual processing*, (ed. M. S. Landy and J. A. Movshon), pp. 359–81. MIT Press, Cambridge, MA. [201]
- Parks, T. E. (1984). Illusory figures: A (mostly) atheoretical review. *Psychological Bulletin*, **95**, 282–300. [77]
- Pastore, N. (1964). Induction of a stereoscopic depth effect. *Science*, **144**, 888. [467]
- Pastore, N. and Terwilliger, M. (1966). Induction of stereoscopic depth effects. *British Journal of Psychology*, **57**, 201–2. [467]
- Patterson, R. (1990). Spatiotemporal properties of stereoaquity. *Optometry and Vision Science*, **67**, 123–8. [170]
- Patterson, R. and Fox, R. (1984a). Stereopsis during continuous head motion. *Vision Research*, **24**, 2001–3. [180]
- Patterson, R. and Fox, R. (1984b). The effect of testing method on stereoanomaly. *Vision Research*, **24**, 403–8. [624]
- Patterson, R. and Fox, R. (1990). Metacontrast masking between cyclopean and luminance stimuli. *Vision Research*, **30**, 439–48. [370]
- Patterson, R. and Martin, W. L. (1992). Human stereopsis. *Human Factors*, **34**, 669–92. [1]
- Patterson, R., Bowd, C., Phinney, R., Pohndorf, R., Barton-Howard, W. J., and Angilletta, M. (1994). Properties of the stereoscopic (cyclopean) motion aftereffect. *Vision Research*, **34**, 1139–47. [571]
- Patterson, R., Hart, P., and Nowak, D. (1991). The cyclopean Ternus display and the perception of element versus group movement. *Vision Research*, **31**, 2085–92. [570]
- Patterson, R., Ricker, C., McGary, J., and Rose, D. (1992). Properties of cyclopean motion perception. *Vision Research*, **32**, 149–56. [590]
- Payne, B. R. (1990). Representation of the ipsilateral visual field in the transition zone between areas 17 and 18 of the cat's cerebral cortex. *Visual Neuroscience*, **4**, 445–74. [130]
- Payne, B. R., Berman, N., and Murphy, E. H. (1981). A quantitative assessment of eye alignment in cats after corpus callosum transection. *Experimental Brain Research*, **43**, 371–6. [425]
- Payne, B. R., Pearson, H. E., and Berman, N. (1984). Role of corpus callosum in functional organization of cat striate cortex. *Journal of Neurophysiology*, **52**, 570–94. [132]
- Peck, C. K. and Blakemore, C. (1975). Modification of single neurons in the kitten's visual cortex after brief periods of monocular visual experience. *Experimental Brain Research*, **22**, 57–68. [635]
- Peckham, R. H. and Hart, W. M. (1960). Binocular summation of subliminal repetitive visual stimulation. *American Journal of Ophthalmology*, **49**, 1121–5. [359]
- Peiperl, A. (1963). *Cerebral function in infancy and childhood*. Pitman, London. [558]
- Pennington, J. (1970). The effects of wavelength on stereoaquity. *American Journal of Optometry*, **47**, 288–94. [172]
- Penrose, L. S. and Penrose, R. (1958). Impossible objects: A special type of illusion. *British Journal of Psychology*, **49**, 31–3. [504]
- Perkel, D. H., Gerstein, G. L., and Moore, G. P. (1967). Neuronal spike trains and stochastic point processes. II. Simultaneous spike trains. *Biophysical Journal*, **7**, 419–40. [612]
- Perrett, D. I., Harries, M. H., Bevan, R., Thoma, S., Benson, P. J., Mistlin, A. J., Chitty, A. J., Hietanen, J. K., and Ortega, J. E. (1989). Framework analysis for the neural representation of animate objects and actions. *Journal of Experimental Biology*, **146**, 87–113. [126]
- Perry, V. H. and Cowey, A. (1985). The ganglion cell and cone distributions in the monkey's retina: Implications for central magnification factors. *Vision Research*, **25**, 1795–1810. [607]
- Perry, V. H., Henderson, Z., and Linden, R. (1983). Postnatal changes in retinal ganglion cell and optic axon populations in the pigmented rat. *Journal of Comparative Neurology*, **219**, 356–68. [607]
- Perry, V. H., Oehler, R., and Cowey, A. (1984). Retinal ganglion cells that project to the dorsal lateral geniculate nucleus in the macaque monkey. *Neuroscience*, **12**, 1101–23. [112]
- Petersik, J. T., Shepard, A., and Malsch, R. (1984). A three-dimensional motion aftereffect produced by prolonged adaptation to a rotation simulation. *Perception*, **13**, 489–97. [565]
- Petrig, B., Julesz, B., Kropfl, W., Baumgartner, G., and Anliker, M. (1981). Development of stereopsis and cortical binoculararity in human infants: Electrophysiological evidence. *Science*, **213**, 1402–4. [620]
- Petrov, A. P. (1980). A geometrical explanation of the induced size effect. *Vision Research*, **20**, 409–13. [283]
- Pettet, M. W. and Gilbert, C. D. (1992). Dynamic changes in receptive-field size in cat primary visual cortex. *Proceedings of the National Academy of Science*, **89**, 8366–70. [129]
- Pettigrew, J. D. (1973). Binocular neurones which signal change of disparity in area 18 of cat visual cortex. *Nature*, **241**, 123–4. [564]
- Pettigrew, J. D. (1974). The effect of visual experience on the development of stimulus specificity by kitten cortical neurones. *Journal of Physiology*, **237**, 49–74. [625]
- Pettigrew, J. D. (1979). Binocular visual processing in the owl's telencephalon. *Proceedings of the Royal Society, London*, **B204**, 435–54. [655]
- Pettigrew, J. D. (1986). The evolution of binocular vision. In *Visual Neuroscience*, (ed. J. D. Pettigrew, K. J. Sanderson, and W. R. Levick), pp. 208–222. Cambridge University Press, London. [645, 655]
- Pettigrew, J. D. (1991). Evolution of binocular vision. In *The evolution of the eye and visual system*, (ed. J. R. Cronly-Dillon and R. L. Gregory), pp. 271–83. CRC Press, Boca Raton, Ann Arbor. [657]
- Pettigrew, J. D. and Dreher, B. (1987). Parallel processing of binocular disparity in the cat's retinogeniculate pathways. *Proceedings of the Royal Society, London*, **B232**, 297–321. [130, 134]
- Pettigrew, J. D. and Konishi, M. (1976). Neurons selective for orientation and binocular disparity in the visual Wulst of the barn owl. *Science*, **193**, 675–8. [655]
- Pettigrew, J. D., Nikara, T., and Bishop, P. O. (1968). Binocular interaction on single units in cat striate cortex: Simultaneous stimulation by single moving slit with receptive fields in correspondence. *Experimental Brain Research*, **6**, 391–410. [24, 133, 140, 625]
- Pettigrew, J. D., Ramachandran, V. S., and Bravo, H. (1984). Some neural connections subserving binocular vision in ungulates. *Brain Behaviour and Evolution*, **24**, 65–93. [657]
- Phillips, S. and Stark, L. (1977). Blur: A sufficient accommodative stimulus. *Documenta Ophthalmologica*, **43**, 65–89. [395]
- Piantanida, T. P. (1986). Stereo hysteresis revisited. *Vision Research*, **26**, 431–7. [324–5]

- Pickersgill, M. J. (1961). On knowing with which eye one is seeing. *Quarterly Journal of Experimental Psychology*, 13, 168–72. [601]
- Pickersgill, M. J. and Jeeves, M. A. (1964). The origin of the after-effect of movement. *Quarterly Journal of Experimental Psychology*, 16, 90–103. [589]
- Pickwell, D. (1984). *Binocular vision anomalies. Investigation and treatment*. Butterworths, London. [388]
- Pickwell, L. D. (1972). Hering's law of equal innervation and the position of the binoculus. *Vision Research*, 12, 1499–1507. [412]
- Pierce, D. M. and Benton, A. L. (1975). Relationship between monocular and binocular depth acuity. *Ophthalmologica*, 170, 43–50. [151]
- Piggins, D. (1978). Moirés maintained internally by binocular vision. *Perception*, 7, 679–81. [43]
- Pinckney, G. A. (1964). Reliability of duration as a measure of the spiral aftereffect. *Perceptual and Motor Skills*, 18, 375–6. [375]
- Pini, A. (1993). Chemoattraction of axons in the developing mammalian central nervous system. *Science*, 261, 95–9. [606]
- Pinter, R. B. and Nabet, B. (1992). *Nonlinear vision: Determination of neural receptive fields, function and networks*. CRC Press, London. [92]
- Pirchio, M., Spinelli, D., Fiorentini, A., and Maffei, L. (1978). Infant contrast sensitivity evaluated by evoked potentials. *Brain Research*, 141, 179–84. [616]
- Pirenne, M. H. (1943). Binocular and unispatial threshold of vision. *Nature*, 152, 698–9. [100, 350]
- Pirenne, M. H. (1970). *Optics, painting and photography*. Cambridge University Press, Cambridge. [9]
- Pitblado, C. B. (1979). Cerebral asymmetries in random-dot stereopsis: Reversal of direction with changes in dot size. *Perception*, 8, 683–90. [625]
- Pittman, R. N. (1985). Release of plasminogen activator and a calcium-dependent metalloprotease from cultured sympathetic and sensory neurons. *Developmental Biology*, 110, 91–101. [606]
- Plateau, J. (1950). Vierte Notiz über neue sonderbare Anwendungen des Verweilens der Eindrücke auf die Netzhaut. *Poggendorff's Annalen der Physik und Chemie*, 80, 287–92. [375]
- Pobuda, M. and Erkelens, C. J. (1993). The relationship between absolute disparity and ocular vergence. *Biological Cybernetics*, 68, 221–8. [403, 406, 408]
- Poggio, G. F. (1984). The analysis of stereopsis. *Annual Review of Neuroscience*, 7, 379–412. [135]
- Poggio, G. F. (1991). Physiological basis of stereoscopic vision. In *Vision and vision dysfunction*, Vol. 9, *Binocular vision*, (ed. D. Regan), pp. 224–38. Macmillan, London. [135]
- Poggio, G. F. and Fischer, B. (1977). Binocular interaction and depth sensitivity in striate and prestriate cortex of behaving rhesus monkey. *Journal of Neurophysiology*, 40, 1392–405. [123, 135, 143, 532, 566]
- Poggio, G. F. and Talbot, W. H. (1981). Mechanisms of static and dynamic stereopsis in foveal cortex of the rhesus monkey. *Journal of Physiology*, 315, 469–92. [135, 143, 532, 564, 566]
- Poggio, G. F., Gonzalez, F., and Krause, F. (1988a). Stereoscopic mechanisms in monkey visual cortex: Binocular correlation and disparity selectivity. *Journal of Neuroscience*, 8, 4531–50. [135]
- Poggio, T., Gamble, E. B., and Little, J. J. (1988b). Parallel integration of vision modules. *Science*, 242, 436–9. [437]
- Poggio, G. F., Motter, B. C., Squatrito, S., and Trotter, Y. (1985). Responses of neurons in visual cortex (VI and V2) of the alert Macaque to dynamic random-dot stereograms. *Vision Research*, 25, 397–406. [135]
- Poggio, T., Fahle, M., and Edelman, S. (1992). Fast perceptual learning in visual hyperacuity. *Science*, 256, 1018–21. [104]
- Pohl, W. (1973). Dissociation of spatial discrimination deficits following frontal and parietal lesions in monkeys. *Journal of Comparative and Physiological Psychology*, 82, 227–39. [127]
- Polak, N. A. and Jones, R. (1990). Dynamic interactions between accommodation and convergence. *IEEE Transactions on Biomedical Engineering*, 37, 1011–14. [398]
- Polat, U. and Sagi, D. (1994). The architecture of perceptual spatial interactions. *Vision Research*, 34, 73–8. [76, 117]
- Pollard, S. B. and Frisby, J. P. (1990). Transparency and the uniqueness constraint in human and computer stereo vision. *Nature*, 347, 553–6. [217]
- Pollard, S. B., Mayhew, J. E. W., and Frisby, J. P. (1985). PMF: A stereo correspondence algorithm using a disparity gradient limit. *Perception*, 14, 449–70. [222]
- Pollen, D. A. and Ronner, S. F. (1981). Phase relationships between adjacent simple cells in the visual cortex of the cat. *Investigative Ophthalmology and Visual Science*, 20 (ARVO Abstracts), 148. [89]
- Polyak, S. (1941). *The retina*. University of Chicago Press, Chicago, Illinois. [106, 111]
- Polyak, S. (1957). *The vertebrate visual system*. pp. 109–110. University of Chicago Press, Chicago. [6, 13, 24, 106, 609]
- Porac, C. and Coren, S. (1984). Monocular asymmetries in vision: A phenomenal basis for eye signature. *Canadian Journal of Psychology*, 38, 610–24. [601]
- Porac, C. and Coren, S. (1986). Sighting dominance and egocentric localization. *Vision Research*, 26, 1709–13. [599]
- Porrill, J. and Mayhew, J. E. W. (1994). Gaze angle explanations of the induced effect. *Perception*, 23, 219–22. [283]
- Porta, G. B. della (1558). *Magiae naturalis*. English edition of 1658, reprinted by Basic Books, New York, 1957. [10]
- Porta, G. B. della (1593). *De refractione. Optices Parte*. Carlinum and Pacem, Naples. [10, 338]
- Porter, J. D. and Baker, R. S. (1992). Prenatal morphogenesis of primate extraocular muscle: Neuromuscular junction formation and fiber type differentiation. *Investigative Ophthalmology and Visual Science*, 33, 657–70. [424]
- Porter, J. D., Guthrie, B. L., and Sparks, D. L. (1983). Innervation of monkey extraocular muscles: Localization of sensory and motor neurons by retrograde transport of horseradish peroxidase. *Journal of Comparative Neurology*, 218, 208–19. [424]
- Porterfield, W. (1759). *A treatise on the eye: The manner and phenomena of vision*. A. Miller, London. [17]
- Post, R. B. and Leibowitz, H. W. (1982). The effect of convergence on the vestibulo-ocular reflex and implications for perceived movement. *Vision Research*, 22, 461–5. [430]
- Potts, M. J. and Harris, J. P. (1979). Dichoptic induction of movement aftereffects contingent on color and on orientation. *Perception and Psychophysics*, 26, 25–31. [379]
- Prazdny, K. (1983). Stereoscopic matching, eye position, and absolute depth. *Perception*, 12, 151–60. [229]
- Prazdny, K. (1985a). Detection of binocular disparities. *Biological Cybernetics*, 52, 93–9. [228]
- Prazdny, K. (1985b). On the disparity gradient limit for binocular fusion. *Perception and Psychophysics*, 37, 81–3. [318]
- Prazdny, K. (1985c). On the nature of inducing forms generating perceptions of illusory contours. *Perception and Psychophysics*, 37, 237–42. [510]
- Prazdny, K. (1986). Three-dimensional structure from long-range apparent motion. *Perception*, 15, 619–25. [527]
- Predebon, J. (1994). Convergence responses to monocularly viewed objects: Implications for distance perception. *Perception*, 23, 303–19. [399]
- Prentice, W. C. H. (1948). New observations of binocular yellow. *Journal of Experimental Psychology*, 38, 284–8. [326]

- Prestrude, A. M. (1971). Visual latencies at photopic levels of retinal illumination. *Vision Research*, 11, 351–61. [545]
- Prestrude, A. M. and Baker, H. D. (1968). New method of measuring visual-perceptual latency differences. *Perception and Psychophysics*, 4, 152–4. [539]
- Prestrude, A. M. and Baker, H. D. (1971). Light adaptation and visual latency. *Vision Research*, 11, 363–9. [547, 549]
- Prévost, A. (1843). *Essai sur la théorie de la vision binoculaire*. Ramboz, Geneva. [18, 50]
- Price, D. J. and Blakemore, C. (1985). The postnatal development of the association projection from visual cortical area 17 to area 18 in the cat. *Journal of Neuroscience*, 5, 2443–52. [611]
- Price, D. J., Ferrer, J. M. R., Blakemore, C., and Kato, N. (1994). Postnatal development and plasticity of corticocortical projections from area 17 to area 18 in the cat's visual cortex. *Journal of Neuroscience*, 14, 2747–62. [611]
- Ptito, M., Lepore, F., and Guillemot, J. P. (1992). Loss of stereopsis following lesions of cortical areas 17–18 in the cat. *Experimental Brain Research*, 89, 521–30. [134, 624]
- Pugh, M. (1958). Visual distortion in amblyopia. *British Journal of Ophthalmology*, 42, 449–60. [631]
- Pulfrich, C. (1922). Die Stereoskopie im Dienste der isochromen und heterochromen Photometrie. *Naturwissenschaften*, 10, 553–64. [535–6, 545]
- Purdy, D. M. (1934). Double monocular diplopia. *Journal of General Psychology*, 11, 311–27. [47]
- Purkinje, J. (1825). *Beobachtungen und Versuche zur Physiologie der Sinne*. Vol. 2, p. 60. J. G. Calve, Prague. [375]
- Quereau, J. (1954). Some aspect of torsion. *AMA Archives of Ophthalmology*, 5, 783–8. [384]
- Quick, M. W., Tigges, M., Gammon, J. A., and Boothe, R. G. (1989). Early abnormal visual experience induces strabismus in infant monkeys. *Investigative Ophthalmology and Visual Science*, 30, 1012–17. [100]
- Quick, R. F. (1974). A vector-magnitude model of contrast detection. *Kybernetik*, 16, 65–7. [632]
- Racanzone, G. H., Schreiner, C. E., and Merzenich, M. M. (1993). Plasticity in the frequency representation of primary auditory cortex following discrimination training in adult owl monkeys. *Journal of Neuroscience*, 13, 87–103. [129]
- Rady, A. A. and Ishak, I. G. H. (1955). Relative contributions of disparity and convergence to stereoscopic acuity. *Journal of the Optical Society of America*, 45, 530–4. [170, 177]
- Raff, M. C., Barres, B. A., Burne, J. F., Coles, H. S., Ishizaki, Y., and Jacobson, M. D. (1993). Programmed cell death and the control of cell survival: Lessons from the nervous system. *Science*, 262, 695–700. [607]
- Rakic, P. (1974). Neurons in rhesus monkey visual cortex: Systematic relation between time of origin and eventual disposition. *Science*, 183, 425–7. [610]
- Rakic, P. (1976). Prenatal genesis of connections subserving ocular dominance in the rhesus monkey. *Nature*, 261, 467–71. [608, 613]
- Rakic, P. (1981). Development of visual centers in the primate brain depends on binocular competition before birth. *Science*, 214, 928–31. [626]
- Rakic, P. (1988). Specification of cerebral cortical areas. *Science*, 241, 170–6. [119, 610]
- Rakic, P. and Riley, K. P. (1983). Overproduction and elimination of retinal axons in the fetal rhesus monkey. *Science*, 219, 1441–4. [606]
- Rakic, P., Bourgeois, J.-P., Eckenhoff, M. F., Zecevic, N., and Goldman-Rakic, P. S. (1986). Concurrent overproduction of synapses in diverse regions of the primate cerebral cortex. *Science*, 232, 232–5. [610]
- Ramachandran, V. S. (1975). Suppression of apparent movement during binocular rivalry. *Nature*, 256, 122–3. [343]
- Ramachandran, V. S. (1976). Learning-like phenomena in stereopsis. *Nature*, 262, 382–4. [192–3]
- Ramachandran, V. S. (1986). Capture of stereopsis and apparent motion by illusory contours. *Perception and Psychophysics*, 39, 361–73. [502–3, 509]
- Ramachandran, V. S. (1987). Visual perception of surfaces: A biological approach. In *The perception of illusory contours*, (ed. S. Petry and G. E. Meyer), pp. 93–108. Springer-Verlag, New York. [509]
- Ramachandran, V. S. (1991). Form, motion, and binocular rivalry. *Science*, 251, 950–1. [377]
- Ramachandran, V. S. and Anstis, S. M. (1986). The perception of apparent motion. *Scientific American*, 254, 102–9. [438]
- Ramachandran, V. S. and Braddick, O. L. (1973). Orientation-specific learning in stereopsis. *Perception*, 2, 371–6. [193]
- Ramachandran, V. S. and Cavanagh, P. (1985). Subjective contours capture stereopsis. *Nature*, 317, 527–30. [502]
- Ramachandran, V. S. and Nelson, J. I. (1976). Global grouping overrides point-to-point disparities. *Perception*, 5, 125–8. [262]
- Ramachandran, V. S. and Sriram, S. (1972). Stereopsis generated with Julesz patterns in spite of rivalry imposed by colour filters. *Nature*, 237, 347–8. [226, 343]
- Ramachandran, V. S., Cobb, S., and Levi, L. (1994a). The neural locus of binocular rivalry and monocular diplopia in intermittent exotropes. *Neuroreport*, 5, 1141–44. [47–8, 334]
- Ramachandran, V. S., Cobb, S., and Levi, L. (1994b). Monocular diplopia and metacontrast in strabismus. *Neuroreport*, in press. [47]
- Ramachandran, V. S., Rao, V. M., and Vidyasagar, T. R. (1973a). The role of contours in stereopsis. *Nature*, 242, 412–14. [200–3]
- Ramachandran, V. S., Rao, V. M., Sriram, S., and Vidyasagar, T. R. (1973b). The role of colour perception and "pattern" recognition in stereopsis. *Vision Research*, 13, 505–9. [221]
- Ramo, A. S., Shadlen, M., and Freeman, R. D. (1987). Dark-reared cats: Unresponsive cells become visually responsive with microiontophoresis of an excitatory amino acid. *Experimental Brain Research*, 65, 658–65. [625]
- Ramón y Cajal, S. (1911). *Histologie du système nerveux de l'homme et des vertébrés*. A. Maloine, Paris. [22, 34, 132]
- Ramón y Cajal, S. (1937). Recollections of my life. (Trans. by E. H. Graige). *Memoirs of the American Philosophical Society*, 3, [12]
- Ransom-Hogg, A. and Spillmann, L. (1980). Perceptive field size in fovea and periphery of the light-and dark-adapted retina. *Vision Research*, 20, 221–8. [114]
- Rao, V. M. (1977). Tilt illusion during binocular rivalry. *Vision Research*, 17, 327–8. [342]
- Rashbass, C. (1970). The visibility of transient changes of luminance. *Journal of Physiology*, 210, 165–86. [362]
- Rashbass, C. (1981). Reflections on the control of vergence. In *Models of oculomotor behavior and control*, (ed. B. L. Zuber), pp. 139–48. CRC Press, Boca Raton. [408]
- Rashbass, C. and Westheimer, G. (1961). Disjunctive eye movements. *Journal of Physiology*, 159, 339–60. [402, 404]
- Ratcliff, F. (1965). *Mach Bands: Quantitative studies on neural networks in the retina*. Holden-Day, San Francisco. [77]
- Rauschecker, J. P. (1991). Mechanisms of visual plasticity: Hebb synapses, NMDA receptors, and beyond. *Physiological Reviews*, 71, 587–615. [615]
- Rauschecker, J. P. and Singer, W. (1981). The effects of early visual experience on the cat's visual cortex and their possible explanation by Hebb synapses. *Journal of Physiology*, 310, 215–39. [628]

- Rauschecker, J. P., Campbell, F. W., and Atkinson, J. (1973). Colour opponent neurones in the human visual system. *Nature*, **245**, 42–3. [334]
- Rawlings, S. C. and Shipley, T. (1969). Stereoscopic acuity and horizontal angular distance from fixation. *Journal of the Optical Society of America*, **59**, 991–3. [59, 159]
- Raybourn, M. S. (1975). Spatial and temporal organization of the input to frog optic tectum. *Brain, Behaviour and Evolution*, **11**, 161–78. [651]
- Raymond, J. E. (1993). Complete interocular transfer of motion adaptation effects on motion coherence thresholds. *Vision Research*, **33**, 1865–70. [375]
- Rayner, A. W. (1966). Aniseikonia and magnification in ophthalmic lenses. Problems and solutions. *American Journal of Optometry and Archives of American Academy of Optometry*, **43**, 617–32. [67]
- Reading, R. W. and Tanalamai, T. (1980). The threshold of stereopsis in the presence of differences in magnification of the ocular images. *Journal of the American Optometry Association*, **51**, 593–5. [156]
- Reading, R. W. and Woo, G. S. (1972). Some of the time factors associated with stereopsis. *American Journal of Optometry and Archives of the American Academy of Optometry*, **41**, 20–8. [171]
- Reading, V. M. (1973). An objective correlate of the Pulfrich stereo-illusion. *Proceedings of the Royal Society of Medicine*, **66**, 1043–4. [550]
- Reading, V. M. (1975). Eye movements and the Pulfrich stereo-illusion. *Journal of Physiology*, **246**, 40P. [550]
- Reed, M. J., Steinbach, M. J., Anstis, S. M., Gallie, B., Smith, D., and Kraft, S. (1991). The development of optokinetic nystagmus in strabismic and monocularly enucleated subjects. *Behavioural Brain Research*, **46**, 31–42. [531]
- Reese, B. E. and Baker, G. E. (1992). Changes in fiber organization within the chiasmatic region of mammals. *Visual Neuroscience*, **9**, 527–33. [608]
- Regal, D. M., Boothe, R., Teller, D. Y., and Sackett, G. P. (1976). Visual acuity and visual responsiveness in dark-reared monkeys (*Macaca Nemestrina*). *Vision Research*, **16**, 523–30. [626]
- Regan, D. (1973). Rapid objective refraction using evoked potentials. *Investigative Ophthalmology*, **12**, 669–79. [145]
- Regan, D. (1977). Speedy assessment of visual acuity in amblyopia by the evoked potential method. *Ophthalmologica*, **175**, 159–64. [145]
- Regan, D. (1982). Visual information channeling in normal and disordered vision. *Psychological Review*, **89**, 407–44. [79]
- Regan, D. (1986a). Form from motion parallax and form from luminance contrast: Vernier discrimination. *Spatial Vision*, **1**, 305–18. [527, 589]
- Regan, D. (1986b). Visual processing of four kinds of relative motion. *Vision Research*, **26**, 127–45. [558]
- Regan, D. (1989a). *Human brain electrophysiology. Evoked potentials and evoked magnetic fields in science and medicine*. Elsevier, New York. [144, 148]
- Regan, D. (1989b). Orientation discrimination for objects defined by relative motion and objects defined by luminance contrast. *Vision Research*, **29**, 1389–400. [589]
- Regan, D. (1991). *Vision and visual dysfunction*, Vol. 9, *Binocular vision* (ed. D. Regan). Macmillan, London. [1]
- Regan, D. (1993). Binocular correlates of the direction of motion in depth. *Vision Research*, **33**, 2359–60. [560-1]
- Regan, D. and Beverley, K. I. (1973a). Some dynamic features of depth perception. *Vision Research*, **13**, 2369–79. [187-90]
- Regan, D. and Beverley, K. I. (1973b). The dissociation of sideways movements from movements in depth: Psychophysics. *Vision Research*, **13**, 2403–15. [190]
- Regan, D. and Beverley, K. I. (1973c). Disparity detectors in human depth perception: Evidence for directional selectivity. *Science*, **181**, 877–9. [566]
- Regan, D. and Beverley, K. I. (1973d). Electrophysiological evidence for existence of neurones sensitive to direction of depth motion. *Nature*, **246**, 504–6. [564]
- Regan, D. and Beverley, K. I. (1978a). Looming detectors in the human visual pathway. *Vision Research*, **18**, 415–21. [558, 565]
- Regan, D. and Beverley, K. I. (1978b). Illusory motion in depth: Aftereffect of adaptation to changing size. *Vision Research*, **18**, 209–12. [101, 558]
- Regan, D. and Beverley, K. I. (1979a). Visually guided locomotion: Psychophysical evidence for a neural mechanism sensitive to flow patterns. *Science*, **205**, 311–13. [559]
- Regan, D. and Beverley, K. I. (1979b). Binocular and monocular stimuli for motion in depth: Changing-disparity and changing-size feed the same motion-in-depth stage. *Vision Research*, **19**, 1331–42. [563]
- Regan, D. and Beverley, K. I. (1980). Visual responses to changing size and to sideways motion: Linearization of visual responses. *Journal of the Optical Society of America*, **11**, 1289–96. [558]
- Regan, D. and Beverley, K. I. (1982). How do we avoid confounding the direction we are looking and the direction we are moving. *Science*, **215**, 194–6. [557]
- Regan, D. and Beverley, K. I. (1984). Psychophysics of visual flow patterns and motion in depth. In *Sensory experience, adaptation and perception*, (ed. L. Spillmann and B. R. Wooten), pp. 215–40. Erlbaum, Hillsdale, N. J. [557]
- Regan, D. and Beverley, K. I. (1985). Postadaptation orientation discrimination. *Journal of the Optical Society of America*, **2A**, 147–55. [79]
- Regan, D. and Cynader, M. (1979). Neurons in area 18 of cat visual cortex selectively sensitive to changing size: Nonlinear interactions between responses to two edges. *Vision Research*, **19**, 699–711. [564]
- Regan, D. and Cynader, M. (1982). Neurons in cat visual cortex tuned to the direction of motion in depth: Effect of stimulus speed. *Investigative Ophthalmology and Visual Science*, **22**, 535–50. [564]
- Regan, D. and Hamstra, S. J. (1993). Dissociation of discrimination thresholds for time to contact and for rate of angular expansion. *Vision Research*, **33**, 447–62. [555]
- Regan, D. and Hamstra, S. J. (1994). Shape discrimination for rectangles defined by disparity alone, by disparity plus luminance and by disparity plus motion. *Vision Research*, **34**, 2277–92. [183]
- Regan, D. and Kaushal, S. (1993). Monocular judgement of the direction of motion in depth. *Vision Research*, **34**, 163–78. [558]
- Regan, D. and Price, P. (1986). Periodicity in orientation discrimination and the unconfounding of visual information. *Vision Research*, **26**, 1299–302. [98]
- Regan, D. and Spekreijse, H. (1970). Electrophysiological correlate of binocular depth perception in man. *Nature, London*, **225**, 92–4. [144, 147, 564]
- Regan, D., Beverley, K. I., and Cynader, M. (1979). The visual perception of motion in depth. *Scientific American*, **241**, 136–51. [559]
- Regan, D., Erkelens, C. J., and Collewijn, H. (1986a). Necessary conditions for the perception of motion in depth. *Investigative Ophthalmology and Visual Science*, **27**, 584–97. [179, 242, 401, 461, 562]
- Regan, D., Erkelens, C. J., and Collewijn, H. (1986b). Visual field defects for vergence eye movements and for stereomotion perception. *Investigative Ophthalmology and Visual Science*, **27**, 806–19. [563]

- Regan, M. P. and Regan, D. (1986). Monocular and binocular nonlinearities in flicker evoked potentials. *Third International Evoked Potential Congress*, Berlin. [146]
- Regan, M. P. and Regan, D. (1988). A frequency domain technique for characterizing nonlinearities in biological systems. *Journal of Theoretical Biology*, 133, 293–317. [92, 146]
- Regan, M. P. and Regan, D. (1989). Objective investigation of visual function using a nondestructive zoom-FFT technique for evoked potential analysis. *Canadian Journal of Neurological Sciences*, 16, 168–79. [146]
- Reichardt, L. F. (1992). Neuronal interactions with the extracellular matrix that regulate axon growth. In *Regeneration and plasticity in the mammalian visual system*, (ed. D. M-K. Lam and G. M. Garth), pp. 59–70. MIT Press, Cambridge, MA. [606]
- Reid, T. (1764). *An inquiry into the human mind. On the principles of common sense*. Miller, Kinnaird and Bell, Edinburgh. [631]
- Reimann, D. and Haken, H. (1994). Stereo vision by self organization. *Biological Cybernetics*, 71, 17–26. [219]
- Reinecke, R. D. and Simons, K. (1974). A new stereoscopic test for amblyopia screening. *American Journal of Ophthalmology*, 78, 714–21. [154]
- Reiter, H. O. and Stryker, M. P. (1988). Neural plasticity without postsynaptic action potentials: Less-active inputs become dominant when kitten visual cortical cells are pharmacologically inhibited. *Proceedings of the National Academy of Science*, 85, 3627–37. [629]
- Reiter, H. O., Waitzman, D. M., and Stryker, M. P. (1986). Cortical activity blockade prevents ocular dominance plasticity in the kitten visual cortex. *Experimental Brain Research*, 65, 182–8. [629]
- Remole, A. (1983). A new eikonometer: The multimeridional apparent frontoparallel plane. *American Journal of Optometry and Physiological Optics*, 60, 519–29. [66]
- Remole, A. (1984). Binocular fixation misalignment measured by border enhancement: A simplified technique. *American Journal of Optometry and Physiological Optics*, 61, 118–24. [389]
- Remole, A. (1985). Fixation disparity vs. binocular fixation misalignment. *American Journal of Optometry and Physiological Optics*, 62, 25–34. [389]
- Remole, A. (1989). Anisophoria and aniseikonia. Part 1. The relation between optical anisophoria and aniseikonia. *Optometry and Vision Science*, 66, 659–70. [62]
- Remole, A. (1991). The tilting keyboard. *Clinical and Experimental Optometry*, 74, 71–9. [67]
- Remole, A. (1992a). New developments in the application of the multimeridional apparent frontoparallel plane. *Optometry and Visual Science*, 69, 193–207. [66]
- Remole, A. (1992b). Multimeridional apparent frontoparallel plane: Relation between stimulus orientation angle and compensating tilt angle. *Optometry and Visual Science*, 69, 544–9. [66]
- Remole, A., Code, S. M., Matyas, C. E., McLeod, M. A., and White, D. J. (1986). Objective measurement of binocular fixation misalignment. *American Journal of Optometry and Physiological Optics*, 63, 63–8. [390]
- Remole, A., Robertson, K. M., and Johnson, B. D. (1993). The multimeridional apparent frontoparallel plane: Introduction of the induced effect. *Optometry and Visual Science*, 70, 792–803. [67]
- Richards, W. (1966). Attenuation of the pupil response during binocular rivalry. *Vision Research*, 6, 239–40. [335]
- Richards, W. (1970). Stereopsis and stereoblindness. *Experimental Brain Research*, 10, 380–8. [487, 583, 623]
- Richards, W. (1971a). Independence of Panum's near and far limits. *American Journal of Optometry and Archives of American Academy of Optometry*, 48, 103–9. [315]
- Richards, W. (1971b). Anomalous stereoscopic depth perception. *Journal of the Optical Society of America*, 61, 410–14. [622]
- Richards, W. (1972). Response functions for sine- and square-wave modulations of disparity. *Journal of the Optical Society of America*, 62, 907–11. [188, 469, 472]
- Richards, W. (1973). Reversal in stereo discrimination by contrast reversal. *American Journal of Optometry and Archives of American Academy of Optometry*, 50, 853–62. [623]
- Richards, W. (1985). Structure from stereo and motion. *Journal of the Optical Society of America*, 2A, 343–9. [441-2, 445-6, 574]
- Richards, W. and Foley, J. M. (1971). Interhemispheric processing of binocular disparity. *Journal of the Optical Society of America*, 61, 419–21. [159]
- Richards, W. and Foley, J. M. (1974). Effect of luminance and contrast on processing large disparities. *Journal of the Optical Society of America*, 64, 1703–5. [159, 168]
- Richards, W. and Foley, J. M. (1981). Spatial bandwidth of channels for slant estimated from complex gratings. *Journal of the Optical Society of America*, 71, 274–9. [234]
- Richards, W. and Lieberman, H. R. (1985). Correlation between stereo ability and the recovery of structure-from-motion. *American Journal of Optometry and Physiological Optics*, 62, 111–18. [527, 584]
- Richards, W. and Miller, J. F. (1969). Convergence as a cue to depth. *Perception and Psychophysics*, 5, 317–20. [427-8]
- Richards, W. and Regan, D. (1973). A stereo field map with implications for disparity processing. *Investigative Ophthalmology and Visual Science*, 12, 904–9. [159, 163, 623]
- Richards, W. J. (1951). The effects of alternating views of the test object on vernier and stereoscopic acuities. *Journal of Experimental Psychology*, 42, 376–83. [187]
- Richmond, B. J. and Optican, L. M. (1987). Temporal encoding of two-dimensional patterns by single units in primate temporal cortex. II. Quantification of response waveforms. *Journal of Neurophysiology*, 57, 147–61. [80]
- Richmond, B. J. and Optican, L. M. (1990). Temporal encoding of two-dimensional patterns by single units in primate visual cortex. II. Information transmission. *Journal of Neurophysiology*, 64, 370–80. [80]
- Richmond, B. J., Optican, L. M., and Spitzer, H. (1990). Temporal encoding of two-dimensional patterns by single units in primate visual cortex. I. Stimulus-response relations. *Journal of Neurophysiology*, 50, 1415–32. [80]
- Richmond, F. J. R., Johnston, W. S. W., Baker, R. S., and Steinbach, M. J. (1984). Palisade endings in human extraocular muscles. *Investigative Ophthalmology and Visual Science*, 25, 471–6. [432, 640]
- Riddell, J. L. (1853). Notice of a binocular microscope. *American Journal of Science and Arts*, 15, 68. [19]
- Riddoch, G. (1917). Dissociation of visual perceptions due to occipital injuries, with especial reference to the appreciation of movement. *Brain*, 40, 15–57. [624]
- Riggs, L. A. and Niehl, E. W. (1960). Eye movements recorded during convergence and divergence. *Journal of the Optical Society of America*, 50, 913–20. [404]
- Rind, F. C. and Simmons, P. J. (1992). Orthopteron DCMD neuron: A reevaluation of responses to moving objects. I. Selective responses to approaching objects. *Journal of Neurophysiology*, 68, 1654–66. [564, 648]
- Rippes, H., Chin, N. B., Siegel, I. M., and Breinen, G. M. (1962). The effect of pupil size on accommodation, convergence, and the AC/A ratio. *Investigative Ophthalmology*, 1, 127–35. [396]
- Ritter, A. D. and Breitmeyer, B. G. (1989). The effects of dichoptic and binocular viewing on bistable motion percepts. *Vision Research*, 29, 1215–19. [570]

- Ritter, M. (1977). Effect of disparity and viewing distance on perceived depth. *Perception and Psychophysics*, 22, 400-7. [458]
- Ritter, M. (1979). Perception of depth: Processing of simple positional disparity as a function of viewing distance. *Perception and Psychophysics*, 25, 209-14. [458]
- Rivest, J., Ono, H., and Saida, S. (1989). The roles of convergence and apparent distance in depth constancy with motion parallax. *Perception and Psychophysics*, 46, 401-08. [447]
- Robb, R. M. and Rodier, D. W. (1987). The variable clinical characteristics and course of early infantile esotropia. *Journal of Pediatrics, Ophthalmology and Strabismus*, 24, 276-81. [637]
- Robb, R. M., Mayer, D. L., and Moore, B. D. (1987). Results of early treatment of unilateral congenital cataracts. *Journal of Pediatrics, Ophthalmology and Strabismus*, 24, 178-85. [632]
- Robertson, R. M. and Johnson, A. G. (1993). Retinal image size triggers obstacle avoidance in flying locusts. *Naturwissenschaften*, 80, 176-8. [555]
- Robertson, V. M. and Fry, G. A. (1937). After-images observed in complete darkness. *American Journal of Psychology*, 46, 265-76. [380s]
- Robinson, S. R. (1991). Development of the mammalian retina. In *Neuroanatomy of the visual pathways and their development*, (ed. B. Dreher and S. R. Robinson), pp. 69-128. Boston CRC Press. [606]
- Robinson, D. A. (1963). A method of measuring eye movement using a scleral search coil in a magnetic field. *IEEE Transactions of Bio-Medical Engineering*, BME-10, 137-45. [419]
- Robinson, D. A. (1981). Control of eye movements. In *Handbook of physiology. The nervous system*, Vol. 2, Sec. 1, pp. 1275-320. American Physiological Society, Bethesda, Maryland. [425]
- Robinson, D. L., Baizer, J. S., and Dow, B. M. (1980). Behavioral enhancement of visual responses of prestriate neurons of the rhesus monkey. *Investigative Ophthalmology and Visual Science*, 9, 1120-3. [128]
- Robinson, D. L., Goldberg, M. E., and Stanton, G. B. (1978). Parietal association cortex in the primate: sensory mechanisms and behavioral modifications. *Journal of Neurophysiology*, 41, 910-32. [129]
- Robinson, D. N. (1968). Visual disinhibition with binocular and interocular presentation. *Journal of the Optical Society of America*, 58, 254-7. [369]
- Rock, I. (1984). *Perception*. Scientific American Library, New York. [578]
- Rock, M. L. and Fox, B. H. (1949). Two aspects of the Pulfrich phenomenon. *American Journal of Psychology*, 62, 279-84. [545-7]
- Rock, I., Hill, A. L., and Fineman, M. (1968). Speed constancy as a function of size constancy. *Perception and Psychophysics*, 4, 37-40. [458]
- Rockland, K. S. and Lund, J. S. (1982). Widespread periodic intrinsic connections in the tree shrew visual cortex. *Science*, 215, 1532-4. [116, 611]
- Rockland, K. S. and Van Hoesen, G. W. (1994). Direct temporal-occipital feedback connections to striate cortex (V1) in the macaque monkey. *Cerebral Cortex*, 4, 300-13. [128]
- Rodieck, R. W. and Dreher, B. (1979). Visual suppression from nondominant eye in the lateral geniculate nucleus: A comparison of cat and monkey. *Experimental Brain Research*, 35, 465-77. [113]
- Roelofs, C. and van der Waals, H. G. (1935). Veränderung der haptischen und optischen Lokalisation bei optokinetischer Reizung. *Zeitschrift für Psychologie*, 136, 5-49. [533]
- Roelofs, C. O. (1959). Considerations on the visual egocentre. *Acta Psychologica*, 16, 226-34. [598, 599]
- Rogers, B. J. (1976). Perceptual consequences of temporal and spatial summation in the human visual system. (Unpublished Ph.D thesis, University of Bristol). [232]
- Rogers, B. J. (1984). Thresholds for discriminating depth differences in motion parallax and stereoscopic surfaces. *Perception*, 13, A20. [584]
- Rogers, B. J. (1986). The perception of surface curvature from disparity and motion parallax cues. *Investigative Ophthalmology and Visual Science*, 27 (ARVO Abstracts), 182. [299, 484, 300]
- Rogers, B. J. (1987). Motion disparity and structure-from-motion disparity. *Investigative Ophthalmology and Visual Science*, 28 (ARVO Abstracts), 233. [447]
- Rogers, B. J. (1992). The perception and representation of depth and slant in stereoscopic surfaces. In *Artificial and biological vision systems* (ed. G. A. Orban and H.-H. Nagel), pp. 241-266. Springer-Verlag, Berlin. [277, 422]
- Rogers, B. J. (1993). Motion parallax and other dynamic cues for depth in humans. In *Visual motion and its role in the stabilization of gaze*, (ed. F. A. Miles and J. Wallman), pp. 119-137. Elsevier, Amsterdam. [573]
- Rogers, B. J. and Anstis, S. M. (1972). Intensity versus adaptation and the Pulfrich stereophenomenon. *Vision Research*, 12, 909-28. [537-38, 540, 546-47]
- Rogers, B. J. and Anstis, S. M. (1975). Reversed depth from positive and negative stereograms. *Perception*, 4, 193-201. [226, 230]
- Rogers, B. J. and Bradshaw, M. F. (1991). Vertical disparities in binocular and monocular depth perception. *Perception* 20 (ECVP Abstracts), 130. [444, 576]
- Rogers, B. J. and Bradshaw, M. F. (1992). Differential perspective effects in binocular stereopsis and motion parallax. *Investigative Ophthalmology and Visual Science*, 33 (ARVO Abstracts), 1333. [281, 290, 576]
- Rogers, B. J. and Bradshaw, M. F. (1993). Vertical disparities, differential perspective and binocular stereopsis. *Nature*, 361, 253-5. [281, 290-5, 305, 576]
- Rogers, B. J. and Bradshaw, M. F. (1994a). Is dif-frequency a stimulus for stereoscopic slant? *Investigative Ophthalmology and Visual Science*, 35 (ARVO Abstracts), 1316. [265, 292]
- Rogers, B. J. and Bradshaw, M. F. (1994b). Disparity scaling and the perception of fronto-parallel surfaces. *Perception*, in press. [292-3, 294, 305]
- Rogers, B. J. and Cagenello, R. (1989). Disparity curvature and the perception of three-dimensional surfaces. *Nature*, 339, 135-7. [142, 253, 298-9, 458, 484, 577, 582]
- Rogers, B. J. and Collett, T. S. (1989). The appearance of surfaces specified by motion parallax and binocular disparity. *Quarterly Journal of Experimental Psychology*, 41A, 697-717. [441, 576]
- Rogers, B. J. and Graham, M. E. (1979). Motion parallax as an independent cue for depth perception. *Perception*, 8, 125-34. [438, 579, 583]
- Rogers, B. J. and Graham, M. E. (1982). Similarities between motion parallax and stereopsis in human depth perception. *Vision Research*, 22, 216-70. [163, 440, 579, 580]
- Rogers, B. J. and Graham, M. E. (1983). Anisotropies in the perception of three-dimensional surfaces. *Science*, 221, 1409-11. [168, 266-8, 462, 480-1, 484, 494, 496, 581]
- Rogers, B. J. and Graham, M. E. (1984). Aftereffects from motion parallax and stereoscopic depth. In *Sensory experience, adaptation and perception*, (ed. L. Spillmann and B. R. Wooten), pp. 603-19, Lawrence Erlbaum, New York. [447]
- Rogers, B. J. and Graham, M. E. (1985). Motion parallax and the perception of three-dimensional surfaces. In *Brain mechanisms and spatial vision*, (ed. D. Ingle, M. Jeannerod, and D. Lee), pp. 95-111. Martinus Nijhoff, The Hague. [163, 273, 491-2, 494, 497, 579]

- Rogers, B. J. and Howard, I. P. (1991). Differences in the mechanisms used to extract 3-D slant from disparity and motion parallax cues. *Investigative Ophthalmology and Visual Science*, 32 (ARVO Abstracts), 695. [277, 280, 421]
- Rogers, B. J. and Koenderink, J. (1986). Monocular aniseikonia: A motion parallax analogue of the disparity-induced effect. *Nature*, 322, 62-3. [266, 275, 286-8, 582]
- Rogers, B. J., Bradshaw, M. F., and Glennerster, A. (1993). Differential perspective, disparity scaling and the perception of fronto-parallel surfaces. *Investigative Ophthalmology and Visual Science*, 34 (ARVO Abstracts), 1438. [293]
- Rogers, B. J., Bradshaw, M. F., and Glennerster, A. (1994). Are eye movements necessary in order to use vertical disparities? *Perception*, 23 (Abstract Supplement), 22. [292, 304]
- Rogers, B. J., Cagenello, R., and Rogers, S. (1988). Simultaneous contrast effects in stereoscopic surfaces: the role of tilt, slant and surface discontinuities. *Quarterly Journal of Experimental Psychology*, 40A (Proceedings), 417. [475, 484]
- Rogers, B. J., Steinbach, M. J., and Ono, H. (1974). Eye movements and the Pulfrich phenomenon. *Vision Research*, 14, 181-5. [536, 542, 549-50]
- Rogers, S. and Rogers, B. J. (1992). Visual and nonvisual information disambiguate surfaces specified by motion parallax. *Journal of Experimental Psychology*, 52, 446-52. [442]
- Rohaly, A. M. and Wilson, H. R. (1993). Nature of coarse-to-fine constraints on binocular fusion. *Journal of the Optical Society of America*, 10A, 2433-41. [175]
- Rohaly, A. M. and Wilson, H. R. (1994). Disparity averaging across spatial scales. *Vision Research*, 34, 1315-25. [233]
- Rohault, J. (1671). *Traité de Physique*. Savreux, Paris. [17]
- Rolls, E. T. (1992). Neurophysiological mechanisms underlying face processing within and beyond the temporal cortical visual areas. *Philosophical Transactions of the Royal Society*, B335, 11-21. [80]
- Rolls, E. T. (1994). Brain mechanisms for invariant visual recognition and learning. *Behavioural Processes*, in press. [78, 126]
- Rolls, E. T. and Cowey, A. (1970). Topography of the retina and striate cortex and its relationship to visual acuity in rhesus and squirrel monkeys. *Experimental Brain Research*, 10, 298-310. [114]
- Romano, P. E., Romano, J. A., and Puklin, J. E. (1975). Stereoacuity development in children with normal binocular single vision. *American Journal of Ophthalmology*, 79, 966-71. [620]
- Rommelteit, R., Toch, H., and Svendsen, D. (1968). Semantic, syntactic, and associative context effects in a stereoscopic rivalry situation. *Scandinavian Journal of Psychology*, 9, 145-9. [347]
- Rosa, M. G. P., Gattass, R., Fiorani, M., and Soares, J. G. M. (1992). Laminar, columnar and topographic aspects of ocular dominance in the primary visual cortex of *Cebus* monkeys. *Experimental Brain Research*, 88, 249-64. [122]
- Rosar, W. H. (1985). Visual space as physical geometry. *Perception*, 14, 403-25. [53]
- Rose, A. (1948). The sensitivity and performance of the human eye on an absolute scale. *Journal of the Optical Society of America*, 38, 196-208. [158]
- Rose, D. (1978). Monocular versus binocular contrast thresholds for movement and pattern. *Perception*, 7, 195-200. [362]
- Rose, D. and Blake, R. (1988). Mislocation of diplopic images. *Journal of the Optical Society of America*, A5, 1512-21. [597]
- Rose, D., Blake, R., and Halpern, D. L. (1988). Disparity range for binocular summation. *Investigative Ophthalmology and Visual Science*, 29, 283-90. [353]
- Rose, L. and Levinson, A. (1972). Anisometropia and aniseikonia. *American Journal of Optometry and Archives of the American Academy of Optometry*, 49, 480-4. [63]
- Rosen, E. (1956). The invention of eyeglasses. *Journal of the History of Medicine and Allied Sciences*, 11, 13-46; 183-218. [9]
- Rosenfeld, A. and Vanderbrug, G. J. (1977). Coarse-fine template matching. *IEEE Transactions on Man, Machine and Cybernetics*, 7, 104-7. [224]
- Rosenfield, M. and Ciuffreda, K. J. (1990). Distance heterophoria and tonic vergence. *Optometry and Vision Science*, 67, 667-9. [388]
- Rosenfield, M., Ciuffreda, K. J., and Hung, G. K. (1991). The linearity of proximally-induced accommodation and vergence. *Investigative Ophthalmology and Visual Science*, 32, 2985-91. [399]
- Ross, J. (1974). Stereopsis by binocular delay. *Nature*, 248, 363-4. [439, 539-40, 551]
- Ross, J. (1976). The resources of perception. *Scientific American*, 234, 80-6. [551]
- Ross, J. and Hogben, J. H. (1974). Short-term memory in stereopsis. *Vision Research*, 14, 1195-201. [186, 538, 551]
- Ross, J. and Hogben, J. H. (1975). The Pulfrich effect and short-term memory in stereopsis. *Vision Research*, 15, 1289-90. [538]
- Ross, J. E. (1983). Disturbance of stereoscopic vision in patients with unilateral stroke. *Behavioural Brain Research*, 7, 99-112. [624-5]
- Rossel, S. (1980). Foveal fixation and tracking in the praying mantis. *Journal of Comparative Physiology*, 139, 307-31. [647]
- Rossel, S. (1983). Binocular stereopsis in an insect. *Nature*, 302, 821-2. [647]
- Rossel, S. (1986). Binocular spatial localization in the praying mantis. *Journal of Experimental Biology*, 120, 265-81. [646]
- Rossel, S. (1991). Spatial vision in the praying mantis: Is distance implicated in size detection? *Journal of Comparative Physiology*, 169, 101-8. [647]
- Rossel, S., Mathis, U., and Collett, T. (1992). Vertical disparity and binocular vision in the praying mantis. *Visual Neuroscience*, 8, 165-70. [646-7]
- Roth, G. (1987). *Visual behavior in salamanders*. Springer, Berlin. [652]
- Rothstein, T. B. and Sacks, J. G. (1972). Defective stereopsis in lesions of the parietal lobe. *American Journal of Ophthalmology*, 73, 281-4. [624]
- Rouse, M. W., Tittle, J. S., and Braunstein, M. L. (1989). Stereoscopic depth perception by static stereo-deficient observers in dynamic displays with constant and changing disparity. *Optometry and Vision Science*, 66, 355-62. [445, 623]
- Rovamo, J. and Virsu, V. (1979). An estimation and application of the human cortical magnification factor. *Experimental Brain Research*, 37, 495-510. [114, 316, 617]
- Rowe, M. H. (1991). Functional organization of the retina. In *Neuroanatomy of the visual pathways and their development*, (ed. B. Dreher and R. S. Robinson), pp. 1-58. CRC Press, Boston. [109]
- Rozhkova, G. I., Nickolayev, P. P., and Shchadrin, V. E. (1982). Perception of stabilized retinal stimuli in dichoptic viewing conditions. *Vision Research*, 22, 293-302. [331]
- Ruddock, K. H. and Wigley, E. (1976). Inhibitory binocular interaction in human vision and a possible mechanism subserving stereoscopic fusion. *Nature*, 260, 604-6. [369]
- Ruddock, K. H., Waterfield, V. A., and Wigley, E. (1979). The response characteristics of an inhibitory binocular interaction in human vision. *Journal of Physiology*, 290, 37-49. [369]
- Rumelhart, D. E., Hinton, G. E., and Williams, R. J. (1986). Learning internal representations by error propagation. In *Parallel distributed processing*, Vol. 1, (ed. D. E. Rumelhart and J. L. McClelland), pp. 318-63. MIT Press, Cambridge, MA. [92]

- Rutstein, R. P. and Fuhr, P. S. (1992). Efficacy and stability of amblyopia therapy. *Optometry and Vision Science*, **69**, 747–54. [634]
- Rutstein, R. P., Marsh-Tootle, W., Scheiman, M. M., and Eskridge, J. B. (1991). Changes in retinal correspondence after changes in ocular alignment. *Optometry and Vision Science*, **68**, 325–30. [47]
- Ryan, C. and Gillam, B. (1993). A proximity-contingent stereoscopic depth aftereffect: evidence for adaptation to disparity gradients. *Perception*, **22**, 403–18. [468, 493–4]
- Sabrin, H. W. and Kertesz, A. E. (1983). The effect of imposed fixational eye movements on binocular rivalry. *Perception and Psychophysics*, **34**, 155–7. [332]
- Sagawa, K. (1982). Dichoptic color fusion studied with wavelength discrimination. *Vision Research*, **22**, 945–52. [327]
- Sagi, D. and Hochstein, S. (1985). Lateral inhibition between spatially adjacent spatial-frequency channels? *Perception and Psychophysics*, **37**, 315–22. [77]
- Saida, S. and Ono, H. (1984). Interaction between saccade and tracking vergence. *Vision Research*, **24**, 1289–94. [412]
- Saito, H., Yukie, M., Tanaka, K., Hikosaka, K., Fukada, Y., and Iwai, E. (1986). Integration of direction signals of image motion in the superior temporal sulcus of the macaque monkey. *Journal of Neuroscience*, **6**, 45–57. [143]
- Sakane I. (1994). The random-dot stereogram and its contemporary significance: New directions in perceptual art. In *Stereogram*, pp. 73–82. Cadence Books, San Francisco. [28]
- Sakata, H., Shibusaki, H., and Tsurugai, K. (1986). Parietal cortical neurons responding to rotary movement of visual stimulus in space. *Experimental Brain Research*, **61**, 658–63. [565]
- Saladin, J. J. and Carr, L. W. (1983). Fusion lock diameter and the forced vergence fixation disparity curve. *American Journal of Optometry and Physiological Optics*, **60**, 933–43. [392]
- Samorajski, T., Keefe, J. R., and Ordy, J. M. (1965). Morphogenesis of photoreceptor and retinal ultrastructure in a sub-human primate. *Vision Research*, **5**, 639–48. [605]
- Sanderson, K. J. and Sherman, M. (1971). Nasotemporal overlap in visual field projected to lateral geniculate nucleus in the cat. *Journal of Neurophysiology*, **34**, 453–66. [130]
- Sanderson, K. J., Darlan-Smith, I., and Bishop, P. O. (1969). Binocular corresponding receptive fields of single units in the cat dorsal lateral geniculate nucleus. *Vision Research*, **9**, 1297–303. [113]
- Sanderson, K. J., Guillory, R. W., and Shackelford, R. M. (1974). Congenitally abnormal visual pathways in mink (*Mustela vison*) with reduced retinal pigment. *Journal of Comparative Neurology*, **154**, 225–48. [642]
- Sanes, J. R. (1989). Extracellular matrix molecules that influence neural development. *Annual Review of Neuroscience*, **12**, 491–516. [606]
- Sarmiento, R. F. (1975). The stereoacuity of macaque monkey. *Vision Research*, **15**, 493–8. [155, 645]
- Sauer, B., Kammradt, G., Krauthausen, I., Kretschmann, H. J., Lange, H. W., and Wingert, F. (1983). Qualitative and quantitative development of the visual cortex in man. *Journal of Comparative Neurology*, **214**, 441–50. [610]
- Saul, A. B. and Cynader, M. S. (1989). Adaptation in single units in visual cortex: The tuning of aftereffects in the spatial domain. *Visual Neuroscience*, **2**, 593–607. [101]
- Savoy, R. L. (1984). "Extinction" of the McCollough effect does not transfer interocularly. *Perception and Psychophysics*, **36**, 571–6. [379]
- Saye, A. and Frisby, J. P. (1975). The role of monocularly conspicuous features in facilitating stereopsis from random-dot stereograms. *Perception*, **4**, 159–71. [193, 218]
- Scammon, R. E. and Wilmer, H. A. (1950). Growth of the components of the human eyeball. II. Comparison of the calculated volumes of the eyes of the newborn and of adults, and their components. *AMA Archives of Ophthalmology*, **43**, 620–37. [604]
- Schaeffel, F., Glasser, A., and Howland, H. C. (1988). Accommodation, refractive error and eye growth in chickens. *Vision Research*, **28**, 639–57. [604]
- Scharff, L. V. and Geisler, W. S. (1992). Stereopsis at isoluminance in the absence of chromatic aberrations. *Journal of the Optical Society of America A*, **9**, 868–76. [207]
- Scheidt, R. A. and Kertesz, A. E. (1993). Temporal and spatial aspects of sensory interactions during human fusional response. *Vision Research*, **33**, 1259–70. [319]
- Schein, S. J. and De Monasterio, F. M. (1987). Mapping of retinal and geniculate neurons onto striate cortex of macaque. *Journal of Neuroscience*, **7**, 996–1009. [111–3, 123, 335]
- Schellart, N. A. M. (1990). The visual pathways and central non-tectal processing. In *The visual system of fish*, (ed. R. H. Douglas and M. B. A. Djamgoz), pp. 345–71. Chapman Hall, London. [649]
- Schiff, B., Cohen, T., and Raphan, T. (1988). Nystagmus induced by stimulation of the nucleus of the optic tract in the monkey. *Experimental Brain Research*, **70**, 1–14. [530]
- Schiff, W. (1965). The perception of impending collision: A study of visually directed avoidant behavior. *Psychological Monographs*, **79**, No. 604. [557]
- Schiff, W. and Detwiler, M. L. (1979). Information used in judging impending collision. *Perception*, **8**, 647–58. [555]
- Schiff, W. and Oldak, R. (1990). Accuracy of judging time to arrival: Effects of modality, trajectory, and gender. *Journal of Experimental Psychology: Human Perception and Performance*, **16**, 303–16. [555]
- Schiff, W., Caviness, J. A., and Gibson, J. J. (1962). Persistent fear responses in rhesus monkeys to the optical stimulus of "looming". *Science*, **136**, 982–3. [557]
- Schillen, T. B. and König, P. (1994). Binding by temporal structure in multiple feature domains of an oscillatory neuronal network. *Biological Cybernetics*, **70**, 397–405. [83]
- Schiller, P. H. (1970). The discharge characteristics of single units in the oculomotor and abducens nuclei of the unanesthetized monkey. *Experimental Brain Research*, **10**, 347–62. [425]
- Schiller, P. H. (1992). The on and off channels of the visual system. *Trends in Neuroscience*, **15**, 86–92. [110]
- Schiller, P. H. and Dolan, R. P. (1994). Visual aftereffects and the consequences of visual system lesions on their perception in the rhesus monkey. *Visual Neuroscience*, **11**, 643–65. [144]
- Schiller, P. H. and Greenfield, A. (1969). Visual masking and the recovery phenomenon. *Perception and Psychophysics*, **6**, 182–4. [369]
- Schiller, P. H. and Lee, K. (1991). The role of the primate extrastriate area V4 in vision. *Science*, **251**, 1251–3. [126, 129]
- Schiller, P. H. and Smith, M. (1968). Monoptic and dichoptic metacontrast. *Perception and Psychophysics*, **3**, 237–9. [370]
- Schiller, P. H. and Wiener, M. (1962). Binocular and stereoscopic viewing of geometrical illusions. *Perceptual and Motor Skills*, **15**, 739–47. [372]
- Schiller, P. H. and Wiener, M. (1963). Monoptic and dichoptic masking. *Journal of Experimental Psychology*, **66**, 386–93. [370]
- Schiller, P. H., Finlay, B. L., and Volman, S. F. (1976). Quantitative studies of single cells in monkey striate cortex. II. Orientation specificity and ocular dominance. *Journal of Neurophysiology*, **39**, 1320–33. [123]
- Schiller, P. H., Logothetis, N. K., and Charles, E. R. (1990). Role of the color-opponent and broad-band channels in vision. *Visual Neuroscience*, **5**, 321–46. [126–7, 144]

- Schiller, P. H., Sandell, J. H., and Maunsell, H. R. (1986). Functions of the on and off channels of the visual system. *Nature*, **322**, 824–5. [110]
- Schirillo, J. A. and Shevell, S. K. (1993). Lightness and brightness judgments of coplanar retinally noncontiguous surfaces. *Journal of the Optical Society*, **10**, 2442–52. [524]
- Schlaer, R. (1972). An eagle's eye: Quality of the retinal image. *Science*, **176**, 920–22. [654]
- Schlagger, B. L. and O'Leary, D. D. M. (1991). Potential of visual cortex to develop an array of functional units unique to somatosensory cortex. *Science*, **522**, 1556–60. [616]
- Schmielau, F. and Singer, W. (1977). The role of visual cortex for binocular interactions in the cat lateral geniculate nucleus. *Brain Research*, **120**, 354–61. [113]
- Schneider, B. and Moraglia, G. (1992). Binocular unmasking with unequal interocular contrast: The case for multiple cyclopean eyes. *Perception and Psychophysics*, **52**, 639–60. [368]
- Schneider, B., Moraglia, G., and Jepson, A. (1989). Binocular unmasking: An analogue to binaural unmasking. *Science*, **243**, 1479–81. [368]
- Schönemann, P. H. and Tucker, L. R. (1967). A maximum-likelihood solution for method of successive intervals allowing for unequal stimulus dispersions. *Psychometrika*, **32**, 403–17. [166]
- Schor, C. M. (1975). A directional impairment of eye movement control in strabismus amblyopia. *Investigative Ophthalmology and Visual Science*, **14**, 692–7. [632]
- Schor, C. M. (1977). Visual stimuli for strabismic suppression. *Perception*, **6**, 583–93. [634]
- Schor, C. M. (1979a). The influence of rapid prism adaptation upon fixation disparity. *Vision Research*, **19**, 757–65. [387, 391, 408]
- Schor, C. M. (1979b). The relationship between fusional vergence eye movements and fixation disparity. *Vision Research*, **19**, 1359–67. [391]
- Schor, C. M. (1983). Fixation disparity and vergence adaptation. In *Vergence eye movements: Basic and clinical aspects*. (ed. M. C Schor, K. J. Ciuffreda), pp. 465–516. Butterworth, Boston. [392]
- Schor, C. M. (1991). Binocular sensory disorders. In *Vision and visual disorders*. Vol. 9, *Binocular vision*. (ed. D. Regan), pp. 179–223. Macmillan, London. [46–7]
- Schor, C. M. (1992). A dynamic model of cross-coupling between accommodation and convergence: Simulations of step and frequency responses. *Optometry and Vision Science*, **69**, 258–69. [398]
- Schor, C. M. and Badcock, D. R. (1985). A comparison of stereo and vernier acuity within spatial channels as a function of distance from fixation. *Vision Research*, **25**, 1113–19. [181]
- Schor, C. M. and Ciuffreda, K. J. (1983). *Vergence eye movements: Basic and clinical aspects*. Butterworths, Boston. [1, 386]
- Schor, C. M. and Heckmann, T. (1989). Interocular differences in contrast and spatial frequency: Effects on stereopsis and fusion. *Vision Research*, **29**, 837–47. [170]
- Schor, C. M. and Horner, D. (1989). Adaptive disorders of accommodation and vergence in binocular dysfunction. *Ophthalmology and Physiological Optics*, **9**, 264–8. [398]
- Schor, C. M. and Howarth, P. A. (1986). Suprathreshold stereodepth matches as a function of contrast and spatial frequency. *Perception*, **15**, 249–58. [175]
- Schor, C. M. and Kotulak, J. C. (1986). Dynamic interactions between accommodation and convergence are velocity sensitive. *Vision Research*, **26**, 927–42. [398, 408]
- Schor, C. M. and Levi, D. M. (1980). Disturbances of small-field horizontal and vertical optokinetic nystagmus in amblyopia. *Investigative Ophthalmology and Visual Science*, **19**, 668–83. [531, 632]
- Schor, C. M. and Tsuetaki, T. K. (1987). Fatigue of accommodation and vergence modifies their mutual interactions. *Investigative Ophthalmology and Visual Science*, **28**, 1250–9. [398]
- Schor, C. M. and Tyler, C. W. (1981). Spatio-temporal properties of Panum's fusional area. *Vision Research*, **21**, 683–92. [320]
- Schor, C. M. and Wood I. (1983). Disparity range for local stereopsis as a function of luminance spatial frequency. *Vision Research*, **23**, 1649–54. [167, 173, 175]
- Schor, C. M., Alexander, J., Cormack, L., and Stevenson, S. (1992). Negative feedback control model of proximal convergence and accommodation. *Ophthalmology and Physiological Optics*, **12**, 307–18. [398–9]
- Schor, C. M., Heckmann, T., and Tyler, C. W. (1989). Binocular fusion limits are independent of contrast, luminance gradient and component phases. *Vision Research*, **29**, 821–35. [317]
- Schor, C. M., Gleason, G., and Horner, D. (1990). Selective nonconjugate binocular adaptation of vertical saccades and pursuits. *Vision Research*, **30**, 1827–44. [414]
- Schor, C. M., Gleason, G., and Lunn, R. (1993b). Interactions between short-term vertical phoria adaptation and nonconjugate adaptation of vertical pursuits. *Vision Research*, **33**, 55–64. [393]
- Schor, C., Landsman, L., and Erikson, P. (1987). Ocular dominance and the interocular suppression of blur in monovision. *American Journal of Optometry and Physiological Optics*, **64**, 723–30. [330]
- Schor, C. M., Gleason, G., Maxwell, J., and Lunn, R. (1993a). Spatial aspects of vertical phoria adaptation. *Vision Research*, **33**, 73–84. [393]
- Schor, C. M., Wesson M., and Robertson, K. M. (1986b). Combined effects of spatial frequency and retinal eccentricity upon fixation disparity. *American Journal of Optometry and Physiological Optics*, **63**, 619–26. [404]
- Schor, C. M., Wood, I. C., and Ogawa, J. (1984a). Spatial tuning of static and dynamic local stereopsis. *Vision Research*, **24**, 573–8. [188, 219]
- Schor, C. M., Wood, I. C., and Ogawa, J. (1984b). Binocular sensory fusion is limited by spatial resolution. *Vision Research*, **24**, 661–5. [316]
- Schor, C. M., Robertson, K. M., and Wesson, M. (1986a). Disparity vergence dynamics and fixation disparity. *American Journal of Optometry and Physiological Optics*, **63**, 611–18. [392]
- Schriever, W. (1924). Experimentelle Studien über stereoskopisches Sehen. *Zeitschrift für Psychologie*, **96**, 113–70. [450]
- Schrödinger, E. (1926). Die Gesichtsempfindungen. In *Mueller-Pouillet's Lehrbuch der Physik*, (11th edn), Book 2, Part 1, pp. 456–560. Vieweg, Braunschweig. [357]
- Schroeder, C. E., Tenke, C. E., Arezzo, J. C., and Vaughan, H. G. (1990). Binocularity in the lateral geniculate nucleus of the alert monkey. *Brain Research*, **521**, 303–10. [113]
- Schumann, F. (1904). Beiträge zur Analyse der Gesichtswahrnehmungen: 1. Einige Beobachtungen über die Zusammenfassung von Gesichtseindrücken zu Einheiten. *Psychologische Studien*, **1**, 1–32. [77]
- Schumer, R. A. and Ganz, L. (1979). Independent stereoscopic channels for different extents of spatial pooling. *Vision Research*, **19**, 1303–14. [165, 440, 481, 495–6]
- Schumer, R. A. and Julesz, B. (1984). Binocular disparity modulation sensitivity to disparities offset from the plane of fixation. *Vision Research*, **24**, 533–42. [163, 481]
- Schuster, H. G. and Wagner, P. (1990). A model for neuronal oscillations in the visual cortex. *Biological Cybernetics*, **64**, 77–82. [83]

- Schwartz, E. L. (1980). Computational anatomy and functional architecture of striate cortex: A spatial mapping approach to perceptual coding. *Vision Research*, 20, 645-70. [115]
- Schwartz, T. L., Dobson, V., Sandstrom, D. J., and Van Hof-van Duin, J. (1987). Kinetic perimetry assessment of binocular visual field shape and size in young infants. *Vision Research*, 27, 2163-75. [605]
- Schwarz, W. (1993). Coincidence detectors and two-pulse visual temporal integration: New theoretical results and comparison data. *Biological Cybernetics*, 69, 173-82. [96, 351]
- Schwarz, U., Busettini, C., and Miles, F. A. (1989). Ocular responses to linear motion are inversely proportional to viewing distance. *Science*, 245, 1394-6. [416]
- Schwassmann, H. O. (1968). Visual projection upon the optic tectum in foveate marine teleosts. *Vision Research*, 8, 1337-48. [649-50]
- Scott, A. B. (1981). Botulinum toxin injection of eye muscles to correct strabismus. *Transactions of the American Ophthalmology Society*, 79, 734-70. [387]
- Scott, T. R. and Wood, D. Z. (1966). Retinal anoxia and the locus of the after-effect of motion. *American Journal of Psychology*, 79, 435-42. [376]
- Sedgewick, H. A. (1986). Space perception. In *Handbook of human perception and performance*, (ed. K. R. Boff, L. Kaufman, and J. P. Thomas), Chap. 21. Wiley, New York. [457, 460]
- Sefton, A. J. (1986). The regulation of cell numbers in the developing visual system. In *Visual neuroscience*, (ed. J. D. Pettigrew and W. R. Levick), pp. 2145-56. Cambridge University Press, London. [607]
- Sekuler, A. B. (1992). Simple-pooling of unidirectional motion predicts speed discrimination for looming stimuli. *Vision Research*, 32, 2277-88. [559]
- Sekuler, R., Pantle, A., and Levinson, E. (1978). Physiological basis of motion perception. In *Handbook of sensory physiology*, Vol. VIII, (ed. R. Held, H. W. Liebowitz, and H. L. Teuber), pp. 67-98. Springer-Verlag, Berlin. [376]
- Selby, S. A. and Woodhouse, J. M. (1981). The spatial frequency dependence of interocular transfer in amblyopes. *Vision Research*, 21, 1401-8. [638, 640]
- Semmlow, J. L. and Heerema, D. (1979). The role of accommodative convergence at the limits of fusional vergence. *Investigative Ophthalmology and Visual Science*, 18, 970-6. [398]
- Semmlow, J. L. and Hung, G. (1979). Accommodative and fusional components of fixation disparity. *Investigative Ophthalmology and Visual Science*, 18, 1082-6. [390]
- Semmlow, J. L. and Hung, G. (1983). The near response. Theories of control. In *Vergence eye movements: Basic and clinical aspects*, (ed. C. Schor and K. Ciuffreda), pp. 175-95. Butterworths, Boston. [394]
- Semmlow, J. L. and Venkiteswaran, N. (1976). Dynamic accommodative vergence components in binocular vision. *Vision Research*, 16, 403-10. [398]
- Semmlow, J. L. and Wetzel, P. (1979). Dynamic contributions of the components of binocular vergence. *Journal of the Optical Society of America*, 69, 639-45. [396]
- Semmlow, J. L., Hung, G., and Ciuffreda, K. J. (1986). Quantitative assessment of disparity vergence components. *Investigative Ophthalmology and Visual Science*, 27, 558-64. [405-6]
- Semmlow, J. L., Hung, G., Horng, J-L., Ciuffreda, K. J. (1994). Disparity vergence eye movements exhibit preprogrammed motor control. *Vision Research*, 34, 335-43. [408]
- Sengelaub, D. R. and Finlay, B. L. (1981). Early removal of one eye reduces normally occurring cell death in the remaining eye. *Science*, 213, 573. [607]
- Sengpiel, F. and Blakemore, C. (1994). Interocular control of neuronal responsiveness in cat visual cortex. *Nature*, 368, 847-50. [345]
- Sengpiel, F., Blakemore, C., and Harrad, R. (1995). Interocular suppression in the primary visual cortex: A possible neural basis of binocular rivalry. *Vision Research*, 35, 179-95. [345-6]
- Servos, P., Goodale, M. A., and Jakobson, L. S. (1992). The role of binocular vision in prehension: A kinematic analysis. *Vision Research*, 32, 1513-21. [2]
- Servos, P. and Goodale, M. A. (1994). Binocular vision and the online control of human prehension. *Experimental Brain Research*, 98, 119-27. [2]
- Sethi, B. (1986). Vergence adaptation: A review. *Documenta Ophthalmologica*, 63, 247-63. [392]
- Sethi, B. and Henson, D. B. (1984). Adaptive changes with prolonged effect of comitant and noncomitant vergence disparities. *American Journal of Optometry and Physiological Optics*, 61, 506-12. [393]
- Sethi, B. and North, R. V. (1987). Vergence adaptive changes with varying magnitudes of prism-induced disparities and fusional amplitudes. *American Journal of Optometry and Physiological Optics*, 64, 263-8. [392]
- Shadlen, M. and Carney, T. (1986). Mechanisms of human motion perception revealed by a new cyclopean illusion. *Science*, 232, 95-7. [343, 568]
- Shapley, R. (1991). Receptive field structure of P and M cells in the monkey retina. In *From pigments to perception*, (ed. A. Valberg and B. B. Lee), pp. 95-104. Plenum Press, New York. [110]
- Shapley, R. and So, Y. T. (1980). Is there an effect of monocular deprivation on the proportions of X and Y cells in the cat lateral geniculate nucleus? *Experimental Brain Research*, 39, 41-8. [627]
- Shatz, C. J. (1983). The prenatal development of the cat's retinogeniculate pathway. *Journal of Neuroscience*, 3, 482-99. [608]
- Shatz, C. J. (1990). Competitive interactions between retinal ganglion cells during prenatal development. *Journal of Neurobiology*, 21, 197-211. [609]
- Shatz, C. J. and Sretavan, D. W. (1986). Interactions between retinal ganglion cells during development of the mammalian visual system. *Annual Review of Neuroscience*, 9, 171-207. [605]
- Shatz, C. J. and Stryker, M. P. (1988). Prenatal tetrodotoxin infusion blocks segregation of retinogeniculate afferents. *Science*, 242, 87-9. [609]
- Shatz, C. J., Ghosh, A., McKonnell, S. K., Allendoerfer, K. L., Friauf, E., and Antonini, A. (1991). Subplate neurons and the development of neocortical connections. In *Development of the visual system*, (ed. D. M-K. Lam and C. J. Shatz), pp. 175-96. MIT Press, Cambridge, MA. [610]
- Shaw, C. and Cynader, M. (1984). Disruption of cortical activity prevents ocular dominance changes in monocularly deprived kittens. *Nature*, 308, 731-4. [629]
- Shaw, W. T. (1861). Description of a new optical instrument called the "Stereotrope". *Proceedings of the Royal Society*, 11, 70-3. [19]
- Shea, S. L., Aslin, R. N., and McCulloch, D. (1987). Binocular VEP summation in infants and adults with abnormal binocular histories. *Investigative Ophthalmology and Visual Science*, 28, 356-65. [620]
- Shea, S. L., Doussard-Roosevelt, J. A., and Aslin, R. N. (1985). Pupillary measures of binocular luminance summation in infants and stereoblind adults. *Investigative Ophthalmology and Visual Science*, 26, 1064-70. [621]
- Shebilske, W. L. and Nice, D. S. (1976). Optical insignificance of the nose and the Pinocchio effect in free-scan visual straight-ahead judgments. *Perception and Psychophysics*, 20, 17-20. [591]

- Sheedy, J. E. (1980). Actual measurement of fixation disparity and its use in diagnosis and treatment. *Journal of the American Optometric Association*, 51, 1079–84. [389]
- Sheedy, J. E. and Fry, G. A. (1979). The perceived direction of the binocular image. *Vision Research*, 19, 201–11. [597]
- Sheedy, J. E., Bailey, I. L., Buri, M., and Bass, E. (1986). Binocular vs. monocular performance. *American Journal of Optometry and Physiological Optics*, 63, 839–46. [2]
- Sheni, D. D. and Remole, A. (1986). Field of vergence limits. *American Journal of Optometry and Physiological Optics*, 63, 252–8. [32]
- Shepard, R. N. and Cooper, L. A. (1982). *Mental images and their transformation*. MIT Press, Cambridge, MA. [588]
- Sherman, S. M. (1973). Visual field defects in monocularly and binocularly deprived cats. *Brain Research*, 49, 25–45. [633]
- Sherman, S. M. and Koch, C. (1986). The control of retino-geniculate transmission in the mammalian lateral geniculate nucleus. *Experimental Brain Research*, 63, 1–20. [113]
- Sherman, S. M. and Stone, J. (1973). Physiological normality of the retina in visually deprived cats. *Brain Research*, 60, 224–30. [626]
- Sherrington, C. S. (1904). On binocular flicker and the correlation of activity of corresponding retinal points. *British Journal of Psychology*, 1, 26–60. [338, 356, 359]
- Sherry, D. F., Jacobs, L. F., and Gaulin, S. J. C. (1992). Spatial memory and adaptive specialization of the hippocampus. *Trends in Neuroscience*, 15, 298–303. [615]
- Shevelev, I. A., Sharaev, G. A., Lazareva, N. A., Novikova, R. V., and Tikhomirov, A. S. (1993). Dynamics of orientation tuning in the cat striate cortex neurons. *Neuroscience*, 56, 865–76. [118]
- Shimojo, S. and Nakayama, K. (1981). Adaptation to the reversal of binocular depth cues: Effects of wearing left-right reversing spectacles on stereoscopic depth perception. *Perception*, 10, 391–402. [488]
- Shimojo, S. and Nakayama, K. (1990). Real world occlusion constraints and binocular rivalry. *Vision Research*, 30, 69–80. [514]
- Shimojo, S., Bauer, J., O'Connell, K. M., and Held, R. (1986). Pre-stereoptic binocular vision in infants. *Vision Research*, 26, 501–10. [618]
- Shimojo, S., Silverman, G. H., and Nakayama, K. (1988). An occlusion-related mechanism of depth perception based on motion and interocular sequence. *Nature*, 333, 265–8. [521]
- Shimojo, S., Silverman, G. H., and Nakayama, K. (1989). Occlusion and the solution to the aperture problem for motion. *Vision Research*, 29, 619–26. [526]
- Shinkman, P. G. and Bruce, C. J. (1977). Binocular differences in cortical receptive fields of kittens after rotationally disparate binocular experience. *Science*, 197, 285–7. [622]
- Shinkman, P. G., Isley, M. R., and Rogers, D. C. (1983). Prolonged dark rearing and development of interocular orientation disparity in visual cortex. *Journal of Neurophysiology*, 49, 717–29. [622]
- Shinkman, P. G., Timney, B., and Isley, M. R. (1992). Binocular depth perception following early experience with interocular torsional disparity. *Visual Neuroscience*, 9, 303–12. [622]
- Shipley, T. (1961). An experimental study of the frontal reference curves of binocular visual space. *Documenta Ophthalmologica*, 15, 321–50. [57]
- Shipley, T. (1971). The first random-dot texture stereogram. *Vision Research*, 11, 1491–2. [455]
- Shipley, T. and Rawlings, S. C. (1970a). The nonius horopter I. History and theory. *Vision Research*, 10, 1225–62. [18, 59–60]
- Shipley, T. and Rawlings, S. C. (1970b). The nonius horopter. II. An experimental report. *Vision Research*, 10, 1263–99. [60]
- Shipley, W. C., Kenney, F. A., and King, M. E. (1945). Beta apparent movement under binocular, monocular and interocular stimulation. *American Journal of Psychology*, 58, 545–9. [567]
- Shipp, S. and Zeki, S. (1985). Segregation of pathways leading from area V2 to areas V4 and V5 of macaque monkey visual cortex. *Nature*, 315, 322–5. [126]
- Shlaer, R. (1971). Shift in binocular disparity causes compensatory change in the cortical structure of kittens. *Science*, 173, 638–41. [621]
- Shortess, G. K. and Krauskopf, J. (1961). Role of involuntary eye movements in stereoscopic acuity. *Journal of the Optical Society of America*, 51, 555–9. [178, 184]
- Shulman, G. L. (1991). Attentional modulation of mechanisms that analyze rotation in depth. *Journal of Experimental Psychology: Human Perception and Performance*, 17, 726–37. [556]
- Siderov, J. and Harwerth, R. S. (1993a). Effects of the spatial frequency of test and reference stimuli on stereo-thresholds. *Vision Research*, 33, 1545–51. [174]
- Siderov, J. and Harwerth, R. S. (1993b). Precision of stereoscopic depth perception from double images. *Vision Research*, 33, 1553–60. [156]
- Siegel, H. and Duncan, C. P. (1960). Retinal disparity and diplopia vs. luminance and size of target. *American Journal of Psychology*, 73, 280–4. [317]
- Sillito, A. M., Jones, H. E., Gerstein, G. L., and West, D. C. (1994). Feature-linked synchronization of thalamic relay cell firing induced by feedback from the visual cortex. *Nature*, 369, 479–82. [33]
- Sillito, A. M., Kemp, J. A., and Blakemore, C. (1981). The role of GABAergic inhibition in the cortical effects of monocular deprivation. *Nature*, 291, 318–20. [629]
- Sillito, A. M., Kemp, J. A., Milson, J. A., and Berardi, N. (1980). A re-evaluation of the mechanisms underlying simple cell orientation selectivity. *Brain Research*, 194, 517–20. [118]
- Silva, L. R., Amitai, Y., and Connors, B. W. (1991). Intrinsic oscillations of neocortex generated by layer 5 pyramidal neurons. *Science*, 251, 432–5. [83]
- Simmons, D. R. and Kingdom, F. A. A. (1994). Contrast thresholds for stereoscopic depth identification with isoluminant and isochromatic stimuli. *Vision Research*, 34, 2971–82. [207]
- Simonet, P. and Campbell, M. C. W. (1990a). The optical transverse chromatic aberration of the fovea of the human eye. *Vision Research*, 30, 187–206. [306]
- Simonet, P. and Campbell, M. C. W. (1990b). Effect of illuminance on the directions of chromostereopsis and transverse chromatic aberration observed with natural pupils. *Ophthalmic and Physiological Optics*, 10, 271–9. [307]
- Simons, K. (1981a). A comparison of the Frisby, Random-Dot, E, TNO, and Random Circles stereotests in screening and office use. *Archives of Ophthalmology*, 99, 446–52. [155]
- Simons, K. (1981b). Stereoacuity norms in young children. *AMA Archives of Ophthalmology*, 99, 439–45. [620]
- Simons, K. (1984). Effects on stereopsis of monocular versus binocular degradation of image contrast. *Investigative Ophthalmology and Visual Science*, 25, 987–9. [170]
- Simons, K. (1993). *Early visual development, normal and abnormal*. Oxford University Press, New York. [604]
- Simons, K. and Reinecke, R. D. (1974). A reconsideration of amblyopia screening and stereopsis. *American Journal of Ophthalmology*, 78, 707–13. [151]
- Simpson, J. I. (1984). The accessory optic system. *Annual Review of Neuroscience*, 7, 13–41. [529]
- Simpson, W. A. (1993). Optic flow and depth perception. *Spatial Vision*, 7, 35–75. [460]

- Simpson, W. A. and Swanston, M. T. (1992). Depth-coded motion signals in plaid perception and optokinetic nystagmus. *Experimental Brain Research*, 86, 447–50. [527]
- Sindermann, F. and Lüddeke, H. (1972). Monocular analogues to binocular contour rivalry. *Vision Research*, 12, 763–72. [334]
- Singer, W. (1970). Inhibitory binocular interaction in the lateral geniculate body of the cat. *Brain Research*, 18, 165–70. [113]
- Singer, W. (1977). Effects of monocular deprivation on excitatory and inhibitory pathways in cat striate cortex. *Experimental Brain Research*, 30, 25–41. [629]
- Singer, W. (1978). The effect of monocular deprivation on cat parastriate cortex: Asymmetry between crossed and uncrossed pathways. *Brain Research*, 157, 351–5. [633]
- Singer, W. (1990). The formation of cooperative cell assemblies in the visual cortex. *Journal of Experimental Biology*, 153, 177–97. [615]
- Singer, W. and Treter, F. (1976). Receptive-field properties and neural connectivity in striate and parastriate cortex of contour-deprived cats. *Journal of Neurophysiology*, 39, 613–30. [625]
- Singer, W., Rauschecker, J., and Werth, R. (1977). The effect of monocular exposure to temporal contrasts on ocular dominance in kittens. *Brain Research*, 134, 568–72. [630]
- Sireteanu, R. (1982). Binocular vision in strabismic humans with alternating fixation. *Vision Research*, 22, 889–896. [634]
- Sireteanu, R. and Fronius, M. (1981). Naso-temporal asymmetries in human amblyopia: consequence of long-term interocular suppression. *Vision Research*, 21, 1055–63. [632]
- Sireteanu, R. and Fronius, M. (1989). Different patterns of retinal correspondence in the central and peripheral visual field of strabismics. *Investigative Ophthalmology and Visual Science*, 30, 2023–33. [46]
- Sireteanu, R. and Fronius, M. (1990). Human amblyopia: Structure of the visual field. *Experimental Brain Research*, 79, 603–14. [633]
- Sireteanu, R. and Hoffmann, K. P. (1979). Relative frequency and visual resolution of X- and Y-cells in the LGN of normal and monocularly deprived cats: Interlaminar differences. *Experimental Brain Research*, 34, 591–603. [627]
- Sireteanu, R. and Maurer, D. (1982). The development of the kitten's visual field. *Vision Research*, 22, 1105–11. [617]
- Sireteanu, R., Fronius, M., and Singer, W. (1981). Binocular interaction in the peripheral visual field of humans with strabismic and anisotropic amblyopia. *Vision Research*, 21, 1065–74. [639–40]
- Sireteanu, R., Fronius, M., and Constantinescu, D. H. (1994). The development of visual acuity in the peripheral visual field of human infants: Binocular and monocular measurements. *Vision Research*, 34, 1659–71. [617]
- Skaliora, I., Scobey, R. P., and Chalupa, L. M. (1993). Prenatal development of excitability in cat retinal ganglion cells: Action potentials and sodium currents. *Journal of Neuroscience*, 13, 313–23. [609, 614]
- Skarf, B. (1973). Development of binocular single units in the optic tectum of frogs raised with disparate stimulation to the eyes. *Brain Research*, 51, 352–7. [652]
- Skottun, B. C. and Freeman, R. D. (1984). Stimulus specificity of binocular cells in the cat's visual cortex: Ocular dominance and the matching of left and right eyes. *Experimental Brain Research*, 56, 206–16. [120]
- Slater, A., Morison, V., and Somers, M. (1988). Orientation discrimination and cortical function in the human newborn. *Perception*, 17, 597–602. [616]
- Slater, A. M. and Findlay, J. M. (1975a). The corneal reflection technique and the visual preference method: Sources of error. *Journal of Experimental Child Psychology*, 20, 240–7. [620]
- Slater, A. M. and Findlay, J. M. (1975b). Binocular fixation in the newborn baby. *Journal of Experimental Child Psychology*, 20, 248–73. [621]
- Sloane, M. and Blake, R. (1984). Selective adaptation of monocular and binocular neurons in human vision. *Journal of Experimental Psychology: Human Perception and Performance*, 10, 406–42. [369]
- Sloane, M. E. and Blake, R. (1987). Perceptually unequal spatial frequencies do not yield stereoscopic tilt. *Perception and Psychophysics*, 42, 569–75. [260]
- Smallman, H. S. and MacLeod, D. I. A. (1994a). Size-disparity correlation in stereopsis at contrast threshold. *Journal of the Optical Society of America*, 11, 2169–83. [169–70]
- Smallman, H. S. and MacLeod, D. I. A. (1994b). Paradoxical effects of adapting to large disparities: Constraining population code models of disparity. *Investigative Ophthalmology and Visual Science*, 35, 1917. [173, 492]
- Smith, A. T. (1983). Interocular transfer of colour-contingent threshold elevation. *Vision Research*, 23, 729–34. [380]
- Smith, D. C. and Holdefer, R. N. (1985). Binocular competitive interaction and recovery of visual acuity in long-term monocularly deprived cats. *Vision Research*, 25, 1783–94. [633]
- Smith, D. C., Lorber, R., Stanford, L. R., and Loop, M. S. (1980). Visual acuity following binocular deprivation in the cat. *Brain Research*, 183, 1–11. [626]
- Smith, D. C., Spear, P. D., and Kratz, K. E. (1978). Role of visual experience in post-critical-period reversal of effects of monocular deprivation in cat striate cortex. *Journal of Comparative Neurology*, 178, 313–28. [628]
- Smith, E. L., Bennett, M. J., Harwerth, R. S., and Crawford, M. L. J. (1979). Binocularity in kittens reared with optically induced squint. *Science*, 204, 875–7. [630]
- Smith, E. L., Harwerth, R. S., and Crawford, M. L. J. (1985b). Spatial contrast sensitivity deficits in monkeys produced by optically induced anisometropia. *Investigative Ophthalmology and Visual Science*, 26, 330–42. [636]
- Smith, E. L., Hung, L.-F., and Harwerth, R. S. (1994). Effects of optically induced blur on the refractive status of young monkeys. *Vision Research*, 34, 293–301. [604]
- Smith, E. L., Harwerth, R. S., Siderow, J., Wingard, M., Crawford, M. L. J., and Noorden, G. K. von (1992). Prior binocular dissociation reduces monocular form deprivation amblyopia in monkeys. *Investigative Ophthalmology and Visual Science*, 33, 1804–10. [633]
- Smith, E. L., Levi, D. M., Harwerth, R. S., and White, J. M. (1982). Color vision is altered during the suppression phase of binocular rivalry. *Journal of Psychology*, 218, 802–4. [635]
- Smith, E. L., Levi, D. M., Manny, R. E., Harwerth, R. S., and White, J. M. (1985a). The relationship between binocular rivalry and strabismic suppression. *Investigative Ophthalmology and Visual Science*, 26, 80–7. [635]
- Smith, J. C., Atkinson, J., Anler, S., and Moore, A. T. (1991). A prospective study of binocularity and amblyopia in strabismic infants before and after corrective surgery: Implications for the human critical period. *Clinical Visual Science*, 6, 335–53. [637]
- Smith, R. (1738). *A compleat system of opticks in four books*. Cambridge. [17, 43]
- Smith, R. A. (1976). The motion/disparity aftereffect, a preliminary study. *Vision Research*, 16, 1507–9. [439, 566]
- Smith, S. (1945). Utrocular or "which eye" discrimination. *Journal of Experimental Psychology*, 35, 1–14. [601]
- Snippe, H. P. and Koenderink, J. J. (1992). Discrimination thresholds for channel-coded systems. *Biological Cybernetics*, 66, 543–51. [97]

- Snow, R., Hore, J., and Vilis, T. (1985). Adaptation of saccadic and vestibulo-ocular systems after extraocular muscle tenectomy. *Investigative Ophthalmology and Visual Science*, **26**, 924–31. [414]
- Snowden, R. J., (1992). Sensitivity to relative and absolute motion. *Perception*, **21**, 563–8. [376]
- Snowden, R. J., Treue, S., and Andersen, R. A. (1992). The response of neurons in areas V1 and MT of the alert rhesus monkey to moving random dot patterns. *Experimental Brain Research*, **88**, 389–400. [99]
- Snyder, A. W. and Miller, W. H. (1978). Telephoto lens system of falconiform eyes. *Nature*, **273**, 127–9. [654]
- Snyder, L. H., Lawrence, D. M., and King, W. M. (1992). Changes in vestibuloocular reflex (VOR) anticipate changes in vergence angle in monkey. *Vision Research*, **32**, 569–75. [416]
- Sobel, E. C. (1990). Depth perception by motion parallax and paradoxical parallax in the locust. *Naturwissenschaften*, **77**, 241–3. [648]
- Sobel, E. C. and Collett, T. S. (1991). Does vertical disparity scale the perception of stereoscopic depth? *Proceedings of the Royal Society, London*, **B244**, 87–90. [289]
- Softky, W. (1994). Sub-millisecond coincidence detection in active dendritic trees. *Neuroscience*, **58**, 13–41. [82]
- Sokoloff, L., Reivich, M., Kennedy, C., Des Rosiers, M. H., Patlak, C. S., Pettigrew, K. D., Sakurada, O., and Shinohara, M. (1977). The [¹⁴C] deoxyglucose method for measurement of local cerebral glucose utilization, procedure, and normal values in the conscious and anesthetized rat. *Journal of Neurochemistry*, **28**, 897–916. [122]
- Solomon, J. S., Doyle, J. F., Burkhalter, A., and Nerbonne, J. M. (1993). Differential expression of hyperpolarization-activated currents reveals distinct classes of visual cortical projection neurons. *Journal of Neuroscience*, **13**, 5082–91. [81]
- Solomons, H. (1975a). Derivation of the space horopter. *British Journal of Physiological Optics*, **30**, 56–80. [48, 51]
- Solomons, H. (1975b). Properties of the space horopter. *British Journal of Physiological Optics*, **30**, 81–100. [51]
- Solomons, H. (1978). *Binocular vision a programmed text*. Heinemann, London. [1]
- Sorsby, A., Leary, G. A., and Richards, M. J. (1962). The optical components in anisometropia. *Vision Research*, **2**, 43–51. [62]
- Sparks, D. L., Mays, L. E., Gurski, M. R., and Hickey, T. L. (1986). Long- and short-term monocular deprivation in the rhesus monkey: Effects on visual fields and optokinetic nystagmus. *Journal of Neuroscience*, **6**, 1771–80. [632]
- Spear, P. D. and Tong, L. (1980). Effects of monocular deprivation on neurons in cat's lateral suprasylvian visual area. I. Comparison of binocular and monocular segments. *Journal of Neurophysiology*, **44**, 568–84. [628]
- Spear, P. D., Langsetmo, A., and Smith, D. C. (1980). Age related changes in effects of monocular deprivation on cat striate cortex neurons. *Journal of Neurophysiology*, **43**, 559–80. [628]
- Spekreijse, H., van der Tweel, L. H., and Regan, D. (1972). Interocular sustained suppression: Correlations with evoked potential amplitude and distribution. *Vision Research*, **12**, 521–6. [146]
- Spencer, R. F. and Porter, J. D. (1988). Structural organization of the extraocular muscles. *Neuroanatomy of the oculomotor system* (ed. J. A. Büttner-Ennever), pp. 33–80. Elsevier, New York. [424]
- Spencer, S. and Willard, M. B. (1992). GAP-43 and regrowth of retinal ganglion cell axons. In *Regeneration and plasticity in the mammalian visual system* (ed. D. M-K. Lam and G. M. Garth), pp. 97–105. MIT Press, Cambridge, MA. [607]
- Sperling, G. (1970). Binocular vision: A physical and a neural theory. *American Journal of Psychology*, **83**, 461–534. [213]
- Sperry, R. W., Minor, N., and Myers, R. E. (1955). Visual pattern perception following subpial slicing and tantalum wire implantations in the visual cortex. *Journal of Comparative and Physiological Psychology*, **48**, 50–8. [119]
- SPIE, (1992). Applications of artificial intelligence X: Machine vision and robotics. SPIE, Volume 1708, [30]
- Spileers, W., Orban, G. A., Gulyás, B., and Maes, H. (1990). Selectivity of cat area 18 neurons for direction and speed in depth. *Journal of Neurophysiology*, **63**, 936–54. [564]
- Spillmann, L. and Redies, C. (1981). Random-dot motion displaces Ehrenstein illusion. *Perception*, **10**, 411–15. [509]
- Sporns, O., Tononi, G., and Edelman, G. M. (1991). Modeling perceptual grouping and figure-ground segregation by means of active reentrant connections. *Proceedings of the National Academy of Science*, **88**, 129–33. [83]
- Springbett, B. M. (1961). Some stereoscopic phenomena and their implications. *British Journal of Psychology*, **52**, 105–9. [372]
- Springer, A. and Gaffney, J. S. (1981). Retinal projections in the goldfish: A study using cobaltous lysine. *Journal of Comparative Neurology*, **203**, 401–24. [649]
- Squires, P. C. (1956). Stereopsis produced without horizontally disparate stimulus loci. *Journal of Experimental Psychology*, **52**, 199–203. [306]
- Srebro, R. (1978). The visually evoked response: Binocular facilitation and failure when binocular vision is disturbed. *AMA Archives of Ophthalmology*, **96**, 839–44. [145]
- Sretavan, D. W. (1990). Specific routing of retinal ganglion cell axons at the mammalian optic chiasm during embryonic development. *Journal of Neuroscience*, **10**, 1995–2007. [607]
- Srinivasan, M. V. and Zhang, S. W. (1993). Evidence for two distinct movement-detecting mechanisms in insect vision. *Naturwissenschaften*, **80**, 38–41. [649]
- St. Cyr, G. F. and Fender, D. H. (1969). The interplay of drifts and flicks in binocular fixation. *Vision Research*, **9**, 245–65. [178]
- Standing, L. G., Dodwell P. C., and Lang, D. (1968). Dark adaptation and the Pulfrich effect. *Perception and Psychophysics*, **4**, 118–20. [545–6]
- Steedman, W. C. and Baker, C. A. (1962). Perceived movement in depth as a function of stimulus size. *Human Factors*, **4**, 349. [555]
- Steinbach, M. J. and Money, K. E. (1973). Eye movements of the owl. *Vision Research*, **13**, 889–91. [655]
- Steinbach, M. J., Howard, I. P., and Ono, H. (1985). Monocular asymmetries in vision: We don't see eye-to-eye. *Canadian Journal of Psychology*, **39**, 476–8. [601]
- Steinbach, M. J., Musarella, M. A., and Gallie, B. L. (1988). Extraocular muscle proprioception and visual function: Psychophysical aspects. In *Strabismus and amblyopia: Experimental basis for advances in clinical management*, (ed. G. Lennerstrand, G. K. von Noorden, and E. C. Campos). Macmillan, New York. [600]
- Steiner, V. and Blake, R. (1994). Interocular transfer of expansion, rotation, and translation motion aftereffects. *Perception*, **23**, 1197–202. [376]
- Steinman, R. M. and Collewijn, H. (1980). Binocular retinal image motion during active head rotation. *Vision Research*, **20**, 415–29. [180, 462]
- Steinman, R. M., Cunitz, R. J., Timberlake, G. T., and Herman, M. (1967). Voluntary control of microsaccades during maintained monocular fixation. *Science*, **155**, 1577–9. [382]
- Steinman, R. M., Cushman, W. B., and Martins, A. J. (1982). The precision of gaze. *Human Neurobiology*, **1**, 97–109. [180]
- Steinman, R. M., Haddad, G. M., Skavenski, A. A., and Wyman, D. (1973). Miniature eye movements. *Science*, **181**, 810–19. [382]

- Steinman, R. M., Levinson, J. Z., Collewijn, H., and van der Steen, J. (1985). Vision in the presence of known natural retinal image motion. *Journal of the Optical Society of America*, **2A**, 226–33. [180]
- Stenton, S. P., Frisby, J. P., and Mayhew, J. E. W. (1984). Vertical disparity pooling and the induced effect. *Nature*, **309**, 622–4. [287]
- Stephens, G. L. and Jones, R. (1990). Horizontal fusional amplitudes after adaptation to prism. *Ophthalmology and Physiological Optics*, **10**, 25–8. [392]
- Sterling, P. (1990). Retina. In *Synaptic organization of the brain*, (ed. G. Shepard), Chap. 6. Oxford University Press, Oxford. [110]
- Stevens, K. A. and Brookes, A. (1987). Detecting structure by symbolic constructions on tokens. *Computer Vision, Graphics, and Image Processing*, **37**, 238–60. [476, 484]
- Stevenson, S. B., Cormack, L. K., and Schor, C. M. (1989). Hyperacuity, superresolution and gap resolution in human stereopsis. *Vision Research*, **29**, 1597–605. [182]
- Stevenson, S. B., Cormack, L. K., and Schor, C. M. (1991). Depth attraction and repulsion in random dot stereograms. *Vision Research*, **31**, 805–13. [234, 470]
- Stevenson, S. B., Cormack, L. K., and Schor, C. M. (1994). The effect of stimulus contrast and interocular correlation on disparity vergence. *Vision Research*, **34**, 383–96. [401]
- Stevenson, S. B., Cormack, L. K., Schor, C. M., and Tyler, C. W. (1992). Disparity tuning mechanisms of human stereopsis. *Vision Research*, **32**, 1685–94. [54, 488]
- Stevenson, T. J. and Sanford, E. C. (1908). A preliminary report of experiments on time relations in binocular vision. *American Journal of Psychology*, **19**, 130–7. [185]
- Stigmar, G. (1970). Observations on vernier and stereo acuity with special reference to their relationship. *Acta Ophthalmologica*, **48**, 979–98. [160]
- Stigmar, G. (1971). Blurred visual stimuli II. The effect of blurred visual stimuli on vernier and stereo acuity. *Acta Ophthalmologica*, **49**, 364–79. [180]
- Stone, J. (1966). The nasotemporal division of the cat's retina. *Journal of Comparative Neurology*, **126**, 585–600. [130]
- Stone, J. and Rapaport, D. H. (1986). The role of cell death in shaping the ganglion cell population of the adult cat retina. In *Visual neuroscience*, (ed. J. D. Pettigrew and W. R. Levick), pp. 157–65. Cambridge University Press, London. [607]
- Stoner, G. R., Albright, T. D., and Ramachandran, V. S. (1990). Transparency and coherence in human motion perception. *Nature*, **344**, 153–5. [527]
- Stork, D. G. and Rocca, C. (1989). Software for generating auto-random-dot stereograms. *Behavior Research Methods, Instruments, and Computers*, **21**, 525–34. [30]
- Stromeyer, C. F. (1978). Form–color aftereffects in human vision. In *Handbook of sensory physiology*, Vol. VII, (ed. H. Teuber and R. Held), pp. 97–142. Springer, New York. [378]
- Stromeyer, C. F. and Julesz, B. (1972). Spatial frequency masking in vision: Critical bands and spread of masking. *Journal of the Optical Society of America*, **62**, 1221–32. [88]
- Stromeyer, C. F. and Mansfield, R. J. W. (1970). Colored aftereffects produced with moving edges. *Perception and Psychophysics*, **7**, 108–14. [379]
- Strong, D. S. (1979). *Leonardo on the eye*. Garland, New York. [14]
- Stryker, M. P. (1991). Activity-dependent reorganization of afferents in the developing mammalian visual system. In *Development of the visual system*, (ed. D. M-K. Lam and C. J. and Shatz), pp. 267–87. MIT Press, Cambridge, MA. [118]
- Stryker, M. P. and Harris, W. A. (1986). Binocular impulse blockage prevents the formation of ocular dominance columns in cat visual cortex. *Journal of Neuroscience*, **6**, 2117–33. [614]
- Stuart, G. W., Edwards, M., and Cook, M. L. (1992). Colour inputs to random-dot stereopsis. *Perception*, **21**, 717–29. [208]
- Sugie, N. (1982). Neural models of brightness perception and retinal rivalry in binocular vision. *Biological Cybernetics*, **43**, 13–21. [343, 359]
- Sumner, F. C. and Watts, F. P. (1936). Rivalry between monocular negative after-images and the vision of the other eye. *American Journal of Psychology*, **48**, 109–16. [380]
- Sundet, J. M. (1972). The effect of pupil size variations on the colour stereoscopic phenomenon. *Vision Research*, **12**, 1027–32. [306]
- Sundet, J. M. (1976). Two theories of colour stereoscopy. *Vision Research*, **16**, 469–72. [307]
- Sutherland, N. S. (1961). Figural aftereffects and apparent size. *Quarterly Journal of Experimental Psychology*, **13**, 222–8. [466]
- Sutterlin, A. M. and Prosser, C. L. (1970). Electrical properties of goldfish optic tectum. *Journal of Electrophysiology*, **33**, 36–45. [649]
- Suzuki D. A. and Keller E. L. (1984). Visual signals in the dorsolateral pontine nucleus of the alert monkey, their relationship to smooth-pursuit eye movements. *Experimental Brain Research*, **53**, 473–8. [530]
- Suzuki, H. and Kato, E. (1966). Binocular interaction at cat's lateral geniculate body. *Journal of Neurophysiology*, **29**, 909–20. [113]
- Swadlow, H. A. (1983). Efferent systems of primary visual cortex: A review of structure and function. *Brain Research Reviews*, **6**, 1–24. [125]
- Swanson, M. T. and Gogel, W. C. (1986). Perceived size and motion in depth from optical expansion. *Perception and Psychophysics*, **39**, 309–26. [555]
- Swanson, M. T. and Wade, N. J. (1985). Binocular interaction in induced line rotation. *Perception and Psychophysics*, **37**, 363–8. [377]
- Swanson, H. A. (1932). The relative influence of accommodation and convergence in the judgment of distance. *Journal of General Psychology*, **7**, 360–80. [429]
- Swets, J. A. (1964). *Signal detection and recognition by human observers*. Wiley, New York. [93]
- Swindale, N. V., Vital-Durand, F., and Blakemore, C. (1981). Recovery from monocular deprivation in the monkey. III. Reversal of anatomical effects in the visual cortex. *Proceedings of the Royal Society, London*, **B213**, 435–50. [636]
- Swindale, N. V., Matsubara, J. A., and Cynader, M. S. (1987). Surface organization of orientation and direction selectivity in cat area 18. *Journal of Neuroscience*, **7**, 1414–27. [124]
- Switkes, E., Bradley, A., and Schor, C. (1990). Readily visible changes in color contrast are insufficient to stimulate accommodation. *Vision Research*, **30**, 1367–76. [395]
- Székely, G. (1971). The mesencephalic and diencephalic optic centres in the frog. *Vision Research*, Supplement 3, 269–79. [651]
- Szentágothai, J. (1973). Neuronal and synaptic architecture of the lateral geniculate nucleus. In *Handbook of sensory physiology*, Vol. VII/3B, (ed. R. Jung), pp. 141–76. Springer-Verlag, New York. [112, 115]
- Tam, W. J. and Ono, H. (1987). Zero horizontal disparity in binocular depth mixture stimuli. *Vision Research*, **27**, 1207–10. [232]
- Tamler, E., Jampolsky, A., and Marg, E. (1958). An electromyographic study of asymmetric convergence. *American Journal of Ophthalmology*, **46**, 174–82. [410]

- Tanaka, K., Saito, H. A., Fukada, Y., and Moray, M. (1991). Coding visual images of objects in the inferotemporal cortex of the macaque monkey. *Journal of Neurophysiology*, 66, 170-89. [126]
- Taylor, J. (1738). *Le mechanisme ou le nouveau Traité de l'anatomie du globe de l'oeil, avec l'usage de ses différentes parties, et de celles qui lui sont contigues*. David, Paris. [12]
- Taylor, M. M. (1962). Figural after-effects: a psychophysical theory of the displacement effect. *Canadian Journal of Psychology*, 16, 247-77. [490]
- Taylor, M. M. (1963). Tracking the neutralization of seen rotary movement. *Perceptual and Motor Skills*, 16, 513-19. [375]
- Taylor, M. M. and Creelman, C. D. (1967). PEST: Efficient estimates on probability functions. *Journal of the Acoustical Society of America*, 41, 782-7. [94]
- Teller, D. Y. (1979). A forced-choice preferential looking procedure: A psychophysical technique for use with human infants. *Infant Behavior and Development*, 2, 135-53. [618]
- Teller, D. Y. and Gallanter, E. (1967). Brightness, luminances, and Fechner's paradox. *Perception and Psychophysics*, 2, 297-300. [357]
- Templeton, W. B. and Green, F. A. (1968). Chance results in utricular discrimination. *Quarterly Journal of Experimental Psychology*, 20, 200-3. [601]
- Templeton, W. B., Howard, I. P., and Easting G. (1965). Satiation and the tilt after-effect. *American Journal of Psychology*, 78, 656-9. [490]
- ten Doeschate, G. (1962). Oxford and the revival of optics in the thirteenth century. *Vision Research*, 1, 313-42. [7, 9]
- ten Doeschate, G. and Alpern, M. (1967). Influence of asymmetrical photo excitation of the two retinas on pupil size. *Journal of Neurophysiology*, 30, 577-85. [621]
- Ternus, J. (1926). Experimentelle Untersuchungen über phänomenale Identität. *Psychologische Forschung*, 7, 81-136. [570]
- Thomas, F. H., Dimmick, F. L., and Luria, S. M. (1961). A study of binocular color mixture. *Vision Research*, 1, 108-20. [326-7]
- Thomas, G. J. (1956). Effect of contours on binocular CFF obtained with synchronous and alternate flashes. *American Journal of Psychology*, 69, 369-77. [360]
- Thomas, J. P. and Gille, J. (1979). Bandwidths of orientation channels in human vision. *Journal of the Optical Society of America*, 69, 652-60. [100]
- Thompson, P. and Wood, V. (1993). The Pulfrich pendulum phenomenon in stereoblind subjects. *Perception*, 22, 7-14. [550]
- Thorn, F. and Boynton, R. M. (1974). Human binocular summation at absolute threshold. *Vision Research*, 14, 445-58. [350, 362]
- Thorn, F., Gwiazda, J., Cruz, A. A. V., Bauer, J. A., and Held, R. (1994). The development of eye alignment, convergence, and sensory binoculararity in young infants. *Investigative Ophthalmology and Visual Science*, 35, 544-53. [621]
- Thorpe, P. A. and Blakemore, C. (1975). Evidence for a loss of afferent axons in the visual cortex of monocularly deprived cats. *Neuroscience Letters*, 1, 271-6. [630]
- Thorpe, S. J., Celebrini, S., Trotter, Y., and Imbert, M. (1991). Dynamics of stereo processing in area V1 of the awake primate. *Journal of Neuroscience*, 4 (Suppl.), 83. [140]
- Tieman, D. G., Tumosa, N., and Tieman, S. B. (1983). Behavioral and physiological effects of monocular deprivation: A comparison of rearing with diffusion and occlusion. *Brain Research*, 280, 41-50. [631]
- Timney, B. (1981). Development of binocular depth perception in kittens. *Investigative Ophthalmology and Visual Science*, 21, 493-6. [618]
- Timney, B. (1988). The development of depth perception, In *Advances in neural and behavioral development*, Vol. 3, (ed. P. G. Shinkman), pp. 153-208. Ablex, Norwood, NJ. [622]
- Timney, B. (1990). Effects of brief monocular deprivation on binocular depth perception in the cat: A sensitive period for the loss of stereopsis. *Visual Neuroscience*, 5, 273-80. [635]
- Timney, B. and Keil, K. (1994). Local and global stereopsis in the horse. *Investigative Ophthalmology and Visual Science*, 35 (ARVO Abstracts), 2110. [657]
- Timney, B., Elberger, A. J., and Vandewater, M. L. (1985). Binocular depth perception in the cat following early corpus callosum section. *Experimental Brain Research*, 60, 19-26. [132]
- Timney, B., Mitchell, D. E., and Cynader, M. (1980). Behavioral evidence for prolonged sensitivity to effects of monocular deprivation in dark-reared cats. *Journal of Neurophysiology*, 43, 1041-54. [635]
- Timney, B., Mitchell, D. E., and Giffin, F. (1978). The development of vision in cats after extended periods of dark-rearing. *Experimental Brain Research*, 31, 547-60. [626]
- Timney, B., Wilcox, L. M., and St John, R. (1989). On the evidence for a 'pure' binocular process in human vision. *Spatial Vision*, 4, 1-15. [340]
- Tittle, J. S. and Braunstein, M. L. (1989). The interaction of binocular disparity and structure-from-motion in determining perceived relative depth. *Investigative Ophthalmology and Visual Science*, 30 (ARVO Abstracts), 263. [445]
- Tittle, J. S. and Braunstein, M. L. (1991). Shape perception from binocular disparity and structure-from-motion. In *Proceedings of the Society of Photo-optical Instrumentation Engineers: Sensor Fusion III: 3-D Perception and Recognition* (ed. P. S. Schenker), pp. 225-34. Society of Photo-optical Instrumentation Engineers, Bellingham. [444]
- Tittle, J. S. and Braunstein, M. L. (1993). Recovery of 3-D shape from binocular disparity and structure from motion. *Perception and Psychophysics*, 54, 157-69. [444-5]
- Toates, F. (1975). *Control theory in biology and experimental psychology*. Hutchinson, London. [87]
- Todd, J. T. (1981). Visual information about moving objects. *Journal of Experimental Psychology: Human Perception and Performance*, 7, 795-810. [441, 555]
- Todd, J. T. (1982). Visual information about rigid and nonrigid motion: a geometric analysis. *Journal of Experimental Psychology: Human Perception and Performance*, 8, 238-52. [574]
- Todd, J. T. and Akerstrom, R. A. (1987). Perception of three-dimensional form from patterns of optical texture. *Journal of Experimental Psychology: Human Perception and Performance*, 13, 242-55. [449]
- Todd, J. T. and Bressan, P. (1990). The perception of 3-dimensional affine structure from minimal apparent motion sequences. *Journal of Experimental Psychology: Human Perception and Performance*, 48, 419-30. [442]
- Todd, J. T. and Norman, J. F. (1991). The visual perception of smoothly curved surfaces from minimal apparent motion sequences. *Perception and Psychophysics*, 50, 509-23. [442]
- Toet, A. and Levi, D. M. (1992). The two-dimensional shape of spatial interaction zones in the parafovea. *Vision Research*, 32, 1349-57. [368]
- Toet, A., van Eekhout, M. P., Simons, H. L. J. J., and Koenderink, J. J. (1987). Scale invariant features of differential spatial displacement discrimination. *Vision Research*, 27, 441-51. [5]
- Tomlinson, R. D., Schwarz, D. W. F., and Fredrickson, J. M. (1978). Cerebellar and brainstem responses to eye muscle stretch in the cat. In *Vestibular mechanisms in health and disease*, (ed. J. D. Hood), pp. 45-51. Academic Press, New York. [640]
- Tong, L., Guido, W., Tumosa, N., Spear, P. D., and Heidenreich, S. (1992). Binocular interactions in the cat's dorsal lateral geniculate nucleus, II: Effects on dominant-eye spatial-frequency and contrast processing. *Visual Neuroscience*, 8, 557-66. [113, 170, 345]

- Tootell, R. B. H., Silverman, M. S., De Valois, R. L., and Jacobs, G. H. (1983). Functional organization of the second cortical visual area in primates. *Science*, **220**, 737–9. [126]
- Tootell, R. B. H., Hamilton, S. L., and Switkes, E. (1988a). Functional anatomy of macaque striate cortex. IV. Contrast and magno-parvo streams. *Journal of Neurophysiology*, **8**, 1594–1609. [115]
- Tootell, R. B. H., Silverman, M. S., Hamilton, S. L., Switkes, E., and De Valois, R. L. (1988b). Functional anatomy of macaque striate cortex. V. Spatial-frequency. *Journal of Neuroscience*, **8**, 1610–24. [123]
- Tootell, R. B. H., Hamilton, S. L., Silverman, M. S., and Switkes, E. (1988c). Functional anatomy of macaque striate cortex. I. Ocular dominance, binocular interactions, and baseline conditions. *Journal of Neuroscience*, **8**, 1500–30. [81, 122]
- Torgerson, W. S. (1958). *Theory and methods of scaling*. Wiley, New York. [93, 95]
- Tovée, M. J., Rolls, E. T., Treves, A., Bellis, R. P. (1993). Information encoding and the responses of single neurons in the primate temporal visual cortex. *Journal of Neurophysiology*, **70**, 640–54. [80]
- Townsend, J. T. (1968). Binocular information summation and the serial processing model. *Perception and Psychophysics*, **4**, 125–8. [355]
- Toyama, K., Komatsu, Y., Kasai, H., Fujii, K., and Umetani, K. (1985). Responsiveness of Clare–Bishop neurons to visual cues associated with motion of a visual stimulus in three-dimensional space. *Vision Research*, **25**, 407–14. [564]
- Treisman, A. M. (1962). Binocular rivalry and stereoscopic depth perception. *Quarterly Journal of Experimental Psychology*, **14**, 23–37. [225–6]
- Treisman, A. M. (1982). Perceptual grouping and attention in visual search for features and for objects. *Journal of Experimental Psychology*, **8**, 194–214. [212]
- Treisman, A. M. (1988). Features and objects. *Quarterly Journal of Experimental Psychology*, **A40**, 201–38. [210]
- Treisman, A. M. and Gelade, G. (1980). A feature–integration theory of attention. *Cognitive Psychology*, **12**, 97–136. [211]
- Tremain, K. E. and Ikeda, H. (1982). Relationship between amblyopia, LGN cell 'shrinkage' and cortical ocular dominance in cats. *Experimental Brain Research*, **45**, 243–52. [627]
- Tresilian, J. R. (1991). Empirical and theoretical issues in the perception of time to contact. *Journal of Experimental Psychology*, **7**, 865–76. [555]
- Tresilian, J. R. (1993). Four questions of time to contact: A critical examination of research on interceptive timing. *Perception*, **22**, 653–80. [555]
- Trick, G. L. and Guth, S. L. (1980). The effect of wavelength on binocular summation. *Vision Research*, **20**, 975–80. [353]
- Tricoles, G. (1987). Computer generated holograms: An historical review. *Applied Optics*, **26**, 4351–60. [26]
- Trincker, D. (1953). Light dark adaptation and space perception: I The Pulfrich effect as an asymmetrical phenomenon. *Pflügers Archiv für die gesamte Physiologie*, **257**, 48–69. [537]
- Tripathy, S. P. and Levi, D. M. (1994). Long-range dichoptic interactions in the human visual cortex in the region of the blind spot. *Vision Research*, **34**, 1127–38. [368]
- Trivedi, H. P. and Lloyd, S. A. (1985). The role of disparity gradient in stereo vision. *Perception*, **14**, 685–90. [222]
- Troelstra, A., Zuber, B. L., Miller, D., and Stark, L. (1964). Accommodation tracking: A trial-and-error function. *Vision Research*, **4**, 585–94. [395]
- Trotter, Y., Celebrini, S., Stricanne, B., Thorpe, S., and Imbert, M. (1992). Modulation of neural stereoscopic processing in primate area V1 by the viewing distance. *Science*, **257**, 1279–81. [84, 136]
- Trotter, Y., Frégnac, Y., and Buisseret, P. (1987). The period of susceptibility of visual cortical binocularity to unilateral proprioceptive deafferentation of extraocular muscles. *Journal of Neurophysiology*, **58**, 795–815. [641]
- Trotter, Y., Celebrini, S., Beaux, J. C., Grandjean, B., and Imbert, M. (1993). Long-term dysfunctions of neural stereoscopic mechanisms after extraocular muscle proprioceptive deafferentation. *Journal of Neurophysiology*, **69**, 1513–29. [641]
- Trueswell, J. C. and Hayhoe, M. M. (1993). Surface segmentation mechanisms and motion perception. *Vision Research*, **33**, 313–28. [527, 454]
- Trusk, T. C., Kaboord, W. S., and Wong-Riley, M. T. T. (1990). Effects of monocular enucleation, tetrodotoxin and lid suture on cytochrome-oxidase reactivity in supragranular puffs of adult macaque striate cortex. *Visual Neuroscience*, **4**, 185–204. [628]
- Tschermak-Seysenegg, A. von (1899). Über anomale Sehrichtungsgemeinschaft der Netzhäute bei einem Schielenden. *Albrecht v. Graefes Archiv für Ophthalmologie*, **47**, 508–50. [47]
- Tschermak-Seysenegg, A. von (1900). Beiträge zur Lehre vom Längshoropter. *Pflügers Archiv für die gesamte Physiologie*, **81**, 328–48. [54–5]
- Tschermak-Seysenegg, A. von (1939). Über Parallaxtoscopie. *Pflügers Archiv für die gesamte Physiologie*, **241**, 455–69. [578]
- Ts'o, D. Y. and Gilbert, C. D. (1988). The organization of chromatic and spatial interactions in the primate striate cortex. *Journal of Neurophysiology*, **8**, 1712–27. [124]
- Ts'o, D. Y., Frostig, R. D., Lieke, E., and Grinvald, A. (1990). Functional organization of primate visual cortex revealed by high resolution optical imaging. *Science*, **249**, 417–19. [122, 124]
- Ts'o, D. Y., Gilbert, C. D., and Wiesel, T. N. (1986). Relationships between horizontal interactions and functional architecture in cat striate cortex as revealed by cross-correlation analysis. *Journal of Neuroscience*, **6**, 1160–70. [116]
- Ts'o, D. Y., Gilbert, C. D., Frostig, R. D., Grinvald, A., and Wiesel, T. N. (1989). Functional architecture of visual area 18 of Macaque monkey. *Society for Neuroscience Abstracts*, **15**, 161. [126]
- Tucker, J. and Charman, W. N. (1979). Reaction and response times for accommodation. *American Journal of Optometry*, **56**, 490–503. [394]
- Tulunay Keesey, U. (1960). Effects of involuntary eye movements on visual acuity. *Journal of the Optical Society of America*, **50**, 769–74. [382]
- Tumosa, N., McCall, M. A., Guido, W., Spear, P. D. (1989). Responses of lateral geniculate neurons that survive long-term visual cortex damage in kittens and adult cats. *Journal of Neuroscience*, **9**, 280–98. [113, 345]
- Twitchell, T. E. (1970). Reflex mechanisms and the development of prehension. In *Mechanisms of motor skill development*, (ed. K. Connolly), pp. 25–37. Academic Press, London. [618]
- Tychsen, L. and Lisberger, S. G. (1986). Maldevelopment of visual motion processing in humans who had strabismus with onset in infancy. *Journal of Neuroscience*, **6**, 2495–508. [531]
- Tyler, C. W. (1971). Stereoscopic depth movement: Two eyes less sensitive than one. *Science*, **174**, 958–61. [187, 189]
- Tyler, C. W. (1973). Stereoscopic vision: Cortical limitations and a disparity scaling effect. *Science*, **181**, 276–8. [155, 161, 318]
- Tyler, C. W. (1974a). Depth perception in disparity gratings. *Nature*, **251**, 140–2. [162, 183, 579]
- Tyler, C. W. (1974b). Induced stereomovement. *Vision Research*, **14**, 609–13. [430]
- Tyler, C. W. (1974c). Stereopsis in dynamic visual noise. *Nature*, **250**, 781–2. [439, 551]
- Tyler, C. W. (1975a). Spatial organization of binocular disparity sensitivity. *Vision Research*, **15**, 583–90. [161, 190]
- Tyler, C. W. (1975b). Characteristics of stereomovement suppression. *Perception and Psychophysics*, **17**, 225–30. [189]

- Tyler, C. W. (1975c). Stereoscopic tilt and size aftereffects. *Perception*, 4, 187-92. [497, 587]
- Tyler, C. W. (1977). Stereomovement from interocular delay in dynamic visual noise: A random spatial disparity hypothesis. *American Journal of Optometry*, 54, 374-86. [551, 552]
- Tyler, C. W. (1980). Binocular Moiré fringes and the vertical horopter. *Perception*, 9, 475-8. [43]
- Tyler, C. W. (1983). Sensory processing of binocular disparity. In *Vergence eye movements: Basic and clinical aspects*, (ed. M. C Schor and K. J. Ciuffreda), pp. 199-296. Butterworth, Boston. [1, 165, 182]
- Tyler, C. W. (1991). Cyclopean vision. In *Vision and visual dysfunction*. Vol. 9, *Binocular Vision*, (ed. D. Regan), pp. 38-74. Macmillan, London. [1, 185, 281, 292, 497]
- Tyler, C. W. (1994). The birth of computer stereograms for unaided stereovision. In *Stereogram*, pp. 86-9. Cadence Books, San Francisco. [152]
- Tyler, C. W. and Cavanagh, P. (1991). Purely chromatic perception of motion in depth: Two eyes as sensitive as one. *Perception and Psychophysics*, 49, 53-61. [190, 208]
- Tyler, C. W. and Clarke, M. B. (1990). The autostereogram. *Proceedings of the International Society for Optical Engineering*, 1256, 182-97. [30]
- Tyler, C. W. and Julesz, B. (1976). The neural transfer characteristic (neuronropy) for binocular stochastic stimulation. *Biological Cybernetics*, 23, 33-7. [214]
- Tyler, C. W. and Julesz, B. (1978). Binocular cross-correlation in time and space. *Vision Research*, 18, 101-5. [214]
- Tyler, C. W. and Julesz, B. (1980). On the depth of the cyclopean retina. *Experimental Brain Research*, 40, 196-202. [162, 178, 229]
- Tyler, C. W. and Raibert, M. (1975). Computer technology: Generation of random-dot stereograms. *Behaviour Research Methods and Instrumentation*, 7, 37-41. [154]
- Tyler, C. W. and Sutter, E. E. (1979). Depth from spatial frequency difference: An old kind of stereopsis? *Vision Research*, 19, 859-65. [256, 262, 339-40]
- Tyler, C. W., Schor, C. M., and Coletta, N. J. (1992). Spatio-temporal limitations of vernier and stereoscopic alignment acuity. *Proceedings of the International Society for Optical Engineering*, 1669, 112-21. [190]
- Tytla, M. E., Lewis, T. L., Maurer, D., and Brent, H. P. (1993). Stereopsis after congenital cataract. *Investigative Ophthalmology and Visual Science*, 34, 1767-73. [626]
- Ullman, S. (1978). Two dimensionality of the correspondence problem. *Perception*, 7, 683-93. [528]
- Ullman, S. (1979). *The interpretation of visual motion*. MIT Press, Cambridge, MA. [527, 573-4]
- Ullman, S. (1980). The effect of similarity between line segments on the correspondence strength of apparent motion. *Perception*, 9, 617-26. [527]
- Ungeleider, L. G. and Mishkin, M. (1982). Two cortical visual systems. In *Analysis of visual behavior*, (ed. D. J. Ingle, M. A. Goodale, and R. J. W. Mansfield), pp. 549-86. MIT press, Cambridge, MA. [126]
- Uomori K. and Nishida, S. (1994). The dynamics of the visual system in combining conflicting KDE and binocular stereopsis cues. *Perception and Psychophysics*, 55, 526-36. [447]
- Updyke, B. V. (1974). Characteristics of unit responses in superior colliculus of the Cebus monkey. *Journal of Neurophysiology*, 37, 896. [563]
- Uttal, W. R. (1987). *The perception of dotted forms*. Lawrence Erlbaum, Hillsdale. [302]
- Uttal, W. R., Davis, S. N., Welke, C., and Kakarala, R. (1988). The reconstruction of static visual forms from sparse dotted samples. *Perception and Psychophysics*, 43, 223-40. [302]
- Uttal, W. R., Fitzgerald, J., and Eskin, T. E. (1975). Parameters of tachistoscopic stereopsis. *Vision Research*, 15, 705-12. [185, 369]
- Valverde, F. (1991). The organization of the striate cortex. In *Neuroanatomy of the visual pathways and their development*, (ed. B. Dreher and S. R. Robinson), pp. 235-77. CRC Press, Boston. [118]
- Van de Castle, R. L. (1960). Perceptual defense in a binocular-rivalry situation. *Journal of Personality*, 28, 448-62. [347]
- Van Essen, D. C. and Zeki, S. M. (1978). The topographic organization of rhesus monkey prestriate cortex. *Journal of Physiology*, 227, 193-226. [131]
- Van Essen, D. C., Anderson, C. H., and Felleman, D. J. (1992). Information processing in the primate visual system: An integrated systems perspective. *Trends in Neuroscience*, 255, 419-23. [125]
- Van Hof, M. W. and Steele Russell, I. (1977). Binocular vision in the rabbit. *Physiology of Behavior*, 19, 121-8. [656]
- Van Hof-van Duin, J. (1976a). Development of visuomotor behavior in normal and dark-reared cats. *Brain Research*, 104, 233-41. [626]
- Van Hof-van Duin, J. (1976b). Early and permanent effects of monocular deprivation on pattern discrimination and visuomotor behavior in cats. *Brain Research*, 111, 261-76. [636]
- Van Hof-van Duin, J. and Mohn, G. (1982). Stereopsis and optokinetic nystagmus. In *Functional basis of ocular motility disorders*, (ed. G. Lennerstrand, D. S. Zee, and E. L. Keller), pp. 113-9. Pergamon Press, New York. [531]
- Van Sluyters, R. C. (1978). Reversal of the physiological effects of brief periods of monocular deprivation in the kitten. *Journal of Physiology*, 284, 1-17. [631]
- Van Sluyters, R. C. and Levitt, F. B. (1980). Experimental strabismus in the kitten. *Journal of Neurophysiology*, 43, 686-99. [641]
- Van Sluyters, R. C. and Stewart, D. L. (1974a). Binocular neurons of the rabbit's visual cortex: Receptive field characteristics. *Experimental Brain Research*, 19, 166-95. [656]
- Van Sluyters, R. C. and Stewart, D. L. (1974b). Binocular neurons of the rabbit's visual cortex: Effects of monocular sensory deprivation. *Experimental Brain Research*, 19, 196-204. [656]
- van Damme, W. J. M., Oosterhoff, F. H., and van de Grind, W. A. (1994). Discrimination of 3-D shape and 3-D curvature from motion in active vision. *Perception and Psychophysics*, 53, 340-9. [582]
- van de Grind, W. A., Koenderink, J. J., and van Doorn, A. J. (1992). Viewing-distance invariance of movement detection. *Experimental Brain Research*, 91, 135-50. [460]
- van den Berg, A. V. (1992). Robustness of perception of heading from optic flow. *Vision Research*, 32, 1285-96. [557]
- van den Enden, A. and Spekreijse, H. (1989). Binocular reversals despite familiarity cues. *Science*, 244, 959-61. [456]
- van der Meer, H. C. (1978). Linear combinations of stereoscopic depth effects in dichoptic perception of gratings. *Vision Research*, 18, 707-14. [261]
- van der Tweel, L. H. and Estévez, O. (1974). Subjective and objective evaluation of flicker. *Ophthalmologica*, 169, 70-81. [360]
- Kruysbergen, N. A. W. H. and de Weert, C. M. M. (1993). Apparent motion perception: The contribution of the binocular and monocular systems. An improved test based on motion aftereffects. *Perception*, 22, 771-84. [377]
- van Kruysbergen, A. W. H. and de Weert, C. M. M. (1994). After-effects of apparent motion: The existence of an AND-type binocular system in human vision. *Perception*, 23, 1069-83. [377]
- van Rijn, L. J. and Collewijn, H. (1994). Eye torsion associated with disparity-induced vertical vergence in humans. *Vision Research*, 34, 2307-16. [417]

- van Rijn, L. J., van der Steen, J., and Collewijn, H. (1992). Visually induced cycloversion and cyclovergence. *Vision Research*, **32**, 1875–83. [421]
- van Rijn, L. J., van der Steen, J., and Collewijn, H. (1994a). Eye torsion elicited by oscillating gratings: Effects of orientation, wavelength and stationary contours. *Vision Research*, **34**, 533–40. [421]
- van Rijn, L. J., van der Steen, J., and Collewijn, H. (1994b). Instability of ocular torsion during fixation: Cyclovergence is more stable than cycloversion. *Vision Research*, **34**, 1077–87. [422]
- Varela, F. J. and Singer, W. (1987). Neuronal dynamics in the visual corticothalamic pathway revealed through binocular rivalry. *Experimental Brain Research*, **66**, 10–20. [113, 345]
- Varner, D., Cook, J. E., Schneck, M. E., McDonald, M. A., and Teller, D. Y. (1985). Tritan discrimination by 1- and 2-month-old human infants. *Vision Research*, **25**, 821–31. [617]
- Vautin, R. G. and Berkley, M. A. (1977). Responses of single cells in cat visual cortex to prolonged stimulus movement: Neural correlates of visual aftereffects. *Journal of Neurophysiology*, **40**, 1051–65. [376]
- Velay, J. L., Roll, R., Lennerstrand, G., and Roll, J. P. (1994). Eye proprioception and visual localization in humans: Influence of ocular dominance and visual context. *Vision Research*, **34**, 2169–76. [432]
- Vereecken, E. P. and Brabant, P. B. (1984). Prognosis for vision in amblyopia after loss of the good eye. *AMA Archives of Ophthalmology*, **102**, 220–4. [633]
- Verhoeff, F. H. (1928). An optical illusion due to chromatic aberration. *American Journal of Ophthalmology*, **11**, 898–900. [307]
- Verhoeff, F. H. (1934). Cycloduction. *Transactions of the American Ophthalmological Society*, **32**, 208–28. [418, 421]
- Verhoeff, F. H. (1935). A new theory of binocular vision. *AMA Archives of Ophthalmology*, **13**, 151–75. [398]
- Verhoeff, F. H. (1942). Simple quantitative test for acuity and reliability of binocular stereopsis. *AMA Archives of Ophthalmology*, **28**, 1000–19. [151]
- Verhoeff, F. H. (1959). Fixation disparity. *American Journal of Ophthalmology*, **48**, 339–41. [389]
- Verstraten, F. A. J., Verlinde, R., Fredericksen, R. E., van de Grind, W. A. (1994). A transparent motion aftereffect contingent on binocular disparity. *Perception*, **23**, 1181–8. [566]
- Victor, J. D. (1979). Nonlinear systems analysis: Comparison of white noise and sum of sinusoids in a biological system. *Proceedings of the National Academy of Science*, **76**, 996–8. [92]
- Videen, T. O., Daw, N. W., and Rader, R. K. (1984). The effect of norepinephrine on visual cortical neurons in kittens and adult cats. *Journal of Neuroscience*, **4**, 1607–17. [63]
- Vidyasagar, T. R. and Mueller, A. (1994). Function of GABA inhibition in specifying spatial frequency and orientation selectivities in cat striate cortex. *Experimental Brain Research*, **98**, 31–8. [118]
- Vidyasagar, T. R. and Stuart, G. W. (1993). Perceptual learning in seeing form from motion. *Proceedings of the Royal Society, B254*, 241–4. [104]
- Vieth, G. A. U. (1818). Über die Richtung der Augen. *Annalen der Physik*, **28**, 233–53. [17]
- Viirre, E., Cadera, W., and Vilis, T. (1987). The pattern of changes produced in the saccadic system and vestibuloocular reflex by visually patching one eye. *Journal of Neurophysiology*, **57**, 92–103. [415]
- Viirre, E., Cadera, W., and Vilis, T. (1988). Monocular adaptation of the saccadic system and vestibulo-ocular reflex. *Investigative Ophthalmology and Visual Science*, **29**, 1339–47. [415]
- Viirre, E., Tweed, D., Milner, K., and Vilis, T. A. (1986). Reexamination of the gain of the vestibuloocular reflex. *Journal of Neurophysiology*, **56**, 439–50. [415]
- Vilis, T., Hepp, K., Schwarz, U., and Henn, V. (1989). On the generation of vertical and torsional rapid eye movements in the monkey. *Experimental Brain Research*, **77**, 1–11. [426]
- Vilis, T., Yates, S., and Hore, J. (1985). Visual patching of one eye produces changes in saccadic properties in the unseeing eye. *Developmental Brain Research*, **17**, 290–2. [415]
- Virsu, V. and Taskinen, H. (1975). Central inhibitory interactions in human vision. *Experimental Brain Research*, **23**, 65–74. [373]
- Vital-Durand, F., Garey, L. J., and Blakemore, C. (1978). Monocular and binocular deprivation in the monkey: Morphological effects and reversibility. *Brain Research*, **158**, 45–64. [627]
- Volchan, E., and Gilbert, C. D. (1995). Interocular transfer of receptive field expansion in cat visual cortex. *Vision Research*, **35**, 1–6. [129]
- Volkmann, A. W. (1836). *Neue Beiträge zur Physiologie des Gesichtssinnes*. Breitkopft, Leipzig. [18]
- Volkmann, F. C., Riggs, L. A., Moore, R. K., and White, K. D. (1978). Central and peripheral determinants of saccadic suppression. In *Eye movements and the higher psychological functions*, (ed. J. W. Senders, D. A. Fisher, and R. A. Monty), pp. 35–54. Erlbaum, Hillsdale, NJ. [386]
- von Bahr, G. (1993). An analysis of the change in perceptual size of the retinal image at correction of ametropia. *Documenta Ophthalmologica*, **20**, 530–6. [63]
- von der Heydt, R., Adorjani, Cs., Hänni, P., and Baumgartner, G. (1978). Disparity sensitivity and receptive field incongruity of units in the cat striate cortex. *Experimental Brain Research*, **31**, 523–45. [134, 140, 272]
- von der Heydt, R., Peterhans, E., and Baumgartner, G. (1984). Illusory contours and cortical neuron responses. *Science*, **224**, 1260–2. [375]
- von Grünau, M., Dubé, S., and Kwas, M. (1993). The effect of disparity on motion coherence. *Spatial Vision*, **7**, 227–41. [527]
- von Hofsten, C. (1979). Recalibration of the convergence system. *Perception*, **8**, 37–42. [433]
- von Holst, E. (1973). *The behavioural physiology of animals and man*. pp. 185–7. Butler and Tanner, London. [427]
- von Seelen, W. (1970). Zur Informationsverarbeitung im visuellen System der Wirbeltiere. *Kybernetik*, **7**, 89–106. [124]
- Vos, J. J. (1960). Some new aspects of color stereoscopy. *Journal of the Optical Society of America*, **50**, 785–90. [307]
- Vos, J. J. (1966). The color stereoscopic effect. *Vision Research*, **6**, 105–7. [307]
- Wade, N. J. (1973). Binocular rivalry and binocular fusion of afterimages. *Vision Research*, **13**, 999–1000. [333]
- Wade, N. J. (1975a). Binocular rivalry between single lines viewed as real images and afterimages. *Perception and Psychophysics*, **17**, 571–7. [344]
- Wade, N. J. (1975b). Monocular and binocular rivalry between contours. *Perception and Psychophysics*, **4**, 85–95. [329, 334]
- Wade, N. J. (1976). On interocular transfer of the movement aftereffect in individuals with and without normal binocular vision. *Perception*, **5**, 113–18. [640]
- Wade, N. J. (1978). Why do patterned afterimages fluctuate in visibility? *Psychological Bulletin*, **85**, 338–52. [331]
- Wade, N. J. (1980). The influence of colour and contour rivalry on the magnitude of the tilt illusion. *Vision Research*, **20**, 229–33. [342]
- Wade, N. J. (1981). A note on the history of binocular microscopes. *Perception*, **10**, 591–2. [19]
- Wade, N. J. (1983). *Brewster and Wheatstone on vision*. Academic Press, New York. [21]
- Wade, N. J. (1987). On the late invention of the stereoscope. *Perception*, **16**, 785–818. [24]

- Wade, N. J. and de Weert, C. M. M. (1986). Aftereffects in binocular rivalry. *Perception*, 15, 419–34. [337]
- Wade, N. J. and Ono, H. (1985). The stereoscopic views of Wheatstone and Brewster. *Psychological Research*, 47, 125–33. [21]
- Wade, N. J. and Wenderoth, P. (1978). The influence of colour and contour rivalry on the magnitude of the tilt after-effect. *Vision Research*, 18, 827–35. [341]
- Wade, N. J., De Weert, C. M. M., and Swanston, M. T. (1984). Binocular rivalry with moving patterns. *Perception and Psychophysics*, 35, 111–22. [331]
- Wade, N. J., Swanston, M. T., and de Weert, C. M. M. (1993). On interocular transfer of motion aftereffects. *Perception*, 22, 1257–82. [375]
- Waespe, W., and Henn, V. (1979). The velocity response of vestibular nucleus neurons during vestibular, visual, and combined angular acceleration. *Experimental Brain Research*, 37, 337–47. [529]
- Wagner, H. and Frost, B. (1993). Disparity-sensitive cells in the owl have a characteristic disparity. *Nature*, 364, 796–7. [655]
- Wagner, H. and Schaeffel, F. (1991). Barn owls (*Tyto alba*) use accommodation as a distance cue. *Journal of Comparative Physiology*, 169, 515–21. [656]
- Wagner, M. (1985). The metric of visual space. *Perception and Psychophysics*, 38, 483–95. [53]
- Wales, R. and Fox, R. (1970). Increment detection thresholds during binocular rivalry. *Perception and Psychophysics*, 8, 90–4. [338]
- Walk, R. D. and Gibson, E. J. (1961). A comparative and analytical study of visual depth perception. *Psychological Monographs*, 75, (Whole No. 15), 1–44. [656]
- Walker, J. T. (1976). Slant perception and binocular brightness differences: Some aftereffects of viewing apparent and objective surface slants. *Perception and Psychophysics*, 20, 395–402. [310]
- Walker, J. T. and Kruger, M. W. (1972). Figural aftereffects in random-dot stereograms without monocular contours. *Perception*, 1, 187–92. [587]
- Walker, P. (1975). Stochastic properties of binocular rivalry alternations. *Perception and Psychophysics*, 18, 467–73. [344]
- Walker, P. (1978a). Orientation-selective inhibition and binocular rivalry. *Perception*, 7, 207–14. [373]
- Walker, P. (1978b). Binocular rivalry: Central or peripheral selective processes? *Psychological Bulletin*, 85, 376–89. [344]
- Walker, P. and Powell, D. J. (1979). The sensitivity of binocular rivalry to changes in the nondominant stimulus. *Vision Research*, 19, 247–9. [336]
- Wallace, G. K. (1959). Visual scanning in the desert locust *Schistocerca gregaria* Forskål. *Journal of Experimental Biology*, 36, 512–25. [648, 460]
- Wallach, H. (1976). On the constancy of visual speed. *Psychological Review*, 46, 5441–52. [460]
- Wallach, H. and Floor, L. (1971). The use of size matching to demonstrate the effectiveness of accommodation and convergence as cues for distance. *Perception and Psychophysics*, 10, 423–8. [428–9]
- Wallach, H. and Goldberg, J. (1977). An exploration of the Pulfrich effect. *Scandinavian Journal of Psychology*, 18, 231–6. [549]
- Wallach, H. and Halperin, P. (1977). Eye muscle potentiation does not account for adaptation in distance perception based on oculomotor cues. *Perception and Psychophysics*, 22, 427–30. [433]
- Wallach, H. and Karsh, E. B. (1963). Why the modification of stereoscopic depth-perception is so rapid. *American Journal of Psychology*, 76, 413–20. [192]
- Wallach, H. and Norris, C. M. (1963). Accommodation as a distance cue. *American Journal of Psychology*, 76, 659–64. [427]
- Wallach, H. and Zuckerman, C. (1963). The constancy of stereoscopic depth. *American Journal of Psychology*, 76, 404–12. [457]
- Wallach, H., Bacon, J., and Schulman, P. (1978). Adaptation in motion perception: Alteration of induced motion. *Perception and Psychophysics*, 24, 509–14. [532]
- Wallach, H., Frey, K. J., and Bode, K. A. (1972a). The nature of adaptation in distance perception based on oculomotor cues. *Perception and Psychophysics*, 11, 110–16. [433]
- Wallach, H., Gillam, B., and Cardillo, L. (1979). Some consequences of stereoscopic depth constancy. *Perception and Psychophysics*, 26, 235–40. [457]
- Wallach, H., Moore, M. E., and Davidson, L. (1963). Modification of stereoscopic depth perception. *American Journal of Psychology*, 76, 191–204. [432]
- Wallach, H., Yablick, G. S., and Smith, A. (1972b). Target distance and adaptation in distance perception in the constancy of visual direction. *Perception and Psychophysics*, 12, 139–45. [430]
- Wallman, J. and Adams, J. I. (1987). Developmental aspects of experimental myopia in chicks: Susceptibility, recovery and relation to emmetropization. *Vision Research*, 27, 1139–63. [604]
- Walls, G. L. (1951). A theory of ocular dominance. *AMA Archives of Ophthalmology*, 45, 387–412. [598]
- Walls, G. L. (1953). Interocular transfer of after-images. *American Journal of Optometry*, 30, 57–64. [363]
- Walls, G. L. (1963). *The vertebrate eye and its adaptive radiations*. Hafner, New York. [34, 650, 653, 657]
- Walraven, J. (1975). Amblyopia screening with random-dot stereograms. *American Journal of Ophthalmology*, 80, 893–9. [154]
- Walsh, G. (1988). The effect of mydriasis on the pupillary centration of the human eye. *Ophthalmic and Physiological Optics*, 8, 178–82. [307]
- Wang, Y. C. and Frost, B. J. (1992). Time to collision is signalled by neurons in the nucleus rotundus of pigeons. *Nature*, 356, 236–8. [555]
- Wang, Y. C., Jiang, S., and Frost, B. J. (1993). Visual processing in pigeon nucleus rotundus: Luminance, color, motion, and looming subdivisions. *Visual Neuroscience*, 10, 21–30. [654]
- Ward, R. and Morgan, M. J. (1978). Perceptual effect of pursuit eye movements in the absence of a target. *Nature*, 274, 158–9. [553]
- Ware, C. and Mitchell, D. E. (1974a). On interocular transfer of various visual aftereffects in normal and stereoblind observers. *Vision Research*, 14, 731–4. [638, 640]
- Ware, C. and Mitchell, D. E. (1974b). The spatial selectivity of the tilt aftereffect. *Vision Research*, 14, 735–7. [485]
- Warren, N. (1940). A comparison of standard tests of depth perception. *American Journal of Optometry*, 17, 208–11. [155]
- Warren, W. H., Morris, M. W., and Kalish, M. (1988). Perception of translational heading from optical flow. *Journal of Experimental Psychology: Human Perception and Performance*, 14, 646–60. [557]
- Washburn, M. F. (1933). Retinal rivalry as a neglected factor in stereoscopic vision. *Proceedings of the National Academy of Science*, 19, 773–7. [338]
- Washburn, M. F., Faison, C., and Scott, R. (1934). A comparison between the Miles A–B–C method and retinal rivalry as tests of ocular dominance. *American Journal of Psychology*, 46, 633–6. [337]
- Wässle, H. and Boycott, B. B. (1991). Functional architecture of the mammalian retina. *Physiological Review*, 71, 447–80. [111]
- Wässle, H., Grünert, U., Röhrenbeck, J., and Boycott, B. B. (1990). Retinal ganglion cell density and cortical magnification factor in the primate. *Vision Research*, 30, 1897–911. [111, 114, 607]

- Wässle, H., Peichl, L., and Boycott, B. B. (1981). Dendritic territories of cat retinal ganglion cells. *Nature, London*, **292**, 344–5. [111]
- Watamaniuk, S. N. J. and Duchon, A. (1992). The human visual system averages speed information. *Vision Research*, **32**, 931–41. [98]
- Watamaniuk, S. N. J., Sekuler, R., and Williams, D. W. (1989). Direction perception in complex dynamic displays: The integration of direction information. *Vision Research*, **29**, 47–59. [98]
- Watanabe, T. and Cavanagh, P. (1992). Depth capture and transparency of regions bounded by illusory and chromatic contours. *Vision Research*, **32**, 527–32. [509]
- Watanabe, T. and Cavanagh, P. (1993). Transparent surfaces defined by implicit X junctions. *Vision Research*, **33**, 2339–46. [455]
- Watson, A. B. and Nachmias, J. (1977). Patterns of temporal interaction in the detection of gratings. *Vision Research*, **17**, 893–902. [362]
- Watson, A. B. and Pelli, D. G. (1983). QUEST: A Bayesian adaptive psychometric method. *Perception and Psychophysics*, **33**, 113–20. [94]
- Watt, R. J. (1987). Scanning from coarse to fine spatial scales in the human visual system after the onset of a stimulus. *Journal of the Optical Society of America*, **A4**, 2006–21. [176]
- Watt, R. J., Morgan, M. J., and Ward, R. M. (1983). Stimulus features that determine the visual location of a bright bar. *Investigative Ophthalmology and Visual Science*, **24**, 66–71. [97]
- Wattam-Bell, J. (1991). Development of motion-specific cortical responses in infancy. *Vision Research*, **31**, 287–97. [617]
- Wattam-Bell, J. (1992). The development of maximum displacement limits for discrimination of motion direction in infancy. *Vision Research*, **32**, 621–30. [617]
- Weale, R. A. (1954). Theory of the Pulfrich effect. *Ophthalmologica*, **128**, 380–8. [536]
- Weinshall, D. (1991). Seeing "ghost" planes in stereo vision. *Vision Research*, **31**, 1731–48. [217, 523]
- Weinshall, D. (1993). The computation of multiple matching of doubly ambiguous stereograms with transparent planes. *Spatial Vision*, **7**, 183–98. [217, 523]
- Weiss, S., Hochman, D., and MacVicar, B. A. (1993). Repeated NMDA receptor activation induces distinct intracellular calcium changes in subpopulations of striatal neurons in vitro. *Brain Research*, **627**, 63–71. [615]
- Weisstein, N. (1972). Metacontrast. In *Handbook of sensory physiology*, Vol. VII/4, (ed. D. Jameson and L. M. Hurvich), pp. 233–72. Springer, New York. [369]
- Wells, W. C. (1792). *An essay upon single vision with two eyes; together with experiments and observations on several other subjects in optics*. T. Cadell, London. [14, 596]
- Welpe, E., von Seelen, W., and Fahle, M. (1980). A dichoptic edge effect resulting from binocular contour dominance. *Perception*, **9**, 683–93. [328]
- Wenderoth, P. M. (1970). A visual spatial aftereffect of surface slant. *American Journal of Psychology*, **83**, 576–90. [486]
- Wenderoth, P. M. (1971). Studies of a stereoscopic aftereffect of a contour slanted in the median plane. *Australian Journal of Optometry*, April, 114–23. [485]
- Wenderoth, P. M., Rodger, R. S., and Curthoys, I. S. (1968). Confounding of psychophysical errors and sensory effects in adjustment measures of spatial aftereffects. *Perception and Psychophysics*, **4**, 133–8. [490]
- Werner, H. (1935). Studies on contour: I. Qualitative analysis. *American Journal of Psychology*, **17**, 40–64. [369]
- Werner, H. (1937). Dynamics in binocular depth perception. *Psychological Monographs*, **49**, 1–120. [466, 469, 484]
- Werner, H. (1938). Binocular depth contrast and the conditions of the binocular field. *American Journal of Psychology*, **51**, 489–97. [466, 476, 484]
- Werner, H. (1940). Studies on contour strobostereoscopic phenomena. *American Journal of Psychology*, **53**, 418–22. [369–70]
- Wertheimer, M. (1912). Experimentelle Studien über das Sehen von Bewegung. *Zeitschrift für Psychologie*, **61**, 161–265. [528]
- Westendorf, D. H. (1989). Binocular rivalry and dichoptic masking: Suppressed stimuli do not mask stimuli in a dominating eye. *Journal of Experimental Psychology: Human Perception and Performance*, **15**, 485–92. [368]
- Westendorf, D. H. and Fox, R. (1974). Binocular detection of positive and negative flashes. *Perception and Psychophysics*, **15**, 61–5. [361]
- Westendorf, D. H. and Fox, R. (1975). Binocular detection of vertical and horizontal line segments. *Vision Research*, **15**, 471–76. [353, 361]
- Westendorf, D. H. and Fox, R. (1977). Binocular detection of disparate light flashes. *Vision Research*, **17**, 697–702. [353]
- Westendorf, D. H., Blake, R., and Fox, R. (1972). Binocular summation of equal-energy flashes of unequal duration. *Perception and Psychophysics*, **12**, 445–8. [361]
- Westendorf, D. H., Blake, R., Sloane, M., and Chambers, D. (1982). Binocular summation occurs during interocular suppression. *Journal of Experimental Psychology: Human Perception and Performance*, **8**, 81–90. [337]
- Westendorf, D. H., Langston, A., Chambers, D., and Allegretti, C. (1978). Binocular detection by normal and stereoblind observers. *Perception and Psychophysics*, **24**, 209–14. [638]
- Westheimer, G. (1965). Spatial interaction in the human retina during scotopic vision. *Journal of Physiology*, **181**, 881–94. [364]
- Westheimer, G. (1978). Vertical disparity detection: Is there an induced size effect? *Investigative Ophthalmology and Visual Science*, **17**, 545–51. [289, 292]
- Westheimer, G. (1979a). Cooperative neural processes involved in stereoscopic acuity. *Experimental Brain Research*, **36**, 585–97. [157, 186]
- Westheimer, G. (1979b). The spatial sense of the eye. *Investigative Ophthalmology and Visual Science*, **18**, 893–912. [180]
- Westheimer, G. (1984a). Line-separation discrimination curve in the human fovea: Smooth or segmented? *Journal of the Optical Society of America*, **1A**, 683–4. [98]
- Westheimer, G. (1984b). Sensitivity for vertical retinal image differences. *Nature*, **307**, 632–4. [286, 290, 292]
- Westheimer, G. (1986a). Panum's phenomenon and the confluence of signals from the two eyes in stereoscopy. *Proceedings of the Royal Society, London*, **B228**, 289–305. [520, 523]
- Westheimer, G. (1986b). Spatial interaction in the domain of disparity signals in human stereoscopic vision. *Journal of Physiology*, **370**, 619–29. [469, 481]
- Westheimer, G. and Hauske, G. (1975). Temporal and spatial interference with vernier acuity. *Vision Research*, **15**, 1137–41. [116, 368]
- Westheimer, G. and Levi, D. M. (1987). Depth attraction and repulsion of disparate stimuli. *Vision Research*, **27**, 1361–8. [470]
- Westheimer, G. and McKee, S. P. (1975). Visual acuity in the presence of retinal-image motion. *Journal of the Optical Society of America*, **65**, 847–50. [382]
- Westheimer, G. and McKee, S. P. (1977). Integration regions for visual hyperacuity. *Vision Research*, **17**, 89–93. [186, 382]
- Westheimer, G. and McKee, S. P. (1978). Stereoscopic acuity for moving retinal images. *Journal of the Optical Society of America*, **68**, 450–5. [155, 186]

- Westheimer, G. and McKee, S. P. (1979). What prior uniocular processing is necessary for stereopsis? *Investigative Ophthalmology and Visual Science*, 18, 614-21. [181]
- Westheimer, G. and McKee, S. P. (1980a). Stereogram design for testing local stereopsis. *Investigative Ophthalmology and Visual Science*, 19, 802-9. [152, 160]
- Westheimer, G. and McKee, S. P. (1980b). Stereoscopic acuity with defocused and spatially filtered retinal images. *Journal of the Optical Society of America*, 70, 772-8. [168]
- Westheimer, G. and Mitchell, A. M. (1956). Eye movement responses to convergence stimuli. *AMA Archives of Ophthalmology*, 55, 848-56. [403, 412]
- Westheimer, G. and Mitchell, D. E. (1969). The sensory stimulus for disjunctive eye movements. *Vision Research*, 9, 749-55. [132, 178, 405, 424]
- Westheimer, G. and Pettet, M. W. (1990). Contrast and duration of exposure differentially affect vernier and stereoscopic acuity. *Proceedings of the Royal Society, London*, B24, 42-6. [180]
- Westheimer, G. and Pettet, M. W. (1992). Detection and processing of vertical disparity by the human observer. *Proceedings of the Royal Society*, B250, 243-7. [294]
- Westheimer, G. and Tanzman, I. J. (1956). Qualitative depth localization with diplopia images. *Journal of the Optical Society of America*, 46, 116-17. [159, 166]
- Westheimer, G. and Truong, T. T. (1988). Target crowding in foveal and peripheral stereoaucuity. *American Journal of Optometry and Physiological Optics*, 65, 395-9. [160]
- Westheimer, G., Shimamura, K., and McKee, S. P. (1976). Interference with line-orientation sensitivity. *Journal of the Optical Society of America*, 66, 332-8. [368]
- Wetherick, N. E. (1977). The significance of the nose for certain phenomena of visual perception. *Nature, New Biology*, 266, 442-3. [591]
- Wheatstone, C. (1838). Contributions to the physiology of vision - Part the first. On some remarkable and hitherto unobserved phenomena of binocular vision. *Philosophical Transactions of the Royal Society*, 128, 371-94. [19, 315, 458]
- Wheatstone, C. (1852). Contributions to the physiology of vision - Part the second. On some remarkable and hitherto unobserved phenomena of binocular vision. *Philosophical Transactions of the Royal Society*, 142, 1-17. [487]
- Wheatstone, C. (1853). On the binocular microscope, and on stereoscopic pictures of microscopic objects. *Transactions of the Microscopical Society of London*, 1, 99-102. [19]
- White, B. L., Castle, P., and Held, R. (1964). Observations on the development of visually-directed reaching. *Child Development*, 35, 349-63. [618]
- White, J. (1967). *The birth and rebirth of pictorial space*. Farber and Farber, London. [9]
- White, K. D. and Odom, J. V. (1985). Temporal integration in global stereopsis. *Perception and Psychophysics*, 37, 139-44. [168, 190]
- White, K. D., Petry, H. M., Riggs, L. A., and Miller, J. (1978). Binocular interactions during establishment of McCollough effects. *Vision Research*, 18, 1201-15. [378-9]
- Whittle, P. (1965). Binocular rivalry and the contrast at contours. *Journal of Experimental Psychology*, 17, 217-26. [328]
- Whittle, P., Bloor, D. C., and Pocock, S. (1968). Some experiments on figural effects in binocular rivalry. *Perception and Psychophysics*, 4, 183-8. [336]
- Wick, B. (1985). Forced vergence fixation disparity at distance and near in an asymptomatic young adult population. *American Journal of Optometry and Physiological Optics*, 62, 591-9. [389, 392]
- Wick, B. (1990). Stability of retinal correspondence during divergence: Evaluation with afterimages and Haidinger brushes. *Optometry and Vision Science*, 67, 779-86. [59]
- Wick, B. and Bedell, H. E. (1989). Magnitude and velocity of proximal vergence. *Investigative Ophthalmology and Visual Science*, 30, 755-60. [399]
- Wick, B. and Cook, D. (1987). Management of anomalous correspondence: Efficacy of therapy. *American Journal of Optometry and Physiological Optics*, 64, 405-10. [387]
- Wickelgren, L. W. (1967). Convergence in the human newborn. *Journal of Experimental Child Psychology*, 5, 74-85. [620]
- Wiesel, T. N. and Hubel, D. H. (1963a). Single cell responses in striate cortex of kittens deprived of vision in one eye. *Journal of Neurophysiology*, 26, 1003-17. [628]
- Wiesel, T. N. and Hubel, D. H. (1963b). Effects of visual deprivation on morphology of cells in the cat's lateral geniculate body. *Journal of Neurophysiology*, 26, 978-93. [626]
- Wiesel, T. N. and Hubel, D. H. (1965a). Extent of recovery from the effects of visual deprivation in kittens. *Journal of Neurophysiology*, 28, 1060-72. [628]
- Wiesel, T. N. and Hubel, D. H. (1965b). Comparison of the effects of unilateral and bilateral eye closure on cortical unit responses in kittens. *Journal of Neurophysiology*, 28, 1029-40. [628]
- Wiesel, T. N. and Hubel, D. H. (1974). Ordered arrangement of orientation columns in monkeys lacking visual experience. *Journal of Comparative Neurology*, 158, 307-18. [613]
- Wiesel, T. N. and Raviola, E. (1979). Increase in axial length of the macaque monkey eye after corneal opacification. *Investigative Ophthalmology and Visual Science*, 18, 1232-6. [604]
- Wiesel, T. N., Hubel, D. H., and Lam, D. M. K. (1974). Autoradiographic demonstration of ocular-dominance columns in the monkey striate cortex by means of transneuronal transport. *Brain Research*, 79, 273-9. [121]
- Wiesenfelder, H. and Blake, R. (1990). The neural site of binocular rivalry relative to the analysis of motion in the human visual system. *Journal of Neuroscience*, 10, 3880-8. [343]
- Wiesenfelder, H. and Blake, R. (1991). Apparent motion can survive binocular rivalry suppression. *Vision Research*, 31, 1589-99. [343]
- Wiggers, W., Roth, G., Eurich, C., and Straub, A. (1994). Binocular depth perception mechanisms in tongue-projecting salamanders. *Journal of Comparative Physiology*, in press. [652]
- Wilcox, L. M., Timney, B., and St John, R. (1990). Measurement of visual aftereffects and inferences about binocular mechanisms in human vision. *Perception*, 19, 43-55. [371, 373-4]
- Wilde, K. (1950). Der Punktreiheneffekt und die Rolle der binokularen Querdisparition beim Tiefensehen. *Psychologische Forschung*, 23, 223-62. [261, 507]
- Williams, D. R. (1988). Topography of the foveal cone mosaic in the living human eye. *Vision Research*, 28, 433-54. [107-8]
- Williams, J. S. (1994). An experimental investigation of depth cue interaction. Unpublished D. Phil. thesis, University of Oxford. [444, 447]
- Williams, J. M. and Lit, A. (1983). Luminance-dependent visual latency for the Hess effect, the Pulfrich effect, and simple reaction time. *Vision Research*, 23, 171-9. [539]
- Williams, R. W., Garraghty, P. E., and Goldowitz, D. (1991). A new visual system mutation. Achiasmatic dogs with congenital nystagmus. *Society for Neuroscience*, 17, 187. [608]
- Williams, R. W., Hogan, D., and Garraghty, P. E. (1994). Target recognition and visual maps in the thalamus of achiasmatic dogs. *Nature*, 367, 637-9. [608]
- Williams, T. D. (1970). Vertical disparity in depth perception. *American Journal of Optometry and Archives of the American Academy of Optometry*, 47, 339-44. [286]

- Wilson, F. A. W., Scalaidhe, P. O., and Goldman-Rakic, P. S. (1993). Dissociation of object and spatial processing domains in primate prefrontal cortex. *Science*, **260**, 1955–7. [127]
- Wilson, H. R. (1976). The significance of frequency gradients in binocular grating perception. *Vision Research*, **16**, 983–9. [262]
- Wilson, H. R. (1977). Hysteresis in binocular grating perception: Contrast effects. *Vision Research*, **17**, 843–51. [170]
- Wilson, H. R. (1986). Responses of spatial mechanisms can explain hyperacuity. *Vision Research*, **26**, 453–69. [98]
- Wilson, H. R. (1988). Development of spatiotemporal mechanisms in infant vision. *Vision Research*, **28**, 611–28. [615]
- Wilson, H. R. (1991). Psychophysical models of spatial vision and hyperacuity. In *Spatial vision*, (ed. D. Regan), pp. 64–86. CRC Press, Boca Raton, FL. [88]
- Wilson, H. R. and Bergen, J. R. (1979). A four mechanism model for threshold spatial vision. *Vision Research*, **19**, 19–32. [259, 491]
- Wilson, H. R. and Gelb, D. J. (1984). Modified line element theory for spatial-frequency and width discrimination. *Journal of the Optical Society of America*, **A1**, 124–31. [100]
- Wilson, H. R. and Giese, S. C. (1977). Threshold visibility of frequency gradient patterns. *Vision Research*, **17**, 1177–90. [259]
- Wilson, H. R., Blake, R., and Halpern, D. L. (1991). Coarse spatial scales constrain the range of binocular fusion on fine scales. *Journal of the Optical Society of America*, **8**, 229–36. [318]
- Wilson, J. A. and Anstis, S. M. (1969). Visual delay as a function of luminance. *American Journal of Psychology*, **82**, 350–8. [539, 545]
- Wilson, J. R. and Sherman, S. M. (1977a). Conditions for dominance of one eye during competitive development of central connections in visually deprived cats. *Brain Research*, **136**, 277–87. [631]
- Wilson, J. R. and Sherman, S. M. (1977b). Differential effects of early monocular derivation on binocular and monocular segments of cat striate cortex. *Journal of Neurophysiology*, **40**, 891–903. [633]
- Wilson, M. A. and Bower, J. M. (1991). A computer simulation of oscillatory behavior in primate visual cortex. *Neural Computation*, **3**, 498–509. [83]
- Wilson, M. E. and Cragg, B. G. (1967). Projections from the lateral geniculate nucleus in the cat and monkey. *Journal of Anatomy*, **101**, 677–92. [132]
- Winkelmann, J. E. (1951). Peripheral fusion. *AMA Archives of Ophthalmology*, **45**, 425–30. [402]
- Winkelmann, J. E. (1953). Central and peripheral fusion. *AMA Archives of Ophthalmology*, **50**, 179–83. [404]
- Winterkorn, J. M. S., Shapley, R., and Kaplan, E. (1981). The effect of monocular paralytic on the lateral geniculate nucleus of the cat. *Experimental Brain Research*, **42**, 117–21. [641]
- Winterson, B. J. and Collewijn, H. (1976). Microsaccades during finely guided visuomotor tasks. *Vision Research*, **16**, 1387–90. [382]
- Wist, E. R. (1968). The influence of the equidistance tendency on depth shifts resulting from an interocular delay in stimulation. *Perception and Psychophysics*, **3**, 89–92. [540]
- Wist, E. R. (1970). Do depth shifts resulting from an interocular delay in stimulation result from a breakdown of binocular fusion? *Perception and Psychophysics*, **8**, 15–19. [540]
- Wist, E. R. and Gogel, W. C. (1966). The effect of interocular delay and repetition interval on depth perception. *Vision Research*, **6**, 325–34. [185]
- Wist, E. R., Brandt, T. H., Diener, H. C., and Dichgans, J. (1977). Spatial frequency effect on the Pulfrich stereophenomenon. *Vision Research*, **17**, 391–7. [544]
- Witazeck, St. (1899). Über die Natur der optischen Täuschungen. *Zeitschrift für Psychologie und Physiologie des Sinnesorgan*, **19**, 81–174. [372]
- Wittenberg, S., Brock, F. W., and Folsom, W. C. (1969). Effect of training on stereoscopic acuity. *American Journal of Optometry*, **46**, 645–53. [191]
- Wohlgemuth, A. (1911). On the after-effect of seen movement. *British Journal of Psychology, Monograph Supplement*. No. 1, 1–117. [375–6, 465, 571]
- Wolf, E. and Zigler, M. J. (1955). Course of dark adaptation under various conditions of pre-exposure and testing. *Journal of the Optical Society of America*, **45**, 696–702. [364]
- Wolf, E. and Zigler, M. J. (1963). Effects of uniconular and binocular excitation of the peripheral retina with test fields of various shapes on binocular summation. *Journal of the Optical Society of America*, **53**, 1199–205. [353]
- Wolf, E. and Zigler, M. J. (1965). Excitation of the peripheral retina with coincident and disparate test fields. *Journal of the Optical Society of America*, **55**, 1517–19. [353]
- Wolf, K. S., Bedell, H. E., and Pedersen, S. B. (1990). Relations between accommodation and vergence in darkness. *Optometry and Vision Science*, **67**, 89–93. [397]
- Wolfe, J. M. (1983a). Afterimages, binocular rivalry, and the temporal properties of dominance and suppression. *Perception*, **12**, 439–45. [333]
- Wolfe, J. M. (1983b). Influence of spatial frequency, luminance, and duration on binocular rivalry and abnormal fusion of briefly presented dichoptic stimuli. *Perception*, **12**, 447–56. [333]
- Wolfe, J. M. (1984). Short test flashes produce large tilt after-effects. *Vision Research*, **24**, 1959–64. [101]
- Wolfe, J. M. (1986a). Briefly presented stimuli can disrupt constant suppression and binocular rivalry suppression. *Perception*, **15**, 413–17. [333]
- Wolfe, J. M. (1986b). Stereopsis and binocular rivalry. *Psychological Review*, **93**, 269–82. [338–40]
- Wolfe, J. M. and Franzel, S. L. (1988). Binocular rivalry and visual search. *Perception and Psychophysics*, **44**, 81–93. [210]
- Wolfe, J. M. and Held, R. (1981). A purely binocular mechanism in human vision. *Vision Research*, **21**, 1755–9. [370–1, 373, 496]
- Wolfe, J. M. and Held, R. (1982). Binocular adaptation that cannot be measured monocularly. *Perception*, **11**, 287–95. [374, 496]
- Wolfe, J. M. and Held, R. (1983). Shared characteristics of stereopsis and the purely binocular process. *Vision Research*, **23**, 217–27. [370, 374, 496]
- Wolfe, J. M. and O'Connell, M. (1986). Fatigue and structural change: Two consequences of visual pattern adaptation. *Investigative Ophthalmology and Visual Science*, **27**, 538–43. [102]
- Wolfe, J. M. and Owens, D. A. (1981). Is accommodation color-blind? Focusing chromatic contours. *Perception*, **10**, 53–62. [395]
- Wolfe, J. M., Held, R., and Bauer, J. A. (1981). A binocular contribution to the production of optokinetic nystagmus in normal and stereoblind subjects. *Vision Research*, **21**, 587–90. [589]
- Wolpert, D. M., Miall, R. C., Cumming, B., and Boniface, S. J. (1993). Retinal adaptation of visual processing time delays. *Vision Research*, **33**, 1421–30. [548]
- Wong, E. and Weisstein, N. (1982). A new perceptual context-superiority effect: Line segments are more visible against a figure than against a ground. *Science*, **218**, 587–9. [524]
- Wong-Riley, M. (1979a). Changes in the visual system of monocularly sutured or enucleated cats demonstrable with cytochrome oxidase histochemistry. *Brain Research*, **171**, 11–28. [123]
- Wong-Riley, M. (1979b). Columnar cortico-cortical interconnections within the visual system of the squirrel and Macaque monkeys. *Brain Research*, **162**, 201–17. [125, 627]

- Wong-Riley, M. T. T. (1989). Cytochrome oxidase: An endogenous metabolic marker for neuronal activity. *Trends in Neuroscience*, 12, 94–101. [123]
- Wong-Riley, M. T. T., Hevner, R. F., Cutlan, R., Earnest, M., Egan, R., Frost, J., and Nguyen, T. (1993). Cytochrome oxidase in the human visual cortex: Distribution in the developing and the adult brain. *Visual Neuroscience*, 10, 41–58. [610, 612]
- Woo, G. C. S. (1974a). The effect of exposure time on the foveal size of Panum's area. *Vision Research*, 14, 473–80. [320]
- Woo, G. C. S. (1974b). Temporal tolerance of the foveal size of Panum's area. *Vision Research*, 14, 633–5. [320]
- Woo, G. C. S. and Reading, R. W. (1978). Panum's area explained in terms of known acuity mechanism. *British Journal of Physiological Optics*, 32, 30–7. [317]
- Woo, G. C. S. and Sillanpaa, V. (1979). Absolute stereoscopic thresholds as measured by crossed and uncrossed disparities. *American Journal of Optometry and Physiological Optics*, 56, 350–5. [155, 166]
- Wood, I. C. J., Fox, J. A., and Stevenson, M. G. (1978). Contrast threshold of random dot stereograms in anisometropic amblyopia: A clinical investigation. *British Journal of Ophthalmology*, 62, 34–8. [634]
- Woodburne, L. S. (1934). The effect of a constant visual angle upon the binocular discrimination of depth differences. *American Journal of Psychology*, 46, 273–86. [155]
- Worth, C. (1903). *Squint*. Blakiston, Philadelphia. [47]
- Wright, M. J. (1986). Apparent velocity of motion aftereffects in central and peripheral vision. *Perception*, 15, 603–12. [375]
- Wright, W. D. (1951). The role of convergence in stereoscopic vision. *Proceedings of the Physics Society*, 64B, 289–97. [177]
- Wu, H. P., Williams, C. V., and McLoon, S. C. (1994). Involvement of nitric oxide in the elimination of a transient retinotectal projection in development. *Science*, 265, 1593–6. [615]
- Würger, S. M. and Landy, M. S. (1989). Depth interpolation with sparse disparity cues. *Perception*, 18, 39–54. [500]
- Wurtz, R. H., Goldberg, M. E., and Robinson, D. L. (1980). Behavioural modulation of visual responses in the monkey: Stimulus selection for attention and movement. *Progress in Psychobiology and Physiological Psychology*, 9, 43–83. [129]
- Xue, J. T., Ramoa, A. S., Carney, T., and Freeman, R. D. (1987). Binocular interaction in the lateral geniculate nucleus of the cat. *Experimental Brain Research*, 68, 305–10. [113, 134]
- Yakovlev, P. I. and Lecours, A. (1967). The myelogenetic cycles of regional maturation of the brain. In *Regional development of the brain in early life*, (ed. A. Minkowski). Blackwell, Oxford. [607]
- Yan, X. X., Zheng, D. S., and Garey, L. J. (1992). Prenatal development of GABA-immunoreactive neurons in the human striate cortex. *Developmental Brain Research*, 65, 191–204. [610]
- Yang, Y. and Blake, R. (1991). Spatial frequency tuning of human stereopsis. *Vision Research*, 31, 1177–89. [176]
- Yang, Y., Rose, D., and Blake, R. (1992). On the variety of percepts associated with dichoptic viewing of dissimilar monocular stimuli. *Perception*, 21, 47–62. [328]
- Yarbus, A. L. (1967). *Eye movements and vision*. (Trans. by L. A. Riggs). Plenum, New York. [412]
- Yates, F. A. (1964). *Giordano Bruno and the hermetic tradition*. Routledge and Kegan Paul, London. [11]
- Yau, K. W. and Baylor, D. A. (1989). Cyclic GMP-activated conductance of retinal photoreceptor cells. *Annual Review of Neuroscience*, 12, 289–327. [109]
- Ye, M., Bradley, A., Thibos, L. N., and Zhang, X. (1991). Interocular differences in transverse chromatic aberration determine chromostereopsis for small pupils. *Vision Research*, 31, 1787–96. [306]
- Ye, M., Bradley, A., Thibos, L. N., and Zhang, X. (1992). The effect of pupil size on chromostereopsis and chromatic diplopia: Interaction between the Stiles–Crawford effect and chromatic aberrations. *Vision Research*, 32, 2121–8. [307]
- Yee, R. D., Baloh, R. W., and Honrubia, V. (1980). A study of congenital nystagmus: Optokinetic nystagmus. *British Journal of Ophthalmology*, 64, 926–32. [643]
- Yellott, J. I. and Kaiwi, J. L. (1979). Depth inversion despite stereopsis: The appearance of random-dot stereograms on surfaces seen in reverse perspective. *Perception*, 8, 135–42. [456]
- Yeshurun, Y. and Schwartz, E. L. (1989). Cepstral filtering on a columnar image architecture: A fast algorithm for binocular stereo segmentation. *IEEE Transactions on Pattern Analysis and Machine Intelligence*, 11, 759–67. [216]
- Yeshurun, Y. and Schwartz, E. L. (1990). Neural maps as data structures. Fast segmentation of binocular images. In *Computational neuroscience*, (ed. E. L. Schwartz), pp. 256–66. MIT Press, Cambridge, MA. [90, 140, 216]
- Yinon, U. (1978). Chronic asymmetry in the extraocular muscles of adult cats: Stability of cortical neurons. *Experimental Brain Research*, 32, 275–85. [641]
- Yinon, U., Auerbach, E., Blank, M., and Friesenhausen, J. (1975). The ocular dominance of cortical neurones in cats developed with divergent and convergent squint. *Vision Research*, 15, 1251–6. [627]
- Yonas, A. and Owsley, C. (1987). Development of visual space perception. In *Handbook of infant perception*, Vol. 3, (ed. P. Salapetek and L. Cohen), pp. 79–122. Academic Press, London. [622]
- Yonas, A., Bechtold, A. G., Frankel, D., Gordon, F. R., McRoberts, G., Norcia, A., and Sternfels, S. (1977). Development of sensitivity to information for impending collision. *Perception and Psychophysics*, 21, 97–104. [557]
- Yonas, A., Oberg, C., and Norcia, A. (1978). Development of sensitivity to binocular information for the approach of an object. *Developmental Psychology*, 14, 147–52. [558, 618]
- Young, F. A. and Leary, G. A. (1991). Refractive error in relation to the development of the eye. In *Vision and visual dysfunction*. Vol. 1, *Visual optics and instrumentation*. (ed. W. N. Charman), pp. 29–44. Macmillan, London. [604]
- Young, L. R. and Sheena, D. (1975). Survey of eye movement recording methods. *Behavior Research Methods and Instrumentation*, 7, 397–429. [383]
- Young, M. J., Landy, M. S., and Maloney, L. T. (1993). A perturbation analysis of depth perception from combinations of texture and motion cues. *Vision Research*, 33, 2685–96. [437]
- Young, M. P., Tanaka, K., and Yamane, S. (1992). On oscillating neuronal responses in the visual cortex of the monkey. *Journal of Neurophysiology*, 67, 1464–74. [83]
- Young, R. W. (1971). Shedding of discs from rod outer segments in the rhesus monkey. *Journal of Ultrastructure Research*, 34, 190–203. [106]
- Young, T. (1802). On the theory of light and colours. *Philosophical Transactions of the Royal Society*, 12–48. [73]
- Youngs, W. M. (1976). The influence of perspective and disparity cues on the perception of slant. *Vision Research*, 16, 79–82. [449]
- Yu, K. and Blake, R. (1992). Do recognizable figures enjoy an advantage in binocular rivalry? *Journal of Experimental Psychology*, 18, 1158–73. [348]
- Yuille, A. L., Geiger, D., and Bülthoff, H. H. (1991). Stereo integration, mean field theory and psychophysics. *Network*, 2, 423–42. [438]
- Yuodelis, C. and Hendrickson, A. (1986). A qualitative and quantitative analysis of the human fovea during development. *Vision Research*, 26, 847–55. [605]

- Zanforlin, M. (1982). Figural organization and binocular interaction. In *Organization and representation in perception*, (ed. J. Beck), pp. 251–67. Erlbaum, Hillsdale, NJ. [452]
- Zee, D. S. and Levi, L. (1989). Neurological aspects of vergence eye movements. *Revue Neurologique*, **145**, 613–20. [408]
- Zee, D. S., Fitzgibbon, E. J., and Optican, L. M. (1992). Saccade-vergence interactions in humans. *Journal of Neurophysiology*, **68**, 1624–42. [411, 413]
- Zee, D. S., Tusa, R. J., Herdman, S. J., Butler, P. H., and Gücer, G. (1987). Effects of occipital lobotomy upon eye movements in primates. *Journal of Neurophysiology*, **58**, 883–906. [530]
- Zeevi, Y. Y. and Geri, G. A. (1985). A purely central movement aftereffect induced by binocular viewing of dynamic visual noise. *Perception and Psychophysics*, **38**, 433–7. [551, 571]
- Zegers, R. T. (1948). Monocular movement parallax thresholds as functions of field size, field position and speed of stimulus movement. *Journal of Physiology*, **26**, 477–98. [579]
- Zeki, S. M. (1974a). Cells responding to changing image size and disparity in the cortex of the rhesus monkey. *Journal of Physiology*, **242**, 827–41. [563–4]
- Zeki, S. M. (1974b). Functional organization at a visual area in the posterior bank of the superior sulcus of the rhesus monkey. *Journal of Physiology*, **236**, 549–73. [125]
- Zeki, S. M. (1978). Uniformity and diversity of structure and function in rhesus monkey prestriate visual cortex. *Journal of Physiology*, **277**, 273–90. [125]
- Zeki, S. M. and Fries, W. (1980). A function of the corpus callosum in the Siamese cat. *Proceedings of the Royal Society, London, B***207**, 249–58. [132]
- Zeki, S. and Shipp, S. (1988). The functional logic of cortical connections. *Nature*, **335**, 311–17. [82]
- Zeki, S. M., Watson, J. D. G., Lueck, C. J., Friston, K. J., Kennard, C., and Frackowiak, R. S. J. (1991). A direct demonstration of functional specialization in human visual cortex. *Journal of Neuroscience*, **11**, 641–9. [126]
- Zhang, Y., Gamlin, P. D. R., and Mays, L. E. (1991). Antidromic identification of midbrain near response cells projecting to the oculomotor nucleus. *Experimental Brain Research*, **84**, 525–8. [45]
- Zhang, Y., Mays, L. E., and Gamlin, P. D. R. (1992). Characteristics of near response cells projecting to the oculomotor nucleus. *Journal of Neurophysiology*, **67**, 944–60. [45]
- Zheng, J. Q., Felder, M., Connor, J. A., and Poo, M. (1994). Turning of nerve growth cones induced by neurotransmitters. *Nature*, **368**, 140–4. [606]
- Zhou, Y. X. and Baker, C. L. (1993). A processing stream in mammalian visual cortex neurons for non-Fourier responses. *Science*, **261**, 98–101. [92]
- Zielinski, B. S. and Hendrickson, A. E. (1992). Development of synapses in macaque monkey striate cortex. *Visual Neuroscience*, **8**, 491–504. [610]
- Zimba, L. D. and Blake, R. (1983). Binocular rivalry and semantic processing: Out of sight, out of mind. *Journal of Experimental Psychology: Human Perception and Performance*, **9**, 807–15. [347]
- Zohary, E. and Sittig, A. C. (1993). Mechanisms of velocity constancy. *Vision Research*, **33**, 2467–78. [460]
- Zohary, E., Celebrini, S., Britten, K. H., and Newsome, W. T. (1994a). Neuronal plasticity that underlies improvement in perceptual performance. *Science*, **263**, 1289–92. [129]
- Zohary, E., Shadlen, M. N., and Newsome, W. T. (1994b). Correlated neuronal discharge rate and its implications for psychophysical performance. *Nature*, **370**, 140–3. [350]
- Zuber, B. L. and Stark, L. (1966). Saccadic suppression: Elevation of visual threshold associated with saccadic eye movements. *Experimental Neurology*, **16**, 65–79. [539]
- Zuber, B. L. and Stark, L. (1968). Dynamical characteristics of the fusional vergence eye-movement system. *IEEE Transactions Systems Science and Cybernetics*, **4**, 72–9. [402]
- Zuidam, I. and Collewijn, H. (1979). Vergence eye movements of the rabbit in visuomotor behavior. *Vision Research*, **19**, 185–94. [656]

Subject Index

- Abathic distance 58
 Absolute disparity 572
 Absolute motion parallax 572
 AC/A ratio 396
 Accommodation 394
 as cue to distance 427
 development 604, 621
 in amblyopia 632
 in animals 647
 Accommodative convergence 396
 Accuracy 93
 Achiastic dogs 608
 Achromatic cells 110
 Action potential 109
 Adaptive field 393
 Adequate stimulus 69
 Adjacency principle 472, 524
 Afocal lens 65
 Airy's disc 87
 Albinism 642
 Aliasing 107
 Alignment detector 77
 All-or-none law 70
 Amacrine cells 109
 Amblyopia 42, 627, 631
 development 633
 strabismic 632
 types 632
 Amblyoscope 388
 Ametropia 62
 Amodal completion 77
 Amphibia 651
 Amplitude spectrum 85
 Anaglyph 26
 Analogue signal 109
 Anatomic position of rest 387
 and binocular summation 359
 and phoria 599
 and visual direction 599
 Angle
 alpha 105, 306, 645
 of anomaly 46
 of declination 61
 Aniseikonia 62, 67, 148, 316, 413
 neural 62
 optical 62
 Anisometropia 634, 63
 types 62
 Anisometric amblyopia 632
 Anisophoria 62, 388, 393
 Anisopia 310
 Anisotropy 267
 Anomalous retinal correspondence 46
 Anterior commissure 132
 Apparent frontal plane 292, 303
 Apparent movement 528
 and binocular rivalry 343
 dichoptic 344
 Area
 17 114, 134, 611
 18 611, 656
 dorsalis 653
 V3 124
 V4 124, 125, 127, 129
 Arousal 128
 Associated phoria 389
 Association fields 76
 Astigmatism 87, 107
 Astrocytes 606, 613
 Astronomy 10
 Attention 103-4, 128
 effects on cortical tuning 129
 Autoradiograph 122, 613, 628
 Autostereograms 28
 Azimuth 38
- Bagolini striated glasses test 46
 Barber-pole illusion 525-26
 Bicuculline 629
 Binaural unmasking 366
 Binding problem 82
 Binocular AND cells 351, 370
 Binocular cells 120
 Binocular colour mixing 325
 Binocular correspondence
 adaptation 621
 Binocular disparity —see Disparity
 Binocular dissociation 630
 Binocular field 3, 645
 of pigeons 653
 of toads 652
 of fixation 32
 Binocular flicker 360, 638
 Binocular lustre 308-9
 Binocular masking-level difference 367
 Binocular perspective 243, 441
 Binocular plane 229
 Binocular rivalry 42, 314, 328-348
 and eye dominance 338
 and eye movements 332
 and meaning 346
 and stimulus duration 333
 and stimulus location 331
 and stimulus motion 341
 and stimulus orientation 332
 models of 343
 neurology of 345
 responses in MT 346
 site of 341
 voluntary control 346
 Binocular stimuli 33
 Binocular subtense 39, 572
 Binocular summation 349, 363
 and amblyopia 634
 in stereoblindness 637
 integration model 352
 of brightness 356
 of suprathreshold discrimination 356
 Binocular suppression 641
 Binocular vision 2
 visual performance in 2
- Binocular zone 512
 Bipolar cells 109
 Bipolar detector 71, 137
 Bipolar response 71
 Bipolar stimulus dimensions. 71
 Blobs 123
 Bloch's law 72, 96, 178, 361
 Brain damage 624
 Broadband-cells 110
- CA/C ratio 397
 Calloectomy 132
 Camera calibration 243
 Camera obscura 7
 Cardboard cut-out phenomenon 297
 Cataract 634, 637
 Cauchy functions 90
 Caudate nucleus 125
 Cepstrum 216
 Cerebellum 125, 640
 Cerebral ventricle 12
 Chameleons
 stereopsis in 653
 Channels 73
 Chiasma 33, 129, 606-7
 Chromatic aberration 306
 and accommodation 395
 Chromatic diplopia 306
 Chromostereopsis 306
 Coding process 72, 74
 Cognitive contours 77, 508, 510
 Collector units 76
 Colour rivalry 325
 Colour-opponent cells 110
 Common fate 526
 Complex cells 118, 138, 141
 Computational theory 236
 Cones 106, 605
 Confusion 634
 Congenital nystagmus 643
 Constant error 92
 Contiguous temporal disparity 539, 541
 Contingent aftereffects 102, 378
 Contrast 465
 Contrast sensitivity
 and amblyopia 632, 635
 development 615
 function 87
 Convergence accommodation 397
 Convergence—see vergence
 Convolution 90, 482
 Coordinate systems 236
 bipolar 40
 cyclopean 38
 for eye movements 383
 for visual direction 236-242
 Copilia 647
 Coplanar retinas 243
 Cornea 105
 Corpus callosum 128, 130-132

- Correctly matched images 42
 Correlation detection 214
 Correspondence problem 43, 212, 241, 527
 in motion 574
 Corresponding points 17, 35-42
 geometrical 36
 physiological 41
 visual 41
 Corresponding visual lines 41, 48
 Cortical plate 610
 Cortical subplate 610
 Craik-O'Brien-Cornsweet illusion 480, 580
 Criterion level 94
 Critical fusion frequency 359
 Critical period 635
 Cross-modulation products 91
 Cross-orientation inhibition 118, 335, 346, 375
 Crowding 368
 Crustacea 64-9
 Cue interactions
 Bayesian model 437
 types of 435
 Cue promotion 436
 Cue trading function 435
 Cüpper's correspondence test 46
 Curvedness 301, 581-2
 Cyclodisparity 417
 Cycloduction 417
 Cyclopean azimuth 39
 Cyclopean direction 240-1
 Cyclopean effects 585-591
 Cyclopean elevation 38
 Cyclopean eye 3, 6, 591
 Cyclopean images 151
 Cyclopean line 593
 Cyclopean motion 589
 Cyclopean point 38
 Cyclopean procedure 4
 Cyclopean shape 586
 Cyclopean stimulus 3, 103
 Cyclophoria 387, 417
 Cyclops 3
 Cyclops effect 595
 Cyclorotation 417
 Cyclovergence 382, 417-424
 and inclination 466
 dynamics 419
 measurement 418
 stimulus 421
 Cycloverversion 382, 417
 Cytochrome oxidase 612, 626
- D10 90
 D6 90
 Dark rearing 625
 Dark vergence 386
 in infants 621
 Dartmouth Eye Institute 389
 De Lange function 360
 Declination 417
 Decussation 33, 130
 Deformation 251, 575, 581
 Deformation disparity 257, 271, 275
 Delta function 85
- Deprivation amblyopia 632
 Depth aftereffects 484-486, 497, 580
 Depth attraction 469
 Depth constancy 300-1, 456
 Depth contrast 462-484
 gradient contrast 474
 long range 467
 mechanisms 481
 short range 469
 successive 484
 Depth discrimination 158
 effects of eccentricity 155
 Depth interpolation 497
 Depth of field 605
 Depth repulsion 469
 Depth reversals 456, 487
 Depth transparency 230
 Detectability 94
 Diastereopsis 182
 Dichoptic apparent motion 568
 Dichoptic composite stimulus 103, 372
 Dichoptic masking
 and amblyopia 635
 in stereoblindness 638
 Dichoptic motion 571, 589
 aftereffect 570
 Dichoptic stimulus 3, 370
 Dichoptic visual beats 638
 Diencephalon 651
 Differential perspective 281
 Dif-frequency disparity 256, 259
 Dif-size disparity 254
 Difference of Gaussians 89, 317
 Differential components 251-2
 Differential invariants 251, 574-5
 Differential transformations 251
 Digital coding 71
 Dioptic stimulus 3, 33
 Dioptrics 6
 Diplopia 35
 Diplopia threshold —see fusion limit 315
 Dipole angle 41
 Directional asymmetry 617
 Directional preponderance 530
 Discrimination 98
 functions 98
 Dishabituation 619
 Disparate images 35
 Disparity 36, 128, 235
 absolute 236, 239-42, 572
 angular 257-8, 271
 averaging 230
 capture 502
 coarse 148
 coding functions 144
 correction 304
 crossed 36
 curvature 253, 296, 458, 577
 detectors 133, 144, 242
 dif-frequency 255, 259
 dif-size 247
 fine 132, 148
 first-order 249, 299, 492
 gradient 40, 222, 250-51, 318, 474
 horizontal 35, 247
 horizontal width 247
- intensity-based 455
 kinetic boundary 448
 masking 469
 normalization 304
 orientation 257, 269, 272-5
 overall 243
 pedestal 150, 155
 polar 271
 receptive fields 482
 relative 236, 239
 scaling 252, 289
 second-order 253, 492
 selectivity 133
 specularity 310
 tuning function 133
 uncrossed 36
 upper limit 150
 vector field 250
 vertical 35, 50
 width 247, 254, 259
 zero-order 492
- Distance paradox 491
 DOG—see Difference of Gaussians
 Dominant stimulus 328
 Double-nail illusion 45
 Duction 382
 Dynamic random-dot correlogram 147
 Dynamic random-dots—see Stereograms
 Dysmetria 413
- Ebbinghaus illusion 587
 Edinger-Westphal nucleus 394
 Egocentre 593
 Eikonometer 64
 Emanation theory 4
 Emmetropization 604
 Epipolar lines 241
 Epipolar meridians 38, 229
 Epipolar plane 241
 Equidistance tendency 463
 Equivalent configurations 575
 Esophoria 387
 Esotropia 387
 Ever-ascending staircase 504
 Evoked potentials—see Visual-evoked potentials
 Exclusive dominance 328, 336
 Exophoria 387
 Exotropia 387
 Extracellular matrix 606
 Extraocular muscles 424
 Eye 105
 development 604
 Eye movements
 types 381
- Falling bead test 151
 Far cells 134
 Far-anchor effect 429
 Feature detector 75
 Fechner's paradox 356
 Feedback 78, 104
 Feedforward 78
 Ferret 609

- Fick system, 237
 Figural aftereffects 101, 132, 520, 587
 Figural induction effects 349, 370
 Figure-ground 507, 524
 Fish
 stereopsis in 649
 Fixation
 disparity 42, 315, 388, 601
 shift 389
 Flicker 633
 Forced-choice procedure 95
 Forced-vergence curve 390
 Fourier transform 85, 91
 Frequency coding 72
 Frisby stereo test 154, 166
 Frogs
 stereopsis in 651
 Frontal lobe 125
 Frontal plane 57
 Frontal vision 645
 Funneling 97
 Fused images 42
 Fusion 314
 Fusion limit 315, 325
 and contrast 316
 and eccentricity 316
 and spatial interactions 318
 for vertical disparity 320
 hysteresis 322
 measurement 315
 temporal factors 320
- GABA, 629
 Gabor function 89
 Gabor patch 89
 Ganglion cells 109-10
 density 607
 receptive field 361
 Gaussian patches 169
 Generic viewpoint 507
 Geometric effect 286-7
 Geometrical illusions 101, 587
 Gestalt 82
 Ghosts, 43
 Glass patterns 591
 Clial cells 606, 613
 Global layer 424
 Global stereopsis 151, 195
 Goat
 stereopsis in 657
 Grasp reflex 618
 Grassmann's third law 79
 Great circle 236
 Growth cone 606
 Gyri 609
- Haploscope 388
 Hawks
 stereopsis in 654
 Headcentric direction 555, 593
 Heading direction 557
 Hebbian synapse 81, 604, 615
 Helmholtz system 238
 Hemidecussation 12, 33
- Hemifield differences 633
 Hemiretina asymmetries 617
 Hering's law 410
 Hering's law of equal innervation 408
 Hering-Bielchowsky afterimage test 46
 Hering-Hillebrand deviation 58
 Herman grid 474
 Hess effect 539
 Heterotropia —see Strabismus
 Higher-order feature 77
 Horizon plane 38
 Horizontal cells 109
 Horizontal disparity 247
 Horizontal size ratio 255, 295
 Horopter 35, 48-62
 anatomical 49
 effects of cyclovergence 51
 effects of gaze elevation 51
 empirical 53
 equal-distance 57
 fusion 53
 history of 15
 horizontal 48
 in oblique gaze 51
 line 52
 nonius 55
 optical 48
 theoretical 48
 vertical 51
 zero-disparity 54
 Horopter default rule 520
 Howard-Dolman test 151, 620
 Hyperacuity 98
 Hyperbolae of Hillebrand 386
 Hypercolumns. 123
 Hypercyclopean level 497
 Hyperphoria 387
 Hypophoria 387
 Hysteresis 91
- Ideal observer 93
 Impact direction 555
 Impulse 85
 Impulse-code 70
 Inclination 417
 Inclined surfaces
 disparities on 268, 280
 Induced effect 285, 464
 in motion parallax 581
 Induced visual motion 377, 466, 532
 Inferotemporal cortex 83, 126
 Interblobs 123
 Interference 107
 Intermediate zone 610
 Intermodal 78
 Interocular axis 38, 48
 Interocular transfer 102, 370-380
 in stereoblindness 637, 639
 of contingent aftereffect 378
 of figural induction effects 370
 of motion aftereffect 375-6, 640
 of tilt aftereffect 640
 of spatial-frequency shift 377
 of tilt contrast 373
 Intracortical inhibition 630
- Intramodal 78
 Inverse cyclopean stimulation 590
 Inverse optics 574
 Inverted image 8, 11
 Irradiation stereoscopy 309-10
 Isoazimuth 236
 Isodisparity circles 248
 Isodisparity cylinder 248
 Isodynamic cells 22, 132
 Isoelevation 236
 Isoluminance 143
 Isovergence locus 385
- Jumping spiders 647
- Kaleidoscope 21
 KDE—see Kinetic depth effect
 Keplerian projection 42, 212
 Kinetic boundary disparity 448
 Kinetic depth effect 442, 527
 Knapp's law 63
 Koffka's ring 476
- Labelled-line code 73
 Lacy depth 230
 Lateral eyes 645
 Lateral geniculate nucleus 33, 83, 111, 124, 346, 626
 binocular interactions 113
 and binocular rivalry 345
 development 608
 and visual deprivation 627
 Lateral suprasylvian area 132
 Law of common binocular directions 594
 Law of common monocular directions 593
 Law of cyclopean projection 594, 598
 Law of headcentric direction 593
 Law of oculocentric direction 593
 Learning 104
 effects on cortical tuning 129
 LGN—see Lateral geniculate nucleus
 Line horopter 48
 Line-spread function 87
 Linear system 84
 Lines of latitude 38
 Lines of longitude 37
 Listing's law 383, 598
 Listing's plane 383
 Local rigidity 574
 Local-sign 73, 97, 103
 exclusion rule 73
 Locus coeruleus 113, 629
 Locus of zero parallax 557
 Locusts 648
 Long-range motion 568
 Long-term potentiation 615
 Looming
 detection in animals 557
 Looming detectors 558
- Mach bands 389, 474
 Mach-Dvorak effect 535, 540

- Macropsia 431
 Maddox-rod test 388
 Magnification factor 114
 Magnocellular laminae 110, 115, 608
 Magnocellular system 112, 126-28, 143
 Mantis 646
 Mantis shrimp 73
 Masking 88, 100, 364
 of stereopsis 176
 Matching disparate images 212-230
 Maxwell's spot 46
 McCollough effect 378
 Medial longitudinal fasciculus 425
 Medial superior temporal area (MST) 126, 530
 Median plane 48
 Meridional afocal lens 65
 Meridional amblyopia 632
 Metacontrast 369, 524
 Metameric matches 96
 Metameric systems 75, 78-9, 98
 Method of constant stimuli 93
 Method of limits 93
 Metre angle 395
 Meynert cells 124
 Micropsia 431
 Middle temporal area 88, 124, 126, 135, 346, 530
 Modal completion 77
 Modulation transfer function 85, 86, 107
 Monocular camouflage 512
 Monocular deprivation 626
 Monocular diplopia 46
 Monocular occlusion 512
 and stereopsis 516
 Monocular rivalry 334
 Monocular zones 220, 512
 Monopolar detector 72
 Mosaic dominance 328
 Motion
 dichoptic 567
 Motion aftereffect 101, 375
 and binocular rivalry 343
 dichoptic 571
 in stereoblindness 639
 Motion coherence 526
 Motion coherence detector 76
 Motion in depth 589, 634
 binocular cues 562
 physiological mechanisms 564
 Motion parallax 430, 571-584, 647-48
 and disparity 578
 contrast effect 580
 individual differences 584
 induced effect 581
 Motion perspective 441
 Motion-defined shape 527
 Motion-distance invariance principle 430
 MST—see Medial superior temporal area
 MT—see Middle temporal area
 MTF 107
 Muller-Lyer illusion 305, 524, 587
 Multichannel models 491-4
 Myelination 607
 Near cells 134
 Near triad 394
 Nearest neighbour rule 220
 Neck-tonic reflex 618
 Nerve growth factor 629
 Neural oscillation 83
 Neural summation 349, 637-38
 Neurotrophic growth factor 606, 613
 Neurotrophins 606
 Newton-Müller-Sudden law 34
 NMDA 614, 629
 Nodal point 31
 Nonius 55, 389, 418
 Nonlinear system 85
 Nonlinearities 91
 Noradrenaline 629
 Normalization 118, 463, 465-8, 490
 Norms 101
 Nyquist limit 97, 107
 Nystagmus
 congenital 608
 Oblique effect 588
 Ocular dominance 633
 Ocular dominance
 columns 120, 122, 126
 development 613
 effects of visual deprivation 628
 scale 122
 Ocular parallax 593
 Oculocentric direction 591
 Oculocutaneous albinism 642
 of disparate images 597
 Oligodendrocytes 607, 613
 Ommatidia 646
 Operant conditioning 619
 Ophthalmoplegia 425
 Opponency 79
 Opponent system 143
 Oppositional stimuli 101
 Optic array 32, 235, 572
 Optic axis 31, 105
 Optic chiasm 12, 131
 Optic flow field 32, 126
 Optic radiations 33
 Optic tectum 649, 651
 Optic tract 33, 132
 Optic vesicle 605
 Optical horopter 48
 Optics 4
 Optokinetic nystagmus 335, 381, 415, 529, 589, 616, 643
 in amblyopia 632
 Optometer 394, 428, 604
 Orbital layer 424
 Orientation columns 119
 Orientation disparity 202, 257, 272-5
 Orientation sensitivity
 development 616
 Orientational selectivity 622
 Orthometria 414
 Orthophoria 387
 Orthotropia 387
 Oscillopsia 643
 Owls
 stereopsis in 655
 Panoramic vision 652
 Panum's fusional area 13, 42, 53, 159, 315
 Panum's limiting case 217, 307-8, 518, 520-23
 Paracontrast 369
 Parallax
 absolute 572
 curvature 577
 Parietal lobe 125-29
 Parvocellular laminae 110, 115, 608
 Parvocellular system 112, 124, 126, 143
 Patent stereopsis 159
 Perception of slant 258
 Perimeter system 383
 Perspective 9, 575
 Perturbation analysis 437
 PET scan 126
 Phantom fringes 378
 Phase-dependent aftereffects 495
 Phase-independent aftereffects 495
 Phase spectrum 85
 Phoria 387
 Phorometer 388
 Photophobia 642
 Physiological nystagmus 382
 Pigeon
 stereopsis in 653
 Pinhole camera 7
 Plane of elevation 38
 Plane of regard 246
 horizontal 38
 monocular 38
 vertical 39
 Plexiform layer. 109
 Poggendorff illusion 305, 587
 Point horopter 48
 Point of subjective equality 93
 Point-spread function 72, 86, 107
 Polar disparities 37, 258, 271
 Pontifical cell 78
 Ponzo illusion 524, 587
 Postcontraction 432
 Postoptic commissures 651
 Postsynaptic potentials 109
 Postural aftereffects 432
 Precision 93
 Preferential looking 618
 Preferred direction 120
 Preferred disparity 133
 Preferred orientation 118
 Prefrontal cortex 127
 Prestriate cortex 124
 Pretegmental 125
 Primary feature 72
 Primary position of gaze 382
 Prism dioptre 396
 Probability summation 100, 350, 440, 637
 Probit analysis 94
 Projection 611
 Projection columns 112
 Proprioception 641
 Protostereopsis 262
 Proximal vergence 398
 Pseudoscopic viewing 456, 487
 Psychometric function 93
 Psychophysical methods 92

- Pulfrich effect 535
 and contrast 548
 and dark adaptation 545
 and dynamic random noise 551
 and eye movements 549
 and stereoblindness 554
 and visual latencies 545
 Pulvinar 125
 Pupils 621
 Pyknostereopsis 182
 Pyramidal cells 116, 125, 611, 613
- Qualitative stereopsis 159
 Quantal efficiency 158
 Quantized signal 70
- Rabbit
 stereopsis in 656
 Random spatial-disparity hypothesis. 552
 Random-dot kinematogram 568
 Random-dot stereogram—see Stereograms
 Range-finder 2, 242
 Rayleigh criterion 97
 Reaching 618
 Receiver operating characteristic 95
 Receptive field 109, 117
 offset 133
 Receptor potential 71, 109
 Rectification 91
 Recurrent inhibition 83
 Relative disparities 243
 Relay cells 111
 Resolution 96
 Reticular formation 425
 Retina 10, 83, 106, 111
 development 605
 Retinoscope 394
 Reverse patching 633
 Reversible perspective 587
 Ricco's law 72, 96
 Rigidity constraint 574
 Rivaldepth 307, 504, 586
 Rivalry contrast threshold 329
 Robotic stereo system 244
 Rod-and-frame effect 524
 Rods 106
 Rotation in depth 565
 Rotundus 653
 Rubin's cross 507, 524
- Saccadic suppression 539
 Salience 472
 Satiation 490
 Scaled relative nearness 305
 Scaling 95
 Scanning retinas 647
 Second-order disparities 253
 Secondary features 74
 Secondary position of gaze 382
 Semantic priming 347
 SfM—see Structure from motion
 Shape index 301-3, 581-2
 Sheep
- stereopsis in 656
 Spherical coordinate system 236
 Shifter circuit 178, 401
 Short-range motion 568
 Siamese cats 132, 642
 Sieve effect 307, 515
 Sighting eye 596
 Signal analysis 87
 Signal detection theory 94
 and binocular summation 351
 Silent eye 123
 Similar-surface default rule 520
 Similarity rule 45
 Simple cells 118, 141
 Simultaneous contrast 465, 580
 Simultaneous spatial disparity 539, 544
 Size-disparity correlation 172
 Slanted surfaces
 disparities on 254, 265
 Smooth-pursuit 530
 Space eikometer 65
 Space horopter 48
 Spatial frequency 100
 discrimination 79
 Spatial zones of binocular rivalry 336
 Spatial-frequency aftereffect 342, 377
 Spatial-frequency masking function 366
 Spatiotemporal averaging 542, 544
 Specific nerve energies 73
 Specific-distance tendency 430
 Speed constancy 458
 Splenium 132
 Staircase method 94
 Station point 31
 Statistical efficiency 158
 Stellate cells 115
 Stereo gain 150
 and spatial scale 175
 Stereoacluity 150
 and colour 172
 and contrast 168
 and disparity modulation 161
 and disparity sign 166
 and eccentricity 159
 and eye movements 177
 and interocular differences 170
 and other acuities 180
 and practice 191
 and spatial scale 173
 and stimulus motion 187
 and stimulus orientation 167
 and stimulus spacing 160
 and temporal modulation of depth
 187
 and vergence 179
 contrast-sensitivity function 169
 tests 151
 types 182
 Stereoanomalies 623
 Stereoblindness 637
 Stereograms
 dynamic random-dot 135, 142, 146,
 589
 random-dot 135, 151, 195,
 Stereomotion scotomata 563
 Stereomovement suppression 189, 208
- Stereopsis
 and disparities of texture 203
 and interocular delay 186
 and interstimulus delay 186
 and isoluminance 206
 and orientation disparity 201
 and vergence 229
 anisotropy 462
 as preattentive feature 209
 disparity limit 159
 from contrast gradients 310
 from geometrical illusions
 from rivalry 307
 processing time 183
 qualitative 159
- Stereoscopes
 polaroid 26
 prism 24
 shutter
 types of 24-30
 Wheatstone 24
- Stereoscopic accuracy 150
 Stereoscopic vision 2
 coarse 132
 development 617
 effects of brain damage 624
 fine 132
 history of 13
 in animals 645
 in the midline 132
 tests 620
- Stiles-Crawford effect 73, 107, 307
 Strabismic amblyopia—see Amblyopia
 Strabismic suppression 634
 Strabismus 46, 637, 387
 comitant 387
 noncomitant 387
- Striate cortex—see Visual cortex
 Stripe of Gennari 114, 610
 Stroboscopic Pulfrich effect 541
 Strong fusion 437
 Structure-from-motion 444
 Structure-from-motion disparity 448
 Subjective contours—see Cognitive
 contours
 Subplate zone 614
 Subthreshold summation 88, 100, 349, 439
 Successive contrast 465, 580
 Sulci 609
 Superior colliculus 113, 125, 627, 640
 Superior temporal sulcus 126, 132
 Superposition 84
 Suppressed stimulus 328
 Suppression theory of binocular vision
 314, 338
 Surface continuity 505
 Surface-in-depth detector 76
 Systems analysis 85
- Tau 554
 Tectum 614
 Telencephalon 651
 Telestereoscope 432
 Temporal coding 80
 Temporal contrast sensitivity

- in stereoblindness 638
function 360
- Temporal disparity hypothesis** 551
- Temporal modulation** 80
- Ternus display** 570
- Tertiary position of gaze** 382
- Tetrodotoxin** 614
- Texture segregation** 506
- Thalamus** 6, 651
- Theta waves** 82
- Threshold-elevation effect** 342, 369, 524
- Tilt aftereffect** 101, 342-43, 373, 485, 639
- Tilt contrast** 343, 373
in stereoblindness 639
- Tilt test** 533
- Time invariance** 84
- Time to impact** 554
- Titmus Fly test** 151, 168, 620, 624
- TNO test** 154, 166, 620
- Toads**
stereopsis in 651
- Tokens for stereopsis** 195-212
- Tonic state of vergence**
and perceived distance 433
- Topographic code** 73
- Torsion** 384
- Trading function** 103, 435
- Transfer function** 84
- Trinocular stereo** 573
- Triplopia** 46
- Troxler effect** 335, 337
- Tuned inhibitory cells** 134
- Tuning function** 75
types 62
- Two-channel models** 490-2
- Unique-matching rule** 217
- Utricular discrimination** 600
- V1** 114
- V2** 125, 134
- Vection** 534
- Venetian blind effect** 310
- Ventricular zone** 610
- VEP**—see **Visual evoked potentials**
- Vergence** 243, 426
and paresis 414
and the vestibuloocular response 415
as cue to distance 428-431
asymmetrical 59
disparity 399
disparity threshold 401
effects on disparity 43
fusion-lock component 404
gain 403
in amblyopia 632
in frogs 651
in rabbit 656
latency 402
models 407
neurology 424
proximal 399
range 400
stability 401
trigger component 404
angle 48, 385
- Vergence burst-tonic cells** 426
- Vergence-angle cells** 425
- Vergence-burst cells** 425
- Vernier acuity**
effects of amblyopia 632
- Version** 382
- Vertical disparity** 135, 247, 280
absolute 281
in frontal surfaces 292
relative 281
- Vertical height disparity** 247
- Vertical horopter** 48, 60
theoretical 50
- Vertical size ratio** 249, 282, 576
- Vestibular nucleus** 530
- Vestibular system** 415
- Vestibuloocular response** 179, 381, 529
and vergence 415
and viewing distance 416
in albinism 643
- Vieth-Muller circle**, 15, 18, 58, 249, 594, 598
- Viewing-system parameters** 243, 283, 285
- Virtual disparity** 543
- Vision**
history 4
- Visual acuity**
and visual deprivation 635
- Visual axis** 31, 105
- Visual beats** 638
- Visual cliff** 618
- Visual cortex** 82, 114, 115-124-25, 127, 609
development 609
horizontal connections 116, 346, 612
lamination 610
- Visual direction** 591
- Visual egocentre** 591
- Visual evoked potentials** 47, 144-148, 616
and binocular rivalry 346
and visual development 620
- Visual field** 32
- Visual latency** 545
- Visual line** 31, 591
- Visual masking** 349
- Visual pathways** 13
in albinism 642
- Visual streak** 645, 656
visual 42
- Visually guided movements** 618
- Visually triggered movements** 618
- Volkmann discs** 60, 418
- W-cells** 608
- Wallpaper illusion** 43, 431
- Wavelet theory** 90
- Weak fusion** 437
- Whole field parameter** 266
- Width resolution** 97
- Wiener kernels** 92
- Wulst** 654
- X cells** 110
- Y cells** 110, 627
- Zero crossings** 90, 197
- Zero-order disparities** 492
- Zöllner illusion** 305, 587
- Zone of clear single binocular vision** 398